ECO STP 2023

6th IWA International Conference on eco-Technologies for Wastewater Treatment

GIRONA- SPAIN
26th-29th June

ICRA Catalan Institute for Water Research

lequia UdG ECO-INNOVATIVE ENVIRONMENTAL SOLUTIONS

Universitat de Girona

CONFERENCE PROCEEDINGS

INDEX

ECOSTP 2023

6th IWA International Conference on eco-Technologies for Wastewater Treatment

GIRONA- SPAIN
26th-29th June

Following the previous successful IWA ecoSTP conferences (Spain 2012, Italy 2014, UK 2016, Canada 2018, Italy 2021), it is our great pleasure to welcome you to the 6th IWA International Conference on eco-Technologies for Wastewater Treatment to be held from June 26th to 29th, 2023 in Girona.

ecoSTP-23 aims to discuss the latest cutting-edge eco-technologies for a sustainable transition in wastewater treatment, reuse, and resource recovery, at urban and industrial scale, giving special attention to the efficient transfer of knowledge into practice. Building a more resilient future for water management needs a transdisciplinary and multi-domain examination, including socio-economic and governance aspects. ecoSTP23 will include hydro-social aspects and the multiple factors that currently frame water management.

Maite Pijuan and Ignasi Rodriguez-Roda

Co-chairs of ecoSTP23

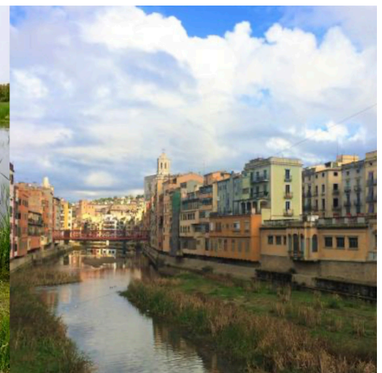

LOCAL ORGANISING COMMITTEE


Gaetan Bladin
(UdG)


Teresa Bosch
(UdG)


Gianluigi Buttiglieri
(ICRA)

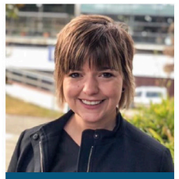
Alba Cabrera
(UdG)

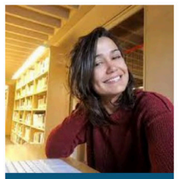
Joana Castellar
(ICRA)


Lluis Corominas
(ICRA)


Joaquim Comas
(UdG/ICRA)


Neus Collado
(ICRA)

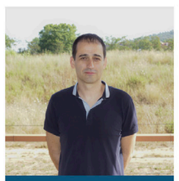
Oriol Gutierrez
(ICRA)


Albert Magrí
(UdG)


Hector Monclus
(UdG)


Luís Rafael López de León
(LEQUIA)


Maite Pijuan
(ICRA)


Alexandra Popartan
(UdG)


Josep Pueyo
(ICRA)


Sebastià Puig
(UdG)


Jelena Radjenovic
(ICRA)


Ignasi Rodriguez-Roda
(UdG)


Sara Rodriguez
(ICRA)

PROGRAM COMMITTEE


Manuela Antonelli
(U. Politec de Milano)


Juan Baeza
(UAB)


Gianluigi Buttiglieri
(ICRA)


Zeynep Cetecioglu
(KTH, Sweeden)


Jesús Colprim
(UdG)


Francesco Fatone
(U. Politec. De la Marche)


Juan Lema
(USC)


Ted Mao
(M W Technologies)


Maite Pijuan
(ICRA)


Manel Poch
(UdG)


Ignasi Rodriguez-Roda
(UdG)


Maria Reis
(UNL)


Ana Soares
(Cranfield Univ.)

SCIENTIFIC COMMITTE

MANUELA ANTONELLI. UNIVERSITÀ POLITECNICA MILANO (ITALY)
STEPHANIE APARICIO ANTON. UV (SPAIN)
CARLOS ARIAS. AARHUS UNIVERSITY (DENMARK)
SERGI ASTALS. UNIVERSITAT DE BARCELONA (SPAIN)
NATASA ATANASOVA. UNIVERSITY OF LJUBLJANA (SLOVENIA)
RAMON BARAT. UNIVERSIDAD POLITÉCNICA DE VALENCIA (SPAIN)
GAETAN BLANDIN. LEQUIA-UDG (SPAIN)
MONICA BRIENZA. UNIVERSITY OF BASILICATA (ITALY)
GIANLUIGI BUTTIGLIERI. ICRA (SPAIN)
ALBA CABRERA. UNIVERSIDAD DE GIRONA (SPAIN)
GABRIEL CAPSON-TOJO. INRAE (FRANCE)
MARTA CARBALLA. UNIVERSIDAD DE SANTIAGO DE COMPOSTELA (SPAIN)
JULIÁN CARRERA. UNIV. AUTÒNOMA DE BARCELONA (SPAIN)
ZEYNEP CETECIOGLU. KTH (SWEDEN)
JOAQUIM COMAS. ICRA (SPAIN)
LLUIS COROMINAS. ICRA (SPAIN)
JESUS COLPRIM. UNIVERSIDAD DE GIRONA (SPAIN)
JAN DRIES. UNIVERSITY OF ANTWERP (BELGIUM)
FERNANDO G FERMOSO. INSTITUTO DE LA GRASA. CSIC (SPAIN)
Mª DEL PILAR FERNÁNDEZ POYATOS. UNIVERSIDAD DE JAÉN (SPAIN)
IVET FERRER. UNIVERSIDAD POLITÈCNICA DE CATALUNYA (SPAIN)
XAVIER FLORES-ALSINA. DANMARKS TEKNISKE UNIVERSITET (DENMARK)
RAMON GANIGUÉ. UNIVERSITY OF GENT (BELGIUM)
JOAN GARCIA. UNIVERSITAT POLITÈCNICA DE CATALUNYA (SPAIN)
WOLFGANG GERNJAK. ICRA (SPAIN)
ORIOL GUTIERREZ. ICRA (SPAIN)
JEREMY GUEST. UNIVERSITY OF ILLINOIS URBANA-CHAMPAIGN (USA)
ALBERT GUISASOLA. UNIVERSITAT AUTÒNOMA DE BARCELONA (SPAIN)
HAORAN DUAN. UNIVERSITY OF QUEENSLAND (AUSTRALIA)
ALMUDENA HOSPIDO. THE UNIVERSITY OF QUEENSLAND (AUSTRALIA)
SHIHU HU. AUSTRALIAN CENTRE FOR WATER AND ENV. BIOTECHNOLOGY (AUSTRALIA)
DAVID IKUMI. UNIVERSITY OF CAPE TOWN (SOUTH AFRICA)
PAUL JENSEN. THE UNIVERSITY OF QUEENSLAND (AUSTRALIA)
ULF JEPPSSON. LUND UNIVERSITY (SWEDEN)
EVINA KATSU. BRUNEL UNIVERSITY (UK)
GÜNTER LANGERGRABER. BOKU UNIVERSITY (AUSTRIA)
RAQUEL LEBRERO. UNIVERSIDAD DE VALLADOLID (SPAIN)
YUEMEI LI. TU DELFT (THE NETHERLANDS)
ELEONORE LOISEAU. INRAE (FRANCE)
MIREILLE MARTENS. RIETLAND (BELGIUM)
FABIO MASSI. IRIDRA (ITALY)
GERTJAN MEDEMA. KWR / DELFT UNIVERSITY OF TECHNOLOGY (NETHERLANDS)
ANNA MIKOLA. AALTO UNIVERSITY (FINLAND)
RAUL MUÑOZ. UNIVERSIDAD DE VALLADOLID (SPAIN)
HECTOR MONCLUS. UNIVERSIDAD DE GIRONA (SPAIN)
ADRIAN OEHMEN. UNIVERSITY OF QUEENSLAND (AUSTRALIA)
KRISHNA PAGILLA. UNIVERSITY OF NEVADA (USA)
DOMINIQUE PATUREAU. INRAE (FRANCE)
MIRA PETROVIC. ICRA (SPAIN)
MAITE PIJUAN. ICRA (SPAIN)
SERGIO PONSÁ. UNIVERSITAT DE VIC (SPAIN)
LUCIA ALEXANDRA POPARTAN. UNIVERSITAT DE GIRONA (SPAIN)
BERNHARD PUCHER. BOKU (AUSTRIA)
SEBASTIÀ PUIG. LEQUIA-UDG (SPAIN)
DANIEL PUYOL. UNIVERSIDAD REY JUAN CARLOS (SPAIN)
JELENA RADJENOVIC. ICRA (SPAIN)
ANACLETO RIZZO. IRIDRA (ITALY)
JORGE RODRIGUEZ. KHALIFA UNIVERSITY (UNITED ARAB EMIRATES)
IGNASI RODRIGUEZ-RODA. UNIVERSIDAD DE GIRONA (SPAIN)
PILAR SÁNCHEZ PEÑA. UAB (SPAIN)
NATALIA SERGIENKO. UNIVERSITY OF CALIFORNIA BERKELEY (US)
THOMAS SEVIOUR. UNIVERSITY OF AARHUS (DENMARK)
ANA SOARES. CRANFIELD UNIVERSITY (UK)
MATHIEU SPERANDIO. INSA-TOULOUSE (FRANCE)
SONIA SUAREZ. UNIV. SANTIAGO DE COMPOSTELA (SPAIN)
ANTONINA TORRENS. UNIVERSITAT DE BARCELONA (SPAIN)
PETER VANROLLEGHEM. UNIVERSITÉ LAVAL (CANADA)
INMA VELO. UNIVERSIDAD DE JAÉN (SPAIN)
BERNARDINO VIRDIS. THE UNIVERSITY OF QUEENSLAND (AUSTRALIA)
EVELINE VOLCKE. UNIVERSITY OF GHENT (BELGIUM)
MARIA WIRTH. ALCHEMIA NOVA (AUSTRIA)
LIU YE. UNIVERSITY OF QUEENSLAND (AUSTRALIA)
SORAYA ZAHEDI. INSTITUTO DE LA GRASA-CSIC (SPAIN)
YAN ZHOU. NANYANG TECHNOLOGICAL UNIVERSITY (SINGAPORE)

LOCAL YWP COMMITTEE


Silvia Bolognesi (LEQUIA)

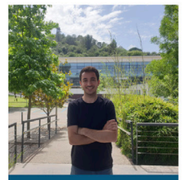
Oriol Carbó Monmany (LEQUIA)


Oriol Casabella Font (ICRA)


Alba Ceballos-Escales López (LEQUIA)


Emma Company Masó (LEQUIA)


Laura Ferrández Galceran (LEQUIA)


Esther Mendoza (ICRA)

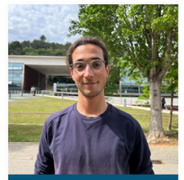
Pere Olives Cegarra (LEQUIA)

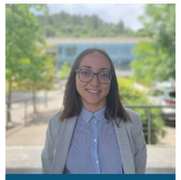
Meritxell Romans Casas (LEQUIA)

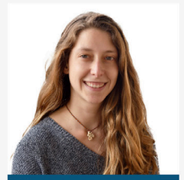
Laura Rovira Alsina (LEQUIA)

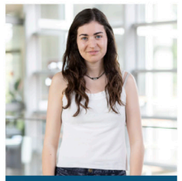
Anna Segués Codina (ICRA)


Bianca Zappulla Sabio (LEQUIA)

PLENARY SPEAKERS

Prof. Zhiguo Yuan

City University of Hong Kong (China)

Exploring New Opportunities for Resource Recovery and Reuse in Wastewater Management

Eva Martinez Diaz

Isle Utilities (united Kingdom)

Navigating towards an innovative and sustainable water industry

Gustaf Olsson

Lund University (Sweden)

Water - key indicator of global warming and basis for energy and food production

Krishna Pagilla

Ralph and Rose Hoeper Engineering Professor

Foundation Professor

Department of Civil and Environmental Engineering Chair

Nevada Water Innovation Institute Director

(United States)

PROGRAM

PRECONFERENCE ACTIVITIES

PC1-PC2 Room	Sala de Graus	Room R1	Room R3
	Urban Biorefineries for circular economy		
Advanced Course Modelling Resource Recovery			
		Workshop: Water reuse and resource recovery at decentralized level in MED area	
Advanced Course Modelling Resource Recovery	Urban Biorefineries for circular economy		
	Urban Biorefineries for circular economy		**Workshop: IWA TG on modelling of phototrophic systems for water treatment**
		Course: Coliphages, the key viral indicator to transform wastewater into reclaimed water	

Room: Sala Sinfònica

Welcome from the Chairs
Maite Pijuan (ICRA) and Ignasi Rodriguez-Roda (UdG)

Conference opening
Catalan Minister of Universities and Research
Hble. Sr. Joaquim Nadal i Farreras
Vicerectora d'investigació i transferència del coneixement (UdG)/
Vice-chancelor for Research and Knowledge Transfer University of Girona
Mrs. Maria Pla de Solà Morales
Sotsdirector (ICRA)/Deputy director (ICRA)
Mr. Sergi Sabater Cortes

Plenary 1
Prof. Zhiguo Yuan (City University of Hong Kong. China)
"Exploring new opportunities for resource recovery and reuse in wastewater treatment"

Plenary 2
Ms. Eva Martínez Diaz (Isle Utilities. UK)
"Navigating towards an innovative and sustainable water industry"

TECHNICAL SESSIONS

T1. N& P recovery

Chairs: Mathieu Sperandio (INSA-Toulouse) & Juan Baeza (Univ. Autonoma of Barcelona)

1.1. Towards a sustainable biorefinery: integrated treatment of the liquid fraction of digestate from the organic fraction of municipal solid waste scale up from laboratory to pilot-scale. Queralt Farras, Eurecat

1.2. Combined water and nutrient recovery from treated wastewater effluents: a case study from Northern Italy. Matia Mainardis, Univ. of Udine

1.3. Recovery of ammonia and phosphate resources from wastewater using gas-permeable membranes. Matias Vanotti, USDA

1.4. Ammonia Removal and Recovery From Municipal Wastewater, Ana Soares, Cranfield Univ.

1.5. NPHarvest efficient nutrient recovery technology for making clean and safe fertilizers. Ana Mikola, Aalto Univ.

1.6. Applying electrodialysis technology for the concentration of nutrients from an anaerobic membrane reactor effluent: operational problems. Patricia Ruiz Barriga. Univ. Valencia

1.7. Pilot Study for Recovery of Phosphate and Ammonia as Struvite from Semiconductor Wastewater. Jhy-Chern Liu. National Taiwan University of Science and Technology.

.8. Effect of suspended solids content on ammonium recovery from pig slurry liquid fraction by liquid-liquid membrane contactors. Rubén Rodríguez-Alegre, LEITAT

T2. N& P recovery II

Chairs: Ana Soares (Cranfield Univ.) & Francesco Fatone (Univ. Polytechnic Marche)

2.1. Optimization of ammonia recovery from urine and digestate using transmembrane chemical absorption. mathieu Sperandio. INSA-TOULOUSE

2.2. Recovery of K-rich struvite after biological nitrogen removal. Emma Company Masó, LEQUIA-UdG

2.3. Phosphorous recovery from waste aerobic granular sludge. Tommaso Lotti. Univ. of Florence

2.4. Recovering vivianite from manure: opportunities and bottlenecks. Sophie Banke. TU Delft

2.5. Nutrient recovery from source separated human urine as vivianite. Chibambila Simbeye. Univ. of Cape Town

2.6. A Comprehensive Assessment of The Opportunities of Integrating a SSSF Into EBPR Systems in view of P Recovery. Mengqi Cheng. Univ. Autonoma of Barcelona.

2.7. Nutrient recovery from hydrolysed urine by Na-chabazite adsorption integrated with ammonia stripping and (K-)struvite precipitation. Haotian Wu. Univ. Laval

2.8. Development and experimental comparison of a precipitation model for struvite using a low-grade magnesium oxide (industrial by-product) as an alternative magnesium source. Beñat Elduayen-Echave. Ceit-BRTA

2.9. BIOFERES: Advanced Recovery of Nutrients from sewage sludge to obtain value-added products for Agriculture: bio-stimulants and liquid fertilizers. Raquel Tamarit Coronado. FACSA

2.10. Continuous bioelectrochemical nitrogen recovery from high N-loaded wastewaters. Zainab Ul. Univ. Autonoma de Barcelona

T3. Water Reuse

Chairs: Jordi Raich (S::can Iberia) & Matia Mainardis (University of Udine)

3.1. Wall2Water, the NAWAMED pilot of living wall for greywater treatment and reuse in Mediterranean countries. Anacleto Rizzo. IRIDRA Srl

3.2. Feasibility assessment of reclaimed wastewater reuse in agriculture: how we do it. Luca Penserini. Politecnico di Milano

3.3. Fertilizer drawn forward osmosis for greywater treatment and subsequent reuse in hydroponics. Esther Mendoza. ICRA

3.4. LIFE AMIA. An innovative combination of wastewater technologies to promote water reuse and sustainable treatment. RUBEN GARCIA TIRADO. Grupo Gimeno

3.5. Towards water self-sufficiency: pilot operation of an off-grid water cycle based on rainwater harvesting and low-tech, biological greywater treatment in an inhabited demonstration house in Switzerland. Devi Bühler. Univ. Gent.

3.6. Tertiary wastewater treatment and natural pigment recovery by cyanobacteria: fate of organic microcontaminants. Marta Bellver Catalá. Univ. Politecnica de Catalunya.

3.7. Plant growth potential of hotel greywater reuse in hydroponic system. Josephine Vosse. ICRA

3.8. Integration of forward osmosis into a granular anaerobic membrane bioreactor for low energy and high quality water reuse and energy production: potential and challenges. Pere Olives. LEQUIA-UdG

T4. WW treament for water reclamation

Chairs: Wolfgang Gernjak (ICRA) & Javier Marugan (URJC)

4.1. Comparing Efficiency in Solar Water Treatment: Photovoltaic-LED vs. Compound Parabolic Collector Photoreactors. MARIA DOLORES MOLINA RAMIREZ. Univ. Rey Juan Carlos

4.2. Peroxymonosulfate/Solar process for the simultaneous disinfection and decontamination of urban wastewater at pilot plant scale. Ilaria Berruti. CIEMAT-PSA

4.3. Chlorine-free inactivation of E. coli in water with manganese oxide-doped graphene-based electrodes. Anna Segués. ICRA

4.4. LIFE RECYCLO: Recycling wastewater from small and medium sized laundries with advanced oxidation process. Baptiste Mathon. Treewater

4.5. Innovative Dual Membrane System for Integrated Water-energy Recovery from Municipal Wastewater. Conghui He. Tsinghua Univ.

4.6. Application of UV-B and UV-C light-emitting diodes (LEDs) for the removal of diclofenac in drinking water. Cristina Pablos Carro. Univ. Rey Juan Carlos

4.7. Natural based solutions combined with solar processes at pilot scale for urban wastewater reclamation. Alba Hernández Zanoletty. PSA-CIEMAT

4.8. Assessment of the Integration of a Vermifilter and a Zooplankton-Based Reactor for the Removal of Microcontaminants to Produce Reusable Water. Manuela Hidalgo. Univ. Girona

T5. Removal of recalcitrant and emerging pollutants

Chairs: Manuela Antonelli (Univ.Politec. Milano) & Sonia Suarez (USC)

5.1. Improvement in the pharmaceutical removal from hospital wastewater in a full-scale hybrid PAC-MBR. Paola Verlicchi, Univ. Ferrara

5.2. Long-term performance of an anaerobic membrane bioreactor amended with graphene oxide treating municipal wastewater. Oriol Casabella, ICRA

5.3. The Study of a Hybrid System - Moving Bed Biofilm Reactor and Nanofiltration for the Elimination of Micropollutants in Wastewater. Muhammad Mukhlis Eshamuddin, Univ. Toulouse

5.4. Presence of Organic Micropollutants and Antibiotic Resistance Genes in an Anaerobic-MBR integrated system (SIAM) treating urban sewage. Matias Rivadulla, Univ. Santiago de Compostela

5.5. Bioreactors for immobilized fungus: Application to long-term continuous pesticides removal by Trametes versicolor. Montserrat Sarra, Univ. Autonoma de Barcelona

5.6. Effect of HRT and dissolved oxygen on the fate of pharmaceutical compounds and antibiotic resistance genes in a high-rate activated sludge reactor. Lorena Gonzalez, Univ. Vigo

5.7. Combining Thermophilic Aerobic Reactor (TAR) with Mesophilic Anaerobic digestion (MAD) to improve sludge reduction and pharmaceuticals degradation, Yolaine Bessiere, INSA-Toulouse

T6. Removal of recalcitrant and emerging pollutants II

Chairs: Paola Verlichi (Univ. Ferrara) & Jelena Radjenovic (ICRA)

6.1. Electrochemical degradation of per- and polyfluoroalkyl substances in real waste streams using boron- and borophene-doped graphene sponge electrode. Nick Duinslaeger. ICRA

6.2. Assessment of PFAS pathways for environmental contamination during landfill leachate treatment. Nicola Lancioni. Marche Polytechnic University

6.3. PFAS in textile wastewater: an integrated approach to reduce the environmental risk for their mixture. Beatrice Cantoni. Politecnico di Milano

6.4. Integration of electrochemical processes in a landfill leachate treatment system for removal of the recalcitrant organic load. Nabil Mostefaqui. Université Gustave Eiffel.

6.5. Effective micropollutant depuration by a novel sustainable approach: coupling solar photo-Fenton with regenerated activated carbon. Paula Núñez-Tafalla. Univ. of Luxembourg

6.6. Boosting active sites of municipal sludge-based biochar for Fenton-like degradation toward phenolic contaminants from water. Battuya Byambaa. Water Cycle Research Center

6.7. Adsorption on activated carbon for PFAS removal: should we act at the source or before the discharge into the environment? Manuela Antonelli. Politecnico di Milano

6.8. Electrochemical removal of antibiotics and multidrug-resistance bacteria using graphene sponge electrodes. Natalia Ormeño. ICRA

6.9. Emerging contaminants in sludge treatment reed beds: degradation or accumulation? Alba Martinez i Quer. Aarhus University

6.10. Developing innovative eco-efficient process for Contaminants of Emerging Concern removal in wastewater reuse applications. Beatrice Cantoni. University of Western Ontario

T7. Algal systems for WW treatment and RR

Chairs: Ramon Barat (Univ. Polytecnic Valencia) & Rosario Rodero Raya (INRAE-LBE & Univ. Valladolid)

7.1. Microalgae Biorefinery for Sustainable Recovery of Bioproducts and Bioenergy from Wastewater. Evelyn Ruales Dávila. Univ. Politècnica de Catalunya

7.2. The Effect of Light Cycling in the Formation of Algae-Bacteria Aggregated Flocs. Holly Stolberg. The Univ. of Queensland

7.3. Anaerobic and microalgae-based treatments: potential for virus inactivation during secondary treatment of municipal wastewater. Andres Torres-Franco. Univ. of Valladolid

7.4. Pilot Scale Wastewater Remediation Using Algae Bacterial Aggregated Flocs (ABAF). Andrew Ward. The Univ. of Queensland

7.5. Comparison of High Rate Algal Pond mesocosm performance using filamentous algae or microalgae. Rupert Craggs. Nat. Inst. Water and Atmospheric Research NZ.

7.6. Wastewater grown microalgae as biofertilizer: Contaminants of Emerging Concern, heavy metals and pathogens assessment. Ana Álvarez González. Univ. Politècnica de Catalunya.

7.7. Effect of veterinary antibiotics and heavy metals in the composition and valorization of a consortium of microalgae and bacteria. Elena M. Rojo. Univ. of Valladolid

7.8. Valorisation of microalgae grown in food waste digestate as biofertilizer. Ana Álvarez González. Univ. Politècnica de Catalunya

T8. Digitalization

Chairs: Rafael Gimenez (CETAQUA) & Paula Carrera (Univ. Ghent)

8.1. Fault-tolerant Control in WRRFs: A Practical Approach Using Case-Based Reasoning for Fault Identification. Sanaz Mohebali. modelEAU - Université Laval

8.2. The use of a low-cost monitoring dataset for sewer model calibration. Paul Schütz. Kompetenzzentrum Wasser Berlin

8.3. Real-time monitoring of adsorption processes in wastewater by innovative spectroscopic sensors: a pilot-scale study. Cecilia Bruni. Univ. Politecnica delle Marche

8.4. Water reuse on the move: decision support for reclaimed water network design solutions. Joaquim Comas. ICRA

8.5. Energy optimization in water distribution systems: Data mining and quality forecasting approach for reducing pumping costs. David Abert. LEQUIA, UdG.

8.6. Design and Deployment of sewage Monitoring Stations to Mine Information from neighbourhoods. Jordi Raich. s::can Iberia

8.7. Intelligent control of wastewater treatment plants by agent reinforcement learning. Oscar Emilio Aponte Rengifo, University of Salamanca

8.8. Sustainable technologies and real-time monitoring for treating industrial wastewater: the case study of Solvay chemical plant at Rosignano Marittimo. Marco Parlapiano, Polytechnic University of Ancona

T9. Modelling

Chairs: Joaquim Comas (ICRA) & Ruben Garcia (Grupo Gimeno)

9.1. A novel methodology for modelling SUDS using SWMM and Giswater: Case study on Montjuic Girona/Spain. Nicole Arnaud, UdG

9.2. Elucidating the field of application of 0D and 1D biofilm models integrated with the hydrodynamics of aerobic granular sludge reactors. Arianna Catenacci, Univ. Politecnico de Milano

9.3. Successful strategies for improving energy self-sufficiency at Grüneck wastewater treatment plant in Germany by improved aeration and food waste co-digestion, Konrad Koch, Tech. Univ.Munich

9.4. Mass-balance-based approach in planning a measurement campaign for energy factory Tilburg. David Ysebaert. U.Gent

9.5. Development of a hydraulic and biological model for trickling filters. Model-based assessment of the 6.6operational strategy. Kepa Olaciregui Arizmendi, Ceit-BRTA

9.6. Model-based assessment of alternative modes of operation in a full-scale industrial wastewater treatment system. Xavier Flores-Alsina, DTU

9.7. Modelling the Metabolism and Population Dynamics of Fermentation-Enhanced EBPR Processes. Rhys Thomson, The Univ. of Queensland

9.8. Mathematical modeling of the long-term dynamics of a sulfate-reducing UASB bioreactor from methanogenic to sulfidogenic conditions. Eric Valdés, Univ. Autonoma de Barcelona

9.9. Influence of substrate characterization on trace metal dosing to improve biogas yield during anaerobic digestion: a dynamic model-based study. Susan George, Instituto de la Grasa CSIC

9.10. CFD modelling as an emerging digital tool for the design and optimization of WWTPs: Learnings from two case studies. Hossein Norouzi Firouz, InsPyro

T10. Membranes

Chairs: Watsa Khongnakorn (Prince of Songkla Univ.) & Vicky Ruano (Univ. Valencia)

10.1. Produced water treatment by membrane aerated biofilm reactors at elevated oxygen partial pressures. Borja Valverde. DTU

10.2. Biological Processes Modelling for Integrated MBR Systems: A Review of the State-of-the-Art. Giorgio Mannina. Palermo University.

10.3. Modelling the impacts of operational conditions on the performance of a full-scale membrane aerated biofilm reactor. Xavier Flores-Alsina, DTU.

10.4. (short presentation, 15:00-15:05) Granular Anaerobic Membrane Bioreactor for low-energy domestic wastewater treatment. Lucie Sanchez. Univ. de Montpellier

10.5. (short presentation, 15:05-15:10)Low temperature anaerobic membrane bioreactor (AnMBR) demonstrator plant: effects of influent characterisation and site operation. Matthew Palmer, Severn Trent

10.6. (short presentation, 15:10-15:15)New framework for standardized notation in membrane filtration modelling for resource recovery from municipal wastewater. Valeria Sandoval. Univ. de València

10.7. (short presentation, 15:15-15:20) Recycled membranes for treating urban wastewater using gravity-driven force. Bianca Zappulla. LEQUIA-UdG

T11. Recovery of added value chemicals

Chairs: Albert Guisasola (UAB) & Tommaso Lotti (Univ. Florence)

11.1. An electrochemical strategy by Lithium recovery from waste battery and brine desalination. Alberto Maimone. CETIM Technological

11.2. From Waste Streams to Platform Chemicals. Isaac Owusu-Agyeman. KTH-Royal Institute of Technology

11.3. High-rate production of carboxylic acids from carbohydrate-rich wastewaters. Ramon Ganigué. Ghent University

11.4. CO2 bioelectrorecycling to butyric acid and its upgrade to butanol. Meritxell Romans Casas. LEQUIA-UdG

11.5. Innovative cell platforms to transform CO2 into fine chemicals for the pharmaceutical industry. Elisa Huang-Lin. Univ. Valladolid.

11.6. Recovery of Cu and Zn from liquid anaerobic digestates via S. pasteurii induced carbonate precipitation: influence of pH and volatile fatty acids on metals precipitation. Ailén Maria Florencia Soto. Spanish National Research Council

11.7. Inhibition limits by undissociated acids in mixed culture fermentation and strategies to increase process capacity. Tomás Allegue. Khalifa University

11.8. Thermal hydrolysis pre-treatment has no positive influence on VFA production from sewage sludge. Ander Castro. CETAQUA

T12. Recovery of PHA and SCP

Chairs: Maria Reis (UNL) & Zeynep Cetecioglu (KTH)

12.1. Volatile fatty acids yield and profile during sludge and food waste co-fermentation at different temperatures. Noemí Pérez i Esteban. University of Barcelona

12.2. Exploring the ammonia presence effect on PHA production of a phototrophic-chemotrophic consortium operated under Light-Feast/Dark-Aerated-Famine. Juliana Almeida. Institute for Health and Bioeconomy and UCIBIO

12.3. Top-down engineering of natural phototrophic microbiomes into stable and productive consortia for the production of bioplastics. Eva Gonzalez Flo. Universitat Politècnica de Catalunya

12.4. Bioconversion of H2 to Single Cell Protein by Purple Bacteria consortia: Influence of environmental conditions on microbial kinetics. Rosario Rodero Raya (INRAE-LBE & Univ. Valladolid)

12.5. The potential of H2S- and CO-tolerant hydrogen-oxidizing bacteria to convert sewage sludge into microbial protein through aerobic syngas fermentation. Vincenzo Pelagalli. Univ. of Cassino and Southern Lazio

12.6. Integration of heterotrophic microalgae beads bioreactor in microbial electrosynthesis for bioelectro-conversion of carbon dioxide into bio-oil and proteins. Silvia Bolognesi. LEQUIA-UdG

12.7. Co-treatment of urban wastewater and municipal solid waste by mixed phototrophic cultures to generate PHA by varying organic carbon loads. Sandra Chacón. Universidad Rey Juan Carlos de Móstoles.

12.8. Maximising the production of composition-specific polyhydroxyalkanoates from volatile fatty acids. Anuska Mosquera. Univ. de Santiago de Compostela

12.9. Resources from wastewater: employment of an advanced strategy for polyhydroxyalkanoates (PHA) synthesis and recovery. Antonio Mineo. Palermo University

12.10. Acidogenic fermentation of model carbohydrate/protein mixtures: how does substrate organic composition impact? Ana Vázquez-Fernández. Univ. Autònoma de Barcelona

T13. Energy Recovery

Chairs: Frank Rogalla (AQUALIA-FCC) & Francisca Sousa Braga (DTU & Skanderborg Spildevand A/S)

13.1. Energy recovery from wastewater: ammonia and hydrogen production from nitrogen-containing waste streams. Ruben Asiain-Mira. AQUALIA-FCC.

13.2. Anaerobic microbial electrochemical fluidized membrane bioreactor for domestic wastewater treatment and reuse with energy recovery. Hari Ananda Rao. KAUST

13.3. Optimising anaerobic digesters with thermal pre-treatment by understanding sludge composition full-scale and laboratory results on trace elements and enzyme supplementation. Yadira Bajon Fernandez. Cranfield University

13.4. High-rate Activated Sludge at very short SRT: key factors for process Stability and Performance of COD fractions removal. Joan Canals GSInima- Lequia UdG

13.5. An integrated system to produce bio-based volatile fatty acids for the industry and biogas from sewage sludge. Ander Castro. CETAQUA

13.6. Influence of carbon-coated zero-valent iron-based nanoparticle concentration on continuous photosynthetic biogas upgrading. Edwin Gilbert Hoyos. Univ. de Valladolid

13.7. Enhancing bioelectrochemical hydrogen production from industrial wastewater in a 150 L microbial electrolysis cell pilot plant. Oscar Guerrero. Univ. Autònoma de Barcelona

13.8. Organic loading rate and pH as optimization parameters for biohydrogen production via dark fermentation coupled with microbial electrolysis cells. Jose Antonio Magdalena. LBE-INRAE

T14. Aerobic granulation

Chairs: Liu Ye (UQ) & Damián Amador (FCC-AQUALIA)

14.1. Unravelling the alpha factor for aerobic granular sludge reactors. Laurence Strubbe. Ghent University

14.2. Determining the causes of the deterioration of granules in an aerobic granular sludge continuous flow system. Anuska Mosquera Corral. Univ. Santigao de Compostela

14.3. A Pilot-Scale Study on the Impact of Aerobic Granular Sludge on Membrane Filtration Performance. Eirini Tsertou. University of Antwerp

14.4. Combined Aerobic Granular Sludge and Gravity-Driven Membrane System for Energy-Efficient Wastewater Treatment and Reuse. Hari Ananda Rao. KAUST

14.5. Getting the most out of existing infrastructure: Denmark and Spain put MABR and AGS technology to the test. Nerea Uri Carreno. VCS Denmark

14.6. Dynamics of antibiotic-resistant genes in aerobic granular systems in aerobic granular reactors treating real wastewater. David Correa-Galeote. Univ. of Granada

14.7. Carbon and nitrogen removal from wastewater in a continuous upflow aerobic granular sludge blanket reactor. Anna Lanzetta. University of Naples

14.8. Kinetic characterization of Phosphorus Accumulating Organisms (PAO) and Glycogen Accumulating Organisms (GAO) anaerobic metabolism in Aerobic Granular Sludge (AGS). Jan Pietro Czellnik. University of Florence

T15. Partial nitritation & anammox

Chairs: Jesús Colprim (LEQUIA-UdG) & Jan Dries (University of Antwerp)

15.1. Energy-efficient nitrogen removal from sewage: achieving mainstream partial nitritation/anammox via recurrent multi-stressor floc treatments. Michiel Van Tendeloo. University of Antwerp

15.2. Sustainable Mainstream Deammonification by Ion Exchange and Bioregeneration via Partial Nitritation/Anammox. Sheldon Tarre. Technion

15.3. Kinetic and stoichiometric characterization of a new thermophilic anaerobic ammonium oxidation culture. Lin Zeng. Ghent University.

15.4. Mainstream Aerobic Granular Sludge start-up from HRAS effluent targeting partial nitritation. Oriol Carbó. GS-Inima

15.5. Sensitivity of anammox bacteria under mainstream conditions: combined effect of low temperature and pH with inhibitory concentrations of free ammonia/free nitrous acid. Alba Pedrouso. Univ. de Santiago de Compostela

15.6. Nitrogen Removal/Recovery in the mainstream of a WWTP including ultrafiltration after the primary treatment: Partial Nitrification+Anammox vs. Ion Exchange+Hollow fiber membrane contactors. Jesús Godifredo. IIAMA

15.7. Influence of free nitrous acid on nitrifiers to introduce shortcut nitrification in the mainstream of WWTP. Edyta Laskawiec. Silesian University of Technology

15.8. When its worthwhile to include the nitrite pathway in a WWTP with C/N/P removal? Àlex Gaona. Univ. Autònoma de Barcelona.

15.9. A novel wastewater treatment process incorporating acidophilic ammonia oxidation. Min Zheng. The University of Queensland.

15.10. Long-term effect of shortcut biological nitrogen removal as energy saving strategy for liquid waste treatment. Laura Palli. GIDA spa

T16. GHG & Microbial community dynamics

Chairs: Adrian Ohemen (UQ) & Evina Katsou (Brunel Univ.)

16.1. The long-term full-scale monitoring of GHG from an Australian WWTP demonstrated the upstream carbon capture can stimulate downstream emissions. Liu Ye, The Univ. of Queensland

16.2. Real-time monitoring and data-driven management of N2O generation in biological reactors. Laura Flores. CETAQUA

16.3. Unraveling the N2O emissions from thermophilic nitrification reactors. Ramon Ganigué. Ghent Univ.

16.4. A laboratory-scale study to mitigate greenhouse gas emissions from open sludge lagoons. Sarah Aucote. Univ. of Queensland.

16.5. Nitrous oxide production for nitrogen valorisation on side stream of an urban waste water treatment plant. Lluc Olmo. Univ. Autònoma de Barcelona.

16.6. Low nitrous oxide emissions and its mechanisms in a pilot-scale mainstream Partial Nitritation/Anammox process. Haoran Duan. The Univ. of Queensland.

16.7. Characterization of hydrogenotrophic methanogenic cultures through a novel pressurized headspace-free Hydrogen Uptake Rate methodology. Manuel Fachal. Univ. Autònoma de Barcelona

16.8. Seasonal microbial community dynamics at Lleida WWTP: filamentous bulking and nitrification deterioration events. Sergi Astals. Univ. de Barcelona.

T17. Nature based solutions

Chairs: Blanca Antizar (Isle utilities) & Silvia Bolognesi (LEQUIA-UdG)

17.1. Framework for a quantification approach of resource streams utilized by nature-based solutions in circular cities. Bernhard Pucher. University of Lisbon

17.2. INTEXT Platforms: Innovative hybrid INTensive EXTensive technologies for wastewater treatment in small communities. Damian Amador Cabezali. AQUALIA-FCC.

17.3. Green solutions for treating nitrate and micropollutants in groundwater to meet drinking standards: one year overview. Belén Fernández. IRTA.

17.4. Nature-Based Solution (NBS) as a tertiary wastewater treatment to reduce antibiotics into the aquatic ecosystems. Edward Jair Pastor López. CSIC-IDAEA

17.5. Organic micropollutant removal from urban waters by MULTISOURCE Enhanced Natural Treatment Solutions. Pedro Carvalho. Aarhus University

17.6. Assessment of intensified constructed wetlands for the attenuation of PMT compounds from groundwater and wastewater. Alicia Cano López. IDAEA-CSIC

17.7. Application of novel filling materials in vertical subsurface flow constructed wetlands to treat the UASB effluent of domestic wastewater. Taxiarchis Seintos. National Technical University of Athens

17.8. Challenges and implementation of Nature-based solutions in Southern European countries. Ivan Blanco. AQUALIA- FCC

17.9. A decision-support tool for Nature-based Solutions selection and pre-sizing using hybrid models. Sophie Guillaume. INRAE

T18. Environmental assessment

Chairs: Bernhard Pucher (BOKU) & Mario Ruiz (Aigües de Barcelona)

18.1. Are circular economy strategies environmentally sustainable? Including the end-of-life stage when assessing seafood plastic packaging. Brais Vázquez Vázquez. Univ. de Santiago de Compostela.

18.2. Environmental assessment of bio based Volatile Fatty Acids production from industrial wastewater. Lucía González. CETAQUA

18.3. Minimal liquid discharge desalination circularity and sustainability assessment. João Ribeiro. Brunel University London

18.4. Analysis and comparison of life cycle assessment approaches in mineral and recovered phosphorus fertilizer production. Lori Manoukian. McGill University

18.5. End-user Perspective Life Cycle Environmental Impacts of Wastewater-derived Phosphorus Products. Ka Leung Lam. Duke Kunshan University

18.6. How sustainable is the digitalization of treatment stages for micropollutant removal? Jueying Qian. University of Kassel

18.7. Utilising sustainable value propositions to understand the value creation of circular actions in wastewater systems. David Renfrew, Brunel University London

18.8. Life cycle assessment of on-site nature-based wastewater treatment and reuse systems. Natasa Atanasova. University of Ljubljana

18.9. Sustainability assessment at early stages of technology development: phosphorus recovery for fertiliser from dairy wastewater. Marta Behjat. Chalmers University of Technology

T19. Decentralized systems

Chairs: Pedro Carvalho (DTU) & Laura Rovira (LEQUIA-UdG)

19.1. Lessons learned from phosphorus chemical precipitation in small wastewater treatment plants. Sophie Besnault. INRAE

19.2. Nitrate electro-bioremediation as a decentralised water treatment: from the proof-of-concept to the on-site technology validation. Alba Ceballos-Escalera. LEQUIA-UdG

19.3. Innovative decentralized wastewater treatment project for 400 households and local industry, combining water, nutrient and energy recovery. Bart De Gusseme. Ghent University

19.4. The third route: Techno-economic analysis of extreme water and wastewater decentralization. Irene Barnosell. LEQUIA-UdG

19.5. Occurrence and fate of Organic Micropollutants and Antibiotic Resistance Genes during Separated Decentralised Treatment of Black Water and Grey Water. Francisco Omil. Univ. Santiago de Compostela

19.6. Decentralized hybrid wastewater treatment system for water reuse on a campsite at Costa Daurada. Queralt Plana Puig, EURECAT

19.7. Biocarriers-facilitated Gravity-driven Membrane Reactor for Decentralized Wastewater Treatment under Cold Climate. Bing Wu. University of Iceland

19.8. Freshwater microbial communities as a potential nature-based solution for wastewater tertiary treatment in small facilities. Lluis Bertrans Tubau. BETA Tech Center- Univ. Vic

Workshops

Workshop I.
Sewer Epidemiology

Chairs: Laura Guerrero Latorre (ICRA) & Jorge Rodriguez (Khalifa University)

Development of a method to detect recent human adenovirus F41 variants in wastewater: Is it linked to the new acute hepatitis? Zeynep Cetecioglu, KTH

SARS-CoV-2 surveillance in the wastewater of Stockholm and Malmö: the Swedish perspective. Mariel Perez-Zabaleta, KTH

Surveillance of SARS-CoV-2 in sewage from buildings housing residents with different vulnerability levels. Anna Pico, ICRA

Workshop II.
Urban Hydrosocial Cycle: Why should engineers care?

Chairs: Alexandra Popartan (LEQUIA-UdG) & Josep Pueyo (ICRA)

Assessment of flood vulnerability through a multidimensional index. Ana Noemi Gomez Vaca. Univ. Girona

Eco-cultural technologies for rural and Maori community on-site wastewater treatment in New Zealand, Rupert Craggs, Nat. Inst. Water and Atmospheric Research NZ

Socio-economic criteria for preventing and controlling phosphorus pollution from municipal wastewater effluents. Edgar Martin Hernandez. Univ. Laval

A hydrosocial approach to domestic water users satisfaction through Agent-Based Modelling. Pol Vidal Lamolla. LEQUIA-UdG

Roadmap and strategic routes to mitigate micropollutant occurrence in surface water bodies through WWTP upgrade. Morgan Abily. ICRA

CLOSING CEREMONY

Chair: Prof. Juan Lema, Univ. Santiago de Compostela

Closing Plenary 1

Prof. Gustav Olson, Lund University (Sweeden): *"Water - key indicator of global warming and basis for energy and food production"*

Closing Plenary 2

Prof. Krishna Pagilla, Nevada Water Innovation Institute (USA): *"Drivers and Strategies of Wastewater Reclamation for Potable Reuse"*

Chairs: *Maite Pijuan (ICRA) & Ignasi Rodriguez-Roda (LEQUIA-UdG)*

Closing remarks, Poster & Platform awards and announcement Next EcoSTP25.

TECHNICAL SESSIONS

T1.

N& P recovery

ECO STP 2023

Towards a sustainable biorefinery: integrated treatment of the liquid fraction of digestate from the organic fraction of municipal solid waste scale up from laboratory to pilot-scale

Q. Farràs[1]*, C. Sielfeld[1], C. Bosch[1], J.R. Vazquez[2], A. Gimenez[2], D. de Wilde[3], W. Naessens[3], G. Sánchez[4], E. Albacete[5], F.X. Prenafeta-Boldú[6], J.M. González[7], F. Pastorino[8]

[1]Eurecat Centre Tecnològic de Catalunya, Spain. [2]FCC Aqualia, Spain. [3]Detricon, Belgium. [4]Àrea Metropolitana de Barcelona, Spain. [5]Ecoparc del Besós, Spain. [6]IRTA, Spain. [7]COGERSA, Spain.[8]AMIU Genova, Italy.

*Corresponding author: queralt.farras@eurecat.org

Abstract

A pilot-scale treatment train based on stripping, thermophilic anaerobic membrane bioreactor (tAnMBR) and membrane contactors was operated for more than 260 days to demonstrate the feasibility of the proposed scheme of technologies to recover energy and fertilisers from organic fraction of municipal solid waste (OFMSW) liquid digestate. Studies at bench scale showed that a stripping process working at 55ºC was needed to remove ammonium (68 %) and avoid ammonia inhibition in the tAnMBR. More than 80% of the total chemical oxygen demand (COD) was removed by the tAnMBR operated at 3.1 kgCOD $m^{-3}\cdot d^{-1}$. Membrane contactors recovered close to 100 % of the residual ammonium. At pilot scale, the two-stage stripping unit allowed ammonia removal at a lower extent (39%) due to temperature instabilities, and the tAnMBR, operated at 1.5 KgCOD $m^{-3}\cdot d^{-1}$, removed 84% of the COD.

Keywords

membrane contactors; stripping; thermophilic anaerobic membrane bioreactor (tAnMBR)

INTRODUCTION

The OFMSW represents about 30-40% of the MSW [1],[2] and, therefore, plays an important role in the transformation towards a circular economy. The most preferred treatment for the OFMSW is anaerobic digestion (AD), which produces biogas and digestate. The digestate is usually separated in liquid and solid fractions for a more sustainable management. The liquid fraction is a challenging wastewater, as it is rich in ammonium and recalcitrant organic compounds [3]. This fraction is conventionally treated by aerobic bioprocesses, which are very energy intensive, and are not designed to recover valuable resources contained in this stream. Thermophilic AD is an interesting option to recover the recalcitrant organic matter in the liquid digestate in form of biogas. If this technology is coupled with an ultrafiltration step, a more robust and efficient technology is obtained: thermophilic anaerobic membrane bioreactor (tAnMBR) [4]. NH_4^+ can be recovered in form of ammonium salts. This can be achieved by using a two-stage stripping process coupled to a scrubber [5]. By stripping CO2, the pH of the liquid current can be increased to benefit the efficiency of ammonia stripping, often completely eliminating the need for caustic dosage. NH_4^+ can also be recovered by novel technologies such as membrane contactors [6]. This work aimed to demonstrate at pilot scale an innovative treatment based on (i) tAnMBR and (ii) ammonium recovery by two-stage stripping and/or (iii) membrane contactors, to valorise the liquid fraction of the OFMSW digestate.

MATERIALS AND METHODS

For the tAnMBR, experiments at bench scale were conducted in a glass reactor of 2 L at 55ºC. The reactor was inoculated with thermophilic anaerobic sludge treating OFMSW from the mechanical and biological treatment plant Can Barba (Terrassa, Catalunya, Spain). Once a day, a peristaltic pump fed the reactor with the liquid fraction of the anaerobic digestate from Ecoparc 2 waste management facility (Montcada i Reixac, Catalunya, Spain). The effluent of the reactor was pumped through a tubular ultrafiltration (UF) membrane (Berghof) of 0.03 µm of pore size and 0.012 m^2 of active area. The concentrate from the UF was recirculated to the reactor and the permeate was collected. Biogas production was measured by means of a Ritter's milligascounter. For stripping, a glass reactor (2 L) was operated in batch mode with 2 h of reaction time. Air was fed from the bottom of the reactor at an aeration rate of 0.25 $L\cdot L^{-1}\cdot min^{-1}$. The permeate of the tAnMBR was treated with a hollow fiber membrane contactor module (HFMC) (MiniModule™ 1x5.5, 3M). Experiments were performed by recirculating an acid solution (H_2SO_4, 0.5M, 0.25L) and the waste (0.5L) through the HFMC. The pH of the effluent was adjusted to 12 prior to the treatment with HFMC, to increase the amount of free ammonia. The overall ammonia mass transfer coefficient was determined according to Licon et al. (2016) [7]. The stripping operation at pilot scale was conducted in a 2.5 m^3 reactor and operated in batch mode at 55ºC with 9 h of retention time. Air was fed from the bottom at an approximate aeration rate of 10 $L\cdot L^{-1}\cdot min^{-1}$. The tAnMBR operation was performed in a 50 m^3 reactor at 55ºC. The reactor was inoculated with centrifuge liquid of anaerobic digestion from Ecoparc 2 waste management facility (mesophilic). The reactor was fed once a day with the effluent of the stripping unit. The effluent of the reactor was pumped through a tubular ultrafiltration (UF) membrane (Pentair) of 0.03 µm of pore size and 4 m^2 of membrane area. The concentrate from the UF was recirculated to the reactor and the permeate was collected.

RESULTS AND DISCUSSION

The tAnMBR was operated at bench-scale for 170 days (Figure 1). During the first 14 days, the reactor was operated at an organic loading rate (OLR) of 0.3 kgCOD $m^{-3}\cdot d^{-1}$, treating directly raw waste, composed by 36.90 $gCOD\cdot L^{-1}$ and 3.80 $gN\text{-}H_4^+\text{-}N\cdot L^{-1}$. Progressive accumulation of COD was observed, which could be related to the high ammonia content in the reactor [7]. To reduce ammonia inhibition, stripping technology was applied to the raw waste, and the effect of temperature on ammonium removal was evaluated (see Fig. 2). Considering technical and economic viability issues, 55ºC was selected as an optimal temperature to remove nitrogen. At this temperature, close to 70% of the NH_4^+ in the influent was removed, producing an influent with suitable characteristics for the tAnMBR (24.50 and 0.82 $g\cdot L^{-1}$ of total COD and NH_4^+-N, respectively). On day 36, continuous operation with the tAnMBR was restarted by feeding the effluent of the stripping process (at 55ºC). A stepwise increase of the OLR was performed, from 0.3 until 3.1 kgCOD $m^{-3}\cdot d^{-1}$, resulting in a progressive accumulation of COD inside the reactor (from 2.64 until 13.63 $gCOD\cdot L^{-1}$). However, the obtained permeate remained stable around 3.50 $gCOD\cdot L^{-1}$, achieving a COD removal above 85%. This behaviour can be explained by the accumulation of highly recalcitrant organic matter inside the reactor that was retained by the UF membrane. Average biogas productivity was 0.05-0.10 $m^3\cdot m^{-3}\cdot d$, which is related to the low COD removal inside the reactor (20-50%).

Based on these results, the tAnMBR at pilot scale was operated with stripped raw waste as influent. However, the temperature operation was unstable until an independent heating system was installed for the stripping unit. This instability during the stripping resulted in lower temperatures of operation, which allowed reduced NH_4^+ removal (39%) (Fig. 2), resulting in an effluent with 19.2 and 1.9 g L^{-1} of total COD and NH4+-N, respectively. The higher $NH4^+$-N of this effluent may have impacted the tAnMBR performance, which achieved lower COD removal (84%) compared to the operation at bench scale. However, the biogas productivity was similar (0.06 $m^3\cdot m^{-3}$ d).

On the other hand, residual NH_4^+ in the wastewater (0.80 $NH_4^+\text{-}N\ g\cdot L^{-1}$) from the bench-scale operation was recovered by HFMC technology. The impact of the pH adjustment on membrane fouling and mass transfer due to the precipitation of salts contained in the effluent was assessed by performing experiments with and without filtration pretreatment (Fig. 3). During the first experiments (Exp. 1), 99.8% of the NH_4^+ was recovered after 105 min. Accumulative fouling after only two cycles without any pretreatment in successive experiments (Exp. 2 and 3) decreased the overall mass transfer coefficient by 35%. These results indicate the importance of including an effective pretreatment step prior to the treatment with HFMC. The performance of HFMC at pilot scale still needs to be evaluated.

ACKNOWLEDGMENTS

This work was funded by the European Commission under the Life Programme, in the frame of the LIFE INFUSION project (Grant agreement nº LIFE 19 ENV/ES/000283).

REFERENCES

[1]European Environment Agency (EEA), 2013. https://www.eea.europa.eu. Last access: 10 December 2021.

[2] https://www.eea.europa.eu/publications/bio-waste-in-europe; EEA Report No 4/2020-Biowaste in Europe.

[3]Chuda, A. & Zieminski, K. 2021. Challenges in treatment of digestate liquid fraction from biogas plant. Performance of nitrogen removal and microbial activity in activated sludge process. Energies **14(21)**, 7321.

[4]Ryue, J., Lin, L., Laqa Kakar, F., Elbeshbishy, E., Al-Mamun, A., Ranja Dhar, B. 2020. A critical review of conventional and emerging methods for improving process stability in thermophilic anaerobic digestion. Energy for Sustainable Development **54**, 72-84.

[5]Palakodeti, A., Azman, S., Rossi, B., Dewil, R., Appels, L. 2021. A critical review of ammonia recovery from anaerobic digestate of organic wastes via stripping. Renewable and sustainable energy reviews **143**, 110903.

[6]Darestani, M., Haigh, V., Couperthwaite, S.J., Millar, G.J., Nghiem, L.D. 2017. Hollow fiber membrane contactors for ammonia recovery: current status and future developments. Journal of Environmental Chemical Engineering **5(2)**, 1349-1359.

[7]Gimenez Lorang, A., Vázquez-Padín, J.R., Dorado-Barragán, C., Sánchez-Santos, G., Vila-Armadas, S., Flotats, X. 2021. Treatment of the Supernatant of Anaerobically Digested Organic Fraction of Municipal Solid Waste in a Demo-Scale Mesophilic External Anaerobic Membrane Bioreactor. Frontiers in Bioengineering and Biotechnology **9** 642747.

[8] Licon Bernal, E.E. Maya, C., Valderrama, C., Cortina, J.L. 2016. Valorization of ammonia concentrates from treated urban wastewater using liquid-liquid membrane contactors. Chemical Engineering Journal **302**, 641-649.

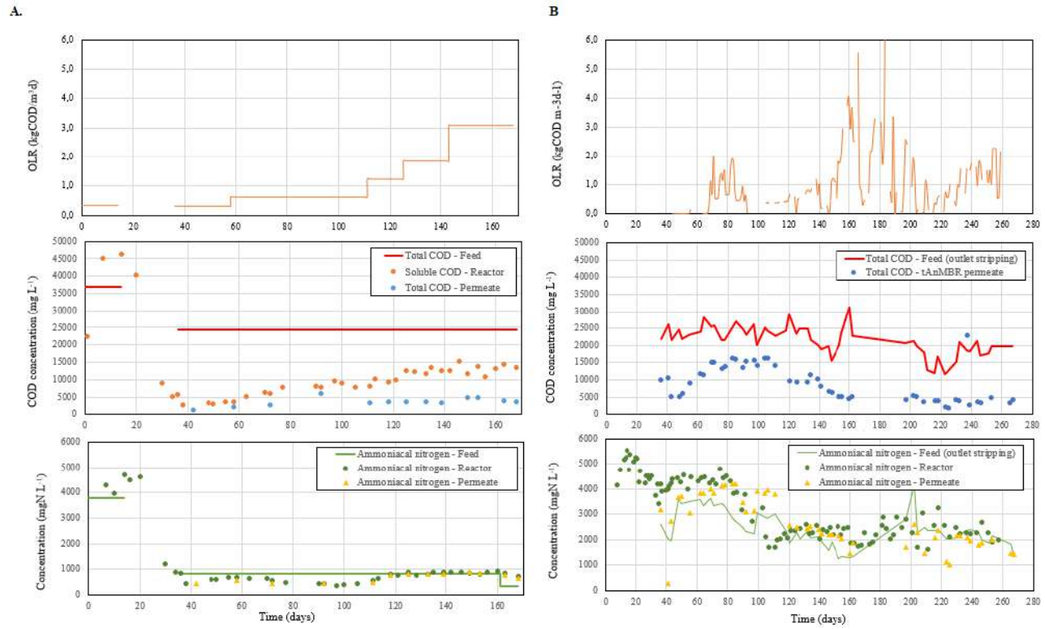

Figure 1. Operation of the thermophilic AnMBR treating the liquid fraction of the anaerobic digestate at bench-scale (left) and at pilot scale (right)

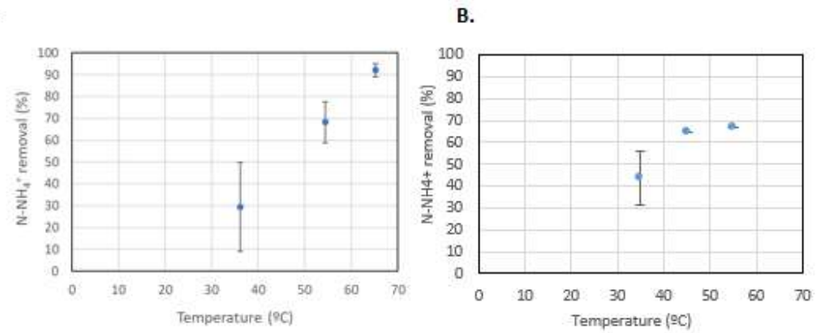

Figure 2. Effect of temperature over the performance of the stripping process at bench scale (A) and at pilot scale (B).

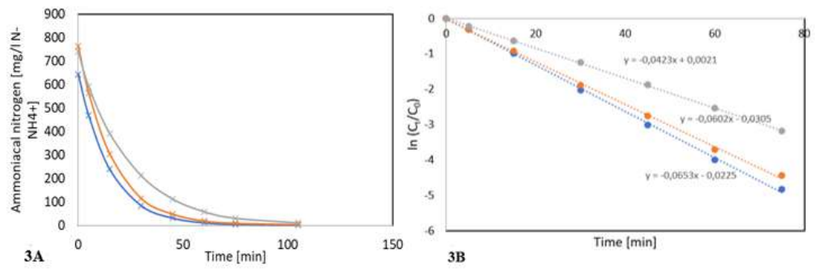

Figure 3. Three HFMC experiments done consecutively at bench scale. In blue experiment 1 (with filtration pretreatment (0,45 µm) after pH adjustment). In orange experiment 2 (no filtration step after pH adjustment). In grey experiment 3 (no filtration after pH adjustment and without cleaning the HFMC module after Experiment 2). **Fig 3A**: NH_4^+ as a function of time. **Fig 3B:** ln (Ct/C0), where C_0 and C_t are the ammonia concentrations at time = t and 0 respectively, was plotted for all experiments to calculate the overall mass transfer coefficient from the slope, according to Licon et al. 2016 [8].

Combined water and nutrient recovery from treated wastewater effluents: a case study from Northern Italy

M. Mainardis*, D. Cecconet**, A. Moretti*, D. Goi*, A.G. Capodaglio**

* Polytechnic Department of Engineering and Architecture, University of Udine, Via del Cotonificio 108, 33100 Udine, IT
(E-mail: *matia.mainardis@uniud.it; moretti.alessandro@spes.uniud.it; daniele.goi@uniud.it)*
** Department of Civil Engineering and Architecture, University of Pavia, Via Adolfo Ferrata 3, 27100, Pavia, IT
(E-mail: *daniele.cecconet@unipv.it; andrea.capodaglio@unipv.it*)

Abstract

Agriculture is the major water consumer sector. Recurring water shortages due to accelerating climate change, which increases the duration of dry periods, boost the exploitation of unconventional water sources. In this framework, treated effluents from wastewater treatment plants can be a reliable and controlled source of water and nutrients for agriculture. A techno-economic assessment methodology was proposed to ascertain the feasibility of reusing effluents from a selected treatment plant in North-eastern Italy to irrigate typical cultivated crops (soybean, maize, rice, vines). A significant reduction in N supply (>40%) could be obtained, while P supply with treated effluents was limited, due to an unbalanced N/P ratio and a lower P use efficiency. As concerns the economic aspects, water saving had a major impact when compared to fertilizer saving. This methodology can be preliminary used in all situations to assess the feasibility of applying fertigation schemes.

Keywords

Agriculture; Fertigation; Nutrient reuse; Techno-economic assessment; Water reuse

INTRODUCTION

Water shortages are increasing worldwide: population growth, climate change, and water quality deterioration are all factors that push for the exploitation of alternative water sources, especially for water-intensive sectors such as agriculture (Jeong, Bhattarai, et al., 2020). Treated effluents from wastewater treatment plants (WWTPs) can be a valuable and controlled water source of water and nutrients for many end-uses, including irrigation.

Through fertigation schemes (combined water and nutrient recovery) from reclaimed wastewater, it is possible to reduce greenhouse gas (GHG) emissions, when compared to traditional fertilization approaches (Jiménez-Benítez, Ferrer, et al., 2020). The nutrients (N, P, K, micronutrients) embedded in treated effluents, in fact, can be recovered, reducing the need for chemical fertilization, showing positive economic, environmental, and sustainability aspects (Chojnacka, Witek-Krowiak, et al., 2020).

However, worldwide the legislative framework for reclaimed wastewater in agriculture is far from being uniform, even if the new European Union Regulation on Reuse (Directive 2020/741) aims to uniformize the requirements for effluents reuse throughout Europe, boosting reuse practices (Mainardis, Cecconet, et al., 2022). Quantitatively, at present the reuse of treated effluents is still limited, accounting for about 0.5% of total freshwater withdrawals, and 2.4% of treated effluents volume in the EU (Gawlik and Alcade-Sanz, 2014), thus further effort is needed to promote this virtuous practice in a safe and controlled way.

In this work, a methodology to preliminary assess the techno-economic feasibility of fertigation practices is proposed and applied to a relevant case study in North-eastern Italy, comparing water and nutrient requirements through traditional irrigation and fertigation and through advanced fertigation. The typical cultivated crops in the area are considered. This simple methodology can be applied in all situations to assess the best match between effluent and crop characteristics.

MATERIALS AND METHODS

The irrigation volumes to be supplied to selected crops were determined based on monthly water balances; Turc equation was employed to determine the effective rainfall from local meteorological data (Trajkovic and Kolakovic, 2009). The net irrigation requirement (L/s ha) was determined by subtracting the effective rainfall from crop evapotranspiration and dividing by the overall irrigation efficiency (Mainardis, Cecconet, et al., 2022).

N and P were considered in the nutrient analysis, due to lack of data concerning K. The specific nutrient requirements of each considered crop (soybean, maize, rice, vines) were used; for the fertigation scenario, the mass balances were drawn considering the volumes of supplied effluents and the nutrient concentration therein. In case the nutrients supplied through fertigation were higher than crop requirement, a limitation was imposed through the reduction of the applied volumes. Two different scenarios were considered in a fit-for-purpose approach (Capodaglio, 2021): actual effluent characteristics and effluent characteristics equal to the legislation standards.

The reduction in CO_2 emissions was calculated by considering emission factors of 5.79 kg CO_2/kg N and 0.633 kg CO_2/kg P for N and P, respectively (Jiménez-Benítez, Ferrer, et al., 2020). A simplified economic analysis was finally conducted to ascertain the savings that could be obtained through fertigation schemes, by considering the cost of commercial fertilizers and water from agricultural consortia.

RESULTS AND DISCUSSION

The investigated crops significantly differed in terms of nutrient and water requirements: maize, soybean and vineyards required irrigation from April to August, while rice required watering from May to September. The maximum water demand was normally encountered in July. The overall water requirements were highest for rice (9,283 m^3/mo ha), followed by maize (10.6% less than rice), grapes (23.2% less than rice) and soybean (29.0% less than rice).

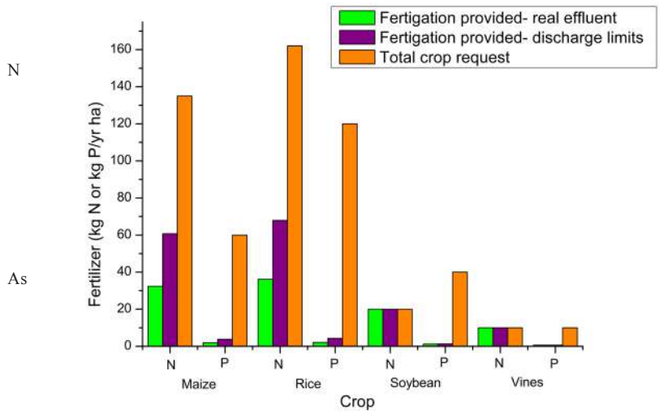

Figure 1. Fertilizers provided by fertigation (kg/ha yr) in comparison with total crop demand.

The amount of nutrients supplied by reclaimed wastewater are shown in Fig. 1. Due to fertigation, a significant reduction in mineral fertilizer dosage could be achieved, while P showed a very limited supply by the effluent. In the second scenario (effluent nutrient concentrations equal to discharge standards), a relevant reduction in mineral N addition (>40%) could be achieved for all crops, while P supply was again extremely low. Soybean and vines, in particular, could be supplied with most of the required N in fertigation schemes. Proper tailoring of wastewater treatment (especially regarding N:P ratio) could lead to improved effluent characteristics for specific crop requirements under a fit-for-purpose approach.

concerns the economic assessment, relevant savings (up to >40%) in mineral fertilizers could be obtained through fertigation. Vines proved to be the most favoured crop, while lower benefits (25%) were calculated for soybean, with maize and rice showing worse performances (respectively 15% and 11% savings). For the two investigated scenarios, the complete results of the economic analysis are summarized in Table 1, while the reduction in nutrients release into the environment and GHG emissions is recapped in Table 2.

Table 1. Water, fertilizers, and total economic savings (€/ha yr) for scenarios 1) and 2).

	Scenario 1 (actual effluent)			Scenario 2 (legislation limits)		
Crop	Water savings (€/ha yr)	Fertilizer savings (€/ha yr)	Total savings (€/ha yr)	Water savings (€/ha yr)	Fertilizer savings (€/ha yr)	Total savings (€/ha yr)
Maize	851	76	927	851	144	995
Rice	952	144	1,096	952	161	1,113
Soybean	526	47	573	281	47	328
Grapevine	263	24	287	140	24	164

Table 2. Saving in fertilizers and GHG emissions for the two analysed scenarios: actual effluent characteristics and legislation limits.

	Scenario 1 (actual effluent)			Scenario 2 (legislation limits)		
Crop	N saving (kg N/ha yr)	P saving (kg P/ha yr)	GHG saving (kg CO_2/ha yr)	N saving (kg N/ha yr)	P saving (kg P/ha yr)	GHG saving (kg CO_2/ha yr)
Maize	32.4	1.9	189	60.7	3.8	354
Rice	36.2	2.1	211	67.9	4.3	396
Soybean	20	1.2	117	20	1.3	117
Grapevine	10	0.6	58	10	0.6	58

Compared to traditional fertilization, fertigation allows a better nutrient use efficiency, improving plant uptake and nutrients availability in the root zone; however, long-term salinity and sodium monitoring is mandatory, due to high sodium adsorption ratio (SAR) levels, sometimes observed in treated effluents.

CONCLUSIONS

The methodological approach developed in the present study can be extremely useful to preliminary ascertain the match between crop water and nutrient requirements and effluent availability and quality in wastewater reuse schemes. The presence/absence of suitable water distribution networks for effluents conveyance to the fields is also an important factor of choice, as well as the availability of appropriate water storage to provide flexibility. The collaboration between stakeholders, from water utilities to agricultural consortia and farmers, is a key point to achieve success. Punctual effluent monitoring and early warning on pollutants and pathogens could reduce the diffused scepticism that still undermines fertigation social acceptance. Further research should involve drawing nutrient balances on monthly bases, considering the different nutrient request throughout plant growing phases, but also considering, besides the positive aspects, the negative factors (such as SAR) that may limit wastewater reuse feasibility.

REFERENCES

Capodaglio, A. G. (2021) Fit-for-purpose urban wastewater reuse: Analysis of issues and available technologies for sustainable multiple barrier approaches. Critical Reviews in Environmental Science and Technology, **51**(15), 1619–1666.

Chojnacka, K., Witek-Krowiak, A., Moustakas, K., Skrzypczak, D., Mikula, K., and Loizidou, M. (2020) A transition from conventional irrigation to fertigation with reclaimed wastewater: Prospects and challenges. Renewable and Sustainable Energy Reviews, **130**, 109959.

Gawlik, B. M. and Alcade-Sanz, L. (2014) Water reuse in Europe: relevant guidelines, needs for and barriers to innovation. Publications Office of the European Union, LU.

Jeong, H., Bhattarai, R., Adamowski, J., and Yu, D. J. (2020) Insights from socio-hydrological modeling to design sustainable wastewater reuse strategies for agriculture at the watershed scale. Agricultural Water Management, **231**, 105983.

Jiménez-Benítez, A., Ferrer, F. J., Greses, S., Ruiz-Martínez, A., Fatone, F., Eusebi, A. L., Mondéjar, N., Ferrer, J., and Seco, A. (2020) AnMBR, reclaimed water and fertigation: Two case studies in Italy and Spain to assess economic and technological feasibility and CO2 emissions within the EU Innovation Deal initiative. Journal of Cleaner Production, **270**, 122398.

Mainardis, M., Cecconet, D., Moretti, A., Callegari, A., Goi, D., Freguia, S., and Capodaglio, A. G. (2022) Wastewater fertigation in agriculture: Issues and opportunities for improved water management and circular economy. Environmental Pollution, **296**, 118755.

Trajkovic, S. and Kolakovic, S. (2009) Wind-adjusted Turc equation for estimating reference evapotranspiration at humid European locations. Hydrology Research, **40**(1), 45–52.

Recovery of ammonia and phosphate resources from wastewater using gas-permeable membranes

M.B. Vanotti*, P.J. Dube**, M.C. Garcia-Gonzalez***, A.A. Szogi*,

*United States Department of Agriculture (USDA), Agricultural Research Service, Coastal Plains Soil, Water and Plant Research Center, 2611 W. Lucas St., Florence, South Carolina 29501, USA. E-mail: Matias.Vanotti@ars.usda.gov

** Water Environment Federation (WEF), Alexandria, VA, USA

*** University of Valladolid, Palencia Campus, Palencia, Spain

Abstract

Phosphorus recovery was combined with ammonia recovery using gas-permeable membranes. In the first step, the ammonia and alkalinity were removed from municipal side-stream wastewater using a gas-permeable membrane manifold. In a second step, the phosphorus was removed using magnesium chloride ($MgCl_2$) and reduced amounts of alkali. The side-stream wastewater contained 730 mg N/L, 140 mg P/L, and 2900 mg/L alkalinity. The process recovered approximately 79-93% of the ammonia and 80-100% of the phosphorus. The phosphates produced were very-high grade (42-44% P_2O_5) with a composition like the bio-mineral newberyite. However, lower-grade phosphate products (27-29% P_2O_5) were produced whenever the N recovery step was bypassed, or carbonate alkalinity was added. Therefore, removing ammonia and alkalinity is important in producing high-grade phosphate products.

Keywords

Ammonia recovery; phosphorus recovery; resource recovery; circular economy

INTRODUCTION

Conservation and recovery of nitrogen (N) and phosphorus (P) from municipal, industrial and agricultural effluents using anaerobic digesters (AD) is important because of economic and environmental reasons.

A promising new method to recover ammonia (NH_3) from wastewater is using gas-permeable membranes (Vanotti and Szogi, 2015). The gas-permeable membrane manifolds are submerged in the liquid manure, and the gaseous NH_3 is removed from the liquid matrix before it escapes into the atmosphere. The N removal is done with low-rate aeration in the reactors that naturally increases the pH of the liquid and accelerates the rate of passage of NH_3 (>96%) through the submerged gas-permeable membrane manifold and further concentration in an acid stripping solution reservoir (Garcia-Gonzalez et al., 2015; Dube et al., 2016). The effluent after ammonia treatment is low in buffering compounds (ammonia and carbonates). In turn, the unbuffered conditions promote phosphorus precipitation reactions.

This work aimed to develop new technology for simultaneous N and P recovery suitable for digester effluents (Vanotti et al., 2018). It combines a gas-permeable membrane technology (N recovery) with P recovery of solid products by precipitation of phosphates. Phosphorus-precipitating compounds such as magnesium chloride (MgCl2) are added to the system after the N removal. Results obtained with municipal side-stream wastewater presented here are consistent with results obtained with livestock wastewater (Vanotti et al., 2017).

MATERIALS AND METHODS

In this example, two steps are used. Ammonia in wastewater is substantially removed in the first step. In the second step, $MgCl_2$ is added to the N-treated effluent in the phosphorus recovery tank (Figure 1). The wastewater was a side stream collected from James River municipal plant, Hampton Roads Sanitation District, Virginia. The side stream wastewater was a centrate effluent from waste sludge subjected to anaerobic digestion and solids separation and contained about 140 mg/L P and 730 mg N/L. The gas permeable membrane module was connected with a stripping solution reservoir containing diluted acid, as described in Dube et al. (2016) and Garcia-Gonzalez et al. (2015). Low-rate aeration was delivered to the bottom of the tank. The gas-permeable membrane was tubular and made of e-PTFE material. A nitrification inhibitor (22 ppm) was added to ensure nitrification inhibition. Concentrated acid was added to the stripping solution to an end-point pH of 1 when the pH increased above about two due to ammonia capture. In a second step, the treated effluent from the N recovery tank was transferred to the phosphorus separation tank, and mixed with $MgCl_2$ and NaOH to obtain a phosphorus precipitate and an effluent without phosphorus or ammonia. $MgCl_2$ was applied to obtain an Mg:P ratio of 1.2:1. Alkali NaOH was applied to pH 9.2. The chemicals were mixed for about one minute. After about a 0.5-hour gravity sedimentation period, the phosphorus precipitate was dewatered using glass-fiber filters and characterized for total N, P, Mg, Ca, and K and plant available phosphorus.

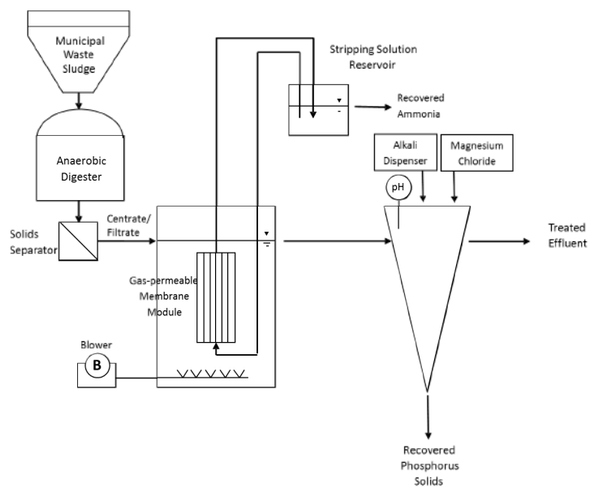

Figure 1. Schematic diagram of nitrogen (N) and phosphorus (P) recovery system using ammonia separation tank and P recovery tank.

RESULTS AND DISCUSSION

Phosphorus recovery of anaerobically digested municipal wastewater via $MgCl_2$ precipitation was enhanced by combining it with the recovery of NH_3 through gas-permeable membranes and low-rate aeration. The low-rate aeration destroyed the natural carbonate alkalinity in the wastewater and increased pH, which accelerated NH_3 uptake in the gas-permeable membrane system (Figure 2). The ammonia capture process substantially reduced carbonate alkalinity, from 2990 mg/L to 90-130 mg/L, and ammonia concentration, from 730 mg N/L to 50 mg/L. These conditions benefited subsequent P recovery. The combined process provided quantitative (ca 100%) P recovery efficiency (Table 1).

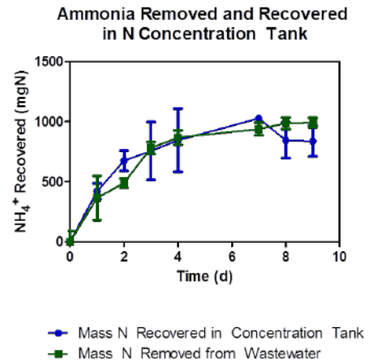

Figure 2. Mass removal and recovery of nitrogen (N) from municipal wastewater using gas-permeable membranes and aeration.

Table 1. Changes in concentration and mass balances for nitrogen (N) and phosphorus (P) using $MgCl_2$ and NaOH. Municipal Wastewater Case 2.

	Influent Concentration	Effluent Concentration	Mass Inflow Initial Manure	Mass Outflow			Total Recovery
				Recovered Solid	Recovered by Membrane	Effluent	
	mg/L			mg (% of initial)			
N	733	60	1100 (100%)	30 (2.73%)	837 (76.09%)	90 (8.18%)	867 (78.82%)
P	133	20	200 (100%)	212 (106.00%)	0 (0%)	30 (15.00%)	212 (106.00%)

With active NH_3 extraction, the magnesium phosphates produced contained higher P_2O_5 grade (42%) with high plant availability (Table 2). The phosphorus product was like the composition of newberyite ($MgHPO_4.3H2O$), a biomineral found in guano deposits, which has approximately 40.8% P_2O_5 and 13.9% Mg composition and a 1:1 P: Mg molar ratio.

Table 2. Composition of recovered solid in the system of Figure 1 using approximately 5.42 mmol/L MgCl2 and about 10 mmol/L NaOH.

N	P (P_2O_5)	Mg	Ca	K	Plant Available P (Citrate soluble)
				%	
2.56	18.30 (42.0)	14.6	1.4	1.9	98.4

However, lower-grade phosphate products (27-29% P_2O_5) were produced whenever the N recovery step was bypassed, or carbonate alkalinity was added (Table 3). Therefore, removing ammonia and alkalinity is essential for making high-grade phosphate products.

Table 3. Effect of ammonia and alkalinity concentration on recovered phosphate minerals.

Conditions before precipitation with $CaCl_2$ (Mg:P = 1.2:1)				NaOH added to pH 9.2 mmol/L	% P recovered by Process	Phosphate mineral composition	
Pre-treatment	NH4-N	Alkalinity	pH			% P_2O_5	% Mg
	mg/L	mg/L					
N recovered	70	90	6.0	8.4	100	42.0	14.6
Added 2 g/L $KHCO_3$, then N recovered	0	1000	8.1	4.4	63	27.4	12.7
None	840	2900	7.6	33.2	99	29.8	10.5

These results showed that it is possible to produce Mg phosphates with high P_2O_5 content by removing the NH_3 from the liquid with the gas-permeable membrane process. This is an important finding because recovered phosphates with high P_2O_5 content are more in line with commercial mineral fertilizers and favored by the fertilizer industry.

REFERENCES

Dube, P. J., Vanotti, M.B., Szogi, A.A., and García-González, M. C. 2016. Enhancing recovery of ammonia from swine manure anaerobic digester effluent using gas-permeable membrane technology. *Waste Management* **49**, 372–377.

García-González, M.C., Vanotti, M.B., and Szogi, A.A. 2015. Recovery of ammonia from swine manure using gas-permeable membranes: Effect of aeration. *J. Environmental Management* ***152***, 19-26.

Vanotti, M.B., and Szogi, A.A. 2015. Systems and methods for reducing ammonia emissions from liquid effluents and for recovering ammonia. U.S. Patent 9,005,333 B1. U.S. Patent and Trademark Office.

Vanotti, M.B., Szogi, A.A., and Dube, P.J. 2018. Systems and methods for recovering ammonium and phosphorus from liquid effluents. U.S. Patent 9,926,213 B2. U.S. Patent and Trademark Office.

Vanotti, M.B., Dube, P.J., and Szogi, A.A. 2017. Recovery of ammonia and phosphate minerals from swine wastewater using gas-permeable membranes. *Water Research* **112,** 137-146.

Ammonia Removal and Recovery From Municipal Wastewater

K.H. Ip*, k, H. Sakar*, M. Palmer **, P. Vale**, A. Soares*,***
*Cranfield Water Science Institute, Cranfield University, Cranfield, MK43 0AL, United Kingdom
** Severn Trent Water, Coventry, CV1 2LZ, United Kingdom
*** a.soares@cranfield.ac.uk, presenting author

Abstract

This study demonstrates the application of ion exchange process to remove and recovery ammonia (NH_4-N) from secondary/anaerobic membrane effluent from a full-scale WWTP. The average NH_4-N concentration fed the IEX was 56.9±9.6 mg N/L at flow if 1 m^3/day, and the IEX process achieved > 90% NH_4-N removal. Four percent NaOH was shown to be the most efficient regenerant for Zeolite-N IEX media used the adsorb the ammonia. The regenerant was used multiple times was able to concentrate ammonia-nitrogen to a high concentration up to 1,750 mg N/L. The ammonia regeneration efficiency peaked at 95.3% and regeneration capacity of 10.0 mg N release/g media. The ammonia was recovered from the regenerant using a hollow fibre membrane contactor (HFMC), and complete recovery of NH_4-N (99.8%) was achieved in the form of ammonium sulphate, which has a potential to be applied as in the production of used for fertilizers, plastics, textile, cleaning products or protein. The obtained data demonstrated that HFMC effectively recovered the ammonia from the regenerant brine establishing the feasibility of IEX-HFMC combined technologies for municipal wastewater treatment, contributing to the circular economy and NET-ZERO targets.

Keywords

exchange; membrane contactors; ammonia recovery

IINTRODUCTION

Ammonia is an essential nutrient in agriculture, with global fertilizer production increasing at around 1.5% per year. Ammonia production to manufacture fertilizers entails 1.5-2.5% of the global energy consumption via Haber-Bosch process. Eventually, ammonia-based fertilizers enter the food and water cycle, ending in wastewater treatment plants. Once there, ammonia is converted into atmospheric N2 in biological processes generating 14-26% of the overall carbon footprint of the wastewater treatment plants (Yea et al., 2018, Cruz et al., 2019). On the other hand, ammonia is a recoverable resource (Darestani et al., 2017). Therefore, developing an effective removal and recovery technology by combination of economic, environmental and energy considerations, would support a sustainable nitrogen cycle.

Ion-exchange process have been tested for ammonia removal and recovery. Despite the potential advantages of ion exchange such as simple operation, high removal efficiency and fast kinetics, regeneration of exhausted zeolite beds produce high concentrated ammonia-nitrogen streams. The feasibility of the process is dependant on the requirement of frequent regeneration periods (with new regenerant solutions each time) and disposal of loaded regenerant as hazardous waste (Lubensky et al., 2019, Huang et al., 2020, Vecinoa et al., 2019). Several processes have been proposed to recover NH4-N from regenerant brines, such as air stripping, steam stripping, and magnesium ammonium phosphate precipitation (Reiga et al., 2021). Among those, membrane contactors provide an attractive alternative due to their simplicity and ability to produce pure product in the form of ammonium sulphate. Regeneration of loaded ammonium zeolites generates rich ammonia concentrates (2–6 g NH_3/L) in brine solutions (NaCl, KCl, NaOH) that is ideal for the integration of hollow fibre membrane contactors (HFMC) (Sancho et al., 2017). HFMC offers a selective ammonia removal with lower energy inputs and without additional chemicals. In HFMCs, volatile free ammonia in the brine transfers across the micro-porous membrane due to a concentration gradient as a driving force provided by reactive acid phase flowing on the lumen side of the membrane, then forming ammonium sulphate upon instantaneous reaction with sulfuric acid on membrane interface (Darestani et al., 2017). The hydrophobicity of the membrane material prevents either liquid from penetrating into the pores, which remain gas-filled, so that only volatile NH_3 transferred across the membrane.

The possibility to recover ammonia from saturated brine promotes a circular approach of resource utilization by enabling the reuse of brine multiple times which decreases the chemical consumption and the production of high purity end product to be used as a fertilizer. The aim of the study is to demonstrate the benefits of ion exchange concentration of NH_4-N in regenerant brine and subsequent ammonia recovery with HFMC in the form of $(NH_4)_2SO_4$.

MATERIALS AND METHODS

For the demonstration scale plant, the AnMBR effluent was obtained from Spernal wastewater treatment plant, 1 m3 a day. The components of the IEX demonstration plant included a compressed air diaphragm pump, a storage tanks for the regeneration chemical 4% NaOH solution), 1 IEX column with zeolite-N for ammonia removal. The IEX columns were filled with 28 L (30 kg) of Zeolite-N. During normal operation, the AnMBR effluent was fed from the top of the IEX column and regenerations were conducted after treating every 2 m^3 of AnMBR effluent. The regenerant flowed into the IEX column from the bottom to give an upward flow for 2 hours. For regeneration of Zeolite-N media, 10 bed volumes (i.e. 278 L). The recovery of ammonia rich brine was performed using an Liqui-Cel 1.7x5.5 MiniModule hollow fibre membrane contactor to obtain ammonia sulphate crystals (Figure 1). The wastewater was analysed with standard methods.

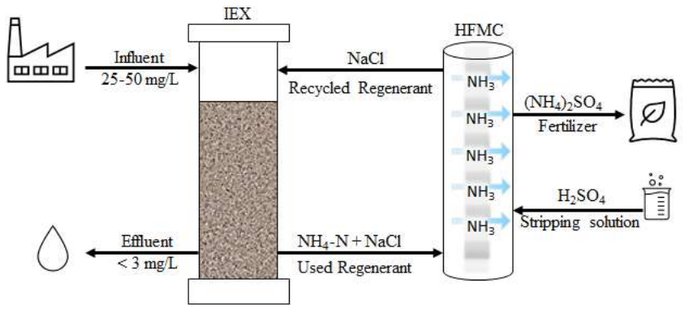

Figure 1 Schematic representation of the IEX and hollow fibre membrane contactor (HFMC) used for ammonia removal and recovery, as ammonium sulphate.

NH_4-N used for fertilizers, plastics, textile, cleaning products or protein production

RESULTS AND DISCUSSION

The influent NH_4-N concentration to the IEX was relatively high at 56.9 ±9.73 mg NH_4-N/L The first 325 bed volumes (BV) operation aimed to reach saturation as far as possible. The effluent NH_4-N concentration increased from 5.3 mg NH_4-N/L and reached 28.6 mg NH_4-N/L, where the peak C/C_0 ratio was 0.6 and the adsorption capacity was 10.6 mg NH_4-N/g media Then the first regeneration was conducted. After the 1st adsorption cycle, the following regenerations were applied after 2 m^3 of AnMBR effluent was treated. Figure 2 shows the IEX influent and effluent NH_4-N concentrations against BV treated from the 2nd to 6th adsorption cycles. Throughout the operation from 1st to 6th adsorption cycles, the average effluent NH_4-N concentration was 1.6 mg NH_4-N/L, with an average removal of 97.3%. When looking at the shape of the curve of the effluent ammonia concentration after regeneration, it is possible to see that concentration took some BV to stabilise, this was likely due to poor rising of the regenerant in between cycles. Nevertheless, the process was efficient and high ammonia removal was achieved.

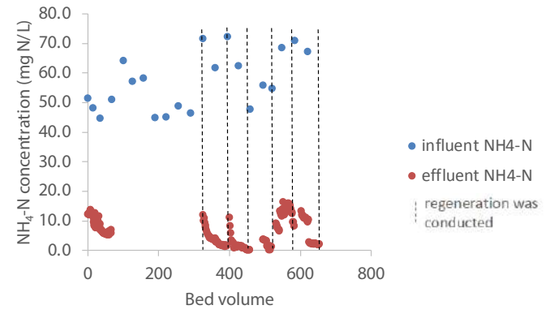

Figure 2 Influent and effluent ammonia concentrations during operation of IEX demonstration plant.

The regenerant accumulated high concentrations of ammonia (Table 1) that could be recovered in the HFMC process. The NH_4-N concentrated in the IEX brine was recovered by HFMC and the recovery efficiency (NaCl 10%, pH 11) reached to 99.8% (complete recovery) after the recirculation of the brine 360 times through the HFMC corresponding to a total operating time of 6.7 hours. In brine with an initial ammonia concentration of 890 mg NH_4^+-N/L was decreased to 25 mg NH_4-N/L after 250 cycles in the HFMC. The dissolved ammonium sulphate that accumulated within the acid side was then recovered as a solid product by evaporation of the acid phase. The chemical characterization of the product recovered from the IEX brine was analysed by energy-dispersive X-ray spectroscopy (EDX) analysis and the elemental composition of ammonium sulphate was identified in atomic percentage which was revealed the purity of the product. The elements comprising ammonium sulphate were solely detected and the proportions were found to be close to the chemical formula of ammonium sulphate (Table 2).

Table 1 Ammonia concentrations in regenerant at the end of each regeneration.

Regeneration cycle	NH_4-N concentration in regenerant (NH_4-N
1st (end)	1,090
2nd (end)	1,540
3rd (end)	1,745
4th (end)	1,750
*5th (end)	334
6th (end)	660

* new regenerant was prepared for the 5th regeneration cycle onwards

Table 2 EDX analysis of the recovered ammonia product.

	Elemental composition (atomic %)		
	N	O	S
Ammonium sulphate (chemical formula)	28.6	57.1	14.2
Ammonium sulphate (recovered product from IEX)	25.5	55.6	18.8

Acknowledgements

We grateful for the funding received funding from the European Union's Horizon 2020 research and innovation program under Grant Agreement No. 777541 (https://nextgenwater.eu).

REFERENCES

Cruz, H., Law, Y.Y., Guest, J.S., Rabaey, K., Batstone, D., Laycock, B., Verstraete, W., Pikaar, I., (2019), Mainstream Ammonium Recovery to Advance Sustainable Urban Wastewater Management, Environ. Sci. Technol., 53(11066/11079).

Darestani, M., Haigh, V., Couperthwaite, S.J., Millar, G.J. and Ngheim, L.D., (2017), Hollow fibre membrane contactors for ammonia recovery: Current status and future developments, J. Environ. Chem. Eng., 5/2(1349/1359).

Guida, S., Van-Peteghem, L., Luquami, B., Sakarika, M., McLeod, A., McAdam, E.J., Jefferson, B., Rabaey, K. and Soares, A., (2021a), Ammonia recovery from brines originating from a municipal wastewater ion exchange process and valorization of recovered nitrogen into microbial protein, Chem. Eng. Sci., 427(130/896).

Guida, S., Conzelmann, L., Remy, C., Vale, P., Jefferson, B. and Soares, A., (2021b), Resilience and life cycle assessment of ion exchange process for ammonium removal from municipal wastewater, Sci. Total Environ., 783(146/834).

Huang, X., Guida, S., Jefferson, B. and Soares, A., (2020), Economic evaluation of ion-exchange processes for nutrient removal and recovery from municipal wastewater, NPJ Clean Water, 3(3079).

Lubensky, J., Ellersdorfer, M., Stocker, K., (2019), Ammonium recovery from model solutions and sludge liquor with a combined ion exchange and air stripping process, J. Water Process. Eng., 32(100/909).

Reiga, M., Vecinoa, X., Giberta, O., Valderrama, C., Cortina, J.L., (2021), Study of the operational parameters in the hollow fibre liquid-liquid membrane contactors process for ammonia valorisation as liquid fertiliser, Sep. Purif. Technol., 255(117/768).

Sancho, I., Licon, E., Valderrama, C., Arespacochaga, N., López-Palau, S., and Cortina, J.L., (2017), Recovery of ammonia from domestic wastewater effluents as liquid fertilizers by integration of natural zeolites and hollow fibre membrane contactors, Sci. Total Environ., 584–585(244/251).

Vecinoa, X., Reiga, M., Bhushana, B., Giberta, O., Valderramaa, C., Cortina, J.L., (2019), Liquid fertilizer production by ammonia recovery from treated ammonia rich regenerated streams using liquid-liquid membrane contactors, Chem. Eng. Sci., 360(890/899).

Yea, Y., Ngo, H.H, Guo, W., Liu, Y., Chang, S.W., Nguyen, D.D., Liang, H.,Wang, J., (2018), A critical review on ammonium recovery from wastewater for sustainable wastewater management, Bioresour. Technol.,268(749/758).

NPHarvest – efficient nutrient recovery technology for making clean and safe fertilizers

J. Uzkurt Kaljunen*, A. Mikola*, R. Al-Juboori**, Hamse Kjerstadius***

*Water and Environmental Engineering Research Group, Department of Built Environment, Aalto University, P.O. Box 15200, Aalto, FI-00076 Espoo, Finland (juho.kaljunen@aalto.fi)

**NYUAD Water Research Center, New York University-Abu Dhabi Campus, P.O. Box 129188, Abu Dhabi, United Arab Emirates

***NSVA, Box 2022, 250 02 Helsingborg, Sweden

Abstract

Nutrients recovery from wastewaters has become a critical issue for European food security. NPHarvest nutrient recovery technology has been developed to provide a profitable pathway to recover nutrients from different waste streams in clean and safe products. The technology was tested with a field scale pilot in RecoLab (Helsingborg, Sweden) with digested black water originating from nearby living areas. P recovery efficiency was 90+% and ammonia recovery in NPHarvest contactor was 70%. The fertilizer products, P-rich solid containing calcium phosphates and liquid ammonium sulphate were analysed for over 300 pollutants, including wide array of heavy metals, pharmaceuticals, and organic pollutants. Despite the digested black water containing significant concentrations of these pollutants, the pollutant contents in the fertilizer products were considerably lower than legislative limits.

Keywords

NPHarvest, nitrogen and phosphorus recovery, recycled fertilizers, wastewater treatment, black water

INTRODUCTION

The nutrients N and P are both a problem and a necessity for us. We would not live without these elements, but we have also changed the natural ecosystems greatly with them (Steffen et al., 2015) by discharging the excess. In addition, the recent developments in the geopolitical landscape, culminating in the Russian attack in Ukraine, have highlighted how vulnerable our food systems are. The EU is especially vulnerable since most of the P used in agriculture is imported (El Wali et al., 2019). This vulnerability culminates in food price volatility, as is the case in the EU in 2022 (Carbonaro, 2022). Nitrogen, on the other hand, is plentiful in the atmosphere. It is bound into reactive forms through the Haber-Bosch process, which consumes a significant amount of global energy (Smith et al., 2020). The top four countries, China, Russia, the United States and India, produced 55% of ammonia in 2021 (Statista, 2022). The energy supply of these countries consists of 76–89% of coal, natural gas, and oil in 2019 or 2020 (IEA, 2022). This leads to significant carbon emissions from N fertilizer production.

Nutrient recovery from waste streams is a viable countering force to these issues. However, wastewaters have a wide variety of pollutants that may be captured with the recovered nutrient products. Currently, the uncertainty of the quantities and effects of these pollutants, especially organic pollutants and pharmaceuticals hinders the use of recycled fertilizers. Thus, it is important to develop nutrient recovery technologies that separate nutrients from pollutants. Furthermore, this should be a cost-effective process to allow wide implementation. NPHarvest technology was developed to be a profitable process (Uzkurt Kaljunen et al., 2021). This study embarked on exploring the quality of NPHarvest end products in detail.

Table 1. NPHarvest product quality compared to municipal wastewater sludge from EBPR plant that is used as fertilizer, commercial struvite made from black water and both Finnish and Swedish legislative limits for fertilizers. b.d.l. = below detection limit.

	Digested black water*	Ammonium salt**	P fertilizer**	Sludge**	Struvite**	Swedish legislation**	Finnish legislation**
Unit	mg/l	mg/kgTS	mg/kgTS	mg/kgTS	mg/kgTS	mg/kgTS	mg/kgTS
Pb	< 0,0050	6,6	0,6	14,6	< 59	100	100
Cd	< 0,0010	b.d.l.	0,11	0,59	< 4	2	1,5
Cu	0,035	3	0,67	348	134	600	600
Cr	< 0,0050	0,3	1,1	29,2	< 4	100	300
Hg	< 0,00010	b.d.l.	b.d.l.	0,45		2,5	1
Ni	0,0082	0,8	5,4	21,1	< 2	50	100
Zn	0,023	149	< 19	497	< 59	800	1500
PAH	0,030	b.d.l.	b.d.l.	0,31			
PCB	0	b.d.l.	b.d.l.	0,04			
Nonylphenols	3,9	b.d.l.	b.d.l.	2,8			
Ibuprofen	350	b.d.l.	0,14	b.d.l.			

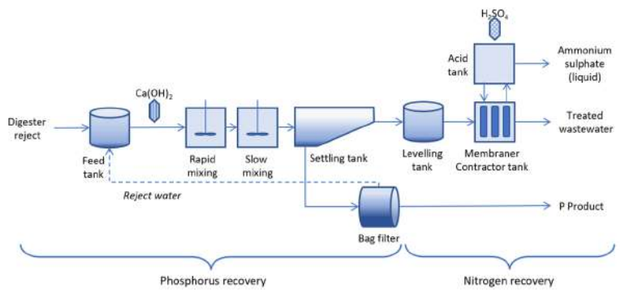

Figure 1. Simplified NPHarvest process schematic.

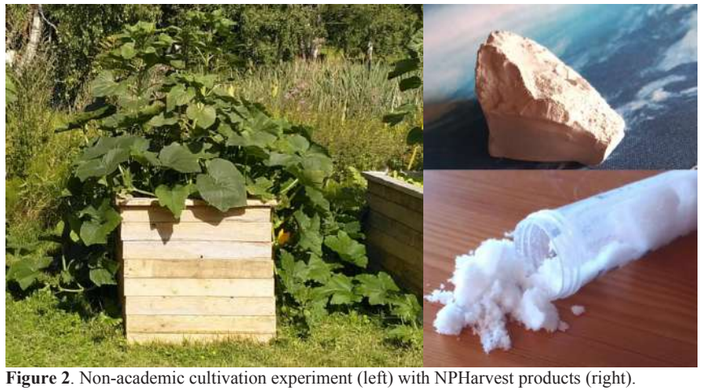

Figure 2. Non-academic cultivation experiment (left) with NPHarvest products (right).

NPHARVEST PROCESS & OPERATIONAL CONDITIONS

Figure 1 presents a simplified process schematic for the NPHarvest process. The process can be divided into two parts: 1) P recovery and pre-treatment and 2) N recovery. In the P recovery phase, the pH of the water is increased to 10+ with Ca(OH)2 which also precipitates P and suspended solids. P-rich sludge is dewatered so that the dry fraction becomes hygienic P fertilizer, and the liquid fraction is returned to the process, so N in the liquid can efficiently be captured. In N

recovery phase the liquid passes through a membrane contactor that has been designed to tolerate relatively high suspended solids concentrations. Hydrophobic membranes passively capture N, in ammonia form, and separate it from the wastewater flow. Ammonia comes in contact with an inorganic acid and reacts forming the N salt products. This product can be crystallized if desired.

The process was continuously operated for two months in Summer 2021 in Recolab, Helsinborg, Sweden. The wastewater was a digested black water collected from nearby apartments. Samples were collected on average 3 times per week from various parts of the process to monitor the process performance. However, detailed pollutant analyses were based on single (but large in mass/volume) samples from influent (digested black water) and recycled products (ammonia salt and P fertilizer).

RESULTS & DISCUSSION

Table 1 summarizes the results of the pollutant analyses, highlighting the most interesting ones out of the over 300 different substances that were analyzed. As can be seen from the first 3 columns, digested black water has noticeable levels of Cu, Ni and Zn. However, the mass concentrations for these metals are not significant in the recycled nutrient products. It is noteworthy that the high Zn concentration in ammonium salt was most likely due to sample contamination. Organic pollutants have also noticeable concentrations in the treated water, but their mass concentrations are below the detection limit for the products. Overall, the product pollutant levels are considerably lower than the legislative limits in Finland or Sweden. Furthermore, they are lower than the fertilizer sludge produced in the same location from municipal wastewater or struvite made from black water (Kern et al., 2008).

During Summer of 2022 we cultivated pumpkin, cauliflower, and sunflower in a non-academic fashion with the produced fertilizers. Inspired by the preliminary results (Figure 2, also showing the fertilizer products), we plan to conduct a proper cultivation test during 2023, focusing on nutrient leaching and growth potential.

CONCLUSIONS

NPHarvest technology has been developed to enhance nutrients recycling possibilities and affordability. The process was operated in a field scale pilot with digested black water and the obtained fertilizer products were thoroughly analyzed. The products, ammonia salt and P-rich solid material have low or non-existent pollutant levels depending on the substance analyzed. Their pollutant levels are lower than competing recycled fertilizers and legislative limits in Sweden and Finland.

REFERENCES

Carbonaro, G., 2022. The rise and rise of Europe's bread prices amid the war in Ukraine [WWW Document]. euronews. URL https://www.euronews.com/my-europe/2022/09/21/the-rise-and-rise-of-europes-bread-prices-amid-the-war-in-ukraine (accessed 10.20.22).

El Wali, M., Golroudbary, S.R., Kraslawski, A., 2019. Impact of recycling improvement on the life cycle of phosphorus. Chinese Journal of Chemical Engineering 27, 1219–1229. https://doi.org/10.1016/j.cjche.2018.09.004

IEA, 2022. Russia - Countries & Regions [WWW Document]. IEA. URL https://www.iea.org/countries/russia (accessed 10.20.22).

Kern, J., Heinzmann, B., Markus, B., Kaufmann, A.C., Soethe, N., Engels, C., 2008. Recycling and Assessment of Struvite Phosphorus from Sewage Sludge. Agricultural Engineering International: CIGR Journal.

Smith, C., Hill, A.K., Torrente-Murciano, L., 2020. Current and future role of Haber–Bosch ammonia in a carbon-free energy landscape. Energy Environ. Sci. 13, 331–344. https://doi.org/10.1039/C9EE02873K

Statista, 2022. Global ammonia production by country 2021 [WWW Document]. Statista. URL https://www.statista.com/statistics/1266244/global-ammonia-production-by-country/ (accessed 10.20.22).

Steffen, W., Richardson, K., Rockström, J., Cornell, S.E., Fetzer, I., Bennett, E.M., Biggs, R., Carpenter, S.R., de Vries, W., de Wit, C.A., Folke, C., Gerten, D., Heinke, J., Mace, G.M., Persson, L.M., Ramanathan, V., Reyers, B., Sörlin, S., 2015. Planetary boundaries: Guiding human development on a changing planet. Science 347, 1259855. https://doi.org/10.1126/science.1259855

Uzkurt Kaljunen, J., Al-Juboori, R.A., Mikola, A., Righetto, I., Konola, I., 2021. Newly developed membrane contactor-based N and P recovery process: Pilot-scale field experiments and cost analysis. Journal of Cleaner Production 281, 125288. https://doi.org/10.1016/j.jclepro.2020.125288

Applying electrodialysis technology for the concentration of nutrients from an anaerobic membrane reactor effluent: operational problems.

P. Ruiz-Barriga*[a], J. Carrillo-Abad [b], A. Bouzas[b], J. Serralta[a], R. Barat[a], José Ferrer[a], A.Seco[b].

a CALAGUA – Unitat Mixta UV-UPV, Institut Universitari d'Investigació d'Enginyeria de l'Aigua i Medi Ambient – IIAMA, Universitat Politècnica de Valencia, Camí de Vera s/n, 46022 Valencia, Spain

*corresponding author. E-mail: patruiba@iiama.upv.es

b CALAGUA – Unitat Mixta UV-UPV, Departament d'Enginyeria Química, Universitat de València, Avinguda de la Universitat s/n, 46100 Burjassot, Valencia, Spain

Abstract

An electrodialysis process (ED) has been applied to the effluent of an Anaerobic Membrane Reactor (AnMBR) as an ion concentration method for the subsequent ammonium and phosphate recovery. Promising results have been obtained regarding ammonium and phosphate concentration efficiencies. However, in areas with high water hardness, precipitation of calcium compounds during the ED process is a bottleneck that avoids the achievement of greater concentration efficiencies needed to the subsequent nutrient recovery. Thus, the objective of this research is to demonstrate the feasibility of the ED process with wastewater with low concentrations of calcium and to deal with precipitation problems when high loads of calcium are present in wastewater.

Keywords

Electrodialysis, nutrient recovery, precipitation, AnMBR effluent.

INTRODUCTION

Nowadays, there is a growing interest in the recovery of nitrogen and phosphorus for fertilizer production from industrial and urban wastewater (Y. Zhang et al., 2013; W. Tarpeh et al., 2018; A. Ward et al., 2018). Currently, different treatments are being used to fertilizer production as crystallization processes for struvite production (L. Pastor et al., 2008; M. Sena and A. Hicks, 2018) or membrane contactors (G. Noriega-Hevia, et al., 2020; W. Rongwong and K. Goh, 2020) for ammonium sulphate and nitrate sulphate production. Nevertheless, the efficiency of these processes would be increased if a previous concentration step was carried out. For that purpose, electrodialysis is a suitable technology. Electrodialysis has been used as an ion concentration method for more than 50 years, mainly to obtain drinking water from brackish water with industrial applicability (H. Strathmann, 2010). Currently, its use has been extended to the treatment of urban and industrial wastewater. Electrodialysis is an electrochemical membrane process based on the electrical field as the electromotive force to separate and/or concentrate anions and cations alternating anion and cation exchange membranes (H. Strathmann, 2010; M. Xie et al., 2016; T.Yan et al., 2018). On the other hand, scaling is a bottleneck on ED processes when high concentrations are reached since the resistance of the system increase significantly due to filter and membrane clogging, leading to a decrease in concentration efficiencies and other operating problems (M. Turek and P. Dydo, 2003; L. Shi et al., 2019). Thus, the main objective of this research is to establish the optimal operating parameters of the ED process to concentrate the ions coming from the effluent of a pilot-scale anaerobic membrane reactor (AnMBR) and, on the other hand, to obtain a dilute stream that reaches discharge limits established in 91/271/EEC Directive concerning urban wastewater treatment. Related to the first purpose of this work, another objective is also to avoid precipitation problems during the concentration process in the way of achieving optimal concentration values of ammonium and phosphate for a subsequent struvite crystallization step and for ammonium sulphate production in membrane contactors.

MATERIAL AND METHODS

The ED equipment was provided by PCCell GmBH (Germany) and consists of a pumping unit (BED 1-2) and a stack of 100 x 100 mm with a maximum of 10 cell pairs (ED 64-002). A PC-SK membrane (PCCell GmbH, Germany) was used as cation exchange membrane and PC Acid 100 OT as anion exchange membrane (PCCell GmbH, Germany), both with an active membrane surface area of 64 cm^2. The main characteristics of membranes are shown in Table 1. Dilute and concentrate streams were fed with 2 L and 1.5 L, respectively, with the effluent of an AnMBR plant, located in the Conca del Carraixet WWTP near Valencia (Spain). The average concentrations of the AnMBR effluent are presented in Table 2. The electrolyte used was 0.01M sulfuric acid with a total volume of 2L. Galvanostatic mode was chosen as work method at 0.24 A. During experiments, conductivity, pH, current and voltage were recorded. Experiments were performed in batch mode, i.e. one cycle was completed when target condition was reached in dilute and concentrate stream. Target condition was a voltage not exceeding 15 V, as they can cause damage to the membranes. After that, dilute tank was fed with fresh AnMBR effluent to complete a new cycle. Flow rate was 50 L/h for dilute and concentrate streams and the electrolyte flow rate was 150 L/h. At the beginning, middle and end of the cycle, samples of each stream were taken to be analysed by ion chromatography (883 Basic IC Plus, Metrohm, Switzerland).

Figure 1. Filter and concentrate tank with $CaSO_4$.

RESULTS AND DISCUSSION

Short-term experiments were done to establish the optimal operating parameters of the ED process. Once these parameters were determined, long-term assays were carried out to demonstrate the feasibility of the ED process for nutrient concentration. The objective was to concentrate up to values around 80-100 ppm of PO_4-P, optimal value for subsequent recovery as struvite (L. Pastor, 2008). During short-term assays high concentrations of NH_4-N were achieved faster than PO_4-P ones, thus no target values of ammonium concentration were established in concentrate stream. pH of concentrate stream was continuously maintained below 3 to avoid salt precipitation. Feed water concentrations, final dilute and concentrate values are shown in Table 3. After 17 cycles, the assay must be stopped due to the precipitation of calcium sulphate, which clogged the system decreasing the flowrate at concentrate stream to 10 L/h (Figure 1). As it can be seen, phosphate target values were not reached in the concentrate stream despite of the high efficiencies obtained. Besides, in dilute stream, phosphate did not reach discharge limits. However, ammonium efficiencies up to 1500% were achieved in concentrate and discharge limits were reached. In order to avoid calcium phosphate precipitation, calcium has to be reduced from the feed stream. Therefore, feed water with a ratio of AnMBR effluent: water of 1:3 was introduced into the system, diluting not only the calcium concentration but also the remaining ionic concentrations. Hence, ammonium and phosphate concentrations were adjusted until typical AnMBR effluent values (Table 4). Results obtained with this influent are shown in Table 3. In this case, both ammonium and phosphate target values were achieved with concentration efficiencies values two and three times higher, for ammonium and phosphate respectively, than the experiment without diluting feed water. Nevertheless, neither ammonium nor phosphate achieved discharge limits, being this last one greater than the one observed in the non-dilute feed water. This can be associated with a shorter duration of cycles due to a decrease in ion concentration in feed water and in consequence to an increase in the resistance of the system. Hence, optimal values of ammonium and phosphate for crystallization process were achieved with higher concentration efficiencies by removing the excess of calcium from feed water. Thus, feasibility of the ED process as concentration method was demonstrated. However, in high calcium loads areas, as the Mediterranean coast, it is necessary to apply an alternative treatment to remove calcium from concentrate stream. Thus, two different options are being studied: i) a previous treatment for ED by cationic exchange resins application or ii) a 3 chamber ED configuration with selective monovalent cation exchange membranes that allows to separate divalent cationic streams from the remaining ones (ED 64004, PCCell GmbH, Germany). Finally, to reach discharge limits in dilute stream, working with several ED stacks in series will be also evaluated.

Table 1. Cationic and anionic membrane characteristics.

Membrane Type	PC SK	PC Acid 100 OT
General use	Standard desalination	Phosphate removal
Composition	Sulfonic acid	Ammonium
Resistance (Ω cm2)	˜ 2.5	˜ 4
pH stability	0-11	0-10
Thickness (µm)	100-120	100-110
Max.Temperature (ºC)	50	40

Table 2. Average of AnMBR effluent concentrations.

pH	6,82	±	0,1
Conductivity (mS/cm)	1,81	±	0,4
NH_4-N (mg/L)	51,6	±	2,4
NO_3-N (mg/L)	0,3	±	0,6
NO_2-N (mg/L)	0,5	±	1,3
PO4-P (mg/L)	8,0	±	2,0
SO4-S (mg/L)	74,0	±	25,6
Cl (mg/L)	204,1	±	36,6
Na (mg/L)	101,6	±	29,4
K (mg/L)	10,4	±	5,9
Mg (mg/L)	32,4	±	11,9
Ca (mg/L)	121,4	±	40,4

Table 3. Long-term experiment results with AnMBR effluent.

	Concentrations (ppm)							Efficiencies (%)	
	Dilute						Concentrate		
	Initial			Final			Final	Dilute	Concentrate
NH_4-N	57.11	±	6.04	11.67	±	2.85	740	79.56	1503.75
NO_2-N	0.35	±	0.87	0.17	±	0.21	2.90	-	-
NO_3-N	0.00	±	0.00	0.08	±	0.15	1.73	-	-
PO_4-P	6.60	±	0.34	2.57	±	0.30	*50*	61.06	1077.48
SO_4-S	98.49	±	13.45	21.39	±	22.00	*1839.01*	78.29	2257.43
Mg	39.81	±	0.37	10.36	±	1.83	*515.62*	73.98	1615.65
Ca	156.81	±	1.10	29.70	±	6.22	*2135.66*	81.06	1556.83

Table 4. Long-term experimental results with diluted AnMBR effluent.

	Concentrations (ppm)							Efficiencies (%)	
	Dilute						Concentrate		
	Initial			Final			Final	Dilute	Concentrate
NH_4-N	62.09	±	4.66	21.84	±	2.82	1600	64.83	3820.61
NO_2-N	0.00	±	0.00	0.00	±	0.00	0	-	-
NO_3-N	0.11	±	0.33	0.19	±	0.30	0	-	-
PO_4-P	7.72	±	1.18	3.41	±	1.13	*130*	55.79	2839.81
SO_4-S	25.42	±	7.34	12.77	±	13.05	*1183.90*	49.77	9155.98
Mg	15.52	±	0.50	6.85	±	2.34	*309.50*	55.86	3390.21
Ca	53.48	±	2.34	22.03	±	7.98	*1189.26*	58.80	3611.52

REFERENCES

Directiva 91/271/CEE del Consejo, de 21 de mayo de 1991, sobre el tratamiento de las aguas residuales urbanas.
G. Noriega-Hevia (2021). Recuperación de nitrógeno mediante contactores de membrana: aplicación, modelación y control. Universitat Politècnica de València.
L. Pastor (2008). Estudio de la precipitación y recuperación del fósforo presente en las aguas residuales en forma de estruvita (MgNH4PO4·6H2O). Universitat Politècnica de València.
W. Rongwong, and K. Goh (2020). Resource recovery from industrial wastewaters by hydrophobic membrane contactors: A review, Journal of Environmental Chemical Engineering, Volume 8, Issue 5.
M. Sena and A. Hicks (2018). Life cycle assessment review of struvite precipitation in wastewater treatment, Resources, Conservation and Recycling,Volume 139, Pages 194-204.
L. Shi, S. Xie, Z. Hu, G. Wu, L. Morrison, P. Croot, H. Hu, X. Zhan. Nutrient recovery from pig manure digestate using electrodialysis reversal: Membrane fouling and feasibility of long-term operation, Journal of Membrane Science, Volume 573.
H, Strathmann (2010). Electrodialysis, a mature technology with a multitude of new applications. Desalination. https://doi.org/10.1016/j.desal.2010.04.069
W. Tarpeh, J. Barazesh, T. Cath and K. Nelson (2018). Electrochemical Stripping to Recover Nitrogen from Source-Separated Urine. Environmental Science and Technology, 52(3), 1453–1460. https://doi.org/10.1021/acs.est.7b05488
M. Turek and P. Dydo (2003). Electrodialysis reversal of calcium sulphate and calcium carbonate supersaturated solution, Desalination, Volume 158, Issues 1–3.
A. Ward, K. Arola, E. Thompson Brewster, C. Mehta and D. Batstone (2018). Nutrient recovery from wastewater through pilot scale electrodialysis. Water Research. https://doi.org/10.1016/j.watres.2018.02.021
M. Xie, H. Shon, S. Gray and M. Elimelech (2016). Membrane-based processes for wastewater nutrient recovery: Technology, challenges, and future direction. In Water Research. https://doi.org/10.1016/j.watres.2015.11.045
T. Yan, Y. Ye, H. Ma, Y. Zhang, W. Guo, B. Du, Q. Wei, D. Wei and H. Ngo (2018). A critical review on membrane hybrid system for nutrient recovery from wastewater. In Chemical Engineering Journal (Vol. 348, pp. 143–156). https://doi.org/10.1016/j.cej.2018.04.166
Y. Zhang, E. Desmidt, A. van Looveren, L. Pinoy, B. Meesschaert and B. van der Bruggen (2013). Phosphate separation and recovery from wastewater by novel electrodialysis. Environmental Science and Technology, 47(11), 5888–5895. https://doi.org/10.1021/es4004476

Pilot Study for Recovery of Phosphate and Ammonia as Struvite from Semiconductor Wastewater

Shao-Hsuan Chang and Jhy-Chern Liu*

* Department of Chemical Engineering, National Taiwan University of Science and Technology, 43 Keelung Road, Section 4, Taipei 10607, Taiwan
(E-mail: *liu1958@mail.ntust.edu.tw)*

Abstract

The pilot-scale study was conducted for converting phosphate (PO_4^{3-})-containing and ammonium (NH_4^+)-containing wastewaters from semiconductor industry to high-purity struvite ($MgNH_4PO_4$). By adding magnesium chloride ($MgCl_2$) at molar ratio of $[PO_4^{-3}]$:$[Mg^{2+}]$:$[NH_4^+]$ of 1:1:1 and pH 9. total of 80-90% of PO_4^{3-} was reacted at initial PO_4^{3-} concentration from 1,000 to 20,000 mg/L. The formation of struvite was confirmed by FESEM, XRD, and wet chemical analysis. Theoretical equilibria were modeled with PHREEQC and compared with experimental results. It was found that initial PO_4^{3-} concentration affected the size and morphology of struvite precipitates. The effluent of the process can be further polished by adding calcium chloride ($CaCl_2$) to induce the formation of hydroxyapatite ($Ca_3(PO_4)_3OH$, HAP). A two-stage process is proposed that ensures resource recovery and meet the effluent standards. The scale-up system was evaluated for potential applications in the factory.

Keywords

Ammonia; phosphate; recovery; semiconductor; struvite; wastewater

INTRODUCTION

Owing to the increasing demand for electronic products worldwide, semiconductor industries have grown rapidly. Semiconductor device fabrication involves a series of complicated processes in which a substantial amount of chemicals, gasses, and ultrapure water are used. It generates significant waste and wastewater (Kuo et al., 2022). Typically, the etching and cleaning processes utilize several chemical compounds, such as ammonium hydroxide (NH_4OH), sulfuric acid (H_2SO_4), phosphoric acid (H_3PO_4), and hydrofluoric acid (HF) (Warmadewanthi and Liu, 2009). Consequently, different streams of wastewater are generated. Among them, the phosphate (PO_4^{-3})-containing wastewater and ammonium (NH_4^+)-containing wastewater received much attention, since the removal of excess PO_4^{-3} is imperative to prevent eutrophication. In this pilot study, we examined the conversion of the two streams of wastewater to struvite ($MgNH_4PO_4$), a valuable fertilizer, by adding magnesium chloride ($MgCl_2$) at molar ratio of $[PO_4^{-3}]$:$[Mg^{2+}]$:$[NH_4^+]$ of 1:1:1, and pH 9.0.

MATERIALS AND METHODS

A semi-batch pilot reactor with diameter of 0.2 m, height of 0.45 m, and total capacity of 12 L was used (**Figure 1**). It is agitated by a multi-impeller composed of anchor and paddles. Three creeping pumps are for the control of $MgCl_2$ dosage, and of pH through a PID controller. Pilot experiments were conducted based on the results of bench-scale experiments using the Jar test apparatus. The PO_4^{-3}-containing wastewater and NH_4^+-containing wastewater were prepared by diluting the concentrated waste H_3PO_4 and NH_4OH from a semiconductor manufacturer. Pilot runs were carried out at molar ratio of $[PO_4^{-3}]$:$[Mg^{2+}]$:$[NH_4^+]$ at 1:1:1, and pH 9.0. Constant flowrate of $MgCl_2$ (Acros) solution was added to induce precipitation. It was stirred at 200 rpm and allowed to react for 5 min, followed by slow mixing at 30 rpm for 30 min. The suspension was sampled and filtered by 0.22 μm PVDF membrane (Advantec) and the filtrate was analysed by ICP-AES (JY 2000) to determine the PO_4^{-3} concentration. The filter cake was dried at 60ºC for at least 48 h and characterized by XRD (G2 Phaser Bruker) and FESEM (JOEL JSM-6500F).

RESULTS AND DISCUSSION

Figure 2 shows that when initial PO_4^{-3} concentration was 1,000, 3,000, 6,000, 12,000, and 20,000 mg/L, the phosphate removal efficiency was 80.1%, 82.5%, 86.8%, 87.1%, and 90.1%, respectively. On the other hand, the ammonium removal efficiency was 80.1%, 82.5%, 86.8%, 87.1%, and 90.1% (Figure not shown), respectively. Compared with the bench-scale system, the removal efficiency was slightly higher since magnesium source of pilot scale system was industrial grade $MgCl_2$. It contained some impurities, which may be beneficial for PO_4^{-3} conversion. It could be proved from wet chemical analysis.

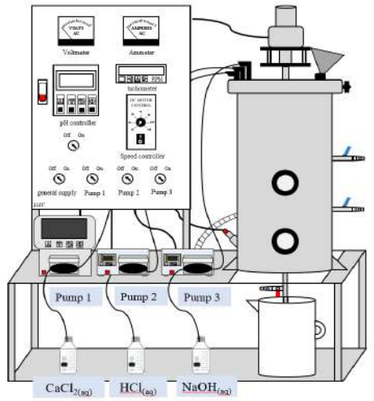

Figure 1 Pilot reactor system

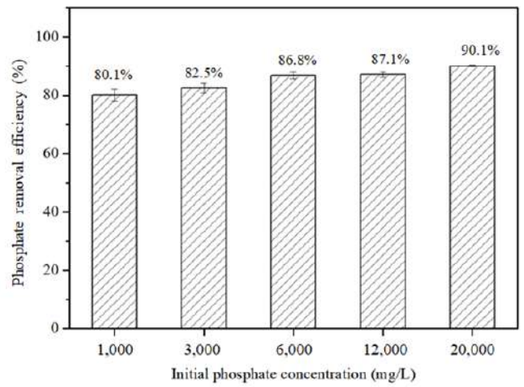

Figure 2 Phosphate conversion as affected by $[PO_4^{-3}]_{initial}$

The preliminary cost analysis was evaluated based on kg P recovered (= kg P_{rec}; = 4.4 kg struvite). The cost of $MgCl_2$ (46.5%) was 3.1 NTD/kg and it needs 12.5kg for kg P_{rec}, while the cost of NaOH was 4.5 NTD/kg and it needs 9.6 kg per kg P_{rec}. For electricity requirement, 5.4 kWh was needed per kg P_{rec}. Total of 38.1 NTD was need for 12.5 kg of $MgCl_2$ per kg P_{rec}, while 43.3 NTD for NaOH. And total electricity was 8.8 NTD per kg P_{rec}. The struvite is priced at 43.7 NTD/kg P recovered as referenced by Berliner Pflanze® and Alibaba. **Table 1** shows the preliminary estimation of profit of 102.1 NTD (ca. 3.3 USD) per kg P_{rec}. The quality the product needs to be further determined, and it is important to carry out more pilot runs and collect related information of the price and specifications of struvite. However, preliminary estimation was positive.

Table 1 Revenue as calculated per kg of P recovered

Resource demand	[NTD/kg P_{rec}]	Energy and water	[NTD/kg P_{rec}]	Product	[NTD/kg P_{rec}]	Revenue (NTD/kg P_{rec})
$MgCl_2$	38.1	Electricity	8.8※	MAP	192.3※※	102.1
NaOH	43.3					

REFERENCES

Kuo, T.C., Kuo, C.Y., Chen, L.W. 2022 Assessing environmental impacts of nanoscale semi-conductor manufacturing from the life cycle assessment perspective. *Resources, Conservation &Recycling* **182**, 106289.

Warmadewanthi, Liu, J.C. 2009 Recovery of phosphate and ammonium as struvite from semiconductor wastewater. *Separation and Purification Technology*, **64**, 368-373.

Effect of suspended solids content on ammonium recovery from pig slurry liquid fraction by liquid-liquid membrane contactors

Rubén Rodríguez-Alegre* **, Julia Zapata-Jiménez*, Laura Pérez Megías*, Carlos Andecochea Saiz*, Montserrat Pérez-Moya**, Julia García-Montaño*, Xialei You*

* LEITAT Technological Center C/ de la Innovació 2, 08225. Terrassa, Barcelona (Spain).
(E-mail: rrodriguez@leitat.org; jzapata@leitat.org; lperez@leitat.org; candecochea@leitat.org; jgarcia@leitat.org; xyou@leitat.org)
** Chemical Engineering Department, Universitat Politécnica de Catalunya, C/ Eduard Maristany 10-14, 08930 Barcelona (Spain)
(E-mail: ruben.rodriguez.alegre@upc.edu; montserrat.perez-moya@upc.edu)

Abstract

The increase in food demand and the resulting intensification in agricultural activities make unsustainable the current linear economy. In this context, it is needed a paradigm shift to a circular economy regarding fertilizers production. Stripping using liquid-liquid membrane contactors reported to be a good alternative for NH_4^+ recovery from waste streams. However, the use of membranes has some limitations such is the fouling issue due to solid presence. In this work, the use of different pre-treatments have been assessed to reduce the content of solids, aimed to expand the lifespan of membranes. As main results, 95% of the ammonium was recovered as ammonium sulphate after 90, 120 minutes centrifuged and sieved samples, respectively, whereas only 55% of recovery was achieved after 150 minutes of experiment for raw sample. The obtained mass transfer coefficient were $1.38 \cdot 10^{-6}$, $1.15 \cdot 10^{-6}$ and $3.03 \cdot 10^{-7}$ m s^{-1} for centrifuged, sieved and raw samples respectively.

Keywords Ammonium sulphate, pig slurry, centrifuge, sieve, liquid-liquid membrane contactor, groundwater

INTRODUCTION

Food demand and its subsequent production have been continuously increased since decades ago due to population growth. In this context, Spain is one of the European countries with the largest production of pork products (19% of the EU production), according to data provided by the European Commission. As a result, livestock farming is becoming more intensive, increasing the environmental issues related to manure management. This manure contains in its composition a high amount of nitrogen, mostly in the form of ammonium (NH_4^+), which can be transformed into N_2O once the manure is directly spread on the soil as fertilizer. This compound can lixiviate and contaminate groundwater. Therefore, it is essential to effectively remove and recover NH_4^+ from pig manure obtaining a valuable subproduct while making an approach to the circular economy.

Ammonium sulphate($(NH_4)_2SO_4$) is a well-known fertilizer used worldwide. This compound can be obtained from the ammonium present in manure by stripping. Previous works reported recovery rates of around 87% (Provolo et al., 2017). This efficiency may be raised by using liquid-liquid membrane contactors (LLMC) as it improves the contact surface between the sample and the stripping acid (Mayor et al., 2020; Reig et al., 2022). Nonetheless, the performance of this membranes-based systems are subject to raw manure characteristics, especially solids presence, as they may cause membrane clogging. In order to limit the membrane contactor's efficiency decrease, the selection of a pre-treatment step is essential (Rongwong & Goh, 2020).

The aim of this study is to assess the effect of suspended solids content in pig slurry liquid fraction (SLF) in the ammonia mass transfer coefficient using LLMC. The studied samples were raw sample and pre-treated samples by centrifugation and sieving.

MATERIALS AND METHODS

For solids removal, centrifugation and sieving were assessed as pre-treatment. Centrifugation was performed using a centrifuge Allegra® 25R (BECKMAN COULTER, Spain) at 5100 rpm and 5ºC for 30 min. Sieving was carried out using a stainless-steel mesh with a mesh light of 106 µm (FILTRA VIBRACIÓN, Spain).

The LLMC for ammonia recovery was performed by using a hollow fibre contactor (MM-1.7x5.5 3M™ Liqui-Cel™, Denmark). Specifications of the device can be found in Table 1.

TABLE 1

Feed and stripping acid were passed respectively through the shell and lumen in countercurrent mode. During experiments, the pH of the stripping acid solution was maintained at 1 by adding sulphuric acid 98% while the feed's pH is maintained at 10 by adding sodium hydroxide 17M, if needed. Both solutions were prepared with reagents from Scharlab (Spain). Acid and feed were used in recirculation with flow rates fixed at 0.5 L min^{-1} at room temperature.

The mass transfer coefficient (K_m) in m s^{-1}, was determined following equation 1 suggested by Licon Bernal et al. (2016) and Hasanoğlu (2013):

$$ln\left(\frac{C_{0(NH_3)f}}{C_{t(NH_3)f}}\right) = \frac{K_{m(NH_3)}\,A_m}{V_f} \cdot t \qquad \text{Equation 1}$$

Where V_f is the total volume of treated feed (L), A_m is the membrane area on the contactor (m^2), $C_{0(NH3)f}$ and $C_{t(NH3)f}$ are the ammonia concentration at the beginning and at the time "t".

The performance of NH_4^+ extraction experiments was carried out in batch mode using the same experimental conditions of pH and temperature. A one-way ANOVA was used to assess whether the effect of these pre-treatments in ammonia extraction is significant.

The chemical composition of the different real samples was measured using colourimetric methods by a spectrophotometer (HACH, Spain), through the analysis of nitrogen in the form of ammonium ($N\text{-}NH_4^+$) based on the Indophenol blue method. pH was determined by using a multimeter coupled with a pH sensor (HACH, Spain) based on standard methods 4500-H+. Finally, the dry matter contents were determined by using method 1684 related to sample evaporation, detailed elsewhere.

RESULTS AND DISCUSSION

In this work, different pre-treatments for total solids removal from SLF and heir effect in the ammonium recovery rate was assessed. Pre-treatments suggested for total solids removal yielded successful results in solids content reduction, obtaining a dry matter reduction of 55,66% in the case of centrifugation and 13.49% in the case of the sieving (Table 2).

TABLE 2

The results obtained from the LLMC experiments are shown in Figure 1 and summarized in Table 3. With an initial NH_4^+ concentration of around 2700 mg L^{-1}, recovery rates of 95% were achieved in 90 and 120 min for centrifuged and sieved samples respectively. On the contrary, in the case of raw SLF, after 150 minutes of experiment, the content of ammonium on the sample remained higher than 1000 mg L^{-1}, which corresponds to a 55% of recovery rate. The difference in experimental times may be explained by the higher solid reduction in the centrifugation step in front of the sieving pre-treatment as when the solid content is higher, the membrane pores are more easily clogged, reducing its mass transfer coefficient. After mass transfer coefficient calculations it was obtained values of $1.38 \cdot 10^{-6}$ m s^{-1} (R^2=0.986), $1.15 \cdot 10^{-6}$ m s^{-1} (R^2=0.972) and $3.03 \cdot 10^{-7}$ m s^{-1} (R^2=0.981) for centrifuged, sieved and raw SLF, respectively. In addition, one-way ANOVA results reported no significant differences between the mass transfer coefficient between centrifuged and sieved samples (p-value = 0.776) while showing significant differences between pre-treated samples and raw SLF as it was reported p-value of 0.009 and 0.022 compared with centrifuged and sieves samples, respectively.

FIGURE 1 | TABLE 3

CONCLUSIONS

This work has studied the effect of total solids removal in the efficiency of ammonium stripping through LLMC after two different pre-treatments: centrifugation and sieving. The obtained results demonstrate the importance of solids removal for improving the performance of LLMC. In addition, obtained results showed the better performance of centrifugation as pre-treatment in front of sieving in terms of total solid removal. However, no significant differences were observed between both pre-treatments in terms of mass transfer coefficient in stripping process.

Table 1. MM-1.7x5.5 LLMC specifications from 3M™ Liqui-Cel™.

Characteristics	Value
Membrane/Potting material	Polypropylene/Polyurethane
Membrane type	X50 Fiber
Flow guidelines	< 2500 ml min^{-1}
Shell side volume	78 ml
Lumen side volume	53 ml
Working temperature/pressure	40°C, 2.1 barg (104°F, 30 psig)

Table 2. Solid content on the samples obtained through dry matter determination.

Pre-treatment	Dry matter	Dry matter	Solid content reduction
	(g L^{-1})	(%)	(%)
No pre-treated	43.80	4.38	-
Centrifuged	19.42	1.94	55.66
Sieved	37.89	3.79	13.49

Table 3. Experimental results from ammonium recovery through LLMC obtained.

Pre-treatment	Experimental time	Initial NH_4^+	Final NH_4^+ in acid	NH_4^+ recovery	R^2	K_m
	(min)	(mg L^{-1})	(mg L^{-1})	(%)	(-)	m s^{-1}
No pre-treated	150.00	2622.00	1539.00	58.70	0.98	$3.03 \cdot 10^{-7}$
Centrifuged	90.00	2710.00	2514.00	96.79	0.98	$1.38 \cdot 10^{-6}$
Sieved	120.00	2720.00	2575.00	94.67	0.97	$1.15 \cdot 10^{-6}$

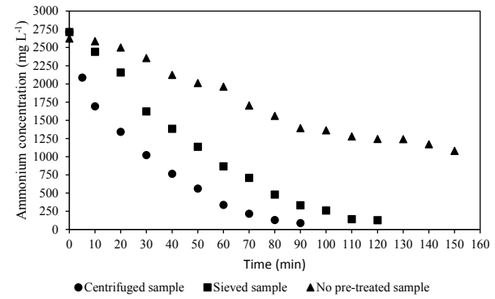

Figure 1. Experimental performance on ammonium extraction from SLF after pre-treatments.

ACKNOWLEDGEMENT

This project has received funding from the European Union's Horizon Europe research and innovation programme under grant agreement No 101081865: NINFA (TakiNg actIoN to prevent and mitigate pollution oF GroundwAter bodies). Also, financial support received from the Spanish "Ministerio de Ciencia e Innovación" and the European Regional Development Fund, both funding the research Project CEPI (PID2020-116051RB-I00) is fully acknowledged.

REFERENCES

Bernal, E. L., Maya, C., Valderrama, C., & Cortina, J. L. (2016). Valorization of ammonia concentrates from treated urban wastewater using liquid–liquid membrane contactors. *Chemical Engineering Journal*, **302**, 641-649.

Hasanoğlu, A., Romero, J., Plaza, A., & Silva, W. (2013). Gas-filled membrane absorption: a review of three different applications to describe the mass transfer by means of a unified approach. *Desalination and Water Treatment*, **51**(28-30), 5649-5663.

Mayor, A., Vecino, X., Reig, M., de Arespacochaga, N., Valderrama, C., & Cortina, J. L. (2020). Ammonium Valorization from Urban Wastewater as Liquid Fertilizers by Using Liquid–Liquid Membrane Contactors. In *Hollow Fiber Membrane Contactors* (pp. 225-240). CRC Press.

Provolo, G., Perazzolo, F., Mattachini, G., Finzi, A., Naldi, E., & Riva, E. (2017). Nitrogen removal from digested slurries using a simplified ammonia stripping technique. *Waste Management*, **69**, 154-161.

Reig, M., Vecino, X., Aguilar-Moreno, M., Valderrama, C., & Cortina, J. L. (2022). Ammonia Valorization by Liquid–Liquid Membrane Contactors for Liquid Fertilizers Production: Experimental Conditions Evaluation. Membranes, 12(7), 663.

Rongwong, W., & Goh, K. (2020). Resource recovery from industrial wastewaters by hydrophobic membrane contactors: A review. *Journal of Environmental Chemical Engineering*, **8**(5), 104242.

TECHNICAL SESSIONS

T2.

N& P recovery II

Optimization of ammonia recovery from urine and digestate using transmembrane chemical absorption

I. Gonzalez-Salgado*, M. Peyre-Lavigne*, G. Nourrit**, C. Guigui*, M. Sperandio*

* TBI, Université de Toulouse, CNRS, INRAE, INSA, Toulouse, France (E-mail: *sperandio@insa-toulouse.fr)*
**NEREUS, Parc d'activité, Dom. des Trois Fontaines, 34230 Le Pouget

Abstract

Nitrogen recycling is one of the major challenges for wastewater management in the future. In this work the optimal conditions for ammonia recovery with gas-permeable membrane absorption are scrutinized. Experiments and modelling works demonstrate the effect of TAN/IC ratio for determining the pH and temperature setpoints, the pretreatment to be applied for minimizing the energy demand.

Keywords

Nitrogen recovery; digestate; urine; wastewater treatment; membrane;

INTRODUCTION

Nitrogen recycling is one of the major challenges for our society. However, nitrogen recovery technologies like stripping, adsorption or reverse osmosis, are still poorly implemented in the water sector, due to capital and operational costs as well as maintenance needs. Biological deammonification (nitrogen conversion into dinitrogen gas through partial nitritation and anammox) is considered as the most cost-effective technology for sidestream systems in treatment plants (…). Besides the scenarios of decentralised management of high strength effluent as urine or liquid digestate encourage nitrogen recovery techniques. Transmembrane chemical absorption process (also called membrane stripping or gas-membrane absorption) is a promising technology to recover ammonia. It consists in transferring ammonia through gas-permeable membrane and capturing it in acid solution. It can be applied on high strength wastewater to produce a liquid fertilizer for agriculture (Richter et al., 2020; Uzkurt Kaljunen et al., 2021; Molinuevo-Salces et al., 2020; Ulbricht et al., 2013). A critical review (Gonzalez-Salgado et al., 2022) has shown the recent progress and pointed out remaining questions regarding this technology and its scale-up: elucidate the effect of ionic strength, reducing the water vapour transport through hydrophobic membranes, optimizing the operating conditions for pre-treatment as well as energy minimization. In this study, transmembrane chemical absorption (TMCS) was applied on digestate, urine, and synthetic wastewater at different scales (lab and industrial pilot). The objective was to support a model describing physical-chemical mechanisms which was used for comparing different scenarios and operational options with a specific focus on energy efficiency.

MATERIAL AND METHODS

The pilot was composed of membrane module (polypropylene, 53 m^2) with pre-treatment processes including aeration, NaOH addition, settling, heat exchanger, and prefiltration (Figure 1). Ammonia was absorbed in sulfuric acid to obtain an ammonium sulphate solution. Ammonia recovery efficiency (ARE) and water vapour transfer were determined through mass balance. A model was developed on Matlab for solving the chemical equilibriums (electroneutrality and thermodynamic constants) and predicting pH variations, mass transfer of ammonia, energy and chemical needs. The primary energy demand of the overall process was calculated using the primary energy factors (PEF) from Ecoinvent database v3.8. Energy saving for producing an equivalent kilogram of nitrogen by Haber-Bosch process was also considered (12.5 kWh kgN^{-1}, Van der Hoek et al., 2018). The ammonia transfer coefficient of the model was determined with experimental results using synthetic wastewater (NH_4Cl) and real effluents (urine, digestate). The influent flow rate varies from 25 to 100 L h^{-1} and influent total ammonium (TAN) concentration ranged from 1 to 4 gN L^{-1}.

RESULTS

Effect of pH, temperature and wastewater composition on performances and energy needs

Ammonia recovery efficiency (ARE) was measured for different hydraulic conditions and varied from 64% to 98%. Results were not significantly different for synthetic wastewater, urine and digestate, despite a small effect of ionic strength. Similar performances (ARE) can be obtained with different couples of pH and temperature in the TMCS process, due to their respective effect on NH_3/NH_4^+ ratios and Henry's law constants of NH_3. Working at lower pH can be compensated by higher temperature. Our results showed that the Nitrogen to Inorganic Carbon ratio (TAN/IC) of the wastewater has a key role in the energy needs for pre-treatments depending on the chosen operational pH for effluent (Figure 2). Aeration (stripping of CO_2) allows to reduce the NaOH consumption for pH rising. The total primary energy requirements per kilogram of nitrogen recovered and the gain in energy saving is more important when the ratio of TAN/IC decreased. The stripping process reduced by 11-23% the use of NaOH and by 8-19% the primary energy. Simulations showed that it is preferable to work at high pH for high TAN/IC (i.e. low IC) whereas it is energetically more efficient to work at lower pH at low TAN/IC (i.e. high IC). The TAN/IC ratio of stored urine ranged from 1.78 to 3.16 whereas a lower TAN/IC was observed for digestate (0.71 to 1.83). Hence different optimal conditions could be chosen for these two types of wastewaters.

Global optimization of primary energy needs

For similar recovery efficiency (ARE=90%) the global primary energy required is also sensitive to the heating source. When TMCS is implemented after anaerobic digestion, methane can be used for heating. In that case the optimal operating condition was found at pH 10 and 35°C whereas the operating conditions of pH 10.5 and 25°C were more suitable for heating with natural fossil gas boiler (Figure 3). When the process operates at ambient temperature, a lower influent flow rate can be applied to increases the ARE and reduce the primary energy requirements (Figure 4). ARE increases from 80% to 92% and up to 98% by dividing the flowrate by 2 and 4 respectively. This would need a higher membrane surface to treat the same effluent flow, but as a consequence the primary energy needs can decrease to less than 15 $kWh_{primary}\ kgN_{recovered}^{-1}$. In that case, considering the energy saving by substituting conventional nitrogen fertilizer from Haber Bosch process (12.5 kWh kgN^{-1}) the energetic needs become lower than partial nitritation – anammox process.

CONCLUSION

TMCS is a mature technology for nitrogen recovery from high strength wastewater. Energy consumption is much lower than conventional stripping. The complete modelling approach shows the influence of TAN/IC ratio on the optimal conditions (pH, T) and associated pre-treatments. This should be taken into consideration for application on urine or digestate. Several choices of temperature and pH, allowed obtaining the same ammonia removal efficiency but the optimization also depends on the heating source (biogas of fossil gas). Working at ambient temperature was the best option for minimising energy needs.

REFERENCES

Gonzalez-Salgado, I., Guigui, C., Sperandio, M., 2022. Transmembrane chemical absorption technology for ammonia recovery from wastewater: A critical review. *Chem. Eng. J.* 444, 136491. https://doi.org/10.3390/membranes12060572

Molinuevo-Salces, B., Riaño, B., Vanotti, M.B., Hernández-González, D., García-González, M.C., 2020. Pilot-Scale Demonstration of Membrane-Based Nitrogen Recovery from Swine Manure. Membranes 10, 270. https://doi.org/10.3390/membranes10100270

Ochs, P., Martin, B., Germain-Cripps, E., Stephenson, T., van Loosdrecht, M., Soares, A., 2023. Techno-economic analysis of sidestream ammonia removal technologies: Biological options versus thermal stripping, Environmental Science and Ecotechnology, Volume 13, 100220, https://doi.org/10.1016/j.ese.2022.100220

Richter, L., Wichern, M., Grömping, M., Robecke, U., Haberkamp, J., 2020. Ammonium recovery from process water of digested sludge dewatering by membrane contactors. Water Pract. Technol. 15, 84–91. https://doi.org/10.2166/wpt.2020.002

Ulbricht, M., Schneider, J., Stasiak, M., Sengupta, A., 2013. Ammonia Recovery from Industrial Wastewater by TransMembraneChemiSorption. Chem. Ing. Tech. 85, 1259–1262. https://doi.org/10.1002/cite.201200237

Uzkurt Kaljunen, J., Al-Juboori, R.A., Mikola, A., Righetto, I., Konola, I., 2021. Newly developed membrane contactor-based N and P recovery process: Pilot-scale field experiments and cost analysis. J. Clean. Prod. 281, 125288. https://doi.org/10.1016/j.jclepro.2020.125288

Van der Hoek, J.P., Duijff, R., Reinstra, O., 2018. Nitrogen Recovery from Wastewater: Possibilities, Competition with Other Resources, and Adaptation Pathways. Sustainability 10, 4605. https://doi.org/10.3390/su10124605

Figure 1. Experimental set-up. A pilot composed of hydrophobic membranes (PP), aeration tank, settler, heat exchanger, NaOH and acid regulation.

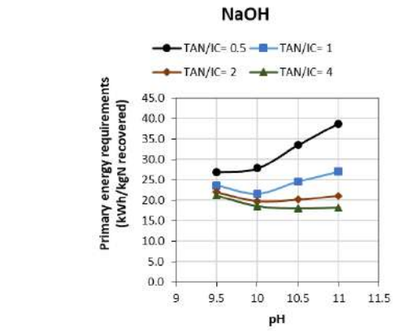

a.

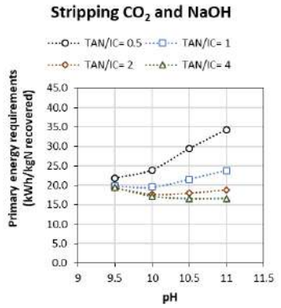

b.

Figure 2. Primary energy requirements per kilogram of nitrogen recovered for different influent compositions and operational pH. Comparison of pH adjustment with a: NaOH addition., b: Stripping + NaOH.

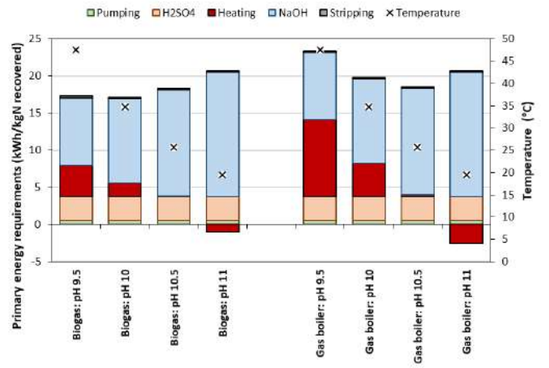

Figure 3. Influent temperature calculation and primary energy requirements per kilogram of nitrogen recovered for a fixed ammonia removal efficiency (ARE) of 90%. Comparison of heating source.

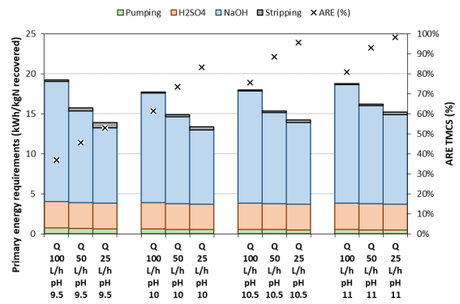

Figure 4. Impact of flow rate in primary energy requirements and ARE at ambient temperature (25 °C)

Recovery of K-rich struvite after biological nitrogen removal

E. Company*, M. Farrés**, J. Colprim* and A. Magrí*
* LEQUIA, Institute of the Environment, University of Girona, Campus Montilivi, Carrer Maria Aurèlia Capmany 69, E-17003 Girona, Catalonia, Spain
(E-mail: emma.company@udg.edu; jesus.colprim@udg.edu; albert.magri@udg.edu)
** Granges Terragrisa SL, Paratge de La Gleva, Camí de Burrissola s/n, E-08508 Les Masies de Voltregà, Barcelona, Catalonia, Spain.
(E-mail: m.farres@grangesterragrisa.es)

Abstract

Swine manure offers mining opportunities for nutrient recovery and subsequent reuse as renewable fertilizer. This research aimed to integrate conventional biological nitrogen removal (BNR) with P and K recovery as K-struvite ($MgKPO_4 \cdot 6H_2O$). The denitrified effluent has an unbalanced Mg/K/P molar ratio of 1.4/9.5/1, so external P and Mg sources should be considered to recover all the K. Waste sludge from the BNR reactor presented a rich and balanced composition (0.7/1.2/1). An acid pre-treatment release PO_4^{3-} and K^+ from the sludge but also Ca^{2+}, which has to be trapped to prevent the formation of calcium phosphates instead of K-struvite. This downstream process allowed for the production of a multi-nutrient fertilizer with 0-1% N, 10-17% P and up to 8% K.

Keywords (maximum 6 in alphabetical order)

EDTA; K_2Na-struvite; Nutrient recovery; Oxalic acid; Waste sludge

INTRODUCTION

Agricultural crop production requires macronutrients such as nitrogen (N), phosphorus (P) and potassium (K) which can be supplied in the form of recovered bio-based fertilizers.

The recovery of P is particularly relevant in the EU framework since P and phosphate rock have been identified as two of 27 critical raw materials (Cordell et al., 2009). Similarly, K is mostly obtained from potash ores, but it is not commonly recovered from wastewater or other similar sources. Thus, there is a need to identify new sources of K (Manning, 2015).

Concerning N, nitrification-denitrification (NDN) is typically applied as a Best Available Technique (BAT) for effective on site biological N removal (BNR) (Giner-Santonja et al., 2017) and the fulfilment of legal criteria in pig production. Under the circular economy framework, after the biological step, innovative procedures for the recovery of P and K as K-struvite (MPP, $MgKPO_4 \cdot 6H_2O$) are of high interest. In the EU, on the basis of the fertilising products regulation (EU) 2019/1009, a legal framework for struvite has already been developed (Huygens et al., 2019).

The waste sludge from the NDN bioreactor (Figure 1) has higher concentration of P than the denitrified liquid effluent, which can be mobilised by acidification. Unfortunately, calcium (Ca^{2+}) will be also mobilised. The crystallisation of K-struvite is disfavoured by high levels of Ca^{2+} due to the formation of calcium phosphates (Ca-P), and thus, the development of new procedures for preventing the interference of Ca during K-struvite formation are needed (Srinivasan et al., 2014).

This study aims to investigate the recovery of K-rich struvite from the denitrified eddluent and the waste sludge of a NDN bioreactor treating pig slurry. Different methods to avoid Ca interference have already tested.

MATERIAL AND METHODS

Samples of denitrified effluent and waste sludge were taken from a NDN treatment plant located in a pig farm from Osona (Spain) and follows the process layout shown in Figure 1.

The denitrified effluent had as soluble Mg/K/P molar ratio 1.4/9.5/1 (136 ±8 mg P/L) whereas the waste sludge had a total Mg/K/P molar ratio of 0.7/1.2/1 (1292 ±8 mg P/L).

When using the denitrified effluent and considering P as the limiting element, magnesium oxide (MgO) and magnesium chloride ($MgCl_2 \cdot 6H_2O$) were dosed as Mg external sources. When considering K as the limiting element, the simultaneous addition of Mg and P was performed with own-synthetized newberyite particles (NP, $MgHPO_4 \cdot 3H_2O$), following Astals et al. (2021). The NP were synthesised with 2.4 g H_3PO_4/g MgO and dried at room temperature.

When using the waste sludge, H_2SO_4, ethylenediaminetetraacetic acid (EDTA) and oxalic acid solutions were used as acidifying agents. All the tests were performed in 1-L glass beakers using a flocculator (mod. JLT6, Velp Scientifica, Italy). NaOH was used to increase the pH. Soluble ionic forms were analysed by ion chromatography. The composition and structure of the precipitate were analysed with inductively coupled plasma (ICP) and X-ray diffraction (XRD), respectively.

RESULTS AND DISCUSSION

Denitrified effluent: As shown in Figure 2A, by considering P as the limiting element, low K recovery efficiencies (KRE) (between 3% and 10%) were reached under different values of pH (from 10 to 12) after 2h mixing. Moreover, the molar removal ratio between Mg and P ($MRR_{Mg:P}$) was slightly above 1 suggesting the co-formation of the magnesium phosphate known as cattiite ($Mg_3(PO_4)_2 \cdot 22H_2O$) (Zhang et al., 2018). By considering K as the limiting element, stable IRE_K were reached after 2 h of reaction (Figure 2B). The higher the dose of NP applied (8-14 g NP/L) the higher K removal efficiency reached, so best results were obtained with the addition of 14 g NP/$L_{effluent}$ (KRE reaching 90%).

Waste sludge: As shown in Figure 3, by adding the acidic agent (H_2SO_4, EDTA or oxalic acid) according to a targeted pH (values from 6 to 4), significant amounts of PO_4^{3-}, Mg^{2+} and, Ca^{2+} were released. In each test, the lower the pH considered, the higher the solubilisation achieved. The concentration of K^+ remained almost invariable during the acidification test because this element was already soluble. The solubilisation efficiencies reached using H_2SO_4, EDTA and oxalic acid at pH 4 were 78%, 70% and 75% for PO_4^{3-} and, 91%, 79% and 83% for Mg^{2+}, respectively. As it was previously reported by Srinivasan et al. (2014), at this pH, the dosage of EDTA and oxalic acid resulted in similar solubilisation efficiencies than H_2SO_4. By adding oxalic acid, any increase in the concentration of Ca^{2+} was observed (Figure 3) due to the formation of calcium oxalate (insoluble). Contrarily, by adding EDTA, an increase in Ca^{2+} concentration was observed (Figure 3) because the interaction between the EDTA and Ca^{2+} ions result in the formation of the complex Ca-EDTA (soluble). Following acidification pre-treatment and solids separation by centrifugation, the pH of the centrate was increased with the addition of NaOH. As shown in Table 1, low calcium removal efficiencies (CaRE) were obtained using EDTA and oxalic acid (i.e., 12% and 0%, respectively) demonstrating the good performance of both as Ca blocking agents. The best KRE (44%) were obtained when using oxalic acid as the acidifying agent.

The analysis of the precipitates formed after raising the pH of the denitrified effluent considering K as the limiting element (using NP) and from the waste sludge using oxalic confirmed in both cases the presence of K_2Na-struvite ($Mg_2KNa(PO_4)_2 \cdot 14H_2O$) with a composition between 10% and 17% for P and 7% to 8% for K (Figure 4).

CONCLUSIONS

This work has proved as feasible the simultaneous recovery of P and K from the denitrified effluent and waste sludge produced in a BNR system treating pig slurry. Concerning the denitrified effluent, limited K recovery was attained y only raising the pH (3-10%). The addition of NP allowed increasing significantly the KRE, reaching 90%. Regarding the waste sludge, an acidifying pre-treatment increased ion availability in the liquid phase, but the use of a Ca-sequestring agent is necessary to prevent the formation of Ca-P compounds. A multi-nutrient valuable product was recovered. Nevertheless, further work is needed to reduce the presence of Na^+ in the recovered precipitate.

FIGURES AND GRAPHICS

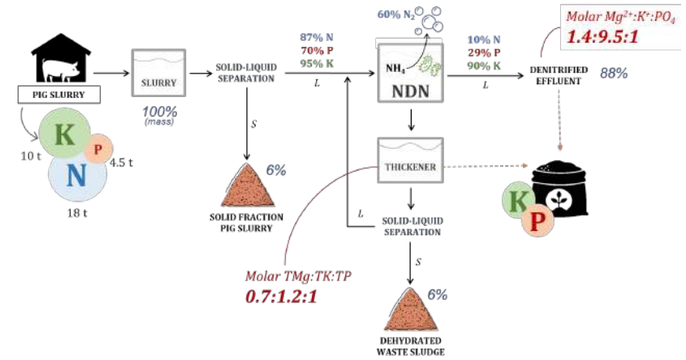

Figure 1. Flow chart of the swine manure treatment plant (Osona).

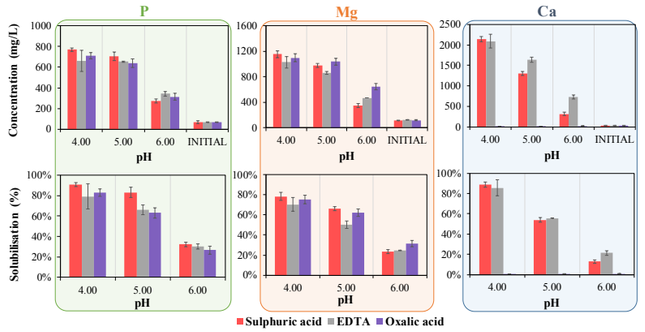

Figure 2. K removal efficiency (IRE_K) from the denitrified effluent considering P as the limiting element (A). Evolution of the K removal efficiency with the addition of different doses of newberyite particles (8, 11 and 14 g NP/$L_{effluent}$) (B). Both tests were performed in 1-L glass beakers.

Table 1. Ion removal efficiencies obtained by adding sulphuric acid, oxalic acid and EDTA. Values are means of three samples ± standard deviation.

Treatment	NaRE (%)	KRE (%)	MgRE (%)	CaRE (%)	PRE (%)
Sulphuric acid	29 ±12	3 ±7	59 ±1	93 ±1	100 ±0
Oxalic acid	32 ±1	44 ±3	98 ±1	0 ±0	77 ±1
EDTA	24 ±6	28 ±2	87 ±5	12 ±3	85 ±2

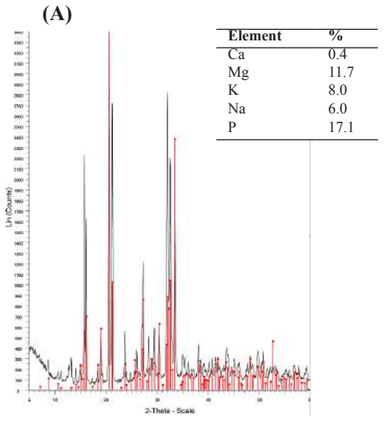

Figure 4. Diffractogram and composition results obtained, respectively, from XRD and ICP analysis of the precipitate obtained from the denitrified effluent considering K as the limiting element (A) and the precipitate obtained from the waste sludge using oxalic acid as acidifying agent. Red colour represents the K_2Na-struvite pattern.

REFERENCES

Astals, S., Martínez-Martorell, M., Huete-Hernández, S., Aguilar-Pozo, V.B., Dosta, J. and Chimenos, J.M., 2021. Nitrogen recovery from pig slurry by struvite precipitation using a low cost magnesium oxide. *Science of The Total Environment*. 768, 144284.
Cordell, D., Drangert, J.O. and White, S., 2009. The story of phosphorus: Global food security and food for thought. *Global Environmental Change*. *19* (2), 292–305.
Giner-Santonja, G., Georgitzikis, K., Scalet, B.M., Montobbio, P., Roudier, S. and Delgado-Sancho, L., 2017. Best Available Techniques (BAT) Reference Document for the Intensive Rearing of Poultry or Pigs. Industrial Emissions Directive 2010/75/EU (Integrated Pollution Prevention and Control). JRC Science for Policy Report, EUR 28674 EN.
Huygens, S., Saveyn, H., Tonini, D., Eder, P. and Delgado Sancho, L., 2019. *Technical Proposals for Selected New Fertilising Materials under the Fertilising Products Regulation (Regulation (EU) 2019/1009 - Process and Quality Criteria, and Assessment of Environmental and Market Impacts for Precipitated Phosphate Salts & Derivates, Thermal Oxidation Material & Derivates and Pyrolisis & Gasification Materials*. JRC Science for Policy Report. *Publications Office of the European Union*. Luxemburg. EUR 29841 EN.
Manning, D.A.C., 2015. How will minerals feed the world in 2050? *Proceedings of the Geologists' Association*. *126*(1), 14–17.
Srinivasan, A., Nkansah-Boadu, F., Liao, P.H. and Lo, K.V., 2014. Effects of acidifying reagents on microwave treatment of dairy manure. *Journal of Environmental Science and Health, Part B: Pesticides, Food Contaminants, and Agricultural Wastes*. *49*, 532–539.
Zhang, C., Xu, K., Zheng, M., Li, J. and Wang, C., 2018. Factors affecting the crystal size of struvite-K formed in synthetic urine using a stirred reactor. *Industrial and Engineering Chemistry Research*. 57, 17301–17309.

Phosphorous recovery from waste aerobic granular sludge

R. Campo**, J.P. Czellnik*, C. Lubello* and T. Lotti*
* Department of Civil and Environmental Engineering, University of Florence, Via di S. Marta 3, Firenze 50139, Italy
(E-mail: *riccardo.campo@unifi.it*)

Abstract

This study aims to investigate phosphorus recovery from waste aerobic granular sludge (WAGS). Phosphorus is an essential element for the growth of all living organisms, but it is a limited and non-renewable resource. It is mainly used as nutrient in the agronomic sector to produce mineral fertilizers and it is included in the list of Critical Raw Materials by the European Commission. Domestic wastewater are streams containing phosphorus that can be recovered from waste activated sludge (WAS) where it is accumulated. Aerobic Granular Sludge (AGS) is a pseudo-spherical biofilm, made of self-aggregated bacteria enriched in slow-growing organisms including phosphorous accumulating organisms (PAOs), applied for biological wastewater treatment. Batch tests have been performed by varying the pH. WAGS was withdrawn from a Granular Sequencing Batch Reactor (GSBR) performing a bioP-removal efficiency of 99%. WAGS was characterized by a VSS/TSS of 84% and a total phosphorus (TP) of 48.8 mgP/gTS, higher than conventional WAS (TP≈14-17 mgP/gTS). The fractionation of TP in WAGS revealed that the 88.6 %wt was inorganic phosphorus (IP), and the 11.4 %wt was organic phosphorus (OP). Preliminary results highlighted a TP-recovery efficiency up to 92% at pH 4 after 12 days. Salts with high P-content, that comply with the EU regulation (2019/1009) on fertilizers, were chemically precipitated from bulk at the end of the tests. These salts could be reused for agronomic applications. Considering an almost complete bioP-removal in a GSBR, the obtained results show the potentials of an attractive side-stream treatment chain with a P-recovery efficiency > 90% of TP contained in raw wastewater.

Keywords (maximum 6 in alphabetical order)

Aerobic granular sludge; phosphorus; resource recovery; wastewater resource recovery facilities

INTRODUCTION

Phosphorus (P) is an essential element for the growth of all living organisms, but it is a limited and non-renewable resource. It is obtained mainly from rocks located in few regions of the world (e.g. about 75% of world's P reserves are in Morocco (Cordell and White, 2015)farmer livelihoods, agricultural productivity and global food security. Yet there is a lack of research and effective governance at global or national scales designed to ensure the future availability and accessibility of this global resource. The world's main source of phosphorus, phosphate rock, is a finite resource that is becoming increasingly scarce, expensive and subject to geopolitical tensions as one country, Morocco, controls three-quarters of the world's remaining high-grade reserves. Given the criticality of phosphorus and the vulnerability of the world's food systems to phosphorus scarcity, there is a strong need to stimulate appropriate sustainable phosphorus practices and technologies, and simultaneously, to initiate effective international governance mechanisms, including policy/research coordination and accountability. Sustainability indicators are increasingly being used as tools to facilitate accountability, implementation, evaluation and communication for global sustainability challenges. This paper presents the first comprehensive set of phosphorus vulnerability and security indicators at global and national scales. Global indicators include: phosphate price, market concentration and supply risk, relative physical phosphorus scarcity and eutrophication potential. National indicators include: farmer phosphorus vulnerability, national phosphorus vulnerability, national phosphorus equity and soil phosphorus legacy. Monitoring and tracking such indicators at the national and global levels can ultimately provide evidence of key phosphorus vulnerabilities or 'hotspots' in the food system, support effective phosphorus governance to stimulate targeted and effective action, raise awareness of this food security challenge, and evaluate the effectiveness and performance of global or national sustainable phosphorus projects.",",author":[{"dropping-particle":"","family":"Cordell","given":"Dana","non-dropping-particle":"","parse-names":false,"suffix":""},{"dropping-particle":"","family":"White","given":"Stuart","non-dropping-particle":"","parse-names":false,"suffix":""}],"container-title":"Food Security","id":"ITEM-1","issued":{"date-parts":[["2015"]]},"title":"Tracking phosphorus security: indicators of phosphorus vulnerability in the global food system","type":"article-journal"},"uris":["http://www.mendeley.com/documents/?uuid=339cdc4e-ad60-4751-9d7f-d35d011b510a"]}],"mendeley":{"formattedCitation":"(Cordell and White, 2015). P is mainly used as nutrient in the agronomic sector to produce mineral fertilizers and it is included in the list of Critical Raw Materials by the European Commission from 2014 (Bobba et al., 2020). Domestic wastewater are alternative sources of P. It was estimated that the total P excreted by humans could meet 22% of global P demand (Mihelcic et al., 2011), and therefore it would be worthwhile to recover it. In this context, a paradigm shift from wastewater treatment plants (WTTPs) to water resource recovery facilities (WRRFs) has taken place over the last few years (Chrispim et al., 2019). P can be mainly recovered from waste activated sludge (WAS) where it is accumulated or precipitated as P-mineral (Chrispim et al., 2019). A novel and promising wastewater treatment technology, named Aerobic Granular Sludge (AGS), is based on pseudo-spherical biofilm made of self-aggregated bacteria enriched in slow-growing organisms including phosphorous accumulating organisms (PAOs) (Pronk et al., 2015) aerobic granular sludge technology has been scaled-up and implemented for industrial and municipal wastewater treatment under the trade name Nereda??. With full-scale references for industrial treatment application since 2006 and domestic sewage since 2009 only limited operating data have been presented in scientific literature so far. In this study performance, granulation and design considerations of an aerobic granular sludge plant on domestic wastewater at the WWTP Garmerwolde, the Netherlands were analysed. After a start-up period of approximately 5 months, a robust and stable granule bed (>8gL-1. The metabolism of PAOs consisted of two phases: in anaerobic conditions, PAOs store volatile fatty acids (VFAs) as polyhydroxyalkanoates (PHAs) inside their cells. The energy that is required to take up VFAs is provided by the hydrolysis of the internally stored glycogen and poly-P thus resulting in PO_4-P release in the bulk. In aerobic/anoxic conditions, PAOs take up the released PO_4-P, thus refilling the internal poly-P pool, using the intracellular PHAs they stored in anaerobic conditions as carbon source and electron donor (Smolders et al., 1995) considering also components like adenosine triphosphate (ATP. Therefore AGS is considerable as an unconventional reservoir of P that is present as poly-P in PAOs and as minerals precipitated on the bacterial surfaces. The aim of this study is to investigate the feasibility of P-recovery from waste aerobic granular sludge (WAGS).

MATERIALS AND METHODS

Anaerobic batch tests were performed by varying the pH of WAGS bulk liquid. pH was regulated by dosing a 1M HCl solution. Throughout all the batch tests duration the following parameters have been monitored: P released (LCK 350 HACH®), heavy metals (ICP-OES), anions/cations (Dionex1100®), total organic carbon (TOC analyser), chemical oxygen demand (COD LCK 614 HACK®), pH. Total Solids (TS) and Volatile Solids (VS) have been analyzed according to standard methods (APHA/AWWA/WEF, 2017)cis-9, cis-12. P fractionation of WAGS was performed according to a protocol named Standards Measurements and Testing (SMT) harmonized procedure (González Medeiros et al., 2005), in order to determine the total P (TP), the inorganic P (IP), as sum of non-apatite-inorganic-P (NAIP, i.e. the forms associated with oxides and hydroxides of Al, Fe, and Mn) and apatite P (AP, i.e. the forms associated with Ca), the organic P (OP, i.e. the P biologically stored inside PAOs cells as poly-P).

RESULTS AND DISCUSSION

WAGS was collected from a Granular Sequencing Batch Reactor (GSBR) performing a bioP-removal efficiency of 99%. WAGS was characterized by a VSS/TSS of 84% and a total phosphorus (TP) of 48.8 mgP/gTS, higher than conventional WAS (TP≈14-17 mgP/gTS) (Cordell et al., 2011; Pokhrel et al., 2018)means phosphorus will also need to be recovered for productive reuse as a fertilizer in food production to replace increasingly scarce and more expensive phosphate rock. Through an integrated and systems framework, this paper examines the full spectrum of sustainable phosphorus recovery and reuse options (from small-scale low-cost to large-scale high-tech. This confirms the high potential of P-recovery from WAGS, at least three times higher than WAS. The fractionation of TP in WAGS revealed that the 88.6 %wt was IP (NAIP+AP) and the 11.4 %wt was OP. These values were comparable with those of WAS that resulted: IP=84.4 %wt, OP=15.6 %wt (Pokhrel et al., 2018) and IP=88.7 %wt, OP=11.3 %wt (González Medeiros et al., 2005). Despite this similar repartition between IP and OP for WAGS and WAS, looking at the IP fractionation some differences are evident. The NAIP fraction for WAGS was considerable higher than WAS (79,6 %wt versus 44.8-48.0 %wt), as visible in Figure 1. This suggested that, due to the biofilm structure of WAGS, in the inner layers of granular sludge the local pH may have favoured the NAIP over the AP precipitation. NAIP fraction is considered the most labile P form, therefore more simple operational conditions are needed to recover it (e.g. pH close to 5-6). Conversely, more severe operational conditions are requested in order to recover AP fraction (e.g. pH close to 4) (Pokhrel et al., 2018). Therefore, a sludge high in NAIP fraction, such as WAGS, will be more promising and less expensive for P-recovery.

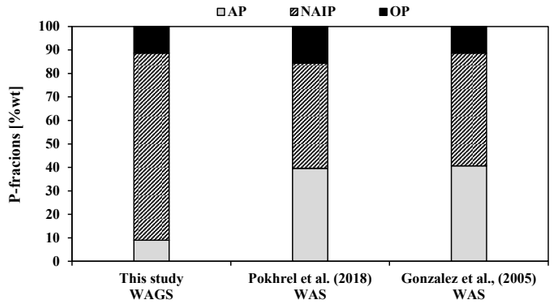

Figure 1: P-fractionation for WAGS (this study) and WAS (reference studies).

Looking at the P-recovery kinetics (Figure 2), it was observed that after 12 days a maximum P concentration of 45.2 mgP/gTS and 37.5 mgP/gTS (92.6 %wt and 76.9 %wt of TP) was reached for pH = 4 and pH = 5 batch tests, respectively. These data suggest that at pH = 4, also a part of AP can be recovered against greater operational complexity, as observed by Pokhrel et al. (2018). However, given the higher NAIP fraction, WAGS permits a significant P-recovery (close to 77% of TP) that would not be obtainable with a WAS under the same operational conditions. Therefore, by its nature, WAGS is in an advantaged position compared to WAS regarding the P-recovery.

Observing the kinetic of the batch test operated without pH control, a dramatic slowdown in P-recovery was registered reaching the maximum concentration of 31.6 mgP/gTS (64.7 %wt of TP) only after 31 days. Therefore, pH control is a key driver in order to maximize the P-recovery in the shortest time, which implies full-scale recovery reactors with smaller volumes. Since all the batch tests were conducted in strictly anaerobic conditions, it is assumed that in all the experiments there was a similar OP recovery.

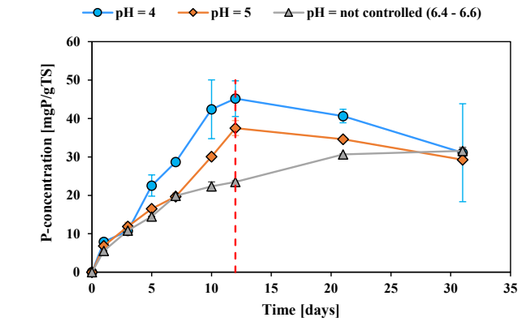

Figure 2: P-recovery kinetics at different pH conditions (fixed WAGS concentration: 2.1 gTS/L).

Salts with high P-content, that comply with the EU regulation (2019/1009) on fertilizers (EC, 2019), were chemically precipitated from bulk at the end of the tests. These salts could be reused for agronomic applications.

In summary, an innovative solution for P-recovery from WAGS is reported in Figure 3.

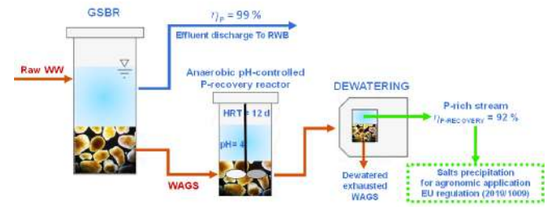

Figure 3: Hypothetical layout of P recovery-chain from WAGS.

Considering that 99% of TP contained in raw wastewater will be removed/accumulated in aerobic granular sludge and hypothesizing to maintain WAGS in anaerobic condition at pH=4, the results obtained in this study highlight that more than 90% of TP contained wastewater can be recovered. This finding places the AGS technology not only as one of the most efficient and promising biofilm technologies for wastewater treatment, but also as a precious mine for resource recovery.

CONCLUSIONS

This study reports on P-recovery from waste aerobic granular sludge. WAGS has higher NAIP fraction then WAS, therefore it offers an easier P-recovery. WAGS was collected from a GSBR performing an almost complete bioP-removal. The maximum P-recovery was achieved after 12 days at pH=4 (92.6% of TP). The obtained results show the potentials of an attractive side-stream treatment chain with a P-recovery efficiency > 90% of TP contained in raw wastewater. P-rich salts, after chemical precipitation from bulk, could be reused for agronomic applications.

ACKNOWLEDGEMENTS

This research was funded by ROP-ESFR Toscana 2014-2022 – IDRO.SMART project (CUP: 3647.04032020.157000040).

REFERENCES

APHA/AWWA/WEF, 2017. Standard Methods for the Examination of Water and Wastewater, 23rd ed., American Public Health Association, Washingto, DC, USA. Am. Public Heal. Assoc. Washingto, DC, USA.

Bobba, S., Carrara, S., Huisman, J., Mathieux, F., Pavel, C., 2020. Critical Raw Materials for Strategic Technologies and Sectors in the EU - a Foresight Study, European Commission.

Chrispim, M.C., Scholz, M., Nolasco, M.A., 2019. Phosphorus recovery from municipal wastewater treatment: Critical review of challenges and opportunities for developing countries. J. Environ. Manage.

Cordell, D., Rosemarin, A., Schröder, J.J., Smit, A.L., 2011. Towards global phosphorus security: A systems framework for phosphorus recovery and reuse options. Chemosphere.

Cordell, D., White, S., 2015. Tracking phosphorus security: indicators of phosphorus vulnerability in the global food system. Food Secur.

EC, 2019. Regulation (EU) 2019/1009 Fertilizer Products. Off. J. Eur. Union.

González Medeiros, J.J., Pérez Cid, B., Fernández Gómez, E., 2005. Analytical phosphorus fractionation in sewage sludge and sediment samples. Anal. Bioanal. Chem.

Mihelcic, J.R., Fry, L.M., Shaw, R., 2011. Global potential of phosphorus recovery from human urine and feces. Chemosphere.

Pokhrel, S.P., Milke, M.W., Bello-Mendoza, R., Buitrón, G., Thiele, J., 2018. Use of solid phosphorus fractionation data to evaluate phosphorus release from waste activated sludge. Waste Manag.

Pronk, M., de Kreuk, M.K., de Bruin, B., Kamminga, P., Kleerebezem, R., van Loosdrecht, M.C.M., 2015. Full scale performance of the aerobic granular sludge process for sewage treatment. Water Res. 84, 207–217.

Smolders, G.J.F., van der Meij, J., van Loosdrecht, M.C.M., Heijnen, J.J., 1995. A structured metabolic model for anaerobic and aerobic stoichiometry and kinetics of the biological phosphorus removal process. Biotechnol. Bioeng.

Recovering vivianite from manure: opportunities and bottlenecks

S. Banke * **, T. Prot *, L. Korving*,C. Schott* ***, and M. C. M. Loosdrecht **

* Wetsus, European Centre of Excellence for Sustainable Water Technology, Oostergoweg 7, 8911 MA Leeuwarden, the Netherlands
(E-mail: *sophie.banke@wetsus.nl)*

** Biotechnology Department, Faculty of Applied Sciences, Delft University of Technology, Van der Maasweg 9, Delft 2629 HZ, The Netherlands

*** Sub-department of Environmental Technology, Wageningen University, P.O. Box 17, 6700AA Wageningen, The Netherlands

Abstract

When dosing iron (Fe) to digested sewage sludge, phosphorus (P) can be magnetically recovered from in form of the paramagnetic mineral vivianite ($Fe_3(PO_4)_2$*8 H_2O). In this presentation we discuss the potential to use a similar approach for recovery of phosphate in manure. The low solubility of vivianite holds perspective to recrystallise other mineral phosphate forms into one recoverable mineral phase. However, while vivianite forms quite efficiently at a Fe/P ratio of 1.5 in sewage sludge, we observed that in pig manure a significant higher Fe dosing of up to Fe/P 4.5 was necessary to form vivianite. Organic matter is known to hinder vivianite formation in lake sediment by complexing Fe. Our first results show although organic ligands can influence vivianite formation and dissolution, the organics found in diluted manure do not have a significant influence. This highlights the necessity of more research on vivianite formation in different environments.

Keywords (maximum 6 in alphabetical order)

Iron complexation, manure organic matter, organic ligands, phosphorus recovery, vivianite

INTRODUCTION

In manure, P is often bound to magnesium (struvite) and calcium phosphates (Pagliari 2012). This makes targeted P recovery difficult because these minerals cannot be retrieved easily. A possible approach to recover P is solubilisation via acidification followed by a solid liquid precipitation and precipitation using alkaline magnesium or calcium salts. This implicates a high use of chemicals, and a more complicated extraction procedure (Tao 2016, Szögi 2015, Schoumans 2014). Therefore, it would be beneficial to have an easier transformation of the phosphorus precipitates in manure to one mineral. Vivianite ($Fe_3(PO_4)_2$*8 H_2O) is a promising mineral for phosphorus (P) recovery from municipal wastewater (Prot et al., 2019). Thanks to its paramagnetic properties it can be recovered magnetically, which has been shown at pilot scale (Wijdeveld et al., 2022). It forms over any other P and Fe-mineral in anaerobic digested sludge, after Fe has bound to sulfur (S). To maximize the transformation of P to vivianite, the stoichiometric dose of Fe/P 1.5 has to be increased depending on the S content of the sludge.(Prot et al., 2020). Vivianite can also be found in lake sediments. Due to similar conditions in sewage sludge and lake sediment, vivianite should also be the most stable mineral P form, which would make it easy to recover.

MATERIALS AND METHODS

Vivianite formation from phosphorus precipitates in manure

One litre of undigested sieved pig manure (< 200 µm) was poured into a sealed Duran bottle of 1.5 L. The bottle with pig manure received iron in three quantities. The quantities were calculated based on the pig manure composition. For the 4 g/L dose the total precipitation of FeS and then 5060 % of the

phosphorus as vivianite; for the 11 g/L, the total precipitation of FeS, then the binding of iron to 25 % of the organic carbon and the precipitation of all phosphorus as vivianite; for the 52 g/L dose a significant excess to maximize the quantity of phosphorus present as vivianite. The iron was added as $FeCl_2$*4 H_2O solution.

Establishing scales of known organic ligands competing with Fe-P bond in vivianite

Vivianite dissolution and formation with commercially available ligands

For vivianite dissolution experiments, vivianite was added to solutions of organic ligands (bipyridine (bipy), citrate, and humate) at a total organic carbon (TOC) content of 330 mg/L. The amount of Fe and P in solution was tracked via ICP-OES over the course of 3 weeks. For the vivianite formation experiment, $FeCl_2$*4 H_2O in solution was added to a solution containing K_2HPO_4 and the above-mentioned organic ligands at the same TOC. Fe and P that did not precipitate after 1 h were determined via ICPOES. The different organic ligands were classified on a scale according to their potential to keep Fe in solution per organic carbon for the dissolution and formation experiment respectively.

Diluted cow manure

Undigested sieved cow manure (< 200 µm) **was diluted to a TOC around 500 mg/L (table 1). Vivianite dissolution and formation experiments were performed according to the procedures described above replacing the organic ligands by the diluted manure. Then the results were compared with the help of the established scales.**

RESULTS AND DISCUSSION

Phosphorus precipitates in manure are transformed to vivianite at higher Fe dosing

For the 4 g/L dose, no vivianite was detected with Mössbauer spectroscopy (figure 1). When dosing 11 g/L a partial transformation of struvite P to vivianite could be seen under the stereoscope, amounting to 80 % of the total P based on calculations from the Mössbauer spectrum. Only in the excess Fe dosing of 52 g/L the complete P transformation to vivianite could be observed. Based on these results, it was estimated that a molar ratio of Fe/P 4.5 would be necessary to transform most of the phosphate into vivianite. This means a lot of Fe in manure stays in the organic material after vivianite recovery, implicating a loss of Fe salt, and making the quality of the organic material questionable for reuse as organic amendment in agriculture (figure 2).

This high surplus of Fe needed cannot be explained by the S content alone. Further explanations could be found in research on vivianite formation in lake sediments. Here, significant losses in vivianite yield have been attributed to 25 % of Fe equivalents binding to sedimentary organic carbon (Kleeberg et al., 2013). Therefore, we hypothesize, that Fe is sequestered by manure organic matter, and hence unavailable for vivianite formation. Therefore, we will study the influence of manure organic matter and compare this with a scale of known organic compounds.

Organics influence vivianite formation and dissolution

Vivianite dissolution (table 1) was observed for citrate, bipy and humate in decreasing intensity. Vivianite formation (table 1) was inhibited by citrate to the biggest extent lesser extent by bipy and humate. The stoichiometric ratio of Fe in solution to the TOC of the organic ligand was plotted on a scale for vivianite dissolution (Figure 3a) and formation (Figure 3b). Based on the hypothesis, manure organics were expected to dissolve vivianite and inhibit its formation to a greater extent. However, this was not the case here. Several factors could explain this unexpected result: low TOC content, the type of animal manure, and kinetic hindrance of the recrystallization from struvite to vivianite. The experiments related to these hypotheses will be performed from February on and the results will be available by June to be presented at the ecoSTP.

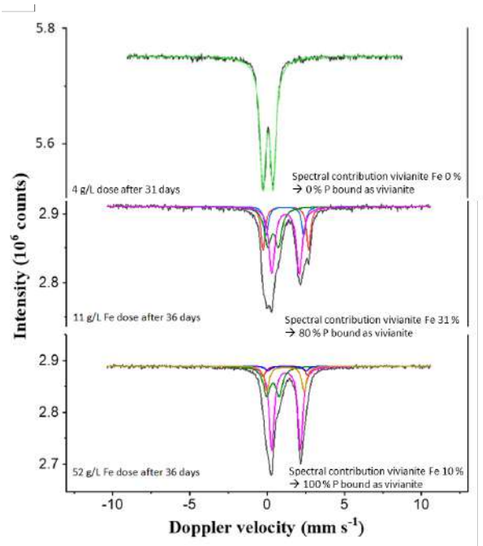

Figure 1. Mössbauer spectra for the samples measured at 300 K with the corresponding amount of P bound as vivianite calculated based on the spectral contribution of vivianite Fe, total amount of Fe, and P. The colors used correspond to, Black: sum of all the contributions, Blue: Vivianite site A, Red: Vivianite site B, Pink: $FeCO_3$, Green: Fe^{3+}/Fe^{II} standing for Fe(III) compounds, and low-spin Fe(II) compounds like pyrite, Yellow: $FeCl_2$*2H_2O.

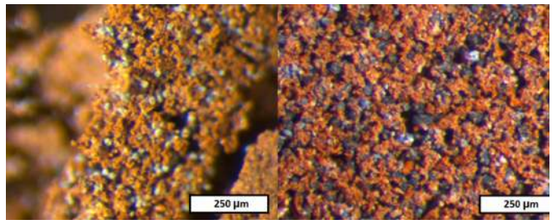

Figure 2. Magnetic fraction after the magnetic separation of the manure treated with 11 g/L (left) and 52 g/L (right) dose of iron. The blue particles observed are vivianite.

Table 1.
Organic ligand with TOC content, relative amount of Fe dissolved from vivianite, and retained in solution after vivianite formation.

	TOC (mg/L)	% Fe dissolved	% Fe in solution after formation
bipy	333	30	37
citrate	324	52	94
humate	294	6	34
diluted cow manure	445	0	12
MiliQ water	-	0	12

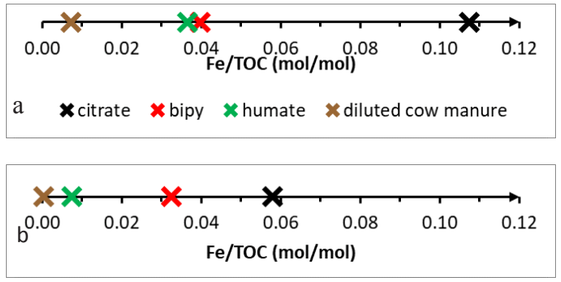

Figure 1. Scale of Fe in solution per TOC of organic ligand for vivianite dissolution (a) and vivianite formation (b).

REFERENCES

Gypser, S., Freese, D., 2020. Phosphorus release from vivianite and hydroxyapatite by organic and inorganic compounds. *Pedosphere* 30.

Kleeberg, A., Herzog, C., Hupfer, M., 2013. Redox sensitivity of iron in phosphorus binding does not impede lake restoration. *Water Research* 47.

Pagliari, P.H.; Laboski, C.A.M; 2012. Investigation of the Inorganic and Organic Phosphorus Forms in Animal Manure. *Journal of Environmental Quality* 41(3), 901-910.

Li, C., Sheng, Y., 2021. Organic matter affects phosphorus recovery during vivianite crystallization. *Water Science and Technology* 83.

Prot, T., Nguyen, V.H., Wilfert, P., Dugulan, A.I., Goubitz, K., de Ridder, D.J., Korving, L., Rem, P., Bouderbala, A., Witkamp, G.J., van Loosdrecht, M.C.M., 2019. Magnetic separation and characterization of vivianite from digested sewage sludge. *Seperation and Purification Technol*ogy 224.

Prot, T., Wijdeveld, W., Eshun, L.E., Dugulan, A.I., Goubitz, K., Korving, L., van Loosdrecht, M.C.M., 2020. Full-scale increased iron dosage to stimulate the formation of vivianite and its recovery from digested sewage sludge. *Water Research* 182.

Schoumans, O. F.; Ehlert, P. A. I.; Nelemans, J. A.; van Tintelen, W.; Rulkens, W. H.; Oenema, O.; 2014. Explorative study of phosphorus recovery from pig slurry. Wageningen UR Alterra Report 2514.

Szögi, A. A.; Vanotti, M. B.; Hunt, P. G.; 2015. Phosphorus Recovery from Pig Manure Solids Prior to Land Application. *Journal of Environmental Management*, 157, 1-7.

Tao, W.; Fattah, K. P.; Huchzermeier, M. P; 2016. Struvite Recovery from Anaerobically Digested Dairy Manure: A Review of Application Potential and Hindrances. *Journal of Environmental Management*, 169, 46–57.

Wijdeveld, W.K., Prot, T., Sudintas, G., Kuntke, P., Korving, L., van Loosdrecht, M.C.M., 2022. Pilot-scale magnetic recovery of vivianite from digested sewage sludge. *Water Research* 212.

Nutrient recovery from source separated human urine as vivianite

C. Simbeye*, C. Courtney*, P. Simha**, N. Fischer*** and D.G. Randall*
* Civil Engineering Department & Future Water Institute, University of Cape Town, 7700 Cape Town, South Africa
(E-mail: *smbchi005@myuct.ac.za*; *crtcai001@myuct.ac.za; dyllon.randall@uct.ac.za)*
** Department of Energy and Technology, Swedish University of Agricultural Sciences, SE-750 07 Uppsala, Sweden
(E-mail: *Prithvi.Simha@slu.se)*
*** Catalysis Institute and DSI-NRF Centre of Excellence in Catalysis c*Change, Department of Chemical Engineering, University of Cape Town, 7700 Cape Town, South Africa
(E-mail: *nico.fischer@uct.ac.za)*

Abstract

Urine contributes up to 70% of the phosphorus load in domestic wastewater, and decentralized sanitation systems and source separation provide an opportunity to recover this phosphorus. In this study, we assessed the feasibility of recovering phosphorus as vivianite from human urine, using thermodynamically modeled and experimentally determined data. We found that type of iron salt used, and also reaction temperature, did not affect yield and purity of vivianite. However, urine pH affected the solubility of vivianite and other co-precipitates, with the highest yield (93 ± 2%) and purity (79 ± 3%) of vivianite obtained at pH 6.0. Yield and purity of vivianite were both maximized when Fe:P molar ratio was greater than 1.5:1, but less than 2.2:1. This molar ratio provided sufficient iron to react with all available phosphorus, while exerting a competitive effect that suppressed formation of other precipitates. Vivianite produced from fresh urine was less pure than vivianite produced from synthetic urine, because of the presence of organics in real urine, but washing the solids with deionized water improved the purity by 15.5% at pH 6.0. Overall, this novel work adds to the growing body of literature on phosphorus recovery as vivianite from wastewater.

Keywords (maximum 6 in alphabetical order)

decentralized sanitation; fertilizers; nutrient recycling; resource recovery; stabilization; wastewater treatment

Note: This work is currently under review for potential publication in *Environmental Science & Technology*

INTRODUCTION

Excess phosphorus (P) in the environment is harmful, as it can cause hypoxia and eutrophication in natural water bodies (Preisner et al., 2020). Domestic wastewater is a major contributor to the global flux of P. Considering that 80% of wastewater produced globally receives no treatment (Connor et al., 2017), it is unsurprising that eutrophication remains a problem worldwide (Hendriks and Langeveld, 2017). This has led to the implementation of stricter effluent standards across the world on discharge of treated wastewater to the environment. However, treatment that only removes P from wastewater is not sufficient and the focus must be shifted to recovering P, as it is a finite resource (Priambodo et al., 2017).

Human urine is rich in P which could be recovered as a valuable solid such as vivianite, which is more valuable than other P-compounds. In freshly excreted human urine, most of the nitrogen present is in the form of urea (Kabdaşlı et al., 2006), which hydrolyses and promotes struvite precipitation. If magnesium does not limit formation of struvite, then all the P in urine is precipitated as struvite (Simha et al., 2022) and no vivianite can form.

In freshly excreted urine not subjected to urea hydrolysis or stabilization treatment, recovery of P as vivianite is likely to be high, as the pH is near-neutral and all phosphate is in solution. In this study, we investigated the feasibility of recovering P in the form of vivianite from source-separated fresh human urine for the first time. We also examined the effects of various process parameters, such as pH, temperature, composition of human urine, and type and dose of iron salts, on precipitation of vivianite. We then compared the yield and purity of vivianite precipitated from synthetic and real urine under different conditions, by combining empirical data with thermodynamic modeling of urine chemistry. This study provides a new eco-friendly and decentralized treatment strategy for P recovery from source separated urine, especially if waste sources of iron are used.

MATERIALS AND METHODS

Both synthetic and real urine were used in this study. Fresh urine was collected from fertilizer-producing urinal developed by Flanagan and Randall (2018).

Thermodynamic modeling was conducted using the Mixed Solvent Electrolyte (MSE) model in OLI Stream Analyzer (OLI System Inc., 2021. The model was used to investigate the effects of type of iron salt used, operating temperature, dose molar ratio (Fe:P), and pH on precipitation and on the yield and purity of vivianite that could be recovered from urine.

All experiments were conducted using 500 mL of urine, which was added to a jacketed crystallizer (GlassChem, Cape Town, South Africa) that was temperature-controlled by water circulation at 25 °C using a chiller (M1907-0156, PolyScience, Illinois, United States). The pH, temperature, and composition of the urine were analyzed before and after iron dosing. A pH probe (HANNA Instrument, Rhodes Island, United States) was used to determine the pH of urine before and after iron dosing, and also during the reaction. Solution pH was controlled by an automated pH controller and logger (GlassChem Instrument, Cape Town, South Africa). A magnetic stirrer (M520, LabCon, California, United States) was set to 150 rpm to keep the solution homogeneous during the experiment. Sodium hydroxide (NaOH, 1 mol L^{-1}) and hydrochloric acid (HCl, 0.5 mol L^{-1}) were used to regulate the pH, at a dosage rate of 51 µL per event. Once the urine solution was dosed with iron salt, the experiments were run for 15 min. All experiments were conducted in triplicate.

RESULTS AND DISCUSSION

Ideal operating conditions for producing vivianite

The iron dose (Fe:P molar ratio) and operating pH were found to have differing effects on the yield and purity of vivianite (Figure 1). It was observed that regardless of iron dose, operation outside the pH range 5.0 - 8.0 adversely impacted the yield of vivianite (Figure 1A). In jar-tests on different wastewaters, (Wu et al., 2019) also found that vivianite formation is generally possible in the pH range 5.0-8.5, although much lower yields have been reported at the extremes of this range (Liu et al., 2018). Reaction pH directly affects the solubility of compounds present in urine.

Iron dose had a direct effect on the amount of vivianite formed at a particular pH, and the concentration of Fe^{2+} in solution also influenced the type and concentration of co-precipitates. It was found that excess Fe^{2+} competed with Ca^{2+} and Mg^{2+} cations for P, hence preventing formation of compounds containing these cations (e.g., hydroxyapatite (HAP), bobierrite), resulting in higher yield and purity of vivianite. In the pH range 5.5-8.5, the highest vivianite yields were achieved when the iron dose was equal to or greater than a Fe:P molar ratio of 1.5. The highest purity was obtained from pH 4.0 (when the solid began to form) to pH 7.0-8.0, depending on the Fe:P dosage ratio. This agrees with findings in the literature that the optimal pH range to maximize the yield and purity of vivianite extraction from wastewater is pH 6.0-8.0 (Wu et al., 2019).

The P in urine can form precipitates of calcium, magnesium, or iron, depending on their concentration and the pH of the urine. Hydroxyapatite begins to form at pH 6.5 and increases in concentration as the pH increases. The solubility of HAP declines as the pH increases, resulting in Ca^{2+} competing with Fe^{2+} for P. The amount of HAP that formed when the urine was underdosed with iron (Figure 1B) was significantly greater than that formed when the Fe:P dosage ratio was 1.5 (Figure 1C) or when iron was overdosed (Figure 1D), in increasing order. Struvite formation was only observed when urine was underdosed with iron (Figure 1B). Excess Fe^{2+} was found to inhibit the formation of calcium and magnesium precipitates at pH values below 8.3.

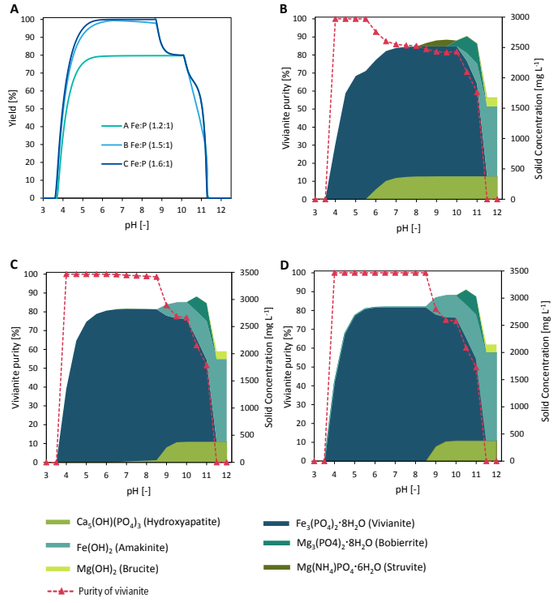

Figure 1. (A) Effect at different pH levels of iron sulfate ($FeSO_4$) dose on yield of vivianite, and effect of pH on vivianite purity and solids concentration when $FeSO_4$ was (B) underdosed [Fe:P ratio 1.2], (C) dosed in the exact molar ratio [Fe:P ratio 1.5], and (D) overdosed [Fe:P ratio 1.6].

Generally, operating in a pH range of 4.0 to 5.5 always produced the highest purity of vivianite, but at the expense of reduced yield due to the relatively higher solubility of vivianite in this pH range (Table 1). Yield of vivianite was maximized between pH 6.0 and 8.3, while the purity depended on the Fe:P ratio. Higher dosages of Fe^{2+} favored formation of vivianite over other precipitates of calcium and magnesium within the pH range 6.0 to 8.3. Within the pH range 4.0 to 8.5, when urine was overdosed with iron (Figure 1D), vivianite was produced in its purest form as the only solid. Above pH 8.5, $Fe(OH)_2$ began to precipitate, consuming Fe^{2+} and reducing the Fe^{2+} concentration in the solution, thus limiting the amount of Fe^{2+} available to form vivianite. This allowed Ca^{2+} and Mg^{2+} ions to form precipitates with the P, resulting in low yield and purity of vivianite (Figure 1D).

This work demonstrated that vivianite can be chemically precipitated from human urine through addition of iron salt, with maximum yield of 93 ± 2 % and maximum purity of 79 ± 3 % obtained at an optimal pH of 6.0.

Type of iron salt used did not affect the yield and purity of the solid fraction obtained, so choice of salt was only influenced by the amount of solid formed and the operating costs. Iron sulfate ($FeSO_4 \cdot 7H_2O$) was found to be the most economical option and is suggested as the preferred iron salt when dosing for vivianite formation from human urine.

Solution pH was found to affect the solubility of vivianite and other co-precipitates of Mg and Ca, and also affected the rate of oxidation of Fe^{2+} when exposed to oxygen in the air. A Fe:P ratio of between 1.5:1 to 2.2:1 was found to maximize yield and purity of vivianite extracted from urine. Overdosing with iron salt provided sufficient Fe^{2+} to react with all P and had a competitive effect that suppressed formation of other co-precipitates of Ca and Mg. Additionally, a small fraction of the Fe^{2+} present oxidized to Fe^{3+}, so excess Fe^{2+} was critical to maximize the yield and purity of vivianite.

Operating temperature had little to no effect on yield and purity of vivianite, and only affected the solubility of Ca and Mg precipitates at pH values above 8.0, which is outside the ideal pH range for vivianite recovery.

The solid fraction obtained from fresh urine contained about 15% organics by mass, regardless of operating pH. Washing this fraction with deionized water improved vivianite purity from 63.1% to 78.6% by mass.

REFERENCES

Connor, R., Renata, A., Ortigara, C., Koncagül, E., Uhlenbrook, S., Lamizana-Diallo, B.M., Zadeh, S.M., Qadir, M., Kjellén, M. Sjödin, J. 2017. The united nations world water development report 2017. wastewater: the untapped resource. The United Nations World Water Development Report.

Hendriks, A.T., Langeveld, J.G. 2017 Rethinking wastewater treatment plant effluent standards: nutrient reduction or nutrient control?. *Environmental Science and Technology* **51**(9), 4735–4737.

Kabdaşlı, I., Tünay, O., İşlek, Ç., Erdinç, E., Hüskalar, S., Tatlı, M. 2006. Nitrogen recovery by urea hydrolysis and struvite precipitation from anthropogenic urine. *Water Science and Technology* **53**(12), 305–312.

Liu, J., Cheng, X., Qi, X., Li, N., Tian, J., Qiu, B., Xu, K., Qu, D. 2018. Recovery of phosphate from aqueous solutions via vivianite crystallization: thermodynamics and influence of pH. *Chemical Engineering Journal* **349**, 37–46.

Preisner, M., Neverova-Dziopak, E., Kowalewski, Z. 2020. Analysis of eutrophication potential of municipal wastewater. *Water Science and Technology* **81**(9), 1994–2003.

Simha, P., Deb, C.K., Randall, D.G., Vinnerås, B. 2022. Thermodynamics and Kinetics of pH-dependent Dissolution of Sparingly Soluble Alkaline Earth Hydroxides in Source-Separated Human Urine Collected in Decentralised Sanitation Systems. *Frontiers in Environmental Science*, **10**, 889119.

Wu, Y., Luo, J., Zhang, Q., Aleem, M., Fang, F., Xue, Z., Cao, J. 2019. Potentials and challenges of phosphorus recovery as vivianite from wastewater: A review. *Chemosphere* **226**, 246–258.

A Comprehensive Assessment of The Opportunities of P Recovery by Integrating a Side-Stream Sludge Fermenter Into EBPR Systems

Mengqi Cheng, Albert Guisasola and Juan Antonio Baeza

GENOCOV. Department of Chemical, Biological and Environmental Engineering, Autonomous University of Barcelona, Campus UAB, Cerdanyola del Vallès, 08193, Spain

(E-mail: *Mengqi.cheng@autonoma.cat; Albert.Guisasola@uab.cat; JuanAntonio.Baeza@uab.cat)*

Abstract

Chemical precipitation as struvite enables phosphorus (P) recovery in wastewater treatment plants (WWTPs). Struvite is generally precipitated using the anaerobic digestion supernatant profiting from its high P concentration. This study shows how the integration of a side-stream sludge fermenter (SSSF), which has been identified as a possible solution to improve the performance of enhanced biological phosphorus removal (EBPR) systems when treating low COD wastewater, opens a pathway for P recovery. The full presentation will detail how, for the first time, incorporating a SSSF into an anaerobic/anoxic/aerobic (A2O) configuration (side-stream EBPR, S2EBPR) can boost P recovery in a 150L pilot plant operated for more than one year. SSSF integration provides a novel location for P-recovery since P concentration in the SSSF can reach values higher than 100 mgP/L, while maintaining excellent P-removal. The S2EBPR performance will also be presented when the SSSF reactor outlet is connected to the anaerobic, anoxic, or aerobic reactor, with the best results obtained for the first case. Moreover, the potential P-recovery opportunities for each of the effluents of the plant under the different scenarios, evaluated using MINTEQ-based simulations, will be presented. These simulations complement the experimental pilot-plant work and will comprehensively show the real possibilities of P-recovery with a S2EBPR configuration.

Keywords

Enhanced biological phosphorus removal (EBPR); P recovery; Side-stream sludge fermenter

INTRODUCTION

Phosphorus (P) is vital to biological processes, but its over-enrichment in water bodies, known as eutrophication, can have detrimental effects on aquatic ecosystems (Suresh Kumar, et al., 2018). Moreover, the demand for P grows yearly with its different applications and depletion. Along with a large amount of P going to WWTPs, P removal and recovery from wastewater become critical, not only for eutrophication control and water reuse initiatives (Nie, Wu, et al., 2019), but also it has been estimated as a suitable solution to meet 15-20% of the global P demand (Venkiteshwaran, et al., 2018).

The anaerobic/anoxic/aerobic (A2O) process is the most accepted EBPR configuration, providing nutrient and organic matter removal, but also high phosphate levels from anaerobic liquors, which is a potential way to implement P recovery (Zhang, et al., 2022). Innovative EBPR configurations are required to move forward from P removal to P recovery. Among them, the integration of a SSSF into a conventional EBPR process (also known as S2EBPR) has recently gained a lot of interest (Onnis-Hayden, et al., 2020). S2EBPR (Figure 1) can overcome the possible bad performance caused by low COD/P ratio input, or excess nitrite returned to the anaerobic reactor (Gu, et al., 2008). There are an increasing number of full-scale applications of S2EBPR facilities worldwide (Tooker, Li, et al., 2017), which have improved P removal performance and stability (Wang, et al., 2019). The possible reasons for the PAO activity increase in S2EBPR are: (1) the biomass fermentation products are mostly VFA, a preferred electron donor for PAO (Wang, et al., 2019); (2) the extended anaerobic phase gives a competitive advantage for PAO with respect to GAO and other heterotrophic organisms (Barnard, et al., 2017) and (3) besides VFA, the SSSF effluent can contain extra readily biodegradable material which could be further fermented to VFA by PAO fermenters such as *Tetrasphaera* (Nielsen, et al., 2019).

The existing knowledge gap in understanding the underlying mechanisms in S2EBPR hampers its further application for P recovery. This work will show the novel results of nearly one-year operation of a 150L S2EBPR pilot plant under different operational conditions. The original idea for S2EBPR was to produce a VFA-rich effluent in the SSSF to improve the whole plant performance. However, PAO activity was so high that all the VFA produced in the SSSF was consumed *in-situ* leading to high levels of P-release and to a high P-concentration effluent. The SSSF P levels (>100 mgP/L, Figure 2) were much higher than those in the anaerobic reactor (>50 mgP/L), opening new scenarios for P recovery.

This observation had two implications that will be fully discussed in the full presentation.

1) The P load to the plant was increased (up to 20%) and, under certain conditions, full P-uptake could be hindered.
2) The high P concentration in the SSSF opened the possibility of recovering P from the SSSF if the purge was located there (more than 25% of the entering P could be recovered). This idea has been experimentally evaluated for the first time under different scenarios of SSSF HRT (0.5 to 2 days) and varied integrated strategies between SSSF and A2O.

We will comprehensively evaluate, for the first time, the opportunities of the S2EBPR system to go beyond P removal and move to P recovery in the full oral presentation. In addition to the one-year experimental measurements, diverse scenarios are simulated using VISUAL MINTEQ (see examples in Figure 3 & 4). For a given scenario, the possibilities of recovering P as struvite from the different effluents of the plant will be shown. Moreover, we will also examine the possibility of subjecting the purge to an extra anaerobic fermentation process to increase the P-levels and, thus, to promote struvite formation and P-recovery. For instance, Figure 3 shows the proportion of different compounds (hydroxyapatite, struvite and $Mg_3(PO_4)_2$) could be precipitated during period I when the purge was subjected to anaerobic digestion with $P\text{-}PO_4^{3-}$, $N\text{-}NH_4^+$ and Mg^{2+} content of 108, 40.3 and 22 mg/L, respectively. It suggests that Ca^{2+} presence limits the P recovery as struvite, as the first option for PO_4^{3-} precipitation is hydroxyapatite (HAP), without being affected by pH. Magnesium will combine with phosphate to produce $Mg_3(PO_4)_2$ at more alkaline pH (>10.4), competing with struvite. With the certain $P\text{-}PO_4^{3-}$, $N\text{-}NH_4^+$ and Mg^{2+} content from conventional EBPR of period I, the purpose of recovering P would be less effective especially in the means of struvite. What we could expect from S2EBPR will be a stronger possibility to recover more P as struvite according to the current data obtained. To better improve the P recovery process with additional dosages, further mathematical simulations have been done. Figure 4 shows that Mg^{2+} addition has a significant effect on P recovery as struvite and correlates closely with the pH. When providing enough NH_4^+ concentration, the struvite formation will be less dependent on the Mg^{2+} supply but on the pH. In this case, adjusting proper pH will be more economical than adding more Mg^{2+}, since its dosage could contribute up to 75% of the total operational cost in some process as reported. More details of different scenarios will be further explained in the presentation.

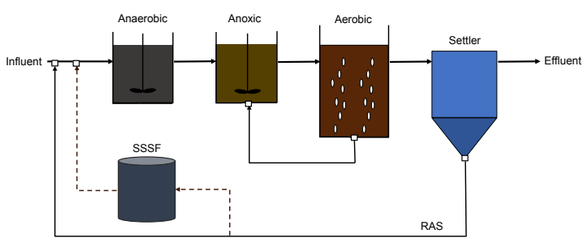

Figure 1. The overview of S2EBPR configuration, obtained by integrating a SSSF reactor into an A2O configuration.

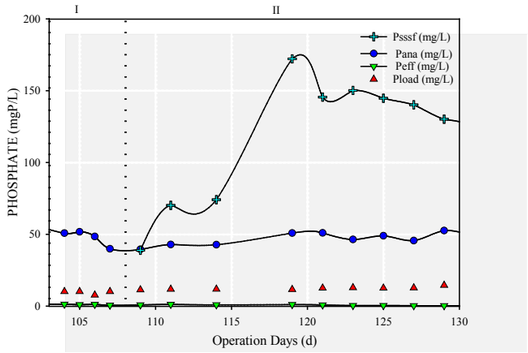

Figure 2. The fate of P and the removal performance of the A2O (Period I) and A2O+SSSF (Period II) systems.

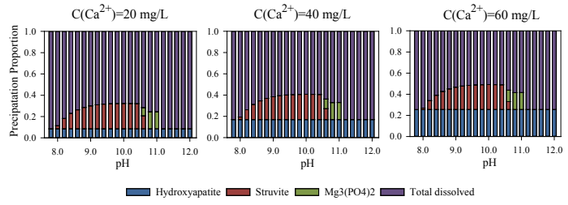

Figure 3. Influence of pH on different P compounds precipitation with the presence of Ca^{2+} (20-60 mg/L) for the supernatant subjected to anaerobic digestion in period I.

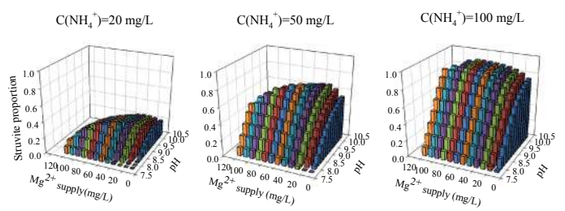

Figure 4. Influence of pH and Mg^{2+} supply on struvite formation for scenarios with different concentration of $N\text{-}NH_4^+$ (20-100 mg/L) and a fixed concentration of Ca^{2+} (20 mg/L) of period I.

REFERENCES

Barnard, J. L., Dunlap, P., and Steichen, M. 2017 Rethinking the Mechanisms of Biological Phosphorus Removal. *Water Environment Research* **89**(11), 2043–2054.

Gu, A. Z., Saunders, A., Neethling, J. B., Stensel, H. D., and Blackall, L. L. 2008 Functionally Relevant Microorganisms to Enhanced Biological Phosphorus Removal Performance at Full-Scale Wastewater Treatment Plants in the United States. *Water Environment Research* **80**(8), 688–698.

Lanham, A. B., Oehmen, A., Saunders, A. M., Carvalho, G., Nielsen, P. H., and Reis, M. A. M. 2013 Metabolic versatility in full-scale wastewater treatment plants performing enhanced biological phosphorus removal. *Water Research* **47**(19), 7032–7041.

Nie, G., Wu, L., Du, Y., Wang, H., Xu, Y., Ding, Z., and Liu, Z. 2019 Efficient removal of phosphate by a millimeter-sized nanocomposite of titanium oxides encapsulated in positively charged polymer. *Chemical Engineering Journal* **360**, 1128–1136.

Nielsen, P. H., McIlroy, S. J., Albertsen, M., and Nierychlo, M. 2019 Re-evaluating the microbiology of the enhanced biological phosphorus removal process. *Current Opinion in Biotechnology* **57**, 111–118.

Onnis-Hayden, A., Srinivasan, V., Tooker, N. B., Li, G., Wang, D., Barnard, J. L., Bott, C., Dombrowski, P., Schauer, P., Menniti, A., Shaw, A., Stinson, B., Stevens, G., Dunlap, P., Takács, I., McQuarrie, J., Phillips, H., Lambrecht, A., Analla, H., Russell, A., and Gu, A. Z. 2020 Survey of full-scale sidestream enhanced biological phosphorus removal (S2EBPR) systems and comparison with conventional EBPRs in North America: Process stability, kinetics, and microbial populations. *Water Environment Research* **92**(3), 403–417.

Suresh Kumar, P., Ejerssa, W. W., Wegener, C. C., Korving, L., Dugulan, A. I., Temmink, H., van Loosdrecht, M. C. M., and Witkamp, G. J. 2018 Understanding and improving the reusability of phosphate adsorbents for wastewater effluent polishing. *Water Research* **145**, 365–374.

Tooker, N. B., Li, G., Bott, C., Dombrowski, P., Schauer, P., Menniti, A., Shaw, A., Barnard, J. L., Stinson, B., Stevens, G., Dunlap, P., Takacs, I., Phillips, H., Analla, H., Russell, A., Ellsworth, A., McQuarrie, J., Carson, K., Onnis-Hayden, A., and Gu, A. Z. 2017 "Rethinking and Reforming Enhanced Biological Phosphorus Removal (EBPR) strategy - Concepts and mechanisms of side-stream EBPR" in Water Environment Federation Technical Exhibition and Conference 2017, WEFTEC 2017. *Water Environment Federation* 4387–4404.

Venkiteshwaran, K., McNamara, P. J., and Mayer, B. K. 2018 Meta-analysis of non-reactive phosphorus in water, wastewater, and sludge, and strategies to convert it for enhanced phosphorus removal and recovery. *Science of the Total Environment* **644**, 661–674.

Wang, D., Tooker, N. B., Srinivasan, V., Li, G., Fernandez, L. A., Schauer, P., Menniti, A., Maher, C., Bott, C. B., Dombrowski, P., Barnard, J. L., Onnis-Hayden, A., and Gu, A. Z. 2019 Side-stream enhanced biological phosphorus removal (S2EBPR) process improves system performance - A full-scale comparative study. *Water Research* **167**, 115109.

Zhang, C., Guisasola, A., and Baeza, J. A. 2022 A review on the integration of mainstream P-recovery strategies with enhanced biological phosphorus removal. *Water Research* **212**, 118102.

Nutrient recovery from hydrolysed urine by Na-chabazite adsorption integrated with ammonia stripping and (K-)struvite precipitation

Haotian Wu [a,b], Xavier Foster [a,b], Hossein Kazemian [c,d] and Céline Vaneeckhaute [a,b] *

[a] BioEngine, Research Team on Green Process Engineering and Biorefineries, Chemical Engineering Department, Université Laval, 1065, avenue de la Médecine, Québec, QC, G1V 0A6, Canada; haotian.wu.1@ulaval.ca, celine.vaneeckhaute@gch.ulaval.ca, xavier.foster.1@ulaval.ca

[b] CentrEau, Centre de recherche sur l'eau, Université Laval, 1065, avenue de la Médecine, Québec, QC, G1V 0A6, Canada; celine.vaneeckhaute@gch.ulaval.ca

[c] Northern Analytical Lab Services, University of Northern British Columbia, Prince George, BC, Canada; hossein.kazemian@unbc.ca

[d] Chemistry Department, Faculty of Science and Engineering, University of Northern British Columbia, Canada; hossein.kazemian@unbc.ca

Abstract

This study investigated the recovery of K^+ along with NH_4^+-N and PO_4^{3-}-P from hydrolyzed urine by technical integration. The K adsorption capacities of biochar, clinoptilolite, artificial zeolite and chabazite were firstly compared. Due to the high K recovery efficiency and additional P recovery capacity, Na-chabazite was selected as the adsorbent in this study. Its kinetics and isotherm analysis indicated that the high molarity of NH_4^+-N seriously hindered the K adsorption onto Na-chabazite in synthetic hydrolyzed urine (SHU). However, this competition between NH_4^+ and K^+ got diminished when their molarity is the same, i.e. in the SHU after ammonia stripping (ASSHU). Based on this key finding, Na-chabazite adsorption was integrated with ammonia stripping and struvite precipitation under different configurations. Simultaneous ammonia stripping was inadequate to diminish the competitive effect of NH_4^+ on K^+ adsorption. Depending on the demand for fertilizer, two sequential configurations were recommended, respectively.

Keywords (maximum 6 in alphabetical order)

Hydrolysed urine; K recovery; K-struvite; Na-chabazite; stripping

INTRODUCTION

Urine has been reconsidered as a renewable resource in the past two decades (Jagtap and Boyer, 2018; Kavvada et al., 2017; Patel et al., 2020). So far, it is typical to hydrolyze urine till 90% of total nitrogen transfers from urea to NH_3/NH_4^+, and then to apply different technologies for nutrient recovery, like struvite precipitation, stripping and adsorption. Currently, most of research focus on nitrogen and phosphate recovery, while potassium (K) recovery is out of main scope despite its huge economic value. Technically, the competitiveness between NH_4^+ and K^+ exists in some nutrient recovery technologies, such as (K-)struvite precipitation. To the best of authors' knowledge, few studies have achieved the efficient recovery of these three macronutrients from hydrolyzed urine. As a result, the current study was undertaken to fill this knowledge gap by selecting a practical adsorbent and integrating it with ammonia stripping and (K-)struvite precipitation.

MATERIALS AND METHODS

K^+ adsorbent selection

In the selection of an appropriate K adsorbent, the tested materials included: 1) sewage sludge derived biochar (1.4 mm); 2) maple biochar (>2 mm); 3) Canada natural clinoptilolite (1 mm); 4) Iran natural clinoptilolite (1.4 mm); 5) Cuba natural clinoptilolite (<0.25 mm); 6) Zeolite 4A China (fine powder); 7) Zeolite 4A Sigma (fine powder); 8) Na-Chabazite (1.4×0.3 mm); 9) Ca/Na-Chabazite (<0.3 mm). These nine candidate adsorbents were added in the KCl solution (1563.92 mg/L) at a dosage of 50 g/L and then shaken at 200 rpm and 25□ for 2h. The supernatant liquid was sampled and filtered through a 0.45 µm membrane before the $[K^+]$ and $[PO_4^{3-}$-P] measurement.

Na-Chabazite (Anhydrous sodium aluminosilicate, natural herschelite-sodium chabazite) was selected as the K adsorbent used in the below sections on Kinetics & isotherm analysis and Technical integration. It was obtained from St. Cloud Mining, USA.

Kinetics and isotherm analysis

In addition to the abovementioned KCl solution, synthetic hydrolyzed urine (SHU) and after-stripping synthetic hydrolyzed urine (ASSHU) were also applied for kinetics and isotherm analysis.

In kinetics analysis, 50 g/L Na-Chabazite was added into SHU, ASSHU and KCl solution and agitated for 8 hours to ensure the equilibrium was reached. The liquid samples were extracted at appropriate time intervals using 0.45 µm syringe filters to detect the change of $[K^+]$ with time. All batch experiments were carried out in triplicate.

For isotherm analysis, SHU, ASSHU and KCl solution were diluted with deionized water to provide a varying initial concentration of K^+. 50 g/L Na-Chabazite was added into diluted batches. The experimental process is consistent with kinetics analysis. All isotherm experiments were also triplicated.

Technical integration

A series of batch experiments was performed to evaluate the nutrient recovery efficiency in different configurations, including:

I) "Stripping + Struvite precipitation + K adsorption";

II) "Stripping → Struvite precipitation + K adsorption";

III) "Stripping → Struvite precipitation → K adsorption".

RESULTS AND DISCUSSION

Selection of K^+ adsorbent

As shown in Figure 1, both natural zeolites, including clinoptilolite and chabazite, and artificial zeolites were able to adsorb K^+ from KCl solution with removal efficiency from 37.3% (Canada natural clinoptilolite) to 93.2% (artificial zeolite 4A Sigma). Sample 7 and 8, namely Sigma artificial zeolite 4A and Na-chabazite, showed an adsorption capacity significantly higher than the other zeolites. On the contrary, maple biochar and sludge biochar desorbed K^+ into KCl solution, improving $[K^+]$ by 1.8% and 4.4%, respectively.

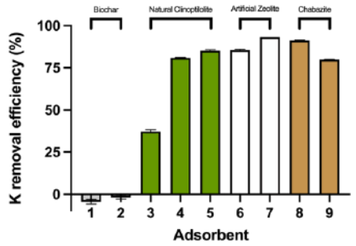

Figure 1. K removal efficiency of different adsorbents in KCl solution

After dropping Na_2HPO_4 solution into their supernatants, precipitation was observed in all batches of natural zeolites, which was not observed in the ones of biochar and artificial zeolites. It indicates that some cations on clinoptilolites and chabazites that could precipitate with PO_4^{3-} got desorbed into supernatant during K^+ adsorption.

Its SEM-EDS spectra indicated that after Na-chabazite adsorption in KCl solution, the content of Na^+, Mg^{2+} and Ca^{2+} decreased from 6.78%, 1.08% and 1.69% to 4.23%, 0.74% and 1.08%, respectively. It suggests that Na^+ was the dominant exchanging cation on Na-Chabazite, and Mg^{2+}/Ca^{2+} also exchanged with K^+, which is consistent with the previous research (Regmi and Boyer, 2021). As to artificial zeolite, in spite of its highest adsorption capacity, sodium was the only exchanging cation, which cannot contribute to PO_4^{3-} recovery (Wang, 2020).

Kinetics analysis

The adsorption of K^+ on Na-chabazite in SHU, ASSHU and KCl solution are presented in Figure 2. As seen, Na-chabazite showed a lower K adsorption capacity in SHU (13.77±0.19 mg/g), compared to the corresponding values in ASSHU and KCl, i.e. 27.11±0.17 mg/g and 27.64±0.17 mg/g, respectively. It suggested that there is a competition between NH_4^+ and K^+ in hydrolyzed urine. Ammonia stripping prior to K adsorption can reduce the competitive effect of NH_4^+ and promote Na-chabazite to adsorb more K^+ from hydrolyzed urine, 5.01 wt% (ASSHU) > 2.88% (SHU). Despite the existence of Na^+ in the effluent of stripping, i.e. 0.108 mol Na^+/L > 0.04 mol K^+/L, it did not cause an obvious decrease to the K adsorption capacity of chabazite, indicating that K^+ has a higher priority to the active sites on chabazite than Na^+.

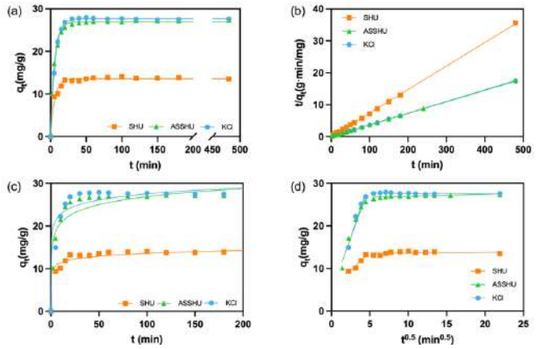

Figure 2. The K^+ adsorption on Na-chabazite in synthetic hydrolyzed urine (SHU), after-stripping synthetic hydrolyzed urine (ASSHU) and KCl solution and their simulation to Pseudo-1st-order (a), Pseudo-2nd-order (b), Elovich (c), and Weber-Morris intra-particle diffusion (d) kinetic models

The regression coefficients of the Pseudo-2nd-order kinetic model revealed to be the best in representing potassium adsorption onto chabazite (>0.99 for all sorts of solution). This could indicate various physical meanings based on different previous research (Esfandiari et al., 2020; Jing et al., 2019; Lalley et al., 2016; Li et al., 2017; Xia et al., 2016; Xiao et al., 2020; Xu et al., 2018). A two-section Weber-Morris IPD kinetics models was observed in Figure 2 (d). It could be stated that the K adsorption on chabazite started with an instant external diffusion followed by intra-particle diffusion, which was the rate-determining step until the equilibrium (Baek et al., 2018; Wu et al., 2009; Zhu et al., 2016).

Isotherm analysis

Figure 3 shows the adsorption behaviour of K^+ by Na-chabazite in SHU (a), ASSHU (b) and KCl (c), when it reached the equilibrium at 25ºC. As the concentration of NH_4^+-N increased from 0 mg/L in KCl solution to 522 mg/L in ASSHU and 6720.5 mg/L in SHU, the maximum quantity adsorbed decreased accordingly, as illustrated in Figure 3(d). The experimental data were well fitted to Langmuir isotherm model, with a coefficient of 0.98 (SHU), 0.93 (ASSHU) and 0.96 (KCl). The value of its parameter, q_m (mg/g), is an indicator of maximum adsorption capacity, which decreased from 75.65 mg/g in KCl to 40.37 mg/g in ASSHU and 11.31 mg/g in SHU. It suggested that the high concentration of NH_4^+-N could restrain the K adsorption capacity of Na-Chabazite in SHU. When it decreased to the same molarity as K^+ in ASSHU by stripping, the adsorption capacity of Na-Chabazite for K^+ got increased.

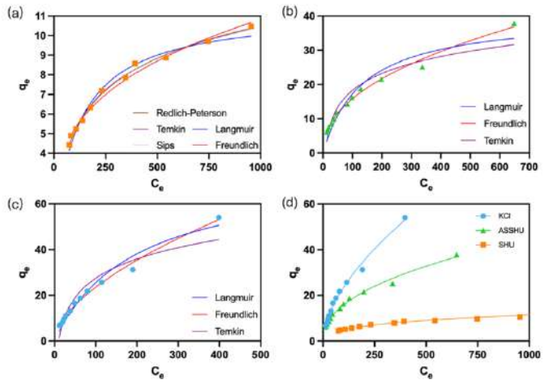

Figure 3. K adsorption onto Na-chabazite at equilibrium in SHU (a), ASSHU (b) and KCl (c) and summary for experimental data and the best-fitting isotherm models (d)

Despite the good fitness to Langmuir isotherm model, those empirical models, i.e. Freundlich model and Langmuir-Freundlich hybrid models, showed a slightly higher correlation coefficient, which is different from the previous research (Leyva-Ramos et al., 2010; Seliman and Borai, 2011). As such, K adsorption on Na-chabazite is supposed to be a heterogeneous process controlled by multiple mechanisms, consistent with the results of kinetics analysis concluded in section 3.2 (Xu et al., 2018).

Comparison of the different configurations of technical integration

To diminish the competitive impact of NH_4^+ on K^+ adsorption and recover all three macronutrients, three different configurations were investigated, and their comparison was shown in Figure 4. As shown, 23.93±2.66% K^+ was removed by simultaneous configuration, significantly lower than the sequential configurations. It indicated that simultaneous stripping has a limited effect on diminishing the competition between NH_4^+ and K^+ for exchanging with Na^+ on Na-Chabazite. As to the reasons behind this observation, the current study infers that despite NH_4^+-N removal through stripping and struvite precipitation, its molarity was still higher than that of K^+ especially at the beginning of the process, hence the competitive effect of NH_4^+-N on K^+ adsorption was not eliminated.

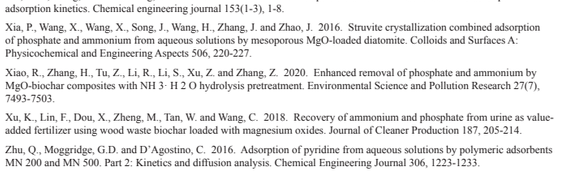

Figure 4. The comparison on nutrient removal efficiency among the different configurations of stripping, K adsorption and struvite precipitation

Both sequential configurations achieved similar recovery efficiency. If pure (K-)struvite is a preferrable end-product, "Stripping → K adsorption → Struvite precipitation" is recommended. In its second step, along with 78.63% K^+, 21.84% PO_4^{3-}-P got recovered in this step even without any addition of Mg source. The ability of both K and P recovery makes Na-chabazite more practical than pristine and surface-modified biochar (Liu et al., 2020).

REFERENCES

Baek, W., Ha, S., Hong, S., Kim, S. and Kim, Y. 2018. Cation exchange of cesium and cation selectivity of natural zeolites: chabazite, stilbite, and heulandite. Microporous and Mesoporous Materials 264, 159-166.

Esfandiari, N., Kashefi, M., Mirjalili, M. and Afsharnezhad, S. 2020. Role of silica mid-layer in thermal and chemical stability of hierarchical Fe3O4-SiO2-TiO2 nanoparticles for improvement of lead adsorption: Kinetics, thermodynamic and deep XPS investigation. Materials Science and Engineering: B 262, 114690.

Jagtap, N. and Boyer, T.H. 2018. Integrated, multi-process approach to total nutrient recovery from stored urine. Environmental Science: Water Research & Technology 4(10), 1639-1650.

Jing, H.-P., Li, Y., Wang, X., Zhao, J. and Xia, S. 2019. Simultaneous recovery of phosphate, ammonium and humic acid from wastewater using a biochar supported Mg(OH)2/bentonite composite. Environmental Science: Water Research & Technology 5(5), 931-943.

Kavvada, O., Tarpeh, W.A., Horvath, A. and Nelson, K.L. 2017. Life-cycle cost and environmental assessment of decentralized nitrogen recovery using ion exchange from source-separated urine through spatial modeling. Environmental science & technology 51(21), 12061-12071.

Lalley, J., Han, C., Li, X., Dionysiou, D.D. and Nadagouda, M.N. 2016. Phosphate adsorption using modified iron oxide-based sorbents in lake water: kinetics, equilibrium, and column tests. Chemical Engineering Journal 284, 1386-1396.

Leyva-Ramos, R., Monsivais-Rocha, J., Aragon-Piña, A., Berber-Mendoza, M., Guerrero-Coronado, R., Alonso-Davila, P. and Mendoza-Barron, J. 2010. Removal of ammonium from aqueous solution by ion exchange on natural and modified chabazite. Journal of environmental management 91(12), 2662-2668.

Li, R., Wang, J.J., Zhou, B., Zhang, Z., Liu, S., Lei, S. and Xiao, R. 2017. Simultaneous capture removal of phosphate, ammonium and organic substances by MgO impregnated biochar and its potential use in swine wastewater treatment. Journal of Cleaner Production 147, 96-107.

Liu, J., Zheng, M., Wang, C., Liang, C., Shen, Z. and Xu, K. 2020. A green method for the simultaneous recovery of phosphate and potassium from hydrolyzed urine as value-added fertilizer using wood waste. Resources, Conservation and Recycling 157, 104793.

Patel, A., Mungray, A.A. and Mungray, A.K. 2020. Technologies for the recovery of nutrients, water and energy from human urine: A review. Chemosphere 259, 127372.

Regmi, U. and Boyer, T.H. 2021. Ammonium and potassium removal from undiluted and diluted hydrolyzed urine using natural zeolites. Chemosphere 268, 128849.

Seliman, A.F. and Borai, E.H. 2011. Utilization of natural chabazite and mordenite as a reactive barrier for immobilization of hazardous heavy metals. Environmental Science and Pollution Research 18(7), 1098-1107.

Wang, Y. 2020. Measurements and modeling of water adsorption isotherms of zeolite linde-type A crystals. Industrial & Engineering Chemistry Research 59(17), 8304-8314.

Wu, F.-C., Tseng, R.-L. and Juang, R.-S. 2009. Initial behavior of intraparticle diffusion model used in the description of adsorption kinetics. Chemical engineering journal 153(1-3), 1-8.

Xia, P., Wang, X., Wang, X., Song, J., Wang, H., Zhang, J. and Zhao, J. 2016. Struvite crystallization combined adsorption of phosphate and ammonium from aqueous solutions by mesoporous MgO-loaded diatomite. Colloids and Surfaces A: Physicochemical and Engineering Aspects 506, 220-227.

Xiao, R., Zhang, H., Tu, Z., Li, R., Li, S., Xu, Z. and Zhang, Z. 2020. Enhanced removal of phosphate and ammonium by MgO-biochar composites with NH 3· H 2 O hydrolysis pretreatment. Environmental Science and Pollution Research 27(7), 7493-7503.

Xu, K., Lin, F., Dou, X., Zheng, M., Tan, W. and Wang, C. 2018. Recovery of ammonium and phosphate from urine as value-added fertilizer using wood waste biochar loaded with magnesium oxides. Journal of Cleaner Production 187, 205-214.

Zhu, Q., Moggridge, G.D. and D'Agostino, C. 2016. Adsorption of pyridine from aqueous solutions by polymeric adsorbents MN 200 and MN 500. Part 2: Kinetics and diffusion analysis. Chemical Engineering Journal 306, 1223-1233.

Development and experimental comparison of a precipitation model for struvite using a low-grade magnesium oxide (industrial by-product) as an alternative magnesium source.

K. Olaciregui-Arizmendi*,** , V. B. Aguilar-Pozo***, S. Astals***, J. M. Chimenos***, A. López****, J. Gómez****, B. Elduayen-Echave*,** and E. Ayesa*,**

*CEIT-Basque Research and Technology Alliance (BRTA), Manuel Lardizabal 15, 20018 Donostia / San Sebastián, Spain. (E-mail: *kolaciregui@ceit.es*)
**Universidad de Navarra, Tecnun, Manuel Lardizabal 13, 20018 Donostia / San Sebastián, Spain.
***Universidad de Barcelona, C/ Martí i Franqués 1, 08028 Barcelona, Spain.
****NILSA, Navarra de Infraestructuras Locales S.A., Av. Barañáin 22, 31008 Pamplona, Spain.

Abstract

In this contribution the development of a precipitation model for struvite precipitation is explained. The main objective of this work is to implement this technology in a real WWTP located in Tudela, Spain. For that reason, a simulation tool is developed in order to help in the definition of the operational strategy. The model replicates how Mg and Ca are dissolved differently depending on the water composition and how it affects the struvite precipitation. The following steps will consist of validating the precipitation model using experiments in several fluidized bed reactors.

Keywords

Low-grade magnesium oxide; Precipitation model; Struvite

INTRODUCTION

Struvite is a salt formed by equimolar quantities of magnesium (Mg), nitrogen (N) and phosphorus (P) which can be used as a slow release fertilizer. Waterways are rich in N and P, but Mg needs to be added externally. Usually, a commercial reactant ($MgCl_2 \cdot 6H_2O$) is used as Mg source, increasing the operational costs of the process. For this reason, magnesium oxide industrial by-products, low-grade magnesium oxide (LG-MgO), obtained from the calcination process of natural magnesite have been suggested as an optimum alternative (Romero-Güiza et al., 2015).

Many factors affect the overall precipitation process, such as reactants concentration, pH or hydrodynamics (Le Corre et al., 2009). Some authors have developed mathematical models where thermodynamic equilibrium or kinetics are studied (Elduayen-Echave et al., 2019) , but to the authors' best knowledge, implications of using LG-MgO have not been modelled.

In this contribution, a new model is developed and calibrated with different experiments. This model includes the effects of using LG-MgO. This precipitation model is a promising tool that may help in the definition of the operation strategy of the process.

MATERIALS AND METHODS

Precipitation model

This model is developed in WEST-DHI simulation platform. The LG-MgO used as a Mg source is a heterogeneous by-product consisting of different compounds, which release Mg^{2+}, Ca^{2+}, CO_3^{2-} and OH^- to the medium. In the model, nine different solid compounds are considered: LG-MgO, struvite, amorphous calcium phosphate (ACP), $Mg(OH)_2$, $MgCO_3$, $Ca(OH)_2$, $CaMg(CO_3)_2$, $CaCO_3$, struvite coating over LG-MgO and ACP coating over LG-MgO. Table 1 includes some of the different transformations considered. Moreover, in the liquid phase: NH_4^+, NH_3, PO_4^{3-}, HPO_4^{2-}, $H_2PO_4^-$, H_3PO_4, $MgPO_4^+$, $MgHPO_4$, $MgH_2PO_4^+$, $MgOH^+$, Mg^{2+}, $CaPO_4^-$, $CaHPO_4$, $CaH_2PO_4^+$, $CaOH^+$ and Ca^{2+} are considered.

The thermodynamic equilibrium is calculated based on the approach by (Ohlinger, Young and Schroeder, 1998). The thermodynamics equations used in the precipitation model can be found in Table 1, whereas the transformations considered in the model are included in Table 2. Only one dissolution process is included in the table. The stoichiometry of the process is defined by a Gujer matrix, see Table 3, as it is often done in wastewater treatment modelling (Lizarralde et al., 2015). The model incorporates saturation index (SI) calculations for each solid compound in each time step, which are the driving force of the precipitation and kinetics, including nucleation and growth.

Experimentation

In order to validate the model, different experimental set-ups have been defined. The main objective of these configurations is to gradually scale up the technology, with the final purpose of applying it in a real plant. Firstly, batch experiments are done, followed by experiments in a pilot fluidized bed reactor of 5 L, a semi-industrial fluidized bed reactor of 80 L and finally, in an industrial reactor located in the WWTP of Tudela, Spain. For an initial validation two different 0.5 L batch experiments are considered. In the first one, the solubility of the LG-MgO is studied for different molar ratios in deionised water. In the second one, struvite precipitation is achieved by adding different concentrations of LG-MgO to a real effluent from a wastewater treatment plant.

RESULTS AND DISCUSSION

From both cases of experiments performed, one of each type has been selected to demonstrate the utility of the model. By now, the model has been heuristically calibrated for each experiment. In the future a more rigorous calibration should be performed. For this purpose, the use of Bayesian Inference techniques is being considered.

In the LG-MgO dissolution experiment considered (209.6 mg/L of LG-MgO, Mg:P molar ratio of 1:1), the pH increased from 6.5 until 10.5 in 30 minutes. After this fast increase, its value remains almost constant during the whole experiment. This pH increase is related to the release of OH^- to the medium. Once pH stabilises, Ca reaches a plateau, no more Ca is released to the deionised water, whereas Mg concentration continues increasing, but at a lower rate. This difference is possibly because of the saturation concentration of Ca is reached, whereas the Mg saturation concentrations is not reached yet. These phenomena are well reproduced by the model, as displayed in Figure 1.

Figure 1. LG-MgO release of Mg and Ca in deionised water.

The precipitation experiments showed a different behaviour. The initial pH is almost the optimum for struvite precipitation (8.5), avoiding the previous effect of a fast release of ions to the medium. For 209.6 mg/L of LG-MgO, the consumption of both species is compensated by the release of Ca and Mg from the LG-MgO. P and N are consumed in the same molar proportion, leading to struvite precipitation. In general, the model is able to predict the release of Mg and Ca ions from the solid and to predict the precipitation of struvite and ACP, Figure 2.

Figure 2. Species behaviour in struvite precipitation using real effluent from WWTP.

CONCLUSIONS AND FUTURE PERSPECTIVES

The simulation results show that the developed precipitation model is able to reproduce correctly the data obtained in the laboratory experiments. Verifying that a useful tool to know if struvite or other compounds will precipitate in real WWTP, with an alternative Mg source, has been developed. However, a standard calibration method should be applied. For that purpose, different experiments are considered in the scaling up process of the technology. The next step is to validate the model using the results obtained from the use of a pilot fluidized bed reactor. Then, this precipitation model could be used to optimize the operation of the process directly and even feed other types of models (CFD or compartmental models) for the design of new reactors.

Table 1. Thermodynamic equations included in the model.

Calculation	Equation	Description
Ionic activity		: ionic activity [mol/L]
Struvite saturation index		: activity coefficient [-]
Ionic strength		: concentration [mol/L]
		: solubility product [mol^3/L^3]
Activity coefficient		: ionic strength [mol/L]
		: valence [-]
		: Debye-Hückel constant [-]

Table 2. Transformations considered in the model.

Reaction	Equation	Description
$Mg(OH)_2$ dissolution		: kinetic constant for dissolution [1/s]
Nucleation		: kinetic constant for nucleation [$mol/L \cdot s$]
Growth		: kinetic constant for growth [1/s]
		: kinetic constant [1/s]
		: kinetic exponent [-]
Coating		: dissolution index [-]
		: saturation index [-]
		: saturation index for coating [-]

Table 3. Example of a Gujer matrix of the model including only Mg compounds precipitation and $Mg(OH)_2$ dissolution.

Species	NH_4^+	Mg^{2+}	PO_4^{3-}	STRU	OH^-	$Mg(OH)_2$	STRU- LG-MgO
Processes							
Struvite precipitation					−	−	−
$Mg(OH)_2$ dissolution	−		−	−			−
Struvite coating		−		−		−	

ACKNOWLEDGMENTS

This research is part of the R&D project RTC2019-007257-5, funded by MCIN/AEI/10.13039/501100011033/. The authors would like to thank the Spanish Science and Innovation Ministry for the Research Project MODYPHOS (PID2019-108378RB-I00) and the Department of Education of the Basque Government for the Predoc Grant (PRE_2022_1_0271).

REFERENCES

Elduayen-Echave, B., Lizarralde, I., Larraona, G.S., Ayesa, E., Grau, P., 2019. A New Mass-Based Discretized Population Balance Model for Precipitation Processes: Application to Struvite Precipitation. Water Res 155, 26–41. https://doi.org/10.1016/j.watres.2019.01.047

Le Corre, K.S., Valsami-Jones, E., Hobbs, P., Parsons, S.A., 2009. Phosphorus recovery from wastewater by struvite crystallization: A review, Critical Reviews in Environmental Science and Technology. https://doi.org/10.1080/10643380701640573

Lizarralde, I., Fernández-Arévalo, T., Brouckaert, C., Vanrolleghem, P., Ikumi, D.S., Ekama, G.A., Ayesa, E., Grau, P., 2015. A new general methodology for incorporating physico-chemical transformations into multi-phase wastewater treatment process models. Water Res 74, 239–256. https://doi.org/10.1016/j.watres.2015.01.031

Ohlinger, K.N., Young, T.M., Schroeder, E.D., 1998. Predicting struvite formation in digestion. Water Res 32, 3607–3614. https://doi.org/10.1016/S0043-1354(98)00123-7

Romero-Güiza, M.S., Tait, S., Astals, S., del Valle-Zermeño, R., Martínez, M., Mata-Alvarez, J., Chimenos, J.M., 2015. Reagent use efficiency with removal of nitrogen from pig slurry via struvite: A study on magnesium oxide and related by-products. Water Res 84, 286–294. https://doi.org/10.1016/j.watres.2015.07.043

BIOFERES: Advanced Recovery of Nutrients from sewage sludge to obtain value-added products for Agriculture: bio-stimulants and liquid fertilizers.

R. Tamarit*, R. Garcia-Tirado*, P. Torrent*, A. Antolí**, J. Herrero**, R. Romaguera*** and R.Hervás***

* Sociedad de Fomento Agrícola, S.A (FACSA), Castelló de la Plana (Castelló), Spain.
(E-mail: *raquel.tamarit@facsa.com; ruben.garcia@grupogimeno.com; paloma.torrent@facsa.com)*
** BIOVIC Consulting, Paterna (València), Spain.
(E-mail: *aantoli@biovic-consulting.es*; *juliana.herrero@biovic-consulting.es)*
***Ingeniería y Desarrollos Renovables, S.L (INDEREN), Silla (València), Spain.
(E-mail: *r.romaguera@inderen.es*; *r.hervas@inderen.es)*

Abstract

The BIOFERES project proposes a new process for advanced nutrient recovery and sewage sludge transformation into high added value products. This new biorefinery concept will bring the wastewater management model closer to the principles of sustainability and circular economy. The project combines the following technologies: (1) Two Phase Anaerobic digestion (TPAD) with co-substrates dosage to increase biogas production and nutrients content in digestate, (2) Production of liquid biofertilizers through advanced nutrient recovery processes using double-stage membrane technologies (ultrafiltration and membrane contactors) and (3) Biostimulant production from the solid fraction of the digested sludge through a solid-state fermentation (SSF) process with bioaugmentation using specific bacterial strains. Results have shown that it is possible to maximize the nutrient content in sludge digestate, reaching values of 5-8 times above the initial ones in the case of P and K, and recovering more than 80% of the nitrogen contained in the liquid fraction.

Keywords

Anaerobic digestion; Biofertilizers; Bioestimulants; Membranes; Sludge.

INTRODUCTION

Traditionally, the sludge from the Wastewater Treatment Plants (WWTP) has been considered the residue produced from the water purification process, so efforts have been mainly focused the reduction of its volume with the objective of reducing management costs from the WWTP to its final disposal.

BIOFERES project has developed and validated a new sewage sludge treatment and valorisation process (Figure 1) that combines different technologies to obtain agronomic products (biofertilizers and bioestimulants), reducing the consumption of raw materials and the carbon footprint, defining a new wastewater management model based on the principles of sustainability and circular economy. The project is led by the company FACSA, together with BIOVIC and INDEREN, and with the participation of the AINIA technology centre and ISIRYM-UPV institute.

MATERIALS AND METHODS

The new process has been studied at lab scale and is currently being validated at pilot scale (Figure 2) in Alcoi WWTP (Alacant, Spain).

Anaerobic co-digestion in double temperature stage and double biological phase (TPAD)

TPAD combines two consecutive reactors for the performance of the hydrolytic-acidogenic and methanogenic steps, respectively, of anaerobic digestion. This allows not only sewage sludge stabilization but also biogas production maximization and nutrients enrichment (including N, P and K) thanks to different organic agrifood wastes used as co-substrates attending to different feeding strategies or diets. Biomethanation potential has been studied at lab scale using BMP tests and TPAD performance and stability has been evaluated using two pilot digesters of 1 and 2,7 m3 that has been operated for several months at thermophilic (55ºC) and mesophilic (35ºC) conditions, respectively, with an organic loading rate ranging from 14,2 to 24,6 gCOD/L·day (Figure 3). Final digestate has been dewatered using an endless screw so solid fraction is taken to SSF and liquid fraction with high nutrients content is derived to the membranes treatment.

Production of liquid biofertilizers through advanced nutrient recovery processes using double-stage membrane technologies

The liquid fraction from digestate dewatering is characterized by containing most of the dissolved nutrient's (N, P and K) and humic and fulvic acids. This fraction is treated using ultrafiltration (UF) to remove solids and pathogens and finally introduced into a membrane contactors stage for N recovery as $(NH_4)_2SO_4$ and remaining a P and K rich liquid biofertilizer. Both UF and membranes contactors has been studied in different lab experiments where different membranes materials (PVDF, PES, PTFE and ePTFE) and operation conditions (TMP (1, 1.5 and 2 bars), pH, time, and acid concentration) has been tested, and finally validated in a pilot prototype treating 110 L/d.

Bio-stimulant production from the solid fraction of the sludge through a solid-state fermentation process and bioaugmentation with specific bacterial strains.

Most of the stabilized organic matter and part of the nutrients, are concentrated in the solid fraction after digestate dewatering. This solid fraction is treated using a SSF process bioaugmented with a specific bacterial strain with biostimulant properties, such as improving nutrients bioavailability and assimilation by crops, so a sludge-based biostimulant is produced. This stage has been studied first using a small solid-state fermenter for sludge-strain compatibility tests and operational conditions definition and is currently being validated in a pilot fermenter of 60L of reacting volume.

RESULTS

Results from BMP of 5 different co-substrates (Co-S) used in the study are summarized in Table 1, where high biogas production potential up to 967±123 NL CH4/kg SV can be observed. During TPAD pilot operation, correct stabilization of both acidogenic and methanogenic reactors have been achieved, reaching more than 11 g/L of Volatile Fatty Acid (VFA) and biogas production with a methane concentration of more than 69% (Figure 4). Moreover, a nutrients concentration increase in P and K of 5-8 times above the initial value has been observed, while N remains constant.

Regarding liquid fraction treatment, best results were obtained with a previous prefiltration (60 microns) and a UF stage with PVDF membrane of 0.03 micron pore size operated at 1 bar. With this membrane, organic matter (COD) and solids removal around 60% and 95%, respectively, has been achieved, but rejection of N, K and P increases above 30%, which could indicate struvite precipitation (Table 2). Membrane contactor selected configuration and conditions were submerged expanded Teflon tubes where 0.1M sulfuric acid was circulated inside the tubes (immersed in the centrifuge drain) and liquid influent pH is adjusted up to 9-10. More than 80% nitrogen recovery was obtained from the liquid fraction (Figure 5).

After the biostimulant strain selection, continuous tests were started to analyse bacterial growth over real dewatered digestate from Alcoi WWTP. After several tests, it was observed that the best strategy was to operate the reactor at 35-37ºC, 16-18%ST concentration, HRT of 5 days and re-inoculate the reactor every 15 days (3 HRT), which allows maintain a strain concentration in the system of the order of 10^6 CFU/ml (Figure 6).

DISCUSSION

With the results obtained so far at lab and pilot scale in BIOFERES project, it has been observed that it is possible to valorise sewage sludge to transform them into biofertilizer and bio-stimulant products that have agricultural applications.

AKNOWLEDGMENT

BIOFERES project has been funded by Agència Valenciana de la Innovació (AVI) under the reference INNCAD/2021/68.

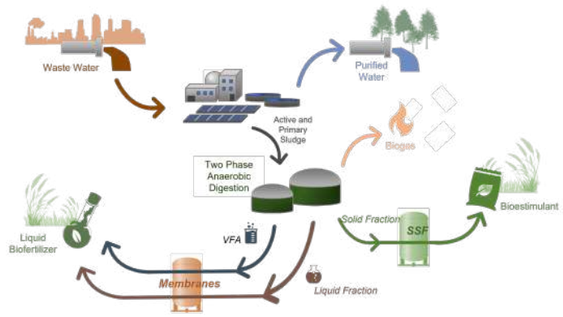

Figure 1. Scheme of the wastewater treatment system proposed in the project.

Figure 2: Pilot stages: a) Two phase anaerobic digestion, b) UF and membrane contactors, c) Solid state fermenter.

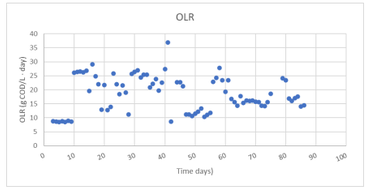

Figure 3: OLR evolution over time.

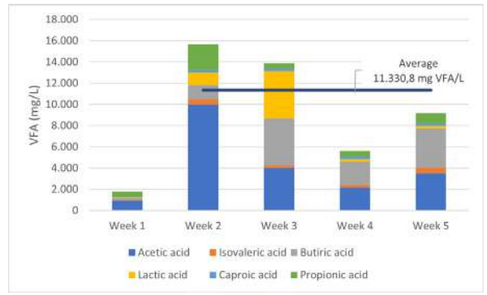

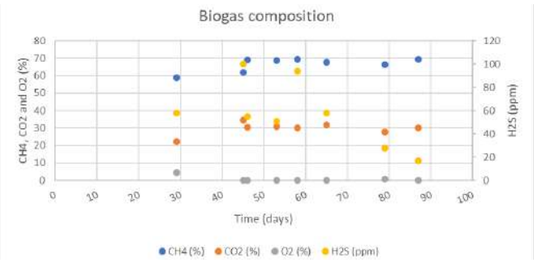

Figure 4: a) VFA evolution over time, b) Composition of biogas produced.

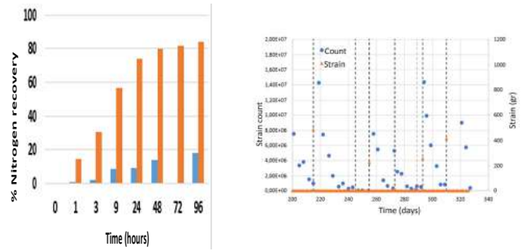

Figure 5: Time course of nitrogen recovery in membrane contactors (PTFE tube in blue, ePTFE tube in brown).

Figure 6: Strain count (blue) and amount of strain added (orange) in SSF

Table 1: Main parameters of the BMP assay of analyzed substrates.

Parameters	*Co-S 1*	*Co-S 2*	*Co-S 3*	*Co-S 4*	*Co-S 5*	*Sludge*
Metane (NL/kgSV)	461 ±36	967 ±123	733 ±81	637 ±1	452 ±11	317
Biogas (NL/kgSV)	646 ±50	1443 ±183	1047 ±115	872 ±71	636 ±16	450
Biodegradability (%)	93%	100%	80%	100%	100%	-
CH_4 (% biogas)	72 ±1	67 ±5	70 ±5	73 ±2	71 ±2	-

Table 2: Characterization of the permeates obtained with the 0.03-micron PVDF UF membrane.

Parameters	*Feeding (After prefiltration at 60 microns)*	*Permeate (P = 1 bar)*	*Permeate (P = 1,5 bar)*
Ammonium (mg/L)	370	227	285
Total phosphorous (mg/L)	96	25	29
Potassium (mg/L)	118	90	76
COD (mg/L)	438	177	189

Continuous bioelectrochemical nitrogen recovery from high N-loaded wastewaters

Zainab Ul, Mira Sulonen, Juan Antonio Baeza, Albert Guisasola

Genocov, Departament d'Enginyeria Química, Biològica i Ambiental, Escola d'Enginyeria, Universitat Autònoma de Barcelona
(E-mail: zainab.ul@uab.cat; mira.sulonen@uab.cat; juanantonio.baeza@uab.cat; albert.guisasola@uab.cat)

Abstract

Microbial electrolysis cells (MECs) enable ammonium recovery from wastewater with low energy requirements. Electric current drives ammonium ion transfer through a cation exchange membrane (CEM) in these systems. Nitrogen can be energy efficiently recovered from the concentrated nitrogen-rich stream by using a hydrophobic membrane. Novel tailor-made cells (0.8 L) were designed to maximize ammonium recovery by reducing dead volumes and improving mass transfer limitations. This work aims to determine the inhibitory effects of ammonium in the range of 0.5 to 2.5 g N-NH_4^+ /L on the performance of current generation and active ammonia recovery from synthetic wastewater. When the ammonium concentration in the feed was increased from 0.5 to 1.5 g N-NH_4^+ /L maximum current density increased to 3.9 A/m^2, but further increase in the concentration had a remarkable effect on the biofilm activity, decreasing the current density to 0.5 A/m^2 at 2.5 g N-NH_4^+/L. The maximum ammonium removal and recovery efficiencies were 67 % and 33 % at 0.5 g N-NH_4^+ /L, respectively. This is the first study of high-purity ammonium recovery using a hydrophobic membrane in a continuously fed MEC with different cathode materials. This in-situ bioelectrochemical ammonium recovery is benchmarked with other current ammonium recovery techniques as leading-edge technology in the current state of the art.

Keywords (maximum 6 in alphabetical order)

Hydrophobic membrane; Microbial electrolysis cells; Nitrogen recovery; Nickel foam; Stainless steel.

INTRODUCTION

In the last decade, much focus has been shifted to channelling energy and nutrients contained in waste streams and reducing the burden and costs of wastewater treatment (Puyol et al. 2017)changing the focus from residues treatment, such as wastewater treatment, toward resource recovery. Biotechnological processes offer an economic and versatile way to concentrate and transform resources from waste/wastewater into valuable products, which is a prerequisite for the technological development of a cradle-to-cradle biobased economy. This review identifies emerging technologies that enable resource recovery across the wastewater treatment cycle. As such, bioenergy in the form of biohydrogen (by photo and dark fermentation processes. Ammonium nitrogen in wastewater has emerged as an appealing compound from the resource recovery point of view. Industrially, ammonia is produced by nitrogen fixation (Haber-Bosch process) (Nancharaiah, et al. 2016) nitrogen removal is practiced through energy intensive biological nitrification and denitrification entailing a major cost in wastewater treatment. Recent innovations in nitrogen removal aim at reducing energy requirements and recovering ammonium nitrogen. Bioelectrochemical systems (BES, which is highly energy intensive and dependent on fossil fuels (Wang et al. 2021). In a conventional wastewater treatment plant, ammonium and nitrate are transformed into nitrogen gas (M. Rodríguez Arredondo et al. 2015), and therefore, they are removed to reduce the risk of eutrophication of receiving water bodies (Georg et al. 2021) but not recovered as valuable products. In contrast, a vast amount of nitrogen-based fertilizers are produced for agriculture (Erisman et al. 2008). Ammonia recovery from wastewater using a bioelectrochemical system (BES) holds promise as a suitable alternative in the circular economy framework.

At the anode of BESs, anode-respiring bacteria oxidize organic matter to carbon dioxide and protons and use a solid anode as a terminal electron acceptor (Kondaveeti et al. 2014). The electrons then flow from the anode to the cathode through an external circuit generating an electric current. At the cathode, the electrons combine with an electron acceptor to form the target product. Ammonium ions can diffuse from the anode chamber into the cathode chamber through a cation exchange membrane (CEM) via diffusion or current-driven migration (Yang and Qin 2021). Diffusion of ammonium ions is induced by the concentration gradient across the CEM, while the aim to achieve electroneutrality after electrons flow from the anode to the cathode also drives the migration of ammonium ions. As a result, ammonium ions are concentrated in the cathode chamber. The ammonium ions have an acid-dissociation constant (pKa value) of 9.25 (at 25ºC) (Wu and Modin 2013). Hence, once the catholyte pH exceeds 9.25 due to e.g., electrochemical hydrogen production, ammonium ions dissociate predominantly as free volatile ammonia (NH_3), which can then be recovered. Dissolved ammonia gas in the catholyte can traverse the pores of the hydrophobic membrane and react with the acidic solution placed on the other side (Kuntke et al. 2016)\n \n The application of a gas-permeable hydrophobic tubular membrane in bio-electrochemical systems enables efficient recovery of ammonia (NH\n 3\n . A high concentration of ammonium in the wastewater can affect the performance of BES because it can inhibit the activity of anode-respiring bacteria. This study assesses the inhibition effects of ammonium on current generation and ammonium recovery in continuously operated microbial electrolysis cells (MECs).We also calculated ammonium and organic removal efficiencies and ammonium recovery rates to compare the performance of different conditions and cells quantitively.

MATERIALS AND METHODS

Each of the two flat plate MECs (0.8 L) used had one anode chamber (400 mL), one cathode chamber (200 mL) separated from the anode chamber by CEM, and one recovery chamber (200 mL) separated from the cathode chamber by a hydrophobic membrane (Figure 1). Anolyte was continuously pumped at 0.5 mL/min through the anode chamber using a peristaltic pump. Two carbon brushes (75 mm length x 50 mm diameter, 7.2 µm fiber diameter, Millrose Co., USA) inoculated with anaerobic sludge were used as the anode. Tyvek was used as hydrophobic membrane (100 cm^2). Two types of cathodes were tested:nickel foam (NF) (purity >99.99%, 600/500 mm width, porosity ≥ 95%; Recemat Ni4753.016) and stainless steel (SS) mesh (304, Feval filtros, Spain). The anolyte was a synthetic medium that contained 111 mg/L CH_3COONa, 104 mg/L Na_2HPO_4, 52 mg/L C_2H_5COONa, 274 mg/L $KHCO_3$, 500 mg/L NH_4HCO_3 152 mg/L $CaCO_3$ and 231 mg/L $MgCl_2 \cdot 6H_2O$. The tested ammonium concentration in the influent ranged from 0.5 to 2.5 g N-NH_4^+ g/L. The catholyte solution was sodium chloride 4 g/L, and the recovery solution was 1% sulphuric acid.

RESULTS AND DISCUSSION

MECs were operated continuously to evaluate the microbial adaptation to high ammonium concentration in the feed. Figure 2 presents the current density obtained at each ammonium concentration for different cathode materials. The current density indicates the amount of electric current flowing through a unit cross-sectional area. Since the area remains the same, the current density reflects the biofilm's ability to generate electrons and, thus, enable ammonium molecules to transfer from the anode chamber to the cathode chamber. To maintain electroneutrality, one cation is transported from the anode chamber to the cathode chamber for each electron passing through the external circuit (Liu et al. 2016)while the generated electrical current through the system tends to acidify (or basify. Therefore, current density correlates with the anodic ammonium removal, indicating the maximum migration rate.

Increasing the ammonium concentration in the influent from 0.5 to 1 g N-NH_4^+ /L led to a slight increase in current density. The maximum current density increased from 2.8 to 3.4 A/m^2 and 3.2 to 3.4 A/m^2 for MEC with NF and SS, respectively. A further increase to 1.5 g N-NH_4^+ /L led to a current density plateau. The highest current density obtained was 3.9 A/m^2 at 2 g N-NH_4^+ /L for the SS cathode. Upon increasing ammonium concentration in the influent to 2.5 g N-NH_4^+ /L, the current density significantly decreased to 0.5 A/m^2. The feed's highest ammonium removal and recovery efficiencies were 66% and 33% obtained with 0.5 g N-NH_4^+ /L, respectively. The maximum ammonium flux from the anode to the cathode was 0.65 g N-NH_4^+ /L/d which led to a maximum recovery flux of 0.41 g N-NH_4^+/L/d (normalized to reactor volume) for 1.5 g N-NH_4^+ /L. The highest final ammonium concentration in the recovery solution obtained was 3.9 g/L.

Recently it was proposed that the ratio between the current density and ammonium loading rates, i.e. the ammonium load ratio (L_n), is vital in determining ammonium recovery and energy input (Rodríguez Arredondo et al. 2017). A L_n below 1 indicates that the current density was insufficient to remove all ammonium from the feed and a L_n above 1 means an excess current concerning the ammonium loading rate. In this study, the L_n was 1.1 for 0.5 g N-NH_4^+ g/L in the feed and decreased to 0.5 for 1.5 g N-NH_4^+ g/L. The decrease in L_n with higher concentrations suggests that the current density was the factor limiting the ammonium recovery.

From a practical point of view of MECs for ammonia recovery, these experimental data demonstrate that wastewaters with high ammonium concentrations can be applied to a continuously fed MEC. The threshold recommendation for maximum ammonium in the wastewater should be around 2 g N-NH_4^+/L or less. The whole presentation will detail the operation of two MECs under different ammonium concentrations in the feed. Electrochemical techniques showed that the decline in the anode performance induced the reduction of the current generation.

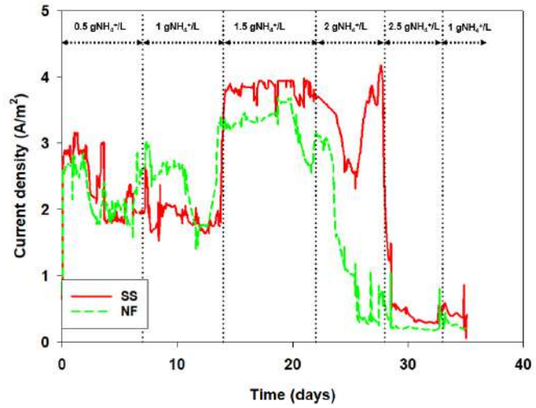

Figure 2. Current density obtained with different N-NH_4^+ concentrations for different cathode materials (SS: Stainless steel, NF: Nickel foam).

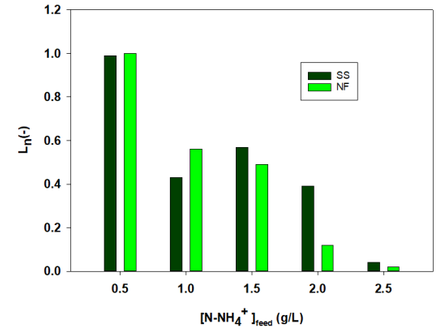

Figure 3. Load ratio calculated for different ammonium concentrations in the feed (SS: Stainless steel, NF: Nickel foam).

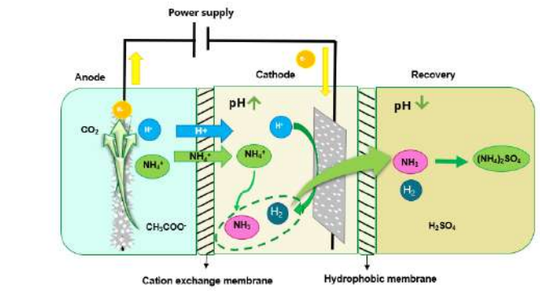

Figure 1. Conceptual diagram illustrating ammonia recovery in MEC with recovery chamber.

REFERENCES

Erisman, Jan Willem et al. 2008. 'How a Century of Ammonia Synthesis Changed the World'. *Nature Geoscience* 1(10): 636–39.

Georg, S. et al. 2021. 'Bio-Electrochemical Degradability of Prospective Wastewaters to Determine Their Ammonium Recovery Potential'. *Sustainable Energy Technologies and Assessments* 47: 101423.

Kondaveeti, Sanath et al. 2014. 'Low-Cost Separators for Enhanced Power Production and Field Application of Microbial Fuel Cells (MFCs)'. *Electrochimica Acta* 132: 434–40.

Kuntke, P. et al. 2016. 'Gas-Permeable Hydrophobic Tubular Membranes for Ammonia Recovery in Bio-Electrochemical Systems'. *Environmental Science: Water Research & Technology* 2(2): 261–65.

Liu, Ying et al. 2016. 'Understanding Ammonium Transport in Bioelectrochemical Systems towards Its Recovery'. *Scientific Reports* 6(1): 22547.

Nancharaiah, Y.V. et al. 2016. 'Recent Advances in Nutrient Removal and Recovery in Biological and Bioelectrochemical Systems'. *Bioresource Technology* 215: 173–85.

Puyol, Daniel et al. 2017. 'Resource Recovery from Wastewater by Biological Technologies: Opportunities, Challenges, and Prospects'. *Frontiers in Microbiology* 7. http://journal.frontiersin.org/article/10.3389/fmicb.2016.02106/full (November 1, 2022).

Rodríguez Arredondo, M. et al. 2015. 'Bioelectrochemical Systems for Nitrogen Removal and Recovery from Wastewater'. *Environmental Science: Water Research & Technology* 1(1): 22–33.

Rodríguez Arredondo, Mariana et al. 2017. 'Load Ratio Determines the Ammonia Recovery and Energy Input of an Electrochemical System'. *Water Research* 111: 330–37.

Wang, Miao et al. 2021. 'Can Sustainable Ammonia Synthesis Pathways Compete with Fossil-Fuel Based Haber–Bosch Processes?' *Energy & Environmental Science* 14(5): 2535–48.

Wu, Xue et al. 2013. 'Ammonium Recovery from Reject Water Combined with Hydrogen Production in a Bioelectrochemical Reactor'. *Bioresource Technology* 146: 530–36.

Yang, Kai et al. 2021. 'The Application of Cation Exchange Membranes in Electrochemical Systems for Ammonia Recovery from Wastewater'. *Membranes* 11(7): 494.

TECHNICAL SESSIONS

T3.

Water Reuse

Feasibility assessment of reclaimed wastewater reuse in agriculture: how we do it

L. Penserini*, A. Moretti**, M. Mainardis**, L. Rizzo***, S. Bozza***, M. Olivieri***, B. Cantoni*, M. Antonelli*

* Department of Civil and Environmental Engineering (DICA) - Environmental Section, Politecnico Milano, Piazza Leonardo da Vinci 32, 20133 Milano, Italy
(E-mail: *luca.penserini@polimi.it; beatrice.cantoni@polimi.it*; *manuela.antonelli@polimi.it)*
** Università degli studi di Udine, Polytechnic Department of Engineering and Architecture (DPIA), Via del Cotonificio 108, 33100 Udine, Italy
(E-mail: *moretti.alessandro@spes.uniud.it; matia.mainardis@uniud.it)*
*** Acque Bresciane S.r.L., Via Cefalonia 70, 25124 Brescia, Italy
(E-mail: *luigi.rizzo@acquebresciane.it; sonia.bozza@acquebresciane.it; mauro.olivieri@acquebresciane.it)*

Abstract

The growing interest towards wastewater (WW) reuse as alternative irrigation source is raised by the worldwide concern on water shortages and enhanced by the new European Directive on water reuse minimum requirements. In this perspective, water utilities and decision makers would benefit from a methodology to evaluate and encourage safe and efficient agricultural WW reuse practices. In this work, we propose a novel approach to identify criteria for assessing and prioritizing WW treatment plants (WWTPs) suitability for WW reuse practices implementation. The developed methodology, coupling WWTPs' characteristics (i.e., flowrate and effluent quality) and features of the local territory (i.e., cultivated crops and climate), is able to quantify the economic savings, in terms of water and nutrients, and avoided environmental impacts, that could be fulfilled from WW reuse, and which WWTPs and territories to prioritize in its implementation.

Keywords (maximum 6 in alphabetical order)

Economic savings; Fertigation; Greenhouse Gas emission; Holistic framework; Nutrients; Sustainability; Wastewater reuse.

INTRODUCTION

The scarcity of fresh water is one of the major challenges faced by humankind today. In this context, agriculture is the sector with the major water demand, accounting for about 70% of global freshwater withdrawals. Water for crops irrigation is typically extracted from natural sources, reducing the freshwater availability and exposing the agricultural sector to a great impact from water shortages (López-Serrano et al., 2020). On the other hand, the reuse of reclaimed municipal wastewater (WW) provides a reliable water source, with continuous and stable production throughout the year. In addition, it is a source of water and nutrients, as nitrogen (N) and phosphorus (P), also contributing to the reduction of green-house gases (GHGs) emissions compared to traditional management approaches, avoiding WW overtreatment and mineral fertilisers addition.

More stringent regulations are continuously proposed on WW quality aimed at direct reuse for irrigation in agriculture, as for the European Union, where the new Directive establishes limits and minimum requirements for reclaimed WW reuse in agriculture (EU Commission, 2020)and in particular Article 192(1. In this perspective, water utilities, often managing hundreds of wastewater treatment plants (WWTPs) of extremely different sizes and characteristics, would benefit from a prioritization methodology, currently missing, that might help them in selecting the most appropriate WWTPs for reuse implementation. This approach should couple both WWTP (i.e., flowrate and effluent quality) and territory (i.e., crops and climate) characteristics. Mainardis et al. (2022) therefore alternatives to use of conventional sources need to be investigated. This paper critically reviews the application of treated wastewater for agricultural fertigation (i.e., water and nutrient recovery proposed a methodological approach to preliminarily assess the techno-economic sustainability and feasibility of WW reuse that was applied to a single case-study.

In this work, the model proposed by Mainardis et al. (2022)therefore alternatives to use of conventional sources need to be investigated. This paper critically reviews the application of treated wastewater for agricultural fertigation (i.e., water and nutrient recovery was upgraded in an holistic framework, including water and nutrients mass balance, economic and environmental impacts assessment. This framework was applied to several Italian WWTPs to: (i) quantify the amount of water and nutrients needed by the crops that could be fulfilled by WW; (ii) evaluate fertigation sustainability over traditional practices; (iii) rank WWTPs and local territory characteristics improving WW reuse feasibility; (iv) determine prioritization criteria for WW reuse practices implementation.

MATERIALS AND METHODS

Irrigation water volumes to be delivered to satisfy crops requirements were estimated based on monthly water balances during the irrigation season (May to September). In the adopted approach, specific crops' evapotranspiration (ET, L s^{-1} ha^{-1}) was considered equal to their water requirement (Mainardis et al., 2022) therefore alternatives to use of conventional sources need to be investigated. This paper critically reviews the application of treated wastewater for agricultural fertigation (i.e., water and nutrient recovery. Thus, the net irrigation requirement (I, L s^{-1} ha^{-1}), which is the necessary fertigation water volume to be provided to the crops, was obtained as reported in Eq. (1):

$$I=(ET-R)/E \quad (1)$$

where R (L s^{-1} ha^{-1}) is the effective rainfall, determined from metereological data through Turc's equation, while E is the overall irrigation efficiency, calculated multiplying (i) irrigation system efficiency, (ii) water distribution efficiency from source to fields, and (iii) application efficiency.

Regarding nutrients, N and P were considered being the ones reported by current reuse regulations. Mass balances were drawn comparing monthly crop nutrient requirements (kg $month^{-1}$ ha^{-1}) and nutrients concentrations of the applied WW volumes, accounting for fertilizer use efficiency. When fertigation-supplied nutrients do not meet crop requirements, mineral fertilizers should be added; in the opposite case, fertigation limitation occurs, resulting in a reduction in the water applied, which should be supplemented with other sources.

Once the amounts of water and nutrients deliverable from the WWTP were calculated, two different outputs were obtained. Firstly, an economic evaluation was performed to quantify water and mineral fertilisers savings. Agricultural water supply cost was considered for water saving estimation. The cost of mineral fertilizers (ammonium nitrate for N, triple super phosphate for P), with their use efficiency were considered. Secondly, the GHGs emission savings due to the reduction of applied mineral fertilisers has been estimated by applying a GHG conversion factor (5.79 kg_{CO2EQ} kg_N^{-1} for N and 0.63 kg_{CO2EQ} kg_P^{-1} for P) (Jiménez-Benítez et al., 2020)by reusing the water and nutrients embedded in the effluent in agriculture (fertigation).

The developed model was applied to 95 municipal WWTPs in two major areas in northern Italy, with a served population equivalent (PE) higher than 2,000 inhab for each WWTP, and close to suitable crop fields. These WWTPs were grouped in different clusters with similar characteristics based on three clusterization parameters: (i) WWTPs size, divided into small (S, PE=2,000-10,000 inhab), medium (M, PE=10,000-70,000 inhab) and large (L, PE>70,000 inhab) WWTPs, (ii) WWTPs nutrient removal, divided into absence of nutrients removal (NO), only N removal (N) and combined N and P removal (NP), and (iii) main crops cultivated nearby the WWTP, divided into seed crops (SEED, maize or soybean) and fruits and vegetables crops (F/V, carrot or vines). The latter parameter was considered due to the significant difference in terms of water required from these two types of crops. One or more representative WWTPs were selected for each cluster, based on the availability and reliability of effluent quality data. For the selected WWTPs, data about median monthly flowrate and N and P concentrations in the effluent, together with the monthly cumulated rainfall and the type of crops nearby the WWTP, were collected.

RESULTS AND DISCUSSION

Ten clusters were determined based on the adopted clusterization parameters, from which the cluster's ID code was derived. Table 1 reports the clusters' characteristics.

For S-WWTPs and M-WWTPs, the evaluation of a single WWTP was sufficient to give a realistic representation of the whole cluster, since the collected data did not show significant differences. Instead, for L-WWTPs' clusters, more than one WWTPs were considered for model application, given the significant variability of the treatment trains; thus, 14 WWTPs were considered in total in the following analysis.

Table 1. Summary of clusters' characteristics: number of available and selected WWTPs, WWTPs flowrate, N and P concentrations, indicated as average and range in brackets.

Cluster ID	#available WWTPs	#considered WWTPs	Flowrate (m^3 day^{-1})	N concentration (mg L^{-1})	P concentration (mg L^{-1})
S-NO-SEED	5	1	1,454 (652 – 9,005)	18.24 (6.8 – 29.2)	1.49 (0.4 – 3.1)
S-NO-F/V	2	1	243 (212 – 249)	11.25 (3.3 – 22.6)	1.57 (0.4 – 2.5)
S-N-SEED	39	1	2,098 (1,337 – 4,144)	9.29 (4.9 – 23.2)	0.68 (0.3 – 1.7)
S-N-F/V	24	1	675 (249 – 1,663)	12.47 (6.1 – 26.2)	2.70 (0.7 – 4.3)
S-NP-SEED	4	1	397 (344 – 442)	6.67 (2.0 – 13.6)	1.19 (0.2 – 2.4)
S-NP-F/V	5	1	323 (137 – 342)	5.97 (1.5 – 17.8)	1.33 (0.1 – 2.7)
M-NP-SEED	6	1	4,176 (1,800 – 11,026)	4.51 (0.3 – 12.9)	0.31 (0.1 – 1.3)
M-NP-F/V	4	1	7,352 (3,647 – 14,465)	9.44 (2.4 – 20.0)	0.68 (0.3 – 2.7)
L-NP-SEED	4	4	19,519 (8,097 – 38,439)	7.40 (1.5 – 16.1)	0.62 (0.1 – 3.3)
L-NP-F/V	2	2	102,229 (7,879 – 176,662)	6.71 (3.4 – 11.0)	0.70 (0.3 – 1.6)

Based on the developed methodology, three outputs were estimated to assess the suitability of the implementation of WW reuse practices: total (i) water and (ii) fertiliser cost savings, and (iii) avoided GHGs emission on the considered period (April to September). For every WWTP, the model was run twice for both types of crops: in SEED for maize and soybean, in F/V for carrots and vines, since they are both present in the WWTPs proximity. As for water, fertilisers and GHG emission savings as a function of different clusters' characteristics (Figure 1), it is evident that different categories of the clusterization parameters affect the distribution of the single clusters' output.

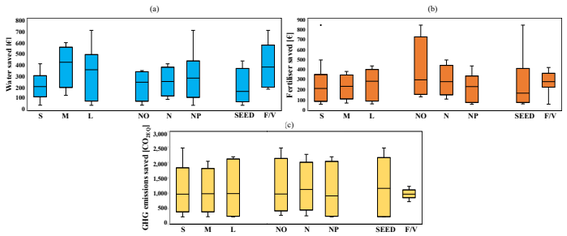

Figure 1. Estimated savings of (a) water, (b) fertilisers and (c) GHG emission differentiated per clusterization parameters.

Regarding the WWTP size, being the size directly proportional to the quantity of treated flowrate (and, thus, of the WW available for reuse), the most affected output is the water cost saving, being on average half for S-WWTPs compared to M- and L-WWTPs. However, conversely to what was expected, L-WWTPs and M-WWTPs water cost savings are not significantly different, due to the limitation in crops nutrients' requirement, which caps the amount of WW deliverable to the crops. For the WWTP's nutrient removal treatment, passing from NO-WWTPs to NP-WWTPs, a slight reduction of the median fertiliser cost savings is observed, and only NO-WWTPs show fertilizers saving over 500 €. This confirms that a lower extent of nutrient removal implies a lower supply of mineral fertilisers to the crops and, thus, a higher saving in fertilisers' cost. Finally, for all the considered outputs, the crop type emerged as the most relevant clusterization parameter. In fact, for each output, the results' distributions vary significantly between SEED-WWTPs and F/V-WWTPs, both in terms of median values and variabilities, meaning that the crops surrounding the WWTP are a fundamental characteristic to consider when a WW reuse practice is evaluated.

The economic savings (given by both water and fertilizers savings) and avoided GHG emissions were plotted in a Pareto chart in Figure 2, for all case studies (14 WWTPs for 2 types of crops), differentiated by cluster. Three distinct groups of WWTPs are evident for GHGs emission savings, which are located on three different horizontal levels. These groups vary only for the specific type of crops, in particular, within SEED-WWTPs, maize-based crops give the best emission savings (mean value of 2,200 kg_{CO2EQ}), but, on the other side, soybean-based crops give the worst ones (mean value of 230 kg_{CO2EQ}). This confirmed the high variability associated with SEED-WWTPs' boxplots in Figure 1b,c. Instead, for F/V-WWTPs, both carrot- and vines-based crops lay on the same horizontal line (mean value of 1,000 kg_{CO2EQ}). Once again, it is confirmed the oustanding relevance of the specific type of crop that is present close to the WWTP in determining WW reuse sustainability. On the other hand, the influence of WWTPs characteristic on economic savings depends on the crop type.

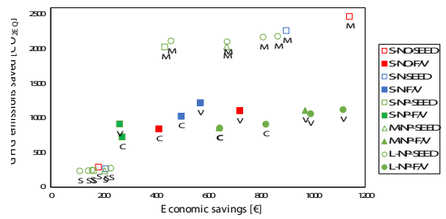

Figure 2. Pareto diagram of all the estimated outputs. The letters refer to the specific crop analysed: M=maize, S=soybean, C=carrots and V=vines.

To conclude, this work highlighted the potential of the developed methodology to rank the characteristics of WWTPs' and their nearby territory for determining useful criteria for the prioritization of WW reuse practices implementation. Further research is needed to validate these results considering other WWTPs, in order to obtain an adaptive methodology that might be applied to a few WWTPs aiming at extending the results to a broader sample of WWTPs.

REFERENCES

EU Commission, 2020. Regulation (EU) 2020/741 of the European Parliament and of the Council of 25 May 2020 on minimum requirements for water reuse. Off. J. Eur. Union 2019, 32–55.

Jiménez-Benítez, A., Ferrer, F.J., Greses, S., Ruiz-Martínez, A., Fatone, F., Eusebi, A.L., Mondéjar, N., Ferrer, J., Seco, A., 2020. AnMBR, reclaimed water and fertigation: Two case studies in Italy and Spain to assess economic and technological feasibility and CO2 emissions within the EU Innovation Deal initiative. J. Clean. Prod. 270. https://doi.org/10.1016/j.jclepro.2020.122398

López-Serrano, M.J., Velasco-Muñoz, J.F., Aznar-Sánchez, J.A., Román-Sánchez, I.M., 2020. Sustainable use of wastewater in agriculture: A bibliometric analysis of worldwide research. Sustain. 12, 1–20. https://doi.org/10.3390/su12218948

Mainardis, M., Cecconet, D., Moretti, A., Callegari, A., Goi, D., Freguia, S., Capodaglio, A.G., 2022. Wastewater fertigation in agriculture: Issues and opportunities for improved water management and circular economy. Environ. Pollut. 296, 118755. https://doi.org/10.1016/j.envpol.2021.118755

Fertilizer drawn forward osmosis for greywater treatment and subsequent reuse in hydroponics

E. Mendoza*,**, J. Vosse*,**, G. Blandin***, L. Alonso*,**, J. Comas*,***, G. Buttiglieri*,**

* ICRA-CERCA. Catalan Institute for Water Research, Girona-Spain (emendoza@icra.cat, jvosse@icra.cat, lalonso@icra.cat, gbuttiglieri@icra.cat, jcomas@icra.cat)
** University of Girona, Girona-Spain
*** LEQUIA, Institute of the Environment, University of Girona, Girona-Spain (gaetan.blandin@udg.edu)

Abstract

Synthetic greywater with 24 organic micropollutants (OMP) was extracted with forward osmosis (FO) technology, using concentrated fertilizers as draw solution (KNO_3 and $(NH_4)_2HPO_4$). Membrane rejection of OMP was high in all cases (>75%, avg. 91%), with negatively charged compounds at the highest rejection rates. Reverse salt fluxes were moderate for monovalent ions and very low for phosphate. The diluted draw solution, which reached similar nutrient concentrations as commercial fertilizing solutions, was applied in hydroponic systems with lettuces. After four weeks of experiment, lettuces grew less than the control plants, presumably due to lack of some nutrients and the presence of sodium coming from the GW in the draw solution but had a healthy appearance. The positive results obtained in these experiments show the potential of FO technology to treat GW and its further application in hydroponic systems, reducing the demand of freshwater for irrigation.

Keywords: forward osmosis, hydroponics systems, lettuce, organic micropollutants, osmotic dilution, water reuse

INTRODUCTION

Forward osmosis (FO) is a membrane technology in which a highly saline solution (draw solution: DS) is diluted by a less saline solution (feed solution: FS), due to their differences in osmotic pressure, which is the driving force of the process (van der Bruggen & Luis, 2015). FO dense membranes have shown good performance regarding pollutant rejection and have low fouling tendency (Achilli et al., 2009), becoming good candidates for the treatment and reuse of wastewater streams. A good example of FO application is fertilizer drawn forward osmosis (FDFO), which uses concentrated fertilizer solutions as draw, and the resulting diluted solution can be applied for irrigation without the need of DS recovery (Chekli et al., 2017; Majeed et al., 2015). An excellent candidate for FS is greywater (GW), as it represents up to 75% of the domestic wastewater and has low levels of pathogens and solids (Sangare et al., 2021). However, it may contain organic micropollutants (OMP: pharmaceuticals, endocrine disruptors, etc.), with reported concentrations sometimes higher than in wastewater (Hernández et al., 2010), which can pose risk for humans and the environment.

Hydroponic systems (soilless culture) can be installed anywhere and could benefit from the diluted DS as a nutritive solution for the growth of the plants. However, plants in hydroponics can take up contaminants that could be present in the solution (Wu et al., 2013).

The aim of this study was to evaluate the treatment of GW with FDFO, focused on OMP rejection, and the application of the diluted fertilizing DS in hydroponic systems with edibles (*i.e.,* lettuces).

MATERIALS AND METHODS

Forward osmosis experiment

Commercial FO hollow fibre modules (HFFO2, Aquaporin A/S, Nikbakht Fini et al., 2020) were used in this study. Synthetic GW (adapted from Hourlier et al., 2010) was used as FS, with the addition of 24 different OMP, spiked at 20 µg/L each. KNO_3 (0.2 M) and $(NH_4)_2HPO_4$ (0.025 M) (common fertilizers) were used as DS.

The test was performed in batch mode, with constant FS (60L as initial volume) and DS (2L as initial volume) recirculation, in counter current, up to 50% of FS recovery (30 L going from FS to DS). The diluted DS was stored in a cold chamber (5ºC) until its application in the hydroponic system (starting the day after the FO test). The water flux crossing the membrane (J_w, from feed to draw) was determined by mass increase of the DS, using a balance connected to a Programmable Logic Controller (PLC).

Hydroponic experiment

Lettuces *(Lactuca sativa)* with 8 to 10 leaves were planted into a controlled hydroponic lab-scale system, divided into two modules (1 per tested condition) of 4 perforated PVC canals, each of which fits 6 plants (adding up to 24 plants per condition). One module was filled with the diluted DS while the other was filled with a commercial nutrient solution (CNS: KNO_3, $Ca(NO_3)_2$, $MgSO_4$, $NH_4H_2PO_4$, and micronutrients) dissolved in deionized water (biotic control). The hydroponic solutions were changed once per week and the experiment lasted 4 weeks.

Sampling and analyses

During the FO tests, samples of FS and DS were taken at the beginning and end of the test to analyse ions and TOC. Samples at the beginning, after 10 and 60 minutes, and at the end of the test were directly analysed for OMP concentrations by UHPLC-MS/MS (Gorga et al., 2013; Gros et al., 2012) without solid-phase extraction (SPE).

For the hydroponic experiment, weekly samples of influent and effluent were used to measure ions, TOC and OMP. As to OMP, 50 ml of sample (25 ml for influent water) were filtered with 0.45 µm PVDF filters, added with 0.1M Na_2EDTA solution, extracted by SPE with Oasis HLB (3 ml, 60 cc.) cartridges, and analysed by the methods cited above.

To assess plant health and growth, the number of leaves were registered weekly. At the end of the experiment, two representative plants of each condition were rinsed with DI water, separated into roots, stems, and leaves, and weighted to determine their fresh mass.

RESULTS AND DISCUSSION

Forward osmosis: water and nutrient fluxes, and fertilizer dilution

The highest recorded water flux of 4.7 L/m²h, was lower than that of other studies using similar modules but is explained by the lower difference in osmotic pressure between FS and DS, caused by the 10x lower DS concentration compared to previous studies (Mirshekar et al., 2021; Ren & McCutcheon, 2018). However, this configuration achieved a DS dilution, in which the final concentrations of the nutrients were similar to those found in the CNS (**Figure 1**). Higher initial DS concentrations would have increased the water flux (Mendoza et al., 2022) but would have required higher water volumes to achieve the desired dilution.

Table 1. Reverse salt fluxes (J_s) and ion migration from DS to FS

ion	J_s mg/(m²h)	ion migration %
$N\text{-}NO_3^-$	16.5	28.1
$P\text{-}PO_4^{3-}$	0.2	1.5
$N\text{-}NH_4^+$	5.6	34.7
K^+	64.1	37.5

Reverse salt fluxes (J_s, from DS to FS) varied between the different ions (**Table 1**), with the highest for K. This is because K is a monovalent ion and positively charged, so it is attracted by the negatively charged membrane (Lotfi et al., 2015; Minier-Matar et al., 2016) and diffused through it to the FS.

Forward osmosis: greywater treatment and membrane rejection

The rejection of the main GW constituents was very high for sulphate (97%) and TOC (83%), while medium for Na (40%), which diffused easily to the DS due to its size and monovalent positive charge (Roy et al., 2016). Na presence in the DS is an issue in case of application in hydroponic systems, as it is toxic for the plants at high concentrations.

Regarding OMP, all of them were well rejected, with almost complete rejection, at 10 and 60 mins, and slightly lower at the end of the experiment (**Figure 2**), with average rejection 100, 99.8 and 91.3 respectively. Higher rejections were found for most of the negatively charged compounds due to their repulsion by the FO membrane (electrostatic interactions). In general, the rejection is driven solely by steric exclusion, *i.e.*, higher rejection for higher MW (**Figure 2**) as previously reported (Sauchelli et al., 2018). Thus, charge and then MW determined the OMP rejection by the membrane in most cases. In any case, the rejection was higher than 75% for all the compounds, with an average 91% OMP rejection at the end of the experiment.

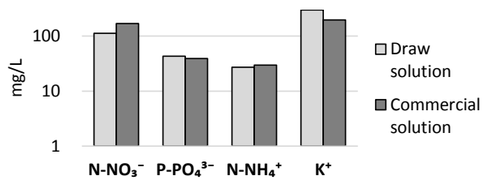

Figure 1. Concentrations of the diluted DS and commercial nutrient solution for their application in hydroponics

Although NH_4 is monovalent, positively charged, and similar to K in size, its J_s was lower because its initial concentration in the DS was around 10x lower than that of K. Thus, initial concentration, charge, and size were responsible for the solute fluxes. The J_s of NO_3 was lower than that of K because it was better repulsed by the membrane. Finally, the J_s of PO_4, due to its nature, was almost negligible. These fluxes led to ion migration from DS to FS, which resulted in nutrient losses, around 30% for monovalent ions and 1.5% for phosphate (**Table 1**).

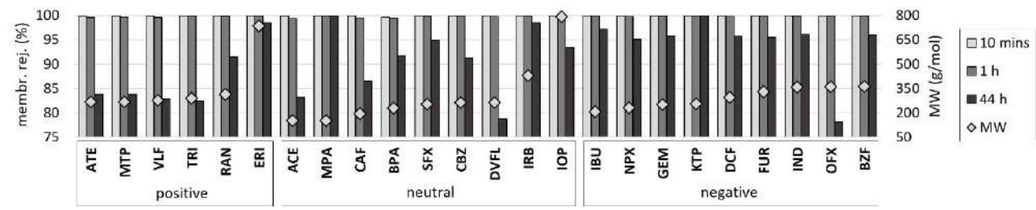

Figure 2. OMP rejection in time periods. OMP: atenolol (ATE), methylparaben (MTP), venlafaxine (VLF), trimethoprim (TRI), ranitidine (RAN), erythromycin (ERI), acetaminophen (ACE), methylparaben (MPA), caffeine (CAF), bisphenol A (BPA), sulfamethoxazole (SFX), carbamazepine (CBZ), desvenlafaxine (DVLF), irbesartan (IRB), Iopromide (IOP); ibuprofen (IBU), naproxen (NPX), gemfibrozil (GEM), ketoprofen (KTP), diclofenac (DCF), furosemide (FUR), indomethacin (IND), ofloxacin (OFX), and bezafibrate (BZF).

Hydroponic system: lettuces grown in the diluted draw solution

The harvested lettuces (4 weeks) growing in DS were slightly darker and had thicker roots than the control ones (**Figure 3**) but looked healthy. Both conditions developed a similar number of leaves along the first three weeks, but the control lettuces had a noticeable higher number of leaves at the end of the experiment (**Figure 4**). Lower leaf and stems fresh mass were measured for DS lettuces, although root mass was similar for both conditions (**Table 1**). This could be explained by the lack of some nutrients in the DS condition (*i.e.,* sulphate, calcium, magnesium, and micronutrients) as well as by the presence of sodium. However, the leaves of the DS lettuces properly grew, suggesting that diluted DS is an appropriate solution to grow lettuces, although nutrients should be balanced.

Figure 3. Lettuces at the end of the experiment, growing in DS (left) and commercial solution (right).

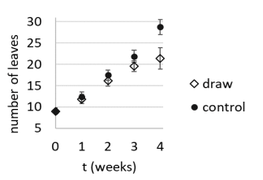

Figure 4. Number of lea-ves along the experiment

Table 2. Fresh mass (g) of the different parts of the lettuces after 4 weeks.

		Lettuces in DS	Control lettuces
Roots	2.2	2.5	
Stems	0.3	1.2	
Leaves	5.7	24.8	

Because of the high rejection in FO, very low OMP concentrations were found in the diluted DS applied in the hydroponic experiment, which ranged from 0.5 to 2.6 µg/L (average 1.4 µg/L). Therefore, the estimated OMP uptake by the lettuces was also very low.

CONCLUSIONS

Forward osmosis technology showed promising results for GW treatment in relation to the rejection of OMP and multivalent ions. Nevertheless, monovalent ion fluxes were medium to high, indicating, on the one hand, loss of nutrients from DS to FS, and on the other hand, sodium fluxes from FS to DS, compromising the quality of the diluted DS.

The lettuces grown in the diluted DS showed a healthy appearance, but grew less than the control, probably due to lack of some nutrients and the presence of sodium in the solution. OMP concentrations in the diluted DS were very low, as well as the estimated OMP uptake by the lettuces. Further studies should focus on decreasing monovalent ion fluxes in FO and optimizing plant growth.

Acknowledgements: *authors acknowledge funding from the Spanish State Research Agency of the Spanish Ministry of Science and Innovation for ReUseMP3 project (PID2020-115456RB-I00 /MCIN/ AEI / 10.13039/501100011033). E. Mendoza and J. Vosse thank Secretariat of Universities and Research from Generalitat de Catalunya and European Social Fund for their FI fellowship (2022FI_B2 00064 and 2022 FI_B 00084, respectively). Gaetan Blandin received the support of a fellowship from "la Caixa" Foundation (ID 100010434), which fellowship code is LCF/BQ/PR21/11840009. Gianluigi Buttiglieri acknowledges Spanish State Research Agency of the Spanish Ministry of Science, Innovation and Universities for the Grant to the Creation of a permanent position Ramon y Cajal 2014 (RYC-2014-16754). ICRA researchers thank funding from CERCA program.*

REFERENCES

Achilli, A., Cath, T. Y., Marchand, E. A., & Childress, A. E. (2009). The forward osmosis membrane bioreactor: A low fouling alternative to MBR processes. *Desalination*, *239*(1–3), 10–21. https://doi.org/10.1016/j.desal.2008.02.022

Chekli, L., Kim, Y., Phuntsho, S., Li, S., Ghaffour, N., Leiknes, T. O., & Shon, H. K. (2017). Evaluation of fertilizer-drawn forward osmosis for sustainable agriculture and water reuse in arid regions. *Journal of Environmental Management*, *187*, 137–145. https://doi.org/10.1016/j.jenvman.2016.11.021

Gorga, M., Petrovic, M., & Barceló, D. (2013). Multi-residue analytical method for the determination of endocrine disruptors and related compounds in river and waste water using dual column liquid chromatography switching system coupled to mass spectrometry. *Journal of Chromatography A*, *1295*, 57–66. https://doi.org/10.1016/j.chroma.2013.04.028

Gros, M., Rodríguez-Mozaz, S., & Barceló, D. (2012). Fast and comprehensive multi-residue analysis of a broad range of human and veterinary pharmaceuticals and some of their metabolites in surface and treated waters by ultra-high-performance liquid chromatography coupled to quadrupole-linear ion trap tandem. *Journal of Chromatography A*, *1248*, 104–121. https://doi.org/10.1016/j.chroma.2012.05.084

Hernández, L., Vieno, N., Temmink, H., Zeeman, G., & Buisman, C. J. N. (2010). Occurrence of xenobiotics in gray water and removal in three biological treatment systems. *Environmental Science and Technology*, *44*(17), 6835–6842. https://doi.org/10.1021/es101509e

Hourlier, F., Masse, A., Jaouen, P., Lakel, A., Gerente, C., Faur, C., & le Cloirec, P. (2010). Formulation of synthetic greywater as an evaluation tool for wastewater recycling technologies. *Environmental Technology*, *31*(2), 215–223. https://doi.org/10.1080/09593330903431547

Lotfi, F., Phuntsho, S., Majeed, T., Kim, K., Han, D. S., Abdel-Wahab, A., & Shon, H. K. (2015). Thin film composite hollow fibre forward osmosis membrane module for the desalination of brackish groundwater for fertigation. *Desalination*, *364*, 108–118. https://doi.org/10.1016/j.desal.2015.01.042

Majeed, T., Sahebi, S., Lotfi, F., Kim, J. E., Phuntsho, S., Tijing, L. D., & Shon, H. K. (2015). Fertilizer-drawn forward osmosis for irrigation of tomatoes. *Desalination and Water Treatment*, *53*(10), 2746–2759. https://doi.org/10.1080/19443994.2014.931524

Mendoza, E., Buttiglieri, G., Blandin, G., & Comas, J. (2022). Exploring the limitations of forward osmosis for direct hydroponic fertigation: Impact of ion transfer and fertilizer composition on effective dilution. *Journal of Environmental Management*, *305*, 114339. https://doi.org/10.1016/j.jenvman.2021.114339

Minier-Matar, J., Santos, A., Hussain, A., Janson, A., Wang, R., Fane, A. G., & Adham, S. (2016). Application of Hollow Fiber Forward Osmosis Membranes for Produced and Process Water Volume Reduction: An Osmotic Concentration Process. *Environmental Science and Technology*, *50*(11), 6044–6052. https://doi.org/10.1021/acs.est.5b04801

Mirshekar, L., Kamarehie, B., Jafari, A., Ghaderpoori, M., Karami, M. A., & Sahebi, S. (2021). Performance evaluation of aquaporin forward osmosis membrane using chemical fertilizers as a draw solution. *Environmental Progress and Sustainable Energy*, *40*(3). https://doi.org/10.1002/ep.13536

Nikbakht Fini, M., Madsen, H. T., Sørensen, J. L., & Muff, J. (2020). Moving from lab to pilot scale in forward osmosis for pesticides rejection using aquaporin membranes. *Separation and Purification Technology*, *240*, 116616. https://doi.org/10.1016/j.seppur.2020.116616

Ren, J., & McCutcheon, J. R. (2018). A new commercial biomimetic hollow fiber membrane for forward osmosis. *Desalination*, *442*(October 2017), 44–50. https://doi.org/10.1016/j.desal.2018.04.015

Roy, D., Rahni, M., Pierre, P., & Yargeau, V. (2016). Forward osmosis for the concentration and reuse of process saline wastewater. *Chemical Engineering Journal*, *287*, 277–284. https://doi.org/10.1016/j.cej.2015.11.012

Sangare, D., Coulibaly, L. S., Andrianisa, H. A., Coulibay, J. Z., & Coulibay, L. (2021). Investigating the capacity of hydroponic system using lettuce (Lactuca sativa L.) in the removal of pollutants from greywater while ensuring food security. *International Journal of Environment, Agriculture and Biotechnology*, *6*(3). https://doi.org/10.22161/ijeab

Sauchelli, M., Pellegrino, G., D'Haese, A., Rodríguez-Roda, I., & Gernjak, W. (2018). Transport of trace organic compounds through novel forward osmosis membranes: Role of membrane properties and the draw solution. *Water Research*, *141*, 65–73. https://doi.org/10.1016/j.watres.2018.05.003

van der Bruggen, B., & Luis, P. (2015). Forward osmosis: Understanding the hype. *Reviews in Chemical Engineering*, *31*(1), 1–12. https://doi.org/10.1515/revce-2014-0033

Wu, X., Ernst, F., Conkle, J. L., & Gan, J. (2013). Comparative uptake and translocation of pharmaceutical and personal care products (PPCPs) by common vegetables. *Environment International*, *60*, 15–22. https://doi.org/10.1016/j.envint.2013.07.015

LIFE AMIA. An innovative combination of wastewater technologies to promote water reuse and sustainable treatment.

E.Zuriaga-Agustí*, C. Pérez*, N. Zamorano-López*, R. García*,F.Valero* J, L. Aranda **., E. Ferrer**, M. Abellán***, C.García****, A.Kenyon*****

*FACSA, SOCIEDAD DE FOMENTO AGRÍCOLA CASTELLONENSE, S.A., C/ Mayor 82-84, 12001, Castellón, Spain, (E-mails: ezuriaga@facsa.com; nuria.zamorano@grupogimeno.com; ruben.garcia@grupogimeno.com; cristian.perez@facsa.com; fvalero@facsa.com)

** EUROFINS- IPROMA, Cno. de la Raya nº 46, 12006, Castellón, Spain, (E-mails: jlaranda@iproma.com; eferrer@iproma.com)

*** ESAMUR, C/ Santiago Navarro, 4, 30100 Espinardo, Spain, (E-mail: manuel.abellan@esamur.com)

**** CEBAS-CSIC,Campus Universitario de Espinardo. Espinardo. Murcia (E-mail: cgarizq@cebas.csic.es)

***** ARVIA, (E-mail: Anna.Kenyon@arviatechnology.com)

Abstract

The water scarcity crisis has led to an increased focus on water reuse and low-energy consumption processes for wastewater treatment. Current technologies for municipal sewage treatment must be transformed to truly shift towards more sustainable approaches. The LIFE AMIA project validates a new concept for Wastewater Treatment Plants that combines a compact Anaerobic-Aerobic treatment, a High-Rate Algal Pond and an Advanced Oxidation Adsorption Process. The aim is to produce high-quality water effluent for reuse in agriculture following the new EU directive. This project achieves obtaining reclaimed water with energy production via biogas production (65±8% CH4) and nutrient recovery of 27.93 g N/m3 and 12.63 g P/m3 treated water. The sludge and microalgae biomass obtained in the treatment process was used as a biofertilizer for degraded soils with positive results. Emerging pollutants removal rates were higher than in conventional WWTP treatment, highlighting the removal of venlafaxine or diclofenac.

Keywords (maximum 6 in alphabetical order)

Advanced Oxidation Process; anaerobic-aerobic treatment; microalgae treatment, nutrients recovery; water reuse; water scarcity

INTRODUCTION

As environmental policies continue to promote high-quality treated and regenerated wastewater, energy efficiency and resource recovery, traditional purification and regeneration technologies based on activated sludge and chlorination or UV are no longer sufficient for meeting these needs, particularly for small and medium populations. In response, the LIFE AMIA project is developing a new combination of technologies that can regenerate municipal wastewater with minimal energy consumption and in accordance with the principles of the circular economy. The results of demonstration plant located in Alhama WWTP treating 12m^3/d are here presented.

MATERIALS AND METHODS

LIFE AMIA pilot plant

The proposed treatment process begins with a compact system that combines a 375L anaerobic stage in the bottom with a 332L aerobic stage at the top in a vertically stacked reactor. The water is introduced into the lower part of the anaerobic chamber, which uses granular biomass in an EGSB-type upflow reactor to produce biogas. After a three-phase separation system, the water is directed to the upper chamber where it is treated with a moving bed technology (MBBR). Figure 2 shows the A2C reactor, anaerobic granular biomass and the carriers holding the aerobic biomass.

After the anaerobic-aerobic compact treatment, the water is introduced into two 28 m^3 microalgae reactors (high-rate algae pond reactors, HRAP) with an HRT in the range of 3-6 days, where photosynthetic autotrophic microorganisms use sunlight to fix dissolved CO2 and assimilate nutrients present in the wastewater, mainly N and P. The system uses a pH regulation system with a CO_2 dosage to maintain pH in the range 7-8. After leaving the HRAP reactor, the microalgae are harvested from the liquid using a dissolved air flotation (DAF) system, obtaining the biomass that can be used as fertilizer due to their high nutrient content. Figure 3 shows the HRAP reactors and the microalgae-bacteria mixed culture.

As the last stage of LIFE AMIA treatment, the purified water undergoes tertiary treatment for regeneration through an adsorption and advanced electro-oxidation process (AOP) powered by solar energy. This novel process uses a 1.6 m^3 NYEX® particles bed to adsorb organic molecules, which are then oxidized to CO2 through the application of a small electrical current (5-15A) that also regenerates the particles. The use of solar power as the main energy source improves sustainability towards the treatment. As a result of this last stage, emerging pollutants removal and disinfection are achieved according to the upcoming EU water reuse directive. Figure 1 presents the LIFE AMIA treatment plant.

Emerging pollutants, pathogens and biofertilizer assessment

In order to assess the emerging pollutants removal in the process, the following species were analysed throughout the process: sulfamethoxazole, venlafaxine, 4-aminoantipyrine, acetaminophen, ketoprofen, diclofenac, trimethoprim and I-V cypermethrin.

A selection of target pathogens was considered in the study as well: F-specific RNA bacteriophages, somatic coliphages, *Clostridium perfringens* spores, total bacteriophages, *Escherichia Coli* and *Salmonella* sp.

Besides, the biomass obtained, including both sludge and microalgae, has been thoroughly tested and assessed for its potential use as a biofertilizer on degraded soils in agriculture. The total organic carbon (TOC) of the potential biofertilizers was studied.

RESULTS AND DISCUSSION

The results of the validation phase are shown follows. Figure 4 shows the evolution of COD removal performance over time in the A^{2}C stage. The anaerobic-aerobic reactor has been in operation for over 700 days, during which time it has maintained stable COD removal yields (74±16%) and has successfully handled COD peaks of up to 1,500 mg/L without significantly affecting the effluent. Figure 5 shows that once stationary conditions were reached, methane production was maintained at an average of 65±8%., resulting in a significant reduction in energy consumption and potential energy recovery.

The HRAP reactors were stabilized with a HRT of 4.5 days and 404 mg TS/L (87% SSV), resulting in COD values below 100 mg/L (75% removal). The average N and P content in the algal biomass was 6.7% N and 3.1% P in dry matter, respectively, and the amount of nutrients recovered from the wastewater in the form of algal biofertilizer was 335.2 gN/d and 156.1 gP/d.

In terms of emerging pollutants, the two compounds with the highest concentration (acetaminophen and 4-aminoantipyrine) were completely eliminated by the LIFE AMIA treatment. The removal of emerging pollutants was greater in the LIFE AMIA treatment compared to conventional activated sludge treatment, ranging from 45.24% to 99.8% after the AOP stage. The most difficult compounds to eliminate were Diclofenac and Venlafaxine, with a better performance compared to conventional treatment. In the pathogens case, the removal was between 94,6-100% for all the samples of the LIFE AMIA treated water. Figure 6 shows the comparison of the micropollutant removal performance between LIFE AMIA and conventional WWTP treatment.

The results of total organic carbon (TOC) of the sludge indicate a 28.1±1.9 and a 27.9±1.6% higher TOC values compared to the control test mineral material used in the study.

ACKNOWLEDGEMENTS

LIFE AMIA project is funded by the LIFE Programme of the European Union under Grant Agreement LIFE18/ENV/ES/000170. The consortium includes 6 partners: FACSA, ESAMUR, EUROFINS-IPROMA, ARVIA, CEBAS-CSIC and ATLANTIS.

FIGURES

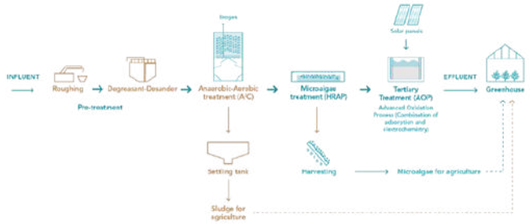

Figure 1. LIFE AMIA treatment scheme.

Figure 2. (a) Compact anaerobic-aerobic treatment (A2C) reactor, (b) anaerobic granular sludge, (c) aerobic biomass held in the biocarriers surface.

Figure 3. (a) HRAP reactors, (b) HRAP mixed culture

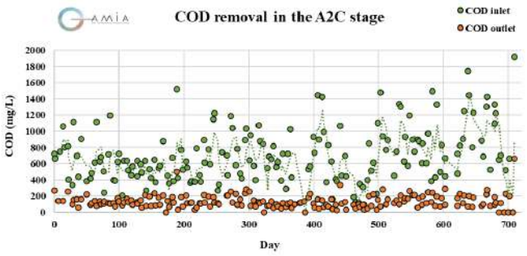

Figure 4. COD removal performance of the A^{2}C treatment.

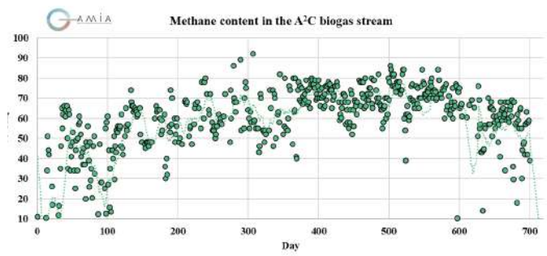

Figure 5. Methane content in the A^{2}C biogas stream.

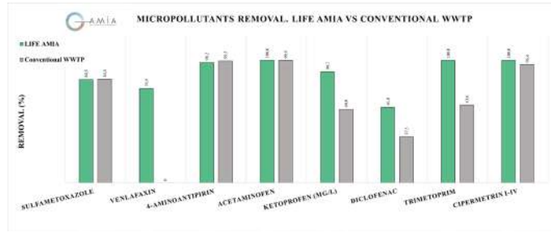

Figure 6. Micropollutants removal of LIFE AMIA vs conventional WWTP.

Towards water self-sufficiency: pilot operation of an off-grid water cycle based on rainwater harvesting and low-tech, biological greywater treatment in an inhabited demonstration house in Switzerland (KREIS-Haus)

D. Buehler*,**, R. Junge** and D. Rousseau*

* Department of Green Chemistry and Technology, Ghent University Campus Kortrijk, Sint-Martens-Latemlaan 2B, 8500 Kortrijk, Belgium (E-mail: *devi.buhler@ugent.be*; *diederik.rousseau@ugent.be*)

** Institute of Natural Resource Sciences, Zurich University of Applied Sciences, Grüentalstrasse 22, 8820 Wädenswil, Switzerland (E-mail: *devi.buehler@zhaw.ch, ranka.junge2@zhaw.ch)*)

Abstract

With the aim to address water scarcity and support the sustainable use and treatment of (waste-) water, this study examines a self-sufficient, off-grid water system in the inhabited demonstration house "KREIS-Haus". The water system is based on rainwater harvesting and greywater treatment with a low-tech treatment implementing submerged, attached biofilm growth. Treated rainwater is used as drinking water and treated greywater is used for the washing machine and irrigation of the rooftop garden. In an experimental period of 17 weeks, several abiotic and biotic parameters were analyzed once per week before and after the rainwater and greywater treatment. Comparing the results to Swiss/EU regulation and literature, the treated greywater is suitable for irrigation and laundry. However, the treated rainwater did not always meet required microbial limit values, indicating insufficient performance of the LED-UV lamp. The greywater treatment unit achieved removal rates of 92% for COD and 98% for turbidity, and no accumulation of substances was observed in the treated greywater. Water self-sufficiency was at 100% over the whole experimental period, and excess water pumped out of the system met the standard for discharge into a water body. While these first results indicate a promising approach to the water concept, more long-term monitoring and testing with higher occupancy is needed.

Keywords

Biological wastewater treatment; greywater treatment, rainwater harvesting, self-sufficiency, wastewater reuse

INTRODUCTION

Freshwater is becoming an increasingly scarce resource due to global trends such as urbanization, climate change and population growth (UNESCO, 2017). Therefore, the 2017 United Nations Global Water Report (2017) highlights the importance of wastewater reuse as a strategy to address water scarcity. A number of studies have examined local greywater treatment and its reuse potential for non-potable applications such as toilet flushing or irrigation (Chrispim & Nolasco, 2017; Masi et al., 2016; Radingoana et al., 2020; Yoonus & Al-Ghamdi, 2020). With the aim to develop fully water self-sufficient systems, greywater treatment and reuse can be combined with rainwater harvesting for drinking water supply. By doing so, no centralized infrastructure for (waste-) water is needed. The inhabited demonstration house "KREIS-Haus" (German for Klima- und Ressourcen-effizientes Suffizienz Haus, English: climate and resource efficient sufficiency house), located in Feldbach Switzerland, implements completely closed resource cycles on building level on approx. 40m^2. The house is built in three parts: the tempered living unit, the adjacent conservatory with rooftop garden, and the technology room. Beside a range of sustainable building materials and an energy system based on solar energy, the house implements an off-grid water system. The aim of this study was to examine the water cycle in KREIS-Haus in terms of treatment performance, output water quality and compliance with legal standards, and degree of water self-sufficiency

MATERIALS AND METHODS

Water supply and management of the examined "KREIS-Haus" is based on rainwater collection and greywater treatment and reuse. Rainwater from the 77m^2 roof is collected in a 3m^3 tank and processed into drinking water by a series of filtration and treatment steps including a particle filter, activated carbon and UV-LED (Figure 1). Thanks to the dry separating toilet, no wastewater is produced from the toilet. All faucets and the shower are highly water efficient. The lightly polluted greywater from the bathroom (sink, shower), washing machine and kitchen is collected in a 1.5m^3 tank. From there, the greywater is pumped once per day into the in-house treatment unit (own development) in the form of a mobile box of 210 x 70 x 150cm (LxWxH). The treatment technology is based on submerged, aerobic, attached biofilm growth in a low-tech process with the aim to require minimal maintenance, energy, as well as investment and running costs. The technology is a further development based on the findings of the previous study of Buehler et al. (2021). The treated greywater is reused in the house for the washing machine and irrigation of the rooftop garden. Not used treated greywater flows back into the greywater tank. When the greywater tank is full, the water flows into the overflow tank (1.5m^3), which needs to be manually emptied. All tanks are located in the ground under the house. Prior to the sampling period of this study, the house was intermittently inhabited, and the treatment system was operational for 9 months. The sampling period was carried from 22 July 2022 to 14 November 2022 (17 weeks). The house was inhabited by changing visitors staying between 2 to 12 days. On average, the house was occupied by 2 people on 3 days per week. Eco-friendly detergents and body care products were provided but their use was not enforced. The abiotic water quality parameters in Table 1 and the microbial parameters in Table 2 were analyzed once per week before and after the rainwater and greywater treatment.

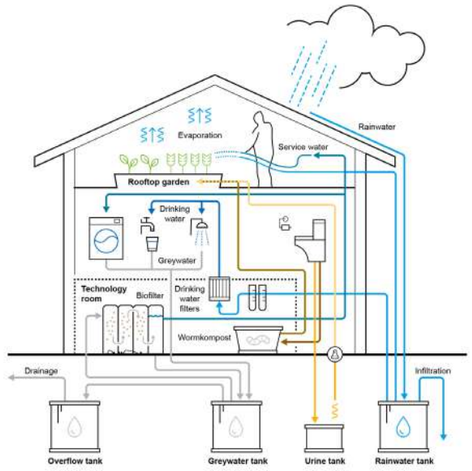

Figure 1. Off-grid water cycle in the KREIS-Haus based on rainwater collection and greywater treatment and reuse

RESULTS AND DISCUSSION

According to the EU regulation 2020/741 for water reuse (European Commission, 2020), the treated greywater is suitable for agricultural irrigation of quality class A in terms of the measured mean values (Table 1, Table 2) for turbidity, BOD$_5$, *E.coli* and Legionella. The treated greywater is also suitable for laundry according to literature values (Ciabatti et al., 2009; Gross et al., 2015; Hoinkis & Panten, 2008) in terms of turbidity, COD, pH and EC. The greywater treatment unit achieved removal rates (92% for COD, 87% for BOD$_5$ and 98% for turbidity) comparable to other well performing attached growth systems (Khalil & Liu, 2021). BOD/COD ratio was before and after the greywater treatment at 0.3, indicating that both biological and physical processes took place. However, biological activity would need to be verified by other methods such as FDA. Figure 1 shows that the pollution loads in greywater fluctuate with the occupancy of the house. Since the values for 'Greywater' do not reflect raw greywater but mixed raw and treated greywater, it is unclear to what extent the treatment system was fed with higher polluted greywater between the sampling times. For an increased stress test, the house should be inhabited permanently over a longer period. Over the experimental period, none of the parameters in the treated greywater showed a trend towards accumulation, one example being COD in Figure 2. This is in contrast to a previous study of the authors on a closed-loop laundry pilot facility with similar technology (Buehler et al., 2021), showing accumulation of COD, TOC and turbidity over time. Even if the two system are not directly comparable, accumulations in the KREIS-Haus should be further observed over a longer period, and if apparent, adequately managed. Assessment of the treated rainwater (drinking water) shows that the values for *E.coli* and Enterococci (Table 2) were at times above the limit values of the Swiss regulation for drinking water (TBDV, 2016) which requires these microbials to be not detectable. This indicates that the UV-LED lamp did not perform sufficiently and needs to be replaced. Over the experimental period, the house was operated 100% water self-sufficiently meaning that no external water supply other than rainwater was used. The overflow tank was emptied twice and contained an average of 52.8 mg/L COD. According to Swiss regulation, the water could have been discharged into a water body (limit value 60mg/L COD) (GSchV, 1998). However, it is unclear if compliance with regulation can be ensured with higher occupancy of the house. These first results indicate that the water concept in KREIS-Haus is a promising approach, but parts as the UV-LED lamp need to be replaced and the greywater treatment needs to be monitored over a longer period with higher occupancy.

Table 1. Mean and standard deviation of abiotic parameters before and after the treatment of rainwater and greywater. Removal rates after the rainwater and greywater treatment.

		Temp. (°C)	Turbidity (FNU)	pH	EC (µS/cm)	O_2 (mg/L)	BOD_5 (mg/L)	COD (mg/L)	TP (mg/L)	TN (mg/L)	TOC (mg/L)	Tensides cationic (mg/L)	Tensides anionic (mg/L)
Rainwater	Mean	18.6	4.0	6.4	24.9	6.1	n.m.	15.9	0.13	0.7	5.0	0.3	0.1
	Std.	2.7	2.6	0.3	6.7	2.6	n.m.	13.6	0.07	0.3	2.9	0.3	0.1
	n	10	16	17	17	17	n.m.	17	15	9	11	15	15
Treated rainwater	Mean	20.7	2.5	6.5	37.2	6.3	n.m.	13.3	0.09	0.6	2.8	0.2	0.0
	Std.	4.6	1.1	0.3	18.6	1.8	n.m.	13.7	0.12	0.2	1.9	0.1	0.0
	n	10	16	17	17	17	n.m.	17	15	12	14	15	15
	Removal		38%					16%	29%	19%	45%	43%	52%
Greywater	Mean	18.6	65.0	6.9	238.0	2.5	42.4	176.6	0.54	3.6	21.3	1.7	8.2
	Std.	3.4	42.3	0.2	41.5	2.6	33.6	96.8	0.32	1.7	6.8	0.6	6.1
	n	10	16	17	17	17	14	17	14	10	12	14	14
Treated greywater	Mean	18.2	1.2	7.3	258.6	6.0	5.3	13.9	0.42	2.1	4.9	0.5	0.3
	Std.	2.7	0.8	0.3	32.7	1.8	2.2	5.3	0.16	1.1	1.4	0.5	0.3
	n	10	16	17	17	17	11	17	15	9	14	15	15
	Removal		98%				87%	92%	22%	41%	77%	74%	97%

Table 2. Mean and standard deviation of microbial parameters before and after the treatment of rainwater and greywater. Removal rates and log reduction after the rainwater and greywater treatment.

		E.coli CFU/100ml	Coliforms CFU/100ml	Enterococci CFU/100ml	Total aerobic count CFU/ml	P.aeruginosa CFU/ml	Legionella CFU/L
Rainwater	Mean	2	219	391	638	19	n.m.
	Std.	7	197	304	408	17	n.m.
	n	14	13	9	13	6	n.m.
Treated rainwater	Mean	1	10	88	32	0	n.m.
	Std.	4	10	118	38	0	n.m.
	n	14	13	8	13	6	n.m.
	Removal	41%	95%	78%	95%	100%	
	Log reduction	0.2	1.3	0.6	1.3		
Greywater	Mean	0	2.00E+07	4.44E+04	2.61E+06	274	<1000
	Std.	0	1.61E+07	2.61E+04	2.05E+06	186	
	n	1	13	4	11	6	2
Treated greywater	Mean	8	4441	1094	566	0	<1000
	Std.	28	4481	603	593	0	
	n	14	9	10	13	7	2
	Removal		100%	98%	100%	100%	
	Log reduction		3.7	1.6	3.7		

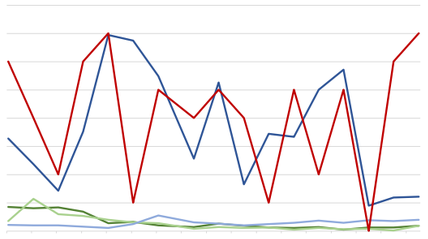

Figure 1. COD over the experimental period before and after the treatment of rainwater and greywater (primary y-axis) and occupancy of the house (secondary y-axis)

REFERENCES

Buehler, D., Antenen, N., Frei, M., Koller, C., Rousseau, D. P. L., Schoenborn, A., & Junge, R. (2021). Towards Water and Energy Self-Sufficiency: A Closed-Loop, Solar-Driven, Low-Tech Laundry Pilot Facility (LaundReCycle) for the Reuse of Laundry Wastewater. *Circular Economy and Sustainability*, *1*(3), 1037–1051. https://doi.org/10.1007/s43615-021-00077-2

Chrispim, M. C., & Nolasco, M. A. (2017). Greywater treatment using a moving bed biofilm reactor at a university campus in Brazil. *Journal of Cleaner Production*, *142*, 290–296. https://doi.org/10.1016/j.jclepro.2016.07.162

Ciabatti, I., Cesaro, F., Faralli, L., Fatarella, E., & Tognotti, F. (2009). Demonstration of a treatment system for purification and reuse of laundry wastewater. *Desalination*, *245*(1), 451–459. https://doi.org/10.1016/j.desal.2009.02.008

Gewässerschutzverordnung, 814.201 (1998).

Verordnung des EDI über Trinkwasser sowie Wasser in öffentlich zugänglichen Bädern und Duschanlagen, 817.022.11 (2016). https://www.admin.ch/opc/de/classified-compilation/20143396/index.html

European Commission. (2020). *Regulation (EU) 2020/741 of the European Parliament and of the Council of May 25 2020 on Minimum Requirements for Water Reuse*. *L*(177), 32–55.

Gross, A., Alfiya, Y., & Friedler, E. (2015). *Greywater Reuse*. CRC Press. https://www.crcpress.com/Greywater-Reuse/Gross-Maimon-Alfiya-Friedler/p/book/9781482255041

Hoinkis, J., & Panten, V. (2008). Wastewater recycling in laundries—From pilot to large-scale plant. *Chemical Engineering and Processing: Process Intensification*, *47*(7), 1159–1164. https://doi.org/10.1016/j.cep.2007.12.010

Khalil, M., & Liu, Y. (2021). Greywater biodegradability and biological treatment technologies: A critical review. *International Biodeterioration & Biodegradation*, *161*, 105211. https://doi.org/10.1016/j.ibiod.2021.105211

Masi, F., Bresciani, R., Rizzo, A., Edathoot, A., Patwardhan, N., Panse, D., & Langergraber, G. (2016). Green walls for greywater treatment and recycling in dense urban areas: A case-study in Pune. *Journal of Water, Sanitation and Hygiene for Development*, *6*(2), 342–347. https://doi.org/10.2166/washdev.2016.019

Radingoana, M. P., Dube, T., & Mazvimavi, D. (2020). Progress in greywater reuse for home gardening: Opportunities, perceptions and challenges. *Physics and Chemistry of the Earth, Parts A/B/C*, *116*, 102853. https://doi.org/10.1016/j.pce.2020.102853

UNESCO. (2017). *The United Nations world water development report, 2017: Wastewater: The untapped resource*. https://unesdoc.unesco.org/ark:/48223/pf0000247153

Yoonus, H., & Al-Ghamdi, S. G. (2020). Environmental performance of building integrated grey water reuse systems based on Life-Cycle Assessment: A systematic and bibliographic analysis. *Science of The Total Environment*, *712*, 136535. https://doi.org/10.1016/j.scitotenv.2020.136535

Tertiary wastewater treatment and natural pigment recovery by cyanobacteria: fate of organic microcontaminants

M. Bellver[1*], E. Ruales[1], R. Díez-Montero[1,2], M. Escolà[3], V. Matamoros[3], I. Ferrer[1**]

[1] GEMMA – Group of Environmental Engineering and Microbiology, Department of Civil and Environmental Engineering. Universitat Politècnica de Catalunya·BarcelonaTech, c/ Jordi Girona 1-3, Building D1, 08034, Barcelona, Spain.

[2] GIA - Group of Environmental Engineering, Department of Water and Environmental Sciences and Technologies. Universidad de Cantabria, Avda. Los Castros s/n, 39005, Santander, Spain.

[3] IDAEA - Department of Environmental Chemistry. CSIC, c/Jordi Girona, 18-26, 08034, Barcelona, Spain.

* Corresponding author: *marta.bellver@upc.edu, ** ivet.ferrer@upc.edu

Abstract

One of the main challenges for wastewater treatment coupled to bioproducts recovery from cyanobacteria is maintaining a stable culture and bioproduct content over time. The aim of the present study was to assess the recovery of bioproducts (natural pigments and biogas) using cyanobacteria as tertiary treatment in a biorefinery approach. Secondary effluent from a municipal wastewater treatment plant was treated with wastewater-borne cyanobacteria (*Synechococcus* sp. and *Synechocystis* sp.) in lab (3 L) and pilot scale (30 L) photobioreactors. Biomass was periodically harvested and pigments (phycobiliproteins) were extracted and quantified over time. Residual biomass was then used to produce biogas. For the first time, the presence of contaminants of emerging concern was analysed in secondary effluent, biomass and pigment extracts. Results showed how both cyanobacteria were able to remove up to 83% of N-NH_4^+ and 97% of P-PO_4^{3-} from secondary effluent. The phycobiliprotein content was up to 214 mg gDW^{-1} for *Synechococcus* sp., while up to 222 NL CH_4 $kgVS^{-1}$ were yielded from residual biomass. For *Synechocystis* sp., a steady phycobiliprotein content around 70 mg gDW^{-1} was maintained over a period of 45 days at pilot scale (30 L). Only 3 out of the 20 contaminants of emerging concern detected in secondary effluent were found in pigment extracts. In conclusion, this research highlights tertiary wastewater treatment with cyanobacteria as a promising strategy for improving the quality of secondary effluents while obtaining bioproducts.

Keywords

Bioproducts; circular economy; cyanobacteria; nutrient recovery; wastewater reuse

INTRODUCTION

The increasing word population, together with climate change and the over-exploitation of freshwater sources, makes it urgent to develop sustainable alternatives for water reuse and everyday goods production. Cyanobacteria are microorganisms capable of accumulating several bioproducts, such as bioplastics, natural pigments and lipids (Senatore et al., 2023), by using sunlight and fixing CO_2. Furthermore, their production may be coupled to wastewater treatment, and their biomass extracted in a biorefinery approach to maximize the profitability of the process. However, the implementation of a wastewater-based cyanobacterial biorefinery is still challenging, as strain stability and bioproduct productivity maintenance over time are difficult to achieve. Thus, the use of strains with environmental plasticity, together with the development long-term experiments are needed. In addition, due to the fact that the social acceptation of wastewater-derived bioproducts is still limited, the tracking of organic microcontaminants in the final product is needed so as to develop realistic applications. This presentation will show a compilation of experiments using wastewater-borne cyanobacteria for tertiary wastewater treatment coupled to the recovery of bioproducts (pigments and biogas) in lab and pilot scale photobioreactors. For the first time, the presence of contaminants of emerging concern (CECs) was tracked over the process.

MATERIALS AND METHODS

Two wastewater-borne cyanobacteria strains (*Synechocystis* sp. and *Synechococcus* sp.) were used for tertiary wastewater treatment and recovery of bioproducts. Firstly, lab scale (3 L) tubular photobioreactors of polymethyl methacrylate were fed with secondary effluent from an activated sludge wastewater treatment plant (WWTP) in semi-continuous mode. Biomass was periodically harvested for pigments extraction and quantification by spectrophotometry following Arashiro et al. (2020). Furthermore, the residual biomass of *Synechococcus* sp. was used in Biochemical Methane Potential (BMP) tests under mesophilic conditions (Table 1). Serum bottles with a total volume of 160 mL and a working volume of 50 mL, were inoculated with 5 g Volatile Solids (VS) L^{-1} of substrate ($VS_{substrate}$), and a $VS_{substrate}$:$VS_{inoculum}$ of 0.5 (Arashiro et al. 2020). Following, as *Synechocystis* sp. showed a more stable phycobiliprotein content over time, it was further scaled-up to a pilot (30 L) tubular photobioreactor. Tubular photobioreactors were mixed either with a magnetic stirrer (200 rpm, 3 L) or paddle (90 rpm, 30 L), and pH was maintained at 7.5-9 by CO_2 injection (HI 8711, HANNA instruments, Italy). Light was provided by cool-white LED lamps. Nutrients (P-PO_4^{3-}, N-NH_4^+, N-NO_3^- and N-NO_2^-) removal and biomass growth (measured as volatile suspended solids, VSS) were monitored following Standard Methods (APHA-AWWA-WPCF, 2017). Finally, the presence of CECs was analysed in the secondary effluent, biomass, and phycobiliprotein extracts as described by Matamoros et al. (2015). Schematic diagrams of the scientific questions and experimental steps are shown in Figure 1 and 2.

RESULTS AND DISCUSSION

Promising cyanobacteria strains for domestic wastewater treatment must have tolerance to high N-NH_4^+ concentration, and this study showed that both wastewater-borne cyanobacteria (*Synechococcus* sp. and *Synechocystis* sp.) were able to treat secondary effluent with an average concentration of 42 mg L^{-1} of N-NH_4^+. Indeed, both of them efficiently removed up to 83% of N-NH_4^+ and 97% of P-PO_4^{3-} (Table 2), reaching stable biomass concentrations around 515 and 494 mg $VSS\ L^{-1}$, respectively. In terms of phycobiliprotein recovery, although *Synechococcus* sp. presented a very high pigment production potential (up to 214 mg gDW^{-1}), phycobiliprotein loss was evidenced over time; whereas in the case of *Synechocystis* sp. it was steadily maintained at concentrations close to 70 mg gDW^{-1} (Figure 3 A, B). Given that N was completely depleted, and under N exhaustion conditions phycobiliproteins are degraded as a cellular N source (chlorosis), it seems that *Synechococcus* sp. is more sensitive to N depletion than *Synechocystis* sp. Thus, when *Synechocystis* sp. was scaled-up to a 30 L photobioreactor, the phycobiliprotein content was maintained over a period of 45 days, reaching up to 74 mg gDW^{-1} (Figure 3 D). Following, the methane production from *Synechococcus* sp. residual biomass after phycobiliproteins extraction by the freeze-thaw methodology was quantified (Table 1). The methane yield reached 222 NL CH_4 $kgVS^{-1}$ (Figure 3 C), which is similar or even higher than the values reported (159-199 mL CH_4 $kgVS^{-1}$) by Arashiro et al. (2020). Regarding CECs, only 3 out of 20 detected in secondary effluent were found in pigment extracts.

In conclusion, this study shows the potential of wastewater-borne cyanobacteria as tertiary wastewater treatment coupled to high-value bioproducts (phycobiliproteins) recovery. Moreover, it highlights the circularity of the process by reusing the residual biomass to recover bioenergy (biogas) in a biorefinery approach. Finally, it evidences the stability of the process at pilot scale (30 L) in the long-term, which is one of the main challenges of nutrient recovery from wastewater coupled to cyanobacterial biomass and derived bioproducts obtention.

TABLES AND FIGURES

Table 1. Experimental conditions, cell disruption methodology and bioproducts recovered over the semi-continuous experiments in secondary effluent. HRT: hydraulic retention time.

Strain	Scale	Days	HRT (d)	Cell disruption	Bioproduct obtained
Synechococcus sp.	3 L	18	6	2 cycles of freeze-thawing (-20 - 4ºC)	Phycobiliproteins and biogas
Synechocystis sp.	3 L	12	5	1cycle of freeze-thawing (-20 - 4ºC) + bead beating (3200 rpm, 10 min at 4ºC)	Phycobiliproteins
	30 L	120	8 and 6		

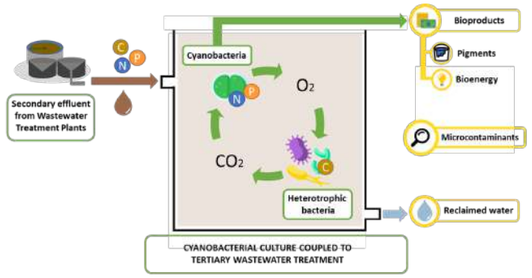

Figure 1. Nutrient recovery from secondary effluents from wastewater treatment plants coupled to cyanobacterial production and bioproduct obtention.

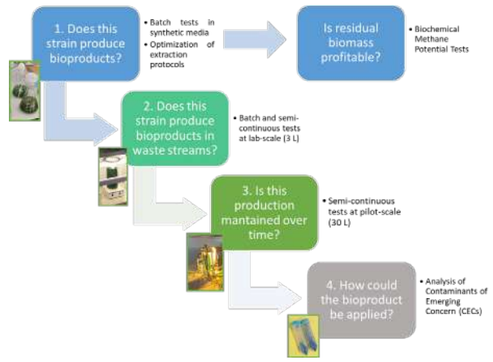

Figure 2. Experimental steps followed to establish a wastewater-based cyanobacterial biorefinery.

Table 2. Average volatile suspended solids (VSS), nitrogen (N-NH_4^+, N-NO_3^-) and phosphorus (P-PO_4^{-3}) content in the secondary effluent (influent) and mixed liquor of the 3L photobioreactor (effluent). HRT: hydraulic retention time.

	Synechococcus sp. (HRT 6 d)			*Synechocystis* sp. (HRT 5 d)		
Parameter	**Influent**	**Effluent**	**Removal efficiency (%)**	**Influent**	**Effluent**	**Removal efficiency (%)**
VSS [mg L^{-1}]	21.1 ± 2.4	515 ±105	-	21.8 ± 2.9	494 ± 124	-
N-NH_4^+ [mg L^{-1}]	41.5 ± 1.3	2.6 ± 7.5	93.9 ± 17.8	42.2 ± 1.2	7.18 ± 9.9	82.9 ± 23.5
N-NO_3^- [mg L^{-1}]	1.3 ± 0.3	3.4 ± 5.9	43.1 ± 34.5	1.2 ± 0.2	4.2 ± 5.2	30.7 ± 34.1
P-PO_4^{-3} [mg L^{-1}]	2.4 ± 0.8	0.02 ± 0.03	99.1 ± 1.1	2.7 ± 0.9	0.05 ± 0.09	97.4 ± 5.3

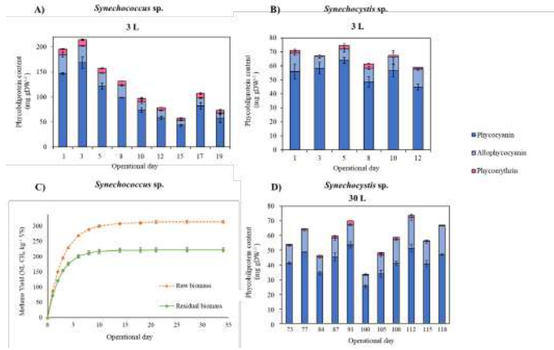

Figure 3. Bioproduct recovery from wastewater-borne cyanobacteria treating secondary effluent. Phycobiliprotein content (mg gDW^{-1}) of the biomass over time (day), during the semi-continuous experiments at lab (3 L) (A, B) and pilot (30 L) scale (D). Methane yields (C).

REFERENCES

APHA-AWWA-WPCF. 2017. Standard Methods for the Examination of Water and Waste Water. In 20th ed. America Public Health Association, Washington DC.

Arashiro, L. T., Ferrer, I., Pániker, C. C., Gómez-Pinchetti, J. L., Rousseau, D. P. L., van Hulle, S. W. H., Garfí, M. 2020. Natural Pigments and Biogas Recovery from Microalgae Grown in Wastewater. *ACS Sustainable Chemistry and Engineering*, **8**(29), 10691–10701.

Matamoros, V., Gutiérrez, R., Ferrer, I., García, J., Bayona, J. M. 2015. Capability of microalgae-based wastewater treatment systems to remove emerging organic contaminants: A pilot-scale study. *Journal of Hazardous Materials*, 288, 34–42.

Senatore, V., Rueda, E., Bellver, M., Díez-Montero, R., Ferrer, I., Zarra, T., Naddeo, V., García, J. 2023. Production of phycobiliproteins, bioplastics and lipids by the cyanobacteria Synechocystis sp. treating secondary effluent in a biorefinery approach. *Science of The Total Environment*, 857, 159343.

Plant growth potential of hotel greywater reuse in hydroponic system

J. Vosse*.**, E. Mendoza*.**, J. Comas*.*** and G. Buttiglieri*.**

* ICRA-CERCA. Catalan Institute for Water Research, Girona, Spain
(E-mail: jvosse@icra.cat; emendoza@icra.cat; gbuttiglieri@icra.cat)
** UdG. University of Girona, Girona, Spain
*** LEQUIA. Institute of the Environment, University of Girona, E-17071 Girona, Spain
(E-mail: joaquim.comas@udg.edu)

Abstract
The potential growth of lettuce (*Lactuca sativa*) and mint (*Mentha Sativa*) in a hydroponic system fed with light greywater, collected from bathroom sinks and showers in Hotel Samba in Lloret de Mar (Spain), was studied. Both types of plants were able to sustain and grow in the channels fed with greywater. However, compared to control plants grown in commercial hydroponic solution, the growth was noticeably smaller. Channels fed with greywater supplemented with the same nutrients on the other hand, produced bigger lettuces as well as mint plants of similar size as the control, showing greywater as a good medium to grow edibles in hydroponics. The present study is part of a more extensive research activity aiming to assess the feasibility of reusing different greywater sources to produce food crops and aromatic herbs.

Keywords
Hydroponic, lettuce, mint, nature-based solutions, plant growth assessment, water reuse

INTRODUCTION

Water reuse has long since been acknowledged to be a necessary measure to counter water scarcity, especially in the Mediterranean region, where touristic activities put additional pressure on decreasing natural freshwater resources. Here decentralised nature-based water treatment and reuse applications (e.g., in hydroponic systems) have been found to be a suitable solution to decrease the fresh water demand in tourist facilities (Estelrich et al., 2021). The agricultural sector has been identified to have the highest potential for water reuse applications (Regulation (EU) 2020/741). An interest to quantify the circularity of water reuse regarding more resources than just the water, by looking into the potential benefit of recovered nutrients from wastewater for plant growth, is rising. Hereby is source separated greywater (GW) an interesting source, as it contains less microbiological contamination than wastewater (Sangare et al., 2021). There is little literature assessing the sufficiency of nutrients in different greywater sources to grow crops. Sangare et al. (2021) found more dry weight production in dishwasher GW irrigated lettuces compared to fresh well water. Conversely, Sawadogo et al. (2014) found that GW constitutes like washing detergent at concentrations <1g/l may negatively affect plant growth. Da Silva Cuba Carvalho et al. (2018) found that treated wastewater only grows plants of comparable size to conventionally grown hydroponic lettuces, if supplemented with nutrients. Similarly due to the lack of essential nutrients, especially nitrogen, for plant growth in treated GW, Eregno et al. (2017) increased their hydroponic lettuce production by using source-separated urine as nutrient solution. This study aims to assess the suitability of hotel light GW (i.e., from bathroom sinks/showers) to grow lettuce and mint plants of marketable size in a hydroponic system. The plant growth assessment is hereby the focus of this abstract.

MATERIALS AND METHODS

The hydroponic system consisted of 15 individual hydroponic PVC channels under controlled environmental conditions (21ºC; 68% relative humidity; 14 light hours, LED lamps). Duplicate channels with either six lettuces or mint plants per channel, were tested per water type. Each channel was fed with 1.5L of either GW, GW plus commercial hydroponic nutrients (GW+), or commercial hydroponic nutrient solution (purchased from groho.es; prepared with deionized water) as control condition (CTRL). Hotel GW was collected weekly and stored at 4ºC in a cold chamber. All water types were renewed twice per week in the system during 4 weeks of experiment. For the plant growth assessment, a minimum of two plants of average representative size (measured by number of leaves and visual appearance) were selected, cleaned with DI water, and separated into functional groups (roots, stems, leaves). The leaf area per plant was measured using the "Easy Leaf Area Free" mobile phone application (last updated 31.07.2015) developed by Hsien Ming Easlon & Arnold J. Bloom. The individual plants parts were dried at 70ºC for 48 hours to calculate average dry weights. The compared plant growth parameters include, next to number of leaves, leaf area and whole plant and leaf dry weight, five traditional plant growth assessment parameters that have been found in guidance literature (Pérez-Harguindeguy et al., 2013; Pandey et al., 2017; van Holsteijn, 1980; Hunt et al., 2002):

$$RGR = \frac{lnW_2 - lnW_1}{t_2 - t_1} \quad (1)$$

Relative growth rate (RGR; g/g/day): Average daily increase in dry matter per unit dry matter per time. Indicates proportionate growth of the plant independent of its size.

$$NAR = \frac{(W_2 - W_1) * (lnLA_2 - lnLA_1)}{(t_2 - t_1) * (LA_2 - LA_1)} \quad (2)$$

Net assimilation rate (NAR; g/cm^2/day) or unit leaf rate (ULR): Increase of plant material per unit of assimilatory material (unit LA) per unit of time. Indicates the daily rate of photosynthesis per unit LA.

$$LWR = \frac{(LW_2/W_2) - (LW_1/W_1)}{2} \quad (3)$$

Leaf weight ratio (LWR; g/g): Ratio of the leaf dry weight (LW) to total plant material dry weight (leaves, stems & roots; W). Indicates the proportion of leaves to the whole plant (i.e., dry weight involved in assimilation).

$$LAR = \frac{(LA_2/W_2) - (LA_1/W_1)}{2} \quad (4)$$

Leaf area ratio (LAR; cm^2/g W): Ratio of leaf area (LA) to total plant dry weight (W). Indicates leafiness of plants (higher LAR indicates more efficient use of dry mass for photosynthesis and respiration).

$$SLA = \frac{(LA_2/LW_2) - (LA_1/LW_1)}{2} \quad (5)$$

Specific leaf area (SLA; cm^2/g LW): Ratio of the leaf area to leave dry weight (LW). A higher SLA indicates less thick and/or dense leaves.

With: W: dry weight of total plant material, LW: dry weight of leaves & LA: total leaf area at t1 & t2: day of planting & harvest of plants each.

RESULTS AND DISCUSSION

GW with and without additional nutrients facilitated plant growth of varying degree (Figure 1).

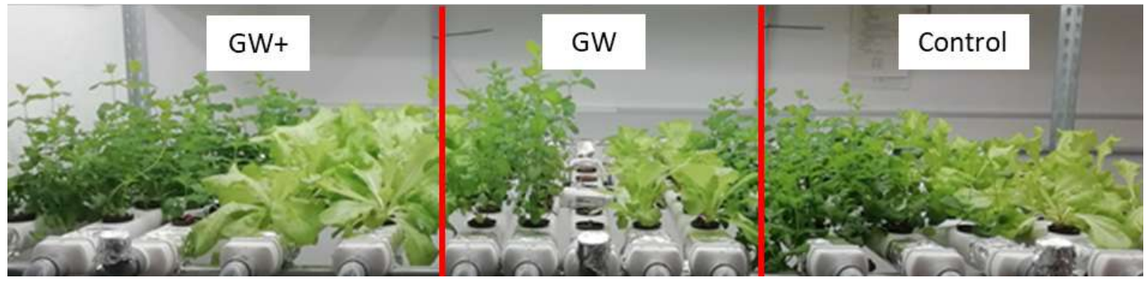

Figure 1. Hydroponic system with mint and lettuce grown in greywater plus nutrients (GW+), greywater (GW) and hydroponic nutrient solution (Control), after week 4 of the experiment.

Comparing the average total nitrogen and total phosphorus influent concentrations (TN (mg/L): 195; 7.7; 199 & TP (mg/L): 35; 0.9; 43) in CTRL, GW, and GW+ respectively, shows that the GW is lacking essential nutrients for plant growth. In the final weeks of the experiment TN & TP concentrations in the GW effluent were depleted below 1 & 0.5 mg/L. The resulting inaccessibility to essential nutrients by the plant explains the limited growth of plants grown in the GW condition.

Figure 2 a & b. Plant growth parameters for lettuce (a) & mint (b); number of leaves, leaf area, and leaf dry weight are provided as additional values produced since the day of planting (t0; initial values indicated as ●).

a. Lettuce. Plant growth parameters in figure 2a show that the control plants grew the same number of leaves as the GW+ condition, which received the same nutrients, but the CTRL leaves were smaller in area and weight. Therefore, while CTRL produced bigger looking plants (higher number and bigger leaves) than GW, plants of both conditions had similarly low RGR (dry weight production). This is because the GW plants grew smaller but thicker leaves indicated by the lower leaf area and SLA, which is a morphological change that has been repeatedly found in GW conditions tested in previous experiments. So, while GW+ and control plants used their dry matter more efficiently for photosynthesis and respiration (higher LAR), GW plants maximized photosynthesis in a smaller area (high NAR). Another typical morphological adaptation to a nutrient scarce environment (Eregno et al., 2017) is the higher ratio of roots to leaves, indicated by the lower LWR. Overall, however, GW+ produced 3 more leaves, 4 times as much leaf area and 3 times as much leaf dry weight as the GW condition. And GW+ was the only condition producing crops of marketable size and form. The control plants did not reach the growth expected, at least as good as GW+. However, this is likely due to their placement in the experimental system, which received the lowest light intensity.

b. Mint. Plant growth parameters in figure 2b show that GW+ and CTRL condition performed similarly well, by multiplying the initial number of leaves by four, the initial leaf area by nine and the initial leaf dry weight by five. While the GW condition only managed to double the number of leaves and triple the leaf area and dry weight compared to t0. Here too the lower LA (SLA) for GW indicates smaller but thicker leaves, to maximize the productivity of the available dry mass (high NAR). While the two other conditions (GW+ and CTRL) used their dry mass more efficiently for photosynthesis and respiration (higher LAR). The lower LWR hints at the adaptation to nutrient scarce environments, through higher root mass, making up 27% of the total GW plant dry weight compared to 14% that it makes up for in control plants. The GW plus additional nutrients, on the other hand, showed growth parameters very similar to the control conditions.

CONCLUSION

The light GW with additional nutrients can be expected to perform similarly well as a conventional nutrient solution prepared with DI water. GW alone did facilitate plant growth, and did not cause visible plant diseases, despite being a raw GW. However, there were noticeable changes in the plant's morphology, and the produced leaf area and dry mass was well below that of the conventional nutrient solution. Therefore, this light greywater source can substitute freshwater in a hydroponic system, however it cannot by itself provide all the necessary nutrients for optimum plant growth.

Acknowledgements: Authors acknowledge funding from the Spanish State Research Agency of the Spanish Ministry of Science and Innovation for ReUseMP3 project (PID2020-115456RB-I00 /MCIN/AEI / 10.13039/501100011033), Project PCI2022-132980 (SAFE) funded by MCIN/AEI/10.13039/501100011033 and the European Union NextGenerationEU/ PRTR. E. Mendoza and J. Vosse thank Secretariat of Universities and Research from Generalitat de Catalunya and European Social Fund for their FI fellowship (2022FI_B2 00064 and 2022 FI_B 00084, respectively). Gianluigi Buttiglieri acknowledges Spanish State Research Agency of the Spanish Ministry of Science, Innovation and Universities for the Grant to the Creation of a permanent position Ramon y Cajal 2014 (RYC-2014-16754). ICRA researchers thank funding from CERCA program.

REFERENCES

da Silva Cuba Carvalho, R., Bastos, R. G., & Souza, C. F. 2018. Influence of the use of wastewater on nutrient absorption and production of lettuce grown in a hydroponic system. *Agricultural Water Management*, *203*(April 2017), 311–321.
Eregno, F. E., Moges, M. E., & Heistad, A. 2017. Treated greywater reuse for hydroponic lettuce production in a green wall system: Quantitative health risk assessment. *Water (Switzerland)*, *9*(7).
Estelrich, M., Vosse, J., Comas, J., Atanasova, N., Costa, J. C., Gattringer, H., & Buttiglieri, G. 2021. Feasibility of vertical ecosystem for sustainable water treatment and reuse in touristic resorts. *Journal of Environmental Management*, *294*(June).
Hunt, R., Causton, D. R., Shipley, B., & Askew, A. P. 2002. A modern tool for classical plant growth analysis. *Annals of Botany*, *90*(4), 485–488.
Pandey, R., Paul, V., Das, M., Meena, M., & Meena, R. C. 2017. Plant Growth Analysis. *Manual of ICAR Sponsored Training Programme on "Physiological Techniques to Analyze the Impact of Climate Change on Crop Plants," January*.
Pérez-Harguindeguy, N., Díaz, S., Garnier, E., Lavorel, S., Poorter, H., Jaureguiberry, P., Bret-Harte, M. S., Cornwell, W. K., Craine, J. M., Gurvich, D. E., Urcelay, C., Veneklaas, E. J., Reich, P. B., Poorter, L., Wright, I. J., Ray, P., Enrico, L., Pausas, J. G., De Vos, A. C., … Cornelissen, J. H. C. 2013. New handbook for standardised measurement of plant functional traits worldwide. *Australian Journal of Botany*, *61*(3), 167–234.
Sangare, D., Coulibaly, L. S., Andrianisa, H. A., Coulibaly, J. Z., & Coulibaly, L. 2021. Investigating the capacity of hydroponic system using lettuce (Lactuca sativa L.) in the removal of pollutants from greywater while ensuring food security. *International Journal of Environment, Agriculture and Biotechnology*, *6*(3), 123–131.
Sawadogo, B., Sou, M., & Hijikata, N. 2014. Effect of Detergents from Greywater on Irrigated Plants : Case of Okra (Abelmoschus esculentus) and Lettuce (Lactuca sativa) *Journal of Arid Land Studies :* 日本沙漠学会誌, *24*(1), 117–120.
van Holsteijn, H. M. C. (1980). *Growth of lettuce - II. Quantitative analysis of growth*. *13*.

Integration of forward osmosis into a granular anaerobic membrane bioreactor for low energy and high quality water reuse and energy production: potential and challenges.

P. Olives*, L. Sanchez**, G. Lesage**, I. Rodriguez-Roda*, G. Blandin*
* LEQUIA, Institute of the Environment, University of Girona, Spain
(E-mail: gaetan.blandin@udg.edu)
** Institut Européen des Membranes (IEM), Université de Montpellier, CNRS, ENSCM, Montpellier, France
(E-mail: *geoffroy.lesage@umontpellier.fr*)

Abstract

Anaerobic membrane bioreactor (AnMBR) is gaining attention for domestic wastewater treatment thanks to the production of high quality permeate and biogas production towards energy positive treatment. Granular sludge based anaerobic membrane bioreactor (G-AnMBR) has gained emphasis in the last decade since granular biotechnology boosts the biomass activity and reduces membrane fouling simultaneously. With the aim to produce higher quality effluent for water reuse applications and improve system efficiency, forward osmosis (FO) system was integrated to a G-AnMBR. Kubota microfiltration modules were step by step replaced by Submerged FO plate and frame modules. Process stability, impact of salinity on biomass, produced water quality and organic matter removal efficiency were assessed and compared for system working in 100% MF, 70%MF/30%FO, 30%MF/70%FO and 10%MF/90%FO respectively. A 15L reactor fed with synthetic wastewater was operated at 25ºC with neither scouring nor relaxation at around 5 L/m2/h permeation flux during at least 10 days. Above 90% COD degradation was observed for all configurations and with a remaining COD content below 50mg/L and below detection limit for MF and FO permeates respectively. Positively, FO membranes proved to be less prone to fouling and increased COD degradation was observed when operating with FO. However, increasing FO share in the reactor, led to salinity increase and to enhanced fouling propensity probably due to salinity shock on the active biomass, releasing extra polymeric substance in the mixed liquor.

Keywords (maximum 6 in alphabetical order)

Water reuse; anaerobic membrane bioreactor; water reuse; fouling

INTRODUCTION

Anaerobic membrane bioreactor (AnMBR) is rising attention for domestic wastewater treatment thanks to the production of high quality permeate and biogas production towards energy positive treatment[1]. Granular sludge based anaerobic membrane bioreactor (G-AnMBR) has gained emphasis in the last decade since granular biotechnology boosts the biomass activity and reduces membrane fouling simultaneously[2,3]during anaerobic digestion of domestic wastewater combined with a submerged ultrafiltration membrane with no gas-sparging. A one-stage submerged granular anaerobic membrane bioreactor (G-AnMBR. A very recent study proved that G-AnMBR applied for domestic wastewater at psychrophilic temperature could achieve high organic matter removal rates, increasing effluent quality, while producing a net energy balance due to the biogas production, derived from the organic matter conversion to methane [2]. In parallel, Forward osmosis (FO) gained some interest since it relies on osmotic gradient, using dense membranes and demonstrated to have lower fouling propensity. Unlike MF and UF membranes, FO retains salts, pesticides, pharmaceutical compounds [4]osmotic membrane systems, such as forward osmosis (FO. Operating AnMBR only with FO membrane (Anaerobic osmotic MBR, AnOMBR) led to high rejection rates, moderate fouling but severe salinity build-up overtime when only a FO membrane is used[5]. Combining FO and MF membrane into the AnOMBR reactor avoided severe salinity build-up while assuring production of high water quality (through the FO membrane), production of biogas and concentration of nutrients (phosphorous in the MF permeate) to facilitate its downstream recovery or reuse[6]ability to efficiently process low ionic strength wastewater and high effluent quality. However, salt accumulation remains a main obstacle for causing severe water flux decline, fouling aggravation and inhibitory on the microbial activity. Here, we report a novel microfiltration (MF. Combining G-AnMBR and AnOMBR may represents some synergy by combining the benefits of both technologies allowing for low fouling propensity, low energy requirements, production of biogas and increasing permeate quality thanks to the high rejection of FO membranes. In this study, we evaluated the progressive substitution of MF membranes by FO membranes in a G-AnMBR to evaluate the concept of Granular Anaerobic Osmotic MBR (G-AnOMBR).

MATERIALS AND METHODS

The G-AnMBR pilot featured a rectangular parallelepiped reactor (282 × 100 × 900 mm) with a working volume of 17L (Figure 1). The reactor was seeded with anaerobic granular sludge obtained from a paper mill factory. Synthetic wastewater was fed to the reactor with COD concentration of 500±200 mg.L^{-1}.The hydraulic retention time (HRT) was set at 10 hours aiming to achieve an optimal organic matter removal of 90%. All experiments were conducted at a temperature of 25°C. The biomass level filled up the bottom part of the reactor up until the bottom part of the membrane modules. A recirculation pump set at 40L.h^{-1} was used to assure a good contact in-between the WW and the biomass and a slight microbial granules fluidization. 3 flat sheet membrane modules (MF and/or FO) with a filtration surface area of 0.1 m^2 each where placed in the reactor. MF and FO modules were operated under negative pumping pressure using 323S peristaltic pumps (Watson-Marlow, UK) without relaxation nor gas sparging. Permeate flows (MF and FO) were monitored by the increase of mass in permeate and draw tanks using Kern EWJ balances. Unless specific conditions, the average targeted permeation flux was of 5 ± 1 L·m^{-2}·h^{-1}. MF permeate flux was controlled by the pump velocity; FO permeation flux was obtained by maintaining constant draw conductivity at 23ms.cm^{-1} (15g.L^{-1} NaCl). The pilot was fully monitored and controlled by a homemade Arduino system. Oxidation-reduction potential, conductivity, temperature, and pH sensors were placed in the G-AnOMBR reactor supernatant.

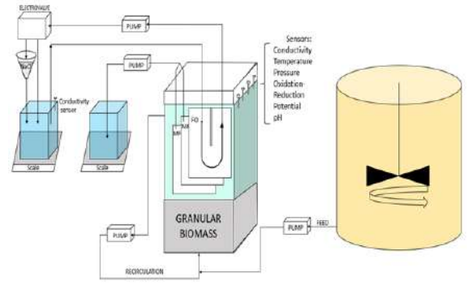

Figure 1. Experimental setup of the G-AnOMBR pilot.

The step-by-step substitution of MF by FO modules led to different hybrid configurations (100%MF, 70%MF, 40-60% MF, 10-20%MF) which were maintained for at least 10 days for each tested conditions. Salinity increase, membrane fouling, organic matter removal, hydraulic retention time, flows were assessed for each operating conditions. MF was operated at constant flux and therefore fouling occurrence was assessed through transmembrane pressure (TMP) increase. MF membranes were cleaned before changing the MF/FO ratio as well as whenever the TMP increased above 300 mbar. FO membrane fouling was assessed through permeation flux reduction; once 30% flux was lost, membranes were cleaned by (1) flushing with 0.5L of DI water followed by osmotic backwashing. For both FO and MF membranes, biofilms removed with the 0.5 L DI flushing of each cleaning were kept for further characterization

RESULTS AND DISCUSSION

Overall, the G-AnOMBR with MF and FO was operated for more than 50 days and with 4 successive steps corresponding to different MF/FO extraction ratio, i.e. 100%MF, 70%MF, 40-60%MF, and 10-20%MF. Hereafter we discuss how this ratio impacts organic matter degradation, salinity and fouling behaviour.

In the initial phase, with 100% MF and 0% FO, COD average removal was of 82.3% (Figure 2). The substitution of MF modules by FO ones into the rector led to an improvement of the overall COD removal well above 90%; leading to average values of 95.9% for 70%MF; 95.0% for 40-60%MF; and 97.2% for 10-20%MF. As such, it indicates first that the integration of FO modules led to an increase of the efficiency of the biological process. Higher COD removal obtained when operating with FO membranes can be explained by the higher retention time of the COD fraction in the reactor; COD rich fraction been extracted only through the MF permeate (fully rejected by FO membrane). As already observed in other studies, FO integration allow for a full dissociation of HRT and SRT, increasing the overall COD fraction degradation.

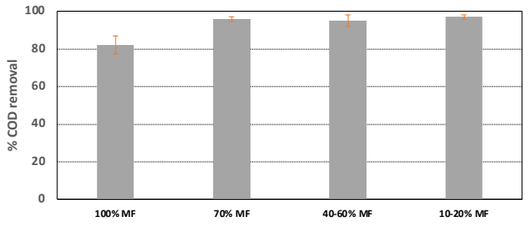

Figure 2. Average % COD removal over 10 days in 100%MF and hybrid MF/FO operation

The integration of FO membranes in the G-AnMBR led to a salinity increase in the reactor (Figure 3a). Conductivity increase was monitored during the study. Initial conductivity operating with 100% MF modules remained around 1.25 mS.cm^{-1} and increased successively up to 2.6, 6.5 and 9 mS.cm^{-1} when increasing the FO extraction rate and consequently decreasing the MF% to 70%, 40-60% and 10-20% MF respectively. Salinity increase was the consequence of (1) high feed solution salt rejection by FO membranes leading to salt accumulation in the reactor and (2) reverse salt diffusion (RSD) from the FO draw solution due to its imperfect salt rejection. Based on conductivity measurement (and theoretical increase due to concentration effect only), it was estimated that RSD was responsible for about half of the salinity increase in the reactor. Developing membranes with higher selectivity and the use of draw solution with lower diffusivity or easily biodegradable organic based draw solutions may help to mitigate this effect.

TMP for MF and permeation flux for FO confirmed the more complicated operation of membrane systems when operation with higher rate of FO membrane. This conclusion was reinforced by the membrane cleaning frequency, which was reduced from 10 days to 7 days, 4-6 days, and 3 days for 100, 70%, 40-60% ad 10-20% MF ratio steps. Interestingly, in 40-60% ratio, FO fouling appeared to less penalizing and MF and FO modules could be operated for a longer time (Figure 3b). Based on biofilm samples collected and dry solids weighted after each cleaning and for each MF/FO ratio, at 70% MF operation, collected amount of biofilm was lower than at 100%, confirming 70% MF as acceptable operating conditions. At higher FO ratio, increased biomass was collected both on FO and MF membranes confirming the higher fouling propensity probably induced by the raised salinity in the reactor which can promote the release of extra polymeric substances (EPS)

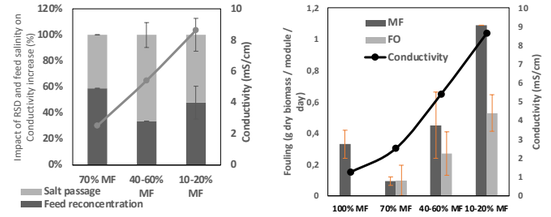

Figure 3. (a) Impact of RSD and concentration effect on salinity increase and (b) total solid (TS) fouling rate (g TS/module/day) attached to the membrane surface for MF and FO modules for various MF/FO operating ratio

REFERENCES

(1) Deng, L.; Guo, W.; Ngo, H. H.; Zhang, J.; Liang, S. 5 - Advanced Anaerobic Membrane Bioreactors: Performance Enhancers and Their Hybrid Systems. In *Current Developments in Biotechnology and Bioengineering*; Ngo, H. H., Guo, W., Ng, H. Y., Mannina, G., Pandey, A., Eds.; Elsevier, 2020; pp 109–142. https://doi.org/10.1016/B978-0-12-819852-0.00005-1.

(2) Sanchez, L.; Carrier, M.; Cartier, J.; Charmette, C.; Heran, M.; Steyer, J.-P.; Lesage, G. Enhanced Organic Degradation and Biogas Production of Domestic Wastewater at Psychrophilic Temperature through Submerged Granular Anaerobic Membrane Bioreactor for Energy-Positive Treatment. *Bioresource Technology* **2022**, *353*, 127145. https://doi.org/10.1016/j.biortech.2022.127145.

(3) Robles, Á.; Ruano, M. V.; Charfi, A.; Lesage, G.; Heran, M.; Harmand, J.; Seco, A.; Steyer, J.-P.; Batstone, D. J.; Kim, J.; Ferrer, J. A Review on Anaerobic Membrane Bioreactors (AnMBRs) Focused on Modelling and Control Aspects. *Bioresource Technology* **2018**, *270*, 612–626. https://doi.org/10.1016/j.biortech.2018.09.049.

(4) Blandin, G.; Ferrari, F.; Lesage, G.; Le-Clech, P.; Héran, M.; Martinez-Lladó, X. Forward Osmosis as Concentration Process: Review of Opportunities and Challenges. *Membranes* **2020**, *10* (10), 284. https://doi.org/10.3390/membranes10100284.

(5) Gu, Y.; Chen, L.; Ng, J.-W.; Lee, C.; Chang, V. W.-C.; Tang, C. Y. Development of Anaerobic Osmotic Membrane Bioreactor for Low-Strength Wastewater Treatment at Mesophilic Condition. *Journal of Membrane Science* **2015**, *490*, 197–208. https://doi.org/10.1016/j.memsci.2015.04.032.

(6) Wang, X.; Wang, C.; Tang, C. Y.; Hu, T.; Li, X.; Ren, Y. Development of a Novel Anaerobic Membrane Bioreactor Simultaneously Integrating Microfiltration and Forward Osmosis Membranes for Low-Strength Wastewater Treatment. *Journal of Membrane Science* **2017**, *527*, 1–7. https://doi.org/10.1016/j.memsci.2016.12.062.

TECHNICAL SESSIONS

T4.

WW treament for water reclamation

Comparing Efficiency in Solar Water Treatment: Photovoltaic-LED vs. Compound Parabolic Collector Photoreactors

M.D. Molina-Ramírez, M. Martín-Sómer, M.L. Perez-Araujo, R. van Grieken, C. Pablos, J. Marugán

* Department of Chemical and Environmental Technology, ESCET, Universidad Rey Juan Carlos, C/ Tulipán s/n, 28933 Móstoles, Madrid, Spain.

(E-mail: *mariadolores.molina@urjc.es; miguel.somer@urjc.es; maria.perezaraujo@urjc.es; rafael.vangrieken@urjc.es; cristina.pablos@urjc.es; javier.marugan@urjc.es)*

Abstract

Seven different solar processes (CPC, PV-UVA LED, PV-UVC LED, CPC+TiO_2, CPC+H_2O_2, PV-UVA LED+TiO_2 and PV–UVC LED+H_2O_2) were investigated, both for the oxidations of chemicals and the inactivation of bacteria. The results showed that, for the oxidation of chemicals, the best photochemical yield (in terms of the use of photons) is achieved by the PV-UVC LED+H_2O_2 process. However, despite being the most effective, the low electrical efficiency of current UVC LED sources makes the CPC+TiO_2 process the most efficient in the use of solar light. In contrast, for bacterial inactivation, the significantly higher effectiveness of the UVC spectral range in damaging DNA makes the PV-UVC LED+H_2O_2 the most efficient in the use of sunlight. When costs are considered, the PV-UVA LED+TiO_2 may be the most efficient process for chemical oxidation, while the PV-UVC LED+H_2O_2 process could be the most efficient for bacterial inactivation.

Keywords (maximum 6 in alphabetical order)

Bacterial inactivation; Chemical pollutant oxidation; Solar CPC photoreactor; Solar PV panel; UVA LED; UVC LED.

INTRODUCTION

Water is a limited resource essential for life and health. In July 2010, the General Assembly of the United Nations recognised through resolution 64/292 the right to drinking water as a fundamental human right (United Nations General Assembly, 2010). However, the availability of water is only legally guaranteed by a few countries. According to a World Health Organization (WHO) report, 29% of the world's population does not have access to drinking water at home. Every year millions of people get diseases such as diarrhoea, cholera, dysentery, typhoid fever, and polio because of the intake of water contaminated by pathogens. It is estimated that only diarrheal conditions cause more than 1.8 million deaths per year, of which 526,000 correspond to children under five years. In addition, many water sources are contaminated with heavy metals, chronic organic pollution, and waste materials that have a destructive effect on public health and the environment. The shortage of drinking water is one of the most transcendental problems worldwide, affecting the most disadvantaged population and decreasing their quality of life. For decades, radiation has been used in water treatment, allowing the inactivation of microorganisms and the removal of chemical pollutants (Pai et al, 2022) One of the key aspects to ensuring the success of the process is the wavelength range of the employed radiation, with the use of UV light being necessary in most cases. The efficiency of UVC light for microorganisms inactivation, by alterations to their DNA chains, has been widely demonstrated (Baldasso et al., 2021). The efficiency of UVA light is too low for this purpose, with UVB being intermediate. In the case of chemical pollutants, for most compounds, the single use of radiation does not produce significant degradation being necessary the use of a catalyst or an additional reactive. These processes are mainly based on the generation of hydroxyl radicals which, through their high oxidising power, can remove a wide range of pollutants in water, either chemical or microbiological (Kebbi et al., 2020).

However, one of the major drawbacks of all the processes described above, and the main reason for their hindered industrial development is their high cost, due to the source of radiation. In recent years, the development of the LED industry has produced a great expansion of UVA LED, and a similar evolution is expected for UVC LED in the forthcoming years (Amano at al., 2020). An alternative is the direct use of solar radiation, since around 6-7% of the light that reaches the Earth's surface is within the UV range (mostly UVA and a small contribution of UVB). To improve the efficiency of the process, it is common to use compound parabolic collectors (CPC) to concentrate the light. Despite the apparent environmental advantage of using direct sunlight to drive the process, the availability of low-cost solar photovoltaic panels (PV) for feeding LED systems increases the interest in alternative solar-powered photochemical water treatment processes due to cost reductions. This work presents a comparative study of solar-driven photo-activated water treatment processes based on the use of three different lighting sources: direct solar light in a CPC photoreactor; UVA LED and UVC LED (both of which are powered by a PV system). Seven different processes involving the potential presence of H_2O_2 and TiO_2 were tested and the efficiency of two test reactions were analysed: oxidation of methanol and inactivation of *E. coli* bacteria, as representatives of water decontamination and disinfection, respectively.

MATERIALS AND METHODS

A solar CPC photoreactor was used for experiments using direct solar light. It consisted of a borosilicate tube 26 mm in inner diameter and 380 mm in length (0.2 L of illuminated volume) located in the optical axis of a CPC aluminium reflector with 358 cm^2 of collection surface area that provides 85% light reflection towards the central pipe. The reactor operates in a closed recirculating circuit with a 1 L reservoir tank of water, driven by a centrifugal pump at a flow rate of 12 L/min.

For experiments based on LED light sources, an annular photoreactor (15 cm long, 3 cm internal diameter and 5 cm external diameter) was used, operating in a closed recirculation circuit with a 1 L reservoir tank, the water being driven by a centrifugal pump with a flow rate of 36 L/min. As an illumination source, two different 8-LED based systems were used. For the experiments carried out with UVA light, LED with a maximum emission peak centred at 365 nm (LedEngin Model LZ1-00UV00) were used, while for the experiments with UVC light, LED with a maximum emission peak centred at 270 nm (Sum Tang ST-POBA20) were used. Total irradiation power was calculated by potassium ferrioxalate actinometry experiments.

To power the LED system, an ATERSA GS 160W Solar PV panel was used, with an output voltage of 12 V and a collection area of 1 m^2. The LED system was connected to an Eleksol Lead-Acid 110Ah battery, as an alternative energy source. The experiments were carried out at Universidad Rey Juan Carlos facilities in Móstoles, Spain (40.33° N, 3.86° W). Both the Solar CPC reflector and the Solar PV panel were placed with an inclination angle corresponding to the local latitude. Solar irradiance was measured using a PCE-UV34 radiometer (290-390 nm). The temperature was monitored, not exceeding 30 ºC in any experiment.

For the comparison of the different treatments, two different test reactions were used. Methanol (Sigma-Aldrich, LC-MS) at an initial concentration of 100 mM was used as an indicator of the efficiency in the oxidation of chemical pollutants. On the other hand, *E. coli* K12 strain (CECT 4624, corresponding to ATCC 23631, where CECT stands for "Colección Española de Cultivos Tipo") was used as a bacterial indicator for water disinfection experiments.

Experiments with H_2O_2 were carried out using an initial concentration of 50 mg/L, ensuring a negligible depletion by using TP01000PX (Scharlab) indicator strips. Sodium sulphite (Na_2SO_3) was added in a Na_2SO_3-to-H_2O_2 molar ratio of 1:1 after sample collection, to stop the oxidative action of H_2O_2. The experiments with H_2O_2 were not carried out in UVA radiation due to the need for a wavelength below 300 nm, to cause the H_2O_2 decomposition. Photocatalytic processes were studied using Evonik P25 titanium dioxide suspensions at a concentration of 0.1 g/L, previously optimised. Dark experiments were carried out both with TiO_2 and H_2O_2 to check if there was any interaction of these compounds in addition to the pure photocatalytic process for any of the pollutants studied.

RESULTS AND DISCUSSION

Methanol oxidation

Results obtained for methanol oxidation are shown in **table 1**. When kinetic constants are calculated for methanol oxidation considering the reaction rate as a function of the number of photons (E) that reached the reactor UVC processes show a significantly higher efficiency in comparison with those based on UVA and direct sunlight due to the high energy of this radiation. The efficiency of the UVC+H_2O_2 process is particularly remarkable, three orders of magnitude higher than that of the TiO_2 based photocatalytic process. On the other hand, if values obtained for the UVA LED and solar radiation are compared, it can be clearly seen that solar UV photons were used to a greater extent than those emitted by the LED source, probably due to the better light distribution throughout the reactor (Martín-Sómer et al., 2017). If kinetic constants are obtained for LED-based systems when the electrical consumption is selected as an independent variable. In this case, the UVA+TiO_2 process is much more efficient than the UVC+H_2O_2 process. The reason for this is that the unquestionably higher photochemical efficiency of UVC photons is counteracted by the very low efficiency in the conversion of electricity into UVC radiation of current UVC LED sources. On the other hand, when kinetic constants are calculated considering solar UV power, coming from the direct use of solar radiation collected in a CPC reactor, or the use of solar radiation in the PV power system to produce electrical energy for the UV LED reactor the results show that, despite the significant increase in the efficiency of UV LED and PV panels in recent years, the use of direct sunlight in a CPC photoreactor is still more efficient. However, another important aspect that must be evaluated when choosing a technology is the cost. In the specific case of the research carried out in this work, the price obtained by adding the different parts purchased for the assembly of the PV+UV LED systems (including solar panel, battery, UV LED, inverter, controller, and annular reactor) was 435 € and 377.8 € for PV+UVA LED and PV+UVC LED, respectively, while the estimated price of the solar collector was 417 €. Investment cost kinetic constants show that the most economic option for carrying out the oxidation process is the PV-UVA LED system with TiO_2.

Table 1. Zero-order kinetic constant for methanol oxidation in the studied processes as a function of time, photons, energy consumption, solar UV radiation and investment cost.

	Photons	Energy	Solar UV	Investment cost
UVA	$(7.58\pm2.15)\cdot10^{-1}$	$(3.68\pm1.05)\cdot10^{-3}$	$(9.21\pm2.61)\cdot10^{0}$	$(2.76\pm0.78)\cdot10^{-1}$
UVA + TiO_2	$(1.68\pm0.69)\cdot10^{1}$	$(8.16\pm3.35)\cdot10^{-2}$	$(2.37\pm0.84)\cdot10^{2}$	$(7.12\pm2.51)\cdot10^{0}$
UVC	$(3.76\pm1.45)\cdot10^{2}$	$(2.23\pm0.45)\cdot10^{-5}$	$(5.58\pm2.15)\cdot10^{-2}$	$(1.93\pm0.74)\cdot10^{-4}$
UVC + H_2O_2	$(1.68\pm0.43)\cdot10^{4}$	$(7.54\pm2.15)\cdot10^{-3}$	$(2.50\pm0.64)\cdot10^{0}$	$(8.61\pm2.22)\cdot10^{-2}$
CPC	$(5.85\pm1.70)\cdot10^{-1}$	-	$(1.17\pm0.34)\cdot10^{1}$	$(1.26\pm0.37)\cdot10^{-2}$
CPC + TiO_2	$(3.79\pm0.53)\cdot10^{1}$	-	$(7.60\pm1.35)\cdot10^{2}$	$(8.64\pm1.13)\cdot10^{-1}$
CPC + H_2O_2	$(2.26\pm0.61)\cdot10^{0}$	-	$(9.69\pm9.85)\cdot10^{0}$	$(8.90\pm3.29)\cdot10^{-4}$

Bacterial disinfection

Experiments similar to those carried out for methanol oxidation were performed for bacterial inactivation and the kinetic constants are shown in **table 2**. When considering the moles of photons (E) reaching the reactors the kinetic constant for UVC LED sources are five orders of magnitude higher, as expected from the selective DNA damaging mechanism. On the other hand, it was possible to verify how direct solar processes are much more efficient than UVA LED-based processes due to the remarkable effect of the UVB fraction of solar light. When referring to the electrical energy consumption, behaviour opposite to that previously described for methanol oxidation can be observed. Due to the great efficiency of UVC light in bacterial inactivation processes, and despite the poor electrical efficiency of UVC LED, the use of this type of radiation represented an energy improvement compared to the use of UVA LED. On the other hand, solar energy efficiency for bacterial inactivation showed that the use of the UVC LED+H_2O_2, powered by a PV system, allowed better use of solar radiation than the processes carried out in the CPC reactor. The sole use of UVC LED showed slightly worse results than the sole use of sunlight in the CPC reactor. However, it is necessary to consider that the electrical efficiency of UVC LED is increasing exponentially, so this result could be reversed very soon. On the other hand, the use of UVA LED for bacterial inactivation does not show these improvements and as seen in methanol oxidation, the use of direct solar light is more efficient. If the efficiency is calculated considering the cost results show an even more remarkable advantage of PV-UVC LED both with and without H_2O_2. Additionally, considering the costs, the use of PV-UVA LED with TiO_2 is now more profitable than the use of direct sunlight. These results highlight that the use of combined systems with PV+UV LED should already be considered when designing solar water disinfection systems.

Table 2. First-order kinetic constant for bacterial inactivation in the studied processes as a function of time, photons, energy consumption, solar UV radiation and investment cost.

	Photons	Energy	Solar UV radiation	Investment cost
UVA	$(1.01\pm0.10)\cdot10^{1}$	$(4.92\pm0.50)\cdot10^{-2}$	$(1.23\pm0.12)\cdot10^{2}$	$(3.69\pm0.37)\cdot10^{0}$
UVA + TiO_2	$(1.13\pm0.08)\cdot10^{2}$	$(5.65\pm0.33)\cdot10^{-1}$	$(1.38\pm0.10)\cdot10^{3}$	$(4.13\pm0.31)\cdot10^{1}$
UVC	$(2.39\pm0.48)\cdot10^{7}$	$(1.42\pm0.29)\cdot10^{0}$	$(3.54\pm0.71)\cdot10^{3}$	$(1.22\pm0.25)\cdot10^{2}$
UVC +	$(5.11\pm0.67)\cdot10^{7}$	$(3.04\pm0.40)\cdot10^{0}$	$(7.59\pm0.99)\cdot10^{3}$	$(2.62\pm0.34)\cdot10^{2}$
CPC	$(2.77\pm1.02)\cdot10^{2}$	-	$(5.52\pm2.04)\cdot10^{3}$	$(5.93\pm2.19)\cdot10^{0}$
CPC + TiO_2	$(2.97\pm0.55)\cdot10^{2}$	-	$(5.93\pm1.09)\cdot10^{3}$	$(6.37\pm1.17)\cdot$
CPC + H_2O_2	$(2.57\pm0.67)\cdot10^{2}$	-	$(5.13\pm1.34)\cdot10^{3}$	$(5.51\pm1.43)\cdot10^{0}$

REFERENCES

C.W. Pai, G.S. Wang, Treatment of PPCPs and disinfection by-product formation in drinking water through advanced oxidation processes: Comparison of UV, UV/Chlorine, and UV/H2O2, Chemosphere. 287 (2022) 132171.

V. Baldasso, H. Lubarsky, N. Pichel, A. Turolla, M. Antonelli, M. Hincapie, L. Botero, F. Reygadas, A. Galdos-Balzategui, J.A. Byrne, P. Fernandez-Ibañez, UVC inactivation of MS2-phage in drinking water – Modelling and field testing, Water Res. 203 (2021) 117496.

Y. Kebbi, A.I. Muhammad, A.S. Sant'Ana, L. do Prado-Silva, D. Liu, T. Ding, Recent advances on the application of UV-LED technology for microbial inactivation: Progress and mechanism, Compr. Rev. Food Sci. Food Saf. 19 (2020) 3501–3527.

H. Amano, R. Collazo, C. De Santi, S. Einfeldt, M. Funato, J. Glaab, S. Hagedorn, A. Hirano, H. Hirayama, R. Ishii, Y. Kashima, Y. Kawakami, R. Kirste, M. Kneissl, R. Martin, F. Mehnke, M. Meneghini, A. Ougazzaden, P.J. Parbrook, S. Rajan, P. Reddy, F. Römer, J. Ruschel, B. Sarkar, F. Scholz, L.J. Schowalter, P. Shields, Z. Sitar, L. Sulmoni, T. Wang, T. Wernicke, M. Weyers, B. Witzigmann, Y.R. Wu, T. Wunderer, Y. Zhang, The 2020 UV emitter roadmap, J. Phys. D. Appl. Phys. 53 (2020) 503001.

M. Martín-Sómer, C. Pablos, R. van Grieken, J. Marugán, Influence of light distribution on the performance of photocatalytic reactors: LED vs mercury lamps, Appl. Catal. B Environ. 215 (2017) 1–7.

Peroxymonosulfate/Solar process for the simultaneous disinfection and decontamination of urban wastewater at pilot plant scale

I. Berruti*, S. Nahim-Granados*, M.J. Abeledo-Lameiro*, I. Oller* and M.I. Polo-López*

* CIEMAT-PSA, Carretera de Senés Km 4, 04200, Tabernas (Almería), Spain

CIESOL, Joint Centre of the University of Almería-CIEMAT, 04120 Almería, Spain.

(E-mail: *ilaria.berruti@psa.es)*

Abstract

The capability of the combination of peroxymonosulfate (PMS) and natural solar radiation as a solar photochemical process for actual urban wastewater (UWW) purification at pilot plant scale has been investigated. A global analysis of the PMS (0-1 mM)/Solar process performance was assessed in a solar Compound Parabolic Collector (CPC) photo-reactor for simultaneous inactivation of naturally occurring bacteria and their antibiotic-resistant (AR) counterparts (*Escherichia coli*, Total coliforms, *Enterococcus* spp. and *Pseudomonas* spp.), the removal of selected antibiotic resistant genes (ARGs) (i.e., 16S rRNA, *intI1, sul1, qnrS, bla*$_{TEM}$, *bla*$_{CTX-M32}$, *tetM*) and the degradation of three contaminants of emerging concern (CECs) (Diclofenac-DCF, Sulfamethoxazole-SMX and Trimethoprim-TMP). An enhancement in the process performance was obtained with increasing oxidant load, obtaining the best results with 1 mM of PMS, at which the inactivation of naturally occurring bacteria and their AR-counterparts (Detection limit of 2 CFU/mL after 30 minutes, 2.6 kJ/L) was achieved, without observing bacterial regrowth after 48h. In addition, CECs (27 minutes, 2.0 kJ/L) were effectively degraded, but it was ineffective for ARGs removal. PMS/Solar process has been demonstrated to be an attractive, suitable and sustainable option as a decentralized system associated to a small volume of water in areas with a high solar radiation incidence, saving energy costs by using natural solar radiation.

Keywords

Antibiotic Resistance; Compound Parabolic Collector; Contaminants of emerging concern; Peroxymonosulfate; Wastewater reclamation.

INTRODUCTION

The reuse of urban wastewater (UWW) in different activities, especially in agriculture, has been gaining attention as a reliable solution to address water scarcity, enhancing water balance, limiting water withdrawal from natural bodies (surface water and groundwater), promoting water savings according to the principle of circular economy, but also ensuring environmental and human health protection (Guerra-Rodriguez et *al.*, 2020). The microbiological quality of secondary UWW effluents does not fit the quality criteria for its direct reuse in irrigation, and, therefore, the application of tertiary treatments is needed to achieve the regulation requirements. Water remediation by peroxymonosulfate (PMS) alone has been considered a promising option, due to its characteristics, such as high water solubility, low cost, easily of storage and its capability to directly oxidize inorganic and organic compounds containing electron-rich moieties (Ding et *al.*, 2020).

In this work, the combination of PMS with natural solar radiation has been investigated at pilot plant scale for the simultaneous inactivation of naturally occurring bacteria (including *E. coli*, *Enterococcus* spp., *Pseudomonas* spp. and Total coliforms), their antibiotic-resistant (ARB) counterparts, the removal of naturally present antibiotic resistant genes (ARGs) and CECs spiked at 100 µg/L each, in UWW.

MATERIALS AND METHODS

Secondary effluents from the urban wastewater treatment plant (UWWTP) of "El Bobar" located in Almería, South East of Spain, were used. Each batch was freshly collected and physicochemical characterized. The enumeration and quantification procedures for bacteria, ARB, ARGs and CECs monitoring were performed as reported by Berruti et al. (Berruti et *al.*, 2021). All assays were performed at the installations of the Plataforma Solar de Almeria (latitude: 37.0909°N, longitude: 2.357°W), starting between 10:30-11:00 am local time and lasting 180 minutes under natural sunlight. Experiments were performed in a Compound Parabolic Collector (CPC) photoreactor with a total water volume of 10 L (50 % illuminated), which consists of a highly reflective anodized aluminium (MiroSun, Alanod, Germany) module and two independent systems with 2 borosilicate-glass tubes (50 mm), each one on a platform titled 37°, 0.44 m^2 of total irradiated surface and a flow rate of 30 L/min. Water temperature ranged between 22 to 39 ºC and solar UV-A irradiance between 25 to 45 W/m^2, while water pH was 8-8.5 in all cases, remaining constant along the treatment time. The accumulative energy per unit of volume (Q_{UV}, kJ/L) received in the photo-reactors was used to compare results under different experimental conditions (Berruti et *al.*, 2021).

RESULTS AND DISCUSSION

The inactivation profiles of the sum of all bacteria by PMS/Solar process with increasing oxidant concentrations (0-1 mM) at pilot plant scale (10-L CPC solar photo-reactor) are shown in Figure 1.

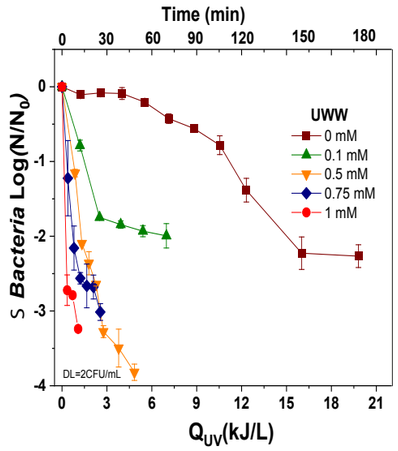

Figure 1. Inactivation profiles of the sum of all bacteria in the presence of increasing concentrations of PMS (0-1 mM) under natural solar radiation in UWW.

An enhancement in process performance was obtained as increasing oxidant concentrations and the best results were obtained with 1 mM, at which detection limit (DL) of 2 CFU/mL was reached for all microbial targets after 15 minutes (1.1 kJ/L of Q_{UV}), compared to 180 minutes with only solar radiation.

Moreover, the absence of bacteria regrowth was observed after 24 and 48 h in the presence of oxidant concentration higher than 0.5 mM, guaranteeing water safety during post-treatment storage.

Figure 2 shows the CEC profiles and a significant enhancement in comparison with only solar radiation (only 40 % of the total CEC removal after 180 minutes or 20 kJ/L of Q_{UV}) was obtained in the presence of added PMS. In addition, more than 80% removal of target CECs was attained with 1 mM after 27 minutes (2 kJ/L of Q_{UV}).

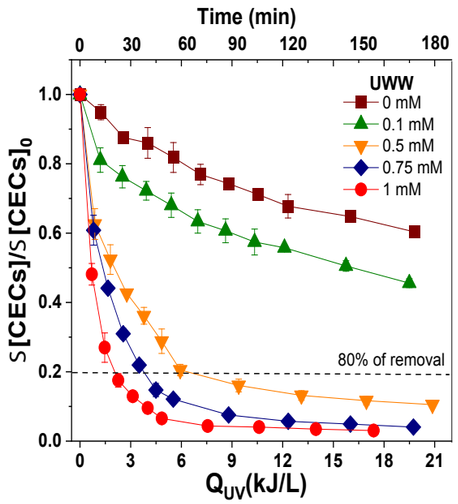

Figure 2. Degradation profiles of the sum of CECs in the presence of increasing concentrations of PMS (0-1 mM) under natural solar radiation in UWW.

In particular, the following CEC reactivity order was found: SMX (17 minutes, Q_{UV}= 1.2 kJ/L) > DCF (30 minutes, Q_{UV}= 2.3 kJ/L) > TMP (40 minutes, Q_{UV}= 3.2 kJ/L).

Moreover, inactivation of naturally occurring ARB, grown in the presence of sub-minimal inhibitory concentrations of three antibiotics (Ampicillin-AMP, Ciprofloxacin-CPX and Trimethoprim-TMP), was monitored in the presence of 1 mM of PMS. No significant differences in the inactivation of wild and AR-bacteria were observed, achieving the DL of 2 CFU/mL within 30 minutes of treatment for all microbial targets, in accordance with a previous study (Michael et *al.*, 2020).

Figure 3 shows ARGs removal in the presence of 1 mM of PMS under natural solar radiation in UWW.

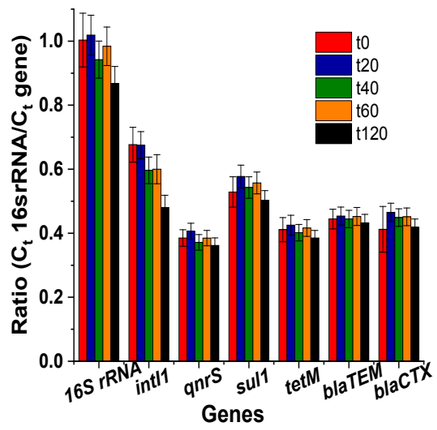

Figure 3. ARGs removal in the presence of 1 mM of PMS under natural solar radiation in UWW.

A decrease of 7 %, 13 % and 30 % was observed after 120 minutes of treatment (11.5 kJ/L of Q_{UV}) for *qnrS*, 16S rRNA and *IntI1*, respectively, while no significant changes in relative abundance were detected for the other genes, highlighting the resistance of this type of pollutants to be removed by this solar processes and being still a challenge to be addressed.

As conclusion, PMS/Solar process has been demonstrated to be an attractive, suitable and sustainable option for UWW reclamation and reuse in agriculture, especially as a decentralized system associated to small volumes of water in areas with a high solar radiation incidence, saving energy costs by using natural solar radiation.

ACKNOWLEDGEMENTS

This work is part of a project that has received funding from the European Union's Horizon 2020 research and innovation programme under the Marie Skłodowska-Curie Grant Agreement No 765860 (AQUAlity). The authors wish to thank also the Spanish Minister of Science and Innovation for funding NAVIA Project (Reference: PID2019-110441RB-C32).

REFERENCES

Berruti, I., Nahim-Granados, S., Abeledo-Lameiro, M.J., Oller, I., Polo-López, M.I. 2021 UV-C peroxymonosulfate activation for wastewater regeneration: Simultaneous inactivation of pathogens and degradation of contaminants of emerging concern. *Molecules* **26**, 4890.

Ding, Y., Wang, X., Fu, L., Peng, X., Pan, C., Mao, Q., Wang, C., Yan, J., 2020. Nonradicals induced degradation of organic pollutants by peroxydisulfate (PDS) and peroxymonosulfate (PMS): Recent advances and perspective. *Sci. Total Environ*. **765**, 142794.

Guerra-Rodríguez, S., Oulego, P., Rodríguez, E., Singh, D.N., Rodríguez-Chueca, J., 2020. Towards the implementation of circular economy in the wastewater sector: Challenges and opportunities. *Water* (Switzerland) **12**.

Michael, S.G., Michael-Kordatou, I., Nahim-Granados, S., Polo-López, M.I., Rocha, J., Martínez-Piernas, A.B., Fernández-Ibáñez, P., Agüera, A., Manaia, C.M., Fatta-Kassinos, D., 2020. Investigating the impact of UV-C/H_2O_2 and sunlight/H_2O_2 on the removal of antibiotics, antibiotic resistance determinants and toxicity present in urban wastewater. *Chem. Eng. J.* **388**, 124383.

Chlorine-free inactivation of *E. coli* in water with manganese oxide-doped graphene-based electrodes

Anna Segues Codina*,**, Natalia Sergienko*,**, Carles M. Borrego*,** and Jelena Radjenovic*,***

* Catalan Institute of Water Research (ICRA), Girona, Spain (E-mail: *asegues@icra.cat)*
** University of Girona, Spain
*** Group of Molecular Microbial Ecology, Institute of Aquatic Ecology, University of Girona, Girona, Spain
**** Catalan Institution for Research and Advanced Studies (ICREA), Barcelona, Spain

Abstract

Thousands of people do not have access to a safe source of water and suffer from water-related diseases. Electrochemistry is a promising technology for decentralized and distributed water treatment. However, this water treatment usually leads to the formation of toxic by-products. In this study, graphene sponge electrodes were synthesized and employed for electrochemical water disinfection without the formation of toxic by-products. Two manganese oxide-based dopants, at two different concentrations of manganese oxide, were studied as anodes. 2-3 log removals of *Escherichia coli* were inactivated at 29 A m^{-2}. Storage experiments conducted with the treated samples demonstrated further inactivation of *E. coli* reaching 4.7 log removal, suggesting irreversible cell damage due to electroporation.

Keywords

Disinfection, electrochemistry, electroporation, reduced graphene oxide

INTRODUCTION

Clean drinking water is essential for the well-being of humans. The World Health Organization estimates that there are 829.000 deaths every year of diarrheal diseases caused by the lack of a safe source of water, sanitation and hygiene (World Health Organisation, 2017). Chlorination, ozonation and UV radiation are common techniques for water disinfection. However, they have important drawbacks: the first two generate toxic disinfection by-products (DBPs) and the latter can lead to microorganism reactivation and regrowth. Also, these systems are usually applied in centralized treatment plants and are not easy to apply on a smaller scale (Huo et al., 2020). Electrochemical systems have attracted attention because they enable a chemical-free water treatment, have a small footprint and modular design, and can be powered with renewable energies; hence, they are very well suited for decentralized water treatment. However, electrochemical disinfection using commercial anode materials is commonly achieved via electro-chlorination, which causes the formation of toxic chlorinated DBPs (Hand et al., 2021)"ISSN":"15205851","PMID":"33616403","abstract":"Electrochemical disinfection - a method in which chemical oxidants are generated in situ via redox reactions on the surface of an electrode - has attracted increased attention in recent years as an alternative to traditional chemical dosing disinfection methods. Because electrochemical disinfection does not entail the transport and storage of hazardous materials and can be scaled across centralized and distributed treatment contexts, it shows promise for use both in resource limited settings and as a supplement for aging centralized systems. In this Critical Review, we explore the significance of treatment context, oxidant selection, and operating practice on electrochemical disinfection system performance. We analyze the impacts of water composition on oxidant demand and required disinfectant dose across drinking water, centralized wastewater, and distributed wastewater treatment contexts for both free chlorine- and hydroxyl-radical-based systems. Drivers of energy consumption during oxidant generation are identified, and the energetic performance of experimentally reported electrochemical disinfection systems are evaluated against optimal modeled performance. We also highlight promising applications and operational strategies for electrochemical disinfection and propose reporting standards for future work.","author":[{"dropping-particle":"","family":"Hand","given":"Steven","non-dropping-particle":"","parse-names":false,"suffix":""},{"dropping-particle":"","family":"Cusick","given":"Roland D.","non-dropping-particle":"","parse-names":false,"suffix":""}],"container-title":"Environmental Science and Technology","id":"ITEM-1","issue":"6","issued":{"date-parts":[["2021"]]},"page":"3470-3482","title":"Electrochemical Disinfection in Water and Wastewater Treatment: Identifying Impacts of Water Quality and Operating Conditions on Performance","type":"article-journal","volume":"55"},"uris":["http://www.mendeley.com/documents/?uuid=16685472-f27d-43e2-b8af-1a58267382e3"]}],"mendeley":{"formattedCitation":"(Hand and Cusick, 2021. The formation of DBPs as well as other chlorinated organic byproducts and highly persistent chlorate and perchlorate, has been a major bottleneck not only of electrochemical disinfection but of electrochemical water and wastewater treatment overall, as chloride is a naturally occurring anion that gets rapidly oxidized at the anode.

To address these shortcomings of commercial electrodes, we have recently developed a low-cost graphene sponge electrode with record low electrocatalytic activity towards chlorine formation (<0.04% of current efficiency in 20 mM NaCl). Furthermore, graphene sponge anode does not form any chlorate and perchlorate (Baptista-Pires et al., 2021). It has shown excellent performance in the degradation of persistent organic pollutants such as PFAS (Duinslaeger et al., 2022), antibiotics (Ormeno-Cano et al., 2022) and the inactivation of *Escherichia coli (E. coli)* ATCC 700078 (Norra et al., 2021). In this study, we synthesised manganese oxide-doped graphene-based sponges and applied them as anodes for the electrochemical disinfection of a resistant strain of *E. coli* (ATCC 25922) in tap water. Manganese-based oxides are very attractive for environmental applications due to their excellent catalytic activity, low-cost and earth abundance. (Zhu et al., 2019) We evaluated the impact of the applied current density on the inactivation of *E. coli*, and their potential re-activation during storage after the electrochemical treatment.

MATERIALS AND METHODS

Graphene sponges were synthesized with a simplified hydrothermal method (Baptista-Pires et al., 2021), where a mineral wool template is coated with reduced graphene oxide (RGO) and a dopant. We tested two types of dopants, manganese oxide (Mn_xO_y) and amino-doped manganese oxide (Mn_xO_y-NH_2), at two different concentrations. The cathodes were nitrogen-doped RGO, as N-doping was found to enhance the production of hydrogen peroxide and its activation to hydroxyl radicals (Farzaneh et al., 2016). The sponges were connected to current feeders and employed for the disinfection in a one-pass, flow-through reactor, using real tap water spiked with 10^7 cfu mL^{-1} of *E. coli 25922*. Samples were taken in open circuit (OC) and galvanostatic mode at three applied current densities, (14, 20 and 29 A m^{-2}). The abundance of the bacteria was determined by membrane filtration using serial dilutions of the samples and Chromocult Coliform Agar. Samples were stored 18 hours at 25 and 37ºC and after, assessed to analyze the potential bacterial regrowth.

RESULTS AND DISCUSSION

Figure 1 shows the electrochemical inactivation of *E. coli* in tap water for the four synthesized graphene sponge anodes, i.e., Mn_xO_y and Mn_xO_y-NH_2 at low and high concentrations. Doping of Mn_xO_y with NH_2 was done to obtain strong covalent bonds between the oxide and RGO, which could enhance the electrochemical performance. (Xu et al., 2019)which is applied extensively in water treatment for disinfection, odor removal and organic pollutants degradation. To improve the performance of catalytic ozonation, we design and synthesize a catalyst of amino-functionalized hybrid of MnO2 and graphene oxide (MnO2-NH2-GO Approximately 0.7 log removal of *E. coli* was achieved in the OC with all four materials, due to the oxidative and membrane stress caused by the RGO coating (Liu et al., 2011)we compared the antibacterial activity of four types of graphene-based materials (graphite (Gt. The inactivation of *E. coli* increased with the application current. Stepwise increase in current density from 20 to 29 A m^{-2} yielded, for the "High Mn_xO_y" anode, an increase in removal from 1.5 to 2.7 log, respectively. After the current was switched off and the reactor returns to the OC mode, the effluent concentration of *E. coli* returned gradually to the initial values. This demonstrated that the removed *E. coli* were inactivated and not simply electrosorbed, which would lead to their accumulation and rise in the final OC concentrations above the initial values. The best-performing anode was the "High Mn_xO_y", which achieved 2.7 log removal at 29 A m^{-2}.

Storage of the electrochemically treated samples for 18 hours at 25 and 37ºC led to further inactivation of *E. coli* (**Figure 2**). This demonstrated that the chlorine-free electrochemical treatment caused irreparable damage to the cell walls of *E. coli*. The highest overall removal (i.e., due to treatment and posterior additional inactivation during storage) was observed for the highest current density (29 A m^{-2}), at the higher storage temperature (37 ºC), reaching 4.7 log removals. Higher quantities of Mn_xO_y-based dopants lead to overall higher inactivation due to having more catalytic active sites. The main mechanism of inactivation was electroporation, as observed by the scanning electron microscopy (SEM) of the treated cells (**Figure 3**). Electroporation is based on the formation of pores in the cell membrane, causing leakage of the intracellular material and cell inactivation (Liu et al., 2013)affordable, and low energy water disinfection methods are in great need to prevent diarrheal illness, which is one of the top five leading causes of death over the world. Traditional water disinfection methods have drawbacks including carcinogenic disinfection byproducts formation, energy and time intensiveness, and pathogen recovery. Here, we report an innovative method that achieves high-efficiency water disinfection by introducing nanomaterial-assisted electroporation implemented by a conducting nanosponge filtration device. The use of one-dimensional (1D. Furthermore, electrogenerated oxidants such as ozone, hydrogen peroxide and hydroxyl radicals were measured in the solution and also contributed to the inactivation of bacteria (Rahmani et al., 2019).

CONCLUSIONS

Manganese oxide-doped reduced graphene oxide sponges inactivated *E. coli* without the formation of toxic chlorinated by-products. The "High Mn_xO_y" anode achieved a 2.7 log removal of *E. coli* at 29 A m^{-2}, whereas storage of the treated samples led to further inactivation and overall removal of 4.7 logs, demonstrating that the electrochemical treatment is causing irreparable damage to the cell walls. This study demonstrates that the low-cost graphene-based sponges doped with manganese oxide could be feasible for point-of-use electrochemical disinfection for water. Studies in the treatment of organic contaminants in real second effluent waters will be performed.

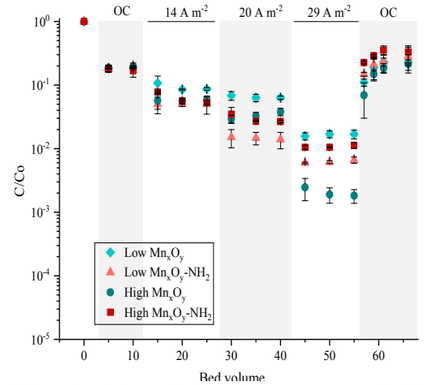

Figure 1. Electrochemical removal of *E. coli* in tap water at current densities of 14, 20 and 29 A m^{-2} for the four reactor configurations: having as anode sponges doped with (1) Low Mn_xO_y, (2) Low Mn_xO_y-NH_2, (3) High Mn_xO_y and (4) High Mn_xO_y-NH_2.

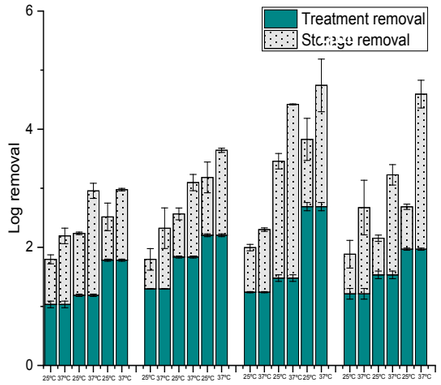

Figure 2. Removal of *E. coli* associated to the electrochemical treatment (green) and the storage effect (grey) for the four systems at 14, 20 and 29 A m^{-2} at 25ºC and 37ºC.

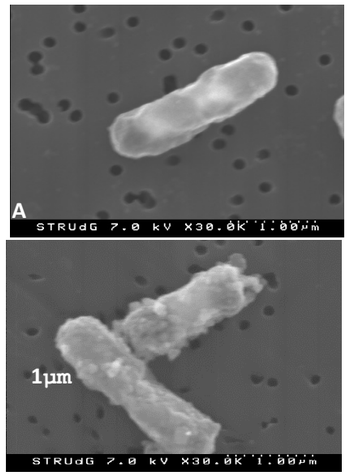

Figure 3. SEM images of (A) an *E. coli* cell before and (B) an *E. coli* cell after the treatment.

ACKNOWLEDGMENTS

The authors would like to thank ERC Starting Grant project ELECTRON4WATER (Three-dimensional nanoelectrochemical systems based on low-cost reduced graphene oxide: the next generation of water treatment systems), project number 714177. ICRA researchers acknowledge the funding from CERCA program.

REFERENCES

Baptista-Pires, L., Norra, G. F., and Radjenovic, J. (2021) Graphene-based sponges for electrochemical degradation of persistent organic contaminants. Water Research, **203**.
Duinslaeger, N. and Radjenovic, J. (2022) Electrochemical degradation of per- and polyfluoroalkyl substances (PFAS) using low-cost graphene sponge electrodes. Water Research, **213**.
Farzaneh, A., Saghatoleslami, N., Goharshadi, E. K., Gharibi, H., and Ahmadzadeh, H. (2016) 3-D mesoporous nitrogen-doped reduced graphene oxide as an efficient metal-free electrocatalyst for oxygen reduction reaction in alkaline fuel cells: Role of π and lone pair electrons. Electrochimica Acta, **222**, 608–618.
Hand, S. and Cusick, R. D. (2021) Electrochemical Disinfection in Water and Wastewater Treatment: Identifying Impacts of Water Quality and Operating Conditions on Performance. Environmental Science and Technology, **55**(6), 3470–3482.
Huo, Z. Y., Du, Y., Chen, Z., Wu, Y. H., and Hu, H. Y. (2020) Evaluation and prospects of nanomaterial-enabled innovative processes and devices for water disinfection: A state-of-the-art review. Water Research, **173**.
Liu, C., Xie, X., Zhao, W., Liu, N., Maraccini, P. A., Sassoubre, L. M., Boehm, A. B., and Cui, Y. (2013) Conducting nanosponge electroporation for affordable and high-efficiency disinfection of bacteria and viruses in water. Nano Letters, **13**(9), 4288–4293.
Liu, S., Zeng, T. H., Hofmann, M., Burcombe, E., Wei, J., Jiang, R., Kong, J., and Chen, Y. (2011) Antibacterial activity of graphite, graphite oxide, graphene oxide, and reduced graphene oxide: Membrane and oxidative stress. ACS Nano, **5**(9), 6971–6980.
Norra, G.-F., Baptista-Pires, L., Lumbaque, E. C., Borrego, C. M., and Radjenovic, J. (2021) Chlorine-free electrochemical disinfection using graphene sponge electrodes. Chemical Engineering Journal, 132772.
Ormeno-Cano, N. and Radjenovic, J. (2022) Electrochemical degradation of antibiotics using flow-through graphene sponge electrodes. Journal of Hazardous Materials, **431**(January), 128462.
Radjenovic, J; Baptista-Pires, L; Norra, G-F; Duinslaeger, N. (2020) Method to prepare a graphene coated sponge-based electrode, electrode obtained there of and use of the electrode for water treatment.
Rahmani, A. R., Samarghandi, M. R., Nematollahi, D., and Zamani, F. (2019) A comprehensive study of electrochemical disinfection of water using direct and indirect oxidation processes. Journal of Environmental Chemical Engineering, **7**(1).
World Health Organisation; UN-Water (2017) *UN-Water Global Analysis and Assessment of Sanitation and Drinking-Water (GLAAS)*,
Xu, J., Li, Y., Qian, M., Pan, J., Ding, J., and Guan, B. (2019) Amino-functionalized synthesis of MnO2-NH2-GO for catalytic ozonation of cephalexin. Applied Catalysis B: Environmental, **256**.
Zhu, L., Scheiba, F., Trouillet, V., Georgian, M., Fu, Q., Sarapulpva, A., Sigel, F., Hua, W., and Ehrenberg, H. (2019) MnO2 and Reduced Graphene Oxide as Bifunctional Electrocatalysts for Li-O2 Batteries. ACS Applied Energy Materials, **2**(10), 7121–7131.

LIFE RECYCLO: Recycling wastewater from small and medium sized laundries with advanced oxidation process

B. Mathon*, B. Cedat*, T. Paulet*, C.L. Franquart*, M. Turull**.***, G. Buttiglieri**.***, S. Insa**.***, L.H.M.L.M. Santos**.***, S. Rodriguez-Mozaz**.***, P. Moretti*

* Treewater, 61 rue de la République, 69002 Lyon, France
(E-mail: *bmathon@treewater.fr*; bcedat@treewater.fr*; tpaulet@treewater.fr; clfranquart@treewater.fr; pmoretti@treewater.fr)*
** Catalan Institute for Water Research (ICRA-CERCA), C/Emili Grahit 101, 17003 Girona, Spain
(E-mail: *mturull@icra.cat*; *gbuttiglieri@icra.cat; sinsa@icra.cat; lhsantos@icra.cat; srodriguez@icra.cat)*
*** University of Girona, Girona, Spain

Abstract

LIFE RECYCLO project aims at setting up a technical solution for the treatment of laundry effluents and water recycling. The present work describes laboratory tests carried out to size this treatment solution and to validate the operating parameters for 3 laundries. This solution includes a coagulation/flocculation step allowing the removal of particulate pollution and about 50% of the COD (initial =0.8-1.2 g/L). A UV/H_2O_2 treatment allows the removal of organic micropollutants and to reach a COD of 200 mgCOD/L (50-70% removal). Finally, adsorption on activated carbon allows to reach a COD of 100 mgCOD/L (50% removal) and to eliminate metals. The overall COD removal is 95 %. This treatment solution has been validated and the deployment of prototypes in 3 laundries is underway. A follow-up of the performance of the prototypes will be carried out for one year to ensure a treated water of sufficient quality to be recycled.

Keywords

Adsorption, Advanced oxidation process, Coagulation flocculation, Laundry, Water recycling

INTRODUCTION

Water is an essential resource for the economies of both industrialised and developing countries. With climate change, more and more regions will be constrained by water scarcity, which could eventually reduce the economic activity of industrial sectors, specifically large water consumers (Van Vliet et al., 2021). Moreover, agricultural, industrial, or urban activities result in the discharge of many emerging pollutants and pathogens into the environment (Schwarzenbach et al., 2006).

The EU laundry industry is a large water consumer with an estimation of 21 L/kg of dry textile (Gooijer et al., 2016). In the EU there are about 11,000 laundries, washing 2.7 billion kg of textiles annually, and using as much as 42 Mm^3 of water per year (Hloch et al., 2012). Moreover, laundries are an emission source of priority substances falling under the Directive 2013/39/EU such as nonylphenols, phthalates (DEHP), PAH and heavy metals with concentrations from ng/L to mg/L (Braga et al., 2014).

Recycling wastewater in laundry is therefore an ideal solution to limit the water consumption, the discharge of emerging pollutants that have an impact on the environment and health and to reduce the cost of water for the laundries (Kumar et al., 2022). Moreover, it sustains access to water for industries.

LIFE RECYCLO is improving water reuse systems by demonstrating the environmental, technical and economic feasibility of recycling laundry wastewater using an innovative advanced oxidation process (AOP) by UV/H_2O_2 combined with a pre-treatment by coagulation/flocculation and a post-treatment by adsorption on activated carbon. A patented 200 L/h pilot will be scaled-up to a pre-market ready prototype. LIFE RECYCLO will offer a water recycling solution to the small and middle size laundries (1 m^3/h to 10 m^3/h). The 3 laundries involved as partners will become a showcase for the textile sector by demonstrating that the system works for different sizes and different wastewater qualities. The results of this paper present the laboratory tests that validated the operating parameters of coagulation/flocculation, AOP and adsorption. These parameters will be used to operate the future prototypes implemented on the 3 laundries.

MATERIALS AND METHODS

Sampling and analysis:

Automatic samplers were set up in 3 laundries: BSJ (France, flow rate = 4m^3/h), KLIN (Luxembourg, flow rate = 2 m^3/h), GRUPFRN (Spain, 0.5 m^3/h). A 24h representative wastewater sample was sampled and homogenized. COD, BOD, TOC, TSS, salts, cationic and anionic surfactants analyses were performed at Treewater lab (DEEP Laboratory – INSA Lyon) as well as metals. All other parameter were analyzed by accredited external laboratories. The results obtained on the raw samples are available in the Table 1.

Pre-treatment by coagulation flocculation:

Lab scale tests were performed to identify a couple of coagulant and flocculant with the highest TSS and COD removal rate. Six Beakers were filled with 200 mL of laundry effluent and mixed at 200 rpm. Then 6 different concentrations of coagulation were injected (from 0.1 to 2.5 mL/L). After waiting time, flocculant concentration (from 0.5 to 3 mL/L) was injected and mixing was decreased to 15 rpm. Mixing was stopped and settling was observed. COD, TSS and pH were analyzed in the supernatant. The best concentration corresponded to the best floc formation and settling as well as turbidity removal. The amount of sludge was also measured to calculate the sludge production rate.

Treatment by H_2O_2/UV:

Advanced oxidation tests were performed to evaluate the degradation efficiency of the H2O2/UV. The tests were performed on a lab-scale pilot with volumes of 3L per test using a 24W low pressure lamp (254 nm). Different UV fluence and hydrogen peroxide concentrations were studied to define the optimal treatment parameters (ratio COD/H_2O_2). The effluent was recirculated in a UV cell for a given time accumulating UV exposure. A defined concentration of H_2O_2 was injected at time zero. COD_t conductimetry, pH and transmittance as well as H_2O_2 consumption were monitored to verify the efficiency.

Post-treatment by adsorption:

Three tests were performed to select the best activated carbon (AC) and determine its COD adsorption capacity:

- A) Adsorption kinetics: to define the maximum performance of different ACs at a given concentration. Six references of AC and biochar (biosourced AC) were tested in parallel: Filtrasorb 400, CycleCarb201, CSC5, GBC 8x30, Terra, Carbo. This test allowed us to identify the best performing reference in terms of improvement of the UV-C transmittance.

The effluent treated by H_2O_2/UV was injected in 6 beakers (500 mL), then mixed at 200 rpm with a reference of AC in each beaker at 30 gCA/L. The duration (contact time) of the test was about 22h, and 4 sample were collected in each beaker to follow pH, conductimetry, and COD.

- B) Isotherm: to determine the maximum loading rate and to pre-select a granular activated carbon, an isotherm of Freundlich is often applied. Several 500 ml beakers were filled with effluent (5 + 1 blank) and AC were added at different concentrations (0.5 to 50 g/L) and mixed continuously at 200 rpm for 18 hours to reach the adsorption equilibrium. Temperature, COD, UV transmittance, and pH were measured at t-0 and t-final.

-C) Dynamic column with CycleCarb201: The column test allows to get closer to a real treatment configuration and to establish a pre-sizing of an activated carbon reactor. This column is continuously fed with a volume of effluent (up to 6 L) with a hydraulic residence time of about 25 min. COD_t, transmittance and metals are measured at the column outlet.

RESULTS AND DISCUSSION

Pre-treatment by coagulation flocculation:

Alopolym 698 (based on cationic polymer, aluminium compound, and iron trichloride) and 632 AP (polymer) were the coagulant and flocculant referent with the best efficiency on the 3-laundry effluents. The selected coagulant concentration was about 0.25 mL/L for BSJ and GRUPFRN, and 0.5 mL/L for KLIN. Flocculant concentration was more variable, with 1.25 to 2.5 mL/L depending on the laundry. Supernatant presented higher UV transmittance, with 43%, 70% and 52% on BSJ, KLIN, and GRUPFRN, respectively, and TSS < LQ. This treatment step was able to remove TSS, turbidity and matter that decreased UVT_{254}. COD removal was 58%, 48% and 45% on BSJ, KLIN, and GRUPFRN, respectively.

Treatment by H_2O_2/UV

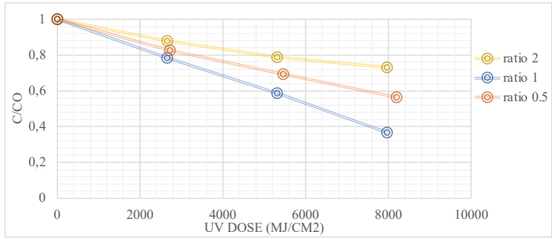

Figure 1 : Evolution of COD (C/C_0) during UV/H_2O_2 treatment of BSJ effluent with different hydrogen peroxide concentrations corresponding to COD/H_2O_2 ratio

The BSJ kinetics tests showed a linear trend for all the COD/H_2O_2 ratio (Figure 1). This reflected a good and constant degradation of organic compounds and no lack of H_2O_2. The degradation coefficients were variable, with the highest at 1 gCOD/gH_2O_2. Higher COD/H_2O_2 ratio was ineffective, with lower COD removal (28%) and lower H_2O_2 consumption (60%). Lower ratio involved higher COD removal with an optimum at 1 gCOD/gH_2O_2 with COD removal of around 44 to 66% (mean of 50%) and final COD is about 200 mgCOD/L. The BSJ tests were replicated on KLIN and GRUPFRN (after coagulation/flocculation treatment). Considering kinetics on each effluent as well as economic considerations, COD removal by AOP has been set at 50 %. The UV Fluence, used to size the UV reactor of the final process was in the range from 8,000 to 10,000 mJ/cm^2 with an associated COD/H_2O_2 rate of 1 gCOD/gH_2O_2.

Post-treatment by adsorption:

Four different AC were tested on the wastewater of the three laundries after AOP treatment to select the best AC reference. CycleCarb201 had clearly the highest COD removal among the AC references. The lowest was La Carbonnerie, which is a non-activated bio-AC. With CycleCarb201, the COD removal was already 45% after 1 h of contact for BSJ and similarly for KLIN and GRUPFRN effluents. CycleCarb201 is a re-activated carbon and has been selected for the 3 laundries. The second step was to determine the loading rate of CycleCarb201 on each effluent. To do so, Freundlich Isotherms were conducted. The calculated maximal loading rates were 223 mgCOD/gAC for BSJ, 343 mgCOD/gAC for KLIN and 220 mgCOD/gAC for GRUPFRN. The sizing of the adsorption step was calculated considering a COD removal of 50 to 60% and an outlet COD concentration targeted of 100 mgCOD/L. This reference value was determined in previous tests and allowed the washing of laundry with sufficient quality. KLIN had the highest loading rate, resulting in a more compact reactor AC volume. The reactor will have to be changed at saturation. Each reactor of AC is sized to be changed once a year.

Performance of the overall process

Laboratory tests with BSJ effluent evaluated the abatement performances on a list of physicochemical parameters and pollutants (Table 1). The results showed excellent removal rates with more than 90% removal of organic and inorganic micropollutants except for aluminum probably due to the contribution of this metal via the coagulant/flocculant. No significant AOX removal was observed. Further studies are needed as good results were obtained on other types of effluent with AOP technology. 95% of the initial COD and 100% TSS were removed. The selected coagulant contains chlorides and therefore an increase was observed. A resin treatment step or the adaptation of the recycling rate is under study. All these results show that the treated water is of very good quality and could be recycled and reused in the laundry washing water. The monitoring of the quality of the linen washed by the water treated by the prototypes will allow to verify this point.

Table 1: Assessment of the physico-chemical parameters of the BSJ laundry effluent before and after the treatment solution by Coagulation/flocculation, AOP, and adsorption

Parameter	Units	Raw water KLIN	Raw water GRUPFRN	Raw water BSJ	Treated water after AC (BSJ)	Removal (%)
pH	/	7.6	9.8	6.81	9.18	
Conductimetry	mS/cm	0.944	0.834	0.492	0.533	
Trans UV	%	12	8.8	0.58	97.9	
COD	mgO_2/L	911	844	922	43.2	95%
TSS	mg/L	51	77	147	0	100%
Ntot	mgN/L	16.2	8	25	11.8	53%
N-NH_4	mgN/L	12.3	4.6	6.97	9.91	-42%
Phosphorus	mg/L		2.4	2.26	0.045	98%
AOX	µg/L	20	110	65	70	-8%
Anionic surfactant	mg/L	21.2	53.2	139	<LD	100%
Cationic surfactant	mg/L	1.3	1.5	0.55	<LD	100%
Chloride (Cl-)	mg/L	2.7	70	23.2	70.0	-202%
Nitrites (NO_2-)		N.M.	1.8	N.M.	<LD	100%
Bromide (Br-)		N.M.	<LQ	N.M.	<LD	100%
Phosphate (PO_4^{3-})		N.M.	<LQ	N.M.	<LD	100%
Sulfates (SO_4^{2-})		38	47	29.5	14.6	51%
Aluminium	mg/L	N.M.	0.47	0.081	0.092	0%
Copper		N.M.	0.18	0.056	<LD	100%
Iron		N.M.	N.M.	0.065	<LD	100%
Zinc		N.M.	0.15	1.48	0.063	96%
BDE 209		<LD	<LD	0.99	<LQ	100%
BDE 47		<LD	<LD	0.016	<LQ	100%
DEHP		0.015	<LQ	6.4	<LQ	100%
Nonylphenols		<LD	<LD	43	0.71	98%
Hydrocarbon index (C10-C40)		18,044	444	5,727	149	97%

***N.M. = not measured**

Conclusion

LIFE RECYCLO will offer a water recycling solution to the small and middle size laundries. The work presented here has validated the proposed technical solution to obtain a water quality compatible with its reuse. The technical solution is composed of a pre-treatment by coagulation/flocculation, a UV/H_2O_2 process and a post-treatment by adsorption on activated carbon. This technical solution has achieved the LIFE RECYCLO objectives of reducing by at least 90% the emission of pollutants. Further studies are needed on AOX abatement performance. The next step of the LIFE RECYCLO project is to set up three prototypes in each laundry and to carry out a performance monitoring over one year.

ACKNOWLEDGMENT

The authors would like to thank all the partners of the LIFE RECYCLO project, especially Pop'Sciences and the 3 laundries (BSJ, GRUPFRN and KLIN). This work was financed by the LIFE Programme. You can find more information about the LIFE RECYCLO project on the website: http://www.treewater.fr/en/recyclo.

REFERENCES

Braga, J. K., & Varesche, M. B. A. (2014). Commercial laundry water characterisation. American Journal of Analytical Chemistry, 2014.

Gooijer, H., & Stamminger, R. (2016). Water and energy consumption in domestic laundering worldwide–a review. Tenside Surfactants Detergents, **53**(5), 402-409.

Hloch, H., Tokos, M., Spettmann, D., den Otter, W.A.J.L., Groosman, M., Vanderhoeven, M., Pušiū, T.,Šostar, S., Fijan, S. & Seite, M. 2012. Sustainable measures for industrial laundry expansion strategies: SMART-laundry-2015. SMILES Report, European seventh framework programme.

Kumar, S., Mostafazadeh, A. K., Kumar, L. R., Tyagi, R. D., Drogui, P., & Brien, E. (2022). Advancements in laundry wastewater treatment for reuse: a review. Journal of Environmental Science and Health, Part A, **57**(11), 927-946.

Schwarzenbach, R.P., Escher, B.I., Fenner, K., Hofstetter, T.B., Johnson, C.A., Von Gunten, U., & Wehrli, B. (2006). The challenge of contaminants in aquatic systems. *Science*, **313**(5790), 1072-1077.

van Vliet, M. T., Jones, E. R., Flörke, M., Franssen, W. H., Hanasaki, N., Wada, Y., & Yearsley, J. R. (2021). Global water scarcity including surface water quality and expansions of clean water technologies. *Environmental Research Letters*, **16**(2), 024020.

Innovative Dual Membrane System for Integrated Water-energy Recovery from Municipal Wastewater

C.H., He*, K., Fang*, K. J., Wang*

* School of environment, Tsinghua university, Beijing, China
(E-mail: *hech19@mails.tsinghua.edu.cn*; *kina_fangkuo@163.com*; *wkj@mail.tsinghua.edu.cn)*

Abstract

This study presents a novel short process consisting of a membrane-based pre-concentration (MPC) module and a reverse osmosis (RO) module. In MPC unit, municipal wastewater (MW) was directly filtrated by a submerged microfiltration module (HRT<1 h, SRT 2-4 days & flux 8-10 LMH), creating a particulate-free permeate and a concentrated organic stream. The permeate was then fed into the RO module (recovery rate of 75%-80%) for water reclamation. The high-concentration organic stream was then redirected into methane production system for energy recovery. A pilot-scale dual membrane system with a treatment capacity of 400 t/d was operated stably for over one year in Beijing. The advantage of this system included: 1) the organic energy was utilized in methane production rather than being mineralized in aerobic degradation; 2) the direct filtration of MW was stabled with the assistance of fouling control methods and therefore the footprint of the complete process is significantly reduced.

Keywords

Energy recovery; Reduced footprint; Water reclamation

INTRODUCTION

Rebranding as integrated resource factories is high on the agenda of the wastewater treatment plants (WWTPs). The membrane-based pre-concentration (MPC) is regarded as a promising approach to recovering organic resources in municipal wastewater (MW). The purpose is to extract the organics before it enters the subsequent treatment processes and redirects them to resource recovery units, such as anaerobic digestion (AD).

Generally, recent focuses in MPC research included: 1) the membrane fouling control, which is a prerequisite for MPC stability, 2) the effluent quality and corresponding subsequent treatment choices, and 3) the quality of recovered organics, usually in terms of methane production capacity.

Based on above background, this study established a pilot-scale MPC-RO system with a treatment capacity of 400 t/d. Main purpose including: 1) testing the effectiveness of fouling control methods combination proposed by our research team earlier on a demonstration scale, 2) investigating the characteristic of MPC effluent and the influence of operating parameters, 3) verifying the feasibility of MPC permeate as RO feed water and the operation performance of RO, and 4) evaluating the stability and technical-economic feasibility during long-term operation over one year.

MATERIALS AND METHODS

The pilot-scale MPC-RO system was in an MW WWTP in northern China. Fig. 1 presents the configuration and photos of the pilot plant. The detail configuration was similar with our previous report (He et al., 2022, 2023). The membrane fouling control methods tested in the MPC plant included on-site coagulation, adsorption, and surface aeration. Table 1 provides detailed operation information. RO system consisted of a security filter (5 μm), a high-pressure pump with variable frequency, a membrane module (18 Dupont Film Tec™ Fortilife™ CR100), a chemical dosing system, and a cleaning in place (CIP) system. The water recovery rate was 75-80% and neither permeate nor concentrate was recycled to the RO feed tank. The flux ranged between 17-18 L/m²/h (LMH).

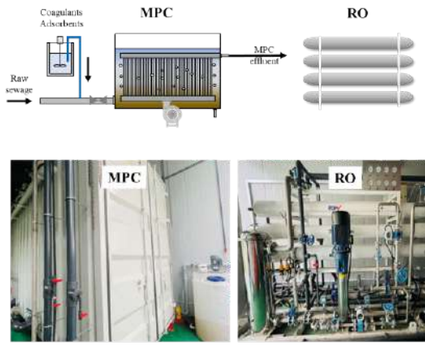

Figure 1. The configuration and photos of the pilot-scale MPC-RO system.

Table 1. Working conditions in the pilot-scale CE-HLMBR

Stages	SRT (Day)	PAC (mg/L)	AC (mg/L)	Aeration strength (%)
C1	4	25	25	100
C2	2	25	25	100
C3		25	0	100
C4		25	25	100
C5		0	25	100
C6	3	25	25	75
C7		25	25	50
C8		25	25	25

RESULTS AND DISCUSSION

The fouling control performance in MPC unit (Fig. 2)

Submerged filtration (8-10 LMH) was stable at SS concentrations of 15-20 g/L. The combination of chemicals and aeration was effective and either one was essential. Coagulation and adsorption have a synergistic effect in two ways: 1) promoting shedding ability and compression resistance of the cake layer and 2) reducing the SMP and especially the carbohydrate concentration. Aeration provided the necessary shear force.

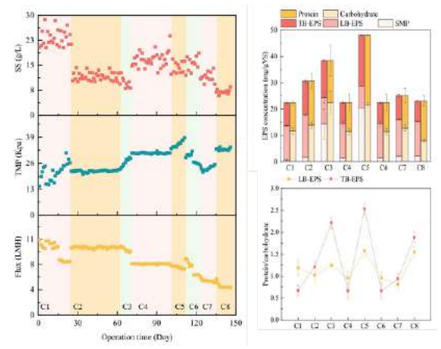

Figure 2. The filtration performance and EPS concentration in 8 stages.

The pollutant removal performance in MPC unit (Fig. 3)

Over 75% soluble organics and 80% sTP were removed in MPC unit via chemical precipitation, adsorption, and bio-degradation pathways. Both nitrification and denitrification occurred simultaneously due to uneven oxygen distribution. Effluent quality, activity tests, and functional microbial analysis all confirmed that nitrogen conversion occurred at 2-3 days SRT. Besides, in another work by our team, the biomethane production from concentrated organic matter was studied.

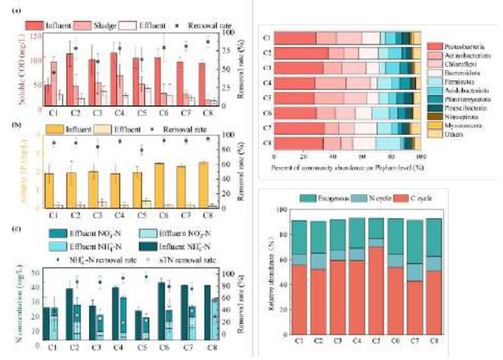

Figure 3. The pollutant removal performance and microbial community in 8 stages.

The performance of RO unit (Fig. 4)

Once the MPC conditions had stabilised, the RO was tested for over 300 days. RO showed a strong removing capacity, with a water recovery rate of 75%–80%. COD, TP, and NH_4^+-N were not detectable in RO effluent. The TOC was below 0.4 mg/L and the conductivity was below 30 μS/cm, which met the NEWater standard in Singapore and environmental quality standards (Class IV) for surface water in China. This study confirmed the feasibility of RO fed with MPC effluent. The changes in the pressure were subjected to a two-stage pattern: an initial negligible rising in 0–60 days followed by a rapid jump (0.15 bar/day) in 60–90 days. CIP was effective that the TMP returned to the low value. Besides, it should be noted that Al^{3+} deposition was observed on the RO membrane surface. Special attention needs to be paid to MPC coagulant overdosing in future studies.

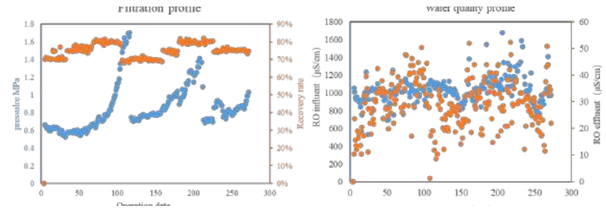

Figure 4. The filtration and water quality profile of RO unit in 300 days.

The technical-economic assessment of the combination system (Fig. 5)

The practical feasibility of "MPC-RO" has been confirmed. Therefore, an integrated "MPC + RO + AD" system for synchronous water-energy reclamation from MW was proposed here. The total energy consumption could be calculated as 0.619 kWh/m³. Considering the electricity recovery potential of AD, the net energy consumption would be as low as 0.273 kWh/m³. The operating costs for MPC and RO were estimated as 1.132 CNY/m³. Considering the typical energy consumption of an MBR-RO system (0.7 kWh/m³) and the price of ultrapure water in China (7.90 CNY/m³), the competitiveness of this proposed new system was emphasized. Compared with traditional double membrane systems such as "conventional activated sludge (CAS) + ultrafiltration + RO" and "MBR + RO". The whole traditional treatment process, including CAS, primary and secondary sedimentation tank, could be compressed into MPC with very short HRT (about 1 hour). Thus, the footprint will be greatly reduced.

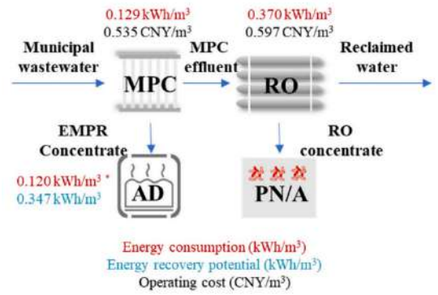

Figure 5. A proposed system for synchronous water-energy reclamation

REFERENCES

He, C. H., Fang, K., Wang, W. C., Wang, Q., Luo. J., Ma, J. Y., Wang, K. J. 2022 Techno-economic feasibility of "membrane-based pre-concentration +post-treatment" systems for municipal wastewater treatment and resource recovery. *Journal of cleaner production*, 375, 134113.

He, C. H., Wang, K. J., Wang, W. C., Luo, J., Fang, K. 2023 Chemically enhanced high-loaded membrane bioreactor (CE-HLMBR) for A-stage municipal wastewater treatment: Pilot-scale experiments and practical feasibility evaluation. Separation and purification technology, 307, 122853.

Application of UV-B and UV-C light-emitting diodes (LEDs) for the removal of diclofenac in drinking water

Raffaella Pizzichetti[*, **, ***], Cristina Pablos[*], Ken Reynolds[**], Simon Stanley[**], Eric Moore[***], Javier Marugán[*]

[*]Department of Chemical and Environmental Technology, ESCET, Universidad Rey Juan Carlos, C/Tulipán s/n, 28933 Móstoles, Madrid, Spain
(E-mail: *raffaella.pizzichetti@urjc.es, cristina.pablos@urjc.es, javier.marugan@urjc.es)*
[**]ProPhotonix IRL LTD, 3020 Euro Business Park, Little Island, Cork, T45 X211, Ireland
(E-mail: *rpizzichetti@prophotonix.com, kreynolds@prophotonix.com, sstanley@prophotonix.com*)
[***]Sensing and Separation Group, School of Chemistry, University College Cork, Cork, Ireland
(E-mail: *121116712@umail.ucc.ie, e.moore@ucc.ie*)

Abstract

In this study, the removal of diclofenac (DCF) was evaluated by using UV-B and UV-C light-emitting diodes (LEDs) alone and in combination with hydrogen peroxide (UV/H_2O_2) and chlorine (UV/Cl). The kinetics followed a pseudo-first-order degradation, and their trend reflected the pattern of the molar extinction coefficients of the DCF and the oxidants, showing great potential for implementing LEDs in water treatments. The UV-LED driven AOPs were superior to the photolysis or the oxidation treatment alone, also confirmed by studies at different intensities. Nevertheless, the electrical energy per order parameter was slightly higher when using the oxidants. Finally, DOC analysis and phytotoxicity assessment were performed to evaluate the by-products' recalcination and potential toxicity.

Keywords

Advanced Oxidation Processes (AOPs), Chlorine, Degradation, Hydrogen Peroxide, Photolysis

INTRODUCTION

In the big challenge of water contamination, contaminants of emerging concerns (CECs) in treated water pose a risk to the safety of the environment and the health of human beings (Villanueva et al., 2014). UV-based light-driven Advanced Oxidation Processes (AOPs) exploit the generation of highly reactive radicals, and they are considered one of the most effective emerging technologies for environmental remediation (Rodriguez-Narvaez et al., 2017). However, a significant drawback is the use of mercury lamps (MPs) since mercury is a hazardous material for the environment and human health and requires a proper disposal protocol. Therefore, a major contribution to UV treatments can be made by the advances in light-emitting diodes (LEDs) in the UV-B and UV-C range. They provide a mercury-free solution other than high design flexibility, tuneable wavelength, and instant on-off. For the AOPs choice, a recent work (Pesqueira et al., 2022) assessed the life cycle impacts of UV-C combined with hydrogen peroxide (H_2O_2), peroxymonosulfate (PMS), and persulfate (PS), and it revealed that H_2O_2 was the best environmental choice. On the other hand, UV/chlorine is an emerging AOP and has become increasingly popular thanks to its low cost and since it is already used in water as a disinfection agent against re-contamination (Wang et al., 2017). Therefore, this study aims to evaluate the efficiency of UV/H_2O_2 and UV/Cl treatment by means of UV-B and UV-C LEDs, by tuning the working wavelength and the intensity to optimise the absorption of the pollutant and the oxidant. Finally, among the CECs, diclofenac (DCF), a non-steroidal anti-inflammatory drug, was selected for the optimisation of the system since it has been added to the first EU Watch List under the Environmental Quality Standards Directive, and it has been detected up to µg/L in water bodies (Sousa et al., 2019).

MATERIAL AND METHODS

Analytical methods

The detection and quantification of DCF were conducted through high-performance liquid chromatography (HPLC) with a reverse C18 column. The optimised mobile phase was acetonitrile and 25 mM phosphate acetate buffer (pH 3) in a ratio of 80:20 v/v. The flow was set to 1 mL/min and the injection volume to 5 µL, the pressure constant at 45 bar and the thermostat at 25 °C. Dissolved organic carbon (DOC) was measured with a TOC-VCPH analyser, and the phytotoxicity was tested for the *Raphanus sativus* (radish) and *Solanum Lycopersicum* (tomato) seeds and evaluated through the germination index (*GI*).

Photoreactor set-up

The reactor employed in the study is shown in Figure 1, where a PID controller was implemented in the Arduino code to work at a constant flow rate. The photoreactor consisted of a quartz tube where the LED lamp was positioned at around 2 mm from the outer diameter of the quartz tube. Chemical ferrioxalate actinometry experiments were carried out as described in the literature (Bolton et al., 2011) to calculate the total irradiation power of the lamps in the system, resulting in 21.98 ± 0.43, 31.18 ± 0.06, and 27.62 ± 0.61 mW/cm² for 265, 285, and 310 nm, respectively.

RESULTS AND DISCUSSION

DCF followed, in all cases, a pseudo-first-order kinetic, which can be described as a function of time (Eq.1) or UV fluence (Eq. 2) and considering the active volume of the reactor (V_R) over the total volume (V_T).

$$\ln\left(\frac{C}{C_0}\right) = -k_{obs,t}\cdot t \ln\left(\frac{C}{C_0}\right) = -k\cdot t\cdot\frac{V_R}{V_T}$$
$$\ln\left(\frac{C}{C_0}\right) = -k\cdot t\cdot\frac{V_R}{V_T} \quad \textit{Eq.1}$$

$$\ln\left(\frac{C}{C_0}\right) = -k_{obs,UV_{fluence}}\cdot UV_{Fluence}$$
$$\ln\left(\frac{C}{C_0}\right) = -k'\cdot UV_{Fluence,T}\cdot\frac{V_R}{V_T} = -k'\cdot UV_{Fluence}$$
$$\ln\left(\frac{C}{C_0}\right) = -k'\cdot UV_{Fluence,T}\cdot\frac{V_R}{V_T} = -k'\cdot UV_{Fluence} \quad \textit{Eq.2}$$

Figure 2 illustrates the degradation of DCF with respect to time and UV fluence via direct photolysis, dark oxidation, and UV-driven AOPs. A removal dependency on the wavelength was found in agreement with the extinction coefficient of the DCF and the oxidant employed, which are shown in Table 1. In almost all cases, except for the 310 nm/H_2O_2, a synergistic effect, measured following Eq. 3, was reached when coupling the UV treatment with the oxidants, Figure3.

$$F_S = \frac{k_{obs,combination}}{k_{obs,LED}+k_{obs,oxidant}} F_S = \frac{k_{UV/oxidant}}{k_{UV}+k_{oxidant}} F_S = \frac{k_{UV/oxidant}}{k_{UV}+k_{oxidant}}$$
Eq. 3

The electrical energy per order (E_{EO}), defined as the electric energy in kWh needed to degrade one order of magnitude of the pollutant in 1 m³ of water, was measured according to Eq. 4.

$$E_{EO} = \frac{P\cdot t}{V\cdot\log\left(\frac{C_0}{C}\right)} E_{EO} = \frac{P\cdot t}{V\cdot\log\left(\frac{C_0}{C}\right)}$$

Despite the higher degradation rate, the electricity demand is similar in almost all cases since the equivalent electric energy consumption to produce the oxidants was also considered. For the UV treatment alone, it was 0.61, 0.58, 0.85 kWh.m^{-3}.order^{-1}. respectively, for 265, 285, and 310 nm. When combined with chlorine, the total E_{EO} was 0.64, 0.56, 0.74 kWh.m^{-3}.order^{-1}, while during the UV/H_2O_2 process, it was 0.62, 0.65, and 1.11 kWh.m^{-3}.order^{-1}.

The DOC decreased only partially by 20-30%, regardless of the degradation process used; it can be concluded that the by-products might be more recalcitrant than DCF itself. Nevertheless, the phytotoxicity studies showed a decrease in toxicity towards tomato and radish seeds; however, the resulting *GI* value was still below the safe phytotoxic value.

CONCLUSIONS

In this study, DCF removal via photolysis alone and coupled with chlorine or hydrogen peroxide was assessed by investigating the advantages of applying different wavelengths. Tuning the wavelength considering the absorption spectra of the contaminants and the oxidants have high potential in water treatments. As expected, in almost all cases, the UV-LED-driven AOPs were superior to the photolysis or the oxidation treatment alone, but the overall treatments have similar energy costs. By-product removal was not achieved completely, and further treatment might need to be implemented for the complete DCF's by-product degradation.

FIGURES AND GRAPHICS

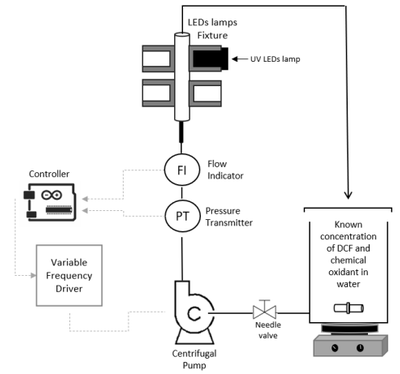

Figure 1. UV-B and UV-C LED reactor employed to evaluate DCF degradation through LED-driven AOPs.

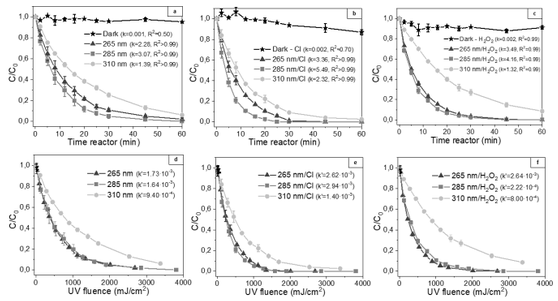

Figure 2. Comparison of time-based (a, b, c) and fluence-based DCF degradation (d, e, f) by UV irradiation alone, dark oxidation and UV coupled with chlorine (20 mg/L), and hydrogen peroxide (20 mg/L).

Table 1. The extinction coefficient of diclofenac (in distilled water, neutral pH), chlorine (used in the form of sodium hypochlorite in distilled water, final pH 8.5), and hydrogen peroxide (in distilled water, final pH 6) measured at the wavelengths of interest.

Wavelength	DCF	Chemical Oxidant	
ε (M^{-1} cm^{-1})		OCl⁻/HOCl	H_2O_2
265 nm	7126.11	173.86	8.58
285 nm	7157.93	388.75	4.24
310 nm	1113.46	300.52	0.62

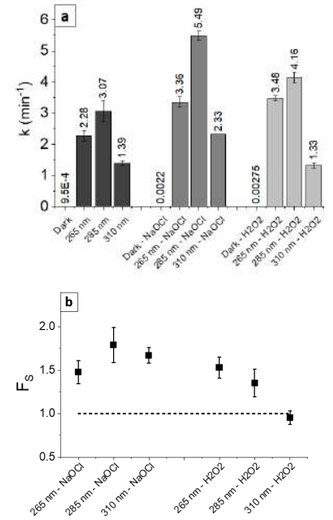

Figure 3. Comparison among the time-based constant *k* by direct photolysis, dark oxidation and UV-driven AOPs (a), and values of the synergist factors (b).

REFERENCES

Bolton, J.R., Stefan, M.I., Shaw, P.S., Lykke, K.R., 2011 Determination of the quantum yields of the potassium ferrioxalate and potassium iodide-iodate actinometers and a method for the calibration of radiometer detectors. *Journal of Photochemistry and Photobiology A: Chemistry* **222**, 166–169

Pesqueira, J.F.J.R., Marugán, J., Pereira, M.F.R., Silva, A.M.T., 2022 Selecting the most environmentally friendly oxidant for UVC degradation of micropollutants in urban wastewater by assessing life cycle impacts: Hydrogen peroxide, peroxymonosulfate or persulfate? *Science of The Total Environment* **808**, 152050

Rodriguez-Narvaez, O.M., Peralta-Hernandez, J.M., Goonetilleke, A., Bandala, E.R., 2017 Treatment technologies for emerging contaminants in water: A review. *Chemical Engineering Journal* **323**, 361–380

Sousa, J.C.G., Ribeiro, A.R., Barbosa, M.O., Ribeiro, C., Tiritan, M.E., Pereira, M.F.R., Silva, A.M.T., 2019 Monitoring of the 17 EU Watch List contaminants of emerging concern in the Ave and the Sousa Rivers. *Science of the Total Environment* **649**, 1083–1095

Villanueva, C.M., Kogevinas, M., Cordier, S., Templeton, M.R., Vermeulen, R., Nuckols, J.R., Nieuwenhuijsen, M.J., Levallois, P., 2014 Assessing exposure and health consequences of chemicals in drinking water: Current state of knowledge and research needs. *Environmental Health Perspectives* **122**, 213–221

Wang, W.L., Wu, Q.Y., Li, Z.M., Lu, Y., Du, Y., Wang, T., Huang, N., Hu, H.Y., 2017 Light-emitting diodes as an emerging UV source for UV/chlorine oxidation: Carbamazepine degradation and toxicity changes. *Chemical Engineering Journal* **310**, 148–156

Natural based solutions combined with solar processes at pilot scale for urban wastewater reclamation

A. Hernández-Zanoletty*, P. Simón**, S. Nahim-Granados*, I. Oller* and M.I. Polo-López*

*Plataforma Solar de Almería-CIEMAT, Carretera de Senés Km 4, 04200, Tabernas (Almería), Spain.
*CIESOL, Joint Centre of the University of Almería-CIEMAT, 04120, Almería, Spain.
**ESAMUR, C. Santiago Navarro, 4 Planta, 1 Complejo Espinardo, 30100, Murcia, Spain.
(E-mail: *ahernandez@psa.es*)

Abstract

The combination between wetlands and raceway pond reactor (RPR) with the addition of hydrogen peroxide (H_2O_2) under natural solar radiation as advanced solar tertiary treatment for urban wastewater (UWW) simultaneous disinfection and decontamination at pilot plant scale has been investigated to determine the optimal water purification conditions for a further test at demonstrative scale. The contaminants of emerging concern (CECs) adsorption/degradation along the wetlands was 88% of average at ng/L concentration level. As a second step, disinfection results for *E. coli* and *Enterococcus* spp. in the RPR, showed that the most efficient oxidant concentration was 25 mg/L of H_2O_2 (<10 CFU/100 mL after 30 minutes, 0.57 kJ/L and 120 minutes, 2.7 kJ/L, respectively). In addition, two different RPR heights were also evaluated (10 cm and 15 cm), preliminarily concluding that the use of higher height was not detrimental, allowing the treatment of higher volumes of water. This combined system has been demonstrated to be an attractive and eco-sustainable alternative to treat large volumes of UWW secondary effluents by using nature based solutions and natural solar radiation.

Keywords

Contaminants of emerging concern; Hydrogen peroxide; Raceway Pond Reactor; Water purification; Wetland system.

INTRODUCTION

The Mediterranean Region is characterized by great water stress and scarcity due to climate change and high water consumption in the agricultural sector. Therefore, the reuse of treated urban wastewater (UWW) is currently considered one of the most promising and suitable water sources to mitigate these problems. Conventional urban wastewater treatment plants (UWTPs) are poorly effective in the removal of contaminants of emerging concern (CECs), pathogenic microorganisms, antibiotic resistant bacteria and genes (ARB and ARGs) and disinfection by-products (Rizzo et al., 2020). Therefore, it is necessary to implement new integrated wastewater technologies that allow improving the quality of water for reusing purposes (Christou et al., 2017). A highly attractive solution are natural based solutions such as wetlands as they are a simple, profitable and low-cost technology, where the purification of pollutants is carried out by natural processes (Haghshenas-Adarmanabadi et al., 2016). The interactions of wetland plants, microorganisms and substrate media allow for obtaining an efficient, eco-sustainable and low-cost reclamation system when compared to conventional wastewater treatment processes (Abuabdou et al., 2020).

On the other hand, solar photochemical processes for the tertiary treatment of UWW have been receiving increasing attention as sustainable and green options (Berruti et al, 2022) and their high efficiency in raceway pond reactors (RPRs), extensive non-concentrating photoreactors, which allow large volumes of water to be treated (Cabrera-Reina et al., 2021). Therefore, combination of solar processes with a wetland system can be an interesting solution to comply with the new 22020/741 EU regulation on minimum requirements for water reuse. This regulation will enter into force in June 2023 and it establishes that the turbidity must be less or equal to 5 NTU and *E. coli* must be at the legislative limit (LL) less or equal to 10 CFU/100 mL.

The aim of this work is to investigate and optimize the advanced solar tertiary treatment based on H_2O_2 and natural sunlight at pilot plant scale (60 and 90 L) for further validation at a demonstrative scale. The DEMO plant consists on an already installed vertical wetland followed by a horizontal one finally connected to a raceway pond reactor (RPR) for wastewater reuse in the urban wastewater treatment plant (UWWTP) of "Blanca" in Murcia, South East of Spain (Figure 1).

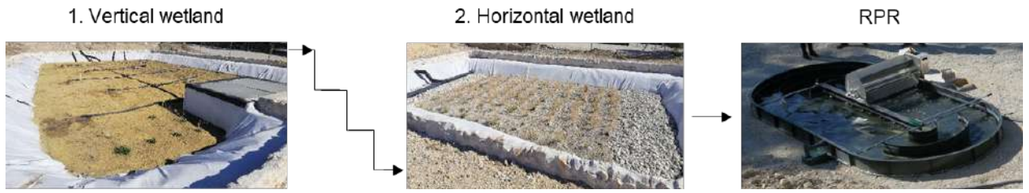

Figure 1. Demonstration system of natural based solutions coupled with advanced solar tertiary treatment in Murcia, Spain.

MATERIALS AND METHODS

Preliminary tests were carried out in a RPR pilot plant under different operating conditions. Three different concentrations of H_2O_2 (25, 50 and 100 mg/L) and two different water column heights in the RPR (10 and 15 cm, 60 L and 90 L of total volume of water, respectively) were tested. Actual secondary effluents from the UWWTP of "Blanca" in Murcia, South East of Spain, were used as a water matrix. In particular, the wastewater effluent from the entrance of the vertical wetland (EVW) and from the outlet of the horizontal wetland (OHW) were used and characterized. A total of 223 CECs along the wetlands were monitored by using an Exion AC UHPLC system (AB Sciex Instruments, Wilmington, DE, USA) coupled to a Triple Quad™ 7500 mass spectrometer (AB Sciex Instruments, Wilmington, DE, USA), including drugs, pesticides, antibiotics, personal care products and their metabolites. The enumeration and quantification of microbial concentration from UWW was performed as reported by Hernández-Zanoletty et al. (2022). Table 1 shows the physicochemical and microbiological characterization of both effluents.

Table 1. Physicochemical and microbiological characterization of the wastewater effluent at the entrance of the vertical wetland (EVW) and from the outlet of the horizontal wetland (OHW).

		Physicochemical	
	Units	(EVW)	(OHW)
Dissolved organic carbon (DOC)	mg/L	41.2 ± 7.9	14.5 ± 3.5
$[HCO_3^-]$	mg/L	713.4 ± 39.0	527.2 ± 33.5
Turbidity	NTU	35.5 ± 9.8	2.21 ± 1.7
pH	-	7.4 ± 0.1	7.5 ± 0.1
Conductivity	mS/cm	3.4 ± 0.4	4.1 ± 0.3
CECs	ng/L	87348 ± 7.6·10³	10088 ± 1.5·10³
		Bacteria	
E. coli	CFU/100mL	540000 ± 7.5·10⁴	70 ± 1.2
Enterococcus spp.	CFU/100mL	80000 ± 5.7·10³	67 ± 3.9

In addition, the following ionic content of both effluents (Table 2) was obtained by using ion chromatograph (Model 850, Metrohm, Herisau, Switzerland in a column METROSEP C4-250/4.0 (250 mm x 4.0 mm ID)).

Table 2. Ionic content of the wastewater effluent at the entrance of the vertical wetland (EVW) and from the outlet of the horizontal wetland (OHW).

		Ionic content	
	Units	EVW	OHW
Cl^-	mg/L	615.1 ± 76.3	730.4 ± 76.3
NO_3^-	mg/L	1.8 ± 0.6	4.3 ± 1.6
NO_2^-	mg/L	0.1 ± 0.0	1.6 ± 1.1
PO_4^{3-}	mg/L	12.5 ± 0.4	6.3 ± 1.7
SO_4^{2-}	mg/L	310.9 ± 58.7	892.0 ± 49.0
Na^+	mg/L	396.6 ± 53.1	567.2 ± 45.5
NH_4^+	mg/L	44.2 ± 2.9	0.84 ± 0.4
K^+	mg/L	21.1 ± 1.5	20.4 ± 3.8
Ca^{2+}	mg/L	218.3 ± 33.2	359.7 ± 64.0
Mg^{2+}	mg/L	95.2 ± 11.5	122.9 ± 12.3

RESULTS AND DISCUSSION

Based on the characterization of EVW and OHW, the purification capability of the wetland systems was set on 88% in the average absorption/degradation of CECs. In terms of disinfection results, *E. coli* reached a 4 logarithm reduction value (LRV) and *Enterococcus* spp. 3 LRV. Therefore, taking into account the EU legislative parameters, the turbidity of water complies with the new legislation (≤ 5 NTU), but the *E. coli* did not, highlighting and justifying the need for an additional treatment step.

Figure 2 shows the inactivation profiles of both bacteria by the additional treatment investigated in this study, i.e., the solar photochemical process based on the use of H_2O_2 as an oxidant and natural solar radiation in RPR. The effect of different H_2O_2 concentrations (from 25 to 100 mg/L) and two different RPR water heights (10 and 15 cm) under natural solar radiation are shown.

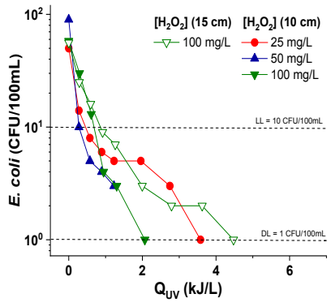

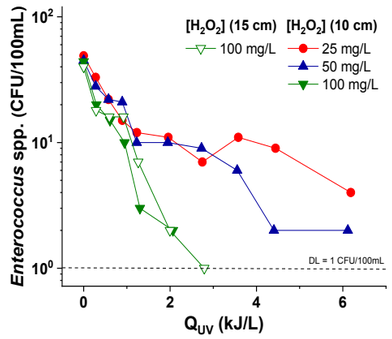

Figure 2. Inactivation profiles of *E. coli* and *Enterococcus* spp. in presence of different oxidant concentrations and different RPR water heights under natural solar radiation.

For *E. coli*, the LL was reached in the presence of all H_2O_2 concentrations, therefore, 25 mg/L of H_2O_2 (after 30 minutes or 0.57 kJ/L of Q_{UV}, accumulated solar UV-irradiance per unit of time and volume) was selected as the best condition. For *Enterococcus* spp., 10 CFU/100 mL was also reached in the presence of the lower oxidant concentration tested, but the LL for these bacteria is not yet regulated. Besides, two different water heights were evaluated in the RPR (in the case of 100 mg/L of H_2O_2), 10 cm and 15 cm (Figure 2), initially the highest H_2O_2 concentration was also tested to analyze its effect on the CECs removal. The bacterial inactivation profiles for both heights are similar, therefore, it is necessary to test the optimal H_2O_2 concentration (25 mg/L) at higher height to see if it is possible to improve the treatment conditions, treating a larger volume of water with the same amount of oxidant. It is important also to highlight that, after each treatment, it is important to evaluate the potential regrowth of inactivated bacteria after 24 and 48 hours, just to assure the safe use of treated wastewater after storage time. Under these experimental conditions, post-treatment regrowth was not observed, so the treatment of solar/H_2O_2 could be considered an effective method for bacterial inactivation. The percentage of CECs removal under the selected operating conditions is being measured.

As conclusion, combined wetland and RPR systems are an effective solution for wastewater purification, CECs average adsorption/degradation along the wetlands was 88% at ng/L concentration level. It was possible to reach concentrations ≤ 10 CFU/100 mL for both tested bacteria with solar and the addition of a low concentration of H_2O_2 (25 mg/L), being able to increase the height of the RPR to treat a greater volume of water, without losing efficiency.

Future research will be focused on the study of the effect of another oxidant (peroxymonosulfate, PMS) and comparison with H_2O_2. Finally, the best-selected operating conditions and oxidant will be evaluated at demo plant scale by monitoring CECs for several months and the presence or not of ARGs and ARB in OHW.

ACKNOWLEDGMENT

The AQUACYCLE project is funded and supported by the European Union through the ENI CBC Mediterranean Sea Basin Programme.

REFERENCES

Abuabdou, S.M.A., Ahmad, W., Aun, N.C., Bashir, M.J.K. 2020. A review of anaerobic membrane bioreactors (AnMBR) for the treatment of highly contaminated landfill leachate and biogas production: effectiveness, limitations and future perspectives. *J. Clean. Prod.* **255**, 1202152.

Berruti, I., Nahim-Granados, S., Abeledo-Lameiro, M.J., Oller, I., Polo-López, M.I., 2022. Recent advances in solar photochemical processes for water and wastewater disinfection. *Chem. Eng. J. Adv.* **10**, 100248.

Cabrera-Reina, A., Miralles-Cuevas, S., Perez, J.A.S., Salazar, R., 2021. Application of Solar Photo-Fenton in Raceway Pond Reactors: A Review. *Science of the Total Environment*, **800**, 149653.

Christou, A., Agüera, A., Bayona, J.M., Cytryn, E., Fotopoulos, V., Lambropoulou, D., Manaia, C.M., Michael, C., Revitt, M., Schröder, P., Fatta-Kassinos, D. 2017 The potential implications of reclaimed wastewater reuse for irrigation on the agricultural environment: The knowns and unknowns of the fate of antibiotics and antibiotic resistant bacteria and resistance genes - A review. *Water Res.* **15**(123), 448- 467.

Haghshenas-Adarmanabadi, A., Heidarpour, M., Tarkesh-Esfahani, S. 2016. Evaluation of Horizontal–Vertical Subsurface Hybrid Constructed Wetlands for Tertiary Treatment of Conventional Treatment Facilities Effluents in Developing Countries. *Water Air Soil Pollut* **227**(1), 28.

Hernández-Zanoletty, A., Oller, I., Polo-López M.I., Blazquez-Moraleja, A., Flores, J., Marín M.L., Boscá, F., Malato, S. 2022, Assessment of new immobilized photocatalysts based on Rose Bengal for water and wastewater disinfection. Catalysis Today. In press.

Rizzo, L., Gernjak W., Krzeminski P., Malato S., McArdell C.S., Sanchez Perez J.A., Schaar H., Fatta-Kassinos, D. 2020. Best available technologies and treatment trains to address current challenges in urban wastewater reuse for irrigation of crops in EU countries. *Science of the Total Environment*. **710**, 136312.

Assessment of the Integration of a Vermifilter and a Zooplankton-Based Reactor for the Removal of Microcontaminants to Produce Reusable Water

A.C. Suñer, V. Salvadó, M. Hidalgo

Department of Chemistry, University of Girona, C/ Maria Aurèlia Capmany, 69, 17003 Girona, Spain
(E-mail: *anacristina.suner@udg.edu; victoria.salvado@udg.edu; manuela.hidalgo@udg.edu)*

Abstract

This research was aimed to provide a system for treatment and reuse of municipal and domestic wastewater based on the combination of nature-based technologies, vermifiltration and a daphnia-based reactor. The study was conducted at pilot-scale (10 p.e.) and particular attention was dedicated to the removal of selected organic micropollutants (PPCPs) and potentially toxic elements. The integrated system delivered an effluent suitable for water reuse for agricultural irrigation and other reuse categories regulated in the Spanish legislation. Regarding metal removal, the integrated system achieved removals of about 30% for Cr, 50% for Zn, 60% for Ni and Cu and close to 100% for Pb. The system demonstrated a good efficiency for the removal of PPCPs with percentages higher than 80% for ibuprofen, naproxen, citalopram, gemfibrozil and triclosan and about 60 % for diclofenac and clofibric acid.

Keywords (maximum 6 in alphabetical order)

Daphnia; earthworms; Pharmaceuticals and Personal Care Products (PPCPs); toxic elements; water reuse

INTRODUCTION

Apart from high nutrient and pathogen loads, urban wastewater may contain thousands of organic micropollutants that are either extensively used on a day-to-day basis or present in products commonly used in industrialized areas. These compounds, also known as contaminants of emerging concern (CECs), comprise pharmaceuticals and personal care products (including antibiotics), perfluorinated compounds, flame retardants, among others. Although metals and metalloids reach the environment mainly through anthropogenic activities such as mining, smelting or excessive use of fertilizers and pesticides, they can also reach sewage treatment plants through paints, ceramics, textiles, pigments, pesticides, or cigarette butts. Micropollutants occur in low ($ng.L^{-1}$) to very low ($pg.L^{-1}$) concentrations in the environment and pose risks to aquatic and terrestrial ecosystems.

These substances are completely out of the ordinary standards of wastewater treatment, and most of the commonly used treatment technologies are ineffective against them. Different technologies are available to ensure that treated effluents achieve high levels of quality. These include physicochemical treatments (coagulation, flocculation, membrane-based treatments, chlorine and ozone disinfection, advanced oxidation, etc.). However, they involve the use of significant energy resources and/or chemicals. In this context, technologies based in natural processes emerge as low-cost and sustainable alternatives to remove micropollutants from wastewater.

Although some systems that mimic natural depuration utilizing solar energy and living organisms (including media filters, lagoons and ponds, aerobic treatments, and wetlands), have proved to be effective, there are still problems in their application due to the maintenance requirements and electricity consumption (media filters and aerobic treatments) while lagoons and wetlands require large areas of land and present difficulties in meeting the discharge criteria across a whole year. Seeking in other alternatives to improve the efficiency of nature-based treatments, the use of earthworms (Jiang et al, 2016) and zooplankton (Pau et al., 2013; Salvadó et al., 2021) has been also considered.

This work discusses novel and relevant results on the removal of metals and pharmaceuticals by the integration of a vermifilter (i.e., primary and secondary treatment) and a zooplankton-based reactor (tertiary treatment).

MATERIALS AND METHODS

The study was conducted at a pilot plant placed adjacent to the municipal WWTP of Quart (Girona, Nord east Spain) that serves approximately 4,000 inhabitants. Inflluent wastewater was taken from the WWTP inlet, passed through a hydraulic circuit to separate coarse solids and grease and pumped to the vermifilters. Vermifiltration was performed in two identical cylindrical reactors working in parallel (1.2 m diameter and 1.7 m height). Filling media was composed of three different layers: river pebbles, pozzolana and woodchip. About 15,000 earthworms (*Eisenia fetida*) were introduced in the reactors. Reactors were operated in fed-batch mode, with 5 min feeding and 25 min drawing. The Daphnia reactor (1,500 L) was fed with the effluent of vermifilters and inoculated with *D.magna* from a laboratory aquarium culture. The integrated system was designed to operate normally at 1,500 L.d-1. Short tests also were performed at 750 $L.d^{-1}$ and 3,000 $L.d^{-1}$.

Additional UV treatment was also available for further polishing of the effluent of the zooplankton reactor.

Influent and effluent samples were collected at the inlet/outlet of the vermifilters and at the outlet of the zooplankton-based reactor over a period of three months. Treatment effectiveness was evaluated in terms of removal of the typical physical and chemical gross parameters, pathogens, and also for the removal of selected PPCPs: sulfamethoxazole (SLF), fluoxetine (FXT), paroxetine (PXT), citalopram (CTP), clofibric acid (CFB), gemfibrozil (GMB), diclofenac (DCF), ibuprofen (IBU), naproxen (NPX), carbamazepine (CBZ), triclosan (TCS), and potentially toxic elements (Cr, Ni, Cu, Zn, As, Cd, Sn, Pb).

RESULTS AND DISCUSSION

The integrated system achieved average removals of 88±7%, 89±8%, 91±8%, 85±19%, 98±3 for COD, TSS, NH4+, BOD5 and pathogen (*E.coli*), respectively, providing an effluent suitable for water reuse for agricultural irrigation and other reuse categories regulated in the Spanish legislation (Pous et al., 2021).

Potentially toxic elements

Table 1 shows the concentration values of the seven potentially toxic elements studied though the different stages of the nature-based treatment. The maximum, minimum and median values are displayed. The joint data for the 750 and 1500 $L \cdot d^{-1}$ flows are shown, because no significant differences were observed in the results obtained at the two different flows (different hydraulic residence time).

Considering the complete process, Lead (Pb) was the metal with the highest removal with more than 95%. Chromium (Cr) and arsenic (As) were the least removed with values lower than 30%. Zinc (Zn) was removed at a value close to 50% and nickel (Ni), copper (Cu) and tin (Sn) at values close to 70%.

Most part of the metals and metalloids were removed in the vermifiltration tank and less than 20% of the total removal took place in the daphnia-based reactor in all cases, except for Cd, with a removal of about 30%.

Table 1. Potentially toxic elements (PTE) concentrations ($\mu g.L^{-1}$) at the different stages of the treatment system. 1: Vermifilter influent; 2: Inlet Daphnia-based reactor influent; 3: Daphnia-based reactor effluent. >LOQ: below limit of quantification.

		Cr	Ni	Cu	Zn	As	Cd	Sn	Pb
1	max	11.9	6.7	47.9	392.2	1.5	0.3	1.1	9.8
	min	5.7	2.7	11.5	41.8	0.7	0.1	0.5	0.8
	median	7.2	4.7	26.1	83.9	1.0	0.1	0.8	2.8
2	max	8.1	2.8	17.8	65.4	1.6	0.2	0.3	1.0
	min	4.2	0.9	4.9	20.1	0.7	<LOQ	0.1	<LOQ
	median	5.5	1.6	7.7	33.4	1.0	0.1	0.2	<LOQ
3	max	7.2	3.0	10.9	65.4	1.5	0.1	0.6	0.2
	min	4.5	1.0	4.1	30.8	0.7	<LOQ	0.1	<LOQ
	median	5.4	1.7	5.8	39.5	1.1	0.1	0.2	<LOQ

Organic micropollutants

The compounds found at higher concentrations were the anti-inflammatory drugs ibuprofen and naproxen, followed to a lesser extent by the lipid regulators gemfibrozil and clofibric acid, in accordance with the consumption pattern for these pharmaceuticals. The antibiotic sulfamethoxazole, and the antidepressants fluoxetine and paroxetine were hardly detected in the influent of the treatment plant.

The results for the removal of the s pharmaceuticals and triclosan in the integrated treatment system at two hydraulic residence times are presented in Figure 1.

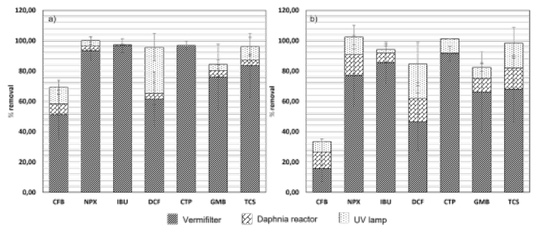

Figure 1. Removal of organic micropollutants by the different treatments integrated in the system.

operating at a) 750 $L.d^{-1}$ and b) 1,500 $L.d^{-1}$.

The efficiency in the removal of organic micropollutants by the integrated nature-based system were similar for the two hydraulic residence times tested, except for clofibric acid. Removals between 80% and 100% were achieved for ibuprofen, naproxen, citalopram, gemfibrozil and triclosan and about 65 % for diclofenac. For clofibric acid, the most polar compound, removals of about 60% were obtained when the system was operated at 750 $L.d^{-1}$, while for the shorter residence time the efficiency decreases, resulting in a removal of about 30%.

By taken a close look at the different treatments, when the system is operated at a nominal load of 750 $L.d^{-1}$, most of the removal takes place at the vermifilter and the daphnia-based reactor only contributes to a small percentage for the removal of gemfibrozil. For the shorter residence time, the contribution of the reactor increases at the expense of the decrease in the efficiency of the vermifilter.

Further treatment of the effluent of the daphnia-based reactor by UV radiation allowed removals higher than 90% for the organic compounds, except for clofibric acid, with maximum total removal of 25%.

This case study demonstrates that the integration of vermifilter and zooplankton- based reactors is a sustainable approach for the removal of micropollutants of different properties while providing reclaimed water that is of a high chemical and biological quality for agricultural irrigation and other non-potable uses. Moreover, this integrated system has a low energy consumption, a minimal maintenance, and a very small sludge production making the system presented here both eco-sustainable and economical.

AGNOWLEDGEMENTS

This research was funded by EU H2020 (INNOQUA Project, GA No 689817) and the Spanish Ministry of Science and Innovation (Projects PID2021-127326OB-100 and TED2021-132721B-100).

REFERENCES

Jiang, L., Liu, Y., Hu, X., Zeng, G., Wang, H., Zou, L., Tan, X., Huang, B., Liu, S. 2016 The use of microbial-earthworms ecofilters for wastewater treatment with special attention to influencing factors in performance: a review. *Bioresource Technology* **200**, 999.

Pau, C., Serra, T, Colomer, J., Casamitjana, X., Sala, L. 2013 *Filtering capacity of Daphnia magna on sludge particles in treated wastewater*. Water Research **47**, 181.

Pous, N., Barcelona, A., Sbardella, L., Gili, O., Hidalgo, M., Colomer, J., Serra, T. Salvadó, V. 2021 Vermifilter and zooplankton-based reactor integration as a nature-based system for wastewater treatment and reuse. *Case Studies in Chemical and Environmental Engineering* **4**, 100153.

Salvadó, V., Hidalgo, M., Pous, N., Serra, T., Colomer, J. 2021 Daphniafilter: A nature-based tertiary treatment *in Innovative wastewater treatment technologies – The INNOQUA Project.* Ed. C. Bumbac, E. Clifford, J.B. Dussaussois, A. Schaal, D. Thompkins. Pp. 192-221. Now Publishers, 2021.

TECHNICAL SESSIONS

T5. Removal of recalcitrant and emerging pollutants

ECOSTP 2023

Improvement in the pharmaceutical removal from hospital wastewater in a full-scale hybrid PAC-MBR

M. Gutiérrez[*,**], D. Mutavdžić Pavlović[**], D. Stipaničev[***], S. Repec[***], F. Avolio[****], M. Zanella[*****], L. Benetti[*****], P. Verlicchi[*]

[*] Department of Engineering, University of Ferrara, Via Saragat 1, 44122 Ferrara, Italy
(E-mail: *marina.gutierrezpulpeiro@unife.it*; *paola.verlicchi@unife.it*)
[**] Department of Analytical Chemistry, Faculty of Chemical Engineering and Technology, University of Zagreb, Marulićev trg 20, 10000 Zagreb, Croatia (E-mail: *dmutavdz@fkit.hr*)
[***] Croatian Waters, Central Water Management Laboratory, Ulica grada Vukovara 220, 10000 Zagreb, Croatia (E-mail: *Drazenka.Stipanicev@voda.hr*; *Sinisa.Repec@voda.hr*)
[****] Asset management, Hera Spa, Ferrara, Italy (E-mail: *francesco.avolio@gruppohera.com*)
[*****] Operation Idrico, Hera SpA, Ferrara, Italy (E.mail: *marcello.zanella@gruppohera.com; linda.benetti@gruppohera.com*)

Abstract

The removal of a selection of organic micropollutants (OMPs) from wastewater was assessed by a hybrid system consisting of an MBR coupled to powdered activated carbon (PAC) added inside the biological tank. Two PAC concentrations were tested (0.1 and 0.2 g/L) in a full-scale MBR treating mainly hospital wastewater. Out of 232 OMPs tested, results of a selection of 25 compounds, mainly antibiotics, is presented regarding their frequency of detection, loadings and removal efficiencies and environmental impact. Results indicate that a PAC concentration of 0.2 g/L reduced the average loads OMPs tested by 77% with respect to MBR alone (41%).

Keywords (maximum 6 in alphabetical order)
Antibiotics, Hospital Wastewater, Hybrid MBR, Organic Micropollutants, Powdered activated carbon, Removal Efficiency

INTRODUCTION

Among the multiple sources of wastewater entering in WWTPs, hospital wastewater has been considered a hotspot for organic micropollutants (OMPs), which may include a variety of pharmaceuticals and their metabolites, contrast media, among others. In particular, antibiotics have drawn the attention since their presence has been associated to chronic toxicity and the prevalence of antibiotic resistant bacteria in aquatic environments (Michael et al., 2013). Despite hospital wastewater is still considered of the same pollutant nature than urban wastewater, it has been an object of research around the globe (Verlicchi et al., 2015) and *in situ* dedicated advanced treatments have been developed (McArdell et al., 2011). Among them, the combination of innovative technologies with advanced biological treatment, as membranes bioreactor (MBR), in the so-called *hybrid MBRs* (Rizzo et al., 2019). In this study, we focus on the use of powdered activated carbon (PAC) added inside the biological tank of an MBR. In this way, the biological degradation is combined with the adsorption process, which results in a synergistic effect that enhances the removal of OMPs from wastewater. Despite the removal of OMPs by PAC-MBR systems has been a matter of interest in recent years, many of the research studies have worked with laboratory- or pilot-scale MBRs using synthetic wastewater, on which the contaminant is spiked at environmental concentrations (Alvarino et al., 2017, 2016; Echevarría et al., 2019; Li et al., 2011; Nguyen et al., 2013; Serrano et al., 2011). In this way, there are knowledge gaps related to the use of PAC under real conditions that hamper the implementation of this technology in the following years. In comparison with other hybrid technologies, PAC added to the biological tank is easy to implement and operate. However, special attention must be paid to ensure a constant concentration of PAC in the system, taking into consideration that many OMPs rely their removal on the adsorption onto fresh PAC (Alvarino et al., 2018).

The present study aims to test the addition of PAC in a full-scale MBR treating mainly hospital wastewater for the removal of OMPs and, in particular antibiotics. For that purpose, three experimental campaigns for a total of one year duration took place testing the MBR in absence and in presence of PAC (at two concentrations, 0.1 g/L and 0.2 g/L).

MATERIALS AND METHODS

Experiments were conducted in a full-scale MBR of a WWTP located in northeastern Italy. The average dry weather flow of the WWTP is 700 m^3/d. The WWTP treats mainly hospital wastewater (75% of the total average flow rate) and urban wastewater (25%). The WWTP consists of a pre-treatment; the MBR, composed by P removal (100 m^3), denitrification (250 m^3) and nitrification (350 m^3) tanks, followed by a tertiary treatment (UV radiation) for disinfection of final effluent. Three treatments were considered, *noPAC*, on which the MBR worked without PAC addition (March - August 2021), *0.1PAC*, where PAC was added and maintained at a concentration of 0.1 g/L inside the biological reactor (September – November 2021), and *0.2PAC*, with a PAC concentration of 0.2 g/L (April – May 2022). The PAC concentration was maintained constant through periodical and controlled additions of PAC to counterbalance the PAC losses associated with the excess sludge withdrawn from the system. WWTP operation was monitored through a set of conventional parameters for water quality. Potential changes in mixed liquor due to PAC addition were evaluated by performing DOC, UV_{254}, TSS measurements.

During the experimental campaigns, a total of 232 OMPs were analysed, from which 25 compounds were selected in the present study. Selected compounds include 17 antibiotics, 4 analgesics, 1 beta-blocker, 2 psychiatric drugs, 1 stimulant and 1 iodinated contrast media. Selection criteria was based on their frequency of detection and research interest. Compounds selected had a frequency of detection greater than 50% in the WWTP influent, and they were present in at least two treatments, thus the treatment efficiency was evaluated with a certain degree of confidence. For OMP analysis, three sampling campaigns took place: *noPAC* treatment (n=5), *0.1PAC* treatment (n=18) and *0.2PAC* (n=12). 24-h time proportional composite wastewater samples were taken once a week by automatic samplers in the influent and MBR permeate. For the permeate samples, the hydraulic retention time was considered. OMPs were determined by UHPLC–QTOF–MS.

RESULTS AND DISCUSSION

Since hospital effluent is considered a point source of OMPs in wastewater, the characterization of the wastewater entering in the WWTP is key to further evaluate the treatment efficiency (Fig. 1a). In this study, 4 OMPs stood out by their high average loads (>1 g/day) in the influent: azithromycin (AZIT) (2.4 g/day), acetaminophen (ACET) (4.4 g/day), caffeine (CAF) (2.2 g/day) and iopromide (IOP) (6.4 g/day). In the case of IOP, its presence is due solely to the hospital wastewater since it is used as a contrast medium for medical exams. In the MBR permeate (Fig. 1b), the OMP load was reduced by one order of magnitude in many cases, with decreasing loads from *noPAC* to *0.2PAC* treatments, indicating the effectiveness of the addition of PAC. Only ofloxacin (OFX) was found at a load higher than 0.1 g/day in *0.2PAC* treatment. Since the addition of PAC seems to reduce the loading of OMPs in the effluent of the WWTP, a risk quotient (RQ) analysis was used to evaluate the impact of the wastewater effluent in the receiving water body (Fig. 1c). Assuming a context of water scarcity with no dilution of the WWTP effluent in the receiving water body, only the *0.2PAC* treatment reduced substantially the RQ of the tested OMPs. 7 pharmaceuticals were found at RQ > 1 (high risk) in *noPAC* and *0.1PAC* treatments, while *0.2PAC* reduced the number to a total of 3 compounds (AZIT, carbamazepine CBZ and OFX). Albeit these OMPs still supposed a high risk, results show that the impact in the receiving water was significantly reduced by increasing PAC concentration for all OMPs except for amoxicillin and IOP. Indeed, the use of risk assessment analysis is a useful tool to evaluate the treatment efficiency of in full-scale investigations. For instance, the frequency of detection of OMPs in the MBR permeate (Fig. 1d) shows that in most of the cases OMPs, even if are highly removed, are still found in the WWTP effluent. The results are not surprising due to the high OMP loads arriving from the hospital effluent and confirms the necessity of *in situ* advanced technologies to deal with their occurrence.

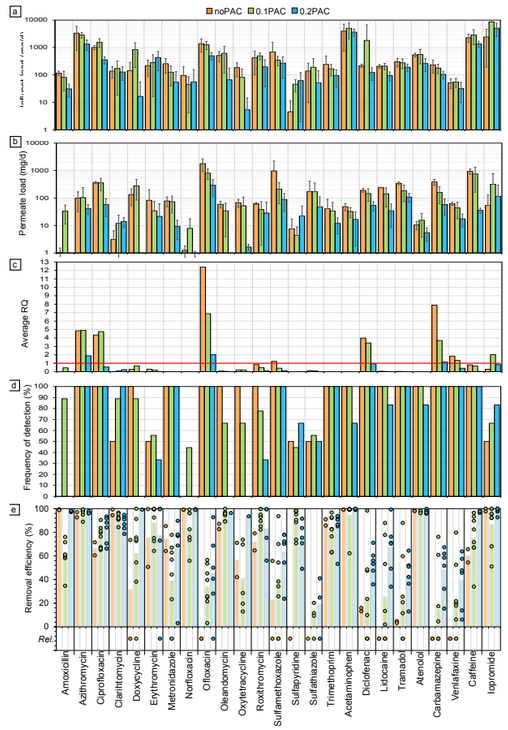

Figure 1. OMP values of a) influent load, b) MBR permeate load, c) average risk quotient and d) frequency of detection (%) in the MBR permeate, e) removal efficiencies (%) for *noPAC*, 0.*1PAC* and *0.2PAC* treatments. Note that bars indicate average values while dots individual measurements.
Rel. indicates release (negative removal efficiency).
Previous studies, with the same treatment configuration as the present work, used a range of PAC concentrations between 0.05 and 2 g/L (Alvarino et al., 2017, 2016; Echevarría et al., 2019; Li et al., 2011; Nguyen et al., 2013; Serrano et al., 2011). Considering the results obtained in those investigations, it was concluded that a PAC dose of 0.1 g/L is sufficient to achieve an 80% of removal for most of the compounds tested. In our study, we confirm that the increase of the PAC concentration up to 0.2 g/L implies a substantial improvement in the removal efficiencies of many recalcitrant OMPs. For antibiotics, the average removal efficiency of 11 out of 17 compounds was improved by the presence of PAC and, for many of them, the increase was correlated to the PAC dose. For instance, doxycycline increased its average removal by 40% and 80% with *0.1PAC* and *0.2PAC*, respectively, while ofloxacin and sulfapyridine went from negative to medium (34% - 45%) and high (74% - 89%) average removal. Some compounds, as sulfamethoxazole, required *0.2PAC* to achieve high removals (up to 72%). It seems that with *0.1PAC* the main removal mechanism is still biodegradation (Alvarino et al., 2017), and thus higher PAC doses are required to obtain synergistic effects of the adsorption and biodegradation processes (OMP biodegraded once it is adsorbed onto PAC surface). Increasing the PAC dose in the bioreactor had also an effect on the analgesics tested. Lidocaine, DCF and tramadol achieved a moderate average removal (43%- 67%) with *0.2PAC* compared to the very low removal or even release in the other treatments. Diclofenac is a recalcitrant compound with very low and variable removal efficiencies in MBR systems (Nguyen et al. 2013). In literature, its increased removal has been associated not only to the PAC dose but to the presence of fresh PAC (Alvarino et al., 2017). Indeed, the presence of PAC greatly influenced the removal of the compounds which rely their removal solely on adsorption. For instance, only moderate removals were achieved with *0.2PAC* for CBZ and venlafaxine. In fact, CBZ has proven to be greatly depends on the presence of fresh PAC, showing an abrupt increment after PAC addition and subsequent decrement over time (Alvarino et al., 2016, Echevarría et al., 2019). In our study, the removal likely varied depending on the sampling day with respect to the addition of fresh PAC.

FUNDING. This work is supported by the European Union's Horizon 2020 research and innovation program under Marie Sklodowska-Curie grant agreement No 81288 – Nowelties ITN-EJD project.

REFERENCES

Alvarino, T., Komesli, O., Suarez, S., Lema, J.M.M., Omil, F., 2016. The potential of the innovative SeMPAC process for enhancing the removal of recalcitrant organic micropollutants. *J. Hazard. Mater.* **308**, 29–36.
Alvarino, T., Torregrosa, N., Omil, F., Lema, J.M., Suarez, S., 2017. Assessing the feasibility of two hybrid MBR systems using PAC for removing macro and micropollutants. *J. Environ. Manage.* **203**, 831–837.
Echevarría, C., Valderrama, C., Cortina, J.L.L., Martín, I., Arnaldos, M., Bernat, X., De la Cal, A., Boleda, M.R.R., Vega, A., Teuler, A., Castellví, E., 2019. Techno-economic evaluation and comparison of PAC-MBR and ozonation-UV revamping for organic micropollutants removal from urban reclaimed wastewater. *Sci. Total Environ.* **671**, 288–298.
Li, X., Hai, F.I., Nghiem, L.D., 2011. Simultaneous activated carbon adsorption within a membrane bioreactor for an enhanced micropollutant removal. *Bioresour. Technol.* **102**, 5319–5324.
McArdell, C.S., Kovalova, L., Siegrist, H., 2011. Input and Elimination of Pharmaceuticals and Disinfectants from Hospital Wastewater - final report.
Michael, I., Rizzo, L., McArdell, C.S., Manaia, C.M., Merlin, C., Schwartz, T., Dagot, C., Fatta-Kassinos, D., 2013. Urban wastewater treatment plants as hotspots for the release of antibiotics in the environment: A review. *Water Res.* **47**, 957–995.
Nguyen, L.N., Hai, F.I., Kang, J., Nghiem, L.D., Price, W.E., Guo, W., Ngo, H.H., Tung, K.-L., 2013. Comparison between sequential and simultaneous application of activated carbon with membrane bioreactor for trace organic contaminant removal. *Bioresour. Technol.* **130**, 412–417.
Radjenovic, J., Matosic, M., Mijatovic, I., Petrovic, M., Barcelo, D., 2008. Membrane Bioreactor (MBR) as an Advanced Wastewater Treatment Technology. Hdb *Env Chem* Vol. **5** (S/2), 37–101.
Rizzo, L., Malato, S., Antakyali, D., Beretsou, V.G., Đolić, M.B., Gernjak, W., Heath, E., Ivancev-Tumbas, I., Karaolia, P., Lado Ribeiro, A.R., Mascolo, G., McArdell, C.S., Schaar, H., Silva, A.M.T., Fatta-Kassinos, D., 2019. Consolidated vs new advanced treatment methods for the removal of contaminants of emerging concern from urban wastewater. *Sci. Total Environ.* **655**, 986–1008.
Serrano, D., Suárez, S., Lema, J.M., Omil, F., 2011. Removal of persistent pharmaceutical micropollutants from sewage by addition of PAC in a sequential membrane bioreactor. *Water Res.* **45**, 5323–5333.
Verlicchi, P., Al Aukidy, M., Zambello, E., 2015. What have we learned from worldwide experiences on the management and treatment of hospital effluent? - An overview and a discussion on perspectives. *Sci. Total Environ.* **514**, 467–491.

Long-term performance of an anaerobic membrane bioreactor amended with graphene oxide treating municipal wastewater

Oriol Casabella[1,2*], Melina Papapanou[1,3], Michele Ponzelli[1,2], Jelena Radjenovic [1,4], Maite Pijuan [1,2] *Corresponding author: *ocasabella@icra.cat*

[1] Catalan Institute for Water Research (ICRA), C. Emili Grahit 101, 17003 Girona, Spain; [2] Universitat de Girona, Girona, Spain; [3] University of Patras, Patras, Greece; [4] Catalan Institution for Research and Advanced Studies (ICREA), Passeig Lluís Companys 23, 08010 Barcelona, Spain

Abstract

The addition of non-biological conductive materials such as graphene oxide (GO) into anaerobic reactors has been suggested to enhance their performance. In this work, an anaerobic membrane bioreactor treating municipal wastewater was operated for 385 days. During its operation, different additions of GO were conducted and its effect on COD and pharmaceutical compounds removal as well as on microbial community composition was monitored. Results showed no effect of GO on the stability of the reactor (e.g. no major changes in alkalinity and COD removal were detected) whereas an enhanced removal of some PhACs, specifically antibiotics was observed. A shift in the archaeal community was also detected after the addition of GO, with an increase in hydrogenotrophic methanogens.

Keywords: Anaerobic treatment, Bio-reduced graphene oxide, Municipal wastewater, Pharmaceuticals

INTRODUCTION

Municipal wastewater (WW) is usually treated using conventional aerobic activated sludge processes, incurring high costs due to aeration and sludge handling. Anaerobic treatment is gaining attention as a low-cost alternative as no oxygen is needed which results in lower sludge production. (Lew et al., 2009)30 and 60 min. During the past decade, increasing research efforts have been directed to study also the fate and removal of pharmaceuticals in WW treatment (Zhang and Li, 2018; Malmborg and Magnér, 2015)alkaline and thermal hydrolysis pretreatment. One of the most worrying groups of pharmaceuticals is that of antibiotics, since their relationship to the potential development of antibiotic-resistant bacteria in WW treatment plants (WWTPs).

The addition of non-biological conductive materials into anaerobic reactors (e.g., GAC, biochar, carbon cloth, carbon nanotubes, and graphene like-materials) has been suggested to enhance the performance of anaerobic processes within WWTP. Syntrophic bacteria can attach to the surface of these conductive materials and use them for electron exchange thus facilitating the direct interspecies electron transfer, enhancing the biotransformation of persistent pharmaceuticals (Lü, et al., 2020; Johnravindar, et al., 2020; Summers, et al., 2010). Nevertheless, there are no studies using graphene oxide in a continuous anaerobic membrane bioreactor (AnMBR), and preliminary studies in batch report contradictory results (Dong, et al., 2019; Bueno-López, et al., 2020). This study investigates the impact of different concentrations of biologically reduced GO in a continuous AnMBR that treats municipal WW supplemented with a mix of pharmaceuticals.

METHODS

Anaerobic Membrane Bioreactor operation

A bench scale AnMBR of 6 L working volume was operated for 385 days at a hydraulic residence time of 24 h to treat real municipal wastewater. An external module of 0.125 m^2 polyvinylidene difluoride hollow fibers membrane (0.4 µm nominal pore size) was connected to the reactor. A mix of seven pharmaceuticals (detailed list in **Figure 1**) was spiked daily to the influent tank in a final concentration of 0.02 µM for each compound. GO was provided from Graphenea (Spain) as a 4 g/L aqueous dispersion. DNA extraction was performed using a commercial kit and sequenced using illumine MiSeq platform.

The reactor operation can be divided into five different stages: i) baseline operation (0 g GO/g VS, days 0-49), ii) pharmaceuticals addition (days 50-175), iii) 1st addition of GO (0.005 g GO/g VS at the beginning of the period days 176-238), iv) 2nd addition of GO (0.05 g GO/g VS at the beginning of the period (days 239-301), and v) 3rd addition of GO (Weekly addition of 0.005 g GO/ g VS until reaching 0.1 g GO/g VS, days 302-385). After each GO addition, the reactor was kept without recirculation nor permeating for 8 hours to ensure GO biological reduction.

RESULTS

COD values for the influent and permeate are summarized in **Table 1**, as well as the COD removal percentage and partial/total alkalinity (IA/TA) ratio. For all five stages with different GO concentrations an average removal of COD higher than 85 % was achieved. This removal was similar to other AnMBR treating municipal WW (Lew et al., 2009). The reactor stability was controlled twice per week with the IA/TA, which had a value lower than 0.3 indicating no accumulation of volative fatty acids (VFA) (**Table 1**). Only during the early stage *i.* (start-up) was detected a slight VFA accumulation.

The different pharmaceutical compounds showed very different results in their removals (**Figure 1**). For four of the compounds monitored an increase in the removal was detected after the addition of GO. Trimethoprim presented an average removal of 64% ± 5% during the baseline operation, rising to 82% ± 2% during stage *v*. The antibiotic with the highest enhancement in removal efficiency was metronidazole, obtaining a removal of 66% ± 4% during de baseline and increasing up to 96% ± 2% after the addition of GO. Other compounds that showed a tendency for higher removal efficiency across the different operational stages were sulfamethoxazole and roxithromycin, reaching maximum values of 81% ± 3% and 51% ± 10%, respectively. However, the removals of other compounds such as naproxen and diclofenac were not enhanced with GO and presented similar removals compared with the literature, even after the addition of particulate activated carbon as carbon-based conductive material (Xiao et al., 2017; Liu et al., 2020).

The addition of GO promoted the enrichment of the hydrogenotrophic and methylotrophic archaea, which use hydrogen as substrate (**Figure 2**). Hypothetically, these microorganisms could be promoted because of the electrons provided through the GO structure. Chloroflexi and Firmicutes were the most common phyla, accounting for more than half of the bacterial population. A previous study reported the presence of GO stimulated the proliferation of many species of these phyla, notably *Rombustia* spp. and *Longilinea* spp.), during the anaerobic digesting process of waste-activated sludge (Casabella et al., 2023). The addition of GO also favored the proliferation of other bacterial genera, such as *Leptolinia* (Chloroflexi) and *Smithella* (Thermodesulfobacteriota).

Conclusions

The addition of GO doesn't have a negative impact on COD removal or reactor stability.

Pharmaceuticals removal from the liquid phase increased for trimethoprim, metronidazole, roxithromycin, and sulfamethoxazole with the highest GO concentration tested.

The addition of GO induced a shift in the microbial community, promoting Firmicutes and Chloroflexi bacteria, and those methanogens that could use hydrogen as substrate.

Acknowledgments: This research is funded by AEI (Agencia Estatal de Investigación, Spanish Government) through project ANTARES (PID2019-110346RB-C22). ICRA researchers also acknowledge the funding from the CERCA program. O. Casabella acknowledges funding from the Secretariat of Universities and Research from Generalitat de Catalunya and European Social Fund for his FI fellowship (2022 FI_B1 00122). M. Ponzelli acknowledges funding from European Union's Horizon 2020 research and innovation program under the Marie Sklodowska-Curie grant agreement – MSCA-ITN-2018 (EJD Nowelties, grant number 812880).

References: Bueno-Lopez, J. I., et al., (2020). Biodegrad., 31(1), 35–45. Dong, B., et al., (2019) Biodegrad., 31(1), 35–45. Johnravindar, D., et al., (2020). Biomass &Bioen., 136, 105543. Lew, B. et al., (2009). Desal., 243(1–3), 251–257. Liu, W. et al., (2020). Env. Tech. & Innov., 17, 100564. Lü, C. et al., (2020). ACS Sust. Chem.Eng., 8(33), 12626–12636. Malmborg, J. and Magnér, J. (2015). J. Env. Man., 153, 1–10. Summers, Z. M., et al., (2010). Science, 330(6009), 1413–1415. Xiao, Y. et al., (2017). Chem. Eng. J., 321, 335–345. Zhang, X. (2018). Biores. Tech., 255, 266–272

FIGURES AND TABLES

Table 1: Results of the parameters monitored during the different operational stages. expressed as the average and standard deviation.

Stage	i.	ii.	iii.	iv.	v.
Influent COD (mg/L)	691 ± 89	709 ± 110	460 ± 102	489 ± 78	594 ± 63
Effluent COD (mg/L)	75 ± 19	79 ± 29	64 ± 9	71 ± 22	69 ± 7
Removal (%)	89% ± 4%	89% ± 4%	85% ± 3%	84% ± 9%	88% ± 1%
IA/TA	0.28 ± 0.03	0.26 ± 0.03	0.23 ± 0.04	0.18 ± 0.07	0.21 ± 0.04
VS (g/Kg)	3.56 ± 0.68	5.44 ± 0.52	5.15 ± 0.42	6.66 ± 0.90	9.98 ± 0.53
TS (g/Kg)	5.54 ± 1.24	8.54 ± 1.00	8.14 ± 1.09	9.67 ± 1.22	13.74±0.21
VS/TS	65% ± 3%	64% ± 5%	64% ± 5%	69% ± 1%	73% ± 4%
Acetic (mg/L)	6.31 ± 8.09	3.36 ± 6.54	<LOD	<LOD	2.87 ± 3.66
Propionic (mg/L)	2.23 ± 4.36	1.26 ± 3.4	<LOD	<LOD	0.74 ± 1.23
Isobutyric (mg/L)	1.67 ± 2.69	1.1 ± 2.19	<LOD	<LOD	0.63 ± 0.41
N-Butiric (mg/L)	1.58 ± 2.47	1.07 ± 2.03	<LOD	<LOD	0.64 ± 0.42

*** The detection (LOD) and quantification (LOQ) limits were: Acetic=0.99 and 3.29 mg/L, Propionic=0.28 and 0.94, Isobutyric=0.47 and 1.56, N-Butyric=0.48 and 1.60, respectively.**

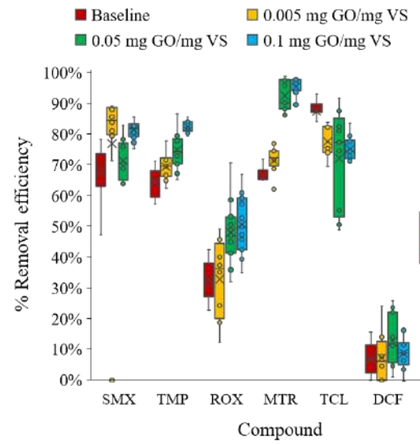

Figure 1. Removal efficiencies for each monitored compound during four (ii.-v.) different stages.

*Baseline-stage *ii.*(0 g GO / gVS), stage *iii.*(0.005 g GO / gVS),stage *iv.* (0.05 g GO / gVS) stage v. (0.1 g GO / gVS).

**Sulfamethoxazole (SMX), Trimethoprim (TMP), Roxithromycin (ROX), Metronidazole (MTR) Triclosan (TCL), Diclofenac (DCF), Naproxen (NPX).

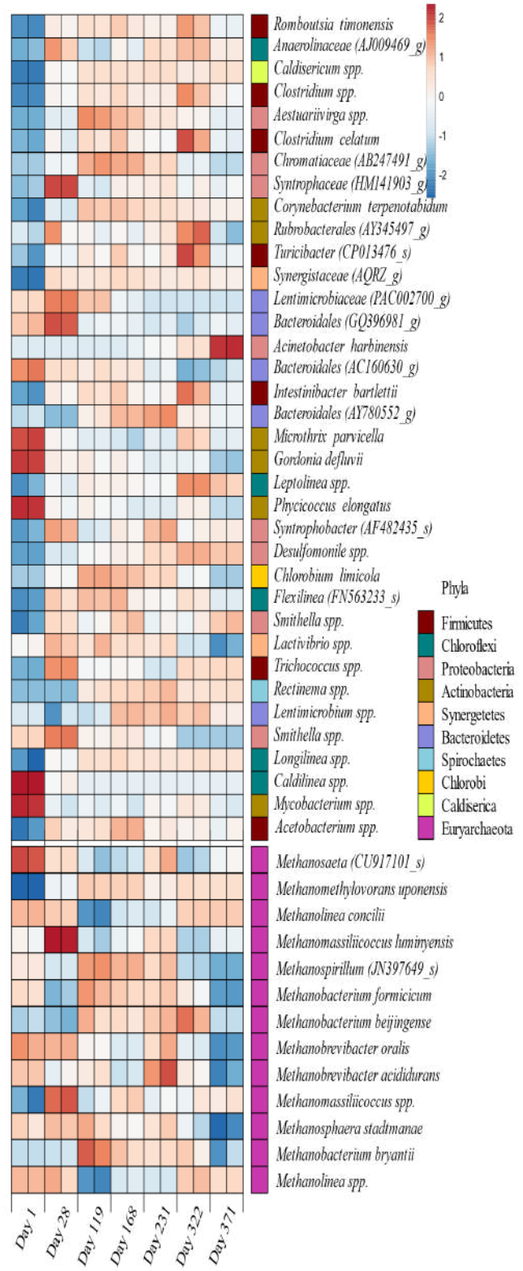

Figure 2. Evolution of the microbial community for archaea and bacteria genera classified in the different phylum.

The Study of a Hybrid System - Moving Bed Biofim Reactor (MBBR) and Nanofiltration (NF) for the Elimination of Organic Micropollutants in Wastewater

M. Eshamuddin*.**, S. Beaufort*, C. Joannis-Cassan*, G. Zuccaro**, G. Nourrit** and C. Albasi*

* Laboratoire de Génie Chimique, Université de Toulouse, CNRS, INPT, UPS, Toulouse, France
(E-mail: *muhammad.eshamuddin@toulouse-inp.fr)*
** Pole Recherche et Développement, NEREUS SAS, 34230 Le Pouget, France

Abstract

The fate of organic micropollutants (MPs) in wastewater treatment plants remains uncertain on various aspects, hence the constant research on its elucidation. This work focuses on the elimination of 19 MPs of different physicochemical properties and the ability of native microbial community to eliminate them in a hybrid system fed with non-conventional wastewater. The hybrid process consists of a Moving Bed Biofilm Reactor (MBBR) coupled with Nanofiltration (NF). Essential process parameters such as chemical oxygen demand, mass of attached biofilm and MPs removal efficiency are comprehensively analysed. This study also strives to establish a correlation between the removals of MPs and the diversity of microbial populations.

Keywords

Biofilm, MBBR, Microbial Community, NF, Organic Micropollutants

INTRODUCTION

The perpetual increase in human activities has resulted in recurrent detections of various organic micropollutants (MPs) particularly at the outlet of wastewater treatment plants (WWTPs). The eventual discharge of such emerging contaminants, e.g., pharmaceutically active compounds, endocrine disrupting chemicals and pesticides, into water bodies remains a worrying issue due to their potential cumulative and toxic effects. Despite their presence at relatively low concentrations (< 1µg/L), the release of these molecules into the environment has been indeed associated with multiple significant risks to human health and aquatic ecosystems (Aemig et al. 2021).

The secondary treatments presently used in most WWTPs display noteworthy removal efficiencies of carbon- and nitrogen-based pollutants but the operating conditions applied in such treatments are not always well adapted for the elimination of MPs. This therefore leads to the implementation of tertiary processes to enhance their removal. Among those processes, the Moving Bed Biofilm Reactor (MBBR) is deemed promising not only for its economic and environmental advantages, but also for its robustness. In fact, biofilm formed on the fluidized plastic carriers has better resistance to constant variations in characteristics of the influent, e.g., organic load, pH, temperature (di Biase et al. 2019); and contributes substantially to the biodegradation of certain MPs (Abtahi et al. 2018).

Currently, on top of quantifying the removal efficiencies of diverse MPs, numerous studies were also conducted to investigate the influence of microbial populations diversity on the degradation of MPs in similar biological processes (Guo et al. 2019). In spite of the persistent progress in research on the characterization of the optimal degradation conditions of MPs and the elucidation of their removal mechanisms, knowledge on the latter is still insufficient due to its complexity.

In this study, the removal efficiency of 19 MPs and the diversity of microbial community in a hybrid system (MBBR + Nanofiltration (NF)) working under different operating conditions were evaluated. Besides, a comparative study of the microbial populations of biomass present in the system (attached and suspended) and those of activated sludge from a WWTP was conducted. The conventional pollution parameters were also analysed to assess the process general performance.

MATERIALS AND METHODS

A hybrid semi-pilot scale MBBR-NF system was operated to treat a non-conventional domestic wastewater from a municipal WWTP in Labège, France. The particularity of this wastewater is its atypically low carbon content, resulting in C/N ratio in the range of 0.8 to 2.0, which is not conventional for biological treatments. The MBBR-NF system presented in figure 1, consisted of an anoxic bioreactor, an aerobic MBBR and a dynamic NF pilot. The treated effluent flowrate varied between 1.5 to 2 l/h depending on the fixed hydraulic retention time. The aerobic MBBR was inoculated with activated sludge from the same WWTP and saddle-shaped, porous carriers (Christian Stöhr GmBH, Marktrodach, Germany) were used as bio-carriers. The carrier filling ratio of the aerobic MBBR was fixed at 44% (v/v).

The analysis of various conventional pollution parameters, i.e., soluble Chemical Oxygen Demand (sCOD), nitrogen based-compounds, mixed liquor suspended solids (MLSS), mass of attached biofilm, were performed systematically throughout the operating period of the hybrid system. MPs were extracted from the collected samples using a modified quick, easy, cheap, effective rugged and safe (QuEChERS) method and analysed by ultra-high-performance liquid chromatography with tandem mass spectrometry (UHPLC-MS-MS) (Cavaillé et al. 2021). DNA extractions were carried out using the procedure provided by DNeasy® PowerSoil® Pro Kit Solution (Qiagen, Germany). The DNA sequencing was executed by the Plateforme Génomique (GeT-PlaGe) - INRA Transfert (Castanet-Tolosan, France).

RESULTS AND DISCUSSION

Physicochemical Analysis

The hybrid system shows good elimination of sCOD with an average removal efficiency of 80.78 ± 3.66%. Moreover, ammonium (NH_4^+) and nitrite (NO_2^-) are almost completely eliminated in the system. However, nitrates accumulation (NO_3^-) is observed in the system due to the low C/N ratio, which hinders the occurrence of denitrification. As regards the core of the biological process, the average mass of biofilm is 12.01 ± 0.66 mg/carrier, thus resulting in a concentration of 10.06 ± 0.55 g/L of attached biomass in the aerobic MBBR (figure 2). The events I-V marked on figure 2 correspond to the different modifications made to the hybrid system.

Micropollutants Analysis

Hitherto, the removal efficiency of detected MPs (figure 3) obtained from a single sampling present compliant results with those from the literature (Blair et al. 2015). Upcoming analyses of the collected samples will be executed using the newly validated method; expected results will be available by May 2023.

Microbiological Analysis

Regarding the diversity of the microbial population at the phylum level, it is observed that the attached biofilm promotes different selectivity of phyla compared to the suspended biomass. Indeed, the abundance of nitrospirae and bacteroidetes varies notably when comparing both forms of biomass but to a lesser extent in respect of proteobacteria. The proliferation of autotrophic nitrifying nitrospirae, is better on the carriers mainly due to a longer contact time between the carriers and the biomass under aerobic condition. Besides, in figure 4, the influence of the hybrid system on the microbial diversity could be noted as the microbial community in the system (attached and suspended biomass) are well distinct from those of the activated sludge used during inoculation. Comprehensive investigations to correlate the influence of MPs are in progress.

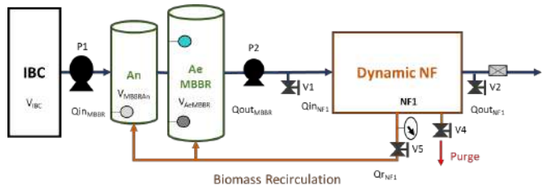

Figure 1. Lab-scale hybrid system (MBBR + NF).

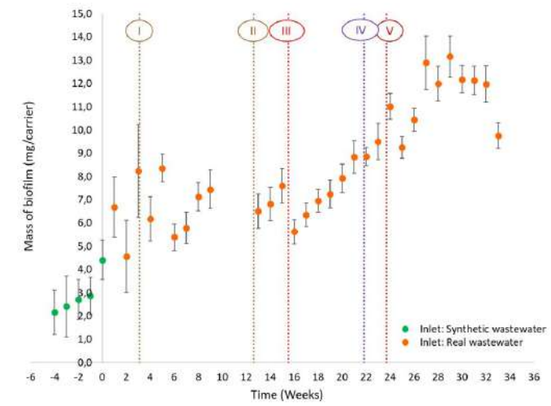

Figure 2. Average mass of the attached biofilm per carrier in the aerobic MBBR.

Abbreviation	Micropollutants
DRN	Diuron
ICP	Imidacloprid
MTC ESA	Metolachlor ESA
BPS	Bisphenol S
ACM	Acetaminophen
CBZ	Carbamazepine
ERY	Erythromycin
KTP	Ketoprofen
MFM	Metformin
OFX	Ofloxacin
SMX	Sulfamethoxazole

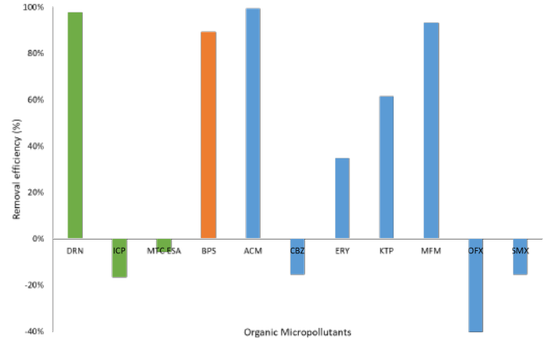

Figure 3. Removal efficiency of detected organic MPs in the hybrid system.

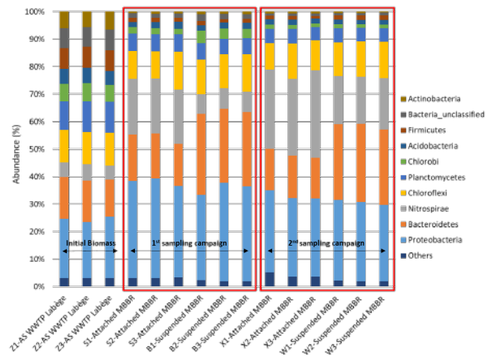

Figure 4. Microbial community profiles of different biomass (initial, attached and suspended) at phylum level.

ACKNOWLEDGEMENT

This research was accomplished under the framework of the SAVE project (https://filiere-save.com/), funded by Agence de l'eau Adour-Garonne and Agence de l'eau Rhône-Méditerranée-Corse.

REFERENCES

Abtahi, S. Mehran, Maike Petermann, Agathe Juppeau Flambard, Sandra Beaufort, Fanny Terrisse, Thierry Trotouin, Claire Joannis Cassan, and Claire Albasi. 2018. 'Micropollutants Removal in Tertiary Moving Bed Biofilm Reactors (MBBRs): Contribution of the Biofilm and Suspended Biomass'. *Science of The Total Environment* 643 (December): 1464–80. https://doi.org/10.1016/j.scitotenv.2018.06.303.

Aemig, Quentin, Arnaud Hélias, and Dominique Patureau. 2021. 'Impact Assessment of a Large Panel of Organic and Inorganic Micropollutants Released by Wastewater Treatment Plants at the Scale of France'. *Water Research* 188 (January): 116524. https://doi.org/10.1016/j.watres.2020.116524.

Biase, Alessandro di, Maciej S. Kowalski, Tanner R. Devlin, and Jan A. Oleszkiewicz. 2019. 'Moving Bed Biofilm Reactor Technology in Municipal Wastewater Treatment: A Review'. *Journal of Environmental Management* 247 (October): 849–66. https://doi.org/10.1016/j.jenvman.2019.06.053.

Blair, Benjamin, Adam Nikolaus, Curtis Hedman, Rebecca Klaper, and Timothy Grundl. 2015. 'Evaluating the Degradation, Sorption, and Negative Mass Balances of Pharmaceuticals and Personal Care Products during Wastewater Treatment', 7.

Cavaillé, L., C. Kim, M. Bounouba, H. Zind, C. Claparols, D. Riboul, E. Pinelli, C. Albasi, and Y. Bessiere. 2021. 'Development and Validation of QuEChERS-Based Extraction for Quantification of Nine Micropollutants in Wastewater Treatment Plant'. *Analytical Bioanalytical Chemistry* 413 (July): 5201–13. https://doi.org/10.1007/s00216-021-03489-z.

Guo, Xuechao, Bing Li, Renxin Zhao, Jiayu Zhang, Lin Lin, Guijuan Zhang, Ruo-hong Li, et al. 2019. 'Performance and Bacterial Community of Moving Bed Biofilm Reactors with Various Biocarriers Treating Primary Wastewater Effluent with a Low Organic Strength and Low C/N Ratio'. *Bioresource Technology* 287 (September): 121424. https://doi.org/10.1016/j.biortech.2019.121424.

Presence of Organic Micropollutants and Antibiotic Resistance Genes in an Anaerobic-MBR integrated system (SIAM) treating urban sewage

M. Rivadulla*, S. Suarez*, F. Omil* and J. M. Garrido*

* CRETUS, Department of Chemical Engineering, Universidade de Santiago de Compostela, 15782 Santiago de Compostela, Galicia, Spain

(E-mail: *matias.cora@usc.es*)

Abstract

The presence of contaminants of emerging concern (CECs) in wastewater, such as organic micropollutants (OMPs) and antibiotic resistance genes (ARGs), entails a current concern in wastewater treatment. Innovative technologies, apart from implying lower operational cost and less environmental impact than conventional ones, are expected to improve the removal of CECs while achieving the discharge limits for conventional pollutants, such as COD, TN, SS. This research analyses the SIAM technology (methanogenic Anaerobic reactor and Membrane bioreactor Integrated System) operating with urban sewage at pilot scale. The aim of this work was to assess the removal of both, conventional and emerging pollutants. The characteristics of the technology enhanced the removal of selected OMPs, due to the presence of different redox conditions and biomass conformation, as well as higher solid retention time (SRT). Compounds like trimethoprim or ciprofloxacin were removed up to 92±3% and 93±13%, respectively. The ultrafiltration membrane achieved 1.78 log maximum reduction of ARGs.

Keywords

Antibiotic resistances, hybrid process, organic micropollutants, real sewage.

INTRODUCTION

The occurrence and fate of organic micropollutants (OMPs) in sewage treatment plants (STPs) has been studied in recent years by the scientific community, since their release to the environment presents a potential toxic risk. Among them, antibiotics are one of the most concerning groups, due to the potential development of antimicrobial resistances in some microorganisms (Phoon et al., 2020). Biological treatment of urban sewage seems to present some conditions that could enhance the spread of ARGs (Manaia et al., 2018).

Innovative wastewater treatment technologies are designed to fulfil the integrated protection of the environment, reducing conventional pollutants load at higher energy efficiency than conventional processes (Lorenzo-Toja et al., 2016). Some of this technologies include different characteristics that may enhance OMPs removal, including alternating redox conditions, a more diverse microbial community, or higher sludge retention times (SRTs)(Alvarino et al., 2018). However, antibiotic resistant genes (ARGs) could be promoted in certain conditions that benefit OMP removal (Karkman et al., 2018). Further research is needed to elucidate whether innovative technologies can achieve a reduction in both, conventional and emerging pollutants, with a better environmental performance than conventional processes.

The objective of this study was to evaluate the performance of an innovative technology treating urban sewage not only in terms of conventional pollutants removal (COD, TN, SS), but also in terms of reduction of the discharge of OMPs and ARGs.

MATERIALS AND METHODS

Experimental setup

The SIAM (patent ES 2 385 002 B2) pilot plant was operated in a NW Spain urban STP at ambient temperature. It consists of two main stages: UASB reactor (120 L); and a hybrid MBR posttreatment (56 L) composed of an anoxic chamber (36 L), aerobic compartment (8 L) and a aerated ultrafiltration chamber (12 L). The UASB contains anaerobic granular biomass, the anoxic and aerobic compartments contain Biochip carriers (20% of working volume), while flocculent biomass flows along the different MBR compartments thanks to the recirculation stream. The membrane chamber contains an ultrafiltration module Zenon ZW-500M-4M. The plant was fed with a mixture of low strength primary treated sewage of the STP and a concentrated medium that contained skimmed milk as extra COD supply and sodium bicarbonate as alkalinity source to ensure the stability of the anaerobic stage. In addition,a mixture of OMPs was added to the feed.

Analytical methods

Conventional parameters. Conventional pollutants (COD, N species, suspended solids, etc.) were determined according to the Standard Methods, and monitored twice a week.

Organic micropollutants. A selection of eight antibiotics was carried out according to the compounds included in the different EU Watch Lists: sulfamethoxazole (SMX), trimethoprim (TMP), erythromycin (ERY), roxithromycin (ROX), azithromycin (AZI), clarithromycin (CLA), ciprofloxacin (CIP). In addition, due to the presence of β-lactam resistances across WWTP in Southern Europe (Cacace et al., 2019), also cefalexin (CFX) was considered. Samples were preconcentrated and analysed according to the methodology presented by Alvarino et al., 2015. Three sampling campaigns were carried out.

Antibiotic resistance genes. A group of ARGs was selected according to their presence in the same WWTP in recent studies (Quintela-Baluja et al., 2019). DNA extractions were performed employing a commercial kit (NucleoSpin Microbial DNA). ARGs were analysed in a SmartChip qPCR (Resistomap). Three sampling campaigns were carried out for biomass samples and two campaigns for liquid streams.

RESULTS AND DISCUSSION

General results

The system was operated for 186 d treating 227.7±8.5 L d^{-1} of primary sewage. HRT was maintained at 12.7±0.5 h in the UASB and 5.9±0.2 h in the MBR posttreatment. Influent sewage contained 540±148 mg COD L^{-1} and 34.9±4.2 mg N L^{-1}. The treatment process obtained a permeate with 12.1±4.8 mg COD L^{-1} and 7.3±2.0 mg N L^{-1}, fulfilling the legal requirements. A 78±9 % removal of the influent COD was achieved in the anaerobic stage. In the MBR posttreatment, nitrogen and dissolved methane maximum removal rates were 124.91 mg N L^{-1} d^{-1} and 119.12 mg CH_4 L^{-1} d^{-1}. The removal efficiencies achieved for these compounds were 78.1±2.5 and 55.8±6.7 % respectively. The obtained results are similar to those observed in a previous study with synthetic wastewater (Silva-Teira et al., 2017).

OMP removal

OMP removal efficiencies achieved are presented in Figure 1. As expected, compounds such as TMP and CIP were mainly removed in anaerobic stage, while others like ERY and CLA were mostly removed in the anoxic/aerobic posttreatment. The overall removal efficiencies are slightly lower than those found in a previous work (Alvarino et al., 2019). In this research, the same system treating synthetic wastewater, at higher metabolic activities than this work: 1020 mg COD L^{-1} d^{-1} (UASB) and 143 mg N L^{-1} d^{-1} (MBR) compared to 786 mg COD L^{-1} d^{-1} (UASB) and 125 mg N L^{-1} d^{-1}. This reduction in the metabolic activity could explain the lower efficiency removal of some compounds found in this research.

ARGs assessment

ARGs analysis showed a different distribution of the ARGs in liquid streams compared to biomass. For biomass samples (Figure 2a), an increase in the concentration of some ARGs (macrolides and TMP) was observed when operating with real sewage. In water samples (Figure 2b), a 1.78 log reduction of the discharge was achieved in the second sampling campaign. Some genes were persistent across the process, like sulphonamide resistant genes *sul1* and *sul2*. This persistence was observed in other MBRs, where the ARGs content in the permeate was related to extracellular DNA (Le et al., 2018).

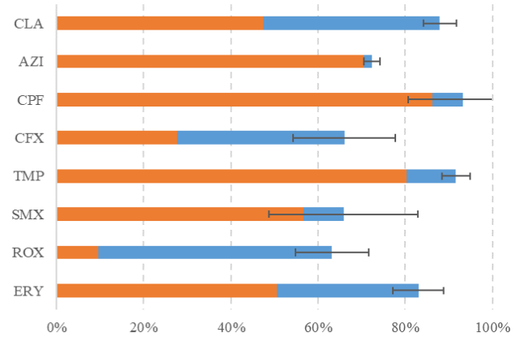

Figure 1. Removal efficiencies of the selected OMPs in the two main stages of SIAM.

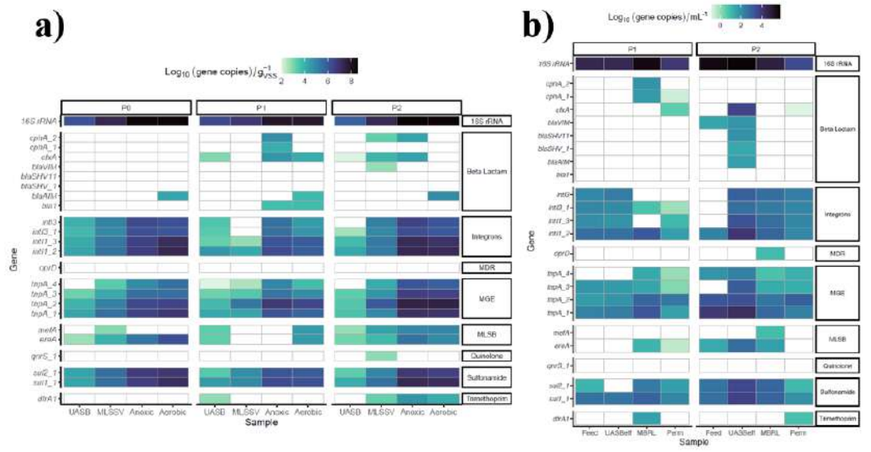

Figure 3. Heatmap of ARGs detected and quantified in the different biomass conformations a) and liquid streams b) for each sampling campaign.

ACKNOWLEDGMENTS

This research was supported by the Spanish State Research Agency (EEA) through ANTARES (PID2019-110346RB-C21) and PRESAGE (PCI2021-121990) projects.

REFERENCES

Alvarino, T. et al. 2019. *Science of the Total Environment*, *671*, 165–174.
Alvarino, T. et al. 2015. *Water Research*, *68*, 701–709.
Alvarino, T. et al. 2018. *Science of the Total Environment*, *615*, 297–306.
Cacace, D., et al. 2019. *Water Research*, *162*, 320–330.
Karkman, A. et al. 2018. *Trends in Microbiology*, *26*(3), 220–228.
Le, T. H. et al. 2018. *Water Research*, *145*, 498–508.
Lorenzo-Toja, Y. et al. 2016. *Science of the Total Environment*, *566–567*, 468–479.
Manaia, C. M. et al. 2018. *Environment International*, *115*(April), 312–324.
Phoon, B. L. et al 2020. *Journal of Hazardous Materials*, *400*(May), 122961.
Quintela-Baluja, M. et al. 2019. *Water Research*, *162*, 347–357.
Silva-Teira, A. et al. 2017. *Chemical Engineering Journal*, *326*, 970–979.

Bioreactors for immobilized fungus: Application to long-term continuous pesticides removal by *Trametes versicolor*

M. Sarrà*, E. Beltran-Flores*, K. Hu**, P. Blánquez*, G. Caminal***

* Department of Chemical, Biological and Environmental Engineering, Universitat Autònoma de Barcelona, Escola d'Enginyeria, Campus Bellaterra 08193 Cerdnyola del Vallès, Spain
(E-mail: Montserrat.Sarra@uab.cat, Eduardo.Beltran@uab.cat, Paqui.Blanquez@uab.cat)
** College of Food Science, Sichuan Agricultural University, Ya'an, Sichuan 625014, People's Republic of China. (E-mail: kaidi666@outlook.com)
*** Institut de Química Avançada de Catalunya (IQAC), Spanish Council for Scientific Research (CSIC). Jordi Girona 18-26, 08034 Barcelona, Spain
(E-mail: gcsqbp@iqac.csic.es)

Abstract
White-rot fungi are versatile in degrading a wide broad of xenobiotic pollutants, but the main problem encountered to real application is the maintenance of the fungal activity over a long period. Immobilization on wood has proven to be a suitable strategy for nutrient supply to the fungus, while reducing the competition with indigenous microorganisms. In this study, the performance of two bioreactors (trickle-bed reactor and rotary drum reactor) filled with colonized holm oak wood chips by *Trametes versicolor* was assessed during a continuous treatment for the removal of pesticides from agricultural wastewater during more than 6 months. The stablished consortia allowed to obtain high removal levels during the entire experimental period.

Keywords (maximum 6 in alphabetical order)
Continuous treatment, Bentazone, Diuron, Rotary drum bioreactor, Trickle-bed bioreactor, Wood chips.

INTRODUCTION

Pesticides are essential to ensure pest control and food production worldwide. Nevertheless, the growing occurrence of pesticides in water resources has become an emerging concern due to their persistence, bioaccumulation and toxicity to human beings and the environment, even at low concentration. Although pesticides are xenobiotic pollutants, bioremediation by white-rot fungi (WRF) can be a promising alternative due to its non-specific intracellular and extracellular enzymatic system, which is able to biodegrade a wide range of persistent organic pollutants including pesticides. Nevertheless, some drawbacks of fungal treatment need to be overcome for full application in a continuous treatment process, such as the maintenance of the fungal metabolic activity and the bacterial competition for nutrients (Mir-Tutusaus et al., 2018).

The fungal degradation of recalcitrant compounds is carried out co-metabolically, which requires nutrient supply, usually a carbon source such as glucose, but this promotes the indigenous microorganism competence by losing fungal biomass and reducing fungal activity. Immobilization of the fungus on lignocellulosic materials, such as wood, is a promising strategy to retain fungal biomass and support fungal growth.

A comparative study between two reactors configurations with *Trametes versicolor* immobilized on wood chips, a trickle-bed reactor (TBR) and a rotating drum bioreactor (RDB), was carried out to assess the continuous treatment of agricultural wastewater spiked with diuron and bentazone during more than six months of operation with a hydraulic retention time of 3 days. In addition to the removal, the key aspect is the persistence of the fungus in the bioreactor during long-term operation, among other practical issues to consider for scaling up the agricultural wastewater treatment, such as the contact time between the fungus and the water to be treated.

MATERIALS AND METHODS

Agricultural wastewater (AW) was collected from an irrigation channel located in Gavà, Parc Agrari Baix Llobregat, corresponding to the Llobregat River Basin (Catalonia, Spain), and stored at 4 ºC until use. To assess the removal capacity of the system by HPLC, AW was spiked with diuron and bentazon, reaching influent concentrations up to 8.43 ± 1.81 mg L^{-1} and 9.51 ± 2.02 mg L^{-1}, respectively.

The TBR was set up with four identical cylindrical methacrylate columns (Ø 11.7 cm, L 50 cm) that were filled with fungal colonized helm oak wood chips and then joined together. At the top of the reactor, fortified AW was loaded into the packing bed through a rotary distributor, and then collected in the reservoir tank placed at the bottom part, in which the liquid volume was kept at around 3.6L. The total height, from the reservoir tank to the distributor, was 2.65 m. The working volume of the packing bed was approximately 17.2L, with a porosity as 60%. The tank was equipped with a stirrer and a pH controller through which the pH of collected water was maintained at 4.5 by adding either 1M HCl or 1M NaOH. Air was introduced from the bottom of the reactor, thereby providing an aeration rate of approximately 0.5L min^{-1}. An external bottom-up recirculation loop was provided with a recirculation ratio between 71 - 284, and new spiked AW was also added via a peristaltic pump, reaching a continuous process with a hydraulic retention time (HRT) of 3 days (Fig. 1).

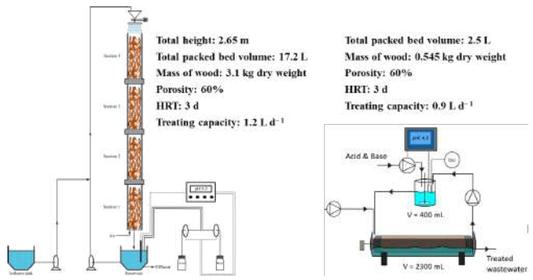

The RDB was constructed with a methacrylate tube supported on a polyvinylchloride gutter. The wastewater was contained within the channel while the colonized wood chips were placed inside the tube. The inner tube contained 1100g DW of colonized wood (2.2g DW·L^{-1} of fungal biomass). Approximately 30 % of the biomass was submerged in the liquid phase, while the rest was in direct contact with air. The inner tube was connected to an electric motor that rotated to alternate the submerged biomass fraction. The RDB was continuously fed with fortified AW to reach 3 days of HRT and a recirculation ratio of 5. The pH was automatically controlled at 4.5 by adding either 1 M HCl or NaOH (Fig.1)

Figure 1. Schematic representation of the TBR and RDB for continuously treating agricultural wastewater spiked with diuron and bentazone during more than 6 months.

RESULTS AND DISCUSSION

Immobilization of *T. versicolor* on wood can be a beneficial option for the treatment of pesticide-contaminated water, in which not only the immobilized biomass amount but also the contact time between the immobilized biomass and liquid phase represent a key factor.
For the TBR, the total contact time is positively related to the recirculation flow rate, but practical concerns such as energy cost, pump workload, biomass washing out, etc. should be taken into consideration. The recirculation rate (RR) is defined as the ratio between recirculation flow rate and the influent flow rate. During the treating process 4 periods were stablished with 3 different RR (71, 142 and 284) with contact times of 5.0, 6.72 and 9.04 h, and liquid hold-up rate of 1.32, 1.78 and 2.39, respectively for a 3 days HRT. Figure 2 shows the removal during the long-term operation with an average removal of 80% and 63% for diuron and bentazone, respectively.
After 186 of operation, fungal biomass increased 4-fold from the initial concentration therefore oak wood was able to support fungal growth in the reactor without nutrient addition. But fungal growth essentially led to enhancing the compactness of packing bed, and it easily caused clogging issue on day 130 of treatment, when it was necessary to reconstitute the packing bed. On the contrary, the bacterial contamination remained low enough to rise the predominance of the fungus *T. versicolor*. This fact overcomes one bottleneck of the fungal treatment which is the bacterial contamination and the consequent reduction of fungal degradation activity (Hu et al., 2022).
The analysis of the fiber content in lignocellulosic carrier evidenced that the consumption rate was constant to 0.35gDWd^{-1} (11% of wood mass/month), suggesting that the packing bed would need to be renovated every 6 months because the lignocellulosic carrier wood would become exhausted.

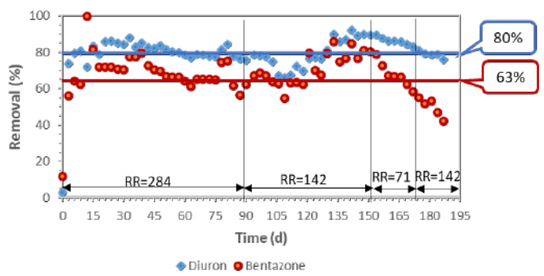

Figure 2. Time-course of the bentazone and diuron removals during the long-treatment in the TBR with an HRT of 3 days.

For the RDB, part of the fungus (approximately 30 %) was submerged in the water and might be limited in dissolved oxygen, hence the fraction of submerged biomass had to be alternated by rotating the inner tube. Two different rotation frequencies were used for each period, 1.5 turns every 4 h and every 24 h for the first and second periods, respectively. Fig. 3 shows the removal during long-term operation in the RDB. Compared to TBR, the average removals of diuron and bentazone were substantially lower in RDB, although this fact was mainly attributed to the lower biomass amount used in the latter case. Fig. 3 also shows that reducing the rotation frequency of the inner tube in the RDB had a positive effect in terms of diuron and bentazone eliminations, maintaining more stable removal yields throughout the second period. This more stable removal was related to a better biomass immobilization on the wood, which reached a 3-fold higher fungal content by the end of the second period compared to the first period. The higher abundance of *T. versicolor* in the second period also contributed to keeping bacterial growth under control. Wood fiber consumption was approximately 1 % wood/month, i.e. substantially lower than that in the TBR, which was associated with the lower *T. versicolor* content present in the RDB (Beltran-Flores, 2022)

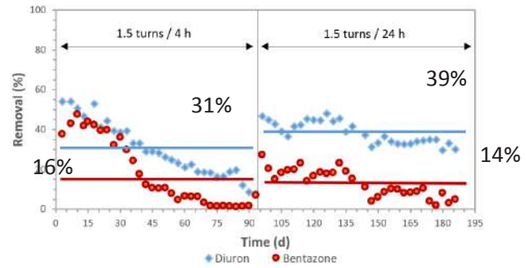

Figure 3. Time-course of the bentazone and diuron removals during the long-treatment in the RDB with an HRT of 3 days.

Table 1. Advantages and limitations of two reactor configurations for the removal of pesticides with fungi immobilized on wood chips.

Trickle bed reactor	
Advantages	**Drawbacks**
✓ Great operational flexibility ✓ Promotes fungal growth ✓ Nature conditions emulated ✓ No oxygen limitation	× Short contact time × Low mass transfer × Risk of clogging × Very high pumping energy × Lack of homogeneity
Rotary drum bioreactor	
Advantages	**Drawbacks**
✓ Reduced bioreactor volume ✓ Low energy demand ✓ Low fungal growth ✓ Low biomass/water relationship ✓ Adaptable for on-site application	× Only 1/3 biomass submerged × Possible oxygen limitation × Required recirculation to maintain homogeneity × Biomass detachment at high rotation speeds

REFERENCES

Beltran-Flores E., Pla-Ferriol, M., Martínez-Alonso, M., Gaju, N., Blánquez, Sarrà M. 2022 Fungal bioremediation of agricultural wastewater in a long-term treatment: biomass stabilization by immobilization strategy. Journal of Hazardous Materials, **439**, 129614

Hu, K, Caminal, G, Sarra, M. 2022. Oak wood provides suitable nutrients for long-term continuous pesticides removal by *Trametes versicolor* in a pilot plant trickle bed reactor. Journal of Cleaner Production, **380**, 135059

Mir-Tutusaus, JA, Baccar, R, Caminal, G, Sarrà, M 2018 Can white-rot fungi be a real wastewater treatment alternative for organic micropollutants removal? A review, Water Research, **138**, 137-151

Effect of HRT and dissolved oxygen on the fate of pharmaceuticalcompoundsandantibioticresistance genes in a high-rate activated sludge reactor

C.Martín-Medrano*,L.González-Gil**,S.Balboa*,J.M.Lema*andM.Carballa*

*CRETUS,DepartmentofChemicalEngineering,UniversidadedeSantiagodeCompostela, 15782 Santiago de Compostela, Spain (E-mail: cinta.martin.medrano@usc.es; sabela.balboa@usc.es; juan.lema@usc.es; marta.carballa@usc.es)

**DefenseUniversityCenter,SpanishNavalAcademy,PlazadeEspaña,36920,Marín,Spain (E-mail: lorena.gonzalez@cud.uvigo.es)

Abstract

High-Rate Activated Sludge (HRAS) reactors could become key units in novel wastewater treatment plants (WWTP) to achieve a net or even positive energy balance. Apart from energy concerns WWTPs must also focus on removing organic micropollutants (OMPs), especially pharmaceutical compounds. Additionally, avoiding the spread of antibiotic resistant genes (ARGs) should also be addressed. HRAS processes are based on high food-to-microorganism ratios, thus they usually operate at low hydraulic retention times (HRT) and low oxygen concentrations(DO). In this contribution it is hypothesized that these operational conditions might affect the biotransformation efficiency of OMPs and the development of ARGs in HRAS reactors. Therefore, in this study, we aim to fill this gap by assessing the fate of OMPs and ARGs in HRAS reactors operating at different DO levels and HRT.

Keywords

Antibioticresistancegenes,emergingcontaminants,high-rateactivatedsludge, organic micropollutants, wastewater

INTRODUCTION

High-Rate Activated Sludge (HRAS) reactors followed by nitrogen removal through partial nitritation and anammox processes are expected to be part of the next generation wastewater treatment plants (WWTP), substituting the conventional treatmentcomposed of a primary clarifier plus an activated sludge unit. The main advantages are the higher quality of the effluent and the increase in the energy efficiency of the plant, since the HRAS systems require less aeration and maximizes the production of sludgeto be transformed into biogas (Taboada-Santos etal., 2020). However, this novel treatment scheme will have to face new challenges, such as the increasing presence of emerging pollutants in wastewater; namely, organic micropollutants (OMPs) and antibiotic resistance genes (ARGs). Unfortunately, the information regarding the behaviour of OMPs in HRAS units is still very limited (Koumaki etal., 2021; Taboada- Santos et al., 2020), and unknown in the case of ARGs.

The objective of this study is to elucidate the influence of two key operational parameters of HRAS systems (i.e., hydraulic retention time -HRT- and dissolvedoxygen levels - DO) in the fate of OMPs and ARGs to find a proper strategy for their mitigation.

MATERIALSANDMETHODS

DescriptionandoperationalconditionsoftheHRASunits

Two HRAS lab-scale systems (2 L reactor + 1 L sedimentation tank) were inoculated with biomass from a conventional activated sludge reactor and operated for ~ 5 months at room temperature, which varied between 18 and 23 ºC. The sludge retention time (SRT) in both HRAS reactors (R1 and R2) was kept at around 4 d. Aeration was monitored and controlled so that the reactors operated at different levels of dissolved oxygen (DO):it was set at a low concentration (1 mg O_2/L) in R1, while in R2 it was maintained at an average value of 6 mg O_2/L (near saturation). The 5-month operationof each HRAS system was divided in 4 periods with different HRT (12 h, 8 h, 4 h and 2 h) to assess the effect of this parameter and DO in the fate of OMPs and ARGs.

The biological reactors were continuously fed with real sewage, taken from the municipal WWTP of Santiago de Compostela (Spain) after the pretreatment step (just before entering the primary clarifier). Due to dilution during rainy periods, the real sewage was supplemented with a mixture of sodium

le 1. List of OMPs spiked into the reactors feeding.

:i-inflammatories (10 µg/L)	Antibiotics (10 µg/L)	Psychiatric drugs (10 µg/L)	Hormones (1 µg/L)
profen (IBP)	Sulfamethoxazole (SMX)	Carbamazepine (CBZ)	Estrone (E1)
›roxen (NPX)	Trimethoprim (TMP)	Diazepam (DZP)	Estradiol (E2)
lofenac (DCF)	Erythromycin (ERY)	Fluoxetine (FLX)	Ethinylestradio
	Roxithromycin (ROX)	Citalopram (CTL)	(EE2)
	Ciprofloxacin (CIP)		
	Azithromycin (AZI)		
	Clarithromycin (CLR)		
	Cefalexin (CEF)		

acetate, acetic acid, yeast extract and several macronutrients to reach a minimum COD concentration of 400 mg O_2/L. Moreover, the reactors feeding was spiked with 18 OMPs (Table 1) including different families of pharmaceutical compounds typically found in WWTPs (Verlicchi etal., 2012).

OMPsandARGssamplingstrategy

Each operational period started with 2 – 3 stabilisation weeks, after which a sampling campaign was carried out. During this week of sampling, triplicate samples were taken in three consecutive days for OMPs and ARGs analyses. Figure 1 shows a scheme ofthe HRAS reactors with the different sampling points for each analysis.

Considering the low sorption coefficients of the selected OMPs and the low concentration of solids in the influent and effluent, OMPs were only measured in the liquid phase of the influent and effluent. Besides, OMPs were measured in the solid purge sludge. To conduct the OMP mass balance in the system, the concentration of OMP in the solid fraction of the reactor sludge was assumed equal to that in the solid purge sludge.

ARGs were determined in the influent and effluent samples, both in liquid and solid phases to study its distribution between both fractions. To further assess the effect of sedimentationonARGsfate,theyweredeterminedinthesolidphasesofthereactorand purge samples.

Analyticalmethods

Conventional parameters. The reactor performance was monitored twice per week in terms of pH, TS, VS, TSS, VSS, COD, NH_4^+, NO_2^- and NO_3^- collecting samples from the influent and effluent and analysing them according to the Standard Methods by triplicate. Sludge from the purge and samples from the reactor were characterised every week in terms of TSS and VSS. Temperature and pH were daily monitored inside the reactor while DO was continuously monitored.

Organic micropollutants. OMPs analyses in the liquid phase were performed via LC- MS/MS after a preconcentration stage using a solid phase extraction protocol in 6 mL Oasis cartridges as described by(Martínez-Quintela etal., 2021). Solid samples were freeze-dried, and after an extraction step, the analytical procedure of liquid samples was applied.

Antibiotic Resistance Genes. ARGs quantification was performed for influent, effluent, reactor and purge samples.Different concentration protocols were followed. Briefly, for reactor and purge samples, 50 mL were collected and centrifuged to obtain a dry pellet was obtained, the extraction Influent (1 L) and effluent (2 L) samples were pre-filtered and subsequently concentrated in dialyzers (Rexeed-25A) and polyamide 0.2 µm filters. DNA extraction from concentrated samples was performed employing a commercial kit (NucleoSpin Microbial DNA) and quantified. ARGs quantification was performed on a SmartChip™ Real-Time PCR by Resistomap (Helsinki, Finland) on a Cycler

RESULTS

HRAS performance

The first two operational periods were carried out at a HRT of 12 h and 8 h (days 1 – 70 and 71 – 90, respectively). The third campaign (HRT 4 h) is ongoing (days 114 – 144) andwillbefollowedbythefourthandlastperiodwithanHRTof2h(expectedondays 145 – 166).

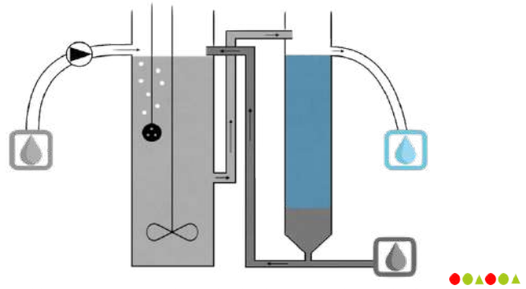

OMP,liquid OMP, solid ARG, liquid ARG, solid

A stable operation was achieved in both reactors during the first two operationalperiods, reaching total COD removals of 80 – 90%, (Figure 2). Soluble COD removal varied between 75 – 95% for both reactors. Low nitrification values were observed through the operation (<1% NO_3^- and <5% NO_2^-). VSS were maintained during the first operational period at 1200 and 1500 mg/L in R1 and R2, respectively. During thesecond period, biomass concentration increased up to 1800 and 2400 mg/L in R1 and R2, respectively.

Figure1.SchemeoftheHRASreactorswithsamplingpointsforOMPsandARGs analyses.

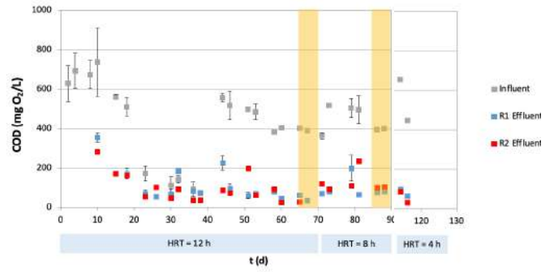

Figure ARGs analyses are in yellow.

Fateof OMPsand ARGs

Samples from the two first sampling campaigns have been processed, but unfortunately the results are not available yet. The last two sampling campaigns will be conducted in February. The data gathered will contribute to confirm some of the following hypotheses:

- **A reduction on HRT could reduce OMPs elimination as microorganisms do not have enough time to biotransform the, or either improve OMPs elimination as microbiological activity increases with a higher food to microorganism (F/M) ratio.**
- **A higher aeration could lead to a faster oxidation, increasing OMPs elimination, although the presence of different microbial communities would suggest alternative metabolic mechanisms that could also alter biotransformation efficiencies.**

Likewise, we expect to establish the effect of these parameters (HRT and DO) on the development of ARGs and determine its relationship with the fate observed for OMPs.

ACKNOWLEGGMENTS

This research was supported by the Spanish Research State Agency (AEI) through ANTARES (PID2019–110346RB-C21) project.

REFERENCES

Koumaki, E., Noutsopoulos, C., Mamais, D., Fragkiskatos, G., & Andreadakis, A. (2021). Fate of Emerging Contaminants in High-Rate Activated Sludge Systems. *International journal of environmental research and public health*, *18*(2).

Martínez-Quintela, M., Arias, A., Alvarino, T., Suarez, S., Garrido, J. M., & Omil, F. (2021). Cometabolic removal of organic micropollutants by enriched nitrite- dependent anaerobic methane oxidizing cultures. *Journal of Hazardous Materials*, *402*.

Taboada-Santos, A., Behera, C. R., Sin, G., Gernaey, K. V., Mauricio-Iglesias, M., Carballa, M., & Lema, J. M. (2020). Assessment of the fate of organic micropollutants in novel wastewater treatment plant configurations through an empirical mechanistic model. *Science of the Total Environment*, *716*, 137079.

Verlicchi, P., Al Aukidy, M., & Zambello, E. (2012). Occurrence of pharmaceutical compounds in urban wastewater: Removal, mass load and environmental risk after a secondary treatment-A review. *Science of the Total Environment*, *429*, 123-155.

Combining Thermophilic Aerobic Reactor (TAR) with Mesophilic Anaerobic digestion (MAD) to improve sludge reduction and pharmaceuticals degradation

Y. Bessiere*, B. Gonzalez Vasquez*, G. Perreira Pantoja*, S. Dubos*, M. Asadi*, M. Bounouba*, L. Cavaillé**, I. Gonzalez-Salgado*, E. Paul*

* TBI, Université de Toulouse, CNRS, INRAE, INSA, Toulouse, France
(E-mail: *ybessier@insa-toulouse.fr; b_gonzal@insa-toulouse.fr; pereira-pant@insa-toulouse.fr; sdubos@insa-toulouse.fr; asadi@insa-toulouse.fr; paul@insa-toulouse.fr*
** SAPOVAL, 51 Rue Isaac Newton 81000 Albi (E-mail*: laetitia.cavaille@sapoval.fr*)

Abstract

A combination of thermophilic aerobic reactor (TAR) with mesophilic anaerobic digestion (MAD) was evaluated for its capacity to enhance the sludge reduction, increase the methane production and improve the efficiency of micropollutant biodegradation when applied to a primary sludge obtained after decantation of urban wastewater.

Higher elimination of organic matter was achieved in MAD-TAR (76% for VSS) compared to conventional MAD (47%). Nevertheless, the measured methane production was comparable for the two processes showing either a contribution of micro-aerobic degradation or a loss of diluted methane in the gas flow.

The removal efficiency of pharmaceutical compounds obtained in the two configurations was compared. The highest removal rates were reported for caffeine (CAF) and sulfamethoxazole (SMX) (>89%) with no significant differences between both processes. MAD-TAR increased significantly the removal for oxazepam (OXA) (73%), propranolol (PRO) (61%) and ofloxacine OFL (41%) and slightly for diclofenac (DIC) (4%) and 2 hydroxy-ibuprofen (2OH-IBP) (5%).

Keywords

Activated sludge treatment; mesophilic anaerobic digestion; pharmaceutical compounds; sludge reduction, thermophilic aerobic reactor;

INTRODUCTION

Wastewater treatment plants (WWTP) are energy-consuming facilities. Management of digested sludge (often referred to as "biosolids") represents a large percentage of a WWTP's operational expenditures, up to 40 %. Anaerobic digestion (AD) reduces the organic matter content of sludge by 40 and 50% and plays a very positive role in the energy independence and the economic balance. Combined with pre- or post-treatment, it enhances the stabilization of sewage sludge and reduces pathogens and odor emissions. Therefore, AD is seen as one of the most sustainable options for sludge treatment. Unfortunately, most conventional AD systems still produce copious amount of biosolids due to limitation in sludge degradation. Advanced Anaerobic Digestion (AAD) has been proposed to create higher quality biosolids and more biogas through higher volatile solids reduction (Guo *et al.* 2013). For example, thermal pre-treatment at high temperature (around 160°C) showed a substantial sludge reduction and increase in biogas (Barber, 2016). However, a significant production of refractory compounds is observed leading to exceeding the standard values for the COD and TKN.

Over the last twenty years, various studies have quantified concentrations and occurrences of pharmaceutical compounds in WWTPs. Depending on the physicochemical properties of the molecules, a significant fraction can adsorb onto the sludge. The evaluation of the degradability of pharmaceutical molecules during digestion is essential for later recovery and valorization of digestates. However, although various studies have investigated the fate of pharmaceutical compounds in the water sector, their behavior during anaerobic digestion has been little studied. In addition, innovation on the process is still needed to improve the degradation of these compounds. Various thermal, chemical and enzymatic processes are known to improve the removal of recalcitrant organic matter (Paul and Liu, 2012). Among all these processes, micro-aeration pretreatment has shown interesting enhancement of particulate matter hydrolysis and substrate solubilization (Johansen *et al.* 2006).

In this work, a combination of two processes, a thermophilic aerobic reactor (TAR) with a mesophilic anaerobic digestion (MAD) is evaluated for its capacity to enhance the sludge reduction, increase the methane production and improve the efficiency of adsorbed micropollutant biodegradation.

MATERIALS AND METHODS

Reactors. The experimental set-up composed of a mesophilic anaerobic digester (MAD) coupled with a thermophilic aerobic digester (TAR). The MAD is a 260 L tank with an agitator and a double jacket connected to the TAR by means of an ALBIN peristaltic recirculation pump (type ALH15), whose flow rate was fixed at 100 $L.h^{-1}$. The TAR, with a volume of 40 L, was also equipped with an agitator and a double jacket. The aeration of the TAR was operated discontinuously to provide a dissolved oxygen concentration, measured by VisiFerm™ DO optical sensor (Hamilton) between 0.2 and 0.5 $mg.L^{-1}$. The two reactors were heated by two independent cryostats in order to maintain the temperatures suitable for aerobic thermophilic (55 °C) and anaerobic mesophilic (35 °C) processes.

The feed was performed with a primary sludge obtained after decantation of urban wastewater (WW) and the duration of feeding, withdrawal and recirculation were adjusted to maintain a total SRT of around 20 days and a residence time in the TAR of 1 day.

Analysis. To evaluate the performances of the two studied processes, daily-composite samples of primary and digested sludge were collected regularly during steady-state periods. Sludge samples were stored at 4 °C and analyzed on the same day. In addition, aliquots of the total and dissolved fractions (obtained after 4500 g centrifugation for 15 minutes) were stored at -20 °C for micropollutants analysis.

The sludge and the supernatants were characterized by Total Suspended solids (TSS), Volatile Suspended Solids (VSS) and Chemical Oxygen Demand (COD).

The degradation of nine compounds (caffeine CAF, ofloxacin OFL, sulfamethoxazole SMX, propranolol PRO, carbamazepine CBZ, oxazepam OXA, diclofenac DIC, ibuprofen IBP and 2 hydroxy-ibuprofen 2OH-IBP) was evaluated. Quantification of micropollutants was performed by UHPLC-MS-MS following a modified QuEChERS extraction.

RESULTS AND DISCUSSION

Performances of digestion

Although the feeding showed fluctuations, as can be expected when working with real WW, the VSS and COD_s concentrations after digestion remained constant with standard deviation below 4%. Considering comparable operating conditions, higher elimination of solid organic matter was achieved in the hybrid MAD-TAR system (around 76% for VSS) compared to the mesophilic one (around 47%) confirming lab results obtained a few years ago (Dumas et al., 2010). Operational conditions and main results are reported in Table 1 and figure 1.

Table 1. Methanisation performance

Operational conditions	MAD	MAD-TAR
OLR ($kgCOD/m^3/day$)	1.2	0.9
OLR ($kgVSS/m^3/day$)	0.8	0.6
SRT (days)	19.6	22.4
Reactor		
TSS (g/L)	11.7±0.5	4.9±0.6
VSS (g/L)	8.3±0.4	3.4±0.4
COD_t (g/L)	14.1±1.4	5.7±0.8
COD_s (g/L)	0.37±0.06	0.36±0.08
Removal efficiencies (%)		
COD	46.7	72.9
VSS	47.0	75.7

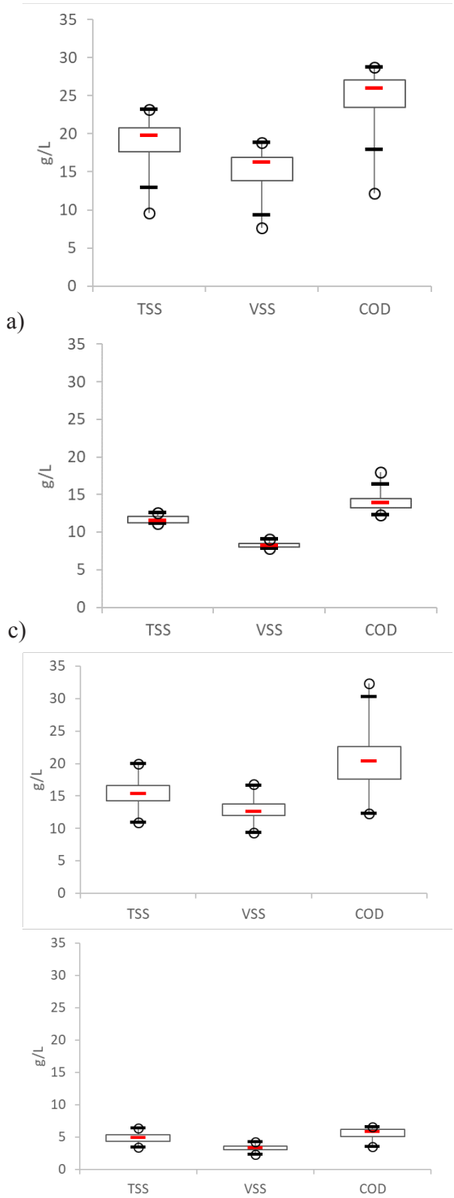

Figure 1. Characteristics of primary sludge (a,c) and digestate (b,d) for MAD (A,b) and MAD-TAR (c,d) configurations., n=17.

Despite the observed sludge reduction, methane production for the hybrid MAD-TAR system was found similar to the one of the conventional MAD. The difference in COD converted to methane could be either due to aerobic degradation or the difficulty to measure methane production in the TAR due to its high dilution in the gas flow. This aspect is still under investigation.

Fate of micropollutants during digestion

All the target molecules were detected and quantified in the primary sludge. Even if some variations have been observed between the two experimental campaigns (-23% in average during the MAD-TAR experiment) the order of magnitude were the same. The highest concentrations of targeted compounds were observed for OFL and CAF (more than 40 µg/L) while medium to low concentrations were reported for SMX, CBZ, PRO, DIC, OXA, IBP and 2OH-IB, around 1.0-10.0 µg/L.

The comparison of removal efficiencies in MAD and MAD-TAR are reported in Figure 1. Compounds placed above the dotted line show better removal efficiency by the innovative process (MAD-TAR) compared to conventional process (MAD). The highest removal rates were obtained for CAF and SMX (>89%) with no significant differences between both processes. The removal of others target compounds was significantly improved by MAD-TAR process. Medium removal ranging between 54% and 75% were observed for OFL and OXA respectively in MAD-TAR compared to only 9% and 49% in MAD. Moreover, while PRO was not removed at all during MAD process, a rate of 69% was achieved in MAD-TAR. DIC and 2OH-IBP present low removal during MADTAR (6-10%) while they were accumulated in MAD. Finally, a negative removal rate was observed for IBP and CBZ in both processes, MAD (-30% and -71%, respectively) and MAD-TAR (-35% and -91%).

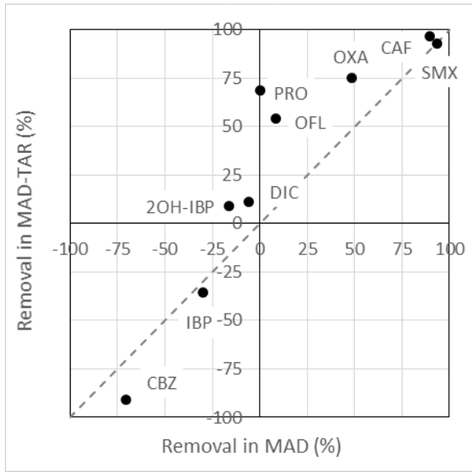

Figure 2. Comparison of compounds removal in conventional vs innovative process

Those experiments are currently being extended to a MAD-TAD (thermophilic anaerobic digestor) hybrid configuration in order to dissociate the respective effects of oxygen and temperature on the removal performances.

ACKNOWLEDGEMENT

This work is part of different projects
- the SMS project "Micropollutant Source Separation for health risks control and preservation of the environment" funded by the Adour-Garonne Water Agency and the French Agency for Biodiversity
- the Ecoval project funded by the Interreg Sudoe Programme through the European Regional Development Fund (ERDF)
- The SAVE project funded by Adour-Garonne and Rhône Alpes Méditérannée Corse Water Agencies, ADEME and Région Occitanie.

REFERENCES

Barber, W.P.F., 2016. Thermal hydrolysis for sewage treatment: A critical review. Water Research **104**, 53–71.

Johansen, J, and Bakke R. 2006. 'Enhancing Hydrolysis with Microaeration'. Water Science and Technology : A Journal of the International Association on Water Pollution Research **53** (February): 43–50.

Guo, W.-Q., Yang, S.-S., Xiang, W.-S., Wang, X.-J., Ren, N.-Q. 2013 Minimization of excess sludge production by in-situ activated sludge treatment processes—A comprehensive review. *Biotechnol. Adv.* 2013, **31**, 1386–1396.

Paul, E., and Liu, Y. 2012. Biological Sludge Minimization and Biomaterials/Bioenergy Recovery Technologies. Wiley InterScience (Online service). Hoboken, N.J.: Wiley InterScience (Online service).

TECHNICAL SESSIONS

T6.

Removal of recalcitrant and emerging pollutants II

ECO STP 2023

Electrochemical degradation of per- and polyfluoroalkyl substances in real waste streams using boron- and borophene-doped graphene sponge electrode

N. Duinslaeger[a], J. Radjenovic[a,b]

[a]Catalan Institute for Water Research (ICRA), c/Emili Grahit 101, 17003 Girona, Spain
(E-mail: nduinslaeger@icra.cat; jradjenovic@icra.cat)
University of Girona, Girona, Spain
[b]Catalan Institution for Research and Advanced Studies (ICREA), Passeig Lluís Companys 23, 08010 Barcelona, Spain

Abstract

Boron- and two-dimensional boron, i.e., borophene-doped graphene sponge anodes were synthesized and applied for the electrochemical oxidation of C4-C8 per- and polyfluoroalkyl substances (PFASs). Borophene-doped graphene sponge was the best performing anode demonstrating removal efficiencies in the range of 30.1-77.1%, obtained in one-pass flow-through mode using low conductivity supporting electrolyte (1 mS cm^{-1}) at 230 A m^{-2} of anodic current density, and with energy consumption of 9.4 ± 0.3 kWh m^{-3}. Moreover, the performance of the borophene-doped graphene sponge was subsequently evaluated using landfill leachate (30 mS cm^{-1}), at higher initial PFASs concentration (2 µM). Enhanced removal % for all target compounds, except PFHxA, were obtained with up to 86.3±7.7% and 71.7±3.0% removal for perfluorooctane sulfonate (PFOS) and perfluorooctanoic acid (PFOA), respectively.

Keywords

Chlorine-free electrochemical system; electrochemical water treatment; PFAS; reduced graphene oxide-coated sponge

INTRODUCTION

Per- and polyfluoroalkyl substances (PFAS) are a class of artificially manufactured compounds which widespread presence in the environment is a topic of major concern for both human health and the environment due to their persistence, bioaccumulation potential, and adverse effects on living organisms. Due to the strength of the C–F bond, currently applied wastewater treatment methods, both conventional and advanced, are not capable of degrading PFASs. Electrochemical oxidation is capable of C-F bond cleavage, but limitations such as high material cost and formation of chlorine, chlorate and perchlorate in the presence of chloride (Radjenovic, Duinslaeger, et al., 2020), are restraining its wider scale application. In our recent study(Duinslaeger and Radjenovic, 2022), we demonstrated that the newly developed boron-doped graphene sponge anode is capable of defluorinating PFAS, while displaying a remarkably low electrocatalytic activity for chloride oxidation, with no chlorate and perchlorate formation, and very low generation of chlorine (i.e., current efficiency of only 0.04% for chlorine production in the presence of 20 mM NaCl)(Baptista-Pires, Norra, et al., 2021). Furthermore, our previous study demonstrated that functionalization of graphene sponge electrodes with two-dimensional (2D) materials can enhance their electrocatalytic activity and modulate the interaction with specific organic contaminants, thus opening new possibilities for designing electrodes tailored to remove specific groups of pollutants(Cuervo Lumbaque, Baptista-Piresa, et al., 2022). In this study, we evaluated the impact of changing to 2D nature of graphene dopant by comparing the performance of boron- and borophene-doped graphene sponge electrode for electrochemical oxidation of six model PFASs, i.e., perfluorooctanesulfonic acid (PFOS), perfluorooctanoic acid (PFOA), perfluorohexane sulfonate (PFHxS), perfluorohexanoic acid (PFHxA), perfluorobutanesulfonic acid (PFBS) and perfluorobutanoic acid (PFBA). The experiments were perfomed using synthetic electrolyte solutions and a highly complex stream of ultrafiltrated (UF) landfill leachate. The obtained results indicate that the developed graphene sponge anode can electrochemically degrade C4-C8 PFAS without forming toxic and persistent organic and inorganic chlorinated by-products.

MATERIALS AND METHODS

Boron- and borophene-doped reduced graphene oxide (RGO) sponge anodes (B-RGO and Bph-RGO, respectively) were synthesized according to the previously published protocols (Cuervo Lumbaque, Baptista-Piresa, et al., 2022), by adding either boric acid or borophene solution to 4 g L^{-1} graphene oxide (GO) dispersion prior to the hydrothermal synthesis method. Borophene solution was obtained through liquid-phase exfoliation from bulk boron (Wang, Li, et al., 2020; Ranjan, Sahu, et al., 2019). All experiments were conducted in a flow-through reactor, operated in one-pass, continuous mode at flow rates of 5 mL min^{-1}. Stainless stell sponge was employed as a flow-through cathode, and leak-free Ag/AgCl as reference electrode. To evaluate possible losses of the target PFASs through adsorption onto the graphene sponge, initial open circuit ($OC_{initial}$) runs were conducted. Electrochemical degradation experiments were conducted in the chronopotentiometric mode at the anodic current density of 230 A m^{-2}. Electrochemical removal of target PFASs was evaluated in synthetic electrolyte solution (10 mM phosphate buffer (PB, 1 mS cm^{-1})) and a highly complex real waste stream of UF landfill leachate (30 mS cm^{-1}), obtained from a near-by landfill in Girona, Spain. In both cases, target PFASs were added at low concentration (0.2 µM) to evaluate their removal, and at higher concentration of 2 µM to evaluate their defluorination. The fluoride, which was determined to be incorporated into the graphene coating due to the high reactivity of the liberated HF (Duinslaeger and Radjenovic, 2022), was quantified using Combustion Ion Chromatography (CIC) of the Bph-RGO anode. At the end of each chronopotentiometric run, the effluent was sampled after the current was switched off (i.e., OC_{final}) to evaluate the loss of the target PFASs due to electrosorption only.

RESULTS AND DISCUSSION

The effluent concentrations were equal to their influent concentrations during the OC_{intial} for the six model PFASs, demonstrating that there was no absorption of PFAS on the graphene sponges or any other part of the reactor. **Figure 1** illustrates the observed removals of the target PFASs at low concentration (0.2 µM) for B-RGO and Bph-RGO in 10 mM PB. Application of 230 A m^{-2} resulted in an average removal efficiency 68.7±2.0% (PFOS), 32.6±5.0% (PFHxS), 26.2±1.8% (PFBS) for the perfluorosulfonic acids (PFSAs) and 41.1±1.5% (PFOA), 23.6±1.9% (PFHxA), 39.4±1.3% (PFBA) for the carboxylic acids (PFCAs). By changing from boron to borophene, the average removal efficiencies were increased for all model PFASs, with 77.1±1.3% (PFOS), 37.5±0.9% (PFHxS), 32.0±1.8% (PFBS) and 57.2±3.1% (PFOA), 30.1±1.7% (PFHxA) and 45.7±2.1% (PFBA) at the same applied current density (230 A m^{-2}). The increase was more pronounced for the perfluorocarboxylic acids (PFCAs) and more prominent with the lengthening of the chain length in the order PFOA>PFHxA>PFBA. This may be a consequence of a lower electrostatic repulsion between borophene active sites and the carboxylic moieties of the PFCAs compared to the perfluorosulfonic acids (PFSAs). In addition, borophene doping was demonstrated to yield an order of magnitude higher concentration of the electrogenerated hydroxyl radicals (OH·) compared with boron-doped graphene sponge anode (Cuervo Lumbaque, Baptista-Piresa, et al., 2022). Electrochemically generated hydroxyl radicals react with PFAS radicals, created after the initial direct electron transfer step from the PFAS to the anode, and assist in the decarboxylation and defluorination. In the OC_{final}, the effluent concentrations for the six studied PFASs rose above their initial concentrations for B-RGO, demonstrating that a fraction of the removed PFAS was only electrosorbed onto the graphene sponge anode and released back into the solution when the current was stopped. The % of the electrosorbed PFASs could be estimated based on the concentrations measured in the fractions in OC_{final} and the total removal efficiencies, and was 35±8.3% (PFOS), 12.1±6.5% (PFOA), 16.1±3.2% (PFHxS), 13.3±3.8% (PFHxA), 13.0±2.6% (PFBS), 7.4±0.5% (PFBA). Thus, the efficiencies of electrochemical degradation for B-RGO were calculated to be 32±4.4% (PFOS), 31.5±9.9% (PFOA), 15.3±6.1% (PFHxS), 10.2±5.9% (PFHxA), 13.7±1.5% (PFBS), and 9.3±1.7% (PFBA). In the case of Bph-RGO, we did not observe any increase in the effluent concentrations of PFAS in the OC_{final}, as they all returned to the initial values immediately after the current was turned off. This suggested that the removed fraction of PFAS was also further electrochemically degraded, evidencing higher electroactivity of the Bph-RGO anode. Doping with borophene lowers the resistance at the electrode-electrolyte interface, increased the material's electrocatalytic activity and enhances the generation of strong oxidants ($HO^{\cdot}$, O_3) (Cuervo Lumbaque, Baptista-Piresa, et al., 2022), thus leading to an improved degradation of the electrosorbed PFAS. The lower resistance at the interface also translates in a decreased overall energy consumption from 10.1 ± 0.7 (B-RGO) to 9.4 ± 0.3 (Bph-RGO) kWh m^{-3}.

Bph-RGO anode was employed for the degradation of single PFAS at high concentration (2 µM) in a real UF landfill leachate (**Figure 2**). For all target compounds, except PFHxA, the removals are higher in landfill leachate. Application of 230 A m^{-2} in 10 mM PB resulted in an ohmic drop-corrected anode potential of 4 V vs Standard Hydrogen Electrode (/SHE), resulted in 59.3±6.2% (PFOS), 53.6±3% (PFOA), 27±2.8% (PFHxS), 36.6±2.6% (PFHxA), 13.5±1.1% (PFBS) and 43.2±1.4% (PFBA) removal of the target PFASs in 10mM PB. We applied an anodic current density of 517.5 A m^{-2} to reach the same ohmic drop-corrected anode potential of 4 V vs Standard Hydrogen Electrode (/SHE) as in the case of 10 mM PB (polarized at 230 A m^{-2}). Despite the complexity of this stream in terms of both organic and inorganic content, we obtained higher removal efficiencies of PFAS, i.e., were 86.3±7.7% (PFOS), 71.7±3.0% (PFOA), 66.9±2.5% (PFHxS), 30.0±3% (PFHxA), 40.5±0.5% (PFBS) and 45.9±8.6% (PFBA). This can be explained by the impact of high leachate conductivity (i.e., 30-fold higher compared to the 10 mM PB). High supporting electrolyte concentration decreases the ohmic drop, minimizes the interfacial impedance between the electrode and the electrolyte, and ensures a more uniform distribution of current in the graphene sponge anode, thus enhancing its electrocatalytic activity. Furthermore, even though the UF leachate concentrate contained □7.3 g L^{-1} of chloride, we did not observe any formation of chlorine, chlorate and perchlorate.

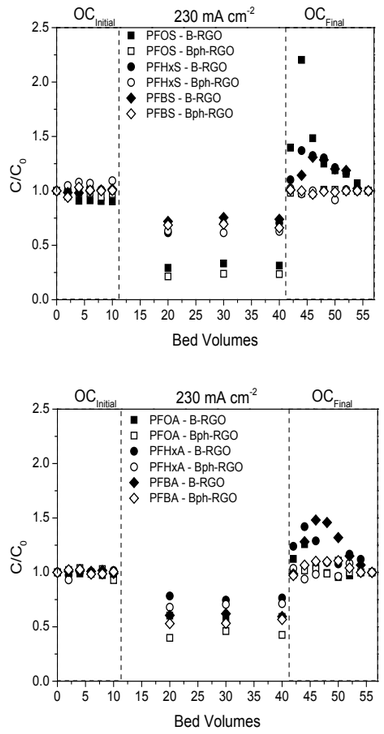

Figure 1. Measured concentrations of perfluorosulfonic acids (PFSAs) (left) and perfluorocarboxylic acids (PFCAs) (right) on B-RGO (full symbols) and Bph-RGO (hollow symbols) normalized to the initial value (C/C0, C0=0.2 µM) at anodic current of 230 A m^{-2} and using a flow rate of 5 mL min^{-1} (i.e., 173 LMH).

As for the determination of defluorination ratios in our previous study (Duinslaeger and Radjenovic, 2022), the Bph-RGO anodes employed for the degradation of individual PFOS and PFOA in both 10mM PB and landfill leachate were subjected to CIC analyses, and the F− concentrations obtained in the combustion of each sponge were used to calculate the fluoride recoveries for both PFASs. The fluoride recoveries in 10mM PB for PFOS (68.6%) and PFOA (81.8%) were comparable to recoveries obtained with B-RGO, 75.3% (PFOS), 74.1% (PFOA). However, in leachate, fluoride recoveries for PFOS and PFOA where 14% and 6.9% respectively. The low recoveries in landfill leachate can be ascribed by the high foam production observed during application of current which negatively impacted the defluorination reaction. The overall defluorination ratio ranged from 40.7±4.2% (PFOS), 43.8±2.5% (PFOA) in 10 mM PB, and 12.1±1.1% (PFOS), 5±0.2% (PFOA) in landfill leachate.

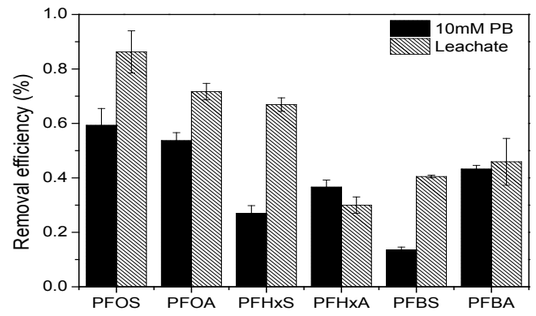

Figure 2. Overall removal efficiency for both perfluorosulfonic acids and perfluorocarboxylic acids in 10mM phosphate buffer (PB) and leachate at 230 A m^{-2} and 517.5 A m^{-2}, respectively.

CONCLUSIONS

In this study we have demonstrated the improved electrochemical removal of six model PFASs when changing from atomic boron to a 2D borophene-doped graphene sponge anode. In the experiments conducted using a Bph-RGO sponge electrode in a low-conductivity supporting electrolyte (1 mS cm^{-1}), and low initial PFASs concentration (0.2 µM), we achieved removal efficiencies with up to 77.1±1.3% for PFOS and 57.2±3.1% for PFOA. The enhanced performance obtained with the introduction of borophene was more pronounced for PFCAs and more prominent with the lengthening of the chain length in the order PFOA>PFHxA>PFBA. We also report an enhanced removal % for nearly all target PFAS in a complex real wastewater matrix, i.e., UF landfill leachate, with 86.3±7.7% and 71.7±3.0% removal observed for PFOS and PFOA respectively. The higher removal % was allocated to the increased electroactivity of the graphene sponge electrode due to the higher conductivity of the electrolytic solution. This study demonstrates that the patented graphene sponge anodes (Radjenović, Baptista-Pires, et al., 2022) effectively enable the degradation of PFAS in high chloride containing streams such as leachate, reverse osmosis concentrate, ion exchange resin regeneration liquids and others. This is a groundbreaking result which opens the door for safe electrochemical treatment of brackish PFAS concentrates using a low cost, easily scalable system.

REFERENCES

Baptista-Pires, 2021, Water Research, 203, 117492.

Cuervo Lumbaque, E., 2022, Chemical Engineering Journal,446, 4, 137057.

Duinslaeger, N. 2022, Water Research, 213, 118148.

Radjenović, J., 2022, European Patent EP3978432A1.

Norra, G. F., 2022, Chemical Engineering Journal, 430, 132772.

Radjenovic, J., 2020, Environ. Sci. Technol., 54, 23, 14815–14829.

Ranjan, P., 2019, 31, 27, 1900353.

Wang, S., 2020, Composites Part A: Applied Science and Manufacturing, 138, 106033.

Yohai, L., 2013, Electrochimica Acta, 102, 88–96.

Assessment of PFAS pathways for environment contamination during landfill leachate treatment

Nicola Lancioni*, Elisa Blumenthal*, Massimiliano Sgroi*, Anna Laura Eusebi*, Giancarlo Cecchini**, Alessandro Filippi**, Alessandro Frugis**, Marco Lazzazzara**, Maria Grazia Asci***, Daniele Matteucci***, Francesco Fatone*.

* Department of Science and Engineering of Materials, Environment and Urban Planning-SIMAU, Marche Polytechnic University (UNIVPM), Via Brecce Bianche, 12, 60131 Ancona, Italy

(E-mail: *n.lancioni@pm.univpm.it*; *m.sgroi@staff.univpm.it)*

** Acea Elabori, gruppo Acea S.p.A., Via Vitorchiano, 165, 00189 Roma, Italy

*** SIMAM S.p.A., gruppo Acea S.p.A., Via Giovanni Cimabue, 11/2, 60019 Senigallia, Italy

Abstract

Per- and poly- fluoroalkyl substances (PFAS), are a group of substances, persistent and potentially dangerous for human health. Landfill leachate contains high concentration of PFAS and may be released into the environment through wastewater treatment plants (WWTPs). Sampling campaigns of three full-scale leachate treatment plants were carried out in Italy, in order to assess the fate of PFASs along the treatment chains. Conventional leachate treatment plants have demonstrated low ability to remove PFAS from landfill leachate. Advanced treatment technologies as reverse osmosis (RO) may provide a permeate "PFAS-free". However, high concentrations of PFAS are found in the treated RO concentrate or in the waste sludges, which resulted important ways for the contamination of the environment by these compounds. Therefore, the development of further technologies is needed in order to reach the aim of "zero pollution".

Keywords (maximum 6 in alphabetical order)

landfill leachate; pathways; per- and polyfluoroalkyl substances; wastewater treatment; zero pollution.

INTRODUCTION

Per- and poly- fluoroalkyl substances, so-called PFAS, are a group of substances, which are used to make fluoropolymers, employed in manufacturing clothing, furniture, adhesives, food packaging. They are persistent and mobile in the environmental medias, and potentially toxic (PM(T)) for human health. Therefore, they are considered among the main obstacles to the development of the circular economy, as the reuse of materials from waste could promote their spread in the environment. The project Horizon2020 PROMISCES (Preventing Recalcitrant Organic Mobile Industrial chemicalS for Circular Economy in the Soil-sediment-water system) aims to identify strategies and solutions for minimizing the occurrence of PFAS in the environment (e.g. surface water and drinking water) as well as in recovered resources (e.g. sludge, wastewater and sediments). The main ambitions of PROMISCES are to contribute to the European ambition of a "toxic free" environment with "zero Pollution" and ensuring the protection of human health during the implementation of circular economy practices. The Italian team partners of the PROMISCES project (UNIVPM, Acea Elabori and Simam) are focusing their research activities on the assessment of PFAS pathways for environment contamination during landfill leachate treatment as well as on the development of sustainable technologies for the separation and destruction of PFAS from sewage sludge and leachate.

Globally, landfills are considered to be one of the major sources of PFAS contamination in the environment. In landfills, PFAS-based products can release these compounds in the leachate and even in the air (ITRC, 2020). It is common practice to discharge landfill leachate, after initial treatment, into municipal wastewater treatment plants. Conventional WWTPs have demonstrated to be ineffective for PFAS removal and the presence of precursors in the influent may lead to an increase of PFAS concentrations in the effluent after biological transformation (Lenka et al., 2021). Thus, PFAS from landfill leachate may be released into the aquatic environment through WWTPs effluents but can also be adsorbed into municipal sewage sludges limiting their agronomic reutilization (Helmer et al., 2022; Fredriksson, et al., 2022).

MATERIALS AND METHODS

Within the context of PROMISCES activities, a first sampling campaign in full-scale leachate treatment plants was carried out in Italy, with the aim of determining the fate of PFAS and its precursors along the treatment chains. A robust and cost-effective methodology for the determination of eighteen target PFAS in complex matrixes, such as leachate, membrane concentrate, and sludge, was developed. Table 1 reports the target PFAS analysed during sampling campaigns and their relative limits of quantification (LOQs) in the investigated matrixes.

Therefore, sampling campaigns for the determination of PFAS fate were implemented in three leachate treatment plants. The first plant includes a conventional treatment with clarifloculation, biologic reactor and ultrafiltration membrane (Figure 1). The second plant is a conventional leachate treatment plant (Figure 2), it is composed of a biologic reactor with intermittent aeration (IA), the waste sludge is digested and dewatered together with municipal sludge of the wastewater treatment plant (WWTP). The last monitored leachate treatment plant (Figure 3) includes several advance treatments: i) pre-treatment sections with flotation and sand filter, ii) double-pass reverse osmosis (RO), and iii) RO concentrate treatment line.

Table 1. Target PFAS analysed (LOQ = limit of quantification)

Target PFAS	LOQ for leachate, concentrate and wastewater	LOQ for sludge	LOQ for permeate
PFBA, PFPeA, PFHxA, PFHpA, PFPeS, PFOA, PFHxS, PFNA, PFHpS, PFDA, PFOS, PFUdA, PFNS, PFDoA, PFDS, PFTrDA, PFTeDA	1.0 µg/L	10 µg/Kg	< 0.015 µg/L

RESULTS AND DISCUSSION

In the leachate treatment plant 1, only the compounds PFBA, PFHxA, PFBS and PFOA were detected in the liquid matrix. The observed concentrations remained more or less constant from the inlet to the outlet of the plant for PFHxA (1.3 µg/L) and PFBS (6 µg/L), whereas the concentration of PFBA and PFOA increased in the effluent suggesting possible release of these substances from sludge or transformation of precursors. Increases were from 1 µg/L to 2.2 µg/L for PFBA, and from 3.3 to 4.1 µg/L for PFOA. In the sludge samples of treatment plant 1 were detected PFBS, PFOA and PFOS. Particularly, PFOS was not detected in the liquid phase. Hence, PFOS may have been absorbed previously in sludge or produced by transformation products. However, release of this compound in the liquid matrix was not observed at concentration higher than LOQ.

In the leachate treatment plant 2, PFBA, PFHxA and PFBS were found in the liquid phase of the leachate at concentration of 3.7, 1.5 and 1.7 µg/L, respectively. In this plant, waste sludges are treated along with the municipal sewage sludge. In this mix of sludge only PFBA was detected at concentration of 11 µg/kg.

The Advanced leachate treatment plant (N°3), which utilize RO treatment, was able to obtain a permeate flux where none of the eighteen target PFAS was detected (LOQ = 15 ng/L). However, the obtained RO concentrate showed a relatively high concentrations of ΣPFAS (97.7 µg/L) and, the implemented concentrate treatment line only partially removed PFAS from the flux (39.8 µg/L). The treated RO concentrate is then discharged into the sewage system together with the RO permeate. Hence, the flux coming from the concentrate treatment line nullified the complete removal of PFAS obtained by RO filtration. Therefore, different treatments of RO concentrate are required for removing per- and polyfluoroalkyl substances and reaching the aim of "zero pollution". Particularly, innovative treatment will be tested within the PROMISCES research activities to obtain the complete destruction/removal of PFAS in RO concentrate.

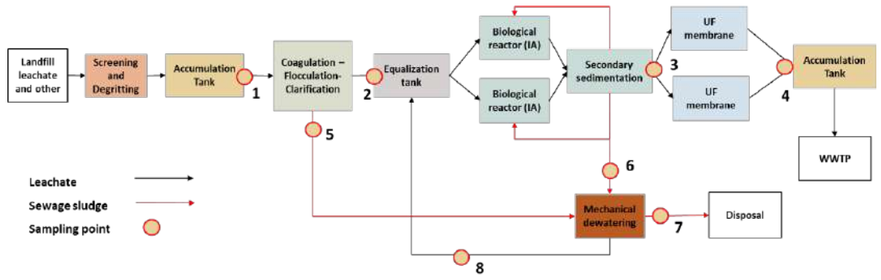

Figure 1. Landfill leachate treatment N°1 (conventional treatment)

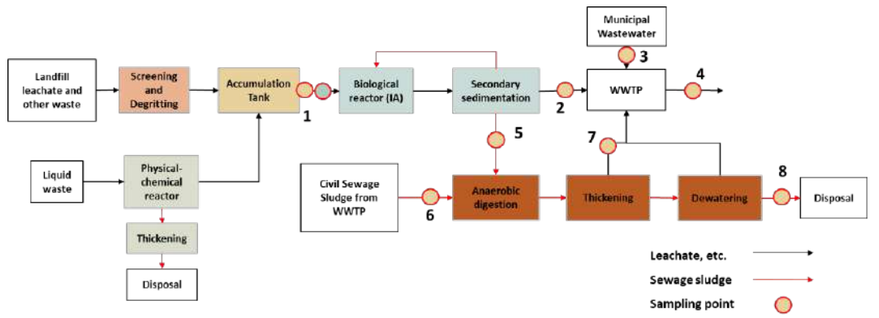

Figure 2. Landfill leachate treatment N°2 (conventional treatment)

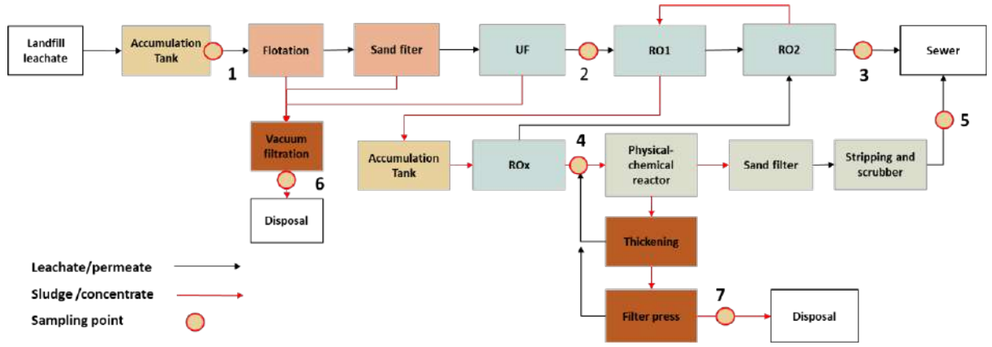

Figure 3. Landfill leachate treatment N°3 (advance treatment)

REFERENCES

Interstate Technology & Regulatory Council (ITRC), updated 2020. PFAS Technical and Regulatory Guidance Document and Fact Sheets PFAS-1. Washington, D.C.: Interstate Technology & Regulatory Council, PFAS Team. [Online]. Accessed Jan 2023

Lenka, S.P., Kah, M., Padhye, L.P. 2021. A review of the occurrence, transformation, and removal of poly- and perfluoroalkyl substances (PFAS) in wastewater treatment plants. *Water Research* **199** (2021) 117187.

Helmer, R.W., Reeves, D.R., Cassidy, D.P. 2022. Per- and Polyfluorinated Alkyl Substances (PFAS) cycling within Michigan: Contaminated sites, landfills and wastewater treatment plants. *Water Research* **210** (2022) 117983.

Fredriksson, F., Eriksson, U., Kärrman, A., Yeung, L.W.Y. 2022. Per- and polyfluoroalkyl substances (PFAS) in sludge from wastewater treatment plants in Sweden - First findings of novel fluorinated copolymers in Europe including temporal analysis. *Science of the Total Environment* **846** (2022) 157406.

PFAS in textile wastewater: an integrated approach to reduce the environmental risk for their mixture

B. Cantoni*, G. Bergna**, E. Baldini***, F. Malpei*, M. Antonelli*

* Department of Civil and Environmental Engineering, Politecnico di Milano, Milan (MI), Italy
(E-mail: *beatrice.cantoni@polimi.it; francesca.malpei@polimi.it; manuela.antonelli@polimi.it;)*
** Lariana Depur s.p.a., Fino Mornasco (CO), Italy (E-mail: g*iovannibergna@lariana.it*)
*** Centro Tessile Serico Sostenibile SRL, Como (CO), Italy (E-mail: *ebaldini@textilecomo.com*)

Abstract

Per- and polyfluoroalkyl substances (PFAS), used in several industrial applications, are gaining increasing concern due to their spread in the environment, their stability and eco-toxicity. To avoid PFAS spread in the environment, reducing the environmental risk on receiving water bodies, removal strategies need to be implemented at both industrial and municipal wastewater treatment plants (WWTP). This study presents a case study in a textile district in northern Italy where PFAS monitoring campaigns were combined with testing at lab and pilot-scale of two promising removal processes (membrane separation, adsorption on activated carbon) and data used for environmental risk assessment. This combination was proved to be useful to support the identification of the optimal combination of prevention and treatment interventions to be applied at different system points to reduce the environmental risk.

Keywords (maximum 6 in alphabetical order)

Adsorption; Environmental risk assessment; Membrane separation; PFAS; Scenarios analysis; Textile Wastewater

INTRODUCTION

Per- and polyfluoroalkyl substances (PFAS) are used in numerous industrial applications, such as in textile manufacturing, for their unique chemical properties. The widespread use of PFAS and their persistence make them ubiquitous compounds of increasing concern due to their eco-toxicity (Lewis et al., 2022). To avoid PFAS spread, both prevention and removal strategies should be implemented at both industrial and municipal wastewater treatment plants (WWTP).
As for the prevention strategies, some studies evaluated the substitution of long-chain PFAS with short-chain ones or with non-fluorinated compounds. As for the treatment of textile industry wastewaters (WW), numerous articles investigated decolorization by several technologies, assessing the removal of dyes or COD from target WW (inter alia, Chollom et al., 2015). However, very few studies can be found on the use of such technologies in removal PFAS in these concentrated streams. Moreover, there are no literature studies comparing PFAS reduction strategies at the sources (i.e. textile industries) and at the centralized municipal WWTP.
Thus, the objective of this study is to combine field monitoring, lab- and pilot-scale experiments, and environmental risk assessment to evaluate the current risk in receiving water body in a textile district in northern Italy and compare prevention and removal strategies for risk minimization.

MATERIALS AND METHODS

The case study is focused on a WWTP collecting WW from textile industries (20-35% of the inlet flowrate) and civil origin. The WWTP comprises pre-treatments, activated sludge biological treatment (pre-denitrification, nitrification/oxidation), tertiary coagulation-flocculation followed by a lamella clarifier and ozonation.

Monitoring campaigns

Three monitoring campaigns have been performed in four textile industries: 1 textile printing, 1 fabric dyeing and 2 yarn dyeing companies. Concerning the WWTP, 11 campaigns have been performed, collecting four samples in each campaign: the WWTP inlet, the biological treatment outlet, the ozonation inlet and the WWTP effluent. Monitored parameters were: 14 PFAS (PFBA, PFHxA, PFBS, GENX, PFPeA, PFHpA, PFOA, PFOS, PFHxS, PFNA, PFDA, PFUnA, PFDoA, PFOSA), pH, conductivity, TSS and COD.

Lab- and pilot-scale experiments

As for textile WW, pressure-driven membrane separation has been tested, assessing both microfiltration (MF) and nanofiltration (NF) and their combination. A SEPA CF Cell cross-flow filtration unit was used in "feed and bleed" mode, under pressure and filtration rate conditions comparable to full-scale ones. Three tests were carried out on a mixture of textile WWs collected from the monitored industries with no PFAS spike. The water matrix was characterized by 23.9 g/L COD, 1440 µS/cm conductivity, pH of 4.5, sum of PFAS equal to 9.5 µg/L.
In the centralized WWTP, adsorption on activated carbon (AC) was tested at lab and pilot-scale. Rapid Small Sale Column Tests (RSSCT) and Field Adsorption Pilot Plant (FAPP) tests have been performed on two water matrices, collected before (IN-O3) and after (OUT-O3) the full-scale ozonation, spiking the samples with 14 PFAS to achieve a concentration of 4 µg/L per single PFAS. The water matrices IN-O3 and OUT-O3 were characterized respectively by: COD of 36 mg/L and 30 mg/L, pH of 7.7 and conductivity around 1350 µS/cm. Both RSSCT and FAPP were sized through the constant-diffusivity down-scaling equation (Crittenden et al., 1987), simulating the performance of full-scale GAC filters with 20 minutes of Empty Bed Contact Time (EBCT). 3 ACs were tested, differing for the porous structure and volume.

Scenarios analysis

To estimate PFAS mass balance throughout the system, the average measured values of flowrate (Q) and PFAS concentrations (C_{PFAS}) (Q_{CIV}=14,240 m^3/d; Q_{TEX}=6,765 m^3/d, $C_{PFAS,CIV}$=0.5 µg/L; $C_{PFAS,TEX}$=0,31 µg/L), and removal efficiencies observed at the lab- pilot-scale were used. The percentage of the total PFAS load leaving the plant through the dewatered sludge, according to the monitoring data, was 0.8%. In scenarios without additional treatments in the WWTP, PFAS concentrations were assumed stable along the treatment train, according to the monitoring data.
The following scenarios have been simulated:
- Scenario 0: Scenario in the current situation (Business As Usual, BAU).
- Scenario 1a: Scenario on voluntary action to reduce total PFAS in textile processes by 35%.
- Scenario 1b: Scenario on voluntary action to replace long-chain PFAS with short-chain PFAS in textile production processes, considering that on average twice the amount of short-chain PFAS is needed to produce fabrics with same performance of long-chain PFAS.
- Scenario 2: Scenario of treatment of textile WW by membrane separation: MF+NF.
- Scenarios 3a and 3b: Scenarios combining scenarios 1a and 2 (3a) and 1b and 2 (3b).
- Scenario 4: Scenario of treatment in the centralised WWTP through adsorption on AC after ozonation, operated for 100,000 bed volumes (BV) (equal to one year operation).
- Scenarios 5a and 5b: Scenarios combining scenarios 1a and 4 (5a) and 1b and 4 (5b).
- Scenarios 6a and 6b: Scenarios combining scenarios 1a, 2 and 4 (6a) and 1b, 2 and 4 (6b).

Environmental risk assessment for PFAS mixture

The environmental risk due to the concentration of the individual PFAS in the effluent of the treatment plant was calculated according to the methodology proposed in the new European Directive proposal for the Environmental Quality Standards (EQS) (European Parliament, 2022). The concentration of each *i-th* PFAS was multiplied by its relative potency factor (RPF_i) to convert it into equivalent concentration of PFOA. The overall concentration of PFAS was calculated as:

$$C_{PFAS,TOT}\ [\mu g/L\ di\ PFOA\text{-}eq] = \frac{\sum_{i=1}^{15} C_{PFAS,i} \times RPF_i}{\sum_{i=1}^{15} C_{PFAS,i} \times RPF_i}$$

The risk of the PFAS mixture was calculated through the risk quotient (RQ), that is the ratio between PFAS concentration, as PFOA equivalent, expected in the river (assuming a dilution factor DF of the discharge equal to 0.1, the default value of the risk assessment), and the EQS for surface water reported by the proposed Directive (0.0044 µg/L of PFOA-eq), with the following formula:

$$RQ_{PFAS,TOT} = \frac{C_{PFAS,TOT} \times DF}{EQS} \quad \frac{C_{PFAS,TOT} \times DF}{EQS}$$

RESULTS AND DISCUSSION

The monitoring campaign was useful to evaluate which PFAS are effectively present and their fate in the WWTP. The textile WW are mainly characterized by short-chain PFAS (91.7% of the total PFAS). In the raw WW a maximum of 7 PFAS was detected over the 14 monitored ones (Figure 1). In the WWTP, the biological treatment increases short-chain PFAS concentration. At the outlet of the final ozonation an average 5% concentration decrease was observed for PFPeA, PFHxA and PFOS, while no effects were observed for PFBA, PFHpA and PFOA. Overall, PFAS sum was not changed throughout the WWTP treatment train.

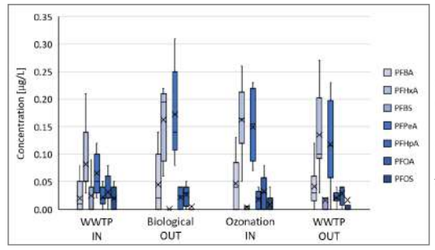

Figure 1. Boxplot of detected PFAS concentrations at each sampling point within the WWTP, for the 11 campaigns carried out.

As for tests on MF and NF on textile WW (Figure 2.a), PFAS rejections by MF were variable; the rejections by NF, fed with the permeate of the MF, were around 80%. Overall, the rejection obtained with the MF+NF sequence was between 88% and 93% and equal to 90% for PFAS sum. In the centralized WWTP, ozonation showed to reduce organic content and improve PFAS removal in the subsequent adsorption step. The breakthrough curves (Figure 2.b) show that AC adsorption improves with PFAS chain length and within 100,000 BV, the average removal for short- and long-chain PFAS is 11% and 56%, respectively.

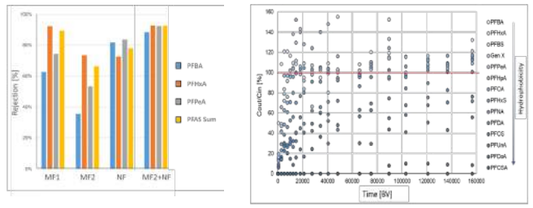

Figure 2. Results of the tests on: (a) PFAS rejections by MF and NF membranes; (b) PFAS breakthrough curves for AC RSSCT tests in OUT-O3.

The overall environmental risk due to the concentrations of each PFAS in the WWTP effluent and the contribution of each PFAS to the risk is depicted in Figure 3.

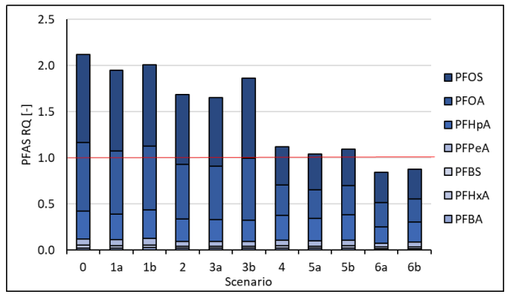

Figure 3. Overall environmental risk due to PFAS mixture for different intervention scenarios (the red line represents the risk threshold RQ=1).

CONCLUSIONS

The mass balance and environmental risk outlined the following evidences:
- Textile WW contribution to the PFAS load entering the WWTP is lower than the civil one.
- In the current scenario (Scenario 0), there is an environmental risk (RQ>1), mainly due to PFOS and PFOA, followed by PFHpA.
- The reduction of 35% of the total PFAS in textile production (Scenario 1a) leads to 8% reduction of the environmental risk, not enough to lower under RQ=1.
- Replacing long-chain with short-chain PFAS in production processes (Scenario 1b) leads to a deterioration in the final effluent quality, due to the higher quantities used.
- The treatment of textile WW through membrane separation (MF+NF) (Scenario 2) reduces by 20% the overall PFAS discharge and environmental risk compared to Scenario 0.
- Combining the reduction or replacement of PFAS in textile production and the treatment via MF+NF (Scenarios 3a and 3b) do not lead to a significant benefit compared to Scenario 2.
- The addition of activated carbon adsorption downstream ozonation in the centralized WWTP (Scenario 4) reduces the discharged PFAS mass by 20% compared to Scenario 0 and 2, and the risk by 50%, because the higher removal of long-chain PFAS that are the most eco-toxic ones. This result highlights that it is important to consider PFAS toxicity (through risk assessment) and not only looking at their sum concentration when prioritizing interventions.
- Combining prevention, treatment at source and treatment at WWTP) interventions (Scenarios 6a and 6b), an acceptable environmental risk is reached (RQ<1), even if it needs attention (RQ>0.1). Finally, to have a more comprehensive assessment and prioritization of the proposed interventions, the proposed environmental risk analysis should be combined with an economic evaluation.

REFERENCES

Chollom, M. N., Rathilal, S., Alfa, D., & Pillay, V. L., 2015. The applicability of nanofiltration for the treatment and reuse of textile reactive dye effluent. Water Sa, 41(3), 398-405.
Crittenden, J.C., Berrigan, J.K., Hand, D.W., Lykins, B., 1987. Design of rapid fixed-bed adsorption tests for nonconstant diffusivities. J. Environ. Eng. (United States) 113, 243–259.
European Parliament, 2022. Proposal for a Directive of the European Parliament and of the Council amending the Water Framework Directive (Directive 2000/60/EC), Groundwater Directive (Directive 2006/118/EC) and Environmental Quality Standards Directive (Directive 2008/105/EC).
Lewis, A., Yun, X., Spooner, D., Kurz, M., McKenzie, E., Sales, C., 2022 Exposure pathways and bioaccumulation of per-and polyfluoroalkyl substances in freshwater aquatic ecosystems: Key considerations. *Science of the Total Environment*, 153561.

Integration of electrochemical processes in a landfill leachate treatment system for removal of the recalcitrant organic load

N. Mostefaoui*, N. Oturan*, S. Bouafia**, Y. Pechaud*, M. Chabani**, B. Tassin***, M.A. Oturan*, C. Trellu*

* Laboratoire Géomatériaux et Environnement, Université Gustave Eiffel, 5 Boulevard Descartes, 77420, Champs-sur-Marne, FRANCE
** Laboratory of Reaction Engineering, University of Sciences and Technology Houari Boumediene, BP 32, El-Allia, Bab-Ezzouar, 16111 Algiers, Algeria
*** Laboratoire Eau Environnement et Systèmes Urbains, LEESU, Ecole des Ponts, Université Paris-Est Créteil, 61 avenue du Général de Gaulle, 94010 Créteil Cedex, France
(E-mail: *nabil.mostefaoui@univ-paris-est.fr, nihal.oturan@u-pem.fr, SC.bouafia@gmail.com,yoan.pechaud@univ-eiffel.fr,bruno.tassin@enpc.fr clement.trellu@u-pem.fr, nihal.oturan@u-pem.fr, mehmet.oturan@u-pem.fr*)

Abstract

Anodic oxidation (AO) was able to achieve 90% mineralization after 6 h of treatment using a boron-doped diamond anode at 42 mA cm^{-2}. The AO process is widely recognized for the non-selective oxidation of organic compounds. However, the main objective of this study was to highlight some drawbacks in order to propose the most suitable way to integrate EAOPs in a full treatment system. Combination of AO with a biological treatment and/or electrocoagulation was investigated. The objective was to reduce the electric charge required during AO in order to lower the energy consumption (EC) as well as the formation of toxic by-products such as ClO_3^- and ClO_4^-. The membrane bioreactor (MBR) operated on-site reduced the organic load and ammonium content. Further treatment by electrocoagulation removed 40% of the remaining organic load with low EC. Therefore, 6 h of treatment by AO at only 8 mA cm^{-2} was then required for achieving similar mineralization yield than for direct treatment of the raw effluent, which corresponds to a 10 times lower EC of the AO process. Recirculation towards the MBR might also be considered based on the biodegradability enhancement of the effluent observed during the treatment by AO.

Keywords (maximum 6 in alphabetical order)

Anodic oxidation, biodegradability enhancement, by-products, combined process, landfill leachate

INTRODUCTION

Electrochemical advanced oxidation processes (EAOPs) are emerging processes with the capacity to achieve full mineralization of organic pollutants in complex effluents (Hien et al., 2022). Particularly, the anodic oxidation (AO) process is based on the generation of hydroxyl radicals (•OH) from water oxidation at the surface of suitable anode materials (Martínez-Huitle et al., 2015)as well as advanced oxidation processes (AOPs. The objective of this study was to compare different EAOPs for the treatment of a real landfill leachate. Several parameters were followed, including total organic carbon (TOC), chemical oxygen demand (COD), turbidity, inorganic ions (NO_3^-, NH_4^+, Cl^-, ClO_3^-, ClO_4^-), energy consumption and effluent biodegradability in order to highlight both advantages and drawbacks (Radjenovic and Sedlak, 2015). The electrocoagulation (EC) process was applied in order to remove a fraction of the organic load with lower energy consumption (EC). The effectiveness of the membrane bioreactor (MBR) operated on-site was also assessed. The objective was to investigate how electrochemical processes might be integrated in a full treatment system for removing the recalcitrant organic load while minimizing the main drawbacks of EAOPs (energy consumption, formation of ClO_3^- / ClO_4^-).

MATERIALS AND METHODS

An open cylindrical undivided reactor (V = 0.18 L) was used to perform EAOPs in batch mode under galvanostatic conditions. For the AO process, the anode was a thin film of boron-doped diamond (BDD) deposited on niobium plate. Results were compared with the use of a dimensionally stable anode (DSA, RuO_2/IrO_2). The cathode was a stainless steel (SS) plate. Results were also compared with the use of the electro-Fenton process (data not discussed in this abstract). The electrocoagulation process was performed in batch configuration in a reactor (V = 2.5 L) made of 10 iron electrodes (S_{tot} = 168 cm^2) placed in parallel.

RESULTS AND DISCUSSION

Characterization of the effluent

The raw leachate was sampled from the leachate storage tank before treatment. A second effluent was collected at the outlet of the MBR operated in the treatment plant. The main characteristics of both effluents are reported in Table 1. The raw leachate was characterized by its (i) high organic load, (ii) high turbidity, (iii) high concentration of N mainly as N-NH_4^+, (iv) high concentration of chloride. The MBR allowed for significant reduction of the organic load and total N (remaining N was mainly N-NO_3^-) and total removal of the turbidity. The biodegradability of the effluent was estimated from the ratio between the ultimate biological oxygen demand (BOD_u, after more than 20 days of incubation) and the COD. This ratio was below 5% at the outlet of the MBR, indicating the low biodegradability of this effluent and the presence of a recalcitrant fraction of the organic load.

Table 1. Main characteristics of (i) raw leachate and (ii) leachate after treatment by membrane bioreactor (MBR)

Sample	$TOC_{dissolved}$ (g/l)	N_{total} (g/l)	Turbidity (NTU)	COD_{tot} (g/l)	BOD_u/COD_{tot} (%)	NO_3^- (mM)	NH_4^+ (mM)	Cl^- (mM)
Raw leachate	1.1	1.0	570	4.0	15	0	68	58
MBR outlet	0.54	0.46	0	1.5	0	33	0.50	66

Treatment of the raw effluent by the anodic effluent process

The BDD anode was the most suitable electrode material for mineralization of the organic load (Fig. 1a). For example, 90% of TOC removal was obtained after 6 h of treatment at 42 mA cm^{-2}, corresponding to an energy consumption of 360 kWh m^{-3}. The DSA was not able to achieve such mineralization (Fig. 1a) because of the lower amount of •OH generated at the electrode surface. However, DSA is widely recognized for its capacity to accumulate active chlorine in the solution, which allowed for removing turbidity through degradation of particulate organic compounds into dissolved by-products (Fig. 2a). The high mineralization yield using BDD anode was accompanied by the formation of large amounts of toxic ClO_3^- and ClO_4^- (Fig. 3), which is one of the most important drawbacks of such EAOP. Partial conversion of ammonium to nitrate was also observed (Fig. 2b). Besides, the evolution of the UV-vis spectra as well as 3D excitation-emission matrices was followed in order to better understand reaction mechanisms in such complex effluent.

Combination with electrocoagulation and biological processes

The application of the EC process was tested on both the raw effluent and the effluent at the MBR outlet. Results reported in Fig. 1c show that application of EC during 20 min was able to remove 40% of the TOC remaining after treatment by the MBR. The corresponding energy consumption was only 0.5 kWh m^{-3}. However, a recalcitrant organic load with low biodegradability (Fig. 4), representing 29% of the initial TOC, was still remaining. Fig. 1d shows that 75% removal of this recalcitrant organic load was finally achieved by application of the AO process during 6 h at only 8 mA cm^{-2}, which correspond to an energy consumption of 36 kWh m^{-3}. This value was ten times lower than the energy consumption required for achieving similar TOC removal yield by using only AO for the treatment of the raw effluent. Moreover, such combined treatment strategy reduced the amount of ClO_3^- and ClO_4^- generated during the AO treatment step (Fig. 3).

Possible synergistic effect between AO and biological treatment was also assessed. AO was able to significantly increase the biodegradability of the effluent after partial removal of the organic load owing to the formation of more biodegradable by-products (Fig. 4). Therefore, treatment strategies might also include a recirculation of the effluent step between the AO treatment step and the MBR.

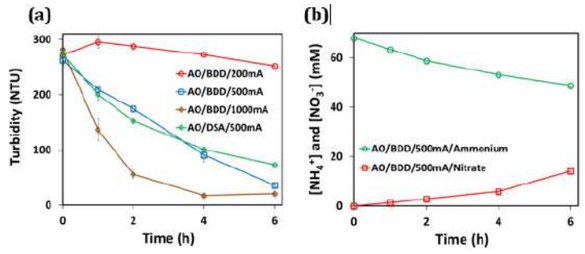

Figure 2. (a) Evolution of the turbidity during treatment of the raw leachate by AO. (b) Evolution of the concentration of ammonium and nitrate during treatment of the raw leachate by AO.

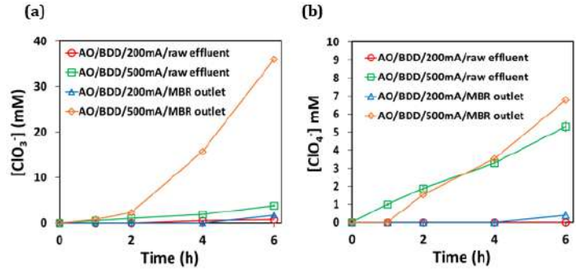

Figure 3. Evolution of the concentration of (a) ClO_3^- and (b) ClO_4^- during the treatment by AO of (i) the raw effluent and (ii) the effluent at the outlet of the MBR.

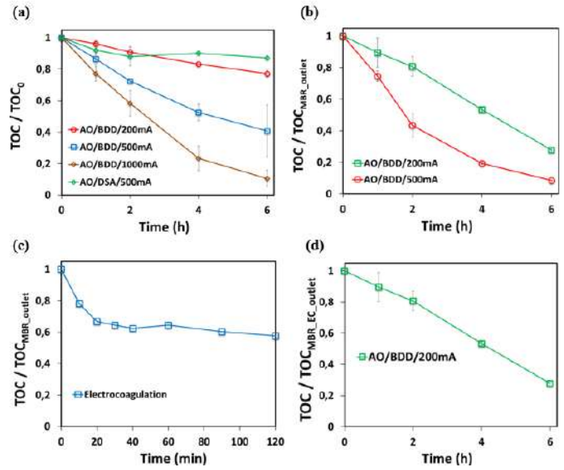

Figure 1. Evolution of the total organic carbon (TOC) during the treatment of (a) the raw effluent (TOC_0 = 1.1 g L^{-1}) by anodic oxidation, (b) the effluent at the MBR outlet (TOC_{MBR_outlet} = 0.54 g L^{-1}) by anodic oxidation, (c) the effluent at the MBR outlet by electrocoagulation and (d) the effluent at the MBR outlet pre-treated by electrocoagulation ($TOC_{MBR\_EC\_outlet}$ = 0.32 g L^{-1})

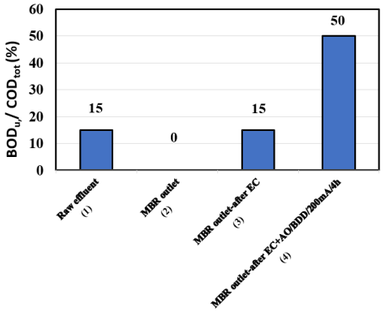

Figure 4. Evolution of the biodegradability of the effluent (ratio between the ultimate BOD and the COD) at different steps of the treatment: (1) raw effluent, (2) MBR outlet, (3), after EC treatment of the effluent at MBR outlet and (4) after EC treatment and 4 h of AO at 8 mA cm^{-2} of the effluent at MBR outlet.

REFERENCES

Hien, S.A., Trellu, C., Oturan, N., Assémian, A.S., Briton, B.G.H., Drogui, P., Adouby, K., Oturan, M.A., 2022. Comparison of homogeneous and heterogeneous electrochemical advanced oxidation processes for treatment of textile industry wastewater. J. Hazard. Mater. 437, 129326.

Martínez-Huitle, C.A., Rodrigo, M.A., Sirés, I., Scialdone, O., 2015. Single and Coupled Electrochemical Processes and Reactors for the Abatement of Organic Water Pollutants: A Critical Review. Chem. Rev. 115, 13362–13407. https://doi.org/10.1021/acs.chemrev.5b00361

Radjenovic, J., Sedlak, D.L., 2015. Challenges and Opportunities for Electrochemical Processes as Next-Generation Technologies for the Treatment of Contaminated Water. Environ. Sci. Technol. 49, 11292–11302. https://doi.org/10.1021/acs.est.5b02414.

Effective micropollutant depuration by a novel sustainable approach: coupling solar photo-Fenton with regenerated activated carbon

P. Núñez-Tafalla*, I. Salmerón*, I. Oller**, S. Venditti*, S. Malato**, J. Hansen*.

* University of Luxembourg, Faculty of Science, Technology and Medicine, Chair for Urban Water Management. 6, rue Richard Coudenhove-Kalergi, L-1359, Luxembourg.
(E-mail: *paula.nunez@uni.lu; irene.salmeron@uni.lu; silvia.venditti@uni.lu; joachim.hansen@uni.lu)*
** CIEMAT-Plataforma Solar de Almería (CIEMAT), 04200 Tabernas, Almería, Spain
(E-mail: *ioller@psa.es; smalato@psa.es*)

Abstract

This work has demonstrated that the coupling of the solar photo-Fenton process and granular activated carbon (GAC) filtration increases the removal of micropollutants (MPs). The solar photo-Fenton process was performed using commercial reagents, obtaining a poor MP removal. Fresh and regenerated GAC were compared with respect to MP adsorption, showing a higher competitive adsorption of the dissolved organic carbon in the regenerated GAC. The close removal rate values can entail an increase in the use of regenerated GAC reducing the carbon footprint of the treatment. The benefit of the coupling of the processes allowed decreasing the treatment time on the solar photo-Fenton reactor and an extension of GAC lifetime between 2 and 3 times magnitude depending on the type of GAC and the water matrix.

Keywords

Advanced oxidation process; Micropollutants; Process combination; Tertiary treatment; Water depuration

INTRODUCTION

Micropollutant (MPs) are continuously discharged on the water bodies in low concentration (order of µg-ng/L) but the potential risk for the ecosystems is very high. Conventional wastewater treatment plants (WWTP) are not designed and resulted not able to remove them, thus a further step is required for their elimination. Advanced oxidation processes are known as a powerful technology, being photo-Fenton one of the most promising processes. The high energy requirements for its operation mainly due to the use of the UV lamps is a drawback, thus the use of solar photo-Fenton (SPF) in raceway pond reactors (RPR) proposed by Carra et al., (2014) resulted as an efficient and lower-cost alternative. Granular Activated Carbon (GAC) filtration is a robust and well-known technology for the removal of MPs. As MPs are adsorbed in the GAC surface, the adsorption capacity decreases until its full exhaustion, needing to be replaced. In recent years the use of regenerated GAC has been widespread to reduce the cost and the carbon footprint (Larasati, Fowler, and Graham 2021).

This work proposes to couple the SPF process with GAC filtration. The goal is to reduce the treatment time on photo-Fenton process, minimizing the surface needed to place the RPR, and to extend the GAC life-time. From the best of our knowledge, the combination of SPF and adsorption process has rarely been performed (Della-Flora et al. 2020), and the combination with GAC filtration in particular never reported. In addition, the viability of commercial reagents instead of analytical quality ones has also rarely been tested.

MATERIALS AND METHODS

Analysis

Iron, H_2O_2, BZT, CBZ and DCF concentrations were quantified as previously described on Sánchez-Montes et al., (2020).

Water matrix

Three different water effluent were used: i) natural water, ii) simulated wastewater and iii) real wastewater. Real wastewater was collected from El Bobar WWTP (Almeria, Spain). The main characteristics of the three water matrices are shown in Table 1.

Table 1. Water matrix characterization.

	Natural water	Simulated water	Real wastewater
pH	7.4-7.5	7.0-7.1	6.3
DOC (mg L^{-1})	48-52	13.7	101
TIC (mg L^{-1})	33-36	0	75
Cl^- (mg L^{-1})	83-100	245-255	486-636
PO_4^{3-}(mg L^{-1})	0.5-0.8	2.4-5.4	3.5-6.8

Experimental set-up

Solar photo-Fenton system. Preliminary tests were performed with a solar simulator reported by Maniakova et al., (2021).Two RPR reactors were used to perform SPF experiments at pilot plant scale with three different depths, 5, 10 and 15 cm. The reactor and the UV irradiation measurement and calculation of UV energy per unit of treated volume (Q_{UV}, kJ L^{-1}) was described by Maniakova et al., (2021).

First tests of SPF were operated with natural water to find the best reagents dose. The natural water results were verified with simulated water, and those were confirmed with actual wastewater. BZT, CBZ and DCF were spiked to the water matrix, to obtain a solution of 100 µg L^{-1} each and homogenized for 5 minutes in dark. After this, the chelated iron ($Fe_3(SO_4)_2$ 12% from Lohmann GmbH and citric acid from Brenntag GmbH at a molar ratio 1:1 or 1:2) was added to the solution and mixed for 5 minutes until homogeneity. Finally, H_2O_2 was added, and the reactor was uncovered, being this time 0, H_2SO_4 was added to the matrix before adding the MPs, in the cases where bicarbonates were reduced

Rapid Small-Scale columns. The breakthrough of the GACs was carried out on rapid small-scale columns (RSSC) with the equipment described on Núñez-Tafalla et al., (2022).

The adsorption tests were performed on simulated and actual wastewater. Each of the columns was filled with a different GAC, one with a commercial fresh GAC, CarboTech DGF 8x 30GL (CarboTech AcGmbh) and the other with the regenerated GAC, CarboTech Pool W1-3 (CarboTech AcGmbh), being operated in parallel to compare with the use of a regenerated GAC source The main characteristics, working conditions and preparation of the GAC were described on Núñez-Tafalla et al., (2022). The selected MPs were added in the tank and mixed to a solution of 100 µg L^{-}1 of each of them. During the test, the samples were taken at defined time intervals.

When SFE and GAC filtration processes where combined, the treatment time by SPF was 5 minutes and this pre-treated water was then filtered through the RSSC.

RESULTS AND DISCUSSION

The best reagents dosage was determined on natural water (Figure 2a) in the solar simulator. Results showed that BZT is the most recalcitrant for SPF. Iron dose was between 1.5 and 6 mg L^{-1} and H_2O_2 between 20 and 40 mg L^{-1}. Initially, the chelating agent molar ratio was 1:1, obtaining a low removal rate probably caused by a limitation in iron availability, so then, the ratio was increased to 1:2. This increment showed a positive effect. High natural concentration of bicarbonates (here 170-180 mg L^{-1}) have been previously reported as hydroxyl radicals' scavengers, thus their concentration was decreased. The decrease of bicarbonates resulted in higher MP removal. Selected reagents dosage to scale-up to the RPR was 6 mg L^{-1} of iron (**molar ratio 1:2**) and 40 mg L^{-1} of H_2O_2. **Under these operating conditions, the removal was 56% for BZF, 61% for CBZ and 70% for DCF after the application of 0.16 KJ L^{-1} (12 min) of accumulated UV energy.**

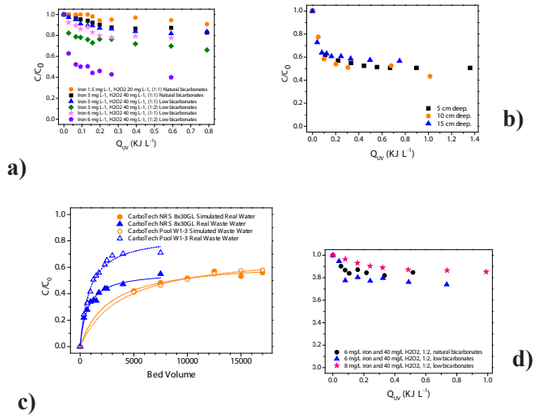

Figure 2. a) BZT removal in natural water by SPF in solar simulator, b) BZT removal in simulated wastewater by SPF in RPR, c) BZT removal in real wastewater by SPF in RPR, d) DCF adsorption.

RPR tests were performed firstly with natural water. Three different depths were tested, showing a similar trend regarding Q_{UV} to reach the desired goal. Thus, the 15cm depth was selected with the objective of increasing the volume of water treated per photoreactor area. The removal achieved on the 15 cm depth after applying 0.16 KJ L^{-1} was 46% for BZF, 50% for CBZ and 62% for DCF. The removal achieved on the 15 cm after applied 0.16 KJ L-1 was 40% for BZF, 44% for CBZ and 55% for DCF (Figure 2b). The results were slightly lower than those obtained with natural water due to the higher complexity of the water matrix. Finally, the removal of the MPs in actual wastewater with 15 cm depth was studied modifying the iron dosage between 4 and 8 mg L^{-1}. The results (Figure 2c) confirmed a dosage of 6 mg L^{-1} of iron and 40 mg/L H_2O_2 as the best. BZT, CBZ and DCF concentration decreased by 21%, 25% and 42%, respectively in 5 minutes. This removal showed the need to combine the SPF process with downstream technologies when using commercial reagents to get a rapid degradation.

The GAC filtration was studied standalone with simulated and actual wastewater since organic background has a high influence competing for active sites. MPs removal was compared taking as reference the 20% breakthrough (20BT) (C/C_0=0.2) meaning to achieve the 80% of MP removal. On simulated wastewater the fresh GAC 20BT was reached 20% and 70% earlier for DCF and BZT respectively in fresh GAC than in regenerated. For CBZ, it was reached a 13% earlier for regenerated GAC than for the fresh (Figure 2d). The similar adsorption capacity of the fresh and the regenerated GAC showed the feasibility of the use of the regenerated GAC. In the case of the real wastewater, the 20BT was achieved 28%, 57% and 85% for DCF, CBZ and BZT respectively for fresh GAC than regenerated. The difference between the water matrix can be associated to the high concentration of DOC (101 mg L^{-1}) in the real wastewater.

The combination was tested in synthetic and actual wastewater under the selected operating conditions. For simulated wastewater, the treatment by SPF reached between 35 and the 45% of MPs removal. In the treatment with GAC, the 80% removal of DCF was achieved till 3900 BV for fresh GAC and 2900 BV for regenerated GAC. Thus, the coupling of technologies allows extending GAC lifetime more than 3 times. The MP removal on SPF in actual wastewater was lower, between 20% and 41%, being BZT the one with lower removal rate and DCF the highest. The 80% removal of DCF in GAC filtration was reached till 910 and 950 BV for fresh and regenerated GAC respectively. Thus, the extended GAC lifetime was between 2 and 3 times.

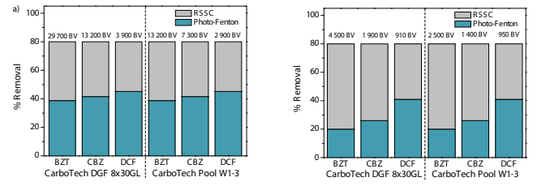

Figure 3. Contribution of each step (till 80%). Above the bars, bed volumes reached at 80% removal. a) Simulated wastewater; b) Real wastewater.

It has been proved that the coupling of processes allows decreasing the hydraulic retention time on the SPF reactor and extending GAC lifetime by 2 and 3 times.

ACKNOWLEGMENTS

The authors wish to thank the Plataforma Solar de Almeria for providing access to its installations, the support of its scientific and technical staff, and the financial support of the SFERA-III project (Grant Agreement No 823802). In addition, the financial support provided by Administration de la gestion de l'eau - Ministère du développement durable et des infrastructures of Luxembourg under the Fentastic Project.

REFERENCES

Carra, Irene et al. 2014. "New Approach to Solar Photo-Fenton Operation. Raceway Ponds as Tertiary Treatment Technology." *Journal of Hazardous Materials* 279: 322–29.

Della-Flora, Alexandre et al. 2020. "Combination of Solar Photo-Fenton and Adsorption Process for Removal of the Anticancer Drug." *Journal of Hazardous Materials* 396(March): 122699.

Larasati, Amanda et al. 2021. "Insights into Chemical Regeneration of Activated Carbon for Water Treatment." *Journal of Environmental Chemical Engineering* 9(4): 105555.

Maniakova, Gulnara et al. 2021. "Simultaneous Removal of CECs and Pathogens from Urban WW by Homogeneous Solar Driven AOP." *Science of the Total Environment* 766: 144320.

Núñez-Tafalla, Paula et al. 2022. "Combinated Treatment of Wastewater Using Photo-Fenton and GAC." *Proceedings of the 39th IAHR World Congress (Granada, 2022)* (June): 2041–46.

Sánchez-Montes, Isaac et al. 2020. "UVC-Based AOP for Simultaneous Removal of MC and Pathogens Pilot Plant." *Environmental Science: Water Research & Technology* 6(9): 2553–66.

Boosting active sites of municipal sludge-based biochar for Fenton-like degradation toward phenolic contaminants from water

B. Byambaa*,** and K.G. Song*,**
* Water Cycle Research Center, Korea Institute of Science and Technology (KIST), Seoul 02792, Republic of Korea
** Division of Energy & Environment Technology, KIST School, University of Science and Technology (UST), Seoul 02792, Republic of Korea
(E-mail: *battuya55@kist.re.kr*; *kgsong@kist.re.kr)*

Abstract

We fabricated the well-structured heterogeneous catalyst from municipal sludge using 2-step thermal modifications and investigated their role in a Fenton-like reaction to degrade emerging organics from water. The reactive sites (graphitic N, edge N species, and carbonyl groups) on the N-doped biochar (NOBC) catalyst heavily dependent on nitrogen precursors were scrutinized in this work. Accordingly, NOBCd exhibited superior catalytic activity in peroxydisulfate (PDS) activation, evidenced by the complete removal of phenolic organic pollutants. The mechanism of the PDS activation on the NOBCd is proposed to be the contribution of radical and non-radical pathways. In terms of practical applications, material stability, the effect of the natural water conditions, and the degradability of the other common organic pollutants were investigated.

The findings of this study suggest that sludge disposal could be turned into an efficient catalyst that boosts the degradation of emerging organics from the water via a Fenton-like reaction.

Keywords (maximum 6 in alphabetical order)

Fenton-like reaction; Metal-free catalyst; Peroxydisulfate; Stoichiometric efficiency; Water remediation; Waste valorization

INTRODUCTION

Massive amounts of municipal sludge waste, rich in nitrogen, phosphorus, heavy metals, organic micro-pollutants, and pathogens, have been released into the environment as humankind shifted to urbanization and industrialization in recent decades (Wu et al., 2019). Therefore, turning sludge waste into different materials has recently become a research hotspot instead of incineration or landfilling, which has caused secondary pollution (Guan et al., 2019). Namely, sludge could be turned into valuable functional carbon material (biochar) and some biofuel through thermal treatment (Hsu et al., 2020; Wu et al., 2019; Zhang et al., 2021). Biochar (BC) is a carbon-rich porous material that can be derived from various biomass and synthesis methods (Byambaa et al., 2023; Hsu et al., 2020; Wang and Wang, 2019; Zhang et al., 2021). Thus, BC helps reduce the leaching of secondary pollutants from sludge disposal into the environment and works as an efficient green catalyst in the Advanced oxidation processes (AOPs). Furthermore, biochar can efficiently activate persulfates as a heterogeneous catalyst, then directly decompose organic pollutants via oxidative species such as hydroxyl radical (•OH), sulfate radical ($SO4^{\bullet-}$), or singlet oxygen ($^1O_2$) are generated in PS-AOPs (Mishra et al., 2017; Wang et al., 2019). However, it is crucial to localize various functional sites on metal-free catalysts to uplift reaction efficiency and avoid blockage of the pristine carbon surface.

In this work, we created N and O co-doped biochar from municipal sludge with different N sources to efficiently remove phenolic compounds via the activation of peroxydisulfate (PDS). The chosen NOBCd nanocomposite has relatively high structure defects and more reactive sites by N and O doping. NOBCd/PDS degraded BPA rapidly without pH adjustment. Moreover, the effects of reaction conditions (pH, ionic strength, and coexistence of the natural organic matter (NOM) on the oxidation of the target pollutant are explored. Classical quenching and electrochemical experiments in NOBCd/PDS are conducted to identify the primary reactive species and reaction mechanism.

MATERIALS AND METHODS

The NOBCs were synthesized according to methods described in the literature (Byambaa et al., 2023) by varying nitrogen precursors, such as ammonium hydrogen phosphate ($(NH_4)_2HPO_4$), urea(NH_2CONH_2), melamine ($C_3H_6N_6$) and dicyandiamide ($C_2H_4N_4$), followed by a thermal treatment in N_2 atmosphere. In detail, sludge powder was added to the N source solution in the weight ratio of 1:3; the suspension was ultrasonicated for 10 min. Then, the mixture was transferred to a Teflon-lined autoclave and heated to 180 °C for 8 h. After the autoclave cooled down to room temperature, the black precipitate was dried in a vacuum oven. Finally, the powder was calcined at 800 °C for 1 h with a heating rate of 15 °C/min under N_2 atmosphere. The obtained sample was named NOBCa, NOBCu, NOBCm, and NOBCd, respectively.

The degradation experiments were conducted at room temperature (25 ± 2 °C) in 100 mL of a solution of targets with the BC, and PDS without pH adjustment. Periodically, the sample was fetched from the reactor, filtered through a 0.22 µm PTFE syringe filter, and terminated the reaction by sodium thiosulfate (0.2 M) immediately before the high-performance liquid chromatography (HPLC) measurement. The PDS concentration was measured by UV–visible absorbance of a yellow-colored solution due to the reaction between PDS and iodide in the presence of bicarbonate at 352 nm. All experiments were conducted in triplicate, and results were reported with error bars.

RESULTS AND DISCUSSION

Carbon skeleton defect was investigated by Raman spectra D-band (~1380 cm−1) and G-band (1607 cm^{-1}) intensity ratios (Wang et al., 2019). As shown in Fig. 1a, NOBCd owns the highest defects (ID/IG = 1.61) compared with NOBCa, NOBCu, and NOBCm. This higher defect might be caused by more active sites fabricated by N and O co-doping is further proven by X-ray photoelectron spectroscopy (XPS) survey and high-resolution spectra analysis. Accordingly, the NOBCd prepared using dicyandiamide as the nitrogen source has a higher nitrogen doping level among created NOBCs samples.

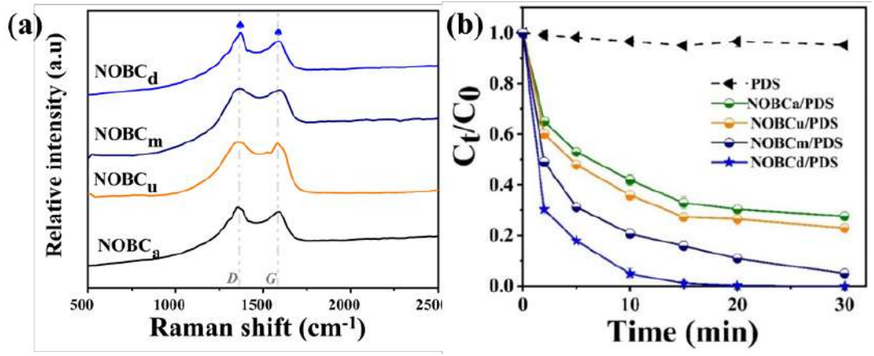

Figure 1. Raman spectra (a), XPS survey (b) of the modified biochar samples, BPA degradation curves in different PDS/NOBCs (c)

The role of structure defect, doped N, and specific active sites on the Fenton-like reaction of NOBCs was investigated through PDS activation to remove phenolic organic contaminants. BPA, one of the widely detected phenolic contaminants, was chosen as the target compound. Because, It is known as a xenoestrogen, an environmental contaminant, a xenobiotic, and an endocrine disruptor. As a chemical compound, BPA is a bisphenol that is 4,4'-methanediyldiphenol in which the methylene hydrogens are replaced by two methyl groups and are assumed to be not easily biodegraded in the environment due to their stability (Chen et al., 2021; Khan et al., 2021).

As shown in Fig. 1b, PDS alone could not degrade BPA without biochar. In comparison, BPA degradation was elevated with NOBC catalysts. Among modified biochar samples, NOBCd outperformed by degrading BPA (within 20 min), and the pseudo-first-order reaction kinetic constant (k_1) of NOBCd/PDS was calculated as 0.37 min^{-1}. Evidently, our optimal NOBCd/PDS system is not only shown superb degration of pollutant (Chu et al., 2019; Zhang et al., 2021), but also the reaction rate was over 10 times folds up the pristine biochar's performance.

Conclusions

Different levels of N-doped biochar (NOBCs) were synthesized by varying the N sources. Selected NOBCd exhibited superb catalytic activity for BPA degradation through PDS activation with huge enhancement compared to the unmodified biochar (SBC) activity. Structure–activity relationship unveils that the carbonyl group and graphitic N were key active sites for BPA degradation. Also, the utilization efficiency of PDS, and relationship between structure and stoichiometric efficiency was revealed in this work. Although the reactive sites on the material circulate both radical and non-radical oxidation during PDS activation, BPA degraded in NOBCd/PDS system via non-radical mechanism is assumed by classical quenching experiments and further investigated in details. As benefiting from the non-radical mechanism, NOBCd/PDS system manifested high resistance to inorganic anions but was still hindered by high concentration of humic acid in water. We believe this work will expand the knowledge of the carbon-assisted PDS activation mechanism, especially in the field of green-catalyst.

REFERENCES

Byambaa, B., Kim, E., Gashaw, M., An, B., Cho, J., Lin, S., Guen, K., 2023. Synthesis of N -doped sludge biochar using the hydrothermal route-enabled carbonization method for the efficient degradation of organic pollutants by peroxymonosulfate activation. Chem. Eng. J. 456, 141037. https://doi.org/10.1016/j.cej.2022.141037

Chen, C.Y., Cho, Y.C., Lin, Y.P., 2021. Activation of peroxydisulfate by carbon nanotube for the degradation of 2,4-dichlorophenol: Contributions of surface-bound radicals and direct electron transfer. Chemosphere 283, 131282. https://doi.org/10.1016/J.CHEMOSPHERE.2021.131282

Chu, C., Yang, J., Huang, D., Li, J., Wang, A., Alvarez, P.J.J.J., Kim, J.-H.H., al., C.C., 2019. Cooperative Pollutant Adsorption and Persulfate-Driven Oxidation on Hierarchically Ordered Porous Carbon. Environ. Sci. Technol. 53, 10352–10360. https://doi.org/10.1021/acs.est.9b03067

Guan, C., Jiang, J., Pang, S., Ma, J., Chen, X., Lim, T.T., 2019. Nonradical transformation of sulfamethoxazole by carbon nanotube activated peroxydisulfate: Kinetics, mechanism and product toxicity. Chem. Eng. J. 378, 122147. https://doi.org/10.1016/j.cej.2019.122147

Hsu, K.Y., Inbaraj, B.S., Chen, B.H., 2020. Evaluation of analysis of cholesterol oxidation products and heterocyclic amines in duck and their formation as affected by roasting methods. J. Food Drug Anal. 28, 322–336. https://doi.org/10.38212/2224-6614.1066

Khan, N.G., Correia, J., Adiga, D., Rai, P.S., Dsouza, H.S., Chakrabarty, S., Kabekkodu, S.P., 2021. A comprehensive review on the carcinogenic potential of bisphenol A: clues and evidence. Environ. Sci. Pollut. Res. 28, 19643–19663. https://doi.org/10.1007/s11356-021-13071-w

Mishra, N., Reddy, R., Kuila, A., Rani, A., Nawaz, A., Pichiah, S., 2017. A Review on Advanced Oxidation Processes for Effective Water Treatment. Curr. World Environ. 12, 469–489. https://doi.org/10.12944/CWE.12.3.02

Wang, H., Guo, W., Liu, B., Wu, Q., Luo, H., Zhao, Q., Si, Q., Sseguya, F., Ren, N., 2019. Edge-nitrogenated biochar for efficient peroxydisulfate activation: An electron transfer mechanism. Water Res. 160, 405–414. https://doi.org/10.1016/j.watres.2019.05.059

Wang, S., Wang, J., 2019. Activation of peroxymonosulfate by sludge-derived biochar for the degradation of triclosan in water and wastewater. Chem. Eng. J. 356, 350–358. https://doi.org/10.1016/j.cej.2018.09.062

Wu, Q., Bao, X., Guo, W., Wang, B., Li, Y., Luo, H., Wang, H., Ren, N., 2019. Medium chain carboxylic acids production from waste biomass: Current advances and perspectives. Biotechnol. Adv. 37, 599–615. https://doi.org/10.1016/J.BIOTECHADV.2019.03.003

Zhang, J., Chen, P., Gao, W., Wang, W., Tan, F., Wang, X., Qiao, X., Wong, P.K., 2021. Melamine-cyanurate supramolecule induced graphitic N-rich graphene for singlet oxygen-dominated peroxymonosulfate activation to efficiently degrade organic pollutants. Sep. Purif. Technol. 265, 118474. https://doi.org/10.1016/j.seppur.2021.118474

Adsorption on activated carbon for PFAS removal: should we act at the source or before the discharge into the environment?

B. Cantoni*, M. Stefanoni*, G. Bergna**, E. Baldini***, M. Antonelli*

* Department of Civil and Environmental Engineering, Politecnico di Milano, Milan (MI), Italy
(E-mail: *beatrice.cantoni@polimi.it; mattia.stefanoni@mail.polimi.it; manuela.antonelli@polimi.it;)*
** Lariana Depur s.p.a., Fino Mornasco (CO), Italy (E-mail: *giovannibergna@lariana.it*)
*** Centro Tessile Serico Sostenibile SRL, Como (CO), Italy (E-mail: *ebaldini@textilecomo.com*)

Abstract

Per- and polyfluoroalkyl substances (PFAS), used in several industrial applications, such as textile production, are gaining increasing concern due to their spread in the environment, their stability and eco-toxicity. To avoid PFAS spread in the environment, removal strategies need to be implemented at both industrial and municipal wastewater treatment plants (WWTP). This study presents a case study in a textile district in northern Italy where PFAS removal in wastewater (WW) through adsorption on activated carbon was tested at lab and pilot-scale at different points of the system (textile companies and municipal WW treatment plant). This lab-testing was proved to be useful to identify where to apply such process in the system and to optimize process configuration and operating conditions.

Keywords (maximum 6 in alphabetical order)

Adsorption; Isotherms; Ozonation; PFAS; Rapid Small-scale Column tests; Textile wastewaters

INTRODUCTION

In the last decades, the presence of per- and polyfluoroalkyl substances (PFAS) in the aquatic environment has become an issue of growing global concern (Griffin et al., 2022). PFAS are ubiquitous and persistent, since they constantly enter the environment through different sources, being the most important the wastewater treatment plants (WWTPs), especially those collecting industrial wastewaters (WW). Worldwide always more stringent limits are posed for PFAS concentration in WW (e.g., the proposed European Directive on Environment Quality Standards (EQS) (European Parliament, 2022)). Thus, to avoid PFAS spread in the environment, treatments need to be implemented at both the industry discharge and municipal WWTPs. As for the industrial discharge, some studies characterized PFAS occurrence in textile industries showing their constant presence at concentrations in the order of µg/L. However, very few studies studied treatment technologies for PFAS removal in these concentrated streams. One of the most successful well-established processes to remove PFAS from water and WW is adsorption onto activated carbon (AC), particularly for long-chain PFAS (Appleman et al., 2014). The majority of the available studies focused on PFOA and PFOS adsorption through lab-scale isotherm tests, and only recently few studies were performed to assess PFAS breakthrough in drinking water through rapid small-scale column tests (RSSCTs) (Cantoni et al., 2021). Finally, activated carbon adsorption directly after ozonation is a process combination extensively applied in drinking water treatment, and less applied for wastewater. Such process combination has been mainly investigated in municipal WW for Pharmaceuticals and Personal Care Products (PPCPs) and in textile WW for dyes, and very few studies analysed the performance of such treatment train towards PFAS. The objective of this study is to assess adsorption performance at the source and at the final WWTP stage through lab- and pilot-scale tests to evaluate where to apply such treatment in a textile district in northern Italy.

MATERIALS AND METHODS

The case study is focused on a textile district composed by 42 textile industries whose WW is discharged in a sewer system together with WW from civil origin. The sewer system conveys WW to a WWTP (20-35% of the inlet flowrate from industrial origin), composed by pre-treatments, activated sludge biological treatment (pre-denitrification, nitrification/oxidation), coagulation-flocculation followed by a lamella clarifier and ozonation.

Lab-scale batch experiments

To assess adsorption performance of different ACs towards PFAS, also considering the interfering action of organic matter, batch isotherm experiments were performed on three water matrices (Table 1): a mix in equal parts of four textile WWs (TWW), treated WW collected at the WWTP before (IN-O3) and after (OUT-O3) the full-scale ozonation unit. The TWW samples, with mean PFAS concentration equal to 4 µg/L, were not spiked. IN-O3 and OUT-O3 samples were spiked with 15 PFAS (from C4 to C12) (PFBA, PFHxA, PFBS, GENX, PFPeA, PFHpA, PFOA, PFOS, PFHxS, PFNA, PFDA, PFUnA, PFDoA, PFOSA, C6O4) to achieve initial concentration of 4 µg/L per single PFAS.

Table 1. Main characteristics (mean value ± standard deviation) of the aqueous matrices used in the experimental tests. UVA_{254} represents the absorbance at 254 nm (1 cm optical path).

Matrix	pH	Conductivity	COD	UVA_{254}
	[-]	[µS/cm]	[mg/L]	[m^{-1}]
TWW	4.4	1589	23900	-
IN-O3	7.7 ± 0.09	1332 ± 4.7	36 ± 1.2	20.5 ± 0.42
OUT-O3	7.8 ± 0.07	1401 ± 3.9	30 ± 1.4	16.0 ± 0.73

Four activated carbons (Table 2) were tested, having different origin, porosity pH of Point of Zero Charge (pH_{PZC}) and applicability (as granules, GAC, and/or powder, PAC, based on their availability on the market), at doses from 3 to 150 mg/L, with 48 h contact time. Only BP2 and G9 were tested for TWWs.

Table 2. Tested adsorbents' main characteristics: origin, iodine number, porosity, pH_{PZC}, applicability (characteristics provided by the AC supplier, Jacobi, except for pH_{PZC} which was determined).

Adsorbent	Origin	Iodine number (mg/g)	Main porosity	pH_{PZC}	Applicability
CP1	Coconut	1,000	Micro	8.0	PAC/GAC
BP2	Bituminous-coal	850	Meso	9.2	PAC/GAC
MP25	Bituminous-coal	1,000	Meso-macro/Macro	9.1	PAC/GAC
G9	Wood	950	Meso-macro/Macro	9.2	PAC

Processed water samples were analysed for PFAS, COD, pH, conductivity, absorbance spectrum, and fluorescence.

Pilot-scale column experiments

Rapid Small Sale Column Tests (RSSCT) and Field Adsorption Pilot Plant (FAPP) tests have been performed at the centralized WWTP on IN-O3 and OUT-O3 matrices. For RSSCT, water matrices were spiked with 15 PFAS at 4 µg/L per single PFAS, while for FAPP tests, no PFAS spike was performed, being the initial concentration of PFAS sum varying from 0.05 to 1.4 µg/L.

In the RSSCT and FAPP, respectively, three ACs (CP1, BP2 and MP25) and two ACs (CP1, BP2) were tested in single column configuration. In addition, RSSCT were carried out in lead-lag configuration: MP25 was selected as "lead", to reduce organic matter and hydrophobic PFAS, while both CP1 and BP2 were tested as "lag", to evaluate the improvement of their performance, especially on hydrophilic PFAS. In these tests, samples were taken at the Lead column inlet, at the Lead column outlet and at the Lag column outlet, to apportion each column contribution to the overall PFAS breakthrough.

Both RSSCT and FAPP, were sized through the constant-diffusivity down-scaling equation (Crittenden et al., 1987) simulating the performance of full-scale GAC filters with 20 minutes of Empty Bed Contact Time (EBCT) and 1.7 mm of AC granules diameter. Thus, RSSCT and FAPP wee characterized respectively by: EBCT of 0.2 min and 3.4 min, AC volume of 0.45 mL and 1.6 L, AC granules diameter of 0.16 mm and 0.5 mm. Based on this design, 100,000 bed volumes (BV) of operation correspond to 7 and 60 days.

RESULTS AND DISCUSSION

Looking at the PFAS removals (Figure 1) achieved by the two ACs for TWW, removal efficiencies are influenced by the type of AC, its dose and the target PFAS. In detail, mesoporous AC (BP2) showed worse adsorption (2-25% on the sum of PFAS) compared to meso/macro-porous AC (G9) (12-34%), due to decreased competition of organic matter. As for municipal WW (Figure 1.b), PFAS hydrophobicity and adsorbent type (porosity, origin) have great influence on the adsorption capacity. In detail, as PFAS hydrophobicity increases (greater Log D_{OW}), the removal increases. For long-chain hydrophobic PFAS (Log D_{OW}>1), efficiencies are higher compared to short-chain PFAS and significantly influenced by the ACs type. The efficiency, in fact, increases with the pore size.

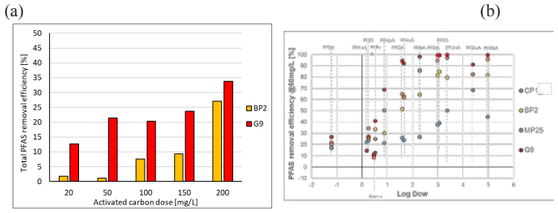

Figure 1. PFAS removal efficiencies for: (a) PFAS sum in TWW as a function of AC type and dose; (b) in IN-O3 at 50 mg/L of different ACs as a function of PFAS hydrophobicity (Log Dow).

Similar results were found with column tests: the breakthrough in RSSCT slows down with the PFAS hydrophobicity (Figure 2). The different porosity of the ACs significantly influences the results: a slower breakthrough of long-chain PFAS is observed as the porosity of the AC increases. For short-chain PFAS, on the other hand, the breakthrough is very rapid, and no significant differences were found between the 3 tested ACs. The competition between PFAS and organic matter for adsorption active sites plays a key role, especially in the case under examination where a real WW is used. Thus, in Figure 2.b it is assessed the effect of both ozonation, comparing IN-O3 and OUT-O3, and lead-lag configuration, comparing MP25 and MP25+CP1, on the adsorption performance. The influence of ozonation is greater than that of the lead-lag configuration in improving adsorption performance. In fact, the AC life (calculated at 100% breakthrough) increases in the OUT-O3 matrix with respect to the IN-O3 matrix by a range between 50,000 BV and more than 100,000 BV, depending on the tested PFAS. Instead, comparing the breakthrough of the single MP25 column with the lead-lag configuration, the AC life increases less significantly, in the range 10,000-25,000 BV, depending on the tested PFAS.

Finally, the correlations between organic matter (as UVA_{254}) removal and PFAS removal, obtained at the three testing scales for the MP25 AC in both tested water matrices, were compared (Figure 3). Despite a certain variability for removal of organic matter and PFAS lower than 30%, the relationships found at the three different scales of tests (batch, RSSCT and FAPP) follow the same trend. This is useful because this relationship can be estimated for the AC to be used at full scale through batch tests, which are faster and simpler to prepare; then, it can adopted in column operations at different scales, simply monitoring organic matter through absorption measurement (faster and cheaper) to estimate the overall removal of PFAS in real time, useful as an early-warning system.

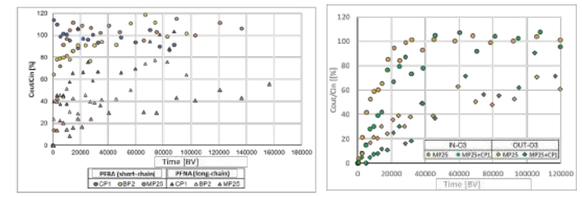

Figure 2. Breakthrough curves in RSSCTs for: (a) PFBA (short-chain) and PFNA (long-chain) with 3 ACs in IN-O3 matrix; (b) for PFNA with MP25 and MP25+CP1 in IN-O3 and OUT-O3 matrices.

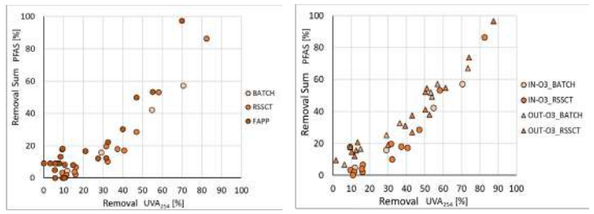

Figure 3. Proxy correlation between removal of UVA_{254} and the sum of PFAS for MP25: (a) in the two matrices for batch tests and RSSCT; (b) in the IN-O3 matrix for batch tests, RSSCT, FAPP.

REFERENCES

Cantoni, B., Turolla, A., Wellmitz, J., Ruhl, A., Antonelli, M., 2021. Perfluoroalkyl substances (PFAS) adsorption in drinking water by granular activated carbon: Influence of activated carbon and PFAS characteristics. Science of The Total Environment, 795, 148821.

Crittenden, J.C., Berrigan, J.K., Hand, D.W., Lykins, B., 1987. Design of rapid fixed-bed adsorption tests for nonconstant diffusivities. J. Environ. Eng. (United States) 113, 243–259.

European Parliament, 2022. Proposal for a Directive of the European Parliament and of the Council amending the Water Framework Directive (Directive 2000/60/EC), Groundwater Directive (Directive 2006/118/EC) and Environmental Quality Standards Directive (Directive 2008/105/EC).

Griffin, E., Aristizabal-Henao, J., Timshina, A., Ditz, H., Camacho, C., Da Silva, B., ... & Bowden, J., 2022. Assessment of per-and polyfluoroalkyl substances (PFAS) in the Indian River Lagoon and Atlantic coast of Brevard County,

Electrochemical removal of antibiotics and multidrug-resistance bacteria using graphene sponge electrodes

Ormeño Cano, N.[1,2], Borrego, C.M[1,3] Balcázar, J.L[1], Radjenovic, J[1, 4]

[1]Catalan Institute for Water Research (ICRA), Emili Grahit 101, 17003 Girona, Spain
(E-mail: normeno@*icra.cat*; *jradjenovic@icra.cat*)
[2] University of Girona, Girona, Spain
[3]Group of Molecular Microbial Ecology, Institute of Aquatic Ecology, University of Girona, Girona, Spain
[4]Catalan Institution for Research and Advanced Studies (ICREA), Passeig Lluís Companys 23, 08010 Barcelona, Spain

Abstract

This study evaluates the performance of graphene sponges doped with atomic sulfur at two S-dopant concentration levels, for electrochemical degradation of six commonly used antibiotics, namely sulfamethoxazole (SMX), trimethoprim (TMP), ofloxacin (OFX), tetracycline (TTC), roxithromycin (ROX) and erythromycin (ERT), as well as for the inactivation of a multidrug-resistant *Escherichia coli (E. coli)*. The experiments were performed in a flow-through, one pass mode, and using real tap water. Highly polar antibiotics such as SMX did not adsorb onto the graphene sponge but were nearly completely removed at very low applied current densities, i.e., 14.5 A m^{-2}. Antibiotics rich in aromatic rings and with high affinity for π-π interactions such as OFX and TTC exhibited removal efficiencies >95% already in the open circuit (OC), whereas the application of current led to further degradation of the adsorbed fraction. S-doped graphene sponge anode with higher concentration of S-dopant resulted in 4.7 log removal of multidrug-resistant *E. coli* at 29 Am^{-2}. No regrowth of bacteria was observed during the storage of the electrochemically treated bacterial suspensions, suggesting that the treatment severely impaired cell viability.

Keywords (maximum 6 in alphabetical order)

Antibiotics, electrochemical oxidation process, graphene-based materials, chlorine-free disinfection, S-doped RGO

INTRODUCTION / MATERIALS AND METHODS / RESULTS AND DISCUSSION

The extensive and misuse of antibiotics for human and veterinary purposes resulted in the pollution of surface waters by antibiotic residues, either partially metabolized or unaltered (Wang, Shi, et al., 2021). This antibiotic pollution has exerted a selective pressure on environmental microbes and stimulated the spread of antibiotic-resistant bacteria (ARB) and their antibiotic resistance genes (ARGs) (Wang, Shi, et al., 2021). According to the latest report of the United Nations (UN), at least 700,000 people die each year due to drug-resistant diseases, and by 2030, antimicrobial resistance could force up to 24 million people into extreme poverty (Bryan-Wilson, 2016). Electrochemical processes are a promising technology for the treatment of contaminated water due to the *in situ* formation of strong oxidant species such as hydroxyl radical (OH•), hydrogen peroxide (H_2O_2), ozone (O_3), just by applying the current, which make them well-suited for decentralized (waste)water treatment (Radjenovic and Sedlak, 2015). However, most commonly used anodes such as e.g., boron-doped diamond (BDD), Magnéli phase and mixed metal oxide (MMO) are limited by a major drawback - the production of chlorine in presence of chloride and, in the case of highly oxidizing anodes (BDD, Ti_4O_7, Ti/SnO_2-Sb), further oxidation of chloride to chlorate (ClO_3^-) and perchlorate (ClO_4^-) (Radjenovic and Sedlak, 2015). In the scope of the ERC-StG ELECTRON4WATER, we have developed three-dimensional (3D), low-cost graphene sponge electrodes that are capable of producing strong oxidant species (e.g., O_3, H_2O_2, OH·) while being electrochemically inert towards chloride, thus avoiding the production of organochlorines, ClO_3^- and ClO_4^- even in the case of high chloride concentrations (i.e., 20–30 mM) (Baptista-Pires, Norra, et al., 2021). In this study, we have synthesized sulfur-doped graphene sponge electrode (SRGO) and used it for electrochemical degradation of sulfamethoxazole (SMX), ofloxacin (OFX), erythromycin (ERT), trimethoprim (TMP), roxithromycin (ROX) and tetracycline (TTC), as well as for the inactivation of a multidrug-resistance *Escherichia coli (E. coli)*, carrying genes as *sul1*, *tetB* and *dfrA16*, which confer resistance to SMX, TTC and TMP, respectively.

MATERIALS AND METHODS

Sulfur (anode) and nitrogen (cathode) -doped graphene sponges were synthesized using previously developed bottom-up synthesis methods (Norra, Baptista-Pires, et al., 2022). S-doped electrodes were synthesized at low and high concentration of S dopant, connected to current feeders, and employed in flow-through reactors in one pass mode, at 5 mL min^{-1}. We used N-doped graphene sponge (NRGO) as flow-through cathode. Target antibiotics were added at low concentration (0.2 µM) to real tap water (0.4-0.5 mS cm^{-1}) to investigate the system performance under realistic conditions of water treatment, where ohmic drop represents a major challenge. To evaluate the disinfection performance of the system, multi-resistant *E. coli* (DSM103246) were added at an initial concentration of 10^7 CFU mL^{-1}. The reactor was operated in chronopotentiometric mode at different applied anodic currents, 14.5 and 29 Am^{-2}. The abundance of *E. coli* was determined using the membrane filtration technique and serial dilutions of collected samples in Chromocult® Coliform Agar medium (Merck). To determine the concentration of target antibiotics from the flow-through reactor, samples were analyzed using an ultraperformance liquid chromatography (UPLC, Waters, USA) with an Acquity UPLC HSS T3 column (2.1×50 mm, 1.8 µm, Waters), coupled to quadrupole linear ion trap mass spectrometer (QqLIT-MS) with a turbo Ion Spray source (5500 QTRAP, Applied Biosystems, USA). The impact of storage was evaluated by storing the electrochemically treated samples at 37ºC for 18h.

RESULTS AND DISCUSSION

Electrochemical removal of antibiotics from tap water

Doping of graphene with heteroatoms such as S and others leads to the introduction of defects and generally enhanced its (electro)catalytic activity. In our previous study, poor adsorption and electrosorption of antibiotics onto graphene sponge electrodes was identified as a major limitation to their electrochemical degradation when working with low conductivity tap water (Ormeno-Cano and Radjenovic, 2022). In an attempt to improve this interaction, we employed S-doping of graphene, previously shown to provide more adsorption sites (i.e., -C-SOx-C-) (Pan, Li, et al., 2022; Omran and Baek, 2022; You, Liu, et al., 2022). **Figure 1** presents the observed removals of target antibiotics at two applied current densities, i.e., 14.5 and 29 A m^{-2}, using *high* and *low*SRGO anode. No significant difference in the antibiotic removal was observed between the two investigated concentration levels of S-dopant, except for TMP for which the removal at 29 Am^{-2} was 66.3 and 88.1 % when *low* and *high*SRGO were used as anode. Compared with our previous study, S-dopant significantly improves the adsorption of contaminants in tap water as electrolyte. E.g. , ERT was adsorbed up to 80 and 50% when sulfur-doped RGO and boron-doped RGO are employed as anodes. (Ormeno-Cano and Radjenovic, 2022) Only in the case of SMX, the removal in the initial OC was similar, with around 12% adsorbed with BRGO anode compared to ~8% in the case of SRGO anode. As expected, very limited removal of SMX was observed in both, *high* SRGO and *low*SRGO -NRGO system in the OC due to the low adsorption affinity of this compound, By contrast, TTC (99% removal in the OC) and OFX (98.5% removal in the OC) are completely adsorbed onto the graphene sponge electrodes due to strong π- π interactions and cation- π bonding between the protonated amino group of both TTC and OFX and the π-electron-rich aromatic structure of graphene (Ai, Liu, et al., 2019). Application of current had a pronounced impact only on the removal of poorly adsorbing SMX and as expected, led to limited increase in removal efficiencies for more strongly adsorbing compounds. Nevertheless, further experiments based on the extraction of the employed graphene sponge anodes with organic solvents will be performed to confirm that the adsorbed antibiotics were also degraded, via direct electrolysis as well as the electro-generated reactive oxygen species (OH•, H_2O_2, O_3).

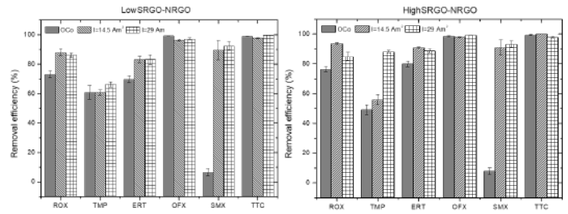

Figure 1. Removal (%) of TMP, ERT, SMX, OFX, ROX and TMP using: A) *low*SRGO anode, and B), *high*SRGO anode at 14.5 and 29 A m^{-2}, *vs.* NRGO cathode.

Electrochemical inactivation of multiresistant *E. coli*

As shown in **Figure 2**, the amount of S-dopant added impacted the extent of *E. coli* removal already in the OC, with 1.8 log removal obtained for *low*SRGO anode to 2.4 log removal for *high*SRGO anode. This effect of the sulfur dopant may be assigned to its bactericide activity, previously reported in other studies (Saedi, Shokri, et al., 2020; Shankar and Rhim, 2018). Application of current further improved the removal efficiency in both systems reaching 3.6 log and 4.7 log removal of *E. coli* when *low*SRGO and *high*SRGO anode, respectively. The highest inactivation of *E. coli* was obtained in *high*SRGO- NRGO system at 29 A m^{-2}. Higher removal of *E. coli* using *high*SRGO anode could be explained by the enhanced electrosorption of the negatively charged bacterial cells onto the anode surface having a greater number of electron-deficient sites after the S doping, and subsequent electroporation of the sorbed bacteria (Norra, Baptista-Pires, et al., 2022; Pan, Li, et al., 2022). Storage of the electrochemically treated bacterial suspensions resulted in an additional 1 log removal, evidencing the irreparable damage of the cells.

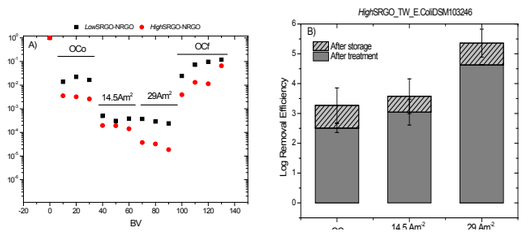

Figure 2. Removal of *E.Coli* in tap water A) for the experimental performed in a flow rate of 5 mL min^{-1}during the initial and final open circuit conditions at two different current 14.5 and 29 A m^{-2} in both *low* and *high*SRGO(A)-NRGO(C) systems B)in *high*SRGO(A)-NRGO(C) system determined after sampling the effluent (e.g "after treatment") and after storing the effluent sample at 37ºC for 18 h (i.e., "after storage"); experiment was performed using tap water at 14.5 and 29 A m^{-2} applied current.

CONCLUSIONS

S-doping of graphene sponge electrodes improved the adsorption of antibiotics onto the graphene sponge in low conductivity tap water. This enabled their further degradation with the application of current, and at very low current densities (i.e., 14.5–29 A m^{-2}). While the amount of the added S-dopant did not impact the removal and degradation of antibiotics, it influenced the extent of inactivation of the multidrug-resistant *E. coli*, with the highest overall removal (i.e., 5 log obtained with "high SRGO" anode at 29 A m^{-2}. Storage experiments confirmed no regrowth of *E. coli* and yielded their further inactivation, evidencing an irreparable damage cell walls caused by the electrochemical treatment.

REFERENCES

Ai, Y., Liu, Y., Huo, Y., Zhao, C., Sun, L., Han, B., Cao, X., and Wang, X. (2019) Insights into the adsorption mechanism and dynamic behavior of tetracycline antibiotics on reduced graphene oxide (RGO) and graphene oxide (GO) materials. Environmental Science: Nano, **6**(11), 3336–3348.

Baptista-Pires, L., Norra, G.-F., and Radjenovic, J. (2021) Graphene-based sponges for electrochemical degradation of persistent organic contaminants. Water Research, **203**(July).

Bryan-Wilson, J. (2016) No time to wait. Artforum International, **54**(10), 113–114.

Norra, G. F., Baptista-Pires, L., Cuervo Lumbaque, E., Borrego, C. M., and Radjenović, J. (2022) Chlorine-free electrochemical disinfection using graphene sponge electrodes. Chemical Engineering Journal, **430**, 132772.

Omran, B. and Baek, K. H. (2022) Graphene-derived antibacterial nanocomposites for water disinfection: Current and future perspectives. Environmental Pollution, **298**(December 2021), 118836. [online] https://doi.org/10.1016/j.envpol.2022.118836.

Ormeno-Cano, N. and Radjenovic, J. (2022) Electrochemical degradation of antibiotics using flow-through graphene sponge electrodes. Journal of Hazardous Materials, **431**(January), 128462. [online] https://doi.org/10.1016/j.jhazmat.2022.128462.

Pan, M., Li, J., and Pan, B. (2022) Identifying the Active Sites of Heteroatom Graphene as a Conductive Membrane for the Electrochemical Filtration of Organic Contaminants. International Journal of Molecular Sciences, **23**(23).

Radjenovic, J. and Sedlak, D. L. (2015) Challenges and Opportunities for Electrochemical Processes as Next-Generation Technologies for the Treatment of Contaminated Water. Environmental Science and Technology, **49**(19), 11292–11302.

Saedi, S., Shokri, M., and Rhim, J. W. (2020) Antimicrobial activity of sulfur nanoparticles: Effect of preparation methods. Arabian Journal of Chemistry, **13**(8), 6580–6588. [online] https://doi.org/10.1016/j.arabjc.2020.06.014.

Shankar, S. and Rhim, J. W. (2018) Preparation of sulfur nanoparticle-incorporated antimicrobial chitosan films. Food Hydrocolloids, **82**, 116–123. [online] https://doi.org/10.1016/j.foodhyd.2018.03.054.

Wang, B., Shi, H., Habteselassie, M. Y., Deng, X., Teng, Y., Wang, Y., and Huang, Q. (2021) Simultaneous removal of multidrug-resistant Salmonella enterica serotype typhimurium, antibiotics and antibiotic resistance genes from water by electrooxidation on a Magnéli phase Ti4O7 anode. Chemical Engineering Journal, **407**(September 2020), 127134. [online] https://doi.org/10.1016/j.cej.2020.127134.

You, J., Liu, C., Feng, X., Lu, B., Xia, L., and Zhuang, X. (2022) Jo ur na of. Carbohydrate Polymers, 119332. [online] https://doi.org/10.1016/j.carbpol.2022.119332.

Emerging contaminants in sludge treatment reed beds: degradation or accumulation?

A. Martínez i Quer*, Gregor Plestenjak**, P. N. Carvalho*,***

* Department of Environmental Science, Aarhus University, Frederiksborgvej 399, DK-4000 Roskilde, Denmark (E-mail: alma@envs.au.dk, pedro.carvalho@envs.au.dk)
** University of Ljubljana, Biotechnical Faculty, Department of Agronomy, Jamnikarjeva 101, 1000, Ljubljana, Slovenia (E-mail: gregor.plestenjak@gmail.com)
*** WATEC - Centre for Water Technology, Aarhus University, Ny Munkegade 120, 8000 Aarhus, Denmark

Abstract
Sludge treatment reed beds (STRBs) are an interesting approach to dewater and mineralize sewage sludge. While these nature-based solutions are robust and efficient to dewater and stabilize activated sludge, they are also promising in providing as final product biosolids that can be used as fertilizer – if legislation allows for it. For this, the quality of the treated sludge is important from two angles: 1) the agricultural use potential based on dry content and nutrients composition, and 2) the content of harmful substances is below threshold limits. One of the critical steps to optimise STRBs performance, and therefore the quality of the final biosolid, is the operation regime which ensures proper sludge dewatering and mineralization. A larger study was carried to compare the performance and efficiency of three types of operation mode: passive aeration, draft aeration or forced aeration). The results herein focus on the different dynamics of degradation and/or accumulation of biocides and pharmaceuticals observed in one of the experiments carried out in Slovenia.

Keywords (maximum 6 in alphabetical order)
Circular economy, Emerging contaminants; Wastewater; Nature-based solutions

INTRODUCTION

Sludge treatment reed beds (STRBs) are an established technology for the management of sludge produced by wastewater treatment plants (Nielsen & Bruun 2015; Brix 2017). Reed beds were used for the first time in Denmark in 1988, when the first sludge processing system was introduced (Nielsen 2003). These systems are now a widespread and common sludge treatment practice in northern Europe, especially in Denmark, and are being used increasingly worldwide. Primary or secondary liquid sludge is loaded on the surface of the reed bed over several years, where long-term (10-12 years) sludge reduction takes place, partly due to dewatering and partly due to decomposition of the organic matter in the sludge (Matamoros et al. 2012).

It is known that the use of sewage sludge or biosolids as agricultural amendments can pose environmental and human health risks related to pathogens and/or antibiotic resistance. A study under Mediterranean climatic conditions demonstrated that the presence of ampicillin-resistant bacteria increased in amended soils 4 months after urban sludge application (Gondim-Porto et al. 2016). The long-term application of sewage sludge and chicken manure significantly increases the abundance and diversity of ARGs in soil (Chen et al. 2016).

In spite of the long-term of mineralization period (10-12 years), STRB operational procedures indicate that the ultimate load should be dewatered and stabilized for 6 months before sludge can be disposed as a biosolid for agriculture (Nielsen & Willoughby 2005). It is uncertain if this time period is enough to ensure the decay of antibiotics and other micropollutants to the environment.

The current project aims to evaluate for the first time the fate of micropollutants, including antibiotics, in STRBs.

MATERIAL AND METHODS

A pilot system was set up at Dragomer, Slovenia (Figure 1) and operated for several experiments until 2022. The pilot contains 9 basins in triplicates for the three of operation mode: passive aeration, draft aeration or forced aeration.

Experimental setup and sampling

Several bags containing the “initial” loading sludge of the beds were wrapped up with a permeable material to replicate natural conditions of water and micropollutant exchange. The bags were left while different sludge loading campaigns were performed onto the STRBs. After each loading campaign, three bags of each bed were pulled off and air dried. The air-dried sludge was used for organic micropollutant quantification.

Analysis

Sludge/biosolids samples were extracted by a two-step process, first water, second methanol, using an ultrasonic bath. The extracts were analysed by LC-MS/MS using two multi-compound methods, one targeting 13 biocides the other 36 pharmaceuticals (Thomsen et al. 2020). Concentrations are reported as dry weight of sludge.

Figure 1. Photo of the pilot at Dragomer, Slovenia in September 2019. The pilot contains 9 basins in triplicates for the three of operation mode: passive aeration, draft aeration or forced aeration.

RESULTS AND DISCUSSION

The biocides irgarol, pyraclostrobin and pirimicarb were detected in the initial sludge, while terbutryn (7 ± 1 ng/g) and the benzalkonium chloride 12-BAC (861 ± 83 ng/g), 14-BAC (210 ± 16 ng/g) and 16-BAC (28 ± 4 ng/g) were quantified. In terms of pharmaceuticals the occurrence was higher than for biocides. The pharmaceuticals tramadol, olmesartan and gabapentin were only detected in the initial sludge, while Azithromycin (75 ± 20 ng/g), Claritromycin (18 ± 4 ng/g), Ciprofloxacin (992 ± 151 ng/g), Propanolol (17 ± 3 ng/g), Carbamazepin (14 ± 1 ng/g), Citalopram (103 ± 13 ng/g), Diclofenac (38 ± 4 ng/g), Phenazone (2 ± 0.2 ng/g), Venlafaxine (21 ± 4 ng/g), Losartan (18 ± 1 ng/g) and Benzotriazole (274 ± 138 ng/g) were quantified.

In terms of fate, we observed three main behaviours of the compounds in time, decrease, no changes and increase in concentration, depending on the compounds (Figure 2). The pesticide terbutryin was stable, 12-BAC and 14-BAC shown a decrease trend, while 16-BAC concentration tended to increase. However, these variations were not significant. For the pharmaceuticals, several compounds showed decrease in concentration such as azithromycin ($p < 0.05$), propranolol, diclofenac ($p < 0.05$), venlafaxine ($p < 0.05$). Carbamazepine, citalopram, and losartan concentration did not change. An increase in concentration was observed for clarithromycin, ciprofloxacin, phenazone ($p < 0.05$) and benzotriazole ($p < 0.05$).

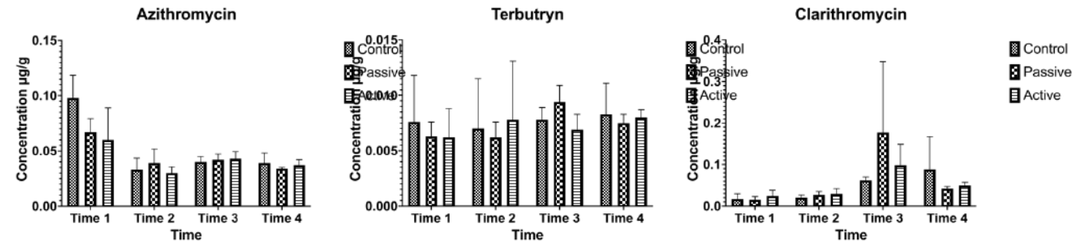

Figure 2. Selected results from representative organic micropollutants showing decrease, no changes and increase in concentration over time.

Statistical tests showed that time was the major variable affecting the micropollutants concentration, while operation mode did not provide any marked difference. It should be noted that the sludge samples in the bags were exposed to x new loadings, thus the increase in concentration. This also implies that a decrease in concentration implies not only biodegradation of the original sorbed compound, but potentially of new amounts that were inserted in the pilots. The experimental setup was considered interesting for understanding removal and accumulation rates in time, but does not allow to perform a mass balance, as the dynamics of a new load implies adding a liquid and a solid fraction and the potential percolation of compounds across de system. Nevertheless, the current results show that emerging contaminants have the potential to be both degraded and accumulated in STRBs in time. This means that it is very important in the future to characterize the stabilization of such systems during the last 6 months of operation without new loads.

REFERENCES

Brix, H. 2017. Sludge Dewatering and Mineralization in Sludge Treatment Reed Beds. *Water* **9**(3), 160

Chen, Q., An, X., Li, H., Su, J., Ma, Y., & Zhu, Y. G. 2016. Long-term field application of sewage sludge increases the abundance of antibiotic resistance genes in soil. *Environment International*, ***92–93***, 1–10.

Gondim-Porto, C., Platero, L., Nadal, I., & Navarro-García, F. 2016. Fate of classical faecal bacterial markers and ampicillin-resistant bacteria in agricultural soils under Mediterranean climate after urban sludge amendment. *Science of The Total Environment*, ***565***, 200–210.

Matamoros, V., Nguyen, L. X., Arias, C. A., Nielsen, S., Laugen, M. M., & Brix, H. 2012. Musk fragrances, DEHP and heavy metals in a 20 years old sludge treatment reed bed system. *Water Research*, ***46***(12), 3889–3896

Nielsen, S. 2003. Sludge drying reed beds. *Water Science and Technology*, ***48***(5), 101–109

Nielsen, S., & Willoughby, N., 2005. Sludge treatment and drying reed bed systems in Denmark. Water and Environment Journal **19**, 296–305.

Nielsen, S., & Bruun, E. W. 2015. Sludge quality after 10–20 years of treatment in reed bed systems. *Environmental Science and Pollution Research*, ***22***(17), 12885–12891.

Silva Thomsen, L. B., Carvalho, P. N., dos Passos, J. S., Anastasakis, K., Bester, K., & Biller, P. (2020). Hydrothermal liquefaction of sewage sludge; energy considerations and fate of micropollutants during pilot scale processing. *Water Research*, ***183***, 116101.

Developing innovative eco-efficient process for Contaminants of Emerging Concern removal in wastewater reuse applications

B. Cantoni*, J. Mata de la vega*, N. Fallah*, C. Diaz Rangel**, T. Vanos**, T. Mao***, D. Santoro*

* Department of Chemical and Biochemical Engineering, University of Western Ontario, London (ON), Canada
(E-mail: *bcantoni@uwo.ca; jmatadel@uwo.ca; naghmeh.fallah@unisalento.it; dsantoro@uwo.ca)*
** Lambton College Research and Innovation, Sarnia (ON), Canada
(E-mail: *carlos.diazrangel@lambtoncollege.ca; teri.vanos@lambtoncollege.ca)*
*** MW Technologies, London (ON), Canada (E-mail: *tedmao@outlook.com)*

Abstract

Increasing water demand is challenging water utilities to find alternative water sources. Interest is growing towards reclaimed wastewater (WW) potable and non-potable reuse. However, the risk for pollution by Contaminants of Emerging Concern (CECs) needs to be faced since current WW treatment plants are not designed to remove CECs. In this study, lab- and pilot-scale experiments were combined and performed at relevant environmental conditions to evaluate the performance of an innovative treatment technology, $MITO_3X$, based on advanced oxidation processes (AOPs), to remove CECs in several water matrices. CECs removal was found to be influenced by CECs properties, water characteristics and $MITO_3X$ operating conditions. Several AOPs configurations were compared taking into account also their energy consumption. Finally, water flowrate was found not to influence the process performance.

Keywords (maximum 6 in alphabetical order)

Advanced Oxidation Processes; Contaminants of Emerging Concern; Design of Experiments; Lab- scale testing; Performance assessment; Wastewater reuse

INTRODUCTION

As a result of population growth, urbanization, cyclical droughts, and climate change, natural water and conventional drinking water (DW) sources (i.e. groundwater and surface water) are expected to be more and more stressed (Van Rossum, 2020). Thus, to meet future water demand in agriculture, industry and to ensure sustainable access to DW, interest is growing towards reclaimed wastewater (WW) potable and non-potable reuse (Tchobanoglous et al., 2015).

However, besides the risk associated with the presence of pathogens, the simultaneous presence of multiple contaminants of emerging concern (CECs) in water has raised the issue of the overall risk of the reused water, since many CECs are not completely removed during conventional WW treatment processes. To avoid CECs spread into the environment, removal strategies need to be implemented at centralised and decentralised wastewater treatment plants (WWTP), being the main sources for CECs in natural resources.

State-of-the-art WW reuse processes are membrane-based filtration (e.g., microfiltration, ultrafiltration, and reverse osmosis), challenged due to their low feasibility and sustainability, and advanced oxidation processes (e.g., UV light/peroxide, UV light/chlorine, ozone (O_3)). Also, other advanced treatment trains have been tested at pilot-scale in the literature combining ozonation and AOPs (e.g. O_3/H_2O_2, granular biofiltration and UV_{254}/H_2O_2) with granular biofiltration (Piras et al., 2020). However, a comprehensive analysis of these processes evaluating and comparing their performance towards CECs in different water matrices and operating conditions is missing.

Thus, the objective of this study is to combine lab- and pilot-scale experiments at relevant environmental conditions to evaluate the performance of an innovative treatment technology, $MITO_3X$, based on advanced oxidation processes, to remove CECs in several water matrices.

MATERIALS AND METHODS

MITO3X is a technology able to dose and mix solid, liquid and gaseous reagents in a liquid flow. The whole system is designed to: (i) aspirate the waters to be treated, (ii) inject the specific reagents required by the process, (iii) mix the water to be treated with the reagents using the centrifuge of the suction pump, (iv) pump the effluent to the next steps of the treatment process. Reducing or oxidizing reagents are injected in 3 distinct points of the process: before ozone, simultaneously with ozone, after ozone to implement several chemical-physical treatment processes. Reagents release occurs through peristaltic dosing double pumps to increase solubility and accelerate reactions.

Two different experimental plans have been designed to test different configurations of $MITO_3X$.

Preliminary lab-scale experiments have been performed on O_3 and O_3/H_2O_2 processes on three water matrices: (i) tap water; (ii) tap water with 5 ppm NO_2 addition; (iii) tap water with 5 ppm NO_2 and 10 ppm TOC addition. Water matrices were spiked prior to the tests with: methylene-blue (5 ppm), pCBA (500 ppb), caffeine and acetaminophen (150 ppb), ciprofloxacin, carbamazepine and sulfamethoxazole (50 ppb). Design of Experiments (DoE) technique has been applied to test $MITO_3X$ configuration at a combination of the following operating conditions: O_3 concentration (0-10 ppm), H_2O_2 concentration (0-5 ppm), water flowrate (30-150 L/min) and pump rate (0-60 Hz). Inlet and outlet samples were collected and the following parameters were measured: residual O_3 and H_2O_2 concentration, target compounds concentration, TOC, NO_2, NO_3, water pressure.

Pilot-scale tests have been performed on a combination of O_3, H_2O_2 and UV processes applied on the effluent of a real WW treatment plant in Italy. The WWTP effluent was characterized by COD of 46.0 mg/L, pH of 7.5, UVT of 61.4%, conductivity of 2907 µS/cm and temperature of 26.5°C. No CECs spike was performed to the water prior to the tests. A total of 36 CECs, mainly pharmaceuticals and personal care products, were detected and average concentration of CECs sum in the tested water was 110 µg/L, with main contribution given by caffeine (24.9 µg/L), diclofenac (18.5 µg/L) and metformin (15.0 µg/L). Design of Experiments (DoE) technique has been applied to test $MITO_3X$ configuration at each combination of the following operating conditions: O_3 concentration (0-9 ppm), H_2O_2 concentration (0-9 ppm), UV dose (0-1 mJ/cm²) and water flowrate (0.6-3 m³/h). Such operating conditions were defined to have comparable energy consumption for O_3 production (440 W) and UV system (400 W). For processes combinations with both O_3 and UV, energy consumption of 840 W was considered for comparison. Inlet and outlet samples were collected and the following parameters were measured: residual O_3 and H_2O_2 concentration, 36 target CECs concentrations, TOC, NO_2, NO_3, water pressure, absorbance and fluorescence.

RESULTS AND DISCUSSION

The preliminary lab-scale tests were useful to evaluate whether water characteristics, CECs properties or $MITO_3X$ operating conditions had the major influence on CECs removal efficiency, displayed in Figure 1 for different target contaminants, as a function of water characteristics.

Figure 1. CECs removal at all $MITO_3X$ operating conditions as a function of CEC and water quality.

Obtained removal efficiencies show that $NaNO_2$ and TOC influence is a function of the contaminant and $NaNO_2$ has more influence than TOC on the final performance. However, for each CEC and water type, high variability can be seen in the obtained removals, especially in tap water (with no $NaNO_2$ and TOC addition). This is due to the different MITO3X operating conditions. Thus, to evaluate what aspect influences the most the performance, a multilinear regression model was build for the removal of CECs sum as a function of pump rate, water flowrate, O_3 and H_2O_2 initial concentrations, TOC and $NaNO_2$ water concentrations, whose results are shown in Figure 2.

Figure 2. Multilinear regression model factorial plots for CECs removal as a function of different operating conditions and water characteristics.

The main influencing factor was found to be $NaNO_2$ concentration followed by O3 initial concentration and the pump rate. Thus, both water characteristics and operating conditions can affect the obtained CECs removal. Low (but significant, p-value<0.05) effect was found for TOC concentration and water flowrate. In particular, an unexpected result showed that an increase in water flowrate do not decrease CECs removal, as it would be expected since the contact time is reduced. Two hypotheses for such a result are: (i) $MITO_3X$ at higher flowrates provides better O_3 mixing and reactivity with compounds, (ii) there is an influence of the water pressure and difference between gas and water pressure on the performance. Finally, no significant effect was found for the addition of H_2O_2 into the system.

To evaluate the validity of these results in more relevant environments, pilot-scale tests were performed. CECs removal results at pilot-scale tests are shown in Figure 3 for different processes combinations and different water flowrates.

(a) (b)

Figure 3. CECs removal as a function of different processes configurations: (a) normalized for the energy consumption, (b) as a function of different water flowrates, where each dot corresponds to one CEC in a specific process operating condition tested at the two flowrate.

When comparing single processes, processes based only on H2O2 or UV showed worse removal compared to O3. Combining two or three processes in the treatment do not provide significant improvement on the energy-normalized CECs removal, even if UV/O_3 and $UV/O_3/H_2O_2$ combinations, characterized by twice the energy consumption, reached always more than 80% removal efficiencies. When looking at Figure 3.b, the following preliminary findings can be summarized:

- Lower CEC removal efficiencies are expected when O_3 is not dosed;
- H_2O_2 alone has the lowest removal efficiencies but improves at higher water flowrates;
- UV and UV/H_2O_2: can reach higher efficiencies only when tested at lower water flowrates;
- When O_3 is dosed the removal improves at higher flowrate with the exception of the O_3/H_2O_2 process, suggesting that further studies need to be done to evaluate this interesting aspect.

REFERENCES

Piras, F., Santoro, O., Pastore, T., Pio, I., De Dominicis, E., Gritti, E., ... & Santoro, D. (2020). Controlling micropollutants in tertiary municipal wastewater by O3/H2O2, granular biofiltration and UV254/H2O2 for potable reuse applications. Chemosphere, 239, 124635.

Tchobanoglous, G., Cotruvo, J., Crook, J., McDonald, E., Olivieri, A., Salveson, A., ... & Vartanian, G. (2015, September). Development of Framework for Direct Potable Reuse Guidelines, Results of the NWRI/WateReuse Association Expert Panel. In WEFTEC 2015. Water Environment Federation.

Van Rossum, T. (2020). Water reuse and recycling in Canada—history, current situation and future perspectives. Water Cycle, 1, 98-103.

TECHNICAL SESSIONS

T7.

Algal systems for WW treatment and RR

ECO STP 2023

Microalgae Biorefinery for Sustainable Recovery of Bioproducts and Bioenergy from Wastewater

E. Ruales*, M. Garfí*, C. Gómez**, C.V. González**, F. G. Acién** and I. Ferrer*

* GEMMA – Environmental Engineering and Microbiology Research Group, Department of Civil and Environmental Engineering, Universitat Politècnica de Catalunya BarcelonaTech, c/ Jordi Girona 1-3, Building D1, E-08034 Barcelona, Spain
(E-mail: *evelyn.ruales@upc.edu*; *ivet.ferrer@upc.edu*)

** UAL – Chemical Engineering Department, Universidad de Almería, Carretera Sacramento s/n, E-4120, Almería, España

Abstract

This study aims to assess the potential of microalgae grown in wastewater to produce biopesticides and biostimulants for crops, along with biogas from residual biomass. Bioassays confirmed the suitability of the microalgae biomass as a biostimulant since gibberellins-like activity, auxins- and cytokinin-like activity was observed in watercress seed germination, mung bean rooting, and wheat leaf chlorophyll retention. Biogas production and the kinetic profile from biostimulant-extracted biomass were 24 and 43% higher than raw biomass, respectively. Co-digestion with primary sludge increased biogas production and showed a positive synergistic effect. The applied downstream processes to get valuable compounds acted as a pre-treatment to enhance the anaerobic digestion performance. The proposed approach is a promising strategy for resource recovery from wastewater in a circular bioeconomy approach.

Keywords (maximum 6 in alphabetical order)

Bioenergy; biorefinery; microalgae; resource recovery; wastewater

INTRODUCTION

During the last decades, microalgae have received focal attention in the biorefinery development, or boosting the plant's natural defense mechanisms. Conversely, antagonistic activity against various phytopathogenic agents, namely *R. solani* and *P. ultimum*, was not observed.

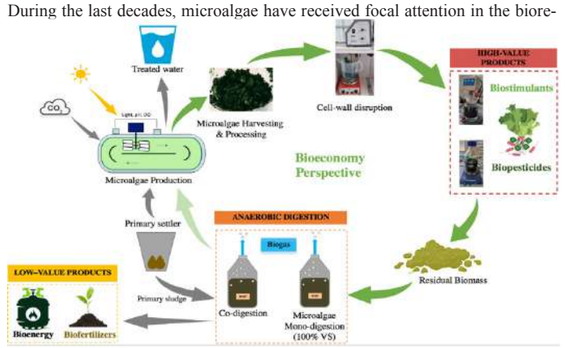

Figure 1. Microalgae biorefinery using microalgae grown in wastewater to produce biostimulants, biopesticides, and biogas. The residual biomass is then co-digested with primary sludge.

MATERIALS AND METHODS

The microalgae biomass was harvested from a pilot-scale raceway pond located at the pilot plant of the University of Almería. The raceway pond (12.6 m^3, 80 m^2) treated the primary effluent from a conventional activated sludge wastewater treatment plant. It was inoculated with *Scenedesmus* sp. and reached a biomass productivity of 23 g m^{-2}·day^{-1}. Downstream processes were applied to extract biostimulants (enzymatic hydrolysis) and biopesticides (organic solvent), with the residual and raw biomass tested for biogas production through anaerobic digestion. Biostimulant activity of microalgae biomass was tested by the gibberellin- auxin- and cytokinin-like effect through the germination index of water creed seeds (0.1 and 0.5 g L^{-1}), the mung beans rooting, and chlorophyll retention in wheat (both at 0.5 and 2 g L^{-1}). Biopesticide activity was detected by the antagonism bioassay with pathogenic fungi (*Rhizoctonia solani* and *Pythium ultimum*) at 1 and 10 g·L^{-1}.

Biogas production was analyzed through Biochemical Methane Potential (BMP) tests under mesophilic conditions (35 °C) and continuous agitation (90 rpm). The raw microalgae biomass (Raw MAB), residual biostimulant-extracted biomass (Stim-E), and residual pesticide-extracted biomass (Pes-E) were employed as substrates to study the effect of the downstream process in the anaerobic digestion performance. The co-digestion of each stream with primary sludge (PS) was also investigated (50:50 on a volatile solid (VS) basis). Mesophilic digested sludge from a wastewater treatment plant was used as inoculum, and microcrystalline cellulose was used as control. The pressure in each bottle (100 ml) was periodically measured with a digital manometer (GMH 3151 Greisinger, Germany), and the composition of the biogas from each batch reactor was analyzed using a gas chromatograph (GC-Trace, Thermo Fisher Finnigan). Specific methane yields were calculated by subtracting the blank (inoculum only) production and normalized to standard conditions. Process kinetics was modelled using a first-order kinetic model as a function of time. Experimental data were statistically assessed via parametric one-way ANOVA test.

RESULTS AND DISCUSSION

Biostimulant and biopesticide activities

Biostimulant activities were detected when two different concentrations of the microalgal extracts (0.1 and 0.5 g DW L^{-1}) were used for seed germination (Figure 2.a). The mung bean rooting tests (Figure 2.b) demonstrated auxin-like activity. Chlorophyll retention was detected when the samples were tested for cytokinin-like activity (Figure 2.c). For both assays, 2.0 g DW L^{-1} was the microalgal extract concentration showing bioactivity compared to the control (distilled water), auxin standard (IBA) and cytokinin standard (BPA).

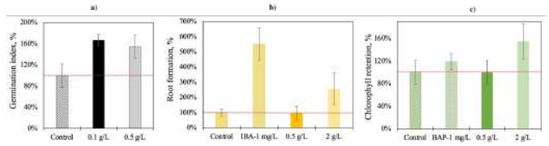

Figure 2. Biostimulant activity from *Scenedesmus* biomass extract, considering distilled water as control. **a)** Gibberellin-like activity through watercress seed germination at 0.1 and 0.5 g L^{-1}. **b)** Auxin-like activity through mung bean rooting at 0.5 and 2 g L^{-1} and indole-3-acetic acid (IBA) as the standard. **c)** Cytokinin-like activity tested using wheat leaf chlorophyll retention at 0.5 and 2 g L^{-1} and 6-benzyl aminopurine (BAP) as standard at 1 mg L^{-1}.

These results highlight the potential of microalgae grown in wastewater as a biostimulant for agriculture applications. Biostimulant microalgal extracts demonstrate the presence of molecules with biological activity that can enhance plant growth and health, often by improving nutrient uptake, promoting root

Biogas production by anaerobic digestion

Figure 3 shows the accumulated methane production of the mono-digestion trials: primary sludge (PS), raw MAB, residual biostimulant-extracted (Stim-E), biopesticide-extracted (Pes-E) biomasses and the co-digestion trials with PS. According to the results from mono-digestion tests, Pes-E achieved the highest methane yield (379 mLCH_4 g^{-1} VS), with an increase of 36% with respect to Raw MAB. Contrariwise, Stim-E achieved the lowest methane yield (251 mL CH_4 g^{-1} VS), corresponding to a decrease of 10% with respect to Raw MAB. This suggests that biostimulant extraction removed a more significant fraction of readily biodegradable organic material, reducing the biogas production. However, the kinetics of Stim-E were significantly higher (by 43%) than with Raw MAB ($p<0.001$), indicating faster hydrolysis due to the enzymatic hydrolysis applied, which increased the digestibility of residual solids.

Upon co-digestion with PS, the methane yield of Raw MAB and Stim-E was improved by 13 and 24%, respectively. Additionally, Raw MAB co-digested with PS improved the kinetics by 25% compared to the anaerobic digestion of Raw MAB. Similarly, the kinetics of Stim-E co-digested with PS showed a significant difference ($p<0.001$) with respect to the kinetics of Stim-E mono-digestion. Besides, Pes-E showed a diauxic behavior, since a sudden increase in methane production was observed after eight days of assay. Indeed, the cumulative methane yield showed two or more distinct growth phases, each one with a different substrate utilization pattern. The remaining organic solvent after biopesticides extraction could explain this behavior in Pes-E. However, the Pes-E biomass co-digested with PS showed a better response and synergetic effect between the two substrates. The double growth in the cumulative curve of Pes-E was diminished through the co-digestion with PS (Figure 3). To summarise, a synergistic effect between all microalgae biomass samples co-digested with PS resulted in improved biogas production and increased methane yield as compared to mono-digestion trials.

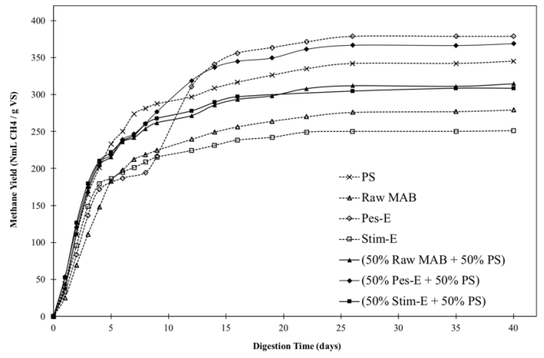

Figure 3. Cumulative methane yield of raw biomass (Raw MAB) and residual biomass after the extraction of biopesticides (Pes-E), and biostimulants (Stim-E), and primary sludge (PS) (mono-digestion and co-digestion).

Table 1. Final methane yield, methane content and first-order kinetic constant of Raw microalgae biomass (Raw MAB), residual biopesticide-extracted (Pes-E) and biostimulant-extracted (Stim-E) biomasses, and co-digestion of each one with primary sludge (PS) (50:50 on VS) (mean values ± stand. dev.; n = 3).

Substrates	Methane Yield, (NmL CH_4 g^{-1} VS)	Methane Content (%)	First-Order Constant Kinetic (day^{-1})
Raw MAB	279.3 ± 1.6 ^{b}	71.1 ± 1.5 ^{a}	0.189 ± 0.0 ^{a}
PS	345.1 ± 2.3 ^{d}	71.7 ± 0.4 ^{a}	0.219 ± 0.0 ^{b}
Pes-E	378.8 ± 4.4 ^{e}	71.8 ± 0.8 ^{a}	-
Stim-E	251.2 ± 3.5 ^{a}	72.0 ± 0.5 ^{a}	0.271 ± 0.0 ^{c}
Raw MAB : PS	314.6 ± 1.0 ^{c}	72.7 ± 0.6 ^{a}	0.237 ± 0.0 ^{b,c}
Pes-E : PS	368.9 ± 3.1 ^{e}	72.9 ± 1.3 ^{a}	0.175 ± 0.0 ^{a}
Stim-E : PS	311.3 ± 4.4 ^{c}	73.5 ± 0.1 ^{a}	0.256 ± 0.01 ^{c,d}

^{a,b,c,d,e} Letters indicate a significant difference between trials after Tukey test ($\alpha = 0.05$).

The kinetics and methane production improvement were attributed to the disruption of the microalgae cell wall upon bioproduct extraction, which acted as a pre-treatment step for the anaerobic digestion. Similar results were found after the extraction of lipids and aminoacids (Markou et al., 2022; Monlau et al., 2021) and natural pigments (Arashiro et al., 2020; van den Hende et al., 2016).

In conclusion, this study showed the possibility of recovering biostimulants for agricultural reuse from microalgae treating wastewater, along with biogas from the residual biomass in the framework of the circular bioeconomy. In this approach, the value-added bioproducts would provide economic profitability, while biogas would alleviate the energy demand of the facility, which in turn would provide sanitation to the population.

Acknowledgements

This research was funded by the AL4BIO project "RTI2018-099495-B-C21" (MCIU/AEI/FEDER, UE). E.R. acknowledges her PhD scholarship (2020 FISDU 00592) and M.G. her MINECO fellowship (RYC-2016-446 20059).

REFERENCES

Arashiro, L. T., Ferrer, I., Pániker, C. C., Gómez-Pinchetti, J. L., Rousseau, D. P. L., van Hulle, S. W. H., & Garfí, M. 2020. Natural Pigments and Biogas Recovery from Microalgae Grown in Wastewater. *ACS Sustainable Chemistry & Engineering*, 8(29), 10691–10701.

Markou, G., Ilkiv, B., Brulé, M., Antonopoulos, D., Chakalis, L., Arapoglou, D., & Chatzipavlidis, I. 2022. Methane production through anaerobic digestion of residual microalgal biomass after the extraction of valuable compounds. *Biomass Conversion and Biorefinery*, 12(2), 419–426.

Monlau, F., Suarez-Alvarez, S., Lallement, A., Vaca-Medina, G., Giacinti, G., Munarriz, M., Urreta, I., Raynaud, C., Ferrer, C., & Castañón, S. 2021. A cascade biorefinery for the valorization of microalgal biomass: biodiesel, biogas, fertilizers and high valuable compounds. *Algal Research*, 59, 102433.

Van den Hende, S., Beyls, J., de Buyck, P.-J., & Rousseau, D. P. L. 2016. Food-industry-effluent-grown microalgal bacterial flocs as a bioresource for high-value phycochemicals and biogas. Algal Research, 18, 25–32.

The Effect of Light Cycling in the Formation of Algae-Bacteria Aggregated Flocs

Holly Stolberg*, Paul Jensen*, and Andrew Ward*

* The Australian Centre for Water and Environmental Biotechnologies, Brisbane, QLD, Australia
(Email: h.stolberg@uq.edu.au, a.ward3@uq.edu.au and p.jensen@uq.edu.au)

Abstract

The formation of algae-bacteria aggregated flocs (ABAFs) allows for fast and cost-effective microalgae harvesting alternative via gravity sedimentation, whilst exploiting the cooperative relationship between algae and bacteria. This leads to rapid nutrient removal and wastewater treatment. However, the key principles surrounding the formation of ABAFs and the conditions that lead to enhanced development of these floccular systems are not fully understood, and thus further investigation is needed. Therefore, in this study the effect of light cycles was investigated to ascertain the effect it has on ABAF formation.

Keywords

ABAF, Gravity Sedimentation, Microalgae, Wastewater

INTRODUCTION

Algae-bacteria aggregated flocs (ABAFs) are an emerging technology where flocs are formed from synergistic algal-bacterial consortia. These flocs exploit the cooperative relationship between algae and bacteria leading to rapid nutrient removal (Bacellar Mendes & Vermelho 2013; Fallahi *et al.* 2021). A major advantage is that ABAFs are able to settle rapidly via gravity allowing for easy separation between the ABAFs and the treated wastewater effluent. Consequently, this form of harvesting eliminates the need for energy intensive and costly separation techniques. However, the key principles surrounding the formation of ABAFs and the conditions that lead to enhanced formation of these flocs are not fully understood, and thus further investigation is needed. One such parameter is the effect light cycling has on the formation of ABAFs. As light availability and duration is considered an important factor in the production of EPS, the major binding factor of ABAFs, it is expected light cycling will effect ABAF formation (Arcila & Buitrón 2017). Therefore, in this study it was investigated whether 24hour light vs. a light and dark exposure (that mimics the daily outdoor day/night light cycle) effected the formation of ABAFs within an upflow column photo-bioreactor (UFCPB).

MATERIALS AND METHODS

Experimental Design

Four up-flow column photo bioreactor (UFCPB) with a working volume of 6L were used throughout. Reactors were operated in batch mode, when NH_3-N reached less than 5mg/L (approximately three days) in the system it indicated batch resolution. Screened raw wastewater was used as the feed. Wastewater was obtained from Luggage Point Wastewater Treatment Plant, Queensland, Australia. Microalgae inoculum during each experiment consisted of a wild-type wastewater algae consortium obtained from high-rate algal ponds located at the Luggage Point Wastewater Treatment Plant in Queensland, Australia. Mixing of the reactors was achieved via a pump that recirculated water from the top of the reactors to the base of the reactor. Upon batch completion, mixing ceased and a 30minute settling period occurred. Following batch completion settleability of algal biomass, and thus ABAF formation, was categorized. This was achieved through measurement of TSS/VSS of the biomass, supernatant and a mixed sample, chlorophyll analysis, microscopy, EPS analysis and algal cell counts. Upon batch restart a portion of the settled inoculum was reintroduced to the reactors with 6L of the screened raw wastewater.

Light Cycling

Reactors were run with 24hour light exposure and were compared to reactors run on 16hours with light on and 8hours without light, mimicking the daily outdoor day / night light cycle.

Wastewater Treatment Capabilities

The wastewater treatment capabilities of the experimental treatments were also determined. The parameters investigated included nitrogen and phosphate removal of the systems.

RESULTS AND DISCUSSION

Results from the experiment indicated that light cycling had a significant impact on the growth rate and formation rate of algae-bacteria aggregated flocs. ABAFs were formed in both treatments and the key indication of this was that >80% of biomass was able to be harvested via gravity sedimentation by batch 7 for both treatments (see Figure 1). This is further evident when looking at the TSS of the effluent from both systems (see Figure 2), which was below the local discharge licence requirements, and contained <1million algae cells/mL. However, the effect of 24-hour light periods is evident when comparing the amount of settled biomass present across the two systems. The systems with 24hour light exposure had ~1.46g/L of settleable biomass, whereas the systems with light cycling had ~0.31g/L of settable biomass upon the completion of batch eight. The amount of biomass, and hence algae present in the system, with 24hour light exposure is almost 5x greater than that of the system with light cycling. Thus, indicating that the light cycling had a significant effect on both the growth rate and formation of ABAFs.

Light cycling also had a detrimental effect on ammonia removal rates of the systems (Figure 3). It can be seen that the system with 24-hour light exposure was able to remove 95% of ammonia from the system during batch seven and eight. Whereas, during the same time frame, the systems with light cycling were removing <30% of the ammonia in the system. This is due to the shorter photosynthetic period occurring in the light cycle reactors. During the dark period the algae were not photosynthesizing nor growing. Consequently, there was less microalgae in the system and therefore ammonia uptake was significantly less in these systems. It is noted that the batch lengths for this experiment were short, three days, as it was in a small reactor with 24hour light exposure. Total ammonia removal from an ABAF system is achievable under light/dark conditions, such as those found in high-rate algal ponds (HRAPs) outside, but a longer batch length is required to achieve >90% ammonia removal rates.

These results indicate that light duration can be factor influencing ABAF formation. Whilst 24hour light periods are not suitable for upscale of ABAFs in outdoor HRAPs, the use of UFCPBs to grow an initial inoculum for HRAPs would allow for shorter start-up time frames. In conclusion, ABAFs were successfully formed, and a stable population cultivated, within the UFCPBs. The formation process was impacted by light cycling, showing that increased light duration increases the growth rate and consequently the formation rate of ABAFs. This research also indicates that whilst light cycling does affect the growth and formation of ABAFs, there are other factors that also lead to ABAF formation as stable ABAF populations were formed in both conditions. This research also highlights ABAFs effectiveness to settle, and thus it's simplified harvesting through gravity sedimentation, hence overcoming a significant bottleneck within the microalgae industry.

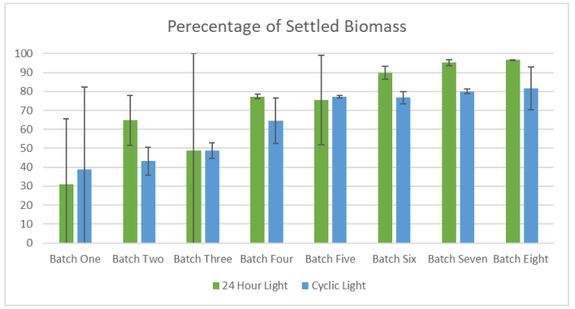

Figure 1. Percentage of biomass harvested via gravity sedimentation.

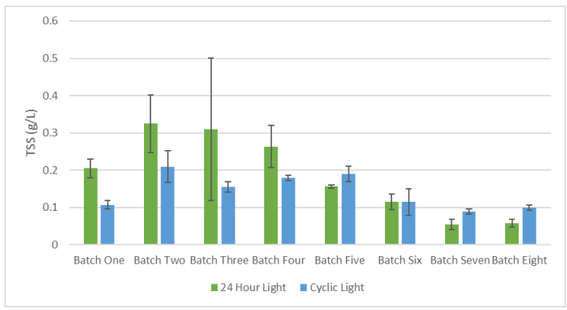

Figure 2. Total suspended solids of effluent.

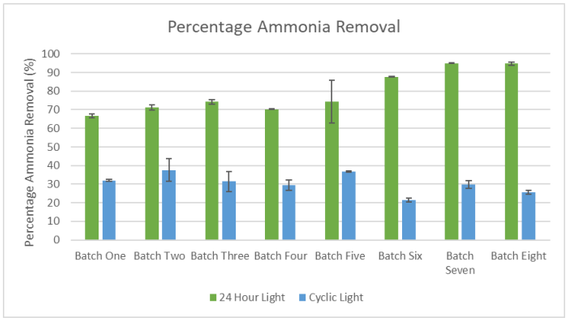

Figure 3. Percentage of ammonia removal for each batch.

REFERENCES

Arcila J. S. and Buitrón G. (2017). Influence of solar irradiance levels on the formation of microalgae-bacteria aggregates for municipal wastewater treatment. *Algal research (Amsterdam)* **27**, 190-7.

Bacellar Mendes L. B. and Vermelho A. B. (2013). Allelopathy as a potential strategy to improve microalgae cultivation. *Biotechnol Biofuels* **6**(1), 152-.

Fallahi A., Rezvani F., Asgharnejad H., Khorshidi Nazloo E., Hajinajaf N. and Higgins B. (2021). Interactions of microalgae-bacteria consortia for nutrient removal from wastewater: A review. *Chemosphere (Oxford)* **272**, 129878.

Anaerobic and microalgae-based treatments: potential for virus inactivation during secondary treatment of municipal wastewater

* Andrés F. Torres-Franco[a,b *], Deborah Leroy-Freitas[a,b], Cristina Martinez-Fraile[a,b], Elisa Rodriguez[a,b], Pedro A. García-Encina[a,b], Raúl Muñoz[a,b*].

[a] Institute of Sustainable Processes, Dr. Mergelina, s/n, 47011 Valladolid, Spain.

[b] Department of Chemical Engineering and Environmental Technology, School of Industrial Engineering, University of Valladolid, Dr. Mergelina, s/n, 47011 Valladolid, Spain.

[*] Corresponding author: e-mail mutora@iq.uva.es (R. Muñoz), andresfelipe.torres@uva.es (A.F Torres-Franco)

Abstract

Anaerobic and microalgae-based technologies for municipal wastewater treatment (MWWT) are sustainable alternatives compared to activated sludge systems due to their lower operating cost and resource recovery potential. Besides, the capacity of treatment technologies to inactivate viruses has been challenged by the COVID-19 pandemic, demanding from emerging technologies a higher potential for virus reduction. To assess virus decay in anaerobic and microalgae-based technologies, and to compare their performance with activated sludge, Phi6 and MS2 bacteriophages were spiked into batch bioreactors treating synthetic municipal wastewater (SMWW). All treatment and control reactors showed relatively similar performance in Phi6 inactivation, which occurred within 48-96h. However, MS2 showed an overall higher survival in all treatments, except in the microalgae-based reactor, which achieved a total removal in the soluble fraction at 96h, likely through photoinactivation and low partitioning to the biomass, thus exhibiting a higher potential to provide by-products of higher sanitary quality during MWWT.

Keywords: activated sludge, anaerobic treatment, bacteriophages, microalgae-based treatment, SARS-CoV-2 surrogate, virus inactivation

INTRODUCTION

The COVID-19 pandemic has questioned the current WWTPs' capacity to inactivate viruses and the underlying mechanisms behind high reductions in virus loads in municipal wastewater. These reductions are mainly achieved during advanced treatment and/or disinfection. However, secondary treatment in activated sludge systems has shown relatively high performance in virus' removal, with several works showing average reductions of up 3 log10 units for viruses such as F+-coliphages, enterovirus, and Norovirus (Delanka-Pedige et al. 2020). Unfortunately, the number of works assessing virus partitioning and survival in emerging wastewater treatment technologies, such as anaerobic and microalgae-based reactors, is scarce (Astals et al. 2012; Delanka-Pedige et al. 2020). These technologies have growing relevance due to their higher sustainability when compared to activated sludge, since they can cost-effectively recover energy and nutrients. However, the content of biological micropollutants, including viruses, is a major constraint during resource recovery from municipal wastewater (Markou et al. 2018).

On the other hand, the viability of viruses in wastewater and WWTPs has been studied using bacteriophages with no biosafety issues, among which Phi6 and MS2 have been more widely applied. Thus, this work assessed the decay of Phi6 (enveloped) and MS2 (non-enveloped) bacteriophages spiked into Activated sludge, Anaerobic digestion, and Microalgae-based treatment batch reactors. The performance of these technologies was compared in terms of bacteriophage reduction and decay kinetics, inactivation, and partitioning to solids during synthetic municipal wastewater treatment.

MATERIAL AND METHODS

Synthetic wastewater, bacteriophages and host strains

Synthetic municipal wastewater (SMWW) was used in this study as a model municipal wastewater. The SMWW was characterized by a pH of 7.39±0.1 and concentrations of dissolved total organic carbon (TOC) of 258.2±12.3 mg L^{-1}, dissolved inorganic carbon (IC) of 5.7±9.9 mg L^{-1}, and 50.7±10.0 mg L^{-1} of dissolved total nitrogen (TN). Bacteriophages Phi6 (DSM-21518) and MS2 (DSM-13767), and their respective hosts *Pseudomonas* sp. (DSM-21482) and *E. coli* (DSM-5695), were purchased from the German Collection of Microorganisms and Cell Cultures (DSMZ). The bacteriophages and their host were revitalized and handled according to DSMZ. High-titer stock solutions were achieved using amplification in plates and the double agar technique was applied to quantify the bacteriophage concentrations (Fedorenko et al. 2020)

Experimental set-up, virus reduction, and decay kinetics

Three batch experiments investigating the decay of Phi6 and MS2 were performed in 2.1 L glass sterile bottles (Fisher) using (i) Activated sludge (ASR), (ii) Anaerobic sludge (ANR), and (iii) a Microalgal-bacterial consortium (MBR). The tests were conducted in duplicate under constant magnetic agitation at 180 rpm (Cimarec I Multipoint, Thermofisher). The reactors were operated in a controlled temperature room at 25° C, 37°C, and 29°C for ASR, ANR, and MBR, respectively. ASR and ANR were inoculated with activated sludge and anaerobic sludge from the local WWTP. MBR used activated sludge and *Chlorella sorokoniana* as inocula. Each reactor was compared to a control reactor (SMWW Control), spiked with bacteriophages, and operated under the same conditions, except bacterial or microalgal inoculation.

The broth of the biodegradation and control reactors was spiked with Phi6 and MS2 suspensions at a ratio 1:1000. Samples were withdrawn at 0, 6, 12, and 24 h after inoculation of the viral suspensions and every 24 h until 96 h for Phi6 monitoring or 144 h for MS2 monitoring. Samples were collected using needles and syringes directly from the reactors and controls under sterile conditions, and were stored in sterile falcon tubes and microtubes. The partitioning to solids and virus reduction capacity of each reactor was estimated based on bacteriophage titers in both soluble and total fractions over time. Furthermore, log-logistic regressions were applied to assess the decay kinetics using the *drc* package in Rstudio (Ritz et al. 2015).

RESULTS AND CONCLUSIONS

Activated sludge, anaerobic and microalgae-based treatments showed high potential in the reduction and inactivation of enveloped Phi6 and nonenveloped MS2 bacteriophages (Table 1, Figure 1). Enveloped Phi6 showed a higher affinity for aerobic solids when compared to nonenveloped MS2, which showed overall low interaction with suspended solids, mainly in activated sludge and microalgae-based treatments (Figure 1). T_{90} values were calculated through log-logistic models, using the titers in the total fraction, showing values of 0.11, 0.17, and 0.39 days for Phi6 and 0.17, 0.98, and 0.44 days for MS2 (Figure 2). Phi6 was completely reduced in 48-96 h in treatment reactors, among which anaerobic treatment produced faster inactivation (before t= 48h). The microalgae-based treatment outperformed the activated sludge and anaerobic processes for the removal of MS2 from the soluble phase, achieving a complete MS2 removal at t=96 h. Photoinactivation and low solid partitioning to the microalgae-bacterial biomass were the main factors favoring bacteriophage inactivation in MBR. Therefore, microalgae-based treatments can potentially provide by-products of higher sanitary quality in terms of virus titers during municipal wastewater treatment.

Table 1. Recovery efficiencies and maximum reductions achieved for MS2 and Phi6 spiked in control and treatment reactors.

Treatment	Virus	Virus Spiked (PFU)		Virus in the inoculum (PFU)	Max Reduction (log_{10} units)		
		Control	Reactor		Control	Reactor	
						Soluble	Total
AS	Phi6	9.1	9.4	0.0	9.1±0.1	9.1±0.1	9.1±0.1
	MS2	11.6	11.9	6.1	4.1±0.1	6.2±0.0	4.8±0.0
AN	Phi6	10.7	11	0.0	10.7±0.0	11.0±0.0	11.0±0.0
	MS2	11.6	11.9	4.7	2.3±0.0	5.7±0.3	5.6±0.2
MB	Phi6	11.6	11.9	0.0	11.6±0.0	11.9±0.0	11.9±0.0
	MS2	11.7	12	6.1	11.7±0.0	12.0±0.0	7.6±0.0

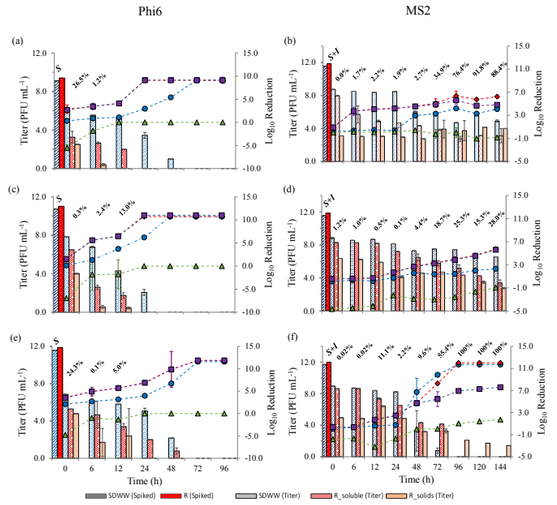

Figure 1. Viral titers (PFU mL^{-1} main y-axis) and log_{10} units reductions (secondary y-axis) for bacteriophages Phi6 and MS2 in (a, b) Activated Sludge, (c, d) Anaerobic treatment and (e, f) Microalgae-based treatment. Viral titers are represented with bars. The larger bars at t=0 show the PFU spiked (S) to each control and biodegradation reactor. For MS2, initial bars include F+-coliphages in the inocula (S + I). Log_{10} unit reductions in total (■) soluble (♦) and solid fraction (▲) of biodegradation reactors, and *SMWW* controls (●) are represented with lines. Negative initial log_{10} unit removals in reactors´ solids fraction denotes the titer increases in t=0 h compared to titers in inocula. Percentages of viral particles attached to solids are written for each time in which titers in solids were detected

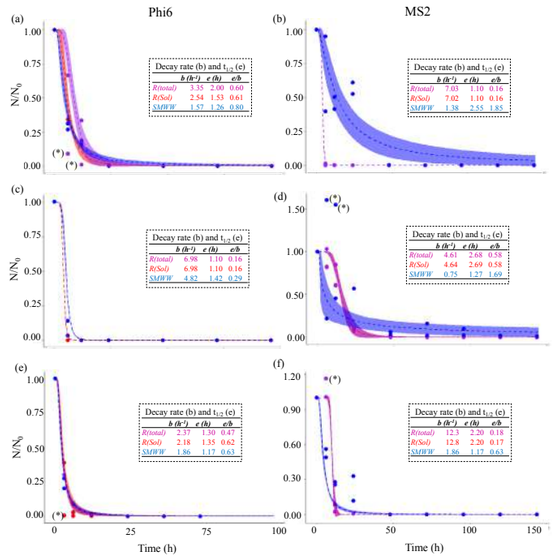

Figure 2. Log-logistic regressions for Phi6 and MS2 decays in total (■) and soluble fractions (■) of biodegradation reactors and *SMWW* controls (■) for (a, b) activated sludge, (b, c), anaerobic and (e, f) microalgae-based trials. Significance intervals were calculated at p<0.1. Points marked as (*) were regarded as outliers and excluded of the model fit.

REFERENCES

Astals, S., Venegas, C., Peces, M., Jofre, J., Lucena, F., & Mata-Alvarez, J. 2012. Balancing hygienization and anaerobic digestion of raw sewage sludge. Water research, 46(19), 6218-6227.

Delanka-Pedige, H. M., Cheng, X., Munasinghe-Arachchige, S. P., Abeysiriwardana-Arachchige, I. S., Xu, J., Nirmalakhandan, N., & Zhang, Y. 2020. Metagenomic insights into virus removal performance of an algal-based wastewater treatment system utilizing Galdieria sulphuraria. Algal Research, 47.

Fedorenko, A., Grinberg, M., Orevi, T., & Kashtan, N. (2020). Survival of the enveloped bacteriophage Phi6 (a surrogate for SARS-CoV-2) in evaporated saliva microdroplets deposited on glass surfaces. Scientific reports, 10(1), 1-10.

Markou, G., Wang, L., Ye, J., & Unc, A. 2018. Using agro-industrial wastes for the cultivation of microalgae and duckweeds: Contamination risks and biomass safety concerns. Biotechnology advances, 36(4), 1238-1254.

Pilot Scale Wastewater Remediation Using Algae Bacterial Aggregated Flocs (ABAF)

A. J. Ward*, Paul Jensen*

* The Australian Centre for Water and Environmental Biotechnology at the University of Queensland, Queensland, Australia
(E-mail: a.ward3@uq.edu.au *and p.jensen@uq.edu.au)*

Abstract

This study demonstrates an innovative biological wastewater treatment process based on an aggregated microbial bio-floc comprising of an algae-bacteria based consortia. The aggregation of the algae-bacteria consortia into a stable floc was successfully demonstrated over a 12-month period in a pilot scale outdoor 4.5m^2 open High-Rate Algae Pond (HRAP) system. The robustness of the algae bacteria aggregated floc (ABAF) was demonstrated through utilisation of existing scalable high-rate algae pond culture techniques with continuous paddle wheel mixing. Results of the 12-month study demonstrate average domestic wastewater nutrient removal efficiencies for NH_4-N, PO_4-P and Total Nitrogen of 98%, 74% and 57% respectively. The HRAPs were operated in a novel process where they were run as a fill and drain sequencing batch reactor with gravitational sedimentation employed to recover biomass.

Keywords (maximum 6 in alphabetical order)

Algae, Aggregated Floc, Algae Harvesting, Bacteria, Wastewater Treatment

INTRODUCTION

Single celled microalgae-based wastewater treatment processes have been extensively researched; however, one of the main factors that limit these systems is the challenge of low-cost efficient biomass harvesting and dewatering. Harvesting microalgal biomass requires efficient solid-liquid separation technologies (Pahl et al. 2013). This technology is often the limiting step due to high equipment costs, excessive energy consumption and high operational costs (Uduman et al. 2010).

Combined algae-bacteria aggregated flocs (ABAFs) can overcome difficult and energy intensive biomass harvesting processes. The formation of bacteria and algae into aggregated flocs allows the ABAFs to settle quickly allowing simple gravitational separation processes for biomass harvesting and dewatering. ABAF systems have the benefits of typical high-rate algae processes whilst also having the potential of a more efficient solution for regional and decentralised wastewater treatment applications. Increased benefits of ABAF systems include the simple separation of the aggregated algal biomass by gravity sedimentation, high removal efficiency for organic carbon and nutrients, independence in terms of oxygen provision through algal photosynthesis and the resource recovery opportunity by producing a valuable biomass feedstock for value added products (Wang et al. 2022; Oswald et al. 1953).

To date no other pilot scale work on ABAFs has been undertaken under Australian climatic conditions. However, limited international laboratory scale studies have demonstrated that algal-bacterial granules / flocs for wastewater treatment can achieve better nutrient removal efficiency than single bacterial or microalgal systems (Muñoz and Guieysse, 2005, 2006; Ramanan et al. 2016; Gutzeit et al. 2004). Results from this initial study identified a novel process that utilises algae and bacteria combined in an aggregated floc to remediate wastewater nutrients.

MATERIALS AND METHODS

The experimental pilot raceways were located at Luggage Point Sewage Treatment Plant located in Pinkenba, Queensland, Australia. Four HRAP (5m L x 2.5m W x 0.4m D) with a surface area of 4.5m^2 each were used for the experimental work. The working volume for the raceways was 1000 litres and paddlewheels were used for culture mixing. The pilot experiment was conducted in unsheltered outdoor conditions over a 12-month period. ABAFs was inoculated into the HRAPs, and the system was then operated in a sequencing batch reactor configuration where the culture was mixed for 5 to 7 days. Following, a 30-minute settling period allowing for ABAF biomass to settle. The treated water was decanted and a percentage of settled biomass removed and used as an inoculum. The HRAPs were then refilled with post screened domestic sewage wastewater and the cycle repeated. The nutrient parameters NH_4-N, PO_4-P, NO_2-N and NO_3-N were analysed using FIA analysis. D.O., pH, turbidity, Soluble COD, TSS and VSS were also analysed over the experimental period. Molecular diversity of Eukaryote and Bacterial diversity was investigated. HRAP were sampled monthly to examine changes in microalgae and bacterial diversity over a 12-month period. This was undertaken by utilising 16s rRNA and 18s rRNA pyrosequencing methods and technologies.

RESULTS AND DISCUSSION

ABAFs industrial biotechnologies developed in this project represent a novel approach to wastewater treatment and algae production. Results demonstrated a stable ongoing 12-month operation of the ABAFs pilot system under outdoor conditions on domestic wastewater. A stable microbial population was also noted over the 12-month period. Average nutrient removal efficiencies achieved over the 12-month experimental period for NH_4-N, PO_4-P and total nitrogen were 98%, 74% and 57% respectively. Monthly average nutrient removal efficiencies are shown in Table 1. Ammonia removal did not show any significant disparity over the 12-month period however, phosphorous removal showed more variation over the experimental period. Total nitrogen removal efficiency reduced over the winter months when compared to the warmer summer months. This could be expected as lower solar radiation is received during the winter months. An average biomass recovery rate of 80% ± 11 % was achieved over the experimental period by using simple gravitational settling process.

CONCLUSION

ABAF biotechnologies developed in this project demonstrate a novel approach to water treatment and algae production. Specifically, the project results to date address major limitations of existing algal technologies by enabling rapid low-cost biomass harvesting. This ABAF technology has demonstrated significant advantages and can eliminate the major limiting step of biomass recovery from algae-based remediation systems.

FIGURES AND TABLES

Table 1: Monthly average removal efficiencies for ammonia and total nitrogen over the 12-month experimental period (N=2) study.

	FEB	MAR	APR	MAY	JUN	JUL	AUG	SEP	OCT	NOV	DEC	JAN
NH_4-N Removal %	95 ± 9	100 ± 1	100 ± 0	100 ± 0	100 ± 0	99 ± 1	100 ± 0	96 ± 7	99 ± 4	99 ± 1	100 ± 1	100 ± 0
PO_4-P Removal %	55 ± 2	70 ± 30	73± 20	70 ± 2	81 ± 21	79 ± 26	82 ± 16	61 ± 39	82 ± 18	89 ± 13	69 ±26	82 ± 24
TN Removal %	67 ± 11	65 ± 21	55 ± 14	35 ± 22	46 ± 10	41 ± 14	45 ± 17	40 ± 12	59 ± 18	61 ± 7	70 ±10	70 ± 9

REFERENCES

Gutziet, G., Lorch, D., Weber, A., Engels, M. and Nies, U. Bioflocculant algal-bacterial biomass improves low-cost wastewater treatment. *IWA 4th World Water Congress* 19-24 sept 2004 (Morroco)

Muñoz, R., Jacinto, M., Guieysse, B., Mattiasson, B., 2005. Combined carbon and nitrogen removal from acetonitrile using algal-bacterial bioreactors. *Applied Microbiological Biotechnology* **67** (5), 699–707.

Muñoz, R., Guieysse, B., 2006. Algal-bacterial processes for the treatment of hazardous contaminants: a review. *Water Research.* **40** (15), 2799–2815.

Oswald, W.J., Gotaas, H.B., Ludwig, H.F. and Lynch, V. (1953). Algae symbiosis in oxidation ponds, III. Photosynthetic Oxygenation. *Sewage and Industrial Wastes* **25**(6), 692-705.

Pahl, S.L., Lee, A.K., Kalaitzidis, T., Ashman, P.J., Sathe, S., Lewis, D.M., 2013. Harvesting, thickening and dewatering microalgae biomass. In: Michael, A.B., Navid, R.M. (Eds.), *Algae for Biofuels and Energy*. Springer, Dordrecht, pp. 165–185.

Ramanan, R., Kim, B.H., Cho, D.H., Oh, H.M., Kim, H.S., 2016. Algae-bacteria interactions:
evolution, ecology, and emerging applications. *Biotechnology Advances* **34** (1), 14–29

Uduman N, Qi Y, Danquah MK, Forde GM, Hoadley A. 2010 Dewatering of microalgal cultures: a major bottleneck to algae-based fuels. *Journal of Renewable Sustainable Energy*. 2:12701.

Wang, S., Mukhambet, Y., Esakkimutha, S. 2022 Integrated microalgal biorefinery – Routes, energy economic and environmental perspectives. *Journal of Cleaner Production* **348**, 131245

Comparison of High Rate Algal Pond mesocosm performance using filamentous algae or microalgae

R. Craggs*, J. Park**, C. Picken*, M. Moshin*, and H. Hariz*

* National Institute of Water and Atmospheric Research, PO Box 1-115 Hillcrest, Hamilton, 3210, New Zealand.
(E-mail: *rupert.craggs@niwa.co.nz)*
**PO Box 20068, Te Rapa, Hamilton 3241, New Zealand.
(E-mail: *jason.park@babbage.co.nz*)

Abstract

Worldwide, the majority of algal wastewater treatment systems have focused on using unicellular or colonial microalgae grown in suspension in either waste stabilisation ponds or more advanced high rate algal ponds. However, challenging operation issues warrant the investigation of filamentous algae instead. This study compared for the first time the nutrient removal performance and algal productivity of native New Zealand (NZ) microalgae and filamentous algae grown on human wastewater in outside high rate algal pond mesocosms. The high rate algal pond mesocosms comprised of 15-L plastic buckets with a 30 cm culture depth which were operated outdoors during summer and winter conditions. The cultures were grown on primary settled domestic wastewater in two mesocosms in series which were operated as continuous cultures each mesocosm with either a 3-day (summer) or 4-day (winter) hydraulic retention time, with hourly wastewater addition into the first mesocosm. The microalgae mesocosms were able to remove over half the influent ammoniacal-N and DRP concentrations. The filamentous algae mesocosms had slightly lower nutrient removal than the microalgae mesocosms under both winter and summer conditions. The microalgae mesocosms had higher productivity than the filamentous algae mesocosms under both winter and summer conditions. These encouraging results suggest that further studies should be undertaken to investigate opportunities to enhance the performance of filamentous algae systems.

Keywords (maximum 6 in alphabetical order)

Ammoniacal-N, Dissolved Reactive Phosphorus, Productivity

INTRODUCTION

Worldwide, the majority of algal wastewater treatment systems have focused on using unicellular or colonial microalgae grown in suspension in either waste stabilisation ponds or more advanced high rate algal ponds (Craggs, 2005; Sutherland 2014). However, challenging operation issues (including lack of process control due to the inability to separate the retention times of the water and microalgae, inefficient and costly harvest of microalgal biomass, and loss of performance due to zooplankton grazing of the microalgae) warrant the investigation of filamentous algae instead. Filamentous algae are comparatively easily harvested there-by enabling algal biomass to be removed and returned to simply adjust its retention time, independently of that of the water. This has the potential to enable much better process control. In addition, filamentous algae don't appear to be as susceptible as microalgae to zooplankton grazing pressure, presumably due to the comparatively much larger size of the algae filaments. However, the larger size of filamentous algae and reduced surface area to volume ratio may result on lower productivity and nutrient removal compared with planktonic microalgae. This study compared for the first time the nutrient removal performance and algal productivity of native New Zealand (NZ) planktonic and filamentous algae grown on human wastewater in outside high rate algal pond mesocosms.

MATERIALS AND METHODS

High rate algal mesocosm setup

This study was conducted outdoors during summer and winter conditions at the Ruakura Research Centre, Hamilton, New Zealand (37°47′ S, 175°190′ E). The high rate algal pond mesocosms comprised of 15-L plastic buckets with a 30 cm culture depth. The buckets were wrapped in opaque

foam to ensure that light entered only from the surface of the water and were placed on individual magnetic stirrer plates and mixed continuously by a novel vertical paddlewheel mixer (4-cm wide blade that hung from a bearing above the water surface to ~1 cm above the bottom of the mesocosm).

The mesocosms were inoculated with wastewater cultures of either mixed planktonic microalgae or mixed filamentous algae. The microalgae culture was dominated by the chlorophyte *Scenedesmus* sp. and Desmodesmus sp. The filamentous algae culture was dominated by *Oedogonium* sp.

Experiment were conducted during summer (22nd November 2021 – 24th January 2022) and winter (25th May to 14th July 2022) conditions and run for a minimum of six weeks. The cultures were grown on primary settled domestic wastewater in two mesocosms in series which were operated as continuous cultures each mesocosm with either a 3-day (summer) or 4-day (winter) hydraulic retention time, with hourly wastewater addition into the first mesocosm.

Dissolved nutrient analysis

For dissolved nitrogen and phosphorus determination, mesocosm culture was sampled twice a week and filtered through Whatman GF/Ffilters, and concentrations of ammonium (NH_4–N), nitrate (NO_3–N) and dissolved reactive phosphorus (DRP) were determined colourimetrically according to standard methods

(APHA 2008).

Biomass determination

For organic matter, a known volume of mesocosm culture was sampled twice a week and filtered through a pre-rinsed, pre-combusted and pre-weighed Whatman GF/F filter, oven dried (105 °C) and weighed, once cooled, to determine the total suspended solids (TSS) concentration. Filters were then combusted at 450 °C for 4 h, cooled in a desiccator, and re-weighed to determine the ash concentration. The organic matter, also referred to as volatile suspended solids, was estimated as the difference between TSS and ash concentrations.

RESULTS

The nutrient removal and algal productivity of the microalgae and filamentous algae mesocosm are compared for both summer and winter conditions in Figures 1 - 4.

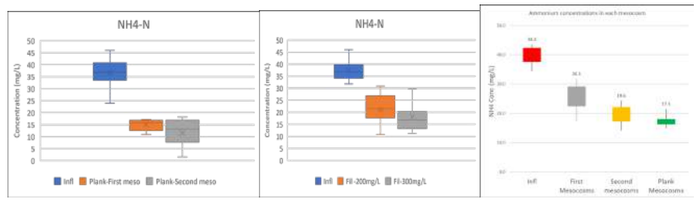

Winter Summer

Figure 1. Ammoniacal-N concentration in microalgae and filamentous algae mesocosms under summer and winter conditions

The microalgae mesocosms were able to remove over half the influent ammoniacal-N concentration. The filamentous algae mesocosms had slightly lower ammoniacal-N removal than the microalgae mesocosms under both winter and summer conditions (Figure 1).

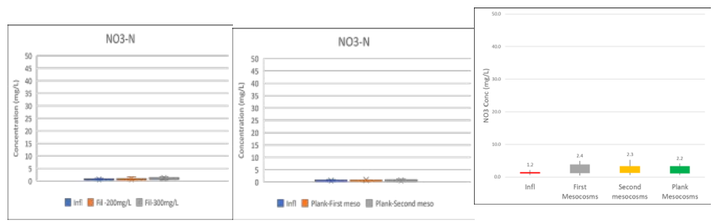

Winter Summer

Figure 2. Nitrate-N concentration in microalgae and filamentous algae mesocosms under summer and winter conditions

Under winter conditions nitrification occurred resulting in slightly elevated nitrate concentrations in both the filamentous algae mesocosms and the microalgae mesocosms (Figure 2). Under summer conditions little nitrification was observed.

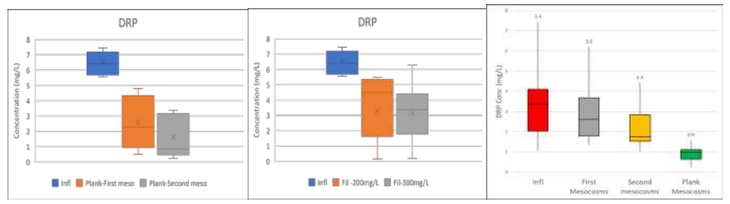

Winter Summer

Figure 3. Dissolved Reactive Phosphate concentration in microalgae and filamentous algae mesocosms under summer and winter conditions

The microalgae mesocosms were able to remove over half the influent DRP concentration. The filamentous algae mesocosms had slightly lower DRP removal than the microalgae mesocosms under both winter and summer conditions (Figure 3).

The microalgae mesocosms had higher productivity than the filamentous algae mesocosms under both winter and summer conditions (Figure 4).

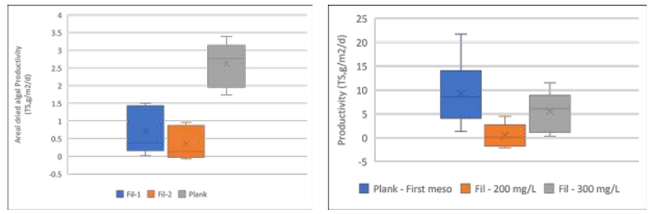

Winter Summer

Figure 4. Biomass productivity in microalgae and filamentous algae mesocosms under summer and winter conditions

DISCUSSION

These results indicate the potential of growing filamentous algae instead of microalgae for wastewater treatment in High Rate Algal Ponds. The performance of the filamentous algae mesocosms was not as good as that of the microalgae mesocosms with respect to both nutrient (Ammoniacal-N and DRP) removal and algal productivity. These encouraging results suggest that further studies should be undertaken to investigate opportunities to enhance the performance of filamentous algae systems.

REFERENCES

Craggs RJ 2005 Advanced integrated wastewater ponds. In: Shilton A(ed) Pond treatment technology. IWA scientific and technical report series. IWA, London, pp 282–310.

Sutherland D, Turnbull M, Craggs R. 2014 The effects of pond operation depth on photosynthesis, algal productivity and nutrient removal in wastewater treatment high rate algal ponds. Water Research **53**, 271–281.

Wastewater grown microalgae as biofertilizer: Contaminants of Emerging Concern, heavy metals and pathogens assessment

Ana Álvarez-González[a], Lydia Serrano[b], Gil Gorchs[b], Mònica Escolà Casas[c], Víctor Matamoros[c], Eva Gonzalez-Flo[c], Rubén Díez-Montero[a,d], Enrica Uggetti[a]

a. GEMMA-Group of Environmental Engineering and Microbiology, Department of Civil and Environmental Engineering, Universitat Politècnica de Catalunya-BarcelonaTech, c/Jordi Girona 1-3, Building D1, E-08034 Barcelona, Spain
b. Department of Agri-Food Engineering and Biotechnology, Universitat Politècnica de Catalunya·BarcelonaTech, C/ Esteve Terrades 8. E-08860 Castelldefels, Spain.
c. GEMMA-Group of Environmental Engineering and Microbiology, Department of Civil and Environmental Engineering, Escola d'Enginyeria de Barcelona Est (EEBE), Universitat Politècnica de Catalunya-BarcelonaTech, Av. Eduard Maristany 16, Building C5.1, E-08019 Barcelona, Spain
d. GIA - Group of Environmental Engineering, Department of Water and Environmental Sciences and Technologies, Universidad de Cantabria, Avda. Los Castros s/n, 39005 Santander, Spain.
e. Department of Environmental Chemistry, IDAEA-CSIC, C/Jordi Girona, 18-26, E-08034, Barcelona, Spain

Abstract

Microalgal biomass cultivated in wastewater was used as biofertilizer for lettuce crop. Pathogens and heavy metals were measured in the biomass and compared to the threshold reported by the EU regulation for fertilizing products. Contaminants of emerging concern (CECs) were monitored in wastewater, microalgal biomass and lettuce leaves. In general, pathogens and heavy metals content of the biomass were below the threshold, except for cadmium. The agronomic assay revealed that microalgal biomass can reduce the use of mineral nitrogen fertilizer, obtaining similar fresh weight. Wastewater presented 25 CECs, which only 3 were found in the biomass in concentrations ranging 0.1 to 25 µg/g_{DM}. Both cadmium and CECs were detected in lettuce crops, but their presence could not be linked to the microalgal biomass.

Keywords

Agronomic tests; Biofertilizer; Circular bioeconomy; Emerging pollutants; Nutrients recovery

INTRODUCTION

In a circular bioeconomy context, the use of wastewater as a source of nutrients for microalgae cultivation has resulted in the reduction of production costs. Moreover, the biomass could be further used as biofertilizer (Ronga et al., 2019). However, wastewater might present contaminants like pathogens, heavy metals and contaminants of emerging concern (CECs). Therefore, it was considered the need to assess the fertilizing capabilities of microalgal biomass grown in wastewater, and at the same time to characterize the microalgal biomass in those terms reported in the European legislation about fertilizing products (European Union, 2019), as well as to track the presence and fate of specific contaminants in the wastewater, microalgal biomass and lettuce plants.

MATERIALS AND METHODS

Biomass cultivation and characterization

Two high rate algal ponds (HRAPs), with a volume of 470 L each, located outdoors in Barcelona (Spain) treated real municipal wastewater. The microalgal biomass from the HRAPs was harvested in secondary settling tanks, thickened in laboratory Imhoff cones at 4ºC, centrifuged and stored at 20ºC until use in agronomic tests.

The characterization of the microalgal biomass consisted in macro- (nitrogen (N), phosphorus (P), potassium (K), magnesium (Mg), calcium (Ca), sulphur (S)) and micronutrients (iron (Fe), sodium (Na)); pathogens (*Salmonella*, *Escherichia coli*, *Legionella* spp. and *Legionella pneumophila*); and heavy metals which include cadmium (Cd), cupper (Cu), chromium (Cr), hexavalent chromium (Cr(VI)), mercury (Hg), nickel (Ni), lead (Pb), zinc (Zn), aluminium (Al), arsenic (As).

Agronomic assay

The agronomic assay was performed in a greenhouse located in Castelldefels (Barcelona, Spain), using Lettuce (*Lactuca sativa* L. cv Maravilla) during November-January. Four treatments were tested: (**C-**) negative control without fertilizer; (**C+**) positive control with NPK 100% inorganic; (**M1**) microalgal biomass + inorganic N (half dose of C+) + inorganic PK (same dose as C+); (**M2**) microalgal biomass + inorganic PK (same dose as C+). Each treatment consisted in 30 pots of 2 L each. At harvest, fresh weight was recorded. Lettuce leaves were analysed in terms of macro- and micronutrients and heavy metals. Contaminants of emerging concern were monitored in wastewater, microalgal biomass and lettuce leaves. A leachate assay was performed after lettuces were harvested. For this, 1 L of tap water was added to each pot and the leachate produced was analysed in terms of water-soluble nutrients (nitrate, ammonium and phosphate).

RESULTS AND DISCUSSION

Biomass characterization

Regarding the nutrient content of the microalgal biomass, N presented the highest content (6.69 %$_{DM}$). It presented a NPK ratio (1:0.25:0.05) which is in accordance with previous studies. Pathogens and heavy metals content (Table 1) were below the threshold of the European regulation, except for Cd, (3.10 mg/kg_{DM} when the limit for organo-mineral fertilizers is 3 mg/kg_{DM}).

Microalgal biomass as biofertilizer: effects in lettuce growth

The agronomic assay revealed that C+ and M1 presented similar shoot fresh weight, with no significant differences ($p < 0.05$), 95.41 g/plant and 93.45 g/plant, respectively (Table 2). However, M2 (43.7 g/plant) presented lower weight than both C+ and M1 (Table 2). These results suggest that the amount of mineral N can be partially replaced with microalgal biomass (M1) without affecting the shoot fresh weight.

The nutrient content measured in lettuce leaves revealed that the nutritional status was similar in C+ and M1 for N and K (Table 2). This result supports the above-mentioned results. In addition, treatment M1 presented significantly higher P and S content ($p < 0.05$) than C+, with an increment of 37 % and 20 %, respectively. In general, M2 showed lower nutrient concentration in leaves, suggesting that the amount of nutrient supplied in this treatment was not enough to support lettuce's growth.

Regarding heavy metals, only Cd was above the threshold given in EU regulation. Therefore, this element was measured in lettuce leaves. There were not significant differences between C+, M1 and M2. This result demonstrates that the source of the metal in lettuce leaves was not linked to the biomass, but probably to the soil, which had a Cd content of 0.5 mg/kg_{DM}.

Contaminants of Emerging Concern: possible transfer to lettuce crops

Although 25 CECs were found in wastewater (Figure 1), only a few presented a concentration higher than 3 µg/L (caffeine, diclofenac, hydrocynamic acid, methyl dihydrojasmonate, and naproxen). In general, the microalgal biomass presented only 3 CECs with concentrations higher than the LOQ (Limit Of Quantification), which where hydrocinnamic acid, caffeine, and bisphenol A (concentration ranging from 0.1 to 25 µg/g_{DM}) (Figure 1). Taking into account these results, CECs were also measured in lettuce leaves. Although some replicates presented concentrations ranging from 0.1 to 0.8 µg/g_{DM} of a few CECs, they were also present in C+ and C- (Figure 1), which demonstrates that the source was not the microalgal biomass.

Nutrient leaching from microalgal-based biofertilizer

At the end of the experiment, after lettuce were harvested, some nutrients (ammonium, nitrate and phosphate) were monitored in the leachate (Table 3). The concentration of the different species of nitrogen in C+ and M1 were different, in spite of receiving the same amount of NO_3-NH_4 23 days prior to the harvest. For instance, C+ presented 128 mg/L N-NO_3^- and 3 mg/L N-NH_4^+ whereas M1 presented 204 mg/L N-NO_3^- and < 0.2 mg/L N-NH_4^+. These results suggest that the microalgal biomass could either promote the presence of soil nitrifying bacteria or provide nitrifying bacteria, which catalyse the oxidation of ammonium to nitrate. Regarding phosphorus, only C+ presented a concentration higher than LOQ in leachate (5 mg/L P-PO_4^{3-}) in spite of being provided with the same dose of P in C+, M1 and M2. This can suggest that microalgal biomass can avoid P leaching.

Table 1. Content of heavy metals (mg/kg_{DM}) and pathogens (CFU/g) in the microalgal biomass cultivated in wastewater. Third column shows the threshold value given in European regulation (EC 2019/1009) for mineral-organic fertilizers.

Heavy metal (mg/kg_{DM})	Microalgal biomass	European regulation limits
Cadmium	3.10	3
Hexavalent chromium	1.31	2
Mercury	0.52	1
Nickel	< 46.5	50
Lead	< 46.5	120
Arsenic	< 18.6	40
Copper	279	600
Zinc	437	1500
Pathogens (CFU/g)	**Microalgal biomass**	**European regulation limits**
Legionella ss	Not detected	-
Salmonella spp	Not detected	Absence
Escherichia coli	400	1000

Table 2. Fresh weight (g/plant) and nutrient content (%$_{DM}$) in the four treatments: C- (negative control), C+ (positive control), M1 (microalgal biomass with N supplement), M2 (microalgal biomass). Standard Error of the Mean is given in brackets (n=30 for fresh weight and n=4 for nutrients). Different letters indicate significant difference ($p < 0.05$).

	C-	C+	M1	M2
Fresh weight (g/plant)	28.28^{c} (0.93)	95.41^{a} (3.53)	93.45^{a} (3.21)	43.7^{b} (1.14)
N (%$_{DM}$)	0.88^{b} (0.03)	3.60^{a} (0.08)	3.69^{a} (0.03)	1.01^{b} (0.02)
P (%$_{DM}$)	0.14^{c} (0.01)	0.18^{bc} (0.01)	0.28^{a} (0.02)	0.19^{b} (0.01)
K (%$_{DM}$)	2.12^{c} (0.07)	5.04^{a} (0.10)	5.24^{a} (0.17)	3.24^{b} (0.09)
S (%$_{DM}$)	0.10^{a} (0.01)	0.24^{c} (0.01)	0.29^{d} (0.01)	0.14^{b} (0.01)

Table 3. Soluble inorganic nutrients concentrations (Ammonium; Nitrate; Phosphate) in the leachate in each treatment: C- (negative control), C+ (positive control), M1 (microalgae biomass with N supplement), M2 (microalgae biomass). Standard Error of the Mean is given in brackets (n=4).

	C-	C+	M1	M2
N-NH_4^+ (mg/L)	<0.02	2.7 (0.6)	<0.2	<0.02
N-NO_3^- (mg/L)	3.0 (0.3)	127.8 (5.5)	204.1 (14.4)	4.4 (0.6)
P-PO_4^- (mg/L)	<0.8	5.4 (1.7)	<0.8	<0.8

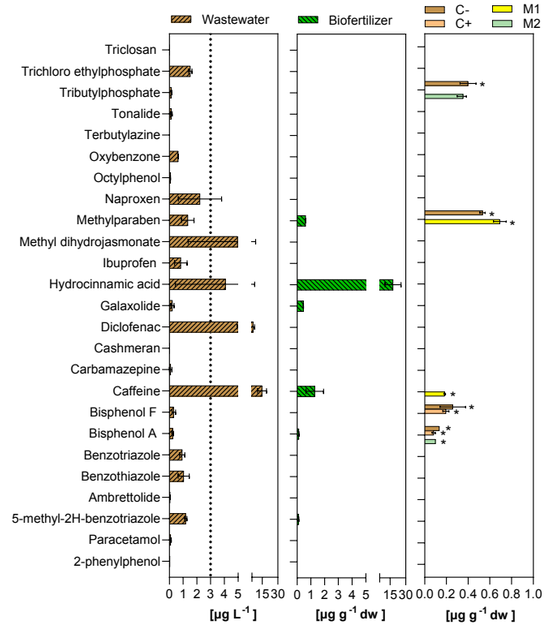

Figure 1. Mean concentrations of the detected CECs (25 out of 29) in the wastewater (n=2), biomass (n=2) and lettuce leaves of each treatment (C-, C+, M1 and M2) (n=4). Values are given in ***µg***/L for water and ***µg***/dDW for biomass or lettuce. Compounds with concentration <LOD in all samples are not plotted. Only replicates with values >LOD were used to calculate means. Error bars show the range of the measurements. *Compounds were detected on two or less replicates.

REFERENCES

European Union 2019. Regulation (EU) 2019/1009 of the european parliament and of the council 2019 laying down rules on the making available on the market of EU fertilising products and amending Regulations (EC) No 1069/2009 and (EC) No 1107/2009 and repealing Regulation (EC) No 2003/2003.

Ronga, D., Biazzi, E., Parati, K., Carminati, D., Carminati, E., Tava, A. 2019. Microalgal Biostimulants and Biofertilisers in Crop Productions. Agronomy 9, 192. https://doi.org/10.3390/agronomy9040192

Effect of veterinary antibiotics and heavy metals in the composition and valorization of a consortium of microalgae and bacteria

Elena M. Rojo*.**, María Hurtado*, A. Alejandro Filipigh*.**, Martina Ciardi***, Francisco Gabriel Acién-Fernández*** and Silvia Bolado*.**

* Institute of Sustainable Processes, University of Valladolid, Dr. Mergelina s/n, 47011 Valladolid (Spain)
(E-mail: *elenamaria.rojo@uva.es)*
** Department of Chemical Engineering and Environmental Technology, School of Industrial Engineering, University of Valladolid, Dr. Mergelina s/n, 47011 Valladolid (Spain)
*** Department of Chemical Engineering, University of Almería, 04120 Almería (Spain)
(E-mail: *Silvia.bolado@uva.es*)

Abstract

Piggery wastewater treatment with microalgae has become a promising process for the treatment and production of valuable biomass, although the presence of emerging contaminants such as antibiotics or heavy metals can influence the biomass composition and the valorization processes. These pollutants affected the protein and carbohydrate solubilisation and recovery yields of different extraction methods. Enzyme activity was inhibited by metals, and the stress generated by combining both types of pollutants decreased the cell wall resistance to chemical treatments.

Keywords (maximum 6 in alphabetical order)

Biomass, carbohydrates, extraction, piggery wastewater, proteins, solubilization.

INTRODUCTION

Pig manure has become a huge source of environmental pollution which must be treated due to its high concentration of organic matter, nitrogen, phosphorus, and ammonium. Bioremediation with microalgae has emerged as a promising technology in terms of efficiency and potential use of generated biomass to produce high-added value products (Saavedra et al., 2019). However, the concern about the presence of certain veterinary antibiotics (used to treat and prevent animal diseases) and heavy metals (present in well water or/and used in animal feed as micronutrients) in piggery wastewater has increased in the last years (López-Serna et al., 2019). These pollutants could affect the biomass composition and the valorization processes. This research is pioneer in the study of the influence of various veterinary antibiotics (VA) and heavy metals (HM) in the extraction of proteins and carbohydrates from microalgal-bacterial biomass grown in a wastewater treatment photobioreactor.

MATERIALS AND METHODS

Three assays were carried out in a thin-layer photobioreactor of 1,200 L with a dilution rate of 0.2 d^{-1} treating 10%-diluted piggery wastewater as feed and inoculated with *Scenedemus almeriensis*. Starting each assay, the photobioreactor was run for 15 days until the steady state was reached to obtain undoped biomasses (UB) as controls. From day 16 to day 36, the feed was doped with three VA (sulfadiazine, tetracycline, and ciprofloxacin (100 µg/L)) in assay 1, three HM (5 mg/L of copper, 15 mg/L of zinc, and 2 µg/L of arsenic) in assay 2 and with both types of pollutants (3 VA and 3 HM) in assay 3 (with the same previous concentrations), to obtain the doped biomasses (DB). The biomass in each period of each assay was harvested, centrifugated, freeze dried, and analyzed.

Several extraction methods were carried out to solubilize proteins and carbohydrates from the different biomasses (UB and DB) collected in the photobioreactor, applying the operational conditions described in Table 1. The residual solids were analyzed to calculate the solubilization of macro-components. The recovery of peptides and monosaccharides was calculated from the analysis of the liquid phase. Protein, carbohydrate, and lipid content were determined using the Total Kjeldahl Nitrogen (TKN), a modified NREL protocol based on an acid hydrolysis and HPLC and the Kochert method respectively. The amino-acid content of the solid and liquid phases was analyzed by HPLC (Rojo et al., 2021). Least significant difference tests (LSD) were carried out to identify the significant statistical differences (95% of confidence level).

RESULTS AND DISCUSSION

Effect of VA and HM on macromolecular biomass composition

Figure 1 shows compositions of the biomasses before and after doping in each assay. VA doping had some influence on the microalgae biomass composition of the assay 1, with significant decreases in protein content (from 56.6% to 52.9%) and glucose content (from 23.6% to 18.1%). In the assay 2, microalgae composition was also altered by the presence of HM, decreasing the carbohydrate content from 25.1% to 19.7%, related to decrease on glucose content from 17.4% to 12.2%. Finally, biomass composition changed significantly in assay 3. The protein content did increase by 45% while carbohydrate content decreased by 29%. The presence of both types of pollutants could produce a big oxidative stress, increasing the protein synthesis to overcome the imbalance due to overproduction of reactive oxygen species (Wang et al., 2022).

Effect of VA and HM on protein and carbohydrate solubilization

Figure 2.A shows the protein and carbohydrate solubilization yields obtained from UB and DB after each extraction treatment in the assay 1. The presence of VA decreased significantly the solubilisation of proteins of the treatments UAEE-P (19%), NaOH 120 (10%) and NaOH 60 (17%). The VA presence also decreased the carbohydrate solubilisation yields when applying UAE (39%), HE-P (42%), NaOH 120 (42%) and NaOH 60 (47%). It was possible that the cell wall became more resistant in response to the presence of VA. Chemical treatments at 120ºC provided the highest recoveries of peptides (55% with NaOH and 50.9% with HCL) and monosaccharides (54.2% of glucose and 46.2% of xylose with HCl) with DB.

The presence of HM decreased significantly the protein, and carbohydrate solubilization yields from biomasses of assay 2 for most of the treatments (Figure 2.B). The decrease on protein solubilization yield resulted remarkable for the physical and biological methods (<35.6%), without significant differences for NaOH 120. Enzymes could be inhibited by the presence of HM, competing for biding sites and interfering the enzymatic activity (Smith et al., 2022). Carbohydrate solubilization were also negatively influenced in the UAE, UAEE-P, HE-P, HCl 120 and NaOH 60 treatments with reductions over 30%. Likewise, the peptide and monosaccharide recoveries obtained from DB were very low in almost all treatments (except for NaOH 120, NaOH 60 and HCl 120) being less than 8%.

Finally, Figure 2.C shows the protein and carbohydrate solubilization yields achieved for biomasses from the assay 3, doped with VA and HM. Protein solubilization yields were influenced by the presence of both pollutants in all experiments except HE-P and HCl 60, while the only treatment that was not affected by these contaminants in the solubilization of carbohydrates was HCl 60. The increase in solubilization yields in the chemical treatments is noteworthy, which could indicate that the cell wall was weaker due to the oxidative stress (Danouche et al., 2022). However, protein solubilization decreased in the UAE and UAEE-P treatments by 24% and 21% respectively. Again, peptide and monosaccharide recoveries were (<10%) in presence of VA and HM, except in HCl 120, where the recoveries yields increased in the DB.

CONCLUSIONS

The presence of veterinary antibiotics and heavy metals influenced significantly the composition of microalgae-bacteria biomass grown in wastewater treatment photobioreactors and the yields of further valorization processes. High negative influence of heavy metals on the enzymatic reactions with both enzymes (metal ions competing for biding sites). Alkaline hydrolysis was affected by the presence of veterinary antibiotics, while acid hydrolysis was mainly affected by heavy metals. The presence of both pollutants reduced the cell wall resistance, improving extraction yields from biomass grown in high stressing environment.

ACKNOWLEDGEMENTS

This work was supported by the "Ministerio de Ciencia, Innovación y Universidades" of Spain (PID2020-113544RB-I00). Elena M. Rojo and A. Alejandro Filipigh would like to thank the "Ministerio de Ciencia, Innovación y Universidades" for their doctorate scholarship (PRE2018-083845 and PRE2021-100176). The authors also thank the regional government of Castilla y León (UIC 338, CLU 2017-09, CL-EI-2021-07) for the financial support of this work.

REFERENCES

Danouche, M., El Ghatchouli, N., Arroussi, H., 2022. Overview of the management of heavy metals toxicity by microalgae. J. Appl. Phycol. 2021 341 34, 475–488.

López-Serna, R., García, D., Bolado, S., Jiménez, J.J., Lai, F.Y., Golovko, O., Gago-Ferrero, P., Ahrens, L., Wiberg, K., Muñoz, R., 2019. Photobioreactors based on microalgae-bacteria and purple phototrophic bacteria consortia: A promising technology to reduce the load of veterinary drugs from piggery wastewater. Sci. Total Environ. 692, 259–266.

Rojo, E.M., Piedra, I., González, A.M., Vega, M., Bolado, S., 2021. Effect of process parameters on the valorization of components from microalgal and microalgal-bacteria biomass by enzymatic hydrolysis. Bioresour. Technol. 125256.

Saavedra, R., Muñoz, R., Taboada, M.E., Bolado, S., 2019. Influence of organic matter and CO_2 supply on bioremediation of heavy metals by Chlorella vulgaris and Scenedesmus almeriensis in a multimetallic matrix. Ecotoxicol. Environ. Saf. 182, 109393.

Smith, D.R., Maroney, M.J., Nordberg, M., Tyson, J.F., 2022. General chemistry of metals, sampling, analytical methods, and speciation. Handb. Toxicol. Met. Vol. I 15–54.

Wang, Y., Li, J., Lei, Y., Li, X., Nagarajan, D., Lee, D.J., Chang, J.S., 2022. Bioremediation of sulfonamides by a microalgae-bacteria consortium – Analysis of pollutants removal efficiency, cellular composition, and bacterial community. Bioresour. Technol. 351, 126964.

Table 1. Operation conditions of the different extraction methods. Extraction time: 1 hour

	T (ºC)	pH	Enzyme/ solvent	Concentration
Ultrasonic assisted extraction (UAE)	50	6.5	-	-
Ultrasonic assisted enzymatic extraction (UAEE-P)	50	6.5	Protamex	1:100 w/w
Enzymatic hydrolysis (HE-P)	50	6.5	Protamex	1:100 w/w
Alkaline hydrolysis (NaOH 120)	120	-	NaOH	2M
Acid hydrolysis (HCl 120)	120	-	HCl	2M
Alkaline hydrolysis (NaOH 60)	60	-	NaOH	2M
Acid hydrolysis (HCl 60)	60	-	HCl	2M

Figure 1. Biomass composition (ash-free dry basis). The data are provided as means ± standard deviations of 2 analytical determinations. Mean values with different letters are significantly different by LSD Test (95% of confidence level).

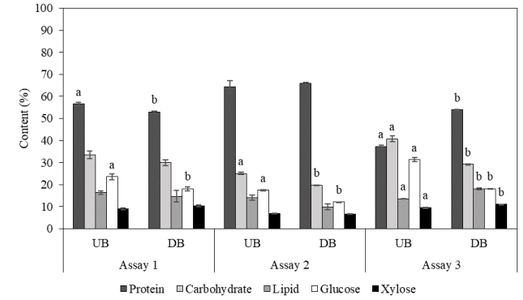

Figure 2. Protein and carbohydrate solubilization yields (%) in reference to the protein and carbohydrate content in the initial microalgal biomass in the assay 1 (A), assay 2 (B) and assay 3 (C). The data are provided as means ± standard deviations of 2 analytical determinations and the standard deviation of the means is represented by vertical interval lines. Different letters denote remarkable differences according to LSD test (95% of confidence level).

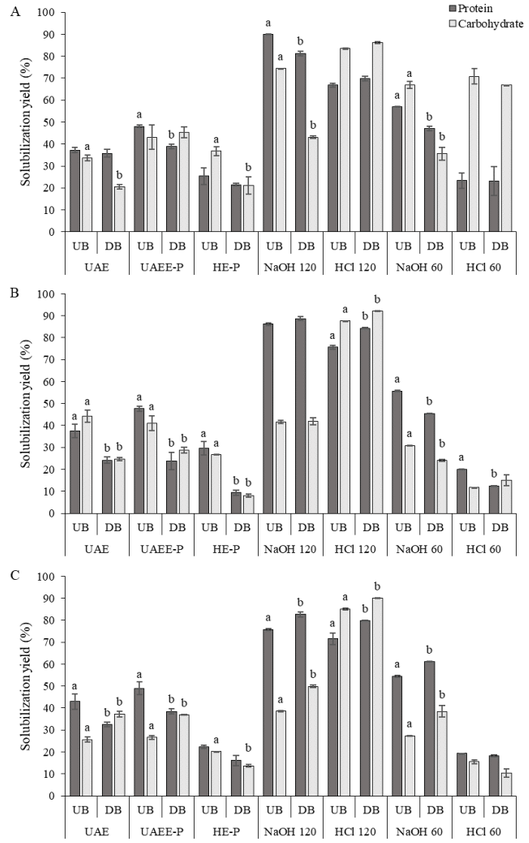

Valorisation of microalgae grown in food waste digestate as biofertilizer

I. M. P. Castro*,**, A.M. Netto***, V.S. Alves*** and F. Passos*,**

* Department of Sanitary and Environmental Engineering. Federal University of Minas Gerais. Av. Antônio Carlos 6627, Campus Pampulha, 31270-901, Belo Horizonte, MG, Brazil.

** Group of Environmental Engineering and Microbiology, Department Civil and Environmental Engineering, Universitat Politècnica de Catalunya·BarcelonaTech, c/ Jordi Girona 1-3, Barcelona 08034, Spain

(E-mail: *iacycastro@ufmg.br*; *fabiana.passos@upc.edu)*

*** Department of Chemical Engineering. Federal University of Viçosa. Av. Peter Henry Rolfs, s/n, Campus Universitario, 36570-900, Viçosa, MG, Braziil.

(E-mail: *vitor.sena@ufv.br, antonio.netto@ufv.br)*

Abstract

The aim of this work was to evaluate the application of microalgae grown in digestate treatment ponds as fertilizer in soil and plant. Harvested biomass was tested before and after anaerobic digestion and co-digestion with food waste as possibilities of valorisation in a treatment plant located in the university campus. The experimental design consisted of applying treatments in randomized pots with hybrid brachiaria *Sabiá* in a greenhouse with three replications each. Assessed parameters showed comparable results on plant growth for fresh and digested microalgal biomass and inorganic fertilizer. Moreover, fresh microalgae provided the highest phosphorus content in the leaf and the also of nitrogen, phosphorus and organic matter in the soil. In conclusion, this study indicates that microalgae-based biofertilizer has potential as a nutrient source and can promote the association in circular valorisation of waste treatment and agriculture.

Keywords

Anaerobic digestion; Circular economy; Fertilizer; High-strength wastewater; Microalgal biomass; Sustainable agriculture

INTRODUCTION

Microalgae has been investigated with successful results for treating high-strength wastewaters, as digestate from organic waste anaerobic digestion (Torres-Franco et al., 2021). In these systems, microalgae produce oxygen needed for heterotrophic bacteria to degrade organic matter, while assimilating macro and micronutrients into their cells. Therefore, harvested microalgal biomass may be further valorized into products, such as biofuels, animal feed and fertilizers.

In particular, the current agricultural sector relies on the use of mineral fertilizers, which are obtained through energy-intensive processes. Moreover, its excessive use generally leads to negative environmental consequences on soil and water bodies (Tilman et al., 2002). In light of these issues, it is urgent to promote sustainable agriculture by applying fertilizer from waste and wastewater. Previous research has demonstrated the potential of microalgae biofertilizer in soil and plant as an alternative to mineral fertilizers (Garcia-Gonzalez e Sommerfeld, 2016; Lorentz et al., 2020; Alvarez-Gonzalez et al., 2022). However, there are still many aspects that require further study and improvement for its full-scale application.

This study was carried out in the context of a demonstration-scale facility implemented in the campus of the Federal University of Minas Gerais (Belo Horizonte, Brazil) for treating food waste, which consists in an anaerobic reactor and a high rate algal pond for post-treating the digestate. Harvested microalgal biomass was investigated as biofertilizer in its natural state and after anaerobic digestion and co-digestion with food waste, in terms of responses in soil and plant. The final goal is to recover resources from food waste and reduce the cost and environmental impacts associated with inorganic fertilizers.

MATERIAL AND METHODS

Food waste (FW) was prepared with rice (20%), beans (20%), meat (15%), lettuce (25%), carrot (10%), and tomato (10%), as determined from monitoring of real food waste composition fed to the demonstration-scale treatment unit at the university campus (UFMG, Brazil) (Figure 1). Microalgal biomass (MB) was collected from the high rate algal pond and was mainly composed of *Scenedesmus* sp. For assessing the microalgae use as biofertilizer after its anaerobic digestion and after co-digestion with food waste (75/25% of food waste and microalgae, in terms of VS), biochemical methane potential tests were carried out in bottles of 500 mL. For that, assays were performed using an inoculum to substrate ratio (ISR) of 2 g VS/g VS and incubated at 35 ºC.

Biofertilization was assessed in soil and plant samples. Productivity of hybrid brachiaria *Sabiá* (forager plant) was conducted in a greenhouse using five treatments: 1) harvested microalgal biomass (MB), 2) microalgal biomass after anaerobic digestion (DM), 3) microalgal biomass and food waste co-digested (MB+FW-dig), 4) urea as inorganic fertilizer (FI) and, 5) soil without fertilization (control). The experiment was set out in a completely randomized block with three replicates per treatment in 4 L capacity pots. For each pot, ten seeds of hybrid brachiaria *Sabiá* were planted at 3 cm profundity. All treatments were dosed at 50 mg N/dm^3 and 100 mg N/dm^3 in the first and second harvested cycle, respectively. For each pot, the source of N was applied into 4 equal parts throughout the 60 and 45 days in cycles 1 and 2, respectively. Fertilizer application was carried out in the soil manually with a graduated cylinder and the pots were irrigated daily.

Chemical properties of the soil were analysed in terms of pH, organic matter and nitrogen (N) as described in EMBRAPA et al. (2009). Phosphorus (P), Potassium (K), Calcium (Ca) and Magnesium (Mg), were determined in a Mehlich extractor and measured in atomic absorption spectrophotometry (Varian Mod. Spect. A 20). Plant parameters monitored were tiller number, fresh and dry matter, Chlorophyll Content Index (Chlorophyll SPAD-502 Meter, MCL502DL Minolta) and macronutrients (i.e. N, P, K, Mg, Ca), which were analysed through nitric-perchloric digestion and measured in optical emission spectrophotometry with inductively coupled plasma (ICP-OES; Perkin Elmer Model Optima 8300 DV).

Experimental data was analysed using with the one-way analysis of variance (ANOVA) test processed by R software, version 4.2.0. Tukey's post hoc test was used to compared different treatments (α = 0.05). Variance normality was tested by Shapiro Willk test and homogeneity by Fligner test. Variance no normality was tested by Kruskal-Wallis test and Dunn's test.

RESULTS AND DISCUSSION

Biofertilization response in plants

Biofertilization was assessed in two cycles with different N dosage (i.e. 50 and 100 mg N/dm^3). Results for plant parameters are summarised in Table 1. As can be seen, when compared to control, all parameters showed an increase in plant productivity after applying inorganic fertilizer or biofertilizer treatments. Especially in C2, when higher N dosage was applied, fertilization and biofertilization increased by 50-60% fresh and dry matter compared to control. Additionally, the leaf chlorophyll content index increased from 13.8 to 25-31, with the highest index found for urea and digested microalgal biomass application.

Although inorganic fertilizer showed the best results for evaluated indicators, results were quite similar to those using biofertilizer based on microalgae, with statistically equal values for almost all parameters. Moreover, plants grown with microalgal biomass after anaerobic digestion exhibited superior performance compared to fresh microalgae. This suggests that probably solubilisation of organic particulates during the biodegradation process led to an enhancement in the availability of compounds for plant uptake.

Macronutrients (N, P, K, Ca and Mg) were measured in the leaf tissue and results are shown in Figure 2. The results revealed that, although control plants had lower growth, those samples showed high content of nutrients, particularly K and Ca. This was probably due to initial conditions of soil. Anyhow, microalgae-based fertilizers revealed high contents of nutrients, with increased values compared to urea for P and K and equal values for Ca and Mg. This result demonstrates how microalgae have a richer diversity and balance in nutrients compared to commercialised fertilizer, as observed in previous studies (Garcia-Gonzalez and Sommerfeld, 2015). Remarkably for P, which is considered a critical nutrient, with lack of natural reserves, values demonstrated that plant was able to uptake the additional P provided by the microalgae-based biofertilizers (Fig. 2B). This result agrees with previously reported studies that found lower N content and higher P content in plants fertilized with microalgae compared to chemical fertilizer (Alvarez-Gonzalez et al., 2022; Lorentz et al 2020).

Biofertilization response in soil

Results for soil parameters are shown in Table 2. Cycles 1 and 2 were in sequence for assessing the recycling and wear of fertilization, as commonly applied in fields. After 60 days of cultivation, the analyses revealed that there were no significant differences among treatments regarding pH, organic matter, N, P and K. In fact, the organic matter content of the soil was found to be significantly higher after 105 days of cultivation when fresh and digested microalgae were applied compared to the control and urea fertilization (8-12% increase). The N and P soil concentrations were also increased after biofertilization, with 8-10% increase for digested microalgae and 10-16% increased for co-digested microalgae and food waste. The results showed that the longer application time of the first to second cycles of biofertilization may have allowed the mineralisation of organic matter from organic compounds in the soil.

CONCLUSIONS

This study assessed the used of microalgae-based fertilizers coming from high-strength wastewater treatment ponds. The results obtained indicated that microalgae-based biofertilizers results in soil and plant were similar compared to the use of inorganic fertilizers, having equal responses in relation to plant growth indicators, foliar macronutrients and soil organic matter and nutrients contents. Besides, this strategy contributes to the circular reuse of resources in organic waste for a sustainable agricultural approach.

ACKNOWLEDGEMENTS

Iacy Castro is grateful for the Brazilian National Council for Scientific and Technological Development (CNPq, Brazil) for the predoctoral scholarship and scholarship for her doctorate stay in the Technical University of Catalonia (Spain).

Figure 1. Waste food treatment system at the university campus (UFMG, Brazil): 1) anaerobic reactor; 2) UASB reactor; 3) solid-liquid separator and; 4) high rate algal pond.

Table 1. Results for Tiller number, fresh matter, dry matter and leaf chlorophyll content (n=12) in hybrid brachiaria *Sabiá* grown with different fertilizer treatments, i.e. Control (without adding fertilizer), IF (inorganic fertilizer), MB (microalgal biomass), DM (digested microalgal biomass) and MB+FW- dig (co-digested microalgal biomass and food waste).

Parameters	Unit	Control	IF	MB	DM	MB+FW--dig
C1 - 50 mg N/dm^3						
Tiller number	n°/plot	16(±2.0)^b	19.5(±2.0)^a	17.6(±2.0)^{ab}	18.8(±2.0)^{ab}	18.9(±2.0)^{ab}
Fresh matter	g/plot	17.5(±3.0)^c	28.5(±4.6)^b	21.5(±3.0)^{bc}	24.7(±3.0)^{ab}	21.2(±3.0)^{bc}
Dry matter	g/plot	4.8(±0.7)^b	6.7(±1.1)^a	5.4(±1.6)^{ab}	5.9(±2.0)^{ab}	5.5(±2.4)^{ab}
C2 -100 mg N/dm^3						
Tiller number	n°/plot	18(±1.5)^c	34.5(±2.9)^a	29.6(±3.0)^b	31.2(±4.0)^{ab}	30.3(±2.9)^{ab}
Fresh matter	g/plot	17.1(±4.0)^c	38.9(±5.8)^a	36.3(±5.2)^{ab}	35.5(±5.5)^{ab}	33.7(±3.2)^b
Dry matter	g/plot	4.4(±0.9)^b	10.2(±0.7)^a	8.8(±1.0)^a	9.4(±2.8)^a	8.3(±0.9)^a
Chlorophyll*	-	13.8(±0.9)^d	31.0(±3.4)^a	25.5(±2.4)^{bc}	28(±2.0)^{ab}	25.3(±1.4)^c

*Note: Different letters indicate significant differences (α < 0.05) according to Tukey's post hoc test or Kruskal-Wallis test (*).

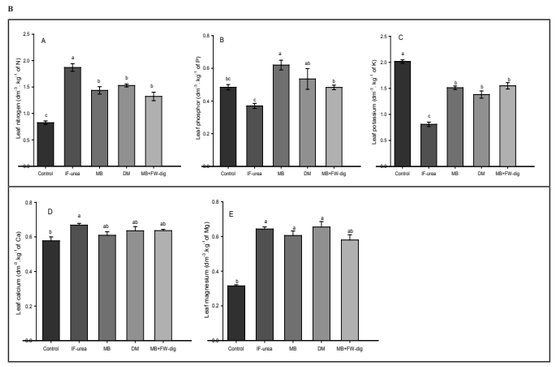

Figure 2. Leaf macronutrient content (N, P, K, Ca, Mg) in hybrid brachiaria *Sabiá* grown with different fertilizer treatments: control (soil without fertilization), IF (inorganic fertilizer), MB (microalgal biomass), DM (digested microalgal biomass), MB+FW-dig (co-digested microalgal biomass and food waste) at 100 mg N/dm^3 dose (C2).

Table 2. Organic matter and macronutrients in soil with different fertilizer treatments**:** control (soil without fertilization), IF (inorganic fertilizer), MB (microalgal biomass), DM (digested microalgal biomass), MB+FW-dig (co-digested microalgal biomass and food waste).

Parameters	Unit	Control	IF	MB	DM	MB+FW-dig
C1 - 50 mg N dm^{-3}						
Organic matter	g/kg	30(±0,2)^a	33(±0,2)^a	31±(0,1)^a	33±(0,2)^a	30±(0,2)^a
N	g/kg	1,2(±0,0)^a	1,2(±0,0)^a	1,3±(0,0)^a	1,3±(0,0)^a	1,3±(0,0)^a
P	g/kg	0,13(±0,01)^a	0,12(±0,01)^a	0,14±(0,01)^a	0,14±(0,01)^a	0,13±(0,01)^a
K	g/kg	0,04(±0,0)^a	0,03(±0,0)^b	0,03±(0,0)^b	0,03±(0,0)^b	0,03±(0,0)^b
C2 -100 mg N/dm^3						
Organic matter	g/kg	33 ±(0,2)^b	34±(0,2)^b	37±(0,1)^a	37±(0,1)^a	36±(0,1)^{ab}
N	g/kg	1,29±(0,0)^b	1,30±(0,0)^b	1,40±(0,0)^{ab}	1,43±(0,0)^a	1,43±(0,0)^a
P	g/kg	0,12 ±(0,02)^{ab}	0,09±(0,02)^b	0,09±(0,01)^b	0,13±(0,02)^a	0,14±(0,02)^a
K	g/kg	0,03±(0,0)^{ac}	0,02±(0,0)^b	0,03±(0,0)^c	0,03±(0,0)^{ab}	0,03±(0,0)^{ab}

REFERENCES

Alvarez-González, A., Uggetti, E., Serrano, L., Gorchs, G., Ferrer, I., Díez-Montero, R. Can microalgae grown in wastewater reduce the use of inorganic fertilizers?, 2022. Journal of Environmental Management 323, 116224.

Garcia-Gonzalez, J., Sommerfeld, M., 2016. Biofertilizer and biostimulant properties of the microalgae *Acutodesmus dimorphus*. Journal of Applied Phycology 28(2), 1051–1061.

Lorentz, J.F., Calijuri, M.L., Assemany, P.P., Alves, W.S., Pereira, O.G., 2020. Microalgal biomass as a biofertilizer for pasture cultivation: plant productivity and chemical composition. J. Clean. Prod. 276, 124130.

Tilman, D., Cassman, K.G., Matson, P.A., Naylor, R., Polasky, S., 2002. Agricultural sustainability and intensive production practices. Nature 418, 671–677.

Torres-Franco, A., Passos, F., Figueredo, C., Mota, C., Muñoz, R., 2021. Current advances in microalgae-based treatment of high-strength wastewaters: Challenges and opportunities to enhance wastewater treatment performance. Reviews in Environmental Science and Bio/Technology 20, 209-235.

TECHNICAL SESSIONS

T8.

Digitalization

ECO STP 2023

Fault-tolerant Control in WRRFs: A Practical Approach Using Case-Based Reasoning for Fault Identification

S. Mohebali* and P.A. Vanrolleghem*

* model*EAU*, Université Laval, 1065, avenue de la Médecine, Québec, QC, G1V 0A6, Canada

(E-mail: *sanaz.mohebali.1@ulaval.ca*; *peter.vanrolleghem@gci.ulaval.ca)*

Abstract

Researchers studying water resource recovery facilities (WRRFs) are putting much effort into improving the control and automation of WRRFs to obtain more robust, efficient, and economic facilities and move towards more sustainable operations. The advances in instrumentation and computer systems provide the opportunity to upgrade WRRF control systems. However, considering the complex, nonlinear, and time-varying nature of wastewater treatment processes, many challenges are still to be addressed. The main objective of this research is to exploit the recent advances in fault identification while utilizing the knowledge of the process in the form of case-based reasoning to improve fault identification and to integrate this information with fault-tolerant control to increase nutrient removal performance of WRRFs and, with it, a decrease in energy and chemical consumption and, thus, the operational cost.

Keywords

Case-based reasoning; fault detection; fault isolation; fault-tolerant control; WRRF

FAULT-TOLERANT CONTROL

Nowadays, efficient automation and control of wastewater treatment facilities are crucial for achieving a reliable and effective facility, increasing the capacity of nutrient removal and/or recovery while reducing energy consumption and greenhouse gas emissions. The changing characteristics of wastewater and the complex nature and dynamical behaviour of Water Resource Recovery Facilities (WRRFs), as well as the relatively low reliability of sensors and actuators, often affect the ideal control and automation of the facility. Considering the harsh environment of wastewater, faulty data due to sensor malfunction is unavoidable and is more challenging to deal with compared to other processes (Alferes et al., 2013). Hence, advanced control and automation of WRRFs still represent a challenging field for research and development.

Faults occurring in sensors, actuators, processes, and the controller can develop into a system failure and plant shutdown. A closed-loop control system can amplify the effect of faults or hide them to the point where complete system failure occurs. Preventing major failures due to simple faults and preserving the system's availability in the event of faults became essential concerns in control engineering (Blanke et al., 2000). A fault-tolerant controller can respond to the presence of the fault by adapting its actions to the plant's malfunctioning behaviour. If these modifications are effective, the system function is maintained even after a fault appears, sometimes after a small performance decay while the control algorithm adapts to the malfunctioning plant. Fault-Tolerant Control (FTC) aims to minimize the catastrophic impacts of failures to preserve acceptable process operation even in the face of severe faults by accommodating the set point or reconfiguring the control system (Blanke et al., 2016).

Two subsystems create a fault-tolerant system: the first system performs fault identification which includes fault detection and fault isolation, i.e. identifying the location of the fault (FDI). The second system redesigns the controller, i.e. adapts the controller to deal with the faulty situation and to keep the entire system accomplishing its objective. After fault identification, signals containing information on the situation will be sent to the supervisory level (fault-tolerant control) to take necessary actions to attenuate the effects of the fault (Figure 1) (Amin & Hassan, 2019; Blanke et al., 2016). Based on the fault type, control reconfiguration will be achieved by accommodating the controller setpoint (Zumoffen and Basualdo, 2008), altering the reference model for monitoring and control, adding soft sensors (Belchior et al., 2018), activating alternate controllers, etc.

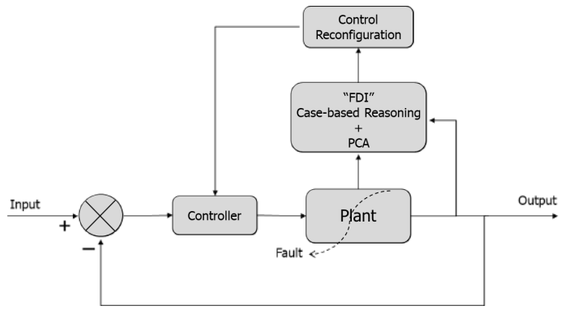

Figure 1. Schematic of fault-tolerant control

FAULT IDENTIFICATION and CASE-BASED REASONING

Fault detection and isolation (identification) are essential for the proper functioning of fault-tolerant control. Statistical and data-driven algorithms (e.g., Principal Component Analysis (PCA) and contribution plots) have already been demonstrated to be effective approaches for real-time monitoring, fault detection, and isolation in wastewater treatment (Nor et al., 2020; Lee et al., 2004). However, considering the time-varying and highly nonlinear characteristics of WRRFs, combined with the fact that some of the operational information in the processes is neither numeric nor quantifiable, such as smells, colors, foam patterns, and the appearance of bulking or floc microscopic characterization, led researchers to exploit the advantages of Knowledge-Based Systems (KBSs). KBSs use a combination of reasoning techniques, collections of facts, heuristics, common sense knowledge, and other types of knowledge to reach inferences. KBSs make an effort to emulate a human expert's thinking pattern in order to deal with the complexity of wastewater treatment systems (Rodriguez-Roda et al., 2001; Sànchez et al., 1997).

Case-Based Reasoning (CBR) is an artificial intelligence knowledge management approach that uses previous experiences to address new problems that emerge in a process. After a fault is identified, CBR retrieves the most comparable experience from an established case library to assist the fault isolation and even diagnosis, i.e. the explanation of the fault (Comas et al., 2006).

This study aims to take advantage of CBR to improve fault detection and isolation and to integrate it into a fault-tolerant control system to maximize the performance of WRRF. The proposed strategy employs PCA to reduce data dimensionality and monitor the process with Hotelling T^2 and Square Prediction Error (SPE) multivariate statistics that allow detecting faults. These monitoring statistics are subsequently used as case descriptors to build the case-based library (Ruiz et al., 2011) during the training of the FTC-system. When the trained FTC is applied, the most similar past experiences are retrieved by evaluating the similarity between a new case and the cases in the library.

APPLICATION OF FTC: an example

A good example that illustrates the role of fault-tolerant control in WRRFs is the practice of the AvN controller at the pilot plant located at Université Laval. The objective of AvN controllers is to maintain an equal concentration of NH_4-N and NO_3-N (NO_x-N preferably) in the effluent by manipulating the extent of aeration in the aerobic reactors. By maintaining this ratio, the effluent is optimized for a downstream deammonification process (anammox treatment). As such, the overall energy budget for aeration required to remove COD and N can be reduced. AvN is a cascade control where the AvN controller uses measurements of both NH_4-N and NO_3-N and cascades the DO controller to manipulate the DO concentration in the aerated tank (Kirim 2022).

The influent load to the WRRF follows a diurnal pattern (Figure 2). The intermittent AvN controller, which is a PID controller, controls NH_4-N and NO_3-N ratio by manipulating the Aeration Fraction (AF) width during the day (i.e., considering a fixed cycle time, the relative duration of the aerobic and anoxic periods is changed). Figure 3 illustrates the aeration pattern obtained. When the AvN controller faces a fault (e.g., the ammonia sensor failure), FTC acts as a system supervisor and replaces the real-time observations to calculate the fractions by historical patterns of aeration fractions such as the one of Figure 3 to fulfil the control goal as close as possible.

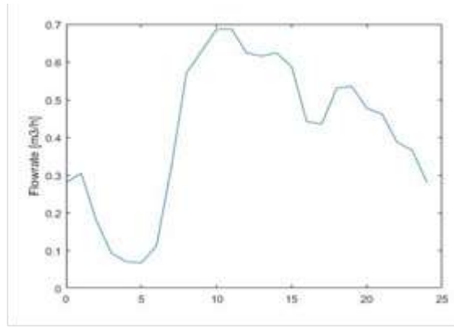

Figure 2. Diurnal pattern of wastewater flow rate

Figure 3. Diurnal aeration pattern

CONCLUSION

The efficient operation of WRRFs heavily relies on the quality of the control system; however, in the event of faults, the common control configurations might not be adequate to deliver the objective of the system. Exploiting the fault-tolerant control technique is a potential solution. Using FTC in the wastewater treatment sector, especially its practical implementation, rarely can be observed in the literature and must thus be considered a line for future research.

Efficient FTC requires powerful fault identification. Although data-driven fault detection and isolation methods have shown promising results, the accumulated knowledge and experience of previous situations (cases) that occurred in the plants can support to achieve more accurate fault identification.

REFERENCES

Alferes, J., Tik, S., Copp, J., Vanrolleghem, P.A., 2013 Advanced monitoring of water systems using in situ measurement stations: Data validation and fault detection. *Water Science and Technology* **68**(5), 1022–1030.

Amin, A.A., and Hasan, K.M. 2019 A review of fault tolerant control systems: Advancements and applications. *Measurement: Journal of the International Measurement Confederation* **143**, 58–68.

Belchior, C.A.C., Araújo, R.A.M., Souza, F.A.A., Landeck, J.A.C. 2018 Sensor-fault tolerance in a wastewater treatment plant by means of ANFIS-based soft sensor and control reconfiguration. *Neural Computing and Application* **30**(10), 3265–3276.

Blanke, M., Frei, C.W., Kraus, F., Pat, R.J., Staroswiecki, M. 2000 What is fault-tolerant control? In: *IFAC Fault Detection, Supervision, and Safety for Technical Processes* Budapest, Hungary.

Blanke, M., Kinnaert, M., Lunze, J., Staroswiecki, M. 2016 Diagnosis and Fault-Tolerant Control, Springer, Third Edition.

Comas, J., Rodriguez-Roda, I., Poch, M., Gernaey, K.V., Rosen, C., Jeppsson, U. 2006 Demonstration of a tool for automatic learning and re-use of knowledge in the activated sludge process. *Water Science and Technology* **53**(4–5), 303–311.

Kirim, G. 2022 Modelling and model-based optimization of N-removal WRRFs: reactive settling, conventional & short-cut N-removal processes. PhD Thesis, Civil and Water Engineering, Université Laval, Quebec, QC, Canada.

Lee, J.M., Yoo, C.K., Choi, S.W., Vanrolleghem, P.A. 2004 Nonlinear process monitoring using kernel principal component analysis. *Chemical Engineering Science* **59**(1), 223–234.

Nor, N.M., Hassan, C.R.C., Hussain, M.A. 2020 A review of data-driven fault detection and diagnosis methods: applications in chemical process systems. *Review in Chemical Engineering* **36**(4), 513–553.

Rodriguez-Roda, I., Comas, J., Poch, M., Sànchez-Marrè, M., Cortés, U. 2001 Automatic knowledge acquisition from complex processes for the development of knowledge-based systems. *Industrial & Engineering Chemistry Research* **40**(15), 3353–3360.

Ruiz, M., Sin, G., Berjaga, X., Colprim, J., Puig, S., Colomer, J. 2011 Multivariate principal component analysis and case-based reasoning for monitoring, fault detection and diagnosis in a WWTP. *Water Science and Technology* **64**(8), 1661–1667.

Sànchez, M.S., Cortés, U., Béjar, J. 1997 Concept formation in WWTP by means of classification techniques: A compared study. *Applied Intelligence* **7**, 147-165.

Zumoffen, D., and Basualdo, M. 2008 Improvements in fault tolerance characteristics for large chemical plants: 1. Wastewater treatment plant with decentralized control. *Industrial Engineering Chemistry Research* **47**(15), 5464–5481.

The use of a low-cost monitoring dataset for sewer model calibration

P. Schütz*, O. Gutierrez**. ***, S. Busquets**. ***, M. Gunkel**** and N. Caradot*

* Kompetenzzentrum Wasser Berlin (KWB), Cicerostr. 24, 10709 Berlin, Germany
(E-mail: *paul.schuetz@kompetenz-wasser.de)*
** Institut Català de Recerca de l'Aigua (ICRA), Edifici H2O, C/ Emili Grahit, 101, 17003 Girona, ES-CT
*** University of Girona, Campus Montilivi, 17003, Girona, Spain
**** Berliner Wasserbetriebe (BWB), Neue Jüdenstraße 1, 10719 Berlin, Germany

Abstract

Urban wastewater management and the associated modelling has become indispensable today. Reliable calibration is essential for these models, and water level data is used as a standard. However, data collection can be limited due to high sensor costs and harsh conditions in the sewer. A novel solution is collecting data using low-cost temperature sensors, placing one in the stream, the other at the crest of the weir. In the case of dry weather, the sensor measures the air phase, whereas, in the case of Combined Sewer Overflow (CSO), the discharged storm and wastewater is measured. Autocalibration was performed using OSTRICH for a SWMM model in Berlin, with water level and fictional temperature data, and various number of measuring sites. Results showed that calibration using temperature data was as good as using water level data, with promising outcomes achieved by using one measuring site, offering a cost-effective alternative for water utilities.

Keywords

Calibration, OSTRICH, SWMM, Temperature data, Water level data

BACKGROUND

The management of urban wastewater systems and the associated modelling of these systems has become indispensable in today's world. In order for these models to represent reality as accurately as possible, a reliable calibration is essential. Water level data is used as a standard, but due to expensive sensors and harsh conditions, data can only be collected at a few key points of the system (DWC, 2022). One method that has experienced an upswing in recent years is data collection using low-cost temperature sensors (Montserrat, 2013, 2015). These sensors are inexpensive and easy to implement at Combined Sewer Overflow (CSO) weirs. Two sensors are needed, one is placed in the stream of the conduit, the other is placed at the crest of the weir. In the case of dry weather, the sensor measures the air phase whereas, in the case of CSO, the discharged storm and wastewater is measured. The start and end of a CSO event can be determined via the merging of measured temperature values in both points of the overflow structure (see Fig. 1a). Due to this method, the duration of CSO events can be detected (DWC, 2022). In this work, the potential benefits of this novel method and the number of measuring sites needed are assessed. This could be of interest for water utilities and practitioners to improve and lower the costs of their calibration of sewer models in the future.

MATERIAL & METHODS

Approach

In order to assess the potential of temperature data for the calibration of sewer models, fictional temperature data had to be created first. This is due to data inaccuracies which were caused in the measuring campaign of the original sensors. Next, the calibration approaches with different data types and different number of measuring sites where carried out by the autocalibration software OSTRICH. Here, an additional 'R-Script' was needed to transfer and evaluate the data generated by SWMM. After the calibration runs, a validation run was needed to ensure comparability for the different approaches. The final assessment was based on the R^2 values of the validation runs.

Study area

The model used is a coarse model of the catchment of *Wilmersdorf*, which is a district in the west of Berlin. It has a size of approximately 1900 ha and around 210.000 inhabitants, which results in a population of 110 person/ha. The catchment area gets represented by 257 subcatchments, which range in size from 0.04 ha up to 177 ha. The model is a combined sewer network, wastewater and rainwater are discharged into a single sewer and pumped to a wastewater treatment plant by pumping stations located in the catchment. In the case of rain events, these pumping stations get overloaded and the system has to discharge into nearby water bodies. In the catchment, three Combined Sewer Outflows are located, which all lead into the nearby *Landwehr Canal* (see Fig. 1c).

Data & Calibration parameters

Two different data types were used for calibration; i.) *water level data*, measured by the Berliner Wasserbetriebe (BWB) at three sites of the modelled catchment area (see Fig. 1c) and ii.) fictional *temperature data*, generated of the water level data of these three sites. Therefore, a threshold was set and the overflow duration, caused by a rain event, was measured when the threshold got exceeded. For calibration, 19 events which occurred from April - May 2021 were used and for validation purposes, 18 events of the period June - August 2021. The calibration parameters used were the roughness of the conduits (*Manning's N*), the roughness of the impervious area of the subcatchments (*Manning's N*) and the slope of the subcatchments (%), chosen based on a sensitivity study carried out and a literature review.

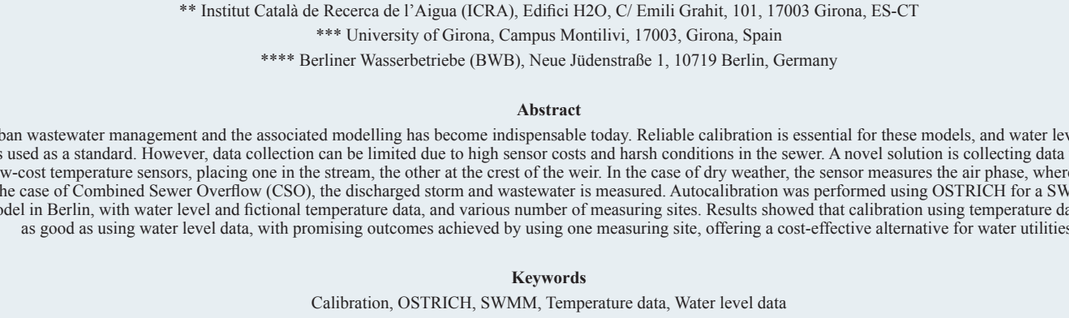

Figure 1. a) Temperature overflow detection concept, b) Calibration set-up and c) Catchment area

Setup

To compare the autocalibration approaches, a triangle relationship of the main components, consisting of OSTRICH, SWMM and an 'R'-Script, was needed (Fig. 1b). OSTRICH is a model-independent multi-algorithm calibration tool (Mattot, 2017). SWMM is a dynamic rainfall-runoff simulation model for single event or long-term simulation (Rossman, 2015). The 'R'-Script was used to convert the results of SWMM from binary to text format first, using the *swmmr*-package (Leutnant, 2019). Next, the Objective Function (OF) was calculated. For this purpose, each event was weighted over the event duration and a total R^2 was calculated. This resulted in the following OF which was to be minimised by OSTRICH:

Thus, a total of four different calibration approaches were carried out: 1.1) water level data, 1 measurement site; 1.2) water level data, 3 measurement sites; 2.1.) temperature data, 1 measurement site; 2.2.) temperature data, 3 measurement sites. Depending on the measuring sites, the OF consisted of 1 or 3 sites. *OSTRICH* completed 100 calibration runs and used the Dynamically Dimensioned Search (DDS) algorithm. After completion, a validation run was carried out for each of the calibration runs. Therefore, the detected calibration parameters were used and evaluated on the basis of the R^2 values of the three measuring sites of the model.

RESULTS & DISCUSSION

Calibration results

OSTRICH is able to perform an autocalibration by using temperature data. An example is shown in Fig. 2: on the left side, the calibration with water level data, and on the right site, with temperature data. It can be seen that the threshold of 31.5 mNN gets exceeded multiple times and therefore, the event has a specific pattern, which OSTRICH tries to fit by adjusting the calibration parameters.

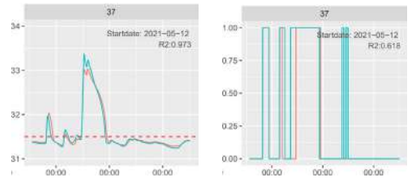

Figure 2. Calibration example for water level & temperature data (red = obs, blue = sim)

Fig. 3 shows the convergence of the calibration approaches 1.1 and 2.1. A convergence was given in all four calibration approaches. This ensures that an improvement or an adjustment of the calibration parameters has taken place and that OSTRICH functions.

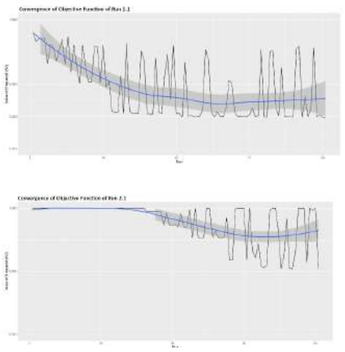

Figure 3. Convergence of Calibration Run 1.1 (left) & 2.1 (right), shown by the value of the OF

Validation results

The validation results for the period June - August 2021 can be seen in Tab.1. The runs 1.1 (water level data, 1 site) and 2.2 (temperature data, 3 sites) show the best results, having an OF value of 1.397. It can be seen that the R^2 of the individual measurement sites are all within the same range. The combined sewer conduit has the highest R^2 (all $R^2 > 0.65$), followed by R^2 of the Inlet Chamber RÜB (all $R^2 > 0.5$). Only the R^2 of the Inlet Chamber Pumphouse is slightly lower with $R^2 < 0.44$. It can be stated, that calibration with temperature data produces as good results as with water level data.

Table 1. Results of the validation runs & final calibration parameters

General Information	Calibration approach	**1.1**	**1.2**	**2.1**	**2.2**
	Data type	Water level	Water level	Temp data	Temp data
	Measurement sites	1	3	1	3
R^2-values of Validation Runs	Value validation function	1.397	1.409	1.411	1.397
	R^2-validation of Inlet Chamber Pumphouse	0.427	0.421	0.416	0.430
	R^2-validation of Inlet Chamber RÜB	0.515	0.517	0.513	0.514
	R^2-validation of Combined Sewer Conduit	0.661	0.653	0.660	0.659
Value calibration parameters	Manning N Conduit [0.005 – 0.4]	0.0076	0.0149	0.0112	0.0063
	Manning N Imperv. Area [0.006 – 0.4]	0.021	0.007	0.017	0.029
	Slope Subcatchments [0.01 - 10]	6.263	9.754	9.968	8.524

These observations are confirmed by similar insights in Montserrat, 2016. Looking at the number of measurement sites needed for a reliable calibration, no conclusion can be made. The water level data performs better with one measurement site, the temperature data with three measurement sites. One reason for these different results could be the lack of spatial distribution of measuring sites in the model. However, looking at the individual calibration parameters, it is noticeable that they are partly unrealistic, i.e. all *Slope* value are > 6%, which is improper for a model located in Berlin. This is caused by the wide boundaries for the calibration parameters given via OSTRICH and has to be adjusted in future calibration runs.

CONCLUSION

It can be stated that similar results can be achieved by autocalibration using temperature instead of flow measurements. This becomes apparent when looking at the value of the validation OF, but also when comparing the individual measuring sites with each other.
It cannot be conclusively clarified whether better calibration results are achieved if several measuring sites are included in the OF instead of just one. One reason for this could be the lack of spatial distribution of the measuring sites in the here used catchment area, as can be seen in Figure 1c.
Above all, the boundaries of the calibration parameters must be realistically defined, otherwise OSTRICH uses unrealistic parameter values to minimise the OF.
It can be stated that using low-cost monitoring methods, such as temperature sensors, could be a cost-effective solution for calibration purposes for water utilities and practitioners.

Currently, the calibration method is applied to real temperature data from a new measuring campaign, which shows appealing results. The fully updated results will be presented at the conference.

ACKNOWLEDGEMENT

The research has been conducted in the frame of the digital-water.city project, which has received funding from the European Union's Horizon 2020 research and innovation programme under grant agreement No 820954.

REFERENCES

DWC, Digital Water.City, (2022): D2.4: Technology Report, Technical documentation of the digital solutions and key requirements for successful deployment
Leutnant D, Döring A, Uhl M (2019). "swmmr - an R package to interface SWMM." *Urban Water Journal*, 16(1), 68-76. https://doi.org/10.1080/1573062X.2019.1611889.
Matott, L.S. 2017. OSTRICH: an Optimization Software Tool, Documentation and User's Guide, Version 17.12.19. 79 pages, University at Buffalo Center for Computational Research, http://www.civil.uwaterloo.ca/envmodelling/Ostrich.html.
Montserrat, A., Gutierrez, O., Poch, M., Corominas, L., (2013). Field validation of a new low-cost method for determining occurrence and duration of combined sewer overflows. Sci. Total Environ. 463-464, 904–912.
Montserrat, A., Bosch, Ll., Kiser, M.A., Poch, M., Corominas, L., (2015). Using data from monitoring combined sewer overflows to assess, improve, and maintain combined sewer systems. Sci. Total Environ. 505, 1053-1061.
Montserrat, A., Hofer, T., Poch, M., Muschalla, D., Corominas, Ll., (2016): Using the duration of combined sewer overflow events for the calibration of sewer hydrodynamic models, Urban Water Journal, DOI: 10.1080/1573062X.2016.1254255
Rossman, L.A. and Agency, U.S. Environmental Protection (2015). Storm Water Management Model User's Manual Version 5.1. url: https://www.epa.gov/water-research/storm-water-management-model-swmm-version-51-users-manual.

Real-time monitoring of adsorption processes in wastewater by innovative spectroscopic sensors: a pilot-scale study

C. Bruni*, M. Parlapiano*, M. Sgroi*, A. L. Eusebi*, F. Fatone*

* Department of Science and Engineering of Materials, Environment and Urban Planning-SIMAU, Marche Polytechnic University, Ancona 60131, Italy
(E-mail: c.bruni@pm.univpm.it; m.parlapiano@pm.univpm.it; m.sgroi@staff.univpm.it; a.l.eusebi@univpm.it; f.fatone@univpm.it)

Abstract

Industrial Symbiosis (IS) is a particular form of Circular Economy applicable to industrial contexts. The H2020 project ULTIMATE is studying IS in different case studies. The Aretusa Italian case study is a successful example of symbiosis which allow 3.8 Mio. m3/y of treated municipal wastewater to be reused by Solvay industry. To increase the quality of the water to be reused, a pilot plant adsorption system has been developed to treat the final wastewater. Real-time monitoring of the pilot has been done through the installation of UV absorbance sensor reading at 254 nm and a fluorescence sensor. UV and fluorescence signals are being tested to monitor the breakthrough curve of organic material (in terms of dissolved organic carbon), but also the adsorption process of organic micropollutants (e.g., pharmaceuticals and personal care products).

Keywords

Fluorescence; Industrial Symbiosis; UV absorbance; Real-time monitoring; Water Reuse

INTRODUCTION

The worldwide concern about the availability of water for a growing world population has led to an awareness of the use of this resource, therefore, water scarcity is a problem affecting both domestic and industrial users which can potentially delay the continuous development of society (Thomé et al., 2019). It is therefore necessary to make the transition from the linear to the Circular Economic (CE) model. CE model is based on increasing resource efficiency, minimizing waste production to separate economic growth from resource use (Arias et al., 2021). Industrial Symbiosis (IS), as a particular form of Circular Economy applicable to industrial contexts, promises a new potential by systematically looking to reuse wastes between industries as raw materials (Daddi et al., 2017). ULTIMATE (indUstry water-utiLiTy symbIosis for a sMarter wATer society) is an Horizon 2020 project introducing a specific type of IS named "Water Smart Industrial Symbiosis" where both water and wastewater play a key role as a reusable sources (https://ultimatewater.eu/water-smart-industrial-symbiosis/). .

The ULTIMATE project in Italy

In Italy the ULTIMATE project is applied in Aretusa Case Study. Aretusa Consortium, established in Tuscany in 2001, is a successful example of industrial symbiosis between a water utility (ASA Livorno), a technology provider (Termomeccanica Ecologia), and an industry (Solvay Chimica Italia). The objective of the Consortium is to treat the effluent coming from the two municipal wastewater treatment plants of Cecina and Rosignano to reach the quality requirements necessary for cooling the towers of Solvay Rosignano Plant or for other forms of reuse. Up to 3.8 Mio. m3/y of treated municipal wastewater is already reused by the industrial partner Solvay, freeing up private industrial wells for drinking water use. Despite this, final quality often overcomes the required limits, mainly in terms of hardness, salinity, and COD concentration. In this context ULTIMATE has the objective of increasing the quality of the final water, maximizing the reuse possibilities in the industrial context, but also for other application, including agricultural irrigation.

MATERIALS AND METHODS

A pilot plant adsorption system has been designed for reducing organic loads from Aretusa effluent wastewater, using innovative materials (e.g., Hydrochar) as well as commercial carbons as adsorbent materials. The main innovations connected with the installation of the adsorption pilot plant are related to the use of alternative adsorbent materials derived by thermal treatment of waste sewage sludge, and on the use of innovative spectroscopic sensors (based on fluorescence measurements) to monitor the organic content in wastewater.
The pilot system has four adsorption columns, two with a bigger size and two smaller, hydraulically connected to be operated in series or in parallel. Considering a design empty bed contact time (EBCT) of 10 min, the big columns can be operated with a flow rate of around 3.5 m3/h, whereas the small columns can treat around 0.5 m3/h of wastewater. The adsorption pilot system has been equipped with different on-line sensors for real-time measurements, which include UV absorbance sensor reading at 254 nm and a fluorescence sensor reading at the excitation/emission couple of 325/445 nm. The main sensors are placed in a monitoring tank. A picture showing all the components of the adsorption pilot plant is shown in Figure 1.

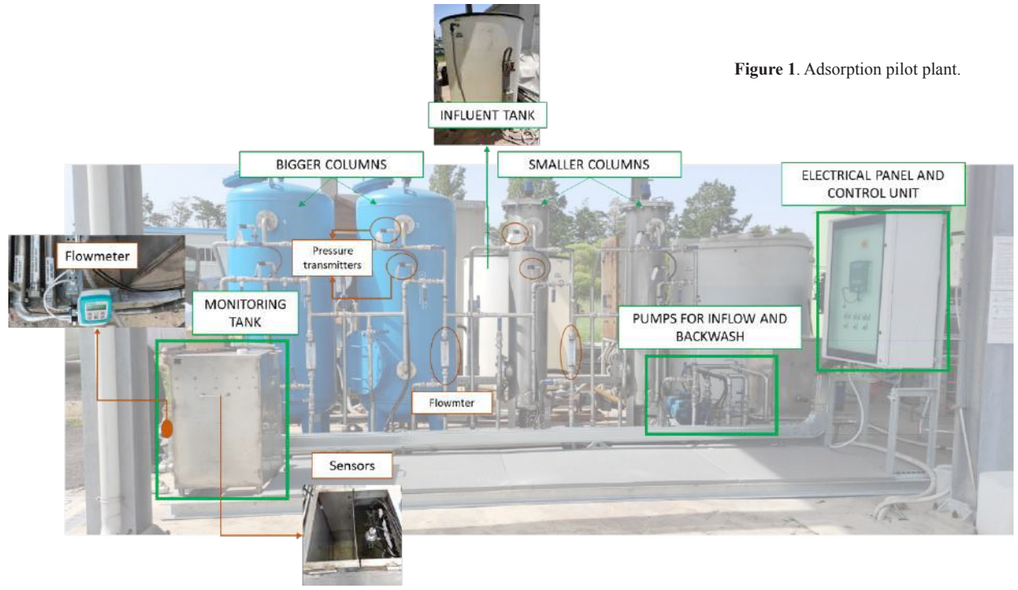

Figure 1. Adsorption pilot plant.

RESULTS AND DISCUSSIONS

Start-up of the pilot system was accomplished in July 2022 and it was focused on the calibration of the fluorescence sensor, which proved to be more sensitive than UV absorbance sensor in monitoring organic matter variation (Figure 2).

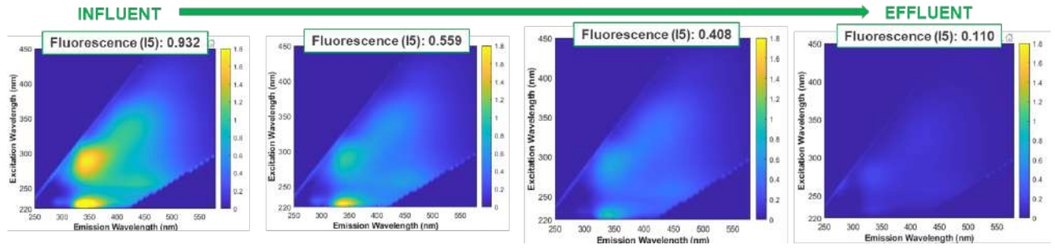

Figure 2. Fluorescence spectra of influent, effluent, and mixed (influent/effluent) samples collected in the monitoring tank of the adsorption pilot plant.

In September 2022 the pilot system was fully operational, and the real-time monitoring activities started. During the monitoring period, two samples per week have been taken to measure UV absorbance and Fluorescence by laboratory instruments for both influent and effluent of the pilot, and to perform comparison between on-line and off-line measurements. Particularly, UV and fluorescence signals are being tested to monitor the breakthrough curve of organic material (in terms of dissolved organic carbon), but also the adsorption process of organic micropollutants (e.g., pharmaceuticals and personal care products).
In Figure 3 is reported the trend observed in the effluent of the adsorption pilot plant for measurements provided by the fluorescence sensor and the UV254 sensor. The trend observed for the two measurements was different, and the fluorescence sensor showed higher performance to detect promptly changes in wastewater organic matter concentration. In addition, probe flurescence measurements showed a high agreement with laboratory measurements. On the contrary, comparison of on-line and off-line measurements of UV absorbance at 254 nm showed often some misalignment.

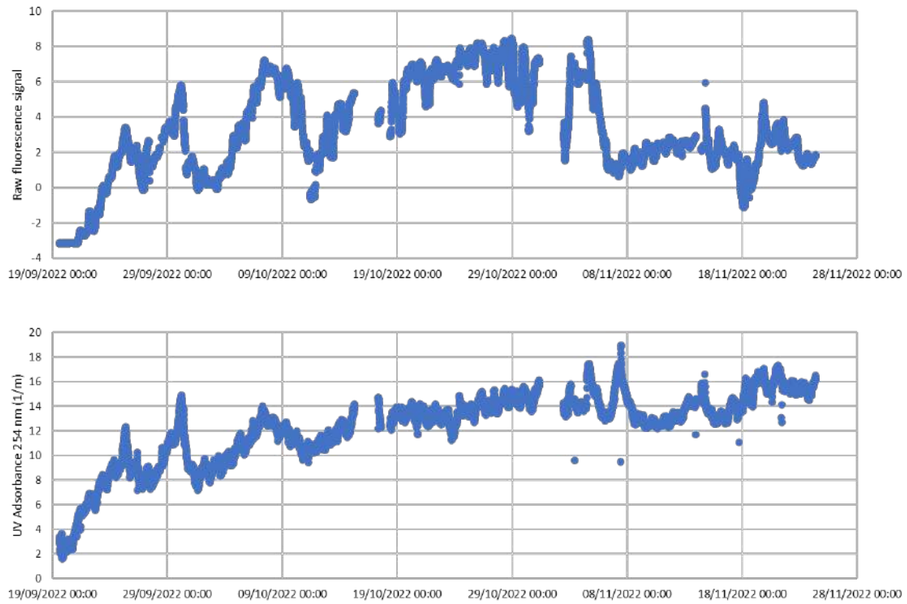

Figure 3. Fluorescence and UV trend.

Furthermore, preliminary data show important correlations between emerging contaminants concentrations in wastewater and fluorescence measurements performed by the on-line probe suggesting important potentialities for the real-time monitoring of the micropollutants.

REFERENCES

Arias, B.G., Merayo, N., Millán, A., Negro, C. 2021 Sustainable recovery of wastewater to be reused in cooling towers: Towards circular economy approach. *Journal of Water Process Engineering* **41**, 275-283.
Daddi, T., Nucci, B., Iraldo, F. 2017 Using Life Cycle Assessment (LCA) to measure the environmental benefits of industrial symbiosis in an industrial cluster of SMEs. *Journal of Cleaner Production* **147**, 157–164.
Thomé, A.C.B., Santos, P.G., Fisch, A.G. 2019 Using rainwater in cooling towers: Design and performance analysis for a petrochemical company. *Journal of Cleaner Production* **224**, 275-283.

Water reuse on the move: decision support for reclaimed water network design solutions

David Martínez[1], Eusebi Calle[1], Gianluigi Buttiglieri[2,3], Lluís Corominas[2,3], Miquel Farreras[1], Joan Saló-Grau[1,2], Pere Vilà[1], Josep Pueyo-Ros[2,3] and Joaquim Comas[2,4]

1 Institute of Informatics and Applications, University of Girona, Girona, Spain.
(E-mail: *david.martineza@udg.edu; eusebi.calle@udg.edu; miquel.farreras@udg.edu; pere.vila@udg.edu)*
2 Catalan Institute for Water Research (ICRA-CERCA), Emili Grahit 101, 17003 Girona, Spain.
(E-mail: *gbuttiglieri@icra.cat; lcorominas@icra.cat; jsalo@icra.cat; jpueyo@icra.cat; jcomas@icra.cat*)
3 University of Girona, Girona, Spain.
4 LEQUIA, Institute of Environment, University of Girona, E-17071, Girona, Spain.

Abstract

Water reuse projects have become essential primarily due to the increasing issue of water scarcity. However, manual or semi-automatic project design approaches are still common. This work makes progress on water reuse network design and planning through a demonstration of the usefulness of the REWATnet decision support tool which, based on open data sources and graph theory coupled with greedy optimization algorithms, is able to automatically compute the optimal reclaimed water network design for a given scenario, including the length and diameter of the pipes, the location of storage tanks, and construction costs. Furthermore, it maximizes the water served on limited budget availability scenarios. The usefulness of the REWATnet tool is illustrated in El Prat de Llobregat, planning the design of a city-wide reclaimed water network. The results demonstrate the fully automatic design of the water reuse network and the optimal limited-budget alternatives, improving current practice significantly.

Keywords (maximum 6 in alphabetical order)

Circular economy; clustering; graph theory; planning; reclaimed water; wastewater treatment

INTRODUCTION

Water scarcity and droughts are an increasing problem in many areas, therefore water reuse is becoming an indispensable alternative measure to complement conventional water resources, especially in the most significant water-consuming sectors on local, regional, and global scales (Masi et al., 2020).

Efficient and sustainable water reuse requires feasible water reuse projects (i.e., water reclamation treatment plants and reclaimed water distribution networks for potential uses). Planning and assessing water reuse projects require decision-makers to answer a number of questions concerning issues such as: (i) the best tertiary/advanced treatment to be implemented, (ii) how much wastewater needs to be reclaimed, and (iii) how to select the optimal water distribution network.

Previous research has been mainly focused on wastewater treatment, i.e., on the selection of the most adequate advanced treatment technologies for water reclamation (Chhipi-Shrestha et al., 2017) and on manual design solutions (Khurelbaatar et al., 2021), or sometimes requiring separating raw greywater from wastewater at the source, which is often not possible in many cities (Yerri and Piratla, 2019).

Water network modelling can be approached through graph theory but has not been used yet for the advanced and automated design optimization of water networks. Given this background, the aim of this paper is to illustrate the usefulness of a decision support tool for optimal planning of water reuse networks in cities. Our approach integrates several algorithms for designing water reuse networks based on graph theory coupled with existent greedy optimization algorithms (Calle et al., 2021; Kesavan and Chandrashekar, 1972; Kou et al., 1981). Our proposal (REWATnet tool), presented for the first time in Calle et al. (2023), uses advanced algorithms to design and optimize large-scale water reuse networks in one single tool, in contrast with the literature, thus avoiding the need for data exchange and thus resulting in potential savings in time and effort. This tool combines city characteristics (i.e., terrain characteristics, including plot and building usages, elevation, and slope) and water consumption rates to automatically propose an optimal network for water reuse. The usefulness of our solution is illustrated in this paper when testing it in El Prat de Llobregat (Catalonia, Spain). Construction costs and benefits in terms of water savings are estimated for each design scenario. Finally, the optimal water network can be provided when only a limited budget is available.

METHODS

Figure 1 describes the innovative REWATnet decision support tool for planning water reuse projects and highlights the steps involved and the outputs produced. First, the scenarios are defined based on the city identifier and cadastral files. With only these inputs information, the tool automatically extracts the initial graph from default values and open data sources, which includes the city street graph with neighbourhoods and node elevations, linked to terrain usages and inhabitants from the cadastral files, water consumptions, and the origin of water and potential destinations of reclaimed water, based on the selected water uses (Gascon et al., 2004).

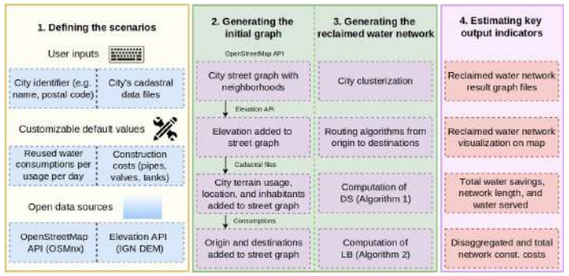

Figure 1. Simplified scheme of the REWATnet decision support tool (Calle et al., 2023).

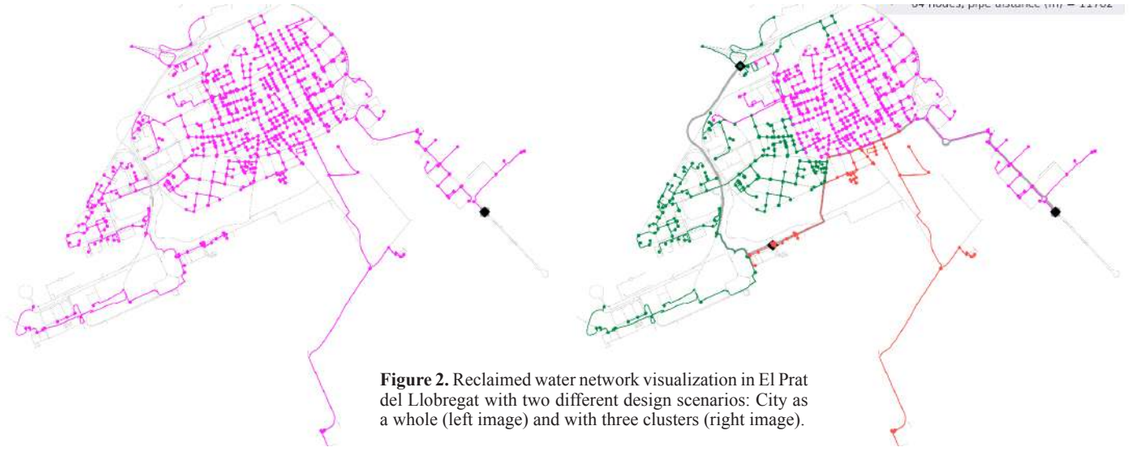

Figure 2. Reclaimed water network visualization in El Prat del Llobregat with two different design scenarios: City as a whole (left image) and with three clusters (right image).

RESULTS AND DISCUSSION

The tool is applied to generate and analyze a potential water reuse project for the city of El Prat de Llobregat, considering all the possible water uses and that the necessary tertiary/advanced treatment is already implemented.

Figure 2 shows the resulting reclaimed water network considering the city as a whole (left image) and with three clusters, each one with an intermediate storage tank (right image). The first scenario results in a 61 km network with a total construction cost of €5,508K. The second scenario results in a 73 km network, a total construction cost of €6,875K. The number of clusters is an input for the tool, allowing users to select the preferred quantity for each scenario based on city characteristics, available budget, or hydraulic constraints. The observed water consumption (i.e., water savings) is 3,418 m^3/d. Note that the whole infrastructure payback period considered is 30 years and the accumulative water savings are 37,427,100 m^3.

The usefulness of the REWATnet tool for network optimization when a limited budget (LB) is available is also illustrated and compared with a semi-manual current practice. The semi-manual approach is an algorithm that simulates the common current practice by adding the closest destination to the reclaimed water network for each potential destination until budget B is reached. As shown in Figure 3, the benefits of the optimal network LB approach are evident as the budget increases. Although this case study has a very similar consumption among all nodes and they are relatively close to each other (which makes the current practice a good approach), the LB algorithm implemented in the REWATnet tool also shows a significant increase in water served compared to the current practice (e.g., water served increased by 50% with a budget of 1M€).

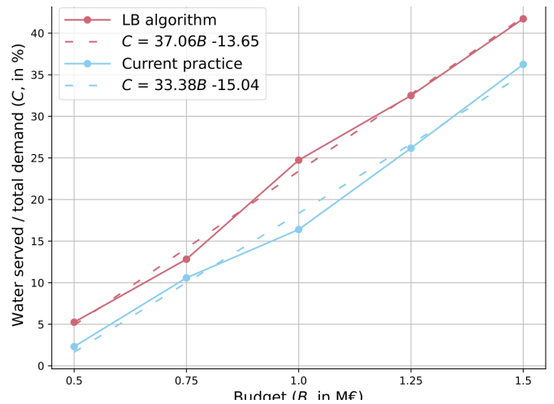

Figure 3. Results of water served with a limited budget: Current practice versus LB algorithm.

Future work

It is expected to improve the tool and its network designs not only by minimizing the cost but also maximizing water availability on destinations (i.e., resilience on failures). It is also expected to include advanced water treatment and network operational costs in the future based on the designs' hydrological validation through EPANET. Furthermore, the estimation of the generated network carbon footprint will be considered. Finally, the hydrological validation will also enable us to automatically detect the minimum number of clusters required for each scenario in order to save additional costs.

REFERENCES

Calle, E., Martínez, D., Buttiglieri, G., Corominas, L., Farreras, M., Saló-Grau, J., Vilà, P., Pueyo-Ros, J. and Comas, J., 2023. Optimal design of water reuse networks in cities through decision support tool development and testing [Manuscript accepted for publication in npj Clean Water]. Institute of Informatics and Applications (University of Girona) and Catalan Institute for Water Research (ICRA-CERCA), Girona, Spain

Calle, E., Martínez, D., Brugués-i-Pujolràs, R., Farreras, M., Saló-Grau, J., Pueyo-Ros, J. and Corominas, L., 2021. Optimal selection of monitoring sites in cities for SARS-CoV-2 surveillance in sewage networks. Environment International, 157, p.106768.

Chhipi-Shrestha, G., Hewage, K. and Sadiq, R., 2017. Fit-for-purpose wastewater treatment: Conceptualization to development of decision support tool (I). *Science of the Total Environment*, *607*, pp.600-612.

Gascon, L., Arregui, F., Cobacho, R. and Cabrera, E., 2004, January. Urban water demand in Spanish cities by measuring end uses consumption patterns. In Proceedings of the Water Sources Conference, Austin, TX, USA (Vol. 11).

Kesavan, H.K. and Chandrashekar, M., 1972. Graph-theoretic models for pipe network analysis. Journal of the Hydraulics Division, 98(2), pp.345-364.

Khurelbaatar, G., Al Marzuqi, B., Van Afferden, M., Müller, R.A. and Friesen, J., 2021. Data Reduced Method for Cost Comparison of Wastewater Management Scenarios–Case Study for Two Settlements in Jordan and Oman. Frontiers in Environmental Science, p.137.

Kou, L., Markowsky, G. and Berman, L., 1981. A fast algorithm for Steiner trees. Acta informatica, 15(2), pp.141-145.

Masi, F., Langergraber, G., Santoni, M., Istenič, D., Atanasova, N. and Buttiglieri, G., 2020. Possibilities of nature-based and hybrid decentralized solutions for reclaimed water reuse. In Advances in Chemical Pollution, Environmental Management and Protection (Vol. 5, pp. 145-187). Elsevier.

Yerri, S. and Piratla, K.R., 2019. Decentralized water reuse planning: Evaluation of life cycle costs and benefits. *Resources, Conservation and Recycling*, *141*, pp.339-346.

Energy optimization in water distribution systems: Data mining and quality forecasting approach to reduce pumping costs.

D. Abert*, F. Valero**, M. Sánchez**, P. Fontanillas,** H. Monclús*

* LEQUIA, Institute of the Environment, Universitat de Girona (UdG), Maria Aurèlia Capmany 69, E-17003, Girona, Catalonia, Spain
** Ens d'Abastament d'Aigua Ter-Llobregat, Sant Martí de l'Erm, 2, 08970, Sant Joan Despí, Catalonia, Spain

Abstract

Since water treatment and distribution is one of the most energy consumption processes all over the world, it is of great interest to develop a methodology to reduce energy costs. In the present work, a tool to reduce these costs was developed based on water quality, supply autonomy and energy costs. The used algorithm was used to modify water tank setpoints. With the proposed changes, significant economic savings were obtained.

Keywords: Costs optimization, water distribution network, energy tariff, water quality, supply autonomy.

INTRODUCTION

One of the most energy demanding in water sector worldwide is the water distribution and treatment. For instance, according to Griffiths-Sattenspiel (2009), the US uses roughly 4% of its total energy consumption in these processes, while Spain uses up to 7% (Hardy et al., 2010). Drinking water and wastewater utilities are primarily owned by local governments, and the energy used to purify the water can account for 30% to 40% of the municipality's energy costs (Copeland & Carter, 2014). In addition, some nations have adopted time-variable energy tariffs, which cause daily fluctuations in energy prices. This situation has increased the need to put initiatives in place to optimize energy expenditures (Chang et al., 2018). The goal of this study is to develop a data mining based solution to reduce the energy expenses associated with the water distribution systems.

METHODOLOGY

Storage tanks from ATL drinking water distribution network (Barcelona, Spain) were used as a case study to develop an energy-optimization methodology. In this study, the supplied water comes from three drinking water treatment plants (DWTP) and two seawater desalination plants. In order to distribute the water along the delivery points, pumps, tanks, and pipes are used. Supplying the water in this network has a variable energy price agreement which takes into account three energy prices throughout the day. Based on each one of these prices, three different time slots are defined. For each one of these time slots, a setpoint level is assigned to the water distribution tanks in order to control the water pumping. The process that makes it possible to cut energy costs is the optimization of the tank setpoints.

There are two restrictions on the tank setpoint configuration: on the one hand, the quality of the water being supplied (i.e., the formation of trihalomethanes (THM)) limits the maximum tank level. Higher tank levels increase hydraulic retention time (HRT), which increases the formation of disinfection by-products (i.e THMs).

On the other hand, tanks must always have a minimum volume to maintain a 24-hour supply of water in non-expected events (i.e. maintenance works).

The developed methodology aimed to increase water pumping in the cheap energy time slots and decrease it in the expensive energy time slots in order to lower energy costs. Also, a water distribution simulation algorithm was created to investigate and assess all potential setpoint levels in an effort to lower energy costs during the medium price energy hours.

To maximise pumping during the period of low energy prices, the maximum values for THMs formation based on tank level were calculated. This was accomplished using a THM predictive model (Godo-Pla et al., 2021). Low energy price timeslots received the highest setpoint level while also taking into account THM potential formation to prevent exceeding the THM concentration limit.

The minimum level that would permit supplying water for 24 hours was determined based on the tanks' capacity and water demand in order to reduce pumping during high-priced time periods.

The general scheme of the algorithm process can be summarized in Figure 1.

RESULTS

Different setpoint levels than those historically used have been suggested by the results obtained using the methodology described. The data obtained through the simulation algorithm was used to assess the economic effectiveness of water pumping. In relation to the electricity price at the time of its execution, the distribution of the pumped water over the hours with various energy prices has been examined.

The methodology that was suggested to optimize the energetic management allowed for either an increase in the proportion of pumped water during the hours with the cheapest energy (Figure 2, Tank 1) or a decrease in the proportion of pumped water during the hours with the highest energy costs (Figure 2, Tank 2). These adjustments were predicted to result in a 5% reduction in the cost of pumping energy overall. The results of the distribution of the consumed kWh in each energetic time slot are shown in Table 1.

DISCUSSION AND CONCLUSION

New tank management configurations could be generated by the tool that was developed. The setpoints produced by this algorithm have demonstrated cutting-edge methods that could lower energy costs related to the distribution of pumping along the various energy prices of the day. The effectiveness of the suggested management could be verified using the creation of a hydraulic simulation algorithm.

FIGURES

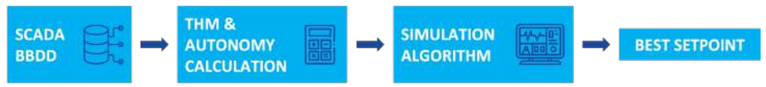

Figure 1: General process scheme of the algorithm.

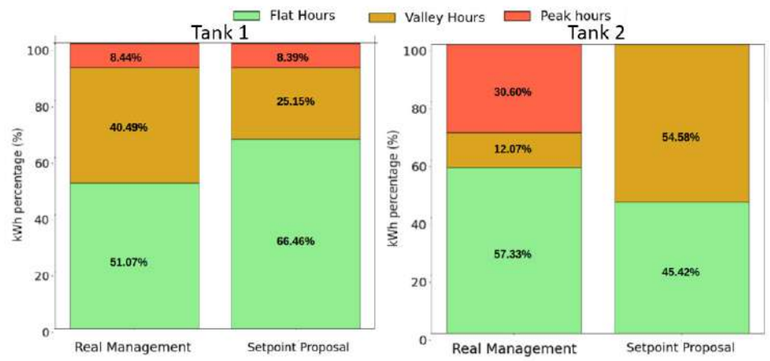

Figure 2: Water pumping distribution along different price hours, for two tanks from the case study.

Table 1. Comparison between the average daily consumed energy according to the three different time slots of energy prices

Energy price time slot	Tank 1 Historical management (kWh)	Tank 1 Proposed management (kWh)	Tank 2 Historical management (kWh)	Tank 2 Proposed management (kWh)
High price	172,47	171,65	148,99	0,00
Medium price	827,41	513,94	58,77	265,75
Low price	1043,62	1358,11	279,14	221,64

REFERENCES

Chang, Y., Choi, G., Kim, J., & Byeon, S. (2018). Energy Cost Optimization for Water Distribution Networks Using Demand Pattern and Storage Facilities. *Sustainability*, *10*(4), 1118. https://doi.org/10.3390/su10041118

Copeland, C., & Carter, N. T. (2014). *Energy-Water Nexus: The Water Sector's Energy Use* (No. R43200; p. 13). https://www.water-energy-food.org/resources/energy-water-nexus-the-water-sector-s-energy-use

Griffiths-Sattenspiel, B. (2009). *The Carbon Footprint of Water* (p. 54). https://www.rivernetwork.org/resource/the-carbon-footprint-of-water/

Hardy, L., Garrido, A., Juana Sirgado, L., & Fundación Marcelino Botín (Santander). (2010). *Análisis y evaluación de las relaciones entre el agua y la energía en España*. Fundación Marcelino Botín. https://agua.org.mx/wp-content/uploads/2019/10/PAV6.pdf

Design and Deployment of sewage Monitoring Stations to Mine Information from neighbourhoods

I. Zammit[1,2], S. Badia[1,2], M.J. Chesa[3], C. Chincolla[3], A. Cuixart[1,2], E. Domene[4], M. Garcia[4], X. Garcia[4], R. Horno[5], A. Martinez[3], A. Llopart-Mascaró[3], J. Pueyo[1,2], Ll. Bosch[1,2], I. Palacin[6], R. Peris[5], J. Raich-Montiu[5], M. Ribalta[6], E. Rubion[6], S. Simon[6], M. Satorras[4], X. Varela[3], Ll. Corominas[1,2]*

1 Catalan Institute for Water Research (ICRA), Emili Grahit 101, 17003 Girona, Spain
2 University of Girona, Plaça de Sant Domènec 3, 17004 Girona, Spain
3 Barcelona Cicle de l'Aigua, SA (BCASA), Carrer de l'Acer, 16, 08038 Barcelona, Spain
4 Barcelona Institute of Regional and Metropolitan Studies, Autonomous University of Barcelona, 08193 Bellaterra, Spain
5 scan Iberia Sistemas de Medición S.L. (s::can), Ciutat de Granada 28 bis, 08005 Barcelona, Spain
6 Eurecat - Technology Centre of Catalonia, Av. Diagonal 177, 08018 Barcelona, Spain

Abstract

Monitoring stations have been built at the neighbourhood level in Barcelona to cover a low, medium and high income neighbourhood. The stations incorporate online sensors to measure COD, pH, temperature, conductivity, and dissolved hydrogen sulfide. Herein we describe how the stations were designed, how they operate and what they can be used for. For example, using these stations dynamics of wastewater generation and pollutant dynamics have been uncovered and related to the usage habits of the inhabitants of these neighbourhoods. The richer neighbourhood generates more wastewater and shows distinct dynamics during the weekend that is attributed to people traveling outside of their residential neighbourhood, something that is not seen in the poor neighbourhood. Other such insights are presented from data collected through the stations.

Keywords (maximum 6 in alphabetical order)
Digitalization, wastewater, flow, intra-urban;

INTRODUCTION

This paper focuses on the real-time dynamics of sewage flow and its concentrations at the intra-urban scale i.e., neighbourhood-level. While there are many real-time applications at wastewater treatment plant (WWTP) level, only a few studies have looked at dynamics at the intra-urban level. Real-time monitoring sewer systems' water quality and flows is more difficult than monitoring of WWTPs because there is no infrastructure in place. Variations in small catchments (primarily residential with minor industrial contributions) have not previously been studied. Furthermore, a long-term assessment has not been carried out using a permanent monitoring station. The goal of this paper is to describe the design and deployment of three wastewater monitoring stations deployed at the neighbourhood level and to evaluate their performance in measuring wastewater flow and pollutant concentrations over a year (to study seasonality effect, mainly winter vs summer). In this paper we describe (1) the rationale for the site selections, (2) the components used and the configuration, (3) results dealing with diurnal flow, COD, TSS, conductivity, HS- concentrations, and (4) some insights into their operation over a year.

MATERIALS AND METHODS

Site selection. The three sites were chosen from the Barcelona sewer system, corresponding to residential areas with little contribution from industrial and commercial activities. Station 1 (S1) covers a catchment area of 0.72 km^2 serving 18,042 inhabitants with a household year income of €25,849; S2 has a catchment of 0.23 km^2 serving 8,914 inhabitants with a household year income of €38,430; S3 is a catchment of 0.18 km^2 serving 5,090 inhabitants with a household year income of €78,476.

Monitoring stations. The setup is shown in Figure 1. All equipment was housed in a stainless cabin measuring 2x1.4x2m and installed at street level near a sewer manhole. A large diameter plastic tube connected a peristaltic pump (Boyser AMP-22) in the cabin to the underground sewer system. The peristaltic pump fed a steady stream of WW to a 12 L acrylic glass reservoir, which is constantly emptied via a drain at the top. WW quality sensors from scan Messtechnik GmbH were installed within this reservoir (condu::lyser, spectro::lyser and pH::lyser –pH). A PLC unit (s::can con::cube) controlled these sensors as well as the actuators for emptying-filling cleaning cycles, allowed remote connection, uploaded data to the platform (via sFTP), and managed other equipment. The spectro::lyser sensor was cleaned automatically using compressed air and mechanical cleaning (s::can ruck::sack – a submersible automatic brush cleaner). In addition, flowmeters were installed directly in the sewer (S1-3 Nivus PCM 4 Nivus GmbH; Eppingen, Germany), S2 - FLO-DAR AV (Hach; Colorado, USA. Radar based sensor – contactless), S3 - NFM-550 (Nivus GmbH) coupled with a Nivus OFR level sensor.. All sensors were calibrated with in-situ measurements.

RESULTS AND DISCUSSION

Flow dynamics. The morning peak of wastewater discharge (WWD) occurs earlier on weekdays than on weekends (Figure 2 Column 1), which is due to people waking up earlier to get ready for work. S1 inhabitants may wake up earlier than in the other neighbourhoods as the morning peak on weekdays is earlier in S1 as compared to S2 and S3; note that the hydraulic residence times between point of WW generation and sampling points are similar across neighbourhoods (around 2 hours on average). Weekend afternoon WWD is higher in low- (S1) and medium- (S2) socioeconomic status neighbourhoods than weekday afternoons at the same time. This could be due to behavioural differences associated with inter-neighbourhood mobility. In S1, residents may find the cost of travelling out of the neighbourhood prohibitive, and staying at home would result in more WW discharged. In S2, the cost of travel is unlikely to be an issue; rather, the observed effect is the result of people visiting the neighbourhood from outside. S2 is a beachfront neighbourhood that probably receives more visitors than S1 and S3, which are highly residential. Figure 2 Column 2 compares summer and winter flow differences between the three neighbourhoods. Summer WWD levels are highest in S2. This is most likely due to S2 being in a popular tourist area, which sees more people during these months. Summer peaks in S1 and S3 are less intense, with moderate WWD observed in the afternoons (in terms of relative level to the morning peak of the same period). This lower summer activity in S3 could be attributed to residents in this high SES having summer homes outside of the Barcelona area; however, it is unclear what causes the lower WWD in S1. Differences in the behaviour of the citizens during different holidays can also be observed in the 3 neighbourhoods with different SES (Figure 2 Column 3).

Conductivity, COD and H_2S. The conductivity patterns (Figure 3) differ greatly between stations. S1 and S3 have the smallest intra-diurnal variation, with minimum-maximum ranges of approximately 500 µS/cm. S2 has much greater intra-diurnal variation, with peaks during the night. S2 is located in a catchment prone to seawater infiltration since it is close to the sea and at more or less sea level. The low flow of WW discharged at night (Figure 2 Column 1) means that seawater infiltration is not flushed away, and as a proportion, seawater infiltration becomes more dominant than during the day, which is then flushed away when WWD is higher, despite the fact that the lowest values at S2 are still higher than either S1 and S3. This is consistent with COD values (Figure 3 Column 2); seawater infiltration would increase conductivity but not COD because seawater contains negligible levels organic oxidisable components. Increased discharged blackwater would raise conductivity and COD. It is unclear why S1 and S3 exhibit opposite trends during the night, i.e. increasing conductivity in S1 and decreasing in S3. An increase in conductivity is expected because the blackwater-to-greywater ratio is higher at night, which would increase conductivity. The decrease in conductivity at night in S3 could be attributed to automatic watering of gardens at night in this high-income neighbourhood, which could partially drain excesses to sewers. WWD levels (Figure 2) at night in S3 are actually higher in summer (when irrigation is required) than in winter.

DISCUSSION

We demonstrate the utility of wastewater monitoring stations and the information that can be extracted from wastewater using online sensors. We see differences in flow patterns that are related to socioeconomic status, as well as differences in conductivity and H_2S that are related to catchment characteristics. According to Enfinger and Stevens (2006), S1 and S2 follow the typical flow pattern of residential areas. The S3 profile falls somewhere between a residential and a Hotel profile for two reasons: (1) the evening peak is much less pronounced than in S1 and S2, and (2) the weekend curve in S3 is never crosses the weekday curve. In terms of concentrations, we find a strong relationship between flows and COD, but no relationship between these variables and pH, H_2S or conductivity. Conductivity dynamics are highly dependent on catchment characteristics; S2 (located 350 m from the sea) received phreatic drains, which significantly influenced conductivity patterns; Atinkpahoun et al. (2018) observed no well-defined variation patterns for pH and conductivity; in our study, we did observe conductivity patterns, but they were not correlated to flows or COD patterns. Finally, H_2S is linked to in sewer-biological processes that are affected by temperature and residence time of wastewater in the sewer system (Zuo et al., 2019). Flow patterns and pollutants dynamics differ between the summer and the winter seasons. Whereas discharged wastewater volumes were lower in the summertime at S1 and S3, they were higher at S2; conductivity was lower at all three stations during the summer, and H_2S increased at S2. In contrast, we found no differences in COD concentrations between summer and winter. The main novelty of this study is the nature of the catchments under study (primarily residential areas with limited industrial activities), the differences in the socioeconomic status of the residents in these catchments, and the long-term (1 year) and high frequency (3 minutes) collection of monitored variables.

REFERENCES

Atinkpahoun, C. N. H., Le, N. D., Pontvianne, S., Poirot, H., Leclerc, J.-P., Pons, M.-N., & Soclo, H. H. (2018). Population mobility and urban wastewater dynamics. Science of The Total Environment, 622-623, 1431-1437. doi:https://doi.org/10.1016/j.scitotenv.2017.12.087
Enfinger, K. L., & Stevens, P. L. (2006). Sewer Sociology – The Days of Our (Sewer) Lives.
Zuo, Z., Chang, J., Lu, Z., Wang, M., Lin, Y., Zheng, M., . . . Liu, Y. (2019). Hydrogen sulfide generation and emission in urban sanitary sewer in China: what factor plays the critical role? Environmental Science: Water Research & Technology, 5(5), 839-848. doi:10.1039/C8EW00617B

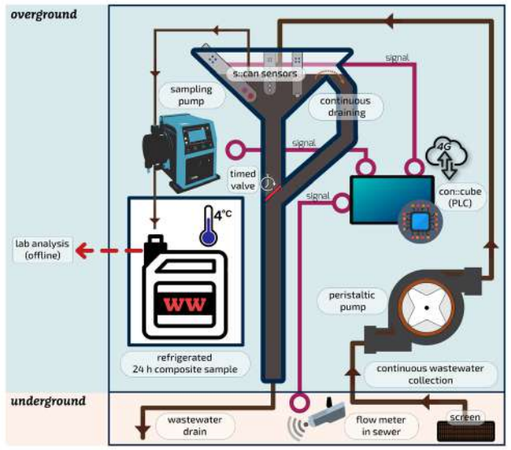

Figure 1 - Overview of the components making up the stations

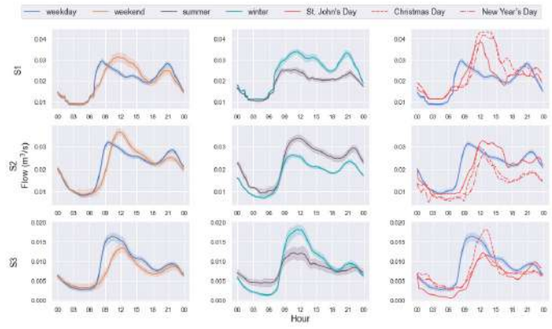

Figure 2 - Flow daily dynamics – each line shows averaged flows of multiple days over 24 h. Column 1 shows differences in dynamics between weekdays and weekends. Column 2 shows differences in dynamics between summer and winter days. Column 3 shows differences between the average of a weekday and holidays (Christmas Day 2021-12-25, New Year's Day 2022-01-01 and St John's Day ('Dia de Sant Joan' 2021-06-24 a very popular holiday in Barcelona)

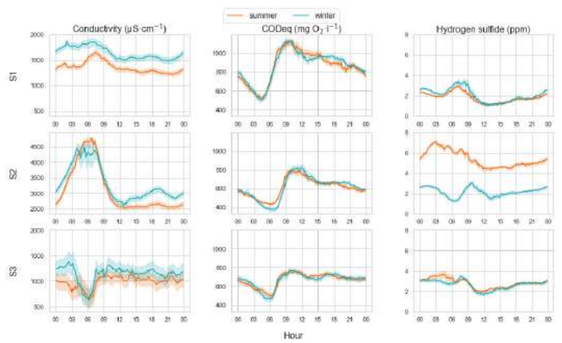

Figure 3 - Dynamics of Conductivity (Column 1), Chemical Oxygen Demand (CODeq) (Column 2), and hydrogen sulfide (Column 3) with station number as rows and each data line showing averaged values of multiple days over 24 h.

Intelligent control of wastewater treatment plants by agent reinforcement learning

O. Aponte-Rengifo*, M. Francisco*, R. Vilanova**, P. Vega*, S. Revollar*.

* Informatics and Automatics Department, University of Salamanca Spain.
(E-mail: *{idu17344, mfs, pvega, srevolla}@usal.es*
** Dept. Telecommunications and Systems Engineering School of Engineering Universitat Autonoma Barcelona, Spain.
(E-mail: *Ramon.Vilanova@uab.cat*)

Abstract

This paper presents deep neural network based Reinforcement Learning (RL) to optimize the aerobic processes of the activated sludge process within an urban wastewater treatment plant (WWTP). The current challenge in WWTP is to obtain accurate models, which is difficult due to the complexity of their biological processes and the uncertainty caused by unforeseen situations. Many advanced control methods are based on plant models, failing in the mentioned situations. Therefore, RL is proposed in this work, which optimizes the process without knowledge of the models and is only driven by the process data. Consequently, the results demonstrate the advantage of RL in achieving the control objectives and adaptability according to the control requirements. Particularly, the trained RL agents aim to set the oxygen setpoint in the aerobic process to optimize the trade-off between environmental impact and operating cost.

Keywords
Wastewater systems, Reinforcement Learning, Intelligent agents, Deep Neural Networks, Effluent Quality.

INTRODUCTION

WWTP modelling has been a very active area and activated sludge models (ASM1, ASM2) are readily available nowadays (Iratni et al., 2019, Revollar et al., 2017). However, they might fail in some real plant situations such as unexpected microorganisms' behaviour due to the intrinsic biologic uncertainty caused by extreme temperatures, peak influent loads, and bulking effects, among others. A possible approach to tackle this issue is the use of artificial neural networks as a methodology to obtain models of complex processes requiring only data, capturing in this way the full plant behaviour.

Deep reinforcement learning (DRL) (Sutton et al., 2018) is a model-free machine learning methodology that employs deep neural networks (DNN) trained by "Trial-Error," like biological brain training. Indeed, DRL algorithms use DNN as an approximation function of the strategy behind its actions, the policy. The Policy Gradient (PG) (Williams 1992) algorithm directly parameterizes policy in large uncertain states and action spaces, performing the gradient ascendent method searching for DNN optimal parameters. These deep neural networks act as intelligent agents (RL Agents), providing the optimal actions to be applied. For example, RL has been applied to provide the oxygen set point during the aerobic process in WWTPs (Hernández-del-Olmo et al., 2018), and in (Chen et al., 2021) optimization from an LCA perspective using RL has also been applied.

This work has developed this strategy with different RL agents trained by PG algorithm to control dissolved oxygen and nitrogen levels in an aerobic process of an activated sludge WWTP, considering environmental impact and operating costs.

MATERIALS AND METHOD

Our controller is trained, implemented, and evaluated in Benchmark Simulation Model n.1 (BSM1) (Alex et al., 2008). BSM1 is a simulation environment that includes a simulation model based on the activated sludge process, a plant design, performance criteria, and procedure evaluations. In the activated sludge process pollutants are removed through nitrification and denitrification processes, occurring in successive anoxic and aerobic bioreactors. In the aerobic zone, where the nitrification process occurs under aerobic conditions, dissolved oxygen (DO) concentration is important since most microorganisms use it to convert organic pollutants into energy and food.

BSM1's Default control strategy (Alex et al., 2008) has two control loops, representing a classical control structure for the plant. The first one controls the level of dissolved oxygen (SO) in the fifth reactor and manipulates the coefficient of aeration (KLa) to maintain a certain level of oxygen (SPSO5). The second loop controls the nitrate level (SNO) in the second reactor by the internal recirculation flow (Qa).

Our proposal aims to minimize the environmental impact and operation cost by manipulating setpoints in the default control strategy. RL Agents has been trained to provide SPSO of reactors 3, 4, and 5 in order to keep effluent ammonia under its limit with an efficient Aeration Energy Cost. For simplicity, $SPSO_3 = SPSO_4 = SPSO_5/2$. Nitrite and nitrate are considered because has an inverse relation with ammonia and have an environmental impact.

Reinforcement Learning Agents

From an RL-WWTP interaction point of view, the RL agent sends an action to the process, and this sends back a state and a reward, both consequences of the action. The action is an increase of $SPSO_5$, [-0.5 0 0.5] with respect to $SPSO_5$ at t-1. The states depend on the controlled variables and the $SPSO_5$. The reward qualifies the action in accordance with the control objectives and is the optimization criteria of PG. Consequently, optimization is driven by actions and states that obtain higher expected cumulative rewards. Therefore, our reward objective seeks that agents minimize environmental impact while reducing operating costs.

Six configurations of RL agents were trained and evaluated. Agents are divided into three groups (Table 1). The Agents differ in the configuration of their states and rewards. In the first and third groups, the states are the normalized errors, which are the difference between the corresponding concentration and its reference, selected as legal limits (4 mg/l for ammonia SNH_5 and 18 for total nitrogen TN) to get reasonable operating costs. In the second group, the states are just the normalized concentrations. As for rewards, in the first and second groups, they are selected heuristically as the weighted sum of squared errors of SNH_5, and SNO_5 with respect to the corresponding legal limit, together with an AE term if aeration costs are considered. The third group considers rewards, the OCI (Operational Cost Index), and the EQ (Effluent Quality). The SNH5 reference is the ammonia limit, while the SNO_5 reference is the total nitrogen limit. SNH_5, SNO_5, SS_5 (Readily biodegradable substrate in reactor 5), AE, EQ, and OCI were normalized to [0 1]. Also, the references were normalized.

RESULTS AND CONCLUSIONS

The results are compared against the default control ($SPSO_3 = SPSO_4 = 1$, $SPSO_5 = 2$) and analyzed using the BSM1 performance indic and time percentages of ammonia and total nitrogen violations of leg limits %VNH and %VN, respectively (Table 2). The evaluation peri considered spans 7 to 14 days, following the benchmark protoc sampling 15 minutes and under dry weather conditions. Episodes t training consisted of 14-day simulations sampling every 15 minutes.

The results are evaluated in terms of the reward objectiv Consequently, agents AG1 and AG2 show the lowest levels of SNl and high levels of AE because their rewards did not include AE. On t other hand. AG1P and AG2P agents display higher SNHe and low AE because their rewards also include AE. SNHe of both groups above the default because the reward was to decrease the margin error concerning its references, not a minimization of both, as in ((Table 2) (Figure 1).

In the case of G3, EQ, and OCI are closest to the default because th reward sought to minimize both, which are competing objectiv Among these results, the lowest %VN and %VNH by G3 is remarkab These improvements do not result in a higher OCI than the defa (Figure 1).

Table 1. Configurations of the RL agents. The episodes column sho the total episodes for training. Objectives within the reward have specific weight obtained heuristically.

Group	Agent	Episodes	Reward	States	Actu...
G1	AG_1	1000	$-(2\,.\,(SNH_5\text{-}4)^2 + 0{,}1\,.\,(SNO_5\text{-}18)^2)$	[(SNH_5-4) (SNO_5-18) $SPSO_5$]	[-0.5 0 0.5]
	AG_{1p}	2000	$-2\,.\,((SNH_5\text{-}4)^2 + 0{,}1\,.\,(SNO_5\text{-}18)^2 + 0{,}1\,.\,(AE)^2)$		
G2	AG_2	1000	$-(0{,}95\,.\,(SNH_5\text{-}4)^2 + 0{,}05\,.\,(SNO_5\text{-}18)^2)$	[SNH_5 SNO_5 $SPSO_5$]	[-0.5 0 0.5]
	AG_{2p}	2000	$-(0{,}9*(SNH_5\text{-}4)^2 + 0{,}05*(SNO_5\text{-}18)^2 + 0{,}05\,.\,(AE)^2)$		
G3	AG_3	1000	$-(2\,.\,EQ + OCI)$	[(SNH_5-4) (SNO_5-18) (SS_5-0.9) $SPSO_5$]	[-0.5 0 0.5]
	AG_{3p}	2000	$-(EQ + OCI)$		

Table 2. Evaluation of agents in dry weather conditions. In addition to the values of each agent, there are differences in percentages (%) with respect to the default control performance. Negative % values indicate that they are below their corresponding default value.

Control	OCI	EQ	SNHe (Effluent ammonia)	TotN (Effluent Total Nitrogen)	AE	% VNH	% VN
		kg poll.units/d	mg N/l	mg N/l			
DEFAULT	17452,94	6016,38	2,03	17,39	4989	14,73	20,98
AG_1	15703,08	6226,46	3,22	16,14	3226,14	28,27	13,54
AG_1%	-10,03	3,49	58,08	-7,2	-35,33	91,92	-35,46
AG_{1p}	15633,41	6280,91	3,48	15,91	3151,9	34,67	12,8
AG_{1p}%	-10,43	4,4	70,83	-8,51	-36,82	135,35	-39,01
AG_2	15952,11	6191,77	2,8	16,79	3485,97	20,98	16,67
AG_2%	-8,6	2,92	37,86	-3,44	-30,13	42,42	-20,57
AG_{2p}	15652,15	6323,06	3,45	16,2	3175,54	35,42	13,54
AG_{2p}%	-10,32	5,1	69,63	-6,86	-36,35	140,4	-35,46
AG_3	16076,73	6144,61	2,61	16,92	3612,53	17,11	17,86
AG_3%	-7,89	2,13	28,3	-2,66	-27,59	16,16	-14,89
AG_{3p}	15905,5	6169,87	2,79	16,7	3437,96	19,05	15,03
AG_{3p}%	-8,87	2,55	37	-3,94	-31,09	29,29	-28,37

Therefore, these results highlight that RL agents minimize environmental impact and operating costs as a function of reward. Specifically, the agents learned without prior knowledge of the model and were only guided by the process data. Moreover, an RL agent is easily adaptable according to requirements. As seen in the results of G1 and G2, which were rewarded with specific objectives, SNH5, SNO5, and AE, while in G3, their targets were global, EQ, and OCI.

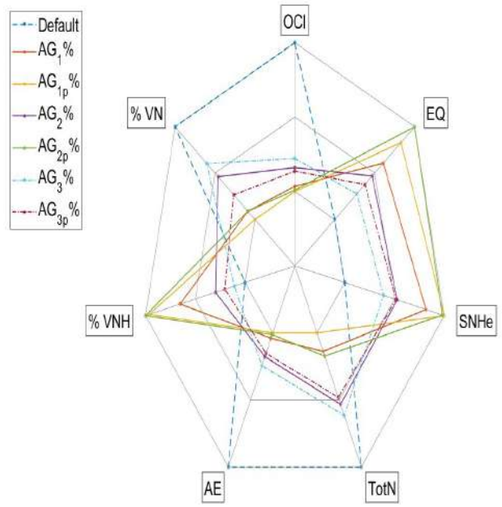

Figure 1. The radar chart displays the percentage difference with respect to the default performance control shown in Table 2. The limits of each axis are its own minimum and maximum values.

ACKNOWLEDGMENTS: This work has been supported by projects PID2019-105434RB-C31 and TED2021-129201B-I00 of the Spanish Government and Samuel Solórzano Foundation Project FS/11-2021.

REFERENCES

Iratni, A., & Chang, N. B. (2019). Advances in control technologies for wastewater treatment processes: status, challenges, and perspectives. IEEE/CAA Journal of Automatica Sinica, 6(2), 337-363.
Revollar, S., Vega, P., Vilanova, R., & Francisco, M. (2017). Optimal control of wastewater treatment plants using economic-oriented model predictive dynamic strategies. Applied Sciences, 7(8), 813.
Sutton, R. S., & Barto, A. G. (2018). Reinforcement learning: An introduction. MIT press.
Williams, R.J. Simple statistical gradient-following algorithms for connectionist reinforcement learning 1992. p. 28.
Hernández-del-Olmo, F., Gaudioso, E., Dormido, R., & Duro, N. (2018). Tackling the start-up of a reinforcement learning agent for the control of wastewater treatment plants. Knowledge-Based Systems, 144, 9-15.
Chen, K., Wang, H., Valverde-Pérez, B., Zhai, S., Vezzaro, L., & Wang, A. (2021). Optimal control towards sustainable wastewater treatment plants based on multi-agent reinforcement learning. Chemosphere, 279, 130498.
Alex, J., Benedetti, L., Copp, J. B., Gernaey, K. V., Jeppsson, U., Nopens, I., ... & Winkler, S. (2008). Benchmark simulation model no. 1 (BSM1). Report by the IWA Taskgroup on benchmarking of control strategies for WWTPs, 1.

Sustainable technologies and real-time monitoring for treating industrial wastewater: the case study of Solvay chemical plant at Rosignano Marittimo

M. Parlapiano*, C. Andreola*, M. Sgroi*, G. Pettinello**, A.L. Eusebi*, F. Fatone*

*Department of Science and Engineering of Materials, Environment and Urban Planning-SIMAU, Marche Polytechnic University, 60131, Ancona, Italy

** Solvay Chimica Italia S.p.A, Via Piave, 6 I-57013, Rosignano SOLVAY LI, Italy

Abstract

This study is focused on the reuse of industrial wastewater (Solvay's peroxides effluent) inside the industry boundaries for the cooling tower needs. The possibility to treat this wastewater, characterized by high recalcitrant COD and relevant amount of Nitrates, by aerobic and anoxic biological processes was tested using a bench scale Sequencing Batch Reactor (SBR). The efficiency of the biological processes was evaluated by varying different parameters, such as Dissolved Oxygen (DO), concentration of Mixed Liquor Suspended Solid (MLSS), Hydraulic Retention Time (HRT), type of external carbon source and COD/N-NO3 ratio. Furthermore, pH and DO were monitored continuously during the bench scale process, while grabbed samples were analysed through UV-Vis and Fluorescence Spectroscopy, gathering relevant information to optimize the operation of the treatment processes increasing its economic abd environmental sustainability.

Keywords: Biological Treatment; Fluorescence Spectroscopy; Industrial wastewater; Industrial reuse; On-line monitoring; UV-Visible Spectroscopy.

INTRODUCTION

It is estimated that 20% of all freshwater consumption globally is used by industry and this share is increased to 50% in industrialized countries. The industrial sector is also a major water polluter, as only up to 60% of industrial wastewater receives treatment before being discharged into the environment (Forster J., 2014). Eco-efficient and sustainable industrial water management is a priority within the integrated water resources management strategy (Agarwal et al, 2000). In many ways, European communities are particularly well-placed to shift from a linear to a circular economy (CE) model. The concept of CE responds to the desire for sustainable growth in the context of increasing pressure on the environment at the global level due to the high demand and consumption of natural resources (Daddi et al., 2017). For this scope, the European Union is funding several research activities under the Horizon 2020 program, which coordinates actions across many policy areas to promote sustainable growth and employment through better use of resources. In light of these, the current study addresses the internal reclamation of wastewater in the Rosignano Solvay chemical plant framed in the H2020 AquaSPICE project. It aims at materializing circular water use in European process industries fostering awareness of resource efficiency and delivering compact solutions for industrial applications. The Rosignano Solvay industrial site is one of the oldest and largest in Italy, where a lot of different chemicals are produced, such as hydrogen peroxide and peracetic acid. In particular, the Solvay peroxides plant produces around 87600 m^3/y of wastewater, characterized by high COD partly recalcitrant, nitrates and sulphates that are subsequently discharged to sea. In this work, this real stream is treated through a biological bench scale Sequencing Batch Reactor (SBR) and the efficiency and feasibility in COD and Nitrates removal are evaluated. This study is supporting the development and design of a sustainable treatment train at the pilot scale (WAPEREUSE) in order to increase energy and carbon-efficient water reuse, and decrease the freshwater intake, the pressure on biodiversity, and the disposal of waste (Solvay One Planet, 2020).

MATERIALS AND METHODS

The biological Sequencing Batch Reactor (SBR), at bench scale, used for the experimental activity, was composed of: a 70L rectangular tank, a vertical mixer (140 rpm), a fine bubble disc diffuser (9 inches), a air blower (4 L/min), a peristaltic pump for influent feeding (26 L/min), a peristaltic pump for effluent discharge (30 L/h), one peristaltic pump for dosing the external carbon source (3 l/h), an on-line pH sensor (SenTix 940 ©, WTW), an on-line DO sensor (LDOsc Hach Lange), and a control&management system (myRIO, NI) to set cycles and to store data. To evaluate the process behaviour and the influence of operative parameters on the treatment efficiency, the following conditions were tested: DO at 8 and 4 mgO_2/L; Mixed Liquor Suspended Solid (MLVSS) between 3.5 and 6 gVSS/L, different COD/N-NO3 ratio (2, 3, 7 and 9), and different types of external carbon source (glycerol and a hydroalcoholic solution). During the experimental activity, the influent on the biological SBR and its performances have been monitored through sampling and analysis of specific parameters, such as alkalinity, COD, Anions, MLSS and MLVSS. Furthermore, UV-Visible and Fluorescence analyses were conducted to study the evolution/transformation of organic matter fraction by parameters that can be used during real-time monitoring

The SBR cycle consists of 1) influent feeding, 2) aeration phase for COD removal, 3) anoxic phase for denitrification, 4) decanting, and 5) effluent discharge.

RESULTS AND DISCUSSION

The characterization of the influent stream is reported in Table 1. The wastewater COD is made of a biodegradable fraction and a recalcitrant part. Volatile substances are also presents and recalcitrant constituents tend to polymerize over time.

Table 1. Characterization of the Solvay industrial stream

Parameter	U. M.	Average	Min	Max	Dev. ST
COD	mg/L	519	109	939	266
Chlorine (Cl)	mg/L	132	49	245	73
Nitrate (NO_3^{2-})	mg/L	969	770	1265	172.5
Phosphate (PO_4)	mg/L	29	2.7	69	23
Sulfate (SO_4)	mg/L	769	631	1007	134
Alkalinity	mg $CaCO_3$/L	92	37	131	27

Increasing DO concentration inside the reactor from 4 to 8 mgO_2/L, the efficiency of the aerobic phase improved from 29 to 47%, respectively (Figure 1). Particulalry, a highest COD removal rate was observed in the first 6 hours of the oxidation phase. Furthermore, most of COD was removed within the first 24 hours of treatment, whereas only an additional removal of 10% was observed if the aerobic oxidation conditions are maintained for two days (Figure 1.a). Otherwise, a higher concentration of biomass didn't lead to higher COD removals (Figure 1.b). Indeed, the obtained results underlined the specific COD composition of the Solvay wastewater: a fraction constituted by biodegradable compounds and a fraction of biological recalcitrant substances. Complete denitrification (around 99%) and a specific removal rate of 1.0 mgN-NO_3/gVSS,h were achieved by dosing glycerol, as an external carbon source, at a COD/N-NO_3 equal to 3. The increase in the COD/N-NO3 ratio, corresponding to higher treatment costs, did not lead to reaction rate improvement (i.e., reduction of HRT for the denitrification) but on the contrary, led to a COD overdose which was then removed by aerobic oxidation. On the other hand, at COD/N-NO3 lower than 3 an incomplete denitrification reaction, revealed by NO_2 accumulation, was detected. Similar denitrification rates were estimated for glycerol and the hydroalcoholic mixture (Figure 1.c). Results were in line with literature values (Cyplik et al, 2013). As a result of oxidation and denitrification reactions, alkalinity inside the reactor increased overtime (Figure 1.d).

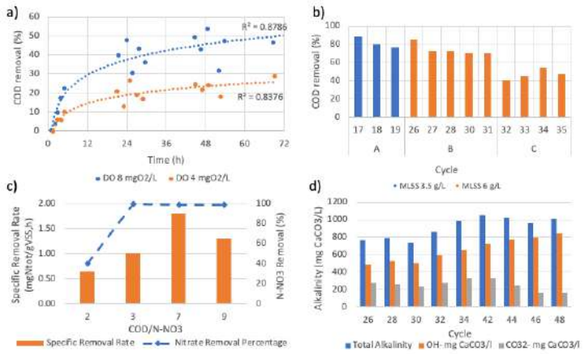

Figure 1. **a)** COD removal percentage at 4 and 8 mgO_2/L of Dissolved Oxygen monitored for 72 hours; **b)** COD removal percentage observed between cycles 17 and 35 at different MLVSS, 3 and 6 g/L; **c)** Comparison of different COD/N-NO3 ratio between specific N-NO3 removal rate (orange bars) and N-NO3 removal percentage (blue dotted line); **d)** Total alkalinity of the SBR effluent (blue), mineral alkalinity (orange) and inorganic alkalinity (grey), between 26 and 48 cycles.

Moreover, relevant information on the COD nature and its behaviour towards the biological SBR was obtained by applying the UV-Visible and Fluorescence spectroscopy. In Figure 2 are highlighted the information obtainable by these two spectroscopic tehniques. UV absorbance measurement resulted a suitable parameter to monitor COD removal during the biological process (Figure 2.a). However, fluorescence spectroscopy offered the advantage to differentiate the removal of the biodegradable and recalcitrant components (Figure 2.b and Figure 2.c). Particularly, Fluorescence spectra identified 3 main peaks: one peak at excitation, and emission wavelength 265/285 nm (I2), and a peak at 300/410 nm (I3). As shown in Figure 2, the peak I2 was removed almost completely, whereas I3 had very low percentage of removals (between 56 and 75%). This peak is mainly constituted by organic matter recalcitrant not easy to be removed biologically (Ou et al, 2014). Hence, treatment monitoring by fluorescence spectroscopy may be very useful strategy to optimize the operation conditions of biological processes since the COD concentration in the influent wastewater is highly variable and affected by the industrial cycle operation.

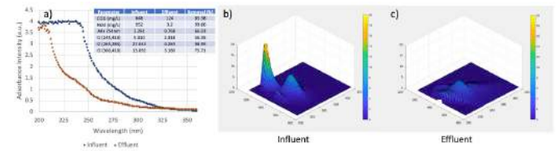

Figure 2. **a)** UV-visible spectra of the SBR influent (blue) and effluent (red); **b)** 3D Fluorescence spectra of the SBR influent and effluent **(c)**.

REFERENCES

Jürgen FÖRSTER, Statistics in focus 14/2014;

https://ec.europa.eu/eurostat/statistics-explained/index.php?title=Water_use_in_industry&oldid=262077

Agarwal et al. Integrated Water Resources Management, TAC Background Papers. No. 4, Global Water Partnership, Stockholm 2000.

Solvay One Planet Policy, 2020;

https://www.solvay.com/en/press-release/2030-sustainability-program-solvay-one-planet

Daddi, T., Nucci, B., & Iraldo, F. 2017. Using Life Cycle Assessment (LCA) to measure the environmental benefits of industrial symbiosis in an industrial cluster of SMEs. J. Clean. Prod. 147, 157–164.

Cyplik, P., Juzwa, W., Marecik, R., Powierska-Czarny, J., Piotrowska-Cyplik, A., Czarny, J., Drozdzyńska, A., & Chrzanowski, Ł. (2013). Denitrification of industrial wastewater: Influence of glycerol addition on metabolic activity and community shifts in a microbial consortium. Chemosphere, 93(11), 2823–2831. https://doi.org/10.1016/j.chemosphere.2013.09.083

Louvet, J. N., Homeky, B., Casellas, M., Pons, M. N., & Dagot, C. (2013). Monitoring of slaughterhouse wastewater biodegradation in a SBR using fluorescence and UV-Visible absorbance. Chemosphere, 91(5), 648–655. https://doi.org/10.1016/j.chemosphere.2013.01.011

Ou, H. S., Wei, C. H., Mo, C. H., Wu, H. Z., Ren, Y., & Feng, C. H. (2014). Novel insights into anoxic/aerobic1/aerobic2 biological fluidized-bed system for coke wastewater treatment by fluorescence excitation-emission matrix spectra coupled with parallel factor analysis. Chemosphere, 113, 158–164. https://doi.org/10.1016/j.chemosphere.2014.04.102

TECHNICAL SESSIONS

T9.

Modelling

A novel methodology for modelling SUDS using SWMM and Giswater: Case study on Montjuic – Girona/Spain

Nicole Aguiar[12], J Comas[12], L Corominas[1], S Busquets[1], J Pueyo[1], M Poch[2]

[1]ICRA, Catalan Institute for Water Research, Scientific and Technological Park of the University of Girona, Emili Grahit 101, E-17003 Girona, Catalonia, Spain (email: infodsu@icra.cat)

[2]LEQUIA, Institute of the Environment, Universitat de Girona, C/Maria Aurèlia Capmany 69, 17003 Girona, Catalonia, Spain (email: nicole.arnaud@udg.edu)

Abstract

The study proposes a more straightforward hydrologic-hydraulic model to assess impact in flow reduction due to improvements in surface hydrology generated by the use of Sustainable Urban Drainage Solutions (SUDS). The result exhibits higher spatial resolution than conventional catchment division models, based in terrain elevation or node-geometric criteria, and is less complex and time-consuming than usual methods for modelling green solutions. The novel approach uses a grid square layer with land use cover to create sub-basin with homogeneous land use type and size. Flow routing from the catchments to the network considers terrain slope and maximum path distance. A SUDS catalog with various techniques and designs was developed for their placement in multiple subcatchments, according to land cover classification. The study was conducted using open-source softwares with spatial data from the Montijuic neighborhood in Girona, Spain.

Keywords: SUDS, SWMM, GISWATER, Hydrology, Hydraulic-Model, catchment division.

INTRODUCTION

Climate change and urbanization pose significant threats to flooding and water quality in urban areas. Urban creep increases the impervious surface and a greater number of hazardous pollutants in water. Flooding has recently caused numerous problems and is one of the potential natural disasters in numerous researches. The lack of stormwater infrastructure also contributes to the increasing volume of Combined Sewer Overflows (CSO), that even as a small proportion of the total annual wastewater discharge, contribute to 30–95% of the annual load for different pollutants (Botturi et al., 2021). To face this scenario, communities must adapt, moving away from only conventional drainage methods that encourage water remotion as quickly as possible and deploy SUDS, solutions that mimic natural processes, controlling flood while also improving runoff water quality. Impacts provided in water quantity and quality by those practices are assisted by hydraulic-hydrological models, which are great tools in the evaluation of runoff generated by a watershed and enable the assessment of the flow effects in various scenarios as well as quantifying the benefits delivered by proposed modifications (Rossman et al., 2016). Usual methods for modelling green solutions (Lee et al., 2018) are time demanding in order to represent terrain, pervious and impervious areas to evaluate baseline properties.

The main goal of this work was to develop a simplified methodology, open source based, to build a high spatial resolution Hydrologic-hydraulic deploying SUDS. The key principles considered in the model include: **(i)** Creating homogeneous subcatchments based on land use type; **(ii)** Flow routing assumes the direction determined by the existence of a minimal surface level difference and maximum flow path distance from catchment areas to the network nodes; **(iii)** Accounting for baseline conditions of surface hydrology inside the catchments by considering flow routing between pervious and impervious areas within sub-basins; and **(iv)** Construction of a SUDS technic Catalog with distinct configurations in accordance with the aimed land use class.

MATERIALS AND METHODS

The model setup uses two main softwares, SWMM (Storm Water Management Model) and a free plugin dedicated to the integral management of the water cycle, named GISWATER, which communicates SWMM to a Spatial database using the interface of QGIS.

In order to establish the hydraulic and hydrological input characteristics of the Combined Sewer System (CSS), it was first necessary to collect network inventory and spatial and temporal data from public domain sources. These activities were followed by six steps, which are illustrated in **Figure 1** and are described in more detail below.

Step 1 – Catchment delineation. To create homogeneous unities with spatially averaged descriptive features, sub-basin delineations were relied on the Copernicus (2018) land use urban atlas data. A designed grid layer with square forms measuring 90 meters on each side was intersected with the land cover. This geoprocessing process intended to generate subcatchments of uniform size and shape (with the exception of building and other eventual cases due to the land use type). Subcatchment with homogeneous land present greater accuracy in their mean hydrological properties. Moreover, sizes with lower discrepancies are excellent to promote model continuity (Lee at al., 2018). Additionally, the grid layer with square shape aimed to estimate a median flow length path, generating median concentration times in accordance with the areas of each catchment, avoiding great discrepancies in peak flow.

Step 2 &3 – Flow routing from the subcatchments to the network and measuring mean values for surface properties. Each subcatchment was connected to the outlet (network nodes) using a QGIS plugin called *Buildings2sewer* developed by ICRA. The use of this plugin enables the sub-basins to be connected to the closest node considering surface elevation criteria and distance. The altitude tolerance was set as 2 meters, and the maximum distance 40 meters (due to the medium distance calculated between the nodes of the CSS). Afterwards, geoprocessing tools were used to calculate mean values for imperviousness and slope of satellite layer in the attribute table of the subcatchments.

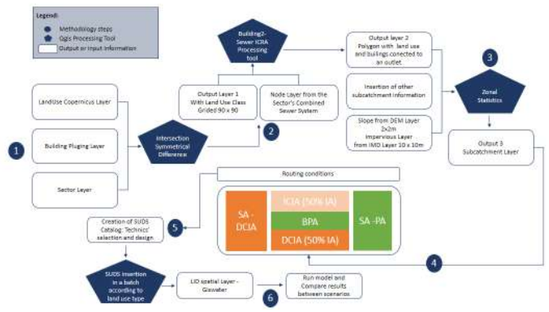

Figure 1. Sequence steps of a novel model methodology for SUDS deployment.

Step 4 – Assumptions about flow routing within the catchment area: The subcatchments delineation made any distinction between directed connected or undirected connected impervious areas. In contraposition, SWMM ability to define routing conditions was used to compensate the counter effects of this model abstraction. It was defined that 50% of the water in the IA (Impervious Area) would be directed to the PA (Pervious Area). In real conditions, flow direction is favourable to the pervious area in function of the natural hydraulic gradient, if considered a flat terrain. The 50% is a mid-value, and good estimation to avoid big deviations from what happens in the field. It means that half of the water is directly connected to the network system and the other 50% of the flow goes to the buffer pervious area. This value is a start point, and in a future calibration, this routing percentage could be changed for less or more, upon the difference between the model water flow and the measured value, if inferior or superior to the measured flow, respectively.

Based on previous basins' classifications (Lee et al., 2018) the routing condition implies three types of subcatchment composition. (**Figure 1, Step4**):

I. Stand Alone Pervious Area (SA-PA): for subcatchments landscape 100% perviousness;

II. Subcatchment with both pervious and impervious area: where pervious area functions as a Buffer Pervious Area (BPA), receiving flow from Indirected Connected Impervious Area (ICIA) and the impervious area directly connected to the outlet (DCIA); and

III. Stand Alone Directed Connect Impervious Area (SA-DCIA): representing landscapes, such as the buildings and streets.

Step 5 – Creation of a SUDS Catalog and their placement in multiple subcatchments according to the land use type: The SUDS selection and its site of installation considered the network surcharge, the existence of CSO that needed to be minimized and hydrogeological aspects. It was designed three different on source SUDS in accordance with the land use type: Permeable Pavement (PP) for the streets, Infiltration Trenches (IT) on parking lots, Rainwater Harvesting (RH) systems for storage of surface runoff from building's rooftops. The latter assumed three different configurations, due to the difference of rooftop sizes (subcatchment geometry): a residential, an institutional and another for commercial sites. Moreover, it was designed infiltration-detention basins upstream outfalls where CSO is a problem. The solutions were placed at once in multiple subcatchments, in accordance with land use classification.

Step 6 – Creation of different scenarios and running the model: In total, it was made nine simulations. Three simulations for each one of the proposed scenarios (SC01: Baseline; SC02: Implementation of on Source SUDS and flow diversion upstream the network study area; SC03: Implementation of on source and two storage SUDS).

RESULTS AND CONCLUSIONS

Subcatchments were represented in sizes of the same order of magnitude, to help maintain hydrologic continuity among them (**Figure 2**, left). The division based on land cover usage as an independent subcatchment helps in decreasing model output uncertainty (Sun et al., 2014).

The adopted methodology allowed an extreme discretization level of the model, counting to 1.570 subcatchments in an urban basin area of 39,12 km². Since buildings and streets were mainly SA-DCIA, it was possible to calculate median rooftop sizes to dimension cistern and propose pavements with the same dimension as the catchment, allowing placing the solutions in a batch (each technique to the proper land use type).

In total the model counted with 169 permeable pavements with, mostly, homogeneous sizes, 771 rain barrels for residential roofs, plus rain barrels for the school and a commercial site. Conventional subcatchment delineation such as the Digital Elevation – Deterministic 8 based and the thiessen - node based geometric method results in subcatchment with heterogeneous land uses (**Figure 2**, right), implicating that surface properties poorly represent hydrologic surface conditions, and impact due green infrastructural changes cannot be properly studied.

For example, considering the case study, using the Thiessen method it was obtained 440 subcatchments, for whom increases in standard deviation represented 57%, 63% and 124% for imperviousness, slope and surface level, respectively, reflecting the poor spatial resolution of those methods in comparison to the land use approach.

Figure 2. Visual comparison for Land Use (left) and Thiessen (right) catchments division methods.

This methodology might reflect unrealistic "green" development baseline conditions, because runoff from 50% of ICIA is evenly distributed throughout the entire PA, which means that all pervious area works like a BPA. On the other side, this impact can be resolved with model calibration and changes in routing percentage to PA.

As for the hydrological and hydraulic quantity impacts evaluated through SUDS usage, the data has shown a reduction in the CSS, an increase in the recharge of the aquifer, and the capacity of the network without having the transport capacity increased using bigger network diameters. The achievement was due to high SUDS efficiencies, ranging from 62 to 100% for a 10-year return rain of 60 minutes. The impact of SUDS usage in a non-calibrated model is still a good preliminary result, since the increased loss due to the new infrastructure does not count with the ones from baseline conditions (that could be over or underestimated in the same proportion in both scenarios). Considering the implementations of the distributed solutions in the terrain, the transition, for example, to permeable payments, could be done in long term period, according to eventual need of reforms on streets pavement.

REFERENCES

Botturi, A., Ozbayram, E.G., Tondera, K., Gilbert, N.I., Rouault, P., Caradot, N., Gutierrez, O., Daneshgar, S., Frison, N., Akyol, Ç., Foglia, A., Eusebi, A.L., Fatone, F., 2021. Combined sewer overflows: A critical review on best practice and innovative solutions to mitigate impacts on environment and human health. Critical Reviews in Environmental Science and Technology 51, 1585–1618. https://doi.org/10.1080/10643389.2020.1757957

Lee, J.G., Nietch, C.T., Panguluri, S., 2018. Drainage area characterization for evaluating green infrastructure using the Storm Water Management Model. Hydrol. Earth Syst. Sci. 22, 2615–2635. https://doi.org/10.5194/hess-22-2615-2018

Rossman, L.A. and Huber, W.C. (2016). Storm Water Management Model Reference Manual, Volume I – Hydrology (Revised). EPA/600/R-15/162A, Revised January 2016. U.S. Environmental Protection Agency, Office of Research and Development, Water Supply and Water Resources Division, Cincinnati, OH.

Sun, N., Hall, M., Hong, B., Zhang, L., 2014. Impact of SWMM Catchment Discretization: Case Study in Syracuse, New York. J. Hydrol. Eng. 19, 223–234. https://doi.org/10.1061/(ASCE)HE.1943-5584.0000777

Elucidating the field of application of 0D and 1D biofilm models integrated with the hydrodynamics of aerobic granular sludge reactors

A. Catenacci*, M. Pesenti*, E. Paini*, L. Formaggia**, G. Rizzardi*, R. Canziani* and A. Turolla*

* Politecnico di Milano, Dipartimento di Ingegneria Civile e Ambientale, Piazza Leonardo da Vinci 32, 20133 Milano, Italy (E-mail: *arianna.catenacci@polimi.it*; *marco4.pesenti@mail.polimi.it; elia.paini@polimi.it; giacomo.rizzardi@polimi.it; roberto.canziani@polimi.it; andrea.turolla@polimi.it)*
** Politecnico di Milano, Dipartimento di Matematica, Piazza Leonardo da Vinci 32, 20133 Milano, Italy (E-mail: *luca.formaggia@polimi.it)*

Abstract
Due to the growing interest that aerobic granular sludge processes are witnessing today, proper modelling is crucial for process optimization and control, but the huge number of parameters and variables involved hinders the spreading of reliable and user-friendly mathematical models. Based on the rule by which "a model should be as simple as possible, and only as complex as needed", this work compares two models developed with different degree of complexity, namely the 0D-B/AGS-SBR and the 1D-B/AGS-SBR. Different process boundary conditions (influent pollutant concentrations, cycle time and phase duration, oxygen dosage) are tested in order to assess the reliability and applicability of both models. Preliminary results motivate the pursuit of this study, primarily aimed at providing wastewater treatment plants operators and modellers with adequate tools for different possible scenarios.

Keywords
Aerobic sludge model; Biofilm; Granular sludge; Half-saturation coefficient; Modelling; Plug-flow feeding.

INTRODUCTION

The advantages of aerobic granular sludge (AGS) technologies are increasingly attracting the scientific community as well as industrial and municipal wastewater treatment plants (WWTPs) operators. Accordingly, the practical implementation of process optimization and control strategies by means of the development of reliable and user-friendly mathematical models is assuming growing relevance (Zaghloul & Achari, 2022). Mechanistic models available in literature show a clear evolution over time towards increased complexity, involving not only biological and physio-chemical transformations as described in the IWA Activated Sludge Models (ASM), but also in terms of granule dynamics (e.g., liquid-granule mass transfer, intragranular transport, attachment/detachment, size distribution) and reactor hydraulics (liquid-phase transport, granule transport, settling) (Baeten et al., 2019).
The detection of a trade-off between model complexity and accuracy is a challenging objective, and although scarcely addressed, this task is of paramount importance for practical purposes, helping modellers to set proper assumptions/simplifications, once defined model goals and system boundary conditions (e.g., reactor size, wastewater characteristics). Recently, in order to simplify model parameter identification, Baeten et al. (2018) demonstrated the possibility of using apparent half-saturation coefficients ($K_{S,app}$) to lump the reaction diffusion process inside granules (zero-dimension biofilm model, 0D-B) in a fully mixed reactor model; on the other hand, a higher complexity model was investigated by Derlon et al. (2022) who integrated a 1D biofilm model (1D-B, with explicit description of diffusion processes) with an SBR (sequencing batch reactor) model explicitly describing plug-flow gradients during feeding.
In this work, two models were developed and compared to assess their accuracy and field of application, and to use them as practical tools for process optimization: i) a 1D-B/AGS-SBR model, where a 1D granule model was coupled to an SBR model including the description of plug-flow anaerobic feeding (AGS-SBR model), and ii) a simplified model (0D-B/AGS-SBR) where apparent half-saturation coefficients were used for biomasses included in the SBR model.

MATERIALS AND METHODS

Model development

The 1D biofilm code was developed in Matlab in spherical coordinates, based on Wanner & Gujer (1986). The system of partial differential equations was solved using a finite-difference method with fixed time step. Variable granule size and number of layers were considered.
The AGS-SBR model was implemented in Matlab-Simulink and simulates a SBR cycle at constant volume: a series of 4 CSTR with a correction code (Derlon et al., 2022) was used to mimic the ideal plug-flow feeding phase with simultaneous discharge. At the end of this phase, a very high recycle flowrate between the four CSTR is applied to create artificial mixing conditions for subsequent aerobic/anoxic phase. Sedimentation and flocs/granules stratification were not modelled, TSS concentration in the reactor was kept at a constant value by removal of excess biomass.
All the biokinetics processes were defined as in Kagawa et al. (2015), applying modified ASM 2d.
The 1D-B/AGS-SBR model was implemented by incorporating the 1D biofilm model into the SBR model and exchanging substrate fluxes between the two models. Flocs were modelled as suspended biomass with intrinsic half-saturation coefficients (K_S) within the SBR reactor.
As regards the 0D-B/AGS-SBR model, apparent half-saturation coefficients were defined as described in Baeten et al. (2018) but, conversely to what explored by the authors, in this case biomasses are subject to plug-flow gradients during anaerobic feeding.

Scenarios selection and research objectives

Different scenarios were selected and simulated using a SBR operated at constant volume (V = 1.45 m^3, h/D = 10, D = 0.57 m, VER = 60%), in order to meet the following targets: (i) verify the effects of using apparent half-saturation coefficients in a system describing the hydrodynamics of aerobic granular sludge reactors; (ii) assess if the use of a 0D biofilm model approach is reliable at varying wastewater strengths (low-medium and high strength wastewater conditions were studied); (iii) support process optimization by testing different operative conditions (e.g., cycle time and phases duration; dissolved oxygen concentration and aeration strategies).

RESULTS AND DISCUSSION

Figure 1 shows simulations obtained by using the 0D-B/AGS-SBR model fed with a low-medium strength wastewater (396 g COD/m^3, 50 g $N\text{-}NH_4^+/m^3$ and 20 g $P\text{-}PO_4^{3-}/m^3$). Different cycle time, phase duration and aeration strategies were tested. In more detail, Figures 1A and 1B compare a 4-hour cycle (C2 = 1 h anaerobic + 1 h aerobic + 1.5 h anoxic + 0.5 h sedimentation) with a 6-hour cycle (C1 = 1.5 h anaerobic + 1.5 h aerobic + 2.5 h anoxic + 0.5 h sedimentation) at same DO dosage and aeration strategy (2 mg DO/L for the aerobic phase and 0.5 mg DO/L for the anoxic phase). As regards effluent COD, ammonium and phosphate, negligible differences were observed, while effluent nitrate concentration was the most sensible variable. Positive effects of testing a different aeration strategy in the SBR cycle C2 are shown in Figure 1C: a linear increase of DO from 0 to 2 mg DO/L during the aerobic phase and a linear decrease from 2 to 0.25 mg DO/L during the anoxic phase, efficiently removes COD, phosphate, ammonium and also nitrate, resulting in an effluent concentration below 1 mg $N\text{-}NO_3^-$/L, compared to a value above 20 mg $N\text{-}NO_3^-$/L using a step aeration strategy (Figure 1A).
Diffusive mechanisms inside granules are shown in Figure 2, where biomass net growth rates and distributions, and substrate concentrations are displayed at increasing the distance from the centre of two differently sized granules. Conversely to heterotrophs (HET), PAO and GAO, the growth of both nitrifiers species (AOB and NOB) and ammonium oxidation are limited by DO penetration through the granule. Besides, for large-size granules, PAO and GAO prevailed on HET at increasing of anoxic and anaerobic conditions. Hence, the integration of the 1D biofilm model with the AGS-SBR model is expected to be of crucial importance, especially when treating high strength wastewater. Authors wish to prove that, for AGS processes too, modelling can be used to fine-tune operative parameters, provided that model complexity has been properly selected and implemented.

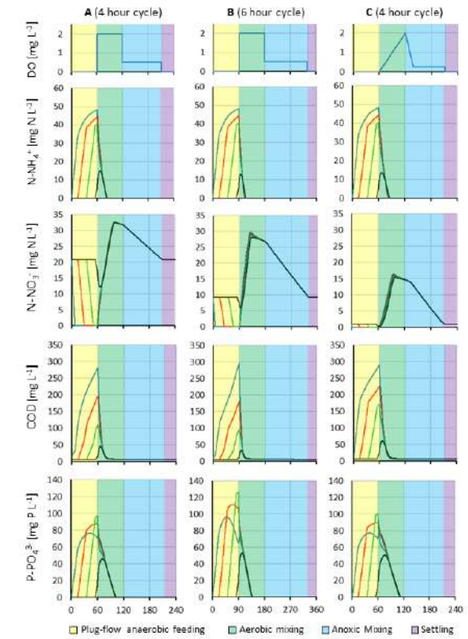

Figure 1. 0D-B/AGS-SBR model simulations at steady state for three cycles with different cycle duration and oxygen dosage strategies. The four lines during the anaerobic phase refer to the four CSTR used to model plug-flow feeding (blue: bottom, red: bottom up, green: top down, black: top).

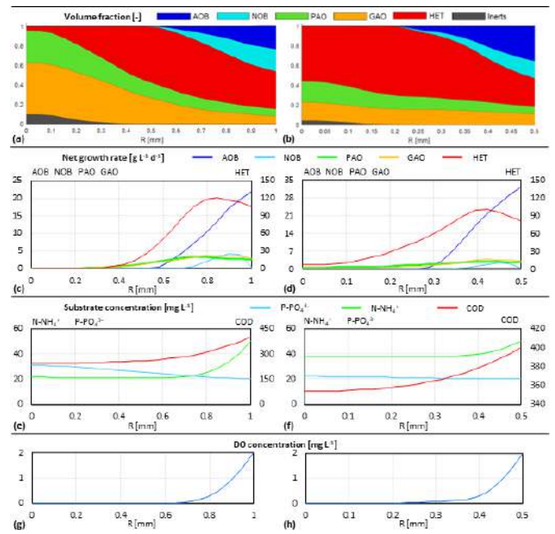

Figure 2. 1D biofilm model simulations at steady state using the SBR cycle C2. Results are shown for two different granule size (on the left, radius R = 1 mm; on the right, R = 0.5 mm).

REFERENCES

Baeten, J. E., van Loosdrecht, M. C. M., Volcke, E. I. P. 2018 Modelling aerobic granular sludge reactors through apparent half-saturation coefficients. *Water Research* **146**, 134–145.
Baeten J. E., Batstone, D. J., Schraa, O. J., van Loosdrecht, M. C. M., Volcke, E. I. P. 2019 Modelling anaerobic, aerobic and partial nitritation-anammox granular sludge reactors - A review. *Water Research* **149**, 322-341.
Derlon, N., Villodres, M.G., Kovács, R., Brison, A., Layer, M., Takács, I., Morgenroth, E. 2022 Modelling of aerobic granular sludge reactors: the importance of hydrodynamic regimes, selective sludge removal and gradients. *Water Science & Technology* **86**(3), 410-431.
Kagawa, Y., Tahata, J., Kishida, N., Matsumoto, S., Picioreanu, C., van Loosdrecht, M.C.M., Tsuneda, S. 2015 Modeling the Nutrient Removal Process in Aerobic Granular Sludge System by Coupling the Reactor- and Granule-Scale Models. *Biotechnology and Bioengineering* **112**.
Wanner, O., Gujer, W. 1986 A multispecies biofilm model. *Biotechnology and Bioengineering* **XXVIII**, 314-328.
Zaghloul, M. S., Achari, G. 2022 A review of mechanistic and data-driven models of aerobic granular sludge. *Journal of Environmental Chemical Engineering* **10**, 107500.

Successful strategies for improving energy self-sufficiency at Grüneck wastewater treatment plant in Germany by improved aeration and food waste co-digestion

K. Koch*, C. Macintosh**.***, C. Sembera*.****, S. Astals**.***

* Chair of Urban Water Systems Engineering, Technical University of Munich, Am Coulombwall 3, 85748 Garching, Germany. (E-mail: *k.koch@tum.de*)
** Australian Centre for Water and Environmental Biotechnology, University of Queensland, St Lucia, QLD 4072, Australia.
*** Council of the City of Gold Coast, Nerang, QLD 4211, Australia.
**** CAS Consulting and Services Inc., 7908 Cameron Road, Austin, Texas 78754, USA.
***** Department of Chemical Engineering and Analytical Chemistry, University of Barcelona, Martí i Franqués 1, Barcelona, 08028, Spain.

Abstract

Population growth, tightening effluent discharge requirements and increasing energy costs are driving the wastewater treatment sector to strive towards energy self-sufficiency. This case study of Grüneck wastewater treatment plant (WWTP) in Germany evaluates the effectiveness of two different energy strategies and quantifies their plant-wide impact. Energy self-sufficiency at Grüneck WWTP increased from 64 to 88% by reducing energy consumption with aeration upgrades (-3.0 kWh PE^{-1} a^{-1}) and increasing energy production with food waste co-digestion (+5.6 kWh PE^{-1} d^{-1}). The increased power production from co-digesting food waste at 0.24 kg_{VS} m^{-3} d^{-1} energetically out-weighed downstream impacts of reduced dewaterability, increased solids accumulation and nitrogen backload. Findings from this case study provide practical knowledge of the trade-offs for different strategies commonly employed to improve energy self-sufficiency at WWTPs.

Keywords

Aeration upgrade; anaerobic digestion, energy self-sufficiency; food waste co-digestion

INTRODUCTION

Population growth and increasingly stringent discharge standards are increasing wastewater treatment energy requirements. This increased energy demand coupled with rising energy costs and environmental concerns is motivating the wastewater treatment sector to strive towards energy self-sufficiency, which can be achieved through a combination of reducing power consumption and increasing on-site power production. Prior to adopting an energy strategy, it is important to understand the plant-wide implications and trade-offs between maximising power savings and minimising process drawbacks. The objective of this full-scale case study was to analyse the effectiveness of two commonly applied strategies, aeration upgrades and co-digestion, to improve energy self-sufficiency and quantify their plant-wide impact.

MATERIALS AND METHODS

5 years of operational data for Grüneck WWTP (2013-2017) was obtained from consultations with the plant operators, annual reports, energy reports and sludge reports. During this period of operation, two energy saving strategies were implemented:

1) In September 2014 the blower system was upgraded from a HV Turbo paddlewheel blower system to an Aerzen rotary lobe blower system.
2) In May 2014, co-digestion with processed food waste commenced at 0.24 ± 0.06 kg_{VS} m^{-3} d^{-1} (20% additional organic load, 5% additional volume).

RESULTS AND DISCUSSION

A process flow diagram with mass balance and energy values from 2016 for Grüneck WWTP is displayed in Figure 1. The specific power consumption throughout the study period was 0.64 ± 0.08 kWh per m^3 wastewater treated. Figure 2 shows the energy consumption for different unit processes. The relatively high specific power consumption at Grüneck WWTP may be attributed to i) high power intensity of headworks and pumping, and ii) energy-intensive advanced treatment with UV disinfection applied during bathing season in the receiving water body.

Upgrading the aeration system reduced the aeration power requirements by 0.03 ± 0.02 kWh m^{-3} (-16 ± 2 %). This improved energy efficiency contributed to a 13 % (350 MWh a^{-1}) reduction in overall plant power consumption and an 8 ± 3 % increase in energy self-sufficiency. Food waste co-digestion boosted the electricity production by 0.11 ± 0.03 kWh m^{-3} (+25 ± 6 %), translating to a 16 ± 5 % increase in energy self-sufficiency. Aeration upgrades and food waste co-digestion successfully increased energy self-sufficiency at Grüneck WWTP from 64 % to 88 % (Figure 3).

The plant-wide analysis indicated that the aeration upgrades did not affect effluent quality. However, co-digesting food waste at 20 % additional organic load caused some minor downstream impacts including reduction in dewaterability (-10 %), fluctuating biogas quality, increased nitrogen backload (+3 t a^{-1}) and solids accumulation (50 kg_{TS} d^{-1}). A solar dryer was installed to manage the increased biosolids production resulting from co-digestion. The dryer reduced biosolids transportation costs by 30 % with minimal increase in total plant energy demand (below 2 %). Overall from an energy perspective, the increased power production from food waste co-digestion energetically out-weighed the downstream impacts.

The capital expenditures for the blower upgrade, food waste acceptance facilities and solar dryer were 50,000 €, 150,000 € and 2,000,000 €, respectively. Based on the current OPEX savings, the blower upgrade and food waste acceptance facilities have payback periods of 10 and 17 months, respectively. However, the solar dryer has a payback period of 30 years. Expanding the energy analysis to incorporate savings from the sludge incineration as well as off-sets associated with other food waste management options revealed that co-digesting food waste and installing the solar dryer save energy in the wider waste management context (Figure 4).

CONCLUSIONS

Grüneck WWTP increased energy self-sufficiency by 24% (from 64% to 88%) through reducing energy consumption with aeration upgrades (8% increase) and increasing energy production with food waste co-digestion (16% increase). This case study demonstrates that there is significant potential for WWTPs to achieve energy self-sufficiency through a combination of strategies, which both reduce energy consumption and increase energy production. Management of plant-wide impacts associated with each strategy however should be considered when selecting the appropriate mix of strategies (Sembera et al., 2019).

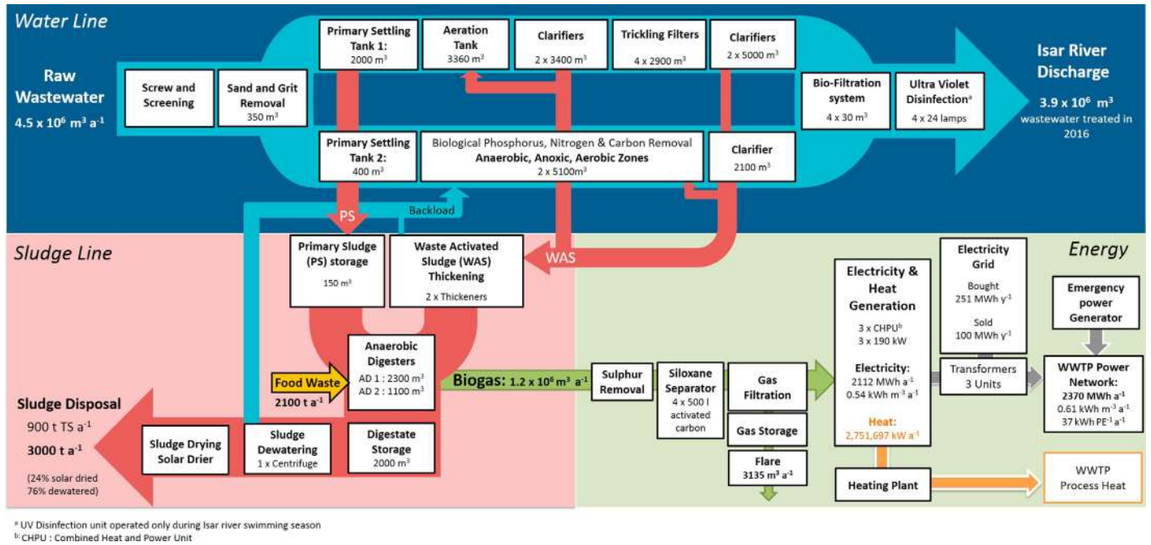

[a] UV Disinfection unit operated only during Isar river swimming season
[b] CHPU : Combined Heat and Power Unit

Figure 1: Grüneck WWTP process flow diagram with mass balance and energy values from 2016 (Macintosh et al., 2019).

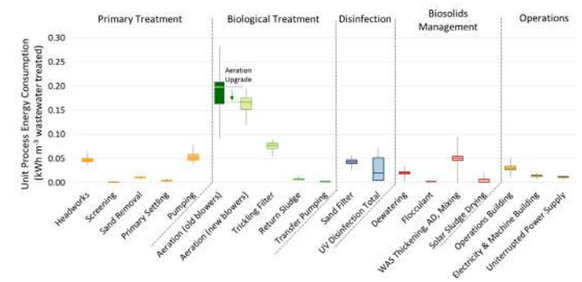

Figure 2: Operational energy consumption for individual processes at Grüneck WWTP (Macintosh et al., 2019).

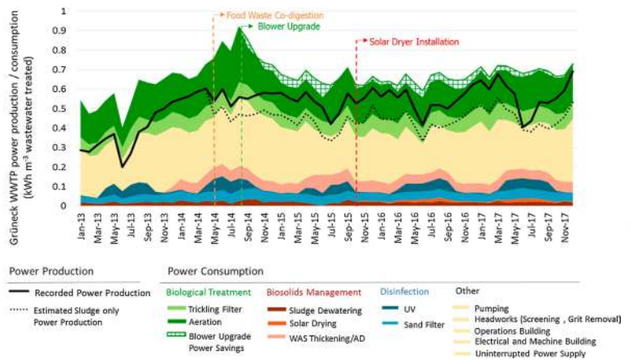

Figure 3: Grüneck WWTP energy balance: power consumption (stacked area) and power production (line) in kWh per m^3 wastewater treated (Macintosh et al., 2019).

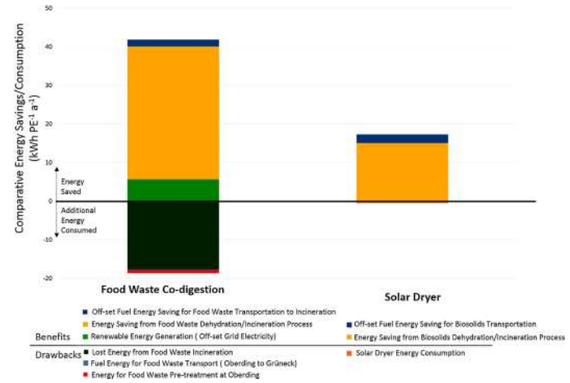

Figure 4: Benefits and drawbacks of food waste co-digestion and solar drying in the wider disposal system context (Macintosh et al., 2019).

REFERENCES

Macintosh, C., Astals, S., Sembera, C., Ertl, A., Drewes, J. E., Jensen, P. D. & Koch, K. 2019 Successful strategies for increasing energy self-sufficiency at Grüneck wastewater treatment plant in Germany by food waste co-digestion and improved aeration. *Applied Energy* **242**, 797–808.

Sembera, C., Macintosh, C., Astals, S. & Koch, K. 2019 Benefits and drawbacks of food and dairy waste co-digestion at a high organic loading rate: A Moosburg WWTP case study. *Waste Management* **95**, 217-226.

Mass-balance-based approach in planning a measurement campaign for energy factory Tilburg

Quan Le*, David Ysebaert*, Stefan Weijers, Ruud Schemen**, Eveline Volcke***
* Dept. Green Chemistry and Technology, Ghent University, Belgium.
(E-mail: HongQuan.Le@Ugent.be; David.Ysebaert@Ugent.be; Eveline.Volcke@Ugent.be)
** Waterschap de Dommel, Boxtel, The Netherlands.
(E-mail: SWeijers@dommel.nl; RSchemen@dommel.nl)

Abstract
Reliable data is important for performance monitoring, production accounting and model development of WWTP's. The aim of this paper was to propose fit-for-purpose measurement layouts/sampling strategies for the Tilburg WWTP that will improve the quality of the collected data by facilitating the mass balance validation and detection of errors for online measurements and grab samples, while keeping in mind the practical and economic feasibility of the measurement lay-out. Mass-balance based experimental design was used to propose these lay-outs and retain the most viable ones. For the Tilburg WWTP this resulted in three viable sampling strategies, each with different accuracies and costs. It could be concluded that a complex WWTP, such as Tilburg, can benefit from mass-balance based experimental design to obtain measurement strategies that can lead to more reliable data.

Keywords
Data collection; Mass balance; Monitoring; Plant-wide modelling

INTRODUCTION

The wastewater treatment plant and "Energy Factory" (EF) Tilburg in the Netherlands was constructed as part of an ambitious Dutch national strategy to exploit the resources of wastewater and to make local water authorities the largest producers of green energy in the Netherlands. In this regard, the majority of the activities of EF Tilburg have focused on the sludge line, which should be considered the production line of the EF. The EF Tilburg produces approx. 6 million m^3 biogas, which makes the plant more energy neutral, and delivers surplus biogas to other facilities in the region. Since 2016, the plant has passed through major and incremental improvements/reconfigurations to optimize treatment, nutrient recovery and energy production.
In order to have reliable data for performance monitoring, production accounting as well as for plant model development, a data collection plan was designed using mass-balance-based experimental design (Le et al., 2018). The project aims to have fit-for-purpose measurement layouts that will improve the quality of the collected data by facilitating the mass balance validation, detection of fault or error of either online measurement and grab samples and at the same time would be practical and economically feasible (Figure 1). The approach of balance-based technique for measurement design was well established in chemical industry for decades (Kretsovalis and Mah, 1987; Madron and Veverka, 1992; Marie Luong Chang Trung Huynh, Jos´e Ragot, 1994) and is recently introduced to waste(water) process monitoring (Spindler, 2014; Villez et al., 2020, 2016).

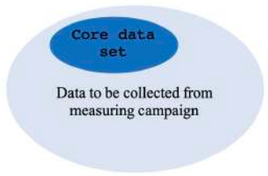

Figure 1. Core data set from mass-balance-based experimental design as a part of the data set to be collected from an extensive measurement campaign.

METHODOLOGICAL APPROACH

The mass-balanced based experimental design procedure of Le et al. (2018) was applied to achieve the main goal. The procedure has seven steps that can be grouped into three parts. The first part is collecting input information including (1) defining the main goal and key variables, (2) setting up mass balancing and (3) data inventory. The second part is finding solutions including (4) feasibility (5) clustering, (6) finding solution. The final part is (7) optimization to deliver optimal solutions in terms of cost and accuracy in the form of a Pareto-front.
Only the first part of collecting input information, the most important and time-consuming part, will be elaborated in this abstract. The second and third parts are automated procedures written in Matlab.

EF Tilburg

EF Tilburg has three main treatment lines. (1) The water line is a conventional activated sludge process. (2) The sludge line has a thermal hydrolysis unit and a digester to treat combined primary sludge and hydrolysed secondary sludge. The plant also receives dewatered sludge from sludge treatment site Mierlo and external secondary sludge from other plants. (3) The side-stream line treats rejected water from the sludge line with the Anammox process.

Collecting input information

The main goal and key variables: The main goal is to obtain improved data using mass-balance based experimental design and data reconciliation for monitoring sludge & biogas production, effluent quality monitoring as well as data for process optimization and modelling: COD mass balances, DO consumption, nitrification, denitrification and phosphorus removal. The main goals are translated into 71 key process variables of flow rate, total COD, nitrogen and phosphorus.
Mass balance setup: The simplified process flow diagram (PFD) of EF Tilburg has 22 (grouped) unit processes and 77 streams. From the PFD, 74 mass balances of total mass flow (22), the mass flow of total phosphorus (17), total COD (17) and total nitrogen (18) were set up including 44 streams and 166 variables.
Data inventory: Measured data were collected from the information system of the plant. The potential new sampling points were chosen taking into account practical aspects such as safety, accessibility and representativeness. The magnitude of standard error of the mean of the variable was estimated from the data set using available data and the set of mass balances. The cost of concentration measurements in each stream is set at 104 EUR/per parameter. The cost of installing a new flow sensor for nine potential streams is about 20,000 EUR/ per stream if flows must be measured in these streams. There are six out of twenty streams that potential sampling points need to be installed for safety reason, which cost 1,000 EUR/ per point.

RESULTS AND DISCUSSION

In the case of EF Tilburg, three different sampling strategies for mass balance validation have been proposed in Table 1. For each strategy, $9x10^{15}$ possible measurement layouts (in terms of flow and concentration) were evaluated, most of them were infeasible and could be quickly removed.

Table 1. Summary of three (03) sampling strategies. '#' denotes 'number of'.

	min cost(1)	max accuracy(1)	A	A+	B+
# improved key variables	69/71	69/71	69/71	69/71	67/71
frequency	1x/week	1x/week	1x/week	1x/week +3x/ week(2)	1x/week +3x/week(2)
# Pareto optimal solution			51	63	72
Selected solution	**#1**	**#51**	**#9**	**#12**	**#9**
total cost	€47,912	€190,680	€49,640	€51,136	€31,136
estimated accuracy	1.93	1.13	1.67	1.5	1.68
# additional variables	30	54	37	35	34
# additional flow sensors	2	9	2	2	1
# sampling points	14	23	16	15	14
# new install sampling point	6	6	6	6	6

(1) Min cost and max accuracy are based on sampling strategy A.
(2) x3 samples per week for specific sampling points

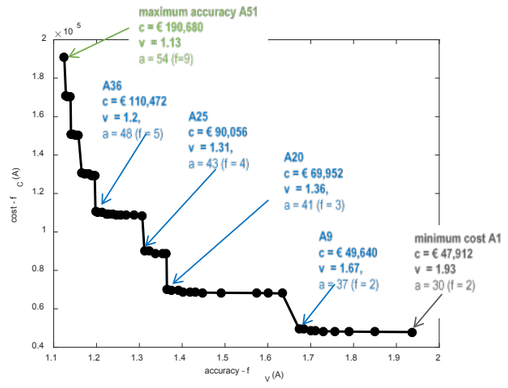

Figure 2. Pareto-front optimal solutions of sampling strategy A. a = number of additional measured variables, v = accuracy and c = cost of additional measurements.

Sampling strategy A is to improve 69/71 specified key variables. Sampling strategy A+ is a more accurate version of sampling strategy A by increasing the frequency of sampling to x3/week in certain streams. Sampling strategy B+ is a cheaper version of sampling strategy A+ with only one additional flow sensor instead of two in strategy A. As a result, B+ only improves 67/71 key variables. An example of a Pareto-front optimal solutions of sampling strategy A is illustrated in Figure 2. Six new sampling points need to be installed, the remain ones were already available as regular sampling points of the plant.
Note that the cost of installing an additional sensor as well as the related cost for maintenance afterward can be greatly reduced by using clamp-on flowmeters for certain streams during the measuring campaign. The accuracy objective function used in the optimization could be replaced by the '*number of redundant variables'* similar to the approach of Villez et al. (2016) that allows errors to be detected in key variables. In the end 3 sampling strategies were proposed. Sampling strategy A was considered

CONCLUSIONS

For such a complex EF as Tilburg, mass-balance based experimental design offers a systematic approach to establishing a core data set that allows the process engineer to validate the collected data, especially those in important streams related to the main goal, using mass balances.
Different sampling strategies were proposed providing a basis for decision-making on the optimal core data set with regard to additional sensors placement.

Opinions

Understanding the plant and setting up a comprehensive PFD are the most time-consuming part of the project in particular and in other similar projects in general.
Prior to mass-balance-based experimental design, data reconciliation of flow measurement should be done to first check the flow sensor availability since flow measurements are important in all mass balances. These additional measurements are very useful to validate the collected data in the sludge line since sludge content will be measured for the first time.

Acknowledgement: The authors thank Peter Dijk, Mark Janssen, Gijs Lavrijsen of Waterschap de Dommel for fruitful help and discussions on data and configuration of EF Tilburg during the project.

REFERENCES

Kretsovalis, A., Mah, R.S.H., 1987. Observability and redundancy classification in multicomponent process networks.
Le, Q.H., Verheijen, P.J.T., van Loosdrecht, M.C.M., Volcke, E.I.P., 2018. Experimental design for evaluating WWTP data by linear mass balances. Water Res. 142, 415–425. https://doi.org/https://doi.org/10.1016/j.watres.2018.05.026
Madron, F., Veverka, V., 1992. Optimal selection of measuring points in complex plants by linear models. AIChE J. 38, 227–236. https://doi.org/10.1002/aic.690380208
Marie Luong Chang Trung Huynh, Jos´e Ragot, D.M., 1994. Observability, redundancy, reliability and integrated design of measurement systems.
Spindler, A., 2014. Structural redundancy of data from wastewater treatment systems. Determination of individual balance equations. Water Res. 57, 193–201. https://doi.org/10.1016/j.watres.2014.03.042
Villez, K., Vanrolleghem, P.A., Corominas, L., 2020. A general-purpose method for Pareto optimal placement of flow rate and concentration sensors in networked systems – With application to wastewater treatment plants. Comput. Chem. Eng. 139. https://doi.org/10.1016/j.compchemeng.2020.106880
Villez, K., Vanrolleghem, P.A., Corominas, L., 2016. Optimal flow sensor placement on wastewater treatment plants. Water Res. 101, 75–83. https://doi.org/10.1016/j.watres.2016.05.068

Development of a hydraulic and biological model for trickling filters. Model-based assessment of the operational strategy.

K. Olaciregui-Arizmendi*,** , S. Jaray-Valdehierro*,**, T. Fernández-Arévalo*,**, A. López***, J. Gómez***, B. Elduayen-Echave*,** and E. Ayesa*,**

*CEIT-Basque Research and Technology Alliance (BRTA), Manuel Lardizabal 15, 20018 Donostia / San Sebastián, Spain. (E-mail: *kolaciregui@ceit.es*)

**Universidad de Navarra, Tecnun, Manuel Lardizabal 13, 20018 Donostia / San Sebastián, Spain.

***NILSA, Navarra de Infraestructuras Locales S.A., Av. Barañáin 22, 31008 Pamplona, Spain.

Abstract

Trickling filters are widely used on large sites. Their robust behaviour and their low economic cost (natural aeration) make them an interesting technology. However, there is no simulation tool (mathematical model) to optimise and fully understand this technology (hydraulics and biology). In this contribution a model considering both hydraulics and biology is shown which is able to reproduce the performance of a real trickling filter. The model-based assessment describes the biomass distribution in a primary and secondary trickling filters, which can help in the definition of the operational strategy of different trickling filters.

Keywords

Biofilm; hydraulics; mathematical model; simulation; trickling filter

INTRODUCTION

Trickling filters are fixed film secondary treatments that are simple and robust to build and have low energy consumption (Ferrer, 2008; Pal, Sarkar and Dasgupta, 2010). The principle of operation of a trickling filter is to pass wastewater through a solid filler that supports the attached bacterial layer. Bacteria attached to this packing (biofilm) feed on the pollutant load and grow on it.

The water quality obtained from this apparently simple operation is in fact a combination of complex internal biological mechanisms described elsewhere (Rauch, Vanhooren and Vanrolleghem, 1999; Almstrand et al., 2011) and an unknown hydraulic behaviour. The uncertainty associated to the combination of both effects has made historically difficult to predict and understand the performance of trickling filters (Saerner, 1986).

NILSA and Ceit-BRTA are collaborating in the construction of a mechanistic mathematical model that describes in detail the hydraulic and biochemical behaviour of trickling filters. This model will help to understand the operation of the technology and will be a useful tool for the design and optimization of new and existing trickling filters. In this contribution, the hydraulic model describing the behaviour of a trickling filter has been calibrated using data from a real WWTP and, in addition, the simulation outputs are compared with experimental tests performed on a real trickling filter with plastic packing media located in Tudela, Navarra. Finally, a first model-based exploration of the biological transformations and water quality has been carried out. This assessment helps in the definition of the operational strategy depending on the water characteristics (raw water or pre-treated water) or in the filling media material (plastic or rocks). In the near future, the model will be calibrated using both hydraulic and water quality data from different trickling filters.

MATERIALS AND METHODS

Experimentation

The experiment used to calibrate the hydraulic model, consisted on introducing a constant flow rate (340 m^3/h) for a given time (60 minutes) and the observing the behaviour of the outflow until the filter was completely emptied, this happened after 200 minutes from the beginning. To obtain the data, flow meters were placed at the inlet and outlet of the trickling filter.

In order to understand the operation of this technology, the compositions of the effluents from the different trickling filters located in Tudela's WWTP are obtained.

Mathematical model

The trickling filter has been divided in 8 virtual tanks. On one hand, the total height of the filter is divided in four levels. On the other hand, the existence of hydraulic short-circuits and retained water makes it necessary to consider in the model a fraction of the circulating water flow that is hardly treated (named circulating path) and another that is retained and biodegraded in the different zones of the biofilm (named retained path), being the effluent a mixture of both. In this way, the heterogeneities that exist in the reactor are represented. Figure 1 shows a schematic diagram, where is the fraction of the water flow that goes to the circulating path, the letter in the subscript ($_C$ for circulating path and $_R$ for retained path) indicates the path and the number the corresponding level.

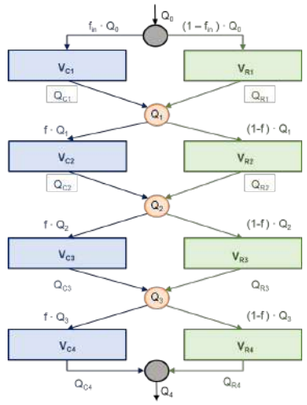

Figure 1. Schematic diagram of the paths and levels described in the hydraulic model.

The mass conservation equation is used to reproduce the variation of the water volume in each tank. This mass balance can be expressed as a volume variation, and considering constant the density of the water, Eq. (1).

Where is the volume of the fluid in the control volume, and the inflow and the outflow rate of the control volume, respectively. The outflows of each tank are modelled by a weir equation, Eq. (2), where is the opening coefficient of the valve and α is the exponent that regulates the emptying of the tank.

The biochemical model used in this contribution is based on the IWA-ASM2d model which is combined with a conventional 10-layer WEST model to describe the bacterial biofilm.

RESULTS AND DISCUSSION

Figure 2 shows the response of the hydraulic model to a pulse of influent flow used in the experiment in Tudela. The calibrated model is able to reproduce the behaviour of both the outlet flow rate and the stored volume. Four sections can be distinguished in the experiment: filling without significant outflow (A), accumulation of water volume (B), fast emptying (C) and slow emptying (D). Once the hydraulic transport model is able to adequately reproduce the hydraulic behaviour of the filter, biochemical model explorations can be performed in WEST. As an example, Figure 3 shows the difference in the effluent characteristics of a primary and a secondary filter. A clear nitrification is observed in the secondary filter, whereas in the primary organic matter is consumed (from 273 g/m^3 to 118 g/m^3). Figure 4 describes the biomass distribution in the biofilm of both trickling filters. As in the primary filter organic matter is removed, heterotroph biomass is predominant. While autotrophs prevail over heterotrophs in the secondary filter. Another important result is the presence of heterotrophic biomass in the outer layers when there is enough organic matter in aerobic conditions, enhancing the growth of heterotrophs. When organic matter is reduced, autotrophs gain importance and they move from inner layers to outer ones. Furthermore, if levels are observed, the presence of biomass in the secondary filter decreases as the water goes down, as ammonium and organic matter are consumed in higher locations.

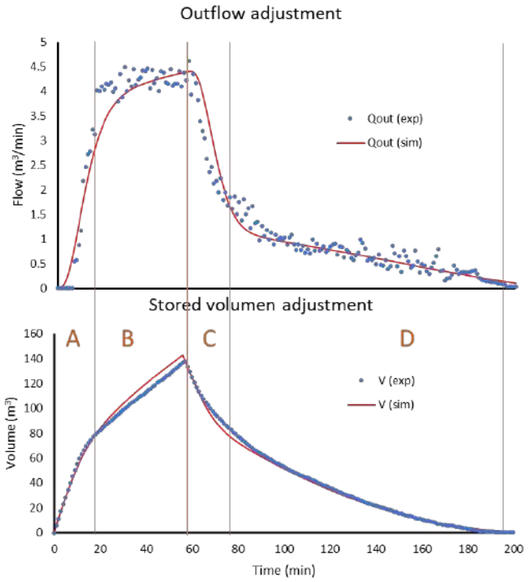

Figure 2. Results of the hydraulic model.

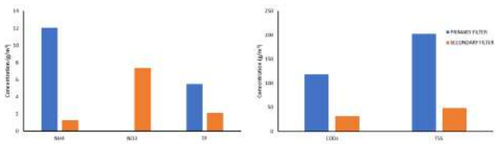

Figure 3. Effluent comparison between a primary and a secondary trickling filter.

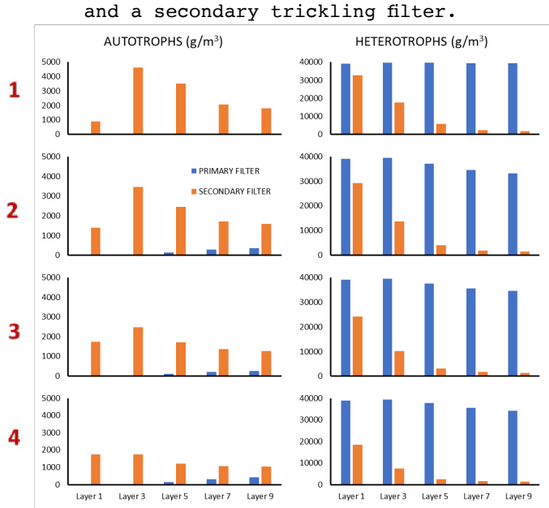

Figure 4. Biomass distribution in the biofilm depending on the trickling filter.

CONCLUSIONS

The new model proposes two routes (circulating and retained) to describe water transport. This provides a satisfactory description of the hydraulic and biochemical behaviour of different trickling filters. With the experimentation done to date, a preliminary replication of the real behaviour of the filters in the mathematical model has been achieved, this model helps in the definition of operational strategies depending on the season of the year or water characteristics. Once the calibration and validation of the model for different operating scenarios has been completed, a very useful tool will be available to optimise the design and operation of NILSA's trickling filters.

ACKNOWLEDGMENTS

The LIFE-IP NAdapta-CC project (LIFE16 IPC/ES/000001) is an integrated strategy for the adaptation to Climate Change of a region, Navarra, and is part of Navarra's contribution to the international commitment to Climate Change. The LIFE-IP NAdapta-CC project has received funding from the European Union's LIFE Programme. The authors would like to thank the Department of Education of the Basque Government for the Predoc Grant (PRE_2022_1_0271) and the Spanish Science and Innovation Ministry for the Research Project MODYPHOS (PID2019-108378RB-I00).

REFERENCES

Almstrand, R., Lydmark, P., Sörensson, F., Hermansson, M., 2011. Nitrification potential and population dynamics of nitrifying bacterial biofilms in response to controlled shifts of ammonium concentrations in wastewater trickling filters. Bioresource Technology 102, 7685–7691. https://doi.org/10.1016/j.biortech.2011.05.066

Ferrer, C., 2008. Procesos de tratamiento de agua. Cepis 1–63.

Pal, S., Sarkar, U., Dasgupta, D., 2010. Dynamic simulation of secondary treatment processes using trickling filters in a sewage treatment works in Howrah, west Bengal, India. Desalination 253, 135–140. https://doi.org/10.1016/j.desal.2009.11.019

Rauch, W., Vanhooren, H., Vanrolleghem, P.A., 1999. A simplified mixed-culture biofilm model. Water Research 33, 2148–2162. https://doi.org/10.1016/S0043-1354(98)00415-1

Saerner, E., 1986. Removal of Particulate and Dissolved Organics in Aerobic Fixed-Film Biological Processes. Journal of the Water Pollution Control Federation 58, 165–172.

Model-based assessment of alternative modes of operation in a full-scale industrial wastewater treatment system.

Vicente Tomas Monje[1], Mikołaj Owsianiak[2], Helena Junicke[1], Kasper Kjellberg[3], Krist V Gernaey[1], Xavier Flores-Alsina[1].

[1] Process and Systems Engineering Centre (PROSYS), Department of Chemical and Biochemical Engineering, Technical University of Denmark. Building, 229, DK-2800, Kgs. Lyngby, Denmark.

[2] Quantitative Sustainability Assessment, Department of Environmental and Resource Engineering, Technical University of Denmark, Produktionstorvet 424, 2800 Kgs. Lyngby, Denmark

[3] Novozymes A/S, Hallas Alle 1, DK-4400, Kalundborg, Denmark.

* Corresponding author: Xavier Flores-Alsina (xfa@kt.dtu.dk)

Abstract: The use of mathematical models is well established procedure in the field of water engineering to "virtually" evaluate the techno-economic feasibility of promising operational strategies. In this way, only options with the highest chance of success are further investigated to be full-scale implemented while less interesting proposals can be disregarded at an early stage. Nevertheless, there is a lack of studies where (plant-wide) comprehensive models are verified with full-scale data and applied in the field. In this paper, a computer simulation model is adjusted to assess alternative modes of operation in the largest industrial wastewater treatment plant (iWTS) in Northern Europe. Multiple economic and technical criteria are defined, verified with plant data and used to test the performance of three types of scenarios:

1) carbon refluxing (CR), 2) change of operational procedures (OP) and 3) the implementation

of new technologies (NT). Life cycle assessment (LCA) quantifies environmental stressors grouped in three categories: human health (HH), environmental qualtity (EQ) and resource scarcity (RS). The presented decision support tool has been used by the biotech company involved in the study on how to handle the future iWTS expansion.

Keywords: Computer Aided Process Engineering, Mathematical Modelling, Multi-criteria evaluation, Plant Wide Optimization, Resource Recovery

INTRODUCION

Although process modelling is a well stablished procedure in wastewater engineering, most of the previously published studies on virtual case studies, dealt with diluted streams, used non-validated models and neglectedprocess economics (Henze et al., 2000, Batstone et al. 2002). In order to circumvent these limitations, we present a model-based evaluation study of plant-wide operational strategies in an industrial water treatment system (iWTS) treating the effluents from two big biotech companies. The case study is the largest iWTS in Northern Europe and handles a pollution load of 2.5 PE in only 10000 m3/day. This will be done using a full-scale validated PWM capable to reproduce and forecast mass and volumetric flows. Finally, special aspects such as energy expenditures, use of chemicals, bio-solids handling and transportation cost, discharge fees and potential (internal / external) energy recovery will be combined with several technical criteria e.g. removal rates, capacity liberation.¨

PLANT CONFIGURATION, MODELS, DATA, SCENARIO & CRITERIA

The flow diagram of the WWTP under study is shown in **Figure 1**. A plant-wide model was developed to describe design / operational conditions. Flow diagram and model parameters were adjusted to reproduce the influent, effluent and process characteristics. A five week measuring campaign was conducted to compare full-scale measurements and model predictions (more details in Monje et al., 2022a,b) . A set of scenarios are defined to assess with multiple criteria (see **Table 1**). The fate of COD and N was quantified using mass balances/ computer simulations. Hence, it is possible to know the amount of a specific compound that can be recovered, removed, captured within the bio-solids and lost with the effluent. In addition, the analysis includes the assumed capacity for three critical units: the anaerobic granular sludge (AnGSR), the activated sludge reactors (ASR) and the inactivation tank (IT). In case of given scenario, the reactor volume is reduced to maintain the same hydraulic retention time (HRT), a certain degree of capacity liberation is obtained. Economic evaluation criteria are divided between *production* and *consumption* indicators. On the one hand, production includes 1) energy recovery (ER) and 2) mass of bio-solids ($M_{biosolids}$). On the other hand, consumption accounts for 1) energy use (EU), 2) quantity of dosed chemicals (CHEM) and 3) volume of bio-solids to be handled and transported ($V_{biosolids}$) and4) volume of treated water released to the environment ($V_{effluent}$). Once *production* and *consumption* indicators are quantified (plant data, model predictions), revenues (REV) and expenditures (COST) can be calculated using appropriate factors.

Table 1. Definition of the scenarios implemented, simulated and evaluated in this study

Scenario code	Scenario title	Description
S0	Baseline scenario	The default scenario representing the current status of the iWTS.
S1 (CR)	SBM dry inactivation + SEC_{WAS} separated dewatering	Around 1/3 of the spent biomass stream is treated with solid CaO. The remaining 2/3 is sent to the inactivation tanks + The WAS stream does not undergo the inactivation step. Instead, it is sent directly to the DEW
S2 (OP)	S1 + BTL + heterotrophic denitrification of liquid influents + AnGSR is operating at full capacity	The buffer tank liquid is made non-reactive by preventing bio-solids accumulation. Heterotrophic denitrification is promoted in the pre-acidification tank by recycling activated sludge liquor. The anaerobic granular sludge reactor is assumed to operate at its full capacity.
S3 (NT)	S2+inactivation with NaOH + anaerobic treatment of reject water	NaOH instead of CaO is used as dosed chemical to rise the pH in the inactivation tanks. Reject water is re-directed to the anaerobic granular sludge reactor instead of being treated aerobically in the ASR
S4 (NT)	S4 + PN/ANX + in-situ feedback control loop	An additional aerobic granular reactor is added running partial nitration/anammox. PAC dosage is based on in-situ phosphate sensors.
S5 (NT)	S3 + inactivation with heat + anaerobic treatment of reject water	Heat instead of chemical is used as inactivation agent. Reject water is re-directed to the anaerobic granular sludge reactor instead of being treated aerobically in the ASR
S6 (NT)	S6 + PN/ANX + in-situ feedback control loop	Aadditional aerobic granular reactor is added running partial nitration/anammox.PAC dosage is based on in-situ phosphate sensors.

RESULTS AND DISCUSSION

Baseline simulations. S0

The results summarized in **Table 2** indicate that for the incoming COD: 32 % is recovered as energy in the anaerobic granular sludge reactor (AnGSR), 23 % is removed in the activated sludge reactor (ASR), 32 % is captured within the bio-solids cake stream (DEW/IT), 12 % is lost during the fermentation process in the buffer (BTL) and pre-acidification tanks (PAT) and 1 % leaves the plant via effluent ($iWTS_{eff}$). With respect to N, 65 % is removed in ASR, 33 % is captured in DEW_{under} and 2 % end up in $iWTS_{eff}$. Finally when it comes to P, 2% leaves the plant via the effluent ($iWTS_{eff}$) and 98% is accumulated in the bio-solids stream ($IT_{EFF\text{-}ext}$, DEW_{under}) as a result of precipitation. **Table 3** includes additional technical criteria: COD/N and VSS/TSS ratio in the activated sludge effluent (ASR_{eff}) and dewatering underflow (DEW_{under}). Hence, one may see the non-standard values resulting from 1) the high organic/inorganic load arriving to the plant and 2) lime use during bio-solids inactivation. With respect to capacity data (**Table 5**), both ASR and inactivation tank (IT) are assumed to operate at 100 % of capacity. Nevertheless, the AnGSR is assumed to be underperforming. Both measurements and computer simulations (**Table5**) show that the plant´s main source of revenues are the income obtained from the (61%) electricity produced in the biogas turbine ($REV_{electricity}$) and (21%) external processing of the inactivated bio-solids (REV_{biogas}). The main expenditures are: the discharge fee (DF) (38 %), transportation and handling of bio-solids ($COST_{biosolids}$) (29 %), dosed chemicals ($COST_{CHEM}$) (19 %) and power consumption ($COST_{electricity}$, $COST_{pumping}$) (14 %).

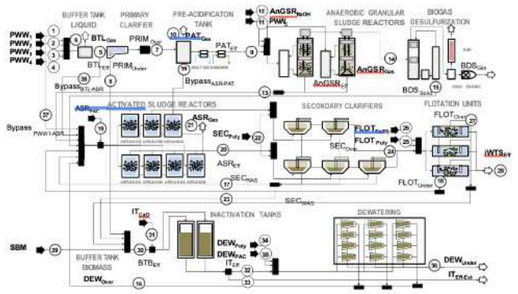

Figure 1. Flow diagram of the iWTS under study: **1–4** Process waste water (PWW_{1-4}), **5,6** - Buffer tank liquid output (BTL_{eff},BTL_{Over}), **7-8** – Primary clarifier overflow and underflow ($PRIM_{Over}$, $PRIM_{Und}$) **9-10** – PAT output (PAT_{eff},PAT_{Und}), **11** - Process waste water (PWW_{1-4}), **12** – Dosing NaOH anaerobic granular sludge reactors ($AGSR_{NaOH}$), **13-14** – anaerobic granular sludge reactors output ($AGSR_{Und}$,$AGSR_{Over}$), **15** – Elemental sulfur recovered (BDS_{Sulf}), **19** – Dosing PAC activated sludge reactors (ASR_{PAC}), **20-21** - activated sludge reactors output (ASR_{Eff},ASR_{Und}), **22** - Polymer dosing secondary clarifiers (SEC_{Poly}), **23,24,17** - secondary clarifiers output (SEC_{Over}, SEC_{Und}, SEC_{RAS}), **25,26** – Polymer and Fe(III) dosing flotation ($FLOT_{Over}$, $FLOT_{FeIII}$), **27,18,28** – Flotation units output ($FLOT_{Over}$, $FLOT_{Under}$, $iWTS_{Eff}$), **29** – Spent biomass stream, **30** - Buffer tank biomass output (BTB_{Eff}), **31** - Quicklime dosing inactivation tanks (IT_{CaO}), **32-33** - Inactivation tanks output (IT_{Eff}, $IT_{Eff,Ext}$), **34,35** – Polymer and PAC dosing dewatering (DEW_{Poly}, DEW_{PAC}), **36,16** - Dewatering under and overflow (DEW_{Under}, DEW_{Over}), **37-39** – Bypasses PWW_1 to ASR, BTL to ASR, ASR to PAT. Considered sub-systems are marked by a dashed line. Black/White arrows are inputs/outputs to the whole system.

Carbon refluxing: S1

As shown in **Table 2**, carbon refluxing increases the accumulation of COD and N in the bio-solids stream (DEW_{under}) up to 38 % and reduces the quantity removed in the ASR (18 % and 59 % respectively). **Table 5** shows that total revenues (REV_{total}) are increased by +9 % due to a higher profit from external treatment of biosolids ($REV_{biosolids}$). Lower energy use (EU), consumption of chemicals (CHEM) and sludge volumes ($V_{biosolids}$) reduce total cost ($COST_{total}$) down to -13 %. Inactivation tank (IT) and ASR capacity is liberated by 50 % and 25 %.

Operational conditions: S2

Change of operational conditions in the buffer tank/anaerobic digester promotes heterotrophic denitrification instead of dissimilatory nitrate reduction to ammonia. Hence, 5 % of the incoming COD is not lost due to fermentative process. COD recovery is increased up to 34 % and 11 % of nitrogen is handled in the pre-acidification tank (see **Table 2**). The latter has implications on $REV_{electricity}$, $COST_{energy}$ and $COST_{biosolids}$ increasing and decreasing REV_{total} and $COST_{total}$ up to + 13 % and down to – 13 %, respectively (see **Table 5**).

New technologies: S3, S4, S5 and S6

Usage of either NaOH or heat (instead of CaO) as inactivation agents allows anaerobic treatment of the reject water, which substantially benefits revenues derived from higher electricity recovery (+44%). However, there is a high toll paid on chemicals (+73%) or heat recovery (-19%) depending on the inactivation technology (see **Table 5**). In addition, partial nitration/anammox and a better poly-aluminum chloride (PAC) dosage strategy is necessary to achieve acceptable (<2%) N and P levels in the effluent (see **Table 2**)

Table 2. Fate of major components within the studied iWTS: plant data, baseline simulation and scenario analysis

	Plant Data	S0	S1	S2	S3	S4	S5	S6	Units
$COD_{recovered}$ – AnGSR	32	32	31	34	45	44	45	44	%
$COD_{removed}$ – ASR	23	23	18	18	13	9	12	9	%
COD_{lost} - BTL/PAT	12	13	12	10	11	12	11	12	%
$COD_{captured}$ bio-solids– DEW/IT	32	31	37	36	30	33	30	33	%
$COD_{effluent}$	1	1	2	1	2	2	2	2	%
$N_{removed}$ - ASR	65	64	59	49	42	52	43	52	%
N_{lost} - BTL/PAT	0	0	0	11	14	13	14	13	%
$N_{captured}$ bio-solids – DEW/IT	33	34	38	38	33	34	33	34	%
$N_{effluent}$	2	2	3	2	11	2	10	2	%
$P_{captured}$ bio-solids – DEW/IT	98	98	93	86	25	98	26	98	%
$P_{effluent}$	2	2	7	14	75	2	74	2	%

Table 3. Additional technical criteria: plant data, baseline simulation and scenario analysis

	Plant Data	S0	S1	S2	S3	S4	S5	S6	Units
COD/N ratio in ASRin	7.3	7.2	6.7	7.7	5.4	5.4	5.4	5.4	g / g
SRT ASR	7.1	7.4	7.2	7.5	7.1	3	7.1	3	days
VSS/TSS in ASR	61.5	58.8	57.1	56.1	54.9	52.5	54.3	52.4	%
VSS/TSS in DEW_{under}	36.7	42.7	51.8	52.3	71.2	71.5	71.1	71.2	%

Table 4. Capacity use: plant data, baseline simulation and scenario analysis

	Plant Data	S0	S1	S2	S3	S4	S5	S6	Units
AnGSR (volume)	65	65	65	100	100	100	100	100	%
ASR (volume)	100	100	75	75	75	79	75	79	%
IT (volume)	100	100	50	50	50	50	50	50	%

Table 5 Main cost and revenues: plant data, baseline simulation and scenario analysis

	Plant dat			S0	S1	S2	S3	S4	S5	S6	
REV_{energy}	6031	6077	€ /d	1	0.0	8.3	44.8	40.0	44.0	40.4	%
$REV_{biosolids}$	1491	1491	€ /d	1	0.0	0.0	0.0	0.0	-18.8	-25.7	%
REV_{total}	3701	3901	€ /d	1	9.5	8.3	-11.1	-2.5	-11.0	-2.7	%
$COST_{energy}$	10707	10691	€ /d	1	0.0	0.0	0.0	0.0	0.0	0.0	%
$COST_{chemicals}$	8064	8299	€ /d	1	-16.9	-18.7	-44.1	-37.4	-44.0	-37.6	%
$COST_{biosolids}$	5053	5278	€ /d	1	-19.3	-18.8	73.4	107.3	-52.6	-18.0	%
DF	3689	3785	€ /d	1	-4.3	-6.7	-23.1	-43.0	-25.5	-43.6	%
$COST_{total}$	11224	11470	€ /d	1	3.2	7.2	19.9	20.3	17.1	17.1	%
savings					-9.2	-10.0	-2.4	3.6	-26.6	-20.3	€ /d
savings					2961.2	3623.2	2966.5	1332.7	9412.9	7648.6	M € /d

Modelling the Metabolism and Population Dynamics of Fermentation-Enhanced EBPR Processes

R. Thomson*, D. Batstone, L. Wang, Y. Zhou, A. Oehmen**

School of Chemical Engineering, University of Queensland, 46 Staff House Rd, St Lucia QLD 4072, Australia
E-mail: * *rhys.thomson@uq.edu.au*, ** *a.oehmen@uq.edu.au*

Abstract

Enhanced biological phosphorus (P) removal (EBPR) processes enable P removal and support resource recovery, but can suffer from low carbon availability. Primary or secondary fermentate dosing can support P removal, with approximately 30% of volatile fatty acids (VFAs) produced consisting of butyrate (HBu), valerate (HVa), and their isomers. These VFAs promote the growth of P accumulating organisms over competitors and produce polyhydroxyalkanoates (PHAs) novel to EBPR. An extended VFA model was developed to capture these dynamics and was compared with existing metabolic models. When compared on P-release predictions, the extended model had a NRMSD of 10% compared to the acetate-only model of 35%. This equates to a 60% over-prediction (50 mg P/L) by the acetate-only model, with clear implications for P removal and recovery. Furthermore, the mechanisms described by the extended VFA model support the performance of fermentation-enhanced EBPR processes and identify conditions to promote novel PHAs such as PH2MH.

Keywords

Enhanced Biological Phosphorus Removal (EBPR), Fermentation, Metabolic Modelling, Polyhydroxyalkanoate (PHA), Resource recovery, Volatile Fatty Acid (VFA)

INTRODUCTION

Enhanced biological P removal (EBPR) processes enable both P removal and support resource recovery. EBPR has been limited due to several factors, namely carbon availability and the resulting process instability. The former can be addressed via dosing of primary or secondary fermentate from on or off-site, however in-situ fermentation is also possible. Of the VFA produced via fermentation, upwards of 30% can consist of butyrate (HBu), valerate (HVa), and their isomers, and could favour the growth of P accumulating organisms (PAOs) over competitors such as glycogen accumulating organisms (GAOs) (Cai, Huang et al. 2019, Gu, Tooker et al. 2019). Mathematical models are used to assist in the design and operation of these processes, however, existing EBPR models describe only acetate (HAc), and occasionally propionate (HPr) uptake. Along with the unique uptake dynamics of these VFAs, this may result in a shift in PHA profile (Wang 2021). This results in a significant shift in predicted process behaviour and therefore undermines the reliability of existing models. The aim of this study was to develop an extended VFA model describing the underlying mechanisms of EBPR when fed these higher order VFAs, and thereby support the design and operation of fermentation-enhanced EBPR and subsequent resource recovery.

MATERIALS AND METHODS

Literature on EBPR process performance, when fed a combination of HAc through to HVa, was used to identify the stoichiometry and kinetics of PAOs and GAOs (Tong and Chen 2007, Wang 2021). Novel PHAs and isomeric VFAs were modelled according to metabolic pathways known to be available in similar organisms. These include the availability of beta-oxidation, conditions for PHA production, redox balancing mechanisms, and VFA uptake. Carbon, energy, and redox balances were conducted over the observed stoichiometry, using modelled pathways and established constraints on metabolite accumulation to identify reaction yields. When conducting these balances, it was identified that further fermentation of HBu and HVa may be occurring, resulting in PAO/GAO uptake of additional HAc and HPr. The stoichiometry of these systems also suggested synergistic uptake of VFAs, acting as a redox balancing mechanism for novel PHA production from HBu/HVa substrates. External fermentation, relative to modelled PAO/GAO populations, and simultaneous substrate uptake was therefore included to capture these dynamics. Furthermore, observed PHA fractions indicated reversible external or internal isomerisation of HBu. This was modelled as a kinetic impact, rather than stoichiometric, given the equivalence of these isomers on metabolite balances. Maintenance, inhibition, sequential use and regeneration of storage products, and state variables to describe PAO/GAO metabolism were modelled according to established methods (Santos, Rieger et al. 2020). The extended model was implemented within Dynamita's Sumo. Model fit was assessed between observed and predicted values via the normalised root mean squared deviation (NRMSD). The extended model was compared to established models over both calibration and validation datasets.

RESULTS AND DISCUSSION

Existing metabolic models were found to over-predict P-release by 35-60% (or 30-50 mg P/L) under fermentation-enhanced EBPR conditions, as shown in **Figure 1**, with the latter representing the more commonly used HAc-only metabolic model. This is compared to the 10-30% (or 10-25 mg P/L) over-prediction by the extended VFA model, with the former more closely representing an acclimatised yield calibration on the full range of VFAs. These discrepancies in P release have direct consequences when modelling P removal and recovery processes, particularly over-time. As shown in **Table 1**, acclimatisation to these VFAs relates to the reliance of the system on external fermentation of HBu and HVa. As shown in **Table 2**, as this reliance declines, and more HBu/HVa is directly consumed by PAOs, the extended VFA model validation fit improves. For GAOs, the acclimatisation process is hindered by their relatively inflexible metabolism. Due to their reliance on glycogen for anaerobic ATP, to consume HAc or HPr, GAOs require electron sinks to balance their internal redox. GAOs achieve this by reducing the products of glycolysis to Pr-CoA, rather than oxidising them to Ac-CoA. As HBu and HVa are more reduced than HAc or HPr, this ratio of reduction to oxidation is increased accordingly. Alternatively, HAc or HPr could be balanced with HBu or HVa uptake to manage reducing equivalents. In contrast, PAOs can freely utilise both balancing mechanisms as required, producing PHAs of PHH/PH4MV from either simultaneous HAc/HBu uptake or glycolysis. Interestingly, the increased production of Pr-CoA required by GAOs with the uptake of HBu is likely what promotes the novel PHA, PH2MH, over the more readily formed PHH/PH4MV.

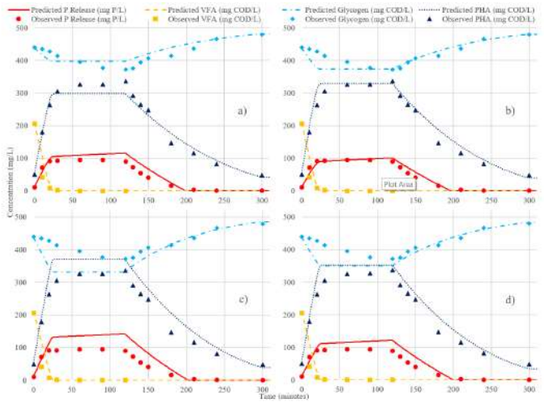

Figure 1. Comparison of extended VFA models (a and b) and existing metabolic models (c and d) on the validation dataset (20 °C, acclimatised to/fed HAc/HPr/HBu/HVa/i-HBu/i-HVa to a ratio of 29:28:9:3:14:17). a) Calibrated yields for SBR acclimatised to HPr feed at 30 °C, fed equal ratio of HAc/HPr/HBu/HVa, b) Calibrated yields for SBR acclimatised to HPr feed at 30 °C, fed equal ratio of HAc/HPr/i-HBu/i-HVa, c) HAc only metabolic model, d) HAc and HPr metabolic models.

Table 1. Calibrated extended VFA model yields (C-mol basis) according to acclimatisation, population, and VFA uptake ratios, compared to existing models. $C_{2\text{-}5}$ refers to equal ratio feed (5.4 C-mmol/L of VFA) of HAc through to HVa, i-$C_{2\text{-}5}$ refers to isomeric HBu and HVa components.

	PAO			GAO		Existing Metabolic Models			
Acclimatised to	HAc	HPr		HAc	HPr	HAc Only		HPr Only	
Fed	i-$C_{2\text{-}5}$	$C_{2\text{-}5}$	i-$C_{2\text{-}5}$	i-$C_{2\text{-}5}$	$C_{2\text{-}5}$	PAO	GAO	PAO	GAO
P-Release/VFA	0.62	0.52	0.42	-	-	0.58	-	0.38	-
PHA/VFA	1.07	1.13	1.25	1.54	1.63	1.33	1.75	1.22	1.5
Glycogen/VFA	0.20	0.23	0.35	0.74	0.85	0.5	1	0.33	0.67
HAc/VFA	0.64	0.40	0.35	0.34	0.55	1	1	-	-
HPr/VFA	0.33	0.39	0.32	0.30	0.45	-	-	1	1
HBu/VFA	0.03	0.21	0.30	0.27	0	-	-	-	-
HVa/VFA	0	0	0.03	0.08	0	-	-	-	-
VFA Up. (C-mmol/L)	4.2	5.4	4.2	4.5	3.1	-	-	-	-
% HBu Ext. Ferm.	91	20	0	0	100	-	-	-	-
% HVa Ex. Ferm.	7	100	0	31	100	-	-	-	-

Table 2. Goodness of fit comparison between extended and existing metabolic models on calibration and validation datasets. Kinetics are calibrated to the associated dataset. A NRMSD of less than 30% indicates a fair fit, 20% a good fit, and 10% an excellent fit.

	Calibration			Validation				
Acclimatised to	HAc	HPr		HAc	HPr		Existing Metabolic Models	
Fed	i-$C_{2\text{-}5}$	$C_{2\text{-}5}$	i-$C_{2\text{-}5}$	i-$C_{2\text{-}5}$	$C_{2\text{-}5}$	i-$C_{2\text{-}5}$	HAc only	HAc and HPr
	NRMSD							
P-Release	5%	3%	6%	31%	17%	10%	35%	22%
PHA	5%	6%	13%	9%	7%	7%	14%	10%
Glycogen	18%	18%	8%	19%	17%	19%	38%	29%

CONCLUSION

These results indicate that existing EBPR models relying on individual HAc or HPr metabolism are inadequate for fermentation-enhanced processes and subsequent P recovery applications, over-predicting P-release by up to 60%. Furthermore, the interactions of substrates and their impact on stoichiometry suggest that individual uptake models are generally insufficient to describe processes with a variety of carbon sources. Acclimatisation to the feed substrate was also shown to impact stoichiometry. This finding demonstrates the importance of metabolic flexibility to fermentation-enhanced process modelling, and highlights the importance of acclimatisation in study design. The improved process stability of fermentation-enhanced EBPR configurations can be partly explained by these findings, as GAOs possess fewer means of adapting to the variety of substrates produced through fermentation and therefore competing with PAOs. Finally, the extended VFA model provided insight into the conditions required to produce PHAs novel to EBPR processes.

REFERENCES

Cai, W., W. Huang, Z. Lei, Z. Zhang, D. J. Lee and Y. Adachi (2019). "Granulation of activated sludge using butyrate and valerate as additional carbon source and granular phosphorus removal capacity during wastewater treatment." Bioresour Technol **282**: 269-274.

Gu, A. Z., N. Tooker, A. Onnis-Hayden, D. Wang, V. Srinivasan, G. Li, I. Takács and E. Vargas (2019). Optimization and Design of a Side-Stream EBPR Process as a Sustainable Approach for Achieving Stable and Efficient Phosphorus Removal. DC, USA, The Water Research Foundation.

Santos, J. M. M., L. Rieger, A. B. Lanham, M. Carvalheira, M. A. M. Reis and A. Oehmen (2020). "A novel metabolic-ASM model for full-scale biological nutrient removal systems." Water Res **171**: 115373.

Tong, J. and Y. Chen (2007). "Enhanced biological phosphorus removal driven by short-chain fatty acids produced from waste activated sludge alkaline fermentation." Environ Sci Technol **41**(20): 7126-7130.

Wang, L. (2021). The metabolism of polyphosphate accumulating organisms (PAOs) and glycogen accumulating organisms (GAOs) in enhanced biological phosphorus removal (EBPR) system under the tropical climate PhD, Nanyang Technological University.

Mathematical modeling of the long-term dynamics of a sulfate-reducing UASB bioreactor from methanogenic to sulfidogenic conditions

Valdés Martín, E.[a], González, D.[a], Munz, G.[b], Gabriel, D[a].

[a] GENOCOV research group, Department of Chemical, Biological and Environmental Engineering, Escola d'Enginyeria, Universitat Autònoma de Barcelona, 08193 Bellaterra, Spain.
(E-mail: *david.gabriel@uab.cat.*)

[b] Department of Civil and Environmental Engineering, University of Florence, Via di S. Marta, 3, 50139, Firenze, Italy
(E-mail: *giulio.munz@unifi.it.*)

Abstract

In this work, a mathematical model was developed to describe the long-term operation of a sulfate-fed 2.5L UASB reactor targeting non-methanogenic, sulfidogenic conditions initially inoculated with methanogenic, non-sulfidogenic sludge. Crude glycerol was used as electron donor to achieve sulfate reduction. The hydraulic model of the UASB was described as a set of CSTRs in series to represent its plug flow-like behavior. The kinetic model included 8 fermentation processes using glycerol as the primary electron source, 5 sulfate-reduction processes using organic and inorganic electron sources, and 2 methanogenic processes. The gradual loss of methane production capacity was described by adding a non-competitive inhibition term as a function of the long-chain fatty acids concentration. A sensitivity analysis and calibration of the most relevant parameters was performed using the experimental data from 300 days of continuous operation of a lab-scale UASB. Carbon and sulfur species profiles as well as microbial dynamics from initial methanogenic conditions to non-methanogenic but sulfidogenic conditions were properly predicted by the model under dynamic simulations.

Keywords

LCFA inhibition; mathematical modeling; model calibration; sensitivity analysis; sulfate reduction; UASB reactor

INTRODUCTION

Treatment of sulfate-rich effluents in sulfidogenic reactors has been proposed as a sustainable alternative for the recovery of metals from S- and metal-rich effluents (SULFATEQ process) as well as the recovery of elemental sulfur from SOx-rich waste gases (SONOVA process, Mora et al., 2020). In such processes, the first stage of the biological treatment is based on sulfate reduction (SR) to sulfide, often carried out in UASB reactors. Amongst others, crude glycerol has been shown as a proper electron donor for SR (Mora et al., 2020). However, Zhou et al. (2022a) reported a progressive loss of performance after 100 days of operation due to degranulation and granule flotation related with the formation of a slime-like substance that contained a high concentration of long-chain fatty acids (LCFA), particularly palmitic acid, which can inhibit methanogenesis (Deaver 2020). In addition, several authors have reported a change in the performance of UASB reactors inoculated with methanogenic sludge when sulfidogenesis becomes a competitive process for the C source. Under certain conditions, methanogenic activity is lost, leading to an increase in the outlet chemical oxygen demand (COD), primarily in the form of volatile fatty acids (VFAs), essentially acetate.

In this work, data from Zhou et al (2022a) from the long-term operation of a lab-scale UASB reactor targeting SR using glycerol as an external carbon source was modeled. A sensitivity analysis of the model was conducted in order to determine the most relevant parameters, and the model was calibrated using the experimental data from the operation of the lab– scale reactor. The model targeted the representation of long-term dynamics of the main C and S species, as well as VSS, including a gradual inhibition of methanogenesis caused by LCFA accumulation inside the reactor.

MATERIALS AND METHODS

The UASB was discretized in a set of *n* mini-CSTRs – vertical layers – in series as previously reported (Rodriguez-Gomez et al., 2014). The kinetic model is based on the anaerobic digestion model no 1 (ADM1, Batstone and Keller 2003) with additional processes accounting for glycerol fermentation and SR, which had been studied and mechanistically determined by Zhou et al. (2022b). The model considers 5 biomass trophic groups (fermentative bacteria X_{FB}; heterotrophic and autotrophic sulfate reducers, X_{HSRB} and X_{ASRB}; hydrogenotrophic and acetoclastic methanogens, X_{HM} and X_{AM}) which carry out 15 biochemical processes: glycerol fermentation and acidogenesis of fermentation products (8), heterotrophic SR (4), autotrophic SR (1), hydrogenotrophic methanogenesis (1) and acetoclastic methanogenesis (1). Consumption rates of a given substrate (S_i) in process *j* followed a Monod – type kinetic equation, which is defined by the maximum specific growth rate km_j (mg S_i mg VSS^{-1} d^{-1}) and the semisaturation coefficient, ks_i (mg S_i L^{-1}). Accumulation of LCFAs and slime formation were simulated according to the experimental results reported by Zhou et al. (2022), and the inhibitory effect of LCFAs on biomass growth was modeled with a non-competitive inhibition term (Ma et al., 2015).

A sensitivity analysis was performed in order to assess the most sensitive parameters of the model by means of a local analysis, i.e., the effect each parameter over the simulated output variables was assessed varying each parameter one at a time, with increments and decrements of ±10%. The local sensitivity of all parameters was evaluated throughout the 300 simulated days of operation. After performing the sensitivity analysis, the most sensitive parameters (i.e., the parameters with the highest relative sensitivities) were selected for calibration. The fitting of the experimental data considered VSS (mg VSS L-1), methane and total inorganic carbon (TIC) flows (mg C d^{-1}) and acetate (mg C L^{-1}) to minimize the objective function. Sulfide was not included in the objective function because the formation of organosulfur compounds experimentally observed was not mechanistically described. Model implementation and calibration was done using MATLAB R2021b.

RESULTS AND DISCUSSION

Prior to the sensitivity analysis, the active fractions of each biomass population were calibrated using the experimental data of the first 30 days of operation. Additionally, other key parameters were pre-calibrated to values within a range known to impact the model in order to improve the reliability of the sensitivity analysis.

The preliminary sensitivity analysis results are shown in Figure 1, which suggest a particularly strong impact of the parameters influencing solids dynamics along the reactor.

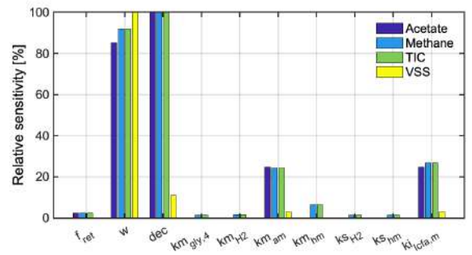

Figure 1. Sensitivity analysis results, where the relative sensitivity of each parameter (%) over a variable is calculated based on the maximum sensitivity value obtained for such variable. Relative sensitivity (%) values of each parameter over acetate, methane, total inorganic carbon (TIC) and volatile suspended solids are represented. Only parameters that displayed a relative sensitivity above 1% over any of the analyzed variables are shown.

After sensitivity analysis, the following parameters were selected for model calibration: *w, dec*, km_{am}, km_{hm}, $ki_{lcfa,m}$. The preliminary calibrated values are shown in Table 1.

Table 1. Calibrated parameters of the model. A brief description of each parameter is shown, as well as the units, the preset value and the final calibrated value.

Parameter	Description	Units	Preset value	Calibrated value
w	Wash-out constant for solids, which factors the flow-rate thus affecting the retention time	-	0.0012	0.0011
dec	Decay rate for all biomass populations	d^{-1}	0.02	0.033
km_{am}	Maximum specific growth rate of acetoclastic methanogens	mg C mg VSS^{-1} d^{-1}	27.6	53.28
km_{hm}	Maximum specific growth rate of hydrogenotrophic methanogens	mg H_2 mg VSS^{-1} d^{-1}	11.28	333.6
$ki_{lcfa,m}$	Inhibition constant of long chain fatty acids over methanogens	mg COD L^{-1}	50	4.5

Figure 2 represents the profiles of TIC, methane, acetate and VSS after model calibration.

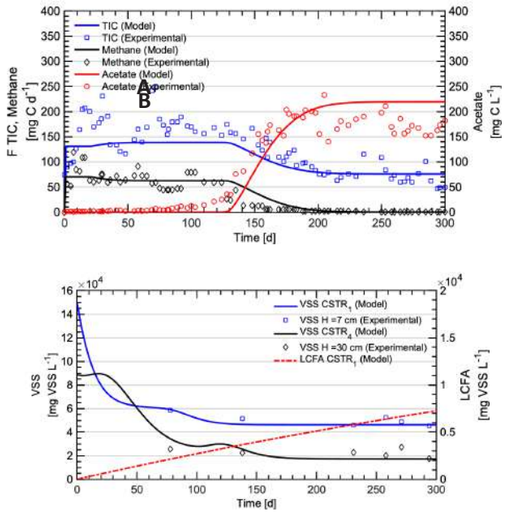

Figure 2. Model calibration results. A) Fit of total inorganic carbon (TIC), methane and acetate outlets (CSTR at the top); B) fit of volatile suspended solids (VSS) at two different heights of the UASB reactor (corresponding to CSTRs 1 and 4), and LCFA at the bottom of the reactor (CSTR 1).

As it can be observed, the model was able to accurately predict the long-term dynamics of these species including acetate accumulation as a result of the loss of methanogenic activity. As shown in the simulated biomass profiles (Figure 3), such inhibition started taking place on day 80 at the bottom of the reactor, with a LCFA concentration around 2 g VSS L^{-1}, which is in agreement with other studies (Ma et al., 2015). Methanogens were washed out from the bottom layer by day 173, whereas a small fraction was still present in CSTR4 (equivalent UASB height = 28 cm), which is in line with the results obtained by Fernández et al. (2022), which showed a total wash-out of methanogens from the system by day 230.

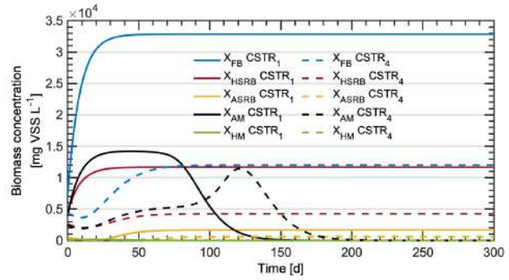

Figure 3. Simulation of the 5 biomass populations at two different heights inside the UASB: 7 cm (CSTR 1) and 28 cm (CSTR 4), after model calibration.

The results from this work, albeit still in process, portray the capacity of the model to predict long-term dynamics of biomass, C and S species in a sulfidogenic UASB accounting for LCFA inhibition.

AKNOWLEDGEMENTS

This project has received funding from the European Union's Horizon 2020 research and innovation programme under the Marie Skłodowska-Curie grant agreement No 872053.

REFERENCES

Mora, M., Fernández-Palacios, E., Guimerà, X., Lafuente, J., Gamisans, X., Gabriel, D. 2020 Feasibility of S-rich streams valorization through a two-step biosulfur production process. *Chemosphere* **253,** 126734.

Zhou, X., Fernández-Palacios, E., Dorado, A.D., Lafuente, J., Gamisans, X., Gabriel, D. 2022a. The effect of slime accumulated in a long-term operating UASB using crude glycerol to treat S-rich wastewater. *Journal of environmental sciences* **Article in press**.

Deaver, J., Diviesti, K., Soni, M., Campbell, B., Finneran, K., Popat, S. 2020 Palmitic acid accumulation limits methane production in anaerobic codigestion of fats, oils and grease with municipal wastewater sludge. *Chemical Engineering Journal* **396**, 125235.

Zhou, X., Dorado, A.D., Lafuente, J., Gamisans, X., Gabriel, D. 2022b Mechanistic modeling of glycerol fermenting and sulfate-reducing processes by granular sludge under sulfidogenic conditions. *Journal of Environmental Chemical Engineering* **10,** 107937.

Batstone, D., Keller, J., Angelidaki, I., Kalyuzhnyi, S., Pavlostathis, S., Rozzi, A., Sanders W., Siegrist, H., Vavilin., V. 2002 The IWA Anaerobic Digestion Model No 1 (ADM1). *Water Science and Technology* **45** (10), 65-73.

Rodríguez-Gómez, R., Gunno, R., Moreno, L., Longcheng,L. 2014 A model to describe the performance of the UASB reactor. *Biodegradation* **25**, 239-25.

Ma, J., Zhao, Q., Laurens, L., Jarvis, E., Nagle, N., Chen, S., Frear, C. 2015 Mechanism, kinetics and microbiology of inhibition caused by long-chain fatty acids in anaerobic digestion of algal biomass. *Biotechnol Biofuels* **8**, 241.

Influence of substrate characterization on trace metal dosing to improve biogas yield during anaerobic digestion: a dynamic model-based study

Susan George*,**, Maria Rosaria Mattei**, Luigi Fruzo** and Fernando G. Fermoso*

* Instituto de la Grasa, Spanish National Research Council (CSIC), Seville, Spain
(E-mail: *susan.george@ig.csic.es*; *fgfermoso@ig.csic.es*)
**Department of Mathematics and Applications, University of Naples Federico II, Naples, Italy
(E-mail: *mariarosaria.mattei@unina.it; luigi.frunzo@unina.it*)

Abstract

Trace metals (TMs) are often dosed into anaerobic digestors to improve biogas yield. TM bioavailability driven by metal speciation influences stimulatory, inhibitory or toxic effects of trace metals on anaerobic digestion (AD) process. Metal speciation is affected by chemical equilibrium and kinetics of physiochemical processes. This study presents a modified Anaerobic Digestion Model 1(ADM1) where the biochemical and physiochemical framework is extended to include trace metal effects on AD. The model includes processes like uptake of metals, precipitation of metals, inorganic complex formation and organic complexation with metabolites. Model results shows influence of trace metal and sulphur concentration present in the substrate on anaerobic digestion process and significance of trace metal dosing to improve the digestor performance.

Keywords

ADM1; bioavailability; metal dosing; anaerobic digestion; trace metal speciation

INTRODUCTION

Anaerobic digestion (AD) is proven to be one of the most economical and effective technologies for the treatment and recovery of waste. AD offers benefits such as biogas production, electricity, heat, high-quality fertilizers, complete recycling of organic waste, greenhouse gas reduction and environmental protection, in addition to reduced operating costs and smaller carbon footprint. Supplementing trace metals (TMs) to enhance AD performance is one such proven technique (Choong et al., 2016; Feng et al., 2010; Thanh et al., 2016). Trace metals are required at optimum concentrations in an AD system as they play an essential role in composition of enzymes and cofactors involved in AD pathways. For example, Iron (Fe) serves as a redox carrier in an AD system and is an important structural component of majority of enzymes present in anerobic digestion processes. Dosing Fe has been discovered to useful in AD for reducing hydrogen sulphide (H2S) formation, increasing propionate conversion rate, accelerating hydrolysis and acidogenesis and reducing volatile fatty acids (VFAs) accumulation (Choong et al., 2016).

Optimum concentration of trace metals (TMs) is essential for an effective operation of an anaerobic digestion system. Metal bioavailability is driven by metal speciation and is influenced by factors like operational conditions (temperature, pH, organic loading rate), reactor type and feedstock. Supplementing TMs can result stimulatory, inhibitory or toxic effects of trace metals on anaerobic digestion (AD) process. Moreover, excess supplementation is costly and causes undesirable metal concentration in the final digestate. Hence, optimisation of TM dosing is significant and a model-based approach will help in obtaining tailor made solutions applicable to each individual case.

Trace metals are commonly supplied to biogas plants through feedstocks and bioavailability of TMs greatly varies with feedstock characterisation, mainly classified as phosphate rich, sulphur rich, lignocellulose rich and lipid rich feedstock (Roussel et al., 2019). Wheat stillage for example has low trace metals with high sulphur concentration and is not an ideal substrate for anaerobic digestion whereas swine wastewater contains high concentrations of Cu and Zn (Thanh et al., 2016). Characterisation of maize silage indicated deficiency of Ni and Co (Evranos & Demirel, 2015). This study evaluates the influence of substrate on trace metal dosing during anaerobic digestion using a dynamic model-based study. The dynamic model is an extension of Anaerobic Digestion Model 1(ADM1) and major process influencing TM speciation are added to capture dynamic behaviour of the metals and its influence on cumulative methane production.

METHODOLOGY

This study presents a modified ADM1 where the biochemical and physiochemical framework is extended to include trace metal effects on AD (Figure 1). Extensions made in biochemical module are according to Frunzo et al. (2019). The physicochemical model includes 13 precipitation/dissolution reactions, 96 aqueous phase reactions (acid-base and complexation reactions) and 4 gas stripping processes. The aqueous phase chemistry module is defined under non-ideal conditions to consider ionic strength effects by considering ion activity instead of molar concentrations. Kinetics of all possible inorganic complex formation and organic complexation with metabolites like volatile fatty acids are also included in the model. Aqueous phase reactions are formulated as nonlinear algebraic equations and modelled as equilibrium reactions as happen very fast and reaches chemical equilibrium rapidly (Barat et al., 2011). Precipitation reactions, biochemical reactions and gas transfer occur relatively slow and are modelled as kinetic reactions. Ordinary differential equations formulated based on mass conservation principle for each of soluble, particulate, gaseous and precipitate components define dynamics of those model components. for soluble (, Eq. (1)), particulate (Eq. (2)), gaseous (Eq. (3)) and precipitate (, Eq. (4)) components.

where is the reactor volume, and are the influent and effluent flow rates, , and are the kinetic rate expressions for biochemical, precipitation, dissolution and gas transfer processes respectively for component *i*. and denote influent concentrations of soluble, particulate and precipitate components. is the volume of reactor headspace and is the gas flow rate. Number of soluble and particulate components is represented as , and , denote number of biochemical processes and precipitation/dissolution processes under consideration. and represent stoichiometric coefficient for biochemical and precipitation/dissolution process *j*. Process equations are implemented in an original MATLAB code and simulations were performed to study influence of substrate type – phosphate rich, sulphate rich and metal concentration in the sludge.

RESULTS AND DISCUSSION

Simulations were performed to test model performance. Figure 2 shows the effect of concentration of trace metal (iron) on cumulative methane production. Methane production increased when iron concentration in the substrate is increased stepwise from 0 µM to 100 µM. This shows stimulatory effects of iron on anaerobic digestion. However, when iron concentration is further increased to 1 mM, methane production drastically decreased. This is due to inhibitory effects of iron on methane production. Similar effects were observed for Co and Ni (plots not shown). Hence concentration level of TMs in substrate is significant during anaerobic digestion. This shows that dosing TM under deprivation during anaerobic digestion can significantly improve yield of the digestor. However, excessive dosing can cause negative effects due to inhibitory and toxic effects. Speciation of iron over time for different iron concentrations is given in Figure 3. For a defined sulphide concentration present in the system, FeS precipitation increases with increase in Fe until no more sulphide is available. Other non-labile Fe species present in the system are negligible. It is evident that sulphide precipitation drives the speciation and bioavailability of iron in the system. Hence, sulphur concentration in the substrate is another important factor and a thorough characterisation of substrate (particularly metal and sulphur concentration) is significant before dosing trace metals. The model is also tested for its adaptability under various scenarios like changing ionic strength, pH and sulphide concentration. Model presented in the study is a good prediction tool to decide metal dosing concentration during metal supplementation.

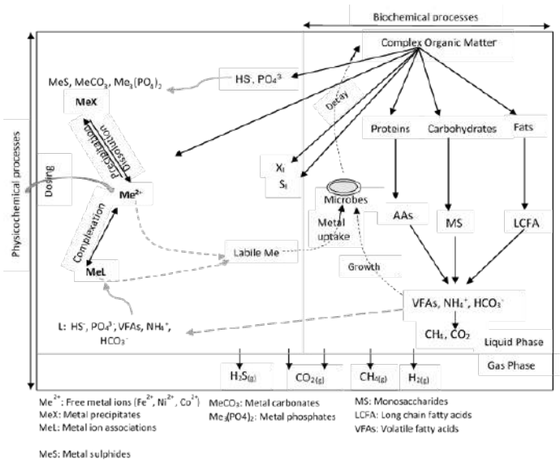

Figure 1. Schematic representation of processes defined in the model

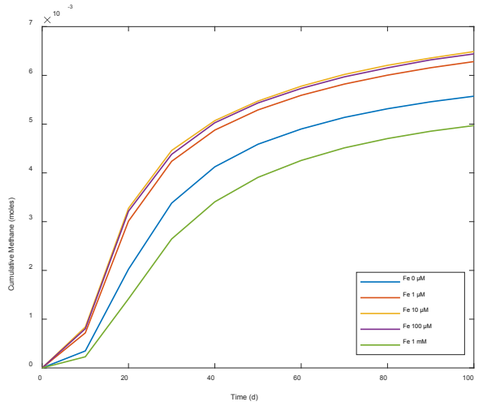

Figure 2. Influence of TM content in substrate on methane production

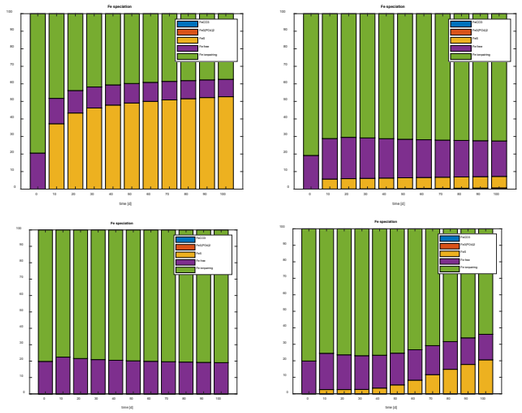

Figure 3. Iron speciation over time under variable concentrations of Fe (a)1 µM (b)10 µM (c)100 µM (d)1 mM

REFERENCES

1. **Barat, R., Montoya, T., Seco, A., & Ferrer, J. (2011). Modelling biological and chemically induced precipitation of calcium phosphate in enhanced biological phosphorus removal systems.** *Water Research*, *45*(12), 3744–3752.

2. **Evranos, B., & Demirel, B. (2015). The impact of Ni, Co and Mo supplementation on methane yield from anaerobic mono-digestion of maize silage.** *Environmental Technology*, *36*(12), 1556–1562.

3. **Feng, X. M., Karlsson, A., Svensson, B. H., & Bertilsson, S. (2010). Impact of trace element addition on biogas production from food industrial waste - Linking process to microbial communities.** *FEMS Microbiology Ecology*, *74*(1), 226–240.

4. **Frunzo, L., Fermoso, F. G., Luongo, V., Mattei, M. R., & Esposito, G. (2019). ADM1-based mechanistic model for the role of trace elements in anaerobic digestion processes.** *Journal of Environmental Management*, *241*, 587–602.

5. **Roussel, J., Carliell-Marquet, C., Braga, A. F. M., Garuti, M., Serrano, A., Fermoso, F. G., van Hullebusch, E., Collins, G., Mucha, A. P., & Esposito, G. (2019).** *Engineering of trace-element supplementation from the book Trace Elements in Anaerobic Biotechnologies*.

6. **Thanh, P. M., Ketheesan, B., Yan, Z., & Stuckey, D. (2016). Trace metal speciation and bioavailability in anaerobic digestion: A review. In** *Biotechnology Advances* **(Vol. 34, Issue 2, pp. 122–136).**

CFD modelling as an emerging digital tool for the design and optimization of WWTPs: Learnings from two case studies

H. Norouzi-Firouz*, S. Arnout*, E. Nagels*, W. Maenhout**, L. Buts** and K. Lenoir**

* InsPyro, Ambachtenlaan 54, 3001 Leuven, Belgium
(E-mail: hossein.norouzi@inspyro.be, sander.arnout@inspyro.be, els.nagels@inspyro.be)
** Aquafin, Dijkstraat 8, 2630 Aartselaar, Belgium

Abstract
This study demonstrates the application of CFD (computational fluid dynamics) modelling for the design optimization of WWTPs through two different case studies. In the first case, three configurations of the aeration system in a tank were investigated by studying the gas hold-up and mass transfer efficiency. A second case is about comparing two mixers' efficiency in a certain sludge buffering tank. Out of each case, one design scenario was selected based on the desired design parameter. As a result, using CFD modelling aided the analysis of various design scenarios with less amount of time, cost and effort.

Keywords
aeration; CFD; digitalization; mixing; sludge buffer; digital design

INTRODUCTION

The smart design of prospective wastewater treatment plants (WWTPs) needs to provide optimal performance in addition to efficiency in energy consumption and low-emission output [1]. Renovation and upgrading of the existing units of a WWTP require fulfilling the same criteria. To achieve these, common methods are investigations on lab or pilot scale and scale-up. However, limitations in the number and type of tests and safety issues as well as the cost and time, call for more promising methods. With the aid of CFD modelling, principally, there is almost no limitation to trying different design scenarios either for optimization or scale-up. At the same time, the costs of simulation are substantially lower especially compared to the build-up of a pilot scale set-up [2]. Moreover, considering the time that it takes from construction to experimentation, CFD results will be available faster. In this paper, design scenarios for two different wastewater treatment units were investigated and aided by CFD modelling: one aeration unit and one sludge buffer tank. Including all the aforementioned advantages, the outcomes assist in selecting a final optimized design.

MATERIALS AND METHODOLOGY

To perform CFD simulations, the first step is making the computational domain which includes the geometry (CAD drawings) and meshing (discretizing the geometry to sufficiently fine cells for the processing phase). The next step is defining settings and methods to run the simulation and finally post-processing to present the results in an illustrative and intuitive form. All these steps were employed for two cases: the design of an aeration tank and the mixing strategy of a sludge buffer.

Aeration tank

Used as the main part of the secondary treatment process, aeration tanks play a vital role in biological wastewater treatment plants. However, due to the high energy demand for providing sufficient air in the tank, an optimal layout of this process is required.
Using CFD modelling, three different setups (Figure 1) as design scenarios are compared for an Aquafin WWTP aeration tank in Belgium. The air flowrate is 800 m^3/h and an assumed bubble size of 2 mm diameter is applied for all configurations to allow for efficiency comparison.

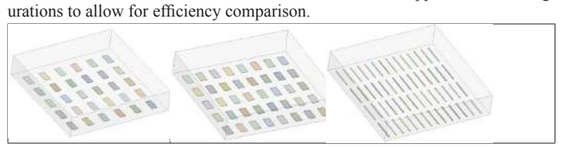

Figure 1. Three configurations of aerators in the same tank: 1) 30 rectangular plates 2) 40 rectangular plates 3) 56 rectangular narrow plates

Sludge buffer tank

The main application of a sludge buffer tank is known to blend and homogenize sludges from different feeds (primary, secondary or digested). Since the content of the tank will be sludge with a high viscosity, a mechanical mixer is needed for better homogenization. Hence, the selection of a fitting mixer design becomes crucial.
In the studied case, Aquafin is designing a sludge buffer and wants to compare two possible types of mixer (Figure 2). In both cases, there is one centrally placed mixer. Its position depends on the type: the top-entry mixer is place 6 meters deep, the hyperboloid mixer at 4 meters deep. The mixing is quantified with the tracer method.

Figure 2. Geometries of two basins with the mixing systems: 1) 2-blade impeller 2) hyperboloid mixer

RESULTS AND DISCUSSION

Aeration tank

The modelling outcomes allow visualizing the flow of both water and air. Water flow profiles at 0.92m from the bottom (Figure 3) imply that the 3rd configuration provides lower velocities, point-wise, but results in more uniform velocity inside the tank with fewer dead zones.
The aeration efficiency is quantified based on the kLa value. As illustrated in Figure 4, for configuration 3 the tank experiences higher kLa overall than other configurations which follow the discussed results of water velocity profiles.
Additionally, based on the gas hold-up and volume-averaged of kLa (Table 1) it can be concluded that configuration 3 performs better with the same air inlet conditions.

Table 1. Gas hold-up and volume averaged of kLa for three configurations

	Gas hold-up [m^3]	kLa * 10^{-3} volume averaged [1/s]
Config. 1	2.7	2.5
Config. 2	2.9	2.6
Config. 3	3.2	2.9

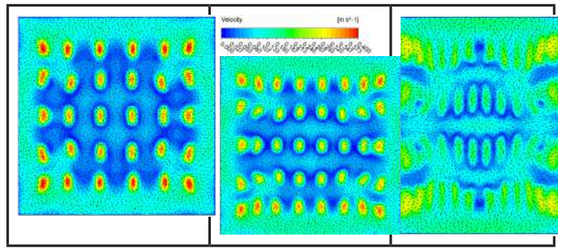

Figure 3. Velocity profiles of water in three different configurations

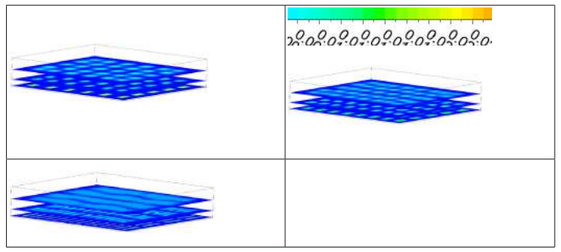

Figure 4. Distribution of kLa at three different depths of the tank for each configuration

Sludge buffer tank

In this case, the simulations aim to compare the performance of two different mixing configurations and check whether both options mix the sludge equally well over the entire volume. For a fair comparison, the mixers' rotation speed was modified with the goal to use the same available power input. Comparing the velocity profiles (Figure 5), it is observed that the 2-blade mixer delivers higher velocity at the top of the tank while the hyperboloid mixer has more impact at the bottom. However, both set-ups aid the recirculation of sludge in the tank. Table 2 gives a better insight into the velocity distribution and mixing by comparing the volume fraction of similar velocities. The 2-blade impeller provides more high-velocity regions than the hyperboloid mixer which implies more active mixing.

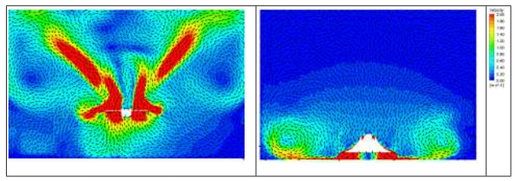

Figure 5. Velocity profiles of sludge at two mixing systems

Table 2. Velocity distribution inside the tank based on volume percentage for two mixing systems

	2-blade imp.	Hyperboloid mix.
Volume % of 0.5 m/s velocity and less	29.3	13.7
Volume % of 0.1 m/s velocity and less	98.1	35.3
Volume % of 0.01 m/s velocity and less	99.9	93.0

Last but not least, doing a virtual tracer test gives an overview of the residence time distribution of each configuration. A Rehman-Nopens (RN) [3] curve (Figure 6) is used for the calculation of the Cumulative Variables Distributions representative of the tank homogeneity. Typically, steep RN curves indicate homogeneous zones in the variable, while less steep slopes indicate a higher degree of heterogeneity. Although both curves are steep, which implies sufficient mixing for both configurations, it is even steeper for the 2-blade mixer which indicates more homogenous mixing. The hydraulic retention time (HRT) has been calculated based on the volume flowrate through the inlet and the volume of the tank. Better performance of the 2-blade impeller is observed again.

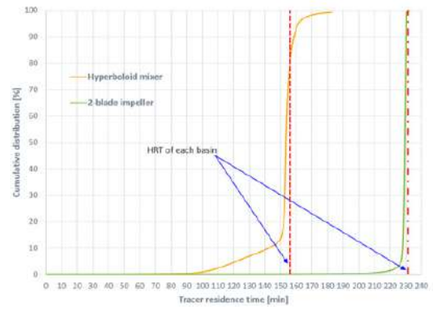

Figure 6. RN curve of residence time distribution based on the tracer test for two mixing systems

CONCLUSION

Two case studies are presented to highlight the potential of CFD modelling for aiding the water technology sector. This helps to achieve optimized designs in a shorter amount of time and at a lower cost. The technique is able to do virtual tracer tests, to observe the velocity magnitude and trajectories at any point in the design. Additionally, extracting local and average gas hold-up and kLa values assist in making design decisions.

REFERENCES

1- Muoio, R., Palli, L., Ducci, I., Coppini, E., Bettazzi, E., Daddi, D., Fibbi, D. and Gori, R., 2019. Optimization of a large industrial wastewater treatment plant using a modeling approach: A case study. Journal of environmental management, 249, p.109436.
2- Patziger, M. (2021). Improving wastewater treatment plant performance by applying CFD models for design and operation: selected case studies. Water Science and Technology, 84(2), 323-332.
3- Rehman, U., Amerlinck, Y., Arnaldos, M. and Nopens, I., 2014, October. CFD and Biokinetic Model Integration applied to a full scale WWTP. In WEFTEC 2014. Water Environment Federation.

1-

TECHNICAL SESSIONS

T10.

Membranes

ECO STP 2023

Produced water treatment by membrane aerated biofilm reactors at elevated oxygen partial pressures

V. Chrysochoidis, X. Lyu, T. Elad, L. M. Skjolding, A. R. Ferreira, H. R. Andersen, B. F. Smets, B. Valverde-Pérez*
Department of Environmental and Resource Engineering, Technical University of Denmark, Bygningstorvet, Building 115, 2800 Kgs., Lyngby, Denmark *(bvape@dtu.dk)

Abstract

Produced water (PW) is a waste stream of crude oil extraction with high content of organic materials, metals and high salinity. Membrane aerated biofilm reactors (MABRs) can be a method to reduce the organic matter and toxicity of this streams prior to discharge in the sea. Given the limited space on offshore platforms, it is preferred to locate the reactor on the seafloor. This could result in energy savings due to more efficient oxygen mass transfer at high pressures. Treatment of PW by three MABRs operating with lumen pressures of 0.2, 0.6 and 1.0 bar oxygen was investigated at laboratory scale. Reactors were fed continuously at hydraulic retention times (HRTs) of 24, 12 and 6 hours. After adaptation, 24 h batch experiments were conducted to assess biokinetics. All reactors removed a large fraction (up to 55 – 75%) of the organic content. The initial toxicity was completely removed with 24 hours.

Keywords

Produced water; membrane aerated biofilm reactors; toxicity removal.

INTRODUCTION

Produced water (PW) is a term used in oil and gas industry, which refers to the water discharged during crude oil extraction. This water typically contains high concentration of organics, metals and other pollutants and is toxic to aquatic ecosystems. Over the years, the amount of PW generated has been steadily increasing with the ageing of oilfield production wells. The nature of PW and the discharge limits in water bodies do not permit its direct disposal into these recipients. The need for effective and efficient treatment is growing significantly. Membrane aerated biofilm bioreactor (MABR) is a compact technology that can effectively treat recalcitrant and toxic organics. In a MABR, a biofilm grows on an oxygen permeable membrane where it is immobilized. Oxygen diffuses through the biofilm from the dry side and pollutants from the water side (i.e., counter diffusion) allowing for water treatment. It is more competitive than other biofilm systems due to high oxygen transfer efficiency, high chemical oxygen demand (COD) removal and energy efficiency. In case offshore crude oil extraction a compact technology with small footprint due to offshore restrictions (weight and space) is needed, preferably operating at seafloor level. Aeration plays a significant role in pollutant removal efficiency in MABRs and its efficiency is affected by pressure. The purpose of this study is to evaluate MABR treatment capacity in terms of organics removal and associated toxicity using PW from an offshore oil field in the North Sea at different oxygen partial pressures.

MATERIALS AND METHODS

The reactors were made of clear acrylic sheets and had a working volume of 250 mL. Thick silicone sheets (Aaa-Acme Rubber Co) were chosen as membranes, placed in-between the acrylic sheets. PVC tubes were used for the influent and effluent from the MABRs while a recirculation line was introduced by using a PharMed® BPT tubing. The influent flow was adjusted to achieve 24, 12 and 6 hours of hydraulic retention time (HRT) respectively. A recirculation flow was set high to ensure complete mixing inside the reactors. Each reactor was aerated from the dry side with different oxygen partial pressures (1.0 bar and 0.6 bar O_2), from cylinders supplied by Air Liquide Danmark A/S, and pressurized air at 0.2 bar. As a result, the simulation of partial pressures at sea level, 40, 20 m below sea water level depths were achieved. The oxygen in the reactors was fed intermittently and the oxygen load was controlled at 0.3 L-O_2/hour, 0.6 L-O_2/hour and 1.2 L-O_2/hour for HRT of 24, 12 and 6 hours respectively, matching the COD load. The inoculum was taken from the detached biomass from biofilm reactors adapted to onshore PW from oil and gas production, adjusted to have similar salinity and organic load as PW from the offshore platform in the North Sea. Both had characteristics which were within the range reported by (Al-Ghouti et al., 2019; Nasiri and Jafari, 2017) for different types of PW (Table 1). The same water was used as a feed to grow the biofilm in the MABRs. In the first month, the reactors run in batch mode with the onshore PW until steady state was reached. Then changed to continuous mode using the same feed. Samples were taken frequently from the reactors to measure the total nitrogen (TN), total phosphorus (TP) and COD (total and soluble). Batch experiments were carried out with PW from the offshore platform in North Sea aiming to understand the organic compound kinetics removal based on soluble COD removal. First, the reactors were adapted to the new feed by operating with continuous flow for 48 hours. Starting batch conditions consisted of half treated and half untreated PW. Each batch lasted 24 h. Samples for pH, TN, TP, conductivity, COD, BTEX (benzene, toluene, ethylbenzene and xylene), VFA (volatile fatty acids) and ecotoxicity were taken from each reactor in predefined times. An air-segmented continuous-flow analyzer (SKALAR San^{++}, Netherlands) was used for colorimetric analysis of dissolved inorganic nutrients. Prior analysis all samples were filtered by nylon 0.2 µm filters (Agilent Technologies). The dissolved oxygen concentration (DO) was monitored with an FDO® 925 sensor attached to a Multi 3430 digital meter. The pH, conductivity, COD, BTEX, VFA and ecotoxicity were measured offline as described by Ferreira et al., (2022). For the soluble COD analysis, the samples were pre-filtered with nylon syringe filters 0.2 µm (Agilent Technologies).

RESULTS AND DISCUSSION

The MABRs were monitored for 66 days at HRT of 24 hours of continuous operation, until steady state in terms of sCOD removal and DO concentration was reached. All three reactors achieved similar removal of organics (Fig.1). The sCOD removal reached 83.3%, 81.0% and 82.8% for the reactors with 0.2 bar, 0.6 bar and 1.0 bar respectively, while the DO remained below 0.5 mg/L. Samples from the feed and reactors effluents were measured for total nitrogen and total phosphorus to evaluate potential nitrification and possible phosphorus precipitation. The influent and effluent total nitrogen were on similar levels with almost all of it being in the form of ammonium, indicating no nitrification by the biofilm. Phosphorous was also on similar level in the influent and effluent. Minor removal of both nutrients occurs mostly via microbial assimilation. The biodegradation curves (Fig. 2) from the batch experiment with offshore PW showed that the partial pressure of oxygen did not have a significant effect. The sCOD degradation followed a 1st order reaction kinetics with total achieved sCOD removal at 74%, 49% and 76% for reactors operating with 0.2 bar, 0.6 bar and 1.0 bar oxygen respectively. The lower removal of the 0.6 bar reactor can be attributed to the less developed biofilm. BTEX were removed by 70% within the first hour and by 96% after 9 hours. VFA are removed by 55% after 3 hours and completely after 9 hours of operation. An ecotoxicity assessment (Fig. 3) showed that the initial toxicity was removed (below the toxicity threshold of 3.3 TU_a) after 24 hours. After adjusting the HRT to 12 hours and doubling the oxygen supply the steady state was reached with sCOD removal at 61.1%, 62.6 and 57.4% for the 0.2 bar, 0.6 bar and 1.0 bar reactors respectively. The batch experiment with offshore PW revealed that the majority of the sCOD degradation started after 12 hours of operation in all three reactors while the sCOD removal in the end was 57%, 51% and 46% for the 0.2 bar, 0.6 bar and 1.0 bar reactors, respectively. The lower removal rate can be either due to having already reached maximum biofilm thickness hampering mass transfer or due to toxic compounds with concentrations above the inhibition level for the biomass. The sCOD degradation in this case did not follow a 1st order reaction kinetics (Fig. 2). After 24 h batch, only the MABR operated with 100% oxygen was able to remove all toxicity. When HRT was at 6 hours, sCOD removal efficiency was at 36%, 41% and 49% for the 0.2, 0.6 and 1.0 bar MABRs, respectively. Again, toxicity was only removed by the MABR operated with highest oxygen pressure. This revealed that at high COD loading rate, higher oxygen partial pressure can lead to better performance. The COD removal percentages in this study are comparable to values reported by (Janson et al., 2015) at 54 – 63% and (Kose et al., 2012) at 80 – 85% for real PW treatment with biological treatment processes. Dong et al., (2011) showed also that lower HRT can affect the COD removal from PW.

Table 1. Produced water characteristics comparison.

Water type	pH	Conductivity (mS/cm)	COD (mg/L)	TN (mg/L)	TP (mg/L)
Onshore PW	7.6	68.1	1223	49.6	7.2
PW from oil platform	6.1-8.7	65.4-114.3	440-1794	41-85	0-0.2
Typical PW	4.3-10	4.2-586	1220-2600	0-92	0

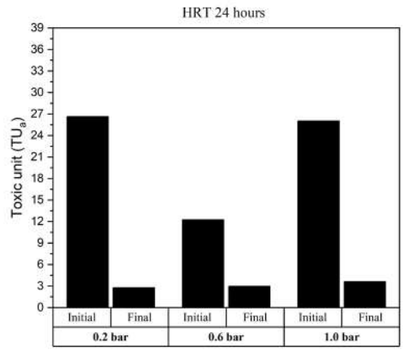

Figure 3. Example of ecotoxicity measurements with photobacterium *Vibrio fischeri* as toxic units TU_a ($100/EC_{50}$(%)) for the three different MABRs in batch experiment with PW from offshore platform in North Sea, at HRT of 24 hours

REFERENCES

Al-Ghouti, M.A., Al-Kaabi, M.A., Ashfaq, M.Y., Da'na, D.A., 2019. PW characteristics, treatment and reuse: A review. Journal of Water Process Engineering **28**, 222–239.

Dong, Z., Lu, M., Huang, W., Xu, X., 2011. Treatment of oilfield wastewater in moving bed biofilm reactors using a novel suspended ceramic biocarrier. J Hazard Mater **196**, 123–130.

Ferreira, A.R., Breinholt, L., Kaarsholm, K.M.S., Sanchez, D.F., Chhetri, R.K., Muff, J., Andersen, H.R., 2022. Feasibility study on PW oxidation as a pretreatment at offshore platform. Process Safety and Environmental Protection **160**, 255–264.

Janson, A., Santos, A., Katebah, M., Hussain, A., Minier-Matar, J., Judd, S., Adham, S., 2015. Assessing the biotreatability of PW from a Qatari gas field. SPE Journal **20**, 1113–1119.

Kose, B., Ozgun, H., Ersahin, M.E., Dizge, N., Koseoglu-Imer, D.Y., Atay, B., Kaya, R., Altinbas, M., Sayili, S., Hoshan, P., Atay, D., Eren, E., Kinaci, C., Koyuncu, I., 2012. Performance evaluation of a submerged membrane bioreactor for the treatment of brackish oil and natural gas field PW. Desalination **285**, 295–300.

Nasiri, M., Jafari, I., 2017. PW from oil-gas plants: A short review on challenges and opportunities. Periodica Polytechnica Chemical Engineering **61**, 73–81.

Biological Processes Modelling for Integrated MBR Systems: A Review of the State-of-the-Art

G. Mannina[1*], B. J. Ni[2], J. Makinia[3], J. Harmand[4], M. Alliet[5], C. Brepols[6], V. Ruano[7], A. Robles[7], M. Heran[7]. I. Smets[9], H. Gulhan[1, 10], I. Rodriguez-Roda[11,12], and J. Comas[11, 12]

[1] Engineering Department, Palermo University, Viale delle Scienze, Ed.8, 90128, Palermo, Italy
[2] Centre for Technology in Water and Wastewater, School of Civil and Environmental Engineering, University of Technology Sydney, Sydney, New South Wales 2007, Australia
[3] Gdańsk University of Technology, Faculty of Civil and Environmental Engineering, ul. Narutowicza 11/12, 80-233 Gdańsk, Poland
[4] LBE-INRAE, Univ. Montpellier, Narbonne, France
[5] Laboratoire de Génie Chimique, Université de Toulouse, CNRS, INPT, UPS, Toulouse, France
[6] Erftverband, Wastewater Department, Am Erftverband 6, 50126 Bergheim, Germany
[7] Departament d'Enginyeria Química, Escola Tècnica Superior d'Enginyeria (ETSE-UV), Universitat de València, Avinguda de la Universitat s/n, 46100 Burjassot, València, Spain
[8] Institut Européen des Membranes, IEM, Univ Montpellier, CNRS, ENSCM, Montpellier, France
[9] Department of Chemical Engineering, KU Leuven, Celestijnenlaan 200F Box 2424, 3001 Heverlee, Belgium
[10] Environmental Engineering Department, Civil Engineering Faculty, Istanbul Technical University, Ayazaga Campus, Maslak, 34469 Istanbul, Turkey
[11] Catalan Institute for Water Research (ICRA), Emili Grahit 101, 17003 Girona, Spain,
[12] LEQUiA, Laboratory of Chemical and Environmental Engineering, University of Girona, Campus Montilivi, 17071 Girona, Spain
[*] Corresponding author: *giorgio.mannina@unipa.it*

Abstract

A mathematical correlation between biomass kinetic and membrane fouling can potentially improve the understanding and the spread of membrane bioreactor (MBR) technology, by solving the membrane fouling issues. On this behalf, this review presents the current state-of-the-art regarding the modelling of biomass kinetic processes, focusing on modelling production and utilization of soluble microbial products (SMP) and extracellular polymeric substances (EPS). The key findings of this work show that the new conceptual approaches focus on the role of different bacterial groups in the formation and degradation of SMP/EPS. There is still a lack of substantial information regarding SMP modelling due to the highly complicated SMP nature. The EPS group has seldom been addressed in the literature, probably due to the lack of knowledge concerning the triggers for production and pathways. Finally, the successful model applications showed that proper estimation of SMP and EPS by modelling approaches can drive the optimization of membrane fouling, which can influence the MBR energy consumption, operating costs, and greenhouse gas emissions.

Keywords
Biomass kinetic models; extracellular polymeric substances; membrane bioreactors; soluble microbial products

INTRODUCTION

Membrane bioreactors (MBR) are widely known as reliable elements of water resource recovery facilities (WRRFs) in terms of effluent quality, low sludge production, well-arranged operation, and spatial requirements (Zuthi et al., 2017). However, membrane fouling issues and, by consequence, high operating costs, are still presented by managers and researchers as significant obstacles to an ever more spread application of this technology (Qin et al., 2018). Studies focusing on experimental data gain to be completed by others using mathematical modelling to obtain answers with less time consuming, predictive possibilities and low cost of implementation (Sun et al., 2016).

The activated sludge model (ASM) family (Henze et al., 2000), formerly developed for conventional activated sludge (CAS) systems, have been expanded to consider the specific biomass kinetics related to MBR bioprocesses. The biomass kinetic models are the modified versions of the ASM-types with the ability to account for the formation and degradation processes of soluble microbial products (SMP) and extracellular polymeric substances (EPS) that are acquainted as being responsible for membrane fouling, which has been one of the main constraints of the MBR technology (Armbruster et al., 2019). Thus, considering the formation/degradation of SMP and EPS is a reasonable approach while assessing the MBR's performance. The aim of this review is to update the findings of the past studies by providing the current state-of-the-art regarding the modelling of biomass kinetic processes, with special attention to the novelties regarding modelling the SMP and EPS formation and degradation processes. Then, the past and current application of hybrid models to MBR is presented with a focus on updates related to bioprocesses. Finally, the main outlooks and conclusions retrieved from the review are presented.

MECHANISMS OF SMP/EPS FORMATION AND UTILIZATION IN MBR

The term SMP has been adopted to define soluble cellular components or debris that are released during cell lysis, lost during synthesis, excreted for some purpose, or diffuse through the cell membrane. SMPs are divided into two groups, as originally proposed by Namkung and Rittmann (1986), including utilization-associated products (UAPs) and biomass-associated products (BAPs). The EPS is a term that encompasses numerous types of organic macromolecules (Gkotsis et al., 2014). They are ensuring the stability and cohesion of the microbial aggregates, such as flocs, granules and biofilms. The EPS can be divided into two fractions, including bound EPS (bEPS) and soluble EPS (sEPS). The first fraction is bound to the sludge flocs, whereas the soluble fraction is able to move freely between sludge flocs and the surrounding liquor. Recognizing SMP and EPS existence and characteristics transformed the mathematical modelling of MBRs since they play an important role in the initial and late fouling stages, respectively (Meng et al., 2017). Despite their importance in membrane fouling, it has to be acknowledged that analytic determination of these compounds is challenging and often inaccurate.

KINETIC MODELS FOR FORMATION AND UTILIZATION OF SMP/EPS

The need to expand the ASM to be applied to MBRs product is based on two rationales: (i) the ASMs were originally designed to address issues related to CAS systems, by considering their specific features (e.g., lower sludge retention time and low organic load with respect to MBR); (ii) they were based on the Monod equations, which are characterized by the prediction that the effluent concentration of the rate-limiting substrate should be independent of the influent substrate concentration (Barker and Stuckey, 1999). A brief historical review of their conceptual approaches is presented in the following section, with a particular attention to the latest progress.

CONCEPTUAL APPROACHES APPLIED TO SMP/EPS FORMATION AND DEGRADATION MODELLING

Historical overview regarding SMP/EPS modelling

The first modelling attempt to estimate SMP was proposed by Luedeking and Piret (1959). The purpose was to characterize microbial product formation from the fermentation of glucose to lactic acid, including the SMP formation as production/utilisation rate based on a growth-associated product (i.e., UAP) and a non-growth associated product (i.e., BAP) (Barker and Stuckey, 1999). Namkung and Rittmann (1986) presented a model in which the UAP formation is controlled by the substrate utilization and the UAPs comprise the direct by-products of substrate utilization and microbial growth. Lu and co-workers (2002) were the first to combine the concepts of SMP presented by Namkung and Rittmann (1986) to the ASMs for MBR studies. Aquino and Stuckey (2008) proposed a new approach to model EPS formation under anaerobic conditions as a non-growth associated process. Jiang et al. (2008) assumed that BAP degradation was the hydrolysis process yielding readily biodegradable substrate (S_s).

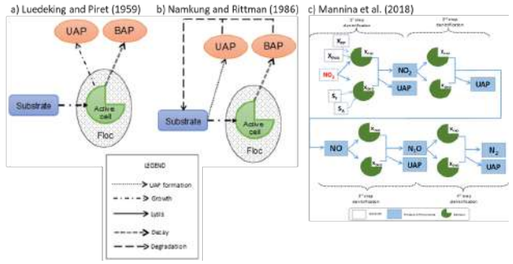

Figure 1. Some conceptual models of the formation/degradation of SMPs used in typical modelling studies (a and b); (c) Four steps of denitrification process considered by Mannina et al. (2018).

New development of conceptual approaches regarding SMP/EPS modelling

This section contains the most recent information regarding modelling SMP and EPS in MBR systems during past ten years. Janus and Ulanicki (2010; 2015) presented ASM-based models being able to account for the formation of SMP and EPS. The work of Janus and Ulanicki (2010;2015) inspired a new model proposal by Mannina et al. (2018), which presented a comprehensive integrated MBR model to assess organic matter, nitrogen and phosphorus biological removal, and greenhouse gas (GHG) formation (Figure 1 c). The processes of SMP formation and degradation and MLSS concentration are considered as an interaction among the biological and physical processes.

PERSPECTIVES

The establishment of modelling approaches is recommended in view of encouraging new findings that may lead to a wider knowledge regarding the EPS formation/degradation. MBR models should be calibrated and validated on the basis of data retrieved from full-scale WRRFs treating real wastewater in order to consider their real response to dynamic changes in influent composition and operating conditions. Finally, the influence of these components on MBR optimization could appropriately be validated provided that, during model simulations, they could be correlated to optimization outputs (e.g., membrane fouling, energy consumption, operating costs, GHG emissions), which has been successfully done before. In practical MBR operations multiple factors may inflict membrane performance. These can be eventually mistaken as genuine fouling but actually may have causes that lie outside the scope of a model. The inevitable but neglected presence of other adverse effects on membrane performance (e.g. coarse fouling, module blocking, filter integrity, uneven flow distribution etc.) which are common at full-scale installations might lead to an overestimation of the role of EPS and SMPs in a model. Thus these modelling approaches have to be used with caution and uncertainties on all stages of the model formulation, data collection, set-up, calibration and validation should be taken into account while rules of good modelling practice are applied.

CONCLUSIONS

- There are some remaining gaps in the literature about SMP and EPS, due to highly complicated nature of SMP and to the lack of information on triggers for EPS production.
- Most of the data used for modelling SMP and EPS from experimental estimation does not represent the dynamic changes in the influent composition and operating conditions.
- The novel conceptual approaches presented focused on the role of each bacterial group in the release of SMP. However, these studies did not consider the direct influence of SMP and EPS over membrane fouling issues, which is an opportunity for future developments.
- Finally, a proper estimation of SMP and EPS can stimulate the optimization of membrane fouling, which directly influence energy consumption, operating costs, and GHG emissions.

REFERENCES

Aquino, S.F., Stuckey, D.C. (2008). Integrated model of the production of soluble microbial products (SMP) and extracellular polymeric substances (EPS) in anaerobic chemostats during transient conditions. *Biochemical Engineering Journal* **38**, 138 - 146.
Armbruster, S., Brochard, A., Lölsberg, J., Yüce, S., Wessling, M. (2019). Aerating static mixers prevent fouling. *Journal of Membrane Science* 570–571, 537–546.
Barker, D. J., Stuckey, D. C. (1999). A review of soluble microbial products (SMP) in wastewater treatment systems. *Water Research* **33**, 3063 – 3082.
Gkotsis, P. K., Banti D. C., Peleka, E. N., Zouboulis, A. I., Samaras, P. E. (2014). Fouling Issues in Membrane Bioreactors (MBRs) for Wastewater Treatment: Major Mechanisms, Prevention and Control Strategies. *Processes* **2**, 795 – 866.
Henze, M., Gujer W., Mino T. and van Loosdrecht M. (eds.) (2000). Activated Sludge Models ASM1, ASM2d and ASM3. Scientific and Technical Report No. 9, IWA Publishing, London (UK).
Janus, T., Ulanicki, B. (2010). Modeling SMP and EPS formation and degradation kinetics with an extended ASM3 model. *Desalination* **261**, 117–125.
Jiang, T., Myngheer, S., De Pauw, D.J.W., Spanjers, H., Nopens, I., Kennedy, M.D., Kennedy, M.D., Amy, G., Vanrolleghem, P.A. (2008). Modelling the production and degradation of soluble microbial products (SMP) in membrane bioreactors (MBR). *Water Research* **42** (20), 4955–4964.
Lu, S. G., Imai, T., Ukita, M., Sekine, M., Higuchi, T. (2002). Modeling prediction of membrane bioreactor process with the concept of soluble microbial product. *Water Science and Technology* **46** (11-12), 63-70.
Luedeking, R., Piret, E.C. (1959). A kinetic study of lactic acid fermentation batch process at controlled pH. *Journal of Microbial and Biochemical Technology* **1**(4), 393–412.
Mannina, G., Cosenza, A., Ekama, G. (2018). A comprehensive integrated membrane bioreactor model for greenhouse gas emissions. *Chemical Engineering Journal* **334**, 1563–1572.
Meng, F., Zhang, S., Oh, Y., Zhou, Z., Shin, H. S., Chae, S. (2017). Fouling in membrane bioreactors: An updated review. *Water Research* **114**, 151-180.
Namkung, E., Rittmann, B. E. (1986). Soluble microbial products (SMP) formation kinetics by biofilms. *Water Research* **20** (6), 795-806.
Qin, L., Zhang, Y., Xu, Z., Zhang, G. (2018). Advanced membrane bioreactors systems: New materials and hybrid process design. *Bioresource Technology* **269**, 476–488.
Sun, J., Liang, P., Yan, X., Zuo, K., Xiao, K., Xia, J., Qiu, Y., Wu, Q., Wu, S., Huang, X., Qi, M., Wen, X. (2016). Reducing aeration energy consumption in a large-scale membrane bioreactor: Process simulation and engineering application. *Water Research* **93**, 205 – 213.
Zuthi, M. F. R., Guo, W., Ngo, H. H., Nghiem, D. L., Hai, F. I., Xia, S., Li, J., Li, J., Liu, Y. (2017). New and practical membrane fouling in an aerobic submerged membrane bioreactor. *Bioresource Technology* **238**, 86-94.

Modellingtheimpactsofoperationalconditionsonthe performance of a full-scale membrane aerated biofilm reactor

X.Flores-Alsina[1],N.Uri-Carreno[2],P.H.Nielsen[2],K.V.Gernaey[1]

[1]PROSYSresearchcenter,DepartmentofChemicalandBiochemicalEngineering,Technical University of Denmark, Søltofts Plads, Building 228A, Kgs. Lyngby, 2800, Denmark

[2]VandcenterSydA/S,Vandværksvej7,Odense,5000,Denmark]

*Correspondingauthor:XavierFlores-Alsina(xfa@kt.dtu.dk)

Abstract: MembraneAeratedBiofilmReactors(MABR)aregainingmoreandmore acceptanceintheplethoraofwastewaterprocessintensificationtechnologies. Computer simulations have contributed to showtheirfeasibility intermsofenergyconsumption and footprint. In this paper, the prediction capabilities of an integrated modelling approach is tested usingfull-scaledatafrom EjbyMølleWWTP+MABRsite(Odense,Denmark).Process performance under two sets of operational conditions could be reproduced with the model. Finally, membrane area is balanced against cost of nitrogen removal for current and future influent loading conditions.

Keywords:processsimulation,nitrificationrates,flowforecasting,sulfideinhibitionand precipitation

INTRODUCION

Mathematical models have proven to be useful tools to virtually study MABRs. The scientific literature offers numerous works dealing with different aspects related to process understanding and optimization. Even though the previous works made a substantial progress in the field of water process systems engineering, there are important aspects that remained untouched. First and foremost, in all these studies, MABR are studied as separate units, but never integrated within the context of a full wastewater treatment plant (WWTP). This is mainly attributed to the softwarelimitation on all these studies (Reichert et al., 2004). The latter made it impossible to study how changes in the operational conditions /control strategies may affect MABR performance (Gernaey et al., 2014). Second of all, previous studies did not includehow water chemistry may change through the biofilm. pH, weak acid/base and precipitation potentially are important aspects when predicting the phosphorus, sulphur and iron cycle (Solon et al., 2017) and the competition between microorganisms and inorganics withinthe biofilm (Feldman et al., 2019). Last but not the least and strongly related to the first point, there are very few references where MABR has been fully modelled as intensification technology given a process layout. Onlyvery fewtheoretical studies have been published up to date (Carlson et al., 2021) . Hence, it is quite difficult to assess the extra value of adding MABR cassettes from a holistic way when it comes to nitrogen removal and/or energy savings

PLANTDESCRIPTION,DATA,MODELS&OPERATIONALCONDITIONS

TheEjbyMølle(EM)Wastewatertreatmentplant(WWTP)inOdense,Denmark,has a 410,000 population equivalent treatment capacity. The MABR is adjacent to an anaerobic zoneat the EM WWTP. Afull-scale hollow-fiber MABR cassette with a total volume of 11.3 $m^3$and a total membrane surface area of 1920 $m^2$is used. External aeration (EA)wasprovidedwithfinebubblediffusers ononesideofthetank to increase the redox conditions inside the reactors. The latter divided the operating space between strategy#1 (#S1) and strategy #2 (#S2). The measured data used in this study comprises 3 years of measurements between June 2018 and December 2020 (1-2 measurementsper week). Samples were taken from 6 locations: 1 point at the raw wastewater inlet, 2 points after the primary (over and underflow), 2 points at the activated sludge section. Hydraulic retention time (HRT), nitrogen load (NL), oyxgen transfer (OTR) and nitrification rate (NR) are obtainedfromtheSCADAsystemandcalculatedasdescribedinUriCarrenoetal.(2021, 2022) and Flores-Alsina et al. (2022). The model is based on the extended version of the ASM2d (with P, S and Fe interactions) (Solon et al., 2017). The multi-scale approach suggested by Feldman et al. (2017) is used to construct the biofilm model. Mass transfer is modified to account for counter-difussional conditions. Biofilm thickness is 1 mm. Steady state is assumed to be achieved after 500 days of simulation. In #S1 and#S2 a PI controller is implemented in order to maintain the DO concentration to 0.01 and 0.15 g/m^3respectively

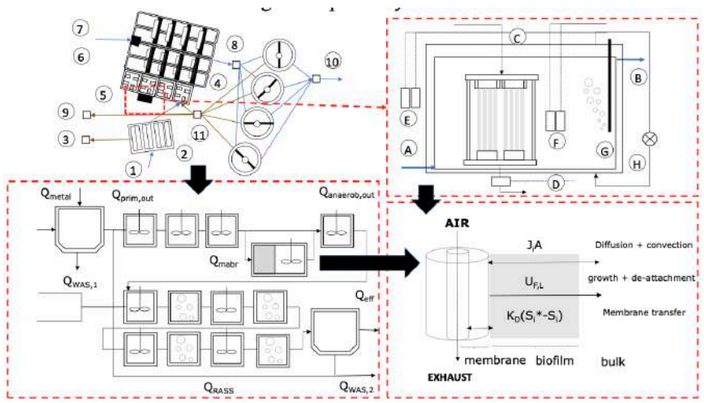

Figure 1. TOP LEFT: Flow diagram of EMWWR (adaptedfrom Google Earth): 1) influent / raw wastewater, 2) and 3) primary clarification under and overflow, 4) input anaerobicsection5) input MABR, 6) and 7)reject water and storm- water stream, 8) oxidation ditch, 9) secondary clarification waste, 10) treated effluent, 11) return activated sludge stream (RASS).

TOP RIGHT:Schematicsofthe MABRunder study:A) influent,B)effluent,C) air injection,D)exhaust,E) influent sensors (ORP, NHX), F) effluent sensors (NHX, ORP), G) micro-aeration, H) internal pumping
BOTTOM LEFT: Schematic representation of reactor hydrodynamics as series of CSTRs with pointing recycle loops and different inputs. The first four tanks are anaerobic, the following tanks are anoxic/aerobic.
BOTTOM RIGHT: Mainprocesses taking placewithin the biofilm:diffusion +convection, growth+ de-attachment and membrane transfer.

RESULTS AND DISCUSSION

Results show a 10% mismatch between flow, COD, N and P predictions and measurements in different plant locations (Figure 2). Using the adopted hydraulic retention time (HRT), nitrogen loading (NL), membrane area (MA) and oxygen transfer rate (OTR) it was possible to predict nitrification rates (NR) within the interquartile range. This has been done under the two considered MABR operational conditions:with (#S1) and without (#S2) external aeration (EA) in the bulk liquid (Figure 3). Both dataand model simulations suggest substantial differences in nitrogen conversion. The proposed approach provides additional insights about process perfomance. More specifically, simulations suggest the potential undesirable effects that sulfate (SRB) and iron (IRB) reducing bacteria may have on the overall process performance under #S1. Thelattercould:1)inhibitAOBduetoH2S,2)decreaseO2availabilityforAOBdue to presence of SOB and 3) increase the volume of inorganics (FeS, HFO and S_0) within the biofilm . Figure 4 (a,d) reveals that the higher content of biomass is found in the inner part of the biofilm (in close contact with the membrane). Inert material resulting from biological activity is generated within the biofilm and pushed towards the bulk by convective movement. Organics are rapidly consumed. Results also show the quantityof precipitates will be higher for #S1. With respect to microbial composition (Figure 4b,e),amoniaoxidizingbacteria(AOB)aredominantinsidethebiofilm.Thisis attributed to high affinity of these microbial groups for O2and the availability of substrategiventhe masstransferlimitations. Ordinaryheterotrophicbacteria(OHO) are clearly favoured in the outer parts of the biofilm. Sulfide oxidizing bacteria (SOB) are only present for #S1 in middle layers. It is important to highlight that phosphorus accumulating organisms (PAO) + sulfate (SRB) and iron reducing bacteria (IRB) are only present in thebulk. Figure 4 c and d shows the changeof inorganicsconcentrations along the horizontal axis. Hydrous ferric oxide (HFO) and mineral sulphur (S_0) will be preferentially formed close to the membrane as a result of the re-oxidation of $Fe^{+2}$and H_2S. The middle and outer parts of the biofilm will favour the accumulation of FeS. EDX and qPCR results will be compared with model predictions (Uri Carreno et al., 2022)

A seconario analysis is included where the performance of the EM WWTP is assessed in terms of kgW.h/kg N removed. This is repeated increasing load up to 50%. Model predictions using baseline conditions can be compared to plant data. Additional are included assuming that 3rd anaeaobic reactor is converted into a full scale MABR (with the same A/V ratio as the pilot). Results show that with an MABR N can be removed with a lower energetic expenditure compared to the default activated sludge configuration (Figure 5a).

Assuming an electricity cost of 0.062 Euro/kWh, it is possible to calculate the yearly savings (in terms of electrical costs) when comparing the two treatment solutions. Hence, at the default loading conditions, the model reveals that the WWTP + MABR implementation would save around 25,000 Euro/year. This difference would be increased up to 70,000 Euro/year in the event of having an increase of the incoming N load. More details in Figure 5b

References
Carlson et al., 2021. Wat Sci & Tech. 83 (6), 1418
Feldman et al., 2017. Water Research. 126, 488
Flores-Alsina et al., 2018. Sci. Tot. Env. 856(1),158980 Gernaey et al., 2014. IWA STR. 23
Reichert . (1994). Water Sci &Tech, 30(2), 21. Solon et al., 2017. Water Research. 113,97
Uri Carreno et al., 2021. Sci. Tot. Env. 779, 146366
Uri Carreno et al., 2022. Chem. Eng, Journal. 451, 138917.

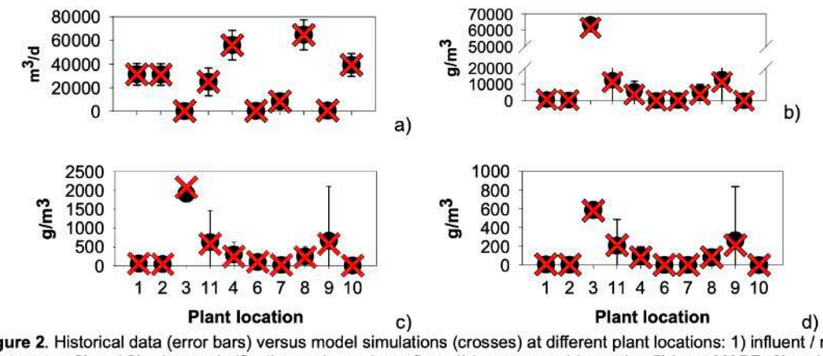

Figure 2. Historical data (error bars) versus model simulations (crosses) at different plant locations: 1) influent / raw wastewater, 2) and 3) primary clarification under and overflow, 4) input anaerobic section 5) input MABR, 6) and 7) reject water and storm-water stream, 8) oxidation ditch, 9) secondary clarification waste, 10) treated effluent, 11) return activated sludge stream (RASS). See Figure 1 for detals.

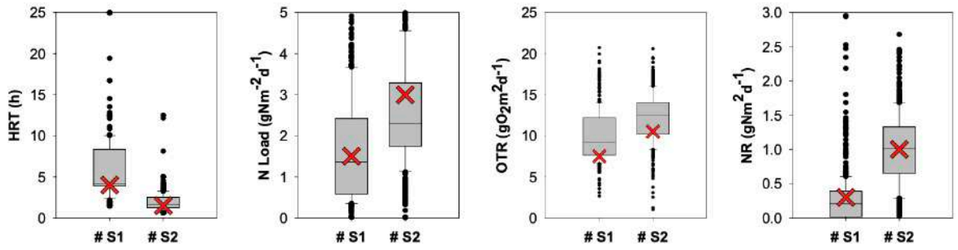

Figure 3. Historical data (error bars) versus model simulations (crosses) of different MABR process variables (#S1 and #S2)

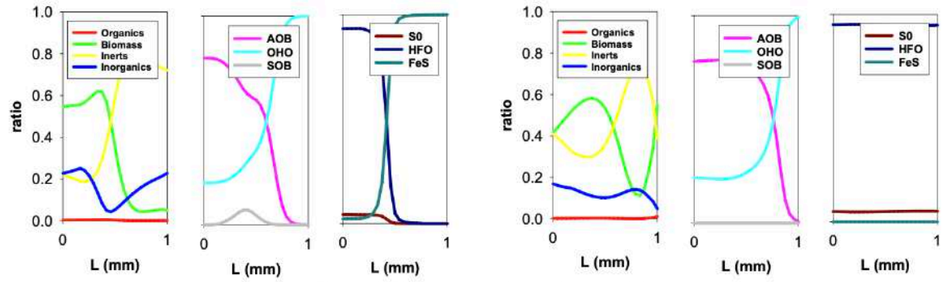

Figure 4. Biofilm composition (#S1 and #S2)

Granular Anaerobic Membrane Bioreactor for low-energy domestic wastewater treatment

L. Sanchez*, M. Heran*, G. Blandin** and G. Lesage*

* Institut Européen des Membranes (IEM), Université de Montpellier, CNRS, ENSCM, Montpellier, France
(E-mail: *geoffroy.lesage@umontpellier.fr*)
** LEQUIA, Institute of the Environment, University of Girona, Spain
(E-mail: *gaetan.blandin@udg.edu)*

Abstract
Optimization of biogas production, limitation of energy requirements as well as innovative fouling control are among the challenges to be studied to allow the expansion of anaerobic membrane bioreactor (AnMBR). In this regard, Granular Anaerobic Membrane Bioreactor (G-AnMBR) is a promising biotechnology that incorporates anaerobic digestion, granular sludge and membrane separation processes. The study revealed the ability of the G-AnMBR to meet excellent treatment performance and to increase the organic to methane conversion rate in comparison to a granular anaerobic digester (i.e. UASB), resulting in a positive net energy balance of 0.58 kWh produced per m3 of treated water. The supernatant fraction (dp < 0.125 mm) was identified as key driver in G-AnMBR fouling, in contrast to the granules (dp ≥ 0.125 mm) whose effect was negligible. Synergetic interactions between granules and supernatant compounds lead to a decrease in both fouling intensity and fouling rate, demonstrating the benefit of using granular biomass. Thus, this research highlights the high potential of G-AnMBR with submerged membrane and without biogas sparging for the treatment of domestic wastewater at ambient temperature.

Keywords (maximum 6 in alphabetical order)
Anaerobic digestion; domestic wastewater; energy recovery; granular sludge; membrane bioreactor

INTRODUCTION

Granular Anaerobic Membrane Bioreactor (G-AnMBR) is a promising bioprocess for energy-positive domestic wastewater treatment through the combination of anaerobic digestion, granular biomass and ultrafiltration membrane separation. If properly exploited, the synergy between these three technologies would allow the implementation of treatment systems that are efficient, energy self-sufficient, low-cost, low-maintenance, low-resource and with a potential for wastewater reuse. Nevertheless, the applicability of G-AnMBR to domestic wastewater treatment is hampered by the difficulty of achieving a positive energy balance (i.e. lower biological activity at ambient temperature, loss of dissolved methane within the effluent, low organic loading rate) and sustaining high filtration fluxes due to membrane fouling. Thus, the overall objective of this study was to implement an innovative G-AnMBR configuration in order to (i) maximize the conversion of organic matter into methane and (ii) minimize energy consumption. This G-AnMBR integrates a granular anaerobic digester (UASB type) combined to an immersed ultrafiltration membrane and does not use gas sparging for fouling mitigation.

MATERIALS AND METHODS

A granular anaerobic membrane bioreactor (G-AnMBR) and an upflow anaerobic sludge blanket (UASB), as a control reactor, were continuously operated in parallel during 120 days. The two reactors were inoculated with granular sludge previously acclimated during 12 months to the domestic wastewater characteristics (i.e. low COD concentration (400 $mg.L^{-1}$) and ambient temperature of 25°C). The two experimental lab-scale reactors had equal working volume of 6.7 L and functioned in the same operating conditions with a hydraulic retention time (HRT) of 13 h and an organic loading rate (OLR) of 0.5 kg $COD.m^{-3}.d^{-1}$. An intermittent filtration cycle of 10 min was operated as follows: (i) 8 min 15 s of filtration, (ii) 30 s of initial relaxation, (iii) 45 s of backwash and (iv) 30 s of final relaxation. The net filtration flux was maintained at 1.45 ± 0.35 $L.m^{-2}.h^{-1}$ (LMH). Treatment efficiencies were evaluated in terms of tCOD, sCOD, DOC, VFA, nutrients and MLSS removals. The granular sludge behaviour was evaluated through particle size distribution (PSD). Transmembrane pressure recording (TMP) and three-dimensional excitation-emission (3DEEM) analysis were performed to evaluate membrane fouling during long-term experiment. In addition, specific analyses were conducted to determine the fouling behaviour of the anaerobic granular sludge. Raw mixed liquor of G-AnMBR was split by sieving at 0.125 mm into granules (d_p ≥ 0.125 mm) and supernatant fractions (d_p < 0.125 mm). Then, the fouling potential and reversibility of the different samples (granules, supernatant and raw mixed liquor) were assessed by filtration tests. Various hydrodynamic conditions, i.e. gas sparging and recirculation, were applied to evaluate the impact of shear stress on fouling propensity. Hence, a liquid recirculation of 24 L/h (RE) and two aeration flow rates of 25 L/h (A25) and 100 L/h (A100) were applied resulting in shear stress of 15, 205 and 409 s-1 respectively.

RESULTS AND DISCUSSIONS

Long-term treatment performances

Following the 12 months of acclimation and the 4 months of operation, it has been demonstrated that:

i. G-AnMBR was stable and efficient almost from the beginning whereas a transient period of 1 month was observed for UASB (Figure 1).

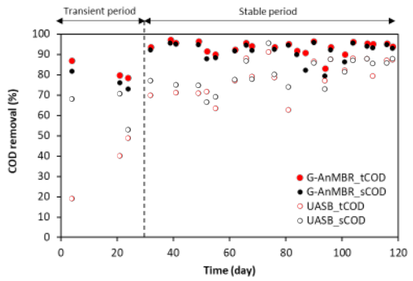

Figure 1. Total and soluble COD removal efficiencies of the UASB and AnMBR during the 120 days of operation.

ii. G-AnMBR performed higher organics and suspended solids removal (92% COD, 98% TOC and 100% MLSS) in comparison to the UASB (79% COD, 86% TOC and 99% MLSS) (Figure 1) due to the UF membrane separation that retains all particulate and colloidal matter and macromolecules.

iii. Higher quantity of methane was produced in the G-AnMBR (0,27 vs 0,22 L-CH_4/kg-$COD_{removed}$). The 3DEEM analysis suggested that the matter retained by the membrane is slowly-biodegradable and non-settleable compounds or by-products that are later converted into biogas thanks to a longer contact time between biomass and organic material. The increase of the organic to methane conversion rate, resulting in a positive net energy balance of 0.58 kWh produced per m^3 of treated water.

iv. The membrane allows to maintain the PSD tendency of the granular sludge within the G-AnMBR while large granules became predominant in UASB sludge bed.

Granular sludge fouling behaviour

Following the filtration tests for the raw granular sludge, the supernatant fraction and the granules fraction, the following conclusions can be drawn:

i. Granules (dp ≥ 0.125) had the lowest fouling potential whatever the hydrodynamic conditions used (Figure 2).
ii. The supernatant fraction, composed of fine compounds and flocs (dp < 0.125), was the key driver of membrane fouling in G-AnMBR (Figure 2).
iii. In the raw mixed liquor, where supernatant and granules are mixed, the fouling rate was lower compared to the supernatant fraction (Figure 2). It is suggested that granules diminished the impact of the fines and micro-particles over membrane permeability through mechanical scouring action and the formation of a more porous and loose cake layer structure.
iv. Hydrodynamic conditions were of high importance in mitigating membrane fouling. In tested conditions, gas sparging was more efficient in limiting membrane fouling than recirculation. However, a plateau was reached in gas sparging rate, above which the increase gas flow does not lead to a decrease in fouling rate.

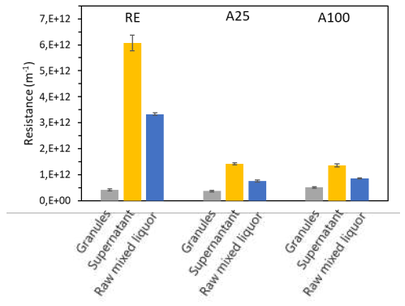

Figure 2. Filtration resistance at the end of the filtration test for the raw mixed liquor and the two fractions at different operating conditions (RE, A25 and A100).

v. Based on the 3DEEM analysis, at least 68% of the fluorescent organic matter from the reversible fouling came from the protein-like region regardless of the fraction. Hence, colloidal proteins seemed to be the main organic foulant in G-AnMBR.

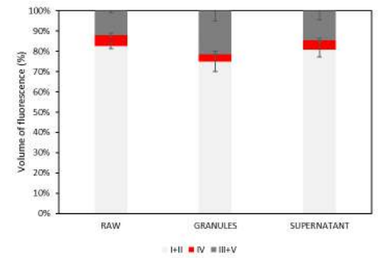

Figure 3. Repartition of the volume of fluorescence within 3DEEM regions of the superficial cleaning for the three fractions.

REFERENCES

Hu Y, Cheng H, Ji J, Li Y-Y. A review of anaerobic membrane bioreactors for municipal wastewater treatment with a focus on multicomponent biogas and membrane fouling control. Environ Sci: Water Res Technol 2020;6:2641–63.
Sanchez, L., Carrier, M., Cartier, J., Charmette, C., Heran, M., Steyer, J. P., & Lesage, G. (2022). Enhanced organic degradation and biogas production of domestic wastewater at psychrophilic temperature through submerged granular anaerobic membrane bioreactor for energy-positive treatment. Bioresource Technology, 353, 127145.
Sanchez, L., Lesage, G., Demiral, Y. O., Rodriguez-Roda, I., Heran, M., & Blandin, G. (2022). Revealing the role of supernatant and granular sludge fractions on granular anaerobic membrane bioreactor fouling. Journal of Water Process Engineering, 49, 103168.
Tomczak W, Gryta M. Energy-Efficient AnMBRs Technology for Treatment of Wastewaters: A Review. Energies 2022;15:4981.
Vinardell S, Astals S, Peces M, Cardete MA, Fernández I, Mata-Alvarez J, et al. Advances in anaerobic membrane bioreactor technology for municipal wastewater treatment: A 2020 updated review. Renewable and Sustainable Energy Reviews 2020;130:109936.

Low temperature anaerobic membrane bioreactor (AnMBR) demonstrator plant: effects of influent characterisation and site operation

M. Palmer*, E. Paissoni **, S. Pitt*, R. Smith*, P. Vale*, A. Soares**

* Severn Trent Asset Intelligence and Innovation, Severn Trent Ltd, 2 St. Johns Street, Coventry, CV1 2LZ
** Cranfield Water Science Institute, Vincent Building, Cranfield University, Cranfield, Beds, MK43 0AL, UK

Abstract

Until recently, application of AnMBRs was limited to tropical climates and only tested at pilot scale in temperate climates. This project scaled up a pilot design to a 500 m^3/d AnMBR demonstrator plant to assess viability when the reactor was fed with primary effluent wastewater. Methane production was highly variable at overall low yield 0.088 ± 0.078 kg CH_4/kg COD. An uncontrolled increase in the influent COD:SO_4 ratio was noticed after day 28 due to a change in the return liquors line. This influenced the methane production, a phenomenon not conventionally expected. The average COD removal (67%) also underperformed compared to pilot scale (90%). This study establishes how influent characterisation changes impacted the overall performance, potentially linked to centrate tank overflow into the return liquors line. This shows that the impact of digestion returns on the AnMBR process needs to be further understood to enable large scale implementation.

Keywords: Anaerobic, Circular economy, Membrane, Sulphate Reducing Bacteria, Wastewater

INTRODUCTION

Transitioning to more circular operation by reducing the amount of energy and chemicals required in treating wastewater and recovering the energy, materials and water is a prescient objective for water utilities. Similarly reducing the emissive footprint of wastewater treatment is vital for achieving net-zero targets.

Anaerobic membrane bioreactors (AnMBRs) allow for wastewater treatment whilst recovering methane, removing organic contaminants, and it does not produce nitrous oxide and allows for nutrient recovery. Research from Cranfield University optimised this process to be viable in northern European climates at pilot scale. To be more energy self-sufficient, a dissolved methane recovery is required at full scale. A demonstrator scale AnMBR was therefore installed as part of the NEXT-GEN horizon 2020 project at Spernal wastewater treatment plant (WWTP) in 2021. This paper discusses the performance of the demonstrator and investigates important factors for interfacing anaerobic treatment with existing wastewater treatment systems.

MATERIALS AND METHODS

AnMBR demonstrator plant

The AnMBR combined an upflow anaerobic sludge blanket reactor (UASB) with physical separation ultrafiltration (UF) membranes for solid-liquid separation and membrane contactor for gas-liquid separation. The UF membrane system was integrated with the UASB through a recirculation line side-stream configuration.

The AnMBR treated 200 m^3/d fixed speed flow (max 500 m^3/d including recirculation) of primary effluent from one of Spernal WWTP primary settlement tanks. The UASB reactor (supplier Waterleau), was inoculated with mesophilic industrial granular sludge (twice during the demonstration, June 2022 for data presented). Recirculation flows (with the UASB effluent and/or from the UF membrane tank) sustained an up-flow velocity of 0.8 m/h and a hydraulic retention time (HRT) of 8-10h. The three-polyethylene hollow fibre ultra-filtration membrane reactor (C-MEM from SFC-Trant) had a total membrane area of 1074 m^2 and was sparged with the biogas produced in the UASB reactor. The HRT in the UF was 1.3h and the flux was 10 LMH.

Operational history of the AnMBR

The UASB was first inoculated in June 2021. Attempts to run the AnMBR system from July 2021 to Dec 2021 were compromised first due to septic influent and then numerous equipment failures across the plant (UASB inlet pump blockage, compressor failure). This resulted in unrepresentative performance and inconsistent operation. Following a plant shutdown to fix mechanical faults, the AnMBR was re-seeded on 08/06/2022 to guarantee fresh active biomass in the reactor and also to ensure that methanogenic activity could be re-established, after the issues with septicity and a long period without any feed or recirculation.

Sampling

Data presented in this report consists of:

- **Wastewater characterisation: instantaneous samples obtained for influent, UASB, UF and degas plant effluent analysed by an external laboratory (ALS, UK).**
- **Gas volumes and composition: instantaneous measurement of UASB, UF and degas plant gas using GFM 436 portable analyser.**

RESULTS AND DISCUSSION

Table 1 summarises the influent concentrations to the AnMBR. The inlet sewage contained high levels of sulphate (111.1 ± 21.9 mg SO_4/L) compared to relatively low levels of COD. A significant range in influent COD was measured.

Table 1: AnMBR influent characterisation

	pH	*COD*	*soluble COD*	*BOD*	*TSS*	*VSS*	*NH_4-N*	*Total P*	*PO_4-P*	*SO_4*	*Alkalinity*	*VFAs*
		mg/L	mg/L	mg/L	mg/L	mg/L	mg/L	mg/L	mg/L	mg/L	mg $CaCO_3$/L	mg/L
Average	7.6	247.5	86.6	91.4	111.4	92.2	28.6	5.4	3.5	111.8	316.7	112.8
STDEV	0.4	85.4	29.2	55.0	117.2	89.0	8.8	2.1	1.8	21.5	62.4	49.5
n	61	60	63	61	62	62	25	25	25	59	58	61

Table 2 summarises the AnMBR effluent concentrations. BOD and TSS concentrations in the effluent (10.3 ± 7 mg TSS/L) were significantly higher than anticipated for a membrane process (pilot <5 mg TSS/L). The discharge quality observed for BOD/COD/SS was 27/81/10. This effluent quality would be insufficient for large scale implementation. The average COD removal was 67%.

Table 2: AnMBR effluent concentrations

	pH	*COD*	*soluble COD*	*BOD*	*TSS*	*VSS*	*NH_4-N*	*Total P*	*PO_4-P*	*SO_4*	*Alkalinity*	*VFAs*
		mg/L	mg/L	mg/L	mg/L	mg/L	mg/L	mg/L	mg/L	mg/L	mg $CaCO_3$/L	mg/L
Average	7.8	80.6	62.3	27.4	10.3	6.5	41.5	5.5	5.3	46.4	401.4	80.8
STDEV	0.3	20.9	14.9	15.3	7.0	5.7	6.1	1.5	1.4	43.6	66.3	45.1
n	44	44	43	44	44	44	17	17	17	44	17	44

An increase in nutrients (ortho-P, NH_4-N) was observed across the UASB. Effluent pH was compliant with UK discharge requirements for recycled wastewater (pH <9). Sulphate removal was significant (58% across the AnMBR). The effluent was compatible with nutrient recovery processes (operated at Cranfield University and not discussed further in this paper).

Methane and gas production

The overall gas production from the UASB and the methane content is shown in figure 1.

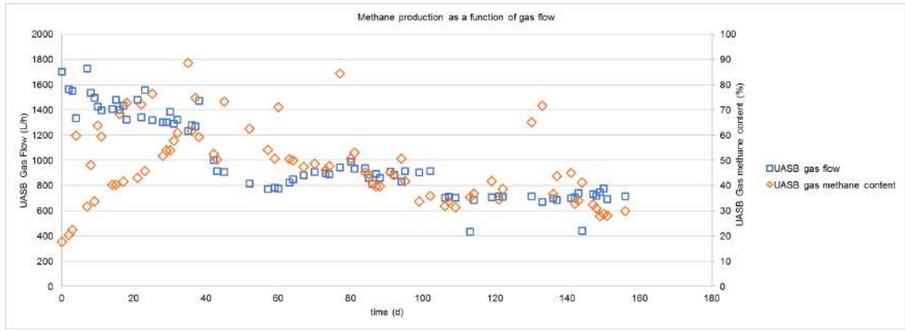

Figure 1: Gaseous methane production

Initial start up (day 0 – 20) showed a relatively stable UASB gas production with the methane content increasing as biological maturation generated methanogenic communities. Day 37 (20/07/2022) demonstrated a decrease in gas production. The gas production from this point reached a lower steady state (~1000 L/h) with a lower gas methane content between 30 – 40% (v/v). The membrane degassing (for gas-liquid separation of dissolved methane post-UF) was not operational due to a water trap on the vacuum side failure due to corrosion. Supply chain and manufacture issues prevented reinstatement of methane gas-liquid separation during the trial phase.

Discussion

Compared to pilot expectations and literature (Aslam et al., (2022) shows multiple references above 80% COD removal), the COD removal was below expectations (Table 1, 67%). The methane yield observed was 0.088 ± 0.078 kgCH_4/kgCOD. Converting this into a gas phase equivalent (i.e. if degassing of dissolved methane was operational and 100% efficient) yields 0.13 ± 0.12 m^3 CH_4/kg COD). Methane production generally declined after day 37 and varied significantly (Figure 1). On certain days, the total production reached ~3 kg CH_4/d. The average total methane production was 1.3 kg CH_4/d.

With degassing assumed operable, the yield is lower than most references though comparable with some reference municipal wastewater AnMBRs (Aslam et al., 2022). This implies that influent characterisation and wastewater site operation impact COD removal and methane performance. Figure 1 shows that the gas production and methane content of the gas decreased after day 37. Figure 2 shows that the influent characterisation and biological behaviour changed after day 28.

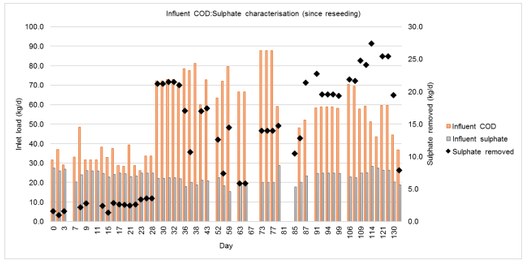

Figure 2: Influent characterisation during trial (COD, sulphate) and sulphate removal.

The trial initially operated at a COD:SO_4 ratio at around 1.5:1. At this ratio, inhibitory effects on the COD removal and methane production would be expected (Song et al., 2018). As can be seen in Figure 2, the influent characterisation (increased COD, COD:SO_4) changed significantly after day 28 – 11/07/2022. Sulphate removal increased from day 30, implying sulphate reducing bacteria outcompeted the methanogenic bacteria intermittently from this point forward despite the increase in COD:SO_4 ratio.

Spernal WWTP post digester centrate balance tank is believed to have intermittently overflowed to the demonstrator plant (not the design intent) from day 28. Limited sampling evidence suggests that the centrate is higher in COD that is not biodegradable (full COD fractionation sampling ongoing at time of writing), explaining the increased COD:SO_4 ratio's lack of impact on methane production. The centrate may have also reduced the oxidation reduction potential (ORP) of the system to prioritise sulphate reducing bacteria (ORP data to be presented in full paper). The trial observed septic conditions caused by very negative ORP feed value due to long retention times in the feed system.

Further work to understand the compatibility of the anaerobic treatment with digester site liquor returns is therefore required to translate the AnMBR demonstrator to full scale.

ACKNOWLEDGMENTS

This project has received funding from the European Union's Horizon 2020 research and innovation programme under grant agreement N°776541.

REFERENCES

Aslam, A., Jamal Khan S., Muhammad Aamir Shahzad H., 2022, Anaerobic membrane bioreactors (AnMBRs) for municipal wastewater treatment- potential benefits, constraints, and future perspectives: An updated review, *Science of the total environment*, **802**.

Song, X., Luo W. et al., 2018, Effects of sulphur on the performance of an anaerobic membrane bioreactor:Biological stability, trace organic contaminant removal, and membrane fouling *Bioresource Technology* **250, 171–177.**

New framework for standardized notation in membrane filtration modelling for resource recovery from municipal wastewater

V. Sandoval García[1], M. Alliet[2], C. Brepols[3], A. Charfi[4], J. Comas[5,6], J. Harmand[7], M. Heran[8], A. Ríos[1], I. Rodriguez-Roda[5,6], M.V. Ruano[1], I. Smets[9], G. Mannina[10], A. Robles[1]

[1] Departament d'Enginyeria Química, ETSE-UV, Universitat de València, Avinguda de la Universitats/n, 46100 Burjassot, Valencia, Spain. (Email: *valeria.sandoval; alejandro.rios; m.victoria.ruano; angel.robles@uv.es*)
[2] Laboratoire de Génie Chimique, Université de Toulouse, CNRS, INPT, UPS, Toulouse, France. (Email*: marion.alliet@ensiacet.fr*)
[3] Erftverband, Am Erftverband 6, 50126 Bergheim, Germany. (Email: *christoph.brepols@erftverband.de*)
[4] Université de Caen Normandie, France. (Email: *amine.charfi@unicaen.fr*)
[5] Catalan Institute for Water Research (ICRA), Emili Grahit 101, 17003 Girona, Spain. (Email: *jcomas@icra.cat; irodriguezroda@icra.cat*)
[6] LEQUiA, Laboratory of Chemical and Environmental Engineering, University of Girona, Campus Montilivi, 17071, Girona, Spain. (Email: *jcomas@icra.cat, irodriguezroda@icra.cat*)
[7] LBE, INRAE, Narbonne, France. (Email: *jerome.harmand@inrae.fr*)
[8] IEM, Univ. Montpellier, CNRS, ENSCM, Montpellier, France. (Email: *Marc.Heran@umontpellier.fr*)
[9] Department of Chemical Engineering, KU Leuven, Celestijnenlaan 200F box 2424, 3001 Heverlee, Belgium. (Email: *ilse.smets@kuleuven.be*)
[10] Engineering Department, Palermo University, Viale delle Scienze, Ed.8, 90128, Palermo, Italy. (Email: *giorgio.mannina@unipa.it*)

Abstract

Membrane filtration models for membrane bioreactors (MBRs) present a lack of homogeneity in the nomenclature used. The main objective of this work is to propose a new notational framework that allows a single and systematic naming. The proposal takes into account the different nomenclature used in literature, trying to minimize specific problems encountered with regards to current notation. An standardized notation for both state variables and model parameters are proposed, including different levels of subscripts to be applied. Standardization within MBR modelling field would allow easily comparing different modelling exercises aimed to advance on the optimization of MBR systems for resource recovery from municipal wastewater.

Keywords

AnMBR; MBR; membrane filtration model; municipal wastewater; standardization.

INTRODUCTION

Due to water stress, the need to recover water for reuse has strongly emerged in the last years. Moreover, wastewater has become in a source of other valuable resources, such as carbon and inorganic nutrients. Therefore, current efforts within the wastewater field focus on transforming the existing wastewater treatment plants into water resource recovery plants. In order to achieve this transition, membrane technology is playing an important role. Mathematical modelling of membrane technology allows advancing on the development and optimization of MBR-bases systems for resource recovery from municipal wastewater (MWW).

Understanding and optimizing membrane-based filtration systems (e.g. MBR and AnMBR) is a complex and time-consuming effort due to the sub-processes that occur simultaneously and are usually correlated. To this aim, mathematical modeling is a key tool that aims to predict and explain the behavior of these systems. Regarding membrane filtration, a several models can be found in literature, most of them having been developed for a given system due to the need of assessing the complexity of membrane fouling phenomenon in each specific scenario. However, there is not consensus regarding their notation and nomenclature.

Hence, it is necessary to propose a new framework for standardized notation in membrane filtration modelling providing the basis for future model developments or that could be applied to existing models in order to compare and implement them in a more consistent way.

MATERIALS AND METHODS

Table 1 shows the relation of models used in this work. An up-to-date review of selected membrane filtration models has been assessed, indicating also the MBR-based technology used to calibrate and validate each model. A matrix summarizing the main parameters of each model was constructed to provide an overview of the symbols and subscripts used in each case. Based on this matrix, a framework for standardized notation has been proposed. The proposal is mainly based on two previous works on standardization in water treatment modelling: Corominas et al. (2010) and Brepols et al. (2020).

RESULTS

In this work, state variables and model parameters have been evaluated individually. For each type of state variable and parameter, the notation for both main symbol and related subscripts has been proposed.

Special attention was put when proposing the notation (symbol or letter) for thickness, specific mass and specific resistance, due to the high variability in the nomenclature found in literature. For instance, the symbol δ was defined for representing thickness (L) as it was widely used in the collection of models studied. In the case of specific mass ($M\ L^{-2}$), ω was selected as reference symbol against *m* or *M* since these are more frequently associated with dry mass and membrane, respectively. For specific resistances ($L\ M^{-1}$), a very similar situation arises, proposing the symbol α instead of *R* and *r*, maintaining *R* for model general resistances (L^{-1}) and *r* for radius (L).

By way of example, Table 2 illustrates the proposed standardized notation for state variables. To establish the subscripts that give rise to the nomenclature, some proposals coming from Brepols *et al.* (2020) have been considered, *e.g.*, *Iv* for irreversible fouling, *M* for membrane, or *PB* for pore blocking. On the other hand, Table 3 shows the proposed subscripts for the state variables shown in Table 2, according to the category they belong to (*i.e.*, mechanisms, location...).

It is important to highlight that differentiation is not considered between AnMBR and MBR neither between other membrane-based systems (e.g. membrane photobioreactors, tertiary filtration, direct membrane filtration, etc.). Thus, the proposed framework aims to provide a general notation for any membrane filtration model applied within the wastewater treatment field. Additionally, a general framework for integrated MBR modelling would be available (examples not shown in this abstract) when combining the current proposal with the work from Corominas *et al*. (2010).

DISCUSSION

The review conducted on MBR filtration models revealed that standardization of membrane filtration modelling is a necessary step in order to advance on the development and optimization of MBR-based systems for resource recovery form MWW. In this respect, a standardized notation framework would improve the exchange of information between modelling professionals and researchers. The parameters included in this work entail those considered to be the most common or general ones. However, from the proposed framework it is possible to easily infer the proposal of other parameters that are case-specific or considered in (more) mechanistic models.

ACKNOWLEDGEMENTS

This research work was supported by the Spanish Ministry of Science and Innovation (Project PCI2020-112218) jointly with The Partnership for Research and Innovation in the Mediterranean Area (PRIMA program, Project EADANMBRT, Reference Number: 2019-SECTION2-10), both of which are gratefully acknowledged. It was also supported by Generalitat Valenciana via a pre-doctoral ACIF fellowship to co-author Valeria Sandoval-García (ACIF/2021/384).

Table 1. Selected models for the standardization proposal

Selected model	*Type of system*
Broeckmann et al. (2006)	SMBR
Busch et al. (2007)	SMBR
Charfi et al. (2014)	SMBR
Charfi et al., (2015)	SMBR
Charfi, Aslam, et al. (2017)	AFMBR GAC
Charfi, Aslam, et al. (2018)	Fluidized MBR
Charfi, Park, et al. (2018)	AFMBR PET
Charfi, Thongmak, et al. (2017)	AnMBR
Giraldo & Lechevallier (2006)	SMBR
Khan et al. (2009)	SMBR
Leeavb et al. (2002)	SMBR
Li & Wang (2006)	SMBR
Ludwig et al. (2012)	SMBR
Mannina et al. (2011)	SMBR
Robles et al. (2013)	AnMBR
Sarioglu et al. (2012)	SMBR
Wintgens et al. (2003)	MBR
Wu et al. (2012)	SMBR
Zarragoitia-González et al. (2008)	SMBR
Zuthi et al. (2017)	SMBR

Table 2. Proposal of main symbols for state variables

Category	Type	Main symbol
Type of compound	Colloidal	C
	Soluble	S
	Suspended	X
Pressure variable	Transmembrane pressure	TMP
Dimension variable	Area	A
Length variable	Thickness	δ
Mass variable	Dry mass	m
	Specific mass	ω
Resistance	Resistance	R
	Specific resistance	α

Table 3. Proposal of subscripts for state variables

Category	Type	Subscript	Category	Type	Subscript
Substance	Non-volatile solids	NVS	**Location**	Biofilm	bf
	Non-volatile suspended solids	NVSS		Bulk	blk
	Total suspended solids	TSS		Cake layer	ck
	Volatile suspended solids	VSS		Membrane	M
	Total solids	TS		Particle	p
	Volatile solids	VS		Pore	po
	GAC	GAC	**Mechanism**	Backwashing	BW
	SMP	SMP		Biofilm formation	BF
Fouling type	Intrinsic	It		Cake layer formation	CF
	Irreversible	Iv		Concentration polarisation	CP
	Irremovable	Im		Pore blocking	PB
	Reversible	Rv		Pore narrowing	PN
Others	Total	Tot		Scouring	SC

REFERENCES

Brepols, C., Comas, J., Harmand, J., Heran, M., Robles, Rodriguez-Roda, I., Ruano, M. v., Smets, I., & Mannina, G. (2020). Position paper - progress towards standards in integrated (aerobic) MBR modelling. Water Science and Technology, 81(1), 1–9. https://doi.org/10.2166/wst.2020.069

Broeckmann, A., Busch, J., Wintgens, T., & Marquardt, W. (2006). Modeling of pore blocking and cake layer formation in membrane filtration for wastewater treatment. Desalination, 189(1-3 SPEC. ISS.), 97–109. https://doi.org/10.1016/j.desal.2005.06.018

Busch, J., Cruse, A., & Marquardt, W. (2007). Modeling submerged hollow-fiber membrane filtration for wastewater treatment. Journal of Membrane Science, 288(1–2), 94–111. https://doi.org/10.1016/j.memsci.2006.11.008

Charfi, A., Aslam, M., & Kim, J. (2018). Modelling approach to better control biofouling in fluidized bed membrane bioreactor for wastewater treatment. Chemosphere, 191, 136–144. https://doi.org/10.1016/j.chemosphere.2017.09.135

Charfi, A., Aslam, M., Lesage, G., Heran, M., & Kim, J. (2017). Macroscopic approach to develop fouling model under GAC fluidization in anaerobic fluidized bed membrane bioreactor. Journal of Industrial and Engineering Chemistry, 49, 219–229. https://doi.org/10.1016/j.jiec.2017.01.030

Charfi, A., Harmand, J., ben Amar, N., Grasmick, A., & Heran, M. (2014). Deposit membrane fouling: Influence of specific cake layer resistance and tangential shear stresses. Water Science and Technology, 70(1), 40–46. https://doi.org/10.2166/wst.2014.186

Charfi, A., Park, E., Aslam, M., & Kim, J. (2018). Particle-sparged anaerobic membrane bioreactor with fluidized polyethylene terephthalate beads for domestic wastewater treatment: Modelling approach and fouling control. Bioresource Technology, 258, 263–269. https://doi.org/10.1016/j.biortech.2018.02.093

Charfi, A., Thongmak, N., Benyahia, B., Aslam, M., Harmand, J., Amar, N. ben, Lesage, G., Sridang, P., Kim, J., & Heran, M. (2017). A modelling approach to study the fouling of an anaerobic membrane bioreactor for industrial wastewater treatment. Bioresource Technology, 245, 207–215. https://doi.org/10.1016/j.biortech.2017.08.003

Charfi, A., Yang, Y., Harmand, J., ben Amar, N., Heran, M., & Grasmick, A. (2015). Soluble microbial products and suspended solids influence in membrane fouling dynamics and interest of punctual relaxation and/or backwashing. Journal of Membrane Science, 475, 156–166. https://doi.org/10.1016/j.memsci.2014.09.059

Corominas, L., Rieger, L., Takács, I., Ekama, G., Hauduc, H., Vanrolleghem, P. A., Oehmen, A., Gernaey, K. v., van Loosdrecht, M. C. M., & Comeau, Y. (2010). New framework for standardized notation in wastewater treatment modelling. Water Science and Technology, 61(4), 841–857. https://doi.org/10.2166/wst.2010.912

Giraldo, E., & Lechevallier, M. (2006). DYNAMIC MATHEMATICAL MODELING OF MEMBRANE FOULING IN SUBMERGED MEMBRANE BIOREACTORS.

Khan, S. J., Visvanathan, C., & Jegatheesan, V. (2009). Prediction of membrane fouling in MBR systems using empirically estimated specific cake resistance. Bioresource Technology, 100(23), 6133–6136. https://doi.org/10.1016/j.biortech.2009.06.037

Leeavb, Y., Cho, J., Sea, Y., Lee, J. W., & Ahn, K.-H. (2002). Modeling of submerged membrane bioreactor process for wastewater treatment. In Desalination (Vol. 146). www.elsevier.com/locate/desal

Li, X. yan, & Wang, X. mao. (2006). Modelling of membrane fouling in a submerged membrane bioreactor. Journal of Membrane Science, 278(1–2), 151–161. https://doi.org/10.1016/j.memsci.2005.10.051

Ludwig, T., Gaida, D., Keysers, C., Pinnekamp, J., Bongards, M., Kern, P., Wolf, C., & Sousa Brito, A. L. (2012). An advanced simulation model for membrane bioreactors: Development, calibration and validation. Water Science and Technology, 66(7), 1384–1391. https://doi.org/10.2166/wst.2012.249

Mannina, G., di Bella, G., & Viviani, G. (2011). An integrated model for biological and physical process simulation in membrane bioreactors (MBRs). Journal of Membrane Science, 376(1–2), 56–69. https://doi.org/10.1016/j.memsci.2011.04.003

Robles, A., Ruano, M. v., Ribes, J., Seco, A., & Ferrer, J. (2013). A filtration model applied to submerged anaerobic MBRs (SAnMBRs). Journal of Membrane Science, 444, 139–147. https://doi.org/10.1016/j.memsci.2013.05.021

Sarioglu, M., Insel, G., & Orhon, D. (2012). Dynamic in-series resistance modeling and analysis of a submerged membrane bioreactor using a novel filtration mode. Desalination, 285, 285–294. https://doi.org/10.1016/j.desal.2011.10.015

Wintgens, T., Rosen, J., Melin, T., Brepols, C., Drensla, K., & Engelhardt, N. (2003). Modelling of a membrane bioreactor system for municipal wastewater treatment. Journal of Membrane Science, 216(1–2), 55–65. https://doi.org/10.1016/S0376-7388(03)00046-2

Wu, J., He, C., & Zhang, Y. (2012). Modeling membrane fouling in a submerged membrane bioreactor by considering the role of solid, colloidal and soluble components. Journal of Membrane Science, 397–398, 102–111. https://doi.org/10.1016/j.memsci.2012.01.026

Zarragoitia-González, A., Schetrite, S., Alliet, M., Jáuregui-Haza, U., & Albasi, C. (2008). Modelling of submerged membrane bioreactor: Conceptual study about link between activated slugde biokinetics, aeration and fouling process. Journal of Membrane Science, 325(2), 612–624. https://doi.org/10.1016/j.memsci.2008.08.037

Zuthi, M. F. R., Guo, W., Ngo, H. H., Nghiem, D. L., Hai, F. I., Xia, S., Li, J., Li, J., & Liu, Y. (2017). New and practical mathematical model of membrane fouling in an aerobic submerged membrane bioreactor. Bioresource Technology, 238, 86–94. https://doi.org/10.1016/j.biortech.2017.04.006

Recycled membranes for treating urban wastewater using gravity-driven force

R. García-Pacheco[a], B. Zappulla[a], A. Galizia[a], N. Navarro[a], P. Vila[a], J. Comas[a,b], G. Blandin[a]

[a] LEQUIA, Institute of the Environment, University of Girona, Spain (E-mail: raquel.garcia@udg.edu)
[b] ICRA, Catalan Institute for Water Research, Emili Grahit 101, 17003, Girona, Spain
[c] ICREA, Catalan Institution for Research and Advanced Studies, Passeig Lluís Companys 23, 08010, Barcelona, Spain

Abstract

Household water treatment and safe storage (HWTS) systems are modular water treatment system used for water sanitation in rural and isolated areas. They provide world health organisation (WHO) water quality standards for families and communities in rural and isolated areas. Membrane technology is used in high-tech HWTS, being numerous commercial systems available in the market. However their configuration is limited to flat sheet and hollow fiber membranes. This work investigated the usage of recycled spiral-wound nanofiltration and ultrafiltration membranes driven by gravity (0.15 bar) to treat part of the secondary effluent of an urban wastewater treatment facility, located in Girona (Spain). From the experiment, initial membrane permeability rapidly decreased when the system was operated continuously (non-stop filtration). Relaxation time followed by flushing helped to partially recover the permeability and control membrane fouling. Membrane permeate achieved the water quality standard for several water reuses according to the Spanish water reuse legislation.

Keywords (maximum 6 in alphabetical order)
Nanofiltration, membrane recycling; membrane regeneration; reverse osmosis, ultrafiltration, water reuse

INTRODUCTION

Household water treatment and safe storage (HWTS) systems are modular devices, designed normally to filter water using the gravity force and to be used for families and communities (having to produce at least 3-15 L day^{-1} per person) [1]the negative impact of exposure of children to fecal bacteria includes long-term consequences on children's physical and mental development, as indicated by undernutrition, poor weight-height ratios, stunting, and Disability Adjusted Life Years (DALY's. HWTS are easy to use, operate, and maintain, which make them interesting for water sanitation and hygiene promotion actions for disease prevention in rural and isolated areas [1]the negative impact of exposure of children to fecal bacteria includes long-term consequences on children's physical and mental development, as indicated by undernutrition, poor weight-height ratios, stunting, and Disability Adjusted Life Years (DALY's.

Ultrafiltration (UF) and microfiltration (MF) membranes are filters frequently used in HWTS as gravity driven membrane (GDM) systems. The pressure-driven is achieved by height difference between the feed tank and the membrane unit (i.e. typically requiring 40-200 mbar of pressure). There is a great spectrum of HWTS commercially available that includes membrane technology. However, the most common membrane configurations for this application are flat sheet and hollow fiber. In fact, GDM systems using spiral-wound nanofiltration (NF) or UF membranes has been only investigated in laboratory scale [4].

On the other hand, in the last two decades, recycling of end-of-life reverse osmosis (RO) membranes from desalination industry into NF and UF membranes has been already proven to be a feasible and green alternative management to avoid landfill deposition and to extend their lifespan [2,3]. García et al. [4] reported that recycled membrane filtering in gravity-driven mode are able to remove low molecular weight and small-sized neutrals organics and, eventually, shows additional high interests such as: large membrane filtration surface area (between 37m^2 and 41m^2), lower cost (between 1 USD m^{-2} [5] and 6 USD m^{-2} [6]), and versatility in terms of system configurations (i.e. used in standard pressure vessels, submerged in deposit or in alternative configuration [4]). Lawler et al. were the first to report the use of recycled UF membranes in flatsheet submerged configuration for HWTS [7].

In the present study, an alternative membrane housing to the standard spiral-wound pressure vessels, recently developed by the authors, was scaled up [4]. The focus of this investigation is on a systematic approach comparing recycled ultrafiltration and nanofiltration membranes (from 8 inches diameter end-of-life RO membranes) for filtering secondary effluent of an urban wastewater treatment plant. Membrane filtration performance and fouling were assessed providing new data set for the GDM field, particularly useful for emergency response and isolated rural areas. This study is part of the OSMO4LIVES project and beneficial for developing compact GDM systems based on recycled spiral-wound membranes for both rural areas and emergency response.

MATERIALS AND METHODS

2.1 Membranes types and recycling process

Discarded RO spiral-wound modules (with 1 m length, 0.2 m diameter and a 37-41 m^2 surface area) were used. Membrane transformation into NF and UF membranes was carried out according to standard protocols already published [4,8,9]end-of-life, reverse osmosis (RO.

2.1 Gravity driven set up

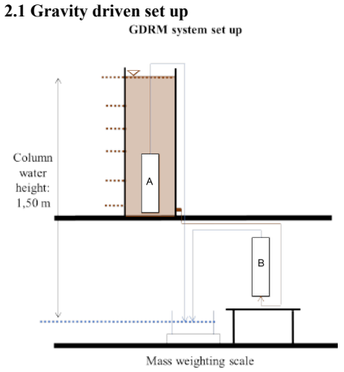

Figure 1. GDM set up for submerged configuration (A) and external (B) configurations

A pilot-scale GDM system was set up for two distinct membrane system configurations: submerged (membrane inside a water deposit) and external (membrane out of the water deposit), as shown in Figure 1. During the experiment, the system was operated under dead-end filtration mode at ambient temperature. Feed water was constantly pumped to the storage tank to keep a constant level of water in the tank, which was 1,50 m above the membrane. Thus, the gravity pressure was constant at 0.15 bar. All the containers were opaque in order to avoid algae growth.

The GDM system was operated in two modes: continuously and intermittently. The continuous mode consisted of cycles of 15 days of filtration, followed by 30 minutes relaxation time, followed by 10 minutes flushing. In the intermittent operation, the filtration cycles, relaxation and flushing were applied every 24 h. No chemical cleaning was applied.

2.1 Membrane performance

The permeate was collected in 2L graduate plastic jars during a given period of filtration. Therefore, the membrane permeability (L m^{-2} h^{-1} bar^{-1}) was obtained by dividing the permeate flow rate by the membrane surface area and the transmembrane pressure (TMP). The TMP was estimated considering the effective water head, which includes the height of the water level of the tank and the height of the end of the permeate tube. Membrane permeability was normalized at 20ºC.

Permeability was measured every day (taking at least 6 L of water). Several samples per week were collected from the feed and permeate to assess water quality according to the Spanish law for water reuse RD1620/2007 (e.g: suspended solid, turbidity and *E.coli*). Rejection coefficients were calculated (% R) following Equation 1, where, C_p and C_f are the specific concentration measured in permeate and feed, respectively.

Eq. 1

RESULTS AND DISCUSSION

Preliminary results using TW30 membrane recycled into UF membrane showed that after 15 days of continuous filtration the membrane was already fouled. The initial permeability declined from 46 to 22 L·m^{-2}·h^{-1}·bar^{-1} (52% reduction, Figure 2) in the firs filtering cycle. In Figure 2 filtering cycles 2, 3 and 4 have dark and light dots representing the measured permeability. Dark colour corresponds to the permeability measurement after 24 h continuous filtration, while the lighter colour shows the permeability after applying relaxation time and flushing. Intermittent operation mode slightly mitigated fouling during the next 18 days (cycle 2 and part of cycle 3), as the permeability dropped from 22 L·m^{-2}·h^{-1}·bar^{-1} to 15 L·m^{-2}·h^{-1}·bar^{-1} (32% reduction). Afterwards the permeability was decreasing up to a minimum of 5 L·m^{-2}·h^{-1}·bar^{-1}. In all the cases, the permeability after applying relaxation and flushing is slightly higher than the value measured after 24 h of filtration. In cycle 4 different frequencies of relaxation and flushing were tested (e.g. after filtering continuously during 2 days, 3 days and 5 days). The observations suggests that relaxation and flushing should be applied at the latest every 3 days.

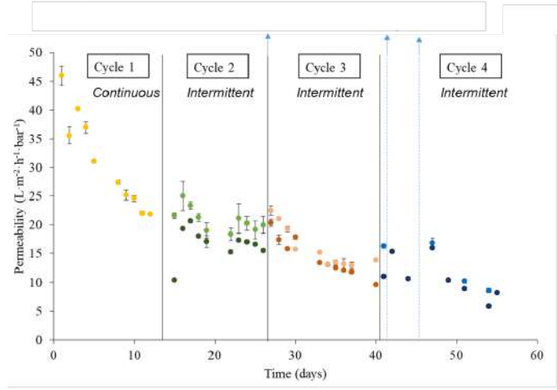

Figure 2. Permeability of TW30 recycled into UF membrane submerged in a water deposit and filtering by gravity-driven conditions. Cycle 1 was continuous (non-stop filtration). Cycles 2 to 4, the membrane was filtrating during 24 h, followed by a relaxing time and flushing.

In average the water quality of the secondary effluent was 1.39 mS/cm, 65.5 ppm COD, 10.7 ppm BDO, 36.5 ppm TKN, 0.3 ppm suspended solids and 3·10^5 CFU/100 mL. The TW30 recycled membrane rejection was: 70% COD, 76% BDO, 9%TKN, 100% suspended solids and 5 LRV of *E.coli*. The regenerated water fulfilled the water quality standards required for several water reuse applications, such as, irrigation without contact with the raw part or in contact with a cooking part, services, industrial cleaning, watering golf courses, ornamental water masses and irrigation of green areas and forest.

CONCLUSIONS

Recycled membranes have shown to be a potential alternative to be reused in gravity-driven filtration systems for tertiary treatment of urban wastewater. Intermittent filtration (regular break and drainage) contributes to control the reduction of permeability, probably resulting from fouling layer detachment from the membrane surface thanks to relaxation and flushing. Flux and permeability were similar within the cycles except for the first cycle, in which the continuous filtration led to higher permeability decrease due to fouling.

A >99.9 %, 100% and >83.7 % of rejection of *E.coli*, suspended solids and organic matter, respectively, was observed; while <2 % of rejection was achieved for nutrients and ions (except N-NO$_2$ and N-NO$_3$, which reach up to >80 % in the first 2 cycles). The values of these parameters, included in the Spanish Royal Decree for water reuse (RD1620/2007) are below range.

The following experiment will apply UF and NF recycled membranes from different brands and origins, aiming at reaching higher recycled membranes permeabilities.

REFERENCES

[1] World Health Organization. Regional Office for the Western Pacific. (2013). Household water treatment and safe storage : manual for the participant. Manila : WHO Regional Office for the Western Pacific. https://apps.who.int/iris/handle/10665/206916, WHO.
[2] R. García-Pacheco, W. Lawler, J. Landaburu-Aguirre, E. García-Calvo, P. Le-Clech, End-of-life membranes: Challenges and Opportunities, in: E. Drioli (Ed.), Compr. Membr. Sci. Eng. II, 2nd ed., Elsevier, 2017.
[3] W. Lawler, Z. Bradford-Hartke, M.J. Cran, M. Duke, G. Leslie, B.P. Ladewig, P. Le-Clech, Towards new opportunities for reuse, recycling and disposal of used reverse osmosis membranes, Desalination. 299 (2012) 103–112.
[4] R. García-Pacheco, Q. Li, J. Comas, R.A. Taylor, P. Le-Clech, Novel housing designs for nanofiltration and ultrafiltration gravity-driven recycled membrane-based systems, Sci. Total Environ. 767 (2021) 144181. doi:10.1016/j.scitotenv.2020.144181.
[5] J. Senán-Salinas, R. García-Pacheco, J. Landaburu-Aguirre, E. García-Calvo, Recycling of end-of-life reverse osmosis membranes: Comparative LCA and cost-effectiveness analysis at pilot scale, Resour. Conserv. Recycl. 150 (2019) 104423.
[6] J. Senán-Salinas, A. Blanco, R. García-pacheco, J. Landaburu-aguirre, E. García-calvo, Prospective Life Cycle Assessment and economic analysis of direct recycling of end-of-life reverse osmosis membranes based on Geographic Information Systems, (2020).
[7] W. Lawler, A. Antony, M. Cran, M. Duke, G. Leslie, P. Le-Clech, Production and characterisation of UF membranes by chemical conversion of used RO membranes, J. Memb. Sci. 447 (2013) 203–211.
[8] R. García-Pacheco, J. Landaburu-Aguirre, S. Molina, L. Rodríguez-Sáez, S.B. Teli, E. García-Calvo, Transformation of end-of-life RO membranes into NF and UF membranes: Evaluation of membrane performance, J. Memb. Sci. 495 (2015) 305–3015.
[9] R. García-Pacheco, J. Landaburu-Aguirre, P. Terrero-Rodríguez, E. Campos, F. Molina-Serrano, J. Rabadán, D. Zarzo, E. García-Calvo, Validation of recycled membranes for treating brackish water at pilot scale, Desalination. 433 (2018) 199–208.

TECHNICAL SESSIONS

T11.

Recovery of added value chemicals

ECO STP 2023

An electrochemical strategy by Lithium recovery from waste battery and brine desalination

A. Maimone*, I. Fernandez* and C. Martinez*
* CETIM Technological. Centre, Parque Empresarial de Alvedro, H20, 15180, Culleredo, A Coruña, Spain.
(E-mail: amaimone@cetim.es)

Abstract

The energy transition of the last decades has as consequence the increase of demand of energy storage systems, lithium batteries being the most important. Therefore, there has been a dramatic rise in the global lithium consumption. At present it is necessary to take advantage of new sources of natural lithium, for which reason alternative methods for lithium recovery are being investigated. Brines with relatively high concentrations of lithium are obtained as waste from desalination plans. In this study, an electrochemical system based on discarded (end of life) batteries is evaluated to recover lithium from desalination brines.

Keywords

Brines; Electrochemical systems; Lithium battery waste; Lithium recovery.

INTRODUCTION

Lithium batteries are the predominant storage system in the automotive and renewable energy market. Currently, the battery sector is supplied by brines and ore, however, in the future it is expected that the increase in lithium demand will lead to shortages. (Srimuk, Su, et al., 2020) The total amount of lithium in seawater reaches 230 billion tons, however, its concentration in seawater is around 0.17 mg/dm^{-3} (Yu, Yuan, et al., 2022). Other alternative sources of lithium are recycling of end-of-life Li-ion batteries and unconventional lithium resources such as jadarite or hectorite,(Tabelin, Dallas, et al., 2021). Additionally, mine drainage/ water, (Mohr, Mudd, et al., 2012) and brines of desalination process are sources of maximum interest.(Flexer, Baspineiro, et al., 2018) with significantly higher concentrations than in seawater. Therefore, the recovery of lithium these currents is a priority for the scientific community.

Several techniques have been studied for lithium extraction from seawater, such as evaporation-based techniques, ionic sieve adsorption, nanofiltration, solvent extraction, electrodialysis, the ionic pump and lithium-ion battery-based electrochemical extraction. Lithium extraction using electrochemical technologies has been shown to be beneficial in aspects such as low energy consumption, versatility and high selectivity. (Zhao, Yang, et al., 2019)

The lithium-ion battery-based electrochemical extraction is based on the application of an electric field to increase the adsorption of lithium and selective materials are used as a working electrode for the lithium embedding/stripping process. (Zhao, Yang, et al., 2023) At present, materials with a spinel and olivine structure are generally used as the cathode of batteries,(Santos and la Mantia, 2022) therefore, using the active material from battery waste to manufacture new electrodes is an interesting alternative. In the present study, new electrodes are synthesized from battery waste cathodes, this active material is pre-treated by chemical and thermal methods and subsequently, the new electrodes are characterized by electrochemical methods, studying the stability and diffusion kinetics of lithium.

MATERIALS AND METHODS

Herein, self-supported LFP electrodes were fabricated from waste batteries. The active material has been immersed in a 0.5 M solution of potassium persulfate at 333 K for 2 hours to favour the release of lithium from the olivine structure and later it was deposited on a conductive sheet using the *doctor blade* technique. To determine the crystalline structure of the electrodes, it was characterized by XRD. Additionally, for the electrochemical characterization, cyclic voltammetry (CV) was performed from which the diffusion coefficient of lithium was obtained.

RESULTS AND DISCUSSION

Figure 1 shows how the diffractogram coincides with the diffraction pattern of the olivine structure (LFP), with peaks that are associated with the planes (200), (101), (210), (111), (211) and (311).

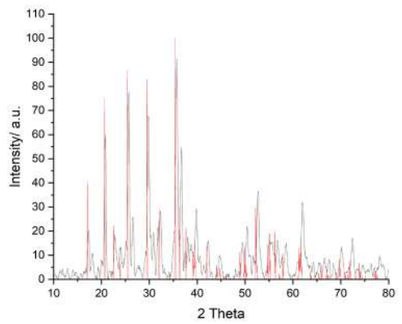

Figure 1. XRD patterns of LFP electrodes synthesized from battery waste. In black, XRD pattern, and in red, olivine diffraction pattern of reference.

Cyclic voltammetry curves are shown in **Figure 2**. One reduction peak appeared near 0 V vs Ag/AgCl, which is associated to intercalation into LFP. Correspondingly, one oxidation peak near 0.2 V is assigned to de-intercalation from LFP. Cyclic voltammetry demonstrated that the embedding/stripping process and transformation were controlled by the diffusion rate. (Takahashi, Tobishima, et al., 2002)

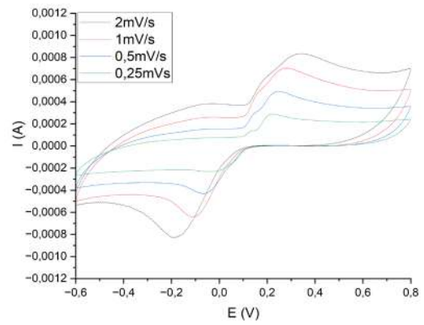

Figure 2. CV of electrode in 0.1 M LiCl solution with different scan rates.

Diffusion coefficients for intercalation/deintercalation were obtained from the CVs, resulting in and , respectively. These values are consistent with literature. (Zhang, Zhang, et al., 2013)

Lithium recovery from brines is possible by using battery waste to synthesize LFPs electrodes. The fabricated electrodes showed high stability and promising Li-ion diffusion kinetics. Finally, the use of battery waste in the synthesis of new electrodes favours the circularity of waste and represents a benefit for the environment.

ACKNOWLEDGMENTS

REWAISE | Resilient Water Innovation for Smart Economy has received funding from the European Union's HORIZON 2020 Research programme under the Grant Agreement no. 869496

REFERENCES

Flexer, V., Baspineiro, C. F., and Galli, C. I. (2018) Lithium recovery from brines: A vital raw material for green energies with a potential environmental impact in its mining and processing. Science of The Total Environment, **639**, 1188–1204.

Mohr, S. H., Mudd, G. M., and Giurco, D. (2012) Lithium Resources and Production: Critical Assessment and Global Projections. Minerals 2012, Vol. 2, Pages 65-84, **2**(1), 65–84. [online] https://www.mdpi.com/2075-163X/2/1/65/htm (Accessed January 31, 2023).

Santos, C. and la Mantia, F. (2022) Recent advances in reactor design and control for lithium recovery by means of electrochemical ion pumping. Current Opinion in Electrochemistry, **35**, 101089.

Srimuk, P., Su, X., Yoon, J., Aurbach, D., and Presser, V. (2020) Charge-transfer materials for electrochemical water desalination, ion separation and the recovery of elements. Nature Reviews Materials, **5**(7).

Tabelin, C. B., Dallas, J., Casanova, S., Pelech, T., Bournival, G., Saydam, S., and Canbulat, I. (2021) Towards a low-carbon society: A review of lithium resource availability, challenges and innovations in mining, extraction and recycling, and future perspectives. Minerals Engineering, **163**, 106743.

Takahashi, M., Tobishima, S. ichi, Takei, K., and Sakurai, Y. (2002) Reaction behavior of LiFePO4 as a cathode material for rechargeable lithium batteries. Solid State Ionics, **148**(3–4), 283–289.

Yu, Y., Yuan, Z., Yu, Z., Wang, C., Zhong, X., Wei, L., Yao, Y., Sui, X., Han, D. S., and Chen, Y. (2022) Thermally assisted efficient electrochemical lithium extraction from simulated seawater. Water Research, **223**, 118969.

Zhang, S. M., Zhang, J. X., Xu, S. J., Yuan, X. J., and He, B. C. (2013) Li ion diffusivity and electrochemical properties of FePO4 nanoparticles acted directly as cathode materials in lithium ion rechargeable batteries. Electrochimica Acta, **88**, 287–293.

Zhao, X., Yang, H., Wang, Y., and Sha, Z. (2019) Review on the electrochemical extraction of lithium from seawater/brine. Journal of Electroanalytical Chemistry, **850**, 113389.

Zhao, X., Yang, S., Hou, Y., Gao, H., Wang, Y., Gribble, D. A., and Pol, V. G. (2023) Recent progress on key materials and technical approaches for electrochemical lithium extraction processes. Desalination, **546**, 116189.

FromWasteStreamstoPlatformChemicals

I.Owusu-Agyeman*,E.Plaza**,Z.Cetecioglu*

*DepartmentofIndustrialBiotechnology,KTH-RoyalInstituteofTechnology,AlbaNovaUniversityCenter,SE- 106 91, Stockholm, Sweden
(E-mail:*isaacoa@kth.se;zeynepcg@kth.se*)
**DepartmentofSustainableDevelopment,EnvironmentalScienceandEngineering,KTH-RoyalInstituteof Technology, SE-100 44, Stockholm, Sweden
(E-mail:*elap@kth.se*)

Abstract

Co-fermentation of primary sludge and external organic waste for volatile fatty acids (VFA) production without pH control was studied using 15 L and 2 m^3bench-scale and pilot-scale reactors, respectively. In the bench-scale experiments, the VFA production reached a maximum of 25,000mg COD/L and a VFA yield of 500 mgCOD/gVSfed. The VFA mixture was dominated by caproic acid with a percentage of ≈ 50%. The pilot-scale reactor showed that substrate variability influences the VFA yield and the individual VFA types. The study also showed that VFA production is feasible with positive economic outlook. In comparison with acetate and methanol, the VFA-rich liquid showed the highest specific denitrification rate and a nitrate equivalent removal efficiency of a maximum of 98% was obtained for the continuous denitrification experiments. VFA separation and purification to obtain pure acid type is being investigated and results will be presented during the conference.

Keywords

Caproicacid;co-fermentation;denitrification;municipalorganicwaste;volatilefattyacids

INTRODUCTION

Waste is seen as a resource which can be processed to produce valuable products. Resource recovery from waste will reduce consumption of primary raw materials and greenhouse gases (GHG) emissions. Thus, recovery of biobased product as an alternative petrochemical will help achieve to achieve a sustainable society.

One of the important bioproducts with a high bioproduction potential from waste streams are volatile fatty acids (VFAs). VFAs are important building block chemicals with a greatly increasing market demand (Atasoy et al., 2018; Bhatt et al., 2020). Despite the promising developments in VFA from waste, there are still challenges to overcomes which include obtaining pure VFA product and increasing production efficiency. On the journey towards full-scale production of VFAs from waste streams, there is the need to ultimately understand how such the waste-based system respond to changes.

The current study has sought to understand the technological and economic feasibility of long-term VFA production from municipal organic wastes. The study elucidated the long-term system resilience and the microbial community dynamics of the VFA production system. The direct application of the waste-derived VFA mixture in the wastewater treatment plants (WWTPs) for denitrificationassustainablealternativetopetroleum-basedcarbonsourceswasexplored.Thestudy also includes the possibility of separation and purification of the VFA mixture to obtained pure biobased product.

MATERIALS AND METHODS

VFA production

In this study, co-fermentation of primary sludge (PS) and external organic waste (OW) for VFA productionwascarriedout. ThePSwasfromHammarbySjöstadverket.ThreedifferentkindsofOW were used which include OW1-organic waste from Himmerfjärden WWTP which ishygienised for 61 minutes at 71°C; OW2-organic waste from Himmerfjärden WWTP which is not hygienised;andOW3-organicwastefromScandinavianBiogas'digestionplantwhichishygienised for 61 minutes at 71°C. The study was carried out two scales: bench scale and pilot scale with afeed consisting of feed of 70% v/v PS and 30% v/v OW. Both experiments were carried out without pH adjustment and at a temperature of 35°C.

The bench scale reactor had a total volume of 15 L with a working volume of 10 L and wasoperated in semi-continuous mode with retention time of 7 days. The bench-scale reactor was operated for 315 days with PS and OW1 as the substrate. The pilot-scale reactor had a total volume of 2 $m^3$with a working volume of 1.5 m^3. The pilot-scale reactor was operated for 264 days in continuous mode with the same conditions as the bench-scale reactor. Unlike the bench-scale reactor, there four different periods of operation for the pilot-scale reactor when different kinds of OW were used as substrates. These included: period I when PS and OW1 were fed; period II when PS and OW2 were fed; period III when only PS was fed; and period IV when PS and OW3 werefed. A limited techno-economic analysis was done for the different periods of the pilot-scale reactor operation.

Denitrification

The VFA-rich liquids were tested for its denitrification potential in comparison with acetate and methanol. Denitrification was done in batch test using the manometric tracking method with different carbon/nitrogen (C/N) ratios (from 0 to 7.5). Furthermore, the denitrification efficacy of the VFA-rich fermentation liquids was explored by operating dentification reactor in a continuous mode with real nitrified wastewater for 63 days. The VFA-rich carbon source was dosed to the continuous denitrification reactor at a C/N ratio of 4.5.

Separation and Purification

Separation of the VFA-mixture with nanofiltration/reverse osmosis technique to obtain one-type VFA with high purity is being done. The study is carried out with FilmTec NF270, NF90, BW30, XUS1207 Acid Stable NF and FilmTec SW30HRLE membranes from Dupont using dead-end stirred cell.

RESULTS ANDDISCUSSION

Volatilefattyacidproductionyieldandcomposition

The VFA production started to increase and peaked at a value of about 18,000 mgCOD/L at day 14 thereafter it began to decrease (Figure 1). The decrease in VFA production was attributed to accumulation of undissociated acid due to a low pH. Accumulation of undissociated acids is known to be toxic to microorganisms (Xiao et al., 2016). However, the system recovered due to acclimatization and increase of pH and the VFA production started

to gradually increase and reached a maximum VFA concentration of 25,000mgCOD/L and a yield of 500 mgCOD/gVS_{fed}on day 98.It was observed that VFA composed of mainly caproic acid with relative abundance of ≈ 50% (Figure 2). Caproic acid is more valuable and has now become the focus of many bioproduction (Angenent et al., 2016).

During the pilot-scale reactor operation, it was revealed that the substrate types influenced the VFA production and composition. The periods with hygienzed OW yielded high VFA and percentage of caproic acid. The pilot-scale reactor had a maximum VFA production of 22,000mgCOD/L with caproicacidpercentageof45%. Thetechno-economicanalysisshowedthatalthoughhyginzationat 71°C added to the cost operation, the economic gains from the yield and VFA types gave a positive economic outlook.

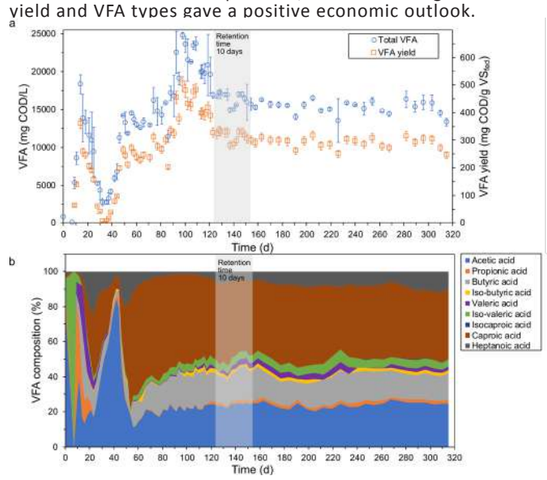

Figure 1. a) VFA production and yield; b) distribution of various VFA components of the bench- scale reactor (Owusu-Agyeman *et al*, 2023)

Denitrificationresults

Denitrification test results showed that the VFA-rich liquid achieved the highest specific denitrification among the three carbon sources (Figure 2). The results also showed that the COD/N ratio of 4.5 is sufficient for complete denitrification with a high denitrification rate. An average nitrate equivalent removal efficiency of 87±14% with a maximum of 98% was obtained for the continuous denitrification experiments. Thus, VFA production from waste has the potential to close the loop for carbon management of WWTPs.

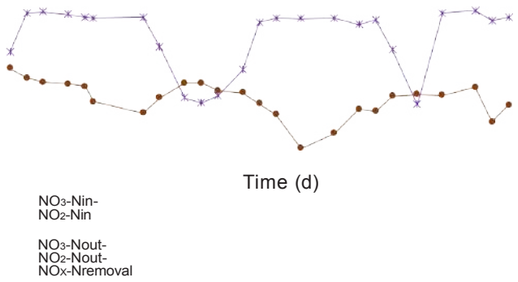

Figure 2. Results of a) batch denitrification experiments and b) continuous denitrification experiment (Owusu-Agyeman *et al*, 2023)

The separation and purification of the VFA to obtained pure products are being worked and the results will be presented in the conference.

The study has revealed the technological and economic feasibility of VFA production through co- fermentation of municipal organic wastes. The finding of the study could be the reference point for full-scale application of VFA

REFERENCES

Angenent,L.T.,Richter,H.,Buckel,W.,Spirito,C.M.,Steinbusch,K.J.J.,Plugge,C.M.,Strik,
D. P. B. T. B., Grootscholten, T. I. M., Buisman, C. J. N., & Hamelers, H. V. M. (2016). Chain Elongation with Reactor Microbiomes: Open-Culture Biotechnology to Produce Biochemicals. *Environmental Science and Technology*, *50*(6), 2796–2810.
Atasoy, M., Owusu-Agyeman, I., Plaza, E., & Cetecioglu, Z. (2018). Bio-based volatile fatty acid production and recovery from waste streams: Current status and future challenges. *Bioresource Technology*, *268*, 773–786.
Bhatt, A. H., Ren, Z. (Jason), & Tao, L. (2020). Value Proposition of Untapped Wet Wastes: Carboxylic Acid Production through Anaerobic Digestion. *IScience*, *23*(6).
Owusu-Agyeman, I., Bedaso, B., Laumeyer, C., Pan, C., Malovanyy, A., Baresel, C., … & Cetecioglu,Z.(2023).Volatilefattyacidsproductionfrommunicipalwastestreamsanduseasa carbon source for denitrification: The journey towards full-scale application and revealing key microbial players. Renewable and Sustainable Energy Reviews, 175, 113163.
Xiao, K., Zhou, Y., Guo, C., Maspolim, Y., & Ng, W. J. (2016). Impact of undissociated volatile fatty acids on acidogenesis in a two-phase anaerobic system. *Journal of Environmental-Sciences*, *42*, 196–201

High-rateproductionofcarboxylicacidsfromcarbohydrate- rich wastewaters

R.Ganigué*,**[a],Q.Mariën*,**,B.Ulčar*,**,E.Hendriks*,B.Vanthuyne*,K.Rabaey*,**,J.M.Carvajal- Arroyo***; P. Candry****
*CenterforMicrobialEcologyandTechnology(CMET),GhentUniversity,CoupureLinks653,Gent,
Belgium
(E-mail:Ramon.Ganigue@UGent.be;Quinten.Marien@UGent.be;Barbara.Ulcar@UGent.be; Eline.Hendriks@UGent.be; Benjamin.Vanthuyne@UGent.be; Korneel.Rabaey@Ugent.be;)
**CenterforAdvancedProcessTechnologyforUrbanResourceRecovery(CAPTURE), FriedaSaeysstraat 1, Gent, Belgium
***Colsen,adviesburovoorMilieutechniek,Kreekzoom3,4561GX,Hulst, TheNetherlands (E-mail: j.carvajal@colsen.nl)
****CivilandEnvironmentalEngineering,UniversityofWashington,201MoreHall,Box352700,Seattle, WA 98195-2700, USA.
(E-mail:pcandry@uw.edu)

aPresentingauthor

Abstract

The conversion of organics in wastewater to added value chemicals, such as medium-chain carboxylic acids (MCCA) has gained increasing attention over the past years. This work investigates the impact of nutritional requirements and operational conditions on the performance of granular fermentations to produce MCCA. First, we show that MCCA selectivity remains unaffected within an influent concentration range of 11-44 gCOD·L^{-1}, and that this selectivity decreases at higher concentrations, likely due to product toxicity. Second, we show that a complex source in the feed is needed for successful MCCA production. Last, we investigate the impact of two critical operational parameters, pH and HRT. Results showed that a mildly-acidic pH (5-5.5) favourschainelongators,andtheseseemtobeinsensitivetochangesinHRTintherange0.25-1

d. This works paves the road to a wider application of granular fermentations for MCCA production from wastewater.

Keywords

Carboxylateplatform;chainelongation;medium-chaincarboxylicacids;wastefermentation

INTRODUCTION

To date, biogas production is the state of the art approach to valorise the carbon and energy present in waste(water). Yet, the small economic margins of biogas installations, coupled to the limited applications for biogas beyond energy production have driven the development of novel technologies for the recovery/valorisation of carbon from wastewater in the form of e.g. bioplastics, biochemicals, new protein sources, etc. (Kleerebezem et al. 2015).

The production of monocarboxylic acids (also known as volatile fatty acids, e.g. acetic acid, propionic acid, butyric acid, etc.) -either as final products or intermediates to a subsequent process (e.g. PHA production)- is central to the majority of these alternative routes (Alloul et al. 2018). Medium-chain carboxylic acids (MCCA) are monocarboxylic acids with a carbon length of 6-12 carbon atoms, and are considered platform chemicals with multitude of applications as feed additives, antimicrobial compounds and can be utilised in production of fragrances, rubbers, dyes and pharmaceuticals (Angenent et al. 2016). Their production from waste streams, including wastewater (Duber et al. 2018) and sludge (Han et al. 2019) has attracted increasing interest due to their higher market value and higher hydrophobicity, which makes their recovery easier and less costly (Carvajal-Arroyo et al. 2021). MCCA are produced via a microbial process called chain elongation, which uses e.g. ethanol, lactic acid, carbohydrates, etc. as an electron and carbon donor to elongate short chain carboxylic acids. As such, acetic acid is elongated to butyric acid that is in turn elongated to caproic acid (Angenent et al. 2016).

Despite their promise, microbial MCCA production is not yet at full scale. Most technological studies have struggled to achieve high production rates, and the few that did achieve high rates eitherusedsyntheticmedia,orusedmethodsthataredifficulttoscaleup(Carvajal-Arroyoetal.

2021). Recently, a novel approach has been developed that uses granular sludge to convert a sugar- richwasteandsidestreamsintocaproicacidinonereactorstep.Inthissystem,productionratesof

0.5 g caproic acid.L.h^{-1}were achieved, the highest reported production rate on an industrial stream without the addition of supplementary substrates such as ethanol, lactic acid or sugars (Carvajal- Arroyo et al. 2019).

In this contribution we explore the development of a fermentative granular technology for the production of MCCA from carbohydrate-rich wastewater and other industrial side-streams, with special focus on the impact of feedstock and operational conditions on the process performance.

MATERIALSANDMETHODS

Experiments were conducted in laboratory-scale expanded granular sludge bed (EGSB) reactors (1.5-2.5L) fed with various watery streams, namely: i) thin stillage; ii) synthetic wastewaters mimicking its composition; or iii) pre-fermented wastewater. Experiments investigated aspects related to the nutritional requirements of the chain elongation microbial community or the effect of target operational parameters (pH & hydraulic retention time (HRT)) on the MCCA productivityand selectivity.

RESULTS AND DISCUSSION

First, we investigated the impact of substrate concentration on product conversion and MCCA selectivity to assess whether or not this technology could be applied to wastewater containing lower or higher COD levels (Figure 1). Experiments were conducted in a fermentative granular system by either diluting thin stillage or supplying additional carbohydrates to it. Results showed that concentrations in the range of 11-44 gCOD·L^{-1}(25-100%) did not have a significant effect on product selectivity, withMCCA representing about 50% of the end products. Selectivity dropped as carbohydrate concentrations increased above 125%, in favour of butyric acid, likely due to MCCA product toxicity (Figure 1.B). We also observed that the higher the concentration, the lower the substrate conversion efficiency and hypothesize this observation was caused by enhanced toxicity due to increasing carboxylic acid concentrations.

Subsequently, we assessed the minimum nutritional requirements to achieve stable MCCA production (Figure 2). We step-wise replaced thin stillage by a mineral medium containing glucose as electron donor. We observed that upon reaching 100% synthetic feed, granules remained but caproic acid production had dropped from 3.5-5 g·$L^{-1}$to 0.3 g·L^{-1}. Caproic acid production wasonly recovered upon adding complex carbon and nitrogen sources such as tryptone to the medium.

Last, we assessed the impact of two key operation parameters, pH and HRT. We observed that pH governed the competition for lactic acid between propionic acid bacteria and chain elongators, with mildly acidic pH (around 5-5.5 favouring the latter) (Figure 3). We also observed it was possible to maintain high MCCA productivities (>10 g·L-1·d-1) throughout the HRT range 1-0.25 d.

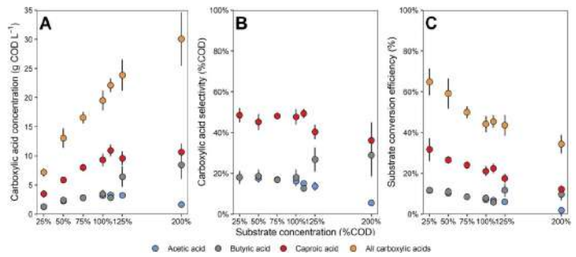

Figure 1. Panel A: Carboxylate concentration in function of substrate concentration. Panel B: Carboxylate selectivity, defined as the ratio of COD of a specific carboxylate to the COD of all produced carboxylates, in function of substrate concentration. Panel C: Substrate conversion efficiency in function of substrate concentration.

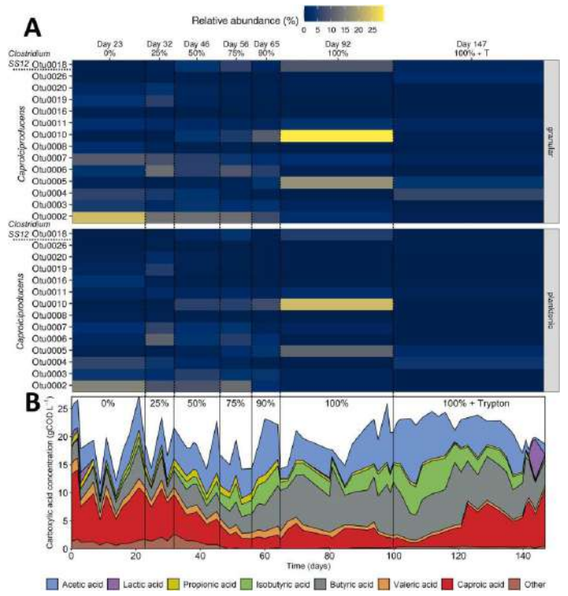

Figure 2. Theeffect ofnutrient composition on theproduction and microbial composition. Panel A: Heatmap of relative abundance in *Caproiciproducens* and *Clostridium sensu stricto 12* OTUs. Only OTUs with a relative abundance above 1% in either planktonic or granular phase are shown. Sampling days for the DNA are shown on top. Panel B: Evolution of the product profile. Shown percentages in bold indicate the volumetric fraction of the medium fed as synthetic medium while the complementary fraction was solids-free thin stillage.

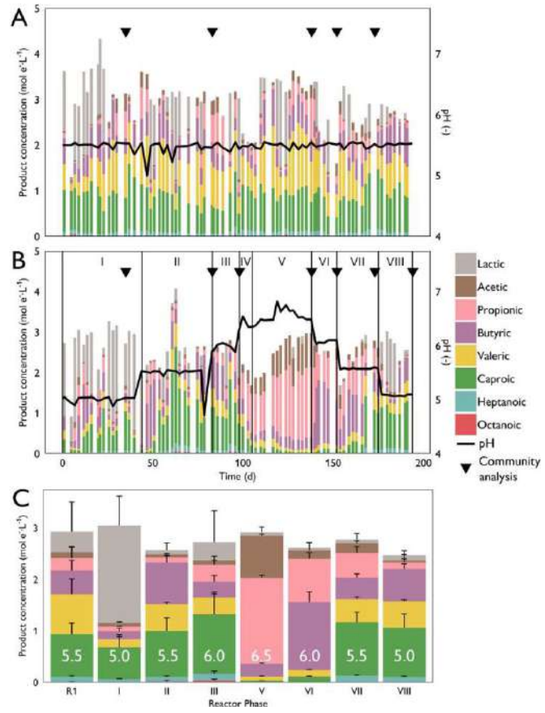

Figure 3. Product profile expressed for long-term reactors at fixed pH 5.5 (R1, Panel A) or varying pH (R2, Panel B) and average over steady state periods (Panel C). Each bar represents the additive product profile, expressed in mol e^-·L^{-1}. In Panel B, full lines indicate shifting of phases.

REFERENCES

Alloul, A., Ganigué, R., Spiller, M., Meerburg, F., Cagnetta, C., Rabaey, K., Vlaeminck, S. 2018. “Capture–Ferment–Upgrade: A Three-Step Approach for the Valorization of Sewage Organicsas Commodities.” Environmental Science & Technology 52 (12): 6729–42.

Angenent, L., Richter, H., Buckel, B., Spirito, C., Steinbusch, K., Plugge, K., Strik, D., Grootscholten, T., Buisman, C., Hamelers, H. 2016. “Chain Elongation with Reactor Microbiomes: Open-CultureBiotechnology to Produce Biochemicals.” Env. Sci. & Tech. 50 (6): 2796–2810.

Carvajal-Arroyo,J.,Candry,P.,Andersen,S., Props,R.,Seviour,T.,Ganigué, R.,Rabaey,K.2019. “Granular Fermentation Enables High Rate Caproic Acid Production from Solid-Free Thin Stillage.” Green Chemistry 21 (6): 1330–39.

Carvajal-Arroyo, J., Andersen, S., Ganigué, R., Rozendal, R., Angenent, L., Rabaey, K. 2021. “ProductionandExtractionofMediumChainCarboxylicAcidsat aSemi-PilotScale.”Chemical Engineering Journal 416 (July): 127886.

Duber,A.,Jaroszynski, L.,Zagrodnik,R.,Chwialkowska,J.,Juzwa,W., Ciesielski,S.,Oleskowicz- Popiel, P. 2018. “Exploiting theReal Wastewater Potential forResourceRecovery-: N -Caproate Production from Acid Whey.” Green Chemistry 20 (16): 3790–3803.

Han, W., He, P., Shao, L., Lü, F. 2019. “Road to Full Bioconversion of Biowaste to Biochemicals Centering on Chain Elongation: A Mini Review.” J. of Env. Sciences (China) 86: 50–64.

Kleerebezem, R., Joosse, B., Rozendal, R., Van Loosdrecht, M.. 2015. “Anaerobic Digestion without Biogas?” Reviews in Environmental Science and Biotechnology 14 (4): 787–801.

CO_2 bioelectrorecycling to butyric acid and its upgrade to butanol

M. Romans-Casas*, L. Feliu-Paradeda**, M. Tedesco***, H. V. M. Hamelers***, L Bañeras**, M.D. Balaguer*, S. Puig*, P. Dessi*

* LEQUiA, Institute of the Environment, University of Girona. Campus Montilivi, Carrer Maria Aurèlia Capmany 69, E-17003 Girona, Spain
(E-mail: *meritxell.romans@udg.edu, dolors.balaguer@udg.edu, sebastia.puig@udg.edu, paolo.dessi@udg.edu*)
** Molecular Microbial Ecology Group, Institute of Aquatic Ecology, University of Girona, Maria Aurèlia Capmany 40, 17003 Girona, Spain.
(E-mail: *laura.feliu@udg.edu, lluis.banyeras@udg.edu*)
*** Wetsus, European Centre of Excellence for Sustainable Water Technology, Oostergoweg 9, 8911, MA, Leeuwarden, The Netherlands
(E-mail: *michele.tedesco@wetsus.nl, bert.hamelers@wetsus.nl*)

Abstract

This study presents the bio-recycling of greenhouse gas carbon dioxide (CO_2) into organic valuable compounds. Low-gap electrically efficient electrolytic cells were operated in order to optimize selective butyric acid production. A selectivity of up to 78% and a production rate of 14.5 g/(m^2·d) were achieved at a remarkably low energy requirement of 34.6 kWh/kg. *Megasphaera* sp. was identified as the key chain elongating player. Besides, the reactor microbiome was capable to trigger butanol production ceasing CO_2 feeding (famine conditions), maintaining pH_2 > 1.5 and pH below 4.8

Keywords

Bioelectrochemistry; Carbon utilisation; Energy; *Megasphera* sp.; Selectivity; Ohmic resistance

INTRODUCTION

The development of carbon capture and utilization (CCU) approaches together with low power demanding processes is compulsory to achieve the sustainable development goal (SDG) 13 on climate change (Ioannou et al., 2023). Microbial electrosynthesis (MES) has emerged as a bio-recycling of carbon dioxide (CO_2) into platform chemicals and alcohols.

MES typically converts CO_2 into short-chain organic products such as acetic acid and ethanol (Blasco-Gomez et al., 2019) which can act as precursors to obtain higher-value products, such as butyric acid (Romans-Casas et al., 2021) which can be further upgraded to butanol, a medium-chain alcohol with large industrial applications (Pinto et al., 2021).

However, previous studies on MES, reported high cell voltages (up to 7 V) and power demand (64.3 kWh/kg of butyric acid) which, besides resulting in unsustainable operation costs, lead to a collateral effect on other SGDs such as population health and water scarcity (Ioannou et al., 2023; Romans-Casas et al., 2023; Jourdin et al., 2018). Thus, testing more efficient cell designs with low ohmic resistance was considered. This study aimed to selectively produce butyric acid from CO_2 through a low-gap electro-cell giving special attention to the conditions that trigger its further conversion to butanol.

MATERIALS AND METHODS

Two commercial MES cells (EC-1 and EC-2) with a total volume of 150 mL per chamber, were assembled and operated in galvanostatic mode. EC-1 was inoculated with a mixed culture dominated by *Clostridium* sp. (Romans-Casas, et al., 2023). CO_2 was periodically fed to the cathode chamber, and operated at different current densities (from 0.3 to 3.0 mA/cm^2). After 110 days of operation, EC-2 was started up using as inoculum the enriched microbial community developed in EC-1. Two tests interrupting the CO_2 supply were done during EC-2 operation to test the impact of hydrogen (H_2) accumulation.

The electrochemical cell characterization was performed through electrochemical impedance spectroscopy (EIS) and cyclic voltammetry (CV). Optical density (OD), pH and electrical conductivity were monitored over time, and samples were collected to determine carboxylic acids and alcohols concentration, gas composition and microbial community.

RESULTS AND DISCUSSION

Figure 1 presents the OD, pH and accumulated concentration of main products throughout the operation of cells (EC-1 and EC-2). During the first days, no products were detected in EC-1. When the current applied was increased 0.6 mA/cm^2 pH decreased, due to acetic acid formation, which was the only carboxylate produced for the first sixty days of operation. It showed a linear production rate up to 10.0 g/(m^2·d) between days 12-19 of operation (Table 1), reaching a concentration of 2.6 g/L at the cathode (Figure 1). Such production rate did not changed after increasing the applied current to 1.0 mA/cm^2. Ethanol was detected from day 30 onwards, probably due to the pH decrease and reached a maximum titer of 0.35 g/L. From day 60 onwards, ethanol and acetic acid concentrations dropped due to the activation of chain elongation reactions. butyric acid was produced with an average production rate of 14.5 g/(m^2·d), reaching a cathodic concentration of 3.6 g/L. Caproic acid was detected from day 70 onwards, obtaining a total amount of circa 0.5 g/L.

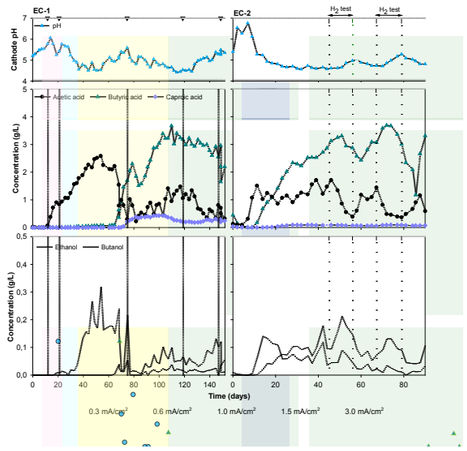

Figure 1. Cathode pH and product concentration in EC-1 and EC-2 along the experimental period under different applied current densities. Inverted triangles mark the changes of applied current.

EC-2 was operated from the beginning at a current density of 1.5 mA/cm^2. The inoculation with an enriched culture, as well as the higher current density, resulted in a lag phase 82% lower than EC-1 for butyric acid production. The production rate obtained for butyric acid was 14.2 g/(m^2·d), similar to the one of EC-1, confirming the replicability of the process. The product selectivity towards butyric acid was 78 % (Table 1), higher than in the few previous studies focusing on the butyric acid production from CO_2 (Ganigué et al., 2015, Raes et al., 2017). According to 16S rRNA metabarcoding analyses of the microbial community, *Megasphaera* sp. appeared as the most abundant genus. Members of this genus have been described as having the ability for chain-elongation (Wang and Yin, 2022).

Besides, the power required to produce the target compound was only 34.6 kWh/kg. This was due to the low ohmic resistance of the cell (15.7 mΩ·m^2) that can be further reduced by using zero-gap configurations (Baek et al., 2022)

Table 1. Average operational and performance parameters of the cells during periods of linear ($R^2 \geq 0.97$) production periods.

		EC-1			*EC-2*			
	Period (days)	12-19	21-54	65-79	7-11	14-28	18-28	46-51
	Main product	Acetate	Acetate	Butyrate	Acetate	Butyrate	Caproate	Butanol
Operation conditions	**Current applied (mA/cm²)**	0.6	1.0	1.0	1.5	1.5	1.5	1.5
	Cell voltage (V)	2.40	2.57	2.58	2.67	2.66	2.67	2.68
	Cathode potential (V *vs* SHE)	-0.55	-0.51	-0.50	-0.42	-0.47	-0.46	-0.40
	pH range	5.4 - 6.1	4.5 - 5.8	4.9 - 5.6	5.3 - 6.8	4.7 - 5.3	4.7 - 4.9	4.6 - 4.7
	pH_2(atm)	0.91	1.14	0.85	1.34	1.38	1.50	1.80
	OD (UA)	0.12	0.11	0.28	0.22	0.38	0.41	0.17
Performance parameters	**Production rate (g/(m²·d))**	10.0	5.5	14.5	27.3	14.2	0.8	2.2
	Production rate (mg/(L·d))	125.4	68.8	181.5	340.9	177.4	10.1	27.0
	Power requirement (kWh/kg)	34.4	111.1	34.6	34.5	65.4	1111.1	416.7
	CE (%)	25.5	7.2	45.3	27.6	24.6	1.7	5.6
	Selectivity (%)	95.8	59.2	74.2	82.6	77.6	4.6	27.9

After accumulating butyric acid in EC-2 catholyte, the CO_2 supply was interrupted (famine conditions) to maintain a high hydrogen partial pressure (pH_2 > 1.5 atm) at the cathode, which favours butanol production via solventogenesis. A butanol production rate of 2.2 g/(m^2·d) was obtained, with up to 28 % selectivity (Table 1). This confirmed that solventogenic pathways were favoured at low pH, low CO_2 concentration and high pH_2.

CONCLUSIONS

This study showed that alternating high pH_2 and pCO_2 promotes butyric acid production from CO_2 in MES cells. The microbial community dominated by *Megasphaera* sp. reached a remarkably high selectivity of 78%. The efficient cell design with low ohmic resistance contributed reducing the electric power requirement to 34.6 kWh/kg of butyric acid. This main compound can be upgraded to butanol by interrupting the CO_2 supply, keeping a high pH_2 and low pH.

AKNOWLEDGEMENTS

This research was carried out in the project "PANGEA – Process intensificAtioN for bioelectroCO2 recyclinG into carbon-nEutrAl products) funded by the Spanish Ministry of Innovation and Science (ref. PID2021-126240OB-I00). MR-C is grateful for the support of the Spanish Government (FPU20/01362). PD is supported by the European Union's Horizon 2020 research and innovation programme under the Marie Sklodowska-Curie grant agreement, project ATMESPHERE, No 101029266. LF-P is grateful for the Catalan Government grant (2021 FISDU 00132). S.P. is a Serra Hunter Fellow (UdG-AG-575) and acknowledges the funding from the ICREA Academia award. LEQUIA and EcoAqua have been recognized as "consolidated research groups" (Ref 2021 SGR01352 and 2021 SGR01142) by the Catalan Agency of Research and Universities.

BIBLIOGRAPHY

Baek, G., Rossi, R., Saikaly, P. E., and Logan, B. E. 2022 High-rate microbial electrosynthesis using a zero-gap flow cell and vapor-fed anode design. Water research, **219**, 118597..

Blasco-Gomez, R., Ramió-Pujol, S., Bañeras, L., Colprim, J., Balaguer, M. D., and Puig, S. 2019 Unravelling the factors that influence the bio-electrorecycling of carbon dioxide towards biofuels. Green Chemistry, **21**, 684–691.

Ganigué, R., Puig, S., Batlle-Vilanova, P., Balaguer, M. D., and Colprim, J. 2015 Microbial electrosynthesis of butyrate from carbon dioxide. Chemical Communications, **51**(15), 3235–3238.

Ioannou, I., Galán-Martín, Á., Pérez-Ramírez, J., and Guillén-Gosálbez, G. 2023 Trade-offs between Sustainable Development Goals in carbon capture and utilisation. Energy and Environmental Science, **16**.

Jourdin, L., Raes, S. M. T., Buisman, C. J. N., and Strik, D. P. B. T. B. 2018 Critical biofilm growth throughout unmodified carbon felts allows continuous bioelectrochemical chain elongation from CO2 up to caproate at high current density. Frontiers in Energy Research, **6**.

Pinto, T., Flores-Alsina, X., Gernaey, K. V., and Junicke, H. 2021 Alone or together? A review on pure and mixed microbial cultures for butanol production. Renewable and Sustainable Energy Reviews, **147**(October 2020), 111244.

Raes, S. M. T., Jourdin, L., Buisman, C. J. N., and Strik, D. P. B. T. B. 201) Continuous Long-Term Bioelectrochemical Chain Elongation to Butyrate. ChemElectroChem, **4**(2), 386–395.

Romans-Casas, M., Blasco-Gómez, R., Colprim, J., Balaguer, M. D., and Puig, S. 2021 Bio-electro CO2 recycling platform based on two separated steps. Journal of Environmental Chemical Engineering, **9**, 105909.

Romans-Casas, M., Perona-Vico, E., Dessì, P., Bañeras, L., Balaguer, M. D., and Puig, S. 2023 Boosting ethanol production rates from carbon dioxide in MES cells under optimal solventogenic conditions. Science of the Total Environment, **856**, 1–8.

Wang, J. and Yin, Y. 2022 Biological production of medium-chain carboxylates through chain elongation: An overview. Biotechnology Advances, **55**, 107882.

Innovative cell platforms to transform CO_2 into fine chemicals for the pharmaceutical industry

E. Huang-Lin[a,b], R. Lebrero[a,b], D.Z. Sousa[c] and S. Cantera[b,c]

[a] Department of Chemical Engineering and Environmental Technology, University of Valladolid, Dr. Mergelina s/n., Valladolid, 47011, Spain. (Email: raquel.lebrero@iq.uva.es; elisa.huang22@estudiantes.uva.es).
[b] Institute of Sustainable Processes, University of Valladolid, Dr. Mergelina s/n., Valladolid, 47011, Spain.
[c] Laboratory of Microbiology, Wageningen University and Research Center, the Netherlands. (Email: sara.canteraruizdepellon@wur.nl; diana.sousa@wur.nl).

Abstract

This study explores a novel biological conversion of CO_2 and H_2 into fine chemicals produced at high salinity, hydroxyectoine and ectoine, that have an important value for the production of pharmaceuticals and cosmetics. Microbial pathways to produce ectoine and hydroxyectoine were investigated in several genomes of halophilic microbes able to use CO_2 (carbon source) and H_2 (energy source) through a novel methodology called genomic mining. A total of 11 species containing these genes were identified and selected for lab tests. Firstly, the species were exposed to H_2/CO_2 to verify their capacity to produce ectoines from CO_2. Further laboratory analyses in bioreactors showed that the most promising bacteria for this bioconversion were *Hydrogenovibrio marinus*, *Rhodococcus opacus* and *Hydrogenibacillus schlegelii*. Overall, these results constituted the first proof of this novel valorisation of CO_2 into pharmaceutical products with high economic and social value.

Keywords: Bio-economy, circular economy, CO_2 abatement, GHG bioconversion, novel cell platforms, pharmaceuticals.

INTRODUCTION

The industrial sector is one of the main sources of anthropogenic CO_2 emissions. Concomitantly, several of these industrial processes generate and store on-site green or blue hydrogen (H_2) with the aim of using it as an alternative energy source. In these scenarios, CO_2 is a perfect feedstock for its *in situ* transformation into chemicals where H_2 can be used as the energetic power to promote this valorization (Nisar et al., 2021). This is possible using biological dark gas fermentation that is based on the biocatalytic action of chemolithotrophic microorganisms able to grow with CO_2 as the only carbon source and valorize this GHG emissions thought out the production of interesting chemicals (Anand et al., 2020). However, current CO_2 bioconversion processes are still not profitable due to the utilization of a small number of model microorganisms and the production of low-price compounds. Therefore, the development of new technologies, which expand microbial catalysts and the portfolio of valuable products synthesized from the abatement of CO_2 is of great interest. Attractive compounds, due to their high market value, include ectoine and hydroxyectoine (1000-1200 € Kg^{-1}), which are small organic molecules that protect the cells under extreme halophilic conditions. Their exceptional properties are already being translated into health-promoting and therapeutic activities. In fact, (hydroxy)ectoines are already being manufactured in the bio-industry using sugars and sold to important pharmaceutical companies (Becker and Wittmann, 2020). However, the potential for generating ectoines from renewable or waste-based carbon sources has remained largely unexplored. Thus, this research aims to identify novel microorganisms capable to produce (hydroxy)ectoines from CO_2 and H_2. To this aim, halophilic chemolithotrophs were first determined through genomic mining and then, the transformation of CO_2 into ectoines was tested in the laboratory for proof-of-concept validation.

MATERIALS AND METHODS

Selection of chemolithoautotrophic organisms able to produce (hydroxy)ectoines

Target genomic mining was used to search for key genes that encode for specific enzymes necessary to produce the target chemicals (considered diagnostic enzymes). To perform these searches, we downloaded all the representative genomes of halophilic chemolithotrophs, able to use H_2 as energy source, from the National Center for Biotechnology Information (NCBI) using Datasets v.10.0.0. Their genomes were screened for genes encoding for enzymes involved in (hydroxy)ectoines synthesis pathways, specifically: *ectA, ectB*, *ectC* and *ectD*, *ectR*, and two genes involved in the production of precursors (*ask* and *asd*). Alignments or profile Hidden-Markov Models for each gene were also retrieved from public databases and searched against the downloaded proteomes using Interproscan. From those analysis, 7 strains were selected for laboratory validation. They were purchased from DSMZ (Brunswick, Germany). Growth tests with H_2/CO_2 were performed in quintuplicate using 100 mL ammonium mineral salt medium (AMS) supplemented with 3% NaCl in 200 mL gas-tight bottles with 10 CO_2: 40 H_2: 50 air (% v/v) in the headspace. 5% of actively grown bacteria was used as inoculum. The experiments lasted until H_2 complete depletion. The biomass dry weight, (hydroxy)ectoines content and gas concentration were monitored for all the strains. The bacteria with the highest productivities was selected for optimization in 1 L gas tight bioreactors.

Analytical methods

CO_2 and H_2 consumption were measured with a gas chromatograph with a TCD detector (Interscience, The Netherlands). Ectoine and hydroxyectoine were extracted following the method of Cantera et al. (2022) and concentrations were measured with a Shimadzu Prominence-i LC-2030C plus HPLC with a UV detector at 210 nm and equipped with a Polaris, NH2, 180Å, 3 µm, 4,6 x 150 mm. For biomass determination, optical absorbance at 600 nm (OD600) was measured using a UV/Vis spectrophotometer. Dry biomass concentration was measured as total suspended solids according to Standard Methods.

RESULTS AND DISCUSSION

Selection of potential chemolithoautotrophic ectoine-producing microorganisms

The genomic mining showed that eleven halophilic chemolithotrophs able to grow with CO_2 as sole carbon source and H_2 as the energy source had the genes to codify the enzymes for ectoine synthesis and six for hydroxyectoine synthesis (Figure 1). Among these, the following aerobic strains were tested for laboratory validation with CO_2 and H_2: *Alkalilimnicola (A.) ehrlichii, Hydrogenovibrio (H.) marinus, Hydrogenibacillus (H.) schlegelii, Pseudonocardia (P.) autotrophica, P. carboxydivorans, P. dioxanivorans, Rhodococcus (R.) opacus*.

Experimental screening for ectoine and hydroxyectoine producers

In our study, we detected chemolithotrophic growth (CO_2/H_2) of *P. autotrophica* and *P. dioxanivoran*s while *P. carboxydivorans* did not grow with these substrates. *P. dioxanivorans* accumulated the highest amounts of hydroxyectoine (41.4 ± 9.1 mg hydroxyectoine g $biomass^{-1}$) of all the tested strains, at the salinity range tested. However, the doubling times obtained for *Pseudonocardia* species in liquid phase were very long, thus process productivities would be low. *A. ehrlichii* did not show activity or growth on CO_2/H_2, despite viability when grown in rich medium. *H. schlegelii, H. marinus,* and *R. opacus* were able to use CO_2 with H_2 with doubling times inferior to 24 hours. The highest ectoine content at 3% NaCl was obtained with *H. marinus*. *R. opacus* and *H. schlegelii* accumulated hydroxyectoine in addition to ectoine. Thus, according to their fast growth and their high ectoines accumulation, these three species were selected for further optimization.

Continuous transformation of CO_2 into ectoines

The implementation of the selected strains in 1 L batch bioreactors was used to determine the optimal production and growth conditions. *H. marinus* accumulated the highest amount of ectoine among the three tested strains at 6% NaCl (79.6 ± 10.5 mg ectoine g $biomass^{-1}$) and had the fastest growth at 6% NaCl with the shortest lag phase. Hydroxyectoine was not detected, which was expected since *H. marinus* lacks the *ectD* gene. Interestingly, ectoine content was similar for *R. opacus* and *H. schlegelii* at all the salinities tested, but hydroxyectoine increased at higher salinities. *R. opacus* accumulated maximum hydroxyectoine values at 7% NaCl (52.1 ± 4.3 mg hydroxyectoine g $biomass^{-1}$) while *H. schlegelii* reached hydroxyectoine contents of 62.0 ± 7.9 mg of hydroxyectoine g $biomass^{-1}$ at 5% NaCl (Figure 2). These hydroxyectoine values are in the range of the hydroxyectoine yields obtained with rich carbon sources, such as glucose.

Our results demonstrate for the first time the feasibility of producing ectoine with CO_2 using relatively low salt concentrations. Additionally, we were able to produce hydroxyectoine using as an isolate osmolyte, which has higher economic value than ectoine and is rarely synthesized separately. Overall, this research set, by means of the use of an innovative genomic technique and laboratory validation, the possibility to find novel microorganisms able to transform CO_2 into fine chemicals with important value for the economy and society. This will impulse the future implementation of CO_2 biotransformation platforms capable of creating value out of CO_2 mitigation.

Figure 1:

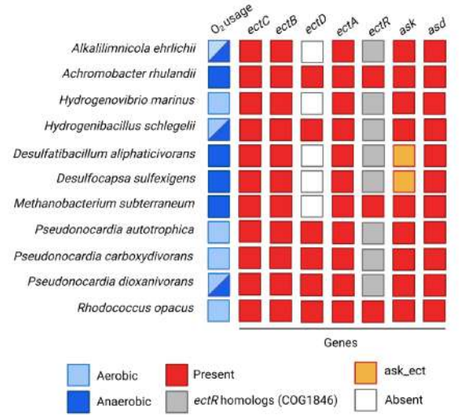

Figure 1. Presence/absence of ectoine and hydroxyectoine genes in halophilic chemolithotrophs that use H_2 as energy source. *ectC*, ectoine synthase (EctC); *ectB*, DABA aminotransferase (EctB); *ectD*, ectoine hydroxylase (EctD); *ectA*, diaminobutyric acid (DABA) acetyltransferase (EctA); *ectR*, MarR-type regulator; *ask*, aspartate kinase (Ask); *ask_ect*, a specialized aspartate kinase (Ask); *asd*, l-aspartate-semialdehyde-dehydrogenase (Asd).

Table 1. Average values (n=5) of the parameters measured for each of the strains growing at 3% NaCl during proof of concept validation

Strain	**Doubling Time** (hours)	**CO_2 removal** ($g_{CO2(g)}$ □ $g_{(i)}^{-1}$)	**Ectoine content** (mg_{Ect} □ g^{-1})	**Hydroxyectoine content** (mg_{HEct} □ g^{-1})
H. schlegelii	25.7 ± 1.0	1.1 ± 0.2	4.1 ± 1.9	18.6 ± 5.6
H. marinus	7.9 ± 0.9	2.3 ± 0.2	26.7 ± 3.1	No detected
P. autotrophica	242.0[a]	0.6 ± 0.1	7.3 ± 5.8	13.4 ± 0.3
P. dioxanivorans	81.3[a]	0.7± 0.1	No detected	41.4 ± 9.1
R. opacus	15.9 ± 3.6	1.1± 0.4	17.8 ± 1.3	5.0± 2.1

[a] The biomass of the replicates was measured filtering the total volume of a bottle at each time point.

Figure 2:

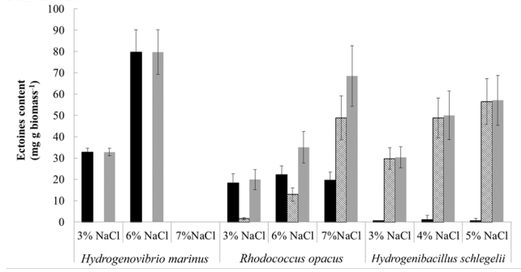

Figure 2. Average ectoine and hydroxyectoine content at different salinities (% NaCl). Black column, ectoine; dashed column, hydroxyectoine, and grey column, total ectoines.

REFERENCES

Anand A., Raghuvanshi S., Gupta S. 2020 Trends in carbon dioxide (CO_2) fixation by microbial cultivations. *Current Sustainable/ Renewable Energy Reports* **7**, 40-47.

Becker J., Wittmann C. 2020 Microbial production of extremolytes—high-value active ingredients for nutrition, health care, and well-being. *Current Opinion in Biotechnology* **65**, 118–128.

Cantera S., Sánchez-Andrea I., Lebrero R., García-Encina P. A., Stams A. J., Muñoz R. 2018 Multi-production of high added market value metabolites from diluted methane emissions via methanotrophic extremophiles. *Bioresource Technology* **267**, 401–407.

Nisar A., Khan S., Hameed M., Nisar A., Ahmad H. and Mehmood S. A. 2021 Bio-conversion of CO_2 into biofuels and other value-added chemicals via metabolic engineering. *Microbiological Research* **251**, 126813.

Recovery of Cu and Zn from anaerobic leachates via *S. pasteurii* induced carbonate precipitation: influence of pH and volatile fatty acids on metals precipitation

A.M.F. Soto*. ***, E.D. van Hullebusch**, C.M.R. Almeida***, F.G. Fermoso*
* Bioprocesses for the Circular Economy, Instituto de la Grasa/Spanish National Research Council (CSIC), University Campus Pablo de Olavide, Building 46, Carretera Utrera, km 1, Seville, Spain
(E-mail: *ailen.soto@ig.csic.es ; fgfermoso@ig.csic.es)*
** Université Paris Cité, Institut de physique du globe de Paris, CNRS, F-75005, Paris, France
(E-mail: *vanhullebusch@ipgp.fr*)
*** Chemistry and Biochemistry Department, Faculty of Sciences of University of Porto and EcoBioTec group, Interdisciplinary Centre of Marine and Environmental Research (CIIMAR), Rua do Campo Alegre, s/n, Porto, Portugal
(E-mail: *calmeida@ciimar.up.pt*)

Abstract

This study explores the feasibility of applying MICP mediated by laboratory cultured *S. pasteurii* to precipitate copper (Cu) and zinc (Zn) from aqueous solutions with similar composition than anaerobic leachates. Solutions containing *S. pasteurii*, urea (20 g L^{-1}), volatile fatty acids (VFAs) (3 g O_2 L^{-1}) and varying concentrations of Cu and Zn (0, 0.5, 1, 5, 10 and 25 mg L^{-1}) at initial pH values adjusted to 5, 6 and 7, were incubated during seven days at 30 °C under aerobic conditions. Results showed that urea degradation led to an increase in NH_4^+ concentration and pH, despite the absence of bacterial growth, indicating urease activity. In the presence of biomass, Cu precipitation yields were higher than 50% for all concentrations tested although significantly lower urea hydrolysis yields were observed at pH=5 and 6, showing that urease activity may not be the only factor explaining Cu precipitation. Zn precipitation yields showed a clear decreasing trend at higher concentrations (i.e. from 100 % to 25 %) indicating a possible toxic effect on *S. pasteurii* activity. Furthermore, precipitation yields of Cu and Zn were lower in the presence of VFAs in all the conditions tested. These results aim to contribute with basic knowledge for next generation waste treatment facilities driven by bioprocesses focused on resource recovery applying technologies that mimic natural biogeochemical cycles

Keywords: Microbial induced carbonate precipitation; metals recovery; Sporosarcina pasteurii; volatile fatty acids; wastewater treatment

INTRODUCTION

There is a growing pressure on finding new sources for metals extraction to overcome a possible shortage of mineral resources in the near future. In this context, the application of biotechnologies for metals recovery can play a major role contributing to the ongoing transition to a circular economy. Among the different biotechnologies currently available for waste treatment and resource recovery, the integration of anaerobic digestion (AD) and microbial induced carbonate precipitation (MICP) pose many advantages.

AD is a well stablished technology commonly used for waste stabilization and biogas generation which can increase its resource exploitation capacity by promoting the formation of volatile fatty acids (VFAs) during anaerobic fermentation to leach metals from organic waste (Molaey et al., 2021)and limited information is available on migration and transformation behavior of potentially toxic metals during anaerobic digestion (AD. On the other hand, ureolysis driven MICP showed to be a novel sustainable alternative to remove metal ions from aqueous solutions via direct precipitation as metal carbonates (Kim et al., 2021; Qiao et al., 2021)four isolates which had the greatest urease production, calcite precipitation, and endurance to the heavy metals were obtained from contaminated areas during the screening steps. These isolates along with Sporosarcina pasteurii were used to bioprecipitate zinc (Zn. Among the extensive variety of microorganisms that hydrolyses urea, the non-pathogenic soil organism *Sporosarcina pasteurii* is widely considered for MICP applications since it has the potential to produce large quantities of active intracellular urease which leads to high yields of carbonate ions within a short time (Stocks-Fischer et al., 1999). The new approach proposed in this study is based on the integration of anaerobic fermentation and carbonate precipitation induced by *S. pasteurii* for metals bioleaching and recovery. To the best of our knowledge the effect of VFAs on MICP has not been studied yet. Therefore, the main objective of this study was to investigate the extent to which *S. pasteurii* can remove Cu and Zn from liquid solutions in the presence of acetate and propionate at acid to neutral pH values (i.e. similar conditions present in liquid anaerobic leachates).

MATERIALS AND METHODS

S. pasteurii culture and growth

S. pasteurii (DSM 33) cultured in an autoclaved growth medium which consisted of brain heart infusion (BHI) (37 g L^{-1}) and urea (20 g L^{-1}). The bacterial suspension was kept at room temperature until use for bacterial growth assays. 1 mL of this suspension was inoculated in a 500 mL liquid growth medium containing yeast extract (15 g L^{-1}) and urea (20 g L^{-1}) at pH=7.5 in a 1L Erlenmeyer. Incubation for growth assays was performed under aerobic conditions at 30 °C for three days before each bio-precipitation assay.

Bio-precipitation assays

After S. pasteurii growth, the complex medium was removed from the bacterial suspension to avoid any bias with metals precipitation. Bio-precipitation assays were performed in 50 mL Falcon tubes with a concentration of biomass of OD_{600} = 0.6 and 20 g L^{-1} of urea as suggested by Duarte-Nass et al (2020)the application of copper precipitation through microbe-induced carbonate precipitation (MICP to ensure maximum urease activity. All Falcon tubes contained varying concentrations of Cu and Zn (i.e. 0.5, 1, 5, 10 and 25 mg L^{-1}), at different initial pH values (i.e. 5, 6 and 7). To study the effect of VFAs on MICP, some samples were spiked with 3 g O_2 L^{-1} of acetic and propionic acid. Samples and controls, tested in triplicates, were **incubated during seven days under aerobic conditions at 30 °C in an incubator shaker at 180 rpm. samples were then centrifuged and filtered for determination of ammonia nitrogen (N-NH_3) and dissolved metals concentration in the supernatant. pH was measured immediately after centrifugation. The concentration of Cu and Zn in solution was analyzed by ICP-OES and the precipitation percentage was calculated from the original concentration of metals in the stock solutions. pH and N-NH_3 concentration were measured as indicators of urease activity. N-NH_3 in samples with S. pasteurii was determined colorimetrically by direct Nesslerization following the Standard test method for ammonia nitrogen in water. The percentage of urea hydrolysis was calculated based on the ammonium (NH_4^+) concentration derived from Nesslerization. Statistical analyses were carried out using one-way analysis of variance (ANOVA) to assess the significance of the results with a confidence level of 95%.**

RESULTS AND DISCUSSION

Urease activity

Final pH values were similar in all the conditions tested, varying between 7.0-9.2 in all the samples where *S. pasteurii* was inoculated except when the initial pH was adjusted to 5 and VFAs were spiked (Figure 1 (a)). These pH values fall into the optimum pH range for urease activity (Stocks-Fischer et al., 1999). A higher pH increase was observed at lower initial metals concentration indicating that urease activity might be affected by metals concentration in solution. A same decreasing trend in the final pH values at higher metals concentration was observed by (Mugwar and Harbottle, 2016)metal toxicity and availability limit the activity and remedial potential of bacteria. We report the ability of a bacterium, Sporosarcina pasteurii, to remove metals in aerobic aqueous systems through carbonate formation. Its ability to survive and grow in increasingly concentrated aqueous solutions of zinc, cadmium, lead and copper is explored, with and without a metal precipitation mechanism. In the presence of metal ions alone, bacterial growth was inhibited at a range of concentrations depending on the metal. Microbial activity in a urea-amended medium caused carbonate ion generation and pH elevation, providing conditions suitable for calcium carbonate bioprecipitation, and consequent removal of metal ions. Elevation of pH and calcium precipitation are shown to be strongly linked to removal of zinc and cadmium, but only partially linked to removal of lead and copper. The dependence of these effects on interactions between the respective metal and precipitated calcium carbonate are discussed. Finally, it is shown that the bacterium operates at higher metal concentrations in the presence of the urea-amended medium, suggesting that the metal removal mechanism offers a defence against metal toxicity.","author":[{"dropping-particle":"","family":"Mugwar","given":"Ahmed J.","non-dropping-particle":"","parse-names":false,"suffix":""},{"dropping-particle":"","family":"Harbottle","given":"Michael J.","non-dropping-particle":"","parse-names":false,"suffix":""}],"container-title":"Journal of Hazardous Materials","id":"ITEM-1","issued":{"date-parts":[["2016"]]},"page":"237-248","publisher":"Elsevier B.V.","title":"Toxicity effects on metal sequestration by microbially-induced carbonate precipitation","type":"article-journal","volume":"314"},"uris":["http://www.mendeley.com/documents/?uuid=7ca9b160-7bd6-4c98-97dd-4772cf809d4a"]}],"mendeley":{"formattedCitation":"(Mugwar and Harbottle, 2016 after seven days of incubation. Samples initially incubated at pH=5 and 6 also stabilized at pH≈7 indicating successful ureolysis driving production of alkalinity, thus implying encouraging results for the application of MICP to recover metals from acid effluents. Similar results were found by Proudfoot et al (2022) in mine waste with an average initial pH=4.4. Figure 1 (b) shows urea hydrolysis percentage of samples and controls after seven days of incubation. By the end of the experiment, ureolysis was observed in all the samples where *S. pasteurii* was inoculated, however, the maximum urea hydrolysis was only found in samples where the initial pH was adjusted to 7. Less than 4% of urea hydrolysis was observed in samples incubated at pH=5 and 6 at the highest metals concentration tested (i.e. 5, 10 and 25 mg L^{-1}) **suggesting a correlation between urease activity and metal tolerance, in agreement with several studies (Kang et al., 2016; Mugwar and Harbottle, 2016; Qiao et al., 2021)the efficiency of Microbially Carbonate Induced Precipitation (MICP.**

Metals precipitation

The precipitation yield of Cu was higher than 50% in all the conditions tested, except for samples spiked with VFAs (Figure 2 (a)). These results correlates well with pH final values found in samples after the incubation period, showing a high dependence of Cu precipitation on the pH of the solution as it was also observed by Duarte-Nass et al (2020)the application of copper precipitation through microbe-induced carbonate precipitation (MICP. In the presence of VFAs, Cu precipitation was significantly lower at the same initial pH, indicating that Cu-VFAs soluble complexes might be formed (Panina et al., 2002). Samples not spiked with VFAs showed significantly higher Zn precipitation yields at lower initial concentrations i.e. 0.5, 1 and 5 mg L^{-1}**, despite the set pH at the beginning of the bio-precipitation assays** (Figure 2 (b)). These results are in line with findings reported by Kim et al. (2021) and Mugwar and Harbottle (2016)metal toxicity and availability limit the activity and remedial potential of bacteria. We report the ability of a bacterium, Sporosarcina pasteurii, to remove metals in aerobic aqueous systems through carbonate formation. Its ability to survive and grow in increasingly concentrated aqueous solutions of zinc, cadmium, lead and copper is explored, with and without a metal precipitation mechanism. In the presence of metal ions alone, bacterial growth was inhibited at a range of concentrations depending on the metal. Microbial activity in a urea-amended medium caused carbonate ion generation and pH elevation, providing conditions suitable for calcium carbonate bioprecipitation, and consequent removal of metal ions. Elevation of pH and calcium precipitation are shown to be strongly linked to removal of zinc and cadmium, but only partially linked to removal of lead and copper. The dependence of these effects on interactions between the respective metal and precipitated calcium carbonate are discussed. Finally, it is shown that the bacterium operates at higher metal concentrations in the presence of the urea-amended medium, suggesting that the metal removal mechanism offers a defence against metal toxicity.","author":[{"dropping-particle":"","family":"Mugwar","given":"Ahmed J.","non-dropping-particle":"","parse-names":false,"suffix":""},{"dropping-particle":"","family":"Harbottle","given":"Michael J.","non-dropping-particle":"","parse-names":false,"suffix":""}],"container-title":"Journal of Hazardous Materials","id":"ITEM-1","issued":{"date-parts":[["2016"]]},"page":"237-248","publisher":"Elsevier B.V.","title":"Toxicity effects on metal sequestration by microbially-induced carbonate precipitation","type":"article-journal","volume":"314"},"uris":["http://www.mendeley.com/documents/?uuid=7ca9b160-7bd6-4c98-97dd-4772cf809d4a"]}],"mendeley":{"formattedCitation":"(Mugwar and Harbottle, 2016 although *S. pasteurii* in this study showed better tolerance to higher concentrations of Zn, even at low initial pH values. The presence of VFAs in samples significantly decreased Zn precipitation yields at all concentrations and pH values tested, as it was also observed in Figure 2 (a). Figure 2 (a) and (b) shows that at pH=7, controls of samples not spiked with VFAs exhibited higher precipitation yields than samples where *S. pasteurii* was inoculated, revealing that metals removal under these conditions might be based on chemical equilibria rather than a microbially-driven mechanism.

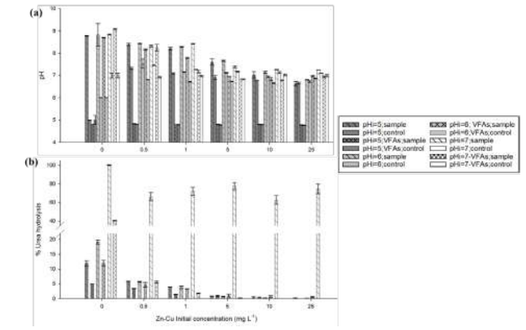

Figure 1. **(a)** pH and **(b)** urea hydrolysis yield after 7 days of incubation at a range of pH and metal concentrations with and without VFAs. Missing data were below the limit of detection

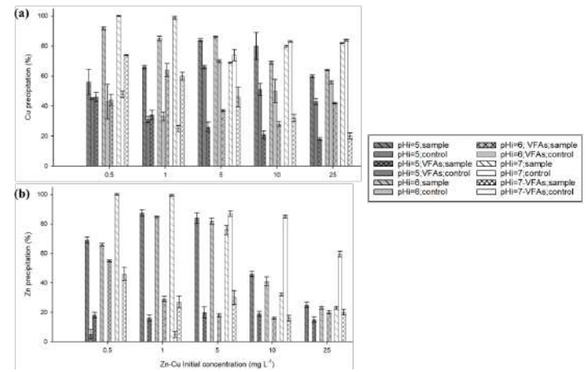

Figure 2. Precipitation yield of **(a)** Cu and **(b)** Zn after 7 days of incubation at a range of pH and metal concentrations with and without VFAs. Missing data were below the limit of detection

REFERENCES

Duarte-Nass, C., Rebolledo, K., Valenzuela, T., Kopp, M., Jeison, D., Rivas, M., Azócar, L., Torres-Aravena, Á., Ciudad, G., 2020. Application of microbe-induced carbonate precipitation for copper removal from copper-enriched waters: Challenges to future industrial application. *Journal of Environmental Management* **256**.

Kang, C., Shin, Y., Anbu, P., Nam, I., So, J., 2016. Biosequestration of copper by bacteria isolated from an abandoned mine by using microbially induced calcite precipitation. *The Journal of general and applied microbiology*, **62**(4) 206–212.

Kim, Y., Kwon, S., Roh, Y., 2021. Effect of Divalent Cations (Cu, Zn, Pb, Cd, and Sr) on Microbially Induced Calcium Carbonate Precipitation and Mineralogical Properties. *Frontiers in Microbiology* **12**, 1–12.

Molaey, R., Yesil, H., Calli, B., Tugtas, A.E., 2021. Influence of volatile fatty acids in anaerobic bioleaching of potentially toxic metals. *Journal of Environmental Management* **285**, 112118.

Mugwar, A.J., Harbottle, M.J., 2016. Toxicity effects on metal sequestration by microbially-induced carbonate precipitation. *Journal of Hazardous Materials* **314**, 237-248.

Panina, N.S., Belyaev, A.N., Simanova, S.A., 2002. Carboxylic acids and their anions. Acid and ligand properties. *Russian journal of general chemistry* **72**, 91-94.

Proudfoot, D., Brooks, L., Gammons, C.H., Barth, E., Bless, D., Nagisetty, R.M., Lauchnor, E.G., 2022. Investigating the potential for microbially induced carbonate precipitation to treat mine waste. *Journal of Hazardous Materials* **424**, 12749.

Qiao, S., Zeng, G., Wang, X., Dai, C., Sheng, M., Chen, Q., Xu, F., Xu, H., 2021. Multiple heavy metals immobilization based on microbially induced carbonate precipitation by ureolytic bacteria and the precipitation patterns exploration. *Chemosphere* **274**, 129661.

Stocks-Fischer, S., Galinat, J.K., Bang, S.S., 1999. Microbiological precipitation of CaCO3. *Soil Biology and Biochemistry* **31**(11), 1563-1571.

Inhibition limits by undissociated acids in mixed culture fermentation and strategies to increase process capacity

Tomás Allegue[1,2], Ramis Rafay[1,2], Sanjana Chandran[1,2], and Jorge Rodríguez[1,2].
(1) Department of Chemical Engineering, Khalifa University, P.O. Box 127788, Abu Dhabi, UAE
(2) Research and Innovation Center on CO_2 and H_2 (RICH), Khalifa University, Abu Dhabi, UAE
(*tomas.martinez@ku.ac.ae*, *ramis_rafay@sfu.ca*, *sanjana.chandran@ku.ac.ae*, *jorge.rodriguez@ku.ac.ae*)

Abstract

High carbohydrate concentrations in mixed culture fermentation (MCF) result in higher products concentration, making the subsequent extraction process more cost-effective. However, this might also result in inhibition by undissociated acids (HA). A concentration threshold of HA inhibiting MCF is determined in this study. A lab-scale fermenter was continuously operated at constant experimental conditions and increasing influent glucose concentrations. The glucose conversion was found to be inhibited repeatedly with concentrations of undissociated acids above 24.9 mM, equivalent to 18.5 g COD L_{Feed}^{-1}. This limit concentration of undissociated acids appears to inhibit carbohydrate conversion. By raising pH to reduce the HA concentration, the inhibition was quickly reversed, and up to 34 g COD L_{Feed}^{-1} of glucose was fully consumed. Using granular biomass also allowed extending carbohydrate conversion above 18.5 g COD L_{Feed}^{-1}.

Keywords

Inhibition; Organic acids; Resource recovery; Short-chain carboxylic acids; Substrate concentration; Undissociated acids.

INTRODUCTION

The application of mixed culture fermentation (MCF) represents an appealing resource recovery strategy to produce valuable chemicals from biowaste (e.g., food waste and industrial wastewater). In MCF, organic substrates are converted into a mixture of CO_2, H_2, solvents, and organic acids. The organic acid produced can be used in several downstream industrial processes: for biological nitrogen removal in sewage treatment; as a substrate for chain elongation processes; for biofuel production; to synthesize biodegradable polymers; and for applications in the pharmaceutical, food, textile and plastics industries The potential for sustainable and economically feasible production and recovery is currently limited at an industrial scale by the inhibition by products accumulation, amongst other challenges.

The suspected mechanism for inhibition by organic acids seems to be linked to the dissociation state. Undissociated acids can freely permeate the cell membrane and dissociate intracellularly at the higher cytosolic pH, which is maintained close to neutral. The uptake of protons lowers the cytosolic pH, increasing the maintenance energy required by the cell to create the transmembrane proton gradient to generate ATP (Booth 1985).

Most studies examining acidic product inhibition in MCF systems were conducted in batch assays, but there is still a lack of understanding about systems operated in continuous mode. In a previous study, we explored the limits and inhibition mechanisms of an MCF operated continuously (Rafay et al. 2022). The maximum concentration of undissociated acids compatible with full glucose conversion was 52 mM, at 38 g COD L_{Feed}^{-1}. However, this high substrate concentration was attained in presence of granules, which might provide protective internal microenvironments such that normal metabolic activities can be sustained even in bulk environments with high acidity. In the present study, the limits of carbohydrate conversion in a continuous MCF system were also explored, but in this case with the presence of only suspended biomass.

MATERIALS AND METHODS

A continuously stirred tank reactor (CSTR)s (Fermac 360, Electrolab), with a working and a headspace volume of 1.5 and 0.5 L, respectively (Figure 1), was operated in continuous mode. Operating parameters such as temperature (30°C), pH (5.4), and HRT (20 h) were kept constant throughout the operating period. pH was monitored and controlled. Glucose was used as the sole carbon source. To identify the limits of fermentation capacity, the feed glucose concentration was increased stepwise (3.8-33.8 g COD L_{Feed}^{-1}) until inhibition by undissociated acids was detected.

RESULTS AND DISCUSSION

The MCF was operated for 310 days with an influent flow rate of 1.81 ± 0.09 L^{-1} d^{-1} corresponding to an HRT of 20.0 ± 1.1 h. The COD balance errors were lower than 6.5 % in all the periods (Figure 2), but in Period XIII (10.3 %), indicating that the main fermentation products were successfully accounted for. Glucose was completely consumed at feed concentrations between 4 and 24 g COD L^{-1} (Figure 3), but with the presence of granular biomass inside the MCF (Periods I-V). In our previous study, using the same reactor configuration and experimental conditions, the accumulation of granular biomass was also observed inside the fermenter at high glucose feed concentrations (Rafay et al. 2022). The limit in the glucose fermentation capacity was found at 33 g COD L_{Feed}^{-1}, with 32 mM of undissociated acids. However, the development of granular biomass led to a significant increase in the fermentation capacity, and full glucose conversions were achieved even at undissociated acids concentrations up to 52 mM, with 38 g COD L_{Feed}^{-1}. Granular biomass is known to be less sensitive to environmental conditions compared to suspended biomass.

In the present study, to avoid granules accumulation, the effluent line was placed at the bottom of the reactor as shown in Figure 1. The vertically positioned effluent tube connected to the effluent pump was previously acting as an in-situ settler. After replacing the effluent line (day 76), a quick granules washout and a high reduction in the glucose conversion capacity were observed. From this moment onwards, granules accumulation was not detected anymore. Along with the washout, lactate started to accumulate in the fermenter, which might be considered a sign of saturation. Due to the lower conversions without granules, the glucose concentration had to be reduced from 24 to 4 g COD L_{Feed}^{-1} (day 100), and once the reactor stabilized, the feed concentration was raised first to 9 and then to 17 g COD L_{Feed}^{-1}, without observing glucose accumulation.

The activity of the suspended biomass was highly inhibited at 23 g COD L_{Feed}^{-1}. Unlike between days 21 and 76, with the same feed glucose concentration, granules were not available to protect the microbes from the high undissociated acids concentration, 29.1 mM (Figure 2). This suggests that the concentration of the acids inhibiting glucose conversion should be found between 17 and 23 g COD L_{Feed}^{-1}. To provide a more accurate inhibition value, the glucose concentration in the feed was raised again but in smaller increments. Glucose accumulated at 21 g COD L_{Feed}^{-1} (Period XII), but this inhibition was quickly reversed by increasing the pH from 5.4 to 6, as higher pH reduces undissociated acids concentration.

At pH 6, up to 33.8 g COD L_{Feed}^{-1} were fully fermented. Further concentration values were not evaluated. Overall, the results achieved strongly suggest that concentrations of undissociated acids above 24.9 mM must be avoided to prevent from possible inhibition events in mixed culture systems with only suspended biomass. Prolonged lactate accumulation could be used as a sign that carbohydrate fermentation is close to saturation, useful for possible full-scale applications. To extend carbohydrate conversion to higher substrate concentrations the formation of granular biomass and the impact of pH control on the accumulation of undissociated acids are determining factors to achieve full carbohydrate conversions in MCF at high acidic conditions.

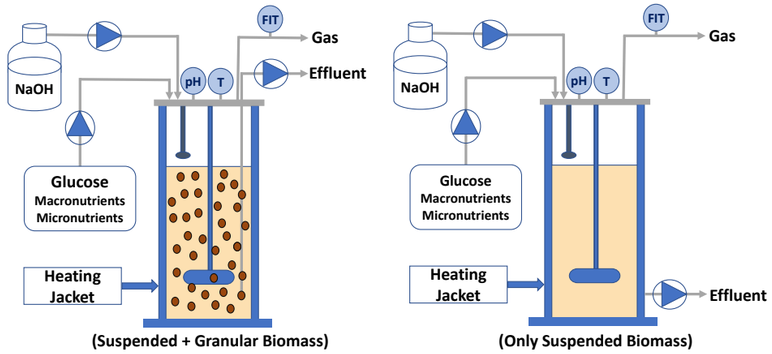

Figure 1. Schematic diagram of the open mixed-culture fermenter (MCF) (1.5 L) operated in continuous mode. Between days 0 and 76, the effluent was collected using a vertical pipeline (*left*), which enabled the accumulation of granular biomass. To promote the granular biomass washout, and keep only suspended biomass, the effluent's line location was shifted and placed at the bottom of the reactor (*right*).

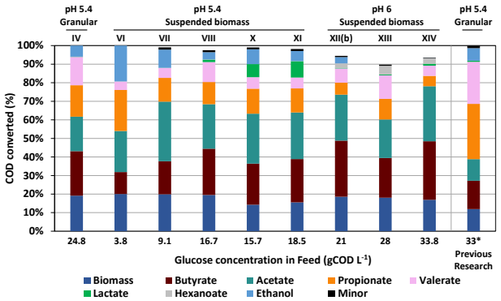

Figure 2. Representative product spectra (%CODproduct/CODglucose consumed), of the different operating periods for the mixed-culture fermenter. Only periods in which steady-state conditions were achieved are represented. The star (*) indicates the results achieved in previous research carried out by Rafay et al. (2022) in which the same reactor setup and operating conditions were used.

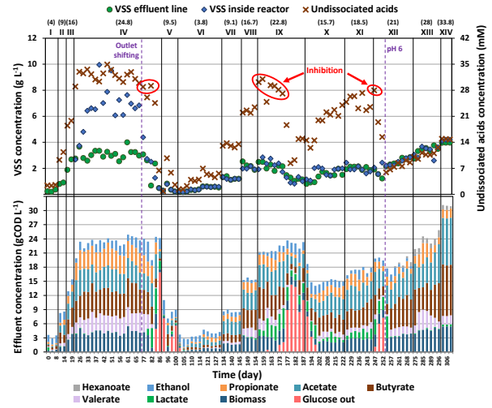

Figure 3. Evolution of the volatile suspended solids (VSS) concentration inside and in the effluent of the mixed culture fermenter (primary axis), and the concentration of the undissociated acid throughout the study (secondary axis) (*top*); and effluent's products concentration (*bottom*). The black vertical lines separate the different periods regarding the COD concentration in the feed. The feed glucose concentration value (gCOD L_{Feed}^{-1}) is indicated at the top part of the graph between (). The pH was increased from 5.4 to 6, from day 145 until the end of the study.

ACKNOWLEDGEMENTS

This study is based upon work supported by Khalifa University's award no. CIRA-2018-84 and the Research and Innovation Center on CO_2 and H_2 (RICH) (RC2-2019-007).

REFERENCES

Booth, I. R. (1985) Regulation of cytoplasmic pH in bacteria. *Microbiological Reviews*, **49**(4), 359–378.

Rafay, R., Allegue, T., Fowler, S. J., and Rodríguez, J. (2022) Exploring the limits of carbohydrate conversion and product formation in open mixed culture fermentation. *Journal of Environmental Chemical Engineering*, **10**(3), 107513.

Thermal hydrolysis pre-treatment has no positive influence on VFA production from sewage sludge

Ander Castro-Fernández*,**, S. Balboa**, M. Tortosa*, Juan M. Lema**, Leticia Rodríguez-Hernández***, C. M. Castro-Barros* and Antón Taboada-Santos*

*CETAQUA, Water Technology Centre, AquaHub - A Vila da Auga, Jose Villar Granjel 33, E-15890, Santiago de Compostela, Spain (E-mail: *ander.castro@cetaqua.com*)

** CRETUS Institute, Department of Chemical Engineering, School of Engineering, Universidade de Santiago de Compostela, E-15782, Santiago de Compostela, Spain

*** ViAQUA, Gestión Integral de Aguas de Galicia, AquaHub - A Vila da Auga, Jose Villar Granjel 33, E-15890, Santiago de Compostela, Spain

Abstract

Fermentation of sewage sludge to produce VFA appears as an alternative of greater value than generating biogas. In order to improve the hydrolytic stage rate, that has been identified as the limiting one, alternatives such as thermal hydrolysis pre-treatment (THP) have been proposed. This work studies the influence of THP on VFA production in batch and continuous operations. In batch mode, the impact of THP was detrimental (maximum VFA yields of about 0.4 g COD-VFA/COD versus 0.3 with raw sludge without pre-treatment). In continuous operation, THP had proved not exerting noticeable influence on the yield nor on the transformation rate of COD on VFA (0.15-0.17 g COD-VFA/g COD substrate). Microbial community analysis showed that phylum *Firmicutes* was the predominant in both reactors and that the enzymes involved in VFA production were very similar regardless of the substrate fed.

Keywords

Sewage sludge, volatile fatty acids, thermal hydrolysis pre-treatment, microbial populations

INTRODUCTION

Sewage sludge has been traditionally valorised by anaerobic digestion (AD) with biogas as the final product. As alternative, VFA are proposed as bioproducts with higher added-value and with an increasing demand in the chemical industry, whose current market is mainly supplied by the petrochemical route.

The most critical stage of fermentation process is the initial hydrolysis, thus affecting the subsequent steps of acidification. To speed-up the process, a wide variety of pre-treatment technologies, such as thermal hydrolysis pre-treatment (THP), have emerged aiming at solubilizing organic matter. Its effect on biogas production has been well documented, showing most authors a positive influence on methane generation; in contrast, the influence of this pre-treatment on VFA production has been less studied.

What has been consistently reported in literature is that biotransformation of organic matter on VFA results always in a much lower yield than the attained when methane is the target product (Liu et al., 2020). Moreover, yields reached in batch tests are normally lower than in continuous operation.

The objectives of this work are: i) to evaluate the effect of the THP on the VFA production from sewage sludge in batch and continuous mode; ii) to identify changes on microbiome after THP and the main key-players.

MATERIAL AND METHODS

The substrate used (raw and pre-treated sludge) was a mix of primary and biological sludge from a Galician WWTP (Table 1). The effect of THP on the higher proportion of soluble COD is clearly observed in pre-treated sludge. The inoculum used was one collected from the anaerobic digester of the same WWTP of the substrates.

Batch acidification experiments were carried out in an adapted AMPTS II device, using bottles with a working volume of 0.5 L (in triplicate) at a temperature of 37 ± 1 °C. Inoculum and substrate amounts were added inside the bottles to achieve a food/microorganism ratio of 2 g COD substrate/g VS inoculum. 2-Bromoethanesulphonic acid sodium salt (BES, 3 g L^{-1}) was also added as inhibitor of methanogenesis. pH was initially adjusted to 8 adding NaOH and blanks were used to study the endogenous VFA production from inocula.

Table 1 Characterization of substrate and inoculum used in the batch acidification experiment

	Raw sludge	Pre-treated sludge	Inoculum
pH	6.12 ± 0.00	6.31 ± 0.01	8.02 ± 0.00
tCOD (g/L)	200.8 ± 2.0	162.5 ± 1.1	58.6 ± 1.0
sCOD (g/L)	9.6 ± 0.2	24.9 ± 0.4	5.4 ± 0.2
TS (g/L)	114.2 ± 1.1	91.0 ± 1.5	46.7 ± 0.3
VS (g/L)	94.0 ± 1.3	73.4 ± 1.4	26.5 ± 0.1
TN (g/L)	14.8 ± 0.1	10.5 ± 0.2	5.4 ± 0.4
TP (g/L)	2.7 ± 0.0	1.9 ± 0.1	2.0 ± 0.2
TAN (g N/L)	0.68 ± 0.03	0.36 ± 0.02	1.52 ± 0.04
$P\text{-}PO_4^{3-}$ (g/L)	0.146 ± 0.001	0.133 ± 0.002	0.094 ± 0.002

Continuous operation was carried out in two CSTR with a working volume of 5 L, which were maintained at 37 °C ± 1 °C with continuous agitation at a speed of 170 rpm. The reactors were initially inoculated with 5 L of inoculum fed with raw (reactor RS) and pre-treated sludge (reactor PS) diluted to 60 g COD/L. Both reactors were operated at a controlled pH of 8.5 at a hydraulic retention time of 10 days during the whole operation period (80 days), with an OLR in the range of 4.8-6.4 g COD $L^{-1}d^{-1}$.

A Hach D43900 spectrophotometer and associated cuvette kits were utilized to monitor the batch test as well as lab-scale reactors and associated experiments. VFA were determined by gas chromatography (Agilent Technologies, model 6850 Series II), equipped with a flame ionization detector (FID). Total genomic DNA was extracted by triplicate using Nucleospin Microbial DNA extraction kit (Macherey Nagel) that were pulled together. The V3V4 hypervariable region for *Bacteria* was sequenced in AllGenetics & Biology SL using an Illumina PE150 platform. The bioinformatic analysis was performed using the Microbial Genomics module workflow (v21.1).

RESULTS AND CONCLUSION

In summary, the acidification test showed that pH 8 was more favorable in terms of VFA yield than pH 10 and that the raw sludge obtained better results. At both pH, acetic acid was predominant in the mix, always exceeding 60% of existence, since alkaline conditions favor the production of this VFA (Fang et al., 2020). Moreover, the addition of the BES salt has not been effective since working at pH 8 the lines begin to decrease once the maximum is reached instead of remaining stable (Figure 1), which indicates that the methanogenic stage took place.

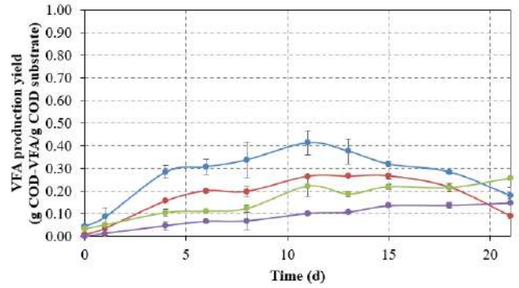

Fig. 1. Acidification yield of raw and pre-treated sludge at pH of 8 and 10. Raw sludge at pH 8 ( ), pre-treated sludge at pH 8 ( ), raw sludge at pH 10 ( ), pre-treated sludge at pH 10 ( ).

Additionally, two CSTR, reactor RS (fed with raw sludge) and reactor PS (fed with pre-treated sludge) were operated (Figure 2). In order to compare the VFA yield and acidification yield in both reactors, the Student's t-test (two independent samples with equal variances with an $\alpha = 0.05$) was used. The statistical analysis concluded that there was no significant difference between the VFA yield obtained with raw and pre-treated sludge (0.15-0.17 g COD-VFA/g COD substrate in both reactors). Therefore, working in continuous mode, THP has no influence on VFA production from sewage sludge. As in the batch tests, the VFA percent composition obtained was practically the same with the two substrates, with acetic acid always having a presence greater than 65% in terms of COD.

A microbiological study of the populations present in both the inlet and outlet streams of the continuous reactors has been carried out by taking samples on six different days. The alpha diversity measures suggest a specialization of the microbial communities present in both reactors converging towards similar hydrolytic and acidogenic populations which give rise to the same VFA yields in continuous operation, independently of the pre-treatment applied to the inlet. The most abundant phyla detected in both reactors was *Firmicutes*, being the enzymes involved in VFA production very similar in both reactors' outlets independently of the pre-treatment of the feeding. This reaffirms the equality both in the production yields and in the selectivity of the acidogenic process, being the same those key-players involved in the VFA production.

In conclusion, raw sludge was compared with thermally pre-treated sludge to see the effect of THP on VFA production in two modes, batch and continuous operation. In batch mode, THP resulted in lower VFA yields at both tested pH, being pH 8 the most favourable in terms of VFA yield. In continuous reactors, the negative effect of THP disappeared, obtaining the same VFA yields and distribution mix independently of the pre-treatment of fed sludge. Continuous mode microbiology analysis confirmed that both reactors converged into similar bacterial populations with *Firmicutes* phylum as the most abundant one.

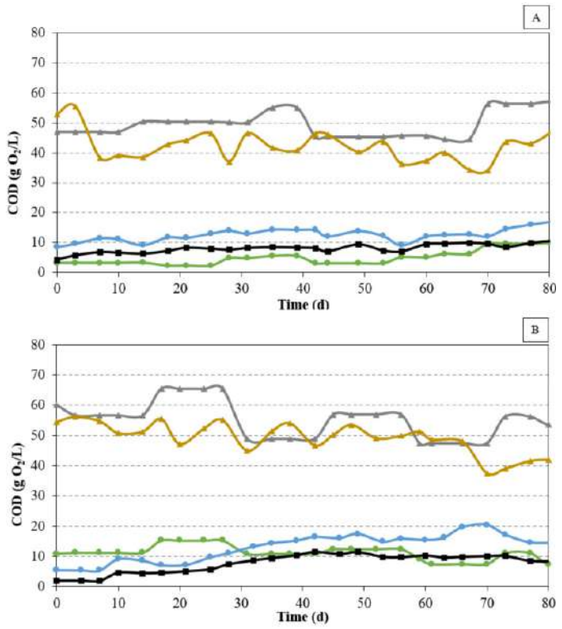

Fig. 2. COD distribution of the inlets (I) and outlets (O) of continuous reactors. A) Reactor RS. B) Reactor PS. tCOD-I ( ), sCOD-I ( ), tCOD-O ( ), sCOD-O ( ), sCOD-I ( ), COD-VFA ( ).

The project was financed by the Xunta de Galicia within the framework of the CIGAT CIRCULAR project and also by INTERREG SUDOE ECOVAL and HOOP (EU's Horizon 2020).

REFERENCES

Fang, W., Zhang, X., Zhang, P., Wan, J., Guo, H., Ghasimi, D. S. M., Morera, X. C., & Zhang, T. (2020). Overview of key operation factors and strategies for improving fermentative volatile fatty acid production and product regulation from sewage sludge. *Journal of Environmental Sciences (China)*, *87*, 93–111. https://doi.org/10.1016/j.jes.2019.05.027

Liu, H., Li, Y., Fu, B., Guo, H., Zhang, J., & Liu, H. (2020). Recovery of volatile fatty acids from sewage sludge through anaerobic fermentation. *Current Developments in Biotechnology and Bioengineering: Resource Recovery from Wastes*, 151–175. https://doi.org/10.1016/B978-0-444-64321-6.00008-2

TECHNICAL SESSIONS

T12.

Recovery of PHA and SCP

ECO STP 2023

Volatile fatty acids yield and profile during sludge and food waste co-fermentation at different temperatures

N. Perez-Esteban*, M. Peces*, J. Vives-Egea*, J. Dosta* and S. Astals*
* Dept. Chemical Engineering and Analytical Chemistry, University of Barcelona, 08028 Barcelona, Spain
(E-mail: *npereziesteban@ub.edu; mpeces@ub.edu; julyvives222@gmail.com; jdosta@ub.edu; sastals@ub.edu*)

Abstract

This study evaluated the effect of temperature (25, 35, 45 and 55 ºC) on waste activated sludge and food waste co-fermentation under continuous conditions. Temperatures had a significant influence on volatile fatty acids (VFA) yield and profile. The highest yield was achieved at 55 ºC followed by 45, and 35 °C. Temperature also had significant influence on VFA profile. High concentrations of acetic and butyric acids were obtained at 55 ºC, while the VFA profile at 35 °C was dominated by acetic, butyric, and propionic acids. At 45 ºC was facilitated the accumulation of caproic acid. Temperature had an influence on the fermenters' microbial community. Two different waste activated sludges were studied at 35 ºC from which different VFA concentration, yield and microbiome were obtained, possibly due to waste activated sludge inherent properties.

Keywords

Fermentation; microbiology; organic waste; sewage sludge; short chain fatty acids; temperature.

INTRODUCTION

Mixed-culture fermentation is an emerging biotechnology to transform organic wastes into easily assimilable organic compounds such as volatile fatty acids (VFAs), lactic acid and alcohols. At wastewater treatment plants, waste activated sludge (WAS) co-fermentation with food waste (FW) is an opportunity to boost VFA and alcohols (X-OH) yields with respect to WAS mono-fermentation. The synergy of this mixture relies on FW high biodegradability and WAS buffer capacity (Perez-Esteban, et al., 2022). Temperature is one of the most influencing parameters on fermentation due to its impact on carbon diversion. The highest fermentation yields have been reported at mesophilic conditions, although optimum performance have also been reported at psychrophilic and thermophilic conditions. However, most of these studies have been carried out in batch assays, which results could be strongly driven by the starting microbial community.

This research evaluates the impact of temperature (25, 35, 45 and 55 ºC) on WAS:FW co-fermentation performance under continuous conditions. The fermenters' microbial community was also assessed to establish links with the obtained VFA yield and profile.

MATERIAL AND METHODS

Substrates

WAS was collected from the secondary clarifier of a municipal WWTP. Synthetic FW was prepared to mimic the composition of household biowaste as for Vidal-Antich et al. (2021).

Experimental platform and methods

The experimental platform consisted of 4 L jacketed reactors equipped with mechanical stirrers. Each fermenter was manually fed once a day with a 70:30 WAS:FW mixture (%VS basis). The organic loading rate was 11 gVS/(L·d) (Hydraulic retention time of 3.3 days). The pH of the fermenters was not controlled. Two different runs (A and B) were carried out in this study. In Run A, the fermenters' temperatures were 25, 35 and 45 ºC, while in Run B, were 35 and 55 ºC. The following parameters were analysed three times per week following the Standard Methods procedures (APHA, 2017): VFA and X-OH, soluble chemical oxygen demand (sCOD), pH, total ammoniacal nitrogen (TAN) and alkalinity. DNA extraction was performed following the MiDAS field guide and the FastDNA® spin kit for soil. The V3-V4 region of 16S rRNA was sequenced by Novogene. Taxonomy was assigned to each amplicon sequencing variant (ASV) using MiDAS 4.8.1 database. Statistical and microbiology analysis were carried out with R studio.

RESULTS AND DISCUSSION

Fermenters' performance

Figure 1 shows significant differences in total VFA concentration depending on the working temperature. At 35 ºC, Runs A and B yielded VFA concentrations statistically different (336 ± 25 and 253 ± 11 mgCOD/gVS, respectively), showing that WAS characteristics had an important impact on fermentation yields (Figure 1a). The VFA concentration values recorded at 55 ºC were the highest (15291 ± 949 mgCOD/L) while at 25 ºC achieved the lowest concentration (8530 ± 398 mgCOD/L) (Figure 1b). These results indicate that thermophilic conditions enhance both the hydrolysis and the acidogenesis step since it showed the highest conversion of sCOD to VFA.

Figure 2 shows that each temperature had distinctive cluster based on the percentage of individual VFA, although the condition 25A, 35A and 35B were very close to each other. This fact indicates that each temperature had a statistically different VFA distribution. It is worth mentioning that 45 and 55 ºC did not enriched propionic acid, while 25 ºC and 35 ºC did. The VFA profile at 55 ºC is enriched in acetic and butyric acid, which is in accordance to Koupaie et al., (2021). 45 ºC led to the enrichment of caproic acid, which was not present in the other temperatures.

Figure 3 shows the monitored parameters of co-fermentation during Run A and B. The pH was slightly higher as the operating temperature increased (Figure 3a). This pH differences may be due to the higher buffering capacity of the fermentation medium at higher temperatures (Figure 3b). This could be partly explained by the higher concentration of ammoniacal nitrogen at higher temperature, indicative of higher organic matter ammonification at higher temperatures (Figure 3c) (Ariunbaatar, et al., 2015; Zhao, et al., 2018). Figure 1d shows that sCOD also increased with temperature, indicating an improvement of hydrolysis capacity at higher temperatures.

Microbial ecology

The indigenous microbial community of the WAS used in Run A and B was different (Figure 4). The genus *Ca.Microthrix,* well-known for causing filamentous bulking in WWTPs (Jiang, et al., 2021), was the most abundant in both WAS. However, the genus midas_g_6 (family *Saprospiracea*), *Amirococcus* and *midas_g_31* (family *midas_f_31*) was more abundant in WAS B than WAS A.

There were significant differences between the microbial community at each temperature (Figure 5). The clusters 35B, 35A and 45A are very close to each other in the PCA, indicating lower differences among their microbial community. At 25 °C predominated the genus *Prevotella*, related with acidogenesis (Shrestha, et al., 2022). At 55 ºC, the microbial community was dominated by the phylum *Firmicute*, including *Ruminococcaceae* (family), *Oscillospirales* (order), *Clostridium sense stricto* (genus). The phylum Firmicute is known to be able to hydrolyse and ferment carbohydrates (Qin, et al., 2021). The microbial community at 35 °C of the Run A and B was quite similar except for the presence of *Actinobacteriota* (phylum) in Run B (Figure 6). The phylum *Actinobacteriota* is reported to have an important role in hemicellulose and lignin degradation (Guo, et al., 2021).

At 35 °C (Run B), a consumption of VFA (mainly acetic acid) was observed, possibly cause by VFA-consuming microorganisms. Microbial ecology suggested that it is not consumed by methanogenic archea since its relative abundance is less than 0.1%. The genera found in the 35 ºC (Run B) were *Methanosphaera*, *Methanobrevibacter* and *Methanosarcina*. These genera stand out for being hydrogenotrophic methanogens.

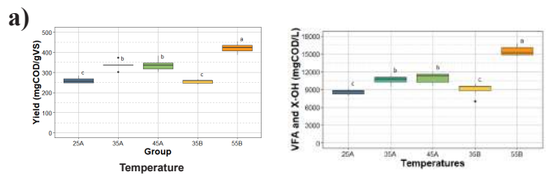

Figure 1. a) Yield boxplot with Tukey Test for Run A and Run B and b) VFA and X-OH concentration boxplot of VFA and X-OH concentration with Tukey Test

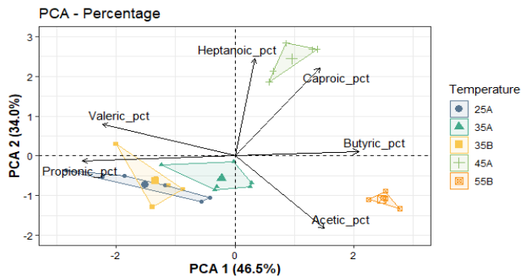

Figure 2. PCA plot of VFA percentage for each temperature studied.

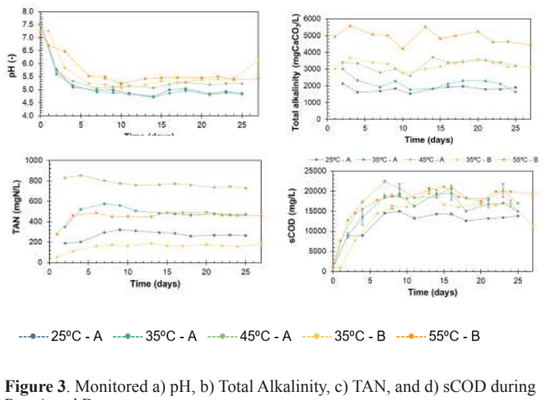

Figure 3. Monitored a) pH, b) Total Alkalinity, c) TAN, and d) sCOD during Run A and B.

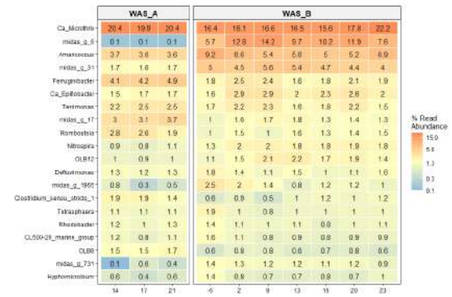

Figure 4. Heatmap showing the 20 top taxa (Genus) waste activated sludge (A or B) at the 3 sampling points for WAS_A and 7 sampling points for WAS_B.

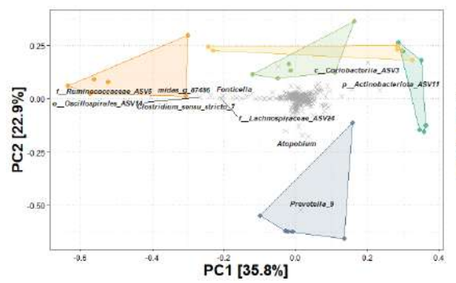

Figure 5. PCA of microbial community profiles at the OUT label (Hellinger transformed) for the 5 conditions at the 6 sampling points.

REFERENCES

APHA (2017) *Standard Methods for the Examination of Water & Wastewater*, American Public Health Association.

Ariunbaatar, J., Scotto Di Perta, E., Panico, A., Frunzo, L., Esposito, G., Lens, P. N. L., and Pirozzi, F. (2015) Effect of ammoniacal nitrogen on one-stage and two-stage anaerobic digestion of food waste. Waste Management, **38**, 388–398.

Guo, Y.-X., Chen, Q.-J., Qin, Y., Yang, Y.-R., Yang, Q.-Z., Wang, Y.-X., Cheng, Z., Cao, N., and Zhang, G.-Q. (2021) Succession of the microbial communities and function prediction during short-term peach sawdust-based composting. Bioresource Technology, **332**, 125079.

Hosseini Koupaie, E., Lin, L., Bazyar Lakeh, A. A., Azizi, A., Dhar, B. R., Hafez, H., and Elbeshbishy, E. (2021) Performance evaluation and microbial community analysis of mesophilic and thermophilic sludge fermentation processes coupled with thermal hydrolysis. Renewable and Sustainable Energy Reviews, **141**, 110832.

Jiang, C., McIlroy, S. J., Qi, R., Petriglieri, F., Yashiro, E., Kondrotaite, Z., and Nielsen, P. H. (2021) Identification of microorganisms responsible for foam formation in mesophilic anaerobic digesters treating surplus activated sludge. Water Research, **191**, 116779.

Peces, M., Pozo, G., Koch, K., Dosta, J., and Astals, S. (2020) Exploring the potential of co-fermenting sewage sludge and lipids in a resource recovery scenario. Bioresource Technology, **300**, 122561.

Perez-Esteban, N., Vinardell, S., Vidal-Antich, C., Peña-Picola, S., Chimenos, J. M., Peces, M., Dosta, J., and Astals, S. (2022) Potential of anaerobic co-fermentation in wastewater treatments plants: A review. Science of The Total Environment, **813**, 152498.

Qin, S., Wainaina, S., Liu, H., Soufiani, A. M., Pandey, A., Zhang, Z., Awasthi, M. K., and Taherzadeh, M. J. (2021) Microbial dynamics during anaerobic digestion of sewage sludge combined with food waste at high organic loading rates in immersed membrane bioreactors. Fuel, **303**, 121276.

Shrestha, S., Colcord, B., Fonoll, X., and Raskin, L. (2022) Fate of influent microbial populations during medium chain carboxylic acid recovery from brewery and pre-fermented food waste streams. Environmental Science: Water Research & Technology, **8**(2), 257–269.

Vidal-Antich, C., Peces, M., Perez-Esteban, N., Mata-Alvarez, J., Dosta, J., and Astals, S. (2022) Impact of food waste composition on acidogenic co-fermentation with waste activated sludge. Science of The Total Environment, **849**, 157920.

Vidal-Antich, C., Perez-Esteban, N., Astals, S., Peces, M., Mata-Alvarez, J., and Dosta, J. (2021) Assessing the potential of waste activated sludge and food waste co-fermentation for carboxylic acids production. Science of The Total Environment, **757**, 143763.

Zhao, J., Liu, Y., Wang, Y., Lian, Y., Wang, Q., Yang, Q., Wang, D., Xie, G.-J., Zeng, G., Sun, Y., Li, X., and Ni, B.-J. (2018) Clarifying the Role of Free Ammonia in the Production of Short-Chain Fatty Acids from Waste Activated Sludge Anaerobic Fermentation. ACS Sustainable Chemistry & Engineering, **6**(11), 14104–14113.

Exploring the ammonia presence effect on PHA production of a phototrophic-chemotrophic consortium operated under Light-Feast/Dark-Aerated-Famine

J.R. Almeida[1,2], E. Serrano León[3], Enrique Lara Corona[3], J.C. Fradinho[1,2], A. Oehmen[2,†], M.A.M. Reis[1,2]

[1] Associate Laboratory i4HB – Institute for Health and Bioeconomy, NOVA School of Science and Technology, NOVA University Lisbon, 2829-516 Caparica, Portugal
[2] UCIBIO – Applied Molecular Biosciences Unit, Department of Chemistry, NOVA School of Science and Technology, NOVA University Lisbon, 2829-516 Caparica, Portugal
(E-mail: *jro.almeida@campus.fct.unl.pt; j.fradinho@campus.fct.unl.pt; amr@fct.unl.pt*)
[3] FCC Servicios Ciudadanos, Av. del Camino de Santiago, 40, edificio 3, 4ª planta, 28050 Madrid, Spain
(E-mail: *esteban.serrano.leon@aqualia.com; ELaraC@fcc.es*)
[†] Present address: School of Chemical Engineering, University of Queensland, Brisbane, QLD, 4072, Australia
(E-mail: *a.oehmen@uq.edu.au*)

Abstract

Availability of ammonia, coupled or uncoupled with carbon feeding, can impact the selection of PHA producing microorganisms in mixed cultures. This research studied this impact on the selection of a PHA accumulating phototrophic mixed culture operated under light-feast/dark-aerated-famine, winter-simulated outdoor conditions, fermented domestic wastewater as feedstock and selected under three ammonia settings: ammonia availability only in light-phase, constant presence, and ammonia availability during dark-aerated-famine phase. Results showed that ammonia presence was required to promote growth of PHA-accumulating bacteria in dark-aerated-famine phase, whereas ammonia absence in the light-period favoured cyanobacteria growth, resulting in decreased phototrophic PHA accumulation capacity. Constant presence of ammonia was the best selection strategy attaining a PHA content of 21.6 %gPHA/gVSS (0.6 gPHA/L.day). Furthermore, light-feast/dark-aerated-famine operation ensured total carbon depletion from wastewater and demonstrated being able to maintain the system PHA accumulation performance under winter conditions, suggesting it can contribute to overcoming the seasonal constraints of outdoor operation.

Keywords

Feast and Famine selection; Polyhydroxyalkanoates; Phototrophic-chemotrophic consortium; Phototrophic Purple bacteria; Transient illumination; Wastewater treatment

INTRODUCTION

Polyhydroxyalkanoates (PHAs) are bio-based and biodegradable polymers that can be internally accumulated as carbon reserves by many bacteria and have similar properties to traditional plastics. Recently, phototrophic mixed cultures (PMC), composed of a consortium of microalgae (oxygen producers) and phototrophic purple bacteria (PPB) (PHA producers), have surged as a new technology in this field. PPB are versatile metabolic bacteria, that are able to remove organic carbon from waste streams using sunlight, as a free energy source, contributing to a reduction of the biopolymer production costs (Capson-Tojo et al. 2020).

Thus far, studies using the conventional selection strategy of carbon feast and famine (FF) on PHA-producing PMCs have achieved PHA storage levels of 30%, using fermented mixtures of wastewater with molasses as feedstock, under open operation, while simulating summer outdoor conditions (Almeida et al., 2021). Previous PMC research has also shown that extended carbon feast phases can improve PPB growth and PHA accumulation potential. However, the existence of an inactive dark phase, due to the absence of oxygen production by microalgae, limits further growth of PPB on accumulated PHA, thus confining both feast and famine phases to the light period. Therefore, it is important to investigate the potential of aerating the night-time to convert it into an active phase and thus enhancing the overall PHA productivity of the system.

Regarding to the organic waste streams used for PHA production, the existing variable nutrient concentrations can directly impact the system performance. In fact, studies with aerobic mixed cultures have shown that uncoupling the ammonia supply from the carbon feeding can promote the culture enrichment in PHA producers and improve PHA productivity (Matos et al. 2021). However, such impact of ammonia supply on PMC selection and PHA production efficiency has never been tested.

The current study aims to determine operational conditions that can improve PHA accumulation in PMCs under outdoor conditions and using real fermented feedstocks. It will be explored the potential of utilizing the full light period as a feast phase for PPB and transforming the dark phase into an active period through mechanical aeration, enabling PPB to consume PHA during a dark-aerated-famine phase, as well as the assessment of different ammonia settings (light-ammonia, constant presence of ammonia and dark-famine ammonia) on the PMC selection and respective PHA productivity.

MATERIALS AND METHODS

A sequencing batch reactor (SBR), with a working volume of 5.8L, was inoculated with sludge from a PMC operated under a FF regime (Almeida et al., 2021). The reactor was operated under simulated outdoor-winter conditions, registered in a paddle wheel high-rate algae pond from Chiclana wastewater treatment plant (Jerez de La Frontera, Spain). At a temperature of 15°C, the PMC was selected under a FF regime, trough a 24 hour light-transient cycle (12h light/12h dark) with a light intensity of 139.5 W/m^2 (0.82 W/L), and externally illuminated by a halogen lamp (60W). During the 12h dark period, the reactor was aerated using an air pump and disperser to ensure the total carbon depletion and guarantee PHA consumption. The air pump switched off when the oxygen concentration reached 2 mg/L. The reactor was fed with a fermented mixture of domestic pre-treated wastewater (de-sanding and degreasing) supplemented with 1% v/v of molasses provided by the Guadalete sugar plant. The evolution of the microbial culture regarding its photosynthetic pigments, such as bacteriochlorophyll *a+b* (absorbance at 775 nm) and chlorophyll *a* (absorbance at 665 nm) pigments was performed by ethanol extraction, as described in Almeida et al. (2021).

RESULTS AND DISCUSSION

A sequencing batch reactor was operated under light-feast/dark-aerated famine and winter outdoor simulated conditions. Along the operation, different settings on the ammonia availability along the SBR cycle were imposed (light-ammonia, constant presence of ammonia and dark-famine ammonia). Figure 1 presents the profile of the PMC selected under each of the three ammonia conditions tested.

In light-ammonia condition (Figure 1.A), ammonia was provided only during the light phase to promote the growth of PPB over other chemotrophic microorganisms by restricting growth during the dark-aerated phase. Results showed that despite the successful PPB growth, a low PHA content was attained (11.2% g PHA/g VSS) and a steady production throughout the cycle, with no accumulation or consumption patterns, was observed. This outcome likely occurred because the bacteria could not utilize the stored PHA for growth without the presence of ammonia during the famine phase.

The operation under constant presence of ammonia was implemented not only to promote PPB growth during the light phase but to allow them to grow on the accumulated PHA during the dark-famine aerated phase. The long-term operation of this condition, also allowed to assess the culture behavior through different feedstock compositions (Figure1.C and Figure 1.D). It was observed that during the light period, less reduce compounds (acetate and propionate) presented higher uptake rates and were preferable for PHA production by PPB. Overall, the microbial culture was able to maintain PHA accumulation efficiency under constant presence of ammonia, regardless of feedstock composition or the feast-phase length imposed by an unfavorable feedstock (higher content of reduced compounds, such as butyrate and valerate), since the dark-aerated phase ensured total carbon depletion and furthered PHA production by aerobic microorganisms.

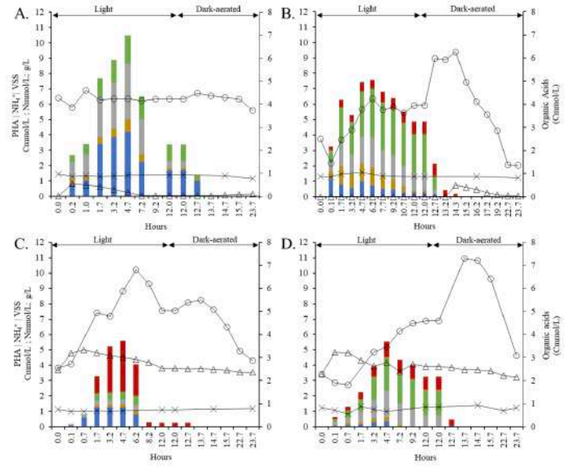

Figure 1. Photosynthetic mixed culture profile. **A.** Light-ammonia condition; **B.** Dark-famine ammonia condition; **C.** Constant presence of ammonia (feedstock with higher content of acetate and propionate); **D.** Constant presence of ammonia (feedstock with higher content of butyrate and valerate); (○) Polyhydroxyalkanoates (PHA) concentration; (×) Total Suspended Solids (VSS); (Δ) Ammonia (NH_4^+); (■) acetate; (■) propionate; (■) butyrate; (■) valerate; (■) ethanol; (■) lactate.

This condition registered the highest PHA content and production rates in both light and dark-aerated periods, indicating that both phototrophic and aerobic microorganisms were able to grow and accumulate PHA effectively in this condition. Under operation with favorable feedstocks the feast phase ended during the light period and a 21.6% g PHA/g VSS at a productivity rate of 0.6 g PHA/L·day was attained. While under unfavorable feedstock operation, carbon content passed to the dark period and the culture achieved a PHA level of 18.5% g PHA/g VSS at a production rate of 1.4 g PHA/L·day.

At last, dark-famine ammonia condition, aimed to study the separation of organic carbon from ammonia to promote the growth of photosynthetic microorganisms that accumulate PHA. During this condition, the selector reactor only achieved a PHA level of 10.4% g PHA/g VSS during the light period, and no further PHA accumulation was observed in parallel accumulation tests performed under increase light intensity (1.9 W/L) or synthetic acetate and propionate feeding. Overall, results show that the absence of ammonia during the light period, thrived the growth of other photosynthetic microorganisms, such as cyanobacteria. However, and despite cyanobacteria being able to accumulate PHA, a decrease in the culture's ability to accumulate PHA during the light period was observed, suggesting that these microorganisms were probably favoring growth through nitrogen fixation instead of PHA accumulation.

Overall, the proposed system operation with extended feast phases coupled to a dark aeration period, is able to ensure the well function of a photosynthetic system under winter conditions. Results showed that despite the existence of an aeration phase led to a drop in PPB pigment concentration (Bchl *a* + *b*), these were being produced, which was confirmed by DNA sequencing results that indicated the prevalence of PPB (Rhodobacter, Chromatiaceae and Rhodopseudomonas) over aerobic microorganisms (Paracoccus, Rhizobium, and Acidovorax). Additionally, and regarding to the system performance, similar PHA productivities were achieved compared to previous reports of PHA production with non-aerated PMC systems operated under the more favorable summer conditions (0.5 g PHA/L.day, Almeida et al. 2021). This suggests that the light-feast/dark-aerated famine system here presented could overcome winter conditions and may be able to ensure a continuous operation of PPB systems across seasons.

ACKNOWLEDGMENTS

This work was supported by national funds from FCT - Fundação para a Ciência e a Tecnologia, I.P., in the scope of the project UIDP/04378/2020 and UIDB/04378/2020 of the Research Unit on Applied Molecular Biosciences - UCIBIO and the project LA/P/0140/2020 of the Associate Laboratory Institute for Health and Bioeconomy - i4HB. Likewise, INCOVER project, that has received funding from the European Research Council (ERC) under the European Union's Horizon 2020 research and innovation programme (grant agreement n° 689242).

REFERENCES

Capson-Tojo, G., Batstone, D. J., Grassino, M., Vlaeminck, S. E., Puyol, D., Verstraete, W., Kleerebezem, R., Oehmen, A., Ghimire, A., Pikaar, I., Lema, J. M., & Hülsen, T., 2020. Purple phototrophic bacteria for resource recovery: Challenges and opportunities. *Biotechnology Advances,* **43**.

Almeida, J.R., Serrano, E., Fernandez, M., Fradinho, J.C., Oehmen, A., Reis, M.A.M., 2021. Polyhydroxyalkanoates production from fermented domestic wastewater using phototrophic mixed cultures. *Water Research*. **197**, 117101.

Matos, M., Cruz, R. A. P., Cardoso, P., Silva, F., Freitas, E. B., Carvalho, G., & Reis, M. A. M. (2021). Sludge retention time impacts on polyhydroxyalkanoates productivity in uncoupled storage/growth processes. *Science of the Total Environment*, **799**.

Top-down engineering of natural phototrophic microbiomes into stable and productive consortia for the production of bioplastics

Eva Gonzalez-Flo*, Beatriz Altamira-Algarra* and Joan García**

* GEMMA-Group of Environmental Engineering and Microbiology. Department of Civil and Environmental Engineering. Escola d'Enginyeria de Barcelona Est (EEBE). Universitat Politècnica de Catalunya-BarcelonaTech. Av. Eduard Maristany 16. Building C5.1. E-08019 Barcelona. Spain

** GEMMA-Group of Environmental Engineering and Microbiology. Department of Civil and Environmental Engineering. Universitat Politècnica de Catalunya-BarcelonaTech. c/ Jordi Girona 1-3. Building D1. E-08034 Barcelona. Spain

Abstract
The utilization of microbiomes for industrial biopolymer production is faced with significant obstacles. However, microbiomes have been observed to be both functionally robust and adaptable to changing environments. The use of cyanobacteria for biopolymer production has been identified as a promising approach as it helps to reduce greenhouse gas emissions and supports the formation of a closed-carbon loop for a circular economy based on polymers. The ultimate goal of this research is to devise a sustainable approach for producing bioplastics with phototrophic microbiomes through the utilization of nutrients present in wastewater. We have developed two strategies to enhance PHB production by utilizing field environmental microbiomes enriched with cyanobacteria. The first approach focuses on optimizing the culture conditions, resulting in a 14% of PHB production. The second strategy promotes the growth of PHB-producing cyanobacteria populations and has been shown to lead to a 22% increase in PHB production.

Keywords (maximum 6 in alphabetical order)
Carbon-based bioproducts; Photosynthethic Microbiome; Polyhydroxybutyrate

INTRODUCTION

Interest in microbial biopolymers is on the rise due to growing consumer demand for eco-friendly and sustainable products as an alternative to chemical-based polymers. One such biopolymer is polyhydroxybutyrate (PHB), a biodegradable polymer produced by various microorganisms for energy and carbon storage. It has potential applications in niche markets such as textiles, food, cosmetics, pharmaceuticals, and medicine (Li M, 2020). Cyanobacteria, a widespread group of photoautotrophic bacteria, can produce PHB using CO_2 and solar energy. The consumption of CO_2 for PHB production not only helps to mitigate greenhouse gases but also contributes to a closed-carbon-loop for a circular economy (Lee J et al., 2021). However, cyanobacterial PHB industrial production and commercialization remains a challenge due to lower productivity compared to PHB synthesis by heterotrophic bacteria (Ansari S, 2016), and high production costs resulting from the use of pure cultures, refined substrates, and sterile conditions, which limit its market potential (Tan D et al., 2020).

To bring PHB production to an industrial scale, phototrophic microbiomes have emerged as a viable alternative to pure-culture methods. Microbiomes have the advantage of not requiring reactor sterilization, having a wider metabolic potential, and expanding feedstock options (Scarborough MJ et al., 2022). A photosynthetic microbiome, which combines the benefits of working with a consortium with those of photosynthetic microorganisms, could use CO_2 and light for growth and bioproduct synthesis. However, research on biopolymer production by photosynthetic microbiomes is limited.

In this study, various photosynthetic microbiomes were evaluated for their ability to produce PHB. These cultures were obtained from environmental samples and enriched with cyanobacteria using low phosphorus concentration as a selective pressure. To boost biopolymer production, two approaches were employed: (1) altering operating parameters known to affect PHB synthesis, and (2) optimizing the culture to increase the presence of PHB-producing organisms. The ultimate goal of this study is to develop a sustainable method for producing PHB using phototrophic microbiomes, by recovering the nutrients present in wastewater. This approach aligns with the principles of circular economy, as it utilizes resources that would otherwise be considered waste, and transforms them into valuable bioproducts.

MATERIALS AND METHODS

Procurement of photosynthetic cultures

Seven samples were collected from four different locations (constructed wetland, river, canal and urban lake) in the metropolitan area of Barcelona, Spain. Samples were grown in laboratory conditions to obtain microbiomes enriched in cyanobacteria. Phosphorus (P) limitation was used to favor the growth of cyanobacteria against other phototrophic organisms (i.e. green algae). Most of the cultures were maintained with a P concentration in the flasks of 0.2 $mg \cdot L^{-1}$.

Microbial identification

The identification and classification of cyanobacteria present in the microbiomes were performed using a combination of morphological observation under a bright light microscope and molecular characterization via clone library analysis of the 16S rRNA gene.

Design of Experiments

The metabolic regime was evaluated by experiments combining three factors: (i) the presence of organic carbon (OC), (ii) inorganic carbon (IC) and (iii) light:dark photoperiods. Multivariable experimental design (DoE) and surface response methodology (SRM) were used to identify the optimal conditions and evaluate their effect on PHB production.

Enriching biomass in PHB-producing cyanobacteria

The Feast and Famine (FF) strategy, commonly used in PHB production by heterotrophic cultures, was implemented for the first time to enhance PHB production in cyanobacteria-enriched microbiomes. The study utilized a Sequencing Batch Reactor (SBR) for 209 days during which cycles of growth and starvation were systematically carried out to selectively enrich the microbiome with microorganisms capable of producing PHB.

RESULTS AND DISCUSSION

Effect of selective pressure on field environmental samples

The effectiveness of the selection pressure applied to favor cyanobacteria over other microorganisms was confirmed through a combination of microscopic observation using both a bright light and fluorescence microscope, as well as molecular analysis of the 16S rRNA gene. The microscopic observations revealed the presence of filamentous and punctate colony-forming cyanobacteria (Figure 1). The results of the 16S rRNA analysis further showed that this selection pressure (P limitation) resulted in a decrease in the number of (heterotrophic) bacterial populations in the environmental samples collected (Figure 2) and a significant increase in the presence of cyanobacteria in the microbiomes.

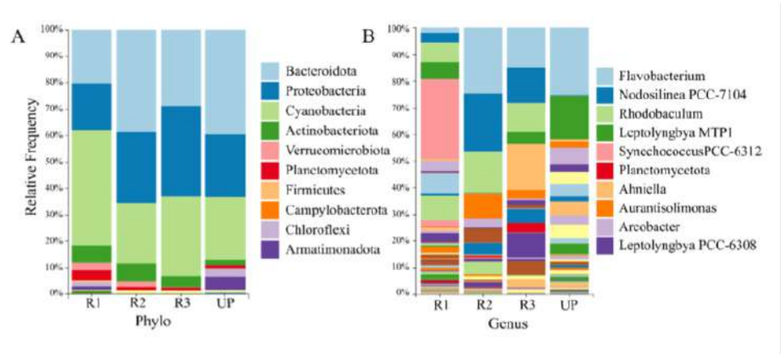

Figure 2. Relative abundance of microorganisms' populations identified in the microbial community at A) phyla level and B) genus level after 5 months of growth with P limitation. The legend shows only the top 10 most abundant taxonomies. Cyanobacteria are represented by light green in A) and dark blue, dark green, pink, and dark purple in B).

Figure 3. PHB evolution over the FF strategy for microbiome optimization on PHB-producer microorganisms for two different photobioreactors. Numbers correspond to the different FF cycles applied. Black arrow indicates the maximum PHB content achieved after 9 FF cycles.

Enhancing PHB production through the optimization of operating conditions

The study found that the optimal conditions for biopolymer synthesis were dependent on the specific microbiome being tested, however, the results from the Design of Experiment (DoE) revealed that higher PHB contents were obtained when the cultures were grown under heterotrophic or mixotrophic conditions. Additionally, the results showed that the addition of organic carbon was the sole factor that had a consistent impact on biopolymer production across all microbiomes tested. The highest PHB content, reaching 14% dry cell weight, was achieved for one specific microbiome by adding 0.6 g of acetate per liter and maintaining a light:dark photoperiod of seven days. Based on these results, the microbiome and the best conditions for bioproduct synthesis were selected for further scaling up.

Enhancing PHB production by enriching biomass in PHB-producer organisms

Glass photobioreactors (PBRs) were operated for 209 days with repeated FF cycles. In addition, the impact of three parameters (nutrient concentration, temperature, and light) on biomass growth and biopolymer synthesis was evaluated beforehand to establish optimal conditions for operating the PBRs. Organic carbon was added in the form of acetate (600 mg/L) at the beginning of the feast phase to stimulate PHB synthesis. Results showed an increase in PHB production from 2% dcw in the initial phase to 22% dcw after 209 days of operation (Figure 3), indicating the development of biopolymer-producing biomass.

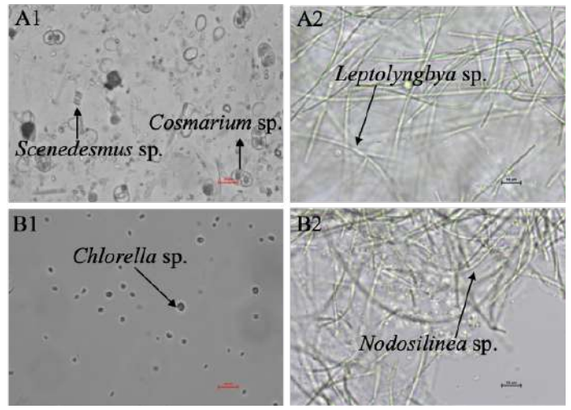

Figure 1. Microscope images of microbiomes under bright light microscopy at 400X. Panel A) corresponds to "microbiome 1" and B) corresponds to "microbiome 2". A1) and B1) correspond to samples of field environmental microbiomes. The scale bar is 20µm. A2) and B2) correspond to cyanobacteria-enriched microbiomes after 5 months of growth with P limitation. The scale bar is 10 µm.

Li M, Wilkins MR. Recent advances in polyhydroxyalkanoate production: Feedstocks, strains and process developments. Int J Biol Macromol 2020;156:691–703. https://doi.org/10.1016/j.ijbiomac.2020.04.082.
Lee J, Park HJ, Moon M, Lee JS, Min K. Recent progress and challenges in microbial polyhydroxybutyrate (PHB) production from CO2 as a sustainable feedstock: A state-of-the-art review. Bioresour Technol 2021;339:125616. https://doi.org/10.1016/j.biortech.2021.125616.
Ansari S, Fatma T. Cyanobacterial Polyhydroxybutyrate (PHB): Screening, Optimization and Characterization 2016. https://doi.org/10.1371/journal.pone.0158168.
Tan D, Wang Y, Tong Y, Chen GQ. Grand Challenges for Industrializing Polyhydroxyalkanoates (PHAs). Trends Biotechnol 2021;39:953–63. https://doi.org/10.1016/j.tibtech.2020.11.010.
Scarborough MJ, Lawson CE, DeCola AC, Gois IM, James M. Microbiomes for sustainable biomanufacturing. Curr Opin Microbiol 2021;2022:8–14. https://doi.org/10.1016/j.mib.2021.09.015

Bioconversion of H_2 to Single Cell Protein by Purple Bacteria consortia: Influence of environmental conditions on microbial kinetics

M. del R. Rodero*, **, J.A. Magdalena*, ***, J. P. Steyer*, N. Bernet* and G. Capson-Tojo*

* INRAE, Univ. de Montpellier, LBE, 102 avenue des Étangs, 11100 Narbonne, France (E-mail: *maria-del-rosario.rodero-raya@inrae.fr; jose-antonio.magdalena-cadelo@inrae.fr, jean-philippe.steyer@inrae.fr; nicolas.bernet@inrae.fr; gabriel.capson-tojo@inrae.fr)*
** Institute of Sustainable Processes, University of Valladolid, 47011, Valladolid, Spain
*** Vicerrectorado de Investigación y Transferencia de la Universidad Complutense de Madrid, 28040 Madrid, Spain

Abstract

Single cell proteins (SCP) have emerged as an alternative protein source to partially alleviate the current problem of food scarcity. However, there is a need to produce SCP from renewable and pathogen-free sources, such as gaseous streams. This study evaluated, for the first time, the use of an enriched phototrophic purple bacteria consortium for SCP production using H_2 and CO_2. The influence of pH (6-8.5), temperature (15-50ºC) and light intensity (0-50 W m^{-2}) on the growth kinetics and biomass yields was investigated. Optimal conditions were found at a pH of 7, temperature of 25ºC and light intensities over 30 W·m^{-2}. High biomass (~ 1 g $COD_{biomass}$ □g^{-1} $COD_{consumed}$) and protein yields of ~4 g protein□g^{-1} H_2 were achieved, regardless of the environmental conditions. The resulted biomass exhibited high protein contents (51–64%w/w), showing its suitability as SCP. The biomass yields obtained herein are amongst the highest ones reported from gaseous streams.

Keywords

Autotrophic growth; environmental conditions; hydrogen; phototrophic purple bacteria; single cell protein

INTRODUCTION

Sustainable food and feed production is nowadays a serious global concern. Ever-growing population, climate change and limited natural resources call for the development of new sustainable food/feed alternatives (Zha et al., 2021). Proteins play a key role in human and animal diet as a source of nitrogen and essential amino acids (Ritala et al., 2017). The use of microorganisms as a protein-rich feedstock, the so-called single cell protein (SCP), is a promising alternative to plant or animal-based proteins, since microorganisms provide higher nitrogen recovery during protein synthesis (Puyol et al., 2017). The production of SCP has many environmental benefits compared to plant/animal proteins, such as lower land requirements and greenhouse gases (GHGs) emissions, or a reduced water footprint (Alloul et al., 2022). Despite these advantages, SCP is currently produced from costly agricultural feedstock or from unsustainable raw materials such as molasses, sucrose, starch, n-alkanes, methanol or natural gas.

Phototrophic purple bacteria (PPB) grown on pathogen-free sources are a potential SCP source, thanks to their high yields and their high amino acids, pigments and vitamins contents. PPB exhibit a highly versatile metabolism, capable of performing anoxygenic photosynthesis, using solar light as energy source, and a wide range of electron/carbon donors such as organic compounds (photoheterotrophic growth), or H_2/H_2S with CO_2 as carbon source (litoautotrophic and photoautotrophic growth) (Capson-Tojo et al., 2020). The resulting H_2 from processes such as dark fermentation of organic waste, syngas, water electrolysis using surplus of electricity from renewable sources, as well as the CO_2 obtained from off-gases, represent promising electron and carbon sources for the sustainable and pathogen-free production of SCP. Spanoghe et al. (2021) proved, for the first time, the feasibility of SCP production from H_2 using pure PPB cultures. However, to the best of our knowledge, the potential of an enriched PPB community (without axenic conditions) growing photoautotrophically with H_2 as SCP source remains unexplored.

Here, the use of an enriched PPB consortium for the bioconversion of H_2 into SCP has been tested for the first time. The influence of environmental conditions (temperature, pH, light intensity) on microbial growth kinetics, protein contents, and microbial population, has been evaluated.

MATERIALS AND METHODS

An enriched photoheterotrophic PPB community grown in continuous photobioreactors treating wastewater was collected in Madrid (Spain) and used as a pre-inoculum. A series of batch enrichments (over 14) in 500 mL Schott flasks were performed to obtain a PPB consortium able to achieve a stable photoautotrophic growth. During each enrichment, aliquots of 20 mL from the previous culture were added to the Schott flasks, together with 230 mL of fresh medium. The medium was based on the mineral synthetic medium (MSM) proposed by Ormerod et al. (1961), modified to ensure photoautotrophic growth. The bottles were closed and the headspace was flushed with N_2 prior to H_2 addition to ensure anaerobic conditions. The initial headspace pressure was adjusted to 1.3 bar. The flasks were covered with UV/VIS filters (Capson-Tojo et al., 2021) and incubated under continuous illumination at ~50 W m^{-2} using infrared LED lights (850 nm) and a temperature of 22±2°C. The flasks pressure was monitored daily. Once the pressure dropped below 1.0 bar, hydrogen was added to reach 1.3 bar. Each enrichment lasted for around one week.

Once the enrichment was stable and showed a constant performance, batch tests at different environmental conditions were tested. Assays at initial pH values of 6, 7 and 8.5, temperatures of 15, 25, 38 and 50°C, and infrared light intensities of 0, 5, 15, 30 and 50 W·m^{-2} were carried out in triplicate, as described above for the enrichments (Figure 1). The gas composition and pressure were monitored 4-5 times per day. These data were used to calculate H_2 consumption rates. Liquid samples were also drawn at the beginning and at the end of each assay in order to determine biomass yields and productivities, crude protein contents, amino acid profiles and microbial communities.

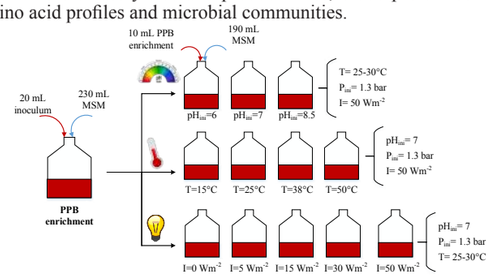

Figure 1. Simplified experimental procedure followed for the evaluation of the influence of environmental conditions (i.e. pH, temperature and light intensity) on the bioconversion of H_2 into SCP using an enriched PPB culture.

RESULTS

After 2-3 enrichments, H_2 consumption was observed, confirming the ability of the mixed PPB culture for growing photoautotrophically. Population analyses (16S r-RNA sequencing) of two enrichment samples after seven cycles confirmed that the consortium was dominated by PPB (> 80%), with *Rhodobacter* sp. and *Rhodopseudomonas* sp. as dominant genera. Consistent biomass yields of 0.9-1.0 g $COD_{biomass}$ □g^{-1} $COD_{consumed}$ were obtained during the last six enrichments.

Environmental conditions had a noticeable impact on H_2 consumption, affecting biomass growth, kinetics and protein production (Figure 2, Table 1). The highest H_2 consumption was observed at initial pH of 7 (with a final value of 8.4 due to CO_2 consumption). The most unfavourable initial pH was 8.5 with a final value of 9.0. The highest H_2 consumption was observed at 25ºC, with 38 and 50ºC decreasing the growth kinetics. Temperatures down to 15ºC also reduced H_2 consumption. Light limitation was observed at intensities lower than 30 W·m^{-2}, but similar results were obtained for both at 30 and 50 W·m^{-2}. Biomass yields close to 1 g $COD_{biomass}$ □g^{-1} $COD_{consumed}$ and protein yields over 4 g protein□g^{-1} H_2 were achieved in almost all the conditions tested (Table 1). These proteins yields were higher than those obtained using pure cultures (Spanoghe et al., 2021). High protein contents (> 50% w/w) were achieved, in agreement with PPB grown photoheterotrophically (Hülsen et al., 2022a, 2022b). Similar C and N contents in the biomass (42 and 9 %w/w) were obtained (Table 1).

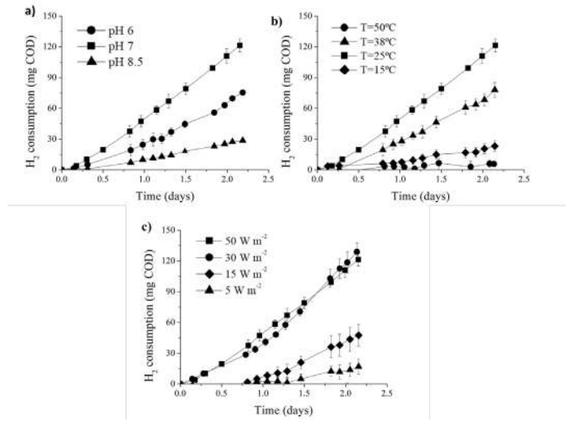

Figure 2. Time course of H_2 consumption by the enriched PPB culture at a) different pH values, b) different temperatures and c) different light intensities. Each data point shows the average and standard deviation (n=3).

Table 1. Main results obtained along with the corresponding standard deviation (n=3) during the batch tests.

	pH		Temperature (°C)		Intensity (W m^{-2})		
	6	8.5	15	38	15	30	50*
Biomass yield (g $COD_{biomass}$ □g^{-1} $COD_{consumed}$)	1.00±0.07	0.93±0.01	0.85±0.07	0.99±0.07	1.02±0.06	1.05±0.01	1.04±0.02
Biomass production rate (mgCOD□L^{-1}□d^{-1})	202±37	77±26	56±44	182±59	110 ±56	378±72	351±60
Protein content of biomass (%w/w)	-	56±5	54±2	51±3	48±7	64±2	51±2
Protein yield (g protein□g^{-1} H_2)	-	3.9±0.3	4.4±0.6	4.3±0.5	4.4±0.2	4.9±0.8	4.2±0.3
C content of biomass (%w/w)	42±1	41±2	41±1	41±1	44±0	43±3	41±2
N content of biomass (%w/w)	8±1	10±0	8±0	9±0	10±0	10±1	10±0

*These values also corresponded to the pH 7 and temperature 25°C tests.

CONCLUSIONS

This study demonstrated that PPB consortia can be efficiently used for production of SCP from H_2. Neutral pH, temperatures of ~25ºC and light intensities higher than 30 W·m^{-2} are the best conditions for biomass growth. **High biomass yields and protein contents were achieved. The high yields and rates achieved confirm the great potential of enriched PPB cultures for H_2 valorisation.**

ACKNOWLEDGEMENTS

The authors acknowledge NextGenerationEU Margarita Salas programme from the European Union for the research contract of María del Rosario Rodero.

REFERENCES

Alloul, A., Spanoghe, J., Machado, D., Vlaeminck, S.E. 2022. Unlocking the genomic potential of aerobes and phototrophs for the production of nutritious and palatable microbial food without arable land or fossil fuels. Microb. Biotechnol. **15**, 6–12.
Capson-Tojo, G., Batstone, D.J., Grassino, M., Vlaeminck, S.E., Puyol, D., Verstraete, W., Kleerebezem, R., Oehmen, A., Ghimire, A., Pikaar, I., Lema, J.M., Hülsen, T. 2020. Purple phototrophic bacteria for resource recovery: Challenges and opportunities. *Biotechnol. Adv.* **43**, 107567.
Capson-Tojo, G., Lin, S., Batstone, D. J., Hülsen, T. (2021). Purple phototrophic bacteria are outcompeted by aerobic heterotrophs in the presence of oxygen. *Water Res.* **194**, 116941.
Hülsen, T., Stegman, S., Batstone, D.J., Capson-Tojo, G. 2022a. Naturally illuminated photobioreactors for resource recovery from piggery and chicken-processing wastewaters utilising purple phototrophic bacteria. *Water Res.* **214**, 118194.
Hülsen, T., Züger, C., Gan, Z.M., Batstone, D.J., Solley, D., Ochre, P., Porter, B., Capson-Tojo, G. 2022b. Outdoor demonstration-scale flat plate photobioreactor for resource recovery with purple phototrophic bacteria. *Water Res.* **216**, 118327.
Ormerod, J.G., Ormerod, K.S., Gest, H. 1961. Light-Dependent Utilization of Organic Compounds Photoproduction of Molecular Hydrogen by Photosynthetic Bacteria ; Relationships with Nitrogen Metabolism. *Arch. Biochem. Biophys.* **94**, 449–463.
Puyol, D., Batstone, D.J., Hülsen, T., Astals, S., Peces, M., Krömer, J.O. 2017. Resource recovery from wastewater by biological technologies: Opportunities, challenges, and prospects. *Front. Microbiol.* **7**, 1–23.
Ritala, A., Häkkinen, S.T., Toivari, M., Wiebe, M.G. 2017. Single cell protein-state-of-the-art, industrial landscape and patents 2001-2016. *Front. Microbiol.* **8**, 2009.
Spanoghe, J., Vermeir, P., Vlaeminck, S.E. 2021. Microbial food from light, carbon dioxide and hydrogen gas: Kinetic, stoichiometric and nutritional potential of three purple bacteria. *Bioresour. Technol.* **337**, 125364.
Zha, X., Tsapekos, P., Zhu, X., Khoshnevisan, B., Lu, X., Angelidaki, I. 2021. Bioconversion of wastewater to single cell protein by methanotrophic bacteria. *Bioresour. Technol.* **320**, 124351.

The potential of H_2S- and CO-tolerant hydrogen-oxidizing bacteria to convert sewage sludge into microbial protein through aerobic syngas fermentation

V. Pelagalli*, S. Matassa**, M. Race*, M. Langone***, S. Papirio**, P. N. L. Lens****, M. Lazzazzara*****, A. Frugis*****, L. Petta******, G. Esposito**

* Department of Civil and Mechanical Engineering, University of Cassino and Southern Lazio, Via Di Biasio 43, 03043 Cassino, Italy (E-mail: vincenzo.pelagalli@unicas.it; marco.race@unicas.it)
** Department of Civil, Architectural and Environmental Engineering, University of Napoli Federico II, Via Claudio 21, 80125 Napoli, Italy (E-mail: silvio.matassa@unina.it; stefano.papirio@unina.it; gioespos@unina.it)
*** Laboratory Technologies for the Efficient Use and Management of Water and Wastewater, Italian National Agency for New Technologies, Energy and Sustainable Economic Development (ENEA), Via Anguillarese, 301, 00123 Rome, Italy (E-mail: michela.langone@ENEA.it)
**** National University of Ireland Galway, University Road, Galway, H91 TK33, Ireland (E-mail: piet.lens@universityofgalway.ie)
***** ACEA ELABORI SpA, Via Vitorchiano 165, Rome, Italy (E-mail: marco.lazzazzara@aceaspa.it; alessadro.frugis@aceaspa.it)
****** Laboratory Technologies for the Efficient Use and Management of Water and Wastewater, Italian National Agency for New Technologies, Energy and Sustainable Economic Development (ENEA), Via Martiri di Monte Sole, 4, 40129 Bologna, Italy (E-mail: luigi.petta@ENEA.it)

Abstract

INTRODUCTION

High volumes of municipal sewage sludge (MSS) are produced worldwide each year (45 dry MT in 2017) (Gao et al., 2020), leading to high management costs for wastewater treatment plants (WWTPs) and serious environmental concerns. The pyrolysis of MSS allows not only its treatment and minimization, but also its conversion into feedstocks such as syngas, a gaseous mixture mainly composed by H_2, CO and CO_2, which could be further valorised into value-added products such as microbial protein (MP) (Sun et al., 2019). MP represents a proteinaceous material (up to 80% of protein content on a weight basis (w/w)) obtained from microbial biomass, and which is employable as alternative protein source for feed and food, as well as for biopolymers and slow-release fertilisers production (Areniello et al., 2022). Hydrogen-oxidizing bacteria (HOB) can ferment gaseous mixtures of H_2, O_2 and CO_2, while accumulating proteins in concentrations up to 75% w/w, and can thus play a key role in the development of a syngas-to-MP route (Matassa et al., 2020). Nevertheless, MSS-derived syngas is characterized by an extremely variable composition, with the H_2/CO_2 volumetric (v/v) ratio varying in the range 0.1-10.0 (Gao et al., 2014; Han et al., 2015), while HOB cultures are generally cultivated by using H_2/CO_2 ratios around 7.0 (Matassa et al., 2015). Potentially inhibitory gases such as H_2S and CO are also present in MSS-derived syngas with concentrations as high as 2000 parts per million by volume (ppmv) and up to 40 % on volume (v/v), respectively (Jaramillo-Arango et al., 2016; Xiong et al., 2013). The potential of HOB to ferment gaseous substrates containing high H_2S concentrations was never assessed before, while a few studies evaluated the performances of pure HOB cultures exposed to CO concentrations as high as 30% v/v (Jiang et al., 2022). In the present study, a mixed culture of HOB was enriched and investigated during the aerobic fermentation of gaseous mixtures simulating realistic MSS-derived syngas, containing H_2, CO_2, CO and H_2S in variable concentrations and ratios. The performance of the HOB culture was evaluated by monitoring gas consumption, biomass concentration as volatile suspended solids (VSS), biomass yield on chemical oxygen demand H_2 equivalents (COD-H_2), biomass volumetric productivity and biomass protein content. Furthermore, the evolution of the enriched HOB culture was evaluated by means of microbial community analysis.

MATERIALS AND METHODS

Active compost was used as source of microorganisms for the enrichment of HOB. The enrichment was performed within 306 mL serum bottles filled with 40 mL of mineral medium prepared according to Yu et al. (2013). The headspace of each bottle was filled with a mixture of $H_2/O_2/CO_2$ in a 65/20/15 volumetric ratio (Matassa et al., 2016), setting an initial pressure of 1.5 bar. The enrichment was incubated at 30 °C and agitated at 600 rotations per minute (rpm). After 5 weeks of enrichment, during which the culture medium and gas headspace were continuously refreshed, the culture showed stable and reproducible growth. The HOB enrichment was then used to perform two different series of batch aerobic fermentation tests, each one aiming to evaluate the effect of a specific syngas composition. In the first tests, a series of short (48 h) batch screening tests were performed to evaluate different syngas mixtures characterized by H_2/CO_2 ratios of 2.0, 4.3 and 10.0, H_2S concentrations from 2000 to 8000 ppmv, and CO concentrations from 10 to 40 % v/v. In the second series of batch tests, the effects of CO concentrations of 10 and 40 % v/v, and those of a mixed condition with CO at 10% v/v and H_2S at 2000 ppmv, were evaluated for a total duration of 30 days by refreshing the liquid and gas phase of each bottle every 48-96 h.

RESULTS AND DISCUSSION

Short-term batch tests

The short-term batch tests allowed to screen the performances of the HOB enrichment in the presence of variable syngas compositions (**Table 1**). No differences were observed for H_2/CO_2 ratios variable between 2 and 10 in terms of biomass concentration and yield (0.53-0.57 g VSS/L and 0.14-0.16 g VSS/g H_2-COD, respectively), as well as for biomass protein content (62-66 %VSS) and H_2 consumption (83-87%). Interestingly, for H_2/CO_2 = 10, a significatively higher CO_2 consumption (90%) was observed, suggesting that higher H_2/CO_2 ratios can lead to a more efficient CO_2 recovery as MP from syngas. Similar values were observed also with the addition of H_2S and CO, without significant differences for concentrations up to 4000 ppmv and 40 % v/v, respectively, thereby showing a remarkable resistance of the HOB enrichment towards these inhibitors. Biomass protein content was not affected by H_2S and CO as well, varying in the ranges of 39-56 %VSS and 53-59 %VSS in the H_2S and CO concentration tests, respectively.

Long-term batch tests

During the long-term batch test, no signs of inhibition were detected with CO as high as 10 and 40 % v/v (conditions CO10 and CO40, respectively) and with the simultaneous exposure to CO and H_2S in concentrations of 10 % v/v and 2000 ppmv, respectively (condition CO10+H_2S) (**Figure 1**). The protein content in biomass was similar in every condition for the entire duration of the test (45-65 %VSS). Biomass yield on H_2 for CO40 was significatively higher with respect to the other conditions, probably due to the H_2-limiting conditions established in the presence of a lower H_2 supply. The analysis of the microbiological composition of the HOB culture before and after the long-term test revealed the determinant role played by the presence of potentially carboxidotrophic HOB in the mixed culture. They might have provided a high degree of resistance to CO, as never shown before in literature for pure HOB cultures. The initial enrichment was mainly composed by representatives of the genus *Paracoccus* (relative abundance of 31.5 %), which were capable of resisting to CO concentrations up to 10 % v/v, but were inhibited by CO concentrations of 40 % v/v. Potentially CO-tolerant HOB, such as *Advenella Kashimrensis*, *Hydrogenophaga*, and *Xanthobacter Autotrophicus,* were instead favoured by the high presence of CO.
Overall, the obtained results suggest that mixed HOB community-driven aerobic syngas fermentation could be performed directly by using raw syngas, delivering high and stable process performances and allowing the production of MP biomass with a protein content of up to 65 % VSS. These findings could have remarkably positive implications in terms of cost and technical feasibility of the overall syngas-to-MP route applied to MSS treatment and valorisation.

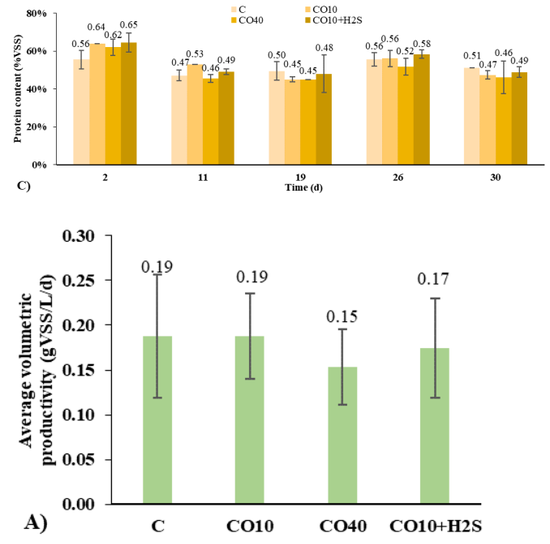

Figure 1. Performances of the HOB enrichment during the long-term batch test. The results are expressed in terms of: **A)** Average volumetric productivity; **B)** Average biomass yield on H_2; **C)** Protein content evolution during the test. *: Statistically different value (*p-value* <0.05).

Table 1. Main results of the short-term batch tests.

	H_2/CO_2		H_2S (ppmv)		CO (% v/v)	
	2, 4.3	10	0 - 4000	6000, 8000	0 - 30	40
H_2 consumption (%)	83 - 87		85 - 97	11* - 0*	82 - 94	
CO_2 consumption (%)	30 - 53	90*	47 - 62	0*	34 - 58	
Final biomass concentration (gVSS/L)	0.53 - 0.57		0.57 - 0.64	0.09* - 0.17*	0.54 - 0.59	
Biomass yield on H_2 (gVSS/gH_2-COD)	0.14 - 0.16		0.13 - 0.17	n.c.	0.13 - 0.20	
Protein content (%VSS)	62 - 66		39 - 56		53 - 59	

*: Statistically different value (*p-value* < 0.05); n.c.: not calculated due to negligible biomass growth.

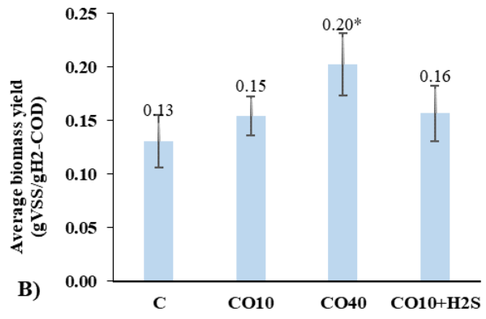

REFERENCES

Areniello, M., Matassa, S., Esposito, G., Lens, P.N.L., 2022. Biowaste upcycling into second-generation microbial protein through mixed-culture fermentation. Trends Biotechnol.
Gao, N., Kamran, K., Quan, C., Williams, P.T., 2020. Thermochemical conversion of sewage sludge: A critical review. Prog. Energy Combust. Sci. 79, 100843.
Gao, N., Li, J., Qi, B., Li, A., Duan, Y., Wang, Z., 2014. Thermal analysis and products distribution of dried sewage sludge pyrolysis. J. Anal. Appl. Pyrolysis 105, 43–48.
Han, R., Zhao, C., Liu, J., Chen, A., Wang, H., 2015. Thermal characterization and syngas production from the pyrolysis of biophysical dried and traditional thermal dried sewage sludge. Bioresour. Technol. 198, 276–282.
Jaramillo-Arango, A., Fonts, I., Chejne, F., Arauzo, J., 2016. Product compositions from sewage sludge pyrolysis in a fluidized bed and correlations with temperature. J. Anal. Appl. Pyrolysis 121, 287–296.
Jiang, Y., Yang, X., Zeng, D., Su, Y., Zhang, Y., 2022. Microbial conversion of syngas to single cell protein: The role of carbon monoxide. Chem. Eng. J. 450, 138041.
Matassa, S., Boon, N., Verstraete, W., 2015. Resource recovery from used water: The manufacturing abilities of hydrogen-oxidizing bacteria. Water Res.
Matassa, S., Papirio, S., Pikaar, I., Hülsen, T., Leijenhorst, E., Esposito, G., Pirozzi, F., Verstraete, W., 2020. Upcycling of biowaste carbon and nutrients in line with consumer confidence: the "full gas" route to single cell protein. Green Chem. 22, 4912–4929.
Matassa, S., Verstraete, W., Pikaar, I., Boon, N., 2016. Autotrophic nitrogen assimilation and carbon capture for microbial protein production by a novel enrichment of hydrogen-oxidizing bacteria. Water Res. 101, 137–146.
Sun, X., Atiyeh, H.K., Huhnke, R.L., Tanner, R.S., 2019. Syngas fermentation process development for production of biofuels and chemicals: A review. Bioresour. Technol. Reports 7, 100279.
Xiong, S., Zhuo, J., Zhang, B., Yao, Q., 2013. Effect of moisture content on the characterization of products from the pyrolysis of sewage sludge. J. Anal. Appl. Pyrolysis 104, 632–639.
Yu, J., Dow, A., Pingali, S., 2013. The energy efficiency of carbon dioxide fixation by a hydrogen-oxidizing bacterium. Int. J. Hydrogen Energy 38.

Integration of heterotrophic microalgae beads bioreactor in microbial electrosynthesis for bioelectro-conversion of carbon dioxide into bio-oil and proteins

Silvia Bolognesi[1], Marcello Gavino Cau[2], Lluís Bañeras[3], Andrea G. Capodaglio[2], Maria Dolors Balaguer[1], Sebastià Puig[1]

[1] LEQUiA, Institute of the Environment, Universitat de Girona, Carrer Maria Aurèlia Capmany 69, Girona 17003, Spain.
[2] Department of Civil Engineering and Architecture, University of Pavia, Via Ferrata 1, 27100 Pavia, Italy.
[3] Group of Molecular Microbial Ecology. Institute of Aquatic Ecology, University of Girona, Carrer Maria Aurèlia Capmany 40, Girona 17003, Spain.

Abstract

Finding new strategies to minimize carbon dioxide (CO_2) emissions impact is at the centre of society interests nowadays. The current fossil fuels crisis motivates both researchers and governments in finding alternative energy sources. Microbial electrosynthesis (MES) for bioelectroCO_2 recycling is an interesting and sustainable opportunity to exploit the spent off-gases from industrial facilities and convert them into valuable products. A novel setup for direct conversion of CO_2 is herein presented: a two-chamber BES coupled with a heterotrophic microalgae beads bioreactor (HMBB) was built and operated in recirculated batch mode. Acetic acid production from CO_2 and electricity was assessed and directly used as feedstock by the microalgae for biodiesel-compatible bio-oil and protein productions.

Keywords

Acetate production; *Auxenochlorella protothecoides*; biocathode; biodiesel; heterotrophic microalgae; microbial electrosynthesis.

INTRODUCTION

In just over a century, human activity significantly played a part in the constantly increasing greenhouse gas (GHG) emissions worldwide (Melillo et al., 2009). Researchers' interest in finding new strategies for GHG emissions mitigation increased sensibly and led governments to encourage to increase in the energy efficiency of productive processes, promote the use of non-fossil fuels, and enhance the capture and storage of carbon dioxide (CO_2) as well as its re-valorization. In this context, microbial electrosynthesis (MES) emerges as a promising technology for CO_2 conversion into multi-carbon products, such as added-value chemicals and biofuels. Being acetate the most abundant product, of scarce economic revenue and challenging downstream process. Further research for strategies to improve the economical sustainability of the process is essential, either by steering production to longer molecules or combining technologies (LaBelle and May, 2017; Dessì 2021). The coupling of MES systems with microalgae is an interesting option to enhance resource recovery by applying a biorefinery approach (Bolognesi et al., 2021; Sevda et al., 2019). Microalgae are considered a resource for GHG emissions mitigation, plus an essential feedstock for microalgal biorefinery products, such as biofuels and food and feed goods. Heterotrophic microalgae, though not directly exploiting CO_2, can use acetate and other short-chain fatty acids for their growth, accumulating lipids in their cells, with no need for light exposure. In the present study, a two-stage process based on coupling MES and a heterotrophic microalgae beads bioreactor (HMBB) is proposed to convert carbon dioxide into biodiesel-compatible oil and proteins. The overall process from CO_2 to bio-oils and proteins includes bioelectroCO_2 conversion into volatile fatty acids (VFAs) and their subsequent conversion into microalgae biorefinery products.

MATERIALS AND METHODS

A two-chambered methacrylate BES was built and operated in recirculated batch mode for 170 days. Cathodic and anodic chambers were separated by a cationic exchange membrane (Membranes International, USA). Carbon cloth (FuelCellsEtc., USA) was used as the cathode while a graphite rod was used as the anode. An Ag/AgCl reference electrode (+0.197 V vs. SHE) was also placed in the cathodic chamber, operating a three-electrode configuration with a potentiostat (Nanoelectra, Spain, E_{cat}=-0.8 V vs SHE). The net liquid volume for both anodic and cathodic chambers was 250 mL. The experiment was conducted at 25±3 °C. The biocathode was inoculated with 100 mL of inoculum from a parent BES (Bolognesi et al., 2022). Both anodic and cathodic chambers were filled with a modified ATCC1754 PETC medium adjusted to pH 6 (Blasco-Gómez et al., 2019). CO_2 (99.9%, Praxair, Spain) was the only carbon source, and it was supplied to the cathodic chamber every 3 days for 1 minute. Before feeding, gas and liquid samples were collected and analyzed to monitor the gas composition and the production of volatile fatty acids (VFAs) and alcohols, as reported in Bolognesi et al. (2022).

The HMBB was prepared by using a glass tube (d_{int}=1.8 cm, h=60 cm) and filled with a 5 cm layer of glass beads (d=0.8 cm) at the bottom, a 50 cm microalgae beads layer, and a 5 cm layer of glass beads to prevent overflow of algae and connected to the cathodic recirculation line (Figure 1). The HMBB was covered to maintain heterotrophic conditions. To prepare the microalgae beads, alginic acid was added to the microalgae solution (1g/100mL) and stirred continuously for one hour. Then, the solution was released drop by drop with a pipette in a $CaCl_2$ solution (0.5g/100 mL) to form the beads. Before the oil extraction, chlorophyll/protein analysis, microalgae beads were dissolved in a 0.1M EDTA solution, and then centrifuged to separate the pellet from the alginate.

Microalgae cultivation, Chlorophyll a analysis, and oil extraction from microalgae were performed as in Bolognesi et al. (2022). Protein extraction and quantification were performed at the beginning and end of each test, using the Bradford protein assay. Figure 2 schematizes the proposed process.

RESULTS AND DISCUSSION

Results obtained in terms of VFAs production and rates were in line with the previous works of our group (Bolognesi et al. 2022). Once the content of acetic acid was sufficient high to sustain the feed for the microalgae, the HMBB was connected to the recirculation line of the biocathode. A series of tests (Table 1) were performed. Table 1 reports initial and final values, but intermediate points for Chlorophyll a, optical density (OD_{540}) and acetate content were taken every second day. The first three tests (Test A, Test B and Test C) were performed with the HMBB disconnected from the MES reactor using a synthetic medium (1.5 g L^{-1} acetate solution) as feedstock. These preliminary tests were conceived to prove the switch from autotrophic to heterotrophic behaviour in algae beads and microalgae growth. All tests confirmed that heterotrophic conditions were reached (linked to the decrease of chlorophyll content) and that encapsulated microalgae were growing. Test B and Test C were performed with replicates algae beads/liquid microalgae to evaluate if using alginate to form the algae beads affected the performance. Test B confirmed that microalgae growth in microalgae beads and liquid microalgae was comparable (+2% for beads). Test C included oil extraction and the oil content detected was low (5%) due to problems with alginate removal compared to the liquid algae control (13%). During the test C, acetate consumption rate was compared between liquid algae and beads, resulting in higher rates for the liquid algae in the first 2 days (436 mg $L^{-1}d^{-1}$ against 371 mg $L^{-1}d^{-1}$), while increased during days 2-5 for the algae beads (168 mg $L^{-1}d^{-1}$ against 205 mg $L^{-1}d^{-1}$). Overall acetate consumption rate was comparable for both configurations.

All the following tests (D, E, F) were performed with the HMBB connected to the MES. During the last tests, both protein and oil contents were analyzed in the liquid algae and microalgae beads, confirming that the alginate does not significantly affect the performance. Oil extracted in test F was analyzed with NMR to compare its profile with other bio-oil compounds available in the literature. Both protein content and oil extracted from the microalgae increase over time using the acetate synthesized in an MES, making the process profitable for biofuel production and synthesis of proteins. The biorefinery potential of MES-HMBB system was assessed, further studies will be performed to test the system under continuous operation and to expand the portfolio of products.

Table 1. Global view of the tests performed with the HMBB. The increment or decrement over time in terms of microalgae growth, acetate content and chloropyll a is reported in parentheses.

	Day	Microalgae growth [g L^{-1}]	Acetate content [g L^{-1}]	Chlorophyll a [mg L^{-1}]	Oil extraction [%]	Protein content [protein/ biomass, %]	HMBB carbon source
Test A	0	0.705	1.437	0.39	-	-	Synthetic
	7	0.793 (+0.088)	0 (-1.437)	0.25 (-0.14)			
Test B	0	1.364	1.441	0.13	-	-	Synthetic
	9	1.707 (+0.343)	0.003 (-1.438)	0.08 (-0.05)			
Test C	0	0.78	1.442		-	-	Synthetic
	10	2.45 (+1.67)	0 (-1.442)	-	5		
Test D	0	0.92	1.442			28.2	Connected to MES
	7	1.51 (+0.59)	0.003 (-1.439)	-	17	37.9	
Test E	0	1.11	1.042			13.2	Connected to MES
	9	1.47 (+0.36)	0.001 (-1.041)	-	17.6	16.1	
Test F	0	1.15	0.359			14.7	Connected to MES
	7	1.39 (+0.24)	0.022 (-0.337)	-	10	22.2	

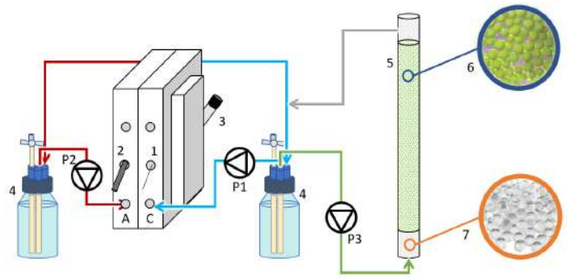

Figure 1. Scheme of the experimental setup. 1) Cathode electrode; 2) anode electrode; 3) reference electrode Ag/AgCl; 4) recirculation buffer tanks; 5) microalgae beads bioreactor; 6) microalgae beads; 7) glass beads. P1, P2 and P3: recirculation pumps.

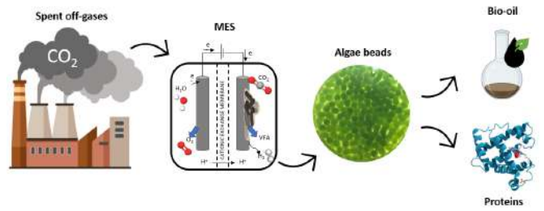

Figure 2. Scheme of the proposed process for CO_2 bio-electro conversion into added value products.

ACKNOWLEDGEMENTS

S.B. is a Juan de la Cierva Formación Fellow (FJC2021-047260-I). S.P. is a Serra Hunter Fellow (UdG-AG-575) and acknowledges the funding from the ICREA Academia award. LEQUIA and EcoAqua have been recognized as "consolidated research groups" (Ref 2021 SGR01352 and 2021 SGR01142) by the Catalan Agency of Research and Universities.

REFERENCES

Melillo, J.M., Reilly, J.M., Kicklighter, D.W., Gurgel, A.C., Cronin, T.W., Paltsev, S., Felzer, B.S., Wang, X., Sokolov, A.P., Schlosser, C.A. 2009 Indirect Emissions from Biofuels: How Important? *Science.* **326**, 1397–1399.

LaBelle, E. V., May, H.D., 2017 Energy efficiency and productivity enhancement of microbial electrosynthesis of acetate. *Frontiers in Microbiology* **8**, 1–9.

Dessì, P., Rovira-Alsina, L., Sánchez, C., Dinesh, G.K., Tong, W., Chatterjee, P., Tedesco, M., Farràs, P., Hamelers, H.M.V., Puig, S. 2021. Microbial electrosynthesis: Towards sustainable biorefineries for production of green chemicals from CO_2 emissions. *Biotechnology Advances* **46,** 107675.

Bolognesi, S., Cecconet, D., Callegari, A., Capodaglio, A.G. 2021 Combined microalgal photobioreactor/microbial fuel cell system: performance analysis under different process conditions. *Environmental Research* **192**, 110263.

Sevda, S., Garlapati, V.K., Sharma, S., Bhattacharya, S., Mishra, S., Sreekrishnan, T.R., Pant, D., 2019 Microalgae at niches of bioelectrochemical systems: A new platform for sustainable energy production coupled industrial effluent treatment. *Bioresource Technology Reports* **7**, 100290.

Bolognesi, S., Bañeras, L., Perona-Vico, E., Capodaglio, A. G., Balaguer, M. D., Puig, S. 2022 Carbon dioxide to bio-oil in a bioelectrochemical system-assisted microalgae biorefinery process. *Sustainable Energy & Fuels*, **6**(1), 150–161.

Blasco-Gómez, R., Balaguer, M.D., Puig, S., Bañeras, L., Colprim, J.Ramió-Pujol, S., 2019 Unravelling the factors that influence the bio-electrorecycling of carbon dioxide towards biofuels. *Green Chemistry* **21**, 684–691.

Co-treatment of urban wastewater and municipal solid waste by mixed phototrophic cultures to generate PHA by varying organic carbon loads

Sandra Chacón-Aparicio[a], John Villamil[a], Raúl Molina[a] & Daniel Puyol[a].

[a] Universidad Rey Juan Carlos de Móstoles. Departamento de Tecnología Química y Ambiental.

sandra.chacon@urjc.es, john.villamil@urjc.es, raul.molina@urjc.es & daniel.puyol@urjc.es

Abstract

Co-treatment of urban wastewater together with pre-treated municipal solid waste for organic matter solubilization has proved to be an optimal environment for mixed phototrophic cultures of PPB. These cultures bacteria, working with an OLR of 0.94, an HRT of 3 days, an SRT of 6 days, 12:12h light cycles, and in a feast/famine regime, have been able to accumulate up to 12% PHA under continuous operation . This work has shown the possibility of co-treating two municipal wastes simultaneously to promote PHA accumulation under microaerophilic conditions.

Keywords

Co-treatment, OFMSW, PHA, Purple phototropic bacteria (PPB), urban wastewater.

INTRODUCCTION

There is increasing interest in looking for sustainable and competitive alternatives to petroleum-based plastics to mitigate the climate change caused by their production. One of the most promising options is bio-polymers of easy degradation, such as polyhydroxyalkanoates (PHA), where microbial biotechnology becomes indispensable for its production (Pilafidis et al., 2022). Several bacteria accumulate this biopolymer as a reservoir of energy. Some cultures capable of producing this bio-plastic include mixed phototrophic cultures of purple phototrophic bacteria (PPB) (Carvalho et al., 2014). However, the problem of extracting the PHA makes these processes very expensive and difficult to include in the commercial market. For this reason, it has been proposed to use waste to reuse it and generate added-value products while simultaneously adding value to these wastes (Carvalho et al., 2014). Several studies use organic wastes for the production of PHA, such as molasses, cheese whey, bio-oil, or industrial wastewater (Pokój et al., 2019), but in most cases, they are diluted to exceed the carbon requirements or supplemented with nutrients to reach the optimum ratio for the growth of PPB. However, co-treatment of wastewater with the organic fraction of municipal solid waste (OFMSW) favors an optimal COD:N:P mixture for growing mixed PPB cultures. In this case, the OFMSW is pre-treated by a steam explosion so that the organic matter is solubilised and can be easily disposed of to the crops, the conditions for which can be found in (Allegue et al., 2022).

In this work, we propose an alternative way of co-treatment of two urban wastes such as domestic wastewater and OFMSW, whose mixture gives rise to the optimal ratio of COD:N:P for the growth and accumulation of PHA by PPB cultures. It should be considered that the metabolic pathway of PHA accumulation in PPB cultures begins with volatile fatty acids (VFA) (Sali & Mackey, 2021), so fermenting the substrates favors this process, and even the presence of sugars in the medium can have a negative effect (Rangel et al., 2023). For this reason, two CSRT reactors are used simultaneously to observe the influence of fermenting LF (CSTR-2) or avoiding fermentation (CSTR-1) and mixing it with DWW. In addition, the inclusion of a hollow fiber membrane in each reactor means that the hydraulic and cell retention times can be separated. Therefore, the volumetric organic load can be optimized since carbon should be in excess, but there needs to be a deficit of one of the nutrients (N or P) (Hülsen et al., 2014). Another novel point of this work is to operate the reactors under microaerophilic conditions, where the ORP of both reactors has been monitored, as it is essential to keep it negative as they are anaerobic cultures (J. Fradinho et al., 2016).

MATERIALS AND METHODS

The co-treatment of the mixed urban wastes has been tested in two 2L cylindrical photobioreactors inoculated with 1% v/v of a mixed culture of PPB and operated in semi-continuous mode, fed during a light cycle of 12/12 h only. The reactors were continuously agitated with a shaker motor at 300 rpm. Two IR-LED lamps (emitting at 850 nm) illuminated the reactors from two sides. Each bioreactor's temperature and oxidation-reduction potential (ORP) were continuously monitored.

Both reactors had worked under microaerophilic conditions opened to the air, simulating the environmental conditions of a scaled-up process. The CSTR-1 was fed using the LF and DWW, and the CSTR-2 was fed using the fermented LF and de DWW (due to operative problems in the UASB, the Stage D was fed using DWW and mix of 50% of synthetic acids Hac:But:Prop and 50% of unfermented LF). The operational stages of both reactors are described in Table 1, where Stage 1 served as acclimatization to obtain a culture enriched in PPB working at an optimal COD:N ratio for its growth. Stage 2 increased the OLR without considering the optimal COD:N ratio for PHA accumulation. Stage 3 focused on PHA accumulation, where only SRT and HRT were fixed by varying OLR. This last stage is still in progress.

Table 1. Operating conditions of CSRT during the whole trial.

	STAGE 1		STAGE 2	STAGE 3		
Sub-Stage	A	B	C	D	E	F
HRT (d)	2,25	1,5	1,5	3	2,25	1,5
SRT (d)	3	2	2	6	6	6
OLR (gCOD/ L*d)	0,36	0,57	0,62	0.94 *Ongoing	*1.5* *To be made	*2 *To be made*
COD:N	100:5		*variable	100:3		
Time (d)	42	37	73	77		
Period (d)	1-42	43-80	81-153	253-330*		

Source of biowaste

The OFMSW came from a municipal waste processing plant in Madrid (Spain). The OFMSW had been thermally hydrolyzed according to previous results (Allegue et al., 2022). This treatment favors the solubilization of organic matter for its following acidification. The liquid fraction of the hydrolysate upon centrifugation was used in this work. *The DWW* came from the outlet of the primary settlers of two domestic wastewater treatment plants (WWTP) located in Estiviel, Toledo (Spain), and Valdebebas, Madrid (Spain).

RESULTS AND DISCUSSION

Values of 12% PHA were achieved in CSTR-2 with an HRT of 3d and an SRT of 6d, setting the OLR at 0.94 gCOD/L*d and, in addition, a more stable PHA production than in CSTR-1 was observed throughout Stage 3 compared to an average of 3.3% PHA in CSTR-1. It is observed that CSTR-2 has a more stable PHA production due to the influence of VFA in the medium and the lower concentration of nutrients in the mixture.

CSTR-1 does not maintain a stable PHA production even though the OLR in the reactor is increased and the solids concentration is similar to that of CSTR-2. A low assimilation of N and P by the PPB does not favor the accumulation of PHA. On the other hand, high organic loads may destabilize the system and promote the accumulation of glycogen instead of PHA, as described in a previous work (Allegue, et al., 2022).

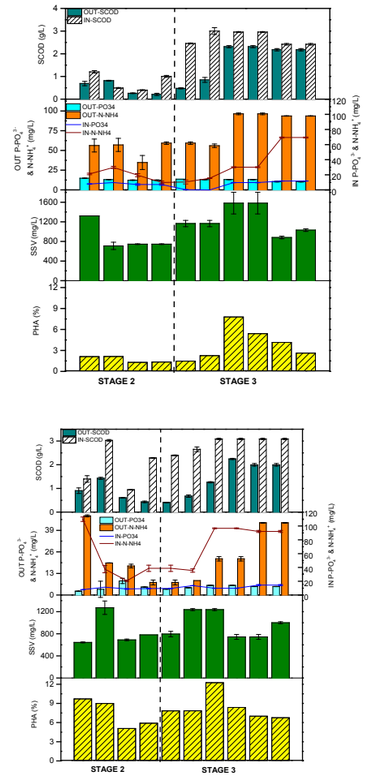

Figure 1. Time course of SCOD, nutrients, volatile solid suspension and PHA accumulation in both reactors at Stage 2 and 3. The graph on the left represents CSTR-1 and the graph on the right represents CSTR-2.

Although in the literature the data on PHA accumulation are higher using fermented DWW (up to 30%), these results are very promising as stability is observed in CSTR-2, which may lead us to believe that the mixed PPB culture developed in the reactor has a better resistance to changes in OLR than that of CSTR-1. In addition, working with the feast/famine strategy under continuous illumination together with external VFA feeding, 20% PHA is feasible (J. Fradinho et al., 2021). Therefore, variations of the HRT and SRT are fundamental, but establishing an optimal COD:N ratio for the operation of these reactors will be crucial for their scale-up. Thus, it is proposed in the following two Stages to decrease the COD:N ratio to 100:2 by fixing the OLR and varying the hydraulic and cell retention times. Increasing the SRT may stabilize more the phototrophic mixed consortia to allow a more positive reaction to carbon overload due to a lower specific loading rate, likely increasing PHA accumulation.

REFERENCIAS

Allegue, L. D., Puyol, D., & Melero, J. A. (2022). Synergistic thermophilic co-fermentation of food and lignocellulosic urban waste with steam explosion pretreatment for efficient hydrogen and carboxylic acid production. *Biofuels, Bioproducts and Biorefining*, *16*(2), 499–509.

Allegue, L. D., Ventura, M., Melero, J. A., & Puyol, D. (2022). Unraveling PHA production from urban organic waste with purple phototrophic bacteria via organic overload. *Renewable and Sustainable Energy Reviews*, *166*, 112687.

Carvalho, G., Oehmen, A., Albuquerque, M. G. E., & Reis, M. A. M. (2014). The relationship between mixed microbial culture composition and PHA production performance from fermented molasses. *New Biotechnology*, *31*(4), 257–263.

Fradinho, J., Allegue, L. D., Ventura, M., Melero, J. A., Reis, M. A. M., & Puyol, D. (2021). Up-scale challenges on biopolymer production from waste streams by Purple Phototrophic Bacteria mixed cultures: A critical review. *Bioresource Technology*, *327*, 124820.

Fradinho, J. C., Reis, M. A. M., & Oehmen, A. (2016). Beyond feast and famine: Selecting a PHA accumulating photosynthetic mixed culture in a permanent feast regime. *Water Research*, *105*, 421–428.

Hülsen, T., Batstone, D. J., & Keller, J. (2014). Phototrophic bacteria for nutrient recovery from domestic wastewater. *Water Research*, *50*, 18–26.

Pilafidis, S., Diamantopoulou, P., Gkatzionis, K., & Sarris, D. (2022). Valorization of Agro-Industrial Wastes and Residues through the Production of Bioactive Compounds by Macrofungi in Liquid State Cultures: Growing Circular Economy. *Applied Sciences 2022, Vol. 12, Page 11426*, *12*(22), 11426.

Pokój, T., Klimiuk, E., & Ciesielski, S. (2019). Interactive effect of crude glycerin concentration and C:N ratio on polyhydroxyalkanoates accumulation by mixed microbial cultures modelled with Response Surface Methodology. *Water Research*, *156*, 434–444.

Rangel, C., Carvalho, G., Oehmen, A., Frison, N., Lourenço, N. D., & Reis, M. A. M. (2023). Polyhydroxyalkanoates production from ethanol- and lactate-rich fermentate of confectionary industry effluents. *International Journal of Biological Macromolecules*, *229*, 713–723.

Sali, S., & Mackey, H. R. (2021). The application of purple non-sulfur bacteria for microbial mixed culture polyhydroxyalkanoates production. *Reviews in Environmental Science and Bio/Technology 2021 20:4*, *20*(4), 959–983.

Maximising the production of composition-specific polyhydroxyalkanoates from volatile fatty acids

Y. López-Garabato*, A. Pedrouso*, ** and A. Mosquera-Corral*

* CRETUS Institute, Department of Chemical Engineering, Universidade de Santiago de Compostela, Rua Lope Gomez da Marzoa s/n, E-15782 Santiago de Compostela, Spain
(E-mail: *yolandalopez.garabato@usc.es; alba.pedrouso@usc.es; anuska.mosquera@usc.es*)
** Department of Biotechnology, Delft University of technology, Van der Maasweg 9, 2629HZ, Delft, The Netherlands.

Abstract

Polyhydroxyalkanoates (PHA) are biodegradable polymers that can be produced by mixed microbial cultures (MMC) from different complex wastes for organic carbon recovery. PHA-accumulating microorganisms were selected in an enrichment sequencing batch reactor (SBR) inoculated with sewage sludge. The SBR was fed with volatile fatty acids and operated in five stages with different fed organic loads, from 2.50 g COD/(L·d) to 5 g COD/(L·d). It was enriched from the first week of operation and reached an average PHA accumulation of 51.9 ± 4.8 % at the end of the feast phase. The biomass concentration increased from 0.8 to 1.5 g VSS/L, which means increase the PHA productivity in the accumulation reactor. Thus, this study demonstrates the rapid MMC enrichment and its excellent performance at high loads, producing PHA with the target composition of 88% PHB and 12% PHV that provide propylene-like properties.

Keywords

Enrichment; fish cannery waste valorisation; mixed microbial culture; PHA; propylene.

INTRODUCTION

Polyhydroxyalkanoates (PHA) are natural, renewable and biocompatible biopolymers with properties similar to petrochemical plastics that can be produced by some microorganisms as energy storage. The PHA production by using pure cultures is expensive due to the need to use specific substrates and to maintain sterile conditions (Raza et al., 2018). These reasons have led to the search for more economic and environmentally sustainable production alternatives.

In this context, the use of mixed microbial cultures (MMC) stands out allowing the use of low-cost substrates (such as wastes from agri-food industries) and operation under non-sterile conditions (Raza et al., 2018). MMC is generally obtained from activated sludge systems from wastewater treatment plants because they contain a wide variety of microorganisms, including those that accumulate PHA (Tu et al., 2019). PHA production by MMC usually involves three steps: the acidogenic fermentation of the feedstock to obtain a stream rich in volatile fatty acids (VFA), the selection and enrichment of PHA-accumulating microorganisms, and the maximisation of PHA accumulation with the enriched biomass (Tu et al., 2019). The composition of the PHA obtained determines their properties and thus their potential applications (Raza et al., 2018).

The present study is part of the project BIOCENPLAS which aims to the production of PHA from acidified fish canning effluents to produce plastic packaging for this industrial sector. This research is focussed on the optimisation of the MMC enrichment step to maximize the productivity of the system on PHA which comply with the desired composition of 88 % PHB and 12 % PHV, that has properties like propylene, one of the most used petrochemical plastics in the agri-food industry.

MATERIALS AND METHODS

A 4-L Sequencing Batch Reactor (SBR) was operated under a dynamic aerobic feeding regime, at 30 ºC and without pH control, to select a MMC enriched in PHA-accumulating bacteria. The SBR operating cycles lasted 12 hours, and the hydraulic and solid retention times were 1 day. The dissolved oxygen (DO) concentration is measured over the cycle.

The SBR operational period lasted 231 days and was divided into five Stages (S) according to the fed organic load: I) 2.5 g COD/(L·d), II) 3.13 g COD/(L·d), III) 3.75 g COD/(L·d), IV) 4.38 g COD/(L·d) and V) 5 g COD/(L·d). The organic feeding consisted of a VFA mixture with a composition of 44% acetic acid, 44% butyric acid, 8% propionic acid and 4% valeric acid (% as COD). VFA and nutrient solutions (Palmeiro-Sánchez et al., 2016) were added simultaneously at the beginning of the cycle. The ammonium solution (165 mg NH4/L) was added uncoupled after 5 hours from the beginning of the cycle, to foster the nitrogen limitation during the feast phase. Nitrogen concentration also varied over Stages proportionally to the organic load increase.

RESULTS AND DISCUSSION

The selection of PHA-accumulating microorganisms was considered reached after 7 days of operation, when the duration of the feast phase (part of the cycle when the DO concentration remains low) was shorter than 20% of the total cycle duration (2.4 hours, Figure 1) according to Dionisi et al. (2007). The fed organic load was progressively increased up to 5 g COD/(L·d) without observing significant influence on the MMC enrichment performance (Figure 1). The values of the feast length that oscillate above the limit of 2.4 hours are ascribed to determination inaccuracies due to fouling of the DO electrode.

The MMC presented a high PHA-accumulation capacity at the end of the feast with average values of 52 ± 5 % (Figure 2), similar to the 51.30 % obtained by Palmeiro-Sánchez et al., (2016). No PHA accumulation data is available for Stage V yet. The targeted PHA composition (88% PHB and 12% PHB), able to potentially substitute the propylene, was obtained and remained stable (Figure 2).

The biomass concentration increased, because of the increase of the fed load, from 0.8 to 1.5 g VSS/L (Figure 3). Having a more concentrated sludge with high PHA-accumulating capacity will boost the productivity of the PHA accumulation reactor. This will allow to have a more compact resource recovery system decreasing not only the CAPEX but also downstream costs.

Acknowledgements

This research was funded by the Spanish Government through the BIOCENPLAS project (2021-PN070). Alba Pedrouso acknowledges the Xunta de Galicia (Spain) for her postdoctoral fellowship (ED481B-2021-041). The authors belong to the Galician Competitive Research Group (GRC D431C-2021/37).

REFERENCES

Dionisi D., Majone M., Vallini G., Gregorio S. D., Beccari M. 2007 Effect

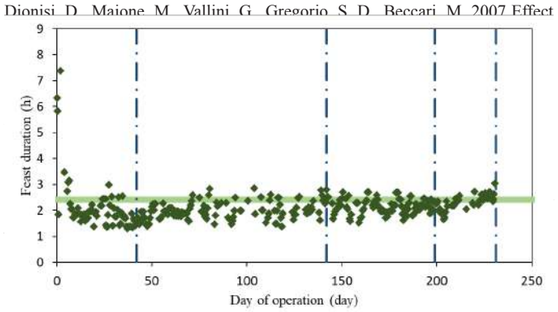

Figure 1. Feast duration all over the different operation cycles. The horizontal line represents the limit of enrichment (20 % of the total cycle duration), and the vertical lines divided the operation in the different stages from the stage I to V.

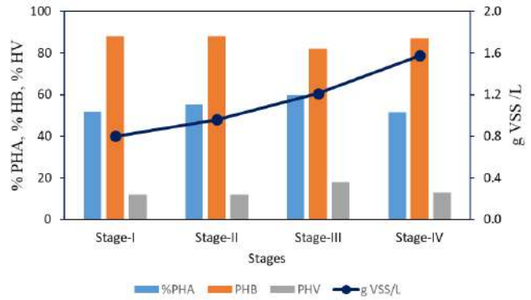

Figure 2. Percentage of polyhydroxyalkanoates (PHA) accumulated at the end of the feast phase, polyhydroxybutyrate (PHB) and polyhydroxyvalerate (PHV) and concentration of biomass all over the operational stages.

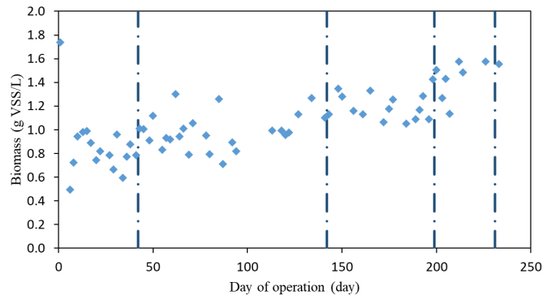

Figure 3. Evolution of the biomass concentration in the enrichment reactor all over time. The vertical lines divided the operation in the different stages from the stage I to V.

Resources from wastewater: employment of an advanced strategy for polyhydroxyalkanoates (PHA) synthesis and recovery

A. Mineo*, L. Isern-Cazorla**, M.E. Suárez Ojeda**, G. Mannina*

* Engineering Department, Palermo University, Viale delle Scienze ed. 8, 90128, Palermo, Italy
(E-mail: *antonio.mineo01@unipa.it; giorgio.mannina@unipa.it)*
**GENOCOV Research Group, Department of Chemical, Biological and Environmental Engineering, School of Engineering, Universitat Autònoma de Barcelona, Escola d'Enginyeria-Edifici Q, Campus UAB, 08193, Bellaterra, Barcelona, Spain.
(E-mail: *Laura.Isern@uab.cat;MariaEugenia.Suarez@uab.cat*)

Abstract
Polyhydroxyalkanoates (PHA) are one of the main resources recoverable from various waste feedstocks such as sewage sludge. Despite the increasing number of papers, sewage sludge based PHA production is still far from the industrial application. The goal of this work, therefore, is to provide experimental data on PHA productivity in the light of a possible scaling up of the process. PHA producers were selected, and it was used to perform several accumulation tests by employing an own-designed software, reaching up to 60 % w/w of PHA contents in the biomass. Finally, an improved PHA extraction protocol was applied obtaining high recovery (78 ± 3 %) and purity (89 ± 2 %) yields.

Keywords Bioplastic production, Polyhydroxyalkanoates, Resource recovery, Sewage Sludge, Wastewater.

INTRODUCTION

Nowadays, despite of research in PHA resource recovery using municipal secondary sewage sludge from wastewater treatment is in the hot spot, still few works focus on improving the crucial stages of PHA accumulation and downstream process even though biopolymer content and quality are pivotal parameters to achieve the economic sustainability of the overall process (Moretto et al., 2020; Pesante and Frison, 2023). However, in the view of industrial PHA production process, other parameters such as the PHA productivity can be also prominent and should be monitored when pilot plant experiments towards scale-up are performed. In this sense, this work proposes a new advanced strategy to enhance the PHA accumulation from domestic wasted sewage sludge by fully automating the process using a newly homemade software. Moreover, the extraction protocol previously described by Mannina et al. (2019) was modified to improve recovery and purity yields.

MATERIALS AND METHODS

The pilot plant experiments were carried out at the Water Resource Recovery Laboratory at Palermo University (Mannina, et al., 2021). Three different selection sequencing batch reactors (S-SBR) were run at three volumetric organic-loading-rates (vOLR) to select PHA producers by adopting the aerobic dynamic feeding (ADF) strategy with a synthetic substrate. Once the selection reached the pseudo steady-state conditions, the biomass was harvested to perform two accumulation tests for each S-SBR at different food to microorganism (F/M) ratio (Table 1). The accumulation tests were run with an automatic pulsate feeding based on the feed-on-demand strategy controlled by a homemade software (Figure 1). Finally, the extraction protocol proposed by Mannina et al. (2019) was modified and applied.

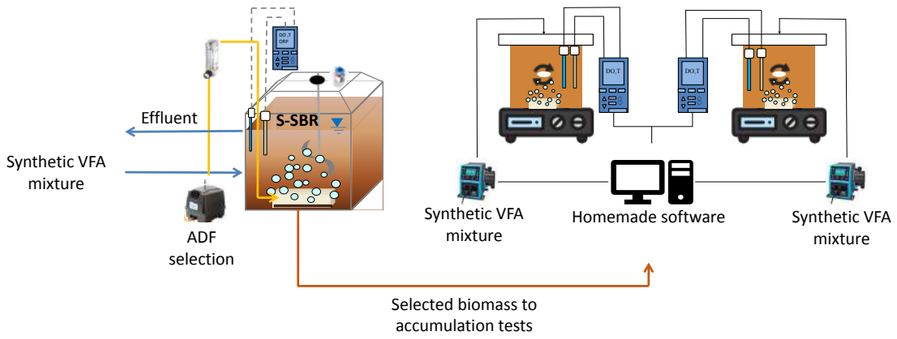

Figure 1. UNIPA pilot plant layout.

RESULTS AND DISCUSSION

Biomass enrichment and PHA accumulation

The highest vOLR applied (1.8 g COD L^{-1} d^{-1}) and feast-to-famine (F/F) ratio (0.28) allowed to obtain the better enrichment in PHA-storage microorganisms, reaching a PHA contents of 13.7 % w/w at the end of the feast phase. In table 1, the F/F ratio indicates that by decreasing the vOLR without changing the cycle length and other operational parameters, lower F/F rate can be achieved. Despite increasing the amount of PHA produced, the higher vOLR, the worse the removal efficiencies of the reactor are. This result suggests that an optimal trade-off for PHA production and reactor performance needs to be evaluated. Once the enrichment in PHA-storage microorganisms was achieved, the biomass was harvested to perform the accumulation tests.
Figure 2 shows the final PHA content achieved for each accumulation test and the PHB:PHV ratio calculated by analysing the lyophilized biomass. When comparing accumulation tests with similar Food-to-Microorganisms (F/M) ratio, it is clear that higher the vOLR during the selection step, the more effective is the enrichment in microorganisms' with PHA storage and production capability, which is mainly related to the PHV synthesis, as can be seen by the PHB:PHV ratio. The PHV:PHB ratio in T6 would suggest that this polymer might be a promising alternative to PHB homopolymers, especially when referring to its industrial applications (de Donno Novelli et al., 2021).
Figure 3 points out the correlation between productivity, PHA contents, vOLR applied in the selection step and F/M ratio used in the accumulation step. When the highest vOLR was used in the selection step, the biomass reaches a low productivity, but with a higher PHA content (Figure 3). On the other hand, there is a direct correlation between the F/M ratio and the enhance in the productivity. This shows that, like vOLR, a medium value of F/M ratio is the best condition to run an accumulation test in order to avoid substrate inhibition due to high F/M ratio while, on the other hand, low PHA content and productivity can be achieved with low F/M ratio (Palmeiro-Sánchez et al., 2019).
These results highlight pivotal parameters that should be taken into account when considering a pilot or full-scale implementation. Still few works focus on optimising the F/M ratio in the accumulation test while considering both PHA concentration and the productivity. These parameters could be used in an energy-mass balance to express, at an industrial level, where it is more convenient to stop the accumulation step and to extract the stored PHA.

PHA extraction

PHA content, purity and recovery were calculated by using a GC equipped with a FID. The protocol used is composed by a two-step solvent extraction: NaClO pre-treatment and non-polymeric cell material (NPCM) destruction by using an organic surfactant (ammonium laureate). The results in table 2 show an overall high purity (89±2%) and recovery (78±3%), proving that the protocol's efficiency is not influenced by the PHA content in the lyophilized samples, up to 32% w/w. The results consistency demonstrates the feasibility of applying this protocol for samples containing different amounts of PHA with different proportions between PHB and PHV monomers.

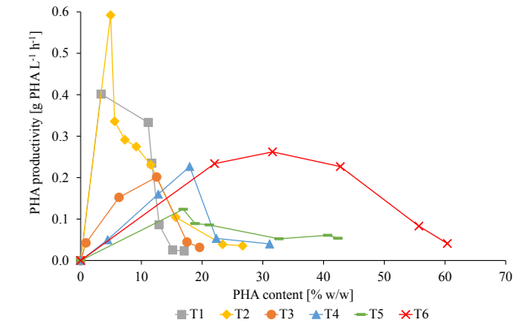

Figure 3. PHA productivity as function of PHA content.

Table 1. Details of S-SBR and accumulation tests.

	OLR (g COD L^{-1} d^{-1})	Feast / famine ratio	PHA at the end of feast (%w/w)	Accumulation tests	F/M (g COD g^{-1} VSS)
S-SBR 1	0.8	0.16	6.0	T1	2.5
				T2	4.5
S-SBR 2	1.3	0.19	6.6	T3	3.1
				T4	5.5
S-SBR 3	1.8	0.28	13.7	T5	3.7
				T6	5.7

Table 2. PHA content, recovery and purity percentage for samples collected from T6.

	Sampling time (h)	PHA content (% w/w)	Purity (%)	Recovery (%)
Sample 1	4.6	31.6	90.1	80.5
Sample 2	7.2	42.8	90.5	74.4
Sample 3	25.5	55.7	87.5	78.0
Sample 4	56.2	60.4	88.8	78.3

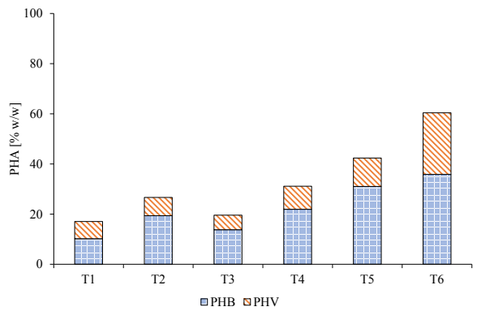

Figure 2. Final PHA amount and PHB:PHV ratio in each accumulation test.

REFERENCES

de Donno Novelli, L., Moreno Sayavedra, S., and Rene, E. R. 2021 Polyhydroxyalkanoate (PHA) production via resource recovery from industrial waste streams: A review of techniques and perspectives. *Bioresource Technology*, **331**, 124985.
Mannina, G., Alduina, R., Badalucco, L., Barbara, L., Capri, F. C., Cosenza, A., di Trapani, D., Gallo, G., Laudicina, V. A., Muscarella, S. M., and Presti, D. 2021 Water resource recovery facilities (Wrrfs): The case study of palermo university (Italy). *Water* (Switzerland), **13**(23).
Mannina, G., Presti, D., Montiel-Jarillo, G., and Suárez-Ojeda, M. E. 2019 Bioplastic recovery from wastewater: A new protocol for polyhydroxyalkanoates (PHA) extraction from mixed microbial cultures. *Bioresource Technology*, **282**, 361–369.
Moretto, G., Lorini, L., Pavan, P., Crognale, S., Tonanzi, B., Rossetti, S., Majone, M., and Valentino, F. 2020 Biopolymers from urban organic waste: Influence of the solid retention time to cycle length ratio in the enrichment of a Mixed Microbial Culture (MMC). *ACS Sustainable Chemistry and Engineering*, **8**(38).
Palmeiro-Sánchez, T., Val del Rio, A., Fra-Vázquez, A., Luis Campos, J., and Mosquera-Corral, A. 2019 High-Yield Synthesis of Poly(3-hydroxybutyrate-co-3-hydroxyvalerate) Copolymers in a Mixed Microbial Culture: Effect of Substrate Switching and F/M Ratio. *Industrial & Engineering Chemistry Research*, **58**(48), 21921–21926.
Pesante G. and Frison N. 2023 Recovery of bio-based products from PHA-rich biomass obtained from biowaste: A review. *Bioresource Technology Reports*, **21**, 101345.

Acidogenic fermentation of model carbohydrate/protein mixtures: how does substrate organic composition impact?

A. Vázquez-Fernández*, M.E. Suárez-Ojeda**, J. Carrera***
GENOCOV research group, Departament d'Enginyeria Química, Biològica i Ambiental, Escola d'Enginyeria, Universitat Autònoma de Barcelona, 08193, Bellaterra, Spain
* ana.vazquez.fernandez@uab.cat, ** mariaeugenia.suarez@uab.cat, *** julian.carrera@uab.cat

Abstract
Acidogenic fermentation is a known process to synthesize value added products such as Carboxylic Acids (CA) and ethanol. However, the impact of the substrate organic composition on the products obtained or process performance is still not clear. Thus, in this work, fermentation experiments were carried out in a sequencing-batch reactor (SBR) to assess the influence of using mixtures of whey protein isolate (as model protein (P)) and food-grade sugar (as model carbohydrate (C)) in different proportions (0% C/100% P; 25% C/75% P; 50% C/50% P; 75% C/25% P and 100% C/0% P) on the fermentation process performance and on the effluent composition. All the experiments were conducted under a volumetric organic loading rate (OLRv) of 6 g COD L^{-1} d^{-1} and a specific organic loading rate (OLRs) of 1.8 g COD g^{-1} VSS d^{-1} Acetic, propionic, butyric and isovaleric acid were present in all the experiments, but the effluent corresponding to a mixture of 75% C/25% P could be considered more convenient for polyhydroxyalkanoates (PHA) synthesis due to the large odd-to-even ratio, the high butyric acid concentration and the high acidified COD. Meanwhile, the effluent corresponding to a substrate of 100% C/0% P would be suitable for medium chain carboxylic acids (MCCA) production as it was the only one containing both CA and ethanol.

Keywords (maximum 6 in alphabetical order)
Acidogenic fermentation; carbohydrates; proteins; sequencing-batch reactor; Volatile Fatty Acids; Carboxylic Acids

INTRODUCTION

Acidogenic fermentation using mixed microbial cultures is a promising process able to produce value-added products such as CA or ethanol. These products can be used as final products or be transformed by subsequent biological processes in another value-added products such as PHA (Matos et al., 2021) or medium chain carboxylic acids (MCCA) (Sarkar et al., 2021). Many authors have performed experiments with numerous types of waste and wastewaters with a high content of organic matter. However, further knowledge about how to control the CA production yield and the effluent composition is needed to be able to scale up this process at the industrial level. In this study, process effectiveness parameters were defined and calculated to evaluate the acidogenic fermentation process performance. Moreover, fermentation experiments in a sequencing-batch reactor (SBR) employing synthetic wastewater containing different proportions of food-grade sugar and whey protein isolate as models compounds of carbohydrates and proteins, respectively, were conducted to analyze the effect of the organic composition of the substrate on the process effectiveness parameters and on the effluent composition.

MATERIALS AND METHODS

The experiments were carried in a SBR with an effective working volume of 2.7 L and a headspace of 1.7 L. The substrate used in the experiment was synthetic wastewater containing mineral salts essential for biomass growth and a total organic matter concentration of 14 g O_2 L^{-1}, in terms of chemical oxygen demand (COD). The substrate was composed by different ratios of food-grade sugar and whey protein isolate, depending on the experimental period (Table 1). The inoculum was acidogenic biomass previously acclimatized to both sucrose and whey protein isolate. The composition of the substrate was modified only after the steady state corresponding to the previous change was reached. The temperature was controlled at 37ºC while the pH was registered on-line. Soluble COD was determined by using COD kits (Lovibond) after filtering effluent samples with 0.45 µm pore filters. CAs (including acetic, propionic, isobutyric, butyric, isovaleric, valeric, isocaproic and caproic acids) and ethanol concentrations were analyzed by gas chromatography (GC, 7820A, Agilent Technologies). Food-grade sugar was measured as glucose and sucrose equivalents. Glucose and lactic acid were measured in a YSI 2950 Biochemistry Analyzer. Sucrose was analyzed by HPLC analysis (HPLC Dionex Ultimate3000). Whey protein isolate was determined using the Bradford method in a spectrophotometer at 595 nm (Bradford, 1976). OLRs and process effectiveness parameters (bioconversion, degree of acidification, acidified COD, CA yield and odd-to-even ratio) were defined and calculated according to the equations presented in Table 2. One-way ANOVA tests ($p<0.05$) were performed to evaluate if the different substrate compositions produced a significant impact on the process effectiveness parameters and the effluent composition.

RESULTS AND DISCUSSION

Figure 1 displays the steady-state effluent composition for the different substrate mixtures tested. The main products obtained for all the conditions were acetic, propionic, butyric and isovaleric acids. Acetic acid was 18%, 22% and 27% for 0% C/100% P, 25%C/ 75% P and 50%C/50% P in the substrate, respectively, showing a significant increase ($p<0.05$) when rising the % of C in the substrate up to the 50%. However, when increasing the C proportion to 75% and to 100%, the acetic acid remained at 20 and 28%, respectively. Propionic acid was 13%, 28%, 21%, 31% and 2% for 0% C/100% P, 25%C/ 75% P, 50% C/50% P, 75% C/25% P and 100% C/0% P in the substrate, respectively. Butyric acid was 15%, 11%, 17%, 34% and 47% for 0% C/100% P, 25% C/75% P, 50% C/50% P, 75% C/25% P and 100% C/0% P in the substrate, respectively, showing a significant increase when rising the % of C from 25% to 100% ($p<0.05$). Isovaleric acid was 17%, 13%, 9%, 5% and 0% for 0% C/100% P, 25% C/75% P, 50% C/50% P, 75% C/25% P and 100%C/0% P in the substrate, respectively, showing a significant decrease ($p<0.05$) as the % of C in the substrate increase. Isocaproic acid, which is considered a MCCA, was found when the substrate contained 0% C/100% P and 25% C/75% P, yielding a 7% and a 5% of the effluent COD, respectively. Ethanol was only detected when the composition of the substrate was 100% C/0% P resulting in an 8% of the effluent COD.

Table 3 shows the process effectiveness parameters obtained for the different substrate mixtures tested. Bioconversion was higher than 94% in all the experiments except for the experiment with 50% C/50% P since in that experiment, there was a significant amount of unconverted protein in the effluent. In relation to the degree of acidification, it was significantly higher ($p<0.05$) when the substrate was a mixture of C and P in different proportions in comparison to the use of a substrate only composed by C or by P or by C and P in equal proportions. The acidified COD was significantly higher ($p<0.05$) when the substrate was composed of 75%C/25% P compared to the rest of the conditions tested unless when the substrate contained 25%C/ 75% P. The CA yield was higher when the substrate was a mixture of C and P in comparison to a substrate composed only by C alone or P alone. Finally, the odd-to-even ratio was significantly higher when the substrate was a mixture of C and P in different proportions compared to the rest of the conditions. In descending order, the following conditions which lead to higher odd-to-even ratios were 50%C/50% P, 0% C/100% P and 100% C/0% P.

It is worth to mention that the effluents obtained when using a substrate with 25% C/75% P and 75% C/25% P are the more convenient ones for a subsequent PHA synthesis since they have the highest odd-to-even ratio (Gameiro et al., 2015) and acidified COD. Between these two, the effluent corresponding to the substrate with 75% C/25% P would be more appropriate as it is richer in butyric acid, which is one of the preferred precursors for PHA production (Matos et al., 2021). Additionally, for MCCA production, the effluent more suitable would be the one obtained with 100% C/0% P in the substrate since, besides CA, it contains ethanol which acts as electron donor in MCCA synthesis (de Groof et al., 2019).

Table 1. Experimental conditions tested in the reactor.

Substrate composition	OLRv	OLRs
% C - % P	g COD L^{-1} d^{-1}	g COD g^{-1} VSS d^{-1}
0% – 100%	6.5 ± 0.6	1.9 ± 0.4
25% – 75%	6.2 ± 0.2	1.8 ± 0.4
50% – 50%	6.1 ± 0.1	1.7 ± 0.5
75% – 25%	6.0 ± 0.2	1.9 ± 0.5
100% – 0%	6.0 ± 0.3	2.2 ± 0.2

Table 2. Equations for calculation of the OLRs and the process effectiveness parameters used in this study.

OLRs	
Bioconversion	
Degree of Acidification	
Acidified COD	
CA yield	
Odd-to-even ratio	

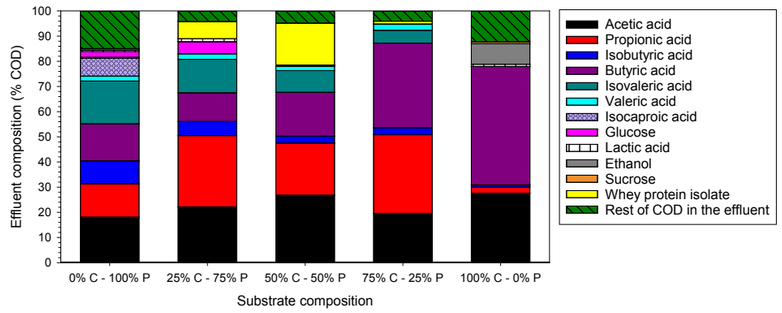

Figure 1. Effect of the substrate composition on the effluent composition.

Table 3. Bioconversion, Degree of Acidification, Acidified COD, Carboxylic Acid yield and odd-to-even ratio for the different substrate compositions tested.

Substrate composition	OLRv	OLRs	Bioconversion	Degree of Acidification	Acidified COD	CA yield	Odd-to-even ratio
%C - %P	g COD L^{-1} d^{-1}	g COD g^{-1} VSS d^{-1}	%	%	%	g COD g^{-1} COD	
0% – 100%	6.5 ± 0.6	1.9 ± 0.4	98.9 ± 1.9	63 ± 3	82 ± 3	0.6 ± 0.1	0.3 ± 0.1
25% – 75%	6.2 ± 0.2	1.8 ± 0.4	94 ± 6	70 ± 3	87 ± 4	0.7 ± 0.1	0.6 ± 0.1
50% – 50%	6.1 ± 0.1	1.7 ± 0.5	87 ± 5	62 ± 5	78 ± 7	0.7 ± 0.1	0.4 ± 0.1
75% – 25%	6.0 ± 0.2	1.9 ± 0.5	99.1 ± 0.7	73 ± 2	95.0 ± 1.7	0.7 ± 0.1	0.6 ± 0.1
100% – 0%	6.0 ± 0.3	2.2 ± 0.2	99.4 ± 0.1	59 ± 7	73 ± 8	0.6 ± 0.1	0.0 ± 0.1

REFERENCES

Bradford, M.M. 1976. A Rapid and Sensitive Method for the Quantitation of Microgram Quantities of Protein Utilizing the Principle of Protein-Dye Binding. *Analytical Biochemistry* **72**, 248-250

Gameiro, T., Sousa, F., Silva, F.C., Couras, C., Lopes M., Louros, V., Nadais, H., Capela, I. 2016. Olive Oil Mill Wastewater to Volatile Fatty Acids: Statistical Study of the Acidogenic Process. Water, Air, & Soil Pollution, 226, 115.

de Groof, V., Coma, M., Arnot, T., Leak, D. J., & Lanham, A. B. 2019. Medium chain carboxylic acids from complex organic feedstocks by mixed culture fermentation. *Molecules*, **24**(3).

Matos, M., Cruz, R. A. P., Cardoso, P., Silva, F., Freitas, E. B., Carvalho, G., & Reis, M. A. M. 2021. Combined Strategies to Boost Polyhydroxyalkanoate Production from Fruit Waste in a Three-Stage Pilot Plant. *ACS Sustainable Chemistry and Engineering*, **9**(24), 8270–8279.

Sarkar, O., Rova, U., Christakopoulos, P., Matsakas, L. 2021. Ethanol addition promotes elongation of short-chain fatty acids to medium-chain fatty acids using brewery spent grains as substrate. *Journal of Environmental Chemical Engineering*, **9**(5).

TECHNICAL SESSIONS

T13. Energy recovery

ECOSTP 2023

Energy recovery from wastewater: ammonia and hydrogen production from nitrogen-containing waste streams

R. Asiain-Mira*,**, P. Zamora*, V. M. Monsalvo*, F. Rogalla*, L. Torrente-Murciano**

* FCC Aqualia, Department of Innovation and Technology, Avda. del Camino de Santiago 40, 28050, Madrid, Spain.
(E-mail: ruben.asiain@fcc.es; patricia.zamora@fcc.es; victor.monsalvo@fcc.es; FRogalla@fcc.es)
** Department of Chemical Engineering and Biotechnology, University of Cambridge, Philippa Fawcett Drive, CB3 0AS, Cambridge, UK.
(E-mail: ra581@cam.ac.uk; lt416@cam.ac.uk)

Abstract

This work presents a new process for the recovery of energy from decentralised wastewater, based on the adsorption of urea from urine and its subsequent decomposition into ammonia and hydrogen. Herein, urea is recovered from urine through adsorption onto commercial activated carbon. Thermal urea desorption and decomposition into ammonia led to the regeneration of the carbon, keeping its adsorption capacity for at least 4 cycles. Finally, when the regeneration and urea decomposition steps are carried out in the presence of an ammonia decomposition catalyst, hydrogen is produced. Energy balances show that this energy recovery system would lead to a hydrogen production of 430 kg/d, with a net energy production of 2850 kWh/d in a city of 160000 inhabitants. In addition, it would cause energy savings of 4600 kWh/day at the wastewater treatment plant, reducing its energy consumption by 35%.

Keywords (maximum 6 in alphabetical order)
Adsorption, ammonia, hydrogen, urea, resource recovery.

INTRODUCTION

Decentralised systems are a novel approach to conventional wastewater treatment that consists of the separation and treatment of wastewater streams directly at their source. Specifically, urine source-separation can be achieved by utilizing urine-diversion toilets to collect undiluted or low diluted urine (Estévez et al., 2022). Despite accounting for less than 1% of the total volume of domestic wastewater, urine contributes to 80% of all the nitrogen, mainly in the form of urea ($(NH_2)_2CO$) (Egle et al., 2015). While urea is traditionally considered a pollutant in this context, it is also a hydrogen-rich compound and a potential source of green energy.

In this work, we present an innovative process for harvesting energy from human urine based on the integration of three different steps. Firstly, urea is recovered from aqueous solution by its adsorption on commercial activated carbon. Secondly, a thermal treatment is used to regenerate the carbon adsorbent leading to the simultaneous decomposition of urea into ammonia and carbon dioxide. And thirdly, hydrogen is produced through the catalytic decomposition of ammonia to be used as an energy fuel.

MATERIALS AND METHODS

Adsorption of urea was carried out in batch systems using commercial activated carbon (Vertex ROX 0.8). The concentration of urea urine was determined by a colorimetric method (With et al., 1961). Temperature programme desorption (TPD) was carried out in a Micromeritics Autochem II chemisorption analyser equipped with a MKS Cirrus 2 mass spectrometer. Decomposition of ammonia into hydrogen was carried out using a Ru (7% wt.) supported on carbon nanotubes catalyst (Hill & Torrente-Murciano, 2014) and measured with a gas chromatographer equipped with a thermo-conductivity detector.

RESULTS AND DISCUSSION

The adsorption capacity of urea in commercial activated carbon was studied by measuring the adsorption isotherm at 30°C using both, synthetic and real human urine samples. The lower adsorption capacity observed when using real urine shows that there are compounds competing for the adsorption sites, presumably proteins and other organic compounds. In both cases, monolayer adsorption dominates the process, following the Langmuir model (Figure 1A). Kinetic experiments show that adsorption was fast, reaching equilibrium in 7 minutes (Figure 1B), and fitting of the data to the Boyd model revealed that the adsorption limiting step was the intraparticle diffusion both using synthetic and real urine samples.

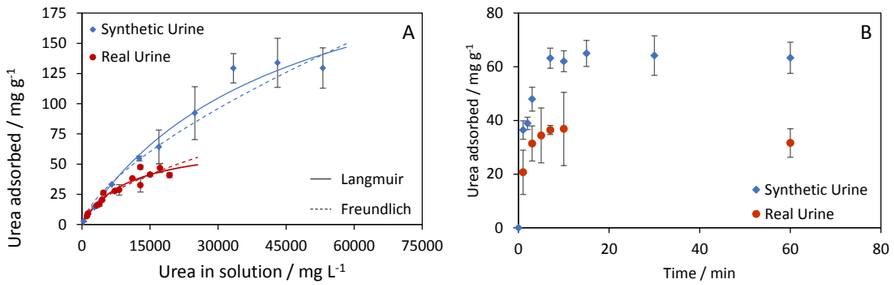

Figure 1. Adsorption of urea onto Vertex ROX 0.8 activated carbon using synthetic and real urine. A: Equilibrium isotherms. B: Kinetic study.

Continuous adsorption of urea was studied to evaluate the influence of different process parameters using synthetic and real urine. The volume of urine treated when the outlet concentration of urea is 50% of the inlet concentration (v_{50}, mL) and the amount of urea adsorbed in the carbon at that moment (q_{50}, mg g^{-1}) are used for comparison.

Firstly, an increase in the inlet concentration of urea presents a negative effect to the adsorption process, as the volume that can be treated is reduced. The urea adsorbed increases just a result of the equilibrium but does not imply a better performing of the system. Secondly, an increase in the mass of activated carbon presents a positive effect, as both the volume and the urea adsorbed raise due to the increase in the contact time between the urine and the adsorbent. Third, a higher flowrate shows a negative effect as can be observed by the lower volume and urea adsorbed, as the contact time is again reduced. Finally, the increase in the inner diameter of the column has a detrimental effect on the adsorption process, decreasing the volume and the urea adsorbed. Similar trends are observed for synthetic and real urine, while with real urine the adsorbed urea is generally lower due to competing adsorption as observed in batch experiments (Figure 2).

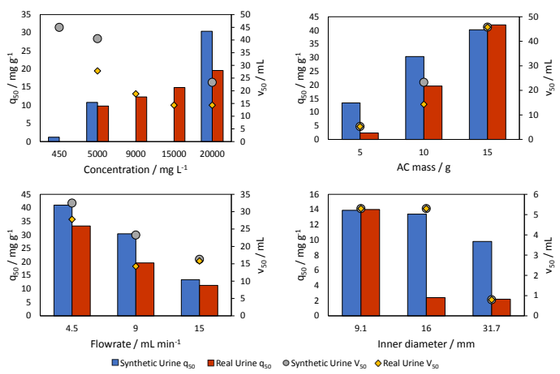

Figure 2. Effect of process parameters on continuous adsorption of urea from synthetic and real urine.

Thermal treatment at 250°C successfully regenerates the saturated activated carbon. The adsorption capacity keeps constant during at least 4 adsorption/desorption cycles when working with synthetic urine (Figure 3A). In the case of real urine samples, the capacity is decreased by 20% in the first cycle, while maintaining a constant value in the next 3 cycles. Temperature programme desorption experiments show adsorbed urea decomposes into NH_3 and HNCO, the latter undergoing further reactions, mainly hydrolysis into more NH_3 and CO_2 (Figure 3B). When the regeneration step is carried out in the presence of an ammonia decomposition catalysts (Ru/CNT), hydrogen is produced. (Figure 3C) (Asiain-Mira et al., 2022).

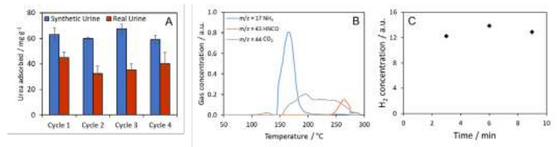

Figure 3. Desorption of urea and regeneration of the carbon. A: Adsorption capacity of activated carbon during 5 adsorption/desorption cycles. B: TPD profile of the activated carbon after adsorption. C: Hydrogen production from adsorbed urea.

An energy balance demonstrates the feasibility of the process for energy recovery. For the analysis, it was assumed that the process is installed in the city of Lleida in Spain, with 160000 inhabitants. Considering a urine production of 1.5 L/person day, the process would produce 430 kg/day of hydrogen, which represent 14225 kWh/day (Figure 4A). Considering the energy requirements of the process (Figure 4B), and the efficiency losses associated to the use of the hydrogen in a PEM fuel cell, the system results in a net electrical production of 2850 kWh/day. Additionally, savings of 4575 kWh/day would be achieved at Lleida's wastewater treatment plant, associated to the reduction on the nitrogen income, which represents more than 35% of its electrical consumption (Asiain-Mira et al., 2022), (Palatsi et al., 2021).

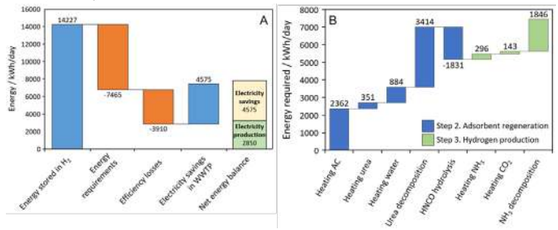

Figure 4. Energy analysis of the process. A: Summary of the energy analysis for the installation of the process in the city of Lleida, Spain. B: Distribution of energy requirements to produce hydrogen from urea in decentralised wastewater systems.

REFERENCES

Asiain-Mira, R., Smith, C., Zamora, P., Monsalvo, V.M., Torrente-Murciano, L., 2022. Hydrogen production from urea in human urine using segregated systems. *Water Research* **222**, 118931.

Egle, L., Rechberger, H., & Zessner, M. 2015. Overview and description of technologies for recovering phosphorus from municipal wastewater. *Resources, Conservation & Recycling* **105**, 325–346.

Estévez, S., Feijoo, G., Moreira, M.T. 2022. Environmental synergies in decentralized wastewater treatment at a hotel resort. . *Journal of Environmental Management* **317**, 115392.

Hill, A. K., & Torrente-Murciano, L. 2014. In-situ H2 production via low temperature decomposition of ammonia: Insights into the role of cesium as a promoter. *International Journal of Hydrogen Energy* **39**(15), 7646–7654.

Palatsi, J., Ripoll, F., Benzal, A., Pijuan, M., & Romero-güiza, M. S. 2021) Enhancement of biological nutrient removal process with advanced process control tools in full-scale wastewater treatment plant. *Water Research* **200**, 117212.

Rossi, L., Lienert, J., & Larsen, T. A. 2009. Real-life efficiency of urine source separation. *Journal of Environmental Management* **90**, 1909–1917.

With, T.K., Petersen, T.D., Petersen, B., 1961. A simple spectrophotometric method for the determination of urea in blood and urine. *J. Clin. Pathol*. **14**, 202–204.

Anaerobic microbial electrochemical fluidized membrane bioreactor for domestic wastewater treatment and reuse with energy recovery

Krishna P. Katuri *, Ananda Rao Hari*, Yogesh Singh*, and Pascal E. Saikaly **

* Water Desalination and Reuse Center (WDRC), King Abdullah University of Science and Technology (KAUST), Thuwal 23955-6900, Saudi Arabia (E-mail: *krishna.katuri@kaust.edu.sa*; *hari.anandarao@kaust.edu.sa*; *Yogesh.singh@kaust.edu.sa*)
**Environmental Science and Engineering Program, Biological and Environmental Science and Engineering (BESE) Division, King Abdullah University of Science and Technology (KAUST), Thuwal 23955-6900, Saudi Arabia (Email: *pascal.saikaly@kaust.edu.sa*)

Abstract
Sustainable supply of clean water and energy has become a global challenge due to population increase. In this study, we demonstrated a photovoltaic powered novel hybrid biotechnology at pilot scale (36 L) to treat domestic wastewater with recovery of resources (reclaimed water for non-potable reuse and energy). In this hybrid system, microbial electrolysis cell (MEC) was integrated with gravity-driven fluidized membrane bioreactor (FMBR) to harness resources from wastewater and mitigate membrane biofouling with minimal energy input. The MEC was coupled with photovoltaic solar panel to improve energy efficiency.

Keywords
MEC; MBR; Resource recovery

INTRODUCTION

Anaerobic microbial technologies hold great promise for resource recovery (energy and nutrients) from wastewater. As such, microbial electrolysis cell (MEC) offers an opportunity to anaerobically treat wastewater with concomitant recovery of energy as methane (double chamber) or hydrogen (single chamber) (Katuri et al., 2019). However, MEC alone cannot generate an effluent suitable for reuse due to the abundance of microbes in the effluents. Therefore, they have to be coupled with micro- or ultra-filtration membranes to effectively block the passage of bacteria and produce high- quality effluent suitable for reuse. Currently, the aerobic membrane bioreactor (AeMBR) technology is the standard technology for wastewater treatment and reuse. However, AeMBR is energy intensive, consumes on average 1–2 kWh/m3, where a large fraction of this energy is used for aeration, filtration process, and scouring of the membranes to minimize fouling. To transform wastewater treatment from an energy-intensive process to an energy-efficient process, we developed a hybrid biotechnology by integrating MEC with gravity-driven FMBR to treat domestic wastewater and recover resources (reclaimed water for reuse and energy).

MATERIALS AND METHODS

The pilot-scale hybrid MEC-FMBR reactor (Figure 1.1) was installed next to the King Abdullah University of Science and Technology (KAUST) AeMBR to treat real wastewater. The primary treated raw wastewater received at the inlet of the KAUST AeMBR has a COD concentration < 200 mg/L. To maintain an influent COD concentration of 450 mg/L, starch and peptone were added to the primary treated wastewater. Four electrode modules were packed in the MEC. Each electrode module contains a carbon-fiber brush anode and nickel mesh cathode, and each module operates independently with a separate power source (powered by a PV cell). The influent wastewater was pumped into the MEC from the bottom the reactor, and the effluent from the top of the MEC flows into the FMBR (through a connection port on the top of the FMBR) for further polishing and water reclamation. The FMBR is equipped with customized hollow fiber microfiltration (pore size 0.1 µm) membrane module with 0.5 m^2 effective membrane surface area (KOLON Industries, Inc., Korea). The water in the FMBR is filtered by gravity. The membrane module was connected to a mass-flow controller (Alicat Scientific) and digital pressure transmitter (LEO3, Keller) to measure flux and FMBR head pressure. Granular activated carbon (GAC, ~1.5 mm) particles pre-enriched with biofilm (with MEC effluent) was added to the FMBR to minimize membrane fouling and promote CH_4 production through methanogens. Microbial community analysis was performed using gene amplicon sequencing targeting the Archaea/Bacteria/Eukarya 16S/18S rRNA gene variable regions 4-8 (abeV48-A). Biogas was analyzed using gas chromatography (SRI Instruments, USA).

RESULTS AND DISCUSSION

The MEC reactor was inoculated with a co-culture of acetoclastic electroactive bacteria (EAB, *Geobacter sulfurreducens* and *Desulfuromonas acetexigens*) and operated in a fed-batch mode of operation at an applied voltage of 1 V for the anodic biofilm development. A synthetic medium containing acetate (10 mM) as a carbon and energy source was used at the beginning of operation to enrich for EAB. A stable current response from each module was observed after few batches of operation. After achieving stable current, the feed was switched to primary treated raw wastewater supplemented with starch and peptone on day 120, and the MEC reactor was operated in batch mode for 40 days (120-160 days) until the reactor produced a reproducible current (Figure 1.2A). A stable current generation from the modules was observed after switching the operation of the MEC to continuous mode (on day 160, Figure 1.2B) with a hydraulic retention time (HRT) of ~14 h and organic loading rate (OLR) of 0.73 ± 0.05 kg COD/m^3/day. During this phase of MEC operation (160-220 days), the COD removal in the reactor was 79 ± 4%, and high purity CH_4 (no CO_2) was produced at a rate of ~0.21 ± 0.002 L CH_4/g COD removed. The H_2 gas concentration in the biogas was below the detection limit. The low CO_2 and H_2 in the biogas are due to hydrogenotrophic methanogens' activity at the cathode of the wastewater-fed MECs. After observing stable reactor performance at OLR of 0.73 ± 0.05 kg COD/m^3/day, the OLR was increased to 1.47 ± 0.07 kg COD/m^3/day (HRT ~7 h, 220-335 days). An increase in current response from the modules (except module 2) was observed after increasing the OLR (Figure 1.2B). However, fluctuations in current generation (240-280 days) occurred due to changes in influent chemical composition (shock-load) associated with repairing and cleaning a central sewer line on campus. Followed by this perturbation phase, the reactor showed a stable performance in terms of CH_4 production (~0.3 ± 0.01 L CH_4/g COD removed) and COD removal (67 ± 6%) and with only ~10% CO_2 gas detected in the biogas.

Further polishing of COD was attained by integrating the MEC with FMBR. The performance of the virgin membrane was assessed at a fixed flux (6 LMH) with clean water (Figure 1.3A) and with effluent from the MEC reactor at 1.47 OLR (Figure 1.3B) without GAC fluidization. A stable water flux was observed with clean water. However, with MEC effluent (i.e., FMBR influent), the flux was dropped by half after one day of reactor operation. Membrane scouring with N_2 gas quickly recovered the desired flux. However, the flux was only sustained for a short time.

The FMBR performance was assessed under GAC fluidization mode (10 min for every two hours interval) with effluent from MEC reactor. Membrane fouling was not noticeable for two months at OLR of 0.73 ± 0.05 kg COD/m^3/day (Figure 1.3C). Constant membrane flux and head pressure were sustained for a prolonged period. Also, the reactor produced clear (zero turbidity) and odorless permeate with <30 mg/L COD at a flux of 6 LMH. More than > 94 ± 2% of bacterial cell removal (i.e., total live cells difference between permeate and MEC effluent) was achieved due to filtration. These results are the first to demonstrate the impact of GAC fluidization on GDM process. When the operation of the MECs was shifted to OLR of 1.47 ± 0.07 kg COD/m^3/day, a stable flux was observed for ten days (Figure 1.3D), and then a gradual drop in flux was observed due to the reactor-head pressure drop, which was associated with the membrane fouling. After subtracting the electrical energy demand from the recovered energy, the energy required to operate the hybrid system was positive (~ 0.1 kWh/m^3). Recovery of reclaimed water for reuse from real wastewater with net positive energy offers a potential advantage of this hybrid configuration over other anaerobic and aerobic MBR systems.

The microbial community analysis of the biomass collected from different components of both reactors confirms the existence of key functional microbiomes responsible for improved reactor performance (Figure 1.4). High relative abundance of the EAB *Geobacter sp.* was observed on the anodic biofilm. The presence of *Methanobacterium sp*. on the cathode (at high abundance) and other locations (anode and suspension) supports hydrogenotrophic methanogenesis in MEC. The presence of *Methanosaeta sp.* supports direct interspecies electron transfer (DIET) or/and acetoclastic methanogenesis at low acetate conditions. The abundance of *Geobacter sp., Methanobacterium sp.,* and *Methanosaeta sp.* on GAC particles in the FMBR may play a crucial role in CH_4 production (via DIET or/and methanogenesis).

Figure 1.1 Photographs showing the pilot-scale MEC-FMBR system (https://drive.google.com/file/d/1sLQwtnwBa_AmqGOqZJaTPPhk2qWnYpV9G/view?usp=share_li nk).

Figure 1.2 The profile of current response from the different electrode modules of MEC operated with sewage in fed-batch mode (A) and continuous operation at different OLRs (B).

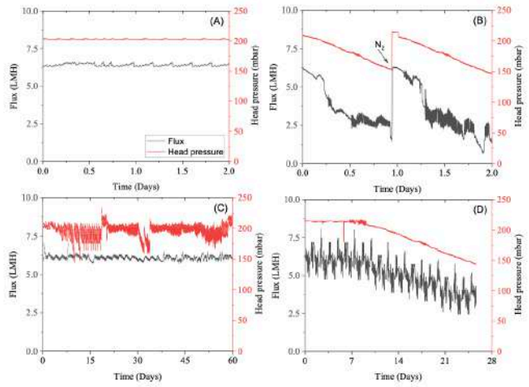

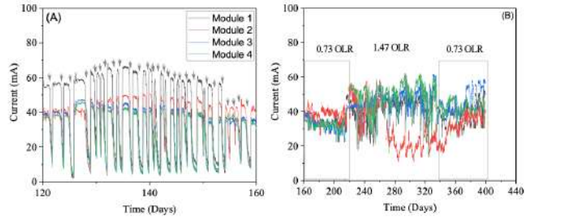

Figure 1.3 FMBR performance at a fixed flux of 6 LMH. Tests with clean water (A) and MEC effluent (B) in the absence of GAC fluidization. Flux and reactor head pressure change with time in the presence of GAC fluidization at 0.73 (C) and 1.47 (D) OLR.

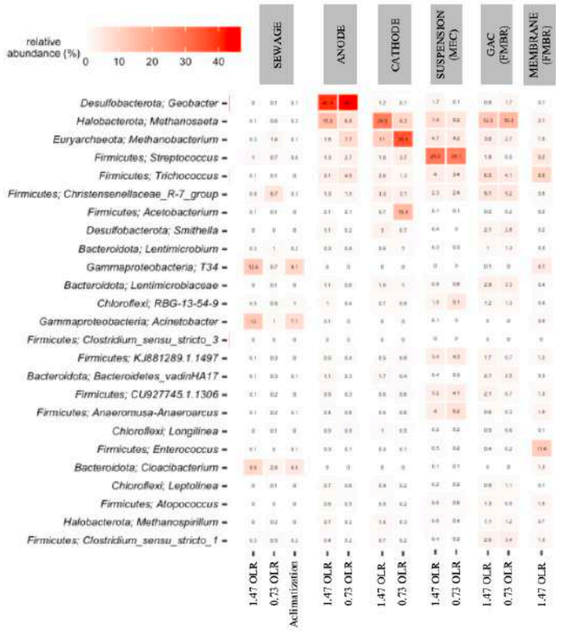

Figure 1.4 Heatmap showing the top 25 operational taxonomic units identified in the MEC and FMBR.

REFERENCES

Katuri, K.P. Muhammad, A. and Saikaly, P.E. (2019), The role of microbial electrolysis cell in urban wastewater treatment: integration options, challenges, and prospects. *Current Opinion in Biotechnology*, 57,101–110.

Optimising anaerobic digesters with thermal pre-treatment by understanding sludge composition – full-scale and laboratory results on trace elements and enzyme supplementation.

N. Nasar*, G. Pizzagalli**, F. Coulon* and Y. Bajón Fernandez*

*Cranfield University, Cranfield, MK430AL, UK (y.bajonfernandez@cranfield.ac.uk)
*Cranfield University, Cranfield, MK430AL, UK (f.coulon@cranfield.ac.uk)
*Cranfield University, Cranfield, MK430AL, UK (Nasreen.nasar@cranfield.ac.uk)
**Anglian Water Services, Greater Cambridge area, UK (gPizzagalli@anglianwater.co.uk)

Abstract

In order to increase the energy recovery potential of the anaerobic digesters (ADs), most UK water utilities have implemented pre-treatment technologies that can aid biological degradation of the sludge with the resulting process being referred to as advanced AD. The predominant technology implemented thus far is thermal hydrolysis process (THP). While plenty of advancements have been made over the past decade, the operational envelopes for THP-ADs are still defined by the feed type, rather than their biochemical composition and fate after pre-treatment and in the digester, which limits optimisation opportunities. Apart from this, Trace elements (TE) also play a significant role in influencing digester performance, especially since THP induces high ammonia concentrations in the digester. This results in very different TE needs for THP-AD compared to conventional digesters to maintain stable conditions. However, the impact of THP on their bioavailability remains underexplored. This paper aims to set a precedent in THP-AD process optimization by profiling sludge composition and TE bioavailability in a full-scale site and informing possible synergistic effects of cost-effective options like enzyme and TE dosing.

Keywords (maximum 6 in alphabetical order)

Augmented treatments; Enzyme dosing; Macromolecules and fate, Thermal hydrolysis; Trace Elements.

INTRODUCTION

In UK, thermal hydrolysis process (THP) is a widely adopted pre-treatment technology in implementing advanced anaerobic digestion (AAD). This is usually done to increase energy recovery potential of the sludge, as well as significantly increasing throughput by enhancing the rate limiting hydrolysis step. THP comprises subjecting the feed sludge to high pressure and temperature to enable solubilization and hydrolysis, while simultaneously overcoming the various constraints imposed by the high sludge bulk viscosity and limited suspended solids (SS) solubility.

While optimization of AAD is usually carried out from an engineering standpoint, their influence on macromolecular composition and fate that predominantly govern the digester's performance is largely unknown, which limits true optimization. This is especially true for THP pre-treatment as it involves the destruction of extracellular polymeric substances (EPS), and enhanced solubilization of suspended matter, rendering substrates with low accessibility for hydrolysis enzymes more accessible. There is also a lack of understanding on how THP pre-treatment impacts the need for trace-element addition in ADs. Moreover, to date, there has not been an integrated approach in understanding the synergistic effects of THP with strategic in-situ options like enzyme and trace element (TE) dosing to enhance digester performance.

Hence, the aim of this study is to set a precedent for THP optimisation, by profiling organics solubilization, macromolecular composition and TE bioavailability throughout a full-scale treatment chain of AADs. Furthermore, this study will inform on optimizing the process through the dosing enzymes and TE to maximise the performance of THP through batch solubilization and BMP tests.

MATERIALS AND METHODS

Macromolecular composition across THP-AD treatment

Sludge was collected before THP pre-treatment, after pre-treatment and after anaerobic digestion from a sludge treatment site processing 21,000 Tons Dry Solids (TDS)/ annum. The sludge is a mixture of primary sludge (PS) and waste activated sludge (WAS) with a combined ratio of 1.5. Protein, lipid and fibre content, as well as trace elements were quantified. Trace element bioavailability was profiled in decreasing order by soluble, exchangeable, carbonates, oxidisable and residual fraction, as described by (Ortner et al., 2014) .

Effect of hydrolysic enzymes on soluble COD release and biogas potential

Five enzymes- Protease 1000 (UB/g)**, Cellulase** (1000 U/g)**, Alpha amylase** (4000 U/g)**, Subtilisin** (2.5 AU-A/g) **and Lipase** (10,000 FIP/g) **were selected to study their effect on solubilization of the pre-treated sludge through batch solubilization tests. The enzymes were dosed at 0.5%,1%,2% and 4% TS (w/w). Best performing enzyme (protease) was then tested in biomethane potential (BMP) tests with sludge collected form the same full-scale site, and its performance compared with control and blank reactors. At present, continuous reactors are running with best conditions from BMP testing.**

RESULTS AND DISCUSSION

Solubilization of macromolecules across full-scale THP-AD

Full-scale profiling evidenced that THP pre-treatment enhances the solubilization of proteins and fibres by 29% and 20% respectively, while not having an impact on lipids (Figure 1). The ineffectiveness of THP at solubilizing lipids has been previously reported (Barber, 2016). Post THP however, the digester achieves the most reduction of volatile suspended solids belonging to lipids at 61% followed by fibres at 47% and proteins at a close 43%. It has been reported that for conventional mesophilic AD treating combined primary and secondary sludge, AD has the least impact on lipids degradation at 25% followed by fibres (Villa et al., 2022). Based on these results, our study suggests that THP pre-treatment, while not necessarily enhancing solubilization of recalcitrant compounds like lipids in the digester feed, may alter their innate composition and biodegradability, making them more amenable to degradation in advanced anaerobic digesters.

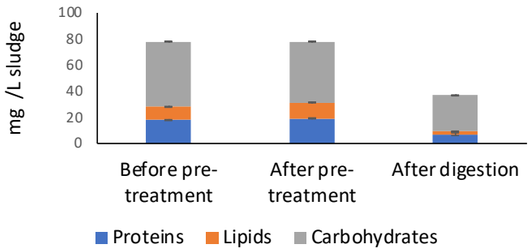

Figure 1. Fate of macromolecule solubilization throughout the THP-AD treatment chain.

Fate of trace element speciation across THP-AD

TE speciation yielded unique distribution patterns for each trace metal (Figure 2a-d). While Se, Co and Ni showed greater mobility towards bioavailable fractions (F1 and F2) after pre-treatment, Zn and Fe showed minimal improvement in bioavailable fractions, while those of Mo were further reduced after pre-treatment. Among all trace elements, THP pre-treatment had the maximum influence on increasing the bioavailable fraction of Se from 1% to 19%.

TE bioavailable concentrations (sum of F1 and F2) were then compared with the minimum free TE requirements for ADs. In general, the required concentration for the micronutrients is very low and in the range between 0.05 and 0.06 mg/l (Weiland, 2010). Only iron is necessary in higher concentration between 1 and 10 mg/l (Weiland, 2010). However, in high-ammonia digesters, like the ones achieved in THP-ADs, sufficient bioavailability of cobalt (0.5 mg/L) and nickel (0.2 mg/L) has been proven to be highly important for good performance of the processes (Westerholm et al., 2016). The study reveals that THP increases Se towards bioavailable limit after pre-treatment while indicating a minor deficiency in the digester (Figure 3a-f). It also shows obvious signs of deficiency in Co and Mo, challenging the general thought that sewage sludge digesters are self-sufficient in meeting their trace element requirements. Our study thus brings into context the bioavailable versus the total concentration of TE in the digesters and the importance of fractionating them to better understand their trace element requirements, especially at high loading rates and high digester ammonia concentrations brought about by THP pre-treatment. The full-scale profiling has informed Co and Mo as possible TE supplements in THP-ADs, with continuous reactors currently in operation.

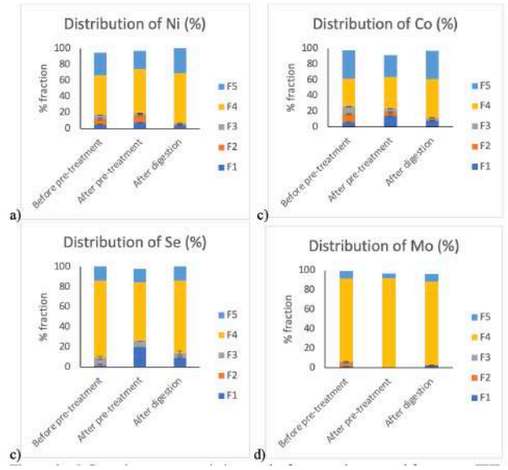

Figure 2a-d. Some important speciation results for trace element and fate across THP-AD treatment with data for Fe and Ni available. (F1 =Dissolved; F2 = Exchangeable; F3 = Carbonates; F4 = Oxidizable fraction; F5 = Residual)

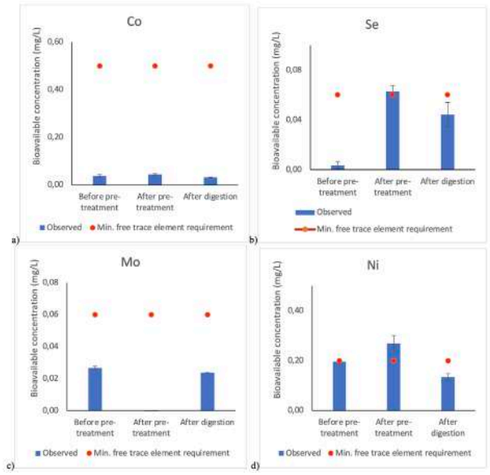

Figure 3a-f. Some important examples of bioavailable trace elements on an indicative basis with data for Fe and Ni available.

Effect of hydrolysis enzymes on soluble COD release

Dosing of different enzymes showed variability in terms of their performance for sCOD release with Cellulase, Alcalase and Lipase restricted to increasing the solubility of organic fraction to within 10% of control. Protease had the highest sCOD release compared to control between 17% and 19% even at low doses, suggesting an opportunity for a synergistic enhancement of AAD performance with the addition of protease. This was further investigated by conducting BMP tests with protease enzyme. Alpha amylase showed a negative performance compared to control , which can be attributed to the flocculation of sludge particles by the enzyme itself (Bonilla et al., 2015).

BMP tests with protease enzyme

The addition of protease in batch THP-AD reactors had a profound impact on enhancing the cumulative methane production, even at the lowest dose (Figure 3). The BMP of control was 431 NmlCH_4/g VS fed or 419 NmL biogas/g TS fed, which is within the range for THP pre-treated digester feed having mixed primary and secondary sludge (400-450 mL biogas/g TS fed) (Barber, 2020). The addition of protease at 0.5%, 1%, 2% and 4% TS (w/w) resulted in an increase in BMP by 22%, 27%, 35% and 36% respectively, indicating that at 2%, the enzyme will no longer be a limiting factor in the reaction. Our results so far show a potential window of opportunity at further enhancing the energy recovery potential of advanced anaerobic digesters at a cost-effective manner and without much investment in infrastructure

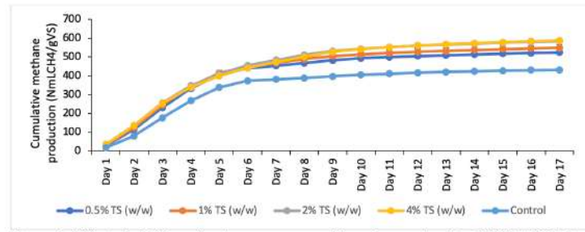

Figure 4. Effect of addition of protease enzyme on biomethane potential of THP-AD sludge.

CONCLUSION

Our study thus far reveals that THP can impact the innate biochemistry of recalcitrant macromolecules like lipids, even if does not lead to solubilization and subsequent hydrolysis but resulting in their enhanced degradation in digesters instead. The unique impact that THP imparts on feed and digester composition is also reflected on trace element speciation and bioavailability. Our study is the first of its kind profiling the influence of THP pre-treatment on bioavailability across a full-scale treatment chain. Results evidence a positive effect of THP on selenium bioavailability and a negative impact on molybdenum and zinc. A deficit of Co and Mo on the full-scale site has informed currently operating continuous AD trials. The BMP tests with protease addition shows that the margin for energy recovery can be pushed further, opening up avenues for augmented treatment with enzyme dosing, with further investigation ongoing for TE supplements as well. Overall, the implementation of THP pretreatment, while greatly enhancing the energy recovery and throughput of sludge treatment sites, could impart a greater benefit to utilities by augmenting with cost effective measures like enzyme and TE dosing to fully realize the potential of advanced anaerobic digesters in achieving higher energy recovery or treatment capacity.

REFERENCES

Surname, N., Surname, N., Surname, N. 2011 Title of the paper. *Water Science and Technology* **28**(11), 11–25.
Barber, W., 2020. Benefits, in: Sludge Thermal Hydrolysis: Application and Potential. IWA Publishing, pp. 137–162. https://doi.org/10.2166/9781789060287_0137
Barber, W.P.F., 2016. Thermal hydrolysis for sewage treatment: A critical review. Water Res 104. https://doi.org/10.1016/j.watres.2016.07.069
Bonilla, S., Tran, H., Allen, D.G., 2015. Enhancing pulp and paper mill biosludge dewaterability using enzymes. Water Res 68, 692–700. https://doi.org/10.1016/j.watres.2014.10.057
Ortner, M., Rachbauer, L., Somitsch, W., Fuchs, W., 2014. Can bioavailability of trace nutrients be measured in anaerobic digestion? Appl Energy 126, 190–198. https://doi.org/10.1016/j.apenergy.2014.03.070
Villa, R., Jantová-Patel, J., Bajón Fernández, Y., 2022. Novel Insight on the Impact of Enzymatic Addition on Organic Loading Rate in Anaerobic Digestion. Waste Biomass Valorization 13, 2109–2120. https://doi.org/10.1007/s12649-021-01662-0
Weiland, P., 2010. Biogas production: current state and perspectives. Appl Microbiol Biotechnol 85. https://doi.org/10.1007/s00253-009-2246-7
Westerholm, M., Moestedt, J., Schnürer, A., 2016. Biogas production through syntrophic acetate oxidation and deliberate operating strategies for improved digester performance. Appl Energy 179. https://doi.org/10.1016/j.apenergy.2016.06.061

High-rate Activated Sludge at very short SRT: key factors for process Stability and Performance of COD fractions removal

Joan Canals[1,2], Alba Cabrera-Codony[1], Oriol Carbó[1,2], Maria Martín[1], Mercè Baldi[2], Belén Gutiérrez[2], Manel Poch[1], Antonio Ordóñez[2], Hèctor Monclús[1*]

[1] LEQUIA, Institute of Environment, Universitat de Girona, M.Aurèlia Capmany 69, 17003, Girona, Catalonia, Spain.
[2] GS Inima Environment, S.A. c/Gobelas 41. 1ª A 28023, Madrid. Spain

Abstract: In high-rate activated sludge (HRAS) processes, reducing the solid retention time (SRT) minimizes COD oxidation and allows to obtain the maximum energy recovery. The aim of this research was to operate a pilot plant (35 m3·d-1) with an automatic control strategy to assure the HRAS process stability and high COD fractions removal efficiency at very low SRT (0.2 d), HRT (0.6h) and DO (0.5 mg·L-1) treating high-strength raw wastewater, at 18-26ºC and at variable influent flow rate. The research includes the effects of temperature, influent concentration and MLSS reactor concentration over the sCOD, cCOD and pCOD removal. The study points out that operating at 2,000±200mg·L-1 assured a stable process despite the large influent variation. Low SVI values of 50-70ml·g-1 indicated the good settling properties of the biomass. With only a 6,9% COD oxidation, a high organic matter removal (57±9% for COD and 56±10% for BOD5), was reached. The high removal efficiencies for pCOD, 74%, compared to the 29% for sCOD and 12% for cCOD also confirmed the importance of settling efficiency and stability in the HRAS.

Keywords: COD fractions removal; HRAS process stability; HRAS pilot plant.

INTRODUCTION

The High rate activated sludge (HRAS) process enhances the removal of particulate and colloidal COD (pCOD, cCOD), and even some of the soluble COD (sCOD) from urban wastewater, with a minimum energy consumption (Carrera et al 2022) by 1) Carbon redirection, where particulate and colloidal fractions are removed by bioadsorption and bioflocculation, and redirected into the sludge matrix, while soluble biodegradable COD is removed by intercellular storage (bioaccumulation), microbial growth and carbon oxidation; and 2) Carbon harvesting, where redirected organic carbon is recovered through settling without having been metabolized by bacteria and sent to anaerobic digestion. One factor that limits carbon harvesting is the settling capability of the biological sludge. Low oxidation of organic matter due to the low sludge retention time (SRT) maximizes the organic matter redirection but decreases the settling of biomass and consequently worsens the harvesting.

The main objective of this study was to evaluate the carbon redirection and the carbon harvesting in a stable operation of a HRAS (SRT< 0.5d, HRT<1h and DO<0.5 mg·L^{-1}) by: i) Evaluating the removal efficiency of each COD fraction and BOD_5 and their correlations with key operational process parameters; ii) Monitoring the influent and effluent COD fractions and BOD_5 in long-term operation; iii) Evaluating the COD oxidation; iv) Comparing the simulated COD fractions removal efficiency with the pilot plant results.

MATERIALS AND METHODS

A HRAS pilot plant was operated during 497 days, running over nine different operational periods treating, the main parameters and conditions of which are summarized in Table 1. The COD mass balance was calculated for each experimental period in order to investigate the efficiency of the process in terms of COD sent to digestion and COD oxidized.

RESULTS AND DISCUSSION

Figure 1 shows the fractions of soluble (sCOD), particulated (pCOD), total COD concentration and BOD_5 at the influent and at the effluent during the HRAS pilot plant operation.

Figure 2 shows the results of the mass balance for each period. The HRAS working at low SRT and high variations in the influent load, permitted to send to digestion an average 55% of the influent COD, with a low average oxidation of 6.9±3.6% and maintaining the COD_{OUT} around 40% for almost every period. Reducing SRT up to 0.2 days and HRT up to 0.6 hours, corresponding to one third of the usual values reported in HRAS operation, allows a high redirection and harvesting of organic matter 57±9% for COD and 56±10% for BOD_5. The different COD fraction removal: 29±12% sCOD, 12±35% cCOD and 74±10% pCOD, highlighted the importance of settling efficiency and stability in the HRAS removal efficiencies.

In order to investigate the sCOD influent concentration effect over the sCOD removal efficiency, Figure 3 shows the relation between COD_{in} fractions and the COD removal at 20 °C corrected temperature (Θ=1.045) (Seeley, 1992) along the nine experimental periods considered. The good correlation indicated that the sCOD removal was controlled by a biological oxidation-storage process according to Hauduc et al. (2019).

Maintaining the biomass concentration in the reactor at 2000±200 mg·L^{-1} as process control strategy assured a very stable process even with the large variations in the influent. So, both in short- and long-term performance the best control parameter at very low SRT to ensure the process stability and minimize COD oxidation was not strictly the SRT but rather the MLSS concentration (Figure 4). The biomass concentration was directly correlated with sCOD and pCOD removal, while the reactor temperature hampered the pCOD removal but increased the sCOD.

The direct relation between influent COD concentration and COD removal makes it advisable to use the HRAS process as a replacement of the PC stage and not as a downstream treatment afterward. Settling efficiency and stability showed a great importance in the HRAS performance. The low SVI30 values of 50-70 mL·g^{-1} showed the exceptional biomass settling properties, while the relatively low SS effluent concentration 50-120 mg·L-1 indicated correct flocculation. HRAS process acts as a filter for the influent COD and pCOD peak loads and, albeit to a lesser extent, for BOD_5, buffering the influent load to the subsequent CAS process. The HRAS-AS process, on the other hand, does not act as a filter for sCOD peak loads, which is important regarding the likely subsequent denitrification process.

Table 1. Reactors and settler operation parameters.

Period	MLSS R2 [mg·L^{-1}]	HRT R1+R2 [hours]	SRT R2 [days]	DO R2 [mg·L^{-1}]	External recycle	OLR-R2 [kgCOD · kgMLSS^{-1}·d^{-1}]	OFR Q_{in} [m·h^{-1}]	SL Q_{in}+Q_R [kgMLSS·m^{-2}·d^{-1}]	SVI_{30} [mL·g^{-1}]	TSS (out) [mL·g^{-1}]
1	3043	1.6	0.2	0.7	73 %	9.9	1.3	164	64	103
2	2577	1.3	0.3	0.4	60 %	8.8	1.6	155	51	92
3	1729	1.2	0.1	0.4	55 %	14.9	1.7	109	55	113
4	2555	1.2	0.2	0.4	54 %	8.5	1.6	156	67	119
5	2508	1.2	0.2	0.4	54 %	9.8	1.6	152	48	91
6	2290	1.2	0.2	0.5	70 %	9.3	0.8	79	55	66
7	2163	0.6	0.1	0.5	70 %	14.6	0.8	75	59	69
8	2010	0.6	0.2	0.5	62 %	10.4	0.8	65	49	65
9	1924	0.6	0.2	1.1	63 %	9.5	0.8	64	49	44

OLR:(organic loading rate); OFR:(over flow rate); SL:(solids loading); SVI_{30}:(sludge volume index 30 min.)

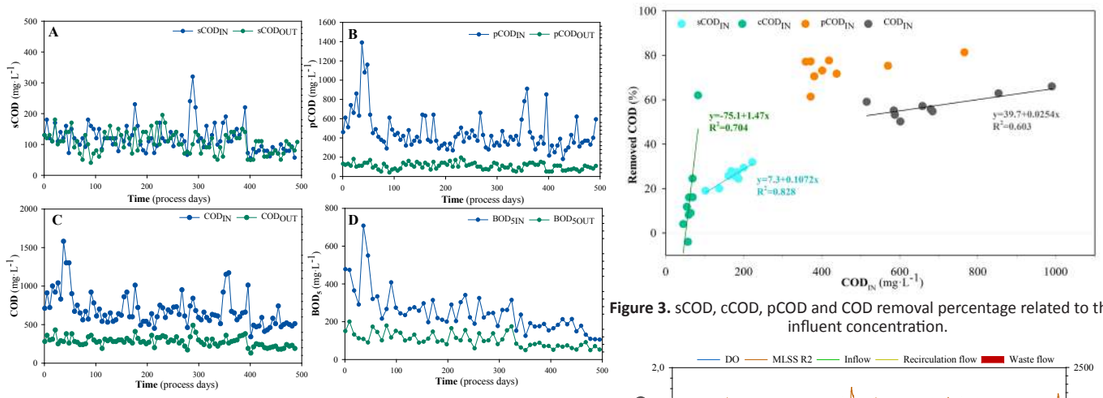

Figure 1. Daily variations of the influent and effluent concentrations of A) sCOD; B) pCOD; C) COD and D) BOD5.

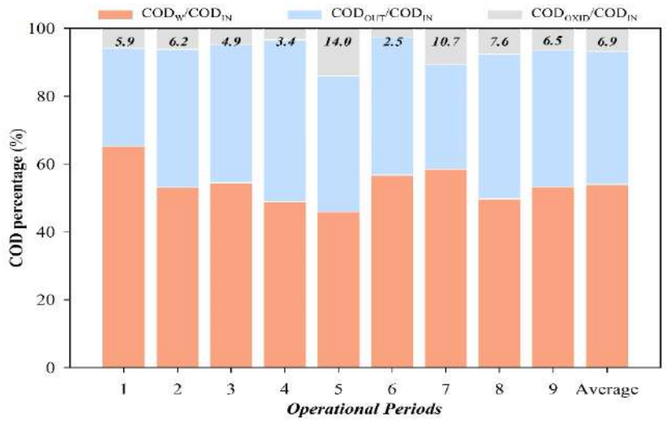

Figure 2. COD influent mass balance distribution: waste, out and oxidized.

Figure 3. sCOD, cCOD, pCOD and COD removal percentage related to their influent concentration.

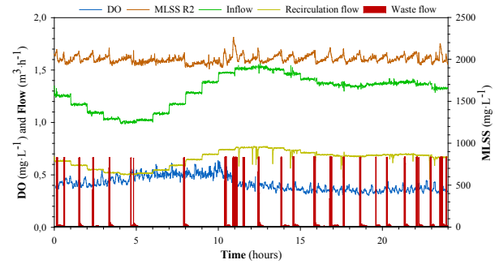

Figure 4. 24h monitoring of the process control parameters: waste sludge flow rate and MLSS concentration in reactor R2, dissolved oxygen (DO) and recirculation flow rate.

REFERENCES

Carrera, J., Carbó, O., Doñate, S., Suárez-Ojeda, M.E., Pérez, J., 2022. Increasing the energy production in an urban wastewater treatment plant using a high-rate activated sludge: Pilot plant demonstration and energy balance. J. Clean. Prod. 354, 131734. https://doi.org/10.1016/J.JCLEPRO.2022.131734

Hauduc, H., Al-Omari, A., Wett, B., Jimenez, J., De Clippeleir, H., Rahman, A., Wadhawan, T., Takacs, I., 2019. Colloids, flocculation and carbon capture – a comprehensive plant-wide model. Water Sci. Technol. 79, 15–25. https://doi.org/10.2166/WST.2018.454

Miller, M.W., Elliott, M., DeArmond, J., Kinyua, M., Wett, B., Murthy, S., Bott, C.B., 2017. Controlling the COD removal of an A-stage pilot study with instrumentation and automatic process control. Water Sci. Technol. 75, 2669–2679. https://doi.org/10.2166/wst.2017.153

Seeley, I.H., 1992. Wastewater Engineering, in: Public Works Engineering. McGraw-Hill, New York, pp. 160–214. https://doi.org/10.1007/978-1-349-06927-9_4

Taboada-Santos, A., Rivadulla, E., Paredes, L., Carballa, M., Romalde, J., Lema, J.M., 2020. Comprehensive comparison of chemically enhanced primary treatment and high-rate activated sludge in novel wastewater treatment plant configurations. Water Res. 169, 115258. https://doi.org/10.1016/j.watres.2019.115258

An integrated system to produce bio-based volatile fatty acids for the industry and biogas from sewage sludge

Ander Castro-Fernández*,**, M. Tortosa*, Juan M. Lema**, Leticia Rodríguez-Hernández***, C. M. Castro-Barros* and Antón Taboada-Santos*

*CETAQUA, Water Technology Centre, AquaHub - A Vila da Auga, Jose Villar Granjel 33, E-15890, Santiago de Compostela, Spain (E-mail: *ander.castro@cetaqua.com*)

** CRETUS Institute, Department of Chemical Engineering, School of Engineering, Universidade de Santiago de Compostela, E-15782, Santiago de Compostela, Spain

*** ViAQUA, Gestión Integral de Aguas de Galicia, AquaHub - A Vila da Auga, Jose Villar Granjel 33, E-15890, Santiago de Compostela, Spain

Abstract

The generation of bioproducts and biogas from sewage sludge is a way to manage it correctly. Specifically, volatile fatty acids (VFA) can be produced through fermentation process when methanogenesis is inhibited. However, the lower yields of the process compared to those from the anaerobic digestion (AD) make necessary to valorise the solid fraction obtained after solid-liquid separation of fermented sludge. In this work, it was proved that it is not feasible to ferment this stream in a second fermentation to produce VFA but it can be converted into biogas, since its biomethane potential is still relevant (184 L (N) CH_4/kg VS). The overall mass balance shows that this process (VFA+AD) achieves the same organic matter conversion as the conventional AD alone. However, the main bottleneck is the VFA concentration; membrane separation and liquid-liquid extraction+distillation are being tested and the overall techno-economic and environmental analysis of the process will be presented.

Keywords

Biogas, hydrolysed sewage sludge, volatile fatty acids

INTRODUCTION

Sewage sludge has been traditionally valorised as biogas through the anaerobic digestion (AD) process. However, if last step of the process (methanogenesis) is inhibited, it can be valorised as volatile fatty acids (VFA), a highly demanded product in several chemical and petrochemical industries that can replace those produced from fossil fuels.

Moreover, in last decades some pre-treatment technologies such as the Cambi™ process prior the AD stage have been developed in order to increase biogas production and to obtain a pathogens free sludge. This technology is currently fully implemented worldwide with more than 70 installations. However, the number of works studying the impact of thermal hydrolysis sludge on VFA production is more limited.

Independently of whether pre-treatment technologies are included in the VFA production or not, the reported conversion yields of sludge into VFA are commonly much lower (20-30% in COD basis) than those of the AD process (50-60%) and reasons for these results are still unclear since VFA are an intermediate of the AD process and a similar yield in both processes could be expected. Therefore, it is essential to post-treat the solid fraction obtained after the VFA production step, since this subproduct still has high proportion of biodegradable organic matter that would damage the soil if used in agriculture.

Moreover, a second bottleneck of the process is the purification and concentration of VFA from the aqueous phase. Several technologies have been or are being developed such as gas stripping with absorption, adsorption, solvent extraction, electrodialysis and membrane separation, but the challenge now is the selection of cost-effective recovery methods which lead to maximum VFA recovery at a minimal cost (Atasoy et al., 2018), since for some applications the VFA must have a very high purity, even above 90%.

Therefore, this work seeks to optimize a fermentative process for the production of VFA on a pilot scale prototype for the obtention of a VFA-rich stream capable of being concentrated, and also a solid cake, whose potential for VFA production was evaluated in a subsequent acidic/alkaline fermentation, as well as its biomethane potential (BMP).

MATERIAL AND METHODS

The work has been carried out in a pilot plant located in Ourense WWTP (Spain), that has the Cambi™ thermal hydrolysis process in its sludge line.

The pilot plant (Figure 1) mainly consists of a 1.5 m^3 volume CSTR fermenter (operated at HRT of 10 days and pH of 8.5), which is fed with thermally hydrolysed sewage sludge stored in a buffer tank. The fermented effluent is fed to a coagulation-flocculation tank and to a subsequent press filter for solid-liquid separation, obtaining a VFA-rich supernatant and a solid residue. The liquid fraction is first purified with the ultrafiltration membrane and then concentrated thanks to the reverse osmosis one, before being subjected to liquid-liquid extraction and distillation.

Figure 1. Pilot plant for the production of VFA operated in the project.

To valorise the solid fraction, it was rehydrated and fed into two acidogenic reactors working at different conditions to determine its potential to be converted to VFA in a second fermentation (at HRT of 6 days and pH of 6 and 8.5). Alternatively, this solid residue was also valorised as biogas in a biomethane potential batch test. To execute this, two semi-continuous 5-L reactors at lab scale and the AMPTS II equipment of the Bioprocess Control brand were used.

The Hach D43900 spectrophotometer and associated cuvette kits were utilized to monitor the pilot plant fermenter, as well as lab-scale reactors and associated experiments. VFA were determined using a gas chromatograph Agilent Technologies (model 6850 Series II), equipped with a flame ionization detector (FID).

Figure 2 shows the proposed technology, a several-stage system which integrates a pilot scale fermentation for the production of VFA with a following valorisation of the press filter cake.

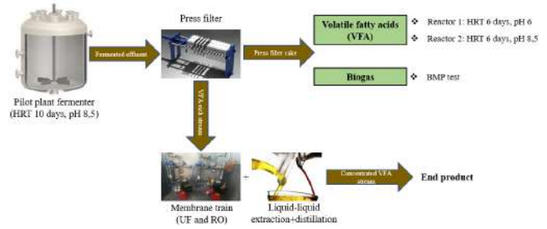

Figure 2. Scheme of the complete proposed system with the applied operating conditions.

RESULTS

Figure 3 exhibits the results obtained in the operation of the pilot plant fermenter. The average production yield of VFA was in the range 0.15-0.20 g COD-VFA/g COD influent, being the VFA mix composed of almost 70% acetic acid (COD-basis), followed by propionic (15%) and butyric acids (10%), in accordance with other authors (Morgan-Sagastume et al., 2011).

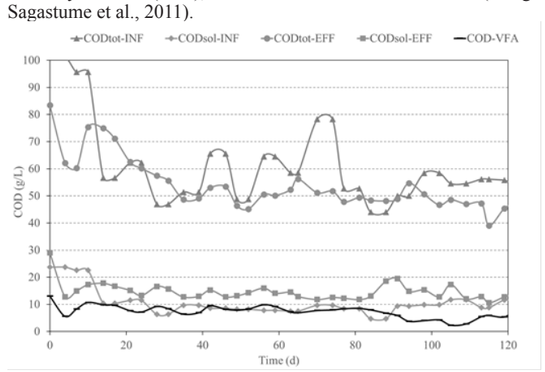

Figure 3. Influent and effluent COD in the fermenter and VFA concentration in the effluent.

As a consequence of the lower yields compared to the conventional AD process, it is necessary to value the solid fraction of the solid-liquid separation due to its still high presence of biodegradable COD. The experiments carried out for the fermentation of the rehydrated solid cake obtained after the first fermentation at alkaline and acidic pH showed negligible transformation, proving that it was not feasible to produce VFA in a second fermentation stage.

However, the BMP test showed that this solid cake has a BMP of 184 L (N) CH_4/kg VS (Figure 4), equivalent to 34% of anaerobic biodegradability, which can be used to partially or totally cover the energetic demand of the whole process.

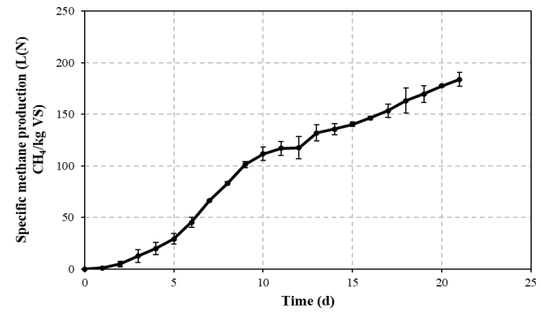

Figure 4. Graph of the BMP test of the solid cake.

The mass balance comparison of the two stages VFA production+AD vs conventional AD shows that per 1 kg of COD of sewage sludge fed into the system, in both cases 0.6 kg of COD as digestate are obtained. However, while conventional AD generates only biogas, with this technological proposal around 0.15-0.20 kg COD-VFA+0.4 kg COD-CH_4 are obtained, being the market value of VFA up to 10 times higher than biogas (Zhou et al., 2018).

CONCLUSIONS

The results show that pilot-scale fermentation can produce an effluent that, after being separated into its solid and liquid fractions, gives rise to a VFA-rich stream and a solid residue that can be converted into biogas. The liquid stream still has to be concentrated to fulfil the requirements of the chemical industry to be used as raw material in biorefineries (purity>90%). Currently, two technologies such as membranes and liquid-liquid extraction+distillation are being tested and the overall technoeconomic and environmental analysis of the process will be presented at the conference, from which the selling price of the obtained bioproducts will be estimated.

The project was financed by the Xunta de Galicia within the framework of the CIGAT CIRCULAR project and also by INTERREG SUDOE ECOVAL and HOOP (EU's Horizon 2020 Nº101000836).

REFERENCES

Atasoy, M., Owusu-Agyeman, I., Plaza, E., & Cetecioglu, Z. (2018). Bio-based volatile fatty acid production and recovery from waste streams: Current status and future challenges. *Bioresource Technology*, *268*(July), 773–786. https://doi.org/10.1016/j.biortech.2018.07.042

Morgan-Sagastume, F., Pratt, S., Karlsson, A., Cirne, D., Lant, P., & Werker, A. (2011). Production of volatile fatty acids by fermentation of waste activated sludge pre-treated in full-scale thermal hydrolysis plants. *Bioresource Technology*, *102*(3), 3089–3097. https://doi.org/10.1016/j.biortech.2010.10.054

Zhou, M., Yan, B., Wong, J. W. C., & Zhang, Y. (2018). Enhanced volatile fatty acids production from anaerobic fermentation of food waste: A mini-review focusing on acidogenic metabolic pathways. *Bioresource Technology*, *248*, 68–78. https://doi.org/10.1016/j.biortech.2017.06.121

Influence of carbon-coated zero-valent iron-based nanoparticle concentration on continuous photosynthetic biogas upgrading

E. G. Hoyos* and R. Muñoz*

* Department of Chemical and Environmental Technology, University of Valladolid, Dr. Mergelina, s/n, 47011, Valladolid, Spain
* Institute of Sustainable Processes, University of Valladolid, Dr. Mergelina, s/n, 47011, Valladolid, Spain

(E-mail: *eghoyosd@funge.uva.es*)

Abstract

The present work investigated the influence of the concentration of carbon-coated zero-valent iron-based nanoparticles (70, 140 and 280 mg L^{-1}) on the continuous biogas upgrading in an algal-bacterial photobioreactor. In addition, the influence of nanoparticle concentrations on the CO_2 liquid-gas mass transfer in the absorption column was investigated. A nanoparticle concentration of 140 mg L^{-1} was the optimal among the concentrations tested, improving almost by 50 % the microalgae productivity compared to the concentration of 70 mg L^{-1}. Concentrations of 280 mg L^{-1} did not entail higher microalgae productivities. The biomethane obtained complied with the European biomethane standard only when nanoparticles were added. Interestingly, none of the nanoparticle concentrations influenced the CO_2 liquid-gas mass transfer in the absorption column.

Keywords

Algal-bacterial photobioreactor; CO_2 liquid-gas mass transfer; microalgae productivity; nanoparticle concentrations; optimization; photosynthetic biogas upgrading

INTRODUCTION

Microalgae are photosynthetic microscopic organisms with a wide variety of applications that contribute to the development of a bioeconomic worldwide. A very interesting application of microalgae that has emerged in recent years is photosynthetic biogas upgrading, where CO_2 is fixed by microalgae via photosynthesis and the O_2 released supports the bacterial oxidation of H_2S (Posadas et al., 2017; Toledo-Cervantes et al., 2016). Nanoparticles can be an effective and promising strategy to enhance photosynthetic biogas upgrading as well as microalgae growth (Vargas-Estrada et al., 2022). The work carried out by Vargas-Estrada et al. (2023) was a preliminary study to evaluate the influence of the addition of carbon-coated zero-valent iron nanoparticles at 70 mg L^{-1} to algal-bacterial cultures devoted to photosynthetic biogas upgrading under continuous operation. The results showed that the addition of nanoparticles significantly boosted the performance of photosynthetic biogas upgrading and microalgae growth. This work aimed at evaluating the effect of nanoparticle concentrations on photosynthetic biogas upgrading under continuous operation. In addition, the influence of nanoparticle concentrations on the CO_2 gas-liquid mass transfer in the absorption column was investigated.

MATERIALS AND METHOD

Figure 1 shows the main experimental set-up, which consisted of a High Rate Algal Pond (HRAP) configuration interconnected to an external CO_2 absorption column (AC) via external liquid recirculation of the supernatant from a settler. Synthetic biogas was used with a composition (% v/v) of 70 % CH_4, 29.5 % CO_2 and 0.5 % H_2S. Centrate was obtained from the wastewater treatment plant of Valladolid, Spain. The carbon-coated zero-valent iron nanoparticles (NPs) (kindly provided by CALPECH) were added to the system and daily to the centrate at the concentrations studied. The operating conditions were: ambient temperature = 26.3 ± 1.6 ºC, HRAP liquid temperature = 31.1 ± 1.2 ºC, photosynthetic active radiation (PAR) = 1405 ± 45 µmol m^{-2} s^{-1}, gas flowrate = 60 L d^{-1}, L/G (external liquid recirculation/gas flowrate) ratio = 2, and centrate feed = 4.3 L d^{-1}. The parameters monitored were: pH, dissolved oxygen, total organic carbon, inorganic carbon, total nitrogen, NH_4^+, NO_2^-, NO_3^-, PO_4^{3-}, SO_4^{2-}, total suspended solids, volatile suspended solids (VSS), gas composition (CH_4, CO_2, H_2S, N_2 and O_2) at the inlet and outlet of the AC, and microalgae population. The influence of NPs concentration on the CO_2 gas-liquid mass transfer in the AC under abiotic conditions was assessed using synthetic centrate mimicking the characteristics of HRAP cultivation broth without biomass at pH = 8 (Figure 2). The composition of the synthetic biogas and the operating conditions were as above described. Four different concentrations of NPs were tested: 0, 70, 150 and 300 mg L^{-1}. Both the gas composition and the pH of the liquid at the outlet of the AC were measured under steady state conditions.

RESULTS AND DISCUSSION

From an initial NPs concentration in the system of 70 mg L^{-1} (stage I), the concentration was increased to 140 and later to 280 mg L^{-1} (stage II and III, respectively) (Figure 3). An increase in the NPs concentration from 70 to 140 mg L^{-1} entailed a rapid increase in pH and VSS in the HRAP (Figure 3a, b), which was mediated by an increase in photosynthetic activity and therefore in algal growth. This phenomenon induced a significant increase in productivity of almost 50 % (from 33 to 48.2 g m^{-2} d^{-1}). During stage II, the CO_2 removal efficiency (RE-CO_2) increased from 90.2 ± 1.8 up to 95.8 ± 1.9 % and thus the CO_2 concentration decreased from 3.6 ± 0.6 to 1.7 ± 0.7 % (Figure 3c), and the CH_4 concentration increased from 91.8 ± 0.8 to 94.2 ± 0.8 % (Figure 3d). The biomethane obtained in stage II complied with the recently enforced European biomethane standard ($CH_4 \geq 90\%$, $CO_2 \leq 2\%$, $O_2 \leq 1\%$ and negligible amounts of H_2S) (Vargas-Estrada et al., 2023). The increase in NPs concentration from 140 to 280 mg L^{-1} led to an initial decrease in algal growth since pH and VSS decreased. However, microalgae activity recovered. This change in conditions did not imply an improvement in microalgae productivity but a change in microalgae population (from *Chlorella sp.* to *Chloroidium saccharophilum*). Due to the increase in pH from 9.2 (stage II) to 9.5 (stage III), the RE-CO_2 increased to 98.1 ± 0.8 % and therefore the CO_2 content decreased to 0.8 ± 0.3 %. Therefore, the CH_4 content slightly increased to 94.4 ± 0.7 %.

Table 1 shows the results of the study of the influence of NPs on the CO_2 gas-liquid mass transfer in the AC. According to the results, the studied nanoparticles at the concentrations tested had no influence on the CO_2 mass transfer in the AC, contrary to the study performed by Jeon et al. (2017) using SiO_2 nanoparticles, which enhanced the CO_2 gas-liquid mass transfer. This finding suggests that the improvement in process performance recorded by the addition of nanoparticles does not rely on an improvement of CO_2 capture in the AC but in the enhancement in photosynthesis.

REFERENCES

Jeon, H-S., Park, S. E., Ahn B., Kim, Y-K. 2017 Enhancement of biodiesel production in *Chlorella vulgaris* cultivation using silica nanoparticles. *Biotechnology and Bioprocess Engineering* **22**, 136-141.

Posadas, E., Marín, D., Blanco, S., Lebrero, R., Muñoz, R. 2017 Simultaneous biogas upgrading and centrate treatment in an outdoors pilot scale high rate algal pond. *Bioresource Technology* **232**, 133-141.

Toledo-Cervantes, A., Serejo, M. L., Blanco, S., Pérez, R., Lebrero, R., Muñoz, R. 2016 Photosynthetic biogas upgrading to bio-methane: Boosting nutrient recovery via biomass productivity control. *Algal research* **17**, 46-52.

Vargas-Estrada, L., Hoyos, E. G., Sebastian, P. J., Muñoz, R. 2022 Elucidating the role of nanoparticles on photosynthetic biogas upgrading: Influence of biogas type, nanoparticle concentration and light source. *Algal Research* **68**.

Vargas-Estrada, L., Hoyos, E. G., Méndez, L., Sebastian, P. J., Muñoz, R. 2023 Boosting photosynthetic biogas upgrading via carbon-coated zero-valent iron nanoparticle addition: A pilot proof of concept study. *Sustainable Chemistry and Pharmacy* **31**.

FIGURES & TABLES

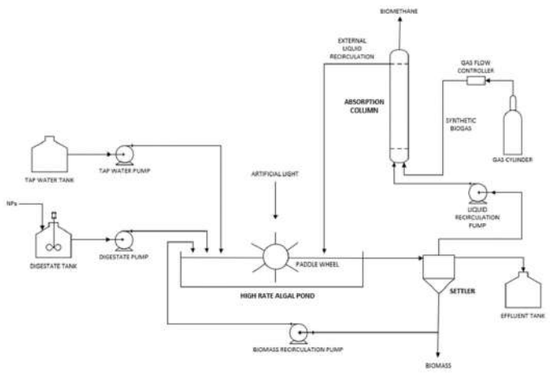

Figure 1. Main experimental set-up.

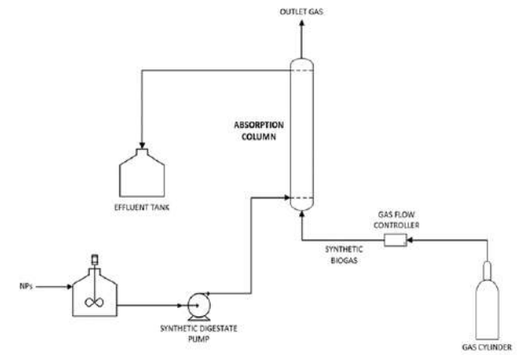

Figure 2. Experimental set-up to assess the influence of NPs concentration on the CO_2 gas-liquid mass transfer.

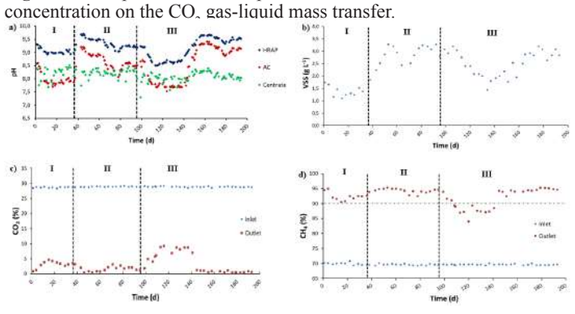

Figure 3. Time course of a) pH, b) VSS in the HRAP, c) CO_2 concentration (% v/v), and d) CH_4 concentration (% v/v) in the treated biogas.

Table 1. Influence of NPs concentrations on the CO_2 gas-liquid mass transfer in the AC.

	Concentration of NPs (mg L^{-1})			
	0	70	150	300
pH	7.59 ± 0.05	7.57 ± 0.03	7.60 ± 0.01	7.58 ± 0.03
CO_2	8.5 ± 0.1	8.2 ± 0.1	8.7 ± 0.1	8.6 ± 0.1
O_2	2.2 ± 0.1	1.7 ± 0.1	1.5 ± 0.1	1.7 ± 0.1
N_2	4.7 ± 0.1	4.1 ± 0.3	3.8 ± 0.2	4.2 ± 0.2
CH_4	84.6 ± 0.1	86.0 ± 0.3	86.0 ± 0.2	85.5 ± 0.3

Organic loading rate and pH as optimization parameters for biohydrogen production via dark fermentation coupled with microbial electrolysis cells

J.A. Magdalena[*,**], M.F. Pérez-Bernal[*], N. Bernet[*], E. Trably[*]

* INRAE, Université de Montpellier, LBE, 102 avenue des Étangs, 11100 Narbonne, France
(E-mail: *jose-antonio.magdalena-cadelo@inrae.fr; maria-fernanda.perez-bernal@inrae.fr; nicolas.bernet@inrae.fr;eric.trably@inrae.fr*)
** Vicerrectorado de Investigación y Transferencia de la Universidad Complutense de Madrid, 28040 Madrid, Spain

Abstract

The present study aims to maximize biohydrogen production from food waste in a two-stage process coupling dark fermentation (DF) and microbial electrolysis cells (MECs). Firstly, the effect of stepwise increases (30, 45, and 60 gVS/Ld) was evaluated in a continuous DF reactor at 37°C and pH 7. Afterwards, the DF effluent was filtered and fed in four two-chamber MECs (Two enriched with *Geobacter sulfurreducens* and two with a mixed consortium). The effluent profile in DF was dominated by acetate (26-30% COD-acetate/COD-metabolites). Interestingly, the butyrate fraction, not easily metabolized by electroactive bacteria, was reduced when increasing the OLR from 25 to 10% COD-butyrate/COD-metabolites. The high acetate content impacted the current densities obtained for both *G. sulfurreducens* and mixed culture-based MECs (7 and 11 A/m², respectively). Overall, the biohydrogen yield in the MEC achieved values of 0.56-0.64 LH_2/ g CODin, whereas considering the coupling the yield was 0.16 LH_2/ g CODin.

Keywords (maximum 6 in alphabetical order)

Biohydrogen; dark fermentation; *G. sulfurreducens*; microbial electrolysis cells; mixed culture; process coupling

INTRODUCTION

Renewable bioprocesses to produce biohydrogen such as dark fermentation (DF) might contribute to the energetic change of paradigm. Nonetheless, the limited hydrogen yields obtained so far still prevent further commercialization of this technology, as most of the organic matter degraded remains in form of volatile fatty acids. A possible strategy to improve the hydrogen yield is to couple the DF process with microbial electrolysis cells (MECs). In this context, the VFAs accumulated during DF can be further metabolized in the MEC to produce biohydrogen at high purity. The abundance of each VFA composing the effluent has a crucial impact on the biohydrogen yields obtained in MECs since some acids are more easily degradable than others. For instance, lactate and acetate showed higher performances in terms of current densities than propionate and butyrate (Flayac, Trably, et al., 2018). Therefore, the increase of the acetate fraction in the digestate, and the reduction of other compounds such as butyrate might enhance the biohydrogen production in MECs. The novelty of this study lies in employing increasing organic loading rates (OLRs) and neutral pH in DF as a tool to promote acetate in DF. Additionally, the effluent was evaluated in MECs with a pure culture of *G. sulfurreducens* and a mixed culture for hydrogen production.

MATERIALS AND METHODS

The aerobic inoculum was subjected to a freeze-drying process. The VS/TS ratio was of 0.97. The FW substrate was stored frozen at -20 °C to avoid changes in its composition over time as described in previous research (Noguer, Magdalena, et al., 2022). FW was thermally pretreated at 70 °C for 1 h and sieved through 2 mm mesh before fermentation. 2 L Fermenters were fed continuously with the FW at controlled pH and temperature (7 and 37.0°C, respectively). Three different stages were distinguished depending on the organic loading rate (OLR) and hydraulic retention times (HRT), namely Stages I, II, and III (30, 45, and 60 g VS/Ld and 1, 1, and 0.75 days, respectively). Effluent from the reactor was recovered and filtered in an ultrafiltration unit (50 nm mesh) composed of a ceramic membrane. Prior to MEC operation, filtered effluents were diluted with distillate water to reach a final acetate concentration of 1 g/L to avoid inhibition of the electroactive bacteria in the MEC (Table 1). MECs consisted of two chambers separated by a cation exchange membrane. MECs were operated using a three-electrode set-up with an anode potential of 0.444 V vs SHE, using a VMP3 potentiostat. An enrichment step with a synthetic medium was conducted in the MEC to create a biofilm using acetate (1 g/L) as a carbon source with the same type of aerobic inoculum used for DF. Concerning *G. sulfurreducens*, the strain was inoculated in 2 MEC reactors using a phosphate-buffered (pH 7) mineral medium with acetate (1 g/L) as a carbon source. Afterward, effluents were adjusted to pH 7 and bubbled with N_2 gas to remove all oxygen and fed into the MEC reactors. MECs were operated at 30 °C and constant stirring of 180 rpm.

RESULTS AND DISCUSSION

The OLRs assessed (30, 45 and 60 g COD/Ld) resulted in average sCOD/tCOD values ranging from 0.51-0.61 corresponding with a COD removal lower than 25%. Hydrogen production was around 0.1 L H_2/Ld regardless of the OLR with increasing hydrogen concentrations in the biogas (from 47±10 to 65±10 %v/v H_2). Nonetheless, hydrogen production was not promoted in this step due to the neutral pH selected, which was set to improve the acidogenic selectivity towards acetate. As a matter of fact, the system showed high robustness to transform organic matter into metabolites at high OLRs maintaining conversion values as high as 41-45% COD-met/CODin (Figure 1) during the experimental time (51 days). Acetate appeared as the most abundant product during the investigation (26 to 30% COD-acetate/COD-metabolites), whereas butyrate was reduced (25 to 10% COD-butyrate/COD-metabolites from Stage I to III).

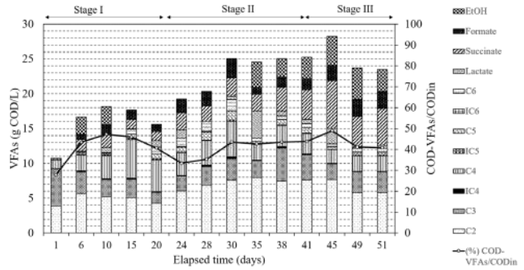

Figure 1. Metabolite analysis at selected experimental points during reactor operation

In the case of *G. sulfurreducens* (R1 and R2_GS, Figure 2) acetate was almost completely consumed by day 4, however high current densities (5 A/m²) were maintained almost until day 5, indicating that other substrates were as well easily consumed. On top of acetate; lactate and formate were completely consumed; while butyrate, valerate and caproate remained unconsumed. On the other hand, succinate was most likely converted into propionate via the succinate pathway, which caused its accumulation. H_2 production in both R1_GS and R2_GS was similar until day 4. Differences from this point were attributed to gas leakage since the CE was similar in both reactors (Table 2). As for the MECs enriched with a mixed culture (R1 and R2_Mixed, Figure 2), the current densities were surprisingly high as well as r_{cat} and r_{H2} (Table 2). Nonetheless, the substrate consumption profile was quite similar than with the pure culture. Differences in current densities were observed between both systems and were attributed to the different ages of the anodic biofilms (15 days and 47 days for the mixed and *G. sulfurreducens* biofilms respectively). The main difference was on valerate formation, while for *G. sulfurreducens* increased only by 0.1 mM for both reactors, in the case of the mixed culture MECs the increases were 0.4 and 0.7 mM. Microbial analysis of the anodic biofilm will be performed to better understand this result.

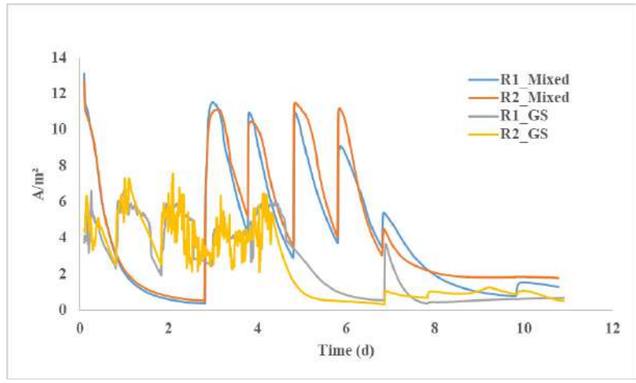

Figure 2. Current density obtained by duplicate in the pure and mixed cultures in the MEC step along the 11 days of experimental time. Pics correspondent to pH adjustment to 7.

CONCLUSION

The OLR was successfully employed as a tool to favor the acetate production as well as a reduction of the butyrate fraction in DF. The subsequent MEC stage benefited due to the acetate-rich DF effluents employed. The enrichment performed with the mixed culture was most likely a key factor for the high process efficiencies obtained in the MEC. Both pure and mixed cultures achieved high VFAs removal and r_{cat}. H_2 production in the MEC step through this strategy contributes to obtaining a highly pure H_2.

Table 1. Initial VFAs concentration fed in the MEC

	Succinate	Lactate	Formate	C2	C3	IC4	C4	IC5	C5	C6
MECs Mixed	7.5	1.8	5.4	16.8	3.8	0.1	3.0	0.1	0.3	0.3
MECs G. sulf	6.9	1.9	4.9	16.0	4.0	0.0	3.8	0.0	0.3	0.1

Table 2. Performance indicators evaluating hydrogen production and VFAs consumption in MECs

	CE	r_{Cat}	r_{H2}	*% e⁻ consumed*
R1_Mixed inoculum	105	89	93	48
R2_Mixed inoculum	88	90	79	44
R1_G. sulfurreducens	88	58*	51	47
R2_G. sulfurreducens	85	94	80	42

CE = Coulombic efficiency (amount of degraded substrate that is converted into current), r_{Cat} = cathode recovery (ratio between the H_2 recovered and the theoretical amount based on the current measured), rH_2 = global H_2 yield (CE*r_{Cat}), *No H_2 recovery after day 6. Electrons for balances were calculated by multiplying the molar amounts of each compound by their electron (Eeq) molar equivalents: Succinate (Eeq = 14), Lactate (Eeq = 12), Formate (Eeq = 2), Acetate (Eeq = 8), Propionate (Eeq = 14), Butyrate and iso-form (Eeq = 20), Valerate and iso-form (Eeq = 26), Caproate (Eeq = 32), H_2 (Eeq = 2).

REFERENCES

Flayac, C., Trably, E., and Bernet, N. (2018) Microbial anodic consortia fed with fermentable substrates in microbial electrolysis cells: Significance of microbial structures. Bioelectrochemistry, **123**, 219–226. [online] https://doi.org/10.1016/j.bioelechem.2018.05.009.
Noguer, M. C., Magdalena, J. A., Bernet, N., Escudié, R., and Trably, E. (2022) Enhanced Fermentative Hydrogen Production from Food Waste in Continuous Reactor after Butyric Acid Treatment. Energies, **15** (11).

TECHNICAL SESSIONS

T14.

Aerobic granulation

Unravelling the alpha factor for aerobic granular sludge reactors

Laurence Strubbe[1], Edward J.H. van Dijk[2,3], Pascalle J.M. Deenekamp[2], Mark C.M. van Loosdrecht[3], Eveline I.P. Volcke[1]

[1] BioCo Research Group, Department of Green Chemistry and Technology, Ghent University, Coupure Links 653, 9000 Gent, Belgium (Laurence.Strubbe@UGent.be and Eveline.Volcke@UGent.be)
[2] Royal HaskoningDHV, Laan1914 35, Amersfoort 3800 AL, the Netherlands, (edward.van.dijk@rhdhv.com and Pascalle.Deenekamp@rhdhv.com)
[3] Department of Biotechnology, Delft University of Technology, Van der Maasweg 9, Delft 2629 HZ, the Netherlands (m.c.m.vanloosdrecht@tudelft.nl)

Abstract

The alpha factor is an important factor influencing the oxygen transfer efficiency and thus the aeration energy costs of water resource recovery facilities. Nevertheless, the dynamic behaviour of the alpha factor has never been studied for aerobic granular sludge reactors. This study showed that the alpha factor increases during the aeration phase of a batch cycle of an aerobic granular sludge plant due to the influence of different process variables. Through a data analysis study of 175 batch cycles of the Prototype Nereda® installation in Utrecht over the summer and winter period of 2020-2021, the exchange ratio and temperature were identified as the main influencing factors on the rate of increase of alpha in a batch cycle. A higher exchange ratio was related to a slower increase in alpha over the aeration phase, while a higher temperature was related to a faster increase in alpha. Moreover, alpha was characterized by a same minimal value at the beginning of every aeration phase, which could be explained by the adsorption of soluble biodegradable organic carbon described by a Langmuir adsorption model. The dynamic behaviour of the alpha factor could be described by a decreasing exponential model as well as by a first order model.. The practical implications of these models are discussed in view of the design and performance optimization of aerobic granular sludge reactors and other batch-wisely operated aerobic wastewater treatment systems.

Keywords

Aeration; aerobic granular sludge (AGS); alpha factor; batch-wise operation; oxygen transfer efficiency; wastewater resource recovery

INTRODUCTION

Water resource recovery facilities (WRRFs) nowadays are not only focusing on wastewater treatment but increasingly aim at recovering resources such as energy. To reach this goal, reducing the energy consumption is paramount. Aerobic granular sludge (AGS) reactors are a most promising technology with low energy consumption (Pronk et al., 2015), but still a relatively high fraction of energy consumption is spent on aeration, which thus holds a strong saving potential. It is known that the alpha factor is an important factor influencing the oxygen transfer efficiency, however its dynamic behaviour has hardly been researched in a batch reactor and never in an AGS reactor.

The alpha factor, αF , lumps the effect of contaminants, biomass and diffuser fouling on the gas-liquid mass transfer coefficient of oxygen, $k_La_{O_2}/k_La_{O_2}$. Cycles of batch reactors show a gradual increase in the $k_La_{O_2}/k_La_{O_2}$ (e.g. Baeten et al., 2021). This is likely due to a slow degradation of surface-active compounds present in the wastewater (Rosso et al., 2006). Because of their amphiphilic nature, they accumulate at the air-liquid interface of bubbles, reducing the mass transfer of oxygen to the liquid.

A lot of research used the influent organics as a proxy for surface-active compounds to express the impact on the alpha factor (e.g. Bencsik et al., 2022; Jiang et al., 2017). Ahmed et al. (2021) were the first to investigate the real-time impact of the degradation of soluble organics on the increase of the alpha factor for an activated sludge batch plant. For the AGS process such an assessment has not yet been performed. Moreover, the influence of process conditions on the observed dynamic behaviour of the alpha factor is still unclear.

MATERIALS AND METHODS

This research was done using the Prototype Nereda® in Utrecht, the Netherlands, which is a full-scale AGS research facility (1050 m^3), operated by Royal HaskoningDHV. The reactor was monitored for liquid and gas phase concentrations during the summer and winter period of 2020-2021. The 175 batch cycles in which the off-gas analyser was active and the exchange ratio met the predefined value were used to calculate the alpha factor over the aeration phase of every cycle.

Soluble organic carbon (estimated through a COD_S measurement) was measured during the aeration phase of one specific cycle on 18 December 2020 at an exchange ratio of 50%. The biodegradable COD_S fraction ($bCOD_S$) at each time instant was determined by subtracting the effluent concentration of COD_S (assumed to be the inert COD_S concentration) from measured total COD_S concentration at that time. This implicitly assumes that the effluent concentration of COD_S is inert, which is reasonable given the long SRT, the plug flow regime in the reactor and full ammonium oxidation.

RESULTS AND DISCUSSION

The oxygen transfer efficiency in a batch-wise operated AGS reactor was scrutinized through the study of the alpha factor during the aeration phase.

The alpha factor increased over the aeration phase length, analogous to the increase along the length of the aeration tank of a continuous fed plug flow reactor (Fig. 1). All aeration cycles had the same value of alpha at the beginning of the aeration phase and the same value of alpha at the end of the aeration phase cycle, independent of the influent load, exchange ratio and temperature. However, a higher exchange ratio was related to a slower increase in alpha over the aeration phase, while a higher temperature was related to a faster increase in alpha (results not shown).

The alpha factor was related to the removal of $bCOD_S$. The relation between αF and the $bCOD_S$ concentration could be described by a decreasing exponential function (Fig 2a). Alternatively, the inverse relation between $bCOD_S$ and the alpha factor could be described by a Langmuir adsorption isotherm for the adsorption of $bCOD_S$ at the air-liquid interface (Fig 2b). The constant initial alpha value is in agreement with the associated concept of a maximum adsorption capacity. Besides, the lower the $bCOD_S$ concentration at the start of the aeration phase, the faster the increase in αF (Fig. 2) and thus the higher the oxygen transfer efficiency over the cycle. It follows that a possible optimization strategy include the trade-off between the exchange ratio and cycle time to influence the $bCOD_S$ concentration at the start of the aeration phase.

Another way to describe the dynamic behaviour of the alpha factor is through a first order relation (Fig. 3), with a fixed gain for all cycles under study and a time constant depending on several factors, such as the initial $bCOD_S$ concentration (in its turn determined by the exchange ratio) and the temperature. The potential of proxies for the initial $bCOD_S$ concentration (e.g. NH_4^+, PO_4^{3-} at the start of the aeration phase) was further investigated to predict the dynamics of alpha over the aeration phase. In contrast to the relation between αF and $bCOD_S$, the first order relation can only be established by first studying the dynamic behaviour of αF over a longer period of time to find a proxy for the $bCOD_S$ concentration. Afterwards, the first order relation could be part of a control strategy to select for the most optimal process performance depending on the incoming load of the specific AGS plant.

CONCLUSION

In light of the growing awareness on energy efficiency, research efforts are underway globally to reduce the energy consumption of WRRFs. However, it is remarkable that an important aspect as the alpha factor is hardly researched while it is well known to affect the aeration energy significantly. In this study, we scrutinized the oxygen transfer efficiency in a batch-wise operated aerobic granular sludge reactor through the study of the alpha factor during the aeration phase. The insights from this study can be used to further optimise the energy efficiency and operation of aerobic granular sludge reactors and other batch-wise operated aerobic wastewater treatment systems.

Further reading

Strubbe, L., Dijk, E.J.H. va., Deenekamp, P.J.M., Loosdrecht, M.C.M. va., Volcke, E.I.P., 2023. Oxygen transfer efficiency in an aerobic granular sludge reactor: Dynamics and influencing factors of alpha. Chem. Eng. J. 452, 139548. https://doi.org/10.1016/J.CEJ.2022.139548

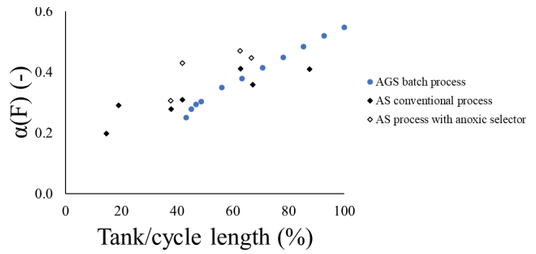

Figure 1. The average αF of 175 cycles over the fraction of the cycle length (%), including feeding and aeration phase, of an aerobic granular sludge (AGS) batch reactor compared to α over the fraction of the aerobic tank length (%) of a continuous activated sludge (AS) plug flow reactor with and without anoxic selector (data obtained from Rosso and Stenstrom (2007)).

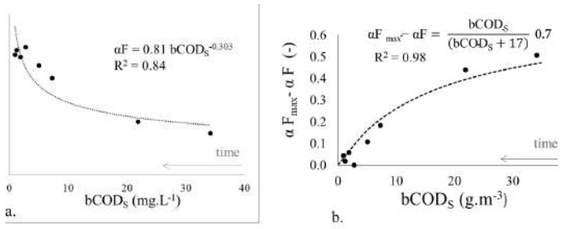

Figure 2. Relation between the alpha factor and soluble biodegradable organic carbon ($bCOD_S$, $mg.L^{-1}$) (a) during the aeration time of an aerobic granular sludge batch reactor. Adsorption isotherms of $bCOD_S$ with $αF_{max}$-αF referring to the adsorption capacity of the air bubbles based on data of a single cycle at 18 December 2020.

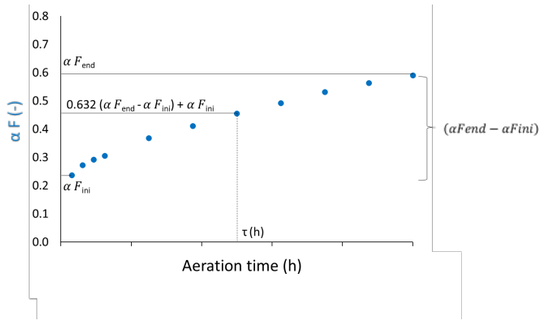

Figure 3. Visualization of the calculation of the time constant $\tau\tau$ (h) for each of the 175 cycles.

The time constant $\tau\tau$ (h) of a first order process is defined as the time at which 63.2% of the final value is reached, upon a step input.

REFERENCES

Baeten, J.E., van Dijk, E.J.H., Pronk, M., van Loosdrecht, M.C.M., Volcke, E.I.P., 2021. Potential of off-gas analyses for sequentially operated reactors demonstrated on full-scale aerobic granular sludge technology. Sci. Total Environ. 787, 147651. https://doi.org/10.1016/J.SCITOTENV.2021.147651

Bencsik, D., Takács, I., Rosso, D., 2022. Dynamic alpha factors: Prediction in time and evolution along reactors. Water Res. 216. https://doi.org/10.1016/J.WATRES.2022.118339

Germain, E., Nelles, F., Drews, A., Pearce, P., Kraume, M., Reid, E., Judd, S.J., Stephenson, T., 2007. Biomass effects on oxygen transfer in membrane bioreactors. Water Res. https://doi.org/10.1016/j.watres.2006.10.020

Gori, R., Jiang, L.M., Sobhani, R., Rosso, D., 2011. Effects of soluble and particulate substrate on the carbon and energy footprint of wastewater treatment processes. Water Res. 45, 5858–5872. https://doi.org/10.1016/J.WATRES.2011.08.036

Jiang, L.M., Garrido-Baserba, M., Nolasco, D., Al-Omari, A., DeClippeleir, H., Murthy, S., Rosso, D., 2017. Modelling oxygen transfer using dynamic alpha factors. Water Res. https://doi.org/10.1016/j.watres.2017.07.032

Leu, S.-Y., Rosso, D., Larson, L.E., Stenstrom, M.K., 2009. Real-Time Aeration Efficiency Monitoring in the Activated Sludge Process and Methods to Reduce Energy Consumption and Operating Costs. Water Environ. Res. https://doi.org/10.2175/106143009x425906

Pronk, M., de Kreuk, M.K., de Bruin, B., Kamminga, P., Kleerebezem, R., van Loosdrecht, M.C.M., 2015. Full scale performance of the aerobic granular sludge process for sewage treatment. Water Res. 84, 207–217. https://doi.org/10.1016/j.watres.2015.07.011

Rosso, D., Iranpour, R., Stenstrom, M.K., 2005. Fifteen Years of Offgas Transfer Efficiency Measurements on Fine-Pore Aerators: Key Role of Sludge Age and Normalized Air Flux. Water Environ. Res. 77, 266–273. https://doi.org/10.2175/106143005X41843

Rosso, D., Stenstrom, M., 2007. Energy-saving benefits of denitrification. Environ. Eng. Appl. Res. Pract. 3.

Determining the causes of the deterioration of granules in an aerobic granular sludge continuous flow system

Alallana E.*, Franchi O.**, Pavissich J.P. **, Crutchik D.**, Da Silva C.*, Guerrero L.*, Pedrouso A.***, Val del Río A.***, Mosquera-Corral A.*** and Campos J.L.**

*Chemical and Environmental Engineering Department, Technical University Federico Santa María, Chile, Ave. España 1680, Valparaíso, Chile (*esteban.alallana.14@sansano.usm.cl; cristopher.dasilva@usm.cl; lorna.guerrero@usm.cl*)
**Facultad de Ingeniería y Ciencias, Universidad Adolfo Ibáñez, Avda. Padre Hurtado 750, Viña del Mar, Chile (*oscar.franchi@edu.uai.cl; juan.pavissich@uai.cl; dafne.crutchik@uai.cl; jluis.campos@uai.cl*)
***Department of Chemical Engineering, Institute of Technology, Universidade de Santiago de Compostela, E-15705 Santiago de Compostela, Spain (*alba.pedrouso@usc.es; mangeles.val@usc.es; anuska.mosquera@usc.es*)

Abstract
The application of the aerobic granular sludge technology in continuous flow systems is still a challenge. In this work, a continuous reactor of 25 L, with six baffles to promote a feast/famine regime, was inoculated with mature granules. When the upflow velocity of 2.9 m/h was imposed in the settler, the flocculent biomass ended up predominating in the system while, when this upflow velocity was increased up to 6.0 m/h, granular biomass maintained its predominance, but its sludge volume index (SVI) worsened along the operation time. This fact could be related to the low substrate concentration present during the feast period. A model to explain the competition between the granular and flocculent biomass was developed. According to this model, the ratio between the solids retention time of granular and flocculent biomass, obtained in each experiment, defines the predominant type of biomass inside the reactor.

Keywords
Continuous flow; feast/HRT ratio; granular biomass; solids retention time; substrate concentration.

INTRODUCTION

The constant increase of the urban population brings with it the need to increase the capacity of the existing wastewater treatment plants (WWTPs). Since, in large cities, the available area to expand the WWTPs is limited, the most suitable alternative to increase their treatment capacity seems to be the change of the conventional activated sludge systems (CAS) by other higher-rate technologies. In this context, a successful alternative technology developed during the last two decades corresponds to the aerobic granular sludge (AGS) (Hamza et al., 2022). AGS offers improved settling properties in comparison to CAS, which allow increasing the suspended solids concentration in aeration tanks and, therefore, increasing the treatment capacity of the system. Although specific conditions to promote aerobic granule formation are well known in sequencing batch reactors (SBR), the conditions to achieve a rapid and stable granulation in continuous flow systems are still under investigation and have been the focus of many AGS studies (Xu et al., 2022). On basis of these observations, the aim of the present work is to define the operating conditions of a continuous flow system that allow maintaining the physical stability of aerobic granules such as in an SBR.

MATERIALS AND METHODS

A continuous reactor of 25 L with six baffles was operated to determine the suitable operational conditions to maintain the long-term stability of granular biomass. Granular biomass taken from a 25 L SBR reactor operated in parallel to the continuous flow reactor was used as inoculum. Both systems were fed with a synthetic medium simulating the composition of domestic wastewater (Jungles et al., 2011). The operating conditions imposed in the continuous flow reactor and the inoculum characteristics of the 3 experiments carried out are detailed in Table 1.

Table 1. Operating conditions and inoculum characteristics of the experiments.

Experiment	Operating conditions			Inoculum	
	Flow rate (L/d)	Upflow velocity in the settler (m/h)	HRT (h)	Initial concentration (TSS/L)	SVI (mL/g TSS)
1	100	2.9	6.0	3.2	26
2	200	6.0	3.0	1.9	56
3	200	6.0	3.5*	1.5	60

*An anaerobic chamber of 4 L was added to the system before the aerobic reactor.

RESULTS

In all the experiments, the system was able to remove more than 95% of the organic matter while nitrogen removal efficiency was around 34% and was due to assimilation, since neither nitrate nor nitrite was detected. None of the operating conditions tested were suitable to maintain the physical stability of the granules for a period longer than 22 days. In the first experiment, the hydraulic selection pressure imposed in the settler was not able to promote the wash-out of the flocculent biomass. Also, since flocs grow faster than granular biomass, its overgrowth probably limited the availability of substrate for granular biomass development. In the case of the second and third experiments, the hydraulic selection pressure imposed was increased and flocculent biomass was successfully washed-out. This promoted the growth of aerobic granules (Figure 1). In the second experiment the average diameter of granular biomass increased from 0.5 up to more than 2.0 mm. Nevertheless, their appearance was fluffy, with an SVI of 109 mL/g TSS. A similar behavior was observed during the third experiment but, in this case, the average diameter and the SVI were lower (1.80 mm and 82 mL/g TSS, respectively) than in the previous experiment. This difference could be attributed to the implementation of an anerobic contact tank during the third experiment.

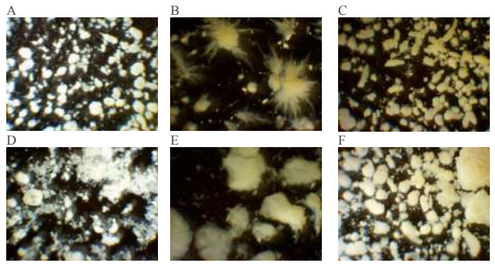

Figure 1. Aspect of biomass. Inoculum: A) Experiment 1; B) Experiment 2; C) Experiment 3. End of the experiment: D) Experiment 1; E) Experiment 2; F) Experiment 3.

In addition to the hydraulic selection pressure, maintaining a suitable feast/famine regime by means of the hydraulic retention time (HRT) is a key operational condition to promote the formation of stable granular biomass. In order to determine if the values of the feast/HRT ratio during the different experiments were suitable to favor the growth of granular biomass over the flocculent one, a conceptual model was developed based on the growth rate of both kinds of biomass. This model allowed calculating the solids retention time (SRT) required by each type of biomass to grow under certain feast/HRT value. The ratio between the SRT values calculated for granular and flocculent biomass (SRT_g/SRT_f) would define the conditions in which the granular biomass would begin to predominate over flocs for a certain value of the feast/HRT ratio (Figure 2). From the COD concentration profile measured along the reactor, a feast/HRT value of 0.14 was determined during the first experiment and of 0.29 during the second and third experiments. Considering the SRT calculated for each type of biomass during the experiments, the model results suggest that the selective hydraulic pressure imposed during the first experiment was not strict enough to achieve the predominance of the granular biomass, while the up-flow velocity imposed in the settler in both experiments 2 and 3 allowed a suitable uncoupling of the SRT of granular and flocculent biomass (Figure 2). However, even though the operating conditions of the two last experiments seemed suitable for the development of the granular biomass, the physical characteristics of the granules generated were not the desired ones (i.e. high SVI, long-term instability). This suggests that the selective hydraulic pressure and the feast/famine regime were suitable for granulation, but not enough to generate granular biomass with good physical characteristics.

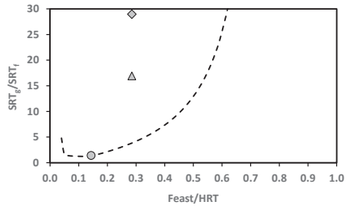

Figure 2. Minimum solid retention time of granular and flocculent biomass ratio required for the predominance of the granular biomass (dashed line); solid retention time of granular and flocculent biomass ratio obtained in: Experiment 1 (◆); Experiment 2 (▲); and Experiment 3 (◆).

Since the deterioration of the physical properties of granules observed during experiments 2 and 3 could be related with the growth of ordinary heterotrophic biomass (X_H) over accumulating heterotrophic biomass (X_{STO}), a simulation based on a diffusion-reaction model was carried to determine how the substrate is consumed inside the granule. The simulation done under the feast phase conditions of both experiments (65 mg COD/L and HRT of 20 minutes) shows that the generation of X_H is 1.46 times higher than that of X_{STO} and, therefore, the granulation process would not be favored. In order to determine the influence of the substrate concentration on the granulation process, a new simulation was performed including the granule size range observed in the experiments (Figure 3). This simulation showed that for a granule diameter of 1.7 and of 3.1 mm substrate concentrations lower than 100 mg COD/L promote the growth of the ordinary heterotrophic biomass over the accumulating heterotrophic biomass (X_H/X_{STO} higher than 1). Also, for these given sizes the X_H/X_{STO} is lower than 1 at substrate concentrations higher than 250 mg COD/L. At higher concentrations the substrate gradient may not limit the growth of accumulating heterotrophs inside the granules. Thus, the configuration of a continuous flow reactor used to generate granular biomass not only should have a suitable feast/famine regime, but also maintain an adequate substrate concentration during the feast period in order to promote the growth of the accumulating heterotrophic biomass.

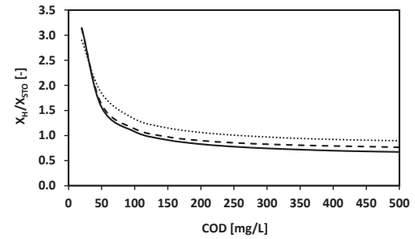

Figure 3. Influence of substrate concentration on the biomass concentration ratio between ordinary heterotrophs and accumulating heterotrophs (granule diameter: 3.1 mm (continuous line); 1.7 mm (dashed line); 0.5 mm (dotted line)).

ACKNOWLEDGEMENTS

This research was funded by the Chilean Government through the Projects ANID/FONDECYT/1200850 and CRHIAM Centre grant number ANID/FONDAP/15130015, and by the European Commission LIFE ZERO WASTE WATER [LIFE19ENV/ES/000631] project. The authors from Universidade de Santiago de Compostela belong to the Galician Competitive Research Group [GRC ED431C-2021/37]. Esteban Alallana would like to acknowledge Postgraduate and Programs Department of Technical University Federico Santa María for their support through a PIIC grant. Alba Pedrouso would also like to acknowledge the Xunta de Galicia for their support through a Postdoctoral Fellowship (ED481B-2021-041).

REFERENCES

Hamza R., Rabii A., Ezzahraoui F.Z., Morgan G., Iorhemen O.T. (2022) A review of the state of development of aerobic granular sludge technology over the last 20 years: Full-scale applications and resource recovery. *Case Studies in Chemical and Environmental Engineering*, 5, 100173.
Jungles M.K., Figueroa M., Morales N., Val del Río A., Costa R.H.R., Campos J.L., Mosquera-Corral and Méndez P. (2011). Start up of a pilot scale aerobic granular reactor for organic matter and nitrogen removal. *Journal of Chemical Technology and Biotechnology*, 86, 763-768.
Xu D., Li J., Liu J., Qu X., Ma H. (2022). Advances in continuous flow aerobic granular sludge: A review. *Process Safety and Environmental Protection*, 163, 27-35.

A Pilot-Scale Study on the Impact of Aerobic Granular Sludge on Membrane Filtration Performance

E. Tsertou*, K. Goossens* and J. Dries

* BioWAVE research group, Faculty of Applied Engineering, University of Antwerp, Groenenborgerlaan 171, 2020 Antwerp, Belgium
(E-mail: eirini.tsertou@uantwerpen.be ; koen.goossens@uantwerpen.be; jan.dries2@uantwerpen.be)

Abstract

This study quantifies the hydraulic performance of pilot-scale ultrafiltration integrated in a full scale industrial aerobic granular sludge (AGS) plant. The treatment plant consisted of parallel AGS reactors, Bio1 and Bio2, with similar initial granular sludge properties. During the 3-month filtration test, a COD overloading episode took place, affecting the settling properties, morphology and microbial community composition in both reactors. The impact on Bio2 was more severe than on Bio1, with higher maximal sludge volume index values, a complete loss of granulation, and the excessive appearance of filamentous bacteria extending from the flocs. The membrane filtration properties of both sludges, with these different sludge qualities, were compared. The permeability in Bio1 varied between 190.8±23.3 and 158.9±19.2 $L.m^{-2}.h^{-1}.bar^{-1}$, which was 50% higher than in Bio2 (89.9±5.8 $L.m^{-2}.h^{-1}.bar^{-1}$). A lab scale filtration experiment using a flux-step protocol showed that the fouling rate remained below 0.5 $mbar.min^{-1}$ for Bio1, but increased in Bio2 resulting in a critical flux of 30-35 $L.m^{-2}.h^{-1}$. The membrane resistance due to pore blocking was three times higher in Bio2 vs. Bio1. This study show the positive impact of granular biomass on the long-term membrane filtration properties, and stresses the importance of granular sludge stability during reactor operation.

Keywords

Feast/famine regime; glycogen accumulating organisms (GAO); nutrient deficient industrial wastewater; sequencing batch reactor; side stream membrane bioreactor (MBR); ultrafiltration

INTRODUCTION

Membrane bioreactors (MBR) combine the biological treatment process with excellent sludge separation. As a result the obtained effluent represents a high potential for reuse, e.g. if followed by reverse osmosis. In addition, MBRs occupy limited space. Despite these advantages, MBR application is limited, because the investment and operating costs are quite high. The main cause of the high operating costs is the mitigation of membrane fouling, leading to loss of permeability and/or increase of transmembrane pressure (TMP) (Le-Clech et al. 2006). An innovative fouling mitigation strategy, related with the morphology and the microbial community of the biomass, is the coupling of aerobic granular sludge (AGS) with a MBR. The dense and compact structure of the more hydrophobic aerobic granules, in comparison to conventional activated sludge, enhances the filtration performance (e.g. Liebana et al. 2018, Campo et al. 2021, Stes et al 2021). To the best of our knowledge there are no studies that evaluate the membrane filtration performance of full scale AGS systems. The first goal of this study was therefore the quantification of the filtration performance of a pilot-scale ultrafiltration unit coupled to a full-scale AGS reactor treating industrial wastewater. The second goal was the evaluation of the effect of the long-term ultrafiltration on the characteristics of the granular sludge.

MATERIALS AND METHODS

Full-scale industrial AGS plant and pilot-scale side-stream ultrafiltration

The biological treatment step in the full-scale installation consists of two parallel AGS SBRs, Bio1 and Bio2 (Caluwé et al. 2022). The nutrient-deficient wastewater originates from a tank truck cleaning (TTC) company, mainly cleaning trucks transporting chocolate and beer. The SBR cycles consisted of 4 h anaerobic feeding, 16 h aerobic reaction, 2 h settling and 2 h discharge.
A pilot ultrafiltration (UF) installation was connected with Bio1 which presented more stable performance. The feed stream for the membranes was mixed liquor pumped for 10h per day during the aerobic reaction phase, hereby producing approximately 50 m^3 permeate. The UF filtration test consisted of three stages. In stage I (approx. 2 months), the membrane unit was connected to Bio1. Then, in stage II (approx. 1 week), it was connected to Bio2 to compare the two sludge systems. After switching back to Bio1, filtration was continued for 11 more days (stage III).

Analyses

Sludge samples derived from both SBRs were delivered frequently and analyzed in the lab. We analyzed the sludge concentration (mixed liquor suspended (volatile) solids, MLSS and MLVSS), morphology (using light microscopy), settleability (sludge volume index, SVI), particle size distribution (using a Malvern Mastersizer), microbial community composition (using 16S rRNA amplicon sequencing), the anaerobic substrate storage capability (as described by Tsertou et al., 2022), and the sludge filterability (using a flux step protocol as described by Stes et al., 2021).

RESULTS AND DISCUSSION

AGS properties at start and overloading episode during the experiment

The granular sludge in the full scale SBRs was formed by introducing an anaerobic mixed feeding step followed by an extended aerated step, without selective discharge, to select for granule-forming slow-growing organisms, as described previously by Caluwé (2022).

Initially, the granular sludge presented a compact structure with excellent settleability, high anaerobic substrate uptake and a high abundancy of glycogen accumulating microorganisms (GAO) (29.8 % and 18.9% for Bio1 and Bio2 respectively). The stability of the granular sludge was however significantly affected by an overloading episode during the experiment. The COD in the influent wastewater on DAY 34 was 7736 $mg.L^{-1}$, and remained high for the next 20 days, whereas the average COD before and after the overloading episode was 4303 ± 160 $mg.L^{-1}$ and 3869 ± 355 $mg.L^{-1}$ respectively. Figure 1 shows the SVI values for both SBRs.

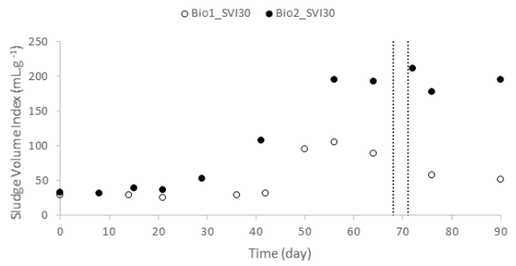

Figure 1. Evolution of the SVI for Bio1 and Bio2 (dashed lines separate the 3 experimental stages).

The SVI value was approximately 33mL.g-1 for both on DAY 0. An increase of SVI30 close to 100 $mL.g^{-1}$ was observed due to the overloading of the two reactors. Bio1 seemed to withstand better the overloading episode. The highest SVI30 value was 105 $mL.g^{-1}$ for Bio1 and 211 $mL.g^{-1}$ for Bio2. Furthermore, Bio1 presented an improvement after DAY 88 but no change was observed for Bio2. Similar observation were done with respect to the anaerobic substrate uptake, particle size distribution, sludge morphology and GAO read abundancies (results available, but not shown, given the page limitation of the abstract).

Pilot-scale filtration performance and lab-scale filterability

Figure 2.a shows the permeability profile obtained from the operation of the pilot ultrafiltration installation.

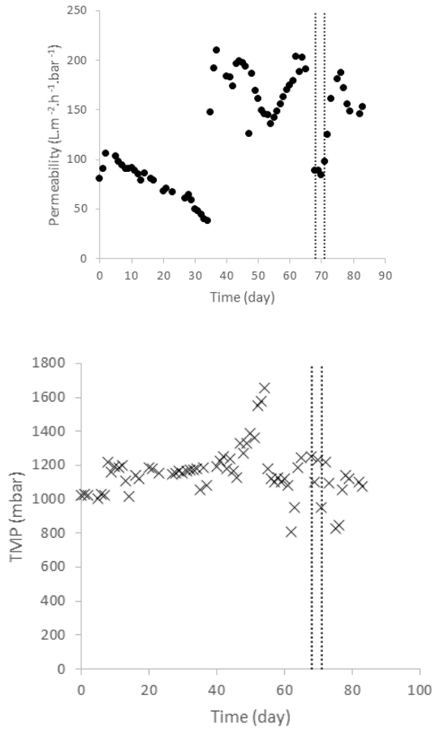

Figure 2. Average permeability profile (a, left), and evolution of the transmembrane pressure TMP (b, right) during the pilot operation (dashed lines separate the 3 experimental stages).

High permeability values (above 80 $L.m^{-2}.h^{-1}.bar^{-1}$) were measured during the start-up of filtration for Bio1. However the permeability continuously declined from DAY 17 until DAY 35, due to an inoperative backwashing. Despite the decreasing trend of permeability, the overall values remained satisfactory since the lowest permeability recorded was 38 $L.m^{-2}.h^{-1}.bar^{-1}$. On DAY 35 cleaning in place (CIP) was performed to restore the membrane permeability. The average permeability was 172.82 ± 23.25 $L.m^{-2}.h^{-1}.bar^{-1}$ for the period after the first CIP, and before switching to Bio2. During the filtration of sludge of Bio2 (stage II), the permeability decreased by almost 50% to an average value of 89.95 ± 5.84 $L.m^{-2}.h^{-1}.bar^{-1}$. Recovery of the permeability was observed when the filtration was switched back to Bio1 (stage III), reaching an average permeability of 158.96 ± 19.21 $L.m^{-2}.h^{-1}.bar^{-1}$. Figure 2.b shows the transmembrane pressure (TMP) profile during the whole operation. Although no backwashing/chemical backwashing was performed in the beginning, the TMP remained almost stable. The TMP stability was interrupted in the period between DAY 45 and DAY 54. Then, elevated TMPs were observed. The increase of TMP was almost linear (R^2= 0.9079). On DAY 55, the membranes were cleaned (CIP). Afterwards, the TMP decreased again.

The lab scale filtration experiment using a flux-step protocol showed that the fouling rate (= slope of the TMP profile as a function of time) remained below 0.5 $mbar.min^{-1}$ for Bio1, but increased in Bio2 resulting in a critical flux of 30-35 $L.m^{-2}.h^{-1}$. The membrane resistance due to pore blocking was three times higher in Bio2 vs. Bio1 (results available, but not shown here).

Discussion

Several studies investigated the filtration performance of conventional activated sludge and aerobic granular sludge, showing the superiority of aerobic granular sludge (Liebana et al. 2018, Stes et al. 2021). Most of these studies attribute the better filtration performance of aerobic granular sludge to their dense structure. In this study, the filtration performance can be related to the sludge morphology. Bio 1 consisted of well-shaped granules, while Bio 2 consisted of more irregular granules with more filaments present. Differences in filtration between Bio1 and Bio2 were observed both in pilot (Figure 2) and lab scale (not shown). In pilot scale, the permeability was more than double in Bio1 vs. Bio2. This confirmed that Bio1 consisted of better quality of granules compared to Bio2.

The maintenance of granular stability is one of the biggest challenges in AGS reactors. The shock load, during stage I, had clearly an impact on sludge settleability, morphology, the ability for anaerobic uptake and the microbial community both in Bio1 and Bio2. Industrial wastewaters present more variable composition compared to municipal wastewater, potentially leading to overloading episodes. This may unsettle the feast (anaerobic)/ famine (aerobic) system that is key to granulation (Tsertou et al. 2022, van Dijk et al. 2022).

Conclusions

The reuse of treated water is imperative because the supply-demand relationship of water has been disrupted. Furthermore, the future solutions should have a limited footprint. The AGS-MBR technology can address both and presents extra advantages compared to conventional MBR such as less fouling. The critical fluxes for aerobic granular sludge were lower in comparison with conventional activated sludge, indicating the possibility of higher applied fluxes and by extension less membrane surface area is required. Further research about long-term filtration operation in full scale and the stability of AGS in overloading episodes is recommended.

REFERENCES

Caluwé, M., Goossens, K., Seguel Suazo, K., Tsertou, E., Dries, J., 2022. Granulation strategies applied to industrial wastewater treatment: from lab to full-scale. Water Science and Technology 85, 2761–2771. https://doi.org/10.2166/wst.2022.129

Campo, R., Lubello, C., Lotti, T., Di Bella, G., 2021. Aerobic Granular Sludge–Membrane BioReactor (AGS–MBR) as a Novel Configuration for Wastewater Treatment and Fouling Mitigation: A Mini-Review. Membranes 11, 261. https://doi.org/10.3390/membranes11040261

Le-Clech, P., Chen, V., Fane, T.A.G., 2006. Fouling in membrane bioreactors used in wastewater treatment. Journal of Membrane Science 284, 17–53. https://doi.org/10.1016/j.memsci.2006.08.019

Liébana, R., Modin, O., Persson, F., Wilén, B.-M., 2018. Integration of aerobic granular sludge and membrane bioreactors for wastewater treatment. Critical Reviews in Biotechnology 38, 801–816. https://doi.org/10.1080/07388551.2017.1414140

Stes, H., Caluwé, M., Dockx, L., Cornelissen, R., De Langhe, P., Smets, I., Dries, J., 2021. Cultivation of aerobic granular sludge for the treatment of food-processing wastewater and the impact on membrane filtration properties. Water Science and Technology 83, 39–51. https://doi.org/10.2166/wst.2020.531

Tsertou, E., Caluwé, M., Goossens, K., Dobbeleers, T., Dockx, L., Poelmans, S., Suazo, K.S., Dries, J., 2022. Is building up substrate during anaerobic feeding necessary for granulation? Water Science and Technology 86, 763–776. https://doi.org/10.2166/wst.2022.236

van Dijk, E.J.H., Haaksman, V.A., van Loosdrecht, M.C.M., Pronk, M., 2022. On the mechanisms for aerobic granulation - model based evaluation. Water Research 216, 118365. https://doi.org/10.1016/j.watres.2022.118365

Combined Aerobic Granular Sludge and Gravity-Driven Membrane System for Energy-Efficient Wastewater Treatment and Reuse

M. Ali[1,2,#], A.R Hari[2], Y. Singh[2], M. Pronk[3], M. Loosdrecht[3], P. E. Saikaly[2]

[1] Department of Civil, Structural & Environmental Engineering, Trinity College Dublin, Dublin 2, Ireland,

[2] Biological and Environmental Science and Engineering Division, Water Desalination and Reuse Center, King Abdullah University of Science and Technology, Thuwal 23955-6900, Saudi Arabia,

[3] Department of Biotechnology, Delft University of Technology, Delft 2629 HZ, The Netherlands,

[#]Corresponding Author E-mail: muhammad.ali@tcd.ie

Abstract

By 2030, the global demand for energy and freshwater is expected to increase by 40% and 50%, respectively (UN-Habitat, 2016). To augment these depleting resources, municipal wastewater cannot be regarded merely as a "waste," but as a valuable resource of energy, material/mineral, and water for reuse (McCarty et al., 2011). The conventional activated sludge (CAS) process has been employed in most wastewater treatment plants (WWTPs) for over a century, where organic matter in municipal wastewater is aerobically converted to biomass and carbon dioxide. Although the CAS process is widely used, it has several significant drawbacks, like poor settling sludge characteristics, limitation to low mixed liquor suspended solids (MLSS) concentrations, and the tendency to develop floating sludge. Additionally, the CAS process is energy-intensive and usually requires 0.3 to 0.6 (typically 0.45) kWh per m^3 of wastewater treated, equivalent to 1620 kJ m^{-3} (US-EPA, 2014). This can be expressed as 324 kJ p^{-1} d^{-1}, assuming a person living in a sewer catchment produces 0.2 m^3 wastewater per day (Chen et al., 2020).

Aerobic granular sludge (AGS) technology can outcompete existing biological wastewater treatment technologies based on CAS, and it can become the standard for biological wastewater treatment in the future because of its small footprint, simultaneous removal of carbon and nutrients (P & N) in a single reactor tank, and ability to withstand toxic shock loading (Ali et al., 2019). The AGS-based system was estimated to have a 40–50% smaller footprint and 23% less electricity requirement than CAS (Bengtsson et al., 2019; Pronk et al., 2015). Currently, there are more than 70 full-scale AGS installations worldwide, and the number is multiplying rapidly (https://www.royalhaskoningdhv.com accessed on 12 May 2022). Nevertheless, to achieve microbiologically safe effluent, further polishing would be required for AGS-treated effluent (van Dijk et al., 2018; 2020). Aerobic membrane bioreactor (AeMBR) technology is currently being used for wastewater treatment and reuse. However, AeMBR process is a highly energy-intensive (energy-driven membrane process) process and on average requires more than 0.6 kWh per m^3 of wastewater treated, equivalent to 2232 kJ m^{-3} (Bengtsson et al., 2019). Here, gravity-driven membrane (GDM) was integrated with AGS system **(Fig. 1)** to reclaim microbiology and chemically safe water for non-potable uses. The GDM filtration is compatible with AGS reactor due to its natural height (tubular shape design). The height of the AGS tank would provide a sufficient water pressure head to drive the GDM filtration process through gravity (without energy input). The GDM-coupled AGS process (AGS-GDM) could easily replace conventional AeMBR technology in the wastewater treatment and reuse market.

The AGS-GDM unit was operated in a sequential batch mode with 2 hours of filling, 1.5 hours of aeration, 10 minutes of settling, and 20 minutes of effluent draw. The AGS tank has a volume of 35 L, and draw and filling were performed with a 50% exchange ratio. Primary treated raw wastewater received at the inlet of the KAUST wastewater treatment plant (GPS coordinates: 22°17′54.3″N 39°07′09.8″E) is diluted, having low concentrations of COD (229±59 mg/L), NH_4^+-N (17±4 mg/L) and PO_4^{3-}P (9±2 mg/L). The raw wastewater was supplemented with synthetic wastewater to make the concentration of COD (450 mg/L), NH_4^+-N (35 mg/L), and PO_4^{3-}P (20 mg/L) more representative of domestic wastewater. The influent wastewater was fed to the AGS tank from the bottom during the filling phase. Then AGS treated effluent was introduced to the GDM tank equipped with customized hollow fiber microfiltration (nominal pore size 0.1 µm) membrane module with a 3.5 m^2 effective membrane surface area (KOLON Industries, Inc., Korea). The AGS-GDM system showed excellent removal performance as the treated effluent has lower residual concentrations of COD (32.6±10.1 mg/L), NH_4^+-N (0.6±1.9 mg/L), NO_2^--N (0.2±0.04 mg/L), NO_3^--N (0.7±0.4 mg/L), and PO_4^{3-}P (1.3±2.6 mg/L) **(Fig. 2)**. The effluent quality of the AGS-GDM system was superior to neighbouring full-scale AeMBR, which generated an effluent with higher concentrations of NO_3^--N (5.6±3 mg/L) and PO_4^{3-}P (7.8±1.5 mg/L). Also, the GDM unit in AGS-GDM showed consistent flux (10 LMH per m hydraulic head) for 50 days without any cleaning **(Fig. 3)**, whereas the AeMBR required constant physical cleaning through aeration blowers and backwashing to control fouling. The AGS-GDM unit consumed significantly lower energy (0.35 kWh/m^3 for pumping and aeration) than the neighbouring full-scale AeMBR (0.82 kWh/m^3 for aeration alone). Taken together, these results demonstrate that the AGS-GDM technology could be a promising viable alternative to AeMBR for energy-efficient wastewater treatment and reuse in water-scarce regions like Saudi Arabia.

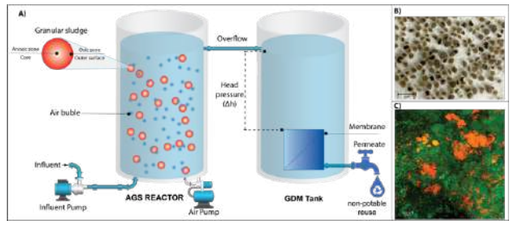

Fig. 1. A) Schematic diagram of the aerobic granular sludge gravity-driven membrane (AGS-GDM) system. B) Photograph of the granular biomass. Scale bars represent 5 mm. C) Confocal laser scanning microscope image of the granular biomass from the AGS reactor: The image shows polyphosphate-accumulating organisms (PAO, orange) and all bacteria (green). Fluorescence in situ hybridization was performed with FITC-labeled EUB mix probe composed of equimolar EUB338I, EUB338II, and EUB338III (green) for most members of Eubacteria and CY3-labeled PAO mix probe composed of equimolar PAO462, PAO651, and PAO846 (red) for *Ca.* Accumulibacter (PAO) bacteria. Scale bars represent 20 µm.

Fig. 2. Water quality from the AGS-GDM system. Nitrite concentration in the effluent was below 1 mg-N/L during this period.

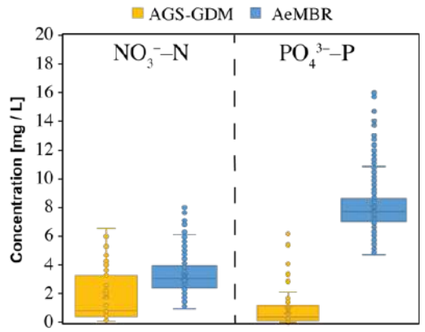

Fig. 3. Variations of specific flux over time. Specific flux presented as litre per m^2 membrane surface area per hour (LMH) per meter hydraulic head of water above the membrane module.

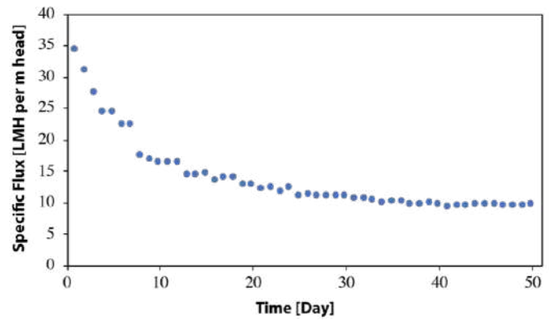

Reference

Ali, M., Wang, Z., Salam, K.W., Hari, A.R., Pronk, M., van Loosdrecht, M.C.M. and Saikaly, P.E. 2019. Importance of Species Sorting and Immigration on the Bacterial Assembly of Different-Sized Aggregates in a Full-Scale Aerobic Granular Sludge Plant. Environ Sci Technol 53(14), 8291-8301.

Bengtsson, S., de Blois, M., Wilen, B.M. and Gustavsson, D. 2019. A comparison of aerobic granular sludge with conventional and compact biological treatment technologies. Environ Technol 40(21), 2769-2778.

Chen, G., Ekama, G.A., Loosdrecht, M.C.M.v. and Brdjanovic, D. (2020) Biological Wastewater Treatment: Principles, Modelling and Design.

McCarty, P.L., Bae, J. and Kim, J. 2011. Domestic wastewater treatment as a net energy producer--can this be achieved? Environ Sci Technol 45(17), 7100-7106.

Pronk, M., de Kreuk, M.K., de Bruin, B., Kamminga, P., Kleerebezem, R. and van Loosdrecht, M.C. 2015. Full scale performance of the aerobic granular sludge process for sewage treatment. Water Res 84, 207-217.

UN-Habitat 2016 Urbanization and Development: Emerging Futures, UN Habitat World Cities Report.

US-EPA, U.S.E.P.A. 2014 Energy Efficiency in Water and Wastewater Facilities: A Guide to Developing and Implementing Greenhouse Gas Reduction Programs.

van Dijk, E.J.H., Pronk, M. and van Loosdrecht, M.C.M. 2018. Controlling effluent suspended solids in the aerobic granular sludge process. Water Res 147, 50-59.

van Dijk, E.J.H., Pronk, M. and van Loosdrecht, M.C.M. 2020. A settling model for full-scale aerobic granular sludge. Water Res 186, 116135.

Getting the most out of existing infrastructure: Denmark and Spain put MABR and AGS technology to the test

N. Uri Carreño*, P.H.Nielsen*, Nicolás Morales**, and J.R. Vázquez Padín**

* VCS Denmark. Vandværskvej 7, Odense 5000, Denmark
(nur@*esss.com*; *stag@bay.matrix.edu.uk)*
** Aqualia, Hangover Square, London NC1 4TS, UK
(E-mail: *jvazquezp@fcc.es*)

Abstract

The ongoing transition in the water sector from wastewater treatment plants to resource recovery facilities is driving change in water management. Biofilm-based technologies are being developed to intensify treatment and reduce environmental impact. The LIFE program project RESEAU is retrofitting two demo sites in Spain and Denmark with MABR (membrane-aerated biofilm reactors) and AGS (aerobic granular sludge) technology to reduce untreated stormwater overflows. The Spanish demo site in Moaña will be retrofitted with AGS reactors to increase capacity by 400%. The Danish demo site in Søndersø will be retrofitted with seven full-scale MABR units, becoming one of the largest MABR installations to date. The implementation will allow a comparison of performance, including capex, opex, capacity increase, energy consumption, and N_2O emissions.

Keywords (maximum 6 in alphabetical order)

INTRODUCTION

The water sector is currently undergoing a revolution, which involves the ongoing transition from the concept of wastewater treatment plants into resource recovery facilities (WRRF), where wastewater is now seen as a matrix containing many resources useful for society: clean water, chemicals, energy, and heat (Garrido-Baserba et al., 2020). Water management is expected to change more in the next twenty years than in the past century (Biswas and Tortajada, 2018) as rapid urbanization, population growth and aging infrastructure will increasingly put pressure on wastewater treatment management (Larsen et al., 2016). The greater frequency of heavy precipitation events due to climate change and stricter effluent requirements increases the need for capacity increase in urban wastewater infrastructure.

On the other hand, utilities around the world are moving toward de-carbonizing their activities. It is therefore of the utmost importance to develop technologies that allow utilities to both intensify treatment and reduce their environmental footprint. More intensive technologies, tend to produce higher N_2O emissions (Figure 1).

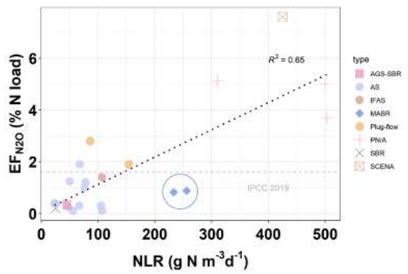

Figure 1. Benchmark of different types of biological N removal technologies according to the % of N load emitted as N_2O-N (y-axis) and the nitrogen loading rate (g N m^{-3} d^{-1}) (x-axis). (Uri-Carreño et al., 2023).

The LIFE program project RESEAU (Retrofitting solution for increasing the resilience of urban wastewater infrastructures in heavy precipitation areas) seeks to reduce by up to 100% the discharge of untreated stormwater overflows from WWTPs in heavy precipitation areas using advanced biofilm technology. Biofilm-based technologies are based on bacteria aggregation either on a carrier material or auto aggregation to form granules. The main benefits include higher nutrient removal rates per reactor volume and a higher level of treatment during loading peaks. Therefore, they will be able to increase the capacity of the WWTPs during high-flow events. Moreover, recent studies have demonstrated the potential of MABR technology to provide nutrient removal intensification with high energy efficiency and maintain low N_2O emissions (Uri-Carreño et al, 2023).

Two demo sites located in Spain in Denmark are being retrofitted with novel biofilm technology, namely MABR (membrane-aerated biofilm reactors) and AGS (aerobic granular sludge). The full-scale implementation of these technologies will allow the comparison of performance in terms of capex, opex, capacity increase, energy consumption and N_2O emissions.

Spanish Demo Site: Moaña WWTP

Located in a coastal region in north-western Spain, close to the Atlantic Ocean. A WWTP of 35,000 population equivalent (P.E.) was built in Moaña in 2001 to improve the wastewater treatment and the effluent quality to Vigo's Estuary, the greatest fishing ground in Galicia (Figure 1). There are currently between 15 and 20 heavy precipitation events per year, causing infiltration/inflow rates of over 80% in the sewer network and stressing the limited hydraulic capacity of the WWTP, which is determined by its unique secondary settler, driving to an estimated discharge of 15,000 m³ of untreated SWOs/year.
The demonstration actions include a retrofit of the existing treatment plant with two AGS reactors of 500 m³ each and liberation of the existing volume of Activated Sludge basins, providing 2,500 m³ to be used as storm tanks. This will increase the WWTP capacity up to 400% (2,000 m³/d).

Danish Demo Site: Søndersø WWTP

Located in Denmark, close to the Baltic Sea. The Søndersø WWTP of 20,000 P.E was built in 1990 and it is heavily loaded with rainwater and infiltration, accounting for two-thirds of the hydraulic loading to the plant (Figure 2). It receives a large quantity of industrial organic load, increasing the aeration/nutrient removal need. During heavy precipitation events, the maximum incoming flow (550 m^3/h) is more than four times the yearly average incoming flow, when the facility is under stress and its performance worsens, resulting in ammonia peaks discharged in the effluent.

The nutrient removal treatment at Søndersø WWTP is configured with two lanes running in parallel, each consisting in two oxidation ditches operated under alternate aerobic/anoxic conditions, as per the so-called BioDenitro process. The MABR upgrade is planned to be installed in one of the two lanes (Figure 3). This will allow for the comparison between the conventional activated sludge lane and the MABR lane.

The demonstration actions include a retrofit of the existing bioreactors with seven units of full-scale MABR technology, therefore becoming one of the largest MABR installations up to date.

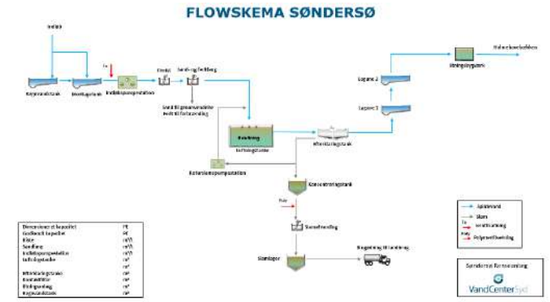

Figure 2. Aerial view and flow scheme of the Søndersø WWTP Danish demo site with MABR technology.

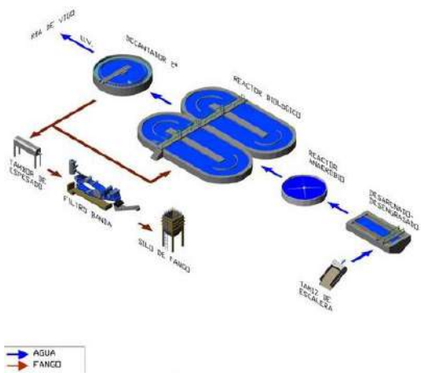

Figure 3. Aerial view and flow scheme of the Moaña WWTP demo site with AGS technology.

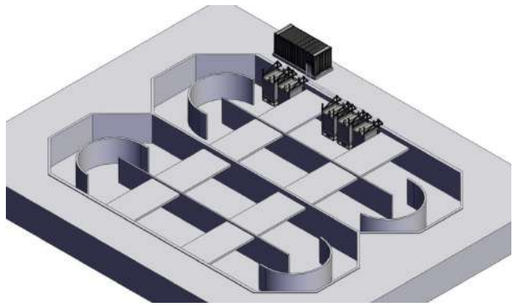

Figure 4. Retrofit of Danish demo site with MABR technology.

REFERENCES

Biswas, A.K., Tortajada, C., 2018. Assessing Global Water Megatrends, in: Biswas Tortajada, Cecilia, Rohner, Philippe, A.K. (Ed.), Water Resources Development and Management. Springer, pp. 1–26. https://doi.org/10.1007/978-981-10-6695-5_1

Garrido-Baserba, M., Corominas, L., Cortés, U., Rosso, D., Poch, M., 2020. The Fourth-Revolution in the Water Sector Encounters the Digital Revolution. Environ. Sci. Technol. 54, 4698–4705. https://doi.org/10.1021/acs.est.9b04251

Larsen, T.A., Hoffmann, S., Lüthi, C., Truffer, B., Maurer, M., 2016. Emerging solutions to the water challenges of an urbanizing world. Science (80-.). 352, 928–933. https://doi.org/10.1126/science.aad8641

Uri-Carreño, N., Nielsen, P.H., Gernaey, K. V., Domingo-Félez, C., Flores-Alsina, X., 2023. Nitrous oxide emissions from two full-scale membrane-aerated biofilm reactors. Submitted to Science of Total Environment. https://papers.ssrn.com/sol3/papers.cfm?abstract_id=4327290

Dynamics of antibiotic-resistant genes in aerobic granular systems in aerobic granular reactors treating real wastewater

L. Perez-Bou, A. Rosa-Masegosa, B. Muñon-Palazon, A. Gonzalez-Martinez, J. Gonzalez-Lopez, D. Correa-Galeote

Microbiology and Environmental Technology Section, Water Institute, University of Granada, 18011 Granada, Spain
(E-mail: lizandrapb@correo.ugr.es; aurorarm@ugr.es; bmp@ugr.es; agon@ugr.es; jgl@ugr.es; dcorrea@ugr.es)

Abstract

Antibiotic-resistance is a growing emergence worldwide promoted by improperly managed wastewater (WW) that results in the dissemination of antibiotic-resistant genes (ARGs) to the environment. Aerobic granular systems in sequential batch reactors (AGS-SBRs) are a promising alternative in WW treatment; however, the removal rates of ARG by these systems are not well known. Hence, the abundances of different ARGs were determined by qPCR in influent, granular biomass, and effluents of a lab-scale AGS-SBR treating real WW for 60 days. Generally considered, high abundances of the different ARGs were found in the biomass, particularly during the granulation period of the operation, highlighting its potential role as antibiotic-resistance hotspots, mainly for *aadA*, *aadB*, and *tetA* genes. Also, generally considered, the average removal rate of ARGs of the bioreactor was very scarce, suggesting that the removal efficiency of ARGs in AGS-SBRs must be optimized to improve the advantages of this technology in WW treatment.

Keywords (maximum 6 in alphabetical order)

AGS-SBR; antibiotic-resistant genes; environmental pollution, qPCR, water bodies, WWTPs

INTRODUCTION

The overuse and improper use of antibiotic substances have led to an increase in the appearance of antibiotic-resistant bacteria (ARBs), resulting in a reduction in the effectiveness of medical treatment against contagious diseases. Particularly, wastewater treatment plants (WWTPs) play potential roles as a transmission route of ARBs via improperly management or treatment of the highly antibiotic-concentrated wastewater (WW), constituting an important antibiotic-resistant genes (ARGs) reservoir (Schages et al., 2021). In addition, the inefficient removal of antibiotics by WWTPs contributes to disseminating ARBs and ARGs to receiving water bodies.

Nowadays, aerobic granular systems in sequential batch reactors (AGS-SBRs) have multiple advantages over conventional WW treatment systems (Cui et al., 2021); however, the effectiveness of AGS-SBRs for the removals of antibiotics, ARBs, and ARGs are largely unknown. Therefore, it is necessary to evaluate the dynamics of the predominant genetic mechanisms that contribute to the antibiotic-resistance phenomenon within the AGS-SBR to prevent the dissemination of ARGs from the effluents generated in these novel engineering systems to the receiving environments.

The general aim of the present research was to determine the absolute abundances of several ARGs in the influent, biomass, and effluent of a lab-scale AGS-SBR fed with real urban WW by qPCR, using a newly developed set of primers covering a higher ARG diversity than the currently available molecular tools.

MATERIAL AND METHODS

A lab-scale AGS-SBR was operated for 60 days to treat real WW sampled from a municipal WWTP (Granada, Spain). The bioreactor was inoculated with activated sludge from the same WWTPs for granule formation. The detailed operational conditions were described in Rosa-Masegosa et al. (2022). Quantification of total abundances of 11 different ARGs was performed by quantitative PCR (qPCR) on a QuantStudio-3 Real-Time PCR system (Applied Biosystems). The different ARG (*aadA*, *aadB*, *ampC*, *blaSHV*, *blaTEM*, *dfrA1*, *ermB*, *fosA*, *mecA*, *qnrS*, and *tetA* genes) analyzed in the influents, granular biomass, and generated effluents are listed in Table 1. In addition, the bacterial 16S rRNA gene was used as a proxy for total *Bacteria* quantification. All reactions were made in triplicate, according to Correa-Galeote et al. (2021). The statistical differences among samples were analyzed using the non-parametric Kruskal–Wallis and Conover–Iman tests (p<0.05 significance level) in XLSTAT v2020 (Addinsoft).

RESULTS AND DISCUSSION

The gene copies of bacterial 16S rRNA genes varied between 1.15×10^5 to 1.87×10^7 gene copies g^{-1} in the influent, 1.42×10^{10} to 2.47×10^{11} g^{-1} in the granular biomass, and 4.98×10^5 to 8.82×10^7 gene copies g^{-1} in the effluents (Fig. 1). These results agree with those of previous work (Rosa-Masegosa et al., 2022). On the other hand, all of the investigated ARGs were detected in the samples except *mecA*, which was removed from further analyses. The abundances of the remaining ARGs oscillated from being below the detection limit (< 0.5×10^3 copies g^{-1}) to 4.55×10^9 gene copies g^{-1} (Fig. 1).

Regarding the influent samples, the average abundance of *tetA* was 2.74×10^6 copies g^{-1}, which was higher than *aadA* (2.05×10^6 copies g^{-1}), *aadB* (1.55×10^6 copies g^{-1}), *blaTEM* (1.11×10^6 copies g^{-1}), *ampC* (4.59×10^5 copies g^{-1}), *qnrS* (1.37×10^5 copies g^{-1}), *drfA1* (1.10×10^5 copies g^{-1}), and *ermB* (9.65×10^4 copies g^{-1}). The *blaSHV* gene was not detected. Hence, the urban WW used in this study presented a high level of ARGs, reinforcing previous reports of its potential to strongly contribute to the phenomenon of antibiotic resistance dissemination (Pantanella et al., 2020).

All the ARGs analyzed in this study were found in the inoculum sample (range 3.76×10^5 - 1.82×10^9 gene copies g^{-1}). On the other hand, the granular biomass harboured a wide variety of ARGs. In this sense, the higher average abundances were found for *aadA* (2.57×10^9 copies g^{-1}), followed by *aadB* (5.88×10^8 copies g^{-1}), *tetA* (2.28×10^8 copies g^{-1}), *drfA1* (9.93×10^7 copies g^{-1}), *blaTEM* (8.34×10^7 copies g^{-1}), *ermB* (6.96×10^7 copies g^{-1}), *qnrS* (4.09×10^7 copies g^{-1}), *blaSHV* (3.97×10^7 copies g^{-1}), and, finally, *ampC* (1.61×10^6 copies g^{-1}). Consequently, great differences in the contribution of the different genes to the total resistome were observed in the granular biomass of the ASG-SBR, being *aadA*, *aadB*, and *tetA* the dominant ARGs. The abundances of the ARGs here analyzed were in the same range than those reported in other WW technologies (Nõlvak et al., 2018; Leroy-Freitas et al., 2022). Also, it is worth mentioning that higher abundances of all the ARGs were found at the beginning of the experiment (day 7) compared to those of days 30 and 60, highlighting the particular extensive potential contribution to the dissemination of ARGs during the start-up periods of AGS-SBRs.

Similarly, higher concentrations of ARGs were present in the final effluents, particularly for *tetA* (4.23×10^6 copies g^{-1}), *blaTEM* (3.72×10^6 copies g^{-1}), *aadA* (1.88×10^6 copies g^{-1}), *aadB* (1.69×10^6 copies g^{-1}), and *ampC* (3.67×10^5 copies g^{-1}). These ARGs were detected in most sampling times. The high prevalence of the ARGs in the effluents is in agreement with Calderón-Franco et al. (2020), which studied the dynamic of ARGs in a full-scale granular sludge WWTP.

Finally, it should be noted that for all the ARGs, except *ermB* and *qnrS*, scarce removal rates in the ARGs were observed when comparing the abundance of ARGs in the influents and those of the effluents. Despite the advantages of AGS-SBR over other technologies in several aspects, the final effluent generated in AGS-SBR could act as an important hotspot in the dissemination of antibiotic-resistances to the receiving water bodies. Therefore, an optimization in the removal of ARG through this promising technology must be addressed.

ACKNOWLEDGMENTS: This research was supported by the Andalusian Government through ECORESISTOME project (A-RNM-62-UGR20).

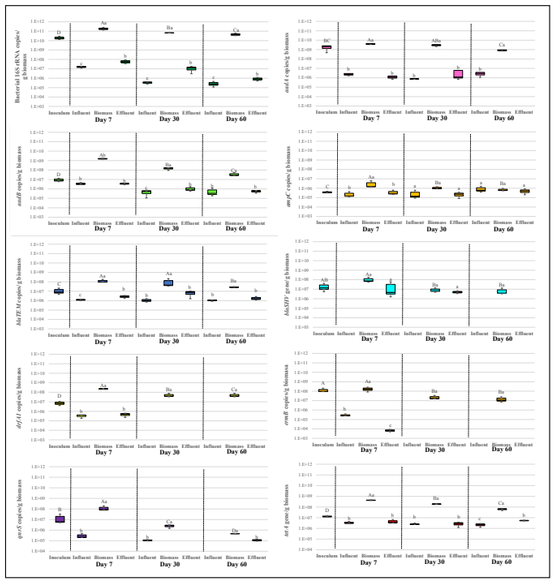

Figure 1. Bacterial 16S rRNA and ARGs genes copies per gram of samples retrieved from a lab-scale AGS-SBR treating real urban WW, determined by quantitative PCR (n = 3). According to Kruskal–Wallis and Conover–Iman tests ($p < 0.05$), different capital letters indicate significant differences among biomass samples (inoculum and granular biomass samples) and different lowercase letters indicate significant differences among samples (influent, biomass, and effluent) for a given sampling time.

Table 1. Antibiotic-resistant genes determined by qPCR in this study, their KEGG orthology numbers, the resistance proteins encoded, and the related antibiotics they confer resistance to.

Gene	KEGG orthology number	Resistance protein encoded	Antibiotics to which the gene confers resistance
aadA	K00984	Streptomycin 3''-adenylyltransferase	Streptomycin
aadB	K17881	Aminoglycoside 2''-adenylyltransferase	Aminoglycoside
ampC	K01467	Beta-lactamase class C	Peniciline
blaSHV	K18699	Beta-lactamase class A SHV	Penicillin and cephalosporine
blaTEM	K18698	Beta-lactamase class A TEM	Penicillin and cephalosporine
dfrA1	K18589	Dihydrofolate reductase	Trimethoprim
ermB	K00561	23S rRNA (adenine-N6)-dimethyltransferase	Macrolide
fosA	K21253	Glutathione S-transferase FosA	Fosfomycin
qnrS	K18555	Fluoroquinolone resistance protein	Fluoroquinolone
tetA	K08151	MFS transporter	Tetracycline

REFERENCES

Correa-Galeote, D., Roibás-Rozas, A., Mosquera-Corral, A., Juárez-Jiménez, B., González-López, J., Rodelas, B. 2021. Revealing the dissimilar structure of microbial communities in different WWTPs that treat fish-canning wastewater with different NaCl content. *Journal of Water Process Engineering* **44**, 102328.

Calderón-Franco, D., van Loosdrecht, M.C., Abeel, T., Weissbrodt, D.G. 2020. A novel method to isolate free-floating extracellular DNA from wastewater for quantitation and metagenomic profiling of mobile genetic elements and antibiotic resistance genes. *Water Research* **189**, 116592.

Cui, D., Chen, Z., Cheng, X., Zheng, G., Sun, Y., Deng, H., Li, W. 2021. Efficiency of sulfamethoxazole removal from wastewater using aerobic granular sludge: influence of environmental factors. *Biodegradation* **32**(6), 663–676.

Nõlvak, H., Truu, M., Oopkaup, K., Kanger, K., Krustok, I., Nehrenheim, E., Truu, J. 2018. Reduction of antibiotic resistome and integron-integrase genes in laboratory-scale photobioreactors treating municipal wastewater. *Water Research* **142**, 363-372.

Leroy-Freitas, D., Machado, E.C., Torres-Franco, A.F., Dias, M.F., Leal, C.D., Araújo, J.C. 2022. Exploring the microbiome, antibiotic resistance genes, mobile genetic element, and potential resistant pathogens in municipal wastewater treatment plants in Brazil. *Science of The Total Environment* **842**, 156773.

Rosa-Masegosa, A., Perez-Bou, L., Muñoz-Palazon, B., Monteoliva-García, A., Gonzalez-Martinez, A., Gonzalez-Lopez, J., Correa-Galeote, D. 2022. Effects of sulphur amino acids on the size and structure of microbial communities of aerobic granular sludge bioreactors. *Amino Acids* **54**(10), 1403–1419.

Pantanella, F., Lekunberri, I., Gagliardi, A., Venuto, G., Sànchez-Melsió, A., Fabiani, M., et al. 2020. Effect of urban wastewater discharge on the abundance of antibiotic resistance genes and antibiotic-resistant Escherichia coli in two Italian rivers. *International Journal of Environmental Research and Public Health* **17**(18), 6813.

Schages, L., Wichern, F., Geisen, S., Kalscheuer, R., Bockmühl, D. 2021. Distinct resistomes and microbial communities of soils, wastewater treatment plants and households suggest development of antibiotic resistances due to distinct environmental conditions in each environment. *Antibiotics* **10**(5), 514.

Carbon and nitrogen removal from wastewater in a continuous upflow aerobic granular sludge blanket reactor

A. Lanzetta*, F. Di Capua**, Davide Mattioli***, Francesco Pirozzi*, Giovanni Esposito* and Stefano Papirio*

* Department of Civil, Architectural and Environmental Engineering, University of Naples Federico II, Via Claudio 21, 80125 Naples, Italy
(E-mail: anna.lanzetta@unina.it; francesco.pirozzi@unina.it; giovanni.esposito1@unina.it; stefano.papirio@unina.it)
** School of Engineering, University of Basilicata, via dell'Ateneo Lucano 10, 85100 Potenza, Italy
(E-mail: francesco.dicapua@unibas.it)
*** Laboratory Technologies for the Efficient Use and Management of Water and Wastewater, Italian National Agency for New Technologies, Energy and Sustainable Economic Development (ENEA), Via M.M. Sole 4, 40129 Bologna, Italy
(E-mail: davide.mattioli@enea.it)

Abstract

In this study, carbon (C) and nitrogen (N) removal from a synthetic urban wastewater was investigated in a continuous double-column upflow aerobic granular sludge blanket (UAGSB) system. The UAGSB reactor was operated under different dissolved oxygen (DO) ranges (0.01-6.00 $mg \cdot L^{-1}$), feed C/N ratios (4.7-13.6), and hydraulic retention times (HRT) (6-24 h). This work shows that at a DO range of 0.01-0.30 $mg \cdot L^{-1}$, a feed C/N ratio of 13.6 and an HRT of 24 h, the UAGSB system achieved the highest chemical oxygen demand, $N\text{-}NH_4^+$ and total inorganic nitrogen removal efficiencies of 86, 99 and 84 %, respectively, representing a potentially valuable and economic alternative to the conventional activated sludge systems for the treatment of municipal or industrial wastewaters.

Keywords

Aerobic granular sludge, carbon and nitrogen removal, denitrification, nitrification, urban wastewater

INTRODUCTION

The biological treatment in municipal wastewater treatment plants (WWTPs) is often accomplished by means of the conventional activated sludge (CAS) process for the removal of organic matter and the modified Modified Ludzack-Ettinger (MLE) process, consisting of separate denitrification and nitrification steps, for combined carbon (C) and nitrogen (N) removal. The simultaneous nitrification and denitrification process (SND) is a promising alternative to the MLE cycle in WWTPs for the concomitant C and N removal from municipal wastewater due to lower carbon demand in denitrification process and sludge production [1], lower energy for aeration [2] and smaller footprint [3]. Generally, the use of biofilm-based systems promotes the coexistence of different microbial communities and allows higher concentration of active biomass, while reducing space requirements and sludge production compared to suspended-cell systems such as CAS and MLE [4]. Aerobic granular sludge (AGS) integrates the characteristics of suspended-growth and biofilm systems, as it leads to the formation of microbial aggregates without any support and having a structure similar to biofilms [5]. Nevertheless, AGS systems have been poorly applied under continuous flow conditions due to system instability and reduced performance [6]. In this study, a continuous double-column upflow aerobic granular sludge blanket (UAGSB) reactor was studied for 306 days for the treatment of synthetic urban wastewater. The effect of different DO concentrations, feed C/N ratios and HRT was mainly assessed in terms of chemical oxygen demand (COD), ammonium nitrogen ($N\text{-}NH_4^+$) and total inorganic nitrogen (TIN) removal as well as the evolution of the different N species.

MATERIALS AND METHODS

The synthetic wastewater used as influent for the UAGSB reactor was prepared as reported by Beun et al. [7]. The influent concentrations are shown in **Table 1**. The inoculum used for the start-up of the bioreactor was an AGS collected from a 1 L lab-scale sequencing batch reactor previously run by Sguanci et al.[8]. The experimental set-up included two laboratory-scale glass columns (0.6 L), one used as the main bioreactor and the other as an aeration column to avoid the loss of biomass from the top of the reactor and prevent damaging of the granules due to impact with air bubbles [9]. A 205S peristaltic pump (Watson-Marlow, UK) was used for influent feeding and effluent suction from the bioreactor. The effluent from the bioreactor was oxygenated in the aeration column and recirculated at the bottom of the bioreactor with a 505U peristaltic pump (Watson-Marlow, UK) at a flow rate between 20 and 40 $mL \cdot min^{-1}$. Air was transferred to the aeration column at a flow rate ranging from 0 to 4.5 L min^{-1} using an aquarium air pump equipped with tubing and a porous stone. DO concentration was continuously monitored using a FDO 925 optical probe (WTW, Germany) connected to a multiparameter benchtop meter inoLab® Multi 9620 IDS (WTW, Germany). A Raspberry PI 3 Model B+ single board computer (Raspberry Pi Foundation, UK) coupled with Python software 3.0 (Python Software Foundation, USA) was used to control and automate aeration in the reactor, as described by Iannacone et al.[10].

RESULTS AND DISCUSSION

The first four periods were aimed at evaluating the effect of different DO concentrations on the removal efficiencies (REs) of COD, $N\text{-}NH_4^+$ and TIN at feed C/N ratios in the range of 12.1-13.5 (**Table 1**). The decrease of DO concentration from period I (4.0-6.0 mg L^{-1}) to period IV (0.02-1.60 mg L^{-1}) resulted in stable (p>0.05) $N\text{-}NH_4^+$, TIN and COD REs of 95 ± 9, 85 ± 8 and 84 ± 5 % (**Fig. 1**), respectively, with a maximum effluent $N\text{-}NO_3^-$ concentration of 10.6 $mg \cdot L^{-1}$. This indicates that the UAGSB reactor could be efficiently operated at low DO conditions, thus entailing low aeration costs for the treatment of municipal wastewater. Periods V and VI were characterized by a similar DO range (**Table 1**) and a decrease of the feed C/N ratio from 13.5 (period IV) to 7.0 and 4.7, respectively. The decrease of the C/N ratio did not negatively affect $N\text{-}NH_4^+$ RE, which remained in the range of 97-99 % (p>0.05) (**Fig. 1**). Nitrification was stimulated as $N\text{-}NO_3^-$ concentration increased from 4.5 ± 2.3 (period IV) to 11.9 ± 5.2 (period V) and 31.1 ± 4.1 mg $N \cdot L^{-1}$ (period VI). The reduction in the feed C/N ratio led to insufficient organic carbon to support denitrification. Consequently, the TIN RE reached a minimum value of 28 ± 8% in period VI (**Fig. 1**) because of the higher effluent $N\text{-}NO_3^-$ concentrations. The COD RE decreased from 84 ± 5% (periods I- IV) to 62 ± 13% (periods V-VI) (**Fig. 1**), while the effluent COD concentration did not change significantly (p>0.05) and averagely remained at 94.7 ± 55.6 $mg \cdot L^{-1}$. Periods VII and VIII were characterized by an increase of the feed COD concentration and, therefore, of the C/N ratio from 4.7 (period VI) to 8.0 and 13.6, respectively, resulting in lower DO concentrations in the bioreactor (below 1 $mg \cdot L^{-1}$ in period VIII), even though the inlet air flow was increased. Interestingly, despite the low DO conditions, $N\text{-}NH_4^+$ RE was not affected (p>0.05) and remained stable at 98 ± 5%. The feed C/N increase resulted in a gradual reduction of the effluent NO_3^- concentration, suggesting an increase in the denitrifying efficiency of the system that could be favoured by the low DO levels in the bioreactor. The results obtained in this stage confirm that the UAGSB reactor works more efficiently at higher C/N ratios, which should be considered in view of future real-scale applications of this system. During the periods IX (day 221) and X (day 259), the HRT was set at 12 and 6 h with the objective to evaluate the COD, $N\text{-}NH_4^+$, and TIN REs at increased organic and nitrogen loading rates. The HRT reduction from 24 to 12 and to 6 h resulted in a significant decrease of $N\text{-}NH_4^+$, TIN and COD REs to 71, 63 and 64 %, respectively (period X). This suggests that the significant increase in the influent organic and nitrogen loads, coupled with the low DO concentrations in the bioreactor, negatively affected nitrification.

Table 1. Operating conditions and duration of each experimental period during the continuous-flow operation of the UAGSB reactor.

Period	Duration (days)	DO range ($mg \cdot L^{-1}$)	HRT (h)	Feed $P\text{-}PO_4^{3-}$ ($mg \cdot L^{-1}$)	Feed COD ($mg \cdot L^{-1}$)	Feed $N\text{-}NH_4^+$ ($mg \cdot L^{-1}$)	Feed C/N
I	0-30	4.0-6.0	24	56.4±25.0	552±55	38.8±6.4	12.1±1.4
II	31-37	2.0-4.0	24	7.5±1.8	604±62	45.3±2.5	13.3±1.4
III	38-65	1.0-2.0	24	8.2±4.8	543±47	43.3±2.9	12.7±1.5
IV	66-87	0.02-1.60	24	6.6±3.1	571±45	42.6±4.3	13.5±1.4
V	88-130	0.12-2.09	24	8.7±3.1	287±141	39.9±8.5	7.0±2.5
VI	131-160	0.10-2.07	24	6.7±2.2	195±30	42.1±2.0	4.7±0.9
VII	161-193	0.03-1.86	24	9.7±2.7	324±47	40.8±2.2	8.0±1.1
VIII	194-220	0.01-0.30	24	10.5±2.9	560±80	41.5±4.3	13.6±2.2
IX	221-258	0.01-1.22	12	12.7±3.6	472±54	41.4±2.1	11.4±1.4
X	259-306	0.01-0.07	6	10.5±1.8	455±30	37.9±3.3	12.1±1.2

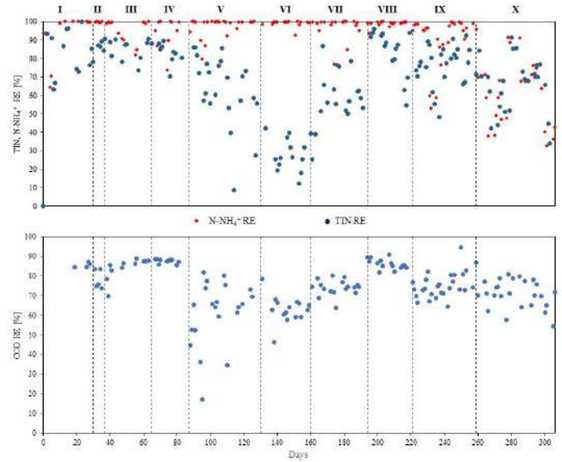

Figure 1. Temporal trend of removal efficiency (%) in terms of $N\text{-}NH_4^+$, TIN and COD from periods I to X.

REFERENCES

[1] Ma, Weiwei, Yuxing Han, Wencheng Ma, Hongjun Han, Hao Zhu, Chunyan Xu, Kun Li, and Dexin Wang. 2017. "Enhanced Nitrogen Removal from Coal Gasification Wastewater by Simultaneous Nitrification and Denitrification (SND) in an Oxygen-Limited Aeration Sequencing Batch Biofilm Reactor." *Bioresource Technology* **244**, 84–91.

[2] A. A. L. Zinatizadeh and E. Ghaytooli. 2015 "Simultaneous nitrogen and carbon removal from wastewater at different operating conditions in a moving bed biofilm reactor (MBBR): Process modeling and optimization," *J. Taiwan Inst. Chem. Eng.*, **53**, 98–111, 2015.

[3] M. Seifi and M. H. Fazaelipoor. 2012 "Modeling simultaneous nitrification and denitrification (SND) in a fluidized bed biofilm reactor," *Appl. Math. Model.*, **36**(11), 5603–5613.

[4] Zhao, Yingxin, Duo Liu, Wenli Huang, Ying Yang, Min Ji, Long Duc Nghiem, Quang Thang Trinh, and Ngoc Han Tran. 2019. "Insights into Biofilm Carriers for Biological Wastewater Treatment Processes: Current State-of-the-Art, Challenges, and Opportunities." *Bioresource Technology* **288** (4), 121619.

[5] F. Wang, S. Lu, Y. Wei, and M. Ji. 2009 "Characteristics of aerobic granule and nitrogen and phosphorus removal in a SBR," *J. Hazard. Mater.*, **164**(2–3), 1223–1227.

[6] D. Xu, J. Li, J. Liu, X. Qu, and H. Ma. 2022 "Advances in continuous flow aerobic granular sludge: A review," *Process Saf. Environ. Prot.*,**163**, 27–35.

[7] J. J. Beun, M. C. M. Van Loosdrecht, and J. J. Heijnen. 2002 "Aerobic granulation in a sequencing batch airlift reactor," *Water Res.*, **36**(3), 702–712.

[8] S. Sguanci, C. Lubello, S. Caffaz, and T. Lotti. 2019 "Long-term stability of aerobic granular sludge for the treatment of very low-strength real domestic wastewater," *J. Clean. Prod.*, vol. **222**, 882–890.

[9] S. Liu, T., He, X., Jia, G., Xu, J., Quan, X., & You. 2020 "Simultaneous nitrification and denitrification process using novel surface-modified suspended carriers for the treatment of real domestic wastewater.," *Chemosphere,* **247**, 125831.

[10] F. Iannacone, F. Di Capua, F. Granata, R. Gargano, and G. Esposito. 2020 "Simultaneous nitrification, denitrification and phosphorus removal in a continuous-flow moving bed biofilm reactor alternating microaerobic and aerobic conditions," *Bioresour. Technol.*, vol. **310**(03), 123453.

Kinetic characterization of Phosphorus Accumulating Organisms (PAO) and Glycogen Accumulating Organisms (GAO) anaerobic metabolism in Aerobic Granular Sludge (AGS)

J.P. Czellnik*, R. Campo*, C. Lubello*, T. Lotti*

* Department of Civil and Environmental Engineering, University of Florence, Via di S.Marta 3, Firenze 50139, IT (E.mail: *janpietro.czellnik@unifi.it; riccardo.campo@unifi.it; claudio.lubello@unifi.it; tommaso.lotti@unifi.it*)

Abstract

This study aims to investigate the anaerobic kinetic parameters and competition between phosphorus and glycogen accumulating organisms in aerobic granular sludge under different substrate concentrations. Several tests were conducted monitoring the concentrations of COD and phosphates, to model the process according to a Monod curve and to evaluate the activities of the accumulating organisms under the different conditions. Results show that the half-saturation constant tends to increase with the maximum specific removal rate, and that a higher GAO activity didn't compromise the biological phosphorus removal process.

Keywords (maximum 6 in alphabetical order)

Aerobic Granular Sludge, Anaerobic metabolism, Enhanced Biological Phosphorus Removal, Phosphorus/Glycogen Accumulating Organisms, Wastewater treatment.

INTRODUCTION

Aerobic Granular Sludge (AGS) is a technological application of biofilm in which microorganisms are aggregated into dense pseudo-spherical shapes. AGS can host different microenvironments with different redox potentials which allows for the simultaneous removal of COD, nitrogen and phosphorus all within a single unit (Pronk et al., 2015). AGS are enriched of Phosphorus Accumulating Organism (PAOs) and Glycogen Accumulating Organisms (GAOs), non-ordinary heterotrophs capable of removing rapidly biodegradable COD anaerobically and storing it in the form of PHA, which can be used as electron donor in the aerobic phase of the cycle. These organisms have a very complex metabolism as it involves the production/consumption of intracellular storage compounds (PHA, polyphosphate and glycogen), which play an essential role in the Enhanced Biological Phosphorus Removal (EPBR) process. The aim of this study is to characterize the anaerobic kinetics of PAOs and GAOs in an AGS reactor fed at different level of COD evaluating the effect on the competition for the common substrate and on the phosphorus removal efficiency.

MATERIALS AND METHODS

The experiments were conducted within a laboratory scale Granular Sequencing Batch Reactor (GSBR) with a useful volume of 5L, operated for seven months as follows: cycle time 6h, HRT=15h, SRT=176±20d, OLR=640mgCOD/Ld, ORE=81%, NLR=80mgN/Ld, NRE=99.5%, PLR=22.4mgP/Ld, PRE=97.5%, T=20±0.5°C and pH=7.5±0.3. The cultivated biomass was mainly granular, with a floccular fraction of about 3% on volatile basis and have been characterized by gravimetric and granulometric analysis: 9.6%gTS/gWW, 6.56gTS/L, 80.1%gVS/gTS, D10=226.4µm, D50=776.9µm and D90=2144.7µm.

The tests were conducted operating the reactor in batch mode after the end of the conventional cycle and all necessary substrates have been supplied through a concentrated solution spike once the Oxidation Reduction Potential (ORP) fell below -200mV, in order to guarantee strict anaerobic conditions. Sodium acetate (HAc) has been used as the sole organic carbon source, with concentrations ranging from 160 to 800 mgCOD/L.

COD and PO_4-P concentrations have been monitored intensively to determine anaerobic kinetics such as the maximum biomass specific COD removal rate (q_{COD}^{max}, [mgCOD/gVSS/h]) and the half-saturation constant (Ks, [mgCOD/L]) to model the process with Monod equation according to the procedure proposed by Smith et al. (1998).

To evaluate PAOs activity a molar ratio of 0.5 Pmol-rel/Cmol-sto (Smolders et al., 1994) has been considered while GAOs activity have been calculated by difference through mass balance on the acetate. Their activity was estimated during the course of the experiments, to evaluate the influence of consumption of internal substrates, and over the whole test time.

RESULTS AND DISCUSSION

Results showed that the removal rates increase with the initial COD concentration, until a plateau is reached for concentrations above 600mgCOD/L (data not shown) when the concentration profile within the biofilm allows for non-limiting conditions even for inner layers. The q_{COD}^{max} recorded for initial concentration of 800mgCOD/L is 157mgHAc/gVSS/h, which is in line with literature values (166mgHAc/gVSS/h, reported by Lopez-Vázquez (2009)) obtained in a flocculent system, showing the high level of PAOs/GAOs enrichment of the GSBR system. The half-saturation constant (Ks), to be considered as "apparent" since bacteria are not in the planktonic state, also increases with increasing initial COD levels (Fig.1).

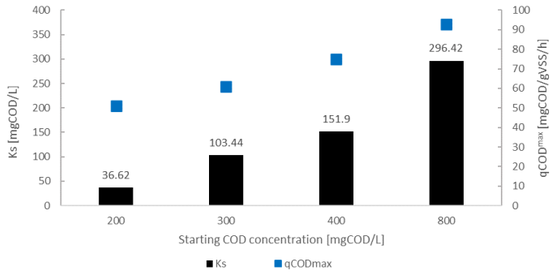

Figure 1. Anaerobic kinetic parameters under different starting COD concentrations.

This is likely due to increasing diffusion limitation inside the biofilm due to higher consumption rate, as proposed by Shaw et al. (2013). Nevertheless, the contribution of limiting availability of internal substrates progressively interesting the microorganisms from the external to the internal layers cannot be excluded.

Regarding the competition between PAOs and GAOs, an increase in phosphates released in the bulk was observed (Fig.2) for increasing COD starting levels, indicating a raising PAO activity. At lower COD concentrations PAOs outcompeted GAOs, but for higher COD levels an increase in GAO activity was registered (Fig.3). Nevertheless, the subsequent aerobic P-removal efficiency was not compromised (data not shown) indicating that GAOs exerted the positive effect of contributing to COD depletion without hampering P-removal efficiency, as stated by Nielsen et al., (2019) for a flocculent system. In Fig.2 the acetate left over at the end of the 800 test shows that the maximum anaerobic uptake capacity of the system was exceeded, which allowed the estimation of the overcapacity of the consortium of 450%, calculated in comparison to a standard cycle.

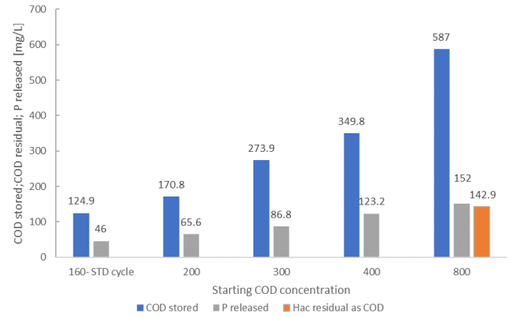

Figure 2. Volumetric concentrations of the stored COD, the residual COD at the end of each test and the PO4_P released with different starting COD concentrations. In the last test the residual HAc as COD is highlighted.

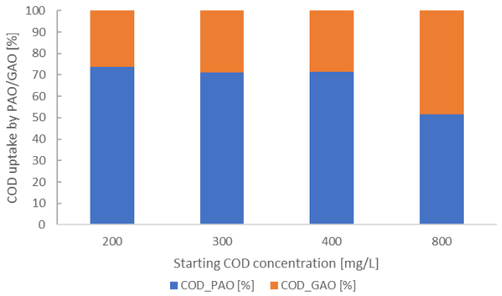

Figure 3. Percentage of activity by PAOs/GAOs over the entire experiment.

During the course of the individual tests, a trend was observed indicating the progressive decrease in PAO activity as the concentrations of COD in the bulk decrease from the starting point, being compensated by higher GAO activity (example reported in Fig.4). As reported by Lopez-Vázquez et al. (2009), the conditions under which the tests took place (T=20°C, pH=7.5 and HAc as sole carbon source) favour PAOs metabolism, which explains the higher activity at the start of the test. To explain the switch from the dominance of PAOs metabolism to GAOs several things need to be taken into account. First, the spatial distribution is important within a biofilm, the species found in the outer layer of the granule detect higher concentrations allowing higher activity and limiting the diffusion of substrate in the inner layers. Then, this initial high PAOs activity is related to a rapid consumption of the internal substrates, which will lead to a progressive slowdown of the metabolism allowing a greater activity of either the microorganisms with lower affinity with the substrate or located in the inside of the granule. In fact, as reported by Lemaire et al. (2008), in AGS PAO Accumulibacter are most likely to be found in the layers penetrated by oxygen in the aerobic period of the SBR operations, corresponding to the external part of the granule.

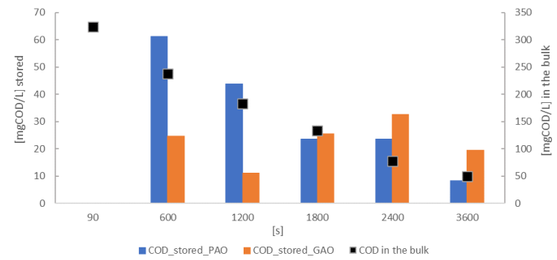

Figure 4. COD concentration in the bulk and its volumetric uptake by PAOs and GAOs in each time interval of the single test.

In summary, the Monod curve turned out to be a good approximation for the modelling of the single tests, but the absence of a constant half-saturation parameter impedes its generalized application to estimate the minimum anaerobic time required in function of the COD fed. Moreover, results show that the enrichment of GAOs in EBPR systems is not necessarily negative since, especially for layered microbial consortium as biofilms, they contribute to face fluctuating COD loads without compromising bio-P removal.

REFERENCES

Pronk, M., De Kreuk, M. K., De Bruin, B., Kamminga, P., Kleerebezem, R. V., & Van Loosdrecht, M. C. M. (2015). Full scale performance of the aerobic granular sludge process for sewage treatment. Water research, 84, 207-217.

Smith, L. H., McCarty, P. L., & Kitanidis, P. K. (1998). Spreadsheet method for evaluation of biochemical reaction rate coefficients and their uncertainties by weighted nonlinear least-squares analysis of the integrated Monod equation. Applied and Environmental Microbiology, 64(6), 2044-2050.

López-V, C. M., Hooijmans, C. M., Brdjanovic, D., Gijzen, H. J., & van Loosdrecht, M. C. (2007, January). A PRACTICAL METHOD FOR QUANTIFICATION OF PAO AND GAO POPULATIONS IN ACTIVATED SLUDGE SYSTEMS. In Nutrient Removal and Recovery Symposium 2007 (pp. 39-63). Water Environment Federation.

Shaw, A., Takács, I., Pagilla, K. R., & Murthy, S. (2013). A new approach to assess the dependency of extant half-saturation coefficients on maximum process rates and estimate intrinsic coefficients. water research, 47(16), 5986-5994.

Nielsen, P. H., McIlroy, S. J., Albertsen, M., & Nierychlo, M. (2019). Re-evaluating the microbiology of the enhanced biological phosphorus removal process. Current opinion in biotechnology, 57, 111-118.

Lopez-Vazquez, C. M., Oehmen, A., Hooijmans, C. M., Brdjanovic, D., Gijzen, H. J., Yuan, Z., & van Loosdrecht, M. C. (2009). Modeling the PAO–GAO competition: effects of carbon source, pH and temperature. Water Research, 43(2), 450-462.

Lemaire, R., Yuan, Z., Blackall, L. L., & Crocetti, G. R. (2008). Microbial distribution of Accumulibacter spp. and Competibacter spp. in aerobic granules from a lab□scale biological nutrient removal system. Environmental Microbiology, 10(2), 354-363.

Smolders, G. J. F., Van der Meij, J., Van Loosdrecht, M. C. M., & Heijnen, J. J. (1994). Model of the anaerobic metabolism of the biological phosphorus removal process: stoichiometry and pH influence. Biotechnology and bioengineering, 43(6), 461-470.

TECHNICAL SESSIONS

T15. Partial nitritation & anammox

ECOSTP 2023

Energy-efficient nitrogen removal from sewage: achieving mainstream partial nitritation/anammox via recurrent multi-stressor floc treatments

M. Van Tendeloo*, M.C. Baptista, T. Van Winckel & S. E. Vlaeminck

Research Group of Sustainable Energy, Air and Water Technology, Department of Bioscience Engineering, University of Antwerp, 2020 Antwerpen, Belgium
* Michiel.VanTendeloo@UAntwerpen.be

Abstract
Implementation of mainstream partial nitritation/anammox for resource-efficient nitrogen removal is important to transition towards energy-autonomous sewage treatment. Its development is challenged by the competitiveness of nitrite-oxidizing bacteria (NOB) scavenging nitrite from anammox bacteria (AnAOB). A unique multi-stressor floc treatment (sulphide-spiked deoxygenated starvation and free ammonia shock) was therefore validated for the first time under lab-scale conditions. A good microbial activity balance was achieved with high AnAOB (71±21 mg N L-1 d-1) and low NOB (4±17% of total nitrite consumption) activity. Recurrent floc treatment was revealed to be an essential strategy. In addition, NOB growth on the biofilm was avoided despite only treating the flocs to safeguard AnAOB activity. Overall, the multi-stressor treatment concept was validated as a useful NOB growth control strategy.

Keywords (maximum 6 in alphabetical order)
Biological nitrogen removal; cold anammox; deammonification; sewage treatment

Introduction
Partial nitritation/anammox (PN/A) is a resource-efficient nitrogen removal pathway. Compared to the conventional nitrification/denitrification process, it offers a 60% reduction in aeration demands (energy consuming) and 100% reduction in COD demands (could be used to produce energy via anaerobic digestion) (Jetten *et al.* 1997). The major challenge for mainstream PN/A implementation is the selective suppression of nitrite-oxidizing bacteria (NOB) over aerobic and anoxic ammonium-oxidizing bacteria (AerAOB and AnAOB). A combination of multiple dedicated control strategies hereby essential (Van Tendeloo *et al.* ; Agrawal *et al.* 2018).

Exposing the sludge to a single biocidal agent or stressor is often applied to selectively suppress NOB activity with for example free ammonia (FA) (Wang *et al.* 2021), sulphide (Erguder *et al.* 2008), or a short substrate starvation (Ye *et al.* 2019). Typically, the concentrated return-sludge stream is periodically treated rather than a continuous exposure in the main tank to reduce the operational cost. Despite promising performance achieved in the lab, long-term and large-scale successes remain scarce. The ability of NOB to adapt to certain control strategies, such as these single-stressor treatments, threatens the implementation of mainstream PN/A (Wang *et al.* 2021). The development of multi-stressor treatments could help to overcome this challenge as they are potentially less susceptible to NOB adaptation (Seuntjens *et al.* 2018).
In this study, the unique multi-stressor treatment concept formulated by Seuntjens *et al.* (2018) was validated under lab-scale conditions, implemented as foreseen in a possible full-scale application. The treatment consisted of sulphide-spiked deoxygenated starvation (2 d) followed by an FA shock (1 h). The main objective was to achieve nitrogen removal via AnAOB with minimal NOB contribution.

Material and Methods
A 4.7L fixed-film activated sludge (IFAS) reactor was operated under mainstream conditions (20±1°C; influent: 49±6 mg NH_4^+-N L^{-1} and 75 mg COD L^{-1}, among others), continuously fed and equipped with a settler (1.0L), pH and DO control. A combination of pre-colonised PN/A carriers (1.3L, from a mainstream lab reactor) and PN/A flocs (< 200µm, from a sidestream DEMON® reactor) was used as inoculum. Floc age was controlled at 8.5 days while the biofilm was not actively wasted. Intermittent aeration (4/8 min on/off at 0.9 mg O_2 L^{-1}) was applied and ammonium limitations (< 5 mg N L^{-1}) were avoided.

Flocs were recurrently exposed to the multi-stressor treatment at a frequency of 0.095 d^{-1} by treating 33% of the flocs every 3.5 days. Deoxygenated conditions were applied by sparging with N_2 gas, and sulphide (157±16 or 305±12 mg S^{2-}-S L^{-1}) was added by a needle. After a 2-day starvation, a short 1-h FA shock was conducted (34±2 mg NH_3-N L^{-1} at pH 8.1).
The performance was evaluated by making a so-called microbial activity balance: all total nitrogen (TN) removal was assumed to originate from AnAOB activity, and subsequently the AerAOB and NOB activity was calculated according to the average stoichiometry(Strous *et al.* 1998; Lotti *et al.* 2014). TN removal by denitrification was assumed to remain limited as oxygen was present for > 81% of the time.

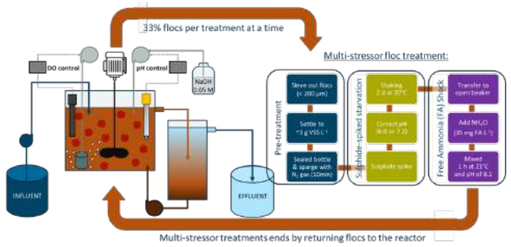

Figure 1 Schematic overview of the reactor and experimental design. Multi-stressor floc treatments were conducted twice a week, treating about 33% of the total flocs, resulting in an overall frequency of 0.095 d^{-1}. Biofilm (both attached and suspended) were excluded from the treatment.

Results and Conclusions
The initially applied operational conditions in Phase Ia were insufficient to maintain a good microbial activity balance with low NOB activity (Figure 2). After doubling the sulphide dose in the floc treatment to 307±15 mg S^{2-} L^{-1} (Phase IIa onwards), a temporal reduction in oxygen levels due to technical difficulties (Phase IIb-IIc), and the addition of extra PN/A carriers in combination with fixing the oxygen control (Phase IIIa), a desired performance was achieved again in Phase IIIa. In the final two phases, the balance deteriorated after removing 57% of the carriers (Phase IIIb), highlighting the importance of sufficient AnAOB activity as nitrite sink(Seuntjens *et al.* 2020; Wang *et al.* 2021), and stopping the recurrent floc treatments, showing the importance of the floc treatment.

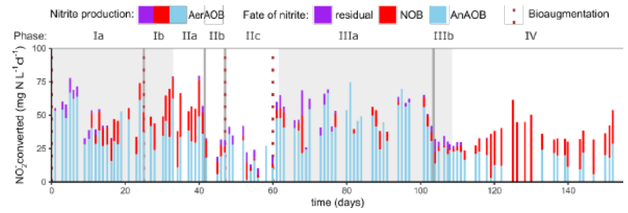

Figure 2 Microbial activity balance in the IFAS reactor during process operation. The nitrite production by AerAOB is visualised as well as the fate of this nitrite: consumed by AnAOB, NOB or remained residual.

This study demonstrated that a clever combination of the recurrent multi-stressor floc treatment and other operational strategies (oxygen availability control, short floc age, and residual ammonium) can result in a good microbial activity balance with high AnAOB (71±21 mg N L^{-1} d^{-1}) and low NOB activity (4±17% of AerAOB) (Figure 2, Phase IIIa). The floc treatment was hereby essential and should be continuously applied to avoid NOB growth. No signs of NOB adaptation were observed over 104 days. Interestingly, NOB growth on the biofilm could successfully be avoided despite solely treating the flocs to safeguard AnAOB activity. The presence of sufficient AnAOB activity was hereby essential. These obtained results ease the implementation of mainstream PN/A, thus advancing the concept of energy neutrality in sewage treatment plants.

Table 1 Summary of the main performance indicators: TN removal rate and efficiency, effluent nitrite concentration, and estimated NOB activity.

Reactor phasing			TN removal		Effluent	Nitrite balance
Reactor	Phase	Period Days	$[NO_2^-]$ mg N L^{-1}	Efficiency %	$[NO_2^-]$ mg N L^{-1}	NOB activity % of AerAOB
R1	Ia	35-60	2.3 ± 0.7	39 ± 15	2.3 ± 0.7	11 ± 24
	Ib	61-68	2.4 ± 0.2	34 ± 8	2.4 ± 0.2	34 ±17
	IIa	69-76	1.8 ± 0.3	12 ± 8	1.8 ± 0.3	45 ± 17
	IIb	77-82	1.2 ± 0.2	14 ± 7	1.2 ± 0.2	33 ± 15
	IIc	83-96	1.8 ± 0.4	18 ± 13	1.8 ± 0.4	10 ± 21
	IIIa	97-138	2.2 ± 0.9	39 ± 9	2.2 ± 0.9	4 ± 17
	IIIb	139-143	3.3 ± 0.9	25 ± 4	3.3 ± 0.9	11 ± 9
	IV	144-188	1.9 ± 0.3	16 ± 13	1.9 ± 0.3	59 ± 35
R2	I	0-40	2.0 ± 0.8	14 ± 11	2.0 ± 0.8	77 ± 38
	IIa	41-59	1.8 ± 0.2	23 ± 4	1.8 ± 0.2	65 ± 12
	IIb	60-67	4.0 ± 1.2	28 ± 9	4.0 ± 1.2	63 ± 20
	IIIa	68-81	2.1 ± 0.7	18 ± 11	2.1 ± 0.7	68 ± 20
	IIIb	82-94	3.1 ± 0.9	19 ± 5	3.1 ± 0.9	53 ± 7
	IV	95-137	5.2 ± 2.0	22 ± 12	5.2 ± 2.0	42 ± 26
	V	138-142	2.2 ± 0.2	37 ± 7	2.2 ± 0.2	19 ± 4
	VI	143-188	2.5 ± 1.0	36 ± 17	2.5 ± 1.0	38 ± 23

REFERENCES

Agrawal S., Seuntjens D., De Cocker P., Lackner S. and Vlaeminck S. E. (2018). Success of mainstream partial nitritation/anammox demands integration of engineering, microbiome and modeling insights. *Current Opinion in Biotechnology* **50**, 214-21.
Erguder T. H., Boon N., Vlaeminck S. E. and Verstraete W. (2008). Partial Nitrification Achieved by Pulse Sulfide Doses in a Sequential Batch Reactor. *Environmental Science & Technology* **42**(23), 8715-20.
Jetten M. S. M., Horn S. J. and vanLoosdrecht M. C. M. (1997). Towards a more sustainable municipal wastewater treatment system. *Water Science and Technology* **35**(9), 171-80.
Lotti T., Kleerebezem R., Lubello C. and van Loosdrecht M. C. M. (2014). Physiological and kinetic characterization of a suspended cell anammox culture. *Water Research* **60**, 1-14.
Seuntjens D., Arroyo J. M. C., Van Tendeloo M., Chatzigiannidou I., Molina J., Nop S., Boon N. and Vlaeminck S. E. (2020). Mainstream partial nitritation/anammox with integrated fixed-film activated sludge: Combined aeration and floc retention time control strategies limit nitrate production. *Bioresource Technology* **314**, 10.
Seuntjens D., Van Tendeloo M., Chatzigiannidou I., Carvajal-Arroyo J. M., Vandendriessche S., Vlaeminck S. E. and Boon N. (2018). Synergistic Exposure of Return-Sludge to Anaerobic Starvation, Sulfide, and Free Ammonia to Suppress Nitrite Oxidizing Bacteria. *Environmental Science & Technology* **52**(15), 8725-32.
Strous M., Heijnen J. J., Kuenen J. G. and Jetten M. S. M. (1998). The sequencing batch reactor as a powerful tool for the study of slowly growing anaerobic ammonium-oxidizing microorganisms. *Applied Microbiology and Biotechnology* **50**(5), 589-96.
Van Tendeloo M., Bundervoet B., Carlier N., Van Beeck W., Mollen H., Lebeer S., Colsen J. and Vlaeminck S. E. Piloting carbon-lean nitrogen removal for energy-autonomous sewage treatment. *Environmental Science-Water Research & Technology*.
Wang Z. Y., Zheng M., Hu Z. T., Duan H. R., De Clippeleir H., Al-Omari A., Hu S. H. and Yuan Z. G. (2021). Unravelling adaptation of nitrite-oxidizing bacteria in mainstream PN/A process: Mechanisms and counter-strategies. *Water Research* **200**, 10.
Ye L. H., Li D., Zhang J. and Zeng H. P. (2019). Start-up and performance of partial nitritation process using short-term starvation. *Bioresource Technology* **276**, 190-8.

Sustainable Mainstream Deammonification by Ion Exchange and Bioregeneration via Partial Nitritation/Anammox

S. Tarre, S. Abasy, L. Gao and M. Green

Faculty of Civil and Environmental Engineering, Technion, Haifa, 32000, Israel
(E-mail: shelly@technion.ac.il; samah@campus.technion.ac.il; ga.lin@campus.technion.ac.il; agmgreen@technion.ac.il)

Abstract

The partial nitritation and anammox (PN/A) process has gained popularity for the treatment of nitrogen removal in wastewater due to significant energy savings and its potentially much lower CO_2 footprint. However, the treatment of mainstream wastewater by PN/A has been limited mainly due to its unsuitable composition. In this research, we apply ion exchange (IX) using a zeolite column to selectively remove and concentrate ammonium from mainstream wastewater. After an absorption phase, the IX column is regenerated using a brine solution. The ammonium rich brine is "bioregenerated" in a PN/A reactor where the ammonium is converted to nitrogen gas allowing the brine to be reused in another cycle of IX regeneration. To successfully remove ammonium from the spent brine, anammox and ammonia oxidizing bacteria (AOB) were first cultivated in separate reactors under saline conditions (4.0%) and later combined in a single PN/A reactor. After continuous operation with sea water, the PN/A reactor treated recirculating brine from the IX column for 48 cycles of ammonium absorption and bioregeneration with minimal blowdown. The various cations of the regenerant solution were stable except for calcium that reached very high values upwards of 3,000 mg/L as Ca^{+2} and finally caused PN/A reactor failure due to mineral precipitation. The build-up of high concentrations of calcium in the regenerant was addressed in two ways: 1) 20% regenerate replacement per cycle, and 2) precipitation of $CaCO_3$ via the addition of sodium carbonate. Both methods were applied to 30 absorption and bioregeneration cycles each and shown to be effective in keeping calcium concentrations from accumulating in the regenerant allowing for stable PN/A reactor operation.

Keywords

INTRODUCTION

While partial nitritation and anammox (PN/A) has been proven as an effective technology for nitrogen removal in municipal wastewater (MWW) side-stream treatment, the technology has not been effectively applied to the much larger market of mainstream MWW treatment. The main reasons for the limited implementation of the PN/A process for mainstream MWW are: 1) high COD/N ratio that encourages heterotrophic microbial growth with the accompanied short sludge age and washout of slow growing autotrophic bacteria, and also competition by denitrifying bacteria for nitrite; 2) lower temperatures with the resulting low conversion rates, and 3) low and fluctuating ammonium concentrations prevalent in mainstream MWW that further limit the extremely slow growing anammox bacteria. On the other side, PN/A offers an enormous potential towards reducing the CO_2 footprint through 1) energy savings for nitrogen removal, 2) better usage of the organic carbon, and 3) reduction of greenhouse gas emissions.

The strategy presented here to overcome the limitations of PN/A is based on an ion exchange (IX) and bioregeneration process for the selective removal and treatment of ammonium from mainstream MWW either before or after carbonaceous removal (see Fig. 1). MWW is passed through an IX column filled with natural zeolite that absorbs ammonium until exhaustion. The IX column is regenerated by passing a cation rich regenerant solution through the column desorbing the ammonium. The ammonium rich regenerant solution is treated in a PN/A biofilm reactor where ammonium is converted to nitrogen gas enabling the reuse and recycling of the regenerant. The premise for this strategy is that selective removal of ammonium from mainstream by IX eliminates competition from carbon removal and provides a desired ratio of COD:N for stable PN/A operation. Moreover, heating a smaller volume of brine to be treated and continually recycled is economically feasible and the much higher ammonium concentration obtained after IX can be used to control nitrite oxidizing bacteria (NOB). In this study, we present results from the operation of a lab scale combined ion exchange and bioregeneration process for ammonia removal from mainstream using partial nitritation/anammox.

Figure 1. Schematic diagram of the ion exchange – bioregeneration process for nitrogen removal. After organic carbon removal, wastewater first passes through the IX column and ammonium is absorbed (left side). After the absorption cycle, the IX column is regenerated with brine (right side). The brine is subsequently treated in a PN/A reactor for ammonium removal and is reused again for another cycle of IX column regeneration.

MATERIALS AND METHODS

Anammox bacteria and AOB biomasses were first enriched separately for treatment of the ammonium rich regenerant solution. Anammox bacteria were enriched under saline conditions (East Mediterranean Sea water, 4.0%) in 6 L continuous flow reactors filled with volcanic scoria and fed with a 1:1 ratio of nitrite to ammonium. Initial inoculum was sludge taken from a denitrification filter treating sea water aquaculture effluent. Growth of AOB for nitritation under saline conditions was carried out in similar reactors with pH control (pH 8.2) and free ammonia concentrations between 5 and 10 mg/L to selectively inhibit NOB. After biomass enrichment, AOB were harvested and added to a 20 L anammox reactor filled with 15 L of volcanic scoria receiving sea water amended with nitrite and ammonium. The feed solution was changed to ammonium only and a mixture of 2.5%/97.5% oxygen/nitrogen gas was sparged to the PN/A reactor to ensure low dissolved oxygen (DO) concentrations. The PN/A reactor temperature was 32°C.

Ion Exchange - Bioregeneration Experimental Setup. IX absorption and regeneration parameters were carried out for a natural zeolite (chabazite) with an IX capacity 2.5 to 3 meq/g (Lahav & Green, 1998). Simulated wastewater with a typical Israeli cation composition was used in the absorption experiments (see Table 1). Regeneration experiments were carried out with same sea water as above. A bench scale IX and bioregeneration system was constructed consisting of an IX column filled with 1 L of chabazite and the PN/A reactor mentioned above. The IX absorption cycle treated 200 L wastewater per cycle (200 bed volumes, BV) and run to maximize NH_4^+ absorption capacity, i.e. complete IX column breakthrough where influent N-NH_4^+=effluent NH_4^+ (higher quality effluent is obtained by running multiple IX columns in series). The IX regeneration cycle used 24 L (24 BV) brine (starting with sea water) per cycle with no blowdown except for the brine remaining in the column at field capacity at the completion of regeneration. Sodium lost during the absorption phase was replaced by adding NaCl to the regenerant and NaOH to the PN/A reactor for nitritation requirements. The IX regenerant was collected and treated batchwise to ensure a constant ammonium concentration. The PN/A reactor was continuously fed with regenerant brine at a flowrate of 10 L/day. Three (3) absorption/regeneration cycles were performed per week.

RESULTS AND DISCUSSION

Table 1 shows the average concentration of IX effluent for 48 absorption cycles of synthetic wastewater after 200 BV. 46.6% of the N-NH_4^+ and 52.5% calcium were removed from the wastewater, resulting in a concurrent rise in sodium by 100 mg/L in the effluent wastewater. This demonstrates the similar affinity ammonium and calcium have for chabazite (1.67 meq NH_4^+ absorbed vs 1.34 meq/L Ca^{+2} absorbed). Wastewater influent and effluent magnesium and potassium concentrations during ion exchange remained largely unchanged.

Fig. 2 shows the ammonium concentration of the ion exchange regenerant before and after treatment in the PN/A reactor throughout the 48 absorption cycles of synthetic wastewater. The average regenerant brine ammonium concentration for synthetic WW was 207.5 ± 12.7 mg/L. The brine regenerant was fed to the PN/A reactor and more than 90% of ammonium was successfully removed (average effluent of 12.7 ± 4.5 mg/L N-NH_4^+) at a removal rate of 0.13 gN/L-reactor/day. The nitrate build up in the recycled regenerant was a result of anammox activity. Microbial community analysis of the PN/A reactor by next generation sequencing (NGS) revealed an obligately halophilic anammox bacteria from the genus *Candidatus Scalindua* and AOB from the halotolerant genus of *Nitrosomonas*. No significant amount of NOB was observed as the ammonium concentration in the PN/A reactor was high enough and DO low enough to maintain inhibitory conditions for their growth. The constant and relatively high influent ammonium concentration allowed for stable PN/A operation for nearly all the experimental period along with stable potassium and magnesium concentrations in the regenerant. However, the build-up of calcium in the recycling regenerant (Fig. 3) to very high concentrations (3000 mg/L as Ca^{+2}) due to its high affinity for chabazite and minimal regenerant blowdown (approximately 1%) led to excessive mineral precipitation in the PN/A reactor and eventually impaired performance as evidenced by the appearance of N-NO_2^- concentrations. Reducing flow to the reactor did not improve reactor performance and the PN/A reactor had to be taken offline for recovery.

Table 1. Chemical composition (average) after 48 cycles of absorption/regeneration using synthetic wastewater and 30 cycles of actual secondary treated wastewater amended with ammonium.

Component	IN synthetic WW	OUT synthetic WW	IN real WW	OUT real WW
N-NH_4 mg/L	50.4 ± 1.9	26.9 ± 2.0	50.2 ± 1.4	30.9 ± 1.5
Ca mg/L as Ca^{+2}	51.0 ± 3.8	24.2 ± 6.9	90.2 ± 3.1	59.6 ± 3.7
Mg mg/L as Mg^{+2}	32.9 ± 4.1	33.4 ± 4.6	30.0 ± 0.7	30.3 ± 0.8
K^+ mg/L	26.7 ± 2.9	25.9 ± 3.5	36.6 ± 0.8	31.2 ± 0.5
Na^+ mg/L	116.4 ± 17.2	213.9 ± 18.0	148.9 ± 2.2	244.7 ± 4.7

The PN/A reactor was reseeded with AOB and anammox bacteria and after a period of continuous operation on sea water, the reactor was again ready to treat the regenerant brine. In this reactor run actual secondary treated wastewater amended with ammonium was used for 30 cycles (Table 1). The average regenerant brine ammonium concentration for real wastewater was 157.8±10.6 mg/L, lower than for synthetic wastewater due to the higher calcium content depressing ammonium absorption. The zeolite showed no reduction in absorption capacity due to potential fouling.

Stabilizing regenerant calcium concentration. Two methods were tested to arrest the increase of calcium in the recirculating regenerant. The first was regenerant replacement, i.e. 20% of the recycling regenerant solution was replaced after treatment in the PN/A reactor with fresh sea water. In this method there was no need to add NaCl to replace sodium lost during IX. The method was run for the 30 cycles when actual wastewater was used. Using regenerant replacement it took 15 cycles for the calcium concentration to increase from 490 mg/L (sea water) and then stabilize at 1879±39 mg/L as Ca^{+2}. The system was run for a further 15 cycles with no problem.

In the second method, calcium removal was carried out by precipitation using sodium carbonate (Zhou *et al.*, 2021). Here a dose of between 0.8 and 1 gram of sodium carbonate per liter of regenerant was given after IX column regeneration just before entering the reactor. The method was run for a further 30 cycles using synthetic wastewater based on the higher Ca^{+2} concentration of actual secondary wastewater used earlier during regenerant replacement. The average Ca^{+2} concentration before IX column regeneration was 1838±42 mg/L and 2130±33 mg/L after regeneration. The average Ca^{+2} after adding Na_2CO_3 was 1858±50 mg/L for an average precipitation of 280±50 mg/L Ca^{+2} per liter regenerant. Excess alkalinity remaining after the addition of sodium carbonate was neutralized to between 40 and 60 mg/L to prevent any further $CaCO_3$ precipitation in the reactor and leave enough inorganic carbon for the autotrophic bacteria. Both methods were shown to be effective in keeping calcium concentrations from accumulating in the regenerant and allowed for stable PN/A reactor performance and continued process operation.

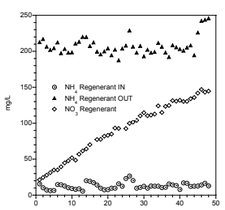

Figure 2. Regenerant N-NH_4 concentration before and after PN/A reactor. Increase in N-NO_3 was due to the anammox activity.

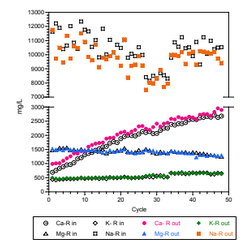

Figure 3. Cation composition of regenerate before and after PN/A reactor treatment.

REFERENCES

Lahav, O., Green, M. 1998 Ammonium removal using ion exchange and biological regeneration. *Water Research* **32**(7), 2019-2028.

Zhou, Z., Wang, K., Qiang, J., Pang, H., Yuan, Y., An, Y., Zhou, C., Ye, J., Wu, Z. 2021 Mainstream nitrogen separation and side-stream removal to reduce discharge and footprint of wastewater treatment plants. *Water Research* **188** (116527), 1-10.

Mainstream Aerobic Granular Sludge start-up from HRAS effluent targeting partial nitritation

O. Carbó*,**, J. Teixidó*, J. Canals*, A. Ordóñez*, A. Magrí**, M. Baldi*, B. Gutiérrez* and J. Colprim**

* GS Inima Environment, S.A. c/ Gobelas 41 1ª 28023, Madrid. Spain
(E-mail: *oriol.carbo@inima.com)*
** LEQUIA. Institute of the Environment. Universitat de Girona. c/Maria Aurèlia Capmany 69, 17003 Girona. Catalonia. Spain

Abstract

Energy efficiency in WWTP can be significantly improved by maximising biogas production while minimising energy demand. One suitable option is a first organic matter redirection to anaerobic digestion followed by autotrophic nitrogen removal using granular biomass. In this paper, the results obtained during the start-up of an AGS reactor fed with a HRAS effluent are presented. Aerobic granulation targeting partial nitritation is addressed by elucidating key operational parameters. The study shows that solids wasting strategy is the key point in aerobic granulation, being a selective purge from the top of the settled sludge bed the best option. Partial nitritation with no nitrate formation is reported, being FNA the main responsible for NOB inhibition.

Keywords

AGS; mainstream, HRAS; energy efficiency; PAO; partial nitritation

INTRODUCTION

Currently, urban wastewater treatment plants (WWTP) are net energy-consumption systems that represent 3% of the global electricity consumption (Li et al. 2015). In the quest to achieve operational self-sufficiency and sustainability, technologies based on a first organic matter redirection to anaerobic digestion (i.e high-rate activated sludge systems, HRAS) followed by autotrophic nitrogen removal using granular biomass have been proposed to maximise biogas production while minimising energy demand (Coma et al., 2011; Cao et al., 2017; Canals et al., 2023). Kosar et al. (2023) coupled HRAS effluent with AGS at lab scale with a good settling property (SVI_{30}=45 mL/gr) but not granular sludge (SVI_5/SVI_{30}=1.44) and focused to achieve full nitrification with nitrogen removal. Efforts have been conducted to achieve autotrophic nitrogen removal in mainstream, where the two-stage process seems to be a more promising option to achieve a successful autotrophic nitrogen removal (Akaboci et al., 2020; Hoekstra et al., 2019)which results in an excess of IC for full nitritation, the oxidized ammonium fully nitrified, and nitrite accumulation was not reached. Limiting influent IC (influent NH4+-N/IC of 0.73 ± 0.03 mg N·mg C−1. The first stage should be devoted to obtain a partial nitritation with a suitable nitrite to ammonia ratio (close to 1.32 $N\text{-}NO_2^-$:$N\text{-}NH_4^+$) while removing the biodegradable organic matter. The second stage should focus on anaerobic autotrophic deamonification (Anammox process). In this paper we present the results obtained during the start-up of an Aerobic Granular Sludge (AGS) fed with the effluent of a HRAS reactor operation at full scale conditions (hourly variation of wastewater quality and temperature for 620 days). First, we address the aerobic granulation process from CAS seeding and secondly the partial nitritation to achieve a suitable anammox reactor influent.

MATERIALS AND METHODS

An 880 L sequencing batch reactor was operated 620 d for AGS development treating the effluent of a HRAS reactor working at real conditions (location: La Garriga WWTP, Catalonia, Spain). Cycle phases comprised i) simultaneous fill/draw (F/D), ii) anaerobic and aerobic reaction and iii) settling. The applied volumetric exchange ratio (VER) was 50%, dissolved oxygen (DO) concentration in aerobic phases was maintained over 2.0 mg/L and total cycle length ranged from 160 to 360 minutes. The SBR was inoculated at day 0 with floccular sludge from a conventional activated sludge system. COD removal efficiency in the HRAS system was 43 ± 15 %. HRAS effluent composition was COD: 406 ± 82 mg/L, NH_4^+-N: 40 ± 14 mg/L, PO_4^{3-}-P: 4.5 ± 1.6 mg/L and alkalinity: 340 ± 56 mg $CaCO_3$/L. No temperature control was applied, ranging from 13 to 26ºC during the whole operation.

RESULTS AND DISCUSSION

To develop AGS, the operation was divided in 3 periods (Table 1). In Period I, granulation strategy was focused in flocs washout during F/D phase by providing an increasing upflow ascensional velocity (v_{asc}) from 2.3 to 4.5 m/h while reducing settling phase from 30 to 5 minutes. Total suspended solids (TSS) in the reactor remained stable around 3 g/L (SRT=4 d) and the sludge volume index (SVI) ranged from 100 to 150 mL/g until day 170, when first granules appeared. Afterwards, TSS increased up to 8 g/L and SVI decreased up to 40 mL/g. First granules were big and had finger-type outgrowth (Figures 1, 2.A and 4). Decreased temperatures due to winter conditions reduced the whole biomass settleability at the end of Period I, which lead to biomass washout (Figures 1 and 4). In order to remove floccular biomass, a once a day manual purge at the end of a settling phase was introduced in Period II. At this time, TSS were low (<2 g/L) while SVI ranged from 50 to 100 mL/g. SRT was as low as 1.1 days. AGS could not develop under these conditions (Figures 2.B and 4) since biomass washout was too severe and unselective. In this context, Period III was characterised by the implementation of an automatic selective purge from the top of the settled sludge bed at the end of every settling phase. At that point, granulation process started and perfect granules were formed (Figure 2.C). TSS reached values of 6 g/L and SVI 20 mL/g. SRT increased to 15-18 d. Moreover, the ratio SVI_5/SVI_{30} reached values of 1.0, being indicative of the high predominance of AGS (Figure 4).

Regarding nitrification, partial nitritation with no nitrate formation was observed in Period I and III. It has been reported the important role and the sensibility of microorganisms to FNA in biological nutrient removal processes (Pijuan et al. 2010)phosphorus removal typically occurs together with nitrogen removal. Nitrite, an intermediate of both the nitrification and denitrification processes, can accumulate in the reactor. The inhibitory effect of nitrite/free nitrous acid (FNA. FNA values of 0.030 mg N/L can lead to a 50% inhibition in nitrite oxidation, according to Blackburne et al. (2007). High FNA concentrations up to 0.075 mg N/L were obtained in the reactor during aerobic phases (Figure 3) and could be responsible for the inhibition of nitrite oxidizing bacteria (NOB) growth in the AGS reactor. Thus, in Period I and III, FNA inhibition to NOB could have prevented nitrate formation in the reactor.

The main outcomes from this paper are: i) selective biomass washout from the top of the sludge bed rather than F/D biomass washout is responsible for a successful aerobic granular formation and ii) partial nitritation can be achieved during aerobic phase if a suitable FNA concentration is achieved to avoid NOB development.

REFERENCES

Akaboci, T. R. V., Ruscalleda, M., Balaguer, M. D., Colprim, J. 2020 Achieving nitratation repression in an SBR at mainstream conditions through inorganic carbon limitation. *International Biodeterioration and Biodegradation*, **147**(November 2019), 104865.

Blackburne, R., Vadivelu, V.M., Yuan, Z., Keller, J. 2007 Kinetic characterisation of an enriched *Nitrospira* culture with comparison to *Nitrobacter*. *Water Research* **41**, 3033–3042.

Canals, J., Cabrera-Codony, A., Carbó, O., Torán, J., Martín, M., Baldi, M., Gutiérrez, B., Poch, M., Ordóñez, A., Monclús, H. 2023 High-rate activated sludge at very short SRT : Key factors for process stability and performance of COD fractions removal. *Water Research* **231**, 119610.

Cao, Y., van Loosdrecht, M.C.M., Daigger, G.T. 2017 Mainstream partial nitritation–anammox in municipal wastewater treatment: status, bottlenecks, and further studies. *Applied Microbiology and Biotechnology* **101**, 1365–1383.

Coma, M. 2011 *Biological Nutrient Removal in SBR Technology: from Floccular to Granular Sludge*. PhD Thesis. University of Girona.

Hoekstra, M., Geilvoet, S. P., Hendrickx, T. L. G., van Erp Taalman Kip, C. S., Kleerebezem, R., & van Loosdrecht, M. C. M. 2019 Towards mainstream anammox: lessons learned from pilot-scale research at WWTP Dokhaven. *Environmental Technology*, **40**(13), 1721–1733.

Kosar, S., Isik, O., Cicekalan, B., Gulhan, H., Cingoz, S., Yoruk, M., Ozgun, H., Koyuncu, I., van Loosdrecht, M.C.M., Ersahin, M.E., 2023 Coupling high-rate activated sludge process with aerobic granular sludge process for sustainable municipal wastewater treatment. J. Environ. Manage. **325**, 116549.

Li, W.-W., Yu, H.-Q., Rittmann, B.E. 2015 Chemistry: Reuse water pollutants. *Nature*, **528**, 29–31.

Pijuan, M., Ye, L., Yuan, Z. 2010. Free nitrous acid inhibition on the aerobic metabolism of poly-phosphate accumulating organisms. *Water Research*, **44**(20), 6063–6072.

Table 1. Relevant SBR phases length and operational parameters applied at the different periods.

Period	Day (d)	SBR phases length (min)				F/D v_{asc} (m/h)	Solids wasting
		F/D	Anaerobic	Aerobic	t_{set}		
I	0 - 300	60 - 30	0 - 30	68 - 105	30 - 5	2.3 - 4.5	Effluent
II	301 - 448	30	30	105 - 100	10	4.5	Lateral
III	449 - 620	30 - 60	0	100 - 269	30	4.5 - 2.3	Selective

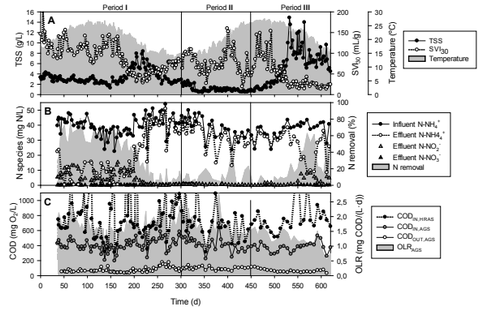

Figure 1. A: TSS, SVI_{30} and temperature in the reactor. B: N species concentration and N removal efficiency in the reactor. C: HRAS influent, AGS influent (HRAS effluent) and AGS effluent COD concentrations and OLR in the AGS reactor.

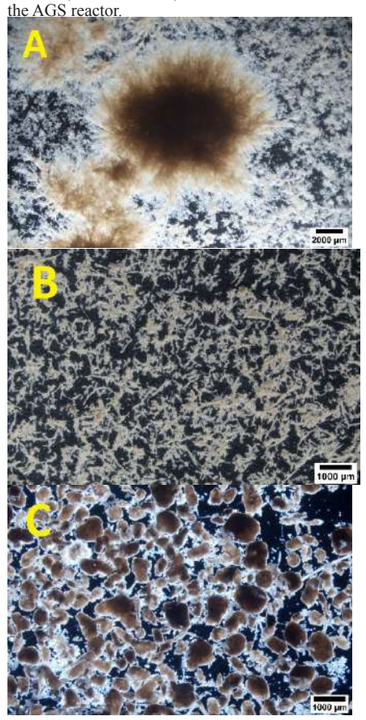

Figure 2. Stereoscopic microscope images of the biomass. A: day 200 (Period I). B: day 344 (Period II). C: day 596 (Period III).

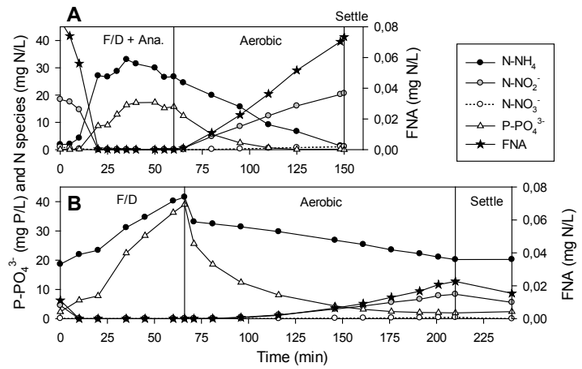

Figure 3. N species and P concentrations at 1/3 reactor's height from representative SBR cycles.
A: day 70 (Period I). B: day 556 (Period III).

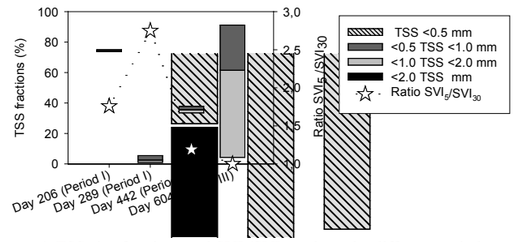

Figure 4. TSS size fractions and SVI_5/SVI_{30} ratio at the different periods.

Sensitivity of anammox bacteria under mainstream conditions: combined effect of low temperature and pH with inhibitory concentrations of free ammonia/free nitrous acid

A. Pedrouso*, J. Blanco*, J.L. Campos**, J.R. Vázquez-Padín***, A. Val del Río* and A. Mosquera-Corral*

* Department of Chemical Engineering, CRETUS Institute, School of Engineering, Universidade de Santiago de Compostela, Rua Lope Gomez de Marzoa, E-15782. Santiago de Compostela, Spain.
(E-mail: *alba.pedrouso@usc.es*; *blancobellon@gmail.com*; *mangeles.val@usc.es; anuska.mosquera@usc.es)*
** Facultad de Ingeniería y Ciencias, Universidad Adolfo Ibáñez, Avda. Padre Hurtado 750, Viña del Mar, Chile.
(E-mail: *jluis.campos@uai.cl*)
*** Aqualia, Av. Del Camino de Santiago, 40, E-28050, Madrid, Spain.
(E-mail: j*vazquezp@fcc.es*)

Abstract
The anammox bacteria (AMX) sensitivity, especially at low temperatures, hinders its application. In this research work the effects of pH and concentrations of ammonium, free ammonia, nitrite and free nitrous acid (FNA) on the specific anammox activity (SAA), at different temperatures were investigated. Results showed a decrease of SAA by 30% per every 5 °C. AMX are particularly sensitive to low pH. At a pH of 6.5, SAA decrease to 50% and 65% at 20 and 30 °C, respectively. FNA plays an important role in the inhibition of SAA, since SAA drops to 65%, at 30 °C and pH 6.5, when using 30 mg N/L as substrate (FNA=18 µg N/L) and to 15% with 70 mg N/L (FNA=54 µg N/L). Therefore, for process robustness, operational strategies should be adapted to avoid feeding acidic nitrified waters into AMX reactors.

Keywords
Activity; anammox; free nitrous acid, inhibition; mainstream; pH.

INTRODUCTION

The combined use of partial nitritation (PN) and anammox (AMX) processes has attracted interest in the search for more energy-efficient nitrogen removal in wastewater treatment plants (WWTPs). Although intensive research has been conducted to implement PN/AMX processes in the mainstream of WWTPs, several issues still need to be addressed. For example, AMX are known to be sensitive and slow growing, especially at low temperatures (Wang et al., 2022).

The two-stage configuration allows the PN and AMX processes to be optimised separately. pH and temperature are two key parameters for the AMX process, as they control the equilibria between ammonium-free ammonia (FA) and nitrite-free nitrous acid (FNA). The effects of FA and FNA on AMX activity have been extensively studied (Carvajal-Arroyo et al., 2014, Fernandez et al. 2012). However, these values vary greatly between studies and have been determined mainly at higher temperatures than those prevailing in the mainstream of a WWTP.

This study aims to research the sensitivity of AMX bacteria to environmental conditions. In particular, this research investigates the effects of pH and ammonium, nitrite, FA and FNA on specific anammox activity (SAA) at different temperatures.

MATERIALS AND METHODS

The SAA, expressed as g N/(g VSS·d), was determined in batch tests, performed in triplicate, in 38 mL-vials with a working volume of 25 mL. The maximum SAA was measured at 30 ºC, pH 7.8 and 70 mg N/L (of each nitrite and ammonium) (Dapena-Mora et al. 2007). First, three temperatures (20, 30 and 35 °C) were tested varying ammonium and nitrite concentrations (30 - 140 mg N/L of each) at pH 7.8 (Table 1). Later, different pH values (6.5 - 8.0; adjusted with phosphate buffer) were tested at 20 and 30 °C and two substrate concentrations (30 and 70 mg N/L of each) (Table 1). AMX-enriched biomass was taken from a lab-scale reactor operated at 30 °C and treating a nitrogen loading rate of 1.13 g N/(L·d). The percentage of activity remaining in the inhibition tests was calculated as %SAA= SAA/SAA_0*100 (where SAA_0 is the maximum SAA measured in a set).

RESULTS AND DISCUSSION

SAA is strongly temperature dependent, with a 33% increase measured from 30 °C (the temperature at which biomass was grown) to 35 °C (Fig. 1). SAA decreased by 61% from 30 to 20 °C. Substrate concentration (30 -140 mg N/L, each) did not significantly affect SAA (Fig. 1). The lowest reported inhibition values, at 30 °C, were 38 mg FA-N/L (50% of SAA loss) and 4.4 µg FNA -N/L (70% of SAA loss) (Fernandez et al. 2012). In these tests, FA concentrations ranged from 0.7 – 9.4 mg N/L and FNA from 0.8 to 5.7 µg N/L (Table 1). Thus, FA is below the inhibition thresholds, but FNA could have negative effects that do not appear to be temperature dependent.

In assays with different pH values performed at 20 and 30 °C, the maximum SAA was measured at pH 7.5 (Fig. 2A). While the loss of SAA at a pH of 8.0 was similar at both temperatures, AMX was more sensitive to a decrease in pH at lower temperatures. Ammonium and nitrite concentrations linearly modify FA and FNA, whereas pH affects them exponentially (low pH favours FNA accumulation and high pH values that of FA) (Table 1). Therefore, it is difficult to determine whether pH or FNA is responsible for the decrease in SAA at low pH. The loss of SAA at pH 6.5 is greater at higher nitrogen concentrations (higher FNA) (Fig. 2. B). For example, at 30 °C, the %SAA is 65% at 30 mg N/L (18 µg FNA-N/L), while it is less than 15% at 70 mg N/L (54 µg FNA-N/L) (Fig. 2B). A clear relationship was observed between the %SAA and FNA concentrations (Fig. 2B), confirming that FNA is mainly responsible for AMX inhibition at low pH.

PN systems often generate wastewater with low pH and moderate nitrite concentrations. Although SAA decreased at low pH, AMX are still active. To ensure the robustness of the process, the operating strategies of the AMX reactors should be adjusted to avoid shocks during feeding.

Acknowledgements
This work was funded by the European Comission (EU) through the LIFE ZERO WASTE WATER project (LIFE19 ENV/ES/000631). A. Pedrouso also acknowledge the Xunta de Galicia (Spain) for her postdoctoral fellowship (ED481B-2021-041). The authors from the Universidade de Santiago de Compostela belong to the Galician Competitive Research Group (GRC D431C-2021/37).

REFERENCES

Carvajal-Arroyo, J.M., Puyol, D., Li, G., Sierra-Alvarez, R., Field, J.A. 2014. The role of pH on the resistance of resting- and active anammox bacteria to NO2 inhibition. *Biotechnology and Bioengineering* **111**(10), 1949-1956.

Dapena-Mora A., Fernadez I., Campos J.L, Mosquera-Corral A., Mendez R. and Jetten M. S. M. 2007. Evaluation of activity and inhibition effects on Anammox process by batch tests based on the nitrogen gas production. *Enzyme and Microbial Technology* **40**(4), 859-865.

Fernandez, I., Dosta, J., Fajardo, C., Campos, J.L., Mosquera-Corral, A., Méndez, R. 2012. Short- and long-term effects of ammonium and nitrite on the anammox process. *Journal of Environmental Management* **95**, 170-174.

Wang, L., Gu, W., Liu, P., Zhang, X., Huang, X. 2022. Challenges, solution and prospects of mainstream anammox-based process for municipal wastewater treatment. *Science of The Total Environment,* **850**, 153351.

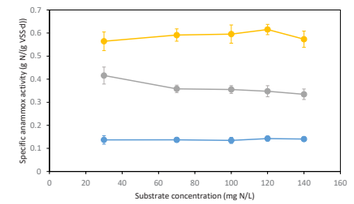

Figure 1. Influence of nitrogen concentration (expressed for ammonium and nitrite, separately) on the specific anammox activity (SAA) at different temperatures: 20 °C (●), 30 °C (●) and 35 °C (●).

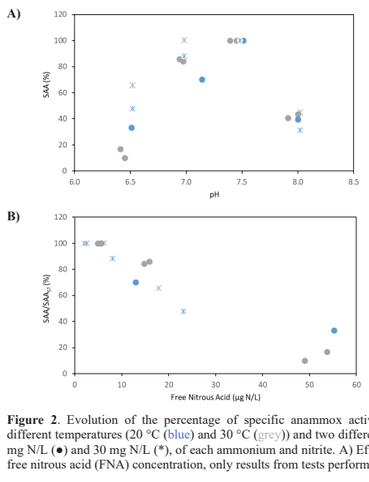

Figure 2. Evolution of the percentage of specific anammox activity that remains (%SAA) at different temperatures (20 °C (blue) and 30 °C (grey)) and two different nitrogen concentrations: 70 mg N/L (●) and 30 mg N/L (*), of each ammonium and nitrite. A) Effect of the pH; B) Effect of the free nitrous acid (FNA) concentration, only results from tests performed at pH ≤ 7.5 were used.

Table 1. Description of the batch activity tests performed and free ammonia (FA) and free nitrous acid (FNA) concentrations at the beginning of the executed tests.

Temperature (ºC)	pH	Ammonium and nitrite (mg N/L)	FA (mg N/L)	FNA (µg N/L)
Effect of temperature and nitrogen concentrations				
20	7.8	30	0.738	1.215
20	7.8	70	1.721	2.835
20	7.8	100	2.459	4.049
20	7.8	120	2.950	4.859
20	7.8	140	3.442	5.669
30	7.8	30	1.468	0.938
30	7.8	70	3.426	2.188
30	7.8	100	4.895	3.126
30	7.8	120	5.874	3.751
30	7.8	140	6.853	4.376
35	7.8	30	2.022	0.829
35	7.8	70	4.719	1.935
35	7.8	100	6.741	2.764
35	7.8	120	8.089	3.317
35	7.8	140	9.437	3.870
Effect of pH value and FA and FNA concentrations				
30	6.5	70	0.180	43.661
30	7.0	70	0.566	13.807
30	7.5	70	1.760	4.366
30	8.0	70	5.279	1.381
30	6.5	30	0.077	18.712
30	7.0	30	0.243	5.917
30	7.5	30	0.754	1.871
30	8.0	30	2.263	0.592
20	6.5	70	0.088	56.558
20	7.0	70	0.279	17.885
20	7.5	70	0.873	5.656
20	8.0	70	2.689	1.789
20	6.5	30	0.038	24.239
20	7.0	30	0.119	7.665
20	7.5	30	0.374	2.424
20	8.0	30	1.152	0.767

Nitrogen Removal/Recovery in the mainstream of a WWTP including ultrafiltration after the primary treatment: Partial Nitrification+Anammox vs. Ion Exchange+Hollow fiber membrane contactors

J. Godifredo*, L. Ruiz*, R. Barat*, J. Ferrer* and A. Seco**

* IIAMA, Universitat Politècnica de València, Camí de Vera, s/n, 46022 Valencia, SP
(E-mail: *jegocal@cam.upv; lruicos@cam.upv.es; rababa@dihma.upv.es; jferrer@hma.upv.es)*
**CALAGUA Mixed research unit UV-UPV, Universitat de Valencia, Avinguda de l'Universitat, 46100 Burjassot, SP
(E-mail: aurora.seco@uv.es)

Abstract
Two new wastewater treatment alternatives focused on resource recovery are proposed. In both scenarios, after the primary treatment, the raw water is treated by means of Ultrafiltration (UF) membrane to increase the organic matter valorisation as biogas in the sludge line. The nitrogen obtained from the permeate can be removed through a Partial Nitrification (PN) process followed by an Anammox stage, allowing the use of existing facilities and reducing the energy consumption of the aeration of the biological treatment. Another alternative consists on the nitrogen recovery in the form of fertilizer. For this purpose, in a first step the ammonium is concentrated in an ion exchange (IE) stage and subsequently valorised by means of a hollow fiber membrane contactor (HFMC).

Análisis de dos alternativas de eliminación de nitrógeno

Keywords
Ammonium removal and recovery, Anammox, Ion exchange, Partial Nitrification, Ultrafiltration, Zeolite

INTRODUCTION

Conventional wastewater treatment plants (WWTPs) has been identified as a process with high energy demand, in addition, a large part of the resources present in the water cannot be recovered following this treatment (McCarty et al., 2011). The growing pressure on water resources, the need to reduce energy consumption and increasingly strict discharge requirements have caused the study of new treatment alternatives to involve transforming WWTPs into water resource recovery facilities (WRRF). However, these alternatives usually imply huge modifications in the present WWTP. In this work, two treatment alternatives are proposed, making modifications to existing infrastructures to enhance the recovery of wastewater resources. Both scenarios (Figure 1) include a Carbon redirection technology (UF process) to maximize biogas production, followed by A) IE-HFMC to recover nitrogen as a fertilizer and B) a Partial Nitrification-Anammox biological stage to remove nitrogen in existing reactors but with lower energy cost.

MATERIALS AND METHODS

Experimental works have been carried out in a pilot plant located in Carraixet WWTP, Valencia. The ultrafiltration plant (0.03 µm pore size) was fed with real wastewater at 320 L/h. The characterization of the inlet water and the permeate obtained are shown in Table 1.

Partial Nitrification was studied in a 15L sequencing batch reactor (SBR) coupled to a 1L UF membrane to decouple the hydraulic and sludge residence time. A diagram of this pilot plant is shown in figure 2. In this reactor, the main mechanisms to stop the oxidation of NH_4 into NO_2 and generate an effluent suitable for the Anammox process were analysed.

According to previous studies and taking into account the high hardness of the working water and the affinity of the different adsorbent materials for ammonium and divalent cations (Zhou et al., 2021), the cation exchange columns were filled with Na-activated natural zeolites (Na-Z). A laboratory-scale set-up of 110ml of Bed Volume (BV) was carried out to evaluate the feasibility of concentrating ammonium from the UF permeate of wastewater. Also, the regeneration phase was studied to obtain a concentrated current in nitrogen valid for the HFMC. The diagram of this set-up is shown in figure 3.

RESULTS AND DISCUSSION

Partial Nitrification

PN could be carried out in the mainstream controlling the nitrite-oxidizing bacteria (NOB) growth to avoid NO_2 oxidation into NO_3. The pH and ammonia inhibition were not used for process control due to the high alkalinity and low ammonia concentration of the working water, which favours the complete oxidation into NO_3 (Pedrouso et al., 2017). Other mechanisms were used to favour ammonium-oxidizing bacteria (AOB) growth over NOB, such as the aerobic phase duration control and maintaining low dissolved oxygen levels between 0.3 -0.6 mg O_2/L. Despite the high accumulation of NO_2 reached (Figure 4), it is necessary a further work to guarantee the process stability.

The viability of this alternative supposes being able to maintain part of the existing biological reactors in the current WWTPs to carry out the PN. In addition, since there is hardly any organic matter to be oxidized and only part of the NH_4 is converted into NO_2, the energy consumption associated with aeration will be significantly reduced. If it is not possible to control the amount of oxidized ammonium during the PN and decreases the NH_4:NO_2 ratio necessary for the Anammox process, a bypass stream can be used in order to adjust the NH_4:NO_2 ratio in the influent to the Anammox process (Figure 1b).

Ion Exchange

Zeolite column proved to be able to concentrate ammonium up to 30 times, obtaining an ammonium stream at a concentration of 760 mg N-NH_4/L treating 180BV until achieva a concentration of 0.5 mg N-NH_4/l in the effluent (Figure 5). In addition, the use of NaOH as a regenerant allows to increase the pH in the concentrated stream above 12, leading the nitrogen to NH_3 form. The high concentration of ammonium and high pH makes this stream an ideal influent for HFMC process, where nitrogen is finally recovered in the form of fertilizer, such as $NH_4(SO_4)_2$ (Figure 1a).

This treatment train not only allows to valorize the nitrogen present in wastewater, but also has other advantages over conventional biological treatment: it is not conditioned by temperature and flow variations due to it is a modular physical-chemical process. However, the consumption of reagents such as NaOH and H_2SO_4 must be taken into account.

ACKNOWLEDGMENTS

The authors would like to acknowledge the Ministry of Science and Innovation for supporting the project "RECREATE" (PID2020-114315RB-C22) and "MEM4REC" (CTM2017-86751-C2-2-R-AR) where this research is framed and the Ministry of Universities for financial the research contract of the first author (FPU17/00540).

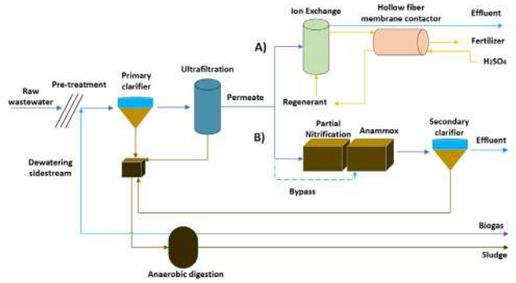

Figure 1. Diagram of the two proposed treatment alternatives A) integrating an IE process, B) transforming the conventional biological process into PN-Anammox stages

Table 1. Characterization of the raw wastewater and Ultrafiltration permeate

Stream	Raw wastewater	Permeate
mg NH_4^+-N/L	27±4	27±4
mg PO_4^{3-} /L	4.5±1.2	3.2±0.9
mg COD/L	172±25	40±20
mg BOD/L	103±13	12±3
mg TSS/L	100±23	N.D.
pH	7.3	7.3

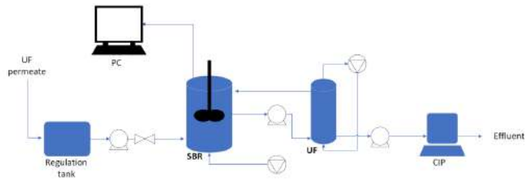

Figure 2. Partial Nitrification pilot plant

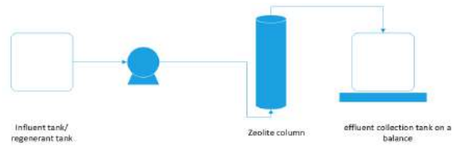

Figure 3. Laboratory set-up of Ion exchange process

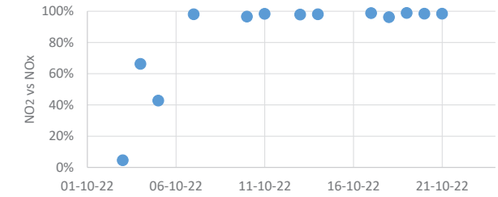

Figure 4. NO_2 accumulation during an experimental test

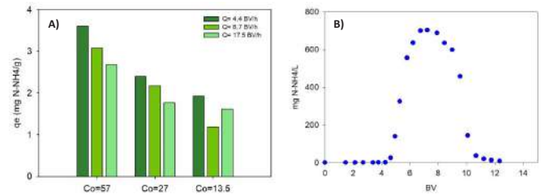

Figure 5. A) Influence of treatment flow and ammonium concentration on the ammonium adsorption capacity and B) Ammonium concentration obtained in the regeneration phase under working conditions with better regenerative capacity (NaOH= 0.1M and Q=4.4 BV/h).

REFERENCES

McCarty, P. L., Bae, J., & Kim, J. (2011). Domestic Wastewater Treatment as a Net Energy Producer–Can This be Achieved? *Environmental Science & Technology*, *45*(17), 7100–7106.

Pedrouso, A., Val del Río, Á., Morales, N., Vázquez-Padín, J. R., Campos, J. L., Méndez, R., & Mosquera-Corral, A. (2017). Nitrite oxidizing bacteria suppression based on in-situ free nitrous acid production at mainstream conditions. *Separation and Purification Technology*, *186*, 55–62.

Zhou, C., An, Y., Zhang, W., Yang, D., Tang, J., Ye, J., & Zhou, Z. (2021). Inhibitory effects of Ca2+ on ammonium exchange by zeolite in the long-term exchange and NaClO–NaCl regeneration process. *Chemosphere*, *263*, 128216.

Influence of free nitrous acid on nitrifiers to introduce shortcut nitrification in the mainstream of WWTP

E. Łaskawiec, F. Gamoń, A. Ziembińska-Buczyńska, M. Ćwiertniewicz-Wojciechowska, Joanna Surmacz-Górska and G. Cema*

* Department of Environmental Biotechnology, Silesian University of Technology, Akademicka 2, Gliwice, Poland
(E-mail: *edyta.laskawiec@polsl.pl*)

Abstract

The paper presents the possibilities of using free nitrous acid (FNA) to conduct the shortcut nitrification process in the mainstream wastewater treatment plant; this will be achieved, among other things, by inhibiting nitrite-oxidizing bacteria (NOB) by FNA in a separate reactor (selector). The effect of free nitrous acid contact time and concentration on the activity of nitrifiers of the first and second nitrification phases is presented. The research subject was samples of activated sludge taken from the municipal sewage treatment plant.

Keywords

Shortcut nitrification; activated sludge; free nitrous acid; nitrite-oxidising bacteria; NOB

INTRODUCTION

Many municipal wastewater treatment plants (WWTPs) receive wastewater with a low C/N ratio; an insufficient carbon source can reduce the denitrification process and leave a relatively high nitrogen load. The use of so-called nitrite pathways represents a modification of biological nitrogen removal processes, as it reduces the need for a carbon source by 40% and aeration by 25% (Rodriguez-Garcia et al., 2014). It is still challenging to achieve a stable performance of the nitrite pathway, i.e., suppressing or leaching nitrite-oxidizing bacteria (NOB) while developing ammonium-oxidizing bacteria (AOB). Shortening the nitrification process in mainstream WWTPs remains challenging due to low nitrogen concentrations and temperatures. However, it has been shown that using FNA allows for maintaining stable development of AOB, unrestricted by aeration systems, and that FNA production from liquid anaerobic digestion is sustainable and economically beneficial (Duan et al., 2018). However, due to low nitrogen concentrations in municipal wastewater, an adequate concentration of FNA cannot be achieved. However, it is possible to produce nitrite in a side stream on the reject water and then mix it with activated sludge in a particular selector reactor (Fig. 1). Such an assumption is being tested in the shortened nitrification in the mainstream results in nitrites instead of nitrates in the outflow of the treatment plant (SNIT) project. The determination of FNA treatment conditions is still unclear, as some studies have shown the adaptation of NOB to FNA in the past (Ma et al., 2017). The study aimed to determine the optimal parameters of NOB inhibition (FNA concentration, contact time, pH) based on activity in short laboratory tests..

MATERIALS AND METHODS

Oxygen uptake rate (OUR) measurements

A conventional fed batch respirometer with a small closed reactor vessel was used for the measurements. The respirometer contained an oxygen electrode connected to a program for automatic recording of readings. The measurement of activity was verified in accordance with the methodology presented in Surmacz-Górska *et al.*, 1995. Allylthiourea (ATU) and sodium azide/sodium chlorate solutions were used as a selective nitrification inhibitors. The activated sludge for OUR measurements was taken from WWTP. Experiments were carried out in the range of pH from 5.5 to 7.0 and FNA concentration 0.004÷2.3 mgHNO_2-N/L. The AOB and NOB activities after FNA treatment were measured. The response of the tested nitrification inhibitors was compared.

Batch tests

The activated sludge collected from municipal WWTP, was treated with 2.3 mgHNO_2-N/L FNA concentration. The test with adding 0 mg HNO_2-N/L was a control test (pH was 7.0±0.2). The pH value was controlled at 6.0±0.2 by adding 1.0 M HCl or 1.0 M NaOH. Experiments of FNA treatment were carried out for 2, 4, 16, 18, 20, 24 h, under anoxic conditions (T=21±2 °C; constant stirring). After FNA batch treatment, activated sludge was washed for three times in a centrifuge at 3600 rpm for 4 min to remove nitrite. Then, in the second part of the experiment the sludge was stirred, in aerobic conditions (DO = 0.5÷1.5 mgO_2/L) with 0.004 mgHNO_2-N/L of FNA (pH was 7.0±0.2), for 2 h. The AOB and NOB activities after FNA treatment were measured and represented as percentage of activities compared to the control test. The effect of FNA treatment time on AOB and NOB was also investigated.

RESULTS AND DISCUSSION

NOB activity expressed as a relative percent activity decreased after sludge FNA treatment. However, also in the case of AOB activity, the value deteriorated. In the low FNA concentration range, it was challenging to demonstrate the effect of contact time on NOB inhibition; for example, at FNA = 0.2 mgHNO_2-N/L and pH=7.0, the extension of the contact time from 1 to 2 h resulted in an increase in relative activity from 86.73 to 64.99%. At the same time, some analyses noted a decrease in AOB activity (Fig. 2a). A major problem of the conducted OUR measurements was the lack of repeatability of the results. The activated sludge for the tests was each time taken from a real facility, so the condition and conditions of the processes could change (Fig 2a-c). Vadivelu et. al. 2007, showed that FNA concentration of 0.40–0.63 mgHNO_2-N/L inhibited NOB culture by 50%. During the measurements of the oxygen uptake rate, the possibility of using various inhibitors of the nitrification process was tested, no significant effect on the final results was demonstrated. OUR tests are quick and easy-to-use tests that report AOB and NOB activity, but the authors have noted big problems with the reproducibility of the results. In batch tests, on the other hand, it has been shown that the most effective contact time for NOB inhibition is 18h, with an FNA concentration of 0.4 mgHNO_2-N/L, which coincides with literature data (Jiang et al., 2018). Studies have shown the potential of FNA in inhibition of NOB while aching still good condition and properties of AOB.

The project was funded by the Polish-Norwegian Research Program operated by the National Centre for Research and Development under POLNOR 2019 in the frame of Project Contract No NOR/POLNOR/SNIT/0033/2019-00

REFERENCES

Duan, H., Wang, Q., Erler, D.V., Ye, L., Yuan, Z. 2018. Effects of free nitrous acid treatment conditions on the nitrite pathway performance in mainstream wastewater treatment, *Science of The Total Environment* **644**, 360-370.
Jiang, C., Xu, Sh., Wang, R., Chau, S-Z., Wu, Sh., Zeng, X., Bai, Z., Zhuang, G., Zhuang, X. 2018. Comprehensive assessment of free nitrous acid based technology to establish partial nitrification. *Environmental Science: Water Research & Technology* **4**(12), 2113.
Ma, B., Yang, L., Wang, Q., Yuan, Z., Wang, Y., Peng, Y. 2017. Inactivation and adaptation of ammonia-oxidizing bacteria and nitrite-oxidizing bacteria when exposed to free nitrous acid. *Bioresources Technology* **245**(Pt A),1266-1270.
Rodriguez-Garcia, G., Frison, N., Vázquez-Padín, J.R., Hospido, A., Garrido, J.M., Fatone, F., Bolzonella, D., Moreira, M.T., Feijoo, G. 2014. Life cycle assessment of nutrient removal technologies for the treatment of anaerobic digestion supernatant and its integration in a wastewater treatment plant. *Science of Total Environment* **490**, 871–879.
Surmacz-Górska, J., Gernaey, K., Demuynck, C., Vanrolleghem, P., Verstraete, W. 1995. Nitrification Process Control in Activated Sludge Using Oxygen Uptake Rate Measurements. *Environmental Technology* **16**(6), 569–577.
Vadivelu, V.M., Keller, J., Yuan, Z. 2007. Free ammonia and free nitrous acid inhibition on the anabolic and catabolic processes of Nitrosomonas and Nitrobacter. *Water Science and Technology* 56(7), 89-97.

Figure 1. Schematic diagram in the project of shortcut nitrification in the mainstream (SNIT).

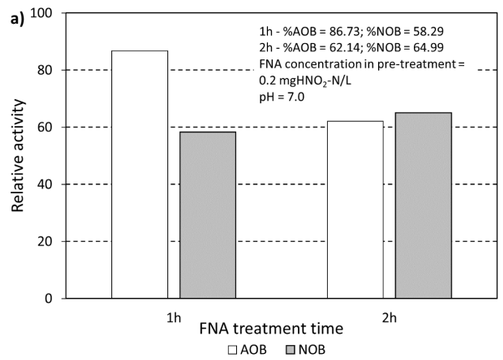

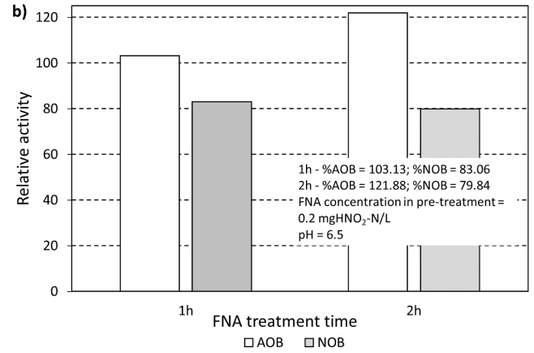

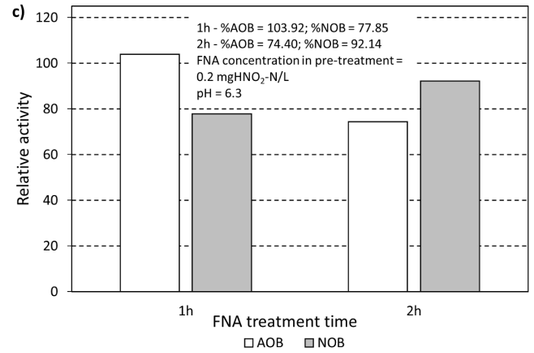

Figure 2. Activity of AOB and NOB bacteria in OUR tests - selected measurements.

When its worthwhile to include the nitrite pathway in a WWTP with C/N/P removal?

À. Gaona, A. Guisasola and J.A. Baeza
GENOCOV, Department of Chemical, Biological and Environmental Engineering, Universitat Autònoma de Barcelona, Spain.
(E-mail: *Alex.Gaona@uab.cat*; *Albert.Guisasola@uab.cat*; *JuanAntonio.Baeza@uab.cat*)

Abstract

Nitrite pathway is often recommended to reduce organic matter requirements. However, no previous studies have been conducted on what the minimum COD requirements would be to meet the total nitrogen and phosphorus discharge limits when integrating enhanced biological phosphorus removal with nitrite pathway. This work is a simulation-based study of a conventional A^2/O WWTP. An ASM2d-N_2O model extended with all the biological and chemical processes involving nitrite and N_2O description was used. This study provides novel correlations and a practical decision tree on the benefits and drawbacks of using nitrite pathway. These correlations are useful for a fast and a priori assessment of the required influent COD/N/P in the ranges of 3-11 mgPO_4^{-3}·L^{-1} and 20-60 mgNH_4^+-N·L^{-1}.

Keywords

Denitritation; enhanced biological phosphorus removal (EBPR); nitritation; nitrite pathway; wastewater; N_2O emissions.

INTRODUCTION

The main pollutants of wastewater are organic compounds and nutrients (N and P). N is removed with biological nitrogen removal (BNR), involving nitrification and denitrification. P removal is based either on chemical precipitation or biological accumulation via enhanced biological phosphorus removal (EBPR). EBPR relies on the enrichment of the sludge with polyphosphate accumulating organism (PAO). Anaerobic-anoxic-aerobic (A^2/O) configuration combines three operating conditions in the simplest way to integrate EBPR with BNR. Various operational A^2/O strategies have been proposed to improve the effluent quality and to reduce the energy requirements. For instance, nitrite pathway, i.e., autotrophic ammonium oxidation to nitrite (nitritation) and posterior heterotrophic nitrite denitrification (denitritation), results in 40% lower COD requirements for denitrification (Xu *et al*. 2021), savings in aeration costs and lower sludge production compared to the conventional processes. On the other hand, when implementing novel strategies, the potential increase of greenhouse gas (GHG) emissions needs to be accounted for. Carbon source limitations or high nitrite concentration can trigger off N_2O emissions. N_2O can be produced by: i) biological reduction of NO to N_2O (hydroxylamine oxidation pathway, NN pathway), ii) N_2O production by AOB in the reduction of nitrite to NO and N_2O (nitrifier denitrification pathway, ND pathway) and iii) heterotrophic denitrification (DEN pathway). Influent COD limitation is nowadays a concern when aiming at integrating BNR and EBPR since an electron donor is required for both processes. The failure due to low influent C/N/P ratios can be overcame with addition of external carbon source at expenses of an increase in the operational cost. In this frame, innovative configurations or strategies are needed to deal with low COD-loaded influents that do not increase neither energy requirements, operational costs nor GHG emissions. Mathematical modelling is a useful tool for the prediction of the WWTP performance under different conditions/configurations. The activated sludge models (ASM) are biokinetic models describing the transformations occurring in the WWTP. Several extended ASM-based models have been proposed to predict the WWTP performance under different scenarios. The ASM2d-N_2O model has been recently proposed and applied to account for N_2O emissions in WWTPs with C/N/P removal (Massara *et al*. 2018; Solís *et al*. 2022).

This work aims to provide plant designers with instantaneous and easy-to-use reference information to help them decide whether nitritation/denitritation nitrogen removal should be implemented in each wastewater scenario.

MATERIALS AND METHODS

A conventional A^2/O configuration is proposed for the biological removal on N, P and organic matter. This configuration combines three different reactors, anaerobic (2800 m^3), anoxic (2800 m^3), aerobic (9000 m^3). The kinetic model used was the ASM2d-N_2O (Massara *et al*. 2018). Nitrate and nitrite pathway were simulated for a wide range of wastewater compositions (3-9 mgP·L^{-1} for P, 20-60 mgN·L^{-1} for N). The minimum amount of organic matter that was necessary to meet the discharge limits for N and P, considering soluble nitrogen (S_{NH4}, S_{NO3}, S_{NO2}) and phosphate (S_{PO4}) was obtained for each pair of N and P concentrations in the wastewater under two different scenarios. In the first scenario, all organic matter was introduced as fermentation products (S_A) to simulate the most favourable organic matter composition for PAO, whereas in the second scenario only slowly biodegradable organic matter (X_S). The effluent legal discharge limits considered were PO_4^{3-} < 1 mg P·L^{-1} and TN < 10 mgN·L^{-1} (ECC Council 1991). The minimum required concentrations of S_A and X_S were estimated using the MATLAB optimisation function *fminbnd*.

RESULTS AND DISCUSSION

Figure 1 shows the minimum S_A (readily biodegradable) and X_S (slowly biodegradable) requirements to meet the legal P and TN effluent limits when operating under nitrate pathway and nitrite pathway conditions. S_A (or X_S) concentration should be high enough to simultaneously accomplish both discharge limits. COD requirements decrease when implementing nitrite pathway for both for N and P-removal. Moreover, higher X_S is required when compared to S_A since the limiting step may be hydrolysis of X_S or fermentation of S_S under anaerobic conditions. These increases are up to 290% for nitrate pathway and 208% for nitrite pathway. Nitrite pathway route has several advantages compared to the nitrate pathway (conventional BNR), such as less aeration needs, less COD demand in the anoxic stage and less sludge production. Therefore, the implementation of the nitrite pathway reduces energy requirements and external COD needs, allowing BNR and EBPR with low COD/N influents.

The full presentation will describe the main outcome of this work, which is the obtainment of general correlations (*Table 1*) to easily quantify the organic matter requirements when implementing either the nitrite or the nitrate pathway scenarios. These correlations can describe S_A and X_S requirements based only on the influent N and P. Correlations for S_A-P [(1) (3)], and X_S-P [(5) (7)] were expressed as linear equations ($y=b_0+b_1·P+b_2·N$), while correlations for S_A-N [(2) (4)] and X_S-N [(6) (8)] were extended with a non-linear summand ($y=b_0+b_1·P+b_2·N+b_3·P·N$) for a better description of the observed N-P dependence. Moreover, *Figure 2* shows a useful decision tree based on these correlations to select the best operational conditions for the proper treatment of a given wastewater under an A^2/O configuration. If the S_A (or X_S) content is too low to meet the desired effluent concentrations, alternatives should be considered: the addition of an external carbon source, the addition of chemicals for phosphate precipitation, or the implementation of the nitrite short-cut pathway. *Figure 3* compares the correlations obtained in this work to those in Metcalf and Eddy (Tchobanoglus *et al*. 2014) in three different case studies. The correlations obtained in this study predict approximately the same S_A requirements under the nitrate pathway. The full presentation will also disclose all the simulations related to the GHG emissions and the operational costs (*Table 2*) for each of the scenarios studied. For example, the nitrite pathway presents lower costs (between 4%-9% less) but a parallel increase of N_2O emissions. The main differences appear in the aeration costs (AE is reduced in the range 36%-37%), and sludge production (SP is reduced 1%-2%). A full discussion on the trade-offs of the nitrite pathway, aiming at reducing operational costs but incrementing the carbon footprint of the WWTP will be provided.

Table 1. Correlations of S_A of X_S requirements for nitrate and nitrite pathway.

	S_A requirements	Equation
Nitrate pathway	S_A-P = 2.51 + 14.03 P + 1.046 N	(1)
	S_A-N = 66.51 – 14.67 P + 4.72 N + 0.600 P·N	(2)
Nitrite pathway	S_A-P = -4.51 + 14.12 P + 0.517 N	(3)
	S_A-N = -32.92 – 3.169 P + 4.144 N + 0.066 P·N	(4)
	X_S requirements	
Nitrate pathway	X_S-P = -7.21 + 31.45 P + 3.22 N	(5)
	X_S-N = -18.73 – 7.67 P + 8.80 N + 0.305 P·N	(6)
Nitrite pathway	X_S-P = -29.52 + 27.67 P + 1.68 N	(7)
	X_S-N = -78.00 – 0.367 P + 5.69 N + 0.008 P·N	(8)

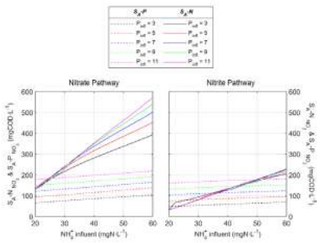

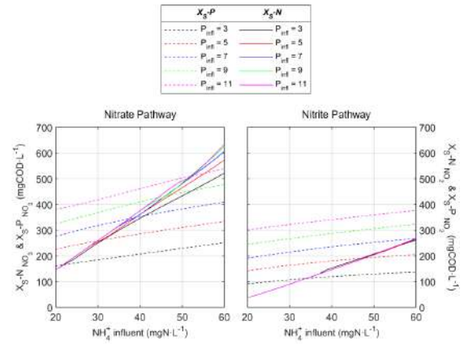

Figure 1. Minimum S_A and X_S requirements to meet the legal P and TN effluent limits (PO_4^{3-} < 1 mgP·L^{-1} and TN < 10 mg N·L^{-1}) when operating under nitrate pathway (left) and nitrite pathway (right) conditions.

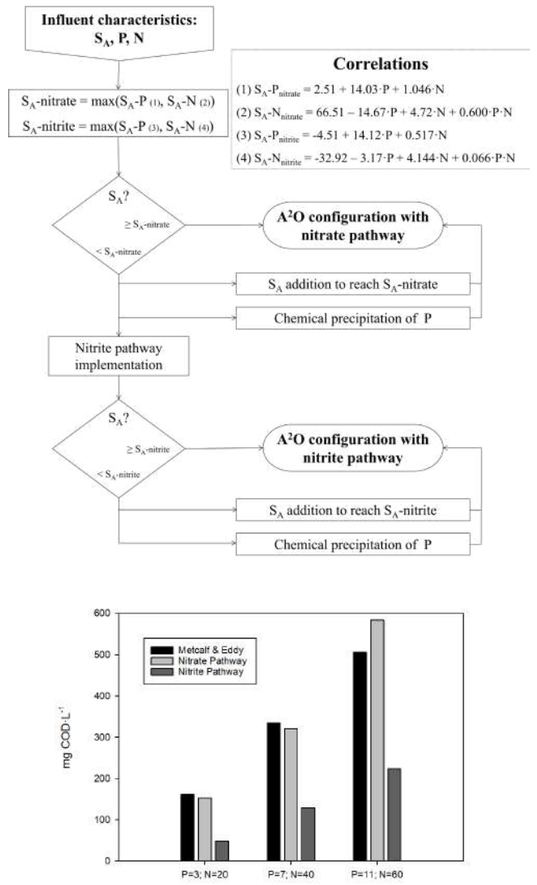

Figure 2. Decision tree for a continuous A^2/O plant to decide whether the implementation of the nitrate or nitrite pathway.

Figure 3. Comparison of the S_A predictions versus Metcalf and Eddy's recommendations on readily biodegradable COD requirements. Three different influent compositions (low, medium and high) are evaluated.

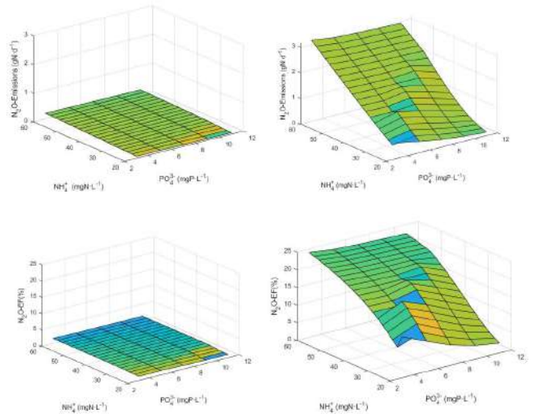

Figure 4. N_2O emissions (top) and N_2O-EF (bottom) for different runs under nitrate (left) and nitrite (right) pathway.

Table 2. Influent conditions and OCI results under nitrate and nitrite pathway

Influent concentrations			
PO_4^{3-} (mgP·L^{-1})	3	7	11
NH_4^{+} (mgN·L^{-1})	20	40	60
S_A (mg·L^{-1})	155	347	590
Nitrate Pathway			
k_a (d^{-1})	25.9	60.2	104.7
AE (kWh·d^{-1})	1447	3600	6786
PE (kWh·d^{-1})	7968	7968	7968
SP (kg·d^{-1})	1836	3065	4647
OCI	14925	20763	28695
Nitrite Pathway			
k_a (d^{-1})	16.6	40.3	71.1
AE (kWh·d^{-1})	910	2318	4337
PE (kWh·d^{-1})	7968	7968	7968
SP (kg·d^{-1})	1797	3017	4596
OCI	14269	19340	26094

REFERENCES

ECC Council, Council Directive of 21 May 1991 Concerning urban wastewater treatment. *Off. J. Eur. Communities.*

Massara, T.M., Solís, B., Guisasola, A., Katsou, E., Baeza, J.A. 2018 Development of an ASM2d-N_2O model to describe N_2O emissions in municipal WWTPs under dynamic conditions. *Chem. Eng. J.* **335** (18), 185–196.

Pocquet, M., Wu, Z., Queinnec, I., Spérandio, M. 2016 A two pathway model for N2O emissions by AOB supported by NO/N2O variation. *Water Res.* **88** (16), 948-959.

Solís, B., Guisasola, A., Pijuan, M., Corrominas, L., Baeza, J.A. 2022 Systematic calibration of N2O emissions from a full-scale WWTP including a tracer test and a global sensitivity approach. *Chem. Eng. J.* **435** (22), 134733

Tchobanoglus, G., Stensel, H.D., Burton, F., Abu-Orf, M., Bowden, G. Pfrang, W. 2014 Metcalf & Eddy. *Treatment and resource recovery, 5th ed,* McFray-Hill Education.

Xu, G., Zhang, Z., Gao, F. 2021 Effect of COD/N ratios and DO concentrations on NOB suppression in a multi-cycle SBR. *J. Environ. Chem. Eng.* **9** (21), 105735.

A novel wastewater treatment process incorporating acidophilic ammonia oxidation

M. Zheng*

*Australian Centre for Water and Environmental Biotechnology, The University of Queensland, St Lucia, Queensland 4072, Australia, (Email: m.zheng@uq.edu.au)

Abstract

Growing interest in achieving energy-neutral wastewater treatment requires a parallel focus on maximizing bioenergy recovery and minimising energy consumption, and the chemical enhanced primary treatment (CEPT) followed by partial nitritation and anammox (PN/A) and anaerobic digestion (AD) is one of the most recognised solutions. However, the acidification of wastewater caused by ferric (Fe^{3+}) hydrolysis in CEPT and the suppression of nitrite-oxidising bacteria (NOB) in PN/A are two major challenges associated with this paradigm in practice. This study proposes a novel wastewater treatment scheme utilising the newly discovered acidophilic ammonia oxidation as a solution to solve these challenges. Long-term demonstration on real domestic sewage showed that, by dosing $FeCl_3$ at 50 mg Fe/L, the CEPT process removed > 60% of COD and > 90% of phosphate, and the molar ratio of $CaCO_3$-alkalinity to ammonium was reduced to below 1. Due to the low alkalinity, stable nitrite accumulation was achieved in an aerobic moving bed biofilm reactor (MBBR) operated at pH of 4.35 aided by the novel acid-tolerant AOB "*Candidatus* Nitrosoglobus". Through the autotrophic nitrogen removal in a following anoxic MBBR (anammox), a satisfactory effluent, containing COD at 41.9 ± 11.2 mg/L, total nitrogen at 5.1 ± 1.8 mg N/L, and phosphate at 0.3 ± 0.2 mg P/L, was achieved. Moreover, the stable performances of this integration (i.e., CEPT, acidic PN and anammox) were well maintained at a low operating temperature (12°C), and ten selected micropollutants were removed from the wastewater with varying degrees. Overall, this integration opens a new avenue for domestic wastewater treatment to achieve energy neutrality

Keywords

Domestic wastewater treatment; CEPT; mainstream anammox; acidophilic ammonia oxidation; low temperature; energy neutrality

Wastewater treatment plants (WWTPs) remove pollutants and protect water bodies while consuming considerable energy, i.e., the electricity consumed can account for about 3% of the total annual electricity demand. In recent years, WWTPs are pursuing technologies to maximise bioenergy recovery and to minimise energy consumption, enabling energy neutrality. It has been recognised worldwide that the widely applied chemical enhanced primary treatment (CEPT) together with anaerobic digestion (AD) is one of the easiest-to-use approaches for bioenergy recovery. However, the maximization of bioenergy recovery by CEPT and the energy-efficient nitrogen removal via partial nitritation and anammox (PN/A) in domestic sewage treatment are both limited by critical issues in practice, as elaborated below.

The CEPT usually uses iron salts (i.e., $FeCl_3$) as the flocculant and is efficient in eliminating organic carbon and phosphorus in wastewater. However, the dosed $FeCl_3$ can cause a secondary effect of decreasing alkalinity via the hydrolysis of metal ions (i.e., Fe^{3+}), probably resulting in the molar ratio of alkalinity (calculated as $CaCO_3$) to ammonium in mainstream wastewater to below 1:1.5. The decrease of wastewater alkalinity is generally neglectable for traditional denitrification but critical to the PN/A process. This is because denitrification can regenerate alkalinity while the anammox process cannot. Moreover, microbial ammonia oxidation in the downstream nitrogen removal process further consumes alkalinity at 1 mol equivalent $CaCO_3$ per mol ammonia oxidized. Therefore, the alkalinity becomes insufficient to maintain the neutral pH of wastewater during the PN/A process, which can drop to below 6 when the alkalinity is depleted and no base is re-supplemented. Such low pH poses adverse effects on the traditional ammonia-oxidizing bacteria (AOB) and anammox bacteria that prefer neutral conditions.

Apart from the issue caused by low wastewater alkalinity, another key challenge for the application of mainstream PN/A is the stable suppression of nitrite-oxidizing bacteria (NOB). Many technologies have been developed to achieve this aim, including the use of low dissolved oxygen (DO), intermittent aeration, shortening sludge retention time (SRT), and sidestream sludge treatment using different strategies. Among all, free nitrous acid (FNA) is known as one of the most effective reagents for NOB inactivation, which is also one of the major reasons for the stable PN achieved in treating high-strength ammonium wastewater (~1 g N/L). However, due to the significantly lower total nitrogen in domestic sewage (40−60 mg N/L) and the generally neutral pH level (> 6) required by traditional AOB, it was deemed impossible to achieve an in-situ FNA level sufficient for NOB suppression under mainstream conditions.

These two issues associated with CEPT and PN/A can be tactfully solved by a novel microbial process: acidophilic ammonia oxidation. This process can be catalysed by the extremely acid-tolerant AOB "*Candidatus* (Ca.) Nitrosoglobus", with the first member discovered from an acidic soil sample recently (Hayatsu et al., 2017). Unlike the AOB *Nitrosomonas* commonly found in wastewater treatment, the novel *Nitrosoglobus*-like AOB (Figure 1.1) are active at pH as low as 2 (Wang et al., 2021). This capability to tolerate acidic condition indicates that a PN process can be operated under slightly acidic condition. By performing the acidic ammonia oxidation, AOB can produce protons and nitrite to lower the wastewater pH and form a high FNA concentration at a parts per million (ppm) level in situ. This technology fundamentally differs from all previous NOB inactivation strategies, which uses in-situ self-sustained stress (i.e., FNA) instead of ex-situ treatment of sludge and is proved energy-efficient and robust. To be noted, it is theoretically only possible to achieve such a low pH for domestic sewage with low alkalinity (i.e., $CaCO_3$-alkalinity/ammonium molar ratio < 1), which perfectly fits the scenario using CEPT for carbon removal (Figure 1.2). Two birds with one stone, the acidic PN process has great potential not only to cope with the low-alkalinity CEPT effluent and also to maintain stable PN for autotrophic nitrogen removal by anammox.

Collectively, this study demonstrated a novel integration of CEPT and PN/A in domestic wastewater treatment by incorporating acidophilic ammonia oxidation. A long-term experiment assessment was conducted in a laboratory system consisting of three units including a CEPT, an acidic PN, and an anammox reactor, which were continuously fed with real wastewater for one year. After the long-term evaluation, the impact of temperature variation mimicking the seasonal change (12−23°C), and the system's removal capacity on selected organic micropollutants were further examined, which were reported for the first time for acidic AOB and would provide a comprehensive assessment of the technology. Throughout the 360-day operation, microbial communities were monitored by 16S rRNA amplicon sequencing. This novel integration of CEPT, acidic PN, and anammox provided a valuable solution to achieve energy neutrality in wastewater treatment (Figures 1.3 and 1.4).

REFERENCES

Hayatsu, M.; Tago, K.; Uchiyama, I.; Toyoda, A.; Wang, Y.; Shimomura, Y.; Okubo, T.; Kurisu, F.; Hirono, Y.; Nonaka, K.; et al. An acid-tolerant ammonia-oxidizing γ-proteobacterium from soil. *ISME J.* **2017**, 11 (5), 1130-1141.

Wang, Z.; Ni, G.; Maulani, N.; Xia, J.; De Clippeleir, H.; Hu, S.; Yuan, Z.; Zheng, M. Stoichiometric and kinetic characterization of an acid-tolerant ammonia oxidizer 'Candidatus Nitrosoglobus'. *Water Res.* **2021**, 196, 117026.

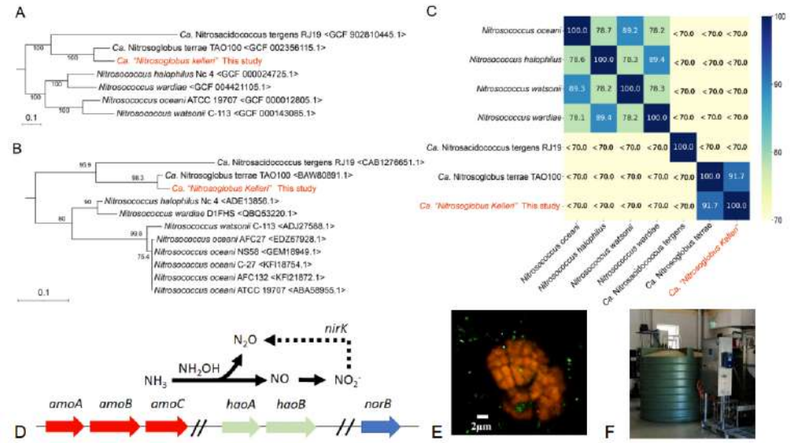

Figure 1.1. Phylogenetic placement of Candidatus (Ca.) Nitrosoglobus kelleri with genome tree (A) and amino acid tree using sequences of AmoA gene (B) inferred using the maximum-likelihood method. Numbers indicate bootstrap values, the scale bars in A and B represent nucleotide and amino acids substitutions, respectively. Heatmap (C) based on average nucleotide identity analysis. (D) The genome contains a complete pathway for ammonia oxidation to nitrite while missing the key nirK gene for N_2O production via the nitrifier denitrification pathway. (E) Fluorescence in Situ Hybridization (FISH) image of this enriched culture in our laboratory. (F) A pilot-scale reactor set-up for obtaining more biomass of Ca. Nitrosoglobus kelleri.

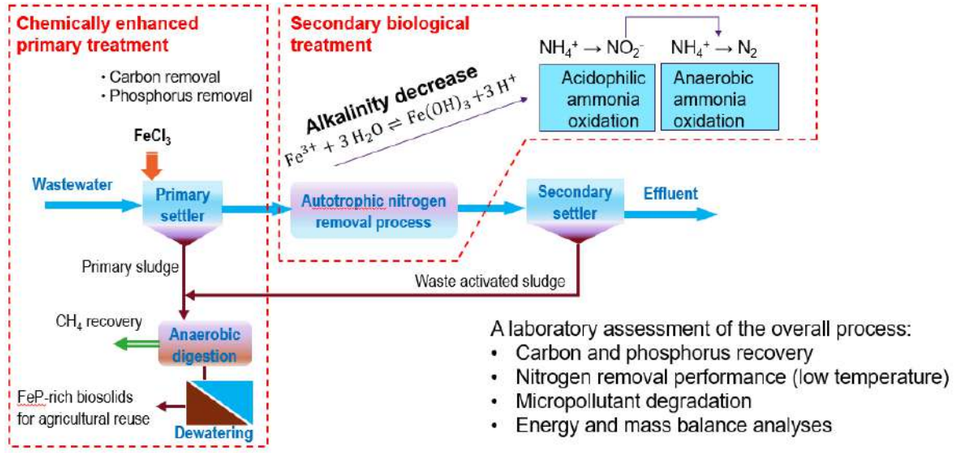

Figure 1.2. Design of a novel wastewater treatment process incorporating acidophilic ammonia oxidation, and an experimental assessment plan

Long-term effect of shortcut biological nitrogen removal as energy saving strategy for liquid waste treatment

L. Palli*, L. Macellaro La Franca*, F. F. Borchi* and D. Daddi*

* G.I.D.A. Spa, Via di Baciacavallo 36, Prato, IT
(E-mail: l.palli@gida-spa.it; l.macellaro@gida-spa.it; f.borchi@gida-spa.it; d.daddi@gida-spa.it)

Abstract

This paper describes a full-scale wastewater treatment plant treating liquid wastes (composed mainly by landfill leachate) by comparing the energy demand before and after a revamp that introduced the shortcut biological nitrogen removal (SBNR) technology. Despite a similar volume of waste treated, after the revamp the total energy consumption was about 29% lower. Energy saving is present in every month of the year but is more evident during the summer period. It is important to underline that this reduction in energy demand has not compromised the performance of the system, which has indeed improved. The new plant has made it possible to reduce the energy requirement by over 220 000 kWh each year, for an overall saving of around 31·000 €/year. This energy saving has led to a reduction in CO_2 emissions equal to 57.6 ton CO_2 per year.

Keywords

Energy; full-scale; liquid waste; membrane; nitrogen removal; SBNR

INTRODUCTION

Aerobic biological treatment for wastewater and/or liquid wastes is an effective yet highly energy-consuming technology (Davery et al, 2019). It estimated that conventional activated sludge (CAS) processes consume about 0.3-0.6 kWh/m^3 of which 50-70% is due to the aeration process (McCarty et al., 2011, Panepinto et al., 2016). In this scenario, improvement in the aeration efficiency and/or changes in the management of the plant aimed at reducing energy requirement of the aeration process liquor has therefore an important impact in the total energy demand of the whole plant. A simple yet efficient technology is the Shortcut Biological Nitrogen Removal (SBNR), which refers to biological nitrogen removal when ammonia is not converted to nitrate, but halts at nitrite to shortcut the conventional nitrification/denitrification process. While full nitrification requires 4.57 mgO_2/mgN, nitritation only requires 3.43 mgO_2/mgN, therefore, suppressing nitratation can save 25% of aeration costs (Winkler and Straka 2019). In order to achieve nitritation only it is necessary to control NOB and enriching AOB and this can be achieved alternating anoxic and oxic conditions in the same biological tank.
In this context, this paper describes a full-scale WWTP treating liquid wastes (composed mainly by landfill leachate) by comparing the energy demand before and after a revamp that introduced the SBNR technology.

MATERIALS AND METHODS

The old plant, a membrane biological reactor (MBR), has been described elsewhere (Coppini et al., 2018) and the treatment train consisted of the following sections: (1) an aerated equalization tank, with a volume of 2000 m^3, where all the leachates are discharged and mixed together; (2) a denitrification tank, with a volume of 2000 m^3, equipped with a dissolved oxygen (DO) probe, a pH probe, and a redox probe; (3) an oxidation/nitrification tank, with a volume of 5000 m^3, equipped with 6 rotor brushes as surface aeration system, a submerged mixing system and probes for the measurement of DO, pH, and redox potential; and (4) two ultrafiltration units placed in an external tank. After the revamping, the treatment train is composed by: (1) six equalizations tanks, with a total volume of about 3900 m^3, where the leachate and the other wastes are discharged and mixed in the desired proportions, (2) two biological tanks, each a volume of 2000 m^3, equipped with one pH probe, two ORP probes, two DO probes and one TSS probe and (3) two ultrafiltration units, not changed after the revamp. Moreover, the aeration system has been changed and fine bubble diffusers has been installed in the biological tanks, together with submerged propeller mixers for the anoxic phase.

RESULTS AND DISCUSSION

For the purpose of energy comparison of CAS and SBNR in the present paper it has been considered the energy consumption related to the biological compartment (meaning energy for aeration and for mixing) and for ultrafiltration, taking into consideration differences due to season (temperature affect greatly the energy demand for aeration) and amount of treated wastes.
Results are presented in the following tables and pictures.

Table 1. Mean treated volume, total and specific energy consumption of the plant before the revamping.

		BEFORE REVAMPING											
		JAN	***FEB***	***MAR***	***APR***	***MAY***	***JUN***	***JUL***	***AUG***	***SEP***	***OCT***	***NOV***	***DEC***
Mean treated volume (m^3/d)		469	548	630	480	510	499	310	275	329	398	624	443
Energy consumption (KWh/month)	***Biological compartment***	56206	47606	38147	48900	46505	53630	61494	48989	54656	69392	69258	74610
	Ultrafiltration unit	10596	12589	9182	11919	9122	9042	7362	5226	6467	5383	8469	7811
	Total energy	66802	60195	47329	60819	55627	62672	68856	54215	61123	74775	77727	82421
Specific consumption (KWh/m^3)	***Biological compartment***	3.87	3.00	1.95	3.40	2.94	3.58	6.39	5.75	5.54	5.63	3.70	5.44
	Ultrafiltration unit	0.73	0.79	0.47	0.83	0.58	0.60	0.77	0.61	0.65	0.44	0.45	0.57
	Total energy	4.60	3.79	2.42	4.22	3.52	4.18	7.16	6.36	6.19	6.06	4.15	6.01

Table 2. Mean treated volume, total and specific energy consumption of the plant after the revamping.

		AFTER REVAMPING											
		JAN	***FEB***	***MAR***	***APR***	***MAY***	***JUN***	***JUL***	***AUG***	***SEP***	***OCT***	***NOV***	***DEC***
Mean treated volume (m^3/d)		632	703	641	518	423	318	319	255	312	271	472	668
Energy consumption (KWh/month)	***Biological compartment***	41266	38000	44300	35500	39200	34400	27200	23500	29100	30200	35833	42167
	Ultrafiltration unit	7750	11307	11454	12230	10723	10983	11485	9800	11986	9961	12419	10794
	Total energy	49016	49307	55754	47730	49923	45383	38685	33300	41086	40161	48252	52961
Specific consumption (KWh/m^3)	***Biological compartment***	2.11	1.93	2.23	2.28	2.99	3.60	2.75	2.97	3.11	3.59	2.53	2.04
	Ultrafiltration unit	0.40	0.57	0.58	0.79	0.82	1.15	1.16	1.24	1.28	1.18	0.88	0.52
	Total energy	2.50	2.50	2.80	3.07	3.80	4.76	3.91	4.21	4.39	4.78	3.41	2.56

Figure 1. Comparison of total energy consumption before and after revamping, divided by month.

Figure 2. Comparison of specific energy consumption before and after revamping, divided by month

As can be seen, despite a similar volume of waste treated (167 922 m^3 per year before revamping and 167 822 m^3 after revamping), the total energy consumption was about 29% lower. Energy saving is present in every month of the year but is more evident during the summer period (July, August and September). Indeed, in this period, the total volume of waste treated is generally lower (since most wastes are represented by landfill leachates which are affected by the amount of rainfall) and the new system is more flexible in adapting the amount of energy used compared to the old system.
It is important to underline that this reduction in energy demand has not compromised the performance of the system, which has indeed improved. In fact, as reported in Table 3 the COD and total nitrogen (TN) in the plant effluent were almost always lower after the revamping.

Table 3. Comparison of COD and Total Nitrogen left in the effluent of the plant before and after the revamping

	BEFORE REVAMPING		AFTER REVAMPING	
Month	**COD (mg/L)**	**TN (mg/L)**	**COD (mg/L)**	**TN (mg/L)**
January	2424	268	1161	76
February	2068	260	1128	90
March	1802	294	1558	183
April	3083	533	1651	113
May	2485	125	1750	100
June	2259	292	1879	156
July	2567	244	1969	211
August	2884	362	2056	202
September	3013	332	2118	347
October	2381	277	2036	447
November	1771	227	2057	442
December	1737	712	1398	264

Conclusions

Considering the reported results, it is possible to conclude that the new plant has made it possible to reduce the energy requirement by over 220 000 kWh each year, while increasing the removal of COD and TN, for an overall saving of around 31 000 €/year (with reference to average price of 2021). Considering the average CO_2 produced per kWh consumed in Italy equal to 260.5 gCO_2/KWh (ISPRA 2022), this energy saving has led to a reduction in CO_2 emissions equal to 57.6 ton CO_2 per year.

REFERENCES

Coppini, E., Palli, L., Fibbi, D., Gori, R., 2018. Long-Term Performance of a Full-Scale Membrane Plant for Landfill Leachate Pretreatment: A Case Study. Membranes. **8** (3) 52.
Davery, A., Pandey, D., Verma, P., et al. 2019 Recent advances in energy efficient biological treatment of municipal wastewater. Bioresource Technology Reports 7, 100252.
ISPRA. 2022. Indicatori di efficienza e decarbonizzazione del sistema energetico nazionale e del settore elettrico. Rapporto 363/2022.
McCarty, P. L., Bae, J., and Kim, J., 2011. Domestic wastewater treatment as a net energy producer can this be achieved? Environ. Sci. Technol. 45, 7100–7106.
Panepinto, D., Fiore, S., Zappone, M., Genon, G., Meucci, L., 2016. Evaluation of the energy efficiency of a large wastewater treatment plant in Italy. Appl. Energy 161, 404–411.
Winkler, M., Straka, L., 2019. New directions in biological nitrogen removal and recovery from wastewater. Current Opinion in Biotechnology, 57C:50–55.

TECHNICAL SESSIONS

T16.

GHG & Microbial community dynamics

ECOSTP 2023

The long-term full-scale monitoring of GHG from an Australian WWTP demonstrated the upstream carbon capture can stimulate downstream emissions

K. Li*, H. Duan*, S. Wang*, Z. Wu*, P. Wardrop**, J. Lloyd** and L. Ye*

* The University of Queensland, Brisbane, QLD, Australia
E-mail: kaili.li@uq.edu.au; h.duan@uq.edu.au *(corresponding author)*; shuting.wang@uq.edu.au; ziping.wu@uq.edu.au; l.ye@uq.edu.au *(corresponding author)*
** Melbourne Water, Melbourne, VIC, Australia
E-mail: peter.wardrop@melbournewater.com.au; james.lloyd@melbournewater.com.au

Abstract

The direct monitoring and quantification of fugitive greenhouse gas (GHG) emissions are essential towards the successful development of mitigation strategies. In this work, an ongoing long-term methane (CH4) and nitrous oxide (N2O) monitoring campaign has been conducted in an Australian wastewater treatment plant (WWTP) where the secondary treatment receives a mixture from anaerobic lagoon effluent and raw sewage. The results showed clear GHG spatial variations due to the step-feed configuration of the plant. N2O is the dominant GHG while CH4 only contribute to 3.43% of the plant fugitive emissions. The assessment of N2O emissions revealed that even in the same reactor with continuous operation, the production pathways and seasonal emission variations can be significantly different in different locations, i.e., AOB and HB respectively dominated N2O productions in different locations. It was revealed that the COD removal in the anaerobic primary treatment leads to insufficient organic carbon for denitrification. The mitigation strategy has been correspondingly developed.

Keywords

Carbon footprint; greenhouse gas; methane; monitoring and mitigation; net zero; nitrous oxide

INTRODUCTION

Greenhouse gas emissions (GHG) must be significantly reduced in the next few decades to minimise the most devastating climate change. Nitrous oxide (N_2O) and methane (CH_4) are the two main fugitive GHG emissions from the sewage treatment processes. The international reporting guideline IPCC has mandated the use of fixed emission factors for the report of these two emissions, which can deviate greatly from the actual emissions and give no incentive to the production pathways and the development of mitigation methods.

In this work, a long-term monitoring approach has been developed to directly measure and quantify the off-gas emissions from an Australian WWTP. The spatial and seasonal variations of fugitive emissions have been assessed. The underlying mechanisms that stimulate the generation of N2O have been analysed and the corresponding mitigation methods have been developed. This is the first long-term (>1 year) GHG monitoring campaign conducted in Australia and the results from which can contribute to the global monitoring inventory.

MATERIALS AND METHODS

The ongoing long-term monitoring campaign has been conducted since October 2021 in a step-feed reactor with four anoxic and aerobic passes, treating a mixture of raw wastewater and anaerobic lagoon effluent with a mixing ratio of 1:4. The wastewater is split into four streams with a splitting ratio of 4:3:2:1 from Pass 1~4. The floating hood systems have been designed to capture off gas to be sent to gas analysers for gas composition analysis. Five gas collection hoods with four hoods are placed in the centre of each aerated pass and one additional hood to assess the spatial variations (Figure 1). Besides, the plant operating information including wastewater characteristics, airflow rates and dissolved oxygen is monitored online. Intensive sampling campaigns were conducted to grab hourly samples for the analysis of potential N2O production pathways. Preliminary mitigation methods have been developed based on model-assisted data analysis.

RESULTS AND DISCUSSION

The GHG emissions from the studied WWTP have been continuously monitored for over a year. The emission patterns for both N_2O and CH_4 have been obtained. Figure 2A and 2B present the daily averaged GHG fluxes. Both N_2O and CH_4 emissions varied substantially over the course of the year. The carbon footprint analysis converted the N_2O and CH_4 fluxes into carbon dioxide equivalent (CO_2-eq). CH_4 only contributes to 3.43% of fugitive emissions from the secondary treatment processes, while N_2O accounts for the majority of the carbon footprint which requires further analysis and mitigation (Figure 2C).

By analysing the influent TKN loading, the daily emission factors of N_2O were shown to vary from 0.22% to 3.88%, with a mean of 1.12%, approximately 30% lower than the fixed emission factor of 1.6% by IPCC. Further investigation of the N_2O emissions from the individual pass showed that Pass 4 made the highest contribution (38.53%) to N_2O emissions (Figure 2D), while Pass 1 which received the most influent contributed to the least (15.92%).

To explore the potential N_2O production pathways, the grab samples from intensive sampling have been analysed for wastewater characteristics, dissolved N_2O and isotope (δ15N abundance). As seen in Figure 3, the dissolved N_2O concentration in each zone was highly correlated with nitrite accumulation. Nitrite accumulated in all 4 aerobic passes. The accumulation of nitrite is known to stimulate N_2O emissions by AOB via the nitrifier denitrification pathway (Foley et al., 2010). In addition, N_2O emissions from aerobic 4 can also be attributed to the accumulated N_2O in the preceding anoxic zone. Anoxic zone 4 exhibited a very different N profile compared to other anoxic zones. High N_2O, as well as NO_2^- accumulation were observed in anoxic zone 4, indicating incomplete denitrification. The above hypotheses were verified by the isotope results where 15N bulk abundance saw an obvious decrease from Pass 1 aerobic to Pass 2 aerobic, and a dramatic increase from Pass 3 aerobic to Pass 4 aerobic, which indicated the nitrous oxide productions were driven by nitrification and denitrification respectively.

The incomplete denitrification in Pass 4 was likely due to the COD deficiency. Assuming a theoretical COD/N ratio of 4.5 for full denitrification (Metcalf et al., 2014), a mass balance analysis during the intensive sampling periods in each anoxic pass showed Pass 4 anoxic is in most deficiency of COD, in at least 30% of COD shortage. It is therefore proposed to alter the mixing ratio between raw wastewater and anaerobic lagoon effluent to above 1:1 to make up for the COD loss in the anaerobic lagoon. The mitigation strategy will be verified through calibrated models and to be implemented at full-scale if working.

Various seasonal variation patterns of N_2O emissions have been reported in previous studies (Daelman et al., 2015; Gruber et al., 2021). However, the cause of different seasonal variation patterns remains unclear. Interestingly, it was observed different N_2O dominant production pathways may lead to different seasonal emission patterns as seen in Figure 3C. The N_2O emission in Pass 4, contributed by denitrification had a high peak in summer and gradually decreased after that with a low peak before winter, while the emission in Pass 1 (contributed more by nitrification) had an earlier high peak and stayed relatively stable for the rest of the year. The different seasonal patterns may be attributed to the different responses of N_2O producing microbes (nitrifiers and denitrifiers) to operating and environmental conditions.

Carbon capture and energy recovery have been increasingly applied in WWTPs to improve energy efficiency (Gu and Liu, 2020). Despite the benefits of carbon recovery, this work showed that there is a potential risk to stimulate N_2O emissions in the nitrogen removal stage due to incomplete denitrification caused by COD deficiency. Therefore, the application of carbon capture and recovery should be considered holistically regarding the overall carbon footprint of the plant.

Figure 1. (A) Plant design and distribution of gas collection hoods (blue circles). The reactor comprises five hoods; one in the centre of each aerated pass and one additional hood in Pass 3 which can be moved to assess spatial variation of emissions. (B) zoom in of the gas collection hood; (C) Horiba VA3000 gas conditioning and analysing system.

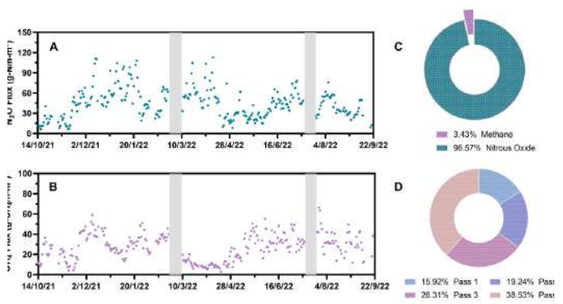

Figure 2. Graphical representation of (A) daily averaged N_2O flux; (B) daily averaged CH_4 flux. Note the grey shaded area in (A) and (B) represents the data missing period due to sensor fault or maintenance. (C) contributions of scope 1 emissions from the studied reactor; (D) contributions of nitrous oxide emissions from the studied reactor.

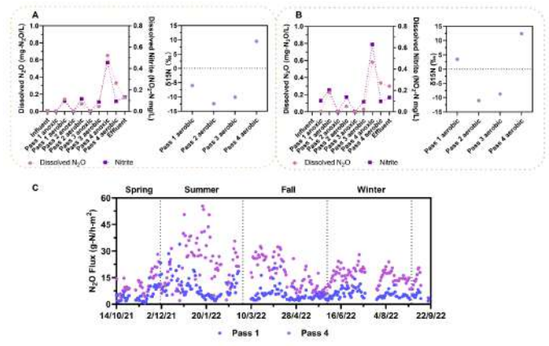

Figure 3. Graphical representation of (A) intensive sampling result from a typical hour; (B) intensive sampling result from another typical hour; (C) seasonal nitrous oxide emission variation pattern for Pass 1 and Pass 4.

REFERENCES

Daelman, M.R.J., van Voorthuizen, E.M., van Dongen, U.G.J.M., Volcke, E.I.P. and van Loosdrecht, M.C.M. 2015. Seasonal and diurnal variability of N2O emissions from a full-scale municipal wastewater treatment plant. Science of The Total Environment 536, 1-11.

Foley, J., de Haas, D., Yuan, Z. and Lant, P. 2010. Nitrous oxide generation in full-scale biological nutrient removal wastewater treatment plants. Water Res 44(3), 831-844.

Gruber, W., von Känel, L., Vogt, L., Luck, M., Biolley, L., Feller, K., Moosmann, A., Krähenbühl, N., Kipf, M., Loosli, R., Vogel, M., Morgenroth, E., Braun, D. and Joss, A. 2021. Estimation of countrywide N2O emissions from wastewater treatment in Switzerland using long-term monitoring data. Water Research X 13, 100122.

Gu, J. and Liu, Y. 2020 Integrated A-B processes for municipal wastewater treatment. Liu, Y., Gu, J. and Zhang, M. (eds), p. 0, IWA Publishing.

Metcalf, Eddy, I., Tchobanoglous, G., Stensel, H.D., Tsuchihashi, R., Burton, F.L., Abu-Orf, M., Bowden, G. and Pfrang, W. (2014) Wastewater engineering treatment and resource recovery, McGraw-Hill Higher Education, New York, NY.

Real-time monitoring and data-driven management of N_2O generation in biological reactors

L. Flores*, K. Kandris**, V. Vasilaki**, P. Tamayo*, Y. Lorenzo-Toja***, A. Vidal****, N. Basset****, M. Bronsoms****, E. León****, E. Katsou**

* Environmental, Economic and Social Sustainability Department, Water Technology Center CETaqua, Carretera d'Esplugues 75, 08040, Cornellà de Llobregat, Spain (E-mail: *laura.flores@cetaqua.com)*
** Department of Civil & Environmental Engineering, Brunel University London, Uxbridge Campus, Middlesex, UB8 3PH, Uxbridge, UK
*** Environmental, Economic and Social Sustainability Department, Water Technology Center CETaqua, Vila da Auga, Rúa de José Villar Granjel 33, Aquahub-A, 15890, Santiago de Compostela, Spain (E-mail: *yago.lorenzo@cetaqua.com)*
**** Aigües de Barcelona, Empresa Metropolitana de Gestió del Cicle Integral de l'Aigua, S.A., Carrer General Batet 1-7, 08028, Barcelona

Abstract

Nitrous oxide (N_2O) is a greenhouse gas (GHG) that contributes significantly to the water sector's carbon footprint. It is estimated that approximately 26% of global emissions from the water sector are from N_2O. The major contribution of N_2O in wastewater treatment plants (WWTPs) is due to nitrification and denitrification processes in biological reactors. This study will assess the impact of environmental stressors under different operational conditions on N_2O generation using supervised and unsupervised modelling techniques. Long-term data collected from a full-scale WWTP are being used to investigate the behaviour of N_2O emissions. To this aim, a low-cost data driven methodology was developed by combining a Bayesian ensemble changepoint detection technique with Random Forest regression and post hoc model interpretation strategies. The results will identify main pathways for N_2O mitigation through the operation and control of the WWTP.

Keywords (maximum 6 in alphabetical order)

INTRODUCTION

Wastewater treatment plants (WWTPs) contribute to global warming through direct emissions of greenhouse gases (GHGs) such as nitrous oxide (N_2O). N_2O emissions from WWTPs increased by 44% from 1990 to 2014, contributing about 3% of total emissions (US EPA, 2016). In addition, these emissions account for up to 26% of GHGs from the entire water supply chain (Vasilaki et al., 2019). N_2O is considered the most ozone-depleting substance of anthropogenic origin, with a global warming potential 265 times greater than that of carbon dioxide (CO_2). The main source of N_2O emissions occurs during the secondary treatment process in the biological reactor, where most of the organic matter and nutrients are removed, contributing up to 75% of the total carbon footprint of a WWTP (Massara et al., 2018).

The methods for measuring N_2O in biological processes have evolved over the years. The most commonly applied method includes offline analysis by gas chromatography with electron capture (GC-ECD) (Saynes and Ramirez, 2018). However, this method can lead to over- or underestimation of the emissions due to daily and seasonal variability, as well as losses during sample transport and handling. Currently, in most cases, the measurement of gas-phase N_2O is performed using gas analyzers based on Fourier transform infrared spectroscopy (FTIR) or non-dispersive infrared (NDIR) sensors (Lebegue et al., 2016). More recently, N_2O emissions are analysed and quantified before they are formed and released into the atmosphere, through their concentrations in the dissolved form. In this case, cathodic Clark-type sensors are gaining interest in this field (Marques et al., 2016; Vasilaki et al., 2020).
The large number of variables that can trigger N_2O emissions makes difficult the establishment of specific mitigation strategies. In addition, correlating emissions with the operating conditions and configuration types of WWTPs and biological reactors in particular remains a challenge (Vasilaki et al., 2019). In this study supervised and unsupervised modelling techniques will be applied to data collected from a long-term monitoring campaign to investigate how environmentally generated stresses of treatment processes (rainfall events, shocks, temperature changes) impact the N_2O generation. The behaviour of N_2O under different operational conditions will be also studied, considering real-time monitored parameters and laboratory analyses. Main pathways for N_2O mitigation through the operation and control of a full-scale WWTP will also be reported.

MATERIALS AND METHODS

Site description and experimental setup

The full-scale WWTP treating domestic wastewater is located in Sant Feliu de Llobregat (Barcelona). The plant consists of an activated sludge process and treats an average influent of 47,000 m^3 day^{-1}. The experimental study is being conducted in one of the biological reactors that applies nitrification-denitrification processes to remove nitrogen. The reactor is a plug flow type divided into a small anoxic compartment and an aerobic one.

The duration of the campaign at Sant Feliu WWTP is planned for 12 months (August 2022-July 2023). Two Clark-type sensors (Unisense, Denmark) are used to continuously measure the dissolved concentration of N_2O in the reactor. In addition, gaseous N_2O emissions are measured online at the reactor surface with a non-dispersive infrared (NDIR) gas analyser (Horiba-VA3116) connected to a floating stainless-steel hood (AC'SCENT Flux Hood, 40L).
The sensors, as well as the floating hood, are placed at various points in the reactor: anoxic zone, anoxic-aerobic transition zone, and different points in the aerobic zone.

Data mining and knowledge discovery

Figure 2 shows the methodology for data analysis that was applied in the project. Data pre-processing comprises all required steps to (a) handle missing data, (b) filter outliers in data, and (c) smooth noisy input. Changepoint detection methods and unsupervised machine learning techniques were applied (Vasilaki et al., 2020) to unveil patterns in (a) environmentally generated stresses of treatment processes, (b) N_2O generation, (c) different operational conditions.

A Bayesian ensemble modelling technique (Zhao et al., 2019) was deployed to detect seasonality, trends, and abrupt changes in time series data of environmental stresses, and N_2O emissions. Random Forests (RFs) were used to identify key variables that impact N_2O emissions under different operational conditions. The RF algorithm assesses the relevance of external forcings in predicting accurately N_2O concentrations through a permutation variable importance metric (VIM). This type of analysis indicates the influence of the predictors in the overall structure of the random forests. Additional interpretability efforts were undertaken to decipher how the model predicts N_2O concentrations. The Shapley values (Lundberg and Lee, 2017) were estimated for the model, and for predictions that correspond to the "highest" observed concentrations of N_2O during each period. The Shapley value of a predictor, evaluates the contribution of the predictor to a prediction. s, by providing an inkling of their relevance in the prediction of extremes.

RESULTS AND DISCUSSION

The performance of the reactor in terms of NH_4-N removal, was stable during the monitoring campaign. The average removal efficiency of COD and NH_4-N, was 97% and 95%, respectively. Influent and effluent concentrations of the system for the duration of the monitoring campaign are given in Table 1.
Figure 3a shows boxplots of typical diurnal profile of the dissolved N_2O concentration during the monitoring campaign. The concentrations follow the diurnal influent and effluent NH4-N profiles in the reactor. The dissolved N_2O concentration ranged between 0.09 and 0.37 mg L^{-1}. Figure 3b illustrates the behaviour of N_2O concentration in respect to NH_4-N and NO_3-N concentrations.

The analysis is ongoing and the final results will be presented in the conference. The applied methodology and key findings contribute significantly towards carbon reduction challenges the water sector currently faces. The study expands the current datasets for long-term N_2O monitoring campaigns in different wastewater treatment processes considering the seasonal variations and plant operational and control strategies. Additionally, a low-cost data driven methodology was developed by combining a Bayesian ensemble changepoint detection technique with RF regression and post hoc model interpretation strategies to (a) understand the influence of the model predictors (operational variables) to model predictions, and (b) unveil why and when the model fails or succeeds to describe the underlying processes. In this case, the benefit is twofold. On one hand, this methodology uncovers potential emission triggering conditions from monitoring data (data valorization) and, on the other hand, it indicates how to improve the models, and, thereby, move from diagnostic levels ("Why something happened?") to predictive ("What is likely to happen?") or even prescriptive ("What to do next?") analytics. Data valorization can be easily adapted in different plants and can support the understanding of the key contributor factors for N_2O generation under different operational and environmental conditions. The methodology facilitates the development of adaptive mitigation options considering different temporal operational conditions and N_2O triggers.

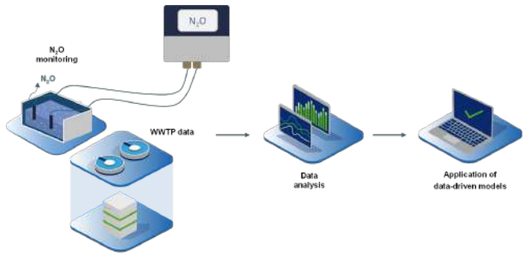

Figure 1. Scheme of the nitrous oxide (N_2O) monitoring and analysis for the identification of mitigation options.

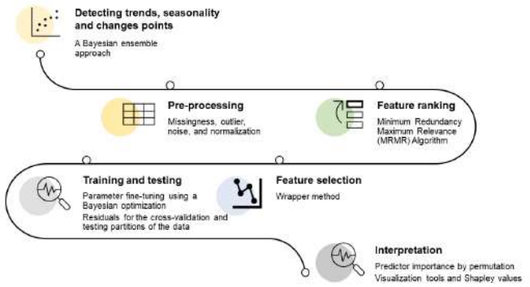

Figure 2. Methodology for data analysis applied.

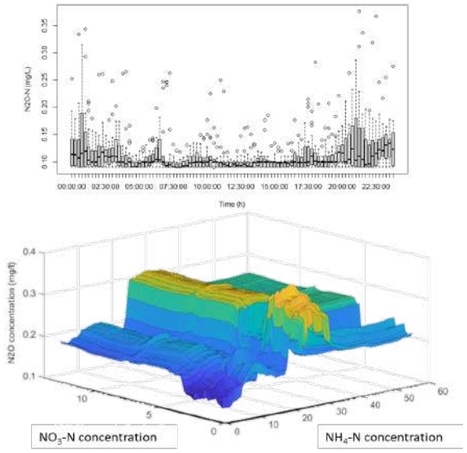

Figure 3. (a) Boxplot of diurnal variation of dissolved nitrous oxide (N_2O) concentration (b) Impact of operational variables on N_2O concentration.

Table 1: Influent and effluent concentrations from the wastewater treatment plant.

	Influent	Biological influent	Effluent
Flow-rate (m^3 day^{-1})	47,000 (±5,200)	7,500 (±880)	-
COD (mg L^{-1})	790.7(±435.4)	349.3 (±109.6)	24.7 (±10.4)
TN (mg L^{-1})	72.8(±12.3)	63.3 (±9.1)	10.5 (±1.2)
NH_4-N (mg L^{-1})	53.5(±9.6)	51.6 (±8.9)	2.8 (±1.27)
TP (mg L^{-1})	9.7(±3.1)	7.90 (±1.4)	1.14 (±0.6)
NO_3-N (mg L^{-1})	-	-	5.0 (±1.3)
NO_2-N (mg L^{-1})	-	-	0.17 (±0.1)

REFERENCES

Lebegue, B., Schmidt, M., Ramonet, M., Wastine, B., Yver Kwok, C., Laurent, O., Belviso, S., Guemri, A., Philippon, C., Smith, J., and Conil, S., 2016. *Atmos. Meas. Tech.*, **9**, 1221–1238,
Lundberg, S. M. and Lee, S. I., 2017. A unified approach to interpreting model predictions. Advances in neural information processing systems. ArXiv, https://arxiv.org/abs/1705.07874
Marques R., Rodriguez-Caballero A., Oehmen A. and Pijuan M., 2016. Assessment of online monitoring strategies for measuring N2O emissions from full-scale wastewater treatment systems. *Water Research* **99**, 171-179.
Massara T., Solís B., Guisasola, A., Katsou, E. and Baeza, J.A., 2018. Development of an ASM2dN2O model to describe nitrous oxide emissions in municipal WWTPs under dynamic conditions. *Chemical Engineering Journal* **335**, 185-196.
Saynes V. and Ramírez E., 2018. The use of gas chromatography in greenhouse gas emission research in the livestocksector. Agroproductividad Vol 11. Mexico D. F. México.
U.S. Environmental Protection Agency (EPA), 2016. International Decontamination Research and Development Conference. U.S. Environmental Protection Agency, Washington.
Vasilaki V., Massara T., Stanchev P., Fatone F. and Katsou E., 2019. A decade of nitrous oxide (N2O) monitoring in full-scale wastewater treatment processes: A critical review. *Water research* **161**, 392-412.
Vasilaki, V., Danishvar, S., Mousavi, A. and Katsou, E., 2020. Data-driven versus conventional N2O EF quantification methods in wastewater; how can we quantify reliable annual EFs?. *Computers & Chemical Engineering*, **141**, p.106997.
Zhao, K., Wulder, M. A., Hu, T., Bright, R., Wu, Q., Qin, H., ... and Brown, M., 2019. Detecting change-point, trend, and seasonality in satellite time series data to track abrupt changes and nonlinear dynamics: A Bayesian ensemble algorithm. *Remote sensing of Environment*, **232**, 111181.

Unraveling the N_2O emissions from thermophilic nitrification reactors

Mingsheng Jia[1,2], Badri Narayan Ravikumar[1,2], Lin Zeng[1,2], Siegfried Vlaeminck[2,3], Nico Boon[1,2], Jose Maria Carvajal Arroyo[1,2], Ramon Ganigué[1,2]

[1] Centre for Microbial Ecology and Technology (CMET), Ghent University, Belgium
(E-mail: mingsheng.jia@ugent.be; badrinarayan.ravikumar@ugent.be; lin.zeng@ugent.be; nico.boon@ugent.be; josemaria.carvajalarroyo@ugent.be; ramon.ganigue@ugent.be)
[2] Centre for Advanced Process Technology for Urban Resource Recovery (CAPTURE), Belgium
[3] Department of Bioscience Engineering, University of Antwerp, Belgium
(Email: siegfried.vlaeminck@uantwerpen.be)

Abstract

Nitrification is a key process in biological nitrogen removal from wastewater. Its first step is ammonia oxidation to nitrite (nitritation) by ammonia-oxidizing bacteria (AOB) or archaea (AOA) or recently identified complete ammonia oxidizers. Most AOB grow optimally at mesophilic temperatures, while thermophilic nitritation in natural and engineered ecosystems is mainly carried out by AOA. This may result in lower N_2O emissions in AOA-dominated thermophilic nitrification compared to AOB-dominated counterparts. Nevertheless, no such information is available yet. We aim to unravel the N_2O from thermophilic nitrification reactors for the first time. The reactors demonstrated stable full nitrification with an influent of 500 mg NH_4^+-N/L and loading rate of 0.5 g N/L/d. The dominating AOA and nitrite-oxidizing bacteria belong to the genera *Candidatus Nitorsosphaera* and *Nitrospira* respectively. Preliminary results showed low N_2O emissions from both the gas and liquid phase of the reactors, indicating a potentially lower carbon footprint of thermophilic nitrification processes.

Keywords (maximum 6 in alphabetical order)

Ammonia oxidizing archaea; Greenhouse gas; Microbial community; Nitrogen removal; Nitrous oxide; Thermophilic nitrification

INTRODUCTION

Anthropogenic alteration of the nitrogen (N) cycle has far exceeded the safety boundaries of our planet, making it one of the major global challenges (Steffen, Richardson, et al., 2015). N removal from wastewater is a key component in sustainable N management. Nitrification is a key process in global nitrogen cycling and for biological N removal from wastewater. It consists of two steps, nitritation (ammonia oxidation to nitrite) by ammonia-oxidizing bacteria (AOB) or archaea (AOA), and nitratation (nitrite oxidation to nitrate) by nitrite-oxidizing bacteria (NOB). Recently discovered complete ammonia oxidizers (Comammox) can perform both steps (Van Kessel, Speth, et al., 2015). Most AOB grow optimally at mesophilic temperatures, while thermophilic nitritation in natural and engineered ecosystems is mainly carried out by AOA instead of AOB (Courtens, Spieck, et al., 2016). Physiological characteristics, including mechanisms for nitrous oxide (N_2O) production, vary within and between AOA and AOB, and AOA usually have a lower N_2O yield (Prosser, Hink, et al., 2020). N_2O is a potent greenhouse gas (about 300 times CO_2) and is among the dominant ozone-depleting substances (Ravishankara, Daniel, et al., 2009). The AOA-dominated thermophilic nitritation may have nitrous oxide (N_2O) emission and, thus, lower carbon footprint compared to AOB-dominated counterparts. Nevertheless, no data on N_2O emissions from the thermophilic nitrification process is available yet, which also hinders the evaluation of the sustainability of rising thermophilic nitrogen removal processes. This contribution aims to unravel the microbial communities and N_2O from two unique thermophilic nitrification reactors.

MATERIALS AND METHODS

Reactor setup and operation

Two lab-scale membrane bioreactors (MBRs, Fig. 1) with a working volume of 2.1L were operated for more than 300 days. The two MBRs were inoculated with the same biomass from previous thermophilic nitrification reactors in the lab (Courtens, Spieck, et al., 2016). The pH was controlled between 6.8 and 7.2 by dosing 0.1 M hydrochloric acid and 0.1 M sodium hydroxide. The temperature was controlled at 49 ± 1 °C by using a heating water jacket connected to a circulating bath. The dissolved oxygen was controlled at a setpoint of 5.0 mg/L (Liquiline CM448, Endress+Hauser, Germany). Both reactors were continuously fed with synthetic medium consisting of $(NH_4)_2SO4$ (up to 500 mg N/L), 12 g $NaHCO_3$/g N, KH_2PO4 (10 mg P/L) and trace elements (Vandekerckhove, Kerckhof, et al., 2019).

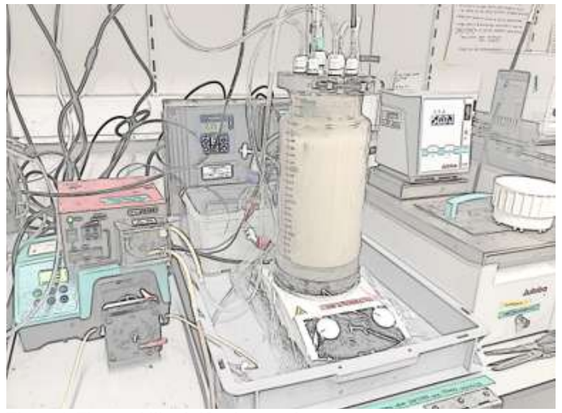

Figure 1. Thermophilic nitrification membrane reactor 1

Liquid, solid, gas and molecular Analysis

Liquid samples were filtered through 0.2 µm disposable filter before measuring the concentrations of ammonium, nitrite, and nitrate. The biomass concentration was determined as total suspended solids (TSS) and volatile suspended solids (VSS) according to standard methods. To systematically quantify the N_2O emissions, online monitoring was set up for both gas phase (gas phase analyser, X-STREAM, EMERSON, Germany) and liquid phase (N_2O-R microsensor, Unisense, Danmark). To infer the microbial community, samples were taken for 16S rRNA gene amplicon sequencing.

RESULTS AND DISCUSSION

Reactor performance

The concentrations of nitrogen compounds in the influent and effluent of the thermophilic nitrification reactor 1 were shown in Figure 2. The results demonstrated stable nitrification activities at influent ammonium concentrations of 500 mg NH_4^+-N/L and a loading rate of 0.5 g NH_4^+-N/L/d. The achieved nitrification rate was two times higher than previous thermophilic nitrification reactors (Courtens, Spieck, et al., 2016; Vandekerckhove, Kerckhof, et al., 2019). Nitrite accumulation was occasionally observed (e.g., day 56, Fig. 2) and effectively eliminated by temporarily lowering the nitrogen loading rate. These results highlight the potential of thermophilic nitrification for biotechnological applications.

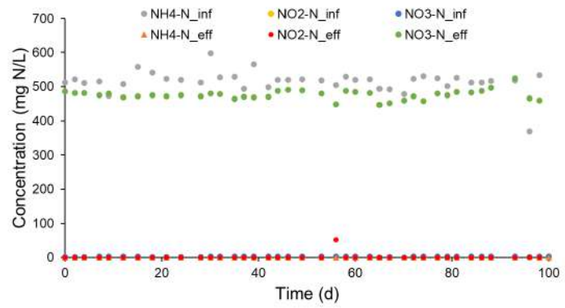

Figure 2. Reactor performance during the stable operation of the thermophilic nitrification reactor 1

Microbial community

The 16S rRNA gene amplicon sequencing indicated that ammonium oxidation was done by AOA belonging to the genus *Candidatus Nitorsosphaera*, with a relative abundance of 56.70%, while no known AOB was detected. Nitrite oxidation was carried out by NOB from the genus *Nitrospira*, accounting for 25.21% of the whole microbial community (Fig. 3). The microbial community was similar to previous studies on thermophilic nitrification in bioreactors (Vandekerckhove, Kerckhof, et al., 2019).

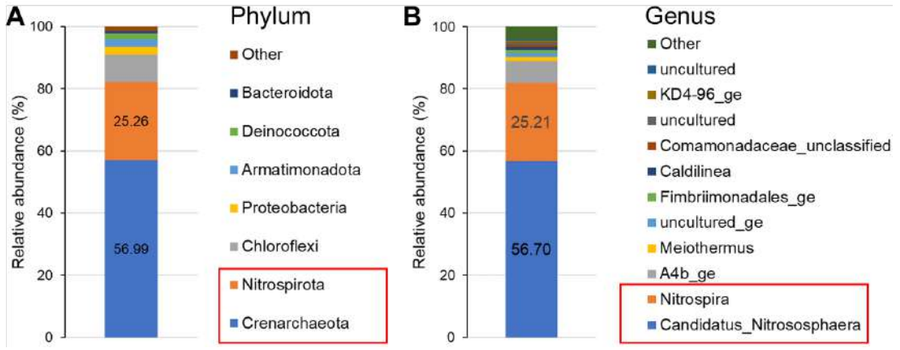

Figure 3. Relative abundance of the top phyla and genera in thermophilic nitrification reactor 1

N_2O emissions

To systematically quantify the N_2O emissions, online monitoring was set up for both the gas and liquid phase. Preliminary results showed no noticeable N_2O in the off-gas of the reactors (ranging between 0-2.3 ppmv, i.e., up to 0.004 mg N_2O/L). Interestingly, the N_2O microsensor showed a relatively stable N_2O concentration of 3.78 ± 0.06 mg N_2O/L in the liquid phase. These preliminary data indicate low N_2O emissions. The online measurement will continue for the following months to quantify N_2O emissions under different operating conditions (e.g., different DO concentrations, and especially with nitrite accumulation while transforming the MBRs from thermophilic full nitrification to yet to-be-reported thermophilic partial nitritation reactors as nitrite accumulation is often associated with high N_2O emissions (Vasilaki, Massara, et al., 2019). This will provide N_2O emission data from AOA-dominated thermophilic nitrification reactors for the first time, which is essential for the holistic evaluation of thermophilic biological nitrogen removal processes, as well as a better understanding of N_2O emissions during the N cycling in thermophilic ecosystems.

REFERENCES

Courtens, E. N., Spieck, E., Vilchez-Vargas, R., Bodé, S., Boeckx, P., Schouten, S., Jauregui, R., Pieper, Di. H., Vlaeminck, S. E., and Boon, N. (2016) A robust nitrifying community in a bioreactor at 50 °C opens up the path for thermophilic nitrogen removal. The ISME Journal, **10**(9), 2293–2303. [online] http://dx.doi.org/10.1038/ismej.2016.8.

Van Kessel, M. A. H. J., Speth, D. R., Albertsen, M., Nielsen, P. H., Op Den Camp, H. J. M., Kartal, B., Jetten, M. S. M., and Lücker, S. (2015) Complete nitrification by a single microorganism. Nature, **528**(7583), 555–559. [online] http://www.nature.com/articles/nature16459 (Accessed August 8, 2019).

Prosser, J. I., Hink, L., Gubry-Rangin, C., and Nicol, G. W. (2020) Nitrous oxide production by ammonia oxidizers: Physiological diversity, niche differentiation and potential mitigation strategies. Global Change Biology, **26**(1), 103–118.

Ravishankara, A. R., Daniel, J. S., and Portmann, R. W. (2009) Nitrous oxide (N2O): The dominant ozone-depleting substance emitted in the 21st century. Science, **326**(5949), 123–125. [online] http://www.ncbi.nlm.nih.gov/pubmed/19713491 (Accessed August 8, 2019).

Steffen, W., Richardson, K., Rockstrom, J., Cornell, S. E., Fetzer, I., Bennett, E. M., Biggs, R., Carpenter, S. R., de Vries, W., de Wit, C. A., Folke, C., Gerten, D., Heinke, J., Mace, G. M., Persson, L. M., Ramanathan, V., Reyers, B., and Sorlin, S. (2015) Planetary boundaries: Guiding human development on a changing planet. Science, **347**(6223), 1259855–1259855. [online] http://www.ncbi.nlm.nih.gov/pubmed/25592418 (Accessed September 4, 2019).

Vandekerckhove, T. G. L., Kerckhof, F.-M., De Mulder, C., Vlaeminck, S. E., and Boon, N. (2019) Determining stoichiometry and kinetics of two thermophilic nitrifying communities as a crucial step in the development of thermophilic nitrogen removal. Water Research, **156**, 34–45. [online] https://linkinghub.elsevier.com/retrieve/pii/S0043135419302192 (Accessed November 5, 2019).

Vasilaki, V., Massara, T. M., Stanchev, P., Fatone, F., and Katsou, E. (2019) A decade of nitrous oxide (N2O) monitoring in full-scale wastewater treatment processes: A critical review. Water Research, **161**, 392–412. [online] https://doi.org/10.1016/j.watres.2019.04.022.

A laboratory-scale study to mitigate greenhouse gas emissions from open sludge lagoons

Sarah Aucote*, Ben van den Akker**, Shihu Hu* and Zhiguo Yuan*

*The University of Queensland, Australia (Email: s.aucote@uq.net.au)
**South Australian Water Corporation, Australia (Email: Ben.vandenakker@sawater.com.au)

Abstract

Open sludge lagoons are employed by wastewater treatment plants (WWTPs) as an economic and efficient means to dewater and stabilise wastewater sludge in countries with an arid climate and inexpensive land. Previous studies revealed that open sludge lagoon methane emissions could contribute one-quarter to two-thirds of the WWTP carbon footprint, highlighting a need for further investigation. Our research aimed to directly quantify methane and nitrous oxide emissions of open sludge lagoons of anaerobically-digested sludge using triplicate laboratory-scale sludge lagoon column incubations. Two different methane emission mitigation strategies were also trialled against an untreated control, whereby sources of nitrate (10 to 15 mg-N/L) and high nitrite (400 to 500 mg-N/L) were continuously applied to the sludge lagoon column natural water-layer. Methane emissions, primarily from ebullitive sources, were the dominant GHG emissions in the control and treated sludge columns. The cumulative methane emission as a percentage of the initial total COD was 23.5 ± 0.5 % in the untreated control after 29 months of incubation. This was reduced by approximately 5.3 % through the high nitrite dosed strategy despite excess nitrous oxide emissions. The nitrate dosed was unable to sufficiently penetrate the sludge-layer to achieve methane emissions reduction, highlighting a limitation that will guide future GHG mitigation strategies. Nitrous oxide emissions that coincided with temporal nitrite accumulation in the water-layer were observed and warrant further investigation. These findings suggest that open sludge lagoons are an overlooked source of GHG emissions that must be considered to achieve sustainable wastewater treatment.

Keywords (maximum 6 in alphabetical order)

Open sludge lagoons; Greenhouse gas emissions; Dewatering; Stabilisation; Wastewater treatment

INTRODUCTION

In countries with an arid climate and inexpensive land, wastewater treatment plants (WWTPs) often employ open sludge lagoons as an economic and efficient means to dewater and stabilise wastewater sludges (Alvarez-Gaitan *et al.* 2016). In Australia, approximately 40% of WWTPs utilise some form of sludge lagoon. Open sludge lagoon operation is highly diverse, where lagoon depths range from 1-3 metres deep and lagoons are operated for months to years. Natural sedimentation of sludge forms distinct water and sludge layers, and in most cases a water-layer is maintained as an odour abatement measure. The high organic matter load of wastewater sludge means that open sludge lagoons are likely sources of greenhouse gas (GHG) emissions. An indirect mass balance assessment of an open sludge lagoon revealed that these systems could contribute one-quarter to two-thirds of the WWTP carbon footprint (Pan *et al.* 2016). However, complementary experiments are required to validate these observations and identify mitigation options. Accordingly, our research employed laboratory scale column incubations for the first direct assessment of methane and nitrous oxide emissions from open anaerobically-digested (AD) sludge lagoons, as well as trialled strategies for the mitigation of methane from AD sludge lagoons.

MATERIALS AND METHODS

Laboratory scale AD sludge column incubations, termed sludge columns, were established in triplicate to mimic the cross-section of a common AD sludge lagoon (Figure 1) and to investigate two separate mitigation options. In the first mitigation strategy, nitrate was dosed to the water-layer of one set of treated sludge columns to a concentration of 10 to 15 mg-N/L to mimic the use of secondary effluent as an alternative water-layer. In the second mitigation strategy, nitrite was dosed to the water-layer of another set of treated sludge columns to a high concentration of 400 to 500 mg-N/L. This nitrite dose was selected to represent partially nitrified centrate that can be available at WWTPs that employ mechanical dewatering alongside open sludge lagoons. Ad hoc dosing of stock concentrations of sodium nitrate and nitrite to the water-layer was performed to maintain the desired treatment range. Direct methane and nitrous oxide emission quantification and physiochemical depth profiling of the ammonium, nitrate, nitrite, methane, nitrous oxide and the soluble chemical oxygen demand was performed during a 29-month incubation period.

RESULTS AND DISCUSSION

Methane emissions were the dominant GHG emission in the untreated control and treatment columns (Figure 2). Nitrous oxide emissions were observed but were small in comparison to methane emissions (Figure 3). After 29 months of incubation, the cumulative methane emission as a percentage of the initial total COD of the untreated control AD sludge columns was 23.5 ± 0.5 %, with approximately one-third of the emissions observed in the first month. Nitrite accumulation in the water-layer was observed inconsistently during the first eight months due to the partial nitrification of ammonium (Figure 4). Periods of nitrite accumulation led to nitrous oxide emissions, while the conclusion of nitrite accumulation coincided with the stabilisation of the ammonium concentration in the water-layer.

The methane emission rate reduced in high nitrite dosed sludge columns, where a decreased rate was observed after three months of incubation (Figure 2). At this time point, the high nitrite treatment permitted nitrite penetration to 15cm below the sludge-water interface. High nitrite presence led to the production of excessive nitrous oxide emissions (Figure 3). After 28 months of nitrite dosing, the cumulative methane emission as a percentage of the initial COD of the control and high nitrite dosed sludge columns were approximately 15.6 ± 0.6 % and 10.3 ± 0.4 %, respectively. However, the cumulative nitrous oxide emission as a percentage of the initial total nitrogen (TN) of the treated columns was exorbitant at 3.7 ± 0.9 %, counteracting the benefits achieved with methane abatement. In the nitrate dosed sludge columns, limited mass transfer of nitrate into the sludge-layer was observed, and as a result, no reduction in methane emissions was observed compared to the control (Figure 2). Interestingly, nitrate dosing increased the extent and duration of nitrite accumulation in the water-layer, which lead to increased nitrous oxide emissions (Figure 3 and 4). After 28 months of dosing, the cumulative nitrous oxide emission as a percentage of the initial TN of the control and nitrate dosed sludge columns was approximately 0.19 % and 0.37 %, respectively (Figure 3). Additionally, nitrate accumulation in the water-layer was observed after 12 months in the control and nitrate dosed sludge columns and nine months in the high nitrite dosed sludge columns (Figure 4). This coincided with the loss of nitrite accumulation, ammonium exhaustion (or ceased ammonium consumption in the untreated control) and increased dissolved oxygen in the water-layer, all of which are indicative of the anaerobic oxidation of ammonium (ANAMMOX) process.

Methane emissions were predominantly ebullitive rather than diffusive in the control and treated sludge columns. Ebullitive methane emissions represented an average of 87 ± 15%, 90 ± 17 % and 88 ± 15 % of the total methane emissions of the control, nitrate-dosed and nitrite-dosed sludge columns, respectively. These findings highlight that unlike the methane mitigation efforts employed here, future emissions reduction strategies must consider ebullitive methane sources.

This research demonstrated that methane emissions in open AD sludge lagoons contribute greatly to the carbon footprint of the WWTPs. While methane mitigation efforts trialled here were unsuccessful at achieving net GHG emission reduction, an invaluable understanding of open sludge lagoons was uncovered that will guide future strategies for methane mitigation. These are currently underway, alongside the assessment of open waste-activated sludge (WAS) lagoons in this context.

Figure 1. Photographs of triplicate 10 L sludge lagoon column incubations containing anaerobically-digested wastewater sludge, including, from left to right, the untreated control, nitrate dosed and high nitrite dosed sludge columns. Columns stand at 1 metre high with water and sludge layers of 40 to 50cm.

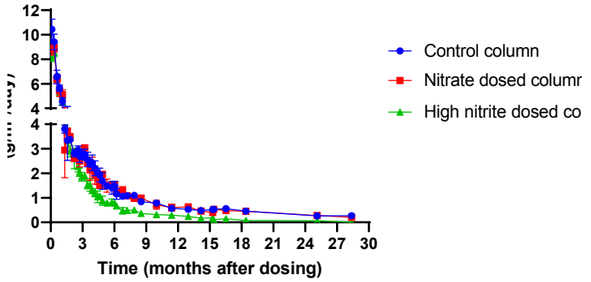

Figure 2. Direct methane emission rate of triplicate AD sludge lagoon column incubations, including the untreated control, nitrate dosed and high nitrite dosed columns, over a 29-month incubation period.

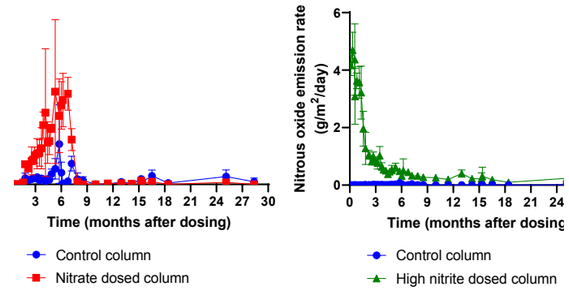

Figure 3. Direct nitrous oxide emission rate of triplicate AD sludge lagoon column incubations, including the untreated control, nitrate dosed and high nitrite dosed sludge columns, over a 29-month incubation period.

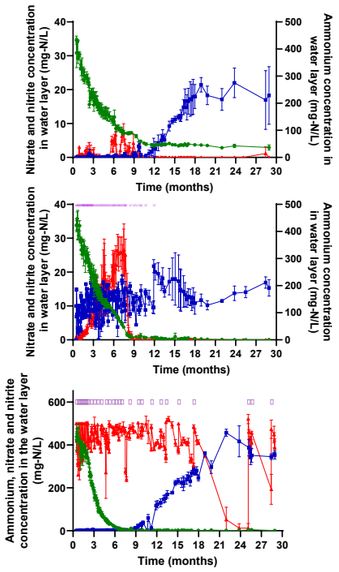

Figure 4. Temporal ammonium (green circle), nitrate (blue square) and nitrite (red triangle) concentration in the water-layer of triplicate sludge lagoon column incubations, including the untreated control (upper), nitrate-dosed water-layer (middle) and high nitrite-dosed water-layer (lower), over a 29-month incubation period, where ad hoc dosing of the treated sludge columns is indicated by a purple arrow.

REFERENCES

Alvarez-Gaitan, J. P., Short, M.D., Lundie, S. & Stuetz, R. 2016 Towards a comprehensive greenhouse gas emissions inventory for biosolids. *Water Research.* **96**: 299-307.

Pan, Y., Ye, L., van den Akker, B., Ganigue Pages, R., Musenze, R. S. & Yuan, Z. 2016 Sludge-drying lagoons: a potential significant methane source in wastewater treatment plants. *Environmental science & technology* **50**: 1368-1375.

Nitrous oxide production for nitrogen valorisation on side stream of an urban waste water treatment plant.

L. Olmo*, J. Pérez* and J. Carrera*

*Department of Chemical, Biological and Environmental Engineering, Universitat Autònoma de Barcelona, Spain.
Corresponding author: *lluc.olmo@uab.cat*

Abstract

Nitrous oxide (N_2O) was monitored in an SBR treating synthetic N-concentrated wastewater through nitritation. N_2O production factors (PF) per ammonium oxidized were quantified depending on the phase where N_2O was found when exiting the reactor. N_2O PF accounted for 18± 4% of total N_2O PF during decanting phase. During aerobic phase, N_2O emissions were found to be heterogeneous along the cycle. An initial N_2O peak was found when transition from anoxic to aerobic conditions took place corresponding to 49±9% of total PF mainly due to hydroxylamine accumulation. In order to maximize N_2O PF, changes in cycle structure will be implemented by adding extra anoxic to aerobic transitional states.

Keywords

Nitrogen valorisation; nitritation; nitrous oxide; waste resource recovery facility.

INTRODUCTION

A waste resource recovery facility (WRRF) is a facility that, while treating wastewater, transforms organic matter and nutrients into energy or various products such as fertilizers, biopolymers, building block chemicals or other advanced bioproducts, that can be used as raw materials and value-added products in other processes (Pott *et al*., 2018). The WRRF proposed here (Figure 1) aims to recover organic matter in form of PHA and biogas, while for nitrogen valorization, nitrite as electron acceptor and nitrous oxide production are considered.

N_2O has been used as a fuel additive in motor racing to increase the power output of engines. Considering the stoichiometric ratio of four (N_2O/CH_4), approximately 37% more energy can be produced using N_2O instead of oxygen during methane combustion. Since anaerobic digestion has been widely stablished for organic matter valorization, it should be noted that nitrogenous compounds contain an estimated value of 0.3 kWh/m^3 that could be recovered. Hence, nitrogen valorization through N_2O has been explored in several studies. The most promising system proposed is the Coupled Aerobic-anoxic Nitrous Decomposition Operation (CANDO) (Scherson, *et al.* 2014). The process involves two reactors for treating the reject water from an urban WWTP: the first stage is a partial nitrification for ammonia oxidation to nitrite; in the second stage, nitrite is reduced to N_2O with organic matter as electron donor (nitrous denitritation). The nitrous denitritation process requires organic matter as electron donor during the second stage, thus the energy gain is compromised since the available organic matter for anaerobic digestion is reduced. To overcome this critical drawback, we propose as a novel alternative the use of nitrifier denitrification, hydroxylamine oxidation and abiotic pathways to produce N_2O so that no organic matter is required.

Hence, the objective of the present study is to investigate the possibility of nitrogen valorization through fully autotrophic pathways. In this presentation, we show a detailed study of the operational parameters affecting the N_2O production in a partial nitritation reactor in view to propose new operational strategies to maximize the N_2O production.

MATERIALS AND METHODS

Reactor configuration and operation phases

A 25 L reactor with a working volume of 20 L was inoculated with sludge from an urban WWTP (Sabadell, Spain). The reactor was operated in SBR mode treating synthetic N-concentrated wastewater (300 mg N-NH_4^+ L^{-1}). The pH was controlled and maintained at 7.8 ± 0.1 throughout the experimental campaign. Compressed air was supplied through an air diffuser placed in the bottom of the reactor at a flow rate of 105 L h^{-1}. During all periods, the cycle length was kept at 6.5 h distributed as follows: 1.14 h of feeding, 4.5 h of aerobic phase, 1 h of anoxic phase, 1 h of settling phase and 0.33 h of decanting phase.

Analytical methods, N_2O measurements and calculations

Ammonium, nitrite and nitrate concentrations in influent and effluent were regularly measured off-line with both, Hach Lange test kits (Hach Lange, Germany) and ionic chromatography using ICS-2000 (DIONEX Corporation, USA) in previously filtered (0.22 µm pore) samples. Hydroxylamine was measured spectrophotometrically after pretreatment with sulfamic acid as in Fear and Burrell (1955). N_2O in the liquid was measured using a Clark type sensor (Unisense, Denmark). N_2O concentration in the gas phase was estimated based on the volumetric mass transfer coefficient.

In the present study, N_2O production factors in relation of the total ammonium oxidized to nitrite were divided into N_2O gas emission factor and N_2O liquid production factor, depending on the phase where N_2O was present when exiting the reactor. The N_2O emitted in the gas phase was quantified as the emission factor (EFgas), while the dissolved N_2O when decanting was quantified as the liquid production factor (PFliq). When necessary, $EFgas_{peak}$ was set in order to estimate the N_2O emission peak contained in EFgas. The total N_2O production factor (PFtot), was calculated by the sum of EFgas and PFliq.

RESULTS AND DISCUSSION

Reactor performance

A stable nitritation operation was required to study the N_2O generation (Figure 2). A start-up process (day 0 to 100) was necessary to enrich the biomass in ammonia oxidizing bacteria (AOB) while supressing the nitrite oxidizing bacteria (NOB). This was possible by maintaining a high free ammonia (FA) concentration during the whole cycle phases as a well-known NOB suppression strategy (Jubany et al., 2009).

Nitrous oxide production

In SBR operation, two main N_2O generation phases are found depending on reactor conditions. In the anoxic phase, N_2O is accumulated in the liquid during decanting which account for an 18±4% of PFtot. In aerobic conditions, EFgas accounted for the remaining 82±4% of PFtot. However, highly heterogeneous emissions were found during aerobic phase with an initial peak which represented the 59±11% of EFgas (set as $EFgas_{peak}$ in Figure3A). Three main processes are reported to be involved in aerobic phase: (I) the accumulation of nitrous oxide during anoxic condition and its subsequent stripping when aeration phase started, which we estimated to be 23±3% of N_2O emitted during peak; (II) the metabolic imbalance caused by the changing conditions that provoked hydroxylamine accumulation (as shown in Figure 3B) thus hydroxylamine oxidation took place and (III) nitrifier denitrification occurring when nitrite acted as final electron acceptor. When stable conditions were stablished (balanced metabolism), hydroxylamine was hardly detected thus, nitrous oxide was produced mainly through nitrifier denitrification.

Finally, in order to maximize N_2O generation of the SBR respect to baseline operation described in this presentation, changes in operational conditions will be implemented. As shown by the results, transition from anoxic to aerobic condition led to a significant N_2O emissions thus, incorporating extra transitional states during the cycle would add extra N_2O production events favouring the PFtot maximization.

Low nitrous oxide emissions and its mechanisms in a pilot-scale mainstream Partial Nitritation/ Anammox process

Y. Zhao*; H. Duan*; S. Hu*; L. Ye* and Z. Yuan*

* The University of Queensland, St Lucia, QLD, Australia 4067 (Email: y.zhao@uq.edu.au; h.duan@uq.edu.au; s.hu@uq.edu.au; l.ye@uq.edu.au; z.yuan@uq.edu.au)

Abstract

Mainstream Partial Nitritation/Anammox (PN/A) has been proposed and dedicatedly investigated for more than a decade for its promising energy potential in wastewater treatment. High nitrous oxide (N_2O) emissions from PN/A are reportedly one of the major challenges hindering its applications. In this work, low N_2O emissions (0.178 ± 0.04%, N_2O-N / NH_4^+-N loading) were observed in a pilot-scale mainstream PN/A operated stably over one-year. Systematic batch tests were designed and conducted to reveal the mechanisms of low N_2O emissions from the process. In the PNA system, flocs were shown to be the major contributor for N_2O emissions, while heterotrophic denitrifiers were the N_2O sink. As a result of FNA side-stream treatment on flocs from PN/A tank, which was applied as a strategy to maintain PN, more resistance to NO_2^- shocks for flocs was found, especially under higher NO_2^--N concentrations, leading to a lower N2O emission factor (5.45% VS 15% at NO_2^--N 10 mg/L, compared with sludge without FNA treatment). Besides, low DO (0.2~0.4 mg/L) and low NO_2^--N concentration (~0.1 mg/L) also contributed to low N_2O emissions from the system, with higher N_2O production as a result of increased nitrifier denitrification pathway observed under higher DO or NO_2^- concentrations. The results of this work will provide guidance to the operation of mainstream PN/A process to minimize N_2O emissions.

Keywords: ***mainstream Partial Nitritation/Anammox; GHG emissions; nitrous oxide.***

INTRODUCTION

Mainstream Partial Nitritation/Anammox (PN/A) is widely recognized as a promising wastewater treatment process. High nitrous oxide (N_2O, a potent greenhouse gas) emissions from PN/A are reportedly one of the major challenges hindering its applications. While anammox process does not generate N_2O, the N_2O emissions from its integration with PN process has great uncertainties. N_2O emissions have been mostly investigated in PN systems receiving high strength wastewater (NH_4^+ > 500 mgN/L). Compared with conventional nitrification and denitrification, higher N_2O emission factors were reported from side-stream PN processes, ranging from 1.7% to 19% of the NH_4^+-N converted [1, 2]. This is mainly caused by the limited DO (i.e. 0.05-1.5 mg/L) [3, 4] to achieve PN and the ensuing NO_2^- accumulation (i.e. 15- 1680 mg/L) [3, 5].

To the best of our knowledge, there is no study on N_2O production from one-stage pilot-scale mainstream PN/A system to date. In this study, we discovered low N_2O emissions from a one-stage pilot-scale mainstream PN/A process during the long-term onsite measurement and investigated the mechanism for the low N_2O emissions from mainstream PNA system. This is the first study reporting the N_2O emissions from one-stage pilot-scale mainstream PNA system, and its mechanism was thoroughly studied.

MATERIAL and METHODS

The pilot-scale mainstream anammox-based system contains high rate activated sludge (HRAS) tank, pre-anammox tank and PN/A tank. The detailed operation conditions of the whole system were described in our recent study [6]. Briefly, the system was operated under a continuous mode based on residual NH_4^+-N control in the PN/A tank; and a portion of the flocs from PN/A reactor was regularly treated by Free Nitrous Acid (FNA, 2 mg N/L) to control the growth of nitrite oxidizing bacteria (NOB). Continuous online N_2O monitoring was carried out in the pilot-scale system. In addition, a series of batch tests were conducted to study the mechanism of N_2O emissions in the pilot mainstream PNA system.

RESULTS and DISCUSSIONS

During the stable state of the pilot reactor operation, the N_2O emissions from the PN/A tank were monitored online continuously, with the representative dynamics shown in Fig. 1. The overall N_2O emissions from the PN/A tank were low during the long-term, ranged between 3-6 ppmv, with an average of 4.25± 0.94 ppm, while the NO was even lower to negligible. Compared with the N_2O emission factor (~1.6% of the nitrogen loading) from the full-scale N/D treatment plant[7], the N_2O emission factor (mass N_2O-N emitted/ NH_4^+-N loading) was lower from our study, averaging at 0.178±0.04%. This was also notably lower than other studies on N_2O emissions from mainstream PN in lab-scale investigations.

Batch test showed flocs contributed to the majority of the N_2O emissions in the PN/A tank. For the N_2O emissions from the three batch tests (carriers only, flocs only, and carriers+ flocs), the highest N_2O emissions occurred from scenario with flocs only (Fig. 2). This finding was in line with the study by Zhuang et al. [8], in which flocs was proposed to be the main source of N_2O in a high-rate anammox granular sludge reactor. One of the possible reasons for the dominant role of flocs for N_2O emission was that AOB was the main species in flocs, acting as the N_2O contributor [9].

Notably, N_2O emission without the presence of COD was 5 times higher than that from with COD from flocs. This was possibly a result of the high abundance of N_2O reducers in flocs. In fact, the emissions from tests with COD were lower than those from without COD (Fig. 2). This is further confirmed with additional experiments showing the addition of external organic carbon reduced N_2O emissions from the PN/A process (Fig. 3). Heterotrophic denitrification is likely a sink for N_2O in the PN/A system.

In addition, the batch tests showed flocs and carriers in PN/A tank have adapted to NO_2^- presence, leading to relatively low N_2O emissions (Fig. 4). N_2O emissions from flocs only, carriers only and normal WAS under elevating NO_2^- concentrations were measured to evaluate its response to NO_2^- concentrations. Significantly different responses of N_2O emissions were observed, which suggested the flocs and carriers in PN/A tank have adapted to NO_2^- presence.

The impacts of operational conditions on N_2O emissions from the mainstream PN/A system was also evaluated in batch tests. The N_2O emissions from different conditions are summarised in Table 1. As can be seen, the total N_2O-N emissions from conditions without COD were all higher than those from with COD (Table 1). These results further confirmed the role of HD as a N_2O sink in the PN/A tank. The promoting effects of nitrite are obvious. Higher DO levels are also found to increase N_2O emissions. The low DO (0.2~0.4 mg/L) and low NO_2^--N concentration (~0.1 mg/L) in the pilot mainstream PNA system also contributed to low N_2O emissions.

Overall, this work reported low N_2O emissions from a pilot-scale mainstream PN/A system and illustrated the underlying mechanisms of the low N_2O emissions. The insights will provide critical guidance for the operation of mainstream PN/A process to minimize the N_2O emissions.

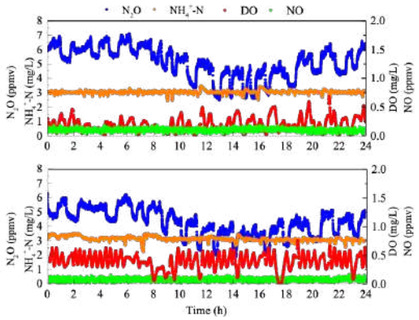

Fig. 1 Performance and N_2O emissions from pilot-scale Anammox based system.

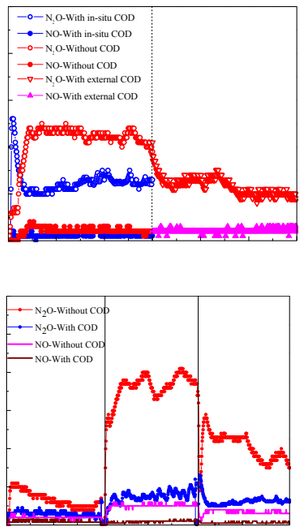

Fig. 2 N_2O emissions from different scenarios

Fig. 3 Reduced N_2O emissions with the addition of external organic carbon.

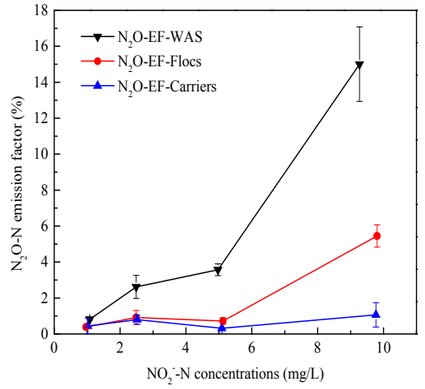

Fig. 4 N_2O emission factors from different scenarios under corresponding NO_2^--N concentrations.

Table. 1 N_2O emissions from different operational conditions

Set	NH_4-N (mg/L)	NO_2-N (mg/L)	DO (mg/L)	With COD		Without COD	
				N_2O-N (mg)	N_2O-N EF (%)	N_2O-N (mg)	N_2O-N EF (%)
1	7.9 ± 0.6	0.9 ± 0.2	0.23 ± 0.06	0.022	0.30 ± 0.05	0.027	0.27 ± 0.04
2	7.2 ± 0.3	1.0 ± 0.3	1.0 ± 0.1	0.047	0.36 ± 0.06	0.048	0.71 ± 0.13
3	7.5 ± 0.8	3.8 ± 0.1	0.25 ± 0.08	0.035	0.32 ± 0.05	0.13	0.47 ± 0.04
4	14 ± 2.5	1.0 ± 0.04	0.22 ± 0.05	0.019	0.11 ± 0.03	0.054	0.23 ± 0.02
5	15 ± 2.1	3.5 ± 0.6	0.22 ± 0.04	0.034	0.19 ± 0.02	0.144	0.38 ± 0.04
6	3.9 ± 0.5	1.1 ± 0.3	0.22 ± 0.06	0.018	0.08 ± 0.03	0.056	0.15 ± 0.06
7	6.4 ± 0.2	3.5 ± 0.6	0.95 ± 0.1	0.23	0.91 ± 0.03	0.24	0.91 ± 0.15
8	7.7 ± 0.2	8.7 ± 0.3	0.27 ± 0.09	0.37	2.00 ±0.23	0.68	7.76± 2.98

Reference

(1) Pijuan, M.; et al. Effect of process parameters and operational mode on nitrous oxide emissions from a nitritation reactor treating reject wastewater. **2014**, *49*, 23-33.
(2) Kampschreur, M. J.; et al.;Dynamics of nitric oxide and nitrous oxide emission during full-scale reject water treatment. **2008**, *42* (3), 812-826.
(3) Terada, A.; et al. Hybrid Nitrous Oxide Production from a Partial Nitrifying Bioreactor: Hydroxylamine Interactions with Nitrite. *Environ Sci Technol* **2017**, *51* (5), 2748-2756.
(4) Lackner, S.; Gilbert, E. M.; Vlaeminck, S. E.; Joss, A.; Horn, H.; van Loosdrecht, M. C. J. W. r. Full-scale partial nitritation/anammox experiences–an application survey. **2014**, *55*, 292-303.
(5) Terada, A. et al. Presence and detection of anaerobic ammonium-oxidizing (anammox) bacteria and appraisal of anammox process for high-strength nitrogenous wastewater treatment: a review. **2011**, *13* (6), 759-781.
(6) Zheng, M.et al. One-year stable pilot-scale operation demonstrates high flexibility of mainstream anammox application. *Water Research X* **2023**, 100166.
(7) IPCC. *2019 Refinement to the 2006 IPCC Guidelines for National Greenhouse Gas Inventories: Wastewater treatment and discharge*; Intergovernmental Panel on Climate Change, Kyoto, Japan, 2019.
(8) Zhuang, J. L. et al. Flocs are the main source of nitrous oxide in a high-rate anammox granular sludge reactor: insights from metagenomics and fed-batch experiments. *Water Res* **2020**, *186*, 116321.
(9) Hubaux, N. et al. Impact of coexistence of flocs and biofilm on performance of combined nitritation-anammox granular sludge reactors. **2015**, *68*, 127-139.

Characterization of hydrogenotrophic methanogenic cultures through a novel pressurized headspace-free Hydrogen Uptake Rate methodology

M. Fachal[a,*], L. R. López[a], E. Valdés[a], M. Deshusses[b], D. González[a] and D. Gabriel[a]

[a] GENOCOV research group, Department of Chemical, Biological and Environmental Engineering, Universitat Autònoma de Barcelona, Spain.
[b] Department of Civil and Environmental Engineering, Duke University, 127C Hudson Hall, Durham, NC 27708
* E-mail: *manuel.fachal@uab.cat*

Abstract

Biomethanation has become an attractive process for biogas upgrading. In this work, a microbial culture with fermentative and homoacetogenic bacteria was enriched in hydrogenotrophic methanogenic archaea. Both cultures were characterized for their microbial diversity and biological activity, the later assessed both in classical serum bottle tests (SBTs) and through a novel methodology to perform pressurized, headspace-free hydrogen uptake rate (PHF-HUR) tests. PHF-HUR under pressure allows increasing H_2 solubility to overcome potential mass transfer limitations of SBTs tests. PHF-HUR tests let us calculate rates and kinetic parameters under a range of conditions by monitoring the dissolved H_2 concentration over time.

Keywords

Biomethanation; hydrogen uptake rate (HUR); microbiological enrichment; yeast extract.

INTRODUCTION

Among different technological innovations and processes tackling the upgrading of biogas to the required methane contents, biogas upgrading using hydrogenotrophic methanogens arises as a key step towards a sustainable model to produce green energy. Hydrogenotrophic methanogenic archaea (H_2-MA) are chemoautotrophic microorganisms capable of converting CO_2 to CH_4 using H_2 as electron donor by a direct reaction (Eq. 1).

$4H_2 + CO_2 \rightarrow CH_4 + 2H_2O$ $\quad \Delta G\square = -130.7$ kJ/mol Eq. 1

$4H_2 + 2CO_2 \rightarrow CH_3COOH + 2H_2O$ $\quad \Delta G°' = -104.5$ kJ/mol Eq. 2

$CH_3COOH \rightarrow CH_4 + CO_2$ $\quad \Delta G°' = -31.0$ kJ/mol Eq. 3

The presence of other microbial populations such as homoacetogenic bacteria, that may compete with H_2-MA for the same e-donor (Eq. 2), and acetoclastic methanogens producing CH_4 (Eq. 3) may lead to apparently unbalanced results with respect to Eq. 1 and to puzzling stoichiometric and kinetic results. Thus, a proper mechanistic characterization of the microbial culture is needed.

Hydrogen Uptake Rate (HUR) tests are a cost-effective tool to characterize the biological activity of hydrogenotrophic cultures and to study the mechanisms, rates, kinetic parameters or growth yields. The conventional approach for a typical H_2-activity test is to use a batch system as serum bottles with a H_2-rich headspace and measuring the headspace pressure to assess H_2 consumption. However, direct measurements of the liquid-phase H_2 concentration by in-situ H_2 probes demonstrated the problems associated with slow and limited H_2 G-L transfer, leading to inaccurate estimation of kinetic parameters. Therefore, a reliable methodology to properly identify hydrogenotrophic cultures rates and kinetic parameters through batch tests is still lacking.

In this sense, a novel methodology is proposed in this work to perform HUR tests avoiding G-L mass transfer limitations. Different selected variables (pH, temperature and the presence of inhibitors such as O_2 or H_2S) were tested. Stoichiometric and kinetic parameters were assessed from the resulting H_2 profiles during the monitoring of the decrease of dissolved H_2 concentration over time. Two microbial populations were assessed through HUR: one fed with mineral medium with yeast extract and an equivalent one enriched without yeast extract. In addition, serum bottle tests and Illumina were used to assess the contribution and role of homoacetogens and fermentative bacteria.

MATERIALS AND METHODS

From one side, characterization of the initial microbial culture with yeast extract in its mineral medium (MM) (not enriched in H_2-MA) as well as without yeast extract in the MM (enriched in H_2-MA) were performed in 250 mL serum bottles (125 mL liquid + 125 mL headspace gas). Preliminary serum bottle tests (SBTs) were performed to assess the contribution of H_2-MA to H_2 consumption vs. that of homoacetogens both in yeast-MM and no-yeast-MM cultures. In addition, a novel pressurized, headspace-free HUR (PHF-HUR) methodology was developed to further assess kinetics of both, enriched and non-enriched cultures. A pressurized 120 mL Miniclave reactor (BuchiGlas, Switzerland) equipped with a dissolved H_2 microsensor (Unisense) was used to perform PHF-HUR tests (Figure 1a). In essence, the liquid phase (with or without biomass) is saturated with H_2 under a selected pressure in a headspace-free reactor. A liquid injection chamber is used to feed either the microbial culture or CO_2, depending on the type of test.

Analyses of total suspended solids (TSS) and volatile suspended solids (VSS) were conducted as described in Standard Methods. Analyses of methane (CH_4), carbon dioxide (CO_2) and hydrogen gas (H_2) were conducted through gas chromatography (GC 7820A, Agilent Technologies). High performance liquid chromatography (Ultimate 3000, Agilent Technologies) was used to measure VFA's accumulation in the liquid phase. Total inorganic carbon (TIC) and Total Organic Carbon (TOC) were measured using a Multi N/C analyzer (Analytikjena). All the samples were filtered with 0.22 µm filters (Millipore). DNA extractions were performed using a Norgen Biotek Corp. Kit to isolate the DNA samples and perform Illumina tests to assess microbial populations.

RESULTS AND DISCUSSION

Methane production pathways were studied for a methanogenic mixed culture with yeast extract in its MM by performing SBTs. Results showed not only the presence of VFAs in the medium, but also an overproduction of CH_4 compared to the inorganic C consumed during the tests. Thus, the presence of acetoclastic methanogens was considered. Feeding composition in the MM was reformulated, removing yeast extract to avoid VFAs production from C sources such as proteins. SBTs in the presence and absence of yeast extract allowed assessing the rates of both biomethanation pathways (H_2-MA and acetoclastic). By removing the yeast extract, the presence of VFAs became negligible and C balances showed an increment in the contribution of the target pathway (H_2-MA) from 69.1 to 82.7% (Table 1). DNA samples were taken after 11 months feeding a yeast extract free medium to observe the evolution of the microbial populations due to the change in the feeding (Figure 2). An enrichment in *Methanobacterium* genus, a H_2-MA , was observed, as expected from the SBTs results.

In parallel, a methodology based on dissolving H_2 under pressure into the liquid medium was used to run several HUR tests. The main characteristic of this methodology is the absence of headspace, thus, avoiding G-L mass transfer limitation of H_2 during the experiment. Different configurations were tested consisting of either injecting bicarbonate to a CO_2-free microbial culture saturated with H_2 or injecting a microbial suspension to a CO_2-rich MM saturated with H_2. In both cases, the liquid phase is first saturated by bubbling H_2, then, the reactor is filled through a pressurized injection chamber ensuring a headspace-free reactor. At that point, the reaction starts and the profile of dissolved hydrogen in the liquid is monitored by the sensor along time. Figure 1b shows the typical profile of dissolved H_2 concentration over time for a PHF-HUR test. In the selected test, H_2 is consumed by the microorganisms at a specific volumetric rate of 24.45 $mmol_{H2}/(gVSS \cdot d)$ when running the PHF-HUR test at 1.5 bars of initial pressure, 37ºC and a pH of 7.6. A battery of PHF-HUR tests were carried out both with the non-enriched and enriched (Table 2) methanogenic cultures under different conditions. Temperature, pH and inhibitory species were assessed through PHF-HUR tests with this novel methodology, thus making possible to study the rates and kinetic parameters of the culture, avoiding potential mass transfer limitations that could occur in the traditional batch tests with serum bottles. These preliminary results show the promising capacity of this methodology as a tool to monitor the culture's hydrogenotrophic activity at different conditions to assess biogas upgrading activity.

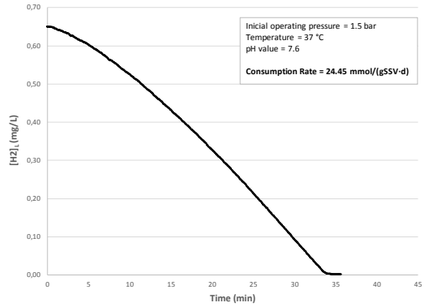

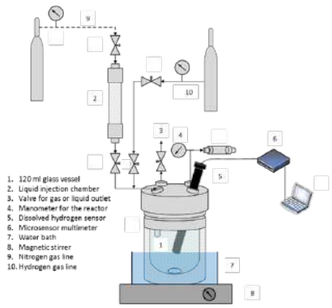

Figure 1. (a) Scheme of the setup for HUR tests: Buchiglas Miniclave reactor. (b) Dissolved H_2 consumption profile in HUR tests.

Table 1. Calculations from activity tests in presence and absence of yeast extract.

CH_4 produced mmol	TIC as CH_4 mmol	TOC as CH_4 mmol	CH_4 Yield %	Pathway's Contribution (%) H2-MA	Acetoclastic	
3,235	2,237	0,918	97,5	69,1	28,4	Yeast Extract Presence

CH_4 produced mmol	TIC as CH_4 mmol	TOC as CH_4 mmol	CH_4 Yield %	Pathway's Contribution (%) H2-MA	Acetoclastic	
3,574	2,956	0,573	98,7	82,7	16,0	Yeast Extract Absence

Table 2. Summary of conditions for the different HUR tests carried out.

Test	Condition	Pressure (bar)	$[0_2]$ (mg/L)	Temperature (° C)	$[H_2S]$ (mg/L)
1	**Abiotic**	3	0	37	0
2	Biotic	**1**	0	37	0
3	Biotic	**2**	0	37	0
4	Biotic	**3**	0	37	0
5	Biotic	3	**1**	37	0
6	Biotic	3	**2**	37	0
7	Biotic	3	0	**27**	0
8	Biotic	3	0	**47**	0
9	Biotic	3	0	37	**50**
10	Biotic	3	0	37	**100**

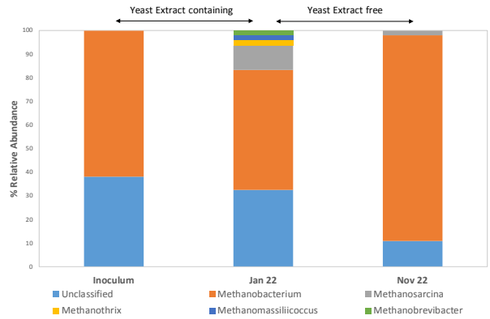

Figure 2. Microbiological enrichment of the culture (Genus level).

ACKNOWLEDGEMENTS

Grant PID2021-126253OB-C21 funded by MCIN/AEI/10.13039/501100011033 and by "ERDF a way of making Europe" by the "European Union".

REFERENCES

Angelidaki, I., Treu, L., Tsapekos, G., Luo, G., Campanaro, S., Wenzel, H., Kougias, P.G. 2018 Biogas upgrading and utilization: current status and perspectives. *Biotechnol. Advances* **36**(2), 452–466.

APHA, AWWA, WPCF, 2005. Standard Methods for the Examination of Water and

Wastewater, 21st ed., Washington, DC.

Kleerebezem, R., Stams, A.J.M. 2000 Kinetics of syntrophic cultures: a theoretical treatise on butyrate fermentation. *Biotechnol. Bioeng.* **67**, 529–543.

Morris, R.L., Tale, V.P., Mathai, P.P., Zitomer, D.H., Maki, J.S. 2016 mcrA Gene abundance correlates with hydrogenotrophic methane production rates in full-scale anaerobic waste treatment systems. *Lett. Appl. Microbiol.* **62**, 111–118.

Seasonal microbial community dynamics at Lleida WWTP: filamentous bulking and nitrification deterioration events

S. Astals*, M. S. Romero-Güiza**, R. Asiain-Mira***, J. Palatsi**, M. Peces*

* Dept. Chemical Engineering and Analytical Chemistry, University of Barcelona, 08028 Barcelona, Spain
(E-mail: *sastals@ub.edu*; *mpeces@ub.edu*)
** Aqualia, Production Area, Cami Sot de Fontanet, 29, 25197 Lleida, Spain
(E-mail: *maycollstiven.romero@fcc.es; jordi.palatsi.civit@fcc.es*)
*** Aqualia, Innovation and Technology Department, Av. Del Camino de Santiago 40, 28050 Madrid, Spain
(E-mail: *ruben.asiain@fcc.es*)

Abstract

Bulking episodes and loss of nitrification capacity are two recurrent issues in municipal WWTPs. This research explores the relation between these phenomena and the dynamic changes of the activated sludge system and the anaerobic digesters microbial community in Lleida WWTP. The decrease of *Nitrosomonas* (AOB) and *Nitrospira* defluvii (NOB) relative abundance was concomitant to the deterioration of the nitrification capacity between March and April 2022. Similarly, the bulking episodes of spring 2022 were associated with an increase of the relative abundance of *Ca. Microthrix* species, which showed a marked seasonal dynamic.

Keywords

Activated sludge; anaerobic digestion; filamentous bulking; microbial time-series; nitrification; wastewater treatment plant.

INTRODUCTION

Wastewater treatment plants rely on complex biological systems for sanitation and resource recovery. However, there is still limited knowledge of the underpinning microbial dynamics on which these mixed-culture biotechnologies performance relies on. This knowledge is essential because uncertainty surrounding the microbial community dynamics is a key barrier preventing the intensification of this biotechnologies and shift the conservative approach of decision-makers.

Bulking episodes and loss of nitrification capacity are two recurrent issues in WWTPs worldwide (Gruber, Niederdorfer, et al., 2021; Johnston, LaPara, et al., 2019; Wágner, Peces, et al., 2022). Between March and April of 2022, the WWT under study experienced a decrease on nitrification activity and a filamentous bulking episode. The latter affected both the activated sludge and the anaerobic digesters. The main goal of this research is to determine whether dynamic changes in the microbial community of the activated sludge system and the anaerobic digesters could explain these two operation issues.

MATERIALS AND METHODS

Lleida WWTP

The WWTP of Lleida (Spain) treats 50,000 m^3/day of municipal sewage (160,000 P.E.). The activated sludge system of the WWTP has biological nitrogen removal and enhanced biological phosphate removal (EBPR). The WWTP has two anaerobic digesters to treat a the primary and waste activated sludge. Further details about the WWTP configuration and operation can be found in Palatsi et al. (2021) and Romero-Güiza et al. (2022).

Microbial community sampling

Activated sludge and anaerobic digestion biomass were sampled weekly from 05-Oct-2021 to 05-Jul-2022. Samples were stored at -20 °C until analysis. Activated sludge samples were collected in the aerobic basin (48 samples), and anaerobic digestion samples were collected in the digesters' recirculation line (40 samples). DNA extraction and sequencing (V3-V4 region of the 16S rRNA) was carried out by Novogene Co. (UK). The ASV (amplicon sequence variants) table was obtained as for Peces et al. (2022). Taxonomy was assigned to each ASV using MiDAS 4.8.1 database.

RESULTS AND DISCUSSION

Microbial ecology results showed that the microbial community of the activated sludge and the anaerobic digesters are dynamic showing a seasonal pattern. The seasonality of the activated sludge microbiome was recently described in Peces et al. (2022). However, the seasonal dynamics of the anaerobic digestion microbiome have not been previously reported. Figure 1 illustrates that temperature have a strong influence on the microbial community beta diversity, although the relative importance of other environmental and operational factors needs further analysis.

Activated sludge microbial community

Nitrosomonas was the only genus of ammonium oxidation bacteria (AOB) detected in the activated sludge microbiome. *Nitrospira* defluvii and an unclassified *Nitrotoga* (ASV12810) were the main nitrite oxidation bacteria (NOB) in the activated sludge microbiome. There was a decline of both *Nitrosomonas* and *Nitrospira* defluvii relative abundance between January and May of 2022, which started two months earlier than noticing a decrease on the nitrification activity (March 2022). These results suggest that microbial community analysis could be used as an early warning, however, further research is required to understand the associations between process performance and microbial dynamics. The nitrification capacity of the system was recovered once the *Nitrosomonas* relative abundance increased.

Tetrasphera, a polyphosphate accumulating organisms, was the main genus with the higher relative abundance in the activated sludge system, as previously reported in Palatsi et al. (2021). The most abundant *Tetrasphera* species (*Tetrasphaera* midas_s_5) also showed a clear seasonal dynamic, with its higher abundance between December 2021 and March 2022 and its lower abundance between May and July 2022. Interestingly, this species did not showed a seasonal dynamic in Danish WWTP plants (Peces, Dottorini, et al., 2022).

Ca. Microthrix (parvicella and subdominans) were the main known filamentous bacteria in the activated sludge, among the over 20 different species detected. Both species have been found to be responsible of bulking episodes in other WWTPs (Nierychlo, Singleton, et al., 2021). The relative abundance of *Ca.* Microthrix species also showed a marked temporal dynamic, with its higher abundance occurring between April and May of 2022 (relative abundance up to 15%), when a severe bulking event occurred at the WWTP.

Anaerobic digestion microbial community

The microbiome of the anaerobic digesters was dominated by *Methanotrix* (a.k.a. *Methanosaeta*), an aceticlastic methanogen. *Methanotrix* is the main methanogen in most WWTP digesters (Jiang, Peces, et al., 2021). Hydrogenotrophic methanogens were also found but at a very low (<1%) relative abundance (e.g. *Ca. Methanofastidiosum*, *Methanospirillum*).

Some putative hydrolytic and fermenting bacteria showed a clear seasonal pattern (*Bacteroidetes* midas_s_19, *Sedimentibacter* midas_s_1214,), while others were washed out from the digesters (e.g. ST-12K33 midas_s_22). However, hydrolytic and fermenting bacteria are considered functionally redundant, hence a decrease of their relative abundance may not imply a lower hydrolytic efficiency. The microbial community of the anaerobic digesters also showed a high diversity of syntrophic bacteria (*Syntrophorhabdus*, *Syntrophomonas*, *Smithella*, *Syntrophobacter* or *Ca. Propionivorax*), indicating a high diversity of the acetogenic degradation pathway.

Several genera from the activated sludge system were detected in high abundance in the anaerobic digesters, despite lacking a role in the anaerobic digestion degradation pathway (e.g. *Tetrasphera*, *Ca. Microthrix*, *Rombustia*), indicating that they are merely immigrating from the activated sludge.

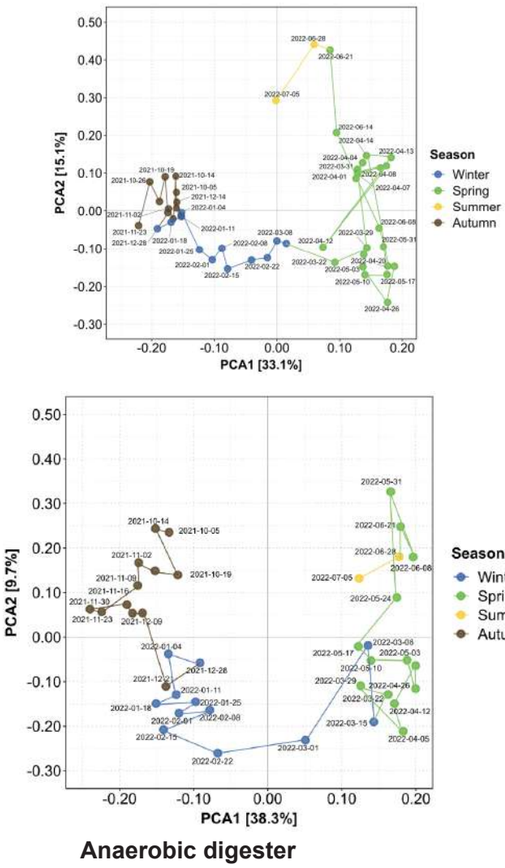

Figure 1. Principal component analysis (PCA) of the microbial community of the (top) activated sludge and (bottom) anaerobic digester. Colours differentiate the seasons of the northern hemisphere (winter, spring, summer and autumn).

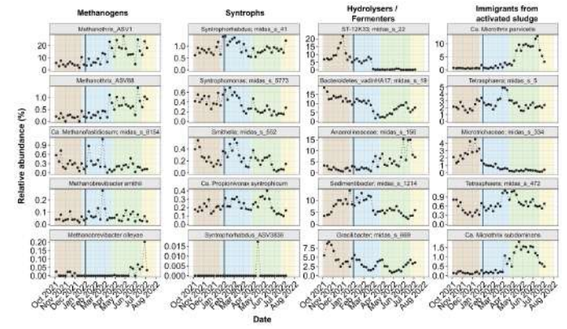

Figure 2. Time-series of the anaerobic digesters' microbial community. The microbial community is clustered in the four functional groups (methanogenesis, acetogenesis, fermenters/hydrolyser and immigrants)

REFERENCES

Gruber, W., Niederdorfer, R., Ringwald, J., Morgenroth, E., Bürgmann, H., and Joss, A. (2021) Linking seasonal N2O emissions and nitrification failures to microbial dynamics in a SBR wastewater treatment plant. Water Research X, **11**, 100098.

Jiang, C., Peces, M., Andersen, M. H., Kucheryavskiy, S., Nierychlo, M., Yashiro, E., Andersen, K. S., Kirkegaard, R. H., Hao, L., Høgh, J., Hansen, A. A., Dueholm, M. S., and Nielsen, P. H. (2021) Characterizing the growing microorganisms at species level in 46 anaerobic digesters at Danish wastewater treatment plants: A six-year survey on microbial community structure and key drivers. Water Research, **193**, 116871.

Johnston, J., LaPara, T., and Behrens, S. (2019) Composition and Dynamics of the Activated Sludge Microbiome during Seasonal Nitrification Failure. Scientific Reports, **9**(1), 4565.

Nierychlo, M., Singleton, C. M., Petriglieri, F., Thomsen, L., Petersen, J. F., Peces, M., Kondrotaite, Z., Dueholm, M. S., and Nielsen, P. H. (2021) Low Global Diversity of Candidatus Microthrix, a Troublesome Filamentous Organism in Full-Scale WWTPs. Frontiers in Microbiology, **12**. [online] https://www.frontiersin.org/articles/10.3389/fmicb.2021.690251 (Accessed January 27, 2023).

Palatsi, J., Ripoll, F., Benzal, A., Pijuan, M., and Romero-Güiza, M. S. (2021) Enhancement of biological nutrient removal process with advanced process control tools in full-scale wastewater treatment plant. Water Research, **200**, 117212.

Peces, M., Dottorini, G., Nierychlo, M., Andersen, K. S., Dueholm, M. K. D., and Nielsen, P. H. (2022) Microbial communities across activated sludge plants show recurring species-level seasonal patterns. ISME Communications, **2**(1), 1–11.

Romero-Güiza, M. S., Flotats, X., Asiain-Mira, R., and Palatsi, J. (2022) Enhancement of sewage sludge thickening and energy self-sufficiency with advanced process control tools in a full-scale wastewater treatment plant. Water Research, **222**, 118924.

Wágner, D. S., Peces, M., Nierychlo, M., Mielczarek, A. T., Thornberg, D., and Nielsen, P. H. (2022) Seasonal microbial community dynamics complicates the evaluation of filamentous bulking mitigation strategies in full-scale WRRFs. Water Research, **216**, 118340.

TECHNICAL SESSIONS

T17.

Nature based solutions

Framework for a quantification approach of resource streams utilized by nature-based solutions in circular cities

B. Pucher[1], M. Radinja[2,3], A. Gholipour[4], F. Chioggia[5], M. Wirth[6], R. Pineda-Martos[7], K. A. Hoffmann[8], A. Canet-Martí[1], P. N. Carvalho[9,10], D.C. Finger[11] and G. Langergraber[1]

[1]University of Natural Resources and Life Sciences, Vienna, Department of Water, Atmosphere and Environment, Institute of Sanitary Engineering and Water Pollution Control, Muthgasse 18, 1190 Vienna, Austria (E-mail: bernhard.pucher@bocu.ac.at, alba.canet@boku.ac.at, guenter.langergraber@boku.ac.at)
[2]Aquafin NV, Dijkstraat 8, B-2630 Belgium (E-mail: matej.radinja@aquafin.be)
[3]University of Ljubljana, Faculty of Civil and Geodetic Engineering, Jamova 2, 1000 Ljubljana, Slovenia (E-mail: matej.radinja@fgg.uni-lj.si)
[4]LEAF – Linking Landscape, Environment, Agriculture and Food, Institute Superior de Agronomia (ISA), University of Lisbon, Tapada da Ajuda, Lisbon 1349-017, Portugal (amirgholipour@isa.ulisboa.pt)
[5]Department of Agricultural and Food Sciences University of Bologna,Viale Fanin 50, 40127, Bologna (Italy) (E-mail: francesco.chioggia2@unibo.it)
[6]alchemia-nova GmbH, Baumgartenstraße 93, 1140 Vienna, Austria (maria.wirth@alchemia-nova.net)
[7]Department of Aerospace Engineering and Fluid Mechanics - Area of Agroforestry Engineering, School of Agricultural Engineering, University of Sevilla, Ctra. de Utrera km. 1, 41013, Sevilla, Spain (E-mail: rpineda@us.es)
[8]Institute of Ecology, Chair of Ecohydrology and Landscape Evaluation, Technische Universität Berlin, Ernst-Reuter-Platz 1, 10587 Berlin, Germany (Email:karin.hofmann@tu-berlin.de)
[9]Department of Environmental Science, Aarhus University, Frederiksborgvej 399, DK-4000 Roskilde, Denmark (e-mail pedro.carvalho@envs.au.dk)
[10]WATEC - Centre for Water Technology, Aarhus University, Ny Munkegade 120, 8000 Aarhus, Denmark
[11]School of Engineering, Reykjavik University, 101 Reykjavik, Iceland (Email: davidf@ru.is)

Abstract
Nature-based solutions (NBS) have the ability to contribute towards the development of circularity for the urban environment. While the qualitative description of the provided functions, processes and benefits is fully available in the literature, there is often a lack of quantification of resource streams and, consequently, of knowledge of the real contribution of NBS. To change this approach, a framework providing guidance on how to achieve the quantification using a simplified and detailed approach is presented in this work. This also includes the description of the actual demands of the urban space for the implementation of NBS as well as their provided services in order to select appropriate NBS units.

Keywords: Circular economy, guidance, nature-based solutions, quantification, resource recovery

INTRODUCTION

The implementation of nature-based solutions (NBS) in the urban context is known to provide multiple benefits towards sustainable development, climate change adaptation, biodiversity improvement, public health, pollution control and resource management. An important aspect, therefore, lies in their application in closing resource cycles and contribute to the transition towards urban circular economy (Langergraber et al., 2021).
Within the COST Action CA17133 Circular City (Langergraber et al., 2020), a set of NBS units, interventions and supporting units was defined to foster the paradigm change towards circularity in the management of natural resources. The work (Langergraber et al., 2021a) evaluated the qualitative potential of NBS to address one or more defined urban circularity challenges (UCC) (Atanasova et al., 2021)resource depletion, climate change, and degradation of ecosystems. To cope with these challenges, the transformation of our cities into sustainable systems using a holistic approach is required. The pathway to this urban transition is adopting the concept of circular economy for resource management. In this way, resources are kept and reused within the city. Nature-based solutions can be implemented for these tasks, and besides the circularity, they can provide additional benefits for the urbanites and the urban environment in general. This paper describes which urban challenges related to circularity can be addressed through nature-based solutions. This systematic review was developed within the COST Action CA17133 Circular City that investigates how nature-based solutions can be used to progress the circular economy in the urban built environment.”,”author”:[{“dropping-particle”:””,”family”:”Atanasova”,”given”:”Nataša”,”non-dropping-particle”:””,”parse-names”:false,”suffix”:””},{“dropping-particle”:””,”family”:”Castellar”,”given”:”Joana A.C.”,”non-dropping-particle”:””,”parse-names”:false,”suffix”:””},{“dropping-particle”:””,”family”:”Pineda-Martos”,”given”:”Rocío”,”non-dropping-particle”:””,”parse-names”:false,”suffix”:””},{“dropping-particle”:””,”family”:”Nika”,”given”:”Chrysanthy Elisabeth”,”non-dropping-particle”:””,”parse-names”:false,”suffix”:””},{“dropping-particle”:””,”family”:”Katsou”,”given”:”Evina”,”non-dropping-particle”:””,”parse-names”:false,”suffix”:””},{“dropping-particle”:””,”family”:”Istenič”,”given”:”Darja”,”non-dropping-particle”:””,”parse-names”:false,”suffix”:””},{“dropping-particle”:””,”family”:”Pucher”,”given”:”Bernhard”,”non-dropping-particle”:””,”parse-names”:false,”suffix”:””},{“dropping-particle”:””,”family”:”Andreucci”,”given”:”Maria Beatrice”,”non-dropping-particle”:””,”parse-names”:false,”suffix”:””},{“dropping-particle”:””,”family”:”Langergraber”,”given”:”Guenter”,”non-dropping-particle”:””,”parse-names”:false,”suffix”:””}],”container-title”:”Circular Economy and Sustainability”,”id”:”ITEM-1”,”issued”:{“date-parts”:[[“2021”,”3”,”17”]]},”title”:”Nature-Based Solutions and Circularity in Cities”,”type”:”article-journal”},”uris”:[“http://www.mendeley.com/documents/?uuid=098ef175-e9bf-43b8-a71a-6cc0f152370c”]}],”mendeley”:{“formattedCitation”:”(Atanasova et al., 2021, namely (1) restoring and maintaining the water cycle, (2) water and waste treatment, recovery, and reuse, (3) nutrient recovery and reuse, (4) material recovery and reuse, (5) food and biomass production, (6) energy efficiency and recovery, (7) building system recovery.
While the qualitative description of the functions, processes and benefits of NBS is generally available, a quantitative determination on the actual extent is often missing. The quantitative assessment would enable evidence-based decision-making. Therefore, it is important to provide this information to 1) inform stakeholders of potential benefits, and 2) provide inputs for commonly applied methods in decision-making (e.g., multi-criteria analysis, cost-benefit analysis). Otherwise, the potential benefits of NBS can be overlooked and not taken into account in the decision-making process, jeopardizing their implementation.
Furthermore, the quantification of NBS processes and subsequent resource streams would enable the implementation of so called NBS systems. These are carefully designed cascade systems of connected NBS units, where each unit provides a service, vital to the functioning of the system. Quantification of NBS streams plays a vital role in an optimal design of NBS systems.
This work provides a framework developed within the COST Action CA17133 Circular City to achieve the needed quantification and subsequently the decision process towards the implementation of NBS within the concept of CE.

MATERIALS AND METHODS

The methodology to develop a framework towards the quantification of resource streams utilized by the implementation of NBS in the urban context includes the following steps: (i) the determination of specific demands based on the description of the defined UCCs (Atanasova et al., 2021)resource depletion, climate change, and degradation of ecosystems. To cope with these challenges, the transformation of our cities into sustainable systems using a holistic approach is required. The pathway to this urban transition is adopting the concept of circular economy for resource management. In this way, resources are kept and reused within the city. Nature-based solutions can be implemented for these tasks, and besides the circularity, they can provide additional benefits for the urbanites and the urban environment in general. This paper describes which urban challenges related to circularity can be addressed through nature-based solutions. This systematic review was developed within the COST Action CA17133 Circular City that investigates how nature-based solutions can be used to progress the circular economy in the urban built environment.”,”author”:[{“dropping-particle”:””,”family”:”Atanasova”,”given”:”Nataša”,”non-dropping-particle”:””,”parse-names”:false,”suffix”:””},{“dropping-particle”:””,”family”:”Castellar”,”given”:”Joana A.C.”,”non-dropping-particle”:””,”parse-names”:false,”suffix”:””},{“dropping-particle”:””,”family”:”Pineda-Martos”,”given”:”Rocío”,”non-dropping-particle”:””,”parse-names”:false,”suffix”:””},{“dropping-particle”:””,”family”:”Nika”,”given”:”Chrysanthy Elisabeth”,”non-dropping-particle”:””,”parse-names”:false,”suffix”:””},{“dropping-particle”:””,”family”:”Katsou”,”given”:”Evina”,”non-dropping-particle”:””,”parse-names”:false,”suffix”:””},{“dropping-particle”:””,”family”:”Istenič”,”given”:”Darja”,”non-dropping-particle”:””,”parse-names”:false,”suffix”:””},{“dropping-particle”:””,”family”:”Pucher”,”given”:”Bernhard”,”non-dropping-particle”:””,”parse-names”:false,”suffix”:””},{“dropping-particle”:””,”family”:”Andreucci”,”given”:”Maria Beatrice”,”non-dropping-particle”:””,”parse-names”:false,”suffix”:””},{“dropping-particle”:””,”family”:”Langergraber”,”given”:”Guenter”,”non-dropping-particle”:””,”parse-names”:false,”suffix”:””}],”container-title”:”Circular Economy and Sustainability”,”id”:”ITEM-1”,”issued”:{“date-parts”:[[“2021”,”3”,”17”]]},”title”:”Nature-Based Solutions and Circularity in Cities”,”type”:”article-journal”},”uris”:[“http://www.mendeley.com/documents/?uuid=098ef175-e9bf-43b8-a71a-6cc0f152370c”]}],”mendeley”:{“formattedCitation”:”(Atanasova et al., 2021)”},{“dropping-particle”:””,”family”:”Andreucci”,”given”:”Maria Beatrice”,”non-dropping-particle”:””,”parse-names”:false,”suffix”:””},{“dropping-particle”:””,”family”:”Langergraber”,”given”:”Guenter”,”non-dropping-particle”:””,”parse-names”:false,”suffix”:””}],”container-title”:”Circular Economy and Sustainability”,”id”:”ITEM-1”,”issued”:{“date-parts”:[[“2021”,”3”,”17”]]},”title”:”Nature-Based Solutions and Circularity in Cities”,”type”:”article-journal”},”uris”:[“http://www.mendeley.com/documents/?uuid=098ef175-e9bf-43b8-a71a-6cc0f152370c”]}],”mendeley”:{“formattedCitation”:”(Atanasova et al., 2021 to give a clearer focus for the implementation of the NBS, (ii) a description of the services required to meet the demand, and (iii) the determination of the NBS units providing the defined service.
All three parts have been determined during two expert workshops. For the demands, (i) the texts of the UCCs have been analysed to extract specific demands to be met by one or multiple NBS. As the determination of the exact NBS unit to be implemented depends on multiple boundary conditions, the term services (ii) was introduced to provide a description of the processes and functions needed to meet the demand. Based on the services, (iii) a list of multiple NBS units capable of providing the required services was defined.
At this stage, the available quantification models for the resource stream were identified. Two complementary approaches were used: (1) a simplified approach based on the demand level and (2) a detailed approach based on the service level.

RESULTS AND DISCUSSION

Framework

The overall approach of the developed framework is illustrated in Figure 1. In order the design a NBS system consisting of one or more NBS to address a specific UCC, a demand has first to be determined. Table 1 provides a preliminary list of demands focusing on key circularity needs. This is by no means a finished list, but includes the main objectives following the work of the COST Action CA17133 Circular City as presented in (Langergraber et al., 2021b, 2021a)and the mainstreaming of NBS in the urban fabric. Existing frameworks describing the use of NBS to address urban challenges do not specifically consider circularity challenges. Thus, the new framework provides the following: (1. Based on the selected demand, the needed services describing e.g. functions or processes, can be identified (Table 1) and reported in detail. Lastly, an expert based ranked list of specific NBS units to provide the required service will be provided and described.

Table 1: Demands (in bold) and needed services determined from the UCCs. The list can be extended based on individual needs. (RW - rainwater; WW - wastewater; FW - food waste; BM - biomass).

Alternative water source RW	**Land restoration**
Collection	Revalorization (Soil)
Treatment (RW)	
Storage (RW)	
	Biomass waste harvesting (from all NBS)
Alternative water source WW	
Collection/Separation	Biomass recovery
Treatment (WW)	
Storage (WW)	
	Urban heat island mitigation and reduction
Alternative nutrient source from Wastewater	
Collection/Separation	Microclimate regulation
Revalorization (liquid)	
Storage	
Alternative nutrient source from bio waste	**Increase energy sufficiency**
Collection (FW)	Increase building insulation
Revalorization (FW)	Energy recovery from BM or FW
Storage	Energy recovery from WW
Food and biomass production	
Production of eatable BM	
Production of non-eatable BM	

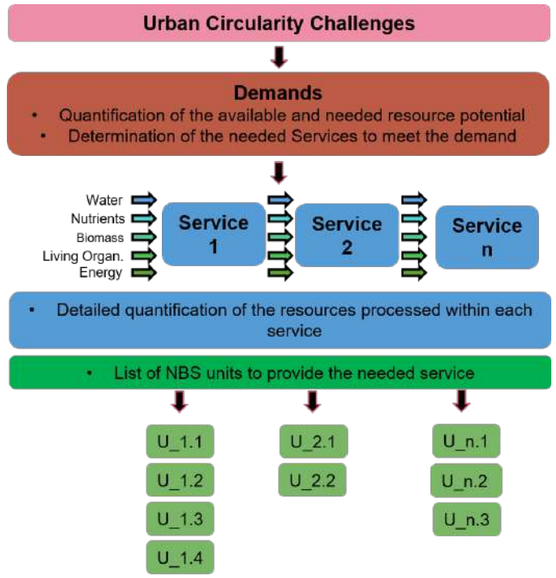

Figure 1: General approach of the framework to identify the needed Demand, Services and NBS units including the steps for resource quantification within the process.

Quantification

The quantification approach also follows the framework (Figure 1) and is split into two parts, namely a simplified approach at the demand level and a detailed approach at the service level. On the demand level, the simplified quantification can illustrate the potential of the available and needed resources to support the decision-making processes. On the service level, the detailed quantification is able to provide input data for the planning and designing of the needed units and thereby support the unit selection process. For example, for the demand “Alternative water source (rainwater)”, a simplified quantification would determine a potential amount of rainwater that could be collected (e.g., from green roof) for future use. While, on service level, a more detail hydological-hydraulic methods would be used to determine water flow through different NBS units.

Next steps

To present the full work, quantification models for the simplified and detailed approach will be generated and tested using case studies. The final product will be embedded in a guidance support system (GSS) using a web-based application providing (i) a descriptive part of the demands, services and units, including their utilization for CE application; (ii) the simplified quantification approach to present the potential of shifting towards CE application for urban resource management using NBS and (iii) the application of the presented framework on multiple case studies.

REFERENCES

Atanasova, N., Castellar, J.A.C., Pineda-Martos, R., Nika, C.E., Katsou, E., Istenič, D., Pucher, B., Andreucci, M.B., Langergraber, G., 2021. Nature-Based Solutions and Circularity in Cities. Circ. Econ. Sustain. https://doi.org/10.1007/s43615-021-00024-1
Langergraber, G., Castellar, J.A.C., Andersen, T.R., Andreucci, M., Baganz, G.F.M., Buttiglieri, G., Canet-Martí, A., Carvalho, P.N., Finger, D.C., Griessler Bulc, T., Junge, R., Megyesi, B., Milošević, D., Oral, H.V., Pearlmutter, D., Pineda-Martos, R., Pucher, B., van Hullebusch, E.D., Atanasova, N., 2021a. Towards a Cross-Sectoral View of Nature-Based Solutions for Enabling Circular Cities. Water 13, 2352. https://doi.org/10.3390/w13172352
Langergraber, G., Castellar, J.A.C., Pucher, B., Baganz, G.F.M., Milosevic, D., Andreucci, M.-B., Kearney, K., Pineda-Martos, R., Atanasova, N., 2021b. A Framework for Addressing Circularity Challenges in Cities with Nature-Based Solutions. Water 13, 2355. https://doi.org/10.3390/w13172355
Langergraber, G., Pucher, B., Simperler, L., Kisser, J., Katsou, E., Buehler, D., Mateo, M.C.G., Atanasova, N., 2020. Implementing nature-based solutions for creating a resourceful circular city. Blue-Green Syst. 2, 173–185. https://doi.org/10.2166/bgs.2020.933

INTEXT Platforms: Innovative hybrid INTensive – EXTensive technologies for wastewater treatment in small communities.

R.Hervas*, A. Petitjean**, S. Troesch ***, G. Solis[+], C.Arias[++], J. Mondejar[+++], L.Herrero[i], P. Otter[ii], T.Moysiadis[iii], I.Blanco*, D. Amador*, E. Lara*, F. Rogalla*, Z. Arbib*

* Department of Innovation and Technology, Aqualia FCC, Avenida Camino Santiago 40, E 28050 Madrid, Spain
Corresponding author email address: hervas.ruben@fcc.es
** Syntea, 10 Lieu-dit Belle-Croix, 33490 Le-Pian-sur-Garonne, France
*** EcoBIRD, 3 route du Dôme, 69630 Chaponost, France
[+]Agencia de Medio Ambiente y Agua de Andalucia, Autovía A49, km28, 41820 Carrión de los Céspedes, Seville, Spain
[++]WATEC - Centre for Water Technology, Aarhus University, Ny Munkegade 120, 8000 Aarhus C, Denmark
+++PROJAR, Polígono Industrial de Quart de Poblet, La Pinaeta s/n, 46930 Quart de Poblet, Valencia, Spain
[i]AIMEN Technology Centre, Polígono Industrial de Cataboi SUR-PPI-2 (Sector 2) Parcela 3, 36418 O Porriño (Pontevedra), Spain
[ii]AUTARCON GmbH, Franz-Ulrich-Str. 18f, 34117 Kassel, Germany
[iii]Future Intelligence, Patriarchou Grigoriou and Neapoleos NCSR Demokritos Technology Park Lefkippos, 15341, Agia Paraskevi, Greece

Abstract

Decentralised EXTensive systems provide adequate sanitation with low operation and maintenance, but require large footprints. The LIFE INTEXT project proposes a reduction in footprint through INTensification into innovative INTEXT technologies. A demonstrative technological platform has been constructed in Talavera de la Reina (Toledo, Spain) to promote innovative sanitation systems (combining extensive and intensified technologies) and demonstrate their economical and treatment efficiencies adapted for small communities as well as awareness through site visits to the facilities. This communication presents a description of the project, the platforms, the INTEXT technologies and the 24 pilots that are part of it.

Keywords (maximum 6 in alphabetical order)

Constructed wetlands, Forced bed aeration, High rate algae ponds, Nature-based solution, Small communities, Wastewater.

INTRODUCTION

Decentralised wastewater systems play an innovative role in delivering sanitation in rural areas. Extensive systems are adequate wastewater treatment technological solutions in rural areas due to their capacity to meet discharge requirements with low operation and maintenance costs, but as a drawback they require relatively large footprints.

Further developments are thus required for these systems to become more compact and efficient while maintaining reasonable investment and operational costs. The LIFE INTEXT project, led by Aqualia, proposes the reduction of this footprint through the INTensification of EXTensive treatment systems into innovative INTEXT technologies. In addition to technical and economic targets, the project has constructed a demonstrative technological platform in Talavera de la Reina (TLR) WWTP (Toledo, Spain) and upgraded the existing Carrión de los Céspedes (CC) WWTP (Seville, Spain) to promote communication and awareness through site visits to the facilities.

This communication describes the innovative INTEXT technologies installed on the INTEXT platforms. The monitoring of performance will allow the validation of the technologies and their optimisation with the target of reducing investment costs, maintenance and footprint (<1m^2/PE).

INTEXT TECHNOLOGIES

The main characteristics and layout of the INTEXT technologies are summarised in Table 1 and Figure 1. Some of the technologies are operated in combination, to evaluate the best wastewater treatment performance and treat onsite the produced sludge.

Anaerobic pretreatment - PUSH® reactor

Upflow Anaerobic Sludge Blanket (UASB) process with pulsed feeding. The PUSH® reactor system has been modified with a top feed that will allow operation during high rainfall events, preventing the biomass to be washed out of the system in an "Imhoff operation mode".

High-Rate Algae Ponds - HRAP

HRAP systems are based on the synergy between microalgae – that produce oxygen through photosynthetic processes – and facultative bacteria that degrade pollutants such as organic matter, nitrogen and phosphorus. Two HRAP have been installed, one with an innovative turbine passive mixing system to evaluate its efficiency against a control.

Constructed wetlands (CW)

Several CWs have been built in the INTEXT platform due to the international recognition of these systems for wastewater treatment: (i) a traditional 2-stage "French system" (Troesch et al., 2014) CW has been built as a control for raw wastewater, (ii) Rhizosph´air® - a one stage CW patented by SYNTEA combining vertical and horizontal flow with forced aeration treating raw wastewater (Petitjean et al. 2022), (iii) Aerated Horizontal Flow CWs (HFCW) with forced aeration or 2nd stage of the "French system" treating effluent from the anaerobic pretreatment (PUSH® reactor), , (iv) floating CWs receiving effluent from PUSH® reactor or Rotating Biological Contactor (RBC), with forced aeration and recirculation, (v) clarifying CW to treat effluent from HRAPs or trickling filter as a polishing step, (vi) sludge drying reed beds treating sludge from PUSH® reactor or activated sludge from the full scale WWTP.

Hybrid secondary treatment

Traditional biofilm systems have been intensified in the project to improve performances and are combined with CWs as a polishing step: (i) RBC intensified with recirculation and a Floating CW for effluent polishing, (ii) Trickling filter intensified with forced aeration (air extraction with fan) and a Sludge Clarifying Drying Reed Beds for sludge dewatering and effluent polishing.

Granular Aerobic Reactor

This system operates in batches, fed sequentially according to the designed loading regime. Alternating anaerobic, anoxic and aerobic cycles allow the removal of organic matter and nutrients, and promotes conditions for granule formation which offer good settlement properties. After the settlement stage there is an emptying cycle, and the process is started again. The INTEXT project will evaluate the best combination of parameters for this technology adapted to small populations.

FINAL REMARKS

The effluent from the INTEXT technologies receives further treatment for: (i) Phosphorus recovery with adsorbent materials, (ii) solar-based disinfection, (iii) water reclamation and reuse with smart irrigation control. The project is also complemented with the evaluation of greenhouse gases emissions, assessment of emerging pollutants and the development of a decision support system (DSS) based on a Life Cycle Analysis (LCA) and Life Cycle Cost Analysis (LCCA).

The fact that the technologies are operated in different climatic conditions (Continental - TLR WWTP, Mediterranean – CC WWTP) allows to determine accurate operating and design parameters that will serve as a base to develop the next generation standards for the treatment of wastewater for small communities in Southern Europe. During the conference, the authors will present results data from the TLR INTEXT platform (Figures 2 and 3).

ACKNOWLEDGEMENTS

The LIFE INTEXT project has received funding under the LIFE financial instrument of the European Union LIFE18 ENV/ES/000233.

REFERENCES

Troesch, S., Salma, F., Esser, D. 2014 Constructed wetlands for the treatment of raw wastewater: the French experience. *Water Practice & Technology* **9**(3), 430-439.

Petitjean, A. Daniau, P., Cano, R., Lara, E., Arbib, Z., Solis, G., Troesch, S. 2022 Intensified French Treatment Wetlands – Influence of operating parameters on nitrogen removal. *Proceedings of the IWA 17th International Conference on Wetland Systems for Water Pollution Control. 6-10 November 2022, Lyon, France*. 477-481.

Table 1. List of treatment technologies, including area, flow treated, PE served and main innovation in the INTEXT platforms

Technology	Area, m^2	Flow, m^3/day	PE served	Innovation
PUSH® reactor	12	72	475	Imhoff mode (rainfall events)
2 x HRAP	500	38	250	Passive mixing
2-stage "French system"	200	19	125	Control
Rhizosph´air®	120	19	125	One-step CW, forced aeration
Rhizosph´air®	130	15	100	One-step CW, forced aeration
2 x Aerated HFCW	72	12	80	Forced aeration
VFCW	50	9	60	Anaerobic pretreatment
4 x Floating CW	500	76	500	Forced aeration, Recirculation
2 x Floating CW	250	25	230	Forced aeration, Recirculation
2 x Clarifying CW	25	12	80	Polishing application for HRAP / Trickling filter
4 x Sludge CW	60	6,5 kg DS		Treatment of anaerobic sludge
RBC	18	19	125	Recirculation
Trickling filter	5	19	125	Forced aeration (fan)
Granular Aerobic Reactor	3	19	125	Application in small populations
Onsite disinfection based on Chlorine Generation	5	50	500	Reuse of treated wastewater Solar Driven

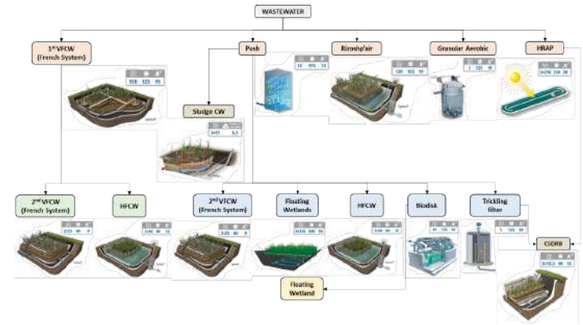

Figure 1. Diagram of the stages, equivalent population, capacity, and surface area of the INTEXT technologies.

Figure 2. Aerial view of the Intext platform at Talavera de la Reina WWTP

Figure 3. INTEXT platform at TLR WWTP (HRAPs, RBC, Clarifying CWs and Floating CWs - left, and French system - right) at different times (construction – top, Summer 2022 – centre, Winter 2023 – bottom)

Green solutions for treating nitrate and micropollutants in groundwater to meet drinking standards: one year overview

J. Pascó1, M. Mendoza1, M. Guivernau1, M. Viñas1, B. Fernández1, R. Trobajo1, V. Matamoros2, J.C. Real3, E. Zuriaga4, R. Garcia4, J. Garcia4, J. Herrero5, C. Biel1*.

1* IRTA - Institute of Agrifood Research and Technology, Torre Marimon, Road C59, km 12, 08140 Caldes de Montbui, Spain. (*carmen.biel@irta.cat*)
2 IDAEA-CSIC Department of Environmental Chemistry, IDAEA-CSIC, c/Jordi Girona, 18-26, 08034 Barcelona, Spain. (*victor.matamoros@cid.csic.es*)
3 PROTECMED S.L., Osona St, 46th, Can Bruguera, 08211 Castellar del Vallès, Spain. (*jcreal@protecmed.com*)
4 FACSA S.A., C/Mayor 82-84, 12001 Castelló de la Plana, Spain. (*ezuriaga@facsa.com*)
5 EURECAT, Carrer de Bilbao, 72, 08005 Barcelona, Spain. (*jofre.herrero@eurecat.org*)

Abstract

The LIFE SPOT project has as main objective to remove groundwater pollution (nitrates, pesticides, antibiotics, and antibiotic resistance genes) to supply drinking water for human and livestock in decentralized areas and prove an alternative water management technology for very small water supplies. For that, a combined photobioreactor and cork-wood pellet filter treatment technology is being assessed at pilot scale in Spain. The added value of the developed SPOT technology is the removal of nitrate and microcontaminants in the groundwater as well as to decrease carbon footprint by enhancing CO2 sequestration and nutrient recovery.

Keywords

Emerging contaminants, groundwater, natural-based treatment, nitrates.

INTRODUCTION

In rural areas, groundwater is used for drinking and for irrigation purposes. Many communities in the Mediterranean area they suffer from severe drinking water shortages due to groundwater pollution or drought. Anthropogenic pollution by nitrate and pesticides is one of the major water quality problems in small and very small water supplies. In fact, approximately 13% of groundwater monitoring stations across Europe exceed the 50 mgNO3/L limit (91/676/EEC), thereby reducing the amount of usable drinking water. In addition, a major public health concern has been raised across Europe during the last years due to the occurrence of antibiotics and antibiotic resistance genes (ARGs) in groundwater, derived from manure application in agriculture. Therefore, the main objective of this work, enclosed in LIFE SPOT project (lifeSPOTproject.eu), is to assess the efficiency of pollution (nitrates/ pesticides/ antibiotics/ ARGs) removal of contaminated groundwater to supply drinking water for livestock in rural areas.

MATERIALS AND METHODS

The scheme of the pilot plant is shown in Figure 1. It combines a continuously stirred photobioreactor (PBR; 15-18 m^3), built with floating light-pits, a clarification step within a dissolved air flotation (DAF) unit, and a corkwood biofilter (CWF; 5 m3) treatment, at field scale (treatment capacity of 1-5 m3/d). The pilot plant is being run under field environmental conditions and assessed by means of a deep physicochemical and microbiological characterization. The real polluted groundwater (Barcelona, Spain) is contaminated due to organic fertilization (manure), which has led to a high level of nitrate, antibiotics, ARGs and pesticides.

RESULTS AND DISCUSSION

The SPOT pilot plant has been working for more than 1 year. The results shown in this work were collected during two periods of continuous and stable operation: summer 2022 (days 222-273) and autumn 2022 (days 343-373), where the average nitrate content in the groundwater was between 162 and 290 mgNO3/L, respectively (Table 1). Micropollutants detected in summer and autumn 2022, were i) 8 antibiotics (sulfonamides and fluoroquinolones) with a concentration from 0.5 to up to 98 ng/L; ii) ARGs (intl1 and sul1 genes) content ranged from 10^4 to 10^5 gene copies/L; and iii) pesticides (desethylatrazine, DEET; surfactants as surfynol 104) with a concentration <20 ng/L.

Table 2 summarizes the average values of operational parameters of the PBR and CWF of the pilot plant at field scale. A natural mixed consortium of bacteria-microalgae, cultivated in conditions like those of the pilot plant, was used to inoculate the PBR in winter 2022. The continuous operation began in spring 2022, when the operation of the PBR and the CWF were synchronized in continuous mode. During the entire operation of the pilot plant, the real polluted groundwater of the site was improved by adjusting its nitrate to phosphate molar ratio (22 and 27 in summer and in autumn, respectively) and by a CO_2 injection (to adjust pH to 7.0-7.5) in the PBR, to enhance the culturing of microalgae and bacterial biomass. The occurrence of Cyanobacteria (Fig.1A) was monitored in the PBR to avoid the presence of cyanotoxins. The biofilter was always operated with a hydraulic residence time (HRT) of 2 days, while the PBR was run with an HRT of 8 days with recirculation of the concentrated biomass from the DAF in summer, and 16 days without recirculation in autumn.

The suspended biomass and microbial biofilms in PBR, DAF and CWF materials were higher in summer than in autumn, in general but with the same tendency. Bacterial biofilms in PBR were ≥10^{11} copies 16SrRNA/mL, composed by 10% of denitrifying bacteria; nonetheless, denitrifiers became 100% of bacterial population in autumn. The flocculated biomass in DAF was like PBR biomass, depicting the same tendency in both seasons. It is noteworthy that denitrifying populations in CWF were highly maintained in both seasons (10^9 *nosZ* copies/g, representing the 95-100% of total population), confirming the important role of nitrate removal by anaerobic denitrifying bacteria. In the CWF, a high abundance of fungal populations was also established growing on corkwood pellets (10^9 ITS copies/g). Therefore, the hydrolysis and fermentation of the filling materials was carried out and controlled by a specific consortium composed of fungi, cellulolytic and bacteria, where volatile fatty acids boosted the denitrifying activity under the saturated water conditions within the CWF.

The denitrifying activity in CWF led to a nitrate removal of 83 and 69 % in-NO_3 in summer and autumn 2022, respectively, but with a higher depletion rate in autumn (28 gNO_3/m^3d) than in summer (20 gNO_3/m^3d) (Table 2). Although denitrifying potential was detected in the PBR (Fig.2), the nitrate removal observed was 19 and 16 % in-NO_3 in summer and autumn 2022, respectively, with a similar depletion rate (4 gNO_3/m^3d) in both seasons (Table 2). The biomass recirculation from DAF in summer negatively affected the removal of nitrates in the PBR (excess flocculant), which affected the microalgae population in summer together with high water temperatures (>27 ºC; Table 2) and light intensity. The planktonic species *Tetradesmus* and *Chlorella* dominated the biomass in suspension (0.15 gTSS/L) in winter-spring but in summer, diatoms and *Tetradesmus* grew in biofilms with a lower planktonic biomass (0.05-0.1 gTSS/L). In autumn, less biofilm was observed and again *Tetradesmus* microalgae presence increased in suspension (0.1 gTSS/L).

Importantly, the whole SPOT plant was shown to be effective for reducing 8 detected antibiotics (ciprofloxacin, sulfamethoxazole, sulfathiazole, sulfadiazine, sulfacetamide, sulfapyridine, sulfamethazine, and sulfamethizole): a depletion of 73 and 78 % was observed in summer and in autumn, respectively, reaching a final concentration <10 ng/L in the treated water (Table 2). The elimination (Fig.3) took place in the the PBR (9 and 40 % in summer and in autumn, respectively), in the DAF (47 and 23 % in summer and in autumn, respectively) and in the CWF (17 and 14% in summer and in autumn, respectively). The higher removal in the DAF can be explained by the coagulation and precipitation of some antibiotics due to the addition of the flocculant agent. In the microalgal biomass, only some sulphonamide was detected (5-20 ng/g-dry weight). The effectiveness of the biofilters can be mainly due to sorption and biodegradation process as it has already been observed in lab-scale cork columns (Rambaldo et al. 2022). ARGs profile is being assessed currently.

CONCLUSIONS

The high content of nitrates and the presence of micropollutants, such as antibiotics and ARGs in the groundwater in rural areas, caused by on-going intensive agriculture and/or organic fertilization, was reduced by the SPOT technology, reaching water quality standards which might allow the supply of drinking water. The on-going work in the SPOT pilot plant (winter-summer 2023) is addressed to validate the usage of the treated water as drinking water for livestock at farm level, the completion of the 2022-23 sampling campaigns and the valorisation of the residual mixed biomass.

Acknowledgements

This work was financed by EU project Life SPOT (LIFE18 ENV/ES/000199). IRTA thanks the financial support of CERCA program (Generalitat de Catalunya). The authors from IRTA of this study belong to the Consolidated Research Group of Sustainability in Biosystems, funded by the AGAUR (Generalitat de Catalunya; ref. 2021 SGR 01568).

REFERENCES

Rambaldo L., H. Ávila, M. Escolà Casas, M. Guivernau, M. Viñas, R. Trobajo, J. Pérez-Burillo, D. Mann, B. Fernández, C. Biel, L. Rizzo, J.M. Bayona, V. Matamoros. (2022) Chemosphere 301, 134777, doi.org/10.1016/j.chemosphere.2022.134777.

Table 1. Average groundwater and treated water in the SPOT pilot plant. Note: *Drinking water must have ≤50 mgNO3/L (91/676/EEC).

	2022 summer		2022 autumn	
Compound	groundwater	treated water	groundwater	treated water
NO_3^- (mg/L)	162 ±37	21 ±13 (*)	313 ±113	64 ±47 (*)
Antibiotics (ng/L)	52±30	9±16	27±20	2±3

Table 2. Summary of parameters during the continuous performance of the SPOT pilot plant in IRTA site (Barcelona, Spain). Mean values of the operation during summer and autumn 2022. Abbreviations: V, working volume; HRT, hydraulic retention time.

		2022 summer	2022 autumn
Photobioreactor PBR	V (m3)	15	18
	HRT (d)	7 ±1	13 ±1
	T ºC (inside)	27 ±2	22 ±3
	load (gNO_3/m^3d)	23 ±11	24 ±9
	NO_3^- removal (%)	19% ±15	16% ±13
	NO_3^- rem rate (gNO3/m3d)	4 ±9	4 ±5
Biofilter CWF	V (m3)	5	5
	HRT (d)	2 ±0	2 ±1
	load (gNO_3/m^3d)	24 ±15	41 ±33
	NO_3^- removal (%)	83% ±9	69% ±32
	NO_3^- rem rate (gNO3/m3d)	20 ±13	28 ±30
SPOT	Total NO_3^- removal (% in-GW)	86%	77%
	(A) PBR	(B) DAF	(C) CWF

Figure 1. Photographs of the SPOT pilot plant. (A) Images of the photobioreactor (PBR) with light-pits and image (light microscopy; x100) of *Tetradesmus obliquus* and presence of cyanobacteria in the form of filaments. (B) Dissolved air flotation (DAF) unit. (C) Corkwood biofilter (CWF) and treated water tank.

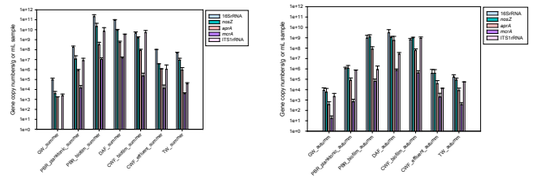

Figure 2. Comparison of qPCR data from the SPOT pilot plant in summer and in autumn. Nomenclature: GW, groundwater; PBR, photobioreactor; DAF, dissolved air flotation unit; CWF, corkwood biofilter; TW, treated water.

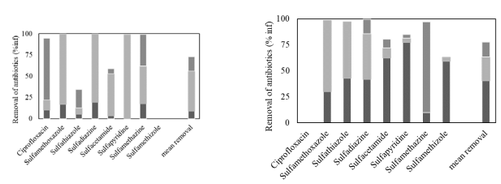

Figure 3. Removal of 8 antibiotics in the SPOT pilot plant. Colours: dark grey, nitrate removal in PBR; light grey, nitrate removal in DAF; grey, nitrate removal in CWF.

Nature-based solutions in Europe and Latin America: A comparative analysis of regional situation and addressed challenges

Yarima Recalde*, Lucia Alexandra Popartán*, Manuel Poch*, Ignasi Rodríguez-Roda*

*LEQUIA, Laboratory of Chemical and Environmental Engineering (LEQUIA), University of Girona, C/Maria Aurèlia Capmany 69, 17003 Girona, Spain

(E-mail: *yarima.recalde@udg.edu; luciaalexandra.popartan@udg.edu; manuel.poch@udg.edu; ignasi.rodriguezroda.udg.edu)*

Abstract

Cities around the world face a number of challenges, including climate change and ecosystem degradation. Nature-based solutions (NbS) can help protect us from the impacts of climate change while also ensuring ecosystem services. However, NbS still face implementation barriers, mainly in developing countries. In order to identify and compare the state of NbS implementation and the main challenges to be addressed in European and Latin American cities, we reviewed and analyzed different case studies and projects published in peer-reviewed articles and gray literature. It was reported that NbS are still evolving as a concept and are not widely implemented in Latin America, mainly due to limited availability of financial resources. There is a marked imbalance in the distribution of studies, with most cases concentrated in the global north, although southern global countries are generally most vulnerable to the impacts of climate change. In Europe, the concept is more integrated into urban planning, however, there are also barriers such as limited understanding of the benefits of NbS by society. The main challenges that Latin American cities aim to address with NbS are agrobiodiversity and improved water management. On the other hand, in Europe, there is a priority to increase urban green infrastructure, as it plays an important role in carbon storage and mitigating the impacts of greenhouse gas emissions in cities.

Keywords

Climate change, Europe, Latin America, Nature-based solutions, Social challenges

INTRODUCTION

Nature-based solutions (NbS) are a concept that is currently gaining ground to address urban challenges. NbS mainly address 7 social challenges including climate change adaptation and mitigation, reduction of natural disaster risk, reversing ecosystem degradation and loss of biodiversity, human health, socio-economic development, food security and water security (IUCN, 2020). In regions with different economic and social realities than developed countries, nature-based solutions are a foreign concept, whose enforcement presents many challenges and limitations. This study aims to describe the state of implementation and challenges that NbS seek to address in Europe and Latin America through a comparative analysis.

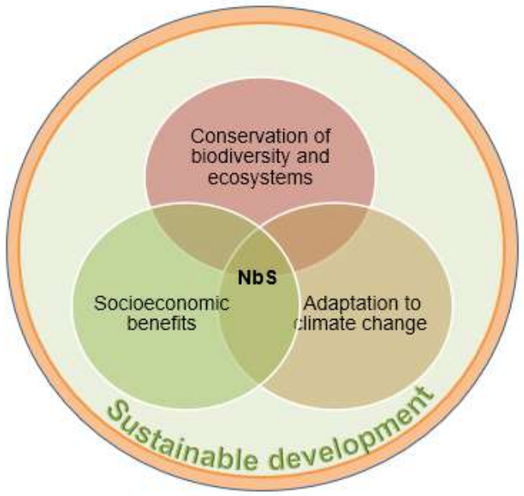

Figure 1. Challenges addressed by NbS

MATERIALS AND METHODS

This work involved a structured search of scientific and grey literature related to Nature-based Solutions (NbS) projects or studies in Europe and Latin America. The obtained literature was analyzed based on the review of the evolution of the NbS topic, its implementation level and the social and environmental challenges to be addressed in these two regions. In addition, limitations, knowledge gaps and opportunities for the implementation of NbS were identified by comparing the literature available in the north and south global. This qualitative method serves as an exploratory tool to achieve a clear picture of the development trajectory of NbS implementation.

RESULTS AND DISCUSSION

The EU has positioned itself as a world leader in NbS research and innovation. Increasingly, European cities are adopting NbS in their public policies, urban plans and programs and their implementation. On the other hand, Latin America society, in general, still does not perceive the importance and benefits of NbS. In this way, public works of another nature associated with the traditional infrastructure are prioritized. Thus, a large part of the projects that are being implemented are still in the phase of preparation and search for financing. One of the main limitations in both Europe and Latin America is the lack of information and data necessary to measure the potential benefits. However, since 2012 the EU has funded multisectoral projects with case studies in Europe and Latin America, which has boosted NbS research in this region as well (Davies et al., 2021). In general, most government objectives for NbS are focused on forests, therefore funding is currently channeled mainly towards tree planting (Seddon et al., 2021). However, this perception is different in Europe and Latin America. The low access of people to green areas is the main challenge in European cities. In Latin America, projects combining conservation and agriculture and solutions focused on improving water management, such as controlling runoff, floods, and rainwater, predominate (Ozment et al., 2021). In general, the social and environmental challenges that NbS are intended to address are different in the two regions. This depends on the local contexts in the environmental, political, economic and social spheres; therefore, more research is needed in terms of cost/benefit analysis and implementation opportunities.

REFERENCES

Davies, C., Chen, W. Y., Sanesi, G., & Lafortezza, R. (2021). The European Union roadmap for implementing nature-based solutions: A review. *Environmental Science & Policy*, *121*, 49–67. https://doi.org/10.1016/J.ENVSCI.2021.03.018

Ozment, S., Schumacher, A., Gonzalez, M., Oliver, E., Morales, G., Gartner, T., Silva, M., Grunwaldt, A., & Watson, G. (2021). Nature-Based Solutions in Latin America and The Caribbean: Regional Status and Priorities for Growth. *Washington, DC: Inter-American Development Bank and World Resources Institute.* https://www.wri.org/research/nature-based-solutions-latin-america-and-caribbean-regional-status-and-priorities-growth

Seddon, N., Smith, A., Smith, P., Key, I., Chausson, A., Girardin, | Cécile, House, J., Srivastava, S., & Turner, B. (2021). *Getting the message right on nature-based solutions to climate change*. https://doi.org/10.1111/gcb.15513

UICN. (2020). Orientación para usar el Estándar Global de la UICN para soluciones basadas en la naturaleza: primera edición. *Orientación Para Usar El Estándar Global de La UICN Para Soluciones Basadas En La Naturaleza: Primera Edición*. https://doi.org/10.2305/IUCN.CH.2020.09.ES

Organic micropollutant removal from urban waters by MULTISOURCE Enhanced Natural Treatment Solutions

V. Kisielius*, L. Zhou*, K. Bester*.**, C.A. Arias**.**** and P.N. Carvalho*.**

* Department of Environmental Science, Aarhus University, Frederiksborgvej 399, DK-4000 Roskilde, Denmark (e-mail pedro.carvalho@envs.au.dk)
** WATEC - Centre for Water Technology, Aarhus University, Ny Munkegade 120, 8000 Aarhus, Denmark
*** Department of Biology, Aarhus University, Ole Worms Allé 1, 8000 Aarhus, Denmark.

Abstract

MULTISOURCE project is operating seven pilots of diverse Enhanced Natural Treatment Solutions (ENTS). The ENTS are treating domestic wastewater, urban surface water runoff or combination of these streams. While the pilots are monitored for conventional water quality parameters by each MULTISOURCE partner, we are supplementing the monitoring activities by performing target and non-target analysis of organic micropollutants. Many of the target compounds (pharmaceuticals, surfactants, pesticides and other) are considered of ecological concern and some are included in current European regulation. Our aim is to provide field-based knowledge about the compound occurrence, removal and transformation in the different ENTS. Our results will later be used for the risk assessment for treated water discharge and potential reuse and contribute to the implementation of ENTS in the future. Monitoring activities are running since the summer of 2022, we will show selected results of the non-target screening analysis, as well as treatment potential of several pilots.

Keywords

Black water; Emerging pollutants; Greywater; Non-target screening; Road runoff; Wastewater

INTRODUCTION

There is a growing demand for water treatment, storage and reuse in urban areas. While the demand can potentially be largely addressed by nature-based solutions, full and pilot scale data about long-term performance of such systems is generally lacking (Yang et al. 2022). MULTISOURCE, the EU Horizon 2020 project exploring ModULar Tools for Integrating enhanced natural treatment SOlutions in URban water CyclEs, aims at addressing this. MULTISOURCE aims to i) demonstrate seven Enhanced Natural Treatment Solutions (ENTS) for a wide range of urban wastewater streams, and ii) develop innovative tools, methods and business models that support implementation of such solutions through a co-creation approach. The pilots are build based on different approaches (green roofs, green walls, raingardens and constructed wetlands) in France, Belgium, Italy, Spain, Norway, Germany and USA (Figure 1).

One of the critical points covered by MULTISOURCE are organic micropollutants, as these can hinder the technology and management options for urban waters. MULTISOURCE investigates the efficiency of seven different Enhanced Natural Treatment Solutions (ENTS) to remove pathogens, priority substances and contaminants of emerging concern, including microplastics. The empirical results will result in recommendations to optimise pilots and their operation for pollutant removal. Long-term monitoring data will be assessed and recommendations for system implementation in urban areas will be proposed.

METHODS

The partners responsible for the pilot plants regularly sample the influent, mid-flow (where relevant) and effluent waters, analyses basic water quality parameters and provides samples to specialised laboratories for microplastic, pathogen and micropollutant analysis. The team from Aarhus University (AU) represented here is responsible for coordinating activities of all pilots, as well as measuring organic micropollutants in their water. For characterizing the pilot performance in terms of the micropollutant removal efficiency, the work is being carried in close collaboration with all partners.

The analytical work includes target analysis by GC-MS and LC-MS/MS, applying three different analytical methods in order to quantify the selected compounds in the different water matrices. Specific methods for wastewater and urban runoff were implemented. For the non-target and suspect-screening approaches we have used high-resolution mass spectrometry (GC-orbitrap and LC-QTOF) and an in-house library of organic pollutants. These results will be further treated for the planned risk assessment analysis by NIVA (Norway). Also, by the different project partners for a detailed characterization of the pilot operation.

RESULTS AND DISCUSSION

The first months of the project have been dedicated to develop a harmonized monitoring plan that ensures comparability of the different ENTS, as well as a tailored approach for each pilot (e.g. type of water, operation mode, seasonality, pollutants of relevance). For the monitoring plan AU has developed *MULTISOURCE suspect screening list* comprising 300 different compounds of relevance for which we will validate their presence or absence in different waters and regions, as well as quantify several. The list includes domestically and industrially applied compounds that are known or suspected to enter environment via wastewater/stormwater streams and cause adverse ecological effects. These include broad range of pharmaceuticals, surfactants, pesticides, combustion products, UV sunscreen agents and other (Figure 2). The *MULTISOURCE suspect screening list* has been combined referring to well-known and emerging micropollutants of environmental concern reported by other studies (Schulze et al. 2019) and European regulation (EU Water Framework Directive 2000/60/EC, EU water policy substances “watchlist” 2018/840), and MULTISOURCE partner consultation.

For quantitation of the organic micropollutants, the wastewater target list includes approx. 90 compounds, majority of which are pharmaceutical compounds representing different therapeutic uses. For the urban runoff, the target list includes approx. 60 compounds, mainly comprising oil and combustion products and urban biocides (Figure 2). Compound quantification lists are updated ongoing based on suspect screening analysis.

The first samples arrived at AU in the spring/summer 2022 and the main commonly found micropollutants have been quantified. The first results indicate that the different MULTISOURCE pilots are receiving a wide variant of organic micropollutants. The French pilots from INRAE have at their inlet several pharmaceutical compounds from different therapeutic classes (antibiotics, anti-inflammatory, antidepressant, anaesthetic anti-convulsant, anti-anxiety, antihypertensive (Figure 3). The Bridger Bowl (Sky Resort) pilot in the USA had at the inlet some biocides and psychotropics, besides several pharmaceutical compounds. Several compounds were measured up to 5 µg/L in the influent.

In terms of first performance results, the Belgium Pilot treating wastewater from a Camping site showed removals above 77% for compounds such as sotalol, venlafaxine, DEET, DDAC or caffeine (Figure 4). Gabapentin, usually showing weak elimination in sewage treatment plants (Herrmann et al. 2015), was removed up to 76% from black water by the phytoparking system. It should also be noted difference in occurrence and treatment between the greywater and black water. Notably we see not only good removal rates, but also concentrations at the effluent bellow PNEC values, for example for venlafaxine (PNEC of 0.1 µg/L).

MULTISOURCE monitoring work keeps developing and new samples are continuously analysed. At ecoSTP2023 we will provide updated results from the monitoring work, as well as the first results from our suspect and non-target screening work that is ongoing. We should also be able to provide data on pilot performance efficiency to remove these compounds.

Figure 1. The wastewater types treated in the project, locations and images/ visualisations of the pilot plants.

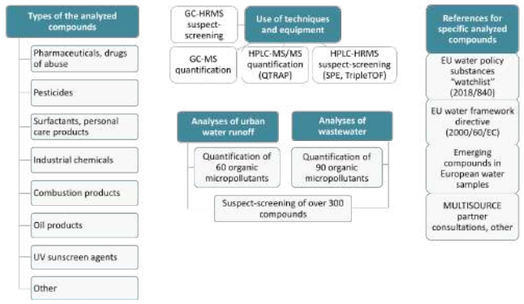

Figure 2. Criteria used for micropollutant inclusion in the risk assessment, and techniques applied at Aarhus University for their detection and quantification.

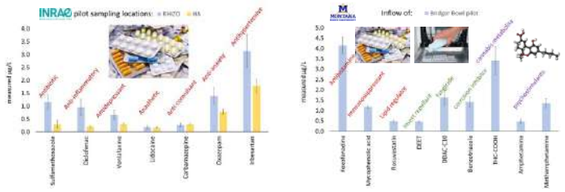

Figure 3. Examples of organic micropollutants found in the inlet of the MULTISOURCE pilots of INRAE (treatment wetland - wastewater) and Montana State University (treatment wetland – high strength wastewater).

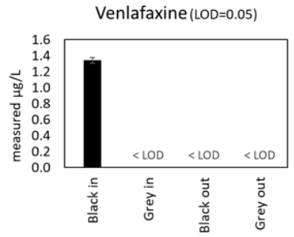

Figure 4. Examples of the removal of organic micropollutants in the MULTISOURCE pilot from Rietland (Phytoparking system, black and greywater)

REFERENCES

Yang F, Fu D, Zevenbergen C, Rene E.R. 2022. A comprehensive review on the long-term performance of stormwater biofiltration systems (SBS): Operational challenges and future directions. *Journal of Environmental Management*. 302, 113956

Schulze S, Zahn D, Montes R, Rodil R, Quintana J.B, Knepper T.P, Reemtsma T., Berger U. 2019 Occurrence of emerging persistent and mobile organic contaminants in European water samples. *Water Research*. 153 (80-90)

Herrmann M, Menz J, Olsson O, Kümmerer K. 2015. Identification of phototransformation products of the antiepileptic drug gabapentin: Biodegradability and initial assessment of toxicity. *Water Research*, 85, (11-21)

Acknowledgements

The MULTISOURCE project has received funding from the European Union’s Horizon H2020 innovation action programme under grant agreement 101003527.

Assessment of intensified constructed wetlands for the attenuationofPMTcompoundsfromgroundwaterand wastewater

AliciaCano-López*,MònicaEscolà-Casas*,JéssicaSubirats*andVíctorMatamoros*

*DepartmentofEnvironmentalPollution&Agriculture,InstituteofEnvironmentalAssessment& WaterResearch (IDAEA), CSIC, Jordi Girona 18-26, 08034 Barcelona, Spain
(E-mail:*aliqam@cid.csic;mecqam@cid.csic.es;jesqam@cid.csic.es;vmmqam@cid.csic.es)*

Abstract
Wastewater and groundwater from industrial areas have been shown to be impacted by the so- called persistent, mobile and toxic (PMT) compounds. This study assessed the capability of using an intensified constructed wetland based on coke for the remediation of 5 PMT compounds (benzotriazole, methyl-benzotriazole, perfluoropentanoic acid, perfluorobutanesulfonic acid, and trifluoromethanesulfonic acid) from both, groundwater and wastewater. The evaluated design parameters inbiofilter packed-columns were: coke granulometric sizes (5-2 mm vs 2-0.5 mm), the presenceofvegetation(*Cyperusalternifolius)*,andhydraulicloadingrate.Thecolumnswere initiallyfedwithrivergroundwater spikedwithdifferentPMTcompoundsat5 and 10µg/L.After 6 operation months, the columns were fed with real secondary-treated wastewater spiked with the same compounds. Both inlet and outlet of the system were analysed by UHPLC-HRMS obtaining removals for benzotriazole and methyl-benzotriazole between 60 and 90%, respectively. Whereas these removal efficiencies were between 20 to 50% for PFAS.

Keywords(maximum6inalphabeticalorder)
Bioremediation;groundwater;industrialareas;NBS;PMT;removal

INTRODUCTION

The occurrence of Persistent, Mobile and Toxic (PMT) substances in groundwater and wastewaters have emerged a big concern due to the capacity of these compounds to travel long distances with water, even throughout bank-filtrate and thus spread over large spatial and temporal scales, posing ecosystem and human health threats (Hale et al., 2022). Some examples of PMTs are organochlorinated compounds, benzotriazoles and per- and polyfluoroalkyl substances (PFAS) which are used by industrial manufacturing processes ending up in wastewater treatment plants (WWTP) and finally into the groundwater (Ateia et al., 2019).

The concern about the widespread presence of PMTs in water bodies has resulted in a common EU strategy to fight against them based on the replacement of these chemicals by more safe and sustainable substances, followed by their minimization and control, and finally, the assessment of advanced technologies for their removal (*EC. Chemicals Strategy for Sustainability Towards a Toxic-Free Environment*, 2021). In this sense, the use nature-based solutions such as constructed wetlands (CWs) have shown to be capable of removing PMTs such as chlorinated solvents or benzotriazoles from wastewater (Hansson, 2019; Shi et al., 2019), but there is low information available of how the use of intensified CWs based on different materials such as coke can be used for removing PMTs from both wastewater and groundwater. In this study we will assess the effectiveness of using coke and vegetation in intensified CWs for removing benzotriazole (BTr), methyl-benzotriazole (MBTr), perfluoropentanoic acid (PFPeA), perfluorobutanesulfonic acid (PFBS) and trifluoromethanesulfonic acid (TFMS) from groundwater and wastewater.

MATERIALSANDMETHODS

The study was conducted in laboratory-scale biofilters under water-saturated conditions duringmore than 200 operational days for the removal of PMTs. Twelve methacrylate columns (43.5mm int.Ø,x-320mmheight)weredesignedandconstructed(Fig.1).Eachcolumnwasfilledwith25mm ofgravel followed by300 mm ofcokeofdifferent granulometricsizes (3columns with particle size of 5-2 mm and 3 columns with 2-0.5 mm) or washed sand (2 mm Ø). 9 of the 12 columns were planted with *Cyperus alternifolius*. All columns were fed with either, groundwater or secondary treated wastewater at a HLR of 70 and 40 mm/d. Plants were acclimatized during 8 weeks and the system started to operate with spiked groundwater at 5 µg/L (BTr and MBTr) and 10 µg/L (TFMS, PFBS and PFPeA) for 8 additional weeks. After that, columns were fed with real secondary treated wastewater spiked with the same PMTs and the performance of the technologywas monitored for 2 additional months. Every week inlet and outlet water samples from each column was collected and analysed for physico-chemical properties (pH, redox, dissolved oxygen) and general quality parameters (chemical oxygen demand, ammonium, nitrates, phosphates, and sulphates). Moreover, same filtrated water samples were injected into a UHPLC-HRMS instrument (Bruker-Impact II) equipped with an Intensity Solo C18-2 column (100 x 2.1 mm, 1.8 µm) for the determination of the selected PMTs and their transformation products.

RESULTSAND DISCUSSION

Preliminary results show that at a HLR of 70 mm/d intensified CW based on coke were able to remove benzotriazoles by more than 60%, and PFAS by 20-50%. from groundwater This can be explained by the capacity of the coke to promote the grow of *Dehalococcoidesspp.*, bacteria which has been observed to enhance the attenuation of organic matter and organic compounds such antibiotics from wastewater (Löffler et al., 2013). The use of wastewater enhanced the attenuation of PMTs by 30 to 50%, probably due to the greater biofilm production and co-metabolism with the organic matter and other constituents of the treated wastewater. In order to enhance the attenuation capacity of the CWs we reduced the HLR to 40 mm/d, achieving removal efficiencies greater than 80%. In the presentation these results will be explained along with the identification of transformation products and the potential ecosystem and human health risk of the treated water. Furthermore, microbial 16S characterization will be used to elucidate the main microbial contributors to the attenuation of PMTs.

CONCLUSIONS

The preliminary results indicate that the use of intensified CW based on coke can be a suitable nature-based solution for removing PMTs from groundwater and wastewater. Future studies will include the long-term performance and scale-up of the technology under real environmental conditions (Technology Readiness Level 5).

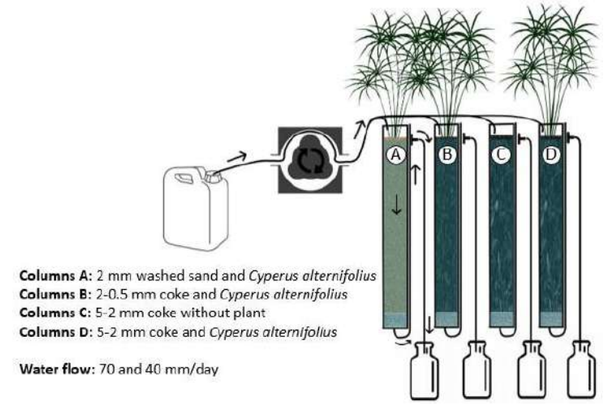

Figure1.PictureofintensifiedCWsystem usingverticalcokepackedcolumns (a)andschemeof the design (b).

ACKNOWLEDGMENTS

The authors want to acknowledge to all the stakeholders involved in PROMISCES that help us to achieve this part of the project. Very grateful to the European funding (grant agreement ID: 101036449) for making this possible.

REFERENCES

Ateia,M.,Maroli,A.,Tharayil,N.,&Karanfil,T.(2019).Theoverlookedshort-andultrashort- chain poly- and perfluorinated substances: A review. *Chemosphere, 220*, 866–882. https://doi.org/10.1016/J.CHEMOSPHERE.2018.12.186
EC.ChemicalsStrategyforSustainabilityTowardsaToxic-FreeEnvironment.(2021).*39*(1),40– 41.
Hale, S. E., Neumann, M., Schliebner, I., Schulze, J., Averbeck, F. S., Castell-Exner, C., Collard, M., Drmač, D., Hartmann, J., Hofman-Caris, R., Hollender, J., de Jonge, M., Kullick, T., Lennquist,A.,Letzel,T.,Nödler,K.,Pawlowski,S.,Reineke,N.,Rorije,E.,...Arp,H.P.H. (2022). Getting in control of persistent, mobile and toxic (PMT) and verypersistent and very mobile (vPvM) substances to protect water resources: strategies from diverse perspectives.
Environmental Sciences Europe, 34(1). https://doi.org/10.1186/s12302-022-00604-4 Hansson,S.O.(2019).BiotechnologyforEnvironmentalPurposes.In *EncyclopediaofFoodand AgriculturalEthics*.https://doi.org/10.1007/978-94-024-1179-9_534
Löffler,F.E.,Yan,J.,Ritalahti,K.M.,Adrian,L.,Edwards,E.A.,Konstantinidis,K.T.,Müller,J. A., Fullerton, H., Zinder, S. H., & Spormann, A. M. (2013). Dehalococcoides mccartyi gen. nov.,sp.nov.,obligatelyorganohalide-respiringanaerobicbacteriarelevanttohalogencycling and bioremediation, belong to a novel bacterial class, Dehalococcoidia classis nov., order Dehalococcoidales ord. nov. and family Dehalococcoidaceae fam. nov., within the phylum Chloroflexi. *International Journal of Systematic and Evolutionary Microbiology, 63*(PART2), 625–635. https://doi.org/10.1099/ijs.0.034926-0
Shi, Z. Q., Liu, Y. S., Xiong, Q., Cai, W. W., & Ying, G. G. (2019). Occurrence, toxicity and transformationofsixtypicalbenzotriazolesintheenvironment:Areview. *ScienceoftheTotal Environment, 661*, 407–421. https://doi.org/10.1016/J.SCITOTENV.2019.01.138

Application of novel filling materials in vertical subsurface flow constructed wetlands to treat the UASB effluent of domestic wastewater

T. Seintos*, A. Koukoura**, E. Statiris*, F. Masi***, C. Noutsopoulos*, S. Malamis*

*Sanitary Engineering Laboratory, Department of Water Resources and Environmental Engineering, School of Civil Engineering, National Technical University of Athens, 5 Iroon Polytechniou, Zografou, 15780, Athens, Greece
**Water and Air Quality Laboratory, Department of Environment, University of the Aegean, 81100, Greece
***Iridra Srl, via la Marmora 51, Firenze 50121, Italy

Abstract
The selection of the appropriate filling material in constructed wetlands (CWs), depends on the required treatment, the cost, availability and the hydraulic behaviour of the system. This work examined material of various origins (sand, recycled glass, biochar and gel beads), that can be used in unsaturated vertical subsurface flow CWs. The suitability of the materials was initially determined by their granulometry and porosity, that affect hydraulic conductivity (sand 0.23, recycled glass 0.16 and biochar 0.04 cm/s). Preliminary results for the treatment of anaerobic effluents produced by a UASB process treating domestic wastewater indicated promising performance of the materials without any clogging issue. Under the so far maximum applied loading (OLR = 8.7 ± 1.8 gCOD m^{-2} d^{-1}, SLR = 3.5 ± 1.5 gTSS m^{-2} d^{-1}, NLR = 2.6 ± 0.4 gNH_4-N m^{-2} d^{-1}), removal efficiency of sand, biochar and glass was greater than 93% for TSS, 86% for COD and 99% for NH_4-N, while gels achieved 83%, 61% and 86%, respectively.

Keywords
Constructed wetlands; filling material; wastewater treatment; hydraulic conductivity

INTRODUCTION

Various materials have been used as an alternative to sand that is usually used as filling material in vertical subsurface flow constructed wetlands (VSSF CWs) such as recycled glass (Humeniuk et al., 2019) and biochar (Gupta et al., 2016). The selection of the filling materials depends on the treatment requirements and therefore the required removal of pollutants e.g., organic matter, nutrients, heavy metals, surfactants and emerging contaminants (Wang et al., 2020) and, thus, the required removal mechanism. The orientation of wastewater treatment has been shifting from safe-to-discharge to safe-to-reuse effluent; the preservation of nutrients in the treated effluent is of crucial importance. Materials that precipitate phosphorus e.g., those that have Ca content >10% (Moreno-Perez et al., 2018) should be avoided. The present work investigated the suitability of three different filling materials (recycled glass, hydrogels and biochar) in comparison to sand for the treatment of anaerobic effluents produced by aUASB) process treating domestic wastewater.

MATERIALS & METHODS

Four columns packed with each substrate were implemented to simulate VSSF unsaturated (UNSAT) CW (Figure 1). Coarse gravel covered the bottom 20 cm as drainage, while 20 cm of finer gravel was placed on top of it to support the main filter media, whose total height was 40 cm. On top of the main filter media 20 cm of the same fine gravel was placed to distribute wastewater uniformly to the filter media. The diameter of each column was 25cm. The first tests of the materials included granulometry, porosity and hydraulic conductivity determination.

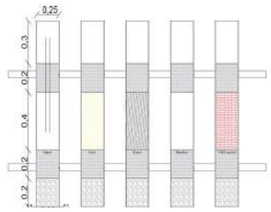

Figure 1. Layout of the four simulation columns (sand, hydrogels, recycled glass, biochar)

Granulometry

Granulometry was carried out for sand, biochar and glass by sieving to produce the granulometric curve. Since fine media was required for VSSF UNSAT CWs, sieves of 2, 1, 0.5, 0.25 and 0.1 mm were used. The gels were commercially available of biodegradable polymer origin and standard uniform size so there was no need for granulometry determination, since the expanded gel (after water absorption) was spherical with 8 – 10 mm diameter.

Porosity calculation (n)

The porosity was calculated according to Eq. 1. Once the sample was dried at 105°C, water was added inside the test device to record added water weight until saturation. Three samples were examined to extract the average value.

$$n = \frac{V_{H_2O}}{V_{sample}} = \frac{w_{H_2O}/\rho_{H_2O}}{A*L} n = \frac{V_{H_2O}}{V_{sample}} = \frac{w_{H_2O}/\rho_{H_2O}}{A*L}$$ Equation 1

where:
A: vessel area (cm^2)
L: vessel length (cm)

w_{H_2O} w_{H_2O} : water weight for saturation of the sample (g)

ρ_{H_2O} ρ_{H_2O} : water density at 20°C (= 0.998 g/cm^3)

Hydraulic conductivity calculation (k)

The hydraulic conductivity was calculated with the variable head method according to Darcy's law. A known volume of water (10 L) was instantly added to the column and the height of the water column above the material was recorded versus time. Hydraulic conductivity was calculated every 1cm drop between the initial 20 cm and last 5 cm, according to Eq. 2 (the bottom 5 cm were not recorded to avoid possible disturbance). Therefore, for each trial k was calculated as an average of 15 values.

$$k = \frac{L}{t_i - t_0} * \ln\left(\frac{h_0}{h_i}\right) k = \frac{L}{t_i - t_0} * \ln\left(\frac{h_0}{h_i}\right)$$ Equation 2

where:
L: filter media height (40 cm)
h_0, h_i initial (20 cm), instant water height above the filter (cm)
t_0, t_i start time (=0 s), time from measurement start for h_i recording (s)
This test was repeated until the pore volume factor (PVF) was equal to 20, as a material is considered to be saturated when PV gets replaced 20 times with new water (Wanigarathna et al., 2013).

Treatment start-up

Plants were not used to avoid the effect of the roots' development. Start-up was performed with UASB effluent and the applied organic loading rate (OLR), solids loading rate (SLR) and nitrogen loading rate (NLR) is given in Table 1. Feeding was intermittent respecting a hydraulic load of the unsaturated beds of 2 cm per flush.

Table 1 VSSF columns operational parameters

Period	Day start	Day end	Q (L/d)	T (°C)	OLR (g_{COD} m^{-2} d^{-1})	SLR (g_{TSS} m^{-2} d^{-1})	NLR (g_{NH4-N} m^{-2} d^{-1})
1	1	101	1	25.5 ± 1.1	4.7 ± 1.2	2.3 ± 0.8	1.1 ± 0.1
2	102	193	2	13.9 ± 2.3	8.7 ± 1.8	3.5 ± 1.5	2.6 ± 0.4

RESULTS & DISCUSSION

Filling material properties

Fine fragments' (<0.3 mm) proportion should not exceed 10% to avoid clogging issues Biochar had similar granulometry with sand (control material) besides the fine fragment (<0.3 mm), that also affected hydraulic conductivity. Both sand and biochar were quite uniform in terms of particle size. Recycled glass was less uniform and fine fragments were present at the range of biochar (Figure 2). Regarding porosity, sand and glass had the same porosity explained by the glass origin that is sand, while biochar had larger porosity. Gels' porosity was almost equal to 1.0, since it was a water absorbent material, which could be expanded more than 100 times in volume terms (Figure 2).

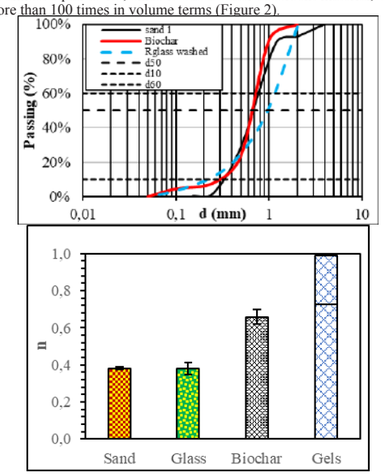

Figure 2. Left: Granulometric curves for the tested materials. Right: Porosity of the tested materials

Hydraulic performance

The hydraulic conductivity of the recycled glass was in the same order of magnitude with sand (0.16 and 0.22 cm/s, respectively), but its reduced percolation was attributed to the presence of very fine fragments in a greater proportion than in sand. Biochar had the slowest percolation (0.04 cm/s), being almost 6 times slower than sand due to the presence of significant amount of fine particles (<0.3 mm) (Figure 3). The test repetition up to PVF 20 indicated that only couple of repetitions are not enough to obtain a steady value which – here – came after PVF 6 -8. This was due to the presence of unsaturated zones inside the material and indicated the need for repetition. Due to the biochar slow percolation volume of added water among PVF 8 and PVF 20 no measurement was performed.

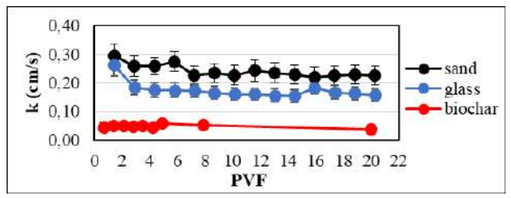

Figure 3. Hydraulic conductivity calculation up to PVF 20

Treatment performance

TSS and COD removal was high for all the tested materials except from gels' COD removal, which was due to the material's self-release of soluble COD (Figure 4). In the latter case, the large deviation of the results was due to the gradual decrease of this COD release, which was less during the second period. Ammonium removal was initially due to adsorption/ion exchange, while nitrification increased relatively fast for sand, biochar and gels. It took more the 100 days for biochar to develop nitrification mechanism and, even after this happened, ammonium adsorption was still a major removal mechanism. The NH_4-N adsorption capacity of sand, glass and gels was almost depleted after the forementioned period and nitrification was the dominant removal (transformation) mechanism thereafter.

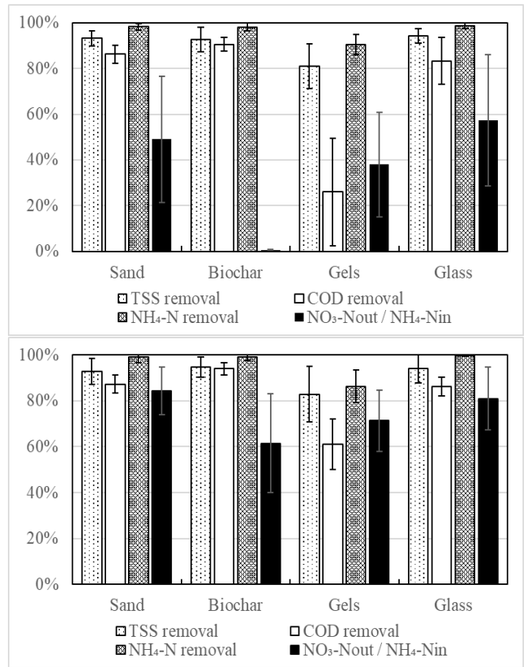

Figure 4 Filling material's performance (average ± st.dev) for period 1 (left) and period 2 (right)

CONCLUSION

All the materials appeared to be suitable to use in unsaturated VSSF CWs applications based on their hydraulic performance and, according to the ongoing results of treatment performance, biofilm growth seemed possible to all materials. However, the leaching of COD is an issue of concern for the gels.

Acknowledgments
This work has received funding from the European Union's Horizon 2020 research and innovation programme under grant agreement No 776643 within the framework of HYDROUSA project.

REFERENCES

Gupta, P., Ann, T.W., Lee, S.M., 2016. Use of biochar to enhance constructed wetland performance in wastewater reclamation. Environ. Eng. Res. 21, 36–44.
Humeniuk, B., Barquero, L.G.C., Wong, C., 2019. Crushed glass as a constructed wetland substrate: Invertebrate community responses to simulated wastewater inputs. Proc 5, 14–27.
Moreno-Pérez, E., Hernández-Ávila, J., Rangel-Martínez, Y., Cerecedo-Sáenz, E., Arenas-Flores, A., Reyes-Valderrama, M.I., Salinas-Rodríguez, E., 2018. Chemical and mineralogical characterization of recycled aggregates from construction and demolition waste from Mexico city. Minerals 8.
Wang, Y., Cai, Z., Sheng, S., Pan, F., Chen, F., & Fu, J. (2020). Science of the Total Environment Comprehensive evaluation of substrate materials for contaminants removal in constructed wetlands. Science of the Total Environment, 701, 134736.
Wanigarathna, D., Sounthararajah, A., Rajeswaran, G., & Kurukulasuriya, C. (2013). Long Term Effect of CaCl2 Solution on Hydraulic Conductivity of Expansive Clays and Expansive Clay-Bentonite Mixtures. Th International Conference on Structural Engineering and Construction Management (ICSECM), Kandy, Sri Lanka, Construction (December).

Challenges and implementation of Nature-based solutions in Southern European countries

I.Blanco*, S. Troesch **, F. Masi***, R. Bresciani***, F.Rogalla*, E.Lara*, R. Hervas*, D. Amador*, Z. Arbib*

*Department of Innovation and Technology, Aqualia FCC, Avenida Camino Santiago 40, E 28050 Madrid, Spain
(E-mail: *ivan.blanco@fcc.es*)
** EcoBIRD, 3 route du Dôme, 69630 Chaponost, France
*** IRIDRA, via Alfondo La Mamora 51, 50144 Florence, Italy

Abstract
Water scarcity in Southern European cities presents challenges for the implementation of Nature-based solutions (NbS) in urban environments, particularly during dry warm periods. The NICE project promotes the use of NbS within the urban water cycle for river basin restauration and the treatment and reuse of wastewater, greywater, stormwater and combined sewer overflow. This communication provides a description of the approach followed to mitigate these challenges in the implementation of NbS pilots in Algeciras and Madrid.

Keywords (maximum 6 in alphabetical order)
Nature-based solution; Sustainable; Grey water; Storm water; Wastewater; Combined Sewer Overflow

INTRODUCTION

Water scarcity in cities may be defined as a structural imbalance between available water and demand, which changes with the seasons and the changing nature of economic activities such as industrial and urban use, including tourism and commercial activities. In Southern Europe, one of the main reasons for water scarcity in cities is the combination of increased demand for water during the warm months due to increased tourism and agricultural production, with a reduced precipitation during this period (EIT Climate-KIC, 2022).

Nature-based Solutions (NbS) are sustainable technologies that are being under consideration for their integration in urban water management transitioning towards more sustainable water, sewerage and storm water systems. NbS can constitute an attractive and integral part of the urban landscape, and provide services such as pollution and runoff mitigation, climate change adaptation, river basin and biodiversity restauration and increasing water availability (Boano et al., 2020).

However, their implementation in Southern European cities faces important challenges. Warm periods with limited rainfall extend several months, increasing the risk of water stress on the plants in the case of lack of water supply for treatment. This may result in an impact on the aesthetic values associated to NbS technologies, reducing their acceptance from the citizens. This communication presents the approach followed by two NbS case studies in Southern Europe in the context of the H2020 NICE project.

H2020 NICE

The NICE project aims to promote the use of NbS as circular urban water solutions. The project will cover the whole urban water cycle: wastewater (WW), greywater (GW), river basins (RB), stormwater runoff (SW) and combined sewer overflow (CSO).

High-potential NbS technologies such as green walls, vegetated rooftops, rain gardens and constructed wetlands will be enhanced with especially tailored bioaugmentation strategies, reactive materials and filling media, novel design and plants in order to obtain highly innovative and efficient NbS for urban water management.

These enhancements will be validated at 11 urban pilots or “Urban Real Labs” (URLs) with a surface of 20-100 m^2. The URLs will be located in 8 countries with different climate, geographical, environmental and socioeconomic characteristics, including large, medium-size and small urban areas. Other pilots will be installed in 4 of the 7 NICE fellow cities.

Five of the URLs will be built and validated in Spain, in order to evaluate NbS under Southern European warm temperate and dry summer climate conditions. AQUALIA will collaborate with EcoBIRD, IRIDRA and other project partners in the design of these systems and will be responsible for their construction and validation. The integration of two of these pilots in the urban environment is provided below.

URL 3: Algeciras

Algeciras is the largest urban area in Campo de Gibraltar (Southwest Spain) with >260.000 inhabitants and the 7th largest port in the EU. Storms are common between autumn and spring, causing severe runoff events from the city to the adjacent port.

A constructed wetland pilot will treat storm water abstracted from the stormwater network in order to demonstrate the potential of NbS to prevent undesired runoff events to the port. The pilot will be built integrated in the surroundings of the Bay of Algeciras boardwalk. The main challenge in the design is the almost absence of rain and the warm temperatures in the period May – September which is likely to cause strong evapotranspiration and hydric stress to the wetland. To prevent this, the project considers the intervention in a local High School next to the location of the pilot, in order to separate and collect up to 2 m^3/day of greywater to be treated in the NbS.

The innovative pilot will be designed as a vertical and horizontal flow constructed wetland combining the treatment of both greywater and stormwater. The discharge will maintain saturated conditions in the filter, allowing enough water for the plants to survive the dry summer period.Plants adapted to the local climate and therefore to periods of water stress will be selected.

URL 6: Madrid

Madrid is a large urban area with >6.3M inhabitants with strong temperature differences between winter and summer. As most of the European cities that has to face with climate change by improving its resilience to extreme events (rain and temperature), NbS will help to mitigate the flooding risk, Heat Island effect, reuse locally stormwater or wastewater and bring many others ecosystem services. Construction of a pilot in a large office building (Aqualia FCC Corporative Offices) will be representative for the future replication of NbS technologies in the urban centre of large EU cities.

New connections in the toilets of the bathrooms within the building will allow the collection of greywater. Two NICE pilots are being considered at this point: a constructed wetland pilot will treat greywater in a plot located at the ground level in the back street of the building, whereas a green rooftop will be used for potential greywater treatment and mitigation of strong temperatures during summer. Greywater treatment and consumption will be monitored to evaluate the reduction in water use for irrigation, and the reduction of water being discharged to the sewer. The regular occupancy of the building even during summer will allow continuous generation of greywater required for the maintenance of the NbS.

ACKNOWLEDGEMENTS

This work has received funding from the European Union´s Horizon 2020 research and innovation program NICE project (GA 101003765). Special acknowledgements to CETIM, coordinator of the NICE project.

REFERENCES

EIT Climate-KIC, 2022. Water scarcity in Southern Europe: Problems and solutions. https://www.climate-kic.org/opinion/water-scarcity-in-southern-europe-problems-and-solutions/

Boano, F., Caruso, A., Costamagna, E., Rifolfi, L., Fiore, S., Demichelis, F., Galvao, A., Pisoeiro, J., Rizzo, A. and Masi, F. 2020 A review of nature-based solutions for greywater treatment: Applications, hydraulic design, and environmental benefits. Science of the total environment **711**, 134731.

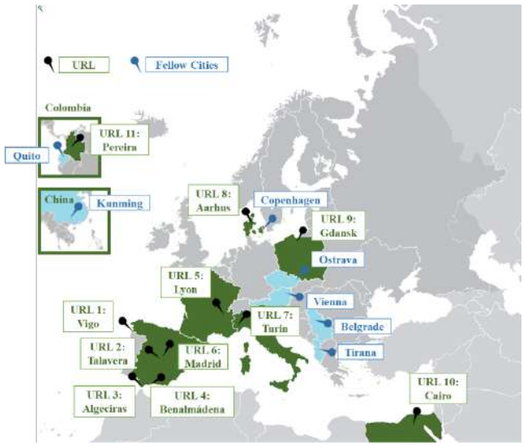

Figure 1. Cities where the 11 Urban Real Labs will be located, and 7 Fellow Cities.

Figure 2. Plot for NbS implementation in the Bay of Algeciras boardwalk

Figure 3. Aqualia FCC Corporative Offices in Las Tablas (Madrid)

Figure 4. Plot for NbS implementation in Madrid at the ground level

A decision-support tool for nature-based solutions selection and pre-sizing using hybrid models

S. Guillaume*, J. Pueyo-Ros**, J. Comas**, N. Forquet *

* Research Unit REVERSAAL, INRAE, 5 rue de la Doua, 69100 Villeurbanne, France
(E-mail: *sophie.guillaume.1@inrae.fr*; corresponding author: *nicolas.forquet@inrae.fr*)
** ICRA, Edifici H2O, C/ Emili Grahit, 101, 17003 Girona (E-mail : *jpueyo@icra.cat, jcomas@icra.cat*)

Abstract

Nature-based Solutions (NBS) become a complementary solution for decentralised water management. They are extensive technologies that require urban planning. The MULTISOURCE decision-support tool will facilitate selection and provide pre-sizing of NBS. The tool will assist decision-makers to choose the best technology for a given scenario regarding wastewater treatment and operational requirements. This study concerns mainly its pre-sizing module.

To mitigate models predictions unacurracies, we test the hypothesis that hybrid modelling can improve model predictions for NBS pre-sizing. We propose a methodology from the gathering and validation of data, to the development and validation of a hybrid model for horizontal subsurface flow TW. Hybridisation is restrained to the use of the tank-in-series model and a learning model.

We expect that this methodolody for hybrid modelling will lead to more reliable predictions of NBS functionning and design, hence better assessment of the feasibility of their implementation.

Keywords

Natural treatment systems, Machine learning, Decision-support systems, Tank-in-series model, Wastewater treatment

INTRODUCTION

Urban water management faces challenges in water resource preservation and pollution control with underground water scarcity and propagation of sanitary and environmental risks. The European regulations 2020/741 offer an alternative to activities consuming water through the controlled use of non-conventional water source, in particular: treated wastewater reuse.

Treatment wetlands for circular cities

Wastewater is conventionally centralised and evacuated towards a treatment plant (WWTP). But in some cases, centralisation has overpassed a threshold where the capacity of the WWTP is overwhelmed and costs in sewer network and pumping "exceed the economies of scale of the WWTP" (Eggimann et al. 2015). A complementary solution to treat wastewater in this context and in case of urban expansion is the use of Nature-Based Solutions (NBS), in particular treatment wetlands (TW). They are extensive but flexible technologies: there exist multiple designs and can be implemented within cities at different scales, providing an alternative source of water and co-benefits (Langergraber et al. 2021).

Decision-making support systems

To facilitate projects of urban wastewater treatment and reuse, decision-making support systems are developed. In particular, SNAPP tool (https://mltsrc-snapp.icradev.cat/) has been implemented by the Catalan Institute for Water Research (ICRA) to ease selection and pre-sizing of all possible NBS (Acuña et al., 2023, IWA 2021). The selection and pre-sizing modules rely on an expert-driven and a data-driven approach respectively. The first module selects among 27 different natural treatment technologies the ones that fulfill a given scenario, based on inlet concentrations and outlet requirements. The data to develop the data-driven pre-sizing module was retrieved from scientific papers (329 papers for all technologies, and ~ 180 case studies for TW).

Further development of SNAPP tool is ongoing in the framework of the MULTISOURCE European project (https://multisource.eu/). New features will include a multi-criteria decision analysis that not only consider treatment performances but also costs (OPEX and CAPEX), environmental impacts based on a life-cycle analysis and multifunctionality in terms of ecosystem services provided. Finally, the pre-sizing module will be also upgraded to mitigate current prediction inaccuracies.

Multiple models

Multiple models are developed for treatment wetlands: from fully expert-driven (mechanistic) for description or design, including hydraulics, transport, microbial growth, pollutant degradation, clogging, etc. (Samsó et al. 2016; Meyer et al. 2015), to fully data-driven (empirical) models (Rousseau et al. 2004).

Models limits.

Learning or data-driven models require data which is difficult and expensive to produce for TW. Often, models developed overfit data leading to bad prediction, and they do not offer a proper physical understanding of the process. Mechanistic models present the drawback of either high mathematical complexity of describing a process, or the oversimplification of the process. Many mechanistic models also rely on experimentally determined parameters.

Hybrid modelling.

Hybrid models are developed such that models can balance out each other's drawbacks. There exist multiple hybridisation methods: corrective, compositional (or serial), embedded (IWA 2020). The hypothesis tested in this project is that following a rigorous methodology for hybrid modelling of TW leads to more reliable predictions than current individual models.

MATERIAL AND METHODS

Dataset construction

A dataset is formed from pollutant removal performances of NBS Technological Units (NBS TU) reported in the scientific literature. Focus is made on horizontal flow TW, however, vertical flow TW and free water surface flow TW were also reported in the final dataset.

Data collection.

Data are extracted from peer-reviewed papers obtained from two rounds of searches (from Web Of Science and from SCOPUS). Papers are downloaded if presenting adequate title and abstract, filtered with a script based on defined terms and selected after full reading.

Dataset storage.

Finally data are aggregated in an online database hosted by ICRA, with a data structure and terminology based on an ontology for TW description.

Data validation and preparation

A script is developed based on data reconciliation methodologies for experimental data (Rieger et al. 2010) to: (i) check unusual/outliers values (concentrations, dimensions) and measuring errors (compounds relationships), (ii) convert concentrations of compounds into N and P-equivalents when applicable, and (iii) impute missing data from other variables and expert knowledge (compounds concentrations, temperature, location coordinates).

Then, Factor Analysis of Mixed Data (FAMD) and Focused-Principal-Component Analysis (F-PCA) are used to determine relevant variables for learning models. FAMD handles continuous and categorical variables and F-PCA visualises variance relative to a given variable.

Model development

Corrective and compositional hybrid modelling is done coupling the tank-in-series (TIS) model to machine learning models. TIS model represents the functioning of a treatment wetland as a series of N Continuously-Stirred Tank Reactors, where N is determined empirically (von Sperling et al. 2023). These models are also compared to data-driven models, i.e. linear, power and exponential regression models where the surface S is predicted from the inlet load L_{in} and the outlet load L_{out} of the TW.

Model validation

The dataset is divided into a train and a test set (0.8:0.2 ratio) and Leave-one-out Cross-Validation is performed on the empirical models with the train set to avoid overfitting. Two efficiency criteria (Hauduc et al. 2015) are used to assess models performances:

- Determination (Nash-Sutcliffe) coefficient (closer to 1^- the better):

$$R^2 = 1 - \frac{\sum_{i=1}^{n} (O_i - P_i)^2}{\sum_{i=1}^{n} (O_i - \bar{O})^2}$$

- Normalised Maximum Error (MEn, closer to 0^+ the better):

$$MEn = max\left|\frac{O_i - P_i}{O}\right|$$

RESULTS AND DISCUSSION

Dataset construction

Data extraction method is described in Figure 1. It resulted in 614 papers downloaded and 381 papers filtered. Some false-negative cases are due to different nomenclature of compounds and non-legible formats of tables/figures for the script. Half of filtered papers are eventually reported in the database. The exclusion of others is notably due to missing elements in the technology description (dimensions, flowrate, concentrations), irrelevant type of water, contaminants and laboratory scale. Struggles to gather data point out the need for more rigorous reporting and characterisation of technologies and study conditions.

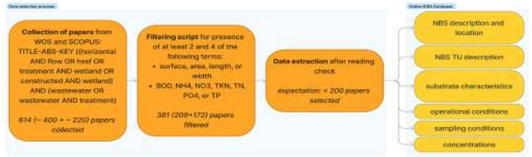

Figure 1. Database creation workflow

Comparison of models

Assessment of prediction performances on a test set for TIS model and regression models is reported in Table 1. Depending on the test set, varying performances are obtained for both types of models on *NO3* outflow predictions, as well as for *TN* and *TP*.

Table 1. Comparison of performances for mechanistic and empirical models on prediction of C_{out} and L_{out} values of a given test set.

		TIS model		Data-driven (linear, power or exponential regression)	
Parameter of interest	**Total number of points in dataset**	$C_{out} = tis(C_{in}, inflow\ rate, surface)$		$L_{out} = m(L_{in}, surface)$	
		R^2 for test set	**MEn for test set**	**R^2 for test set**	**MEn for test set**
BOD	87	0.66	1.90	0.83 exp	5.99..
NH4	65	0.98	0.86	0.85 lin	3.99
NO3	38	0.54	1.42	0.65 exp	1.41
TN	81	0.72	0.96	0.94 exp	3.61
TP	57	0.24	1.93	0.99.. lin	0.26

Variables selection

In cases where model performances vary greatly, other potential explanatory variables are assessed for development of new learning models. These models will be coupled with TIS model. Exploratory tools are used on *NO3* dataset. Figure 2. shows variance described according to quantitative and categorical variables using FAMD.

Figure 2. Variance of *NO3* dataset explained by ~ 50% by two principal components using FAMD.

Future hybrid models

The objective of the methodology is to propose a flexible and adequate modelling of TW according to available knowledge and data. This ongoing study shows that with limited data and TIS model available, a regularisation with a hybrid model provides more reliable predictions. Further research will be done for the cases in-between and testing other hybrid models. We aim at a rigorous methodology for hybrid modelling leading to more reliable predictions of NBS functioning and surface area requirements, hence better assessment of the feasibility of the NBS implementation.

ACKNOWLEDGEMENTS

This project is part of MULTISOURCE European project, which has received funding from the European Union's Horizon H2020 innovation action programme under grant agreement 101003527. This particular research in collaboration between INRAE and ICRA has also received fundings from the International School of Research of Agreenium Alliance (EIR-A) and from H2O'Lyon university school of research on water and hydrosystems sciences.

REFERENCES

Acuña, V. et al., 2023. « Development of a decision-support system to select nature-based solutions for domestic wastewater treatment ». *Blue-Green Systems* (submitted).

Eggimann, S., et al. 2015. « To Connect or Not to Connect? Modelling the Optimal Degree of Centralisation for Wastewater Infrastructures ». *Water Research* 84 (november): 218-31.

Hauduc, H., et al. 2015. « Efficiency Criteria for Environmental Model Quality Assessment: A Review and Its Application to Wastewater Treatment ». *Environmental Modelling & Software* 68 (june): 196-204.

IWA. 2021. *Nature-Based Solutions for Wastewater Treatment - A series of factsheets and case studies*. IWA Publishing, UK.

IWA. 2020. « Hybrid Models in Wastewater Merging Mechanistic with Data-driven ». Webinar (november).

Langergraber, G., et al. 2021. « A Framework for Addressing Circularity Challenges in Cities with Nature-Based Solutions ». *Water* 13 (17): 2355.

Meyer, D., et al. 2015. « Modelling Constructed Wetlands: Scopes and Aims – a Comparative Review ». *Ecological Engineering* 80 (july): 205-13.

Rieger, L., et al. 2010. « Data Reconciliation for Wastewater Treatment Plant Simulation Studies-Planning for High-Quality Data and Typical Sources of Errors ». *Water Environment Research* 82 (5): 426-33.

Rousseau, D. P.L., et al. 2004. « Model-Based Design of Horizontal Subsurface Flow Constructed Treatment Wetlands: A Review ». *Water Research* 38 (6): 1484-93.

Samsó, R., et al. 2016. « Modelling Bioclogging in Variably Saturated Porous Media and the Interactions between Surface/Subsurface Flows: Application to Constructed Wetlands ». *Journal of Environmental Management* 165 (january): 271-79.

Sperling, M. von, et al. 2023. « Representing Performance of Horizontal Flow Treatment Wetlands: The Tanks In Series (TIS) and the Plug Flow with Dispersion (PFD) Approaches and Their Application to Design ». *Science of The Total Environment* 859 (february): 160259.

TECHNICAL SESSIONS

T18. Environmental assessment

ECO STP 2023

Are circular economy strategies always environmentally sustainable? Including the end-of-life stage when assessing seafood plastic packaging

Jessica Pérez-García, Brais Vázquez-Vázquez and Almudena Hospido

CRETUS, Department of Chemical Engineering, Universidade de Santiago de Compostela, 15782, Santiago de Compostela, Spain

Abstract

Plastic litter is known to be one of the main global environmental concerns currently. Life Cycle Assessment (LCA) is the appropriate method to assess the environmental performance, nevertheless all process stages must be covered. To date, LCA does not normally include the impacts of the end-of-life (EoL) phase, in particular the unmanaged flows (i.e. direct plastic leak on the environment). By developing the characterization factors for two plastic packaging prototypes for the seafood industry, this study can cover the full life cycle of both materials. Results show that the inclusion of uncontrolled plastic waste causes significant impact on the environment.

Keywords:

Characterization factor; end of life; environmental impact, life cycle assessment, oil-based plastic

INTRODUCTION

The fish processing industry in Spain, and in particular Galicia, which accounts for 80% of total national production, it plays an important role in the world market. It is known that the activities seafood processing sector generate a complex wastewater with high pollutant load, so its correct treatment is essential (Roibás-Rozas et al., 2021)PHA accumulating capacity was below 10%, so several strategies were tested. In the acidification unit, Na(HCO3. Furthermore, this industry is highly dependent on oil-based plastic for use in the packaging of its products; polyethylene and polypropylene (PE and PP, respectively) are the most demanded plastics by this industry (Plastics Europe, 2021).

The national funded project BIOCENPLAS put together the National Association of Manufacturers of Canned Fish and Shellfish (ANFACO-CECOPESCA), the Galician Water Technology Centre (CETAQUA) and the academia (USC) to materialize circular strategies of waste valorization by means of transforming effluents rich in lipids from the seafood canning industry into biopolymers able to replace oil-based plastic (i.e. conventional plastic).

Over the last decades, it has become undeniable the significant impact of oil-based plastic in the ecosystem and the human health (Saling et al., 2020)the impacts of marine plastic debris are not considered. However, this type of particulates can be assessed like other emissions with the systematic and quantifiable approach in life cycle assessment (LCA. Currently, there are numerous studies addressing the environmental assessment of conventional plastics, but them only consider the stages cradle to gate, including raw material extraction, plastic production and moulding and waste management (landfill, incineration and recycling), regardless of plastics leakage associated with the use and the end-of-life stage (Figure 1) regardless of plastics leakage associated with the end-of-life stage (Marie et al., 2021; Saling et al., 2020){“id”:”ITEM-2”,”itemData”:{“DOI”:”10.1007/s11367-020-01802-z”,”ISSN”:”16147502”,”abstract”:”Purpose: Plastic pollution in marine environments is a severe problem in the world due to misuse and mismanagement of the materials. Microplastics are a specific form of pollutants in this context and its handling is very difficult due to its very small size of particulates. Currently, the impacts of marine plastic debris are not considered. However, this type of particulates can be assessed like other emissions with the systematic and quantifiable approach in life cycle assessment (LCA. So the aim of this work is to integrate the complete EoL stage in the life cycle environmental evaluation of two food packaging items, i.e. a sheet of polyethylene (PE) (120 x 120 mm) with a thickness of 100 µm which contains as a chemical additive bis(2-ethylhexyl) phthalate, and a tray of polypropylene (PP) (228 x 145 x 30 mm) with a thickness of 450 µm which contains dibutyl phthalate, selected as representative by the seafood.

METHODS

Life Cycle Assessment (LCA) is a standardized method (ISO 14040 and 14044) where inputs and outputs are transformed into potential environmental impacts by means of a four-stage procedure.

At the inventory stage, data were collected from companies of the sector, national and region al statistics of plastic waste management and secondary data (i.e. background processes for plastic production, transport, and so on) come from the Ecoinvent v3 database (Bishop et al., 2021)inventory completeness (e.g. inclusion of additives. According to Jambeck et al. (2015) the total uncontrolled waste depends on the country´s waste management systems, being estimated to be around 4% for Spain. For the EoL stage, the Plastic Leak Project (PLP) is, to the best of our knowledge, the only initiative that has developed a standardised methodology to quantify the plastic flows to each compartment environmental (Peano et al., 2020) and is the one followed here. So, the release rate of the plastic litter to the marine and terrestrial compartments are estimated based on the size of the material and its residual value, is defined as the probability of waste being reintroduced back into the value chain (Table 1), both materials are small size, and it has been assumed that PE has a low residual value while PP has a medium residual value.

At the impact assessment stage, impacts related to chemical released are measured as in eq. 1 where IS is the impact score, CF is the characterization factor, and M is the mass of substance emitted. Then, the CF is calculated considering the principal cause−effect chains; thus, through fate, exposure, and effect factors (FF, XF, and EF, respectively), according to eq. 2 (Rosenbaum et al., 2008).

$$IS = CF \cdot M \quad \text{(eq. 1)}$$

$$CF = FF \cdot XF \cdot EF \quad \text{(eq. 2)}$$

The FF is associated to the plastic transport and their fragmentation and degradation, it represents the residence time of the plastic in the compartments and is expressed in days, and it was modelled according Corella-Puertas et al., 2022, where the rate of degradation involves mass loss in each compartment calculated by a kinetic of first order. The EF deals with the sensitivity of the species to the released pollutant and is expressed in PAF m^3/kg. EF is modelled under the USEtox perspective by Species Sensitivity Distribution (SSD) curve that is determined by the concentration of the pollutant released in relation to the variation of the affected species studied (Rosenbaum et al., 2008). The USEtox model considers both the exposure and the concentration of the pollutant in the final compartment, considering the effect on the species affected by the exposure. The XF states the probability of exposure of living organisms by the release of the pollutant into the final compartment.

Recipe 2016 v1 was the chosen impact assessment method as it addresses the most appropriate categories for this system (Bishop et al., 2021)inventory completeness (e.g. inclusion of additives, complemented with the development of specific CF for plastic materials leakage in the natural environment following Corella-Puertas et al. (2022).

RESULTS & DISCUSSION

The contribution of each stage of the process (excluding EoL) to the selected impact categories is presented in the Figure 2 for each material. Both plastic items have similar environmental profiles, with significant contribution observed from the production and moulding stages in all categories, followed by intermediate transport (includes all transport of packaging and plastic waste). In terms of waste management, it is worth highlighting the environmental benefit derived from recycling, negatives values in the Figure 2, and the low contribution of incineration and landfilling.

Concerning EoL stage, the results of CFs are shown in Table 2. The higher values of the FF are linked to a slow degradation of plastic in each compartment mainly due to increased persistence. Regarding EF, it is observed in the SSD curves (Figure 3) that when the additives concentration present in the plastic increases the effect in the species is higher.

The impacts caused by plastic leakage are relevant (Table 3) and the inclusion of theses environment impacts contribute up to 40% of quality ecosystem. Therefore, this work shows that incorporating impacts caused by plastic leakage can aid in addressing these environmental problems.

Taking everything into account, there is an uncertainty in the development of characterization factor for the quantification of environmental impacts that need more research.

REFERENCES

Bishop, G., et al. (2021). https://doi.org/10.1016/j.resconrec.2021.105451
Corella-Puertas, E., et al. (2022). https://doi.org/10.1111/jiec.13269
Marie, A., et al. (2021). https://doi.org/10.1007/s11367-021-01975-1
Jambeck, R,. et al. (2015). https://science.sciencemag.org/CONTENT/347/6223/768
Peano, L., et al. (2020). https://doi.org/10.32964/tj19.4
Plastics Europe. (2021). https://plasticseurope.org/knowledge-hub/plastics-the-facts-2021/
Roibás-Rozas, A., et al. (2021). https://doi.org/10.1016/j.biortech.2021.124964
Rosenbaum, R., et al. (2008). https://doi.org/10.1007/s11367-008-0038-4
Saling, P., et al. (2020).. https://doi.org/10.1007/s11367-020-01802-z

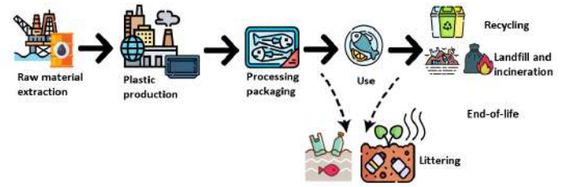

Figure 1. Life cycles stages of plastic packaging, being the discontinuous lines the focus of this contribution.

Table 1. Release rates (Rel) to the marine and terrestrial compartment. Peano et al., 2020.

	Small size (<5 cm)		Medium size (5-25 cm)		Large size (>25 cm)	
LRV[a]	40%	60%	25%	75%	5%	95%
MRV[b]	25%	75%	15%	85%	5%	95%
HRV[c]	15%	15%	10%	5%	1%	1%

[a]Low residual value; [b]Medium residual value; [c] High residual value

Figure 2. Characterization results for the PE sheet (left) and for PP tray (right) for the impact categories: global warming (GWP), ozone depletion (ODP), terrestrial acidification (AP), eutrophication (EP), human toxicity (HTP), photochemical oxidant (POCP), ecotoxicity (TETP), and Fossil depletion (DAR).

Table 2. Fate, effect and exposure factors for the PE film and PP tray for each environmental compartment.

	PE sheet		PP tray	
	Marine	Terrestrial	Marine	Terrestrial
FF (year)	4.10	106.26	11.31	34.42
EF (PAF m^3/kg)	11.08	21.01	14.90	18.65
XF	1	1	1	1
CF (PAF m^3 year /kg)	45.44	2232.47	114.58	641.96

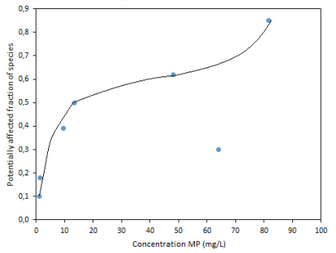

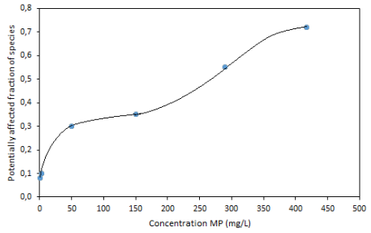

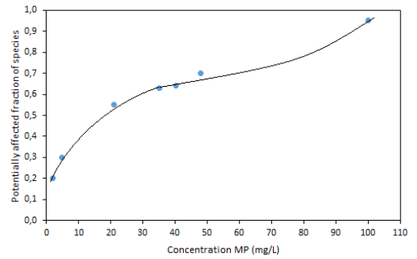

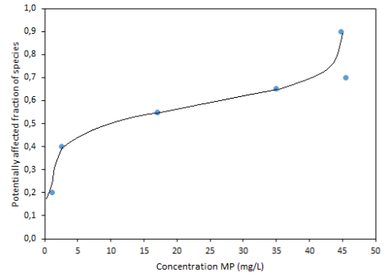

Figure 3. Species Sensitivity Distribution curves for a) PE sheet in the marine compartment b) PE sheet in the terrestrial compartment c) PP tray in the marine compartment and d) PP tray in the terrestrial compartment

Table 3. Impacts of the emissions of plastic leakage in the ecosystem quality.

	PE film		PP tray	
IS	Marine	Terrestrial	Marine	Terrestrial
Damage to ecosystem quality (PAF m^3 day)	$1.89 \cdot 10^4$	$2.78 \cdot 10^6$	$4.18 \cdot 10^4$	$9.07 \cdot 10^5$

Environmental assessment of bio – based Volatile Fatty Acids production from industrial wastewater

L. González- Monjardin*, T. Casero*, M. Tortosa*, C. Castro-Barros*, Y. Lorenzo* and A. Hospido**

*CETAQUA, Water Technology Centre, AquaHub - A Vila da Auga, José Villar Granjel 33, E-15890, Santiago de Compostela, Spain.
(E-mail: lucia-jimena.gonzalez@cetaqua.com, tamara.casero@veolia.com, maria.tortosa@cetaqua.com, celia-maria.castro@cetaqua.com, yago.lorenzo@cetaqua.com)
** CRETUS, Department of Chemical Engineering, Universidade de Santiago de Compostela, E-15782, Santiago de Compostela, Spain
(E-mail: almudena.hospido@usc.es)

Abstract
The production of Volatile Fatty Acids (VFA) from wastewater is an interesting process that contributes to the transition of Wastewater Treatment Plants (WWTP) into resource recovery facilities. This transition needs to be supported by a better environmental performance, so Life Cycle Assessment (LCA) was used to evaluate the production of VFA from dairy wastewaters and to compare it to the actual treatment process. Two major limitations were identified in that comparison: i) a fermentation yield of at least 0.34 g VFA-COD/ g CODin is required to be environmentally competitive; and ii) the use of ethyl acetate as extraction solvent is a significant bottleneck due to its high environmental cost across all evaluated impact categories. Although this technology was proven not mature enough to replace the business-as-usual approach at this stage, these results will help shaped the next steps of its development.

Keywords
Environmental performance, Life Cycle Assessment, Resource recovery

INTRODUCTION

To address the challenges faced by society, including climate change, and environmental degradation, and ensure the sustainability of further generations, a paradigm shift from linear economy (extract-use-dispose) to circular economy (extract-use-recycle) must occur. In the case of wastewater (WW) management, moving from the simple treatment and discharge alternative to the recovery of valuable substances strategy, is an interesting, and usually more sustainable approach. Wastewater from food processing industries often contains high amounts of organic matter and nutrients such as Nitrogen (N) and Phosphorous (P). Although research shows the potential for resource recovery in food-processing WW, this practice is not commonly applied in industrial settings apart from anaerobic digestion to obtain biogas (Stasinakis et al., 2022).

Volatile Fatty Acids (VFA) production is among the innovative routes of valorisation being studied because of their high demand and market value and for its potential to displace their petro-chemical analogues (Atasoy et al., 2018). These new valorisation approaches present great interest due to their perceived lower environmental impact; however, this needs to be assessed and proved, as not all circular economy initiatives are intrinsically contributing positively to sustainability. Life Cycle Assessment (LCA) is presented as a systematic methodology capable of quantifying the environmental burdens associated with products, processes, and services along their respective life cycle and is widely used at an early stage of technology development (van der Giesen et al., 2020).

The dairy industry is a key sector of the Spanish economy with an approximate turnover of 9,500 million euros per year (FENIL, n.d.). Dairy processing plants generate significant amounts of wastewater. Around 4.6 L/kg of WW are generated in fermented milk products and up to 3.25 L/kg in cheese production. Although dependent on the production processes, organic loads are often high enough to merit some form of treatment before discharge (Stasinakis et al., 2022).
The purpose of this work is twofold: firstly, to quantify the environmental impacts associated with a novel technology to produce VFA from dairy wastewater and secondly, to compare the environmental performance of this valorisation strategy to the environmental impacts of the current treatment option in the dairy industry.

SELECTED CASE STUDY

Wastewater from a dairy industry located in Pontevedra (NW Spain) that produces yoghurt and cheese was selected as feed because it presented not only a higher VFA potential production on laboratory scale test but also better technical viability in terms of feed availability and stability than the other industrial WW tested. The characteristics of this particular waste stream (i.e., virtually all its COD is soluble, and no significant amount of fats are present) favour the anaerobic fermentation of this stream and thus VFA production.

The selected feed is an ultrafiltration (UF) permeate that is separated at the dairy industry and managed as a residual stream (Figure 1a) where some low-value added valorisation occurs: the UF permeate is sent to a nanofiltration (NF) unit, and the retentate is sent to evaporation to obtain a powder that is then converted into animal feed, while the permeate is treated in an industrial wastewater treatment plant (IWWTP) before being discharge to the sewage.

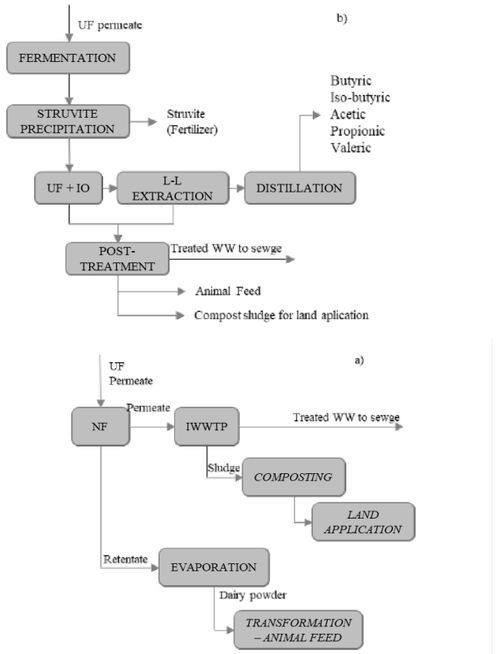

Figure 1: Process schemes for current treatment (a) and novel VFA production (b)

The novel valorisation scheme (Figure 1b) consists of the fermentation of the UF permeate to inhibit methane production and obtain VFA. Afterwards, VFA are separated, concentrated, and purified to recover the different acids individually and other added value products (e.g., struvite). Along the VFA downstream train, several residual streams are generated that will need further treatment before being ready for discharge.

The function of both processes is to manage the UF permeate produced at the dairy industry, so the functional unit (FU) has been defined based on its daily production (34 m^3) and stated in terms of organic load (1882.73 kg of $COD_{soluble}$/ day). No environmental loads were allocated to the UF permeate as it is considered a residual stream and all the burdens were then allocated to the main products of the dairy industry (yoghurt and cheese). Additionally, only the operation stage was considered. Given the significant uncertainty associated with these activities in this early stage of technology development (van der Giesen et al., 2020), the construction and dismantling of the required facilities, the distribution, commercialization, and use of all the obtained products in both scenarios were left outside the scope of the study.

INVENTORY STRATEGY AND IMPACT ASSESSMENT METHOD

Different sources of data were used to compile both scenario life cycle inventories. Primary data from the operation of the dairy plant was used, alongside with the results from operating pilot plants of the novel technology. Additionally, lab-scale tests combined with computer simulation were used for modelling the liquid-liquid extraction and distillation stage, as no pilot scale results were available at the time. Finally, other necessary information was obtained from bibliographical sources as well as LCA databases.

ReCiPe 2016 was chosen as the impact assessment method and the selected categories were: Global Warming Potential (GWP), Terrestrial Acidification (TA), Freshwater Eutrophication (FE), Marine Eutrophication (ME) and Fossil Resource Scarcity (FRS).

RESULTS

The results show that with the average fermentation yield obtained in the VFA production pilot plant (0.16 gCOD-VFA/$gCOD_{in}$), the novel technology presents higher environmental impacts in 4 of the 5 studied impact categories (Figure 2). The main reasons behind this are the low fermentation yield and the use of ethyl acetate as solvent for the liquid-liquid extraction stage. Meaning at this point the current scheme is more sustainable. Different additional scenarios were analysed to determine the technology hotspots and possible solutions.

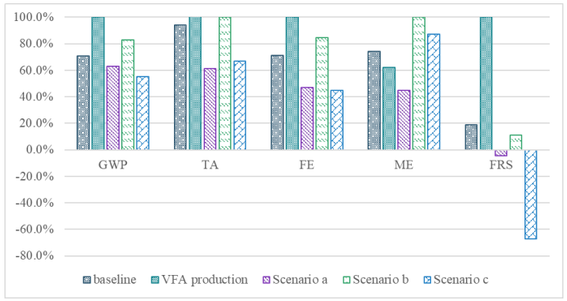

Figure 2: Normalized life cycle characterization results for the evaluated scenarios.

When the highest reported fermentation yield for dairy WW was used (i.e., 0.39 g VFA-COD/g COD_{in}) according to Magdalena et al., 2019 the production of VFA has a lower environmental impact across all categories regardless of the type of solvent use (Figure 2, scenario a).

As mentioned before, the use of ethyl acetate as solvent implies significant environmental loads. A scenario involving the use of a "bio ethyl acetate" produced by esterification of acetic acid with bioethanol instead of the petro-based was analysed (Figure 2, scenario b). The results showed a reduction of the environmental impact across categories. However, these impacts are still higher than the baseline in all but the FRS category. This result reinforces the hypothesis that although ethyl acetate places an important role in the environmental performance of the VFA production the biggest challenge is still unconverted COD and its means of treatment.

The use of a bio-solvent reduces the environmental burden of the VFA production in the GWP, TA, FE and FRS impact categories (Figure 2, scenario b). For the ME impact category, the trend reverses from the original setting (where the VFA production had a lower impact than the baseline). This occurs, because the bioethanol process used for the assessments is obtained from the fermentation of rye and carries a significantly bigger impact in this category that is then transferred to the Bio ethyl acetate. Even when the highest yield obtained in the pilot plant (i.e., 0.334 g VFA-COD/g COD_{in}) is combined with bio-based solvent the ME category continues to have a larger impact than the baseline (Figure 2, scenario c). Showing that not always the bio – product is the most sustainable choice, and that a detailed and holistic study of each situation is needed.

CONCLUSIONS

The production of VFA from dairy industry WW is shown to have the potential to be a more sustainable approach than treatment once certain challenges are overcome. Mainly higher fermentation yields are necessary and further research into alternative extraction solvents.

The results obtained in the pilot plant show that it is possible to reach the breakpoint of the technology. The conclusions of this LCA can now inform further pilot tests and assist in decision making surrounding the next steps in the technology development.

ACKNOWLEDGMENT

The project was financed by the Xunta de Galicia within the framework of the CIGAT CIRCULAR project (IN853C2022/03) and EC-INTERREG CONSERVAL (0679_CONSERVAL_1_E). Acknowledgements also to HOOP (EU's Horizon 2020).

REFERENCES

Atasoy, M., Owusu-Agyeman, I., Plaza, E., & Cetecioglu, Z. (2018). Bio-based volatile fatty acid production and recovery from waste streams: Current status and future challenges. *Bioresource Technology* **268**, 773–786.
C. van der Giesen, S. Cucurachi, J. Guinée, G.J. Kramer, A. Tukker (2020). A critical view on the current application of LCA for new technologies and recommendations for improved practice. *Journal of Cleaner Production* **259**.
FENIL. (n.d.). Datos generales del sector. Retrieved December 30, 2021, from http://fenil.org/sector-lacteo-espana/datos-generales-del-sector/
Magdalena, J. A., Greses, S., & González-Fernández, C. (2019). Impact of Organic Loading Rate in Volatile Fatty Acids Production and Population Dynamics Using Microalgae Biomass as Substrate. *Scientific Reports*, **9**(1).
Stasinakis, A. S., Charalambous, P., & Vyrides, I. (2022). Dairy wastewater management in EU: Produced amounts, existing legislation, applied treatment processes and future challenges. *Journal of Environmental Management*, **303.**

Minimal liquid discharge desalination circularity and sustainability assessment

J.M. Ribeiro*, C.E. Nika*, R. Ktori**, G. A. Tsalidis*, M. Ghafourian*, D.F.C. Dias*, D. Xevgenos**, E. Katsou*

* Department of Civil & Environmental Engineering, Institute of Environment, Health and Societies, Brunel University London, Uxbridge Campus, Middlesex, UB8 3PH, Uxbridge, UK

(E-mail: joao.ribeiro@brunel.ac.uk; elisa.nika2@brunel.ac.uk; george.tsalidis@brunel.ac.uk; matia.ghafourian2@brunel.ac.uk; daniel.dias@brunel.ac.uk; evina.katsou@brunel.ac.uk)

** Faculty of Applied Sciences, Delft University of Technology, Lorentzweg 1, 2628 CJ Delft, the Netherlands

(E-mail: r.ktori@tudelft.nl; d.xevgenos@tudelft.nl)

Abstract

Desalination sector faces environmental and economic challenges due to brine discharge. Treating brine and recovering valuable materials from it, potentially brings environmental and economic benefits. This is addressed by the Minimal Liquid Discharge (MLD) and Zero Liquid Discharge (ZLD) approaches; however, to analyse the full potential, a sustainability assessment is required. Additionally, as both, MLD and ZLD, approaches are based on circular economy model, it is also important to ensure a sustainable transition from linear to circular practices in the desalination sector by measuring the circularity level. The preliminary Life Cycle Assessment (LCA) results show that the water produced by the MLD has overall higher environmental impacts compared to the reverse osmosis, mainly due to the higher energy consumption. On the other hand, the minerals production shown a significant lower impact compared to mining scenarios, showing that brine as a secondary source could reduce environmental pressure caused during the mineral's extraction stage.

Keywords (maximum 6 in alphabetical order)

Assessment; Circularity; Minimal Liquid Discharge; Sustainability

INTRODUCTION

Desalination technologies has received increased attention in recent years as a viable option to meet the fresh water domestic and municipal needs, however they face challenges due to certain barriers related with relatively high economic costs and diverse environmental problems (Jones et al., 2019). Desalination plants produce a saline wastewater, brine, as a by-product, resulting from separating water from the salts, and therefore it is seen as a waste that desalination plants should further deal with. The amount of global brine produced by desalination plants was calculated to be around 129 000 000 m^3/d (IDA, 2019), and coastally-located desalination plants and facilities usually discharge brine back into the sea, potentially causing issues with the ecosystem and the environment (Ogunbiyi et al., 2021). Treating brine is seen as a beneficial option to eliminate its impact, increasing the water production yield, and extracting valuable materials (Panagopoulos and Haralambous, 2020). The brine contains a mixture of metals and minerals at various concentrations with recovery potential, and economic advantages. Salts, such as NaCl, Na_2SO_4, $Mg(OH)_2$ and $Ca(OH)_2$ are potentially recoverable resources from the brine (Morgante et al., 2022; Culcasi et al., 2022). This practice is in line with the circular economy model that has been promoted by European Union (Panagopoulos and Haralambous, 2020), therefore measuring and assessing the circularity level (e.g. minimal or no waste, limited emissions and efficient resource utilization) is an important step to ensure a sustainable transition from linear to circular practice. Recent works have evaluated different Minimal Liquid Discharge (MLD) and Zero Liquid Discharge (ZLD) concepts from a techno-economic point of view (Morgante et al., 2022; Panagopoulus, 2022), however we still lack a comprehensive circularity and sustainability assessment. Therefore, the objective of this work is to measure and assess the circularity and sustainability level of a MLD system configuration that desalinates seawater and produces water, while recovering valuable materials like NaCl, Na_2SO_4, $Mg(OH)_2$ and $Ca(OH)_2$. To address this, a methodology has been used to measure the circularity and sustainability performance of the MLD at a process and product level.

MATERIALS AND METHODS

MLD description

The system under investigation has been operated at pilot-scale in the Lampedusa (Italy) desalination plant, therefore the full-scale scenario was modelled. The MLD is composed of 7 technologies (Figure 1) – i.e. Multimedia filtration (MMF) Nanofiltration (NF), Multi-effect distillation (MED), Thermal crystallizer (TC), Multiple feed plug flow reactor (MF-PFR), Eutectic freeze crystallizer (EFC) and Electrodialysis with bipolar membrane (EDBM). The resulting products are: Industrial water, NaCl, $Mg(OH)_2$, $Ca(OH)_2$ and Na_2SO_4. The EDBM produces NaOH and HCL, and both are used onsite in the process. The flowrate of raw seawater is 3000 m^3/d, and the thermal energy consumed by the MED and TC is supplied by Lampedusa power station. Additionally, antiscalant and NaOH are sourced externally. The NaOH produced in the EDBM is not enough to cover the demand for $Mg(OH)_2$ and $Ca(OH)_2$. The ions composition of the streams and flowrates of products are given in Table 1 and 2.

Circular and sustainable measurement and assessment

The scope of the assessment is to measure the circularity and sustainability of the MLD products (Industrial water, NaCl, $Mg(OH)_2$, $Ca(OH)_2$ and Na_2SO_4) and to compare them with conventional productions (e.g. seawater reverse osmosis (SWRO), mining). Data for the conventional production (e.g. mining) scenarios are collected from the Ecoinvent database v3.8. The system boundaries are cradle-to-gate, i.e., they include the MLD system, production and transportation of the MLD products. Therefore, the functional unit of the assessment is 1 kg of each MLD product. The circular measurement and assessment are based on the methodology developed by Nika et al., 2022 (figure 2). The methodology includes the system development that identifies the information needed for indicator selection, the type of measurements and models required, while also resulting in a system testing of the indicators (sensitivity to changes), and finally, the circularity assessment. The selected circularity indicators focus on the resources, water and energy categories at product level (e.g. energy intensity per product). The objective is to assess and compare the resources demand (e.g. Na, Cl, K, Mg, Ca, SO4, others) for the MLD products, and compare with the conventional products, e.g. how much virgin non-renewable resources are required per product. Moreover, with a similar objective, water and energy related circularity indicators have been calculated for the MLD products and conventional products. The sustainability assessment is performed through established methodologies, such as Life Cycle Assessment (LCA), Life Cycle Costing (LCC) and social LCA (sLCA).

RESULTS AND DISCUSSION

Figures 3, 4 and 5 show the LCA results (the $Mg(OH)_2$ and Na_2SO_4 results will be presented in the full manuscript) for the reference products. The industrial water produced by the MLD system results in higher environmental impacts than the SWRO. The global warming impact score is close to 80% reduction for SWRO. Energy requirements of the MED can be 5-6 times higher than the conventional SWRO (Raluy et al., 2006), and because the source of electrical energy in the current study are the diesel engines, this explains the higher impact on global warming. Additionally, as the MED receives the permeate from the MF-PFR and NF processes, a fraction of energy consumption of these processes is allocated to the water production. A climate change impact reduction is expected if solar-driven is integrated with the MED (Alhaj et al., 2022). On the other hand, the MLD production of NaCl and $Ca(OH)_2$ results in environmental benefits when compared with conventional production of these products. Regarding the production minerals and metals, studies have demonstrated that the mining and beneficiation (separation/concentration processes before refining) stages contribute significantly to the environmental performance (Marmiroli et al, 2022). Despite, the use of secondary sources (e.g. brine) will not fully cover the demand for minerals (Marmiroli et al, 2022), the MLD shows a significantly smaller impacts on minerals production. Similar results are seen for $Mg(OH)_2$ and Na_2SO_4.

A detailed circularity and sustainability assessment will be further presented in the full manuscript, and the results will be discussed.

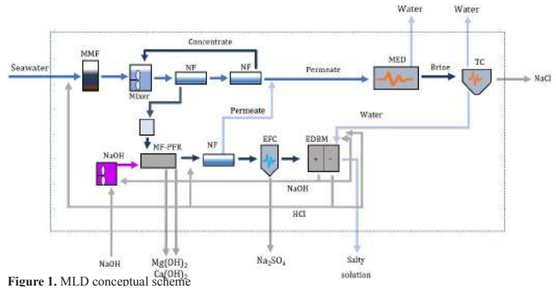

Figure 1. MLD conceptual scheme

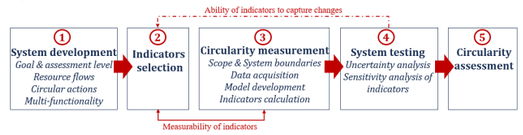

Figure 2. Methodological steps of the circularity assessment

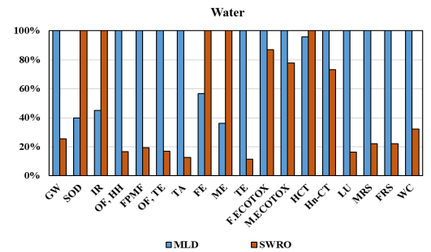

Figure 3. Mid-point LCA impacts: MLD vs SWRO for 1 kg of water produced.

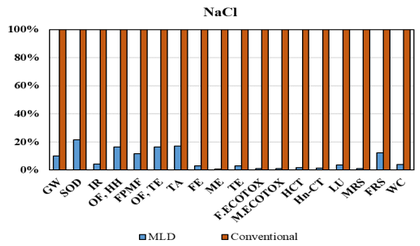

Figure 4. Mid-point LCA impacts: MLD vs conventional for 1 kg of NaCl.

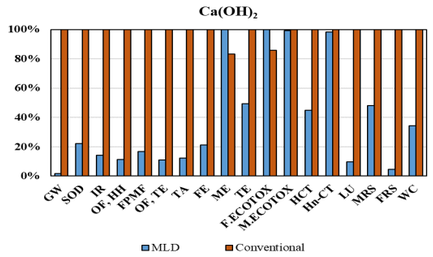

Figure 5. Mid-point LCA impacts: MLD vs conventional for 1 kg of $Ca(OH)_2$.

Table 1. Ions composition of the MLD flows

Ions	MMF feed	NF feed	NF retentate	NF permeate	MED feed	MED brine	MF-PFR effluent	NF retentate	EFC effluent	EDBM effluent
	Concentration [g/L]									
Na^+	11.90	11.90	15.18	10.75	12.18	103.53	18.08	19.95	9.65	7.33
Cl^-	21.80	21.80	34.34	17.40	18.42	156.55	21.59	24.23	39.54	36.80
K^+	0.40	0.40	0.63	0.32	0.32	2.75	0.39	0.47	0.80	0.79
Mg^{2+}	1.40	1.40	5.29	0.03	0.025	0.21	0.00	0.00	0.00	0
Ca^{2+}	0.40	0.40	1.47	0.03	0.04	0.37	0.43	0.92	1.53	1.53
SO_4^{2-}	3.20	3.20	12.30	0.01	0.08	0.07	7.73	18.59	6.03	6.03
Flowrate [m3/d]	3000	3000	779	2221	2976	299	1239	503	303	303

Table 2. Products flowrate of the MLD

	Products								
	Water (MED)	Water (TC)	NaCl	$Mg(OH)_2$	$Ca(OH)_2$	Na_2SO_4	Ice	NaOH	HCl
Flowrate	2678 m^3/d	199 m^3/d	99682 kg/d	9899 kg/d	1128 kg/d	25099 kg/d	186102 kg/d	30 m^3/d	30 m^3/d

REFERENCES

Alhaj, M., Tahir, F., Al-Ghamdi, S. G. 2022 Life-cycle environmental assessment of solar-driven Multi-Effect Desalination (MED) plant. *Desalination* **524**, 115451.

Cipolleta, G., Lancioni, N., Akyol, Ç., Eusebi, A. L., Fatone, F. 2021 Brine treatment technologies towards minimum/zero liquid discharge and resource recovery: State of the art and techno-economic assessment. *Journal of Environmental Management* **300**, 113681.

Culcasi, A., Ktori, R., Pellegrino, A., Rodriguez-Pascual, M., van Loosdrecht, M. C. M., Tamburini, A., Cipollina, A., Xevgenos, D., Micale, G. Towards sustainable production of minerals and chemicals through seawater brine treatment using Eutectic freeze crystallization and Electrodialysis with bipolar membranes. *Journal of Cleaner Production* **368**, 133143.

IDA. 2019 The IDA Water Security Handbook, IDA and GWI DesalData.

Jones, E., Qadir, M., van Vliet, M. T. H., Smakhtin, V., Kang, S. 2019 The state of desalination and brine production: A global outlook. *Science of the Total Environment* **657**, 1343–1356.

Marmiroli, B., Rigamonti, L., Brito-Parada, P. R. Life Cycle Assessment in mineral processing – a review of the role of flotation. *The International Journal of Life Cycle Assessment* **27**, 62-81.

Morgante, C., Vassallo, F., Xevgenos, D., Cipollina, A., Micari, M., Tamburini, A., Micale, G. 2022 Valorisation of SWRO brines in a remote island through a circular approach: Techno-economic analysis and perspectives. *Desalination* **542**, 116005.

Nika, C. E., Vasilaki, V., Renfrew, D., Danishvar, Echchelh, A., Katsou, E. 2022 Assessing circularity of multi-sectoral systems under the Water-Energy-Food-Ecosystems (WEFE) nexus. *Water Research* **221**, 118842.

Ogunbiyi, O., Saththasivam, J., Al-Masri, D., Manawi, Y., Lawler, J., Zhang, X., Liu, Z. 2021 Sustainable brine management from the perspectives of water, energy and mineral recovery: A comprehensive review. *Desalination* **513**, 115055.

Panagopoulos, A., Haralambous, K. 2020 Minimal Liquid Discharge (MLD) and Zero Liquid Discharge (ZLD) strategies for wastewater management and resource recovery – Analysis, challenges and prospects. *Journal of Environmental Chemical Engineering* **8**, 104418.

Panagopoulos, A. 2022 Techno-economic assessment of zero liquid discharge (ZLD) systems for sustainable treatment, minimization and valorization of seawater brine. *Journal of Environmental Management* **306**, 114488.

Raluy, G., Serra, L., Uche, J. 2006 Life cycle assessment of MSF, MED and RO desalination technologies. *Energy* **31**, 2361-2372.

Analysis and comparison of life cycle assessment approaches in mineral and recovered phosphorus fertilizer production

L. Manoukian*, E. Martín Hernández**, J. Morris***, C. Vaneeckhaute**, D. Frigon**** and S. Omelon*

* Department of Mining and Materials Engineering, McGill University, Montréal, Canada
(E-mail: *lori.manoukian@mail.mcgill.ca*; *sidney.omelon@mcgill.ca)*
** BioEngine - Research Team on Green Process Engineering and Biorefineries, Chemical Engineering Department, Université Laval, 1065 Ave. de la Médecine, Québec, QC, G1V 0A6, Canada
(E-mail: *edmah2@ulaval.ca*, *celine.vaneeckhaute@gch.ulaval.ca*)
***Leibniz Institute of the Ecological Urban and Regional Development, Weberplatz 1, 01217 Dresden, Germany (E-mail: j.morris@ioer.de)
* Department of Civil Engineering, McGill University, Montréal, Canada
(E-mail: dominic.frigon@mcgill.ca *)*

Abstract

Phosphorus (P) is an essential agricultural nutrient. Mineral P fertilizers are produced from phosphate rock; the associated environmental impacts have been assessed with life cycle analysis (LCA) studies. LCAs quantify the impacts of a product or process based on a functional unit for a defined system boundary. LCAs have also assessed processes that recover P as a fertilizer from municipal wastewater treatment facilities. Only a few LCA studies compare mineral and recovered P fertilizer production processes simultaneously. This work reviews, compares, and contrasts the functional units, impact categories, and system boundaries of peer-reviewed LCAs for mineral and/or recovered P fertilizer production. Variances in the functional units, impact assessment categories, and system boundaries limit meaningful comparisons. A metric tonne of P and/or P_2O_5 functional unit would improve LCA comparisons. Reasons for improbable standardization of impact criteria or system boundaries for mineral and recovered P-fertilizer are discussed.

Keywords (maximum 6 in alphabetical order)

INTRODUCTION

Phosphorus (P) is a vital nutrient for agricultural productivity, second only to nitrogen (N) in importance (Sharma, Sayyed, Trivedi, & Gobi, 2013)in both organic and inorganic forms, its availability is restricted as it occurs mostly in insoluble forms. The P content in average soil is about 0.05 % (w/w. Soluble phosphate is a component of fertilizers that is critical for global food production. Unlike ammonia production from N and hydrogen gases with the Haber-Bosch process, phosphate cannot be synthetically produced (Cordell, Drangert, & White, 2009)-- it is refined from mined "phosphate rock". P-rich ores are primarily located in Morocco, China, and the US. Global P supply chains and food security are therefore vulnerable to geopolitical instability (Rosemarin & Ekane, 2016)within the monitoring and regulation of these components, and surrounding the role of stakeholders in the process. As a result the intrinsic objectives of a governance system for P are not well formulated and yet to be implemented. Phosphorus is a mineral and is produced and marketed much like other minerals. But since P is also an essential element in our food systems, critical for all forms of life and very dispersed in different products, it requires special attention concerning data collaboration especially regarding rock phosphate (RP. Environmental concerns associated with mineral P fertilizer production include air and water emissions, eutrophication, and soil contamination with cadmium and uranium from sedimentary-type phosphate rock deposits (Lottermoser, 2010). Some mineral P demand may be replaced with P recovered from municipal wastewater treatment plants (WWTP) as struvite ($NH_4MgPO_4{\cdot}6H_2O$) or calcium phosphate (Egle, Zoboli, Thaler, Rechberger, & Zessner, 2014).
Effective comparisons of P-fertilizer production by primary (linear) technologies or secondary (circular) technologies can be undertaken with life cycle analyses (LCAs). LCAs require defined functional units (FU), impact categories (IC), and system boundaries. This work reviews and compares published LCAs for mineral P-fertilizer production and technologies for P-recovery for reuse as P-fertilizer. Significant variation in FU, IC, and system boundaries between and within LCAs for mineral P-fertilizer production and P-recovery processes prevents meaningful comparisons. The P-community may consider a standardized LCA approach to assess P-fertilizer production to guide the generation of future, comparable, LCA analyses.

MATERIALS AND METHODS

This review work was completed in two steps. The first step was a literature search using the keywords "life cycle analysis" and one or more of phosphorus, phosphorus recovery, phosphorus fertilizer, phosphorus processing, phosphate rock processing, wastewater treatment plant, wastewater, nutrient recovery, sewage sludge, struvite, and enhanced biological phosphorus removal (EBPR). The search engines Web of Science, Scopus, and Google Scholar identified 31 publications (Fig. 1). The second step compared, contrasted, and identified gaps between the FUs, ICs, and system boundaries in the LCA publications identified in Step 1.

RESULTS AND DISCUSSION

The subjects of the identified LCAs, and selected references, are presented in Fig. 1. Mineral P and recovered P fertilizer processes were compared with respect to LCA FUs, ICs, and system boundaries.

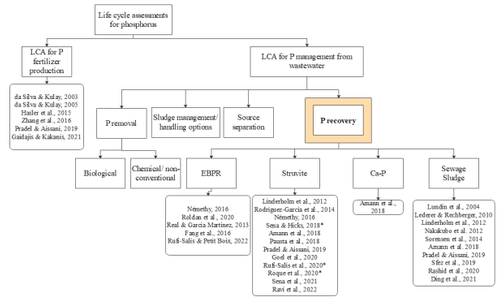

Figure 1. Themes identified in LCA studies of mineral P fertilizer production and P recovery from municipal wastewater. Review articles are indicated with *.

FUs for P fertilizers were masses of fertilizer (ex: monoammonium phosphate (MAP)), and/or P, and/or $\%P_2O_5$. FUs for recovered P from WWTP varied by definition and units. 25% of studies used the volume of treated wastewater as an FU. The recovered P mass (kg, ton, tonne, unspecified if metric or US short or long ton) or recovered rate (mass per year) was used for ~40% of LCAs. The P-product bioavailability was not assessed in any of the reviewed LCA studies. Other FUs for recovered P technologies included person equivalents and eutrophication potential reduction with respect to P removed. FUs used in thermal P-recovery technologies included "dry matter mass recovered" (40% of studies). The balance was "recovered P mass" or "annual P production". These different FUs limit meaningful LCA study comparisons.
Six IC methods were identified in the LCAs (Fig. 2A). The most common IC methods were ReCiPe (impact characterization factoring) and CML (product environmental impact). 47 specific ICs and their use frequency are presented in Fig 2B. Nearly 70% of the LCAs used global warming potential as an IC. Acidification and eutrophication were the next most frequent ICs.

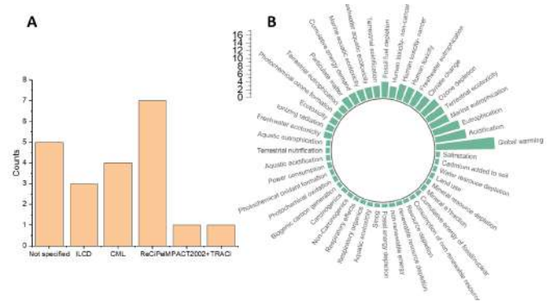

Figure 2.A LCA frameworks used in the studies assessed. **B** All impact assessment outcomes from the selected studies and the number of times they were studied.
System boundaries for LCAs of P fertilizer production are presented in Fig. 3. Most LCAs focused on mineral P production processes from phosphate rock. Mining and wastewater treatment were not included in all studies. LCA system boundaries for **P recovery from WWTP included P-recovery processes as struvite or calcium phosphate from water, sludge, and incinerated sludge ashes (Fig. 4).** The system boundaries covered P-fertilizer manufacture, field application, consumption, and wastewater treatment (Pausta, Razon, Promentilla, & Saroj, 2018), to smaller studies of a municipal wastewater treatment process (Zhou, Remy, Kabbe, & Barjenbruch, 2019). Few LCA studies directly compared mineral P production and recovered P-fertilizer production (Goel, Kansal, & Pfister, 2021; Linderholm, Tillman, & Mattsson, 2012).

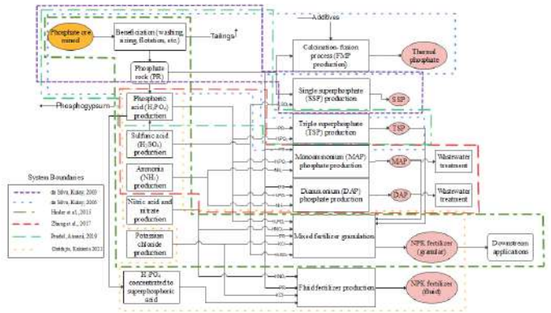

Figure 3. LCA system boundaries of different mineral P fertilizer production processes.

P-fertilizer LCA comparisons also have different inventory data types and qualities. Some LCAs analysed commercial, full-scale processes, others assessed pilot plant data or model data. Overall, this study shows how most mineral and recycled P-fertilizer production LCAs are not easily comparable due to different FUs, ICs, and system boundaries. A recommended general and potentially translatable FU for future LCAs across different P-fertilizer production options could be a metric tonne of P or P_2O_5. The wide range of options for ICs and system boundaries may preclude a common set for P-fertilizer production LCA studies.

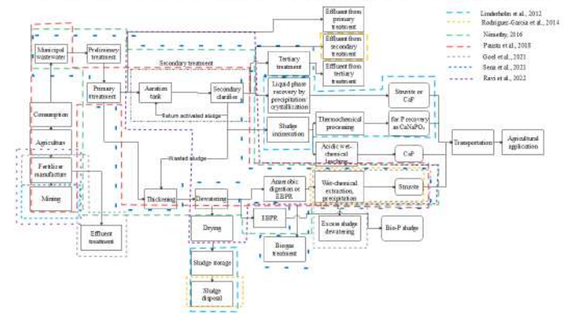

Figure 4. LCA system boundaries for P recovery from municipal wastewater solutions or solids.

REFERENCES

Cordell, D., Drangert, J., & White, S. 2009 The story of phosphorus : Global food security and food for thought. *Global Environmental Change* **19**, 292–305.
Egle, L., Zoboli, O., Thaler, S., Rechberger, H., & Zessner, M. 2014 The Austrian P budget as a basis for resource optimization. *Resources, Conservation and Recycling* **83**, 152–162.
Goel, S., Kansal, A., & Pfister, S. 2021 Sourcing phosphorus for agriculture: Life cycle assessment of three options for India. *Resources, Conservation and Recycling* **174**, 105750.
Linderholm, K., Tillman, A. M., & Mattsson, J. E. 2012 Life cycle assessment of phosphorus alternatives for Swedish agriculture. *Resources, Conservation and Recycling* **66**, 27–39.
Lottermoser, B. G. 2010 Waste of phosphate and potash ores. In *Mine Wastes (Third Edition): Characterization, Treatment and Environmental Impacts*, 313–333.
Pausta, C. M. J., Razon, L. F., Promentilla, M. A. B., & Saroj, D. P. 2018 Life cycle assessment of a retrofit wastewater nutrient recovery system in metro Manila. *Chemical Engineering Transactions* **70,** 337–342.
Rosemarin, A., & Ekane, N. 2016 The governance gap surrounding phosphorus. *Nutrient Cycling in Agroecosystems* **104**(3), 265–279.
Sharma, S. B., Sayyed, R. Z., Trivedi, M. H., & Gobi, T. A. 2013 Phosphate solubilizing microbes: Sustainable approach for managing phosphorus deficiency in agricultural soils. *SpringerPlus* **2**(1), 1–14.
Zhou, K., Remy, C., Kabbe, C., & Barjenbruch, M. 2019Comparative environmental life cycle assessment of phosphorus recovery with different generations of the AirPrex® systems. *International Journal of Environmental Science and Technology* **16**(5), 2427–2440.

End-user Perspective Life Cycle Environmental Impacts of Wastewater-derived Phosphorus Products

K. L. Lam

Division of Natural and Applied Sciences, Duke Kunshan University, 8 Duke Avenue, Kunshan, 215316, China

(E-mail: *kaleung.lam@dukekunshan.edu.cn)*

Abstract

Recovering phosphorus from wastewater in more concentrated forms has potential to sustainably recirculate phosphorus from cities to agriculture. This study assessed life cycle environmental impacts of substituting half of the conventional phosphorus rock-based fertilizers used in an average U.S. soybean production system with wastewater-derived phosphorus products (i.e., struvite, Ca-P, rhenania phosphate-like product, single superphosphate-like product) from six recovery pathways. The results show that the substitution reduces global warming, smog formation, acidification, eutrophication, and ecotoxicity potential of the assessed crop production system in most recovery pathways and scenarios. As more wastewater-derived products being available, this perspective contributes toward better understanding the potential systemic environmental consequences of a broader uptake of these products.

Keywords

Agricultural land application; environmental impacts; life cycle assessment; phosphorus recovery; resource recovery; wastewater

INTRODUCTION

Resource recovery from wastewater is gaining increasing attention, especially phosphorus recovery (Kehrein *et al.*, 2019). Depleting phosphate rock reserves is becoming a driver for phosphorus recovery. In wastewater treatment plants, phosphorus can be recovered in different concentrated forms (Harder *et al.*, 2019). The recovered phosphorus products can be used as fertilizers. Life cycle assessment (LCA) has been used to evaluate the potential environmental impacts of various wastewater-based phosphorus recovery and reuse opportunities (Diaz-Elsayed *et al.*, 2020; Lam *et al.*, 2020). Most LCA studies related to wastewater-based phosphorus recovery used the *process perspective* or the *product perspective* in their assessments (Figure 1) (Lam *et al.*, 2022).

This study assesses the life cycle environmental impacts of the agricultural use of wastewater-derived phosphorus products in an average U.S. soybean production system. It demonstrates the application of the *end-user perspective* to understand the life cycle environmental consequences of substituting conventional inputs with recovered products at the end user's product system.

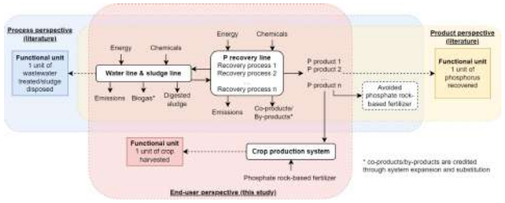

Figure 1. Process, product, and end-user perspectives of phosphorus recovery (Lam *et al.*, 2022).

MATERIALS AND METHODS

Goal and Scope

The primary goal of this study is to assess life cycle environmental impacts of substituting conventional phosphate rock-based fertilizers with wastewater-derived phosphorus products in crop production systems from the end-user perspective via six recovery pathways (Figure 2). Each pathway was modelled considering three different influent wastewater compositions, three alternative sludge disposal methods (incineration, landfill, land application), and three carbon intensity levels of grid electricity (low, medium, high).

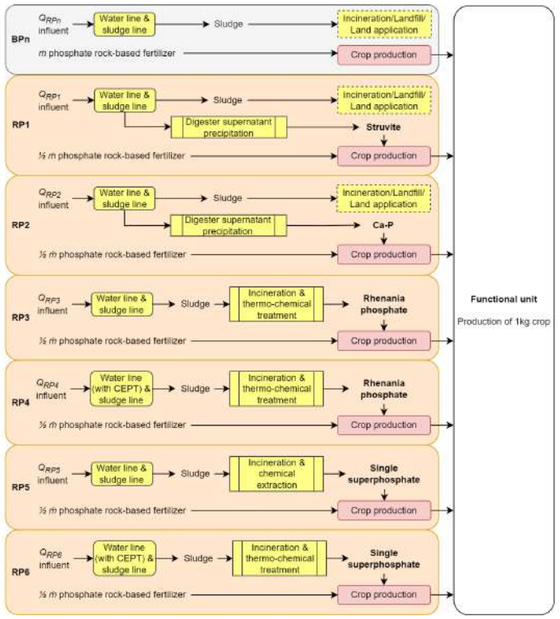

Figure 2. Baseline pathways (BPn) without P recovery and six possible P recovery pathways (RP1-RP6), differing in the recovered phosphorus products (i.e., struvite, Ca-P, rhenania phosphate-like product or single superphosphate-like product) and the possible inclusion of chemically enhanced primary treatment (CEPT) in the treatment line. For all RPs, the wastewater-derived phosphorus product was assumed to substitute half (½ ṁ) of the conventional phosphate rock-based fertilizers used in the baseline pathways (BPn). (Modified from Lam *et al.*, 2022).

Life Cycle Inventory

This study is based loosely on the U.S. context. The recovered phosphorus product inventory is from Lam *et al.* (2022), while the U.S. soybean production inventory is from Ecoinvent 3.6.

Impact Assessment

The Tool for Reduction and Assessment of Chemicals and Other Environmental Impacts (TRACI 2.1) was used as the impact assessment method. The LCA results are presented as the changes in impacts compared to those in the baseline scenarios.

RESULTS AND DISCUSSION

Life Cycle Environmental Impacts of Applying Wastewater-Derived Phosphorus Products

The LCA results are presented as the changes of life cycle environmental impacts compared to the baseline pathways (Figure 2). Substituting half of the conventional phosphate rock-based fertilizers originally used in the soybean production system with wastewater-derived phosphorus products from RP1, RP2, RP3, and RP4 reduces the assessed life cycle environmental impacts of these production systems in most scenarios. RP3, RP5, and RP6 would increase global warming potential in all scenarios, while RP3 and RP6 are mostly favourable for reducing eutrophication potential and acidification potential.

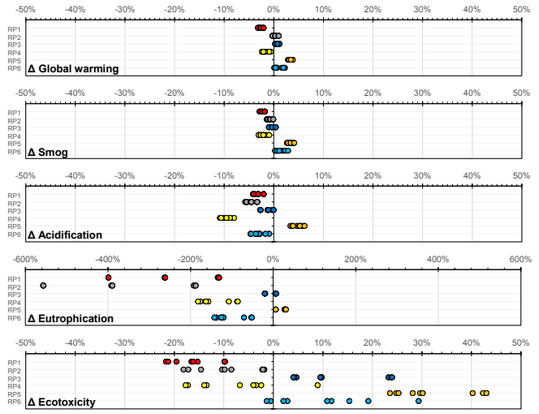

Figure 3. Changes in global warming, smog, acidification, eutrophication, ecotoxicity potential for six different recovery pathways (RPs), compared to the baseline pathway. Within a recovery pathway (RP), each dot is a scenario – one of the 27 combinations of influent pollutant concentration, sludge disposal method, and carbon intensity of grid electricity.

The Role of End-user Perspective

Life cycle assessments of wastewater-based resource recovery could generally be categorized as the *process perspective*, the *product perspective*, and the *end-user perspective* (Figure 1) (Lam *et al.*, 2022). The *process perspective* (also called the waste management perspective) evaluates the integration of resource recovery processes into conventional wastewater treatment plants. This perspective often aims to quantify and optimize the influence of resource recovery processes to the overall environmental performance of wastewater treatment plants. The focus is on the primary functionality of wastewater treatment and sludge disposal. The *product perspective* shifts attention from wastewater treatment plants to wastewater-derived products. This perspective often aims to evaluate and compare potential environmental impacts of the wastewater-derived products derived from different recovery approaches.

The *end-user perspective* extends on the *product perspective*. It centers on how the application of wastewater-derived products impacts on the overall environmental performance of the end users' product system (i.e., in this study, the end user is the agricultural sector using wastewater-derived phosphorus products). One major difference between the *product perspective* and the *end-user perspective* is that the *product perspective* typically credits the recovered phosphorus products for avoiding an assumed conventional phosphate-rocked fertilizer production, while the *end-user perspective* only implicitly considers that when there is a baseline of using conventional fertilizer (i.e., not being considered for a new crop production system).

This study demonstrates the application of the *end-user perspective* for conducting life cycle assessments of "downstream" product systems that utilize wastewater-derived products as inputs. The *end-user perspective* can serve three major purposes. First, the *end-user perspective* can complement with the process perspective and the product perspective to give a more holistic picture of environmental impacts along the "circular economy value chains" of wastewater-based resource recovery. Second, the *end-user perspective* is essential to evaluate system-wide environmental impacts of wide uptake of wastewater-derived products at downstream product systems. Third, the *end-user perspective* has an advantage of drawing more attention to the need of understanding the long-term environmental impacts and agronomic effectiveness of applying wastewater-derived phosphorus products (e.g., soil context, phosphorus uptake, contaminants). As more wastewater-derived products being available, this *end-user perspective* is becoming more important.

REFERENCES

Diaz-Elsayed, N., Rezaei, N., Ndiaye, A., Zhang, Q. 2020 Trends in the environmental and economic sustainability of wastewater-based resource recovery: A review. *Journal of Cleaner Production* **265**, 121598.

Harder, R., Wielemaker, R., Larsen, T.A., Zeeman, G., Öberg, G. 2019 Recycling nutrients contained in human excreta to agriculture: Pathways, processes, and products. *Critical Reviews in Environmental Science and Technology* **49**(8), 695-743.

Kehrein, P., Van Loosdrecht, M., Osseweijer, P., Garfí, M., Dewulf, J., Posada, J. 2020 A critical review of resource recovery from municipal wastewater treatment plants-market supply potentials, technologies and bottlenecks. *Critical Reviews in Environmental Science and Technology* **6**(4), 877-910.

Lam, K.L., Zlatanovic, L., van der Hoek, J.P. 2020 Life cycle assessment of nutrient recycling from wastewater: A critical review. *Water Research* **173**, 115519.

Lam, K.L., Solon, K., Jia, M., Volcke, E.I.P., van der Hoek, J.P. 2022 Life Cycle Environmental Impacts of Wastewater-Derived Phosphorus Products: An Agricultural End-User Perspective. *Environmental Science & Technology* **56**(14), 10289-10298.

How sustainable is the digitalization of treatment stages for micropollutant removal?

Jueying Qian*, Hana Atallah Al-asad*,**, Janna Parniske*, Jens Alex**, Martin Möller***, Steffen Metzger****, Tobias Morck*

* University of Kassel, Department of Urban Water Engineering, Kurt-Wolters-Street 3, 34125, Kassel, Germany
(E-mail: *qian@uni-kassel.de*; *parniske@uni-kassel.de*; *morck@uni-kassel.de*)
** ifak - Institute for Automation and Communication, Werner-Heisenberg-Str. 1, 39106, Magdeburg, Germany
(E-Mail: *hana.alasad@ifak.eu*; *jens.alex@ifak.eu*)
*** Öko-Institut e.V. Merzhauser Straße 173, 79100, Freiburg, Germany
(E-mail: *m.moeller@oeko.de*)
**** Weber-Ingenieure GmbH, Bauschlotter Straße 62, 75177 Pforzheim, Germany
(E-mail: *steffen.metzger@hamburgwasser.de*)

Abstract

This study focuses on the sustainability assessment of the digitalization technology applied in the advanced wastewater treatment stage aimed at eliminating organic micropollutants using activated carbon. Powdered activated carbon is currently dosed proportional to the inflow volume in a wastewater treatment plant (WWTP 1, Germany, 55.000 population equivalent). A mathematical model-based dosing strategy will be implemented in the WWTP 1 to improve the treatment efficiency and reduce PAC consumption. Comparing the reference technology (volume-proportional dosage) and the new digitalization technology, digitization technology can save ca. 4 % PAC and lower the carbon footprint of the PAC treatment stage by ca. 8000 kg CO_{2e}/a in WWTP 1. The reduction of CO_{2e} emissions after implementing the new control technology at WWTP1 will be evaluated. More potential systematical benefits of mathematical model-based dosage are recognized. Detailed ecological, economic, and social aspects based on life cycle analysis will be carried out.

Keywords (maximum 6 in alphabetical order)

carbon foodprint; digitalization technology; organic micropollutant; powdered activated carbon; wastewater treatment plant

INTRODUCTION

Organic micropollutants can be removed from wastewater treatment plants by applying activated carbon or ozone. In the wastewater treatment plant (WWTP) investigated in this study, powdered activated carbon (PAC) is dosed proportionally to inflow volume (such as 8 mg PAC/L), regardless of the wastewater characteristics. In the planning digitalization technology, PAC is dosed according to a mathematical model-based regulation. The mathematical model calculates the necessary PAC dosage to achieve a mean removal of more than 80% for a selection of micropollutants.

The digitalization technology incorporating the mathematical model-based dosing strategy can potentially reduce PAC consumption and improve the removal efficiency of micropollutants. However, the new digitalization technology involves additional production of hardware such as PCs and power consumption due to the usage of the additional hardware. The objective of the study is to compare the sustainability of the reference technology (current volume-proportional PAC dosage) and the digitalization technology (mathematical model-based dosage) by qualitative assessment and life cycle assessment (carbon footprint).

MATERIALS AND METHODS

Sustainability assessment on a qualitative level

A working hypothesis concerning the potential benefits and drawbacks of the digitalization technology is identified based on the three orders of the environmental impact: 1) first-order effect or direct effect: e.g., resource and energy consumption due to digitalization infrastructure and equipment; 2) second-order effect or indirect effect: e.g., immediate positive/negative effects of the new technology; and 3) third-order effect or systematic effect: e.g., mission statements, values, acceptance (Kampffmeyer & Gensch, 2019).

Sustainability assessment through the evaluation of carbon footprint

The carbon footprint of reference technology (volume-proportional PAC dosage) and digitalization technology (mathematical model-based dosage) used in WWTP 1 was compared. The mathematical model for WWTP 1 (Germany, 55.000 population equivalent) has been developed based on a published model (Atallah Al-asad et al., 2022). The model simulates the adsorption competition between background organic matter and micropollutants, and calculates the necessary PAC dosage. The developed mathematical model will soon be coupled into the IT infrastructure of WWTP 1. The calculation in this paper is based on a case study and not real data yet.

In a case study, benzotriazole was used as a reference substance for the mathematical model to calculate the required PAC dose to remove 80% of benzotriazole. The model was simulated on a time scale of 31 days using dynamic inflow (Figure 1) and inflow UVA_{254}. The concentration of benzotriazole corresponded to the same dynamics as soluble inert organics according to DWA-A 131 (DWA, 2016). The carbon footprint was calculated based on a tool developed by Öko-Institut in Germany (Gröger, 2020; Öko-Institut, 2020).

RESULTS AND DISCUSSION

Qualitative sustainability assessment: potential benefits and drawbacks

By replacing the volume-proportional PAC dosage with model-based PAC dosage, additional materials and resources are consumed for the production of extra servers and computers, which in turn increases the carbon footprint of WWTPs. This is recognized as a potential drawback of digitalization technology (direct first-order effect). However, the process reduces the amount of operational material (e.g., PAC) needed in the improved process control, a potential benefit of digitalization technology (indirect second-order effect). Moreover, the application of the model-based control strategy will improve the elimination efficiency of organic micropollutants, which results in many potential benefits such as protection of the ecosystem, reduction of diseases, and increase in the acceptance of the reuse of the treated wastewater (Table 1)

Comparison of the carbon footprint in both technologies

Comparing the reference technology and digitalization technology:

- Extra hardware is produced in digitalization technology: 500GB of online data storage and 2.5 GB/month of data exchange is needed. PCs are already equipped in WWTP 1.
- Additional power consumption due to the extra hardware mentioned above.
- PAC is supposed to be saved in the digitalization technology.

Case study

A case study has been carried out for WWTP 1, which applies PAC as an advanced treatment step. Results show that the reference technology involving volume-proportional dosage consumes averagely 70.02 kg PAC/day. The mathematical model-based dosage reduces the average PAC consumption to 67.51 kg/day, around 3.6% lower compared to volume-proportional dosage. The greenhouse gas emission of fresh activated carbon from hard coal is 8.7 kg CO_{2e}/kg PAC (Mousel et al., 2017). The annual reduction of carbon footprint due to saving of PAC is 7970 kg CO_{2e} when digitalization technology is used. The additional energy consumption of the 500 GB online data storage and the extra data transfer for the digital twin causes only 6.5 kg CO_{2e} per year (Table 2). The annual carbon footprint reduction is therefore 7963.5 kg CO_{2e}/a according to the calculation.

In general, digitization can reduce the carbon footprint of the advanced wastewater treatment stage using PAC. The reduction of CO_2e emissions after implementing the new control technology at WWTP1 will be evaluated. More potential benefits of mathematic-model-based dosage are recognized in the study, such as improved micropollutant removal and protection of the ecosystem.

Table 1. Three orders of the environmental impact regarding digitalization technology, including analysis of the contributions to the Sustainable Development Goals (SDGs) formulated by the United Nations General Assembly.

	Potential benefits		Potential drawbacks	
	Effect	SDG	Effect	SDG
First-order effect (direct)			Resource consumption for the production of digitization technologies (e.g., computers, servers)	SDG 8.4
			Power consumption for the operation of digitization techniques (e.g., processing, transfer, and storage of data)	SDG 7.3
Second-order effect (indirect)	Saving of operating materials in the process control (e.g., activated carbon)	SDG 8.4		
	Reduction of the energy requirement in the process control	SDG 7.3		
	Waste avoidance (e.g., by saving activated carbon and thus reduction of sludge production)	SDG 8.4		
Third-order effect (systematic)	Reduction of pollutants in water, soil, and air	SDG 3.9 SDG 6.3 SDG 12.4		
	Reduction of diseases (e.g., due to hazardous chemicals)	SDG 3.9		
	Increase in the acceptance of the reuse of the treated wastewater	SDG 6.3 SDG 6.4 SDG 12.2 SDG 6.6		
	Protection of the integrity of ecosystems (e.g., surface water)	SDG 14.2 SDG 15.1		

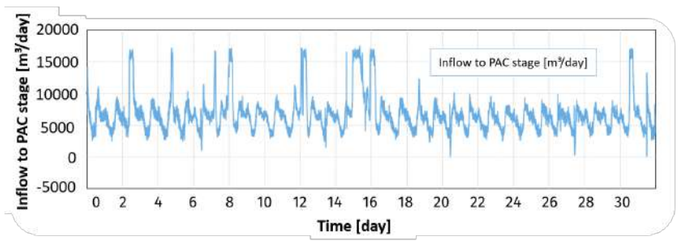

Figure 1. The inflow of the PAC treatment stage in the case study.

Table 2. Calculation of the increase and decrease of carbon footprint when using digitalization technology in a case study.

Items	Additional CO_{2e}-emission [kg CO_{2e}/a]
Online data storage (500GB)	+6,0
Data exchange (2.5 GB/month)	+0,5
PAC dosage	-7970
Sum	-7963.5

REFERENCES

Atallah Al-asad, H., Parniske, J., Qian, J., Alex, J., Ramaswami, S., Kaetzl, K., & Morck, T. (2022). Development and application of a predictive model for advanced wastewater treatment by adsorption onto powdered activated carbon. *Water Research*, *217*(April), 118427. https://doi.org/10.1016/j.watres.2022.118427

DWA. (2016). *Working Paper DWA-A 131: Design of single-stage activated sludge plants (in German: Arbeitsblatt DWA-A 131: Bemessung von einstufigen Belebungsanlagen)*.

Gröger, J. (2020). *Digital carbon footprint Data collection to estimate production costs, energy consumption and use of digital devices and services (in German: Digitaler CO2-Fußabdruck: Datensammlung zur Abschätzung von Herstellungsaufwand, Energieverbrauch und Nutzung dig*. https://www.oeko.de/publikationen/p-details/digitaler-co2-fussabdruck

Kampffmeyer, N., & Gensch, C.-O. (2019). *Working Paper: Sustainable consumption through digitization?(in German: Nachhaltiger Konsum durch Digitalisierung?)*.

Mousel, D., Palmowski, L., & Pinnekamp, J. (2017). Energy demand for elimination of organic micropollutants in municipal wastewater treatment plants. *Science of the Total Environment*, *575*, 1139–1149. https://doi.org/10.1016/j.scitotenv.2016.09.197

Öko-Institut. (2020). *Online-Tool: Digital Carbonfootprint*. https://www.digitalcarbonfootprint.eu/

Utilising sustainable value propositions to understand the value creation of circular actions in wastewater systems

D. Renfrew*, V. Vasilaki*, E. Nika*, G. Tsalidis*, E. Katsou*

* Department of Civil & Environmental Engineering, Institute of Environment, Health and Societies, Brunel University London, Uxbridge Campus, Middlesex, UB8 3PH, Uxbridge, UK
(E-mail:david.renfrew@brunel.ac.uk)

Abstract

Value propositions are used to link the strategic goals of an organisation with the circular actions of innovative wastewater technologies. The value proposition canvas 'gains creators' are used to identify value creating actions of the circular solution for selecting relevant performance indicators, these indicators then guide complementary sustainability indicator selection to quantify value creation for stakeholders. The method developed is applied to a small-scale wastewater treatment plant with a novel photobioreactor technology that produces biofertilizer. The indicators show that all strategic and value creating goals were achieved and resulted in sustainable value creation across all pillars of the triple bottom line.

Keywords (maximum 6 in alphabetical order)

Abstract; circularity assessment, indicator selection, sustainable value creation, value propositions

INTRODUCTION

The circular use of wastewater has attracted significant attention in recent years, shifting the focus from treatment to recovery. There are already many circular technologies available to the wastewater sector for resource recovery and water recycling, but implementation is limited through lack of planning and performance analysis (Smol and Koneczna, 2021). It has been shown that technological aspects are not barriers to the circular transition, rather a company culture stemming from the view these investments are not economically favourable in the short term (Kirchherr, Piscicelli, et al., 2018), and is compounded with limited research on how the circular economy (CE) provides a competitive advantage (Lahti, Wincent, et al., 2018). Currently, assessment frameworks focus on measuring material flows, with circularity indicators aligned against triple bottom line (TBL) dimensions to evidence that sustainability is adequately measured. This results in patchy assessments and consequences such as impact leakage (Chen, 2021). For sustainable innovations, a lack of similar market options creates difficulties when assessing aspects such as acceptability, therefore the creation of customer value should be emphasised (da Luz Peralta, Echeveste, et al., 2020)especially in startups, where the degree of uncertainty is high, and the business model has no consolidation. To this end, different approaches, which are mostly supported by learning cycles of experimentation, have emerged to assess customer and stakeholder value in innovation projects. To understand how these approaches and practices represents an alternative for value identification and proposition, this study aims to demonstrate a method to conduct practices and techniques in innovative solutions to anticipate customer value during the front-end phases of a sustainable product. The main contribution is the application of the framework in the case of a startup focused on agriculture for the development of a grain drying machine. The main technology behind this innovation is the drying through oxyhydrogen burn, which is extracted from the water. The framework proved to be useful for organizing market-bound information to form customer value proposition. The results allow the startup to reduce or solve uncertainties in its business model, which are challenges inherent to the innovation market. The learning from the application of the framework resulted in a remodeling of the business model to achieve a broader public as the startup pivoted initial customer needs into product requirements."

title":"Applying the framework to identify customer value: A case of sustainable product in agriculture","type":"article-journal","volume":"270"},"uris":["http://www.mendeley.com/documents/?uuid=96f01471-1750-468b-8213-dcf68d8c64ad"]}],"mendeley":{"formattedCitation":"(da Luz Peralta, Echeveste, et al., 2020. It has been shown that sustainable value is created when societal level aims are addressed using circular business models (Tapaninaho and Heikkinen, 2022)this article utilises stakeholder theory to conceptualise value creation as a relational, systemic activity involving multiple stakeholder relationships. We conduct a case study of the CE business development of a Finnish energy company and offer novel insights by identifying five joint value creation activities: sharing the CE story, co-constructing knowledge for political decision-making, developing the industry, creating local CE ecosystems and refining the business model. Additionally, we define the concept of multidimensional value, which acknowledges multifaceted, subjective stakeholder value expectations and enables the engagement of stakeholders in joint value creation activities. We conclude that the stakeholder relationship perspective on CE business value creation allows for the creation of the synergy necessary to advance CE business and sustainability.","author":[{"dropping-particle":"","family":"Tapaninaho","given":"Riikka","non-dropping-particle":"","parse-names":false,"suffix":""},{"dropping-particle":"","family":"Heikkinen","given":"Anna","non-dropping-particle":"","parse-names":false,"suffix":""}],"container-title":"Business Strategy and the Environment","id":"ITEM-1","issue":"6","issued":{"date-parts":[["2022"]]},"page":"2728-2740","title":"Value creation in circular economy business for sustainability: A stakeholder relationship perspective","type":"article-journal","volume":"31"},"uris":["http://www.mendeley.com/documents/?uuid=40072da5-1b6d-47dd-9314-4b1e60073938"]}],"mendeley":{"formattedCitation":"(Tapaninaho and Heikkinen, 2022, and as wastewater decision makers have set targets at this level (including carbon neutrality, water provision and energy security), sustainable value creation should be used as a holistic indicator of circular business model performance for wastewater systems. In this work, a method for selecting indicators to assess the value creating circular actions of wastewater systems is provided, and how this can guide the use of complementary sustainability analysis for quantifying the resultant sustainable value created.

MATERIALS AND METHODS

To understand the physical impacts of circular actions to wastewater systems, the circular solution should be modelled to facilitate resource flow analysis as this is a key aspect of any circularity assessment. For the first step of indicator selection, the method of da Luz Peralta et al. (2020)especially in startups, where the degree of uncertainty is high, and the business model has no consolidation. To this end, different approaches, which are mostly supported by learning cycles of experimentation, have emerged to assess customer and stakeholder value in innovation projects. To understand how these approaches and practices represents an alternative for value identification and proposition, this study aims to demonstrate a method to conduct practices and techniques in innovative solutions to anticipate customer value during the front-end phases of a sustainable product. The main contribution is the application of the framework in the case of a startup focused on agriculture for the development of a grain drying machine. The main technology behind this innovation is the drying through oxyhydrogen burn, which is extracted from the water. The framework proved to be useful for organizing market-bound information to form customer value proposition. The results allow the startup to reduce or solve uncertainties in its business model, which are challenges inherent to the innovation market. The learning from the application of the framework resulted in a remodeling of the business model to achieve a broader public as the startup pivoted initial customer needs into product requirements."

title":"Applying the framework to identify customer value: A case of sustainable product in agriculture","type":"article-journal","volume":"270"},"uris":["http://www.mendeley.com/documents/?uuid=96f01471-1750-468b-8213-dcf68d8c64ad"]}],"mendeley":{"formattedCitation":"(da Luz Peralta, Echeveste, et al., 2020 is recommended for value proposition canvas (VPC) development which requires the views of stakeholders to understand their desires and the obstacles for implementation, and linking this with 'gain creators' and 'pain relievers' to show how a technology aims to create value (identifying the goals of the circular solution). To create the VPC, workshops with relevant stakeholders are needed to create a Lean Canvas, revealing how the circular solution creates value for stakeholders, and an Empathy Map for what they wish to accomplish (da Luz Peralta, Echeveste, et al., 2020)especially in startups, where the degree of uncertainty is high, and the business model has no consolidation. To this end, different approaches, which are mostly supported by learning cycles of experimentation, have emerged to assess customer and stakeholder value in innovation projects. To understand how these approaches and practices represents an alternative for value identification and proposition, this study aims to demonstrate a method to conduct practices and techniques in innovative solutions to anticipate customer value during the front-end phases of a sustainable product. The main contribution is the application of the framework in the case of a startup focused on agriculture for the development of a grain drying machine. The main technology behind this innovation is the drying through oxyhydrogen burn, which is extracted from the water. The framework proved to be useful for organizing market-bound information to form customer value proposition. The results allow the startup to reduce or solve uncertainties in its business model, which are challenges inherent to the innovation market. The learning from the application of the framework resulted in a remodeling of the business model to achieve a broader public as the startup pivoted initial customer needs into product requirements.","author":[{"dropping-particle":"","family":"Luz Peralta","given":"Carla Beatriz","non-dropping-particle":"da","parse-names":false,"suffix":""},{"dropping-particle":"","family":"Echeveste","given":"Marcia Elisa","non-dropping-particle":"","parse-names":false,"suffix":""},{"dropping-particle":"","family":"Martins","given":"Vera Lúcia Milani","non-dropping-particle":"","parse-names":false,"suffix":""},{"dropping-particle":"","family":"Lermen","given":"Fernando Henrique","non-dropping-particle":"","parse-names":false,"suffix":""}],"container-title":"Journal of Cleaner Production","id":"ITEM-1","issued":{"date-parts":[["2020"]]},"page":"122384","title":"Applying the framework to identify customer value: A case of sustainable product in agriculture","type":"article-journal","volume":"270"},"uris":["http://www.mendeley.com/documents/?uuid=96f01471-1750-468b-8213-dcf68d8c64ad"]}],"mendeley":{"formattedCitation":"(da Luz Peralta, Echeveste, et al., 2020.

To link the goals identified from VPCs with relevant action indicators, they are grouped based on circular strategic goals. Strategic goals are the high level aims of the project, commonly defined as quantitative targets, such as a reducing waste or emissions production by a certain percentage. These are used to create generic CE actions that are initiated by the circular solution, which can be found in literature (such as recycling or renewable energy generation). Simultaneously, VPC development recognises how the circular solution aims to create sustainable value for stakeholders, by using 'gain creators' to highlight technology expectations. These are combined with the CE actions to create circular value creating actions that are specific to the project. Lastly, the specific circular actions are used to select appropriate indicators for the assessment of system performance to achieve the defined goals. A summary of these steps is provided in Figure 1 and are applied to the example of a novel photobioreactor (PBR) (H2020 Deep Purple) for treatment of wastewater in rural Spain for a population equivalent of approximately 10,000 to produce biofertilizer. The results provided by these indicators will show whether the goals are met, and the circular actions of the technology have been successful at generating sustainable value for stakeholders.

RESULTS AND DISCUSSION

The strategic goals of the technology were taken from H2020 Deep Purple project documentation and website (Deep Purple, 2019). The terminology of minimising, maximising and reducing several operational constraints such as cost, waste, GHG emissions and energy demand, reveals the strategic goal of *optimising the performance of supply chains*. The emphasis on generating economic value from bioproducts and recovering energy from waste stream means that the technology must also have the ability to *cascade biomaterials*. Recovering the organic and nutrient contaminants in wastewater and minimising waste production is achieved through the action of *recycling* wastewater resources. Therefore, three strategic goals were identified, and these must then be combined with the outcomes from a sustainable VPC to select relevant indicators. The stakeholders used to generate the VPC in this example were the PBR technology developers. The resultant Lean Canvas is presented in Figure 2 with the 'gain creators' category used to understand the PBR's individual value creating actions. The four 'gains creators' identified were related to cost, carbon footprint, sludge valorisation and energy consumption.

A summary of the step to select indicators including the gains creators, CE actions and value creating actions is provided in Table 1, with results provided as the percentage change compared with a conventional small-scale wastewater process. Results show that nearly all of the indicators highlight an improvement in performance of the PBR technology versus conventional treatment (except waste eco-efficiency due to the increase of pretreatment solids captured). This is attributed to a reduction in grid electricity demand and direct emissions, resulting in a significant decrease to carbon footprint. Also, material and energy consumption reduction lowers costs, and biofertilizer sales increases revenue streams from sludge. Therefore, the PBR technology is effective at achieving the defined value creating goals. Additionally, action indicator calculations provide insights into which complementary sustainability indicators are required to quantify the value creation of the system. It is clear from the results that the photobioreactor technology instigates economic, environmental and social value creation, as shown in Table 2.

CONCLUSIONS

The method described selected indicators for the assessment of a small-scale wastewater treatment plant with a novel PBR for producing biofertilizer. The indicator results show that all strategic and value creating goals were achieved and resulted in sustainable value creation across the TBL.

Figure 1. Steps for selecting indicators to assess the actions of a circular solution.

Figure 2. Lean canvas of the PBR technology based on figure from da Luz Peralta et al. (2020)especially in startups, where the degree of uncertainty is high, and the business model has no consolidation. To this end, different approaches, which are mostly supported by learning cycles of experimentation, have emerged to assess customer and stakeholder value in innovation projects. To understand how these approaches and practices represents an alternative for value identification and proposition, this study aims to demonstrate a method to conduct practices and techniques in innovative solutions to anticipate customer value during the front-end phases of a sustainable product. The main contribution is the application of the framework in the case of a startup focused on agriculture for the development of a grain drying machine. The main technology behind this innovation is the drying through oxyhydrogen burn, which is extracted from the water. The framework proved to be useful for organizing market-bound information to form customer value proposition. The results allow the startup to reduce or solve uncertainties in its business model, which are challenges inherent to the innovation market. The learning from the application of the framework resulted in a remodeling of the business model to achieve a broader public as the startup pivoted initial customer needs into product requirements

Table 1. Action indicators selected and with results compared against a conventional process.

Gains Creators	General CE Action	Value Creating Action of Circular Solution	Indicators Associated	Results
Lower Energy Consumption	2. Development of New Processes for Supply Chain Optimisation	Reduction of Energy Intensity	Circular Process Energy Intensity (kWh/kg Carbon)	-67.6 %
			Self-sufficiency (%)	58.8 %
			Demand Minimisation (kWh/d)	13.4 %
Lower Carbon Footprint		Achieving Decarbonisation	Carbon footprint ($kgCO_2$ eq)	- 66.3 %
			Emissions Eco-efficiency Emissions Eco-efficiency (€/kg)	+ 97.7 %
Savings on Logistics and Infrastructure		Reducing CAPEX and OPEX	Yearly Cost (€)	- 44.6 %
Valorisation of Sludge	Cascading of Biomaterials	Extraction/Generation of Value Added Bio-products	Waste Eco-efficiency (€/kg)	- 34.5 %
			Value Added per Functional Unit (€/ m^3)	+ 1152 %
		Renewable Resource Use (energy recovery, nutrients from fertilisation)	Substitution Factor of Virgin Materials –Fertiliser N	+ 345.0 %
	Recycling	Retain Nutrients in Wastewater for Fertiliser Production and Return to Soil	Recovery Rate - Nutrients NPC (%)	+ 165.3 %
				+ 195.0 %
				+ 15.5 %

Table 2. Sustainability indicators identified to quantify the value created by the circular solution.

Environmental		Economic	
Carbon Footprint	-66 %	Total Value Added (M€/y)	0.49
Acidification (kg SO2 eq)	-15 %	**Social**	
Eutrophication (kg PO4 eq)	-41 %	Human health (DALY)	58 %
Photochemical Oxidation (kg NMVOC)	-20 %	Ecosystems(species.yr)	46 %
Abiotic Depletion, elements (kg Sb eq)	-20 %	Resources (USD2013)	35 %
Abiotic Depletion, fossil fuels (MJ)	-19 %	Employment (No. of people)	100 %
Water Consumption (m^3 eq)	0 %	Local economy Contribution (€/pe)	1151 %
Ozone Layer Depletion (kg CFC^{-11} eq)	-34 %		

REFERENCES

Chen, C.-W. (2021) Clarifying rebound effects of the circular economy in the context of sustainable cities. Sustainable Cities and Society, **66**, 102622. [online] https://www.sciencedirect.com/science/article/pii/S2210670720308398.

Deep Purple (2019) Recover Energy & Valuable Resources from urban waste streams in Photobiorefineries with the help of purple phototropic bacteria. [online] https://deep-purple.eu/ (Accessed January 30, 2023).

Kirchherr, J., Piscicelli, L., Bour, R., Kostense-Smit, E., Muller, J., Huibrechtse-Truijens, A., and Hekkert, M. (2018) Barriers to the Circular Economy: Evidence From the European Union (EU). Ecological Economics, **150**, 264–272. [online] https://www.sciencedirect.com/science/article/pii/S0921800917317573.

Lahti, T., Wincent, J., and Parida, V. (2018) A Definition and Theoretical Review of the Circular Economy, Value Creation, and Sustainable Business Models: Where Are We Now and Where Should Research Move in the Future? Sustainability, **10**(8). [online] https://www.mdpi.com/2071-1050/10/8/2799.

da Luz Peralta, C. B., Echeveste, M. E., Martins, V. L. M., and Lermen, F. H. (2020) Applying the framework to identify customer value: A case of sustainable product in agriculture. Journal of Cleaner Production, **270**, 122384. [online] https://www.sciencedirect.com/science/article/pii/S0959652620324318.

Smol, M. and Koneczna, R. (2021) Economic Indicators in Water and Wastewater Sector Contributing to a Circular Economy (CE). Resources, **10**(12). [online] https://www.mdpi.com/2079-9276/10/12/129.

Tapaninaho, R. and Heikkinen, A. (2022) Value creation in circular economy business for sustainability: A stakeholder relationship perspective. Business Strategy and the Environment, **31**(6), 2728–2740. [online] https://onlinelibrary.wiley.com/doi/abs/10.1002/bse.3002.

Life cycle assessment of on-site nature-based wastewater treatment and reuse systems

D. Istenič[1,3], S. Morera[2], J. Comas[4,5], T. Griessler Bulc[1,3], N. Atanasova[1]

[1] Faculty of Civil and Geodetic Engineering, University of Ljubljana, Jamova c. 2, 1000 Ljubljana, Slovenia (E-mail: darja.istenic@fgg.uni-lj.si; natasa.atanasova@fgg.uni-lj.si)
[2] Plaça de l'Església, 20, 25125 Alguaire, Lleida, Spain (E-mail: serni.morera@gmail.com)
[3] Faculty of Health Sciences, University of Ljubljana, Zdravstvena pot 5, 1000 Ljubljana, Slovenia (E-mail: tjasa.bulc@zf.uni-lj.si)
[4] Catalan Institute for Water Research (ICRA-CERCA). Carrer Emili Grahit 101, 17003 Girona, Spain (E-mail: jcomas@icra.cat)
[5] Laboratory of Chemical and Environmental Engineering (LEQUIA), Institute of the Environment, University of Girona. Plaça de 7 Sant Domènec 3, 17004 Girona, Spain

Abstract

This research extends the system boundaries of life cycle assessment (LCA) of wastewater treatment technologies, which typically focus on construction, operation, and maintenance, to include resource recovery. LCA of three different nature-based wastewater treatment solutions (treatment wetland, evapotranspirative willow system and high-rate algae pond) were compared with and without the use of recovered resources. The results showed that despite the higher use of some materials (e.g., irrigation system) LCA results were in favour of the systems with reuse of resources. Treatment wetland with the use of reclaimed water provided the best results in 4 of the 6 categories studied (climate change, freshwater eutrophication, water depletion, and metal depletion). Considering CO_2 uptake as a positive impact, evapotranspirative willow system showed the best results due to the greatest carbon storage in woody biomass compared to the treatment wetland and the high-rate algae pond.

Keywords

high-rate algae pond, LCA, reclaimed water, system boundaries, treatment wetland, willow system

INTRODUCTION

Resource recovery is a response to increasing demand for resources and increasing waste production due to increasing economic and population growth. The circular approach to wastewater management has been studied mainly for cities, where nature-based solutions (NBS) are gaining attention (Atanasova et al. 2021). Robust NBS for wastewater treatment are an even more appealing solution for rural areas, where space is not as critical as in urban areas. To reduce the environmental impact as much as possible, a suitable wastewater treatment technology must be selected and the life cycle assessment of the technology and the reuse (irrigation) system must be evaluated.

In the field of wastewater treatment, LCA focuses mainly on the construction and operation of wastewater treatment plants (Morera et al. 2017, Morera et al. 2020), while the system boundaries do not consider the circularity in terms of capturing the reuse of recovered wastewater treatment products. This can significantly change the outcome of the LCA analysis and the environmental performance of a wastewater treatment solution. In particular, the outcome may be different when NBS are evaluated and their co-benefits are included in the assessment.

The objective of this study was to evaluate and compare the environmental impacts of constructing and operating three different NBS for wastewater treatment for small volumes of water (5 PE). Treatment wetland (TW), high-rate algae pond (HRAP) and evapotranspirative willow system (EWS) with different resource recovery options, namely discharge of water to a nearby river or reuse of treated water for irrigation in the case of TW and HRAP, and in the case of EWS, reuse of the woody biomass produced as woodchip for soil amendment or composting.

MATERIALS AND METHODS

The LCA methodology followed ISO 14040-14044. The LCA study considered the extraction of resources needed for the construction, operation and to produce the products (treated water and recovered resources).

Goal and scope definition

The functional unit of the study is the volume of water treated by the treatment and recovery plants during the 20-year operation, including the construction of these plants and the maintenance of the main equipment. The life of the NBS treatment systems tested was assumed to be 20 years for the entire plant; however, we considered the life of individual components and considered replacement with shorter lives (e.g., pumps). Whenever possible, real data from the technologies tested were used, but when this was not possible, information from other studies or from the manufacturers was used. 20 years was used for all the civil works, 5 years for aluminum pumps, and 15 years for the ultrasound unit and engine.

A total of seven scenarios were analyzed:

- **Scenario A: TW to treat domestic wastewater; treated water is discharged to a nearby stream; reeds produced are harvested and used as structural material for composting.**
- **Scenario B: same water treatment as in Scenario A, but treated water is reused to irrigate a lawn; reeds produced are treated as in Scenario A.**
- **Scenario C: EWS to treat domestic wastewater; all influent is used for evapotranspiration; woody biomass produced is used as woodchip for soil amendment or composting.**
- **Scenario D: aboveground HRAP to treat domestic wastewater; the pond is made of polystyrene; the treated water is discharged to a nearby stream; the produced algae-bacteria biomass is used as fertilizer.**
- **Scenario E: same water treatment as in Scenario D; the treated water is used to irrigate a lawn; the algae-bacteria biomass produced is used as fertilizer as in Scenario D.**
- **Scenario F: same as Scenario D, but the HRAP is constructed as an earthen pond sealed with an EPDM liner.**
- **Scenario G: same as Scenario E, but the HRAP is constructed as in Scenario F.**

Inventory phase

In the inventory phase, data on the type and quantity of the system's inputs (materials, energy, resources, etc.) and outputs (emissions to air, water and soil) were collected through direct measurements related to construction and operation. The inventory obtained was then compared with background information from the Ecoinvent database (version 3.3). Some assumptions were necessary because the Ecoinvent database did not have information on all the materials used (e.g., due to no data on EPDM it had to be replaced by polyethylene membrane) and in some cases equivalent materials were used (e.g., chromium steel for stainless steel).

Impact assessment

Environmental impacts were calculated based on previously collected inventory data using ReCiPe 1.13 in the midpoint version. This method considers 18 midpoint impact categories, although only 6 were selected in this case: climate change, freshwater eutrophication, marine eutrophication, water depletion, metal depletion and fossil depletion.

Interpretation

Interpretation of the results followed the recommendations of ISO 14044: analyzing the most important aspects for each environmental impact, looking for possible solutions to reduce the environmental impact, performing an additional sensitivity analysis of the results considering different processes.

RESULTS AND DISCUSSION

Figure 1 shows the overall results (construction and operation combined) for all scenarios studied for the three treatment technologies. Scenario B provides the best results in 4 of the 6 categories studied, namely climate change, freshwater eutrophication, water depletion and metal depletion. Scenario C, on the other hand, provides the best results for marine eutrophication, and finally, Scenario A is the best for fossil depletion.

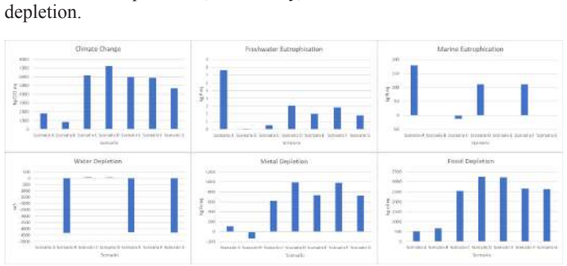

Figure 1. Total impact results for all categories for all the scenarios considered.

Figure 2 shows the same results, but differentiated by construction and operation. These results show that the scenarios with water reuse have positive effects on the impact categories of climate change, water depletion, metal depletion, and fossil depletion, since water reuse can save the use of potable water for gardening. In terms of eutrophication categories, Scenario C has the best results for marine eutrophication, as the reuse of willow woodchip saves the production of this material. In terms of freshwater eutrophication, Scenario B is the best, also because of the positive effect of water reuse. In general, construction is a relatively large contributor to impacts compared to operation, which is in contrast to activated sludge technologies where construction accounts for only about 10% of impacts (Morera et al., 2017). This is due to the fact that nature-based treatment systems have very low energy requirements for operation compared to conventional technologies.

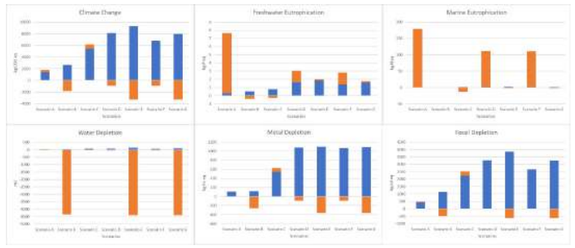

Figure 1. Impact results for all the scenarios considered differentiating between construction (blue) and operation (orange).

Sensitivity analysis

Impacts on the climate change category were analysed when CO_2 uptake is considered a positive effect or not, which is common practice as the CO_2 from the biogenic cycle is considered neutral and positive if it is stored in woody biomass for longer period. The EWS (Scenario C) shows the best results in terms of CO_2 uptake by plants, with a value of -17324.80 kg CO_2 eq (Table 1), which means that this wastewater treatment technology plays a positive role for the climate change impact category because it eliminates CO_2 eq from the atmosphere.

Table 1. Comparison of the climate change impact considering or not the effect of CO_2 uptake.

Scenario	Positive effect of CO_2 uptake	No consideration of CO_2 uptake
A	1166.29	1792.74
B	192.47	818.92
C	-17324.80	6172.85
D	3170.84	7222.51
E	1946.71	5998.38
F	1845.43	5897.09
G	621.30	4672.96

CONCLUSIONS

In general, the results were better when the system boundaries included the use of reclaimed water despite the installation of an irrigation system. Scenario B (TW with water reuse) is the best scenario because it provides the best results for 4 of the 6 categories analysed (climate change, freshwater eutrophication, water depletion, and metal depletion) and the second best for the other two categories (marine eutrophication and fossil depletion). This is due to the positive effects of water reuse and the fact that this scenario consumes less energy compared to the other treatment technologies. The contribution of construction to the total impact is relatively high for all the technologies studied which is due to the low energy required for operation. Considering the absorption of CO_2 by the plants as a positive effect in the climate change category, the EWS is the best solution.

REFERENCES

Atanasova, N., Castellar, J.A.C., Pineda-Martos, R., Nika, C.E., Katsou, E., Istenič, D., Pucher, B., Andreucci, M.B., Langergraber, G. 2021 Nature-based solutions and circularity in cities. *Circular Economy and Sustainability* **1**, 319-332.

Morera, S., Santana, M.V.E., Comas, J., Rigola, M., Corominas, L. 2020. Evaluation of different practices to estimate construction inventories for life cycle assessment of small to medium wastewater treatment plants. *Journal of Cleaner Production* **254**, 118768.

Morera, S., Corominas, L., Rigola, M., Poch, M., Comas, J. 2017 Using a detailed inventory of a large wastewater treatment plant to estimate the relative importance of construction to the overall environmental impacts. *Water Research* **122**, 614-623.

Sustainability assessment at early stages of technology development: phosphorus recovery for fertiliser from dairy wastewater

M. Behjat*, M. Svanström and G. Peters

Department of Environmental System Analyses, Chalmers University of Technology, Gothenburg SE-412 96, Sweden

*Corresponding author: [marta.behjat@chalmers.se]

Abstract

A reduction in the availability of phosphate rock resources for fertiliser production coincides with an increase in phosphorus-rich dairy wastewater in Europe. Interest into the development of technologies for phosphorus recovery from wastewater and the use of the products as fertilisers in agriculture has increased. The dairy wastewater is a potential waste stream for these technologies. This work aims to contribute both to the technical development of this emerging technical system and methodological development of assessing the sustainability of it with regard to (1) the identification and selection of sustainability indicators, and (2) the assessment of life cycle environmental impacts. The work describes an approach developed for identifying and selecting the indicators as well as an approach employed for performing a meta-analysis of previously published life cycle assessment results to cope with lack of inventory data.

Keywords

dairy wastewater, meta-analysis, LCA, phosphorus recovery, sustainability indicator, wastewater treatment

INTRODUCTION

In abiotic systems, phosphorus (P) does not occur naturally other than in the form of phosphate rock. Phosphate rock is a finite, non-renewable resource that is largely needed for fertiliser production. Also considering the lack of exploitable phosphate mineral reserves in Europe (Schröder et al., 2010), the European Union (EU) has prioritised the recovery and safe reuse of P from food and municipal waste flows through its circular economy package (European Commission, 2016). This confluence of events has led to the development of technologies for phosphorus recovery from dairy wastewater and the use of the products as fertilisers in agriculture. An emerging technology combines dairy wastewater treatment (DWWT) with the recovery of P-rich products for such products to be used as fertilisers in agricultural activities. The purpose of this research was to contribute to both the technical development and methodological development of assessing the sustainability of this innovative technology. This work provides guidance on methods to partially overcome the lack of information by contributing to (1) the selection of a broad range of sustainability indicators for assessing impacts of the recovery system of P from DWW to produce fertilisers for agricultural activities and to (2) the environmental assessment by a meta-analysis, or rather, the mining and refining of information from previous life cycle assessment (LCA) studies.

MATERIALS AND METHODS

The overall methodological approach of this research work is represented in Figure 1.

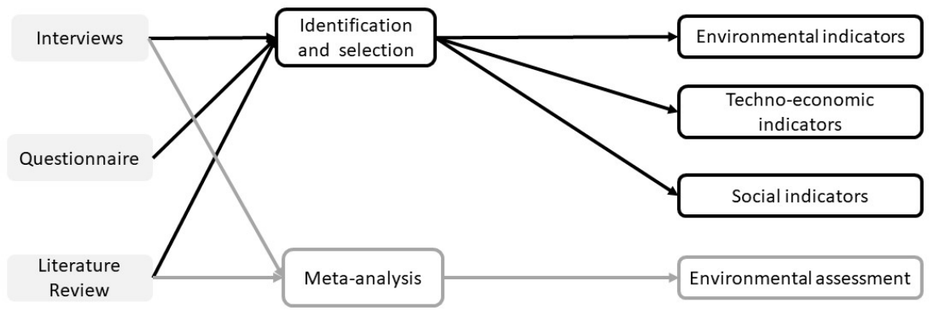

Figure 1 Workflow of the research. This figure represents how the research could achieve its aim by obtaining the listed expected results: sustainability indicators and the environmental impacts.

The research work was supported by three research tools: interviews, questionnaire, and literature review. The information collected by using these tools was used to (1) identify and select a list of sustainability indicators and to (2) perform a meta-analysis focused on life cycle environmental impacts.

Interviews

The interviews aimed to provide information about the innovative technologies that constitute the system. This information includes material flow data, actors, and EU policies and contributes to the development of a conceptual system description as well as to the development of a framework used in indicator selection. The framework highlights elements of the system and maps correlations between elements.

Questionnaire

The questionnaire is a form developed to gather information about actor priorities with regard to various aspects of sustainability in relation to the considered system. The approached actors evaluated these aspects, which are referred to the environment, economy and society. These aspects were graded from “not important” to “very important”.

Literature review

Different documents were selected and reviewed for various parts of the research to collect information to contribute to both methodological development and sustainability assessment.

Identification and selection of sustainability indicators

Specific documents were consulted for identifying an initial list of sustainability indicators (382). However, a practical subset of this long list of indicators was selected using three screening processes. The first screening process consisted of comparing the indicators found in the literature with the elements that constitute the developed screening framework. Next, the list of indicators obtained from the first screening was filtered based on the actors’ interests collected through the results of the questionnaire. Finally, a further screening was applied based on the indicator selection criteria proposed in literature.

Meta-analysis

With the meta-analysis, literature results were extracted and recalculated owing to the lack of published LCAs on P recovery from DWWTs. The information on environmental impacts was rescaled to the same FU (1 kg of P recovered). Impacts of the DWWT, as gathered from the dairy LCAs, was recalculated to relate to the P in the DWW. The extracted and rescaled environmental impact results of the DWWT process were related to those of the P recovery process in the conceptual combined system.

RESULTS AND DISCUSSION

The results presented in this study, apart from the methodological contributions, is a set of 26 sustainability indicators screened from an initial set of 382. Furthermore, according to the results presented in this study, installing P recovery as part of or after DWWT would normally not incur large additional environmental costs compared to the current DWWT with regard to climate impact or energy use; in general, the processes recovering from a liquid flow have a lower impact than when sludge is the P source.

REFERENCES

Behjat, M., Svanström, M., Peters, G., 2022. A meta-analysis of LCAs for environmental assessment of a conceptual system: Phosphorus recovery from dairy wastewater. Journal of Cleaner Production 369, 133307.

European Commission, 2016. Circular economy: New Regulation to boost the use of organic and waste-based fertilisers (MEMO/16/826). Brussels.

Schröder, J.J., Cordell, D., Smit, A., Rosemarin, A., 2010. Sustainable Use of Phosphorus. Wageningen UR.

TECHNICAL SESSIONS

T19.

Decentralized systems

Lessons learned from phosphorus chemical precipitation in small wastewater treatment plants

Sophie Besnault*, Stéphanie Prost-Boucle*, Luc Seranne*, Alan Le Bouder**, Jean-Marc Choubert*, Sylvie Gillot* and Pascal Molle*

* INRAE UR REVERSAAL, 5 rue de la Doua, CS 20244, F-69625 Villeurbanne, France
(E-mail: *sophie.besnault@inrae.fr)*
** Conseil Général of Gironde department, SATESE 33, Esplanade Charles de Gaulle, 33074 Bordeaux Cedex, France

Abstract
Feedback from 46 small to medium wastewater treatment plants equipped with chemical precipitation with iron chloride for phosphorus removal was gathered. Chemical precipitation with iron chloride is efficient to reach the phosphorus levels required for all the processes studied, except when the requirements are too low (< 1 mg TP/L). But an injection of iron chloride in a small WWTP requires a more complex and more frequent follow-up and significantly increases the operation costs.

Keywords (maximum 6 in alphabetical order)
Iron chloride; phosphorus removal; rotating biological contactors; vertical flow treatment wetlands; trickling filters

INTRODUCTION

The accumulation of phosphorus discharged in the environment by wastewater treatment plants (WWTPs) is one of the main causes of eutrophication. As a consequence, in France, an increasing number of small WWTPs are required to treat phosphorus, sometimes to reach very low levels, under 1 mg Total Phosphorus (TP)/L. Conventional processes installed to treat wastewater in small plants such as vertical flow treatment wetlands (VFTWs), rotating biological contactors (RBC) or trickling filters are not designed to remove phosphorus (Cramer et al., 2016). Chemical precipitation is then often implemented in order to reach the required levels of phosphorus in treated wastewater (Di Capua et al., 2022). This process is very frequent in large WWTPs, in particular in activated sludge systems (Strom, 2007). However, there is a lack of feedback on the use of chemical precipitation for phosphorus removal associated with technologies for small WWTPs (Bunce et al., 2018). Implementing chemical precipitation on smaller treatment plants presents new challenges as they cannot benefit from economies-of-scale, rigorous monitoring and in-house operating expertise as the larger WWTPs. For this reason, the French national working group Epnac (www.epnac.fr, gathering all the public organisms working on wastewater treatment in France) started a study in 2020 on phosphorus chemical precipitation implemented in different treatment technologies in small WWTPs. The objectives were to evaluate the performance of phosphorus treatment and to identify potential bottlenecks.

MATERIALS AND METHODS

The first step of the study was a national survey to collect data (water treatment regulatory monitoring, information on the phosphorus removal process selected at the plant, feedback from the operation of this process...) from the members of the Epnac group. Specific sites were then selected to proceed to extended monitoring in order to evaluate the performance of the process for phosphorus removal using a common experimental methodology.

Data from 367 regulatory monitoring (24-hour-flow composite samples) in 46 WWTPs treating phosphorus with a capacity of 260 to 8 000 Population Equivalents were gathered. The processes implemented at the studied plants were activated sludge systems (9 treatment plants), rotating biological contactors (16), vertical flow treatment wetlands (4), VFTWs with forced aeration (5) and trickling filters combined with VFTWs (12). All these WWTPs are equipped with a chemical precipitation unit using iron chloride ($FeCl_3$) to reach the low levels of phosphorus required at the outlet.

31 specific 24-hour-flow composite samples monitoring were produced for this study with additional parameters in regard to the classical parameters followed during the mandatory self-monitoring of the WWTP. The extended monitoring consisted in flow proportional sampling at each treatment steps in order to analyse global parameters as well as additional relevant parameters regarding phosphorus chemistry (iron, bicarbonate ions, volatile fatty acids…).

RESULTS AND DISCUSSION

Global performance of chemical precipitation for phosphorus removal in small WWTPs

Chemical precipitation with iron chloride is efficient to reach the phosphorus levels required except when they are too low (lower than 1 mg TP/L) as shown in Table 1. This confirms that levels of total phosphorus under 1 mg/L are hard to reach with chemical precipitation alone and require additional techniques such as filtration (Bunce et al., 2018).

Table 1. Percentage of 24-hour-flow composite samples meeting the phosphorus levels required at the outlet of the WWTPs according to the TP level required

Phosphorus level required (mg TP/L)	Number of 24-hour-flow composite samples	Percentage of samples under the required phosphorus level
>=0.7 and <=1	7	43%
>1 and <=1.5	34	85%
>1.5 and <=2	235	88%
>2 and <=4	62	69%
>4	26	77%

As seen in Table 2, the activated sludge system seems to be the most reliable process as 97% of the samples are below the required phosphorus level. Other processes such as trickling filters + VFTWs or VFTWs with forced aeration allow a good compliance with the total phosphorus discharge requirements (compliance over 75%).

Table 2. Percentage of 24-hour-flow composite samples meeting the phosphorus levels required at the outlet of the WWTPs according to the process

Process	Number of 24-hour-flow composite samples	Percentage of samples under the required phosphorus level
Activated sludge	117	97%
Rotating biological contactors	135	61%
Trickling filters + VFTWs	76	75%
VFTWs	30	70%
VFTWs with forced aeration	10	80%

As shown in Figure 1, TP removals above 67% were obtained for all the processes. Concentrations of phosphorus in treated water were the lowest with activated sludge. Low concentrations could also be obtained with VFTWs with forced aeration. Lower levels of total suspended solids (TSS) are associated with a better removal of phosphorus as around 2-3% of organic solids is phosphorus (Strom, 2007).

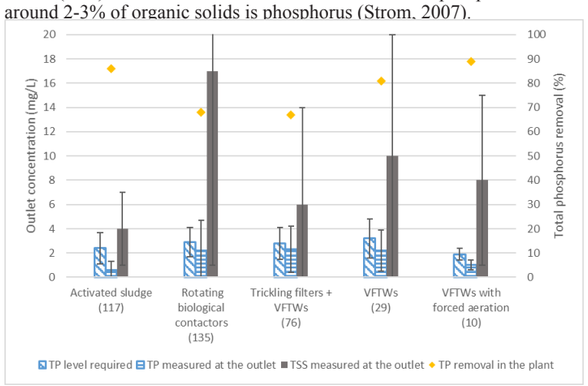

Figure 1. Comparison of processes for phosphorus removal.

Lessons learned

As chemical precipitation and sludge management can be implemented differently, even in a particular biological treatment technology, it is interesting to analyse more deeply the effect of the choice of the precipitation step implementation on efficiencies. A comparison of the different configurations for each process allowed to draw conclusions. For rotating biological contactors for example, 3 of the 16 WWTPs had an injection of iron chloride inside the biological rotating disc tank as shown in Figure 2. A similar removal of phosphorus (77%) was measured for these plants. In comparison with WWTPs where iron chloride was injected before or after the rotating discs tanks, a similar performance was obtained while lower iron chloride dosage was used (226 mg/l of commercial iron chloride for the injection inside the rotating discs, 98 mg/l for the injection before the rotating discs). The rotation of the discs is very slow and does not allow a good mixing of iron chloride, necessary to precipitate P. Iron chloride, as in activated sludge systems, should be injected in the most turbulent part of the tanks.

Figure 2. Injection of iron chloride inside the biological rotating disc tank.

Trickling filters followed by VFTWs can have 1 stage of filters, 2 stages or a lamella clarifier as a second stage. Iron chloride is injected before or after the first stage of VFTWs, as shown in Figure 3. The WWTP with no second stage did not remove as much phosphorus (48%) and suspended solids as the WWTPs with the two other configurations (78% removal for total phosphorus). This configuration without a second stage should be selected only when higher levels of phosphorus are required at the outlet.

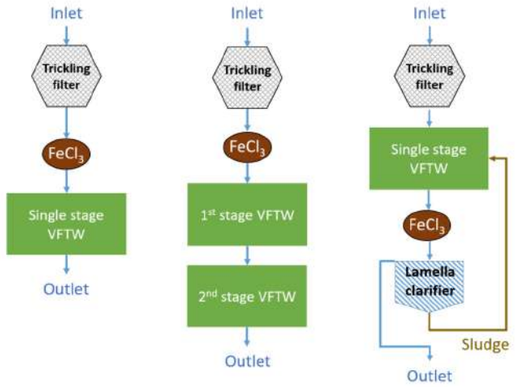

Figure 3. Three configurations for phosphorus removal by chemical precipitation for trickling filters followed by VFTWs.

Application of iron chloride in excess is frequent in small WWTP due to a less frequent follow-up, generating high reagent costs. Based on the data gathered in this study, the consumption of iron chloride for a theoretical 1 000 PE WWTP can vary from 4.3 to 11.4 tons per year. The quantity depends on the inlet phosphorus concentration, the removal objective and the regulation of the injection. Iron chloride can represent a cost of 0.8 to 5.7 euros per year per PE excluding taxes (up to +114% on operation costs of the plant in comparison with a similar plant without P precipitation).

Conclusions

Multiple systems exist for chemical precipitation of phosphorus in small WWTP (injection point, regulation of the injection, separation of the resulting solids residuals…) and can be efficient. It is not necessary to choose activated sludge if low levels of phosphorus are required in a small WWTP, other processes can be combined with chemical precipitation. But an injection of iron chloride in a small WWTP requires a more complex and more frequent follow-up in comparison with a classical plant without P precipitation and increases the operation costs. Phosphorus removal with iron chloride should only be implemented if the aquatic ecosystem really requires it, alternative to treatment should be considered (infiltration in the ground, reuse, evaporation…) to limit the discharge of P in superficial water.

REFERENCES

Bunce, J.T., Ndam, E., Ofiteru, I.D., Moore, A. and Graham, D.W. 2018 A Review of Phosphorus Removal Technologies and Their Applicability to Small-Scale Domestic Wastewater Treatment Systems. *Frontiers in Environmental Science* **6**(8).

Cramer, M., Koegst, T., Tränckner, J. 2016 Cost-efficient Phosphorus removal in rural WWTPs. 13th IWA specialized conference on small water and wastewater systems proceedings

Di Capua, F., de Sario, S., Ferraro, A., Petrella, A., Race, M., Pirozzi, F., Fratino, U., Spasiano, D. 2022 Phosphorous removal and recovery from urban wastewater: Current practices and new directions. *Science of the Total Environment* 823

Strom, P. F. 2007 Technologies to remove phosphorus from wastewater. *Rutgers University*, 1–8.

Nitrate electro-bioremediation as a decentralised water treatment: from the proof-of-concept to the *on-site* technology validation

Alba Ceballos-Escalera, Narcís Pous, M. Dolors Balaguer, Sebastià Puig

LEQUiA, Institute of the Environment, University of Girona, C/ Maria Aurèlia Capmany, 69, E-17003, Girona, Spain
(E-mail: *alba.ceballosescalera@udg.edu; narcis.pous@udg.edu; dolors.balaguer@udg.edu; sebastia.puig@udg.edu*)

Abstract
Up to 40% of rural areas cannot afford drinking water services due to the cost and difficult implementation of conventional centralised water treatments. Nitrate electro-bioremediation is emerging as an accessible decentralised treatment to increase drinking water availability in rural areas, where nitrate-contaminated groundwater is a widespread problem. This study moved towards scaling up the technology, including its validation in a relevant environment. The results validated the technology as a decentralised treatment in a rural area and paved the ground for further implementation.

Keywords:
Bioelectrochemical system; Biological denitrification; Groundwater; Microbial electrochemical technology; Reactor scaling up; Water recovery

INTRODUCTION

United Nations adopted the 2030 Agenda with the goal of universal access to safe drinking water (SDG 6, A/RES/70/1) since 2 billion people in 2020 still lacked safely managed drinking water. The high cost and complex implementation of conventional centralised water treatments in rural areas mean that up to 40% of these areas cannot afford drinking water services. A particularly exacerbated problem in rural areas is connected to agricultural and livestock production activities that often lead to nitrate contamination of groundwater (Yu et al., 2020). Because nitrates threaten groundwater potability, the European Directive 2020/2184 sets a safety concentration limit of 50 mg NO_3^- L^{-1}.

Many microorganisms have the ability to exchange electrons with solid electron conductors or other cells (electroactive microorganisms). This ability contributed to developing a broad range of practical applications, from bioenergy and bioelectronics to water treatment. In this area, electro-bioremediation is emerging as a decentralised and sustainable water treatment to increase the availability of treated water in rural areas (Pous et al., 2018). This treatment harnesses the capacity of electroactive microorganisms to perform selective oxidation and reduction reactions with solid electron conductors (i.e., electrodes), overcoming the lack of electron donors/acceptors. In nitrate-contaminated sites, these bioelectrochemical systems (BESs) could perform a selective nitrate reduction using the cathode as an inexhaustible electron donor and inorganic carbon as a carbon source (Clauwaert et al., 2007). The main advantages of this approach are: (i) independence of chemical reagents; (ii) modular reactor that provides flexible treatment capacity (iii) low operational cost; (iv) low environmental impact (e.g., no generation of brine); and (v) non-invasive and selective dosing of electron donors/acceptors avoiding side reactions.

Nevertheless, the technology is still in the transition from technology validated in the laboratory to a relevant environment. Against this backdrop, this study moved towards scaling up the technology using know-how on electro-bioremediation at a laboratory scale. For instance, it was noted that the low electrical conductivity of groundwater hinders the mass transfer (i.e., protons), requiring an external recirculation to minimise this limitation (Ceballos-Escalera et al., 2021). In addition, water softening was demonstrated to be a prerequisite to prevent scale formation in the reactor and increase treatment life in high-hardness groundwater (Ceballos-Escalera et al., 2022). The developed pilot plant was installed in a rural region (Navata, Spain), treating *on-situ* nitrate-contaminated groundwater for 3 months.

MATERIALS AND METHODS

A compact tubular bioelectrochemical fixed-bed reactor (**Figure 1**) was built with PVC (6.0 cm diameter and 1.7 m length). The cathode (inner part) and anode compartments (outer part) were separated with a tubular cation-exchange membrane (CEM, CMI-7000, Membranes Int., USA). Both compartments were filled with granular graphite (average diameter of 3.25 mm, enViro-cell, Germany) with a bed porosity of 50 %, resulting in a net cathode volume (NCC) of 1.2 L. The cathode electrode was previously inoculated with a denitrifying community obtained in the laboratory, dominated by *Sideroxydans* sp. (Ceballos-Escalera et al., 2021). The system was electrically operated in a two-electrode configuration, fixing the cell potential between 1.2 to 1.7 V by an external power supply.

The groundwater was treated with a commercial ion exchange softener to reduce the hardness from 300 to 45 ± 25 mg $CaCO_3$ L^{-1}. The main influent characteristics were a pH of 8.1, a conductivity of 0.8 ± 0.1 mS cm^{-1} and 92 ± 7 mg NO_3^- L^{-1}. The softened groundwater was pumped directly through the bottom of the cathode compartment and spilt over the top into the anode compartment towards the bottom, where the outlet was located. A fraction of the cathodic effluent was recirculated at a flow rate of 150 L d^{-1} to the influent. The reactor was operated at a room temperature of 30 ± 5ºC.

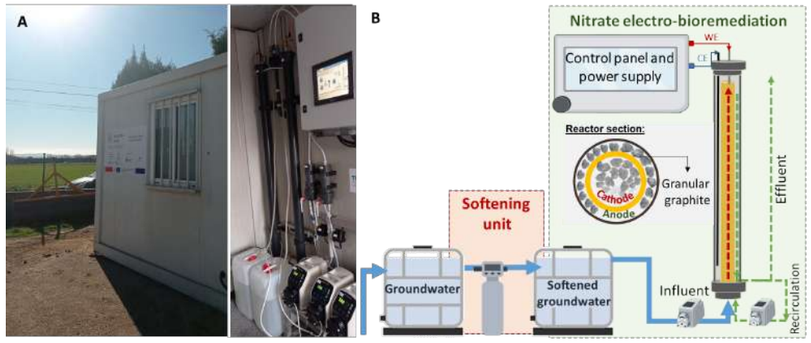

Figure 1. (A) Images of the pilot plant placed in Navata (Spain) (left) and bioelectrochemical reactors (right). (B) Process outline and scheme of the reactor.

RESULTS AND DISCUSSION

A nitrate electro-bioremediation pilot plant was operated for the first time with promising results. The pilot plant was tested in continuous flow mode for 3 months, decreasing the HRT_{cat} from 10.0 to 2.0 h (**Table 1**), corresponding to a flow rate from 2.9 to 14.3 L d^{-1}. Consequently, the nitrate reduction rate was increased to a maximum rate of 0.84 ± 0.11 kg-NO_3^- m^{-3} d^{-1} at the lower HRT_{cat}. In all HRT_{cat} tested, the nitrate removal efficiencies were higher than 90 % except for the lower HRT_{cat} of 2.0 h with an efficiency of 78 ± 11%. Even so, the effluent reached the drinking water quality in the whole operational time in terms of nitrate and nitrite concentration (> 50.00 mg-NO_3^- L^{-1} and >0.50 mg-NO_2^- L^{-1}, European Directive 2020/2184). Inclusive at the lower HRT_{cat}, the effluent kept a safe concentration of 20.16 ± 9.87 mg-NO_3^- L^{-1} and 0.00 ± 0.01 mg-NO_2^- L^{-1}. The results did not differ from those obtained on a laboratory scale, where the maximum rate of 2.28 ± 0.23 kg-NO_3^- m^{-3} d^{-1} was reached at HRT_{cat} of 1.5 h (Ceballos-Escalera et al., 2021).

Finally, the nitrate electro-bioremediation was energetically competitive with an average energy consumption of 0.31 ± 0.01 kW m^{-3} (**Table 1**) compared with conventional nitrate treatments, some of them with higher environmental impacts. For instance, reverse osmosis consumes between 0.9 - 2.2 kWh m^{-3} (Twomey et al., 2010), while generating nitrate-concentrated brines that must be treated afterwards. This evidenced the successful transition from the laboratory to the pilot scale and the technology validation in a real environment.

Table 1. Treatment performances and water characteristics according to the different HRT_{cat} tested (n ≥ 3). The table was coloured based on efficiency and water quality, where green is the best performing and yellow is the least performing.

Period	HRT_{cat}	Process efficiency			Effluent characteristics	
		Nitrate removal rate	Nitrate removal percentage	Energy consumption	Nitrate	Nitrite
(day)	(h)	(kg-NO_3^- m^{-3} d^{-1})	(%)	(kW m^{-3})	(mg-NO_3^- L^{-1})	(mg-NO_2^- L^{-1})
0-17	10.0	0.22 ± 0.02	94 ± 6	0.32 ± 0.02	5.64 ± 5.31	0.44 ± 0.23
17-28	8.0	0.28 ± 0.01	100 ± 0	0.31 ± 0.02	0.13 ± 0.22	0.09 ± 0.51
28-35	6.3	0.36 ± 0.02	100 ± 0	0.34 ± 0.01	0.17 ± 0.21	0.00 ± 0.00
35-42	5.1	0.43 ± 0.01	99 ± 0	0.30 ± 0.01	0.48 ± 0.24	0.19 ± 0.33
42-49	3.1	0.65 ± 0.07	93 ± 10	0.32 ± 0.02	6.11 ± 8.91	0.12 ± 0.33
49-85	2.0	0.84 ± 0.11	78 ± 11	0.30 ± 0.04	20.16 ± 9.57	0.00 ± 0.01

CONCLUSIONS

The present work validated nitrate electro-bioremediation in a relevant environment and paved the ground to move towards further scaling up the technology. Furthermore, the encouraging results demonstrated its applicability and evidenced the potential of the decentralised treatment to increase safely managed drinking water services in rural areas.

ACKNOWLEDGEMENTS

This work was funded through the European Union's Horizon 2020 project ELECTRA [no. 826244]. A.C-E. was supported by a PhD grant from the University of Girona (IF_UDG2020). Sebastià Puig is a Serra Hunter Fellow (UdG-AG-575) and acknowledges the funding from the ICREA Academia award. LEQUIA has been recognised as a "consolidated research group" (Refs 2021 SGR01352) by the Catalan Ministry of Research and Universities.

REFERENCES

Ceballos-Escalera, A., Pous, N., Balaguer, M. D., and Puig, S. 2022 Electrochemical water softening as pretreatment for nitrate electro bioremediation. Science of The Total Environment, 806, 150433.

Clauwaert, P., Rabaey, K., Aelterman, P., De Schamphelaire, L., Pham, T. H., Boeckx, P., Boon, N., and Verstraete, W. 2007 Biological denitrification in microbial fuel cells. Environmental Science & Technology, 41(9), 3354–3360.

Pous, N., Balaguer, M. D., Colprim, J., and Puig, S. 2018 Opportunities for groundwater microbial electro-remediation. Microbial biotechnology, 11(1), 119–135.

Twomey, K. M., Stillwell, A. S., and Webber, M. E. 2010 The unintended energy impacts of increased nitrate contamination from biofuels production. Journal of Environmental Monitoring, 12, 218–224.

Yu, G., Wang, J., Liu, L., Li, Y., Zhang, Y., and Wang, S. 2020 The analysis of groundwater nitrate pollution and health risk assessment in rural areas of Yantai, China. BMC Public Health, 20(1), 1–6.

Zhang, Y. and Angelidaki, I. 2014 Microbial electrolysis cells turning to be versatile technology: Recent advances and future challenges. Water Research, 56, 11–25.

Innovative decentralized wastewater treatment project for 400 households and local industry, combining water, nutrient and energy recovery

B. De Gusseme*,**, D. Seuntjens***, L. Demolder***, W. Jacobs** and P. De Smet***

* Center for Microbial Ecology and Technology (CMET), Ghent University, Coupure Links 653, B-9000 Gent, Belgium
(E-mail: *bart.degusseme@ugent.be)*
** Department Innovation, FARYS|TMVW, Stropstraat 1, 9000 Gent, Belgium
(E-mail: *wim.jacobs@farys.be*)
*** Clean Energy Innovative Projects cvba (CEIP), Drève des Soupirs 9, 1430 Rebecq, Belgium
(E-mail: *dries.seuntjens@ducoop.be; lieven.demolder@cleanenergyinvest.be; peter.de.smet@cleanenergyinvest.be)*

Abstract

An innovative decentralized wastewater treatment and resource recovery project has been set up for 400 households (1265 IE) in Belgium, based on source separation of grey and black wastewater. The segregated black water is mixed with collected kitchen waste and treated anaerobically in an UASB reactor, followed by phosphorus recovery. Grey water has the highest energy potential to recover. Separate collection and heat recovery through heat exchangers allows to transfer most of the energy to the district heating system. Together with energy recovery through biogas, almost 1/3 of the total heat demand of the urban area is provided by the decentralized reuse plant. Using UF-RO membrane filtration, the treated effluent is entirely recovered as process water for a local industry, and district heating allows recovery of the excess heat of the plant. As such, this remarkable demonstration project for sustainable transition in wastewater treatment in the city of the future combines water, energy and nutrient recovery, and contributes to the public acceptance of new urban resource recovery schemes. The project was part of the European projects Run4Life (H2020) and NEREUS (Interreg) and is in full operation now, at one fourth of its maximum design capacity. Hence, EcoSTP23 is the first opportunity to share the full-scale technical results, together with the importance of the socio-economic and governance aspects to be considered to set up such a project for cutting-edge ecotechnologies at the urban scale.

Keywords

decentralized wastewater treatment; nature-based solutions for urban resource recovery; nutrient and energy recovery; public acceptance for reuse; source separation and treatment; water reuse

THE NEED FOR DECENTRALIZED WASTEWATER TREATMENT AND RESOURCE RECOVERY IN THE CITIES OF THE FUTURE

When dealing with the urban metabolism, there is an urgent need to rethink and redesign the currently used treatment lines, in the perspective of a sustainable bio-economy (Verstraete & De Gusseme, 2011). For example, the scarcity of water is no longer a problem relevant to arid zones only, but it occurs globally, even in regions considered water-rich (e.g. Belgium). A paradigm shift is needed to cope with these challenges and the sewage treatment plants (STPs) in the cities of the future should be regarded as an integral part of the municipal water production process of the 21st century (Qin et al., 2004). We have to reconsider the actual sanitation approach, which is entirely based on flushing excrements out of the city surroundings by use of ample amounts of water. Instead of centralizing the sewage treatment in major STPs considered as a cost factor, one should dare to examine the possibility to decentralize municipal waste treatment and to develop local water resource recovery facilities or biorefineries, making use of the resources in domestic wastewater, including water, nutrient, and energy recovery (Kisser et al., 2020).

To demonstrate the potential of urban resource recovery, a remarkable decentralized wastewater treatment project is set up in 2020, in a former harbor dock in Ghent, Belgium, called the "Nieuwe Dokken". An innovative multi-step treatment concept, referred to as ZeroWasteWater (Verstraete & Vlaeminck, 2011), is implemented with a total design capacity for 400 households (1265 IE). The approach brings new eco-technologies for STPs into practice, based on source separation of the grey (GW, sanitary) and black (BW, toilet) wastewater, with the overarching goal of recovering the maximum of its energy potential and redistribute it by means of a district heating system, and closing the water cycle by capturing >35.000 m^3/j treated effluent directly and reuse it as process water for the industry.

SOURCE SEPARATIONS AND ECOTECHNOLOGIES ALLOWING ENERGY AND NUTRIENT RECOVERY

The BW is collected undiluted by means of vacuum toilets and a vacuum collection system. The segregated BW is mixed with collected kitchen waste (KW) and treated anaerobically in an anaerobic digester (UASB). The system is designed to handle a maximum influent COD load of 165 kg O_2/d, which is degraded for 70% (COD_{sol} for >80% and COD_{SS} for 60%), resulting in a biogas production of max. 45 Nm^3/d. Biogas energy is recovered as heat (50-100 MWh_{th}/y at full capacity) and distributed back to the households by a district heating system. The UASB effluent is further treated in a struvite crystallization reactor, allowing phosphate recovery and reuse as fertilizer in the local green areas and urban farming projects.

GW has the highest temperature and energy potential to recover, about 700 MWh_{th}/y at full capacity, by collecting it at 25-28°C using isolated buffers and pressurized sewerage. Separate collection and heat recovery through heat exchangers allows to transfer most of the energy to the district heating system. Together with the energy recovery through biogas, almost 1/3 of the total heat demand of the urban area (2,1 GWh/y) will thus be provided by the WWTP. The GW is further treated in a nitrifying/denitrifying membrane bioreactor (MBR), together with the effluent of the BW treatment.

The MBR consists of two membrane units of 90 m^2 total membrane surface each, using newly developed PVDF ultrafiltration (UF) membranes (80 nm). The integrated permeate channel membranes are the first fully back-washable flat sheet membranes, especially designed to operate at high fluxes up to 40 L/m^2.h. The resulting excess sludge of the aerobic treatment is digested in the aforementioned UASB together with the BW and KW, to valorize its organic content and to increase energy production.

FIRST RESULTS AND ENERGY RECOVERY

The development of a new urban district goes in phases. To date, one of the three building areas is completely finished and in the second one, the first residents are arriving as well. As a result, respectively 88 and 30 housing units are already occupied on November 25th, 2022, with an average population density of 1,75 IE per unit. This results in an occupation of about 206 IE as continuous residents in the district, but also the local school and sports facilities of the City of Ghent are already connected to the decentralized WWTP. As a result, the system is operated at one fourth of its maximal capacity now, in November 2022. Two more large buildings are expected to be finished in early 2023, thus scale-up is expected very soon.

In Figure 1, the daily treated water flows in 2022 are shown as a function of time. On average, 12,73 ± 6,82 m^3/d is treated, of which 20,9% is black water. From January 1st up till November 25th, 3743 m^3 of wastewater was treated, of which 783 m^3 black water. For 2022, this already resulted in a total energy recovery of 15.352 kWh in the form of biogas. The struvite precipitation reactor was put in operation as well, resulting in an average struvite production of 175 g/day, which allowed to recover the first 50 kg of fertilizer for the local farming projects. A further update of the increasing full-scale technical results with the increasing number of residents in the district will be presented at EcoSTP23.

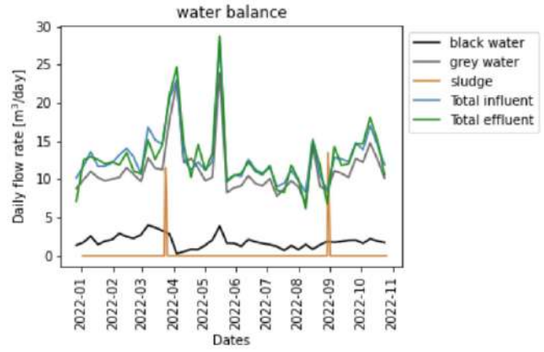

Figure 1. The daily flow rates of the separated streams treated in the decentralized WWTP at the Nieuwe Dokken in 2022. Excess sludge was removed two times, which resulted in the two peaks.

SAFE WATER REUSE FOR THE LOCAL INDUSTRY

Close to the newly developed urban area, a hygiene chemicals producing factory is located. The production process requires >35.000 m^3/y softened process water and 15.000 m^3/y demineralized water (<20 µS/cm). This need for water can be partially met by the reuse of the treated effluent. To meet the quality requirements, reverse osmosis (RO) is the key technology after the pretreatment by ultrafiltration in the aerobic MBR.

High quality water, free of pathogens, nutrients and hardness is achieved and completely reused in the factory. Hence, the decentralized water reuse plant can be considered as a zero-liquid discharge installation, as the RO concentrate is completely reused as well. Specific attention is given to the fate of organics during membrane filtration, since 25,79 ± 7,79 mg COD/L is still present in the effluent after the aerobic MBR. Therefore, organic carbon and specific organic compounds creating discoloring and bad odor of the final water are monitored.

To date, the first batches of reclaimed WWTP effluent have been produced and reused for the full-scale production of hygiene chemicals by the factory. Figure 2 shows the resulting waters after the different treatment steps, from UF filtrate to softened process water (< 0,3 °F).

Figure 2. The resulting waters after the different treatment steps in the water reuse process: (L) UF filtrate, (M) after organics removal with activated carbon, and (R) softened process water after ion exchange, ready to be used in the full-scale industrial process.

Moreover, the factory produces a lot of excess heat in the air chillers and heat exchangers of the production process. This heat will be recovered by coupling it to the district heating system in the urban area, thus meeting the remaining 2/3 of the total heat demand. This demonstration project of innovative STP layouts for the city of the future thus combines water, energy and nutrient recovery.

SOCIO-ECONOMIC MODEL AND GOVERNANCE: INVOLVEMENT OF THE LOCA COMMUNITY AND NEW BUSINESS MODEL

One of the most important aspects to remove the roadblocks for implementing new reuse schemes in an urban settlement, is the integration of the local community and a sound business model within the boundaries of the current legal framework for resources recovery. Therefore, an Energy Service Company (ESCO) has been set up to organize the technical maintenance and district services. This ESCO is a mixed private-public-citizens initiative in which the local inhabitants are represented, together with investors and public stakeholders such as the local water utility FARYS.

The local community benefits directly from the revenues of the recovered products and the local district heating system. This integrated approach in combination with the scale of the project will significantly contribute to the public acceptance of new urban water reuse schemes and the believe in the opportunities to turn STPs into profitable decentralized water resource recovery facilities, allowing affordable water reuse and resource recovery in the cities of the future.

The Nieuwe Dokken project was part of the Run4Life project, funded by the EU H2020 program CIRC-01-2016-2017 - "Systemic, eco-innovative approaches for the circular economy: large-scale demonstration projects", and the "New Energy and Resources from Urban Sanitation" (NEREUS) project, funded by the EU Regional Development Fund (Interreg 2 Seas). Prof. B. De Gusseme takes part in the EU COST action CA17133 "Circular City" – WG3: Resource recovery.

REFERENCES

Kisser, J., Wirth, M., De Gusseme, B., Van Eekert, M., Zeeman, G., et al. 2020 A review of nature-based solutions for resource recovery in cities. *Blue-Green Systems* **2**(1), 138–172.

Qin, J. J., Oo, M. H., Lee, H. & Kolkman, R. 2004 Dead-end ultrafiltration for pretreatment of RO in reclamation of municipal wastewater effluent. *Journal of Membrane Science* **243**, 107-113.

Verstraete, W. & De Gusseme, B. 2011 Visions about water and sanitation for the cities of the future: time to rethink environmental microbial processes. *Microbial Biotechnology* **4**(2), 131-132.

Verstraete, W. & Vlaeminck, S.E. 2011 ZeroWasteWater: Short-cycling of Wastewater Resources for Sustainable Cities of the Future. *International Journal of Sustainable Development and World Ecology* **18**(3), 253-264.

The third route: Techno-economic analysis of extreme water and wastewater decentralization

Manel Garrido-Baserba[1,2], Irene Barnosell[3], David L. Sedlak[4], Korneel Rabaey[5], Diego Rosso[2,6], Maria Molinos-Senante[7], Oliver Schraa[1], Manel Poch[3]

[1] inCTRL Solutions Corp., Salt Lake City, UT 84102, USA
[2] Water-Energy Nexus Center, University of California, Irvine, CA 92697, USA.
[3] LEQUiA, Institute of the Environment, University of Girona, Spain
[4] Department of Civil and Environmental Engineering, University of California, Berkeley, CA 94720, USA
[5] Center for Microbial Ecology and Technology, Ghent University, Belgium
[6]Department of Civil and Environmental Engineering, University of California, Irvine, CA 92697, USA
[7]Department of Hydraulic and Environmental Engineering, Pontificia Universidad Católica de Chile

Abstract

Decentralized treatment and source separation hold the potential to drastically improve the technical, environmental, and economic performance of current technologies. This research assesses the techno-economic feasibility of implementing independent and community-level decentralized systems for rainwater harvesting, potable and wastewater treatment, and resource recovery in five main types of buildings (e.g., household, townhouse, high rise, etc.). Five different treatment layouts under five different climatic conditions were evaluated per each type of building. The proposed layouts consider varying levels of source separation (i.e., black, grey, yellow, brown, and, even, typical wastewater) using the corresponding toilet types (vacuum, urine-diverting, and conventional) and the necessary pipeline and pumping requirements. We show that the proposed layouts could satisfy 100% of the water demand in most of the scenarios (e.g., medium-sized buildings in wetter climates) while the worst scenario (i.e., high-rise building in arid climate) could satisfy up to 75% of the water demand. A comprehensive economic analysis considering CapEx and OpEX yielded that the cost of upgrading the buildings to become water and wastewater independent is 5.6-11.6% of the total construction cost of the building for larger buildings and individual dwellings, respectively, with relatively low space requirements. For buildings or combined water systems with more than 300 people, the total price of water (including harvesting, treatment, recycling, and monitoring) could range between $1.5/m3 and $2.7/m3 in comparison to the current $4-3.5/m3 in the USA and western Europe. Our results indicate that extreme decentralization is not only technically feasible but also has the potential to reduce the cost significantly and environmental impact of water services, improving the marginal cost of water and other societal benefits, which could facilitate the necessary transition in the urban water system.

Keywords: Decentralization, resilience, source separation, source recovery, modelling

Introduction

The push toward a transition in the urban water system keeps increasing as freshwater resources are under unprecedented pressure due to over-consumption from a growing population, climate degradation, and poor management (Daigger et al., 2019; IPCC, 2022; Olsson, 2015; Sedlak, 2014; van Loosdrecht and Brdjanovic, 2014). Traditional water and wastewater supply infrastructures, which involve centralized treatment and the energy-intense activated sludge (AS) process (which follows a disposal-oriented approach), are being questioned because of their environmental and economic underperformance and their low resilience against extreme natural events due to climate change. Alternatively, a decentralized system based on the source separation of grey (GW) and brown and yellow (BW+YW) water, together with rainwater capture and state-of-the-art resource recovery technologies, has the potential to improve the efficiency of the urban water system by reducing both energy consumption and greenhouse gas emissions, while allowing nutrient and energy recovery. Thus, extreme decentralization coupled with source separation and resource recovery is a potential venue towards sustainability, reliability, and resilience of the water system (Garrido-Baserba et al., 2018; Larsen et al., 2016; Peter-Varbanets et al., 2009; Piratla and Goverdhanam, 2015; Remy, 2010; Roefs et al., 2017).

Material and Methods

To evaluate the technical feasibility of implementing decentralized systems, this study covers the theoretical implementation (using state-of-the-practice technologies and methodologies) of an online monitoring and control system coupled with a real-time model-based digital twin. The digital twin corresponds to one of the treatment configurations applied to five housing types (i.e., from low-rise dwellings and high-rise buildings to city blocks). Creating a digital twin of one of the most cost-effective, sustainable, and resilient alternatives enabled: (i) a deeper understanding of all the required processes and steps (while confirming effluent water quality), (ii) improved reactor and equipment seizing to calculate the required space better, (iii) using resource models (aka LCA) for a detailed environmental and economic analysis, (iv) incorporate economic benefits (i.e., resource and energy recovery).

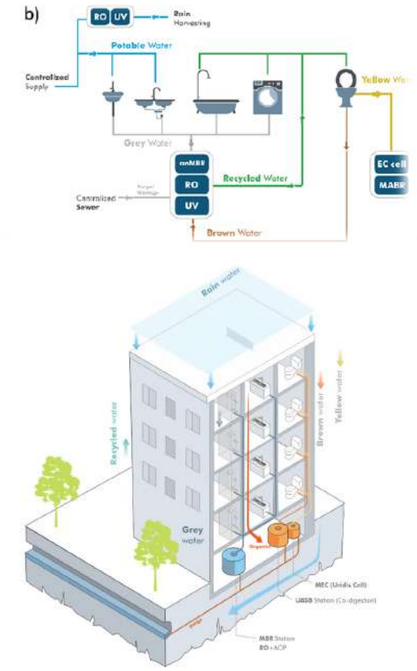

Figure 1. The upper flow diagram represents one of the fully decentralized approaches correspondings to the urine-diverting layout (b), and the larger is a conceptual 3D representation of the flows within one of the studied buildings (i.e., Medium-size)

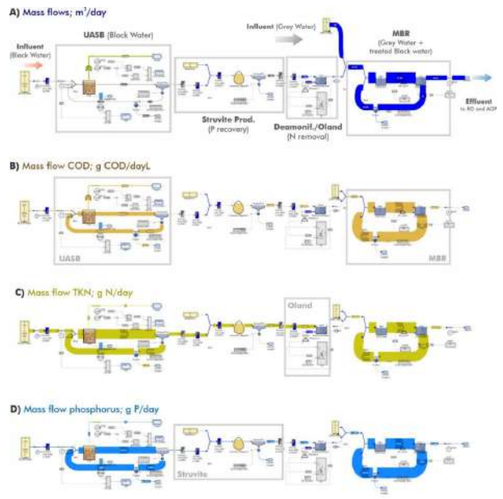

Figure 2. Model of the V1 layout with its corresponding Sankey diagrams obtained by the modeling software SIMBA#. The Sankey diagrams represent a) Blue, m3/day; b) Brown COD, mg COD/L; c) Green, TKN, mg N/L; and d) Light blue, Phosphorus, mg P/L. Five other models corresponding to the five scenarios under consideration were built and tested.

Results and Discussion

The modelling of the proposed decentralized systems confirmed the technical feasibility of extreme decentralization, and we made several observations:

- The simulations indicated that all the different effluents meet current quality regulations in terms of greywater reuse and drinking water. Existing institutional barriers (or non-technical barriers) are slowly adapting to new frameworks and financing schemes, facilitating the path toward a potential adoption.
- New developed models (i.e., anMBRs, UASB and biofilm reactors, and an improved co-digestion-biogas model) helped confirm their adequacy and identify the most cost-effective alternatives.
- A sewer model helped identify potential sewer management strategies that, coupled with a theoretical future large-scale decentralization adoption (reducing sewage from urban areas), could be used to ameliorate the effects of the changing climate; sewers could be used to better manage the alarming decrease in the return period of extreme events due to climate change.
- The use of resource models (SIMBA# nomenclature for LCA sub-models) helped evaluate environmental impacts and supported the creation of an inventory for operational costs calculations. Operational costs were added to capital costs, and it was identified that during the construction of new residential blocks, only 5.6-11.6% of additional investment would be required to deploy the required equipment and pipeline network.
- A digital twin of the most favorable alternative was built and implemented to a remote monitoring platform, enabling exhaustive and remote monitoring and control of the operations.

Conclusion

Extreme decentralization coupled with source separation is technically and economically feasible. Thanks to the most recent advances in modelling (e.g., biofilm and anaerobic processes, co-digestion for biogas, system-wide evaluations, rain harvesting & management, biogas, etc.) and new control tools (e.g., digital twins, predictive models), is possible to explore and study in great detail those treatment configurations better suited to tackle current climate challenges, which are aligned with key concepts such as resilience, circular economy, resource recovery, and sustainability. The most sustainable and decentralized treatment configurations (from an LCA perspective and top expert opinions) were implemented using modelling software. A digital twin was developed for the most economical and sustainable treatment configuration.

This study found that extreme decentralization has the potential to reduce the cost and environmental impact of water services significantly. In the upcoming years, the total cost (and amount) of water may well increase when considering the cost of maintaining the legacy of the centralized and the new decentralized infrastructure. However, this study shows that decentralization could improve the marginal cost of water (i.e., cheaper than building new reservoirs and desalination plants) and other societal benefits, facilitating the necessary transition in the urban water system.

The modelling of extreme decentralization enabled us to put numbers on some of the key concepts towards a potential transition towards source and energy efficiency, such as 92-98% of water recycling capacity (either rain harvesting or direct potable reuse), energy-neutral (Anaerobic-based plus co-digestion instead of the current aeration-based CAS, which is highly energy inefficient), resource production (Biogas or hydrogen and high-quality fertilizer), better integration with the whole urban sewer and wide-system management (i.e., resilience sewer strategies), and resilient (designed to be independent of the potable system and the electric grid, if needed).

REFERENCES

Daigger, G.T., Voutchkov, N., Lall, U., Sarni, W., 2019. *The Future of Water: A Collection of Essays on "Disruptive" Technologies that may Transform the Water Sector in the Next 10 Years*. Washington, D.C.

Garrido-Baserba, M., Vinardell, S., Molinos-Senante, M., Rosso, D., Poch, M., 2018. The Economics of Wastewater Treatment Decentralization: A Techno-economic Evaluation. *Environmental Science and Technology 52*, 8965–8976.

IPCC, 2022. IPCC Sixth Assessment Report: Impacts, Adaptation, and Vulnerability.

Larsen, T.A., Hoffmann, S., Lüthi, C., Truffer, B., Maurer, M., 2016. Emerging solutions to the water challenges of an urbanizing world. *Science* 352, 928–33.

Larsen, T.A., Udert, K.M., Lienert, J., 2015. Source Separation and Decentralization for Wastewater Management, Source Separation and Decentralization for Wastewater Management.

Olsson, G., 2015. Water and energy: threats and opportunities, *Water Intelligence Online*. IWA publishing.

Peter-Varbanets, M., Zurbrügg, C., Swartz, C., Pronk, W., 2009. Decentralized systems for potable water and the potential of membrane technology. Water Research 43, 245–265.

Piratla, K.R., Goverdhanam, S., 2015. Decentralized Water Systems for Sustainable and Reliable Supply. *Procedia Engineering* 118, 720–726.

Remy, C., 2010. Life cycle assessment of conventional and source separation systems for urban wastewater management. Technischen Universität Berlin 340.

Roefs, I., Meulman, B., Vreeburg, J.H.G., Spiller, M., 2017. Centralized, decentralised, or hybrid sanitation systems? Economic evaluation under urban development uncertainty and phased expansion. *Water Research* 109, 274–286.

Sedlak, D., 2014. Water 4.0: the past, present, and future of the world's most vital resource.

van Loosdrecht, M.C.M., Brdjanovic, D., 2014. Anticipating the next century of wastewater treatment. *Science* (1979) 344, 1452–1453..

Occurrence and fate of Organic Micropollutants and Antibiotic Resistance Genes during Separated Decentralised Treatment of Black Water and Grey Water

M. Rivadulla*, A.X. Elena**, S. Suarez*, T.U. Berendonk**, F. Omil* and J. M. Garrido*

* CRETUS, Department of Chemical Engineering, Universidade de Santiago de Compostela, 15782 Santiago de Compostela, Galicia, Spain
**Technische Universität Dresden, Institute of Hydrobiology, Dresden, Germany.

(E-mail: *matias.cora@usc.es*)

Abstract

Decentralised wastewater treatment is becoming a suitable strategy to reduce cost and environmental impact. Besides, it presents a potential on reducing the release of contaminants of emerging concern (CECs) such as organic micropollutants (OMPs), antibiotic resistance genes (ARGs). In this research, a characterization of the performance of two technologies treating black water (BW) and grey water (GW) fractions of urban sewage is carried out in a decentralised treatment of the wastewater produced in three office buildings in NW Spain. An anaerobic membrane bioreactor (AnMBR) treating BW and a hybrid anoxic/aerobic membrane bioreactor (H-MBR) treating GW were operated at pilot scale. Their operation was characterised in terms of removal of conventional pollutants, such as COD, TN, TP, and CECs. Preliminary results showed a stable operation in both systems in terms of COD and TN removal in AnMBR and H-MBR, respectively. The behavior of selected OMPs was analysed in a first sampling campaign, in which it was found a different distribution of compounds among sewage fractions. A initial characterization of ARGs was carried out to select a list of genes to be monitored by q-PCR. Final results are expected to be received in the coming weeks.

Keywords (maximum 6 in alphabetical order)

Antibiotic resistances, decentralised treatment, membrane processes, organic micropollutants.

INTRODUCTION

Wastewater treatment is being adapted to achieve sustainability goals, such as resource recovery and water reuse. The conventional wastewater treatment strategy consists on the centralised treatment of the sewage produced by a certain populated area, which means high construction (sewers and full-scale plants) and operational (high flows and energy demanding technologies) costs. Currently, decentralised treatment is becoming an interesting alternative to achieve sustainability, by treating wastewater in its source of production and selecting the most suitable technologies according to its characteristics (Arias et al., 2020). Regarding contaminants of emerging concern (CECs), such as organic micropollutants (OMPs) and antibiotic resistance genes (ARGs), decentralised treatment is a promising strategy to reduce *in situ* their load released to the environment by implementing the most suitable technology for each matrix. Despite its potential, there is still a lack of knowledge in this topic (Hube & Wu, 2021), since the actual implementation of decentralised treatment is challenging yet.

The aim of this work is to characterize the decentralised treatment of three office buildings in NW Spain regarding conventional pollutants removal, OMPs presence and fate, and ARGs distribution.

MATERIALS AND METHODS

Experimental setup

The black water (BW) generated in the three office buildings was treated in an anaerobic membrane bioreactor (AnMBR) pilot plant. BW are collected after grit removal in a non-stirred equalization tank of 2 m^3. From this unit is fed to a digester of 2.4 m^3, where anaerobic digestion of organic matter takes place. The filtration step is carried out in a separated compartment of 1 m^3, where the produced biogas in the digester is recirculated to prevent membrane fouling. The AnMBR permeate comes from a 6.25 m^2 ultrafiltration plate membrane module. The generated grey water (GW) was collected in a non-stirred equalization tank of 1 m^3, and fed to a hybrid anoxic/aerobic membrane bioreactor (H-MBR, patent EP 1484287 B1). H-MBR consist of three compartments: a continuously stirred anoxic compartment (17.8 L), an aerobic compartment (20.2 L) and a filtration compartment (9.5 L). Both anoxic and aerobic chambers contained suspended biomass and Biochip carriers (20% of working volume each). The filtration chamber contains a hollow fibre membrane module of 0.6 m2. Suspended biomass is recirculated from the filtration compartment to the anoxic chamber.

Analytical methods

Conventional parameters. COD, N species, total and volatile suspended solids (TSS, VSS), etc. were monitored twice a week, according to the Standard Methods.

Organic micropollutants. A selection of eight relevant compounds was carried out. First, according to the latest EU Watch Lists (2020, 2022), three antibiotics were selected: sulfamethoxazole (SMX), trimethoprim (TMP) and ciprofloxacin (CIP). Then, another six compounds were selected due to their presence in the BW of the site: two anti-inflammatories, ibuprofen (IBP) and naproxen (NPX); and three hormones, estrone (E1), β-estradiol (E2) and α-ethinylestradiol (EE2). The selected compounds were not spiked to the system. OMP samples were preconcentrated by solid phase extraction (SPE) and determined by LC-MS/MS.

Antibiotic resistance genes. Initial information on ARGs was obtained using a chip-based HT-qPCR approach. This screening was carried out on biomass and water streams of the plants. For this procedure, different criteria were applied to select an initial list of 34 genes. According to these results and the ARGs health risk classification proposed by Zhang et al. (2021), a subset of genes (n=7) was selected for further quantification via qPCR

RESULTS AND DISCUSSION

General results

The decentralised system was operated for 226 d. AnMBR hydraulic retention time (HRT) was maintained at 2.36±0.19 d. Since the production of GW during weekends was not enough to maintain a continuous operation, H-MBR was operated 5 days a week, with a HRT of 4.71±0.03 h. The anaerobic treatment of BW efficiently removed COD, as shown in Figure 1a. Total nitrogen (TN) was not removed in this stage: 124.5±27.7 mg N L^{-1} at the influent and 115.4±20.1 mg N L^{-1} at the permeate. In BW treatment line, the COD removal efficiency achieved was 89.7±3.5 %. TN removal efficiency and nitrogen species concentration in this system are displayed in Figure 1b. Despite the relatively low influent TN concentration in BW, 4.1±1.1 mg N L^{-1}, it was achieved a removal efficiency up to 54 %.

OMPs behavior

Two sampling campaigns were carried out in each plant to characterize the occurrence and fate of the selected OMPs in the decentralised system. The concentrations of the different compounds found in the influent of both BW and GW treatment lines in the first sampling campaigns are gathered in Table 1. As expected, the occurrence of the selected OMPs is higher in BW than GW, where only TMP and IBP were detected at relatively low concentrations. The removal of these compounds in the H-MBR was 9.8±17 % and 22.5±5.3 %, respectively. The removal efficiencies of the detected compounds in BW line are shown in Figure 2. Although the low influent concentrations, compounds such as TMP and NPX were moderately removed in the AnMBR, which could be expected since both compounds are easily biodegradable in anaerobic environments (Alvarino et al., 2018).

ARGs characterization

The characterization of the ARGs present in the system was carried out in two sampling campaigns at the beginning and at the end of the operation. The initial characterization using HT-PCR resulted in a preliminary overview of the 34 selected genes SmartChip q-PCR. From this list, a final selection was chosen, considering the most relevant gene of each analysed class according to the methodology proposed by Zhang et al., 2021. The final selection is presented in Table 2. The normalised (-log) relative abundances of the final selection are presented in Figures 3a (BW treatment line) and 3b (GW treatment line). Lower relative abundances were found in the GW line, as expected. The results of the final characterization are still pending.

ACKNOWLEDGEMENTS

This research was supported by the Spanish State Research Agency (EEA) through ANTARES (PID2019-110346RB-C21) and PRESAGE (PCI2021-121990) projects.

Table 1. Influent concentrations of the selected OMPs in the decentralised system

Compound	BW (ng L^{-1})	GW (ng L^{-1})
SMX	n.d.	n.d.
TMP	1.07±0.34	1.03±0.59
CIP	n.d.	n.d.
IBP	23799.02±6276.90	18.57±6.05
NPX	175.22±65.29	n.d.
E1	19.16±1.71	n.d.
E2	197.03±20.64	n.d.
EE2	n.d.	n.d.

Table 2. Final selection of ARGs to be quantified by q-PCR.

Class	Gene
Class 1 integron integrase	*intl1*
Sulfonamides	*sul1*
Beta-Lactams	$bla_{CTX\text{-}M}$
Colistin	*mcr*
Macrolides	*ermB*
FluoroQuinolones	*qnrS*
Bacteria taxonomic	*dll*

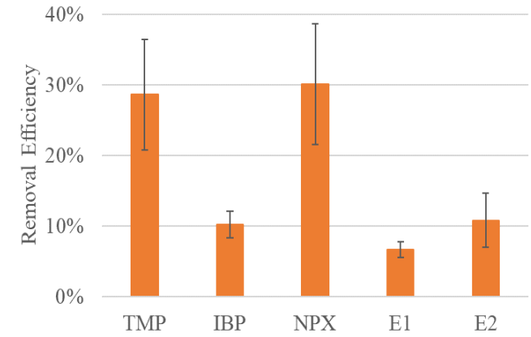

Figure 2. Removal efficiencies of the detected compounds in the AnMBR.

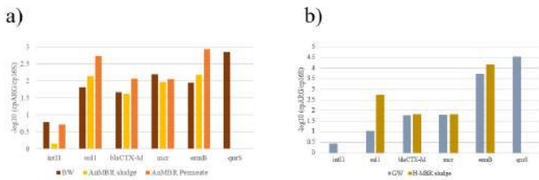

Figure 3. Normalised relative abundances of the selected genes in the initial characterization of the BW (a) and GW (b) lines.

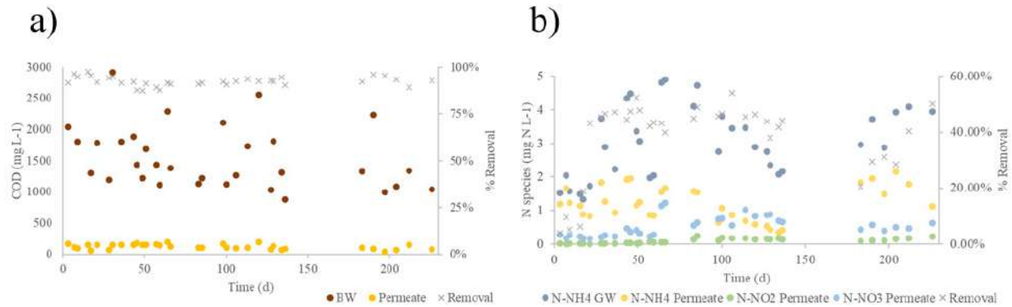

Figure 1. COD removal in AnMBR (a) and TN removal in H-MBR (b).

REFERENCES

Alvarino, T. et al. 2015.. *Water Research*, *68*, 701–709.
Alvarino, T. et al. 2018. *Science of the Total Environment*, *615*, 297–306.
Arias, A. et al. 2020. *Current Developments in Biotechnology and Bioengineering: Advanced Membrane Separation Processes for Sustainable Water and Wastewater Management - Case Studies and Sustainability Analysis*, 259–287.
Hube, S., & Wu, B. 2021. *Science of the Total Environment*, *779*, 146545.
Zhang, A. N. et al. 2021. *Nature Communications*, *12*(1), 1–11.

Decentralized hybrid wastewater treatment system for water reuse on a campsite at Costa Daurada

J. Llimós*, M. Casademont*, J. Herrero*, Q. Plana* and S. Casas*

* Eurecat, Water Air and Soil (WAS) Unit, Plaça de la Ciència, 2, 08242 Manresa, Barcelona, Spain
(E-mail: *Jordi.llimos@eurecat.org)*

Abstract
The risk of water scarcity in Spain is the highest among European countries. Wastewater reuse through decentralized systems could improve the sustainability of the water systems. Producing high-quality water effluent that can be used for a wide diversity of non-potable uses, can increase the water availability. In this context, a decentralized hybrid wastewater treatment system for water reuse is going to be implemented in the Tamarit Beach Resort Campsite at the Costa Daurada. It is expected to obtain a high-quality water for irrigation and cleaning purposes inside the campsite and a treatment system that could be applied to other similar campsite from the Mediterranean coast.

Keywords (maximum 6 in alphabetical order)
Water reuse; Decentralized system; Climate resilience; Upflow anaerobic sludge blanket

INTRODUCTION

Spain has the highest risk for water scarcity and aridification among European countries. Catalonia, in particular its coastline, is a region that struggles with the supply of potable water. Thus, since the early 2000's the Catalan government has made significant progression implementing water management strategies.

Campsites along the Catalan coast use commonly the public drinking water network for potable and non-potable uses. Alternatively, some of them used other sources, such as their own wells or rainwater tanks. Last decades, campsite resorts applied water-saving measures (WSMs) motivated by competitiveness, legitimation, and ecological responsibility (Llausàs et al., 2020). Wastewater segregation and reuse is one of the alternative and emerging approaches to cope up with sustainable and integral water management where the population faces acute water shortages (Ofori et al., 2021). However, some risks may arise when wastewater is reused. Among them, major constraints are associated with microbiological risks, and the impact of detergents and xenobiotic organic compounds and their toxic effects on the environment, on humans, and wildlife (Eriksson et al., 2002).

The wastewater treatment to be implemented depends on the reclaimed water uses and their specific requirements according to water quality standards and guidelines such as WHO and UNEP (2006); USEPA (2012); Real Decreto 1620/2007. For example, the previously studied aerobic and anaerobic biological wastewater treatment technologies including the sequencing batch reactor (SBR), the membrane bioreactor (MBR) and the upflow anaerobic sludge blanket (UASB) (Khalil & Liu, 2021) could be used to produce reclaimed water. The lower cost of anaerobic treatment compared to aerobic treatment, presents the anaerobic reactor as a suitable technology to be implemented.

In the context of the European project IMPETUS, the challenge addressed is to develop and implement, in the Tamarit Beach Resort Campsite, a decentralised hybrid water reclamation system to increase water availability for non-potable uses within the installations. The objective of the demonstration is to prove the economic, social and environmental benefits of wastewater reuse in the context of campsites on the Catalan coast.

MATERIALS AND METHODS

Lab-scale experimental design

The proposed treatment approach will be adapted to the production peaks during vacation period and weekend peaks during the mid-season. In addition, wastewater treatment will be adapted to the strict legislation for water reuse (i.e., Real Decreto 1620/2007) and the foreseen use for green zones and other cleaning purposes. Figure 1 shows the scheme for the proposed treatment. Three steps are foreseen: 1) dissolved organic carbon by UASB with ultrafiltration, 2) nutrients removal by a biofilter/NBS solution and 3) polishing step, with a disinfection. The UASB have an approximated working volume of 12 L and is coupled to a submerged ultrafiltration membrane. The concentrate of the ultrafiltration is recirculated to the anaerobic reactor in a relation of 6:1 respect the feed flowrate.

Scale-up of the treatment process on site

The proposed UASB treatment process tested at a bench-scale experiments will be implemented on the campsite installations, to treat between 0,5-1 m^3/h of wastewater. The final process design will be scaled-up from the results obtained in the bench-scale set-up maintaining the operating conditions selected during the experiments.

RESULTS AND DISCUSSION

Consumption data from the public network of the campsite

The initial data available from the campsite was used to study the seasonality of water consumption.
Water consumption is heavily dependent on the drinking water network, with a percentage that has been increasing steadily (data not sown). Furthermore, the water consumption from the public network clearly shows the seasonality of consumption and how it is highest in the summer season and lowest in the winter season (Figure 2), due to the vacation's period.

Initial characterization of the wastewater

First of all, an initial screening of 3 different point to characterize the water that will be treated was performed, as presented in table 1. Point 1 (P1) and point 2 (P2) seems to have a lower COD concentration than Point 3 (P3). The microbiological content (E.coli concentration) from the P3 is higher than P1 and P2. Also, the chloride concentration in P2 is high because some pool water is collected in this point. Due to the characterization performed, the results obtained and the amount of flow available during the year in each point, P3 water was selected to be treated.

Initial AnMBR (UASB) performance

Currently, the UASB with ultrafiltration is at the granulation stage of the biomass. To promote the granulation calcium sulfate was added in an approximated concentration of 200 mg/L Ca^{2+}. It was achieved up to 80% of COD removal during this initial stage performance. Due to that granulation has not yet been fully reached, the nutrients' removals are around 50%, but it is expected to have better nutrients removals when the granulation is achieved, and mature granules are formed. In addition, the biofilter/NBS and the disinfection steps have not been considered at the lab scale tests, and improved removal efficiencies are expected once the system is implemented on site.

Conclusions

The UASB reactor have high COD removal efficiencies even during the initial stage of the performance. When the biofilter/NBS steps coupled to the disinfection unit will be implemented it is expected to obtain a high-quality reclaimed water for self-consumption at the campsite.

Acknowledgement

The authors wish to acknowledge the Eurecat's sustainability laboratory, the Tamarit Beach Resort Campsite and the Catalan Office for the Climate change (OCCC). The work has been financially supported by the European Union's Horizon 2020 research and innovation program under grant agreement No. 101037084.

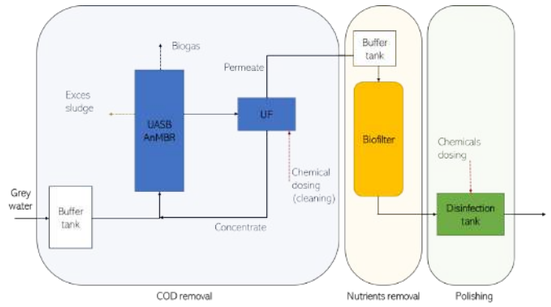

Figure 1: Proposed scheme for wastewater treatment

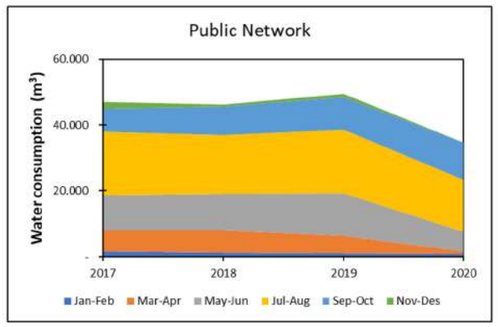

Figure 2: Water consumption from the public network of the campsite

Table 1: Initial characterization of three water points.

Parameter	P1	P2	P3
COD (mg/L)	363	296	3619
Total P (mg/L)	1,42	3,30	23,39
pH	6,96	6,97	6,34
CE (mS/cm)	1,17	8,29	2,73
Turbidity (NTU)	103,8	94,58	1521,6
TSS (mg/L)	56	240	2185
Oils and fats (mg/L)	50,8	215,7	1063,2
E.coli (ufc/ml)	959,0	7490,0	> 2,42 E+05
N Kjeldahl (mgN/L)	14,6	32,1	219
Microtox (equitox/m3)	13,1	<4	24,5
Surfactant (mg/L)	1,11	0,17	0,86
Chlorure (mg/L)	150	2350	444
Sulfate (mg/L)	22	476	114
Fosfate (mg/L)	<0,5	60	30
Nitrate (mg/L)	<0,2	<2,0	<0,5
Amonia (mg/L)	11	27	107

REFERENCES

Eriksson, E., Auffarth, K., Henze, M., & Ledin, A. (2002). Characteristics of grey wastewater. Urban Water, 4(1), 85–104. https://doi.org/10.1016/S1462-0758(01)00064-4
Khalil, M., & Liu, Y. (2021). Greywater biodegradability and biological treatment technologies: A critical review. International Biodeterioration & Biodegradation, 161, 105211. https://doi.org/10.1016/J.IBIOD.2021.105211
Llausàs, A., Padullés Cubino, J., Ribas Palom, A., Padullés, J., Anna, C., & Palom, R. (2020). Small and medium sized accommodation managers and opportunities for water conservation. PASOS. Revista de Turismo y Patrimonio Cultural, 18(1), 129–142. https://doi.org/10.25145/J.PASOS.2020.18.008
USEPA, 2012. Guidelines for Water Reuse. Environmental Protection Agency, Office of Wastewater Management, Office of Water, Washington, D.C.
Ofori, S., Puškáčová, A., Růžičková, I., & Wanner, J. (2021). Treated wastewater reuse for irrigation: Pros and cons. Science of The Total Environment, 760, 144026. WHO, U.N.E.P., 2006. Guidelines for the Safe Use of Wastewater, Excreta and Greywater, WHO Policy and Regulatory Aspects 1.
Boletín Oficial del Estado, Real Decreto 1620/2007, de 7 diciembre por el que se establece el régimen jurídico de la reutilización de las aguas depuradas. Nº 294 de 8 diciembre 2007, 2007, p. 50639.

Biocarriers-facilitated Gravity-driven Membrane Reactor for Decentralized Wastewater Treatment under Cold Climate

Selina Hube, Ihtisham Ul Haq Shami, Bing Wu

Faculty of Civil and Environmental Engineering, University of Iceland, Hjardarhagi 2-6, IS-107, Reykjavik, Iceland; (E-mail: *seh34@hi.is; iuh1@hi.is; wubing@hi.is)*

Abstract

This study investigated the effects of reactor configuration, operation temperature, and periodically cleaning protocol on the performance of biocarrier-facilitated gravity-driven membrane (GDM) reactors in treating municipal wastewater. The results indicated that (1) the cake layer fouling was predominant, regardless of reactor configuration and operation conditions; (2) decreasing operation temperature had negligible effect on fouling resistance distribution patterns and permeate quality; (3) in the presence of periodic cleaning (at 50°C), the cleaning effectiveness followed a sequence as ultrasonication-enhanced water flushing > two-phase flow cleaning > chemical-enhanced water flushing > water flushing, regardless of GDM operation temperature. Furthermore, the wastewater treatment costs of the GDM reactors were estimated at ~0.3 Euro/m^3, which was lower than that of conventional membrane bioreactors under lower population scenarios.

Keywords (maximum 6 in alphabetical order)

Biocarriers; Gravity-driven membrane filtration; Low temperature; Membrane fouling; Periodic membrane cleaning; Permeate quality

INTRODUCTION

Recently, gravity-driven membrane (GDM) filtration has received great attention as an alternative decentralized wastewater treatment process. The advantages of the GDM process include that (1) it can produce superior treated water due to high membrane separation efficiency; (2) it is an economic process due to its lower capital cost (no permeate suction pump) and operation cost (without requiring physical and chemical cleaning) compared to the conventional activated sludge process and other membrane processes such as membrane bioreactors (MBRs) (Pronk et al., 2019).

However, a major challenge of GDM-based wastewater treatment process is its low permeate flux (< 5 L/m^{2}h without applying any cleaning protocols) due to limited driving force (< 1 m water head). To further improve GDM membrane performance and permeate quality, the biocarriers (such as granular activated carbon) were integrated with the GDM systems (Lee et al., 2019, 2021), aiming to pre-treat the wastewater before its permeating the membrane. However, there is still a lack of knowledge on the optimization of periodic cleaning protocols and fundamental mechanisms relating to flux enhancement in GDM systems operated under low-temperature conditions. Especially, the economic feasibility of GDM systems with periodically chemical cleaning has not been well illustrated.

This study aims to investigate membrane performance and permeate quality in lava stone facilitated GDM systems under combined effects of temperature and periodic cleaning. Several cleaning strategies at various cleaning frequencies were applied, such as geothermal water flushing, two-phase flow cleaning, ultrasonication- and chemical-enhanced physical cleaning. The membrane fouling mechanism was illustrated by fitting experimental permeate flux data with a previously reported constant pressure filtration model. The effects of temperature on biodegradation behaviours of biofilms and membrane separation efficiency were illustrated by periodically examining water quality in the GDM reactor and permeate.

MATERIALS AND METHODS

Reactor setup and operation conditions

In Stage 1, the effect of biocarrier types on the GDM performance was investigated. In detailed. R1, R2, R3 (Figure 1) with microfiltration membrane modules (0.2 µm) were operated at ~10°C in parallel, with periodic chemical (NaClO; 0.5%, 50°C) cleaning (60 min per 3-4 days). Synthetic fibers (~0.93 m), lava stones (~1 kg), and sands (~1 kg) were used as biocarriers for R1, R2, and R3, respectively. The water head was variable at 0.22-0.25, 0.22-0.25 m, and 0.24-0.34 m for R1, R2, and R3, respectively. In Stage 2, two identical R4 were setup and operated at ~8°C and ~22°C, respectively, to investigate the effect of temperature and periodic cleaning approaches on the GDM performance. Lava stones were used as biocarriers and microfiltration membrane (0.08 µm, with 0.6 m water head) was placed in the filtration cell. The operation conditions were described in Table 1. The feed wastewater (taken from wastewater treatment plant at Klettagarður, Reykjavík, Iceland). was delivered to the tank via a feed pump, and its flowrate was periodically regulated based on permeate flowrate. The permeate was collected and weighted periodically by a digital balance.

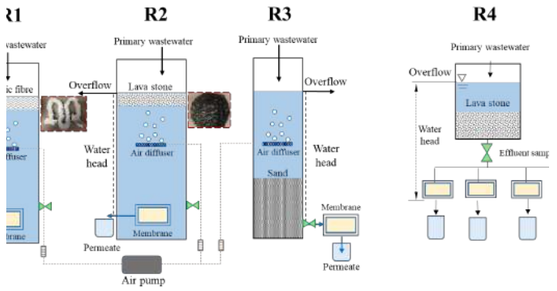

Figure 1. Schematic diagram of the GDM reactors.

Biofilm reactor operation time	Membrane cleaning condition	Membrane module			
		M1	M2	M3	M4
Day 0-15	**Phase I:** Geothermal water flushing (50°C)	No cleaning	10 min	30 min	60 min
Day 16-32	**Phase II:** Air sparging-enhanced geothermal water flushing (50°C)	0.3 L/min (60 min)	0.3 L/min (30 min)	0.6 L/min (30 min)	0 L/min (30 min)
Day 35-52	**Phase III:** PMS in geothermal water (50°C) for 30 min flushing	10 mg/L PMS	50 mg/L PMS	100 mg/L PMS	0 mg/L PMS
Day 56-66	**Phase IV:** No cleaning	No cleaning	No cleaning	No cleaning	No cleaning
Day 70-86	**Phase V:** Ultrasonication (50°C)	10 min	30 min	60 min	No cleaning
Day 90-108	**Phase VI:** Ultrasonication with flushing (50°C) for 30 min	Ultrasonication	Ultrasonication-enhanced geothermal water flushing	Ultrasonicated geothermal water flushing	No cleaning
Day 109-128	**Phase VII:** Comparison of physical and chemical cleaning (50°C, 30 min)	PMS (50 mg/L) in geothermal water flushing	Ultrasonication + geothermal water flushing	Air sparging (0.3 L/min) + geothermal water flushing	No cleaning

Table 1. A summary of membrane cleaning protocols in R4.

RESULTS AND DISCUSSION

The water qualities of feed, reactor effluent and membrane permeate in R4 are summarized in Figure 3. Both biofilm reactors achieved comparable COD removals, TN removals, and TSS removals, but increasing temperature significantly promoted biodegradable organic (BOD_5) removals in the biofilm reactors (56 ± 27% at 22°C *vs.* 47 ± 26% at 8°C, p<0.05).

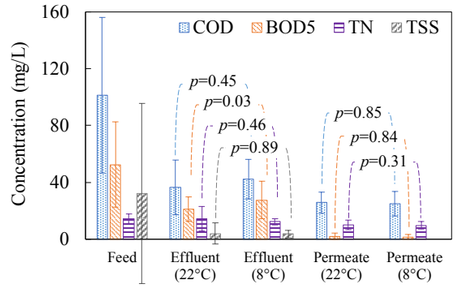

Figure 3. Water quality in feed, effluent and permeate (n=10-15).

The water production cost of R1-R3 ranged from 0.31 to 0.37 EUR/m^3, in which aeration energy cost (~70-83%) and membrane cost (~12-28%) were major cost items (Figure 4a). In MBR systems, the water production cost significantly dropped with population size and appeared to be constant above ~500 population condition, while in GDM reactors, there was almost no influence of population size on the water production cost (Figure 4b).

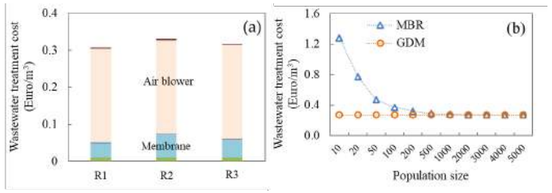

Figure 4. (a) Water production cost of R1-R3; (b) Comparison of water production cost in GDM and MBR systems.

As shown in Figure 5, extending cleaning duration benefited for fouling reduction. The cleaning effectiveness followed a sequence as "ultrasonication-enhanced water flushing" (~87% at 22°C and ~88% at 8°C) > "two-phase flow cleaning" (~67% at 22°C and ~81% at 8°C) > "chemical-enhanced water flushing" (~32% at 22°C and ~31% at 8°C). The operation temperature of the GDM system displayed insignificant effects on the fouling removal ratio (52 ± 21% at 22°C and 54 ± 23% at 8°C; p>0.05) and water productivity (0.28 ± 0.08 L/day at 22°C and 0.28 ± 0.08 L/day at 8°C; p>0.05). Cake layer resistances were dominant (>95%) in the GDM systems with periodic cleaning.

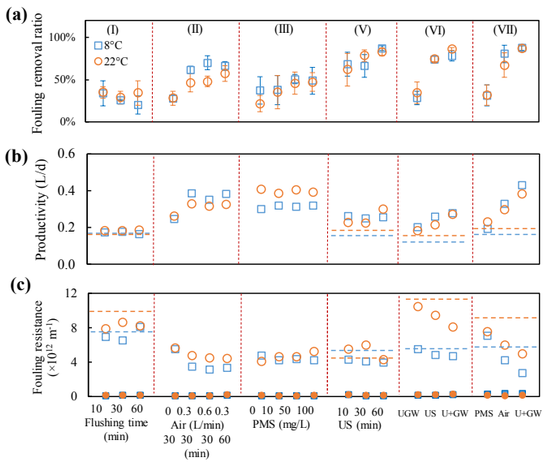

Figure 5. (a) Fouling removal ratio, (b) water productivity, and (c) fouling resistance (non-fill symbols represent cake layer fouling, solid-fill symbols represent irreversible fouling) in R4 with different periodic cleaning protocols. The dash line indicated the level in the control membrane module without periodic cleaning. "UGW" represents ultrasonicated geothermal water flushing; "US" represents ultrasonication; "U+GW" represents ultrasonication-enhanced geothermal water flushing.

REFERENCES

Pronk, W., Ding, A., Morgenroth, E., Derlon, N., Desmond, P., Burkhardt, M., Wu, B., Fane, A.G. 2019 Gravity-driven membrane filtration for water and wastewater treatment: A review. *Water Research* **149**, 553-565.

Lee, S., Badoux, G.O., Wu, B., Chong, T.H. 2021 Enhancing performance of biocarriers facilitated gravity-driven membrane (GDM) reactor for decentralized wastewater treatment: Effect of internal recirculation and membrane packing density. *Science of the Total Environment* **762**, 144104.

Lee, S., Sutter, M., Burkhardt, M., Wu, B., Chong, T.H. 2019 Biocarriers facilitated gravity-driven membrane (GDM) reactor for wastewater reclamation: Effect of intermittent aeration cycle. *Science of the Total Environment* **694**, 133719.

Freshwater microbial communities as a potential nature-based solution for wastewater tertiary treatment in small facilities

L. Bertrans-Tubau*, M. Abril*, J. Lopez-Doval*, S. Ponsá*, A.C. Suñer**, V. Salvadó**, M. Hidalgo**, L. Proia*
* BETA Technological Center- University of Vic- Central University of Catalonia, Carretera de Roda 70, 08500, Vic, Barcelona, Spain
(E-mail: *lluis.bertrans@uvic.cat*)
** Department of Chemistry, University of Girona, Campus Montilivi, 17071, Girona, Spain

Abstract

The combination of micro and macro-scale experimental approaches focusing on the role of natural freshwater microbiota was assessed as a highly nature-based solution to be implemented in wastewater tertiary treatment in small facilities (<10,000 PE). Both experiments were focused to evaluate removal efficiencies of nutrients, fecal bacteria (*E.coli*) and contaminants of emerging concern. Additionally, we tested the contribution of natural inoculum affected by treated wastewater release to reduce economical costs in the upscaling process that under laboratory-controlled conditions performed irrelevant differences compared to non-inoculum effect. Previous results demonstrated high removal capacity on nutrients (over 65% in laboratory conditions versus 25-70% in a real scenario).

Keywords

Freshwaters; microbiota; nature-based solution; small facilities; wastewater treatment

INTRODUCTION

The treatment of sewage waters has improved significantly in last decades achieving a general reduction of the impacts generated by wastewater (WW) release to the environment. However, treated and untreated sewage waters are still one of the main sources of nutrients and pollutants to the environment worldwide. Current technologies adopted in wastewater treatment facilities generally focus on the reduction of suspended solids and organic matter to achieve the reduction of biological oxygen demand. In some cases, an additional step follows the secondary treatment with the main goal to reduce the high amount of nitrogen (N), phosphorus (P) and carbon (C) still present in treated sewage water. Small water treatment facilities rarely include this additional treatment step because of financial and infrastructural constraints. Moreover, this kind of wastewater treatment plant (WWTP) normally release its treated effluents to low-order streams with reduced dilution capacity. This can be a relevant issue particularly in arid and semi-arid zones (like Mediterranean area) subjected to long dry period that provoke water scarcity problems and frequent droughts in streams. Consequently, it is not rare to have streams in which the total amount of flowing water comes from WWTP effluents during droughts. It is therefore important to investigate the potential development of innovative low-cost technologies which implementation could be assumed by managers of small WWTP facilities in order to improve the quality of the treated wastewaters released to the ecosystem. This study aims to investigate the efficiency of freshwater microbial communities as potential nature-based solution for tertiary treatment in small WWTP facilities. To achieve this aim, two experiments were carried out at microcosms and macrocosm scale in order to test the removal efficiency of nutrients loads and fecal bacteria released to the aquatic environment. We hypothesize that microbial communities could have the capacity to obtain high nutrient removal in both conditions investigated. We also expected a rapidly growth of microbiota associated to maximal removal efficiency performance. These steps were essential before considering its implementation in a real scenario.

MATERIALS AND METHODS

We carried out two different experiments, one in microcosms under strictly controlled conditions (laboratory-scale) and the other in a pilot plant (mesocosm) installed in a WWTP. In the first case, a factorial experimental design was performed with benthic (B) and planktonic (P) compartments, separately and in combination (B+P), treating a secondary effluent of a WWTP (<10,000 PE) for 39 days. The effect of the addition of natural inoculum from an ecosystem affected by treated WW release was also assessed (BI, PI and BI+PI). In the second experiment, the pilot plant consisted in two connected modules in which benthic and planktonic microbial communities were growing for 49 days, respectively. In both conditions, the sampling collection was performed twice per week. The bioreactor received water from the effluent of a WWTP to reduce nutrients, fecal bacteria, and contaminants of emergent concern (CECs) before its release to the freshwater receiving ecosystem.

In both experiments, different water quality indicators (nutrients such as $N\text{-}NH_4$, $N\text{-}NO_3$, $N\text{-}NO_2$, TDN, $P\text{-}PO_4$, TDP and TP, faecal bacteria (*E.coli*) abundance, and CECs) were monitored to calculate and compare the removal efficiency of the respective bioreactor. A set of biological parameters of benthic and planktonic communities (total biomass (OM), algal biomass (Chlorophyll-*a*), microbial composition and photosynthetic efficiency) were also monitored simultaneously to be related with the removal performance in the bioreactor. The hydraulic retention time (HRT) was 3 and 1.6 days in microcosm and macrocosm experiments, respectively.

RESULTS AND DISCUSSION

Preliminary results were focused on phosphorus and nitrogen removal efficiencies in laboratory and WWTP conditions.

Laboratory bioreactor efficiency (microcosms)

Total phosphorus (TP) and total dissolved nitrogen (TDN) were strongly reduced over time in benthos (B) and combination with plankton reactors (B+P) in which the lowest removal efficiencies were obtained on WW impacted inoculum (BI and BI+PI) (>50%) (Figure 1).

Respect to biotic indicators we specifically focused on benthic algal biomass (which resulted highly correlated with total biomass $r = 0.81$; $p < 0.001$). In general, a significant negative non-parametric relation was obtained between chlorophyll-*a* and total phosphorus concentration in most of the treatments highlighting an important effect of algal biomass over the reduction of phosphorus (Figure 2.a) that was not detected for nitrogen reduction (Figure 2.b).

Macroscale pilot bioreactor optimisation

In real WWTP conditions high reduction of *E.coli* and nitrogen was observed (84.7 ± 30.8% and 72.5 ± 9.3% respectively) compared to phosphorus (23.8 ± 29.4%). Benthic algal biomass presented a clear increment in the first two weeks with a degradation of their composition after a month of the system operation. However, in the planktonic compartment the algal biomass peaked after two weeks and the gradually decreased until the end of the experiment (Figure 3). Additionally, the benthic algal biomass did not show any significant correlations with TDN and TDP concentrations. Nevertheless, in the planktonic compartment the increment of nitrogen was related to higher concentration of algal biomass (Figure 4).

Upscaling the process should be the last step before the implementation of this nature-based solution in small WWTPs, specifically below 10,000 PE in which European Legislation was less restrictive (European Commission 1998). Further research in incrementing the treated WW capacity of this bioreactor was required before its implementation in real conditions.

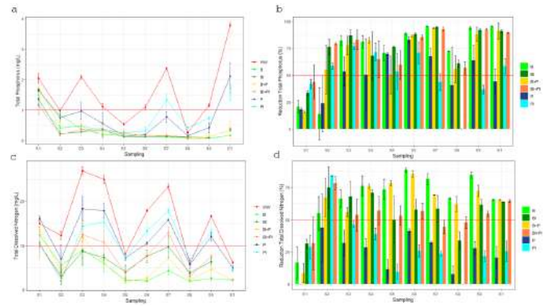

Figure 1. Total phosphorus and total dissolved nitrogen concentration over different sampling dates (a,c), red horizontal line fixed the limit of urban wastewater release by 98/15/CE UE Commission Directive of 27th February,1991. Reduction of total phosphorus and total dissolved nitrogen over different sampling dates (b,d), red horizontal line fixed the 50% attenuation efficiency of each nutrient.

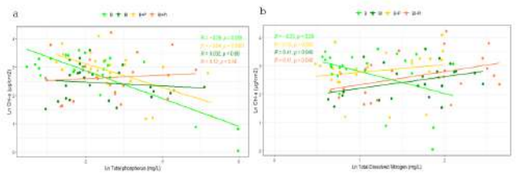

Figure 2. Lineal correlation of ln chlorophyll- *a* and ln total phosphorus (a) and ln chlorophyll- *a* and ln total dissolved nitrogen (b) with different benthic compartments in both cases with the auto determination coefficient and *p*-value.

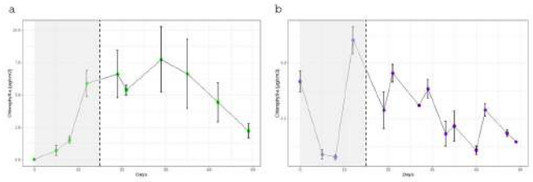

Figure 3. Chlorophyll- *a* represented by days in benthos (a) and plankton (b) compartments in the macrocosm scale experiment. Grey transparency related to the colonization phase of benthos and plankton communities.

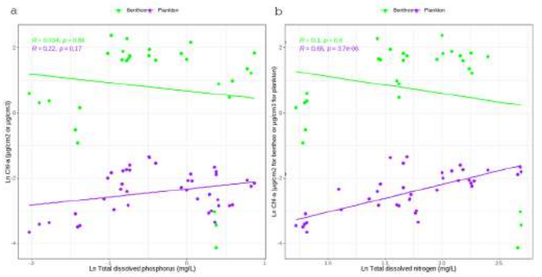

Figure 4. Lineal correlation of ln chlorophyll- *a* and ln total dissolved phosphorus (a) and ln chlorophyll- *a* and ln total dissolved nitrogen (b) with benthic and planktonic compartments in both cases with the auto determination coefficient and *p*-value.

REFERENCES

European Commission. UWWTD - Amendment 1998 (98/15/EC). *Off J Eur Communities* 1998:29–30.

WORKSHOPS

Workshop I.
Sewer Epidemiology

Chairs: Laura Guerrero Latorre (ICRA) & Jorge Rodriguez (Khalifa University)

Development of a method to detect recent human adenovirus F41 variants in wastewater: Is it linked to the new acute hepatitis? Zeynep Cetecioglu, KTH

SARS-CoV-2 surveillance in the wastewater of Stockholm and Malmö: the Swedish perspective. Mariel Perez-Zabaleta, KTH

Surveillance of SARS-CoV-2 in sewage from buildings housing residents with different vulnerability levels. Anna Pico, ICRA

Workshop II.
Urban Hydrosocial Cycle: Why should engineers care?

Chairs: Alexandra Popartan (LEQUIA-UdG) & Josep Pueyo (ICRA)

Assessment of flood vulnerability through a multidimensional index. Ana Noemi Gomez Vaca. Univ. Girona

Eco-cultural technologies for rural and Maori community on-site wastewater treatment in New Zealand, Rupert Craggs, Nat. Inst. Water and Atmospheric Research NZ

Socio-economic criteria for preventing and controlling phosphorus pollution from municipal wastewater effluents. Edgar Martin Hernandez. Univ. Laval

A hydrosocial approach to domestic water users satisfaction through Agent-Based Modelling. Pol Vidal Lamolla. LEQUIA-UdG

Roadmap and strategic routes to mitigate micropollutant occurrence in surface water bodies through WWTP upgrade. Morgan Abily. ICRA

WORKSHOPS

WI.

Sewer Epidemiology

Development of a method to detect recent human adenovirus F41 variants in wastewater: Is it linked to the new acute hepatitis?

Mariel Perez-Zabaleta[a], Cecilia Williams[b], Zeynep Cetecioglu[a]
a Department of Industrial Biotechnology, KTH Royal Institute of Technology, AlbaNova University Center, SE-10691, Stockholm, Sweden.
b Department of Protein Science, KTH Royal Institute of Technology, Science for Life Laboratory, Solna, Sweden.
zeynepcg@kth.se (Z. Cetecioglu)

Abstract
Human adenovirus type F-41 has been pursued as one of the potential reasons for the new acute hepatitis cases of unknown cause in young children. Tracking its spread in the population using wastewater can help clinical investigations. In this study, methods to detect human adenovirus type F and specifically type F41 were designed and implemented to quantify the amount of these pathogens in wastewater. An assay based on RT-qPCR reaction using TaqMan technology and primers targeting the three main capsid genes of adenoviruses: hexon, penton, and fiber, was designed. The hexon primers were specific to adenovirus F41, while fiber primers could quantify both adenoviruses, F40 and F41. Wastewater samples from Stockholm were used to validate the designed assay.
Our results can contribute to a better understanding of the possible causes of new cases of acute hepatitis.

Keywords
Acute hepatitis, human adenovirus F41 (HAdV-F41), human adenovirus F40 (HAdV-F40), wastewater-based epidemiology (WBE).

INTRODUCTION

Human adenoviruses are nonenveloped DNA viruses and are classified into seven species (A to G) and at least 104 genotypes [1]. Adenoviruses can cause respiratory illness, gastroenteritis, conjunctivitis, or cystitis in young children [2]. Adenovirus type F (40 and 41) usually causes acute gastroenteritis in children and cases of hepatitis have been reported in immunocompromised children associated with adenovirus type 41 (HAdV-F41) infection [2].

A sudden increase in acute hepatitis cases of unknown cause was reported to the World Health Organization (WHO) in 2022. Between April 5 and July 8, 2022, 1 010 probable cases and 22 deaths were reported by 35 countries, including five pediatric patients with severe hepatitis of unknown origin identified at a children's hospital in Alabama, U.S., in early October 2021 [3]. Of the 1 010 probable cases, 5% of the children required a liver transplant, and almost half of the cases (48%) were reported from European countries. The children were under 16 years old, had liver inflammation (including some with liver failure), and tested negative for hepatitis A to E (WHO, 2022). The cases were not associated with travel, and most children tested positive for adenovirus, in which type 41 was predominant. Of 251 cases tested for adenovirus in the UK, 68% gave positive results against this pathogen [4]. In Alabama, HAdV-F41 was detected in all five infected patients [5].

Wastewater-based epidemiology (WBE) is a useful tool to detect the occurrence of viruses in a population, as viruses do not possess the ability to grow outside their host and their concentration in wastewater can be representative of the infection rate [6]. Simultaneous detection of different adenoviruses genotypes was previously investigated to determine the removal efficiency of "generic" adenoviruses through the wastewater treatment process [7–9]. Few studies were able to specifically identify HAdV-F41 [10–12], and previously designed primers to detect HAdV-F41 can be less specific for emergent variants. According to Götting and colleagues (2022), HAdV-F41 has evolved significantly over the past decade, which possibly has resulted in altered virulence of this pathogen. The emergence of a novel strain of HAdV-F41 could be suspected, which may be causing hepatitis.

In this study, the gene sequences of these three major capsid genes, hexon, penton and fiber, were used to design the primers and probes for the quantification of adenovirus type F by RT-qPCR. The difference between the specificity of the primers was tested. In silico and in vitro validations were performed and wastewater samples from Stockholm were used to validate the designed methods.

MATERIALS AND METHODS

Primers and probes targeting the main capsid genes of adenovirus: hexon, penton and fiber, were designed using recently published genome sequences of HAdV-F41 variants current in 2021 and 2022: MW567962.1 (March 2021), ON532826.1 (May 2022) and OP174922.1 (August 2022). The primers were analyzed in silico using Basic Local Alignment Tool (BLAST) from the National Center for Biotechnology Information (NCBI) and the sequences of the three primer sets were confirmed to match HAdV-F41. Then, the primer sequences were aligned against twenty HAdV-F41 species and two HAdV-F40 species from NCBI GenBank. The alignments were performed using DNASTAR Bioinformatics Software. Subsequently, the hexon, penton, and fiber primers were evaluated against thirteen genotypes of human adenovirus for species A, B, C, D and E and three positive controls of adenovirus type F. The adenovirus species were provided by the Norrlands Universitetssjukhus (Klinisk Mikrobiologi, Umeå, Sweden).

RT-qPCR assays were performed using TaqMan Reliance One-Step Multiplex Supermix (BioRad, Cat # 12010221). 1 µL of 20 mg/ml Bovine Serum Albumin (BSA) (Thermo Scientific, Cat # B14) was added to reduce PCR inhibitors and enhance efficacy, for a final reaction volume of 20 µL. Reactions were considered positive if the cycle threshold (Ct) was below 42 cycles. Amplifications were carried out on the FAM channel. Standard curves were created using constructed plasmids containing appropriate regions for hexon, penton, and fiber (IDT, Custom MiniGene 25-500 bp).

Wastewater samples from Stockholm were used to validate the method. Approximately 500 ml of wastewater samples from each inlet were taken over a period of 24 hours from Monday to Tuesday, using a flow-proportional composite sampler. Wastewater samples were transported to the laboratory on ice and kept at 4°C until further analyses. Wastewater sample concentration and TNA extraction were performed using Maxwell RSC Enviro TNA Promega Kit and Maxwell RSC Instrument (Promega Biotech AB, Sweden). Two independent replicates were analyzed for each sample and tap water was used as a negative control for viral concentration and DNA extraction steps. The PCR amplicons from the wastewater samples obtained after RT-qPCR were purified using GeneJET PCR Purification Kit (ThermoFisher Scientific, Cat # K0701). Two pure PCR products per sample were sent for Sanger sequencing, which has been performed by Eurofins.

RESULTS AND DISCUSSION

In silico and in vitro validation of primer sets

The primers and probes were designed to be specific to adenovirus type F. To test their specificity, different adenovirus species (A, B, C, D and E) were used as negative controls. The three sets of primers (hexon, penton and fiber) gave negative results for species A to E, confirming that the primers are specific towards HAdV-F. Subsequently, the primers were in vitro tested against one positive control of HAdV-F40 (strain HoviX) and two variants of HAdV-F41 (strain Tak and strain isolated from a Swedish patient). Fiber and penton primer sets detected the HAdV-F40 (strain HoviX), while hexon primers gave negative results, showing no specificity towards HAdV-F40 (Figure 1a). The primers targeting the hexon region could not detect adenovirus F41 (strain Tak) (Figure 1b). However, the HAdV-F41 variant previously isolated from a Swedish patient was detected by all three primer sets, which quantified similar amounts of the virus, with no significant difference (P-value = 0.35, Figure 1c). The validation of primers in silico and in vitro showed that hexon primers are selective for recent HAdV-41 strains evolved in lineage 2. Fiber and penton primers can be used to detect both HAdV-40 and HAdV-41 variants. However, penton is less sensitive against HAdV-40 than fiber primers, but both primer sets can detect similar amounts of HAdV-41 strains.

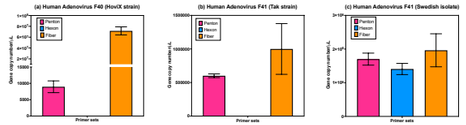

Figure 1. Analysis of positive controls for human adenovirus F40 and F41 using primers-sets for hexon, penton and fiber regions. Quantification of HAdV-F40 and F41 determined by RT-qPCR analysis of the hexon, penton or fiber region in three controls (a) Prototype HAdV-F40 HoviX strain (b) Prototype HAdV-F41 Tak strain (c) and an HAdV-F41 strain isolated from a patient in Sweden.

Validation of primer sets using wastewater samples

After in silico and in vitro validation, the primer sets were evaluated with raw wastewater from Stockholm. The results showed that primers targeting the hexon region detected lower amounts of adenovirus compared to penton or fiber primers (Figure 2). These results are in line with the outcomes obtained in the specificity study since hexon primers were more specific to HAdV-41 lineage 2 and did not detect HAdV-F40 or HAdV-F41 Tak strain. Fiber primers detected higher levels of adenovirus compared to penton primers in all the samples (Figure 2b). Fiber and penton assays detected the same trends of increasing or decreasing amounts of virus, whereas the hexon primers detect a different trend. The fiber and penton assays detected about 100 times more viral DNA copies (around 10^{17}) than the hexon primer (10^{15}). A recent study showed an increasing detection of HAdV-F40/41 in wastewater, which correlates to the increasing number of clinical cases in Northern Ireland [14]. In this study, statistical correlations were not performed due to the lack of clinical surveillance of adenovirus in Sweden.

Furthermore, Hexon, penton and fiber PCR products were analyzed by Sanger sequencing. The obtained sequences were compared in the NCBI databases by BLAST and Hexon PCR products showed specificity for HAdV-F41. In the case of penton and fiber, the DNA sequences were not specific to HAdV-F41 and a double detection of HAdV-F40 and HAdV-F41 can be suspected.

Clinical surveillance of adenovirus in the population is challenging because symptoms may not always be specific and laboratory tests are only performed after severe symptoms. Therefore, WBE could be a valuable tool for community surveillance of HAdV-F41 and for monitoring the newly evolved variants by sequencing. Furthermore, this study confirms the growing evidence that WBE can be used as an effective public health strategy for the surveillance of pathogens in addition to SARS-CoV-2.

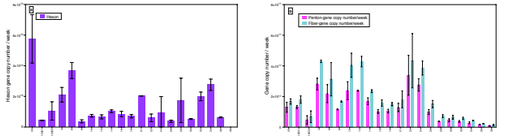

Figure 2. Quantification of HAdV- F40 and F41 using primers-sets for hexon, penton and fiber regions in wastewater samples. Gene copy numbers of HAdV-F41 and F40 per µL were determined by targeting (a) hexon region (purple), (b) penton (pink) and fiber (green) regions. Two biological replicates were analyzed for each sampling point.

REFERENCES

1. HAdV Working Group. Human Adenovirus genotypes. http://hadvwg.gmu.edu/ (2022).
2. Ikner, L. A. & Gerba, C. P. Adenoviruses. in *International Encyclopedia of Public Health (Second Edition)* (ed. Quah, S. R.) 5–9 (Academic Press, 2017). doi:https://doi.org/10.1016/B978-0-12-803678-5.00004-7.
3. WHO. Severe acute hepatitis of unknown aetiology in children - Multi-country. https://www.who.int/emergencies/disease-outbreak-news/item/2022-DON400 (2022).
4. UK Health Security Agency. *Investigation into acute hepatitis of unknown aetiology in children in England.* (2022).
5. Baker, J. M. *et al.* MMWR, Acute Hepatitis and Adenovirus Infection Among Children — Alabama, October 2021–February 2022. (2021) doi:10.1128/CMR.5.3.262.
6. Xagoraraki, I. & O'brien, E. Wastewater-Based Epidemiology for Early Detection of Viral Outbreaks. (2020) doi:10.1007/978-3-030-17819-2_5.
7. Quintão, T. S. C. *et al.* Detection and molecular characterization of enteric adenovirus in treated wastewater in the Brazilian Federal District. **3**, 691 (2021).
8. Carducci, A. *et al.* Study of the viral removal efficiency in a urban wastewater treatment plant. *Water Science & Technology* (2008) doi:10.2166/wst.2008.437.
9. Hata, A., Kitajima, M. & Katayama, H. Occurrence and reduction of human viruses, F-specific RNA coliphage genogroups and microbial indicators at a full-scale wastewater treatment plant in Japan. (2012) doi:10.1111/jam.12051.
10. Heim, A., Ebnet, C., Harste, G. & Pring-Åkerblom, P. Rapid and quantitative detection of human adenovirus DNA by real-time PCR. *J Med Virol* **70**, 228–239 (2003).
11. Kuo, D. H. W., Simmons, F. & Xagoraraki, I. A new set of PCR assays for the identification of multiple human adenovirus species in environmental samples. *J Appl Microbiol* **107**, 1219–1229 (2009).
12. Tiemessen, C. T. & Nel', M. J. *Detection and typing of subgroup F adenoviruses using the polymerase chain reaction. Journal of Virological Methods ELSEVIER Journal of Virological Methods* vol. 59 (1996).
13. Götting, J., Cordes, A. K., Steinbrück, L. & Heim, A. Molecular Phylogeny of human 1 adenovirus type 41 lineages 2 3. (2022) doi:10.1101/2022.05.30.493978.
14. Reyne, M. I. *et al.* Detection of human adenovirus F41 in wastewater and its relationship to clinical cases of acute hepatitis of unknown aetiology. *Science of The Total Environment* **857**, 159579 (2023).

SARS-CoV-2 surveillance in the wastewater of Stockholm and Malmö: the Swedish perspective

Mariel Perez-Zabaleta[a,b], Amena Archer[c], Kasra Kathami[a,b], Mohammed Hakim Jafferali[c], Prachi Nandy[b], Merve Atasoy[b], Madeleine Birgersson[c], Cecilia Williams[c,1], Zeynep Ceteciogl[a,b]
a Department of Industrial Biotechnology, KTH Royal Institute of Technology, AlbaNova University Center, SE-10691, Stockholm, Sweden.
b Department of Chemical Engineering, KTH Royal Institute of Technology, SE-10044, Sweden.
c Department of Protein Science, KTH Royal Institute of Technology, Science for Life Laboratory, Solna, Sweden

Abstract
Wastewater-based epidemiology (WBE) has been used to track the spread of SARS-CoV-2 in several countries since the beginning of the pandemic. SARS-CoV-2 levels were monitored from April 2020 in Stockholm and August 2021 in Malmö, providing extensive information about the spread of Covid-19 in two of the biggest cities of Sweden.
During this long-term surveillance, two sampling protocols, two RNA concentration/extraction methods, two calculation approaches, and normalization to the RNA virus Pepper mild mottle virus (PMMoV) are presented and discussed. In addition, a storage condition study was performed, and we demonstrate that the decay of virus RNA (Nucleocapsid gene and PMMoV) was lower when glycerol was added to the wastewater before storage at -80°C. Furthermore, SARS-CoV-2 variants were detected using hpPCR and next-generation sequencing. Our results can contribute to a greater understanding of the multiple factors affecting SARS-CoV-2 surveillance in wastewater and provide valuable information that can be used in further investigations and by health public agencies to incorporate WBE as a prediction tool for possible future outbreaks and in preparations for future pandemics.

Keywords
Covid-19; Sewage surveillance; Severe Acute Respiratory Syndrome Coronavirus 2 (SARS-CoV-2); Wastewater-based epidemiology (WBE).

INTRODUCTION

The emergence of Severe Acute Respiratory Syndrome Coronavirus 2 (SARS-CoV-2), known as Coronavirus Disease 2019 (Covid-19), has been one of the major threats to public health in the recent century. This virus was initially identified in Wuhan, China in December 2019, and in March 2020, COVID-19 was categorized as a global pandemic by the World Health Organization(WHO, 2020). The rapid spread of SARS-CoV-2 resulted in unprecedented measures imposed by different governments such as lockdowns, closure of borders and travel restrictions. While the Swedish approach mostly relied on voluntary social distancing guidelines, creating a unique scenario compared to most parts of the world. The first case of Covid-19 in Sweden was confirmed in the city of Jönköping on February 4, 2020, and since then 2,7 million confirmed cases have been reported by the Swedish Public Health Agency. The Swedish capital, Stockholm, accounts for 23% and Malmö for approximately 10% of the total cases of Covid-19 in Sweden (Swedish Public Health Agency, 2022).

The concept of wastewater-based epidemiology (WBE) was initially perceived in 2001(Daughton C.G. and Jones-Lepp T.L., 2001) and applied in 2005 for the detection of illegal substance uses (Zuccato et al., 2005). WBE has been successfully implemented as a tool to grasp the circulation of viruses in previous outbreaks and during the Covid-19 pandemic, WBE has become an important tool to track Covid-19 prevalence in a population and approximately 72 countries (COVIDPoops19, 2021) implemented it as routine monitoring.

In this study, we present the outcome and analysis of long-term monitoring of SARS-CoV-2 in municipal wastewater of Stockholm and Malmö, where no stringent lockdowns or restrictive methods were enforced. Moreover, we also present the impact of sample storage conditions on the SARS-CoV-2 stability over prolonged time periods as this is one of the unsolved challenges of WBE. Furthermore, hpPCR and next-generation sequencing were used to analyze the different variants of concern for SARS-CoV-2. The outcomes of this long-term project can provide fruitful lessons on the application of WBE for the potential emergence of other public health challenges in the future.

MATERIALS AND METHODS

Long-term monitoring of the wastewater of Stockholm was performed for more than 33 months while Malmö wastewater has been monitored for more than 16 months. Stockholm is Sweden's capital and largest city with a population of approximately 1.6 million. Malmö is the third-largest city in Sweden, with a population of 350 647.
For Stockholm, samples are received from three different municipal wastewater treatment plants (WWTP), Stockholm Vatten och Avfall Bromma (377 500 inhabitants), Stockholm Vatten och Avfall Henriksdal (862 100 inhabitants), and Käppala WWTP (700 000 inhabitants). For Malmö, weekly samples are received from VA SYD (350 000 inhabitants).

Approximately, 500 ml of raw wastewater samples (prior to any biological or chemical treatment) from each WWTP were transported to the laboratory on ice. During the monitoring period, two sampling protocols were used. In the first protocol, an equal volume of flow-proportional-composite samples was collected each day for one week, stored at 4°C and then mixed prior to transfer to the laboratory. In the second protocol, representative samples (500 ml) were taken over a period of 24 hours from Monday to Tuesday every week, using flow-proportional composite samplers, which were flow compensated.

Two different protocols were used and compared for SARS-CoV-2 concentration and RNA extraction. In the first protocol, 10 ml of wastewater was concentrated through double filtration on the same day the samples were received, as previously described by Jafferali et al., (2021). In the second protocol, the viral total nucleic acid (TNA) was concentrated from raw wastewater samples using Maxwell RSC Enviro TNA Promega Kit and then RNA was extracted using Maxwell RSC Instrument (Promega Biotech AB, Sweden) following the manufacturer's instructions. In both protocols, two independent replicates were analysed for each sample and tap water was used as the negative control.

Reverse transcriptase quantitative polymerase chain reaction (RT-qPCR) was performed as previously described by Jafferali et al., (2021). The reaction was performed using SYBR Green one-step kit (Bio-Rad) according to the manufacturer's instructions, with the modification of adding 2 µL of 4 mg/ml Bovine Serum Albumin (BSA). N3 primers targeting the Nucleocapsid gene (N-gene) were used for the quantification of SARS-CoV-2 and Pepper mild mottle virus (PMMoV) was quantified for normalization purposes (Perez-Zabaleta et al., 2023). Reactions were considered positive if the cycle threshold (Ct) was below 40 cycles with a single melting peak at the correct temperature. The hpPCR analysis for the detection of SARS-CoV-2 variants of concern was performed using a custom kit assembled by APLEX Bio AB (Solna, Sweden) (Perez-Zabaleta et al., 2023).

RESULTS AND DISCUSSION

Statistical analyses between positive clinical cases number in Stockholm and Malmö area and the Total-gene copy number of SARS-CoV-2 detected per week correlated significantly with each other until week 6-2022 (Figure 1 and Figure 2). From this week, free Covid-19 tests were no longer offered to the Swedish population, and large-scale testing ceased. All Pearson correlations until week 6-2022 were equal or higher than 0.84 and considered statistically significant with a p-value < 0.001. Early warnings were observed in all the waves before week 6-2022 in both cities (Figure 1 and Figure 2). The measured values in the wastewater during the long monitoring were used to estimate the number of positive cases. This estimation revealed a significant positive Pearson correlation of 0.97 and this strong correlation confirms the high potential of WBE as a tool to estimate the infection rate in a region.

Few studies have monitored SARS-CoV-2 in wastewater over long periods of time. One study in Brazil presented 10-month data, while another study in Germany showed 6-month data (Agrawal et al., 2021; Claro et al., 2021). Our current study presents over two years of monitoring, which is a sufficient number and time frame to draw more certain conclusions about factors influencing SARS-CoV-2 wastewater surveillance.

Technical parameters relating to sampling protocols, RNA concentration/extraction methods, normalization/calculation approaches, and storage conditions were evaluated and discussed. Both RNA-isolation methods generated equally accurate data and no significant difference between the protocols was found. However, the Promega kit generated a higher yield enabling lower variations at low levels. Also, both tested sampling protocols and normalization/calculation methods worked well with different strengths and limitations. The storage study has demonstrated that wastewater samples can be stored for up to 18 weeks, if kept at -80°C with glycerol added, and still generate similar results to the ones obtained with fresh wastewater samples. Furthermore, hpPCR showed the potential to expand the WBE capacity by allowing highly multiplexed viral variant analysis on a routine basis, providing higher sensitivity and faster turnaround (within one workday).

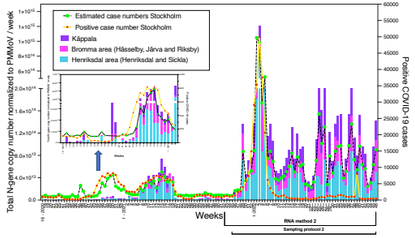

Figure 1. SARS-CoV-2 monitoring in the Stockholm region. Three major plants in Stockholm were monitored, Käppala WWTP (purple bar), Bromma WWTP (pink bar) and Henriskdal WWTP (light-blue bar). SARS-CoV-2 content was expressed as the Total N-gene copy number per week, which has been normalized with PMMoV content and flow rate. For the same monitoring period, the positive case numbers in Stockholm based on laboratory-confirmed PCR (yellow line/red dots) are plotted as well as the estimated case numbers based on SARS-CoV-2 measurements in wastewater (black interrupted line/green dots). Two RNA methods and two sampling protocols were applied.

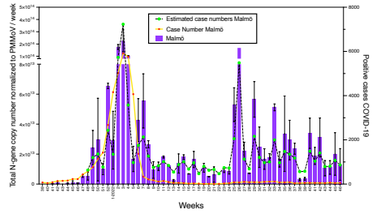

Figure 2. SARS-CoV-2 monitoring in the Malmö region. SARS-CoV-2 content was expressed as the Total N-gene copy number per week (purple bar), which has been normalized with PMMoV content and flow rate. For the same monitoring period, the positive case numbers in Malmö based on laboratory-confirmed PCR (yellow line/red dots) are plotted as well as the estimated case numbers based on SARS-CoV-2 measurements in wastewater (black interrupted line/green dots).

Our study shows the feasibility of tracking the spread of Covid-19 in a population, the ability to provide early warnings, and the accuracy of the method. The data generated here is published and updated weekly on a Covid-19 data portal (SciLifeLab Data Centre, 2022), and has become an important tool to allow both the healthcare sector, authorities, and the Swedish population to track changes in SARS-CoV-2 content in the wastewater.

REFERENCES

Agrawal, S., Orschler, L., Lackner, S., 2021. Long-term monitoring of SARS-CoV-2 RNA in wastewater of the Frankfurt metropolitan area in Southern Germany. Sci Rep 11, 5372. https://doi.org/10.1038/s41598-021-84914-2
Claro, I.C.M., Cabral, A.D., Augusto, M.R., Duran, A.F.A., Graciosa, M.C.P., Fonseca, F.L.A., Speranca, M.A., Bueno, R. de F., 2021. Long-term monitoring of SARS-COV-2 RNA in wastewater in Brazil: A more responsive and economical approach. Water Res 203. https://doi.org/10.1016/j.watres.2021.117534
COVIDPoops19, 2021. COVIDPoops19 Summary of Global SARS-CoV-2 Wastewater Monitoring Efforts by UC Merced Researchers [WWW Document].
Daughton C.G., Jones-Lepp T.L., 2001. Pharmaceuticals and care products in the environment: Scientific and regulatory issues. American Chemical Society.
Jafferali, M.H., Khatami, K., Atasoy, M., Birgersson, M., Williams, C., Cetecioglu, Z., 2021. Benchmarking virus concentration methods for quantification of SARS-CoV-2 in raw wastewater. Science of the Total Environment 755. https://doi.org/10.1016/j.scitotenv.2020.142939
Perez-Zabaleta, M., Archer, A., Khatami, K., Jafferali, M.H., Nandy, P., Atasoy, M., Birgersson, M., Williams, C., Cetecioglu, Z., 2023. Long-term SARS-CoV-2 surveillance in the wastewater of Stockholm: What lessons can be learned from the Swedish perspective? Science of The Total Environment 858, 160023. https://doi.org/10.1016/J.SCITOTENV.2022.160023
SciLifeLab Data Centre, 2022. Covid-19 Data Portal Sweden [WWW Document].
Swedish Public Health Agency, 2022. Number of cases of COVID-19 in Sweden at regional level [WWW Document]. https://experience.arcgis.com/experience/19fc7e3f61ec4e86af178fc2275029c5.
WHO, 2020. Novel Coronavirus (2019-nCoV) Situation Report - 1. WHO Bulletin 1–7.
Zuccato, E., Chiabrando, C., Castiglioni, S., Calamari, D., Bagnati, R., Schiarea, S., Fanelli, R., 2005. Cocaine in surface waters: a new evidence-based tool to monitor community drug abuse. Environmental Health 4, 14. https://doi.org/10.1186/1476-069X-4-14

Surveillance of SARS-CoV-2 in sewage from buildings housing residents with different vulnerability levels

Anna Pico-Tomàs [1,2], Cristina Mejías-Molina[3,4], Ian Zammit[1,2], Marta Rusiñol[3,4], Silvia Bofill-Mas[3,4], Carles M. Borrego[1,5], Lluís Corominas[1,2]

[1] Catalan Institute for Water Research (ICRA), Emili Grahit 101, 17003 Girona, Spain
[2] University of Girona, Plaça de Sant Domènec 3, 17004 Girona, Spain
[3] Laboratory of Viruses Contaminants of Water and Food, Genetics, Microbiology & Statistics Dept., Universitat de Barcelona. Barcelona, Catalonia, Spain
[4] The Water Research Institute (IdRA), Universitat de Barcelona, Barcelona, Catalonia, Spain
[5] Group of Molecular Microbial Ecology, Institute of Aquatic Ecology, University of Girona, Girona, Catalonia, Spain

Abstract
Human monitoring sewage as a way to track COVID-19 infection prevalence is by now ubiquitous. In this study, we sampled sewage from different buildings (a school, a university campus, a university residence, and an elderly residence) that host residents of different levels of vulnerability. Our main goal was to evaluate the efficacy and utility of sewage surveillance when implemented in buildings hosting communities of different ages, COVID-19 vulnerability, social habits, and case reporting. At the elderly's residence we used two sampling methods, passive and active, the latter of which was more sensitive. The other buildings were sampled using passive sampling. Altogether, we were able to detect the virus in all the buildings even when no cases were reported using clinical-based surveillance, demonstrating the potential of this method to provide cheap SARS-CoV-2 monitoring at building level.

Keywords (maximum 6 in alphabetical order)
COVID-19, passive sampling, wastewater-based epidemiology, wastewater surveillance

INTRODUCTION

The COVID-19 pandemic caused a global crisis since it was challenging to maintain economic activity without being able to work and interact physically together. For this reason, building managers had an interest to provide protective measures to enter a "co-existing with the virus" scenario phase. The measures were adapted to the building's hosts or visitors. The measures included the use of protective equipment, limiting the number of people in common spaces, and surveillance of the cases based on clinical testing. massive random screening to detect mild and asymptomatic cases has been common in some vulnerable communities but not applied at large scale (i.e., cities) because of its cost[1]. Wastewater-based epidemiology (WBE) has been demonstrated to be a non-invasive, cost-effective tool to track the circulation of SARS-CoV-2 by sampling influent wastewater at Wastewater Treatment Plants (WWTPs) but also in neighborhoods, hospitals, universities, schools, and households. Now the main challenge is to make the method cost-effective, and installation-friendly, thus finding an alternative to the autosamplers. Passive samplers are exposed to the wastewater over a known time, and it entraps the analytes of interest (i.e., SARS-CoV-2 RNA)[2]. Massive random screening to detect mild and asymptomatic cases has been common in some vulnerable communities but not applied at large scale (i.e., cities) because of its cost[1]. Wastewater-based epidemiology (WBE) has been demonstrated to be a non-invasive, cost-effective tool to track the circulation of SARS-CoV-2 by sampling influent wastewater at Wastewater Treatment Plants (WWTPs) but also in neighborhoods, hospitals, universities, schools, and households. Now the main challenge is to make the method more cost-effective, and installation user-friendly, thus by finding an alternative to the use of autosamplers. Passive samplers are exposed to the wastewater over a known timeframe, and it entraps the analytes of interest (i.e., SARS-CoV-2 in this case)[2]. While the results obtained using passive samplers are only qualitative, they are still comparable to those obtained using active sampling for the detection/non-detection of the virus.

Our main goal was to evaluate the efficacy and utility of sewage surveillance when implemented in buildings hosting communities of different ages, COVID-19 vulnerability, social habits, and case reporting. These were an elderly peoples' residence (*ElderlyRes*), a university residence (*UnivRes*) a university campus (*UniCamp*), and a school (*School*) For that purpose, we monitored one outbreak in four buildings using passive sampling. Additionally, in *ElderlyRes*, we also used active sampling to compare both protocols.

MATERIALS AND METHODS

Four buildings were sampled using passive sampling in a weekly basis between November 2021 and March 2022. The *ElderlyRes* was also sampled using active sampling. Samples were analyzed using qPCR for the SARS-CoV-2 targets N1 and N2. Wastewater results were compared with clinical data provided by the building managers.

RESULTS AND DISCUSSION

The high frequency of clinical testing and case reporting at the *ElderlyRes* allowed us to obtain a reliable comparison between the number of cases and sewage signals (Fig 1). We observe a good and significant correlation between the mean concentration of N1 and N2 and the number of clinically confirmed cases, with a Pearson coefficient of 0.61. This result guarantees the active sampling as a good validator.

To assess the validity of passive sampling, we compared the results to those from composite samples in the *ElderlyRes*. Results from composite samples were also converted into a binary outcome (values above the detection limit were considered "detected" and those below the detection limit were considered "non-detected"). Overall, we observed a good match between the detection of SARS-CoV-2 by both approaches since 14 out of 18 samples showed a perfect match. The mismatch came for samples collected during dates of low COVID-19 prevalence, with SARS-CoV-2 results from composite samples close to the limit of detection. The prevalence detection limit (PLD) in the *ElderlyRes* is 0.4% for active sampling and 1.5% for passive sampling, both values are close to the ones observed in other studies[3,4]. Passive samplers to those from composite active samples in the *ElderlyRes*. Results from composite samples were also converted into a binary outcome (values above the detection limit were considered "detected" and those below the detection limit were considered "non-detected"). Overall, we observed a good match between the detection of SARS-CoV-2 by both approaches since with 14 out of 18 samples showed a perfect match. The mismatch came for samples collected during dates of low COVID-19 prevalence, with SARS-CoV-2 results from composite samples close to the limit of detection. The prevalence detection limit in the *ElderlyRes* is 0.4% for active sampling and 1.5% for passive sampling.

As for the other buildings (Fig 2), *UnivRes* and the *ElderlyRes,* we consistently observed positive detection during the 6th wave period (January to February 2022). For the non-residential buildings (*UniCamp* and *School*), the detection was rather intermittent which probably reflects the fact that these buildings hosted a lot of temporary visitors, that are less likely to defecate there. Our study has revealed that sewage surveillance can also uncover blind spots in monitoring strategies implemented in different facilities to track and report COVID-19 cases among vulnerable populations. Sewage surveillance provides anonymous and cost-effective data on the communal circulation of the virus, allowing the fast implementation of protective measures should they be deemed desirable.

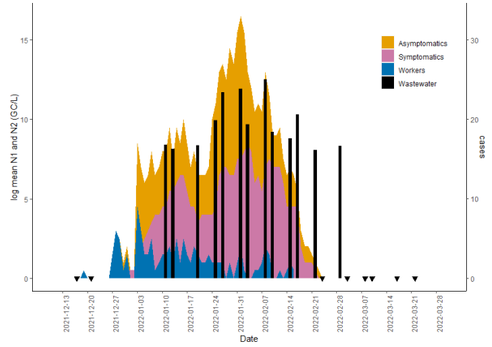

Figure 1. Geometric Mean concentration of gene targets N1 and N2 (black bars, in log of GC·L-1) and COVID-19 cases (shaded areas that are color-coded by subpopulation, see legend) in the elderly's residence during the studied period (December 2021-March 2022). Inverted black triangles show the dates where both gene targets were below the limit of detection.

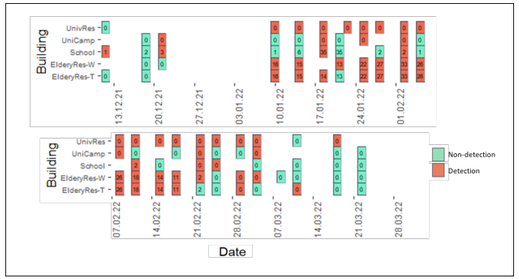

Figure 2. Detection of N1 or N2 in the wastewater of the studied buidings using passive samplers in all cases except for ElderlyRes-W, where an autosampler was used. Red cells indicate the dates where detection was positive and green cells when negative. The numbers inside the cells are the reported clinical cases in the corresponding building.

REFERENCES

1. Hassard, F., Lundy, L., Singer, A. C., Grimsley, J. & Di Cesare, M. Innovation in wastewater near-source tracking for rapid identification of COVID-19 in schools. *The Lancet Microbe* **2,** e4–e5 (2021).
2. Schang, C. *et al.* Passive Sampling of SARS-CoV-2 for Wastewater Surveillance. *Environ. Sci. Technol.* **55,** 10432–10441 (2021).
3. Corchis-Scott, R. *et al.* Averting an Outbreak of SARS-CoV-2 in a University Residence Hall through Wastewater Surveillance. *Microbiol. Spectr.* **9,** e00792-21 (2021).
4. Spurbeck, R. R., Minard-Smith, A. & Catlin, L. Feasibility of neighborhood and building scale wastewater-based genomic epidemiology for pathogen surveillance. *Sci. Total Environ.* **789,** 147829 (2021).

WORKSHOPS

WII.

Urban Hydrosocial Cycle: Why should engineers care?

Assessment of flood vulnerability through a multidimensional index

A.N. Gomez, L.AS. Popartan, M. Poch, and I. Rodriguez-Roda

LEQUIA. Institute of the Environment, Universitat de Girona, C/ Maria Aur˙elia Capmany, 69, 17003, Girona, Spain

Abstract:
The vulnerability assessment is considered key to reducing the risk of floods, and the most widespread methodology for characterizing vulnerability is the creation of an index. However, the indices that have been obtained so far are fragmented or follow a very complicated methodology. To overcome the challenge of floods, urban planning must take into account innovative and simple strategies to achieve resilient and sustainable cities. This document addresses these gaps and proposes a methodology to simplify and holistically evaluate the vulnerability to floods in cities through a multidimensional index based on indicators that take into account five dimensions: social, economic, infrastructure, environmental and institutional.
The proposed methodology allows us to identify the sources of vulnerability and their causes by dimension, which contributes to improving flood risk management and encourages decision makers to formulate vulnerability reduction strategies.

Keywords
Cities, GIS, floods, indicators, multidimensional index, vulnerability

INTRODUCTION

Flooding in urban areas is associated with pluvial flooding that occurs when rainfall intensity exceeds the infiltration and conveyance capacity of the storm sewer system. (Bulti & Abebe, 2020; Tanaka et al., 2020). They account for approximately one-third of all global hazard events, and the number of extreme flooding incidents has increased significantly over the past decade (Tsatsaris et al., 2021). In addition, climate change, urbanization, the reduction of urban green spaces and the deterioration of urban water management infrastructures increase the risk of pluvial flooding (Kaykhosravi et al., 2019; Rangari et al., 2018).

Cities with complex hydro-meteorological environments may face multiple hazards from various types of urban flooding such as pluvial and fluvial flooding (Wu et al., 2018). Flood risk and vulnerability for different types of floods have been addressed in several studies (Pacetti et al., 2022; Tanaka et al., 2020; Tapia et al., 2017). The results show that the contribution of pluvial flooding should not be ignored, even in a basin where fluvial flooding is the main cause of flood damage. (Muthusamy et al., 2019). There is a need to improve our current understanding of the extent and impact of pluvial flooding in urban areas and how risks can be reduced.

Risk assessment along with its geolocation and flood mapping is an essential step to identify potential flood risk areas under rainfall events. Geographic information systems (GIS) are an important tool for mapping flood risk (Mudashiru et al., 2021; Quesada-Román, 2022).
The integration of remote sensing and GIS techniques together with the analytical hierarchical process (AHP) are the best techniques to assess flood risk and vulnerability (Ikirri et al., 2022).

On the one hand, flood risk maps represent areas that may be at various levels of flood hazard, identifying areas of low and high risk (Yang et al., 2015). As noted by Mutusamia (2019), modeling the spatial distribution of pluvial and fluvial floods using a 2D model based on a high-resolution digital elevation model (DEM) and developing a 2D model in HEC-RAS (v.5) can be a good alternative to generate flood risk maps.

In addition, vulnerability assessment must be multidimensional and integrated (Aroca-Jiménez et al., 2022; Birkmann et al., 2013). Vulnerability analysis is often driven by the derivation of vulnerability indices (Moreira et al., 2021). The most considered dimensions are: the social (Oulahen et al., 2015), physics (Papathoma-Köhle et al., 2019), economic (Veen & Logtmeijer, 2005), institutional (Papathoma-Köhle et al., 2021) and environmental (Damm, 2010).

The motivation of this study is to propose a simple evaluation methodology and apply it to a case study. First, we intend to model the spatial distribution of pluvial and fluvial floods using a 2D model based on digital elevation models (DEM) with hydro-geomorphological data that affect extreme events (altitude, mean annual precipitation, slope, distance to rivers, soil type and drainage density). Second, to assess flood vulnerability in five dimensions: social, economic, environmental, physical (infrastructure) and institutional, for the creation of a multidimensional index, using multi-criteria decision analysis (MCDA) and analytic hierarchical process (AHP) to delineate scenarios that reduce the risk and vulnerability associated with floods. Finally, adaptation/mitigation strategies to the effects of urban flooding are proposed through structural and non-structural measures, according to the most vulnerable dimensions or areas, which allow for more resilient and sustainable cities.

RESULTS

The proposed methodology for calculating a vulnerability index, shown in *Figure 1*, consists of two sections:

Hazard: development of a flood map that considers fluvial and pluvial floods in the case study, for different return periods. With the flood map we identify potentially flooded areas.

Vulnerability: This section is divided into five dimensions that can be defined as:

Social dimension. propensity for human well-being to be damaged by the disruption of individual (mental and physical health) and collective (health services, education, etc.) social systems and their characteristics (e.g. gender, marginalization of social groups) (Birkmann et al., 2013), describing the capabilities, knowledge and behaviors of the affected persons and/or organizations (Balica & Wright, 2010). Indicators: age, income, gender, employment, population density, nationality.

Economic dimension. reflects the income of the affected area, propensity for loss of economic value due to damage to physical assets and/or interruption of production capacity (Birkmann et al., 2013), that could be caused by flooding. Indicators: municipal debt, municipal budget, number of businesses, cafeterias, and restaurants.

Infrastructure dimension: potential for damage to physical assets, including built-up areas, infrastructure and open spaces (Birkmann et al., 2013). Indicators: hospitals, education centers, sewage infrastructure, drinking water infrastructure, monuments, and museums.

Environmental dimension: potential for damage to all ecological and biophysical systems and their different functions, including particular ecosystem functions and environmental services (Birkmann et al., 2013) that may be caused by floods or the interference of human activities on the natural environment, which may increase vulnerability in certain areas (Balica & Wright, 2010). Indicators: nature reserve, green areas, land use, quality of surface and subway water bodies.

Institutional dimension: potential for damage to governance systems, organizational form and function, as well as to formal/legal and informal/customary governing norms, any of which may be forced to change the following weaknesses exposed by the disaster and response (Birkmann et al., 2013). Indicators: availability of emergency plans, level of understanding of the national household warning system, warnings about recent floods.

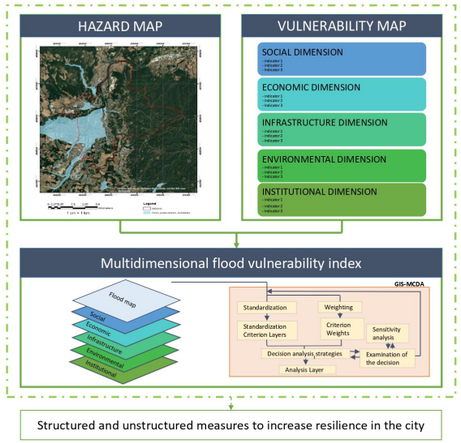

Figure 1 Methodology proposal

The indicators for each dimension will be considered based on context, as well as exposure, sensitivity, and adaptive capacity for better understanding.
The proposed index method is through GIS-MCDA consisting of criteria standardization, criteria weights, strategy analysis, sensitivity analysis and a layer analysis.
This methodology allows us to calculate a flood vulnerability index in cities in a simplified and holistic manner, as well as the most vulnerable dimensions according to the case study.

REFERENCES

Aroca-Jiménez, E., Bodoque, J. M., García, J. A., & Figueroa-García, J. E. (2022). Holistic characterization of flash flood vulnerability: Construction and validation of an integrated multidimensional vulnerability index. *Journal of Hydrology*, *612*, 128083. https://doi.org/10.1016/j.jhydrol.2022.128083
Birkmann, J., Cardona, O. D., Carreño, M. L., Barbat, A. H., Pelling, M., Schneiderbauer, S., Kienberger, S., Keiler, M., Alexander, D., Zeil, P., & Welle, T. (2013). Framing vulnerability, risk and societal responses: The MOVE framework. *Natural Hazards*, *67*(2), 193–211. https://doi.org/10.1007/s11069-013-0558-5
Moreira, L. L., De Brito, M. M., & Kobiyama, M. (2021). Review article: A systematic review and future prospects of flood vulnerability indices. *Natural Hazards and Earth System Sciences*, *21*(5), 1513–1530. Scopus. https://doi.org/10.5194/nhess-21-1513-2021
Mudashiru, R. B., Sabtu, N., Abustan, I., & Balogun, W. (2021). Flood hazard mapping methods: A review. *Journal of Hydrology*, *603*, 126846. https://doi.org/10.1016/j.jhydrol.2021.126846
Pacetti, T., Cioli, S., Castelli, G., Bresci, E., Pampaloni, M., Pileggi, T., & Caporali, E. (2022). Planning Nature Based Solutions against urban pluvial flooding in heritage cities: A spatial multi criteria approach for the city of Florence (Italy). *Journal of Hydrology: Regional Studies*, *41*, 101081. https://doi.org/10.1016/j.ejrh.2022.101081
Papathoma-Köhle, M., Schlögl, M., & Fuchs, S. (2019). Vulnerability indicators for natural hazards: An innovative selection and weighting approach. *Scientific Reports*, *9*(1), Article 1. https://doi.org/10.1038/s41598-019-50257-2
Rangari, V. A., Gonugunta, R., Umamahesh, N. V., Patel, A. K., & Bhatt, C. M. (2018). 1d-2d Modeling of Urban Floods and Risk Map Generation for the Part of Hyderabad City. *The International Archives of Photogrammetry, Remote Sensing and Spatial Information Sciences*, *XLII–5*, 445–450. https://doi.org/10.5194/isprs-archives-XLII-5-445-2018
Tanaka, T., Kiyohara, K., & Tachikawa, Y. (2020). Comparison of fluvial and pluvial flood risk curves in urban cities derived from a large ensemble climate simulation dataset: A case study in Nagoya, Japan. *Journal of Hydrology*, *584*. Scopus. https://doi.org/10.1016/j.jhydrol.2020.124706
Tapia, C., Abajo, B., Feliu, E., Mendizabal, M., Martinez, J. A., Fernández, J. G., Laburu, T., & Lejarazu, A. (2017). Profiling urban vulnerabilities to climate change: An indicator-based vulnerability assessment for European cities. *Ecological Indicators*, *78*, 142–155. https://doi.org/10.1016/j.ecolind.2017.02.040
Veen, A. V. D., & Logtmeijer, C. (2005). Economic Hotspots: Visualizing Vulnerability to Flooding. *Natural Hazards*, *36*(1), 65–80. https://doi.org/10.1007/s11069-004-4542-y

Eco-cultural technologies for rural and Māori community on-site wastewater treatment in New Zealand

R. J. Craggs, J. Sukias, Valerio Montemezanni, C. Picken, A. Dakers, and C. Tanner

* National Institute of Water and Atmospheric Research, PO Box 1-115 Hillcrest, Hamilton, 3210, New Zealand. (E-mail: *rupert.craggs@niwa.co.nz)*

Abstract
This multi-disciplinary research programme is focused on partnering with indigenous Māori communities in New Zealand to co-develop, eco-cultural wastewater treatment technologies (ECWT) that incorporate mātauranga Māori (Māori indigenous knowledge) and cutting-edge science to address current barriers to ecotechnology implementation. ECWT provide cost-effective and culturally acceptable "natural" options to upgrade failing rural wastewater infrastructure. This talk will discuss the co-design process and preliminary performance of:

Intensified wetland filters (IWF) for marae and papakāinga (māori housing development) wastewater treatment, using and intermittent dosing to enhance treatment performance in terms of nutrient and faecal indicator bacteria removal.

Final effluent wetlands (FEW) that provide habitat for native plants and animals and revitalise mauri (life force) and health (hauora) of water, the environment (taiao), and people (tangata) that depend on them.

Accumulating volume sludge digestion ponds (AVSDP) that reduce the volume of wastewater sludge requiring disposal.

Sludge treatment wetlands (STW) that convert wastewater sludge into a soil amendment, reducing Māori concerns and costs of sludge transport and disposal.

Affordability and sustainability of ECWT will be enhanced by co-development of culturally appropriate and resource recovery (biogas energy, bioproducts, and treated water).

Keywords
Biogas recovery, Māori co-development, Onsite sludge treatment, Wetland filters

INTRODUCTION

Limits to reduce water pollution and support iwi taiao kaitiakitanga (environmental stewardship) of freshwaters, being set under New Zealand's National Policy Statement for Freshwater Management (NPS-FM) require a significant upgrade of failing rural wastewater infrastructure. The estimated capital investment required to upgrade rural on-site treatment systems (OSTS) using advanced tank-based mechanical treatment (AMT) is NZ$20-40 million.

Ecotechnologies offer substantial advantages in affordability, cultural acceptability, energy efficiency and resilience compared to advanced mechanical WWTP upgrade options and hold great promise for sustainable development world-wide. However, they have yet to be widely implemented, and require further development in NZ to:
a) fully align with Māori cultural values for wastewater management and address stakeholder barriers to implementation;
b) improve treatment effectiveness, particularly during winter, to reduce land area requirements.
c) improve treatment resilience (maintain effectiveness) under highly variable wastewater loads, common for rural systems, to future-proof for population growth and climate change, and.
d) recover resources to accelerate transition to a circular economy.

The main barriers hindering the uptake of innovative wastewater treatment ecotechnologies have been identified (Etnier et al. 2007) as:
• decreased financial reward for engineering consultancies.
• lack of knowledge and experience of ecotechnologies, leading to the perception that they have greater risk and inflated costs.
• an unfavourable regulatory environment and,
• lack of holistic systems thinking and whole-of-life assessment.

These barriers tend to be propagated within the mindset of local government implementors, and the engineering consultancies that they depend on, resulting in preference for traditional advanced mechanical treatment solutions.

This project has partnered with indigenous Māori communities in New Zealand to co-develop four innovative, cost-effective and culturally acceptable eco-cultural wastewater treatment technologies (ECWT). ECWT are wetland and pond-based innovations that incorporate mātauranga Māori (Māori indigenous knowledge) and address barriers to ecotechnology implementation.

Intensified wetland filters (IWF)

Intensified wetland filters (IWF) have been co-developed for marae and papakāinga (māori housing development) septic tank effluent treatment. They are a substantial improvement on vertical flow constructed wetlands. Treatment performance and resilience to variations in wastewater load is enhanced by incorporating different active media and using intermittent wastewater dosing to cycle aerobic/anoxic conditions. IWF incorporate Mātauranga related to:

- Locally available media and indigenous wetland plants with potential resource recovery co- benefits.
- Passage through Papatūānuku (mother earth) to revitalise the mauri of the water.

IWF require less land (reducing costs) for effluent infiltration than that required for existing vertical-flow wetlands (Sukias et al. 2018).

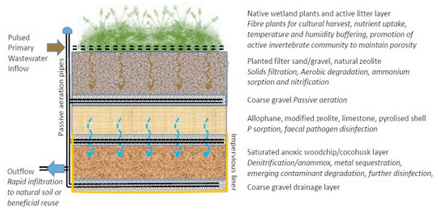

Figure 1 Intensified wetland filter concept.

Final effluent wetlands (FEW)

Final effluent wetlands (FEW) provide final cleansing of treated wastewater prior to discharge, since direct discharge of even highly treated wastewater into surface waters is abhorrent to Māori. FEW co-development has been guided by tikanga and Mātauranga Māori. The use of soils/rocks, landscaping and planting ensures provision of habitat for native plants and animals and the revitalisation of the mauri (life force) of the wastewater and protection of Te Hauora (health) of the waterbody, local environment, and associated community. Colonisation by taonga (culturally treasured) species physically indicate to Māori the efficacy of the system and limited open water habitat prevents waterfowl from re-polluting treated effluent.

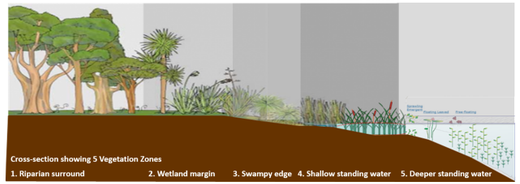

Figure 2 Final Effluent Wetland concept.

Accumulating volume sludge digestion ponds (AVSDP)

Accumulating volume sludge digestion ponds (AVSDP) substantially reduce the volume of, and recover energy from, wastewater sludge prior to disposal. Treatment, transport and disposal of septage and wastewater sludge is an expensive step in rural wastewater treatment and does not align with tikanga Māori (Ihaka et al. 2000). AVSDPs have extended residence times (~1Y), that promote similar biogas recovery under ambient conditions to conventional heated, mixed sludge digesters, but have much simpler operation because of annual (compared to daily) sludge handling.

Sludge treatment wetlands (STW)

Sludge treatment wetlands (STW) convert wastewater sludge into a soil amendment, reducing Māori concerns and costs of sludge transport and disposal. This co-design combines established designs from European and Australian industry partners (Orbicon Ltd and Wetland Ecological Systems Ltd) with Mātauranga Māori and knowledge of NZ soils and plants.

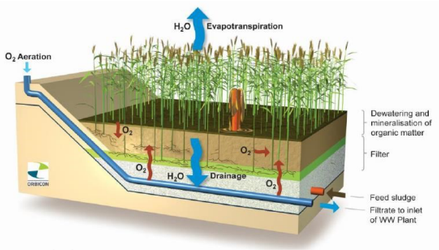

Figure 3 Sludge treatment wetland concept

Affordability and sustainability of ECWT is enhanced by co-development of culturally appropriate and resource recovery (biogas energy, nutrients, bioproducts, and treated water).

The co-design of ECWT ensures that they incorporate Mātauranga Māori and address ecotechnology implementation barriers (particularly the current preference of endusers for hard-engineered solutions) to promote widespread uptake. Hui and workshops using cross-cultural participatory methods have promoted understanding of linkages between western science and mātauranga Māori.

Successful ECWT co-development will enable Māori to achieve their objectives for WWT and overcome barriers to ecotechnology uptake identified by wastewater industry stakeholders. Widespread implementation of ECWT will benefit rural economies; reduce pollution of freshwater resources; and improve Te Mana o te Wai (the holistic well-being of freshwater).

REFERENCES

Etnier, C., Pinkham, R., Crites, R., Johnstone, D., Clark, M., Macrellis, A. 2007 Overcoming barriers to evaluation and use of decentralized wastewater technologies and management. Report 04-DEC-2 issued by the Water Environment Research Federation (WERF), Alexandria, USA.
Ihaka, M., Awatere, S., and Harrison, D. 2000 Tangata Whenua Perspectives of Wastewater. Report prepared for Gisborne District Council, NZ by Te Kauere Partnership. 57p.
Sukias, J., Park, J., Stott, R., and Tanner, C. 2018 Quantifying resilience of constructed wetland and denitrifying bioreactor treatment systems to shock loadings. *Water Research* **139**, 450-461.

Socio-economic criteria for preventing and controlling phosphorus pollution from municipal wastewater effluents

E. Martín Hernández*, C. Vaneeckhaute*,** and G.J. Ruiz-Mercado***,****

* BioEngine - Research Team on Green Process Engineering and Biorefineries, Chemical Engineering Department, Université Laval, 1065 Ave. de la Médecine, Québec, QC, G1V 0A6, Canada (E-mail: *edmah2@ulaval.ca*; *celine.vaneeckhaute@gch.ulaval.ca)*
** CentrEau, Centre de recherche sur l'eau, Université Laval, 1065 Avenue de la Médecine, Québec, QC, G1V 0A6, Canada (E-mail: *celine.vaneeckhaute@gch.ulaval.ca)*
*** Center for Environmental Solutions and Emergency Response (CESER), US Environmental Protection Agency, 26 West Martin Luther King Drive, Cincinnati, Ohio 45268, United States (E-mail: *ruiz-mercado.gerardo@epa.gov)*
**** Chemical Engineering Graduate Program, Universidad del Atlántico, Puerto Colombia 080007, Colombia (E-mail: *ruiz-mercado.gerardo@epa.gov)*

Abstract
In this work, we assess the techno-economic and social performance of preventing and controlling phosphorus releases from municipal wastewater effluents in local communities. This multicriteria assessment framework accounts for the effects of the economies of scale and the population economics across the United States by considering geospatial public access information. The economies of scale have a significant impact on the costs of phosphorus removal, resulting in considerable increases in phosphorus removal costs in areas where small population centers are predominant due to the lack of economies of scale in their wastewater treatment plants. Additionally, the average per capita income of these areas is generally lower than large cities and their metropolitan areas. Therefore, the economic impact of requiring phosphorus removal systems to meet water quality criteria in local communities is crucial information to be considered in designing adequate incentive policies for supporting such water pollution control and prevention efforts.

Keywords (maximum 6 in alphabetical order)
Nutrient pollution, Wastewater, Phosphorus removal, Sustainability, Social impact

INTRODUCTION

Phosphorus pollution is an environmental concern impacting ecosystems and communities worldwide. The effects of phosphorus pollution include harmful algal bloom events, hypoxia of waterbodies, and impairment of drinking water sources. Therefore, to prevent these harmful effects, phosphorus removal or recovery operations must be implemented in point source releases like wastewater treatment plant effluents (Ansari, 2010).

In the United States, nutrient removal treatments are often installed in wastewater treatment plants (WWTPs) equipped with advanced treatments, which in turn are usually those serving large urban areas. These facilities are benefited from the economies of scale and can remove or recover phosphorus at a competitive cost for the served users. Conversely, WWTPs serving smaller population centers are usually limited to primary and secondary treatments. However, the lack of economies of scale hinders the adoption of phosphorus removal and recovery processes. Also, implementing countrywide regulations similar to the Urban Waste Water Treatment Directive (UWWTD 91/271) from the European Union will lead to adopting phosphorus removal processes at large and small scales (ESSP, 2023). However, removing and recovering phosphorus in these smaller facilities would result in large costs due to the lack of economies of scale. Therefore, the economic impact of requiring phosphorus removal systems to meet water quality criteria in local communities is crucial information to be considered in designing adequate incentive policies for supporting such water pollution control and prevention efforts.

MATERIALS AND METHODS

Technical information describing the WWTPs across the contiguous U.S. was retrieved from the HydroWASTE database (Ehalt Macedo et al., 2022). Such information includes the spatial location, treatment level, treatment design capacity, and served population. The HydroWASTE database reports the treatment level at each WWTP as primary, secondary, or advanced treatments. We consider that only WWTPs with advanced treatments have specific processes for removing phosphorus since secondary wastewater treatment systems do not limit nutrient releases considering the water quality criteria definition reported by the U.S. Environmental Protection Agency. Instead, it limits biological oxygen demand, total suspended solids, and pH. Thus, for these advanced treatment facilities, we assume a phosphorus removal efficiency of 88% (U.S. Environmental Protection Agency, 2015), while the phosphorus removal efficiency associated with primary and secondary treatments are assumed to be 23% and 40% respectively (Venkatesan et al., 2016; Shi, 2011). As a result, this study assesses 14,639 WWTPs reported in HydroWASTE.

The cost of phosphorus removal processes implemented in WWTPs is estimated based on the cost information reported by U.S. Environmental Protection Agency (2015). This report surveys numerous phosphorus removal systems installed in WTTPs throughout the U.S., with treatment design capacities ranging from 0.14 to 943.6 million cubic meters per year. Correlations in the form of exponential functions, as shown in Figure 1, are developed based on these data to estimate the cost of implementing phosphorus removal technologies in WWTPs as a function of their treatment design capacity. Thus, these correlations provide the capital and operating costs of phosphorus removal for WWTPs with primary or secondary treatment levels. For advanced WWTPs, the capital costs of implementing the phosphorus removal process are zero since we assumed they already have some installed phosphorus removal technology, and we only consider their operating costs.

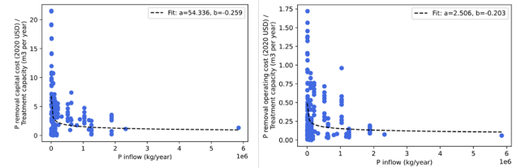

Figure 1. Capital and operating costs of phosphorus removal systems in WWTPs (U.S. Environmental Protection Agency, 2015).

We estimate the total removal costs as the sum of the annual operating and the annualized capital costs. The annualized capital cost was estimated through the annual capital charge ratio assuming an interest rate of 7% and a lifetime of 20 years.

RESULTS AND DISCUSSION

This population distribution is directly related to the average size of the WWTPs, whose average size is large in counties densely populated, as shown in Figure 2. Comparing the average size of WWTPs and their treatment level, we observe a predominance of WWTPs with more advanced treatments in the more populated areas, which are counties with larger WWTPs. As a result, we can establish a direct relationship between the population characteristics, the scale of the WWTPs, and the treatment level. Figure 3 describes the economies of scale for the operating expenses of WWTPs.

Figure 4 shows the phosphorus removal cost at WWTPs. Comparing the spatial distribution of removal cost with the WWTPs' average size shown in Figure 2, we can observe that they present opposite distribution patterns, confirming the significant impact of the economies of scale in phosphorus removal.

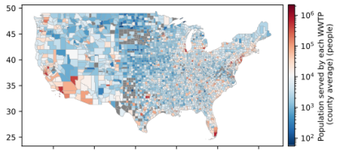

Figure 2. Average size of WWTPs in the contiguous U.S. at county level.

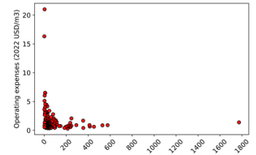

Figure 3. Estimated operating expenses of WWTPs in the U.S. for 2022, based on data reported by AWWA and RFC (2011).

Additionally, we estimate the economic impact of implementing P removal systems in all WTTPs on the users. Figure 5 collects the P removal cost per capita, and Figure 6 shows the household affordability index of P removal. These figures present opposite distribution patterns than the distribution of the WWTPs average size, resulting in a significant impact on the economy of the WTTPs users. In this regard, the U.S. Environmental Protection Agency recommends that wastewater treatment costs not exceed 2% of the household income (U.S. Environmental Protection Agency, 1997).

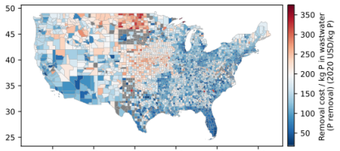

Figure 4. Spatial distribution of phosphorus removal costs.

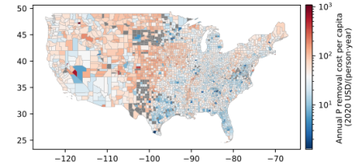

Figure 5. Annual phosphorus removal cost per capita.

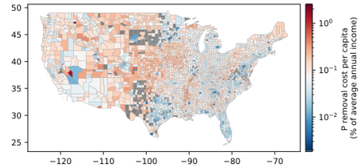

Figure 6. Household affordability index for phosphorus removal.

Therefore, this information is crucial for designing fair policies that balance environmental protection needs and financial equity for WWTP users. Also, it supports the design of WWTPs considering current phosphorus removal criteria. However, we aim to assist decision-makers in developing policies to incentivize water resource recovery facilities (WRRFs) with more advanced systems to recover and recycle valuable resources like phosphorus and transition from a linear to a circular economy paradigm.

REFERENCES

Ansari, A. 2010. Eutrophication: causes, consequences and control. *Springer Science+Business* Media, New York.

Ehalt Macedo, H., Lehner, B., Nicell, J., Grill, G., Li, J., Limtong, A., Shakya, R., 2022. Distribution and characteristics of wastewater treatment plants within the global river network. *Earth System Science Data* **14**, 559–577.

ESSP, 2023. Draft revision of EU Urban Waste Water Treatment Directive. *European Sustainable Phosphorus Platform*.

Shi, C.Y., 2011. Mass flow and energy efficiency of municipal wastewater treatment plants. *IWA Publishing*.

U.S. Environmental Protection Agency, 1997. Combined Sewer Overflows: Guidance for Financial Capability Assessment and Schedule Development.

U.S. Environmental Protection Agency, 2015. A Compilation of Cost Data Associated with the Impacts and Control of Nutrient Pollution.

Venkatesan, A.K., Hamdan, A.H.M., Chavez, V.M., Brown, J.D., Halden, R.U., 2016. Mass balance model for sustainable phosphorus recovery in a US wastewater treatment plant. *Journal of Environmental Quality* **45**, 84–89.

A hydrosocial approach to domestic water users' satisfaction through Agent-Based Modelling

Pol Vidal-Lamolla* **, Manel Poch*, Jordi Fontana**, Eduardo Martínez-Gomariz**

* LEQUIA, Institute of the Environment, University of Girona, Girona, Catalonia 17004, Spain
(E-mail: *pol.vidal@udg.edu; manuel.poch@udg.edu)*
** Aigües de Barcelona, Empresa Metropolitana de Gestió del Cicle Integral de l'Aigua, Barcelona, Spain
(E-mail: *pol.vidal@aiguesdebarcelona.cat; jordi.fontana@aiguesdebarcelona.cat; eduardo.martinez@aiguesdebarcelona.cat)*

Abstract
While the need of more sustainable and environment-preserving technologies is a consensus among the scientific community, that is not guaranteed when it comes to the whole society. Economic feasibility and efficient management are no longer the only criteria to ensure the success for the implementation of new eco-technologies and policies. It is becoming mandatory considering the social aspects implied in the whole process as well. That is, how the end users' satisfaction is being fulfilled. Therefore, it is necessary to have an insight in the socio-cognitive processes that mediate between the social perception on utility management, emerging technologies or policies and the satisfaction that is translated into, as well as the effects caused by different degrees of acceptance. Tools relying on artificial intelligence, such as agent-based models, can be extremely useful to deepen in the modelling of social acceptance processes as well as performing social simulations.

Keywords:
Agent-based modelling; artificial intelligence; satisfaction; social acceptance; socio-cognitive

INTRODUCTION

Classical offer-demand schemes considered customers' satisfaction as a matter of offering them a good quality-price relationship. Nevertheless, in recent years there has been increasing evidence that many other factors play a role in this sense. In the case of utilities such as domestic water, with the need to incorporate technical, environmental and social variables, complexity raises. To reflect this complexity, the "hydrosocial cycle" (Boelens, 2014) is a concept which aims to overcome the artificial separation between environment society and envisions the circulation of water as a combined physical and social process.

Thus, it is necessary to study the socio-cognitive framework of users, looking at how the relationship between perception and both conscious and unconscious reasoning, leading to different degrees of satisfaction or acceptance of water-related technologies and policies. Situations that can also lead to distinct decisions and behaviour of users. Demographic factors also play an important role in the perception of users when deciding, for instance, between tap water vs bottled water (Doria, 2010, March et al., 2020).

Studying final users' satisfaction and acceptance of innovative technologies, requires considering a wide range of factors, as there is a broad diversity among domestic water users. For this purpose, Agent Based Modelling (ABM) can be an advantageous tool which helps to capture differences between users, including demographic variables, housing types and even their mental frameworks or values driving their behaviour (Perelló-Moragues, 2020). Once the model is built, it can later be used to perform Agent-Based Social Simulations (ABSS) of different scenarios to analyse the effects and tendency changes in agents' behaviour caused by introducing new policies, ways of management or technologies.

This paper will use an ABM approach to study how the satisfaction of domestic water users —from Barcelona and its Metropolitan Area— is formed and to which extent the multiple factors implied in this process are important. Most studies taking an insight into water users satisfaction rely on a survey performed in a punctual time, which only permits analysing a specific picture. We aim to fathom in users' perception to unbox the processes implied in the definition of their satisfaction by using data gathered from wider time series of: i) satisfaction surveys, ii) water analysis results, iii) demography and adding a socio-cognitive factor through iv) value profiles.

MATERIALS AND METHODS

ABM models rely on a set of multiple computational entities: agents. Each agent can be programmed with specific features and Artificial Intelligence (IA), which will both guide actions pursuing their goals. At the same time, agents can form a network, being influenced by other agents. This architecture allows to study at the same time: how different individuals act and effects on the environment caused by aggregated activity of all individuals.

Nevertheless, the flexibility provided by ABM can become an issue when the process following the modelling is not transparent enough. Leading to difficulties in re-implementation or cases where similar models sharing the studied phenomena bring out completely different results (Daly et al., 2022). This situation has been assessed by raising different standardization approaches for developing and explaining ABM (Daly et al., 2022, Grimm et al., 2020).

In water use related ABM, each agent most commonly represents a household (Perelló-Moragues et al., 2021, Athanasiadis et al., 2005, Koutiva & Makropoulos, 2016), as that is the basic unit for billing and that scale has many information available. Such as consumption patterns and their changes easier to track trough water (smart)meters. As this simplification is assumed, it is necessary taking that in consideration to accurately represent in the model the variability and distribution of those variables relevant in the studied phenomena (i.e., values, age, gender, income, education…).

With the aim of studying users' satisfaction through an ABM, it was previously necessary to build a model which represented the case study —the Metropolitan Area of Barcelona— with the needed accuracy. For that purpose, the first step for building the ABM was a bibliographical review to choose the relevant variables necessary for the model and then obtaining that data to enter it to the ABM environment (see Table 1).

Table 1. Different variables considered to model the Metropolitan Area of Barcelona, their function and source.

	Purpose	Source
Supply zones	defining the zones with different water sources	GIS dataset
Municipalities inhabs.	distributing agents according to population	GIS dataset
Water analysis results	assigning different parameters to water depending on its source	Water company dataset
Demography	distributing age, income, house members, etc. according to reality	Public datasets
Users' value profiles	representing diversity of mental frameworks	Brouwer et al., 2019

Once all data was gathered the environment of the model was built using the integrated development environment (IDE) NetLogo. First step was loading the intersection of supply zones and municipalities GIS datasets, in order to delimitate the simulated physical space where households can be placed. Also, their quantity based on the relative population on each municipality. After that, demographic information was treated with R for clustering households in a few household types to be distributed in the model. Water analysis results were loaded to the environment and given to households as an input according to the supply zone they are placed in. Finally, value profiles —based on the segmentation of drinking water customers proposed by Brouwer et al., 2019— are randomly distributed. There was no data available which could be used to set a criterion for the proportion and placement of each of the value profiles used (aware & committed, down on earth & confident, egalitarian & solidary, quality & health concerned).

RESULTS

The work explained led to the first layer of the model expected to develop, the environment (see Figure 1). The following steps will be defining the rules which guide households' behaviour according of the variables defining them (age, income, education…).

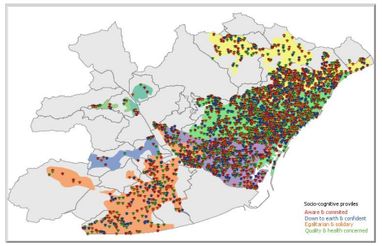

Figure 1. ABM interface representing the Metropolitan Area of Barcelona with 3 000 agents loaded. The legend distinguishes socio-cognitive profile of agents according to their colour.

Once agents' behaviour has been calibrated, the model should be able to become a useful tool to test how the satisfaction of users from Barcelona and its metropolitan area could vary under certain scenarios. For instance, variations leading to changes in water quality, the implementation of new technologies, or awareness campaigns.

DISCUSSION

While the use of the presented ABM can be advantageous for studying how satisfaction and social acceptance work in the hydrosocial cycle, human behaviour and reasoning are complex and diverse processes. Because of this, working on this kind of ABM requires simplifications and the results cannot be expected to be the exact reproduction of reality.

With that in mind, model will help to a better comprehension of the internal dynamics of the social phenomena studied —perception, satisfaction and social acceptance—and improving their understanding. Thus, the actual value of ABM is reached by answering the questions *Why agents are not behaving the way we expected them to do?* and *What do we need them to make different to achieve so?*

Studying these complex processes trough ABM additionally benefits from the multidisciplinary they require. The incorporation of multiple insights to address the issue eases the deeper perspective of factors involved and their interrelations.

REFERENCES

Athanasiadis, I. N., Mentes, A. K., Mitkas, P. A., & Mylopoulos, Y. A. (2005). A Hybrid Agent-Based Model for Estimating Residential Water Demand. Simulation, 81(3), 175–187. https://doi.org/10.1177/0037549705053172

Boelens, R. (2014). Cultural politics and the hydrosocial cycle: Water, power and identity in the Andean highlands. Geoforum, 57, 234–247. https://doi.org/10.1016/j.geoforum.2013.02.008

Brouwer, S., Pieron, M., Sjerps, R., & Etty, T. (2019). Perspectives beyond the meter: A Q-study for modern segmentation of drinking water customers. Water Policy, 21(6), 1224–1238. https://doi.org/10.2166/wp.2019.078

Daly, A. J., de Visscher, L., Baetens, J. M., & de Baets, B. (2022). Quo vadis, agent-based modelling tools? In Environmental Modelling and Software (Vol. 157). Elsevier Ltd. https://doi.org/10.1016/j.envsoft.2022.105514

Doria, M. F. (2010). Factors influencin public perception of drinking water quality. Water Policy, 12(SUPPL. 1), 1–19. https://doi.org/10.2166/wp.2009.051

Grimm, V., Railsback, S. F., Vincenot, C. E., Berger, U., Gallagher, C., DeAngelis, D. L., Edmonds, B., Ge, J., Giske, J., Groeneveld, J., Johnston, A. S. A., Milles, A., Nabe-Nielsen, J., Polhill, J. G., Radchuk, V., Rohwäder, M.-S., Stillman, R. A., Thiele, J. C., & Ayllón, D. (2020). The ODD Protocol for Describing Agent-Based and Other Simulation Models: A Second Update to Improve Clarity, Replication, and Structural Realism. Journal of Artificial Societies and Social Simulation, 23(2). https://doi.org/10.18564/jasss.4259

Koutiva, I., & Makropoulos, C. (2016). Modelling domestic water demand: An agent based approach. Environmental Modelling and Software, 79, 35–54. https://doi.org/10.1016/j.envsoft.2016.01.005

March, H., Garcia, X., Domene, E., & Sauri, D. (2020). Tap water, bottled water or in-home water treatment systems: Insights on household perceptions and choices. Water (Switzerland), 12(5). https://doi.org/10.3390/W12051310

Perello-Moragues, A. (2020). A value-based approach to agent-based simulation for policy assessment: an exploration in the water domain [Doctoral dissertation, Universitat Autònoma de Barcelona]. https://digital.csic.es/handle/10261/235635

Perello-Moragues, A., Poch, M., Sauri, D., Popartan, L. A., & Noriega, P. (2021). Modelling domestic water use in metropolitan areas using socio-cognitive agents. Water (Switzerland), 13(8), 1024. https://doi.org/10.3390/w13081024

Roadmap and strategic routes to mitigate micropollutant occurrence in surface water bodies through WWTP upgrade

Abily M.*, Acuña V. *, Corominas L.*, Rodríguez-Roda I. *-**, Gernjak W.*-***

* Catalan Institute for Water Research (ICRA). Carrer Emili Grahit 101, 17003 Girona, Spain.
**Laboratory of Chemical and Environmental Engineering (LEQUiA), Institute of the Environment, University of Girona, 17071 Girona, Spain.
*** Catalan Institution for Research and Advanced Studies (ICREA), Passeig Lluis Companys 23, 08010 Barcelona, Spain.

Abstract
Contaminants of emerging concern (CEC) occurrence in river is a key challenge that the European Union is eager to address by 2027. We propose here a strategic foresight exercise to build a roadmap aiming to envision potential strategic routes for EU goal fitting WWTP treatment upgrades favouring CEC removal. Exercise starts with a screening and ranking of WWTP tertiary and advanced treatment technology upgrades in the context of the Shared Socioeconomic Pathways (SSPs) global change narratives interpretation for the EU region. Then, envisioned strategic routes allowed identifying and confronting core challenges such as the CEC removal agenda, technologies' performance, requirements for CEC removal and water scarcity. Results shaw that: (i) achieving CEC related EU water quality goals is unlikely before 2040 in all SSPs, (ii) enhancing circular economy solutions in WWTP, (iii) water reclamation, and (iiii) accelerated increase of the technology readiness level of nature-based will be key.

Keywords
Advanced treatment processes; contaminants of emerging concern; Foresight exercise; shared socioeconomic pathways

INTRODUCTION

The European Commission's ambitious target to attain by 2027 good chemical and ecological status in all EU surface water bodies (SWBs), therefore, puts the emphasis on monitoring and addressing contaminants of emerging concern (CEC) occurrence in SWBs. Indeed, the previous EU River Basin Management Plan reporting period (2015-2021), the number of SWB failing to reach a good chemical status rose from 3% to 34% when CEC are considered in the chemical status assessment (EEA, 2018). The chemical status being part of the assessment of the ecological status or potential of SWB, CEC impose decisive limitations on the ecological status of EU SWB. Consequently, the EU Commission's target to attain good ecological status in all SWB already appears challenging (Posthuma et al., 2020); and the situation will be even worse due to climate change (Abily et al., 2021).

The quality of the released urban wastewater concentrating these CEC is a trade-off between investment in wastewater treatment operation and infrastructure, and acceptable released pollutant concentration to comply with established contaminant threshold values. While a broad range of possible tertiary treatment technological solutions upgrades exists (CTO, 2021), envisioning the future of wastewater treatment to specifically target and control CEC release remains challenging. This is due to the complexity and variation in CEC behaviour, to the demanding assessment of the maturity and evolution of technologies toward this specific removal purpose and lastly, due to dependency upon political, environmental, economical and social drivers.

A strategic technological roadmap is a future mapping approach often based on scenario planning to cover a range of uncertain futures. At a practical level, scenario planning and strategic road-mapping approaches have been implemented in a broad range of fields to draw several projected sets of future conditions (Reardon et al., 2013; Rulleau et al., 2020), or to test the viability of strategies under variable circumstances, aiming to foresee and analyse a priori their success and failure potentials.

In this work, we chart and rank WWTP upgrade technologies' characteristics and merits to address the CEC removal goals. Moreover, because (i) the EU agenda for 2027 is expected to be unlikely attainable, and (ii) the WWTP upgrade technologies have a multi-decade lifespan, we matched in a tailormade roadmap these technologies charting and Shared Socioeconomic Pathways (SSP) narratives interpretation at the regional level (via performance, scalability, energy, sustainability, and economy dimensions). Following this, strategic routes are built for SSP narratives. The cross-analysis of the resulting strategic routes highlights common core challenges to be addressed and key opportunities to strengthen the shaping of WWTP technological upgrade investments targeting CEC removal.

It is expected that the key messages regarding challenges and opportunities stressed in this work will be a reference among the urban water sector's various stakeholders (urban planners, technologies providers, water utilities' decision-makers, academics, *etc.*) on the potential directions to prioritize technological development and their implementation direction favoring WFD goals achievement.

METHOD

The conducted approach for the strategic foresight exercise is summarised below.

- A generic roadmap framework was constructed with a structured framed as follow. The time horizon was set, up to 2080 which would represent the expected optimal lifespan of a WWTP upgrade implementation, then key layers of the roadmap were build up:
  - Policy objectives for CEC removal layer.
  - Trends and drivers. This layer is directly framed by our EU regional interpretation for the SSP of interest (O'Neill et all, 2017). The SSP storylines are in that case interpreted specifically for the EU region
  - Function/capability layer. This layer reflects key functions and capabilities in the wastewater treatment utilities/services, potentially developed as a result of technological upgrades.
  - WWTP upgrade technologies layer. This technological layer of the roadmap combines the selected technological upgrades with the appropriate SSP narratives upgrades.
- Screening process. Screening of WWTP technologies for treatment upgrade was conducted via:
  - A series of collaborative workshops, produce a technological layer definition for the roadmap with WWTP technologies upgrade enumeration and evaluation based on twenty criteria. The result of this process is synthetised in Figure 1.
  - A technology selection process where dimension reduction was used to gage the technologies level of performance toward five dimensions: Performance of CEC removal, Economical aspect of the technology, sustainability, energy and scalability performances
- A horizon scanning process has been conducted based on SSP narrative interpretation for the EU region. These interpretations were performed for namely: SSP1 ('Taking the green road'), SSP2 ('Taking the middle road') and SSP5 ('Taking the highway'). We looked at these future changes naratives in terms of (i) in water resource availability and (ii) in CEC levels of production and excretion. Changes in (i) and (ii) are driven by climate change impacts, policy, social behaviour, demographic changes such as urbanisation, population growth and evolution of demographic pyramids in member states and, for example, associated changing pharmaceutical use patterns.
- Strategic routes assessment based on the interdependency between established layer assessment within an iterative process and an adaptation of the framework for the different selected SSPs.

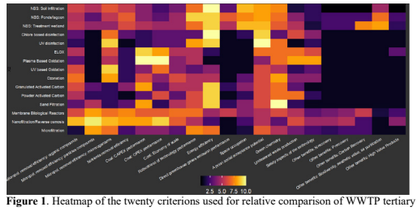

Figure 1. Heatmap of the twenty criterions used for relative comparison of WWTP tertiary treatment technology upgrade (the closer the value to ten, the more performant toward the criteria).

	Microfiltration	Nanofiltration / Reverse osmosis	Membrane Biological Reactors	Sand Filtration	Powder Activated Carbon	Granulated Activated Carbon	Ozonation	UV based Oxidation	Plasma Based Oxidation	EO/EL	UV disinfection	Chlore based disinfection	NBS: Treatment wetland	NBS: Ponds/ lagoon	NBS: Soil infiltration
Performance	3.0	8.0	7.0	3.0	3.0	4.0	3.0	3.0	3.0	4.0	3.0	4.0	3.0	4.0	3.0
Economy	9.0	3.0	3.0	3.0	3.0	4.0	3.0	4.0	3.0	3.0	7.0	7.0	5.0	9.0	9.0
Sustainability	4.0	3.0	5.0	5.0	3.0	4.0	4.0	3.0	3.0	3.0	4.0	3.0	5.0	8.0	8.0
Energy	7.0	3.0	4.0	6.0	6.0	6.0	5.0	4.0	3.0	3.0	9.0	10.0	9.0	9.0	10.0
Scalability	3.0	4.0	3.0	4.0	3.0	4.0	4.0	3.0	3.0	3.0	3.0	3.0	4.0	4.0	8.0

Figure 2. Heatmap of the twenty criterions used for relative comparison of WWTP tertiary treatment technology upgrade (where the closer the value to ten, the more performant the technology toward the criteria).

RESULTS

The presented result focusses only on the SSP5 ('Taking the highway') to illustrate the type production in a concise manner. In the Figure 3, the roadmap is the same for all the SSPs, but only the layer *Trends for drivers 'level of change* (in dashed) is adapted for each SSP. Then based on this roadmap of a potential future, a strategic road is built up to tentatively reach set goals (Figure 4). With an analysed summarized below, a strategic routes explains as follow: *The goal in the SSP5 driven roadmap is to match with the 2027 EU WFD ecological status objective. The need to do so would be a minimum of 85-90% CEC removal for 85-90% of the WWTP volume. As per interpretation of the narrative (IPCC6), temporality to reach these objective will be economically driven. The clear intent to achieve these goals will not start until the economic penalties and the environmental impacts become concerning for society. This ambition would translate into the late implementation of high and holistically performant CEC removal technology, accompanied by specific upgrades directly targeting selective CEC removal as a reactive remediation process. In terms of a technological upgrade selection (from Figure 4), the performance dimension of the technologies and the scalability of the processes are envisioned to favoured due to the increased urbanisation projections. The capabilities to be enhanced in such a scenario would be (i) holistic CEC removal, (ii) ease of implementation in an urban environment and, (iii) capability of the upgrade to combine with other tertiary treatments already in place. Microfiltration, nanofiltration, reverse osmosis and membrane biological reactors are seen as the most applicable for WWTP technological upgrades for this narrative.*

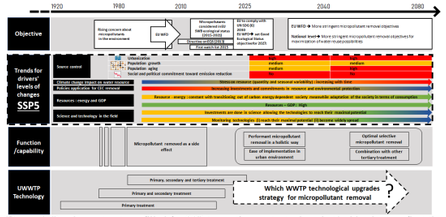

Figure 3. Roadmap structure, filled for SSP5 narrative context where hot/cold colours reflect the drivers' condition evolution

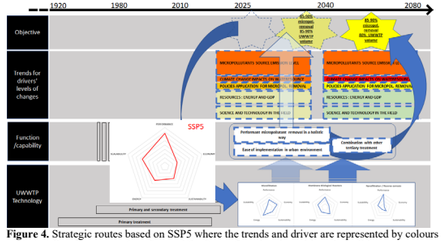

Figure 4. Strategic routes based on SSP5 where the trends and driver are represented by colours palette scaling from green (good) to red (bad) to reflect the given drivers' condition.

REFERENCES

Abily, M., Acuña, V., Gernjak, W., Rodriguez-Roda, I., Poch, M., & Corominas, L. (2021). Climate change impact on EU rivers' dilution capacity and ecological status. Water Research, 199, 117166.

CTO, Finding the right combinations for micropollutant treatment in Europe, Global Water Intelligence, 22(4), 22 April 2021, 47-51.

European Environmental Agency (2018). Chemical Status of Surface Water Bodies. Dashboard DAS-42-en. Accessed from internet on 02-06-2022. https://www.eea.europa.eu/ds_resolveuid/199fc5a57d5540ce99fcf20479530a09

O'Neill, B. C., Kriegler, E., Ebi, K. L., Kemp-Benedict, E., Riahi, K., Rothman, D. S., van Ruijven, P.J., van Vuuren, DP., Birkmann, J., Kok, K., Levy, M., & Solecki, W. (2017). The roads ahead: Narratives for shared socioeconomic pathways describing world futures in the 21st century. Global environmental change, 42, 169-180.

Posthuma, L., Zijp, M. C., De Zwart, D., Van de Meent, D., Globevnik, L., Koprivsek, M., ... & Birk, S. (2020). Chemical pollution imposes limitations to the ecological status of European surface waters. Scientific reports, 10(1), 14825.

Reardon, R., Davel, J., Baune, D., McDonald, S., Appleton, R., & Gillette, R. (2013). Wastewater treatment plants of the future: current trends shape future plans. Florida Water Resources Journal, 10, 8-14.

Rulleau, B., Salles, D., Gilbert, D., Le Gat, Y., Renaud, E., Bernard, P., ... & Stricker, A. E. (2020). Crafting futures together: scenarios for water infrastructure asset management in a context of global change. Water Supply, 20(8), 3052-3067.

ECO STP 2023

6th IWA International Conference on **eco-Technologies for Wastewater Treatment**

GIRONA- SPAIN
26th-29th June

ABSTRACTS BOOK
PART 2
POSTERS

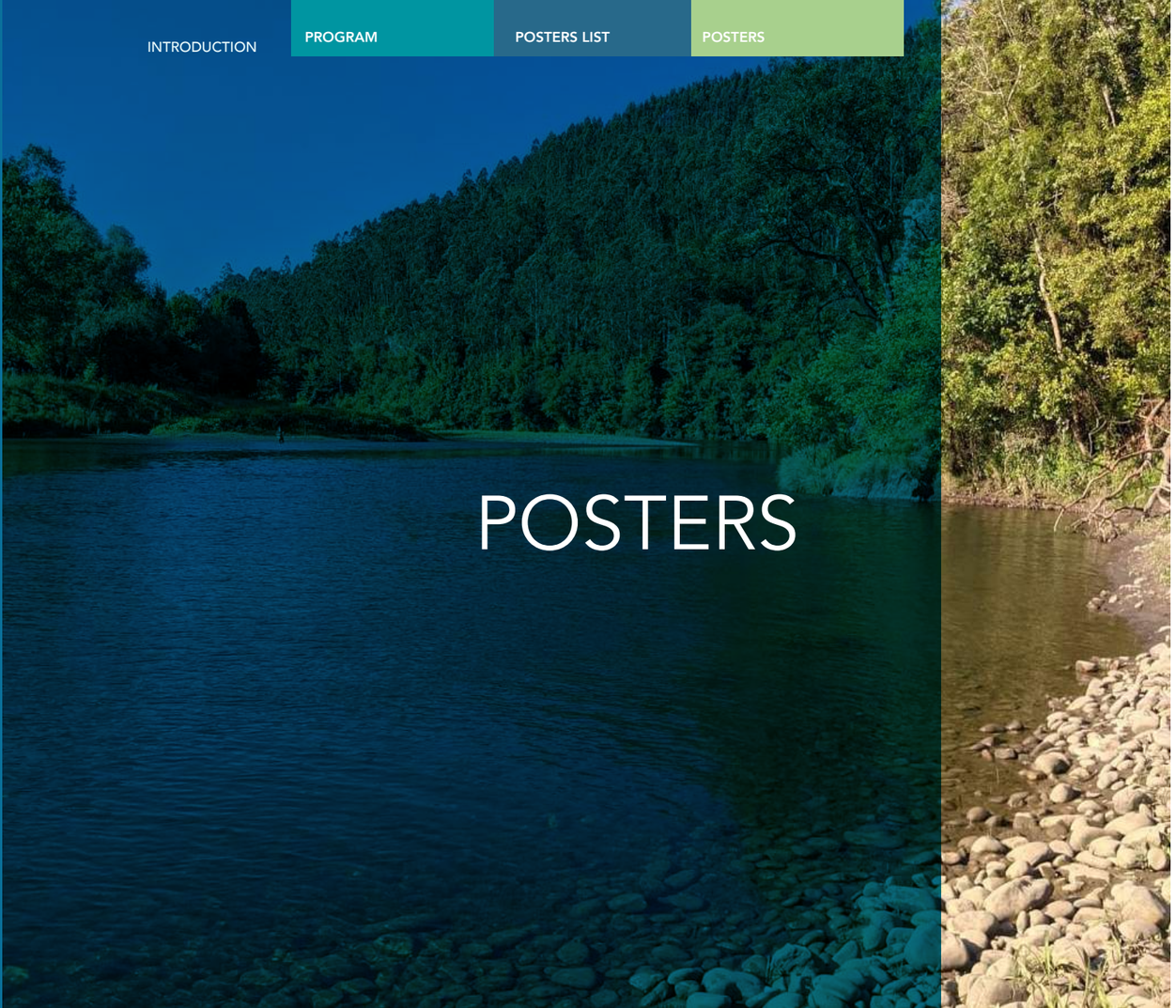

POSTERS

ECO STP 2023
6th IWA International Conference on eco-Technologies for Wastewater Treatment
GIRONA- SPAIN
26th-29th June

1. Emerging Technologies and Processes

POSTER No.	TITLE	PRESENTING AUTHOR	AFFILIATION
1.1	CFD analysis for membrane distillation optimization for wastewater treatment	Morgan Abily	ICRA
1.2	Activated Sludge Model No.1 Calibration and Data Analysis for a Paper Mill Wastewater Treatment Plant	Hussain Ahmed	Tampere University
1.3	In-situ production of H2O2 to enhance electrochemical advanced oxidation efficiency for treatment of pharmaceutical compounds	Izba Ali	Inopsys
1.4	The status of urine recycling as a niche and pathways for development	Abdulhamid Aliahmad	Swedish University of Agricultural Sciences
1.5	Assessing the biodegradability of monoethanolamine for industrial wastewater treatment applications	Tomas Allegue Martinez	Khalifa University
1.6	Pre-enrichment of electrodes with acetoclastic electroactive bacteria and hydrogenotrophic methanogens and external voltage application promotes the performance of anaerobic digestion	Hari Ananda Rao	KAUST
1.7	Photocatalysts for Chemical-free PFOA Degradation – What we know and where we go from here?	Jan Max Arana Juve	Aarhus University
1.8	EPC-EqTech: an innovative turnkey solution to process spent caustic in the Oil&Gas industry	Oscar Arumi Arderiu	CETAQUA
1.9	Cost-effective sorption materials for the removal of pharmaceuticals from aqueous medium	Tomasz Bajda	AGH University of Science and Technology in Krakow
1.10	Activated biochar from rice husk for the removal of micropollutants: Characterization and application in real wastewater	Bernardí Bayarri Ferrer	Universitat de Barcelona
1.11	LIFE Zero Waste Water: from the WWTP to the WRRF treating UWW and bio-waste	Alberto Bouzas	University Of Valencia
1.12	Development of a continuous flow MEC-AD system with autonomous feeding control and performance optimisation.	Kyle Bowman	WASE & University of Westminster
1.13	Natural Clay-Based Materials for the Removal of Antibiotics from Contaminated Water	Monica Brienza	University of Basilicata
1.14	Towards next generation LUCAS® technology for cost-efficient municipal wastewater treatment plants	Michel Caluwé	Waterleau Group NV
1.15	Industrial scale-up, automatization and validation of high-performance multi-stage anaerobic reactor for treatment of wastewater from food and drink SMEs	Jose B. Carbajo	AEMA
1.16	Phase separation in anaerobic fixed-film reactor for wastewater treatment: biomethane production and pharmaceutical compounds removal	Rodrigo Carneiro	Univeristy of Sao Paulo
1.17	Can graphene oxide enhance methane production and pharmaceutical removal under anaerobic digestion?	Oriol Casabella	Catalan Institute for Water Research
1.18	Partially saturated vertical surface flow constructed wetland for emerging contaminants and antibiotic resistance genes removal from wastewater: The effect of bioaugmentation with Trichoderma fungus	Serge Chiron	University of Montpellier

1.19	Treatment of polymer-containing oilfield wastewater by ionizing radiation: demulsification, sterilization and enhancement to oil removal	Libing Chu	Tsinghua University
1.20	Cyanobacteria for heavy metals removal: from pure metal solutions to electroplating industry wastewaters	Matilde Ciani	University of Florence
1.21	Reusability of cyanobacteria-based biosorbents through consecutive adsorption-desorption cycles of bivalent metals	Matilde Ciani	University of Florence
1.22	Pulsed light degradation of pesticides: optimisation & metabolites	François Clavero	Sanodev / Université de Bordeaux
1.23	Simplified design approach supports avenue for selection of complementary P removal mechanisms in return sludge sidestream processes	Kylie Close	The University of Queensland
1.24	Fate of PPCPs within biofilters based on hazelnut shell/sawdust and fed with domestic wastewater	Kennedy Costa da Conceicao	Universidad de Santiago de Chile
1.25	Fabrication of Fouling Resistant and Operationally Stable Nanocomposite Membranes for Refinery Wastewater Treatment	Ngozi Enemuo	University of the Witwatersrand
1.26	Fenton pre-treatment combined with an activated sludge system for carbamazepine removal	Chihhao Fan	National Taiwan University
1.27	Metabolic Modelling of a Designed Bacterial Consortium to Evaluate its Capability for In-situ Removal of Contaminants from Biogas	David Gabriel Buguña	Universitat Autonoma Barcelona
1.28	Anticancer Drugs Affect the Performance and Microbiome in an Aerobic Granular Sludge System Operated in Sequential Batch Reactor	Manuel Jesús Gallardo Altamirano	University of Granada
1.29	Microbial Fuel Cells for Energy Production and Treatment of Industrial Saline Wastewater: Effect of Hydraulic Retention Time	Manuel Jesús Gallardo Altamirano	University of Granada
1.30	Tertiary treatment of nitrite-containing wastewater in a denitrification filter - preliminary studies	Filip Gamon	Silesian University of Technology
1.31	Performance, resilience and energetic balance in ElectroStimulated Anaerobic Reactor (ELSAR®) vs. anaerobic fluidized bed reactor	Antonio Giménez Lorang	FCC Aqualia
1.32	Implementing Ozone/Ultrasound for Trimethoprim and Sulfamethoxazole removal and reducing antibiotic resistance in Finnish reject waters.	Ksenija Golovko	Aalto University
1.33	Microalgal photobioreactor systems for urban wastewater treatment and removal of emerging contaminants	FÉLIX GONZALO IBRAHIM	University of Valladolid
1.34	Anaerobic valorisation of process water from waste sludge hydrothermal carbonization: insights into volatile fatty acids and biomethane production	Matteo Grana	Politecnico di Milano
1.35	Low Cost, Zero Chemical and Energy Efficient Municipal Wastewater (Pre-)Treatment with Electrocoagulation-Floatation	Nazia Hassan	Ghent University
1.36	On-site Regeneration of A modified Activated Carbon by Ozone	Chihpin Huang	National Yang Ming Chiao Tung University
1.37	Flotation and Fenton Process Pilot Technology for the treatment of Real Olive Mill Waste Water	Inês Inocêncio	ADVENTECH
1.38	Isolation of acid tolerant bacteria capable of metal adsorption from acid mine drainage without neutralization	Sohei Iwama	Hokkaido university
1.39	Characterization of iron-rich particles assisted anammox granules: Extracellular Polymeric Substance (EPS) tell the story	Sohee Jeong	Chungnam National University
1.40	Granulation characteristics of the high saline anammox bacteria.	Sohee Jeong	Chungnam National University
1.41	Algal-Bacterial Biofilms to Purify Wastewater, Reduce Power Consumption, and Minimize Carbon footprint.	Daniel Johnson	Algaewheel
1.42	Analyzing the impact of salt concentration on the activity of enriched N-damo bacteria biomass	Garrido Juan M.	Universidade de Santiago de Compostela
1.43	Photo-Membrane Reactor (PMR) for Removal of Per- and Polyfluoroalkyl Substances (PFAS)	Allyson Junker	Aarhus University
1.44	Electrochemical degradation of amoxicillin: Operational parameters optimization and degradation mechanism	Bhavana Kanwar	Indian Institute of Technology Bombay
1.45	Investigating nutrient removal capacity of nature-based solutions (NbS) for eutrophic brackish water	Ece Kendir Cakmak	KTH
1.46	Performance of In-house Photocatalytic Membrane on Hormone Removal	Watsa Khongnakorn	Prince of Songkla University
1.47	Functionalized CNTs-coated carbon electrodes to improve desalination battery performance: Comparison with thermally oxidized carbon electrode	SANGGYUN KIM	Pusan National University
1.48	Removal of Organic Dyes Through Polymer Inclusion Membrane Based on Perbenzylated-β-Cyclodextrin	Jakub Lagiewka	Jan Dlugosz University in Czestochowa
1.49	Feammox biofilm formation to enhance ammonium removal from wastewater	Eduardo Leiva	Pontificia Universidad Católica de Chile
1.50	Fe- and Zn-biochar mediated carbamazepine removal via heterogeneous Fenton process	Anita Leovac Macerak	University of Novi Sad, Faculty of Sciences
1.51	WATER QUALITY AND QUANITY, FRESH WATER SOURCES SUITABLE FOR CREEK RIDGE INFILTRATION IN THE BRAAKMAN ZUID REGION (NL)	Bart Letterie	HZ University of Applied Sciences
1.52	Use of a packed-bed biofilm reactor to achieve rapid formation of anammox biofilms for high-rate nitrogen removal	Yingyu LI	The University of Hong Kong
1.53	Implementing the use of pure oxygen to expand the Integrated Fixed-film Activated Sludge (IFAS) at the Monteagudo (Navarra) Waste Water Treatment Plant (WWTP)	Andrea Lopez	NILSA
1.54	OPFRs degradation by White Rot Fungi: Screening of degraders and approach to the degradation mechanism	Diana Losantos	Universidad Autónoma de Barcelona
1.55	Removal of paracetamol, amoxicillin and triclosan through hazelnut shell biochar used as support medium in filtration processes	Paula Madariaga	University of Santiago of Chile
1.56	Overview of methodologies for evaluating the energy efficiency of the wastewater treatment plant.	Desara Malluta	University of Genova
1.57	Reduction of high concentrations of ammonium nitrogen on a laboratory scale using the activated sludge method.	Kinga Marek	Wroclaw University of Environmental and Life Sciences
1.58	Simultaneous Removal of Zinc and Tetracycline Using Low Methoxyl Pectin Cross-linked by Calcium and Europium	Javier Martinez Sabando	Centro de Física de Materiales (CSIC-UPV/EHU)-Material Physics Centre (MPC)
1.59	Investigation of potential synergistic effect between three different UV wavelengths in water photodisinfection	JAVIER MARUGAN	UNIVERSIDAD REY JUAN CARLOS
1.60	Nature-based solutions to reduce antibiotics and antimicrobial resistance in aquatic ecosystems	Víctor Matamoros	IDAEA-CSIC
1.61	Circular Water Management Opportunities for Wineries Using Novel Thermal Process	Václav Miklas	Brno University of Technology
1.62	Lab Scale Study of Wastewater Treatment using Nano-bubble Aeration in the Activated Sludge Process	Mohamed Mohamed	United Arab Emirate University
1.63	Removal of pharmaceutical compounds from food-processing digestate	Nazanin Moradi	IHE-Delft Institute for water education
1.64	Assessing the feasibility of different membrane technologies for dissolved methane capture from AnMBR effluents	Kristel Moyano	Universitat de Valencia
1.65	The emerging concern of hospital wastewaters: their treatment using aerobic granular sludge technology	Bárbara Muñoz Palazón	Universidad de Granada
1.66	Development and characterization of a new sol-gel coating for anti-scaling properties	Soumaya NOUIGUES	SORBONNE UNIVERSITE
1.67	Characterization of biochar obtained from recovered cellulose and its potential for the removal of pollutants in water	Paula Núñez-Tafalla	University of Luxembourg
1.68	Seasonal changes of waste activated sludge methane potential and its susceptibility to mid-temperature alkaline disintegration	Piotr Oleskowicz-Popiel	Poznan University of Technology
1.69	Impact of Polyethylene terephthalate (PET) degradation products on Mixed Purple Phototrophic Bacteria (PPB) metabolism	Miguel Palhas	NOVA School of Science and Technology - UCIBIO/i4HB
1.70	Valorisation of saline wastewater to produce added-value organic acids of industrial interest	Lidia Paredes	Fundació Universitaria Balmes
1.71	Activated carbon from banana peel: an emerging bio-based material for adsorption of diclofenac	SIVCHHENG PHAL	INSA Toulouse
1.72	CFD Modelling of CP in Roto-dynamic RO System at Seawater Salinity During Turbulent Cross Flow.	NITIKESH PRAKASH	Indian Institute of Technology, Madras
1.73	Industrial wastewater treatment by integrated processes: coupling Fenton with biological	João Ribeiro	Centre for Environmental and Marine Studies - University of Aveiro
1.74	Recovery and valorisation of iron sludge from Fenton processes	João Ribeiro	Centre for Environmental and Marine Studies - University of Aveiro
1.75	Upscaling Anaerobic Reactors using Purple Phototrophic Bacteria for low-cost wastewater reuse and resource recovery	Frank Rogalla	Aqualia
1.76	Mechanisms involved in veterinary antibiotics removal by microalgae-bacteria consortia	Elena M. Rojo	University of Valladolid
1.77	Evaluation of a single-chamber continuous-flow bioreactor to treat urban wastewater with aerobic granular sludge	Aurora Rosa Masegosa	University of Granada
1.78	Use of Atmospheric Dissolved Air Flotation (DAF) in Removal of Surfactants	Ali Rostamiiranagh	Azarbaijan Shahid madani university
1.79	Use of wetlands for wastewater treatment in iran	Ali Rostamiiranagh	Azarbaijan Shahid madani university
1.80	The fate of microplastics in mesophilic anaerobic digestion combined with ultrafiltration membrane.	Patricia Ruiz Barriga	IIAMA (Universitat Politècnica de València)
1.81	BIODAPH20 – Eco-efficient system for wastewater tertiary treatment and water reuse in the Mediterranean region	Victoria Salvadó	University of Girona
1.82	Specific Hydrogenotrophic Methanogenic Activity test: the role of operating conditions	Anna Santus	Politecnico di Milano

1. Emerging Technologies and Processes

1.83	Study of the key parameters influencing ammonium removal from wastewaters by Fe(III)-mediated anaerobic ammonium oxidation (Feammox) microbial communities.	Jennyfer Serrano	Universidad Mayor
1.84	Metal Biosorption from Wastewater under Acidic Environment	Chikara Takano	Hokkaido University
1.85	Application of MABR to Japanese Municipal Sewage Treatment	Hideharu Tanaka	Sanki Engineering Co.,Ltd
1.86	Evapotranspiration toilet: a safe and sustainable treatment for black water	Adriano Luiz Tonetti	Unicamp
1.87	Prospecting Microbial Consortia for high yield Polyhydroxyalkanoates production	Maria Reis	UCIBIO-i4HB/FCT NOVA
1.88	Transformation products generated by oxidation of carbamazepine during various wastewater treatment processes – review and modelling	Jeanne TROGNON	Laboratoire de Génie Chimique
1.89	The impact of high and low temperatures on Candidatus Competibacter fed with industrial wastewater	EIRINI TSERTOU	University of Antwerp
1.90	Phosphorus extraction from sewage sludge ashes and subsequent co-precipitation with other nutrients: insight into factors favouring a beneficial recovery	Andrea Turolla	Politecnico di Milano
1.91	Aquafarm: Biological sludge degradation, nutrient removal and greenhouse gas reduction by macroinvertebrates and macrophytes	Tom van der Meer	Wageningen Environmental Research
1.92	Removal of nanomaterials from wastewater by Microbial Fuel cell – Current knowledge and future direction	Divya Vempati	Indian Institute of Technology Delhi
1.93	Microbial-Mediated Biological Treatment of Wastewater Containing Arsenic (III) and Arsenic (V)	Manoj Kumar Verma	Indian Institute of Technology (BHU)
1.94	Innovative solutions to minimize brine discharges in the mining & metallurgy industry	Alejandro Vilar	Cetaqua
1.95	Atmospheric water harvesting – a case study in South Africa	Frans Waanders	North-West University
1.96	Coal derived PAH removal from various water sources using photo catalytic degradation	Frans Waanders	North-West University
1.97	Chemical-free vacuum UV processes for PFAS abatement	Yicheng Wang	Wetsus
1.98	Fenton self-cleaning MOF and MOF-derived porous carbons modified ceramic membrane towards highly efficient for oil/water emulsion separation	Pei Wang	The University of Hong Kong
1.99	BioPhree: Reversible phosphate adsorption for phosphate removal to ultra-low levels and recovery. Demonstrations and perspectives	Wokke Wijdeveld	Wetsus
1.100	Reactor designs to increase photocatalytic degradation of organic trace substances for improved water protection	Julia Wolters	RWTH Aachen University
1.101	Biochar-nano zero-valent iron composite membrane for the degradation of carbamazepine by activation of persulfate	Yongtao Xue	Ku Leuven
1.102	Convergence of bioreduction process and ICT for practical use of biosorption technology	Hanui Yang	Yonsei University
1.103	Development of a new bioreduction process for the treatment of chromium wastewater	Hanui Yang	Yonsei University
1.104	Novel ceramic SnO2 electrocatalytic membrane for advanced wastewater treatment and water reuse	Chao Yang	The university of Hong Kong
1.105	High-Rate Post-treatment of Sewage from Residential Community by the Down-flow Hanging Sponge System	WILASINEE YOOCHATCHAVAL	Kasetsart University
1.106	Microbial-fuel-cell driven intermitted aeration enhanced the removal of organic matter and nitrogenous compounds	Naoko Yoshida	Nagoya Institute of Technology
1.107	Giving four lives to osmotic membranes with innovative recycling processes (Osmo4Lives)	Bianca Zappulla Sabio	Lequia
1.108	Photocatalysis as a Remediation Technology for Wastewaters Containing Organic Dye Compounds	Elnaz Zehtab Lotfi	East azarbaijan Shahid madani university
1.109	Periodate activation with copper oxide nanomaterials for the degradation of ciprofloxacin-A new insight into the efficiency and mechanisms	Xi Zhang	KU Leuven
1.110	In-situ Fabrication of Titanium Suboxide-Laser Induced Graphene Composites with Enhanced Electrochemical Activity for Environmental Remediation	Ashish Kumar	Indian Institute of Technology Bombay
1.111	The new Hot Bubble Pilot Plant (HBPP) for water sterilisation and desalination.	Adrian Garrido Sanchis	University of New South Wales
1.112	Electrochemical oxidation of ammonia in aqueous solution using high catalytic CuCo bimetallic catalyst supported on Ni foam	Chih-Chao Wu	Feng Chia University

2. Decentralized Strategies

POSTER No.	TITLE	PRESENTING AUTHOR	AFFILIATION
2.1	Light greywater quality consistency: challenge for their treatment and reuse. Study case: Colombia	Jessica Burgos Arias	Universidad Industrial de Santander
2.2	Organic micropollutants in a Euro-Mediterranean resort: occurrence in the water cycle	Gianluigi Buttiglieri	ICRA
2.3	Earthworms influence on macroporosity and biofilm in constructed wetland	Siriane Cazaux	Laboratoire Écologie Fonctionnelle et Environnement
2.4	Industrial-urban symbiosis waste treatment for regional development in Alcoy region (Spain)	Raquel Tamarit	FACSA
2.5	Identifying substrates for greywater treatment in a novel green wall system based on trickling filters	Maximilian Grau	Zurich University of Applied Sciences
2.6	Fuzzy Risk Assessment for Hydraulic Detention Time in UASB Reactors	DAYANE LIMA	Universidade de Aveiro
2.7	Evaluation of a low-tech, passively solar-driven pilot plant for nutrients recovery from source-separated urine on household level	Laila Lüthi	Zurich University of Aplied Science
2.8	Multidimensional assessment of a Nature-based Solution for decentralized small-scale greywater treatment in Costa Rica	Maria Perez Rubi	Leibniz Universität Hannover(LUH)
2.9	Anaerobic digestion effluent treatment in constructed wetlands for agricultural reuse	Pau Porras i Socias	Universidade do Porto
2.10	Comparison of engineered, natural and hybrid wastewater treatment schemes for the removal of nanoparticles from wastewater	Radhika	Indian Institute of Technology, Delhi
2.11	Performance of Multi-module Biochar Filter for Onsite Wastewater Treatment System	Makoto Shigei	Uppsala University
2.12	Potential of integrated membrane and TiO?-based advanced oxidation processes for greywater reclamation	Haruka Takeuchi	Kyoto University
2.13	Nutrients and characterization of greywater from rural households	Adriano Luiz Tonetti	Unicamp
2.14	Adsorption of cadmium on raw and base treated Bolivian natural zeolite	Lisbania Velarde Arnez	Luleå University of Technology
2.15	Surfactant elimination in horizontal and vertical-flow constructed wetlands for greywater treatment	Karen Midori Takahashi	Federal University of Mato Grosso do Sul

3. Resource recovery and safe reuse

POSTER No.	TITLE	PRESENTING AUTHOR	AFFILIATION
3.1	Seasonal accumulation of pharmaceuticals in soils from a full-scale horticultural system irrigated with reclaimed water.	Lucas Alonso	ICRA
3.2	Effective radiation transfer as a major element for the optimized design and operation of purple phototrophic bacteria photobioreactors	Ali Amini	Politecnico di Milano
3.3	Bioelimination of different arsenic species by microalgae and bacteria grown in wastewater treatment plants	Beatriz Antolín Puebla	Institute of Sustainable Processes
3.4	Protein recovery from algal biomass grown in piggery wastewater using deep eutectic solvents	Beatriz Antolín Puebla	Institute of Sustainable Processes
3.5	Use of Industrial Magnetite in Wastewater Treatment	Yara Arbid	Ecole Nationale Supérieure de Chimie de Rennes
3.6	FlashPhos: The complete thermochemical recycling of sewage sludge	Sander Arnout	InsPyro
3.7	Study of struvite precipitation in a fluidised bed reactor using synthetic supernatant	Sergi Astals Garcia	Universitat de Barcelona
3.8	Integrated Resource Recovery from Aerobic Granular Sludge Plants	Nouran Bahgat	Wetsus/TU Delft
3.9	Design of a decision support system for wastewater sanitation in small population centers in the Besòs-Tordera Consortium	Aldo Barahona	Universidad de Barcelona
3.10	Assessment of the role of the solubilization time in the P-recovery process in the Murcia-Este WWTP	Ramon Barat	Polytechnic University of Valencia
3.11	FORWARD-FACTORY: Integrating forward osmosis and advanced biological reactor for water reuse and resource recovery factory	Gaetan blandin	University of Girona
3.12	Novel concentration process based on membranes for volatile fatty acids concentration (ConcentrA)	Gaetan blandin	University of Girona
3.13	Resource recovery from aerobic granular sludges: Gel-forming biopolymers extraction, fractionation and gelling capacity	Abdo BOU SARKIS	Laboratoire de Biotechnologies Agroalimentaire et Environnementale
3.14	Stabilization of sewage sludge in constructed wetlands for reuse in agriculture	Ana Cano	Universitat Politècnica de Catalunya
3.15	Toluene valorization into PHA by Rhodococcus opacus	Sara Cantera	Valladolid University
3.16	Modelling H2 conversion by purple bacteria enriched cultures: evaluating kinetics of gas-fed processes to assess feasibility	Gabriel Capson Tojo	INRAE
3.17	Biological Methanation of WWTP biogas with green H2 for sustainable mobility	Oriol Casal	Cetaqua Centro Tecnológico del Agua
3.18	Nitrogen recovery to produce Smart Fertilisers from wastewater	Oriol Casal	Cetaqua Centro Tecnológico del Agua
3.19	Pharmaceuticals occurrence in water bodies of Catalonia in the last decade, which are the most ubiquitous compounds?	Marc Castaño	ICRA
3.20	Enhancing reactive species exposure in a dielectric barrier discharge plasma reactor through lava rock packing in view of phosphonate-contaminated wastewater treatment and subsequent phosphorous recovery	Changtao Chen	Ghent university
3.21	Analysis of the enrichment in PHA-accumulating bacteria in mixed microbial communities fed with fish-canning waste	David Correa-Galeote	University of Granada
3.22	WATER-MINING Project: La Llagosta Case Study, a flexible fit-for-use wastewater treatment scheme for resource recovery	Teresa de la Torre	Sorigué
3.23	Development of methodologies and tools of risk assessment for wastewater and stormwater reuse	Lucia De Simoni	Polytechnic University of Marche (UNIVPM)
3.24	Degradation and erosion of polymers in alkalised fresh human urine collected in source-separating sanitation systems	Anuron Deka	Swedish University Of Agricultural Sciences
3.25	Drinking Water Treatment Residuals: from waste to a new promising adsorbent of emergent compounds	Rita Dias Santos	CENSE - Center for Environmental and Sustainability Research, School of Science and Technology, NOVA University Lisbon
3.26	Valorisation of the liquid waste of distilled gin production through high rate anaerobic co-digestion and biogas production	Rubén Díez Montero	Universidad de Cantabria
3.27	Enhancing Carbon recovery compromises low N2O emissions: example of a new municipal wastewater treatment.	Carlos Domingo Felez	University of Glasgow
3.28	Sustainability assessment framework and circular diagnosis of water treatment plants	Sofía Estévez Rivadulla	University of Santiago de Compostela
3.29	Exploiting the DO Profile for the Mathematical Modelling of a Mixed PHA-accumulating Microbial Community	Serena Falcioni	Universitat Autonoma de Barcelona
3.30	Improvement of activated sludge systems: should we pay more attention to the role of EPS?	Zoé FAU	INRAE
3.31	BIOUP – Biomethane production through the integration of renewable energy surpluses in WWTP	federico ferrari	acciona agua
3.32	Energy recovery from olive mill waste streams	Ivet Ferrer	Universitat Politècnica de Catalunya
3.33	From removal to recovery: opportunities for bioelectrochemical ammonia recovery from wastewater	Mariella Belén Galeano López	Universitat Autònoma de Barcelona
3.34	Effects of direct filtration of wastewater in anaerobic digestion	Jesús GODIFREDO CALVO	IIAMA (Universitat Politécnica De Valencia)
3.35	Simulation of outdoor conditions for the cultivation of microalgae in a small-scale photobioreactor for wastewater treatment	Félix Gonzalo Ibrahim	University of Valladolid
3.36	Polyhydroxyalkanoates production by mixed microbial cultures from fermented cheese whey under high salinity conditions	Matteo Grana	Politecnico di Milano
3.37	New modelling methodogy to improve phosphorus recovery in WWTPs	Tamara Guijarro	Depuración de Aguas del Mediterraneo
3.38	Upgrading of biogas produced from anaerobic digestion of sewage sludge through in-situ biological hydrogen methanation in mesophilic CSTR system	Mohamed Hellal	Silesian University of Technology
3.39	Development of copper-substituted Prussian blue analog immobilized ion exchange resins for high-performance ammonium recovery from wastewater	Seongwon Im	Korea institute of civil engineering and building technology
3.40	Effect of enhanced hydrolysis of a lipid-rich wastewater on the acidogenic fermentation	Montserrat Jiménez Urpí	VEnvirotech Biotechnology
3.41	Heavy metals uptake with energy crops biomass depending on soil amendment	Mykola Kharytonov	Dnipro State Agrarian and Economic University
3.42	Is bioaugmentation a successful strategy to manipulate biopolymer production from wastewater?	Kasra Khatami	KTH Royal Institute of Technology
3.43	Fate of pollutants in overloaded Wastewater Stabilization Pond (WSP) system	Szymon Kilian	Wroclaw University of Environmental and Life Sciences
3.44	Effect of extracellular polymeric substances (EPS) content on sludge dewaterability using filter-press	Sujin Lee	Pusan National University
3.45	Temperature effect over the PHA:TAG accumulation ratio with mixed microbial cultures and oily substrates	José Ramón Lorenzo Llarena	Universidade de Santiago de Compostela
3.46	Impact of high-rate activated sludge system on WWTP energy balance: Effect of HRT and dissolved oxygen	Cinta Martín Medrano	USC
3.47	Evaluation of the potential of carbon recovery from sewage sludge plus organic wastes by anaerobic co-fermentation in a region	Miguel Mauricio-Iglesias	Universidade de Santiago de Compostela
3.48	Mechanisms of Hexavalent Chromium Reduction by Rhodococcus qingshengii strain SC26	Alice Melzi	University of Milan
3.49	Vinyl Chloride Biodegradation In Contaminated Aquifer Undergoing Stimulation Treatment	Alice Melzi	University of Milan
3.50	Thermal treatment assessment to improve the phosphorus recovery as struvite from olive mill wastes	Marlene Del Mar Mendoza	IRTA
3.51	Starting points for the management of sewage sludge's digestate for phosphorus recovery in the concept of a circular economy	Vesna Mislej	JP VODOVOD KANALIZACIJA SNAGA d.o.o.
3.52	Gas-permeable membranes for the reduction of ammonia emissions in pig farms: A global approach.	Beatriz Molinuevo Salces	Agricultural Technological Institute of Castilla y Léon.
3.53	Production of Volatile Fatty Acids and Kinetic Study of the Anaerobic Digestion of Cheese whey	Beatriz Molinuevo Salces	Agricultural Technological Institute of Castilla y Léon.
3.54	Treatment of pickling waste liquors using a thraustochytrid for removal of organic carbon and nitrogen and simultaneous production of polyunsaturated fatty acids	Satoshi Nakai	Hiroshima University
3.55	Metabolic network reconstruction providing insights into the metabolism relevant for resource recovery in Rhodobacter sphaeroides	Adrian Oehmen	The University of Queensland
3.56	Onsite Sanitation Disinfection: A Modeling Approach for Lime Treatment of Fecal Matter Containing Viruses	Wakana Kaneko	Tohoku University
3.57	Insights on the Agronomic Potential of Structural Extracellular Polymeric Substances (sEPS) from Aerobic Granular Sludge	Benedetta Pagliaccia	University of Florence
3.58	Influence of system geometry and substrate on the removal of linalool and geraniol in zero-liquid discharge unplanted-NBS	Paula Paulo	UFMS
3.59	Reclaimed wastewater reuse impacts: from literature data gaps to integrated risk modelling	Luca Penserini	Politecnico of Milan
3.60	LIFE HIDAQUA: Sustainable water management in high water demanding industries	Queralt Plana	Fundació Eurecat
3.61	Valorizing Methane: Methanotrophs based Biorefinery for Extracellular Biopolymers Production (CH4-BIOPOL)	David Primo Catalunya	Institut Català de Recerca de l'Aigua
3.62	Monitoring and thorough behaviour of volatile methylsiloxanes through a wastewater treatment plant	Nuno Ratola	ALICE - LEPABE - Faculty of Engineering of the University of Porto
3.63	Volatile methylsiloxanes (VMSs) in biogas generation in WWTPs – a mass balance	Nuno Ratola	ALICE - LEPABE - Faculty of Engineering of the University of Porto
3.64	Green roofs and green walls for greywater treatment and reuse: a review of design and operational conditions	Anacleto Rizzo	IRIDRA Srl
3.65	Protein and carbohydrate recovery from secondary sludge biomass generated in wastewater treatment plant	Elena M. Rojo	University of Valladolid
3.66	Towards a more sustainable water treatment and reuse through brines valorisation	Adriana Romero	Cetaqua. Water Technology Center
3.67	Proteins: How electrochemistry can drive the food future of Microbial Protein production	Laura Rovira Alsina	LEQUiA / University of Girona

3.68	Low-cost natural by-products: an efficient way to improve emerging contaminants removal in Nature-based Solutions	Daiane Ruwer	CETIM
3.69	Preliminary study of anaerobic digestion of olive oil industry wastewaters in a conical spouted bed digester	Maria J San Jose	University of the Basque Country UPV/EHU
3.70	Dietary exposure and human health risk assessment of wastewater-derived organic contaminants in leafy vegetables irrigated with treated wastewater under real agricultural field conditions	Lúcia Santos	Catalan Institute for Water Research (ICRA)
3.71	Biofiltration of odorous emissions in WWTPs through the reuse of by-products of the integral water cycle	Lidia Saúco Bozic	DAM Aguas
3.72	LIFE REPTES - Renewable bio-hydrogen production technologies from lignocellulosic waste and sewage sludge co-fermentation	Lidia Saúco Bozic	DAM Aguas
3.73	New advanced applications of compost from sewage sludge. Compost-UP! Project	Lidia Saúco Bozic	DAM Aguas
3.74	Micropollutant uptake in lettuce irrigated with UASB-CW reclaimed wastewater in a water scarce area	Sofia Semitsoglou Tsiapou	Institut Català de Recerca de l
3.75	Soil contamination due to reuse of ZnO nanoparticles contaminated wastewater effluent	Radhika	Indian Institute of Technology, Delhi
3.76	Innovative and versatile integrated solution to remove contaminants of emerging concern in water treatment systems	Aina Soler-Jofra	Acciona
3.77	"Can Peracetic Acid disinfect wastewater?		
3.77b	A Portuguese pilot installation in a WWTP says it can	Diogo Sousa	CENSE - Center for Environmental and Sustainability Research, School of Science and Technology, NOVA University Lisbon
3.78	Enhancing purple phototrophic bacteria granulation by size classification	Samuel Stegman	The University of Queensland
3.79	Evaluation of emerging micropollutants presence in laundry greywater facilities for recycling	Marta Turull	Catalan Institute for Water Research (ICRA)
3.80	Aerobic biodegradability of fat, oil and grease wastes	Carlota Ucha	Universidade de Santiago de Compostela
3.81	Optimization of high rate algal ponds design and operation to enhance biomass production for biofertilizer application	Enrica Uggetti	Universitat Politècnica de Catalunya
3.82	The GAIA project: Bioelectroconversion of orGAnic waste streams and C02 into sustaInAble fuels	Maria Vega	Leitat Technological Center
3.83	Determination of microplastics in three wastewater treatment plants in north-western Spain	Carlota Vijande	Universidade de Santiago de Compostela
3.84	Synergistic cytotoxicity of specific combination of water disinfection by-products assessed by bacterial reverse mutation tests	Laura Vinardell	Eurecat
3.85	Enantioselective uptake, distribution, and biotransformation of chiral pharmaceuticals venlafaxine and O-desmethylvenlafaxine in hydroponic lettuces	Zhen Wang	Catalan Institute for Water Research
3.86	Contactless membrane distillation for effective ammonia recovery from waste sludge	Lei WEN	The University of Hong Kong
3.87	Gravity-driven Membrane Filtration Primary Wastewater Effluent for Irrigating Soil-plants and Hydroponic-plants	Bing Wu	University of Iceland
3.88	Regeneration of high-quality water for reuse by forward osmosis-reverse osmosis system treating urban wastewater	Xuefei Yang	CETIM Technological Centre
3.89	Exploring the potential of olive by-products: antioxidants, sugars, contaminants and energy	Soraya Zahedi Diaz	Instituto Grasa CSIC
3.90	Exploring veterinary drug and resistance genes in livestock manure and their removal by biomethanisation	Soraya Zahedi Diaz	Instituto Grasa CSIC
3.91	Implementation of a municipal wastewater treatment technology to eutrophic environments: Ammonium nitrogen dosing strategy for developing phosphorus recovery from marine sediments	Fengyi Zhu	KTH Royal Institute of Technology
3.92	Application of electrocoagulation treatment to meat industry wastewater	Nataša Dudukoviċ	University of Novi Sad
3.93	Applying helium within a hot-bubble pilot plant to enhance the recovery of pure water from supersaturated air	Thi Thuy Nguyen	University of New South Wales

4. Digitalization

No.	TITLE	PRESENTING AUTHOR	AFFILIATION
4.1	Modelling salinity effects on aerobic granular sludge treating fish-canning wastewater	Paula Carrera Fernández	Ghent University
4.2	SADAR: a digital predictive system with photonic pathogen biosensors for safe water reclamation in WWTP	Ruben Garcia Tirado	FACSA
4.3	Real-time, in-situ nitrite and nitrate analyser for process control within wastewater treatment facilities	Meritxell Grau Butinyac	TE Laboratories
4.4	Prediction of methane production of co-digestion of pig manure in WWTP based on metabolic and machine learning models	Mª Jose Tárrega Martí	GLOBAL OMNIUM MEDIOAMBIENTE, S.L.
4.5	Aerial Mapping of Pollution and Odour in a Wastewater Treatment Plant: the SNIFFIRDRONE project	Lidia Saúco Bozic	DAM Aguas
4.6	Study of atmospheric pollutants generated in wastewater treatment plants using Artificial Intelligence	Lidia Saúco Bozic	DAM Aguas
4.7	Effect of temperature on the kinetics of methane production in the co-digestion of manure and agri-food waste in WWTP	Mª Jose Tárrega Martí	GLOBAL OMNIUM MEDIOAMBIENTE, S.L.
4.8	Digital Water at Consorci Besòs Tordera	Jackson Tellez Alvarez	Consorci Besós Tordera 7 Ccb Serveis Mediambientals, Sau
4.9	Quantitative Image Analysis of Biosolids: Evaluating morphological parameters versus visual features	Sebastian Topalian	Technical University of Denmark
4.10	HADES: a digital twin for the optimization of WWTP performance	Carla Vázquez	ACCIONA
4.11	4SM Project. Spread sewer sensing for sustainable management: advanced tools for optimal sewer management	Oriol Gutiérrez	ICRA
4.12	Comparative modeling of SMP product/utilization on membrane fouling in submerged membrane bioreactor system using MES, PLS, MLR, PCA and ANN techniques	Hana Benaliouche	University of Constantine 3
4.13	Smart sensor monitoring and prediction for safe wastewater reuse: Development of an early Warning System tool	Francesto Fatone	Università Politecnica delle Marche

5. Economics and environmental/social footprint

POSTER No.	TITLE	PRESENTING AUTHOR	AFFILIATION
5.1	Lowering of groundwater levels and their effect on Water, Sanitation and Hygiene services in the Savelugu District, Northern Region of Ghana	Albert Acheampong	KNUST (WORLD VISION GHANA)
5.2	Theoretical feasibility assessment of water loops in the Balearic Islands of Mallorca, Cabrera, and Formentera	Gianluigi Buttiglieri	ICRA
5.3	The uncertainty of N2O emissions is underestimated and hampers accurate comparison of WWT technologies.	Carlos Domingo Felez	University of Glasgow
5.4	Re-thinking industrial wastewater treatment using advanced mathematical modelling.	Xavier Flores-Alsina	Danmarks Tekniske Universitet
5.5	Distinct characteristic pollution and systematical ecological risk assessment of microplastic in the Yangtze River	Qianen Huang	Northwest A&F University
5.6	Case Study of Climate Change Countermeasures (Jeju Island in South Korea)	Jinkeun Kim	Jeju National Univ.
5.7	Social footprint evaluated within Chilean rural wastewater treatment plants	Paula Madariaga	University of Santiago of Chile
5.8	Stakeholders' attitudes towards acceptance in the use of nutrient reuse technologies and decentralised systems in four case studies in Europe	Beatriz Medina	WE&B
5.9	Monitoring of odorous emissions in WWTPs: proposal for a simple procedure	Laura Palli	GIDA spa
5.10	The effect of liquid wastes on a full-scale WWTP nitrogen removal performance	Laura Palli	GIDA spa
5.11	Nature-based solutions in Europe and Latin America: A comparative analysis of regional situation and addressed challenges	Yarima Recalde	University of Girona
5.12	Emerging contaminants occurrence in an urban wastewater impacted aquifer: The Onyar River basin study case	Nonito Ros Berja	ICRA
5.13	Effects of Environmental and Social Factors on Eutrophication in Tonle Sap Lake	Vouchlay Theng	Institute of Technology of Cambodia
5.14	Monitoring and study of specified metals' behaviour in a large Italian wastewater treatment plant	Francesca Tuci	Università degli Studi di Firenze
5.15	The challenges of the indigenous perspective on water security in the Amazon region	Antonina Torrens	Universitat de Barcelona
5.16	Bioplastics accelerated degradation under simulated conditions: generating data for including their end-of-life in LCA studies	Brais Vázquez Vázquez	Universidade de Santiago de Compostela

1. Emerging Technologies and Processes

CFD analysis for membrane distillation optimization for wastewater treatment

A. Tizchang*, T. Tan**, M. Abily* and W. Gernjak*, ***

* Catalan Institute for Water Research (ICRA), C. Emili Grahit 101, 17003 Girona, Spain; Universitat de Girona, Girona, Spain (E-mail: atizchang@icra.cat and mabily@icra.cat)

** Université Côte d'Azur, Polytech Nice Sophia 930 Route des Colles, 06410 Biot, France (E-mail: tian.tan@etu.univ-cotedazur.fr)

*** Catalan Institute for Water Research (ICRA), C. Emili Grahit 101, 17003 Girona, Spain; Catalan Institution for Research and Advanced Studies (ICREA), Passeig Lluís Companys 23, 08010, Barcelona, Spain. (E-mail: wgernjak@icra.cat)

Abstract: In the context of circular economy and of decarbonisation of the society, one of the uprising techniques for industrial wastewater treatment is the use of Membrane distillation (MD) system, because of its capabilities such as low carbon footprint, and being able to be coupled with waste thermal energies. However, the main drawback of these systems is the temperature polarization phenomenon which can lead to performance reduction. To overcome this problem, geometry modifications such as adding spacers in the system is considered. Thus, a simple geometry is built to study the thermal distribution through the system, and then the effects of adding spacers with different configurations is here investigated using Computational Fluid Dynamics (CFD) analysis. The different spacer configurations are characterised and their effect on MD performance are tested. The optimal configuration will be used, via 3D printing to confirm finding on an experimental setup on upcoming study.

Keywords
Computational Fluid Dynamics, Membrane Distillation, OpenFOAM

INTRODUCTION

Among all the potential techniques for industrial wastewater treatment, membrane separation technology is considered one of the promising ways for this goal due to its smaller footprint and higher energy efficiency (Kalla, 2021; Yao et al., 2020). Particularly when the wasted heat source can be accessible as it is the case in many industrial sectors. Unlink most of the membrane separation processes that are pressure driven such as Microfiltration (MF), Ultrafiltration (UF), Nanofiltration (NF) and Reverse Osmosis (RO), the driving force in the membrane distillation (MD) process is partial pressure difference of water vapor across membrane pore caused by the temperature difference (Kim et al., 2017; Martõ Ânez-Dõ Âez et al., n.d.; Shirazi et al., 2015). Hence, MD processes can be regarded as an adequate choice for challenging wastewater since they will not require high pressures (Yao et al., 2020).

However, one of the drawbacks of using MD systems is temperature polarization which is caused due to the difference of the temperature at the membrane interface in the bulk temperature and in the channel (Eykens et al., 2016). To overcome this drawback, modification of geometry using spacers in the feed and permeate channels has been suggested to promote mixing and enhance the mass and heat transfer, which finally will result in reduction of concentration and temperature polarization (Shakaib & Haque, 2019). One of the ways that we can investigate different configurations of spacers to find the optimum configuration for achieving the best performance of the MD is through computational fluid dynamics (CFD) analysis (Kuang et al., 2019; Tan et al., 2019; el Kadi et al., 2020; Hasani et al., 2019).

Thus, in this study, 3D geometries of the MD system with different spacers' configurations are prepared, and after generating the proper mesh, CFD analyses are performed to assess the MD system's performance.

METHODS

A new CFD model is developed to study the thermal and velocity distributions in the MD system. First, 3D structures of membrane distillation system with and without spacers will be designed using open-source CAD software: Salome 9.8 (SALOME Version 9.8.0 Released in December 2021., n.d.). After defining the whole geometry, a suitable mesh will be implemented to the structures. The created meshes will be exported to the OpenFOAM10 (Https://Openfoam.Org/, n.d.), an open-source CFD simulation tool, to study the characteristics of the system in the defined computational domain.

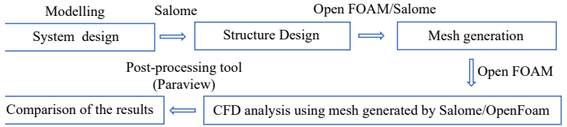

Figure 1. The schematic workflow of the study

PRELIMINARY RESULTS AND DISCUSSION

Fig.2 shows the 3D designed geometry of the MD system with spacers in both feed and permeate channels. As it is shown in the Fig.2, the spacers have a 45◦ angle with the feed and permeate flows. To understand the dimensions of the figure, Table 1. represents the dimensions of this basic case.

As part of this research, different configurations/dimensions of the spacers will be designed for CFD analysis, and after investigating mass, heat and momentum phenomena in each case, the best configuration will be selected to achieve the best MD performance.

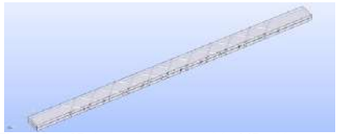

Figure 2. A 3D designed geometry of the MD with spacers.

Table 1. the dimensions of the MD geometry

Parameter	Value
Block length	200 mm
Block width	10 mm
Block height	2 mm
Initial distance	30 mm
Filament radius	0.499 mm
Filament distance	10 mm
Filament amount	11

Fig.3 shows the initial result of the thermal distribution along the MD system without spacers. As it is illustrated in the figure, the feed channel is shown on the bottom, and it has an initial feed temperature of 330◦ C, and as feed flow goes along the channel, the temperature decreases to approximately 312◦ C. The permeate channel is shown on the top, and permeate initial temperature is 290◦ C, and as it travels through the channel, the temperature increases to around 314◦ C.

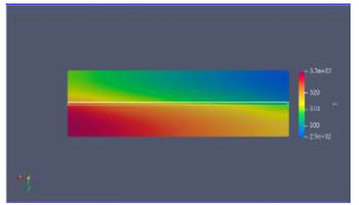

Figure 3. Thermal distribution along the MD module

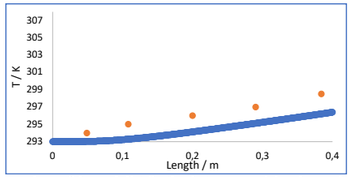

Figure 4. Comparison of thermal distribution between model and experimental results

The initial obtained CFD results showed compatibility with the previous experimental results by Harandi's group (Harandi et al., 2021), therefore for the following studies, other configurations with spacers will be designed and investigated by CFD analysis.

REFERENCES

el Kadi, K., Janajreh, I., & Hashaikeh, R. (2020). Numerical simulation and evaluation of spacer-filled direct contact membrane distillation module. Applied Water Science, 10(7). https://doi.org/10.1007/s13201-020-01261-9

Eykens, L., de Sitter, K., Dotremont, C., Pinoy, L., & van der Bruggen, B. (2016). How to Optimize the Membrane Properties for Membrane Distillation: A Review. Industrial and Engineering Chemistry Research, 55(35), 9333–9343. https://doi.org/10.1021/ACS.IECR.6B02226/SUPPL_FILE/IE6B02226_SI_001.PDF

Harandi, H. B., Asadi, A., Fathi, H., & Sui, P. C. (2021). Combined macroscopic and pore scale modeling of direct contact membrane distillation with micro-porous hydrophobic membranes. Desalination, 514, 115171. https://doi.org/10.1016/J.DESAL.2021.115171

Hasani, S. M. F., Sowayan, A. S., & Shakaib, M. (2019). The Effect of Spacer Orientations on Temperature Polarization in a Direct Contact Membrane Distillation Process Using 3-d CFD Modeling. Arabian Journal for Science and Engineering, 44(12), 10269–10284. https://doi.org/10.1007/s13369-019-04089-x

https://openfoam.org/. (n.d.).

Kalla, S. (2021). Use of membrane distillation for oily wastewater treatment – A review. Journal of Environmental Chemical Engineering, 9(1), 104641. https://doi.org/10.1016/J.JECE.2020.104641

Kim, A. S., Ki, S. J., & Kim, H. J. (2017). Research perspective of membrane distillation: multi-scale and multi-physics phenomena. Desalination and Water Treatment, 58, 351–359. https://doi.org/10.5004/dwt.2017.11423

Kuang, Z., Long, R., Liu, Z., & Liu, W. (2019). Analysis of temperature and concentration polarizations for performance improvement in direct contact membrane distillation. International Journal of Heat and Mass Transfer, 145. https://doi.org/10.1016/j.ijheatmasstransfer.2019.118724

Martõ Ânez-Dõ Âez, L., Va Âzquez-Gonza Âlez, M. I., & Florido-Dõ Âaz, F. J. (n.d.). Study of membrane distillation using channel spacers.

SALOME version 9.8.0 released in December 2021. (n.d.).

Shakaib, M., & Haque, M. E. ul. (2019). Numerical simulations for fluid dynamics and temperature patterns in membrane distillation channels. Heat and Mass Transfer/Waerme-Und Stoffuebertragung, 55(12), 3509–3522. https://doi.org/10.1007/s00231-019-02678-y

Shirazi, M. M. A., Mahdi, M., Shirazi, A., & Kargari, A. (2015). A Review on Applications of Membrane Distillation (MD) Process for Wastewater Treatment. Journal of Membrane Science and Research, 1(3), 101–112. https://doi.org/10.22079/JMSR.2015.14472

Tan, Y. Z., Ang, E. H., & Chew, J. W. (2019). Metallic spacers to enhance membrane distillation. Journal of Membrane Science, 572, 171–183. https://doi.org/10.1016/j.memsci.2018.10.073

Yao, M., Tijing, L. D., Naidu, G., Kim, S. H., Matsuyama, H., Fane, A. G., & Shon, H. K. (2020). A review of membrane wettability for the treatment of saline water deploying membrane distillation. Desalination, 479, 114312. https://doi.org/10.1016/J.DESAL.2020.114312

Activated Sludge Model No. 1 Calibration and Data Analysis for a Paper Mill Wastewater Treatment Plant

H. Ahmed*, H. Pörhö**, E. Toivonen***, E. Räsänen***, J. Tomperi**, M. Vilkko*

* Automation Technology and Mechanical Engineering, Tampere University, P.O. Box 589, FI-33014 Tampere, Finland
(E-mail: *hussain.ahmed@tuni.fi; matti.vilkko@tuni.fi*)
** Environmental and Chemical Engineering Research Unit, Control Engineering Research Group, P.O. Box 8000, 90014 University of Oulu, Finland.
(E-mail: *henri.porho@oulu.fi; jani.tomperi@oulu.fi*)
*** Computational Physics Laboratory, Tampere University, P.O. Box 692, FI-33014 Tampere, Finland
(E-mail: *esko.toivonen@tuni.fi; esa.rasanen@tuni.fi*)

Keywords (maximum 6 in alphabetical order)
activated sludge model; aeration; optimal operation; cost-effective.

INTRODUCTION

Pulp and paper mills discharge large amounts of wastewater that contains various pollutants. Hence, wastewater treatment plants (WWTP) are employed with the aim to remove the maximum amount of these pollutants with minimal operational cost before discharging the wastewater into water basins. With constantly tightening environmental regulations, and the need to optimize the WWTP for economic gains, WWTPs need modern tools to improve their operation and provide cost-effectiveness.

Wastewater treatment is a complex industrial process, as shown in Figure 1. In this process, aeration treatment is used to remove organic substances from the wastewater. The concentration of the organic substances in the aeration treatment is measured as the amount of oxygen required for its oxidization, commonly called Chemical Oxygen Demand (COD). The COD in the aeration process resides in various forms that interact with each other in a complex manner (Osipchuk O. 2020). Moreover, this COD is typically dependent on the wastewater type, weather, or other environmental issues; thus, operating the WWTP without a deep understating of the aeration process may result in a higher amount of effluent COD and poor WWTP operation. The COD in aeration changes with change in the product quality and operating conditions. Additionally, the aeration process requires continuous air pumping that requires extensive energy. As the current global trend is that energy costs will continue to increase, stakeholders are keen to find new cost-effective solutions for the WWTP.

For understanding and analyzing the aeration process, one useful tool is Activated Sludge Model No. 1 (ASM1) (Orig. Henze *et al.* 1987). Such in-depth analysis of the aeration process can help the process operators to make more accurate decisions that could increase the effluent quality and reduce the energy requirement, thus reducing the economic and environmental footprint.

MATERIALS AND METHODS

For modeling the aeration process, ASM1 is considered a reference model (Mulas, M. 2006). This model is widely used in research applications and is developed primarily for municipal wastewater treatment. A typical ASM1 model consists of two parts: an anoxic part for removing nitrogen and an aeration part for oxidizing organic substances from the influent wastewater. In this study, the WWTP processes paper mills wastewater, which is nitrogen deficient. Therefore, nitrogen removal is not the primary objective here; thus, the ASM1 is modified by removing the anoxic part, and only the aeration part is considered. A schematic diagram of the ASM1 model is shown in Figure 2. A comprehensive description of the ASM1 is given in (Henze *et al.* 1987, Jeppsson, U. 1996).

ASM1 model considers that the influent COD consists of biodegradable substances, non-biodegradable substances, and two types of microorganisms. This model has 13 local processes that represent the change in the number of COD substances (Alex *et al.* 2008). In each local process, various organic substances interact with each other with varying reaction rates. The complete list of ASM1 parameters and their default values can be found in (Henze *et al.* 1987).

ASM1 requires details of the influent COD. For this purpose, a sampling campaign was performed in which the wastewater samples were taken at two points: before entering the aeration pool and after the secondary clarifier (Mustonen S. 2022). This sampling campaign was conducted during weeks 22-24, and one composite sample was taken per week. For sampling, composite samplers (HACH AS950) are used that grab a wastewater sample every 4 hours and 40 min and then combined those samples to form a composite sample. These samples were analyzed in the laboratory, and the concentration of various substrates is calculated. Details about the sampling campaign are given in Table 1 (Mustonen S. 2022). For ASM1 calibration, we used the hit-and-trial method. In model calibration, the aim is to find the appropriate model parameter values so that the model result matches the sample results that were taken during the campaign period. In the hit-and-trial method, the model is tested for various combinations of parameters, so that the model results match the benchmark results.

Data generated by the automatic measurement system in the WWTP was utilized. The dataset includes data from 2022-05-01 to 2022-09-16. Selected variables are presented in Figure 3 and the basic statistical properties of these variables are presented in Table 2. The COD and phosphorus measurements were preprocessed with the Potts functional (Weinmann *et al.* 2015) to extract the piecewise-constant functions caused by the sampling method. For outlier removal we used an approach based on running median. Removed values were replaced with linear interpolation. We analyze the delays between wastewater variables by calculating the Time-Lagged Windowed Cross-Correlation (TLWCC) matrices (Boker *et al.* 2002) and finding the lag that maximizes the average correlation coefficient.

RESULTS

The ASM1 model is simulated for the given data using the calibrated parameter, and the results are shown in Figure 4. The COD in the Pulp and Paper WWTP is composed of carbon-based substrates; therefore, only carbon-based substrates are shown here. Figure 4 shows that the model prediction matches the result of the sampling period; therefore, the calibrated model is ready to predict COD concentration in the aeration process for any given data set.

Based on the TLWCC analysis, the average correlation coefficient between influent and effluent COD is maximized with a lag of 16 hours; that is, the influent COD leads the effluent by 16 hours. However, with a larger dataset covering the whole year 2021 (not shown), the average correlation coefficient was maximized with a lag of 23 hours. When comparing effluent COD and BOD, the correlation coefficient was maximized with zero lag.

DISCUSSION

Future work includes creating comprehensive imaginary data for the ASM1, tuning and testing the ASM1 for a larger data set and integrating the secondary clarifier to the new tuned ASM1 model. Future work also includes analyzing the wastewater variables with advanced time series analysis methods.

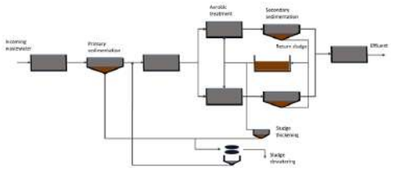

Figure 1. Simplified layout of the studied wastewater treatment plant.

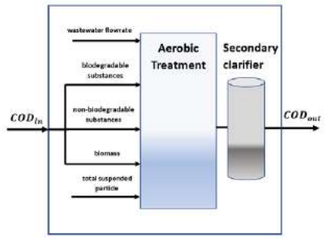

Figure 2. Schematic diagram of ASM1.

Table 1. Composition of influent ($gCOD/ml$)

Week No.	S_I	S_S	X_S	X_I
22	254.4	778.6	404.4	558
23	347.3	855.1	506.6	259
24	263	767.1	386.6	220.3

Table 2. Basic statistical properties of wastewater variables. μ = mean, σ = standard deviation, N = number of datapoints.

	μ	σ	N	Min	Max
COD, aeration influent (mg/L)	2000	480	712	120	3337
COD, effluent (mg/L)	220	51	712	8.9	352
Total phosphorus, effluent (mg/L)	0.7	0.2	712	0.2	1.2
Soluble phosphorus, effluent (mg/L)	0.3	0.1	712	0.06	0.8
BOD_7, effluent (mg/L)	4.5	1.7	16	2.6	8.2
Urea load (kg/d)	590	170	125	0	1100

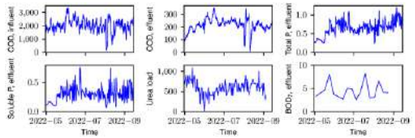

Figure 3. Selected wastewater parameters.

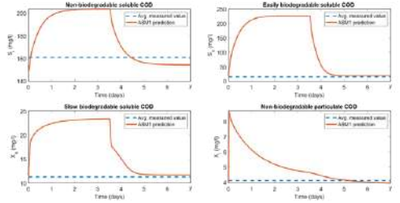

Figure 4. Simulation results.

REFERENCES

Alex, J., Benedetti, L., Copp, J., Gernaey, K., Jeppsson, U., Nopens, I., Pons, MN., Rieger, L., Rosen, C., & Steyer, J-P. (2008). Benchmark Simulation Model no. 1 (BSM1). *Report by the IWA Taskgroup on Benchmarking of Control Strategies for WWTPs*.

Boker, S. M. , Xu, M. , Rotondo, J. L. & King, K. (2002). Windowed Cross-Correlation and Peak Picking for the Analysis of Variability in the Association Between Behavioral Time Series. Psychological Methods, 7 (3), 338-355.

Henze, M., Grady Jr, L., Gujer, W., Marais, G., & Matsuo, T. (1987). Activated Sludge Model No 1. Wat Sci Technol, 29.

Jeppsson, U. (1996). Modeling aspects of wastewater treatment processes. Ph.D. Thesis, *Lund Institute of Technology, Lund.*

Mulas, M. (2006). Modelling and Control of Activated Sludge Processes. PhD. Thesis, *University of Cagliari.*

Mustonen S. (2022). COD fractionation of pulp and paper mill wastewaters. MSc. Thesis, *Tampere University.*

Osipchuk, O. (2020). Use of activated sludge process models. Application at small-scale wastewater treatment plant in Finland. BSc. Thesis, *South-Eastern Finland University of Applied Sciences.*

Weinmann, A., Storath, M., & Demaret, L. (2015). The L^1-Potts functional for robust jump-sparse reconstruction. *SIAM Journal on Numerical Analysis, 53(1), 644-673.*

In-situ production of H_2O_2 to enhance electrochemical advanced oxidation efficiency for treatment of pharmaceutical compounds

Izba Ali*, Raf Dewil** and Kwinten Van Eyck*

*InOpSys - Mobiele waterzuivering voor chemie en farma, Zandvoortstraat 12a, 2800 Mechelen, Belgium
(E-mail: izba.ali@inopsys.eu)
**Department of Chemical Engineering - Process and Environmental Technology Lab, KU Leuven, Sint-Katelijne-Waver, Belgium
(E-mail: raf.dewil@kuleuven.be)

Abstract
The presence of micropollutants in wastewater effluents is a topic of major concern, as these pollutants end up in surface and ground water. The electrochemical advanced oxidation processes (eAOP) have shown a great ability to remove these recalcitrant compounds from water. However, in eAOP the degradation of pollutants is mainly caused by oxidation at anode. Whereas, the cathodic part of the cell does not play a significant role in pollutant oxidation. Recently, there has been an increase in the research interest to generate H_2O_2 at the cathode by supplying air/oxygen. Hydrogen peroxide (H_2O_2) is often used for the treatment of (waste)water due to its highly oxidative and non-polluting nature as it breaks down to harmless compounds (i.e., water and oxygen). H_2O_2 is mainly produced in industrial settings which are relatively expensive and demands extreme care with handling, shipping and storage. Therefore, it is important to devise an in-situ, decentralized H_2O_2 generation and utilization facility for the purpose of water treatment. Electrochemical production of H_2O_2 has become an attractive option as it can be instantaneously brought into utilization for in-situ treatment of water in an eAOP system.
In an electrochemical system, H_2O_2 is produced at cathode surface via oxygen reduction. Various carbonaceous catalyst and electrode materials have been developed over the past decade to enable H_2O_2 production at the cathode. In this study, a carbonaceous cathode material has been prepared and coated with a novel carbon black catalytic coating to efficiently generate H_2O_2. Furthermore, H_2O_2 generated in the system was utilized in-situ for the treatment of pharmaceutical compounds losartan and irbesartan which are often detected in wastewater effluents. The new cathode composition prepared in this study, was found to produce H_2O_2 with >80 % faradaic efficiency. Furthermore, the degradation rate of losartan and irbesartan was increased 6 folds by activating the in-situ produced H_2O_2. In conclusion, the results from this study illustrate that a novel inexpensive carbonaceous catalytic coating for cathode can greatly enhance the efficiency of an eAOP.

Keywords
Carbonaceous cathode; electrochemical advance oxidation; hydrogen peroxide; in-situ water treatment; irbesartan; losartan

INTRODUCTION

The increasing accumulation of parameters compounds in natural waters has led the researcher to devise efficient tertiary treatments for the removal of such compounds from the water before it is being discharged into the aquatic environment. Recently, electrochemical advanced oxidation processes (eAOP) have emerged as efficient and environmentally friendly technology for tertiary treatment. In a traditional eAOP, the degradation of pollutants is mainly caused by their oxidation at the anode, whereas at the cathode H_2 gas is produced which doesn't help in pollutant removal. Therefore, recently there has been an increase in research interest in inducing the oxygen reduction at the cathode to produce H_2O_2. This way, the in situ produced H_2O_2, after activation, can further enhance the pollutant oxidation. In the present study, a carbonadoes cathode is prepared by coating carbon black catalytic ink onto the reticulated vitreous carbon (RVC) surface. The cathode is tested for the production of H_2O_2. Two pharmaceutical compounds, losartan (LST) and irbesartan (IBT) have been have been selected to treat in the electrochemical system because of their frequent detection in water bodies (Khosravi et al. 2021) and resistance towards biological treatment (Tran et al. 2015). The H_2O_2 produced in the system is activated with the help of cobalt ferrite ($CoFe_2O_3$) particles as a catalyst to enhance the degradation of LST and IBT as compared conventional electrooxidation.

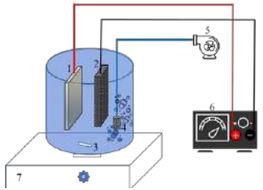

Figure 1. Schematic of the electrochemical system used in the study. 1. BDD anode 2. fabricated cathode 3. magnetic stirrer 4. air diffuser 5. air pump 6. Potentiostat 7. Stirring plate

MATERIALS AND METHODS

All the chemicals were purchased from Sigma Aldrich (Overijse, Belgium), BDD plate electrode from NeoCoat (La Chaux-de-Fonds, Switzerland), and Ag/AgCl reference electrode was purchased from redox.me (Norrköping, Sweden). The working volume was 400 mL, where anode was BDD and cathode was RVC coated with carbon black ink prepared in the lab. RVC was prepared by polymerization of poly-furfuryl alcohol on a polyurethane sponge as a template followed by carbonization at 900-1300°C. The catalytic ink was prepared by mixing carbon black with water, methanol and polytetrafluoroethylene in certain ratios. Air was continuously purged with the help of an aerator. The production of H_2O_2 was monitored by potassium titanium oxalate spectrophotometric method stated elsewhere and the degradation of LST and IBT was tracked by Agilent 1260 Infinity II Prime Online HPLC System (Agilent Technologies, Waldbronn, Germany).

RESULTS AND DISCUSSION

The removal of LST and IBT is represented by C/C_0 in figure 2, where C is the concentration of the compound at any time (t) and C_0 is the concentration at the start of the experiment. Furthermore, in figure 3 the degradation rate (k) is calculated by taking natural log of C/C_0. Since, the graphical plot between "ln C/C_0" and "t" is a straight line with $R^2 > 0.99$, it suggests that the process follows pseudo first order kinetic. The results, as shown in Figure 2 and 3, show that the degradation of LST and IBT in the electrochemical system was enhanced in the presence of $CoFe_2O_3$. The increase in degradation rate indicates the production and activation of H_2O_2 in the system which improved the degradation rate by around 6 times.

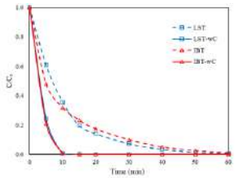

Figure 2. The removal of LST and IBT in the presence and absence of CoF_2O_3 catalyst.

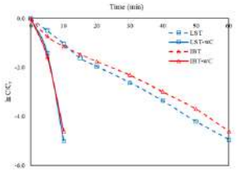

Figure 3. The degradation rate of LST and IBT in the presence (wC) and absence of CoF_2O_3 catalyst.

REFERENCES

Khosravi, A., Saghafi, S., Zolgharnein, J. 2021. Presence of pharmaceuticals in the aquatic environment: A review study. Chemosphere, 273, 129645.
Tran, N. H., Urase, T., Kannan, K. 2015. Occurrence and removal of pharmaceuticals and personal care products in wastewater treatment plants in Vietnam. *Science of the Total Environment*, 527-528, 357-366.

The status of urine recycling as a niche and pathways for development

Aliahmad, A.*, Harder, R., Simha, P., Vinnerås, B., & McConville, J.

Swedish University of Agricultural Sciences, Department of Energy and Technology, Box 7032, Uppsala, SE-750 07, Sweden (E-mail: Abdulhamid.aliahmad@slu.se)

INTRODUCTION

In recent years, there has been a growing call for a paradigm shift toward circular nutrient management [1]. This call is a response to the biogeochemical planetary boundary being pushed beyond its threshold, mainly due to the release of anthropogenic reactive nitrogen (N) and phosphorus (P) into the environment [2]. Environmental impacts are apparent in eutrophication and algae blooms in various water bodies worldwide [3]. Synthetic fertilizers have frequently been associated with these environmental impacts. Additionally, most nutrients that enter the human food chain end up in wastewater and are either partly removed in wastewater treatment plants or discharged directly into water bodies [4]. One approach to enable the recovery of nutrients is urine source separation [5]. Recently, several urine recycling technologies (URTs) have emerged [6]. However, despite their high potential for advancing circularity and relieving ecological perils, these technologies have not yet advanced into large scale implementation/diffusion [7].

In the early stages of adoption, emerging technologies are sheltered from mainstream competition in niches i.e., protected breeding spaces for radical innovations (e.g., labs, etc) [8]. Niches gain momentum as they mature and become technological innovation systems (TISs) with a more shaped structure of actors, networks, rules and regulations [9]. In order to understand why the diffusion of emerging technologies has been delayed a TIS analysis needs to be conducted. This paper therefore aims to explore why URTs failed to catch on and diffuse in terms of large-scale implementation after more than two decades since their introduction. We will examine the state of urine recycling in Sweden and Switzerland, as well as the fundamental processes responsible for its development and diffusion. Our objective is to identify blocking mechanisms that may have hindered the expansion and to formulate recommendations targeting actors and entities, illustrate scenarios for future implementations and pinpoint where change has the most potential for creating the most effects.

METHODOLOGY

The TIS performance is evaluated in relation to a group of essential functions (entrepreneurial experimentation, knowledge development and diffusion, guidance of search, market formation, resource mobilization, and legitimacy creation) [10]. Scholars regard these functions as critical processes within the TIS necessary for the successful development and diffusion of emerging technologies. A TIS analysis identifies lagging functions and their blocking mechanisms.

An essential function in developing TISs, especially early in the formative phase, is "knowledge development and diffusion" [11]. This function is considered to be the most critical system function as it reflects the breadth and depth of the knowledge base and how knowledge is diffused within the TIS [12]. To evaluate this function, we developed a novel multi-criteria framework Table 1. The other functions have been evaluated using a list of indicators Table 2 generated by the co-authors through an iterative process. Subsequently, the Delphi method was followed to perform the evaluation, i.e., the evaluation was conducted by professionals in the field rather than the analyst to prevent any possible bias from occurring.

RESULTS AND DISCUSSION

The knowledge function was rated weak to moderate in terms of innovation in scientific research and diversification of emerging technologies into the TIS, with a tendency for strong publication rate growth and diffusion between countries. For the first criterion results in **¡Error! No se encuentra el origen de la referencia.** showed that the rate of growth in urine recycling publications was between 5 and 10 folds over the decades thus it was deemed high and scored 4. The second criterion revealed very few pilot-scale implementations per technology around the globe thus the criterion was deemed weak and scored 2. From the temporal changes in publications on urine technologies, it is evident that new technologies have been incorporated into the urine recycling TIS over the past three decades. Thus, the third criterion was deemed moderate and scored 3. Based on temporal and spatial changes in publications on urine technologies **¡Error! No se encuentra el origen de la referencia.**, 10 to 30 countries entered the urine recycling TIS in the past two decades (2000-2021) thus the fourth criterion was deemed high and scored 4. For the fifth and sixth criterion, urine recycling was placed in a broader context, i.e., in relation to existing conventional systems. A Scopus search, limited to the same timeframe 1990-2021 and study areas as the comprehensive mapping, was performed results showed that source separation made up a relatively small proportion of total wastewater publications. Urine recycling is a subset of source separation, meaning urine recycling-related publications are less than 1%. As regards the proportion of relevant conferences, mapping of IWA conferences showed that urine recycling TIS conferences made up less than 10% of total conferences in the wastewater sector from 1990-2021. The fifth criterion was therefore deemed weak and scored 1. Despite the low proportion of urine recycling in wastewater publications, looking at the progression of urine recycling TIS over time shows an increasing trend thus the sixth criterion was rated high.

The evaluation of the other functions identified various blocking mechanisms the urine recycling TIS faced, ranging from lack of knowledge, technological advancement, investment, and legal support. Recycling urine goes beyond simply diverting urine; it encompasses the entire value chain, from diversion and collection to post-treatment and application. This was one of the main challenges facing the industry in the 1990s when the value chain was lagging behind [13]. There were issues with urine collection, the technology used was poor, and end users were untrained in handling urine. A robust system was not implemented and responsibilities between the actors were vaguely distributed i.e., it's not clear who and how urine should be collected, treated and handled. To kick off urine recycling and increase its market share and reputation, actors need to work collectively. The direction of intervention needs to be a combination of a top-down and a bottom-up movement; what matters most is that all involved actors are equally motivated. Equally engaged and motivated actors are essential to developing a robust value chain. The absence of government intervention (top-down movement) and reliance only on grass-roots initiatives (bottom-up movement) is a major reason why the current value chain lags behind its potential - the Swedish experience during the 1990s is a relevant example. **¡Error! No se encuentra el origen de la referencia.** below shows our scenarios and combinations for diffusing today's urine recycling TISs.

Table 1: The multi-criteria framework utilized for evaluating the knowledge development and diffusion function in the urine recycling technological innovation system (TIS). The analysis is based on the urine-recycling technologies.

	Evaluation criterion	(1-5) scale Evaluation		
		1-2 (Weak)	3 (Moderate)	4-5 (High)
F1- Knowledge development and diffusion	**Growth in scientific publications within the TIS per decade**	TIS publications increased zero-fold* per decade. TIS publications increased < 2-fold* per decade. (Less than double)	2-fold* ≤ TIS publications growth < 4-fold* per decade. (More than double)	4-fold* ≤ TIS publications growth > 8-fold* per decade. TIS publications increased ≥ 8-fold*.
	Innovation in scientific research per technology within the TIS	Zero pilot-scale trials, and follow-up publications per technology. < 5 pilot-scale trials, and follow-up publications per technology.	5-10 pilot-scale trials, and follow-up publications per urine technology.	11-30 pilot-scale trials, and follow-up publications per technology. >30 pilot-scale trials, and follow-up publications per technology.
	Diversification of emerging technologies into the TIS	Zero new technologies entering the TIS per decade. < 5 new technologies entering the TIS per decade.	5-10 new technologies entering the TIS per decade.	11-30 new technologies entering the TIS per decade. >30 new technologies entering the TIS per decade.
	Diffusion of knowledge between countries	Zero new countries entering the TIS per decade. < 5 new countries entering the TIS per decade.	5 - 10 new countries entering the TIS per decade.	11 - 30 new countries entering the TIS per decade. >30 new countries entering the TIS per decade.
	TIS knowledge volume compared with conventional systems	TIS publications < 1% of conventional systems & TIS conferences < 5% of total conferences /year. 1% ≤ TIS publications ≤ 2% of conventional systems & 5% ≤ TIS conferences < 8% of total conferences /year.	3% ≤ TIS publications ≤ 5% of conventional systems & 8% ≤ TIS conferences < 10% of total conferences /year	6% ≤ TIS publications ≤ 9% of conventional systems & 10% ≤ TIS conferences < 12% of total conferences /year. 12% ≤ TIS publications ≤ 15% of conventional systems & 12% ≤ TIS conferences ≤ 15% of total conferences /year.
	Development of urine recycling publications over time compared to conventional systems **Actors' engagement in knowledge generation**	Negative trend i.e., the progression of urine recycling publications compared to conventional systems is decreasing over time. Not yet defined	Static trend i.e., the progression of urine recycling publications compared to conventional systems is not changing over time. Not yet defined	Positive trend i.e., the progression of urine recycling publications compared to conventional systems is increasing over time. Not yet defined

Table 2: TIS functions and the indicators used for the evaluation.

	Indicators
F1- Entrepreneurial experimentation	▲ The diversity level in the TIS ▲ The engagement and activeness level in the TIS ▲ The experimentation rate in the TIS
F3- Knowledge development	▲ The engagement in knowledge generation in the TIS
F4- Guidance of the search	▲ National strategy for nutrient recovery from wastewater ▲ National policy / incentives enabling urine recycling ▲ Vision and expectations of the sanitation system
F5- Market formation	▲ The number of urine diversion toilets ▲ The number of pilot-scale projects ▲ The price for urine diversion installation ▲ The service fees for urine recycling ▲ The agricultural sector attitudes toward urine-based fertilizer
F6- Resource mobilization	▲ The availability level of human resources in the TIS ▲ The availability level of infrastructure in the TIS
F7- legitimacy creation	▲ The level of lobbying activities against urine recycling ▲ The level of lobbying activities to legitimize urine recycling ▲ The willingness of conventional systems to adopt urine recycling ▲ Users acceptance of urine recycling

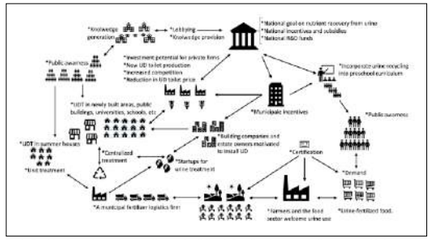

Fig 1: Combination on how urine recycling can be diffused. One direction arrow indicates a one-sided relationship, two directions arrow indicates a two-sided relationship. This illustration shows both bottom-up and up-bottom interventions .

REFERENCES

1. Cordell, D., J.-O. Drangert, and S. White, *The story of phosphorus: Global food security and food for thought.* Global Environmental Change, 2009. **19**(2): p. 292-305.
2. Rockström, J., W. , et al., *Planetary Boundaries: Exploring the Safe Operating Space for Humanity.* Ecology and Society 2009. **14**.
3. Sutton, M.A., et al., *The European Nitrogen Assessment* Cambridge University Press , 2011.
4. Powers, S.M., et al., *Global Opportunities to Increase Agricultural Independence Through Phosphorus Recycling.* Earth's Future, 2019. **7**(4): p. 370-383.
5. Larsen, T.A. and W. Gujer, *Separate management of anthropogenic nutrient solutions (human urine).* Water Science and Technology, 1996. **34**: p. 87-94.
6. Macura, B., et al., *Effectiveness of ecotechnologies in agriculture for the recovery and reuse of carbon and nutrients in the Baltic and boreo-temperate regions: a systematic map.* Environmental Evidence, 2019. **8**(1).
7. Aliahmad, A., et al., *Knowledge evolution within human urine recycling technological innovation system (TIS): Focus on technologies for recovering plant-essential nutrients.* Journal of Cleaner Production, 2022. **379**.
8. Schot, J. and F.W. Geels, *Strategic niche management and sustainable innovation journeys: theory, findings, research agenda, and policy.* Technology Analysis & Strategic Management, 2008. **20**(5): p. 537-554.
9. Markard, J., R. Raven, and B. Truffer, *Sustainability transitions: An emerging field of research and its prospects.* Research Policy, 2012. **41**(6): p. 955-967.
10. Bergek, A., et al., *Analyzing the functional dynamics of technological innovation systems: A scheme of analysis.* Research Policy, 2008. **37**(3): p. 407-429.
11. Hekkert and Negro, *Functions of innovation systems as a framework to understand sustainable technological change: Empirical evidence for earlier claims.* Technological Forecasting and Social Change, 2009. **76**(4): p. 584-594.
12. Hekkert, et al., *Functions of innovation systems: A new approach for analysing technological change.* Technological Forecasting and Social Change, 2007. **74**(4): p. 413-432.
13. Johansson, M., *Urine separation- closing the nutrient cycle.* 2001.

Assessing the biodegradability of monoethanolamine for industrial wastewater treatment applications

Tomás Allegue[1,2] and Jorge Rodríguez[1,2].

(1) Department of Chemical Engineering, Khalifa University, P.O. Box 127788, Abu Dhabi, UAE
(2) Research and Innovation Center on CO_2 and H_2 (RICH), Khalifa University, Abu Dhabi, UAE
(*tomas.martinez@ku.ac.ae*, *jorge.rodriguez@ku.ac.ae*)

Abstract
Wastewater containing monoethanolamine (MEA) is generated in nuclear power plants as it is used to minimize metal pipes' corrosion in steam cycles. If not treated, it can cause environmental problems due to its COD and nitrogen content. Physicochemical processes have traditionally been used to treat MEA, but a more sustainable and cost-effective alternative is possible through biological means. Research on MEA biodegradability is limited to determine if bioprocesses could be a viable option for treating MEA at large-scale. The effect of different MEA concentrations on aerobic MEA degradation is examined using discontinuous tests to evaluate if high concentrations could inhibit biomass activity. The highest removal rate was found with 3 g COD L^{-1} of MEA, 6.2 g COD g VSS^{-1} d^{-1}. The removal rates decreased by 2 and 4 times in tests with 6 and 9 g COD L^{-1}, respectively, attributed to the accumulation of intermediary MEA degradation products.

Keywords
Biodegradation; Monoethanolamine; Industrial wastewater treatment; Batch-test assays.

INTRODUCTION

Wastewater containing monoethanolamine (MEA) is generated in nuclear power plants (NPPs) with pressurized water reactors. MEA is used in the steam cycle of NPPs to minimize the metal corrosion of pipes. If not treated, MEA can lead to serious environmental problems in the receiving water bodies due to its chemical oxygen demand (COD) and nitrogen content. To date, the degradation of wastewater containing MEA has been addressed using expensive physicochemical processes. MEA might be also treated at lower costs and in a more sustainable way by biological means. There are studies assessing the biodegradability of MEA at different redox conditions: aerobic and anoxic (Kim et al. 2010) and anaerobic (Wang et al. 2013). However, the knowledge is limited and the information available is still insufficient to assess if using biological processes might be a feasible alternative to treat this wastewater at an industrial scale. This study is aimed to evaluate if MEA could inhibit biomass activity at high concentrations. For this purpose, the impact of different MEA concentrations on the activity of biomass highly enriched in aerobic MEA degraders is evaluated employing discontinuous batch-test assays.

$$C_2H_7ON + 2.5O_2 \rightarrow CO_2 + H_2O + NH_4^+ + HCO_3^- \qquad (1)$$

MATERIALS AND METHODS

The short-term impact of different MEA concentrations (0.4, 1, 3, 6, and 9 g COD L^{-1}) on the activity of aerobic MEA degraders was examined for 8 h using discontinuous batch-test assays with constant experimental conditions (pH 7; 25°C; O_2 saturation) (Figure 1a). 200 mL of suspended biomass enriched in aerobic MEA degraders was added to each bottle. The biomass used as inoculum was taken from a sequencing batch reactor (SBR) highly enriched in MEA degraders with a specific activity of 4.9 g COD g^{-1} VSS d^{-1} and a concentration of 1.2 g VSS L^{-1}.

RESULTS AND DISCUSSION

The maximum MEA removal rate, 6.2 g COD g VSS^{-1} d^{-1}, was achieved for the assay with an MEA concentration of 3 g COD L^{-1}. In contrast, concentrations above 3 g COD L^{-1} resulted in decreasing removal rates (Figure 1b). For the 6 and 9 g COD L^{-1} tests, removal rates of 3.0 and 1.6 g COD g VSS^{-1} d^{-1} were observed, values which are 2 and 4 times lower compared to the maximum accomplished at 3 g COD L^{-1}, respectively. This drop might be attributed to the accumulation of intermediary MEA degradation products. The initial MEA hydrolysis step, where NH_4^+ and acetaldehyde are produced, seems to be faster than the oxidation of acetaldehyde or other intermediary products. This is supported by the high accumulation of NH_4^+ measured, which does not correspond to the expected ammonium production considering the observed COD removal (Figure 1c) and the negligible nitrification rates accomplished. The maximum rate achieved in the present study is three times higher than the 1.9 g COD g VSS^{-1} d^{-1} reported by Kim et al. (2010) with 1 g COD L^{-1} of MEA. Despite the high rates attained in this study, it is suggested that high concentrations of MEA might negatively affect short-term biomass activity and they should be preferably avoided inside bioreactors treating this type of wastewater. Further research is needed to determine if this inhibition could be reversed through biomass adaptation (long term).

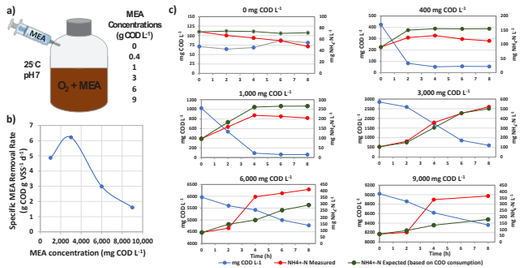

Figure 1. a) Batch-tests experimental set-up and conditions; b) maximum specific MEA removal rates at different MEA substrate concentrations; and c) evolution of the ethanolamine concentration (COD), and the measured and expected ammonium (based on COD consumption observed and stoichiometry of Equation 1) concentrations.

ACKNOWLEDGEMENTS

This study was supported by the Emirates Nuclear Energy Company (ENEC) under Award no. 8434000451, the Emirates Nuclear Technology Center (ENTC) (EX2020-024) and the Research and Innovation Center on CO_2 and H_2 (RICH) (RC2-2019-007).

REFERENCES

Kim, D. J., Lim, Y., Cho, D., and Rhee, I. H. (2010) Biodegradation of monoethanolamine in aerobic and anoxic conditions. *Korean Journal of Chemical Engineering*, **27**(5), 1521–1526.

Wang, S., Hovland, J., and Bakke, R. (2013) Anaerobic degradation of carbon capture reclaimer MEA waste. *Water Science and Technology*, **67**(11), 2549–2559.

Pre-enrichment of electrodes with acetoclastic electroactive bacteria and hydrogenotrophic methanogens and external voltage application promotes the performance of anaerobic digestion

Hari Ananda Rao*, Krishna P. Katuri*, and Pascal E. Saikaly**

*Water Desalination and Reuse Center (WDRC), King Abdullah University of Science and Technology (KAUST), Thuwal 23955-6900, Saudi Arabia (*hari.anandarao@kaust.edu.sa, krishna.katuri@kaust.edu.sa*)
**Environmental Science and Engineering Program, Biological and Environmental Science and Engineering (BESE) Division, King Abdullah University of Science and Technology (KAUST), Thuwal 23955-6900, Saudi Arabia
(Email: *pascal.saikaly@kaust.edu.sa*)

Abstract

Studies have shown that anaerobic digestion (AD) performs significantly better when integrated with microbial electrolysis cell (MEC). However, the role of MEC in enhancing the performance of AD is still not well understood. In this study, five sets of reactor conditions based on introducing a virgin electrically conductive electrode, pre-enriching electrically conductive electrodes with a culture of *Geobacter sulfurreducens* (anode) and hydrogentrophic methanogens (cathode) and operating the MEC-AD reactors with or without power supply (0.8 V) were examined for their role in enhancing the efficiency of methane production in AD. The findings offer new insight for pre-enriching the electrically conductive electrodes and applying external voltage (0.8V), both of which are essential for improving resource recovery (CH_4) from wastewater.

Keywords

Pre-enrichment; *Geobacter sulfurreducens;* hydrogentrophic methanogens; microbial electrolysis cell; anaerobic digestion

INTRODUCTION

Anaerobic digestion (AD) is an effective process for recovering resources as CH_4 from wastewater, but stable performance necessitates a longer hydraulic retention time. In AD, syntropy between fermenters and methanogens is required for the complete breakdown of organic compounds to CH_4. However, the buildup of H_2 and volatile fatty acids (VFAs) at high organic loading rates is harmful for AD process. Therefore, for AD to function properly, the concentration of H_2 and VFAs must be reduced. It has been reported that the overall AD performance has been enhanced by the incorporation of microbial electrolysis cells (MEC) (i.e., insertion of electrically conductive electrodes into AD) (De Vrieze et al., 2014). In the MEC-AD system, the anode enriches electroactive bacteria (EAB) to oxidize organic compounds and reduce the concentration of VFAs, while the cathode promotes the enrichment of hydrogenotrophic methanogens (1) and/or electromethanogens (2) to convert H_2 and/or electrons to CH_4. As a result, MEC-AD systems have shown to be more effective at removing organic matter and producing CH_4 than AD systems alone (Feng et al. 2015).

$4H_2 + CO_2 \rightarrow CH_4 + 2H_2O$ (1)

$8H^+ + 8\,e^- + CO_2 \rightarrow CH_4 + 2H_2O$ (2)

Despite the advantage of this integration, the role of MEC in enhancing the performance of AD is still not well understood. For instance, it is not clear which of the following factors has the greatest influence in improving the performance of AD: i) bioelectrochemical processes at the bioanode and biocathode, ii) biomass retention due to the additional surface area of electrodes, or iii) direct interspecies electron transfer (DIET) between EAB and methanogens at the electrode in the absence of current generation. Therefore, to assess the effect of electrodes in MEC in enhancing the overall performance of AD, five sets of reactor conditions were examined in this study.

MATERIALS AND METHODS

Four sets of MEC-AD reactors (EE-O.C, EE-0.8 V, VE-O.C, VE-0.8 V) and one set of AD reactors (NE-AD) were constructed to test five different start-up strategies (Fig. 1). In EE-O.C, duplicate reactors were started with pre-enriched electrodes (i.e., anode and cathode were pre-enriched with *Geobacter sulfurreducens* PCA and mixed culture of hydrogenotrophic methanogens, respectively) and operated under open circuit mode. In EE-0.8 V, duplicate reactors started similarly as EE-O.C reactors but 0.8 V was applied using a power source (3645 A, Array, Inc.). In VE-O.C, duplicate reactors were started with virgin electrodes (i.e., no pre-enrichment of anode and cathode) and operated under open circuit mode. In VE-0.8 V, duplicate reactors started similarly as VE-O.C reactors but 0.8 V was applied using a power source. The NE-AD reactors represent conventional AD reactors without electrodes. All reactors were made of glass bottles filled with 300 ml of liquid and they had 20 ml of headspace. The reactors were sealed with a bromobutyl rubber stopper held on with an open top screw cap. Gas bags (0.5 L) were connected to the top of the rubber stopper to collect more volume of gas. The anodes in MEC-AD reactors were carbon felt (8 cm L X 6 cm W). The cathodes were nickel mesh (8 cm L X 6 cm W). Sludge collected from an existing lab-scale AD reactor operated at 30°C was used as the inoculum. The sludge composition was: total chemical oxygen demand of 18000 ± 600 mg/L, soluble COD (SCOD) of 310 ± 40 mg/L, total suspended solids of 15400 ± 650 mg/L, and a volatile suspended solids of 11300 ± 400 mg/L. The anaerobic growth medium (pH 8.0) used for the experiments consisted of glucose (2.5 g/L) as the sole carbon source, bicarbonate buffer (80 mM), nutrients (6.71 g/L NaH_2CO_3, 0.31 g/L NH_4Cl, 9.2 g/L Na_2HPO_4, 4.9 g/L NaH_2PO_4, 0.3 g/L KCl, Wolfe's vitamin (10 mL/L)), and trace mineral (10 mL/L) solution. For the first cycle, a growth medium with 20% (V/V) of inoculum was used. The reactors were operated in a fed-batch mode by replacing 60% of the liquid with fresh medium at the end of each cycle. The duration of each cycle was determined based on low current or end of gas production from all reactors. All reactors were operated in a temperature-controlled room at 30 °C. The current in the circuit was determined by measuring the voltage across a resistor (10 Ω) in the circuit using a data acquisition system (Pico data logger, UK), at 15 minutes intervals. Biogas was analyzed using a gas chromatography (SRI Instruments, USA). The SCOD was analyzed using standard methods (Hach Company). The concentrations of glucose and VFAs (acetate, propionate, and butyrate) were analyzed by a high-performance liquid chromatograph (HPLC) (Agilent, USA). The total and suspended solid concentrations were measured according to a standard method (Associations et al., 1920). All chemical analyses were performed in duplicate. The performance of the MEC-AD reactors was evaluated on the basis of the current density of the reactor, I (A/m^2); methane production volume (mL) per fed-batch; coulombic efficiency, CE (%); and COD removal (%). Microbial community analysis was performed using gene amplicon sequencing targeting the Archaea/Bacteria/Eukarya 16S/18S rRNA gene variable regions 4-8 (abeV48-A).

RESULTS AND DISCUSSION

The electrodes were pre-enriched with *G. sulfurreducens* (anode) and mixed culture of hydrogenotrophic methanogens (cathode) in a dual-chamber MEC configuration. The pre-enriched electrodes were then switched to single chamber MEC-AD reactors (EE-O.C and EE-0.8 V) following successful pre-enrichment (reproducible current or CH_4 production). Regardless of the tested conditions, pre-enriched anode (EE-0.8 V) and virgin anode reactors (VE-0.8 V) produced reproducible current after several fed-batch cycles (Fig. 2). Additionally, both the pre-enriched anode reactors and the virgin anode reactors displayed peak current densities of about 5 A/m^2 (Fig. 2). However, compared to the virgin anode (VE-0.8 V) (batch time:~100 hours), the pre-enriched anode (EE-0.8 V) demonstrated more steady and reproducible current generation and a longer batch time (~120 hours) (Fig. 2). Moreover, the CE was higher in EE-0.8 V (60 %) than VE-0.8 V reactors (46 %) (Table 1). The methane accumulation volume per batch was highest in EE-0.8 V (445 ± 16ml) followed by VE-0.8 V (391 ± 15ml), EE-O.C (388 ± 14ml), VE-O.C (342 ± 19 ml) and NE-AD (325 ± 21ml). The COD removal followed a similar trend like methane accumulation where EE-0.8 V reactors exhibited the highest COD removal efficiency of 86±6% (Table 1). The VFAs profile analysis revealed that acetate, propionate and butyrate were produced from glucose and used for CH_4 production (data not shown). Overall, EE-0.8 V reactors showed the best reactor performance (i.e., CH_4 production and COD removal efficiency) compared to the other tested conditions which shows that pre-enriching the electrodes and applying a voltage (0.8 V) improved the MEC-AD performance.

Following 90 days of reactors operation, the microbial community at the anode, cathode, and suspension was characterized with 16S rRNA gene sequencing. PCA analysis showed that the pre-enriched anode and cathode were clustered separately from other samples and they were clustered according to the sample type (i.e., pre-enriched anode and pre-enriched cathode) (Fig. 3). Additionally, samples from the duplicate reactors were clustered together indicating similar microbial composition which is consistent with the identical reactor performance seen between the duplicate reactors operated under the same conditions (Fig. 3). The most abundant 20 operational taxonomic units (OTUs) in each sample were presented in a heatmap with their relative abundance and taxonomic classification at the genus and phylum level. Higher abundance of EAB belonging to *Geobacter* sp. was observed in the anode of EE-0.8 V (24±2%) compared to other reactors which showed lower abundance of *Geobacter sp.* (< 1.5%) (Fig. 4). Higher abundance of *Streptococcus sp.* (2.4- 27.4%) and *Enterococcus sp.* (1.6-20.8%) were observed in the anode and suspension of pre-enriched reactors (EE-O.C & EE-0.8V). However, they were absent from the inoculum (Fig. 4). Higher fraction of fermenters, such as *Trichococcus* sp. (13.7-40%) in the anode and suspension and Chloroflexi (4-13.4%) in the suspension, along with the detection of VFAs in the suspension, suggest their fermentative role in MEC-AD. Acetoclastic methanogens (*Methanosarcina sp.* & *Methanosaeta sp.*) and hydrogentrophic methanogens (*Methanobacterium sp.*, & *Methanospirillum* sp.) were observed in the anode, cathode, and suspension of all tested conditions. The dominant methanogen family varied depending on the biomass type (i.e., anode, cathode, or suspension). For example, *Methanobacterium sp.*, (2-34.5%) was dominant in the cathode and suspension of the reactors. This is expected given the availability of H_2 through the hydrogen evolution reaction at the cathode which provides a better niche for their growth at the cathode. Hydrogenotrophic methanogens also contribute to CH_4 generation by utilizing the H_2 generated through fermentation of complex organics. In contrast, the acetoclastic methanogens, *Methanosaeta sp.,* and *Methanosarcina sp.,* were dominant in the anode of MEC-AD reactors. The existence of *Methanosaeta* sp. at the anode support their role in converting a portion of acetate generated from fermentation to CH_4. In comparison, higher abundance of *Methanosaeta* sp. was observed in the virgin anode reactors (VE-0.8 V &VE-O.C) than pre-enriched anode reactors. This could be explained by the relatively higher abundance of acetoclastic EAB, *Geobacter sp.* on the anode of pre-enriched reactors (EE-0.8 V), outcompeting *Methanosaeta sp.* for acetate. These findings demonstrate that pre-enriching the electrodes with acetoclastic EAB and hydrogenotrophic methanogens and applying external voltage (0.8 V) are successful operating strategy for enhancing the overall performance of AD.

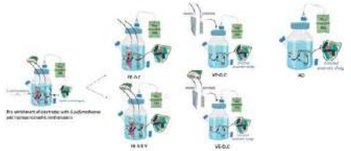

Figure 1. Different sets of reactors. EE-O.C, enriched electrodes operated as open circuit condition; EE-0.8 V, enriched electrodes operated with applied voltage of 0.8 V; VE-O.C, virgin electrodes operated as open circuit condition; VE-0.8 V, virgin electrodes operated with applied voltage of 0.8 V; and AD, anaerobic digester as control.

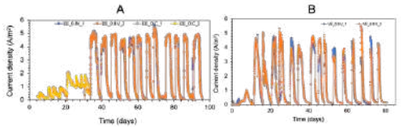

Figure 2. Current generation of pre-enriched (A) and virgin electrodes (B) of MEC-AD reactors.

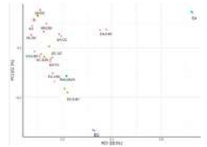

Figure 3. Principal Components Analysis (PCA) of microbial communities based on unweighted UniFrac distance matrix. EA- Pre-enriched anode; VA-virgin anode; EC-pre-enriched cathode; VC-virgin cathode; ES-pre-enriched reactors suspension; VS- virgin reactors suspension; O.C-open circuit; AD-anaerobic digestion

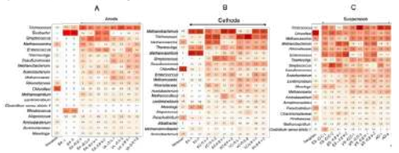

Figure 4. Heatmap showing the top 20 operational taxonomic units identified in the anode (A), cathode (B), and suspension (C). PEA- pre-enriched anode; VA-virgin anode; PEC-pre-enriched cathode; VC- virgin cathode; PES-pre-enriched reactors suspension; VS- virgin reactors suspension; O.C- open circuit; AD-anaerobic digestion

Table 1. Performance of five set of reactors

Reactors	Methane volume (mL/batch)	COD removal (%)	CE%
EE-O.C	388 ± 14	78 ± 4	
EE-0.8V	445 ± 16	86 ± 6	60 ± 7
VE-O.C	342 ± 19	75 ± 7	
VE-0.8V	391 ± 15	82 ± 4	46 ± 5
NE-AD	325 ± 21	70 ± 7	

REFERENCES

De Vrieze, J. , Devooght, A. , Walraedt, D. , Boon, N. , 2016. Enrichment of Methanosae- taceae on carbon felt and biochar during anaerobic digestion of a potassium-rich molasses stream. Appl. Microbiol. Biotechnol. 100 (11), 5177–5187 .

Feng, Y. , Zhang, Y. , Chen, S. , Quan, X. , 2015. Enhanced production of methane from waste activated sludge by the combination of high-solid anaerobic digestion and microbial electrolysis cell with iron–graphite electrode. Chem. Eng. J. 259, 787–794 .

Photocatalysts for Chemical-free PFOA Degradation – What we know and where we go from here?

Jan-Max Arana Juve*,**, Juan A. Donoso Reece**, Michael S. Wong**, Zongsu Wei* and Mohamed Ateia***

* Department of Biological and Chemical Engineering, Aarhus University, Universitetsbyen 36, 8000 Aarhus C, Denmark (*arana@bce.au.dk, zwei@bce.au.dk*)
** Department of Chemical and Biomolecular Engineering, Rice University, Houston, TX, USA (*jad15@rice.edu; mswong@rice.edu*)
*** Center for Environmental Solutions & Emergency Response, US EPA, Cincinnati, OH, USA (*Ibrahim.Mohamed@epa.gov*)

Abstract
Perfluorooctanoic acid is a toxic and recalcitrant perfluoroalkyl substance commonly detected in environmental samples. Recent advances in chemical-free photocatalysis emerge for the sustainable degradation of PFOA. This work (I) classifies the state-of-the-art of chemical-free photocatalysts for PFOA degradation in families of materials, (II) describes the evolution of catalysts and discusses the strategies to enhance their performance, and (III) identifies current research gaps and future research opportunities. This study will assist researchers and practitioners to develop rational photocatalyst designs for green degradation.

Keywords
Chemical-free, Near-zero PFAS discharge, Photodefluorination, PFAS perspectives

INTRODUCTION

Photocatalysis has emerged as a viable option for PFOA degradation due to its free chemical additives, low cost, and production of different reactive spices. The recent upgrowth in the number of works, the different parameters, and the variety of catalysts developed challenge their comparison to optimize the photocatalytic degradation of PFOA. It is therefore critical to structure the main families of materials, compare their performance, practical strengths, and drawbacks, and provide insights for future research trends.

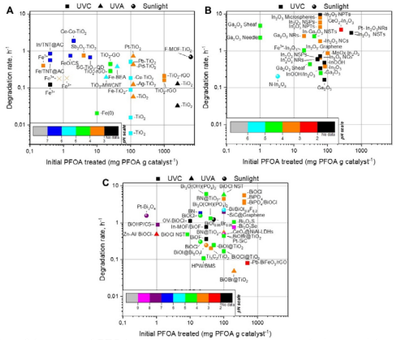

Figure 1. Map of the reported PFOA treatment efficiency of photocatalytic materials, a) Ti and Fe-based materials, b) In and Ga-based materials, c) Bi and novel materials.

CHEMICAL-FREE PHOTOCATALYSTS FOR PFOA DEGRADATION

We extended the PFOA-degrading materials classification (Xu, Ahmed, et al., 2017) to 7 families (Ti, Fe, Ga, In, Bi, Si, and BN, Figure 1). From our evaluations, the defluorination is not the only important parameter of photocatalyst performance, while the catalyst stability, solution pH, and irradiation energy are also critical. Novel photocatalysts have also been devloped to overcome the limitations of Ti-based materials, the catalyst recovery, and the scarcity and high cost of the post-transition catalysts. Technoeconomic analysis is an underdevelopment tool to compare materials and technologies.

WHAT DO WE KNOW AND WHERE DO WE GO FROM HERE?

Highly efficient photocatalysts are produced, although complete defluorination in a time-feasible frame has not been achieved yet. The improvement of the materials design (electropositive materials, oxygen vacancies, amination), effective heterojunctions (Type II p-n materials), electron trapping strategies (Pt, graphene), and reactive species production (facet engineering, crystal phase tunning) can realize the chemical-free zero PFAS discharge. Practical inconveniences such as low concentrations, light spending, and complex matrixes can be overcome by developing adsorptive photocatalysts (Arana Juve, Li, et al., 2022) and further understanding of the role of coexisting species. Additionally, the material stability, irradiation parameters (photon flux, fluence dose), energy input, and mass balances need to be further discussed to solve the global PFAS problem.

REFERENCES

Arana Juve, J.-M., Li, F., Zhu, Y., Liu, W., Ottosen, L. D. M., Zhao, D., and Wei, Z. (2022) Concentrate and degrade PFOA with a photo-regenerable composite of In-doped TNTs@AC. Chemosphere, 300, 134495. https://doi.org/10.1016/j.chemosphere.2022.134495.

Li, F., Duan, J., Tian, S., Ji, H., Zhu, Y., Wei, Z., and Zhao, D. (2020) Short-chain per- and polyfluoroalkyl substances in aquatic systems: Occurrence, impacts and treatment. Chemical Engineering Journal, 380(2019).

Xu, B., Ahmed, M. B., Zhou, J. L., Altaee, A., Wu, M., and Xu, G. (2017) Photocatalytic removal of perfluoroalkyl substances from water and wastewater: Mechanism, kinetics and controlling factors. Chemosphere, 189, 717–729. https://doi.org/10.1016/j.chemosphere.2017.09.110.

EPC-EqTech: an innovative turnkey solution to process spent caustic in the Oil&Gas industry

E. Mundaray*, O. Arumi*, M. Pastur*, C. Pastor*, B. Lefevre**, V. Almirall**, S. Arca***, F. Senol***, B. Vlkcan***, O. Sahin***, C. Echevarria*, J. Tobella*

* Cetaqua, Cornellà de Llobregat, Carretera d'Esplugues, 75, 08940, Spain
(E-mail : *eleana.mundaray@cetaqua.com; oscar.arumi@cetaqua.com; mateo-bruno.pastur@cetaqua.com; claudia.pastor@cetaqua.com; carlos.echevarria@cetaqua.com; joana.tobella@cetaqua.com*)
** AQUATEC, proyectos para el sector del agua, S.A.U. Passeig Zona Franca, 48, 08038, Barcelona, Spain
(E-mail: *blefevre@aquatec.es; valmirallh@agbar.es*)
*** Tüpras Güney Mah Petrol Cad. No: 25 41790. Kâfkez/Kocaeli, Turkey
(E-mail: *SERHAT.ARCA@tupras.com.tr; Feriye.SenolKapti@tupras.com.tr; Ocan.Sahin@tupras.com.tr; BekirVolkan.Sisman@tupras.com.tr*)

Abstract
Spent Caustic from petrochemical industries is a complex concoction of various pollutants, not only making it a threat to the environment, but also very difficult to treat using conventional treatment processes. EPC-EqTech creates a novel solution capable of processing spent caustic at low-cost and within regulatory parameters. Different laboratory scale experiments have been performed obtaining a degradation of more than 80% COD and 100% sulphide. The obtained results allow to design a prototype (1 m^3/h) based on a pre-peroxidation step followed by Electro-peroxicoagulation (EPC) unit that will be operated for 12 months to demonstrate a cost-effective spent caustic processing solution for the Oil&Gas sector that minimises environmental impact and enables refineries to meet ever tightening regulations. The prototype will be located in an oil refinery of Tupras company, Turkey.

Keywords:
Electro-peroxicoagulation; Electrochemical technology; Oil&Gas; Petrochemical; Spent Caustic

INTRODUCTION

In the petrochemical industry, alkaline washing processes for oil product desulphurisation purposes result in spent alkaline solutions, known as spent caustic (SC) or sour water, which contains very high Chemical Oxygen Demand (COD) levels and several other hazardous contaminants such as sulphides, mercaptans, etc. Due to these contaminants, these wastewaters are difficult to treat and very harmful and toxic to the environment. Consequently, SC wastewater treatment can be both challenging and expensive.

Today, the global Oil&Gas industry spends ~3.5 bn€ p.a. to process spent caustic making it a critical challenge [1]. However, due to regulatory tightening designed to reduce environmental impacts, costs are now climbing further. These complex wastewaters are difficult to treat using conventional processes. Traditionally, various SC disposal techniques were adopted for disposal such as: deep well injection, biological treatment with careful dosage, incineration, wet air oxidation or disposal off-site. Many of these traditional spent caustic treatment processes have proven to be unattractive due to key issues: (i) difficult operation; (ii) significantly cost prohibitive; (iii) damaging to the environment (i.e. toxic volatile organic compounds, air contamination and soluble mobile organics) and/or (iv) inability to treat extremely hazardous materials meaning they do not meet regulations [2].

Since 2016 Cetaqua and Aquatec have been collaborating in the development of an innovative solution: "EPC-EqTech" – a plant that combines three electrochemical technologies to create a novel solution capable of processing SC at low-cost and within regulatory parameters.
EPC-EqTech technology demonstration is within FTI-H2020 project that focuses on the adaptation of the EPC technology for suitability with spent caustic, the novel materials selection required for reactors and other equipment and, the adaptation to the layout design; process configuration and combination of processes to achieve optimal processing capability.

This present study, based on the EPC-EqTech project, is focused on the optimization of the process, to ensure both, a cost-effective spent caustic processing solution for the Oil&Gas sector that minimises the environmental impact and enables refineries to meet ever tightening regulations, and the safety of the process, taking into account the gas generation, and the temperature stream regulation.

MATERIALS AND METHODS

The stream selected for treatment has a high COD - range of 60-85 g/L - an average pH of 11.5 ± 0.2, a conductivity of 223 ± 0.5 mS/cm, and highly odorous reduced sulphur compounds, such as sulphides (average concentration of 3 ± 0.5 g/L) and mercaptans, as well as corrosive organic species.

The variables for process optimization were the reaction time, the H_2O_2 dosage, and the electrical current during the EPC process. Calorimetry tests were carried out in conditions equivalent to those that the system will be operating in the final design of the plant. Last, respirometry tests were performed varying the pH and the amount of treated spent caustic that is introduced in the biological reactor.

RESULTS AND CONCLUSIONS

During the laboratory phase, the key goals of the project were achieved by degrading more than 80% of COD and 100% of the sulphides (Figure 1). Removal efficiencies and costs seemed to be better compared with other techniques used for eliminating spent caustic. There have also been identified other benefits such as treatment on site, eliminating the need for transport, possibility of roving units to be used by the same client at different sites, etc. In addition, the technology is modular, so reactors and pumps can be added and can be scaled up for different customer size.

Apart from the tests performed to optimize the process itself, calorimetry and respirometry tests have been carried out to optimize the cooling system and the effluent pH adjustment and flow conditions respectively. Based on theoretical calculations and laboratory tests, two parallel heat exchangers are needed to dissipate the energy generated during the reaction and to maintain the spent caustic stream at about 30-35ºC (Figure 2). The effluent conditions have been determined through respirometry trials. It has been concluded that the optimal option is to adjust the pH of the treated spent caustic to 10.5-11 and discharge it upstream to biological treatment at a flow rate of 1 m3/h (Figure 3).

On the other hand, to ensure safe operation from the point of view of health and safety, a gas treatment ventilation has been added. The forced ventilation installed in the main reaction tank will allow the dilution and dispersion of the hydrogen generated during the process. The minimum air flow has been calculated for the worst case scenario, in which the generation of hydrogen and hydrogen sulphide (generated in uncontrolled acid pH events) gases are maximized.

The results obtained from the laboratory scale tests allowed to optimize the operational and safety design of the plant. Once the pilot of the EPC process has been constructed, commissioning will be performed. At this point the system will be operating at design conditions. Finally, 12-months of commercial trials at Tüpraş technically will validate the processing capability of the plant and the materials capability to withstand spent caustic. As an output a case study of results will be produced that will be used to prove the capability and commercial benefit potential of EPC-EqTech to our stakeholders.

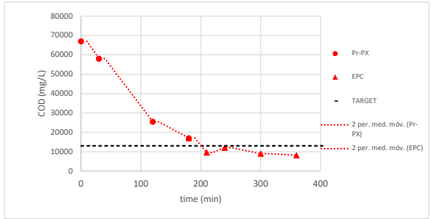

Figure 1. Operation conditions: Pre-peroxidation (Pr-PX), ElectroPeroxiCoagulacion (EPC).

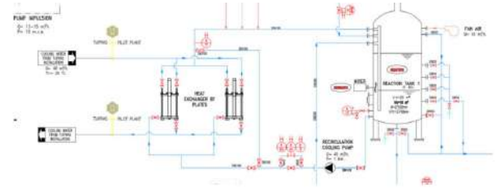

Figure 2. Cooling system and reaction tank.

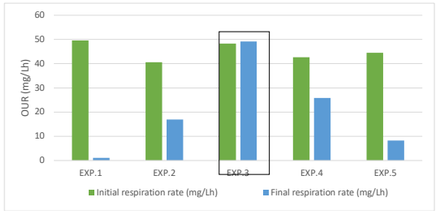

Figure 3. Impact of biomass in WWTPi:

REFERENCES

1. Siemens Energy I-WS. Water Recycling Efficiency In Ethylene Spent Caustic Treatment, Part I: Cost. Water Online. https://www.wateronline.com/doc/water-recycling-efficiency-in-ethylene-spent-caustic-treatment-part-i-cost-0001. Published 2018.

2. Seyedin S, Hassanzadeganroudsari M. Evaluation of the Different Methods of Spent Caustic Treatment. Int J Adv Res Sci Eng Technol. 2018;5(2):5275-5283.

Cost-effective sorption materials for the removal of pharmaceuticals from aqueous medium

Tomasz Bajda*, Agnieszka Grela*,**, Joanna Kuc*,***, Agnieszka Klimek*, Jakub Matusik*, Justyna Pamuła**, Wojciech Franus ****

* Faculty of Geology, Geophysics and Environmental Protection, AGH University of Science and Technology, 30-059 Cracow, Poland (E-mail: *bajda@agh.edu.pl, agrela@agh.edu.pl, jkuc@agh.edu.pl, aklimek@agh.edu.pl, jmatusik@agh.edu.pl*)
** Department of Geoengineering and Water Management, Faculty of Environmental and Power Engineering, Cracow University of Technology, 31-155 Cracow, Poland (E-mail: grela@pk.edu.pl, justyna.pamula@pk.edu.pl)
*** Faculty of Chemical Engineering and Technology, Cracow University of Technology, 31-155 Cracow, Poland (E-mail: joanna.kuc@pk.edu.pl)
**** Department of Construction Materials Engineering and Geoengineering, Faculty of Civil Engineering and Architecture, Lublin University of Technology, 20-618 Lublin, Poland (E-mail: w.franus@pollub.pl)

Abstract
Erythromycin (ERY), colistin (KOL), fluoxetine (FLUO), amoxicillin (AMO) and 17-alpha-ethinylestradiol (EST) are pharmaceuticals (PhCs) whose concentrations in water and wastewater have been reported to exceed normative levels. As the methods used so far to remove ERY, KOL, FLUO, AMO, and EST from aquatic environments have not been effective, it is necessary to develop effective methods for their removal. In the present study, fly ash (FA)-based zeolite materials that have not been previously investigated as ERY, KOL, FLUO, AMO, and EST sorbents, were used. The effects of adsorbent mass, contact time, and initial concentration of PhCs on the removal of ERY, KOL, FLUO, AMO, and EST were analysed. The analysed PhCs were removed within the first 2 min of reaction with efficiencies above 85%. The most efficient sorption was obtained at a sorbent dose of 1-2 g L-1. The removal efficiency of PhCs decreases according to the order: EST>AMO>COL>FLUO>ERY. A five-fold regeneration of the sorbents showed no significant loss of adsorption efficiency. These results indicate that zeolite materials effectively remove ERY, KOL, FLUO, AMO, and EST and can be further investigated for removing other pharmaceuticals from water and wastewater.

Keywords
adsorption; zeolite; carbon–zeolite composite; wastewater; antibiotics

INTRODUCTION

Pharmaceuticals are among the pollutants that are often found in wastewater but also surface water. This is because conventional wastewater treatment processes using mechanical, chemical and biological processes are not designed to remove PhCs (Park et al., 2020). In addition, various chemical reactions during wastewater treatment can produce metabolites and transformation products of PhCs, making the treated wastewater a source of surface water pollution (Tarpani, Azapagic, 2018). Therefore, the search is for advanced materials and technologies that can eliminate PhCs in wastewater or water treatment. PhCs and their metabolites can be removed by adsorption or photocatalytic degradation (Mansouri et al., 2021). The adsorption efficiency depends on the sorbents' surface properties, the PhCs' physico-chemical properties and the environmental conditions in the aqueous phase. The present work reports the results of adsorption efficiencies from solutions through selected PhCs: ERY, KOL, FLUO, AMO, and EST. Their occurrence dictates the selection of these compounds in wastewater and that these PhCs should be monitored, so that surface water quality does not deteriorate. ERY, KOL and AMO are different-generation antibiotics, while FLUO is an antidepressant and EST is a hormonal drug. Synthetic zeolites and zeolite-carbon composites were used as sorbents.

MATERIALS AND METHODS

Sorbents

Zeolites are tectosilicates consisting of about 50 minerals with synthetic analogues. Their structure is formed by three-dimensional networks of Al/Si tetrahedrons arranged in channels containing water and exchangeable alkali metal or alkaline earth metal cations. Due to these particular structural features, they are widely used in the separation and refining industry as catalysts, adsorbents and ion exchangers (Novembre et al., 2021). Zeolite NaP1_FA was produced by hydrothermal synthesis from fly ash (FA). Hydrothermal synthesis of the zeolite-carbon composite NaP1_C was obtained using carbon-rich FA fly ash. The main difference between the sorbents used is the use of FA with different carbon contents as substrate in the synthesis reaction. Thus, the carbon content of NaP1_FA is 5.5% and that of NaP1_C is 42.2%.

Adsorption and desorption experiments

Static sorption experiments were performed to examine the effect of the initial PhCs concentrations, adsorbent dosage, and contact time on adsorption performance. The samples from the experiment of the initial concentration influence were subjected to desorption using ethanol. Five subsequent cycles of regeneration were performed. PhCs were determined using a Modular (U) HPLC system - Nexera (LC-40) series, Shimadzu, with a triple quadrupole analyzer and a QTrap 3200 reaction chamber (AB Sciex). Electrospray ionization (ESI) and multiple reaction monitoring were applied.

RESULTS AND DISCUSSION

The effect of the initial concentrations

The sorbents NaP1_FA and NaP1_C achieve high FLUO and KOL sorption efficiencies (70 to 100%) over the entire range of initial concentrations tested, 0.1 - 200.0 mg L^{-1}. In the case of ERY, a high 90% sorption efficiency was achieved for the NaP1_C sample, only in the concentration range from 0.1 to 2.5 mg L^{-1}. In contrast, for higher ERY concentrations, the sorption efficiency is a few percent. Comparing the sorption efficiency of ERY on NaP1_FA and NaP1_C sorbents, it can be seen that about 30% less ERY is removed by NaP1-FA. The reason for this may be the higher porosity of NaP1_C, resulting in a higher sorption capacity of the sample. In the case of FLUO, which is a smaller molecule than ERY and KOL, the sorption capacity of the sorbents is the highest (already at the lowest FLUO concentrations, sorption reaches 90% efficiency).

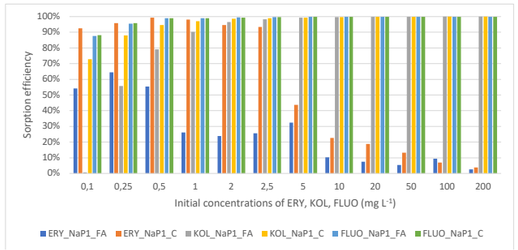

Fig. 1. Influence of the initial concentration of ERY, KOL, and FLUO on the sorption efficiency.

The effect of dosage

Adsorbent doses of 1 and 2 g L^{-1} resulted in the removal of PhCs to the greatest extent (Fig. 2). The initial concentration of ERY, KOL, FLUO, AMO, and EST was 100 µg L^{-1}. The concentrations after adsorption decreased to 35 µg ERY L^{-1} for NaP1_C and 23 µg ERY L^{-1} for NaP1_C, and 3.5 µg AMO L^{-1} for NaP1_C and 3.6 µg AMO L^{-1} for NaP1_FA. In the adsorption of KOL and EST on NaP1_C, the best removal results were obtained using a dose of 2 g L^{-1}, while the sorbent NaP1_FA was most effective using a dose of 1 g L^{-1}. After using a 2 g L^{-1}, NaP1_C reduced the concentration of KOL to 7.1 µg L^{-1} and EST to 2.2 µg L^{-1}. In contrast, the concentrations after adsorption using a dose of 1 g L^{-1} and NaP1_FA decreased to 5.7 µg KOL L^{-1} and 2.7 µg EST L^{-1}, respectively. A dose of 1 g L^{-1} of NaP1_C sorbent and 2 g L^{-1} of NaP1_FA sorbent results in the most effective removal of FLUO. The concentrations after adsorption are 7.5 µg L^{-1} for NaP1_C and 10.8 µg L^{-1} for NaP1_FA, respectively.

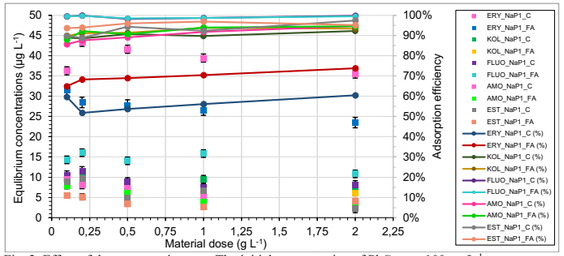

Fig. 2. Effect of dose on sorption rate. The initial concentration of PhCs was 100 µg L^{-1}.

The effect of time reaction

Pharmaceuticals are effectively removed after 2 minutes of reaction. Four kinetic models were analysed to determine the sorption mechanism of selected PhCs on NaP1_C and NaP1_FA sorbents: pseudo-zero-order, pseudo-first-order, pseudo-second-order and the Behnajada-Modirshahl-Ghanbery (BMG) kinetic model. The coefficient of determination (R^2) was used to measure the quality of model fit. It was determined that the NaP1_FA sorbent should exhibit the lowest contaminant degradation efficiency of 84% during AMO adsorption, and the NaP1_C sorbent should exhibit the highest efficiency of over 99% during ERY adsorption.

Regeneration

Differences in the strength of methanol-analyte interaction for individual pharmaceuticals depend primarily on the desorbed substance's chemical properties and the sorbent-analyte bond's strength. Exemplary differences in the desorption capacity of pharmaceuticals with methanol from the NaP1_FA and NaP1_C sorption materials are presented in Fig. 3. Methanol, as a polar-protic solvent is the most commonly used extraction solvent due to its high polarity. Due to its high volatility, it can extract lipophilic and hydrophilic substances and remove them easily at room temperature. The high efficiency of desorption of analytes (ERY, FLUO) from sorbents occurs practically in the first regeneration cycle. The results show that methanol can be successfully used as a reagent to remove residues of adsorbed pharmaceuticals in sorption materials.

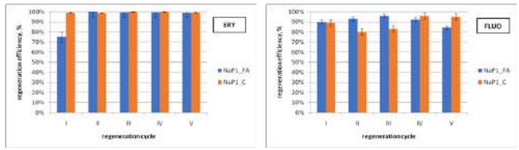

Fig. 3. The ERY and FLUO efficiency of NaP1_FA and NaP1_C after regeneration cycles.

CONCLUSIONS

The removal efficiency of pharmaceuticals depends on several factors, both physical (related to the degree of physical (associated with the degree of wastewater treatment) and chemical (related to the composition of the water matrix). However, the most critical parameter in pharmaceutical adsorption methodology is the selection of the appropriate adsorbent composition and process conditions. We have conducted numerous laboratory experiments that confirm that the zeolite NaP1 and the NaP1-C composite can effectively remove pharmaceuticals from aqueous solutions.

REFERENCES

Tarpani, R. R. Z., Azapagic, A. 2018. Life cycle environmental impacts of advanced wastewater treatment techniques for removal of pharmaceuticals and personal care products (PPCPs). *Journal of Environmental Management* **215**, 258–272.

Park, J., Kim, Ch., Hong, Y., Lee, W., Chung, H., Jeong, D-H, Kim, H. 2020. Distribution and Removal of Pharmaceuticals in Liquid and Solid Phases in the Unit Processes of Sewage Treatment Plants. International Journal of Environmental Research and Public Health **17**(3), 687.

Mansouri, F., Chouchene, K., Roche, N., Ksibi, M. 2021. Removal of Pharmaceuticals from Water by Adsorption and Advanced Oxidation Processes: State of the Art and Trends. Applied Sciences **11**(14), 6659.

Novembre, D., Gimeno, D., Del Vecchio, A. 2020. Synthesis and characterization of Na-P1 (GIS) zeolite using a kaolinitic rock. Scientific Reports 11.

Activated biochar from rice husk for the removal of micropollutants: Characterization and application in real wastewater

B. Bayarri*, A. Sales*, P. Llopart* and C. Sans*

* Department of Chemical Engineering and Analytical Chemistry, Chemistry Faculty, Universitat de Barcelona C/Martí i Franquès, 1 – Barcelona (SPAIN)

Abstract
Biochar derived from husk rice was synthesized and activated with CO2 to be used as adsorbent of micropollutants present in wastewater. Physical and chemical characterization showed that it was an alkaline solid, with good porosity (380 m^2 g^{-1}) and low density of functional groups. Biochar was tested for the removal of three different pesticides obtaining that it could adsorb between 100 and 260 µmol g^{-1} of biochar. pH did not affect greatly the biochar performance but when testing with real wastewater adsorption performance decreased.

Keywords
Activated Carbon, Adsorption, Biochar, Micropollutant, Wastewater

INTRODUCTION

Water scarcity has become one of the major issues that human being has to face this century. To respond to this challenge the scientific community is increasing efforts to develop safe water treatment methods with low environmental impact. Among these methods, adsorption is a well-known, effective technology widely tested in several wastewater treatment plants. Related to it, biochar (BC) is being considered as a good precursor to create activated carbon capable of adsorbing several of pollutants present in current wastewater. BC can be generated from organic waste by pyrolysis, thus reducing its carbon footprint and making this material very appealing.

In this work, BC from a common waste, rice husk, was synthesized. Then it was activated with CO_2 to improve its adsorption capacities. The final goal was to obtain and characterize an activated carbon and assess its capacity to adsorb different micropollutants present in wastewater.

MATERIAL AND METHODS

Rice husk was milled and 250 µm fraction was washed with $NaCO_3$ and water, and then dried and pyrolyzed in a tubular oven under a N_2 atmosphere at 500ºC for 4 hours. Then, it was activated in the same oven under a CO_2 atmosphere, at 800º during 1 hour. In both steps, the temperature ramp was fixed at 5 ºC $minute^{-1}$.

Obtained BC was characterized by different techniques. Physical parameters (moisture, ashes, fixed carbon) were determined by proximate analysis [1], surface morphology was investigated by field emission scanning electron microscope (FESEM), Fourier-transform infrared spectroscopy (FTIR) was used to determine the presence of functional groups on the surface of the material, surface area was estimated by BET analysis, C-H-N-O was monitored by elemental analysis and surface charge was determined by the pH drift method.

Biochar adsorption capacity was assessed by the adsorption of three micropollutants, all pesticides, with different octanol-water distribution coefficients (K_{ow}): clothianidin (CTD, K_{ow} =0.7), thiacloprid (TCP, K_{ow} =1.26) and atrazine (ATZ, K_{ow} =2.61). Solutions of these compounds were prepared in deionized water at different pH with concentrations between 20 and 200 µM. Experiments were carried out in 100 mL glass vials by adding 5 or 20 µmol L^{-1} of micropollutant solution and 50 mg L^{-1} of BC. Then vials were agitated at 330 rpm up to 145 hours at the dark at 22 ºC. Micropollutants concentration was monitored by an Infinity 1260 HPLC provided by Agilent Technologies (USA) equipped with a C-18 Tecknokroma column. Some of the experiments were carried out spiking the micropollutants in wastewater (pH= 7.6, TOC= 25 mg L^{-1}, total suspended solids = 38 mg L^{-1}) obtained from the secondary effluent of a WWTP in the area of Barcelona.

RESULTS AND DISCUSSION

Characterization results

Table 1 shows the main values of the BC characterization. Material before and after activations are listed.

Table 1. Main properties of the synthesized biochar, activated with CO_2 and non-activated. *H* refers to humidity, *VM* to volatile matter, C_{fixed} to the fixed carbon, *EC* to electrical conductivity, *pH pzc* to the point of zero charge, *BET* to the surface area, *PV* to pore volume and *PS* to the pore size.

	Yield	H	VM	Ash	C_{fixed}	pH	EC	pH pzc
	%	[%]	[%]	[%]	[%]		[mS cm^{-1}]	
ACTIVATED BC	26.95	1.57%	45.89%	43.21%	9.32%	11.06	8.01	10.2
NON Activated BC	40.09	0.64%	59.32%	36.28%	3.76%	10.73	5.82	-

	BET [m^2/g]	PV [cm^3/g]	PS [nm]	% C	% H	% O	% N	% S
ACTIVATED BC	379.95	0.123	5.56	37.83	0.00	5.18	0.27	0.08
NON Activated BC	1.22	4.48 . 10^{-4}	65.78	56.31	1.76	7.48	0.40	0.00

Values obtained are aligned with similar materials reported in literature [2]. Remarkable is the amount of ashes in the sample, about 40%. In spite of the previous washing with $NaCO_3$, the percentage of mineral compounds was very high, far away from the optimum 6-8% recommended for obtaining the best adsorption capacities [2]. Thus, further reduction of the amount of ashes could greatly improve the BC properties. Obtained material was alkaline with a pH = 11, indicating the absence of acidic groups on the surface and linked to the high amounts of ashes. BET analysis was carried out, showing a remarkable surface area close to 400 m^2/g for the activated BC. Before activation, BC surface area was only 1.22 m^2/g proving the efficiency of the activation step in spite of the high presence of ashes. Activated BC presented an adsorption isotherm of type II: most of the adsorption took place at low relative pressure but adsorption still went on when increasing relative pressure, confirming the presence of mesoporous which are very interesting for adsorption of big pollutants molecules presents in wastewater. Elemental analysis reported the low presence of oxygen and almost null presence of hydrogen or other atoms. This indicates that pyrolysis was long enough to volatilize most of common functional groups. This point was confirmed with the FTIR analysis showed in figure 1 for the activated BC. The typical peaks for hydroxyl groups or C-H bonds were not observed, which is in agreement with the % of hydrogen measured. This fact corroborates a low polarity of the BC. Detected peaks are proposed to correspond to C-O or C=C (1430 cm-1) bonds or even Si-O bond (1047 cm-1) and Si-O-Si (618 cm-1). Si presence can be explained because it is the main compound of the ashes.

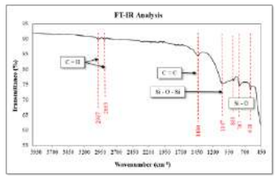

Figure 1. FTIR spectra of rice husk biochar activated with CO_2 at 800 ºC for 1 h.

Figure 2 presents FESEM images of the activated and non-activated BC. As it can be observed, after the activation with CO2, most of pore-blocking substances were driven off, appearing well-developed porous, honeycomb-like structures. These images confirm the important increasing in the surface area detected by BET analysis.

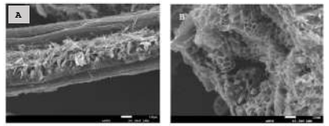

Figure 2. FESEM images of (A) non activated and (B) activated rice husk BC at x850 magnifications.

Adsorption results

Firstly, the activated BC was tested as adsorbent of three micropollutants (CTD, TCP and ATZ) dissolved in deionized water at different pHs, as described in figure 3. . Despite each micropollutant owns different K_{ow} and pK_a, no big differences were observed for the different pHs tested. For example, it was expected that there would be electrostatic repulsions to CTD in the pH between 2 and 10, since the point of zero charge for the BC was determined to be 10.23 and pKa for CTD was 11.09. Thus, both species would be positively charged hindering the adsorption process. However, experimental results showed that adsorption was relatively stable for all the tested conditions. The same can be said for ATZ and only TCP showed a higher adsorption at pH 12. Therefore, it seems that pH and electrostatic interactions do not play a key role in the adsorption mechanism of these species.

Adsorption performance of biochar was also tested spiking the same micropollutants in the effluent from a WWTP, and results are shown in figure 4. TCP and CTD presented similar adsorption rates, despite having different K_{ow} and polarity. ATZ adsorption was quite slower, and less amount was eliminated. Results show how important is the matrix for the adsorption process.

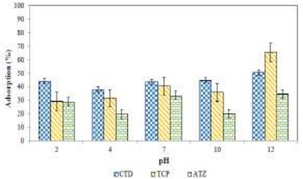

Figure 3. Adsorption in activated BC after 74 hours for solutions of micropollutants in deionized water at different pH values. $[ATZ]_0$= $[CTD]_0$= $[TCP]_0$= 20 µmol L^{-1}, $[BC]_0$= 50 mg L^{-1}, T=22 ºC

In previous experiments working with deionized water, the amount of micropollutants retained was about 3-5 times higher. Real matrix contains several compounds which are competing with the micropollutants for the adsorption site. Thus, it seems clear that new materials must be tested in real conditions to understand properly their real potential and more selective materials must be designed.

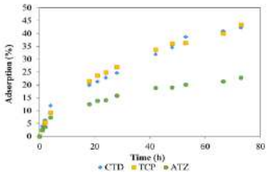

Figure 4. Adsorption profile of CTD, TCP and ATZ simultaneously on BC with wastewater matrix. $[ATZ]_0$= $[CTD]_0$= $[TCP]_0$= 2 µmol L^{-1}, $[BC]_0$= 50 mg L^{-1}, T=23 ºC, pH_0=7.6

CONCLUSIONS

BC derived from rice husk has proved to be a valid material for the adsorption of organic micropollutants in water. Even in real wastewaters it shows a good capacity to retain these compounds. Activation with CO_2 has demonstrated to be a valid procedure to significantly/enormously increase the adsorption properties of the biochar.

BIBLIOGRAPHY

[1] European Council of Chemical Manufacturers' Federations, "Test Methods for activated carbon", 1986

[2] Pan, X., Gu, Z., Chen, W., & Li, Q. 2021 Preparation of biochar and biochar composites and their application in a Fenton-like process for wastewater decontamination: A review. Science of the Total Environment, 754, 142104

LIFE Zero Waste Water: from the WWTP to the WRRF treating UWW and bio-waste

M. Roldán*, J. Bautista-Giménez*, A. Mosquera**, L. Sáez***, A. Seco*, J.R. Vázquez**** and J. Ribes*

*CALAGUA – Unidad Mixta UV-UPV, Departament d'Enginyeria Química, Escola Tècnica Superior d'Enginyeria, Universitat de València, Av. De la Universitat s/n, 46100, Burjassot (València)
(E-mail: miguel.roldan@uv.es; juan.b.gimenez@uv.es; aurora.seco@uv.es; josep.ribes@uv.es)
** Departamento de Ingeniería Química, Universidad de Santiago de Compostela, 15782 Santiago de Compostela.
(E-mail: anuska.mosquera@usc.es)
*** Canal de Isabel II. Calle de Santa Engracia, 125. 28003 Madrid.
(E-mail: lsaez@canal.madrid)
**** FCC Aqualia. Dpto. Innovación y tecnología. Calle Federico Salmón 13, 28016 Madrid
(E-mail: jvazquezp@fcc.es)

Abstract
Anaerobic membrane bio-reactors (AnMBR) arise as a key technology to reduce the environmental impacts of the present-day wastewater treatment plants (WWTPs) while promoting the obtention of biogas, digestate for composting or agricultural use and permeate enriched in nutrients suitable for irrigation from urban wastewater (UWW). Its co-treatment together with the food waste fraction from the municipal solid waste (MSW) is an opportunity to achieve the net production of energy during the process whilst meeting the legal targets of reduction in landfilling and incineration and preparation for re-use and recycling of the MSW. Coupling the co-treatment of both fractions in AnMBR system with the use of food waste disposers (FWDs) to grind the food waste before its transportation through the sewerage can be an efficient integrated urban sanitation system to facilitate the fulfilment of recycling targets with a low environmental impact related to transport, since it overcomes the low citizen participation in the selective collection of MSW and reduces the content of impurities in the final compost.
In the LIFE Zero Waste Water project (LZWW), an AnMBR-based Water Resource Recovery Facility (WRRF) has been built to treat 50 m^3/d UWW and 125 kg/d bio-waste in the Valdebebas WWTP. The treatment train is completed with an AQU-ELAN system, a nutrient extraction and recovery unit and a smart water monitoring and control system.

Keywords
AnMBR, bio-waste, food waste, integrated urban sanitation system, WRRF

INTRODUCTION

The upgrade of already built WWTPs, mostly based on energy demanding processes, to convert them into WRRFs plays an essential role in the reduction of the worst effects of the challenging scenarios of climate change and resources scarcity. In this context, the AnMBR process arises as an opportunity to reduce or even remove the energy requirement for the organic matter removal from UWW whilst producing valuable products such as biogas, a reduced amount of digested sludge suitable for composting or agricultural application and an effluent suitable for irrigation free of pathogens without requiring any tertiary treatment (Jiménez-Benítez et al., 2020). Moreover, including the separately collected food waste, which accounts for up to the 77% of the bio-waste fraction and more than the 30 % of the MSW production in Spain (Favoino & Giavini, 2020), in the influent stream together with UWW entails an opportunity to convert WRRFs into net energy producers. Additionally, the joint management of both fractions is an opportunity to meet the legal targets of preparation for re-use and recycling and the ban on the disposal of the separately collected bio-waste required in the Waste Framework Directive (2018/851/CE).

Within the LZWW project, besides the co-treatment of UWW and food waste in an AnMBR-based WRRF, the environmental aspects of using FWDs located under the kitchen sink to grind the food leftovers before its transportation from households together with UWW through the sewerage towards WRRFs will be also studied, as an alternative to conventional systems of bio-waste collection in specific bins located in the street, which have shown problems to reach a high enough citizen participation, or door-to-door collection, which requires high efforts from operators and municipalities and is related to higher environmental impacts related to waste transportation (Rossi et al., 2022).

MATERIALS AND METHODS

In the Valdebebas WWTP (Spain) a demo-scale WRRF (300 P.E.) has been built to treat an average of 50 m^3/d of UWW and 125 kg/d of separately collected food waste (see Figure 1). The food waste will be firstly provided from nearby HoReCa services and subsequently from brown bins and door-to-door collection systems (see Figure 2a) to study the influence of the collection system on the co-treatment process and the quantity and quality of the recycled materials obtained.
The WRRF treatment train comprises 1) a reception site and dosing system for the bio-waste, 2) a 100 m^3 AnMBR reactor, 3) an AQU-ELAN system for partial nitritation-Annamox nitrogen removal in the main stream, 4) a nutrient extraction and recovery unit, and 5) a Smart Water Monitoring and Control System for the WRRF management according to the nutrient content in the effluent, depending on the end-user demand and regulations (see Figure 2b).

RESULTS AND DISCUSSION

The real advantages of the joint management of both fractions in the Valdebebas WRRF will be quantified during the plant operation under stable conditions. However, some of them have already been quantified separately in previous studies. Among these advantages are: 1) the reduction in the environmental impact of food waste management due to its transportation through the sewer system, 2) a positive energy balance with an average production of 1.0 kWh per m^3 of treated UWW, 3) the possibility of 95 % of UWW reclamation, 4) around 50 % reduction in sludge production and 5) 150 % in the CO_2 emissions related to the operation in comparison to conventional activated sludge-based WWTPs (see Table 1).

REFERENCES

Favoino, E., & Giavini, M. (2020). Bio-waste generation in the EU : Current capture levels and future potential, 50. Retrieved from https://biconsortium.eu/sites/biconsortium.eu/files/documents/BIC-ZWE report - Bio-waste generation in the EU - current capture and future potential.pdf

Jiménez-Benítez, A., Ferrer, J., Rogalla, F., Vázquez, J. R., Seco, A., & Robles, Á. (2020). Energy and environmental impact of an anaerobic membrane bioreactor (AnMBR) demonstration plant treating urban wastewater. In *Current Developments in Biotechnology and Bioengineering: Advanced Membrane Separation Processes for Sustainable Water and Wastewater Management - Case Studies and Sustainability Analysis* (pp. 289–310). https://doi.org/10.1016/B978-0-12-819854-4.00012-5

Rossi, M., Papetti, A., & Germani, M. (2022). A comparison of different waste collection methods: Environmental impacts and occupational risks. *Journal of Cleaner Production*, *368*(June), 133145. https://doi.org/10.1016/j.jclepro.2022.133145

ACKNOWLEDGEMENTS

LIFE+, the European Financial Instrument for the Environment, supported and co-financed this study as part of the ZERO WASTE WATER Project (LIFE19 ENV/ES/000631).

Figure 1. a) FWDs implemented in the demo plant and b) food waste dosing and AnMBR system in the Valdebebas WRRF

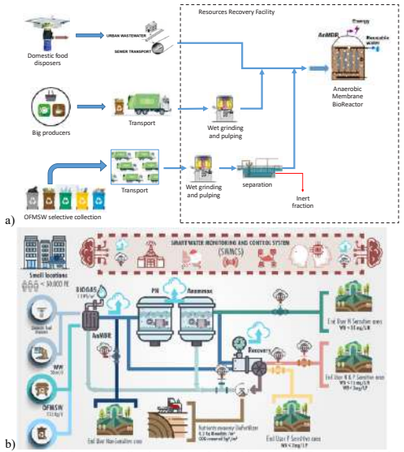

Figure 2. a) Separate collection system for the biowaste. b) Treatment train for resource recovery.

Table 1. Comparison between conventional activated sludge and LZWW WRRF expectation.

	Conventional activated sludge	LZWW WRRF expectation
Energy consumption (kWh/m^3)	0,5	-1,0
Energy consumption related emissions (kgCO_2 eq./m^3)	0,15	-0,30
Biosolids production (kg/kg COD removed)	0,4 (not stabilized)	0,2 (stabilized)
UWW reclamation (%)	0 (without considering tertiary treatments)	95% (does not require tertiary treatment)

Development of a continuous flow MEC-AD system with autonomous feeding control and performance optimisation.

K. Bowman[a], H. Rutland[a,c,d], J. You[c], H. Liu[c], T. Fudge[a], G. Kyazze[b]

[a] WASE, Midland Road, Bristol BS2 0NS, United Kingdom;
Kyle.Bowman@WASE.co.uk
[b] University of Westminster, 115 New Cavendish St, London W1W 6UW, United Kingdom;
[c] University of West England, Coldharbour Ln, Bristol BS16 1QY, United Kingdom;
[d] University of Bristol, Beacon House, Queens Rd, Bristol BS8 1QU, United Kingdom,

Abstract
Microbial Electrochemical Cells coupled with Anaerobic Digestors (MEC-AD) improve upon the performance of conventional AD systems, allowing shorter hydraulic retention times and higher organic loading rates due to enriched biofilm bound microbial consortia and bioelectrochemical catalysis of key process reactions. MECs have been used as biosensors to sense VFA concentrations but have not yet been utilised as a control sensor for MEC-AD.

A small scale (2L) continuous flow MEC-AD reactor was designed and constructed to operate autonomously treating high strength simulated brewery wastewater (10-30 g/L tCOD). The feed rate of the MEC-AD reactor was modulated by using the electrodes as a biosensor, utilising the current response of the system as a performance indicator and control parameter. Autonomous feed rate control was implemented using a threshold-based algorithm to interpret trends in current output and control feed pump speed - allowing the reactor to feed itself as it requires.

We investigate whether stable operation at loading rates between 2-8 kgCOD/m^3/d can be effectively maintained by adjusting feed rate in response to the current draw of the MEC reactor. The system performance and stability will be evaluated to determine the effectiveness of such autonomous control and the effect on reactor health over time. The ability of the system to respond to changing influent characteristics will be tested to simulate real world operation.

Development of biosensor led, autonomous feed rate control will allow reduced laboratory testing and operator burden on commercial scale MEC-AD systems. This may reduce downtime while increasing waste treatment rates and methane yields, improving the commercial viability of the technology. This will enable the implementation of MEC-AD systems in remote areas or in response to humanitarian crises to provide sanitation and renewable energy without the need for skilled operators.

Keywords
electromethanogenesis; resource recovery; microbial electrochemical technology; wastewater treatment.

Natural Clay-Based Materials for the Removal of Antibiotics from Contaminated Water

1. Introduction

Environmental pollution by emerging contaminants is one of the hot spot problems. Many pollutants released into the environment are very easily found in aquatic compartments, both in drinking water (Benotti et al., 2009) and in wastewater (Pascale et al., 2020). Major pollutants include heavy metals, organic micropollutants, personal care products, and pharmaceuticals (Nielsen and Bandosz, 2016). Among the latter, two of the most detected compounds are trimethoprim and sulfamethoxazole (Figure 1). The first one is a synthetic antimicrobic molecule belonging to diaminopyrimidine class (Wróbel et al., 2020). The second one is an antimicrobic belonging to the sulphonamides family and acts as a competitive inhibitor of the enzyme dihydropteroate synthase (Gupta et al., 2013). The persistence of these hazardous compounds in the environment is very concerning because trace levels, such as µg/L (Nielsen and Bandosz, 2016), can promote the formation of antibacterial resistance genes (Yang et al., 2017). Considering their potential impacts on environment and health, additional treatments have to be applied to drastically reduce the load of such molecules in dis-charged effluents and best achieve non-detectable concentrations. Several technologies have already proven to be effective for this purpose such as activated carbon adsorption as well as advanced oxidation processes. In the last decade, hybrid configurations (adsorption/oxidation) have been extensively studied for the degradation of organic compounds. Recently, a hybrid process of classical adsorption of pollutants on a fixed bed of activated carbon followed by batch wet catalytic oxidation at higher temperature and pressure on the same bed of activated carbon, which is then regenerated in situ, has been also evaluated for the remediation of phenols. The drawback of the mentioned technologies is the high cost and the low applicability at large scale. However, natural-based solutions can be a promising alternative. In this context, the present paper has two objectives related to the remediation of selected antibiotics: first, to characterize the natural soil from Mt Vulture volcano (Basilicata, Italy); second, to test its capacity to adsorbed/oxidate contaminants.

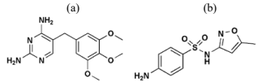

Figure 1: Chemical structure of a) trimethoprim and b) sulfamethoxazole

Experimental work on the oxidative process is still in progress and is focused on degradation mediated by sulphate radicals to remove sulfamethoxazole. Laboratory batch experiments were (and are) performed in order to study the adsorption kinetics.

2. Materials and methods

Analytical grade standards of trimethoprim, sulfamethoxazole (purity <=100 %) and potassium peroxymonosulfate, with the commercial name of Oxone ® (PMS, KHSO5, 0.5 KHSO4, 0.5 K2SO4), were purchased from Sigma Aldrich (St. Louis, USA). For chemical analysis acetonitrile and formic acid were HPLC grade from Honeywell (Wabash, Indiana, US). Water was ultrapure Milli-Q grade (18.2 MΩ cm-1 resistivity at 25 °C). Stock solutions 1,000 mg/L were prepared in methanol (LC-MS grade) provided by Carlo Erba reagents (Milano, Italy). The natural soil adsorbent used within this work is from Mt. Vulture volcano (Basilicata, Italy) was characterized by XRPD and XPS analysis.

2.1 XPS analysis

XPS analysis was carried out by spectrometer (Phoibos 100- MCD5, SPECS) operating at 10 kV and 10 mA, in medium area (Θ=2 mm) mode, using achromatic MgKα (1,253.6 eV) radiation and a pressure in the analysis chamber higher than 10^{-9} mbar. Wide spectra were collected in fixed analyser transmission (FAT) with a constant pass energy of 20 eV and channel widths of 1.0.

2.2 HPLC-DAD analysis

The concentrations of trimethoprim and sulfamethoxazole were monitored by a high-performance liquid chromatography (HPLC) system (Agilent Technologies 1200 series, USA) equipped with a Kinetex C18 100Å column (250 x 4.6 mm i.d., 5 µm particle size) and a diode array detector (DAD), set at λ = 270 nm. The mobile phase consisted of biphasic gradient using water acidified with 0.1% formic acid (A) and acetonitrile (B), structured as follows: 0-2 min 100 % A, 2-3 min. from 100 % A to 60 % A, 3-8 min 60 % A, 8-9 min. from 60 % A to 0% A, 9-12 min 0 % A, 12-15 min from 0 % A to 100 % A and finally, 15-18 min 100 % A.

2.3 Batch adsorption and catalytic degradation experiments

Batch adsorption experiments were carried out whit different solid-to-liquid ratio in flasks containing 100 mL of liquid solutions at different concentration of trimethoprim (TRM); they were continuously mixed with magnetic stirrer. The initial and final concentrations of TRM were measured regularly for each experiment. The equilibrium experiments were performed by stirring 100 mL of TRM solution with initial concentration of 4 mg/L as optimum condition. The aqueous samples were taken at fixed times. After adsorption, the adsorbent samples were separated by filtration at 0.2 µm, and the supernatants were analysed for residual TRM by HPLC-UV.
Preliminary, batch oxidative processes were performed in 100 mL of solution containing SMX 5 mg/L and 800 µM of PMS as oxidant agent. The amount of adsorbent material was 28.2 g.

3. Results and discussion

3.1 Characteristics of volcanic soil

Mt. Vulture volcano is a large volcano of post-Calabrian age, located near the western edge of the Bradanica trench in Southern Apennine chain, Basilicata, Italy (Fiore et al., 1992). Inside the crater of a minor cone, there are the two natural lakes of Monticchio (Basilicata). Soil present in this area have different characteristics, many of them exhibiting andic properties and is the largest hydrocarbon reservoir in continental Europe (Gizzi et al., 2029). XPS analysis of samples showed different signals, including the Si 2s (153.6 eV), which is attributable to a pyroxene and olivine structure according to Seyama and Soma (1985) (Table 1). The signal Si 2p (103.6 eV), according to Wagner et al. (1982), is attributable to pyroxene. Noteworthy are also the signals of Al 2p (74.0 eV) that, according to Seyama and Soma (1985) are attributable to pyroxene and the signal of Fe 2p (710.6 eV) attributable to the presence of olivine (Seyama and Soma, 1987).

Table 1: Results of XPS analysis

Element	eV	Reference
Si 2s	153.6	Seyama H, 1985 olivine, piroxeno
Si 2p	103.6	Wagner C.D., 1982 piroxeno
Mg 2s	93.6	
Al 2s	128.6	
Al 2p	74.0	Seyama H., Soma M., 1987 piroxeno
Fe2p	710.6	Seyama H., Soma M., 1987 olivina
Ca 2p	350	
K 2p	293.6	
O1s	553.6	
O2s	33.6	

3.3 Effect of contact time

The effect of contact time on the rate of removal of trimethoprim was investigated. In batch adsorption experiment, all of the parameters including solid/liquid ratio (0.02 ÷ 0.04 g/mL), agitation speed (450 ÷ 750 rpm), initial contaminant concentration (4 ÷ 8 mg/mL), were considered. From the data shown in the table 2, it can be seen that the variation in contact time is closely related to molecule concentrations. Indeed, while at a concentration of TRM 4 mg/L, all other parameters being constant, the variation of contact time determines a variation of absorption ranging from 7 to 13.21 %, while at a concentration of 8 mg/L it is registered a variation ranging from 4.3 to 15.28 %. In a more evident way, it can be observed that at a concentration of 6 mg/L a variation of 30 min of adsorption time determines a variation of 36 % of adsorbed molecule.

Table 2: Effect of contact time on the rate of removal of trimethoprim

C_0 (mg/L)	v (rpm)	t (min)	Solid/Liquid (g/mL)	% of adsorption
4	450	20	0.02	51.66
4	450	50	0.02	62.17
4	750	20	0.02	56.52
4	750	50	0.02	69.73
4	450	20	0.04	64.26
4	450	50	0.04	72.95
4	750	20	0.04	65.08
4	750	5	0.04	72.08
6	600	5	0.03	34.87
6	600	35	0.03	70.81
6	600	65	0.03	75.75
8	450	20	0.02	44.08
8	450	50	0.02	59.15
8	750	20	0.02	52.44
8	750	50	0.02	56.74
8	450	20	0.04	56.58
8	450	50	0.04	69.94
8	750	20	0.04	57.86
8	750	50	0.04	73.14

3.4 Catalytic oxidation in the adsorption processes

The natural presence of metals into the natural adsorbent allows the material to exhibit excellent capacity to be used for catalytic applications. During the adsorption processes, a known amount of PMS (800 µM) was added into the reaction systems with 4 mg/L of sulfamethoxazole. Benefiting from the effective transfer of electrons on volcanic soil/PMS, the degradation rate of SMX was significantly faster than its adsorption rate and its oxidation by Fenton processes. The blank test showed that 43 % of the SMX was removed from water using only PMS or Fenton like process (PMS/Fe). It can be seen from Figure 2 that SMX degradation rate in the volcanic soil/PMS was efficient and could be completely removal within 2 h.

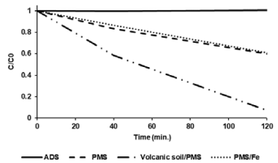

Figure 2: Sulfamethoxazole degradation profiles in the adsorption process using Fenton like oxidation based on PMS activation

4. Conclusion

The application of natural based material for the removal antibiotics from contaminated water was successfully investigated using abundantly available low-cost adsorbents. Preliminary results showed that the tested volcanic soil is an effective adsorbent for the removal of trimethoprim from aqueous solutions. Batch adsorption experiments showed that volcanic soil was efficient to remove trimethoprim, but did not show any appreciable ability in taking out sulfamethoxazole. In contrast, its ability to activate oxidant agent such as peroxymonosulfate demonstrated to be very effective in oxidation of sulfamethoxazole.
The results of the tests carried out on this innovative material are very encouraging. Obviously, as these are preliminary studies, it is necessary to investigate variables such as treatable pollutants, interferences, conditions (pH, temperature, pollutant concentration, etc.), optimal dosages as well as the engineering solutions to be adopted in order to ensure its safe use in real-scale plants. Additionally, experiments should be scheduled to test the natural activation of different oxidant agents; it would be interesting to extend the ability of this natural material as a potential disinfection treatment.

Acknowledgements

XPS data were provided by Dr. F. Langerame and Prof. A. M. Salvi at ESCA Laboratory, University of Basilicata.

References

Benotti M.J., Trenholm R.A., Vanderford B.J., Holady J.C., Stanford B.D., Snyder S.A., 2009, Pharmaceuticals and Endocrine Disrupting Compounds in U.S. Drinking Water, Environmental Science & Technology, 43, 597-603.
Directive 2000/60/EC of the European Parliament and of the Council of 23 October 2000 establishing a framework for Community action in the field of water policy, Official Journal, L 327, 0001 – 0073.
Fiore S., Huertas F., Linares J., 1992, Mineralogy and geochemistry of some “so-called” paleosols from Mt. Vulture volcano (southern Italy), Chemical Geology, 99, 237-252.
Gizzi F. T., Proto M. & Potenza M. R. 2019, The Basilicata region (Southern Italy): a natural and ‘human-built’ open-air laboratory for manifold studies. Research trends over the last 24 years (1994–2017), Geomatics, Natural Hazards and Risk, 10(1), 433-464
Gupta R., Kazmi I., Afzal M., Khan R., Chauhan M., Al-Abbasi F.A., Ahmad A., Anwar F., 2013, Combination of sulfamethoxazole and selenium in anticancer therapy: a novel approach, Molecular and Cellular Biochemistry, 384, 279–285.
Nielsen L., Bandosz T.J., 2016, Analysis of sulfamethoxazole and trimethoprim adsorption on sewage sludge and fish waste derived adsorbents, Microporous and Mesoporous Materials, 220, 58-72.
Pascale R., Bianco G., Coviello D., Lafiosca M.C., Masi S., Mancini I.M., Bufo S. A., Scrano L., Caniani D., 2020, Validation of a liquid chromatography coupled with tandem mass spectrometry method for the determination of drugs in wastewater using a three-phase solvent system, Journal of Separation Science, 43, 886–895.
Seyama H., Soma M, 1985, Bonding-state characterization of the constitutent elements of silicate minerals by X-ray photoelectron spectroscopy, Journal of Chemical Society, Faraday Transaction 1: Physical Chemistry in Condensed Phase, 81, 485–495.
Seyama H., Soma M., 1987, Fe 2p spectra of silicate minerals, Journal of Electron Spectroscopy and Related Phenomena, 42, 1, 97-101.
Wagner C.D., Passoja D.E., Hillery H.F., Kinisky T.G., Six H.A., Jansen W.T., Taylor J.A., 1982, Auger and photoelectron line energy relationships in aluminum–oxygen and silicon–oxygen compounds, Journal of Vacuum Science and Technology, 21, 933,
Wróbel A., Arciszewska K., Maliszewski D., Drozdowska D., 2020, Trimethoprim and other nonclassical antifolates an excellent template for searching modifications of dihydrofolate reductase enzyme inhibitors, The Journal of Antibiotics volume, 73, 5–27.
Yang Y., Jiang J., Ma J., Liu G., Cao Y., Liu W., Li J., Pang S., Kong X., Luo C., 2017, Degradation of sulfamethoxazole by UV, UV/H_2O_2 and UV/persulfate (PDS): formation of oxidation products and effect of bicarbonate, Water Research, 118, 196-207.

Towards next generation LUCAS® technology for cost-efficient municipal wastewater treatment plants

S. Wyffels*, H. Stes*, N. Calabuig* and M. Caluwé*

* Waterleau Group NV, Nieuwstraat 26, 3150 Wespelaar, Belgium
(E-mail: *stijn.wyffels@waterleau.com; michel.caluwe@waterleau.com)**

Abstract
By adopting novel insights in the activated sludge process and embracing hydrodynamic engineering aspects, Waterleau's continuous flow SBR technology branded as LUCAS®, has been future proofed. Featuring a construction footprint reduction of 44% and an energy consumption saving of 41% compared to conventional variable volume SBRs, the next generation LUCAS® becomes an interesting alternative to serve the secondary biological treatment of large municipal wastewater treatment plants. A sludge densification strategy is added primarily selecting for better settling sludge, and inclined tube settlers further support the solid-liquid separation during the clarification and settling process. Plant developers and plant operators choosing for reliable and affordable technology may count on a dual improved functionality and a combined cost reduction of 13% compared to conventional continuous flow activated sludge systems.

Keywords
continuous flow SBR; hydrodynamics; sludge densification; treatment cost; tube settlers

INTRODUCTION

Over the last two decades various types of SBRs have been reported and applied successfully in municipal wastewater treatment plants worldwide (Wilderer et al., 2001; Dutta et al., 2015). UNITANK and LUCAS® systems are truly continuous flow, fixed volume SBR configurations consisting of hydraulically connected compartments undergoing periodic and cyclic steps of feed to biomass accumulation, biomass regeneration, effluent withdrawal, sludge settling and sludge wasting without any additional pumping nor external sludge recirculation, which are therefore considered amongst the more advanced activated sludge SBR technologies (Bui et al., 2022). LUCAS® technology developed by Waterleau generally features a lower construction footprint compared to conventional continuous flow activated sludge systems and a lower energy consumption compared to conventional variable volume SBRs (Gerards et al., 2005). Recently developed control strategies for sludge densification aiming to select for aerobic granular sludge (AGS) in industrial wastewater treatment plants (Caluwé et al., 2022), together with the integration of inclined tube settlers improving solid-liquid separation and promoting selective sludge retention (Kent et al., 2018), has allowed to gear up the LUCAS® technology for further application into today's eco(nomic)-efficient municipal wastewater treatment plants.

MATERIALS AND METHODS

A pilot-scale LUCAS® reactor is operated during a 200-days period to study the metabolic strategy for sludge densification under continuous flow conditions. The reactor consists of three compartments with constant volume of 40 L that are interconnected with three control valves. Each compartment is equipped with influent control valves, effluent control valves, mechanical stirring, diffused aeration, and measurement devices for dissolved oxygen, pH, ORP, turbidity and conductivity. Control loops based on OUR and pH/ORP slope are implemented to dynamically adjust the time-controlled LUCAS® process steps. In addition, a full-scale LUCAS® reactor is modelled with the aid of Computational Fluid Dynamics (CFD) to investigate the hydrodynamic effect of inclined tube settlers on the sludge settling process. After adoption of the sludge densification strategy and incorporation of the inclined tube settlers, the novel LUCAS® technology is benchmarked high-level with other state-of-the-art secondary biological treatment technologies.

RESULTS AND DISCUSSION

Sludge densification

The continuous flow LUCAS® reactor configuration has been studied to impose subsequent and pronounced feast and famine conditions enabling the selection of slow-growing organisms (SRT > 30 days) that are understood to produce extracellular polymeric substances (EPS) and induce sludge densification and to a further extent, sludge granulation, and thus contribute to a better sludge settling behaviour (SVI_{30}< 100 mL/g). With a three compartment set-up it was possible to build up a substrate gradient in the feeding compartment under non-mixed anaerobic conditions, followed by a sudden mixing step promoting the substrate accumulation by the facultative anaerobic organisms and thereby preventing the degradation of readily biodegradable carbon by fast-growing heterotrophic organisms, and to regenerate the accumulated biomass in the adjacent second compartment under aerated aerobic conditions, whilst the third compartment was taking part in the sludge settling process and enabling further hydraulic selection for fast settling sludge. The time-controlled feeding, mixing, aeration and settling steps and rotation of biological treatment and settling functions between the compartments, allowed to progressively grow, select, and maintain dense sludge flocs and small granules in the range of 200–400 µm in the LUCAS® system consistently. Operational data further show the feasibility of the LUCAS® system as a continuous flow densified sludge reactor: MLSS are in the range of 7.0–7.7 g/L with SVI_{30}/SVI_{10} ratio > 0.71.

Sludge settling

The LUCAS® sludge settling process consists of a batch settling step with supernatant clarification followed by a dynamic settling step with clean effluent flowing over from the surface and without the need for an external recirculation of the settled sludge, thereby allowing to increase the sludge bed over time (Figure 1). When dealing with diluted or primary treated sewage and when facing a peak flow regime, the hydraulic load factor on the secondary settling function becomes more important than the organic and nutrient load factor on the biological treatment function. Means to improve solid-liquid separation may contribute to the performance of the settling process.

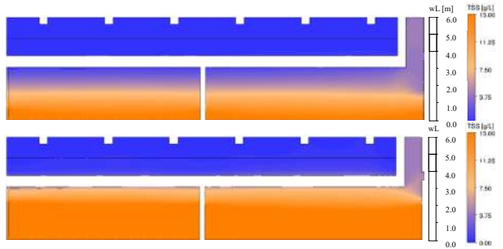

Figure 1. LUCAS® compartment (24.4 m W x 24.4 m L x 6.0 m wL) with settling function showing the settled sludge bed height after 60 minutes of batch settling (top) and after 180 minutes of subsequent dynamic settling with production of 1,080 m^3/h solids-free treated effluent (bottom). The inclined tube settlers have a height of 1 m and are positioned between the 5 – 6 m water level.

Inclined tube settlers. During batch settling, the tube settlers show to act as 'flocculator', promoting collision, cohesion and drag of the sludge particles into the settling sludge bed. During dynamic settling, the tube settlers work as 'polisher', inducing re-flocculation of fragmented sludge particles and a downward solids flow whilst the treated supernatant flows up (Figure 2). The clean effluent is collected from a series of overflow weirs evenly distributed at the tank surface with a surface overflow rate (SOR) of 1.81 $m^3/m^2/h$ at average flow conditions. During peak flow at SOR = 2.86 $m^3/m^2/h$ – when some solids may be allowed to wash out temporarily with effluent TSS < 30 mg/L – the tube settlers may act as 'selector' for larger and dense sludge aggregates versus smaller flocculent particles, and thus retain selectively the best settling sludge fraction.

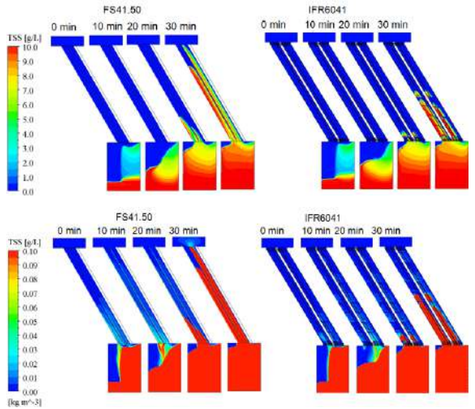

Figure 2. Two different types of inclined tube settlers type FS41.50 (equidistant, chevron shape, 11 m^2/m^3 sedimentation area) and type IFR6041 (non-equidistant, trapezoid corrugated shape, 9.5 m^2/m^3 sedimentation area) compared at the same hydraulic rate of 6.64 10^{-4} m/s during the final 30 minutes of a dynamic settling step at peak flow regime, thereby reaching critical bi-directional flow inside the tube settlers with solids building up and sloughing-off to the sludge bed underneath (top) and with clean effluent moving up to the collecting overflow weirs above (down). Although the flow pattern is laminar in the tube settlers of type FS41.50 and irregular in the tube settlers of type IFR6041 because of wave-like internal structures, there was no significant difference in solid-liquid separation efficiency between the two different types.

Cost performance indicators

A theoretical comparative design using BioWin and a cost benchmark performed on a municipal wastewater treatment plant with a 100 MLD capacity of the water line, consisting of pre-treatment, primary settling, secondary treatment, and tertiary treatment, allowed to assess the economic efficiency of next generation LUCAS® technology in relation to other frequently applied secondary treatment technologies, being Continuous Flow Activated Sludge technology (CF-AS), Integrated Fixed Film Activated Sludge (IFAS) technology, and Variable Volume Sequencing Batch Reactor (VV-SBR) technology (Table 1). Enabling the lowest combined cost of secondary treatment within this exercise, LUCAS® technology may become an interesting biological treatment alternative for future municipal wastewater treatment plants. Current examples include the incorporation of LUCAS® technology within the Independent Sewage Treatment Plants (ISTPs) of Taif (100 MLD), Tabuk (90 MLD), Buraidah (150 MLD) and Madinah (200 MLD) in the Kingdom of Saudi Arabia.

Table 1. Comparison of secondary treatment technologies treating influent loads of 38,584 kg COD/day, 18,200 kg BOD/day, 13,416 kg TSS/day, 4,685 kg TN/day, 634 kg TP/day, and wet weather peak flow up to 8,000 m^3/h. Process volume and footprint accounts for the sum of volumes and construction footprint for pre- and post-buffer tanks, reactor tanks and settling tanks. Energy consumers include equalization pumps, excess sludge pumps, sludge recycle pumps, submersible mixers and blowers for diffuser aeration. Capital expenditures and combined cost of secondary treatment are relative numbers within the cost context of a municipal WWTP in the Middle East North Africa (MENA) region. Combined cost of secondary treatment (CC) is calculated using Net Present Value (NPV) method including CAPEX and OPEX during 20 years of design flow.

	Volume	Footprint	Power consumption	CAPEX		CC
	(m^3)	(m^2)	(kWh/m^3)	(% E&M)	(% Civil)	(%)
CF-AS	73,845	16,664	0.26	100	100	100
IFAS	77,848	18,865	0.28	135	102	115
VV-SBR	94,000	15,667	0.25	92	128	103
LUCAS®	53,000	8,833	0.15	113	72	87

REFERENCES

Wilderer, P., Irvine, R., Goronszy, M. 2001 *Sequencing Batch Reactor Technology*. IWA Scientific and Technical Report No. 10. IWA, London.

Dutta, A., Sarkar, S. 2015 Sequencing Batch Reactor for wastewater treatment: recent advances. *Curr Pollution Rep* **1**, 177–190.

Bui, X., Nguyen, D., Nguyen, P., Ngo, H., Pandey, A. 2022 *Current Developments in Biotechnology and Bioengineering: advances in biological wastewater treatment systems. Chapter 3 - Activated sludge processes and recent advances*. Elsevier, Amsterdam.

Gerards, R., Gils, W., Vriens, L. 2005 Upgrading of existing aerobic plants with the LUCAS® anaerobic system based on full-scale experiences. *Water Science and Technology* **52**(4), 39– 46.

Caluwé, M., Goossens, K., Seguel Suazo, K., Tsertou, E., Dries, J. 2022 Granulation strategies applied to industrial wastewater treatment: from lab to full-scale. *Water Science and Technology* **85**(9), 2761–2771.

Kent, T., Bott, C., Wang, Z. 2018 State of the art of aerobic granulation in continuous flow bioreactors. *Biotechnology Advances* **36**, 1139–1166.

Industrial scale-up, automatization and validation of high-performance multi-stage anaerobic reactor for treatment of wastewater from food and drink SMEs

J. B. Carbajo[a], M. Navajas[a], B. Goicoechea[a], A. Torres[a]
C. Bengoechea-Cuadrado, A. Martínez[b], M. Miana[b], S. Izquierdo[b]
O. G. Chenaru[c], G. Florea, L. Ocheana[c]
A. Domínguez[d]

[a] AEMA, Agua, Energía y Medio Ambiente, Polígono Industrial El Pilar, C/ Fitero 9, 26540 Alfaro (Spain). Email address: jbcarbajo@aemaservicios.com (J. B. Carbajo).
[b] ITAINNOVA, Aragon Institute of Technology, C/ María de Luna 7, 50118, Zaragoza (Spain).
[c] SIS, Societatea de Ingineria Sisteme, Soseaua Electronicii 22, Bucuresti (Rumania).
[d] EGA, Energygreen Gas Almazan, Carretera de Gómara, km 2,8, 42200-Almazan (Spain).

Abstract

Food and drink small and medium enterprises (SMEs) are highly water-intensive sector, that urgently needs an eco-efficient solution to treat their wastewater and decrease the associated energy costs. Being aware of the gap in the market, LIFE Multi-AD consortium scaled-up and automatized a high-performance multiphase anaerobic reactor. Multi-AD devise was industrial-scale installed in the winery WWTP and has been validated in continuous operation. The results show that Multi-AD reactor is capable of achieving COD removal higher than 93%, as well as biogas production of 3.6 m^3/m^3·d for organic load rate up to 10 kg COD/m^3·d. The ground-breaking reactor design, based on 4 chambers, achieves that organic matter is degraded in a stepwise conversion, fact that may make it more effective than conventional reactors. Multi-AD innovative solution allows SMEs to count with decentralized, automatized and eco-innovative technology for treatment of their wastewaters, allowing them to save 60% of energy and 34% of operational expenditures.

Keywords (maximum 6 in alphabetical order)

Biogas, Decentralized strategy, Economic viability, Technical viability, Small and medium enterprise, Winery

INTRODUCTION

The food and drink (F&D) industry, the largest manufacturing sector in the EU, is comprised of 290,000 small and medium enterprises (SMEs) – making up 99% of the entire industry [1]. F&D SMEs are highly water-intensive sector worldwide, producing significant volume of wastewater. These industrial effluents are characterized by high concentration of biodegradable organic matter, which results a significant environment pressure [2]. Thus, they are most commonly treated by aerobic biological system at the industrial facility where the wastewater is generated. Due to the typical process selection, aerobic biological treatment, relative energy consumption is high [3]. Moreover, due to typical on- or near- site disposal of biosolids without biogas recovery, there is little or no opportunity for carbon emission offset [4].

On the other hand, anaerobic system appears as a more environmentally friendly and economical process for treatment high-load wastewater [2,4]. However, high-rate anaerobic reactors already on the market (*e.g.*, UASB, EGSB or IC) are optimised for large enterprises (>1,000 m^3/d, being 2,500 m^3 a standard capacity) where economies of scale make vast technology investment affordable. In contract, the F&D sector, dominated by SMEs, does not discharge an enough organic load for existing anaerobic reactors to prove economically viable.

Being aware of the gap in the market, AEMA developed and patented a 100 L prototype of a high-performance multiphase anaerobic reactor (ES-2541078-B1). The continuous operation of the ground-breaking anaerobic reactor with winery wastewater showed COD removal efficiency higher than 90%, as well as an average biogas conversion of 0.45 m^3 biogas/kg COD removed [5]. With this experience, AEMA decided to lead LIFE Multi-AD project (LIFE17 ENV/ES/000331) in cooperation with four more partners in order to demonstrate the technical, economic and environmental viability of a high-performance multiphase anaerobic reactor at industrial scale.

The aim of this study was the industrial scale-up, automatization and validation of a ground-breaking high-performance multiphase anaerobic reactor for treatment of industrial wastewater from food and drink sector.

MATERIAL AND METHODS

Industrial wastewater

Industrial wastewater to be treated by Multi-AD reactor was produced by a winery located in Fuenmayor (Spain), which discharges around 40,000 m^3 per year through different seasons. Physico-chemical characteristics of wastewater sampled from July until November are shown in Table 1. Analytical determinations were carried out using standard methods [6]. Produced wastewaters are characterized by variable flow rates (as they are seasonal in nature), high organic loading, the low pH and nutrient levels as the bibliography shows [7].

Demonstration plant

Multi-AD technological solution is industrial-scale installed in the current WWTP of the cited winery, which is based on aerobic process by membrane bioreactor. Figure 1 shows the lay-out of Multi-AD technology, which is mainly composed of a water and gas line. The water line consists of conditioning physico-chemical (*i.e.*, sieving, equalization, settling, pH, nutrient and temperature adjustment), as well as anaerobic biological processes, which takes place in the Multi-AD reactor.

Multi-AD reactor is a multi-stage anaerobic reactor with a volume of 110 m^3 (9.1 m of height and 8.5 m of diameter at the bottom) that has a maximum OLR of 20 kg COD/m^3 d and is capable of treating up to 200 m^3/d of wastewater. Multi-AD device is made up of an influent system distribution, an anaerobic reactor core (4 chambers bordered by 3 baffles) and a three-phase separator. It is important to note that Multi-AD reactor was scaled-up from the 100 L prototype. The upscale process was supported by simulation results in order to predict the performance of the new design, as well as reducing the risk and costs associated with uncertainty. The CFD model developed was used for optimizing the design of the 110 m^3 demo unit, with special emphasis being placed on influent, chamber baffles and three-phase separator.

Thus, in the Multi-AD reactor, the wastewater is pumped from the bottom, uniformly into the reactor, where it moves upwards through the granular sludge bed (20 kg TS/m^3) located along the different chambers. At the top of the reactor, sludge, biogas and treated effluent are separated in a three-phase separator. On the one hand, treated water is sent to an aerobic process for a polishing treatment before it is discharged into the Ebro River, and, on the other hand, biogas is used as fuel in a boiler after desulfurization process by means of bio-scrubber system.

Multi-AD technological solution has an intelligent optimized control thanks to the development of a heuristic automation solution integrating current innovative technologies like Industry 4.0 [8] and Internet of Things. This was achieved through a two-level decision approach ready to be adopted by F&D SMEs: one local and one for remote monitoring and control [9].

RESULTS

Scaling-up

An analysis of numerical simulations showed that different modifications should be done in designing the industrial-scale Multi-AD reactor in order to achieve a cost-effective technological solution. The most significant modifications of the 1:1 industrial-scale Multi-AD reactor over the 100 L prototype were *i)* elimination of external biogas recirculation, *ii)* increment of diameter/height ratio (*i.e.*, reactor geometry) *iii)* reduction of number of chambers, as well as *iv)* new design of feed distribution pipping and three-phase separator.

Automation

An advanced control system was designed and developed in order to optimise Multi-AD reactor performance by adjusting the controllable output variables such as temperature, pH (DRD1R5.99, Hach), total solids (LXV424.99.00100-Solitax, Hach), ORP (DRD1R5.99, Hach), COD (SP-1-001-p0-s-NO-075 spectro::lyserTM, s::can) and biogas (EHS 9G3B25-1LJ1/0, Endress-Hauser).

The control logic was developed using a "cause-effect" approach by means TIA Portal V16 software. The logic was implemented on a Siemens S7-1500 PLC with analog and digital IO modules. This approach allows to operate the innovative solution at constant organic load by means of a mass balance over the Multi-AD reactor. Two continuous COD-analyzer were situated inline at the inlet of the conditioning tank and the outlet of the effluent tank, respectively. The analysers produce a continuous measurement value every 2 minutes, that allows the PLC tunes raw wastewater flow to be treated by means a group of flowmeters (MAG 5100, Siemens) and flow control valves (SIPART PS2 electropneumatic positioner, Siemens).

The architecture to carry out the monitoring and control of Multi-AD technology was developed in order to achieve an unattended and fully automated operation. Equipment and instrumentation of demo unit were connected to the power and automation-control panel. The control panel, which integrates the PLC and HMI, was connected to the power panel and the remote-control centre using a SCADA application developed in PcVue.

Validation

Multi-AD innovative solution was operated in continuous mode for four months. During this period, the anaerobic reactor treated more than 5,000 m^3 of winery wastewater at increasing organic load rate (OLR) (Figure 2). Despite influent variability, OLR was gradually increased from 0.5 to 10 kg COD/m^3·d thanks to COD based control strategy.

The planned increase in OLR took place once anaerobic reactor reaches the steady state. Thus, the values of the following process parameters were evaluated: pH, alkalinity, VFA and COD. pH, alkalinity and VFA had optimal values for the anaerobic digestion process, which shows that Multi-AD devise did not have any episodes of destabilisation or overloading. It is worth to note that the effluent COD concentration was usually lower than 600 mg/L during the validation period. This fact, taking into account the influent COD concentration, results in degradation efficiencies above 93%. These results are in line with previous study with this kind of wastewater [3,5].

Figure 3 shows that there is a decrease in soluble organic matter through Multi-AD reactor chambers. It can be seen, therefore, that there is a stepwise conversion, chamber by chamber, in line with the design propose of a multi-stage reactor, where each chamber behaves as a CSTR. This fact may indicate that Multi-AD reactor is capable to achieve better degradation rates for the same volume than a conventional anaerobic reactor such as UASB.

Anaerobic degradation of winery wastewater generated biogas conversion of 0.4 m^3/kg COD removed, with a biogas production of 3.6 m^3/m^3·d at the highest studied OLR (*i.e.*, 10 kg/m^3 d). The combustible gas generated after Multi-AD technological solution was characterized by a methane mean value of 71%. Moreover, it is important to highlight that hydrogen sulfide concentration was lower than 10 ppm after bio-scrubber system.

Economic assessment

Finally, a comprehensive process design was performed in this study to investigate the economic viability of Multi-AD innovative solution. Two different scenarios were selected for treatment of 100 m^3/d of winery wastewater: baseline, based on aerobic process, and Multi-AD scenario, based on anaerobic system coupled with post aerobic treatment.

As indicated in the Table 2, the Multi-AD scenario would achieve savings in OPEX around 50,000 €/y comparted to base line baseline scenario. This one-third potential reduction in operational costs is mainly due to energy saving. The integration of anaerobic process in the WWTP allows to save 175,000 kWh/y, *i.e.*, 60%. On the other side, a notable reduction in biosolid management cost line was also achieved by Multi-AD scenario due to the significant reduction in sludge produced by the anaerobic reactor operation.

CONCLUSION

Multi-AD reactor allows SMEs to count with decentralized, automatized and eco-innovative technological solution for treatment of their wastewaters, allowing them to save energy and operational costs.

REFERENCES

[1] Data & Trends: EU Food and Drink Industry. 2022 Edition. Food Drink Europe, Belgium. Available at: www.fooddrinkeurope.eu (last visit: 10/01/2023).
[2] Vitezova, M., Kohnotova, A., Vitez, T., Hanisakova, N., Kisjlevych, I. 2020. Methanogenic Microorganisms in Industrial Wastewater Anaerobic Treatment. *Processes* **8**, 1546.
[3] Ngwenya, N., Gaszynski, C., Ikumi, D. 2022. A review of winery wastewater treatment: A focus on UASB biotechnology optimisation and recovery strategies. *Journal of Environmental Chemical Engineering* **10** (4), 108172.
[4] Wu, Z., Duan, H., Li, K., Ye, L. 2022. A comprehensive carbon footprint analysis of different wastewater treatment plant configurations. *Environmental Research* **214**, 113818.
[5] Petropoulos, E., Cuff, G., Huete, E., Garcia, G., Wade, M., Spera, D., Aloisio, L., Rochard, J., Torres, Weichgrebe, D. 2016. Investigating the feasibility and the limits of high-rate anaerobic winery wastewater treatment using a hybrid-EGSB bio-reactor. *Process Safety and Environmental Protection* **102**, 107–118.
[6] APHA, AWWA, WEF, 1998. Standard Methods for the Examination of Water and Wastewater, 20th Edition. American Water Works Association, Water Environment Federation, Washington DC.
[7] Bolzonella, D., Papa, M., Da Ros, C., Muthukumar, L.A., Rosso, D. 2019. Winery wastewater treatment: A critical overview of advanced biological processes. *Critical Reviews in Biotechnology* **39** (4), 489–507.
[8] Cheah, C. G., Chia, W. Y., Lai, S. F., Chew, K. W., Chia, S. R., Show, P. L., 2022. Innovation designs of industry 4.0 based solid waste management: Machinery and digital circular economy. *Environmental Research* **213**, 113619.
[9] Pandey, S., Twala, B., Singh, R., Gehlot, A., Singh, A., Montero, E. C., Priyadarshi, N. 2022. Wastewater treatment with technical intervention inclination towards smart cities. Sustainability **14**, 11563.

FIGURES

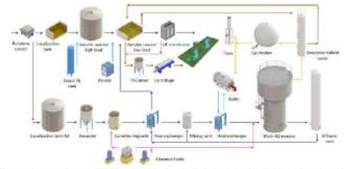

Figure 1. Lay-out of current WWTP and Multi-AD technological solution installed in a winery located in Fuenmayor (Spain).

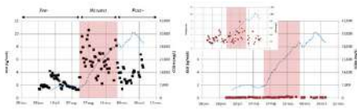

Figure 2. Evolution of COD in the influent (dark square) and effluent (red square) with the OLR (blue dash line) throughout continuous operation time in the Multi-AD technological solution.

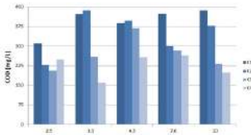

Figure 3. Evolution of soluble COD of wastewater throughout Multi-AD reactor (*i.e.*, chambers) at different OLR.

TABLES

Table 1. Main physico-chemical parameters of winery wastewater.

Parameter	Unit	Mean
pH	upH	5.29
Suspended solids	mg/L	648
Soluble chemical organic demand	mg/L	11,025
Chemical organic demand	mg/L	13,450
Total Kjeldahl total	mg/L	52.2
Orthophosphate	mg/L	22.8
Sulphate	mg/L	165

Table 2. Operational expenditures for base line and Multi-AD scenario considering wastewater flow of 100 m^3/d.

Cost line	Baseline (aerobic process)		Multi-AD (anaerobic+aerobic process)		Savings	
	(€/m^3)	(€/y)	(€/m^3)	(€/y)	(€/y)	(%)
Chemicals	0.40	14,931	0.33	12,194	2,737	18
Energy	2.03	73,364	0.81	29,526	43,838	60
Biosolids	0.39	14,021	0.03	1,697	12,324	88
Analysis	0.05	1,686	0.12	4,385	-2,699	-160
Taxes	0.26	9,500	0.26	9,500	0	0
Staff	0.83	29,802	1.02	36,788	-6,986	-23
Total	**3.96**	**143,304**	**2.57**	**94,090**	**49,214**	**34**

Phase separation in anaerobic fixed-film reactor for wastewater treatment: biomethane production and pharmaceutical compounds removal

R. B. Carneiro*, G. M. Gomes**, M. Zaiat** and A. J. Santos-Neto*

* Laboratory of Chromatography (CROMA), Institute of Chemistry of São Carlos, University of São Paulo (USP), 400, Trabalhador São-Carlense Ave., São Carlos, São Paulo, 13566-590, Brazil
(E-mail: *rodrigocarneiro@sc.usp.br; alvarojsn@iqsc.usp.br*)
** Laboratory of Biological Processes (LPB), São Carlos School of Engineering, University of São Paulo (USP), 1100, João Dagnone Ave., Santa Angelina, 13563-120, São Carlos, São Paulo, Brazil
(E-mail: *gisele.gomes@usp.br; zaiat@sc.usp.br*)

Abstract In this work, new configurations of anaerobic fixed-film reactors were operated under conventional methanogenic conditions (single phase - SP-R, M1), and in a sequential two-phase system, acidogenic reactor followed by methanogenic reactor (TP-R, Ac+M2), in order to verify the impact of the phase separation on the biomethane production and some target pharmaceutical compounds removal - sulfamethoxazole, diclofenac, carbamazepine, and metoprolol. The results found evidenced that the TP-R enhances significantly the volumetric methane production rate (182 ± 45 and 312 ± 47 $mLCH_4 \cdot L^{-1} \cdot d^{-1}$, respectively for M1 and M2), and the biotransformation of pharmaceutical compounds. The reduction of the drugs load driven by the acidogenic reactor contributed to the optimization of the methanogenic activity on the bioconversion of the pharmaceutical compounds in the reactor.

Keywords
Acidogenesis; Anaerobic reactor; Bioenergy; Biofilm; Methanogenesis; Micropollutants

INTRODUCTION

There is a growing trend to face municipal wastewater as a potential source of value-added products that can be recovered, such as biomethane in the form of bioenergy (Kong et al., 2021). The pharmaceutical compounds are micropollutants frequently detected in municipal wastewater around the world, and in many cases they are not effectively removed in conventional biological treatment processes (Mejías et al., 2021). Recent studies have shown that the different stages of anaerobic digestion, e.g., acidogenesis and methanogenesis, may act differently on the biotransformation of organic micropollutants (Carneiro et al., 2020). Thus, this work intends to promote the phase separation of anaerobic digestion in order to enhance the biomethane production and the pharmaceutical compounds removal in wastewater treatment plants.

MATERIAL AND METHODS

The experimental apparatus comprises two anaerobic digestion (AD) systems: a single-phase methanogenic reactor (SP-R - M1), and a two-phase reactor - acidogenic followed by a methanogenic reactor (TP-R - Ac + M2). The bench scale anaerobic reactors (useful volume of 2 L) are fixed bed with polyurethane foam as support material for biofilm formation. The operation is carried out continuously at 30 °C and the applied organic loading rate is 2 $kgCOD\ m^{-3}\ d^{-1}$. For M1 and M2, the inoculum biomass was a granular methanogenic sludge from a full-scale UASB bioreactor (Tietê, São Paulo, Brazil). For Ac reactor, the same sludge was pretreated at pH 3 with HCl 5M. The reactors were fed with a lab-made municipal wastewater (1 $gCOD\ L^{-1}$) spiked with 10 $\mu g\ L^{-1}$ of some target pharmaceutical compounds belonging to different classes - the antibiotic sulfamethoxazole (SMX), the anti-inflammatory drug diclofenac (DCF), the neurodrug carbamazepine (CBZ), and the beta-blocker metoprolol (MTP). The analytes were quantified by using column-switching online solid phase extraction coupled with liquid chromatography / hybrid triple quadrupole-linear ion trap mass spectrometer. The performance assessment of the reactors was monitored in terms of COD (chemical oxygen demand) removal efficiency, and volumetric methane production rate (VMPR, in $mLCH_4 \cdot L^{-1} \cdot d^{-1}$, Equation 1). Q_{biogas} is the biogas flow rate in $mL \cdot d^{-1}$ and X_{CH4} is the percentage of methane in biogas; and $V_{reactor}$ is the reactor volume in L.

$$VMPR = \frac{Q_{biogas} \cdot X_{CH_4}}{V_{reactor}} \quad (1)$$

RESULTS AND DISCUSSION

Both treatment systems showed excellent performance in terms of COD removal - SP-R - 86 ± 16%, TP-R - 92 ± 7%. Fig. 1 shows the average results obtained during the operation bioreactors. It can be noticed a better performance of TP-R compared to SP-R evidenced by the higher VMPR in M2 (Fig. 1a - 182 ± 45 and 312 ± 47 $mLCH_4 \cdot L^{-1} \cdot d^{-1}$, respectively for M1 and M2). The percentage of methane in biogas (X_{CH4}) was significantly higher in M2 (89 ± 6%) compared to M1 (76 ± 7%). The biomethane production was potentiated by feeding the methanogenic reactor from the acidogenic effluent. Fermentation products from acidogenesis facilitated the bioconversion and organic matter removal kinetics in TP-R. Regarding the pharmaceutical compounds removal, the results (Fig. 1b) suggest that the two phase system considerably improves the bioconversion of the compounds carbamazepine, metoprolol and diclofenac: SP-R removal - CBZ = 74%, MTP = 58%, DCF = 56%; and TP-R removal – CBZ = 55%, MTP = 44%, DCF = 29%. The sulfamethoxazole removal was complete in both systems, being fully biotransformed both in methanogenic and acidogenic conditions. It can be concluded that acidogenesis acts as a key factor in the biotransformation of microcontaminants during anaerobic digestion. The reduction of the applied load of the xenobiotics on the populations of methanogenic archaea in M2 reactor and the presence of short-chain volatile fatty acids readily bioavailable for acetogenesis/methanogenesis may have contributed to the enhancement of the methanogenic enzymatic activity, facilitating the biotransformation of the pharmaceutical compounds. The results indicate that the anaerobic fixed-film reactors system with phase separation (acidogenesis / methanogenesis) is a promising biotechnology for optimizing the biomethane production and the removal of pharmaceutical compounds in municipal wastewater from biological treatment plants.

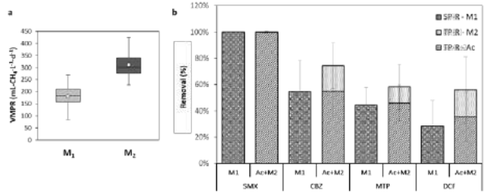

Figure 1. Boxplot of VMPR (a) and removal efficiencies of the pharmaceutical compounds (b) in SP-R and TP-R.

REFERENCES

Carneiro, R.B., Gonzalez-Gil, L., Londoño, Y.A., Zaiat, M., Carballa, M., Lema, J.M., 2020. Acidogenesis is a key step in the anaerobic biotransformation of organic micropollutants. J. Hazard. Mater. 389, 121888. https://doi.org/10.1016/j.jhazmat.2019.121888

Kong, Z., Li, L., Wu, J., Wang, T., Rong, C., Luo, Z., Pan, Y., Li, D., Li, Y., Huang, Y., Li, Y.Y., 2021. Evaluation of bio-energy recovery from the anaerobic treatment of municipal wastewater by a pilot-scale submerged anaerobic membrane bioreactor (AnMBR) at ambient temperature. Bioresour. Technol. 339. https://doi.org/10.1016/j.biortech.2021.125551

Mejías, C., Martín, J., Santos, J.L., Aparicio, I., Alonso, E., 2021. Occurrence of pharmaceuticals and their metabolites in sewage sludge and soil: A review on their distribution and environmental risk assessment. Trends Environ. Anal. Chem. 30. https://doi.org/10.1016/j.teac.2021.e00125

Can graphene oxide enhance methane production and pharmaceutical removal under anaerobic digestion?

O. Casabella-Font*, J. Radjenovic** and M. Pijuan*

* Catalan Institute for Water Research (ICRA), C. Emili Grahit 101, 17003 Girona, Spain; Universitat de Girona, Girona, Spain (E-mail: ocasabella@icra.cat and mpijuan@icra.cat)

** Catalan Institute for Water Research (ICRA), C. Emili Grahit 101, 17003 Girona, Spain; Catalan Institution for Research and Advanced Studies (ICREA), Passeig Lluís Companys 23, 08010, Barcelona, Spain. (E-mail: jradjenovic@icra.cat)

Abstract: Graphene oxide (GO) has been studied as conductive material during anaerobic digestion. The methane production and pharmaceutical removal kinetics were assessed by adding 0.075 g GO/g VS to the anaerobic digestion process using the biochemical methane potential test as a methodologic approach. The results obtained demonstrated that the formation of biologically reduced GO enhanced the methane production rates by 40%, although an adaptation period was necessary that compromised the specific methane production in the first ten days. In general, the removal of persistent pharmaceuticals was improved in those tests with GO (e.g. Carbamazepine removal was enhanced by 60% with GO). A microbial population change was detected in those cultures in the presence of GO, with enrichment of the hydrogenotrophic archaea. According to this study, the addition of GO improves methane production kinetics and pharmaceutical removal during the anaerobic digestion process.

Keywords biotransformation; bio-reduced GO; carbamazepine; kinetics; micropollutants

INTRODUCTION

Anaerobic digestion is a more economical alternative method to conventional aerobic treatment in the wastewater treatment process, with lower energy requirements and greater energy and resource recovery (Li et al., 2022). Increasing research efforts have been directed over the last decade to study the fate and removal of pharmaceuticals (PhAC) in aerobic treatment reactors, as many of these compounds are adsorbed in the sludge and can be released during the anaerobic digestion process of waste-activated sludge (Zhang and Li, 2018). This biological process consists of four steps and involves a heterogenous consortium of microorganisms, which can be understood as an electron flux between bacteria and archaea genera. The addition of carbon-based materials into anaerobic digestion reactors has been studied as a methodology to enhance microbial activity in anaerobic environments. Syntrophic bacteria can use these conductive materials for electron exchange, thus facilitating direct interspecies electron transfer (DIET). This resulted in increased methane production kinetics and enhanced biotransformation of organic micropollutants (Johnravindar, et al., 2020).

MATERIALS AND METHODS

To assess the impact of graphene oxide (GO) on anaerobic digestion the biochemical methane potential test methodology was used with an inoculum/substrate ratio of 2. The impact of 0.075 g of GO and hydrothermally reduced GO (rGO) (Baptista-Pires, et al., 2021) per g of inoculum volatile solid (VS) on specific methane production (SMP) and PhAC removal was assessed using cellulose as substrate and the fed-batch strategy: GO or rGO was only added at the beginning, while 3 pulses of cellulose were added (day 0, day 15 and day 30 resulting in 3 sets of consecutive batch tests: FB1, FB2, and FB3). The SMP was monitored online using a Gas Endeavour instrument (BPC Instruments, Sweden). Twelve PhACs were spiked to a final concentration of 1 µM at the beginning of the BMP tests.

RESULTS AND DISCUSSION

Impact of graphene oxide on methane production

Although there are some studies published in the literature there is no agreement concerning the effect of the addition of graphene oxide on methane production (Dong, et al., 2019; Muratçobanoğlu, et al., 2021). The fed-batch strategy allowed us to assess the impact of GO on methane production and compare the methane production kinetics of three sequential batches in the presence and absence of GO and hydrothermally reduced GO. The methane production rate (μ_{max}) was not affected by the presence of GO/rGO in the first batch (FB1), with values ~140 mL CH_4/ g VS · d in all conditions (**Figure 1**), but a reduction in the total amount of methane produced (~22% mL CH_4/ g VS), as well as a longer lag phase, was detected in the presence of GO (**Figure 2**). Once the GO was biologically reduced and incorporated into the sludge matrix, a significant enhancement ($p < 0.05$) in the μ_{max} was detected in the GO batch tests as well as in the rGO tests (~37% and ~50%, respectively) after adding the 2nd pulse of cellulose (FB2), whereas in the Control condition was not detected a significant enhancement ($p > 0.05$) (**Figure 1**). In the third addition of cellulose (FB3), the GO-batch tests and the rGO-batch tests increased the methane production rate up to 234.79 ± 16.59 and 243.75 ± 24.41 mL CH_4/ g VS · d respectively, which means the production rate was ~40% faster than the Control (**Figure 1**). We hypothesize that the addition of GO produces electron scavenging during the first days of the anaerobic digestion process (1st addition of cellulose). Once GO is bioreduced, the sludge recovers the same specific methane potential as the control as it is shown in **Figure 2**.

Impact of graphene oxide on pharmaceuticals removal

The removal kinetics of twelve PhACs were monitored (**Figure 3**) during the first (FB1) and third (FB3) sets of batch tests. Carbamazepine (CBZ) presented the highest removal enhancement in the tests conducted with GO as compared to the other conditions tested. No variation along the time was detected in the Control condition and was poorly removed in presence of rGO (13 ± 8%). Regarding the removal in presence of GO, 22 ± 1% removal was detected after 24 hours by the addition of GO and was enhanced up to 63 ± 1% by the end of the first batch. The detected removal could be associated with biological transformation since no adsorption was detected in the blank conditions measured after 48 hours (**Figure 3**). Trimethoprim (TMP) transformation was highly influenced by the addition of GO and rGO, with removals of 90 ± 2% and 79 ± 2% respectively, in just 24 hours. At the same time, only 13 ± 3% was removed in the Control condition. Iohexol presented high removal rates at the beginning of the experiment (FB1) but stopped after 36 h of reaction.. Tetracyclines showed a high tendency to adsorb on both materials (GO and rGO) and were associated with chemical interaction as π-π interactions and hydrogen bonds.

Additional experiments are being conducted to determine the different mechanisms that involve the GO on the removal of the different pharmaceuticals.

Conclusions: The addition of GO enhances the methane production rate by ~40%, and pharmaceutical removal. The results obtained determine the specific methane production is reduced during the biological reduction of GO but once reduced, the same methane production as the control or the rGO tests is obtained.

Acknowledgments

This research is funded by AEI (Agencia Estatal de Investigación, Spanish Government) through project ANTARES (PID2019-110346RB-C22). ICRA researchers also acknowledge the funding from the CERCA program. O. Casabella acknowledges funding from the Secretariat of Universities and Research from Generalitat de Catalunya and European Social Fund for his FI fellowship (2022 FI_B1 00122).

References

Baptista-Pires, L. et al., (2021). Water Research, **203**, 117492. Dong, B. et al., (2019). Science of the Total Environment, **646**, 1376–1384. Johnravindar, D. et al., (2020) Biomass and Bioenergy, **136**, 105543. Li, L. et al., (2022). Environmental Science and Ecotechnology, **11**, 100180. Lü, C. et al., (2020). ACS Sustainable Chemistry and Engineering, **8**(33), 12626–12636. Muratçobanoğlu, H. et al., (2021). Biochemical Engineering Journal, **173** 108080. Summers, Z. M. et al., (2010). Science, **330**(6009), 1413–1415. Zhang, X. et al., (2018). Bioresource Technology, **255**, 266–272.

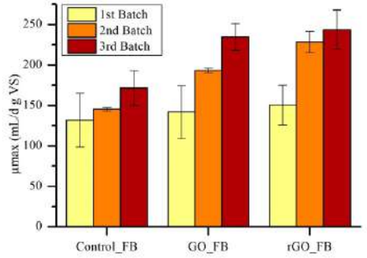

Figure 1. Specific methane production rates (μ_{max}) of the different conditions were tested for the different sequential batches.

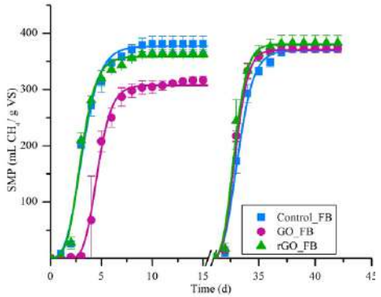

Figure 2. Experimental specific methane production (SMP) during the first (days 0-15) and third (days 30-45) batch for each condition assessed (symbols) and Gompertz model curve (lines).

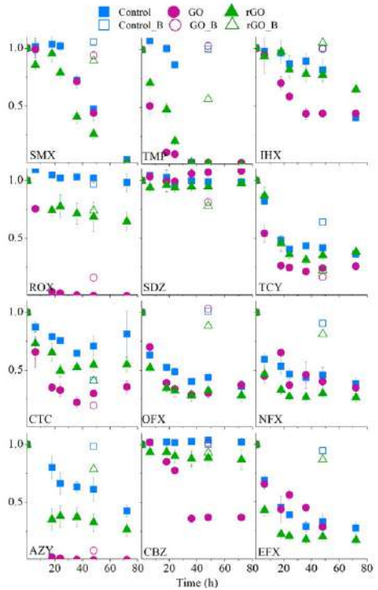

Figure 3. Removal profiles for the different pharmaceuticals in presence of GO, rGO, and Control. Adsorption blanks are represented in hollow symbols with the same colors.

Partially saturated vertical surface flow constructed wetland for emerging contaminants and antibiotic resistance genes removal from wastewater: The effect of bioaugmentation with *Trichoderma* fungus.

D. Tadić*, A. Sauvêtre**, F. Lestremau**, N. Ait-Mouheb***, S. Chiron*

*UMR HydroSciences Montpellier, University of Montpellier, IRD, CNRS, 15 Av. Charles Flahault 34093 Montpellier cedex 5, France (E-mail: *serge.chiron@umontpellier.fr)*
** UMR HydroSciences Montpellier, University of Montpellier, IMT Mines Alès, Ales, France (E-mail: andre.sauvetre@mines-ales.fr)
***UMR G-eau, University of Montpellier, INRAE, 361 rue Jean-François Breton, 34196 Montpellier cedex 5, France (E-mail: nassim.ait-mouheb@inrae.fr)

Abstract
The removal of contaminants of emerging concern (CECs) and antibiotic resistance genes (ARGs) were investigated at pilot-scale with partially saturated vertical flow constructed wetland bioaugmented or not with the *Trichoderma asperellum* (strain T34) by means of the non-target liquid chromatography high-resolution mass spectrometry and SmartChip™ Real-Time PCR methodological approaches. Bioaugmentation testing was successful as *Trichoderma* was able to grow in competitive conditions resulting from the use of secondary treated domestic wastewater. The most significant beneficial effect was observed with benzotriazole and diclofenac. High variability in removal efficiency (RE) along a four-week experiment remained the chief constraint for the proper assessment of treatment performances. There was a clear relationship between the RE and the biodegradability as well as the sorption capacity of the identified compounds. Sorption prevailed over biodegradation for hydrophobic (log Dow > 3) and slowly biodegradable compounds. For moderate hydrophobic compounds (0 < log D_{ow} > 3), the RE appeared to be dependent on functional groups and transformation reactions. But RE higher than 65% was obtained for selected slowly biodegradable compounds. The most difficult compounds to be eliminated were the most polar ones (log Dow < 0). Transformation products (TPs) were also investigated. N-oxide TPs and 14-hydroxyclarithromycin were formed in wetland treatment while TPs which were prone to undergo further N-dealkylation or hydroxylation reactions were partly eliminated. Bioaugmented wetland treatments have cause a shift in the ARGs composition but there was no statistical difference in average ARGs removal rates.

Keywords: Antibiotic resistant genes; bioaugmentation; constructed wetlands; contaminants of emerging concern; transformation products; *Trichoderma*

INTRODUCTION

The so-called partial saturated vertical subsurface flow CW (VSSF-CW) has shown enhanced removal of total nitrogen and selected CECs without the requirement of external energy input. This result was mainly assigned to a more diverse and metabolically versatile bacterial communities. However, saturated conditions and anaerobic conditions, despite favoring the elimination of certain antibiotics, may result in the spread of ARGs in bacterial communities. VSSF-CW could remove ARGs from wastewater by directly eliminating microorganisms. Bioaugmentation has appeared to be a promising approach to improve the functioning of wetland treatments, considering that natural mycorrhization has been detected in wetlands. However, little evidence exists to show that bioaugmentation of CW through bacterial or fungal inoculation substantially improves their efficiency in CECs and ARGs removal. In this context, we decided to inoculate at a pilot scale VSSF-CW with *Trichoderma* fungi because (i) they are known to be plant symbionts which might promote plant performances and contaminants plant uptake and (ii) they possess a machinery of unspecific enzymes (e.g., laccase and peroxidase enzymes), similarly to *Trametes Versicolor,* which makes their application in CECs removal attractive.

MATERIALS AND METHODS

Experimental set-up: The CW consisted of three lines of three CW units each and operated in parallel. Each unit has been designed to treat 96 L/d distributed in 8 batches along the day and was partially saturated with water (0.2 out of 0.6 m height), allowing for a combination of oxic and anoxic conditions. The first line consisted of substrate and plant, while in the second line *Trichoderma asperellum* (strain T34) was inoculated. A third line without plant was also implemented as a reference system. The CW was fed with secondary treated wastewater.
CECs analysis in wastewater: SPE and non-target liquid chromatography-high resolution mass spectrometry (LC-HRMS) screening.
ARGs: analysis: A SmartChip™ Real-Time PCR methodological approach.

RESULTS AND DISCUSSION

This study provided additional data on the capacity of VSSF- CW units to eliminate a large array of CECs. The most easily eliminated compounds were those which are known to be readily biodegradable (e.g., nicotine). Interestingly, from 22 compounds with RE > 65%, 17 compounds have a log Dow between 0 and 3 (optimal plant uptake). The most difficult compounds to be eliminated were the most polar ones (log Dow < 0) such as melamine. Our treatment wetland also generated TPs. Interestingly, N-oxide TPs of tertiary amines and 14-hydroxyclarithromycin were frequently detected in effluent. Attempts in bioaugmentation with *Trichoderma* were successful since the fungus was able to grow in competitive conditions. However, the high range of standard deviation values associated with RE values resulted to be the main issue for a proper assessment of treatment efficiency. This calls for more fundamental research into the mechanisms of compound attenuation to find strategies to limit fluctuating RE. None of the wetland treatments (with and without bioaugmentation) was able to significantly reduce the overall bacterial and ARGs loads. Hybrid treatment systems combining CW and advanced oxidation processes are currently implemented in our research group to avoid antibiotic resistance spreading.

Acknowledgements: This research was supported by the EU PRIMA program through the research project SAFE - Sustainable water reuse practices improving safety in agriculture, food and environment.

Treatment of polymer-containing oilfield wastewater by ionizing radiation: demulsification, sterilization and enhancement to oil removal

L. Chu* and L. Fang*
* Institute of Nuclear and New Energy Technology (INET), Tsinghua University, Beijing 100084, P. R. China
(E-mail: *chulibing@tsinghua.edu.cn; 2547149337@qq.com)**

Abstract
Ionizing radiation by γ-ray was applied to treat the real polymer-containing oilfield produced wastewater with high viscosity and emulsification. The viscosity decreased rapidly from initial 3.7 mPa s to 1.5 mPa s with the absorbed dose of 1.0 kGy, and then gradually to reach the level of pure water at 5.0 kGy. The produced wastewater was negatively charged and the absolute value of zeta potential diminished stepwise during γ-irradiation, indicating the stability of oil/water emulsion was destroyed. γ-ray radiation pretreatment contributes to the oil removal by coagulation. The efficiency of oil removal raised remarkedly from 47% by coagulation alone to 85% with 1.0 kGy of γ-ray pretreatment at the same flocculant dosage of 100 mg/L. γ-irradiation is also effective to disinfect the three typical bacteria in oilfield wastewater, saprophytic bacteria (TGB), sulfate-reducing bacteria (SRB) and iron bacteria (IB). With the absorbed dose of 1.0 kGy, more than 99.8% of TGB, SRB and IB were killed and a complete deactivation was observed at 2.5 kGy. Oxidation by ·OH formed in water radiolysis is the major pathway to reduce viscosity and kill bacteria, while the direct γ-ray irradiation also plays a role. The members belonging to genera *Thauera*, *Defluviimonas* and *Comamonadaceae* were predominant in the produced wastewater. Based on PICRUSt analysis, the function genes related to metabolism exhibit the highest abundance (25%) and their abundance increased at the low dose of 1.0 kGy and declined at 10 kGy. This suggests that ionizing radiation at low dose might stimulate the bacterial activity for metabolism. In practical application, ionizing radiation by electron accelerator can be added before coagulation in the conventional produced wastewater treatment processes for reinjection.

Keywords
advanced oxidation; oilfield produced wastewater; oil removal, demulsification, sterilization.

INTRODUCTION

Petroleum is an important and nonrenewable energy source. Among the enhanced oil recovery (EOR) methods, polymer flooding is the most often used and efficient method (Pogaku et al., 2018). The wastewater produced during polymer flooding with huge amount has become a challenging issue in the oilfield. Partially hydrolyzed polyacrylamide (HPAM) is one of the most popular polymer. HPAM has extreme high molecular weight (MW) of several to dozens million Daltons. HPAM can increase the viscosity of produced wastewater significantly and leads to high emulsification and stability (Gao, 2013). As a result, the oil droplet and particles exist stable in the produced wastewater and are hard to be removed by the gravity or coagulation.

The advanced oxidation processes (AOPs) are developed to decompose the polymer and reduce viscosity. Ionizing radiation involving γ-ray and electron beam (EB) is a novel AOPs. Under both the direct adsorption of high-energy ray/EB and the oxidation and reduction of active species involving ·OH, e_{aq}^- and ·H formed in water molecule's radiolysis, a variety of recalcitrant pollutants are able to be degraded effectively. (Wang and Chu, 2016). Ionizing radiation might be a promising option to treat the polymer-containing produced wastewater to decompose polymers, reduce viscosity, break emulsion and kill bacteria simultaneously.

The objective of the study was to treat the real oilfield produced wastewater from polymer flooding by ionizing radiation. The effect of ionizing radiation on viscosity reduction, the changes in wastewater characteristics and inactivation of three typical bacteria were evaluated. The enhancement of ionizing radiation as pretreatment to flocculation for oil removal was investigated. This research provides a new strategy for treating the polymer-containing produced wastewater with high viscosity and emulsification by ionizing radiation.

MATERIALS AND METHODS

The produced wastewater was taken from an oilfield wastewater treatment plant in north China. Table 1 shows the characteristics of the produced wastewater. The experiments of ionizing radiation were conducted using gamma-ray derived from the radioisotope ^{60}Co with radioactivity of 7.4×10^{14} Bq. Around 50 mL of wastewater were put into tubes and delivered for γ-ray irradiation at ambient temperature of around 25 °C. The dose rate maintained at 11.5 kGy/h. After γ-ray irradiation, the wastewater samples were analyzed directly for the parameters involving COD, oil, HPAMzeta potential, number of saprophytic bacteria (TGB), sulfate-reducing bacteria (SRB) and iron bacteria (IB), and the bacterial community and function, etc.

RESULTS AND DISCUSSION

Viscosity reduction and demulsification

Figure 1 depicts the changes in solution viscosity, HPAM content and zeta potential during γ-radiation. The viscosity declined sharply from initial 3.7 mPa s to 1.5 mPa s with the absorbed dose of 1.0 kGy and then gradually with rising the absorbed doses, reaching to the level of pure water under the same temperature at 5.0 kGy. The HPAM decomposition rate is lower than viscosity reduction rate. The efficiency of HPAM removal was around 22% at 2.0 kGy and increased to 35% at 10 kGy. the produced wastewater was negatively charged and the absolute value of zeta potential declined stepwise during γ-irradiation. This implies that γ-irradiation is efficient to decrease the stability of emulsion of the produced wastewater.

Organics and oil removal

Figure 2 presents the changes in COD, TOC and oil content in the produced wastewater during gamma irradiation. The concentration of COD and TOC decreased slowly with increasing the adsorbed doses. The removal percentage of COD and TOC was 5.5%-10.7% at 1.0 kGy and reached 11.0%-22.7% at 10 kGy. The reduction of oil content is higher than COD/TOC removal. Oil removal reached 24.6% with the absorbed dose of 1.0 kGy and rose to 40.3% at 10 kGy.

Deactivation of TGB, SRB and IB

With the absorbed dose of 1.0 kGy, more than 99.8% of TGB, SRB and IB were killed and a complete deactivation was observed as increasing the dose to 2.5 kGy (Fig. 3). This is beneficial for treating the produced wastewater for reinjection because the consumption for germicidal agent is going to be saved.

Changes in bacterial community and predictive function

The bacterial diversity of the oilfield produced wastewater was relatively low. At the phylum level, *Proteobacteria* was predominant remarkable with the relative abundance of 94.5%, followed by *Campilobacterota* (2.0%), *Firmicutes* (0.8%) and *Desulfobacterota* (0.4%). At the genus level, the members *Thauera*, *Defluviimonas* and *Comamonadaceae* were predominant.

Based on PICRUSt analysis (Fig. 4), the function gene related metabolism exhibits the highest abundance (25%), followed by environmental and genetic information processing (8.4% and 6.8%). The abundance of almost all the genes coding for metabolism increased with the low absorbed dose of 1.0 kGy and then declined with increasing the dose to 10 kGy. This suggests that ionizing radiation at low dose might stimulate the bacterial activity for metabolism.

Enhancement of γ-radiation pretreatment to coagulation for oil removal

γ-ray pre-treatment with the low absorbed dose of 1.0 kGy improved oil removal by coagulation remarkably. The efficiency of oil removal was 39-47% by coagulation alone and reached 73-85% with γ-ray pre-treatment at PFAC dosages of 50 mg/L and 100 mg/L (Fig. 5).

Table 1. Characteristics of oilfield produced wastewater

Parameters	Values	Parameters	Values
pH	7.92~7.99	SS (mg/L)	85.0 ± 5.0
COD (mg/L)	629 ± 12	CH_3COOH (mg/L)	37.3 ± 0.6
TOC (mg/L)	311 ± 1.5	C_3H_7COOH (mg/L)	60.0 ± 0.3
Oil (mg/L)	295 ± 36	$C_5H_{11}COOH$ (mg/L)	18.3 ± 1.0
HPAM (mg/L)	334 ± 17	Cl^- (mg/L)	887 ±15
Viscosity (mg/L)	3.7 ± 0.1	SO_4^{2-} (mg/L)	9.0 ± 0.9
Salinity (mg/L)	4226 ± 20	S^{2-} (mg/L)	2.84 ± 0.1

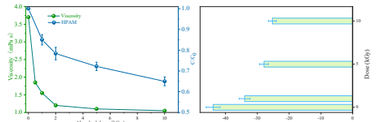

Figure 1. Changes in viscosity, HPAM content and zeta potential during γ-irradiation

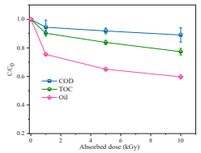

Figure 2. Removal of COD, TOC and oil during gamma irradiation of the produced wastewater

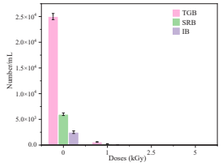

Figure 3. Changes in the number of three typical bacteria during γ-irradiation

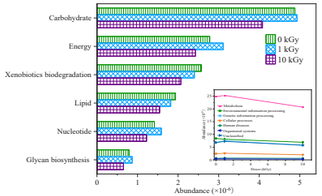

Figure 4. Variation in function genes related metabolism during γ-irradiation

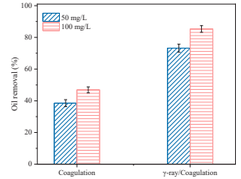

Figure 5. Oil removal by coagulation and γ-ray pretreatment (1.0 kGy) combined with coagulation with two PFAS dosages of 50 mg/L and 100 mg/L, the pictures of coagulation without (beaker 2) and with γ-ray pretreatment (beaker 4) were present

REFERENCES

Gao, C. 2013 Viscosity of partially hydrolyzed polyacrylamide under shearing and heat. *J. Pet. Explor. Prod. Technol.* **3**, 203-206.
Li, C., Li, J., Wang, N., Zhao, Q., Wang, P. 2021 Status of the treatment of produced water containing polymer in oilfields: A review. *J. Environ. Chem. Eng.* **9**, 105303.
Pogaku, R., Mohd Fuat, N.H., Sakar, S., Cha, Z.W., Musa, N. Awang Tajudin, D.N.A., Morris, L.O., 2018 Polymer flooding and its combinations with other chemical injection methods in enhanced oil recovery. *Polym. Bull.* **75**, 1753-1774.
Wang, J., Chu, L. 2016 Irradiation treatment of pharmaceutical and personal care products (PPCPs) in water and wastewater: An overview. *Radiat. Phys. Chem.* **125**, 56-64.

Cyanobacteria for heavy metals removal: from pure metal solutions to electroplating industry wastewaters

M. Ciani*, C. Capelli*, G. Daly*, R. De Philippis* and A. Adessi*

* Department of Agriculture, Food, Environment and Forestry (DAGRI), University of Florence, Piazzale delle Cascine, 18, Florence, IT
(E-mail: *matilde.ciani@unifi.it; chiara.capelli@stud.unifi.it; giulia.daly@unifi.it; roberto.dephilippis@unifi.it; alessandra.adessi@unifi.it)**

Abstract
Cyanobacteria are photoautotrophic microorganisms able to adsorb and/or accumulate heavy metals. Thus, they can be exploited as eco-friendly tools to remove and recover metal ions from wastewater. In this work, we evaluated the biosorption ability of three marine cyanobacteria in laboratory-prepared three-metal solutions and real electroplating wastewaters containing mainly Cu, Ni, Zn, Au, Pd, and Cr. We found that the pre-treatment influences the performances of the biosorbents, with a strain-specific effect. Furthermore, the feasibility of the process is strongly influenced by the concentration of the metals and the composition of wastewater.

Keywords
Biosorption; electroplating wastewaters; heavy metals; marine cyanobacteria; precious metals

INTRODUCTION

Cyanobacteria are cosmopolitan photoautotrophic microorganisms able to survive in extreme conditions, comprising environments containing pesticides, petroleum by-products, xenobiotics, and heavy metals. This ability has risen the attention for their possible exploitation as a clean green technology for the degradation or detoxification of contaminants (Gehlot et al., 2022; Zanganeh et al., 2022). Cyanobacteria have been proposed as biosorbents for heavy metal remediation from contaminated waters thanks to their ability to passively bind positively charged ions on the cell's surface (Singh, 2020). Many cyanobacteria are able to produce a high amount of exopolysaccharides (EPS), which are heteropolymers characterized by six or more different types of monosaccharides and strong anionic nature that may help chelating positively charged heavy metals (Cui et al., 2021; De Philippis and Micheletti, 2017).
Biosorption by cyanobacteria may represent an eco-friendly approach for heavy metal remediation. Additionally, metal ions can be recovered from cyanobacteria biomass to enter again into the productive cycle of the industries. Otherwise, metal-organic materials can be valorized as hybrid catalysts or antimicrobials (Gandolfi et al., 2022; Netanel Liberman et al., 2021). The possibility to recover and reuse these compounds may represent an economic opportunity for the industry sustaining the "end of waste". Previous studies mainly focused on the use of cyanobacteria with single-metal solutions. Nevertheless, the biosorption process is strongly influenced by the composition of the water and the presence of other ions that can cooperate in a competitive or synergistic way (Aranda-García et al., 2020; Zinicovscaia et al., 2018).
This study aims to evaluate the biosorption ability of three selected cyanobacteria strains in *i)* laboratory-prepared three-metal solutions comparing a different pre-treatment and *ii)* real electroplating wastewater adopting confined whole cultures.

MATERIALS AND METHODS

Cyanobacteria and growth conditions

Two unicellular marine cyanobacteria, namely *Cyanothece* sp. CE 4 and *Dactyloccocopsis salina* sp. 16Som2, and a co-culture of *Halothece/Euhalothece* spp named VI 22M, previously selected for their ability to produce EPS and remove Cu, Ni, Zn from single-metal solutions, were grown in 1-L glass bottles with enriched seawater medium (De Philippis et al., 1993), under continuous illumination (200 µmol m^{-2} s^{-1}) and insufflation of CO_2-enriched air.

Biosorption assays

One week-grown cultures were harvested, confined in dialysis tubing (MW cut-off 12-14 kDa) and pre-treated to remove the excessive salts contained in the cultivation medium, with deionized water and HCl or NaOH 0.1M. The same pre-treatments were carried out with dialysis tubing only containing the culture medium (blank). Next, the confined pre-treated cultures or the blank were dipped in the metal containing solutions with a ratio 1:10 (v:v, biosorbent and metal solution, respectively) and maintained under continuous agitation at 25°C. Three replicates were set for each condition. After 24 h the dyalisis tubings were removed and residual metals concentration in the solutions was determined by ICP-OES. The specific metal uptake was expressed as mmol of metal g^{-1} DW. Biomass dry weight (DW, g L^{-1}) was determined by filtering cell suspension after the pre-treatment on pre-weighted 0.45 µm filters and drying the filters at 105°C per 4 hours.

Three-metal solution

A starting solution containing 10 mg L^{-1} of Cu ($CuCl_2$), 10 mg L^{-1} of Ni ($NiCl_2$), and 10 mg L^{-1} of Zn ($ZnCl_2$) was prepared. The cyanobacteria were tested evaluating the effect of both acid and basic pre-treatment (HCl and NaOH 0.1M, respectively). The trial was set as described above maintaining the pH at 5.0 ± 0.3.

Electroplating water

Five wastewaters from electroplating baths were provided by Galvanica Aricci Srl (Ghisalba, BG, Italy) and characterized (table 1). A mixed solution (E1) and the other three solutions (E2, E3, E4) were adopted to verify the biosorption capability of cyanobacteria in real electroplating wastewater. Acid or basic pre-treatment was chosen based on the pH of the solutions to not affect the solubility of the metals. The trial was set as described above.

Table 1. pH and metal composition of five wastewaters provided by Galvanica Aricci Srl

Main metal of electroplating bath	pH	Au	Cr	Cu	Ni	Pd	Zn	Reference name for the assay
		mg L^{-1}						
Cu	1.66	<0.01	0.01	29.52	0.29	nd[a]	21.19	E1[b]
Ni	6.67	nd	nd	0.19	747.22	nd	0.75	E1[b]
Ni	4.11	nd	nd	0.67	386.94	nd	1.01	E2
Pd	7.19	<0.01	0.16	7.31	0.64	24.55	0.14	E3
Au	5.30	7.22	4.49	0.25	6.30	nd	1.66	E4

[a] nd not detected; [b] The first two wastewaters were mixed 1:4 (v:v) to increase the pH of the first solution while decreasing the concentration of Ni in the second solution and named E1.

RESULTS AND DISCUSSION

Three marine cyanobacteria able to produce high amounts of EPS were adopted as biosorbents for heavy metal removal from multi-metal solutions.

Three-metal solution

At the end of the pre-treatment, the cultures had a pH of 3.1 ± 0.3, or 10.1 ± 0.2 when treated with HCl or NaOH 0.1M, respectively. All the cyanobacteria highlighted a stronger affinity towards Cu with acid pre-treatment. VI 22M showed a slightly higher total specific uptake compared to the other strains both with acid and basic pre-treatment (1.30 and 2.19 mmol metal g^{-1} DW, respectively), mainly due to greater Ni removal (figure 1a, 1b). Basic pre-treatment appeared more efficient in Ni and Zn uptake, this statement is particularly evident for VI 22M and 16Som2 (average increment percentage of Ni and Zn uptake within the range of 134% for VI 22M and 243% for 16Som2 with basic pre-treatment), whereas acid pre-treatment improved Cu uptake for CE 4 (+187%). The different behaviour based on the pre-treatment may be explained by different EPS composition (Philippis & Micheletti, 2017).

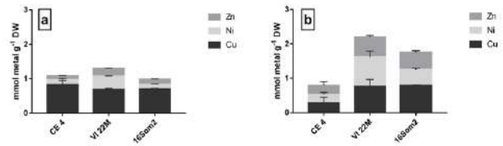

Figure 1. Specific uptake (mmol metal g^{-1} DW) by CE 4, VI 22M, and 16Som2 after 24h contact with three-metal solution (mean ± sd): a) acid pre-treatment, b) basic pre-treatment.

Electroplating water

According to the pH of the wastewater provided by Galvanica Aricci Srl, we adopted basic pre-treatment for E1 and E2, acid pre-treatment for E3 and E4. We compared Ni uptake in E1 and E2 since these solutions were characterized by an extremely high Ni concentration (table 1). VI 22M and 16Som2 showed higher Ni uptake in E2 compared to E1 (figure 2), despite the lower initial concentration of the metal in E2, whereas CE 4 showed a slightly higher uptake in E1. The comparison of Ni uptake per gram of biomass between electroplating water and three-metal solution assays (figure 1b) revealed higher uptake in real electroplating water by all the cyanobacteria, that may be explained by a higher Ni content in the solutions.

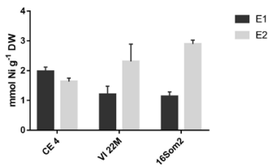

Figure 2. Ni uptake (mmol Ni g^{-1} DW) by CE 4, VI 22M, and 16Som2 after 24h contact with E1 and E2 effluents (mean ± sd).

The possibility to recover precious metals like Au and Pd is extremely important for the industry sector. We evaluated the biosorption ability from palladium and gold-plating bath's wastewater (E3 and E4). The specific uptake considering a single metal was always lower than 80 µmol metal g^{-1} DW (data not shown). The highest Pd and Au uptake was shown by CE 4. Additionally, CE 4 showed a total metal uptake in E4 roughly 4 times greater than VI 22M and 16Som2.
Plating baths containing precious metals are usually rich in conductive salts to reduce the resistance of the solutions, the presence of coexisting ions can negatively affect the biosorption of the metal of interest (Aranda-García et al., 2020), probably reducing the uptake in E3 and E4 solutions.
Exopolysaccharide-producing cyanobacteria may represent an eco-friendly strategy to remove and recover metal ions from wastewater. Nevertheless, we found that the feasibility of the process is strongly influenced by the concentration of the metals and the composition of wastewater.

REFERENCES

Aranda-García, E.. Chávez-Camarillo. G. M.. & Cristiani-Urbina. E. 2020 Effect of Ionic Strength and Coexisting Ions on the Biosorption of Divalent Nickel by the Acorn Shell of the Oak Quercus crassipes Humb. & Bonpl. *Processes*, **8**(10), Article 10.

Bhatt. P.. Bhandari. G.. Bhatt. K.. & Simsek. H. 2022 Microalgae-based removal of pollutants from wastewaters: Occurrence, toxicity and circular economy. *Chemosphere*, **306**, 135576.

Cui. J.. Xie. Y.. Sun. T.. Chen. L.. & Zhang. W. 2021 Deciphering and engineering photosynthetic cyanobacteria for heavy metal bioremediation. *Science of The Total Environment*, **761**, 144111.

De Philippis. R.. Margheri. M. C.. Pelosi. E. & Ventura. S. 1993 Exopolysaccharide production by a unicellular cyanobacterium isolated from a hypersaline habitat. *Journal of Applied Phycology*, **5**, 387-394.

De Philippis. R.. & Micheletti. E. 2017 Heavy Metal Removal with Exopolysaccharide-Producing Cyanobacteria. In *Handbook of Advanced Industrial and Hazardous Wastes Management*.

Gandolfi. R.. Facchetti. G.. Cavalca. L.. Mazzini. S.. Colombo. M.. Coffetti. G.. Borgonovo. G.. Scaglioni. L.. Zecchin. S.. & Rimoldi. I. 2022 Hybrid Catalysts from Copper Biosorbing Bacterial Strains and Their Recycling for Catalytic Application in the Asymmetric Addition Reaction of B2(pin)2 on α,β-Unsaturated Chalcones. *Catalysts*, **12**(4), 433.

Gehlot. P.. Pareek. N.. & Vivekanand. V. 2022 Cyanobacterial and microalgal bioremediation: An efficient and eco-friendly approach toward industrial wastewater treatment and value-addition. In *Microbial Biodegradation and Bioremediation: Techniques and Case Studies for Environmental Pollution* (pp. 343–362).

Netanel Liberman. G.. Ochbaum. G.. Bitton. R.. & (Malis) Arad. S. 2021 Antimicrobial hydrogels composed of chitosan and sulfated polysaccharides of red microalgae. *Polymer*, **215**, 123353.

Potnis. A. A.. Raghavan. P. S.. & Rajaram. H. 2021 Overview on cyanobacterial exopolysaccharides and biofilms: Role in bioremediation. *Reviews in Environmental Science and Bio/Technology*, **20**(3), 781–794.

Singh. S. 2020 Biosorption of Heavy Metals by Cyanobacteria: Potential of Live and Dead Cells in Bioremediation. In M. P. Shah (Ed.), *Microbial Bioremediation & Biodegradation* (pp. 409–423). Springer.

Zanganeh. F.. Heidari. A.. Sepehr. A.. & Rohani. A. 2022 Bioaugmentation and bioaugmentation–assisted phytoremediation of heavy metal contaminated soil by a synergistic effect of cyanobacteria inoculation, biochar, and purslane (Portulaca oleracea L.). *Environmental Science and Pollution Research*, **29**(4), 6040–6059.

Zinicovscaia. I.. Cepoi. L.. Povar. I.. Chiriac. T.. Rodlovskaya. E.. & Culicov. O. A. 2018 Metal Uptake from Complex Industrial Effluent by Cyanobacteria Arthrospira platensis. *Water, Air, & Soil Pollution*, **229**(7), 220.

Reusability of cyanobacteria-based biosorbents through consecutive adsorption-desorption cycles of bivalent metals

M. Ciani*, A. Adessi*, C. Capelli*, G. Daly* and R. De Philippis*

* Department of Agriculture, Food, Environment and Forestry (DAGRI), University of Florence, Piazzale delle Cascine, 18, Florence, IT
(E-mail: matilde.ciani@unifi.it; alessandra.adessi@unifi.it; chiara.capelli@stud.unifi.it; giulia.daly@unifi.it; roberto.dephilippis@unifi.it)*

Abstract
Effective management of heavy metal pollution requires a multi-faceted approach that includes regulations, monitoring, and remediation efforts. Cyanobacteria are photosynthetic prokaryotes that can be exploited for water remediation of heavy metals through the biosorption process. The aim of this study was to evaluate the ability of two halotolerant cyanobacteria to adsorb Cu^{2+}, Ni^{2+}, and Zn^{2+} from aqueous solutions adopting confined systems. Additionally, in order to improve the feasibility of the system, the use of cyanobacteria-based biosorbents in consecutive adsorption cycles was also assessed.

Keywords
Adsorption; desorption; halotolerant cyanobacteria; heavy metals

INTRODUCTION

The negative effects of population growth, industrialization, and resource overuse on ecosystems have prompted the search for effective and eco-friendly strategies for their restoration. Heavy metals can be released into the environment through industrial activities, agricultural practices, and natural processes and can have several negative effects on the environment and human health (Briffa et al., 2020). Biosorption, which utilizes biological materials to remove pollutants, can be used for heavy metal remediation and supports the principles of the circular economy by allowing the recovery and reuse of the absorbed materials. During biosorption, ions from aqueous solutions passively bind onto the functional groups on the surface of the biomass, thus, the cells are not affected by heavy metal concentration and can undergo several adsorption/desorption cycles (Bashir et al., 2019; Paperi et al., 2006). Halotolerant cyanobacteria are particularly promising in this regard as most of them are able to produce a large amount of exopolysaccharides around their cells which possess strong anionic properties, making them effective chelating agents for positively charged heavy metals (Al-Amin et al., 2021; Gehlot et al., 2022).
The aim of this study was to evaluate i) the ability of two halotolerant cyanobacteria to adsorb Cu^{2+}, Ni^{2+}, and Zn^{2+} from aqueous solutions, ii) the stability of the binding in water, and iii) the possibility to use the cultures for a second consecutive adsorption cycle.

MATERIALS AND METHODS

Two halotolerant cyanobacteria strains belonging to *Cyanothece* cluster 3 of *Halothece* and named CE 4 and 16Som2, were grown in 1-liter glass bottles adopting enriched seawater medium. The cultures were managed in semi-continuous mode, replenishing half-culture weekly with fresh medium. Harvested cultures were confined in dialysis tubings (12-14 KDa, MW cut-off), pre-treated with HCl 0.1M solution, and adopted for the assays. Each week, a different metal was tested, namely Cu^{2+}, Ni^{2+}, Zn^{2+}. Firstly, metal uptake was determined after 24 hours of contact with lab-made solutions containing 10 mg L^{-1} of metal, then the stability of the binding between biosorbents and adsorbed metals in the water was evaluated while maintaining the confined cultures in agitation with distilled water for 3 hours. Finally, in order to check the possibility to use the cyanobacteria-based biosorbents for a second adsorption cycle, a test based on consecutive adsorption (I cycle) – desorption – adsorption (II cycle) was performed. HCl 0.1M was adopted as desorbing agent. Metal quantification from water solutions was carried out by adopting an adaptation of the bicinchoninate, 1-(2-pyridylazo)-2naphthol and Zincon method (HI 93702, HI93740 and HI93731 reagents kit, respectively, Hanna Instruments Srl, Italy) following manufacturer's instructions.
Metal uptake was expressed as mg metal g^{-1} DW (dry weight) of biomass.

RESULTS AND DISCUSSION

We observed stronger stability of Cu-biomass complexes. Indeed, the percentage of Cu released in water by the biosorbents was 4-6% of the previously adsorbed amount (data not shown). This percentage increased up to 73% for the other metals, suggesting a stronger affinity of the biosorbents toward Cu. To evaluate the possibility to reuse the cyanobacteria-based biosorbents, two consecutive adsorption cycles were carried out. Generally, metal (mainly Cu and Ni) uptake in the second adsorption cycle was reduced compared to the first adsorption cycle (Figure 1). On the contrary, we found Cu uptake by CE 4 in the second adsorption cycle even higher (+53%) than in the first cycle, probably suggesting that two acid treatments, carried out for pre-treatment and desorption, may improve Cu adsorption by CE 4.

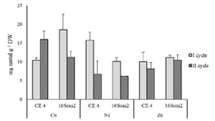

Figure 1. Cu, Ni, Zn uptake (mg metal g^{-1} DW) by confined cultures of CE 4 and 16Som2 in a first adsorption cycle (I cycle) and second adsorption cycle (II cycle).

Cu, Ni, and Zn are common metals in the industry. Thus, they can easily be found in industrial effluents. The biosorption of these metals with halotolerant cyanobacteria may represent a valid bioremediation approach. The use of confined systems promotes easy management of the biosorbents that can be used in consecutive adsorption cycles increasing their shelf-life and economic value, while adsorbed metals can be recovered to enter again in the productive cycle.

REFERENCES

Al-Amin, A., Parvin, F., Chakraborty, J., Kim, Y.-I. 2021 Cyanobacteria mediated heavy metal removal: A review on mechanism, biosynthesis, and removal capability. *Environmental Technology Reviews* **10**(1), 44–57.
Bashir, A., Malik, L. A., Ahad, S., Manzoor, T., Bhat, M. A., Dar, G. N., Pandith, A. H. 2019 Removal of heavy metal ions from aqueous system by ion-exchange and biosorption methods. *Environmental Chemistry Letters* **17**(2), 729–754.
Briffa, J., Sinagra, E., Blundell, R. 2020 Heavy metal pollution in the environment and their toxicological effects on humans. *Heliyon* **6**(9), e04691.
Gehlot, P., Pareek, N., Vivekanand, V 2022 Cyanobacterial and microalgal bioremediation: An efficient and eco-friendly approach toward industrial wastewater treatment and value-addition. In *Microbial Biodegradation and Bioremediation: Techniques and Case Studies for Environmental Pollution* (pp. 343–362). Scopus.
Paperi, R., Micheletti, E., De Philippis, R. 2006 Optimization of copper sorbing–desorbing cycles with confined cultures of the exopolysaccharide-producing cyanobacterium Cyanospira capsulata. *Journal of Applied Microbiology* **101**(6), 1351–1356.

PULSED LIGHT DEGRADATION OF PESTICIDES : OPTIMISATION & METABOLITES

F. Clavero*,**, R. Ghidossi*, N. Picard **, F. Meytraud** G. de Revel* and C. Franc*

* ISVV, UMR OENO, University of Bordeaux, 210 Chem. de Leysotte, 33882 Villenave-d'Ornon, France (E-mail: *francois.clavero@u-bordeaux.fr)*

** *SANODEV, 1, Avenue d'ESTER - 87 100 LIMOGES (E-mail: nicolas.picard@sanodev.com, fanny.meytraud@sanodev.com)*

Abstract

The use of pesticides for agricultural purposes is responsible for generating an important volume of wastewater. In 2009, 13 treatment processes were authorized but they are expensive and the toxicological impact of the secondary metabolites that are formed is not clearly established. In this field, Pulsed Light (PL) seems to be an interesting alternative to modify pesticide structure. Optimization of operating parameters was carried out in terms of intensity and flash number for 20 pesticide molecules. The untargeted analysis identified 118 secondary metabolites and 53 structure hypotheses were proposed. Then, a quantitative method was developed to quantify the secondary metabolites and the parent compounds.

Keywords (maximum 6 in alphabetical order)

Degradation, pulsed light, pesticides, secondary metabolites

INTRODUCTION

According to the FAO (Food and Agriculture Organization), the total pesticides use increased in the most recent decade by nearly 50 percent compared to the 1990's. Statistically, more than 300 liters per hectare of pesticide preparations are sprayed each year. This use is directly linked to an important production of wastewater. Indeed, each year, the cleaning of the sprayers generates a volume of effluent ranging from 400,000 to 900,000 m^3. Recently photodecomposition processes have been studied and proved an effectiveness to degrade pesticides (Martínez-López *et al.,* 2018 ; Gómez-Morte *et al.,* 2020 ; Fortunato *et al.,* 2021). Organic molecules absorb UV light and therefore are impacted and modified (Coly and Aaron, 1994; Patria et al., 1995). Among these techniques, pulsed light has shown its efficiency (Baranda et al., 2012, 2014, 2017). Pulsed light (PL) is a non-thermal technology based on the accumulation of high discharge voltage in a capacitor where the stored electrical energy is delivered as intermittent short pulses through a light source filled with xenon gas. PL relies on a wide wavelength range from 200 to 1000 nm. However, research focusing on the degradation of phytosanitary products by PL (Baranda et al., 2012, 2014, 2017) or UV-C (Maheswari *et al.,* 2010, Lassale *et al.,* 2014) was carried out on a few number of pesticides. Moreover, these experiments did not study toxicity through in-vivo biotoxicity assay. Therefore, the aim of this work was to investigate the PL technology as a new process for the degradation of pesticides. The degradation parameters for 20 pesticides and the formation of their metabolites were studied. The optimization of operating parameters was achieved for each pesticide.

MATERIALS AND METHODS

Pesticide Selection : 20 pesticides (Tab. 1) widely used in viticulture were selected according to their high toxicity, with a low LC50 (Lethal concentration 50) for *Daphnia Magna*.

LP Box : The LP Box is a compact and ergonomic machine, in "office" format (fig 1). As mentioned above, the principle of pulsed light is based on the emission of polychromatic light covering a wide spectrum (200 to 1000 nm, UVC 20%, UVB 10%) by light flashes (between 1 µs and 100 ms per flash).

Untargeted Analysis : Each pesticide was prepared in aqueous solution at a concentration of 10 mg/L, 10 ml of the mix were placed into glass petri dishes, PL fluence values ranged from 19 J/cm^2 to 153 J/cm^2. After treatment, the samples were analyzed in scan mode with a HPLC/MS-MS (HPLC 1260 infinity coupled to a triple quadrupole 6430 from Agilent) in reverse phase with a Poroshell 120 CS-C18 column (2.1×150 mm, 2,7µm). The electrospray ionization was performed in positive mode (ESI$^+$).

Quantitative analysis: The quantification method was developed using the same conditions than for the untargeted analysis but in MRM mode (Multiple Reaction Monitoring). For the specific purpose of developing a method for absolute quantification of the 20 pesticides chosen (Tab.1), a quantitation range from 1 to 200 µg/L was validated (linearity $r^2 > 0.98$, accuracy 70-120%) and limits of quantification were determined by the regression line method.

Fragmentation experiments were performed between 5 and 50 eV on each metabolite previously identified in order to determine 2 transitions per compound and create a relative quantification method for these molecules.

Degradation study :

In order to study the degradation ability of LP Box on pesticides, 7 pesticides were selected because of their rapid degradation with PL. An optimization was made to identify the number of pulses needed to degrade each one of the 7 pesticides. This study used increasing flashes on solutions at LC50 (*Daphnia Magna*) until obtaining concentrations below the LOQs. The samples were analyzed after each 100 flashes of treatment to identify the fluence needed to totally degrade pesticides.

RESULTS AND DISCUSSION :

Untargeted analysis : The aim of this part was to identify secondary metabolites of pesticides and to elucidate their structures. High concentrations were used with the aim of having strong signals in order to detect all metabolites produced during PL degradation. The untargeted analysis showed that PL was able to degrade all pesticides tested. It also demonstrated that HPLC coupled to a triple quadrupole was an effective tool to detect secondary metabolites in treated samples and to make structural hypotheses about them. This study allowed to detect 118 metabolites and 53 hypotheses of structures were proposed using m/z, isotopic patterns of the molecules containing halogens as well as results previously obtained in the literature (fig. 2 and 3). The reactions mainly observed are halogen losses if they are presents in the parent compounds or an addition/substitution of an hydroxyle group.

Quantitative analysis : A MRM method was built for the 20 studied pesticides and for the compounds previously identified as secondary metabolites. Two transitions per compound were used following fragmentation experiments. The developed MRM method allows absolute quantification of the parent molecules and relative quantification of 87 secondary metabolites.

Degradation study :

These experiments show that LP Box is able to degrade pesticides from their LC50 (*Daphnia Magna)* to a concentration lower than their LOQ (fig. 4). These experiments also demonstrated that it was possible to relatively quantify secondary metabolites of pesticides after PL degradation (fig.5). This study also permitted to determine the fluences needed to degrade pesticides from their LC50 to a concentration lower than the LOQ (Tab.2).

CONCLUSION

In conclusion, our results proved that pulsed light has an effective impact on all pesticides treated although the fluence needed is molecule-dependent. Metabolites were detected and a method was built to absolutely quantify 20 pesticides and relatively quantify 87 secondary metabolites. An optimization in terms of fluence showed that it was possible to degrade 7 pesticides from a toxic concentration to a concentration below the LOQ.

Table 1. Pesticide list

Ametoctradin	Azoxystrobin	Benalaxyl	Boscalid	Chlorantraniliprole
Cyprodinil	Difenoconazole	Dimethomorph	Fenbuconazole	Fenhexamid
Fludioxonil	Iprovalicarb	Kresoxim-Methyl	Mandipropamid	Metrafenone
Pyraclostrobin	Pyrimethanil	Tebuconazole	Tebufenozide	Tetraconazole

Figure 1. LP Box

Figure 2. Chromatograms of fenhexamid (10 mg/L in aqueous solution) treated with increasing flashes of PL.

Figure 3. Structure hypothesis for the metabolite 4 of fenhexamid.

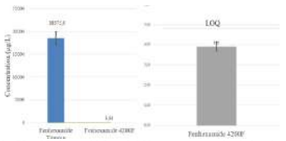

Figure 4. Degradation by PL of fenhexamid from LC50 to a concentration below its LOQ.

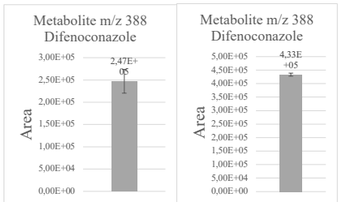

Figure 5. Relative quantification of difenoconazole metabolites

Table 2. Fluences needed to degrade pesticides (J/cm^2)

Chlorantraniliprole	Difénoconazole	Fenbuconazole	Fenhexamide	Kresoxim-Me	Mandipropamide	Tétraconazole
6,706	47,9	210,76	421,52	38,32	28,74	57,48

REFERENCES

1. FAO. 2022. Pesticides use, pesticides trade and pesticides indicators – Global, regional and country trends, 1990–2020. FAOSTAT Analytical Briefs, no. 46. Rome. https://doi.org/10.4060/cc0918en
2. Martínez-López, S.; Lucas-Abellán, C.; Serrano-Martínez, A.; Mercader-Ros, M. T.; Cuartero, N.; Navarro, P.; Pérez, S.; Gabaldón, J. A.; Gómez-López, V. M. Pulsed Light for a Cleaner Dyeing Industry: Azo Dye Degradation by an Advanced Oxidation Process Driven by Pulsed Light. *Journal of Cleaner Production* **2019**, *217*, 757–766. https://doi.org/10.1016/j.jclepro.2019.01.230.
3. Gómez-Morte, T.; Gómez-López, V. M.; Lucas-Abellán, C.; Martínez-Alcalá, I.; Ayuso, M.; Martínez-López, S.; Montemurro, N.; Pérez, S.; Barceló, D.; Fini, P.; Cosma, P.; Cerón-Carrasco, J. P.; Fortea, M. I.; Núñez-Delicado, E.; Gabaldón, J. A. Removal and Toxicity Evaluation of a Diverse Group of Drugs from Water by a Cyclodextrin Polymer/Pulsed Light System. *Journal of Hazardous Materials* **2021**, *402*, 123504. https://doi.org/10.1016/j.jhazmat.2020.123504.
4. Fortunato, L.; Yarali, E.; Sanchez-Huerta, C.; Anthopoulos, T. D. Rapid Photodegradation of Organic Micro-Pollutants in Water Using High-Intensity Pulsed Light. *Journal of Water Process Engineering* **2021**, *44*, 102414. https://doi.org/10.1016/j.jwpe.2021.102414.
5. Coly, A.; Aaron, J.-J. Photochemical–Spectrofluorimetric Method for the Determination of Several Aromatic Insecticides. *Analyst* **1994**, *119* (6), 1205–1209. https://doi.org/10.1039/AN9941901205.
6. Patria, L.; Merlet, N.; Dore, M. Degradation D'un Herbicide, La Flurochloridone, Par Hydrolyse et Photolyse Hydrolysis and Photodegradation of the Herbicide Flurochloridone. *Environmental Technology* **1995**, *16* (4), 315–327. https://doi.org/10.1080/09593330.1995.9618233.
7. Baranda, A. B.; Barranco, A.; de Marañón, I. M. Fast Atrazine Photodegradation in Water by Pulsed Light Technology. *Water Research* **2012**, *46* (3), 669–678. https://doi.org/10.1016/j.watres.2011.11.034.
8. Baranda, A. B.; Fundazuri, O.; Martínez de Marañón, I. Photodegradation of Several Triazidic and Organophosphorus Pesticides in Water by Pulsed Light Technology. *Journal of Photochemistry and Photobiology A: Chemistry* **2014**, *286*, 29–39. https://doi.org/10.1016/j.jphotochem.2014.03.015.
9. Baranda, A. B.; Lasagabaster, A.; de Marañón, I. M. Static and Continuous Flow-through Pulsed Light Technology for Pesticide Abatement in Water. *Journal of Hazardous Materials* **2017**, *340*, 140–151. https://doi.org/10.1016/j.jhazmat.2017.07.012.
10. Maheswari, M. A.; Lamshöft, M.; Sukul, P.; Spiteller, P.; Zühlke, S.; Spiteller, M. Photochemical Analysis of 14C-Fenhexamid in Aqueous Solution and Structural Elucidation of a New Metabolite. *Chemosphere* **2010**, *81* (7), 844–852. https://doi.org/10.1016/j.chemosphere.2010.08.013.
11. Lassalle, Y.; Kinani, A.; Rifai, A.; Soussi, Y.; Clavaguera, C.; Bourcier, S.; Jaber, F.; Bouchonnet, S. UV-Visible Degradation of Boscalid - Structural Characterization of Photoproducts and Potential Toxicity Using *in Silico* Tests: UV-Visible Degradation of Boscalid. *Rapid Commun. Mass Spectrom.* **2014**, *28* (10), 1153–1163. https://doi.org/10.1002/rcm.6880.

Simplified design approach supports avenue for selection of complementary P removal mechanisms in return sludge sidestream processes

K. Close*, L. Ye*, D. Wang**, A. Z. Gu***, A. Oehmen*

* School of Chemical Engineering, The University of Queensland, St Lucia, Queensland, 4072, Australia (Email: k.close@uq.edu.au; l.ye@uc.edu.au; a.oehmen@uq.edu.au)
** State Key Laboratory of Eco-hydraulics in Northwest Arid Region, Xi'an University of Technology, Xi'an, Shaanxi 710048, China (Email: higher1983@outlook.com)
*** School of Civil and Environmental Engineering, Cornell University Ithaca, New York 14853, United States (Email aprilgu@cornell.edu)

Abstract
Limited design information hampers applications of the return sludge side-stream (RSS) process to promote enhanced biological phosphorus removal. Extended anaerobic batch tests were carried out to examine phosphorus release profiles commonly associated with polyphosphate accumulating organism (PAO) activity for the selection of a side-stream tank (SST) hydraulic retention time (HRT). 16 hours was selected and employed in a lab scale RSS system which demonstrated stable long-term N&P removal. A combination of *Tetrasphaera* and *Accumulibacter* PAOs were observed, where both groups played a key role in P removal as assessed by Raman-FISH. A high abundance of GAOs were also observed, although phosphorus removal was not impacted. The multiple PAOs with synergistic removal mechanisms are likely advantageous towards ensuring phosphorus removal stability in RSS systems. Follow up extended anaerobic batch tests with RSS biomass support 16-24 hours as an appropriate SST HRT for the enrichment of *Tetrasphaera*. This simplified approach highlights the potential for SST HRT to be designed and selected by assessment of phosphorus release exhaustion.

Keywords (maximum 6 in alphabetical order)
Polyphosphate accumulating organisms (PAOs), phosphorus, return sludge sidestream (RSS); sidestream enhanced biological phosphorus removal (S2EBPR); *Tetrasphaera*

INTRODUCTION

Anaerobic side stream tank (SST) hydraulic retention times (HRT) in return activated sludge side-stream (RSS) systems have been observed to range from 1-60 hours (Jonsson and Jansen, 2006; Onnis-Hayden et al., 2020; Vale et al., 2008; Vollertsen et al., 2006). This range can be considered extremely broad, with the fundamental rationale for SST HRT selection unclear. For the RSS processes to be applied more widely, particularly outside of Denmark and in variable climates, a clearer understanding of design parameters such as SST HRT needs to be developed for designers. It is hypothesised that if there is an advantage for both VFA consuming and fermenting PAOs under extended anaerobic conditions, pinpointing where phosphorus (P) release is exhausted should elucidate the optimal time range for SST HRT, as no additional substrate storage by PAOs would be possible after this point. In this work, extended anaerobic batch tests were carried out with waste activated sludge (WAS) from the Luggage Point sewage treatment plant (STP) to examine initial P release dynamics. Based on these results, a SST HRT was selected and implemented in a lab scale RSS sequencing batch reactor (SBR) to assess if the design methodology was valid. A range of advanced microbial techniques were applied to assess the contribution and mechanism of different PAOs. This work furthers our understanding for RSS process design, particularly on how to actively select and enrich for *Tetrasphaera*.

MATERIALS AND METHODS

Waste activated sludge (WAS) collected from Luggage Point Sewage Treatment Plant, in Brisbane, Australia was used for the extended anaerobic batch tests. Each reactor had a working volume of 1 litre and was continuously mixed and sparged with nitrogen gas to ensure anaerobic conditions. Samples were collected at the start of each batch test and subsequently at 8-hour intervals up to 48 hours and analysed accordingly for NH_4-N, PO_4-P, COD, sCOD, TSS/VSS and VFAs. The RSS sequencing batch reactor was operated with a working volume of 4L and inoculated with WAS from Luggage Point STP. The system was operated on a 12-day solids retention time (SRT), a SBR HRT of 16 hours and an SST HRT of 16 hours. 2L of feed per cycle, comprising average influent COD, NH_4-N and PO_4-P concentration of 494.5±16.4mg COD/L, 55.6±5.1 mgN/L and 10.9±0.8 mgP/L was fed to the reactor. The COD was a mixture of glucose, casein amino acids, glycerol, acetate and propionate proportioned to mimic real wastewater. Each cycle lasted 8 hours (3 cycles per day) and comprised four main phases where alternating anoxic/aerobic conditions were employed, followed by a waste, settle, and decant phase. 200mL of RAS (10%) was transferred to the sidestream tank after the decanting phase mixed and then 200mL returned to the SBR for the next cycle.

RESULTS AND DISCUSSION

Extended anaerobic batch tests highlighted P release occurring within 16-24 hours of extended anaerobic conditions (**Figure 1a**). The initial rate of orthophosphate release (PO_4-P) was determined to be inconsistent with both PAO maintenance and general biomass decay. P release associated with substrate uptake was assessed to be occurring during the first 16-24 hours, after which a transition occurs to a constant rate likely associated with cell decay. Synergistically, the VFA concentration also appears to increase at this transition point (**Figure 1b**). These observations suggested an SST HRT of 16-24 hours could be optimal for enabling efficient RSS performance. An RSS SBR system was then implemented and operated with an SST HRT of 16 hours to test the substrate related P exhaustion hypothesis.

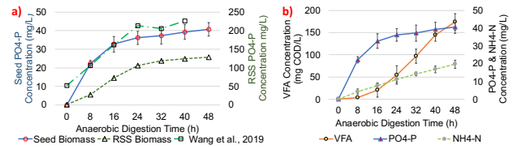

Figure 1. a) Phosphorus release profiles from extended anaerobic batch tests with seed biomass taken from a 5 stage Bardenpho bioreactor (Luggage Point STP), biomass acclimated in an RSS SBR system and P release from Wang et al., 2019. b) VFA, PO4-P and NH4-N concentration profiles from the extended anaerobic batch tests with seed biomass.

The RSS SBR system reached steady state within 3 SRT's and was operated for a total of 180 days. The effluent NH_4-N, NO_x-N and & PO_4-P effluent concentrations measured 0.10±0.14 mgNH_4-N/L, 6.45±0.14 mgNO_x-N/L and 0.35±0.43 mg PO_4-P/L, respectively. Microbial community analysis through FISH, 16s rRNA sequencing and Illumina metagenomics analysis indicated that operational conditions implemented in the RSS SBR were able to enrich for *Tetrasphaera* and maintain a stable presence in the system for the duration of the reactor operation, as highlighted in **Table 1.** Contrary to full-scale studies showing GAOs in lower abundance in full scale RSS systems, *Competibacter*, *Defluviicoccus* and *Micropruina* (not shown in **Table 1** but validated through metagenomics) were observed to be in high abundance in the lab scale RSS system. It is not currently clear if this observation is due to the SST HRT or due to other unknown factors. Nevertheless, it does highlight that both VFA driven and fermenting GAOs did not impact P removal stability in the RSS system. RSS can likely rely on two or more P removal mechanisms occurring in tandem, the fermentative PAO metabolism (e.g. *Tetrasphaera*) and VFA-driven PAO metabolism (e.g. *Accumulibacter*) supporting P removal. *Ca*. Microthrix were not observed in this study, unlike Petriglieri et al. (2022), who identified this group as a contributor to P removal in some RSS plants. A follow up extended anaerobic batch test was conducted using acclimated biomass from the RSS reactor. In agreement with the original batch tests (**Figure 1a**), P release associated with substrate uptake appears to occur within 16-24 hours before transitioning to a slower constant rate.

Table 1. FISH quantification for RSS system day 63 and day 137 (biovolume ± standard error of the mean).

Target Organism Probe Mix	Day 63 %vol fraction	Day 137 %vol fraction
Tetrasphaera TetMix	24.7±10.3	18.2±5.1
Accumulibacter PAOMIX	4.7±2.7	2.3±1.6
Competibacter GAOMix	6.4±1.9	7.1±1.6
Defluviicoccus DEFMix	7.4±2.4	8.1±1.9

Single cell Raman spectroscopy (SCRS) was also performed on samples from the main RSS reactor and the SST before RAS fermentation to ascertain intracellular polyP content within *Tetrasphaera* and *Accumulibacter*. **Figure 2** highlight changes in intracellular polyP content (expressed as Raman peak intensity, CCD counts) across key SBR phases. Results indicate *Tetrasphaera* released most of their polyP reserves during the anaerobic phase in the SST rather than in the mainstream system, which is in agreement with Fernando et al. (2019). Moreover, despite the substantially higher abundance of *Tetrasphaera*, both *Tetrasphaera* and *Accumulibacter* activity were instrumental towards achieving P removal, with 57% of the P stored by *Tetrasphaera* and 43% stored by *Accumulibacter*.

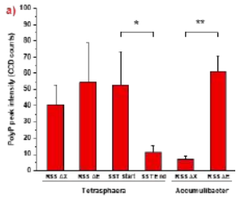

Figure 2. Intracellular polyP content (expressed as Raman peak intensity) in FISH-identified *Tetrasphaera* and *Accumulibacter* cells in different samples (error bars represent standard error, *p<0.05, **p<0.01).

CONCLUSIONS

Outcomes from this work highlights how the enrichment of both PAO groups can be beneficial for stable P removal performance and supports the hypothesis that intracellular polyP exhaustion associated with substrate uptake can be used a selection tool for SST HRT in applications of RSS. It also validates that an SST HRT between 16-24 hours could be used as a design basis for RSS applications to enrich for *Tetrasphaera* PAOs. It is suggested further work should be carried out to examine the influence of temperature on the SST HRT range.

REFERENCES

Fernando, E.Y., McIlroy, S.J., Nierychlo, M., Herbst, F.A., Petriglieri, F., Schmid, M.C., Wagner, M., Nielsen, J.L. and Nielsen, P.H. 2019. Resolving the individual contribution of key microbial populations to enhanced biological phosphorus removal with Raman-FISH. *ISME J* 13(8), 1933-1946.

Jonsson, K. and Jansen, J. 2006. Hydrolysis of return sludge for production of easily biodegradable carbon: effect of pre-treatment, sludge age and temperature. *Water Sci Technol* 53(12), 47-54.

Onnis-Hayden, A., Srinivasan, V., Tooker, N.B., Li, G., Wang, D., Barnard, J.L., Bott, C., Dombrowski, P., Schauer, P., Menniti, A., Shaw, A., Stinson, B., Stevens, G., Dunlap, P., Takacs, I., McQuarrie, J., Phillips, H., Lambrecht, A., Analla, H., Russell, A. and Gu, A.Z. 2020. Survey of full-scale sidestream enhanced biological phosphorus removal (S2EBPR) systems and comparison with conventional EBPRs in North America: Process stability, kinetics, and microbial populations. *Water Environ Res* 92(3), 403-417.

Petriglieri, F., Petersen, J.F., Peces, M., Nierychlo, M., Hansen, K., Baastrand, C.E., Nielsen, U.G., Reitzel, K. and Nielsen, P.H. 2022. Quantification of Biologically and Chemically Bound Phosphorus in Activated Sludge from Full-Scale Plants with Biological P-Removal. *Environmental Science & Technology* 56(8), 5132-5140.

Vale, P., Barnard, J.L., Thomas, D. and Dold, P.L. 2008 RAS Fermentation to Enhance Biological Phosphorus Removal, pp. 1775-1789, *Water Envrionment Federation*.

Vollertsen, J., Petersen, G. and Borregaard, V.R. 2006. Hydrolysis and fermentation of activated sludge to enhance biological phosphorus removal. *Water Sci Technol* 53(12), 55-64.

Fate of PPCPs within biofilters based on hazelnut shell/sawdust and fed with domestic wastewater.

K.C. Conceicao[1,3], L. S. Freitas[2] and C. A. Villamar-Ayala[3*]

[1]Facultad de Ingeniería, Departamento de Ingeniería Civil Química, Universidad de Santiago de Chile (USACH), Santiago, Chile (email: *kennedy.costa@usach.cl*)
[2]Departamento de Química, Universidade Federal de Sergipe, São Cristóvão, Brasil (email: *lisiane@academico.ufs.br*)
[3*]Facultad de Ingeniería, Departamento de Ingeniería Civil en Obras Civiles, Universidad de Santiago de Chile (USACH), Santiago, Chile (E-mail: *cristina.villamar@usach.cl*)

Abstract
Pharmaceutical and personal care products (PPCPs) consumption was increased mainly during COVID-19 pandemic. Nature-based solutions, such as biofilters could be a technological alternative for rural areas and developing countries. The objective of this study was to evaluate the fate of PPCPs within biofilters based on hazelnut shell/sawdust and fed domestic wastewater. Wastewater (influent/effluent), plant, and soil samples were collected for PPCPs analysis from 4 biofilters. Chromatographic analysis (LC-DAD-MS) used C18 column and with/without clean-up method's extraction. Caffeine (CAF), losartan (LOS), ibuprofen (IBU) and triclosan (TRI) were monitored. The results showed that PPCP concentrations at influents and effluents were between 0.35 and 4.57 µg/L and from 0.01 to 0.48 µg/L, respectively. In plants, PPCPs (LOS, IBU and TRI) accumulated at concentrations between 0.02 and 1.68 µg/L; while that, soil concentrated between 0.02 and 9.08 µg/L. Therefore, soil was the main fate of lipophilic PPCPs and plants when PPCPs are more mobile.

Keywords
Biofiltration; PPCPs, Plant; Soil; Treatment; Wastewater

INTRODUCTION

Pharmaceuticals and personal care products (PPCPs) are among the relatively new and concerning contaminants detected around the world (Almeida et al., 2021). Caffeine (CAF, $C_8H_{10}N_4O_2$), Ibuprofen (IBU, $C_{13}H_{18}O_2$), Losartan (LOS, $C_{22}H_{23}ClN_6O$) and Triclosan (TRI, $C_{12}H_7Cl3O_2$) were studied, due to the high rate of usual consumption and during the COVID-19 pandemic (Buchan and Quiñones et al., 2016; Chicaiza et al., 2020). The fate and time half-lives of PPCPs are variable when assessing environmental risk by the influence of dispersion, degradation, or sorption (O´Malley et al., 2021). For the antibiotics, NSADs, and physical stimulants class, maximum concentrations of 0.0199 µg/mL were detected in influent and effluent samples, respectively (Papageorgiou et al., 2016; Dhangar and Kumar, 2020). Furthermore, during the confinement due to the SARS-CoV-2 pandemic, the consumption of PPCPs was high (<0.1–1.19 µg/mL), and it becomes necessary the treatment, as using biofilters that are nature based on solutions. Biofilters based on plant–earthworms–microorganisms are particularly interesting for developing countries, due to their easy operation and low-cost (Tejedor et al., 2019). Support materials are extremely important when using this technology since they impact in the treatment-cost. Technologies that utilize plants (as constructed wetlands) remove contaminants associated rhizosphere, have a pronounced ability for uptake and phyto-depuration that function as a media nature and biological. Ibuprofen has reported being removed using plants at concentrations to up 0.06 µg/mL within WWTPs (He et al., 2017). In this work, we study the evaluation of 4 biofilters typologies (BM, BEM, BH and BPM) in lab-scale, as a natural environment of removal of PPCPs, and identify the mechanisms involved in biotic components/support, to establish the fate and mobility of the PPCPs studied, from rural domestic wastewater Chilean.

MATERIALS AND METHODS

Materials

Hight Performance Liquid Chromatography (HPLC) grade methanol (99%, CH_3OH), water (100%, H_2O) and acetonitrile (99%, CH_3CN) were obtained from Sigma-Aldrich (Santiago, Chile), Hydrochloric acid (32%, HCl) and Ammonium hydroxide (92%, NH_4OH) were obtained from Spectrum (Santiago, Chile). Analytical-grade formic acid (88%, CH_2O_2) was obtained from Merck (Brazil). Caffeine (99%, $C_8H_{10}N_4O_2$, CAF), Ibuprofen (98%, $C_{13}H_{18}O_2$, IBU), Losartan (99%, $C_{22}H_{23}ClN_6O$, LOS) and Triclosan (99%, $C_{12}H_7Cl_3O_2$, TRI) standards were purchased from Sigma–Aldrich (Santiago, Chile). Oasis HLB cartridge-SPE (6 cc, 200 mg) were purchased from Waters Corp., Milford, USA. Fiberglass filters (ø = 0.45 µm) and nylon syringe filters (ø = 0.22 µm) were obtained from Millipore, Billerica, MA.

Experimental models

The domestic wastewater samples to feed the biofilter systems were taken in situ at a domestic wastewater treatment plant (WWTP), located in the Santiago Metropolitan Region, Chilean. The location of this plant corresponds to the coordinates (33°0'29.41"S.; 70°53'21.50"W), WGS-84 datum. The material used in the active layer of the biofilters was a mixture of hazelnut shells and sawdust. The shell was crushed and sieved in 2 mm. The proportion used was 75% sawdust and 25% hazelnut shells (v/v). *Eisenia feotida* Saving earthworms were used with 57 individuals per biofiltration column, following the density recommended by the literature of 10,000 individuals/m^3 (Kumar et al., 2016). The plants *Zantedeschia aethiopica* L., 1 individual per column was used, according to Vera-Puerto et al., (2021). The physical model consisted of 4 biofiltration typologies. Each column was divided into 3 different horizontal layers: active (sawdust/hazelnut shell, 0.6 m high), medium (gravel sand, 0.2 m high) and support (gravel, 0.1 m high). The columns used were polyvinyl chloride (PVC), with a diameter of 0.11 m and a height of 0.9 m. The hydraulic load rates used corresponded to a nominal value of 2 (m^3/m^2 d) and applied to 4 biofilters of different types operating. The typologies used were: biofilter based on microorganisms (BM), on earthworms (BEM), on plants (BPM), and hybrid microorganism+earthworms+plants (BH). The feed with the wastewater was applied to each biofilter a regimen of 2 hours of flow and 2 hours of rest, during 5 day/week from March to December of 2022. In this way, the corresponding nominal flow for rate 2 biofilters was 9.5 (L/d).

Analytical methods

Wastewater samples (influent) from rural WWTP (33°00'29.7"S 70°53'22.7"W) located close to Santiago city, which uses vermifiltration technology as secondary phase. Biofilters wastewater samples (effluent) at lab-scale was collected using an aliquot of 0.5 L each typology biofilters (BM, BEM, BPM, y BH) by 24 hours of end a cycle operational (2 m^3/ m^2 d). In lab, centrifugation (5000 rpm, 25 min) and vacuum filtration (fiberglass filters: 0.45 µm (GF/B, Whatman, UK), nylon syringe filters: 0.22 µm (Millipore, Billerica, MA) were applied prior to SPE/HLB (Solid Phase Extraction–Hydrophilic Lipophilic Balance) extraction method. Finally, wastewater samples were stored/kept refrigerated under dark conditions at 4 °C. Root and Sheets/Stem tissue were extracted from 0.5 g of frozen plant tissue. Samples were ground to a fine powder in liquid nitrogen and mixed with 1 mL of 0.1 M HCl/acetonitrile (50/50, v/v) by vortexing, and after centrifugation at 12 000 rpm for 15 min under 4 °C. Solid phase extraction (SPE) was performed with Oasis HLB cartridges (6 cc/200 mg), preconditioned with 6 mL methanol, and equilibrated with 6 mL deionized water. After loading 1200 µL sample, the cartridge was washed with 12 mL deionized water and eluted with 12 mL of 25% NH_4OH: MeOH (8/92, v/v). To determine the PPCPs concentration in soil samples, solid-liquid extraction method. 2 g of soil (organic support of biofilters in different points) were weight in plastics tubes with lids. Subsequently, 10 mL of methanol were used for the extraction method. The mixture was stirred for 1 h and centrifuged at 15,000 rpm for 20 min at 4◦C.

Chromatographic analysis

Wastewater, plant, and soil samples concentrations were determined by LC-DAD-MS (Schimadzu, Kyoto, Japan). The column was a Cl Kinetex C18 (2,6 um, 100 mm x 2,1 mm). The wavelength for the quantification were 205 nm (CAF) and 223 nm (LOS, IBU and TRI), in PDA. MS were evaluated in Full Scan mode (m/z) of the PPCPs, in ESI (+) and (-). In (+): CAF (195), LOS (423); (-) IBU (205), TRI (289). The PPCPs compounds were determined in gradient condition using formic acid 0.2% (A) and acetonitrile (B). Flow was set at 0.2 mL/min. The column was thermostated at 35 °C The retention times under these conditions were 4.322, 15.910, 17.557, and 18.616 min for CAF, LOS, IBU and TRI, respectively.

Data analysis

Data were acquired by means of Postrum and processed/recollected applying Microsoft Excel Software. The contaminant removal behavior was obtained as a linear function, where the independent variable is the concentrations of each system and adjusted for the statistical measurement of R^2.

RESULTS AND DISCUSSION

Table 1 shows the occurrence data of the 4 selected PPCPs inside wastewater (influent/effluent), plant and soil samples from biofilters based on hazelnut shell/sawdust (4 typologies). Within each biofilter (BM, BEM, BH and BPM) they present very high concentrations, with respect to the PPCPs/Matrices, in values of up to 0.722, 0.424, 0.424, 0.612 µg/mL, respectively. In wastewater, results were obtained from biofilters versus PPCPs (CAF, LOS, IBU and TRI) presenting a concentration variation in ug/mL from (0.023–0.722, BM), (0.299–0.424, BEM), (0.198–0.424, BH) and (0.392–0.612, BPM). Meanwhile, plant reported values in BH and BPM of 0.010 to 0.754 µg/L, and 0.017 to 0.318 µg/L for the PPCPs, respectively. LOS, IBU and TRI were very prevalent concentrations ranging between 0.01 and 1.68 µg/L in the biofilters of plants and hybrid. Soil sample concentration were between (0.027-0.362, BM), (0.015-0.353, BEM), (0.021-0.720, BH), (0.024-9.082, BPM) for biofilters. Caffeine was analysed low with quantification (<LQ) and detection limit (<LD). Losartan presented concentrations from up to 0.054 µg/mL in within biofilters analysed. In the case Ibuprofen presented high concentration in the soil with 9.082 µg/mL due influence the sorption. Triclosan were the range of 0.021 to 0.031 in within biofilters analysed.

Table 1. Wastewater, plant, and soil with total range of concentrations (min–max in µg/mL) with mean values in brackets and limit of detection/quantification. LQ: is the limit of the calibration curve; LD: the limit is 3.3x lower than that of the calibration curve.

Matrices	PPCPs	BM	BEM	BH	BPM
Wastewater	CAF	<LD	<LD	<LD	<LD
	LOS	(0.023-0.475)	(0.299-0.401)	(0.198-0.424)	(0.392-0.423)
	IBU	0.722	0.424	0.234	0.612
	TRI	<LD	<LD	<LD	<LD
Plant	CAF			<LD	<LD
	LOS			(0.010-0.016)	<LQ
	IBU			(0.156-0.754)	(0.156-0.318)
	TRI			0.017 – 0.018	0.017
Soil	CAF	<LD	<LD	<LD	<LD
	LOS	(0.030-0.054)	(0.015-0.038)	(0.029-0.044)	(0.024-0.039)
	IBU	(0.161-0.362)	0.353	0.720	(0.615-9.082)
	TRI	(0.025-0.027)	(0.023-0.026)	(0.021-0.027)	(0.024-0.031)

For caffeine and triclosan, their concentration (µg/L) ratio in domestic wastewater/soil was consistently higher, with from 0.02–0.452 (TRI) and 0.006–0.070 (CAF) in agriculture sectors and from irrigation of treated effluents with concentration of 0.116–3.529 (TRI) and 0.0179–0.178 (CAF), suggesting that these compounds might be unsuitable as chemical markers of wastewater leakage (Tran et al., 2019; Mojiri et al., 2021). Moreover, triclosan is a broad-spectrum antibacterial agent present as an active ingredient in some personal care product such as soaps, toothpastes and sterilizers, with and low average in effluents (<40 µg/L) (Olaniyan et al., 2016). Losartan is among the most prescribed drugs in Chile in people with high blood pressure (ISP, 2022). According to He et al., (2017), concentrations of ibuprofen was analysed in the liquid medium with plants, that an immediate exponential-wise decline of IBU contaminant was observed with 0.45 ± 0.10 µg/mL.

Acknowledgements

This researcher was supported by the Fondecyt (project grant 11190352). Authors thank the facilities provided to this research by Chilean rural WWTPs. Moreover, authors thank the Interdisciplinary Lab of Water and Sciences Technology (Ko-Yaku Lab, Chile), to CLQM (Center of Multi-users Chemistry Laboratories) from Federal University of Sergipe for the analysis support and the Chromatographic Analysis Lab (LAC Lab, Brazil).

REFERENCES

Almeida-Naranjo, C. E., Frutos, M., Tejedor, J., Cuestas, J., Valenzuela, F., Rivadeneira, M. I., Villamar, C. A., Guerrero, V. H. 2021 Caffeine adsorptive performance and compatibility characteristics (Eisenia foetida Savigny) of agro-industrial residues potentially suitable for vermifilter beds. *Science of The Total Environment*, **801**, 149666.
Buchan S.J., Quiñones R.A. 2016 First insights into the ocean-graphic characteristics of a blue whale feeding ground in Northern Patagonia, Chile, 183–199.
Chicaiza, C., Huaraca, L., Almeida-Naranjo, C. E., Guerrero, V. H., Villamar, C. A. 2020 Improvement of organic matter and nutrient removal from domestic wastewater by using intermittent hydraulic rates on earthworm–microorganism biofilters. *Water Science and Technology*, **82**(2), 281-291.
Dhangar, K., Kumar, M. 2020 Tricks and tracks in removal of emerging contaminants from the wastewater through hybrid treatment systems: A review. *Science Total Environment*, 140320.
He, Y., Langenhoff, A. A., Sutton, N. B., Rijnaarts, H. H., Blokland, M. H., Chen, F., Huber, C., Schröder, P. 2017 Metabolism of ibuprofen by Phragmites australis: uptake and phytodegradation. *Environmental science & technology*, **51**(8), 4576-4584.
Instituto de Salud Pública – ISP 2023 ISP entrega antecedentes de decomiso de más de 10 mil kilos de medicamentos, Chile, https://www.ispch.cl/noticia/isp-entrega-antecedentes-de-decomiso-de-mas-de-10-mil-kilos-de-medicamentos/ (accessed on January 28, 2023).
Kumar, T., Hari Prasad, K. S., Singh, N. K. 2016 Substrate removal kinetics and performance assessment of a vermifilter bioreactor under organic shock load conditions. *Water Science and Technology*, **74**(5), 1177-1184.
Mojiri, A., Baharlooeian, M., Kazeroon, R. A., Farraji, H., Lou, Z. 2020 Removal of pharmaceutical micropollutants with integrated biochar and marine microalgae. *Microorganisms*, **9**(1), 4.
O'Malley, E., McLachlan, M. S., O'Brien, J. W., Verhagen, R., Mueller, J. F. 2021 The presence of selected UV filters in a freshwater recreational reservoir and fate in controlled experiments. *Science Total Environment.*, **754**, 142373.
Olaniyan, L. W. B., Mkwetshana, N., Okoh, A. I. 2016 Triclosan in water, implications for human and environmental health. *Springerplus*, **5**, 1-17.
Papageorgiou, M., Kosma, C., Lambropoulou, D. 2016 Seasonal occurrence, removal, mass loading and environmental risk assessment of 55 pharmaceuticals and personal care products in a municipal wastewater treatment plant in Central Greece. *Science Total Environment*, **543**, 547-569.
Tejedor J., Cóndor V., Almeida-Naranjo C.E., Guerrero V.H., Villamar C.A. 2020 Performance of wood chips/peanut shells biofilters used to remove organic matter from domestic wastewater. *Science of The Total Environment*, **738**, 139589.
Tran, N. H., Reinhard, M., Khan, E., Chen, H., Nguyen, V. T., Li, Y., Goh, S.G., Nguyen, Q.B., Saeidi, N., Gin, K. Y. H. 2019 Emerging contaminants in wastewater, stormwater runoff, and surface water: Application as chemical markers for diffuse sources. *Science of the Total Environment*, **676**, 252-267.
Vera-Puerto, I., Escobar, J., Rebolledo, F., Valenzuela, V., Olave, J., Tijaro-Rojas, R., Arias, C. 2021 Performance comparison of vertical flow treatment wetlands planted with the ornamental plant *zantedeschia aethiopica* operated under arid and Mediterranean climate conditions. *Water*, **13**(11), 1478.

Project title: Fabrication of Fouling Resistant and Operationally Stable Nanocomposite Membranes for Refinery Wastewater Treatment

N. D. Enemuo*, M. Daramola**, H. L. Richards* and A. Etale***

* Department of Chemistry, University of the Witwatersrand, 1 Jan Smuts Avenue, Braamfontein, Johannesburg, South Africa
(E-mail: *828645@students.wits.ac.za)*
** Department of Chemical Engineering, University of Pretoria, Lynnwood Road, Hatfield, Pretoria, South Africa
(E-mail: *michael.daramola@up.ac.za*)
* Department of Chemistry, University of the Witwatersrand, 1 Jan Smuts Avenue, Braamfontein, Johannesburg, South Africa
(E-mail: *heidi.richards@wits.ac.za)*
*** Department of Chemistry, University of Bristol, BS8 1TL, Bristol, United Kingdom
(E-mail: anita.etale@bristol.ac.uk)

Abstract
Benzene, Toluene, Ethylbenzene, and Xylene (BTEX) are among the major contaminants in refinery wastewater, and they pose serious detrimental effects on both human and environmental health. Although there are existing treatment methods targeting the removal of BTEX such as coagulation and filtration, there is still a need to improve the treatment scheme to ensure a safer and more effective process for their removal. In this study, green-synthesized iron oxide nanoparticles were used to improve the physical properties and performance of PVDF ultrafiltration membranes, and further functionalization using polyvinyl alcohol (PVA) was performed. The BTEX rejection of the optimum modified membrane (PVDF-1%wt.Fe_3O_4) was 80% which increased to 94% upon further functionalization using PVA. The Flux Recovery Ratio (FRR) of the pristine membrane was 62% while that of the optimum modified membrane was 81% and increased further to 92% when blended with PVA, thus indicating a significant improvement in its antifouling capacity. The modified membranes also showed improvement in other properties such as mechanical, chemical, and thermal stability which is ideal for withstanding the operational conditions during the wastewater treatment process. Therefore, the modified membranes have good potential in providing an alternative means of removing BTEX from refinery wastewater before discharge to any receiving water body.

Keywords
BTEX; Green-synthesized Fe_3O_4; Nanoparticles; PVA; Ultrafiltration membrane; Wastewater

INTRODUCTION

The global water challenge that mainly originates from perilous human activities requires continuous approaches to tackle it. Emerging membrane technology offers possible solutions to ensure wastewater is properly treated before being discharged into the water bodies (Zhang et al., 2016). Functionalized PVDF membranes provide a safe and effective means to treat refinery wastewater to ensure their safe discharge into water bodies.

MATERIALS AND METHODS

All the chemicals used for synthesizing the nanoparticles, preparing the membranes, and analyzing the prepared membranes were purchased from Sigma Aldrich. Iron (III) chloride was used as the precursor for the green synthesis of the iron oxide nanoparticles. PVDF was adopted as the base membrane material. N-methyl-2-pyrrolidone (NMP) was used as the solvent for the preparation of the dope solutions. PVA was also used for the second step functionalization of the membranes and maleic acid was utilized as the cross-linking agent in this step. The rejection and antifouling capacity of the membranes were tested using Humic Acid (HA) and BTEX solutions. The chemical stability of the membranes was tested using BTEX, sodium hypochlorite, and chlorine solutions.
The iron oxide nanoparticles were synthesized using the green route by reducing the metal precursor with the aqueous extract of pomegranate leaves. The membranes were prepared with varying amounts of the green-synthesized Fe_3O_4 and cast through the phase inversion method and the second step functionalization of the membranes was also performed by phase inversion after blending the PVA into the dope solution, followed by subsequent cross-linking using maleic acid.

RESULTS AND DISCUSSION

A few of the results of the properties and performance of the green-synthesized nanoparticles and membranes are shown in Fig. 1. The XRD shows characteristic peaks indicating that the synthesized nanoparticles are Fe_3O_4 and the noisy patterns seen in the spectra reveal the presence of organic components in the synthesized nanoparticles. The FTIR confirms that the organic component has hydroxyl functional group which further contributed to improving the hydrophilicity of the membranes and enhanced the membranes' performance. The antifouling ability of the membranes significantly improved but reached an optimum at 1wt.%- Fe_3O_4.

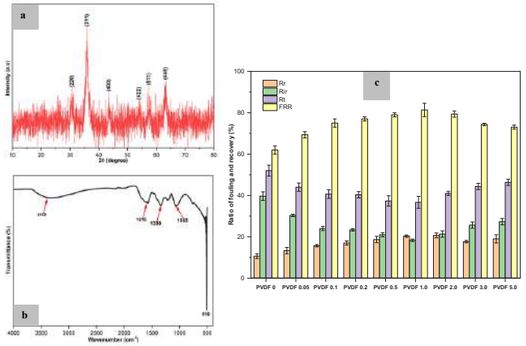

Figure 1. The properties of the green-synthesized nanoparticles and the membranes: (a) XRD of the green-synthesized nanoparticles; (b) FTIR of the green-synthesized nanoparticles; (c) antifouling behavior of the membranes

REFERENCE

Zhang, R., Liu, Y., He, M., Su, Y., Zhao, X., Elimelech, M., & Jiang, Z. (2016). Antifouling membranes for sustainable water purification: Strategies and mechanisms. *Chemical Society Reviews*, *45*(21), 5888–5924.

Fenton pre-treatment combined with an activated sludge system for carbamazepine removal

Y.-Y. Lee* and C. Fan**

* Department of Bioenvironmental Systems Engineering, National Taiwan University, No. 1, Sec. 4, Roosevelt Rd., Da-An District, Taipei, 10617, Taiwan
(E-mail: *youyilee0603@gmail.com*)*
** Department of Bioenvironmental Systems Engineering, National Taiwan University, No. 1, Sec. 4, Roosevelt Rd., Da-An District, Taipei, 10617, Taiwan
(E-mail: *chfan@ntu.edu.tw*)*

Abstract
Carbamazepine (CBZ) is one of the most frequently detected pharmaceuticals in various waters due to its extensive utilization and persistence in the environment. This study aimed to evaluate the CBZ removal through the Fenton process followed by a sequencing batch reactor (SBR). The results showed that CBZ mineralization was facilitated by subsequent biological treatment following the Fenton pre-treatment, supporting the hypothesis that the degradation intermediates from the Fenton process were more biodegradable. The CBZ removal by the Fenton process at neutral pH remained at 76.05%, implying that the combined system for CBZ removal may work at a neutral pH range. The blue-shifted signal in EEM spectra indicated the decomposition of the aromatic structure and the formation of molecular fractions. Due to the low biodegradability of CBZ, using the Fenton process as a pre-treatment for SBR-AS is a possible way to improve the aqueous CBZ removal efficiency.

Keywords
Activated sludge treatment; Advanced oxidation process; Carbamazepine; Fenton process; Sequencing batch reactor

INTRODUCTION

Carbamazepine (CBZ), a widely used anticonvulsant and mood-stabilizing drug for the treatment of epilepsy and bipolar disorder, has been one of the most frequently detected pharmaceutical compounds in the environment (Ferrer & Thurman 2012). Due to its molecular structure and chemical characteristics, CBZ showed persistence in conventional treatment processes (Hai *et al.* 2018). Although the CBZ removal tests by several well-known advanced technologies were reported previously, none of them was regarded as an effective treatment in WWTPs (Zhang *et al.* 2008). Thus, the discharge of CBZ residual through wastewater effluents leads to its widespread occurrence in natural water bodies, making CBZ one of the emerging and concerning contaminants. CBZ has been proposed as an anthropogenic marker of sewage contamination to assess water treatment quality (Kumar *et al.* 2016; Marcelo *et al.* 2017).

The Fenton process generates the hydroxyl radical which has a strong oxidizing ability without selectivity. It can decompose organic compounds easily to form oxidation intermediates or CO_2 as the end product. Although the contaminants may be fully degraded by the Fenton process, the mineralization rate remains relatively low (Mirzaei *et al.* 2017). The metabolites formed following the AOPs, such as ozonation and sonolysis, have been reported to be readily mineralized by the bioreactor (Prado *et al.* 2017). Along with the context, AOPs may not mineralize CBZ completely, but they shall reduce the toxicity and increase biodegradability, implying that the AOP may act as a pre-treatment process before biological treatment. It is noted that some resulting (by-)products of CBZ, such as acridine, may have higher toxicity than the parent compound when CBZ is only partially mineralized (Vogna *et al.* 2004). Therefore, effective pre-treatment should be capable of reducing the toxicity and enhancing the biodegradability of the effluents that can be effectively treated by conventional activated sludge. This study aimed to explore the feasibility of the Fenton process as a pre-treatment, followed by a biological sequencing batch reactor (SBR) for CBZ removal.

MATERIAL AND METHODS

The Fenton pre-treatment was conducted in a 1 L beaker under ambient temperature (22±1°C). The initial concentration of CBZ was 50 μM. The H_2SO_4 and NaOH were used for pH control. The Fenton pre-treatment started with the addition of H_2O_2 into the $FeSO_4$ solution, and the process was quenched after 30 minutes and the pH value was adjusted to around 7 for subsequent biological reaction. The pre-treated solution was introduced to the influent tank of the biodegradation treatment in SBR. Samples were collected at the beginning, 1, 2, 3, 4 hours after the biological process started. They were analyzed for CBZ residuals, TOC, EEM spectra, mass spectra and COD after 0.22 μm filtration.

RESULTS AND DISCUSSION

CBZ removal by combined Fenton process and activated sludge treatment

The CBZ removal results by the combined Fenton process and activated sludge treatment system of different pre-treatment conditions are shown in Figure 1. The biodegradability was evaluated using CBZ removal experiment by activated sludge without Fenton pre-treatment. The low degradation rate indicated that the biological treatment was not efficient in removing CBZ from wastewater. Since CBZ is moderately hydrophobic, its removal via sorption onto activated sludge has been reported in the range between 5 to 20% only (Zhang *et al.* 2008; Wijekoon *et al.* 2013). In addition, CBZ contains an amide group in structure, which is an electron-withdrawing functional group that makes CBZ resistant to biodegradation (Tadkaew *et al.* 2011). In short, the removal of CBZ by activated sludge was mostly via sludge sorption rather than biodegradation, and the removal was poor and unstable.

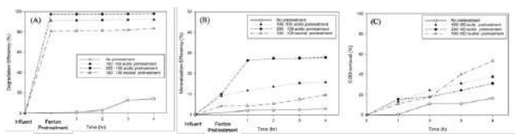

Figure 1. The (A) degradation, (B) mineralization, and (C) COD removal efficiencies of CBZ by combined Fenton pretreatment and activated sludge treatment.

Alternatively, the Fenton process was utilized as a pre-treatment to decompose CBZ before biodegradation. In Figure 1, the degradation, mineralization, and COD removal showed the activated sludge treatment was able to further degrade the CBZ oxidation by-products after Fenton pre-treatment. The pre-treatment with 200 μM H_2O_2 and 100 μM Fe^{2+} in acidic condition showed the highest relative degradation and mineralization of 97.90% and 28.87%, indicating the oxidation by-products of CBZ was more readily biodegradable than the parent compound CBZ.

The Zahn-Wellens test of CBZ and its oxidation (by-)products for evaluating their inherent biodegradability was performed by Monsalvo et al. (2015), showing that CBZ inhibited microbial activity, and the biodegradability of CBZ oxidation products by the Fenton process was enhanced and their toxicity was reduced. The Fenton oxidation was used to decompose the non-biodegradable organic compounds into fragments which were much more easily degraded by microorganisms. In this study, the Fenton process was found effective as a pre-treatment before activated sludge treatment to improve aqueous CBZ removal efficiency.

EEMs for CBZ degradation by the combined system

The excitation-emission matrix (EEM) fluorescence spectrometry was employed to characterize dissolved organic matters in water. The EEM spectra of different pre-treatment conditions were shown in Figure 2, and the original CBZ EEM features and the positions of fluorophores were sketched in Figure 2 (A). In Figure 2 (D), (G), and (J), signal C (HA-like, $\lambda_{ex}/\lambda_{em}$ = 300-370 nm/ 400-500 nm) was an apparent peak after the Fenton oxidation compared to Figure 2 (A), indicating the oxidation by-products contained HA-like structures which were likely to form in CBZ degradation.

The pre-treated solution was introduced into the activated sludge aeration tank for biological treatment, and the intensity of signal C in Figure 2 (E), (H), and (K) decreased because of the dilution effect. Signals A (FA-like, $\lambda_{ex}/\lambda_{em}$ = 220-270 nm/ 380-550 nm), B (Tyrosine-like, $\lambda_{ex}/\lambda_{em}$ = 225-237 nm/ 309-321 nm), and T (Tryptophan-like, $\lambda_{ex}/\lambda_{em}$ = 225-237 nm/ 340-381 nm) shown in Figure 2 (B) were the background resulting from the existence of activated sludge. Slight biodegradation was found without the Fenton pre-treatment in Figure 1 and the EEM in Figure 2 (B) and (C) also showed a similar result. With the Fenton pre-treatment, the biological removal of CBZ shifted the fluorescence signals towards a shorter wavelength (Figure 2 (F), (I), and (L)). To be more specific, signals A and C were blue-shifted along the excitation and emission axes. The phenomenon of EEM signal blue-shifting may be associated with the following reasons: (i) the decomposition of aromatic moieties, (ii) the breakage of large molecules into smaller fragments, (iii) the decrease in the number of aromatic rings, (iv) the decrement of conjugated bonds in a chain structure, (v) the conversion of a linear system to a non-linear system, and (vi) the elimination of particular functional groups including carbonyl, hydroxyl, and amine groups (Valencia *et al.* 2013). The blue-shifted results of EEM indicated the decomposition of the aromatic structure of CBZ and the resulting molecular fractions after activated sludge treatment. Tyrosine- and tryptophan-like (peaks B and T) compounds are small organic matters suitable for microbial activity and are predominant in wastewater (Henderson *et al.* 2009). The occurrence of signal T represented the organics under microbial oxidation emerging after SBR treatment, confirming the enhancement of the overall biodegradability of CBZ and its fractions.

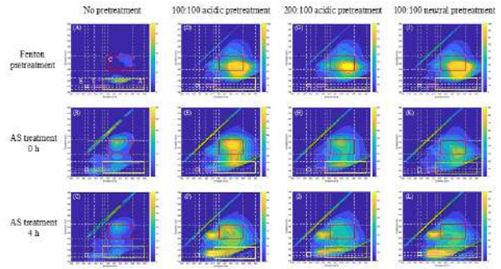

Figure 2. The EEM fluorescence spectrometry of the CBZ degradation by Fenton process in different stages of the combined Fenton process and activated sludge treatment.

CONCLUSION

CBZ possessed resistance to direct biodegradation due to its physicochemical properties, and the result showed that only 14.21% of CBZ and 2.86% of TOC were removed when CBZ was directly treated by SBR for four hours. The combined system in this study, in which CBZ was pre-treated with the Fenton process and the resulting by-products were introduced into the sequencing batch reactor, was able to remove CBZ. The almost complete removal of CBZ and up to 27.87% TOC removal were found when CBZ was pre-treated by the Fenton process. Moreover, the CBZ degradation efficiency by Fenton in neutral conditions remained at 76.05%, implying that it is feasible to combine the Fenton pre-treatment and biological treatment for CBZ removal in a neutral environment, which may solve the practical problem of pH adjustment when applying classic Fenton process to treat real wastewater. The blue-shifted EEM signal inferred the decomposition of aromatic rings and the smaller fragments' formation. Tyrosine- and tryptophan-like signals that represented the organics under microbial oxidation appeared after SBR treatment, enhancing the overall CBZ biodegradability. This study showed the possibility of using the Fenton process as a pre-treatment before conventional biological treatment when treating recalcitrant emerging contaminants. The removal efficiency of CBZ in the real wastewater by the combined system needs further study to evaluate the impact of co-dissolved molecules on the wastewater treatment performance.

REFERENCES

Ferrer I. and Thurman E. M. (2012). Analysis of 100 pharmaceuticals and their degradates in water samples by liquid chromatography/quadrupole time-of-flight mass spectrometry. *J Chromatogr A* **1259**, 148-57.
Hai F., Yang S., Asif M., Sencadas V., Shawkat S., Sanderson-Smith M., Gorman J., Xu Z.-Q. and Yamamoto K. (2018). Carbamazepine as a Possible Anthropogenic Marker in Water: Occurrences, Toxicological Effects, Regulations and Removal by Wastewater Treatment Technologies. *Water* **10**(2).
Henderson R. K., Baker A., Murphy K. R., Hambly A., Stuetz R. M. and Khan S. J. (2009). Fluorescence as a potential monitoring tool for recycled water systems: A review. *Water Research* **43**(4), 863-81.
Kumar A., Batley G. E., Nidumolu B. and Hutchinson T. H. (2016). Derivation of water quality guidelines for priority pharmaceuticals. *Environ Toxicol Chem* **35**(7), 1815-24.
Marcelo V. O., Salette R., Jose L. F. C. L. and Marcela A. S. (2017). Analytical Features of Diclofenac Evaluation in Water as a Potential Marker of Anthropogenic Pollution. *Current Pharmaceutical Analysis* **13**(1), 39-47.
Mirzaei A., Chen Z., Haghighat F. and Yerushalmi L. (2017). Removal of pharmaceuticals from water by homo/heterogonous Fenton-type processes - A review. *Chemosphere* **174**, 665-88.
Monsalvo V.M., Lopez J., Munoz M., de Pedro Z.M., Casas J.A., Mohedano A.F., Rodriguez J.J. (2015). Application of Fenton-like oxidation as pre-treatment for carbamazepine biodegradation. Chemical Engineering Journal 264, 856-862.
Prado M., Borea L., Cesaro A., Liu H., Naddeo V., Belgiorno V. and Ballesteros F. (2017). Removal of emerging contaminant and fouling control in membrane bioreactors by combined ozonation and sonolysis. *International Biodeterioration & Biodegradation* **119**, 577-86.
Tadkaew N., Hai F. I., McDonald J. A., Khan S. J. and Nghiem L. D. (2011). Removal of trace organics by MBR treatment: The role of molecular properties. *Water Research* **45**(8), 2439-51.
Valencia S., Marín J. M., Restrepo G. and Frimmel F. H. (2013). Application of excitation–emission fluorescence matrices and UV/Vis absorption to monitoring the photocatalytic degradation of commercial humic acid. *Science of The Total Environment* **442**, 207-14.
Vogna D., Marotta R., Andreozzi R., Napolitano A. and d'Ischia M. (2004). Kinetic and chemical assessment of the UV/H2O2 treatment of antiepileptic drug carbamazepine. *Chemosphere* **54**(4), 497-505.
Wijekoon K. C., Hai F. I., Kang J., Price W. E., Guo W., Ngo H. H. and Nghiem L. D. (2013). The fate of pharmaceuticals, steroid hormones, phytoestrogens, UV-filters and pesticides during MBR treatment. *Bioresource Technology* **144**, 247-54.
Zhang Y., Geissen S. U. and Gal C. (2008). Carbamazepine and diclofenac: removal in wastewater treatment plants and occurrence in water bodies. *Chemosphere* **73**(8), 1151-61.

Metabolic Modelling of a Designed Bacterial Consortium to Evaluate its Capability for In-situ Removal of Contaminants from Biogas

R. Peighami*, D. Gabriel** and F. Zolfagharzadeh***

* Biotechnology Group, Department of Chemical Engineering, Tarbiat Modares University, Tehran, Iran
(E-mail: *rezapeighami@gmail.com; r.peighami@modares.ac.ir*)
** GENOCOV Research Group, Department of Chemical, Biological and Environmental Engineering, Escola d'Enginyeria, Universitat Autònoma de Barcelona, 08193 Bellaterra, Spain
(E-mail: *David.Gabriel@uab.cat*)
*** Department of Energy and Environment, Petroleum University of Technology, Iran
(E-mail: fahameh.zolfagharzadeh@gmail.com)

Abstract
Removing contaminants from biogas is an important step in making biogas a usable product. On current work a genome scale metabolic model was developed for a designed consortium of bacteria containing both methanogenic and sulfur oxidizing bacteria (SOBs) to analyse the consortium capability of removing H_2S and reducing CO_2 concentration in produced biogas. Results show that by using such a consortium, H_2S could be consumed nearly completely by SOBs and CO_2 concentration decreases by 0.67 in comparison to the culture without SOBs as chemolithoautotrophic bacteria utilize CO_2 as carbon source and H_2S as energy source. Due to anaerobic digestion, for using such a consortium, it is necessary to integrate the process with nitrate stream as final electron acceptor. The model predicts that H_2S post-treatment process from produced biomass is capable of being removed by using the consortium.

Keywords (maximum 6 in alphabetical order)
Biogas treatment; microbial consortium; genome scale metabolic model; sulfur oxidizing bacteria

INTRODUCTION

Biogas is a valuable renewable energy source that is produced due to anaerobic digestion of wastes and wastewater (De Arespacochaga, Valderrama et al. 2014). The obtained biogas from anaerobic digestion is a mixture of different components whose composition depends on the source and varies over time due to the variation in substrate (Pirolli, da Silva et al. 2016). The main components of the biogas are methane (CH_4: 50-60 % vol.), carbon dioxide (CO_2: 34-38 % vol.) and traces of other compounds such as hydrogen sulfide (H_2S: 500-20000 ppm). To further use biogas as a fuel, biogas upgrading is needed. Among the contaminants, H_2S has received the most attention for biogas use for electricity production due to its high corrosivity. Numerous methods have been developed for H_2S removal from biogas that could be categorised in physical, chemical and biological methods. In all cases, an extra step is added to the biogas production process, which introduces extra costs and operational complications to the system(Torres, Marín et al. 2020). Although H_2S is sometimes completely removed, there is still a significant amount of CO_2 (about 30%), which strongly reduces the specific heat value of the biogas and must be removed for obtaining biomethane. Thus, finding new methods to reduce costs and operational issues by removing H_2S and CO_2 from biogas streams is desirable.

In the current study, modelling tools were used to investigate the following hypothesis: as sulfur oxidizing bacteria (SOB) are chemolitoautotrophs that consume CO_2 as carbon source and H_2S as energy source, a consortium of SOB and methanogenic bacteria would lead to a simultaneous reduction in the content of both contaminants in biogas. In this way, a genome scale metabolic model for a methanogenic bacterium was reconstructed and modified as a consortium genome scale model containing the core metabolism of chemolitoautotrophs to analyse the behaviour of the consortium in producing methane and removing H_2S and CO_2.

MATERIALS AND METHODS

For developing a genome scale metabolic model in order to analyse the behaviour of bacterial consortium in anaerobic digestion, the genome scale metabolic model reported for methanogenic bacteria *Methanosarcina barkeri* (Feist, Scholten et al. 2006) was modified to be used as a multi-cell model. The consortium is assumed to contain methanogen and sulfur oxidizing bacteria. To reconstruct the multi-cell model, the core metabolism of SOB represented in databases e.g., KEGG, UNIPROT, BIGG and biochemical reactions that are reported in literature, were added to the *Methanosarcina barkeri* model. All the data were gathered in a spreadsheet.

The metabolic network was processed using linear programming and constraint-based modelling concepts as mathematical tool. Calculations were done using MATLAB software, COBRA toolbox and the glpk (GNU Linear Programming Kit) package. The methane production was defined as objective function and Flux Balance Analysis (FBA) was used to find the fluxes of all reactions. All the calculations of FBA are simplified if Eq. (1):

$$\text{Max } Z = c \cdot v \qquad S \cdot v = b \qquad v_{min} < v < v_{max} \qquad \text{Eq. 1}$$

where Z is the objective function which is methane production in here, c is the coefficients of objective function, S is the stochiometric matrix of the metabolism (number of metabolites × number of reaction fluxes (unknown)), b is the right-hand side vector which is known reaction fluxes and v_{min} and v_{max} are the upper and lower bounds of fluxes. For proceeding FBA calculations for H_2S and CO_2 removal, the fluxes are multiplied by ratio of reported mean maximum specific growth rate of SOBs to methanogens. Considering the anaerobic, nitrate was introduced as final electron acceptor for SOB. The results of FBA were analysed in order to investigate the capability of consortium for in-situ H_2S and CO_2 removal. Also, for further investigation, Dynamic FBA was run for the model to see how the concentrations change with time.

RESULTS AND DISCUSSION

The initial network for *Methanosarcina barkeri* had 690 reactions and 215 reactions containing C, S, and N metabolic pathways, were added for building the multi-cell model. The reactions were categorised in 8 metabolic pathways among which 21% of reactions were in cofactor metabolism category. There were 52 non-gene associated reaction and the metabolite counts involved in model was 932. The results of model characteristics are illustrated in Table 1 and Figure 1.

Table 1. Detailed information about the metabolic network reconstructed for multi-cell model.

	Features	Model
Reactions	Total Reactions	905
	Metabolic Reactions	820
	Gene Associated Reactions	853
	Non-gene Associated reactions	52
	Exchange Reactions	14
	Transport Reactions	71
Metabolites	Number of Metabolites	932

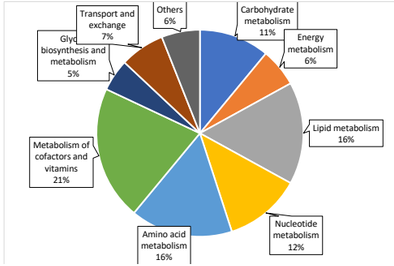

Figure 1. Contribution of pathways in metabolic model.

Model evaluation for methane production and H_2S and CO_2 Removal

The μ_{max} for methanogens is reported to be between 0.015 to 0.022 h^{-1} (Sowers, Nelson et al. 1984) and the FBA prediction for biomass growth is 0.025 h^{-1} that shows model has an acceptable prediction rate, of course with an over prediction which is reported to be accepted in FBA. Results of CH_4 production and concentrations of H_2S and CO_2 at the end of a batch culture is represented in Table 2. Produced H_2S in anaerobic digestion could be nearly completely consumed by SOBs because of the higher growth rate of SOBs (μ_{max} = 0.055) in comparison to slowly growing methanogens (μ_{max} = 0.025). Also, Table 2 shows that the CO_2 production by the consortium culture is reduced by 67% in comparison to that of a SOB-free methanogenic culture.

Table 2. Results of CH_4 production and concentrations of H_2S and CO_2 at the end of a batch culture.

Condition	Methane Production (mmol/L)	H_2S Production (mmol/L)	CO_2 Production (mmol/L)
Experiment	120	0.001	65
Methanogenic model	128	0.0012	69
Consortium model	116	$7 \cdot 10^{-7}$	22

Results of dynamic FBA are also illustrated in Figure 2a for methane and CO_2 and in Figure 2b for H_2S. In the methanogenic culture, the H_2S and CO_2 concentration increased over time. However, concentrations are predicted to be much lower in the consortium culture. The reduction of CO_2 is caused by the chemolithoautotrophic behaviour of SOBs as CO_2 is consumed as carbon source.

CONCLUSIONS

From the results of the reconstructed metabolic model for a consortium of methanogenic and SOB bacteria, the consortium is capable of in-situ removing H_2S while reducing the CO_2 concentration. Then, an external biogas treatment step can be removed to reduce costs while increasing safety. Model-based testing on the hypothesis of chemolithoautotrophic behaviour of SOBs proved successful.

a)

b)

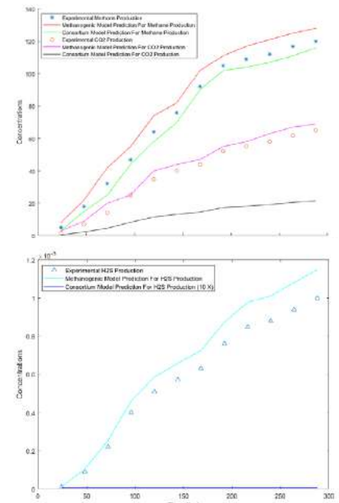

Figure 2. Experimental results and model prediction of the methanogenic model vs consortium culture model for a) methane and CO_2 production and b) H_2S production

REFERENCESç

Arespacochaga, N., Valderrama, C., Mesa, C., Bouchy, L., Cortina, JL. 2014. Biogas deep clean-up based on adsorption technologies for Solid Oxide Fuel Cell applications. *Chemical Engineering Journal* **255**, 593-603

Feist, AM., Scholten, JCM., Palsson, B., Brockman, FJ., Ideker, T. 2006. Modeling methanogenesis with a genome-scale metabolic reconstruction of *Methanosarcina barkeri*. *Molecular Systems Biology* **2**, 2006.0004

Pirolli, M., Da Silva, M., Mezzari, MP., Michelon, W., Prandini, JM., Soares, HM. 2016. Methane production from a field-scale biofilter designed for desulfurization of biogas stream. *Journal of Environmental Management* **177**, 161-168

Sowers, KR., Nelson, MJ., Ferry, JG. 1984. Growth of acetotrophic, methane-producing bacteria in a pH auxostat. *Current Microbiology* **11**, 227-229

Anticancer Drugs Affect the Performance and Microbiome in an Aerobic Granular Sludge System Operated in Sequential Batch Reactor

A. Castellano-Hinojosa*, M. J. Gallardo-Altamirano*, J. González-López*, A. González-Martínez*

* Department of Microbiology, Institute of Water Research, University of Granada, 4 Ramon y Cajal, Granada, 18071, Spain
(E-mail: *ach@ugr.es;manujga@ugr.es;jgl@ugr.es;agon@ugr.es)*

Abstract
The consumption of anticancer drugs (also known as chemotherapy drugs or antineoplastic drugs) has augmented over the last decades due to increased cancer incidence. Although there is an increasing concern about the presence of pharmaceutical compounds in natural environments and urban/domestic wastewater, anticancer drugs used in chemotherapy and anticancer medication have received less attention. We found three anticancer drugs commonly detected in influents of WWTPs can significantly reduce the efficiency of nitrogen removal and decrease the abundance of bacterial, archaeal, and fungal communities in an aerobic granular sludge (AGS) operated in sequential batch reactor. These results were observed at concentrations commonly detected in wastewater influents suggesting increased attention should be paid in the future for removing these substances from wastewater as they may impact overall´s system wastewater treatment performance and microbial communities.

Keywords
Cytotoxic; Bacteria; Fungi; Microbial diversity; Wastewater

INTRODUCTION

Cancer is a significant global health concern responsible for approximately 10 million deaths and almost one out of every six deaths in 2022 according to the World Health Organization (WHO). This increase in cancer incidence has led to a significant increase in the use of drugs that combat cancer (referred to as anticancer drugs, chemotherapy drugs or antineoplastic drugs) over the past two decades. A recent review study showed that anticancer drugs can pass through the entire water system in urban areas, from hospitals and wastewater treatment plants (WWTPs) to rivers and groundwater (Castellano-Hinojosa et al. 2023). Membrane bioreactors (MBR) is the main biological technology that has been examined for removing anticancer drugs from wastewater with removal efficiencies ranging from 20-90% depending on the type of anticancer drug and treatment concentration. New biological techniques such as aerobic granular sludge (AGS) systems are being explored and improved for the removal of common contaminants [e.g., organic matter and nitrogen (N)] and emerging hazardous pollutants (e.g., pharmaceutical compounds such as antibiotics). However, it is unknown how the presence of these substances at different concentrations may impact overall system´s performance in terms of removal of carbon (C) and N and the microbiome (abundance and diversity of bacterial, archaeal and fungal communities). Therefore, we examined the effect of three anticancer drugs commonly detected in influents of WWTPs applied at three different representative concentration levels (low, mid, and high) on the physicochemical performance and abundance of total bacterial, archaeal, and fungal communities in a AGS operated in sequential batch reactor (SBR).

MATERIALS AND METHODS

The bioreactor had a height of 45 cm and a diameter of 9 cm and an operational volume of 2.5 L, of which 50% was exchanged per cycle. The hydraulic retention time was 8 h and the cycles, and each cycle consisted of four stages: 3 minutes for adding synthetic water, 240 minutes of constant aeration, 3 minutes for decantation of the granules, and 4 minutes for discarding the effluent. Air was supplied to the bottom of the bioreactor through fine bubbles. The bioreactor was firstly inoculated with 1 L of activated sludge from Los Vados (Granada, Spain) WWTP. The bioreactor was fed from the top of the bioreactor using a peristaltic pump (Watson Marlow, UK) with synthetic wastewater simulating urban sewage: CH_3COONa 1.5 g L^{-1}, NH_4Cl 0.25 g L^{-1}, $MgSO_4{\cdot}7H_2O$ 0.1 g L^{-1}, K_2HPO_4 0.085 g L^{-1}, KCl 0.04 g L^{-1}, and KH_2PO_4 0.03 g L^{-1}. The bioreactor operated for a month as a steady-state phase until it reached stable conditions. Then, four consecutive phases with different levels of anticancer drug concentration were run as follows: control without anticancer drugs, low (x1), mid (x10), and high (x100) concentration levels. Each phase had a duration of 30 operational days. Finally, the bioreactor was operated for an additional 30 days during which it was feed with synthetic wastewater without anticancer drugs to investigate whether the performance and microbial community of the system would return to initial levels; this phase was named as "residual". Cyclophosphamide (CP), tamoxifen (TMX), and methotrexate (MTX) were selected for this study as they are the most studied and frequently reported anticancer drugs in hospital effluents and wastewater influents and effluents (Castellano-Hinojosa et al. 2023). Low levels were 60, 1.5, add 40 ng L^{-1} for CP, TMX, and MTX, respectively. Physicochemical analysis was carried out two times per week during the experimental period. The concentration of acetate (CH_3–COO^-), ammonium (NH_4^+), nitrite (NO_2^-), and nitrate (NO_3^-) were analyzed using an ion chromatograph (Metrohm Ion Chromatograph, AG, Switzerland). Total nitrogen (TN) removal efficiency (%) was calculated as the difference in the concentration of $NH_4^+ + NO_2^- + NO_3^-$ between the influent and effluent. Granular biomass (50 mL) was collected in duplicate after 5, 15, and 30 days of operation for each the control, low, mid, high, and residual phases and the abundance of total bacterial, archaeal, and fungal communities quantified via quantitative PCR (qPCR).

RESULTS AND DISCUSSION

Application of anticancer drugs at different levels had no impact on the efficiency of acetate removal (Fig. 1A). However, anticancer drugs at mid and high concentrations levels significantly reduced efficiency of TN removal (Fig. 1B) to return to normal levels afterward at the residual phase. The application of anticancer drugs at mid and high levels significantly decreased the abundance of total bacterial, archaeal, and fungal communities compared to control and low phases but they recovered afterward at the residual phase. Overall, we found the effect of anticancer drugs on N removal and microbiome may depend on the concentration of anticancer drugs in wastewater.

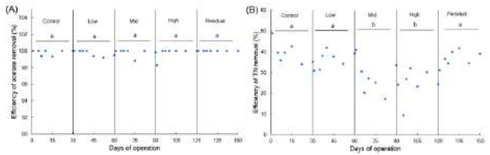

Figure 1. Efficiency of acetate (A) and total nitrogen (B), removal during the experimental period (Tukey's HSD, $p \leq 0.05$).

REFERENCES

Castellano-Hinojosa, A., Gallardo-Altamirano, M.J., González-López, J., González-Martínez, A. 2023. Anticancer drugs in wastewater and natural environments: A review on their occurrence, environmental persistence, treatment, and ecological risks. *Journal of Hazardous Materials* **447**, 130818.

Microbial-fuel-cell driven intermittent aeration enhanced the removal of organic matter and nitrogenous compounds

Naoko Yoshida*, Kyosuke Mitsuoka, Ayano Shimidzu, Fumichika Tanaka, Xie Li

* Dept. Civil Eng., Nagoya Institute of Technology (Nitech), yoshida.naoko@nitech.ac.jp

Abstract

This study optimized electricity recovery and the secondary use strategy for twelve tubular air-cathode microbial fuel cells (MFCs) in a 245L-scale reactor. The twelve pairs of MFC and ADP5090 in 245L wastewater can lighten two LEDs; each can provide 56-70 lx of illuminance at 15 cm of distance from the light and 0.39L/h (1.6L/h/m3) of aeration flow in wastewater. The time required to meet the planned effluent quality of BOD was 41 hours without aeration and decreased to 23 hours by the intermittent aeration driven by MFC power. The intermittent aeration also grew anammox and slightly enhanced ammonia removal. However, the improvement of individual MFCs is still required for the effective energy utilization of wastewater biomass.

Keywords

Microbial fuel cell, intermittent aeration, 1ow-voltage boosting, Anammox

INTRODUCTION

Microbial fuel cells (MFCs) have been applied in municipal wastewater treatment, however, the secondary use of recovered electricity has been rarely investigated. A simple strategy to boost the output voltage from MFCs involves connecting multiple MFCs in series or parallel. However, the MFCs connected in series often failed to boost the voltage due to voltage inversion (Oh and Logan, 2007) and a parallel connection has helped successfully boost the voltage; although, the voltage has never exceeded the theoretical voltage (Aelterman et al., 2006). Another way of boosting voltage using MFCs is by voltage multiplier circuits. So far, various DC/DC converters have been used to boost the voltage of MFCs and the input and output voltages range from 0.2 to 0.4 V and 3.3 to 2.0 V. The boosted electricity has been used as a power source for light-emitting diodes (LEDs) (Kim et al., 2019), pumps (Ge and He, 2016), and for charging a mobile phone battery (Prasad and Tripathi, 2021).

Here, we examined the applicability of a DC/DC converter, ADP5090, to boost tubular air-cathode MFCs using an anion exchange membrane (AEM) as the separator, which is superior to an MFC with a cation exchange membrane (CEM) in terms of power recovery (Itoshiro et al., 2022), and which was successfully scaled up to 226 L (Sugioka et al., 2022). First, the connection of 1–12 MFCs was evaluated based on the electricity produced and the electricity density; thereafter, the MFCs were boosted using two DC/DC converters, and the secondary use of the electricity was evaluated.

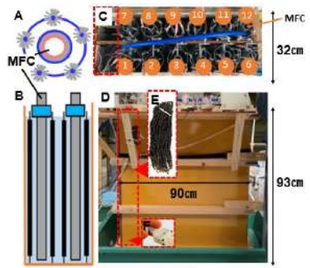

Fig. 1 Apparatus and illustration of MFC cores and reactor. Panels A and B illustrate the top and side views of MFC cores with CBs, respectively. Panels C and D show the top and side views of the reactor, respectively. Panels E and F indicate the sponges hang in aeration part and a mini-air pump driven by MFC.The numbers in panel B indicate the MFC numbers.

MATRIALS AND METHODS

MFC and the operation of a continuous flow of sewage wastewater

A cylindrical MFC core (diameter: 5 cm; length: 1 m) with an air cathode made of a stainless-steel mesh surrounded by a carbon-based cathode was used, along with an AEM and nonwoven graphite fabric. As an anode, five carbon brushes (CBs) (ϕ 4 cm × 1 m) were placed around the MFC core in addition to the nonwoven graphite fabric. Twelve sets of an MFC core with five CBs were installed in a cuboid reactor (32×90×93cm) made of polyvinyl chloride and reinforced with wood (Fig.1) and were filled with 246 L of the effluent from a primary sedimentation tank (PST). The reactor was operated in a sewage wastewater treatment plant and continuously supplied with the PST effluent using a tubing pump for a hydraulic retention time (HRT) of 48 h. The MFC was connected to a 1:1 boost circuit ADP5090 (Linear Technology, MA, USA).

Boosting voltage by DC/DC converters for the secondary use

Six different connections by changing the number of a DC/DC converter, ADP5090 (Analog Devices, Norwood, MA, USA) per MFC were evaluated while a capacitor (1F) was charged;12P-4ADP was the connection of 12 MFCs in parallel, and it was connected to four ADP5090; (2P-ADP) × 6, was that connecting each of two MFCs in parallel to six ADP5090; (1MFC-ADP) × 12 and (1MFC-ADP) × 6 were those connecting twelve and six MFCs to DC/DC converters, respectively; and (1MFC-2ADP) × 6 was that connecting six sets of a connection of single MFCs to two ADP5090. A mini air pump (KPM130B-3A), fan (YDM2507C05F), or white LED (osw5dk5b62a-5v) were connected to the output. To evaluate the effect of the MFC's driven aeration on the removal of organic matter and nitrogenous compounds, the reactor was partitioned to have an aeration part (8% of total reactor) with hanging of 380 polyurethane (PU) sponges (1 cm^3) exposure with intermittent aeration by a mini air-pump driven by MFC. The cell voltage between the anode and cathode with the boost circuit connected was recorded every hour.

RESULTS AND DISCUSSION

Performance of individual and multiple-connected MFCs

The single MFC showed 16 mW of maximum electric power and the parallel connection of eight MFCs showed 3.5-fold higher increase to 58 mW, although the power density was the best from single MFC or two MFCs showed 0.104 and 0.11W/m^2 (Fig.2). The comparison of electricity recovery from MFCs with changing the combination ratio of MFC and a DC/DC converter, ADP5090, showed the highest efficiency of electricity recovery (60%) in the connection of the single MFC and ADP5090 one by one.

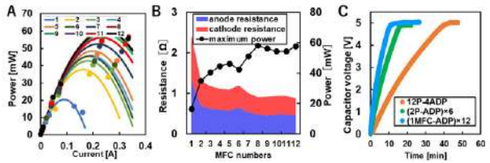

Figure 2. The effect on electric power by connecting MFCs and the ratio of the number of MFCs and ADP5090s. Panels A and B indicate the effect on power density and electrode resistance, respectively. The panel C indicates the effect of the ratio of the number of MFCs and ADP5090s on the charging time of a 1F capacitor.

Secondary use of boosted power

The MFCs were applied as the power source for the three devices. The twelve MFCs continuously lit up two white LEDs, but not three LEDs. A DC fan worked for 45 s every eight minutes and provided 12.8 L/h/reactor of airflow. Approximately 2 L of air was exchanged through the air flow every 2 h. A mini air pump could run intermittently for 30 s every 4.5 min (**Fig. 3A**); furthermore, this corresponded to give 0.45 L/h of aeration rate at a depth of 50 cm. The aeration provided 0.54 mg/L of average dissolved oxygen (DO) above the air pump (**Fig. 5B**); although, the average DO values decreased to 0.39 and 0.14 from 10 cm and 20 cm horizontal distances, respectively.

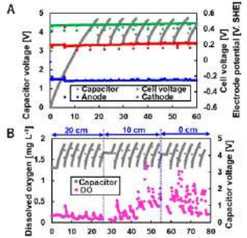

Fig. 3 The driving of a mini air-pump by twelve MFC units. Panels A shows the resulting change in voltage in response to the charge and driving of mini air pump. Panel B indicates the resulted change in dissolved oxygen. The length values on the top of graph in panel B indicates the horizontal distance from a mini-air pump.

Effect of the impact of intermittent aeration on organic matter and NH_4^+ removal

The degradation of organic matter (COD and BOD) was determined using mono-exponential regression with the concentration in influent and effluent at different HRTs, and resulted in $C_{COD}=183e^{-0.048t}$ and $C_{BOD}=75e^{-0.069t}$, respectively, under the intermittent aeration. The higher degradation rate constants for COD (0.048) and BOD (0.069) than the values without aeration (0.039 and 0.044, for COD and BOD, respectively) indicate the facilitation of organic matter degradation by MFC-driven aeration (**Fig. 4AB**). The time required to meet the planned effluent quality of BOD was 41 hours without aeration and decreased to 23 hours by the intermittent aeration driven by MFC power.

The removal of NH_4^+ was slightly facilitated by the MFC-driven aeration to have $C_N=35e^{-0.005t}$ in comparison of $C_N=35e^{-0.002t}$ without aeration (**Fig. 4C**). However, the combination of MFC and MFC-driven aeration required 112 hours to meet the planed discharge standard of total nitrogen. The DO that resulted by intermittent aeration was far lower than the minimum DO for ammonia oxidization

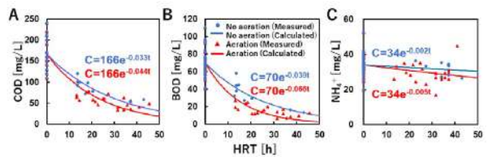

Figure 4 The effect of MFC-driven aeration on organic matter and ammonia removal. Panels A, B, and C shows the changes of COD, BOD, and NH4+ at different HRT, respectively.

(0.5 mg L^{-1}) (Hanaki et al., 1990) but similar values that observed in the partial anammox and nitrification process with intermittent aeration (0.01-0.05 mg/L) (Qiu et al., 2019).

3.4 Microbial community analysis

The 16SrRNA gene amplicon analysis showed the carbon brush was mostly dominated by the genus *Longilinea* at 12-14% and secondary with genera *Syntrophus* (3.5-5.3%) and *Methanobacterium* (2.4-4.3%), suggested the mutualistic relationship between these bacteria to provide/consume fatty acids and provide H_2/formate for methanogen. *Geobacter* species were relatively lower (1.5-1.3 %) suggesting the main energy conversion on CB was the symbiotic digestion to methane and a relatively minor contribution to recovering electric current. In contrast, *Geobacter* was more in GNWF-anode surrounding air-cathode (5.3%) and anolyte (9.2%). Interestingly, the sponge includes 2.7% of "*Candidatus Brocadia*" known as anaerobic ammonium oxidation (anammox) - bacteria together with aerobic ammonia-oxidizing bacteria of *Nitrospira* (0.7 %) (data not shown), suggested that the intermittent aeration facilitated the aerobic oxidization of ammonia to nitrite and the anammox reaction using the nitrite.

Table 1 Representative genera detected in MFC. SP1,2: sponge at the top (1) and bottom (2), CB-T, M, B: carbon brush at top (T), middle (M) and bottom (B), GNWF: GNWF-anode nearby air-cathode

	Relative proportion in total reads(%)						
Genus	SP1	SP2	CB-T	CB-M	CB-B	GNWF	Anolyte
Methanobacterium	1.1	0.1	2.4	4.7	4.3	1.9	0.0
Longilinea	12	3.3	12	12	14	0.3	0.1
"Candidatus Brocadia"	0.5	2.7	0.0	0.0	0.0	0.0	0.0
Geobacter	0.9	0.3	1.5	1.7	1.3	5.3	9.2
Syntrophus	2.9	3.7	3.5	4.5	5.3	0.2	0.3
Syntrophobacter	0.5	0.3	1.0	0.9	0.9	0.1	0.0
Arcobacter	0.5	0.1	0.1	0.1	0.1	0.6	12

Conclusion

The combined system of MFC and MFC-driven aeration reduced BOD to the planned discharge standard after 23 hours of operation without introducing external energy for aeration, but the MFC's energy was secondarily used for aeration rather than electricity recovery. However, the energy consumption for total nitrogen (TN) removal consumes 6.08 W h/g-TN, which indicates that MFC needs improvements to meet the discharge standards for both organic and nitrogenous compounds and more advantage in the removal of TN rather than energy recovery.

References

Aelterman, P., Rabaey, K., Pham, H.T., Boon, N., Verstraete, W., 2006. Continuous electricity generation at high voltages and currents using stacked microbial fuel cells. *Environ. Sci. Technol.* **40**, 3388–3394.

Ge, Z., He, Z., 2016. Long-term performance of a 200 liter modularized microbial fuel cell system treating municipal wastewater: Treatment, energy, and cost. *Water Res. Technol.* **2**, 274–281.

Hanaki, K., Wantawin, C., Ohgaki, S., 1990. Nitrification at low levels of dissolved oxygen with and without organic loading in a suspended-growth reactor. *Water Res* 24, 297–302.

Itoshiro, R., Yoshida, N., Yagi, T., Kakihana, Y., Higa, M., 2022. Effect of ion selectivity on current production in sewage microbial fuel cell separators. *Membranes*, **12**, 183.

Kim, T., Yeo, J., Yang, Y., Kang, S., Paek, Y., Kwon, J.K., Jang, J.K., 2019. Boosting voltage without electrochemical degradation using energy-harvesting circuits and power management system-coupled multiple microbial fuel cells. *J. Power Sources* 410–411, 171–178.

Oh, S.E., Logan, B.E., 2007. Voltage reversal during microbial fuel cell stack operation. *J. Power Sources* **167**, 11–17.

Prasad, J., Tripathi, R.K., 2021. Scale-up and control the voltage of sediment microbial fuel cell for charging a cell phone. *Biosens. Bioelectron.* **172**, 112767.

Sugioka, M., Yoshida, N., Yamane, T., Kakihana, Y., Higa, M., Matsumura, T., Sakoda, M., Iida, K., 2022. Long-term evaluation of an air-cathode microbial fuel cell with an anion exchange membrane in a 226L wastewater treatment reactor. *Environ Res* **205**, 112416.

Tertiary treatment of nitrite-containing wastewater in a denitrification filter - preliminary studies

F. Gamoń*, A. Ziembińska-Buczyńska*, G. Cema*

* Department of Environmental Biotechnology, Silesian University of Technology, Akademicka 2, Gliwice, Poland
(E-mail: *filip.gamon@polsl.pl)**

Abstract
Increasing environmental requirements for wastewater treatment plants (WWTPs) make it necessary to search for new wastewater treatment technologies. One such solution may be the implementation of shortcut nitrification in the mainstream of WWTPs. However, the use of shortened nitrification in the mainstream results in nitrite instead of nitrate present in the outflow of the treatment plant. Due to strict regulation of nitrite concentration in the effluent, additional removal of nitrite, for example in a variety of filters, is necessary. For this reason, denitrification filters can be used, in which wastewater is treated by flowing through a column reactor filled with a bed inoculated with activated sludge. In this study, three ways of inoculation such filters were investigated (inoculation from the top of the filters, from the bottom, and mixing the activated sludge with the bed). The best results in nitrite and COD removal were obtained for the reactor with mixed bed with the sludge reaching nitrites and COD removal efficiency even 100% and 82%, respectively.

Keywords
Denitrification filter; halloysite; nitrite; wastewater

INTRODUCTION

Reducing the operating cost of wastewater treatment plants (WWTPs) exploitation, while maintaining the high efficiency of the WWTPs operating combined with a reduction in greenhouse gas emissions, is one of the major challenges facing WWTPs. The presented research is a part of an international project to develop a technology for the utilization of free nitrous acid (FNA) for mainstream shortcut nitrification and sludge disintegration for higher energy production. This technology will provide significant savings of energy (25% reduction of aeration needs) at WWTP as well as other environmental positive impacts such as lower nitrogen discharge and carbon footprint. Since the regulations for nitrite concentration are very strict and in the outflow from the treatment plant its concentration must not exceed 1 g/m^3 this will require additional treatment of the outflow from the treatment plant of nitrite nitrogen. For this purpose, denitrification filters will be used. This technology was widely applied for nitrate removal (Gou et al., 2021; Wang et al., 2021), however, its usage for nitrite reduction from wastewater is hardly described. Thus, three ways of filter inoculation by activated sludge are presented in this study.

MATERIALS AND METHODS

The experiment was conducted in three denitrification filters (R1 – reactor inoculated from the top of filters; R2 - reactor inoculated from the bottom of filters; R3 – inoculation by mixing activated sludge with bed) with an active volume of 500 mL filled with expanded clay and halloysite. The reactors were inoculated with activated sludge (7.8 mg TSS/L) and the ratio of activated sludge to halloysite was 30% (v/v). The hydraulic retention time (HRT) was 2 h, while the concentration of nitrite was 10 mg/L and the concentration of COD was 90 mg/L. The experiment was conducted at room temperature (~ 20˚C) and pH 7.0.

RESULTS AND DISCUSSION

The obtained results (Figure 1) show that R3 presented the highest level of COD, as well as nitrite removal, and reached 100% efficiency for nitrite removal between 8 and 10 days, while in the same period, COD removal was approximately 80%. Similar results were obtained for R2. In R1, the removal efficiency of nitrite was increased from 10% on day 4 to 70% on day 8 and then maintained until day 14 when reached 97%. It can be suspected that the transfer of seeding sludge from the top needs more time for adaptation for microorganisms. Similarly, Zhang et al. (2018) obtained stability work of denitrification filters filled from the top after 20 days. In each reactor increase in the removal efficiency of both nitrite and nitrate was observed after day 10 and slightly decreased till the end of the experiment. This situation may be caused by the desorption of both nitrite and nitrate from the halloysite, however, this thesis required further analysis.

CONCLUSION

Denitrification filters seem to be a good technology for nitrite removal in tertiary treatment. As the most effective method of inoculating the bed seems to be its complete mixing of the halloysite with the sludge. Moreover, studies have shown that it only takes 8 days to achieve stable system operation. It is worth to noted that further research focusing on nitrogen load, temperature and HRT is ongoing.

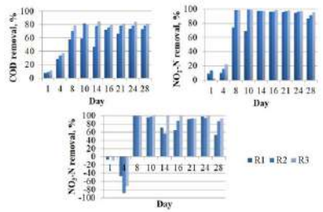

Figure 1. COD, nitrite and nitrate removal efficiency in the tested denitrification filters. R1 – reactor inoculated from the top of filters; R2 - reactor inoculated from the bottom of filters; R3 – inoculation by mixing activated sludge with bed.

The project was funded by the Polish-Norwegian Research Programme operated by the National Centre for Research and Development under POLNOR 2019 in the frame of Project Contract No NOR/POLNOR/SNIT/0033/2019-00

REFERENCES

Wang, S.S., Cheng, H.Y., Zhang, H., Su, S.G., Sun, Y.L., Wang, H.C., Han, J.L., Wang, A.J. Guadie, A. (2021). Sulfur autotrophic denitrification filter and heterotrophic denitrification filter: Comparison on denitrification performance, hydrodynamic characteristics and operating cost. Environmental Research, 197, 111029

Guo, Q., Yang, Z., Zhao, Q., Chen, J., Li, J., Chen, L., Shi, W., An, P., Wang, G., Xu, G. (2021). A pilot-scale study of a novel two-stage denitrification filter. Journal of Water Process Engineering, 39, 101873.

Zheng, X., Zhang, S., Zhang, J., Huang, D., Zheng, Z. (2018). Advanced nitrogen removal from municipal wastewater treatment plant secondary effluent using a deep bed denitrification filter. Water Science and Technology, 77(11), 2723–2732.

Tertiary treatment of nitrite-containing wastewater in a denitrification filter - preliminary studies

F. Gamoń*, A. Ziembińska-Buczyńska*, G. Cema*

* Department of Environmental Biotechnology, Silesian University of Technology, Akademicka 2, Gliwice, Poland
(E-mail: *filip.gamon@polsl.pl)**

Abstract
Increasing environmental requirements for wastewater treatment plants (WWTPs) make it necessary to search for new wastewater treatment technologies. One such solution may be the implementation of shortcut nitrification in the mainstream of WWTPs. However, the use of shortened nitrification in the mainstream results in nitrite instead of nitrate present in the outflow of the treatment plant. Due to strict regulation of nitrite concentration in the effluent, additional removal of nitrite, for example in a variety of filters, is necessary. For this reason, denitrification filters can be used, in which wastewater is treated by flowing through a column reactor filled with a bed inoculated with activated sludge. In this study, three ways of inoculation such filters were investigated (inoculation from the top of the filters, from the bottom, and mixing the activated sludge with the bed). The best results in nitrite and COD removal were obtained for the reactor with mixed bed with the sludge reaching nitrites and COD removal efficiency even 100% and 82%, respectively.

Keywords
Denitrification filter; halloysite; nitrite; wastewater

INTRODUCTION

Reducing the operating cost of wastewater treatment plants (WWTPs) exploitation, while maintaining the high efficiency of the WWTPs operating combined with a reduction in greenhouse gas emissions, is one of the major challenges facing WWTPs. The presented research is a part of an international project to develop a technology for the utilization of free nitrous acid (FNA) for mainstream shortcut nitrification and sludge disintegration for higher energy production. This technology will provide significant savings of energy (25% reduction of aeration needs) at WWTP as well as other environmental positive impacts such as lower nitrogen discharge and carbon footprint. Since the regulations for nitrite concentration are very strict and in the outflow from the treatment plant its concentration must not exceed 1 g/m^3 this will require additional treatment of the outflow from the treatment plant of nitrite nitrogen. For this purpose, denitrification filters will be used. This technology was widely applied for nitrate removal (Gou et al., 2021; Wang et al., 2021), however, its usage for nitrite reduction from wastewater is hardly described. Thus, three ways of filter inoculation by activated sludge are presented in this study.

MATERIALS AND METHODS

The experiment was conducted in three denitrification filters (R1 – reactor inoculated from the top of filters; R2 - reactor inoculated from the bottom of filters; R3 – inoculation by mixing activated sludge with bed) with an active volume of 500 mL filled with expanded clay and halloysite. The reactors were inoculated with activated sludge (7.8 mg TSS/L) and the ratio of activated sludge to halloysite was 30% (v/v). The hydraulic retention time (HRT) was 2 h, while the concentration of nitrite was 10 mg/L and the concentration of COD was 90 mg/L. The experiment was conducted at room temperature (~ 20˚C) and pH 7.0.

RESULTS AND DISCUSSION

The obtained results (Figure 1) show that R3 presented the highest level of COD, as well as nitrite removal, and reached 100% efficiency for nitrite removal between 8 and 10 days, while in the same period, COD removal was approximately 80%. Similar results were obtained for R2. In R1, the removal efficiency of nitrite was increased from 10% on day 4 to 70% on day 8 and then maintained until day 14 when reached 97%. It can be suspected that the transfer of seeding sludge from the top needs more time for adaptation for microorganisms. Similarly, Zhang et al. (2018) obtained stability work of denitrification filters filled from the top after 20 days. In each reactor increase in the removal efficiency of both nitrite and nitrate was observed after day 10 and slightly decreased till the end of the experiment. This situation may be caused by the desorption of both nitrite and nitrate from the halloysite, however, this thesis required further analysis.

CONCLUSION

Denitrification filters seem to be a good technology for nitrite removal in tertiary treatment. As the most effective method of inoculating the bed seems to be its complete mixing of the halloysite with the sludge. Moreover, studies have shown that it only takes 8 days to achieve stable system operation. It is worth to noted that further research focusing on nitrogen load, temperature and HRT is ongoing.

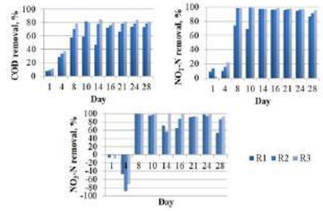

Figure 1. COD, nitrite and nitrate removal efficiency in the tested denitrification filters. R1 – reactor inoculated from the top of filters; R2 - reactor inoculated from the bottom of filters; R3 – inoculation by mixing activated sludge with bed.

The project was funded by the Polish-Norwegian Research Programme operated by the National Centre for Research and Development under POLNOR 2019 in the frame of Project Contract No NOR/POLNOR/SNIT/0033/2019-00

REFERENCES

Wang, S.S., Cheng, H.Y., Zhang, H., Su, S.G., Sun, Y.L., Wang, H.C., Han, J.L., Wang, A.J. Guadie, A. (2021). Sulfur autotrophic denitrification filter and heterotrophic denitrification filter: Comparison on denitrification performance, hydrodynamic characteristics and operating cost. Environmental Research, 197, 111029

Guo, Q., Yang, Z., Zhao, Q., Chen, J., Li, J., Chen, L., Shi, W., An, P., Wang, G., Xu, G. (2021). A pilot-scale study of a novel two-stage denitrification filter. Journal of Water Process Engineering, 39, 101873.

Zheng, X., Zhang, S., Zhang, J., Huang, D., Zheng, Z. (2018). Advanced nitrogen removal from municipal wastewater treatment plant secondary effluent using a deep bed denitrification filter. Water Science and Technology, 77(11), 2723–2732.

Performance, resilience and energetic balance in ElectroStimulated Anaerobic Reactor (ELSAR®) vs. anaerobic fluidized bed reactor

A. Giménez-Lorang*, Y. Asensio-Ramírez*, N. Hernández-Ibáñez*, X. Tomás-Ortiz*, V.M. Monsalvo-García*, F. Rogalla*

* FCC Aqualia, Innovation & Technology Department, Av. Camino de Santiago, 40, Building #3, 4th floor. 28050 - Madrid (Spain). *Email : antonio.gimenez@fcc.es ; yeray.asensio@fcc.es ; naiara.hernandez@fcc.es ; xavier.tomas@fcc.es ; victor.monsalvo@fcc.es ; frogalla@fcc.es

Abstract

Pilot tests of the ELSAR® (ElectroStimulated Anaerobic Reactor) technology applied to the treatment of brewery wastewater showed significant improvements compared to conventional anaerobic fluidized bed reactor (AFBR), like better organic matter removal performance, higher biogas production productivity, higher calorific potential of biogas as a consequence of a higher biohydrogen content and better microbial response to sudden changes (reactor's temperature, organic loading rate or addition of inhibitors). The energy consumption of the treatment in lab-scale tests has been below 0.4 kWh·removed kg COD^{-1}, regardless of the organic loading rate of the reactor. Given these promising results, Aqualia has decided to scale up the technology, which can already be considered, according to the literature, a technical milestone. An ELSAR®-based wastewater treatment plant is being built with a treatment capacity up to 2000 kg COD·day^{-1}.

Keywords

bioelectrochemistry; fluidized; industrial wastewater treatment, electrostimulation

INTRODUCTION

Coupling anaerobic digestion with electrochemistry have shown promising results and opens a wide spectrum of possibilities in the wastewater sector (particularly in the food and beverage sector, where wastewaters tend to present high dissolved and biodegradable organic matter contents) due, among others, to the extra methane production that takes place thanks to bioelectrochemical electron transfer pathways on electrodes (Park et al., 2020).

The use of a microbial electrochemical fluidized bed reactor (registered as Electro-Stimulated Anaerobic Reactor (ELSAR®)) has been reported as a suitable solution where electron transfer by Geobacter stains (along with other anaerobic bacteria) allows to stimulate the degradation of organic matter (Tejedor-Sanz et al., 2018). ELSAR® (EP 2927196 A1) combines a classic fluidized reactor and a bioelectrochemical system: electroactive bacteria grow in a fluidized bed of activated carbon. These bacteria transfer the electrons from the oxidation of the organic matter present in wastewater to the activated carbon, which acts as an electroconductive material that stores electrons. After charging, the capacitive granules can be discharged at a current collector, which is poised at a higher potential than the granules. Consequently, power is produced (Figure 1).

To validate ELSAR® as a competitive solution for the wastewater market, the system has been compared to high-rate conventional existing anaerobic technologies (anaerobic fluidized bed reactors, AFBR), in terms of performance, resilience and energetic balance. This paper compiles the main results with regard to this comparison.

MATERIALS AND METHODS

In the frame of the LIFE Answer project (http://life-answer.eu/), a tubular-shaped lab-scale (1.2L capacity) ELSAR® has been operated under the following conditions:

- organic loading rates between 0.23 kg COD·m^{-3}·day^{-1} and 23.60 kg COD·m^{-3}·day^{-1}
- anode potential from +200 mV to + 800 mV vs Ag/Ag/Cl

Pilot-scale (5.4L capacity) ELSAR® and AFBR were run, monitored and compared under steady and stress conditions (described in the next chapter). All tests were done in the mesophilic range.

RESULTS AND DISCUSSION

Under steady conditions long-term bench-scale tests showed that ELSAR® outperformed anaerobic fluidized bed reactor (AFBR) in terms of COD removal and CH_4 production. Furthermore, hydrogen content (average 154 mg H_2·L^{-1}) was observed in the biogas produced by ELSAR®, while no H_2 was detected in the AFBR biogas. The consequence of this generated hydrogen is a significant increase in the calorific power of the produced biogas, meaning an improvement on the energetic balance of the system (Table 1).

Under stress conditions, a more resilient behaviour has been observed in ELSAR® compared to AFBR under the following stress operational tests: COD overload, biocide dosing, long starvation periods and operation at low temperatures (Table 1). The bioelectrochemical system achieves a higher maintenance of the process stability, which is in concordance with was widely reported in several references (Park et al., 2020).

Energy consumption on ELSAR® lab-scale tests treating real brewery wastewater has been always below 0.4 kWh·kg^{-1} removed COD, not depending on the applied organic loading rate. The mentioned value is ca. 10 times lower in comparison to typical energetic requirements of aerobic conventional activated sludge systems.

All these promising results motivated the upscaling of ELSAR® up to an industrial scale. In the frame of the EU project ULTIMATE (https://ultimatewater.eu/), Aqualia is designing and building the industrial-scale ELSAR® (treatment capacity 20 m^3·h^{-1} wastewater or 2.000 kg COD·day^{-1}) in the Mahou San Miguel brewery in Lleida (Spain) (expected commissioning mid-2023) (Figure 2).

AKNOWLEDGEMENTS

The authors would like to thank the European Union's Horizon 2020 research and innovation programme, which provided the needed funding under the Grant Agreement No 869318.

REFERENCES

Asensio, Y., Llorente, M., Fernández, P., Tejedor-Sanz, S., Ortiz, J.M., Ciriza, J.F., Monsalvo, V.M., Rogalla, F., Esteve-Núñez, A. Upgrading fluidized bed bioelectrochemical reactors for treating brewery wastewater by using a fluid-like electrode. *Chemical Engineering Journal*, Volume **406**, 2021a

Asensio, Y., Llorente, M., Tejedor-Sanz, S., Fernández-Labrador, P., Manchon, C., Ortiz, J.M., Ciriza, J.F., Monsalvo, V.M., Rogalla, F., Esteve-Núñez, A. Microbial electrochemical fluidized bed reactor (ME-FBR): An energy-efficient advanced solution for treating real brewery wastewater with different initial organic loading rates. *Journal of Environmental Chemical Engineering*, Volume **9**, Issue 6, 2021b

Park, J-G., Jiang, D., Lee, B., Jun., H-B. Towards the practical application of bioelectrochemical anaerobic digestion (BEAD): Insights into electrode materials, reactor configurations, and process designs. *Water Research*, Volume **184**, 2020

Tejedor-Sanz, S., Fernández-Labrador, P., Hart, S., Torres, C.I., Esteve-Núñez, A. 2018. Geobacter Dominates the Inner Layers of a Stratified Biofilm on a Fluidized Anode During Brewery Wastewater Treatment. **Front. Microbiol**. **9**:378.

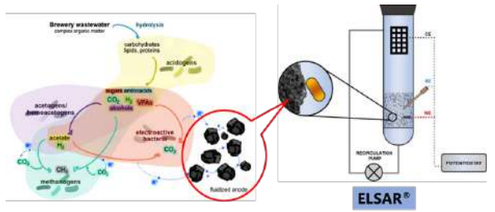

Figure 1. Schematic of the different anaerobic communities that might coexist within the ELSAR® and the possible competitive reactions among them for the electron donors. The discontinuous lines indicate the electric connections. WE = Working Electrode. RE = Reference Electrode. CE = Counter Electrode. Adapted from Asensio et al. (2021b) and Tejedor-Sanz et al. (2018).

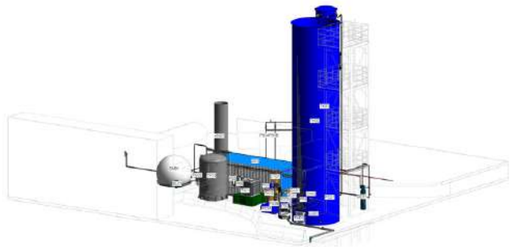

Figure 2. 3D view of the industrial-scale WWTP based on ELSAR®.

Table 1. Parameters comparison ELSAR® vs. anaerobic fluidized bed reactor. Adapted from Asensio *et al.*, 2021a.

Parameter	Difference ELSAR® vs. AFBR	Operating conditions
COD removal [%]	+10% vs. AFBR	OLR 6.0–7.1 kg COD·m^{-3}·d^{-1}, HRT 9h
Energy production associated to generated biogas [kWh·treated m^{-3}]	+30% vs. AFBR	
COD removal reduction after starvation period [%]	70% vs. 70%	OLR 0 kg COD·m^{-3}·d^{-1} during 20 days;
Recovery period to normal performance after starvation period [number of days]	20 days vs. 40 days	OLR 0 kg COD·m^{-3}·d^{-1} during 20 days; then OLR 6.0–7.1 kg COD·m^{-3}·d^{-1}
COD removal after biocide dosing [%]	10% vs. 55%	OLR 6.0–7.1 kg COD·m^{-3}·d^{-1}, HRT 9h
COD removal 1 month after temperature drop [%]	70% vs. 35%	Sudden temperature drop from 35 to 25ºC, OLR 6.0–7.1 kg COD·m^{-3}·d^{-1}, HRT 9h

Implementing Ozone/Ultrasound for Trimethoprim and Sulfamethoxazole removal and reducing antibiotic resistance in Finnish reject waters.

K. Golovko*, A. Kruglova*, K. Tsytlishvili*, R. Al-Juboori**, M. Valtari*, T. Tuhkanen*** and A. Mikola*

* Department of Built Environment, Aalto University, PO Box 15200, FI-00076, AALTO, Finland
(E-mail: ksenija.golovko@aalto.fi, antonina.kruglova@aalto.fi, kateryna.tsytlishvili@aalto.fi, maria.valtari@aalto.fi, anna.mikola@aalto.fi)

** NYUAD Water Research Center, Experimental Research Building (C1), NYU Abu Dhabi, Saadiyat Campus, PO Box 129188, Abu Dhabi, United Arab Emirates
(E-mail: ra9914@nyu.edu)

*** University of Jyväskylä, Survontie 9 C, Ylistönrinne, Building YK, PO Box 35, FI-40014
(E-mail: tuula.a.tuhkanen@jyu.fi)

Abstract
Antibiotic resistant bacteria and active pharmaceutical compounds such as antibiotics constitute a menace to environmental sustainability. The biodegradability of various pharmaceutical micropollutants is of concern due to the complexity of solutions used in medicine. Furthermore, conventional biological wastewater treatment plants have been revealed to be hot spots for antibiotic resistant bacteria development and accumulation. Internal recycling of sludge thickening, and dewatering reject water creates a path for non-degraded antibiotics to impact the wastewater treatment plant's overall load. This study focuses on side-stream treatment (e.g., reject wastewater) to investigate advanced oxidation processes' combination impact on antibiotics removal, antibiotic resistant bacteria reduction, and biodegradability of wastewater. Trimethoprim (TMP) and Sulfamethoxazole (SMX) mix represented the target group of antibiotics for removal efficiency and resistant bacteria reduction tests. The combination of Ozonation (O_3) and ultrasound (US) techniques was used, and different types of reject wastewater were tested. Different reject wastewater samples of full-scale Finnish plants with and without implemented side-stream deammonification were analyzed and used to collect data on the typical composition of antibiotic resistant genes. Advanced oxidation process regimes were adjusted for reject wastewater treatment considering wastewater quality: thus, ozone concentration, ultrasound frequency, and contact time were adapted. In the end, substantial antibiotic resistant bacteria reduction was achieved. In contrast, more research on biodegradability improvement should be conducted to customize the location of the advanced oxidation process in the side-stream treatment.

Keywords
Antibiotic resistant bacteria; trimethoprim; sulfamethoxazole; advanced oxidation process; reject wastewater; ANITA™ Mox.

INTRODUCTION

Advanced oxidation processes (AOP) are often implemented at wastewater treatment plants (WWTP) in the effluent of the process, particularly for disinfection purposes if WWTP effluent is considered a water source for reuse (Sgroi et al., 2021). Environmental permits regulate effluent quality regarding microbiological contamination after the biological treatment at the plant. Nevertheless, full-scale investigation and implementation of AOP should be considered to provide the most efficient removal of antibiotics and ensure antibiotic resistant bacteria (ARB) accumulation prevention (Rodriguez-Chueca et al., 2019). Previous studies show potential biosorption for some of the micropollutants performed by activated sludge (Yang et al., 2011). TMP/SMX mix appears to be among the most common antibiotics in Finnish municipal wastewaters compared with a wide selection of antibiotic groups (Kortesmäki et al., 2020). Therefore, the trimethoprim (TMP) and sulfamethoxazole (SMX) combination creates potential hazards for the environment since antibiotic compounds could be released in the environment if further sludge treatment is not implemented. Moreover, the contribution of side-stream recycling is still unclear, and more data on antibiotic concentration and the presence of ARB are required to fulfill the picture of the wastewater treatment process with additional factors. The more information needed such as the impact of anaerobic digestion on the degradation of antibiotics and possible positive outcome of sides-stream pre-treatment with advanced oxidation processes. Thus, more studies should be conducted to investigate the best approach for antibiotic resistance prevention with possible positive side effects for biological treatment after AOP implementation.

Antibiotic removal and Antibiotic resistant bacteria

TMP and SMX presence is primarily studied in the effluent from wastewater treatment plants. In contrast, potential hot spots for resistance development and antibiotic impact on the treatment process are located within biological treatment reactors and anaerobic digestors (Wu et al., 2022). TMP and SMX are mentioned to have a high excretion rate, solubility, and persistence (Chen, 2020). Therefore, a significant fraction of the total load consumed enters the bioreactors. Antibiotic removal can be achieved to a certain extent. However, most of the biological municipal WWTPs could not provide prevention of ARB accumulation (Rodriguez-Chueca et al., 2019). Accumulation leads to the development of antibiotic resistance of microorganism groups that potentially could enter the environment after releasing effluent from WWTP.

Reject wastewater and ANITA™ Mox

Reject wastewater from sludge thickening and dewatering after anaerobic digestion significantly contributes to the total nitrogen and COD load when recycling back to the WWTP influent (Koskue et al., 2021). Therefore, this side-stream wastewater was a subject for implementing specific nitrogen load reduction processes. Few plants in Finland have incorporated ANITA™ Mox Anammox-based moving bed biofilm reactor (MBBR) deammonification process from Veolia Environnement SA for reject wastewater treatment. However, the presence of antibiotic-resistant bacteria in reject wastewater and the effect of the ANITA™ Mox process on ARB reduction have not been extensively studied. Anammox bacteria involved in the ANITA™ Mox process are microorganisms with low growth rates, sensitive to low substrate concentrations and temperature decrease (Yuan et al., 2023). All factors included are essential to prevent possible intrusion of high concentrations of micropollutants to achieve the highest treatment efficiency. Moreover, pre-treatment of reject water could improve COD fractions favorable for biological treatment.

MATERIALS AND METHODS

A combination (figure 1) of ozonation and ultrasound (O_3/US) was used with reactor volume 1.5 L, ozonizer 300.5 (Erwin Sander), ultrasonic system (Meinhardt® Ultrasonics, ultrasound transducer E 805/T/M, glass reactor UST 02/500-03/1500). Three sets of experiments were held with two repetitions of each, and the main operation parameters are described in table 2.
Reject water quality testing was performed according to the methods described in table 1. In addition, reject water quality before and after the use of AOPs was compared to define the impact on reject water suitability to recycle to the influent of WWTP.
Antibiotic resistant bacteria growth preliminary check-up was performed with the plating method by (Chen, X. S., 2020) using Mueller Hinton agar (Oxoid) and TMP/SMX concentrations 10/50 mg/l of agar (TMP/SMX, respectively).
Antibiotic concentration measurements were done at Jyväskylä University using Hewlett-Packard Agilent 1100 HPLC (Agilent Technologies).
Antibiotic resistant gene testing was performed using SmartChip qPCR (Resistomap Oy).

RESULTS AND DISCUSSION

Reject water types (impact on AOP efficiency)

Water quality parameter values of reject water used for the testing are presented in table 3. ANITA™ Mox from WWTP (2) was still in the start-up process, and the sample was collected only for the actual AOP process testing. Thus, the sample number was limited to define standard deviation. Reject water samples before and after AOP are presented in figure 2.

AOP impact on reject water biodegradability

AOP treatment could be considered a feasible pre-treatment of reject water to increase soluble biodegradable fraction of COD and improve biological side-stream treatment efficiency to remove nitrogen while reducing the impact of antibiotic resistant bacteria.

Antibiotic resistant bacteria reduction

ARB reduction was detected already during the preliminary plating tests, where a lower concentration of ARB was observed in the plated after AOP treatment, especially in the case of higher ozone dosage (test 3 in table 2).

TMP/SMX removal

A combination of higher frequency ultrasound and ozone dosage is preferred in the TMP/SMX mix degradation due to the high suspended, and total solids concentration in dewatering reject waters. In the case of antibiotic removal as a primary goal, the main challenges will be the energy efficiency of the treatment process, the risk of ultrasound equipment overheating, and extensive foaming of dewatering reject water due to the reaction with ozone.

Table 1. Reject water quality parameters methods.

Parameter	Method
COD	SFS 3036 (dated 1981)
BOD_5	OxiTop manual, SFS-EN 1899-1
Total Nitrogen	SFS-EN ISO 11905-1
Total Phosphorus	ISO 6878 (dated 2004)
Total Iron	SFS 3028 (dated 1976)
Total suspended solids	SFS-EN 872
Volatile suspended solids	SFS-EN 872
Total solids	SFS 3008
Volatile solids	SFS 3008
pH	SFS-EN ISO 10523 (dated 2012)

Table 2. O3/US main operation parameters

Test	O_3 (mg/l), voltage level	US frequency (kHz), power levels (%)	Operation time, US mode
1	4.5 mg/l	865 kHz	30 min
	58%	90%	continuous
2	4.5 mg/l	1144 kHz	15 min
	58%	90%	continuous
3	7 mg/l	865 kHz	30 min
	70%	90%	continuous

Table 3. Reject water quality parameter values (± standard deviation) from Finnish WWTPs

Sample	COD (mg/l)	Total Nitrogen (mg/l)	Total Phosphorus (mg/l)
WWTP (1) reject water before ANITA™ Mox	2195.0 ± 3.7	964.9 ± 14.5	13.2 ± 1.5
WWTP (1) reject water after ANITA™ Mox	1668.2 ± 331.0	321.0 ± 26.7	12.2 ± 1.6
WWTP (2) thickening reject water before digestion	582.1 ± 0.8	80.0 ± 30.6	3.1 ± 1.8
WWTP (2) dewatering reject water after digestion	3024.5 ± 101.4	1398.0 ± 89.1	14.0 ± 2.5
WWTP (2) reject water after ANITA™ Mox	1259.8	187.1	2.9

Figure 1. O_3/US combination experimental setup.

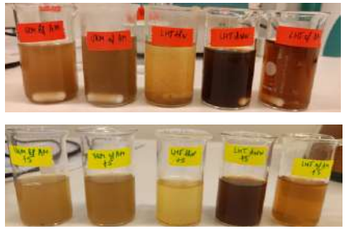

Before AOP treatment

After AOP treatment

Figure 2. Reject waters before and after AOP treatment.

REFERENCES

Chen, X. S. (2020). Development of antibiotic resistance detection method for the express analysis of wastewater effluents. Master's Thesis, Aalto University, Department of Built Environment.

Kortesmäki, E., Östman, J.R., Meierjohann, A., Brozinski, J.-M., Eklund, P., Kronberg, L. (2020). Occurrence of Antibiotics in Influent and Effluent from 3 Major Wastewater-Treatment Plants in Finland. *Environmental Toxicology and Chemistry*, **39**(9), 1774-1789.

Koskue, V., Freguia, S., Ledezma, P., Kokko, M. (2021). Efficient nitrogen removal and recovery from real digested sewage sludge reject water through electroconcentration. *Journal of Environmental Chemical Engineering*, **9**(5), 106286.

Rodriguez-Chueca, J., Giustina, S. V. d., Rocha, J., Fernandes, T., Pablos, C., Encinas, A., Barcelo, D., Rodriguez-Mozaz, S., Manaia, C. M., Marugan J. (2019). Assessment of full-scale tertiary wastewater treatment by UV-C based-AOPs: Removal or persistence of antibiotics and antibiotic resistance genes? *Science of The Total Environment*, **652**, 1051-1061.

Sgroi, M., Snyder, S.A., Roccaro, P. (2021). Comparison of AOPs at pilot scale: Energy costs for micro-pollutants oxidation, disinfection by-products formation and pathogens inactivation. *Chemosphere*, **273**, 128527.

Wu, Q., Zou, D., Zheng, X., Liu, F., Li, L., Xiao, Z. (2022). Effects of antibiotics on anaerobic digestion of sewage sludge: Performance of anaerobic digestion and structure of the microbial community. *Science of The Total Environment*, **845**, 157384.

Yang, S.-F., Lin, C.-F., Lin, A. Y.-C., Hong, P.-K. A. (2011). Sorption and biodegradation of sulfonamide antibiotics by activated sludge: Experimental assessment using batch data obtained under aerobic conditions. *Water Research*, **45**(11), 3389-3397.

Yuan, Q., Jia, Z., Roots, P., Wells, G. (2023). A strategy for fast anammox biofilm formation under mainstream conditions. *Chemosphere*, pre-print, 137955.

Microalgal photobioreactor systems for urban wastewater treatment and removal of emerging contaminants

Félix Gaspar Gonzalo Ibrahim*, Rebeca López Serna**, Raúl Muñoz Torre**, Ignacio de Godos Crespo*
*Department of Chemical Engineering and Environmental Technology. School of Forestry, Agrarian and Bioenergy Engineering; Campus Duques de Soria, University of Valladolid, Spain and ISP, University of Valladolid
**Department of Chemical Engineering and Environmental Technology, University of Valladolid, School of Industrial Engineering, Valladolid, Spain and Institute of Sustainable Process, University of Valladolid

Abstract
Microalgae cultivation offers a low-cost wastewater treatment for domestic effluents. This work evaluated the performance of an integral microalgae-based domestic wastewater treatment system was conducted in lab-scale photobioreactors under the conditions prevailing in outdoor HRAP reactors. For this purpose, seasonal and daily variations of light intensity were essayed in an open reactor with similar mass transfer characteristic that a conventional HRAP. Wastewater treatment was evaluated in terms of nutrient, organic matter, bacteria pathogen, and emerging contaminants. The photobioreactors demonstrate a very high efficiency in removal and, therefore, in the permitted water reuse.

Keywords
Biotransformation; Emerging contaminants; Microalgae; Pharmaceutical removal; Photobioreactor; Wastewater treatment.

1- INTRODUCTION

The photosynthesis reaction of these microorganisms releases the oxygen needed for organic matter oxidation while nutrients are assimilated into algae biomass, allowing for nitrogen and phosphorous recovery into biomass. Experimental set-ups must be carefully designed to simulate the conditions as close as possible to those found in outdoor photobioreactors. In this context, research studies can be differenced in two main strategies: outdoors demonstration essays conducted in long-term operation and lab-scale systems addressed to study specific issues of the bioprocess: such as rates of pollutant removal or biomass characteristics.

2- MATERIALS AND METHODS

Experimental set up

The experimental set up was located indoors, at the laboratory in Campus of Soria - Valladolid University. The system was integrated by two 2.15 L cylindrical PVC photobioreactors connected to each photobioreactor (Fig. 1).

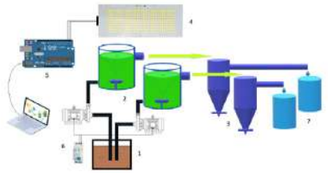

Figure 1. Schematic diagram of the experimental setup. (1) Wastewater, INLET (2) Photobioreactor for wastewater treatment, (3) Conical settler, (4) LED module, (5) Illumination program System of Arduino (6) Pumps programmed system, (7) OUTLET.

The system treated real wastewater from the municipal WWTP of Garray (Soria, Spain). The photobioreactors were illuminated with a day simulator program consisting in two LED module PHILIPS 94V covering a total surface of 0.16 m^2. The illumination was programmed with Arduino device (IDE) that modulated the light intensity by means of a Pulse Width Modulation (PWM). Reactor's temperature was controlled by thermostatic bath fixed at (20° C) in summer and (10° C) in winter (Frigiterm-SELECTA). However, light irradiation created temperature fluctuations in the bulk liquid. The photobioreactors were fed with two pumps (WATSON MARLOW 313S) at an inlet flowrate of 0.7 L d^{-1} from a 5 L homogenization tank resulting in a hydraulic retention time of 3 days. Evaporation rates were determined by the measurement of the decrease in depth in batch mode experiments. The rates of evaporation were used in every calculation for mass balances and biomass productivity (de Godos et al., 2016). The rates of oxygen exchange between the bulk liquid and the atmosphere were determined following a standard procedure of volumetric mass transfer coefficient.

Analytical methods

In order to evaluate the wastewater treatment efficiency, the following parameters were analysed: COD, NH_4^+, PO_4^{3-} total suspended solids (TSS), according to Standard Methods (APHAAWWA-WEF, 2012). All the analyses were done in duplicate and results are given as average values. Biomass productivity was determined by the measurement of total suspended solids (TSS) considering the outlet flow. In calculations of biomass production, the TSS parameter and the total surface of the photobioreactor were used. Organic matter removal was measured with Chemical Oxygen Demand (COD) concentration, total and soluble. Soluble COD was measured after the filtration through a 0.45 µ of nylon filter. The concentrations of the following parameters were determined: total suspended solids (TSS) and volatile suspended solids (VSS). Samples were collected every two days to perform the chemical analyses that were carried out on filtered samples using spectrophotometric quantitative measurements.

E. coli and coliform concentration in influent and effluent of the photobioreactors were determined using the protocol described in the ISO 9308-1:2014 (ISO, 2014) with Chromocult® Coliform Agar (CCA). The method is based on membrane filtration for 100 ml and Petri dishes cultivation, subsequent culture on a chromogenic coliform agar medium, and calculation of the number of target organisms in the sample. The method was used for detection and enumeration of *Escherichia coli* and coliform bacteria.

Fifty-nine pharmaceutical residues were measured following the analytical methodology. The CEC samples were performed according to (López-Serna et al., 2011, López-Serna et al., 2019a, López-Serna et al., 2019b). In brief, 100 mL of each sample (filtered through a 0.45 µm filter) were spiked with a 0.1% Na2EDTA solution and 1000 ng L−1 of internal standard, before solid phase extraction (SPE) using Oasis HLB cartridges (Water Chromatography, Spain). Then, the cartridges were eluted with 6 mL of acetonitrile, and the resulting solution was evaporated and reconstituted in 1 mL of 0.1% formic acid (FA) in H2O/MeOH (95:5). Finally, the extracts were analysed by ultra-high performance liquid chromatography (UHPLC) – tandem mass spectrometry (MS/MS) in selected reaction monitoring (SRM) mode. More specifically, chromatographic separation was carried out by a Sciex Exion UHPLC and a Phenomenex reversed-phase column Kinetex EVO C18 (2.1 mm × 50 mm, particle size 1.7 µm), making use of H2O- and MeOH-based mobile phases containing 0.1% FA as modifier. Mass detection was performed by the triple quadrupole Sciex 6500+ QqQ.

3- RESULTS AND DISCUSSION

The values found for the aeration coefficient (0.393 h^{-1}) were considerably lower than the reported values for similar systems. The seasonal variations, without any modification in the HRT, were particularly relevant the productivity of biomass per surface area. The production during summer conditions in two photobioreactor: photobioreactor 1 operated at 2.99 ± 0.26 days of HRT, 21.98 ± 2.58 $g \cdot m^{-2} \cdot d^{-1}$ (measured as VSS) and photobioreactor 2 operated at 2.96 ± 0.23 days of HRT, 25.09 ± 0.73 $g \cdot m^{-2} \cdot d^{-1}$ (measured as VSS). During the winter conditions the pond presented a decrease in productivity: photobioreactor 1 operated at 3.16 ± 0.40 days of HRT, 5.68 ± 2.58 $g \cdot m^{-2} \cdot d^{-1}$ (as VSS) and photobioreactor 2 operated at 3.23 ± 0.26 days of HRT, 6.75 ± 2.13 $g \cdot m^{-2} \cdot d^{-1}$ (as VSS).
The photobioreactors demonstrate a very high efficiency in removal of COD, SST, N-NH^+_4 and P-PO_4^{-3} despite the different conditions applied. Table 1 shows the results obtained from the analysis of the influents and effluents of different seasonality of two photobioreactors.

Comparison analysis of the influents and the effluents of the different seasonality in the photobioreactor experiment.

Parameter (units)	Sample point				Removal efficiency %	
	Winter		Summer			
	IN	OUT	IN	OUT	Winter	Summer
COdt (mg/L)	181.72 ± 92.83	31.13 ± 11.84	387.37 ± 85.28	80.06 ± 31.71	81.59 ± 9.32	78.08 ± 8.61
COds (mg/L)	113.88 ± 81.99	5.22 ± 2.87	177.21 ± 23.62	18.66 ± 7.36	82.837 ± 10.73	89.18 ± 4.60
N-NH^{+4} (mg/L)	24.59 ± 10.61	0.68 ± 0.36	16.47 ± 7.05	0.47 ± 0.13	97.00 ± 2.01	96.64 ± 1.60
P-PO_4^{-3} (mg/L)	9.38 ± 5.22	0.90 ± 0.07	7.19 ± 6.87	0.86 ± 0.06	83.20 ± 10.91	79.19 ± 6.87
TSS (mg/L)	157.78 ± 7.03	16.47 ± 7.04	248.5 ± 88.80	35.34 ± 13.28	94.26 ± 3.49	83.72 ± 8.54
E. Coli (CFU/100mL)	1.98E+4 ± 1.59E+3	212.50 ± 17.68	6.28E5+ ± 1.30E+5	24.93 ± 1.62	98.93 ± 4.98E-1	100.00 ± 3.51E-3
Enterobacter A.(CFU/100mL)	1.09E+4 ± 1.34E+4	232.50 ± 84.11	5.07E+5 ± 1.49E+5	28.00 ± 9.02	99.79 ± 4.35E-2	99.98 ± 4.80E-3
Enterococcus F.(CFU/100mL)	8.31E+3 ± 3.80E+3	290.00 ± 14.14	2.32E+5 ± 5.66E+4	9.42 ± 0.31	94.84 ± 2.51E-1	99.95 ± 2.36E-2

Table 1. Comparison analysis of the influents and effluents of different seasonality in the photobioreactors.

The photobioreactors obtained removal efficiencies above 80% in all measured parameters both winter and summers, except for CODt and P-PO_4^{-3} in summer conditions. Then, in both winter and summer conditions, the microalgae experimental systems comply with the regulation, except the TSS in summer conditions. The TN (removal efficiency 63% or 32 ± 16 $mg \cdot L^{-1}$) and the TP (removal efficiency 84% or 2 ± 2 $mg \cdot L^{-1}$) is lower than this experiment due to temperature and solar radiation. The TSS (removal efficiency 95% or 24 ± 26 $mg \cdot L^{-1}$) is constantly but in this experiment, there are different variations from summer to winter conditions.

Algae based systems provides pathogen bacteria removal as consequence of the environment created by microalgae and the light exposition. In this way, secondary and tertiary treatment take place simultaneously and final effluents can be used as reused water. High levels of disinfection were achieved in both conditions. Summer conditions resulted in a effluent with a *E. coli* concentration of 24.93 ± 1.62 CFU·100 ml^{-1}, while winter conditions decreased the level of disinfection with average value of 212.50 ± 17.68 CFU·100 ml^{-1}. Some authors suggest that UV light exposition is the main mechanism of pathogen removal, since most of bacteria are sensible to DNA damage mediated by UV light. However, light source used in this experiment only provides light in the visible spectrum.
In this experiment, in summer conditions, the class are B of the reclaimed water quality classes and the permitted uses and irrigation methods, *E. coli* (number/100 ml) was, nevertheless in winter conditions, the class are C due to *E. coli* (number/100 ml) was 212.50 ± 17.68 CFU·100 ml^{-1}. The reclaimed water quality classes and the permitted uses and irrigation methods for each class and the minimum requirements for water quality are in the Regulation (EU) 2020/741 of the European Parliament and of the Council of 25 May 2020 on minimum requirements for water reuse and the current Spanish regulation RD 1620/2007.

The removals efficiency of progesterone, caffeine, fenbendazole, clarithromycin, atorvastatin and dexamethasone in the photobioreactors (Fig. 4) were similar in both stages of operation (> 97,00 %). The CECs mass balance calculations revealed that biodegradation/biotransformation was the main removal mechanism in two conditions.

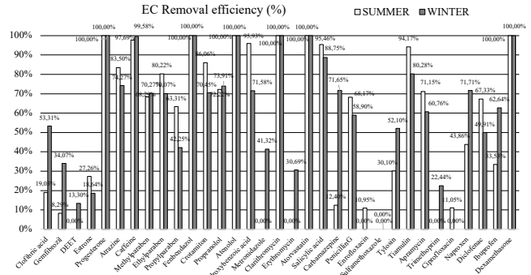

Figure 4. Removal efficiency (%) of thirty-three compounds.

In conclusion, the photobioreactors demonstrate a very high efficiency the permitted reuses with irrigation methods reducing pathogens and emerging contaminants.

References

de Godos, I., Arbib, Z., Lara, E., & Rogalla, F. (2016). Evaluation of High Rate Algae Ponds for treatment of anaerobically digested wastewater: Effect of CO2addition and modification of dilution rate. *Bioresource Technology*, *220*. https://doi.org/10.1016/j.biortech.2016.08.056
López-Serna et al., 2011. López-Serna, M. Petrović, D. Barceló. Development of a fast instrumental method for the analysis of pharmaceuticals in environmental and wastewaters based on ultra high performance liquid chromatography (UHPLC)-tandem mass spectrometry (MS/MS)Chemosphere, 85 (2011), pp. 1390-1399, 10.1016/j.chemosphere.2011.07.071

Anaerobic valorisation of process water from waste sludge hydrothermal carbonization: insights into volatile fatty acids and biomethane production

M. Grana[1], G. Riboli[1], M. Mantovani[2], A. Turolla[1], E. Ficara[1]

[1] Politecnico di Milano, Dipartimento di Ingegneria Civile e Ambientale, Piazza Leonardo da Vinci 32, 20133 Milano, Italy (E-mail: matteo.grana@polimi.it; giorgia.riboli@mail.polimi.it; andrea.turolla@polimi.it ; elena.ficara@polimi.it)
[2] Università degli studi di Milano-Bicocca, Dipartimento di scienze dell'ambiente e della terra (DISAT), P.zza della Scienza 1, 20126 Milano, Italy (E-mail: m.mantovani10@campus.unimib.it)

Abstract
Acidogenic fermentation for volatile fatty acids production, anaerobic digestion for biomethane production, and thermochemical conversion are among the main strategies to promote the sustainable management of waste sludge produced in wastewater treatment plants. In this study, hydrothermal carbonization (HTC) was studied as pre-treatment to enhance anaerobic degradability of mixed waste sludge. The HTC process was effective in the particulate COD solubilization. BOD_{20}/COD ratio resulted in the range 67%-93%, thus showing a good degradability of the HTC process water. Batch fermentability tests showed similar results as the untreated sludge, while the biomethane potential of HTC process water was 30% higher than the untreated sludge.

Keywords
Fermentation; biomethane; hydrothermal carbonization; sewage sludge; volatile fatty acids

INTRODUCTION

Waste sludge produced in wastewater treatment plants – WWTP – is traditionally one of the main issues in plant operation, as its treatment and disposal requires a proper management. Resource and energy recovery are key strategic elements to ensure environmental and economic sustainability of sludge management, being carried out mainly through biological treatments, direct land application, and thermochemical conversion (Bora et al., 2020). Traditionally, anaerobic digestion was one of the first processes developed, allowing to reduce the amount of sludge to be disposed and to recover energy in the form of biogas. Similarly, acidogenic fermentation designed for volatile fatty acids – VFAs – production was developed more recently in the view of applying VFAs as external carbon source for biological nutrient removal processes in the WWTPs or for the production of polyhydroxyalkanoates – PHA (Atasoy et al., 2018). Regarding thermochemical conversion, hydrothermal carbonization – HTC – is gaining attention lately as a process able to convert a high moisture stream into a carbonaceous product, the hydrochar, and a process liquid rich in organic compounds. The temperature of the process is relatively low, usually in the range 160 - 250°C, while the retention time strongly influences the process output (Chen et al., 2021). Coupling pre-treatment of sludge via HTC with the subsequential valorisation through anaerobic processes has been investigated as an opportunity for enhancing biogas production, while limited data is available on the possibility of using HTC for promoting VFAs production via fermentation (Chen et al., 2021).

The aim of the study is to assess the biological treatability and fermentability of mixed wasted sludge collected in a WWTP after pre-treatment with HTC process; the pre-treatment goal is to improve and speed-up the hydrolysis of the particulate matter, eventually to achieve a faster VFAs synthesis.

MATERIALS AND METHODS

The waste sludge was sampled in a WWTP located in northern Italy. The sludge was a mixture of primary and secondary sludge (80% and 20% w/w, respectively), and it was collected after the co-sedimentation of both streams in the primary settler.
HTC was carried out in a high-pressure laboratory reactor (BR-700, BERGHOF). After the HTC process, the liquid fraction (or process water) used for all the subsequent tests, was obtained by centrifuging at 3000 rpm the treated sludge. Preliminary screening was done testing two operative temperatures, namely 170°C and 190°C, and three residence times, namely 30, 60, and 150 minutes. Batch tests for fermentability were set up using 0.5 L bottles, magnetically stirred at 250 rpm, and maintained at the temperature of 30 ± 1 °C by means of a thermostatic chamber. Tests were run for 5 days and sludge from a full-scale fermenter (HRT = 4 d T = 27 ± 1 °C) was used as inoculum. Mesophilic BMP tests were carried out using a volumetric device (AMPTS II, Bioprocess Control®). BOD tests were performed by means of the manometric system (OxiTop Control from WTW).

RESULTS AND DISCUSSION

Experimental results from the preliminary tests indicated that the lower temperature tested, namely 170 °C, showed a better solubilization of the COD (8.0 g/L - 11.7 g/L and 7.3 g/L - 8.5 g/L respectively). Among the different residence times in the reactor, higher values resulted in a limited increase in sCOD while consuming a higher amount of energy for the reaction. Thus, 170 °C and 30 minutes were the operative conditions chosen for biological tests.
For BOD tests, two HTC runs (HTC-A and HTC-B) were performed on waste sludge sampled approximately 1 month apart. 50% v/v dilution conditions were also applied for HTC-A. Experimental results are shown in Table 1. The BOD_{20}/COD ratio showed a good degradability for both HTC-A and HTC-B, with HTC-B characterized by higher ratio. This is likely due to a lower synthesis of toxic or inhibiting compounds during HTC. The same explanation is also suggested by higher BOD_{20}/COD for diluted HTC-A in comparison with non-diluted HTC-A, that might imply a dilution of inhibiting compounds.
Results from fermentability batch tests are shown in Table 2. The inoculum used was sampled in a full-scale fermenter located in the same WWTP and thus acclimatized with the same waste sludge. HTC-B did not result in a better fermentability in comparison with the untreated sludge, while the diluted HTC-B was slightly higher than the latter. Nevertheless, acclimatization for the HTC process water might be needed to adapt the biomass to a very different substrate than the one usually fed to the full-scale reactor. Furthermore, potential inhibitory effects might occur, as suggested by the result of the diluted HTC-A, that might as well be mitigated by the biomass adaptation. Regarding the VFAs composition, HTC pre-treatment favoured more complex VFAs synthesis, as butyric and valeric (and their isomers) content increased, as shown in Figure 1. This is relevant for possible downstream applications such as PHA production (Albuquerque et al., 2011). On the other hand, BMP tests showed a greater degradability for HTC-B than untreated sludge, being BMP values respectively 106 ± 4.6 $NmlCH_4/gCOD_{in}$ and 81.2 ± 3.2 $NmlCH_4/gCOD_{in}$. The higher BMP productivity for HTC-B suggests that methodological improvements (such as biomass adaption and higher inoculum content) for the fermentability tests might lead to a higher VFAs production as well.
Currently ongoing activities include semi-continuous tests for HTC process water fermentation.

FIGURES AND TABLES

Table 1. Average (and standard deviations) sCOD (mg/L), BOD_5 (mg/L), BOD_{20} (mg/L), and $BOD_{5:20}$/COD ratios for HTC process water a, b, and a diluted 50% v/v.

	HTC-A		HTC-A dil. 50%		HTC-B	
	Mean	St.Dev	Mean	St.Dev	Mean	St.Dev
sCOD	8800	[-]	4400	[-]	2700	[-]
BOD_5	4900	127	2600	[-]	1960	28
BOD_5/sCOD	56%	1%	59%	[-]	73%	1%
BOD_{20}	5900	113	3300	[-]	2510	85
BOD_{20}/sCOD	67%	1%	75%	[-]	93%	3%

Table 2. Average (and standard deviation) specific net VFAs production ($g_{VFA\text{-}COD}/g_{COD,substrate}$) for untreated waste sludge, HTC-B process water, and HTC-B process water diluted 50% v/v.

Untreated. sludge	HTC-B dil. 50%	HTC-B
412 ± 114	470 ± 119	302 ± 112

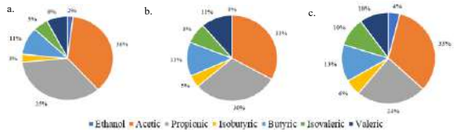

Figure 1. VFAs composition after the fermentation batch test for untreated sludge (a.), diluted HTC-B (b.) and HTC-B (c.)

REFERENCES

Albuquerque, M. G. E., Martino, V., Pollet, E., Avérous, L., and Reis, M. A. M. (2011) Mixed culture polyhydroxyalkanoate (PHA) production from volatile fatty acid (VFA)-rich streams: Effect of substrate composition and feeding regime on PHA productivity, composition and properties. Journal of Biotechnology, **151**(1), 66–76.

APHA (2005) *Standard Methods for the Examination of Water and Wastewater*, Washington DC, USA, APHA 2005 Standard Methods American Public Health Association/American Water Works Association/Water Environment Federation.

Atasoy, M., Owusu-Agyeman, I., Plaza, E., and Cetecioglu, Z. (2018) Bio-based volatile fatty acid production and recovery from waste streams: Current status and future challenges. Bioresource Technology, **268**, 773–786.

Bora, R. R., Richardson, R. E., and You, F. (2020) Resource recovery and waste-to-energy from wastewater sludge via thermochemical conversion technologies in support of circular economy: a comprehensive review. BMC Chemical Engineering, **2**(1), 8.

Chen, Z., Rao, Y., Usman, M., Chen, H., Białowiec, A., Zhang, S., and Luo, G. (2021) Anaerobic fermentation of hydrothermal liquefaction wastewater of dewatered sewage sludge for volatile fatty acids production with focuses on the degradation of organic components and microbial community compositions. Science of The Total Environment, **777**, 146077.

Low Cost, Zero Chemical and Energy Efficient Municipal Wastewater (Pre-)Treatment with Electrocoagulation-Floatation

Nazia Hassan**, Dries Parmentier***, Stijn Wim Henk Van Hulle*

*Laboratory for Industrial Water and Ecotechnology (LIWET), Department of Green Chemistry and Technology, Ghent University Campus Kortrijk, Sint-Martens-Latemlaan 2B/5, 8500 Kortrijk, Belgium
(Email: nazia.hassan@ugent.be; dries.parmentier@ugent.be; stijn.vanhulle@ugent.be;)
**Environmental Science Discipline, Khulna University,Khulna-9208, Bangladesh
(Email: nazia02ku@es.ku.ac.bd)
***Noah Water Solutions bvba, Burchtweg 7, B-9890 Gavere, Belgium
(Email: d.parmentier@noahws.be)

Abstract
Iron (Fe) electrocoagulation-floatation (EC-F) technology was investigated in view of zero chemical municipal wastewater (MWW) (pre-)treatment. Eleven operational settings were evaluated employing various current densities (CDs) in continuous mode using a flow through and a recirculation mode, various current supply systems, and various cathode materials (Cu, SS). The optimum operation was when recirculation was used (with two EC-F runs (2R)) at a CD of 12 A/m^2. Maximum Faraday efficiency, good total chemical oxygen demand (tCOD) (i.e.,78%) and total phosphate (TP) (i.e.,85%) removal and low OPEX were taken into consideration for this. Furthermore, using SS as cathode material was found beneficial to remove heavy metals (93±9 % Zn, 70±15% Pb and Cu 49±10%). As such the EC-F technology was demonstrated to be a green and feasible technology for facilitating zero chemical use and energy efficient MWW pre-treatment around the world.

Keywords: Electrocoagulation-Floatation; energy efficiency; heavy metal; low-cost; phosphate removal; total COD removal.

INTRODUCTION

Municipal wastewater (MWW) treatment technology application depends on efficient operation at low energy and chemical costs. Electrocoagulation (EC) can effectively remove total chemical oxygen demand (tCOD), total phosphate (TP), suspended solid (SS), turbidity, and heavy metal from a myriad of wastewater types with a variety of anode and cathode materials(Chen *et al.* 2004; Mollah *et al.* 2004; Elazzouzi *et al.* 2020). During EC-F electro-chemical reactions are triggered by electricity without adding any chemicals as dissolution of a sacrificial anode (e.g. iron (Fe) or aluminum (Al)) occurs as well as hydrogen gas production at the cathode.

In the last two decades, electrocoagulation-flotation (EC-F) was investigated with either synthetic MWW or with adjusted pH and conductivity, utilizing different current densities (CDs) and current supply mode, electrode gap and flow rate in batch mode (Merzouk *et al.* 2009; Que *et al.* 2021; Vasudevan and Lakshmi, 2011; Devlin *et al.* 2019; Ebba *et al.* 2021). Research on continuous EC-F systems in view of operational optimization is rarely found with MWW treatment (López-Guzmán *et al.* 2021). As such, this study aimed to optimize EC-F for a low-cost treatment of real MWW in a continuous operating mode. Different operational settings are investigated, focusing on increasing floatation, lower coagulant dose, electrode life, and energy efficiency to enhance reactor design efficiency (Parmentier *et al.* 2020; Moussa *et al.* 2016; Yang *et al.* 2020). Single pass operation or multiple recirculation at low operational CD, alternating pulsed current (APC) mode, and choice of cathode material are looked at in view of optimal pollutant removal and operational expenses.

MATERIALS AND METHODS

An EC-F set-up with an iron (Fe) sacrificial tubular metal anode was used to treat freshly collected MWW at a flow rate of 10L/h. Single pass EC-F treatment (1R) compared to two or three sequential EC-F passes (2R and 3R) and alternating pulsed current (APC) supply versus direct current (DC) supply mode and different cathode materials (copper (Cu) and stainless steel (SS))were considered as different operational experimental settings (Exp) for optimization at various CDs (i.e., 12, 40, 80, 120, and 160 A/m^2). Duplicate experiments were performed using various grab MWW samples from a MWW treatment plant (Kortrijk, Belgium).

Common physical-chemical parameters, i.e. pH, dissolved oxygen (DO), electrical conductivity (EC) and oxidation reduction potential (ORP) before and after each experiment was determined. Optimized performances were evaluated based on removal of tCOD, TP, total nitrogen (TN), Faraday efficiency (FE)(i.e., applied CD efficiency to dissolved metal from anode) and total operational expenses (OPEX) (i.e., sum of energy and electrode consumption) according to Parmentier *et al.* (2020).Sludge production were calculated from volume of sludge produced and measured total solid (TS) contains. TS and dry solid (DS) contains of EC-F sludge were measured following standard methods. Heavy metals analysis were also performed according to Lakho *et al.* (2020).

RESULTS AND DISCUSSION

Operation of Fe EC-F unit with 2R at 12 A/m^2 (experiment #2) resulted in optimized treatment performance, i.e., 78±11 % tCOD, 85±0.5 % TP and 32±22%TN removal at the second lowest total OPEX (i.e., 0.215±0.014 €/m^3) at a FE 1.08±0.32 (Figure 1 and Table 1). Maximum pollution removal and FE were obtained with 1R at 80A/m^2 (experiment #5) while the total OPEX was 3 times higher than with 2R at 12A/m^2 (experiment #2) (Figure 1 and Table 1).

Recirculation increases the contact time for electrochemical reactions and floc formation to increase floating, which is good for more pollutant removal at optimal OPEX with the studied EC-F unit at lower CD. The lowest sludge volume production were also obtained with 0.097±0.01 mg/L TS and 0.023% DS at experiment#2. The effluent quality were suitable with higher DO, and similar ORP in comparison to 1R 40 A/m^2 (experiment #4) and 1R 80 A/m^2 (experiment #5) (Table 1). Effluent obtained when operating with 2R Fe EC-F at CD 12 A/m^2 contained biodegradable matter and TN, suitable for subsequent simple biological treatment.

Interestingly with 3R at 12 A/m^2 (experiment #3), and 2R 120 A/m^2 (experiment #10) resulted in anodic passivation demonstrated lower FE at the final recirculation step (Table 1). Green flocs (GR) were visible in all experimental condition at different operational step up (experiment #2 to experiment #11) and CDs, except at (experiment #1) with 1R with at 12 A/m^2. Among single pass (1R) operation, using 40 A/m^2 (experiment #4) resulted in comparable removal performances and resulted in half the OPEX compared to using 80 A/m^2 (experiment #5). DC mode operation (experiment #5) was found suitable for higher pollutant removal efficiency and minimal operational cost differences in comparison to APC mode operation (experiment #7). Fe EC-F with SS cathode were found beneficial to remove heavy metals (93±9 % Zn, 70±15% Pb and Cu 49±10%).

Table 1. Quality of effluent of Fe EC-F and Faraday efficiency at different operational experimental settings(Exp).

Sample ID & Exp No.	EC-F Setup	CD A/m^2	pH	DO mg/L	EC µS/cm	ORP mv	FE
Influent Effluent	--		7.8±0.2	3.6±2.7	1165±361	21±99	--
1	1R	12	8±0.1	2.2±0.7	1279±272	-232±11	0.90±0.27
2	2R	12	8.1±0.1	4.4±0.8	1263±260	-223±23	1.08±0.32
3	3R	12	8.3±0.1	2.8±0.2	1237±250	-246±44	0.26±0.02
4	1R	40	8.3±0.0	1.6±0.1	990±252	-202±4	0.90±0.03
5	1R	80	9±0.23	2.4±0.6	1138±270	-266±21	0.91±0.04
6	2R	80	9.8±0.0	2.3±0.2	1426±43	-142±21	1.10±0.07
7	*APC	80	8.7±0.6	3.2±0.6	1243±11a	-265±26	0.88±0.05
8	**Cu	120	9.42±0.2	2.4±1.5	862±256	-495±97	0.82±0.12
9	1R	120	9.5±0.2	4.4±0.9	868±345	-262±45	0.89±0.15
10	2R	120	10.1±0.4	5.19±1.6	690±358	-311±72	0.48±0.28
11	1R	160	9.2±0.4	1.8±0.1	1355±334	-425±32	0.89±0.01

Note:* APC is alternated pulsed power supply mode, while all other tests are at continuous direct current mode; **Cu as cathode material instead of SS. Experimental results from different optimization settings of EC-F unit (n=11) using various CD and various operational parameter.

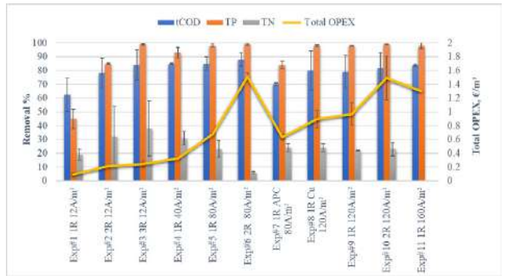

Figure 1. Removal of pollution and total OPEX of Fe EC-F for the treatment of MWW with several operational experimental settings (Exp) (n=11) at various Applied CD(A/m^2). Following as Exp #1 1R 12A/m^2, Exp#2 2R 12A/m^2, Exp #3 3R 12A/m^2, Exp #4 1R 40A/m^2, Exp #5 1R 80A/m^2, Exp #6 2R 80A/m^2, Exp #7 APC 80A/m^2, Exp #8 Cu 120A/m^2, Exp #9 1R 120A/m^2; Exp #10 2R 120A/m^2 and Exp #11 1R 160A/m^2. Exceptionally in Exp #7 APC current mode were used with single pass, and in Exp #8 copper (Cu) used as cathode material instead of DC current mode and stainless steel(SS) cathode with Fe anode respectively.

REFERENCES

Chen, G. 2004 Electrochemical technologies in wastewater treatment. *Separation and Purification Technology* 38(1), 11–41.
Devlin, T.R., Kowalski, M.S., Pagaduan, E., Zhang, X., Wei, V., Oleszkiewicz, J.A. 2019 Electrocoagulation of wastewater using aluminum, iron, and magnesium electrodes. *Journal of Hazardous Materials* 368,862–868.
Ebba, M., Asaithambi, P., Alemayehu, E. 2022 Development of electrocoagulation process for wastewater treatment: optimization by response surface methodology. *Heliyon*, *8*(5).
Elazzouzi, M., Haboubi, K., Elyoubi, M.S. 2017 Electrocoagulation flocculation as a low-cost process for pollutants removal from urban wastewater. *Chemical Engineering Research and Design* 117, 614–626.
Parmentier, D., Manhaeghe, D., Baccini, L., van Meirhaeghe, R., Rousseau, D.P.L., van Hulle, S.W.H. 2020 A new reactor design for harvesting algae through electrocoagulation-flotation in a continuous mode. *Algal Research* 47(101828), 1-7.
Lakho, F.H., Le, H.Q., van Kerkhove, F., Igodt, W., Depuydt, V., Desloover, J., Rousseau, D.P.L., van Hulle, S.W.H. 2020 Water treatment and re-use at temporary events using a mobile constructed wetland and drinking water production system. *Science of the Total Environment* 737(139630),1-9.
Moussa, D. T., El-Naas, M. H., Nasser, M., Al-Marri, M. J. 2017 A comprehensive review of electrocoagulation for water treatment: Potentials and challenges. *Journal of Environmental Management*,*186*, 24–41.
Merzouk, B., Gourich, B., Sekki, A., Madani, K., Chibane, M. 2009 Removal turbidity and separation of heavy metals using electrocoagulation-electroflotation technique. A case study. *Journal of Hazardous Materials*, *164*(1), 215–222.
Que, N. H., Kawamura, Y., Watari, T., Takimoto, Y., Yamaguchi, T., Suematsu, H., Niihara, K., Wiff, J. P., Nakayama, T. 2021 Nanosecond pulse used to enhance the electrocoagulation of municipal wastewater treatment with low specific energy consumption. *Environmental Technology (United Kingdom)*, *42*(14), 2154–2162.
Vasudevan, S., Lakshmi, J. 2011 Effects of alternating and direct current in electrocoagulation process on the removal of cadmium from water - A novel approach. *Separation and Purification Technology*, *80*(3), 643–651.
López-Guzmán, M., Flores-Hidalgo, M. A., & Reynoso-Cuevas, L. 2021 Electrocoagulation process: An approach to continuous processes, reactors design, pharmaceuticals removal, and hybrid systems—a review. *Processes*, 9(10),1831.
Mollah, M. Y. A., Morkovsky, P., Gomes, J. A. G., Kesmez, M., Parga, J., Cocke, D. L. 2004. Fundamentals, present and future perspectives of electrocoagulation. *Journal of Hazardous Materials*, *114*(1–3), 199–210.
Yang, J., Liu, F., Bu, Y., Wei, N., Liu, S., Chang, J., Chen, X., Zhang, W., Zhou, R., Zhang, C. 2020. Cd removal by direct and positive single pulse current electrocoagulation: Operating conditions and energy consumption. *Environmental Technology and Innovation*, *20*.

On-site Regeneration of A modified Activated Carbon by Ozone

Chihpin Huang and Shanshan Chou

Environmental Technology and Smart System Research Center
National Yang Ming Chiao Tung University
Hsinchu, Taiwan
huang@nctu.edu.tw

In recent years, due to stricter environmental regulations, the global demand for granular activated carbon (GAC) has increased. Therefore, the reuse of GAC has become an important effective method to save cost. At present, thermal regeneration of saturated activated carbon is the only large-scale and commercialized way of reusing activated carbon. However, it has several drawbacks such as high energy consumption and large space, besides, the adsorption capacity of GAC drops rapidly after thermal regeneration because of the serious carbon loss and destroyed GAC structure. Therefore, this study evaluates the regeneration efficiency of a polymetallic metal oxide modified activated carbon (mGAC) by ozone. The surface of mGAC is loaded with noble metal ruthenium (Ru), Ru in mGAC is turned into higher oxidation states after oxidized by ozone. The high valance Ru compound can act as a strong oxidant to oxidize organic matter, and it can also be used as a catalyst for catalyzing ozone to generate hydroxyl radicals.

In this study, firstly, 1 gram of mGAC is in equilibrium at benzoic acid solution. Then comparing the regeneration efficiency (RE) under different parameters. The results show that the optimal RE condition is at pH 9 or above, 80°C, and regeneration time of 4 hr. After getting the optimal RE parameter, we compare RE with GAC after multi-cycle batch adsorption/regeneration experiments. Secondly, mGAC stability is evaluated. Conducting mGAC adsorption in continuous flow mode and observing the changes in adsorbed amount and surface characteristics after several adsorption/regeneration cycles. The results show that after 4 cycles, BET specific surface area drops from 1060 to 698 m^2/g. Accumulated adsorbed amount decreases a little at cycle 2 to 4. it is speculated that some of the noble metal Ru active sites, which are not shielded by carbon deposition, still remain their high valence state to mineralize part of the adsorbate as well as promote ozone to generate hydroxyl radicals.

The results show that mGAC by ozone regeneration can maintain the adsorption capacity after a prolonged period, and has a strong ability to remove adsorbate, indicating that the application of mGAC in the industrial wastewater treatment can effectively reduce the cost of replacing activated carbon and achieve the goal of circular economy.

$RE = \frac{q_{reg}}{q_{fresh}} \times 100\ \%$, in which q_{reg} and q_{fresh} means the adsorption capacity of regenerated mGAC and fresh mGAC, respectively.

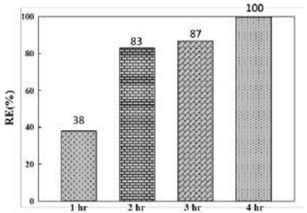

Fig. 1. Effect of regeneration time with ozone on RE of mGAC at pH 9 and 80°C.

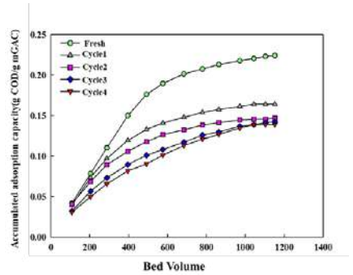

Fig. 2. Changes in accumulated adsorption capacity of mGAC in continuous flow mode with 12 BV/h after several adsorption/regeneration cycles. Regeneration condition is pH 9, 80°C and 4 hrs with 0.024 mg/L of ozone.

Flotation and Fenton Process Pilot Technology for the treatment of Real Olive Mill Waste Water

I. Oliveira-Inocêncio*, M. Silva*, A. G. Nogueira*, S. Castro-Silva*

* ADVENTECH – Advanced Environmental Technologies, Lda. Rua de Fundões 151, 3700-121 São João da Madeira, Aveiro, Portugal
(E-mail: *ines.inocencio@adventech.pt*; id*@adventech.pt)**

Abstract
Waste water from an olive pomace extractor factory, equivalent to 3- stage centrifugal OMW, was treated using flotation and Fenton Process. Influence of flocculant, coagulant and flocculant dosage and pH was assessed for the flotation unit. Influence of Fe:H2O2 ratio, reaction time, pH control and iron reagent was evaluated for Fenton process. The best flotation results were obtained with 1.2 L/m3 of PAX18 and 33 L/m3 of AS01. In the Fenton, pH control and reaction time do not affect COD removal significantly. Best results were obtained for 8:16 ratio, with FeSO4.7H2O during one hour, with 58 % COD removal and 89 % TPh removal. Further tests with the Fenton pilot will be performed aiming the hydrogen production through steam reforming after membrane distillation.

Keywords (maximum 6 in alphabetical order)
Fenton Process, Flotation, Olive-mill waste water, Pilot Technology

INTRODUCTION

Olive oil industry is a significant sector at a worldwide level. About 2.7 million tons of olive oil were produced in the 2022/2023 campaign, of which 55 % in the EU (Council, 2022). About 0.5 to 1.68 cubic meters of waste water are produced for each ton of olives processed (Amor, 2019, Paraskeva, 2006). These effluents contain heavy loads of COD, BOD, TSS and different phenolic compounds, along with high EC, acidic pH and dark brown colour (Amor, 2019, Papaphilippou, 2013).

The commonly investigated pre-treatment processes for these WW are advanced oxidation processes (AOP) and physical-chemical treatments.

The aim of this work is to study the combined process, in pilot units, of flotation and Fenton Process, using real OMW from an olive oil pomace extractor factory in the Center of Portugal. The influence of coagulant and flocculant concentration was assessed in flotation, and the influence of the Fe:H_2O_2 ratio in the Fenton Process. The effluent produced after Fenton will be used in a membrane distillation and reforming unit at pilot scale in future work.

MATERIALS AND METHODS

Tests were performed in 600 mL beacons using a jar-test. For the pilot scale, two pilot units were used: the flotation unit for the treatment of 1 m^3/h and the Fenton process unit to treat 400 L/h in semi-discontinuous mode, used sequentially.

Flotation was performed with coagulant Kemira PAX18 and AS01 flocculant, prepared at 2 g/L, from SNF. Fenton process was performed with ferrous sulfate ($FeSO_4.7H_2O$), richness higher than 87.6 %, from Sociedade Portuense de Drogas, or $FeCl_3$, and hydrogen peroxide 49.5 %. pH adjustment was made with sulfuric acid 30 % and sodium hydroxide 48-50 %, all 4 from Brenntag.

Trials were executed between April 2022 and January 2023. For the Fenton trials, the inlet was the outlet of the flotation unit.

RESULTS AND DISCUSSION

Coagulation/Flocculation – Flotation

The best results were obtained, at laboratory scale, with anionic flocculant, showing a more consistent COD removal for lesser amounts of flocculant. It stayed between 44 and 51 %.

In the pilot unit, flotation efficiency varied significantly along the trials, showing lower removals than the ones obtained at laboratory scale. The best results showed COD removals of about 30 %, at the waste water's initial pH, with AS01. pH adjustment showed no significant correlation with treatment efficiency, as did the variability of the waste water's initial COD.

The increase of PAX18 dosage seemed to have a positive impact in COD removal, with the highest removals of above 28 % for 1 and 1.2 L/m^3. AS01 concentration seems to be optimum around 30 L/m^3, decreasing efficiency for lower and higher concentrations.

Fenton Process

The efficiency of Fenton was assessed essentially at laboratory scale. The variable with highest influence in COD removal was the Fe:H_2O_2 ratio. The increase in reaction time for 2 hours did not have a significant impact in COD or TPh removals, with some efficiency decrease. pH control in the acid stage did not show relevant changes. The exchange of reagent to $FeCl_3$ showed lesser COD removal, but slightly higher TPh removals.

The best results were obtained for 8:16 g_{Fe}/g_{H2O2}, with COD removal of 58 % and TPh removal of 89 %. Further pilot tests will be performed in the future.

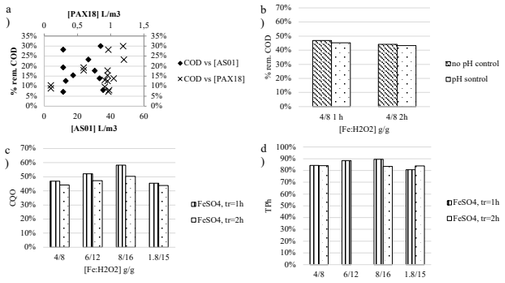

Figure 1. Flotation: a) COD removal related with coagulant and flocculant concentration; Fenton: b) COD removal with pH control, c) COD removal with different Fe:H2O2 ratios and reaction times and d) TPh removal with different Fe:H2O2 ratios and reaction times.

REFERENCES

Council, I. O. O. (2022) Huiles D'Olives – Olive Oils, [online] https://www.internationaloliveoil.org/wp-content/uploads/2022/12/HO-W901-13-12-2022-P.pdf (Accessed January 30th, 2023)

Amor, C;, Marchão, L.; Lucas, M. S.; Peres, J. A. (2019); Application of advanced oxidation processes for the treatment of recalcitrant agro-industrial wastewater: a review. *Water*, **11**, 205-236.

Paraskeva, P.; Diamadopolous, E. (2006) Technologies for olive mill wastewater (OMW) treatment: a review. *Journal of Chemical Technology and Biotechnology* **81**, 1475-1485.

Papaphilippou, P. C.; Yiannapas, C.; Politi, M.; Daskalaki, V. M.; Michael, C.; Kalogerakis, N.; Mantzavinos, D.; Fatta-Kassinos, D. (2013) Sequential Coagulation/flocculation, Solvent Extraction and Photo-Fenton oxidation for the Valorization and Treatment of Olive Mill Effluent. *Chemical Engineering Journal* **224**, 82-88.

ACKNOWLEDGMENTS: The authors are thankful to European Regional Development Funds (ERDF) through COMPETE2020 for the financial support under the VERPRAZ project (NORTE-01-0247-FEDER-039789).

Isolation of acid tolerant bacteria capable of metal adsorption from acid mine drainage without neutralization

Sohei Iwama*, Chikara Takano**, Kazunori Nakashima**, Hideki Aoyagi***, Satoru Kawasaki**

* Graduate School of Engineering, Hokkaido University, Sapporo, Hokkaido 060-8628, Japan.
(E-mail: k1445@eis.hokudai.ac.jp)
** Faculty of Engineering, Hokkaido University, Sapporo, Hokkaido 060-8628, Japan.
(E-mail: takano.chikara@eng.hokudai.ac.jp, k.naka@eng.hokudai.ac.jp, kawasaki@geo-er.eng.hokudai.ac.jp)
*** Faculty of Life and Environmental Sciences, University of Tsukuba, Tsukuba, Ibaraki 305-8572, Japan.
(E-mail: aoyagi.hideki.ge@u.tsukuba.ac.jp)

Abstract
Acid mine drainage (AMD) is serious problem in mining industry because of generating waste harmful water. Once AMD is generated, it will discharge even mining site is closed. Neutralization using slaked lime is generally applied to deal with AMD. It generates heavy metal sludge which should be disposed as industrial waste. Metal removal before neutralization is efficient to decrease the industrial waste. Thus, we proposed a novel process using bacteria which can tolerate and adsorb metals under AMD conditions. In this study, acid and metal tolerant bacteria were isolated from closed mining site and neutral environmental soil. Isolated strain *Paenarthrobacter* sp. removed 42% arsenic and 8.7% iron from the AMD in Horobetsu sulphur mine (pH 1.95, initial concentrations were 5.75 and 301 [mg/L], respectively). Although further research is required to improve removal efficiency, this study potentially contribute to achieve sustainable AMD treatment.

Keywords
Acid mine drainage; acid tolerant bacteria; biosorption

INTRODUCTION

Acid mine drainage (AMD) is generated in not only operating mining sites but also mines closed decades ago. Due to the abundant heavy metals, AMD discarded into rivers is harmful for ecosystems and people who use the river water. Currently, neutralization and precipitation treatment with addition of neutralizer like slaked lime is applied to remove heavy metals from AMD before discarding. With this process, mixture of iron, arsenic, and calcium is generated as waste sludge. It should be treated as industrial waste. Considering the limitation of industrial waste deposit, it is desired to reduce amount of generated waste from both an environmental and economical point of views. Recently, passive treatment and biosorption are studied as an alternative technology to remove metals. However, passive treatment also generates metal-rich residues ([1]Marouen *et al.* 2019) and most of current biosorption research are mainly conducted under neutral pH conditions. Considering this situation, we devised the concept of novel AMD treatment process using acid tolerant bacteria (**Fig. 1**). In this process, bacterial biosorption is performed under acidic conditions before neutralization to reduce sludge generation. In this study, we attempted to obtain bacteria that can selectively adsorb metals under acidic conditions as an environmentally friendly metal adsorbent.

MATERIALS AND METHODS

Material

Environmental water and soil for bacterial isolation were sampled from some mining sites and Hokkaido University Sapporo campus. AMD was collected from several Japanese mining sites. Metal concentrations was quantified using inductively coupled plasma atomic emission spectroscopy (ICPE-9820, Shimazu, Kyoto, Japan, ICP-AES) and standard curve prepared using ICP standard solution IV (Merck, Germany) and Arsenic standard solution (Fujifilm Wako pure chemical Co. Ltd., Japan). Specialized cellulose film (SCF, [2]Aoyagi *et al*, 2022) and non-woven fabric were purchased from Futamura Chemical Co. Ltd. (Japan). Nutrient Broth (Becton, Dickinson and Company, U.S.A.) and R2A medium (Fujifilm Wako pure chemical) were applied to bacterial isolating cultivation.

Isolation of acid and metal tolerant bacteria

SCF was placed on non-woven fabric which was soaked with mixture (1:1) of AMD and NB medium (**Fig. 2**). Environmental samples (70 µL) were inoculated on the surface of SCF and incubated (30°C, 19 days). To obtain pure bacterial strain, formed colonies were isolated and streaked on agar plate (AP) of R2A medium. After overnight incubation, formed colonies were steaked on fresh AP again. This purification process was repeated 5 times. Isolated strains were identified using 16S rRNA gene sequences and evaluated growth ability under neutral pH conditions.

Evaluation of metal biosorption ability

Isolated bacterial strain was cultured (30°C, 160 rpm) in 50 mL R2A medium until reached to stationary phase. Then, bacterial cell was harvested by centrifugation and suspended into filtered 50 mL AMD of Horobetsu mining site (pH 1.95). Biosorption treatment was conducted for 3 h (30°C,160 rpm) and bacterial cell was removed. One mL of initial and treated solutions were collected and 25 times diluted with 1% nitric acid. Metal adsorption abilities of each strain were evaluated based on metal concentrations quantified using ICP-AES.

RESULTS AND DISCUSSION

Isolation of acid and metal tolerant bacteria

Three acid and metal tolerant bacterial strains were isolated and identified as *Paenarthrobacter* sp. and *Bacillus* sp. (**Table 1**). All strains were classified as biosafety level 1. These bacteria can be cultivated under neutral pH conditions and survived under acidic metal existing conditions. This means that acidic wastewater is not generated by biomass production. According to these results, isolated bacteria are potentially available for metal biosorption process under acidic conditions.

Evaluation of metal biosorption ability

All isolated strains adsorbed arsenic and iron from AMD of Horobetsu mining site (**Fig. 3**) The strain H1 showed the highest adsorption ratio of arsenic 40% and iron 8.77%, respectively (Initial concentrations were 5.83 [mg/L] and 295 [mg/L], respectively, pH 1.95). Comparing the metal adsorption ability [mg/g-dry cell], the strain H2 showed the highest ability that arsenic 1.95 [mg/g-dry cell] and iron 14.0 [mg/g-dry cell] (**Table 2**). These results indicate that arsenic and iron in AMD can be adsorbed by acid tolerant bacteria under strongly acidic conditions. In Japan, arsenic concentration standard of discharged AMD is generally 1 [mg/L]. Although adsorption efficiency was not satisfied the standard in this study, it was succeeded to remove arsenic from AMD without generating waste sludge.

Conclusion

In this study, acid tolerant bacteria were isolated which can adsorb arsenic and iron from AMD under strongly acidic conditions. With those bacteria, it was achieved to remove metals from AMD without generating waste sludge. This is the first step to establish environmentally friendly AMD treatment process.

Table 1. Bacterial strains and their growth abilities under neutral pH condition.

Strain number	Strain	Biomass [g/L]
H1	*Paenarthrobacter* sp.	1.04
H2	*Paenarthrobacter* sp.	0.596
H3	*Bacillus* sp.	0.706

Table2. Metal adsorption abilities of isolated bacterial strains [mg/g-dry cell]

Strain number	Arsenic	Iron
H1	1.43	10.5
H2	1.95	14.0
H3	1.34	13.3

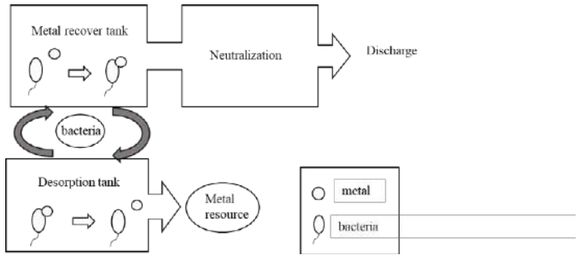

Figure 1. Novel AMD treatment process using acid tolerant bacteria.

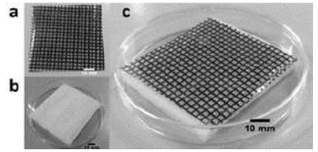

Figure 2. Specialized cellulose film method.
a: Specialized cellulose film b: Non-woven fabric c: Combined

Figure 3. Horobetsu mine site. (Geospatial Information Authority of Japan)

Reference
[1] Jouini, M., Rakotonimaro, T., Neculita, C., Genty, T., Benzaazoua, M., 2019 Prediction of the environmental behavior of residues from the passive treatment of acid mine drainage. Applied Geochemistry 110, 104421.
[2] Aoyagi, H., Saitoh, R., Murayama, K., 2022 Development of a device for cultivation and isolation of microbes using a specialized cellulose film. Journal of Microbiological Methods 195, 106450.

Characterization of iron-rich particles assisted anammox granules: Extracellular Polymeric Substance (EPS) tell the story

Sohee Jeong[1], Haejun Jeon[1], Schwa Bae[1], Victory Fiifi Dsane[2], Younggyun Choi[1,†]

[1]Dept. Env. Eng., Chungnam National University, 99 Daehak-ro, Yuseong-gu, Daejeon, Republic of Korea
[2]BKT Co. Ltd, Sinseong-dong, Daejeon, Republic of Korea
(E-mail: *youngchoi@cnu.ac.kr*†)

Abstract
Iron-rich carrier particles can be ionized into Fe^{2+} and Fe^{3+} which improves the activity and aggregation of anammox bacteria. Three samples from a carrier assisted granulation reactor with size groups including Flocs, FL (0 – 300μm), Small Granules, SG (300 – 500μm) and Large Granules, LG(500 – 1000μm) were used in this study. It was observed that as the granule size increased, the iron rich carrier content increased, and their active crystals improved the microbial cell density. Specific anammox activity (SAA) was 34.63 ± 5.02, 55.29 ± 5.14, and 63.81 ± 7.50 mg-N/g-VSS/d for FL, SG and LG, respectively. In addition, in heme c content of LG was 31.5% higher than SG and 62.9% higher than FL. An in-depth study into the extracellular polymeric substances (EPS) showed that the secretion intensity of essential proteins followed the order of FL<SG<LG in LB-EPS and FL>SG>LG in TBEPS. Functional group analysis confirmed that the hydrophobic C-N and N-H stretching vibration band had almost 3.5 times higher transmittance intensity in LG than the other sizes and the corresponding ratio of α-helix/(β sheet + random coil) in secondary derivative proteins analysis showed tightness in the protein structures of FL. The relative abundance of Brocadia Sinica increased from 0% in FL to a high of 20.46% in LG. This study aims to communicate the essence of in-depth EPS analysis beyond the usual EPS yield and major contents of proteins (PN) and polysaccharides (PS) analysis..

Keywords
Anammox, agglomeration, EPS, granule size, hydrophobicity, hydrophilicity

INTRODUCTION

In this study, a detailed characterization of three distinct sizes (0~300μm, 300~500μm, 500~1000μm) of iron-rich carrier assisted granules was carried out focusing on nitrogen removal activity, Heme c production, sectional and total EPS secretion and its importance in maintaining the granules stability and performance. Specific microbial species and enzyme response for each granule size is also looked at to help identify the overall optimal granule size and performance in the anammox process when iron rich particles are employed as carrier.

MATERIALS AND METHODS

The three distinct anammox sludge sizes used in this study were taken from a 2.3 L lab-scale sequencing batch reactor (SBR) that has been operated with the addition of 0.5 g/L iron-rich carrier particles (45-75μm) to enhance granulation. The nitrogen loading rate (NLR) of the SBR reactor was 0.96 gN/L/d. The three kinds of EPS (S-EPS, LB-EPS and TB-EPS) were extracted using the modified heat extraction method (Wang et al. 2020c). To measure the heme c contents of each granule size, the uniformly homogenized samples were centrifuged at 12,000 rpm for 10 min. The supernatants were collected and used in the measurement of heme c concentration according to the methods stipulated in Ma et al. (2019) and using a millimolar extinction coefficient of 23.97. Extraction of DNA was carried out using a PowerSoil DNA kit (Mobio Laboratories Inc., USA) following keenly the manufacturers protocol. For each granule size, 2 mL of settled sludge sample was collected for the extraction of DNA.

RESULTS AND DISCUSSION

(Size effect of Anammox activity) In the anammox study, microbial activity is measured through the specific substrate consumption of a unit cell per day as well as through the production of the heme variant (heme c) that remains bounded to the holoprotein and cytochrome c to promote multiple electron transfer reactions (Jetten et al. 2009). In order to accurately characterize the different granule sizes, the variation in their activity was measured and presented together with the microscopic representative granules of each size in Figure 1. It can be seen that as the granule size increases, the core encompassed iron-rich carrier contents increase and hence provides the attraction force to enable additional subunits adhesion and thereby increase the granule's size.

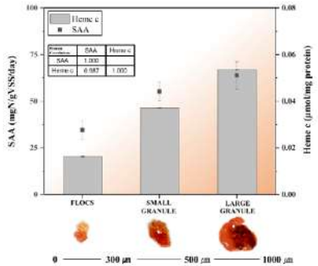

Figure 1. Anammox Activity and heme c production for the three distinct size granules

(Anammox Extracellular Polymeric Substances (EPS)) In Figure 2, the extracted EPS for all three anammox sizes is presented in the sectional and total form. For all sizes, the PN contents didn't not show any significant differences when observed as individual EPS types. Therefore, the total PN showed an infinitesimal difference between SG and LG and just slightly higher in FL.

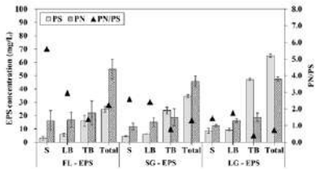

Figure 2. EPS and PN/PS ratio for FL, SG and LG

(Anammox size and microbial consortia) The relative abundance of the three distinct microbial sizes at the phylum and class level is shown in Figure 3. From the Figure 3, the general decrease in microbial diversity as iron-rich particles and granule size increase is emphasized through the class level obervation.

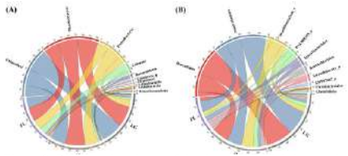

Figure 3. Relative abundance of the three microbial sizes at the Phylum (A) and Class (B) level

Acknowledgemnet: This research was funded by the National Research Foundation (NRF) of Korea (project number: RS-2023-00208398)

Granulation characteristics of the high saline anammox bacteria

Sohee Jeong[1], Jongeun Park[1], Yonghun Cho[1], Victory Fiifi Dsane[2], Younggyun Choi[1,†]

[1]Dept. Env. Eng., Chungnam National University, 99 Daehak-ro, Yuseong-gu, Daejeon, Republic of Korea
[2]BKT Co. Ltd, Sinseong-dong, Daejeon, Republic of Korea
(E-mail: *youngchoi@cnu.ac.kr*†)

Abstract
The growing interest in the anaerobic ammonium oxidizing (AMX) process in treating high nitrogen containing wastewaters and a comprehensive study into the granulation mechanism of these bacteria under diverse environmental conditions over the years have been unequal. To this effect, the distinctive differences in saline adapted AMX (S_AMX) and non-saline adapted AMX (NS_AMX) granules are presented in this study. It was observed that substrate utilisation profiles, granule formation mechanism, and pace towards granulation differed marginally for the two adaptation conditions. The different microbial dominant aggregation types aided in splitting the 471 days operated lab-scale SBRs into three distinct phases. In both reactors, phase III (granules dominant phase) showed the highest average nitrogen removal efficiency of 87.9% ± 4.8% and 85.6% ± 3.6% for the S_AMX and NS_AMX processes, respectively. It was observed that granules of the S_AMX reactor were mostly loosely and less condensed aggregates of smaller sub-units and flocs while those of the NS_AMX reactor were compact agglomerates. The ionic gradient in saline enrichment led to an increased activity of the Na + /K + – ATPase, hence enriched granules produced higher cellular adenosine triphosphate molecules which finally improved the granules ac-tive biomass ratio by 32.96%. Microbial community showed that about three to four major known AMX species made up the granules consortia in both reactors.
Keywords
Anammox, enzyme analysis, EPS, floc, granule

INTRODUCTION

In this study, we tried to provide an in-depth differentiation between the granulation profiles of the S_AMX and NS_AMX granules through adapting physiological and morphological analysis techniques. It focuses and highlights the differences in the general granule health in terms of microbial energy production and maximum specific activity. Also, the disparities in settleability and granules floatation mechanisms as well as the expression of major proteins and functional genes are summarized and discussed in detail. Practically, understanding and realizing these differences can help wastewater treatment plants operators identify the occurrence of unexpected nutrient conditions that may gradually lead to domi- nance shift if not curtailed in time.

MATERIALS AND METHODS

Two water jacketed sequencing batch reactors (SBR) with 2.3 L and 1.8 L operational and effective volume, respectively were used for the granulation profile determination. The reactors were installed side by side and labelled S_AMX and NS_AMX for saline adapted and non-saline adapted AMX process, respectively. The bioreactor operation was similar for both reactors except for the gradual NaCl injection into the S_AMX reactor. The reactors were operated with 4 cycles per day and the treatment capacity was fixed at 2 L/day. The hydraulic retention time (HRT) was there- fore 21.6 hr and the average operational temperature (35 ±1.1°C) and pH (7.75 ±0.8) were maintained with a thermostatic water bath and intermittent CO_2 supplied when the reactors' pH surpasses 8.1.

RESULTS AND DISCUSSION

(**Substrate utilization & removal**) Table 1 summarizes in details the characteristics of the different phases in both reactors. Salinity in the form of NaCl was introduced from a minimum of 0 to 10 g/L into the S_AMX re- actor in phase I. After the initial stepwise increase of saline levels, a longer duration of 86 days was maintained for the 5 g/L NaCl injection in phase I on account of reports that saline inhibition of freshwater AMX species is mostly experienced at this salt concentration.

Table 1. Average performance characteristics of the AMX reactors at the different enrichment phases

Phase	S_AMX					NS_AMX				
	Period (day)	NLR (kg-N/m³/day)	SNLR (kg-N/kg-VSS/day)	NRE (%)	Rs:Rp 0.26:1.32*	Period (days)	NLR (kg-N/m³/day)	SNLR (kg-N/kg-VSS/day)	NRE (%)	Rs:Rp 0.26:1.32*
I	0 ~ 273	0.32 ± 0.07	0.123 ± 0.028	71.4 ± 9.2	0.42: 1.04	0 ~ 201	0.46 ± 0.11	0.163 ± 0.037	77.3 ± 8.7	0.35: 1.04
II	274 ~ 375	0.23 ± 0.01	0.091 ± 0.004	66.3 ± 12.8	0.50: 1.01	202 ~ 256	0.68 ± 0.01	0.182 ± 0.001	84.4 ± 10.0	0.21: 1.02
III	376 ~ 471	0.32 ± 0.03	0.159 ± 0.013	87.9 ± 4.8	0.27: 1.13	257 ~ 471	1.16 ± 0.30	0.339 ± 0.088	85.6 ± 3.6	0.24: 1.11

* Theoretical values calculated from Eq. (1); Rs is the molar ratio of NO_3^- – N depleted to NH_4^+ – N depleted, Rp is the molar ratio of NO_3^- – N produced to NH_4^+ – N consumed.

(**Granule morphology and characteristics**) In order to comprehend the apparent differences in the granules formed in the saline and non-saline enriched environments, it is important to consider comprehensively the mi- nor but essential physiological and morphological factors and characteristics of the two distinct granules and their granulation techniques. Fig. 1 shows the physical appearance of the S_AMX and NS_AMX granules and the annotated granulation mechanism for the two different AMX adaptation conditions.

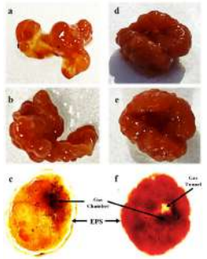

Figure 1. observation of the S_AMX (a-c) and NS_AMX (d-f) granules

(**Community and functional genes expressions**) In a typical AMX process, an analyses of the major microbial proteins and functional genes expressions enhances the understanding of the metabolic activities and correlates this to the performance of the granules in a specific enrichment environment. Several important proteins and enzymatic functional genes based on the distinct expressions between the two differently enriched environments are summarised as a heat map in Fig. 2. The dominant AMX species in all three samples (Inoculum, S_AMX and NS_AMX) expressed these proteins and functional genes in accordance to their abundance in the extracted DNA samples. A close observation of Fig. 2 also shows that the ATPase genes responsible for the intracellular transportation of Na+ and K+ were expressed distinctively different for all samples.

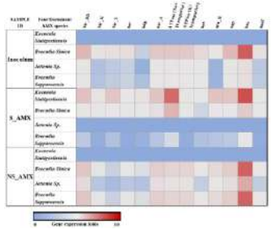

Figure 2. Heat-map of the gene expressions of selected major proteins and enzymes

Acknowledgemnet: This research was funded by the National Research Foundation (NRF) of Korea (project number: RS-2023-00208398)

Algal-Bacterial Biofilms to Purify Wastewater, Reduce Power Consumption, and Minimize Carbon footprint.

D.B. Johnson*

* Algaewheel Inc, 180 Tower Rd Cary NC, 27512
(E-mail: *dan.johnson@algaewheel.com)**

Abstract

Hybrid algal-bacterial wastewater systems are effective natural solutions to decentralized wastewater purification, reducing electrical usage by 75% and greenhouse gas emissions by 87%. Algaewheel functions similarly to a river in a box. The rotating algal contactors combine the synergistic performance benefits of algae, and bacterial biofilm to oxidize COD and ammonia while directly assimilating carbon dioxide, nitrogen, and phosphorus. Algaewheel can meet permit limits as stringent as 5 $CBOD_5$ and <1 NH_3-N. The low energy requirement makes the system favorable for rural decentralized, or developing areas where it is impractical to have complicated systems or pump waste. Algaewheel has few mechanical moving parts, reducing maintenance, and making it easier to operate than activated sludge processes. Algaewheel treatment results in a large reduction of CO_2 emissions, less complexity, and high-quality effluent. This presentation will review existing facility data and processes in the US, Mexico, and MENA region.

Keywords (maximum 6 in alphabetical order)
Algae, Wastewater, Hybrid biofilms, Sustainable wastewater, Water reuse, Rotating Algal Contactors

Analyzing the impact of salt concentration on the activity of enriched N-damo bacteria biomass

R. Fariñas, F. Omil, J.M.Garrido*

* CRETUS. Department of Chemical Engineering, Universidade de Santiago de Compostela, 15782 Santiago de Compostela, Galicia, Spain

(E-mail: raquel.farinas@usc.es ;francisco.omil@usc.es ; *juanmanuel.garrido@usc.es*)

Abstract
N-damo bacteria are microorganisms that could be used in innovative processes for the removal of dissolved methane and total nitrogen present in the effluents of anaerobic bioreactors treating municipal wastewater. Sewage treatment plants in coastal areas suffer seawater intrusion. There are few studies on the possible inhibitory impact of N-damo bacteria under saline conditions, which should be evaluated for practical application at industrial scale. In this study, batch tests have been carried out to evaluate the impact of salt concentration on the activity of N-damo bacteria. The preliminary results of this study indicate that salinity may have a profound impact on the activity of these microorganisms.

Keywords (maximum 6 in alphabetical order)
Anaerobic methane oxidation; batch assays; N-damo bacteria; nitrite removal; salinity.

INTRODUCTION

The presence of dissolved methane and nitrogen compounds in liquid effluents from anaerobic bioreactors in water treatment plants is an issue, currently being studied to reduce greenhouse gas emissions [1]. In order to diminish the negative impact of anaerobic treatment, the use of N-damo microorganisms could be an alternative [1]. These microorganisms, discovered in 2010, are capable of simultaneously removing nitrite and dissolved methane under anaerobic conditions [2]. They are characterised by their low activity and slow doubling times, which makes their practical application difficult [2]. Previous studies, in which the role of NaCl on N-damo biomass was determined by He et al. [3], found that increased salinity had a negative impact on N-damo activity. However, biomass with a very low N-damo specific activity was used, less than 2-3 mg $N{\cdot}g\text{-}VSS^{-1}{\cdot}d^{-1}$, which is significantly lower than that found in our laboratories, of around 95 mg $N{\cdot}g\text{-}VSS^{-1}{\cdot}d^{-1}$[1]. Therefore, it is important to corroborate the impact of salinity with biomass of greater specific activity, using not only NaCl but other ions. The aim of this study is to analyse the effect of salt concentration on N-damo biomass with high specific activity.

MATERIALS AND METHODS

The assays were carried out in 500 mL Pyrex bottles with screw cap and teflon septum, with biomass from an enriched N-damo MBR bioreactor [1]. For the preparation of the necessary solutions, 120 mL glass bottles with metal septum and washer were used. The bottles were filled with the base medium described by Allegue et al. [1] and the following elements: $NaHCO_3$ (100 mg L^{-1}) acting as a buffer element, $Na_2S_2O_3$ 0,4 mM to maintain reducing conditions, 10 mg L^{-1} NO_2^--N as a nitrogen source and different concentrations of salt solution prepared from a stock of 33 g L^{-1} NaCl in base medium (5%, 20% y 50% v/v). In the gas phase, 20 mL of CH_4 and CO_2 are added under overpressure from a gas mix 90% CH_4 10% CO_2. This volume of CH_4 establishes a concentration that is in excess which allows the limiting reagent to be nitrite.
A stream of argon was passed through the solutions for 10 min to desorb oxygen and maintain anoxic conditions. The different solutions were added to the assays through the septum via syringes. The assays were inoculated with a concentration of 0.077 g L^{-1} N-damo biomass and placed on a thermostatic shaker (125 rpm) at 28° C in the dark. Liquid and gas phase sampling were performed at time zero and periodically every 24 h until the end of the assays. At the time of sampling, the same extracted volume of inert gas Argon is injected to maintain the pressure inside the bottle. Measurements of pH, conductivity, nitrite concentration and biogas composition are carried out.

RESULTS AND DISCUSSION

The inoculum comes from a enriched N-damo culture grown in a membrane bioreactor (MBR) as described by Allegue et al. [1]. The concentration of volatile suspended solids in the mixing liquor was 4.85 g MLVSS L^{-1}. The system operated at 29º C with a permeate flow rate of 5.54 ± 0.50 L d^{-1}, maintaining a hydraulic retention time of 1.21 ± 0.09 d. The nitrite load in the feed ranges between 112 and 123 mg NO_2^--N L^{-1} reaching average nitrite concentrations at the permeate of 0.05 with minimum values of 0 and maximum values of 0.21 mg NO_2^--N L^{-1}.
During the experimental period the nitrite removal rate of the MBR was 95.8 ± 8 mg NO_2^--N L^{-1} d^{-1}, achieving a maximum nitrite removal rate of 117 mg NO_2^--N L^{-1} d^{-1}, similar to the maximum values reported previously by Allegue et al. [1]. The apparent specific activity resulting from the N-damo was 20 ± 1.8 mg NO_2^--N g^{-1} MLVSS d^{-1}, lower than those of 95.5 mg NO_2^--N g^{-1} MLVSS d^{-1} reported by Allegue et al. [1]. This lower specific activity rates of the N-damo bacteria could be explained by the increase of the biomass concentration accumulated in the MBR.
Figure 1 shows the preliminary results obtained in the first activity experiments, and showed a remarkable stimulation in N-damo activity using the lowest salt concentration (5% or 1.65 $g{\cdot}L^{-1}$ NaCl) with respect to the test in in which salt was not added. The 5% salt test consumed almost all the nitrite in 96 h, with specific activity values at this adaptation stage of 23.4 mg NO_2^--N g^{-1} MLVSS d^{-1}. At 168 h a second pulse of 20 mg NO_2^--N L^{-1} was added, increasing the activity to 51.7 mg NO_2^--N g^{-1} MLVSS d^{-1}. On the other hand, the activity measured with intermediate salt concentration (20% or 6.6 $g{\cdot}L^{-1}$ NaCl) was similar to that without any salt addition (Biotic 0%). Nevertheless, in the 50% test (16.5 $g{\cdot}L^{-1}$ NaCl) N-damo denitrifying activity was almost negligible. These preliminary results, using N-damo biomass with high activity, indicate that the impact of NaCl is similar to that previously reported by He et al. [3]. However, unlike this study, it has been found that a lower concentration of 1.65 $g{\cdot}L^{-1}$ NaCl could be stimulatory for the N-damo activity. Thus, low saline concentrations could have a positive effect on the N-damo process.

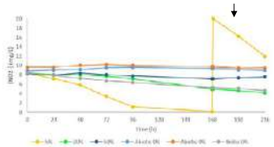

Figure 1. Evolution of the NO_2^- concentration obtained in the activity assays (with the different % salt and the abiotic controls with and without salt). The arrow indicates the addition of a new pulse of 20 mg NO_2^--N L^{-1} for the 5% salinity test.

Acknowledgements: To the project Antares (PID2019-110346RB-C21), co-funded by FEDER. The authors belong to the Galician Competitive Research Groups (GRC) ED431C-2021/37, a program co-funded by FEDER.

REFERENCES

[1] Allegue, T. et al. 2018 *Chem. Eng. J.* **347**, 721–730.
[2] Ettwig, K., Butler, M., Le Paslier, D. *et al.* 2010. *Nature* **464**, 543-548.
[3] He, Z., Geng, S., Shen, L., Zheng, P., Xu, X., Hu, B. 2015. *Water Research* **68**, 554-562.

Photo-Membrane Reactor (PMR) for Removal of Per- and Polyfluoroalkyl Substances (PFAS)

A. L. Junker & Z. Wei*

*Department of Biological and Chemical Engineering, Aarhus University, 36 Universitetsbyen, 8000 Aarhus, Denmark (Email: *ajunker@bce.au.dk*; *zwei@bce.au.dk*)

Abstract
A novel technology combines membrane separation and advanced oxidation processes in a single photomembrane reactor to safely and effectively "concentrate and destroy" aqueous micropollutants. The reactor operates with an adsorptive photocatalyst immobilized on the membrane surface. The membrane and adsorptive photocatalyst both promote the concentration of PFAS at the membrane surface, where it is mineralized under UV irradiation mediated by the photocatalyst.

Keywords
Membrane separation; PFAS degradation; photocatalysis; zero pollution

INTRODUCTION

Persistent micropollutants, such as per-and polyfluoroalkyl substances (PFAS), endanger society due to their mobility in the environment and resistance to degradation, posing long-term exposure risk if not effectively eliminated during wastewater treatment. While conventional treatment methods are ineffective, reverse osmosis and activated carbon can remove PFAS from water but generate contaminated waste streams. Advanced oxidation processes (AOPs) and thermolysis treatments show potential to mineralize PFAS into benign compounds; however, these methods are expensive, energy intensive, and difficult to scale up. By combining membrane separation and AOPs, a single-step reactor can efficiently concentrate and destroy PFAS, without harmful waste products and under the same mild conditions normally found at WWTPs.

MATERIALS AND METHODS

Four adsorptive photocatalysts were synthesized via hydrothermal process from inexpensive base materials: carbon, titanium dioxide, and post-transition metals. The catalysts were evaluated for PFAS removal, degradation and defluorination rates, after exposing them to UVC irradiation. Catalyst trials were conducted in both a slurry suspension and immobilized on a membrane. PFOA was selected as a model PFAS.
Catalyst loadings and membrane coating methods were tested and compared. The samples were analysed for fluorine ion and PFAS content via ion chromatography (IC) and ultra-performance liquid chromatography with a quadruple mass spectrometer (UPLC-MS/MS), respectively. The results of the heterogeneous catalyst were compared with PFAS degradation via UV/sulfite treatment, with sulfite added as a photosensitizer in lieu of the photocatalyst.
The most effective catalyst was immobilized on ultrafiltration and nanofiltration membranes, which were then placed into the photo-membrane reactor (PMR) system. Reactor conditions were optimized for flow mode, pressure and permeate flux. The system was run continuously for 8 hours, with samples taken every 2 hours. At the end of the run time, the catalytic membrane was sonicated in a 100 mM ammonium acetate in methanol solution, and the supernatant was analysed for PFAS extracted from the solid phase. In addition, the degradation of five pharmaceuticals (e.g. carbamazepine, trimethoprim, diclofenac, sulfamethoxazole, and propranolol) were tested in the same setup.

RESULTS AND DISCUSSION

A simple method was developed for immobilizing the catalyst on membranes. Short-chain PFAS species and fluorine ion observed during sample analysis are indicative of PFAS degradation and high rates of defluorination. In slurry, the photocatalysts removed > 99.9% of PFOA in 4 hours, with an overall defluorination rate of up to 57% at an initial concentration of 100 ppb, and even higher at lower concentrations. The iron-doped titanium nanotubes on activated carbon (Fe/TNT@AC) showed the highest defluorination rates, although all synthesized catalysts had a similar adsorption capacity. Comparatively, the UV/sulfite system exhibited very low defluorination rates, less then 3%.
During the static membrane tests, the catalyst removed up to 46% of PFOA, even though only a tenth of the catalyst (by weight) was used to treat the same sample volume of water. However, the membrane's removal abilities diminished when reused cyclically.
In the PMR system, up to 87% of PFOA was removed by the coated ultrafiltration membrane operating at low pressure. Meanwhile, the nanofiltration membrane was able to exclude up to 100% of PFOA from the permeate, when operated at a low pressure and permeate flux. The analysis of the extracted solid phase revealed that only 33 – 46% of the initial PFOA loading was still adsorbed to the catalytic membranes at the end of the run, indicating a significant portion of PFOA had been captured and destroyed in the PMR. The PMR system was less effective at removing the pharmaceuticals from the water, with only sulfamethoxazole and diclofenac showing any significant removal.

Take-home message

The adsorptive photocatalyst, Fe/TN@AC, is effective at removing PFAS, even when immobilized on a membrane. The PMR technology easily combines membrane and AOP treatment processes in a single-step, making its scale up viable. Initial testing indicates excellent removal rates and high degradation rates in the PMR system. However, improving the photocatalytic effect of the membrane could improve its lifetime, resulting in a system that could completely breakdown PFAS.

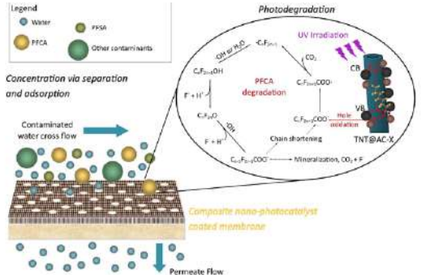

Figure 1. Schematic of the photocatalytic membrane's "concentrate and destroy" mechanism.

REFERENCES

Arana Juve, J.-M., et al. 2022. "Concentrate and degrade PFOA with a photo-regenerable composite of In-doped TNTs@AC." *Chemosphere* **300**: 134495.

Fischer, K., et al. 2018. "Synthesis of high crystalline tio2 nanoparticles on a polymer membrane to degrade pollutants from water." *Catalysts* **8**(9).

Li, C., et al. (2019). "Systematic evaluation of TiO2-GO-modified ceramic membranes for water treatment: Retention properties and fouling mechanisms." *Chemical engineering journal* **378**: 122138.

Li, F., et al. (2020). "A concentrate-and-destroy technique for degradation of perfluorooctanoic acid in water using a new adsorptive photocatalyst." *Water Research* **185**: 116219.

Electrochemical degradation of amoxicillin: Operational parameters optimization and degradation mechanism

Bhavana Kanwar[1], Mitil M. Koli[1], and Swatantra P. Singh[1,2,3]*

[1] Environmental Science and Engineering Department (ESED), Indian Institute of Technology Bombay, Mumbai 400076, India

[2] Centre for Research in Nanotechnology & Science (CRNTS), Indian Institute of Technology Bombay, Mumbai 400076, India

[3]Interdisciplinary Program in Climate Studies, Indian Institute of Technology Bombay, Mumbai 400076, India

*Corresponding author's e-mail: swatantra@iitb.ac.in

Abstract

The detection of emerging contaminants (ECs) in our water environment is a serious concern for the whole ecosystem as these can cause known or presumed adverse ecological and/or health impacts. ECs consist of pharmaceutical compounds, personal care products, pesticides, microplastics, industrial chemicals, synthetic dyes, surfactants, etc. Amoxicillin (AMX) is an antibiotic used to treat a variety of bacterial infections and is one of the widely prescribed antibiotics around the world for both human and animal medicine. AMX is an EC, and its impact on the environment and health is still uncertain. Due to its common use, traces of AMX have been detected in rivers, lakes, groundwater, drinking water, coastline water, urban effluents, water, and wastewater treatment plants, etc. The conventional wastewater treatment plants are comparatively ineffective in achieving complete removal of AMX, so there is an urgent need for advanced technology. Electrochemical oxidation (EO) is a very promising technology for wastewater treatment in which electro-generated radicals result in the complete mineralization of organic pollutants. This study is aimed to evaluate the EO of AMX and analyse its removal efficiency. The AMX Concentration has been detected by reverse phase HPLC with an ultraviolet-visible (UV-Vis) detector spectroscopy and the degradation by-products through QE Orbitrap LC-MS. Under the optimal conditions, the removal rates of AMX reached 99.1% after 3 hours of treatment at 7.5 voltages in 0.05M Na_2SO_4 solution. The results indicated that the electrochemical degradation of AMX fitted first-order reaction kinetics.

Keywords: Emerging contaminants, amoxicillin, antibiotic, wastewater, electrochemical oxidation

MATERIALS AND METHODS

Amoxicillin Trihydrate ($C_{16}H_{19}N_3O_5S.3H_2O$) has been purchased from Zeta Scientific for amoxicillin (AMX) source. Sodium sulphate (Na_2SO_4) have been purchased from EMPARTA® ACS. HPLC-grade methanol, used for HPLC analysis, have been obtained from Merck. Ultra-purified water obtained from Millipore-Q system for all the solutions. All the chemicals are analytical grade and used without further purification in this study. Fresh electrolyte solution with 0.05M Na_2SO_4 and DI water and 0.05M NaCl and DI water has been prepared at room temperature for each electro-oxidation experiment. The electrodes were characterized using a scanning electron microscope (SEM) and Raman spectroscopy of the graphite electrode for physical and chemical characteristics and performance. The electro-oxidation experiments were performed in a 100 ml cylindrical rector. Voltage-controlled conditions for electrolysis were maintained using a regulated D.C. power supply (HTC Instruments; DC POWER SUPPLY DC3005; 0-30 V, 0-5 A). Electrooxidation reactions began when the power supply was switched on.

RESULTS

In all electrochemical processes, the applied voltage is one of the important parameters to control reaction rate in electrochemical reactors. It manages the flow of the electron transfer, the capability of ‘OH generation, and determines the energy efficiency concerning the size of a reactor, resistance of the materials, etc. (Pan et al., 2020; Sopaj et al., 2015; Xu et al., 2019). Electrochemical experiments have performed using 1 mg/L of Amoxicillin (AMX) with variable voltage conditions and the analysis performed in HPLC. The results showed that the removal efficiency increased from 60.3 to 98.7% (Figure 1) as the voltage increases and the pseudo-first-order rate constant (k_{obs}) increased from 0.3977 to 0.9025 min^{-1} and the k_{obs} had excellent corelations with the voltage (R^2=0.991).

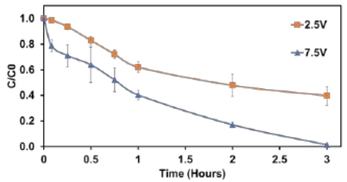

Figure 1: Removal efficiency for 1mg/L AMX initial concentration at different time intervals for different voltage.

References:

Pan, G., Sun, X., & Sun, Z. (2020). Fabrication of multi-walled carbon nanotubes and carbon black co-modified graphite felt cathode for amoxicillin removal by electrochemical advanced oxidation processes under mild pH condition. *Environmental Science and Pollution Research*, *27*(8), 8231–8247. https://doi.org/10.1007/S11356-019-07358-2/FIGURES/12

Sopaj, F., Rodrigo, M. A., Oturan, N., Podvorica, F. I., Pinson, J., & Oturan, M. A. (2015). Influence of the anode materials on the electrochemical oxidation efficiency. Application to oxidative degradation of the pharmaceutical amoxicillin. In *Chemical Engineering Journal* (Vol. 262, pp. 286–294). https://doi.org/10.1016/j.cej.2014.09.100

Xu, L., Ma, X., Niu, J., Chen, J., & Zhou, C. (2019). Removal of trace naproxen from aqueous solution using a laboratory-scale reactive flow-through membrane electrode. *Journal of Hazardous Materials*, *379*, 120692. https://doi.org/10.1016/J.JHAZMAT.2019.05.085

Investigating nutrient removal capacity of nature-based solutions (NbS) for eutrophic brackish water

E. Kendir Cakmak*-**, M. Hartl***, T. Centofanti***, Z. Cetecioglu** and J. Kisser***

* Department of Environmental Engineering, Hacettepe University, 06800, Ankara, Turkey
** Department of Industrial Biotechnology, KTH Royal Institute of Technology, AlbaNova University Center, SE-11421, Stockholm, Sweden
(E-mail: *ece2@kth.se, zeynepcg@kth.se*)
***Institute for Circular Economy & Nature-based Solutions, alchemia-nova GmbH, 1140 Vienna, Austria
(E-mail: *marco.hartl@alchemia-nova.net, tiziana.centofanti@alchemia-nova.net, jkl@alchemia-nova.net*)

Abstract
Marine ecosystems are facing eutrophication problem due to intensive accumulation of nutrients mainly from wastewater discharge and agricultural runoff. Nature-based solutions (NbS) are promising in terms of in-situ treatment eutrophic marine waters in a sustainable way. The aim of this study is to assess nutrient removal from eutrophic brackish sea water (the Baltic Sea) via lab-scale NbS systems mimicking conditions in the envisioned floating vertECO© raft constructed wetland technology. Six lab scale systems containing substrate mixture (zeolite, pumice and biochar) and two different plants (*Bolboschoenus maritimus* and *Schoenoplectus tabernaemontani*) as triplicates and one control system with substrate mixture (without plants) were operated with eutrophic brackish sea water. The results showed that lab-scale vertECO© wetland systems could remove nutrients and the systems with *Bolboschoenus maritimus* had a better performance.

Keywords (maximum 6 in alphabetical order)
Eutrophication; floating wetland; nature-based solutions; nutrients

INTRODUCTION

Marine eutrophication is a global concern that has adverse effects on both ecosystem and human services. It is stated that 762 coastal areas are impacted by eutrophication and/or hypoxia (World Resources Institute, 2013). For managing marine eutrophication, the strategies should include in-situ/ex-situ engineering approaches to remove nutrients in addition to nutrient input reduction strategies on wastewater discharge and agricultural runoff (Kendir Cakmak *et al*, 2022). Nature-based solutions (NbS) can provide a sustainable way to tackle eutrophication and floating wetlands are one of the successful examples commonly applied on freshwater sources. However, the main application of coastal/marine areas is erosion control, food web support, sediment trapping and aesthetic enhancement (Takavakoglu *et al*, 2021) and knowledge gap is huge for treatment of eutrophic waters.

MATERIALS AND METHODS

Seven lab-scale constructed wetland systems (open-air) were constructed in the premises of alchemia-nova (Vienna, Austria). The eutrophic sea water was collected from the Stockohlm Archipelago, the Baltic Sea. The systems included triplicates with two different local plant species (*Schoenoplectus tabernaemontani* and *Bolboschoenus maritimus*) and one control system without plants. Horizontally placed plastic columns (inner Ø:15 cm, height:1 m, total volume:18 L) were modified by cutting the top open and inserting an outlet pipe to control the water level. The plastic columns were filled with a substrate mixture (zeolite:30%, pumice:60%, biochar:10%). 5 bunches of the plants (roots were pre-washed) were planted except the control system. The systems were fed from a 250L storage tank by a submerged pump. Graduated buckets were placed at the outlet to collect the outlet water and measure the actual flow. During an initial acclimation phase, the systems were firstly fed with i) 20 days with artificial sea water (6 psu salinity, 0.55 mg/L NO_3-N, 0.06 mg/L PO_4^{3-} and 0.03 mg/L NH_4^+-N mimicking the collected Baltic Sea water). Later, the systems were fed with ii) higher concentrated eutrophic artificial sea water (0.831 mg/L PO_4^{3-} and 1.968 mg/L NH_4^+-N mimicking an eutrophic bay in the Baltic Sea as stated in Rydin *et* al, 2017) to assess nutrient removal under higher eutrophic inflows. The average initial nutrient concentrations of this artificially prepared water were 0.875 mg/L PO_4^{3-}, 2.675 mg/L NH_4^+, 0.55 mg/L NO_3-N and 0.006 mg/L NO_2-N. After the acclimation phase, the systems were fed with iii) the real Baltic Sea water set to higher eutrophic conditions as stated above for 9 days. Both outlet and inlet samples were analysed for pH, conductivity (EC), NH_4^+ NO_3-N, NO_2-N and PO_4^{3-}. The plant growth was visually monitored. One-way ANOVA was performed to compare the effect on treatment (with/without plants) on nutrient removal.

RESULTS AND DISCUSSION

The average NH_4^+ and PO_4^{3-} removal efficiencies were highest with *Bolboschoenus maritimus* (99.9% for NH_4^+ and 54.6% for PO_4^{3-}). PO_4^{3-} removal was lowered after 4 days due to the saturation of the adsorption sites of substrates (Dotro *et al* 2012). For PO_4^{3-} and NH_4^+ removal, the differences between plant treatments as well as control and treatment with *Bolboschoenus maritimus* were significant ($p<0.05$). The differences between control and treatment with *Schoenoplectus tabernaemontani* were insignificant ($p>0.05$). NO_3-N and NO_2-N were not removed in the systems. pH values increased from 8.07 to 8.55-8.73 and EC was also measured as 9.38-9.79 mS/cm. The height of the both plants increased and the new shoots were grown during experiments. The growth of *Bolboschoenus maritimus* was better. To conclude, lab-scale vertECO© wetland systems could remove nutrients from the brackish eutrophic sea water and *Bolboschoenus maritimus* showed better nutrient removal performance. The combined effect of plants and substrates was not considerably more effective than the effect of substrate uptake itself. As sorption sites will be saturated over time (especially for the PO_4^{3-}), the role of the plants might increase over time if managed properly through regular plant harvesting. Future designs can focus on enhanced nutrient removal and plant performance and beneficial use of harvested plants.

REFERENCES

Dotro, G., Langergraber, G., Molle, P., Nivala, J., Puigagut, J., et al. 2017. *Biological Wastewater Treatment Series,Treatment Wetlands (Volume 7)*.
Kendir-Cakmak, E., Hartl, M., Kisser, J., Cetecioglu, Z., 2022. Phosphorus Mining from Eutrophic Marine Environment towards a Blue Economy: The Role of Bio-based Applications. *Water Research* **219**, 118505.
Rydin, E., Kumblad, L.,Wulff, F., and Larsson, P. 2017. Remediation of an eutrophic bay in the Baltic Sea. *Environmental Science & Technology* **51** (8), 4559-4566.
Takavakoglou, V. Georgiadis, A. Pana, E. Georgiou, P.E. Karpouzos, D.K. et al. 2021. Screening Life Cycle Environmental Impacts and Assessing Economic Performance of Floating Wetlands for Marine Water Pollution Control. *Journal of Marine Science and Engineering*, **9**, 1345.
World Resource Institute, 2013. https://www.wri.org/data/eutrophication-hypoxia-map-data-set. Accessed date. 03.03.2023

ACKNOWLEDGEMENTS

The first author was funded by i) the COST Action CA1713 to conduct Short Term Scientific Mission in the alchemia-nova, ii) the Scientific and Technological Research Council of Turkey (TUBITAK) via 2219, Grant Agreement No:1059B192000320.

Performance of in-house photocatalytic membrane on hormone removal

W. Khongnakorn*, N. Karnjanamit*, and C. T. Buranachai**

*Center of Excellence in Membrane Science and Technology and Department of Civil and Environmental Engineering, Faculty of Engineering, Prince of Songkla University, Songkhla, 90110, Thailand.
(E-mail: *wats.k@psu.ac.th*; *nichakkar@gmail.com*)*
** Center of Excellence for Trace Analysis and Biosensor and Division of Physical Science, Faculty of Science, Prince of Songkla University, Songkhla, 90110, Thailand.
(E-mail: *chongdee.t@psu.ac.th*)

Abstract
The micropollutant is high effect and accumulate in the aqua system. The almost widely used 17α-methyltestosterone (MT) and 17β-Estradiol (E2) for Nile tilapia productivity and female hormone increasing. This study is focused on MT and E2 removal via the photocatalytic process using in-house PVDF membrane modified by nanomaterials (either 1%TiO_2 or TiO_2/α-Fe_2O_3). The membranes were characterized for water contact angle (WCA), morphology analysis, permeability and salt rejection. The membrane permeability results of PVDF, PVDF-TiO_2, and PVDF-TiO_2/α-Fe_2O_3 were 4.5 x 10^{-11}, 6.1 x 10^{-11} and 6.3 x 10^{-11} m/s.Pa, respectively. The optimum removal time with UV light is 20 min and 60 min for MT and E2, respectively. The MT removal is 100% removal performance for all membrane. The performance of E2 removal by PVDF, PVDF-TiO_2, and PVDF-TiO_2/α-Fe_2O_3 were 65%, 95%, and 72%, respectively. The addition of nanomaterials, both TiO_2 and α-Fe_2O_3, enhanced the water flux. However, the removal efficiency of E2 less than MT according to the chemical bond and structure of E2 is stronger than MT. The addition of α-Fe_2O_3 showed the high permeability but less removal performance consistent with the surface roughness which inhibited the catalytic activity.

Keywords (maximum 6 in alphabetical order)
Photocatalytic membrane (PMR); hormone; 17β-Estradiol (E2); 17α-methyltestosterone (MT); titanium dioxide (TiO_2); Hematite (α-Fe_2O_3)

INTRODUCTION

Endocrine-disrupting compounds (EDCs) are micropollutants and bioaccumulate that can cause widespread environmental. 17 α-methyltestosterone (MT) and 17β-Estradiol (E2) for Nile tilapia productivity and female hormone increasing. Conventional wastewater treatment technology is inefficient completely in the removal of hormone such as adsorption, biodegradation, bio-sorption (Tagliavini and Schäfer 2018; Vieira et al. 2021). It requires longer operational time and is less efficient. Nanomembrane filtration process and advanced oxidation processes (AOP) had been presented a high performance but high pressure and energy demand. Hence, the coupling technique and mechanism of membrane sieving and photocatalytic which can oxidize pollutants quickly and enhance the presence of irradiation light to improve process performance. The performance of the photocatalytic membrane system was investigated the MT and E2 removal at source to use for the surface water management around agriculture fish floating case and wastewater treatment plant effluent in Songkhla lake, Songkhla, Thailand.

MATERIALS AND METHODS

Synthesis of TiO_2 was carried out following methods published in previous studies (Bootluck et al., 2021). The TiO_2 powder was obtained after calcinated at 450°C for 2 h. α-Fe_2O_3 and Ti/α-Fe_2O_3 samples were fabricated by the hydrothermal method following the previous method (Bootluck et al., 2021). The preparation process of the in-house photocatalytic membrane was fabricated is shown in **Figure 1**. The control PVDF was prepared as following in-house fabricated and named PVDF, PVDF-TiO_2, and PVDF-Ti/α-Fe_2O_3 membranes. For the PVDF-TiO_2 used 1 wt% TiO_2 and was mixed with 0.1 wt% PVP and 17 wt% PVDF and dissolved in NMP under a magnetic stirrer for 5 h at 60°C (Subramaniam et al., 2020). PVDF-Ti/α-Fe_2O_3 membranes, either adding 1 wt% Ti/α-Fe_2O_3 and followed the previous method. Then, the homogeneous solution was sonicated for 30 min by sonication (GT sonic, China). The membrane casting was done on a glass plate using phase inversion method. The membrane was dried for 5 min at 70 °C and was stored in DI water until used.

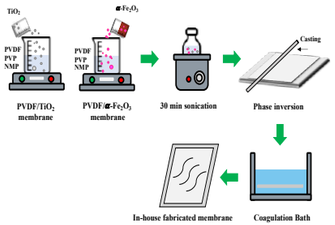

Figure 1. The schematic diagram of the fabrication process of photocatalytic membranes

Membrane surface and morphology were characterized by water contact angle (WCA) measurement and scanning electron microscope (SEM, SU 3900, Hitachi, Japan). The membrane permeability and salt rejection were test as following ASTM D4516 method (ASTM, 2002).
The 5 mg/L of MT and E2 concentration removal performance were test by the crossflow unit cell assembly for 3 hrs for with and without UV_{95W} condition. The photocatalytic kinetics were determined and the first-order rate constant (k) was calculated following Dzinun et al. (2015).

RESULTS AND DISCUSSION

The contact angle of PVDF, PVDF-TiO_2, and PVDF-TiO_2/α-Fe_2O_3 membranes are 84°, 78° and 71°, respectively. The WCA decreases when added TiO_2 and TiO_2/α-Fe_2O_3 which relatives with the increasing of permeability. The results of membrane permeability of PVDF, PVDF-TiO_2, and PVDF-TiO_2/α-Fe_2O_3 were 4. 5 x 10^{-11}, 6.1 x 10^{-11} and 6.3 x 10^{-11} m/s.Pa, respectively. The morphology showed two-layered the sponge-like structure and macro voids to carry the high-water flux. The water flux for 180 min operation, PVDF-TiO_2 membrane was the highest (573 LMH). PVDF-TiO_2 and PVDF-TiO_2/α-Fe_2O_3 membranes showed similar permeate flux. The results showed that the PVDF-TiO_2 membrane showed the highest flux, meaning water flux is not correlated to WCA.

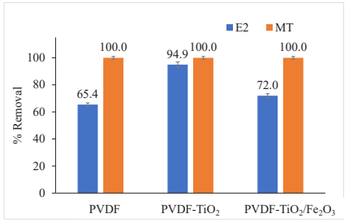

Figure 2. The hormone removal performance of PVDF, PVDF-TiO_2, and PVDF-TiO_2/α-Fe_2O_3 membrane.

From Figure2. the hormone removal of MT and E2 found that the E2 (82%) is less performance than MT (100%) due to the strong chemical bond of E2. The optimum time with UV light is 20 min and 60 min for MT and E2 removal, respectively. The kinetic degradation of MT and E2 are first-order reaction. There have rough spots on the surface membrane after adding TiO_2 and α-Fe_2O_3 catalyst, and the membrane pores of cross-section became wider upon catalyst but effect on its performance. However, the high pH is more OH ions available on the TiO_2 surface which it is easier to generate OH• and improves process efficiency.

REFERENCES

ASTM D4516, 2002 Standard Practice for Standardizing Reverse Osmosis Performance Data, ASTM Vol. 11.02

Bootluck W., Chittrakarn T., Techato K., Panitan, J., Khongnakorn, W. 2021 Modification of surface α-Fe_2O_3/TiO_2 photocatalyst nanocomposite with enhanced photocatalytic activity by Ar gas plasma treatment for hydrogen evolution. *Journal Environmental Chemical Engineering* **9**:105660. https://doi.org/10.1016/j.jece.2021.105660.

Dzinun, H., Othman, M. H. D., Ismail, A. F., 2015 Photocatalytic degradation of nonylphenol by immobilized TiO_2 in dual layer hollow fibre membranes. *Chemical Engineering Journal* **269**:255–261. https://doi.org/10.1016/j.cej.2015.01.114

Tagliavini, M., and Andrea, I. S. 2018 Removal of Steroid Micropollutants by Polymer-Based Spherical Activated Carbon (PBSAC) Assisted Membrane Filtration. *Journal of Hazardous Materials* **353**:514–21. doi: 10.1016/j.jhazmat.2018.03.032.

Wang, B., Li, C., Cui, H. 2013 Fabrication and enhanced visible-light photocatalytic activity of Pt-deposited TiO_2 hollow nanospheres. *Chemical Engineering Journal* **223**:592-603. http://dx.doi.org/10.1016/j.cej.2013.03.052

Vieira, W. T., Marina, B. D. F., Marcela, P. S., Meuris, G., Carlos, D. S., Melissa, G. A. V. 2021 Endocrine-Disrupting Compounds: Occurrence, Detection Methods, Effects and Promising Treatment Pathways - A Critical Review. *Journal of Environmental Chemical Engineering* **9**(1) 104558.

Subramaniam, M. N., Goh, P. S., Lau, W. J., Abidin, M. N. Z., Mansur, S., Ng, B. C., Ismail, A. F. 2020 Optimizing the spinning parameter of titania nanotube-boron incorporated PVDF dual-layered hollow fiber membrane for synthetic AT-POME treatment. *Journal of Water Process Engineering* **36**:101372.

Functionalized CNTs-coated carbon electrodes to improve desalination battery performance: Comparison with thermally oxidized carbon electrode

S. G. Kim*, J. H. Kim **, H. Y. Choi*, S. J. Lee * and I. G. Byun***

* School of Civil and Environmental Engineering, Pusan National University, 2, Busandaehak-ro 63beon-gil, Geumjeong-gu, Busan, Republic of Korea (E-mail: *ksg584875@gmail.com, gydud9270@pusan.ac.kr, mwls172@pusan.ac.kr*)
** School of Civil and Environmental Engineering, Pusan National University, 2, Busandaehak-ro 63beon-gil, Geumjeong-gu, Busan, Republic of Korea (E-mail: *hyeon@pusan.ac.kr*)
***Institute for Environment and Energy, Pusan National University, 2, Busandaehak-ro 63beon-gil, Geumjeong-gu, Busan, Republic of Korea (E-mail: *big815@pusan.ac.kr*)

Abstract
The purpose of this study is to apply a desalination battery as a method to remove NaCl in food wastewater and to improve the performance of a desalination battery by introducing a carbon-based electrode. Carbon felt(CF), graphite felt(GF), and carbon felt coated with functionalized MWCNTs(CNT-CF) were tested as target electrodes. MWCNTs were coated using the electrophoresis method. CF showed the lowest chloride ion removal performance, and the time required to achieve a chloride ion removal rate of over 85% was reduced by about 7.7 times for GF and 3.6 times for CNT-CF compared to CF.

Keywords
Carbon Felt; Carbon nanotubes; Chloride ion removal; Desalination; Electrode; Graphite Felt

INTRODUCTION

Food wastewater is one of the wastes inevitably discharged from human life, and the amount of it is increasing due to the increase in population and economic activity. Anaerobic digestion is being considered as a method for treating food wastewater [1]. However, a large amount of NaCl is contained in food wastewater, which reduces the stability of anaerobic digestion [2]. Desalination batteries can be a way to remove NaCl and store some of the energy used for NaCl removal. Desalinated battery has a section for desalination between the anode and cathode, and the cation exchange membrane and the anion exchange membrane are designed to form an interface with the desalination section. In desalination, sodium ions and chlorine ions in the desalination chamber are separated and transported to the anode and cathode. The electrochemical reaction during charging is as shown in Equations (1) to (3) [3].

Anode Part: $Na^+ + e^- \rightarrow Na(s)$ (1)
Desalination Part: $NaCl(aq) \rightarrow Na^+ + Cl^-$ (2)
Cathode Part: $2H_2O(l) \rightarrow 4H^+ + O_2(g) + 4e^-, H^+ + Cl^- \rightarrow HCl(aq)$ (3)

The electrochemical redox reaction on the surface of the electrode should be encouraged in order to improve battery performance. Large-surface-area oxide electrodes generally offer high catalytic activity [4]. Carbon materials can be thermally oxidized to increase their surface area and make them advantageous for use in aqueous solutions. Because of these advantages, research on CF and GF electrodes is in progress. One of them is to improve the electrochemical reaction by coating the carbon-based electrode with other materials. Carbon nanotubes are being studied as electrode coating materials and are characterized by high tensile strength, high electrical conductivity and large surface area [5].

In this study, multi-walled carbon nanotubes were attached to CF by electrophoresis, and it was named CNT-CF. In addition, CNT-CF was applied as electrodes to a desalination battery and their performance was compared with CF and GF.

MATERIALS AND METHODS

Preparation of electrodes

CF(CNF Co. Ltd., Republic of Korea) and GF(CeTech Co. Ltd., Taiwan) were thermally oxidized at 500 °C for 4 hours to improve surface wettability. MWCNTs (Sigma Aldrich) with a diameter of 10 to 20 nm and a length of 5 to 15 nm were added to a mixed solution of sulfuric acid and nitric acid (3:1) for impurity removal and functionalization. The functionalized MWCNTs were ultrasonically dispersed in ethanol to form a uniform suspension. 25 mg $ZnSO_4 \cdot 7H_2O$ was added into the suspension to improve the deposition rate and the adhesion of the MWCNTs to electrode [6]. Electrophoretic deposition was performed by applying a voltage of 30 V for 10 minutes. CF was used as coating substrates to connect to the negative potential, and the counter electrode was made of the same material as the substrate. The distance between the electrodes was maintained at 10 mm.

Assembly of the desalination battery module

The desalination battery is assembled with SWB2464 coin cell(4toone Co., Ltd., Republic of Korea), seawater battery housing kit(4toone Co., Ltd., Republic of Korea), anion exchange membrane(fumatech Co., Ltd., Germany), and desalination compartment. The desalination compartment is made of polycarbonate material and designed with an internal volume of up to 3.4 ml.

Electrode performance test

In experiments No.1 to No.3, 5,000 mg/L as Cl synthetic wastewater was prepared by adding 8.242 g of NaCl to 1 L of deionized water. The value of 5,000 mg/L as Cl refers to the concentration of chlorine compounds in effluents in 2017 and 2019 investigated by the Ministry of Environment of the Republic of Korea. 3 ml of synthetic wastewater was injected into the desalination compartment, and the compartment was separated with an anion exchange membrane before assembly. All of test electrodes were connected to the cathode compartment and an external voltage of 9 V was applied. Chlorine ion concentrations were measured by sampling samples in the desalination compartment at specific times.

Table 1. Experimental condition of desalination test by seawater battery

No.	Conc. (mg Cl^-/L)	External voltage (V)	Cathode materials	Initial cell voltage (V)
1	5,000	9	CF(3cm×3cm)	1.305
2			GF(3cm×3cm)	1.827
3			CNT-CF(3cm×3cm)	1.116
4	302		CF(3cm×3cm), CNT-CF(3cm×3cm)	1.218, 1.240

RESULTS AND DISCUSSION

When CF was used as the cathode electrode, 86.7% of chlorine ions were removed in 165.5 hours. As shown Fig. 2, the voltage change of the cell was divided into a phase in which the voltage rapidly increased(A-stage) and a phase in which the voltage increased slowly(B-stage). The A-Stage shows a sharp slope due to the adsorption behavior of sodium ions on the Na metal of the anode, and the stable slope at the B-Stage is due to the intercalation of sodium ions in the Na metal [7]. The chlorine ion removal rate in the A-Stage section showed a relatively insignificant tendency compared to the B-Stage.

Figure 3 shows the chlorine ion removal experiment by applying GF to the cathode electrode. During the operating time of 21.5 hr, the chlorine ion removal rate achieved 92.6%. By replacing the cathode electrode from CF to GF, the time required to achieve a chlorine ion removal rate of over 85% was reduced by about 7.7 times (165.5 hr → 21.5 hr). The better chlorine ion removal of GF than the CF can be explained by the difference in oxidation degree between the two electrodes. During the heat treatment process for use as an electrode, hydrophilic functional groups (C-O, C=O, etc) are created on the electrode surface [8],[9].

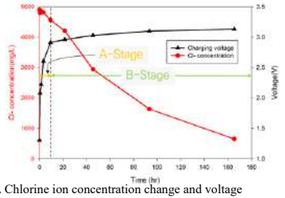

Figure 2. Chlorine ion concentration change and voltage change according to operating time of seawater battery using CF as cathode electrode

In Figure 4, a chloride ion removal experiment was performed using the CNT-CF electrode coated with MWCNT on the CF applied in Figure 1 as a cathode electrode. During the operating time of 45.5 hr, the voltage rose from 1 V to 3 V, and the chlorine ion removal rate reached 98.0%. This means that CNT-CF in Fig. 4 has an improved electrochemical redox reaction than CF in Fig. 2. This result can be explained by the difference in electrical conductivity between CF and MWCNT. The electrical conductivity of CF (PAN-based) is 588 S/cm, and the electrical conductivity of MWCNT is 104 to 105 S/m, so MWCNT has about 17 to 170 times the electrical conductivity of CF [10],[11].

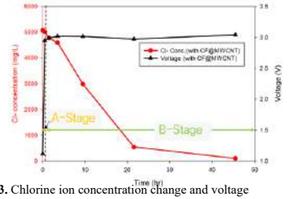

Figure 3. Chlorine ion concentration change and voltage change according to operating time of seawater battery using GF as cathode electrode

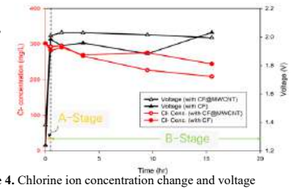

Figure 4. Chlorine ion concentration change and voltage change according to operating time of seawater battery using CNT-CF as cathode electrode

CONCLUSION

To improve the performance of the desalination battery, a carbon-based electrode was applied as a negative electrode. The electrodes used in the experiment were CF, GF, and CNT-CF, and GF took the shortest time when comparing the time required to achieve 85% chloride ion removal rate.

Comparing the performance of CNT-CF and CF, CNT-CF showed better performance, and similar results were obtained when CNT-CF and CF electrodes were applied to thermal power plant floor ash washing water. It was found that MWCNTs had a positive effect on the redox reaction rate of the electrode. In the future, the desalination of actual food wastewater will be tested and the interfering effect of other substances will be identified.

ACKNOWLEDGEMENTS

This work supported by the Korea Environment Industry & Technology Institute (KEITI) through the Development of Demonstration Technology for Converting Unconventional Waste Biomass to Energy, funded by the Korea Ministry of Environment (MOE) (2022003480001).

REFERENCES

[1] Shin, S. G., Han, G., Lee, J., Cho, K., Jeon, E. J., Lee, C., & Hwang, S. (2015). Characterization of food waste-recycling wastewater as biogas feedstock. Bioresource Technology, 196, 200-208.
[2] Zhao, J., Liu, Y., Wang, D., Chen, F., Li, X., Zeng, G., & Yang, Q. (2017). Potential impact of salinity on methane production from food waste anaerobic digestion. Waste Management, 67, 308-314.
[3] Kim, N., Park, J. S., Harzandi, A. M., Kishor, K., Ligaray, M., Cho, K. H., & Kim, Y. (2020). Compartmentalized desalination and salination by high energy density desalination seawater battery. Desalination, 495, 114666.
[4] Kim, K. J., Park, M. S., Kim, Y. J., Kim, J. H., Dou, S. X., & Skyllas-Kazacos, M. (2015). A technology review of electrodes and reaction mechanisms in vanadium redox flow batteries. Journal of materials chemistry a, 3(33), 16913-16933.
[5] Spitalsky, Z., Tasis, D., Papagelis, K., & Galiotis, C. (2010). Carbon nanotube–polymer composites: chemistry, processing, mechanical and electrical properties. Progress in polymer science, 35(3), 357-401.
[6] Wang, L., Chen, Y., Chen, T., Que, W., & Sun, Z. (2007). Optimization of field emission properties of carbon nanotubes cathodes by electrophoretic deposition. Materials Letters, 61(4-5), 1265-1269.
[7] Zhang, B., Ghimbeu, C. M., Laberty, C., Vix-Guterl, C., & Tarascon, J. M. (2016). Correlation between microstructure and Na storage behavior in hard carbon. Advanced Energy Materials, 6(1), 1501588.
[8] Han, J., Hwang, S. M., Go, W., Senthilkumar, S. T., Jeon, D., & Kim, Y. (2018). Development of coin-type cell and engineering of its compartments for rechargeable seawater batteries. Journal of Power Sources, 374, 24-30.
[9] Zhang, H., Chen, N., Sun, C., & Luo, X. (2020). Investigations on physicochemical properties and electrochemical performance of graphite felt and carbon felt for iron-chromium redox flow battery. International Journal of Energy Research, 44(5), 3839-3853.
[10] Jang, J., Lee, C. H., Park, K. H., & Ryu, S. K. (2006). Physical Properties and Electrical Conductivity of PAN-based Carbon Fiber Reinforced Paper. Korean Chemical Engineering Research, 44(6), 602-608.
[11] Wang, Y., & Weng, G. J. (2018). Electrical conductivity of carbon nanotube-and graphene-based nanocomposites. In Micromechanics and nanomechanics of composite solids (pp. 123-156). Springer, Cham.

Removal of Organic Dyes Through Polymer Inclusion Membrane Based on Perbenzylated-β-Cyclodextrin

J. Łagiewka*, A. Nowik-Zajac*, K. Witt^, M. Drapała*, Magdalena Drapała, and I. Zawierucha*

* Institute of Chemistry, Jan Dlugosz University in Czestochowa, 42-200 Czestochowa, Poland
(E-mail: *jakub.lagiewka@doktorant.ujd.edu.pl, a.zajac@ujd.edu.pl, magdadrappa77@gmail.com, i.zawierucha@ujd.edu.pl*)
^ Faculty of Chemical Technology and Engineering, Bydgoszcz University of Science and Technology, 3 Seminaryjna Street, PL 85326 Bydgoszcz, Poland
(E-mail: *wittkatarzyna@pbs.edu.pl*)

Abstract
Industrial development leads to the generation of effluents, wastewater and contaminated water. It is caused by increased demand for production of clothing and improving the quality of health. The organic dyes are a threat to aquatic ecosystems due to their carcinogenic and mutagenic properties which are harmful for the fauna living in contaminated water. Herein, the polymer inclusion membranes (PIMs) containing a cyclodextrin (CD) ligand which characterizes strong affinity for organic pollutants, seems to be a perfect material for wastewater treatment. The novel PIM containing CD ligand was studied for separation of organic pollutants from aqueous solutions. Influence of different parameters was studied to determine optimal conditions for removal of Acid Orange 7 (AO7) and Methylene Blue (MB). The driving force of dye transport across PIM was based on pH gradient and RF values were 97,6% and 96,5% for AO7 and MB, respectively.

Keywords
Cyclodextrins; Membrane Processes; Organic Dyes; Polymer Inclusion Membrane

INTRODUCTION

Recently, an increase in the concentration of various chemicals such as dyes, pharmaceuticals, detergents, pesticides in water and sewage has been observed. This is caused by the increased demand for the production of clothing and improving the quality of health, which also leads to the discharge of this type of substances with industrial or municipal wastewater as a result of dyes production, clothing colouring and washing clothes. Dyes as organic compounds are a threat to aquatic ecosystems due to their carcinogenic and mutagenic properties, which affects the health of the fauna living in contaminated water. In addition, it results in limited visibility, which disturb the functioning of the fishes (*Berradi et al. 2019*). The processes of photosynthesis under such conditions are inhibited and the production of oxygen in water is reduced. There are known some treatment methods for removal organic dyes from (waste)water: membrane separation, adsorption, advanced oxidation processes, photocatalysis, biological treatment. One of the simple, cost-effective and safe alternative for colour removal are membrane processes for instance with application of polymer inclusion membranes (PIMs). The PIMs are obtained as a result of mixing and immobilization of doped carrier together with plasticizer in polymer matrix. The doped carrier is responsible for recognition and transport of pollutant molecule/ion from source phase into feeding phase (*Ma et al. 2017*). Nowadays most studies focused on ion carriers which are applied in PIMs for separation of heavy metals from aqueous solutions, but only some consider application of organophillic carrier like cyclodextrins (CDs).
The CDs are group of macrocyclic oligosaccharide family composed mostly with 6, 7 or 8 glucose units, well known as α-, β-, and γ-CD respectively. These compounds are derived from cellulose through biocatalytic synthesis with specific cyclodextrin glycosyltransferase (CGTase), The most interesting ability of CDs is formation of inclusion complex with organic molecules like ibuprofen, this ability was applied in drug delivery. However, it seems a promising strategy to obtain separative materials containing CDs (*Jambhekar et al. 2016*).
The application of CDs for organic pollutants removal is promising but also problematic by reason of their high solubility in water due to carbohydrate core. In turn, the preparation of PIM with CDs is an issue due to their low solubility in organic solvents. On the other hand, the most research around CDs in PIMs focused mostly on metal ion removal. Therefore, the application of CDs in removal of organic pollutants from aqueous solutions is not fully checked field in spite of remarkably promising properties.
In this study, we analyzed the removal of organic dyes (AO7 and MB) from aqeous solutions using PIMs containing a perbenzylated β-CD derivative as the carrier. To evaluate the performance of organic dyes separation, we used the following parameters: the impact of the carrier concentration, the quantity of plasticizer in the membrane, the acidity of the source phase as well as receiving phase, and the feasibility of reusing the membrane.

MATERIALS AND METHODS

Reagents

Inorganic reagents, i.e., sodium chlorides (NaCl), magnesium sulphate ($MgSO_4$), hydrochloric acid (HCl) and sodium hydroxide (NaOH), potassium hydroxide (KOH) provided by POCh (Gliwice, Poland) and organic chemicals, i.e., crystalline β-Cyclodextrin, benzyl chloride, Methylene Blue, Acid Orange 7 were obtained from MERCK (Darmstadt, Germany); and cellulose triacetate (CTA), *o*-nitrophenyl octyl ether (*o*-NPOE) and chloroform were obtained from Fluka (Seelze, Germany).

Synthesis of the perbenzylated β-CD derivative and preparation of PIM

Native β-CD was dissolved in distilled water and then activated to form an oxyanion by 4M aqueous solution of potassium hydroxide (KOH). Benzyl chloride was introduced into the reaction mixture. The reaction mixture was heated at 65°C for 24 h. After cooling, the mixture was extracted with chloroform, then the organic layer was washed with distilled water. The organic layer was dried with anhydrous $MgSO_4$, then separated by filtration and concentrated. The synthesis protocol was slightly modified according to (*Bouzitoun et al., 2006)*.
PIM was prepared, according to previously designed protocol (*Zawierucha et al., 2022)*, from a chloroform solution containing: a matrix (cellulose triacetate (CTA)), a plasticizer (*o*-nitrophenyl octyl ether) and a carrier (perbenzylated β-CD derivative). The glass ring attached to the glass plate by a CTA-chloroform based adhesive was filled with the appropriate dosage of the organic solution. The mixture was left overnight at room temperature to evaporate the chloroform. The resulting membrane (Figure 1) was separated from the glass plate by wetting with cold water. The thickness of the membrane was measured with an ultrameter.

Transport studies

Transport studies were carried out in special two-chamber permeation vessels at room temperature. The membrane was placed between two chambers containing feeding and receiving phases. The feeding phases contained aqueous solutions (50 cm^3) of MB or AO7. Both of phases were continuously stirred at 600 rpm, whereas the sample were periodically collected. The concentrations of dyes in the samples were quantified by UV-VIS Shimadzu 2401 spectrophotometer.
The removal efficiency was described by the recovery factor (*RF*) as followed in equation:

$$RF = \frac{c_0 - c}{c_0} \times 100\% \quad (1)$$

where c_o and c are initial concentration of dyes in source phase and feeding phase at given time (mg/l).

RESULTS AND DISCUSSION

Kinetics of dyes transport through PIM

The kinetics of dye transport was analysed for the MB and AO7 through PIM containing perbenzylated β-CD derivative. The analysis was performed for changes of concentration in the feeding and receiving phase.

The kinetic curves on Figure 2 express exponential nature of relationship: c/c_0 in the function of time. The presented kinetic model is similar to primary transport proposed for supported liquid membranes (*Danesi et al. 1984)*.

Influence of initial concentration on transport through PIM

According to the Figure 3, the RF value is highly maintained in range 10-100 mg/l of AO7 for around 98%. The RF value for 500 mg/l was decreased to 92% and may be caused by precipitation of dye molecules on membrane surface or clogging of membrane pores.

Mechanism of dyes transport through PIM

The driving force of transport is based on pH gradient between two phases. The dyes are carried from feeding phase to receiving phase through formation of inclusion complex with CD inside PIM. The mechanism of transport is presented on Figure 4.

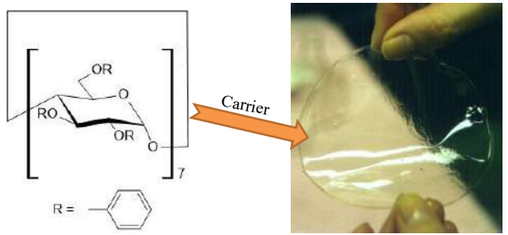

Figure 1. The structure of perbenzylated β-CD (the carrier) and the PIM with doped carrier.

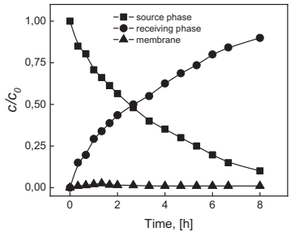

Figure 2. The profile of AO7 (100 mg/l) concentrations in source, membrane and receiving phases during the transport process across PIM.

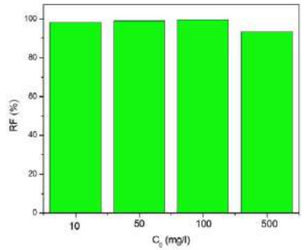

Figure 3. The RF profile depending on initial concentrations of AO7 in feeding phase.

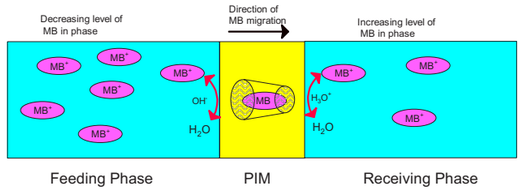

Figure 2. The mechanism of separation of MB through PIM containing perbenzylated β-CD carrier.

REFERENCES

Berradi, M., Hsissou, R., khudhair, M., Assouag, M., Cherkaoui, O., Bachiri, A. E., Harfi, A. E. 2019 Textile finishing dyes and their impact on aquatic environs. *Helyion* 5, e02711.
Bouzitoun, M., Mlika, R., Gam, H., Ben Ouada, H., Majdoub, M., Sfihi, H. 2006 A non-water-soluble modified β-cyclodextrin for sensitive electrode. *Materials Science and Engineering C* **26**, 481 – 485.
Danesi, P. R.. 1984-1985 Separation of metal species by supported liquid membranes, Separation of Science and Technology. *Separation of Science and Technology* **19**, 857–894.
Jambhekar, S.S., Breen, P. 2016 Cyclodextrins in pharmaceutical formulations I: structure and physicochemical properties, formatiosn of complexes, and types of complex. *Drug Discovery Today* **21**(2), 356-362.
Ma, X., Chen, P., Zhou, M., Zhong, Z., Zhang, F., Xing, W. 2017 Tight Ultrafiltration Ceramic Membrane for Separation of Dyes and Mixed Salts (both NaCl/Na_2SO_4) in Textile Wastewater Treatment. *Industrial & Engineering Chemistry Research* **56**(24), 7070-7079.
Zawierucha, I., Nowik-Zajac, A., Lagiewka, J., Malina, G. 2022 Separation of Mercury(II) from Industrial Wastewater through Polymer Inclusion Membranes with Calix[4]pyrrole Derivative. *Membranes* **12**, 492.

Feammox biofilm formation to enhance ammonium removal from wastewater

A. S. Cerda*, M. D. Gonzalez*, C. A. Rodríguez*, J. S. Serrano** and E. D. Leiva*, ***

* Department of Inorganic Chemistry, Faculty of Chemistry and Pharmacy, Pontificia Universidad Católica de Chile, Avenida Vicuña Mackenna 4860, Macul, Santiago 7820436, Chile. (*ascerda@uc.cl; m.gonzalezbustos@uandresbello.edu; cnrodriguez@uc.cl; ealeiva@uc.cl*)
** School of Biotechnology, Universidad Mayor, Camino La Pirámide 5750, Huechuraba, Santiago 8580745, Chile. (*jennyfer.serrano@umayor.cl*)
*** Department of Hydraulic and Environmental Engineering, Pontificia Universidad Católica de Chile, Avenida Vicuña Mackenna 4860, Macul, Santiago 7820436, Chile. (*ealeiva@uc.cl*).

Abstract
Excessive deposition of reactive nitrogen in the environment has led to loss of biodiversity, eutrophication and acidification of ecosystems. Recently, bacteria capable of anaerobically metabolizing ammonium through the reduction of iron III, a biological process called Feammox, have been discovered. The formation of biofilms of Feammox bacteria in hollow-fiber membrane bioreactor (HFMB) was evaluated as an efficient and sustainable alternative for ammonium removal in from wastewater.

Keywords
Ammonium, biofilms, Feammox, HFMB, nitrogen, wastewater.

INTRODUCTION

Human activities coupled with the growth of industrialization have generated high levels of reactive nitrogen (Nr) pollution in the form of ammonium (NH_4^+) (Galloway and Cowling, 2002). Consequently, excessive Nr deposition in the environment has caused biodiversity loss, eutrophication and soil acidification (Yang et al., 2014).

Biological nitrogen removal is mainly based on the use of activated sludge, which corresponds to a heterogeneous set of microorganisms categorized as bacterial consortia (BC) (Yang et al., 2011). However, biofilm formation is more effective for biological nitrogen removal (Li et al., 2021). For example, hollow-fiber membrane bioreactors (HFMB) integrating a selective membrane and biological treatment based on biofilm formation of bacterial communities have been widely used for NH_4^+ treatment (Razaviarani et al., 2019; Wu et al., 2020).

In 2005, a bacterial process called Feammox, discovered in a forested riparian wetland soil in New Jersey (USA), was identified as capable of anaerobically metabolizing NH_4^+ through the reduction of ferric iron (Fe^{+3}) (Clément et al., 2005). In this context and based on the favorable growth conditions of Feammox bacteria, it is established that this biological process could have a significant impact on improving autotrophic nitrogen removal from wastewater, optimizing removal efficiency, reducing energy costs and organic carbon requirements of conventional nitrification-denitrification processes.

MATERIALS AND METHODS

The anaerobic sludge sample was obtained from the sewage system of a brewery treatment plant (IC) located in Santiago, Chile. The sludge sample inoculum was added to a Feammox pathway enriched medium, with sodium bicarbonate ($NaHCO_3$) or sodium acetate (CH_3COONa) at pH 7 and under anaerobic conditions (20 ± 2°C). Samples were monitored every 7 days for 28 days, measuring NH_4^+ and ferrous iron (Fe^{+2}). Cultures inoculated with pre-enriched bacterial consortia (EBC) were also evaluated under optimized growth conditions.

Pieces of 10 cm hollow-fiber (0.4 - 2.6 mm diameter) were incubated with 20mL of the culture medium inoculated with the sludge sample (after 28 days of growth), in a Petri dish, under anaerobic conditions, at 20 ± 2°C, for 10 days and analyzed by scanning electron microscopy (SEM).

RESULTS AND DISCUSSION

Figure 1 shows the results of the measurements obtained from the batch reactor treatment. Four samples were evaluated: IC sludge, Feammox selective medium and $NaHCO_3$ (Treatment. 1); IC sludge, Feammox selective medium and CH_3COONa (Treatment 2); EBC, Feammox medium and $NaHCO_3$ (Treatment 3); and EBC, Feammox medium and CH_3COONa (Treatment. 4). In all samples, Figure 1A [Fe^{+2}] and 1B [NH_4^+] were measured. Treatment 2 increases its concentration steadily, reaching a +Δ84.6 mg/L of [Fe^{+2}]. In Treatment. 2, a NH_4^+ removal % of 20.37% is obtained with respect to the initial [NH_4^+]. The degradation of CH_3COONa could release protons, reducing the pH of the medium, generating a favorable environment for the Feammox reaction (Xia et al., 2022), which would explain the positive results obtained with CH_3COONa. This is the reason why CH_3COONa is proposed as the most efficient carbon source for the Feammox process.

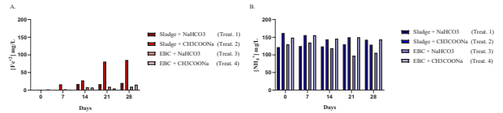

Figure 1. A. Fe^{+2} and B. NH_4^+ concentrations of the samples $NaHCO_3$ sludge (Treatment.1), CH_3COONa sludge (Treatment 2), EBC $NaHCO_3$ (Treatment 3) and EBC CH_3COONa (Treatment. 4)

In Figure 2, SEM images of the hollow-fiber samples are shown. The results show the formation of biofilm networks between Feammox bacteria on the fibers exposed to the sludge samples with $NaHCO_3$ and CH_3COONa. Working with biofilm formation is more convenient as it allows obtaining a higher biomass concentration, a denser sample structure and a higher resistance to shock loads (Hassard et al., 2015).

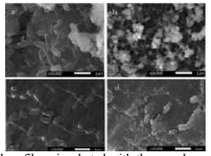

Figure 2. SEM images of hollow-fibers incubated with the samples a. $NaHCO_3$ sludge (Treatment 1), b. CH_3COONa sludge (Treatment 2), c. EBC $NaHCO_3$ (Treatment 3) and d. EBC CH_3COONa (Treatment 4).

These results would support the use of HFMB, based on biofilm formation, as an efficient method for Nr removal from wastewater.

REFERENCES

Clément, J. C., Shrestha, J., Ehrenfeld, J. G., and Jaffé, P. R. 2005 Ammonium oxidation coupled to dissimilatory reduction of iron under anaerobic conditions in wetland soils. Soil Biology and Biochemistry 37(12), 2323-2328. https://doi.org/10.1016/j.soilbio.2005.03.027

Galloway J. N., Cowling E. B. 2002 Reactive Nitrogen and The World: 200 Years of Change. AMBIO: A Journal of the Human Environment 31(2), 64-71. https://doi.org/10.1579/0044-7447-31.2.64

Hassard, F., Biddle, J., Cartmell, E., Jefferson, B., Tyrrel, S., & Stephenson, T. (2015). Rotating biological contactors for wastewater treatment–a review. Process Safety and Environmental Protection, 94, 285-306. https://doi.org/10.1016/j.psep.2014.07.003

Li, X., Hou, L., Liu, M., Zheng, Y., Yin, G., Lin, X., ... & Hu, X. 2015 Evidence of nitrogen loss from anaerobic ammonium oxidation coupled with ferric iron reduction in an intertidal wetland. Environmental Science & Technology 49(9), 11560-11568. https://doi.org/10.1021/acs.est.5b03419

Li, Y. Y., Huang, X. W., & Li, X. Y. (2021). Use of a packed-bed biofilm reactor to achieve rapid formation of anammox biofilms for high-rate nitrogen removal. Journal of Cleaner Production, 321, 128999. https://doi.org/10.1016/j.jclepro.2021.128999

Razaviarani, V., Ruiz-Urigüen, M., & Jaffé, P. R. 2019 Denitrification of nitric oxide using hollow fiber membrane bioreactor; effect of nitrate and nitric oxide loadings on the reactor performance and microbiology. Waste and Biomass Valorization 10(7), 1989-2000. https://doi.org/10.1007/s12649-018-0223-z

Visvanathan, C., Aim, R. B., and Parameshwaran, K. 2000 Membrane separation bioreactors for wastewater treatment. Critical reviews in environmental science and technology 30(1), 1-48. https://doi.org/10.1080/10643380091184165

Wu, W., Zhang, X., Qin, L., Li, X., Meng, Q., Shen, C., and Zhang, G. 2020 Enhanced MPBR with polyvinylpyrrolidone-graphene oxide/PVDF hollow fiber membrane for efficient ammonia nitrogen wastewater treatment and high-density Chlorella cultivation. Chemical Engineering Journal 379, 122368. https://doi.org/10.1016/j.cej.2019.122368

Xia, Q., Ai, Z., Huang, W., Yang, F., Liu, F., Lei, Z., & Huang, W. (2022). Recent progress in applications of Feammox technology for nitrogen removal from wastewaters: A review. Bioresource Technology, 127868. https://doi.org/10.1016/j.biortech.2022.127868

Yang, C., Zhang, W., Liu, R., Li, Q., Li, B., Wang, S., ... & Mulchandani, A. 2011 Phylogenetic diversity and metabolic potential of activated sludge microbial communities in full-scale wastewater treatment plants. Environmental science & technology 45(17), 7408-7415. https://doi.org/10.1021/es2010545

Yang G., Nianpeng H., Xinyu Z. 2014 Effects of reactive nitrogen deposition on terrestrial and aquatic ecosystems, Ecological Engineering 70, 312-318. https://doi.org/10.1016/j.ecoleng.2014.06.027

Zhou, H., & Xu, G. 2019 Integrated effects of temperature and COD/N on an up-flow anaerobic filter-biological aerated filter: Performance, biofilm characteristics and microbial community. Bioresource technology 293, 122004. https://doi.org/10.1016/j.biortech.2019.122004

Fe- and Zn-biochar mediated carbamazepine removal via heterogeneous Fenton process

A. Leovac Maćerak*, A. Kulić Mandić*, T. Tunić**, M. Bečelić-Tomin*, V. Pešić*, D. Tomašević Pilipović*, Đ. Kerkez*

*Department of Chemistry, Biochemistry and Environmental Protection, University of Novi Sad, Trg Dositeja Obradovica 3, Republic of Serbia
(E-mail: anita.leovac@dh.uns.ac.rs)
** Department of Biology and Ecology, University of Novi Sad, Trg Dositeja Obradovica 2, Republic of Serbia*

Abstract
In this work, the removal of carbamazepine in an aqueous solution was performed using the Fenton process catalyzed with Fe-BC and Zn-BC. The research included synthesis of catalysts and optimization of pharmaceutical removal conditions using the *Definitive screening design* statistical method in order to achieve the maximum efficiency of the mentioned treatment. Both materials showed good catalytic performance in the applied treatment (~98%). Obtained effluents showed high toxicity inhibition percent (~80%), as well as mineralization measured as TOC~80%. The further step is characterization of effluents using ultra-performance liquid chromatography (UPLC)–high-resolution mass spectrometry (HRMS) method.

Keywords
biochar-based catalyst; degradation; Fenton; carbamazepine;

INTRODUCTION

Carbamazepine (CBZ) is classified as a persistent organic pollutant, because its removal efficiency in water treatment plants is about 10%. It is toxic even at concentrations below 100 mg/l. Therefore, there is a need to find an efficient technology for its removal from the aquatic environment.
The Fenton process is one of the most effective advanced oxidation processes and is used to treat water with a high content of complex organic matter, as well as other no biodegradable compounds. The use of Fenton's reagent increases the degradability of complex organic compounds in wastewater, which results in their conversion into organic compounds of low molecular weight, or complete mineralization, until the formation of carbon dioxide and water. Increasing attention is focused on the use of biochar as a catalyst in order to use sewage sludge as a resource, not the waste. Due to its low cost, large specific surface area and good stability, biochar is a promising material that can be compared with other carbon materials. It has been often applied as carrier to improve the performance of iron and other ions impregnated in the carbon matrix. In this work, the removal of carbamazepine was performed using the Fenton process catalyzed by modified biochars, Fe-BC and Zn-BC. The test included the synthesis of biochar and the optimization of the conditions for the degradation of CBZ, using the Fenton process, with varying doses of hydrogen peroxide, CBZ and prepared catalysts, as well as pH and reaction time.

MATERIALS AND METHODS

For the synthesis of biochar, the final sludge from the wastewater treatment plant in the settlement of Kovilj (near Novi Sad), Autonomous Province of Vojvodina, Republic of Serbia was used. The biochar preparation procedure was performed according to Chen et al. (2020). Impregnation with iron and Zn onto biochar was performed according to the conventional method (Iurascu et al., 2009; Azmi et al., 2014). A BET analyzer (AutoSorb iQ2) was used to characterize the synthesized materials in order to test the specific surface area. To optimize the process conditions, the statistical method of *Definitive screening design (DSD)*, was assessed in order to achieve the maximum efficiency of the applied treatment and the degradation of the selected pollutant. The tests were carried out by a series of experiments on JAR test apparatus (FC6S Velp scientific, Italy). The absorbance (A) was measured at a wavelength of CBZ λ_{max} = 285 nm. Determining the absorption maxima (λ_{max}) by recording the spectrum of the CBZ solution, as well as monitoring the change in absorbance during the experiments, was performed using a UV-VIS spectrophotometer. Toxicity of samples was tested with the Aliivibrio fischeri bacteria bioluminescence test according to protocol ISO 11348-3 (2007). The principal of the test is to measure the bioluminescence of the bacteria before and after the addition of test samples, compared to control, at different time rates, 5, 15 or 30 minutes. The mineralization of effluents was determined using TOC analyzer (liquiTOC II, Elementar, Germany) (SRPS ISO 8245:2007).

RESULTS AND DISCUSSION

The impregnation of the pristine biochar with Fe (III) (BET= 3.807 m^2/g) and precipitation with Zn (II) ions (BET= 104.7 m^2/g) influenced the increase of the specific surface areas of the pristine material (BET= 57.83 m^2/g). The basic scheme of the experiment, obtained by applying the DSD model with 5 numerical factors, consists of 12 experiments and 2 central points (Table 1).

Table 1. Matrix of experiment with achieved CBZ removal efficiencies

Sample	Removal efficiency (%)	
	Fe-BC	Zn-BC
1	78	79
2	87	85
3	88	58
4	84	79
5	1	81
6	88	85
7	83	87
8	7	90
9	0.2	95
10	79	85
11	79	88
12	88	93
13	96	96
14	96	98

The results of testing the efficiency of the Fenton process in the removal of carbamazepine are shown in Table 4, where the range of removal efficiency was established from 0.2% to 96% for Fe-BC, from 58% to 98% for the Zn-BC catalyst. The achievement of maximum and minimum removal efficiency in the Fenton process at different set of process conditions is observed, thus confirming the assumption that the drug removal process itself largely depends on the applied experimental conditions, as well as on the applied materials. During the experiment, very significant removal efficiency was observed in the Fenton process at a different set of process conditions, which established that the removal process itself depends on the applied experimental conditions and used catalysts. An exception exists in 3 experiments in the case of Fe-BC, when the efficiency was low (up to 7%).
Optimization diagrams of the Fenton process are shown in Figures 1 and 2. They give a clear insight into how the selected process parameters affect the dependent variable, i.e. drug removal efficiency. The statistical model within the Fenton process for Fe-BC suggests a high carbamazepine removal efficiency of 95.885% under the following optimal conditions: pH=5.5, drug concentration of 5.5 mg/l, catalyst concentration of 60 mg/l, hydrogen concentration -peroxide of 10.5 mM and a reaction time of 105 min.

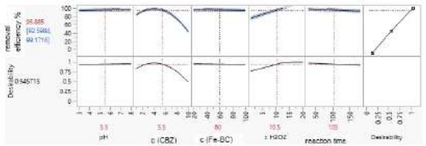

Figure 1. Optimization diagram of the Fenton process catalyzed by Fe-BC

Additionally, the statistical model within the Fenton process for Zn-BC suggests a high carbamazepine removal efficiency of 97.09% under the following optimal conditions: pH=5.5, drug concentration of 5.5 mg/l, catalyst concentration of 60 mg/l, concentration of hydrogen peroxide of 10.5 mM, while the reaction time is not proposed by the model, assuming that it does not have a large effect on the efficiency of the removal of the selected drug, under the investigated conditions (Figure 2).

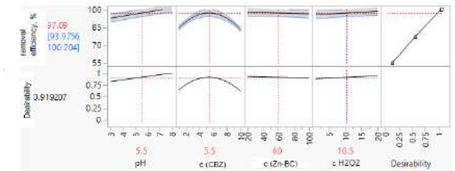

Figure 2. Optimization diagram of the Fenton process catalyzed by Zn-BC

It can be concluded that both biochars showed good catalytic performance under the applied conditions of the Fenton process. Toxicity measurements showed high inhibition percent (~85%) in both cases, pointing out on formation of toxic intermediates after Fenton reaction of 105 minutes. Further investigation will be conducted for longer reaction time, aiming on decreasing the effluent toxicity. Also, significant mineralization, measured as TOC, was achieved (~80%). The next step that will be implemented is the characterization of the obtained effluents after the optimal conditions using ultra-performance liquid chromatography (UPLC)–high-resolution mass spectrometry (HRMS) method.

REFERENCES

Azmi N.H.M., Ayodele O.B., Vadivelu V.M., Asif M., Hameed B.H. 2014. Fe-modified local clay as effective and reusable heterogeneous photo-Fenton catalyst for the decolorization of Acid Green 25. *Journal of the Taiwan Institute of Chemical Engineers*, **45**, 1459-1467.

Chen, Y., Duan, X., Zhang, C., Wang, S., Ren, N., Ho, S. 2020 Graphitic biochar catalysts from anaerobic digestion sludge for nonradical degradation of micropollutants and disinfection. *Chemical Engineering Journal*, 384, 123244.

Iurascu B., Siminiceanu I., Vione D., Vicente M.A., Gil A. 2009. Phenol degradation in water through a heterogeneous photo-Fenton process catalyzed by Fe-treated laponite. *Water Research*, **43**, 1313-1322.

International Organization for Standardization (2007). ISO 11348-3: Water quality — Determination of the inhibitory effect of water samples on the light emission of *Vibrio fischeri* (Luminescent bacteria test) — Part 3: Method using freeze-dried bacteria.

SRPS ISO 8245:2007, Water quality - Guidelines for the determination of total organic carbon (TOC) and dissolved organic carbon (DOC).

This project has received funding from the *European Union's Horizon Europe research and innovation programme, Horizon Europe - Work Programme 2021-2022 Widening participation and strengthening the European Research Area, HORIZON-WIDERA-2021-ACCESS-02*, under grant agreement No [101060110], SmartWaterTwin

WATER QUALITY AND QUANITY, FRESH WATER SOURCES SUITABLE FOR CREEK RIDGE INFILTRATION IN THE BRAAKMAN ZUID REGION (NL)

B.Letterie

Water Technology Research Group, HZ University of Applied Sciences, Edisonweg 4, 4382 NW Vlissingen the Netherlands (E-mail: *lett0009@hz.nl)**

Abstract

The Dow facility located in Terneuzen currently uses water of drinking water quality which is transported over a large distance. Dow want to use a water source closer by and not compete with drinking water. Dow needs ca. 400 Nm^3/y. Creek Ridge Infiltration can be used as a methodology to store water during the wet season and extract it during the dry season, with a 50% efficiency. The water quality and water quantity of the water source used for infiltration is key and needs to be examined. In this research several fresh water sources have been evaluated, both on quantity (1 mNm^3/y needed) and quality for infiltration, following local regulations. The results show that especially the quality of surface water is insufficient in the Terneuzen area, mainly caused by pesticides from agriculture. There is the need to pre-treat the water before infiltration, preferably using a NBS like a wetland (to be tested in a following up project). Also the water quantity available for infiltration shows great variation over the year, but also between the years, making is a necessity to consider the usage of several sources in the surroundings rather than focus on one source with the best quality.

Keywords

Water quantity, water quality, managed aquifer recharge, legislation, fresh water source

INTRODUCTION

The FRESH4Cs project focusses on the second Europe 2020 priority of sustainable growth, by demonstrating the provision of alternative and sustainable fresh water resources for lowland coastal regions. Traditional water resources are under pressure, and this problem is even more prominent in lowland coastal regions due to salinization of (near) surface waters. These same coastal lowlands drain vast amounts of water towards the sea at moments of water surplus (seasonal). Where water consumption has often been reduced to economic feasible levels, a second step in efficient water resource management is providing alternative and more sustainable resources, which is the focus of this project.

Dow is a partner in the FRESH4Cs project and the aim for Dow is to become resilient to climate change and independent of remote fresh water supply originating from the Biesbosch, 120 km away. Therefore Dow actively works on water savings, recycling and multi-sourcing. In 2008 the concept of a Robust Water System in the area of Zeeuws-Vlaanderen was initiated. It pursues collaborations with local governments and other end users in industry and agriculture to find regional solutions. DOW has invested over the past years in this robust water system for the region, not only in providing for its own water resources but also in aiding other regional water users.

In the current project there is an interest in exploring underground fresh water storage capabilities within the Braakman South region (cross-border Netherlands/Belgium). Excess rain precipitating in winter months, can be captured and temporarily stored for usage by agriculture and industry during periods of shortage. Dow would benefit from such a feasibility study, as it might provide solutions for its own water resources. Additionally, it will also strengthen Dow's cooperation with other regional water users that will benefit directly from the project (mainly farmers).

This report is written under work package 3 of the project, where Dow is preparing for investments, articulating the volumes and quality of water to be supplied to Dow and local farmers. In this report the water quality and water quantity of water sources in the area will be examined for suitability for infiltration. The ultimate goal is to find a suitable fresh water source for the infiltration of 1 Mm^3 annually during the winter months.

METHODOLOGY

In this chapter the methodology used to examine the suitability regarding both the water quality and the water quantity of the three potential fresh water sources will be described.

Isabellakanaal

The Isabellakanaal receives less fresh water from the Belgium polders since 2015 and therefore it is plausible that the chloride concentration of the Isabellakanaal has become too high over the past few years to be used for infiltration. Therefore the water quality was first tested on electrical conductivity (EC), a substitute for the chloride concentration.

For the duration of one year, starting on September 2020 until august 2021, the EC has been measured on a monthly basis on different locations along the Isabellakanaal starting at the Braakman and following the channel until past the Isabella gemaal, just across the Belgium border.

Leopoldkanaal

To determine the water quality parameters that are relevant for infiltration into the groundwater the Nota Grondwater is applicable (*Waterschap Scheldestromen, 2019*). The water quality of the Leopoldkanaal has been determined by the external laboratory Aqualab Zuid B.V., accredited conform NEN-EN-ISO/IEC 17025 (nl) under the number L387. The analysis have been performed conform NEN 6600-2, in compliance with the Nota Grondwater. The parameters that have been monitored have been discussed with the waterboard Waterschap Scheldestromen and are mostly in line with the Nota Grondwater. WSSS has agreed with deviating slightly from the Nota Grondwater regarding the list of pesticides and herbicides since the monitoring of the water quality regarding pesticides and herbicides was already ongoing for several years on the water coming from the Belgium Zwarte Sluispolder and the Isabellapolder by Evides, and measuring the same parameters on the Leopoldkanaal enabled us to make a solid comparison while still taking the major pesticides and herbicides into account.

Zwarte Sluispolder and Isabellapolder

Also for the Zwarte Sluispolder and for the Isabellapolder the water quality has been determined by Aqualab Zuid B.V. The water samples have been taken from the Evides basins whose are only fed by water coming from both polders. The same parameters have been analysed as for the Leopoldkanaal.

Of both the Zwarte Sluispolder and the Isabellapolder, an analysis has been done how much water would potentially be available for infiltration. The water of both polders comes together in a ditch and is discharged over the Boekhoute weir towards the Leopoldkanaal. The water from the Leopoldkanaal finally flows into the North Sea where it is mixed with the sea water.

To calculate the volume of water that flows over the weir data from the Boekhoute weir has been used (*Vlaanderen Waterinfo Kaartencatalogus*). The data provides information about the water level upstream of the weir and of the level of the weir itself, both TAW corrected. By using the Rehbock formula (Boiten *et al.*, 1995) the flowrate over the weir can be calculated. The data at the Boekhoute weir is logged every 15 minutes which makes it possible to calculate the volume that flows over the weir for every quarter of an hour. Finally the volume has been calculated on a monthly basis.

RESULTS AND DISCUSSION

In this chapter the results of the measurements of the water quality will be presented and compared with the thresholds mentioned in the Nota Grondwater. Also the calculated water quantities will be presented and discussed.

Water quality

The water quality of the Isabellakanaal, the Leopoldkanaal and the water from the Evides basins that comes from the Belgium Zwarte Sluispolder and the Isabellapolder has been measured and analysed. In the next subchapter the water quality analysis of the three possible sources of freshwater will be presented. The raw data and the processed data can be found in Appendix **¡Error! No se encuentra el origen de la referencia..**

Isabellakanaal

For the Isabellekanaal the water quality was first tested on electrical conductivity (EC), a substitute for the chloride concentration. In the Nota Grondwater, a threshold for chloride for infiltration in groundwater is stated of 160 mg/l. Also the Nota Grondwater states formula (1) and (2) for converting EC into the of concentration chloride in mg/l.

$$EC < 4mS/cm \ / \ Cl < 1000 \ mg/l: EC = (Cl + 188.5) / 286 \quad (1)$$

$$EC > 4mS/cm \ / \ Cl > 1000 \ mg/l: EC = (Cl + 450) / 360 \quad (2)$$

Using formula (1) it is determined that an upper threshold of 1.22 mS/cm can be used, all values below the threshold represent chloride concentrations lower than 160 mg/l. The results of the EC measurements at the different location is shown in Figure 1.

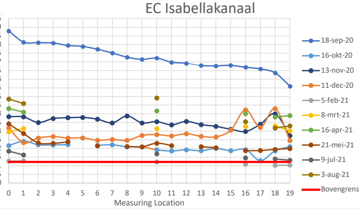

Figure 1: EC measurements Isabellakanaal

From Figure 1 it can be derived that only on February the 5th from location 10 to the Belgium border the EC was sufficiently low to meet the threshold for chloride of 160 mg/l. All other measurements show an exceedance of the norm for chloride. This would mean that the Isabellakanaal can only provide fresh water for infiltration during a very limited timeframe of the year.

Leopoldkanaal

The results of the analysis of the water quality of the Leopoldkanaal are shown in Table 1

Table 1: Results water quality analysis Leopoldkanaal

Parameter	Unit	Nota Grond-water	2-11-2021	6-12-2021	3-1-2022	7-2-2022	7-3-2022	4-4-2022
Chloride (Cl^-)	mg/L	160	140	150	290	130	160	1000
Total Phosphorous	mg/L-P	2	0,49	0,49	0,44	0,69	0,25	0,25
Nitrate (NO_3^-)	mg/L-N	50	12	26	21	21	26	<0,2
Arsenic (As)	µg/L	13,2	2,2	2,5	2,4	3,2	1,2	4,2
Cadmium (Cd)	µg/L	0,35	<0.2	<0,2	<0,2	<0,2	<0,2	<0,2
Copper (Cu)*	µg/L	2,4	<5	5,1	<5	5,1	<5	<5
Lead (Pb)	µg/L	7,4	<1	1,4	<1	4,6	<1	<1
Manganese (Mn)*	µg/L	31	380	150	190	160	220	130
Nickel (Ni)	µg/L	20	2,3	2,9	2,6	3,5	2,1	2,1
Total sum of Pesticides**	µg/L	0,5	1,43	0,96	0,83	0,75	0,80	0,80
Naphthalene	µg/L	0,01	<0.05	<0,05	<0,05	<0,05	<0,05	<0,05
Anthracene	µg/L	0,0007	<0.005	<0,005	<0,005	<0,005	<0,005	<0,005
Phenanthrene	µg/L	0,003	<0.005	0,0096	<0,005	0,0091	0,0056	<0,005
Crysene	µg/L	0,003	<0.005	<0,005	<0,005	<0,005	<0,005	<0,005
Fluoranthene	µg/L	0,003	<0.005	<0,005	<0,005	0,0056	<0,005	<0,005
Benzo (a) anthracene	µg/L	0,0001	<0.005	<0,005	<0,005	<0,005	<0,005	<0,005
Benzo (k) fluoranthene	µg/L	0,0004	<0.005	<0,005	<0,005	<0,005	<0,005	<0,005
Benzo (a) pyrene	µg/L	0,0005	<0.005	<0,005	<0,005	<0,005	<0,005	<0,005
Benzo (ghi) perylene	µg/L	0,0003	<0.005	<0,005	<0,005	<0,005	<0,005	<0,005
Indeno (123cd) pyrene	µg/L	0,0004	<0.005	<0,005	<0,005	<0,005	<0,005	<0,005

* Only for biological agriculture
**If the sum is exceeded, a threshold of 0.1 µg/l for the individual substances are applicable

The chloride concentration of the Leopoldkanaal is mainly in compliance with the threshold of 160 mg/l as described in the Nota Grondwater. During the infiltration the EC will be continuously monitored and when the threshold is exceeded, the infiltration will be stopped if water the Leopoldkanaal would be used.

For the metals, cupper exceeds the upper limit in two of the six measurements, and manganese is structurally to high. For both cupper and manganese, the norm is only applicable if the water will be used for biological agriculture. Since it is assumable that one of the potential farmers will practice biological agriculture, it is desirable that both cupper and manganese meet the threshold mentioned in the Nota Grondwater if water of the Leopoldkanaal would be used for infiltration.

Also for the total sum of pesticides, the values structurally exceed the threshold of 0.5 µg/l. Conform the Nota Grondwater, the individual pesticides have been analysed and it was concluded that 2,6-Dichlorobenzamide (BAM), Glyphosate (commonly used in Roundup and nowadays also in other brands) and Aminomethylphosphonic acid (AMPA, a breakdown product of glyphosate) exceed the threshold of 0.1 µg/l for all analysis. For infiltration the pesticides are too high if water from the Leopoldkanaal would be used.

For the polycyclic aromatic hydrocarbons (PACs) phenanthrene exceeds the threshold in three out of 6 analysis. Phenanthrene is released by burning hydrocarbons like natural gas and gasoline, and is considered to be carcinogenic. Also one analysis showed an exceedance of fluoranthene. For both phenanthrene and fluoranthene the limit for drinking water is 0.1 µg/L (*RIVM Zoeksysteem van stoffen, 2022*). It can be assumed that there is no health risk involved when water from the Leopoldkanaal is used for infiltration, but to avoid accumulation of the PACs in the groundwater the limit as described in the Nota Grondwater will be followed meaning that the values for PACs are too high for infiltration when water from the Leopoldkanaal would be used.

Zwarte Sluispolder and Isabellapolder

The results of the water quality analysis of the Zwarte Sluispolder and the Isabellapolder are show in Table 2.

Table 2: Results water quality analysis Zwarte Sluispolder and Isabellapolder

Parameter	Unit	Nota Grondwater	14-12-2020	18-1-2021	15-2-2021	15-3-2021	19-4-2021	17-5-2021	21-6-2021	15-11-2021	20-12-2021	17-1-2022	21-2-2022	21-3-2022
Chloride (Cl^-)	mg/L	160	83	81	81	80	78	81	81	84	77	77	78	80
Total Phosphorous	mg/L-P	2	0,1	0,1	0,1	0,1	<0,1	<0,1	<0,1	0,024	0,036	<0,1	<0,1	<0,1
Nitrate (NO_3^-)	mg/L-N	50	3,2	6,4	6,1	6,4	28	25	21	13	20	26	26	24
Arsenic (As)	µg/L	13,2	1	1	1	1	<1	<1	<1	<1	<1	<1	<1	<1
Cadmium (Cd)	µg/L	0,35	0,2	0,2	0,2	0,2	<0,2	<0,2	<0,2	<0,2	<0,2	<0,2	<0,2	<0,2
Copper (Cu)*	µg/L	2,4	5	5	5	5,1	<0,005	<0,005	<0,005	<0,005	<0,005	<0,005	<0,005	0
Lead (Pb)	µg/L	7,4	1	1	1	1	<1	<1	<1	<1	<1	<1	<1	<1
Manganese (Mn)*	µg/L	31	25	63	62	60	<10	<10	13	52	82	98	78	63
Nickel (Ni)	µg/L	20	2	2,2	2,1	2,5	2,0	2,3	2,1	2,1	2,5	2,6	2,1	2,4
Total sum of Pesticides**	µg/L	0,5	0,677	0,024	0,493	0,67	0,691	0,63	0,37	1,085	1,242	0,635	0,613	0,598
Naphthalene	µg/L	0,01	<0,05	<0,05	<0,05	<0,05	<0,05	<0,05	<0,05	<0,05	<0,05	<0,05	<0,05	<0,05
Anthracene	µg/L	0,0007	<0,005	<0,005	<0,005	<0,005	<0,005	<0,005	<0,005	<0,005	<0,005	<0,005	<0,005	<0,005
Phenanthrene	µg/L	0,003	0,0064	0,0072	0,009	0,006	<0,005	<0,005	<0,005	0,0052	0,007	0,0077	0,0062	0,0055
Crysene	µg/L	0,003	<0,005	<0,005	<0,005	<0,005	<0,005	<0,005	<0,005	<0,005	<0,005	<0,005	<0,005	<0,005
Fluoranthene	µg/L	0,003	<0,005	<0,005	<0,005	<0,005	<0,005	<0,005	<0,005	<0,005	<0,005	<0,005	<0,005	<0,005
Benzo (a) anthracene	µg/L	0,0001	<0,005	<0,005	<0,005	<0,005	<0,005	<0,005	<0,005	<0,005	<0,005	<0,005	<0,005	<0,005
Benzo (k) fluoranthene	µg/L	0,0004	<0,005	<0,005	<0,005	<0,005	<0,005	<0,005	<0,005	<0,005	<0,005	<0,005	<0,005	<0,005
Benzo (a) pyrene	µg/L	0,0005	<0,005	<0,005	<0,005	<0,005	<0,005	<0,005	<0,005	<0,005	<0,005	<0,005	<0,005	<0,005
Benzo (ghi) perylene	µg/L	0,0003	<0,005	<0,005	<0,005	<0,005	<0,005	<0,005	<0,005	<0,005	<0,005	<0,005	<0,005	<0,005
Indeno (123cd) pyrene	µg/L	0,0004	<0,005	<0,005	<0,005	<0,005	<0,005	<0,005	<0,005	<0,005	<0,005	<0,005	<0,005	<0,005

* Only for biological agriculture
**If the sum is exceeded, a threshold of 0.1 µg/l for the individual substances are applicable

The concentration of chloride meets the requirement of 160 mg/l. For cupper some measurements exceed the threshold, as well as for manganese. Although this only applies for biological agriculture, it is desirable that both cupper and manganese meet the threshold mentioned in the Nota Grondwater if water of the Belgium polders would be used for infiltration.

Also for the total sum of pesticides, the values mostly exceed the threshold of 0.5 µg/l. Conform the Nota Grondwater, the individual pesticides have been analysed and it was concluded that BAM, Glyphosate and AMPA exceed the threshold of 0.1 µg/l for most of the analysis. For infiltration the pesticides are too high if water from the Belgium polders would be used for infiltration.

Comparable with the Leopoldkanaal, also the PAC phenanthrene exceeds in many of the measurements the threshold mentioned in the Nota Grondwater.

Water quantity

The volume of the water flowing from the Zwarte Sluispolder and the Isabellapolder over the Boekhoute weir has been calculated on a monthly basis. The results are show in Table 3.

As is shown in Table 3 there are huge differences in the volume that flows over the weir between the different months in one year, but also between the various years. In 2021 21M m^3 was discharged to the Leopoldkanaal, while in 2018

s flown over the weir at all, while in the month March alone more than 6M m^3
d flow over the weir, more in one month than in the entire year of 2018.

e 3: Calculated volume over the Boekhoute weir

	Jan	Feb	Mar	Apr	Mei	Juni	Juli	Aug	Sept	Okt	Nov	Dec	Totaal
Volume over stuw (m3):	3.697.693	3.078.252	919.178	256.584	1.238.819	1.152.604	1.760.280	1.314.739	1.033.880	738.849	1.079.524	4.595.146	20.865.548
Max Debiet (m3/s)	13,59	6,67	2,34	0,93	4,04	1,60	12,97	1,32	1,06	2,30	4,13	8,29	
Gem Debiet (m3/s)	1,38	1,27	0,34	0,10	0,46	0,44	0,66	0,49	0,40	0,28	0,42	1,72	0,66
95 percentiel Debiet (m3/s)													2,34
Neerslag (mm)	120,3	45,1	36	36,7	90,1	114,1	55,8	46,8	15,7	102,1	97,9	93,3	853,9
Volume over stuw (m3):	0	2.551.010	6.284.489	0	32.881	1.741.292	446.407	0	120.141	2.732.506	569.953	1.230.126	15.708.804
Max Debiet (m3/s)	0,00	9,05	28,00	0,00	1,51	22,28	22,89	0,00	3,38	1.51 4,50	1,28	16,99	
Gem Debiet (m3/s)	0,00	1,02	2,35	0,00	0,01	0,67	0,17	0,00	0,05	1,02	0,22	0,46	0,50
95 percentiel Debiet (m3/s)													1,37
Neerslag (mm)	33,4	133,2	82,6	16,1	15,8	108,9	65,8	54,2	134,2	102,1	34,4	71,7	852,4
Volume over stuw (m3):	178.840	375.808	1.778.668	91.770	292.442	617.714	188.957	53.827	3.990	24.689	97.599	152.243	3.856.548
Max Debiet (m3/s)	1,42	2,23	3,38	1,52	1,68	1,15	0,85	0,71	0,45	1,07	1,26	2,68	
Gem Debiet (m3/s)	0,07	0,16	0,67	0,04	0,11	0,24	0,07	0,02	0,00	0,01	0,04	0,06	0,12
95 percentiel Debiet (m3/s)													0,60
Neerslag (mm)	68,7	44,6	80,2	20,9	36,3	90,2	60,2	39,6	55,6	98,3	84,3	79,2	758,1
Volume over stuw (m3):	1.719.797	299.661	596.908	159.074	96.295	48.003	812	0	903	7.288	37.742	7.283	2.973.767
Max Debiet (m3/s)	5,53	2,44	1,68	0,36	0,31	0,22	0,16	0,00	0,10	0,22	0,28	0,19	
Gem Debiet (m3/s)	0,64	0,12	0,22	0,06	0,04	0,02	0,00	0,00	0,00	0,00	0,02	0,00	0,09
95 percentiel Debiet (m3/s)													0,26
Neerslag (mm)	83,2	33,8	93,3	61,7	38,5	14,6	4,4	54,6	36,8	60,3	35,3	85,7	602,2
Volume over stuw (m3):	705.650	298.434	462.288	2.863	0	0	0	24.541	92.174	4.801	80.744	1.963.187	3.634.682
Max Debiet (m3/s)	2,04	1,65	2,38	0,14	0,00	0,00	0,00	2,04	0,25	0,15	1,17	6,55	
Gem Debiet (m3/s)	0,26	0,12	0,17	0,00	0,00	0,00	0,00	0,01	0,04	0,00	0,03	0,73	0,11
95 percentiel Debiet (m3/s)													0,41
Neerslag (mm)	72,1	43,6	51,8	21	32,4	15,4	134,8	77,7	75,4	76,7	90	128,9	819,8
Volume over stuw (m3):	2.311.822	1.280.006	578.480	226.568	150.779	506.727	157.983	72.988	43.466	16.688	154.007	42.420	5.541.934
Max Debiet (m3/s)	6,25	5,69	2,25	2,61	0,79	0,61	0,32	0,23	0,16	0,24	5,03	19,27	
Gem Debiet (m3/s)	0,86	0,51	0,22	0,09	0,06	0,20	0,06	0,03	0,02	0,01	0,06	0,02	0,18
95 percentiel Debiet (m3/s)													0,48
Neerslag (mm)	146,3	85,5	76	43,2	79,4	104,4	24,7	54,6	23,6	55,9	119,9	19,2	832,7

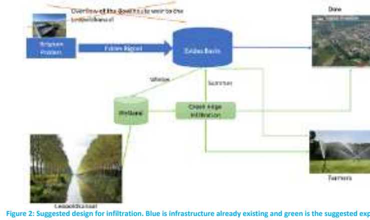

Figure 2: Suggested design for infiltration. Blue is infrastructure already existing and green is the suggested expansion.

Refferences

Waterschap Scheldestromen. (2019). *Nota Grondwater.* Version db 2 juli 2019. Reg nr. 2019005935. 13 juni 2019

RIVM Zoeksysteem van stoffen, Geraadpleegd op 20-06-2022, van http://rvszoeksysteem.rivm.nl

Vlaanderen Waterinfo Kaartencatalogus, Geraadpleegd op 23-05-2022, van https://www.waterinfo.be/kaartencatalogus

Boiten, W., Dommerholt, A. en Soet, M., 1995. Handboek debietmeten in open waterlopen. *Vakgroep Waterhuishouding, rapport 51, Wageningen*

Waterschap Scheldestromen. (2015). *Watergebiedsplan Braakman e.o. Planvorming wateropgave.* Reg nr. 2015033897. 28 October 2015.

CONCLUSIONS

The water EC of the water of the Isabellakanaal shows values varying from 8 mS/cm to 1 mS/cm. However, the measurements show that only for circa six weeks in one year time the values were under the threshold of 1.22 mS/cm representing the chloride concentration of 160 mg/l. From these measurements it can be concluded that the water of the Isabellakanaal contains a to high chloride concentration to be used as a reliable source of fresh water for infiltration into the groundwater.

The water of the Leopoldkanaal showed to be fresh enough for infiltration. However, the metals cupper and manganese exceed the threshold for infiltration, 2.4 µg/l and 31 µg/l respectively, when biological agriculture would be performed. Also the total sum of pesticides exceeds the threshold of 0.5 µg/l with the individual pesticides BAM, glyphosate and AMPA exceeding the threshold of 0.1 µg/l. Finally the PACs phenanthrene and fluoranthene also exceed the threshold for infiltration of 0.003 µg/l. The water quality of the Leopoldkanaal is therefore insufficient for infiltration in the groundwater.

The water of the Zwarte Sluispolder and the Isabellapolder seems slightly better than the water of the Leopoldkanaal, however also cupper, manganese, BAM, AMPA, glyphosate and phenanthrene exceed the thresholds mentioned in the Nota Grondwater. The water of the polders is of a slightly better quality then the water of the Leopoldkanaal, however the substance mentioned above exceeding the Nota Grondwater make this water, not suitable for infiltration.

The water quantity of the Zwarte Sluispolder and the Isabellapolder available for infiltration shows variations over the months in one year, but also between the various years. To have access to a source that can supply a constant amount of water, the water from the Zwarte Sluispolder and the Isabellapolder can provide a substantial part of the water, but it cannot be guaranteed that the water will be available all the time.

Seen the varying effect of infiltrating water of different quality into the groundwater as mentioned above, it cannot directly be concluded that the infiltration pilot has positively or negatively changed the quality of the groundwater. It should be noticed that the pilot was small scale, and only has occurred for a period of one year. To gain more insight in the effect of the infiltration pilot, a longer period of experimenting for at least 5 years with additional monitoring is advised to be able to draw conclusions regarding water quality effects of infiltration on the groundwater quality.

RECOMMENDATIONS

Since the infrastructure of Evides that is already installed to transport the water of the Zwarte Sluispolder and the Isabellapolder to the basins, and the water quality seems the most suitable, the water from the Belgium polders is the most preferred option for infiltration. However, the quantity is not always adequate for continues infiltration. Therefore a second water source may be considered. Since the chloride concentration of the Leopoldkanaal is much lower than the Isabellakanaal, and mostly in compliance with the Nota Grondwater, the Leopoldkanaal seems most suitable as a second water source.

The quality of both the water from the Belgium polders and from the Leopoldkanaal do not meet the requirements of the Nota Grondwater for all the substances. Therefore it is recommended to do research towards suitable technologies to treat the water in the most cost and energy efficient way. During the course of this project, the follow up project Aquatuur has been initiated where several constructed wetlands , whether or not combined with activated carbon filters, will be tested on removal efficiencies of the substances found in this research that now exceed the thresholds of the Nota Grondwater.

Since the water can be transported using the Evides infrastructure, it would be beneficial to discuss the options, possibilities, challenges and limits of the infrastructure with Evides. Also the management of the basins, possibilities to store additional water for infiltration in the basins and monitoring possibilities could be discussed with Evides as well as the common interest Dow, Evides and local farmers would experience for infiltration additional water that later can be extracted.

The VMM controls the level of the Boekhoute weir, and decides when the weir will be lowered or raised, in consultation with the owners of the Zwarte Sluispolder and the Isabellapolder. Therfore it is also recommended to start communications with these stakeholders to discuss the possibilities of pumping more water from the polders, and measures that allow more extraction without changing the groundwater level in the polders. The ideal situation would be that all the water that in the current situation flow over the Boekhoute weir is used for infiltration via the Evides infrastructure, including the basins.

As a design for the extraction of the fresh water source, infrastructure needed to transport and pump the water to the infiltration location and after extraction of the groundwater to the water consumers, a schematic overview is suggested in Figure 2.

Use of a packed-bed biofilm reactor to achieve rapid formation of anammox biofilms for high-rate nitrogen removal

Ying-yu Li*, Xiao-yan Li

* Environmental Engineering Research Centre, Department of Civil Engineering,
The University of Hong Kong, Pokfulam, Hong Kong, China
(E-mail: yingyuli@connect.hku.hk)

Abstract
Anammox (AMX) is an efficient and carbon-saving process for biological nitrogen removal; however, the long start-up period hinders its application in wastewater treatment. In this study, an innovative packed-bed biofilm reactor (PBBR) was developed for the rapid enrichment of AMX biofilms. With a greatly reduced fluid turbulence in the PBBR, the attachment and growth of AMX biofilms were found to be accelerated and the specific AMX biofilm formation rate was 60% faster than that in the conventional moving-bed biofilm reactor and the nitrogen removal capacity of the PBBR increased rapidly from 77.6 to 876.8 mg N/(L·d) in 2 months.

Keywords (maximum 6 in alphabetical order)
Anammox, autotrophic nitrogen removal, biofilms, start-up, wastewater treatment

INTRODUCTION

Fluid turbulence and mechanical collision between biocarriers are the main detrimental factors that restrict the biomass attachment to the carriers. The successful start-up of Anammox (AMX) bioreactors commonly requires 150–500 d (Yu et al., 2013; Zekker et al., 2013). In this study, a new bioreactor configuration, packed-bed biofilm reactor (PBBR), in which plastic carriers were tightly packed in the bioreactor, was developed for the rapid start-up of AMX biofilm reactors. With the significantly reduced fluid turbulence and no mechanical collisions between the biocarriers, the PBBR provided a more favorable condition for AMX biofilm formation and growth. Besides, the AMX biofilm pre-acclimated in the PBBR was found to have a much higher nitrogen removal capacity and more stable nitrogen removal performance in the practical wastewater treatment than the AMX biofilm enriched in the conventional moving-bed biofilm reactor (MBBR).

MATERIALS AND METHODS

A column-type reactor made of polymethyl methacrylate with a height of 50 cm, diameter of 8 cm, and working volume of 2.5 L was used. The PBBR column was filled with 2 L of commonly used plastic K1 carriers (AnoxKaldnesTM, Veolia, Sweden). The top of the biocarriers was capped with a coarse screen to keep the carriers tightly packed in the PBBR. Experimental studies were conducted to investigate the biofilm development and the nitrogen removal performance of the PBBR system.

RESULTS AND DISCUSSION

Rapid AMX biofilm formation in the PBBR

The confocal laser scanning microscopy (CLSM) was used for monitoring and visualization of biofilm development in the PBBR (Fig.1). Different from the suspension in the conventional MBBR (> 30/s), biocarriers in the PBBR would experience a much lower shear intensity (< 1/s) during its operation. With a greatly reduced fluid shear in the mild flow of PBBR, biomass would settle on the biocarriers and readily colonize on the carrier surface. Under the nearly quiescent fluid environment, the rate of AMX biofilm formation in PBBR was significantly promoted, and the biofilm biomass content in the bioreactor rapidly increased to 4,047 ± 333 mg VSS/m^2 after 100-d acclimation, with an average biofilm thickness of 182.5 ± 44.1 μm. In comparison with the conventional MBBR, the doubling time of the AMX biofilm in the PBBR was greatly shortened from 34.0 d to 21.7 d. The PBBR which can effectively facilitate the formation and growth of AMX biofilms on the biocarriers can be used as a source and supplier of healthy AMX biofilms.

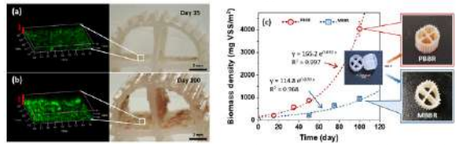

Figure 1. Biofilm formation in the PBBR: CLSM and stereoscopic images of the enriched AMX biofilms on (a) day 35 and (b) day 100; (c) biomass density and biofilm growth on the K1 carriers in the PBBR (vs. the MBBR).

Nitrogen removal performance of the PBBR

In addition to being an excellent reactor for AMX biofilm enrichment, the PBBR also showed an excellent autotrophic nitrogen removal performance. The nitrogen removal capacity slowly increased from the initial level of 77.6 to 106.0 mg N/(L·d) during Stage I (Fig. 2). In Stage II, with the adjustment of the feeding scheme, the free ammonia (FA) and free nitrous acid (FNA) contents in the PBBR were maintained at a low level by decreasing the exchange ratio and extending the hydraulic retention time in operation. Maintaining a low FA (< 2.7 mg/L) and FNA (< 5.8 μg/L) concentrations in the early stage was found to play a critical role in the AMX biofilm development, particularly when the biofilm was thin (<100 μm). As the biofilm thickened, the AMX bacteria embedded in the thick biofilm were well-protected from FA and FNA, and the biofilm became more robust against inhibitors in the suspension. Overall, by using the optimized operating strategy for the PBBR, the AMX biofilm growth was accelerated and the nitrogen removal capacity of the PBBR could increase rapidly from 77.6 to 876.8 mg N/(L·d) in 2 months, significantly shortening the start-up period of the AMX-based bioreactors.

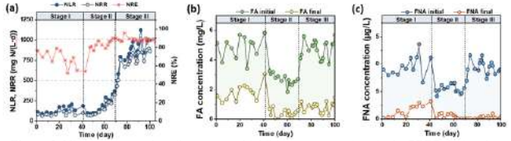

Figure 2. Nitrogen removal performance and inhibitor concentrations in the PBBR during the experimental period: (a) nitrogen loading rate (NLR), nitrogen removal rate (NRR), and nitrogen removal efficiency (NRE); (b) FA concentration at the beginning and the end of each SBR cycle; and (c) FNA concentration at the beginning and the end of each SBR cycle.

REFERENCES

Yu, Y.C., Gao, D.W., Tao, Y., 2013. Anammox start-up in sequencing batch biofilm reactors using different inoculating sludge. Applied Microbiology and Biotechnology, **97**(13), 6057–6064.

Zekker, I., Rikmann, E., Tenno, T., Kroon, K., Vabamäe, P., Salo, E., Loorits, L., dC Rubin, S.S.C., Vlaeminck, S.E., Tenno, T., 2013. Deammonification process start-up after enrichment of anammox microorganisms from reject water in a moving-bed biofilm reactor. Environmental Technology, **34**(23), 3095–3101.

Implementing the use of pure oxygen to expand the Integrated Fixed-film Activated Sludge (IFAS) at the Monteagudo (Navarra) Waste Water Treatment Plant (WWTP)

I. Ilzarbe*, M. de Gracia**, A. López* and J. Gómez*

* Navarra de Infraestructuras Locales S.A. (NILSA). Av. de Barañáin, 22, 31008 Pamplona, Navarra
(E-mail: *ilzarbe@nilsa.com*)
** Nippon Gases. Poligono Akarregi, 10, Oficina 306, 20120 Hernani
(E-mail: *monica.degracia@nippongases.com*)

Abstract
The Monteagudo WWTP faces a major challenge during four months of the year when a temporary agro-industrial discharge increases the average treated load from 2500 equivalent-inhabitants to six times that amount. To address this issue, a study to test the feasibility of pure oxygen as an alternative to increasing the volume of the IFAS process was conducted. The study was performed from 2017 to 2022, during which the use of pure oxygen was tested and subsequently verified. The results of the study showed that the use of pure oxygen effectively increased the capacity of the WWTP's treatment process reaching removal values up to 9 kgCOD/m^3/d. This approach not only improved the capacity to handle temporary industrial discharge but also avoided the need for an important investment in the expansion of the WWTP. The treatment in question is currently applied on an annual basis during the season of agro-industrial discharges.

Keywords
IFAS; MBBR; pure oxygen; temporary industrial discharge

INTRODUCTION

The Monteagudo (Navarra) Waste Water Treatment Plant (WWTP) is responsible for treating the discharge of an average of 2500 equivalent inhabitants throughout most of the year. However, during the four months of August to November, the treated load is significantly increased to 15000 eq-inhabitants due to a temporary agro-industrial discharge. This presents a significant challenge for the WWTP in terms of maintaining the effectiveness of the treatment process. The treatment plant consists of Integrated Fixed-film Activated Sludge (IFAS) as biological process, followed by a trickling filter and final lagooning. The volume of the biological process was designed for the usual load, having difficulties during the high load period to guarantee the quality of the treated water.

An alternative method for increasing the capacity of the biological process is to utilize liquid oxygen injection in place of traditional aeration. This approach relies on the ability to transfer oxygen to microorganisms at a significantly higher rate. While aeration using air bubbles can transfer a maximum of 1500-2000 mgO$_2$/m^3/day, the use of pure oxygen can transfer up to 7500-9000 mgO$_2$/m^3/day. According to Skouteris *et al.* (2020), pure oxygen achieves faster treatment rates at higher biomass concentrations and shorter hydraulic retention times (HRT). The WWTP receives up to 1800 kg/day of COD in 800 m^3/day during peak months, which requires more than 600 kgO$_2$/day. Given the volume of the IFAS is 135m^3, the necessary oxygen transfer rate (OTR) is estimated to be more than 4000 gO$_2$/m^3/day. Therefore, replacing air with pure oxygen could expand the WWTP capacity to effectively treat the received load. Furthermore, the use of pure oxygen also increases its diffusion in the biofilm of moving bed-based processes, thus it would be possible to increase the attached biomass (Salvetti *et al.*, 2006).

The current study shows the experimental research carried out on a real WWTP during a high load period, with the aim of evaluating the effects of replacing the electrical consumption of blowers through the utilization of pure oxygen injection. The assessment will cover the examination of the treatment capacity, the quality of the final discharge and the energy and consumable costs.

MATERIALS AND METHODS

Influent water and operating parameters.
Table 1 summarizes the characteristics of the influent water at average and high load. **Table 2** shows the expected operating parameters in each of the seasons.

Pure oxygen injection equipment and monitoring.
Exclusive technology from Nippon Gases was installed, including specific injection equipment, a cryogenic tank and control panels. Additionally, the MiruGas® system was implemented for process remote monitoring, automation and control. This APC tool is specifically designed for the operation of biological processes. Through its calculation algorithm for Oxygen Utilization Rate (OUR - gO$_2$/m^3/d), the tool is capable of continuously monitoring microbial activity (Irizar *et al.*, 2009). Additionally, other key variables including water flow, gas flow, dissolved oxygen and turbidity at the outlet, were also tracked. During the testing period, an intensive analytical monitoring was carried out to verify the performance of the pure oxygen application.

RESULTS AND DISCUSSION

During the high load experimental period shown in the following graphs, the operating conditions of blowers together with the pure oxygen were changed until the combination that managed to treat the entire load at minimum cost was obtained: finally, a fixed blower input was established, being the injection of pure oxygen regulated (ON-OFF control) by the Dissolved Oxygen (DO) value.

Figure 1 shows the flow rate and the organic input load. Typical values were ranging between 1200 and 1500 kg COD/day, which are up to 5 times greater than the load for the rest of the year. **Figure 2** shows the COD concentration values at the inlet of the WWTP, at the secondary clarifier, and the final outlet after the trickling filter. Most of the COD removal occurs in the IFAS process with pure oxygen. The trickling filters have acted as a refining process. The best results in terms of water quality were obtained during the last part of the period, when the sludge was already acclimatised to pure oxygen, and the air and oxygen configuration was optimal. This configuration has been repeated in subsequent years. It has been proved that the correct application of pure oxygen in moving bed processes achieves significant improvements in the suspended solids, facilitating their settling and significantly reducing the COD of the output water associated with suspended solids.

It is important to find the optimal balance between both air/oxygen systems, as an excess of air can lead to an undesired stripping of the injected oxygen bubbles. On the other hand, a minimum but continuous supply of air is recommended to ensure agitation. This saves a lot of cryogenic oxygen consumption while still achieving high Oxygen Transfer Efficiency (OTE) values, which are impossible to achieve with air bubbles alone. The volumetric load that the expanded IFAS process was capable of treating with pure oxygen and proper operation and control is shown in **Figure 3**, reaching values of up to 9 kgCOD/m^3/d. With this data, it can be concluded that excellent process efficiencies and greater stability were achieved. The operational cost comparison of this configuration versus the amortisation and operating cost of the increased IFAS volume and blowers clearly showed the convenience of pure oxygen injection considering 4 months campaigns. With the implementation of pure oxygen, NILSA had two benefits: it required no fixed installation, thus eliminating risk of a costly investment in case of company closure. Secondly, was ready for use when needed and avoided the need for major construction work in time for the following season. Additionally, for Nippon Gases, this presented a chance to evaluate and enhance their new special injection equipment for moving bed processes.

Table 1. Characteristics of the influent water at average load associated with most of the year, and the high load expected between August and November

Parameter		AVERAGE	HIGH
Flow	m^3/d	**500**	**800**
TSS	gSS/m^3	250	500
COD_{total}	gCOD/m^3	600	2250
$COD_{soluble}$	gCOD/m^3	303	1655
BOD_5	gCOD/m^3	400	1595
$COD_{T\ inert}$	gCOD/m^3	50	80
Resulting loads			
COD load	kgCOD/d	300	1800
SS load	kgSS/d	125	400

Table 2. Expected operating parameters in each of the seasons.

Operational parameters		AVERAGE	HIGH
IFAS volume	m^3	135	135
HRT	h	6	4
F/M	$gCOD_{in}$/SSV/d	0,63	**3,09**
Volumetric load	kgCOD/m^3/d	2,2	13,3
SRT	day	5,3	0,8
COD_{total} effluent	mg/l	42	40
SOUR	mgO$_2$/gSSV/h	14,8	47,8
OUR	gO$_2$/m^3/d	1940	**4943**
Total O_2 requirements	kgO$_2$/d	328	834
Sludge produced	kgSS/d	122	862
Sludge temperature	ºC	25	25

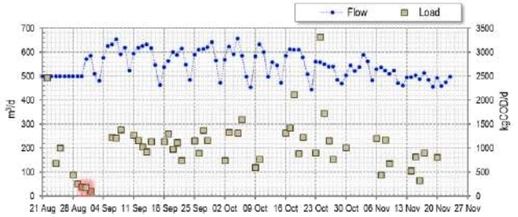

Figure 1. Flow rate (m^3/d) and the organic input load (kgCOD/d).

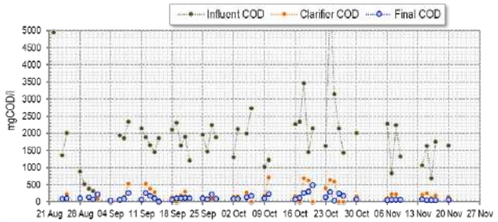

Figure 2. COD concentration values (mg/l) at the inlet of the WWTP, at the secondary clarifier, and the final outlet after the trickling filter.

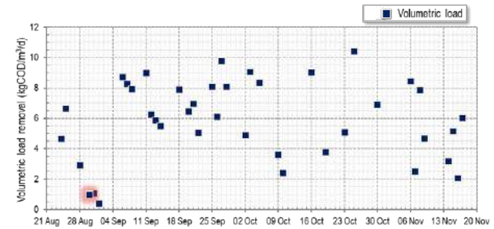

Figure 3. Volumetric load (kgCOD/m^3/d) removed at the IFAS process.

REFERENCES

Irizar, I., Zambrano, J.A., Montoya, D., De Gracia, M., García, R., 2009. Online monitoring of OUR, K_La and OTE indicators: practical implementation in full-scale industrial WWTPs. Water Sci Technol 60, 459–466. https://doi.org/10.2166/wst.2009.363

Salvetti, R., Azzellino, A., Canziani, R., Bonomo, L., 2006. Effects of temperature on tertiary nitrification in moving-bed biofilm reactors. Water Res 40, 2981–2993. https://doi.org/10.1016/j.watres.2006.05.013

Skouteris, G., Rodriguez-Garcia, G., Reinecke, S.F., Hampel, U., 2020. The use of pure oxygen for aeration in aerobic wastewater treatment: A review of its potential and limitations. Bioresource Technology 312, 123595. https://doi.org/10.1016/j.biortech.2020.123595

OPFRs degradation by White Rot Fungi: Screening of degraders and approach to the degradation mechanism.

D. Losantos*, M. Sarrà*, S. Tayar*, G. Caminal**

* Department of Chemical, Biological and Environmental Engineering, Universitat Autònoma de Barcelona, Escola d'Enginyeria, Campus Bellaterra 08193 Cerdanyola del Vallès, Spain
(E-mail: diana.losantos@uab.cat, montserrat.sarra@uab.cat, ghamim.tayar@uab.cat)
** Institut de Quimica Avançada de Catalunya (IQAC), Spanish Council for Scientific Research (CSIC). Jordi Girona 18-26, 08034 Barcelona, Spain
(E-mail: gcsqbp@iqac.csic.es)

Abstract
OPFRs are emergent, toxic, and persistent pollutants that can easily diffuse in water, and that are only partially removed in wastewater treatment plants. Ligninolytic white rot fungi (WRF) can constitutively, and co-metabolically degrade a series of contaminants through non-specific extracellular enzymes and a versatile intracellular system. An initial screening for evaluating the ability of six different WRF and one non- ligninolytic fungus to degrade TEP, TBP, TCEP and TBEP is reported. WRF showed to be better degraders than *A. niger*, which can grow in the medium but not degrade OPFRs. TEP was not removed at all, while only 47% of TCEP could be removed by *G. lucidum* under nutrient limiting conditions. TBP and TBEP were completely degraded by *G. lucidum*, *P. sanguineus* and *T. versicolor* after 3 days. We theorize that OPFRs with larger structures are more easily degraded as it is easier for the fungi to take radicals of them. Biodegradation was the main mechanism of OPFRs removal, but its contribution depends on each fungus and each contaminant.
Keywords: emerging pollutants, flame retardants, fungal degradation, laccase, removal.

INTRODUCTION

Organophosphate flame retardants (OPFRs) are alkyl esters of phosphoric acid which are used as additives in a variety of commercial products due to their ability to act as flame retardant barriers. These high-production-volume compounds are not chemically bonded to their host materials and can easily diffuse in water compartments, being only partially removed in wastewater treatment plants (WWTPs) (Reemtsma et al., 2008). Bioremediation progressively appears as an appealing degradation method for persistent contaminants as it is simple, efficient and economically feasible.
The microbial degradation of some OPFRs has been studied (Dunyu et al., 2021). However, it implies the need for an adaptation period for bacteria to efficiently degrade the contaminant and a substrate's concentration "response threshold", below which bacteria cannot degrade the contaminant (Chaudhari et al., 2012). Ligninolytic white rot fungi (WRF) can overcome these concerns as they can constitutively, and co-metabolically degrade a series of contaminants through non-specific extracellular ligninolytic enzymes and a versatile intracellular system.
The present work reports an initial screening for evaluating the ability of six different WRF and one non- ligninolytic fungus to degrade four OPFRs, known to be soluble in water and usually detected in WWTPs effluents. Additionally, performance of two chosen fungi was further studied in the degradation of a well-degraded contaminant, to elucidate the contributions of physical adsorption and biodegradation to this removal. As a part of an ongoing project, it is expected that the results of this work pave the way for deeper studies on the degradation of soluble OPFRs through WRF.

MATERIALS AND METHODS

Four different OPFRs were tested: triethyl phosphate (TEP), tributyl phosphate (TBP), trichloro ethyl phosphate (TCEP) and tributoxy ethyl phosphate (TBEP). Six WRF: *Ganoderma lucidum, Pleorotus ostreatus, Phanerochaete velutina*, *Pycnoporus sanguineus*, *Trametes versicolor,* and *Trichoderma viride* and one non-ligninolytic fungus (*Aspergillus niger,* as we intend to degrade real wastewaters with elevated COD in the future) were tested. Pellet fungal biomass was used in all cases.
For the initial screening, 250 mL Erlenmeyer flasks with 50 mL of maintenance medium were used. The medium was spiked with a mixture of the four OPFRs at a concentration of 10 ppm for each compound and inoculated with pellets equivalent to 3.5 g/L of dry biomass. Experiments were conducted for 15 days, in a dark controlled environment at 25ºC, with continuous shaking (135 rpm).
Duplicates were performed for each fungus. Samples were taken at t_0 and after 3 days of experiment, to evaluate immediate degradation. Afterwards, 3 g/L of glucose were added, and final samples were taken at day 15 to assess fungal performance under nutrient-limiting conditions. To assess the contribution of each degradation mechanism, *Ganoderma lucidum* and *Trametes versicolor* were inoculated in maintenance medium spiked with TBP at 10 ppm. In this case, ~3.5 g/L of dry biomass of heat-killed pellets were inoculated to evaluate physical adsorption. Experiments were conducted in triplicate for 7 days, in the same environmental conditions as before. Samples were taken at t_0 and after 3 and 7 days of experiment. TBP concentrations were quantified for each experimental time.

RESULTS AND DISCUSSION

Initial fungal screening

T. viride and *A.niger* were the least suitable candidates to remove OPFRs, thus showing that ligninolytic fungi have a better degradation capacity in this case. TEP was the most recalcitrant compound because no degradation was detected. TCEP is also very difficult to remove, with *G. lucidum* being the only fungus able to remove 47% of the contaminant, only under nutrient limiting conditions, which would indicate that the enzymes involved in this degradation may be different than the ones that degrade TBP or TBEP. These two last contaminants were easily removed by *G. lucidum, P. sanguineus* and *T. versicolor*, which were able to remove 100% of the contaminants after 3 days of treatment. However, *P. sanguineus* and *T. versicolor* would be more efficient in this specific case, as they are able to remove the same amount of TBP and TBEP as *G. lucidum* but with ~50% less of biomass (as measured by final dry weight determination). By looking at each of the contaminant's structure, we theorize that WRF degrade OPFRs by taking radicals of them, which would explain why contaminants with larger structures are more easily degraded. Further research into specific enzymatic activities and transformation products should be carried to validate our hypothesis.

Results of control experiment with thermal inactivated biomass after 3 days, showed that adsorption contributed to 31% of the removal for *G. lucidum,* and 21% for *T. versicolor.* This parameter was maintained until the end of the experiment, which shows that there is no desorption of the contaminant afterwards. As for the results, we can conclude that biodegradation is the main mechanism of OPFRs removal. Nevertheless, the contribution of adsorption as a removal mechanism will depend on each fungus and each contaminant, so further research is necessary.

ACKNOWLEDGEMENTS:
Diana Losantos would like to acknowledge support from the doctoral research grant from project PID2019-103989RB-100 financed by MCIN/ AEI /10.13039/501100011033.

REFERENCES

Reemtsma, T., Quintana, J. B., Rodil, R., García, M., & Rodríguez, I. (2008). Organophosphorus flame retardants and plasticizers in water and air I. Occurrence and fate. *TrAC Trends in Analytical Chemistry*, *27*(9), 727-737.
Dunyu, S. U. N., Shaogui, Y. A. N. G., Weiming, X. I. A. N. G., Wenwu, Z. H. O. U., Xiaohan, W. A. N. G., Huan, H. E., & Shiyin, L. I. (2021). Research progress on degradation methods of organophosphorus flame retardants. *Environmental Chemistry*, (2), 474-486.
Chaudhari, T. D., Melo, J. S., Fulekar, M. H., & D'Souza, S. F. (2012). Tributyl phosphate degradation in batch and continuous processes using Pseudomonas pseudoalcaligenes MHF ENV. *International Biodeterioration & Biodegradation*, *74*, 87-92.
Mir-Tutusaus, J. A., Baccar, R., Caminal, G., & Sarrà, M. (2018). Can white-rot fungi be a real wastewater treatment alternative for organic micropollutants removal? A review. *Water research*, *138*, 137-151.

Removal of paracetamol, amoxicillin and triclosan through hazelnut shell biochar used as support medium in filtration processes.

P. J. Madariaga[1], C. A. Villamar[2*]

[1]Facultad de Ingeniería, Departamento de Ingeniería Química, Universidad de Santiago de Chile (USACH), Santiago, Chile (E-mail: *paula.madariaga@usach.cl*)
[2*]Facultad de Ingeniería, Departamento de Ingeniería Civil en Obras Civiles, Universidad de Santiago de Chile (USACH), Santiago, Chile (E-mail: *cristina.villamar@usach.cl*)

Abstract
Emerging contaminants such as pharmaceuticals and personal care products (PPCPs) have increased their use during the COVID-19 pandemic. Nature-based solutions, such as biofiltration are a good alternative for their removal. The use of hazelnut shells and its biochar is a cheap support material. Thus, this work is focused on the evaluation of the adsorption processes within biofiltration, optimizing variables for the removal of paracetamol, amoxicillin and triclosan. Biochar was produced from 3 different particle sizes. The removal process was evaluated in columns continuously until saturation. Results with biochar reported removals up to 100% for the 3 contaminants, optimizing the parameters of adsorbent dose (0.5-12 g/L) and agitation time (5-180 minutes). The use of smaller particle sizes (<355 µm) showed higher removals at lower doses of material (74-100%, 2 g/L). The biochar significantly improved the removal up to 200%, being its use is recommended at ratios 1:0.25 with hazelnut shells.

Keywords
Adsorption, amoxicillin, biochar, paracetamol, superficial area

INTRODUCTION

Nature-based solutions, such as biofilter-based technologies have a biotic component (plants, earthworms and/or microorganisms) and a support medium. The latter is a fundamental part of these technologies and will favor the adsorption and biodegradation (support biotic component) processes to be carried out in the emerging contaminants removal (Deng et al., 2021). In these technologies, adsorption has proven to be highly effective in removing emerging contaminants but conventional support materials, such as gravel, can account for up to 50% of the investment cost. Various materials have been studied for this purpose, such as zeolite, sand, construction waste, activated carbon, among others (Chang et al., 2019; Thuptimdang et al., 2021; Wang et al., 2013). Activated carbon as an adsorbent has been highlighted, but its investment costs are high (~21 USD/kg). For this, the use of organic residues is an alternative that benefits this type of technology as it is sustainable, economical, and effective. These have functional groups that benefit interactions with contaminants, as well as being easily modifiable to biochar, benefiting their porosity and surface area for the contaminant's removal (Maleki & Mao, 2022; Mohanty et al., 2018).

In recent times, due to the COVID-19 pandemic, drug consumption and use of personal care products has been on the rise. These can cause negative effects on human and animal health when discarded into the environment, causing alterations in the endocrine system and antibacterial resistant pathogens (García-Gómez et al., 2011). This study proposes the use of hazelnut shell and its biochar to study their potential use in support media, evaluating their ability to remove 3 emerging contaminants: paracetamol, amoxicillin and triclosan.

MATERIALS AND METHODS

Adsorbent material

Hazelnut shells were crushed, sieved, and divided into 3 granulometries: large (<2 mm and >600 µm), medium (<600 µm and >355 µm) and small (<355 µm and >150 µm). For biochar generation, approx. 15 g of hazelnut shell was placed in a 50 mL crucible with a lid, which was inserted into another 150 mL crucible. The smallest was covered with sand to reduce the entry of air into the sample. Crucibles were introduced into the muffle with a heating rate of approximately 20 °C/min, up to a temperature of 900 °C.

Experimental model

Adsorption was evaluated with different doses of adsorbent for each size: between 1 and 64 g/L for hazelnut shell and 0.5 a 12 g/L for biochar. These tests were carried out separately for each contaminant, for concentrations of 20 ppm in 20 mL of solution. The solutions were added to beakers covered with aluminum foil which were installed on an orbital shaker at 150 rpm for 1 hour. After contact time, the samples were centrifuged and filtrated. The concentration of each contaminant was determined before and after the tests, thus determining the percentage of removal. After selecting the most favorable working point, the optimal stirring time (between 5-180 minutes) for the adsorbent dose determined for each particle size was evaluated. Finally, the removal percentages were determined through the same procedure mentioned.

For the continuous test, to determine the optimal proportion of biochar and shell necessary in a continuous process, the rupture curves were carried out in 10 x 0.8 cm columns. 20 ppm of each contaminant was evaluated, using a flow rate of 9.3 m^3/m^2d. The evaluated shell:biochar ratios were 1:0, 1:3, 1:1, 3:1, 0:1.

Analytical method

For determination of the concentration of each contaminant, ultraviolet visible light spectroscopy (UV-Vis) was used through Hanon i5 UV-Vis Spectrophotometer with 1 cm wide quartz cells. The respective calibration curves were generated at wavelengths of 243, 228 and 292 nm for paracetamol, amoxicillin and triclosan, respectively.

RESULTS AND DISCUSSION

For the tests only with hazelnut shell, the removals of none of the contaminants exceeded 27% for the ranges evaluated, this value being reached only by the smallest sizes of adsorbent in the removal of paracetamol. In the case of biochar, removals increased significantly. For example, removal was 86% for triclosan with biochar from a large shell size. In any case, smaller sizes of the material required lower doses, reaching removals of 100% paracetamol, 98.7% triclosan and 73.7% amoxicillin with only 2 g/L of adsorbent in 1 hour of contact. The greater superficial area that this material has, agrees with the high removals at low doses and times.

Regarding the continuous process, amoxicillin columns were the first to saturate (5 days). It is possible to relate the shortest saturation time with the adsorption capacity of the adsorbent. The ratios of 1:1 and 1:3 showed similar results, reaching a C/C_0 for paracetamol on the 9th and 10th days of operation, respectively. Although a greater amount of biochar can allow a longer operating time for this type of filter, it is preferred to accompany the material with a certain percentage of shell. This since it generates a similar operation and allows a more economical replacement of adsorbents, requiring less treatment for the hazelnut shell for its use compared to biochar.

Table 1. Comparative removal percentage of amoxicillin, paracetamol and triclosan through biochar of different particle sizes with an adsorbent dose of 2 g/L

	% Removal	
Contaminant	Large particle size	Small particle size
Amoxicillin	13.69	73.65
Paracetamol	18	100
Triclosan	16.51	98.70

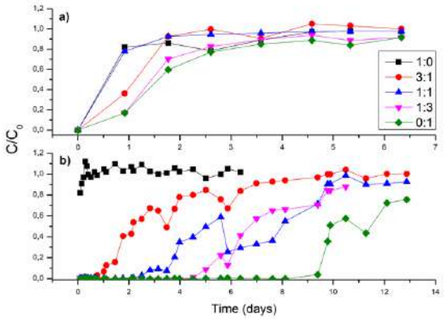

Figure 1. Breakthrough curve of continuous adsorption test with hazelnut shell: biochar columns. a) Amoxicillin b) Paracetamol

Acknowledgements

This researcher was supported by the Fondecyt (project grant 11190352). Moreover, authors thank the Interdisciplinary Lab of Water and Sciences Technology (Ko-Yaku Lab, Chile).

REFERENCES

Chang, J., Mei, J., Jia, W., Chen, J., Li, X., Ji, B., & Wu, H. 2019. Treatment of heavily polluted river water by tidal-operated biofilters with organic/inorganic media: Evaluation of performance and bacterial community. *Bioresource Technology* **279**, 34-42.

Deng, S., Chen, J., & Chang, J. 2021. Application of biochar as an innovative substrate in constructed wetlands/biofilters for wastewater treatment: Performance and ecological benefits. *Journal of Cleaner Production* **293**, 126156.

García-Gómez, C., Gortáres-Moroyoqui, P., & Drogui, P. 2011. Contaminantes emergentes: efectos y tratamientos de remoción. *Química Viva* **10**(2), 96-105.

Maleki Shahraki, Z., & Mao, X. 2022. Biochar application in biofiltration systems to remove nutrients, pathogens and pharmaceutical and personal care products from wastewater. *Journal of Environmental Quality* **51**, 129-151.

Mohanty, S. K., Valenca, R., Berger, A. W., Yu, I. K. M., Xiong, X., Saunders, T. M., & Tsang, D. C. W. 2018. Plenty of room for carbon on the ground: Potential applications of biochar for stormwater treatment. *Science of the Total Environment* **625**, 1644-1658.

Thuptimdang, P., Siripattanakul-Ratpukdi, S., Ratpukdi, T., Youngwilai, A., & Khan, E. 2021. Biofiltration for treatment of recent emerging contaminants in water: Current and future perspectives. *Water Environment Research* **93**(7), 972-992.

Wang, Z., Dong, J., Liu, L., Zhu, G., & Liu, C. 2013. Study of oyster shell as a potential substrate for constructed wetlands. *Water Science and Technology* **67**(10), 2265-2272.

Overview of methodologies for evaluating the energy efficiency of the wastewater treatment plant

D. Malluta*, E. Gagliano*, M. Gallo*, A. Del Borghi*

* Department of Civil, Chemical and Environmental Engineering, University of Genova, Via All'Opera Pia, 15, Genoa, Italy
(E-mail: *desara.malluta@edu.unige.it*; *erica.gagliano@unige.it; michela.gallo@unige.it; adriana.delborghi@unige.it)**

Abstract
Wastewater treatment plants (WWTPs) play a crucial role in protecting the environment and public health by removing pollutants. However, the energy consumption of these facilities can be significant, making it important to evaluate their energy efficiency. To date, a comprehensive methodology for energy audit at WWTP is still missed. This paper provides an overview of the methodologies currently used for evaluating the energy efficiency of WWTPs highlighting their advantages and limitations. The information will be useful to guide future research on this topic helping WWTP utilities to reach the energy audit goals in accomplishment of EU directives. The present overview pointed out that the obtained findings from benchmarking are often limited and fragmented and energy evaluation based on data envelopment analysis (DEA) depends on the selection of proper parameters. Consequently, further investigations are advised to develop standard procedures for data acquisition and online monitoring.

Keywords
Benchmarking; Energy efficiency; key performance indicator (KPIs); methodology; wastewater treatment plants (WWTPs)

INTRODUCTION

The main priority at wastewater treatment plants (WWTPs) is the attainment of high quality of treated effluent ensuring high effective removal of pollutants and protecting the environment and public health. However, WWTPs consist of energy-consumptive stages and the energy consumption mainly depends on the implemented technologies, on the plant size (in terms of population equivalent) and on the differences on target effluent quality among several countries (Gu et al. 2017). For instance, in medium and large WWTPs with conventional activated sludge (CAS), the aeration is the highest energy-consuming component (~60% of the total electricity consumption) as shown in Figure 1. As whole, the specific energy demand in WWTPs might decrease with the increase of inflow volume while it might increase with increasing concentration of pollutants in the influent (measured in terms of COD, BOD_5, and nitrogen) (Gu et al., 2017).
Therefore, the optimization in terms of removal efficiency and energy savings is essential to ensure the WWTPs performance that is both environmentally sustainable and economically viable (Sabia et al., 2020).
As recently advised by the European Commission, further efforts are needed to decrease the energy consumption in the wastewater sector which accounts for ~0.8% of the total energy use in the EU. In this regard, energy audit of WWTP could help to identify the significant energy consumers (such as processes and equipment) including the evaluation of the needed maintenance practices and their lifespan. However, further investigations are required to develop a comprehensive methodology for energy audit at WWTP (Sabia et al., 2020).

The aim of the present article is to provide an overview of the methodologies available in literature to assess the energy efficiency of WWTPs highlighting their advantages and limitations. The information will be useful to guide future research on this topic helping WWTP utilities to reach the energy audit goals in accomplishment of EU directives.

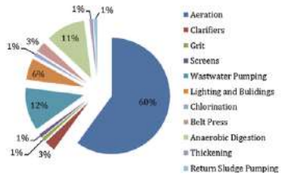

Figure 1. Percentages of energy use related to different compartments of CAS system (Gu et al., 2017).

METHODOLOGIES OVERVIEW

Table 1 provides a brief survey of main available methodologies to assess WWTPs energy performance. As a whole, they can be categorized in a) benchmarking; b) energy management tools; c) decision support tools.
The former, benchmarking, represents the first analysis aimed at understanding the energy consumption at WWTPs and it is based on Key Performance Indicator (KPI). Among the most reliable water-energy indexes, the total energy consumption (kWh) could be related to the treated wastewater volume (kWh/m^3), the plant size expressed as served PE per year (kWh/PE*y), and the amount of COD removed (kWh/kg COD). Several studies have performed the energy benchmarking using different KPIs. For instance, ENERWATER is an energy benchmarking model based on identification of KPIs that reflect the operational efficiency. While other studies have been performed by linearly aggregating the KPI values using the weights derived by Factorial analysis (F.A.) and consequently calculating the Global Energetic Index (GEI) in order to obtain a single indicator (Sabia et al., 2020).
However, the obtained findings from benchmarking are often limited and fragmented since they are strongly influenced by characteristics of treated wastewater and data are locally collected showing some differences at different geographical areas.
Among energy management tools, data envelopment analysis (DEA) is a mathematical programming technique that allows the analysis of processes that involve various inputs (e.g., costs for energy, waste management, and chemical) generating several outputs (amount of TSS, COD and BOD removed) (Hernández-Sancho et al., 2011). Moreover, DEA output could be related to environmental impacts in the framework of life cycle assessment (LCA) providing a broader performance evaluation of WWTPs.
Lastly, limited studies have been performed in order to develop decision support tools which could help WWTP managers to identify all possible strategies and actions for the optimization.

Table 1. Overview of methodologies for the evaluation of energy efficiency.

Methodology	Description	Limitations	References
KPI based on volume of treated water, PE, COD removed, BOD removed , TN removed, TSS removed	Determines evaluation of energy performance through a specific energy consumption and by using a set of indicators.	KPI for volume and PE assumes that the pollutant concentration are constant; KPI for COD, BOD, TN, TSS neglects the volume of WW and the other pollutants to be treated.	(Vaccari et al., 2018), (Di Fraia et al., 2018), (Zaborowska et al., 2017)
GEI (Global Energetic Index)	Was performed by linearly aggregating the KPI values using the weights derived by factorial analysis	Small number of WWTPs for the development of this methodology.	(Sabia et al., 2020)
EI (Energy Intensity)	A novel approach to evaluate the influence of the aging factor on energy use in WWTPs.	Are evaluated the economic cost of the energy used rather than the quantity of energy consumed in WWTPs.	(Longo et al., 2016)
ENERWATER	Standard method and online tool for assessing and improving the energy efficiency of wastewater treatment plants	The availability of data observation should be large to be representative of all the European WWTPs.	(Longo et al., 2016), (Longo et al., 2019)
DEA (Data envelopment analysis)	Non-parametric model, that calculates rather than estimates, the frontier using programming techniques. Widely applied for eco-efficiency assessment.	Not robust, no allowance for stochastic factors, heterogeneity across units of assessment not considered.	(Hernández-Sancho et al., 2011), (Lorenzo-Toja et al., 2015)

CONCLUSION AND FINAL REMARKS

WWTPs energy consumption depend on several factors including influent flowrate, pollutant load, WWTP size, type of the treatment technologies implemented. COD, suspended solids, nitrogen and phosphorus are the main parameters that influence the energy consumption and the treatment efficiency. Assessing the energy efficiency of WWTPs is essential to reduce the energy consumption and operational costs meanwhile improving the environmental sustainability and optimizing WWTPs performance. Benchmarking based on single KPI is suitable for WWTPs operated at similar conditions (e.g., same installed technologies). However, findings are strongly related to wastewater characteristics. Findings obtained by applying DEA depend on the proper selection of input and output variables. Further investigations should address the development of standard procedures for data acquisition and collection and the implementation of online monitoring.

REFERENCES

Belloir, C., Stanford, C., Soares, A., 2015. Energy benchmarking in wastewater treatment plants: The importance of site operation and layout. Environ. Technol. (United Kingdom) 36, 260–269.
Di Fraia, S., Massarotti, N., Vanoli, L., 2018. A novel energy assessment of urban wastewater treatment plants. Energy Convers. Manag. 163, 304–313.
Gude, V.G., 2015. Energy and water autarky of wastewater treatment and power generation systems. Renew. Sustain. Energy Rev. 45, 52–68.
Gu, Y., Li, Y., Li, X., Luo, P., Wang, H., Robinson, Z.P., Wang, X., Wu, J., Li, F., 2017. The feasibility and challenges of energy self-sufficient wastewater treatment plants. Appl. Energy 204, 1463e1475
Hernández-Sancho, F., Molinos-Senante, M., Sala-Garrido, R., 2011. Energy efficiency in Spanish wastewater treatment plants: A non-radial DEA approach. Sci. Total Environ. 409, 2693–2699.
Longo, S., d'Antoni, B.M., Bongards, M., Chaparro, A., Cronrath, A., Fatone, F., Lema, J.M., Mauricio-Iglesias, M., Soares, A., Hospido, A., 2016. Monitoring and diagnosis of energy consumption in wastewater treatment plants. A state of the art and proposals for improvement. Appl. Energy 179, 1251–1268.
Longo, S., Mauricio-Iglesias, M., Soares, A., Campo, P., Fatone, F., Eusebi, A.L., Akkersdijk, E., Stefani, L., Hospido, A., 2019. ENERWATER – A standard method for assessing and improving the energy efficiency of wastewater treatment plants. Appl. Energy 242, 897–910.
Lorenzo-Toja, Y., Vázquez-Rowe, I., Chenel, S., Marín-Navarro, D., Moreira, M.T., Feijoo, G., 2015. Eco-efficiency analysis of Spanish WWTPs using the LCA+DEA method. Water Res. 68, 651–666.
Molinos-Senante, M., Gómez, T., Garrido-Baserba, M., Caballero, R., Sala-Garrido, R., 2014. Assessing the sustainability of small wastewater treatment systems: A composite indicator approach. Sci. Total Environ. 497–498, 607–617.
Sabia, G., Luigi, P., Avolio, F., Caporossi, E., 2020. Energy saving in wastewater treatment plants: A methodology based on common key performance indicators for the evaluation of plant energy performance, classification and benchmarking. Energy Convers. Manag. 220.
Vaccari, M., Foladori, P., Nembrini, S., Vitali, F., 2018. Benchmarking of energy consumption in municipal wastewater treatment plants - A survey of over 200 plants in Italy. Water Sci. Technol. 77, 2242–2252.
Zaborowska, E., Czerwionka, K., Makinia, J., 2017. Strategies for achieving energy neutrality in biological nutrient removal systems – a case study of the Slupsk WWTP (northern Poland). Water Sci. Technol. 75, 727–740.

Reduction of high concentrations of ammonium nitrogen on a laboratory scale using the activated sludge method.

Kinga Marek*, Katarzyna Pawęska* and Aleksandra Bawiec*

* Institute of Environmental Engineering, Wroclaw University of Environmental and Life Sciences, Grunwaldzki Square 24, 50-363 Wroclaw
(E-mail: kinga.marek@upwr.edu.pl; katarzyna.paweska@upwr.edu.pl; aleksandra.bawiec@upwr.edu.pl)*

Abstract
An experiment was carried out to check the effectiveness of ammonium nitrogen removal from synthetic wastewater using the activated sludge method and a structure supporting biofilm settling. The cleaning process was carried out in 6 cylinders with a capacity of 4 liters. Three of them were filled with synthetic sewage with a composition similar to domestic sewage. In addition, an increased dose of ammonium nitrogen was used in 3 cylinders. The hydraulic retention time was set at 36 hours. The most optimal conditions for microorganisms were provided by constant temperature of the wastewaterand aeration. Four cylinders are equipped with a specially prepared insert made of plastic, which largely contributed to better contact of activated sludge with synthetic sewage. The other two unfilled cylinders were treated as a comparative level. In the first group of cylinders, the reduction of ammonium nitrogen remained at the level of 58.51 - 77.96%. However, in the second group, the efficiency of purification processes was much lower and the average ranged from 27.64 to 33.43%.The final comparison of the cleaning effects in each of the cylinders shows that the increased content of ammonium nitrogen does not inhibit the process, but only slows it down.
Keywords
activated sludge, ammonium nitrogen, wastewater treatment

INTRODUCTION

Wastewater characterized by a high content of ammonium nitrogen comes from, among others, Motor Rest Area facilities. These facilities very often do not have a local wastewater treatment plant, due to the fact that previous experience in the wastewater management sector in Motor Rest Area facilities indicates serious operational problems during biological wastewater treatment. The main reason for the failure of the biological treatment of this type of wastewater is the too high content of ammonium nitrogen, significantly exceeding the range of concentrations of this pollutant in typical domestic wastewater, which ultimately leads to the inefficiency of the treatment systems. Therefore, measures were taken to check the level of ammonium nitrogen reduction in wastewater heavily loaded with this pollutant using the activated sludge method.

MATERIALS AND METHODS

The test stand was equipped with 6 cylinders with the same capacity of 4 liters. Activated sludge was obtained from the Municipal Sewage Treatment Plant located in the city of Świdnica (Poland)., Each of the cylinders was filled with activated sludge to the level of 1.5 liters. The remaining capacity was supplemented with specially prepared synthetic sewage, according to the source [1,2,3,4]. Each cycle required a freshly prepared synthetic wastewater just before the end of the hydraulic retention time, so the synthetic sewage was prepared on an ongoing basis due to the risk of putrefaction caused by the presence of nutrients in the recipe. For this reason, the parameters of synthetic wastewater did not differ much from each other. Monitoring of wastewater quality was carried out during each cycle.
The cylinders were divided into two groups. The first of the three were flooded with sewage of the basic composition. The remaining cylinders (the second group) received wastewater with an increased concentration of ammonium nitrogen. The concentration level was determined on the basis of literature, but also own research of wastewater from Motor Rest Area facilities. In addition, in each group of cylinders, two of them are equipped with a proprietary fluid bed made of plastic.
Each of the cylinders was equipped with an aeration system, and the aeration time was set at 12 hours, as well as the rest time, which was also 12 hours. The hydraulic retention time of sewage was set at 36 hours.

Wastewater samples for testing were taken at the beginning of each cycle in the 1st hour, the second batch was taken in the 2nd hour to control the treatment process. The third batch of samples taken in he 36th hour represented the end of each cycle. The test results obtained from the last batch of samples were compared to the initial one, which was the reference point. Thanks to this, it was possible to assess the level of ammonium nitrogen reduction.

RESULTS AND DISCUSSION

The used filling of the cylinders improved the cleaning process by deposition of biofilm in the free spaces of the material. In the cylinders in which the filling was present throughout the experiment, it supported the growth of biomass. This is due to the better contact between wastewater and activated sludge, and consequently faster reduction of ammonium nitrogen. This is evidenced by the better efficiency of cleaning in filled cylinders. The first three cylinders, where the composition of synthetic sewage was similar to the composition of domestic wastewater show a greater range of ammonium nitrogen reduction in the range of 58.51-77.96%. However, the last three, to which wastewater representing higher concentrations was delivered, were worse at reducing ammonium nitrogen in the range of 27.64-33.43%. Due to the fact that the first three cylinders shown in the diagram show a wider range of reduction, it is concluded that the purification process is much more intensive at lower concentrations of ammonium nitrogen. On the other hand, the results of the experiment prove that, contrary to the thesis adopted so far, that the processes of nitrogen transformation are inhibited by the concentration of ammonium nitrogen equal to 150 mg NH_3/dm^3 [5], but even at high concentrations (used in the experiment), deviating from the norm assigned to domestic sewage, there is still reduction, and the purification processes are not inhibited, but only slowed down.

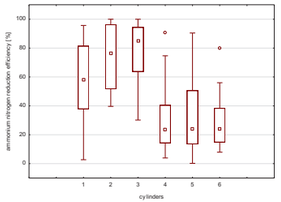

Figure. 1. Reduction of ammonium nitrogen in the cylinders at HRT of 36 hours.

REFERENCES

[1] Choi H., Zhang K., Dionysiou D. D., Oerther D. B. & Sorial G. A. (2006). Effect of activated sludge properties and membrane operation conditions on fouling characteristics in membrane bioreactors. Chemosphere, 63(10), 1699-1708.
[2] Figdore B. A., Stensel H. D. & Winkler M. K. H. (2018). Bioaugmentation of sidestream nitrifying-denitrifying phosphorus-accumulating granules in a low-SRT activated sludge system at low temperature. Water research, 135, 241-250.
[3] Hassan G. K. & El-Gohary F. A. (2021). Evaluation of partial nitritation/anammox process for reduction of pollutants from sanitary landfill leachate. Water, Air, & Soil Pollution, 232, 1-12.
[4] Wang J., Yang H., Zhang F., Su Y. & Wang S. (2020). Activated sludge under free ammonia treatment using gel immobilization technology for long-term partial nitrification with different initial biomass. Process Biochemistry, 99, 282-289.
[5] Fux C, Boehler M, Huber P, Brunner I. 2002. Biological treatment of ammonium-rich wastewater by partial nitritation and subsequent anaerobic ammonium oxidation (anammox) in a pilot plant. J.Biotechnol. 99, 295–306.

Simultaneous Removal of Zinc and Tetracycline Using Low Methoxyl Pectin Cross-linked by Calcium and Europium

Javier Martínez-Sabando[1], Francesco Coin[1], Jorge H. Melillo[2] and Silvina Cerveny[1,2]

[1] Centro de Física de Materiales (CSIC-UPV/EHU)-Material Physics Centre (MPC), Paseo Manuel de Lardizabal 5 (20018), San Sebastián, Spain (E-mail: *jmartinez240@ikasle.ehu.eus*; *fcoin001@ikasle.ehu.eus)**
[2] Donostia International Physics Center, Paseo Manuel de Lardizabal 4 (20018), San Sebastián, Spain (E-mail: *jorge.melillo@dipc.org*, *silvina.cerveny@ehu.es*)

Abstract
Nowadays, contamination is observed in almost all sources of available water bodies. A fundamental environmental challenge is the so-called emerging contaminants (EOCs) previously not known to be significant in freshwater. EOCs appear from products typically used in everyday life, including persistent organic pollutants, veterinary medicines, pharmaceuticals, and personal care products. These EOCs are gaining notable prominence in water remediation research because they possess an intricate molecular nature and are very hard to detect and remove.
This talk will present a new pectin-based adsorbent to simultaneously remove heavy metals and antibiotics. We will show that by changing the traditional way to crosslink pectin, we can adsorb big quantities of Zn2+ and tetracycline. We will discuss the application of pseudo first- and second-order models to understand the adsorption kinetics and the Langmuir isotherm model to describe adsorption onto pectin.

Keywords (maximum 6 in alphabetical order)
Adsorption; Pectin; Tetracycline; Water Remediation, Zinc

INTRODUCTION

Access to clean water for human consumption is becoming a significant challenge worldwide because around 14000 people die daily because of water pollution[1]. Water contaminants are classified into different groups regarding their nature: organic, inorganic radioactive, suspended solids, pathogens, and nutrient contaminants. In particular, heavy metals can reach water via natural sources such as volcanic eruption or anthropogenic activities like mining, causing different diseases by bioaccumulation in the target organs. Each metal type has different target organs and an accumulation limit before being fatal for the individual. On the other hand, antibiotics can only reach aquatic media from human activities (hospitals, domestic or veterinary uses). These contaminants are present in the water bodies of numerous countries in the range of ng/L to µg/L. The problem created by antibiotics is the coexistence of antibiotics and bacteria in the aquatic media, dramatically elevating the probability of developing antibiotic resistance genes by these bacteria, resulting in a public health issue[2].
The principal problem with these pollutants is that they escape from the methods used in most wastewater treatment plants. Different strategies have been developed to overcome this problem; the most popular are chemical precipitation, coagulation/flocculation, ionic interchange, or membrane technologies. Among them, we chose bio-sorption because it is a convenient method, as it is metabolically passive, does not need any external energy (cost-effectiveness) and is sustainable.
In this work, we have used citrus pectin to develop an adsorbent with the abovementioned characteristics. Pectin is discarded from the juice industry and can be isolated by green extraction methods. Pectin has been used as an absorbent of heavy metals when it is cross-linked with Ca^{+2} [3]. However, in this work, we will present a new cross-linking system based on lanthanides. We will show in this talk that we can adsorb heavy metals and antibiotics simultaneously.

MATERIALS AND METHODS

Materials: Pectin with low DE (9.9%) was gently delivered from Herbstreith & Fox. Glycerol (≥ 99%), calcium chloride anhydrous granular (≥ 93%), europium chloride hexahydrate (99.99%), tetracycline, and Zinc solutions were purchased from Merck.
Film preparation and dual cross-link: 3 wt% of LM pectin was dissolved and stirred in Milli Q water and 6 wt% of glycerol solution at 70 C and consequentially casted into a petri dish at room temperature to obtain thin film hydrogel membrane. Hydrogel crosslinking was performed in two steps exploiting the batch method; firstly into a 500 ppm of Ca^{2+} solution for 40 min (LMP-Ca). Therefore, the LMP-Ca hydrogel was washed with Milli Q water and secondly cross-linked with Eu^{3+} solution at the same conditions (LMP-Ca+Eu). Both the hydrogels cross-linked only with Ca^{2+} (LMP-Ca) and those cross-linked with the dual system (LMP-Ca+Eu) will be used to analyse the adsorption capacity against heavy metals and antibiotics.
Batch adsorption experiments: Kinetic adsorption experiments, were performed at fixed initial concentration of 150 mg/L for Zn^{2+}, 50 mg/L for TC, and 30 mg/L for TC/Zn^{2+} simultaneous removal. Metal ion concentration a specific time (C_t) were measured by an inductively coupled plasma atomic emission spectrometer (ICP-AES) (Horiba Yobin Yvon Activa), whereas the tetracycline concentration was determined by UV-Vis spectra. We measured the heavy metal concentration at different times ranging from 10 min to 24 h. The adsorbent dosage was fixed to 2.5 g/L, and a constant pH = 7 was kept for all the experiments.
C_t were measured by an inductively coupled plasma atomic emission spectrometer (ICP-AES) (Horiba Yobin Yvon Activa), whereas the tetracycline concentration was determined by UV-Vis spectra. Aliquots were taken at a specific time and were used to measure the C_t. The adsorption capacity (q_t) (mg/g) was calculated as follows:

$$q_t = \frac{C_0 - C_t}{d} \quad (1)$$

where C_0 and C_t represent the initial and after soaking concentrations of a given pollutant (mg/L), respectively and d is the adsorbent dose (g/L).
The removal efficiency (R%) was calculated as follows:

$$R\% = \left(\frac{(C_0 - C_t)}{C_0}\right) \times 100\% \quad (2)$$

RESULTS AND DISCUSSION

Figure 1 shows the calcium (a), europium (b) and calcium-europium (c) uptake capacities of LM-pectin films determined by ICP-AES. These kinetic experiments allow determining the cross-link density of these films after 40 minutes. The sorption of Eu^{3+} (Fig 1b) was fast in the first 30 min. After that, it proceeded at a relatively slower rate and finally reached equilibrium after ~200 min. The same behaviour is observed using calcium as a crosslinking agent (Fig. 1a). In addition, Fig. 1c shows the kinetic when the pectin is cross-linked with calcium and then with europium. In this last case, the crosslinking is even more effective than that produced only with Eu^{+3}. In pure water with pH of 7, LM-pectin has a large number of negative centres, because pKa of pectin is about 3.5. The degree of esterification has a crucial importance for an electrostatic interaction between pectin and ions. The low degree of esterification causes a high available number of acidic groups, which can bind with a higher amount of cations. Thus, the lower the degree of esterification of pectin, the higher number of junction zones. Therefore, the formed film is stable.

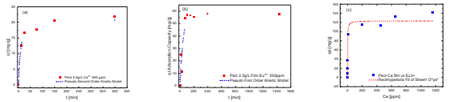

Figure 1. Adsorption kinetics of LM-pectin cross-linked by Ca^{2+} (a), Eu^{3+} (b) and with the dual system (Ca^{2+} and Eu^{3+}).

The adsorption kinetics was investigated for tetracycline (TC). The experiments for the effects of contact time were carried out at varying contact times ranging from 10 min to 1500 min at an adsorbent dose of 2.5 g/L, at room temperature (25 °C), and pH = 7. Optimization of contact time is essential for the adsorption studies to ensure complete equilibrium between the film and TC. Fig. 2 shows the effect of the contact time of the pectin cross-linked with Eu^{3+} film and TC. It was found that TC removal was fast during the first 100 min reaching the equilibrium after ~500 min. This may be because, in the initial stage, adsorption sites are highly available, but over time, there is a depletion of the adsorption sites. Fig. 2b shows the amounts of removal rate corresponding to the different equilibrium concentrations. The results showed that the percentage of tetracycline removed is maximum (68 %) at 10 ppm of TC. It is also expected to increase at lower concentrations of TC in water.

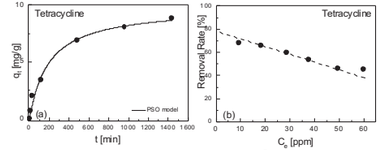

Figure 2. Adsorption kinetics of pectin cross-linked with Eu^{3+}. Initial tetracycline concentration was 50 mg/L and pH 7. Dashed line represents the fitting using the PSO model.

Fig. 3 shows the kinetic experiments (a) and the removal rate (b) for adsorption of tetracycline on pectin films cross-linked with the dual system (Eu^{3+} and Ca^{2+}). The adsorption capacity of TC is higher for the dual crosslinking system. The q value for the TC removal is 57% higher for the dual system (14 mg/g) than the Eu^{3+} cross-linked film (8 mg/g).

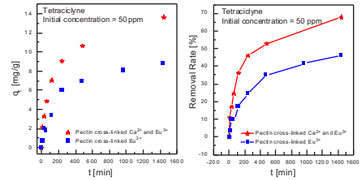

Figure 3. Adsorption kinetics (a) and removal rate (b) of pectin film cross-linked with the dual system (black points) and cross-linked only with Ca^{2+}. Initial tetracycline concentration was 50 ppm, pH = 7 was fixed using a HNO_3 solution and the dose was 2.5 g/L.

Finally, Fig. 4 shows the kinetic experiments (a) and the removal rate (b) for adsorption of the two pollutants (tetracycline and Zinc) simultaneously. The removal rate is very high in both cases as seen in Fig. 4b.

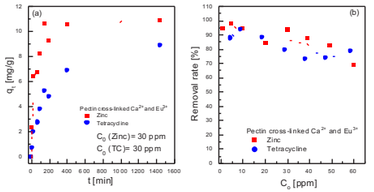

Figure 4. Adsorption kinetics (a) and removal rate (b) of pectin film cross-linked with the dual system (black points). Initial concentration was 30 ppm for tetracycline and for Zinc respectively. pH = 7 was fixed using a NaOH and HNO_3 solutions. The dose was 2.5 g/L.

In conclusion, we have shown a novel way to crosslink pectin with a low degree of methoxylation via Eu^{3+}. Moreover, we can use a dual crosslinking system of Eu^{+3} and Ca^{2+}. With this strategy, we can reach remarkable pharmaceuticals and heavy metals adsorption.

REFERENCES

1. FN, C. and MF, M. 2017 Factors Affecting Water Pollution: A Review, *Journal of Ecosystem & Ecography*, **07**(01), pp. 6–8.
2. Patel, M., Kumar, R., Kishor, L., Mlsna, T., Pittman, C.U., Mohan, D., 2019 Pharmaceuticals of Emerging Concern in Aquatic Systems: Chemistry, Occurrence, Effects, and Removal Methods, *Chem. Rev.* **119**, 3510−3673.
3. Cao, L., Lua, W., Mataa, A., Nishinarib, K., Fanga, Y., 2020 Egg-box model-based gelation of alginate and pectin: A review, *Carbohydrate Polymers* **242**, 116389.

Investigation of potential synergistic effect between three different UV wavelengths in water photodisinfection

A P. Uppinakudru*,**, M. Martín-Sómer*, M.D. Molina-Ramírez*, Cristina Ramírez-Miguel*, K. Reynolds**, S. Stanley**, C. Pablos* and J. Marugán*

* Department of chemical and environmental technology, ESCET, Universidad Rey Juan Carlos, C/ Tulipán s/n, 28933, Mostoles, Madrid, Spain
(E-mail: *adithya.uppinakudru@urjc.es, miguel.somer@urjc.es, mariadolores.molina@urjc.es, cristina.ramirezm@urjc.es, cristina.pablos@urjc.es , javier.marugan@urjc.es*)
** ProPhotonix IRL LTD, 3020 Euro Business Park, Little Island, Cork, T45 X211, Ireland
(E-mail: *kreynolds@prophotonix.com, sstanley@prophotonix.com*)

Abstract
The development of UV LEDs in the past decade has led to significant research in water disinfection. The possible synergy between multiple wavelengths in the UV range has been widely debated. Some researchers have concluded the existence of synergy, while others have discarded it. This study analyses the use of three UV light sources with different wavelengths (265, 275, and 310 nm) on the inactivation of *Escherichia coli* bacteria. A fixture to accommodate up to 8 high power light sources has been designed and used in the tests. This study proves that combinations of 310 nm with 265nm or 275 nm devices present a significant synergy. The observed synergistic effect has been correlated to the emission spectra of the respective LEDs to elucidate the possible mechanism of inactivation in combination.
Keywords
E. coli; disinfection; spectrum; synergy; ultraviolet light; wastewater

INTRODUCTION

There exists a controversy on the possibility of a combination of wavelengths and its resultant effect on different applications [1,2]. In all the studies on synergy so far, authors have had little to no control over the light sources used. In the author's opinion, factors like emission spectrum, type of device, and contribution of each wavelength, when combined, plays a key role in comprehensively evaluating possible synergistic effect between multiple wavelengths for the inactivation of microorganisms. This study attempts to fill these knowledge gaps and take advantage of establishing complete control over the light source to study its resulting effect on the inactivation of *E. coli K12*.

MATERIALS AND METHODS

The LEDs used in this study result from extensive market research and characterisation, thus enabling a good understanding of its behaviour. 13 possible combinations of the wavelengths on the fixture, as seen in figure 1 (a-d), have been studied. Experiments have been conducted in a single pass flow type system (figure 1e) at two different intensities to estimate the overall UV dose response.

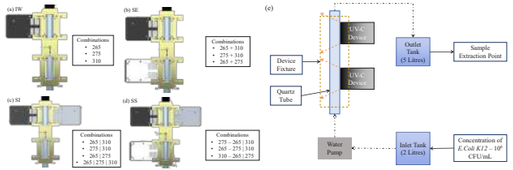

Figure 1. Combinations on UV fixture – (a) Individual wavelengths (IW), (b) Sequential Mode (SE), (c) Simultaneous Mode (SI), (d) Sequential + Simultaneous Mode (SS), and (e) Experimental set-up

RESULTS AND DISCUSSION

Individual disinfection experiments in a single pass, at a flow rate of 2 L/min and contact time of 0.753 seconds, confirmed the 265 nm light source to be most effective in the inactivation of E. coli (2.793 ± 0.173 log units), while the 310 nm led to the lowest disinfection (0.0003 ± 0.00008 log units). Due to the similar inactivation mechanism of wavelengths in the 250-280 nm range, the observed log reduction for 265 nm and 275 nm (2.448 ± 0.244 log units) were similar within the experimental error. Also, resulting from a different inactivation mechanism, the 310 nm light source was ineffective in a single-pass system due to short contact time. When a combination of the three wavelengths was used, an average log reduction of 5.408 ± 0.314 was observed. Under combined irradiation experiments, the average log reductions were similar to the sum of individual log reductions of the respective wavelengths for combinations of 265 nm and 275 nm attempted. For combinations involving the use of 310 nm, a possible synergistic effect was seen.

Table 1. Synergy of inactivation at 50% and 100% dose with error representing the 95% confidence interval obtained by t-student analysis. (LRV – Log reduction value)

UV	At 50% Dose		At 100% Dose	
Combination	Theoretical LRV	Actual LRV	Theoretical LRV	Actual LRV
265|275	2.640 ± 0.091	2.722 ± 0.088	5.241 ± 0.092	5.281 ± 0.038
265|310	1.514 ± 0.035	1.781 ± 0.124	2.794 ± 0.053	2.944 ± 0.047
275|310	1.127 ± 0.084	1.850 ± 0.141	2.448 ± 0.075	3.047 ± 0.157
265|275|310	2.641 ± 0.091	2.801 ± 0.071	5.242 ± 0.092	5.408 ± 0.115
265+275	2.640 ± 0.091	2.783 ± 0.109	5.241 ± 0.092	5.231 ± 0.076
265+310	1.515 ± 0.035	1.772 ± 0.086	2.794 ± 0.053	2.945 ± 0.085
275+310	1.127 ± 0.084	1.277 ± 0.059	2.448 ± 0.075	2.647 ± 0.119

To further evaluate the synergistic effect of the wavelengths, a robust statistical analysis using three different techniques has been conducted. T-student, ANOVA, and Codified ANOVA (2 factor, 2 level) analysis showed significant synergy for the combinations highlighted in blue in Table 1. This is mainly due to the emission spectra of the 310 nm LEDs, wherein about 26% of the light emission occurs after 320 nm. In this range, the inactivation shifts to another mechanism leading to a synergistic effect [3].
Finally, the electrical energy per order of inactivation has been calculated to evaluate if the synergistic effect is energy efficient as well.

REFERENCES

1. Beck, S.E., Ryu, H., Boczek, L.A., Cashdollar, J.L., Jeanis, K.M., Rosenblum, J.S., Lawal, O.R., Linden, K.G. 2017. Evaluating UV-C LED disinfection performance and investigating potential dual-wavelength synergy. Water Res. **109**, 207–216.
2. Nyangaresi, P.O., Qin, Y., Chen, G., Zhang, B., Lu, Y., Shen, L. 2018. Effects of single and combined UV-LEDs on inactivation and subsequent reactivation of E. coli in water disinfection. Water Res. **147**, 331–341.
3. Ashkenazi, H., Malik, Z., Harth, Y., Nitzan, Y. 2003. Eradication of Propionibacterium acnes by its endogenic porphyrins after illumination with high intensity blue light. FEMS Immunol. Med. Microbiol. **35**, 17–24.

Nature-based solutions to reduce antibiotics and antimicrobial resistance in aquatic ecosystems

V. Matamoros [1*], Mònica Escolà [1], Edward Pastor-López[1], Pedro Carvalho[2], Vaidotas Kisielius[2], Carlos Arias[2], Rene Kilian[3], Jens Chr. Pors[3], Dominik Hellmann[4], Jochen A. Mueller[4], Eberhard Kuester[5], C. Marisa R. Almeida[6], Ana M. Gorito[6], Laura Guimarães[6], Sandra Ramos[6], Vânia Freitas[6], Abdoulaye Diawara[7], Sidy Ba [7]

[1] Institute of Environmental Assessment and Water Research, Barcelona, Spain (*E-mail: victor.matamoros@cid.csic.es; edward.pastor@ cid.csic.es; monica.escola@ cid.csic.es*)

[2] University of Aarhus, Aarhus, Denmark (*E-mail: pedro.carvalho@envs.au.dk; vk@envs.au.dk; carlos.arias@envs.au.dk*)

[3] Killian water, Aarhus, Denmark (*E-mail: ens@kilianwater.com; info@kilianwater.com*)

[4] Karlsruhe Institute of Technology, Karlsruhe, Germany (*E-mail: jochen.mueller@kit.edu; dominik hellmann@student.kit.edu*)

[5] Helmholtz-Centre for Environmental Research, Leipzig, Germany (E-mail: eberhard.kuester@ufz.de)

[6] Interdisciplinary Centre of Marine and Environmental Research (CIIMAR), Porto, Portugal (*E-mail: calmeida@ciimar.up.pt; guimlid@gmail.com; up201104215@fe.up.pt; ssramos@ciimar.up.pt; vpfreitas@ciimar.up.pt)*

[7] Ecole Nationale d'Ingénieurs Abderhamane Baba Touré, Bamako, Mali (*E-mail: Sidy.Ba@usherbrooke.ca; abdoulaye.diawara.ad9@gmail.com*)

Abstract

The NATURE project (https://www.natureproject.eu/) aims to explore the use of nature-based solutions (NBS), especially wetlands, as management option for reducing the presence of antibiotics (ABs) and antimicrobial resistance (AMR) at the river catchment scale, from wastewater treatment to estuarine areas in four countries (Denmark, Spain, Portugal, and Mali). The results show the presence of several classes of ABs (fluoroquinolones, lincosamides, macrolides, sulfonamides, and rifamycin) and AMRs in wastewater and surface water samples, but their concentration and abundance were highly variable (ranging from 4 to 760 ng/L). Overall, our study demonstrate that the implementation of NBS at different river catchment levels (wastewater treatment, river stream or estuarine area) can improve the attenuation of ABs and AMR from 30 to 50%, in comparison to a reference approach without vegetation.

Keywords

Antibiotics; ecosystems; nature based solutions; removal; constructed wetlands; saltmarshes.

INTRODUCTION

Antibiotics (ABs) have been found in 2/3 of the world's rivers and experts expect a 65% increase of drug concentration in water by 2050. Once in the environment, ABs can promote antimicrobial resistance (AMR) which creates resistant microbial strains posing a risk to ecosystems and human health (Murray, Ikuta, et al., 2022). AMR is already responsible for an estimated 33,000 deaths per year in the EU and costs €1.5 billion per year in healthcare costs and productivity losses. The NATURE project (https://www.natureproject.eu/) aims to explore the use of nature-based solutions (NBS), especially wetlands, as management option for reducing the presence of ABs and AMR at the river catchment scale, from wastewater treatment to estuarine areas in four countries (Denmark, Spain, Portugal, and Mali).

RESULTS AND DISCUSSION

The results show the presence of several classes of ABs (fluoroquinolones, lincosamides, macrolides, sulfonamides, and rifamycin) and AMRs in wastewater samples, but their concentration and abundance were highly variable(ranging from 4 to 760 ng/L), at least in small decentralized wastewater treatment NBS monitored in Denmark (10 to 100 PE). Trimethoprim was the most abundant AB in the pre-settled wastewater from Denmark, whereas in the case of the Spanish site, clindamycin and azithromycin were the most abundant compounds in secondary treated wastewater effluents. The main results achieved so far demonstrate that the use of NBS as secondary or tertiary wastewater treatments results in a greater removal of ABs and AMR than conventional wastewater treatment solutions. For example, average removal of identified ABs and AMR (intI1 and sul1) in conventional tertiary wastewater treatment was of 40% and 1.5 log units, whereas these removals increased up to 70-80% and 2-3 log units by using NBS, respectively. Similarly, the renaturalization of river streams has been observed to enhance the attenuation of antibiotics by 30-40%. Several micropollutants have been detected in water of a Portuguese river estuary, all at low amounts (concentrations lower than 5 ng/L except for trimethoprim, which was detected up to 100 ng/L). However, the most abundant compounds were anti-inflammatory and analgesic compounds (up to 2,700 ng/L for acetaminophen). The potential of the estuarine saltmarsh to remove these pollutants is being evaluated. Results from Mali indicate that hospital wastewater effluents discharging into the Niger river are a very important source of ABs, reaching concentration levels greater than 30,000 ng/L (ciprofloxacin and acetyl-sulfamethoxazole). Therefore, we expect that the implementation of NBS at these sites would aid to reduce the impact of ABs and AMR into the Niger river.

CONCLUSIONS

Overall, the results demonstrate that the implementation of NBS at different river catchment levels (wastewater treatment, river stream or estuarine area) can improve the attenuation of ABs and AMR.

Acknowledgments

The authors would like to thank the European Commission (AEI, IFD, BMBF, FCT, and Sida) for funding in the frame of the collaborative international consortium (NATURE) financed under the 2020 AquaticPollutants Joint call of the AquaticPollutants ERA- NET Cofund (GA Nr. 869178). This ERA-NET is an integral part of the activities developed by the Water, Oceans and AMR JPIs

References

Murray, C. J. et al (2022) Global burden of bacterial antimicrobial resistance in 2019: a systematic analysis. The Lancet. 10.1016/S0140-6736(21)02724-0.

Circular Water Management Opportunities for Wineries Using Novel Thermal Process

V. Miklas*, M. Miklasová**, M. Touš*, M. Vondra*, J. Buzík***, V. Máša*

* Institute of Process Engineering & NETME Centre, Brno University of Technology, Technická 2896/2, 616 69, Brno, Czech Republic
(E-mail: *vaclav.miklas@vut.cz; tous@fme.vutbr.cz; m.vondra@vut.cz; masa@fme.vutbr.cz*)*
** Institute of Chemistry and Technology of Environmental Protection, Brno University of Technology, Purkyňova 464/118, 612 00, Brno, Czech Republic
(E-mail: *marta.miklasova@vutbr.cz*)
*** HUTIRA s.r.o., Vintrovna 398/29, 664 41, Popůvky, Czech Republic
(E-mail: *jiri.buzik@hutiravision.com*)

Abstract
Wine making is a water-intensive industry, with an estimated water footprint of up to 1,000 L per 1 L of wine. Most of the footprint is associated with irrigation, which essentially narrows the opportunities for circular water management to wineries. The water used by wineries, however, becomes highly contaminated with sugars, alcohols, carboxylic acids, etc. The organic loads of winery wastewater (WWW) are not only high, but also extremely fluctuating, e.g. chemical oxygen demand can vary by multiple orders of magnitude throughout a year. Wineries have limited possibilities to dispose the wastewater legally. An investment into their own wastewater treatment plant is frequently too high for the often family-owned small and medium wineries, therefore they are dependent on external facilities whose services are costly. Given these challenges and the growing legislation pressure, there is an increasing demand for cost-effective, robust and compact wastewater treatment technologies that would allow for water reuse and/or secondary products. One such technology, which is investigated in this work, is a combination of evaporation and stripping. Laboratory tests with real WWW from the Czech Republic have shown that the original wastewater volume can be reduced by 90 % using evaporation with the ethanol yield being virtually 100 % in the distillate. The distillate can be further processed in a stripping column to obtain recycled water with over 99.99 wt.% purity, with ethanol being either recovered or discarded based on the market situation. It was also demonstrated that the storage period affects the technology performance, therefore the storage time can be optimized to achieve specific technological goals. These promising results confirm that the innovative technology configuration has the potential to not only be competitive against the conventional WWW treatment technologies, but also redefine the water management in wineries by turning what was originally a waste stream into usable and/or marketable products.

Keywords
Circularity; ethanol; evaporation; stripping; wastewater recycling; winery

INTRODUCTION

Wineries produce significant amounts of wastewater, with an estimated specific winery wastewater (WWW) production of 0.5–14 L per 1 L of wine (Ioannou et al., 2015). The main contaminants are ethanol, organic acids (mostly acetic acid) and unfermented sugars (glucose, fructose) (Malandra et al., 2003). These can result in chemical oxygen demand (COD) over 100,000 mg/l particularly in the vintage period (grape crushing), during which the wastewater is extremely difficult to treat (Mosse et al., 2011). Given the limitations of the conventional technologies (high capital cost and spatial footprint, low turndown ratio), there is a number of emerging technologies which have been of research interest and allow not only for WWW treatment, but also water management circularity. The three most prominent are membrane bioreactor, reverse osmosis and evaporation (Miklas et al., 2022b), the last of which is the subject of this study. As the authors previously revealed, there have been limited research efforts targeting ethanol, despite it being the primary contaminant. This creates an apparent research gap to assess the possibilities of 'closing the loop' using an evaporation process. This is complemented by an investigation of the effect of storage prior to treatment, as storage time affects the composition of the WWW and can thus be used to optimise the process.

METHODOLOGY

The methodology consists of two parts:
a) simulated storage (Figure 1),
b) operating test (Figure 2).

In both parts, analytical chemistry methods are used to determine COD and concentrations of ethanol, acetic acid, glucose and fructose. COD was measured photometrically using COD cell test, fructose and glucose was determined by high-performance liquid chromatography, ethanol by gas chromatography with flame ionization detector, and acetic acid by ionic chromatography.

WWW samples for this research are taken from a winery in South Moravian region in the Czech Republic during the critical period of the vintage season and analysed at biweekly (14 days) intervals for 1 month (see Figure 1) before the follow-up testing takes place.

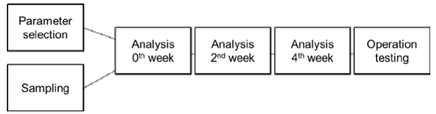

Figure 1. Methodology of the storage period investigation.

The operating test consists of two steps: evaporation in a multi-stage flash evaporator with nominal heat output of 40 kW and air stripping in a small-scale column (700 mm tall, 100-mm diameter) as shown on Figure 2.

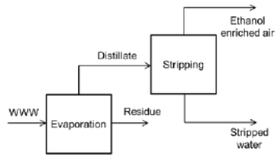

Figure 2. Operating test sequence.

The methodology allows for three key results: a) the effect of storage time effect on contaminant levels, b) volume reduction capabilities and product purities from the proposed process configuration, c) the relationship between the two to determine strategy for operation testing, including a potential chemicals dosage.

RESULTS AND DISCUSSION

The sample was taken on October 7th, 2022 and the first test was carried out immediately. The sugars' concentration was already negligible as alcohol fermentation had probably already converted them to ethanol. The COD value was relatively high (8,310 mg/l) and only slightly decreased over the 4-week period. Ethanol concentration, on the other hand, decreased significantly from 3.914 g/l to 1.890 g/l. The related acetic acid formation was evident as its concentration increased from 0.649 g/l to 3.733 g/l during the monitoring period. The ethanol and acetic acid concentrations can be seen on Figure 3.

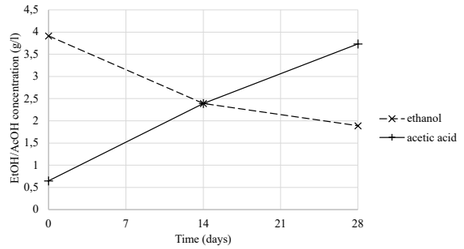

Figure 3. Ethanol and acetic acid concentration over the storage period.

During WWW storage, sugars are first transformed to ethanol during alcohol fermentation, followed by acetic fermentation consuming ethanol to form acetic acid. During evaporating, the volatility of ethanol makes it concentrate in the distillate, while the concentration of acetic acid is significantly lower and sugars are to be found exclusively in evaporation residue. The stripping column effectively separates ethanol from water, but the presence of acetic acid contaminates both potential products (ethanol solution and stripped water).

The evaporation test started with 182.5 L of WWW, which was circulated in a closed loop until a volume reduction of 90 % was achieved (less than 20 L as the evaporation residue). Figure 4 shows the difference between the distillate and residue.

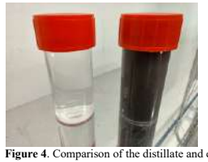

Figure 4. Comparison of the distillate and evaporation residue.

Based on the storage period investigation, sodium hydroxide was dosed during operating tests to stabilize acetic acid in the evaporation residue, which eliminated the distillate contamination. This has proven to be successful as the distillate contained only 8.8 mg/l of acetic acid. Simulation results (see Figure 5) show that the concentration would be 200 times higher without NaOH. Also, once around 50 % of the WWW is evaporated, basically no ethanol is left in the residue.

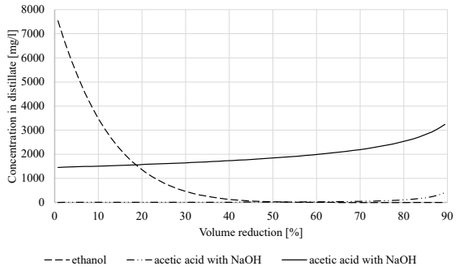

Figure 5. Simulation results from a model validated by the evaporation test.

The stripping test was carried out with extremely dry air, which resulted in an underwhelming ethanol removal of around 15 % per pass. The previous experiment with ambient air suggests that the removal can be close to 50 % (Miklas et al., 2022a), potentially resulting in sub-100 mg/l ethanol concentration and allowing for a more meaningful water reuse. This is the point for future validation and/or other technology consideration (e.g. membrane distillation).

CONCLUSION

The presented work expanded the opportunities for circular water management in wineries by demonstrating the potential of evaporation coupled with stripping as a means to obtain clean water and ethanol. Results suggest that up to 90 % of WWW can be recycled using the technology, with the possibility to recover ethanol as a by-product. The effect of storage period on the technology performance was also investigated. It is advisable to process WWW as soon as possible (sugars dominance) if water recycling is the main priority, as this leads to the lowest distillate contamination. If ethanol recovery is desirable, a prolonged storage period can be beneficial. Very long storage periods are related to acetic acid formation, which is mostly undesirable. However, the acid stabilization using sodium hydroxide can prevent distillate contamination and potentially leads to the recovery of sodium acetate as an additional product.

REFERENCES

Ioannou, L. A., Puma, G. L., Fatta-Kassinos, D. 2015 Treatment of winery wastewater by physicochemical, biological and advanced processes: A review. *Journal of Hazardous Materials*, **286**, 343–368.
López-Pérez, P. A., Cuervo-Parra, J. A., Robles-Olvera, V. J., del C Rodriguez Jimenes, G., Pérez España, V. H., Romero-Cortes, T. 2018 Development of a Novel Kinetic Model for Cocoa Fermentation Applying the Evolutionary Optimization Approach. *International Journal of Food Engineering*, **14**(5–6).
Malandra, L., Wolfaardt, G., Zietsman, A., Viljoen-Bloom, M. 2003 Microbiology of a biological contactor for winery wastewater treatment. *Water Research*, *37*(17), 4125–4134.
Miklas, V., Touš, M., & Máša, V. 2022a Winery Wastewater Treatment: Synergy Between Model and Experiment for Air Stripping Unit. *Book of Abstracts of the Energy, Sustainability and Climate Change Conference*, **7**, 102.
Miklas, V., Touš, M., Miklasová, M., Máša, V., Horňák, D. 2022b Winery Wastewater Treatment Technologies: Current Trends and Future Perspective. *Chemical Engineering Transactions*, **94,** 847–852.
Mosse, K. P. M., Patti, A. F., Christen, E. W., Cavagnaro, T. R. 2011 Review: Winery wastewater quality and treatment options in Australia. *Australian Journal of Grape and Wine Research*, **17**(2), 111–122.

Lab Scale Study of Wastewater Treatment using Nano-bubble Aeration in the Activated Sludge Process

M. Mohamed, M.I. Kizhisseri, M. Sakr, M. Maraqa, M. Hamouda

* Department of Civil and Environmental Engineering, United Arab Emirates University, Al Ain, UAE
(E-mail: m.mohamed@uaeu.ac.ae)*

Abstract
The most widely used method in municipal wastewater treatment is activated sludge process (ASP). For an ASP system, oxygen level in the aeration tanks is a critical factor in improving the removal efficiency of organic matter. Nano-bubbles are expected to be effective in increasing the levels of oxygen in comparison with conventional macro-bubbles used for aeration. This study aims to determine the feasibility of using nano-bubble aeration to replace macro-bubble aeration in a conventional ASP system. In this study, a hybrid method of aeration in which a nano-bubble generator and ultrafine diffusers with compressed air were operated intermittently to generate nano-bubbles. Two identical ASP systems; one with nano-bubble and the other with macro-bubble were tested. The treatment efficiency was determined by measuring the COD of the influent and effluent samples. Results indicate that nano-bubble aeration has a great potential in enhancing the biological treatment efficiency of ASP wastewater treatment systems.

Keywords
Activated sludge process, aeration, bubble size distribution, nanobubbles, wastewater treatment.

INTRODUCTION

The major biological processes prevalent in the Middle East region for municipal wastewater treatment are found to be the conventional activated sludge process and membrane bioreactor. At domestic WWTPs in the UAE, wastewater is treated to tertiary level to produce treated effluent (Statistics Centre - Abu Dhabi, 2015, 2018). A major challenge encountered in the ASP wastewater plants is attributed to power consumption during the aeration process of the activated sludge system. Usually, aeration in activated sludge systems is achieved by bottom diffusers. The efficiency of diffusors of macro bubbles is very low and ranges between 6-30%, which results in huge quantities of air that needs to be pumped to achieve the required treatment level. A critical factor in enhancing the efficiency of wastewater treatment is the transfer of oxygen in water. The aerobic biodegradation capacity is related to the growth of site specific microorganisms, which is significantly affected by the oxygen content in water (Song and Katayama, 2010). Thus, there is a need to improve oxygen transfer in the aeration tanks of activated sludge system not only to cut down on energy consumption but also to reduce the carbon footprint associated with the process.

Conventional techniques can produce macro-bubbles with diameters of millimetres or centimetres. Macrobubbles stay in water for short times and are inefficient for oxygen transfer process, leading to a small zone of influence and low activity of aerobic microorganism (Agarwal et al., 2011). An effective technique for increasing the oxygen transfer in water would be MNBs injection compared with the traditional technologies with macrobubbles (H. Li et al., 2013). Microbubbles with 30 μm radius were first found by Turner (Turner, 1961) in water and they were found to exist for long periods of time. Nanobubbles stay in water for longer periods and their stability can be attributed to electrically charged liquid–gas interface, which creates repulsion forces that prevent the bubble coalescence (Ushikubo et al., 2010). MNBs are tiny bubbles with diameters on the order of micrometers and nanometers, showing great potential in environmental remediation (H. Li et al., 2013).

Application of MNBs has drawn recent interest in various environmental applications due to its special characteristics, such as large specific surface area, negatively charged surface, long residence time in water, high mass transfer efficiency, and the generation of highly reactive free radicals (H. Li et al., 2013). (H. Li et al., 2013) showed that MNBs would greatly enhance bioremediation by accelerating oxygen transfer process. Enhanced aerobic degradation technologies aim mainly on increasing oxygen levels which can increase biodegradation rates by several orders of magnitude (Mohamed et al., 2010; Mohamed and Hatfield, 2011). These technologies operate by providing a supply of oxygen, which becomes available to bacteria (Mohamed, 2011). Micro and nano bubbles have been in use for various environmental engineering applications in the past twenty years because of various characteristics they possess (Movahed and Sarmah, 2021; Xia and Hu, 2018; Yang et al., 2017).

Based on the differences in their sizes, bubbles were categorized as macrobubbles, microbubbles (MBs), and sub-micro or nano bubbles (NBs) for conventional or big bubbles, fine bubbles, and ultrafine bubbles, respectively (Agarwal et al., 2011; Pérez-Garibay et al., 2012). Garibay et al. (Pérez-Garibay et al., 2012) employed the term conventional bubbles to describe the bubbles with sizes ranging between 600–2500 μm. In 2017, Temesgen et al. (2017) suggested the size boundaries of the MBs, with a minimum size of approximately 10 μm, while the maximum size suggested was 100 μm; and the diameters below 200 nm represent the NBs. The bubble size ranges and their associated properties can be summarized as shown in Figure 2. The most typical tools used for measuring the size and size distribution of the MBs and NBs are the laser-diffraction particle-size analyzer (Agarwal et al., 2011), atomic force microscope (Parmar & Majumder, 2013), and image analysis (Kim et al., 2012). The size and size distribution of the MBs and NBs are affected by the design and operation conditions. Kim et al. (2012) demonstrated that the size and fraction of the MBs mainly depend on the pressure differences across the nozzle system such as higher pressure would produce smaller bubbles because of an increase in air density and at pressures above approximately 3.5 atm, the sizes of the MBs were almost constant.

As MNBs have higher surface area/volume ratio as compared to macro air bubbles and they tend to reside longer before they burst on the liquid surface (Sakr et al., 2022). Thus, we hypothesized that nanobubbles (NBs) will be more efficient to use than macro air bubbles, leading to reduced pumping volume to the reactor and a consequent cut down on the pumping cost. To test our hypothesis, we carried out lab-scale experiments to characterize NBs size and size distribution which leads to optimization of operating conditions with respect to NBs size.

This study aims to determine the feasibility of use of nanobubble aeration to replace macro bubble aeration in a pilot-scale conventional ASP system. The process was evaluated by its capacity to reduce the soluble organic matter at increased loading rates, as well as the DO levels of the aeration tank.

MATERIALS AND METHODS

The study involved the construction of lab-scale activated sludge systems and experiments on biological treatment of wastewater. Two identical ASP systems were operated; one with nanobubble aeration and the other with macro bubble aeration, and tested as bench scale systems for treating 60 liters of wastewater per day. The schematic of experimental set up is shown in Figure 1.

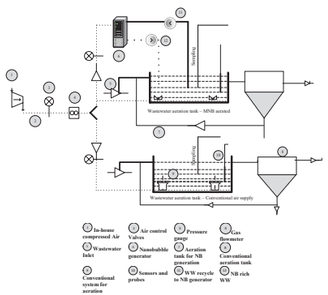

Figure 1. Experimental set-up of the bench-scale activated sludge process systems

Domestic wastewater after primary settling and return activated sludge (RAS) were collected from the nearest municipal wastewater treatment plant (WWTP), Al Saad WWTP in Al Ain, United Arab Emirates. The primary settled wastewater was stored in a tank, and pumped into the aeration tank, which is also activated with RAS from the sludge settling tank (Figure 1). Experiments were conducted with a hydraulic retention time(HRT) of 8 hours, mixed-liquor suspended solids of 2000-3000 mg/L and RAS circulation of 20%. These operating conditions were as close as the conditions at Al Saad WWTP. The MNB aeration system differed from the conventional system only on the air delivery system. The wastewater was aerated at constant air flowrate using in-house compressed air, to keep the oxygen level above 2 mg O_2/L. In this study, for the MNB aeration ASP system, nanobubbles were produced by a nanobubble generator (N2BG, Newmantech Co. Ltd., Korea) in addition to compressed air introduced into the aeration tank through ultrafine diffusers. In N2BG generator, air was injected to a cylinder inside the generator along with the wastewater, and thus nanobubbles are generated in the liquid. The macro bubbles for the experiments were produced by air compressor and induced into the system through a pipe with inner diameter of 5mm. In both the systems, the air inflow rate was kept same to ensure the similar condition. The treated water was transferred to the sedimentation tank, where the sludge was allowed to settle. The RAS was pumped to the aeration tank (sludge return) from the sedimentation tank. For each experiment run, the continuous flow ASP systems were run for 8 hours and required measurements were made.

The online measurements in the aeration tanks included temperature, pH, dissolved oxygen levels and TDS levels. In addition, chemical oxygen demand (COD) was analyzed at regular intervals from the beginning of the experiment to the end of the experiment run. The COD was analyzed to assess the effectiveness of treatment in removing organic compounds. The bubble size distribution, dissolved oxygen levels, and zeta potential were analyzed at regular intervals to understand the change in DO transfer efficiency of both the types of aeration.

RESULTS AND DISCUSSION

The quantity and size of the MNBs affect their mass transfer efficiency. Larger amounts of the NBs result in larger total surface area and increases the mass transfer flux from bubbles to solution, and smaller bubble size results in higher internal pressure and larger specific area. Analysis results showed that the hybrid method followed for nanobubbles generation for the experiments was successful in generating nanobubbles. MRB's NANOTRAC Wave II Particle Analyzer (Germany) was used to analyze the MNB characterization and bubbles distribution at regular intervals. Nanoparticle analyzer results showed that the microbubble generator produced a good concentration of bubbles with the diameter size in the range 10 -500nm. Also, the zeta potential values showed relative stability of the bubbles. The particle distribution curve obtained for a case of 1hr NB aeration is shown in Figure 2 (a). The trend of the concentration nanobubbles present in the aeration tank because the NB generation is depicted in the Figure 2 (b). It showed that a high concentration of the nanobubbles of the order of the 10^{-} 8 numbers/ml were maintained throughout the experiment run. However, it was noted that the concentration of nanobubbles reached a peak immediately after the run of nanobubble generator (N2BG, Newmantech Co. Ltd., Korea). However, when the samples from aeration tank with conventional aeration were analyzed, no significant concentration of NBs were detected.

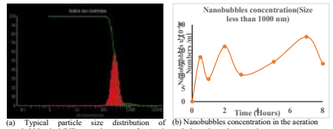

(a) Typical particle size distribution of nanobubbles in MNB aerated system, after (at 1 hr)

(b) Nanobubbles concentration in the aeration tank throughout the operation

Figure 2. Properties of the nanobubbles generated in the aeration tank

The average values of characteristics of wastewater influent into the aeration tanks are measure as shown in the Table 1.

Table 1. Characteristics of wastewater used for the experiments

Characteristics of influent to aeration tank	Values
pH @ 25°C	7.3
COD (mg/L of O_2)	185
Conductivity (μS /cm)	1385
Total dissolved Solids (mg/l)	2663.5
DO (mg/l O_2)	0.97
Temperature	20.2 ° C
Nanobubbles concentration (< 1000nm)	Not Detected

In the NBs based ASP system, the concentration of DO showed a rapid increase in first 30 minutes, which was high when compared with DO values of the conventional aeration (Figure 3). The average DO during the first 30 minutes increased by more than 4 mg/l while it was only about 2.5 mg/l by conventional aeration. The concentration of dissolved ozone increased along with the time initially, and remained relatively constant after 2 hours of operation.

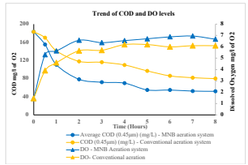

Figure 3. Dissolved oxygen and COD changes with time.

The treatment efficiency was determined by measuring the COD of the influent and effluent samples. The concentrations of COD in different times showed significant differences. The values of CODs of the effluent from aeration tanks at regular time periods of treatment is shown in Figure 3. The removal efficiency values were calculated relative to the concentration COD in the influent to the aeration tank. It was noted that the COD removal was more efficient throughout the operation. Most of the COD removal was achieved within 6-7hrs of operation in both the systems. The performance of MNB aerations system exceeded the conventional system at all times of the experiment run, and achieved a COD removal of about 72% in comparison to an average COD removal of 56%. Another significant observation was that a quick COD reduction occurred in the first 1-2 hrs of NB aeration, and this could be because of oxidation ability of nanobubbles to produce better oxidation effect, but the efficiency is limited by the quantity of oxygen transfer. Also, the observed overall improved efficiency of NB system could be because of their ability to maintain electron acceptors for microorganisms for their metabolic, and longer life in water system contributing to oxygen transfer efficiency.

CONCLUSIONS

In this study, application of nano bubble aeration in biological wastewater treatment as an efficient aeration technique for organic removal is proposed. The initial results showed significant increase in DO transfer capacity and COD removal efficiency for nanobubble aeration. Therefore, the nanobubble aeration has a great potential in enhancing the biological treatment efficiency of ASP wastewater treatment plants.

REFERENCES

Agarwal, A., Ng, W.J., Liu, Y., 2011. Principle and applications of microbubble and nanobubble technology for water treatment. Chemosphere 84, 1175–1180. https://doi.org/10.1016/j.chemosphere.2011.05.054.

H. Li, L. Hu, Z. Xia, Impact of groundwater salinity on bioremediation enhanced by micro-nano bubbles, Materials (Basel) 6 (9) (2013) 3676–3687.

Kim, T. il, Kim, Y. ha, Han, M., 2012. Development of novel oil washing process using bubble potential energy. Mar. Pollut. Bull. 64, 2325–2332.

M Mohamed , Guidelines for optimal design of electron acceptor injection wells to enhance bioremediation of contaminated groundwater, 2011,IAHS-AISH publication 342, 346-349.

M Mohamed, K Hatfield ;Dimensionless parameters to summarize the influence of microbial growth and inhibition on the bioremediation of groundwater contaminants, 2011, Biodegradation 225, 877-896.

M Mohamed, NE Saleh, MM Sherif, Modeling in situ benzene bioremediation in the contaminated Liwa aquifer (UAE) using the slow-release oxygen source technique, 2010, Environmental Earth Sciences 61 (7), 1385-1399

Movahed, S.M.A., Sarmah, A.K., 2021. Global trends and characteristics of nano- and micro-bubbles research in environmental engineering over the past two decades: A scientometric analysis. Science of The Total Environment 785, 147362.

Parmar, R., Majumder, S.K., 2013. Microbubble generation and microbubble-aided transport process intensification-A state-of-the-art report. Chem. Eng. Process: Process Intensification 64, 79–97.

Perez-Garibay, R., Martínez-Ramos, E., Rubio, J., 2012. Gas dispersion measurements in microbubble flotation systems. Miner. Eng. 26, 34–40.

Sakr, M., Mohamed, M. M., Maraqa, M. A., Hamouda, M. A., Aly Hassan, A., Ali, J., & Jung, J. (2022). A critical review of the recent developments in micro–nano bubbles applications for domestic and industrial wastewater treatment. Alexandria Engineering Journal, 61(8), 6591–6612.

Song, D., Katayama, A., 2010. Approach for estimating microbial growth and the biodegradation of hydrocarbon contaminants in subsoil based on field measurements: 1. Model development and verification. Environ. Sci. Technol. 44, 767–773.

Statistics Centre - Abu Dhabi, 2015. Statistical Yearbook of Abu Dhabi - 2015. https://www.scad.gov.abudhabi/en/pages/GeneralPublications.aspx?

Statistics Centre - Abu Dhabi, 2018. Statistical Yearbook of Abu Dhabi -2018. https://www.scad.gov.abudhabi/en/pages/GeneralPublications.aspx?pubid=79&themeid=7.

Temesgen, T., Bui, T.T., Han, M., Kim, T. il, Park, H., 2017. Micro and nanobubble technologies as a new horizon for water-treatment techniques: a review. Adv. Colloid Interface Sci. 246, 40–51.

Ushikubo, F.Y., Furukawa, T., Nakagawa, R., Enari, M., Makino, Y., Kawagoe, Y., Shiina, T., Oshita, S., 2010. Evidence of the existence and the stability of nanobubbles in water. Colloid. Surface. Physicochem. Eng. Aspect. 361, 31–37.

Xia, Z., Hu, L., 2018. Treatment of Organics Contaminated Wastewater by Ozone Micro-Nano-Bubbles. Water 11, 55.

Yang, Y., Ok, Y.S., Kim, K.-H., Kwon, E.E., Tsang, Y.F., 2017. Occurrences and removal of pharmaceuticals and personal care products (PPCPs) in drinking water and water/sewage treatment plants: A review. Science of The Total Environment 596–597, 303–320.

Removal of pharmaceutical compounds from food-processing digestate

N. Moradi*, F. Rubio Rincon**, C.M. Lopez-Vazquez **, H. Garcia Hernandez**, D. Brdanovic**, Mark van Loosdrecht***

* Department of Water Supply, Sanitation and Environmental Engineering. IHE Delft Institute for Water Education, 2611 AX Delft, The Netherlands. Department of Biotechnology, Delft University of Technology. (*Email: n.moradi@un-ihe.org*)
** Department of Water Supply, Sanitation and Environmental Engineering. IHE Delft Institute for Water Education, 2611 AX Delft, The Netherlands.
***Department of Biotechnology, Delft University of Technology, the Netherlands.

Abstract
Digestate sludge coming from the anaerobic digestion (AD) plants is a rich source of nutrient that can be used for agriculture. However, due to the presence of emerging contaminants, and among them pharmaceuticals, a post- AD treatment would be required. In this research four treatment including RO, ozonation, adsorption and UV-based AOP were compared in terms of efficiency and cost for pharmaceutical removal. The highest removal efficiency was obtained with the RO treatment followed by O_3, activated carbon and UV/H_2O_2. However, by considering the cost, ozone treatment seems to be the most cost-effective post-AD treatment.

Keywords
Pharmaceutical removal; advanced oxidation; Digestate

INTRODUCTION

Organic waste represents an average of 46 % of global waste, resulting in GHG emissions that poses a serious climate change thread (Worldbank.org). Anaerobic digestion (AD) can contribute to recover valuable renewable energy and nutrients from multiple organic waste streams. However, the use of active pharmaceutical compounds including antibiotics and hormones for animal farming limits the direct application of food-processing digestate. As such, there is a need for cost-effective solutions for the removal of pharmaceuticals from digestate.

MATERIALS AND METHODS

Food processing digestate was collected from a biogas plant in Malta. Four methods (RO, ozonation, adsorption and UV/H_2O_2) were evaluated in terms of efficacy for pharmaceutical removal. In all the experiments, the digestate supernatant was spiked with a final concentration of 10 mg/L salicylic acid (SA) as a surrogate for pharmaceutical compounds. The four treatments were conducted as following:

For filtration via reverse osmosis (RO), a cross-flow RO membrane unit coupled with Diaphragm Booster pump (OsmoPure, model 75) was used. The ozone treatment were carried out in a plexiglass bubble column reactor with the capacity of 2.7 L equipped with stirrer and diffuser. Adsorption experiments were conducted in 250 ml glass stoppered bottles by using acid-washed steam-activated powder of activated carbon (AC) (DARCO@G-60) in different ratio of AC:DOC. The UV and UV/H_2O_2 treatments were done using a PearlLab beam device, and adding certain amount of H_2O_2.

The reported capital and operational cost (CAPEX and OPEX) of the four treatment were compared to find the most cost-effective treatment.

RESULTS AND DISCUSSION

Figures 1a to 1d show the results of the four experiments:

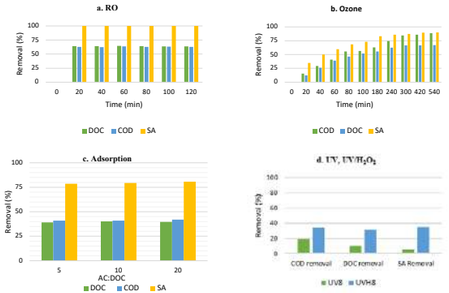

Figure 1. COD, DOC and SA removal efficiency from the digestate during (a) RO, (b) ozone, (c) adsorption, and (d) UV and UV/H_2O_2 treatment (UV8 is UV experiment in 8 hours and UVH8 is the same experiment by adding H2O2).

In the RO system, the flux remained constant (32.1 LMH) in the two-hour experiment, meaning that no fouling occurred. Data obtained from Figure 1a shows a similar removal efficiency for all the samples collected every 20 min, which again confirms that the RO treatment can produce a permeate free of SA without fouling despite the complex matrix and high load of organic matter.

In ozone treatment, SA removal of 83 % was achieved after 180 min (Figure 1b). However, as the key parameters (COD, DOC) were still high (with COD:DOC ratio of 3.7), the experiment continued for 540 min. SA removal did not show any significant changes after 180 min, also full mineralization did not happen even after 540 min. These can be related to the higher refractory compounds in the matrix that cannot be oxidized under this operational condition.

Results for the adsorption experiment in figure 1c shows a maximum of 35% DOC removal. Yet, almost 80 % of SA was removed after 2 hours in all AC:DOC ratios. The high removal of SA is likely due to its hydrophobic nature. K_{OW} for SA is 2.26 which indicates its affinity to attach to the floc, particles and adsorbed by activated carbon.

In UV treatment, the UV-LED machine offers intensities that are lower than what has previously been used for the treatment of pharmaceuticals and organic materials, even for simpler and less concentrated matrices. Therefore, this system cannot handle an organic load higher than 150 mg/L of COD per 272.9 µW/cm². As shown in Figure 1d, less than 6 and 36% of SA was removed after 8 hours treatment with UV and UV/H_2O_2, respectively. The higher removal efficiency by adding H_2O_2 is contributed to the formation of active OH radicals.

Table 1.1 shows the capital, operational and maintenance cost related to the four treatment reported in pervious researches for advance wastewater treatment in view of water reclamation and reuse (McGivney & Kawamura, 2008; Plumlee et al., 2014).

Table 1. CAPEX and OPEX of the four treatments

Treatment	CAPEX ($M/MGD*)	OPEX and maintenance ($M/MGD)
RO	7.14 (a)$^{-0.22}$	0.44 × (a)$^{-0.13}$
Ozone	2.26(a)$^{-0.54}$	0.0068(a)-$^{0.051}$
Activated carbon (AC)	3.03 (a)$^{-0.54}$	0.085 (a)$^{-0.16}$
UV/H_2O_2	0.474 (a)$^{-0.056}$	0.038 (a)$^{-0.052}$

*Million US dollars per million gallons per day of treated flow. a: Plant capacity in MGD

As the table shows, the cost related to the four treatment is in the following order:

Capital cost: UV/H_2O_2<O_3<AC< RO

Operation and maintenance cost: O_3<UV/H_2O_2< AC<RO

Although RO leads to full removal of pharmaceutical compounds, by taking the cost into account, ozonation seems to be the most cost-efficient treatment for pharmaceutical removal from digestate.

REFERENCES

Surname, N., Surname, N., Surname, N. 2011 Title of the paper. *Water Science and Technology* **28**(11), 11–25.
McGivney, W., Kawamura, S. 2008 Cost estimating manual for water treatment facilities. doi:10.1002/9780470260036
Plumlee, M., Stanford, B., Debroux, J.-F., Hopkins, Snyder, S. 2014. Costs of advanced treatment in water reclamation. ozone: science and engineering, **36**. doi:10.1080/01919512.2014.921565
worldbank.org. trends in solid waste management.

Assessing the feasibility of different membrane technologies for dissolved methane capture from AnMBR effluents

K. M. Moyano*, P. Sanchis-Perucho*, V. Sandoval-Garcia*, R. Serna-Garcia* and A. Robles*

* CALAGUA - Unidad Mixta UV-UPV, Departament d´Enginyeria Química, Universitat de Valencia, Spain
(E-mail: kristel.moyano@uv.es; pau.Sanchis-Perucho@uv.es; valeria.sandoval@uv.es; rebecca.serna@uv.es; angel.robles@uv.es)

Abstract

Direct greenhouse gas (GHG) emissions due to methane stripping from AnMBR effluents is still a key issue that limits the full-scale application of this technology. Degassing membrane (DM) technology has been extensively applied in several industries for dissolved gasses removal/recovery from liquid streams. In this study, the performance of three different DM systems are compared at different operational conditions, such as liquid flow rate (Q_L), operating temperature, and diving force intensity (i.e. transmembrane pressure, TMP). Overall, the highest methane recoveries (up to 50%) were achieved when operating at low Q_L (200-250 L/h) and high TMPs (0.6-0.8 bar). However, the estimated overall mass transfer coefficient was significantly hindered as the Q_L was increased.

Keywords
Anaerobic effluent; AnMBR; Degassing membrane; Dissolved methane recovery.

INTRODUCTION

Anaerobic systems are an excellent alternative for sustainable municipal wastewater treatment. However, effluents with a significant concentration of dissolved methane are produced. Methane losses in anaerobic effluents can reach up to the 80% of the overall production when operating at low temperatures (under 15ºC) (Giménez et al., 2014), resulting in dramatic reductions in process feasibility. Additionally, methane emissions produce a significant environmental impact due to the high global warming potential of this gas (more than 25 times than CO_2) (EPA 2022), representing a key limitation for the applicability of anaerobic processes at full-scale.

Degassing membrane (DM) technology is a promising alternative for dissolved methane capture from anaerobic effluents, boosting the applicability of high-rate anaerobic treatment (e.g. municipal wastewater) at ambient temperature. However, further work is needed to minimize membrane resistance in order to maximize methane recovery while minimizing total costs.

This work aims to evaluate the potential of three DM technologies for dissolved methane recovery from AnMBR effluents, i.e. non-porous polydimethylsiloxane (PDMS) membranes, non-porous polymethylpentene (PMP) membranes, and porous hydrophobic polypropylene (PP) membranes. Different operational conditions (e.g. treatment flow rate (Q_L), operating temperature, and transmembrane pressure (TMP) applied as driving force) are evaluated in order to maximize energy recovery and reduce greenhouse gas (GHG) emissions.

MATERIALS AND METHODS

Figure 1 shows a picture of the pilot plant used in this study, which includes Three parallel commercial DM systems for recovering the methane dissolved in the effluent from a pilot-scale AnMBR system: i.e. non-porous PDMS membranes (PERMSELECT ®, MedArray Inc. USA), non-porous PMP membranes (Separel ®), and porous PP membranes (3M™ Liqui-Cel™). Table 1 shows different characteristics of the membranes used.
By way of example, results from the performance of the PDMS unit are presented in this abstract. This unit was operated in shell-side mode to avoid lumen clogging problems, applying vacuum in the lumen side to generate the driving force necessary for gas recovery.

RESULTS AND DISCUSSION

Fig. 2 shows the methane recovery efficiencies reached in the PDMS DM unit at different TMP and Q_L. The highest methane recovery efficiencies were reached when applying low Q_L since low flow rates results in high contact times between liquid and membrane (i.e. high hydraulic retention times). On the other hand, methane recovery raised as TMP was increased since raising the driving force in the system resulted in a greater flux of gas through the membrane, enhancing thereby methane capture efficiency.

The global mass transfer coefficient (K) was evaluated to determine the effect of the studied operating conditions (Q_L and TMP) on the total system resistance (see Fig. 3). The estimated K indicated that increasing liquid flow rate significantly hindered the mass transfer efficiency. This was related to the liquid velocities reached in the DM unit, which could favour the generation of dead zones causing undesirable effects on K. Moreover, this effect may be amplified when operating at shell-side mode since the fibres may suffer some kind of shakings, deforming, and compression, reducing overall effectivity. On the other hand, increasing the TMP resulted in beneficial effects on K. This was attributed to a possible increase in membrane permeability as the operating driving force was raised. Consequently, operating the DM unit at moderate Q_L and high TMP could be recommended to boost the methane recovery efficiency of PDMS membranes.

CONCLUSIONS

Methane recovery was maximized at high TMP and low Q_L. Maximum methane recovery efficiencies of around 50% were achieved when operating at 0.8 bar and 200 L/h. Increasing TMP resulted in an improvement on K, whilst increasing Q_L results in unfavourable effects on methane recovery due to reduced K values.

REFERENCES

Cookney, J., Mcleod, A., Mathioudakis, V., Ncube, P., Soares, A., Jefferson , B., & McAdam, E. (2016). Dissolved methane recovery from anaerobic effluents using hollow fibre membrane contactors. J Membr. Sci. 502 , 141-150.
Environmental Protection Agency. (2022). EPA. Retrieved January 31, 2023, from https://www.epa.gov/gmi/importance-methane
Giménez, J., Matí, N., Robles, A., Ferrer, J., & Seco, A. (2014). Anaerobic treatment of urban wastewater in membrane bioreactors: evaluation of seasonal temperature variations. water Sci. Technol. 69 (7), 1581-1588.
Heli, S., Chernicharo, C., Brandt , E., & Mc Adams, E. (2017). Dissolved gas separation for engineered anaerobic wastewater systems. Separ. Purif. Technol. 189, 405-418.
Henares, M., Izquierdo, M., Marzal , P., & Matrínez-Soria, V. (2017). Demethanization of aqueous anaerobic effluents using a polymethylsiloxane membrane module mass transfer, fouling and energy analysis. *Separ. Purif. Technol. 186*, 10-19.
Stanojevic, M., Lazarevic, B., & Radic, D. (2003). Review of membrane contactors desing and applications of different modules in industry. *FME Trans 31*, 91-98.
Wickramasinghe, S., Semmens, M., & Cussler, E. (1992). Mass transfer in various hollow fiber geometries. *J. Membr Sci. 69 (3)*, 235-250.

FIGURES AND TABLES

Table 1. Main characteristics of the DM units evaluated.

	3M LIQUI-CEL	PERMSELECT	SEPAREL
Type of membrane	Hollow fiber	Dense Hollow Fiber	Hollow Fiber
Configuration	Lumen side Liquid Flow /parallel flow	Tube side (liquid pressure> 1bar)	
Material	PP Polypropylene/polyurethane X50	PDMS (Silicone) Polydimethyl siloxane	PMP Poly 4Methylpenten-1
Membrane area (m^2)	-	1.0*	1.8
Max liquid flow rate (l/h)	<180	30-360**	6-300
Max liquid pressure (bar)	2.1***		
Max vacuum pressure (bar)	<4.1 bar	2	0-1

*Based on fiber OD
** Typical flow
***working pressure lumen side

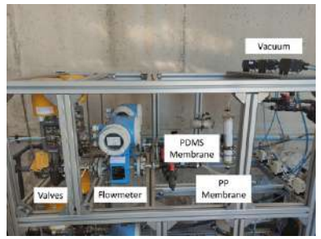

Figure 1. Prototype plant of degassing membranes

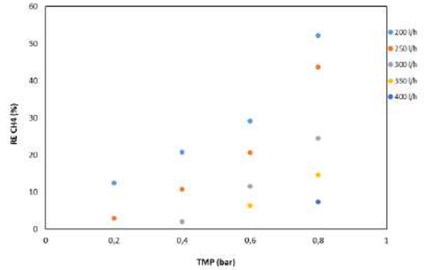

Figure 2. Effect of transmembrane pressure (TMP) and liquid flow rate (Q_L) on the Methane recovery efficiency

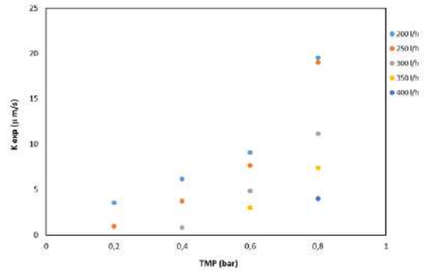

Figure 3. Effect of transmembrane pressure (TMP) and liquid flow rate (Q_L) on the overall mas transfer coefficient (K).

The emerging concern of hospital wastewaters: their treatment using aerobic granular sludge technology

B. Muñoz-Palazón*,**, A. Rosa-Masegosa*,**, Lizandra Perez-Bou*,**, A. Gonzalez-Martinez*,** and J. Gonzalez-Lopez*,**

* Institute of Water Research, University of Granada, C/Ramón y Cajal, 4, 18071 Granada, Spain (E-mail: bmp@ugr.es; aurorarm@ugr.es; lizandraph@correo.ugr.es; agon@ugr.es;jgl@ugr.es)*
** Faculty of Pharmacy, University of Granada, Campus de Cartuja, s/n, 18071 Granada, Spain (E-mail: bmp@ugr.es; aurorarm@ugr.es; lizandraph@correo.ugr.es; agon@ugr.es;jgl@ugr.es)

Abstract
Aerobic granular sludge technology was used for treating wastewater from a hospital for 150 days. The abrupt changes in the influent characteristics did not significantly affect the organic matter and nutrients removal. The granular conformation suffered modifications in settle ability and size, but the granular shape was never compromised by the influent nature. The capability to remove pharmaceuticals was linked to absorption-desorption processes over the operation. Cyclophosphamide, triclosan, naproxen and ketoprofen were removed with success, diclofenac and carbamazepine had oscillation in removal ratios and, trimethoprim could remove until day 60. The study of microbial populations of bacteria, archaea, and fungi supported the variations in performance because the diversity increased notably at day 60. The fungi and PAO organisms were depleted from day 120 to day 140 linked with higher toxics loads in influent, but later they proliferated again.

Keywords
Aerobic granular sludge; hospital effluent; microbial ecology; pharmaceuticals; wastewater.

INTRODUCTION

Environmental pollution by pharmaceutical compounds (PhCs) is become a problem that concern the regulatory agencies since these chemical compounds negatively affect to aquatic wildlife generating neuroendocrine problems and mutagenic effects, as well as the depletion of quality of water by exposure at small doses, which are bioaccumulative and persistent even at low concentration. The consumption of PhCs has increased drastically for human health and veterinary control worldwide. Hospital activities have been pointed out as a relevant source of pharmaceutical compounds via wastewater discharges due to the use of PhCs, even those that are not commonly dispensed. In most countries, hospital discharges without previous treatment are introduced into urban wastewater networks and are treated together with other effluents. This fact entails less efficiency for removal PhCs on WWTPs, it will trigger the release of these compounds to receiving water bodies. WWTPs located in Spain usually encompass exclusively primary and secondary treatments, with biological treatment based on conventional activated sludge, while other technologies are rarely applied. Wastewater treatment plants appear unequipped to remove effectively remove PhCs because they were designed to biodegrade carbon, nitrogen, and phosphorous.

Different wastewater technologies have been analyzed to determine the efficiency to remove PhCs. Díaz-Garduño et al., 2017 showed a deep study of WWTPs located in southern of Spain taking into account different real scenarios. They compared effluents after photobiotreatment based on microalgae and effluents after multibarrier treatment. Results showed that the most effective way was multibarrier treatment. However, the high economic and energy costs are a big disadvantage. Aerobic granular sludge (AGS) technology is postulated as an alternative energetically sustainable, which is extremely resistant to drastic changes in the characteristics and loads of influents. This distinctive is marked by the compact biofilm in spherical conformation, encouraged by shear force in circular and continuous movement. The tridimensional matrices allow the co-existence of aerobic-anoxic-anaerobic niches to promote diverse metabolic pathways both for organic matter and inorganic nutrients and for the various needs to degrade PhCs. This technology has been tested using simulated hospital wastewater (Muñoz-Palazon et al., 2022), but the microbial load and changes in the influent characteristics are key aspects to evaluate the capability of treatment of AGS. In this research, we have studied the capacity of AGS to remove, degrade and transform pollutants from real hospital wastewater.

MATERIALS AND METHODS

Determination of physic-chemical parameters

The BOD_5, COD, inorganic nitrogenous ions (NH_4^+, NO_2^- and NO_3^-) and phosphate ion (PO_4^{3-}) were measured in duplicate. The granular properties were analysed by mean size and settling time using n=35±5 pieces. The samples of effluent and influent were subjected to solid phase extraction and eluted in methanol. The pre-concentrated samples were used to measure PhCs using UHPLC 1260 Infinity II - 6470 LC/TQ.

Biological studies

Then, DNA from biological samples was extracted and was used to quantify the absolute number of genes through qPCR and to identify the bacterial, archaeal and fungal communities by means of massive parallel sequencing(Muñoz-Palazon et al.,2022). The pipeline of raw bioinformatic data from Illumina was done using mothur software.

Statistical studies

Analyses of diversity were calculated with PAST. SIMPER analyses were done to evaluate the contribution to dissimilarities among periods and PERMANOVA to analyse the significance of variables. The treated bioinformatic data were employed to calculate analysis based on compositional statistics (PCA and Expected effect size). Multivariate analyses were done to link microbial communities and performance.

RESULTS AND DISCUSSION

The AGS operated in sequential batch cycles showed robustness during the whole experimentation time (150 days), because great changes were detected in the influent in terms of composition, loads and toxic substances. Despite oscillations in COD concentration (Figure 1A), the removal ratio was higher than 70% since operational day 50. In terms of inorganic nutrients, the total nitrogen removal achieved values of 91% of removal ratio, and until 52% of phosphate removal (Figure 1B). The biomass granular changed their size and decrease their settle ability but the conformation was not compromised (Figure 1C, 1D).
Related to PhCs, the trend could not be defined because the results pointed out a bioadsorption-desorption processes related to their attachment to granular biomass. Although, AGS demonstrated high capacity to retain and/or removal these PhCs and not release them in discharges. The most abundant PhCs received in hospital sewage were trimethoprim, carbamazepine, naproxen and diclofenac, followed by ketoprofen. Both cyclophosphamide and triclosan had the lowest concentration. The removal ratio of all PhCs is shown in Figure 2, where it is observed higher ratios for naproxen, cyclophosphamide, triclosan and ketoprofen.

In terms of microbial population, continuous changes were detected over the operation, because the real wastewater from the hospital supposed a relevant load of external microorganisms within the system. In fact, this event was more notorious between days 60 and 140, depending on the domain, as could be in the absolute quantification genes of interest, especially highlighted for PAO and *Fungi*. In general, *Donkdonella*, *Thauera* and *Hyphomicrobium* were the most ubiquitous bacteria (Figure 3). *Nectriaceae* and *Trichosporonaceae* were the most abundant fungal phylotypes and *Bathyarchaeaota* and *Euryarchaeaota* phyla as the most abundant archaeal OTUs.

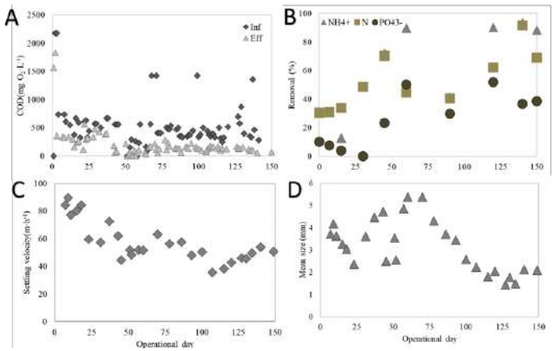

Figure 1. Chemical oxygen demand (COD) concentration for influent and effluent(A); removal ratio of ammonium, total nitrogen and phosphate (B); Settling velocity (C); and mean size (D)

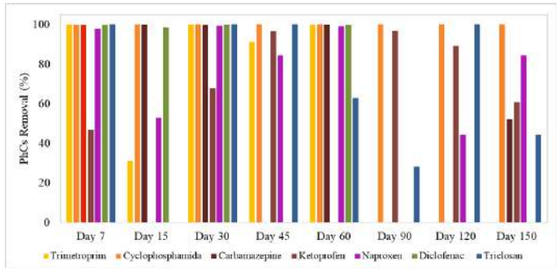

Figure 2. Pharmaceuticals removal ratio for whole experimentation.

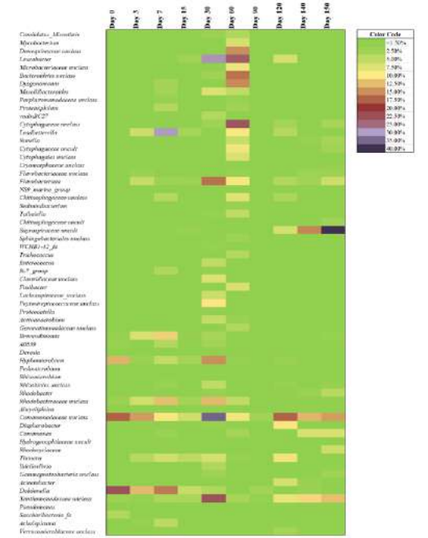

Figure 3. Heat map of bacterial communities with more than 1.5% of relative abundance.

REFERENCES

Muñoz-Palazon, B., Rosa-Masegosa, A., Vilchez-Vargas, R., Link, A., Gorrasi, S., Gonzalez-Lopez, J., Gonzalez-Martinez, A. 2022. Biological removal processes in aerobic granular sludge for treating synthetic hospital wastewater: Effect of temperature. *Journal of Water Process Engineering*, **47**, 102691.
Díaz-Garduño, B., Pintado-Herrera, M. G., Biel-Maeso, M., Rueda-Márquez, J. J., Lara-Martín, P. A., Perales, J. A., Martín-Díaz, M. L., 2017. Environmental risk assessment of effluents as a whole emerging contaminant: Efficiency of alternative tertiary treatments for wastewater depuration. *Water research*, **119**, 136-149.

We would like to acknowledge the Project A-RNM-62-UGR20 of Junta de Andalucia

Development and characterization of a new sol-gel coating for anti-scaling properties

S. Nouigues*, H. Cheap-Charpentier**, Y. Ben Amor***, C. Laberty-Robert**** and H. Perrot*

* LISE, Sorbonne Université, CNRS 4 place Jussieu, 75005 Paris-France
(E-mail : *soumaya.nouigues@sorbonne-universite.fr* ; *hubert.perrot@.sorbonne-universite.fr)*
** EPF, Engineering school, 55 Av. du Président Wilson, 94230 Cachan-France
(E-mail : *helene.cheap-charpentier@epf.fr)*
*** ISTEUB, Carthage University, Tunis-Tunisia
(E-mail : Yasser.benamor@isste.u-carthage.tn*)
****LCMCP, Sorbonne Université, 4 place Jussieu, 75005 Paris-France
(E-mail : christel.laberty@sorbonne-universite.fr)

Abstract
In this study, the efficiency of a scale inhibitor, the diethylene triamine penta (methylene phosphonic acid) (DTPMPA) has been investigated. The results obtained showed that DTPMPA can inhibit $CaCO_3$ formation in solution and on a metallic surface at very low concentration in solution. A hydrophobic sol-gel film has been developed and presented interesting scale inhibition properties.

Keywords
Electrochemical quartz crystal microbalance; fast controlled precipitation; Scale inhibition; Sol-gel coating

INTRODUCTION

Scaling phenomenon, principally formed by calcium carbonate $CaCO_3$, leads to technical and economic problems in industry. Environmental and health issues lead laboratories to seek new methods of detection to determine and to quantify the calcium carbonate $CaCO_3$ crystals in water.
The aim of this study is to develop a new hybrid sol-gel coating able to inhibit scale formation. An inhibitor, namely diethylene triamine penta (methylene phosphonic acid) (DTPMPA) will be impregnated at the surface of the sol-gel coating. Firstly, the scale inhibition properties of DTPMPA, on the nucleation/growth processes of $CaCO_3$, have been studied in bulk and on a metallic surface using fast controlled precipitation and electrochemical quartz crystal microbalance respectively. Secondly, the scale inhibition properties have been studied when a sol-gel coating has been applied to the metallic surface. The evaluation of its antiscale effectiveness has been followed by quartz crystal microbalance.

MATERIALS AND METHODS

Fast controlled precipitation

The fast controlled precipitation (FCP) method is based on the moderate degassing of CO_2 gas dissolved in water, which generates an increase of pH leading to the $CaCO_3$ precipitation. This method is generally used to evaluate the efficiency of scale inhibitors (Peronno 2015). The precipitation time and the crystal growth kinetics were followed by measuring simultaneously the pH and resistivity of the solution over time.

Electrochemical quartz crystal microbalance (EQCM)

The electrochemical quartz crystal microbalance (EQCM) was performed to measure the mass change of $CaCO_3$ deposited on an active surface and to assess the scaling rate in the absence and presence of inhibitor (Gabrielli 1998). The working electrode, a 5 mm diameter gold disc deposited in a quartz crystal resonator, was adapted in a submerged impinging jet cell. The electrochemical potential was maintained at -1 V/SCE, corresponding to the reduction of the dissolved dioxygen. The formed hydroxyl ions increased the local pH near the electrode surface up to 11.2 and if no chemical reaction contributed to the consumption of OH^-, it leads to $CaCO_3$ precipitation. The current and the frequency change Δf as function of time were recorded simultaneously. The frequency change Δf of the quartz resonator was proportional to the mass change (Δm), due to the $CaCO_3$ deposition on the working electrode, according to Sauerbrey equation (Eq. 1) (Gabrielli 1998, Cheap-Charpentier 2018):

$$\Delta f = -K_S \Delta m \quad (1)$$

Quartz crystal microbalance (QCM)

Finally, a quartz crystal microbalance (QCM) was used to measure the mass of $CaCO_3$ deposited on the surface of the electrode and to follow its kinetic of growth, scale particles being generated by the FCP method. The mass deposited was measured over time according to Sauerbrey equation typically at 9 MHz, 1,22 ng mass change corresponds to 1 measured Hz. Different metallic surfaces (aluminum alloy, stainless steel) were used in this study, with or without sol-gel coating.

The synthesis of the sol-gel coating

The procedure used for the synthesis of mesoporous silica films was similar to the earlier procedure described by Zhao et al. (D. Zhao 1998). Various formulations were tested according to the nature of the precursors to study their different characteristics (hydrophobicity, roughness ...) and then, to evaluate their anti-scaling action. The precursors used are: Tetraethylorthosilicate (TEOS), 3-(Trimethoxysilyl)propyl methacrylatele (MEMO) and Methyltrimethoxysilane (MTEOS). Two sol-gels were tested here: S1 (TEOS:MEMO) and S2 (TEOS:MTEOS).

CHARACTERIZATION OF THE SOL-GEL LAYER BY SEM

The sol-gel layer S2 deposited on a gold surface has been characterized by scanning electronic microscopy (SEM) and its thickness is about 0.5 µm (Figure 1).

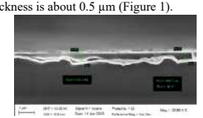

Figure 1. SEM image of the sol-gel S2 (TEOS: MTEOS) deposited on the gold electrode.

The hydrophobicity of the film was determined by determining the contact angle for the sol-gel films S1 and S2 (Figure 2).

Sol-gel	S1 (TEOS:MEMO)	S2 (TEOS:MTEOS)
Contact angle (°)		

Figure 2. Contact angle for the sol-gel films S1 and S2.

The addition of precursors with methyl groups (MTEOS) increases the hydrophobic character of the film. This is shown by the increase of the contact angle in the sol-gel S2.

RESULTS AND DISCUSSION

Evaluation of the effect of the inhibitor in solution by FCP

To determine the inhibition effect of the DTPMPA towards $CaCO_3$ precipitation in solution, the tests were carried out using FCP method.

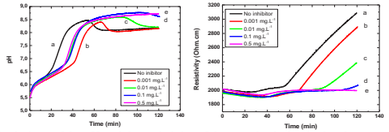

Figure 3. Evolutions of the pH and the resistivity of the tested solution in the absence and presence of DTPMPA: (a) 0 (b) 0.001, (c) 0.01, (d) 0.1 and (e) 0.5 $mg.L^{-1}$ at 30 °C, hardness 25 °F (containing initially 100 $mg.L^{-1}$ Ca^{2+}).

Without inhibitor, during the first nucleation phase, the pH increases until a maximum value that marks the time of precipitation (T_p), before decreasing until a constant value, which indicates the re-establishment of the chemical equilibrium. The resistivity-time curve exhibits an increasing slope that indicates a homogeneous precipitation stage. The precipitation time increases from 57 min without inhibitor to 86 min with 0.01 ppm of inhibitor until a total inhibition for 0.5 ppm of DTPMPA (Figure 3). The results show that DTPMPA can inhibit efficiently the $CaCO_3$ formation at very low concentration.

Evaluation of the effect of the inhibitor on a metallic surface by EQCM

To facilitate the comparison between the different experiments, the current is normalized by I_0, the initial reduction current. The scaling time, t_s, is defined as the intersection of the tangent at the inflexion point of the curve I/I_0 vs time and the time axis. The scaling rate, r_s, is determined according the slope of the linear part of the falling current. A low value of the residual current (I/I_0 close to 0) indicates that the $CaCO_3$ layer formed on the metallic surface is insulating and compact (Figure 4, right).

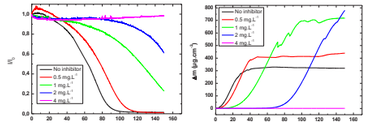

Figure 4. Evolutions of the relative current and the deposited mass of the tested solution in the absence and presence of DTPMPA, T = 30 °C, hardness 25 °F, E = -1 V/ECS.

The $CaCO_3$ deposit progressively covers the entire surface of the metal, then isolates it from the water, avoiding the electrochemical formation of scale. The mass increases over time with the surface coverage and the corresponding slope gives a comparative idea of the scaling rates in the absence and presence of DTPMPA. Without inhibitor, the mass does rapidly increase until its stabilization which corresponds to the full coverage of the electrode surface.
With inhibitor (Figure 4, right), a decrease of the slope and an increase of the scaling time is observed, indicating that inhibitor delays the formation of scale. For [DTPMPA] at 1 and 2 ppm, the scaling rate decreases but the mass continues to increase, this is due to the porosity created in the layer of scale by the inhibitor. For [DTPMPA]=4 ppm, no change in mass and current is observed, showing an absence of scale deposition on the electrode surface. This corresponds to a total inhibition of scale.

Study of the sol-gel coating

A hybrid sol-gel layer was deposited onto a metallic electrode to evaluate its anti-scaling by QCM (Figure 5).

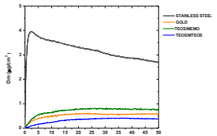

Figure 5. Curves of the evolution of the deposited mass according to the nature of the surface

The mass of scale deposited on stainless steel is twice as high as the one measured on the sol-gel layer made from TEOS and MEMO. To improve the scaling effect, the hydrophilicity of the sol-gel layer was measured by modifying its composition using MTEOS with methyl groups. This layer efficiently inhibits scale formation.

CONCLUSION

The DTPMPA inhibits perfectly the scale formation in solution and on a metallic surface. By controlling the hydrophilicity of the sol-gel coating, this film presented very interesting anti-scaling properties. To totally inhibit the scale formation, the impregnation of the inhibitor on the surface of the hybrid sol-gel coating will be performed. This approach, maintaining the inhibitor attached to the surface, is very important to preserve the water quality.

REFERENCES

Cheap-Charpentier, H., Horner, O., Lédion, J., Perrot, H., 2018. Study of the influence of the supersaturation coefficient on scaling rate using the pre-calcified surface of a quartz crystal microbalance. *Water Res.* **142**, 347-353.
Deslouis, C., Frateur, I., Maurin, G., Tribollet, B., 1997. Interfacial pH measurement during reduction of dissolved oxygen in a submerged impinging jet cell. *Journal of Applied Electrochemistry* **27**, 482 – 492.
Gabrielli, C., Keddam, M., Khalil, A., Maurin, G., Perrot, H., Rosset, R., Zidoune, M., 1998. Quartz crystal microbalance investigation of electrochemical calcium carbonate scaling. *J. Electrochem. Soc.* **145**, 2386-2396.
Peronno, D., Cheap-Charpentier, H., Horner, O., Perrot, H., 2015. Study of the inhibition effect of two polymers on calcium carbonate formation by fast controlled precipitation method and quartz crystal microbalance. *J. Water Process Eng.* **7**, 11-20
Tlili, M.M., Benamor, M., Gabrielli, C., Perrot, H., Tribollet, B., 2003. Influence of the interfacial pH on electrochemical $CaCO_3$ precipitation. *Journal of the Electrochemical Society* **150**, C765-C771.
Zhao, D., Yang, P., Melosh, N., Feng, J., Chmelka, B.F., Stucky, G., 1998. Continuous mesoporous silica films with highly ordered large pore structures. *Adv. Mater.* **10**, 1380-1385.

Characterization of biochar obtained from recovered cellulose and its potential for the removal of pollutants in water.

I. Salmerón*, P. Nuñez-Tafalla*, S. Venditti* and J. Hansen*

* Faculty of Science, Technology and Medicine, Chair for Urban Water Management, University of Luxembourg, 6, rue Richard Coudenhove-Kalergi, L-1359, Luxembourg
(E-mail: irene.salmeron@uni.lu, paula.munez@uni.lu, silvia.venditti@uni.lu, joachim.hansen@uni.lu)*

Abstract
Cellulose can be recovered from sewage to develop valuable bioproducts. This study aims to assess the suitability of biochar produced via carbonisation from recovered cellulose as an absorbent for pollutants removal. 3 types of biochar were tested: 100% cellulose, 50% cellulose-50% straw and 50% cellulose-50% wood. Despite the physical characterization showed that the mix with wood had the higher surface area, adsorption test revealed that it had the lower absorption capacity. The most satisfactory results were obtained with 100% cellulose and will be verified by the analysis of the biologically activated biochar.

Keywords
Bio-based products, Circular Economy, Raw materials, Water depuration

INTRODUCTION

Wastewater contains a huge number of substances with the potential to be transformed into raw materials for bio-based products. Cellulose from toilet paper is one of the most relevant representing between 40 and 50% of the total suspended solids in several countries (Liu et al., 2022). In this context the INTERREG-WOW! project aims to recover that cellulose to produce activated biochar to be used as a substrate for additional treatment for the removal of pollutants (e.g. in Constructed Wetlands (CW)). Cellulose from Ede wastewater treatment plant (WWTP) influent (The Netherlands) was collected and dried by Cirtec B.V. (Khan et al., 2022) and pre-processed by Klimafarmer who obtained 3 types of non-activated biochar: 100% cellulose, 50% cellulose-50% straw and 50% cellulose-50% wood. The main target of this study was to assess their pollutants adsorption capacity to choose the most suitable for the application as additional treatment step.

MATERIALS AND METHODS

Physical characterization of biochar

Material characterization was performed by 3P INSTRUMENTS. Density was determined by Helium pycnometry following DIN 66137-2. BET surface area and micropore analysis were performed with CO_2 at 273 K.

Evaluation of the adsorption capacity

Biochar preparation for analysis. As absorption capacity is dependent on the particle size, to make an adequate comparison, the material was crushed and washed obtaining three different fractions (Fig. 1): pellets, 100-500 µm and powder below 100 µm.

Figure 1. Fractions of 100% cellulose biochar. a) pellets, b) 100 - 500µm c) powder <100µm.

Batch mode test. This is the most common setup for kinetics experiments. In this study brown-glass bottles containing 1 g/L of biochar were used and filled with 250 mL of a solution of 5 mg/L of indigo carmine (model compound) in ultrapure water and placed on a shaking table for 10 days.

Continuous mode test. As an alternative to conventional lab-scale columns systems that needs several months to reach the saturation, a rapid small-scale columns (RSSCs) system was used for this work. The equipment had two columns operated in parallel with 10 mm of internal diameter and filled with 400 mg of biochar, obtaining 0.8 mL of bed volume. They were fed from a storage tank containing a 5mg/L solution of indigo carmine at a flow of 10 mL/min.

RESULTS AND DISCUSSION

Materials Characterization

Results obtained from biochar characterization showed that Helium density was similar for all of them. The main difference was the BET surface area. 50% cellulose-50% wood has the best conditions regarding adsorption, with 280 m^2/g while 100% cellulose and 50% cellulose-50% wood have 211 and 249 m^2/g respectively, thus the mix of cellulose with other conventional sources of biochar entailed an increase in the area, that could improve the adsorption capacity.

Adsorption capacity

The profiles of indigo carmine adsorption for the fraction between 100-500 µm of each non-activated biochar is presented in Figure 2. From the material characterization, the 50% cellulose-50% wood biochar was expected to present a higher adsorption capacity. Nevertheless, this material showed the lowest one in all cases. In batch, 50% cellulose-50% straw showed slightly better yield (10% higher) than 100% cellulose. However, in continuous 100% cellulose took longer to reach saturation. In powder, it was the most evident reaching the 80% of saturation after 32, 80 and 101 BV for the mix of wood, the mix of straw and pure cellulose respectively.

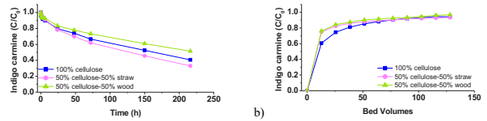

Figure 2. Adsorption of the indigo carmine by the 100-500µm fraction of each biochar mix in a) batch mode b) continuous mode.

This first assessment with non-activated biochar showed that 100% cellulose had great potential as an adsorbent. The next step will evaluate the surface changes due to the biological activation of the material and will verify if 100% cellulose is the most suitable biochar for CW substrate.

ACKNOWLEGMENTS

The authors wish to thank North-West Europe Interreg for funding this research under the WOW! project (Wider business Opportunities for raw materials from Wastewater), grant number 619.

REFERENCES

Khan, M.N., Lacroix, M., Wessels, C., Van Dael, M., 2022. Converting wastewater cellulose to valuable products: A techno-economic assessment. J. Clean. Prod. 365, 132812.
Liu, R., Li, Y., Zhang, M., Hao, X., Liu, J., 2022. Review on the fate and recovery of cellulose in wastewater treatment. Resour. Conserv. Recycl. 184, 106354.

Seasonal changes of waste activated sludge methane potential and its susceptibility to mid-temperature alkaline disintegration

M. Komorowska-Kaufman*, A. Cydzik-Kwiatkowska**, W. Pomian***, M. Florczyk**, M. Budych-Górzna***, S. Ciesielski**, P. Oleśkowicz-Popiel*

* Poznan University of Technology, Faculty of Environmental Engineering and Energy, Institute of Environmental Engineering and Building Installations, Berdychowo 4, 60965, Poznan, Poland, (E-mail: *malgorzata.komorowska-kaufman@put.poznan.pl; piotr.oleskowicz-popiel@put.poznan.pl*)
** University of Warmia and Mazury in Olsztyn, Faculty of Geoengineering, Department of Environmental Biotechnology, Słoneczna 45G, 10709 Olsztyn, Poland (E-mail: *agnieszka.cydzik@uwm.edu.pl; maciej.florczyk@uwm.edu.pl; slavcm@uwm.edu.pl*)
*** AQUANET S.A., Dolna Wilda 126, 61492 Poznań, Poland (E-mail: *weronika.pomian@aquanet.pl; m.budych_gorzna@wp.pl*)

Abstract
The aim of this work was to investigate the effect of mid-temperature alkaline pre-treatment with NaOH on waste activated sludge (WAS) disintegration and methane yield (Y_{CH4}) increase. The use of a small dose of 16 g NaOH/kg TS and 30 minutes of heating at 60°C allowed to obtain the average degree of sludge disintegration of 29% and Y_{CH4} increase of 30%. The obtained results varied significantly during the year. The highest Y_{CH4} increase (71%) was achieved in summer when the raw WAS Y_{CH4} was the lowest. Changes in WAS Y_{CH4} were correlated to its composition, which was noticed in extracellular polymeric substances (EPS) formation.

Keywords
alkaline pre-treatment; extracellular polymeric substances; methane potential; waste activated sludge disintegration

INTRODUCTION

During the wastewater treatment processes significant amounts of sewage sludge are formed and must be disposed of. Nowadays, the most common method used for sludge treatment is anaerobic digestion (AD), where the mass of sludge is reduced and energy is recovered in form of biogas (methane). Increasing the efficiency of biogas production to achieve energy self-sufficiency in a municipal wastewater treatment plant (WWTP), and even to become an energy producer, is recently one of the key aims for WWTP operators.

An effective way to increase biogas production at WWTP is the co-digestion of sewage sludge with agro-industrial waste (Budych-Górzna et al., 2016). Case studies of co-digestion of biosolids with organic wastes at full scale showed that the use of co-digestion could overcome significant economic challenges including higher methane yield (Y_{CH4}), more efficient digester volume utilization, and reduced biosolids production (Shen et al., 2015). However, the use of co-digestion is possible only if the WWTP has an excess volume of digesters. Otherwise, the focus should be on increasing the production of biogas from sludge generated at WWTP and improving its degradation rates, allowing full-scale plants to reduce the size of digesters (Souza et al., 2013). One way to achieve this is to enhance the digestibility of waste activated sludge (WAS) via a variety of pre-treatment methods (e.g. Zhen et al., 2017).

Microorganisms responsible for aerobic wastewater treatment tend to aggregate by forming flocs, biofilms, and granules thanks to extracellular polymeric substances (EPS). EPS are the predominant constituents of activated sludge and represent up to 80% of its mass (Tian et al., 2006). The EPS matrix may serve as a multipurpose functional element of microbial communities, including adhesion, protection, structure, recognition, and physiology. The temperature, rather than wastewater composition, significantly influences the content and chemical constituents of different EPS fractions (Zhang et al. 2015). Although EPS are essential for proper activated sludge functioning, they have a negative impact on the AD process (Peng et al., 2020).

Alkaline pre-treatment (APT) is relatively simple to implement in the full-scale WWTP (Zhen et al., 2017) because it does not require sophisticated devices and it is easy to operate. Among the alkaline reagents, NaOH was found to be the most effective in sludge solubilization and enhancing biogas production. The combination of APT together with mid-temperature (<100°C) conditions could potentially lead to an even doubling of methane production (Liu et al., 2019). Toutian et al. (2021) recommended keeping alkali dosage during ATP below 80 mg NaOH per g TS of WAS.

The aim of this work was to investigate the effect of mid-temperature (60°C) APT with NaOH on WAS disintegration, EPS composition, and methane yield changes during the yearly operation of WWTP. Low alkaline doses were chosen to lower potential operational costs, eliminate the need for pH correction, avoid salinity increase and enable potential implementation at the industrial scale.

MATERIALS AND METHODS

Mechanically thickened WAS for batch tests was collected in different months from the Central WWTP (1,200,000 people equivalent, Poznan, Poland). Portions of 1.5 kg of WAS diluted to 5% TS were put into 2 L beakers with a mechanical agitator (140 rpm) and doses of NaOH were added. The initial dose of 2 mL 30% NaOH/L (i.e. 16.0 g NaOH/kg TS) was chosen according to the previous studies (Budych-Górzna et al., 2021, Komorowska-Kaufman et al. 2022). Tests were carried out in temperatures of 20°C and 60°C, with a time of 30 minutes. The pH and temperature were measured every 5 minutes. Soluble chemical oxygen demand (SCOD) was analysed in all samples to calculate DD according to the equation presented by Kim et al. (2013). Basic wastewater sludge parameters were measured according to APHA (2017).

Y_{CH4} was measured in triplicates with a blank sample with Automatic Methane Potential Test System (AMPTS, BPC Instruments AB, Sweden). The inoculum (I) was taken from a full-scale AD mesophilic reactor. The WAS without pre-treatment (WAS_o), after APT (WAS_A) and after mid-temperature APT (WAS_{MA}) were used as a substrate (S). The AD batches lasted 21.5 days at a temperature of 36°C, the I/S ratio was equal to aprox.1.

From WAS, three fractions of EPS were extracted: soluble (SOL), loosely bound (LB), and tightly bound (TB) (Pellicer-Nàcher et al., 2013). The total quantity of extracted EPS was expressed as TOC and measured with an Elementar High TOC (Shimadzu TOC-L, Japan).

RESULTS AND DISCUSSION

The characteristics of WAS used in batch tests were as follows: TS=4.9±0.2%, VS=78.7±1.0% TS, COD=57000±13130 mg/L, SCOD=231±88 mg/L, pH=6.9±0.2, N-NH_4=17.3±14.8 mg N/L, and soluble TP=55.1±10.9 mg P/L. All reagent doses increased the sludge pH to about 10.0, although after dosing 16 g NaOH/kg TS after approx. 30 min it decreased to 8.7 in 20°C and to 7.6 in 60°C, so no pH correction prior AD process was needed. APT with an initial dose at 20°C caused DD of 4.6±1.4%, additional implementation of heating (60°C) allowed to achieve DD of about 28.6±7.8%. It was noticed that obtained DD varied depending on the quality of the raw WAS. The less biodegradable during AD it was, the higher DD was achieved for the same process conditions. Therefore, for comparison of the disintegration process, WAS was seasonally collected in a sufficient amount for the necessary trials. The use of heating alone resulted in a reduction of the obtained DD in relation to the value after APT with an initial NaOH dose at 60°C by 4.8-18.5%. On the other hand, the use of heating and a high dose of 64 g NaOH/kg TS resulted in a 3.0-4.9% higher DD compared to that achieved in the process with a low dose. This confirms the validity of using a lower dose of the alkalizing agent.

The DD was not the main factor influencing the increase in methane production in the 21.5-day AD trials. The Y_{CH4} of raw WAS turned out to be the most important (Fig.1). If its value was over 210 NmL CH_4/g VS, which is close to the maximum value for WAS, the use of APT increases methane production only by a few percent. Kim et al. (2013) achieved maximum Y_{CH4} after disintegration with 0.1 M NaOH at 75°C (191.4 NmL CH_4/g VS). When Y_{CH4} of raw WAS was lower, the use of any disintegration method greatly increased methane production. In samples from summer, the increase in Y_{CH4} obtained with the low-dose mid-temperature APT was as high as 70.7%.

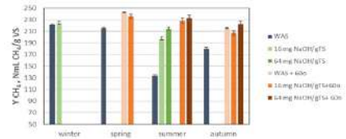

Figure 1. Changes in raw and pre-treated WAS during the year.

Similar conclusions were reached by Toutian et al. (2020) showing that thermal APT led to a higher biogas yield increase in summer (+42%) and a lower increase in winter (+3%). In the examined samples of raw WAS (Fig.1), COD was similar, although differences in the amount of EPS were noticed (Fig.2). The concentration of TB EPS was the highest in the June sample of WAS. Disintegration turned them into SOL EPS, resulting in an amount almost twice higher than in the other samples. Li et al. (2022) indicated that after EPS layer delamination, the Y_{CH4} in AD increased by 32.2% compared to the raw WAS.

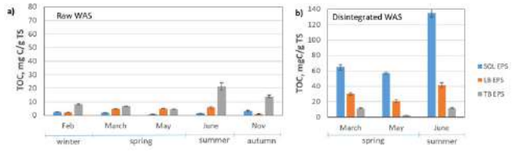

Figure 2. EPS concentration measured as TOC in raw WAS (a) and in WAS after disintegration with mid-temperature alkali pre-treatment with 16 g NaOH/kg TS and 60°C (b).

CONCLUSIONS

It was indicated that a low dose of 16 g NaOH/g TS and mid-temperature (60°C) was sufficient to achieve a significant DD of up to 45%. However, the DD under the same conditions depended on the properties of the raw WAS, which varies throughout the year. In addition, the methane production increase is not proportional to the achieved DD. It depends mainly on the Y_{CH4} of raw WAS, which was found to be correlated to the content of various EPS forms. The lowest raw Y_{CH4} for WAS was noticed in a summertime, and it was recommended to use during that period of a year heat pretreatment with alkaline addition. In many cases, in summer there is excess heat at the WWTP from combined heat and power units for which there is no direct application. Whereas, during winter, excess heat is often used for heating purposes of digesters and other facilities. It was indicated that during that period, solely alkaline is sufficient to boost Y_{CH4}. It is concluded that in order to best use energy and resources, the pretreatment should be adapted to seasonal changes in WAS. Overall economic and energy balance will be carried out to find best-case scenarios.

Acknowledgments: This work was financially supported by Polish National grant NOR/POLNOR/SIREN/0069/2019 'Integrated system for SImultaneous Recovery of Energy, organics and Nutrients and generation of valuable products from municipal wastewater (SIREN)'

REFERENCES

APHA, 2017. Standard Methods for the Examination of Water and Wastewater, 23st ed. American Public Health Association/American Water Works Association/Water Environment Federation, Washington DC.
Budych-Górzna, M., Jaroszyński, Ł., Oleskowicz-Popiel, P. 2021 Improved Energy balance at a municipal wastewater treatment plant through waste activated sludge low-temperature alkaline pretreatment. *Journal of Environmental Chemical Engineering* **9**, 106366
Budych-Górzna, M., Smoczyński, M., Oleskowicz-Popiel, P. 2016 Enhancement of biogas production at the municipal wastewater treatment plant by co-digestion with poultry industry waste. *Applied Energy* **161**,387–394
Kim, J., Yu, Y., Lee C. 2013.Thermo-alkaline pretreatment of waste activated sludge at low-temperatures: Effects on sludge disintegration, methane production, and methanogen community structure. *Bioresource Technology* **144**, 194–201
Komorowska-Kaufman, M., Budych-Górzna, M., Oleśkowicz-Popiel, P. 2022 Effect of mid-temperature alkaline pre-treatment on disintegration of waste activated sludge, methane yield and digestate dewatering. Conference materials of 11th IWA International Symposium on Waste Management Problems in Agro-Industry, Gdańsk, Poland
Li, S., Zhang, Y., Duan, W., Deng, R.,Gu, L., Shi, D. 2022 Insights into the resistance of different extracellular polymeric substance (EPS) layers to the fermentation environment in sludge anaerobic digestion. *Chemical Engineering Journal* **449**, 137844
Liu, X., et al. 2019 Thermal-alkaline pretreatment of polyacrylamide flocculated waste activated sludge: process optimization and effects on anaerobic digestion and polyacrylamide degradation. *Bioresource Technology* **281**, 158–167
Pellicer-Nàcher, C., Domingo-Félez, C., Mutlu, A.G., Smets, B.F. 2013 Critical assessment of extracellular polymeric substances extraction methods from mixed culture biomass. *Water Research*, **47(15)**, 5564–5574.
Peng, M, Xu, J., Yang, G., Xu, H. 2020 Digestion Properties of Intracellular Polymers and Extracellular Polymeric Substances and Influences of Extracellular Polymeric Substances on Anaerobic Digestion of Sludge. *Journal of Environmental Engineering* **146**(10), doi:org/10.1061/(ASCE)EE.1943-7870.0001787
Shen, Y., Linville, J.L., Urgun-Demirtas, M., Mintz, M.M., Snyder, S.W. 2015 An overview of biogas production and utilization at full-scale wastewater treatment plants (WWTPs) in the United States: Challenges and opportunities towards energy-neutral WWTPs. *Renewable and Sustainable Energy Reviews* **50**, 346–362
Souza, T.S.O., Ferreira, L.C., Sapkaite, I., Pérez-Elvira, S.I., Fdz-Polanco, F. 2013 Thermal pretreatment and hydraulic retention time in continuous digesters fed with sewage sludge: Assessment using the ADM1. *Bioresource Technology* **148C**(5), 317–324
Tian, Y., Zheng, L., Sun, D. 2006 Functions and behaviors of activated sludge extracellular polymeric substances (EPS): a promising environmental interest. *Journal of Environmental Sciences* **18**(3) 420–427
Toutian, V., Barjenbruch, M, Loderer, C., Remy, C. 2020 Pilot study of thermal alkaline pretreatment of waste activated sludge: Seasonal effects on anaerobic digestion and impact on dewaterability and refractory COD. *Water Research* **182**, 115910
Toutian, V., Barjenbruch, M, Loderer, C., Remy, C. 2021 Impact of process parameters of thermal alkaline pretreatment on biogas yield and dewaterability of waste activated sludge. *Water Research* **202**, 117465
Zhang, W., Yanga, P., Xiao, P., Xu, S., Liu, Y., Liu, F., Wang, D. 2015 Dynamic variation in physicochemical properties of activated sludgefloc from different WWTPs and its influence on sludge dewaterabilityand settleability. *Colloids and Surfaces A: Physicochem. Eng. Aspects* **467**, 124–134
Zhen, G., Lu, X., Kato, H., Zhao, Y., Li, Y.-Y. 2017 Overview of pretreatment strategies for enhancing sewage sludge disintegration and subsequent anaerobic digestion: current advances, full-scale application and future perspectives. *Renewable and Sustainable Energy Reviews*, **69**, 559–577

Impact of Polyethylene terephthalate (PET) degradation products on Mixed Purple Phototrophic Bacteria (PPB) metabolism (max: 15 words)

M. Palhas*[1,2], D. Puyol**,J. Fradinho*[1,2] and M.A.M Reis*[1,2]

*[1]Associate Laboratory i4HB – Institute for Health and Bioeconomy, NOVA School of Science and Technology, NOVA University Lisbon, 2829-516 Caparica, Portugal
*[2] UCIBIO – Applied Molecular Biosciences Unit, Department of Chemistry, NOVA School of Science and Technology, NOVA University Lisbon, 2829-516 Caparica, Portugal
(E-mail: *m.palhas@campus.fct.unl.pt; j.fradinho@campus.fct.unl.pt; amr@fct.unl.pt)**
** Group of Chemical and Environmental Engineering (GIQA), Higher School of Experimental Sciences and Technology (ESCET), Universidad Rey Juan Carlos, 28933 Móstoles, Madrid, Spain
(E-mail: daniel.puyol@urjc.es)

Abstract (max: 150 words)
Plastics and their degradation products are almost everywhere nowadays, even in traditional waste streams. These streams can be treated by multiple technologies, such as purple phototrophic bacteria (PPB). Current knowledge on PPB and plastic interaction is scarce. The study aimed to investigate the impact of plastic degradation compounds (PDCs) on the metabolism of PPB. Batch tests were performed on 100mL flasks under an irradiance of 160 ± 10 W/m^2 in the presence of butyric acid at different concentrations of PDCs (1, 2.5, and 5 gCOD/L), composed of half ethylene glycol and half terephthalic acid. Results indicate that PPB can tolerate PDCs concentrations of up to 5 gCOD/L without significant adverse effects on growth and activity but with a slight lag phase at higher concentrations simultaneously with EG consumption. Further research is needed to understand the upper tolerance limit for PDCs and their long-term effects on the bacteria.

Keywords (maximum 6 in alphabetical order)
Purple Phototrophic Bacteria; Plastic Degradation Products; Polyethylene terephthalate

INTRODUCTION

A significant quantity of non-biodegradable plastics is being used daily, such as polyethylene, polypropylene, and polyethylene terephthalate (PET); e.g., in Europe, more than 50 million metric tons of plastic is consumed every year. These plastics pose a significant environmental impact. This has led to unprecedented concerns about plastic pollution and a growing need for solutions to manage plastic waste and alternatives to traditional plastics [1]. These plastics often find their way into various aquatic environments, including oceans, rivers, and lakes, and can ultimately flow into crucial natural water sources. Furthermore, the presence of these compounds can have a detrimental impact on wastewater treatment plants by clogging filters and reducing the efficiency of the biological treatment processes [2].

Purple phototrophic bacteria (PPB) are a diverse group of organisms with a wide range of metabolic capabilities, including the ability to grow aerobically and anaerobically and utilize carbon-based organics as energy and carbon sources. They can also store carbon as polymers called polyhydroxyalkanoates (PHAs), fully biodegradable biopolymers with thermoplastic properties that are useful as a sustainable alternative to traditional plastics in multiple applications. In addition, PPB have also been shown to consume hydrocarbons and aromatic compounds. As such, PPB have been the subject of considerable study in recent years for their potential use in the bioremediation and biodegradation of multiple substrates [3-4].

This study aims to investigate the impact of plastic degradation compounds (PDCs), which includes Ethylene glycol (EG) and the aromatic compound terephthalic acid (TPA), derived from the degradation of PET, on the activity and growth of PPB. Studies have yet to be made with the PPB metabolism on the presence of such compounds despite their significant presence in our daily lives and on waste streams that PPB can treat. By understanding the influence of these compounds on the metabolism of PPB, we hope to gain insights into the potential toxicity to these microorganisms so crucial in the future of waste treatment. With further research, PPB are another valuable tool in the bioremediation of plastic pollution and for developing sustainable alternatives to traditional plastics.

MATERIALS AND METHODS

Origin of Culture. The culture used for the batch tests was selected in a continuous Sequence Batch Reactor (SBR) with a working volume of 4.2 L. The reactor was submitted to cycles of 24 hours, fed once per cycle with all the nutrients required using butyric acid as the organic carbon source and $NaCO_3$ as the inorganic carbon (IC) source. The end of the cycle was characterized by an IC famine phase that lasted from 3 to 5 hours. The reactor was continually illuminated with four halogen lamps with a Visible light cut filter, allowing only the Infrared wavelength to pass to the inside of the reactor, giving an approximated volumetric irradiance of 2.25 W/L.

Batch Tests. The batch tests were operated with an initial working volume of 100 mL under an irradiance of 160 ± 10 W/m^2 after the Visible light cut filter in a 150-rpm shaker with a temperature of 34 °C ± 2ºC and with the initial pH fixed at 6.6. The inoculum of each flask started with an optical density (OD) of 0.067 ± 0.002. All flasks were fed with 8.4 mmol/L of carbonate, 10.71 mmol/L of ammonia, 10.02 mmol/L of phosphate, 0.11 mmol/L of sulfate, and a standard mineral solution. In the study, three different concentrations of PDCs were examined, all with the same molar ratio of EG to TPA of 1:1. The concentrations were 1, 2.5, and 5 g COD/L, and the experiments were performed in the presence of butyric acid at 2 gCOD/L, the sole organic source in the origin reactor, to evaluate the activity of the PPB culture. Two control conditions were also evaluated: one in which only butyric acid was present at 2 gCOD/L and the other in which a combination of EG and TPA was present at a total concentration of 1 g COD/L. A spike of butyric acid and carbonate to reach 2 gCOD/L and 8.4 mmol/L in the flasks, respectively, was introduced at 1.7 days post-inoculation to prevent the culture from reaching a starvation phase. On the 4th day, except for PDCs control, all flasks were reinoculated to restart to the initial condition. Each condition was carried out in triplicates.

RESULTS AND DISCUSSION

The experiment started at a low biomass concentration hence with a colorless solution. Throughout the study, with the increase of biomass concentration, followed by the OD (Figure 2. A), the flasks acquired the typical reddish color specific to PPB culture enrichment and prominent absorption peaks at 805 and 865 nm, corresponding to the presence of bacteriochlorophyll a.

The results indicate that the butyric acid consumption rate was similar in the control (Figure 1. A) and the condition with 1 g COD/L of PDCs. (Figure 1. C) However, as the concentration of PDCs increased on conditions 2 and 3 up to 2.5 and 5g COD/L (Figure 1. D and E), there was a noticeable reduction in the butyric acid consumption rate on the first day, a 30% reduction in 5 g COD/L of PDCs condition. No increase was seen in EG or TPA consumption to compensate for this reduction, indicating the existence of a lag phase at these concentrations. After the butyric spike, the consumption of butyric acid increased in the conditions with higher concentrations of PDCs, namely at 2.5 and 5 g COD/L of PDCs (Figure 1. D and E, black arrow) when compared with the butyric control (Figure 1. A). This suggests that PPB required some time to adapt to PDCs at higher concentrations but did not seem to affect the overall activity of butyric consumption.

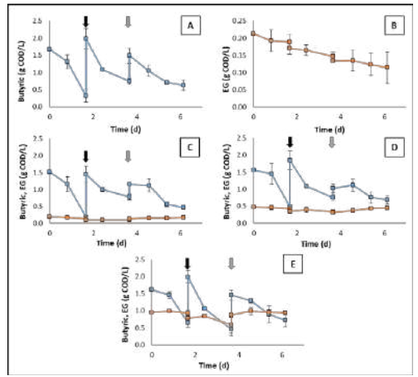

Figure 1. Evolution of butyric or EG concentration trough time for each condition. For each data point the average of triplicates is represented with the correspondent standard deviation. A – Control with butyric only (1 gCOD/L). B – Control with PDCs at 1 gCOD/L (TPA not shown). C – Condition 1: started at 1 gCOD/L of PDCs and 2 gCOD/L of butyric. D - Condition 2: started with 2.5 gCOD/L of PDCs and 2 gCOD/L of butyric E – Condition 3: started at 5 gCOD/L and 2 gCOD/L of butyric. Black and grey arrows showing the time of butyric spike and reinoculation respectively.

The PPB demonstrated the capability to consume EG, particularly in the control flasks containing only PDCs (EG and TPA) as sole organic source (Figure 1. B) and at 5 g COD/L of PDCs (Figure 1. E). EG maximum consumption of 109 mg COD/L.d was achieved at the highest concentration of PDCs. This was also associated with the highest biomass concentration suggesting that, in addition to the butyric acid, the extra carbon from EG might be used for growth (Figure 2 B). The growth rate seems not to be affected by the presence of the PDCs in the medium, except for a higher hindrance on growth at the beginning of the test at higher concentrations of PDCs, namely 2.5 and 5 gCOD/L as we have seen with the butyric acid uptake, being both related (Figure 2. A).

TPA was not consumed at a measurable rate without acclimatization or pre-selection of bacteria. This may be due to the aromatic nature of TPA and the metabolic requirements it poses (results not shown). Further research is needed to fully understand the upper tolerance limit for PDCs and the potential long-term effects on the bacteria.

Conclusion. Overall, the results suggest that PPB can tolerate concentrations of PDCs up to 5 g COD/L without significant negative effects on growth and activity, except for a slight lag phase at the beginning of the test at higher concentrations. The capability of PPBs to consume EG without previous adaptation is worthy of notice. This study demonstrated promising results relating PPB and plastic tolerance and their great potential for plastic bioremediation. Gradual acclimatization of PPB to PDCs will be further tested to increase the capacity of PPB to consume PDCs and evaluate their use for PHA production.

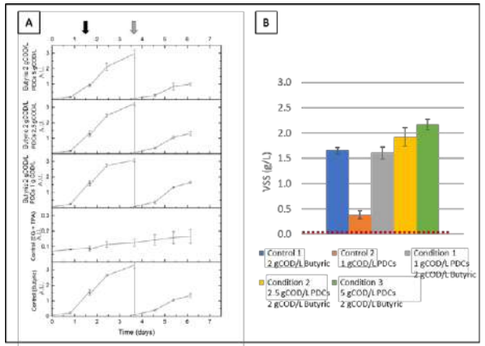

Figure 2. Growth of PPB at the different conditions and controls. A – Evolution of optical density at different conditions, average of triplicates with standard deviations. Black and grey arrows correspond to the time of butyric acid spike and reinoculation, not applying to PDCs Control. B – VSS values at the end of the first inoculum (grey arrow on Figure 2. A), average values from triplicates with standard deviation. Red dashed line showing the initial value of VSS in day 0.

REFERENCES

[1] Butler, E., Devlin, G. & McDonnell, K. 2011 Waste polyolefins to liquid fuels via pyrolysis: Review of commercial state-of-the-art and recent laboratory research. *Waste and Biomass Valorization* 2, 227–255.
[2] Zhang, Z. & Chen, Y. 2020 Effects of microplastics on wastewater and sewage sludge treatment and their removal: A review. *Chem. Eng. J.* 382, 122955.
[3] Fradinho J., Allegue, L.D., Ventura, M., Melero, A., Reis, M.A.M., Puyol, D. 2021 Up-scale challenges on biopolymer production from waste streams by Purple Phototrophic Bacteria mixed cultures: A critical review, *Bioresource Technology*, Volume 327, May 2021, 124820
[4] Harwood, C. S. 2009 Degradation of Aromatic Compounds by Purple Nonsulfur Bacteria. in 577–594 (Springer, Dordrecht,. doi:10.1007/978-1-4020-8815-5_29

Valorisation of saline wastewater to produce added-value organic acids of industrial interest

L. Paredes, M. Martínez-Quintela, G. Casas, E. Vega, L. Llenas

BETA Technological Center (TECNIO Network). University of Vic - Central University of Catalonia (UVic-UCC), Carretera de Roda 70, 08500 Vic, Spain
(E-mail: lidia.paredes@uvic.cat, miguel.martinez@uvic.cat, gemma.casas.papell@uvic.cat esther.vega@uvic.cat, laia.llenas@uvic.cat)

Abstract
The proper management of meat brines is associated to high costs for the meat processing industries. Consequently, exploring alternatives for their valorisation is essential to increase the competitiveness and circularity of the meat sector. In that sense, this study proposes the valorisation of meat brines for the production of volatile fatty acids of industrial interest by means the application of anaerobic fermentation coupled with electrodialysis.

Keywords
Anaerobic fermentation; brines; electrodialysis; meat industry; organic acids

INTRODUCTION

The meat industry is one of the pillars of the food sector in Europe and the main industry of the agri-food sector in Catalonia with a turnover of 8,453 M€. During the preparation of processed products such as fuet and cured ham, the meat processing industry generates large volumes of high salinity wastewater (brines) due to the use of sodium chloride as preservative agent. Considering the high environmental impact which could cause their discharge in water bodies, brines must be properly managed by food industries either on-site or through external management companies. The current management costs for brines (up to 100€/m^3) are forcing companies to explore alternative processes oriented not only to treat them properly, but also valorise them with the purpose of approaching the circular economy model. To address this challenge, this study proposes the valorisation of high salinity wastewater generated in the meat processing industry to produce volatile fatty acids (VFAs) of industrial interest. The proposed technological approach is based on the application of a fermentation process under anaerobic conditions using mixed microbial culture as inoculum combined with electrodialysis as a suitable technology to recover the VFAs in the permeate and concentrate the salts in a more reduced volume.

MATERIALS AND METHODS

Acidification batch test were conducted to identify the optimal operating conditions to maximize the production of VFAs during the valorisation of 2 types of brines generated in the meat processing industries (Brines A-fuet production (λ: 107 mS/cm) and Brines B-cured ham production (λ: 220 mS/cm)) and a mixture 50:50 (vol.) of Brines A and B. The inoculum used for the batch test was enriched in acidogenic microorganisms in an anaerobic fermenter of 10 L operated in continuous mode under an HRT of 6 d and fed with saline wastewater (λ: 35 mS/cm). The test were carried out in 200 mL bottles during a period of 7 days at 37°C, evaluating the influence of the inoculum-substrate ratio for each type of brine to simulate an HRT of 3 and 6 days. The production of VFAs (acetic, propionic, butyric, iso-butyric, valeric, iso-valeric and 4-methylvaleric acid) was monitored periodically by the analysis of samples from the liquid phase by means of Gas Chromatography.

The effluent obtained in the anaerobic fermenter (Figure 1) was subsequently treated in an electrodialysis unit in order to evaluate its potential to separate the VFAs produced during the valorisation of brines and the salts, trying to maximise their recovery in the permeate.

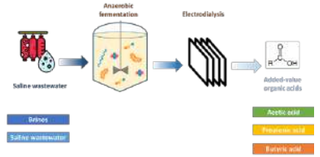

Figure 1. Production of volatile fatty acids from meat brines.

RESULTS AND DISCUSSION

The results obtained during the acidification batch test show the conductivity of the brines significantly affects to the percentage of acidification, ranging from 30% for Brine B to 80% from Brine A. In addition, higher HRT are associated to higher percentages of acidification. Figure 2 shows the composition of the VFAs produced during the anaerobic fermentation depends not only on the initial composition of the brines, but also on the operating conditions applied during the anaerobic fermentation.

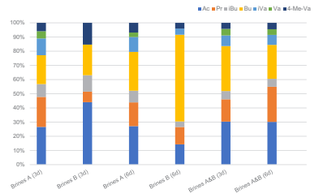

Figure 2. Composition of volatile fatty acids produced during the valorisation of meat brines.

The application of the electrodialysis allowed to efficiently recover (up to 95%) the volatile fatty acids produced during the anaerobic fermentation in the permeate and concentrate the salts (mainly sodium chloride) in a more reduced volume (~30% of the initial volume).

ACKNOWLEDGMENTS

The VASAL project is linked to the Knowledge Industry grants (Llavor i Producte) and has the support of the Department of Research and Universities of the Generalitat de Catalunya. Nº exp 2021 LLAV 00067.

REFERENCES

Fra-Vázquez, A., Pedrouso, A., Del Rio, A. V., Mosquera-Corral, A., 2020. Volatile fatty acid production from saline cooked mussel processing wastewater at low pH. *Science of the Total Environment*, 732, 139337.

Activated carbon from banana peel: an emerging biobased material for adsorption of diclofenac

S. Phal* **,R.Tan*,Y.Bessiere**, and C. Guigui**

* RIC, Institute of Technology of Cambodia, Russian Federation Blvd., P.O. Box 86, Phnom Penh (E-mail: *rtan@itc.edu.kh*)*
** TBI, INSA CNRS UMR 5504, INRA UMR 792, Université de Toulouse, 31077 Toulouse (E-mail: *phal@insa-toulouse.fr; yolaine.bessiere@insa-toulouse.fr ;guigui@insa-toulouse.fr*)

Abstract
Characteristics of activated carbon from banana peel and its adsorptive performance on diclofenac were studied to evaluate the potential of using banana peel as low-cost adsorbent as an alternative to conventional activated carbon for removal of micropollutants. Equilibrium was reached after 1000-1500 min and adsorption capacity was 93mg.g^{-1}. The kinetics were best fitted with a pseudo-second-order model indicating chemisorption and multiple diffusion steps. The adsorption isotherm was best fitted with Langmuir corresponding to homogenous sorption. Increasing pH from 6 to 10 caused gradual reduction in the adsorption capacity as electrostatic repulsion occurred due to both negative charge of diclofenac and activated carbon. This new adsorbent could be comparable with other adsorbent in previous studies. Based on the result, activated carbon produced from biowaste can be relevant to improve the wastewater treatment while preventing the negative side effect of using conventional activated carbon.

Keywords
Activated carbon; adsorption; banana peel; diclofenac; low-cost adsorbent

INTRODUCTION

The presence of persistent micropollutants cause a negative effect on aquatic organisms and human health. One of the reasons for their occurrence in environment is inefficient processes in conventional wastewater treatment plants (Carvalho et al., 2022). Pharmaceutical compounds are the subject of attention because of their intrinsic biology activity which can lead to fetal consequences. For instance, diclofenac (DCF) seems to be the compound with the highest acute toxicity among non-steroidal and anti-inflammatory drugs (Nadour et al., 2019). A concentration of several ng.l^{-1} DCF can change the cellular in the bronchi and kidney of rainbow trout (Zyłła et al., 2019). DCF has been detected in the Asian, European and American continents between 1998 and 2020 in the surface waters, raw and treated sewage in the water treatment plant with a wide range of concentrations from 0.04 ng.l^{-1} to 11 mg.l^{-1} (Carvalho et al., 2022).

Adsorption process with high dose activated carbon or combination with advanced wastewater treatment method might improve removal of micropollutant (Guillossou et al., 2019). Due to the large amount of activated carbon (AC) demand, using activated carbon produced from non-renewable sources such as coal, or lignite causes environmental pollution and enhances greenhouse gas emission (Hagemann et al., 2020). Hence, replacing fossil feedstocks of AC with sustainably and locally low-cost waste would contribute to waste management, circular economy, and removal of emerging contaminants. In this context, AC from banana peels may be a relevant alternative for water treatment. AC from banana peel was used for treatment of the methylene blue or heavy metal (Maia et al., 2021; Thuan et al., 2016), but its application to remove DCF has been little studied and the mechanisms involved remain poorly understood. Therefore, the objectives of this study are to: (i) investigate the adsorption characteristic by using kinetic, isotherm and intra-particle modelling, (ii) investigate the mechanisms involved by evaluating the effect of pH on adsorption in link with the change of activated carbon's characteristics.

MATERIALS AND METHODS

Activated carbon production

Banana peels were cut into 3 pieces around 4cm and washed with distilled water and dried at 105°C for 24h. They were ground into pieces from 254µm-2mm. Activated carbon was produced under chemical activation at impregnation ratio 1:1.5 (Banana peel: H_3PO_4, w:w) and kept overnight at room temperature. The material was placed in a muffle furnace with heating program for 4h at 200 °C followed by 2h at 500 °C. After the pyrolysis, it was washed with NaOH solution (1mol.l^{-1}) and then with distilled water up to pH 7. The obtained material was dried at 105°C for 14h and then it was sieved to gather particle with size from 75µm to 106µm and stored for characterization and adsorption tests. Commercial activated carbon Norit SAE 2 was used for comparison purposed as it has been proven to effectively remove the majors micropollutants (NORIT SAE SUPER, 2023).

Activated carbon characterization

Size distributions were determined by the Granulometer Malvern M3000. For the size distribution in volume, D10, D50, D90 of AC from banana peel were 7.32µm,73.6µm and 141µm respectively. In addition, commercial AC contained D[v,0.1] 4.24µm, D[v,0.5] 26.86µm and D[v,0.9] 136.41µm. The size distribution in number of both activated carbon were similar with small particle below 11µm.
Zeta potential of AC was measured by Malvern zetameter (Nano Zetasizer). Suspensions of 0.025g of AC in 200mL of 0.01M NaCl under different initial pH (2,3,4,5,6,7,8,10) were submitted to orbital shaker at 150rpm for 24h to reach equilibrium and measure the zeta potential.

Adsorption studies

The batch experiments (in triplicate) were carried out at 20°C by using a Jar test for constant agitation at 150rpm. Samples were filtered by a 0.45µm nylon membrane and DCF concentrations were determined by a UV-VIS spectrophotometer at 274nm.
The kinetic study was conducted to know the contact time effect on adsorption. Tests were conducted with 100mg.l^{-1} DCF solution and 0.5g.l^{-1} of AC. The pseudo-first-order, pseudo-second order, and intraparticle diffusion models were adjusted (Table 1).
Isotherm shows the relationship between the equilibrium concentration of the analytes (Ce) and the adsorbents uptakes (q_e) and it can provide insights into the nature of the biosorption phenomenon (Li et al., 2019). Equilibrium isotherms were obtained after 24h at different DCF concentrations from 1 to 10 mg.l^{-1} with 0.2 g.l^{-1} of AC. Langmuir, and Freundlich models were fitted (Table 1)
Effect of pH. The solution pH effect on the amount of DCF adsorbed was evaluated after 22h with 0.5g.l^{-1} of the adsorbent in 100mg.l^{-1} DCF solution with pH 6,7,8,9 and 10.

Table 1. Adsorption kinetic and isotherm model used

Model	Non-linear form	Linear form	Phenomena
Pseudo-first order	$q_t=q_e(1-e^{-k_1 t})$	$\log(q_e-q)=\log q_e-\left(\frac{k_1}{2.303}\right)t$	Physisorption
Pseudo-second order	$q_t=\frac{k_2 q_e^2 t}{1+k_2 q_e t}$	$\frac{t}{q}=\frac{1}{k_2 q_e^2}+\left(\frac{1}{q_e}\right)t$	Chemisorption
Intraparticle diffusion	$q_t=K_{id}t^{\frac{1}{2}}+C_e$		Mass transfer
Langmuir	$q_e=\frac{q_m K_L C_e}{1+K_L C_e}$	$\frac{C_e}{q_e}=\frac{1}{K_L q_m}+\frac{C_e}{q_m}$	Homogeneous
Freundlich	$q_e=K_F C_e^{\frac{1}{nF}}$	$\ln(q_e)=\frac{1}{n}\ln(C_e)+\ln(K_f)$	Heterogeneous

RESULTS AND DISCUSSION

Adsorption kinetic

Fig. 1a showed that the speed of adsorption was very fast in the early stage (0min- 90min) and reached equilibrium at 1000-1500 min. The experimental maximum adsorption capacity was 93mg.g^{-1}. Pseudo-second order model was the best fitted to experimental data with R^2=0.999 (Fig. 1b). This model indicated that the adsorption could be controlled by a chemisorption process that occurred with electrons sharing between molecules of DCF and AC's surface group. Moreover, experimental kinetic data was plotted by using intraparticle diffusion modelling in Fig.1c. It might be not rate-limited step in this process but it might involve multi stage adsorption where the initial stage (1st linear section) occurred (0-90 minutes) and represented the external mass transfer resistance involving the particle's surface. The second step (2nd linear section) (90-600 min) indicated a more gradual adsorption, characteristic of the adsorbate transport through the adsorbent inner surface. Finally, the third stage (3rd linear section) (600-3060 min) represented to the adsorption equilibrium.

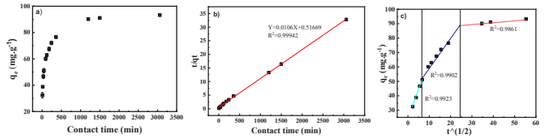

Figure 1. (a) Kinetic adsorption curves; (b) Pseudo-second order model of kinetic study and (c) Intraparticle diffusion kinetic plot

Isotherm study

Experimental data were fitted with Langmuir and Freundlich model with R^2 of 0.9901 and 0.9644 respectively (Figure 2a). K_L (Langmuir) and 1/n (Freundlich) values are 0.9572 and 0.593 below 1, so the diclofenac adsorption was favourable in the adsorbents of activated carbon from banana peel. These results suggested that the diclofenac adsorption took place onto a homogenous surface

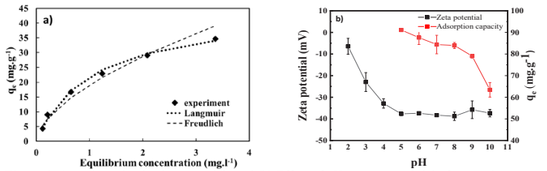

Figure 2. (a) Adsorption isotherm models and (b) Effect of pH on zeta potential of AC and resulting DCF adsorption capacity

Effect of adsorption pH

Fig. 2b showed about zeta potential of AC from banana peel with different pH. Within the pH range in which the adsorption capacity was evaluated, the activated carbon was negatively charged. Indeed, when the suspension alkalized, the particle tended to have more negative charge and zeta potential reach a plateau value of -40mV from pH 5 to 10. Concomitantly, adsorption capacity gradually decreased when increasing the pH from 6 to10 possibly due to an increase number of deprotonated species (-COO and O-) of DCF (pKa= 4.15) inducing electrostatic repulsion at high pH between negative charges of DCF and AC.

Comparison with commercial activated carbon

The commercial activated carbon adsorption capacity was 195mg.g^{-1} thus well above that of the banana peel AC (93mg.g^{-1}). However, the banana peel AC showed comparable adsorption capacities than other alternative adsorbent such as activated carbon tea waste (91.2 mg.g^{-1}), coco shell (63.47 mg.g^{-1}) (Malhotra et al., 2018, Saucier et al., 2015) and thus represent a potentially sustainable alternative.

REFERENCES

Carvalho, A. De, Matias, H., Fernandes, B. S., Motteran, F., Luiz, A., Paiva, R. De, Joaquim, J., & Cabral, P. 2022 Efficiency of the bank filtration technique for diclofenac removal. *Environmental Pollution*, 300, 0269–7491.

Guillossou, R., Le, J., Mailler, R., Vulliet, E., Morlay, C., Nauleau, F., Gasperi, J., & Rocher, V. 2019 Chemosphere Organic micropollutants in a large wastewater treatment plant : What are the bene fi ts of an advanced treatment by activated carbon adsorption in comparison to conventional treatment ? *Chemosphere*, 218, 1050–1060.

Hagemann, N., Schmidt, H., Kägi, R., Böhler, M., Sigmund, G., Maccagnan, A., Mcardell, C. S., & Bucheli, T. D. 2020 Wood-based activated biochar to eliminate organic micropollutants from biologically treated wastewater. *Science of the Total Environment*, 730, 138417.

Li, Y., Taggart, M. A., Mckenzie, C., Zhang, Z., Lu, Y., Pap, S., & Gibb, S. 2019 Utilizing low-cost natural waste for the removal of pharmaceuticals from water : Mechanisms , isotherms and kinetics at low concentrations. *Journal of Cleaner Production*, 227, 88–97.

Maia, L. S., Duizit, L. D., Pinhatio, F. R., & Mulinari, D. R. 2021 Valuation of banana peel waste for producing activated carbon via NaOH and pyrolysis for methylene blue removal. *Carbon Letters*.

Malhotra, M., Suresh, S., & Garg, A. 2018 Tea waste derived activated carbon for the adsorption of sodium diclofenac from wastewater : adsorbent characteristics , adsorption isotherms , kinetics , and thermodynamics. *Environmental Science and Pollution Research*, 32210–32220.

Nadour, M., Boukraa, F., & Benaboura, A. 2019 Removal of Diclofenac, Paracetamol and Metronidazole using a carbon-polymeric membrane. *Journal of Environmental Chemical Engineering*, 7(3),103080.

NORIT SAE SUPER, 2023, Dolder AG. Retrived from https://www.dolder.com/fr/filtration-purification/noritr-sae-super/ on 31 Jan 2023

Saucier, C., Adebayo, M. A., Lima, E. C., Catalu, R., Thue, P. S., Prola, L. D. T., Machado, F. M., Pavan, F. A., & Dotto, G. L. 2015 Microwave-assisted activated carbon from cocoa shell as adsorbent for removal of sodium diclofenac and nimesulide from aqueous effluents. *Journal of Hazardous Materials*, 289, 18–27.

Thuan, T. Van, Thi, B., Quynh, P., Duy, T., & Thanh, V. T. 2016 Response surface methodology approach for optimization of Cu^{2+}, Ni^{2+} and Pb^{2+} adsorption using KOH-activated carbon from banana peel. *Surfaces and Interfaces*, 0, 1–9.

Zyłła, R., Boruta, T., Gmurek, M., Milala, R., & Ledakowicz, S. 2019 Integration of advanced oxidation and membrane filtration for removal of micropollutants of emerging concern. *Process Safety and Environmental Protection*,130, 67–76.

CFD Modelling of CP in Roto-dynamic RO System at Seawater Salinity During Turbulent Cross Flow.

Nitikesh Prakash *, Abhijit Chaudhuri *, Shyama Prasad Das **

* Department of Applied Mechanics, Indian Institute of Technology Madras, Chennai 600036, India.
(E-mail: nitikeshprakash@gmail.com ; abhijit.chaudhuri@iitm.ac.in)
** Department of Mechanical Engineering, Indian Institute of Technology Madras, Chennai 600036, India.
(E-mail: spdas@iitm.ac.in)

Abstract
Concentration polarization (CP) is the major drawback in reverse osmosis (RO) system for brackish/seawater desalination. The present study aims to understand the effect of induced shear stress and enhanced flow dynamics on CP. We have numerically modelled the salt precipitation and CP with CFD, and for turbulent flow additional eddy viscosity and RSM equations are added in the solver. In case of turbulent flow CP is significantly reduced at the membrane surface, which may increase the longevity and overall performance of the membrane.

Keywords
CFD, concentration polarization, Roto-dynamic RO system, Turbulence Modelling.

INTRODUCTION

Today, RO filtration is the most used technology in the world for desalination. However, conventional spiral would RO modules (SWRO), face operational difficulties such as CP, which increases the internal friction and cause decline of permeate flux. Study [1-6] shows that cross flow increases the shear rate over the membrane, enhances the mass transfer coefficient and reduces the mineral concentration over the membrane. Dynamic filter [1-10] creates several wave forms that assist increasing cross flow, shear and mixing along the membrane surface which ensure the lower accumulation of solute and reduce the species transfer towards the permeate out. Such dynamic filter also disjoints the drop in pressure and shear rates. The performance analysis of roto-dynamic system proposed by Chaudhuri et al. [4] is considered for the present study, have a spinning disk over the membrane surface which creates axisymmetric flow structure, which enhances the shear and species transport over the membrane. The flow dynamics and precipitation rate [11-12], depend on feed concentration of salts, feed pressure and nature of flow (i.e., laminar/Turbulent) over the membrane surface. The CP is analysed for low and high shear region along the membrane surface at different feed pressure and spinning speed of rotor, which changes the flow patterns and concentration profiles as flow changes from laminar to turbulent.

METHODS AND RESULTS

To establish the numerical frame-work, we have used Ansys (fluent) as CFD solver for simulation of fluid flow, species transport, salt precipitation, and CP. We have used multiple UDFs to imposed different boundary and initial conditions.

Performance of roto-dynamic RO system in turbulent regime: Turbulence modelling and measurement of the turbulent flow along with species precipitation over the porous membrane is of great challenge. Therefore, first we stabilised the turbulence model used for the analysis (i.e., SST-Kω and RSM) in Ansys (fluent), validated with the existing experimental results of Poncet et al. [13], for non-dimensional velocity profile along the radial and azimuthal direction at different cross flow as shown in figure2.

The referred flow cavity [13] consist of a fixed disk (the stator) and a smooth rotating disk (the rotor). A fixed shroud encloses the cavity. The rotor and the central hub attached to it rotate at the uniform angular velocity Ω. The mean flow is mainly governed by three control parameters: the aspect ratio G, the Reynolds number (Re) based on the outer radius of the rotor, and the flow-rate coefficient C_w, defined as follows:

$G = h/R_2$; $R_e = \Omega R_2^2 / \nu$,$C_w = Q / \nu R_2$
where ν is the kinematic viscosity of water and Q is the imposed throughflow.

Table 1. Geometrical Parameters

Description	Symbol	value	unit	Source
Inlet Radius	R_1	38	mm	[13]
Outlet Radius	R-R_2	3	mm	[13]
Membrane to disk height	h	9	mm	[13]
Outer Radius	R_2	250	mm	[13]

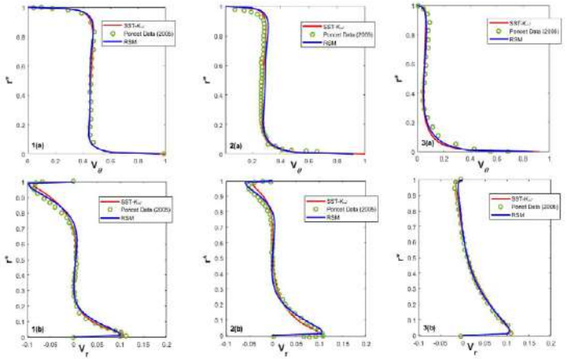

Figure 2. Mean velocity profiles for Re = 4.15 ⨯ 10^6, G = 0.036 at r* = 0.44 for SST-kω, RSM model and experimental data from poncet et al. [13], (1) C_w=0, (2) C_w=2579, (3) C_w = 5159.

This validated turbulence model is then used, to simulate the turbulent flow combined with the concentration polarization and particle precipitation behavior of salt in rotor-dynamic system. The dimensional specifications of rotor-dynamic system are taken same as rotor-stator cavity [Table 1] with same Reynolds number of 4.15 ⨯ 10^6. However, the stator is now being replaced with a porous membrane and a high pressure of 70 Bar with seawater salinity are applied as feed to simulate the CP of salt over membrane.

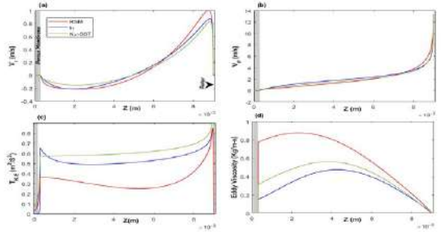

Figure 3. (a) Radial velocity, (b) Tangential velocity, (c) Turbulent kinetic energy and (d) Eddy viscosity profile along the domain perpendicular to membrane surface.

The high turbulent kinetic energy and turbulent viscosity over the membrane can be seen in the results (figure 3), which induces a high shear and recirculation over the membrane, increasing the transport of salt species.

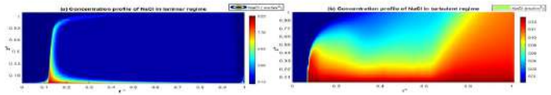

Figure 4. Concentration Polarization (CP), of NaCl over RO membrane in (a) laminar and (b) Turbulent flow.

In figure 4(a), we can see a pick in concentration near inlet of laminar flow due to presence of stagnation point. But, as we increase the rotor speed, due to the flow dynamics no such point exists in turbulent flow regime (figure 4(b)). Another important point is the concentration value over the membrane, as discussed, due to high turbulent kinetic energy, strain rate and eddy-viscosity the concentration polarization (CP) value is very less in case of turbulent flow.

CONCLUSION

Turbulence modelling equations is performed to study the CP of RO membrane during seawater desalination in turbulent regime after validating the model with the existing literatures.

The study shows that, it is possible to significantly reduce the CP propensity of the RO membrane, by maintaining a high shear and diffusion rate over the membrane with dynamics of fluid. Therefore, we can conclude that turbulent flow could be very beneficial for roto-dynamic system in order to mitigate the CP of desalinating membranes by enhancing the flow structure over the membrane.

REFERENCES

1. N Prakash, A Chaudhuri, S.P Das, Numerical modelling and analysis of concentration polarization and scaling of gypsum over the RO membrane during sea water desalination, Chemical Engineering Research and Design, Doi: https://doi.org/10.1016/j.cherd.2022.12.050.
2. Uppu, A. Chaudhuri, S.P. Das, N. Prakash, CFD modelling of Gypsum scaling in cross-flow RO filters using moments of particle population balance, Doi: HTTPs: //doi.org/10.1016/j.jece.2020.104151.
3. A. Jogdand, A. Chaudhuri, Modeling of concentration polarization and permeate flux variation in a roto-dynamic reverse osmosis filtration system, Desalination 375 (2015) 54–70, https://doi.org/10.1016/j.desal.2015.07.011
4. A. Chaudhuri, A. Jogdand, Permeate flux decrease due to concentration polarization in a closed roto-dynamic reverse osmosis filtration system, desalination. Doi: HTTP://dx.doi.org/10.1016/j.desal.
5. Radu, L. Bergwerff, M. van Loosdrecht, C. Picioreanu, A two-dimensional mechanistic model for scaling in spiral wound membrane systems, Chem. Eng. J. (2014) Doi: HTTPs: //doi.org/10.1016/j.cej.2013.12.021.
6. A. Uppu, A. Chaudhuri, S.P. Das, Numerical modelling of particulate fouling and cake-enhanced concentration polarization in roto-dynamic reverse osmosis filtration systems, Desalination 468 (2019), Doi: HTTPs://dx.doi.org/10.1016/j.desal. 2019.06.019.
7. A. Karabelas, M. Kostoglou, S. Mitrouli, Incipient crystallization of sparingly soluble salts on membrane surfaces: The case of dead-end Filtration with no agitation, desalination (2011) 105–. Doi: HTTPs://dx.doi.org/10.1016/j. 636 desal.2010.10.057.
8. A. Uppu, A. Chaudhuri, S. P. Das, Numerical modeling of particulate fouling and cake-enhanced concentration polarization in roto-dynamic reverse osmosis filtration systems, desalination (2019). Doi: HTTPs://dx.doi.org/10.1016/ j.desal.2019.06.01.
9. M. Y. Jaffrin, Dynamic shear-enhanced membrane filtration: a review of rotating disks, rotating membranes, and vibrating 704 systems, Journal of Membrane Science (2008). Doi: HTTPs://dx.doi.org/10.1016/j.memsci.2008.
10. M. Y. Jaffrin, Dynamic Filtration with rotating disks, and rotating and vibrating membranes: an update, Current Opinion in Chemical Engineering. Doi: HTTPs://dx.doi.org/10.1016/j.
11. R. Sheikholeslami, H. Ong, Kinetics and thermodynamics of calcium carbonate and calcium sulfate at salinities up to 1.5 m, Desalination (2003) Doi: HTTPs://dx.doi.org/10.1016/S0011-9164(03)00401-6.
12. M. Kostoglou, A. Karabelas, On modelling incipient crystallization of sparingly soluble salts in frontal membrane filtration, Journal of colloid and interface science (2011) Doi: HTTPs://dx.doi.org/10.1016/j.jcis.2011. 06.040.
13. S. poncet, R.Schiestel, M.P. Chauve, Centrifugal Flow in a Rotor-Stator Cavity, Journal of fluids Engineering, 2005, Vol.127, DOI: 10.1115/1.1949645.

Industrial wastewater treatment by integrated processes: coupling Fenton with biological

J. P. Ribeiro*, C. P. Morim*, F. C. Silva* and M. I. Nunes*

*CESAM – Centre for Environmental and Marine Studies, Department of Environment and Planning, University of Aveiro, 3810-193, Aveiro, Portugal
(E-mail: joaoperes@ua.pt; carolinapedrosamorim@ua.pt; flavio.silva@ua.pt; isanunes@ua.pt)*

Abstract
This work describes the sequential coupling of Fenton and aerobic biological process to treat pulp bleaching wastewater. Focus was put on the removal of chemical oxygen demand (COD) and adsorbable organic halides (AOX), under two treatment setups: Fenton followed by biological process; and biological followed by Fenton process. Aerobic biological treatment was performed in 2 L batch bioreactors, at room temperature, for 48 h. Fenton experiments were performed in 0.5 L batch reactors, using hydrogen peroxide as oxidant and Fe^{2+} as catalyst. Under optimal operating conditions, sequential treatment by Fenton followed by biological process yielded global removal of 71.9 % of COD and 89.6 % of AOX. The inverse sequence (biological followed by Fenton process) yielded global removal of COD and AOX of 82.6 % and 89.5 %, respectively.

Keywords
AOX; COD; process optimisation; pulp bleaching wastewater; response surface methodology.

INTRODUCTION

Aerobic biological wastewater treatment is based on the oxygen-assisted degradation of organics by microorganisms, yielding biomass, carbon dioxide, and water, among others (Suhr, Klein, et al., 2015). It is broadly used due to its lower cost, simpler operation, and less secondary pollution, when compared with physical and chemical technologies (Crini and Lichtfouse, 2019). Nonetheless, it is widely accepted that the toxic and recalcitrant nature of some industrial wastewaters render biological processes insufficient for pollution abatement (Hubbe, Metts, et al., 2016). Fenton process is a feasible alternative, known for its fast and effective abatement of recalcitrant pollution from wastewaters. It is based on the catalytic (Fe^{2+}) dissociation of H_2O_2 into •OH radical, which is a strong and non-selective oxidant (Brink, Sheridan, et al., 2017). For some wastewaters, the combination of these processes may be more efficient than the single application of any of them.

This work aimed to study the coupling of both processes: aerobic biological and Fenton, to maximise the global treatment performance in chemical oxygen demand (COD) and adsorbable organic halides (AOX) abatement. The goal was to address a major issue in this field of research: how to implement a setup in wastewater treatment plants that effectively reduces recalcitrant compounds, without compromising the effectiveness of conventional bioprocesses.

MATERIALS AND METHODS

Pulp bleaching wastewater served as case-study in this work, showing high levels of COD and AOX. The latter are recalcitrant compounds of environmental hazard. Wastewater was sampled at a pulp mill, after the first bleaching stage with ClO_2, which is the stream with higher concentration of AOX. Biocatalyst used in the bioprocess consisted of aerobic sludge collected at the wastewater treatment plant of the same mill. Two treatment setups were studied: (i) Fenton followed by aerobic biological process (activated sludge), and (ii) aerobic biological process followed by Fenton.

Fenton followed by biological process

Fenton process was carried out in 0.5 L batch with 6.0 mM of Fe^{2+} (as $FeSO_4.7H_2O$), 139 mM of H_2O_2 (30 % w/v), and treatment time (t) of 10 min. These operating conditions aimed to maximise AOX removal, as described elsewhere (Ribeiro, Marques, et al., 2020), since Fenton process is especially suitable to remove recalcitrant compounds. Wastewater temperature (T) and pH were set at 60 ºC and 2.48 ± 0.20, respectively, which are the values at which this wastewater stream is usually generated at this mill. At the end of treatment, wastewater samples were collected for determination of COD and AOX. The remaining wastewater was neutralised to 6.5 < pH < 7.5 with 9 M NaOH and proceeded for biological treatment. Nutrients N (as NH_4Cl) and P (as KH_2PO_4) were added to ensure COD:N:P of 100:7:1. Initial load of volatile suspended solids (VSS) of 3.60 $g \cdot L^{-1}$ was used according to preliminary tests. Preliminary experiments were also performed under different dilutions of the wastewater, showing that the biological sludge was able to cope with the Fenton by-products and the remaining recalcitrant compounds (Ribeiro, Morim, et al., 2021). Therefore, in this work, biological process was conducted directly on the Fenton-treated wastewater in 2 L glass reactors – 1.6 L of working volume, including wastewater, sludge, and micronutrients – under 400 rpm magnetic stirring, at room T, for 48 h.

Biological process followed by Fenton

In this treatment setup, aerobic biological treatment of raw wastewater was performed under similar conditions to those described for the inverse treatment sequence. Afterwards, biologically treated wastewater was centrifuged to remove the sludge, and reacidified to 2.5 < pH < 3.0 using a 32.5 % (v/v) HNO_3 solution. This procedure was adopted to perform Fenton process at the most favourable pH range (Ribeiro and Nunes, 2021). Response surface methodology (RSM) was used to find the optimal operating conditions of Fenton process, aiming to maximise the removal of AOX after the biological abatement of readily biodegradable compounds. Central composite experimental design was used to plan the experiences (Rodrigues and Iemma, 2015). The factors studied were the concentration of H_2O_2 (in the range 150 – 450 mM) and Fe^{2+} (4 – 10 mM), plus the treatment time (25 – 65 min). Three repetitions of the central point were performed, totalling 17 assays. Experiments were run at room T, to simulate what would happen at full-scale. After the established time for each experiment, samples were collected and immediately quenched with sodium sulphite.

Analytical methods

AOX content was quantified following EN 16166:2012, ISO 9562:2004 and EPA Method 1650C. COD and VSS were measured following Standard Methods 5220D and 2540E, respectively (Greenberg, Clesceri, et al., 1999). To support RSM analysis of the Fenton trials, four mathematical models were fitted to the experimental data: linear and second-order polynomial equations, with and without the terms describing the interaction between factors. 95 % confidence level was adopted.

RESULTS AND DISCUSSION

Fenton followed by biological process

Fenton process removed 50.2 % of COD and 65.0 % of AOX from the raw pulp bleaching wastewater (Figure 1). These results showcase the efficacy of Fenton process on the removal of recalcitrant compounds. The observed decrease in COD was in accordance with the observations of Van Aken et al. (2013), who reported 67 % COD removal from graphical industry wastewater under oxidant dose ranging 0.2 – 2 $g_{H2O2} \cdot g^{-1}_{COD}$ (in this work, 1.78 $g_{H2O2} \cdot g^{-1}_{COD}$ were used).

Biological treatment removed 37.3 % COD and 41.8 % AOX from the already Fenton-treated wastewater, leading to global removal from the coupled treatment of 71.9 % COD and 89.6 % AOX (Figure 1). These results highlight the advantage of coupling the treatments, achieving much higher removal of pollutants than by any of the processes applied individually. In a comparable work, Li et al. (2023) studied the sequential conjugation of Fenton process followed by activated sludge applied for treatment of mixed wastewater from different industries. The authors reported a maximum contribution of 20.9 % from Fenton process to the COD removal. Conversely, biological treatment contributed the most to the removal of the targeted pollutants, showing that its coupling with Fenton process may be especially suitable when recalcitrant compounds are found in the wastewater.

Biological process followed by Fenton

In this treatment setup, activated sludge removed 36.4 % of COD and 20.2 % of AOX. The removal of COD by biological treatment was similar between treatment setups, whilst the removal of AOX was about half of the value achieved under the inverse sequence. This suggested that the AOX compounds remaining in the wastewater after Fenton process may have been converted into less recalcitrant and more easily biodegradable compounds. When biological process is applied first, the recalcitrant nature of the raw wastewater is stronger and AOX removal is hindered.

The biologically treated wastewater was then subjected to Fenton process, which was optimised. Second-order quadratic model without interaction terms was selected as the best-fitting one, after checking the normality and randomness of the residuals, and analysing R^2 and adjusted R^2 (Rodrigues and Iemma, 2015). Lack-of-fit test for the two models (COD and AOX removal) yielded $p > 0.05$, meaning both models fitted well to the experimental data. Fe^{2+} concentration was the main factor statistically influencing the removal of COD and AOX. Optimal operating conditions to maximise COD removal from the wastewater were modelled to be 286 mM H_2O_2, 17 mM Fe^{2+}, and 83.3 min, yielding removals of 97.6 % COD and 12.3 % AOX. To maximise the removal of AOX, 489 mM H_2O_2, 9.3 mM Fe^{2+}, and 49.2 min should be adopted, yielding removals of 82.7 % AOX and 68.9 % COD. The latter set of operating conditions presents the best combined performance, reaching overall removal of 82.6 % COD and 89.5 % AOX. Abedinzadeh et al. (2018) used a sequential batch bioreactor followed by Fenton process (6.0 mM H_2O_2 and 3.0 mM Fe^{2+}) to remove COD from pulp wastewater. Overall COD removal of 98 % was achieved, which is higher than the one obtained in this work, using considerably less chemicals. This may be due to the lower initial COD (1.50 $g_{O2} \cdot L^{-1}$ against 2.14 $g_{O2} \cdot L^{-1}$) and higher biodegradability (0.37 against 0.08).

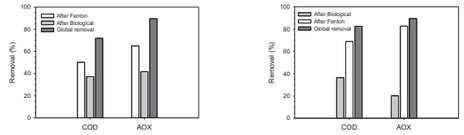

Figure 1. Removal of COD and AOX from the wastewater by the coupled treatments: (a) Fenton followed by biological process; (b) biological process followed by Fenton.

CONCLUSIONS

Fenton and aerobic biological (activated sludge) processes were successfully coupled in the treatment of pulp bleaching wastewater, maximising the removal of COD and recalcitrant AOX. When applied first, Fenton process removed 50.2 % of COD and 65.0 % of AOX from the raw wastewater, with biological treatment increasing the overall removal to 71.9 % of COD and 89.6 % of AOX. Under the inverse sequence, activated sludge removed 36.4 % of COD and 20.2 % of AOX from raw wastewater. Fenton process was optimised under RSM, allowing for global removal of COD and AOX of 82.6 % and 89.5 %, respectively. Therefore, this appeared to be the most suitable treatment setup for combined abatement of COD and AOX. Further research is still needed aiming at the full characterisation of the treated wastewater, to assess possible increase on toxicity.

ACKNOWLEDGEMENTS

Thanks are due to FCT/MCTES for the financial support to CESAM (UIDP/50017/2020 + UIDB/50017/2020 + LA/P/0094/2020), through national funds. João P. Ribeiro acknowledges FCT for his PhD Grant SFRH/BD/141133/2018. F.C. Silva acknowledges national funds (OE) under the contract framework foreseen in art. 23º DL57/2016 (nº 4, 5, 6) August 29th, amended by DL57/2017 July 19th.

REFERENCES

Abedinzadeh, N., Shariat, M., Monavari, S. M., and Pendashteh, A. (2018) Evaluation of color and COD removal by Fenton from biologically (SBR) pre-treated pulp and paper wastewater. Process Safety and Environmental Protection, **116**, 82–91.

Van Aken, P., Van Eyck, K., Degrève, J., Liers, S., and Luyten, J. (2013) COD and AOX Removal and Biodegradability Assessment for Fenton and O3/UV Oxidation Processes: A Case Study from a Graphical Industry Wastewater. Ozone-Science & Engineering, **35**(1), 16–21.

Brink, A., Sheridan, C. M., and Harding, K. G. (2017) The Fenton oxidation of biologically treated paper and pulp mill effluents: A performance and kinetic study. Process Safety and Environmental Protection, **107**, 206–215. [online] http://dx.doi.org/10.1016/j.psep.2017.02.011.

Crini, G. and Lichtfouse, E. (2019) Advantages and disadvantages of techniques used for wastewater treatment. Environmental Chemistry Letters, **17**(1), 145–155. [online] https://doi.org/10.1007/s10311-018-0785-9.

Greenberg, A., Clesceri, L., and Eaton, A. (eds.) (1999) *Standard methods for the examination of water and wastewater*, Baltimore, American Public Health Association; American Water Works Association; Water Environment Federation.

Hubbe, M. A., Metts, J. R., Hermosilla, D., Blanco, M. A., Yerushalmi, L., Haghighat, F., Lindholm-Lehto, P., Khodaparast, Z., Kamali, M., and Elliott, A. (2016) Wastewater treatment and reclamation: A review of pulp and paper industry practices and opportunities. BioResources, **11**(3), 7953–8091.

Li, X., Yang, H., Pan, J., Liu, T., Cao, X., Ma, H., Wang, X., Wang, Yi-fan, Wang, Yifan, Lu, S., Tian, J., Gao, L., and Zheng, X. (2023) Variation of the toxicity caused by key contaminants in industrial wastewater along the treatment train of Fenton-activated sludge-advanced oxidation processes. Science of The Total Environment, **858**(August 2022), 159856. [online] https://doi.org/10.1016/j.scitotenv.2022.159856.

Ribeiro, J. P., Marques, C. C., Portugal, I., and Nunes, M. I. (2020) Fenton processes for AOX removal from a kraft pulp bleaching industrial wastewater: Optimisation of operating conditions and cost assessment. Journal of Environmental Chemical Engineering, **8**(4), 104032. [online] https://doi.org/10.1016/j.jece.2020.104032.

Ribeiro, J. P., Morim, C. P., Silva, F. C., and Nunes, M. I. (2021) "Coupling of Fenton and biological processes for pulp bleaching wastewater treatment" in Proceedings of the 7th World Congress on New Technologies., 1–8. [online] https://avestia.com/NewTech2021_Proceedings/files/paper/ICEPR/ICEPR_118.pdf.

Ribeiro, J. P. and Nunes, M. I. (2021) Recent trends and developments in Fenton processes for industrial wastewater treatment – A critical review. Environmental Research, **197**(110957).

Rodrigues, M. I. and Iemma, A. F. (2015) *Experimental design and process optimization*, CRC Press - Taylor Francis Group.

Suhr, M., Klein, G., Kourti, I., Rodrigo Gonzalo, M., Giner Santonja, G., Roudier, S., and Delgado Sancho, L. (2015) *Best Available Techniques (BAT) Reference Document for the Production of Pulp, Paper and Board*, Luxembourg.

Recovery and valorisation of iron sludge from Fenton processes

J.P. Ribeiro*, C.C. Marques*, H.G.M.F. Gomes*, M.C. Neves**, L. Sarinho*, L.A.C. Tarelho* and M.I. Nunes*

* CESAM – Centre for Environmental and Marine Studies, Department of Environment and Planning, University of Aveiro, Aveiro, Portugal
(E-mail: joaopcres@ua.pt; m.catarina@ua.pt; helenagil@ua.pt; l.sarinho@ua.pt; ltarelho@ua.pt; isanunes@ua.pt)*
** CICECO – Aveiro Institute of Materials, Department of Chemistry, University of Aveiro, Aveiro, Portugal
(E-mail: mcneves@ua.pt)

Abstract
This work proposes a route to valorise the iron sludge from Fenton process, turning it into a heterogeneous Fenton catalyst. The sludge was produced after the treatment of pulp bleaching wastewater by Fenton process catalysed by (i) iron sulphate (homogeneous Fenton), and (ii) residual iron dust from the metallurgic industry (heterogeneous Fenton). The generated sludges were collected and thermochemically treated under nitrogen atmosphere aiming to promote the transition from ferric hydroxide to phases of higher catalytic activity towards Fenton process, mainly magnetite. Suitable temperatures of the thermochemical treatment were defined ($500 \leq T \leq 700$ ºC) by thermodynamic calculations based on the change of standard-state Gibbs energy of the iron reduction reactions. Chemical and structural characterisation of the thermochemically treated sludges will support the study of their performance as Fenton catalyst.

Keywords
AOX; catalyst; iron; magnetite; residual iron dust; wastewater.

INTRODUCTION

It is widely accepted that biological treatment is sometimes insufficient to remove toxic, recalcitrant compounds. Fenton processes are well-studied options to degrade recalcitrant compounds, based on the Fe-catalysed dissociation of hydrogen peroxide (H_2O_2) into hydroxyl radical, a strong non-selective oxidant (M'Arimi, Mecha, et al., 2020; Ribeiro, Marques, et al., 2020). Despite their numerous advantages, Fenton processes are usually linked to two main drawbacks: high exploitation of iron and production of iron sludge requiring management (e.g. Ribeiro and Nunes (2021)).

This work aimed to valorise the Fenton sludge as a catalyst of Fenton process applied to industrial wastewater treatment. To that end, industrial wastewater was treated by homogeneous and heterogeneous Fenton processes, and the resulting sludges were recovered and thermochemically treated. This way, a circular solution was sought to reduce the demand for iron and the amount of iron sludge to manage, by converting it into a waste-derived heterogeneous Fenton catalyst.

MATERIALS AND METHODS

Materials

Pulp bleaching wastewater was collected from a Portuguese pulp industry, after the first bleaching stage with ClO_2, since that stream is usually associated with considerable concentration of recalcitrant adsorbable organic halides (AOX) (Toczyłowska-Mamińska, 2017). H_2O_2 was used as received (30 % m/v solution); Fe^{3+} was supplied from a 184 mM aqueous solution of $Fe_2(SO_4)_3.5H_2O$; sodium hydroxide (NaOH) was used as a 2 M aqueous solution.

Iron sludge production

Wastewater was treated by Fenton processes catalysed by: (i) iron sulphate (homogeneous Fenton), and (ii) residual iron dust (RID) from the metallurgic industry (heterogeneous Fenton). Homogeneous Fenton process was performed with 170 mM H_2O_2, 5.5 mM Fe^{3+}, and reaction time of 10 min. These conditions were found in preliminary trials to maximise the removal of AOX (≈ 80 %) from the wastewater. In the heterogeneous Fenton process, RID was first added to the wastewater at 1:200 (g:mL) ratio and contacted for 30 min. At that point, 100 mM H_2O_2 was added, and further 10 min were allowed (Ribeiro, Sarinho, et al., 2022). For both Fenton processes, wastewater temperature (T) and pH were set at 60 ºC and 2.6, respectively, which are the values at which this wastewater stream is usually generated. After treatment, wastewater was always aerated with compressed air to eliminate residual H_2O_2, and alkalised to pH > 9 with NaOH to precipitate the iron sludges (Zhu, Xia, et al., 2021). The sludges were separated from the treated wastewater by decantation and dried at ≈ 60 ºC.

Thermochemical treatment of iron sludge

For both types of Fenton process, the resulting iron sludges were thermochemically treated in a fixed-bed tubular quartz reactor with 20 mm internal diameter and 350 mm length, under N_2-atmosphere. A type K thermocouple located at the central region of the tubular reactor allowed the monitoring of T, which was regulated by a control and data acquisition electronic system. In this work, 10 ºC·min^{-1} heating rate was adopted in all experiments. Treatment time (t) of 15, 30, and 60 min was tested. Most suitable T were defined by thermodynamic calculations, based on the change of standard-state Gibbs energy of the iron reduction reactions, described in Eq. (2)-(5).

RESULTS AND DISCUSSION

Fenton iron sludge production

Homogeneous Fenton process allowed for 83.4 ± 3.0 % removal of AOX from the wastewater, validating the choice of operating conditions. Heterogeneous RID-catalysed Fenton process yielded AOX removal from the wastewater of 66.2 ± 2.2 % under the chosen operating conditions.

The yield of iron sludge was higher in the homogeneous Fenton process, since the concentration of iron supplied to the wastewater was also higher: 5.5 mM in the homogeneous process, against 1.41 ± 0.11 mM after 30-min contact at 1:200 ratio (g:mL) in the heterogeneous process (Ribeiro, Sarinho, et al., 2022). In the latter, some RID particles were also inevitably collected with the sludge. In both processes, solids and fibres originally present in the wastewater were also collected with the sludge, due to the simple precipitation and decantation recovery procedure. Overall, the recovery of sludge was 2.55 g·L^{-1} and 1.75 g·L^{-1} for the homogeneous and heterogeneous Fenton processes, respectively.

Thermochemical treatment of iron sludge

Iron in the raw Fenton sludge consists mainly on ferric hydroxide $Fe(OH)_3$ or goethite (α-FeOOH) at high pH (Zhu, Xia, et al., 2021). Above 300 ºC, dehydration is expected to drive the conversion of goethite to hematite (α-Fe_2O_3) (Eq. (1)) (Gialanella, Girardi, et al., 2010). Depending on T and organic matter content, CO and/or H_2 may convert hematite to magnetite (Fe_3O_4) (Eq. (2)-(3)), which in turn may be reduced to Fe^0 (Eq. (4)-(5)) (Ye, Zhou, et al., 2022). To find adequate T to drive the reactions in these directions, thermodynamic calculations were made aiming to determine the change of standard-state Gibbs energy of the reactions (ΔG_R^0) described in Eq. (2)-(5). ΔG_R^0 is a state-function incorporating entropy and enthalpy to describe equilibrium and spontaneity of a reaction (Chang and Thoman Jr., 2014). It can be calculated from Eq. (6), where ΔH_R^0 and ΔS_R^0 are the changes of the standard-state enthalpy and entropy of the reaction, respectively.

$$2FeOOH_{(s)} \rightleftharpoons Fe_2O_{3(s)} + H_2O_{(g)} \quad (1)$$

$$3Fe_2O_{3(s)} + CO_{(g)} \rightleftharpoons 2Fe_3O_{4(s)} + CO_{2(g)} \quad (2)$$

$$3Fe_2O_{3(s)} + H_{2(g)} \rightleftharpoons 2Fe_3O_{4(s)} + H_2O_{(g)} \quad (3)$$

$$Fe_3O_{4(s)} + 4CO_{(g)} \rightleftharpoons 3Fe^0_{(s)} + 4CO_{2(g)} \quad (4)$$

$$Fe_3O_{4(s)} + 4H_{2(g)} \rightleftharpoons 3Fe^0_{(s)} + 4H_2O_{(g)} \quad (5)$$

$$\Delta G_R^0 = \Delta H_R^0 - T\Delta S_R^0 \quad (6)$$

The values of ΔG_R^0 for the formation of magnetite and Fe^0 (Eq. (2)-(5)) are compiled in Table 1 for T ranging 500 – 985 ºC. For all temperatures, reactions (2) and (3) present $\Delta G_R^0 < 0$, meaning that both reactions are favoured towards the formation of magnetite from hematite at those conditions. Regarding the reduction of magnetite to Fe^0, reactions (4) and (5) presented $\Delta G_R^0 > 0$ up to, at least, 800 ºC, favouring the occurrence of reaction in the reverse direction. Therefore, relatively low temperatures may be sufficient to drive the system towards the formation of magnetite, with high catalytic performance towards Fenton process (Adityosulindro, Rahdhani, et al., 2021). To drive reactions (4)-(5) towards the production of Fe^0, T ≥ 985 ºC could be required, implying higher energy consumption. Moreover, magnetite presents an advantage compared with Fe^0: the easier magnetic separation of spent catalyst from the wastewater. Considering these data, $500 \leq T \leq 700$ ºC was chosen as suitable range to treat the Fenton sludges, aiming to maximise magnetite formation.

Table 1. ΔG_R^0 of the reactions yielding magnetite and metallic iron.

Reaction	ΔG_R^0 (kJ·mol^{-1})				
	500 ºC	600 ºC	700 ºC	800 ºC	985 ºC
(2)	-81.7	-85.1	-88.7	-92.6	-100.3
(3)	-71.3	-78.2	-85.1	-92.2	-105.6
(4)	3.46	6.7	10.1	13.8	20.9
(5)	44.9	34.4	24.6	15.5	-0.02

The yields of char from the treatment of sludges are compiled in Table 2. Regardless of Fenton process, lower T (≤ 600 ºC) allowed for a higher recovery of solid, reaching 73.6 % in homogeneous Fenton, and 69.2 % in heterogeneous Fenton. These values express mainly the recoverability of solid, rather than an actual difference in its production compared with gas or oil fractions. Increasing T led to increasing encrustation of the sludge on the quartz reactor. This behaviour may have been driven by slagging/fouling phenomena, which are usually favoured by high concentrations of low melting point elements, like Na, K, S, Cl (alkali or chloride sulphates), and unfavoured by high melting point ones like Ca, Mg, Si (calcium or magnesium silicates) (García, Pizarro, et al., 2015). The chemical and structural characterisation of the obtained solids is currently being performed. This will allow the verification of the distribution of the expected iron phases in the solids and the evaluation of their real catalytic performance in (heterogeneous) Fenton process.

Table 2. Solid yield (%) of thermochemically treated Fenton sludges at the different operating conditions studied.

T (ºC)	Homogeneous Fenton			Heterogeneous Fenton		
	t (min)			t (min)		
	15	30	60	15	30	60
500	71.5	71.7	73.6	69.2	68.7	69.2
600	70.8	70.5	70.3	66.3	65.1	66.2
700	26.6	32.3	29.2	60.5	55.2	54.4
800	6.3	~0	~0	45.5	40.3	34.9

CONCLUSIONS

This work proposed a circular solution to valorise the main by-product – iron sludge – of Fenton processes applied to remove AOX from pulp bleaching wastewater. The spent iron catalyst was recovered by precipitation after homogeneous and heterogeneous Fenton processes. The recovery of iron sludges reached 2.55 g·L^{-1} and 1.75 g·L^{-1} for the homogeneous and heterogeneous Fenton processes, respectively. Thermodynamic calculations were made and indicated $500 \leq T \leq 700$ ºC as suitable conditions to treat the Fenton sludges aiming at the formation of magnetite, due to its known catalytic activity and magnetic properties. Thermochemical treatment in N_2 atmosphere was used at those conditions to produce a waste-derived Fenton catalyst, yielding 73.6 % in homogeneous Fenton, and 69.2 % in heterogeneous Fenton.

ACKNOWLEDGEMENTS

Thanks are due to FCT/MCTES for the financial support to CESAM (UIDP/50017/2020 + UIDB/50017/2020 + LA/P/0094/2020) and CICECO (UIDB/50011/2020 & UIDP/ 50011/2020), through national funds. This work was developed in the scope of INOVC+ (CENTRO-01-0246-FEDER-000044), co-funded by Centro2020, Portugal2020 and the ERDF. J.P. Ribeiro, C.C. Marques, and H.G.M.F. Gomes acknowledge FCT for their PhD Grants SFRH/BD/141133/2018, 2021.08959.BD, and 2020.09864.BD, respectively. M.C. Neves acknowledges FCT for the research contract CEECIND/00383/2017 under the CEEC Individual 2017.

REFERENCES

Adityosulindro, S., Rahdhani, A., and Hartono, D. M. (2021) Heterogeneous Fenton Oxidation Catalysed by Rebar Flakes Waste for Removal of Methyl Orange in Water. Journal of Applied Science and Engineering, **25**(3), 381–388.

Chang, R. and Thoman Jr., J. W. (2014) *Physical chemistry for the chemical sciences*, Canada, University Science Books.

García, R., Pizarro, C., Álvarez, A., Lavín, A. G., and Bueno, J. L. (2015) Study of biomass combustion wastes. Fuel, **148**, 152–159.

Gialanella, S., Girardi, F., Ischia, G., Lonardelli, I., Mattarelli, M., and Montagna, M. (2010) On the goethite to hematite phase transformation. Journal of Thermal Analysis and Calorimetry, **102**(3), 867–873.

M'Arimi, M. M., Mecha, C. A., Kiprop, A. K., and Ramkat, R. (2020) Recent trends in applications of advanced oxidation processes (AOPs) in bioenergy production: Review. Renewable and Sustainable Energy Reviews, **121**, 109669. [online] https://doi.org/10.1016/j.rser.2019.109669.

Ribeiro, J. P., Marques, C. C., Portugal, I., and Nunes, M. I. (2020) Fenton processes for AOX removal from a kraft pulp bleaching industrial wastewater: Optimisation of operating conditions and cost assessment. Journal of Environmental Chemical Engineering, **8**(4), 104032. [online] https://doi.org/10.1016/j.jece.2020.104032.

Ribeiro, J. P. and Nunes, M. I. (2021) Recent trends and developments in Fenton processes for industrial wastewater treatment – A critical review. Environmental Research, **197**(110957).

Ribeiro, J. P., Sarinho, L., Neves, M. C., and Nunes, M. I. (2022) Valorisation of residual iron dust as Fenton catalyst for pulp and paper wastewater treatment. Environmental Pollution, **310**(119850).

Toczyłowska-Mamińska, R. (2017) Limits and perspectives of pulp and paper industry wastewater treatment - A review. Renewable and Sustainable Energy Reviews, **78**, 764–772.

Ye, G., Zhou, J., Huang, R., Ke, Y., Peng, Y., Zhou, Y., Weng, Y., Ling, C., and Pan, W. (2022) Magnetic sludge-based biochar derived from Fenton sludge as an efficient heterogeneous Fenton catalyst for degrading Methylene blue. Journal of Environmental Chemical Engineering, **10**(2), 107242. [online] https://doi.org/10.1016/j.jece.2022.107242.

Zhu, R., Xia, J., Zhang, H., Kong, F., Hu, X., Shen, Y., and Zhang, W. H. (2021) Synthesis of magnetic activated carbons from black liquor lignin and Fenton sludge in a one-step pyrolysis for methylene blue adsorption. Journal of Environmental Chemical Engineering, **9**(6), 106538. [online] https://doi.org/10.1016/j.jece.2021.106538.

Upscaling Anaerobic Reactors using Purple Phototrophic Bacteria for low-cost wastewater reuse and resource recovery

Patricia Zamora*, Eugenio Marín*, Victor Monsalvo*, Daniel Puyol and Frank Rogalla***

* Aqualia, Innovation and Technology Department, Avda. Camino de Santiago, 40, 28050 Madrid, Spain, patricia.zamora@fcc.es

** Universidad Rey Juan Carlos, Chemical and Environm. Tech., Campus Bldg. I/234. 28933 Móstoles, Spain

Abstract:

Efficient resource recovery from domestic wastewater by low-cost technologies, achieving a reduced-carbon footprint and affordable wastewater reuse in small populations, remains a key challenge to ensure sustainable and cost-effective resource management. In this study, a novel and disruptive technology for low-cost domestic wastewater reuse in anaerobic photobioreactors using purple phototrophic bacteria is proposed. This process is aimed at small population areas, due to reduced energy consumption and simple operation, as well as a biomass rich in polyhydroxyalkanoates (PHAs) available for beneficial use in bioplastics or fertilisers.

After thorough investigation and development, the technology has been scaled to two demonstrative photobioreactors of 150 m^3 each at the wastewater treatment plant (WWTP) Linares in Jaén, Spain. With a maximum treatment capacity of 350 m^3/d, the treated water complies with limits for agricultural reuse, reaching average concentrations of 55 mgCOD/L, 12 mgBOD5/L and 10 mgTSS/L. To allow maintaining nutrients as fertilizer in the effluent during irrigation season, the removal of nitrogen and phosphorus can be optimized due to the alternance of aerobic and anaerobic conditions in the raceway reactors, varying hydraulic retention times and operational conditions. This article describes the control parameters to obtain optimised process benefits.

Keywords: PPB, small populations, photobioreactors, nutrient recovery, water reuse.

Introduction

The traditional and centralized concept of wastewater treatment (WWT) has been successfully applied during the last decades in highly populated and industrialized areas. Conventional WWT is characterized by high energy consumption related to aeration and coupled to limited nutrient recovery. Since the approval of the Directive Urban WWT 91/271/CEE more than 30 years ago, WWT has been applied to municipalities of more than 2000 population equivalent (p.e.). However, a recent revision of this Directive now lowers its applicability to small populations areas (> 1000 p.e.), and proposes energy neutrality of the WWT process, making it extremely challenging to an economically viable implementation using conventional technologies. Considering that 25% of the EU population lived in rural areas in 2021 (The World bank, 2021), this leads to the need to develop low-cost decentralized wastewater reuse that provides high quality treated water without significant carbon footprints.

The present study focuses on the development of a novel and disruptive single-step wastewater reuse concept based on Purple Phototrophic Bacteria (PPB) in anaerobic raceways or photobioreactors (PBR). The versatile metabolism of PBBs by assimilation of carbon and nutrients opens new possibilities for domestic WWT and the recovery of resources such as polyhydroxyalkanoates (PHAs), single-cell-proteins (SCP) and hydrogen, among others – as published by Puyol et al. 2020 showing the initial process evolution.

After this detailed development with King Juan Carlos University (URJC) since 2015, full scale anaerobic photobioreactors using PPB photobioreactors with solar radiation have been commissioned at the WWTP Linares (Jaén, Spain), under the name ANPHORA® (ANaerobic PHOtotrophic RAceways), scaling it to Technology Readiness Level (TRL) 7.

Material and Methods

The demonstrative PBRs have a treatment capacity of 350 m^3/d (approximately 1500 p.e.) (Figure 1), made up of two anaerobic raceways with a surface area of 465 m^2 each, and a volume of 149.5 m^3 each, coupled to two secondary clarifiers with a volume of 80 m^3 each. The PBRs are equipped with paddle wheels to keep the phototrophic biomass in suspension and in contact with solar radiation. To enhance the growth of PPBs, the photobioreactors are covered by filters that allow only the passage of infrared radiation.

Figure 1 (A) ANPHORA® demonstrative photobioreactors; (B) Secondary clarifiers at WWTP Linares.

Start-up of the PBRs was carried out in August 2022 and since then they have been operated in batch mode to enhance the growth of the PPB biomass, feeding the different batches with primary settled wastewater from Linares WWTP with the average composition (SD in brackets): BOD_5: 134 (31), TCOD: 241 (34), TSS: 85 (10), TN: 45 (9), TP: 4 (1), BOD/COD: 0.6 (0.1), pH: 7.7 (0.1) and conductivity: 659 (61) μScm^{-1}.

NH_4^+, PO_3^{4-}, total and soluble COD, TN and TP concentrations were determined by commercial colorimetric kits (Hach Lange, Spain). TSS, VSS and BDO5 were measured according to standard methods (Standard Methods, 2005). The phototrophic activity ratio was calculated according to the relationship between the absorbance measurement of the biomass at 850 nm and at 660 nm.

Results and Conclusions

During the start-up the PBRs were operated in batch mode for more than three months, achieving the removal efficiencies of the soluble components (sCOD, NH^{4+} and PO_4^{3-}) as shown in Table 1. Soluble COD removal was maintained at a range from 30 to 50% to keep PPB in a constant exponential growth phase. Within the batch periods, NH^{4+} and PO_4^{3-} removal efficiencies have steadily increased up to almost 100% and 25%, respectively.

This increasing removal efficiency is a clear indication of the growth of PPB biomass within the PBRs. Figure 2 shows the evolution in the concentration of MLSS, as well as the evolution of the ABS850/ABS660 ratio. The concentration of the MLSS followed a positive evolution but stagnated at the end due to intense rains lowering the organic load of the feed. Regarding the ABS850/ABS660 ratio, a positive evolution over time can be clearly seen, reaching values above 1.1, indicating that the biomass is enriched in PPB.

Table 1 Average removal efficiencies in demonstrative PPB photobioreactors.

Batch number	Duration	sCOD (%)	NH^{4+} (%)	PO_4^{3-} (%)
1	8	29.8	35.9	2.2
2	5	30.3	71.7	3.5
3	6	36.9	47.4	3.7
4	7	77.6	72.0	4.1
5	6	43.6	99.8	5.6
6	6	34.6	54.9	6.0
7	9	55.4	76.0	25.8
8	11	37.4	99.6	14.9
9	8	38.5	98.6	10.9
10	5	27.9	42.8	23.7
11	5	26.8	99.9	21.0

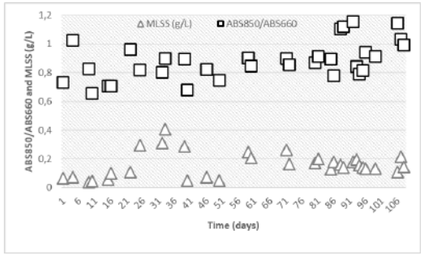

Figure 2 Time course of MLSS and ABS850/ABS660 ratio in demostrative PPB photobioreactors.

At the end of each batch, the photobioreactors are emptied and the biomass is conducted by gravity to the secondary clarifiers. There, the separation of the liquid and solid phases is carried out, the biomass being recirculated back to the PBRs and the treated effluent sent by gravity to the discharge of Linares WWTP. The treated water was compared to the Spanish discharge limits for areas without nutrient removal (COD, BOD5 and TSS). Figure 3 depicts the evolution of water quality treated by demonstrative PBRs using PPB, which consistently complied with discharge limits, with average concentrations of 55 mg COD/L, 12 mg BOD5/L and 10 mg TSS/L, respectively.

As shown in Table 1, the elimination of N and P is depending on operational parameters, and can be adapted to various requirements. For water reuse during irrigation periods, the nutrients can be maintained to bring fertilizers for crop watering, while for sensitive receiving waters low nutrient limits can be achieved.

Once the PPB biomass has been established (Abs 850/Abs 660 > 0.9) and the optimal MLSS (0.5-0.6 g/L) concentration has been reached, the operation mode will be switched to continuous mode with the aim to increase overall treatment capacity. Biomass characteristics also depend on operational parameters, and enrichment of PHA are observed at higher COD influent loadings. The fertilizer value of the biomass and the options of bioplastics extraction were evaluated, to complete a cost/benefit analysis and Life Cycle Assessment, and achieve an energy positive balance and a favourable carbon footprint for water reuse applications.

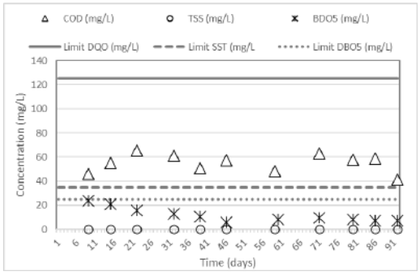

Figure 3 Time course of COD, TSS and BDO5 concentrations in treated water against discharge limits by Spanish regulation (EU Urban WWTD).

References

Puyol, D., Monsalvo, V.M., Marín, E., Rogalla, F., Melero, J.A., Martinez-Castillejo, F., Hülsen, T. and Batstone, D.J. 2020 Purple phototrophic bacteria as a platform to create the next generation of wastewater treatment plants: Energy and resource recovery. In book: *Wastewater Treatment Residues as Resources for Biorefinery Products and Biofuels*, 250-280.

Standard Methods for the Examination of Water and Wastewater. Method 2540 D, APHA, 21st Edition, 2005.

The world data Bank. Rural population (% of total population) – European Union from 1960 to 2021.

Acknowledgements

This project has received funding from the Bio Based Industries Joint Undertaking (JU) under the European Union's Horizon 2020 research and innovation programme under grant agreement No 837998. The JU receives support from the European Union's Horizon 2020 research and innovation programme and the Bio Based Industries Consortium.

Mechanisms involved in veterinary antibiotics removal by microalgae-bacteria consortia

Johanna Zambrano[a,b], Pedro Antonio García-Encina[a,b], Félix Hernández[c], Ana M. Botero-Coy[c], Juan J. Jiménez[a,d], Rubén Irusta-Mata[a,b,*]

[a] Institute of Sustainable Processes. University of Valladolid. Dr. Mergelina s/n, 47011 Valladolid. Spain
[b] Department of Chemical Engineering and Environmental Technology, School of Industrial Engineering, University of Valladolid, Dr Mergelina s/n 47011 Valladolid, Spain.
[c]Environmental and Public Health Analytical Chemistry, Research Institute for Pesticides and Water, University Jaume I, Avda. Sos Baynat s/n, 12071 Castellón, Spain
[d] Department of Analytical Chemistry, University of Valladolid, Campus Miguel Delibes, Paseo Belen 7, 47011 Valladolid, Spain
*Corresponding author. E-mail: *ruben.irusta@uva.es*

Abstract

The mechanisms involved in the removal of a mixture of four veterinary antibiotics (VA) – tetracycline (TTC), ciprofloxacin (CPF), sulfadiazine (SDZ) and sulfamethoxazole (SMX) – in synthetic wastewater using microalgae-bacteria consortia (MBC) dominated by Scenedesmus almeriensis was studied at different initial concentrations of 1000, 500, 100 and 20 µg/L per antibiotic. Ultra-high performance liquid chromatography and tandem mass spectrometry (UHPLC-MS/MS) were used to determine the removal of the VA for each mechanism. For a hydraulic retention time of 4 days, the overall removal of antibiotics by the MBC was 99.9% for TTC, 78.0% for CPF, 52.6% for SDZ and 5.0% for SMX. A pseudo-first order irreversible model was applied to best fit the experimental data. The degradation constant rates were 0.136 h^{-1} for TTC, 0.012 h^{-1} for CPF, 0.010 h^{-1} for SDZ and 0.0007 h^{-1} for SMX. Under all the evaluated conditions, CPF and TTC exhibited the highest removal efficiency. Biosorption was the main mechanism for all four antibiotics, followed by biodegradation in the cases of TTC and SDZ. CPF did not show removal via biodegradation. SMX did not show removal via hydrolysis or photolysis. This study i) integrates and evaluates individually the mechanisms involved in VA removal using an MBC; ii) determines an overall removal rate constant for a wide array of TTC, CPF, SDZ and SMX concentrations; and iii) demonstrates the high removal capacity and potential use of microalgae as an ecofriendly wastewater treatment process.

Keywords
Biodegradation; Biosorption; Hydrolysis; Microalgae; Photolysis

INTRODUCTION

The fate of antibiotics in microalgae-based systems is largely unknown. In order to broadly use microalgae in wastewater treatment applications for the removal of antibiotics it is critical to assess the mechanisms involved in this process. With this objective, the aim of this study was to determine the mechanisms of TET, CIP, SDZ and SMX removal using a microalgae-bacteria consortium from a high-rate algae pond (HRAP) used for piggery wastewater treatment. The four antibiotics were chosen as representative compounds of three families of antibiotics most found in water samples (fluoroquinolones, sulfonamides and tetracyclines). Different initial concentrations were analyzed, similar to those found in real water samples.

MATERIALS AND METHODS

Tests were performed in 1 L glass beakers containing 1 L Milli-Q water spiked with a mixture of 4 antibiotics to a final concentration of 1000, 500, 100 or 20 µg/L per antibiotic. After taking a first sample to determine the initial antibiotic concentration in each reactor, the microalgae-bacteria consortium were added (on selected reactors for biosorption and biodegradation) under continuous mixing to obtain a concentration of 1 g/L. Samples were taken at different time intervals until 4 days of operation. Experiments were conducted in triplicate.

RESULTS AND DISCUSSIONS

Removal of VA by the MBC

The whole process for VA removal using a MBC was studied in batch experiments for 96 h. For a mixture of the four aforementioned VA, the initial concentration decreased over time. The removal efficiency of VA by the MBC is highly dependent on the antibiotic classes, as was indicated by other authors (Leng et al., 2020). In all the conditions studied, only TTC was completely removed. In order to understand the mechanisms of VA removal, hydrolysis, photolysis and biodegradation were studied. As biosorption was expected to be the most important removal process, biosorption data was reported separately in a previous study (Zambrano et al., 2021). Data showed biosorption as the main removal process for CPF and TTC; however, it was not significant for SDZ and SMX removal. Batch experiments without algae under dark conditions indicated that antibiotic hydrolysis took place. The initial concentration decreased over time for three antibiotics, except for SMX which was not removed by hydrolysis in any of the studied conditions. Antibiotic photolysis was studied in batch experiments without algae under illuminated conditions. SMX was not removed by photolysis in any of the studied conditions. For the other three antibiotics, a decrease in the initial concentration over time was more prominent for 20 µg/L. VA biodegradation was also studied in batch experiments for 96 h. CPF did not biodegrade under any of the studied conditions. From the four antibiotics, SMX had the highest biodegradation capacity, possible due to a good adaptation of S. almeriensis to this antibiotic because other algae of the genus Scenedesmus, such as Scenedesmus obliquus, have been shown to have an efficient adaptation mechanism for SMX (Leng et al., 2020). In the following sections, the kinetics of the removal of VA using a MBC and each of the removal modes involved in this process will be determined.

Kinetics for the removal of VA using MBC

The removal of TTC, CPF, SDZ and SMX was investigated with zero-order and pseudo-first order kinetic models (the latter being both an irreversible and a reversible reaction). R^2 values closer to unity were presented by the pseudo-first order irreversible kinetic model (Fig.1). This model fit the best to the experimental data for the whole process of VA removal via the MBC as well as for hydrolysis, photolysis and biodegradation. In the whole process of VA removal it was observed that TTC, CPF and SDZ were removed faster than SMX. The highest rate constant was presented by TTC. The pseudo-first order irreversible rate constant for the removal of VA by the MBC were 0.1362 h^{-1} for TTC, 0.0119 h^{-1} for CPF, 0.0098 h^{-1} for SDZ and 0.0007 h^{-1} for SMX. The pseudo first-order irreversible rate constant k for the removal of VA by hydrolysis were 0.0001 h^{-1} for TTC, 0.0002 h^{-1} for CPF and 0.0004 h^{-1} for SDZ. The pseudo first-order irreversible rate constant k for the removal of VA by photolysis were 0.0011 h^{-1} for TTC, 0.0012 h^{-1} for CPF and 0.0005 h^{-1} for SDZ. On the other hand, k values found for biodegradation were 0.0018 h^{-1} for TTC, 0.0026 h^{-1} for SDZ and 0.0006 h^{-1} for SMX. In our previous work, biosorption kinetics were evaluated and a pseudo second-order kinetic model best fit the biosorption experimental data. The results suggested that the rate constant increased with a decrease in the initial VA concentration and that CPF presented the highest k value (Zambrano et al., 2021).

Removal of VA using MBC

The removal of the four VA MBC is shown in Fig. 5B. The VA results are consistent with the ones previously reported in the literature. In the present study, TTC removal was complete after 5.7 days. Current results showed that CPF removal was complete after 15 days. In the case of SDZ, removal was 88.3 and 92.5% after 9 and 12 days, respectively. Finally, SMX removal was 10.9, 16.6 and 20.6% after 7, 11 and 14 days, respectively. The comparison of the results obtained in the present study with those previously reported in the literature showed that the VA removal efficiency is highly dependent on the algae strain used for the water treatment process and that the S. almeriensis algae-bacteria consortium presented good removal efficiencies. For comparison purposes, removal efficiencies are reported in Table 1. Biosorption data was reported in our previous study (Zambrano et al., 2021), where CPF and TTC exhibited the highest removal efficiencies. Removal efficiencies of biosorption ranged between 74.6 – 81.5% for TTC, 43.5 – 100% for CPF, 11.6 – 30.4% for SDZ, and 0 – 31.5% for SMX. The removal of the four VA by hydrolysis is shown in Fig. 6B. SMX was not removed by hydrolysis. Using the kinetic parameters obtained in the previous section, it can be estimated that the complete removal of TTC, CPF and SDZ using only hydrolysis could be achieved after 1204, 956 and 400 days, respectively. In view of these results, and due to the hydrophobic characteristics of the four antibiotics analyzed in this study, hydrolysis is not representative in VA removal. The removal of the four VA using a MBC by photolysis is shown in Fig. 7B. The complete removal of TTC, CPF and SDZ can be achieved after 162, 125, and 311 days, respectively, while SMX was not removed by photolysis. The removal of the four veterinary antibiotics using a microalgae-bacteria consortium by biodegradation is shown in Fig. 8B. The complete removal of TTC, SDZ and SMX can be achieved after 125, 31 and 292 days, respectively. CPF was not removed by biodegradation.

CONCLUSIONS

To our knowledge, the mechanisms involved in the removal of TTC, CPF, SDZ and SMX in synthetic wastewater using a Scenedesmus almeriensis microalgae-bacteria consortia, as well as the determination of their rate constants by fitting experimental data over a wide range of concentrations to a single general equation, were analyzed for the first time. Working with a pH of 8 and a mixture of low concentrations of four VA that resemble the characteristics of real water samples, the MBC proved to be highly efficient in the removal of a mixture of VA. The overall removal of the four VA followed a pseudo-first order irreversible kinetic. Biosorption turned out to be the most important removal process for the four antibiotics while hydrolysis was insignificant. Hydrolysis and photolysis took place in the removal of the VA except for SMX. Biodegradation was an important mechanism for TTC, SDZ and SMX but was not present in CPF removal. Further investigations must focus on the optimization of operational parameters to improve photolysis and biodegradation in order to increase VA degradation. Additionally, studies should be done on byproduct formation in pursuit of a widely used industrial scale implementation of microalgae-based technology for the removal of VA.

Table 1. Efficiency for the different removal mechanisms of veterinary antibiotics in synthetic wastewater using microalgae-bacteria consortia (4 day hydraulic retention time)

Compound	Removal (%)				
	Global process	Hydrolysis	Photolysis	Biodegradation	Biosorption*
Tetracycline	99.93	1.03	6.83	14.29	74.61 - 81.53
Ciprofloxacin	78.01	1.39	7.29	0	43.45 - 100
Sulfadiazine	52.58	2.94	3.94	9.94	11.62 - 30.35
Sulfamethoxazole	5.01	0	0	5.01	0 - 31.48

*Data reported in a previous study (Zambrano et al., 2021).

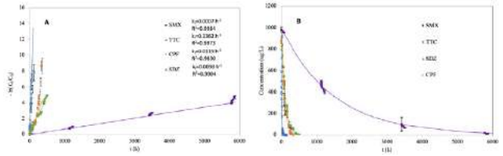

Fig. 1. (A) Linear representation of pseudo-first order kinetics for VA removal using MBC. (B) VA concentration variation using MBC along time. Each data point represents the mean and standard deviation from triplicate assays.

REFERENCES

Botero-Coy, A.M., Martínez-Pachón, D., Boix, C., Rincón, R.J., Castillo, N., Arias-Marín, L.P., Manrique-Losada, L., Torres-Palma, R., Moncayo-Lasso, A., Hernández, F., 2018. 'An investigation into the occurrence and removal of pharmaceuticals in Colombian wastewater.' Sci. Total Environ. 642, 842–853. https://doi.org/10.1016/j.scitotenv.2018.06.088

Hom-Diaz, A., Norvill, Z.N., Blánquez, P., Vicent, T., Guieysse, B., 2017. Ciprofloxacin removal during secondary domestic wastewater treatment in high rate algal ponds. Chemosphere. https://doi.org/10.1016/j.chemosphere.2017.03.125

Leng, L., Wei, L., Xiong, Q., Xu, S., Li, W., Lv, S., Lu, Q., Wan, L., Wen, Z., Zhou, W., 2020. Use of microalgae based technology for the removal of antibiotics from wastewater: A review. Chemosphere 238, 124680. https://doi.org/10.1016/j.chemosphere.2019.124680

Norvill, Z.N., Toledo-Cervantes, A., Blanco, S., Shilton, A., Guieysse, B., Muñoz, R., 2017. Photodegradation and sorption govern tetracycline removal during wastewater treatment in algal ponds. Bioresour. Technol. https://doi.org/10.1016/j.biortech.2017.02.

Zambrano, J., García-Encina, P.A., Hernández, F., Botero-Coy, A.M., Jiménez, J.J., Irusta-Mata, R., 2021. Removal of a mixture of veterinary medicinal products by adsorption onto a Scenedesmus almeriensis microalgae-bacteria consortium. J. Water Process Eng. 43, 102226. https://doi.org/10.1016/j.jwpe.2021.102226

Evaluation of a single-chamber continuous-flow bioreactor to treat urban wastewater with aerobic granular sludge

A. Rosa-Masegosa*, B. Muñoz-Palazon*, D. Correa-Galeote*, M. Gallardo-Altamirano*, A. Castellano-Hinojosa*, A. Gonzalez-Martinez* and J. Gonzalez-Lopez*

* Institute of Water Research, University of Granada, C/ Ramón y Cajal, 4, 18071 Granada, Spain
(E-mail: *aurorarm@ugr.es; bmp@ugr.es; dcorrea@ugr.es; manujga@ugr.es; ach@ugr.es; agon@ugr.es; jgl@ugr.es)**

Abstract
Aerobic granular sludge is an advantageous technology for wastewater treatment, however its actual operating mode by cycles is inefficient if used at full scale. The design of continuous-flow reactors could improve the application of this technology. We designed and evaluated a single-chamber continuous-flow reactor at lab-scale with the aim to know if it could maintain a good granulation while achieve a successful organic matter removal rate. After the operation, it could be concluded that the new reactor was able to adapt the microbial community to the new conditions, leading to compact and well-structured biomass able to reach a 90% of organic matter remotion. The presented design could be an optimal alternative to implement at full scale.

Keywords
Aerobic granular sludge; biological treatment; continuous-flow reactor; organic matter removal; single-chamber reactor

INTRODUCTION

Aerobic granular sludge technology (AGS) is an advantageous biological system for wastewater treatment. It is based in the formation of dense spherical biofilms, which are responsible of the technology's advantages over other systems (Nancharaiah and Kiran Kumar Reddy, 2018). The high density of granules promotes high concentrations of biomass. Moreover, granules are able to withstand toxic substances and influent changes. Furthermore, there is a redox gradient along the granule, that promotes the selection of different microorganisms, which makes possible the simultaneous removal of diverse pollutants. Additionally, the excellent settleability properties avoid the implantation of a secondary settling tank. All these advantages improve the water quality and lead to energy and cost savings. Traditionally, AGS has been operated in sequential batch reactors. However, this mode of operation has difficulties when it is implemented in wastewater treatment plants (WWTPs) at full-scale, due to the continuous character of the wastewater's arrival to the WWTPs. For that reason, the use of continuous-flow reactors (CFRs) improve the application of AGS at full-scale, because it allows easier operation, technology compaction and the treatment of larger volumes of wastewater (Kent, 2018). But CFRs have traditionally two disadvantages, on one hand, the low retention capacity and, on the other side, the accumulation of fluffy aggregates that destabilize the system. Recent investigations are being made to avoid these drawbacks, but, until this moment, an efficient single-chamber reactor had not been implemented.

Our research group designed and evaluated a single-chamber CFR for treating wastewater with AGS, with the aim to create an alternative to implement at full scale and improve de biological treatment.

MATERIALS AND METHODS

The bioreactor consisted on a cylinder of 10 cm of diameter and 72 cm of height with an eccentric cone where the air diffuser was placed. The operative volume was 6 L. The influent was introduced incessantly at mid-height of bioreactor, while effluent overflowed continuously by the output which was located at the top. To avoid the loss of granules, a decanter of 6.3 cm of diameter was placed in the water discharge zone. With this element, granular biomass could not reach the outlet zone while floc biomass could. The influent was a synthetic medium that simulated urban wastewater. The bioreactor was inoculated with 600 mL of granular sludge from a sequential batch reactor, and it was operated for 55 days with a hydraulic retention time of 6 h.

During the experimentation, chemical oxygen demand (COD) and biological oxygen demand (BOD_5) were quantified to evaluate the removal rate of organic matter. Moreover, to control the biomass, mix liquor suspended solids (MLSS), mean size and settling velocity of granules were determined. On the other hand, next generation sequencing was made for Prokarya and Eukarya. The raw data were analysed and sequences were classified against SiLVA nr v132 database and clustered into operational taxonomic units (OTUs).

RESULTS AND DISCUSSION

Granular characteristics

Granules increased their mean size and achieved a value around 12 mm. In terms of MLSS, reactor stabilized at 2.5 $g \cdot L^{-1}$, but at the end of experimentation, biomass concentration reached 3.5 $g \cdot L^{-1}$. Regarding the settling velocity of granules, they reached more than 100 $m \cdot h^{-1}$, which meant that granules had high density, a key parameter to reach the optimum purpose of AGS. In terms of organic matter removal performance, the system achieved around a 90%. These values do not differ from those obtained from sequential batch reactors, so the CFR could be implemented in WWTPs.

Microbial community dynamic

Microbial community dynamic showed that the dominant OTUs of the inoculum were displaced and other OTUs dominated the system, due to the change in operational conditions and reactor configuration. In this way, the most dominant phylotype of prokaryotic community in the inoculum was OTU02, which belonged to the *Chitinophagaceae* family, with a 8.8% of total relative abundance, followed by OTU04 (8.3%), OTU01 (7.1%) and OTU06 (5.9%), affiliated to the *Allorhizobium-Neorhizobium-Pararhizobium-Rhizobium* genus, the *Brevundimonas* genus and the *Xanthobacteraceae* family, respectively. After the operation in the novel CFR, OTU01, and OTU06 suffered a sharp reduction until 0.6% and 1.4% of total relative abundance respectively at day 55. On the contrary, OTU03 increased its total relative abundance until 11.1%. It belonged to the *Xanthomonadaceae* family, a group of microorganisms with extracellular polymeric substances excretion activity. On the other hand, for eukaryotic community, OTU01 was the dominant phylotype in the inoculum with a 63.3% of total relative abundance, followed by OTU02 (13.1%) and OTU04 (12.5) belonging to the *Ascomycota* phylum, the *Hypocreales* order and the *Trichosporonaceae* family respectively. While at the end of the experiment with the new bioreactor, the dominant phylotypes were OTU01, with 62.1% of total relative abundance, OTU03 affiliated to the *Peronosporomycetes* class with a 15.8% and OTU07, an unclassified *Eukaryota* with 8.1%.

REFERENCES

Nancharaiah, Y.V., Kiran Kumar Reddy, G. 2018 Aerobic granular sludge technology: Mechanisms of granulation and biotechnological applications. *Bioresource Technology* **247**, 1128–1143.
Kent, T.R., Bott, C.B., Wang, Z.W. 2018 State of the art of aerobic granulation in continuous flow bioreactors. *Biotechnology advances* **36**(4), 1139–1166.

We would like to acknowledge the project B-RNM-137-UGR18 FEDER/Junta de Andalucía.

Use of Atmospheric Dissolved Air Flotation (DAF) in Removal of Surfactants

Ali Rostamiiranagh*, Elnaz Zehtab Lotfi**

* Expert of sewage studies and technical inspection office water and sewage co, eastazarbaijan, Iran, alirostamiiranagh@ yahoo.com

** Expert of water studies and technical inspection office water and sewage co, eastazarbaijan, Iran, elnazzlo@yahoo.com

Abstract
Surfactants are among the most widely disseminated xenobiotic that contribute significantly to the pollution profile of sewage and wastewaters of all kinds. Among the currently employed chemical unit processes in the treatment of wastewaters, coagulation-flocculation has received considerable attention for yielding high pollutant removal efficiency. Dissolved Air Flotation-DAF, is a well-established separation process that employs micro-bubbles as a carrier phase.DAF can be divided into three group. pressure atmospheric & vacuum . In this work effect of aeration rate & retention time were investigated on COD removal of detergent industries wastewater.
Keywords: surfactant; wastewater; air flotation

Introduction

For many applications of flotation in the wastewater treatment field, it is more efficient to use micro-bubbles generated by nucleation of dissolved air, rather than the dispersed air method used for minerals. Flotation offers process advantages over sedimentation, including better treated-water quality, rapid startup, high rate operation, and thicker sludges. DAF is considered not only an alternative to sedimentation plants, but also a clarification method to improve filtration. In this work we tried to remove surfactant with air flotation. DAF tests were carried out using pilot units (Figure 1). The operational specification of system is according to table 2 and physicochemical characteristic of effluents is shown in table 1. Process efficiency was evaluated by measuring COD removal. We find that increase in aeration rate up to 200 ml/min will remove surfactant but after more increase in rate COD removal will reduce. It is because of reduce in bubbles retention time, increase in wet bubbles & reduce solution height which cause solution of more foam. According to the results, in short retention time, aeration rate of 250 ml/min has the best recovery for COD removal. But with increasing in retention time ,aeration rate of 200 ml/min has the best recovery.(figure2)

Table 1 Physicochemical characteristics of effluents

Parameters	range	Iranian guide level (agriculture)
pH	7.00 – 7.60	6-8.5
color	Light green	-
Turbidity(NTU)	20-25	50
Sulphate (mg/L)	43-49	-
Pt (mg/L)	1.2-1.4	-
NTK (mg/L)	41.5-48.8	-
COD (mg/L)	1500	200
BOD_5 (mg/L)	412	100
Temperature(℃)	15	-
BOD_5/COD	0.3	-

Table 2 Operational of specification of DAF

Parameters	range
Shape	cylinder
H(cm)	60
$\varphi_{cylinder}$(cm)	15
φ_{pipe}(cm)	2
$V_{reactor}$(L)	10.6
$V_{wastewater}$(L)	6
Material	PVC

Figure 1 Pilot plant of dissolved air flotation

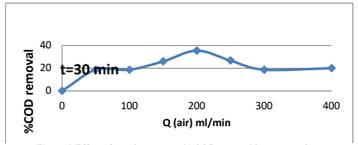

Figure 2 Effect of aeration rate on % COD removal in constant time

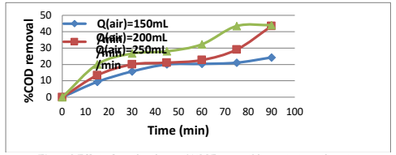

Figure 3 Effect of aeration time on % COD removal in constant aeration rate

1. Crockett, J. and Muntisov, M., Potable water treatment by dissolved air Flotation/Filtration, *in*: L. O. Kolarik; A. J. Priesley (Eds.) 'Modern Techniques in Water and Wastewater Treatment', East Melbourne, Vic., Australia (1995).
2. Dupre, V., Ponasse, M., Aurelle, Y. and Secq, A., Bubble Formation by Water Release in Nozzles-II. Influence on various parameters on bubble size, Water Research, 32, No.8, pp. 2498-2506 (1998).
3. Takahashi, T., Miyahara, T., Mochizuki, H., Fundamental Study of Dissolved Air Pressure Flotation, J. Chem. Engng. Japan, v.12, pp. 275-280 (1979).
4. Aboulhassan, MA, Souabi, S, Yaacoubi, A & Baudu, M 2006, 'Removal of surfactant from industrial wastewaters by coagulation flocculation process', Int. J. Environ. Sci. Tech., vol. 3, no. 4, pp. 327-332.
5. Lee EJ, Kim HS, Jang A. Application of dissolved air flotation (DAF) with coagulation process for treatment of phosphorus within permeate of membrane bioreactor (MBR). Desalination Water Treat. 2016;57(19):9043-50.
6. El-Gohary F, Tawfik A, Mahmoud U. Comparative study between chemical coagulation/precipitation (C/P) versus coagulation/dissolved air flotation (C/DAF) for pre-treatment of personal care products (PCPs) wastewater. Desalination. 2010;252(1-3):106-12.

Use of wetlands for wastewater treatment in iran

Ali Rostamiirangh*, Elnaz Zehtab Lotfi**

* Expert of sewage studies and technical inspection office water and sewage co, eastazarbaijan, Iran, alirostamiiranagh@ yahoo.com

** Expert of water studies and technical inspection office water and sewage co, eastazarbaijan, Iran, elnazzlo@yahoo.com

Abstract
Many challenges are decelerating solving the global sanitation problem , such as the financial limitations and lack of technical capacities. Parallel to this, many countries are facing a growing demand on their limited water resources. There is a growing interest in finding low-cost, easy-to-operate and sustainable sanitation solutions. Constructed wetlands (CWs) in recent years have proved their capability in the sanitation sector as an appropriate sanitation system in different contexts, CWs have proved their ability to treat several types of wastewaters for several decades. Several benefits and facts, such as the low construction and operational costs of CWs, low-energy, and less operational requirements, have raised the interests in CWs as a treatment technology. Several studies have investigated CWs suitability based on different sustainability indices (technical,social, environmental, etc.). In this paper we tried to investigate the experiments about the use of wetlands for wastewater treatment in iran.

Keywords
wetland; wastewater treatment; Iran

The utilization of environmentally friendly and eco-safe wastewater treatment plan is nowadays widespread. There are the different conventional methods for wastewaters treatment such as active sludge process (ASP), rotating biological contactor (RBC), stabilization ponds, oxidation ditch, trickling filter (TF), sequence batch reactors (SBR), lagoons and up flow anaerobic sludge blanket (UASB), Micro-algae techniques etc.. These methods having the limitations like energy, economic, complex construction and operation, sensitive to temperature and excessive sludge. Currently, the global interest for simple, safe, cost-effective and green technology has been developed. Constructed wetland as a natural process, environmentally friendly, eco-friendly with simple construction and low maintenance is one of the interested technique. Constructed wetlands (CWs) as human made basin according to engineering design that create ecological condition same to natural wetlands for treating wastewater in different physical, chemical and biological conditions. Figure1.

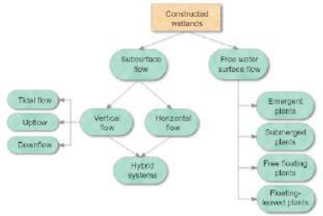

Figure 1. Classification of constructed wetlands for wastewater treatment

The effect of artificial wetland treatment of Qasr-e-shirin in Kermanshah province on water quality, growth performance and biochemical composition of fish body for optimal use in the aquaculture industry was investigated. In this study, water quality parameters including turbidity, DO, COD,MPN total coliform, nitrate, phosphate, and experiments in sections of bioassay, monitoring of aquatic tissue due to the presence of pathogens were satisfactory.The results show that the COD, turbidity and MPN values of the total effluent from the treatment plant are 33 mg/L, 13.4 NTU and 230,000, respectively. Effluent analysis took place after passing through the UV pool. and complete dewatering of the pool with treated and disinfected effluent; COD, turbidity and MPN values of total coliform were 25 mg/L, 13 NTU and 8000, respectively. The microbial load of the effluent is dramatically reduced by passing through the UV pool.figure2.

Figure 2. pool dewatered by wastewater treated by wetland method

The applications of constructed horizontal surface flow (HF-CW) wetland with two different local plants (Louis latifoila and Phragmites -australis (Cav.) Trin) at the wastewater treatment plant in Babol city Iran was investigated. This system was designed as an advanced treatment unit in field scale after the treatment plant. Parameters such as Total Dissolved Solid (TDS), Total Suspended Solid (TSS), Turbidity, Biological Oxygen Demand (BOD) and Chemical Oxygen Demand (COD), were investigated. The result shows that treatment efficiency increases with the passage of time. The efficiency of Phragmites planted setups in open environment was fairly good for all studied parameters (28.6% of TDS, 94.4% for TSS, 79.8% for turbidity, 93.7% for BOD and 82.6% for COD). The efficiency of the latifoila set up was also good, but lower than that of Phragmites (26.5% of TDS, 76.9% for TSS, 71.5% for turbidity, 79.1 for BOD and 68.8% for COD).figure 3.

Figure3. Set up of constructed wetland built in an open field environment.

As alternative to the conventional treatment systems, the constructed wetlands are man-made systems implemented for the control of environmental pollution control by natural treatment of a variety of wastewaters including industrial effluents, domestic, municipal, agricultural, livestock wastewaters, sludge, and landfill leachate.
Wastewater treatment is achieved in constructed wetlands through a combination of biological, physical and chemical interactions between plants, substrate and microorganisms. Vegetation plays a vital role in the treatment, because it provides surfaces and a suitable environment for microbial growth and filtration. A wide variety of contaminants, such as suspended solids, organic compounds, nutrients, pathogens, metals, and emerging contaminants are effectively removed in constructed wetlands.

REFERENCES

Sayadi, M. H., Kargar, R., Doosti, M. R., & Salehi, H. (2012). Hybrid constructed wetlands for wastewater treatment: A worldwide review. Proceedings of the international academy of ecology and environmental sciences, 2(4), 204.
Shahamat, Y. D., Asgharnia, H., & Kalankesh, L. R. (2018). Data on wastewater treatment plant by using wetland method, Babol, Iran. Data in Brief, 16, 1056-1061.
Shahrezaei, F., Pakravan, P., Pouria, M. 2022. "Investigating the possibility of using the effluent of Qasr-e-shirin wastewater treatment plant in aquaculture" Journal of Water and Wastewater, 33(2), 62-74.
Vymazal, J. (2010). Constructed wetlands for wastewater treatment. Water, 2(3), 530-549.

The fate of microplastics in mesophilic anaerobic digestion combined with ultrafiltration membrane.

M. Lera*, A. Ruiz*, A. Jiménez-Benítez**, J.F. Ferrer***, N. Martí*, J. Serralta** and A. Seco*

* CALAGUA – Unidad Mixta UV-UPV, Departament d'Enginyeria Química, Universitat de València, Av. de la Universitat s/n, 46100 Burjassot, Valencia, Spain. (E-mail: *maria.lera@uv.es; ana.ruiz-martinez@uv.es; nuria.martí@uv.es; aurora.seco@uv.es*)
** CALAGUA – Unidad Mixta UV-UPV, Institut Universitari d'Investigació d'Enginyeria de l'Aigua i Medi Ambient – IIAMA, Universitat Politècnica de Valencia, Camí de Vera s/n, 46022 Valencia, Spain. (E-mail: *anjibe1@upvnet.upv.es; jserralt@hma.upv.es*)
*** AIMPLAS – Instituto Tecnológico del Plástico. València Parc Tecnològic. Carrer Gustave Eiffel 4, 46980 Paterna, Valencia, Spain. (E-mail: *jferrer@aimplas.es*)

Abstract

This study focuses on evaluating the fate of microplastics retained in the sludge during mesophilic anaerobic digestion. For this purpose, two laboratory-scale digesters were operated in parallel; the first one is a conventional anaerobic digester and was operated at 20 days hydraulic and sludge retention time (HRT and SRT, respectively). The second reactor was an anaerobic membrane bioreactor (AnMBR) equipped with an ultrafiltration membrane which allowed the decoupling of the HRT and SRT values, thus increasing the retention of biomass to 40 days. Both digesters were continuously fed with a combination of primary and secondary sludge from a wastewater treatment plant. The results obtained show that the AnMBR is more efficient than the conventional digester in terms of biomethanization (58 % vs. 39 %), methane production (0.20 L CH_4·g COD^{-1} vs. 0.16 L CH_4·g COD^{-1}) and microplastics removal (89 % vs. 62 %).

Keywords: anaerobic digestion, AnMBR, biodegradability, membrane, methane production, microplastics.

INTRODUCTION

The inefficient end-of-life management of diverse plastic materials represents a global environmental challenge that affects the quality of human life, wildlife, and ecosystems (Cazaudehore et al., 2022). One of the greatest concerns regarding plastic pollution comes from the so-called "microplastics" (MPs), i.e. plastic particles with sizes smaller than 5 mm that account for up to 90% of total microlitter (ML) present found in waters (OSPAR Commission, 2014). MPs may be vectors for toxic micropollutants (originally present in their production processes or subsequently adsorbed on their surface), for priority pollutants (i.e., organochlorine pesticides, polycyclic aromatic hydrocarbons, polychlorinated biphenyls, and polybrominated diphenyl ethers) and pathogens (Gatidou et al., 2019). Some of these MPs are directly released into the environment (primary MPs) but most result from the deterioration and fragmentation of coarser plastic pieces subjected to physical, chemical, and biological processes (secondary MPs). Many MPs are found in urban and industrial wastewater and thus wastewater treatment plants (WWTPs) act as the final barriers to reduce MPs emissions into the aquatic environments, with efficiencies of over 90 % (Edo et al., 2020). As a result, MPs are mainly transferred from wastewater to the sludge. Therefore, sludge management is of great importance to reduce or even avoid the spread of the retained MPs, especially when digested sludge is used for agricultural soil amendment (Cesaro et al., 2022). Anaerobic digestion (AD) is the most common process applied in medium-large WWTPs to stabilize waste sludge, but only a few studies have investigated the fate of MPs in anaerobic digesters (Chand et al., 2021; Mahon et al., 2016). This work aims to assess the MPs removal in two laboratory-scale mesophilic anaerobic digesters (one conventional anaerobic digester (AnR) and the other one equipped with an ultrafiltration membrane) fed with mixed sludge from a conventional WWTP. Moreover, COD removal, methane production and microbial population are also evaluated to compare the effect of the ultrafiltration membrane on the AD process.

MATERIALS AND METHODS

Inoculum and mixed sludge characterization

The reactors were inoculated with sludge from the anaerobic digester of an urban WWTP and were fed with mixed sludge from the same WWTP. The characteristics of the substrate and inoculum used are shown in Table 1.

Experimental set-up and operating conditions of continuous anaerobic digesters at lab-scale

The experimental set-up consisted of two cylindrical methacrylate tanks with a total volume of 14 L and a working volume of 8 L (Figure 1). Both systems were equipped with a data acquisition program used to monitor pH, redox, and temperature through electrodes, headspace pressure using a pressure transducer and volumetric biogas production using a milligas counter. In addition, the anaerobic membrane bioreactor (AnMBR) was equipped with an external hollow-fiber ultrafiltration membrane module (PURON Koch membrane systems, 0.03µm pore size) with a surface area of 0.42 m^2, installed in a membrane tank with a total volume of 1 L and a working volume of 0.9 L. The permeate pump was programmed to operate the membrane in three different modes: filtration, backwash, and relaxation. Regarding the operating conditions, both reactors were maintained for 130 days in mesophilic conditions and they were operated at an organic loading rate (OLR) of 1.69 g $COD{\cdot}L^{-1}{\cdot}d^{-1}$. The SRT and HRT were set at 20 days in the AnR reactor. The AnMBR reactor was operated at an SRT of 40 days and an HRT of 20 days.

AD performance analyses

Samples from both reactors, the AnMBR permeate and the feed sludge were analyzed weekly to evaluate the biological process performance. The following parameters were analyzed in duplicate and using standard methods (APHA, 2017): total and soluble COD (T-COD and S-COD, respectively), total solids (TS), volatile solids (VS), total suspended solids (TSS), volatile suspended solids (VSS), volatile fatty acids (VFA), alkalinity (ALK), total nitrogen (T-N), ammonium (NH_4-N), total phosphorus (T-P), phosphate (PO_4-P), and sulfate (SO_4-S). Biogas samples from the reactor headspace were collected three times a week, and the methane content was analyzed by a gas chromatograph fitted with a flame ionization detector.

Microbial population analyses

Three samples were collected from the AnMBR and the AnR in the pseudo-steady period when COD, TS and biogas production showed variations lower than 10% and were therefore considered biological replicates. Following the E.Z.N.A. ® Soil DNA Kit-Protocol the nucleic acid material was extracted from all the samples and sequencing was performed during the Illumina sequencing platform.

Microplastic analyses

MPs were extracted from sludge during a three-step process, including sludge purification by adding 30% hydrogen peroxide (H_2O_2) to oxidize the organic material, density separation using sodium chloride (NaCl) (1.2 g/mL), and filtration through stainless steel grids of different mesh sizes (500, 104 and 41 µm). The quantification of microplastics was carried out by gravimetric analysis and samples of the particles retained by the larger mesh were collected for analysis by FTIR-Attenuated Total Reflectance (FTIR-ATR) to identify genuine MPs particles from other microlitter (i.e. other inorganic and organic materials such as metals, wood, rubber, glass and paper) that can be extracted with the MPs during the experimental procedure.

RESULTS AND DISCUSSION

Table 2 shows the sludge characterization of both digesters at the end of the experimental period when a pseudo-steady state was reached. The higher SRT in the AnMBR resulted in higher biomethanization (58% vs. 39%) (Figure 2) and higher methane production (0.20 L CH_4·g COD^{-1} vs. 0.16 L CH_4·g COD^{-1}) (Table 3) than in the AnR. Regarding MPs biodegradation, the results obtained again suggest a higher removal efficiency in the AnMBR (89 %) than in the AnR (62 %) (Table 4). It is yet to be determined whether the higher removal rates observed in the AnMBR are due to the degradation obtained from the longer SRT, or due to the adsorption of MPs on the biomass cake layer of the membrane. Also, as other authors have stated (Chand et al., 2021), MPs reduction in the digesters could have been caused by plastic degradation, depolymerization or fragmentation of the particles to sizes below 41 µm (i.e. the detection limit for the applied analytical method). Differences between microbial populations in both digesters are being assessed.

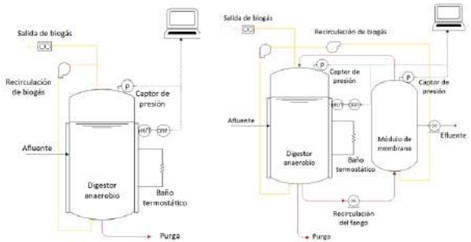

Figure 1. The layout of the anaerobic digestion system shows the anaerobic reactor (AnR) and the anaerobic membrane bioreactor (AnMBR).

Table 1. Characterization of inoculum and mixed sludge used as feed substrate. (Mean values ± standard deviation)

	Inoculum	Mixed sludge
TSS (mg TSS·L^{-1})	17605 ± 1110	27984 ± 10344
VSS (%)	81 ± 14	70 ± 14
T-COD (mg COD·L^{-1})	21738 ± 2082	33926 ± 4675
S-COD (mg COD·L^{-1})	-	3749 ± 834
VFA (mg $CH_3COOH{\cdot}L^{-1}$)	-	1868 ± 707
ALK (mg $CaCO_3{\cdot}L^{-1}$)	-	262 ± 122
SO_4-S (mg S·L^{-1})	128 ± 3	12 ± 2

Table 2. Digested sludge characterization. (Mean values ± standard deviation)

	AnMBR	AnR
TSS (mg TSS·L^{-1})	22234 ± 1766	18300 ± 2307
VSS (%)	60 ± 6	62 ± 6
T-COD (mg COD·L^{-1})	24379 ± 2307	21056 ± 2615
S-COD (mg COD·L^{-1})	1177 ± 680	1131 ± 562
VFA (mg $CH_3COOH{\cdot}L^{-1}$)	109 ± 75	108 ± 72
ALK (mg $CaCO_3{\cdot}L^{-1}$)	3507 ± 466	3071 ± 455
TP (mg P·L^{-1})	207 ± 57	188 ± 26
PO_4-P (mg P·L^{-1})	10 ± 4	16 ± 8
TN (mg N·L^{-1})	1434 ± 446	1258 ± 377
NH_4-N (mg N·L^{-1})	862 ± 147	733 ± 181
SO_4-S (mg S·L^{-1})	29 ± 10	28 ± 11
pH	6.86 ± 0.22	7.17 ± 0.12

Table 3. Methane production in both reactors. (Mean values ± standard deviation)

	AnMBR	AnR
Methane yield (L CH_4·g COD^{-1})	0.20 ± 0.02	0.16 ± 0.01
CH_4 in biogas (%)	63 ± 6	60 ± 2
Biogas flow (L/week)	19.3 ± 4.0	25.5 ± 5.0

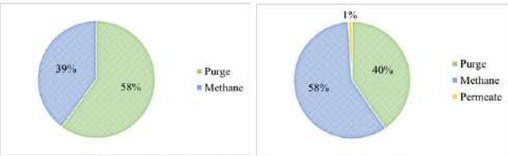

Figure 2. COD balance in the AnR (left) and AnMBR (right).

Table 4. Microplastics (MPs) removal during anaerobic digestion at laboratory scale. (Mean values ± standard deviation)

		MPs removal (%)	
		AnMBR	AnR
Filter size (µm)	< 500	92 ± 5	69 ± 11
	500 - 104	89 ± 7	62 ± 29
	104 - 41	77 ± 14	50 ± 28
	Global	89 ± 7	62 ± 23

ACKNOWLEDGEMENTS

This research work was supported by the Agencia Valenciana de la Innovació (AVI) and by the European Union through the European Regional Development Fund (ERDF) Operational Program of the Generalitat Valenciana (Spain) through the Project PREVENPLAST (INNEST/2021/168 and INNEST/2021/150) which is gratefully acknowledged.

REFERENCES

Cazaudehore, G., Guyoneaud, R., Evon, P., Martin-Closas, L., Pelacho, A. M., Raynaud, C., & Monlau, F. (2022). Can anaerobic digestion be a suitable end-of-life scenario for biodegradable plastics? A critical review of the current situation, hurdles, and challenges. *Biotechnology Advances*, 56, 107916.

Cesaro, A., Pirozzi, F., Zafirakou, A., & Alexandraki, A. (2022). Microplastics in sewage sludge destined to anaerobic digestion: The potential role of thermal pretreatment. *Chemosphere*, 309.

Chand, R., Rasmussen, L. A., Tumlin, S., & Vollertsen, J. (2021). The occurrence and fate of microplastics in a mesophilic anaerobic digester receiving sewage sludge, grease, and fatty slurries. *Science of the Total Environment*, 798.

Edo, C., González-Pleiter, M., Leganés, F., Fernández-Piñas, F., & Rosal, R. (2020). The fate of microplastics in wastewater treatment plants and their environmental dispersion with effluent and sludge. *Environmental Pollution*, 259.

Gatidou, G., Arvaniti, O. S., & Stasinakis, A. S. (2019). Review on the occurrence and fate of microplastics in Sewage Treatment Plants. *Journal of Hazardous Materials*, 367, 504–512.

Mahon, A. M., O'Connell, B., Healy, M. G., O'Connor, I., Officer, R., Nash, R., & Morrison, L. (2016). Microplastics in Sewage Sludge: Effects of Treatment. *Environ. Sci. Technol*, 51, 810−818

OSPAR Commission (2014). Regional Action Plan for Prevention and Management of Marine Litter in the North-East Atlantic.

Rice, E. W., Baird, R. B., Eaton, D. (2017). Standard Methods for the Examination of Water and Wastewater, 23rd Edition. Washington, D.C. *American Public Health Association*.

BIODAPH$_2$O – Eco-efficient system for wastewater tertiary treatment and water reuse in the Mediterranean region

V. Salvadó [1], T. Serra[1], E. Nyktari[2], V. Matamoros[3], A. Amengual[4], T. de la Torre[5]

[1]University of Girona, C/ Maria Aurèlia Capmany, 69, 17003 Girona, Spain (victoria.salvado@udg.edu; teresa.serra@udg.edu)
[2] Department of Water Resources an Environmental Engineering. National Technical University of Athens Iroon Polytechniou St 5, 15780 Zografou Campus, Athens, Greece.) (gleninyktari@mail.ntua.gr)
[3]Dpt. of Environmental Chemistry. IDAEA-CSIC, Jordi Girona, 18-26, 08034. Barcelona, Spain (vmmqam@cid.csic.es)
[4] Catalan Water Partnership. C/ Emili Grahit, 17003 Girona, Spain. (aina.amengual@cwp.cat))
[5] ACSA-Sorigué, Ronda del Guinardó, 99, 08041 Barcelona, Spain (t.delato@sorigue.com)

Abstract
LIFE BIODAPH$_2$O is a demonstration project that has the main objective of scaling-up and implementing an eco-efficient nature-based tertiary wastewater treatment (BIODAPH) at two demo sites located in two water-stressed regions of the Mediterranean area, Quart WWTP (Spain) and Antissa WWTP (Greece). During the execution of the project, the impact of the implementation of this technology on the ecological and chemical status of the receptor aquatic media in Spain and the irrigated agroforestry media in Greece will be assessed. The BIODAPH system is based on the depuration capacity of biological organisms: water fleas (*Daphnia*), microalgae and biofilms for removing pollutants (nutrients, organic carbon, suspended solids, pathogens, heavy metals, emerging and priority pollutants, and micro plastics). This compact and low-energy consumption system does not produce sludge nor uses chemicals.

Keywords: Daphnia; nature-based tertiary system, water reclamation, micropollutant removal.

INTRODUCTION

The project aims to demonstrate the effectiveness of BIODAPH technology, an eco-efficient and nature-based wastewater tertiary treatment, in producing reclaimed water while at the same time reducing dependence on conventional energy sources, in accordance with circular and green economy criteria. This will be applied in wastewater treatment plants to diminish discharges of pollutants and pathogens in freshwater ecosystems and promote agricultural reuse of the reclaimed water. The BIODAPH technology combines the filtration capacity of zooplankton (*Daphnia*) with the capacity of bacterial and algal biofilm to remove nutrients. In previous studies, we have demonstrated that *Daphnia* can remove particles <35 µm that do not settle in secondary clarifiers or do so slowly. The removal of solids is associated with a decrease in organic matter and pathogens such as coliforms and *E. coli* from secondary wastewater. However, *Daphnia* is sensitive to common contaminants when they are at raw wastewater levels (e.g. organic matter, ammonium and nitrite, and metals) and, thus, the integration of zooplankton in wastewater treatment lines is limited to a tertiary treatment (Pous et al., 2020). With regard to organic micropollutants, *Daphnia* filtration had shown high efficiencies (80% average) in the removal of pharmaceuticals and personal care products (Matamoros et al., 2012). As for microplastics, given that *Daphnia* are efficient filters for suspended solids, it can be expected that they are also efficient filters for microplastics; a hypothesis that has received support in as laboratory experiments (Colomer et al., 2019). Up to now, no results have been published regarding the capacity of *Daphnia* to remove perfluoroalkyl substances (PFAs) and antibiotic resistant genes (ARGs).

METHODOLOGY

The project aims to design a 100 m^3 reactor, scaling up from the 1.5 m^3-cylindric reactor previously developed within the framework of the INNOQUA project (https://innoqua-project.eu/). Two of these large-scale reactors will be connected to an activated sludge secondary treatment at Quart (Spain) to treat 200 m^3/d, whereas in the case of Antissa (Greece), a reactor that is able to treat a maximum of 50 m^3/d will be connected to a treatment system that combines an upflow anaerobic sludge blanket reactor (UASB) with constructed wetlands (https://www.hydrousa.org/).

The optimisation of the key design factors of the BIODAPH reactor will be carried out by monitoring its efficiency in terms of the biological, microbiological and chemical quality of the effluent to meet the standards set out in the Water Framework Directive (Directive 2000/60/EC) and the requirements for agricultural irrigation (EU Directive 2020/741) as well as to reduce the discharge of emerging contaminants such as pharmaceuticals and microplastics into the aquatic media. The sustainability assessment impacts of the technology will be assessed (environmental LCA, techno-economic LCC, and socio-economic S-LCA). The feasibility of the process will be evaluated using environmental technology verification (ETV). An economic validation, including the exploitation and the business plan and the assessment of the transferability and replicability of the BIODAPH technology, will also be performed.

EXPECTED RESULTS

- Demonstration of the capacity of the BIODAPH technology to remove emerging pollutants: ~70%, for pharmaceuticals, ~90% for antibiotic resistant genes (ARGs), ~80% for microplastics, and ~60% for perfluoroalkyl substances (PFAs).
- Demonstration of the capacity of the BIODAPH system to reach the standards set in national wastewater reuse guidelines and recent EU regulations (2020/741 of the European Parliament) on minimum requirements for water reuse (PE/12/2020/INIT). To recover and recycle resources by discharging reclaimed water with low nutrient content (~50%) and reduce the regulated microbiological parameters by between 90 and 99%.
- Production of reclaimed water with improved quality to reduce the impact generated by the discharge of treated sewage waters in the River Onyar at the Spanish site. At the Greek site, a reduction in the use of freshwater and potable water for agricultural irrigation, which will also reduce the environmental impacts associated with wastewater release into the aquatic media.
- Energy consumption reduction of more than 90% and a carbon footprint and greenhouse gas production reduction of more than 80% in comparison with conventional tertiary wastewater treatments.
- Significant reduction in operating costs (OPEX) as the treatment is free from chemicals and is less energy intensive.

AGNOWLEDGEMENTS

This research is co-funded by the European Union Life Programme under Grant Agreement nº 101074191 - LIFE21-ENV-ES-BIODAPH2O and the Spanish Ministry of Science and Innovation (Project TED2021-132721B-100).

REFERENCES

Pous N., Hidalgo M., Serra T., Colomer J., Colprim J., Salvadó V. 2020. Assessment of zooplankton based eco-sustainable wastewater treatment at laboratory scale. *Chemosphere*, 238, 124683.

Matamoros V., Sala L., Salvadó V. 2012. Evaluation of a biologically based filtration water reclamation plant for removing emerging contaminants: A pilot plant study. *Bioresource Technology*, 104, 243.

Colomer J., Müller M.F., Barcelona A., Serra T. 2019. Mediated food and hydrodynamics on the ingestion of microplastics by Daphnia magna. *Environmental Pollution*, 252, 434.

Specific Hydrogenotrophic Methanogenic Activity test: the role of operating conditions

A. Santus*, M. Trionfini*, A. Catenacci*, F. Malpei*

* Department of Environmental and Land Planning Engineering, Politecnico di Milano, Piazza Leonardo da Vinci 32, Milano (MI), 20133
(E-mail: *anna.santus@polimi.it)**

Abstract
This work is focused on the study of Specific Hydrogenotrophic Methanogenic Activity (SHMA) tests, as a practical tool for the monitoring and optimization of biological biogas upgrading process. In view of the development of a standardized protocol, the influence of three main test operating conditions (mixing speed, liquid working volume, and initial H_2 partial pressure) was investigated by analysing data from a total of 42 SHMA tests. Operating conditions were varied to assess their role on the estimation of the SHMA value. Preliminary analyses on data show that SHMA is strongly influenced by mixing speed (in relation to gas-liquid mass transfer process) and by the liquid working volume adopted (affecting hydrodynamics of the test).

Keywords
Anaerobic activity test, anaerobic processes, bioenergy production, biological biogas upgrading, hydrogenotrophic methanogens

INTRODUCTION

Chemoautotrophic biological biogas upgrading is attracting significant attention in order to yield high quality biomethane to be used as an alternative energy source to natural gas. Carbon dioxide and hydrogen can be converted into methane by Archaea hydrogenotrophic methanogens (HM) and the relation describing the metabolic reaction is reported in literature as in eq.1 (Speece, 1983):

$$H_2 + 0.256CO_2 + 0.004HCO_3^- + 0.004NH_4^+ \rightarrow 0.239CH_4 + 0.004C_5H_7O_2N + 0.517H_2O \quad \text{eq.1}$$

This process is naturally carried out during anaerobic digestion at low yield and rate, depending on digester environmental conditions and on the abundance of HM over other microbial species. The opportunity to exploit and boost hydrogenotrophic methanogenesis in order to engineer and optimize CO_2 conversion into CH_4 makes biological biogas upgrading an interesting solution to recycle and reduce carbon emissions to the environment (Zabranska & Pokorna, 2018). Hence, the need for a measuring method of the hydrogenotrophic methanogenesis activity is becoming essential for process monitoring, optimization, and control.

The Specific Hydrogenotrophic Methanogenic Activity test (SHMA) indirectly measures H_2 consumption and thus, methane-specific production rate mediated by HM microorganisms. It is a key tool to evaluate possible inhibition effects or supporting the monitoring of an operating plant. Scientific literature reports about SHMA test results, but, due to the lack of a standardized protocol (Ripoll et al., 2020) the use of SHMA remains a prerogative of the research world. In order to exploit and export this tool for process monitoring at the full-scale, a standardized method needs to be developed. A first step towards this objective is provided by this study, which aims at investigating the role of test operating conditions on SHMA results.

MATERIALS AND METHODS

Guidelines proposed by Coates et al. (1996) and Ripoll et al. (2020) were taken as reference to carry out SHMA tests. MethanTUBE® (Biological Care, IT) instrumentation was used: each 3.76 L reactor is equipped with a digital pressure manometer, temperature regulation system, screws, and gaskets to ensure sealed anaerobic conditions. A total number of 42 trials was performed. Each set of trials included duplicate blank bottles (tests performed with inoculum only) and duplicate activity test bottles. As inoculum, an enriched hydrogenotrophic methanogens culture previously collected from a biological biogas upgrading ex-situ pilot plant, after 300 days of operation, was used. Bottles were fed with inoculum and nutrients. The concentration of inoculum in the reactor on a volatile solids basis (C_{vs}) was kept at 1.52 ± 0.26 g VS·L^{-1}. As soon as the bottle reached the operating temperature, the headspace (V_{gas}) was flushed with a mixture of H_2:CO_2 (80:20 v/v) for 10 minutes (total gas replacement is verified) and, finally, the desired overpressure was set. During the test pressure was continuously measured over time, thus allowing the estimation of H_2 consumption rate and, in turn, of CH_4 production. SHMA is expressed as mL_N CH_4·g VS^{-1}·d^{-1} and is calculated as follows (eq.2), by selecting the maximum slope of the linear part of the curve, before elbow occurred:

$$SHMA = max\left(\frac{\Delta p}{\Delta t} \cdot \frac{V_{gas} \cdot VM}{VS \cdot R \cdot T_{op}} \cdot s\right) \quad \text{eq.2}$$

Where:

- Δp is the pressure increase/decrease at a generic time interval Δt;
- VM is the molar volume at standard conditions (22.414 L_N·mole^{-1});
- VS is the total mass of volatile solids, expressed as g_{VS};
- R is the ideal gas constant (0.0083145 L_N·bar·mole^{-1}·K^{-1});
- T_{op} is the operating temperature of the test (310 ± 0.5 K);
- *s* is the stoichiometric methane production, *s* = 0.239 (eq.1).

Three parameters (values reported in **Table 1**) were selected to elucidate the role of operating conditions on test results: the initial overpressure in the headspace ($p_{gas,0}$, absolute bar), the mixing speed (rpm), and the working volume (V_{liq}). Those parameters have been selected according to their role in gas-liquid mass transfer theory (Jensen et al., 2021; Whitman, 1962).

Table 1. Operating conditions of the tests.

Parameter		Values
$p_{gas,0}$	(absolute bar)	1.2 – 1.6 – 2.0
Mixing speed	(rpm)	0 – 400 – 800
V_{liq}	(mL)	200 – 400 – 600

The combination of tested operating conditions is selected according to a Box-Behnken design of experiments (**Figure 1**), plus an extreme of interest ($p_{gas,0}$ = 2.0 bar, V_{liq} = 200 mL and mixing speed = 800 rpm).

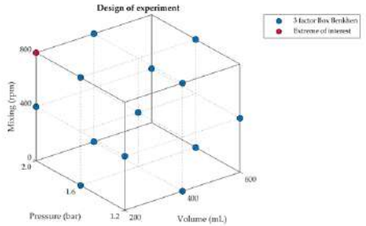

Figure 1. Box-Benkhen DOE graphical representation.

RESULTS

The minimum value of SHMA obtained is 118 mL_N CH_4·g_{SV}^{-1}·d^{-1} and the maximum is 5'709 mL_N CH_4·g_{SV}^{-1}·d^{-1}, showing an order of magnitude variation in the SHMA value. The mean value is 1'622 mL_N CH_4·g_{SV}^{-1}·d^{-1}, the median 1'115 mL_N CH_4·g_{SV}^{-1}·d^{-1}, and a standard deviation of 1'627 mL_N CH_4·g_{SV}^{-1}·d^{-1} which highlights the high variation between SHMA values.

Figure 2 shows the results in form of boxplots. A liquid volume increase results in an average decrease of SHMA values, contrarily to what observed for an increase of mixing speed and initial overpressure (except for $p_{gas,0}$ = 1.6 bar). Possible explanations for these trends are summarized as follows:

1. An increase of mixing speed and, hence, of system turbulence, improves gas-liquid mass transfer rates, allowing for increased concentrations of dissolved H_2 that can be up taken by microorganisms. This means that at high stirring speed, the process rate is limited by gas-liquid mass transfer efficiency to a lower extent, hence resulting in more reliable SHMA values, actually describing the kinetic behavior of biomass;
2. An increase of starting overpressure positively affects substrate availability (Henry's law), hence increasing the amount of hydrogen that can be dissolved in the liquid phase;
3. A liquid volume decrease leads to an increase in both substrate availability (V_{gas} increase) and the turbulence hydrodynamics and, as for the first two points the whole mass transfer of hydrogen.

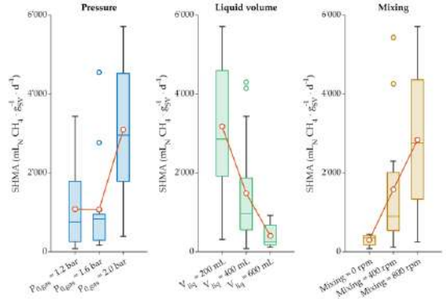

Figure 2. SHMA boxplots at varying of operative parameters. Line connected dots represent mean values for each category.

CONCLUSIONS AND FUTURE DEVELOPMENTS

This work confirms that SHMA values obtained are highly influenced by the operating conditions, varying by more than one order of magnitude. The general conclusion is that SHMA results are influenced by operating conditions which influence the transfer rate (k_La) of the test. As future development, it is necessary to measure also the k_La of the test. Knowing this parameter is fundamental to understanding the SHMA test according to user interests. Moreover, support of data interpretation by means of batch test modelling will be implemented to get more insights.

REFERENCES

Coates, J. D., Coughlan, M. F., & Colleran, E. (1996). Simple method for the measurement of the hydrogenotrophic methanogenic activity of anaerobic sludges. *Journal of Microbiological Methods*, *26*(3), 237–246. https://doi.org/10.1016/0167-7012(96)00915-3

Jensen, M. B., Ottosen, L. D. M., & Kofoed, M. V. W. (2021). H2 gas-liquid mass transfer: A key element in biological Power-to-Gas methanation. *Renewable and Sustainable Energy Reviews*, *147*, 111209. https://doi.org/10.1016/j.rser.2021.111209

Ripoll, E., López, I., & Borzacconi, L. (2020). Hydrogenotrophic activity: A tool to evaluate the kinetics of methanogens. *Journal of Environmental Management*, *270*, 110937. https://doi.org/10.1016/j.jenvman.2020.110937

Speece, R. E. (1983). Anaerobic biotechnology for industrial wastewater treatment. *Environmental Science & Technology*, *17*(9), 416A-427A. https://doi.org/10.1021/es00115a725

Whitman, W. G. (1962). The two film theory of gas absorption. *International Journal of Heat and Mass Transfer*, *5*(5), 429–433. https://doi.org/10.1016/0017-9310(62)90032-7

Zabranska, J., & Pokorna, D. (2018). Bioconversion of carbon dioxide to methane using hydrogen and hydrogenotrophic methanogens. *Biotechnology Advances*, *36*(3), 707–720. https://doi.org/10.1016/j.biotechadv.2017.12.003

Study of the key parameters influencing ammonium removal from wastewaters by Fe(III)-mediated anaerobic ammonium oxidation (Feammox) microbial communities.

J. Cisternas*,** C. A. Rodríguez**, J. S. Serrano* and E. D. Leiva **, ***

* Biotechnology School, Faculty of Science, Engineering and Technology, Universidad Mayor, Santiago, Chile (*jennyfer.serrano@umayor.cl, jaime.cisternas@mayor.cl*).
** Department of Inorganic Chemistry, Faculty of Chemistry and Pharmacy, Pontificia Universidad Católica de Chile, Santiago, Chile. (*cnrodriguez@uc.cl; ealeiva@uc.cl*).
*** Department of Hydraulic and Environmental Engineering, Pontificia Universidad Católica de Chile, Santiago, Chile. (*ealeiva@ing.puc.cl*).

Abstract

Nitrogen biogeochemical cycling have been one of the most important nutrient cycles in terrestrial environments. By their agriculture and economical importance, there are an excessive nitrogen use in soils that infiltrate to water bodies. Recently, a new biological pathway involved the anaerobic ammonium oxidation coupled with iron reduction and has been called Feammox, has been described. We study the effect of several abiotic and biotic conditions to determine their impact on the Feammox process enriched from wastewater sludges. In this way, parameters such as iron source, temperature, carbon source, pH, and sludge inoculum are tested to determine which conditions allow the best reduction of ferric iron along with the oxidation of NH_4^+.

Keywords
Feammox, iron, ammonium removal, NGS, nitrogen, wastewater.

INTRODUCTION

Recently, a new biological pathway of nitrogen cycle called Feammox, has received significant research attention (Clément et al., 2005). This process occurs in anoxic, iron-rich, and water-saturated systems such as riparian, forested, coastal wetlands, and and wastewater sludge (Kappler et al., 2021). Feammox is a process that can be described as the oxidation of NH_4^+ under iron-reducing conditions, with iron oxides [Ferric iron, Fe(III)] as the electron acceptor (Huang et al., 2016). Fe(III) is reduced to ferric iron Fe(II), while NH_4^+ is transformed to N_2, NO_2^- or NO_3^- (Huang and Jaffé, 2015). As Feammox is related to a particular group of microorganisms, it is evident that the conditions in which they are found will affect their development. Thus, essential factors such as iron source, pH, temperature, and carbon source will affect the microbial composition (Yao et al., 2019; Zhu et al., 2021).

MATERIALS AND METHODS

The Feammox enrichment process was carried out using the two sludge sources collected from two wastewater treatment plants, both located in Santiago, Chile as from anaerobic reactors (EGSB and IC). The cultures were enriched with variable iron sources, initial pH, temperature, and different organic and inorganic carbon sources to determine the optimal conditions for Feammox activity by 42 days. A sequential enrichment process (56 days) was carried out using the best enrichments resulting from the previous stage as inoculum for the next one, discarding the less favorable environmental conditions. For molecular analysis DNA extraction from the sludge and enrichments was performed using the DNeasy® PowerSoil® Pro kit (QIAGEN)). Phylogenetic analysis of the sludge samples and enrichments at the end of incubations were performed by 16S rRNA gene sequencing (V3/V4 region) at Genoma Mayor, Universidad Mayor, Chile. The amplicons were purified, quantified, pooled, and then sequenced on the NovaSeq 6000 platform (Illumina, USA), in 250 pair-end (PE) mode. The DADA2 bioinformatics protocol on the R platform was used for sample analyses (Callahan et al., 2016).

RESULTS AND DISCUSSION

The first enrichments carried out by 42 days with $FeCl_3$ presented better results associated with Feammox activity than Ferrihidrite and Goethite (data non shown). These enrichments were used as inoculum to study the effect of environmental conditions on crop performance in a second step of enrichment by 56 days. Figure 1 summarizes the best conditions related to the Feammox process in a second enrichment. The variable conditions that allowed the optimal Feammox response are constituted by a common culture medium, having $FeCl_3$ as Fe source, sodium acetate as carbon source, at initial pH 7.0 and purged with CO_2 (Figure 1).

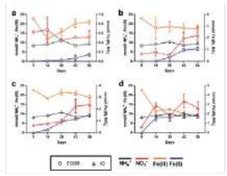

Figure 1. Study of environmental conditions using FeCl3 as iron source: (a) EGSB enrichment as inoculum at room temperature (EGSB 2.1); (b) EGSB enrichment as inoculum at 35°C (EGSB 2.2); (c) IC enrichment as inoculum at room temperature (IC 2.1); and (d) IC enrichment as inoculum at 35°C (IC 2.2). The left and right Y-axes show the concentrations in millimols per liter (mmol/l) of the different chemical species.

The results obtained from the enrichment steps show the importance of incubation temperature and inoculum type. Although the candidates did not show a tendency to decrease the ammonium level, they behaved in the same way in terms of the other parameters NO_3^-, Fe (II) and Fe (III) according to the Feammox process (320% increase in NO_3^- and 1.67 mmoles/l of Fe (II)). On the other hand, it was possible to enrich cultures that can carry out the Feammox process in a period of 56 days. behavioural that are supported by other similar results presented in the literature (Feng et al., 2020; Le et al., 2021).

Given that there is evidence of the occurrence of the Feammox process in our enrichments and sludge, a massive sequencing analysis was carried out to determine the composition of the microbial community. From the sequencing, a total of 1,198,557 reads were obtained from the total of the 8 samples, which indicates an average of 149,820 reads per sample. A total of 1844 ASVs were identified from the data analysis for the 8 samples. The graphs below present the results of the microbial community diversity analysis (relative abundance). Sludge, enrichments, and environmental conditions study samples are reported by Phylum and Class.

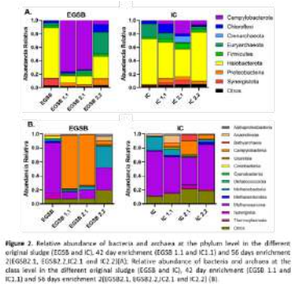

Figure 2. Relative abundance of bacteria and archaea at the phylum level in the different original sludge (EGSB and IC), 42 day enrichment (EGSB 1.1 and IC1.1) and 56 days enrichment 2(EGSB2.1, EGSB2.2,IC2.1 and IC2.2)(A). Relative abundance of bacteria and archaea at the class level in the different original sludge (EGSB and IC), 42 day enrichment (EGSB 1.1 and IC1.1) and 56 days enrichment 2(EGSB2.1, EGSB2.2,IC2.1 and IC2.2) (B).

REFERENCES

Callahan, B.J., McMurdie, P.J., Rosen, M.J., Han, A.W., Johnson, A.J.A., Holmes, S.P., 2016. DADA2: High-resolution sample inference from Illumina amplicon data. Nat. Methods 2016 137 13, 581–583

Clément, J.C.; Shrestha, J.; Ehrenfeld, J.G.; Jaffé, P.R. Ammonium oxidation coupled to dissimilatory reduction of iron under anaerobic conditions in wetland soils. Soil. Biol. Biochem. 2005, 37, 2323–2328.

Feng, L., Li, J., Ma, H., Chen, G., 2020. Effect of Fe(II) on simultaneous marine anammox and Feammox treating nitrogen-laden saline wastewater under low temperature: Enhanced performance and kinetics. Desalination 478, 114287.

Huang, S., Chen, C., Peng, X., Jaffé, P.R., 2016. Environmental factors affecting the presence of Acidimicrobiaceae and ammonium removal under iron-reducing conditions in soil environments. Soil Biol. Biochem. 98, 148–158

Huang, S., Jaffé, P.R., 2015. Characterization of incubation experiments and development of an enrichment culture capable of ammonium oxidation under iron-reducing conditions. Biogeosciences 12, 769–779

Kappler, A., Bryce, C., Mansor, M., Lueder, U., Byrne, J.M., Swanner, E.D., 2021. An evolving view on biogeochemical cycling of iron. Nat. Rev. Microbiol. 2021 196 19, 360–374.

Yao, Z., Wang, F., Wang, C., Xu, H., Jiang, H., 2019. Anaerobic ammonium oxidation coupled to ferric iron reduction in the sediment of a eutrophic lake. Environ. Sci. Pollut. Res. 26, 15084–15094.

Zhu, J., Li, T., Liao, C., Li, N., Wang, X., 2021. A promising destiny for Feammox: From biogeochemical ammonium oxidation to wastewater treatment. Sci. Total Environ. 790, 148038.

Metal Biosorption from Wastewater under Acidic Environment

C. Takano*, K. Nakashima*, S. Kawasaki* and H. Aoyagi**

* Faculty of Engineering, Hokkaido University, Sapporo, Hokkaido 060-8628, Japan.
(E-mail: takano.chikara@eng.hokudai.ac.jp, k.naka@eng.hokudai.ac.jp, kawasaki@geo-er.eng.hokudai.ac.jp)
** Faculty of Life and Environmental Sciences, University of Tsukuba, Tsukuba, Ibaraki 305-8572, Japan.
(E-mail: aoyagi.hideki.ge@u.tsukuba.ac.jp)

Abstract
Metal removal from acidic solution is an important issue to deal with both industrial wastewater and environmental pollution. Conventionally, chemical neutralization and precipitation process is applied widely. However, it requires considerable amount of neutralizer and generates waste sludge. Considering this, we proposed a novel concept of bacterial sequential biosorption process under acidic condition. Here, we established a model process using 5 bacterial strains and evaluated metal adsorption abilities from metal solution (pH 1.5, containing 100 mg L^{-1} each of Co, Cu, Li, Mn, and Ni). Among 5 strains, *Priestia* sp. Mn7 was regarded as the most efficient adsorbent. Using the strain, same process was performed, and dynamics of various metals were evaluated. These results suggest metal biosorption of the strain was related to K and Mg release. Although further experiments are expected, this study potentially contributes to develop a sustainable metal removal process by reducing the required additives and generated waste.

Keywords (maximum 6 in alphabetical order)
Acid tolerant bacteria, Acidic hydrosphere, Biosorption, Heavy metal

INTRODUCTION

Rapid spread of information technologies and electric vehicles causes increased metal consumption. Due to this, treatment of wastewater containing various heavy metals is becoming an important issue from both industrial and environmental aspects. To prevent waste metal pollution of hydrosphere and human health problems, various metal removal processes have been proposed. However, there are serious drawbacks in conventional neutralization and precipitation process since they consume large amount of neutralizer and generate a large amount of waste sludge. To improve sustainability and reduce effort and waste generation, biosorption process has been studied, and bacteria, plants, and other biomass have been applied as metal adsorbent (Wang and Chen 2009, Rizvi *et al.* 2020). Although it is an environmentally friendly process, most of the studies on biosorption are performed under neutral pH conditions. On the other hand, metal containing wastewater is mainly acidic pH due to the solubility. Considering this situation, we focused on acid tolerant bacteria as an expected adsorbent that can work under strongly acidic conditions and developed a novel screening method (Takano and Aoyagi 2022). Using this method, acid tolerant metal adsorbing bacteria were isolated. In this study, those strains were applied for a sequential metal biosorption process under acidic condition.

MATERIAL AND METHOD

Material

Four previously isolated bacterial strains and a model bacterial strain *Micrococcus luteus* JCM1464 were used in this study. These strains have exhibited acid tolerance and metal adsorbing abilities under acidic conditions. Considering the wastewater containing metals from waste lithium-ion battery and printed circuit board, simulated metal solution was prepared by dissolving Co, Cu, Li, Mn, and Ni ions in distilled water (pH was modified by using 10× H_2SO_4). Inductively coupled plasma atomic emission spectroscopy (ICPE-9820, Shimazu, Kyoto, Japan, ICP-AES) was applied to metal ions quantification. Standard curves were prepared using ICP multi-element standard solution IV (Merck, Germany).

Sequential metal biosorption process

Adsorbents were prepared by cultivating the 5 bacterial strains overnight (30°C, 160 rpm). According to their metal adsorption ability and selectivity, reaction conditions of sequential metal biosorption process was designed (**Table 1**). The first strain was centrifuged and suspended into simulated metal solution containing 1 g L^{-1} each metal ion. Metal biosorption reaction was performed and bacterial cells were removed. Then, the second strain was suspended to adsorb metals. This process was repeated for 5 strains sequentially. Metal adsorption ability and selectivity of each strain was quantified based on the metal concentrations after each step using ICP-AES. To improve the metal removal efficiency, the same sequential process was performed using the single strain *Priestia* sp. Mn7, the most effective adsorbent.

Evaluation of metal ions dynamics

To clarify the bacterial response to simulated metal solution, dynamics of 23 metal species during the sequential metal adsorption process using the strain *Priestia* sp. Mn7 was quantified using ICP-AES. Same sequential process was performed using acidic solution without metal ions (pH 1.5) to evaluate effect of acidic environmental stress. Bacterial response against the metal solution was estimated based on adsorbed and released metal ions. All experiments were performed in triplicate.

RESULT AND DISCUSSION

Sequential metal biosorption process

The sequential metal biosorption process with 5 bacterial strains adsorbed 6.99% total metal ions from the simulated metal solution (**Table 2**). Although the metal adsorption under strongly acidic conditions was achieved, the efficiency of the process was impractical, and it has a long reaction period. In this study, *Priestia* sp. Mn7 was regarded as the most effective adsorbent considering its high adsorbing efficiency and the highest cell productivity. Using this strain, reaction period was shortened from 6 h to 2.5 h, and metal adsorption efficiency was not affected significantly (7.04%). Although the efficiency of the process is still lower than conventional chemical process (>40%, Provazi *et al.* 2011), metal biosorption process without neutralization was established.

Evaluation of metal ions dynamics

Metal concentration dynamics was evaluated for 23 metal species during the biosorption process. In the acidic solution not containing metal ions, Ca, K, Mg, and Na were released from bacterial cell (Ca: 0.36, K: 13.40, Mg: 2.18, and Na: 1.36 mg g^{-1}-dry cell) compared to the initial acidic solution. Under metal containing conditions, K and Mg concentrations were significantly increased (24.43 and 2.70 mg g^{-1}-dry cell, respectively) after the sequential biosorption process (**Figure 1**). These results indicate that *Priestia* sp. Mn7 releases K and Mg ions to deal with high metal concentrations. Similar response was observed during bacterial enhanced expression of metal efflux pump (Huang *et al.* 2018). Further experiments are required to understand bacterial metal adsorbing mechanisms and to improve the metal biosorption efficiency.

In this study, metal biosorption process under strongly acidic conditions was established using the acid tolerant metal adsorbing bacteria *Priestia* sp. Mn7. The strain can adsorb 5 metals and release K and Mg ions in response to metal existing acidic environment. Although further studies are required, this is the first step to establish a treatment process for metal containing wastewater without neutralization.

Table 1. Reaction order and period of bacterial strains applied to the sequential metal biosorption process and their growth abilities under neutral pH condition.

Order	Strain	Reaction period [h]	Growth ability [g-dry cell L^{-1}]
1	*Coma monas* sp. HTL	1.5	0.55
2	*Micrococcus luteus* JCM1464	0.5	0.32
3	*Pseudomonas* sp. MS3	0.5	0.93
4	*Enterobacter* sp. MnA	3.0	0.67
5	*Priestia* sp. Mn7	0.5	0.63

Table 2. Reaction period [h] and metal adsorption ratio (%) of sequential metal biosorption process using 5 bacterial strains and 5 cycles of *Priestia* sp. Mn7.

	Reaction period [h]	Co	Cu	Li	Mn	Ni	Total
5 bacterial strains	6.0	7.23	6.82	7.52	5.85	7.64	6.99
Priestia sp. Mn7	2.5	6.76	8.11	7.52	6.29	6.47	7.04

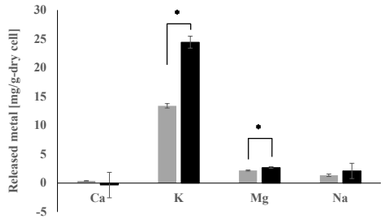

Figure 1. Comparison of released cations concentrations [mg L^{-1}] during sequential metal biosorption process. Gray: Without metal. Black: Containing 1 g L^{-1} of 5 metal species.
*: Significant difference (n=3, $p<0.05$).

REFERENCES

Huang, F., Wang, Z., Cai, Y., Chen, S., Tian, J., Cai, K. 2018 Heavy metal bioaccumulation and cation release by growing Bacillus cereus RC-1 under culture conditions. *Ecotoxicology and Environmental Safety* **157**(15), 216-226.
Provazi, K., Campos, B., Espinosa, D., Tenorio, J. 2011 Metal separation from mixed types of batteries using selective precipitation and liquid–liquid extraction techniques. *Waste Management* **31**(1), 59–64.
Takano, C., Aoyagi, H. 2022 Screening and isolation of acid-tolerant bacteria using a novel pH shift culture method. *Journal of Bioscience and Bioengineering* **134**(6), 521-527.
Rizvi, A., Ahmed, B., Zaidi, A., Khan, M. 2020 Biosorption of heavy metals by dry biomass of metal tolerant bacterial biosorbents: an efficient metal clean-up strategy. *Environmental Monitoring and Assessment* **192** (12), No. 801.
Wang, J., Chen, C. 2009 Biosorbents for heavy metals removal and their future. *Biotechnology Advances*, **27**(2), 195-226.

Application of MABR to Japanese Municipal Sewage Treatment

H. Tanaka*, S. Cho* and R. Tsujibayashi*

* Research & Development Center, Sanki Engineering Co., Ltd., 7-10-1 Chuorinkan, Yamato, Kanagawa 242-0007, Japan
(E-mail: *hideharu_tanaka@eng.sanki.co.jp)*

Abstract
The first pilot scale test of Membrane Aerated Biofilm Reactor (MABR) in Japan was conducted. The MABR total working volume of 14 m^3 was installed at a municipal wastewater treatment plant (WWTP). The operation started with hydraulic retention time (HRT) of 8.4 hours, and the loading rate was stepwise increased, finally the highest load of HRT 1.6 hours was kept for more than 218 days. The MABR showed remarkable performance of COD, S-COD and NH_4^+-N removal, the mean removal rates were 77 %, 63 % and 90 %, respectively. T-N removal rate by simultaneous nitrification- denitrification was 44 %, with a maximum of 73%.

Keywords
MABR; municipal sewage treatment

INTRODUCTION

Membrane Aerated Biofilm Reactor (MABR) is a promising wastewater treatment technology because of its advantages such as energy saving based on high oxygen-supplying ability, a small footprint of reactor, and simultaneous nitrification-denitrification, therefore, applications of MABR to sewage are increasing around the globe (He *et al*. 2021; Lu *et al*. 2021). However, there are only some lab-scale studies reported in Japan so far. This report describes the first result of pilot scale MABR applied to sewage in a major Japanese city.

MATERIALS AND METHODS

Pilot plant setup and operational conditions

A reactor, total working volume of 14 m^3 with a couple of membrane module was installed at a municipal wastewater treatment plant (WWTP) in Yokohama city, Japan. The reactor was divided into two stages for each module. The system was a pure biofilm reactor, without suspended activated sludge. The effluent of primary settlement of the WWTP was pumped through 1 mm mesh screen to the reactor. **Table 1** shows the specifications and operational conditions of the membrane module.

Water quality and sludge analysis

Influent and effluent of the MABR were grab sampled at least once a week to determine COD, S-COD, NH_4^+-N, T-N. From 118 days, the excess sludge generated in the scouring process of the membrane was also sampled to determine its amount, and sludge yield was estimated with COD removal rate once a month. COD and S-COD was determined by spectrometry (DR400, Hach, USA). Others were analyzed according to *Standard Methods for the Examination of Water and Wastewater* (2017).

Table 1. Specifications and operational conditions of the membrane module.

Membrane			Process/Mixing Air		Scour air			
Type	Material	Diameter	Surface area	Flowrate	Pressure	Flowrate	Duration	Frequency
-	-	mm	m^2/module	Nm^3/(hr・module)	kPa (G)	Nm^3/(reactor・hr)	min./module	times/ (day・module)
Hollow fiber	PDMS	OD 0.5	2200	10	20-25	180	1-2	1-4

Energy requirement

The required energy of blowers for the operation was calculated based on the actual air flow rate and pressure with assuming overall efficiency of the blower as 68%.

RESULTS AND DISCUSSION

Sewage load and water wuality

The operation of the MABR was started with hydraulic retention time (HRT) of 8.4 hours, without seeding activated sludge etc. The loading rate was stepwise increased and finally 1.6 hours of HRT, the highest load, was kept for more than 218 days.

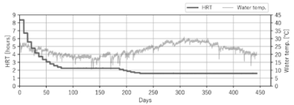

Figure 1. Time course of HRT and temp. of the reactor.

The MABR showed remarkable performance of COD, S-COD and NH_4^+-N removal through whole period of the operation. The mean removal rates of them were 77 %, 63 % and 90 %, respectively. Regarding T-N removal by simultaneous nitrification- denitrification, the removal rate was 44 % as mean values, with a maximum of 73%.

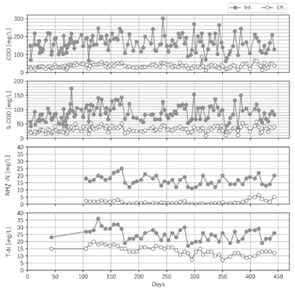

Figure 2. Time course of water quality.

Excess sludge production

The sludge yield was estimated as 0.2-0.5 kg $_{SS}$ per kg $_{COD\ removal}$. It tended to be lower in the period of high water temperature and higher in the period of low temperature.

Energy requirement

The required energy for air supply (including process air, mixing air and souring air) during the period of the highest load was calculated as 0.04 kWh per m^3 of sewage loading.

CONCLUSION

The advantages of MABR, such as small footprint based on high performance of sewage treatment, simultaneous nitrification-denitrification and low energy were demonstrated.

ACKNOWLEDGEMENT

We are grateful to Yokohama city for providing the site and sewage for this study.

REFERENCES

He, H., Wagner, B. M., Carlson, A. L., Cheng, Y., Daigger, G. T., 2021 Recent progress using membrane aerated biofilm reactors for wastewater treatment. *Water Science and Technology* **84**(9), 2131–2157.

Lu, D., Bai, H., Kong, F., Liss, S. N., Liao, B., 2021 Recent advantages in membrane aerated biofilm reactor. *Critical Reviews in Environmental Science and Technology* **51**(7), 649–703.

Evapotranspiration toilet: a safe and sustainable treatment for black water

Tonetti, A. L.*, Figueiredo, I. C. S., Almeida, M. E. P., Leonel, L. P., Portela, D. G., Miyazaki, C. K., Barbosa, A. C.

School of Civil Engineering, Architecture and Urban Design – FECFAU, Sanitation and Environment Department, University of Campinas – UNICAMP, PO box 6021, 13083-830, Campinas (SP), Brazil. (E-mail: tonetti@unicamp.br).

Abstract
In this work, we evaluated the evapotranspiration toilet (EVT), which is one of the possible solutions for sewage treatment in rural communities or isolated areas. Although, the system is still poorly widespread, it stands out for not generating final effluent or large amounts of sludge. Thus, it is possible for plants to use most of the nutrients contained in domestic wastewater, without the need of post treatments or human contact with the effluent. We found that the systems' removal efficiency is over 90% for COD and BOD, above 98% for turbidity and Total Suspended Solids and 58% for phosphorus.
Keywords
Decentralized strategies; Decentralized treatment; Ecological sanitation; Reuse.

INTRODUCTION

Nutrient removal in the effluent of isolated communities is a challenge since most of decentralized wastewater treatment systems has low efficiency to remove it. The evapotranspiration toilet (EVT) is one of the existing alternatives for this purpose. The EVT is a waterproof tank filled with different layers of filter material and covered with several plant species (Figure 1).

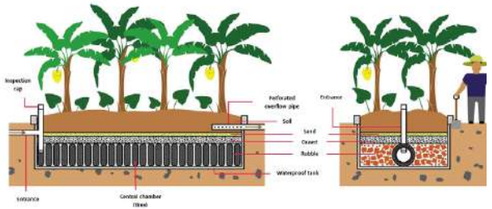

Figure 1 Evapotranspiration toilet system. Source: Translated from Tonetti et. al. (2018).

Natural processes occur within the tank, among them degradation of organic matter, absorption of nutrients and the evapotranspiration through the soil and plants into the atmosphere. An important advantage of the system is that it provides water and nutrient recycling through biomass and food production. Moreover, the system avoids human contact with the effluent, lowering the risk of contamination by pathogens.

MATERIALS AND METHODS

In this work, we monitored for eight months an EVT installed in a rural site in Campinas (Brazil). Banana trees and taioba growth was visually monitored and the effluents were collected in two points of the system, before and after the treatment, for which the parameters were measured: turbidity, pH, COD, BOD, total phosphorous (P_{total}), E-coli, and Total Suspended Solids (TSS).

RESULTS AND DISCUSSION

The plants above the tank shown a regular growth. Three banana trees fructified during the period of the project and taioba leafs were harvested and consumed. The results of the parameters monitored are in Table 1 and removals over 90% efficiency for TSS, turbidity, BOD and COD were registered, while the removal of P_{total} was of 58%.

Table 1 Physiochemical characterization on EVT

Parameter	Sample size	Influent	Effluent	Efficiency (%)
BOD (mg O_2 L^{-1})	8	1009 ± 813*a*	64 ± 48*b*	93.6
COD (mg O_2 L^{-1})	17	2375 ± 1652*a*	220 ± 116*b*	90,7
P_{total} (mg P L^{-1})	7	23.1 ± 13.7*a*	9.7 ± 4.8*b*	58.0
TSS (mg L^{-1})	16	2817 ± 2710*a*	42.9 ± 21.6*b*	98.5
Turbidity (UT)	17	1511 ± 1268*a*	26 ± 20*b*	98.3
pH	17	7.60 ± 0,13*a*	7.76 ± 0.5*a*	-
E. *coli* (MPN 100 mL^{-1})	7	4.0 x 10^7*a*	7.6 x 10^5*b*	-

MPN – most probable number *Different lowercase letters on the same line may differentiate between media (Mann-Whitney, p<0.05).

This result indicates a high removal rate and a high efficiency of physical filtration process inside the tank. An analogous trend was found for BOD removal, with an efficiency of 93,6%. This value far exceeds the minimum of 60% required by the Brazilian law of discharge pattern of treated effluent into water bodies. The efficiency removal of 58% total phosphorus was 20% higher than that found by Galbiati (2009) in a similar setting. The removal of this nutrient can be explained by the plant's high absorption during their grow phase. Regarding E. coli, the removal rates we found are compatible removal with the rates of typical anaerobic reactors, which usually vary from 70 to 90% (Von Sperling, 2014). However, as the effluent is trapped within the tank, there is no risk of contact with the residents or even with the underground aquifer. This feature can demonstrate that EVT would be a great alternative to the cesspool pit, a system traditionally used in rural areas in Brazil (Tonetti et al., 2018).

AKNOWLEDGEMENTS

We thank CAPES and CNPq (311275/2015-0) for the master and doctoral scholarships received and Fapesp (Process 2017/07490-4) for the research grant.

REFERENCES

Galbiati, A, F, (2009) Tratamento domiciliar de águas negras através de tanque de evapotranspiração, Master Dissertation, Universidade Federal de Mato Grosso do Sul, Campo Grande,

Tonetti, A. L., Brasil, A.L., Madrid, F.J.P.L., Figueiredo, I.C.S., Schneider, J., Cruz, L.M.O., Duarte, N.C., Fernandes, P.M., Coasaca, R.L., Garcia, R.S., Magalhães, T.M (2018) In: Tratamento de esgotos domésticos em comunidades isoladas: referencial para a escolha de soluções, Biblioteca/Unicamp, ISBN 978-85-85783-94-5.

Von Sperling, M. (2014) In: Introdução à qualidade das águas e ao tratamento de esgoto, Editora UFMG, ISBN: 9788542300536.

Prospecting Microbial Consortia for high yield Polyhydroxyalkanoates production

Marta Catalão*,**, Cristiana A.V. Torres*,** Mara A M Reis*,**, Filomena Freitas*,**

* Associate laboratory i4HB – Institute for Health and Bioeconomy, School of Science and Technology, NOVA University Lisbon, Caparica, Portugal
** UCIBIO – Applied Molecular Biosciences Unit, Department of Chemistry, School of Science and Technology, NOVA University Lisbon, Caparica, Portugal
(E-mail:m.catalao@campus.fct.unl.pt/ amr@fct.unl.pt)

Abstract

Microorganisms live in Nature in complex communities, the microbiomes. This allows them to cooperate with each other by intra and interspecies interactions, performing tasks not possible for a single organism to do on its own and conferring them robustness and metabolic diversity. Thanks to that, mixed microbial consortia derived from different ecosystems are powerful tools for harnessing Nature's potential for producing metabolites with commercial interest, like biopolymers. Whitin biopolymers, are the polyhydroxyalkanoate (PHAs) that are biodegradable and biocompatible biopolyesters, whose physical-chemical properties makes them sustainable alternatives to petroleum-based plastics. This work aims to study the evolution of a natural microbiomes collected from distinct habitats towards polyhydroxyalkanoates (PHAs) enriched consortia. Therefore, sediments from different habitats (forest soil, sediments from marine environments (sand and mud) and, plant roots) were collected and subjected to feast and famine alternate cycles for the selection of PHA-storing microorganisms. The different microbiomes evolved into consortia containing PHA-storing bacteria. The microbiomes from forest soils and river marshland yielded the higher PHA content. The different abilities to accumulate PHA presented by the different microbiomes are a result of the initial microbial population of each community, since the same metabolic pressure was imposed to the all the original microbiomes. This work is being performed within the European project PROMICON – Harnessing the power of nature (GA 101000733).

Keywords (maximum 6 in alphabetical order):
Biopolymers, microbiome, natural habitats, polyhydroxyalkanoates

MATERIALS AND METHODS

Samples collection and processing

Seven sites from two main areas (Setúbal and Aveiro) were chosen to collect the environmental samples (Figure 1). These areas are exposed to different environmental and climate conditions.
Plant, forest soil and aquatic sediments were collected. The soil (~500 g) and root (~250 g) samples were collected into clean bags, while the sediments (~1 L) were collected into clean flasks. All the samples were stored at 4 ºC and processed within 24 h after collection. The different sites were chosen to provide natural microbiomes samples of higher microbial diversity given the different geographical origin and diverse ecosystems' characteristics. The seven collected samples were characterized for their physical-chemical characteristics, including pH, conductivity, total suspended solids (TSS), volatile suspended solids (VSS), and nutrients. Prior to the analyses, samples were pre-treated to remove large fragments (solid microbiomes), root samples were milled. All samples were mixed with milli-Q water to obtain suspensions of similar solids content (30 wt.%).

Selection assays

Aiming to select for PHA-producing bacteria, a strategy of alternate feast-and-famine periods was imposed to each of the environmental microbiomes' samples. During the feast phase, the culture was fed with a suitable carbon source to promote cell growth, while during the subsequent famine phase the bacteria able to synthesize PHA will thrive, using the accumulated biopolymer as a source of carbon and energy. By imposing consecutive feast-and-famine cycles, a culture enriched in PHA-accumulating organisms is selected from the initial microbiome (Albuquerque et al. 2010).
The experiments were performed in 500 mL baffled shake flasks with a working volume of 200 mL. The pH value was adjusted to 7.0 before autoclaving. To each collected microbiome sample (160 mL), 40 mL of cultivation medium were added to give an initial acetate concentration of 20 g/L. Samples (40 mL) were periodically collected from each flask over the experiments, and replaced by the same volume of fresh medium, thus creating periods of alternate feast and famine conditions. At each sampling time, the pH was measured and adjusted to 7.0 ± 0.2 by the addition of 5 M NaOH or 5 M HCl. The culture broth samples were used for determination of the total suspended solids (TSS) and the volatile suspended solids (VSS), according to the Standard Methods (APHA, 1995). The supernatant obtained by centrifuging the broth samples (8000×g, 15 min, 4 ºC) was used for the quantification of acetate (by HPLC). The resulting pellet was washed twice with deionized water, lyophilized and used for PHA quantification by gas chromatography (GC).

Optimizing Culture Conditions

From the microbiome screening tests, the marshland sediments consortium was selected. To enrich the microbiome in PHA producer's microorganisms, the strategy of feast and famine was used, and shake flask studies at different pH, temperature and initial acetate concentration were performed to optimize the cultivation conditions. For these experiments fresh sediments of the selected microbiome were collected, in order to evaluate the impact of different cultivation parameter on sample from nature effectively. Assays were done at 2 different pH values, namely 7, and 8 and at 20 ºC and 30ºC, with an initial acetate concentration of 20 g/L for each cycle.

Samples' microbiological characterization

The general microbial composition of the Marshland microbiome (fresh samlple) and after cultivation at certain condition was assessed by Fluorescence in Situ Hybridization (FISH). Aiming to characterize the bacteria present in each condition, several oligonucleotide probes were applied Fluorescein isothiocyanate (FITC)-labelled EUBmix probe for all Bacteria (mixture of EUB338, EUB338-II and EUB338-III and Cyanine 3 (Cy3)-labelled ALF969 for *Alphaproteobacteria*, BET42a for *Betaproteobacteria* and GAM42a for *Gammaproteobacteria*, Delta495a for *Deltaproteobacteria,* BAC303 for *Bacteroidaceae* and *Prevotellaceae* families; LGC0354 and LGC355 for *Firmicutes*. The oligonucleotide probes are specifically detailed in probeBase. The slides were observed using an epifluorescence microscope, and the images were analyzed by Zeiss Imager D2 at 1000x.

RESULTS AND DISCUSSION

Seven environmental samples originating from two different geographical areas, and encompassing distinct habitats, namely, marshland, forest soil, river sediments and plant roots, were collected and characterized. Each environmental sample was subjected to a selective pressure, aiming to select for PHA-accumulating microorganisms. The microbiomes, both the environmental collected samples and those obtained during the selection assays, were characterized for their potential for the production of PHA (Table 1).
For all the microbiomes tested the microbial content increased, however the population diversity decreased (data not shown), as a result of the selective pressure imposed. Further all the microbiome showed the ability to accumulate PHA (Table 1). However, during the duration of the assays the marshland microbiome was the one that achieved faster the feast and famine conditions, achieving also higher PHA contents, which demonstrated a higher capacity to adapt to the conditions imposed to the system.

Table 1. Results obtained in the shake flask microbiome selection assays: VSS (g/L), PHA_{max} (mg_{PHA}/g_{VSS}).

Microbiome	Max VSS (g/L)	mg PHA/g VSS
River Sediments	9.54 ± 0.35	17.83 ± 0.48
Marshland Sediments	17.31 ± 6.69	46.70 ± 3.78
Dunes plant roots	17.45 ± 3.28	7.69 ± 2.44
Forest soil (Caparica)	25.89 ± 0.28	18.56 ± 1.43
Forest soil (Bussaco)	26.39 ± 4.65	9.14 ± 0.66
Fenal roots	21.55 ± 3.43	11.14 ± 0.77
Lima bean roots	14.14 ± 0.31	14.55 ± 0.51

Therefore, marshland sediments microbiome was chosen to study the effect of different environmental condition (pH and temperature) on the population evolution and PHA accumulation capacity. Assays were done at 2 different pH values, namely 7, and 8, at 20 ºC and 30ºC, with an initial acetate concentration of 20 g/L for each cycle.

After microbiome characterization, the 30 days' experiments started. At pH 7 and 20 ºC (Figure 1) the acetate uptake was almost complete on the first cycle (between day 1-5) and on the 6th cycle (day 15-17). On the rest of the cycles the acetate uptake was never complete, this may indicate that the time of feast and famine cycles needs to be higher or the changes that were observed on the initial microbiome influence its performance. The overall acetate uptake was 177.55 g/L. Regarding, nitrogen consumption it varied between 0.30±0.01 g/L and 0.71±0.05 g/L with the exception of the fifth cycle (between day 13 and 15) where no nitrogen uptake was observed.

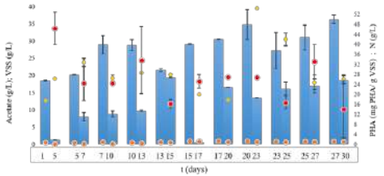

Figure 1 Microbiome cultivation at pH 7 and 20ºC for 30 days. Blue columns: acetate; Red dots: PHA (mg PHA/mg VSS); Orange dots: N (g/L); Yellow dots: VSS (g/L).

Across the 30 days the ratio between VSS/TSS increase across the assay (from 8.58 wt.% and 82.61wt.%), meaning that the inorganic content of microbiome is being substituted by organic content (biomass). PHA was always present in the samples, indicating that there was no famine phase that lead to PHA consumption and therefore enrichment of biomass on PHA producers.
The microbiome was also cultivated at pH 8 and 20 ºC. The acetate uptake was complete between day 1 and 5(first cycle). Thereafter, the consumption varied across the cycles however there was a continuous availability of acetate across the experiment that led to no need of PHA accumulation by the selected bacteria. For the assays at 30ºC pH 7 and pH 8 the behaviour for acetate uptake is similar to the prior assays with the acetate not being consumed for all the cycles and therefore impacting the ability of microbiome to accumulate PHA.
From the condition tested seemed that the time cycle (2 or 3 days) were not enough to exhaust the media in acetate and therefore select the bacteria with PHA producing ability. However, taking in consideration the performance of microbiome at the different conditions tested, the 20ºC seems better than the 30ºC, since the increase in VSS was higher. Further, at 20ºC and pH 8 there was PHA consumption at the end of the experiments while that behaviour was not observed at pH 7. Thus, it was decided to perform the next cultivations at 20 ºC and pH 8.

FISH of fresh microbiome and selected populations

FISH results of initial marshland sediments microbiome shown the presence of major bacterial groups of *Alphaproteobacteria, Bacteroidaceae, Betaproteobacteria, Gammaproteobacteria, Deltaproteobacteria and Firmicutes* identified by the positive fluorescent signal of the oligonucleotide probes. No dominant bacteria group was observed in microbiome, but some abundant populations were identified, which is the case, for instance, of the *Alphaproteobacteria, Deltaproteobacteria and Firmicutes* population, targeted by the Cy3 and FITC labelled (Figure 2).

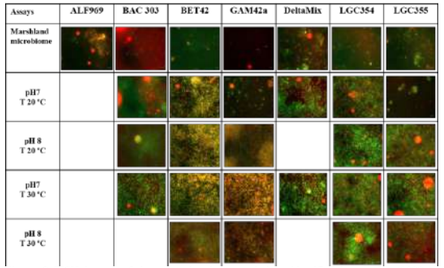

Figure 2 FISH images of the most abundant populations identified in samples (1000x): fresh marshland microbiome; population selected after 30 days at pH 7/ pH8 and 20 ºC; population selected after 30 days at pH 7/ pH 8 and 30 ºC. The images show bacteria hybridized with Cy3-labelled ALFA969, BAC303, BET42, CF319a; DELTA495; GAM42a; HGC69a and LGC0355.

After the 30 days of selection it is observed that population of the assay at pH 7 and 20ºC is enriched in *Betaproteobacteria*, identified by the abundant positive signal of the BET42a probe, *Deltaproteobacteria* (DeltaMix) *and Firmicutes* (LGC354 andLGC35). At the same pH but 30 ºC the population is enriched in the same bacteria but also *Bacteroidaceae* (BAC 303) and *Gammaproteobacteria* (GAM42a). At pH 8 and different temperatures the *Deltaproteobacteria* disappeared and at 30 ºC the *Bacteroidaceae* also disappeared. At pH 8 and 20 ºC the culture is enriched in *Betaproteobacteria*, identified by the abundant positive signal of the BET42a and *Firmicutes* (abundant positive signal LGC354) (Figure 2).
Results of FISH showed that the different conditions of temperature and pH enriched the bacterial population in different families.

REFERENCES

Albuquerque M.G., Martino V., Pollet E., Avérous L., Reis M.A.M. 2011. Mixed culture polyhydroxyalkanoate (PHA) production from volatile fatty acid (VFA)-rich streams: effect of substrate composition and feeding regime on PHA productivity, composition and properties. J Biotechnol. 151(1):66-76.

APHA, 1995. Standard Methods for the Examination of Water and Wastewater, American Public Health Association, Washington DC.

Transformation products generated by oxidation of carbamazepine during various wastewater treatment processes – review and modelling

J. Trognon*, C. Albasi* and J.M. Choubert**

* Laboratoire de Génie Chimique, Université de Toulouse, CNRS, INPT, UPS, Toulouse, France
(E-mail: *jeanne.trognon@toulouse-inp.fr; claire.albasi@toulouse-inp.fr;**
** INRAE UR REVERSAAL, Villeurbanne, France
(E-mail: *jean-marc.choubert@inrae,fr*)

Abstract
Carbamazepine is removed by most oxidative processes, however, they generate various transformation products, which might be even more hazardous for aquatic environment than carbamazepine itself. The prediction of such molecule formation by computer-based modelling thus appears as a relevant solution for risk evaluation and processes design assessment. In this context, this work aims to improve the knowledge on the nature, fate and dynamics of carbamazepine and its transformation products by an extensive literature analysis and computer modelling. Preliminary literature review and model calibration show promising results concerning transformation products prediction.

Keywords (maximum 6 in alphabetical order)
Carbamazepine, Modelling, Oxidation, Processes, Transformation products, Wastewater

INTRODUCTION

Carbamazepine (CBZ) is an anticonvulsant drug, derived from dibenzazepine, mainly used for the treatment of epilepsy, bipolar disorder and trigeminal neuralgia (Hai *et al*., 2018). This drug is released in domestic and hospital wastewater and then reaches wastewater treatment plants (WWTP). CBZ is one of the most detected drugs in surface water (Luo *et al*., 2014), even in areas with low anthropogenic pressure (Wilkinson *et al*., 2022). Indeed, CBZ global consumption is estimated at 1000 tons per year (Zhang *et al*., 2008) and is poorly removed (< 25%) by conventional secondary processes (Joss *et al*., 2006). Moreover, CBZ is also known for its toxicity on aquatic organisms such as green algae, daphnia or fishes (ECOSAR, 2022).

In order to achieve CBZ removal, polishing treatment processes, such as ozone or advanced oxidation processes (AOP) and water disinfection processes (drinking water), have been studied for several years (Mathon *et al*., 2017; Bourgin *et al*., 2017). However, many unknowns remain about the fate of this molecule. Indeed, the diversity of degradation mechanisms involved in these processes implies a multitude of reaction pathways leading to many transformation products (TPs). TPs display different physicochemical properties and their structures are still poorly identified (Bonnot *et al*., 2022). Therefore, the behavior of TPs is not fully understood and the anticipation of their removal seems even more complex than MPs. Recently, computer-based modelling emerges as a promising tool to predict the fate of MPs and their TPs. Indeed, considering the technological advances made in MPs monitoring and quantification, model predictions can be used for both risk evaluation and processes design improvement (Delli Compagni *et al*., 2020; Plósz *et al*., 2013)).

This work aims to improve the knowledge on the nature, fate and dynamics of CBZ and its TPs. In this context, the objectives of this study are: 1) to identify and model the transformation pathways of CBZ in various oxidation processes and 2) to suggest classification criteria for these processes.

MATERIALS AND METHODS

The project is based on an extensive literature review of more than 80 scientific papers published between 2000 and 2022. The abatement of CBZ in various processes as well as the measured TPs resulting from its degradation have been determined. The data collected were processed using RStudio interface [v2022.07.2] and Gephi software [v0.9.5]. CBZ and TPs modelling was performed using a Python encoded program through the Spyder interface [v5.1.5]. This program uses the Symfit library for the resolution of ordinary differential equations (ODE) based on formation and degradation kinetic equations. Indeed, equations were written from mass balance performed thanks to CBZ degradation reactions.

RESULTS AND DISCUSSION

Literature review

More than 100 different TPs have been identified after the degradation of CBZ (Figure 1). They have very different chemical properties (molecular weight, pKa, LogD) leading to resistance mechanisms towards degradation specific to each molecule. Thus, a review of the degradation pathways for each identified TPs has been performed as shown in Figure 1. We have shown a very complex network of possible reactions. Some degradation reactions of CBZ were common to all studied processes, and therefore, resulting primary TPs appear to be very important. Furthermore, results highlight the relevance to study intermediary TPs such as acridine and acridone, which appears to be responsible for a high number of final products. Indeed, the great diversity of these TPs as well as the multiplicity of the reactions involved make it difficult to follow them in the water cycle and molecules of interest need to be targeted. Moreover, most of the TPs from CBZ show a significant toxicity on aquatic organisms (United Nations GHS report, 2011) pointing out the importance of improving our knowledge on the fate of this micropollutant, its degradation or its accumulation potential.

Modelling

From the transformation pathways of CBZ found in literature, we have set-up a numerical model (Figure 2). Calibration was performed using different data sets (i.e quantified concentration versus time in batch test conditions) published in literature. Various CBZ degradation processes were studied such as TiO_2 photocatalysis (Franz *et al.,* 2020; Jelic *et al*., 2013), UV-Cl (Pan *et al.,* 2017; Suara & Bezares-Cruz., 2022), UV-H_2O_2 (Lu & Hu, 2019) or UV-NH_2Cl (Wang *et al*., 2022). Overall, we obtained a good fit of the CBZ degradation model with experimental data ($R^2 > 85\%$). Concerning TPs modelling, quality of the model is highly variable ($14 < R^2 < 98\%$), most likely because of the diversity of reaction mechanisms involved in TPs formation and the differences in experimental conditions between studies. However, due to the very low concentration (ng.L^{-1}) of some TPs, the R^2 might not be the most adapted quality descriptor. The assessment method of our model might therefore be improved by calculation of other criteria. For model validation, there is a lack of experimental data on TPs quantification. Indeed, there is a need for further TPs studies in various water treatment processes, which is still a challenge due to poor reference standards availability.

CONLUSIONS AND PERSPECTIVES

Our knowledge of the fate and dynamics of CBZ in wastewater is still incomplete, particularly concerning its various transformation products. This is why comprehensive studies through modelling are needed, but the lack of TPs quantification remains an important challenge.

Therefore, the perspectives of this work consist of carrying a series of batch tests for biological and oxidative processes for micropollutant degradation. The chemical analysis is under process. The results might be presented during the conference.

ACKNOWLEDGMENT

The authors thank the French National Research Agency (ANR) for funding this project "TRANSPRO".

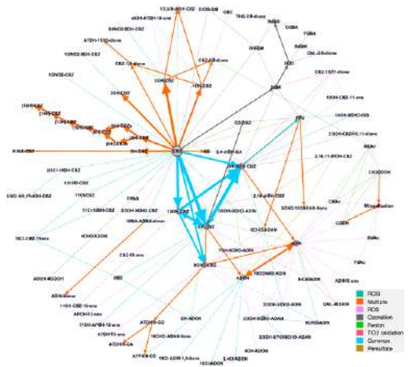

Figure 1. Maps of CBZ degradation pathways leading to TPs formation, classified by tertiary processes. Chemical reactions are symbolized by directed arrows, which are colored by processes.

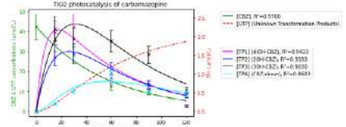

Figure 2. Modelling of CBZ degradation by TiO2 photocatalysis (data used for the model were extracted from Jelic *et al.,* 2013)

REFERENCES

Hai F. I., Yang S., Asif M. B., Sencadas V., Shawkat S., Sanderson-Smith M., Gorman J., Xu Z. and Yamamoto K. Carbamazepine as a Possible Anthropogenic Marker in Water: Occurrences, Toxicological Effects, Regulations and Removal by Wastewater Treatment Technologies. *Water*, **2018**(10).

Luo Y., Guo W., Ngo H. H., Nghiem L. D., Hai F. I., Zhang J., Liang S. and Wang X. C. A review on the occurrence of micropollutants in the aquatic environment and their fate and removal during wastewater treatment. *Science of the Total Environment*, **2014**, 619–641.

Wilkinson J. L., Boxall A. B. A., Kolpin D. W., Leung K. M. Y. *et al.* Pharmaceutical pollution of the world's rivers. *PNAS,* **2022**(119).

Zhang Y., Geißen S. and Gal C. Carbamazepine and diclofenac: Removal in wastewater treatment plants and occurrence in water bodies. *Chemosphere*, **2008**(73), 1151–1161.

Joss A., Zabczynski S., Göbel A., Hoffmann B., Löffler D., McArdell C. S., Ternes T. A., Thomsen A. and Siegrist H. Biological degradation of pharmaceuticals in municipal wastewater treatment: Proposing a classification scheme. *Water research*, **2006**(40), 1686– 1696.

United State Environmental Protection Agency, ECOSAR Predictive Model, https://www.epa.gov/tsca-screening-tools/ecological-structure-activity-relationships-ecosar-predictive-model, Last updated on August 8, 2022.

Mathon B., Coquery M., Miege C., Penru Y. and Jean-Marc Choubert J. M. Removal efficiencies and kinetic rate constants of xenobiotics by ozonation in tertiary treatment. Water Science and Technology, **2017**(75.12), 2727-2746.

Bourgin M., Borowska E., Helbing J., Hollender J., Kaiser H., Kienle C., McArdell C. S., Simon E. and von Gunten U. Effect of operational and water quality parameters on conventional ozonation and the advanced oxidation process O3/H2O2: Kinetics of micropollutant abatement, transformation product and bromate formation in a surface water. *Water Research,* **2017**(122), 234-245.

Bonnot K., Benoit P., Mamy L., and Patureau D. Transformation of PPCPs in the environment: Review of knowledge and classification of pathways according to parent molecule structures. *Critical Reviews in Environmental Science and Technology*, **2022.**

Delli Compagni R., Gabrielli M., Polesel F., Turolla A., Trapp S., Vezzaro L., and Antonelli M. Advances in Chemical Pollution, Environmental Management and Protection, Chapter six: Modeling tools for risk management in reclaimed wastewater reuse systems: Focus on contaminants of emerging concern (CECs), **2020**, ISSN: 2468-9289.

United Nations, Globally Harmonized System of classification and labelling of chemicals (GHS), Fourth revised edition, **2011**, ISBN: 978- 92-1-117042-9

Franz S., Falletta E., Arab H., Murgolo S., Bestetti M. and Mascolo G. Degradation of Carbamazepine by Photo(electro)catalysis on Nanostructured TiO2 Meshes: Transformation Products and Reaction Pathways. *Catalysts*, **2020**(10).

Jelic A., Michael I., Achilleos A., Hapeshi E., Lambropoulou D., Perez S., Petrovic M., Fatta-Kassinos D. and Barcelo D. Transformation products and reaction pathways of carbamazepine during photocatalytic and sonophotocatalytic treatment. *Journal of Hazardous Materials*, **2013**, 177–186

Pan Y., Cheng S., Yang X., Ren J., Fang J., Shang C., Song W., Lian L., Zhang X. UV/chlorine treatment of carbamazepine: Transformation products and their formation kinetics. *Water Research*, **2017**(116), 254-265.

Suara M. A. and Bezares-Cruz J. C. Synergistic effect of nitrate on UV-chlorine photochemical degradation of carbamazepine. *Environmental Science and Pollution Research*, **2022.**

Lu G. and Hu J. Effect of alpha-hydroxy acids on transformation products formation and degradation mechanisms of carbamazepine by UV/H2O2 process. *Science of the Total Environment,* **2019**(689), 70–78.

Wang X., Ao X., Zhang T., Li Z., Cai R., Chen Z., Wang Y., Sun W. Ultraviolet-Light-emitting-diode activated monochloramine for the degradation of carbamazepine: Kinetics, mechanisms, by-product formation, and toxicity. *Science of the Total Environment,* **2022**(806).

The impact of high and low temperatures on *Candidatus* Competibacter fed with industrial wastewater

E. Tsertou*, K. Goossens*, K. Seguel Suazo* and J. Dries*

* Research group BioWaVE, Biochemical Wastewater Valorization & Engineering, Faculty of Applied Engineering, University of Antwerp, Groenenborgerlaan 171, 2020 Antwerp, Belgium
(E-mail: Eirini.Tsertou@uantwerpen.be; Koen.Goossens@uantwerpen.be; karina.seguelsuazo@uantwerpen.be; ian.dries2@uantwerpen.be)

Abstract
The goal of this study was the investigation of the impact of high and low temperatures on biomass anaerobic metabolism, when the biomass is exposed to them both in long-term and short-term. Furthermore, the settleability and the structure of the sludge as well as the carbon removal efficiency is evaluated. All in all, the high temperatures (above 38°C) had irreversible negative impact on *Ca.*Competibacter. The low temperatures (11°C) was the reason that *Ca.*Competibacter decreased in number and the uptake capacity deteriorated but not at an alarming level.

Keywords
Aerobic granular sludge; feast/famine feeding strategy; sequencing batch reactor; slow growing microorganisms; substrate consumption rate, tank truck cleaning

INTRODUCTION /

Aerobic granular sludge is considered a novel biological treatment technology because it improves the settleability of the biomass without carrier materials (de Kreuk, 2005). De Kreuk et al. (2004) showed that the selection of slow growing microorganisms such as the phosphate accumulating organisms (PAO) and glycogen accumulating microorganisms (GAO) improves the stability of the aerobic granular sludge. GAO will proliferate under certain circumstances. Both the wastewater composition and the feeding strategy play crucial role on GAO selection. Feast (anaerobic)/ famine (aerobic) regime as feeding strategy and wastewater poor in nutrients have been proved perfect conditions for GAO enrichment both in lab and full scale (Caluwé, 2022) (Tsertou, 2022) (Tsertou, 2023 submitted). Temperature is another factor that has strong impact on the growth rate of the microorganisms. Low temperatures slow down the growth rate and high temperatures accelerate it. However, it is believed that there is an upper limit-temperature above which the rate is decreasing, probably because of the destruction of enzymes at higher temperatures (Lopez-Vazquez, 2009). The temperature effect on GAOs has been studied before but with synthetic wastewater. This research focus on the impact of temperatures on enriched *Candidatus* Competibacter biomass which is fed with industrial wastewater, which is derived from the cleaning of trucks transporting chocolate and beer.

MATERIALS AND METHODS

The investigation of temperature impact was done with two different set ups. First experiment was about the investigation of high temperatures (range from 25 to 40°C) and the second one about the low temperatures (range from 25 to 10°C). Each set up was consisted of two Sequencing Batch Reactors (SBR); the reference and the experimental. The temperature was held at 25°C for the reference reactor and was changed for the experimental reactor (Figure 1).The anaerobic feast/aerobic famine regime was applied in both experiments. The 24 h SBR cycle consisted of a prolonged anaerobic feeding (4h slow feeding) followed by 0.5h mixing, aeration (approx.18h), settling (1h) and discharge.
MLSS, MLVSS and SVI were performed in accordance with Standard Methods (APHA, 1998). Sludge morphology was observed using an Olympus B310 light microscope with phase contrast illumination (Ph1) and a total magnification of 2 times.

16S RNA gene amplicon sequencing is the molecular technique that was used for identification of the microbial community. A detailed description can be found in the study by Tsertou et al. (2022). The long term anaerobic uptake (in-situ measurement) was determined during an ordinary SBR cycle as described by Tsertou et al. (2022). The short term anaerobic uptake (ex-situ measurement) was determined by collecting endogenous sludge in the end of the experimental and reference SBR cycle as described by Tsertou et al. (2023). For the ex-situ measurements only two extreme temperatures were selected (10°C and 40°C). The test started only when the endogenous sludges reached the temperature setting and after increasing the pH of the wastewater up to 7 with NaOH.

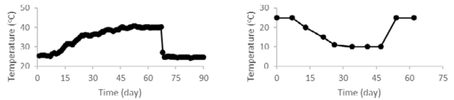

a. b.

Figure 1. Temperature profile for the experimental reactor. Experimental design of high (a) and low (b) temperatures.

RESULTS AND DISCUSSION

Part A. Impact of High Temperatures on settleability, morphology, bacteria abundancies, anaerobic metabolism, carbon removal efficiency.
% COD removal was 97.4 ±1.5 for the EXP and 98.2±0.3 for the REF reactor. Despite the high efficiency of both reactors in COD removal, only the REF reactor complied always with the Flemish discharge limits (COD <125 mg.L^{-1}). Regarding the settling performance, SVI 30 remained always below 70 mL.g^{-1} for the REF reactor. On the other hand, the SVI 30 deteriorated after DAY 41 (approx. 38°C) in the EXP reactor. SVI 30 peaked at 94 mg.L^{-1}. The evolution of the structure of the sludge is similar in both reactors (Figure 3). The size of the granules increased in function of time. During the long term operation of the reactors, the anaerobic metabolism of *Ca.* Competibacter was very sensitive to temperatures changes above 37°C. Consequently, % anaerobic uptake and % abundance of *Ca*. Competibacter dropped to zero (Figure 2). On the contrary, the REF reactor had av. 89.4 ± 6.4 % anaerobic uptake and 18.1 ± 5.6 % abundance of *Ca.* Competibacter. The abundance of *Ca.* Competibacter in the EXP reactor was not restored even when the temperature was set back at 25°C. The results from ex-situ anaerobic test showed that the REF reactor had higher uptake capacity than the EXP reactor either at 25°C or 40°C. Furthermore, both reactors had slightly higher uptake rate at 40°C (Figure 4).

Part B. Impact of Low Temperatures on settleability, morphology, bacteria abundancies, anaerobic metabolism, carbon removal efficiency.
% COD removal was 96 ± 1.7 for the EXP and 98± 0.6 for the REF reactor. REF reactor complied most of the time with the discharge limits (102.4±33.5 mg.L^{-1} av.COD) but EXP reactor did not (179.8±90.5 mg.L^{-1} av.COD). SVI 30 was below 35 mg.L^{-1} for both reactors. The microscopic examination showed similar structures for the two reactors (Figure 6). The long term operation under low temperatures affected negatively the % anaerobic uptake (Figure 5.a) and the % abundancies (Figure 5.b). The average uptake was 82.7±15.6% and 94.7±1.8% for the EXP and REF reactor respectively. The average read abundance of *Ca.*Competibacter was 18.7±6.6% and 20.8±2.9% for the EXP and REF reactor respectively. The high deviations in the EXP reactor is because of measured values during the operational period at low T. The short term experiments showed clearly that the low Temperature decreased the uptake rate in both reactors (Figure 7).

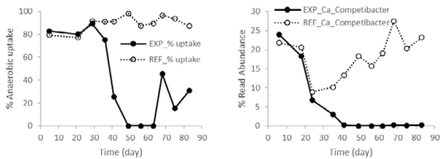

a. b.

Figure 2. a. In situ measurement of % DOC uptake during the anaerobic phase. b. % Relative read abundancy of *Candidatus* Competibacter.

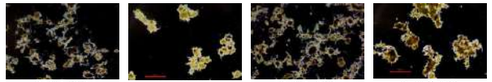

Figure 3. Microscopic examination of the biomass structure. Bar indicates 500µm.

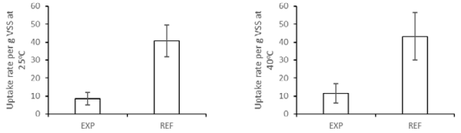

a. b.

Figure 4. Substrate Anaerobic uptake rate (mg DOC.g^{-1}VSS.h^{-1}) at 25°C (a) and 40°C (b).

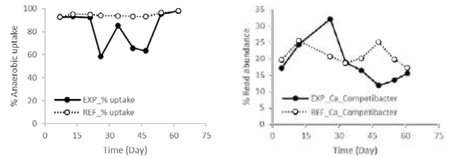

a. b.

Figure 5. a. In situ measurement of % DOC uptake during the anaerobic phase. b. % Relative read abundancy of *Candidatus* Competibacter.

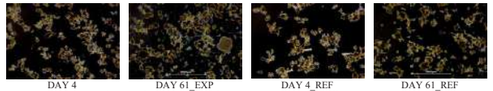

Figure 6. Microscopic examination of the biomass structure. Bar indicates 1000 µm.

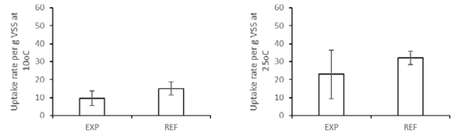

a. b.

Figure 7. Substrate Anaerobic uptake rate (mg DOC.g^{-1}VSS.h^{-1}) at 10°C (a) and 25°C (b).

To sum up, the results indicate a strong sensitivity of Ca.Competibacter at high T (above 37°C). The decrease of temperature had also a negative impact. However, Ca.Competibacter was not hindered completely as it happened with the high temperatures' experiment. In addition, it seems that the recovery from the exposure to low temperatures is fast enough.

REFERENCES

APHA/AWWA/WEF 1998 Standard Methods for the Examination of Water and Wastewater, 20th edn. APHA/AWWA/WEF, Washington, DC, USA.
Caluwé M., Goossens K., Seguel Suazo K., Tsertou E., Dries J., 2022, Granulation strategies applied to industrial wastewater treatment: from lab to full-scale, Water Science and Technology, **85** (9), 2761–2771
de Kreuk M.K., McSwain B.S., Bathe S., Tay S.T.L., Schwarzenbeck and Wilderer P.A. 2005 "Discussion outcomes". Ede. In: *Aerobic Granular Sludge*. Water and Environmental Management Series. IWA Publishing. Munich, 165–169.
de Kreuk M.K. and van Loosdrecht M.C.M., 2004, Selection of slow growing organisms as a means for improving aerobic granular sludge stability, Water Science and Technology, **49**, 9–17
Lopez-Vazquez C.M., Hooijmans C.M., Brdjanovic D., Gijzen H.J., van Loosdrecht M.C.M., 2009, Temperature effects on glycogen accumulating organisms, Water Research, **43**, 2852-2864
Tsertou E., Caluwé M., Goossens K., Dobbeleers T., Dockx L., Poelmans S., Seguel Suazo K., Dries J., 2022, Is building up substrate during anaerobic feeding necessary for granulation? Water Science and Technology, **86** (4), 763–776
Tsertou E., Caluwé M., Goossens K., Seguel Suazo K., Dries J., 2023, Performance of aerobic granular sludge membrane filtration at a full scale industrial plant, Water Science and Technology, (submitted)

Phosphorus extraction from sewage sludge ashes and subsequent co-precipitation with other nutrients: insight into factors favouring a beneficial recovery

G. Boniardi*, T. Seljak**, R. Canziani*, A. Turolla*

* Department of Civil and Environmental Engineering, Politecnico di Milano, Piazza Leonardo da Vinci, 32, Milano, IT (E-mail: gaia.boniardi@polimi.it; roberto.canziani@polimi.it; andrea.turolla@polimi.it)
** Faculty of Mechanical Engineering, University of Ljubljana, Askerceva 6, Ljubljana, SI (E-mail: tine.seljak@fs.uni-lj.si)

Abstract
The present works, representing the first outcome of the ERA-MIN 3 "PHOSTER" project, investigates the most relevant factors affecting nutrient recovery from ashes in the view of providing preliminary guidelines for process development. In detail, the work is focused on the assessment of two process steps, poorly investigated so far, namely incineration and co-precipitation of phosphorus with other nutrients (i.e., K and Mg). Experimental results demonstrated that incineration phase is fundamental, with the addition of calcium-based additives in the combustion chamber strongly affecting the pH of ashes and hindering the subsequent phosphorus extraction. Furthermore, precipitation tests indicated best conditions for phosphorus precipitation, with 100% recovery at pH 9.5 with a molar ratio of K:Mg:P=1:2:2. Cattiite was the main crystalline compound in the solid product, while K was mostly present in amorphous form.

Keywords
Co-precipitation; critical raw materials; incineration; nutrients; sewage sludge ashes; wet chemical extraction

INTRODUCTION

Phosphorus (P) is considered a primary resource for life on earth. It is an irreplaceable element in agricultural activities, especially in the production of fertilizers, because it is essential for crops growth (Meng et al., 2019). Phosphate rocks are the most important source of P, being non-renewable resources concentrated in limited countries (e.g., Morocco, Western Sahara, China). Because of excessive exploitation of natural reserves and excessive use of P in agriculture, the world is heading towards P scarcity. Thus, the recovery of P from alternative sources such as sewage sludge and derived ashes is emerging as a key element for the development of circular and sustainable systems. Even if lot of research has been conducted during the past years to recover P via wet chemical extraction (Liang et al., 2019; Fang et al., 2020; Baldi et al., 2021; Liu et al., 2021), high operational costs and quality of the recovered material are the main issues to tackle. This works, which is part of the ERA-MIN 3 "PHOSTER" project, primarily investigates the impact of incineration process on ashes composition and thus on P extraction, providing guidelines for optimizing the extraction process. In addition, the influence of operating conditions on the co-precipitation of P in multi-nutrient high-value products is assessed for enhancing the overall quality of recovered material.

MATERIALS AND METHODS

Sewage sludge ashes (SSA) samples (S1-S7) were collected from bag filters of a pilot-scale fluidized bed (FB) incinerator at the wastewater treatment plant (WWTP) of Milano San Rocco (IT). To assess the influence of incineration process conditions on SSA composition, 3 different feed type were tested: (1) dewatered sewage sludge (DSS), (2) DSS with a Ca-based additive, and (3) a mixture of DSS and dried sewage sludge. A reference sample S0 was taken from electro-filters of a full-scale incineration plant (Werdhölzli, CH). Characterization was conducted for total solid (TS) content, volatile solid (VS) content and pH as in Bontempi et al. (2010). Grain size distribution was determined as in ASTM 2020 and ISO 3310–1:2016. Al, Ca, Fe, K, Mg and As, Cd, Cr, Cu, Ni, Pb, Zn were measured with ICP-MS after aqua regia digestion (UNI EN ISO 17294-1:2007), while P was determined after mineralization (EN 15959:2011) with UV-Vis method (Hach LCK 348). After preliminary experiments, P extraction for S1-S7 was performed with the following operating conditions: 1 M H_2SO_4, liquid-to-solid ratio of 20:1, 2-h contact time, room temperature. For S0, instead, 0.2 M H_2SO_4 was used. Extraction procedure details are in Boniardi et al. (2021).

Precipitation tests were conducted with synthetic P solution (H_3PO_4 or KH_2PO_4), leachate with high PEE from S1-S7 and leachate from S0. K (from leaching of carbonized biomass) was added to P leachate, while Mg was added as $MgCl_2$. Nutrients were added to have molar ratio K:Mg:P=1:1:1 and 1:2:2. pH was then increased till 3.5, 5, 8, 9, 9.5, 10 and 11 with 0.1 M NaOH. P precipitation efficiency (PPE) and K precipitation efficiency (KPE) were determined, XRD was used to detect crystalline structures.

RESULTS AND DISCUSSION

pH of S1-S7 varied between 12.6 and 12.8, pH of S0 was 7.1. This can be explained by the different incineration process conditions and treatment layouts. At San Rocco WWTP, $CaCO_3$ was dosed in the incineration chamber so that S1-S7 have a higher Ca content (16.4-23.5%) compared to S0 and literature (Krüger et al., 2014). The higher buffer capacity may hinder the subsequent acid extraction suggesting that SSA collection point and type of flue gas treatment are of paramount importance. S1-S7 showed lower P content (5.6-6.6%) compared to S0 (8.6%) but a similar K and Mg content (**Table 1**). Instead, Al and Fe were higher in S0 (5.2-17.5%) due to chemical P removal. To optimize the P recovery, guidelines are provided on (i) WWTP layout and treatment capacity, (ii) type of incinerator and process conditions (e.g., temperature, contact time, additives), (iii) flue gas treatment layout, (iv) SSA collection point, (v) pH of SSA and grain size. In summary, most suitable SSA for P recovery were obtained in case of enhanced biological P removal, FB technology without direct Ca-based addition, multi-step flue gas treatment to reduce the metal content in P-rich SSA, SSA collection point located along the flue gas treatment train allowing for minimization of metals presence, SSA characterized by neutral SSA and fine size (D50 < 100-200 µm).

PEE ranged between 57.4% and 91.5%, achieving its maximum for sample S2 (91.1%) and S6 (91.5%) as shown in **Figure 1**, suggesting that the type of incinerator feed may not affect the subsequent extraction. Similar extraction efficiency was obtained from S0 (91.1%) with much lower acid consumption, therefore suggesting the high importance of SSA pH.

Results from synthetic solutions showed that the addition of K increased the PPE (except at pH 9) (**Figure 2**). Maximum PPE (85%) and KPE (68%) were achieved at pH 10, suggesting the occurrence of P and K co-precipitation resulting in P and K content in the solid of 15.2% and 15.3%, respectively. Results from leachate confirmed high PPE (97%) and KPE (28%) at pH 9 with K:Mg:P=1:2:2 (**Figure 3**). XRD identified cattiite ($Mg_3(PO_4)_2(H_2O)_{22}$) as the main crystalline phase, while K was mainly present as amorphous phase. These results suggest that the addition of other nutrient besides the available P may be beneficial for the quality of the final solid product.

In conclusion, to optimize the P recovery several parameters besides P extraction must be considered. Experimental results showed that nearly 100% of P can precipitate at pH 9 from leachate with K:Mg:P=1:2:2, resulting in a P and K content in the final solid of 14% and 3% respectively. Cattiite was the main crystalline compound present, while K was mostly present in amorphous form. Additional experimental activities are planned to understand the effect of incineration process conditions and the role of heavy metals in the co-precipitation process within the ERA-MIN 3 "PHOSTER" project framework.

ACKNOWLEDGMENTS
The present work was partly funded by the ERA-MIN 3 "PHOSTER" project (https://phoster-project.eu/). The authors would like to thank Rea Dalmine (Greenthesis group) for granting the PhD of Ms Gaia Boniardi, and Prof. Elza Bontempi and Dr. Laura Fiameni for the analytical support.

Table 1. Most abundant element in SSA (samples S0-S7) (value±uncertainty). Estimated uncertainty: 10% for ICP-MS, 15% for UV-Vis spectrometry (P). N.A. = not available.

Sample	P	Al	Ca	Fe	K	Mg
S0	8.63±1.30	17.46±1.75	11.11±1.11	5.20±0.52	N.A.	1.24±0.12
S1	5.64±0.85	2.31±0.23	21.87±2.19	0.57±0.06	0.82±0.08	0.90±0.09
S2	5.04±0.76	2.87±0.29	30.15±3.02	0.62±0.06	0.83±0.08	0.88±0.09
S3	6.36±0.95	2.11±0.21	17.52±1.75	2.76±0.28	0.80±0.08	0.96±0.10
S4	6.27±0.94	2.42±0.24	20.66±2.07	2.42±0.24	0.83±0.08	1.00±0.10
S5	6.22±0.93	2.67±0.27	16.39±1.64	2.78±0.28	0.71±0.07	0.98±0.10
S6	6.35±0.66	2.61±0.26	23.50±2.35	2.67±0.27	0.97±0.10	1.19±0.12
S7	6.56±0.84	2.47±0.25	22.76±2.28	2.62±0.26	0.72±0.07	1.17±0.12

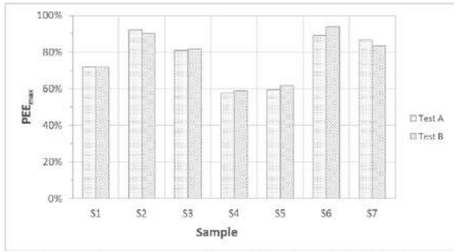

Figure 1 Maximum phosphorus extraction efficiency (PEE_{max}) for samples S1-S7. Leaching conditions: 1 M H_2SO_4, liquid-to-solid ratio of 20:1, 2-h contact time, room temperature.

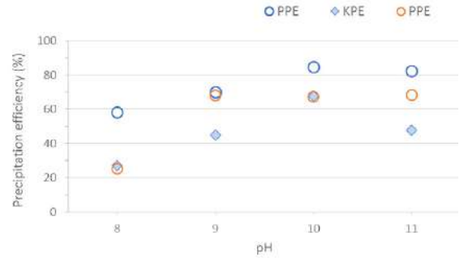

Figure 2. Phosphorus and potassium precipitation efficiency (PPE and KPE) from synthetic solutions. Blue dots and diamonds refer to tests with KH_2PO_4 and $MgCl_2$ as K, P and Mg source, while orange ones to tests with H_3PO_4 and $MgCl_2$ as P and K sources.

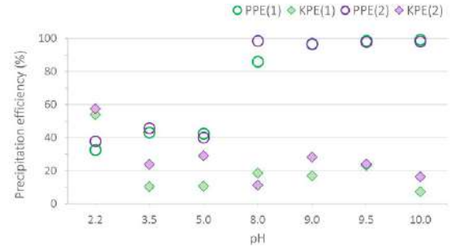

Figure 3. Phosphorus and potassium precipitation efficiency (PPE and KPE) from leachate solution. Green dots and diamonds refer to molar ratio of K:Mg:P=1:1:1, while violet ones to molar ratio of K:Mg:P=1:2:2 (2).

REFERENCES

ASTM International 2020. ASTM E-11: Standard Specification for Woven Wire Test Sieve Cloth and Test Sieves.

Baldi, M., Martinotti, A., Sorlini, S., Katsoyiannis, I., Abbà, A., Carnevale Miino, M., Collivignarelli, M. 2021 Extraction and purification of phosphorus from the ashes of incinerated biological sewage sludge. *Water* **13**, 1102.

Boniardi, G., Turolla, A., Fiameni, L., Gelmi, E., Malpei, F., Bontempi, E. & Canziani, R. 2021 Assessment of a simple and replicable procedure for selective phosphorus recovery from sewage sludge ashes by wet chemical extraction and precipitation. *Chemosphere* **285**, 131476.

Bontempi, E., Zacco, A., Borgese, L., Gianoncelli, A., Ardesi, R. & Depero, L. E. 2010 A new method for municipal solid waste incinerator (MSWI) fly ash inertization, based on colloidal silica. *Journal of Environmental Monitoring* **12**, 2093.

European Committee for Standardization 2011, EN 15956 Fertilizers – extraction of phosphorus soluble in mineral acids.

Fang, L., Wang, Q., Li, J., Poon, C. S., Cheeseman, C. R., Donatello, S. & Tsang, D. C. W. 2020 Feasibility of wet-extraction of phosphorus from incinerated sewage sludge ash (ISSA) for phosphate fertilizer production: a critical review. *Critical Reviews in Environmental Science and Technology* **51**, 1–33.

International Organization for Standardization (ISO) 2016 Test Sieves – Technical Requirements and Testing Test Sieves of Metal Wire Cloth (ISO 3310-1:2016).

Krüger, O., Grabner, A. & Adam, C. 2014 Complete survey of German sewage sludge ash. *Environmental Science & Technology* **48**, 11811–11818.

Liang, S., Chen, H., Zeng, X., Li, Z., Yu, W., Xiao, K., Hu, J., Hou, H., Liu, B., Tao, S. & Yang, J. 2019 A comparison between sulfuric acid and oxalic acid leaching with subsequent purification and precipitation for phosphorus recovery from sewage sludge incineration ash. *Water Research* **159**, 242–251.

Liu, H., Hu, G., Basar, I. A., Li, J., Lyczko, N., Nzihou, A. & Eskicioglu, C. 2021 Phosphorus recovery from municipal sludge-derived ash and hydrochar through wet-chemical technology: a review towards sustainable waste management. *Chemical Engineering Journal* **417**, 129300.

Meng, X., Huang, Q., Xu, J., Gao, H., Yan, J., 2019. A review of phosphorus recovery from different thermal treatment products of sewage sludge. *Waste Disposal & Sustainable Energy* **1**, 99–115.

UNI EN ISO 17294-1, 2007. Water Quality - Application of Inductively Coupled Plasma Mass Spectrometry (ICP-MS) - Part 1: General Guidelines (ISO 17294-1:2004).

Aquafarm: Biological sludge degradation, nutrient removal and greenhouse gas reduction by macroinvertebrates and macrophytes

T.V. van der Meer*/****, L. Hendriks**, F. van Schie***, P.F.M. Verdonschot*, M.H.S. Kraak****, A.J.P. Smolders**, L.P.M. Lamers**, A.J. Veraart**

* Wageningen Environmental Research, Wageningen UR, P.O. Box 47, 6700 AA, Wageningen, The Netherlands
(*tom l.vandermeer@wur.nl; piet.verdonschot@wur.nl*)
** Department of Aquatic Ecology and Environmental Biology, Radboud Institute for Biological Sciences, Radboud University, P.O. Box 9010, 6500 GL, Nijmegen, The Netherlands
(*Lisanne.Hendriks@ru.nl; Fons.Smolders@ru.nl; Leon.Lamers@ru.nl; Annelies.Veraart@ru.nl*)
*** Hoogheemraadschap Hollands Noorderkwartier, P.O. Box 250, 1700 AG, Heerhugowaard, The Netherlands
(*f.vanschie@hhnk.nl*)
**** Institute for Biodiversity and Ecosystem Dynamics, University of Amsterdam, P.O. Box 94240, 1090 GE, Amsterdam, the Netherlands
(*m.h.s.kraak@uva.nl*)

Abstract
There is an urgent need for new wastewater treatment techniques that reduce the amount of sludge produced, and lower effluent nutrient concentrations, while greenhouse gas emissions are limited. In an Aquafarm-system, macroinvertebrates degrade sludge, while aquatic plants take up and assimilate nutrients, thereby minimizing effluent nutrient concentrations and maximizing CO_2 uptake. Biomass produced in this way may have applications in the circular economy. To test the efficiency of the Aquafarm principle, we performed several experiments on sludge degradation by macroinvertebrates, and nutrient removal by macrophytes, while also measuring GHG fluxes. The results revealed that macroinvertebrates increased sludge degradation, and floating plants effectively removed nutrients, while taking up CO_2, without emitting GHGs. Sludge degradation, nutrient removal, as well as GHG reduction depended on the macroinvertebrate taxa or plant species. Thus, it is concluded that the treatment of municipal wastewater sludge and effluent by macroinvertebrates and macrophytes is a promising treatment technique.

Keywords
Floating plants; macroinvertebrates; municipal wastewater; self-purification; nature-based solution

INTRODUCTION

Wastewater treatment plants (WWTPs) are often a point-source of nutrients, and contaminants, and produce excess sludge and greenhouse gasses (GHGs). Meanwhile 48% of global wastewater is not treated at all, leading to poor surface water quality and associated human and environmental health risks (Jones et al., 2021). Therefore, there is an urgent need for affordable WWTP and (post-)treatment techniques that further reduce the nutrient concentrations in wastewater effluent, as well as the amount of produced sludge, while having a minimal GHG footprint (European Commission, 2022). We here argue that utilizing the self-purifying capacity of surface waters may pave the way to such a futureproof wastewater treatment system, since aquatic organisms have the potential to aid in the degradation of sludge and nutrient removal, as they also degrade organic matter and take up nutrients in their natural environment. Indeed, multiple species of macroinvertebrate collector-gatherers can feed on WWTP sludge (van der Meer et al., 2022) and macrophytes and especially floating plants can effectively remove nutrients from WWTP effluent (Hendriks et al., under review). During these processes, the organisms grow and reproduce, and thus produce biomass. Nutrients can be permanently extracted from the system by removing the produced biomass, preventing nutrient discharge into the environment. Utilizing the removed biomass for products, would also aid in the ambition to achieve 100% circularity in terms of resource use which has been agreed upon in the Paris Agreement. Furthermore, the interactions between these organisms in their natural environment may enhance these functions. Therefore, a cascade of monocultures of aquatic invertebrates and plants may serve as a WWTP (post-) treatment step to combat eutrophication, excess sludge production and GHG emissions from WWTPs. An Aquafarm cascade would aim to provide the optimal conditions for each monoculture in the cascade, thus achieving optimal functioning of the organisms, therewith fuelling the processes. In contrast to some other nature-based treatment techniques, the harvesting of biomass allows permanent removal of nutrients from the system and benefits the circular use of resources.

MATERIALS AND METHODS

In the first part of this project, several experiments have been performed assessing the capability of sludge degradation by (combinations of) multiple species of macroinvertebrates. Furthermore, multiple species of submerged, emerged, and floating plants have been cultured on WWTP effluent to assess their nutrient uptake, growth and effects on GHG emissions. Here, we have highlighted two of these experiments. In the first experiment, all possible combinations of 3 taxa of detritivorous macroinvertebrates; worms, chironomids and snails have been grown on sludge from three WWTPs differing in contaminant loads. After 7 days, the amount of degraded sludge was determined. In the second experiment, eight species of floating plants (*Eichhornia crassipes*, *Pistia stratiotes*, *Stratiotes aloides*, *Salvinia molesta*, *Azolla filiculoides*, *Azolla pinnata*, *Lemna minuta*, *Trapa natans*) were grown on effluent for two weeks, and nutrient uptake, biomass production and GHG fluxes were measured.

RESULTS

Macroinvertebrates can stimulate sludge degradation (Fig. 1)

The results of the macroinvertebrate experiment showed that these could stimulate the degradation of sludge from all three WWTPs, regardless of contaminant level. The least contaminated WWTP was Rhenen, followed by Mijdrecht and then Alkmaar. Sludge degradation did differ between taxa and WWTP site, with % of degraded sludge being highest in Rhenen (18.5%), and lowest in Alkmaar and Mijdrecht (7.4%). Degradation by invertebrates could be as high as 39.2% of initial sludge in 7 days. However, the sludge degradation of the multispecies treatments was only higher than expected based on the single-species treatments in Alkmaar, indicating that positive species interactions may only occur in higher stressed/contaminated environments.

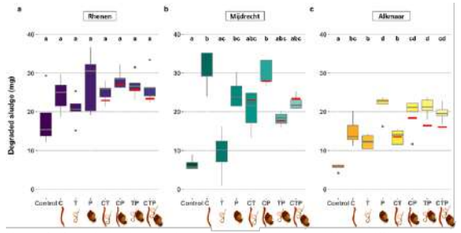

Figure 1. Degradation (mg) by (combinations of) chironomid larvae (C), worms (T), and snails (P) of sludge from the WWTPs of Rhenen (a), Mijdrecht (b), and Alkmaar (c). Boxes show interquartile range, bold lines represent the median, whiskers indicate the lowest and highest values within a 1.5x interquartile range from the box, dots represent outliers. Letters indicate significant ($p < 0.05$) differences between species (combinations). Two outliers at Mijdrecht (C-treatment: 50.1 mg; CP-treatment: 66.0 mg) are not shown to increase figure readability. Red lines indicate the median of the predicted degradation by multi-taxa assemblages based on single-taxa degradations.

Floating macrophytes stimulate nutrient removal while taking up GHGs (Fig. 2)

All of the tested plants were able to completely remove ammonium, most likely by stimulating nitrification. Only *E. crassipes*, *P. stratiotes* and *S. molesta* were able to lower nitrate concentrations to the limits set for natural waterbodies. *A. filiculoides* and *A. pinnata* were the only plants lowering phosphate concentrations. CH_4 and N_2O emission were lowest in treatments with *A. filiculoides*, *A. pinnata*, *L. minuta* and *T. natans*. CO_2 was sequestered in all treatments, but *A. filiculoides* showed the highest uptake. Both *Azolla* species had the highest biomass gain.

DISCUSSION

The present experiments have shown that aquatic macroinvertebrates are able to enhance sludge degradation, and that the efficiency of these processes are taxa and WWTP specific. We also showed that floating macrophytes increase the nutrient removal from the effluent, and can limit GHG emissions during wastewater treatment. The efficiency of these processes depends on different plant traits, like growth rate.

The present results indicate that the use of a cascade of aquatic organisms may offer promising future-proof solutions to the challenges of the creation of circular and zero emissions systems. The Aquafarm cascades degraded excess sludge and reduced nutrient concentrations in the effluent to be within the limits set for natural waterbodies, while also resulting in a net uptake of GHGs. During these processes, the organisms converted sludge and nutrients into biomass, which may be harvested, and possibly applied for other uses such as fish feed and fertilizer. This will aid the goal of a circular treatment process. The next step in the development of such a well-functioning treatment-process is the scaling of these processes and making them robust for different climates is. However, as different organisms have different traits in terms of sludge degradation and nutrient transformations, selection and combining the right species depending on the type of WWTP, and providing the appropriate conditions for the organisms to grow, is needed to optimize further wastewater treatment and effluent polishing. In this way, wastewater treatment using macroinvertebrates and macrophytes contributes to a circular economy and energy-neutrality of wastewater treatment, but mostly to the urgently needed decrease in eutrophication.

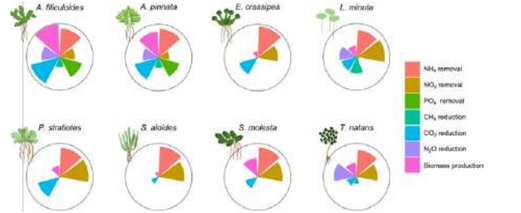

Figure 2. Efficiency of the eight measured floating plant species in nutrient removal, biomass production and greenhouse gas reduction when grown on municipal wastewater effluent. Data are normalized to the highest removal, reduction or biomass production, i.e. they were expressed as a fraction of the highest removal rate, reduction potential and biomass production, where the black line depicts 1.

REFERENCES

European Commission (2022). European Green Deal: Commission proposes rules for cleaner air and water. Press release, 26 October 2022, Brussels.

Hendriks, L., Smolders, A.J.P., van den Brink, T., Lamers, L.P.M., Veraart, A.J. (under review). Low-emission plant-based municipal effluent polishing: Floating plants perform better than submerged plants in both nutrient removal and reducing greenhouse gas emission. *Under review.*

Jones, E.R., van Vliet, M.T.H., Qadir, M., Bierkens, M.F.P. (2021). Country-level and gridded estimates of wastewater production, collection, treatment and reuse. *Earth System Science Data*, **13**, 237-254.

Van der Meer, T.V., Verdonschot, P.F.M., van Eck, L., Narain-Ford, D.M., Kraak, M.H.S. (2022). Wastewater treatment plant contaminant profiles affect macroinvertebrate sludge degradation. *Water Research*, **222**, 118863.

Removal of nanomaterials from wastewater by Microbial Fuel cell – Current knowledge and future direction

D. Vempati* and A. Kumar*

* Department of Civil Engineering, Indian Institute of Technology Delhi, Hauz Khas, New Delhi, India
(E-mail: divyavs23@gmail.com; arunku@civil.iitd.ac.in)

Abstract
The use of engineered Nanoparticles (NPs) is increasing across all domains – from personal care products to medical purposes and currently, treatment plants are not equipped to remove these. Microbial Fuel Cell (MFC) uses microorganisms to degrade wastewater and generate electricity, with lower cost, lesser space requirement and minimal chemical usage. NPs exist as a mixture of ions and particles in water – of which ions have been removed in MFCs. To use this technology for NP removal, it is imperative to understand the possible interactions in the system. NPs have been reported to adversely affect biofilm, but there is a lack of studies in the context of anode biofilm. This study thus summarises the knowns of NPs with biofilm and MFC to draw out the course of future research in this direction.

Keywords – Biofilm; Microbial Fuel cell; Nanoparticle; Toxicity

INTRODUCTION

With advent of technology and development, newer contaminants, aka emerging contaminants, are becoming concerning. Within this category, contaminants in particulate form, especially in nano size range are rapidly increasing. Broadly classified as "nanoparticle (NP)", it refers to any particle whose size is within 100 nm. Several types of NPs are in existence – carbon-based (carbon nano tubes, fullerene, etc.), metal-based (nano Ag, metal oxides etc.), nano plastics, etc. Personal care products, health sector, electronics, paints, petrochemical industry are major contributors to these NP wastes. The nano size facilitates easy penetration into cells of living organisms, causing many harmful effects.

Recent years have seen increased exploration in the usage of Microbial Fuel Cell (MFC) for treating wastewater due to possibility of simultaneous clean energy generation and wastewater treatment – catering to 2 of the Sustainable Development Goals by the UN. A keyword search of "Nanoparticle; MFC" on Scopus yielded 427 research publications over the last decade, with over half of studies emerging in the last 4 years. Majority of the 427 studies have employed nanomaterials for enhancement of electrode surface or as mediators. On the other hand, only 5 studies were obtained on keyword search of "Nanoparticle; toxicity; MFC", indicating that very few studies have focused on NP as a contaminant in MFC. This study forms a preliminary assessment for understanding (i) removal of NPs in MFC and (ii) NP effect on anode biofilm and then presents a hypothesis of NP induced toxicity to biofilm.

RESULTS

NP removal in MFC

As the occurrence of NPs in wastewater will inevitably rise exponentially in the coming years, the need to understand their impact on bio-electrochemical treatment technologies becomes important. Due to limited prior knowledge in this domain, the effect of NPs on different components of the MFC was explored. The anode biofilm is the main reaction site of the MFC where the electrogenic microbes colonise, degrade organic matter and release electrons. Biofilm directly influences the MFC performance, thus studying the impact of NPs on biofilm can be a reliable estimate. In solution, NPs occur in both particle and ion form – of which the latter has been extensively investigated in the context of MFC. MFC has achieved high removal efficiencies for several heavy metal ions. The phenomena such as biosorption, electrochemical reduction, etc. which have been attributed to their removal can also be extrapolated for the NP derived ion. A brief literature review covering these aspects is shown in Table 1. The major shortcoming that emerged from the literature study is that no study has targeted the removal of NPs using MFC. Further, most bioreactor experiments focus on a single type of NP with substrate. Along with that, other contaminants and constituents will also influence the impact NPs will have on the overall treatment process. More research is required to understand the realistic wastewaters where a mixture of NPs will occur.

Table 1. Summary of findings of studies on metal/ NP removal in MFC (studies using NP is shown as italicized texts)

Reference	Experimental design	Results	Reported gaps
Li, Wu et al., 2014	Single chamber; electron acceptor: 50mg/L Fe(III); 10mg/L Cr(VI)	Max power generation= 658 mW/m^2 (50mg/L Fe) and 419 mW/m^2 (10mg/L Cr); metal removal range: 97-98%	Need for continuous flow studies
Touach, Ortiz-Martínez, et al., 2016	Single chamber; real wastewater; MnO_2 based cathode	MnO_2/CNT/PTFE resulted in best performance - 511 mW/m^2 max power; 78% COD removal; 59-97% heavy metal removal	Heavy metal removal mechanisms
Zakaria and Dhar, 2020	*Community change study due to 50mg/L Ag NPs in Microbial Electrolysis Cell*	*Reduction in current density and COD removal; NP removal; NP attachment to EPS layer*	*Effect of Ag NPs in real wastewater*
Han et al., 2013	*MB dye degradation in presence of Au NP (as e- relay) and H_2O_2 in MFC cathode.*	*98% MB degradation; 96% COD removal (max electricity 36.56 mW/m^2)*	*Extension of use of Au NPs as mediator*
Gupta et al., 2017	*Double chamber MFC; Alumina (AA) Nickel NP dispersed CNF electrodes for 100 mg/L Cr (VI)*	*100% Cr removal (max power density =1540 mW/m^2); AA NPs improved the electrical conductivity of electrode; Ni NPs catalysed the Cr reduction*	*Scaling up of the modified electrode material for larger reactors*

Impact of NP on anode biofilm

The biofilm over an anode consists of numerous microbial colonies interlinked in a matrix of extracellular polymeric substances (EPS). With time, the biofilm thickens, which gives rise to a concentration gradient of substrate across the depth. The presence of NPs in the wastewater can disrupt this process in different ways – inhibition of initial surface attachment and growth, cell penetration and destruction, deterioration of biofilm structure etc. The studies covering these aspects are described in Table 2 and the same is illustrated in Fig 1. Most of the NP biofilm toxicity studies have scrutinized pure culture biofilms, which is not the case for real wastewaters that contain mixed culture of microbes. Although, entrapment of NPs in biofilm is desired for its removal, its further implications on the performance of MFC has to be delved into.

Table 2. Literature review on effect of NPs on biofilm

Reference/ NP type	NP concentration (mg/L)	Biofilm culture	Nature of impact on biofilm
Kalishwaralal et al. 2010/ Ag	0.00107 - 0.0107 mg/L	*Pseudomonas aeruginosa; Staphylococcus epidermidis*	Suppression of formation of exopolysaccharide by bacteria. Eradication of biofilm at higher NP concentrations
Maurer-Jones et al. 2013/ TiO_2	1 -100 mg/L	*Shewanella oneidensis*	Decreased growth rate possibly due to adsorption of substrate on NP
Awasthi et al. 2020/ ZnO	500 and 1000 mg/L	*Bacillus subtilis*	Reduction in initial surface attachment of bacteria and biofilm density; formation of empty pockets in EPS matrix
Zakaria et al. 2020/ Ag	Ag; 50 mg/L	Mixed culture	Decreased bacterial cell count (> 90%); NP Infiltration of NP in bacterial cell and cell destruction
Alizadeh et al. 2019/ PVP coated Ag NPs	0.0108, 0.131, and 0.631 mg/L	Mixed culture	Biofilm detachment and re-release of trapped NPs. Antimicrobial action of NPs after penetration into deeper layers of biofilm

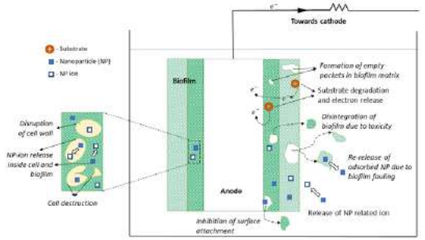

Figure 1. Hypothesized possible impacts of nanoparticles (NP) to anode biofilm. The effects written in italics indicate the NP-induced effects

CONCLUSIONS

MFC has the potential to become an in-situ treatment facility for industries with high concentration of NPs in effluent or even central treatment facilities with mixed, NP-containing wastewaters. There are very few studies in the context of NP and anode biofilm – which plays a pivotal role both for treatment and electricity generation. In ion form, similar to heavy metal ions, NP ions can be removed by biosorption, reduction. Once entrained in the biofilm, adverse impacts such as reduction in growth and viability, destruction of microbial cell and fouling can occur. For future studies, the incorporation of the following points can lend an enhanced perspective in this ambit:

- To study the effect of NP-inducted impacts on biofilm on the performance of MFC
- Use of realistic wastewaters considering co-existence of NPs with other contaminants in MFC studies for facilitating field adoption of this technology.
- To study MFC performance using mixed culture biofilms and NPs.

ACKNOWLEDGEMENTS

The authors would like to thank Indian Institute of Technology (IIT Delhi), India for providing support for this study and acknowledge the Prime Minister Research Fellowship (PMRF), the Government of India for providing fellowship.

REFERENCES

Alizadeh, S., Ghoshal, S., and Comeau, Y. 2019 Fate and inhibitory effect of silver nanoparticles in high rate moving bed biofilm reactors. *Science of the Total Environment*, **647**, 1199–1210.

Awasthi, A., Sharma, P., Jangir, L., Kamakshi, Awasthi, G., Awasthi, K. K., and Awasthi, K. 2020 Dose dependent enhanced antibacterial effects and reduced biofilm activity against Bacillus subtilis in presence of ZnO nanoparticles. *Materials Science and Engineering C*, **113**.

Gupta, S., Yadav, A., and Verma, N. 2017 Simultaneous Cr(VI) reduction and bioelectricity generation using microbial fuel cell based on alumina-nickel nanoparticles-dispersed carbon nanofiber electrode. *Chemical Engineering Journal*, **307**, 729–738.

Han, T. H., Khan, M. M., Kalathil, S., Lee, J., and Cho, M. H. 2013 Simultaneous enhancement of methylene blue degradation and power generation in a microbial fuel cell by gold nanoparticles. *Industrial and Engineering Chemistry Research*, **52**(24), 8174–8181.

Kalishwaralal, K., BarathManiKanth, S., Pandian, S. R. K., Deepak, V., and Gurunathan, S. 2010 Silver nanoparticles impede the biofilm formation by Pseudomonas aeruginosa and Staphylococcus epidermidis. *Colloids and Surfaces B: Biointerfaces*, **79**(2), 340–344.

Li, Y., Wu, Y., Puranik, S., Lei, Y., Vadas, T., and Li, B. 2014 Metals as electron acceptors in single-chamber microbial fuel cells. *Journal of Power Sources*, **269**, 430–439.

Maurer-Jones, M. A., Gunsolus, I. L., Meyer, B. M., Christenson, C. J., and Haynes, C. L. 2013 Impact of TiO2 nanoparticles on growth, biofilm formation, and flavin secretion in Shewanella oneidensis. *Analytical Chemistry*, **85**(12), 5810–5818.

Touach, N., Ortiz-Martínez, V. M., Salar-García, M. J., Benzaouak, A., Hernández-Fernández, F., de los Ríos, A. P., Labjar, N., Louki, S., el Mahi, M., and Lotfi, E. M. 2016 Influence of the preparation method of MnO2-based cathodes on the performance of single-chamber MFCs using wastewater. *Separation and Purification Technology*, **171**, 174–181.

Zakaria, B. S. and Dhar, B. R. 2020 Changes in syntrophic microbial communities, EPS matrix, and gene-expression patterns in biofilm anode in response to silver nanoparticles exposure. *Science of the Total Environment*, **734**.

Microbial-Mediated Biological Treatment of Wastewater Containing Arsenic (III) and Arsenic (V)

Manoj Kumar Verma [1] and Vishal Mishra [1]
[1] School of Biochemical Engineering, Indian Institute of Technology (BHU), Varanasi, Uttar Pradesh, India 221005
E-mail: manojkverma.rs.bce18@itbhu.ac.in

Abstract

Biological treatments for arsenic and other pollutant removal from wastewater involve using microorganisms, such as bacteria, to convert the contaminant into a less toxic form. Microbe-mediated bioaccumulation provides cost-effective and eco-friendly technology for removing heavy metals and other pollutants from water. *Kurthia gibsonii* strain MKVVM3 IITBHU was shown to be capable of adsorbing and accumulating, including both As (III) and As (V) from the contaminated water. Arsenic resistance gene expression from MKVVM3 IITBHU was regulated by various mechanisms, including gene regulation and metabolic adaptation conferring bacterial resistance against arsenic. These include arsenate reductase and arsenite oxidase, which play a role in arsenic detoxification. In the SEM study, the bacteria appeared to be long and rod-shaped cells. AFM analysis revealed that MKVVM3 IITBHU accumulated arsenic in its cell walls, increasing its surface area in aqueous solutions. XRD confirmed the isolates' size and shape conformation and indicated amorphous nature. EDS and Elemental mapping were conducted to infer the presence and distribution of elements in the sample. The combined study of these techniques provides the bioremediation potential of MKVVM3 IITBHU in removing arsenic. The process of using bacteria to bind the arsenic to their cell surface, thus preventing it from entering the environment. It further provides researchers with a deeper understanding of the pathways of how these bacteria utilize their energy for wastewater treatments.

Keywords: *Kurthia gibsonii* strain MKVVM3 IITBHU, Bioremediation, As (III) and As (V), Wastewater treatment

INTRODUCTION

Arsenic (As) groundwater contamination is caused by the weathering of rocks, water pH, competing ions' presence, biological alteration of minerals, and other anthropogenic sources. As poisoning in people can lead to illnesses such as skin rashes, neurological and respiratory issues, and various cancers. (Chung et al., 2014). Several countries, including Argentina, Bangladesh, China, Chile, Canada, Japan, Vietnam, Taiwan, India, Mongolia, Nepal, and the United States, have reported elevated As levels in their drinking water. (Smith et al., 2009). This research aims to characterize arsenic-resistant bacteria and establish their role in arsenic bioremediation.

MATERIALS AND METHODS

Bacterial coevolved genes were investigated to identify gene expressions that support resistance. To evaluate the isolate's effectiveness in the bioremediation of As (III) and As (V), biochemical and morphological analysis was also carried out using SEM and AFM.

RESULTS AND DISCUSSION

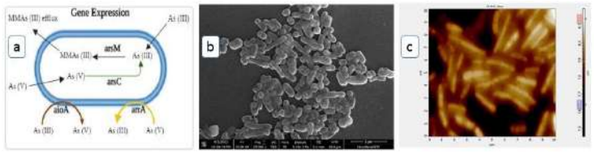

Figure 1. *Kurthia gibsonii* strain MKVVM3 IITBHU (a) Gene expression, (b) SEM and (c) AFM

In the present work, *the Kurthia gibsonii strain MKVVM3 IITBHU (NCBI accession no. - ON248393.1) w*as Gram-positive. Oxidizing, reducing, methyltransferase, and respiring gene expressions suggested that it can play an essential role in the biogeochemical cycle of As. These include genes involved in producing the arsenate-reducing enzyme, ArsC and aioA gene responsible for As (III) transformation by oxidation Fig.1(a). Rod-shaped species of bacteria Fig. 1(b) that SEM has identified. Surface morphology investigations using AFM Fig. 1(c) provided insight into how adhesion forces supported As adsorption on bacterial surfaces to remove metalloid contaminants.

REFERENCES

Chung, J. Y., Yu, S. Do, & Hong, Y. S. (2014). Environmental Source of Arsenic Exposure. *Journal of Preventive Medicine and Public Health*, *47*(5), 253.
Smith, E., Kempson, I., Juhasz, A. L., Weber, J., Skinner, W. M., & Gräfe, M. (2009). Chemosphere Localization and speciation of arsenic and trace elements in rice tissues. *Chemosphere*, *76*(4), 529–535.

INNOVATIVE SOLUTIONS TO MINIMIZE BRINE DISCHARGES IN THE MINING & METALLURGY INDUSTRY.

Carlos Echevarria*, Alejandro Vilar*, Claudia Pastor*, Celia Castro*, Marina Arnaldos*, Reyes Parga**, Guillermo Ferrero**, Estela Gonzalez**.

* CETAQUA, Water Technology Center, Ctra d'Esplugues 75, 08040, Cornellà de Llobregat (Barcelona), Spain.
** SANDFIRE MATSA, Ctra Hu-7104 km 12, Amonaster la Real (Huelva), Spain.

Abstract
An innovative water solution, to improve and minimise brine discharges in the mining and metallurgy industry, is demonstrated in a mineral processing industry with the aim of reduce brine discharges applying innovative technologies getting salts as valuable by-products and a clean water ready to reuse it. A prototype (10 m^3/h) based on a softening step, followed by nanofiltration, reverse osmosis, electrodialysis and evaporation will be operated for 18 months in a real environment in order to gather the operational data to assess from a technical, economic and environmental point of view the feasibility of scaling up this system.

Keywords
AMD, brine discharges, membranes, mining wastewater, water reuse

Introduction

The application of dense membrane-based technologies such as nanofiltration (NF) or reverse osmosis (RO) to remove sulphates in acid mine drainage (AMD) from the mining industry has grown in the last few years to bring water quality in line with these new regulations (Masisdi et al, 2017). Membrane processes allow a lower consumption of chemicals than physico-chemical systems, a fixed removal rate of the target parameters and the possibility to produce purified water, suitable for reuse or to improve discharge water quality. Nevertheless, the rejection of dissolved salts and the consequent generation of brines needs to be managed, especially in inland areas where marine discharge is not a possibility.

LIFE REMINE WATER project aims to demonstrate an alternative treatment train for sulphates removal and deploy innovative solutions for brine concentration in the mining sector, in which water can be recovered to enhance water quality discharged and boost the recovery of valuable by-products. Additionally, the use of renewable energies such as solar-thermal systems to reduce the carbon footprint and OPEX associated to evaporation will be assessed.

Material and Methods

The project is carried out in an ore treatment plant (copper, zinc and lead) located in the south-west of Spain. Industrial wastewater is currently derived to an iWWTP based on a physico-chemical system. Table 1 shows the intake water characterization for the pilot plant. An innovative integrated solution has been designed to remove effectively sulphates in AMD and minimize the generated brines volume in a cost-efficient way.

Table 1. Intake water characteristics

Parameters	Units	Raw water
pH	-	2.27 ± 0.10
conductivity	mS/cm	7.94 ± 0.99
Sulphates	mg/l	3763 ± 173
Ca	mg/l	660 ± 79
Mg	mg/l	223 ± 27

Firstly, a NF unit treats 7 m^3/h with the goal of eliminate the sulphates and the remaining divalent elements that are present in the raw water. Before the NF, a softening stage (based on CO_2 and NaOH) is applied to ensure the maximum removal of calcium and magnesium to minimize the risk of membranes scaling due to an uncontrolled precipitation of $CaSO_4$, pH is neutralized with HCl addition and a sand filter is used as pretreatment to avoid that suspended matter can provoke membrane clogging.

The NF (DK-400, Veolia Water Technology) has been designed to operate at a maximum recovery of 80%. The unit was composed by a single pressure vessel containing 7 membrane elements. The obtained permeate can be directly used to improve the water discharge; nevertheless, in this research a further step of RO will be applied to reduce TDS concentration and produce process water for it reuse. The rejection will be recirculated to one of the buffer ponds of the mine.

The RO stage (AG8050F-100, Veolia Water Technology) will treat 5,6 m^3/h and the goal of this stage is to remove the monovalent elements to reduce the conductivity and obtain a permeate ready to reuse it or discharge. The permeate will be reused in industrial uses, and the brine (0.7 m^3/h), which contains 36 g/L of TDS, will feed an Electrodialysis (ED) unit.

ED-BC (electrodialysis brine concentration) allows without applying pressure as a driving force, to concentrate the brine up to 150 g/L TDS. The brine feeds the stack composed by anionic and cationic membranes. The concentrated brine (0.05 m^3/h) is accumulated and will feed a low temperature evaporator coupled with solar thermal collectors.

The low temperature evaporator is based on Multi Effect Distillation to concentrate the brine up to 250 g/L TDS. Once water has been recovered, the remaining concentrate stream is derived to a crystallizer to obtain a solid waste. In this research, a four stages distillation has been designed. One of the main advantages of low temperature evaporation is that can be coupled with renewable energies. Solar thermal collectors will be used to provide this heat and thus reduce the OPEX and carbon footprint of the process.

Results and Conclusions

The pilot plant has been operating for almost 4-5 months, in these months the different stages have been started up in cascade. Once we obtain the expected results, we move on to the next one and so on with all the stages. Currently the pretreatment, NF and RO are under operation, and it is expected that in the following months the ED-BC and the evaporator will be fully demonstrated.

The pretreatment has been carried out with a Ca/CO_2 mass ratio of 2 and a pH on the settler between 10-10,5. The average calcium removal obtained is 70%, even reaching removals of 96%. Regarding magnesium, the average removal obtained is 60% reaching removals of 90% in a few days. The next step in this stage is to optimize the process by using less CO_2 and consequently reducing the consumption of NaOH.

The NF has been operated with a pressure of 7 bar and an antiscaling concentration (MDC776, Veolia Water Technology) of 4 ppm, obtaining sulphate removals over 95%, an average removal conductivity of 60% and calcium concentration at the outlet for below 25ppm. The quality of the permeate obtained is sufficient (even with better quality than what is needed) for most of the production stages of a mine, and it also has the quality that will allow it to be discharged in compliance with the current limits (and in the coming years) of discharge.

The RO has been operated like the NF with a pressure of 7 bar and an antiscaling concentration (MDC776, Veolia Water Technology) of 5 ppm. The average conductivity removal obtained is over 96% with an outlet calcium concentration of less than 10 ppm. This permeate can be used in all the industrial processes of a mine (reducing the consumption of fresh water). In the event of a discharge, this current will comply with the current limits and with the most stringent discharge limits that may arise. The next step at the membrane stages is to optimize the operation by reducing antiscaling consumption and improving recovery through the use of recirculation in the membranes.

If the abstract is accepted detailed results (including the ED-BC and the evaporator) of the prototypes performance will be shared in the conference.

Figure 1. LIFE REMINE WATER pilot plant.

REFERENCES

V.Masindia, M.S.Osmana, A.M.Abu-Mahfouza (2017). Integrated treatment of acid mine drainage using BOF slag, lime/soda ash and reverse osmosis (RO): Implication for the production of drinking water. Desalination 424 (2017) 45–52

Atmospheric water harvesting – a case study in South Africa

Palesa Moji*, Frans Boudewijn Waanders*, Elvis Fosso-Kankeu**, Ali Al Alili***

* Centre of Excellence in Carbon- based Fuels, School of Chemical and Minerals Engineering, North-West University, Potchefstroom, 2520, South Africa
(E-mail: frans.waanders@nwu.ac.za)
** Department of Mining Engineering, College of Science Engineering and Technology, University of South Africa, Florida Science Campus, South Africa
*** Department of Mechanical Engineering, Khalifa University of Science and Technology, P O Box 127788, Abu Dhabi, United Arab Emirates

Abstract

Water shortages occur in semi-arid countries, mainly due to their geographical location, climate change, droughts, urbanisation, and pollution of existing water resources. Alternative technologies, not depending on surface water sources, should be investigated in these regions, with atmospheric water harvesting (AWH) a possible approach. The successful application of this technology mainly depends on the weather parameters, such as temperature (T) and relative humidity (RH). In this study, the performance of atmospheric water generators (AWGs) to produce water, was assessed during the four seasons in a remote town in the Gauteng Province of South Africa. The results show that the highest production of water was during summer and autumn seasons, whilst limited or no water production was recorded on some days in the winter and spring months. AWGs could be considered as an alternative source of water, during specific seasons of the years.

Keywords
Atmospheric water generators, Climate change, Water harvesting

INTRODUCTION

Essential to life is to have a sustainable fresh water supply to satisfy the needs of society. Atmospheric water harvesting (AWH) should be seen as an alternative technology for drinking water supply. The water formation within the air is dependent on the temperature (T) and relative humidity (RH) of the air with the suitability of AWH dependent on the thermodynamic principles of an active cooling, condensation, vapour compression cycle, technique. At the AWH location, the 1st annual rains occur during spring, at a minimal rate, with most of the rain falling during the summer season and no rain falls in autumn and winter, hence it is classified as a "semi-arid" region. Careful assessment of the performance of the technology at high altitude, semi-arid regions, is thus needed. In this paper the case study outcomes of the use and performance of atmospheric water generators (AWGs) was investigated to address the challenges of drinking water security [1].

MATERIALS AND METHODS

Atmospheric water generators

Two atmospheric water generators (AWGs), each with a maximum production capacity of 10 000 L per day, were used. The generators are installed at the Ga-Rankuwa site with geographical location coordinates 25°33'24.43'' S, 28°0'5.75'' E in the Gauteng Province, South Africa. The AWGs draw air from the atmosphere, filter it, and condenses it below its dew point temperature for water generation, typically when T≥ 15°C and RH≥ 30%.

Operating Data Recording and Capturing

The control of the AWGs consisted of a human interface screen, that displays the operating conditions, such as the T and RH, and when AWH commences. From 1/1/2020 until 31/1/2021, T and RH were recorded daily to ensure seasonal coverage and behavioural performance of the generators through the different seasons. Concurrently to the recording, weekly average weather forecast from the South African Weather Services (SAWS) [2] were added to the manual collected data on an Excel spread sheet to conduct an analysis of deviation from the climate to predict and optimise water productivity by the AWGs. A 3rd party forecast tool, Meteoblue [3], was later introduced and provided more accurate, hourly forecasts for up to 2 weeks at a time.
All data were recorded manually, including the water production from the AWGs, which was measured from the internal flowmeters near the final water collection tank within the AWGs.

RESULTS AND DISCUSSION

The performance of the AWGs was assessed by plotting water harvested (Litres), T (°C) and RH(%) over a period of one year. For the cold season (winter) and the warm seasons (summer, spring, autumn) a considerable influence on the water production was observed (Figure 1). The average weather forecasts from the SAWS used, showed significant deviations, and thus the hourly weather forecast tool, Meteoblue, was subsequently used to close the water production gap between the SAWS forecasts and site expectation outcomes from the AWGs.

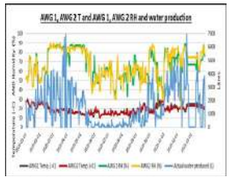

Figure 1: AWGs temperatures and relative humidities with water production for the study year.

The highest water production was observed during the autumn season; March - May 2020. Water production picked up again in the middle of spring (starting in September) towards the summer season (December - February 2021), in a range of about 5000 L to 7000 L water production per day, with less water harvested from the atmosphere during the winter season, where the lowest average T was 9°C with RH being around 17%, as was observed between June and August 2020. A total of almost 60 000L of water production was recorded within the year studied.

CONCLUSION

The results showed that atmospheric water harvesting in a semi-arid, high altitude region using AWGs may be sustainable during autumn and summer seasons as these generators can only perform at their maximum under favourable ambient conditions; implying that T and RH are continually within a specified range. This study provides information that will be useful during the implementation of AWH in remote areas lacking a conventional water supply in South Africa.

REFERENCES

1. P. T. Moji, 2023. Potential of atmospheric water harvesting in South Africa, PhD submitted to the North-West University, Potchefstroom, South Africa. pp118.
2. Department of Forestry, F. a. (2020-2021). *https://www.weathersa.co.za/home/sevendaysdetailed*. Retrieved January 2020-2021, https://www.weathersa.co.za/home/sevendaysdetailed.
3. Meteoblue, E. (2020). *Meteoblue*. Retrieved January-January, 2020-2021, from https://www.meteoblue.com/en/weather/week/ga-rankuwa_republic-of-south-africa_1002851.

Coal derived PAH removal from various water sources using photo catalytic degradation.

F.B. Waanders*, J-B Mougnol* and E. Fosso-kankeu**

* Centre of Excellence in Carbon- based Fuels, School of Chemical and Minerals Engineering, North-West University, Potchefstroom, 2520, South Africa
(E-mail: frans.waanders@nwu.ac.za)
** Department of Mining Engineering, College of Science Engineering and Technology, University of South Africa, Florida Science Campus, South Africa

Abstract
Polycyclic Aromatic Hydrocarbons (PAHs), derived from coal-tar pollution in water, remain in the water for very long, creating hazards to the environment. A need arose to develop and implement an effective technique that will remove these pollutants in polluted water sources.
A self-made flatbed photoreactor was built to degrade, under visible light, the PAHs in acidic-alkaline mine drainage, and sewage wastewater. Zinc oxide (ZnO) and silver (Ag) solutions, functionalised with the agrowastes moringa oleifera seed (MO), groundnut shells (GS) and apatite (A), to obtain a novel heterogeneous photocatalysts, were used in the photo degradation process.
Less than 65% removal of PAHs in 60 min for the different wastewaters when using only the flatbed photoreactor, but the photocatalyst combination of MO/GS/A/ZnO/Ag in a 1:1:1 ratio, removed almost 100% of PAHs from the different water sources for a 60 min period.

INTRODUCTION

Water is a valuable resource for humans; therefore, it is essential to have a sustainable fresh water supply to satisfies the society. The water crises, in particular occurring in South Africa, has exacerbated and major concerns are raised regarding the pollution of the environment from various industries [1,2], with coal conversion, petroleum refining, processing of organic chemicals, among others, responsible for the degradation of water qualities through releasing organic pollutants such as polycyclic aromatic hydrocarbons (PAHs) into the receiving waters [3].
The PAHs remain in the water for very long, creating various hazards, resulting in a need to develop and implement an effective technique that will remove these pollutants in the water sources. In the present investigation a flatbed photoreactor was designed and built to degrade, under visible light, the PAHs in acidic-, alkaline mine drainage, and sewage wastewater.

MATERIALS AND METHODS

The coal-tar used in this study was obtained from a coal coking plant and the interaction of the coal tar with acid mine drainage (pH 2.77), alkaline mine drainage (pH 7.95) and sewage wastewater (pH 6.70) was used to simulate the release of PAHs from the coal tar into the environment. A mass of 116.3 mg coal tar with 2 mL of hexane added, was used to extract, and analyse the PAHs using GC-MS.
For leaching, 5 grams of coal tar was added to a glass column, containing 300mL of either one of the solutions mentioned, with the leaching process conducted over a period of 8 weeks.
The three water sources containing the PAHs were left in solar radiation to determine the degradation efficiency and subsequently a flatbed photoreactor, made of Perspex glass (dimensions: length 40 cm, width 35 cm and height 15 cm) was designed and built to degrade, under visible light, the PAHs in the acidic-, alkaline mine drainage, as well as sewage wastewater. Zinc oxide (ZnO) and silver (Ag) solutions, functionalised with three agrowastes, moringa oleifera seed (MO), groundnut shells (GS) and apatite (A) were used in the final photodegradation process to obtain a higher removal efficiency of PAHs.
Analytical techniques used, included photoluminescence (PL), scanning electroscopic microscopy (SEM), X-ray diffraction (XRD), energy-dispersive X-ray spectroscopy analysis (EDS), gas chromatography-mass spectrometry (GC-MS) and Fourier transform infrared analyses (FTIR).

RESULTS AND DISCUSSION

Leaching of PAHs

The coal tar contained 2917 mg/L of PAHs, with the most abundant PAHs being naphthalene (788 mg/L), phenanthrene (632 mg/L), fluoranthene (395 mg/L), acenaphthylene (356 mg/L), fluorene (327 mg/L), pyrene (266 mg/L), and anthracene (245 mg/L).
After 8 weeks of leaching, 19.3 mg/L, 1.62 mg/L and 1.81 mg/L PAHs were released from the acidic mine drainage, alkaline mine drainage, and sewage wastewater respectively. The release of PAHs from the coal tar was observed to increase over time. The PAHs with lower weight, between 2 to 4 rings, were observed to be highly dissolved in the samples.

Photodegradation of PAHs

The photodegradation of the PAHs in the three water sources (acidic-, alkaline mine drainage, and sewage wastewater) was significantly influenced by time, irradiation method used, i.e., without the flatbed reactor, with the flatbed reactor and with the addition of a heterogeneous photobiocatalyst.
The degradation of PAHs via solar energy only, was proven to be spontaneous in the acidic mine drainage, followed by alkaline mine drainage and lastly the sewage wastewater, with a reduction of PAHs obtained for the three water sources investigated, to be 53%, 33% and 39% respectively over time [1].
It was observed that the use of only a flatbed photoreactor was effective in achieving the photodegradation efficiency of 64%, 58% and 55% under solar irradiation for 60 min for the acidic, alkaline and sewage wastewater [1].
The added agrowastes (groundnut shells (GS), *moringa oleifera* seed (MO) and apatite (A)), including silver to enhance the properties of the ZnO semiconductor, were used to make a heterogeneous photobiocatalyst, with the MO/GS/A/ZnO/Ag photobiocatalyst, mixed in a ratio of 1:1:1, resulted in the best properties and lowest bandgap of 1.96 eV compared to the parental ZnO bandgap, which was found to be 3.35 eV and 2.96eV for ZnO/Ag respectively.
The ZnO/Ag photocatalyst showed a decrease in photodegradation over time in the acid mine drainage, although the removal efficiency increased over time, in contrast to the MO/GS/A/ZnO/Ag in the acidic water, that showed an increase in photodegradation with an almost constant removal efficiency occurring over time, removing 100%, 97% and 98% of PAHs in the acidic, alkaline and sewage wastewater for a 60 min period, respectively [1].

CONCLUSION

The application of green synthesis, using plant materials, functionalised on the semiconductors, could add value to the green synthesis of the metal oxides ZnO or TiO_2 on the photodegradation of PAHs in wastewater with an almost 100% removal in the photodegradation process.

REFERENCES

1. Mougnol, J-B. B. 2023. Degradation of polycyclic aromatic hydrocarbons from coal tar aqueous solutions using photo-biocatalysts. PhD submitted to the North-West University, Potchefstroom, South Africa. pp218.
2. Giri, S. 2021. Water quality prospective in twenty first century: Status of water quality in major river basins, contemporary strategies and impediments: A review. *Environmental Pollution*, 2021 Feb 15;271:116332. doi: 10.1016/j.envpol.2020.116332. Epub 2020 Dec 16. PMID: 33383423.
3. Wasi, S., Tabrez, S. and Ahmad, M. 2013. Toxicological effects of major environmental pollutants: An overview. *Environmental monitoring and assessment*, *185(3)*, 2585-2593.

Chemical-free vacuum UV processes for PFAS abatement

Y. Wang[1,2], D. Santoro[3], K. Bell[4], M. Stefan[5], B. Martijn[6], B.A. Wols[1,7], W. Gernjak[8,9]

[1]Wetsus, Leeuwarden, 8911MA, the Netherlands
[2]University of Girona, 17004 Girona, Spain
[3]USP Technologies, 3020 Gore Rd, London, ON N5V 4T7, Canada
[4]Brown and Caldwell, Walnut Creek, California, United States
[5]Trojan Technologies, 3020 Gore Rd, London, ON N5V 4T7, Canada
[6]PWNT water technology, Rijksweg 501, P.O Box 2046, 1990 AA Velserbroek, The Netherlands
[7]KWR, Groningenhaven 7, 3433 PE Nieuwegein, the Netherlands
[8]Catalan Institute for Water Research (ICRA), 17003 Girona, Spain
[9]Catalan Institution for Research and Advanced Studies (ICREA), 08100 Barcelona, Spain
(E-mail: *yicheng.wang@wetsus.nl*)

Abstract
Per- and polyfluoroalkyl substances (PFAS) are one of the most persistent pollutants in the environment and recent research points to human health risks at low concentrations in environmental media. Hydrated electrons (e^-_{aq}) generated from H_2O under vacuum UV (VUV) irradiation can cleave C-F, leading to the PFAS transformation. Six types of PFASs with two different head groups and various chain lengths were investigated in a specialized VUV reactor to assess removal efficiency. Without additional chemicals, four perfluoroalkyl carboxylic acids (PFCA, CF_3-$(CF_2)_n$-COOH) were transformed at both neutral and alkaline conditions, while one perfluoroalkyl sulfonate (PFSA, CF_3-$(CF_2)_n$-SO_3) was abated at a high pH condition. Elimination of dissolved oxygen improved PFAS transformation using VUV irradiation.

Keywords
Vacuum UV, PFAS, hydrated electron

INTRODUCTION

Per- and polyfluoroalkyl substances (PFAS) have been widely used for industrial applications and consumer products due to their properties. Because of their widespread use, PFAS are frequently detected in surface water and drinking water. PFAS are bioaccumulative and toxic, which poses risks to human health and the environment. Due to the stability of the C-F bonds, PFAS is highly persistent in the environment. Physical treatments, e.g., membrane filtration and ion exchange, separate PFAS from contaminated water into a more concentrated waste stream, and do not destroy the target PFAS compounds (Bentel et al., 2019). Hydrated electrons (e^-_{aq}), with a reduction potential (E^0) of -2.9 V, can cleave the C-F bond (Buxton et al., 2009). UV-based methods, e.g., UV/sulfite, have been used to generate e^-_{aq} for halogenated compound degradation. The obvious disadvantages of applying chemicals are undesired by-products and additional post-treatment. Vacuum UV (VUV) at 185 nm photolyzes water molecules into various radicals, including e^-_{aq}, requiring no additional chemical addition. Apart from e^-_{aq}, hydroxyl radicals ($HO\cdot$) are generated during water ionization and further assist oxidation of defluorinated PFAS products. Simultaneous reduction and oxidation reactions provide a promising alternative for PFAS degradation. Existing studies on PFAS degradation have primarily focused on PFOA and PFOS. Few studies have investigated multiple PFAS at the same time. In this study, we used four perfluoroalkyl carboxylic acids (PFCA, carbon number = 4, 7, 8, 10) and two perfluoroalkyl sulfonates (PFSA, carbon number = 4, 8) to examine their removal performance with VUV irradiation.

MATERIALS AND METHOD

PFBA ($CF_3(CF_2)_2COOH$, 99.5%), PFHpA ($CF_3(CF_2)_5COOH$, 97%), PFOA ($CF_3(CF_2)_6COOH$, 95%), PFDA ($CF_3(CF_2)_8COOH$, 98%), PFBS ($CF_3(CF_2)_3SO_3H$, 97%), PFOS ($CF_3(CF_2)_7SO_3H$, 40% in water), NaOH (1 mol/L), and H_2O_2 (30%) were purchased from Sigma Aldrich. All experimental solutions were made by spiking Milli-Q water with PFAS. NaOH was used for pH adjustment. The experiment was conducted in a collimated beam with a low-pressure mercury UV/VUV lamp. Light intensity at 254 nm on the reactor surface was measured at 6.5×10^{-4} (W cm^{-2}), using a NIST Traceable Light Measurement System from International Light Technologies. The intensity of 185 nm was calculated at 1.3×10^{-4} (W cm^{-2}). The depth of the reactor cell was 10 mm. Control experiments under UV, UV/H_2O_2, and dark conditions were conducted to assess the role of HO-, only, on PFAS removal. To eliminate dissolved oxygen (DO), nitrogen gas (N_2) was used to purge the solution and reactor. LC-MS was used to analyze PFAS concentrations.

RESULTS

- Four PFCAs were transformed at all three pH conditions after 5 min VUV treatment (Figure 1). After 810 min treatment, PFCAs abatement exceeded 90%. PFDA (carbon number = 10) evaluated, which is the longest PFCA, had the highest decay rate at three pH conditions.
- The degradation rates of PFCAs improved with increasing pH (Figure 1). At pH 11, the decay rates of PFCAs improved by approximately 60% compared to pH 7.
- Short-chain PFBS (carbon number = 4) did not degrade in any of the three pH conditions. Long-chain PFOS (carbon number = 8) showed moderate removal (~60%) at pH 11 after 810 min treatment.
- Eliminating DO improved the removal of PFBA, PFHpA, and PFOA by approximately 20%, while the abatement of PFDA was only slightly improved (~3%, Figure 2).
- Oxidation via $HO\cdot$ (Figure 2) or direct photolysis at 254 nm (not shown in the figures) did not initiate PFAS abatement.

DISCUSSION

- The degradation of PFAS depends on the functional group and chain length. PFAS with sulfonate groups were more refractory to VUV irradiation than carboxylic acids groups. In general, long-chain PFAS compounds were less persistent than short-chain compounds and showed higher transformation in the VUV system.
- PFAS had better abatement at high pH because alkaline conditions favored the generation and accumulation of e^-_{aq}. At 185 nm, the quantum yield of e^-_{aq} from OH^- is 0.11, while from H_2O is 0.045 (Dainton et al., 1965; Gonzalez et al., 2004). Moreover, alkaline conditions suppress e^-_{aq} scavenging by H^+ and promote the transformation of $H\cdot$ to the stronger reductive radical - e^-_{aq} (Gonzalez et al., 2004).
- DO in solution is a scavenger for e^-_{aq}, thus eliminating DO enhanced PFAS degradation. But the difference in PFAS transformation with and without purging N_2 gas was not drastic, which may result from the long experimental time and/or direct photolysis at 185 nm. DO could be transformed into different forms (e.g., $O_2^{\cdot-}$) under 185 nm irradiation, leading to decreased DO concentration at a later reaction time (Heit et al., 1998). Besides, the direct photolysis of PFAS at 185 nm could reduce the impact of DO on PFAS removal.

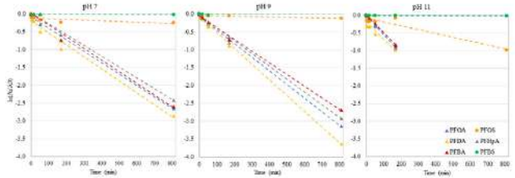

Figure 1. Degradation of six PFAS in VUV processes vs. time. N_2 gas was prior purged into the solution. Reaction time = 5, 17, 52, 170, 810 (min). The initial concentration was 0.1 umol/L for each PFAS. The concentration of PFCAs at pH 11 and 810 mins were lower than detection limits (0.05 ng/L).

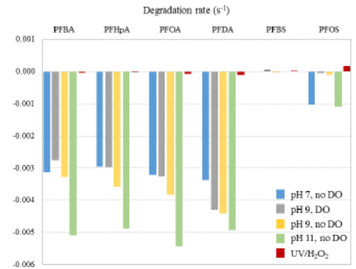

Figure 2. Comparison of the PFAS degradation rates in VUV processes. The initial concentration was 0.1 umol/L for each PFAS. [H_2O_2] = 0.15 mmol/L.

REFERENCES

Bentel, M. J., Yu, Y., Xu, L., Li, Z., Wong, B. M., Men, Y., & Liu, J. (2019). Defluorination of Per- and Polyfluoroalkyl Substances (PFASs) with Hydrated Electrons: Structural Dependence and Implications to PFAS Remediation and Management. *Environmental Science and Technology*, *53*(7), 3718–3728. https://doi.org/10.1021/acs.est.8b06648

Buxton, G. v., Greenstock, C. L., Helman, W. P., & Ross, A. B. (2009). Critical Review of rate constants for reactions of hydrated electrons, hydrogen atoms and hydroxyl radicals (·OH/·O− in Aqueous Solution. *Journal of Physical and Chemical Reference Data*, *17*(2), 513. https://doi.org/10.1063/1.555805

Dainton, F. S., F.R.S, & Fowles, P. (1965). The photolysis of aqueous systems at 1849 Å II. Solutions containing Cl-, Br-, SO2-4 or OH- ions. *Proceedings of the Royal Society of London. Series A. Mathematical and Physical Sciences*, *287*(1410), 312–327. https://doi.org/10.1098/RSPA.1965.0182

Gonzalez, M. G., Oliveros, E., Wörner, M., & Braun, A. M. (2004). Vacuum-ultraviolet photolysis of aqueous reaction systems. *Journal of Photochemistry and Photobiology C: Photochemistry Reviews*, *5*(3), 225–246. https://doi.org/10.1016/J.JPHOTOCHEMREV.2004.10.002

Heit, G., Neuner, A., Saugy, P. Y., & Braun, A. M. (1998). Vacuum-UV (172 nm) actinometry. The quantum yield of the photolysis of water. *Journal of Physical Chemistry A*, *102*(28), 5551–5561. https://doi.org/10.1021/JP980130I/ASSET/IMAGES/LARGE/JP980130IF00012.JPEG

Fenton self-cleaning MOF and MOF-derived porous carbons modified ceramic membrane towards highly efficient for oil/water emulsion separation

Pei Wang and Xiao-yan Li

Department of Civil Engineering, the University of Hong Kong, Pokfulam, Hong Kong, China (E-mail: *u3007979@connect.hku.hk)**

Abstract
A novel catalytic flat sheet ceramic membrane (CFSCM) is fabricated that is integrated with the advanced oxidation process (AOPs) to achieve a synergistic effect on the mitigation of membrane fouling and removal of organic pollutants from wastewater. With the increased hydrophilicity, higher electronegativity, and narrowed pore size, NPC-MIL-53(Fe)-functionalized catalytic ceramic membrane (NPC53@CM) exhibited a more effective antifouling capability during its application in oil removal from an oily wastewater. The CFSCM performed particularly well in the cleaning and regeneration of fouled membranes, which might be attributed to its increased hydrophilicity and Fenton reaction activity of the coated catalysts.

Keywords
Antifouling, Flat sheet ceramic membrane, Fenton self-cleaning, MOF-derived porous carbon, Oil-in-water emulsion separation

RESULTS AND DISCUSSION

Antifouling performance of the ceramic membrane

Membrane fouling is still one of the greatest challenges for membrane applications, especially in the oil/water separation process. In this work, a MIL(Fe)-type metal-organic framework (MOF) and its calcination yielded MOF-derived N-doped porous carbon were grown in situ on the CFSCM surface to obtain the NH_2-MIL-53(Fe)-functionalized catalytic ceramic membrane (NM53@CM) and NPC-MIL-53(Fe)-functionalized catalytic ceramic membrane (NPC53@CM). The antifouling performance and self-cleaning function of the membranes in the oil emulsion removal from water were investigated.

Under the similar permeability coefficient and separation efficiency conditions (NM53@CM and NPC53@CM had oil removals of 96.4% and 96.9%, respectively), NPC53@CM had a more effective antifouling capability during its application in oil/water emulsion treatment, as shown in Fig. 1. This is likely due to the enhanced hydrophilicity and higher electronegativity of the CFSCM. According to the membrane fouling model analysis, the fouling behavior, including adsorption, deposition, pore blockage, and cake layer formation were alleviated with NPC53@CM owing to the increased hydrophilicity and oleophobicity of the membrane surface. Assessed by extended Derjaguin-Landau-Verwey-Overbeek (XDLVO) theory, NPC53@CM exhibited a higher energy barrier and a powerful repulsive force for foulants to overcome to attach onto membrane surface.

Self-cleaning function of the ceramic membrane

During a long operating period, membrane fouling remains inevitable for CFSCM. The catalytic cleaning performance by Fenton reagent was investigated to evaluate the self-cleaning function of the membrane. As shown in Fig. 2b, the NPC53@CM showed a good catalytic performance in the cleaning and regeneration of the fouled membranes with a flux recovery ratio of 98.8%, which is likely attributed to its increased membrane hydrophilicity and Fenton reaction activity of the coated catalysts. In addition, NPC53@CM maintained a good stability and recyclability after multiple cleaning cycles, indicating its excellent application potential. The research work provides a new technical strategy for modification of ceramic membranes with Fe-based MOFs to achieve antifouling and Fenton self-cleaning function of the membranes for water purification and wastewater treatment.

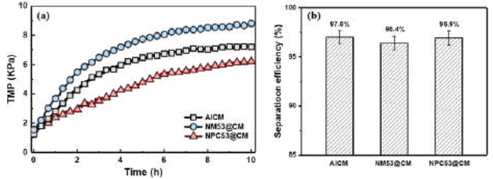

Figure 1. The antifouling performance of different ceramic membranes in treating the oil/water emulsion wastewater: (a) transmembrane pressure (TMP) variation, (b) the oil removal efficiency.

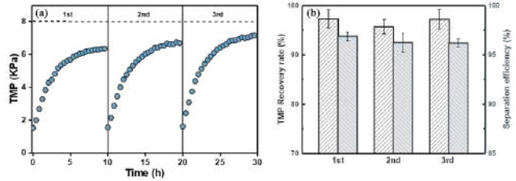

Figure 2. The multiple filtration-cleaning cycle performance of the NPC53@CM membrane treating the oil/water emulsion wastewater: (a) the TMP variation, and (b) the TMP recovery ratio and oil removal efficiency.

REFERENCES

Li, N., Lu, X., He, M., Duan, X., Yan, B., Chen, G., & Wang, S. (2021) Catalytic membrane-based oxidation-filtration systems for organic wastewater purification: A review. Journal of Hazardous Materials, 414, 125478.

Liu, K., Qiao, Y., Shi, T., & Zhou, Q. (2021) Study on coupling coordination and spatiotemporal heterogeneity between economic development and ecological environment of cities along the Yellow River Basin. Environmental Science and Pollution Research, 28, 6898-6912.

Ye, Z., Padilla, J. A., Xuriguera, E., Brillas, E., & Sirés, I. (2020) Magnetic MIL (Fe)-type MOF-derived N-doped nano-ZVI@ C rods as heterogeneous catalyst for the electro-Fenton degradation of gemfibrozil in a complex aqueous matrix. Applied Catalysis B: Environmental, 266, 118604.

Zhang, T., Zhang, J., Wang, Q., Zhang, H., Wang, Z., & Wu, Z. (2022) Evaluating of the performance of natural mineral vermiculite modified PVDF membrane for oil/water separation by membrane fouling model and XDLVO theory. Journal of Membrane Science, 641, 119886.

BioPhree: Reversible phosphate adsorption for phosphate removal to ultra-low levels and recovery. Demonstrations and perspectives

W.K. Wijdeveld*, C. Belloni*, P. de Jager**, R. Buliauskaite**

*Wetsus, European Centre of Excellence for Sustainable Water Technology, Oostergoweg 9, Leeuwarden 8911MA, the Netherlands
(E-mail: wokke.wijdeveld@wetsus.nl; carlo.belloni@wetsus.nl)
**Aquacare Europe B.V., Graaf van Solmsweg 56, 5222 BP, 's Hertogenbosch, the Netherlands
(E-mail: pdjager@aquacare.nl; r.buliauskaite@aquacare.nl)

Abstract
Phosphorus (P) in the effluent of wastewater treatment plants (WWTPs) and agricultural run-off is a major cause for eutrophication of freshwater bodies and should be sufficiently removed. Removal of phosphorus to ultra-low levels is also becoming more important to prevent/minimize biofouling when wastewater effluent is treated with membrane technologies. BioPhree is a technology which uses iron (hydr)oxide-based adsorbents to remove P to ultra-low levels. This presentation shows past and present demonstrations of the technology on freshwater and urban wastewater, including an overview of different pilot tests, performance data and lessons learnt. Finally, it will provide an overview of future demonstrations and perspectives for this adsorption technology.

Keywords (maximum 6 in alphabetical order)
Adsorption; Biofouling; Demonstration; Eutrophication; Mossbauer; Phosphorus

INTRODUCTION

Eutrophication and algal blooms are an increasing threat for water bodies and can cause huge environmental and economic damages. Phosphorus (P) in the effluent of wastewater treatment plants (WWTPs) and agricultural run-off is a major cause for eutrophication in freshwater bodies and should be sufficiently removed. P concentrations greater than 100 µg/L are commonly considered high enough to cause eutrophication (Vollenweider R.A., 1980; Dodds et al., 1998; Richardson et al., 2007; Lurling and Oosterhout, 2013). However, the strictest regulations target 10 µg/L as a good ecological level for fresh waterbodies (Carvalho et al., 2013.)
Removal of phosphorus to ultra-low levels is also becoming more important to combat biofouling when wastewater effluent is treated with membrane technology (Vrouwenvelder et al., 2010). With a trend of complete re-use of wastewater (zero-liquid discharge), Nano Filtration (NF) and Reverse Osmosis (RO) membranes are applied more often to remove pollutants and recover nutrients and salts.
Adsorption is a suitable method for P removal in terms of performances and economics, with a low footprint (Kumar et al, 2019). Some of the most promising adsorption media are iron (hydr)oxide granules and hybrid ion exchange resins (HAIX) with ferric oxide nanoparticles embedded in the structure (Huang et al., 2020). These adsorbents can be regenerated many times with an alkaline solution from which the phosphorus can be subsequently recovered. BioPhree is a technology which uses iron (hydr)oxide-based adsorbents to remove P to ultra-low levels. This presentation shows past and present demonstrations of the technology on freshwater and urban wastewater, including an overview of different pilot tests, performance data and lessons learnt. Finally, it will provide an overview of future demonstrations and perspectives for this adsorption technology.

GEORGE BARLEY PRIZE

The BioPhree technology was demonstrated for 3 months in eutrophicated marsh water in Canada in the George Barley Water Prize contest in 2018. The BioPhree technology treated up to 32 m3/day of water with ortho-P (oP) and particulate-P (pP) concentrations of 0.177 mg/L and 0.220 mg/L respectively. The installation consisted of an advanced filtration stage for particulate P-removal, followed by an iron oxide-based resin adsorbent system for ortho-P adsorption. The total oP and pP removal was 97% and 78% respectively. The adsorbent could be regenerated and re-used and P could be recovered from the regenerant solution as raw material for fertilizer application. The regeneration is a key factor which considerably decreases operational cost of adsorption systems.

H2020 WATER-MINING

In the H2020 Water-Mining project, Wetsus is demonstrating reversible P-adsorption on pilot-scale at two case study sites in Cyprus and Catalonia. At these sites, effluent wastewater from the WWTPs is reused for irrigation purposes. Due to salinity concerns of the water in Cyprus, a desalination pilot plant is demonstrated at the wastewater treatment plant of Larnaca. Biofouling of membranes is a common occurrence when treating wastewater and can seriously limit the efficiency of such processes. BioPhree is implemented before the desalination process system to remove P down to ultra-low levels, thus limiting biofouling. Moreover, the irrigation water in Larnaca is stored in a lagoon before use. This lagoon is heavily eutrophied and can lead to clogging of the irrigation system with algae. Especially for drip irrigation this can be problematic. By removing phosphorus down to ultra-low levels BioPhree has the benefit of preventing eutrophication in storage lagoons. The BioPhree system in Larnaca is currently operational for over a year with effluent quality <50 ug/L demonstrated and repeated regenerations performed. In the spring of 2023, the pilot system will be moved and demonstrated in La Llagosta, Catalonia, for another year. In La Llagosta, Wetsus will also demonstrate a vivianite crystallization technology named ViviCryst to remove the bulk of phosphorus as a post-precipitation method, before polishing the effluent with BioPhree.

ADSORBENT SPECIATION WITH MOSSBAUER SPECTROSCOPY

One of Wetsus' greatest tools in studying and developing P adsorbents is Mossbauer Spectroscopy (MB). It was observed that many adsorbents lack in terms of speciation characterization (Kumar et al., 2019) and that especially during regeneration, the iron oxide species in the adsorbent can transform or sinter, thus impacting the performances (Kumar et al., 2018). MB is a non-destructive nuclear technique, which works with few elements, among which Fe is the most widely investigated. It provides information on the oxidation state, structural properties, magnetic properties, particle size, and can provide a quantitative speciation of the iron species in the sample. MB allows us to fully characterize iron oxide-based adsorbents, identifying and quantifying the different Fe species, both crystalline and amorphous, monitoring their transformations throughout the process.
MB provides the chance to investigate and monitor the properties of our adsorbents and the regeneration thereof on a fundamental level, understanding their behavior throughout the process, to further improve adsorbent stability for P-recovery. For example, MB has been applied in our group to develop innovative doped iron-based nanoparticles with improved stability.

PERSPECTIVES

Adsorption is a promising technology to recover P. Precipitations becomes too expensive when aiming at ultra-low P removal (Kumar et al., 2019). Current P-removal technologies to prevent eutrophication consist of (coated) sand filtration, which does not efficiently remove oP or makes it impossible to recover it, and constructed wetlands, which have a considerable footprint and eventually turns in P hotspots for downstream waterbodies (Bishop & Szafraniec, 2019). An adsorption plant requires tens to hundreds of times less area than wetlands, allows recovery of P and regeneration of the adsorbent, decreasing the OpEx. Too little attention on adsorption to target P sources (as WWTP effluent or agricultural runoff) to prevent eutrophication of freshwater bodies and for lake remediation has been spent. In fact, in-lake treatments like P precipitation with Al or La based chemicals are still widely preferred (Mucci et al., 2019), despite the former revealed to be ineffective for long-term P-blocking and to affect the waterbody pH, while the latter effectively blocks P without allowing its recovery and regeneration of the adsorbent.

Biophree has proven its efficacy to fill the gap between current regulations limits (which are not always met) and actual good ecological quality of water, meeting the circularity targets as environmental impact (eutrophication prevention), nutrients and resources recovery (P), and reusability of materials (adsorbent) with a low footprint.

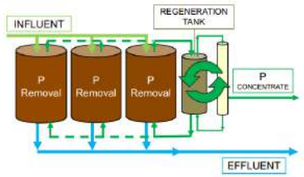

Figure 1. BioPhree concept

Figure 2. Water-Mining pilot installation in Cyprus

REFERENCES

Bishop, W.M., Szafraniec, M.L., 2019, November 11-15. Mitigating Internal Nutrient Loading in a Florida Treatment Wetland [Conference presentation]. NALMS 2019, Burlington, Vermont, United States
Carvalho, L., Mcdonald, C., de Hoyos, C., Mischke, U., Phillips, G., Borics, G., Poikane, S., Skjelbred, B., Solheim, A.L., Van Wichelen, J., Cardoso, A.C., 2013. Sustaining recreational quality of European lakes: Minimizing the health risks from algal blooms through phosphorus control. J. Appl. Ecol. 50, 315–323. https://doi.org/10.1111/1365-2664.12059
Dodds, W.K., Jones, J.R., Welch, E.B., 1998. Suggested classification of stream trophicstate: distributions of temperate stream types by chlorophyll, total nitrogen, and phosphorus. Water Res. 32 (5), 1455-1462.
Huang, X., Guida, S., Jefferson, B., Soares, A., 2020. Economic evaluation of ion-exchange processes for nutrient removal and recovery from municipal wastewater. npj Clean Water 3. https://doi.org/10.1038/s41545-020-0054-x
Kumar, P.S., Korving, L., van Loosdrecht, M.C.M., Witkamp, G.J., 2019. Adsorption as a technology to achieve ultra-low concentrations of phosphate: Research gaps and economic analysis. Water Res. X 4, 100029. https://doi.org/10.1016/j.wroa.2019.100029
Kumar, P., Ejerssa, W.W., Wegener, C.C., Korving, L., Dugulan, A.I., Temmink, H., van Loosdrecht, M.C.M., Witkamp, G.J., 2018. Understanding and improving the reusability of phosphate adsorbents for wastewater effluent polishing. Water Res. 145, 365–374. https://doi.org/10.1016/j.watres.2018.08.040
Lurling, M., Oosterhout, F., 2013. Controlling eutrophication by combined bloom precipitation and sediment phosphorus inactivation
Mucci, M., Waajen, G., Lürling, M., 2019, November 11-15. Managing Eutrophication Through Chemical Inactivation of Phosphate [Conference presentation]. NALMS 2019, Burlington, Vermont, United States
Murad, E., Cashion, J., 2004. Mössbauer spectroscopy of environmental materials and their industrial utilization. Kluwer Academic Publishers, DOI 10.1001/978-1-4419-9040-2
Richardson, C.J., King, R.S., Qian, S.S., Vaithiyanathan, P., Qualls, R.G., Stow, C.A., 2007. Estimating Ecological Thresholds for Phosphorus in the Everglades. Environ. Sci. Technol. 41 (23), 8084-8091
Vrouwenvelder J.S., Beyer F., Dahmani K., Hasan N., Galjaard G., Kruithof J.C., van Loosdrecht M.C.M., 2010. Phosphate limitation to control biofouling. Water Res. 44: 3454–3466. https://doi.org/10.1016/j.watres.2010.03.02
Vollenweider RA, K.J., 1980. Background and summary results of the OECD cooperative program on eutrophication. Proceedings of an International Symposium on Inland Waters and Lake Restoration 26-36.

Reactor designs to increase photocatalytic degradation of organic trace substances for improved water protection

J. Wolters*, A. Alves Cardoso*, D. Daskalova**, G. Aguila**, B. M. Aumeier*, U. Plachetka** and T. Wintgens*

* Institute of Environmental Engineering (ISA) of RWTH Aachen University, Mies-van-der-Rohe-Str. 1, 52074 Aachen, Germany (E-mail: wolters@isa.rwth-aachen.de)
** AMO GmbH, Otto-Blumenthal-Str. 25, 52074 Aachen, Germany

Abstract
Among advanced oxidation processes (AOPs) – key technologies for the degradation of persistent trace substances in wastewater (WW) treatment – photocatalysis shows great promise, but needs improvement in efficiency. In this study, we investigated the influence of improved catalyst material and adapted reactor geometry on the photocatalytic degradation of organic trace substances. In particular, we studied the extent to which mixing reduced mass transport limitations and thus increased the efficiency of the process. Kinetic rate constants were determined and compared well to data from other studies These comprehensive investigations and promising results are the prerequisites for up-scaling the process and hence contribute to narrowing the gap between fundamental research and industrial application of photocatalysis in WW treatment.

Keywords
Advanced oxidation process; micropollutants; pilot plant; rapid prototyping; wastewater treatment

INTRODUCTION

A good ecological and chemical status of water bodies - set as a target by the Water Framework Directive - has not been achieved in many rivers (Land.Nrw, 2023). One reason are substance inputs from point sources like municipal WW treatment plants, which can be reduced by advanced treatment (Rizzo et al. 2020). Photochemical AOP derive energy from light radiation and photocatalysts can be used to promote the formation of the reactive OH radicals. Due to this high reactivity, critically persistent substance groups such as PFAS can also be eliminated (Leonello et al., 2021). The efficiency of this process depends on the reactor setup, the catalyst material and the light transmission and chemical composition of the water matrix (Venieri et al., 2020). In this study, we holistically investigated these influencing factors at lab-scale, with a view to operating a pilot plant at a WW treatment plant.

MATERIALS AND METHODS

The methodology of the preliminary study is based on DIN 52980 to determine the photocatalytic activity of surfaces (10^{-5} mol L^{-1} methylene blue as test substance). A collimated beam device was uses with λ = 365 nm and E = 15.000 µW cm^2. Pseudo-first-order rate constant was used for evaluation.
Different reactor variants were produced with 3D printing.

Figure 1. Lab set-up: (a) pump; (b) control box of irradiation unit (c) PearlLab Beam™ and (d) reactor.

RESULTS AND DISCUSSION

The effectiveness of the catalyst under UV radiation could be increased by various structural modifications. In addition, a shift in the absorption spectrum from the UV range to the visible light range could be achieved. (Daskalova et al. 2022 preprint) Figure 2 shows how our preliminary results outperform the rate constants of many other laboratory studies.

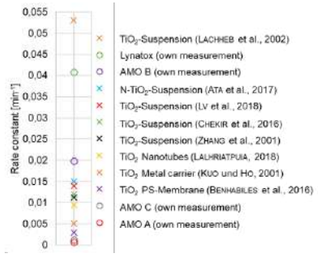

Figure 2. Efficiency of different UV catalyst systems for water purification. AMO B is currently the best self-made catalyst (immobilized: plasmonic structure of gold and ammonil with TiO2 coating on quartz glass carrier).

In addition to these nanoscopic but far-reaching material changes, the meaningful use of these advantages requires changes in the reactor design. In the reactor, the catalyst is irradiated with light while the WW to be cleaned moves over the reactive surface. Consequently, mixers have to be introduced into the used flat-bed and tubular reactors in order to maximize the contacts of reactants by minimizing the laminar boundary layer. (Chong et al. 2010) The first attempts at mixing by means of overflow and the resulting reduction in mass transport limitations are presented in Figure 3.

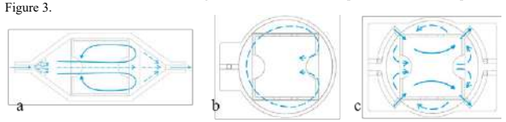

Figure 3. Reactor designs: (a) loop reactor; (b) aereation reactor and (c) flow through reactor - The flow through reactor achieved the best degradation performance with 91.8%, followed by the aeration reactor with 74.7% and the circulation reactor with 59.9%. The degradation performance could be improved by additional ventilation.

ACKNOWLEDGEMENTS

The authors thank the Federal Ministry of Education and Research of Germany (BMBF; grant number 02WCL1019A) and the PEPcat project partners.

REFERENCES

Chong et al. 2010 Recent developments in photocatalytic water treatment technology: A review. *Water Research*, **44**(10), 2997–3027.
Daskalova et al. (n.d.) Combined Structural and Plasmonic Enhancement of Thin Film Photocatalysis for Solar-Driven Wastewater Treatment. doi.org/10.48550/arXiv.2212.04465.
Land.NRW 2023
Leonello et al. 2021 Light-Induced Advanced Oxidation Processes as PFAS Remediation Methods: A Review. *Applied Sciences*, **11**(18), 8458.
Rizzo, L. et al. 2020 BAT and treatment trains to address current challenges in urban wastewater reuse for irrigation of crops in EU countries. *STOTEN* **710**, 136312
Venieri et al. 2020 Solar Photocatalysis for Emerging Micro-Pollutants Abatement and Water Disinfection: A Mini-Review. *Sustainability,* **12**(23), 10047.

Biochar-nano zero-valent iron composite membrane for the degradation of carbamazepine by activation of persulfate

Yongtao Xue *, Mohammadreza Kamali * and Raf Dewil **

* KU Leuven, Department of Chemical Engineering, Process and Environmental Technology Lab, J. De Nayerlaan 5, 2860 Sint-Katelijne-Waver, Belgium (E-mail: *Yongtao.xue@kuleuven.be*; *Mohammadreza.Kamali@kuleuven.be)*
** University of Oxford, Department of Engineering Science, Parks Road, Oxford OX1 3PJ, United Kingdom (E-mail: *raf.dewil@kuleuven.be*)

Abstract
In this study, novel walnut shell biochar-nano zero-valent iron nanocomposites (WSBC-nZVI) were synthesized using a combined pyrolysis/reduction process. The WSBC-nZVI displayed a high removal efficiency (85%) for carbamazepine (CBZ) compared with WSBC (70%) and nZVI (77%) in the presence of persulfate. Subsequently, WSBC-nZVI was applied for the fabrication of the membrane using a phase inversion method. The membrane demonstrated an excellent degradation efficiency (91%) for CBZ in a dead-end system. In addition, the effect of different operating parameters on the degradation efficiency in the membrane/persulfate system was investigated. The optimum pH was achieved under near-neutral conditions and by increasing the concentration of CBZ a drop in the efficiency of the system was observed. The degradation mechanisms and degradation products were also investigated, and the possible degradation pathways and the predicted toxicity of intermediates were proposed. Furthermore, the feasibility of this membrane technology was examined by the treatment of real wastewater.
Keywords
catalytic membrane; mechanisms; nano zero-valent iron; persulfate; walnut shell biochar

MATERIALS AND METHODS

The walnut shell was obtained from Matthys Bvba (Belgium) with a particle size ranging from 450 µm to 800 µm. A controlled pyrolysis process was implemented for the preparation of the walnut shell biochar. In detail, 20 g of the walnut shell was impregnated with 100 mL H_3PO_4 (0.6 M) at 90 °C for 3 h, then dried at 80 °C overnight. Subsequently, the obtained precursor was pyrolyzed at 520 °C for 2 h with a heating rate of 10 °C/min. The entire pyrolysis process was carried out under the nitrogen atmosphere. The prepared black powder was collected and labelled as WSBC for further characterization and use. The WSBC-nZVI was synthesized using a liquid phase reduction process. Typically, 0.4 g WSBC and 6 g $FeSO_4{\cdot}7H_2O$ were dispersed in 400 mL distilled water under the stirring and nitrogen atmosphere for 30 min. Then, 200 mL $NaBH_4$ solution with a concentration of 20g/L was added into the mixture drop by drop with the flowing nitrogen. After 1 h of reaction, the final black powder was collected and washed with distilled water three times. Finally, the nanomaterial was dried at 60 °C overnight under the nitrogen atmosphere. The nZVI was also synthesized through the same method without the WSBC.

The WSBC-nZVI membrane was fabricated by a phase inversion method. In a typical process, the WSBC-nZVI nanomaterial (2%) was dispersed into a DMF solution (70%), then it was distributed uniformly under ultrasound conditions for 30 min. Subsequently, the PES (16%) and PEG (12%) were added to the above solution. The mixture was heated at 60 °C for 6 h under continuous stirring conditions. The obtained homogenous solution was degassed under ultrasound conditions for 30 min to remove bubbles in the solution. Then, the solution was evenly spread onto a glass plate using a casting knife (Elcometer 3580, Netherlands) to set a wet membrane thickness of 200 µm. Thereafter, the glass plate was immediately immersed in a distilled water bath at room temperature until the membrane spontaneously detached from the glass plate. The membrane was stored in the distilled water under an N_2 atmosphere to remove the residual organic solvent.

RESULTS AND DISCUSSION

Characterization of the nanomaterials and membrane

Fig. 1a demonstrates the vesicle-type morphology of WSBC with a porous structure. The nZVI presents as agglomerated spherical particles. The aggregation of the nanosized particles is due to the Van der Waals effects between the nano-size magnetic particles. In Fig. 1d-e, the morphology of WSBC-nZVI clearly confirms that the nZVI particles are well dispersed on the surfaces and pores of WSBC. In addition, the mapping of WSBC-nZVI proves the presence of C, O, and Fe in the composition of the materials, as indicated in Fig. 1e-i. Furthermore, the presence of WSBC-nZVI particles on the flat surface of the membrane is evident from Fig. 1j. The cross-sectional images of the membrane (Fig. 1 k-m) also reveal its porous and spongy morphology. Formation of the porous structures is due to the use of PEG as a pore-forming agent in the membrane fabrication process. In addition, the presence of hydrophilic oxygen-containing groups (such as -COOH, C-O) on the surface of WSBC-nZVI nanoparticles can improve the diffusion rate of water into the membrane during the fabrication process of the membrane, which results in the formation and development of pores.

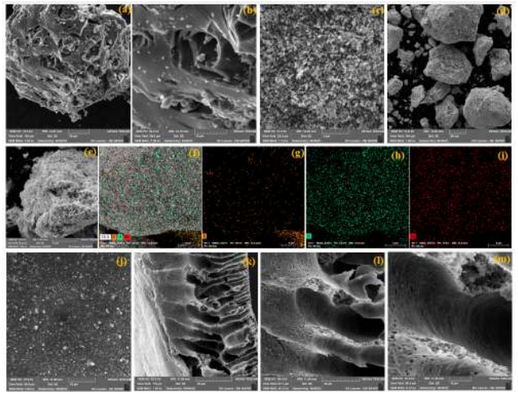

Figure 1. SEM images of WSBC (a-b), nZVI (c), WSBC-nZVI nanocomposite (d-e), mapping (f-i) of WSBC-nZVI nanocomposite, surface (j), and cross-section (k, l, m) of the WSBC-nZVI membrane.

Degradation of CBZ

Fig. 2a indicates that WSBC exhibits the highest adsorption capacity for CBZ (75%) among the studied materials This can be attributed to the presence of surface functional groups such as -COOH, -N-H on the surface of WSBC which can provide more active sites for the adsorption of pollutants, and may also promote the formation of hydrogen bonds between adsorbent and the contaminant. In addition, the adsorption capacity of WSBC-nZVI for CBZ was slightly increased (9%) compared to nZVI (4%), which can be related to the surface functional groups still remained at the surface of BC after loading of nZVI. Furthermore, the addition of PS had no significant effect on the removal of CBZ with WSBC (Fig. 2 b). In this situation, the competitive adsorption occurs between CBZ and PS, and a part of the adsorption sites of WSBC is occupied by PS. On the other hand, the WSBC can't efficiently activate PS to degrade CBZ. As indicated in Fig. 2b, both nZVI and WSBC-nZVI demonstrated high CBZ degradation efficiencies of 86% and 76%, respectively, indicating that these nanomaterials can efficiently activate PS for the degradation of CBZ. In addition, the WSBC-nZVI exhibits a higher degradation efficiency than nZVI, which can be attributed to the high surface area high porosity, and abundant functional groups of WSBC-nZVI.

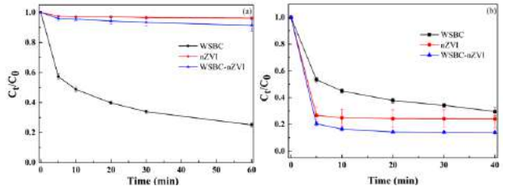

Figure 2. Adsorption (a) and degradation (b) kinetics of CBZ by different nanomaterials (conditions: 0.5 g/L catalyst, 10 mg/L CBZ, 1mM PS).

Degradation mechanisms

Fig. 3 illustrates the reaction mechanism for the WSBC-nZVI membrane/PS system proposed according to the results achieved by the scavenging experiments. The Fe species (Fe^{2+}) is quickly generated from WSBC-nZVI via different routes, such as the direct reaction of Fe^0 with PS, indirect reaction of Fe^0 with oxygen, the indirect reaction of Fe^0 with water molecular. Subsequently, Fe^{2+} can react with PS to produce Fe^{3+} and $SO_4^{\cdot-}$. A part of $SO_4^{\cdot-}$ is converted into SO_4^{2-} and ·OH by the reaction of H_2O or OH^-. In addition, $O_2^{\cdot-}$ can be produced from two routes including the reaction between Fe^{2+} and O_2 and the reaction between O_2 and electrons. The $^1O_2$ can also be generated from the reaction between $O_2^{\cdot-}$ and water (or H^+). Meanwhile, Fe^{3+} can be reduced into Fe^{2+} through the reaction of Fe^0 and Fe^{3+}, which is a key reaction for the degradation of CBZ. Moreover, WSBC as a supporter can not only prevents the agglomeration of nZVI but also promotes the conversion of Fe^{3+} to Fe^{2+} by supplying electrons. The abundant functional groups (such as -COOH, C-O) of WSBC can improve the adsorption capacity for CBZ and boost the activation efficiency of PS for the degradation of organic pollutants. In a conclusion, the CBZ can be firstly adsorbed on the surface of the membrane, then it's decomposed in the presence of active species (e.g. ·OH, $SO4^{\cdot-}$, $O_2^{\cdot-}$, $^1O_2$). Finally, the CBZ can be further oxidized into small molecular intermediates, CO_2, and H_2O (Fig. 4).

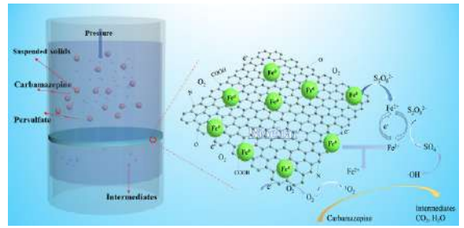

Figure 3. The possible reaction mechanism for degradation of CBZ by WSBC-nZVI membrane.

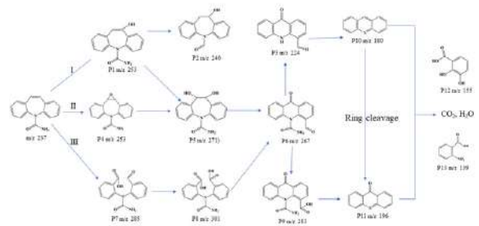

Figure 4. Proposed degradation pathways of CBZ in the membrane/PS system.

REFERENCES

Xue, Y., Kamali, M., Yu, X., Appels, L., Dewil, R.2022. Novel CuO/$Cu_2(V_2O_7)$/V_2O_5 composite membrane as an efficient catalyst for the activation of persulfate toward ciprofloxacin degradation. *Chemical Engineering Journal*, 140201.
Xue, Y., Guo, Y., Zhang, X., Kamali, M., Aminabhavi, T. M., Appels, L., Dewil, R. 2022. Efficient adsorptive removal of ciprofloxacin and carbamazepine using modified pinewood biochar–A kinetic, mechanistic study. *Chemical Engineering Journal* **450**, 137896.

Convergence of bioreduction process and ICT for practical use of biosorption technology

Hanui Yang*, Donghee Park*

* Department of Environmental Engineering, Yonsei University, 1 Yonseidae-gil, Wonju 26493, Republic of Korea
(E-mail: *gksml506@naver.com*; *dpark@yonsei.ac.kr)**

Abstract
A previous study has developed a new bioreduction process for the continuous treatment of chromium wastewater by predicting the effluent concentration of Cr(VI). In this study, we introduce the ICT-Brduction process that measures the influent characteristics in real-time by applying information and communication technology (ICT) and calculates the Cr(VI) concentration of the influent through machine learning. In addition, the bioreductant used in this process can be recovered as Cr_2O_3, which has a high recycling value. Therefore, the ICT-Bioreduction process applying biosorption technology has a high value in the ESG industry because it can purify the chromium wastewater using biowaste and recover chromium resources therefrom.

Keywords
Biosorption; Chromium; ESG; ICT; Machin learning; Sensor

INTRODUCTION

In previous studies, we developed a new bioreductant and bioreduction process that simultaneously remove Cr(VI) and Cr(III). In addition, for practical process development, a new model suitable for the bioreduction process was developed to predict the effluent concentration of Cr(VI). In this model, the values of influent Cr(VI) concentration and the pH determine the effluent concentration of Cr(VI). Therefore, to put the bioreduction process to practical use, it is necessary to measure the Cr(VI) concentration and pH value of the influent in real-time. The influent concentration of Cr(VI) was calculated in real-time through OPR, EC, and RGB sensors, and the pH value was measured in real-time through the pH sensor. In addition, this study aims to suggest the possibility of using biosorption technology in the field of environmental society and governance (ESG) by researching on the disposal or recycling of bioreductants treated with Cr(VI) wastewater.

MATERIALS AND METHODS

Information and communication technology (ICT)

Arduino (Arduino Uno SMD R3, arduino. cc), which is a single-board microcontroller for building a digital device, was used as ICT to predict the influent concentration of Cr(VI) in real-time. An automatic measurement system that consisted of five sensor devices: pH (SEN0161-V2, DFRobot, China), oxidation-reduction potential (ORP) (SEN0165, DFRobot), electrical conductivity (EC) (DFR0300, DFRobot, China), temperature (KIT0021, DFRobot, China), and color (RGB) (SEN0212, DFRobot, China) sensor connected to one Arduino was developed to measure the properties of Cr(VI) wastewater influent in real-time. The sensors were installed in two cylindrical reactors with a volume of 500 mL. The reactor equipped with the RGB sensor was wrapped with black insulating tape to block ambient light. The data measured through the sensors were programmed to be monitored in real-time using Tkinter, which is a module used for graphical user interface programming.

Bioreduction process

Bioreduction process incorporates an up-flowed fixed-bed column with inlet and outlet ports. Acrylic columns with an internal diameter of 2 cm and a length of 17 cm were connected in series to facilitate their replacement. The column was moderately densely packed with a bioreductant (500 g/L) composed of pine bark and alginate. Thin cotton was placed in the bottom of the column to ensure uniform distribution of influent across the entire cross-section of the column. A top layer of thin cotton was used to minimize washing out of the bioreductant. The process was operated in an up-flow mode at a constant temperature.

RESULTS AND DISCUSSION

To predict the influent concentration of Cr(VI), chromium synthesis wastewater was prepared under 46 conditions and the characteristics of the chromium synthesis wastewater were measured using the automatic measurement system. As a result of convolution neural networks (CNN) of about 7,000 measurement data collected from the automatic measurement system, RGB values showed a very high correlation with Cr(VI) concentration. Therefore, an empirical model for calculating the Cr(VI) concentration was derived using the RGB values (Fig. 1). Thus, the Cr(VI) concentration of influent can be calculated in real-time using machine learning, and the Cr(VI) concentration of effluent can be predicted from the concentration and pH of influent measured through the automatic measurement system. The ICT-Bioreduction process is a process that can be put to practical use in actual processes by continuously treating Cr(VI) wastewater through ICT convergence.
Table 1 shows the XRF results of components after incinerating the bioreductant treated with Cr(VI)wastewater at 1100 °C. The incinerated bioreductant was mainly composed of Cr and O, which was composed of Cr_2O_3 molecular structure as a result of XRD analysis. Cr_2O_3 is used in various industrial fields such as links, glasses, paints, and ceramics. Therefore, chromium can be recovered by incineration of the bioreductant, and can be recycled in other industries.

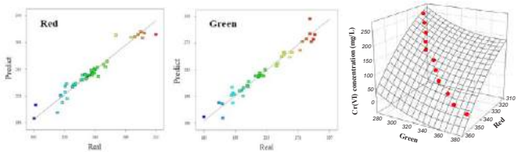

Figure 1. RSM diagnostics plot for predicting verse real of RGB.

Table 1. XRF result of bioreductant ash incinerated at 1100 ℃

Atomic content (mass %)				
Cr	O	C	Ca	Etc. (Al,Si)
62.8	36.1	0.8	0.1	0.2

ACKNOWLEDGMENT

This research was supported by Basic Science Research Program through the National Research Foundation of Korea (NRF) funded by the Ministry of Education (2022R1A6A3A0108699211).

REFERENCES

Park, D., Yun, Y.-S., Jo, J.H., Park, J.M. 2005a. Mechanism of hexavalent chromium removal by dead fungal biomass of Aspergillus niger. *Water Res*. **39**(4), 533-540.

Development of a new bioreduction process for the treatment of chromium wastewater

Hanui Yang*, Donghee Park*

* Department of Environmental Engineering, Yonsei University, 1 Yonseidae-gil, Wonju 26493, Republic of Korea
(E-mail: *gksml506@naver.com*; *dpark@yonsei.ac.kr*)*
*

Abstract
A bioreduction process was composed by filling the column with a new bioreductant capable of simultaneously removing Cr(VI) and Cr(III) using natural biomass. The bioreduction process is in the form of connecting several columns in series, that continuously treat Cr(VI) wastewater by the column rotation system. A new mathematical model was applied to this process to predict the concentration of Cr(VI) in the effluent. As a result of simulating the process using the mathematical model, the predicted value and the experimental value of the effluent concentration showed similar tendencies. In addition, this process is very economical when compared to chemical treatment. This study shows the possibility of applying biosorption technology to the actual process for Cr(VI) wastewater treatment.

Keywords
Biomass; Bioreductant; Bioreduction process; Biosorption; Chromium

INTRODUCTION

Biosorption, one of the Cr(VI) removal methods, is dominated by oxidation-reduction reaction, which has been recognized as 'adsorption-coupled reduction' (Park et al., 2005a). Over the past decades, many researchers have tested various biomass for the removal of toxic Cr(VI) from aqueous solutions. However, research on the practical use of Cr(VI) wastewater treatment using biosorption technology is still insignificant. This study introduces a bioreductant developed using abiotic biomass and shows a new bioreduction process developed for practical use and the results of the process simulation.

MATERIALS AND METHODS

Bioreductant

The abiotic biomass, pine bark (*Pinus sp.*), is a biowaste from a sawmill. The pine bark was sun-dried, then cut into pieces approximately 2–3 cm in size. The small pieces were dried at 100 °C for 24 h, after which they were ground into smaller particles and then sieved to select finer particles between 38–106 μm in diameter. The fine particles were immobilized by entrapment in alginate polymeric matrices. The immobilization content ratio is 4.8 g of fine particles to 2 g of sodium alginate in 100 mL of DI water. The alginate-bark slurry was extruded into 0.1 M $CaCl_2$ to form of unbreakable fiber using a 1 mm diameter of syringe for polymerization. The polymerized resultant formed a skein shape. The skein-bioreductant was washed several times, and the water was wiped off the surface. This bioreductant contained approximately 80% water.

Bioreduction process

Bioreduction process incorporates an up-flowed fixed-bed column with inlet and outlet ports. Acrylic columns with an internal diameter of 2 cm and a length of 17 cm were connected in series to facilitate their replacement. The columns were packed moderately densely with the bioreductant (500 g/L). Thin cotton was placed in the bottom of the column to ensure uniform distribution of influent across the entire cross-section of the column. A top layer of thin cotton was used to minimize washing out of the bioreductant. The process was operated in an up-flow mode at a constant temperature.

RESULTS AND DISCUSSION

Bioreduction process was configured to continuously treat Cr(VI) wastewater by recovering the first column before the Cr(VI) concentration in the effluent was detected above the standard value and installing a new column behind the last column (Figure 1). The Cr(VI) concentration of effluent was predicted through a mathematical model when determining the value of Cr(VI) concentration and pH in influent. The mathematical model was developed by expanding of 'modified dose-response' model. The mathematical model simulated the Cr(VI) concentration in the effluent of each column in the process and obtained the replacement period of the column.
Table 1 shows the required amount of $FeSO_4 \cdot 7H_2O$ and $Ca(OH)_2$ to remove 1 ton of 1 mM Cr(VI), which was calculated from the batch experiment result. The bioreduction process was simulated through the expanded modified dose-response model to calculate the required amount of the bioreductant to treat 1 ton of 1 mM Cr(VI). The bioreduction process reduced costs by 86% compared to the chemical treatment.

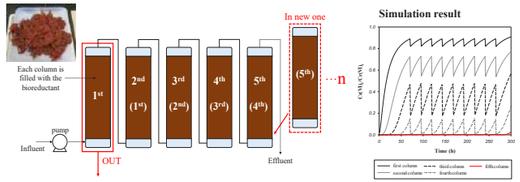

Figure 1. Schematic of bioreduction process.

Table 1. Comparison of the economic value of chemical treatment and bioreduction process for treatment of the 1 ton of 1 mM Cr(VI) wastewater at pH 2.

		Price (won/g)	Required amount (g)	Required cost (won)	Total cost (won)
Chemical treatment	$FeSO_4 \cdot 7H_2O$	4.16	845	3,515	3,996
	$Ca(OH)_2$	0.69	697	481	
Bioreduction process	Bark	-	235	-	565
	Alginate	5.5	98	539	
	$CaCl_2$	0.48	55	26	

ACKNOWLEDGMENT

This research was supported by Basic Science Research Program through the National Research Foundation of Korea (NRF) funded by the Ministry of Education (2022R1A6A3A0108699211).

REFERENCES

Park, D., Yun, Y.-S., Jo, J.H., Park, J.M. 2005a. Mechanism of hexavalent chromium removal by dead fungal biomass of Aspergillus niger. *Water Res.* **39**(4), 533-540.

Novel ceramic SnO_2 electrocatalytic membrane for advanced wastewater treatment and water reuse

Chao Yang[1*] and Xiao-yan Li[1]

[1] Department of Civil Engineering, The University of Hong Kong, Pokfulam, Hong Kong.
[#]Corresponding Author E-mail: yangchao90@connect.hku.hk

Abstract
A novel freestanding ceramic SnO_2-Sb electrocatalytic membrane is developed, which functions as both an anode and a membrane for advanced wastewater treatment, including emerging organic pollutant removal and high-rate virus disinfection. Nearly 100% removal of the pollutants can be achieved by the charged SnO_2-Sb anode membrane in a single-pass treatment.

Keywords (maximum 6 in alphabetical order)
Disinfection; electrochemical oxidation; electroactive membrane; emerging organic pollutants, water treatment

INTRODUCTION

Emerging organic pollutants in wastewater, which are commonly resistant to conventional biological wastewater treatment, have not only posed considerable risks to the eco-system but also worsened the water scarcity problem. Meanwhile, viruses in wastewater are also causing more concerns on human health. Thus, there is an urgent demand of effective technologies for advanced wastewater treatment and water reuse. Electrochemical technology is a promising method for the removal of emerging contaminants from wastewater, due to its strong oxidation capability and environmental compatibility (Radjenovic & Sedlak, 2015). However, the practical application of electrochemical oxidation processes has been hindered by the mass-transfer-limited kinetics and high energy consumption. Reactive electrochemical membrane, also named electrocatalytic membrane, is an innovative strategy to overcome the challenges in electrochemical water treatment (Guo et al., 2016). The porous electrodes simultaneously serve as an electrocatalytic electrode and a membrane filter, which can substantially increase the electroactive surface area of the electrode and improve the mass transport of the process for efficient wastewater treatment (Yang et al., 2021). Herein, a novel freestanding and permeable SnO_2-Sb electrocatalytic membrane was fabricated for electrochemical oxidation and wastewater treatment. The anode was operated in the single-pass flow-through pattern for the removal of emerging organic pollutants and the inactivation of viruses in wastewater. The robustness, feasibility, and stability of the SnO_2-Sb electrocatalytic membrane system was also evaluated in this experimental study.

RESULTS AND DISCUSSION

The schematics of the electrochemical wastewater treatment system equipped with the SnO_2-Sb membrane are shown in Figure 1. The porous and permeable 3D reactive membrane allows wastewater to flow depth-wise through the anode, thus providing a multitude of active sites for direct organic oxidation and reactive radical generation. The treated effluent can be collected for reuse.

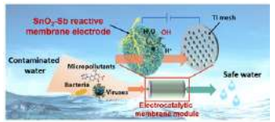

Figure 1. Schematic illustration of the novel electrochemical treatment system equipped with a SnO_2-Sb electrocatalytic membrane for wastewater treatment and reuse.

Performance of the electrocatalytic membrane for antibiotics degradation and virus disinfection

Ciprofloxacin (CIP) was used as a model emerging organic pollutant to evaluate the effectiveness of the ceramic SnO_2-Sb electrocatalytic membrane-based treatment system (Figure 2). In the conventional flow-by configuration, the electrochemical treatment removed approximately 48.0% of the CIP. In the flow-through mode with the electrocatalytic membrane, the CIP removal efficiency increased significantly to 92.1% under the same experimental conditions. The rate constant k_{obs} of CIP degradation for the flow-through anode (0.077 min^{-1}) was more than five times that of the flow-by anode (0.014 min^{-1}). The power consumption of CIP degradation for the flow-through mode was 0.31 kWh g^{-1} CIP, significantly lower than that for the flow-by mode (2.43 kWh g^{-1} CIP).

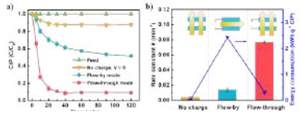

Figure 2. ECO experiments in the flow-by and flow-through configurations: (a) CIP degradation, (b) pseudo-first-order degradation rate constants and energy consumption (conditions: [CIP] = 10 μM, cell potential = 4.0 V, pH = 6.0).

Bacteriophage MS2 was selected as a model virus in this study because its similarity to human pathogenic viruses. Figure 3 shows the virus removal efficiencies of the electrochemical treatment. Nearly no MS2 removal was observed under the non-charged conditions (0 V), as the size of MS2 (20–30 nm) was too small to be removed by membrane filtration. In the conventional flow-by mode with an applied voltage of 3.5 V, a 2.6-log inactivation of MS2 was obtained, with a large amount of MS2 virus remaining in the effluent (10^5–10^6 PFU mL^{-1}). Using the reactive membrane in the flow-through mode, the MS2 virus removal efficiency significantly increased to 100% (> 8.3-log inactivation), and no live MS2 virus was detected in the treated effluent.

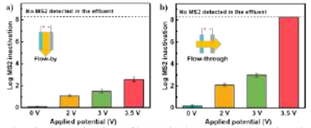

Figure 3. The electrochemical inactivation of bacteriophage MS2: (a) using the conventional flow-by operation and (b) the SnO_2-Sb catalytic membrane flow-through operation with a feed of ~1.5 × 10^8 PFU mL^{-1} of MS2 in 0.05-M Na_2SO_4 at a flux of 54 LMH.

These results prove the superiority of the electrocatalytic SnO_2-Sb membrane in the electrochemical treatment of emerging organic contaminants and viruses within a short period of only about 1.7 min through the membrane anode. The improved mass transport and enlarged electroactive surface area facilitated the direct oxidation and reactive radical generation for organic degradation, resulting in the excellent treatment performance. Overall, this research provides a new strategy for the design and operation of ceramic electrocatalytic membrane systems to achieve effective and reliable purification and disinfection of water and wastewater in decentralized applications.

REFERENCES

Guo L., Jing Y. and Chaplin B.P. (2016) Development and characterization of ultrafiltration TiO_2 Magneli phase reactive electrochemical membranes. Environ. Sci. Technol. 50(3), 1428-1436.
Radjenovic J. and Sedlak D.L. (2015) Challenges and opportunities for electrochemical processes as next-generation technologies for the treatment of contaminated water. Environ. Sci. Technol. 49 (2015) 11292-11302.
Yang C., Fan Y., Shang S., Li, P. and Li, X.Y. (2021) Fabrication of a permeable SnO_2-Sb reactive anodic filter for high-efficiency electrochemical oxidation of antibiotics in wastewater. Environ. Int. 157, 106827.

High-Rate Post-treatment of Sewage from Residential Community by the Down-flow Hanging Sponge System

W. Yoochatchaval*, C. Yensuang*, N. Boonprom *, Y. Takemura** and K. Syutsubo**.***

Department of Environmental Engineering, Faculty of Engineering, Kasetsart University, 50 Ngamwongwan, Ladyao, Chatuchak, Bangkok, 10900, Thailand (E-mail: fengwny@ku.ac.th; ghollapin.y@ku.th; patpaphat.b@ku.th)
** Regional Environment Conservation Division, National Institute for Environmental Studies, 16-2 Onogawa, Tsukuba-City, Ibaraki, 305-8506, Japan (E-mail: takemura.yasuyuki@nies.go.jp; stubo@nies.go.jp)
***Research Center for Water Environment Technology, School of Engineering, The University of Tokyo, Japan (E-mail: stubo@nies.go.jp)

Abstract
This research investigates the process performance of down-flow hanging sponge reactor (DHS) for the post-treatment of effluent from activated sludge process. The reactor was operated under high flow rate condition and low hydraulic retention time (HRT) at 0.5-1 hour for one year. At the shortest HRT of 0.5 hour, the BOD and ammonium loading was 0.96±0.26 kg BOD/m^3/day and 0.30±0.08 kg N/m^3/day, respectively. The reactor illustrated effective performance with respect to high removal efficiency of organic matter (86±7% of BOD removed) without excess sludge treatment. Inorganic nitrogens (ammonium, nitrite, and nitrate) were effectively eliminated (46±19% removal efficiency). The *E. coli* log reduction was 2.2±0.7. So, it is possible to use this reactor as an energy efficiency technology for the post-treatment of domestic wastewater from residential building with HRT of 0.5-1 hour.

Keywords
DHS, Energy efficient; Inorganic nitrogen; Post-treatment; Sponge; Trickling filter

INTRODUCTION

Insufficient aeration process of decentralized wastewater treatment plant is one of the reasons that Bangkok water resources were deteriorated. Installation of post-treatment system is required to improve the organic matter and nitrogen reduction from the discharge. However, huge area (due to the longer retention time) is required which is unfavorable for the space limit area like Bangkok. The down-flow hanging sponge (DHS) technology is one of alternative wastewater treatment technology with the compact size and energy efficient (Tandukar *et al.*, 2005). Because of the self-aeration, the electricity consumption is about 68% reduction from conventional activated sludge process (Yoochatchaval *et al.*, 2014). So, it is an attractive technology for developing countries where are facing with the limitation on budget and space. The DHS system was developed as an aerobic trickling filter using polyurethane sponge media where the oxic and anoxic zone are available. As a result, there are nitrification and denitrification reaction occur. Moreover, the snails (macrofauna) were present on the surface of the sponge resulted to the small excess sludge generated from this system (Onodera *et al.*,2015). From previous research, DHS reactor explicated the significant organic matter removal efficiency under HRT of 1-5 hours (Danshita *et al.*, 2020; Takemura *et al.*, 2022). In this study, the investigated HRT was 0.5- 1 hour. The treatment efficiency of DHS as a post-treatment was observed about 370 days.

MATERIALS AND METHODS

A pilot-scale DHS reactor has been setup at Bongai national housing, in Bangkok area. This cylinder shape reactor has a diameter at 40 cm. The reactor has 4 segments inoculated with sponge media followed by clarifier unit. The total height is 4.12 m. The total volume of sponge media was 175 L with 8,000 pieces of the sponge media. To simulate insufficient water quality of decentralized wastewater treatment plants' effluent, the effluent from Bongai's activated sludge process has been collected and mixed with raw sewage from the national housing at mixing ratio of 2:1. Then, it flowed through the reactor under ambient temperature condition. The operating HRT was set at 1 hour for 170 days. As a result, the BOD and ammonium loading rate were 0.83±0.34 kg BOD/m^3/day and 0.36±0.11 kg N/m^3/day, respectively. At HRT of 0.5 hour (from day 171), the mixing ratio of AS effluent and fresh sewage was changed to 5:1. Then, the BOD and ammonium loading rate were 0.96±0.26 kg BOD/m^3/day and 0.30±0.08 kg N/m^3/day, respectively. The DHS reactor's process performance was investigated routinely by the composite sampling technique. The water quality parameters such as temperature, oxidation reduction potential (ORP), DO and pH were measured onsite. The following parameters were analyzed at laboratory; total suspended solids (TSS), volatile suspended solids (VSS), biochemical oxygen demand (BOD), chemical oxygen demand (COD), total nitrogen (TN), ammonium, nitrite, nitrate (inorganic nitrogen, sum of ammonium, nitrite, and nitrate) and *Escherichia coli* (*E. coli*). The tracer experiment was conducted to confirm the actual HRT. In this experiment, saturated NaCl concentration has been used as the tracer mineral. The NaCl was loaded from the top of the reactor. Then the conductivity of the effluent from DHS reactor was determined.

RESULTS AND DISCUSSION

According to the water quality data, the DHS reactor showed effective process performance. For physical treatment capacity, sponge media was able to trap the suspended solid on the surface area of sponge. As a result, the TSS removal efficiency was more than 85% throughout the experiment. The excess sludge generation was low as compare with other aerobic process. The retained sludge concentration was about 4.7-13.0 kg VSS/m^3-sponge. Because of the long sludge retention time and sufficient oxygen supply, the DHS reactor can successfully treat the organic matter (BOD). The BOD removal efficiency was 86±7% at HRT of 0.5 hour. The DO concentration of the effluent was about twice as compare with the influent (Table 1). The water samples were collected from onsite wastewater treatment plant which located nearby the dense population community. So, fresh sewage was predominated with the pathogens which impacted to human health. *E. coli* could be classified as a sanitation indicator. Interestingly, the DHS reactor can supply enough oxygen and the *E. coli* reduction achieved at 2.2 $\log_{10}$.

Table 1. The water quality data of post-treatment DHS reactor

	HRT 1 hour (day 0-170) AS Effluent: fresh sewage = 2:1			HRT 0.5 hour (day 171-370) AS Effluent: fresh sewage = 5:1		
BOD loading (kg BOD/m^3/day)	0.83±0.34			0.96±0.26		
Ammonium loading (kg N/m^3/day)	0.36±0.11			0.30±0.08		
	Influent	Effluent	Removal	Influent	Effluent	Removal
DO (mg/L)	2.5±0.8	5.2±0.8		3.2±1.0	5.4±0.4	
TSS (mg/L)	20±5	3±3	85±12%	11±4	1±1	91±4%
Total COD (mg/L)	88±23	22±18	76±10%	52±18	13±10	76±13%
Total BOD (mg/L)*	34±14	4±2	87±5%	20±5	3±1	86±7%
Ammonium (mgN/L)	14.9±4.1	2.5±2.4	84±14%	6.4±1.7	0.5±0.4	93±4%
Inorganic N. (mgN/L)	15.8±4.0	3.84±1.80	46±18%	6.46±2.78	3.63±1.93	46±19%
E. coli (CFU/mL)	4.5 E+04	3.1 E+02	2.16 $\log_{10}$	1.7 E+04	1.2 E+02	2.17 $\log_{10}$

*The BOD measurement with additional of allylthiourea (ATU)

The DHS reactor has high potential for nitrification process. As a result, ammonium concentration of the effluent is very low (0.5-2.5 mgN/L). From previous research the removal efficiency of ammonia was 79% at 0.046 kg N/m^3 day loading and HRT of 1.5 hour (Onodera *et al.*, 2016). Interestingly, this experiment confirmed the super high rate of ammonia removal at 93±4% with the loading of 0.30±0.08 kg N/m^3/day under HRT of 0.5 hour. So, short HRT condition did not significantly impact to the nitrification process. Also, the inorganic nitrogen removal efficiency was about 45% of both HRT. This evidence confirmed that the DHS reactor is possible for application as the post-treatment system.

The information of retained sludge concentration is shown in figure 1. When the HRT reduced to 1 hour, the sludge was washed out from the first segment due to effect of wastewater volume and hydraulic impact. As a result, the concentration of retain sludge reduced in segment 1-4. However, the reduction of sludge concentration was not obvious in segment 2-4 due to the lower hydraulic impact and higher growth of biomass. Finally, the retained sludge in segment 4 remained at 13.0 kg VSS/m^3/sponge. The retained sludge concentration of segment 2-4 is similar to previous research.

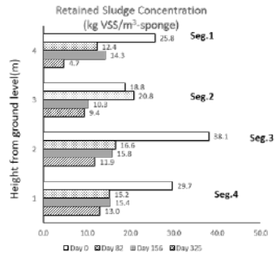

Figure 1. Retained sludge concentration

CONCLUSIONS

A pilot-scale DHS reactor was installed at a small-scale wastewater treatment plant. This reactor has been used as the post-treatment system of sewage from residential area (Bangai community, Bangkok). The DHS reactor illustrated the effective process performance at HRT of 0.5 hour. The organic matter and inorganic nitrogen could be treated sufficiently by this reactor. BOD removal efficiency reached 86±7%. The inorganic nitrogen removal efficiency was 46%. The energy consumption for this system is for the purpose of water lift up (self-aeration). Sponge media can retain the sludge in sufficient concentration. Sludge deterioration and washed out slightly occurred resulting to long sludge retention time. So, the DHS reactor is possible to apply for post-treatment of onsite wastewater treatment plant.

ACKNOWLEDGMENT

We wish to thank the Bangkok Metropolitan Administration for providing space for the installation of the DHS reactor. This research project was supported by the NIES Research Funding (Type A) of the National Institute for Environmental Studies; Japan

REFERENCES

Danshita, T., Yoochatchaval, W., Takemura, Y., Miyaoka, Y., Kada, M., Tepjun, W., Thonglee, S., Sonaka, H., Yamaguchi, T., Tomioka, N., Banjongproo, P., Okadera, T., Ebie, T., Syutsubo, K. 2020 Performance evaluation of a down-flow hanging sponge (DHS) reactor as a decentralized domestic wastewater treatment system in tropical regions. *Journal of Environmental Science and Health: Part A (Toxic/Hazardous Substances and Environmental Engineering)* https://doi.org/10.1080/10934529.2020.1748472 , **55**(7), 847-857.

Onodera, T., Syutsubo, K., Yoochatchaval, W., Sumino, H., Mizuochi, M., Harada, H. 2015 Protection of biomass from snail overgrazing in a trickling filter using sponge media as a biomass carrier: down-flow hanging sponge system. *Water Science & Technology*, **71**(4), 518-523.

Onodera, T., Okubo, T., Uemura, S., Yamaguchi, T., Ohashi, A., Harada, H. 2016 Long-term performance evaluation of down-flow hanging sponge reactor regarding nitrification in a full-scale experiment in india. *Bioresource Technology*, **204**, 177-184.

Takemura, Y., Yoochatchaval, W., Danshita, T., Miyaoka, Y., Aoki, M., Thao Tran, P., Tomioka, N., Ebie, Y., Syutsubo, K. 2022 A pilot-scale study of a down-flow hanging sponge reactor as a post-treatment for domestic wastewater treatment system at short hydraulic retention times 2022 *Journal of Water Process Engineering* volume 50 https://doi.org/10.1016/j.jwpe.2022.103313.

Tandukar, M., Uemura, S., Machdar, I., Ohashi, A., Harada, H. 2005 A low-cost municipal sewage treatment system with a combination of UASB and the "fourth-generation" downflow hanging sponge reactors, *Water Science and Technology* **52** (1-2), 323-329.

Yoochatchaval, W., Onodera, T., Sumino, H.,Yamaguchi, T., Mizuochi, M., Okadera, T., Syutsubo, K. 2014 Development of a down-flow hanging sponge reactor for the treatment of low strength sewage. *Water Science & Technology*, **7**(4), 656-663.

Giving four lives to osmotic membranes with innovative recycling processes (Osmo4Lives)

B. Zappulla[a], R. García-Pacheco[a], W. Gernjak[b,c], G. Blandin[a]

[a] LEQUIA, Institute of the Environment, University of Girona, Spain (E-mail: bianca.zappulla@udg.edu)
[b] ICRA, Catalan Institute for Water Research, Emili Grahit 101, 17003, Girona, Spain
[c] ICREA, Catalan Institution for Research and Advanced Studies, Passeig Lluís Companys 23, 08010, Barcelona, Spain

Abstract

The interest on membrane recycling has been growing in the last 20 years. Environmental Directives (such as waste management and circular economies), public grants (e.g. in Europe LIFE and Horizon H2020 programs) and private funding (mainly from water management utilities) promote the investigation of alternatives regarding end-of-life membrane management. Recently published literature indicates that the design of reusable and recyclable membranes is being investigated. Research carried out over the last decade has been focused on restoring reverse osmosis (RO) membrane performance or their recycling through transformation as other membrane types. The study of how an RO membrane is affected by oxidizing agents and/or by drying conditions is one of the topics that is still not fully understood. This lack of knowledge, along with the need to push membrane recycling concept towards the implementation of a cascade recycling cycle with RO membrane end-of-life to give them more than one recycled lives, is being studied in this project called Osmo4Lives.

Keywords (maximum 6 in alphabetical order)
Desalination; membrane drying; membrane oxidation; recycling; regeneration; reverse osmosis

INTRODUCTION

Membrane processes are key elements for water reuse and desalination. They can be classified by membrane type (dense/porous), removal mechanisms, driving force used and/or industrial application. In terms of seawater desalination, reverse osmosis (RO) is the fastest growing technique and has taken the leading position thanks to its lower water production costs compared to thermal desalination processes. Globally, in 2025 to combat water scarcity, 75 Mm^3/day of water will be treated with RO membranes[1]. This number represents the 77% of the total desalinated water, showing the consolidation of the RO technology. Nanofiltration (NF) membranes were recognized in the late 80's as a process intermediate between RO and ultrafiltration (UF) which was developed in the late 1960s[2]. Those technologies have been continuously developed being applied in different fields such as chemical compounds recovery, water treatment, WW reclamation, juice concentration, dairy industry or medical usage. Other processes such as forward osmosis (FO) gained interests for the two decades following the commercialization of the first dedicated FO membrane by Hydration Technologies. Both for RO and FO, thin-film composite (TFC) most available commercial membranes are thin-film composite (TFC). Both TFC FO and RO membranes, feature a selective polyamide (PA) layer formed by interfacial polymerization on top of a porous substrate (polysulfone (PSF) typically).

At the end of their life (typically 5-10 years for seawater and brackish water desalination processes), membranes are discharged, leading the production of waste. The interest on membrane recycling has been growing in the last 20 years. Environmental Directives, public grants and private funding promoted the investigation of alternatives regarding end-of-life membrane management. Recently published literature indicates that the design of reusable and recyclable membranes is possible. Research carried out over the last decade has been focused on restoring reverse osmosis (RO) membrane performance or their recycling through transformation as other membrane types (UF, NF…). Still, how an RO membrane is affected by oxidizing agents and/or by drying conditions is one of the topics that is still not fully understood. This lack of knowledge, along with the need to push membrane recycling concept towards the implementation of a cascade recycling cycle with RO membrane end-of-life to give them more than one recycled lives, is being studied in this project called Osmo4Lives. Apart from new alternatives for RO membrane recycling, Osmo4Lives propose to better understand how dense membrane (FO, RO) and especially their PA layer are affected by oxidising agents and drying that can occur during their usage or storage so to extend their life and favour their recycling.

MATERIALS AND METHODS

The study of the impact on membrane properties at laboratory scale is organized in three principal tasks (T): evaluate various oxidizing agents and tests their impact on PA active layer (T1), evaluate the impact of drying on membrane characteristics (T2) and cascade recycling of membrane coupons (T3).

During T1, the exposure time and dose and the impact on permeability and selectivity as a result of this exposition for several oxidation agents such as chlorine will be studied. T2 evaluates the impact of drying conditions (temperature, time…) on membrane characteristics (permeability, pore size) and the impact of various solvents (as water, seawater, ethanol…) on rehydration/recovery of membranes. T3 will consists of standardizing oxidizing protocols for membrane surface modifications and optimize it based on results from T1 using innovative protocols. RO membrane coupons will be tested and characterized before and after applying any treatment using a standard saline solution[3]. A flat-sheet membrane cell testing equipment will be used to assess the permeability and the rejection of the membranes, to identify properly the impact of each treatment. Advanced characterization will be performed in collaboration with Khalifa University (EAU) and The University of New South Wales (Australia) to better evaluation of treatment impacts on membrane surface and structure. Finally, the cascade recycling process will consist on gradually degrading SWRO performance as shown in Figure 1. At each step, membranes will be characterized and the cascade recycling process will be compared with one step process.

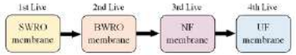

Figure 1. Cascade recycling process

RESULTS AND DISCUSSION

Initial results of the Osmo4Lives project including the impact of drying conditions, solvents and contact time on membrane properties, as well as their potential recovery will be presented. First results showed that full recovery of permeability and selectivity is observed in some membrane brands when using Ethanol as a soaking solution.

REFERENCES

(1) Markets, R. *FOCUS DECK GWI MARKET FOCUS DECK : DESALINATION & REUSE MARKETS July 2020*; 2020; Vol. 44.
(2) M. Cheryan*: Ultrafiltration Handbook. 374 Seiten, Zahlr. Abb. Und Tab. Technomic Publishing Co., Inc., Lancaster, Basel 1986.*; Inc.
(3) García-Pacheco, R.; Landaburu-Aguirre, J.; Molina, S.; Rodríguez-Sáez, L.; Teli, S. B. ; García-Calvo, E. Transformation of End-of-Life RO Membranes into NF and UF Membranes: Evaluation of Membrane Performance. *J. Membr. Sci.* **2015**, *495*, 305–315.
(4) Meño, C. G.; Hernández, P.; Cos, D.; Pérez, J. J. Presupuesto y Gasto Público 101-(4/2020). El Agua En España: Economía y Gobernanza. *J. Econ. Lit.* **2020**, *31* (1), 392–393.

Photocatalysis as a Remediation Technology for Wastewaters Containing Organic Dye Compounds

Ali Rostamiirangh*, Elnaz Zehtab Lotfi**

* Expert of sewage studies and technical inspection office water and sewage co, eastazarbaijan, Iran, alirostamiiranagh@ yahoo.com

** Expert of water studies and technical inspection office water and sewage co, eastazarbaijan, Iran, elnazzlo@yahoo.com

Abstract
In many nations, particularly those experiencing water scarcity, novel approaches are being applied to clean wastewater. Heterogeneous photocatalysis is the most widely used of these approaches because it entails the decomposition of organic molecules into water and carbon dioxide, which is a more ecologically benign process. In our study, we studied the photocatalytic degradation process of organic pollutant in wastewater.
Keywords
Organic pollutant; Photocatalyst; wastewater

Introduction

With increasing worldwide interest in environmental issues such as global warming, water/air pollution and waste management, many efforts are being made to find cost effective and sustainable processes for energy production, pollution elimination or recycling. The most abundant energy source available on earth is sunlight. Consequently, engineering efficient solar technologies is a critical step towards carbon-free energy production. photocatalytic materials are materials that are able to convert an incident photon into a consumable or storable energy source, through the creation of an electron/hole pair at the photocatalyst level. Various types of pollutants have contaminated water resources in recent decades. Emerging organic pollutants and resistant organic and inorganic compounds are among the pollutants that conventional water and wastewater treatment processes have a hard time removing with suitable efficiency. New, and sometimes costly methods, are being explored to remove these pollutants, highlighting the need for economical and effective solutions. Thus far, the application of photocatalytic methods to remove pigments, phenols, nitrogen compounds, sulfur compounds, pharmaceutical compounds, pesticides and many other compounds has been investigated.

$ZnTiO_3$ has high thermal and chemical stability, a wide energy gap, high electron mobility, high reduction potential, and low oxidation potential, plus it is cost-effective and environmentally friendly. In recent years, $ZnTiO_3$ has been investigated for application in many fields, such as regenerable sorbent for desulfurization of hot coal gases,gas sensor, humidity sensor, paint pigment, microwave dielectric material, antibacterial agent, and as photocatalyst . It is well known that the photocatalytic activity of semiconductors is closely related to physical properties such as crystalline phase, particle size, crystallinity, and morphology.

Therefore, at present, several methods have been used to obtain $ZnTiO_3$ of controlled shape and size with high purity and low cost. To synthesize $ZnTiO_3$ particles, various techniques have been reported, including conventional solid-state reaction, spin coating, chemical vapor deposition, spray pyrolysis, sputtering, laser sintering, sonochemistry, co-precipitation, hydrothermal/ion exchange process, sol-gel process, chemical bath deposition and Pechini method. Among these methods, the sol-gel process was chosen as a well-established green chemistry technique. The photocatalytic activity of the compounds was evaluated by the photocatalytic degradation of methylene blue under solar light radiation.Figure1 shows the Schematic diagram of the principle of photocatalysis.

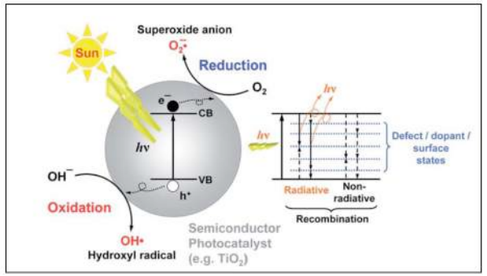

Figure 1. Schematic diagram of the principle of photocatalysis

Result and disscution

Characterizations of photocatalysts

X-ray diffraction (XRD) patterns of the synthesized perovskites were collected to by D8 Advance, Bruker (Germany), diffractometer with monochromatic high-intensity Cu Kα radiation (l = 1.5406˚A), an accelerating voltage of 40 kV and current of 30 mA. Field emission scanning electron microscopy (FESEM) images, Energy-dispersive X-ray spectroscopy (EDX) patterns and elemental mapping analysis were achieved by Mira 3, Tescan (Czech Republic) microscope. Transmission electron microscopy (TEM) was carried out using CM30, Philips (Netherlands) microscope.figure2

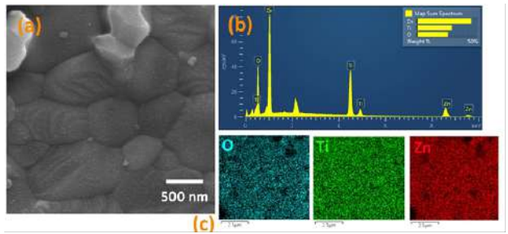

Figure 2. . FESEM images and EDX spectrum accompanied by EDX mapping for $ZnTiO_3$

photocatalytic activity

The photocatalytic activity of the ZnTiO3 was determined by decomposition under visible light irradiation of Methylene Blue (MB) in wastewater. The results obtained in the present study clearly indicate that ZnTiO3 possesses excellent photocatalytic performance. Figure 3. Shows the photocatalytic activity of $ZnTiO_3$ in dark and in presence of visible light. The degradation efficiency was defined as $X=(A_0-A)/A_0$, where X is the degradation efficiency, A_0 is the initial absorbance and A_t is the absorbance of the solution at t min. During the photocatalysis, samples (3 mL) were taken from the reactor every 15 min.

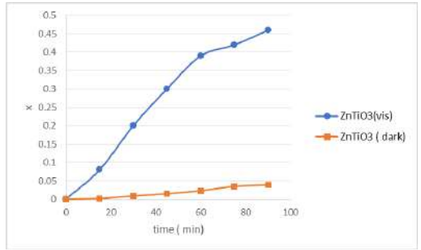

Figure 2. photocatalytic activity of $ZnTiO_3$ for degradation of methylene blue

REFERENCES

Ameta R, Ameta SC. Photocatalysis: Principles and Applications: CRC Press LLC, Boca Raton, Florida, United States, 2019

El Mouzdahir, Y.; Elmchaouri, A.; Mahboub, R.; Gil, A.; Korili, S.A. Adsorption of methylene blue from aqueous solutions on a Moroccan clay. J. Chem. Eng. Data 2007, 52, 1621–1625

Jing, G.; Sun, Z.; Ye, P.; Wei, S.; Liang, Y. Clays for heterogeneous photocatalytic decolorization of wastewaters contaminated with synthetic dyes: A review. Water Pr. Technol. 2017, 12, 432–443.

Makama, A.B.; Salmiaton, A.; Saion, E.B.; Choong, T.S.Y.; Abdullah, N. Synthesis of CdS sensitized TiO2 photocatalysts: Methylene blue adsorption and enhanced photocatalytic activities. Int. J. Photoenergy 2016, 2016, 1–14.

Umar, K.; Haque, M.; Muneer, M.; Harada, T.; Matsumura, M. Mo, Mn and La doped TiO2: Synthesis, characterization and photocatalytic activity for the decolourization of three different chromophoric dyes. J. Alloy. Compd. 2013, 578, 431–438, doi:10.1016/j.jallcom.2013.06.083.

Vasilachi IC, Asiminicesei DM, Fertu DI, Gavrilescu M. Occurrence and Fate of Emerging Pollutants in Water Environment and Options for Their Removal. Water2021; 13(2): 181.

.

Periodate activation with copper oxide nanomaterials for the degradation of ciprofloxacin - A new insight into the efficiency and mechanisms

Xi Zhang*, Deirdre Cabooter** and Raf Dewil*

* KU Leuven, Department of Chemical Engineering, Process and Environmental Technology Lab, J. De Nayerlaan 5, 2860 Sint-Katelijne-Waver, Belgium
(E-mail: xi.zhang@kuleuven.be; raf.dewil@kuleuven.be)*
** KU Leuven, Department of Pharmaceutical and Pharmacological Sciences, Pharmaceutical Analysis, Herestraat 49, 3000, Leuven, Belgium
(E-mail: Deirdre.cabooter@kuleuven.be)

Abstract
In this study, CuO was synthesized using a facile precipitation method and was characterized using various techniques for the efficient activation of periodate (PI). Compared to systems consisting of PI alone (0.5 mM) and CuO alone (0.5 g/L), the CuO (0.5 g/L)/PI (0.5 mM) process exhibited improved degradation performance for ciprofloxacin (CIP), a widely used refractory antibacterial drug, with 98% of this pollutant (20 mg/L) removed in a reaction time of 30 min. Both radical and nonradical degradation pathways were identified to play a significant role in the developed CuO/PI system, where the nonradical pathway (holes and electrons) played the most important role in the degradation of CIP. Under both acidic (pH = 3) and near-neutral (pH = 6) conditions, the system showed an improved efficiency for the degradation of CIP in comparison with alkaline conditions (pH = 10). This was attributed to a more facile adsorption of the PI ions onto the surface of the CuO nanoparticles, induced by the electrostatic attraction between the PI ions and the CuO nanomaterial. Analysis of the degraded samples with ultrahigh-performance liquid chromatography quadropole time-of-flight mass spectrometry (UHPLC Q-TOF MS) demonstrated that cleavage of the piperazine ring and defluorination were the primary degradation pathways of CIP under this oxidation process. The CuO/PI system also showed an excellent removal efficiency for other refractory organic contaminants, such as sulfamethoxazole (SMX) and methylene blue (MB), in various water matrices, including real wastewater. Moreover, respiration tests revealed that the toxicity of the effluents was reduced after the treatment process. In conclusion, this research presents a novel, promising periodate activation technique for the removal of refractory organic contaminants in wastewater treatment.
Keywords (maximum 6 in alphabetical order)
CuO nanomaterials; degradation mechanism; periodate activation; pharmaceutical micropollutants; toxicity analysis

MAJOR HEADINGS FOR INTRODUCTION

The discharge of antibiotic drugs into natural waters due to their widespread use in medical therapy has sparked serious global concerns. Among them, ciprofloxacin (CIP), a fluoroquinolone antibiotic, is widely used to cure a wide range of microbial diseases in both animals and humans. It has also been discussed in the literature that the migration and transformation of these antibiotic compounds in water bodies can result in the formation of toxic intermediates with the potential to pose a serious threat to both ecosystem safety and public health [1]. Moreover, antibiotic compounds can exert selective pressure on microbes, resulting in antibiotic-resistant bacteria in water bodies [2].
Hence, it is critical to develop wastewater treatment techniques that can deal with a wide range of environmental pollutants, such as antibiotics and dyes, before being discharged into natural waters. To address this need, various advanced oxidation processes (AOPs) have been developed in recent years [3]. The basis of these methods is the generation of oxidative agents (such as $^{\bullet}OH$, $O_2^{\bullet-}$, and $SO_4^{\bullet-}$), which can strongly attack and decompose a wide range of complex organic compounds. Among AOPs, the activation of oxidation agents (such as persulfate, peroxymonosulfate, periodate, and chlorine) using various physical or chemical techniques has received much interest in recent years [4,5].
Periodate (PI, IO_4^-) is a relatively novel oxidation agent that has recently been used for the degradation of various types of recalcitrant organic contaminants. It has some advantages over other oxidation agents, such as being stable and easy to ship and store [6]. PI with a reduction potential of +1.60 V is able to produce a plethora of different radicals and highly reactive substances, such as $IO_3^{\bullet}$, $IO_4^{\bullet}$, $O(^3P)$, $^{\bullet}OH$, and $^1O_2$ [7], when activated with different techniques, such as UV light [8], ultrasound [9], microwaves [10] and freezing [11]. However, the need for an external source of energy for most of these techniques has restricted their wider application [12]. PI can also be activated by chemicals, such as hydrogen peroxide [13] and hydroxylamine [14]. Additionally, there is an interest in the application of carbonaceous materials (such as activated carbon [14]) or transition metals and metal oxides as catalysts for the generation of powerful oxidation agents from PI, with advantages such as low cost, energy savings and ease of use [15,16].
Copper oxide (CuO) is one of the most popular transition metal oxides, widely used in AOPs, such as the photocatalytic degradation of organic compounds [17], and very recently used for the activation of oxidation agents (OAs), such as persulfate (PS) and peroxymonosulfate (PMS) [18] to generate oxidative radicals. However, to the best of our knowledge, it has not been used for the activation of novel OAs, such as PI. Copper is a cheap, eco-friendly, and abundant element in nature that is present in the Earth's crust at concentrations ranging from 146 g/t to 60 g/t [19]. Furthermore, copper oxide nanomaterials normally have a large specific surface area and porous structure, which makes them ideal candidates for surface oxidative reactions [20,21].
In this study, a facile precipitation method was employed to prepare CuO nanomaterials for the activation of PI. The prepared materials were used in a novel CuO/PI activation system for the degradation of pharmaceuticals, including CIP and sulfamethoxazole (SMX).

MATERIALS AND MATHODS

Experimental procedures

The removal of CIP was investigated in a 500 mL glass Erlenmeyer flask containing a 200 mL reaction solution. The initial pH of the solution was adjusted to the required pH (3–10) with diluted H_2SO_4 and NaOH solutions. Because only a small volume was required for the pH adjustment, the volume increase of the reaction volume was negligible. During the reaction, a magnetic stir bar was used to constantly stir the reaction medium. The preferred concentration of PI and the dosage of CuO were mixed in a conical flask to start the reaction. Liquid (1.5 mL) was collected with a syringe at specific time intervals and instantly filtered by a 0.45 µm membrane filter into a clear tube. To halt the oxidation reactions, 1.5 mL of the collected sample was mixed with 50 µL of $Na_2S_2O_3$ (0.1 M). After that, the solution was analysed with HPLC to determine the concentration of the remaining CIP.
For the respirometry experiments, 250 mg/L sodium acetate (NaAc) was chosen as the reference control substrate [22,23]. The activated sludge was received from a sewage treatment plant (Aquafin, Mechelen-Noord, Belgium) and was mixed with water to ensure a biomass concentration of 2.5 g/L MLVSS (mixed liquid volatile suspended solids) for respirometry experiments.

RESULTS AND DISCUSSION

Degradation of CIP and identification of active species in the CuO/PI system

CuO nanoparticles were tested for their catalytic activity as a PI activator for the removal of CIP from aqueous solutions. Fig. 3(a) shows the removal efficiency of 20 mg/L CIP under control conditions (i.e., CuO alone or PI alone) and using the CuO/PI system within 30 min of reaction. CuO alone removed only 37% of CIP in the absence of PI. Here, it is suggested that adsorption is the main mechanism for the removal of CIP, which is supported by the relatively large BET surface area (36 m^2 g^{-1}) of the material [24]. A very low degradation efficiency was also observed for PI alone (28%, within 30 min), which can be attributed to the low oxidation potential of PI. The combination of CuO and PI, on the other hand, exhibited a significant enhancement in CIP removal. The degradation rate reached 53% after 2 min and 92% after 30 min, with a mineralization rate of 44%. The CIP removal kinetics were subsequently fitted to a pseudo-first-order model to further investigate the catalytic performance of the system [8]. The rate constant (k) of the CuO/PI system was calculated to be 0.11 min^{-1}, which is much higher than that of CuO alone (0.011 min^{-1}) and PI alone (0.021 min^{-1}). As shown in Fig. 3(b), the leaching rate of copper in CuO/PI system is less than 0.65 mg/L, which is lower than the discharge limit of copper ion in industrial wastewaters set by the United States Environmental Protection Agency (US-EPA, 1.3 mg/L) [25]. The contribution of leached Cu^{2+} to PI activation was also tested. As we can see from Fig. 3(c), Cu^{2+} can activate PI and 49% of CIP was removed in 2 min. After that, the degradation rate remains almost unchanged. The PI activation efficiency of Cu^{2+} is lower than that of CuO with the same molar mass (6.29 mM). We also used 0.65 mg/L (0.01 mM) Cu^{2+} to simulate the released Cu^{2+} to activate PI. After 30min, the degradation efficiency of CIP reached only 8.86%, which was similar to that of PI alone system. It shows that in CuO/PI system, the activation effect on PI can be ignored because the concentration of leached Cu^{2+} is too low.
Quenching tests were subsequently conducted to determine the main active species involved in the degradation of CIP using the CuO/PI system. For this purpose, hydroxyl radicals (·OH) and $O(^3P)$ were quenched with 2-propanol, and iodate (IO_3^-), periodate radicals ($IO_4^{\bullet}$) and ·OH were quenched with phenol [26]. The contribution of these different active species to the degradation of CIP using the CuO/PI system is indicated in Fig. 3(d) and 3(e). The addition of 2-propanol had almost no effect on the CIP removal efficiency (Fig. 3(d)), implying that ·OH and $O(^3P)$ do not play a role in CIP removal in the CuO/PI system. Because the interference of ·OH has been eliminated by 2-propanol, phenol was added to the system to explore the effect of $IO_3^{\bullet}$ and $IO_4^{\bullet}$. The quenching studies indicated that the kinetics of CIP removal decreased by 54% when phenol was added, revealing that $IO_3^{\bullet}$ and $IO_4^{\bullet}$ effectively contribute to the removal of CIP in the CuO/PI system. Extra analysis was also performed to exclude the effects of the addition of the scavenger on the adsorption of CIP and the consumption of PI, as shown in Fig. 3(f). The results indicated that the addition of phenol can inhibit a bit the adsorption of CIP by CuO probably because of occupying the available active area on the surface of CuO. There are also reports in the literature to support such a statement, for instance by Liao et al. [27].
The possible mechanisms involved in the degradation of CIP using the PI/CuO system were explored using the results obtained from the scavenging experiments and XPS results. The peaks for the used CuO nanomaterial undergo a slight negative shift of 4eV, revealing that CuO acts as an electron acceptor and Cu(II) valence state decreases. It is speculated that the periodate molecules are first adsorbed onto the CuO surface. Then, the interaction between CuO and PI leads to the formation of surface-bonding active complexes, which facilitate electron transfer from PI to Cu(II). In this process, PI and Cu(II) act as the electron donor and the electron acceptor, respectively. As a result, $^{\equiv}Cu^{+}$ and $IO_4^{\bullet}$ are formed according to Eq. 1. In the presence of H^+ and e^-, IO_3^- and $IO_4^{\bullet}$ can be formed for the efficient degradation of CIP (Eq. 2, 3 and 4).

$$\equiv Cu^{2+} + IO_4^- \rightarrow \equiv Cu^{2+} + IO_4^{\bullet} \quad \text{(Eq. 1)}$$

$$IO_4^{\bullet} + 2H^+ + e^- \rightarrow IO_3^- + H_2O \quad \text{(Eq. 2) [12,28]}$$

$$IO_4^{\bullet} + IO_3^- \rightarrow IO_4^- + IO_3^{\bullet} \quad \text{(Eq. 3) [12]}$$

$$IO_4^{\bullet} + \text{pollutants} \rightarrow IO_3^- + \text{products} \quad \text{(Eq. 4) [28]}$$

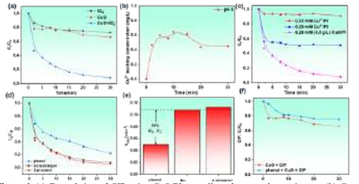

Figure 1. (a) Degradation of CIP using CuO/PI as well as the control experiments. (b) Copper leaching rate from CuO/PI system. (c) Degradation of CIP using Cu^{2+}/PI system. (d) The impact of various scavengers on CIP removal in the CuO/PI process. (e) The impact of various scavengers on CIP removal kinetics in the CuO/PI process. (f) The influence of phenol on the adsorption of CIP by CuO. Conditions: [CuO] = 0.5 g/L (6.29 mmol/L), [CIP]$_0$ = 20 mg/L (0.06 mM), [PI]$_0$ = 0.5 mM, pH = 6.

REFERENCES

[1] J. Kang, C. Jin, Z. Li, M. Wang, Z. Chen, Y. Wang, Dual Z-scheme MoS2/g-C3N4/Bi24O31Cl10 ternary heterojunction photocatalysts for enhanced visible-light photodegradation of antibiotic, J. Alloys Compd. 825 (2020) 153975. https://doi.org/10.1016/j.jallcom.2020.153975.
[2] I. Michael-Kordatou, P. Karaolia, D. Fatta-Kassinos, The role of operating parameters and oxidative damage mechanisms of advanced chemical oxidation processes in the combat against antibiotic-resistant bacteria and resistance genes present in urban wastewater, Water Res. 129 (2018) 208–230. https://doi.org/10.1016/j.watres.2017.10.007.
[3] Y. Pan, R. Qin, M. Hou, J. Xue, M. Zhou, L. Xu, Y. Zhang, The interactions of polyphenols with Fe and their application in Fenton/Fenton-like reactions, Sep. Purif. Technol. 300 (2022) 121831. https://doi.org/10.1016/j.seppur.2022.121831.
[4] Z. Bu, M. Hou, Z. Li, Z. Dong, L. Zeng, P. Zhang, G. Wu, X. Li, Y. Zhang, Y. Pan, Fe3+/Fe2+ cycle promoted peroxymonosulfate activation with addition of boron for sulfamethazine degradation: Efficiency and the role of boron, Sep. Purif. Technol. 298 (2022) 121596. https://doi.org/10.1016/j.seppur.2022.121596.
[5] N. Han, S. Wang, Z. Yao, W. Zhang, X. Zhang, L. Zeng, R. Chen, Superior three-dimensional perovskite catalyst for catalytic oxidation, EcoMat. 2 (2020) e12044. https://doi.org/10.1002/eom2.12044.
[6] Y. Zong, Y. Shao, Y. Zeng, B. Shao, L. Xu, Z. Zhao, W. Liu, D. Wu, Enhanced Oxidation of Organic Contaminants by Iron(II)-Activated Periodate: The Significance of High-Valent Iron–Oxo Species, Environ. Sci. Technol. (2021). https://doi.org/10.1021/acs.est.1c00375.
[7] Y.-C. Lee, M.-J. Chen, C.-P. Huang, J. Kuo, S.-L. Lo, Efficient sonochemical degradation of perfluorooctanoic acid using periodate, Ultrason. Sonochem. 31 (2016) 499–505. https://doi.org/10.1016/j.ultsonch.2016.01.030.
[8] X. Zhang, X. Yu, X. Yu, M. Kamali, L. Appels, B. Van der Bruggen, D. Cabooter, R. Dewil, Efficiency and mechanism of 2,4-dichlorophenol degradation by the UV/IO4- process, Sci. Total Environ. (2021) 146781. https://doi.org/10.1016/j.scitotenv.2021.146781.
[9] O. Hamdaoui, L. Merouani, Improvement of sonochemical degradation of Brilliant blue R in water using periodate ions: Implication of iodine radicals in the oxidation process, Ultrason. Sonochem. 37 (2017) 344–350. https://doi.org/10.1016/j.ultsonch.2017.01.025.
[10] A.M.S. Mohammadi, G. Asgari, A. Poormohammadi, M. Ahmadian, Oxidation of Phenol from Synthetic Wastewater by a Novel Advance Oxidation Process: Microwave-Assisted Periodate, 75 (2016) 7.
[11] Y. Choi, H.-I. Yoon, C. Lee, L. Vetráková, D. Heger, K. Kim, J. Kim, Activation of Periodate by Freezing for the Degradation of Aqueous Organic Pollutants, Environ. Sci. Technol. 52 (2018) 5378–5385. https://doi.org/10.1021/acs.est.8b00281.
[12] L. He, C. Yang, J. Ding, M.-Y. Lu, C.-X. Chen, G.-Y. Wang, J.-Q. Jiang, L. Ding, G.-S. Liu, N.-Q. Ren, S.-S. Yang, Fe, N-doped carbonaceous catalyst activating periodate for micropollutant removal: Significant role of electron transfer, Appl. Catal. B Environ. 303 (2022) 120880. https://doi.org/10.1016/j.apcatb.2021.120880.
[13] N.E. Chadi, S. Merouani, O. Hamdaoui, M. Bouhelassa, M. Ashokkumar, H2O2/periodate (IO4−): a novel advanced oxidation technology for the degradation of refractory organic pollutants, Environ. Sci. Water Res. Technol. 5 (2019) 1113–1123. https://doi.org/10.1039/C9EW00147F.
[14] X. Li, X. Liu, C. Qi, C. Lin, Activation of periodate by granular activated carbon for acid orange 7 decolorization, J. Taiwan Inst. Chem. Eng. 68 (2016) 211–217. https://doi.org/10.1016/j.jtice.2016.08.039.
[15] J. Du, G. Xiao, Y. Xi, X. Zhu, F. Su, S.H. Kim, Periodate activation with manganese oxides for sulfanilamide degradation, Water Res. 169 (2020) 115278. https://doi.org/10.1016/j.watres.2019.115278.
[16] W. Li, Y. Li, D. Zhang, Y. Lan, J. Guo, CuO-Co3O4@CeO2 as a heterogeneous catalyst for efficient degradation of 2,4-dichlorophenoxyacetic acid by peroxymonosulfate, J. Hazard. Mater. 381 (2020) 121209. https://doi.org/10.1016/j.jhazmat.2019.121209.
[17] M. Li, N. Han, X. Zhang, S. Wang, M. Jiang, A. Bokhari, W. Zhang, M. Race, Z. Shen, R. Chen, M. Mubashir, K.S. Khoo, S.S. Teo, P.L. Show, Perovskite oxide for emerging photo(electro)catalysis in energy and environment, Environ. Res. 205 (2022) 112544. https://doi.org/10.1016/j.envres.2021.112544.
[18] J. Yang, H. Ma, C. Wang, H. Liu, Bromate formation during oxidation of bromide-containing water by the CuO catalyzed peroxymonosulfate process, Chin. Chem. Lett. (2022). https://doi.org/10.1016/j.cclet.2022.01.008.
[19] V. Rajput, T. Minkina, B. Ahmed, S. Sushkova, R. Singh, M. Soldatov, B. Laratte, A. Fedorenko, S. Mandzhieva, E. Blicharska, J. Musarrat, Q. Saquib, J. Flieger, A. Gorovtsov, Interaction of Copper-Based Nanoparticles to Soil, Terrestrial, and Aquatic Systems: Critical Review of the State of the Science and Future Perspectives, in: P. de Voogt (Ed.), Rev. Environ. Contam. Toxicol. Vol. 252, Springer International Publishing, Cham, 2020: pp. 51–96. https://doi.org/10.1007/398_2019_34.
[20] N. Baylan, İ. İlalan, İ. İnci, Copper Oxide Nanoparticles as a Novel Adsorbent for Separation of Acrylic Acid from Aqueous Solution: Synthesis, Characterization, and Application, Water. Air. Soil Pollut. 231 (2020) 465. https://doi.org/10.1007/s11270-020-04832-3.
[21] A. El-Trass, H. ElShamy, I. El-Mehasseb, M. El-Kemary, CuO nanoparticles: Synthesis, characterization, optical properties and interaction with amino acids, Appl. Surf. Sci. 258 (2012) 2997–3001. https://doi.org/10.1016/j.apsusc.2011.11.025.
[22] A. Gupta, A. Garg, Degradation of ciprofloxacin using Fenton's oxidation: Effect of operating parameters, identification of oxidized by-products and toxicity assessment, Chemosphere. 193 (2018) 1181–1188. https://doi.org/10.1016/j.chemosphere.2017.11.046.
[23] X. Yu, M. Kamali, P. Van Aken, L. Appels, B. Van der Bruggen, R. Dewil, Advanced Oxidation of Benzalkonium chloride in Aqueous Media Under Ozone and Ozone/UV Systems – Degradation kinetics and toxicity evaluation, Chem. Eng. J. (2020) 127431. https://doi.org/10.1016/j.cej.2020.127431.
[24] T. Yang, S. Fan, Y. Li, Q. Zhou, Fe-N/C single-atom catalysts with high density of Fe-Nx sites toward peroxymonosulfate activation for high-efficient oxidation of bisphenol A: Electron-transfer mechanism, Chem. Eng. J. 419 (2021) 129590. https://doi.org/10.1016/j.cej.2021.129590.
[25] M. Arbabi, N. Golshani, Removal of copper ions Cu (II) from industrial wastewater: A review of removal methods, Int. J. Epidemiol. Res. 3 (2016) 283–293.
[26] C. Ling, S. Wu, J. Han, T. Dong, C. Zhu, X. Li, L. Xu, Y. Zhang, M. Zhou, Y. Pan, Sulfide-modified zero-valent iron activated periodate for sulfadiazine removal: Performance and dominant routine of reactive species production, Water Res. 220 (2022) 118676. https://doi.org/10.1016/j.watres.2022.118676.
[27] R. Liao, S. Wen, Q. Feng, J. Deng, H. Lai, Activation mechanism of ammonium oxalate with pyrite in the lime system and its response to flotation separation pyrite from arsenopyrite, Int. J. Miner. Metall. Mater. (2022). https://doi.org/10.1007/s12613-022-2505-5.
[28] L. He, L. Lv, S.C. Pillai, H. Wang, J. Xue, Y. Ma, Y. Liu, Y. Chen, L. Wu, Z. Zhang, L. Yang, Efficient degradation of diclofenac sodium by periodate activation using Fe/Cu bimetallic modified sewage sludge biochar/UV system, Sci. Total Environ. 783 (2021) 146974. https://doi.org/10.1016/j.scitotenv.2021.146974.

In-situ Fabrication of Titanium Suboxide-Laser Induced Graphene Composites with Enhanced Electrochemical Activity for Environmental Remediation

A. Kumar*, N. H. Barbhuiya* and S. P. Singh**

* Environmental Science and Engineering Department (ESED), Indian Institute of Technology Bombay, Mumbai 400076, India
(E-mail: ashish1503@iitb.ac.in; ashish.enano15@gmail.com; najmul@iitb.ac.in)*
** Environmental Science and Engineering Department (ESED), Indian Institute of Technology Bombay, Mumbai 400076, India
(E-mail: swatantra@iitb.ac.in; swatantra.esed@gmail.com)

Abstract
Titanium suboxides (TSO) are identified as a series of compounds showing excellent electro- and photochemical properties. TSO composites with carbon-based materials such as graphene have further improved water splitting and pollutant removal performance. However, their expensive and multistep synthesis limits their wide-scale use. Furthermore, recently discovered laser-induced graphene (LIG) is a facile and less expensive fabrication method for graphene-based composites having various environmental application such as anti-microbial, anti-biofouling, and pollutant sensing. Moreover, various heteroatoms doping in LIG are done to enhance their catalytical performance in pollutant decontamination. Here, we demonstrate the single-step in-situ fabrication of TSO-doped LIG composites as electrodes and porous conductive filters on polymer sheets using a CO_2 infrared laser. The various spectroscopic and electron microscopic techniques confirmed the successful fabrication of TSO doped LIG on the polymer surface. Moreover, the TSO-LIG composite has enhance electrochemical activity as demonstrated using cyclic voltammetry and electrochemical impedance spectroscopy. Furthermore, the TSO-LIG composite surfaces were tested for electrochemical application as electrodes and filters. The composite electrodes exhibit enhanced degradation performance for removing emerging pollutant due to the in-situ hydroxyl radical generation. Additionally, the TSO-LIG conductive filters showed the complete 6-log microbial killing in flow-through filtration mode and showed ~ 2.5-log more killing compared to undoped LIG filers. Nevertheless, the performance of these LIG composites was examined on various doping concentrations and applied potentials.

Keywords
Antimicrobial, Conductive filters, Laser-induced graphene, Electrochemical decontamination, Titanium suboxide

MATERIALS AND METHODS

All chemicals for electrochemical testing was purchased from Sigma-Aldrich and Merck life science Pvt Ltd., India. Nutrient broth and Luria Bertani agar were purchased from HiMedia Laboratories, India. Unless specified, all chemicals were dissolved in distilled water from the distillation unit.
The LIG composites with different concentration of heteroatom were fabricated by irradiating the titanium oxide doped polymer precursor using a 10.6 µm CO_2 pulse laser. All characterisation was done in the central facility of Indian Institute of Technology Bombay, India.

RESULTS

The laser-induced formation of TSO, along with graphene was achieved in a chemical-free, facile, and cost-efficient method using CO_2 infrared laser. The graphene formation was confirmed is using various characterisation techniques such as Raman in Figure 1a. Moreover, the insertion of TSO in the surface was confirmed with the presence of characteristic Ti2p peak in XPS spectrum as shown in Figure 1b.
Moreover, the TSO-LIG composite had enhanced electrochemical activity as demonstrated by electrochemical characterisation with increase cyclic voltammetry curve area of TSO-LIG as compared to the non-doped LIG electrodes (Figure 2a). Furthermore, the in-situ generation of •OH enhanced the pollutants removal efficiency of the TSO-LIG electrodes against MB, giving the best results in the case of 10% doping of TSO at 2.5 V (Figure 2b). Nonetheless, the degradation efficiency of the TSO-LIG electrodes is proportional to the applied voltage and doping concentration.

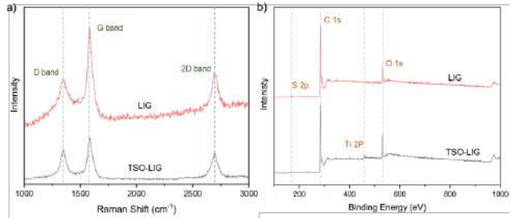

Figure 1. (a) Raman spectrum of the LIG and TSO-LIG composite showing the graphene formation on the surface. (b) XPS spectrum of the LIG and TSO-LIG composite indicating the present of various element on the surface.

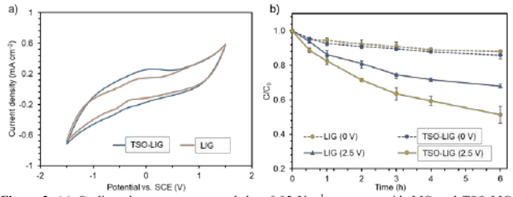

Figure 2. (a) Cyclic voltammograms recorded at 0.05 V s^{-1} scan rate with LIG and TSO-LIG composite electrodes. (b) Electrochemical removal of methylene blue using LIG and TSO-LIG composite electrodes at 0 V and 2.5 V applied voltage.

REFERENCES

Singh, S.P., Li, Y., Be'Er, A., Oren, Y., Tour, J.M., Arnusch, C.J., 2017. Laser-Induced Graphene Layers and Electrodes Prevents Microbial Fouling and Exerts Antimicrobial Action. ACS Appl Mater Interfaces 9, 18238–18247. https://doi.org/10.1021/acsami.7b04863

Singh, S.P., Li, Y., Zhang, J., Tour, J.M., Arnusch, C.J., 2018a. Sulfur-Doped Laser-Induced Porous Graphene Derived from Polysulfone-Class Polymers and Membranes. ACS Nano 12, 289–297. https://doi.org/10.1021/acsnano.7b06263

Singh, S.P., Ramanan, S., Kaufman, Y., Arnusch, C.J., 2018b. Laser-Induced Graphene Biofilm Inhibition: Texture Does Matter. ACS Appl Nano Mater 1, 1713–1720. https://doi.org/10.1021/acsanm.8b00175

Kumar, A., Barbhuiya, N.H., Singh, S.P., 2022. Magnéli phase titanium sub-oxides synthesis, fabrication and its application for environmental remediation: Current status and prospect. Chemosphere 307, 135878. https://doi.org/10.1016/J.chemosphere.2022.135878

The new Hot Bubble Pilot Plant (HBPP) for water sterilisation and desalination.

Adrian Garrido Sanchis*, Rui Wei**

*University of New South Wales, Canberra, ACT, Australia, a.garridosanchis@adfa.edu.au
**University of New South Wales, Canberra, ACT, Australia, r.wei@adfa.edu.au

Abstract:
The potential use of hot combustion gas to produce hot bubbles in a bubble column reactor, as a new water sterilization and desalination process on farms offers a new attractive energy-efficient alternative to disinfecting wastewater from the agricultural industry while producing pure condensed water. Many industries, such as pig farms, landfills, biogas power plants, and coal power plants, emit large amounts of hot combustion gases. This work investigates the potential use of these hot combustion gases (waste) to create hot bubbles in a bubble column reactor, as a new water sterilization and desalination process on farms. This new technology fits within the circular economy principles by using waste gases as an input for the system at 0 running cost.
The use of hot combustion gases as the main input makes this new process highly energy efficient, with potentially no energy requirements (0 kWh/m3).

Keywords:
Combustion gas; Pilot plant; sterilisation; water reuse

INTRODUCTION

The new HBPP transfers heat from the hot gas bubbles of 1-3 mm diameter to the surrounding solution (effluent or sea water). The heat transfer rate between liquid and gas is 100 times more efficient in a gas-liquid bubble column than in a single-phase flow according to Deckwer [1].

This is because the hot bubble surface acts as a natural semi-permeable membrane to purify ions, pollutants, and microorganisms while allowing the heat transfer and mass transfer of the evaporated water vapor [2]. The improved evaporation efficiency of the bubble column, compared with the other thermal process, can sterilise and produce pure condensed water from wastewater. In addition, the use of combustion gas and low-quality waste heat can further reduce the energy consumption of the BCE process [4].

MATERIAL AND METHODS

The exhaust pipe of a gas generator was attached to the inlet of the HBPP. Then hot gases traveled through the sinter into the effluent in the form of hot gas bubbles, inactivating different types of pathogens and producing two potentially valuable water products (Stream 1 and 2). See Figure 1.

- Stream 1, pure condensed water (pure distilled water).
- Stream 2, sterilized water (disinfected water from the HBPP reactor).

RESULTS

Sterilised water

The new HBPP offers a viable water sterilization technology that can sterilize different types of bacteria [3] and protozoa spores in the most heavily infected piggery effluent (see Table 1) using hot combustion gases at 115°C and hot air at 175°C. Inlet gas temperature is the key variable needed to improve the performance of the plant.

Pure condensed Water

The results prove that the new HBPP can evaporate brackish water and piggery effluent at virtually no cost when operated with exhaust gases producing high-quality water condensed water that fits within different international drinking water quality standards such as the European Drinking Water Directive (EU 2020), the Guidelines for Drinking-water Quality from the World Health Organisation (WHO 2011), and the Australian and New Zealand Guidelines for Fresh and Marine Water Quality (ANZECC 2000). Values of conductivity, chloride, sulfate, total nitrogen, calcium, magnesium, and sodium are much lower than the acceptable level for drinking water proving that the HBPP can provide high-quality condensed water (see Table 2).

CONCLUSION

Many industries, such as pig farms, landfills, biogas plants, and coal power plants, emit large amounts of hot combustion gas bubbles in the new HBPP for water-desalination and water-sterilisation processes offers an attractive new energy-efficient technology that produces high quality condensed and desalinated water which complies with international standards.

Figure 1. Picture of the mobile BCE prototype set up on a trailer for field experiments.

Table 1: First pathogen inactivation results from the HBPP after 20 minutes of treatments at the farm using piggery effluent [4].

			Pilot Plant Treatments			
Pathogens	**Units**	**Raw Piggery Water**	**175°C inlet Air**	**115°C inlet Combustion gas**	**Inactivation factor hot air**	**Inactivation factor combustion gas**
Thermotolerant Faecal Coliforms	*CFU/100mL*	179000	< 100	159000	-3.26	-0.05
Salmonella VIDAS	*NONE*	Detected	Not Detected	Detected		
E.coli	*CFU/100mL*	179000	<100	159000	-3.26	-0.05
Cyanophyta	*Cells/mL*	35600	7800	30800	-0.66	-0.06
Giardia	*cysts/L*	50	30	50	-0.22	0.00
Cryptosporidium	*oocysts/L*	6960	1480	6960	-0.67	0.00

Table 2. Comparison of 14 different water quality variables to evaluate the purity of the condensed water after treating synthetic piggery effluent with combustion gas or air at 90ºC.

	Water Quality Variables	Units	Untreated Piggery Effluent	Treated with Combustion gas	Treated with Air	Acceptable Level
	pH	pH Unit	7.18	7.65	7.61	6.5 - 8.5 [5]
	Conductivity	µS/cm	8,960	21	65	2,500 [6]
	Turbidity	NTU	4.9	1.2	0.7	0.5 [7]
	Total Organic Carbon	mg/L	1,490	18	5	NAS*
Anions	Chloride	mg/L	2,730	5.3	5.6	250 [7]
	Sulphate	mg/L	193	2.8	3	250 [7]
	Phosphate as P	mg/L	40.3	<0.4	<0.4	NAS*
	Suspended Solids (SS)	mg/L	139	-	3	NAS*
	Total Nitrogen	mg/L	2,280	112	10.7	50 [5]
	Total Phosphorus	mg/L	52.9	0.12	0.06	NAS*
Total Metals	Calcium	mg/L	167	3.08	1.58	200 [5]
	Magnesium	mg/L	63.9	0.21	0.22	150 [5]
	Potassium	mg/L	112	0.2	0.2	NAS*
	Sodium	mg/L	1040	2.8	2.8	180 [7]

** No Available Standard (NAS)*

REFERENCES

1. Deckwer, W.D., *On the mechanism of heat transfer in bubble column reactors.* Chemical Engineering Science, 1980. **35**(6): p. 1341-1346.
2. Garrido, A., R.M. Pashley, and B.W. Ninham, *Water sterilisation using different hot gases in a bubble column reactor.* Journal of Environmental Chemical Engineering, 2018. **6**(2): p. 2651-2659.
3. WHO, *Chapter 8. Algae and cyanobacteria in fresh water*, in *Guidelines for safe recreational water environments.* 2003, WHO.
4. Garrido Sanchis, A. and L. Jin, *Evaluation of the new energy-efficient hot bubble pilot plant (HBPP) for water sterilization from the livestock farming industry.* Water Resources and Industry, 2020. **24**: p. 100135.
5. WHO, *Guidelines for Drinking-water Quality, Fourth Edition.* 2011.
6. EU, *European Drinking Water Directive*, E.E.A. (EEA), Editor. 2020: European Commission.
7. ANZECC, *Australian and New Zealand Guidelines for Fresh and Marine Water Quality*, A.a.N.Z.E.a.C.C.a.A.a.R.M.C.o.A.a.N. Zealand., Editor. 2000: Canberra.

Electrochemical oxidation of ammonia in aqueous solution using high catalytic CuCo bimetallic catalyst supported on Ni foam

Ming-Han Tsai*, Tzu-Chiang Chen*, Chih-Chao Wu**, Chihpin Huang*

*Institute of Environmental Engineering, National Yang Ming Chiao Tung University, Hsinchu 300, Taiwan (E-mail: *minghan102018@gmail.com)*
**Department of Environmental Engineering and Science, Feng Chia University, Taichung 400, Taiwan

Abstract
As part of ongoing efforts to effectively remove ammonia from industrial wastewater, electrochemical oxidation has become an alternative to conventional biological treatment due to its easier operation and better tolerance of toxic pollutants. This study aims to prepare CuCo/nickel foam (CuCo/NF) electrodes by depositing different ratios of Cu and Co as catalysts and investigate their performance for ammonia electrooxidation (AEO). Under optimum conditions (pH 11 and applied voltage of 1.1 V vs Ag/AgCl), excellent ammonia removal was obtained using the $Cu_{0.5}Co_{0.5}$/NF electrode system, with 93% removal after 5 h for a low level of ammonia loading (50 mg-N/L), which was superior to the performance of the bare NF electrode (only 54%). The $Cu_{0.5}Co_{0.5}$/NF electrode also had a higher current efficiency of 34% and lower energy consumption of 0.11 kWh g^{-1} compared to the bare NF and single metal Cu (Cu/NF) or Co (Co/NF) electrodes. The high catalytic performance of the $Cu_{0.5}Co_{0.5}$/NF electrode towards ammonia indicates that a CuCo bimetallic catalyst on a NF substrate is a promising solution for effective removal of ammonia from industrial wastewater.

Keywords
Ammonia; CuCo catalyst; Electrooxidation; Nickel foam

INTRODUCTION

Ammonia discharged in wastewater is a major cause of eutrophication, which is a concern in aquatic ecosystems. Electrochemical method, as one of potential eco-technologies, applied in the ammonia removal from wastewater has several advantages over conventional biological treatment, such as easier operation, greater environmental friendliness, and a higher tolerance to pollutants. Pt-based electrodes have been the most widely studied due to their low overpotential and high activity towards ammonia electrooxidation. However, Pt is quite expensive to commercialize and is susceptible to poisoning by N_{ads} during ammonia electrooxidation (AEO). Therefore, the development of a low-cost electrode material with high electrocatalytic performance and low overpotential is highly desirable.

Nickel foam (NF) electrodes have been promoted as an alternative to Pt-based materials for AEO because of their three-dimensional porous structure and relatively high specific area. It has been reported that the addition of a catalyst (e.g. Co, Cu) on the NF substrate can enhance the current density and activity of the electrode (Yan et al., 2012). Copper in particular is one of the most active catalysts for AEO due to its highly conductive nature and abundant active sites. However, the binding of Cu to N atoms is weak, somewhat limiting its performance for AEO. To solve this problem, it is proposed to add cobalt because Co combines a low onset potential with high stability for the electrochemical process. Co is also a low-cost and highly active catalyst. Bimetallic catalysts involving transition metals Ni-Cu and Ni-Co on a NF substrate have shown potential for urea electrooxidation and hydrogen evolution (Wu et al., 2019). It is therefore expected that the combination of conductive Cu and active Co deposited on NF could produce a synergistic catalytic effect to enhance AEO. To further test this hypothesis, bimetallic catalysts with different ratios of Cu and Co (Cu_xCo_y) were prepared on a NF substrate (Cu_xCo_y/NF) as novel anodes for AEO. The electrochemical properties and surface characteristics of these catalytic Cu_xCo_y/NF electrodes were investigated. In addition, the effects of the different atomic ratios of Cu and Co in the Cu_xCo_y/NF electrodes on both removal efficiency and product selectivity were studied.

MATERIALS AND METHODS

The Cu_xCo_y/NF electrodes were prepared by electrodeposition of Cu and Co using different concentration ratios in the plating solution. The variables x and y in Cu_xCo_y (i.e. Cu_1Co_0, $Cu_{0.75}Co_{0.25}$, $Cu_{0.5}Co_{0.5}$, $Cu_{0.25}Co_{0.75}$ and Cu_0Co_1) represent the concentration ratio of $Cu(NO_3)_2$ and $Co(NO_3)_2$ in the plating solutions. The electrodeposition was conducted by adding $Cu(NO_3)_2$ and $Co(NO_3)_2$ with 0.5 M Na_2NO_3 as an electrolyte using a current of 3 mA and 3 C. As a result, Cu_xCo_y film was deposited on the NF substrate (thickness: 1.7 mm, area density: 320 g/m^2, effective area: 6 × 6 cm^2) to form different Cu_xCo_y/NF electrodes.

The synthetic ammonia-containing wastewater was prepared by adding NH_4Cl at low and high concentrations (50 mg/L and 450 mg/L). Na_2SO_4 was used as the electrolyte, and the initial pH was adjusted to 11 using NaOH (0.5 M). CuCo/NF, Pt, and Ag/AgCl were used as the working, counter, and reference electrodes, respectively. The performance of the Cu_xCo_y/NF electrodes for ammonia electrooxidation was investigated over a period of 5 h. The electrochemical characterization and batch AEO experiment were conducted using an Autolab Potentiostat/Galvanostat 302N. The surface properties, and chemical composition of the electrode were analyzed by scanning electron microscopy (SEM), energy-dispersive X-ray analysis (EDX), and X-ray photoelectron spectroscopy (XPS). The electrooxidation performance was assessed by evaluating the ammonia removal efficiency, product selectivity, current efficiency (CE) and energy consumption (EC).

RESULTS AND DISCUSSION

Fig. 1 shows the SEM images of CuCo deposited NF electrodes. Bare NF (**Fig. 1a**) had a porous and/or a mesh structure with a smooth surface. For Cu/NF, Cu was homogeneously distributed on the NF substrate (**Fig. 1b**). Cu tended to agglomerate, which resulted in large particle sizes ranging from 6 to 21 μm, leading to the formation of a thicker surface. Compared to Cu, the Co particles were smaller and more widely dispersed on NF (**Fig. 1c**). For $Cu_{0.5}Co_{0.5}$/NF, the surface of the NF was thicker and rougher (compared to bare NF) due to the electrodeposition of the CuCo bimetallic material, typically by the agglomeration of Cu (**Fig. 1d**). Furthermore, EDS mapping confirmed that Cu and Co had been successfully deposited on the NF substrate.

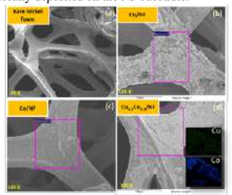

Figure 1. SEM images of (a) bare NF, (b) Cu/NF, (c) Co/NF, (d) $Cu_{0.5}Co_{0.5}$/NF.

The cyclic voltammograms of the NF, Cu/NF, Co/NF, and $Cu_{0.5}Co_{0.5}$/NF electrodes in the absence and presence of NH_3 are illustrated in **Fig. 2**. For NF, Cu/NF, and Co/NF electrode, the current density increased slightly in the presence of NH_3 (**Figs. 2a-2c**). These observations demonstrated the low catalytic activity of monometallic catalyst towards NH_3 (Xu et al., 2017). For $Cu_{0.5}Co_{0.5}$/NF in the absence of NH_3 (**Fig. 2d**), an oxidation peak occurred at 0.42 V vs Ag/AgCl, indicating the oxidation of β-$Ni(OH)_2$ to NiOOH. Astonishingly, the $Cu_{0.5}Co_{0.5}$/NF electrode exhibited a significant increase in current density (from 2 to 9 mA cm^{-2}) in the presence of NH_3 at 0.47 V. The faradaic reaction at this potential was similar to that without NH_3 addition where β-$Ni(OH)_2$ was oxidized to NiOOH. To conclude, the catalytic effect of the $Cu_{0.5}Co_{0.5}$/NF electrode is activated when interacting with NH_3.

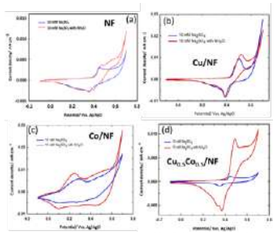

Figure 2. Cyclic voltammograms of (a) NF, (b) Cu/NF, (c) Co/NF, (d) $Cu_{0.5}Co_{0.5}$/NF in the absence and presence of ammonia (NH_3: 0–0.01 M, electrolyte: 10 mM of Na_2SO_4, scan rate: 10 mV/s).

The chemical composition of the $Cu_{0.5}Co_{0.5}$/NF electrode before and after the electrochemical treatment (ECT) was analysed using XPS (**Fig. 3**). Before the ECT, Ni existed in the form of Ni^0, NiO and β-$Ni(OH)_2$ (**Fig. 3a**). After the ECT, Ni^0 and Ni^{2+}oxidized to Ni^{3+} in the form of β-$Ni(OH)_2$ and NiOOH (**Fig. 3d**). The presence of active NiOOH could mediate the electron transfer of the NF-based electrode during AEO (Shih et al., 2018). For Cu, the peak of Cu_2O was transformed to $Cu(OH)_2$ after the ECT (**Figs. 3b and 3e**). Like Cu, CoO was transformed to $Co(OH)_2$ after the ECT (**Figs. 3c and 3f**). In addition, the formation of oxyhydroxide CoOOH was observed. To sum up, the metal oxides, whether Cu, Co, or Ni, were oxidized to metal hydroxides after ECT. The formation of active metal hydroxides and oxyhydroxide on the $Cu_{0.5}Co_{0.5}$/NF electrode is responsible for its superior performance toward AEO.

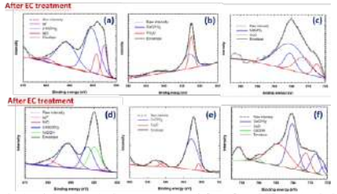

Figure 3. XPS analysis of the chemical composition of $Cu_{0.5}Co_{0.5}$/NF electrode before and after the electrochemical treatment: (a, d) Ni, (b, e) Cu, (c, f) Co.

NF and CuCo/NF electrodes with different CuCo ratios were tested for AEO at pH 11 using 1.1 V vs Ag/AgCl of applied potential. **Fig. 4a** shows that the highest NH_3 removal was obtained with $Cu_{0.5}Co_{0.5}$/NF (93%) followed by $Cu_{0.75}Co_{0.25}$/NF (84%), $Cu_{0.25}Co_{0.75}$/NF (78%), Cu_1Co_0/NF (64%), bare NF (58%), and Cu_0Co_1/NF (44%). Although $Cu_{0.5}Co_{0.5}$/NF provided the highest NH_3 removal, the N_2 selectivity was only 15.3%. By contrast, the highest N_2 selectivity (48.2%) was obtained by Cu_0Co_1/NF, which however showed less capability towards the removal of NH_3 (**Fig. 4b**). **Fig. 4c** shows the EC and CE for different electrodes at pH 11 and 1.1 V vs Ag/AgCl of applied potential. It can be seen that $Cu_{0.5}Co_{0.5}$/NF with a low NH_3 concentration had the highest CE (34%) and lowest energy consumption (0.11 kWh g^{-1}) compared with the bare NF, Cu/NF and Co/NF systems. At a high NH_3 concentration of 450 mg-N/L, although the NH_3 removal efficiency of the $Cu_{0.5}Co_{0.5}$/NF electrode decreased to 72%, its CE substantially increased (77%) with an energy consumption of only 0.03 kWh g^{-1}. This corresponds to better N_2 selectivity with 57% of N_2 being selected (i.e. 3.8 times higher than in the low NH_3 concentration case).

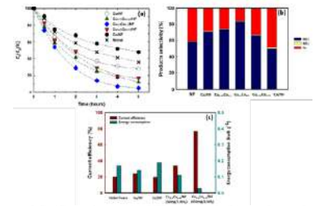

Figure 4. The effects of Cu/Co ratios on (a) NH_3 removal, (b) product selectivity after 5 h (50 mg/L NH_3, 10 mM Na_2SO_4, pH 11, 1.1 V vs Ag/AgCl), (c) comparison of different electrode systems on CE and EC.

CONCLUSION

This study demonstrates that the $Cu_{0.5}Co_{0.5}$/NF electrode is effective for AEO in terms of ammonia removal efficiency, current efficiency and energy consumption compared to the bare NF, Cu/NF, and Co/NF electrodes. The increase in catalytic activity towards ammonia is attributed to the formation of active CuCo oxyhydroxide. However, the main product is NO_3^- instead of the more desirable N_2 gas. Further investigations into the effect of pH and applied voltage should be conducted to achieve higher N_2 selectivity.

REFERENCES

Yan, W., Wang, D., Botte, G.G. 2012 Nickel and cobalt bimetallic hydroxide catalysts for urea electro-oxidation. *Electrochimica. Acta* **61**, 25–30.
Wu, M. S., Sie, Y. J., Yang, S. B. 2019 Hollow mesoporous nickel dendrites grown on porous nickel foam for electrochemical oxidation of urea. *Electrochimica. Acta* **304**, 131–137.
Xu, W., Lan, R., Du, D., Humphreys, J., Walker, M., Wu, Z., Tao, S. 2017 Directly growing hierarchical nickel-copper hydroxide nanowires on carbon fibre cloth for efficient electrooxidation of ammonia. *Applied Catalyst. B* **218**, 470–479.
Shih, Y. J., Huang, Y. H., Huang, C. P. 2018 In-situ electrochemical formation of nickel oxyhydroxide (NiOOH) on metallic nickel foam electrode for the direct oxidation of ammonia in aqueous solution, *Electrochimica. Acta* **281**, 410–419.

2. Decentralized Strategies

Light greywater quality consistency: challenge for their treatment and reuse. Study case: Colombia

Jessica Burgos-Arias*, Daniela Rey-Romero*, Lizeth Fernández*, and Edgar Ricardo Oviedo-Ocaña*

*Escuela de Ingeniería Civil, Universidad Industrial de Santander, Bucaramanga 680002, Colombia (E-mail: *jessica2218409@correo.uis.edu.co; daniela2208106@correo.uis.edu.co; lizeth2172083@correo.uis.edu.co; eroviedo@uis.edu.co)*

Abstract
Onsite domestic reuse of light greywater (LWG) for non-potable uses is an alternative to fulfill water demand worldwide. However, the main challenge for its reuse is the selection of appropriate treatment technologies, given the high variability in its quality. This study analyzed the physicochemical characteristics of LGW in a household from Colombia to propose potential treatment processes. We found high variability of LWG quality compared with data reported in the literature. Biological processes are not recommended for treating LWG, due to their low nutrient content, while filtration in granular media or membranes is highly recommended.

Keywords
Light greywater quality; light greywater treatment; reuse.

INTRODUCTION

Onsite domestic greywater (GW) reuse, specifically light greywater (LWG), is currently one of the most studied alternatives to mitigate water scarcity scenarios worldwide. According to Noutsopoulos et al. (2018), the main advantage of LWG reuse is its relatively low pollutant load compared with other domestic wastewater. Therefore, its treatment could be achieved with lower costs and level of complexity. Previous studies in Colombia show social acceptance of LWG reuse from potential end-users (Domínguez et al., 2017; Oviedo-Ocaña et al., 2018). However, the lack of knowledge about LWG quality in that context makes it a challenge to select appropriate treatment technologies to apply such reuse. While many studies have assessed the quality characteristics of LGW, most of them have been conducted in high-income countries (Eriksson et al., 2009; Ziemba et al., 2018), and have shown the high variability in LWG quality. Given the knowledge gap about LWG in low- and middle-income countries like Colombia, and the high variability their characteristics may have, in this study, we analyze physicochemical quality from a Colombian household to determine its consistency and explore potential treatments for countries from a similar context.

MATERIALS AND METHODS

Study area

The study was conducted in a household located in a residential area of Bucaramanga (Colombia) with 100% coverage of potable water supply, sewage, and solid waste management services. The residence is a family house of four people whose ages are 52, 32, 27, and 12 years old. The household has a total built area of 133.5 m^2 and has a living room, a kitchen, four bedrooms, three bathrooms, and a patio.

Sample collection

We collected 16 LGW samples produced in the household during September and December of 2022. We adopted a protocol based on those implemented in other studies (Shaikh & Ahammed, 2022; Teh et al., 2015) for sample collection. Due to the impossibility of accessing the shower's outflow pipes, each family member was asked to collect the greywater generated while showering using a 59-L plastic tub. Greywater from hand basins was collected directly from the outflow pipe with a 1-L plastic graduated cylinder. From previous studies in the house, we concluded that 94% of the daily production of LGW occurs from 5:00 to 14:00 h. Therefore, on each sampling day, LWG collected from both sources during that period was emptied and thoroughly mixed in a 55-gal plastic barrel.

Laboratory analysis

LGW samples for analysis were collected from the barrel and transported to the laboratory for immediate analysis of physicochemical parameters. Based on the literature review, the main physic-chemical parameters of the GW were identified and used in this study, i.e., pH, electrical conductivity (EC), turbidity, total phosphorous (TP), total nitrogen (TN), total suspended solids (TSS), total chemical oxygen demand (COD) and biochemical oxygen demand (BOD_5). TN was measured according to the persulfate digestion method proposed by Hach®, whereas other quality parameters were analyzed following the standard methods (APHA-AWWA-WEF, 2017). The results of the physicochemical characterization were analyzed with descriptive statistics and contrasted with values found in the literature for LGW in other geographical contexts.

RESULTS AND DISCUSSION

Table 1 presents descriptive statistics for each quality parameter analyzed for LGW samples and data reported in the literature. We found that LGW analyzed in this study gives pH values close to neutrality (7.46 ± 0.15), which is similar to data reported in the literature. Turbidity values were relatively high (242.90 ± 45.12) compared to those found by other authors (Jamrah et al., 2006), which could be related to the use of solid soaps. TSS values (214.57 ± 54.38) were close to values reported in the literature (Friedler, 2004; Teh et al., 2015) and may be associated with hair strands and skin cells. EC values (191.69 ± 9.35) were similar to those found in other contexts (Morandi et al., 2021; Santos et al., 2014) and could be related to the use of personal care products with high salt concentration.

LGW from our study household has a high organic pollutant load in terms of COD and BOD_5 with values of 874.54 ± 161.75 mgO_2/L and 397.88 ± 78.04 mgO_2/L, respectively, which is contrasting to most of the values found in the literature (Jamrah et al., 2006; Morandi et al., 2021; Noutsopoulos et al., 2018), but similar to results found for LWG in Turkey (Oktor & Çelik, 2019). Kadewa et al. (2020) explain that high organic matter concentration in LWG is related to the presence of fatty alcohols used as emollients in personal care products. In addition, the high COD and BOD_5 concentrations in LGW from our study could be attributed to the tendency of less water consumption in low- and middle-income countries compared to high-income countries (Khanam & Patidar, 2022). As our studied LWG showed a BOD_5:COD ratio of 0.45 and neutral pH, it would be acceptable to consider the biological process for its treatment. However, the LWG low nutrient content could compromise biological treatment efficiency, with TN and TP concentrations of 6.17 ± 1.73 and 0.88 ± 0.38, respectively. Furthermore, as the recommended COD:TN:TP ratio for biological treatment is 100:5:1 (Jefferson et al., 2004; Ziemba et al., 2018), the nutrients deficiency is also evident for our studied LWG whit a ratio of 381.90:2.85:1.

With the measured turbidity, TSS, COD, and BOD_5 values, and for LGW decentralized reuse for non-potable uses, we suggest considering granular media filtration, which in previous studies have reported remotion efficiencies of 88%, 76%, 52%, and 20% for COD, BOD_5, turbidity, and TSS, respectively (Ghaitidak & Yadav, 2016; Shaikh & Ahammed, 2021). In addition, the use of ultrafiltration membranes and inverse osmosis is also recommended based on organic matter remotion efficiency above 50%, achieved in other studies (Kant et al., 2018). This study shows the need to deepen the aspects that affect the variability of LWG quality, and to continue monitoring the quality of LWG (i.e., in one and several households) to establish typical characteristics in the context of low- and middle-income countries such as Colombia.

Table 1. Quality parameters LGW measured in this study and reported in literature.

Parameter	Unit	Values in this study				Values reported in literature						
		n	Average	SD	CV	Jordan[1]	Malaysia[2]	Germany[3]	Turkey[4]	Israel[5]	Greece[6]	Portugal[7]
pH		16	7.46	0.15	2%	7.42	6.13	8.4	-	7.43	7.5	6.7
EC	µS/cm	16	191.69	9.35	5%	-	-	737	-	-	318	94.6
Turbidity	NTU	16	242.90	45.12	19%	35.2	-	-	-	-	-	-
TN	mgN/L	16	6.17	1.73	28%	10.92	-	28.3	14.13	-	-	-
TP	mgP/L	13	0.88	0.38	43%	1.12	-	1.9	2.25	-	-	-
TSS	mg/L	14	214.57	54.38	25%	-	81	-	-	303	73.5	-
COD	mgO_2/L	16	874.54	161.75	18%	77	445	328	1171	645	390	540
BOD_5	mgO_2/L	16	397.88	78.04	20%	40.2	349	-	568	424	263	-

n: Number of samples; *SD:* standard deviation; *CV:* coefficient variation
[1] (Jamrah et al., 2006); [2] ((Teh et al., 2015); [3] (Morandi et al., 2021); [4] (Oktor & Çelik, 2019); [5] (Friedler, 2004); [6](Noutsopoulos et al., 2018); [7] (Santos et al., 2014)

REFERENCES

APHA-AWWA-WEF. (2017). *Standard Methods for the Examination of Water and Wastewater* (E. W. Rice, R. B. Baird, & A. D. Eaton, Eds.; 23rd ed.). American Public Health Association, American Water Works Association, Water Environment Federation.

Domínguez, I., Ward, S., Mendoza, J. G., & Rincón, C. I. (2017). End-user cost-benefit prioritization for selecting rainwater harvesting and greywater reuse in social housing. *Water*, *9*(7), 1–18. https://doi.org/10.3390/w9070516

Eriksson, E., Andersen, H. R., Madsen, T. S., & Ledin, A. (2009). Greywater pollution variability and loadings. *Ecological Engineering*, *35*(5), 661–669. https://doi.org/10.1016/j.ecoleng.2008.10.015

Friedler, E. (2004). Quality of individual domestic greywater streams and its implication for on-site treatment and reuse possibilities. *Environmental Technology*, *25*(9), 997–1008. https://doi.org/10.1080/09593330.2004.9619393

Ghaitidak, D. M., & Yadav, K. D. (2016). Greywater treatment for reuse: Comparison of reuse options using analytic hierarchy process. *Journal of Water Reuse and Desalination*, *6*(1), 108–124. https://doi.org/10.2166/wrd.2015.177

Jamrah, A., Al-Omari, A., Al-Qasem, L., & Ghani, N. A. (2006). Assessment of availability and characteristics of greywater in Amman. *Water International*, *31*(2), 210–220. https://doi.org/10.1080/02508060.2006.9709671

Jefferson, B., Palmer, A., Jeffrey, P., Stuetz, R., & Judd, S. (2004). Grey water characterisation and its impact on the selection and operation of technologies for urban reuse. *Water Science and Technology*, *50*(2), 157–164.

Kadewa, W. W., Knops, G., Pidou, M., Jeffrey, P., Jefferson, B., & le Corre, K. S. (2020). What is the impact of personal care products selection on greywater characteristics and reuse? *Science of the Total Environment*, *749*. https://doi.org/10.1016/j.scitotenv.2020.141413

Kant, S., Jaber, F. H., & Karthikeyan, R. (2018). Evaluation of a portable in-house greywater treatment system for potential water-reuse in urban areas. *Urban Water Journal*, *15*(4), 309–315. https://doi.org/10.1080/1573062X.2018.1457165

Khanam, K., & Patidar, S. K. (2022). Greywater characteristics in developed and developing countries. *Materials Today: Proceedings*, 1494–1499. https://doi.org/10.1016/j.matpr.2021.12.022

Morandi, C., Schreiner, G., Moosmann, P., & Steinmetz, H. (2021). Elevated vertical-flow constructed wetlands for light greywater treatment. *Water (Switzerland)*, *13*(18). https://doi.org/10.3390/w13182510

Noutsopoulos, C., Andreadakis, A., Kouris, N., Charchousi, D., Mendrinou, P., Galani, A., Mantziaras, I., & Koumaki, E. (2018). Greywater characterization and loadings – Physicochemical treatment to promote onsite reuse. *Journal of Environmental Management*, *216*, 337–346. https://doi.org/10.1016/j.jenvman.2017.05.094

Oktor, K., & Çelik, D. (2019). Treatment of wash basin and bathroom greywater with Chlorella variabilis and reusability. *Journal of Water Process Engineering*, *31*. https://doi.org/10.1016/j.jwpe.2019.100857

Oviedo-Ocaña, E. R., Domínguez, I., Ward, S., Rivera-Sanchez, M. L., & Zaraza-Peña, J. M. (2018). Financial feasibility of end-user designed rainwater harvesting and greywater reuse systems for high water use households. *Environmental Science and Pollution Research*, *25*(20), 19200–19216. https://doi.org/10.1007/s11356-017-8710-5

Santos, C., Matos, C., & Taveira-Pinto, F. (2014). A comparative study of greywater from domestic and public buildings. *Water Science and Technology: Water Supply*, *14*(1), 135–141. https://doi.org/10.2166/ws.2013.181

Shaikh, I., & Ahammed, M. M. (2021). Coagulation Followed by Continuous Sand Filtration for Treatment of Greywater. *Journal of Hazardous, Toxic, and Radioactive Waste*, *25*(4). https://doi.org/10.1061/(asce)hz.2153-5515.0000640

Shaikh, I., & Ahammed, M. M. (2022). Quantity and quality characteristics of greywater from an Indian household. *Environmental Monitoring and Assessment*, *194*(3). https://doi.org/10.1007/s10661-022-09820-0

Teh, X. Y., Poh, P. E., Gouwanda, D., & Chong, M. N. (2015). Decentralized light greywater treatment using aerobic digestion and hydrogen peroxide disinfection for non-potable reuse. *Journal of Cleaner Production*, *99*, 305–311. https://doi.org/10.1016/j.jclepro.2015.03.015

Ziemba, C., Larivé, O., Reynaert, E., & Morgenroth, E. (2018). Chemical composition, nutrient-balancing and biological treatment of hand washing greywater. *Water Research*, *144*, 752–762. https://doi.org/10.1016/j.watres.2018.07.005

Organic micropollutants in a Euro-Mediterranean resort: occurrence in the water cycle

Gusmaroli, L.*,**,***, Vosse, J. *,**, Mendoza, E.*,**, Rodriguez-Roda, I.*,****, Ferrero, G.*****, Buttiglieri, G.*,**

* Catalan Institute for Water Research (ICRA-CERCA), C. Emili Grahit 101, 17003 Girona, Spain
** Universitat de Girona, Girona, Spain
*** Catalan Water Partnership, Girona, Spain
**** LEQUiA, Institute of the Environment, University of Girona, E-17071 Girona, Spain
***** IHE Delft Institute for Water Education, Westvest 7, 2611 AX Delft, Netherlands
(E-mail: gbuttiglieri@icra.cat)

Abstract
Touristic facilities located in water scarce areas of the Euro-Mediterranean are simultaneously facing growing incoming numbers of tourists and decreasing availability of water resources. Decentralised water reuse has become one of the most promising practices for insuring dramatic reduction of water consumption in the touristic sector. Different targets in terms of water quality requirements are established by national and international regulations. However, emerging micropollutants have not yet been included in such policies, partially because of the lack of information on their occurrence. This article investigates the occurrence of a set of OMP in the water cycle of a large resort located in Lloret de Mar, Spain. It hereby considers tap and pool water, as well as the separate wastewater streams: black water and kitchen, laundry, and bathroom greywater, where part of the greywater is reused for toilet flushing.

Keywords
Endocrine disrupting compounds; greywater; hotel; micropollutants; pharmaceuticals; tourism

INTRODUCTION

Global water use has tripled in the last 50 years due to population increase, economic growth, changes in lifestyle, technologies, and international trade. Fresh water availability is unevenly distributed between countries and within countries and water scarcity may exist at the regional and local scale. High and concentrated tourism may exceed the levels of consumption of water resources in arid and water-stressed regions, some of which have already needed water transfers to prevent salinization (Cazcarro et al., 2014). Increasing water consumption and intensity as well as tourist numbers and tourism activities standards are expected. Tourism water consumption is typically below 5 % of domestic water use, but can be as high as 40 % (e.g., Mauritius; Gössling et al., 2012). Additionally, touristic nuclei can have a strong impact on water quality and have been considered as probable sources of micropollutants in seawater especially during the high season (Moreno-Gonzalez et al., 2015). At present, there is a general lack of studies addressing the occurrence of organic micropollutants (OMP) such as personal care products, pharmaceuticals (PhACs), and endocrine-disrupting compounds (EDCs) in closed water cycles.
This study aims at filling a knowledge gap on OMP in tourist facilities in a water-scarce area. A large resort located in Lloret de Mar (NE Spain) that implements a partially closed water cycle was chosen as study site to assess the occurrence of OMP in the water cycle, comprising different water streams, including greywater, in the high and low tourist season. The data gathered may prove useful to evaluate future reuse opportunities and for policy makers and public health authorities.

MATERIALS AND METHODS

Hotel Samba is in an extremely touristic area of the North-Eastern Mediterranean coast of Spain, where dramatic water demand increase coincides with water scarcity events during the summer months. Hotel Samba is a large 3-star resort with 441 air-conditioned rooms, green areas and exterior pools, conference rooms, bar, and restaurant. Water use reported by the hotel ranges from 25,000 to 34,000 m^3/year (100-135 L/person/day). Two sampling campaigns have been performed in the high season (June, with 76-99% of rooms occupied) and in the low season (November, with 35-67% of rooms occupied). The sampling points are presented in Figure 1. Different chemical, physical and microbiological parameters were analyzed as well as 39 OMP: 10 endocrine disruptors and related compounds (EDCs) and 29 pharmaceuticals (PhACs).

RESULTS AND DISCUSSION

It emerged an important seasonal variation in water consumption per use (Figure 1) with a 48% total tap water reduction during low season (128 vs 67 m^3/day in high and low season, respectively).

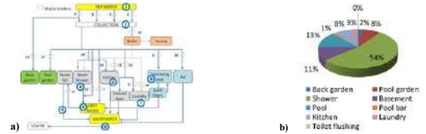

Figure 1. a) Sampling points. b) Tap water consumption by use during the high season.

Overall, the present study evidences a knowledge gap regarding the occurrence of micropollutants in closed water cycles, especially laundry and kitchen greywater, and in relation to tourism. Further studies are needed to be able to choose adequate reuse trains without disregarding important sources of contamination. The load of micropollutants is as variable in different GW sources as it is in different blackwater sources. The provided differentiation of loads by GW streams helps to deepen the understanding of the reuse and treatment potential of the different wastewater streams, besides the commonly reported standard parameters, as well as shining a light on the impact of seasonality on compound distribution in the different water streams, in the context of tourism.

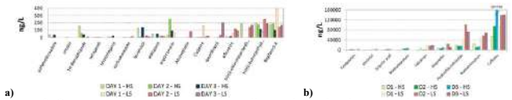

Figure 2. Occurrence of a selection of micropollutants in the hotel water cycle (HS: high season; LS: low season; a) greywater, b) wastewater).

REFERENCES

Cazcarro I., Hoekstra A.Y., Sánchez Chóliz J. (2014), The water footprint of tourism in Spain. Tourism Management, 40, 90-101.
Gössling, S., Peeters, P., Hall, C. M., Ceron, J.-P., Dubois, G., Lehmann, L. V., & Scott, D. (2012). Tourism and water use: Supply, demand, and security. An international review. Tourism Management, 33, 1–15. https://doi.org/10.1016/j.tourman.2011.03.015
Moreno-González R., Rodriguez-Mozaz S., Gros M., Barceló D., León V.M. (2015), Seasonal distribution of pharmaceuticals in marine water and sediment from a Mediterranean coastal lagoon. Environ. Res. 13, 326-344.

ACKNOWLEDGMENTS

This work was funded by the European Union's Horizon 2020 Research and Innovation programme (HYDROUSA, GA N° 776643). G.B. acknowledges Spanish State Research Agency of the Spanish Ministry of Science, Innovation and Universities (Grant RYC-2014-16754) and 2021 SGR 01283.

Earthworms influence on macroporosity and biofilm in constructed wetlands

S. Cazaux*, **, A. Lacou*,***, C. Gontié*, P. Duru**, M. Alliet***, C. Albasi***, A-L. Pablo****, E. Ortega****, S. Canovas*, D. Orange**** and M. Gerino*

* Laboratoire Ecologie Fonctionnelle et Environnement, Université Paul Sabatier, 118 route de Narbonne, 31062 Toulouse Cedex 9, France
(mail : magali.gerino@univ-tlse3.fr ; alexandre.lacou@univ-tlse3.fr)
** Institut de Mécanique des Fluides de Toulouse, Université de Toulouse, CNRS, INPT, UPS, Toulouse, France
(mail : paul.duru@imft.fr ; siriane.cazaux@toulouse-inp.fr)
*** Laboratoire de Génie Chimique, Université de Toulouse, CNRS, INPT, UPS, Toulouse, France
(mail : marion.alliet@ensiacet.fr ; claire.albasi@toulouse-inp.fr)
**** Eco&Sols, IRD, Université Montpellier, CIRAD, INRA, Montpellier SupAgro, Montpellier, France
(mail : didier.orange@ird.fr ; anne-laure.pablo@ird.fr)

Abstract
Constructed wetlands (CW) are one of the nature-based solutions for wastewater treatment. The main drawback of CW is their large footprint, which is due to both clogging problems and purification efficiency that requires long retention times. In order to improve the process, we are studying the potential of introducing earthworms into CW such as bioaugmented filters. These invertebrates are known for their ability to lower the clogging process, facilitate oxygen penetration into the substrate, increase the bioavailability of organic matter through molecular simplification and influencing microbial biodiversity. Our working hypothesis is to reduce the space requirement of the CW by introducing earthworms in the system. In continuity with the O'BIOM project (French ANR) carried out during 2022, two Ph-D projects have just started with the objective to describe and to perform the earthworms' influence on the porosity of the filtering substrate and on the biofilm microbial communities' structure at larger spatial and temporal scales through a CW living lab. The galleries network of different functional groups of earthworms (anecic, epigeic, endogeic) will be assessed via X-ray tomography image analysis to estimate the macroporosity dynamics. And the OTUs richness of the interstitial biofilm will be compared in order to seek the temporal evolution of the microbial composition under earthworm feeding pressure.

Keywords
Biodiversity ; biofilm ; constructed wetland ; earthworms ; macroporosity ; water flow

INTRODUCTION

This work is based on a biomimetic approach of the natural service of water-quality regulation. The constructed wetlands (CWs) require more space than conventional wastewater treatment systems, and the main lock of this system is their large footprint, which is due to both clogging problems[1] and purification efficiency that requires long retention times[2]. In order to improve the process efficiency, from a microbial and hydrological point of view, we are studying the potential of introducing earthworms into CW. Earthworms are known for their ability to stem the clogging process[3], facilitate oxygen penetration into the substrate[4], increase the bioavailability of organic matter through molecular simplification[5] and increase microbial biodiversity in the biofilm[6]. On the one hand, the biophysical relationship between the 3D galleries network and the water infiltration in the macroporous soil system is investigated for a better description of the water flow in these unsteady conditions. On the other hand, the challenge is to identify the dynamics of microbial communities in relation to the biodiversity involved in the filters (invertebrates and plants) and the substrate.

EXPERIMENTAL PROTOCOL

The preliminary results presented here have been provided by experiments at microcosm scale for 2 months with synthetic water. They are 40 cm high and 12.5 cm diameter cylindrical cores, made of a combination of filter sand and white peat, and inoculated with 3 earthworms species (the control microcosm excepted). The biofilm was sampled for eDNA metabarcoding sequencing with the Nanopore MinIon technology, and the microcosms were scanned by X-ray tomography. Image processing is carried out with Matlab and Avizo to make 3D volume renderings and extract salient features of the spatial arrangement of the network.

RESULTS

Influence of earthworms on the macroporosity of constructed wetlands

At a microscopic scale, we study the impact of the earthworms' galleries network on the residence time of wastewater in CW, thus optimising the use of the volume of the filtering substrate. To visualise both the substrate natural macroporosity and the network of earthworms' galleries, high spatial resolution X-ray tomography will be used extensively.

Influence of earthworms on biofilm of constructed wetlands

The partially recovered results allowed us to see slight differences in biofilm microbial community structure in presence of earthworm. A new sequencing run is scheduled to go further into the interpretation of these results. The comparison of the microbial species richness in the interstitial biofilm with and without earthworms provides evidence of these invertebrate influences on the biofilm composition. It is suggested that this biofilm biocontrol by the invertebrate increases the adaptation to pollutants occurrence.

PERSPECTIVES AND ON-GOING RESEARCH WORK

Together, these experimental works will demonstrate the existence of a combination of earthworms/substrates and plants that optimises the retention time of the wastewater and the level of wastewater purification in the filter. It should be noted that the preliminary study was carried out at a short time scale (2 months), which does not allow to obtain a mature state of the ecosystem. It is therefore necessary to extend the study duration, in order to reach a steady state. Two PhD thesis projects have just started, with the objective of continuing the assessment of the impact of earthworms on the porosity of the filtering substrate and on the biofilm microbial communities' structure at larger spatial and temporal scales. The experiments will be carried out at mesocosm and pilot scales through a CW living lab collecting domestic wastewaters from UT3 University (2,5 to 10 EqInhab). The water treatment efficiency will be controlled by analysing physico-chemical parameters (BOD_5, COD, NO_3^-, PO_4^{3-}, TSS). And the permeability will be monitored.

ACKNOWLEDGEMENT *: O'BIOM project was publicly funded through ANR under the "investissements d'avenir" programme with the reference ANR-10-LABX-04-01 LabexCEMEB and coordinated by the University of Montpellier.*

REFERENCES

[1] Wang, et al. 2021 Clogging mechanisms of constructed wetlands. *J. Clean. Prod.* **295**.
[2] Lee, et al. 2009 Nitrogen removal in constructed wetland systems. *Eng. Life Sc.* **9**, 11–22.
[3] Gilibert O, Gérino M, …… Orange D. 2022 Density effects of Eisenia sp. epigeic earthworms on the hydraulic conductivity …. *Water*, **14** (1048).
[4]Hoang T. K., Probst A., Orange D., ……, Gerino M., 2018. Bioturbation effects on bioaccumulation of Cadmium in the wetland plant Typha latifolia. *STOTEN*, 618 : 1284-1297..
[5] Li et al. 2011 A practical method for the restoration of clogged rural vertical subsurface flow constructed wetlands f. *Water Sc. & Tech.* **63**(2).
[6] Gérino M., Orange D., Sanchez-Perez JM., Buffan-Dubau E., Canovas S., Monfort B., Albasi C., Sauvage S. 2022 What inspiring elements from natural services of water quality regulation could be applied to water management? *Water*, **14** (3030).

Industrial-urban symbiosis waste treatment for regional development in Alcoy region (Spain).

N. Zamorano-López*, R. Tamarit*, E. Zuriaga*, F. Valero*, E. Pérez**, M. Blanes**.

*FACSA, SOCIEDAD DE FOMENTO AGRÍCOLA CASTELLONENSE, S.A., C/ Mayor 82-84, 12001, Castellón, Spain, nuria.zamorano@grupogimeno.com; ezuriaga@facsa.com; raquel.tamarit@facsa.com; favlero@facsa.com.
** AITEX, ASOCIACION DE INVESTIGACION DE LA INDUSTRIA TEXTIL. Plaza Emilio Sala, 1, 03801, Alcoy, Spain. eperez@aitex.com; mblanes@aitex.com

Abstract
The main goal of SYMSITES is to implement the regional industrial-urban symbiosis in four European regions different in socio-economic and environmental aspects, from the north of Denmark, through the centre, Austria to the south, Spain, and Greece. The Spanish Ecosite consists of an urban organic waste management plant coupled to anaerobic treatment of urban wastewater by an Anaerobic Membrane Bioreactor (AnMBR). Biogas production will be upgraded into hydrogen using protonic membranes. Also, new anti-fouling membrane technologies are developed such as magnetic vibration systems and corrugated membranes. The microbial risk associated with the effluent of the plant will be analysed using viral infectivity and bacterial activation assays. The contribution of this project for Alcoy region sustainable development and industrial-urban symbiosis is here presented highlighting the innovative technologies that are being developed and implemented to maximize resource recovery using AnMBR systems.

Keywords (maximum 6 in alphabetical order)
AnMBR; hydrogen; industrial-urban symbiosis; regional development; wastewater; water reuse.

INTRODUCTION

Transition into a circular economy requires the development of multidisciplinary approaches and can be a strategy for sustainable regional development. Hydrogen production should be implemented in WWTP to guarantee their positive carbon footprint. Also, water reclamation and reuse for industrial purposes should be facilitated. The aim of this project is to develop and prove the concept of Industrial-Urban Symbiosis (IU-S) in Alcoy region (textile, and cosmetic industries). The technologies will include: (i) AnMBR with magnetically induced membrane vibration (MMV) for advanced antifouling control without biogas sparging, (ii) adsorption column-based of antibacterial and antiviral lignin nanoparticles (LigNP) for antibacterial and antiviral treatment (Morena et al., 2022), (iii) pyrolysis of textile and cosmetic non-recyclable wastes (NRW) and (iv) hydrogen from protonic membrane reformer (PMR) for biogas upgrading (Clark et al., 2022).

MATERIALS AND METHODS

Urban and industrial biowastes

Urban wastes are collected through two strategies: organic wastes container and on-source household separation. After separation of non-organic wastes, the biowaste is grinded and shrived up to 0.1 mm in wet conditions. The resulting bio-pulp is fed into the AnMBR based pilot plant as a co-substrate. Industrial wastes from textile and cosmetic facilities are treated in a pyrolysis system operated at 650-850°C, to produce char and pyrolysis oils. Analytical measurements of pH, COD, solids, nutrients and VFA have been carried out to characterize the resulting slurries and pyrolysis inputs. Biomethane Potential (BMP) tests have been carried out following standard UNI/TS 11703.

AnMBR with MMV pilot plant and hydrogen production

The plant is designed for treating 4m^3/day when operating at 70d Solids Retention Time (SRT), 12h Hydraulic Retention Time (HRT) at ambient temperature (15-25°C). The external membrane modules are equipped with submerged membranes: (i) 0.03µm ultrafiltration hollow fibre membrane (Pulsion, KOCH) with biogas sparging and (ii) 0.1µm microfiltration flat corrugated membranes of micro-patterned PVDF with MMV anti-fouling control (Ilyas et al., 2022). PMR technology is being applied to the resulting biogas from the AnMBR to produce, separate and compress hydrogen in a single-step reaction. In this process, CO_2 is captured through a steam methane reforming reaction. Before PMR the H_2S fraction is removed from the biogas using water scrubbing methods at different efficiency ratios to optimise the process and reduce purification efforts towards the minimum energy requirements.

Water reuse

AnMBR effluent is being used for liquid fertilizer in ammonia sulphate form using a membrane contactor (Accurel PP 300/1200, Germany). The microbial risk assessment analysis of this effluent is being analysed using the standards: EN ISO 19458, EN ISO/IEC-17025, UNE-EN ISO 8199:2019, UNE-EN ISO 15216-1:2017 and ISO 9308-1:2014 according to European Regulation (EU) 2020/741. Analysis of the AnMBR effluent for circular reuse in textile and cosmetic water demands is being carried out analysing parameters like pH, conductivity, turbidity, chemical oxygen demand, total nitrogen, phosphates, chloride, total solids, Fe, and microbial parameters such as Escherichia coli.

RESULTS AND DISCUSSION

The pilot-plant is expected for 2023 but on-going work is being carried out for biowastes characterization. Future work would be presented including the results of BMP tests over the different mixtures of biowastes retrieved from the municipality, textile, and cosmetics industrial wastewater effluents. Ratio adjustment for the conversion of these wastes into energy is necessary before pilot plant operation. The expected outcome of the project is achieving a 90% COD removal with a pathogen elimination over 4.0 log10 levels. Also, the sludge reduction capacity will be analysed and adjusted to achieve values over 80% which is feasible through the application of anaerobic processes in membrane bioreactors. The biomethane obtained and biogas composition will be used to simulate its conversion into hydrogen also in CSIC pilot plant facilities. Theoretical energy recovery values will be obtained in the batch and laboratory stage that is being carried out and will be used as a baseline before pilot plant start-up.

ACKNOWLEDGEMENTS

SYMSITES project is funded by the European Union under HORIZON-CL4-2021-TWIN-TRANSITION-01 call (Grant Agreement 101058426). Partners contributing to the EcoSite Spain are fully acknowledged: Fomento Valencia Medioambiente SL; Greene Waste to Energy; Universitat Politecnica de Catalunya; Agencia Estatal Consejo Superior de Investigaciones Cientificas (CSIC centres ITQ, IATA and CEBAS); Germaine de Capuccini SAU, Francisco Jover SA, and Katholieke Universiteit Leuven.

REFERENCES

Clark, D., Malerød-Fjeld, H., Budd, M., Yuste-Tirados, I., Beeaff, D., Aamodt, S., Nguyen, K., Ansaloni, L., Peters, T., Vestre, P. K., Pappas, D. K., Valls, M. I., Remiro-Buenamañana, S., Norby, T., Bjørheim, T. S., Serra, J. M., & Kjølseth, C. 2022. Single-step hydrogen production from NH3, CH4, and biogas in stacked proton ceramic reactors. *Science*, 376 (6591), 390–393.

Ilyas, A., Timmermans, L., Vanierschot, M., Smets, I., Vankelecom, I. F. J. 2022. Micro-patterned PVDF membranes and magnetically induced membrane vibration system for efficient membrane bioreactor operation. Journal of Membrane *Science*, 662, 120978.

Morena, A. G., Pérez-Rafael, S., & Tzanov, T. 2022. Lignin-Based Nanoparticles as Both Structural and Active Elements in Self-Assembling and Self-Healing Multifunctional Hydrogels for Chronic Wound Management. *Pharmaceutics*, 14 (12), 2658.

Truchado, P., Gil, M. I., López, C., Garre, A., López-Aragón, R. F., Böhme, K., & Allende, A. 2021. New standards at European Union level on water reuse for agricultural irrigation: Are the Spanish wastewater treatment plants ready to produce and distribute reclaimed water within the minimum quality requirements? *International Journal of Food Microbiology*, 356, 109352.

Identifying substrates for greywater treatment in a novel green wall system based on trickling filters

M.G.P. Grau*, N. Krähenbühl*, N. Antenen*

* Institute of Natural Resource Sciences, Zurich University of Applied Sciences, Grüentalstrasse 14, 8820 Wädenswil, Switzerland (E-mail: *maximiliangerdphilipp.grau@zhaw.ch)*

Abstract
Green walls with greywater treatment capabilities can play a key role to close water cycles in growing cities worldwide. Most green wall systems for greywater treatment apply a similar process as in constructed wetlands, where the substrate acts as plant substrate and to treat the polluted water. A novel green wall system is in development that separates the plant layer from the greywater treatment, by introducing a setup similar to a trickling filter. In a first step, various commercial substrates were tested for their suitability in terms of treatment performance at two different hydraulic loading rates over a 10-week period, using synthetic greywater. Measured parameters for determining pollutant removal were turbidity, chemical oxygen demand (COD), and others over a treatment time of seven days, measuring concentrations at the beginning, after three days and at seven days. The first substrate, expanded shale, performed best, achieving removal rates up to 60% for COD, closely followed by the other two substrates, plastic Hel-x and foam carriers. Generally, most pollutants were removed within the first three days of treatment. Even though plastic Hel-x carriers were not as efficient in pollutant removal as expanded clay, the carrier will be used for planned pilot trials of the novel green wall system due to their lower weight.

Keywords
Green walls; greywater treatment; substrate tests; trickling filter; water re-use

INTRODUCTION

The urbanization of the world's population is steadily increasing. 68% of people are projected to live in urban areas by 2050 (United Nations 2019), which will increase the pressure on water supply and sanitation. It is essential that water resources are managed sustainably, and also the use of alternative water sources must be considered (Bahri 2012). Greywater has shown great potential for re-use, however treatment technologies on household level need to be developed (Ghaitidak and Yadav 2013). In recent years, nature-based solutions have emerged as potential treatment options for greywater treatment in urban settings, especially green roofs and green walls, demonstrating high removal efficiencies of up to 80% for organic matter (Boano et al. 2020). Additionally, green walls have the potential to address other pressing issues of growing cities, such as the heat island effect (Pucher et al. 2022). Most green wall systems with integrated greywater treatment are designed similarly to constructed wetlands, where the substrate in pot-based, vertical systems acts as the substrate for the plants and also for greywater treatment, optimized for pollutant removal (Masi et al. 2016; Prodanovic et al. 2017). Also other processes such as trickling filters have been demonstrated to be suitable for greywater treatment (Ghaitidak and Yadav 2013; Gross, Kaplan, and Baker 2007). However, trickling filters have hardly been developed in the form of a green wall. In this study, a novel, layered green wall system, that separates the greywater treatment from the plant section is being developed. A filter system operates like a trickling filter on the back of the module, with a separate plant part in the front layer. The focus of this study was to test various commercially available substrates for their application as filter media for the green wall system in development.

MATERIALS AND METHODS

In order to find the most suitable substrate for the back layer of the green wall, the pollutant removal efficiency of three commercially available substrates (i.e., expanded shale, plastic Hel-x carriers, and foam carriers) were investigated in a column experiment over a period of 10 weeks under controlled climate conditions (25 °C and 60 % rH). Each column contained 2 L of a single substrate and was operated as a trickling filter under either a fast (34 l m-2 h-1) or slow (8 l m-2 h-1) hydraulic loading rate (HLR). Each column had a separate bucket for the greywater that was continuously recirculated through the columns with an aquarium pump. Each substrate and hydraulic loading regime was performed in triplicate, resulting in a combined setup of 18 columns. Prior to the experiment, each substrate was inoculated by being submerged in real greywater for 1 month. Every week each replicate was dosed with 15 ml of synthetic greywater and tap water was added to maintain a starting volume of 20 litres. The greywater addition was approximated to contain 300 mg/l chemical oxygen demand (COD), 14 mg/l total nitrogen (TN) and 3.5 mg/l total phosphorus (TP). This addition was maintained throughout the trial regardless of the concentrations remaining from the previous week. To determine the pollutant removal efficiency of the substrate and general conditions several parameters relevant to water quality were measured 2 hours (Day 0), 3 and 7 days after synthetic greywater addition. Removal rates were calculated compared to day 0 measurements. Measured parameters were pH, dissolved oxygen, temperature and conductivity, turbidity, COD, TP, total organic carbon (TOC) and TN.

RESULTS AND DISCUSSION

Expanded shale consistently exhibited the highest removal across all examined parameters, followed by Hel-x carriers, reaching removal efficiencies for COD up to 60% (Figure 1). Foam carriers generally performed either similar or worse than the Hel-x counterparts. A slower HLR showed partially better treatment performance compared to the faster HLR, while still preventing excessive biofilm formation that could clog the trickling filter. Particularly changes in TP highlighted the benefit of utilising complex materials containing natural adsorption sites, such as expanded shale for phosphorus removal. Apart from TOC most of the removal for various pollutants occurred within the first 3 days after greywater addition (up to: 80% for turbidity, 60% for TN, 40% for TP). This highlights the importance of biofilm establishment and adaptation to the pollutants present in greywater when in operation. Even though expanded shale demonstrated the best treatment performance, plastic Hel-x will be considered for the use in a pilot installation of the novel green wall system, mainly due to its lower weight of the material, thus achieving a lighter weight per m^2 green wall installed.

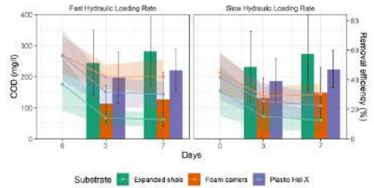

Figure 1. Treatment efficiency for COD of the three substrates; Average COD concentrations plotted as lines at the beginning and after 3 and 7 days over a 10-week period on the left axis. Average COD removal efficiency % plotted as bar graphs on the right axis.

REFERENCES

Bahri, Akiça. 2012. 'Integrated Urban Water Management'. Stockholm: Global Water Partnership (GWP). http://dx.doi.org/10.13140/RG.2.1.4187.0160.

Boano, Fulvio, Alice Caruso, Elisa Costamagna, Luca Ridolfi, Silvia Fiore, Francesca Demichelis, Ana Galvão, Joana Pisoeiro, Anacleto Rizzo, and Fabio Masi. 2020. 'A Review of Nature-Based Solutions for Greywater Treatment: Applications, Hydraulic Design, and Environmental Benefits'. *Science of The Total Environment* 711 (April): 134731. https://doi.org/10.1016/j.scitotenv.2019.134731.

Ghaitidak, Dilip M., and Kunwar D. Yadav. 2013. 'Characteristics and Treatment of Greywater—a Review'. *Environmental Science and Pollution Research* 20 (5): 2795–2809. https://doi.org/10.1007/s11356-013-1533-0.

Gross, Amit, Drora Kaplan, and Katherine Baker. 2007. 'Removal of Chemical and Microbiological Contaminants from Domestic Greywater Using a Recycled Vertical Flow Bioreactor (RVFB)'. *Ecological Engineering* 31 (2): 107–14. https://doi.org/10.1016/j.ecoleng.2007.06.006.

Masi, F., R. Bresciani, A. Rizzo, A. Edathoot, N. Patwardhan, D. Panse, and G. Langergraber. 2016. 'Green Walls for Greywater Treatment and Recycling in Dense Urban Areas: A Case-Study in Pune'. *Journal of Water, Sanitation and Hygiene for Development* 6 (2): 342–47. https://doi.org/10.2166/washdev.2016.019.

Prodanovic, Veljko, Belinda Hatt, David McCarthy, Kefeng Zhang, and Ana Deletic. 2017. 'Green Walls for Greywater Reuse: Understanding the Role of Media on Pollutant Removal'. *Ecological Engineering* 102 (May): 625–35. https://doi.org/10.1016/j.ecoleng.2017.02.045.

Pucher, Bernhard, Irene Zluwa, Philipp Spörl, Ulrike Pitha, and Günter Langergraber. 2022. 'Evaluation of the Multifunctionality of a Vertical Greening System Using Different Irrigation Strategies on Cooling, Plant Development and Greywater Use'. *Science of The Total Environment* 849 (November): 157842. https://doi.org/10.1016/j.scitotenv.2022.157842.

United Nations. 2019. 'World Urbanization Prospects The 2018 Revision (ST/ESA/SER.A/420)'. New York: United Nations.

Fuzzy Risk Assessment for Hydraulic Detention Time in UASB Reactors

D. A. Lima*, M. H. Nadais* D.A. Lima** and F.J.A. da Silva**

*Corresponding author: Environment and Planning Department, University of Aveiro, Campus de Santiago, 3810-193 Aveiro, Portugal Phone: +351 234 370 349 Email: d*ayane.lima@ua.pt) / nadais@ua.pt*

** Corresponding author: Department of Hydraulic and Environmental Engineering, Federal University of Ceará, Campus do Pici, Bloco 713. Pici. CEP: 60455-900. Fortaleza – Ceará – Brazil. Phone/Fax: +55 85 3366-9490. Email: *fjas@deha.ufc.br*

Abstract
Continuous monitoring of treatment plants can be costly and is essential to guarantee the proper functioning of these systems. For the case of UASB reactors hydraulic retention time, up flow velocity and volumetric organic loading can be controlled via triangular fuzzy numbers. In this sense it is possible to compute risk of failure. This paper shows the potential of a fuzzy approach to improve operational control of full-scale plants.

Keywords: Fuzzy risk; UASB reactors; Hydraulic Retention Time.

INTRODUCTION

The UASB reactors are applied for different types of effluents, from domestic to industrial and are especially suitable for regions with warm climate. However, many treatment plants may show performance below the design considerations due to the fact that they are poorly operated and monitored. Operational problems alert to the fact that although UASB reactors are considered robust they require adequate monitoring, control and optimization strategies. The risk of failure must be interpreted over an interval or under measurable conditions. A marginal risk of failure can undergo a better scrutinization via triangular fuzzy numbers (TFN) and represent operating conditions. For such cases TFN numbers provide a process mapping based (Kaufmann and Gupta, 1991) on typical flow variation profiles throughout the day, as well documented in the technical and scientific literature (*e.g.* CAMPOS; VON SPERLING, 1996; METCALF; EDDY, 2016; QASIM; ZHU, 2018). The present paper approaches the monitoring and operational diagnosis based on the fuzzy risk assessment for hydraulic retention time in UASB reactors.

MATERIAL AND METHODS

Operational Fuzzy Risk

The study was based on regular monitoring data from 19 full-scale UASB operating in the Ceará State, Brazil. Treatment plants were located in the polygon formed by 3º26' to 4º13' South and 38º28' to 39º02' West, 45 m asl. Local air temperature ranged from 23.8 to 31.5º C. Flow rate (Q) was measured at the Parshall flume including flow charts at the preliminar treatment unit of the plants. Chemical oxygen demand (COD) was analised in grab samples collected at 10 am. Triangular fuzzy numbers (TFN) were considered according to the minimum, most probable (represented by average) and maximum values of Q and COD. These numbers were used to compute fuzzy functions to estimate hydraulic retention time (HRT), up flow velocity (V_{UF}) and applied organic load (L_V). Classification of operational fuzzy risk followed rules for mapping marginal fuzzy intervals as showed in Table 1.

Table 1 – Intervals for mapping Fuzzy Risk (F_R) regarding to HRT, V_{UF} and L_V.

Marginal *Fuzzy* Risk	HRT (h)	V_{UF} (m/h)	L_V (kg DQO/m³.dia)
Very Low to Low	HRT ≥ 10	$V_{UF} \leq 0,7$	$L_V \leq 3,5$
Low to Medium	$10 \geq HRT \geq 6$	$0,7 \leq V_{UF} \leq 1,1$	$3,5 \leq L_V \leq 7,0$
Medium to High	$6 \geq HRT \geq 4$	$1,1 \leq V_{UF} \leq 1,5$	$7,0 \leq L_V \leq 9,0$
High to Very High	HRT ≤ 4	$V_{UF} \geq 1,5$	$L_V \geq 9,0$

Fonte: adapted from Mara (2003) and von Sperling and Chernicharo (2005).

RESULTS AND DISCUSSION

The complement of the marginal fuzzy risk (F_R) is the marginal fuzzy guarantee (F_G), and the summation is equal to 1. From this logical reasoning Table 2 shows F_G according to the fuzzy number resulted from dilation of the crisp average value of Q. The results point out that higher peaks over average flow rate may reduce significantly the F_G.

Table 2 – Fuzzy state guarantee, based on NFT, regarding the mapping of hydraulic detention time in UASB reactors treating domestic wastewater.

HRT (h)	Ranges of flow rate (m³/h)			
	0.25 to 2Q	0.25 to 3Q	0.25 to 3.5Q	0.25 to 4Q
≥ 10	0.720	0.688	0.679	0.672
10 to 6	0.244	0.241	0.240	0.239
6 to 4	0.036	0.060	0.064	0.067
≤ 4	0.000	0.011	0.017	0.022

Same reasoning was confirmed in relation of V_{UF} and L_V. Although organic overloading appeared to show more sensitivity in respect to reactor stability, the limits of V_{UF} can be considered more relevant in terms of sludge washout. In this sense F_G for V_{UF} control is more relevant in terms of performance.

CONCLUSIONS

The described behavior referring to the increase of the flow of 2 times the average flow, is repeated for the other flows of 3; 3.5 and 4 times, disregarding the times where the flows have a 4-fold increase and consequently a reduction in HRT, the fuzzy guarantee is reduced and the fuzzy risk increased. The HRT variation combined with COD (*i.e.* organic loading) followed the same pattern. However, fluctuation of V_{UF} is an excellent indicator for the stability control because it is a simple physical variable.

REFERENCES

CAMPOS, H.M.; VON SPERLING, M. Estimation of domestic wastewater characteristics in a developing country based on socio-economic variables. *Water Science and Technology* v. 34, n. 3-4, 71-77, 1996.

KAUFMANN, A.; GUPTA, M.M. *Introduction to Fuzzy Arithmetic: theory and applications*. Van Nostrand Reinhold, New York, p. 321. 1991.

METCALF & EDDY. *Wastewater Engineering: Treatment and Reuse*. McGraw Hill, 5th edition, 1980p. Inc. (2016).

QASIM, S.R.; ZHU, G. *Wastewater treatment and reuse – theory and design examples*. Volume 1. Taylor and Francis. CRC Press. Boca Raton, FL, 2018. 1160 p.

Evaluation of a low-tech, passively solar-driven pilot plant for nutrients recovery from source-separated urine on household level

L. Luethi*, D. Buehler*

*Institute of Natural Resource Sciences, Zurich University of Applied Science, Grüentalstrasse 14, 8820 Wädenswil (E-mail: *laila.luethi2@zhaw.ch, devi.buehler@zhaw.ch)*

Abstract
This study presents a pilot-scale technology for solar-driven evaporation of human urine, and investigates its feasibility for nutrient recovery and use as fertilizer. A field experiment was conducted at Zurich University of Applied Sciences in Switzerland, in which source-separated urine was stabilized with acetic acid to suppress hydrolysis by the enzyme urease and associated ammonia outgassing, while also promoting pathogen inactivation by bringing the pH below 4.
The stabilized urine was then passed through a six-piece tube system that was oriented towards the sun, with a black-lined housing and Plexiglas windows to create a greenhouse effect, and air holes to allow air flow and therefore increased evaporation rate. The powder obtained from evaporation was analyzed for nutrient content and compared with conventional fertilizers in a hydroponic growth experiment with basil.
The stabilization process was successful, with evaporation rates of up to 1.7 L/m²/d and an average recovery of 24 g/L nitrogen, 17.7 g/L phosphorus, and 55 g/L potassium oxide. The use of evaporated urine as a fertilizer at a dilution rate of 2 g/L resulted in plant growth comparable to that of conventional fertilizers. This demonstrates the feasibility of utilizing urine as a resource while also positively contributing to sustainable agriculture without the need for additional energy inputs (for the production of mineral fertilizer) or incurring high costs.

Keywords
Acid stabilization, hydroponic planting trials, nutrient recovery, passive evaporation, solar energy, source-separated urine

INTRODUCTION

The natural availability of nutrients, such as nitrogen, phosphorus, and potassium, needed for conventional fertilizer in agriculture, is limited (Mehta et al., 2015). Since human urine contains most of the excreted nutrients, fertilizer from urine has the potential to replace conventional fertilizers (Bischel et al., 2015; Martin et al., 2022). The use of urine as a fertilizer can not only conserve scarce resources, but also reduce the need for synthetic fertilizers, help to conserve water, decrease disruption of planetary biogeochemical cycles, and reduce the amount of waste sent to landfills (Escher et al., 2006; Larsen & Gujer, 2001; Reynaert et al., 2020). Previous laboratory studies (Bethune, 2015; Mayer, 2002) and field trials (Antonini et al., 2012; Simha et al., 2020) indicate that urine evaporation is a viable option for nutrient recovery. However, research on urine evaporation has been limited and most solutions are either technologically demanding, require high use of energy, or the use of chemicals (Ek et al., 2006; Maurer et al., 2003 & 2006). The aim of this study was to develop and test a low-tech urine evaporation system that can be implemented on household level in order to locally close the nutrient cycle. The study examined the functionality of the evaporation module, dosage and amount of acid with varying urine volumes, and long-term stabilization success to prevent nitrogen loss in order to produce a fertilizer that is comparable to conventional fertilizers.

MATERIALS AND METHODS

In the experimental setup (Figure 1), the urine was separately collected from feces using a dry toilet system based on a conveyor belt (Figure 1, no 1). Driven by gravity, the urine was led to and collected in a tank under the toilet (Figure 1, no 1, 2). A light sensor above the toilet was used to detect use of the toilet in order to trigger a pump to feed acetic acid into the urine tank for its stabilization (Figure 1, no 3). The stabilized urine was manually fed onto the evaporation module where weekly evaporation rates were measured and compared to temperature, solar radiation, and humidity (Figure 1, no 4). Samples of the urine residue were collected weekly and analyzed for nutrient content (ammonium, calcium, chloride, magnesium, nitrate, nitrite, phosphate, potassium, sodium, sulfate), pH, and electrical conductivity (Figure 1, no 5). The urine residue was diluted in water to be used as fertilizer (2g/l and 0.2g/l). Plant growth in a hydroponic culture of the two urine fertilizer dilutions was compared to a conventional fertilizer and a commercially available urine fertilizer (Figure 1, no 6).

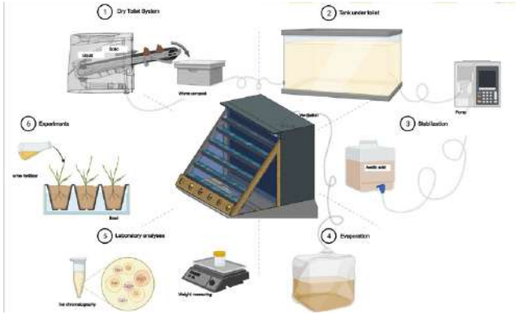

Figure 1: Experimental setup for the production and analysis of urine fertilizer from a urine evaporation module

RESULTS AND DISCUSSION

The stabilization in the urine tank functioned effectively with automatic dosing, however, the pH level in the evaporation module increased. Other experiments have confirmed a slight increase in pH level in vinegar-stabilized urine (Boncz et al., 2003). Our results indicate that the increase in pH could potentially rise exponentially rather than linearly. With a surface area of 0.47 m², it took approximately 21 days to achieve complete evaporation of the liquid fraction of approximately 18L undiluted urine. This corresponds to an average evaporation rate of 1.7 l/m²/d. The end product of the urine had an average of 24 g/l TN (ammonium and nitrate only), 18 g/l P_2O_5, and 55 g/l K_2O. The plant growth experiments confirmed the suitability of urine as a fertilizer when diluted at a ratio of 2g/l. The results of this study indicate that urine evaporation on household level holds great potential as a viable option for nutrient recovery. However, for further experiments, more stable constructions materials should be used to build the evaporation module, and its design should be simplified to improve operation and monitoring. Since accurate data for evaporation over time could not be collected, the exact dependence of evaporation rate on temperature, solar radiation, and humidity could not be determined. However, it was observed that the evaporation rate increased with rising temperatures and decreasing humidity. Previous studies (Joyce et al.,1996; Ren et al., 2021) have shown that solar radiation can kill pathogens in urine. Therefore, solar disinfection should also be further investigated in this type of technology.

REFERENCES

Antonini, S., Nguyen, P. T., Arnold, U., Eichert, T., & Clemens, J. (2012). Solar thermal evaporation of human urine for nitrogen and phosphorus recovery in Vietnam. *The Science of the Total Environment*, *414*, 592–599. https://doi.org/10.1016/j.scitotenv.2011.11.055

Bethune, D. (2015). *A Novel Urine Evaporation and Collection System for Dry Toilets*. https://doi.org/10.11575/PRISM/24932

Bischel, H. N., Duygan, B. D. Ö., Strande, L., McArdell, C. S., Udert, K. M., & Kohn, T. (2015). Pathogens and pharmaceuticals in source-separated urine in eThekwini, South Africa. *Water Research*, *85*, 57–65.

Ek, M., Bergström, R., Bjurhem, J. E., Björlenius, B., & Hellström, D. (2006). Concentration of nutrients from urine and reject water from anaerobically digested sludge. *Water Science and Technology: A Journal of the International Association on Water Pollution Research*, *54*(11–12), 437–444. https://doi.org/10.2166/wst.2006.924

Escher, B. I., Pronk, W., Suter, M. J.-F., & Maurer, M. (2006). Monitoring the Removal Efficiency of Pharmaceuticals and Hormones in Different Treatment Processes of Source-Separated Urine with Bioassays. *Environmental Science & Technology*, *40*(16), 5095–5101. https://doi.org/10.1021/es060598w

Larsen, T. A., & Gujer, W. (2001). Waste design and source control lead to flexibility in wastewater management. *Water Science and Technology: A Journal of the International Association on Water Pollution Research*, *43*(5), 309–317.

Maurer, M., Pronk, W., & Larsen, T. A. (2006). Treatment processes for source-separated urine. *Water Research*, *40*(17), 3151–3166. https://doi.org/10.1016/j.watres.2006.07.012

Maurer, M., Schwegler, P., & Larsen, T. A. (2003). Nutrients in urine: Energetic aspects of removal and recovery. *Water Science and Technology*, *48*(1), 37–46. https://doi.org/10.2166/wst.2003.0011

Mehta, C. M., Khunjar, W. O., Nguyen, V., Tait, S., & Batstone, D. J. (2015). Technologies to Recover Nutrients from Waste Streams: A Critical Review. *Critical Reviews in Environmental Science and Technology*, *45*(4), 385–427. https://doi.org/10.1080/10643389.2013.866621

Ren, J., Hao, D., Jiang, J., Phuntsho, S., Freguia, S., Ni, B.-J., Dai, P., Guan, J., & Shon, H. K. (2021). Fertiliser recovery from source-separated urine via membrane bioreactor and heat localized solar evaporation. *Water Research*, *207*, 117810. https://doi.org/10.1016/j.watres.2021.117810

Reynaert, E., Greenwood, E. E., Ndwandwe, B., Riechmann, M. E., Sindall, R. C., Udert, K. M., & Morgenroth, E. (2020). Practical implementation of true on-site water recycling systems for hand washing and toilet flushing. *Water Research X*, 100051 (13 pp.). https://doi.org/10.1016/j.wroa.2020.100051

Simha, P., Karlsson, C., Viskari, E.-L., Malila, R., & Vinnerås, B. (2020). Field Testing a Pilot-Scale System for Alkaline Dehydration of Source-Separated Human Urine: A Case Study in Finland. *Frontiers in Environmental Science*, *0*. https://doi.org/10.3389/fenvs.2020.570637

Multidimensional assessment of a Nature-based Solution for decentralized small-scale greywater treatment in Costa Rica (max. 250 characters)

M. Perez Rubi and J. Hack

Institute for Environmental Planning, Leibniz University Hannover, Herrenhäuser Str. 2, Hannover, Germany
(Email: *perez@umwelt.uni-hannover.de*)

Abstract

In Costa Rica, water supply networks cover more than 94% of the country; however, it is estimated that only 10% of wastewater receive proper treatment. The lack of centralized sanitation infrastructures has led to the implementation of domestic septic tanks for blackwater disposal and the discharge of greywater into rivers without any treatment, hence, causing environmental degradation of surface waters. Retrofitting conventional centralized sewerage networks and treatment plants into the existing urban grid implies extensive social, economic and technical challenges. Since greywater has potentially less pollutants than mixed wastewaters, there is an intrinsic opportunity in the current situation for a leapfrogging toward onsite treatment and resource recovery. In this sense, proposing decentralized technologies for greywater treatment contributes to reducing pollutant loads being discharged, therefore, improving the environmental status of water resources. In this study, we assess the performance of a small-scale horizontal flow constructed wetland, called "Biojardinera" in Costa Rica, as a Nature-based Solution prototype for decentralized domestic greywater treatment. Organic matter, nutrients and microbiological water quality standards are being analysed and compared with reported removal efficiencies from other case studies in the country. Furthermore, economic, social and legal aspects for the implementation of this low-cost ecotechnology are evaluated for the context of Costa Rica. The results contribute to the understanding of performance and application potential which is needed to adopting this type of Nature-based Solution for water quality improvement, not only in Costa Rica, but also other areas in the region where a comparable sanitation situation prevails.

Keywords (maximum 6 in alphabetical order)

Decentralized greywater treatment, Latin America, Nature-based Solutions, onsite resource recovery

Anaerobic digestion effluent treatment in constructed wetlands for agricultural reuse

Pau Porras Socias[1,2,3], Gavin Collins[3], Alexandre B. De Menezes[3], Carlos R. Gomes [1,2], C. Marisa R. Almeida[1,2] and Ana Paula Mucha[1,4]

[1]EcoBioTec - Bioremediation and Ecosystems Functioning, Interdisciplinary Centre of Marine and Environmental Research, University of Porto, Matosinhos, Portugal.
(E-mail: pporras@ciimar.up.pt; calmeida@ciimar.up.pt; amucha@ciimar.up.pt)
[2]Chemistry and Biochemistry Department, Faculty of Sciences, University of Porto, Porto, Portugal.
(E-mail: crgomes@fc.up.pt)
[3]Microbiology, School of Natural Sciences and Ryan Institute, University of Galway, Galway, Ireland.
(E-mail: gavin.collins@universityofgalway.ie; alexandre.demenezes@universityofgalway.ie)
[4]Biology Department, Faculty of Sciences, University of Porto, Porto, Portugal.

Abstract
Anaerobic digestion effluents can be a reservoir of pollutants and need effective treatment strategies to avoid dissemination to the environment and associated risks to public health. This study aims to determine the potential of constructed wetlands (CWs) to eliminate metals, antibiotics and ARG, from the liquid fraction of the digestate for agricultural reuse.

Twelve laboratory scale vertical subsurface flow CWs systems were assembled with gravel, light expanded clay aggregate and sand planted with *Sparganium erectum* testing four different treating conditions (liquid digestate dosed with oxytetracycline or with sulfadiazine or with ofloxacin or without dosing).

Removal of Fe, Zn, Cu, Pb and Cr were always > 92 % and Mn removal was between 82 and 94 %. In addition, high organic matter and nutrients removal were reported (69-99.8 %). No significant differences between presence or absence of antibiotics were observed.

Acknowledgments - This project has received funding from the European Union's Horizon 2020 research and innovation programme under the Marie Skłodowska-Curie grant agreement No 861088.

Keywords (maximum 6 in alphabetical order)
Antibiotics, antimicrobial resistant genes, constructed wetlands, liquid digestate, metals.

INTRODUCTION

Constructed wetlands (CWs) are nature-based solutions that can be used to treat liquid effluents from different industries. These biotechnological tools can eliminate a wide range of pollutants from nitrogen nutrients or trace metals to contaminants of emerging concern from water through different physical, chemical and biological reactions (Gorito et al., 2017).

Anaerobic digestion is a well-known process to valorise organic waste into bioenergy products. A byproduct is the digestate, a complex matrix of biosolids rich in organic matter and nutrients that has conventionally been disposed by landspreading as a fertilizer (Wang et al., 2023). However, the digestate can be a reservoir of metals, antibiotics, and antimicrobial resistant genes (ARG) and it is necessary to implement efficient treating methods to prevent their diffusion to the environment (Venegas et al., 2021).

There are several studies investigating the capacity of CWs to remove the high nutrient content of liquid digestates, but studies focusing on the removal of other contaminants from this complex matrix are scarce (Maucieri et al., 2016; Zhou et al., 2020; Wu et al., 2016).

The objective of this study is to evaluate the potential of CWs, at a microcosm scale, to remove metals, antibiotics and ARG, from the liquid fraction of the digestate to valorise the effluent in fertigation.

MATERIALS AND METHODS

Twelve laboratory scale vertical subsurface flow CWs systems were assembled with gravel, light expanded clay aggregate and sand planted with *Sparganium erectum* testing four different treating conditions (liquid digestate dosed with oxytetracycline, or dosed with sulfadiazine, or dosed with ofloxacin or without dosing) in a four-month period. The digestate was recirculated over 14 days, then removed from the systems and replaced with a new influent with the same conditions. Samples of all effluents were collected for analysis of nutrients and metals and for quantification of *intI1*, *tetA, tetW, sul1* and *qnrS* genes. The removal efficiencies of the pollutants were calculated according to the following equation:

$$Removal\ efficiency\ (\%) = \frac{C_{in} - C_{out}}{C_{in}} \times 100$$

RESULTS AND DISCUSSION

The initial concentration of Fe, Mn, Zn, Cu and Cr in the liquid digestate before the treatment in the CWs was much higher than levels reported in guidelines for irrigation water. Removals of organic matter, and ammonium, nitrate, nitrite and phosphate ions ranged between 69 and 99.8 % with no significant differences between the presence or absence of antibiotics. Removal efficiencies of Fe, Mn, Zn, Cu, Pb and Cr reached over 82 %. An increase in relative abundance of the *intI1*, *tetA* and *sul1* genes was observed in the effluent after the CWs treatment, while a decrease in *tetW* was noticed.

CONCLUSION

Overall, CWs are a suitable alternative to valorise the liquid effluent of anaerobic digestors using it in fertigation, closing the loop of circular bioeconomy. However, ARGs dissemination in the environment remains a grand challenge that needs further understanding and management for their proper removal and wastewater treatment solutions must take that into consideration.

REFERENCES

- Gorito, A. M., Ribeiro, A. R., Almeida, C. M. R., Silva, A. M. T. (2017). A review on the application of constructed wetlands for the removal of priority substances and contaminants of emerging concern listed in recently launched EU legislation. *Environmental Pollution,* 227: *428–443*
- Maucieri, C., Mietto, A., Barbera, A. C., & Borin, M. (2016). Treatment performance and greenhouse gas emission of a pilot hybrid constructed wetland system treating digestate liquid fraction. *Ecological Engineering*, *94*, 406-417.
- Venegas, M., Leiva, A. M., Reyes-Contreras, C., Neumann, P., Piña, B. & Vidal, G. (2021). Presence and fate of micropollutants during anaerobic digestion of sewage and their implications for the circular economy: A short review. *Journal of Environmental Chemical Engineering*, 9(1): 104931.
- Wang, W., Chang, J. S., & Lee, D. J. (2023). Anaerobic digestate valorization beyond agricultural application: Current status and prospects. *Bioresource Technology*, 128742.
- Wu, S., Lei, M., Lu, Q., Guo, L., & Dong, R. (2016). Treatment of pig manure liquid digestate in horizontal flow constructed wetlands: Effect of aeration. *Engineering in Life Sciences*, *16*(3), 263-271.
- Zhou, S., Wang, C., Sun, H., Zhang, J., Zhang, X., & Xin, L. (2020). Nutrient removal, methane and nitrous oxide emissions in a hybrid constructed wetland treating anaerobic digestate. *Science of The Total Environment*, *733*, 138338.

Comparison of engineered, natural and hybrid wastewater treatment schemes for the removal of nanoparticles from wastewater

R. Sharma* and A. Kumar*

* Department of Civil Engineering, Indian Institute of Technology Delhi, Hauz Khas, New Delhi, India (E-mail: *r.bwn24@gmail.com*; *arunku@civil.iitd.ac.in)*

Abstract
The advancement in the field of nanotechnology has led to their wide usage in commercial products, leading to their disposal in environmental waters. The use of both engineered treatment technologies and nature-based treatment technologies, such as constructed wetlands, soil aquifer treatment have been explored for the removal of nanoparticles from raw wastewater. In this work, various wastewater treatment schemes including engineered and/or nature-based treatment technologies were envisaged. Published literature data was then utilized to find the removal of Ag nanoparticles through each of these treatment schemes. Monte Carlo simulation approach was utilized to generate a large dataset for probabilistic computations & avoid point calculation. The nanoparticles' concentration in the effluent were calculated and compared with regulatory guidelines. Probability of exceedance was used to compare and rank the treatment schemes for removal of Ag nanoparticles. The treatment scheme involving both engineered and nature-based treatment technologies was ranked one. Treatment schemes involving only the engineered treatment technologies were ranked last. Hence, the use of nature-based solutions along with the existing treatment infrastructure is required for the effective removal of nanoparticles. The decision-making framework presented here, can be utilized to identify suitable treatment schemes for treatment of wastewater laden with metal nanoparticles.

Keywords
Decision making; nanoparticles; constructed wetlands

INTRODUCTION

Nanotechnology has enabled the integration of metal & metal-based nanoparticles (NPs) into our daily-usage products (cosmetics, antibacterial paints & fabrics, paints, electronics etc.). Their frequent usage implies their frequent detection in environmental waters, as has been now detected frequently by researchers around the world (Gagnon, Turcotte, et al., 2021). Both engineered wastewater treatment units and nature- based treatment technologies [such as vertical scale subsurface flow Constructed Wetlands (VSSF CW) and Soil Aquifer Treatment (SAT)] have been explored for removal of nanoparticles, with latter showing immense scope despite their low operating costs (Huang, Xiao, et al., 2019). Nature-based solutions can be used in combination with the existing wastewater treatment infrastructure, for removal of nanoparticles. The objective for this work is to compare different treatment schemes (engineered, natural or hybrid) for efficient removal of Ag nanoparticles from wastewater. Literature data already published was searched and utilized in this work to calculate the concentration of Ag NPs in effluent of the derived treatment schemes. The decision-making framework developed here for finding the top 3 treatment schemes for Ag NPs removal can be further utilized for other metal or metal-based nanoparticles as well.

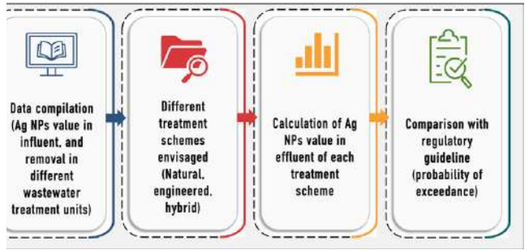

ıre 1. Illustrative schematic of the framework developed in this work.

TERIALS AND METHODS

erature review was carried out to compile the following data:
'oncentration of Ag NPs in influent wastewater
Removal of Ag NPs in different treatment units of a WWTP [Primary treatment unit (1°), ndary treatment unit (2°) and Tertiary treatment unit (3°)]
Removal of Ag NPs in natural treatment technologies- VSSF CW (Vertical Sub-Surface structed Wetlands) and SAT (Soil Aquifer Treatment).

normal distributions were derived for each of the variable. As part of uncertainty analysis, Monte-o simulation was used to generate 20,000 numbers of each variable. Various treatment schemes : then envisaged involving either the engineered treatment units of a WWTP or the natural ment technologies or a hybrid of both. Then, effluent concentration of Ag NPs was computed for chemes using the distributions developed. The effluent was then compared with regulatory elines. For Ag NPs, only recommended value of 21 mg/L was found (Parsai and Kumar, 2021), no other regulatory authority guideline. Regulation for Ag ions were then searched for, with the mption that Ag NPs disassociate as silver ions completely. Australian guidelines recommend a µg/L value for silver ion in freshwater systems. Corresponding to this, discharged effluent elines was computed as 10 µg/L, back-calculating using a dilution ratio (D) of 99:1 (Tyagi et al.,).

a conservative approach, 10 µg/L was selected to compare the different treatment schemes. ulative probability for remaining Ag NPs conc in effluent was computed for each scheme using bull formulae. Probability of exceedance from the guideline value was calculated and used to pare the treatment schemes with each other. The overall methodology is pictorially depicted in l. Table 1 depicts the different treatment schemes that were envisaged in this work.

ULTS AND DISCUSSION

rage value for all treatment schemes were found to be less than guideline value 10 µg/L (Table Hybrid treatment schemes (i.e., involving both engineered and natural treatment technologies) : the top 2 ranked, T7 and T8, and natural treatment scheme T2 was ranked 3. The treatment mes T7 and T8 showed little difference with respect to average Ag NPs in effluent & probability ceedance.

Table 1. Different engineered, natural and hybrid treatment schemes envisaged

	Treatment Scheme	Type (Engineered, natural or hybrid)
T1	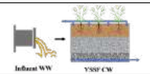	Natural
T2	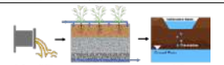	Natural
T3	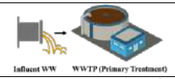	Engineered
T4	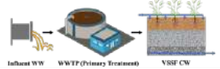	Hybrid
T5	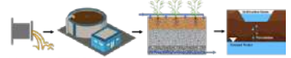	Hybrid
T6	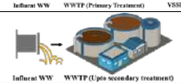	Engineered
T7	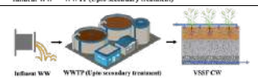	Hybrid
T8	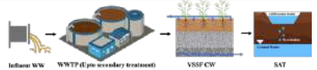	Hybrid
T9	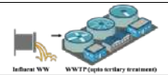	Engineered

Table 2. Statistical summary for the Ag NPs concentration in effluent (Ce) of various treatment schemes, associated probability of exceedance in percentage and ranking

	Treatment Scheme	Average value of Ag NP conc in effluent, µg/L	% Prob of exceedance from guideline value	Ranking
T1	Influent WW→VSSF CW	0.51	0.767	6
T2	Influent WW→VSSF CW→SAT	0.13	0.140	3
T3	Influent WW→WWTP (1°)	8.67	10.997	9
T4	Influent WW→WWTP (1°) →VSSF CW	0.47	0.708	5
T5	Influent WW→WWTP (1°) →VSSF CW→SAT	0.12	0.141	4
T6	Influent WW→WWTP (1°+ 2°)	0.77	1.254	7
T7	Influent WW→WWTP (1°+ 2°) → VSSF CW	0.06	0.071	2
T8	Influent WW→WWTP (1°+ 2°) → VSSF CW→SAT	0.02	0.000	1
T9	Influent WW→WWTP (1°+ 2°+ 3°)	1.41	1.652	8

As many of the existing wastewater treatment plants have only up to secondary treatment (Jamwal, Mittal, et al., 2008), hence retrofitting such plants with low-cost nature-based treatment technologies like VSSF CW and SAT will help in effective removal of nanoparticles. The treatment scheme T3 was ranked the last, due to high probability of exceedance compared to the guideline value, implying that disposal of only primary treated NPs laded WW may invite regulatory actions.

CONCLUSIONS

Only primary treatment of NPs laded wastewater was found to have the highest probability to exceed the regulatory guideline. Hybrid treatment scheme (Secondary treatment in WWTP followed by treatment using CW and SAT) was ranked first for removal of silver nanoparticles from raw WW, based its least probability of exceedance with respect to the guideline value. For effective removal of nanoparticles from wastewater, the idea of retrofitting the existing wastewater treatment plants with nature-based technologies like constructed wetlands and soil aquifer treatment will also offer additional benefits of overall low cost. For wastewater treatment plants receiving wastewater from industries manufacturing or fabricating nanoparticle-enabled products, the presented methodology can be adapted for design or selection of a treatment scheme (natural, engineered or hybrid) for removal of metal/metal-based nanoparticles by utilizing published literature

REFERENCES

Gagnon, C., Turcotte, P., Gagné, F., and Smyth, S. A. 2021. Occurrence and size distribution of silver nanoparticles in wastewater effluents from various treatment processes in Canada. *Environmental Science and Pollution Research*.

Huang, J., Xiao, J., Chen, M., Cao, C., Yan, C., Ma, Y., Huang, M., and Wang, M. 2019. Fate of silver nanoparticles in constructed wetlands and its influence on performance and microbiome in the ecosystems after a 450-day exposure. *Bioresource Technology*, **281**, 107–117.

Parsai, T. and Kumar, A. 2021. Setting guidelines for co-occurring nanoparticles in water medium. *Science of the Total Environment*, **776**.

Jamwal, P., Mittal, A.K. and Mouchel, J.M. 2009. Efficiency evaluation of sewage treatment plants with different technologies in Delhi (India). *Environmental Monitoring and Assessment*, **153**(1), pp.293-305.

Performance of Multi-module Biochar Filter for Onsite Wastewater Treatment System

M. Shigei*, R. Herbert*, and S. Dalahmeh*

* Department of Earth Sciences, Uppsala University, Villavägen 16, 752 36 Uppsala, Sweden
(E-mail: makoto.shigei@geo.uu.se; Roger.Herbert@geo.uu.se, sahar.dalahmeh@geo.uu.se)

Abstract
In this study, an innovative onsite wastewater treatment system (OWTS) using a multi-module biochar filter was tested. The system comprised six modules with different biochar and bark sizes constructed vertically. It was composed of saturated/anaerobic modules and unsaturated/aerobic modules. Water samples of the influent and the filter effluent were analyzed to investigate the treatment efficiency of organic matter (COD), nitrogen, phosphate, and *Escherichia coli* (*E. coli*). The results showed a relatively high average removal of organic matter (COD: 82.7%) and moderate nitrogen removal (Tot-N: 40.1 %). The phosphate removal was varied and had an analytical uncertainty. The removal of *E. coli* (2.44 Log_{10} CFU mL^{-1}) was higher than the levels reported in conventional OWTS. Further investigation of the filter design is planned to enhance denitrification and phosphorus removal.

Keywords
Biochar; *E. coli*; Multi-module systems; nitrogen; onsite wastewater treatment

INTRODUCTION

Approximately 1,000,000 onsite wastewater treatment systems (OWTS) have been implemented in Sweden, but some OWTSs are insufficient to meet environmental standards. The issues vary in each system/region, including groundwater ingress, inadequate soil conditions of the site, and insufficient maintenance regulation. The effluent remains a significant source of eutrophication even after the treatment (Roth et al., 2016). Swedish EPA reported that only 66 % of OWTSs comply with Environmental Code Standards (Naturvårdsverket, 2014). In this study, an alternative treatment system using biochar has been tested. Biochar is a carbon-rich product made by the anoxic thermal conversion of biomass. It is advantageous as a filtration medium because of its lighter weight for transportation and high adsorption capacity due to the porous structure with a large surface area (Xiang et al., 2020). In addition, biochar is produced from biowaste and can be used as a fertilizer after its use as a wastewater adsorbent (Li et al., 2020; Werner et al., 2018). Biochar contributes to a sustainable future as a wastewater treatment and soil amendment. Although the potential of biochar-based systems has been studied, few studies have used pilot-scale biochar filtration systems. Hence this study aimed to investigate the performance of a multi-module biochar filter to be operated after the sedimentation unit for OWTS.

MATERIALS AND METHODS

Three identical multi-module filters composed of six modules were constructed, and each module was constructed from plastic boxes (Figure 1). Modules 1-5 were filled with biochar, while module 6 was filled with a pine bark layer topped with biochar. The bark enhances bacterial die-off due to tannins released from the bark (Kaczmarek, 2020). The three filters were placed at the Uppsala wastewater treatment plant (WWTP) to be operated with municipal wastewater. Raw wastewater which passed the rough screen at the wastewater treatment plant was used to feed the filters by the wastewater distribution system operated by peristaltic pumps and timers. Particle density, bulk density, and porosity of solids were determined, and SEM analyzed the morphology of the biochar with X-ray microanalysis.

The removal efficiency of pollutants in the system was investigated during the period between 1st February (day 1) to 7th April 2021 (day 66). The water samples were collected for the influent from the sedimentation tank (Figure 2) and the effluent from the bottom module 6. The following parameters were analyzed for each sample: chemical oxygen demand (COD), ammonium (NH_4-N), Nitrate (NO_3-N), total nitrogen (Tot-N), phosphate (PO_4-P), and *Escherichia coli (E. coli).*

RESULTS AND DISCUSSION

Figure 3 shows the influent and effluent concentration of COD (mg L^{-1}), Nitrogen (mg L^{-1}), phosphate (mg L^{-1}), and *E. coli* (log_{10}CFU mL^{-1}) of each filter 1 to 3. Organic matter was well removed in terms of COD reduction by 82.7%. However, the reported influent COD concentration coming to the WWTP from 2018 to 2020 was 760 - 890 mg L^{-1} (Uppsala Vatten, 2019), so the present influent concentration data (239.0 ± 70.6 mg L^{-1}) is uncertain. This uncertainty might happen due to the test kit's low detection ranges, which were 10-150 mg L^{-1} for both influent and effluent. Though each influent sample was diluted twice, it was not sufficient, and the removal efficiency could even be better regarding the possibility of higher influent concentration. Ammonium was consistently transformed to nitrate at nearly 100 %, while total nitrogen removal was 40 %. Incoming wastewater had a phosphate concentration of 1.3 ± 1.6 mg L^{-1}, but the reported Tot-P influent concentration from WWTP from 2018 to 2020 was 5.9 – 6.3 mg L^{-1} (Uppsala Vatten, 2019), so the influent concentration is uncertain due to the analytical error which could also affect to the effluent concentration. Nevertheless, the metal ion composition of the biochar used in this filter was only 0.24% of Potassium and 0.42% of calcium, which could influence the low removal ratio of PO_4-P.

The process of bacteria treatment was planned to be performed in the last module with biochar and bark. The bark is the primary source of antibacterial phenolic compounds called tannin, so it was expected to inactivate the bacteria coming to the last module (Das et al., 2020; Kaczmarek, 2020). Biochar could also retain the bacteria by physical removal through filtration since it could provide micropores in the module. There were few visible colony units in the effluent sample plates for *E. coli,* which resulted in a reduction rate of 2.44 log_{10}CFU mL^{-1}. It is higher performance than the conventional onsite treatment system. Harrison et al. (2000) reported the reduction rate of fecal coliform treated by OWTS designed with a septic tank and soil drainage field as 0.75-1.86 log_{10} CFU mL^{-1}. Suppose it is only a septic tank; the reduction rate of *E. coli* was reported as 0.14 - 1.05 log_{10} CFU mL^{-1} (Wang et al., 2021)

In summary, the multi-module biochar filter system performed well for organic matter removal, nitrification and *E. coli* removal, and the further filter-design update will enhance the denitrification and phosphorus removal.

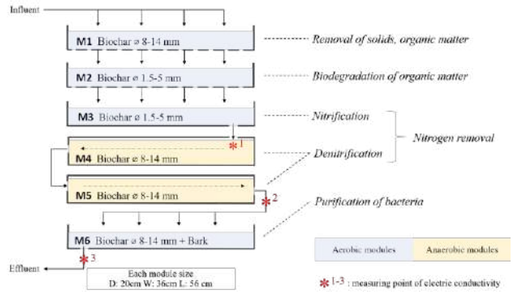

Figure 1. Multi-module filter (side view) with the contents and aim of each module, *1-3 shows the measuring points of electric conductivity during the tracer test. The aerobic modules (M1-3, 6) have a downflow (unsaturated), and the anaerobic modules (M4, 5) have a horizontal flow (saturated).

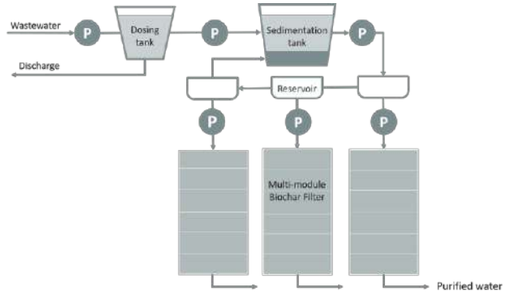

Figure 2. Schematic image of the experimental setup; wastewater flows and distribution system with three identical multi-module biochar filters.

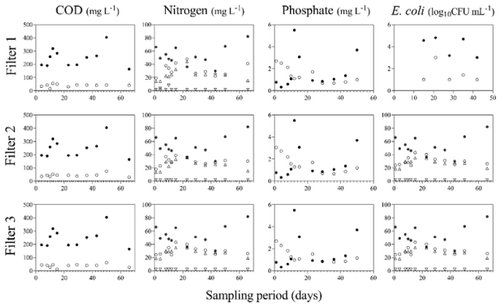

Figure 3. Concentration of different parameters in influent and effluent of filter 1 to 3. (●, ○ = influent and effluent concentration of COD, Tot-N, phosphate, and *E. coli*; ▽=NH_4-N effluent concentration; △=NO_3-N effluent concentration)

REFERENCES

Harrison, R.B., Turner, N.S., Hoyle, J.A., KrejsL, J., Tone, D.D., Henry, C.L., Isaksen, P.J., Xue, D., 2000. Treatment of Septic Effluent for Fecal Coliform and Nitrogen in Coarse-textured Soils: Use of Soil-only and Sand Filter Systems. Water, Air, & Soil Pollution 124, 205–215. https://doi.org/10.1023/A:1005298932244

Kaczmarek, B., 2020. Tannic Acid with Antiviral and Antibacterial Activity as A Promising Component of Biomaterials—A Minireview. Materials (Basel) 13, 3224. https://doi.org/10.3390/ma13143224

Li, S., Chan, C.Y., Sharbatmaleki, M., Trejo, H., Delagah, S., 2020. Engineered Biochar Production and Its Potential Benefits in a Closed-Loop Water-Reuse Agriculture System. Water 12, 2847. https://doi.org/10.3390/w12102847

Naturvårdsverket, 2014. Wastewater treatment in Sweden. Naturvårdsverket, Stockholm.

Roth, S., Ejhed, H., Olsson öberg, M., Hansson, K., Dorgeloh, E., Herschl, B., Plaza, G., 2016. Maintenance regulation of small wastewater treatment facilities. IVL Svenska Miljöinstitutet, Stockholm.

Uppsala Vatten, 2019. MILJÖRAPPORT 2019. Uppsala Vatten, Uppsala.

Wang, M., Zhu, J., Mao, X., 2021. Removal of Pathogens in Onsite Wastewater Treatment Systems: A Review of Design Considerations and Influencing Factors. Water 13, 1190. https://doi.org/10.3390/w13091190

Werner, S., Kätzl, K., Wichern, M., Buerkert, A., Steiner, C., Marschner, B., 2018. Agronomic benefits of biochar as a soil amendment after its use as waste water filtration medium. Environmental Pollution 233, 561–568. https://doi.org/10.1016/j.envpol.2017.10.048

Xiang, W., Zhang, X., Chen, J., Zou, W., He, F., Hu, X., Tsang, D.C.W., Ok, Y.S., Gao, B., 2020. Biochar technology in wastewater treatment: A critical review. Chemosphere 252, 126539. https://doi.org/10.1016/j.chemosphere.2020.126539

Potential of integrated membrane and TiO_2-based advanced oxidation processes for greywater reclamation

H. Takeuchi*, R. Homma**, Y. Onodera***, A. Noda***, S. Sameshima****, Y. Arai**** and F. Nishimura*

* Research Center for Environmental Quality Management, Kyoto University, 1-2 Yumihama Otsu, Shiga, Japan
(Email: *takeuchi.haruka.6m@kyoto-u.ac.jp*)
** Graduate School of Engineering, Kyoto University, Katsura, Nishigyo-ku, Kyoto, Japan
(Email: *homma.ryosuke.6j@kyoto-u.ac.jp*)
*** Advanced Science, Technology & Management Research Institute of KYOTO (ASTEM), 134 Chudoji Minamimachi, Shimogyo-ku, Kyoto, Japan
(Email: *onodera@astem.or.jp*)
**** MEIDENSHA CORPORATION, 2-1-1 Osaki, Shinagawa-ku, Tokyo, Japan
(Email: *sameshima-s@mb.meidensha.co.jp*)

Abstract
Greywater reclamation has increasingly been recognized as an alternative water resource for non-potable or potable use. Laboratory-scale experiments were conducted to evaluate the removal performances of membranes and TiO_2-based advanced oxidation processes (AOP). The membrane processes include a flat sheet ceramic microfiltration (MF), a nanocomposite nanofiltration (NF) and a polyamide reverse osmosis (RO) membrane. The AOP system consisted of a flat sheet ceramic MF with TiO_2 cake layer on its surface, and low-pressure mercury lamps with 254 nm wavelength as a radiation source. Although the RO process provided high removal rates for salts and organic matters, membrane fouling was formed quickly. On the other hand, the NF process exhibited high removal rates for salts and moderate removal rates for organic matters. The residual organic matters in NF permeate were further decomposed by the following TiO_2-based AOP. Since membrane fouling was less significant in the NF process than the RO process, the integrated NF and TiO_2-based AOP processes can be a viable option for sustainable system operation and greywater reclamation.
Keywords
Greywater reclamation; membrane technology; photocatalyst

INTRODUCTION

Greywater reclamation has increasingly been recognized as an alternative water resource for non-potable or potable use. While membrane processes have become key components of greywater reclamation, studies on their combination with advanced oxidation processes (AOP) for greywater reclamation are still limited. This study aimed to evaluate removal performance of membrane technologies and TiO_2-based AOP for greywater reclamation. Laboratory-scale experiments were conducted using three greywater samples for assessing the qualities of reclaimed water from the membrane and AOP treatments.

MATERIALS AND METHODS

Domestic greywater samples were collected from a tub shower and a washing machine (denoted as GW1 and GW2) by a resident. Another greywater sample was collected at a complex commercial building (denoted as GW3), in which greywater consists of wastewater from tub showers and washbasins in a hotel, offices and commercial facilities. Tap water was also collected to compare the water qualities with greywater samples.

Laboratory-scale experiments were conducted to investigate the performances of microbubble floatation, membrane processes and a TiO_2-based AOP for greywater reclamation. Greywater samples were first treated by microbubble floatation (MBF) to remove suspended solids which can cause severe membrane fouling in the following membrane processes. The membrane processes include a flat sheet ceramic microfiltration (MF) with membrane pore size of 0.1 μm, a nanocomposite nanofiltration (NF) and a polyamide reverse osmosis (RO) membrane with salt rejection of 40% and 99.7%, respectively. The MBF effluents were supplied to either of the membrane processes to compare their removal performances. After the membrane processes, treated water samples were further fed to a TiO_2-based AOP to decompose the residual components. The AOP system consisted of a flat sheet ceramic MF with 2.0 mg/cm^2 of TiO_2 cake layer on its surface, and UV-LED with 310 nm wavelength as a radiation source (irradiation intensity: 10 mW/cm^2). Water qualities of the samples were assessed by measuring their excitation emission matrix (EEM), total organic carbon (TOC), turbidity, salt concentrations, and surfactant concentrations.

RESULTS AND DISCUSSION

By the MBF process, turbidity of the greywater samples was decreased from 33.0 to 18.5 NTU for GW1, from 18.3 to 8.1 NTU for GW2, and from 19.4 to 7.0 NTU for GW3. The removal rate ranged from 44% to 64%, which may reduce membrane fouling and membrane damage in the following membrane treatments.

While the MF process provided limited removal rates for TOC and salts, the NF and RO processes exhibited high removal rates for TOC (>82%) and salts (>70%) for all greywater samples. As a result, salt levels in NF (GW1: 4.7 mg/L, GW2: 3.8 mg/L and GW3: 14.6 mg/L) and RO permeate (GW1: 1.5 mg/L, GW2: 1.2 mg/L and GW3: 2.6 mg/L) were lower than the value in tap water (21.8 mg/L) (Figure 1). TOC level in RO permeates (GW1: 1.9 mg/L, GW2: 2.0 mg/L and GW3: 0.6 mg/L) was also lower than that in tap water (2.2 mg/L). Even though the NF process gave higher TOC level than tap water, the following TiO_2-based AOP further decreased the TOC levels (GW1: 1.4 mg/L, GW2: 2.0 mg/L and GW3: 0.8 mg/L). The same tendency was observed with the EEM analysis (Figure 2). Since membrane fouling progressed faster with the RO process than the NF process, the integrated NF and TiO_2-based AOP processes can be a viable option for greywater reclamation in terms of water quality and continuous system operation.

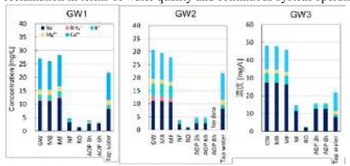

Figure 1. Salt concentrations in greywater and reclaimed water samples.

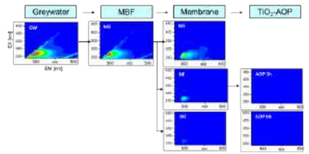

Figure 2. EEM fluorescence spectrum of GW1 before and after the water reclamation processes.

ACKNOWLEDGEMENT

This study was supported by the funding from Kyoto city. We acknowledge Mr. Tanimura (NITTOSEIKO CO., LTD.) for his advice and supports on microbubble generator.

Nutrients and characterization of greywater from rural households

Tonetti, A. L.; Figueiredo, I. C. S, Almeida, M. E. P.; Portela, D.G., Miyazaki, C. K.

*School of Civil Engineering, Architecture and Urban Design – FECFAU, Sanitation and Environment Department, University of Campinas – UNICAMP, PO box 6021, 13083-830, Campinas (SP), Brazil. (E-mail: tonetti@unicamp.br).

Abstract
It was found that in a rural area of Campinas (SP), over 90% of households segregated greywater. The source of greywater generation had a great influence on its composition, especially due to cleaning products in it. Greywater from showers presented higher NTK concentration, due to the habit of urinating in the shower.

Keywords (maximum 6 in alphabetical order)
Greywater; Nitrate; Phosphorus; Source Separation.

INTRODUCTION

Greywater composition and generation depend on factors such as the finality and quantity of clean water used, which are directly influenced by regional and cultural characteristics (Boyjoo et al., 2013). Greywater can contain organic matter, chemicals, fat, soap, fibers, and hair, with different compositions due to their origin (Paulo et al., 2018).

There are little data available about greywater composition from rural households in Latin America. Thus, the present study evaluated the composition of segregated greywater from Campinas (SP) rural area and characterized samples of this specific wastewater fraction.

MATERIALS AND METHODS

Source-separation of water is very common in the study area. About 91% of households separate the water from laundry tub and washing machine, 83.2% separate kitchen water and 63.2% separate shower water (Madrid et al., 2015). The quality analysis results followed the methods described in APHA et al. (2012).

RESULTS AND DISCUSSION

According to Table 1, COD and total suspended solids (TSS) concentration in kitchen water were higher than the typical value for domestic sewage (Von Sperling, 2014), linking these parameters values with food waste. The higher pH average of effluents from shower and laundry probably occurred due to sodium hydroxide-based soaps and bleach laundry uses, which raised the water pH (Morel and Diener, 2006).

Shower samples presented high concentrations of total phosphorus (Pt), which were near to the 7 mgL^{-1} typical sewage levels (Von Sperling, 2014). A possible explanation for this is the use of shampoos, sunscreen, and liquid soap, which have phosphates in their composition to fulfil the function of foam stabilizers. Regarding nitrogen analysis, shower samples presented the highest concentration in comparison with the other sources. The results are probably associated with to the habit of peeing in the shower. However, this habit is not common for all residents, causing a variation of NTK concentration (126.0 ± 132.0 mgN L^{-1}). Thus, NTK values from the shower became comparable to those values from other sources. The nitrogen concentration of laundry and mixed water were significant due to the large variation of NTK concentration in all samples. Nitrogen presence in laundry and mixed water had contributions from the disinfectants and cleaning products use, which have ammonia-based composition.

Table 1. Quality analysis of the different greywater sources.

Parameter	Kitchen	Mixed	Shower and washbasin	Laundry
COD (mgO2L-1)	2331±308 a	1296±565 b	611±723 c	748±519 c
TSS (mgL-1)	1109±706 a	318±283 ab	178 + 158 bc	93±78 c
NTK (mgN L-1)	9.5±4.9 a	24.5±15.1 ab	126.0±132.0 b	22.5±18.9 ab
Ptot (mgL-1)	3.4±2.1 a	5.3±8.7 a	6.9±11.3 a	3.7±2.1 a
pH	5.5±0.5 a	6.0±0.6 ab	7.1±0.2 b	8.6±1.4 b
Conductivity (mS cm-1)	0.4±0.1 a	0.5±0.1 a	0.6±0.4 a	2.1±1.3 b
Turbidity (uT)	242±106 a	179±95 a	154±185 ab	66±42 b

The statistical study presented indicate the absence of a relationship between the analysed parameters. Thus, it was produced wastewater with different characteristics, despite all wastewaters have been called greywater. Bakare et al. (2016) found similar results after evaluating greywater samples from 75 households in South Africa. Jefferson and Jeffrey (2013) also found that greywater variability depends on people's activities, and is a consequence of geographic, economic, and social factors.

AKNOWLEDGEMENTS

We thank CAPES and CNPq (311275/2015-0) for the master and doctoral scholarships received and Fapesp (Process 2017/07490-4) for the research grant.

REFERENCES

APHA. Standard methods for the examination of water and wastewater. 22ª ed. Washington: American Public Health Association. 2012.
Bakare, B. F.; Mtsweni, S.; Rathilal, S. (2016) Characteristics of greywater from different sources within households in a community in Durban, South Africa, Journal of Water Reuse and Desalination, 7, 520-528.
Boyjoo, Y.; Pareek, V. K.; Ang, M. (2013) A review of greywater characteristics and treatment processes, Water Science & Technology, 67, 1403-1424.
Paulo, P.L.; Galbiati, A.F.; Magalhães, F.J.C. (2018), In: CataloSan: Catálogo de soluções sustentáveis de saneamento - gestão de efluentes domésticos. Ministério de Saúde. Fundação Nacional de Saúde. ISBN: 978-85-63202-07-9
Jefferson, B.; Jeffrey, P. (2013) In: Source separation and decentralization for wastewater management, IWA Publishing, ISBN 9781780401072.
Madrid, F. J. P Y L, Figueiredo, I. C. S., Ferrão, A. M. De a., Tonetti, A. L. (2015) Metodologia de desenvolvimento eco-sistêmico aplicado ao paradigma do saneamento descentralizado, Revista Monografias Ambientais - REMOA, 14, 101-105.
Morel A.; Diener, S. (2006) In: Greywater Management in Low and Middle-Income Countries, Review of different treatment systems for households or neighbourhoods. Swiss Federal Institute of Aquatic Science and Technology (Eawag). ISBN: 3-906484-37-8978-3-906484-37-2.
Von Sperling, M. (2014) In: Introdução à qualidade das águas e ao tratamento de esgoto, Editora UFMG, ISBN: 9788542300536.

Adsorption of cadmium on raw and base treated Bolivian natural zeolite

L. Velarde*, E. Escalera**, and Farid Akhtar*

* Division of Materials Science, Department of Engineering Sciences and Mathematics, Luleå University of Technology, SE-971 87 Luleå, Sweden
(*E-mail:* lisbania.arnez@associated.ltu.se; farid.akhtar@ltu.se;)
** Department of Chemistry, Faculty of Science and Technology, San Simon University, UMSS, Cochabamba, Bolivia
(*E-mail:* escalera.edwin@gmail.com)

Abstract

In recent times, population growth has implied a higher generation of wastewater and contamination of water resources. The country of Bolivia has not been the exception. Thus, methods and materials for wastewater treatment suitable for Bolivian society should be studied. Bolivian natural zeolite (BZ) was selected as an adsorbent for the removal of cadmium. Likewise, BZ was converted to Na-form (NaBZ) by a treatment in a solution of 2M NaCl. BZ and NaBZ were characterized by XRD, scanning electron microscope SEM, and N_2 adsorption-desorption measurements. Additionally, the techniques of XPS and FT-IR were used to study the adsorption mechanism. Cadmium adsorption on BZ and NaBZ was described by Langmuir model, which provided considerable values of maximum cadmium adsorption capacity of 20.2 and 25.6 mg/g for BZ and NaBZ, respectively. The adsorption data followed the pseudo-second-order model. Additionally, the effect of pH (5-11), temperature (25-60 °C), contact time (5-180 min), and desorption test was studied. Moreover, a study of the adsorption of heavy metals (As, Cd, Cu, Co, Ni, Pb, and Zn) from an actual sample (Brine from Uyuni salt flat) was studied. The obtained results in this study show the efficacy of Bolivian natural zeolites in the adsorption of heavy metals.

Keywords (maximum 6 in alphabetical order)
Adsorption; cadmium; clinoptilolite; heavy metals; natural zeolites

INTRODUCTION

Nowadays, pollution is one of the biggest problems around the world. Remove of toxic heavy metal ions from wastewater has received significant attention due to their harmful impact on the environmental and public health (Anbia & Amirmahmoodi, 2016). Within the group of heavy metals is cadmium which is carcinogen and can produce a damage in the kidney, bones and respiratory system (Godt et al., 2006).According to the literature, many conventional approaches have been used to reduce concentrations of heavy metals from wastewater, such as coagulation, flocculation, chemical precipitation, flotation, reverse osmosis, ion exchange, and ultra-filtration (Da'na, 2017). Among the many methods available, adsorption is considered a very promising technique for metals removal, due to its high efficiency, easy operation, low cost, and the availability of different adsorbents (Fu & Wang, 2011; Prelot et al., 2012). The natural zeolites are one of the adsorbents with high availability, mainly due to zeolites are undoubtedly the most inexpensive alternative adsorbents compared to others. Additionally, natural zeolites have been reported as a good adsorbents for the retention of heavy metal ions due to their open pore structure, accessible adsorption sites, regeneration ability (Babel & Kurniawan, 2003; Da'na, 2017; De Gisi et al., 2016; Zhao, 2011) . Moreover, pretreatment of natural zeolites by NaCl was highly reported due to the increase in the heavy metals removal(Cortés-Martínez, R., Martínez-Miranda, V., Solache-Ríos, M., & García-Sosa, 2004; Gedik & Imamoglu, 2008; Giornoa & Driolia, 1997; Lonin et al., 2018).
Bolivia is a rich country in the mineralogical field (Valle & Holmes, 2013). The availability of nonmetallic minerals is a good alternative to using them and transforming them in specialized products (Zeballos et al., 2017). One of the mineral available are natural zeolites, thus their application in the adsorption of heavy metals will be suitable and useful for the treatment of water sources of communities and wastewater from industries.
Currently, the application of Bolivian natural zeolites and their application in the removal of heavy metals has not been reported. Therefore, the aim of the present study is the application of raw and NaCl-treated Bolivian natural zeolites in the adsorption cadmium. Furthermore, a study of heavy metals adsorption from the brines of Salar de Uyuni, Bolivia has been developed.

MATERIALS AND METHODS

Bolivian natural zeolite (BZ) of Clinoptilolite type was provided from Sucre, Bolivia. Firstly, BZ was crushed and sieved through meshes in the range of 45-500 µm, then washed with abundant distilled water and dried at 105 °C for 24 h. The brine to be treated was obtained from the salt flat of Salar de Uyuni, located in Potosi, Bolivia. The brine was collected in September 2019 (geographical coordinates: 20° 17' 22" S 67°04'35" W).

2.1. Bolivian Natural Zeolite Pretreatment

Na-form was prepared similar to the procedures reported in the literature (Bektaş & Kara, 2004; Semra Çoruh & Osman Nuri Ergun, 2008). 100 g of BZ was added to a solution of 2M NaCl, and the solution was stirred at 120 rpm, 25 °C for 24 h, then was filtered and washed with plenty of distilled water to remove the chloride ions (Cl^-) completely. The resultant pretreated zeolite was labeled as NaBZ. To ensure that the Cl^- has been eliminated, the verification of the presence of Cl^- was performed by the silver nitrate ($AgNO_3$) (0.1 M) test.

2.2. Characterization of zeolites

The mineralogical composition of BZ and NaBZ was determined by X-ray powder diffraction (XRD) by (ADP 2000 Pro X-ray diffractometer, Italy) with Cukα radiation (λ=1.5418Å) in the 2Θ range of 5-50 between with a step of 0.02. The microstructure was characterized by scanning electron microscope (JSM-IT 300 SEM JEOL, Japan). The characterization of BZ and NaBZ before and after the adsorption of cadmium by Fourier transform infrared spectroscopy FT-IR (Vertex 70v vacuum-based, USA), and X-ray photoelectron spectroscopy (Kratos Analytical Ltd., UK) were used to study the mechanism.

2.3. Batch adsorption experiments

The adsorption of cadmium on BZ and NaBZ was carried out using the batch method. 1 g of zeolite was added to 50 mL of 500 ppm of Cd. The solution was stirred at 200 rpm, for 24 h. Once the equilibrium was achieved, the solution was filtered with a syringe filter of 0.45 µm to collect the final solutions. Cadmium adsorption was determined by the difference between initial and final metal concentrations in the solution. The concentration of initial and final of cadmium solutions was measured by inductively coupled plasma sector field mass spectrometry (ICP-SFMS, USA).
Moreover, the adsorption isotherms and kinetics were obtained varying the initial concentration in the range of 10 to 500 mg/L and stopping the time each 5, 10, 15, 30 ,60 ,120, and 180 min), respectively. Additionally, the effect of temperature (25-45 °C), and pH (5.5-11) were studied.

2.4. Desorption test

The desorption test was performed adding a cadmium saturated BZ and NaBZ in a solution of HCl 0.1 M, at RT and 24 h. After the desorption process, samples were washed with distilled to remove the excess of Cl^- ions. The desorption process was conducted three times to verify the regeneration process of BZ and NaBZ.

2.5. Adsorption of heavy metals from Salar de Uyuni

The adsorption of heavy metals from brine of Uyuni salt flat on BZ and NaBZ was carried out similarly to the procedure of section 2.3. 1 g of zeolite was added to 50 mL of brine, solutions were stirred at 200 rpm, pH 6, and 25 °C for 24 h. After, the adsorption process, samples were filtrated with a syringe filter of 0.45 µm to recover BZ and NaBZ and measure the final concentrations by atomic absorption spectrophotometer (AA500, England).

RESULTS AND DISCUSSION

Firstly, BZ and NaBZ were characterize, after characterization the results showed no change in the crystallography structure, however an increase in the textural properties after the treatment by NaCl was detected. The obtained values were to surface area (25.93 to 30.94 m^2/g), pore diameter (13.88 to 15.83 m^2/g) and pore volume (0.0051 to 0.0091 cm^3/g). The increase in the textural properties are consistent with previous literature reports (Bektaş & Kara, 2004; Gedik & Imamoglu, 2008).

Subsequently, an adsorption test was performed to analyse the adsorption capacity of BZ and NaBZ towards cadmium. 1 g of zeolite was added to a solution of 500 mg/L of Cd and stirred until reach the equilibrium. The cadmium adsorption process on BZ and NaBZ has been studied using the adsorption isotherms of Langmuir and Freundlich. Between the two models, the Langmuir model was the best fit to the adsorption data obtained, with values of 20.2 and 25.6 mg/g for BZ and NaBZ, respectively. The obtained results showed a higher cadmium adsorption in comparison to some studies which reported lower cadmium adsorption on different natural zeolites from the world such as Ukrainian clinoptilolite (4.22 mg/g) (Sprynskyy et al., 2006), Iranian clinoptilolite (4.00 mg/g) (Merrikhpour & Jalali, 2013), Australian clinoptilolite (1.32 mg/g) (Taamneh et al., 2012).

Furthermore, the adsorption rate was studied through kinetics of pseudo-first and second order. The kinetic data was obtained by stirring Cd concentrations in a range of concentration of 5 to 180 min. According to the obtained data pseudo-second order fitted well with a correlation factor of 1 and similar data than the obtained experimentally.

Subsequently, a desorption process was carried out to verify the regeneration capacity of BZ and NaBZ. The upload zeolites were stirred in a solution of HCl 0.1 M. After, the desorption process percentage of 52.5 and 45.6 for BZ and NaBZ respectively.

Additionally, BZ and NaBZ were applied in the adsorption of heavy metals from a real water source (Brine from Uyuni salt flat, Bolivia). The application of BZ and NaBZ showed effective removal towards heavy metals. The removal percentage in BZ was for As (46 %), Cd (84.8 %), Cu (73.6 %), Co (67.5 %), Ni (85.7%), Pb (33.5%), Zn (12.4 %), and for NaBZ was for As (51.9 %), Cd (73.3 %), Cu (79 %), Co (69.4 %), Ni (96.6 %), Pb (55.9 %), Zn (81.8 %).

CONCLUSION

According to the obtained results, the adsorption capacity of BZ and NaBZ towards cadmium from synthetic solutions and heavy metals from real brine has been effective. Thus, Bolivian natural zeolites should be considered as a suitable candidate for the adsorption of heavy metals from polluted sources which will be a benefit for the Bolivian communities due to the use of own resources which will imply a low-cost method and improvement in the access to drinking water and quality of life.

ACKNOWLEDGEMENTS

This work was supported by Swedish International Development Cooperation Agency, SIDA), contribution No. 13486.

REFERENCES

Anbia, M., & Amirmahmoodi, S. (2016). Removal of Hg (II) and Mn (II) from aqueous solution using nanoporous carbon impregnated with surfactants. *Arabian Journal of Chemistry*, *9*, S319–S325. https://doi.org/10.1016/J.ARABJC.2011.04.004

Babel, S., & Kurniawan, T. A. (2003). Low-cost adsorbents for heavy metals uptake from contaminated water: a review. *Journal of Hazardous Materials*, *97*(1–3), 219–243. https://doi.org/10.1016/S0304-3894(02)00263-7

Bektaş, N., & Kara, S. (2004). Removal of lead from aqueous solutions by natural clinoptilolite: Equilibrium and kinetic studies. *Separation and Purification Technology*, *39*(3), 189–200. https://doi.org/10.1016/j.seppur.2003.12.001

Cortés-Martínez, R., Martínez-Miranda, V., Solache-Ríos, M., & García-Sosa, I. (2004). Evaluation of natural and surfactant-modified zeolites in the removal of cadmium from aqueous solutions. *Separation Science and Technology*, *39*(11), 2711–2730. https://doi.org/10.1081/SS-200026766

Da'na, E. (2017). Adsorption of heavy metals on functionalized-mesoporous silica: A review. *Microporous and Mesoporous Materials*, *247*, 145–157. https://doi.org/10.1016/J.MICROMESO.2017.03.050

De Gisi, S., Lofrano, G., Grassi, M., & Notarnicola, M. (2016). Characteristics and adsorption capacities of low-cost sorbents for wastewater treatment: A review. *Sustainable Materials and Technologies*, *9*, 10–40. https://doi.org/10.1016/J.SUSMAT.2016.06.002

Fu, F., & Wang, Q. (2011). Removal of heavy metal ions from wastewaters: A review. *Journal of Environmental Management*, *92*(3), 407–418. https://doi.org/10.1016/J.JENVMAN.2010.11.011

Gedik, K., & Imamoglu, I. (2008). Affinity of Clinoptilolite-based Zeolites towards Removal of Cd from Aqueous Solutions. *Http://Dx.Doi.Org/10.1080/01496390801888060*, *43*(5), 1191–1207. https://doi.org/10.1080/01496390801888060

Giornoa, L., & Driolia, E. (1997). Catalytic Behaviour of Lipase Free and Immobilized in Biphasic Membrane Reactor with Diþerent Low Water-Soluble Substrates. *J. Chem. T Ech. Biotechnol*, *69*, 11–14. https://doi.org/10.1002/(SICI)1097-4660(199705)69:1

Godt, J., Scheidig, F., Grosse-siestrup, C., Esche, V., Brandenburg, P., Reich, A., & Groneberg, D. A. (2006). *Journal of Occupational Medicine The toxicity of cadmium and resulting hazards for human health*. *6*, 1–6. https://doi.org/10.1186/1745-6673-1-22

Lonin, A. Y., Levenets, V. V., Omelnik, O. P., & Shchur, A. O. (2018). Comparison of the sorption properties of natural and synthetic zeolites for the purification of aqueous solutions from cobalt: sorption of the cobalt from aqueous solutions in dynamic conditions and the quantitative determination of cobalt by the PIXE method. *Journal of Radioanalytical and Nuclear Chemistry*, *315*(2), 163–169. https://doi.org/10.1007/S10967-017-5676-1/FIGURES/11

Merrikhpour, H., & Jalali, M. (2013). Comparative and competitive adsorption of cadmium, copper, nickel, and lead ions by Iranian natural zeolite. *Clean Technologies and Environmental Policy*, *15*(2), 303–316. https://doi.org/10.1007/S10098-012-0522-1/FIGURES/8

Prelot, B., Einhorn, V., Marchandeau, F., Douillard, J. M., & Zajac, J. (2012). Bulk hydrolysis and solid–liquid sorption of heavy metals in multi-component aqueous suspensions containing porous inorganic solids: Are these mechanisms competitive or cooperative? *Journal of Colloid and Interface Science*, *386*(1), 300–306. https://doi.org/10.1016/J.JCIS.2012.07.045

Semra Çoruh & Osman Nuri Ergun. (2008). Ni (II) Removal from Aqueous Solutions Using Conditioned Clinoptilolites: Kinetic and Isotherm Studies. *Environmental Progress & Sustainable Energy*, *33*(3), 676–680. https://doi.org/10.1002/ep

Sprynskyy, M., Buszewski, B., Terzyk, A. P., & Namieśnik, J. (2006). Study of the selection mechanism of heavy metal (Pb2+, Cu2+, Ni2+, and Cd2+) adsorption on clinoptilolite. *Journal of Colloid and Interface Science*, *304*(1), 21–28. https://doi.org/10.1016/J.JCIS.2006.07.068

Taamneh, Y., Reyad, •, & Dwairi, A. (2012). The efficiency of Jordanian natural zeolite for heavy metals removal. *Applied Water Science 2012 3:1*, *3*(1), 77–84. https://doi.org/10.1007/S13201-012-0061-2

Valle, V. M., & Holmes, H. C. (2013). Bolivia's Energy and Mineral Resources Trade and Investments with China: Potential Socioeconomic and Environmental Effects of Lithium Extraction. *Latin American Policy*, *4*(1), 93–122. https://doi.org/10.1111/LAMP.12007

Zeballos, A., Weihed, P., Blanco, M., & Machaca, V. (2017). Characterization of some nonmetallic resources in Bolivia: an overview of their potentiality and their application in specialized formulations. *Environmental Earth Sciences*, *76*(22). https://doi.org/10.1007/s12665-017-7094-7

Zhao, G. (2011). Sorption of Heavy Metal Ions from Aqueous Solutions: A Review. *The Open Colloid Science Journal*, *4*(1), 19–31. https://doi.org/10.2174/1876530001104010019

Surfactant elimination in horizontal and vertical-flow constructed wetlands for greywater treatment

C. G. Morandi*, K. M. Takahashi*,**, P. Paulo**, H. Steinmetz*

* Department for Resource-Efficient Wastewater Technology, Rheinlandpfälzische Technische Universität Kaiserslautern-Landau, Kaiserslautern, Germany
(E-mail: carlo.morandi@bauing.uni-kl.de; heidrun.steinmetz@bauing.uni-kl.de)
** Faculty of Engineering, Architecture and Urbanism and Geography, Federal University of Mato Grosso do Sul, Campo Grande, MS, 79070-900, Brazil. (E-mail: paula.paulo@ufms.br)

Abstract
Surfactants are among the main chemical contaminants in greywater and can pose risks to humans and the environment. This study assessed the surfactant removal capacity of 9 different constructed wetland systems for greywater treatment that differed with respect to design and operation as well as input greywater. Anionic surfactants could be detected in all greywaters studied at much higher concentrations than nonionic or cationic surfactants. It was shown that several investigated VFCW systems were suitable for extensive surfactant removal. This is mainly due to the required complete aerobic biodegradability of surfactants to be placed on the market. The investigated HFCW may only be suitable for extensive surfactant removal by operation at considerably lower hydraulic and organic loading rates and thus higher hydraulic retention times and reactor volumes. Based on the results shown, it is advisable to employ aerobic vertical-flow constructed wetlands for surfactant removal for safe greywater reuse.

Keywords (maximum 6 in alphabetical order)
Biodegradability, greywater reuse, HFCW, VFCW, nature-based solution, treatment wetland.

INTRODUCTION

Greywater is household wastewater that excludes urine and faecal wastewater. Given their widespread applicability, surfactants (emulsifiers or surface-active agents that allow two immiscible liquids to mix) are among the main chemical contaminants in greywater and are generally found not only in wastewater but also in natural waters (Ramprasad and Philip 2016). Surfactants usually enter the wastewater stream due to high solubility, without undergoing any metabolic changes. As a result, these compounds persist in the discharged environment for a long time, resulting in many adverse effects. Surfactants can cause increased environmental pollution, specially negative changes in soil properties, e.g., hydrophobicity in soil (Gross *et al.* 2015). In humans, they mostly cause skin irritation and allergic dermatitis, but in chronic conditions they can lead to more severe disorders, such as cancer (Ramprasad and Philip 2016). Conventional wastewater treatment plants (WWTPs) are ineffective at completely removing surfactants (Ramprasad and Philip 2016). Furthermore, surfactants enter greywater predominantly through the use of detergents and cleaning products; typically, anionic surfactants are used to remove dirt particles, nonionic surfactants are employed to eliminate grease, and cationic surfactants are used as fabric softeners (Gross et al. 2015). In the European Union and elsewhere, legislation usually requires proof for both the primary degradability and the complete aerobic biodegradability of surfactants to be placed on the market (EC Detergents Regulation 2004). Due to their linear carbon chains, easily biodegradable anionic surfactants are predominantly used in cleaning products (Gross *et al.* 2015). Hereof, linear alkyl benzene sulfonate (LAS) is the most commonly used surfactant in laundry and dishwashing agents, accounting for approx. 80 % of all household cleaning agents (Venhuis and Mehrvar 2004). In washing machine wastewater, pollutants in the laundry and the ingredients of the detergents, including surfactants, sometimes lead to very high COD concentrations (Friedler 2004; Weingärtner 2013). Due to the use of personal care products, light greywater from showers usually contains compounds that are difficult to biodegrade, such as synthetic surfactants. The presence of surfactants usually reflects in relatively high COD to BOD_5 ratios [COD/BOD_5 = 2.8 ± 1.0 (Jefferson *et al.* 2004); 2.5 ± 0.5 (Gethke *et al.* 2007)]. According to Keysers *et al.* (2008), a concentration range for anionic surfactants of 0.46-0.83 mg/l and for nonionic surfactants of 1.4-1.7 mg/l was found in shower greywater generated at a German WWTP. Cationic surfactants were below the quantitative limit of detection (< 0.05 mg/l).
Nature-based solutions as biological treatment offer a promising approach that benefits both human and environmental health at little cost. For greywater treatment, specially constructed wetlands (CWs) seem to be an adequate treatment option (Boano *et al.* 2020).
This study assessed the surfactant removal capacity of 9 different constructed wetlands that differed with respect to design (horizontal-flow or vertical-flow) and operation (variation in loading rate) as well as input greywater (washing machine greywater or light greywater from showers and hand wash basins with and without kitchen wastewater shares).

MATERIALS AND METHODS

Experimental setup and design

The investigated horizontal-flow constructed wetland (HFCW) showed the dimensions 1.00 m × 1.00 m × 0.70 m (L × W × D) and treated a mean flow of 150 L/d [HLR = 392 ± 272 L/(m^2·d)] greywater generated by two showers, two lavatories, two laundry basins, and one washing machine within an experimental bathroom at UFMS Campus in Campo Grande, Brazil. The system is described in Filho *et al.* (2018) and was monitored for 497 d.
Two investigated pilot-scale vertical-flow constructed wetlands (VFCW) are described in Morandi *et al.* (2021). They consisted of 2.5 m^2 filter area each and were filled either with common fluviatile sand (0 – 2 mm) or lava sand (0 – 4 mm), acquired from a quarry in Rhineland-Palatinate in Germany. The pilot-scale VFCW treated greywater from showers and hand wash basins at a temporary construction workers' housing in Stuttgart, Germany. The hydraulic loading rate to the lava sand VFCW amounted to 65.3 ± 16.2 L/(m^2·d), whereas it corresponded to 75.4 ± 17.2 L/(m^2·d) for the fluviatile sand compartment. The systems were investigated for 446 d.
Moreover, six small-scale VFCW columns S1 to S6 (Ø = 29 cm) made of acrylic glass with inclined bottom and slotted drainage pipe (8 mm) were investigated for the removal of surfactants (see Figure 1). The systems were operated at the facilities of the RPTU Campus in Kaiserslautern, Germany, and filled either with fluviatile sand (0 – 2 mm) or lava sand (0 – 4 mm) as filter layer. The drainage layer of S3, S4, and S6 was functionalized with anthracite coal for enhanced phosphorus removal, which is beyond the scope of this study. The systems were fed with light greywater from showers and hand wash basins with kitchen wastewater shares from students' dormitories in Birkenfeld, Germany, and investigated for 530 d. The HLR varied, depending on the system, from 69 ± 13 L/(m^2·d) [S4] up to 82 ± 21 L/(m^2·d) [S1].

Figure 1. Small-scale VFCW after start-up with greywater (left) and after approx. one and a half years of operation (right) in Kaiserslautern, Germany.

RESULTS AND DISCUSSION

Table 1 illustrates the removal efficiency in terms of COD and surfactants for the 9 constructed wetlands studied. Anionic surfactants could be detected in all greywaters studied, as these readily biodegradable surfactants are predominantly used over nonionic or cationic surfactants due to legal regulations (EC Detergents Regulation 2004). Cationic surfactants, on the other hand, were hardly detected or only in low concentrations, which is in accordance with Keysers *et al.* (2008). The reason for this was the exclusion of washing machine wastewater in all VFCW systems investigated. For the HFCW, neither cationic nor nonionic surfactants were analyzed. The highest concentrations for anionic surfactants with 28 ± 10 mg/l LAS were found to be upstream of the HFCW in mixed greywater after pretreatment. This can be ascribed especially to the washing machine greywater contribution. Also, greywater from the workers' housing showed 12.8 mg/l anionic surfactants. This can be attributed to the regular cleaning of shower stalls (two to three times per week) with an alkaline high-concentrate cleaning agent. Greywater from the student dormitories exhibited 12.1 mg/l anionic surfactants, which can also be found in shampoo formulations (Trüeb 2007). With regards to nonionic surfactants, it is possible that they were introduced into the kitchen wastewater in Birkenfeld via the use of dishwashing detergents as grease solvents, while at the pilot plant they enter the greywater via the bath cleaning agent in the same way as the anionic surfactants.

Table 1. Mean values ± SD for loading rates, COD, and surfactants concentrations in the influent as well as corresponding removal efficiencies in horizontal and vertical-flow constructed wetlands.

Constructed wetland	Hydraulic loading rate in L/(m^2·d)	Organic loading rate in g COD/(m^2·d)	Influent concentration in mg/l	Removal in % or effluent concentration in mg/l
HFCW	392 ± 272	36 ± 30	282 ± 100 (COD) 28 ± 10 (LAS) 270 ± 137 (COD) 3.9 ± 3.7 (nonionic surfactants) 0.7 ± 0.3 (cationic surfactants) 12.8 ± 3.2 (anionic surfactants)	38 ± 16 % COD 35 ± 23 % LAS 97.0 ± 1.6 % COD ; 95.9 ± 1.8 % anion. surf.; < 0.2 (LoD) – 0.57 mg/l cationic surf.; < 0.2 (LoD) – 0.24 mg/l nonionic surf.
VFCW, pilot-scale, Rhine sand	75.4 ± 17.2	16.4 ± 5.5		
VFCW, pilot-scale, lava sand	65.3 ± 16.2	19.0 ± 6.2		98.2 ± 0.7 % COD 96.4 ± 1.5 % anion. surf. < 0.2 (LoD) – 0.73 mg/l cationic surf.; < 0.2 (LoD) – 0.26 mg/l nonionic surf.
S1	82 ± 21	19 ± 8.8	277 ± 148 (COD) 2.5 ± 1.9 (nonionic surfactants) < 0.2 (LoD) – 5 (cationic surfactants) 12.1 ± 18.5 (anionic surfactants)	97.5 ± 1.2 % COD 0.33 ± 0.36 mg/l (anion. surf.)
S2 (lava)	79 ± 11	18 ± 7.4		97.4 ± 1.2 % COD 0.33 ± 0.30 mg/l (anion. surf.)
S3	76 ± 7.8	17 ± 6.7		97.0 ± 1.3 % COD 0.31 ± 0.30 mg/l (anion. surf.)
S4	69 ± 13	16 ± 7.1		96.9 ± 1.2 % COD 0.33 ± 0.32 mg/l (anion. surf.)
S5	71 ± 9.3	16 ± 7.0		97.5 ± 1.2 % COD 0.30 ± 0.19 mg/l (anion. surf.)
S6 (lava)	76 ± 17	17 ± 7.2		97.8 ± 1.1 % COD 0.25 ± 0.12 mg/l (anion. surf.)

< 0.12 mg/l (LoD; cationic surfactants). Predominantly < 0.2 mg/l (LoD; nonionic surfactants)

In contrast to the HFCW, it can be inferred from Table 1 that both the lava and Rhine sand VFCW removed surfactants extremely well. Previous studies have shown that vertical flow is more efficient than horizontal flow for surfactant removal in treatment wetlands (Tamiazzo *et al.* 2015). For instance, Fountoulakis *et al.* (2009) reported a LAS removal efficiency of 55% (inlet concentration 7.17 mg/l) in a 45 m² full-scale HFCW. The results of this study also suggest that higher COD eliminations significantly contribute to higher surfactant removal. Regarding the removal of anionic surfactants, regardless of the VFCW filter material, the influent value was reduced to very low concentrations (see Table 1). In the effluent, the values for cationic and nonionic surfactants fell mostly under 0.20 mg/l (LoD). This indicates a high treatment efficiency also for more recalcitrant substances, such as cationic and nonionic surfactants. It can be concluded that several VFCW investigated were suitable for surfactant removal. The main reason for that is that aerobic biodegradability is a prerequisite for surfactants to be placed on the market (EC Detergents Regulation 2004). An aerobic biodegradability does not, however, necessarily imply a corresponding anaerobic biodegradability. HFCW, in which anaerobic conditions prevail, may only be suitable for surfactant removal by operation at considerably lower hydraulic and organic loading rates and thus higher hydraulic retention times and reactor volumes. Based on the results shown, it is advisable to employ aerobic vertical-flow constructed wetlands for surfactant removal for safe greywater reuse.

REFERENCES

Boano, F., Caruso, A., Costamagna, E., Ridolfi, L., Fiore, S., Demichelis, F., Galvão, A., Pisoeiro, J., Rizzo, A. and Masi, F. 2020 A review of nature-based solutions for greywater treatment: Applications, hydraulic design, and environmental benefits. *The Science of the total environment*, **711**, 134731.
EC Detergents Regulation 2004 *REGULATION (EC) No 648/2004 OF THE EUROPEAN PARLIAMENT AND OF THE COUNCIL of 31 March 2004 on detergents.*
Filho, F. J. C. M., Sobrinho, T. A., Steffen, J. L., Arias, C. A. and Paulo, P. L. 2018 Hydraulic and hydrological aspects of an evapotranspiration-constructed wetland combined system for household greywater treatment. *Journal of environmental science and health. Part A, Toxic/hazardous substances & environmental engineering*, **53**(6), 493–500.
Fountoulakis, M. S., Terzakis, S., Kalogerakis, N. and Manios, T. 2009 Removal of polycyclic aromatic hydrocarbons and linear alkylbenzene sulfonates from domestic wastewater in pilot constructed wetlands and a gravel filter. *Ecological Engineering*, **35**(12), 1702–1709.
Friedler, E. 2004 Quality of Individual Domestic Greywater Streams and its Implication for On-Site Treatment and Reuse Possibilities. *Environmental technology*, **25**(9), 997–1008.
Gethke, K., Herbst, H., Keysers, C. and Pinnekamp, J. 2007 Grey water reuse in hotel and catering industry. *6th IWA Specialist Conference on Wastewater Reclamation and Reuse for Sustainability*, **9–12 Oktober, 2007**.
Gross, A., Maimon, A., Alfiya, Y. and Friedler, E. 2015 *Greywater Reuse.* CRC Press, Boca Raton, FL.
Jefferson, B., Palmer, A., Jeffrey, P., Stuetz, R. and Judd, S. 2004 Grey water characterisation and its impact on the selection and operation of technologies for urban reuse. *Water Science and Technology*, **50**(2), 157–164.
Keysers, C., Gethke, K. and Pinnekamp, J. 2008 Grauwassernutzung im Hotel- und Gaststättengewerbe: (German: Greywater reuse in the hotel and catering industry). *GWA Tagungsband (German: GWA proceedings)*, 1–20.
Morandi, C., Schreiner, G., Moosmann, P. and Steinmetz, H. 2021 Elevated Vertical-Flow Constructed Wetlands for Light Greywater Treatment. *Water*, **13**(18), 2510.
Ramprasad, C. and Philip, L. 2016 Surfactants and personal care products removal in pilot scale horizontal and vertical flow constructed wetlands while treating greywater. *Chemical Engineering Journal*, **284**, 458–468.
Tamiazzo, J., Breschigliaro, S., Salvato, M. and Borin, M. 2015 Performance of a wall cascade constructed wetland treating surfactant-polluted water. *Environmental science and pollution research international*, **22**(17), 12816–12828.
Trüeb, R. M. 2007 Shampoos: ingredients, efficacy and adverse effects. *Journal der Deutschen Dermatologischen Gesellschaft = Journal of the German Society of Dermatology : JDDG*, **5**(5), 356–365.
Venhuis, S. H. and Mehrvar, M. 2004 Health effects, environmental impacts, and photochemical degradation of selected surfactants in water. *International Journal of Photoenergy*, **6**(3), 115–125.
Weingärtner, D. E. 2013 *Greywater characteristics, biodegradability and reuse of some greywaters,* Schriftenreihe SWW, **144.** Verl. Siedlungswasserwirtschaft, Karlsruhe.

3. Resource recovery and safe reuse

Seasonal accumulation of pharmaceuticals in soils from a full-scale horticultural system irrigated with reclaimed water.

Alonso L.L.[1,2], Salvoch, M.[1,2], Startiris, V. [3], Malamis, S. [3], Buttiglieri, G. [1,2], Rodriguez Mozaz, S.R. [1,2]

[1] ICRA-Catalan Institute for Water Research, Girona, Catalonia, 17003, Spain
[2] University of Girona (UdG), Girona, Spain
[3] National Technical University of Athens, Athens, 10682, Greece.

(Email: lalonso@icra.cat, msalvoch@icra.cat, vagstatiris@gmail.com, malamis.simos@gmail.com, dbarcelo@icra.cat, gbuttiglieri@icra.cat, srodriguez@icra.cat)

Abstract
In the present study, plots from a horticultural field were irrigated with reclaimed water, and the accumulation of pharmaceuticals in the bulk and rhizosphere soils was studied. Analgesics and non-steroidal anti-inflammatories represented the major fraction of the initial pharmaceutical mass load, while irbesartan, hydrochlorothiazide were the most detected compounds after the irrigation. Rhizosphere soils exhibited a greater number of analytes and higher concentrations than bulk soils. Further studies will include the analysis of antibiotic resistant genes and the evaluation of the whole water-soil-plant system, to assess potential human risks.

Keywords (maximum 6 in alphabetical order)
Antibiotics, Rhizosphere, Soil pollution, Soil-plant system, Water treatment.

INTRODUCTION

Freshwater scarcity in times of climate change is a global concern that needs urgent attention. Island communities, especially those receiving high influxes of tourists, demand the availability of fresh water enough to satisfy not only the domestic usage, but for agricultural purposes. The circular economy processes intend to provide alternative solutions to address this situation, such as the application of wastewater treatment systems to obtain water suitable for irrigation. One of the major challenges involves the effective removal of organic pollutants, especially the so-called emerging ones, such as pharmaceuticals (drugs, antibiotics, among others). After passing through the system, these pollutants can reach the soil, generating potential human and environmental health risks, from the promotion of antimicrobial resistance in soils, toxic effects on the edaphic biota, and even a food safety risk, if crops can uptake them into their edible parts. Within the framework of the H2020 EU HYDROUSA project, we studied the accumulation of pharmaceuticals on agricultural soils after two seasonal periods of irrigation with reclaimed water. The study was performed during the growth period of a regular crop (lettuce), at full-scale under environmental conditions.

MATERIALS AND METHODS

The study was performed in Lesvos, a touristic island from Greece, where a demonstration-scale treatment plant was installed. The system consists of an upflow anaerobic sludge blanket reactor, a constructed-wetland system, and finally a tertiary treatment (UV). The reclaimed water is collected in storage tanks and applied for irrigation on adjacent horticultural fields. The field was divided into 2 plots: one irrigated with the reclaimed water (RW) and another with tap water (TW). Common lettuce (*Lactuva sativa*) was grown in both plots for c.a. 45 days (growing period of the crop) in two different seasons: autumn (2021) and summer (2022). Bulk soil samples were collected at 10 cm depth in the proximity of the crop, near the drippers before planting (initial time), and at harvesting time (final time). Additionally, the soil attached to the roots (rhizosphere soil) was collected at the final time by manual shaking of the roots (Shen et al., 2021).

Solid samples were extracted according to Gros et al., (2019). Briefly, 1 gram of freeze-dried soil was extracted with a buffer McIlvaine/MeOH solution in an ultrasound bath, followed by SPE (Oasis HLB) for clean-up. The analytes were eluted with MeOH, the solvent was evaporated, and the sample was reconstituted in LC mobile phase. Before injecting, samples were spiked with isotopically labelled standards. The quantification of samples was performed with a matrix-matched calibration curve, and recovery tests were performed to assess the extraction efficiency. The samples were analyzed in a quadrupole linear ion trap tandem mass spectrometry (UHPLC-QqLIT, SCIEX), following a total of 64 compounds in target mode.

RESULTS AND DISCUSSION

Pharmaceuticals were detected in the TW and RW soils before and after the growth periods. Overall, a higher number of compounds and a total mass load of pharmaceuticals were found in the RW, when compared to the TW soils. The non-steroidal analgesics and anti-inflammatories comprised more than the 90% of the mass burden at the initial time in autumn for both plots, with acetaminophen (max: 15.8 ug/kg), ketoprofen (max: 18.6 ug/kg), and the ibuprofen metabolite 2-OH ibuprofen (max: 23.9 ug/kg) all three with detection frequencies >80%. The same pattern was found in summer, though for the RW soils the fraction of NSAAI was lower (54%), as other groups such as antihypertensive and psychiatric drugs exhibited higher concentrations.

The number of compounds detected in the bulk soils of the RW plots at the final time (harvest) increased at both campaigns (autumn and summer). More pharmaceuticals were detected after the irrigation period in the summer season (n=27) than in the autumn (n=11). Hydrochlorothiazide and irbesartan were the compounds detected at the highest concentrations, at 59.4 and 62.5 µg/kg, respectively (Fig 1). Psychiatric drugs such as venlafaxine, its metabolite O-desmethyl-venlafaxine, and carbamazepine were also detected in the bulk soil in a range of 3.8-17 µg/kg.

Higher numbers of compounds as well as higher concentrations were found in the rhizosphere soil compared to the bulk soil in both seasons. The drugs found at higher concentration levels presented a similar profile in both soils (Fig 2). It is notable that three extra antibiotics were only found at rhizosphere soils (sulfamethazine, sulfamethoxazole, and trimethoprim). Since the soil organic matter did not differ between both types of soils, it is expected that other inherent physicochemical properties (pH, soil texture, among others) might provide better conditions for the sorption and accumulation of these compounds.

CONCLUSIONS

Pharmaceuticals were detected in soils after irrigation with reclaimed water. Although the control plots irrigated with tap water also showed the presence of several compounds (mainly analgesics and non-steroidal anti-inflammatories), reclaimed water for irrigation lead to detections of up to 33 compounds in the soil surrounding the rhizosphere of the lettuce crops. Several metabolites were found, such as the 2-OH ibuprofen and O-desmethyl-venlafaxine. The detection of compounds such as antibiotics in these soils is also relevant from the microbiological point of view. Further studies will include the analysis of antibiotic resistant genes and the evaluation of the whole water-soil-plant system, to assess potential human risks.

ACKNOWLEDGEMENTS

This study has received funding from the Spanish State Research Agency of the Spanish Ministry of Science and Innovation for ReUseMP3 project (PID2020-115456RB-I00 /MCIN/AEI / 10.13039/501100011033). Authors also acknowledge funding from the European Union's Horizon 2020 Research and Innovation programme (HYDROUSA, grant agreement N° 776643). The ICRA researchers are thankful for funding from the CERCA Program, Generalitat de Catalunya.

REFERENCES

Gros, M., Mas-Pla, J., Boy-Roura, M., Geli, I., Domingo, F., Petrovic, M. 2019. Veterinary pharmaceuticals and antibiotics in manure and slurry and their fate in amended agricultural soils: Findings from an experimental field site (Baix Empordà, NE Catalonia). *Science of the Total Environment*. **654**, 1337-1349.

Shen, Y., Li, H., Ryser, E.T., Zhang, W. 2021. Comparing root concentration factors of antibiotics for lettuce (Lactuca sativa) measured in rhizosphere and bulk soils. *Chemosphere*. **262.**

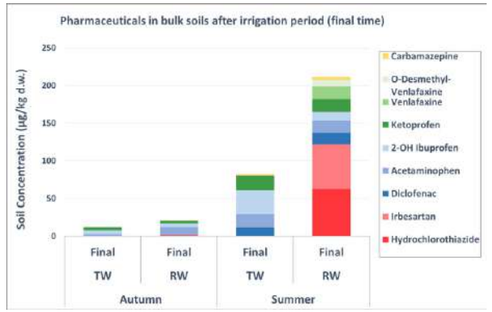

Figure 1. Soil concentrations in bulk soils at the harvesting time, on each season. TW: tap water irrigated plots; RW: reclaimed water irrigated plots.

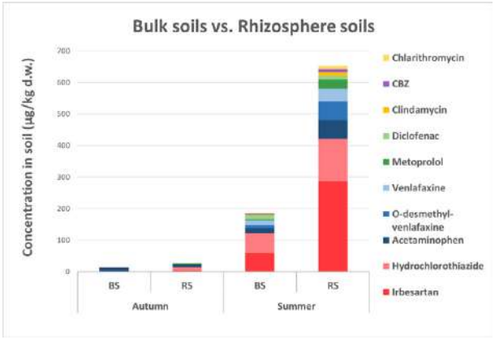

Figure 2. Soil concentrations in bulk (BS) and rhizosphere (RS) soils at the harvesting time, on each season. Only the RW (reclaimed water irrigated plots) are presented.

Effective radiation transfer as a major element for the optimized design and operation of purple phototrophic bacteria photobioreactors

A. Amini*, E. Porciatti*, M. Greco*, S. Rossi*, E. Ficara*, A. Turolla*

*Department of Civil and Environmental Engineering (DICA), Politecnico di Milano, Piazza Leonardo da Vinci 32, 20133, Milan, Italy (E-mail: ali.amini@polimi.it; elisa.porciatti@mail.polimi.it, michael.greco@mail.polimi.it; simone.rossi@polimi.it; elena.ficara@polimi.it; andrea.turolla@polimi.it)

Abstract

The cultivation of purple phototrophic bacteria (PPB) in photobioreactors (PBRs) using different waste streams offers a promising opportunity for resource recovery. Effective reactor system design and mathematical modeling are crucial for maximizing PPB growth and optimizing the design and operation of PBRs. Insufficient research has been done on radiation transfer in mixed cultures of PPB, despite the fact that scaled systems require a thorough understanding of this phenomenon. In this work, laboratory-scale batch experiments were conducted to study the effect of light intensity on PPB growth. Based on experimental data, light distribution in PBRs was modeled using the most relevant approaches. Results showed that PPB scattering cannot often be ignored under conventional operating conditions. The Aiba model emerged as the best option for predicting the influence of light intensity on kinetic parameters. Guidelines for the optimized design and operation of PBRs were identified in the view of process scale-up.

Keywords

Photobioreactors; purple phototropic bacteria; radiation transfer; resource recovery

INTRODUCTION

Purple phototrophic bacteria (PPB) are among the species in nature with the widest variety of metabolisms (Fradinho et al., 2021). PPB are considered a promising phototrophic mediator for resource recovery from wastewater to produce value-added products (Capson-Tojo et al., 2021). Under photoheterotrophic growth conditions, PPB can use light as energy source for assimilative pollutant removal and maximizing the resource recovery potential (Capson-Tojo et al., 2022).

One of the key factors to be accounted for PPB growth is the light supplied by irradiation sources (artificial, sunlight) in photobioreactors (PBRs). Low light intensity might hinder microbial growth, while high values of light intensity can lead to photooxidation and photoinhibition phenomena (Carvalho et al., 2011). Furthermore, design, operation, and control of PBRs require accurate determination of light distribution within the PBRs (Wágner et al., 2016; Naderi et al., 2017) in order to provide valuable inputs to mathematical models that are able to predict PPB growth.

This work is primarily aimed at (i) the detailed modeling of radiation transfer in PBRs by the most relevant light propagation approaches, namely the Beer-Lambert law and the two-flux approximation model, and (ii) the assessment of the light intensity effect on PPB growth. Modeling results were applied for identifying guidelines for PBR optimized design and operation.

MATERIALS AND METHODS

Laboratory batch experiments were set up using flat-plate PBRs with a volume of 316 mL to assess the effect of different light intensities (10, 20, 40, and 60 W/m^2) on PPB growth at 30 °C and light distribution within the PBR. During the experiments, the light was supplied from one side as monochromatic radiation at 850 nm, and the pH was kept between 6.8 and 7.2. Light distribution within the PBR was evaluated at different biomass concentrations (ranging from 40 to 350 mgTSS/L) by applying the Beer-Lambert law and the two-flux approximation model, and the average light intensity was calculated based on the integration of the models used over the culture depth. Moreover, the kinetic parameters for PPB growth were obtained by fitting the experimental data with appropriate models for describing photooxidation and photoinhibition phenomena. With the aim of further investigating the scattering effect, optical properties were characterized by a spectrophotometer equipped with an integrating sphere over the spectral range of 300 to 1100 nm.

RESULTS AND DISCUSSION

Figure 1 shows the light intensity profiles inside the PBRs for different PPB concentrations at various incident light intensities by applying the Beer-Lambert law. As light passes through the PBR containing a PPB suspension, there is a strong reduction in the light intensity with increasing depth. For concentrations lower than 80 mgTSS/L every point of the reactor is illuminated, while for concentrations higher than 320 mgTSS/L half of the reactor is in the dark.

By comparing the average light intensities between the Beer-Lambert law and the two-flux approximation model, it can be seen that the scattering effect for PPB concentrations up to 500 mgTSS/L is not negligible (Figure 2). Results showed that neglecting scattering phenomena led to discrepancies of 33% and 24% for PPB concentrations of 160 and 320 mgTSS/L, respectively. Moreover, the optical properties confirmed the fact that scattering is a relevant phenomenon (Figure 3-a). As shown in figure 3-b, regarding the absorption peaks in the near-infrared region, for incident light intensities higher than 40 W/m^2 a downward shift in the light absorption of PPB was observed, indicating an adaptation in the pigment content of PPB for facing high light intensities.

The kinetic parameters of PPB in a batch PBR were obtained with particular emphasis on the effect of different light intensities. Experimental data from batch tests evidenced the occurrence of photoinhibition phenomena. The Aiba model emerged as the best modeling solution. As shown in Figure 4, the model correctly described the experimental data for each light intensity investigated. This resulted in a half saturation coefficient in the range of 3.82-4.63 W/m^2.

Modeling results were finally applied to the optimization of PBR design and operation, especially looking for the best geometrical configuration for flat-plate PBRs (in terms of thickness) as a function of PPB concentration, which in turn usually depends on the operating conditions of continuous flow systems (e.g., irradiation intensity, HRT, influent substrate concentration).

CONCLUSIONS

The results indicated that (i) light distribution is fundamental for PPB growth, (ii) scattering is important under certain operating conditions, (iii) light distribution has to be optimized to maximize energy absorption and minimize detrimental phenomena, (iv) it is necessary to design and operate reactors with an accurate assessment of radiation transfer, and (v) this work is paving the way to the scale-up of the technology as much higher productivity is granted by an effective use of radiation.

REFERENCES

Capson-Tojo, G., Batstone, D. J., Grassino, M., Vlaeminck, S. E., Puyol, D., Verstraete, Kleerebezem, R., Oehmen, A., Ghimire, A., Pikaar, I., Lema, J.M., & Hülsen, T. (2020). Purple phototrophic bacteria for resource recovery: Challenges and opportunities. Biotechnology Advances, 43, 107567.

Capson-Tojo, G., Batstone, D. J., Grassino, M., & Hülsen, T. (2022). Light attenuation in enriched purple phototrophic bacteria cultures: implications for modelling and reactor design. Water Research, 118572.

Carvalho, A. P., Silva, S. O., Baptista, J. M., & Malcata, F. X. (2011). Light requirements in microalgal photobioreactors: an overview of biophotonic aspects. Applied microbiology and biotechnology, 89(5), 1275-1288.

Fradinho, J., Allegue, L. D., Ventura, M., Melero, J. A., Reis, M. A., & Puyol, D. (2021). Up-scale challenges on biopolymer production from waste streams by Purple Phototrophic Bacteria mixed cultures: A critical review. Bioresource Technology, 327, 124820.

Naderi, G., Znad, H., & Tade, M. O. (2017). Investigating and modelling of light intensity distribution inside algal photobioreactor. Chemical Engineering and Processing: Process Intensification, 122, 530-537.

Wágner, D. S., Valverde-Pérez, B., Sæbø, M., de la Sotilla, M. B., Van Wagenen, J., Smets, B. F., & Plosz, B. G. (2016). Towards a consensus-based biokinetic model for green microalgae–The ASM-A. Water research, 103, 485-499.

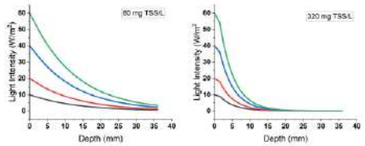

Figure 1. Light attenuation profiles at different biomass concentrations and incident light intensities by applying the Beer-Lambert law.

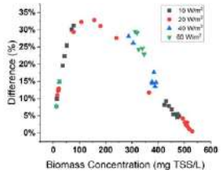

Figure 2. Comparison of average modeled light intensity in the PBR by the Beer-Lambert law and the two-flux approximation model for different PPB concentrations.

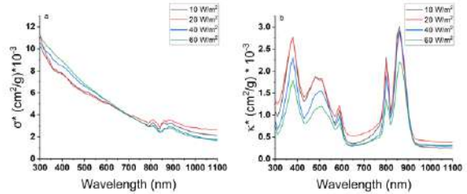

Figure 3. (a) specific scattering coefficient and (b) specific absorption coefficient of PPB determined at four different PPB concentrations at the wavelengths from 300 to 1100 nm.

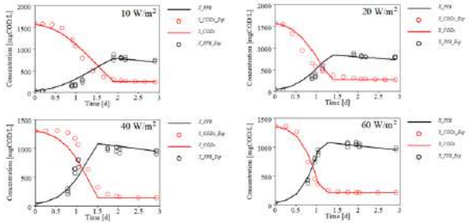

Figure 4. Experimental and modeled data for PPB growth and substrate (acetate) consumption.

Bioelimination of different arsenic species by microalgae and bacteria grown in wastewater treatment plants

B. Antolín[1,2], D. Moldes[1,2], E. Sánchez[2], P. García-Encina[2,3], M. Vega[1,2]

[1]Institute of Sustainable Processes, University of Valladolid, Dr. Mergelina s/n, 47011 Valladolid, Spain
[2]Dept. of Analytical Chemistry, University of Valladolid, Paseo de Belén 7, 47011 Valladolid, Spain
[3]Dept. of Chemical Engineering and Environmental Technology, University of Valladolid, Dr. Mergelina s/n, 47011 Valladolid, Spain)
(E-mail: beatriz.antolin@uva.es)

Abstract
Livestock farming is a relevant economic sector in many countries, generating large amounts of highly polluting wastes loaded with nutrients, organic pollutants and toxic trace elements which cause serious environmental issues if not properly treated. Piggery wastewater treatment in photobioreactors has shown great potential for nutrients recovery and removal of heavy metals. In this work, the removal capacity and biotransformation of arsenic species by microalgae and bacteria grown in photobioreactors treating piggery wastewater is investigated. The effect of contact time and metal concentration on the biosorption of As(III), As(V) and DMA on green microalgae *Scenedesmus almeriensis* and on bacteria from activated sludge were investigated, using batch photobioreactors fed with synthetic wastewater simulating the composition (C, N, P) of piggery wastewater. The maximum biosorption capacity of both biomasses for each metal at 1 and 72 h contact time were obtained from the adsorption isotherms.

Keywords
Arsenic, biosorption, heavy metals, *Scenedesmus almeriensis,* activated sludge, wastewater

INTRODUCTION

Contamination of soil and groundwater by arsenic has become a severe health and environmental concern worldwide due to the toxicity, mobility and persistence of this element. Prolonged exposure to arsenic species through drinking water and food develops cancer and other serious diseases. In water, the primer source of this toxic element to humans, arsenic occurs mainly as inorganic As(III) and As(V), but also organic dimethylarsinic acid (DMA) or monomethylarsonic acid (MMA) species may be present. Wastewater, specially from livestock farming using feed and/or water containing arsenic, is another important source of arsenic and values up to 690 µg/L as total arsenic have been reported (Gao et al., 2018). Bioremediation using microorganisms arises as a promising methodology to eliminate simultaneously organic and inorganic pollutants from wastewater and extensive research is being carried out on the use of this technique for the treatment of water contaminated with heavy metals and metalloids (Benis et al., 2020). Large amounts of valuable biomass are generated in this process and efforts are being carried out to recover nutrients and other high value biomolecules for new applications (fertilizers, feed, industrial applications…) within the context of the circular economy (Bădescu et al., 2018). This work addresses the capability of green microalgae and aerobic bacteria, usually employed in wastewater treatment plants, to remove inorganic and organic arsenic species (As(III), As(V) and DMA).

MATERIALS AND METHODS

Biosorption experiments were carried out with two biomasses of green microalgae *Scenedesmus almeriensis* and bacteria from an activated sludge, grown in a culture medium simulating the composition of piggery wastewater, spiked with 0.1 and 0.5 mg/L of As(III), As(V) or DMA, concentrations adopted from reference values reported for total arsenic in pig manure (ASAE, 2003). The synthetic wastewater was prepared dissolving per litre of deionised water,: 30 mg urea, 32.5 mg KNO_3, 4 mg $CaCl_2 \cdot 2H_2O$, 7 mg NaCl, 2 mg $MgSO_4 \cdot 7\ H_2O$, 110 mg peptone and 160 mg of meat extract (Sigma Aldrich, Germany) (Alcántara et al., 2015). Initial biomass concentration of 2 and 4 g/L of microalgae and activated sludge, respectively, was treated at 25°C under continuous stirring in orbital shaker at 250 rpm and LED lightening at 1200 $\mu E \cdot m^{-2} \cdot s^{-1}$ in 12:12 h light-darkness periods. Bioelimination percentages of arsenic species were determined at different contact times from 8 h to 15 days. The concentration of As species in the filtered supernatant was determined by HPLC-ICP-MS (Agilent 2200 HPLC system coupled to Agilent 7800 ICP-MS). Maximum biosorption capacities of both biomasses for each As species at 1 and 72 h contact time were obtained from the respective adsorption isotherm constructed at concentrations of As species ranging from 1 to 500 $mg \cdot L^{-1}$, using Langmuir and Freundlich approximations.. The biomass growth was determined gravimetrically, measuring the variation in biomass weight after the biosorption experiments.

RESULTS AND DISCUSSION

The adsorption capacities of both microorganisms are depicted in Table 1.

Table 1. Adsorption capacity of As(III), As(V) and DMA species on *Scenedesmus almeriensis* and activated sludge at 1 and 72 h.

1h		Langmuir-1h		Langmuir-72h	
		q_{sat} mg/g	K_L L/mg	q_{sat} mg/g	K_L L/mg
As(III)	*Scenedesmus Al.*	**0.40**	0.021	**9.52**	0.010
	Activated sludge	**1.90**	0.023	**23.15**	0.002
As(V)	*Scenedesmus Al.*	**0.18**	0.032	**4.9**	0.0029
	Activated sludge	**2.46**	0.117	**34.7**	0.0004
DMA	*Scenedesmus Al.*	**0.39**	0.010	**37.0**	0.0007
	Activated sludge	**0.58**	0.156	**3.16**	0.0038

At 1 h contact time, the best adsorption capacity was achieved for As(V) with *activated sludge* (2.46 mg/g) whereas for 72h of contact time DMA showed the maximum adsorption capacity of 37.0 mg/g on *Scenedesmus almeriensis*. The dimensionless separation coefficient R_L was calculated according to the following expression:

$$R_L = \frac{1}{1 + K_L \cdot c_0}$$

R_L between 0 and 1 where obtained which is indicative of a favourable adsorption process (Liu et al., 2011). On the other hand, n values from Freundlich linear fit were higher than 1, which again demonstrates the adsorption process as favorable.

Figure 1 shows the bioremoval efficiency of both microorganisms as a function of the contact time. At short contact times, between 8 and 72 h, the microalgae shows a higher affinity for the more toxic inorganic species As(III) and As(V), with a moderate bioelimination of 13 and 27%, respectively. However, a progressive increase in the bioelimination of the organic species with time is observed, reaching a maximum up to 80% elimination of DMA after 10 days of contact. On the other hand, for activated sludge, the highest affinity for tri- and pentavalent inorganic species is confirmed, resulting in bioelimination percentages up to 80% at a contact time of 1 day for both 0.1 and 0.5 mg/L initial concentrations of arsenic species.

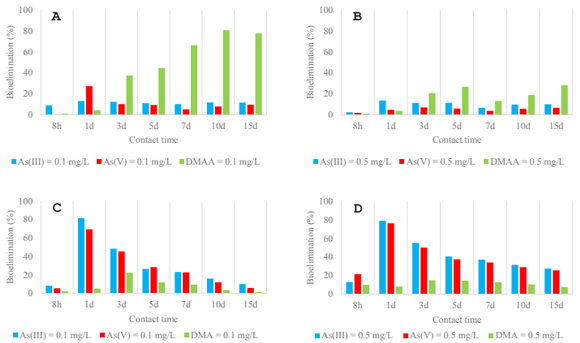

Figure 1. Bioelimination percentages for As(III), As(V) and DMA with the two biomasses tested, *Scendesmus almeriensis* (**A** and **B**) and activated sludge (**C** and **D**) for 0.1 and 0.5 mg/L as initial concentration.

Figure 2 depicts the effect of the arsenic species and concentration on the viability of the biomasses. After 15 days of contact with As species, a progressive growth of microalgae biomass has been observed without causing apparent cell death, while for activated sludge a much faster growth is observed, not needing an acclimatization time as the microalgae exhibits. Maximum biomass concentrations of 2.65 and 4.79 g/L were reached for microalgae and activated sludge, respectively.

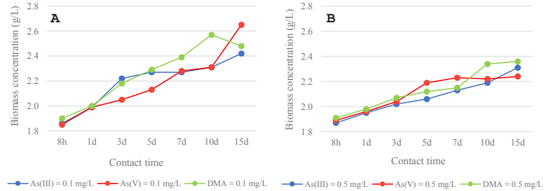

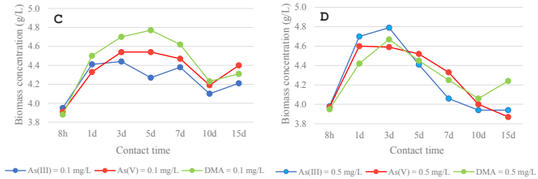

Figure 2. Biomass concentration for the experiments spiked with As(III), As(V) and DMA with the two biomasses tested, *Scendesmus almeriensis* (**A** and **B**) and activated sludge (**C** and **D**) for 0.1 and 0.5 mg/L as initial concentration of each arsenic species.

After 15 days of contact time of both biomasses with arsenic species it was observed the complete oxidation of As(III) to As(V) in the presence of microalgae, while in the solutions spiked with As(V) and DMA arsenic speciation remained unchanged. For the activated sludge biomass, the conversion of added As(III) into As(V) and DMA is observed, although the latter in lower proportion. When the initial species is As(V), no significant transformation is observed. Finally, when the initial species is DMA between 20-45% is transformed into inorganic As(V).

Acknowledgments
This work was supported by the Spanish "Ministerio de Ciencia e Innovación" (PID2020-113544RB-I00) and the doctorate scholarships of B. Antolín and D. Moldes. The authors also thank the financial support from Regional Government of Castilla y León - FEDER (CL-EI-2021-07).

REFERENCES

Alcántara, C., Muñoz, R., Norvill, Z., Plouviez, M., Guieysse, B. 2015. Nitrous oxide emissions from high rate algal ponds treating domestic wastewater. *Bioresource Technology* **177**, 110–117.
ASAE, 2003. Manure Production and Characteristics American Society of Agricultural Engineers. *American Society of Agricultural Engineers* 682–685.
Bădescu, I.S., Bulgariu, D., Ahmad, I., Bulgariu, L. 2018. Valorisation possibilities of exhausted biosorbents loaded with metal ions – A review. *Journal of Environmental Management* **224**, 288–297.
Gao, S., Hu, C., Sun, S., Xu, J., Zhao, Y., Zhang, H. 2018. Performance of piggery wastewater treatment and biogas upgrading by three microalgal cultivation technologies under different initial COD concentration. *Energy* **165**, 360–369.
Liu, C., Yuan, H., Yang, J., Li, B. 2011. Effective biosorption of reactive blue 5 by pH-independent lyophilized biomass of Bacillus megaterium. *African Journal of Biotechnology* **10**, 16626–16636.

Protein recovery from algal biomass grown in piggery wastewater using deep eutectic solvents

D. Moldes[1,2], B. Antolín[1,2], P.F. Requejo[1,2], M. Vega[1,2] and S. Bolado[1,3]

[1] Institute of Sustainable Processes, University of Valladolid, Spain
(E-mail: *david.moldes@uva.es; beatriz.antolin@uva.es; patricia.fernandez.requejo@uva.es; mariasol.vega@uva.es; silvia.bolado@uva.es)*
[2] Department of Analytical Chemistry, Faculty of Sciences, University of Valladolid, Spain
[3] Department of Chemical Engineering and Environmental Technology, Industrial Engineering School, University of Valladolid, Spain

Abstract

Photobioreactors are a sustainable wastewater treatment alternative capable of removing nutrients and pollutants. Microalgae are photosynthetic microorganisms that, if grown in wastewater with high nitrogen loads, contain a high percentage of protein and could be a promising alternative to the increasing demand for this nutrient. New sustainable solvents are needed to extract the proteins from microalgal biomass selectively. Deep eutectic solvents (DES) are a promising green alternative to traditional protein extraction methodologies using classical organic solvents or alkaline/acidic conditions, which are detrimental to protein stability and planet health. In this work, protein extraction from green microalgae *Scenedesmus almeriensis* grown in swine wastewater has been investigated using DES. The response variables measured were the protein yield and the protein/carbohydrate partition ratio. The effects of the solvent used (choline chloride:glycerol [1:2], choline chloride:urea [1:2], and only water) and the amount of water added to the solvent-biomass suspension (0, 3, 6, and 20 g) were investigated through a full factorial design and quantified by ANOVA.

Keywords
Deep Eutectic Solvents; Extraction with solvents; Microalgae biorefinery; Photobioreactors; Protein recovery

INTRODUCTION

Wastewater pollution is a severe socio-sanitary problem requiring efficient and economically sustainable solutions capable of simultaneously removing water pollutants and converting them into reusable materials while decreasing energy consumption (Zhang et al., 2018). Photosynthetic reactors are emerging as a cost-effective alternative to conventional biological wastewater treatment with promising results. These photobioreactors are based on the cultivation of microalgae, which consume CO_2, produce O_2 and assimilate nutrients from the wastewater (García et al., 2019), converting them into potentially valuable compounds (proteins, sugars, bioactive compounds, or oils). The protein fraction of the grown biomass is a source of peptides, valuable as bio-stimulants in agriculture or as amino acids for animal feed (Gao et al., 2020). However, obtaining proteins from microalgae is a complex process, as they must be separated from the rest of the biomass components. Classical methods employ toxic substances and harsh conditions, which are detrimental to the planet's health and protein stability. Thus, new efficient, selective, and sustainable methodologies for protein recovery from biomass are needed. In this context, deep eutectic solvents (DES) prepared from natural compounds are a promising option as extraction agents since they present a lower environmental impact than conventional solvents (Mehariya et al., 2021).

MATERIALS AND METHODS

Protein recovery from the algal biomass based on *Scenedesmus almeriensis* grown in swine wastewater has been investigated. The effect of water on the extraction of protein has been evaluated, as it is present in fresh microalgal biomass and can reduce solvent viscosity, which might improve the extraction performance. A full factorial experimental design has been carried out studying two factors: the type of solvent (choline chloride:glycerol [1:2], choline chloride:urea [1:2] and only water), and the amount of water added to the solvent-biomass suspension (0, 3, 6, and 20 g). The extraction experiments were performed in duplicate on lyophilized biomass for 1 hour at 25 ºC, with the solvent-to-biomass ratio fixed at 9:1 (in mass). The research aims to maximize the recovery of proteins while reducing carbohydrate extraction, as they may hinder later protein applications. Therefore, two response variables were monitored: the protein recovery yield (PRY) and the protein/carbohydrate partition ratio (PCR). Quantification of proteins and carbohydrates in the extracts was carried out spectrophotometrically using the BCA protein assay and the phenol-sulfuric acid method, respectively. An Analysis of Variance (ANOVA) was performed at a significance level of 0.05 to evaluate the significant factors for each response variable. Subsequently, post hoc pairwise multiple comparisons of means using the Fisher's Least Significant Difference (LSD) test was applied to identify the optimal levels of the factors causing significant differences in the response variables.

RESULTS AND DISCUSSION

The ANOVA of the results showed that the type of solvent and the amount of added water were factors with a significant effect on PRY and PCR (p-values < 0.05). The use of DES increased significantly, and simultaneously, the yield and selectivity of the protein extraction with respect to the values obtained when water was the only extractant. The improvement in PCR was attributed to the increased polarity of the extraction media containing DES. Adding water to the DES-biomass suspension also improved PRY and PCR and facilitated the handling of the samples during the extraction process. The optimum extraction conditions were choline chloride:glycerol (1:2) with 20 g of water, achieving 20.8 of PRY and 1.6 of PCR. Only a few works published to date use DES to extract proteins from microalgae, obtaining similar or lower recoveries even using ultrasonication or ball milling as extraction aids (Cicci et al., 2017). Therefore, despite the low PCR values obtained, our results are promising, and further research is in progress to improve the selectivity and yield of protein extraction using DES.

Acknowledgments
This work was supported by the "Ministerio de Ciencia e Innovación" of Spain (PID2020-113544RB-I00) and the doctorate scholarships of D. Moldes and B. Antolín. The authors also thank the regional government of Castilla y León (CL-EI-2021-07) for the financial support.

REFERENCES

Cicci, A., Sed, G., Bravi, M., 2017. Potential of choline chloride-based natural deep eutectic solvents (NaDES) in the extraction of microalgal metabolites. Chem. Eng. Trans. **57**, 61–66.
Gao, J., Weng, W., Yan, Y., Wang, Y., Wang, Q., 2020. Comparison of protein extraction methods from excess activated sludge. Chemosphere **249**.
García, D., de Godos, I., Domínguez, C., Turiel, S., Bolado, S., Muñoz, R., 2019. A systematic comparison of the potential of microalgae-bacteria and purple phototrophic bacteria consortia for the treatment of piggery wastewater. Bioresour. Technol. **276**.
Mehariya, S., Fratini, F., Lavecchia, R., Zuorro, A., 2021. Green extraction of value-added compounds from microalgae : A short review on natural deep eutectic solvents (NaDES) and related pre-treatments. J. Environ. Chem. Eng. **9**, 105989.
Zhang, W., Alvarez-Gaitan, J.P., Dastyar, W., Saint, C.P., Zhao, M., Short, M.D., 2018. Value-added products derived from waste activated sludge: A biorefinery perspective. Water (Switzerland).

Use of Industrial Magnetite in Wastewater Treatment

Y. Arbid*, B. Mathon**, B. Cedat**, K. Hanna*

*Université Rennes, Ecole Nationale Supérieure de Chimie de Rennes, CNRS, ISCR-UMR 6226, Rennes F-35000, France (E-mail: yara.arbid@ensc-rennes.fr; khalil.hanna@ensc-rennes.fr)
**Treewater, 61 rue de la République, 69002 Lyon, France (E-mail: bmathon@treewater.fr; bcedat@treewater.fr)

Abstract
In this work, the efficiency of an industrial magnetite (M1) produced from ferrous wastes to catalyze Fenton reactions in laundry wastewater at pH 6 was investigated. Its reactivity was assessed towards the degradation of two environmental compounds, ciprofloxacin and phenol, under UVC and UVA irradiation, and then compared with that of a synthetic magnetite (SM) and zerovalent iron (ZVI). M1 enhanced ciprofloxacin and phenol degradations under UVC and UVA irradiation respectively. Fe (II)/Fe (III) ratio played a key role while the size and surface area of the particles seemed to be less important. ZVI was found efficient in all cases but its rapid passivation might restrict its application. In addition to being easily magnetically separated, a promoter to photo-Fenton reactions even under circumneutral pH, this "industrial" magnetite made from ferrous wastes can be a promising catalyst in wastewater treatment applications.

Keywords
Ciprofloxacin; industrial magnetite; phenol, photo-Fenton; water treatment

INTRODUCTION

Magnetite is a natural magnetic mineral extensively used as a heterogeneous Fenton catalyst in the Advanced Oxidation Processes (AOPs) [1]. Several studies show that the Fe (II)–Fe (III) mixed valence oxide is a good iron source in the heterogenous Fenton reactions where Fe (II) plays a principal role in their initiation [2]. Its redox properties contribute to its high activity; and its ability to catalyze the oxidative degradation of organic pollutants have attracted the scientific community. Since industrial wastewaters hold a variety of toxic, non-biodegradable organic pollutants, magnetite can be a promising catalyst in Fenton/ photo-Fenton reactions aiming at their removal [3].

Magnetite can be synthesized by many biotic and abiotic pathways in the laboratory; however, to our knowledge, few data exist on the reactivity of magnetites produced from ferrous or steel wastes. Wastes produced from steel industries are abundant in iron oxides; 50 % of the iron is either disposed outside of the companies or accumulated in sedimentation ponds leading to the deterioration of the environment. Hence, recycling and reusing useful parts of the wastes are of pronounced concern [4].

In our experiments, we studied the reactivity of a magnetite produced from steel wastes in the Fenton/ photo-Fenton reactions in laundry wastewater. Laundering processes use large amounts of water; households, hotels, and hospitals pollute water with high COD values [5]. The removal of phenol, a model pollutant, and ciprofloxacin (CIP), a pharmaceutical compound under different conditions (UVC and UVA irradiation) was investigated in the presence of H_2O_2 and magnetite. The reactivity of this magnetite was compared to that of a synthetic magnetite produced in the laboratory via co-precipitation and zerovalent iron (ZVI). Furthermore, TOC of the wastewater was measured before and after the reactions.

MATERIALS AND METHODS

Experiments were conducted on 2 magnetites (M1 and SM) and zerovalent iron (ZVI). M1 was provided by Hymag'in, SM and ZVI were prepared in the lab as explained in detail in previous works [6][7].

Magnetites were characterized by XRD to identify the crystal structures, TEM to obtain information regarding morphology and size of particles, and N_2–BET analysis to determine their specific surface areas. The Fe (II) content in the oxide structure was determined by chemical analysis after acid dissolution with HCl. Ferrous and total iron concentrations were determined using a modified 1,10-phenanthroline method.

In a glass reactor (20 ml), the target compounds (20 µM) and H_2O_2 (25 mM) as well as the magnetites/ ZVI (0.1 g/L) were added to the laundry wastewater (pH ~ 7, TOC= 54 mgC/L, COD= 891 mgO_2/L of the raw wastewater). The pH was adjusted to 6 and irradiation took place under UVA (365 nm, 0.55 mW/cm^2) or UVC (254 nm, 0.87 mW/cm^2) lamps. Samples taken at specific time intervals were analyzed by HPLC-UV to monitor P and CIP degradations. After that, TOC was measured by a TOC analyzer. Solutions of spiked laundry wastewater, magnetite/ ZVI, and H_2O_2 (50 mM) were irradiated under UVA or UVC for 2 days.

Table 1. Some properties of the magnetite samples used in this study.

Magnetites	Specific surface area	Particle size	Fe (II)/Fe(III)
	(m^2/g)	(nm)	-
M1	18,5	100-600	1
SM	89	10-15	0,48

RESULTS AND DISCUSSION

Characterization of magnetites

Magnetite purchased from Hymag'in is called M1 (industrial magnetite) while the lab-synthesized magnetite is called SM (synthesized magnetites). Table 1 shows that they exhibit different specific surface areas and particle sizes. The ratio Fe (II)/Fe (III) was determined and reported in the table as it is a key parameter in heterogeneous Fenton reactions. SM has a high ratio of ~0.5 "stoichiometric magnetite" since it was prepared in a glove box by co-precipitation. However, M1 has a much higher ratio (i.e.1), which is probably due to the presence of elemental metal traces including Fe (0).

Photo-Fenton degradation of ciprofloxacin and phenol

Preliminary experiments showed that the photo-Fenton system with magnetite had an optimal loading of 0.1 g/L, and that 25 mM H_2O_2 was efficient for a complete degradation of 20 µM ciprofloxacin and phenol. Therefore, such conditions were chosen to compare the behavior of different magnetite samples and ZVI.

Photo-Fenton degradation of ciprofloxacin. **Fig.1** reports the time trend of ciprofloxacin degradation in the photo-Fenton system under UVC (left-hand side) and UVA (right-hand side) irradiation at pH ~6 in the presence and absence of magnetites/ZVI.
The left-hand side of the figure shows that almost complete ciprofloxacin degradation was achieved in 2 h in the presence and absence of magnetite. However, ciprofloxacin degradation was faster in the presence of magnetite especially in the first 40 min before the slowing down of the reaction. Although the kinetic behavior was similar, ciprofloxacin degradation after 2 h-irradiation was slightly faster with M1. Experiments with ZVI induced effective degradation.

Experiments under UVA irradiation showed that ~60 % of ciprofloxacin after 4 h was degraded in the presence of M1 and SM while ~80% was observed after 4 h in the presence of ZVI. Unlike experiments under UVC irradiation, the graph shows no difference in CIP degradation in the presence or absence of magnetite. The variation in the degradation profiles may be due to the nature of the laundry wastewater. It contains organic matter (TOC 54 mgC/L), metals, anions, etc.

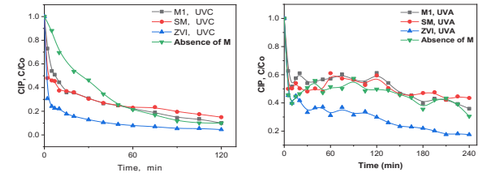

Figure 1 Time trend of ciprofloxacin (initial concentration 20 µM, pH 6 by $HClO_4$) under photo-Fenton conditions (ciprofloxacin + H_2O_2 + magnetite/ ZVI + UVC/UVA) and in the

Photo-Fenton degradation of phenol. **Fig.2** shows that in the presence or absence of magnetites/ ZVI, a high phenol degradation was achieved in less than 2 h. The reaction between phenol and $^{\bullet}OH$ has a high rate constant ≈ 6.6 x 10^9 M/s and the presence of UVC (energetic light) produces a high concentration of radicals that can directly degrade the pollutant. Magnetite had a slight screening effect.

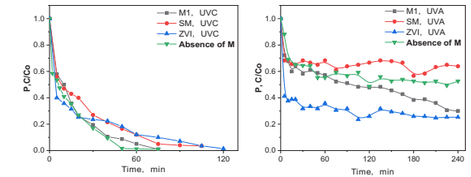

Figure 2 Time trend of phenol (initial concentration 20 µM, pH 6 by HClO4) under photo-Fenton conditions (phenol + H2O2 + magnetite/ ZVI + UVC/UVA) and in the absence of magnetite/ ZVI.

Under UVA, (right-hand side of **Fig.2**), phenol degradation was clearly enhanced in the presence of M1 and ZVI compared to that in the absence of a catalyst. SM, in this case, might have a screening effect. This could be due to the high Fe (II)/ Fe (III) ratio of M1 compared to SM and to the ZVI high reductive capacity. In all cases, a 60-90 % degradation was achieved with a higher removal of phenol under UVC light than under UVA.

TOC measurement. Preliminary experiments with SM (0.1 g/L), ciprofloxacin (20 µM), H_2O_2 (50 mM) under UVC irradiation at pH 6 showed almost complete mineralization in 2 days. The TOC was halved in around 1 day, TOC values decreased from 54 mgC/L to around 20 mgC/L. These experiments can show how the photo-Fenton reaction can progress over time.

The AOPs, specifically photo-Fenton, are effective in removing pollutants from wastewaters. In our experiments, M1 was a good catalyst to the reaction inducing a higher degradation than in the presence of SM or absence of catalyst; especially with ciprofloxacin (under UVC irradiation) and phenol (under UVA irradiation). Although ZVI greatly enhanced the removal of both pollutants, its rapid passivation limits possible applications. Besides being accessible and produced from ferrous/ steel wastes M1showed a promising reactivity to be used for high-scale applications.

Further experiments will focus on the TOC measurement to better understand the evolution of the photo-Fenton reaction with time as well as the metals adsorption before and after the treatment. Fe leaching and H_2O_2 consumption will also be monitored.

REFERENCES

[1] Rahim Pouran S., Abdul Raman A. A., Wan Daud W. M. A. 2014 Review on the application of modified iron oxides as heterogeneous catalysts in Fenton reactions. *J. Clean. Prod.*, vol. 64, 24–35.

[2] Minella M..Marchetti G., De Laurentiis E., Malandrino M., Maurino V., Minero C., Vione D., Hanna K. 2014 Photo-Fenton oxidation of phenol with magnetite as iron source. *Appl. Catal. B Environ.*, vol. 154–155, 02–109.

[3] De Jesus J. H. F., Lima K. V. L., Pupo Nogueira R. F., 2022 Copper-containing magnetite supported on natural clay as a catalyst for heterogeneous photo-Fenton degradation of antibiotics in WWTP effluent. *J. Environ. Chem. Eng.*, vol. 10, 107765.

[4] Somova Y. V., Sviridova T. V., Alekseeva P. A., Nekerov E. A., Schwabecher D. 2021 Analysis of methods for processing oily mill scale and oily sludge for iron and steel production. *IOP Conf. Ser. Earth Environ. Sci.*, vol. 839.

[5] Šostar-Turk S., Petrinić I., Simonič M. 2005 Laundry wastewater treatment using coagulation and membrane filtration. *Resour. Conserv. Recycl.*, vol. 44, 185–196.

[6] Cheng W., Marsac R., Hanna K. 2018 Influence of Magnetite Stoichiometry on the Binding of Emerging Organic Contaminants. *Environ. Sci. Technol.*, vol. 52, 467–473.

[7] Bae S., Gim S., Kim H., Hanna K. 2016 Effect of NaBH4 on properties of nanoscale zero-valent iron and its catalytic activity for reduction of p-nitrophenol. *Appl. Catal. B Environ.*, vol. 182, 541–549.

FlashPhos: The complete thermochemical recycling of sewage sludge

S. Arnout*, M. Rapf**, A. Kotze*, Y. Cryns*, D. Messina* and E. Nagels*

* InsPyro, Ambachtenlaan 54, 3001 Leuven, Belgium
(E-mail: *sander.arnout@inspyro.be*; *andrea.kotze@inspyro.be; yannick.cryns@inspyro.be; davide.messina@inspyro.be; els.nagels@inspyro.be)*
** University of Stuttgart, Institute for Sanitary Engineering, Water Quality and Solid Waste Management, Bandtäle 2, 70569 Stuttgart
(E-mail: *matthias.rapf@iswa.uni-stuttgart.de*)

Abstract
Elemental white phosphorus is a strategic raw material, while sewage sludge is a P-rich waste material abundantly available in Europe. FlashPhos intends to be the first technology in Europe producing white phosphorus from sewage sludge, with a high energetic efficiency and zero waste production. This paper discusses the process, the planned pilot plant, and the initial lab scale results.

Keywords
Phosphorus recovery; sewage sludge; thermal process; white phosphorus

INTRODUCTION

Elemental white phosphorus is a strategic raw material with high criticality due to its irreplaceability for key industries, for example in the food, pharmaceutical and electronic sector. Currently, the European Union is completely dependent on white phosphorus imports from Kazakhstan, Vietnam and China. Yet, there are enough phosphorus reserves in Europe veiled in sewage sludge to cover the EU's whole demand on white phosphorus plus up to 25% of the phosphate consumed in the EU for other applications.

Sewage sludge, on the other hand, is a waste inevitable in every industrial country. In the EU it is forbidden to landfill sewage sludge due to its high organic content. Thermal treatment is not an alternative for many countries due to high costs, so most of the European sewage sludge is used as fertiliser or soil enhancer. However, regarding soil application, it must not be forgotten that sewage sludge is the sink for all contaminants removed from sewage, including microplastics and pharmaceuticals.

Hence, in several European countries, soil application of sewage sludge is already forbidden or will be stopped in a few years. Also in the EU, there are efforts to reduce this practice, which will require viable solutions in the medium term. The new FlashPhos process can offer a solution to sustainably dispose of sewage sludge and recover phosphorus from it. Accepting mechanically dewatered sludge as it comes from sewage plants, and being attached to industries available all over Europe, FlashPhos will be applicable also in countries still far from fulfilling present or coming EU sludge regulations.

FlashPhos intends to be the first technology in Europe producing white phosphorus for the chemical industry, providing at the same time a solution for the problematic sewage sludge disposal. It is expected that FlashPhos plants will be able to cover 50% of the European P_4-demand by 2040. This will be possible by recycling 15% of the sludge currently generated in Europe.

FlashPhos will significantly contribute to major objectives of the European society:

- **Recover a critical raw material (CRM)**, white phosphorus (P_4). The P_4 produced following FlashPhos' principles will avoid that equivalent P_4 will be produced in other places, consuming natural mined Phosphate Rock, which is a finite world resource. P_4 from FlashPhos will consume less energy and have a higher purity than the P_4 currently available on the market.
- **Reduce the emission of CO_2** by substituting cement clinker – one of the products with the highest CO_2-production worldwide – by alternative cement materials. FlashPhos will be connected to cement plants that will use FlashPhos' fuel gas and waste heat to replace fossil fuels, without disturbing the cement process with phosphorus, which has a negative influence on cement quality. This will increase the cement industry's capability of substituting fossil energy by wastes and still comply with coming phosphorus regulations.
- **Reduction of waste generation** and contributing to reliable long-term-available waste treatment capacities by thermally treating sewage sludge, safely removing the sludge's contaminants from the biosphere.

THE FLASHPHOS PROCESS

The first step of the FlashPhos process is an innovative dryer-grinder, producing fine and dry materials as an input to the Flash reactor.

The second step, the actual "Flash" process, is a high temperature entrained flow (flash) gasification of sewage sludge, and other phosphate-containing waste streams such as meat-and-bone meal. The organic components of the sewage sludge serve as fuel for the gasification, in which they are converted into heat and a combustible gas. This gas and excess heat can be used in cement plants to substitute fossil fuels. The inorganic waste components are melted or evaporated.

The molten inorganic materials are then treated further in a refiner reactor to produce recycled P_4 as the main product. Other output materials of the process are a climate-friendly alternative cement raw material, an iron alloy and a heavy metal concentrate as valuable raw materials for the metal industry. Consequently, practically no solid wastes are produced by the FlashPhos process.

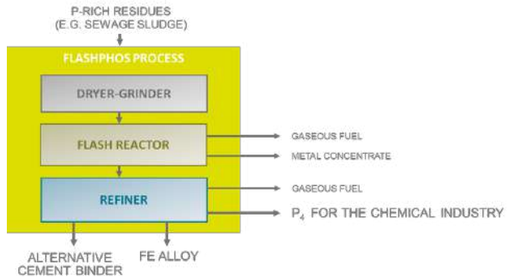

Figure 1. All figures should be embedded correctly positioned within your Word file.

During the four-year innovation action, the industrial FlashPhos process will be demonstrated in a pilot plant with up to 250 kg/h sewage sludge throughput. The first full-scale FlashPhos pilot plant in Europe will be built by 2025 and will provide the basis for industrial scale white phosphorus production. The industrial scale market introduction is expected by 2028.

Currently, the process is in the design and commissioning phase, with extensive support from work packages providing modelling, experimental results, and risk analysis. As part of the experimental work, the thermal behaviour of sewage sludge is investigated on lab scale by InsPyro. These results, discussed in the next paragraph, are important to select process conditions to design the pilot plant and optimize its operations.

EXPERIMENTAL RESULTS

Thermal behaviour

Combustion, melting and reduction of sludge from different sources are studied both theoretically and experimentally in DSC-TGA and lab furnaces. Theoretical values from thermodynamic calculations, such as the expected melting point, gas-metal-slag equilibria and enthalpies corroborate the results. The P-yield is further evaluated in larger scale experiments, in which the behaviour of impurity elements is studied as well. These results are crucial to the quality of the end products: elemental phosphorus, iron alloy and supplementary cementitious material.

In this paper, the focus is on the behaviour of the combusted sludge (ash). The melting behaviour (weight loss and heat of melting) of the ash is shown in Figure 2. Melting is found to occur between 1100 - 1250°C and is accompanied by a small weight loss (possibly loss of oxygen, e.g. Fe_2O_3 to FeO), as well as an endothermic reaction from which the melting enthalpy can be derived.

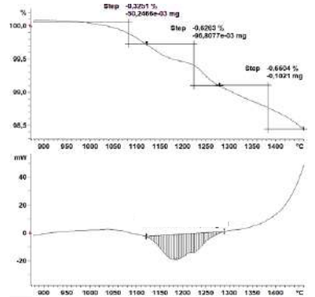

Figure 2: Melting behaviour of ash in an inert atmosphere.

The reduction of the ash is shown in Figure 3. From the curve, it can be observed that the reaction with carbon speeds up around 1300°C. After some 15 min, while reaching 1400°C, limited further reduction is observed. The continued decrease of the sample weight is also due to the minor but continuous loss of carbon to the gas phase. The influence of different temperatures, basicities and carbon particle size is also evaluated but not included in this article.

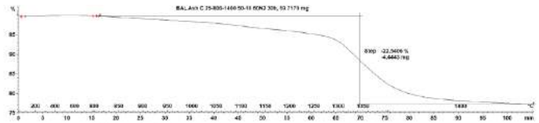

Figure 3: Reduction of ash with carbon in inert N_2 atmosphere.

The results from the DSC-TGA are also compared with thermodynamic calculations conducted in FactSage 8.2. The calculated melting temperature of the combusted slag are in line with those measured in Figure 2. Reduction calculations indicate vapour formation, because of the formation of mainly CO and P_2 gas, of up to 20% of the initial mass, which is in line with the results in Figure 3. These thermal behaviour experiments and calculations determine the optimal operating conditions for the sludge combustion and the refining process. The experiments confirmed recovery of between 50-80% of the phosphorus depending on the sludge origin, which is in line with thermochemical models.

CONCLUSIONS

The FlashPhos process targets the recovery of white phosphorus from sewage sludge, thereby providing a European source of a critical raw material for the chemical industry, and providing a valuable waste-free outlet for sewage sludge. The pilot scale plant will be constructed in the next few years. Initial results at smaller scale define the needed temperatures and confirm the expected recovery yields.

ACKNOWLEDGMENT

This project has received funding from the European Union's Horizon 2020 research and innovation programme under grant agreement No. 958267.

Study of struvite precipitation in a fluidised bed reactor using synthetic supernatant

V. B. Aguilar-Pozo*,**, S. Peña-Picola**, J. M. Chimenos* and S. Astals**

* Department of Materials Science and Physical Chemistry, University of Barcelona, 08028 Barcelona, Spain (E-mail: veronicaguilar@ub.edu, chimenos@ub.edu)
** Department of Chemical Engineering and Analytical Chemistry, University of Barcelona, 08028 Barcelona, Spain
(E-mail: *spenapicola@ub.edu, sastals@ub.edu)*

Abstract
Struvite precipitation in wastewater treatment plants could solve the rapid depletion of phosphorus in the world. This process requires a magnesium source and an alkaline reagent, which limit the process economically. This study used a magnesium oxide by-product as the sole reagent to precipitate struvite in a laboratory-scale fluidized-bed reactor. By-product quantity, feed inlet positions and recycle flow rates were studied. The results showed a struvite content higher than 75%. There were two configurations that reached a struvite percentage of 90%, the only different variable being the recirculation flow rate (215.86 and 907.07 mL/min).

Keywords
Fluidized-bed reactor, magnesium oxide by-product, phosphorus, recovery and struvite.

INTRODUCTION

High phosphorus (P) concentrations in Anaerobic Digester (AD) supernatant from wastewater treatment plants (WWTP) (Peng et al., 2018a) could solve the rapid depletion of P rocks and meet 15-20% of global demand (Peng et al., 2018b). P precipitation as struvite has gained interest since it can be used as a slow release fertilizer and simultaneously recovers phosphorus and nitrogen (N). Besides that, controlled precipitation could prevent the auto-precipitation in pipes and elbows of WWTP (Ye et al., 2018). However, this process requires the addition of magnesium (Mg) and alkaline chemicals to increase pH (Ye et al., 2018). The magnesium and other reagents (NaOH) utilized may account for 75% of the overall costs of struvite production (Peng et al., 2018a). For this reason, inexpensive magnesium sources are studied.

This work shows a study of the MAGNYFOS project (RTC2019-007257-5). Where an industrial magnesium oxide by-product (LG-MgO) is used as a Mg source and alkaline reagent for the struvite precipitation in a laboratory-scale fluidized-bed reactor (FBR). LG_MgO has around 56% of MgO and others as $MgCO_3$, $CaMg(CO_3)_2$. Its price is 10 times cheaper than $MgCl_2$ (pure reagent). The use of LG-MgO can reduce reagent costs and revalue an industrial by-product.

MATERIALS AND METHODS

Synthetic supernatant and industrial by-product of magnesium oxides

Synthetic supernatant was prepared using distilled water, dipotassium hydrogen phosphate (K_2HPO_4) and ammonium chloride (NH_4Cl). The concentrations in solution were 80 mg/L of P-PO_4 and 600 mg/L of N-NH_4, respectively. The pH of the solution was not adjusted.
LG-MgO was provided by Magnesitas Navarras, S.A. (Navarra, Spain). This is a by-product from the natural magnesite calcination process. LG-MgO has 56.04% of MgO, 12.04% of $MgCO_3$, 11.59% of $CaCO_3$, 8.55% of $CaMg(CO_3)_2$, 3.75% of $Mg(OH)_2$, 2.24% of $Ca(OH)_2$ and others. The mean diameter was 12 µm.

Experiment set-up

The struvite precipitation was carried out in a laboratory-scale FBR. The glass reactor was designed with two sections of increasing diameter and three sampling points (Figure 1). The working volume was 4,89 L and the hydraulic retention time (HRT) was 2.5 hours. Two peristaltic pumps were used to feed the reactor and control the recycle flow rate.
Twelve experiments were performed to study the most suitable configuration for precipitating struvite. The study variables were molar ratios between P and Mg (magnesium concentration was calculated from LG-MgO composition), feed inlet positions, and recycle flow rates.
The procedure was (i) addition of the LG-MgO into the reactor, (ii) start-up of the feed pump, (iii) start-up of the recycle pump, (iv) stopping both pumps after 5 hours and (v) recovering the solid. The sample interval was 0, 30, 60, 120, 180, 240, and 300 minutes and 4mL of liquid was withdrawn. Initial conditions for each experiment are shown in Table 1.

Analytical methods

The samples were filtered using a 0.45 µm regenerated cellulose syringe filter. Then pH, anions (P-PO_4) and cations (Ca^{2+}, Mg^{2+} and N-NH_4) were measured.
The precipitated solid was dried at 25 ºC. After the solid was characterised by thermogravimetric analysis (TGA), X-ray diffraction (XRD) and particle size distribution (PSD).

RESULTS AND DISCUSSION

Figure 2 shows the P and Mg concentrations in the effluent (reactor outlet stream). The addition of a 1:3.3 molar ratio (P:Mg) succeeded in continuously decreasing the P concentration to values of about 3-4 mg/L. However, high concentrations of Mg were lost to the effluent. The experiments with a 1:1 ratio showed that the P concentration decreased during the first 30 minutes (10.12 mg/L), then remained constant until minute 180, then increased and reached concentrations of 17-19 mg/L. Mg loss decreased over time and concentrations reached of around 31 mg/L. When the molar ratio was 1:0.5, there was a continuous loss of P between 20 and 30 mg/L. Mg was also detected in the effluent, although the amount added was less than the amount necessary for struvite formation.

XRD diffractograms of the 12 experiments showed the presence of struvite, MgO, $MgCO_3$, $CaMg(CO_3)_2$ and $Mg(OH)_2$. Bhuiyan et al. (2008) reported that the decomposition reaction of struvite (Eq. 1) began at around 55 ºC ended around 250 ºC. In this study, the results of the TGA showed that the decomposition temperature range was 60 to 200 ºC. The weight loss percentage of struvite was followed through NH_3 and H_2O (Ray L. et al., 2004). The struvite percentage in each experiment was estimated (Table 2). When the ratio was 1:0.5, a high recycle flow rate favoured the formation of struvite (Ex. 2 and 4), reaching 85%. This may be due to a higher homogeneity of Mg in the reactor. If one wants to work with low recycle flow rates, the feed inlet should be at the bottom of the reactor. The feed comes into direct contact with the LG-MgO particles, since at low recycle flow rates they mostly fluidise in the lower part of the reactor. At a 1:1 molar ratio and bottom feed position, the highest percentage of struvite formation was achieved (91-92%) and the variation of the recycle flow rate had almost no influence. When there was an excess of Mg (1:3.3), the percentage of struvite in the precipitate decreased (ex. 9, 10, 11 and 12), this may be due to the higher amount of undissolved LG-MgO.

$$MgNH_4PO_4 \cdot 6H_2O \rightarrow MgHPO_4 + NH_3 + H_2O \qquad \textbf{Eq. 1}$$

Configurations with low recycle flow rates had larger particle sizes than high flow rate configurations, except for configuration 4 with respect to configuration 3 (Table 2). A higher mixing intensity reduces induction time and particle size (Elduayen-Echave, 2020).

Table 1. Initial conditions of the twelve experiments in the FBR.

Nº	Feed position	P:Mg^{2+}	LG-MgO (g/L)	Recycle flow rate (mL/min)	Feed flow rate (mL/min)
1	Side	1:0.5	0.08	215.86	32.60
2	Side	1:0.5	0.08	907.07	32.60
3	Bottom	1:0.5	0.08	215.86	32.60
4	Bottom	1:0.5	0.08	907.07	32.60
5	Side	1:1	0.16	215.86	32.60
6	Side	1:1	0.16	907.07	32.60
7	Bottom	1:1	0.16	215.86	32.60
8	Bottom	1:1	0.16	907.07	32.60
9	Side	1:3.3	0.50	215.86	32.60
10	Side	1:3.3	0.50	907.07	32.60
11	Bottom	1:3.3	0.50	215.86	32.60
12	Bottom	1:3.3	0.50	907.07	32.60

Table 2. Struvite percentage and mean diameter of the recovered solid for the 12 experiments.

Nº	Struvite (%)	Mean diameter (µm)
1	78.42	37.45
2	85.93	37.17
3	83.00	26.94
4	84.55	51.09
5	87.01	47.63
6	87.89	32.6
7	91.28	32.97
8	92.50	16.77
9	78.16	14.37
10	75.16	14.36
11	76.97	17.14
12	83.97	15.98

Figure 1. Laboratory-scale fluidized-bed reactor.

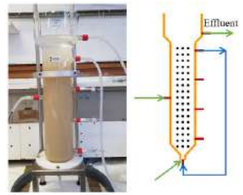

Figure 2. Experimental results of Mg and P monitoring in the effluent of the twelve experiments.

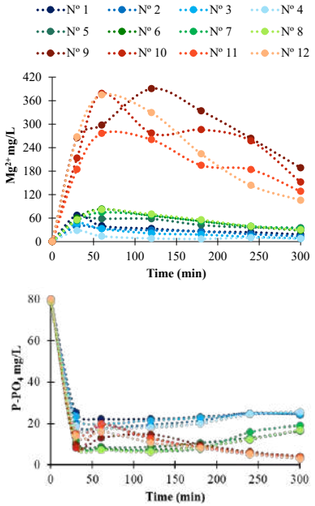

REFERENCES

Bhuiyan, M.I.H., Mavinic, D.S., Koch, F.A. 2008 Thermal decomposition of struvite and its phase transition. *Chemosphere* **70**, 1347–1356.
Elduayen-Echave, B., Azcona, M., Grau, P., Schneider, P.A. 2020 Effect of the shear rate and supersaturation on the nucleation and growth of struvite in batch stirred tank reactors *Journal of Water Process Engineering* **38,** 101657.
Peng, L., Dai, H., Wu, Y., Peng, Y., Lu, X. 2018a A Comprehensive Review of the Available Media and Approaches for Phosphorus Recovery from Wastewater *Water Air Soil Pollut* **229**, 115.
Peng, L., Dai, H., Wu, Y., Peng, Y., Lu, X. 2018b A comprehensive review of phosphorus recovery from wastewater by crystallization processes *Chemosphere* **197**, 768–781.
Ye, Y., Ngo, H.H., Guo, W., Liu, Y., Chang, S.W., Nguyen, D.D., Liang, H., Wang, J. 2018 A critical review on ammonium recovery from wastewater for sustainable wastewater management *Bioresource Technology* **268**, 749–758.

Integrated Resource Recovery from Aerobic Granular Sludge Plants

Nouran T. Bahgat [a,b,⋆], Philipp Wilfert[b], Leon Korving[a], MarkC.M. van Loosdrecht[b]
[a] Wetsus, European Centre Of Excellence for Sustainable Water Technology, Oostergoweg 7, 8911 MA, Leeuwarden, The Netherlands
[b]Dept. Biotechnology, Delft University of Technology, Van der Maasweg 9, 2629 HZ Delft, The Netherlands
⋆ Corresponding author: Phone: +31(0)582843000; E-mail: t.m.s.m.bahgat@tudelft.nl

Abstract
This study evaluated the combined phosphorus, nitrogen, methane, and extracellular polymeric substances (EPS) recovery from aerobic granular sludge wastewater treatment plants. The study showed that 30% of sludge organics are recovered as EPS, and 25-30% can be recovered through integrated alkaline anaerobic digestion (AD) producing ≈260 ml methane/g VS. It also showed that 20% of excess sludge total phosphorus (TP) ends in the EPS, 20-30% in the acidic liquid by-product stream (≈600 mg PO_4-P/L), and 15% in the AD liquid effluent (≈800 mg PO_4-P/L) which can be recovered through an integrated chemical precipitation unit. Ammonium recovery from the alkaline high-temperature liquid stream is attractive but it is not feasible for existing large-scale established technologies because of low concentrations. However, ammonium concentration in AD liquid effluent was calculated to be 2600 mg NH_4-N/L and ≈20% of total nitrogen in sludge, making it feasible for recovery. The methodology used in this study consisted of three main steps. The first step was developing a laboratory protocol mimicking large-scale EPS extraction conditions. The second step was establishing mass balances over EPS extraction on laboratory and demonstration scales within a full-scale AGS WWTP. Finally, the feasibility of resource recovery was evaluated based on concentrations, loads, and integration of existing technologies for resource recovery.

Keywords: Nereda®, mass balances, phosphate, methane, ammonium

INTRODUCTION

A Dutch public-private partnership led to the development of the full-scale aerobic granular sludge technology, also known as "Nereda technology" for wastewater treatment. The study of AGS not only opened a door for a new, more resource-efficient wastewater treatment technology (Pronk et al., 2015) but also created new opportunities for resource recovery, with the recovery of extracellular polymeric substances (EPS) as a successful example. EPS is a polymeric gel material produced by bacteria during cell metabolism that consists of proteins, polysaccharides, DNA, lipids, glycoproteins, and humic substances that form the matrix in which the cells are immobilized as granular particles (Seviour et al., 2019). Recovered EPS from aerobic granular sludge are flexible, practical, versatile, and valuable in agriculture, building, textile, and paper industries (Feng et al., 2019). The Netherlands has the world's first two demonstration-scale installations to extract EPS polymers from Nereda® granules under the product name "Kaumera".

The fate of nutrients through the EPS extraction process is unknown. A careful analysis of the EPS production process is vital to identify the best synergies to combine these elements' recovery within the EPS extraction process. Mass balances can provide insight into how and what to expect from integrated recovery technologies to evaluate these synergies. Mass balances are a robust decision tool to estimate quantities of elements of interest in all relevant streams and recovery potential, make value chains, and evaluate market potential. Concentrations are also crucial in technology selection and its efficiency. This study used mass balances over the EPS extraction in the lab and demonstration scale plant in municipal sewage Epe WWTP to evaluate combined recovery. We aim to set the foundation for future AGS-based resource factories by answering two main research questions. The recovery% potential of combined phosphorus, nitrogen, EPS, and methane from AGS is the first question. To answer that, a modified laboratory protocol for EPS extraction was developed to mimic demonstration-scale conditions, and mass balances were established both on laboratory and demonstration scales in Epe and extrapolated to a full-scale Nereda AGS WWTP. The second question is about the possible existing technologies that can be applied to have a fully integrated AGS WWTP to recover these elements. To address this, concentrations, stream composition, speciation of nutrients, and loads were used to evaluate the feasibility of existing technologies.

MATERIALS AND METHODS

Laboratory EPS extractions were performed using AGS surplus sludge samples collected from Epe AGS WWTP. Extractions were performed based on a newly developed modified protocol adapted from demonstration-scale practices in Epe and Zutphen, The Netherlands.

The resemblance/differences between laboratory extractions and Epe demonstration extraction installations were assessed. Epe WWTP was the first full-scale domestic wastewater treatment plant in the Netherlands to install the innovative Nereda (AGS) sewage treatment technology, and its EPS extraction process installation is the second installation in the Netherlands. Sampling for this mass balance study was performed on a continuous process with a capacity equal to 0.5 m^3 thickened AGS/hour. Mass balances of carbon, phosphorus, and nitrogen were established based on samples analysis and flows, and Epe demonstration-scale mass balances were extrapolated within the context of Epe AGS WWTP. Mass flows were depicted by Sankey diagrams, where flow sizes are proportional to the waste sludge (lab) and wastewater influent (Epe) mass flow expressed in %.

RESULTS AND DISCUSSION

The resemblance between modified lab protocol and demonstration extractions

The total solids, TCOD, total nitrogen, total phosphorus, and dissolved species relevant for nutrient recovery as phosphate, ammonium, calcium, and magnesium ions in the alkaline and acidic liquid streams were compared between the original, modified lab protocol developed in this study and Epe demonstration. Unlike the original laboratory protocol, the new modified laboratory protocol concentrations are comparable and have the same order of magnitude as the demonstration-scale concentrations.

Carbon Recovery

COD balances showed a 30% EPS yield in the lab and Epe demonstration scales. 50-60% of organics end in the alkaline sludge residue by-product stream, and 25-30% of sludge TCOD can be recovered as methane by AD technology. The AD process is proposed to be mesophilic (35°C) and alkaline (pH=9-11), similar to the characteristics of the alkaline sludge residue after solid-liquid separation. Alkaline conditions are used as an effective pretreatment step for better degradability, higher biogas production, and methane-rich biogas. The potential of methane production using the alkaline sludge residue is calculated to be ≈260 ml/g VS. The first proof of principle batch experiments on digestion of this residue under mesophilic alkaline conditions showed that the methane yield was equal to 200-240 ml/g VS, and the substrate recovered as methane was about 40-50% (unpublished results), which is in line with the calculations in this study. The same experiments also showed that methane content was around 98%, with 2% CO_2.

Phosphorus Recovery

According to the established mass balances, phosphorus recovery is realized in two ways during the EPS chemical extraction process.

Phosphorus Recovery in the EPS

EPS-Kaumera from AGS is a potential example of upcycling P-recovery products as it can substitute some P_4 derivatives, i.e., as flame retardant. Kim et al., 2020 reported that EPS-Kaumera acts as a high-performance bio-based flame retardant as it shows self-extinguishing properties attributed to phosphorus present in the EPS.

Ortho-phosphorus recovery from alkaline, acidic, and digestate liquid streams

Around 25%-20% of TP in sludge on the lab scale and 35%-30% of Epe sludge ends in the alkaline, acidic liquid streams, respectively, as orthophosphates. The phosphate concentration is 600 mg PO4-P/L, comparable to concentrations reported for mature technologies of the full-scale phosphate recovery processes for municipal and industrial wastewater (Desmidt et al., 2015). Chemical precipitation by metal addition as magnesium, calcium, and iron is the most common straightforward technology for orthophosphate recovery from liquid streams. The acidic stream has a low pH=2.2, requiring intensive chemical addition for pH adjustment to form commercial P-recovery products such as struvite, calcium phosphates, or vivianite. On the other side, it is a byproduct stream that would not interfere with the Kaumera production as the EPS is already removed, and the organics interference with the final P-recovery product would be minimal compared to the alkaline liquid stream. The acidic stream seems more promising, so current research is ongoing to validate the possibility of phosphorus recovery in the acidic stream. Orthophosphate fraction in the AD effluent was calculated to be 12% (Epe)-15% (lab) of sludge TP with concentrations ≈700-900 mg PO_4-P/L, showing feasible recovery.

Ammonium Recovery

The concept of recovering ammonium from the alkaline liquid stream is attractive since it has high pH and high temperature, which are required for commercial ammonium recovery technologies as air stripping and membrane stripping. Ammonium recovery should not require more energy than ammonium production by the Haber-Bosch process, so it is highly dependent on concentration. Ammonium concentration in the alkaline supernatant at pH=9 is 105 mg NH4-N mg/L which is too low to be energy efficient recovered (Maurer et al., 2006). However, the ammonium fraction in the anaerobic digestion effluent was calculated to be 17% (Epe) and 25%(lab) of TN in sludge with a concentration of around 2600 mg NH4-N/L, which would make it feasible for nitrogen recovery.

CONCLUSIONS

The modified laboratory protocol developed in this study is an excellent base to predict demonstration /large-scale practice. It can be used for futural experimental work focused on nutrient recovery or to test the effect of different extraction conditions and predict the consequences on a large scale. Mass balances allowed for the quantification of recoverable products, and concentrations allowed for evaluating the technology selection. It was shown that combined EPS, methane, phosphorus, and nitrogen recovery is promising in AGS WWTPs by integrating anerobic digestor, P-chemical precipitation unit and air/membrane stripping for ammonium recovery.

Figure 1. Potential of carbon, phosphorus, and nitrogen recovery from AGS WWTP

Acknowledgments
This work is part of the Water Mining EU project; it has received funding from the European Union's Horizon 2020 research and innovation program under grant agreement No 869474'

REFERENCES

1. Pronk, M., de Kreuk, M. K., de Bruin, B., Kamminga, P., Kleerebezem, R., & van Loosdrecht, M. C. M. (2015). Full-scale performance of the aerobic granular sludge process for sewage treatment. *Water Research*, *84*.https://doi.org/10.1016/j.watres.2015.07.011
2. Seviour, T., Derlon, N., Dueholm, M. S., Flemming, H. C., Girbal-Neuhauser, E., Horn, H., Kjelleberg, S., van Loosdrecht, M. C. M., Lotti, T., Malpei, M. F., Nerenberg, R., Neu, T. R., Paul, E., Yu, H., & Lin, Y. (2019). Extracellular polymeric substances of biofilms: Suffering from an identity crisis. In Water Research (Vol. 151). https://doi.org/10.1016/j.watres.2018.11.020
3. Feng, C., Lotti, T., Lin, Y., & Malpei, F. (2019). Extracellular polymeric substances extraction and recovery from anammox granules: Evaluation of methods and protocol development. *Chemical Engineering Journal*, *374*. https://doi.org/10.1016/j.cej.2019.05.127
4. Kim, N. K., Mao, N., Lin, R., Bhattacharyya, D., van Loosdrecht, M. C. M., & Lin, Y. (2020). Flame retardant property of flax fabrics coated by extracellular polymeric substances recovered from both activated sludge and aerobic granular sludge. *Water Research*, *170*. https://doi.org/10.1016/j.watres.2019.115344
5. Desmidt, E., Ghyselbrecht, K., Zhang, Y., Pinoy, L., van der Bruggen, B., Verstraete, W., Rabaey, K., & Meesschaert, B. (2015). Global phosphorus scarcity and full-scale P-recovery techniques: A review. *Critical Reviews in Environmental Science and Technology*, *45*(4). https://doi.org/10.1080/10643389.2013.866531
6. Maurer, M., Pronk, W., & Larsen, T. A. (2006). Treatment processes for source-separated urine. In *Water Research* (Vol. 40, Issue 17). https://doi.org/10.1016/j.watres.2006.07.012

DESIGN OF A DECISION SUPPORT SYSTEM FOR WASTEWATER SANITATION IN SMALL POPULATION CENTERS IN THE BESÒS-TORDERA CONSORTIUM.

A. Barahona*, M. Folch** and M. Salgot**.

*University of Barcelona, Faculty of Chemistry, Department of Analytical Chemistry and the Environment, Martí i Franquès, 1, 08028 Barcelona (E-mail: abarahqu18@alumnes.ub.edu)
** University of Barcelona, Faculty of Pharmacy, Pedology and Agricultural Chemistry, Av. Joan XXIII 27-3108028 Barcelona (E-mail: mfolch@ub.edu; salgot@ub.edu)

Abstract
The sanitation problem in the small population centers in the Consorci Besòs Tordera (CBT) presents various problems due to the diversity of parameters that govern these systems: the changing orography throughout the basins, the isolation in the headwaters in mountainous relief, among other issues. A set of methods are used that can give us answers to the difficulties presented. Decision support systems (DSS) that produce synergy between the experience of experts and varied information such as that of a database, in silico systems to work this information efficiently.

KEYWORDS
CBT, DSS, environmental management, small population centers, wastewater.

INTRODUCTION

Our priority is the CBT and to analyze the sanitation problem of its small population centers. For this, it is important to identify these nuclei in their varied orography, especially in the mountainous area where the headwaters of the basins are located (ecologically sensitive areas). These nuclei are normally isolated and dispersed, these particularities are what delimit the action of any type of sanitation, which constitutes a challenge to adapt to the relief and isolation. On the other hand, there are other characteristics such as the seasonality of the population, that presents an increase in the number of inhabitants throughout the year (weekends, summer, winter holidays, etc.) which considerably alter the characteristics of the discharges; such as in restaurants and hotels.
This environmental problem has led to the application of a set of tools that, under the heading DSS propose an improvement to decision-making.
It should be added that wastewater treatment will be Nature-based solution systems (NBS) innovating in wastewater treatment in small population centers.

THEORETICAL BACKGROUND

In the 1980s, and due to the complex problem posed by an environmental system with biological variables, DSS were perceived as a tool that offered a large degree of freedom, since it took it to a higher level than where computer models were at that time. At that time, since they did not integrate qualitative knowledge, they presented limitations when dealing with knowledge referred to in situ practice. Today, all the models are integrated, mathematical, statistical, and emerging technologies, as well as artificial intelligence applied to the DSS. In all his context, we are designing a customized DSS for the small nuclei in the CBT through the search for NBS, which are designed systems that imitate and use natural environments with a minimum dependence on mechanical elements, to carry out the water sanitation process.

OBJECTIVES

-Design a decision support system for wastewater treatment in small seasonal population centers in the Consorci Besòs-Tordera.
-Exclusively use the NBS for the treatment of wastewater treatment systems.

METHOD

The database of the CRAI (Learning and Research Resource Center) of the University of Barcelona is used as the main tool to identify relevant publications, while academic search engines are used to complete the search for possible non-inventoried works. In addition, the data from the Catalan Water Agency (ACA) website is used to have an updated base of the CBT nuclei.

DISCUSSION

After the characterization, it is necessary to find out what is done with the tributary: do we pour it into the river? (In one place or in several), do we pour them on the ground? What kind of soils do we have? Agricultural soils or riverside soils? We will also consider a recharging of aquifers and for this it is necessary to know the type of soils and subsoils that exist, ideally gravel, or think about infiltration-percolation systems. In an ideal scenario, it is necessary to look for floodplains that are close to the treatment plants. The problem arises when it arises in the headwaters of the rivers where there is not plain. On the other hand, by eliminating the effluent we have positive and negative impacts that need to be quantified. Among the positives, we have the Ecosystem Services that provide less erosion capacity, bring more clean flow to the river, recover the riverside forest, floodplain and maintenance or formation of lateral wetlands.
In relation to economic considerations, it is necessary to ask about the type of treatment plant. If an aeration system is developed, it could be economically unaffordable because there are few inhabitants. Therefore, we must consider NBS or others. It is necessary to consider parameters such as the price of the analysis and confirm if the reuse or controlled application to the medium is feasible. With this, the SAD is built, which will take into account the main thing that is debugging, as well as all these secondary parameters.

Finally, it is necessary to carry out a scientific diffusion, such as, for example, through nearby schools where the SAD is explained and the motivations for their choice and its benefits are expressed. The general population must be provided with training, information, and communication, also considering the cost that this has.

In summary, with the design and evolution of the SAD, it is concluded that it must go beyond the choice of wastewater treatment technology, and that, in addition, it will have a favorable environmental effect that contributes to the development of more resilient.

Assessment of the role of the solubilization time in the P-recovery process in the Murcia-Este WWTP

M. Roldán*, A. Bouzas*, A. Seco*, E. Mena**, A. Romero*** and R. Barat****

*CALAGUA – Unidad Mixta UV-UPV, Departament d'Enginyeria Química, Escola Tècnica Superior d'Enginyeria, Universitat de València, Av. De la Universitat s/n, 46100, Burjassot, València, Spain
(E-mail: miguel.roldan@uv.es; alberto.bouzas@uv.es aurora.seco@uv.es)
** EMUASA, Plaza Circular, 9, 30008, Murcia, Spain.
(E-mail: eva.mena@emuasa.es)
***Cetaqua, Water Technology Centre, Carretera d'Esplugues, 75, 08940 Cornellà de Llobregat, Barcelona, Spain
(E-mail: adrianalucia.romero@cetaqua.com
****CALAGUA – Unidad Mixta UV-UPV, Insituto de Ingeniería del Agua y Medio Ambiente -IIAMA, Universitat Politècnica de València, Camí de Vera s/n, 46022, València, Spain
(E-mail: rababa@dihma.upv.es)

The adaptation of already existing wastewater treatment plants (WWTP) aiming phosphorus (P) recovery from sewage is an essential strategy considering its limited mineral reserves and its key role in the food supply chain. The already full-scale implemented recovery systems are mainly focused on the recovery after anaerobic digestion. However, they are limited due to the uncontrolled precipitation of P in the digesters. In the Murcia-Este WWTP (Spain) this limitation was overcome by implementing a two-step process in the sludge line to promote the solubilization of the polyphosphate (poly-P) stored in the sludge and the obtention of liquid stream enriched in orthophosphate (PO_4) after elutriation in the gravity thickening together with the primary sludge. After six months of operation under stable conditions, with 47.8% of average enhanced biological phosphorus removal, the 18.8 ± 6.9 % of the WWTP influent P load was extracted through the recovery stream with a PO_4-P concentration of 41,1 ± 8.8 mg L^{-1}. The sludge retention time (SRT) during the solubilization stage was pointed as a hot spot of the process as longer SRT promoted the fermentation and the poly-P solubilization but also reported a decrease in the settling rate in the gravity thickening.
This affection to the settleability after mixing both sludges in the gravity thickening was found to play a key role in the successful operation of this WWTP.

Keywords: Elutriation, Fermentation, Full-scale, Phosphorus recovery, Settleability

INTRODUCTION

The upgrade of already existing WWTPs with the arising technologies plays a key role in the mitigation of the worst effects of the current scenario of climate change and resources depletion (Robles et al., 2020). Regarding to P, it is an essential raw material for the food supply chain and is expected to deplete in the next decades and because of this was included in the last List of Critical Raw Materials. This situation has driven to a broad agreement among the different stakeholders about the relevance of its recovery from wastewater as a promising strategy to improve its sustainability.
Most of the full-scale implemented technologies are focused on the recovery from the centrifuge centrate after the anaerobic digestion, however, the efficiency of these technologies is limited by the uncontrolled precipitation in the digestersAiming the recovery before anaerobic digestion is considered as an option to increase the efficiency whilst mitigating the uncontrolled precipitation issue (Roldán et al., 2020)..
The sludge line of the Murcia-Este WWTP (Spain) was modified to promote the obtention of a PO_4-enriched liquid stream before anaerobic digestion for its subsequent recovery. This work resumes the main operation results and the influence of the SRT during the solubilization in the global process performance.

MATERIALS AND METHODS

The new sludge line of the Murcia-Este WWTP was implemented to enable the bio-sludge distribution between the original and the new sludge management handlings. During the 6 months period of operation under stable conditions a flow-rate of 100,000 m^3 d^{-1} was treated with a low EBPR efficiency of 47.8 ± 20.6 %. The PO_4 extraction was carried out in a two steps process: 1) bio-sludge storage in the 'Elutriation Tank' under anaerobic conditions to promote the poly-P solubilization after volatile fatty acids uptake (VFA) and 2) elutriation of the resulting and the primary sludges over gravity thickeners to obtain the PO_4-enriched liquid overflow. The whole sludge line was controlled with a new fuzzy-logic control system whose core relied on controlling the sludge blanket level in the gravity thickening by wasting and controlling the bio-sludge distribution between the current and the previous configurations before anaerobic digestion (see Figure 1).
In lab-scale tests, the effect of the duration of the poly-P solubilization in the VFA production, the PO_4 concentration in the bio-sludge and the settleability in the gravity thickening were studied in order to understand the affection of this parameter to the proper WWTP operation.

RESULTS AND DISCUSSION

Figure 2 shows the ability, during a representative 24 h period under stable conditions, of the fuzzy logic based-control system to keep the sludge blanket level in the gravity thickening near to the setpoint by wasting from the bottom of the thickener and opening the control valve to reduce the bio-sludge flow entering into the elutriation tank at excessive blanket levels. After operating the new sludge line for 6 months, the PO_4-P concentration in the overflow increased from 6.7 ± 0.7 mg L^{-1}, (represents the 3.0 ± 0.5 % of the influent P load operating the original configuration), to 41.1 ± 8.8 mg L^{-1} (represents the 18.8 ± 6.9 % of the influent P load). This concentration occasionally increased up to 60 mgP L^{-1}.
In lab-scale tests was observed the VFA accumulation in the elutration tank (Figure 3), whose concentration increased up to 410.1 ± 94.2 mg L^{-1} after 22-24 h. This fermentation promoted the poly-P solubilization and the increase of the PO_4-P concentration in the bio-sludge stream (see Figure 4) from 88.0 ± 49.2 mg L^{-1} to 277.0 ± 59.8 mg L^{-1} in this period.
A negative effect was observed in the settleability when increasing the solubilization HRT, which led to a higher fermentation but also to slower settling rates. Despite the lack of differences between 12 and 24 h of solubilization, a significantly slower settling rate was observed at 40 h of solubilization (see Figure 5).

ACKNOWLEDGEMENTS

The LIFE program, the European Financial Instrument for the Environment, supported and co-financed this study as part of the LIFE ENRICH Project (LIFE16 ENV/ES/000375).

REFERENCES

Robles, Á., Aguado, D., Barat, R., Borrás, L., Bouzas, A., Giménez, J. B., Martí, N., Ribes, J., Ruano, M. V., Serralta, J., Ferrer, J., & Seco, A. (2020). New frontiers from removal to recycling of nitrogen and phosphorus from wastewater in the Circular Economy. In *Bioresource Technology* (Vol. 300). Elsevier Ltd. https://doi.org/10.1016/j.biortech.2019.122673

Roldán, M., Bouzas, A., Seco, A., Mena, E., Mayor, & Barat, R. (2020). An integral approach to sludge handling in a WWTP operated for EBPR aiming phosphorus recovery: Simulation of alternatives, LCA and LCC analyses. *Water Research*, *175*. https://doi.org/10.1016/j.watres.2020.115647

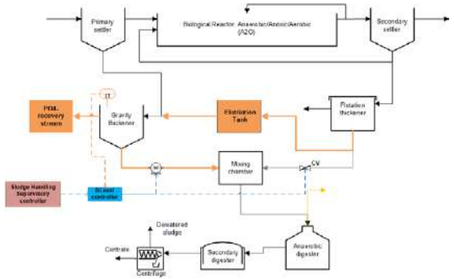

Figure 1. New sludge line configuration and control of the sludge blanket height during the gravity thickening in the Murcia-Este WWTP.

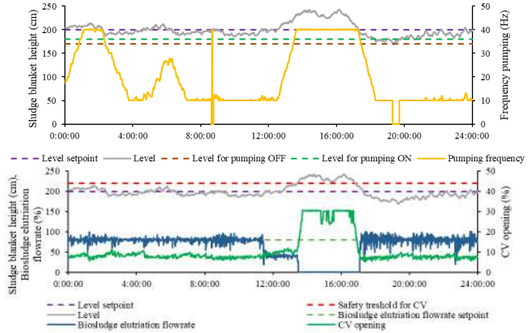

Figure 2. Sludge blanket level control in the gravity thickening.

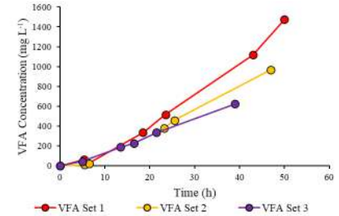

Figure 3. VFA concentration during the poly-P solubilization.

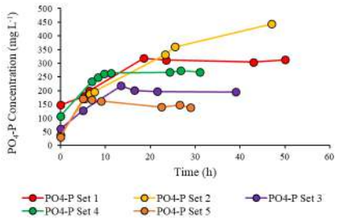

Figure 4. PO4 concentration during the poly-P solubilization.

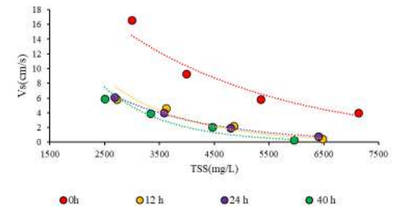

Figure 5. Effect of the solubilization time in the settleability of the mixed sludge.

FORWARD-FACTORY: Integrating forward osmosis and advanced biological reactor for water reuse and resource recovery factory

G. Blandin*, R. Yalamanchili*, P. Olives*, C. Padilla Gallegos*, I. Rodriguez-Roda*

* LEQUIA, Institute of the Environment, University of Girona, Spain
(E-mail: gaetan.blandin@udg.edu)

Abstract
FORWARD-FACTORY project aims at transforming urban wastewater treatment (WWTP) into a resource recovery factory (RRF) to foster and reinforce the resource revolution thanks to forward osmosis (FO) combined with advanced biological processes. Seawater (SW) is used as draw solution to make use of osmotic driving force for water extraction and nutrients concentration. Then diluted SW is passed through reverse osmosis process allowing for combining desalination and water reuse at lower energy costs. Our recent works studied various aspects of the proposed concept. It was demonstrated that FO could improve anaerobic digestion efficiency (with granular biomass), could be used for microalgae concentration with limited fouling propensity and allow for retrofitting of existing desalination plant allowing production of pure water at lower than 1kWh.m^{-3}.

Keywords
Forward osmosis; nutrients recovery; microalgae treatment; water reuse; desalination

INTRODUCTION

The conventional urban wastewater treatment WWTP apply activated sludge systems which are energy intensive and current approach is limited to the removal of valuable nutrients from the water stream, not optimizing their recovery. FORWARD-FACTORY project aims at transforming WWTP into a resource recovery factory (RRF) to foster and reinforce the resource revolution. FORWARD FACTORY proposes (1) to move from WW discharge to water recovery and reuse, (2) to promote to organic matter value recovery processes (to produce biogas, valuable organic compounds and/or fertilizers) and (3) to move towards nutrients recovery (especially N and P). One limitation for RRF concept is the low concentration of organic matter, nitrogen and phosphorus and the high inflow rate to be treated which negatively impact the efficiency of resource recovery bioprocesses (fermentation, anaerobic digestion, microalgae production). Thus, a pre and post-concentration step are required. Forward osmosis (FO), an innovative membrane technology, features unique properties by combining high rejection rate, low fouling propensity and driven by salinity gradient energy. Seawater is used as extracting solution for the FO steps allowing also to dilute the seawater stream and therefore the energy costs for downstream desalination. As such, the forward factory concept also allows for integration of water reuse and desalination (Figure 1).

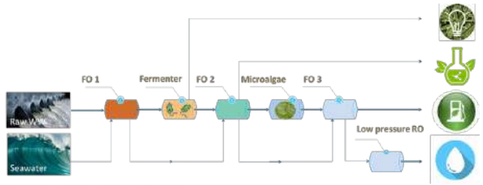

Figure 1: FORWARD-FACTORY concept.

MATERIALS AND METHODS

To validate this concept, our recent work focused on the integration and evaluation of FO with biological processes such as granular anaerobic bioreactor (G-AnMBR) and microalgae photobioreactor. Also, a design study was performed to evaluate the potential of FO to dilute seawater and decrease desalination energy costs below 1kWh.m^{-3} so to assure safe water production at affordable costs. Granular anaerobic membrane bioreactor (G-AnMBR): Forward osmosis membrane were integrated to a G-AnMBR. Kubota microfiltration modules were step by step replaced by FO Submerged FO plate and frame modules. Microalgae cultivation and concentration: Chlorella vulgaris was grown in a BG11 media under controlled illumination and CO_2 injection. Then, 8L batches of microalgae suspension were concentrated 4 times through submerged FO and MF membrane to evaluate fouling propensity and impact of aeration. Retrofitting of RO desalination plant: LewaPlus (Lanxess) water treatment design package was used for simulation work. As a reference, a baseline desalination plant (with 35 g/l feed salinity) was modelled to a capacity of 1,800 m3/h of permeate production. The same plant design was simulated with varying salinity (5, 10, 20 g/l) in the feed to evaluate the impact of required energy for water production, water quality and potential increase in water production.

RESULTS AND DISCUSSION

G-AnMBR: FO membranes proved to be less prone to fouling and increased COD degradation was observed when operating with FO (above 90%). However, increasing FO membrane share in the reactor, led to salinity increase and to enhanced fouling propensity probably due to salinity shock on the active biomass, releasing extra polymeric substance in the mixed liquor.

Microalgae concentration: Both MF and FO submerged membrane led to a complete rejection of chlorella vulgaris. Under aeration, negligible fouling was observed for both membranes leading to a microalgae recovery above 90%. Fouling layer removal proved to be easily reversible in FO thanks to osmotic backwash allowing for almost full recovery of microalgae biomass.

The simulation results from LewaPlus states that, thanks to FO predilution of SW (down to 5g/L), an existing desalination plant could be retrofitted allowing for decrease of energy consumption by 65.5% (below 1kwh/m^3) and leading to potential competitive advantages like significant reduction of the Total Dissolved Salt content (TDS) and Boron in the permeate stream.

CONCLUSION

Tests with G-AnMBR and microalgae demonstrated the capacity to concentrate WWTP streams and optimise biological reactor efficiency. However, salinity increase remains a limiting factor that should be considered for optimised biological reactor and efficient resource recovery. Using SW as extracting solution in FO before RO desalination demonstrated several advantages both in terms of energy savings and produced water quality and the potential for FO-RO hybrid to combine water reuse and desalination.

ACKNOWLEDGMENTS

Gaetan Blandin received the support of a fellowship from “la Caixa” Foundation (ID 100010434). The fellowship code is LCF/BQ/PR21/11840009.

Novel concentration process based on membranes for volatiles fatty acid concentration (ConcentrA)

C. Ramos[a], Pere Olives[a,b], G. Blandin[b], Ignasi Rodriguez-Roda[b], J. Margarit[a]

[a] VEnvirotech Biotechnology, Spain (E-mail: carlos.ramos@venvirotech.org)
[b] LEQUIA, Institute of the Environment, University of Girona, Spain

Abstract

New technologies you be implemented to the concentration of volatile fatty acids (VFAs) produced from organic waste. This fact is related to the current commercial processes presented several drawbacks, such as (i) several ions compete with the VFAs to be adsorbed onto the matrix, reducing the effectiveness of the adsorption and (ii) high energy requirements for heating to achieve VFAs separation by distillation and evaporation. To solve these problems, membrane technologies appear as a important player, due to low energy demand, specific separation and easy scalability. To develop a concentration process based on membranes, VEnvirotech Biotechnology and Lequia joint efforts to develop and implement an innovative technology for VFAs concentration. Preliminary results show that VFAs concentration by membrane is technically feasible and nanofiltration, reverse osmosis and forward osmosis processes have the capacity to concentrate a solution of volatile fatty acids. The effects of different operational conditions are under study.

Keywords (maximum 6 in alphabetical order)
Concentration; forward osmosis; membrane; purification; volatile fatty acids; reverse osmosis

INTRODUCTION

Nowadays, volatile fatty acids production from organic waste is attracting great interest as a sustainable approach for implementation of circular economy. VFA are a subgroup of fatty acids, ranging from 2 to 5 carbon atoms, including acetic, propionic, isobutyric, butyric, isovaleric and valeric acids. Its current main applications are related to building blocks in several industries, such as pharmaceutical, food and chemical[1]. In recent years, VFAs have become important players in the production of bioplactics, such as polyhydroxyalkanoates (PHA). Thus, it is expected that the market will increase. The current commercial production of VFAs is based on chemical synthesis from petroleum-based compounds. Thus, economic and environmental issues are related to this production pathway. To move forward a circular economy approach, new technologies should be considered to apply organic waste.

VEnvirotech Biotechnology is a Spanish company devoted to the sustainable transformation of organic waste into bioplactics and it's developing a revolutionary (bio)technology to produce bioplastics using VFAs as building block. The current technology under development needs high concentrations of VFAs to achieve feasible technical, environmental and economic benefits.

On a commercial scale, the current concentration technologies for VFAs are adsorption, distillation and evaporation. However, these processes presented several drawbacks, such as (i) several ions compete with the VFAs to be adsorbed onto the matrix, reducing the effectiveness of the adsorption process and (ii) high energy requirements for heating to achieve VFAs separation by distillation and evaporation processes.

Due to the detected limitation of the current technologies, new processes should be studied and developed for VFA concentration. The mentioned drawback can be solved by the implementation of membranes, including electrodialysis (ED), microfiltration (MF), ultrafiltration (UF), nanofiltration (NF), reverse osmosis (RO) and forward osmosis (FO)[2]. Membrane technology allows the use of different kinds of effluent to be treated, lower energy demand in comparison to current concentration technologies, specific separation and easy scalability[2].

Currently at full-scale, membrane processes are key elements for water reuse and desalination. RO is a consolidated technology for seawater desalination. Another developed membrane technologies are NF and UF and they have been applied in different fields such as chemical compounds recovery, water treatment, WW reclamation, juice concentration, dairy industry or medical usage. Other membrane processes is forward osmosis (FO), it is a novel technology in comparison to the other processes and it had gained interest in the last two decades.

Nowadays the implementation of membranes, such as RO and NF, are mainly related to desalination and water reused. However, for VFA concentration the investigation is limited. Thus, research should be applied to evaluate membrane technology as a potential key player in the concentration field. Thus, researchers and engineers from VEnvirotech Biotechnology and Lequia are working together for the implementation of a novel process based on membrane to achieve concentration of VFAs from biotransformed waste. The joint efforts from both entities have been achieved in the implementation of the ConcentrA project, to study, develop and scale-up a membrane-based technology for VFAs concentration. To achieve this goal, different membranes and operational parameters will be evaluated.

MATERIALS AND METHODS

The study has two main tasks. The first one will be performed at bench-scale in Lequia facilities, where different membranes at laboratory scale (0.01 m^2 of filtration area) will be tested. A flat-sheet membrane cell testing equipment will be used to assess the permeability and the rejection of the membranes. In this way, different kinds of membranes can be characterized to evaluate their potential implementation and to identify properly their concentration capacities. At the same time, operational conditions for each membrane will be determined with synthetic and real effluents. The focus will be on the flux, pressure, conductivity, temperature, pH and water concentration factor. Thus, design parameters can be obtained. Besides, knowing the capacity of the membranes, a concentration train can be defined and proposed for scale-up.

The second task of the project is the scale up of the membrane technology for VFA concentration. The proposed technology will use commercial membrane modules (2-3 m^2 of filtration area) and will be tested on a real environment at VEnvirotech facilities.

RESULTS AND DISCUSSION

The ConcentrA project is ongoing, and the first task is under development. Preliminary results show that VFAs concentration by membrane is technically feasible and nanofiltration, reverse osmosis and forward osmosis processes have the capacity to concentrate several times a solution of volatile fatty acids. The effects of different operational conditions are under study.

ACKNOWLEDGMENTS

ConcentrA project is funded by the catalan agency for business competitiveness (ACCIÓ) through the NUCLIS call.

REFERENCES

(1) Agnihotri, S.; Yin, D.-M.; Mahboubi, A.; Sapmaz, T.; Varjani, S.; Qiao, W.; Koseoglu-Imer, D. Y.; Taherzadeh, M. J. A Glimpse of the World of Volatile Fatty Acids Production and Application: A Review. *Bioengineered 13* ***2022***, 1, 1249–1275.
(2) Blandin, G.; Ferrari, F.; Lesage, G.; Le-Clech, P.; Héran, M.; Martinez-Lladó, X. Forward osmosis as concentration process: review of opportunities and challenges. *Membranes* **2020**, 10 (10), 284.

Resource recovery from aerobic granular sludges: Gel-forming biopolymers extraction, fractionation and gelling capacity

Abdo BOU-SARKIS*, **, Etienne PAUL**, Yolaine BESSIERE**, Nicolas DERLON***, Elisabeth GIRBAL-NEUHAUSER*.

* Université de Toulouse; UPS, LBAE, Laboratoire de Biotechnologies Agroalimentaire et Environnementale, URU 4565, Institut Universitaire de Technologie, 24 rue d'Embaquès, 32000 Auch, France. (E-mail: *abdo.bou-sarkis@iut-tlse3.fr; elisabeth.neuhauser@iut-tlse3.fr*)
** TBI, Université de Toulouse, CNRS, INRAE, INSA, Toulouse, France. (E-mail: *etienne.paul@insa-toulouse.fr; yolaine.bessiere@insa-toulouse.fr*)
*** EAWAG, Swiss Federal Institute of Aquatic Science and Technology, Department of Process Engineering, CH-8600, Dübendorf, Switzerland (E-mail: *Nicolas.Derlon@eawag.ch*)

Abstract

Gel-forming extracellular polymeric substances (EPS) were extracted from aerobic granular sludge, then fractionated according to their net surface charge using preparative anionic exchange chromatography. The fractions eluted by increased NaCl concentrations were collected and their gel formation capacity was analyzed using a gelling factor (GF) obtained through a miniaturized screening test based on the level of the molecular interactions and the volume of gel formed after calcium-induced gelation. Initial EPS solution extracted from granules exhibited interesting gelling capacity, approximately half of that of alginate (GF of 0.2 ± 0.02 and 0.45 ± 0.06 respectively). The GF correlated with the polymer's charge: a GF of 0,04 ± 0.03 was measured for the first eluted molecules (with NaCl 0,25M) and a GF of 0,26 ± 0.1 for the lastly eluted molecules (with NaCl 0,75M). The size distribution of the molecules participating in the gelation was analyzed by Size Exclusion Chromatography allowing the determination of the % of reactivity corresponding to the area that disappeared from the chromatograms. High molecular weights were implied in the gelation whatever the charge of the polymers was (between 65% and 100% of reactivity). Concerning low molecular weights their participation was limited (<40%). Therefore, the obtained results show that both charge and molecular size are important factors for gelation. With the goal of selecting gel-forming EPS, these results underline the necessity to modulate the extraction and purification methods towards the selection of molecules having the appropriate negative charge and also towards the preservation of their molecular weight during the extraction steps.

Keywords

Aerobic granular sludge; calcium-induced hydrogels; gel-forming EPS; molecular weight; resource recovery; surface net charge

INTRODUCTION

Polymers with gelling properties, in presence of divalent cations, can be extracted from aerobic granular sludge which are emergent promising biofilms that are used in wastewater treatment [1]. These polymers called gel-forming Extracellular Polymeric Substances (EPS) are interesting because they are from renewable sources and fall within the circular economy concept. Using alkaline and heating treatments, gel-forming EPS can be recovered from granules as a mix of biopolymers (proteins and polysaccharides are the major ones) with yields representing 23% of the total organic matter. Therefore, wastewater treatment plants using aerobic granular sludge technology treating domestic wastewater (COD ≈ 600 mg/L), with a flow rate of approximately 3.0 m^3/s, could produce approximately 1 ton/day of gel-forming EPS [2]. Bio-hydrogels are valuable materials with diversified mechanical properties and their characteristics are influenced by the molecular properties of the involved biopolymers. In the case of alginates from seaweed, a higher molecular weight was shown to improve gel formation kinetics and to increase fluid hydrogels viscosities [3]. It was also observed that the charge of molecules influences their gelling capacity[4]. However, there is a lack of knowledge concerning molecular weight and/or net surface charge involvement in the gelling process of the very complex EPS fraction extracted from aerobic granules. The implication of these two factors in the gelation will be addressed in this study.

MATERIALS AND METHODS

Biomaterial and gel-forming EPS extraction

Aerobic granular sludge was recovered from sequencing batch reactors fed with synthetic wastewater (equal COD fractions of acetate and propionate) [5]. After freeze-drying, aerobic granules were solubilized at 80°C in Na_2CO_3 0.2 M and gel-forming EPS were precipitated by reducing the pH to 2 [6].

Preparative Liquid Chromatography

EPS fractionation according to their net surface charge was performed using a Resource™ Q column grafted with a quaternary ammonium ligand. Equilibration was done by using Tris HCl 50 mM pH=12±0.02, and elution was performed by the sequential addition of NaCl 1 M. Absorbance was monitored at 280 nm and peak areas (mAU×mL) were processed using the UNICORN 5.31 software. The fractions were collected, dialyzed against distilled water and then freeze-dried for further analysis. Fractions from the Resource Q column were prepared at 0.5% (w/v) volatile solids (VS), incubated without or with 0.1 M calcium for one hour. Then the supernatant was collected after a 15 min centrifugation at 14 000 g for further analysis by SEC using a Superdex 200 column as described in [6]. The MW reactivity (%) for each MW group was calculated using the formula 1.1:

$$MW\ reactivity\ (\%) = \frac{(total\ area\ without\ calcium - total\ area\ with\ calcium)*100}{total\ area\ without\ calcium} \quad (1.1)$$

Test for evaluation of gelling capacity

Dialyzed solutions at a final concentration of 1 % (w/v) VS were incubated for 1h with 0.1 M calcium chloride then centrifuged at 14 0000g for 15 min. The volume of the supernatant was measured and therefore the gel volume (Vg) for samples with calcium was deduced allowing to calculate a gel volume percentage (%Vg). UV-vis spectra between 220 and 500 nm were measured to determine a reactivity (%R) corresponding to the percentage of area that disappeared from the spectra after addition of calcium. Both factors were combined to obtain a gelling factor (GF), as seen in equation 1.2, that help in comparing solutions capacities to form hydrogels.

GF = % Vg * %R (1.2)

This method allows the detection of gelation using only 2 mg of the sample to be tested and could be very beneficial in lab scale experiments where this material availability is limited.

RESULTS AND DISCUSSION

What are the effects of the net negative surface charge on the gelling capacity?

As shown in figure 1, the fractionation of gel-forming EPS through a sequential elution strategy (NaCl steps with increasing concentrations from 0 to 1 M) allowed to clearly separate groups of molecules with different negative surface charges. It can be noticed that the majority (91.5 ± 5 %) of the molecules present within the EPS solution are negatively charged (figure 1) similarly to other studies [7].

The collected fractions were analyzed for their gelling capacity using a miniaturized method based on the analysis of the soluble molecules remaining in the supernatant after addition of 0,1 M calcium. As shown in Table 1, the initial EPS solution extracted from granules by sequential alkaline and acidic treatment exhibited interesting gelling capacity, corresponding approximately half of that of alginate (GF of 0.2 ± 0.02 and 0.45 ± 0.06 respectively). In order to select biopolymers with interesting gelling capacities the fractions eluted from the anionic exchange column were screened for their gelation capacity after calibration at 1% VS. As shown in Table 1, the unbound Cat/N exhibited the highest GF at 0.37 ± 0.03 due to a good %R to calcium and a high %Vg. Further analysis showed that in fact Cat/N fraction has a global neutral charge (data not shown) and this neutral charge is due to the formation of strong associations between positively and negatively charged polymers, these anionic polymers being able to react with calcium and form hydrogels. Concerning the negatively charged polymers, the GF increased with charge from 0.04 ± 0.03 for LAC to 0.26 ± 0.1 for HAC. However, upon reaching a very high negative charge (i.e., VHAC) the gelling capacity decreased abruptly reaching 0.02 ± 0.0005. Indeed, the presence of a lot of negatively charged polymers could hinder the hydrogel formation capacity due to an increased repulsion of polymers as described for carrageenan hydrogels [8,9].

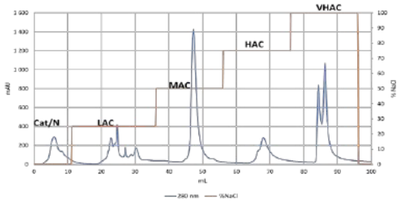

Figure 1. Anionic Exchange Chromatography of gel-forming EPS extracted from aerobic granules and eluted with gradual NaCl concentrations. Cat/N=cationic/neutral molecules, LAC= low anionic charge molecules, MAC= medium anionic charge molecules, HAC= high anionic charge molecules and VHAC= very high anionic charge molecules.

Table 1. The gel volume (%Vg), reactivity (%R) and gelation capacity (GF) of the different samples. The results were obtained through three gelation replicates.

sample	%Vg	%R	GF
Alginate	54.2 ± 5.2	83.3 ± 2.5	0.45 ± 0.06
Unfractionated EPS	30 ± 2.5	65.4 ± 1	0.2 ± 0.02
Cat/N	41.7 ± 1.4	87.90 ± 4.6	0.37 ± 0.03
LAC	12.33 ± 4.5	32.08 ± 10.1	0.04 ± 0.03
MAC	19.83 ± 0.3	54.73 ± 1.9	0.11 ± 0.00
HAC	34.67 ± 10.7	74.38 ± 6.6	0.26 ± 0.10
VHAC	2.50 ± 0.0	97.62 ± 2.1	0.02 ± 0.00

Which molecular weight groups are the ones responsible for the gelation?

No matter what the net negative surface charge is, the HMW group always participates in the gelation with a % of reactivity going from 65% for the MAC fraction to values as high as 100% for the LAC fraction (figure 2). On the contrary, participation of MMW molecules to the hydrogel formation is dependent on the net negative surface charge. Indeed, for the LAC and MAC, the % of reactivity is below 25% while for the fractions with high negative charge (HAC and VHAC), the participation of MMW is above 95%. Surprisingly the Cat/N fraction has a % of reactivity for MMW at 87%. When it comes to LMW molecules, their participation is always limited, reaching 27%, 14% and 11% respectively for Cat/N, LAC and MAC and around 40% for HAC and VHAC.

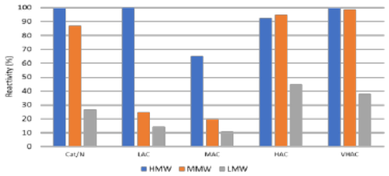

Figure 2. The % of reactivity for Molecular weight groups showing their respective participation in the gelation.

CONCLUSION

The miniaturized screening method is capable of comparing gelling capacities of different solutions obtained either by different processes/extraction protocols/fractions of EPS... Fractions of gel-forming EPS from aerobic granular sludge obtained through anionic exchange chromatography showed that both the charge and size of the polymers are essential factors for the gelation of EPS. Different gelling capacities were nevertheless measured for polymers exhibiting more or less important anionic charges indicating that a process based on anionic exchange is relevant for further purification of these valuable biopolymers.

REFERENCES

[1] C.M. Schambeck, E. Girbal-Neuhauser, L. Böni, P. Fischer, Y. Bessière, E. Paul, R.H.R. da Costa, N. Derlon, Chemical and physical properties of alginate-like exopolymers of aerobic granules and flocs produced from different wastewaters, Bioresour. Technol. 312 (2020) 123632.
[2] T.J. Tavares Ferreira, S. Luiz de Sousa Rollemberg, A. Nascimento de Barros, J.P. Machado de Lima, A. Bezerra dos Santos, Integrated review of resource recovery on aerobic granular sludge systems: Possibilities and challenges for the application of the biorefinery concept, J. Environ. Manage. 291 (2021).
[3] I. Fernández Farrés, I.T. Norton, Formation kinetics and rheology of alginate fluid gels produced by in-situ calcium release, Food Hydrocoll. 40 (2014) 76–84.
[4] M. Beaumont, R. Tran, G. Vera, D. Niedrist, A. Rousset, R. Pierre, V.P. Shastri, A. Forget, Hydrogel-Forming Algae Polysaccharides: From Seaweed to Biomedical Applications, Biomacromolecules. 22 (2021) 1027–1052.
[5] M. Layer, A. Adler, E. Reynaert, A. Hernandez, M. Pagni, E. Morgenroth, C. Holliger, N. Derlon, Organic substrate diffusibility governs microbial community composition, nutrient removal performance and kinetics of granulation of aerobic granular sludge, Water Res. X. 4 (2019) 100033.
[6] A. Bou-sarkis, B. Pagliaccia, A. Ric, N. Derlon, E. Paul, Y. Bessiere, E. Girbal-neuhauser, Effects of alkaline solvents and heating temperatures on the solubilization and degradation of gel-forming Extracellular Polymeric Substances (EPS) extracted from aerobic granular sludge, Biochem. Eng. J. 185 (2022) 108500.
[7] C. Caudan, A. Filali, D. Lefebvre, M. Spérandio, E. Girbal-Neuhauser, Extracellular polymeric substances (EPS) from aerobic granular sludges: Extraction, fractionation, and anionic properties, Appl. Biochem. Biotechnol. 166 (2012) 1685–1702.
[8] E.R. Morris, Polysaccharide Conformation and Interactions in Solutions and Gels. In: Gettins, W.J., Wyn-Jones, E. (eds) Techniques and Applications of Fast Reactions in Solution. NATO Advanced Study Institutes Series, vol 50. Springer, Dordrecht., 1979.
[9] S. Liu, L. Li, Thermoreversible gelation and scaling behavior of Ca2+-induced κ-carrageenan hydrogels, Food Hydrocoll. 61 (2016) 793–800.

Stabilization of sewage sludge in constructed wetlands for reuse in agriculture

A. Cano*, R. Castellnou***, L. Colomer****, G. Gorchs**, R. Moreno****, L. Serrano** and E. Uggetti*

* Department of Civil and Environmental Engineering, Polytechnic University of Catalonia, Jordi Girona street, 31, 08034, Barcelona, Spain (E-mail: ana.maria.jose.candelaria.cano@upc.edu; enrica.uggetti@upc.edu)
** Department of agri-food engineering and biotechnology, Polytechnic University of Catalonia, Esteve Terradas street, 8, 08860, Barcelona, Spain (E-mail: gil.gorchs@upc.edu; lydia.serrano@upc.edu)
*** Depuradores d'Osona S.L., Carrer de Valls, 19, 08500 Vic, Barcelona
(E-mail: rcastellnou@depuradoresosona.cat)
**** Osona County Council, Historiador Ramon d'Abadal i de Vinyals, 5 08500, Vic, Barcelona, Spain (E-mail: lcolomerc@ccosona.cat; rmorenob@ccosona.cat)

Abstract
Globally, a large amount of solid waste is produced, including sludge generated in wastewater treatment plants (WWTP). Due to the high production of sludge, different strategies have been proposed to enhance its reuse, preferably with low-cost strategies friendly to the environment. For this reason, constructed wetlands (CWs) have been proposed as a solution indeed, in such systems, sludge can be treated to obtain a dry, mineralized by-product (biosolid) that can be reused. Two CW facilities were studied by measuring biological and physicochemical parameters to check the stabilization and hygienization of these biosolids. Dry biosolids content of 50% total solids (TS) was obtained, with a decrease in organic matter between 38% and 49% volatile solids (VS); a decrease in pathogenic microorganisms, and a high content of essential nutrients for plant growth respect to the influent. According to these properties, biosolids could be reused in agriculture as a possible organic fertilizer, potentially increasing crop yield and replacing commercial fertilizers.

Keywords
Agriculture, constructed wetlands, sludge, sludge drying beds, wheat

INTRODUCTION

The global population has led to an increase in solid waste production from industrial, residential, and public sources. Every year, 4 billion tons of waste are generated, and municipal waste accounts for 1,6 to 2 billion tons. Wastewater treatment facilities produce sludge, which is a type of solid waste containing organic and inorganic materials. The amount of sludge produced depends on the parameters of the effluent and the type of treatment used, typically ranging from 60-80 g TS/person/day when using standard activated sludge processes (Andreoli, et al., 2007). Stabilized sludge (also known as biosolid) typically has between 50-70% organic matter, 3-4% nitrogen, 1-3% phosphorous, and trace levels of heavy metals like Cr, Zn, Pb, Ni, and Cd. Sludge management strategies should focus on both pollutant removal and biosolids reuse to reduce potential health and environmental risks and make the material harmless and more reusable.

Developed and developing countries are searching for ways to manage sludge produced in WWTP. Solutions such as thermal processing, composting, disposal, and agricultural use are being explored. Agricultural use is gaining more attention since sludges contain components that can act as soil conditioners or fertilizers, providing an alternative to commercial fertilizers and adding value to wastewater treatment by-products. However, the sludge must be treated before to be reused. For these reasons, constructed wetlands (CWs) are gaining more attention as a solution due to their ability to treat sludge in a sustainable, low-energy, and low-maintenance manner and obtain a by-product suitable to be reused in agriculture. The aim of this study was to evaluate the capacity of CWs to generate stabilized biosolids after different periods of rest (without feeding) and to test their compliance with the requirements established by European legislation for agricultural reuse (European Commission 2000). Moreover, agronomic essays were carried out in agronomic crops (i.e. wheat) to test biosolids properties as organic fertilizer.

MATERIALS AND METHODS

The facilities studied in this work are located in the WWTP Sentfore-La Guixa (1000 PE) and the WWTP Santa Eulàlia de Riuprimer, (2000 PE), both located in Vic (Barcelona, Spain). **Sampling methods and sludge characterization**

Three sampling campaigns have been carried out during 6 months starting one week after the CWs received the last feeding (June 2022). Samplings were carried out in June 2022, September 2022, and December 2022. In order to obtain a composite sample of the sludge, in each facility one representative bed was selected and divided into 4 sections, 1 sample was collected in each section and then carefully mixed. Samples were analysed in triplicate using standard techniques in accordance with the Standard Methods (APHAAWWA-WPCF, 2001). The following parameters were analysed: pH, Electrical Conductivity (EC), Total and Volatile Solids (TS and VS), Chemical Oxygen Demand (COD), Total Kjehldahl Nitrogen (TKN), nutrients, heavy metals, faecal bacteria indicators (*Salmonella spp*, *E. coli*, faecal coliform and nematode eggs).

Experimental design of the agronomic essay

The agronomic essay was carried out at the Tona WWTP located in the Osona region of Barcelona province. Three fertilizer treatment were considered: biosolids from CW applied directly to the soil (T1), biosolids from CW after crushing (T2) and commercial inorganic fertilizer (T3). The doses of sludge and commercial fertilizer were calculated with respect to the nutritional needs of the crop and the concentrations of total nitrogen in biosolids and fertilizer. For biosolids, 2 $t \cdot ha^{-1}$ of T1 and 3 $t \cdot ha^{-1}$ of T1 and T2 were applied in the agronomic assay. Each treatment was carried out in triplicate in smallholdings of 3x8 m^2 (figure 1). All fertilizers were homogeneously mixed with the soil at the beginning of the experiment, then 200 Kg ha^{-1} of wheat seeds (KWS ultim) were planted in each smallholding. During the testing period (6 months), samples of the plants and soil were taken to measure the different parameters stablished by the directive AAA/1072/2013 (MAGRAMA 2013).

RESULTS AND DISCUSSION

The physicochemical characterization of the sludges from CW during three sampling campaigns is shown in table 2. The pH and EC values were similar to those previously reported for biosolids quality (Stehouwer et al. 2022). The sludge after 6 months without feeding has reduced its moisture from 33%TS to 50%TS in the system of La Guixa and 35%TS to 50%TS in St. Eulàlia. The organic content of the biosolids in all basins studied was quite uniform (40-49%SV) and in accordance with previous studies (Uggetti et al., 2009). Biosolids contain a large amount of nutrients (4,6% TKN/TS for La Guixa and 5,7%TKN/TS for St. Eulàlia).

Finally, the concentration of the heavy metals was evaluated to verify their potential in agricultural application (table 3). In all basins there was a small accumulation of metals, such as Cu, As, and Mn in the three basins; and Zn and Cr in the St. Eulàlia basin. However, despite the slight accumulation of these metals, concentrations do not exceed the thresholds established in the European Directive (European Commission 2000). Lastly, indicators of faecal contamination were analysed, in particular to evaluate the quality of the final product for its application in agriculture. According to the results, *Salmonella spp* was not detected in any samples. *E. coli* was present in the three sampling campaigns and their presence increased along the sampling period. Nematode eggs were present just in the first campaign, but in the third campaign it was not detected (table 3).

Crop trials are currently taking place, and it is expected that the sludge will favour the wheat crop performance due to its high content of nitrogen and other nutrients, thus it could be considered as an organic fertilizer. It is expected that, the addition of biosolid (organic fertilizer) will increase the plant weight compared to the inorganic fertilizer as reported by Bouzerzour et al. (2002) in their pot studies. Indeed, they detected an increase in leaf diameter, leaf area index, accumulated dry matter on the soil, tiller number, and plant height of crops such as barley and oats. Latare et al.(2014) reported a wheat yield of 39.21 $g \cdot pot^{-1}$ using a sludge concentration of 40 $t \cdot ha^{-1}$. According to these studied, good results are expected with biosolids from CW.

Table 1. Physiochemical characterization of sludge in rest for 6 months in CW.

Parameters	Unity	Campaign I June 2022		Campaign II September 2022		Campaign III December 2022	
		La Guixa	St. Eulàlia	La Guixa	St. Eulàlia	La Guixa	St. Eulàlia
pH		5,6	6,4	5,2	5,7	5,0	5,4
EC	dS/m	0,3	0,5	0,3	0,5	2,17	2,75
TS	%	33	35	53	47	50	50
VS	% TS	43	41	40	41	38	49
DQO	g/kg TS	1502	1488	1044	1143	911	1125
NKT	%TS	-	7,2	4,6	5,9	-	5,7
P_2O_5	%TS	9	7	9	7	8,74	6,91
K_2O	%TS	1	1	1	1	0,75	0,85

Table 2. Heavy metals (mg/kg TS) in biosolids from the 3 STW of the resting period.

		Cd	Cu	Hg	Ni	Pb	Zn	As	Cr	Cr VI	Mn
Campaign I June 2022	La Guixa	0,6	406	0,4	27,3	72,9	597	14,6	60,2	0,5	310
	St. Eulàlia	0,8	354	0,4	36,3	77,5	893	11,5	50,9	0,5	310
Campaign II September 2022	La Guixa	0,5	339	0,4	29,3	66,9	630	13,5	52,6	10	325
	St. Eulàlia	0,6	304	0,4	36,9	93	808	12,6	46,6	10	260
Campaign III December 2022	La Guixa	< 0,5	356,5	0,4	26,85	64,1	627, 5	13,9	49,9	10	360
	St. Eulàlia	0,6	345,5	0,4	36,1	79	869	12,5	50,2	0,5	345
3rd Draft EU Working Document		10	1000	10	300	750	2500	-	800	-	-

Table 3. *Salmonella spp, E. coli,* faecal coliform and nematode eggs in biosolids from 3 STW of the resting period.

Parameters	Unity	Campaign I June 2022		Campaign II September 2022		Campaign III December 2022	
		La Guixa	St. Eulàlia	La Guixa	St. Eulàlia	La Guixa	St. Eulàlia
Salmonella spp	Absence/ Presence in 25 g	Absence	Absence	Absence	Absence	Absence	Absence
E. coli	UFC/g	650	11,850	500	1,300	<100	37,050
Faecal coliform	UFC/g	34,050	665,000	49,300	48,500	140,000	427,350
Nematode eggs	in L	<1	<1	Absence	Absence	Absence	Absence

Figure 1. Schematic image of the experimental design.

REFERENCES

Andreoli, C., M. Von Sperling, and F. Fernandes. 2007. *Sludge Treatment and Disposal*. IWA publishing.

Bouzerzour, H., L. Tamrabet, and M. Kribba. 2002. "Response of Barley and Oat to the Wastewater Irrigation and to the Sludge Treatment. In: The Proc. Int. Seminar: Biol. Environ. University Mentouri, Consantine, Algeria, p. 71." *Curso Teórico Práctico De Inseminaciónartificial En Bovinos* 1.

European Commission. 2000. "Working Documento on Sludge 3rd Draft." 80(April):1–19.

Latare, A. M., Omkar Kumar, S. K. Singh, and Archana Gupta. 2014. "Direct and Residual Effect of Sewage Sludge on Yield, Heavy Metals Content and Soil Fertility under Rice-Wheat System." *Ecological Engineering* 69:17–24. doi: 10.1016/j.ecoleng.2014.03.066.

MAGRAMA. 2013. "Orden AAA/1072/2013, de 7 de Junio, Sobre Utilización de Lodos de Depuración En El Sector Agrario." *Boletín Oficial Del Estado* 44966–73.

Stehouwer, Richard, Leslie Cooperband, Robert Rynk, Johannes Biala, Jean Bonhotal, Susan Antler, Tera Lewandowski, and Hilary Nichols. 2022. "Chapter 15 - Compost Characteristics and Quality." Pp. 737–75 in *The Composting Handbook*, edited by R. Rynk. Academic Press.

Uggetti, Enrica, Esther Llorens, Anna Pedescoll, Ivet Ferrer, Roger Castellnou, and Joan Garcia. 2009. "Sludge Dewatering and Stabilization in Drying Reed Beds: Characterization of Three Full-Scale Systems in Catalonia, Spain." *Bioresource Technology* 100(17):3882–90. doi: 10.1016/j.biortech.2009.03.047.

Vázquez, M. A., R. Sen, and M. Soto. 2015. "Physico-Chemical and Biological Characteristics of Compost from Decentralised Composting Programmes." *Bioresource Technology* 198:520–32. doi: 10.1016/J.BIORTECH.2015.09.034.

Toluene valorization into PHA by *Rhodococcus opacus*

R. Lebrero*, S. Cantera*, S. Rodríguez* and R. Pérez*

* Institute of Sustainable Processes, University of Valladolid, Dr. Mergelina s/n., Valladolid 47011, Spain
(E-mail: raquel.lebrero@uva.es; sara.canteraruizdepellon@wur.nl; silvia.rodriguez.francos@alumnos.uva.es; rebeca.perez@iq.uva.es)

Abstract
Volatile organic compounds emitted by anthropogenic sources contribute to increasing tropospheric ozone concentration and the formation of secondary organic aerosols, as well as being harmful to human health. This work presents a novel solution for the removal of these pollutants, based on their biotransformation into market value compounds: polyhydroxyalkanoates (PHAs), expanding their production beyond conventional organic feedstock and making use of the gaseous pollutants while supporting their mitigation. Different nitrogen limitation strategies were tested for the continuous abatement of toluene and PHA synthesis. Promising results have been obtained so far, achieving PHA accumulation values of 25-30% (w/w) and up to 53% (w/w) under nitrogen feast-famine cycles of 24:48h.

Keywords (maximum 6 in alphabetical order)
Atmospheric pollution, polyhydroxyalkanoates, *Rhodococcus opacus*, volatile organic compounds, waste gas valorization.

INTRODUCTION

Atmospheric pollution has a massive impact on human health, causing millions of deaths every year along with imposing a heavy burden on ecosystems and social resources (Almetwally et al. 2020). Volatile organic compounds such as benzene, toluene, ethylbenzene, xylene and styrene (namely BTEXS) are among the most harmful pollutants emitted by anthropogenic sources.

Although environmental strategies promote preventive measures, they are often insufficient or technically and/or economically unfeasible, thus it is necessary to implement end-of-pipe treatment solutions. Biological treatments have been promoted in recent decades for air pollution control as they present lower investment and operating costs and lower environmental impacts. In addition, these biological technologies are capable of partially or totally degrading the pollutants into biomass, CO_2 and water, and not merely transferring them from one phase to another (Alfonsín et al., 2015; Mudliar et al., 2010). Numerous studies have demonstrated the ability of several bacterial strains to degrade BTEXS, however, scarce studies have investigated their potential bioconversion to valuable end products (Akmirza et al. 2017).

In this context, the valorization of BTEXS via bioconversion into polyhydroxyalkanoates (PHAs), a group of biodegradable and biocompatible polymers that can substitute oil-based plastics, appears as an attractive alternative due to their environmental and commercial interest (4-20 € kg^{-1}_{PHA}). The industrial manufacture of PHAs currently relies on the use of refined agricultural feedstock, such as glucose or fatty acids from sugar cane and palm oils, with high associated costs that can reach up to 40-50% of the total production costs, limiting PHA industrialization due to a low competitive price. Thus, the development of cost-effective technologies for the production of biodegradable and biocompatible polymers from waste sources could alleviate our heavy dependence on fossil plastics (Borrero et al. 2022).

However, only few studies have investigated to date the feasibility of bacterial conversion of BTEXS into biopolymers. For example, *Rhodococcus Aetherivorans IAR1* has been shown to accumulate short-chain-length PHA during degradation of aromatic compounds (Hori et al. 2009). Similarly, *Pseudomonas* genus synthesizes medium-chain-length PHA using BTEX as substrate (Narancic et al., 2012; Ni et al., 2010). Nevertheless, despite the promising results obtained so far, the potential of continuous removal of BTEX coupled with PHA synthesis has never been investigated. This work reports for the first time a comparative analysis of different nitrogen supply strategies to optimize PHA production by *Rhodococcus Opacus* using gaseous toluene as the only carbon source.

MATERIALS AND METHODS

Inoculum and mineral medium

Rhodococcus opacus (DMS 43205, Leibniz-Institut DSMZ, Germany) was cultivated in 120 mL serological bottles with mineral medium supplemented with 20 mL L^{-1} of a glucose solution (200 g L^{-1}). The mineral medium was composed of (g L^{-1}): NH_4Cl, 5; Na_2HPO_4, 75.2; KH_2PO_4, 30; NaCl, 5; 1 mL L^{-1} of a $MgSO_4{\cdot}7H_2O$ solution (1M); 0.3 mL L^{-1} of a $CaCl_2{\cdot}2H_2O$ solution (1M); 10 mL L^{-1} of a trace element solution composed of (g L^{-1}): EDTA, 5; $FeCl_3 \cdot 6H_2O$, 0.83; $ZnCl_2$, 0.168; $CuCl_2{\cdot}2H_2O$, 0.13; $CoCl_2{\cdot}2H_2O$, 0.01; HBO_3, 0.01; $MnCl_2 \cdot 4H_2O$, 0.0016; 1 mL L^{-1} of a biotine solution (1 g L^{-1}) and 1 mL L^{-1} of a thiamine solution (1 g L^{-1}). After growth, this pre-inoculum was transferred to 1.2 L bottles and growth in 200 mL of mineral medium also supplemented with glucose. The bottles were incubated under controlled temperature of 25ºC and continuously agitated at 200 rpm.

Experimental setup and operating procedure

An automatic stirred tank reactor (Biostat ® A, Sartorius Stedim Biotech GmbH, Germany) was used for the degradation of toluene and the production of PHA. The working volume was 2 L. The reactor was continuously stirred at 300 rpm, maintained at a constant temperature of 25ºC and the pH of the cultivation broth was controlled at 7 using a 4 M NaOH solution.

The toluene laden stream was obtained by injecting toluene with a syringe pump (Chemyx, Fusion 100) using a 5 mL syringe (Hamilton 1005RN) into an air inlet flow of 200 mL min^{-1}. Thus, the final inlet concentration was ~4 g m^{-3} and the gas residence time 30 s. The polluted stream was continuously fed to the bioreactor via a stainless steel fine bubble diffuser with a pore size of 2 µm. The reactor was filled with MSM and inoculated with the pre-inoculum to an initial concentration of 0.24 g L^{-1}. The reactor was then operated for 95 days in three different stages, as described in Table 1.

Table 1. Description of the different N-limitation strategies during the experimental period.

Stage	Days	N-feeding regime	N load
I	1-14	N added at the beginning of the stage (6 days limitation)	-
II	15-41	N addition upon depletion in the cultivation broth	Days 15-27: 100 mg N Days 28-41: 2.5 g N
III	42-95	Feast-famine N cycles	Days 42-68: 24h:48h (feast-famine, continuous N feeding) Days 69-88: 24:72 h (feast-famine, pulse N-feeding) Days 89-95: 120 h famine

Analytical methods

The concentration of VOCs was daily analysed by gas chromatography in a GC-FID (GC-FID Agilent 8860). Biomass concentration was quantified using Standard Methods (APHA 2018) as total suspended solids (TSS) and culture absorbance using a UVmini-1240 spectrophotometer at 600 nm (Shimadzu, Japan). pH measurements were performed using a pH meter Basic 20 (Crison, Spain), inlet pressure was daily monitored by an electronic pressure sensor PN7097 (Ifm Electronic, Germany), and gas flowrates were verified using the water displacement method. Total organic carbon (TOC) and total nitrogen (TN) concentrations were determined in a Shimadzu TOC-LCSH/CSN analyser equipped with a TNM-1 unit (Shimadzu, Japan).

Biomass samples were collected and refrigerated for preservation prior to extraction and PHA characterization. For extraction, 10 mL of sample was taken, centrifuged at 9000 rpm for 10 min at 4°C, with the resulting biomass pellet washed and dried for 12 h at 90°C. Then, 4 mL of pure chloroform was used for extraction by incubation for 4 h at 100°C, to finally recover the solvent and quantify PHA. The bacterial PHB content was measured using a GC–MS (GC System 7820A MSD 5977E, Agilent Technologies, Santa Clara, USA) equipped with a DB-wax column.

RESULTS AND DISCUSSION

After the initial acclimation period, complete toluene removal was recorded under N-sufficient conditions regardless of the operating stage. During N limitation, a slight deterioration of the toluene removal performance was observed, with minimum values of 92% (Figure 1). During stage I, a maximum PHB concentration of 39.7% (w/w) was obtained after 5 days of N limitation. On the contrary, feeding N upon depletion during stage II did not result in a significant accumulation of PHB, with maximum values of 28.2% recorded by day 27. It is also worth to mention that the biomass concentration during these stages was relatively low, reaching maximum values of ~1.7 g TSS L^{-1}. Biomass concentration significantly increased during stage III, with average values of 3.2 g TSS L^{-1}. The maximum PHA concentration of 53.0% (w/w) was also recorded in this stage when N was supplemented during 24h followed by a 48h famine period.

Overall, the capacity of *Rhodococcus Opacus* to continuously biodegrade toluene from a gaseous stream and produce PHB was demonstrated. Further optimization of the N-feeding strategy is being performed to promote biopolymers synthesis.

REFERENCES

Akmirza I., Pascual C., Carvajal A., Pérez R., Muñoz R., Lebrero R. 2017. Anoxic biodegradation of BTEX in a biotrickling filter. *Science of the Total Environment* **587-588**, 457-465.

Alfonsín, C., Lebrero, R., Estrada, J. M., Muñoz, R., Kraakman, N. J. R., Feijoo, G., Moreira, M. A. T. 2015. Selection of odour removal technologies in wastewater treatment plants: A guideline based on Life Cycle Assessment. *Journal of Environmental Management* **149**, 77–84.

Almetwally, A. A., Bin-Jumah, M., Allam, A. A. 2020. Ambient air pollution and its influence on human health and welfare: an overview. *Environmental Science and Pollution Research* **27,** 24815–24830.

Borrero-de Acuña, J.M., Rohde, M., Saldias, C., Poblete-Castro, I. 2021. Fed-Batch mcl-Polyhydroxyalkanoates Production in Pseudomonas putida KT2440 and ΔphaZ Mutant on Biodiesel-Derived Crude Glycerol. *Frontiers in Bioengineering and Biotechnology* **9**, 1–10.

Hori, K., Kobayashi, A., Ikeda, H., Unno, H. 2009. Rhodococcus aetherivorans IAR1, a new bacterial strain synthesizing poly(3-hydroxybutyrate-co-3-hydroxyvalerate) from toluene. *Journal of Bioscience and Bioengineering*, **107**(2), 145–150.

Mudliar, S., Giri, B., Padoley, K., Satpute, D., Dixit, R., Bhatt, P., Vaidya, A. 2010. Bioreactors for treatment of VOCs and odours - A review. *Journal of Environmental Management* **91**(5), 1039–1054.

Narancic, T., Kenny, S. T., Djokic, L., Vasiljevic, B., O'Connor, K. E., Nikodinovic-Runic, J. (2012). Medium-chain-length polyhydroxyalkanoate production by newly isolated Pseudomonas sp. TN301 from a wide range of polyaromatic and monoaromatic hydrocarbons. *Journal of Applied Microbiology*, **113**(3), 508–520

Ni, Y. Y., Kim, D. Y., Chung, M. G., Lee, S. H., Park, H. Y., Rhee, Y. H. 2010. Biosynthesis of medium-chain-length poly(3-hydroxyalkanoates) by volatile aromatic hydrocarbons-degrading Pseudomonas fulva TY16. *Bioresource Technology*, **101**(21), 8485–8488.

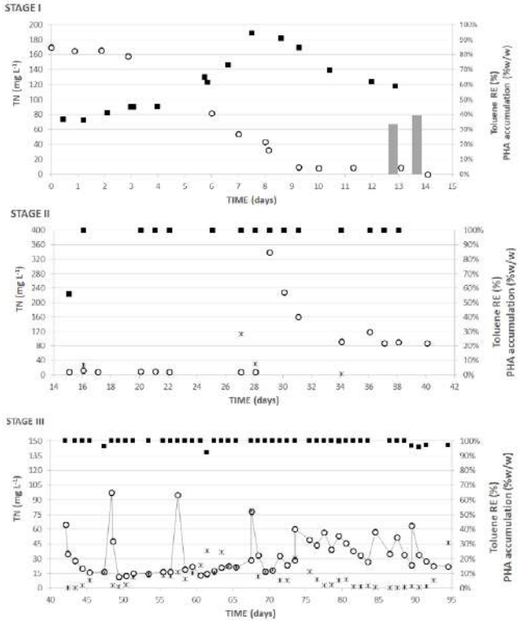

Figure 1. Time course of the total nitrogen concentration (white circles), toluene removal efficiency (black squares) and PHA accumulation (grey bars in figure 1A, and asterisks in figures 1B and 1C) during the different operating stages.

Modelling H_2 conversion by purple bacteria enriched cultures: evaluating kinetics of gas-fed processes to assess feasibility

G. Capson-Tojo*, J. P. Steyer*, N. Bernet* and M. del R. Rodero*,**

* INRAE, University Montpellier, LBE, 102 avenue des Étangs, 11100 Narbonne, France
(E-mail: *gabriel.capson-tojo@inrae.fr*; *jean-philippe.steyer@inrae.fr*; *maria-del-rosario.rodero-raya@inrae.fr*)
** Institute of Sustainable Processes, University of Valladolid, 47011, Valladolid, Spain

Abstract
Purple phototrophic bacteria (PPB) can be used to convert gaseous streams (e.g., H_2 and CO_2) into single-cell protein. Here we have determined, for the first time, the specific uptake rates of enriched PPB cultures under different environmental conditions (i.e., temperatures, pH and light intensities), using a mechanistic model considering relevant biological and physico-chemical processes. The model accurately represented results from batch tests with different gas-transfer kinetics (i.e., k_La values), providing similar biological uptakes rates. Optimal rates of 1.9-2.0 g COD·g COD^{-1}·d^{-1} were reached at pH 7, 25 ºC and light intensities over 30 W·m^{-2}, with biomass yields of ~1 g COD·g^{-1} COD. The influence of light and temperature on the uptake rates was modelled using the Steele's equation and the cardinal temperature model with inflection. The obtained rates are similar to those for pure PPB cultures and those achieved via photoheterotrophy.

Keywords
Autotrophy; gas valorisation; modelling; purple phototrophic bacteria; resource recovery; single-cell protein

INTRODUCTION

Processes based on purple phototrophic bacteria (PPB) are a promising option for resource recovery due to the high biomass yields that their phototrophic metabolism allows. PPB can efficiently generate a wide range of value-added products (*e.g.*, single-cell protein (SCP), fertilisers, or polyhydroxyalkanoates) at biomass yields up to 1 g COD·g COD^{-1} (Capson-Tojo et al., 2020).

While their photoheterotrophic capabilities have been considerably studied in the past few years for resource recovery from wastewater (Hülsen et al., 2022a, 2022b, 2022c), their photoautotrophic capabilities have barely been researched. PPB grown autotrophically could allow the efficient conversion of H_2 and CO_2 into SCP, generating a pathogen-free high value-added product usable as feed/food (Delamare-Debouteville et al., 2019). If the H_2 and nutrient sources are sustainable (e.g., from bioH_2 and anaerobic digestate), this approach could be a game changer for valorising gaseous effluents in a biorefinery, while recovering remaining nutrients. The proof of concept of H_2 conversion by PPB has been recently realised using pure cultures (Spanoghe et al., 2021). Recent results from our group have shown than enriched PPB cultures can valorise H_2 and CO_2 at higher yields than pure cultures (unpublished). The specific rates (crucial for implementation) are still to be determined using dedicated models.

The mechanistic models available to represent resource recovery by PPB are the Photo-anaerobic model (PAnM) (Puyol et al., 2017) and its extension, the ePAnM (Capson-Tojo et al., 2023), which have been successfully applied for wastewater treatment. Photoautotrophic uptake is included in both models, but they do not consider detailed gas-transfer kinetics. This is essential for modelling gas-fed processes, as models must account for rate limitation by mass transfer due to the low solubility of gaseous substrates.

Results from dedicated batch tests have been used here to calibrate a mechanistic model considering PPB as biomass component. Once we confirmed that the model could account for both physical and biological rate limitations, the model was used to determine the specific uptake rates of enriched PPB cultures under different environmental conditions (e.g., pH, temperature (T) and light intensities). The impact of these variables on the rates was studied and modelled.

MATERIALS AND METHODS

Photoautotrophic enrichments were grown in Schott flasks of 500 mL using the mineral synthetic medium (MSM) proposed by Ormerod et al. (1961) but modified to provide CO_2 as C source (as carbonate) and providing H_2 in the headspace. The flasks were filled with 190 mL of MSM and 10 mL of PPB enrichment as inoculum. After, they were closed and the headspace was flushed with N_2 prior to H_2 addition. The initial headspace pressure was adjusted to 1.30-1.35 bar. The flasks were covered with UV/VIS filters (Hülsen et al., 2022c) and incubated under continuous illumination using infrared LED lights (850 nm). Two tests at different mixing intensities (and thus gas transfer rates) were performed, at 150 and 600 rpm. Assays at initial pH values of 6, 7 and 8.5, T of 15, 25, 38 and 50 °C, and light intensities of 0, 5, 15, 30 and 50 W·m^{-2} were carried out at 600 rpm (in triplicate). Gas composition and pressure were monitored 4-5 times per day. Liquid samples were drawn to determine biomass yields, crude protein contents and microbial communities.

The model considered PPB as single biomass component and growth on H_2 and CO_2 and biomass death as biological processes. Table 1 shows the corresponding Petersen matrix. Mass transfer processes and chemical equilibria were modelled as in the ADM1 (Batstone et al., 2002), modifying the model to account for gas consumption and for relevant chemical species for pH calculation. The model was structured following IWA standards. Stoichiometric parameters were either determined experimentally (yields) or gathered from the literature. Matlab was used to perform the simulations. Estimation of parameters related to H_2 uptake (K_m and K_{H2}) was performed as in Puyol et al. (2017). The effect of T and light on uptake rates was modelled using the cardinal temperature model with inflection (CTMI) (Ruiz-Martínez et al., 2016) and The Steele's equation (Wágner et al., 2018).

Table 1. Petersen matrix of the proposed model. The nomenclature is the same as in Capson-Tojo et al. (2023).

Component →	i	1	2	3	4	5	6	Rate (mg COD·L^{-1}·d^{-1})
j	**Process ↓**	S_{IC}	S_{H2}	S_{IN}	S_{IP}	X_{PB}	X_C	
1	Autotrophic uptake of H_2 by PPB	-$f_{IC,au}$	1	-$\sum_{i=1\text{-}2,4\text{-}6} N_i \cdot \nu_{i,1}$	-$\sum_{i=1\text{-}3,5\text{-}6} P_i \cdot \nu_{i,1}$	$Y_{PB,au}$		$k_{dis} S_{IC}/(K_{IC}+S_{IC}) \cdot S_{H2}/(K_{H2}+S_{H2}) \cdot X_{PB} \cdot I_{INC} \cdot I_{IP}$
2	Decay of X_{PB}					-1	1	$k_{dec,PB} \cdot X_{PB}$
Units		mol C·L^{-1}	mg COD·L^{-1}	mg N·L^{-1}	mg P·L^{-1}	mg COD·L^{-1}	mg COD·L^{-1}	

RESULTS

Figure 1 shows, as example, the results for one of the batch tests at 150 rpm. Despite the change in limiting rates, the model was able to represent the whole process, predicting accurately biomass and hydrogen concentrations. Before 0.9 d, H_2 was sufficient, and the consumption rates were limited by biological uptake (typical exponential curve, soluble H_2 concentrations much higher than the saturation constant for H_2 (K_{H2}; below 0.05 mg COD·L^{-1} in all experiments) and uptake rates increased with supply). After 0.9 d, the H_2 transfer rate became limiting due to the high biomass concentration and the low k_La (28.7 d^{-1}), a situation that did not change despite the injection of extra H_2 in the headspace. After this point, the concentration of H_2 in the liquid was always close to zero, the growth curve became linear, and the uptake rate was limited by the supply rate. The model predicted accurately this behaviour, confirming its applicability for rate determination.

The tested environmental conditions affected considerably the H_2 uptake rates. Optimal rates of 1.9-2.0 g COD·g COD^{-1}·d^{-1} were achieved at initial pH values of 7, 25 ºC, and light intensities over 30 W·m^{-2} (Table 2). Lower or higher pH values and T resulted in decreased rates (Table 2, Figure 2). No photoinhibition was observed at 50 W·m^{-2}. With R^2 values of 0.97 and 0.91, the Steele's equation and the CTMI when able to represent these impacts accurately (Figure 2). The biomass yields close to 1 g COD·g^{-1} COD confirmed effective phototrophic growth. The optimal conditions are similar to those reported for photoheterotrophic PPB growth, confirming these values and suggesting that the growth mode does not affect optimal conditions (Capson-Tojo et al., 2022, 2020). Optimal specific uptake rates are close to those for photoheterotrophic processes (2.3-2.7 g COD·g COD^{-1}·d^{-1}; (Capson-Tojo et al., 2023; Puyol et al., 2017)) and similar to those reported for pure PPB cultures grown autotrophically (below 2.3 g COD·g COD^{-1}·d^{-1}; (Spanoghe et al., 2021)).

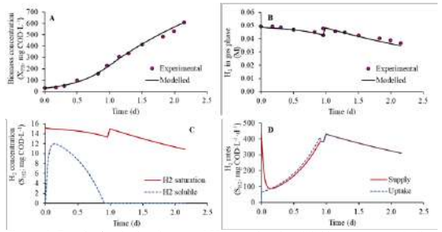

Figure 1. Results for the batch test at 150 rpm, showing (A) biomass concentrations, (B) H_2 gas concentrations, (C) H_2 liquid concentrations, and (D) H_2 supply and uptakes rates.

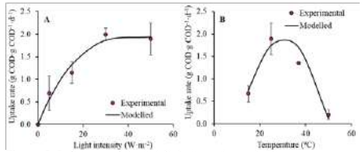

Figure 2. Influence of the (A) light intensity and (B) temperature on the specific H_2 uptake rates. Average and confidence intervals are shown (95%; n=3). The modelled results correspond to the Steele's equation (light intensity) and the cardinal temperature model with inflection (temperature).

Table 2. Main biomass yields and uptake rates from the batch tests.

	Mixing (rpm)		pH		Temperature (°C)		Intensity (W·m^{-2})		
	150[1]	600[1]	6	8.5	15	38	15	30	50[2]
Biomass yield (g $COD_{biomass}$·g $COD_{consumed}^{-1}$)	1.01± 0.03	1.01± 0.01	1.00± 0.07	0.93± 0.01	0.85± 0.07	0.99± 0.07	1.02± 0.06	1.05± 0.01	1.01± 0.01
Specific uptake rates (g COD·g COD^{-1}·L^{-1})	2.01± 0.50	1.89± 0.35	1.50± 0.05	0.83± 0.02	0.66± 0.18	1.35± 0.04	1.15± 0.24	2.00± 0.14	1.89± 0.35

1. k_La_{H2} of 28.7 d^{-1} at 150 rpm and 70.4 d^{-1} at 600 rpm.
2. Results also for the tests at pH 7 and 25 ºC.

CONCLUSIONS

Here we show for the first time that enriched PPB cultures can be grown autotrophically from H_2 at similar rates than pure cultures, proving that axenic conditions are not needed. Optimal values of 1.9-2.0 g COD·g COD^{-1}·d^{-1} were reached at pH 7, 25ºC and light intensities higher than 30 W·m^{-2}. The developed model was able to represent the overall kinetics of the process, accurately predicting rate limitations. The Steele's equation and the CTMI represented accurately the variations in the specific uptake rates due to light and T. The high yields and rates achieved confirm the great potential of enriched PPB cultures for H_2 valorisation. Volumetric production rates must be assessed and the model must be validated using continuous bioreactors.

REFERENCES

Batstone, D.J., Keller, J., Angelidaki, I., Kalyuzhny, S. V, Pavlostathis, S.G., Rozzi, A., Sanders, W.T.M., Siegrist, H., Vavilin, V.A., 2002. Anaerobic digestion model no. 1 (ADM1). IWA Publishing.

Capson-Tojo, G., Batstone, D.J., Grassino, M., Vlaeminck, S.E., Puyol, D., Verstraete, W., Kleerebezem, R., Oehmen, A., Ghimire, A., Pikaar, I., Lema, J.M., Hülsen, T., 2020. Purple phototrophic bacteria for resource recovery: Challenges and opportunities. *Biotechnol. Adv.* **43**, 107567.

Capson-Tojo, G., Batstone, D.J., Grassino, M., Hülsen, T., 2022. Light attenuation in enriched purple phototrophic bacteria cultures: implications for modelling and reactor design. *Water Res.* **219**, 118572.

Capson-Tojo, G., Batstone, D.J., Hülsen, T., 2023. Expanding mechanistic models to represent purple phototrophic bacteria enriched cultures growing outdoors. *Water Res.* **229**, 119401.

Delamare-Debouteville, J., Batstone, D.J., Kawasaki, M., Stegman, S., Salini, M., Tabrett, S., Smullen, R., Barnes, A.C., Hülsen, T., 2019. Mixed culture purple phototrophic bacteria is an effective fishmeal replacement in aquaculture. *Water Res. X* **4**, 100031.

Hülsen, T., Barnes, A.C., Batstone, D.J., Capson-Tojo, G., 2022a. Creating value from purple phototrophic bacteria via single-cell protein production. *Curr. Opin. Biotechnol.* **76**, 102726.

Hülsen, T., Stegman, S., Batstone, D.J., Capson-Tojo, G., 2022b. Naturally illuminated photobioreactors for resource recovery from piggery and chicken-processing wastewaters utilising purple phototrophic bacteria. *Water Res.* **214**, 118194.

Hülsen, T., Züger, C., Batstone, D.J., Solley, D., Ochre, P., Porter, B., Capson-Tojo, G., 2022c. Outdoor demonstration-scale flat plate photobioreactor for resource recovery with purple phototrophic bacteria. *Water Res.* **216**, 118327.

Ormerod, J.G., Ormerod, K.S., Gest, H., 1961. Light-Dependent Utilization of Organic Compounds and Photoproduction of Molecular bHydrogen by Photosynthetic Bacteria; Relationships with Nitrogen Metabolism. *Arch. Biochem. Biophys.* **94**, 449–463.

Puyol, D., Barry, E.M., Hülsen, T., Batstone, D.J., 2017. A mechanistic model for anaerobic phototrophs in domestic wastewater applications: Photo-anaerobic model (PAnM). *Water Res.* **116**, 241–253.

Ruiz-Martínez, A., Serralta, J., Seco, A., Ferrer, J., 2016. Modeling light and temperature influence on ammonium removal by Scenedesmus sp. under outdoor conditions. *Water Sci. Technol.* **74**, 1964–1970.

Spanoghe, J., Vermeir, P., Vlaeminck, S.E., 2021. Microbial Food From Light, Carbon Dioxide And Hydrogen Gas: Kinetic, Stoichiometric And Nutritional Potential Of Three Purple Bacteria. *Bioresour. Technol.* **337**, 125364.

Wágner, D.S., Valverde-Pérez, B., Plósz, B.G., 2018. Light attenuation in photobioreactors and algal pigmentation under different growth conditions – Model identification and complexity assessment. *Algal Res.* **35**, 488–499.

Biological Methanation of WWTP biogas with green H_2 for sustainable mobility

O. Casal*, C.M. Castro-Barros*, J. Tobella*, M. Poch**, O. Guerrero***, D. Gabriel***, J.A. Baeza***, A. Guisasola ***, M. Canet****

* Cetaqua Centro Tecnológico del Agua, Carretera d'Esplugues 75, 08940 Cornellà de Llobregat, Barcelona, Spain (E-mail: oriol.casal@cetaqua.com)
**Aigües de Barcelona, Empresa Metropolitana de Gestió del Cicle Integral de l'Aigua, S.A., Carrer General Batet 1-7, 08028, Barcelona, Spain
***GENOCOV Research Group, Department of Chemical, Biological and Environmental Engineering, School of Engineering, Universitat Autònoma de Barcelona, Escola d'Enginyeria. Edifici Q Campus UAB, 08193, Bellaterra, Barcelona, Spain
****Transports Metropolitans de Barcelona, Carrer 60, 21-23, Sector A, 08040, Barcelona, Spain

Abstract
Biological methanation is seen as one key technology which might enable long-term renewable energy storage in the chemical form. When applied to a WWTP biogas stream, it is capable of substituting a conventional upgrading step, with the advantage of increasing the total biomethane produced by 40 to 80%. An ex-situ biological methanation process is tested at demonstration scale to supply biomethane to a public transportation bus.

Keywords (maximum 6 in alphabetical order)
Biomethane, biological methanation, green hydrogen, power-to-gas, regenerated water, sustainable mobility

INTRODUCTION: THE NEED OF ENERGY STORAGE IN THE PATH OF DECARBONIZATION

As Europe progresses towards de-carbonization of the energy sectors as well as invests in renewable investments, the gap between instantaneous production and consumption of electricity becomes more crucial and harder to manage for grid operators. Storage of surplus renewable electricity in the chemical form is expected to be a key bridge in the decarbonization of the several sectors, transportation among them. Hydrogen has been gaining most of the attention since it can be readily produced out of water and electricity, however, it is well known that storing energy in the form of hydrogen comes with a number of unsolved issues, among them: low energy volumetric density, high corrosivity, high fugacity and very high explosive mixtures range with air.

Processing the H_2 molecule into another species is seen as the next logical step, in spite of the potential losses. Among the candidates, there is methanol, ammonia, synthetic long hydrocarbon chains as well as methane. Methane, or biomethane, has the advantage that it can be readily injected into existing infrastructure, however, in order to produce methane, as the reaction of Sabatier shows (see Equation 1), CO_2 is needed as a reactive, and, if possible, biogenic CO_2.

$$CO_{2(g)} + 4\,H_{2(g)} \rightarrow CH_{4(g)} + 2H_2O_{(g)}$$

Equation 1. Sabatier methanation reaction

Biogas upgrading to biomethane consists of the separation of CO_2 from CH_4, either by membrane separation, or chemical or physical absorption, or pressure swing adsorption, or cryogenically. In the case of methanation, hydrogen can be directly injected into the biogas for its methanation and upgrading into biomethane. The volume of biomethane obtained is also increased compared to conventional upgrading, in-between 40% and 80% depending on the on-site composition of the biogas.

Methanation can either be carried out biologically or catalytically. Catalytic methanation requires high temperature and pressure (pressure enhances reaction kinetics due to Le Chatelier's principle) which leads to very low residence times and enables coupling with heat integration (district heating, steam generation, etc.). However, although the maturity of catalytic methanation is very high, it has a weak point: catalyst poisons quickly due to remaining pollutants such as H_2S in the biogas, ppb traces accumulate over processed volume flows and render the operation inviable.

Biological methanation on the other hand, is at a lower degree of maturity and requires much longer residence times, but it does not suffer from catalyst poisoning, as microbes regenerate and are much more tolerant to pollutants. Pressure and temperature requirements are lower, which ease construction of reactors although it makes heat integration less attractive. Biological methanation can be done ex-situ (on a separate reactor) or in-situ (in the anaerobic digester itself). Literature seems to suggest that in-situ methanation is limited in terms of the maximum achievable concentration of methane in the off-gas.

MATERIALS AND METHODS

In the LIFE NIMBUS (LIFE19 ENV/ES/000191, http://www.life-nimbus.eu) project a biological methanation ex-situ process has been developed to upgrade on-site biogas produced in an anaerobic digester of WasteWater treatment plant sludge at the Baix Llobregat WWTP. The process has been scale up to build a demonstration plant with a nominal capacity of 7,4 Nm^3/h of biomethane, enough to cover the daily needs of a urban transportation bus which covers a distance of 150km daily. The biogas is scrubbed of H_2S and pressurized into the reactor up to 4 barg, where it mixes with the hydrogen and CO_2 reacts to CH_4. The biomethane is conditioned and pressurized up to 300 bars for its storage and refuelling of a public transportation bus (see Figures 1 and 2).

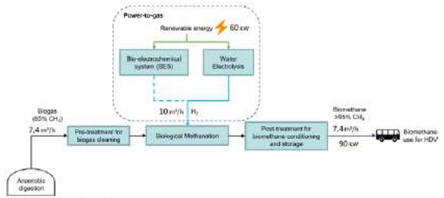

Figure 1. Flowchart of the biological methanation implemented process.

This process is not only presented as an alternative to a conventional biogas upgrading to biomethane such as membrane upgrading or chemical absorption; it really is a hybrid between a biogas upgrading process as well as a power-to-gas process, for it stores renewable electrical surplus energy in the form of biomethane. The hydrogen necessary to methanate the biogas will be supplied by an on-site alcaline electrolyzer (60 kWe, 10 Nm^3/h H_2) powered by renewable electricity. A Biological Electrochemical System is also implemented at pilot scale. This type of electrolyzer obtains part of its energy needs from organic matter from a wastewater stream, greatly improving the efficiency of electrolysis. The electrolyzer requires deionized water with a very high purity (no salts nor organic content), regenerated water will be treated so as to obtain this demineralized water.

Figure 2. Public transportation bus from TMB fuelled by biomethane produced in the LIFE NIMBUS project

Both the methanation plant (see Figure 3) as well as the Biological Electrolyzer System pilot plants have been designed based on laboratory experimental data on microbial activity as well as other aspects such as mass and heat transfer, which can become limiting when scaling up from laboratory/bench scale. Both pilot plants will start its operation in February 2023, and operational data will be collected to assess both technically as well as economically the scale-up of the process to commercial nominal capacities, in order to determine the technology viability. Furthermore, the bus engine and tanks will be analysed to see any detrimental effects by remaining Siloxanes and H_2 traces.

Figure 3. View of the biological methanation plant

RESULTS AND DISCUSSION

The first results of the operation of the pilot plant will be presented at the congress.

ACKNOWLEDGEMENTS

The LIFE NIMBUS project is led by Cetaqua together with Aigües de Barcelona, Universitat Autònoma de Barcelona and Transports Metropolitans de Barcelona. It is financed by the EU under the LIFE programme (LIFE19 ENV/ES/000191).

Besides the LIFE NIMBUS project, Cetaqua is also developing biological methanation in the project HORIZON EUROPE project SEMPRE-BIO: SEcuring doMestic PRoduction of cost Effective BIOmethane, grant nº 101084297

Nitrogen recovery to produce Smart Fertilisers from wastewater

G. Noriega-Hevia*, A. González-Miguez*, A. Mayor*, L. Rodríguez-Hernández** and C.M. Castro-Barros*

* CETAQUA- Water Technology Centre,
(E-mail: guillermo.noriega@cetaqua.com; alicia.gonzalez@cetaqua.com; amayor@cetaqua.com; celia-maria.castro@cetaqua.com)
** VIAQUA
(E-mail: leticia.rodriguez@agbar.es)

Abstract
Nitrogen recovery from wastewater appears as a feasible alternative to produce ammonia fertilisers with a lower impact than the conventional process, increasing the nutrient circularity and reducing the external EU dependence on fertilisers. For that aim, a treatment train formed by an ion exchange unit and a hollow fibre membrane contactor unit was evaluated in this work for the recovery of nitrogen from wastewater. The results show its capacity to recover nitrogen as marketable ammonium salts with high efficiencies (91%) which will be blended with recovered struvite and Plant Growth Promoting Bacteria to produce a Smart Bio-based fertiliser.

Keywords
Biofactory; circular economy; hydrophobic membrane; ion exchange; nitrogen recovery; smart fertiliser.

INTRODUCTION

Nitrogen is an essential nutrient for plant growth. Its demand to produce fertilisers to be applied in agriculture has increased drastically in the last decades. Conventional production of nitrogen as fertiliser is carried out by the Haber-Bosch process, which is an energy-intensive process and fossil fuel dependent. More sustainable ways to obtain nitrogen fertilisers have been developed recently. In this framework, Horizon 2020 WalNUT project came out, developing new alternatives to produce fertilisers from wastewater and brine, increasing the nutrients' circularity as well as reducing the external EU dependence of these products by the application of different technologies to recover nitrogen, phosphorus and salts such as sodium, chloride or potassium.

Nitrogen is usually removed from wastewater treatment plants (WWTPs) by the nitrification-denitrification process. This two-step process has high energy requirements in terms of aeration to oxidise ammonium to nitrate, and also needs organic matter to reduce the nitrate to nitrogen gas. A more sustainable alternative is to recover the nitrogen from wastewater instead of removing it. In particular, nitrogen can be recovered from reject water, which is the most nitrogen rich stream from WWTPs, reducing the energy demand and the carbon footprint from WWTPs (Noriega-Hevia et al., 2021). For that purpose, gas-permeable hollow fibre membrane contactors (HFMC) are one of the best technologies to applied because of its low energy requirements, modularity, high ammonia selectivity and its hydrophobicity, which avoid the pass of hazardous substances such as heavy metals or organic micropollutants (Licon Bernal et al., 2016). These membranes offer a surface to favour the pass of free ammonia gas from a feed solution with a high ammonia concentration to an acid solution, usually sulphuric acid or nitric acid. This free ammonia is captured in the acid solution due to the low pH producing an ammonia salt which is marketable as fertiliser. The driven force is the free ammonia concentration in both sides of the membrane. In some applications it is advisable to add a unit of ion exchange to concentrate the ammonia of the reject water before feeding the membranes in order to maximise the salt production.

Although the ammonia salt produced is a marketable as fertiliser, in this project the final aim is to produce a NPK smart bio-based fertiliser (BBF), that is, a nitrogen, phosphorus and potassium fertiliser in which is possible to modify the release of the nutrients by biological or chemical techniques (Raimondi et al., 2021). This fact favours an adaptive application of fertilisers depending on the soil requirements, increasing the sustainability and improving its management. In this case, selected Plant Growth Promoting Bacterias (PGPBs) are going to be added to the NPK fertiliser. In this work, it is shown the performance of the nitrogen recovery process from reject water by the application of HFMC and IE jointly as the first step to produce a smart BBF in the framework of WalNUT project. Different operational conditions have been tested to determine the optimum conditions in terms of recovery efficiency, recovery rate and ammonia content in the acid tank.

MATERIAL AND METHODS

The treatment train applied for the recovery of nitrogen consisted of two units: an ion exchange unit, to concentrate the ammonia content of the reject water; and two hollow fibre membrane contactors in series to extract the ammonia of the feed and to produce an ammonia sulphate solution (Figure 1). Ion exchange columns have a bed volume of 1 litre using natural zeolites (ZEOCAT- 0-1 mm) as exchangers. HFMC were two modules of Liqui-Cel® 3M with an unitary surface of 1.4 m2.

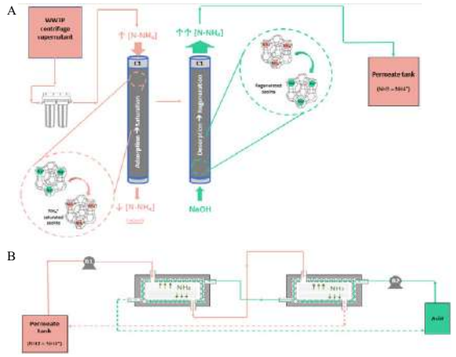

Figure 1. Nitrogen recovery set-up: A) ion exchange unit; B) membrane unit.

The feedstock was reject water from the full-scale Ourense WWTP located in the Northwest of Spain. This stream has an ammonia concentration of 1307±146 mg NH4-N/l and a SST of 2.3±0.3 g/l. Although the amount of solids of this stream is not dangerous, a pre-treatment of two filters in series (20 µm + 5 µm), was also included in order to remove the big solids that could be present.

Different tests were carried out to characterise and evaluate the performance of the treatment train to define the optimum operational conditions in each part of it. Regarding the IE unit, to obtain the maximum concentration of ammonia in the regeneration with the minimum losses and, in the case of the HFMC unit, the maximum recovery efficiency to obtain a concentrated ammonium salt.

RESULTS AND DISCUSSION

The treatment train proposed in this research has been validated, proving its capacity to recover nitrogen from wastewater. In this section, the results obtained in the different units are shown.

Ion exchange unit

Different operational conditions have been tested in order to characterise the column and to determine the optimised operating conditions. Figure 2 presents the ammonia evolution in the column outflow with an HRT of 23 minutes. The cation exchange capacity (CEC (mg/g)) obtained by the zeolites in the different tests carried out was 15 mg N-NH_4/g zeolite.

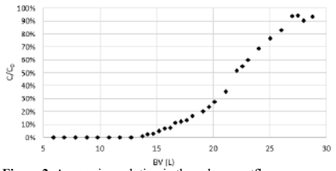

Figure 2. Ammonia evolution in the column outflow.

Another important parameter to evaluate is the concentration of the regenerant, in this case sodium hydroxide. Different concentrations were tested. A more concentrated solution reduced the regeneration time and offered the possibility to obtain higher ammonia concentrations (Figure 3). However, a higher concentration of NaOH led to a higher pH, which increases the risk of free ammonia losses by stripping. This is an important parameter to evaluate for the best performance of the treatment train due to the reagents costs.

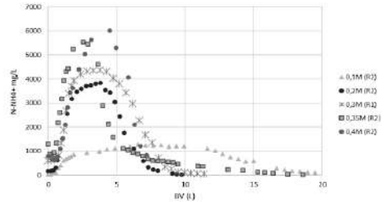

Figure 3. Effect of NaOH solution in the regeneration.

Membrane unit

Regarding the membrane, different flow rates were tested to evaluate the effect of this parameter on the recovery rate. Figure 4 shows the ammonia evolution in the feed tank during the recovery process.

The feed concentration was 1285±102 mg N-NH_4/l and pH was 12.4±0.2. As it can be seen, an increase in flow rate leads to a higher recovery rate but, at values higher than 400 ml/min, the rate is similar. These results suggest that applying a higher flow rate, the turbulence reduces the boundary layer resistance but, at a certain flow rate, this resistance is minimum, and the turbulence could not be more reduced. In these tests, the recovery efficiency was 91±3%. The nitrogen recovered was stored in the acid tank as sulphuric acid. At this moment, only a sulphuric acid concentration of 0.09M has been tested, obtaining an ammonia sulphate solution with 2.5 g N-NH_4/l.

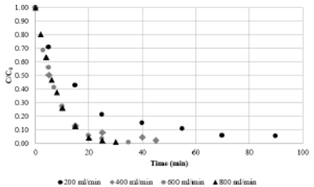

Figure 4. Ammonia evolution during the recovery rate at different flow rates.

Next steps will be focused on the increase of the ammonia sulphate nitrogen concentration and the optimization of both units jointly as the previous step of the production of a NPK Smart fertiliser in the WalNUT project framework. This Smart fertiliser will be the blend of recovered ammonia salt and struvite with a selected PGPB to maximise the soil nutrient uptake.

CONCLUSIONS

The treatment train proposed is able to work as a unique unit maximising the nitrogen recovery and reducing costs due to the previous concentration with the IE. Furthermore, it presents high recovery efficiencies (91%) producing a concentrated ammonia sulphate solution. However, the optimization of both units working together as well as the raised product ammonia concentration will be aspects to work on to produce the final Smart BBF.

REFERENCES

Licon Bernal, E.E,. Maya, C., Valderrama, C., Cortina, J.L. 2016 Valorization of ammonia concentrates from treated urban wastewater using liquid-liquid membrane contactors. Chemical Engineering Journal **302**, 641-649.

Noriega-Hevia, G., Serralta, J., Seco, A., Ferrer, J. 2021 Economic analysis of the scale-up and implantation of a hollow fibre membrane contactor plant for nitrogen recovery in a full-scale wastewater treatment plant. Separation and Purification Technology **275**, 119128.

Raimondi, G., Maucicri, C., Toffanin, A., Renella, G., Borin, M., 2021 Smart fertilizers: What should we mean and where should we go?. Italian Journal of Agronomy **16**, 1794

ACKNOWLEDGEMENTS

The authors are grateful to the European Commission, specifically to the Horizon 2020 Programme, which funds WalNUT project (H2020-RUR-2020-2 101000752).

Pharmaceuticals occurrence in water bodies of Catalonia in the last decade, which are the most ubiquitous compounds?

M. Castaño-Trias*,, S. Rodriguez-Mozaz*,**, G. Buttiglieri*,****

* Catalan Institute for Water Research (ICRA-CERCA), C/Emili Grahit 101, 17003 Girona, Spain
** University of Girona, Girona, Spain
(E-mail: m.castano@icra.cat; lalonso@icra.cat; srodriguez@icra.cat; gbuttiglieri@icra.cat)

Abstract: Pharmaceutical active compounds (PhACs) have been detected in the environment for several years. These substances, even at low concentrations can have an impact in the ecosystems. Therefore, it is crucial to develop new methodologies to track these concentrations in the environment. A suitable selection of pharmaceuticals is a critical step and it can be achieved through a prioritisation strategy. In this work, PhACs occurrence data were obtained from monitoring studies of our group in the last 10 years in hospital and urban wastewater, river, and sea. The data were used to determine the most relevant pharmaceuticals in terms of occurrence and an analytical method upgrade to analyse them was performed. The new methodology was then applied and validated with water (wastewater, river, and sea water), soil, and crops samples from Greece and Spain suffering from water scarcity.

Keywords: Emerging contaminants; Hospital wastewater; Transformation Products; Wastewater.

INTRODUCTION

Pharmaceutical active compounds (PhACs) have been widely detected in wastewater. Wastewater treatment plants may not achieve their total degradation and, therefore, they are released in the environment (Čelić *et al.*, 2019). These compounds, even at low concentrations, can have an impact in the ecosystems. Thus, it is critical to develop up-to-date analytical methods to determine their occurrence. To obtain accurate information a target analysis is required. Nonetheless, the fact that analytes must be selected in advance is a major drawback, and, in some cases, no-preselected analytes could remain unspotted while other selected ones might not be present. Therefore, properly selecting the most relevant analytes through a prioritisation is a critical step. In this work, an occurrence-based prioritization was performed using an in-house research group database of 30 publications in hospital and urban wastewater, river, and sea. A new multi-residue analytical methodology was upgraded, applied, and validated with wastewater, river, and sea water from Catalonia and Greece, areas suffering from water scarcity (EU HYDROUSA project, www.hydrousa.org).

MATERIALS AND METHODS

Studies performed by the group in the last 10 years in river, hospital, and urban wastewater in Catalonia (NE Spain) were gathered. The generated database (30 publications) provided the occurrence data of 157 pharmaceuticals and transformation products (TPs). Compounds were ranked based on their mean concentrations and 4 different lists were generated (hospital and urban wastewater, treated wastewater, and river water). A list of 50 compounds was generated combining the 4 lists considering each compound ranking. Current analytical methodologies of the institution based on SPE and UHPLC-MS/MS (5500 QTRAP hybrid triple quadrupole-linear ion trap mass spectrometer) were combined to obtain an upgraded method for the analysis of the selected compounds in both positive (HSST3 column) and negative (BEH column). The methodology was validated with real samples from Spain and Greece.

RESULTS AND DISCUSSION

Therapeutic classes with the highest concentrations in water bodies of Catalonia in the last 10 years were analgesics and antiinflammatories (30%), antibiotics (24%), and psychiatric drugs (20%). Other compounds with high concentrations in water belong to β-blockers, histamine receptor antagonists, or calcium channel blockers. On the other hand, 12 TPs were detected and represented 24% of the 50 more ubiquitous compounds, highlighting how important it is to include them in monitoring programs. Figure 1 depicts the 25 compounds occupying the first positions of the selection.

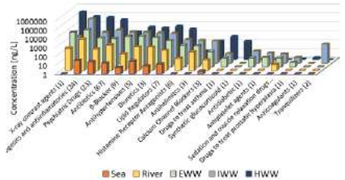

Figure 1: Concentration (ng/L, logarithmic scale) of the first 20 occurrence based prioritised PhACs in IHWW, IWW, EWW, and river water.

Sampling campaigns were carried out in Catalonia and Greece water samples (2019-2020) with the upgraded analytical method. Similar concentration profiles were observed in both areas in influent wastewater (338 and 351µg/L in Greece and Catalonia, respectively). Furthermore, the concentrations did not strongly differ in most of the therapeutic classes. Nevertheless, some compounds presented different concentrations in wastewater influent: levamisole, gemfibrozil, and iopromide were detected at higher concentration levels in Catalonia; whereas ranitidine, venlafaxine, and valsartan presented higher values in the Greek Islands. These results may suggest there might be some preference in the usage of certain pharmaceuticals based on the country. Results obtained in Catalonia followed the same patterns of the in-house database but with higher concentrations for some TPs, especially of ibuprofen.

CONCLUSIONS

Data coming from 30 publications in the last 10 years in Catalonia was gathered to select the 50 most ubiquitous pharmaceuticals in surface and wastewater. More than 20% of the selected compounds correspond to TPs. A new analytical method was developed based on the in-house methods for these 50 compounds and applied to water samples of Catalonia and Greece. Both countries showed similar therapeutic classes concentration profiles, with some differences for some compounds: levamisole, ranitidine, gemfibrozil, venlafaxine, iopromide and valsartan. Further studies are required to confirm the hypothesis of different prescription/use/preferences in the usage of certain pharmaceuticals in different countries.

ACKNOWLEDGEMENTS

This study has received funding from the European Union's Horizon 2020 Research and Innovation programme (HYDROUSA, grant agreement N° 776643). Marc Castaño-Trias acknowledges his PhD scholarship from AGAUR2020FI_B00711.

REFERENCES

Čelić, M., Gros, M., Farré, M., Barceló, D., & Petrović, M. 2019. Pharmaceuticals as chemical markers of wastewater contamination in the vulnerable area of the Ebro Delta (Spain). *Science of the Total Environment*, **652**, 952–963.

Pantanella, F., Lekunberri, I., Gagliardi, A., Venuto, G., Sànchez-Melsió, A., Fabiani, M., Balcázar, J. L., Schippa, S., De Giusti, M., Borrego, C., & Solimini, A. 2020. Effect of Urban Wastewater Discharge on the Abundance of Antibiotic Resistance Genes and Antibiotic-Resistant Escherichia coli in Two Italian Rivers. *International Journal of Environmental Research and Public Health*, **17**(18), 6813.

Enhancing reactive species exposure in a dielectric barrier discharge plasma reactor through lava rock packing in view of phosphonate-contaminated wastewater treatment and subsequent phosphorous recovery

Changtao Chen *, Kristof Demeestere **, Anton Nikiforov ***, Stijn Van Hulle *

* LIWET, Laboratory for Industrial Water and EcoTechnology, Department of Green Chemistry and Technology, Faculty of Bioscience Engineering, Ghent University, Campus Kortrijk, Sint-Martens-Latemlaan 2B, B - 8500 Kortrijk, Belgium (changtao.chen@ugent.be, stijn.vanhulle@ugent.be)
** EnVOC, Research Group Environmental Organic Chemistry and Technology, Department of Green Chemistry and Technology, Faculty of Bioscience Engineering, Ghent University, Coupure Links 653, B - 9000, Ghent, Belgium (kristof.demeestere@ugent.be)
*** RUPT, Research Unit Plasma Technology, Department of Applied Physics, Faculty of Engineering and Architecture, Ghent University, Sint-Pietersnieuwstraat 41, B4, B - 9000 Ghent, Belgium (anton.nikiforov@ugent.be)

Abstract
Phosphonate contamination of water bodies has drawn much attention. Advanced oxidation combined with phosphorus recovery from phosphonate-contaminated waste water bodies is considered as a promising solution to but the development of a cost-efficient process remains challenging. This work demonstrates an effective two-step process including a plasma degradation step followed by granular filtration with iron-coated sand (ICS). In the first step, a tandem reactor configuration, which consists of a dielectric barrier discharge (DBD) plasma chamber and an ozonation chamber was used to transform 1-hydroxyethane-1,1-diphosphonic acid (HEDP), a phosphonate widely used in textile industry, to Ortho-phosphate (Ortho-P). Ozone gas produced in the dielectric barrier discharge (DBD) reactor was introduced in the ozonation chamber. Experiments were performed with and without lava rock packing in the ozonation chamber. The addition of lava rock as packing material increased the Ortho-P production efficiency by 15-35%, because the presence of lava rock increased the exposures of reactive species (O_3, ·OH and $O_2^{\bullet-}$) by 120%, 20% and 30%, respectively. The effects of carrier gas composition as well as waste water composition was also evaluated in the operational model of plasma & packed ozonation chamber. The use of O_2 resulted the highest Ortho-P production efficiency (86 %), followed by Ar (48%), N_2 (21%) and air (13%). Humic acids present in waste water can compete with phosphonates for reactive species, decreasing the Ortho-P production efficiency by 30%. In the second step, ICS granules were used to adsorb produced Ortho-P. The final recover efficiency of Ortho-P from real textile and synthetic wastewater was 53% and 85%, respectively.

Keywords
Exposure of reactive species, Lava rock, Phosphonates, Nonthermal plasma

Analysis of the enrichment in PHA-accumulating bacteria in mixed microbial communities fed with fish-canning waste

D. Correa-Galeote*, B. Juarez-Jimenez*, A. Mosquera-Corral**, B. Rodelas and J. Gonzalez-Lopez*

* Microbiology and Environmental Technology Section, Water Research Institute, University of Granada, 18011 Granada, Spain
(E-mail: *dcorrea@ugr.es; belenjj@ugr.es; mrodelas@ugr.es; jgl@ugr.es)*
** Department of Chemical Engineering, CRETUS Institute, University of Santiago de Compostela, 15782 Santiago de Compostela, Spain
(E-mail: *anuska.mosquera@usc.es*)

Abstract
The biosynthesis of polyhydroxyalkanoates (PHAs) from fish-canning wastes by mixed microbial cultures is a promising technology to replace conventional plastics. However, the dynamics of the key populations involved in the PHA are not well known, limiting the feasibility of PHA yield. Hence, the aim of this study was to determine the shifts in the bacterial communities in lab-scale sequencing batch reactors (SBRs) fed with fish-canning waste under a double growth limitation (DGL) strategy. The analysis of the bacterial communities was determined by Illumina sequencing of 16S rRNA genes, and the bioaccumulation of PHA was measured by gas chromatography in two SBRs using different NaCl concentrations (SBR-N, 0.5 g NaCl/L, and SBR-S, 10 g NaCl/L). The imposition of the DGL strategy resulted in broad successions of the dominant genera, being *Calothrix*, *Gordonia*, and *Chryseobacterium* the most abundant PHA-accumulating bacteria in the SBR-N, whereas *Qipengyuania, Corynebacterium*, and *Dokdonella* those in SBR-S.

Keywords (maximum 6 in alphabetical order)
Bacterial diversity; fish-canning waste; Illumina sequencing; mixed microbial cultures; PHA accumulation; sequencing batch reactors

INTRODUCTION

The production of conventional plastics, which involves the use of crude oil and natural gas, produces major damage to the environment due to its high CO_2 emissions. Hence, there is an urgent need to develop biodegradable, compostable, and environmentally friendly substitutes for traditional petroleum-based plastics. In this sense, bioplastic production is the most promising strategy in the replacement of the high contaminant conventional plastics. Among the different alternatives, polyhydroxyalkanoates (PHAs) production by mixed microbial communities (MMC) using industrial wastes stands out as a promising biotechnology against fossil-fuel-derived plastics. In this regard, the PHA biosynthesis by using an MMC requires a robust enrichment in the bacterial populations carrying the enzymatic machinery to achieve a high level of synthesis and accumulation of PHAs. However, the successional patterns of the key genera involved in the effective establishment of PHA-accumulating communities are not well known. Hence, the main objective of this work was to determine the dynamics of PHA-accumulating bacteria within the MMCs in two SBRs using fish-canning waste as a substrate using two different levels of salinity.

MATERIALS AND METHODS

Two lab-scale (4 L) sequencing batch reactors (SBRs) were operated using two different levels of salinity (SBR-N, 0.5 g NaCl/L, and SBR-S, 10 g NaCl/L) for the enrichment of PHA-accumulating bacteria for 331 and 122 days, respectively. Both SBRs were operated under a double growth limitation (DGL) strategy, in which C (added in the feast phase) and N (added in the famine phase) were incorporated separately. The accumulation of PHAs was determined by gas chromatography in biomass samples (Argiz et al., 2021). High-throughput Illumina MiSeq sequencing of the V3-V4 region of the 16S rRNA gene was performed according to Correa-Galeote et al. (2022). The corresponding statistical analyses were carried out in the XLSTAT software (Addinsoft, USA).

RESULTS AND DISCUSSION

The main physicochemical parameters showed few statistical differences among sampling times and reactors. Regarding the PHA accumulation, the maximum yields were 22.03 wt% and 26.33% for SBR-N and SBR-S, respectively, without statistical differences in the PHA yield between reactors. Regardless of the SBR and sampling time, the most abundant bacteria were *Gordonia* (8.88%), *Qipengyuania* (6.19%), and *Acidovorax* (5.65%). Significant differences of the relative abundances of several main bacterial genera were found after the imposition of DGL strategy in both bioreactors. The broad successions of the dominant bacteria found throughout the operational time in both SBRs, suggest that the DGL strategy for the enrichment in PHA-accumulating bacteria strongly affected the structure of the bacterial communities. In this sense, *Calothrix* (20.88%), *Gordonia* (18.15%), and *Chryseobacterium* (7.72%) were the PHA-accumulating bacteria with higher-than-average relative abundance at the end of the operation of SBR-N; whereas, *Qipengyuania* (57.09%), *Corynebacterium* (17.33%) and *Dokdonella* (11.62%) were the most abundant genera at the end of the experiment for SBR-S. According to these results, the operation strategies imposed resulted in the implementation of different well-established PHA-accumulating potential capacities in each SBR. This suggests a broad functional redundancy in the PHA accumulating capacity within the bacterial communities of both SBRs. Finally, the multivariate statistical analysis carried out showed that increasing the salt concentration from 0.5 g NaCl/L to 10 5 g NaCl/L had no influence on the PHA-accumulating capacity.

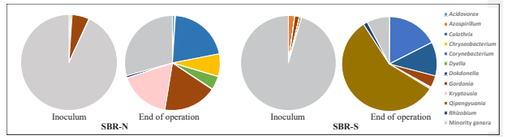

Figure 1. Structure of the dominant bacterial genera (relative abundance > 0.5%) from two PHA-accumulating SBR reactors operated using two different levels of salinity (SBR-N, 0.5 g NaCl/L, and SBR-S, 10 g NaCl/L).

ACKNOWLEDGMENTS: This research was supported by the Spanish Ministry of Science and Innovation through (PID2020-112550RB-C22) project.

REFERENCES

Argiz, L., et al. 2021. Open-culture biotechnological process for triacylglycerides and polyhydroxyalkanoates recovery from industrial waste fish oil under saline conditions. *Separation and Purification Technology*. **270**, 118805.

Correa-Galeote, D., Argiz, L., Val del Rio, A., Mosquera-Corral, A., Juarez-Jimenez, B., Gonzalez-Lopez, J., Rodelas, B. 2022. Dynamics of PHA-accumulating bacterial communities fed with lipid-rich liquid effluents from fish-canning industries. *Polymers,* **14**(7), 1396.

WATER-MINING Project: La Llagosta Case Study, a flexible fit-for-use wastewater treatment scheme for resource recovery

T. de la Torre*, C. Sielfeld,**, R. Rafecas**, W. Wijdeveld***. L. Korving***, G. Gamboa****

* Department of Innovation, Sorigué, Ronda Guinardó, 99, 08041, Barcelona, Spain
(E-mail: t.delato@sorigue.com, r.rafecas@sorigue.com)
**Eurecat, Water Air and Soil (WAS) Unit, Plaça de la Ciència, 2, 08242 Manresa, Barcelona, Spain
***Wetsus, European Centre of Excellence for Sustainable Water Technology, 8911MA Oostergoweg 9, Leeuwarden, The Netherlands
****Institute of Environmental Science and Technology, Universitat Autònoma de Barcelona, C/ de Les Columnes s/n, Campus de La UAB, 08193, Cerdanyola del Vallès, Barcelona, Spain

Abstract
A next-generation fit-for-use water reclamation treatment scheme is being operated since January 2023 with the aim of demonstrating innovative technologies to treat and valorize urban wastewater in the form of energy, nutrients and water for different purposes. The pilot plant is treating 400 L/h of wastewater coming to La Llagosta WWTP (Barcelona, Spain) using a treatment train composed of an anaerobic membrane bioreactor followed by a partial nitritation reactor and an anammox reactor. In May 2023, additional units will be in place to incorporate phosphorous recovery in the form of vivianite and a reverse osmosis module using recycled membranes. The design of the plant has followed the Value Sensitive Design (VSD) principles. Interested stakeholders have been involved in the project from its beginning through meetings of the so-called "Community of Practice" (CoP) where topics related to the implementation of the Water Mining technologies are analysed and expertise is exchanged.

Keywords (maximum 6 in alphabetical order)
Water, reuse, phosphorous, anammox, recovery, social innovation

INTRODUCTION

The Water-Mining project is a H2020 funded project started in September 2020 with the aim of contributing to the circular economy in the water sector. It is a highly collaborative project (38 partners) coordinated by Technical University of Delft, The Netherlands) (www.watermining.eu. The different technologies that will be demonstrated within the project are spread into different case studies and living labs in five European countries. In this abstract, Case Study 5 is presented, which is taking place in a pilot plant located in the wastewater treatment plant (WWTP) of la Llagosta (Barcelona, Spain). In this plant, the recovery of nutrients, energy and water for different purposes will be evaluated using novel technologies.

THE PILOT PLANT

The CS5 Water-Mining pilot plant is being commissioned in January 2023 and will be in operation for 18 months. It will be treating 400 L/h municipal wastewater using a flexible wastewater reuse treatment scheme described in Fig. 1. The first unit of the treatment train consists on a granular anaerobic membrane bioreactor (AnMBR) with the configuration of an EGSB (expanded granular sludge bed) reactor followed by two hollow fiber ultrafiltration modules (Thermally Induced Phase Separation (TIPS) PVDF UF membranes from Scinor, China). From this unit, biogas will be produced and quantified and the water coming from it could be either directly applied to agriculture in the form of fertirrigation or pass the N and/or the P removal systems located afterwards. The N removal is comprised by a granular partial nitritation reactor and an anammox reactor. Anammox is the oxidation of ammonium with nitrite as the electron acceptor and dinitrogen gas as the product (Kumar *et al.*, 2017). In the partial nitritation reactor, approximately 50% of the ammonium contained in the influent will be oxidized to nitrite. Afterwards, the ammonium and nitrite of the influent will be converted into nitrogen gas via an anammox reactor where anammox bacteria will be cultivated in the form of granules.

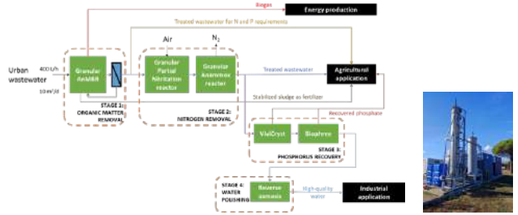

Figure 1. Water-Mining CS5 treatment scheme (left) and picture of the pilot (right).

After the N removal step, the ViviCryst and Biophree technologies from Wetsus will be operated in order to recover P in the form of vivianite ($(Fe)_3(PO_4)_2$ $8H_2O$) via precipitation (ViviCryst unit) and to eliminate the remaining P using adsorption (Biophree unit) that can lead to severe fouling in the RO membranes afterwards. The RO modules will be recycled using oxidative treatment by Eurecat (Fig. 2).

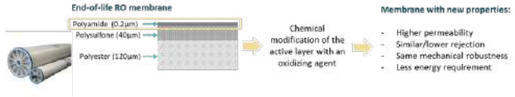

Figure 2. Regeneration process of the RO membranes.

SOCIAL INNOVATION: THE COMMUNITIES OF PRACTICE

A group of relevant stakeholders was selected at the beginning of the project that included water authorities, NGOs, private water companies and research centres. This group conform the so-called "communities of practice" (CoP), which participate in meetings along the project in order to incorporate their opinions, values and expertise in the design of the technologies and their further applications. Two meetings have been held to date, where approximately 15 people have given their insights about the Water-Mining project analysing the market, policy, technological and economical barriers of the implementation of the technologies and provided recommendations for optimization.

REFERENCES

Kumar, M., Daverey, A., Gu, J. D., & Lin, J. G. 2017 Anammox processes. *Current developments in biotechnology and bioengineering*, 381-407.

AKNOWLEDGEMENTS

The authors would like to thank the Consorci Besòs Tordera for the use of their installations and support.

Development of methodologies and tools of risk assessment for wastewater and stormwater reuse

L. De Simoni[1], S. Radini[1], A. Foglia[1], M. Sgroi[1], D. J. Magna[1], B. Szelag[2], A. Kiczko[3], A. L. Eusebi[1], F. Fatone[1]

[1] Department of Science and Engineering of Materials, Environment and Urban Planning-SIMAU, Faculty of Engineering, Polytechnic University of Marche, Ancona, Italy
[2] Department of Geotechnics and Water Engineering, Kielce University of Technology, Kielce, Poland
[3] Department of Hydraulic and Sanitary Engineering, Warsaw University of Life Sciences, Warsaw, Poland
(E-mail: *l.desimoni@pm.univpm.it, s.radini@pm.univpm.it, a.foglia@univpm.it, m.sgroi@staff.univpm.it, debora.jaretamagna@phd.unict.it, bartoszszelag@op.pl, adam_kiczko@sggw.edu.pl, a.l.eusebi@staff.univpm.it, f.fatone@staff.univpm.it)*

Abstract
Climate change and environmental degradation increasingly represent a threat to the entire world, and therefore the safe recovery of resources is crucial in order to encourage the use of what is now considered as waste as a real resource. In this context, risk analysis is the main element to ensure the safe reuse of wastewater and grey water. For this purpose, a semi-quantitative approach was followed for risk assessment in wastewater reuse, while a QMRA calculation tool was developed for a quick assessment of the risk of re-use to support stakeholders in making decisions about possible restrictions.

Keywords (maximum 6 in alphabetical order)
FMEA; QMRA; risk assessment; run-off; stormwater management; water reuse.

INTRODUCTION

Water scarcity and water stress are issues of growing concern at international and European level (Delli Compagni et al., 2020). Freshwater availability is getting scarcer due to effects related to climate change issues, like heatwaves or drought periods. Apart from limiting water resources for human consumption, water scarcity implies some environmental impacts such as increasing contaminants concentration and water pollution. Potential contamination sources include also diffuse inputs, such as urban and agricultural run-offs, which may occur during precipitation and flooding events. Extreme rainfall events may impact on sewer overflows and thus on surface water quality, since they may increase bacterial loads and concur in environmental contamination, affecting both human health and ecosystem. Reclaimed wastewater and greywater can contribute to compensate water needs, providing regular supply (Deviller et al., 2020), reducing the exploitation of natural water resources and alleviating the pressures of wastewater treatment plants (WWTP) discharges into sensitive areas. In this context, risk assessment represents a crucial task to ensure health and environmental protection for water reuse applications. Regulatory frameworks are including this aspect, even if detailed procedures are still lacking, especially for alternative sources, such as greywater. The work carried out aimed to face risk assessment, both for wastewater and for run-off water reuse.
Considering wastewater reuse, a semi-quantitative risk assessment has been developed and detailed for a full-scale water reuse system in Italy. Moreover, a specific methodology has been developed for safe stormwater management and reuse of greywater, during the European project WATERUN.

MATERIALS AND METHODS

Risk assessment has been developed according to existing international guidelines, such as Australian Guidelines and WHO Manuals (QMRA 2016).

Table 1. QMRA methodology.

Step	Description	Formulas
1	**Dose-response relationship** (dose of pathogens with which the exposed group enter in contact)	*d = pathogen concentration × log reduction × exposure* *Exposure/event = volume (mL) with which people enter in contact in a single event of exposure during a certain activity*
2	**Probability of infection** (Pinf) related to each event of exposure to the target pathogen	$P_{inf} = 1 - (1-d/\beta)^{(-\alpha)}$ *Beta Poisson model* α,β = dose response constants
3	**Total probability of infection in one year** (of each pathogen)	$P_{inf\,(year)} = 1-(1-P_{inf})^{N}$ 1 activity N=number of exposures/year
4	**Probability of illness** (Pill) in one year	$P_{illness\,(year)} = P_{inf\,(year)} \times$ ratio of illness to infection
5	**Disability-adjusted life years (DALYs)**	DALY/year = $P_{illness\,(year)} \times$ DALY per case × susceptibility fraction

Risk assessment includes uncertainties, due to not reliable data or lack of information, which might lead to errors in the overall result (WHO, 2016). Data analysis may support the development of a robust dataset, which allows to increase the numerosity but also to include extreme events characterised by lower probability of occurrence, which are more difficult to detect by standard measures. Literature research may also be useful to define typical ranges of concentration and characteristic ratios between parameters, in case local measures are not available, not sufficient or not trustable. Models and analysis, such as multi-criteria decision analysis, fuzzy and stochastic analysis or Monte Carlo based models can help to deal with uncertainty, but their application requires specific skills. Simpler models, such as Failure Mode and Effects Analysis (FMEA) can also be used to assess water systems. FMEA analysis allows to identify the critical parameters that may have an impact on water quality, by comparing the 95th percentile with intervals defined between the lab detection limits and quality standards (ISS, 2019). The approach and the level of detail are strictly dependant from the site-specific characteristics, the available information and the required results. The methodology for risk assessment should thus be flexible and reshaped to be fitted with the specific application in exam.

Wastewater reuse

The water utility ACEA manages the territorial district of ATO2 in Lazio, Italy, and Fregene WWTP was selected to provide safe reclaimed water for irrigation purposes, since the surrounding area is voted to horticultural cultivation. The WWTP is characterised by pre-treatment, biologic CAS process, secondary sedimentation, sand filtration and UV disinfection. Data from the routinary lab analysis for the characterisation of influent and effluent wastewater were acquired, together with information on the design and operative parameters of each unit.

Run-off reuse

In order to support risk assessment for run-off water reuse, an innovative tool for stormwater management, based on a risk-based approach, is being implemented, in the context of the EU project WATERUN. Hence, a python tool (β -version) for QMRA calculation has been developed, which is able to calculate the microbiological risk for specific reuse scenarios (e.g., garden irrigation, toilet flushing) and for three different pathogens (Campylobacter, Rotavirus, Cryptosporidium). Furthermore, a preliminary version of a graphical user interface (GUI) has been created to allow the communication of a stormwater management model (SWMM) outputs with the phyton tool.

RESULTS AND DISCUSSION

Proposed methodology for risk assessment

A detailed and specific methodology for risk assessment has been developed to be implemented in water reuse applications.
The steps detailed for safe wastewater reuse (Figure 1) included a preliminary phase of system description and asset management, where the design and operative parameters of each operative unit were verified and compared with the literature working ranges, in order to define indicators for the resilience of the treatment layout. Then, a phase of data analytics was performed, in order to detect anomalies or critical conditions occurred in the plant. Once all the information was elaborated, risk assessment must be performed. A first semi-qualitative approach has been carried out, with the definition of a risk matrix that included all the hazardous events identified for each unit, according to the evaluations of the previous data analysis. A quantitative approach could be furtherly performed, in case from the previous phase a deeper analysis would be required. In that case, QMRA and QCRA could be performed to evaluate microbial and chemical risks, respectively. After that, control measures and digital support tools could be applied and implemented in the monitoring. Finally, communication and emergency procedures should be implemented.

Figure 1. Proposed methodology for risk assessment.

The presented approach has been followed to perform the risk assessment of Fregene water reuse system. Data from the WWTP has been analysed and the possible hazardous events have been identified. The FMEA has been then implemented, in order to evaluate effluent quality and identify the most critical parameters. A semi-quantitative approach was followed and a risk matrix has been developed. Scores have been attributed to the probability and the severity of each identified hazardous event, according to the results of data analysis, expertise judgement and considering the control measures applied in the plant.

A more detailed approach has been followed to assess the risks for run-off reuse. In order to provide a more quantitative information on the health outcomes from run-off water reuse and since information on pathogens in urban stormwater were available from literature, a quantitative assessment has been developed and implemented into a tool that could support users to perform a QMRA. More in detail, the developed tool allowed to perform QMRA for each pathogen and for each rainfall event that generate overflow (DWA A-118 (2006) guidelines), implementing Monte Carlo analysis for statistical reliability. This tool will provide information about water quality, indication for safe reuse practices and thus restrictions needed in the districts of the urban catchment for reuse or recreational activities after the simulated storm water event. Moreover, this risk-based tool will allow to evaluate the reduction of the health-risk after the implementation of different preventive measures through the application of different log removals.
This tool will enable stakeholders to quickly assess the risk for different activities following weather events and thus make decisions on possible reuse.

Figure 1. GUI interface for QMRA calculation.

REFERENCES

R. Delli Compagni, M. Gabrielli, F. Polesel, A. Turolla, S. Trapp, L. Vezzaro, M. Antonelli, 2020 Risk assessment of contaminants of emerging concern in the context of wastewater reuse for irrigation: An integrated modelling approach, *Chemosphere* 242. https://doi.org/10.1016/j.chemosphere.2019.125185.

G. Deviller, L. Lundy, D. Fatta-Kassinos, 2020 Recommendations to derive quality standards for chemical pollutants in reclaimed water intended for reuse in agricultural irrigation, *Chemosphere* 240. https://doi.org/10.1016/j.chemosphere.2019.124911.

World Health Organization, 2016 Quantitative Microbial Risk Assessment: Application for Water Safety Management. https://apps.who.int/iris/handle/10665/246195 (accessed January 10, 2023).

Lucentini L, Achene L, Fuscoletti V, Nigro Di Gregorio F, Pettine P (Ed.). Linee guida per la valutazione e gestione del rischio nella filiera delle acque destinate al consumo umano secondo il modello dei Water Safety Plans. Roma: Istituto Superiore di Sanità; 2014. (Rapporti ISTISAN 14/21).

Degradation and erosion of polymers in alkalised fresh human urine collected in source-separating sanitation systems

Anuron Deka*, Prithvi Simha*, Rupam Kataki**, Björn Vinnerås*

* Department of Energy and Technology, Swedish University of Agricultural Sciences, Undervisningsplan 7H, 75651 Uppsala, Sweden
** Department of Energy, Tezpur University, Department of Energy, Tezpur University, Napaam, Tezpur, Assam, India. Post code- 784028

Abstract
Recovering plant essential nutrients from wastewater and converting them to value-added products is an important step for society to transition to circular nutrient management. We have developed a process that separately collects human urine and converts it into solid bio-based fertilizers containing >10% N, 1% P & 4% K. It involves adding alkaline chemicals to freshly excreted urine to stabilise nutrients like urea and ammonia so that they are not lost when urine is concentrated by evaporation. In this study, our objective was to evaluate the possibility of formulating alkaline chemicals into a multilayer tablet that is enclosed using a water-soluble or water-swellable polymer layer. We evaluate the degradation and erosion of Polypropylene (PP), Polylactic Acid (PLA), Polycaprolactone (PCL) and Polyvinyl Alcohol (PVOH) in two types of urine: $Ca(OH)_2$ treated fresh urine and $Ca(OH)_2$ treated concentrated urine, with a control using Milli-Q water. We performed destructive sampling on days 1, 2, 4, 8, 16 and 32, and analysed COD, pH and EC as proxy parameters for the degradation of polymers. Further tests such as ICP, FTIR, DSC, GPC and SEM were also conducted to determine the degradation mechanisms. PLA and PVOH were identified as the most promising polymers for urine treatment. A follow-up investigation was also done to evaluate the effect of the thicknesses of PLA films (0.05 mm to 0.25 mm) on the breakthrough time at two temperatures, 21 °C and 45 °C. Here, we demonstrated that polymer films with lesser thickness and kept at a higher temperature degraded the fastest in urine.

Keywords
Polymer degradation, Human urine, Nutrient recovery, Source separation, Wastewater treatment

INTRODUCTION

Domestic wastewater fractions such as human urine contain plant-essential nutrients that can be recovered and recycled as crop fertilizers. Recovering nutrients from waste and converting them to value-added products is an important step for society to transition to circular nutrient management. Irrespective of the type of sanitation system, today most of the nutrients, energy, and water present in human urine are not recovered. A better approach to valorise resources present in human urine is to first collect urine and faeces separately using a urine-diverting toilet. When the collected urine is treated further by alkaline dehydration, a solid bio-based fertilizer with the following composition can be produced: 10% N, 1% P & 4% K on a dry matter basis (Simha et al., 2020).

To prevent urease-catalysed hydrolysis of urea present in human urine, the pH of fresh human urine needs to be increased. Several different alkaline chemicals can be added to urine to achieve this and many have already been evaluated (Simha et al., 2018). However, in present system designs, the chemicals must be added manually from time to time to a urine stabilisation reactor. These chemicals could be can be formulated into a multilayer tablet (e.g., dishwasher detergent) and enclosed using a water-soluble or water-swellable polymer layer. The dissolution rate of polymers depends on their chemical composition, properties, and thickness, as well as the composition of the solution in which they are placed. Therefore, the objective of this study was to evaluate the degradation and erosion rates of different polymers when they are added to alkalised fresh human urine.

MATERIALS AND METHODS

Fresh human urine was collected anonymously in 500 mL polypropylene bottles. The donors were both male and female and aged between 20-65 years. The total number of donations was 51 which were collected over 3 days. The total volume of urine collected was 25 L (pH= 6.05, EC= 13.7 mS/cm). To the collected urine, 10 g/L of $Ca(OH)_2$ was added and mixed for 30 min using a mechanical stirrer until the urine pH was >12. The $Ca(OH)_2$ treated urine was then put in two separate buckets, buckets A and B. Bucket A contained 8 L of the alkalised fresh urine. Bucket B contained 17 L of alkalised concentrated urine and was dried in a CO_2-free dryer (Electrolux Day Care Eco) for 48 h at 40 °C till the volume was reduced to 9.04 L. The concentrated urine (CONCU) thus produced had a concentration factor of 1.88, pH of 12.5 and EC of 26.1 mS/cm.

Laboratory grade Polypropylene (PP) pellets, Poly Caprolactone (PCL) flakes, Poly Vinyl Alcohol (PVOH) powder and Poly Lactic Acid (PLA) pellets were used to fabricate 2 mm thick polymer samples. PP, PCL and PLA samples were prepared by heat. PVOH samples were fabricated via solution polymerization technique using deionised water as the solvent. No additives were used during the fabrication process. The samples were then cut into 2 cm diameter pieces and weighed.

A follow-up experiment was conducted using a PLA sheet with 0.05 mm thickness. The sheet was moulded into 2 different thicknesses (0.1 mm and 0.25 mm) using the pressure moulding technique. CU was the only media used for the follow-up investigation and milli-Q water was used as a control. The investigation was carried out at two different temperatures: 21 °C and 45 °C.

Experimental Setup

The experiment evaluated the degradation and/or erosion kinetics of polymers in different types of urine over 32 days. All the samples were made into duplicates. 80 mL of urine was put in Petri dishes using a pipette, after which the polymer samples were placed. The setup was then kept undisturbed and covered with opaque boxes. Destructive sampling was done on every sampling day, namely day 1, day 2, day 4, day 8, day 16 and day 32, respectively.

The follow-up experiment evaluated the effect of the temperature and thickness of the polymer film on the breakthrough time and erosion. 100 mL urine was put in an airtight container containing the polymer samples. The containers that were kept at 21 °C were kept undisturbed and covered with opaque boxes. The containers that were kept at 45 °C were put in an incubator. Destructive sampling was done on every sampling day, namely day 2, day 4 and day 8.

RESULTS AND DISCUSSIONS

In the first experiment involving 2 mm thick polymer samples, there was no visually noticeable degradation or erosion. However, evaluating the proxy parameters showed signs of erosion and degradation of the samples in both types of urine concentration of COD in both types of urine. There was also loss of sample weight and a decrease in thermal properties for every polymer on every sampling day.

The second experiment demonstrated the effect of temperature and pH on the breakdown of PLA films. Films with 0.05 mm thickness broke down in 2 days at both the evaluated temperatures in CU, while 0.1 mm and 0.25 mm thick films broke down in 4 days at 45 °C (H) but did not break down at 21 °C (R). In milli-Q water, none of the polymers broke down. However, there was a decrease in the transparency of the film and they became more brittle. All the samples have been sent for further analyses, namely FTIR and GPC to gain more insight into the degradation mechanism, and the results will be presented at the conference.

PP break down into a mixture of alkanes and alkenes which will further undergo reduction due to the presence of ammonia and other ionic salts to form alkanes which are slightly basic (Gewert et al. 2015). PLA is most likely to degrade into the oligomers and monomers such as lactic acid or other compounds such as sodium lactate. These compounds are slightly acidic (pH ~ 6.5 to 7.3) (Siddiqui et al. 2020). PCL degrades to carboxylate anion and diloxanide which have a pH close to 7 (Bartnikowski et al. 2019). PVOH degrades to various hydrolases, ketones and acetic acid. While hydrolases and ketones do not change the pH or EC of a media unless introduced in a significant amount, acetic acid is a weak acid and can reduce the pH of the media (Halima, N. B. 2016).

Li et al. studied the effect of pH on the erosion and degradation of PLGA films. At pH 10.1, the breakdown of the polymer was the fastest but the decrease in molecular weight was slower than in acidic conditions. This explains the breakdown of the PLA films in urine (pH >12) evaluated in this study, and also why they are intact in milli-Q water. Literature also points to faster degradation of PLA at higher temperatures. This is because at elevated temperatures (close to the glass transition temperature of PLA) the coils of the polymer start to untangle, making it more susceptible to water intake (Teixeira et al. 2021). This explains the breakdown of all PLA films, irrespective of their thicknesses at 45 °C, while 0.1 mm and 0.25 mm thick films do not break at 21 °C. All the samples collected in our experiments have been sent for FTIR, GPC, DSC and SEM analysis, and the results will be presented at the conference.

REFERENCES

Simha, P., Lalander, C., Nordin, A., & Vinnerås, B. (2020). Alkaline dehydration of source-separated fresh human urine: Preliminary insights into using different dehydration temperature and media. Science of the Total Environment, 733, 139313.

Simha, P., Senecal, J., Nordin, A., Lalander, C., & Vinnerås, B. (2018). Alkaline dehydration of anion–exchanged human urine: Volume reduction, nutrient recovery and process optimisation. Water research, 142, 325-336.

Gewert, B., Plassmann, M. M., & MacLeod, M. (2015). Pathways for degradation of plastic polymers floating in the marine environment. Environmental science: processes & impacts, 17(9), 1513-1521.

Siddiqui, M. N., Kolokotsiou, L., Vouvoudi, E., Redhwi, H. H., Al-Arfaj, A. A., & Achilias, D. S. (2020). Depolymerization of PLA by phase transfer catalysed alkaline hydrolysis in a microwave reactor. Journal of Polymers and the Environment, 28(6), 1664-1672.

Bartnikowski, M., Dargaville, T. R., Ivanovski, S., & Hutmacher, D. W. (2019). Degradation mechanisms of polycaprolactone in the context of chemistry, geometry and environment. Progress in Polymer Science, 96, 1-20.

Halima, N. B. (2016). Poly (vinyl alcohol): review of its promising applications and insights into biodegradation. RSC advances, 6(46), 39823-39832.

Li, J., Jiang, G., & Ding, F. (2008). The effect of pH on the polymer degradation and drug release from PLGA-mPEG microparticles. Journal of applied polymer science, 109(1), 475-482.

Teixeira, S., Eblagon, K. M., Miranda, F., R. Pereira, M. F., & Figueiredo, J. L. (2021). Towards controlled degradation of poly (lactic) acid in technical applications. C, 7(2), 42.

Drinking Water Treatment Residuals: from waste to a new promising adsorbent of emergent compounds

R. Dias *, D. Sousa *, M. Bernardo **, P. Fontes*** and R. Maurício *

* CENSE – Center for Environmental and Sustainability Research & CHANGE - Global Change and Sustainability Institute; NOVA School of Science and Technology, NOVA University Lisbon, Portugal
(E-mail: ra.dias@campus.fct.unl.pt; db.sousa@campus.fct.unl.pt; rmr@fct.unl.pt)
**LAQV/REQUIMTE, School of Science and Technology, NOVA University Lisbon, 2829-516 Caparica, Portugal
(E-mail: maria.b@fct.unl.pt)
***EPAL – Empresa Pública de Águas Lives S.A.,- AdP – Grupo Águas de Portugal
(E-mail: p.fontes@adp.pt)

Abstract
The use of drinking water treatment residuals (DWTR) as an adsorbent has raised attention as a sustainable option to remove emergent compounds (EC). The objective of this study was to analyse a DWTR with high activated carbon content, without any reactivation process, as adsorbent of estrone, 17β-estradiol and 17α-ethinylestradiol. The DWTS characterization results showed that it is a heterogenous material with high surface area and pore volume, which may suggest high adsorption potential. Adsorbent dosage study suggested that 0.2 g guarantees high adsorption capacity with the possibility of compounds quantification. Adsorption kinetics study points to an adsorption equilibrium at 24 h contact time. The concentrations tested for adsorption isotherm modelling where not enough to reach the maximum adsorption capacity, implying the need of further analysis with higher concentrations. DWTR showed promising results, already supported by the literature, to adsorb estrogens, and to be further tested with other types of EC.

Keywords
Adsorption processes; drinking water treatment residuals; emergent contaminants; estrogens

INTRODUCTION

The presence of emergent contaminants (EC) in aquatic environment has raised global concern. Among this group of compounds, estrogenic action hormones, such as estrone (E1), 17β Estradiol (E2) and 17α Ethinylestradiol (EE2) have been detected in concentrations ranging from ng/L to mg/L in water bodies and wastewater discharges (Tran et al., 2018). These compounds enter into the aquatic environment mainly through wastewater treatment plants (WWTP), since these are excreted through urine and faeces (Martins et al., 2022). Their presence in the aquatic environment has been well documented due to observed adverse consequences, such as the feminization of male fish and the induction of vitellogenin synthesis in fish plasma (Kasonga et al., 2021). Even though hormones are normally detected in low concentrations, these cannot be removed by conventional wastewater treatment systems, becoming crucial the development of new, easy to implement, environmentally friendly and affordable technologies to ensure their removal (Tiwari et al., 2017). According to recent reviews there is a scientific consensus which settles adsorption process as the most promising one, since it does not entail the operational and energetic costs of other treatments such as the advanced oxidation processes or the membrane processes (Rout et al., 2021). Within the scope of adsorption processes and the vast possibilities of low-cost materials for this purpose, drinking water treatment residuals (DWTR) have been tested as a suitable adsorbent material for estrogens (Dias et al., 2021; Martins et al., 2022). The objective of this study was to analyse a DWTR with high content of activated carbon (resulting from the raw water treatment and subsequent decantation), further on referred as PAC-DWTR, as adsorbent of three estrogen compounds, E1, E2 and EE2 that are commonly present in water bodies and wastewater effluents.

MATERIALS AND METHODS

Drinking water treatment residuals preparation and characterization

DWTR from a Portuguese drinking water treatment plant was used to assess their adsorption potential of E1, E2 and EE2. The procedure and results were presented by Dias et al. (2021) where the sample was air-dried and sieved to obtain a particle size of 45/60 mesh. Within the DWTR characterisation, the determination and results of elemental analysis, ash content, the pH at point zero charge and thermogravimetric analysis procedures were presented by Dias et al. (2021). The BET surface area (S_{BET}), the total pore volume (V_{total}), microporosity (V_{micro}) and mesoporosity (V_{meso}) volumes were determined according to the methodology presented by Bernardo et al.(2020). The elemental composition and surface morphology of the PAC-DWTR were analyzed by Scanning Electron Microscopy with Energy Dispersive Spectroscopy (SEM-EDS) and energy dispersive X-ray spectrometer light elements detector attachments. Functional surface groups were analyzed by Fourier Transform Infrared Spectroscopy (FTIR).

Stock Solution and Determination of The Emerging Pollutants

The stock solution preparation and the determination of the estrogens followed the procedures reported by Dias et al. (2021), where the extraction and detection of the target compounds was performed using solid-phase extraction (SPE), with Oasis HLB cartridges (200 mg, Waters), and high-performance liquid chromatography tandem mass spectrometry (HPLC-MS-MS), respectively.

Analysis of the adsorbent dosage

Four PAC-DWTR doses were prepared, 2.5 g/L, 1 g/L, 0.5 g/L, 0.2 g/L and 0.05 g/L, in 250 mL flasks, in horizontal agitation (160 rpm) to which distilled water spiked with 1000 ng/L of the stock solution was added. The adsorption capacity (*qe*) that is the amount of estrogen absorbed (ng) per mass of PAC-DWTR (g).

Adsorption kinetic and isotherms

The adsorption kinetic study was performed using a PAC-DWTR dose of 0.2 g/L in 250 mL flasks, in horizontal agitation to which milli-Q water spiked with 1000 ng/L of the stock solution was added. The adsorption kinetics was evaluated at 0, 0.08, 0.25, 0.5, 1, 2, 6, 8, 18, 24, 48, and 72 h. The kinetic data were modelled through pseudo-first-order (PFO) and pseudo-second-order (PSO) rate equations to describe adsorption data obtained under non-equilibrium as described in the methodology presented by Bernardo et al.(2020). The adsorption isotherm study was performed using a PAC-DWTR dose of 0.2 g/L in 250 mL flasks, for 24 h contact time to which milli-Q water spiked with 200, 400, 600, 800 and 1000 ng/L of the stock solution was added. The data was analysed through Langmuir and Freundlich nonlinear models to describe the maximum adsorption capacity of the material.

RESULTS AND DISCUSSION

Drinking water treatment residuals characterization

Surface characterization parameters, such S_{BET} stood out with 352 m^2/g, higher than the one presented by Martins et al (2022), without any type of structural modification. However, V_{total} obtained was lower 0.174 (cm^3/g), though 66% of the V_{total} corresponds to V_{micro}. In SEM image (Figure 1- a)) it is possible to observe the PAC-DWTR heterogeneity and the rough surfaces, which may indicate the presence of mineral matter at their surface. Which is in accordance with the PAC-DWTR's high ash content and mineral composition (Dias et al., 2021). EDS analysis to the selected area within the particle (Figure 1 – b)), indicates four major peaks, corresponding to higher percentages of oxygen (O), carbon (C), aluminium (Al) and silica (Si). Carbon high percentage could be related to the presence of PAC in the DWTR, as corroborated by Lee et al. (2020). The FTIR spectrum shows four major peeks. The stretching of -OH functional group emerged at 3436 cm-1 and in the 1638 cm-1 the bending vibrations of HO-H, due to adsorbed water molecules and hydroxyl groups presence, respectively (El-Kammah et al., 2022). The 1421 cm^{-1} stretching can be related to C=C double bond of aromatic organic matter (He et al., 2022). The peak identified at 968 cm^{-1} band can be related do OH bending or with structures bonded with Al (Lee et al., 2020) and finally, an O-Al-O stretching at 543 cm^{-1} (Hamadeen et al., 2021).

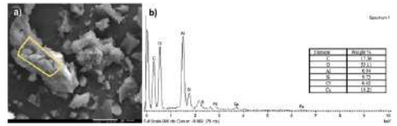

Figure 1. SEM-EDS results: a) SEM image; b) EDS spectra of the selected area of the SEM image.

Analysis of the adsorbent dosage

The three target compounds presented greater adsorption capacities at the lowest adsorbent dosage (0.05g). This behaviour is expected due to mass transference phenomena (El-Kammah et al., 2022; Martins et al., 2022). Even though, the selected adsorbent dosages for the subsequent experiments was 0.2 g, to allow full quantification of the selected compounds.

Adsorption kinetic and isotherms

The results obtained using PFO and PSO models for the three compounds showed similar determination coefficients (R^2). However, for both E1 and E2, the equilibrium time was obtained slightly sooner (around 20 h) than EE2 (closer to 24h). Therefore, the contact time selected for the adsorption isotherm study was 24 h. Different initial concentrations were not tested, and so the difference between models could not be addressed, since PFO is normally related to adsorption processes with initial concentration dependence and PSO to chemisorption processes (Martins et al., 2022). The results obtained showed that the concentrations used for each of the three compounds, where not sufficient to reach the maximum adsorption capacity. Nevertheless, the R^2 was also similar for both models (for each compound). A similar situation was described by Martins et al. (2022), who used heterogenicity parameter of the Sip isotherm model for adjustments to the Langmuir (monolayer adsorption) and Freundlich (multilayer adsorption) model. If the parameter is closer to one, the phenomena is described by Langmuir, and the opposite is related to Freundlich. Further assessment is needed within the adsorption isotherms modelling to reach maximum capacity and to better relate each adsorption model to each compound.

Though there are aspects on isotherm modelling still under assessment, this material showed to have potential for adsorption of estrogens, which is also supported by the study developed by Martins et al. (2022) and therefore, provides a possible sustainable wastewater treatment option, especially when considering wastewater reuse. Nevertheless, the use of low-cost adsorbents should always be assessed due to their leaching potential and possible ecotoxicological risks.

REFERENCES

Bernardo, M., Correa, C. R., Ringelspacher, Y., Becker, G. C., Lapa, N., Fonseca, I., Esteves, I. A. A. C., & Kruse, A. (2020). Porous carbons derived from hydrothermally treated biogas digestate. *Waste Management*, *105*, 170–179. https://doi.org/10.1016/j.wasman.2020.02.011

Dias, R., Sousa, D., Bernardo, M., Matos, I., Fonseca, I., Cardoso, V. V., Carneiro, R. N., Silva, S., Fontes, P., Daam, M. A., & Maurício, R. (2021). Study of the potential of water treatment sludges in the removal of emerging pollutants. *Molecules*, 1–11. https://doi.org/https://doi.org/10.3390/ molecules26041010

Du, B., Fan, G., Yu, W., Yang, S., Zhou, J., & Luo, J. (2020). Occurrence and risk assessment of steroid estrogens in environmental water samples: A five-year worldwide perspective. *Environmental Pollution*, *267*, 115405. https://doi.org/10.1016/j.envpol.2020.115405

El-Kammah, M., Elkhatib, E., Gouveia, S., Cameselle, C., & Aboukila, E. (2022). Enhanced removal of Thiamethoxam from wastewater using waste-derived nanoparticles: Adsorption performance and mechanisms. *Environmental Technology and Innovation*, *28*. https://doi.org/10.1016/j.eti.2022.102713

Hamadeen, H. M., Elkhatib, E. A., Badawy, M. E. I., & Abdelgaleil, S. A. M. (2021). Novel low cost nanoparticles for enhanced removal of chlorpyrifos from wastewater: Sorption kinetics, and mechanistic studies. *Arabian Journal of Chemistry*, *14*(3). https://doi.org/10.1016/j.arabjc.2020.102981

He, L., Chen, Y., Li, Y., Sun, F., Zhao, Y., & Yang, S. (2022). Adsorption of Congo red and tetracycline onto water treatment sludge biochar: characterisation, kinetic, equilibrium and thermodynamic study. *Water Science and Technology*, *85*(6), 1936–1951. https://doi.org/10.2166/WST.2022.085

Kasonga, T. K., Coetzee, M. A. A., Kamika, I., Ngole-Jeme, V. M., & Benteke Momba, M. N. (2021). Endocrine-disruptive chemicals as contaminants of emerging concern in wastewater and surface water: A review. *Journal of Environmental Management*, *277*(May 2020), 111485. https://doi.org/10.1016/j.jenvman.2020.111485

Lee, Y. E., Shin, D. C., Jeong, Y., Kim, I. T., & Yoo, Y. S. (2020). Pyrolytic valorization of water treatment residuals containing powdered activated carbon as multifunctional adsorbents. *Chemosphere*, *252*. https://doi.org/10.1016/j.chemosphere.2020.126641

Martins, D. S., Estevam, B. R., Perez, I. D., Américo-Pinheiro, J. H. P., Isique, W. D., & Boina, R. F. (2022). Sludge from a water treatment plant as an adsorbent of endocrine disruptors. *Journal of Environmental Chemical Engineering*, *10*(4), 108090. https://doi.org/10.1016/J.JECE.2022.108090

Rout, P. R., Zhang, T. C., Bhunia, P., & Surampalli, R. Y. (2021). Treatment technologies for emerging contaminants in wastewater treatment plants: A review. *Science of the Total Environment*, *753*, 141990. https://doi.org/10.1016/j.scitotenv.2020.141990

Tiwari, B., Sellamuthu, B., Ouarda, Y., Drogui, P., Tyagi, R. D., & Buelna, G. (2017). Review on fate and mechanism of removal of pharmaceutical pollutants from wastewater using biological approach. *Bioresource Technology*, *224*, 1–12. https://doi.org/10.1016/j.biortech.2016.11.042

Tran, N. H., Reinhard, M., & Gin, K. Y. H. (2018). Occurrence and fate of emerging contaminants in municipal wastewater treatment plants from different geographical regions-a review. *Water Research*, *133*, 182–207. https://doi.org/10.1016/j.watres.2017.12.029

Valorisation of the liquid waste of distilled gin production through high rate anaerobic co-digestion and biogas production

R. Diez-Montero*, J.A. Montes*, A.L. Esteban-García*, A. Lobo* and C. Rico*

* Group of Environmental Engineering, Department of Water and Environmental Sciences and Technologies, Universidad de Cantabria, Avda. Los Castros s/n, 39005 Santander (Spain)
(E-mail: *ruben.diezmontero@unican.es)*

Abstract
In this study, it has been tested the treatability of gin spent wash in UASB reactors through anaerobic co-digestion, as a way to recover bioenergy by the production of biogas. Results showed that gin spent wash can be efficiently treated by anaerobic co-digestion with wastewaters that provide alkalinity and nutrients. At the same time, the spent wash was valorised through an efficient and stable production of biogas. Overall, this process can contribute to the generation of energy in the distilled gin industry, turning an environmental problem into a recoverable resource.

Keywords (maximum 6 in alphabetical order)
Anaerobic co-digestion; biogas; distillery wastewaters; gin spent wash; over-acidification; UASB

INTRODUCTION

The industry of production of alcoholic beverages is a very important source of wastes worldwide. In particular, distillery spent wash (DSW, the liquid fraction of the residual waste after distilled liquor production) is considered the major liquid stream from the distilled beverage production due to its high Chemical Oxygen Demand (COD) and low pH (Acharya et al., 2008). Anaerobic digestion has been suggested as a feasible treatment process for DSW, since its organic content is highly biodegradable, and in addition the spent wash is produced at high temperature (70-80ºC) (Goodwin et al., 2001). On the other hand, distilleries are high energy demanding factories, mainly for heating purposes, which increases the motivation for producing valuable biogas through the anaerobic digestion of the organic pollution of the DSW. Thus, anaerobic treatment could become of crucial interest for the distillery industry, in order to valorise the organic matter of waste, recovering resources as bioenergy in a circular economy approach.
The aim of this study was to evaluate the valorisation of DSW through biogas production in Upflow Anaerobic Sludge Blanket (UASB) reactors. The spent wash was co-digested with swine wastewater (SWW) in order to provide nutrients and alkalinity to help the anaerobic process avoiding external chemicals and alkalinity supplementation.

MATERIALS AND METHODS

Experimental setup

A cylindrical lab-scale UASB reactor with a useful volume of 1 L, made of PMMA, was used for the experiments. The reactor was maintained at 36±1ºC and the produced biogas was collected in gas bags for the determination of gas volume and methane concentration. Granular sludge from an industrial UASB reactor was used as inoculum. More details about the experimental setup and methodology can be found in Montes et al. (2019).

Substrates and mode of operation

The DSW was collected at a local gin distillery while the SWW was obtained from a closed-cycle pig farm. The UASB reactor was fed in a semi-continuous mode with a constant HRT of 3.3 days. The feed consisted of a mixture of SWW (16.7%), diluted DSW (33.3%), and effluent recycled from the UASB effluent (50%) to dilute the influent and to reuse alkalinity. The DSW was diluted with dechlorinated tap water. The experiment was divided in 8 experimental periods, increasing the organic loading rate (OLR) by increasing the content of DSW in the diluted DSW, starting from 10% dilution in period 1 and eventually achieving an 80% dilution in period 8.

RESULTS AND DISCUSSION

Biogas and methane production

The production of methane over the experimental period is shown in Figure 1(a), as the volumetric methane production rate (VMPR) versus the OLR. A very good correlation was obtained between the OLR and the VMPR until period 7, indicating that the efficiency of the process did not decrease with the increasing OLR up to 28.5 kgCOD m^{-3} d^{-1}. The reactor was able to produce a maximum stable mean VMPR yield of 8.4 m^3CH_4 m^{-3} d^{-1}, when it was fed with a highly concentrated DSW (70% dilution). When the last period was set (80% DSW in the diluted DSW), the biogas and methane production started to drop and fell to minimal values.

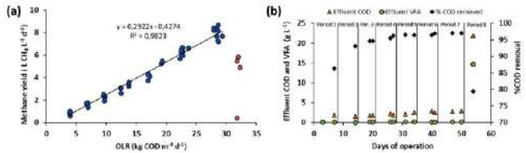

Figure 1. (a) Volumetric methane production rate (VMPR) at different organic loading rates (blue circles represent operation for periods 1–7; red circles represent the period 8); (b) COD and COD_{VFA} in the effluent and removal percentage of COD

COD removal efficiency

The content of acetic and propionic acids in the effluent, during experimental periods 1-7, was minimal with concentrations lower than 200 mgCOD_{VFA} L^{-1}, while the effluent COD ranged between 1.5 and 2.8 gCOD L^{-1}, as shown in Figure 1(b). The COD removal efficiency increased with the OLR because of the higher biodegradability of the DSW compared to that of the SWW, eventually achieving a removal efficiency of 97%. In period 8, the VFA concentration in the effluent raised to 14.7 gCOD_{VFA} L^{-1}, evidencing that the reactor failure was due to over-acidification. The last increment in the OLR caused an organic overloading that could not be compensated with the alkalinity in the medium, causing VFA accumulation, along with a big drop in the pH and inhibition of methanogenesis. To keep reactor stability, additional alkalinity should be provided by increasing the proportion of SWW in the feed or by increasing the effluent recirculation to influent ratio. In a different approach, the operational conditions of period 8 could be explored to produce and recover VFA as another valuable resource from the spent wash.

REFERENCES

Acharya, N.K., Mohana, S., Madamwar, D. 2008. Anaerobic treatment of distillery spent wash – A study on upflow anaerobic fixed film bioreactor. *Bioresour. Technol.* 99, 4621–4626.
Goodwin, J.A.S., Finlayson, J.M., Low, E.W. 2001. A further study of the anaerobic biotreatment of malt whisky distillery pot ale using an UASB system. *Bioresour. Technol.* 78, 155–160.
Montes, J.A., Leivas, R., Martínez-Prieto, D., Rico, C. 2019. Biogas production from the liquid waste of distilled gin production: Optimization of UASB reactor performance with increasing organic loading rate for co-digestion with swine wastewater. *Bioresour. Technol.* 274, 43–47.

Enhancing Carbon recovery compromises low N_2O emissions: example of a new municipal wastewater treatment.

C. Domingo-Felez*,**, Marlene M. Jensen*, Anders Bang***, and Barth F. Smets**

* Department of Environmental and Resource Engineering, Technical University of Denmark, Miljøvej, Building 115, 2800 Kgs., Lyngby, DK (E-mail: *mmaj@dtu.dk; bfsm@dtu.dk)*
** Current address: Infrastructure and Environment, School of Engineering, University of Glasgow, University Avenue, Glasgow G12 8QQ, UK (E-mail: *carlos.domingo-felez@glasgow.ac.uk*)
*** Assens Forsyning A/S, 5610 Assens, DK (E-mail: *aba@assensforsyning.dk*)

Abstract
WWTPs aim to remove and redirect nutrients from wastewater to energy generating processes efficiently. A newly built WTTP with capacity of 480 m^3/d was operated to maximize Carbon recovery while minimizing GHG (N_2O) emissions. Briefly, the plant consisted of: HRAS Biosorption, BNR, MBR for solids separation, and MBBR for pharmaceutical removal. The impact of autotrophic-driven denitrification (Anammox) and heterotrophic denitrification (conventional AS) was evaluated against the C-recovery load. Excessive C-recovery (>70% influent) lead to significantly higher N_2O emission factors (0.35 – 0.89%), compared to lower C-recovery loads (0.01 – 0.09%). Full-scale results agreed with offline analysis of specific activity for key N-removing microbes and Biomethane potential tests.

Keywords (maximum 6 in alphabetical order)
Carbon recovery; GHG; HRAS; Net-zero; nitrous oxide;

INTRODUCTION

The ambitious target for net-zero in 2030 in the water industry remains challenging. The positive effect of energy and nutrient recovery are insufficient if greenhouse gas emissions are not targeted. Within the HEPWAT national project, the municipality of Assens (AssensForsyning, Denmark), built and operated a 3.000 PE WWTP to investigate novel strategies for resource recovery, and nutrient, pathogen, and pharmaceutical removal. Experience and results would inform the design of a new 100.000 PE WWTP for the region, currently under construction. The objective of this study was to quantify N_2O emissions and the potential C-recovery as CH_4. The influent to the WWTP lies within a catchment that receives mainly municipal but also industrial wastewater (Dairy, and potentially also a brewery). The hypothesis was that increasing C-recovery also increases N_2O emissions as denitrification becomes C/N-limited (Peng, Carvajal-Arroyo, et al., 2017). Also, while autotrophic N-removal would maximize C-recovery it also poses the largest threat for high N_2O emissions. Focusing on the BNR processes the aims of this study were:

- Maximize the C-recovery load while minimizing N_2O emissions targeting either autotrophic or heterotrophic nitrogen removal.
- Perform offline analysis to elucidate the effect of operating variables for maximum C-recovery on N_2O production, on the potential N-removing activity (AOB, NOB, Anammox), and on the potential for C-recovery via Biomethane Potential tests.

MATERIALS AND METHODS

WWTP configuration

A WWTP was operated for over 300 days treating 15-20 m^3/h (3000 PE) and process performance was monitored online, and 24h samples several times per week (**Figure 1**). *BioSorption HRAS*: Aerobic MBBR (50 m^3, K5-carriers) followed by Fe and polymer dosing, and primary solids retained by a drum filter (40 µm). *IFAS*: The operational strategies adapted to lower aeration, intermittent aeration, and lower biomass set points compared to conventional activated sludge processes. *Anammox*: The filling ratio of K5 carriers was 9%, significantly lower than conventional biofilm systems (30-40%), economic reasons. *MBR*: The solids separator (52 m^3, 1500 m^2, 0.4 µm).

Experimental campaign: N_2O monitoring and offline analysis

N_2O production: The N_2O measuring campaign lasted 260 days while operation strategies for C-recovery were implemented. Two variables varied during the campaign: the total flow of wastewater treated, and the fraction of the flow considered for C-recovery in the BioSorption unit. N_2O was measured in the liquid phase in two of the Activated Sludge / IFAS reactors. Additionally, the influent, effluent, and BioSorption effluent were monitored with a lab-scale N_2O liquid sensor. The kLaO2 was estimated from the online DO data (corrected for the response time of the DO sensor) and percentage of valve opening from the blower, which was then converted into kLaN2O values. *qPCR*: Functional genes were quantified for total bacteria, 16S AOB, 16S Anammox, 16S Nitrobacter, 16S Nitrospira, Typical nosZII Atypical nosZII. *C-recovery*: The COD content was analysed for different particle sizes (<0.45, 0.45-0.70, >0.70 µm). The quantity of COD to be recovered as methane (CH_4) was studied via biomethane potential (BMP) tests after incubation period of 40 days at 35 °C and volatile fatty acids (VFA). *Offline tests*: Test the effect of (BOD/N ≫ 1) and (BOD/N ≈ 1) on the N_2O production (aerobic), and N_2O consumption (anoxic). Standardized batch tests at varying temperatures (10 – 20 – 30 °C) to monitor changes in potential Anammox activity, AOB, NOB and OUR activity.

RESULTS AND DISCUSSION

Key process performance and nutrient removal parameters

Industrial wastewater: The industrial wastewater contributed to 10% of the influent but 30-35% of COD and TN load. The COD load was comprised of particulate (39%), colloidal (18%) and soluble (43%). The BMP potential of industrial origin (dairy and brewery) was higher than that of the BioSorption unit, on-site recovery was recommended.
Anammox and IFAS: Because of the low Anammox biomass mass abundance the contribution of Anammox to the overall Nitrogen removal was difficult to distinguish and was significantly dependent on temperature (**Figure 5**), while no significant specific activity was lost for four months. Specific nitrification rates decreased over time as the Bypass flow increased, because more COD was loaded, and heterotrophic bacteria increased. The nitrifying capacity remained in excess and the total nitrogen removing capacity also increased. A 25-75% ration of Bypass-Biosorption flows at maximum influent rate (20 m^3/h) allowed for good removal of COD, BOD, SS, TP and TN (< 8.5 mgN/L). The membrane bioreactor (MBR) (TSS > 7gSS/L) acted as solids retention unit and additional nitrifying reactor (DO > 4mg/L) and hampers NOB suppression.

Nitrous oxide emissions

Increasing N_2O concentrations were observed when aeration occurred and NH_4^+ concentration was higher than ≈ 2 mgN/L (**Figure 2**). With respect to N_2O consumption, aerobic conditions slowed down, but not stopped, N_2O reduction, indicating the possibility of simultaneous N_2O production and consumption (Domingo-Félez and Smets, 2019). The daily-average N_2O emissions varied significantly, from below the detection signal of the sensor (≈ 0% emission factor) to 8.31% during an MBR process malfunction. During 41% of the days analysed N_2O emissions in the MBR were larger than in the Activated Sludge reactors, indicating that, contrary to settling tanks, MBRs are hotspots of N_2O emissions and should be considered in new WRRF designs. The higher the ratio [Bypass / Total flow], the lower the C-recovery of the process, where the [Bypass/Total flow] is, approximately, an indicator of the C/N levels in the influent to the Activated Sludge reactors (**Figure 3**). The N_2O emission factor was significantly higher when the influent to the Activated Sludge reactor consisted of C-depleted wastewater from the Biosorption unit (0.35 – 0.89%), compared to when a fraction of the raw influent was bypassed (0.01 – 0.09%). Also, the higher the wastewater load was, the higher the N_2O emission factor (**Figure 4**). Additionally, the highest N_2O emission factors corresponded to periods with the lowest TN removal efficiency. Hence, a balance between efficient C-recovery and low N_2O emissions must be found.

Conclusion: Regardless of the total flow rate treated, a C-recovery flow ratio of more than 30% resulted in high TN removal efficiencies (> 80%) and low N_2O emission factors (< 0.1%).

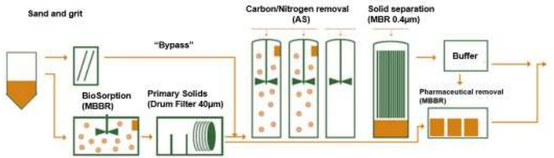

Periods	days	28	41	22	27	20	5	3	7	9	20	9	4	13
BioSorption	m^3/h	15	17	17	15	12	5	10	9	9	12	13	15	10
Bypass	m^3/h	0	0	3	5	8	5	5	6	11	8	7	0	7
Bypass / Total	(-)	0%	0%	15%	25%	40%	50%	33%	40%	55%	40%	35%	0%	41%
Total	m^3/h	15	17	20	20	20	10	15	15	20	20	20	15	17

Figure 1. Layout of the HEPWAT WWTP and Flow distribution BioSorption – Bypass, during selected periods.

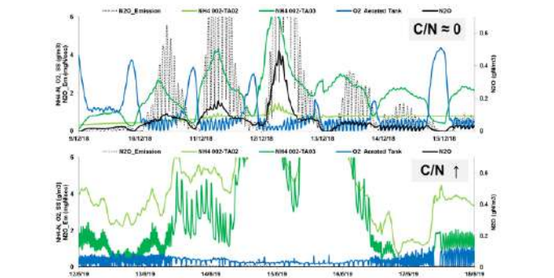

Figure 2 – Liquid concentrations in a BioTank of NH_4^+ (green), N_2O (black), DO (blue) and N_2O emissions (black, dashed) during a period of no Bypass flow (C/N ≈ 0), and 35% [Bypass / Total flow].

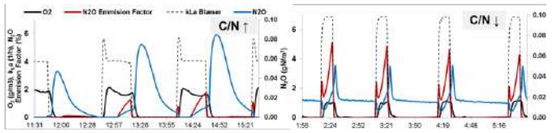

Figure 3 – Liquid concentrations in a BioTank of N_2O (blue), DO (black), N_2O EF (red), and O_2 mass transfer coefficient (black, dashed) during high (left) and low (right) [Bypass / Total flow].

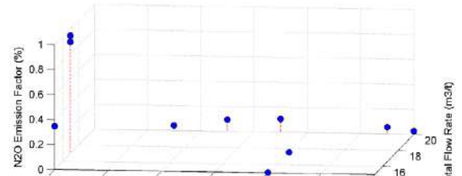

Figure 4 – Average N_2O emission factor of the HEPWAT WWTP for the different periods tested with varying ratios of Bypass to Total flow rate, and Total flow rate treated.

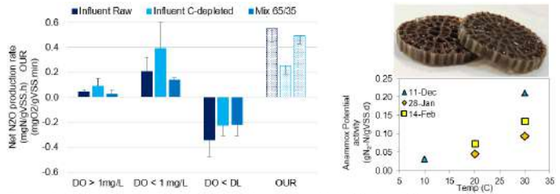

Figure 5 – Offline tests. Left: N_2O production rates at high DO, low DO, and anoxic conditions, and OUR, fed on Raw influent, C-removed influent, and a mixture 65%/35%. Right: Temperature dependence of potential Anammox activity from carriers.

REFERENCES

Domingo-Félez, C. and Smets, B. F. (2019) Regulation of key N2O production mechanisms during biological water treatment. Current Opinion in Biotechnology, **57**, 119–126. [online] https://linkinghub.elsevier.com/retrieve/pii/S0958166918301265.
Peng, L., Carvajal-Arroyo, J. M., Seuntjens, D., Prat, D., Colica, G., Pintucci, C., and Vlaeminck, S. E. (2017) Smart operation of nitritation/denitritation virtually abolishes nitrous oxide emission during treatment of co-digested pig slurry centrate. Water Research, **127**, 1–10.

Sustainability assessment framework and circular diagnosis of water treatment plants

S. Estévez*, D. Sastre Quemada*, G. Feijoo*, M.T. Moreira*

* Department of Chemical Engineering, University of Santiago de Compostela, Rúa Lope Gómez de Marzoa, 15782, Santiago de Compostela, Spain (E-mail: *sofia.estevez.rivadulla@usc.es; daniel.sastre@usc.es; gumersindo.feijoo@usc.es; maite.moreira@usc.es*)

Abstract
Legislative developments are triggering a race against time to upgrade and optimize technologies in the wastewater treatment sector. Detailed diagnosis of aspects such as greenhouse emissions, elimination of emerging pollutants, resource recovery and energy efficiency are central elements in wastewater management. Based on this premise, this study advances a roadmap for the evaluation of the operation of wastewater treatment plants under circularity indicators.

Keywords
Circular economy; Wastewater treatment performance; Indicators; Roadmap

INTRODUCTION

The updating of Directive 91/271/EEC has just started with the aim of extending its scope and aligning it with current sustainable and circular actions. The most recent proposal was revised in October 2022 to include aspects related to greenhouse gas emissions, removal of emerging micropollutants, efficient use of energy, water reclamation and recovery of valuable resources (i.e., organic matter and nutrients) (European Commission, 2022). In this context, wastewater treatment facilities are nowadays considered not only as the focus of wastewater treatment but also the recovery of nutrients as biofertilizers and water reclamation. To this end, facilities must be subjected to rigorous scrutiny in order to obtain a complete diagnosis of their performance. Indicators can be useful as tools for the measurement of the circularity as they can be used at various implementation scales. Since the indicators provide a single score result, they are not able to provide full insight of a treatment process and the analysis should be encompassing different understandings (Moraga et al., 2019). Therefore, a system of indicators is required to assess the successful development and implementation of CE. Other studies related wastewater treatment have tried to provide a background for evaluation within the sector. For example, Preisner et al. (2022) have collected indicators for resource recovery in wastewater treatment, but they have not created a thorough framework beyond that application. Kayal et al. (2019) have designed a composite indicator monitoring the 3Rs and Kakwani et al. (2022) another one for the urban water cycle. It is perhaps the study of Nika et al. (2022) the one providing a full multi-indicator analysis (17 indicators). However, they have taken an approach very linked to the specific design of facilities and does not advocate for a top-down approach to detect needs from the legislation and the state-of-the art. For this reason, this study provides a review and roadmap based on holistic criteria extracted from legislation aimed at the quantitative measurement of the circular economy performance of wastewater treatment plants under different topic areas (i.e., water quality and energy efficiency).

MATERIALS AND METHODS

The circularity assessment can be approached on the basis of a multidisciplinary analysis, so that it is possible to identify a set of circular indicators that would quantify various dimensions of a wastewater treatment plant or technology. The assessment tool is based on three different steps: (1) review, classification and adaptation of water sector indicators for the purposes of wastewater treatment facilities, (2) identification of all possible inflows and outflows of the selected scenarios, as well as the variables needed to calculate each selected indicator, and (3) gaps and proposal of new indicators to fulfil the circular actions and products. The analysis was framed for the operational phase of wastewater treatment facility, leaving the construction and long-term maintenance of the infrastructure outside the system boundaries. It should be noted that the study provides a process or mesoscale perspective, therefore, the indicators related to the transport, storage and consumption of drinking water or those associated with the sewerage system were disregarded.

RESULTS AND DISCUSSION

Bibliographic data analysis and classification of indicators

Two types of documents were considered for revision: grey literature (reports and initiatives) and scientific articles. The result was a total of 103 water-oriented indicators (76 for the environment, 15 for economy and 12 for governance), being around 87% of them from papers. The truth is that, despite the large efforts of OECD to compiled 474 indicators different sectors (report "The OECD Inventory of Circular Economy indicators"), the concept of circular economy and the increase of interest of the scientific community in the measurement of the circular actions taken for the processes has led to a blooming of ideas and creation of indicators. In fact, by the end of 2022 the Scopus database shown that around 56% of the articles associated to the keywords of "circular economy" and "wastewater treatment" belong to the last two years. On the other hand, consensus has not been reach regarding to the classification of the indicators. The report of the OCDE arranged the indicators into 5 categories and 27 subcategories while Seghezzo et al. (2014) proposed 20 different criteria grouped within the three pillars of sustainability (5 environmental, 7 social and 4 economic) and technical aspects (4). Singhirunnusorn y Stenstrom (2009), instead, grouped them in 7 principles allocated within the technical, socioeconomic and environmental pillars and 14 more specific criteria. It is also worth mentioning the document named as "*Categorization system for circular economy*", which highlighted 14 categories assembled in circular design and production, circular value of the recovery, circular use and support. The thing is, in relation to the outcomes of this study, the quantitative indicators measuring the circularity of the wastewater sector facilities can be classified according to the pillar of sustainability around topics of design, water quality, water reclamation, energy performance nutrient traceability, sludge valorization, waste treatment, product quality, employment, education, perception and innovation. Some examples of circular economy indicators are shown in Table 1 for the theme of water quality.

Identification of inflows and outflows

The study had a two-side approach: top-down regarding to the collection of indicators and bottom-up to consider the specific needs to the facilities (both novel and conventional design) which helps detect gaps while adjusting the assessment to the process. The registered indicators required the measurement of a total of 100 variables to complete the estimation of the indicators. Some of them such as the plant influent flow rate or nitrogen and phosphorus content of the wastewater are already quantified to comply with legislation while others like the content of Al_2O_3 and the total incomes from the produced bio-based products are not usually provided.

Detection of gaps and new indicators

A list of principles, criteria and sub-criteria were extracted from 17 European directives and regulations (shown in Table 2) with the main goal to verify if the actual legislation in force, very oriented to performance and sustainability, is also adapted to the upcoming circular economy framework for indicators. The directive 86/278/EEC for the protection of the soil against sewage sludge, 2020/741 related to minimum requirements for water reclamation, 2010/75/EU about industrial emissions were the 3 of the 17 analyzed showing some advancements in circular economy. However, their focus is on monitoring (establishment on management plans, awareness campaigns, traceability of the documentation and prevention and recovery programs, among others) which is more related to a qualitative measurement than quantitative. Besides, and from the second stage of the assessment provided within this study (identification of in-out flows of wastewater treatment plants), gaps have been detected in the current dataset of indicators from literature regarding to human health and biodiversity as well as other topic under assessment for the proposal of the new wastewater treatment directive: emerging micropollutants and resource recovery (i.e., polyhydroxyalkanoates, volatile fatty acids for butanol manufacturing and celluloses).

Table 2. List of principles, criteria and sub-criteria from directives and regulations.

Pillars	Principles	Criteria	Sub-criteria
Environment	Protection of ecosystems	Conservation of the biological diversity	Ecosystems diversity Diversity of species Presence of invasive species
		Maintenance of the health and vitality of the ecosystems	General Soil quality Water quality Air quality
		Conservation and management of air	Protective function
		Conservation and management of water	Protective function
		Conservation and management of soil	Protective function
	Improvement of resources	Management and monitoring	-
		Use of resources	-
		Management and monitoring	-
Socio-economic	Improvement and maintenance of the socioeconomic benefits to satisfy social needs	Production and consumption	-
		Investment	-
		Added value	Finance management Security
		Basic community needs	Potable water Waste treatment Health
		Working conditions	-
		Tourism and entertainment	-
		Management and monitoring	-
Governance	Design of the wastewater infrastructure	Treatment system	Catchment design Installation capacity
		Facilities	Installation location Technologies and infrastructure Operation and maintenance
		Water catchment	-
		Monitoring	-
Circularity	Waste management	Reuse and recycling of resources	Water recovery Sludge valorisation
		Treatment strategies	-
	Monitoring	-	-

Table 1. Example of some of the environmental indicators used for the circular wastewater treatment diagnosis.

Category	Theme	Indicator	Code	Units	Equation	Level	Objective	Reference
Environmental	Water quality	Reduction of the contaminant load of effluents	A1	Dimensionless	$A1 = \frac{MW_{SS} + MW_{BOD} + MW_P}{6} + \frac{MW_{NO3-} + MW_{NO2-} + MW_{NH4+}}{6}$	Meso	Compliance with environmental legislation	Kiselev et al. (2019)
Environmental	Water quality	Organic matter removal efficiency	A2	Dimensionless	$A2 = \frac{Q_{in} \cdot (COD_{in} - COD_{out})}{10^6}$	Meso	Optimization (maximize)	Preisner et al. (2022)
Environmental	Water quality	Net eutrophication environmental impact	A3	Dimensionless	$A3 = \frac{EP_{in} - EP_{process} - EP_{out}}{EP_{in} - EP_{out,maximum}}$	Meso	Minimization	Lorenzo-Toja et al. (2016)
Environmental	Water quality	Wastewater reclamation for irrigation	A4	%	$A4 = \frac{Q_{reclaimed\ irrigation}}{Q_{out}} \cdot 100$	Meso	Optimization (minimize up to 100%)	Preisner et al. (2022)
Environmental	Water quality	Global index for water reuse	A5	%	$A5 = \frac{Q_{reclaimed\ and\ reused}}{Q_{out}} \cdot 100$	Meso	Optimization (minimize up to 100%)	Kiselev et al. (2019)

Acronyms: Q: Flowrate; COD: Chemical Oxygen demand; in: Input/Influent; out: output/effluent; EP: Eutrophication potential; MW: Multiplicity weight; SS: Suspended Solids; BOD: Biological Oxygen Demand and P: Phosphorus.

REFERENCES

European Commission 2022. Proposal for a revised Urban Wastewater Treatment Directive. (Visited 25 of December of 2022). Available online on: https://environment.ec.europa.eu/publications/proposal-revised-urban-wastewater-treatment-directive_en

Kakwani, N.S., Kalbar, P.P., 2022. Measuring urban water circularity: Development and implementation of a Water Circularity Indicator. *Sustainable Production and Consumption*, **31**, 723-735.

Kayal, B., Abu-Ghunmi, D., Abu-Ghunmi, L., Archenti, A., Nicolescu, M., Larkin, C., Corbet, S., 2019. An economic index for measuring firm's circularity: The case of water industry. *Journal of Behavioral and Experimental Finance*, **21**, 123-129.

Lorenzo-Toja, Y., Vázquez-Rowe, I., Amores, M.J., Termes Rifé, M., Marín-Navarro, D., Moreira, M.T., Feijoo, G., 2016. Benchmarking wastewater treatment plants under an eco-efficiency perspective. *Science of the Total Environment*, **566-567**, 468-479.

Moraga, G., Huysveld, S., Mathieux, F., Blengini, G.A., Alaerts, L., Van Acker, K., de Meester, S., Dewulf, J., 2019. Circular economy indicators: What do they measure? *Resources, Conservation and Recycling*, **146**, 452-461.

Nika, C.E., Vasilaki, V., Renfrew, D., Danishvar, M., Echchelh, A., Katsou, E., 2022. Assessing circularity of multi-sectoral systems under the Water-Energy-Food-Ecosystems (WEFE) nexus. *Water Research*, **221**, 118842.

OECD. (2021) The OECD Inventory of Circular Economy indicators. (Visited 25 of December of 2022). Available online on: https://www.oecd.org/cfe/cities/InventoryCircularEconomyIndicators.pdf

Preisner, M., Smol, M., Horttanainen, M., Deviatkin, I., Havukainen, J., Klavins, M., Ozola-Davidane, R., Kruopiene, J., Szatkowska, B., Appels, L., Houtmeyers, S., Roosalu, K., 2022. Indicators for resource recovery monitoring within the circular economy model implementation in the wastewater sector. *Journal of Environmental Management*, **304**, 114261.

Seghezzo, L., van Vliet, B., Zeeman, G., Lettinga, G., 2014. Assessment of the sustainability of anaerobic sewage treatment in northwestern Argentina

Singhirunnusorn, W., Stenstrom, M.K., 2009. Appropriate wastewater treatment systems for developing countries: criteria and indictor assessment in Thailand. Water Science and Technology, 59, 9, 1873-1884.

Exploiting the DO Profile for the Mathematical Modelling of a Mixed PHA-accumulating Microbial Community

S. Falcioni*, D. Gabriel**, M.E. Suárez-Ojeda**, G. Munz*,

* Dept. of Civil and Environmental Engineering, University of Florence, Via di S. Marta 3, 50139 Florence, IT (E-mail: *serena.falcioni@unifi.it; giulio.munz@unifi.it)*
**GENOCOV Research Group, Dept. of Chemical, Biological and Environmental Engineering, School of Engineering, Universitat Autònoma de Barcelona, Escola d'Enginyeria. Edifici Q Campus UAB, 08193, Bellaterra, Barcelona, ES (E-mail: *David.Gabriel@uab.cat; MariaEugenia.Suarez@uab.cat)*

Abstract
A two-population model, implemented by modifying the Guyer matrix of the model 2C in Sumo software, was calibrated through the experimental dissolved oxygen (DO) profile to highlight the mechanisms of microbial competition and selection occurring in a mixed microbial community (MMC) comprising PHA-accumulating heterotrophic and ordinary heterotrophic microorganisms. The model takes its cue from the work of Marang et al. (2015), and further details the biomass decay processes to better represent experimental data obtained from monitoring a lab-scale bioreactor set to select PHA storing microorganisms. The model made it possible to hypothesise new control strategies for effective selection of PHA storing rich cultures.

Keywords
Calibration; dissolved oxygen; mixed microbial community; modelling; polyhydroxyalkanoates

INTRODUCTION

Polyhydroxyalkanoates (PHAs) are a wide category of bio-based and biodegradable polymers, produced intracellularly by several microorganisms, as a carbon and energy storage compounds. Currently, its industrial production process consists of using pure cultures of natural or genetically modified microorganisms as they can accumulate high amounts of PHA (up to 90% of their cell dry weight), but the costs are also high, and not competitive with conventional plastics. To reduce process costs and with the perspective of valorising specific wastes, mixed microbial communities (MMCs) instead of pure cultures are a promising alternative. Lab-scale trials have demonstrated that the MMCs can achieve cellular PHA content comparable to that of pure cultures, depending also on the complexity of the substrate. Nevertheless, the overall yields are still lower, probably due to the lower cell density (or biomass concentration) of the MMC compared to the pure one. The selected MMCs presumably consist of both conventional and PHA-accumulating heterotrophic bacteria. So far, the most robust strategy to select PHA-accumulating bacteria is the alternation of feast and famine phases, in aerobic conditions, and using selected volatile fatty acids (VFA) as substrates (Estévez-Alonso et al., 2021). To better highlight the dynamics between PHA-accumulating and ordinary heterotrophic populations and as a basis for the development of future control selection strategies, in the present study a two-population ASM-like model was developed and calibrated using of experimental data collected from a laboratory-scale sequencing batch reactor (SBR) and data taken from literature (Dias et al., 2005, Jiang et al., 2011, Marang et al., 2015). This study aims to extend the two-population model developed by Marang et al. (2015) by detailing the decay processes on the basis of preliminary experimental results reporting non-negligible concentrations of slowly-biodegradable residual-soluble organic matter (in terms of chemical oxygen demand-COD-) and predation phenomena.

MATERIALS AND METHODS

Experimental set up

An aerobic lab-scale SBR with a maximum working volume of 1.4 L has been running from 6 months. It was fed with 1 gCOD $L^{-1}d^{-1}$ of VFAs (80% acetate and 20% propionate), 30 mgN_NH_4^+ $L^{-1}d^{-1}$ of ammonium and 7 mgP_PO_4^{3-} $L^{-1}d^{-1}$ (C:N:P =100:6:1.5 in w/w proportion). The reactor operates with 12 h cycles, for a hydraulic retention time (HRT) of 1 day and with a volume exchange ratio (VER) of 50%. The feast-famine (F/F) ratio was set to 0.3 and an intermediate settling and effluent discharge has been introduced between feast and famine phases. Selection was forced by applying an uncoupled feeding: the VFA solution was dosed at the beginning of the feast while the nutrient solutions (N, P and micro-nutrients) were dosed at the beginning of the famine. The sludge withdrawal was made at the end of the cycle under mixing conditions (in the represented model, due to the need to respect the constraints imposed by the model structure, purging is immediately following the supernatant discharge) to maintain the sludge retention time (SRT) at 3.6 d. The temperature in the reactor was controlled at 27 ±0.5 °C, while pH varied between 8.4 and 8.9. The dissolved oxygen (DO) profile, obtained by monitoring with an optical probe (S423/C/OPT/T, Chemitec), has been used to calibrate the model.

Activated sludge model

The model Sumo 2C, developed by Sumo (Dynamita S.A.R.L., France), was modified for including the PHA-storage heterotrophic organisms (X_{PHO}), not available in the library (different from the polyphosphate- and glycogen-accumulating organisms, PAO and GAO, respectively), to simulate the competition with the ordinary heterotrophic organisms (X_{OHO}). In the modified model X_{OHO} and X_{PHO} populations are the only two microbial populations. The reactions involved are as follows and represented in the schematic in Figure 1: storage of VFAs (S_{VFA}), growth on VFAs, growth on PHA (X_{PHA}) and decay for X_{PHO}, growth on S_{VFA}, growth on readily and soluble biodegradable substrate (Ss) and decay for X_{OHO}.

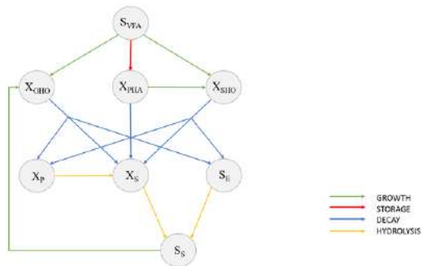

Figure 1. Schematic of the processes involved in the model (only the carbon cycle is reported).

Both X_{PHO} and X_{OHO} decay were defined in three different compounds: particulate slowly hydrolysed (X_P), particulate readily hydrolysed (X_S) and soluble-decay-products slowly-biodegradable (S_E) compounds. The hydrolysis processes convert X_P in X_S and both X_S and S_E in S_S. Table 1 shows the stoichiometric and kinetics parameters picked up for the simulations.

Table 1. Overview of the model input: stoichiometric and kinetic parameters for OHO and PHO.

Stoichiometric parameters	**Description**	**Value**		**Reference**
$Y_{PHO,VFA}$	Yield of PHO on VFA	0.4	g COD. g COD-1	Dias et al., 2005
$Y_{PHA,VFA}$	Yield of PHA on VFA	0.55	g COD. g COD-1	calibrated
$Y_{PHO,PHA}$	Yield of PHO on PHA	0.55	g COD. g COD-1	calibrated
$Y_{OHO,VFA}$	Yield of OHO on VFA	0.6	g COD. g COD-1	default Sumo
$Y_{OHO,Ss}$	Yield of OHO on Ss	0.67	g COD. g COD-1	default Sumo
Kinetic parameters PHO	**Description**	**Value**		**Reference**
μ_{PHO}	Max specific growth rate	4.5	d^{-1}	calibrated
q_{VFAmax}	Rate of VFA storage into PHA	80	d^{-1}	Marang et al., 2015
$K_{VFA,PHO}$	Half-saturation of VFA	8.4	mgCOD L^{-1}	Marang et al., 2015
$K_{PHA,PHO}$	Half-saturation of PHA	0.1	mgCOD L^{-1}	calibrated
$Ki_{PHA,PHO}$	Half-inhibition of max PHA	10	g COD.g COD-1	calibrated
$Ki_{VFA,PHO}$	Half-inhibition of VFA	5	mgCOD L^{-1}	calibrated
b_{PHO}	Decay rate	0.8	d^{-1}	calibrated
Kinetic parameters OHO	**Description**	**Value**		**Reference**
μ_{OHO}	Max specific growth rate	4.5	d^{-1}	calibrated
$K_{Ss,OHO}$	Half-saturation of Ss	20	mgCOD L^{-1}	calibrated
$Ki_{VFA,OHO}$	Half-inhibition on VFA	5	mgCOD L^{-1}	calibrated
$K_{VFA,OHO}$	Half-saturation of VFA	8.4	mgCOD L^{-1}	calibrated
b_{OHO}	Decay rate	0.8	d^{-1}	calibrated
Kinetic parameters BIO	**Description**	**Value**		**Reference**
$K_{NHx,BIO}$	Half-saturation of NHx	0.1	mgN L^{-1}	calibrated

RESULTS AND DISCUSSION

Figure 2 shows the calibration results of a simulated DO profile along the experimental one. The VFA and ammonium concentration profiles reflect experimental trends, while PHA concentration has a profile consistent with that predicted; VFA decreases and it is totally consumed before the end of the feast phase, meanwhile accumulating PHA and consuming oxygen. During the famine phase, after ammonium dosing, PHO grow on stored PHA, consuming nutrients and oxygen (Fig. 3). The volatile suspended solids (VSS) concentration provided by the model are approximately 430 mg L^{-1} (consistent with the experimental value, 490 mg L^{-1} ca.). The most abudant population selected on average is that of PHA-accumulating microorganisms (250 mgCOD L^{-1}), the rest are OHOs (200 mgCOD L^{-1}). The effluent mostly contains both S_E and S_S (for a total of 70 mg sCOD L^{-1}), representative of the residual experimental COD measured at the end of the famine phase. Calibrating the model on the basis of the experimentally monitored DO profile seems to achieve the purpose. Moreover, many DO data are easily obtained from the bioreactor monitoring; collecting several DO values over time is relatively simple, provided the bioreactor is equipped with a DO probe. Several insights emerge from the results of the simulations. For instance, the feast and famine phases duration is not perfectly optimised, thus still favouring the OHO rather than the PHO. Adjusting the duration of the two phases could lead to richer communities of accumulating PHA microorganisms.

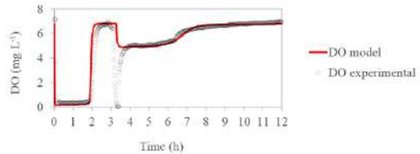

Figure 2. Model calibration results: comparison between experimental and modelled DO profile.

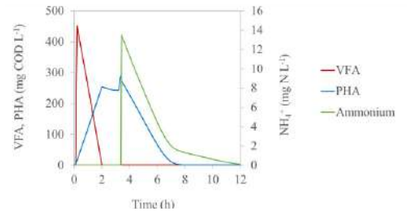

Figure 3. Results of the simulation: VFA, PHA and ammonium (as representative nutrient) profiles along one cycle.

ACKNOWLEDGEMENTS

This project has received funding from the European Union's Horizon 2020 research and innovation programme under grant agreement No. 872053.

REFERENCES

Dias, J. M., Serafim, L. S., Lemos, P. C., Reis, M. A., & Oliveira, R. (2005). Mathematical modelling of a mixed culture cultivation process for the production of polyhydroxybutyrate. *Biotechnology and bioengineering*, *92*(2), 209-222.
Estévez-Alonso, A., Pei, R., van Loosdrecht, M. C., Kleerebezem, R., & Werker, A. (2021). Scaling-up microbial community-based polyhydroxyalkanoate production: status and challenges. *Bioresource Technology*, *327*, 124790.
Jiang, Y., Hebly, M., Kleerebezem, R., Muyzer, G., & van Loosdrecht, M. C. (2011). Metabolic modeling of mixed substrate uptake for polyhydroxyalkanoate (PHA) production. *Water research*, *45*(3), 1309-1321.
Marang, L., van Loosdrecht, M. C., & Kleerebezem, R. (2015). Modeling the competition between PHA-producing and non-PHA-producing bacteria in feast-famine SBR and staged CSTR systems. *Biotechnology and bioengineering*, *112*(12), 2475-2484.

Improvement of activated sludge systems: should we pay more attention to the role of EPS?

Z. Fau*, A. Azaïs*, S. Gillot* and F. Chazarenc*

* INRAE, UR REVERSAAL, Villeurbanne F-69625, France (zoe.fau@inrae.fr, antonin.azais@inrae.fr, sylvie.gillot@inrae.fr, florent.chazarenc@inrae.fr)

Abstract
Understanding links between bioflocculation, settling and extracellular polymeric substances (EPS) in activated sludge (AS) systems presents a challenge, but is necessary to describe and optimize bioprocesses. This study provides a comprehensive approach, including new insights to characterize the role of EPS in AS systems, to reduce energy and environmental treatment costs. AS samples were taken in a wide range of full-scale facilities including conventional AS (CAS), high rate AS (HRAS) and densified sludge processes. Complementary and innovative protocols were selected to analyse EPS content and nature, as well as bioflocculation and settling efficiencies. Links between EPS, bioflocculation and settling were observed under different operating conditions. One sampling and analysis campaign on two full-scale plants and a pilot plant is presented in this abstract. More investigations on six other processes will be scheduled in four sampling campaigns in the forthcoming months.

Keywords: Bioflocculation, Biological process, EPS, Settling

INTRODUCTION

The transition from wastewater treatment plant to wastewater resource recovery facilities requires solutions to optimize energy efficiency of activated sludge (AS) processes and to reduce their overall environmental footprint. Current solutions such as carbon capture and valorisation (using chemically enhanced primary treatment and/or high rate activated sludge) or the use of sludge densification enable to reduce treatment costs, but there is still a need to maximise organic matter capture for recovery and to reduce energy needs. Better understanding the role of extracellular polymeric substances (EPS) and their link with bioflocculation and settling mechanisms was recently highlighted as a way to optimize AS processes (Ngo et al., 2022; Van Winckel, 2022, Yang and Li, 2009). EPS are produced by bacteria, they are composed mainly of proteins and sugars that form a matrix around cells, which interact with the external environment. Results related to the role of EPS in AS available in literature show no consensus. Some studies demonstrate that EPS are responsible for good bioflocculation (Ngo et al., 2022; Van Winckel, 2022), others that EPS generate poor settling (Liao et al., 2001), and a study even conclude that there is no link between EPS and process performances (Kinyua et al., 2017).

The first challenge is to quantify EPS concentrations, which is linked to their complexity and the lack of standardised protocols. This explains the difficulty to reach a consensus in addition to the very large range of experimental conditions (scale, processes and wastewater types).

The objective of this study was to analyse samples of mixed liquor simultaneously for EPS characterisation, bioflocculation and settling with the aim to develop complementary insights.

A comprehensive approach has been followed, consisting of:

- Selection of robust and easily applied protocols accepted by the scientific community as well as recently developed ones to a general understanding of the mechanisms;
- Sampling of full-scale systems to characterise processes ongoing under real conditions;
- Sampling of a large panel of AS processes (CAS, HRAS, densified sludge) in several campaigns to characterise mechanisms under a wide range of conditions.

One sampling and analysis campaign on two full-scale plants and on one pilot plant is presented in this abstract. A full series of data including six more plants investigated with four more campaigns as well as several other parameters measured will be available in June 2023.

MATERIALS AND METHODS

Biological processes

AS samples were collected from the biological reactor of one full-scale CAS system, one full-scale densified AS system and one HRAS pilot plant (as presented in Table 1) and analysed for bioflocculation and settling within 30 minutes and for EPS within 4 hours after sampling.

EPS

Total EPS (EPSt) were extracted by using the cation exchange resin (CER) extraction method developed by Frølund et al. (1996). This protocol enables a good extraction while limiting cell lysis. Loosely Bound (LB) and Tightly Bound (TB) EPS were extracted by using a heat extraction method modified based on Li and Yang (2007). This method is complementary to the first one by giving information on EPS structure; both are easily performed even under field conditions. Once extracted, EPS were quantified by measuring the total COD content using WTW® micro-methods.

Bioflocculation and settling

Conventional methods as diluted Sludge Volume Index (dSVI), Effluent Suspended Solids (ESS) measured by the TSS (Total Suspended Solids) of the dSVI supernatant, and initial settling velocity were determined with standards methods (APHA 2005). Limit Of Stokesian Settling (LOSS) was determined by using the method of Mancell-Egala et al. (2017). LOSS provides the minimal sludge concentration at which flocculent settling transitioned into hindered settling. The combination of these macroscopic physical behaviours of sludge with the biochemical characterisation of EPS enable to better understand the link between EPS, bioflocculation and settling mechanisms.

RESULTS AND DISCUSSION

As expected, HRAS sludge presents the lowest settling velocity and the largest ESS reflecting the presence of weak flocs having a low density (Table 1). The observed dSVI and LOSS of HRAS are in between those measured for CAS and densified process.

Densified sludge presents a low dSVI and a high LOSS, corresponding to a good compression capacity, and a high settling velocity. This can be the consequence of a greater sludge density that settles faster with higher compression capacity. ESS is not significantly different from that of CAS.

Table 1. Operating parameters, bioflocculation and settling performance of full scale and pilot reactors

	CAS	Densified	HRAS
SRT (d)	15	20	1.5
Organic loading rate (gDBO/gVSS/d)	0.09	0.18	3
TSS (g/L)	2.97	2.94	2.30
VSS (g/L)	2.39	2.43	1.92
dSVI (mL/g)	151	81	129
ESS (g/L)	0.005	0.010	0.061
Settling velocity (m/h)	1.8	4.1	1.2
LOSS (mg/L)	1060	1580	1079

EPSt concentrations (Figure 1) are similar to those obtained in other comparable studies (Ngo et al., 2022; Van Winckel, 2022).

EPSt and LB-EPS are larger for HRAS. As LB-EPS make flocs less dense, their settling velocity is lower. LB-EPS have relatively low cohesion strengths. Their high concentration makes flocs more sensitive to deflocculation, they can break down easily, which is likely to corroborate the high ESS. The positive correlation between LB-EPS and ESS was also observed by Yang and Li (2007) in a 2 L AS reactors (SRT ~ 5-20 d) fed with synthetic water.

With this high LB-EPS, one can expect a larger dSVI and a lower LOSS. Therefore, the following hypothesis can be formulated: the good compressibility observed is related to isolated particles, generated by deflocculation, rather than diffuse flocs. This initial floc structure is due to the short sludge retention time, which does not allow flocs to aggregate strongly.

More TB-EPS would be expected in the densified sludge, as TB-EPS are presumably responsible for strong aggregation. However, there is no significant difference in the concentration and structure (i.e. TB and LB-EPS) of the EPS between densified and CAS sludge. This can be a consequence of EPS extraction. The protocol developed for flocs may have limits to extract EPS from robust aggregates. More aggressive methods might be required. Therefore, there is still a need to develop a method enabling to compare EPS in flocs and granules.

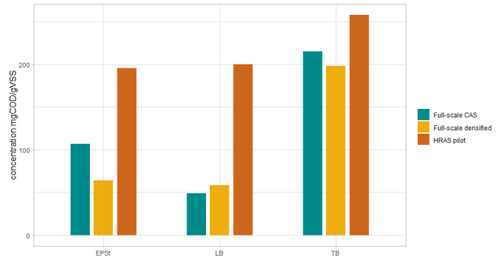

Figure 1. EPSt, LB-EPS and TB-EPS concentration in full-scale and pilot reactors

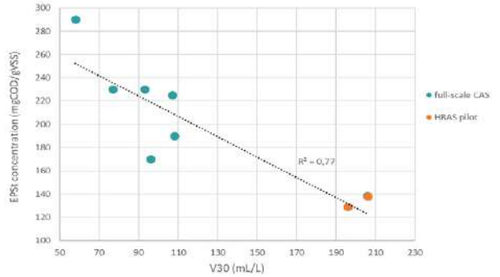

Figure 2. Relation between V30 and EPSt in HRAS pilot and CAS processes

Results were analysed to draw correlations between EPS, bioflocculation and settling efficiencies. As an example, a correlation was observed between V_{30} and EPSt (Figure 2). This suggests that the presence of more EPSt increases the capacity of flocs to aggregate and, therefore, the overall compressibility. Investigations are still under progress, a larger set of data will enable to perform more statistical tests and to highlight other potential correlations.

CONCLUSION

These preliminary investigations provide the following conclusions:

- Links between EPS, bioflocculation and settling can be observed under different operating conditions.
- Protocols for EPS extraction still need to be adapted for specific sludge types (e.g. densified sludge).

Other results are expected both in terms of investigated parameters, such as bioflocculation characterisation (e.g. Threshold of Flocculation (TOF)), EPS composition (e.g. ratio protein/sugar), floc investigation (particle size and morphology analysis) and additional data sets in the upcoming campaigns.

REFERENCES

Frølund, B., Palmgren, R., Keiding, K., Nielsen, P.H., 1996. Extraction of extracellular polymers from activated sludge using a cation exchange resin. Water Res. 30, 1749–1758.

Kinyua, M.N., Elliott, M., Wett, B., Murthy, S., Chandran, K., Bott, C.B., 2017. The role of extracellular polymeric substances on carbon capture in a high rate activated sludge A-stage system. Chem. Eng. J. 322, 428–434.

Li, X.Y., Yang, S.F., 2007. Influence of loosely bound extracellular polymeric substances (EPS) on the flocculation, sedimentation and dewaterability of activated sludge. Water Res. 41, 1022–1030.

Liao, B.Q., Allen, D.G., Droppo, I.G., Leppard, G.G., Liss, S.N., 2001. Surface properties of sludge and their role in bioflocculation and settleability. Water Res. 35, 339–350.

Mancell-Egala, W.A.S.K., De Clippeleir, H., Su, C., Takacs, I., Novak, J.T., Murthy, S.N., 2017. Novel Stokesian Metrics that Quantify Collision Efficiency, Floc Strength, and Discrete Settling Behavior. Water Environ. Res. 89, 586–597.

Ngo, K.N., Tampon, P., Van Winckel, T., Massoudieh, A., Sturm, B., Bott, C., Wett, B., Murthy, S., Vlaeminck, S.E., DeBarbadillo, C., De Clippeleir, H., 2022. Introducing bioflocculation boundaries in process control to enhance effluent quality of high-rate contact-stabilization systems. Water Environ. Res. 94.

Van Winckel, T., 2022. Enhancing bioflocculation in high-rate activated sludge improves effluent quality yet 2increases sensitivity to surface overflow rate.

Yang, S., Li, X., 2009. Influences of extracellular polymeric substances (EPS) on the characteristics of activated sludge under non-steady-state conditions. Process Biochem. 44, 91–96.

BIOUP – Biomethane production through the integration of renewable energy surpluses in WWTP

F. Ferrari*, I. Diaz**,***, M.L. Ruiz****, R.I. Esteban****, M.M Micó*, J. Malfeito*

* Innovation department of Acciona Agua S.A.U, Parc de Negocis Mas Blau II, Avda. de les Garrigues, 22, 08820 El Prat de Llobregat, Barcelona, Spain
** Department of Chemical Engineering and Environmental Technology, School of Industrial Engineering, University of Valladolid, Dr. Mergelina, s/n, 47011 Valladolid, Spain
*** Institute of Sustainable Processes, Dr. Mergelina s/n, 47011 Valladolid, Spain
**** Advanced Biofuels and Bioproducts Unit, Department of Energy, Research Centre for Energy, Environment and Technology (CIEMAT), Avda. Complutense 40, 28040 Madrid, Spain

(E-mail: *fferrari@acciona.com*; *israel.diaz@uva.es*; *marisa.rlorenzo@ciemat.es*; *raquel.iglesias@ciemat.es*; *mariamar.mico.reche@acciona.com*; *jorgejuan.malfeito.sanchez@acciona.com*)

Abstract
The new European policies to achieve a carbon neutral Europe in 2050 are increasingly strict and call for increasing the use of renewable energy and implementing technologies based on hydrogen, biogas and biomethane. The BIOUP project will offer a "power-to-gas" solution for the use in the form of biomethane ((above 90% in CH_4 content) of green hydrogen from surplus renewable energy, which cannot be used at certain times of the day. For this purpose, an in situ pilot plant and ex situ pilot plant (biotrickling filter) will be integrated into the sludge line of a WWTP. Thus, the conversion of biogas into biomethane will be studied and optimized, evaluating a series of scenarios, also studying the different energy supply options for the generation of green hydrogen through the HOMER and XENDEE energy simulators.

Keywords (maximum 6 in alphabetical order)
Anaerobic digestion; biogas; ex situ; in situ; power-to-gas

INTRODUCTION

The new European and national policies to achieve a carbon neutral Europe in 2050 are increasingly strict and call for increasing the use of renewable energy and implementing technologies based on hydrogen (H_2), biogas and biomethane. The BIOUP project will offer a "power-to-gas" solution not available until now, for the use in the form of CH_4 of green H_2 from surplus renewable energy, that may exceed conventional demand at certain times of the day. To this end, it will develop a technology that will biologically enrich WWTP anaerobic digested sludge biogas (60% in CH_4) from the anaerobic digestion of sewage sludge through the biomethanation of CO_2 contained in it, with renewable H_2, so that the upgraded biomethane generated have sufficient quality to be injected into the natural gas network (> 95% in CH_4) or used directly in transport vehicles (> 90% in CH_4). The BIOUP project aims to develop and validate a technology for the biological transformation into CH_4 of H_2, from renewable sources, and carbon dioxide (CO_2), generated in the anaerobic digestion of organic matter. This technology fits the particularities of WWTP, which have large volumes of anaerobic digestion of sludge and a clear need to increase the energy efficiency of their operation.

MATERIAL AND METHODS

BIOUP will address the assessment of in situ and ex situ biomethanation technologies. In the case of the in situ technology, laboratory tests will be carried out to determine the technical feasibility and the optimal design conditions and parameters of the biomethanation process, in order to determine the best operating conditions, together with the potential effect of the codigestion and different alternatives to improve H_2 transfer. The study of microbial populations of the processes will also take place through the project, in order to offer a deeper insight of the biodynamics of the system. Subsequently, with the data obtained, a 5m^3 prototype will be designed and built for the validation of the technology on a pilot scale. It will be installed in a real WWTP, to use real sludge to feed the in situ biomethanation digester. For ex situ biomethanation, biotrickling filter (BTF) technology will be assessed as a way to support the specialized biomass that will metabolize the H_2 and CO_2 contained in the biogas, potentially coming from a conventional digester, or in the eventually poor biomethane coming from a previous in situ system with incomplete conversion. Again, the study of this technology will be addressed from lab and pilot scales approaches. To start with, the feasibility of using the centrate from the AD of sludge, rich in ammonium and micronutrients, as nutrient source for ex situ biomethanation will be evaluated so that the use of chemicals for biomass subsistence is minimized. Together with this one, other operational conditions will be explored to obtain the best operational strategy and design for a 150L pilot plant that will also be installed in a real WWTP. In this case, biogas coming from the real scale anaerobic digestion or the eventually poor biomethane produced in the in situ pilot plant with incomplete conversion would be fed to the pilot BTF. Daily monitoring of the pilots will be carried out, analysing the critical physicochemical parameters to know the evolution of the process, measuring the quality of the biogas obtained. Thus, the conversion of biogas into biomethane will be studied and optimized. In parallel to the empiric work to be carried out in the project, BIOUP will also study the different energy supply options for the generation of green H_2 through HOMER and XENDEE energy simulators, in order to design a competitive strategy to implement this kind of technology in a real scale, depending on the renewable energy scenario of different locations.

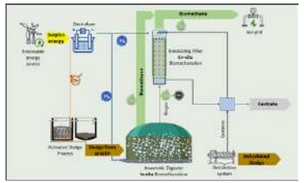

Figure 1. Concept of the BIOUP project for the generation of CH_4 in the WWTP.

EXPECTED RESULTS

The conclusions obtained in the project will make it possible to establish the application settings of the BIOUP technology in a real environment in existing or newly built WWTP. Among the main aspects and improvements to be achieved with the project, the following stand out:

- Through one stage or two stage strategies, to produce biomethane that meets the specifications for use as transportation fuel (>90% CH_4) and for injection into the network (>95% CH_4).
- Obtain a "power-to-gas" system that allows improving the energy performance of the WWTPs, generating 0.4 kW/m^3, with the aim of promoting the energy self-sufficiency of these facilities or becoming a source of extra income by injecting biomethane (which price ranges between 50 and 150 €/MWh) into the gas network.
- Demonstrate that an energy improvement of up to 25% per kg of TSS treated can be achieved compared to conventional systems by enriching the biogas stream and reducing the aeration needs to remove nitrogen.
- Contribute to the circularity of water sector by boosting the energy recovery of WWTP sludge, producing an energy vector from residual biomass that helps the use and production of renewable energy in a WWTP.
- Advance in the decarbonization of the energy system and the water treatment sector.
- Expand the portfolio of ACCIONA technologies applicable in a WWTP, which allow flexibility and maximize the use and recovery of resources.

Energy recovery from olive mill waste streams

S. Correa*, M. Llamas**, F. Passos*, F.G. Fermoso** and I. Ferrer*

* Group of Environmental Engineering and Microbiology, Department Civil and Environmental Engineering, Universitat Politècnica de Catalunya BarcelonaTech, 1-3 Jordi Girona, Barcelona 08034, Spain
(E-mail: *sandra.corre@upc.edu; fabiana.passos@upc.edu; ivet.ferrer@upc.edu*)
** Group of Bioprocesses for the Circular Economy, Department of Food Biotechnology, Instituto de la Grasa, Spanish National Research Council (CSIC), Campus Universitario Pablo de Olavide – Ed. 46, Ctra. de Utrera, km1, Sevilla 41013, Spain
(E-mail: *mllamas@ig.csic.es; fgfermoso@ig.csic.es*)

Abstract
The lack of cost-effective strategies for the treatment of Olive Mill Waste Streams (OMW) compromises the sustainability of the olive oil sector and hinders the transition towards a circular economy. In the present study, the anaerobic digestion of OMW and its co-digestion with pig manure were investigated in semi-continuous reactors. Results showed that the co-digestion with pig manure improved the methane yield 3.5-fold, which was attributed to an increase in the buffer capacity, dilution of phenolic compounds concentration and nutrients balance. Moreover, an energy balance showed the feasibility of scaling-up the process. Therefore, this consolidated technology appears as a promising solution for the co-treatment and bioenergy recovery from agro-industrial waste streams.

Keywords (maximum 6 in alphabetical order)
Agro-industrial residues; anaerobic co-digestion; bioenergy; biogas; circular bioeconomy

INTRODUCTION

Olive oil production is of great economic importance for the Mediterranean region. However, this agro-industrial sector still lacks sustainable, cost-efficient strategies for the management of generated waste streams (OMW). In Spain only, being the first olive oil producer worldwide, over 10 million tons of olive mill by-products are generated every year (ANEO 2019).

Anaerobic digestion arises as an effective technology for the treatment of organic wastes, such as OMW, with the added benefit of renewable energy generation in the form of biogas. Nonetheless, specific characteristics of OMW, i.e., high concentration of solids and lignin presence, phenolic content, low alkalinity, and high C/N ratio, can constrain the anaerobic digestion performance. Thus, anaerobic co-digestion with nitrogen-rich co-substrates has been investigated to enhance the process stability and biogas outcome.

Despite the energy production from agro-industrial waste streams is not a new process, the industrial implementation and execution continue to be a challenge. The aim of this work is to evaluate the anaerobic digestion of OMW and co-digestion with pig manure in terms of biogas production using semi-continuous lab-scale reactors and the feasibility scaling-up the process.

MATERIALS AND METHODS

OMW and pig manure were obtained from an integrated storing and drying facility and a local farm, respectively, located in Seville, Spain. The physicochemical characterization of both substrates is shown in **Table 1**.

Two semi-continuous reactors with 1.7L of effective volume were inoculated with an adapted inoculum and operated for 126 days. The reactors were operated at an organic loading rate of 1 g VS/L·d, a hydraulic retention time of 21 days and mesophilic temperature (37°C), in accordance with previous experiments (Serrano et al., 2017).

The methane production was daily measured by water displacement, after removing CO_2 from the biogas stream using a 3N NaOH solution. The pH was daily monitored, but not controlled. Soluble samples of the digester effluents were analyzed in terms of chemical oxygen demand (sCOD) by the colorimetric standard method 5220D (APHA 2017) (daily) and volatile fatty acids (VFA) by gas chromatography (three times per week). Effluent samples were also analyzed two times per week in terms of total alkalinity (TA) using pH titration to 4.5; total and volatile solids (TS and VS) by APHA procedure 2540G; ammonia nitrogen by APHA 4500-NH_3 C; and total and soluble phenols following the Folin-Ciocalteu method (Box 1983; APHA 2017).

Experimental results were used to perform a feasibility study for an industrial scale plant for the co-treatment of both residues. Theoretical energy balances considered thermal and electric power requirements of the proposed system (anaerobic digestion coupled to a 120kW combined heat and power (CHP) facility), and the energy produced upon steady-state operation of lab-scale reactors.

RESULTS AND DISCUSSION

OMW anaerobic mono-digestion

During the first experimental period (day 1 to 63) the anaerobic mono-digestion of OMW was evaluated. The methane yield was in average 51 mL CH_4/g VS (**Figure 1a**), a poor value resulting from low organic matter removal (11%), as indicated by the accumulation of VS and sCOD towards the end of this experimental period. These results are far below those reported for the anaerobic digestion of OMW in batch reactors, i.e. 321 mL/g VS (Fernández-Rodríguez et al. 2014) and semi-continuous reactors, i.e. 220 mL/ g VS (Stoyanova et al. 2017).

Process instability was suggested by low pH values (5.5-6) (**Figure 1a**) and a concomitant increase in VFA concentration, which raised from 3,731 to 6,053 mg COD/L (**Figure 1b**), acetic and propionic acid being the most abundant. Moreover, the average concentration of total phenols in the reactor was 1,406 mg gallic acid/L, which is close to the proposed methanogenic activity inhibition threshold of 1,500 mg/L (Monlau et al. 2014).

OMW anaerobic co-digestion with pig manure

During the second experimental period (days 64 to 126) the co-digestion of OMW with pig manure was assessed. The results showed that the methane yield increased by 3.5-fold as compared to the mono-digestion (from 50 to 175 mL CH_4/g VS). This was attributed to the alkalinity increment, the balance of nutrients (C/N ratio decreased from 33 to 28) and dilution of phenolic compounds by 70%.

Energy balance

Based on experimental data, it was estimated that the proposed digester produced 966 Nm^3 CH_4/day to be fed to a CHP plant. The energy balances showed that the CHP plant was able to provide enough thermal and electric energy for the anaerobic digestion facility to be self-sufficient and excess green electricity to be fed to the grid (**Figure 2**). Moreover, the stabilized digestate could re-enter the olive oil production cycle as a biofertilizer or be used in different agro-industrial applications.

These findings support the anaerobic digestion technology as a promising solution for the sustainable co-treatment of OMW along with other agro-industrial waste streams in Mediterranean countries, and contribute to the transition towards a circular economy in the olive oil sector.

Table 1. Physicochemical characterization of the substrates (olive mill waste stream (OMW) and pig manure)

Parameter	OMW	Pig manure
pH	4.58 ± 0.10	6.53 ± 0.12
Total alkalinity (mg $CaCO_3$/L)	n/a	25.79 ± 1.01
Electrical conductivity (mS/cm)	1.41 ± 0.03	1.29 ± 0.02
Total solids (g/L)	252.60 ± 3.00	374.44 ± 4.65
Volatile solids (g/L)	236.85 ± 3.12	218.43 ± 10.01
Chemichal Oxygen Demand (g O_2/L)	351.17 ± 3.55	263.62 ± 4.58
Soluble chemical oxygen demand (g O_2/L)	135.35 ± 1.75	51.96 ± 4.88
C/N	34.59 ± 1.18	16.89 ± 1.17
N-NH_4^+ (g /L)	147.93 ± 7.85	832.85 ± 24.98
Total phenols (g gallic acid/L)	10.18 ± 0.35	n/a
Soluble phenols (g gallic acid/L)	4.82 ± 0.58	n/a
3,4-dihydroxyphenylglycol (mg/L)	295.80 ± 5.79	n/a
Hydroxityrosol (mg/L)	2749.65 ± 64.75	n/a
Tyrosol (mg/L)	798.63 ± 10.64	n/a

n/a: not applicable

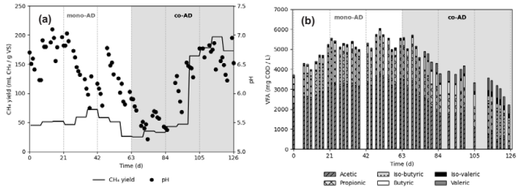

Figure 1. (a) Methane yield and pH throughout experimental periods 1 (mono-AD) and 2 (co-AD); (b) VFA concentration and profile throughout experimental periods 1 (mono-AD) and 2 (co-AD).

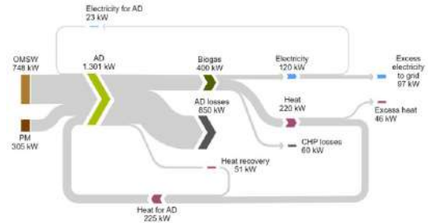

Figure 3. Sankey diagram for the energy flows representation for an industrial scale anaerobic digestion facility co-treating olive mill waste streams (OMW) and pig manure (PM).

ACKNOWLEDGEMENTS

This research was funded by the PRIMA Foundation (4BIOLIVE project PCI2021-121979). S. Correa is grateful to the Generalitat de Catalunya for her predoctoral scholarship (2021 FISDU 00057). F. Passos is grateful to the Spanish Ministry of Universities (MIU) for her Maria Zambrano 2021 Fellowship.

REFERENCES

ANEO. 2019. El Futuro Del Alperujo En Extremadura.

APHA. 2017. *Standard Methods for the Examination of Water and Wastewater*. 23rd ed. Washington, DC: American Public Health Association.

Box, J. D. 1983. Investigation of the Folin-Ciocalteau Phenol Reagent for the Determination of Polyphenolic Substances in Natural Waters. *Water Research* **17** (5): 511–25.

Fernández-Rodríguez, M. J., B. Rincón, F. G. Fermoso, A. M. Jiménez, and R. Borja. 2014. Assessment of Two-Phase Olive Mill Solid Waste and Microalgae Co-Digestion to Improve Methane Production and Process Kinetics. *Bioresource Technology* **157** (April): 263–69.

Messineo, Antonio, Manfredi Picciotto Maniscalco, and Roberto Volpe. 2020. Biomethane Recovery from Olive Mill Residues through Anaerobic Digestion: A Review of the State of the Art Technology. *Science of the Total Environment*. Elsevier B.V.

Monlau, F., C. Sambusiti, A. Barakat, M. Quéméneur, E. Trably, J. P. Steyer, and H. Carrère. 2014. Do Furanic and Phenolic Compounds of Lignocellulosic and Algae Biomass Hydrolyzate Inhibit Anaerobic Mixed Cultures? A Comprehensive Review. *Biotechnology Advances* **32** (5): 934–51.

Serrano, Antonio, Fernando G. Fermoso, Guillermo Rodríguez-Gutierrez, Juan Fernandez-Bolaños, and Rafael Borja. 2017. Biomethanization of Olive Mill Solid Waste after Phenols Recovery through Low-Temperature Thermal Pre-Treatment. *Waste Management* **61** (March): 229–35.

Stoyanova, Elitza, Tserennyam Lundaa, Günther Bochmann, and Werner Fuchs. 2017. Overcoming the Bottlenecks of Anaerobic Digestion of Olive Mill Solid Waste by Two-Stage Fermentation. *Environmental Technology* **38** (4): 394–405.

FROM REMOVAL TO RECOVERY: OPPORTUNITIES FOR BIOELECTROCHEMICAL AMMONIA RECOVERY FROM WASTEWATER

M. B. Galeano, M. Sulonen, J. A. Baeza, A. Guisasola

GENOCOV, Department of Chemical, Biological and Environmental Engineering, Universitat Autònoma de Barcelona, Cerdanyola del Vallès 08193, Barcelona, Spain
(E-mail: *mariella.galeano@autonoma.cat*; *albert.guisasola@uab.cat*; *juanantonio.baeza@uab.cat*; *mira.sulonen@uab.cat*)

Abstract
Technologies for nutrient recovery have generated industrial and academic interest as part of the circular economy strategy, since they contribute to an efficient management of available resources and to the environmental sustainability. Among the different technologies to recover ammonia, bioelectrochemical systems (BESs) are innovative systems with lower energy consumption and less chemicals requirements than traditional methods. Nevertheless, several limitations may hinder its industrial development such as the development of a resilient electroactive biofilm on the electrode surface with tolerance to high ammonia concentrations, and the need for electrode and membrane materials that could perform at long term operation and at high current density. This research seeks to provide information on the progress made in recent years to obtain high performance BESs for ammonia recovery. Details of the different configuration of the reactors and main performance parameters are described. Finally, this work will provides conclusions and future perspectives of this technology when compared to the current state-of-the-art.

Keywords
Ammonia recovery; Bioelectrochemical systems; Bioelectroconcentration cells; Microbial Electrolysis Cells; Microbial Fuel Cells

INTRODUCTION

The fundamental transformation towards a circular economy creates a demand for an efficient recovery of energy and nutrients (e.g. N, P) from wastewater. In urban and industrial wastewaters, the inorganic nitrogen is mainly represented by total ammonia nitrogen (TAN) in two forms of reactive nitrogen, NH_3 and NH_4^+ (Kuntke et al., 2018). The different approaches used to recover TAN from wastewater can be classified into chemical, physical, and biological processes. The chemical and physical processes include struvite precipitation (Li et al., 2012), ammonia stripping (Kim et al., 2021), reverse osmosis (Shin et al., 2021), ion exchange (Ding & Sartaj, 2016) and the use of gas-permeable membranes (Hou et al., 2018). Biological processes for NH_3 recovery are based on the use of BESs (Kuntke et al., 2018). BESs are biologically catalyzed electrochemical systems that consist of two connected electrodes. The biological catalysts are electroactive microorganisms capable of exchanging electrons with a solid electrode. The electrons released in the organic matter oxidation on the anode surface travel through an external circuit to the cathode and the electrons are donated to a terminal electron acceptor. The electron flow can drive the transport of TAN through a cation exchange membrane (CEM) and thus allow its recovery with a minimal dosage of chemicals for pH control and with simultaneous production of other valuable compounds such as electricity or hydrogen (Kuntke et al., 2018; Rodríguez Arredondo et al., 2015). The most relevant BESs configurations for TAN recovery are the Microbial Fuel Cells (MFCs), Microbial Electrolysis Cells (MECs), Microbial Desalination Cells (MDCs) and Bioelectroconcentration Cells (BECs) (Figure 1). If the oxidation and reduction reactions are spontaneous and electrical energy is produced, this system is called MFC. In MECs, external energy is applied to drive the oxidation and reduction reactions. MDCs are MFCs modified with an anionic and a cationic membrane placed between the cathode and anode chamber, which allows ionic species to be recovered in a middle chamber without electrical energy input (Cao et al., 2009). BECs are similar to MDCs, with the major difference that BECs require electrical energy input that can be used to recover ionic species in a concentrate chamber. The bioelectrochemical NH_3 recovery in BESs occurs in three main steps (Iddya et al., 2018) (Figure 1): i) the electric current resulting from the microbial oxidation drives the transport of NH_4^+ cations from the anode to the cathode chamber to maintain the charge neutrality; ii) conversion of NH_4^+ to NH_3, since the reduction reaction on the cathode surface increases the pH above 10, where NH_3 dominates *vs* NH_4^+ (pKa 9.24 at 25 °C); and iii) NH_3 is recovered, e.g. by stripping and gas diffusion membranes (Kuntke et al., 2018).

Many advances have been made with the reactor configurations, scaling up and recovery/removal efficiencies and new challenges have been encountered (Lee et al., 2022, Kuntke et al., 2018; R. Sharma et al., 2022; Xiang et al., 2020) since previous reviews focusing on bioelectrochemical NH_4^+removal and recovery were published. The aim of this work is to provide a comprehensive overview of the current state of these systems, benchmark them with other existing methodologies for TAN recovery and to provide recommendations for its design. This work revises the last manuscripts related to bioelectrochemical NH_3 recovery and focuses on comparing its performance results obtained in the past studies as a function of the configuration of the reactors and the influent wastewater. The focus is set to TAN recovery (e.g. stripping or precipitation) and the inclusion of innovative materials as gas diffusion electrodes.

RESULTS AND DISCUSSION

Forty-eight manuscripts related to bioelectrochemical NH_3 recovery in two scientific databases (Web of Science and Scopus) between 2019-2023 were reviewed. Most of them were related to MECs. MECs require an energy input, but the NH_3 recovery rate can be increased in this configuration using different strategies (Kelly & He, 2014). For example, Cerrillo et al. (2021) reported a NH_3 recovery rate of ~36 g N m^{-2} d^{-1}, coupling a MEC and a hydrophobic membrane. So, the use of this hydrophobic membranes could be an interesting strategy for the improvement of NH_3 recovery in MECs reactors. About the electrical current density produced in MECs, Wu & Modin (2013) reported a high electrical current produced in MECs (28 A m^{-2}) with an ammonia recovery efficiency of 94 %. This value could be considered interesting, nevertheless, more efforts should be done to improve the electrical current density produced in MECs, as the NH_4^+ transport through the CEM is driven by the current that is produced in the reactor. Regarding MFCs, the highest NH_3 recovery rate reported for Kuntke (2013) was 9.6 g N m^{-2} d^{-1} with an electrical current density of 2.6 A m^{-2}. However, this MFC rate was less than a half of the MEC rate reported by Cerrillo et al (2021). Zhang et al. (2022) reported an MFC coupling with a stripping unit for NH_3 recovery with a current density of 1.2 A m^{-2} and a NH_3 recovery rate of 6.9 g N m^{-2} d^{-1}. Low NH_3 recovery rates in MFCs can be increased by changing them into MECs, which produce more current due to the applied power (Kuntke et al., 2014).

Finally, innovative configurations such as MDCs and BECs have gained interest for nutrient recovery. Particularly, the BECs used mainly with urine for NH_3 recovery shows an interesting performance. Ledezma et al. (2017) reported an ammonia recovery rate of 430 g N m^{-2} d^{-1}, which is the highest value of NH_3 recovery determined until today for BESs. This high value is related to the high current density of 37.8 A m^{-2} reached by the system. MDCs reactors have also achieved high recovery rates. Zhang et al. (2015) reported a recovery rate of 80 g N m^{-2} d^{-1} using a novel submersible MDC. In this case, an electrical current density of 2.85 A m^{-2} was produced. All these results are interesting in comparison with the values obtained for the other configurations reviewed. Moreover, more critical analysis will be presented about other parameters related to the performance of BESs. For example, the electrode materials. Electrodes with high conductivity and biocompatibility allows to reduce the internal resistance in the system. The NH_3 concentration is relevant since high concentrations can be toxic. Thus, acclimation of the biofilm may be necessary. The load ratio (ratio between the current density and the TAN loading rate) shows whether the current density of the system is limiting NH3 transfer rate. Finally, the presence of other cations that can compete with ammonium when balancing electroneutrality will be detailed and discussed.

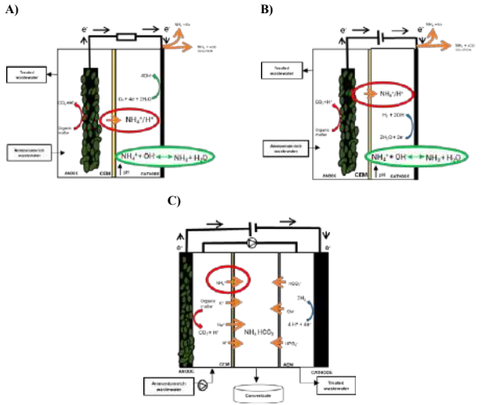

Figure 1. Bioelectrochemical systems for NH_3 recovery. A) MFC, B) MEC and, C) BEC.

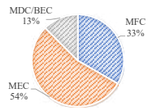

Figure 2. Percentage of research papers of the different BESs configuration (MEC: Microbial Electrolysis Cells; MFC: Microbial Fuel Cells; MDC/BEC: Microbial Desalination Cells/Bioelectroconcentration cells) included in the Web of Science database related to bioelectrochemical systems for NH_3 recovery.

REFERENCES

Cao, X., Huang, X., Liang, P., Xiao, K., Zhou, Y., Zhang, X., & Logan, B. E. (2009). A new method for water desalination using microbial desalination cells. *Environmental Science and Technology*, *43*(18), 7148–7152. https://doi.org/10.1021/es901950j

Cerrillo, M., Burgos, L., Serrano-Finetti, E., Riau, V., Noguerol, J., & Bonmati, A. (2021). Hydrophobic membranes for ammonia recovery from digestates in microbial electrolysis cells: Assessment of different configurations. *Journal of Environmental Chemical Engineering*, *9*(4), 1–12. https://doi.org/10.1016/j.jece.2021.105289

Ding, Y., & Sartaj, M. (2016). Optimization of ammonia removal by ion-exchange resin using response surface methodology. *International Journal of Environmental Science and Technology*, *13*(4), 985–994. https://doi.org/10.1007/s13762-016-0939-x

Hou, D., Iddya, A., Chen, X., Wang, M., Zhang, W., Ding, Y., Jassby, D., & Ren, Z. J. (2018). Nickel-Based Membrane Electrodes Enable High-Rate Electrochemical Ammonia Recovery. *Environmental Science and Technology*, *52*(15), 8930–8938. https://doi.org/10.1021/acs.est.8b01349

Iddya, A., Hou, D., Khor, C. M., Ren, Z. J., Tester, J., Posmanik, R., Gross, A., Jassby, D., Carrera, J., Jubany, I., Carvallo, L., Chamy, R., Lafuente, J., Cerrillo, M., Burgos, L., Serrano-Finetti, E., Riau, V., Noguerol, J., Bonmati, A., … Kuntke, P. (2018). Hydrophobic Gas Transfer Membranes for Wastewater Treatment and Resource Recovery. *Environmental Science and Technology*, *2*(20), 11618–11635. https://doi.org/10.1021/acs.est.9b00902

Kelly, P. T., & He, Z. (2014). *Bioresource Technology Nutrients removal and recovery in bioelectrochemical systems : A review*. *153*, 351–360.

Kim, E. J., Kim, H., & Lee, E. (2021). Influence of ammonia stripping parameters on the efficiency and mass transfer rate of ammonia removal. *Applied Sciences (Switzerland)*, *11*(1), 1–13. https://doi.org/10.3390/app11010441

Kuntke, P. (2013). Nutrient and energy recovery from urine: PhD thesis, Wageningen University, Wageningen, NL . 168 p.

Kuntke, P., Rodrigues, M., Sleutels, T., Saakes, M., Hamelers, H. V. M., & Buisman, C. J. N. (2018). Energy-Efficient Ammonia Recovery in an Up-Scaled Hydrogen Gas Recycling Electrochemical System. *ACS Sustainable Chemistry and Engineering*, *6*(6), 7638–7644. https://doi.org/10.1021/acssuschemeng.8b00457

Kuntke, P., Sleutels, T. H. J. A., Arredondo, M. R., Georg, S., Barbosa, S. G., & Heijne, A. (2018). (Bio) electrochemical ammonia recovery : progress and perspectives. *Applied Microbiology and Biotechnology*, *2*(102), 3865–3878.

Kuntke, P., Sleutels, T. H. J. A., Saakes, M., & Buisman, C. J. N. (2014). *Hydrogen production and ammonium recovery from urine by a Microbial Electrolysis Cell*. *9*(0), 2–9.

Ledezma, P., Jermakka, J., Keller, J., & Freguia, S. (2017). Recovering Nitrogen as a Solid without Chemical Dosing: Bio-Electroconcentration for Recovery of Nutrients from Urine. In *Environmental Science and Technology Letters* (Vol. 4, Issue 3, pp. 119–124). https://doi.org/10.1021/acs.estlett.7b00024

Lee, Y., Lin, B., Xue, M., & Tsunemi, K. (2022). Ammonia/ammonium removal/recovery from wastewaters using bioelectrochemical systems (BES): A review. *Bioresource Technology*, 127927. https://doi.org/10.1016/j.biortech.2022.127927

Li, Z., Ren, X., Zuo, J., Liu, Y., Duan, E., Yang, J., Chen, P., & Wang, Y. (2012). Struvite precipitation for ammonia nitrogen removal in 7- aminocephalosporanic acid wastewater. *Molecules*, *17*(2), 2126–2139. https://doi.org/10.3390/molecules17022126

Rodríguez Arredondo, M., Kuntke, P., Jeremiasse, A. W., Sleutels, T. H. J. A., Buisman, C. J. N., & Ter Heijne, A. (2015). Bioelectrochemical systems for nitrogen removal and recovery from wastewater. *Environmental Science: Water Research and Technology*, *1*(1), 22–33. https://doi.org/10.1039/c4ew00066h

Sharma, R., Kumari, R., Pant, D., & Malaviya, P. (2022). Bioelectricity generation from human urine and simultaneous nutrient recovery: Role of Microbial Fuel Cells. *Chemosphere*, *292*(December 2021), 133437. https://doi.org/10.1016/j.chemosphere.2021.133437

Shin, C., Szczuka, A., Jiang, R., Mitch, W. A., & Criddle, C. S. (2021). Optimization of reverse osmosis operational conditions to maximize ammonia removal from the effluent of an anaerobic membrane bioreactor. In *Environmental Science: Water Research and Technology* (Vol. 7, Issue 4, pp. 739–747). https://doi.org/10.1039/d0ew01112f

Wu, X., & Modin, O. (2013). Ammonium recovery from reject water combined with hydrogen production in a bioelectrochemical reactor. *Bioresource Technology*, *146*, 530–536. https://doi.org/10.1016/j.biortech.2013.07.130

Xiang, S., Liu, Y., Zhang, G., Ruan, R., Wang, Y., Wu, X., Zheng, H., Zhang, Q., & Cao, L. (2020). New progress of ammonia recovery during ammonia nitrogen removal from various wastewaters. *World Journal of Microbiology and Biotechnology*, *36*(10), 1–20. https://doi.org/10.1007/s11274-020-02921-3

Simulation of outdoor conditions for the cultivation of microalgae in a small-scale photobioreactor for wastewater treatment.

C. Ruiz[1,2], A. García[1,2], F.G. Gonzalo[1,2], I. de Godos[1,2]

[1]School of Forestry, Agronomic and Bioenergy Industry Engineering (EIFAB), University of Valladolid, Campus Duques de Soria, 42004, Soria, Spain.
[2]Institute for Sustainable Processes, University of Valladolid, 47011, Valladolid, Spain
Email: César.ruiz.palomar@uva.es, agarcia@uva.es, felixgaspar.gonzalo@uva.es, ignacio.godos@uva.es.

Abstract

Alterations in the parameters that allow controlling the quality of the water, such as excess contaminants in it, appear more and more frequently. There are many areas with problems of excess concentration of nitrates, nitrites, phosphates, ammonia, etc., which reach concentration levels higher than those allowed and which can affect human health. As well as potentially toxic elements (PTEs) V, Cr, Zn, Co, Pb, Ni, Cu, As and Cd. In addition, there are cases of contamination with Enterobacteria and Coliform bacteria, present in the aquifers used for crop irrigation and in the food itself.
In this study, the potential of microalgae for the elimination of contaminants and pathogens in wastewater has been simulated. For this, a photobioreactor has been used, simulating temperature and light conditions similar to those existing outside.
The concentration of the main contaminants in the water at the entrance and exit of the photobioreactor has been monitored. It has been analyzed: COD, phosphates, ammonium, organic matter. The disinfection capacity of microalgae has been studied by analyzing pathogens such as E. coli and total coliforms present in the water. As well as monitoring the algar biomass concentration.

Keywords
Contaminants; disinfection; microalgae; pathogens; photobioreactor; simulation.

INTRODUCTION

There is an increasing deficit of pure water suitable for consumption, as a result of climate change, which is affecting temperature and rainfall. Greenhouse gases are the main drivers of global climate change (Hu et al., 2021). There is less and less rainfall or it is in the form of a storm, affecting the availability of pure water. The main causes of contamination depend on human use in mining and the misuse of commercial fertilizers applied in agriculture and intensive agriculture (Liu et al., 2021). Alterations in the parameters that allow controlling the quality of the water, such as excess contaminants in it, appear more and more frequently. In drinking water, problems of excess concentration of nitrates, nitrites, phosphates, ammonia, etc. appear in many places, which reach concentration levels higher than those allowed and which can affect human health (Wang et al., 2022). As well as potentially toxic elements (PTEs) V, Cr, Zn, Co, Pb, Ni, Cu, As and Cd (Liu et al., 2021). In addition, there are cases of contamination with Enterobacteria and Coliform bacteria, present in the aquifers used to irrigate crops and in the food itself. According to the WHO, it is estimated that one in ten people contract diseases from eating spoiled food. Every year 420,000 people die from consuming food contaminated by microbial agents (Bari & Yeasmin, 2018). By the year 2050, it is expected that the demand for water will increase by 40%, and the demand for energy will increase by 50%, this is influenced by the need to increase food production by 60% (FAO, 2015).
That is why it is necessary to apply an economical and more environmentally friendly solution, using purification systems with low energy consumption (Chong et al., 2021). The cultivation of microalgae for wastewater treatment can be an alternative solution to conventional purification systems, since it can remove inorganic nutrients such as nitrogen and phosphorus present in wastewater through photosynthetic activity (Dolganyuk et al., n.d.). In addition, in this process it is possible to fix carbon dioxide (CO_2), the main compound that causes the greenhouse effect. (Fthenakis & Kim, 2012). The digestate from anaerobic digestion can be used for the cultivation of microalgae since it has nutrients that allow the growth of microalgae (Chong et al., 2021).

MATERIALS AND METHODS

The cultivation of microalgae is carried out in a continuous photobioreactor. Using pig slurry diluted with distilled water with a concentration between 1:20 and 1:40 as a substrate to adjust the concentration in order to maintain a COD in the range of 0.5 and 1.0 g/l.
The photobioreactor is a stainless-steel cuvette that simulates a small-scale raceway-type photobioreactor. It can work at different heights of water column 20, 25 and 30 cm deep. Simulating standard conditions in microalgae lagoons. This has a pump programmed for the introduction of residual water. And a pumping agitation system, to maintain the homogeneity of the microalgae culture.
As a light source for the development of photosynthetic activity and growth of microalgae, a Philips LED light source is used, simulating the intensity of sunlight. For this the lamp is connected to a microcontroller. In addition to light, in order to simulate outdoor conditions, a SELECTA Frigiterm brand thermoregulator is used, through which the temperature can be adjusted to simulate the desired season of the year.
In addition, different parameters are monitored by sensors: temperature, pH, dissolved oxygen (D.O), solar irradiation (PAR).

Figure 1. Stainless steel photobioreactor for microalgae cultivation with light and temperature simulation.

RESULTS AND DISCUSSION

Under winter conditions, a lower elimination of ammonia 20.72% is achieved than in summer conditions 78.26%. Regarding the elimination of phosphorus, a greater elimination is achieved in summer 69.83% than in winter 34.83%. This is since algar biomass grows faster with high temperatures such as those typical of summer. However, higher total solids and COD removal values are reached in winter than in summer. The percentage of elimination of total solids in winter and summer is 96.20% and 50.18% respectively. And the COD removal percentage in winter and summer is 91.08% and 65.34% respectively.
Under winter conditions, a lower elimination of ammonia is achieved, 21% than in summer conditions, 78%. Regarding the elimination of phosphorus, a greater elimination is achieved in summer 70% than in winter 35%. This is since the algar biomass has greater activity and greater growth with high temperatures such as those typical of summer. Achieving a greater absorption of nutrients by the algar biomass. However, slightly higher values, although not very significant, of organic matter removal are reached in winter than in summer. Being the percentage of COD removal in winter and summer of 91% and 65% respectively. In summer there is greater bacterial activity in the wastewater compared to winter, due to the temperature. In both conditions, high disinfection values are reached. To determine the level of disinfection, the regulations focus on the presence of E. coli bacteria, resulting in this study an elimination percentage of 99.6% and 100% in winter and summer respectively.

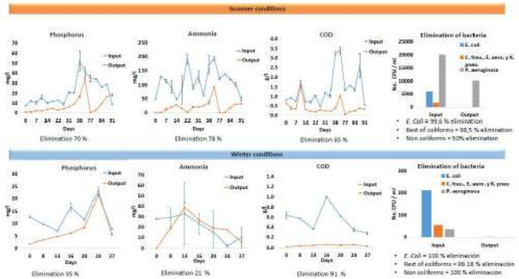

Figure 2. Results in inlet and outlet water of the concentration of phosphorus, ammonium, COD and elimination of coliform bacteria, in summer and winter conditions.

REFERENCES

1. Hu, X. M., Ma, J. R., Ying, J., Cai, M., & Kong, Y. Q. (2021). Inferring future warming in the Arctic from the observed global warming trend and CMIP6 simulations. Advances in Climate Change Research, 12(4), 499–507. https://doi.org/10.1016/J.ACCRE.2021.04.002.
2. Liu, Y., Wang, P., Gojenko, B., Yu, J., Wei, L., Luo, D., & Xiao, T. (2021). A review of water pollution arising from agriculture and mining activities in Central Asia: Facts, causes and effects. Environmental Pollution, 291, 118209. https://doi.org/10.1016/J.ENVPOL.2021.118209
3. Wang, C., Zhang, H., Xin, X., Li, J., Jia, H., Wen, L., & Yin, W. (2022). Water level–driven agricultural nonpoint source pollution dominated the ammonia variation in China's second largest reservoir. Environmental Research, 114367. https://doi.org/10.1016/J.ENVRES.2022.114367
4. Bari, Md. L., & Yeasmin, S. (2018). Foodborne Diseases and Responsible Agents. Food Safety and Preservation, 195–229. https://doi.org/10.1016/B978-0-12-814956-0.00008-1
5. Chong, C. C., Cheng, Y. W., Ishak, S., Lam, M. K., Lim, J. W., Tan, I. S., Show, P. L., & Lee, K. T. (2021). Anaerobic digestate as a low-cost nutrient source for sustainable microalgae cultivation: A way forward through waste valorization approach. Science of The Total Environment, 150070. https://doi.org/10.1016/J.SCITOTENV.2021.150070
6. Dolganyuk, V., Belova, D., Babich, O., Prosekov, A., Ivanova, S., Katserov, D., Patyukov, N., & Sukhikh, S. (n.d.). biomolecules Microalgae: A Promising Source of Valuable Bioproducts. https://doi.org/10.3390/biom10081153
7. Fthenakis, V. M., & Kim, H. C. (2012). Environmental Impacts of Photovoltaic Life Cycles. Comprehensive Renewable Energy, 1, 143–159. https://doi.org/10.1016/B978-0-08-087872-0.00107-4

Polyhydroxyalkanoates production by mixed microbial cultures from fermented cheese whey under high salinity conditions

M. Grana[1,*], B.C. Marreiros[2,3], M. Carvalheira[2,3], E. Ficara[1], and M. A. M. Reis[2,3]

[1] Politecnico di Milano, Dipartimento di Ingegneria Civile e Ambientale, Piazza Leonardo da Vinci 32, 20133 Milano, Italy; matteo.grana@polimi.it
[2] Associate Laboratory i4HB—Institute for Health and Bioeconomy, NOVA School of Science and Technology, NOVA University Lisbon, 2819-516 Caparica, Portugal
[3] UCIBIO—Applied Molecular Biosciences Unit, Department of Chemistry, NOVA School of Science and Technology, NOVA University Lisbon, 2819-516 Caparica, Portugal

Abstract
Polyhydroxyalkanoates (PHAs) are biopolymers synthesised by microorganisms in the presence of nutrient-limiting environments that are suitable as source for bioplastics production. To make to overall process economically and environmentally sustainable, waste streams are often evaluated as feedstock for PHAs production. The aim of this study is the use of a real fermented cheese whey feedstock as carbon source for the selection of a PHA-accumulating mixed microbial culture, operating under a saline concentration equal to 30 gNaCl/L. A stable and acclimatized culture was obtained in a sequence batch reactor operating in a Feast/famine regime with an organic loading rate of 60 Cmmol/(L d). The accumulation capacity of the culture was tested, reaching a maximum content of 76.5% (weight/weight, on volatile suspended solids basis).

Keywords
Acidogenic fermentation; Cheese whey; Halotolerant microorganisms; Mixed microbial cultures; Polyhydroxyalkanoates; Saline wastewaters.

INTRODUCTION

Sustainable industrial practices such as circular economy are nowadays primary important to reduce the environmental impact of human activity. Resource recovery from waste streams is strongly encouraged to reduce raw material extraction and processing as well as to limit the impact of waste disposal. Saline side streams from agri-food industries are characterized by a high cost in their treatment for safe disposal, as the conventional biological processes are often inhibited by the high saline concentration. Among others, fishery and dairy industry are a relevant source of saline wastewaters (Lefebvre and Moletta, 2006; Chen et al., 2018). Therefore, the development of biological processes able to produce secondary raw materials from saline wastewaters as feedstock is favourable to promote both environmental and economic sustainability for the agri-food industry.

PHAs are biodegradable polymers produced by certain microorganisms as intracellular energy and carbon reserves. The production of this polymer is of growing interest as they are viable substitutes of conventional plastics (Kourmentza et al., 2017). Nevertheless, PHA production process is characterized by high costs that make bioplastics more expensive that petroleum-based polymers.
PHA production by open mixed microbial cultures (MMC) comprises three distinct stages: (i) acidogenic fermentation, where the organic matter is converted into Volatile Fatty Acids (VFAs) which are the PHA precursors; (ii) culture selection, where the aerobic MMC is enriched with PHA-storing organisms under selective pressure conditions; (iii) PHA production, where PHA accumulation is carried out using the culture selected in stage (ii) and fed with fermented stream produced from stage (i). The use of industrial by-products or waste streams as feedstock for VFAs production and thus for PHA synthesis is being investigated for the overall process cost reduction. In this framework, saline conditions might be applied as a direct consequence of using salty waste streams or, in the cost reduction and environmental perspectives, due to the use of seawater for dilution instead of freshwater.

In the present study, the valorisation of salted fermented cheese whey, a by-product from the dairy industry into PHA by MMC was investigated. The main challenges were to enrich an efficient PHA-accumulating MMC and attain good PHA productivities under high salinity (30 g_{NaCl}/L). In addition, PHA accumulation batches using the salted fermented stream supplemented with valeric acid as feedstock was investigated.

MATERIALS AND METHODS

A sequence batch reactor (SBR) with a 2 L working volume was used for the culture selection. The culture was enriched with PHA-accumulating organisms by applying a F/f regime strategy as selective pressure. The SBR was operated with 3 cycles/day of 8 hours each, with a hydraulic retention time (HRT) and a solids retention time (SRT) of 14.5 h and 3 d, respectively. The pH was controlled bellow 8.5 through automatic dosing of 0.5 M HCl . The reactor was operated under aerobic conditions, with mechanical stirring (150 RPM) and at room temperature (20°C ± 1.5 °C). The organic loading rate – OLR – was set at 60 Cmmol/(L d), and the C/N/P ratio selected was 100/5/2. The feed solution was obtained from an acidogenic fermenter reactor, with the typical composition reported in Tab.1. As the C/N/P ratio of the fermented solution was 100/1/2, the remaining amount of ammonia was fed after the exogenous carbon was depleted (uncoupled feeding), approximately one hour after the carbon feed. Together with the fermented stream, a mineral solution with allitiourea, to inhibit nitrification, and micronutrients was fed to the SBR as described in (Carvalho et al., 2022). The salted conditions (30 g_{NaCl}/L) were artificially imposed to SBR, through salt addition in the fermented and mineral solutions, to mimic a real salted fermented stream.The feeding was composed of 111 mL carbon solution and 889 mL dilution mineral solution. . PHA-accumulation performance of the culture was assessed through a pulse-wise feeding strategy in a 2 L reactor. Accumulation-A was carried out with the same fermented stream used in the operation of the selection reactor, while the feed of Accumulation-B was supplemented with valeric acid (H.Va) to reach a relative concentration of 30% $Cmmol_{H.VA}/Cmmol_{VFA}$.
Total and volatile solids (TS, VS) and total and suspended solids (TSS,VSS) were determined according to standard methods (APHA, 2005). Volatile fatty acids (VFAs) were quantified in filtered samples (0.20 µm) using a high-performance liquid chromatography (HPLC) in a VWR Hitachi Chromaster chromatographer. Ammonia and phosphate concentrations were determined in filtered samples (0.20 µm) using a segmented continuous flow analyzer (Skalar SNA++). Lyophilized biomass was weighted and incubated with 1 mL chloroform and 1 mL acidic methanol (20% H_2SO_4) through digestion at 100 °C for 3.5 h. After the digestion, the organic phase was extracted and injected into a gas chromatograph (GC-FID, Brucker).

RESULTS AND DISCUSSION

The results obtained in the culture selected with PHA-accumulating organisms are summarized in Tab.2 while in Fig.1 and Fig.2 is depicted a representative F/f cycle. A complete VFA consumption was observed after ~ 0.6 h, with a greater preference for the consumption of butyric acid (-qBut = 0.397 ± 0.055 Cmol/Cmol X.h). This resulted in a F/f ratio equal to 0.076 ± 0.016 on average, which is considered adequate to boost the selection of a good PHA-storing biomass (Kourmentza et al., 2017). At the end of the feast phase, it is reached the maximum PHA content (39 ± 5 %wt., VSS basis), where the co-polymer accumulated was composed of 94% of 3-hydroxybutirate and 6% of 3-hydroxyhexanotate. Overall, a stable halotolerant PHA-accumulating mixed culture with a good PHA storing capacity ($Y_{PHA/S}$ = 0.75 ± 0.03 Cmol/Cmol X.h) was selected under high salinity.

Regarding PHA accumulation, Accumulations A (fermented stream) and B (fermented stream + 30% H.Va) showed a good storing capacity of the culture as it was reached a maximum PHA content of 73.0% and 76.5% (wt., on VSS basis), respectively. For Acc-A the maximum storing capacity was reached after 4 pulses while for Acc-B after 5 pulses. It is worth noting that even though the culture was selected without the presence of H.Va, a higher maximum PHA content was observed under the presence of this VFA. The capacity of the biomass of consuming the H.Va. in Acc-B was showed also by its consumption rate (qSvale) greater than acetic and hexanoic acids

FIGURES AND TABLES

Table 1 Average VFAs composition of the fermented stream

	H.Acet	H.iBut	H.But	H.Hex	Et.OH	SUM
Cmmol/l	109	2	206	26	10	352
	31%	1%	58%	7%	3%	
gCOD/l	3.5	0.1	8.2	11.0	0.5	13.4
	26%	1%	62%	8%	3%	

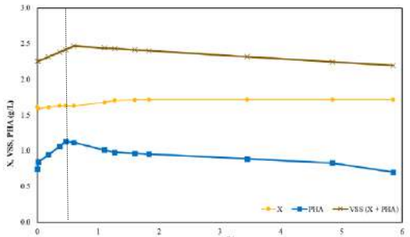

Figure 1 Biomass (X), volatile solids (VS) and PHA composition in a reference cycle

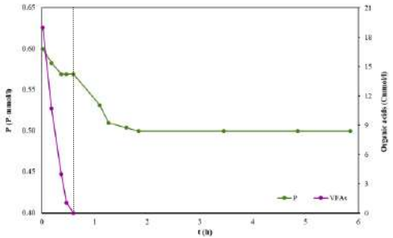

Figure 2 Phosphate (P), expressed as P, and VFAs in a reference cycle

Table 2 Main parameters of reference cycles

Parameter	Average ± Standard Deviation
Feast/famine [h/h]	0.076 ± 0.016
X @famine [g-X/L / Cmol-X/L]	1.61 ± 0.16 / 63.4 ± 6.2
Max PHA content [%wt., VSS basis]	39 ± 5
ΔPHA [%wt., VSS basis]	11.0 ± 2.2
HB:HHex ratio [wt. basis]	94 ± 1: 6 ± 1
qPHA feast [Cmol-PHA/(Cmol-X.h)]	0.40 ± 0.05
-qS feast [CmolS/ (Cmol$_X$.h)]	0.67 ± 0.09
$Y_{PHA/VFA}$ [Cmol-PHA/(Cmol-S)]	0.75 ± 0.03
$Y_{X/VFA}$ [Cmol-X/Cmol-S]	0.18 ± 0.05
-qPHA famine [Cmol-PHA/(Cmol-X.h)]	0.17 ± 0.03

Table 3 Accumulation-A and Accumulation-B results

	Parameter	Average	Unit
Accumulation-A	Max PHA	73.0	%wt., VSS basis
	HB:HHx	94:6	%wt
	(-)qacet	0.23 ± 0.04	Cmol/Cmol X.h
	(-)qbuty	0.46 ± 0.04	Cmol/Cmol X.h
	(-)qhexa	0.08 ± 0.02	Cmol/Cmol X.h
	(-)qS	**0.77 ± 0.10**	**Cmol /Cmol X.h**
	qX|feast	0.33 ± 0.04	Cmol-X/Cmol-X h
	qHB	0.45 ± 0.07	Cmol/Cmol X.h
	qHHx	0.03 ± 0.01	Cmol/Cmol X.h
	qPHA	**0.48 ± 0.07**	**CmolPHA/Cmol X.h**
Accumulation-B	Max PHA	76.5	%wt., VSS basis
	HB:HV:HHx	66:30:4	%wt
	(-)qacet	0.16 ± 0.05	Cmol/Cmol X.h
	(-)qbuty	0.26 ± 0.05	Cmol/Cmol X.h
	(-)qvale	0.23 ± 0.05	Cmol/Cmol X.h
	(-)qhexa	0.03 ± 0.01	Cmol/Cmol X.h
	(-)qS	**0.68 ± 0.13**	**Cmol /Cmol X.h**
	qX|feast	0.22 ± 0.06	Cmol-X/Cmol-X h
	qHB	0.32 ± 0.05	Cmol/Cmol X.h
	qHV	0.26 ± 0.03	Cmol/Cmol X.h
	qHHx	0.03 ± 0.01	Cmol/Cmol X.h
	qPHA	**0.61 ± 0.08**	**CmolPHA/Cmol X.h**

REFERENCES

APHA (2005) *Standard Methods for the Examination of Water and Wastewater*, Washington DC, USA, APHA 2005 Standard Methods American Public Health Association/American Water Works Association/Water Environment Federation.

Atasoy, M., Owusu-Agyeman, I., Plaza, E., and Cetecioglu, Z. (2018) Bio-based volatile fatty acid production and recovery from waste streams: Current status and future challenges. Bioresource Technology, **268**, 773–786.

Carvalho, J. M., Marreiros, B. C., and Reis, M. A. M. (2022) Polyhydroxyalkanoates Production by Mixed Microbial Culture under High Salinity. Sustainability, **14**(3), 1346.

Chen, G. Q., Talebi, S., Gras, S. L., Weeks, M., and Kentish, S. E. (2018) A review of salty waste stream management in the Australian dairy industry. Journal of Environmental Management, **224**, 406–413.

Kourmentza, C., Plácido, J., Venetsaneas, N., Burniol-Figols, A., Varrone, C., Gavala, H. N., and Reis, M. A. M. (2017) Recent Advances and Challenges towards Sustainable Polyhydroxyalkanoate (PHA) Production. Bioengineering, **4**(2), 55.

Lefebvre, O. and Moletta, R. (2006) Treatment of organic pollution in industrial saline wastewater: A literature review. Water Research, **40**(20), 3671–3682.

New modelling methodogy to improve phosphorus recovery in WWTPs

Tamara Guijarro*, Sofia Grau*, Silvia Doñate*, Juan Manuel Ayllon*

*Depuración de Aguas del Mediterráneo (DAM). Avenida Benjamín Franklin, 21. 46980 Parque Tecnológico, Paterna, Valencia, Spain
(E-mail: tamara.guijarro@dam-aguas.es)

Abstract
Modelling wastewater treatment plants (WWTP) is a very extended and useful tool for the analysis, management and optimisation of urban WWTP. However, the development of new innovative processes and technologies urges to adapt and validate these models to simulate the innovative technologies. Based on the results from the PHERTILIZER project, the software BioWin® was used in the study to simulate different WWTP configurations to increase phosphorus (P) recovery as struvite, yielding up to 119 kg/d of recovered struvite and reducing almost all of the uncontrolled precipitation inside the anaerobic digestion process, thus optimising the related operational processes. Additionally, this study offers a new methodology that can be transferred to other WWTPs to optimise the phosphorus recovery plant location in a WWTP to minimise associated problems with uncontrolled precipitation and hydrogen sulphide (H_2S) emissions.

Key words
WWTP, struvite, phosphorus, nutrient recovery, simulation

INTRODUCTION

Phosphorus (P) is an essential nutrient and limited resource. With an increasing demand for P, therefore, the PHERTILIZER project has the objective of recovering P as struvite from WWTPs and increasing its value as fertiliser. Moreover, the uncontrolled precipitation of P in the anaerobic reactors in WWTPs leads to operational problems and increases operational costs. It has been demonstrated that these problems can be reduced by the implementation of phosphorus precipitation and its recovery as struvite (De-Bashan and Bashan, 2004), obtaining a product not only rich in P but also with nitrogen (N).

In order to recover P as struvite from WWTPs, it is imperative to obtain a flow with a high concentration of P. Therefore, the study of the optimal P-recovery plant location is critical in order to obtain the highest efficiency. Likewise, the elutriation of the sewage sludge process reduces up to 43% of the P loses by uncontrolled precipitation (Bouzas, et al., 2019). Hence, all the WWTP configurations studied are based on the elutriation of sludge flows to produce a high P concentrated flow to be fed into the crystallizer to produce a controlled precipitation. The simulation study of these configurations allows determining the optimal location and the evaluation of the side effects related to the implementation of P-recovery technologies.

METHODS

The simulation model (figure 1) developed with the BioWin® software was based on the experience and results from the P-recovery plant used in the PHERTILIZER project. In order to get representative results, the model was calibrated and validated with the results from the experience at the WWTP, with and without the crystallization process.

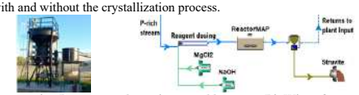

Figure 1. Demonstration P-recovery plant, picture and layout on BioWin software.

Using this model, the study of the different scenarios was focused on comparing the optimal location for the P-recovery plant, the effects and the recommendation of including the elutriation process to improve the results, and the effects of each configuration on the whole WWTP. Three different configurations were compared: Layout 1: elutriation of mixed sludge in primary thickener; Layout 2: elutriation of mixed sludge on secondary thickener; Layout 3: elutriation of secondary sludge in secondary thickener.

RESULTS AND DISCUSSION

The main difference in between the three scenarios was the elutriation of the sludge. Consequently, this is the critical point to control the P-recovery process and improve the WWTP operation. Thus, the combination of elutriation and a P-recovery process results in a reduction of between 11-18% of the total sludge production and 10% of the aeration ratio.

Table 1. Significant parameters obtained for each scenario.

		Layout.0	**Layout.1**	**Layout.2**	**Layout.3**
Biogas	m^3/h	61.39	50.85	53.37	57.40
H_2S MC	kg/d	27.41	28.39	3.90	0.01
H_2S Digestion	kg/d	24.83	20.14	22.84	37.74
Sludge production	kgDM/d	1,850	1,514	1,644	1,594
Aeration energy ratio	kWh/m^3	0.21	0.18	0.18	0.18
P-precipitation in anaerobic digestion	kg/d	181	143	142	0.23
Struvite recovery	**kg/d**	**-**	**98.03**	**71.18**	**118.85**

However, in addition to a remarkable struvite production (almost 119kg/d) in Layout 3, it is important to emphasise the reduction of uncontrolled precipitation of P in the digester by almost 100% and the minimisation of H_2S emissions in the plant (figure 2). These H_2S emissions, linked to elutriation, will be favoured if the WWTP initially had this problem.

Figure 2. Operational results. (A) H_2S emissions (kg/d). (B) P distribution in the WWTP (kg/d).

From this study, the simulation methodology is transferred to other WWTPs, analysing the combination of sewage sludge elutriation and struvite recovery process to validate the optimal location and the most favourable configuration for P-recovery and WWTP management. To this end, improving the biological P removal process at the WWTP and having anaerobic conditions along the sludge line to increase P-release is essential. Moreover, simulation studies are useful to validate the design of the P-recovery process including not only the volume of the crystalliser but also the addition of reactants.

CONCLUSIONS

The recovery of P combined with the elutriation of the sewage sludge increases the amount of struvite recovered and decreases the operational costs at WWTPs. In addition, if only the secondary sludge is elutriated, the uncontrolled precipitation of P will be almost totally reduced. This study shows a new simulation methodology transferable to other WWTPS for evaluation.

REFERENCES

Bouzas, A., et al. (2019). Implementation of a global P-recovery system in urban wastewater treatment plants. Journal of Cleaner Production, 227, 130-140.
De-Bashan L.E., Bashan Y. (2004). Recent advances in removing phosphorus from wastewater and its future use as fertilizer (1997–2003). Water Research, 38 (19): 4222–4246.

Upgrading of biogas produced from anaerobic digestion of sewage sludge through in-situ biological hydrogen methanation in mesophilic CSTR system

M.S. Hellal*,**, G. Cema*, K K. Kadimpati*, A. Ziembińska-Buczyńska*, J. Surmacz-Górska*

*Environmental Biotechnology Department, Faculty of Energy and Environmental Engineering, Silesian University of Technology, Akademicka St. 2, 44-100 Gliwice, Poland (mohamed.saad.hellal@polsl.pl; grzegorz.cema@polsl.pl; kishore.kumar.kadimpati@polsl.pl; aleksandra.ziembinska-buczynska@polsl.pl; joanna.s.gorska@polsl.pl)

** Water Pollution Research Department, National Research Centre, 33 El-Bohouth St., Dokki, Giza 12622, Egypt.

Abstract

This study is focusing on evaluation in-situ biological hydrogen methanation in mesophilic continuous stirred-tank reactor (CSTR) for biogas upgrading. Two CSTRs was installed with effective capacity of 5 L and loaded with inoculum sludge with VS concentration of 1.5% and fed with mixed waste sludge with organic loading rate (OLR) of 1.9 g VS/L and sludge retention time (SRT) of 14 days at mesophilic condition with temperature of 37 °C. One of the reactor was operated as control while the other one was injected with H_2 through micro-ceramic membrane diffuser at H_2:CO_2 ratio of 4:1. The quantity of produced biogas was monitored continuously via gas counters and gas chromatography. The results showed a good performance of bio-methanation process in the upgraded CSTR as the average methane yield increased to 215 mL/g VS compared with 135 mL/g VS methane yield in the control reactor. Also, gas constituent analysis showed good improvement of biogas quality as the % CH_4 reached 68% starting from 52% without H_2 injection. The results showed also utilisation of about 88% of the hydrogen injected to the reactor in the bio-methanation process. Based on this results, the upgrading of biogas produced from sewage sludge is promising and furthers studies will be carried out on the effect of gas recirculation and the performance in thermophilic conditions to reach maximum utilisation of H_2 for high performance bio-methanation.

Keywords

Anaerobic digestion; biogas; Bio-methanation; CSTR; hydrogen

INTRODUCTION

Biogas is a product of anaerobic digestion process (AD) of organic wastes and it is composed of methane (CH_4) with about 50–70% and carbon dioxide (CO_2) with 25–45% while minor amounts of other compounds, such as nitrogen (N_2) (0–3%), oxygen (O_2) (0–1%), and hydrogen sulfide (H_2S) at concentrations of 0-4% (Golmakani, et al., 2022). Except CH_4, the other gasses in biogas are not wanted and are considered as biogas pollutants and this reduce the energy content of biogas described by lower calorific value (LCV) from 36 to 20 MJ/m^3. The biogas could be utilized as an alternative of natural gas. However, European Commission has recently issued a mandate for determining harmonized standards for gas quality which must contain about 95% methane (Angelidaki, et al., 2018). Accordingly, the biogas should be treated to increase the methane content through conversion of CO_2 contained in the raw biogas to CH_4 by reaction with H_2 (Kougias, et al., 2017). The biogas can be upgraded in the same reactor through injection of H_2 during the AD process and it is called in-situ upgrade. The other method is ex-situ upgrade in which the mixing of biogas and H_2 in another external anaerobic reactor is occurred. The aim of this study is to evaluate in-situ upgrade of biogas produced from anaerobic digestion of sewage waste sludge by H_2 injection inside CSTR system.

MATERIALS AND METHODS

Reactors set-up and operation

Two laboratory-scale AD reactors were fabricated with a capacity of 5 L for each one of the reactors is injected with H_2 gas while the other acts as control. The reactors were stirred with the use of paddle-type mixers, and the temperature was kept at level of 37–38 °C by means of a water jacket connected to circulating water baths with digital temperature controller (VWR International, USA). For H_2 supply inside one of the reactors a precision digital mass flow controller (MFC) model DPC07 (AALBORG, USA) was used to inject the H_2 through a ceramic membrane micro-bubble diffuser ED 60 (Enviro Ceramic Co., Ireland) made from ultra-fine nano porous aluminum oxide. The reactors were loaded with inoculum from anaerobic digester of a municipal waste water treatment plant (WWTP) from southern part of Poland with VS content of 1.5 % while substrate used was collected from the mixed sludge waste at the same treatment plant with average VS contents of 2.7%. Both reactors were operated at OLR of 1.9 g VS/L and fed with sewage sludge substrate every 24h and SRT of 14 days. Figure 1. Shows the reactors configurations.

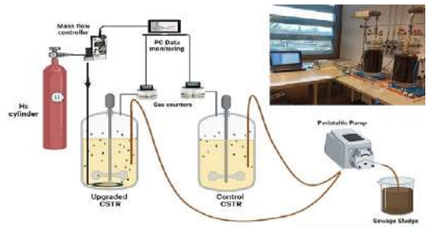

Figure 1. Schematic diagram of in-situ methanation system

Analysis and measurements

pH and temperature measurements were carried out in the reactors on daily basis. The volume of produced biogas was measured continuously with use of gas counter (RITTER MGC-1 V3.4, Germany) PC software. The composition of biogas was measured by collecting gas in Tedlar bags and injection to gas chromatography (Agilent). Also, the composition of substrate and digestate from each reactor was monitored weekly in terms of soluble COD, TS, VS, TN, ammonia, VFA and alkalinity.

RESULTS AND DISCUSSION

Reactor operation

The operation of the reactors was started in normal mode and same conditions for both reactors for three months till reaching the steady state. During this period, the performance of both reactors was monitored for gas quality and quantity as well as analysis of digestate effluent. The results of this stage showed stable pH value in the reactors (6.9-7.1) and the produced gas ranged between 240-280 mL/g VS. The gas contents in both reactors were 50-55% CH_4, 25-32% CO_2, 5-11% N_2 and 2-4% O_2. After the steady state, the hydrogen was injected to one of the reactors through micro-ceramic membrane diffuser. The amount of H_2 injected to the reactor was calculated to be H_2:CO_2 ratio of 4:1 based on literature studies on biological hydrogen methanation (Wahid and Horn, 2021). To reach this ratio, gradual increase in the amount of H_2 injected to the reactor was performed starting from 1:1 then 2:1 and 3:1 till 4:1. It was noticed that the %CH_4 was slightly increasing with increasing the H_2: CO_2 ratio with the sequence of 55%, 57% and 60%.

Evaluation of in-situ hydrogen bio-methanation

The H_2 was injected to the CSTR reactor with a flow rate of 1.4-1.5 mL/min according to the gas flow rate of the control reactor to achieve H_2: CO_2 ratio of 4:1. Table 1 summarizes the performance of bio-methanation process during the study period. The average amount of hydrogen added was 3150 mL/d and the average produced biogas in the control reactor was 2510 mL/d. The average amount of upgraded biogas from bio-methanation process is 3100 mL/d of which 11 % H_2. The results depicted in Figure 2 showed the variation of CH_4 yield over time in the control and upgraded CSTRs. The results showed an increase in CH_4 yield by 59% (from 135 to 215 mL/g VS) and the methane production rate was 415 mL/L_{VT} .d compared to 260 mL/L_{VT}. d without hydrogen addition. Also, the H_2 conversion rate high and ranged from 83 to 92% with average rate of 88%. Analysis of gas composition showed acceptable increase in the % CH_4 (Figure 3) as it reached to 68 % compared with 52% in the control reactor. The achieved yield was satisfactory compared to similar studies on in-situ bio-methanation in CSTR reactor. Luo and Angelidaki (2013) investigated the biogas upgrading by hydrogen bio-methanation in 1L CSTR for digestion of manure at thermophilic condition (55 °C) with H_2: CO_2 ratio of 4:1. They obtained CH_4 content of 68% at retention time 92h and methane production rate of 1.2 L/L_{VT}.d which considered high production rate due to the high organic load and thermophilic conditions. The achieved results in our study could be improved through investigation the increase of H_2 to CO_2 ratio to more than 4:1 via circulation a part of biogas in the reactor headspace and application of thermophilic conditions in the reactor.

Table 1. Process performance variables in control CSTR and upgraded CSTR with H_2 addition.

Reactors	Control CSTR	Upgraded CSTR
H_2 addition	No	Yes
H_2:CO_2 ratio	--	4:1
H_2 added (L/L_{gas}. d)	-	1.3
% CH_4	52	68
% CO_2	32	18
%H_2	--	1
CH4 production rate (L/L_{VT}.d)	260	415
CH_4 yield (mL/g VS)	135	215
% H_2 consumption	-	88

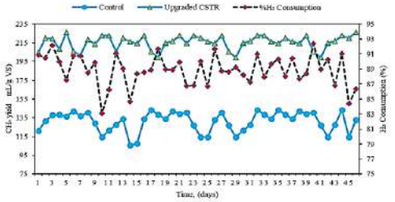

Figure 2. Variation of methane yield and hydrogen consumption in control and upgraded CSTR.

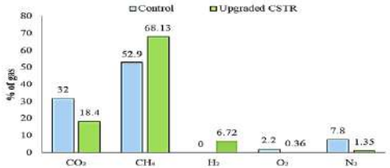

Figure 3. Biogas composition from control and upgraded CSTR.

CONCLUSION

This study demonstrated the feasibility of biogas upgrading through in-situ biological hydrogen methanation using a two CSTRs system where one was control, and the other was injected with hydrogen with H_2: CO_2 ratio of 4:1 through ceramic diffuser. The results showed a good performance of bio-methanation process in the upgraded CSTR as the average methane yield increased to 215 mL/g and the gas constituent analysis showed good improvement of biogas quality as the % CH_4 reached 68% with utilisation of about 88% of the hydrogen injected to the reactor. Based on these results, the upgrading of biogas produced from sewage sludge is promising and furthers studies will be carried out on the effect of gas recirculation and the performance in thermophilic conditions to reach maximum utilisation of H_2 for high performance bio-methanation.

AKNOWLAGEMENT

This work is within the framework of project WasteValue funded by Norway grant No. (NOR/POLNOR/WasteValue/0002/2019-00)

REFERENCES

Angelidaki, I., Treu, L., Tsapekos, P., Luo, G., Campanaro, S., Wenzel, H., and Kougias, P. G. 2018 Biogas upgrading and utilization: Current status and perspectives. *Biotechnology Advances*, **36**(2), 452–466.

Golmakani, A., Ali Nabavi, S., Wadi, B., and Manovic, V. 2022 Advances, challenges, and perspectives of biogas cleaning, upgrading, and utilisation. *Fuel*, **317**, 123085. [online] https://linkinghub.elsevier.com/retrieve/pii/S0016236121029458.

Kougias, P. G., Treu, L., Benavente, D. P., Boe, K., Campanaro, S., and Angelidaki, I. 2017 Ex-situ biogas upgrading and enhancement in different reactor systems. *Bioresource Technology*, **225**, 429–437.

Luo, G. and Angelidaki, I. 2013 Co-digestion of manure and whey for in situ biogas upgrading by the addition of H2: Process performance and microbial insights. *Applied Microbiology and Biotechnology*, **97**(3), 1373–1381.

Wahid, R. and Horn, S. J. 2021 The effect of mixing rate and gas recirculation on biological CO2 methanation in two-stage CSTR systems. *Biomass and Bioenergy*, **144**, 105918. [online] https://linkinghub.elsevier.com/retrieve/pii/S0961953420304517.

Development of copper-substituted Prussian blue analog immobilized ion exchange resins for high-performance ammonium recovery from wastewater

S. Im*, B. Lee*, K. Ahn*, T.-H., Kim**, Y. Hwang** and S. Kang*

* Department of Environmental Research, Korea Institute of Civil Engineering and Building Technology, 283 Goyang-daero, Ilsanseo-gu, Goyang-si, Gyeonggi-do 10223, Republic of Korea
(E-mail: *seongwonim@kict.re.kr*; *bjdream@kict.re.kr*; *khahn@kict.re.kr*; *kangsw93@kict.re.kr)*
** Department of Environmental Engineering, Seoul National University of Science and Technology, 232 Gongneung-ro, Nowon-gu, Seoul 01811, Republic of Korea
(E-mail: *th.kim@seoultech.ac.kr*; *yhhwang@seoultech.ac.kr*)

Abstract
Ammonia (NH_3) is a valuable resource used in various industries and is commonly produced from H_2 and N_2, while researchers have tried to recover directly from wastewater. In this study, a facile synthesis procedure was developed for preparing high-performance ammonium adsorbent via in-situ immobilization of Prussian blue analog, viz. copper hexacyanoferrate (CuHCF) on a weakly acidic cation exchange resin (WAC). From the analysis of the physicochemical properties of the synthesized CuHCF-based adsorbents, it was confirmed that CuHCF was successfully immobilized on the surface of WAC, allowing access to NH_4^+ for adsorption. The maximum equilibrium adsorption capacity was 47.07 mg NH_4^+ per g of WAC-CuHCF at pH 6.5 by fitting the Langmuir isotherm model. The optimal pH was 8, and the competition effect of K^+ and Na^+ on the capacity was not severe (<10%). The ability of WAC-CuHCF to regenerate was assessed in the column test, and the regenerated adsorbent was found to adsorb and desorb NH_4^+ to essentially the same extent.

Keywords
Ammonium recovery; Copper hexacyanoferrate; Prussian blue analog; Regeneration; Weakly acidic cation exchange resin

INTRODUCTION

Ammonia is a useful chemical substance in various industrial fields but could be a problematic pollutant causing eutrophication and so on when emitted into nature. Various technologies have been developed to remove it, but a significant amount of energy is required. Therefore, numerous studies for recovering ammonia from wastewater have been performed using non-biological methods. Adsorption is preferred because of its environmental sustainability and economic feasibility. Prussian blue (PB) and its analogs (PBAs) are materials in which metal ions and metal cyanide ions combine in a specific ratio to form a lattice structure that is known to capture monovalent cations (Cs^+ of which ionic radius is similar to ammonia). In this study, we aimed to develop a method for producing CuHCF-based composites as adsorbents for the adsorption of ammonium ions from wastewater. In this case, the production process was simplified using a commercial IX resin rich in carboxyl groups as the substrate for PBA immobilization.

MATERIALS AND METHODS

Copper sulfate pentahydrate and potassium hexacyanoferrate trihydrate were coated on the surface of weakly acidic cation exchange resin (WAC). The physicochemical properties of the synthesized CuHCF-based adsorbents were analysed using various methods (PXRD, FT-IR, BET, HR-SEM etc.). To evaluate the ammonium ion adsorption characteristics of the synthesized CuHCF-based adsorbents for ammonium ions in water, batch and column tests were performed. The experimental results were fitted by the kinetics equations, adsorption isotherms, and Thomas model.

RESULTS AND DISCUSSION

The WAC-CuHCF was successfully prepared with the facile preparation method suggested in this study. The BET surface area of WAC-CuHCF decreased by 16 %, but its average pore size increased to 282.3 Å compared to one of WAC. The WAC-CuHCF exhibited different thermal behavior and fewer intra-particle pores than WAC and WAC-Cu. The ammonium adsorption capability of WAC-CuHCF was approximately 62 and 7 times higher than one of WAC and WAC-Cu, respectively. It was revealed that the primary adsorption mechanism for WAC-CuHCF was the chemical action of the monolayer, and its maximum adsorption capacity was 47.07 mg/g, which was significantly higher than one of the other adsorbents in the previous studies (Table 1). Within the pH range of 4–9, the optimal pH for ammonium adsorption was 8.0, and the competition effects of K^+ and Na^+ against ammonium ions were not severe (<10 %). The adsorption-regeneration process was successfully demonstrated in the continuous column test with high ammonium loading conditions (1,200 mg/L). Furthermore, the amount of ammonium from the regeneration process was similar to the amount of removed ammonium by adsorption, implying outstanding recyclable performance and high stability. The WAC-CuHCF may be a promising candidate for highly effective ammonium recovery from wastewater. Ammonia, which gains attention as a hydrogen carrier in the future society, is highly likely to be produced in specific regions, so long-distance transportation to the consumer is inevitable.

Table 1. The maximum ammonium adsorption capacity of various ammonium adsorbents reported in the literature.

Material	Sample type	Adsorption capacity (mg/g)	Initial ammonium concentration (mg/L)	Sample dosing (g/L)	Contact time (h)	Ref.
Bentonite/chitosan	Bead	15.9	~26.4	15	3	Gaouar Yadi et al., 2016
Zeolite/PVA-Alginate	Bead	28.17	20-400	20	3	Zhang et al., 2016
KCuHCF	Bead with binder	37.04	100-4,000	10	24	Sinha et al., 1993
PES-Zn-HCF	Bead with binder	27.26	~200	2.5	48	Nativ et al., 2021
WAC-CuHCF	Bead	47.07	10-1,000	1	24	This study

REFERENCES

Gaouar Yadi, M., Benguella, B., Gaouar-Benyelles, N., Tizaoui, K. 2016 Adsorption of ammonia from wastewater using low-cost bentonite/chitosan beads. *Desalination and Water Treatment* **57**(45), 21444-21454.

Nativ, P., Ben-Asher, R., Fridman-Bishop, N., Lahav, O. 2021 Synthesis and characterization of zinc-hexacyanoferrate composite beads for controlling the ammonia concentration in low-temperature live seafood transports. *Water Research* **203**, 117551.

Sinha, P.K., Amalraj, R.V., Krishnasamy, V. 1993 Flocculation studies on freshly precipitated copper ferrocyanide for the removal of caesium from radioactive liquid waste. *Waste Management* **13**(4), 341–350,

Zhang, H., Li, A., Zhang, W., Shuang, C. 2016 Combination of Na-modified zeolite and anion exchange resin for advanced treatment of a high ammonia–nitrogen content municipal effluent. *Journal of Colloid and Interface Science* **468**, 128–135.

Effect of enhanced hydrolysis of a lipid–rich wastewater on the acidogenic fermentation

M. Jiménez-Urpi [1], G. Baquerizo [2], M. Suárez-Ojeda [3], G. Montiel-Jarillo [1]
[1] Vervirotech Biotechnology, Santa Perpetua de Mogoda, Spain, montserrat.jimenez@vervirotech.com
2 Eurecat Sostenibilidad, Manresa, Spain.
3 GENOCOV Research Group, Department of Chemical, Biological and Environmental Engineering, Universitat Autonoma de Barcelona, Barcelona, Spain.

Abstract
The hydrolysis of a lipid-containing wastewater was studied using two different hydrolytic strategies, enzymatic and alkaline. The enzymatic hydrolytic strategy achieved a 98% triglycerides (TAG) hydrolysis, and it was used in an acidogenic fermentation process performed in a lab-scale stirred, temperature and pH-controlled reactor, obtaining a maximum yield of 0.46 g short-chain carboxylic acids (SCA)/g chemical oxygen demand (COD).

Keywords
Acidogenic fermentation, enzymatic hydrolysis, lipid-rich wastewater, SCA production,

INTRODUCTION

In a circular economy process, the treatment of industrial wastewaters is aimed at generating products of interest while, at the same time, preserving the environment from receiving damaging substances. Conventional biological technologies, including anaerobic digestion, have been satisfactorily used for treating high-strength waste streams generated, for example, from food manufacturing industries (Mendes et al., 2006). The first step of an anaerobic digestion process involves hydrolysis and acidogenic fermentation of the feeding stream to generate short-chain carboxylic acids (SCA) to be used in a second step by methanogenic bacteria. Recently, the hydrolysis-fermentation step, namely acidogenic fermentation, has been seen as a promising alternative itself inside a circular economy process as it is able to efficiently manage high-strength waste streams, and also to obtain high-value by products (SCA) that can be used as a carbon source for producing, for example, polyhydroxyalkanoates (PHA), a high-value bioplastic (Silva et al., 2013). On the other hand, the management of high-strength wastewaters from food manufacturing industries involves some inconveniences, such as a high fats concentration, that affects negatively the acidogenic fermentation due to mass transfer limitations that will affect the hydraulic retention time (HRT) and will promote the formation of fat scum at the surface of the reactors, resulting as the rate limiting step of the process. High fat concentrations can also affect the use of some industrial equipment, for example, by pipe clogging. To overcome such limitations, several hydrolytic strategies have been proposed, in order to degrade the lipid content prior to an acidogenic fermentation process. On the one hand, some authors report chemical strategies, such as lipid saponification as an effective way to improve anaerobic digestion by increasing the bioavailability of fatty wastes. On the other hand, biological-based strategies, such as the use of enzymes that specifically hydrolyze complex organic matter have gained interest over the last years (Domingues et al., 2015). Lipases (triacylglycerol ester hydrolases EC 3.1.1.3) are able to catalyze the hydrolysis of triacylglycerides (TAG) into glycerol and free fatty acids (FFA). For this reason, these enzymes seem to be a promising alternative to efficiently achieve the degradation of lipid-rich waste streams (Cammarota et al., 2001). Regarding the acidogenic fermentation, there are several parameters that influence the SCA yield, such as the pH, the temperature or the volumetric organic loading rate (vOLR) (Vázquez-Fernández et al., 2022). It has been reported that increasing the vOLR raises the VFA production. However, at very high vOLR the acidogenic fermentation process is unstable, affecting the acidogenic microbial communities. For this reason, determining the optimal vOLR is important to assess a high SCA yield. In this sense, the aim of this work is to compare two different hydrolytic strategies, an alkaline and an enzymatic one, to hydrolyze the lipid content of a lipid-rich wastewater. The hydrolyzed wastewater was then used as the substrate to obtain an SCA-rich effluent through acidogenic fermentation in order to evaluate its effect over the SCA yield.

MATERIALS AND METHODS

A wastewater liquid waste stream was obtained from a food processing industry located in Vic (Girona). The characterization of the wastewater is shown in Table 1.

Daily samples were stored in the fridge (4ºC) for further analysis and the parameters of interest were analyzed. Commercial lipase obtained from a non-GMO strain. The optimal enzyme conditions were pH between 7 and 11, and temperature in a range between 25 and 65ºC, being its optimal at 40ºC. Anaerobic sludge was obtained from acidogenic fermentation reactors previously adapted to the wastewater tested and it was used as inoculum for the acidogenic fermentation.

Table 1. Characteristics of the wastewater. pCOD: particulate Chemical Oxygen Demand; sCOD: soluble COD; tCOD: total COD; TAG: triacylglycerides; TSS: Total Suspended Solids: TS: Total Solids.

Parameter	Value	Unit
pCOD	76.5 ± 12.9	g L^{-1}
sCOD/tCOD	33.0 ± 2.2	%
TAG	19.7 ± 0.1	g L^{-1}
TSS/TS	44.6 ± 3.0	%
Protein	3.00	g Kg^{-1}
Density	1000.0	g L^{-1}

Alkaline hydrolysis was carried out in 3L stirred reactors and the temperature was controlled at 37ºC. Raw wastewater was added to the reactors and pH was adjusted to 12 using NaOH (25%w/v). The optimal alkaline conditions, regarding the optimal dose, time and temperature were found in previous experiments (data not shown). Enzymatic hydrolysis was also performed in 3L reactors. The pH and temperature were adjusted according to the optimum for the enzyme activity stated by the manufacturer, and it was dosed at 1% w/v, as found in previous experiments (data not shown). Samples were taken at the beginning and at the end of each experiment for the quantification of TAG, total and soluble Chemical Oxygen Demand (tCOD and sCOD). The hydrolysis of the organic matter was determined as sCOD/tCOD, and the TAG hydrolysis was analyzed and quantified according to the initial and final concentrations. The pH of the hydrolyzed effluent was adjusted to 8 before starting the acidogenic fermentation.

Acidogenic fermentation was performed in lab-scale mechanically stirred reactors, mesophilic conditions were maintained, and pH was controlled at 8. Previously acclimated anaerobic sludge was used as inoculum, and the enzymatic hydrolyzed wastewater was used as substrate. Sludge retention time (SRT) was set in 10 days. The test was carried out over 46 days, maintaining the same conditions, except the organic vORL, that was adjusted in order to maximize the production yield. The vORL was defined as the amount of organic material fed, quantified as Total Solids (TS) per volumetric unit of the reactor per unit of time. Concentrations of TAG, SCA, tCOD and sCOD were analyzed periodically to determine the stability of the process and the fermentation yield. The production yield or SCA yield (Yp/s) was calculated as SCA produced in terms of sCOD per tCOD fed into the system (Ramos-Suarez et al., 2021). Degree of acidification (DA) was calculated as the amount of SCA produced in terms of COD over sCOD of the fermented broth (Girotto et al., 2017).

TS and COD were determined according to the procedures described in the Standard Methods of Water and Wastewater (APHA, 2012). Concentration of SCA was determined using an HPLC SCA analyzing method (Agilent Hi-plex H column). Six types of metabolites and SCA were analyzed: lactic acid (HLac), acetic acid (HAc), propionic acid (HPr), iso-butyric acid (HiBt), n-butyric acid (HBt) and valeric acid (HVc).The SCA concentrations were expressed as theoretical equivalents of COD (Naresh Kumar & Venkata Mohan, 2018). TAG concentration was analyzed performing a lipid extraction and determined using RMN.

RESULTS AND DISCUSSION

Hydrolysis of wastewater

Enzymatic and alkaline hydrolytic strategies were carried out in order to evaluate the most convenient hydrolytic strategy. Table 2 shows the composition of the hydrolyzed wastewater and samples were obtained after 24h assays. Initial and final TAG concentrations are shown, and TAG hydrolysis was also calculated from the concentration difference.

The sCOD/tCOD is also represented to assess the reached solubility. An increase of the soluble fraction (sCOD/tCOD) from a 33% to a 59% and 54% in the alkaline and enzymatic strategies, respectively, was observed. These results showed that both strategies are able to solubilize the organic matter present in the wastewater, by achieving almost the same solubilization. On the other hand, the TAG hydrolysis was also quantified. Total TAG concentration decreased up to 24% in the alkaline strategy, while 98% TAG concentration decrease was obtained in the enzymatic pretreated wastewater. The TAG hydrolysis is credited to the effect of the lipase in the enzymatic strategy. This behavior was not observed in the alkaline strategy, as little TAG hydrolysis was achieved.

Table 2. Hydrolytic strategies results

Assay	TAG			
	Initial concentration (g L^{-1})	Final concentration (g L^{-1})	TAG hydrolysis (%)	sCOD/tCOD (%)
Alkaline hydrolyzed wastewater	19.97 ± 0.23	15.39 ± 0.62	24%	59%
Enzymatic hydrolyzed wastewater	19.97 ± 0.23	0.45 ± 0.05	98%	54%

The solubilization of the pCOD, involving an increased in the sCOD/tCOD ratio, can be attributed to the pH effect, as both the alkaline and enzymatic pretreatment were adjusted to pH 10 and 12, respectively, involving the addition of NaOH (Li et al., 2012). However, the TAG hydrolysis can only be related to the lipase action, as the alkaline hydrolysis has no potential effect in the lipid hydrolysis, and only the lipases hydrolyze specifically the TAG present in the wastewater. Based on the results presented herein, the enzymatic pretreatment was significantly more effective for the TAG hydrolysis, achieving an equal percentage of sCOD solubilization. For this reason, this enzymatically hydrolyzed residue was chosen to be used as the substrate in the subsequent acidogenic fermentation, in order to study the SCA yield obtained from this residue.

Acidogenic fermentation results

The acidogenic fermentation of the enzymatic hydrolysate to produce SCA from lipid-rich wastewater was performed, and the fermentation parameters were set according to the literature (Yin et al., 2016). DA (%), SCA concentration (gCOD L^{-1}) and SCA yield (Yp/s) are shown in Figure 1A, as well as the vOLR of each period. The vOLR was set at 22.1 g TS L^{-1} d^{-1} during the first days of the acidogenic fermentation (day 0 to day 16, period 1). During this period, the SCA yield was, on average, 20 ± 8 % and the total SCA concentration achieved was 24 ± 6 gCOD L^{-1}. Since operation during this period was very unstable regarding the Yp/s and SCA concentration, the vOLR was therefore reduced. According to the literature, vOLR higher than 16 g TS L^{-1} d^{-1} was considered to cause instability in the process, while lower vOLR, such as 5 or 11g TS L^{-1} d^{-1} was considered optimal for SCA production from food wastes (Jiang et al., 2013). Therefore, the vOLR was set at 12.6 g TS L^{-1} d^{-1} from day 16 to the end of operation (Period 2). After the vORL adjustment, the production yield increased up to 38 ± 5%. In this second period, which lasted 30 days, the average SCA concentration was 30 ± 3 gCOD L^{-1}. In comparison to the first stage, the DA increased from 29 ± 6% to 62 ± 8%, showing the vOLR adjustment had an effect on the process performance. Regarding the sCOD/tCOD, it was 48 ± 9 % during period 1, and then it was 47 ± 7 % for the rest of the acidogenic fermentation process. No significant variation was observed as the sCOD/tCOD parameter depends on both the hydrolytic strategy and the characteristics of the substrate itself. Moreover, no variation in this parameter shows stability in the hydrolytic process. Regarding the TAG concentration, and due to a high hydrolytic yield in the enzymatic pretreatment strategy prior to the acidogenic fermentation, it was 0.49 ± 0.05 g L^{-1}, showing that the low TAG concentration is preserved during the fermentation stage. Modifying the vOLR affects the acidogenic fermentation performance in terms of SCA concentration, and subsequently, the SCA yield and DA, indicating that vOLR is a key parameter to consider to achieve high production yields.

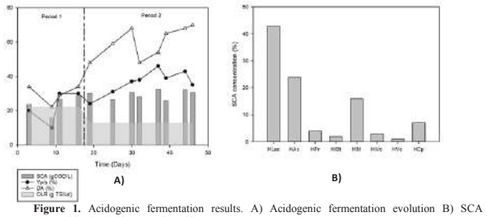

Figure 1. Acidogenic fermentation results. A) Acidogenic fermentation evolution B) SCA composition in the fermentation effluent

In case of a subsequent PHA production, the composition of the SCA obtained is a parameter of paramount importance as a direct correlation between SCA and the type of PHA biosynthesized can be predicted. In general, it is expected that fermented SCA-effluents with higher odd equivalent acids, such as propionic or valeric, lead to higher Hydroxy-valerate (HV) composition in the final PHA (Albuquerque et al., 2011). In this sense, Figure 1B shows the SCA composition (%) in the acidogenic reactor, during the second period of the fermentation. The most abundant SCAs in the second period were lactic acid (43%), acetic acid (24%) and butyric acid (16%). In this fermentation effluent, low concentration of propionic (4%) and valeric acids (1%) were detected, leading, in principle, into hydroxy-butyrate (HB) polymers. A modification of the operational parameters should be considered in order to modify the SCA composition to drive the PHA production into PHV. Acidogenic fermentation of high-strength wastewaters can be limited by the lipid hydrolysis. In this work, the use of a commercial lipase has shown to promote a great TAG hydrolysis, enhancing also the solubilization of the particulate organic matter. Moreover, the acidogenic fermentation of the enzymatic hydrolyzed waste was studied, and, by adjusting the vOLR, better acidogenic yields were achieved. The results show that coupling the enzymatic hydrolysis with an acidogenic fermentation done at an appropriate vORL might be an attractive alternative for the valorization of lipid-rich waste streams.

REFERENCES

Albuquerque, M. G. E., Martino, V., Pollet, E., Avérous, L., & Reis, M. A. M. (2011). Mixed culture polyhydroxyalkanoate (PHA) production from volatile fatty acid (VFA)-rich streams: Effect of substrate composition and feeding regime on PHA productivity, composition and properties. *Journal of Biotechnology*, *151*(1), 66–76.

APHA. (2012). *Standard Methods for the Examination of Water and Wastewater, 23rd Edition.*

Bengtsson, S., Hallquist, J., Werker, A., & Welander, T. (2008). Acidogenic fermentation of industrial wastewaters: Effects of chemostat retention time and pH on volatile fatty acids production. *Biochemical Engineering Journal*, *40*(3), 492–499.

Cammarota, M. C., Teixeira, G. A., & Freire, & D. M. G. (2001). Enzymatic pre-hydrolysis and anaerobic degradation of wastewaters with high fat contents. In *Biotechnology Letters* (Vol. 23).

Domingues, R. F., Sanches, T., Silva, G. S., Bueno, B. E., Ribeiro, R., Kamimura, E. S., Franzolin Neto, R., & Tommaso, G. (2015). Effect of enzymatic pretreatment on the anaerobic digestion of milk fat for biogas production. *Food Research International*, *73*, 26–30.

Girotto, F., Lavagnolo, M. C., Pivato, A., & Cossu, R. (2017). Acidogenic fermentation of the organic fraction of municipal solid waste and cheese whey for bio-plastic precursors recovery – Effects of process conditions during batch tests. *Waste Management*, *70*, 71–80.

Jiang, J., Zhang, Y., Li, K., Wang, Q., Gong, C., & Li, M. (2013). Volatile fatty acids production from food waste: Effects of pH, temperature, and organic loading rate. Bioresource Technology, 143, 525–530

Mendes, A. A., Pereira, E. B., & de Castro, H. F. (2006). Effect of the enzymatic hydrolysis pretreatment of lipids-rich wastewater on the anaerobic biodigestion. Biochemical Engineering Journal, 32(3), 185–190

Naresh Kumar, A., & Venkata Mohan, S. (2018). Acidogenesis of waste activated sludge - Biohydrogen production with simultaneous short chain carboxylic acids. Journal of Environmental Chemical Engineering, 6(2), 2983–2991.

Ramos-Suarez, M., Zhang, Y., & Outram, V. (2021). Current perspectives on acidogenic fermentation to produce volatile fatty acids from waste. In Reviews in Environmental Science and Biotechnology (Vol. 20, Issue 2, pp. 439–478). Springer Science and Business Media B.V.

Silva, F. C., Serafim, L. S., Nadais, H., Arroja, L., & Capela, I. (2013). Acidogenic fermentation towards valorisation of organic waste streams into volatile fatty acids. Chemical and Biochemical Engineering Quarterly, 27(4), 467–476.

Vázquez-Fernández, A., Suárez-Ojeda, M. E., & Carrera, J. (2022). Review about bioproduction of Volatile Fatty Acids from wastes and wastewaters: Influence of operating conditions and organic composition of the substrate. Journal of Environmental Chemical Engineering, 10(3).

Yin, J., Yu, X., Wang, K., & Shen, D. (2016). Acidogenic fermentation of the main substrates of food waste to produce volatile fatty acids. International Journal of Hydrogen Energy, 41(46), 21713–21720.

Heavy metals uptake with energy crops biomass depending on soil amendment

M. M. Kharytonov*, M.G.Babenko* and N.V. Martynova**

* Department of Soil Sciences and Farming, Dnipro State Agrarian and Economic University, 25 Serhii Yefremova st. Dnipro, 49600, Ukraine (E-mail: *kharytonov.m.m@dsau.dp.ua)*
** Department of Nature Flora, Botany Garden, Dnipro National University, 72 Gagarin Avenue, Dnipro, 49044, Ukraine (E-mail: *nadiamartbg@gmail.com*)

Abstract
The application of various amendments leads to an increase in the parameters of vertical and horizontal growth from 2% to 40%. The greatest effect is the use of sewage sludge. The content of heavy metals in the above-ground biomass is quite low and varies from 4.2-4.5 to 129.5-159.9 mg kg^{-1}. The content of heavy metals in the biomass of Miscanthus was higher than in Switchgrass by 20-30%.
Keywords: energy crops, sewage sludge, heavy metals.

INTRODUCTION

The issues with utilization of wastewater sludge are not resolved for decades in Ukraine. Hygienic properties and high content of heavy metals in wastewater sewage sludge are the main problems that hinder the use of biosolids in agriculture, including technical crops for production of biofuels (Singh and Agrawal, 2008; Stietiya and Wang, 2011; Antonkiewicz et al., 2018). Main objective of this case study was to estimate heavy metals uptake with energy crops biomass depending of kind and rate of soil amendment.

MATERIALS AND METHODS

The field experiment was established on phytomeliorated loess-like loam at the DSAEU research station located in the south of Ukraine (47°39′N, 34°08′E). The following five amendments were used to determine the effect of various additional fertilizers: ash of sunflower husk in amount 10 t ha^{-1}, municipal sewage sludge (10 t ha^{-1}), mixture of ash and sewage sludge (10 t ha^{-1}), a double rate of sludge (20 t ha^{-1}) and mineral fertilizer with a balance of nutrients $N_{60}:P_{60}:K_{60}$ kg ha^{-1}. All amendments were put into the soil in dry form annually once in spring. The biometric parameters and biomass productivity were defined at the end of vegetation season (second part of September).

RESULTS AND DISCUSSION

The application of amendments led to an increase in the parameters of vertical and horizontal growth from 2% to 40%. The use of ash had the least effect, and the influence of double dose of sewage sludge was the strongest. The thickness of the shoots has also increased. In Switchgrass, the stem diameter under the influence of ash and a mixture of ash and sludge changed slightly, up to 5%. The application of sewage sludge and mineral fertilizer increased this indicator by 11-18%. In Miscanthus, only a double dose of sludge had an improving effect (13.9%), other amendments did not have a significant impact (1-1.6%). In this way, the response of Switchgrass plants to amendment application was better than Miscanthus, which contributed to an increase in biomass yield from 7 t DM ha^{-1} (control) to 15-17 t DM ha^{-1} (sewage sludge). In Miscanthus, the maximum yield (12.4-13.3 t DM ha^{-1}) was achieved using mineral fertilizer and double dose of sludge. Thus, for Switchgrass, the most promising amendment is only sewage sludge. For Miscanthus, the use of sewage sludge in amount of 10-20 t ha^{-1} and mineral fertilizers is optimal. In the control plot, the content of heavy metals in the biomass of Miscanthus was higher than in Switchgrass by 20-30%. On the plots with amendments, the content of Mn and Zn was also higher in Miscanthus. At the same time, Cu and Pb accumulated more intensively in Switchgrass biomass. It was detected that the amendment application modified the physicochemical properties of soil, thereby enhancing the availability of heavy metals in the soil and increasing their accumulation in biomass. The mineral fertilizer use had the least effect (from 0.1% to 90% for Miscanthus and from 32% to 48% for Switchgrass). The addition of double dose of sewage sludge had the most significant effect and caused an increase in content of heavy metals by 90-165% for Miscanthus and by 124-333% for Switchgrass compared to the control. It was detected during analyzing heavy metals content in the Miscanthus biomass that amendments affect Mn accumulation most intensively. Greatest effect was noted for Cu in the Switchgrass biomass. The application of the amendments led to an increase in heavy metal uptake by the Miscanthus and Switchgrass biomass (Fig. 1).

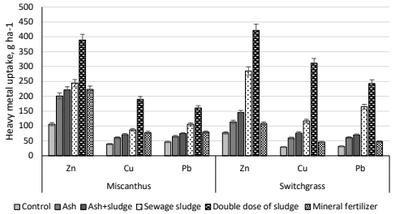

Fig.1. Heavy metal uptake (Cu, Zn and Pb) by the 3-year-old plants of Miscanthus and Switchgrass

In control, the level of heavy metals uptake was higher in Miscanthus compared to Switchgrass. The introduction of amendments has changed this ratio. The introduction of mineral fertilizers, ash and mixture of ash and sewage sludge contributed to an increase in the uptake of Zn, Cu and Pb by the biomass of both plant species on average 1.5-2.6 times. The application of single dose of sewage sludge enhanced the uptake of these metals by the Miscanthus 2.2-2.7 times, whereas for Switchgrass the uptake level increased 3.7-5.2 times. The applying of double dose of sewage sludge had the greatest effect. However, while in Miscanthus the uptake capacity was increased by 3.4-4.8 times, in Switchgrass it was augment by 5.5 (Zn), 7.7 (Pb) and 10.6 (Cu) times.

REFERENCES

Antonkiewicz J., Pełka R., Bik-Małodzińska M., Żukowska G., Gleń-Karolczyk K. The effect of cellulose production waste and municipal sewage sludge on biomass and heavy metal uptake by a plant mixture. Environmental Science and Pollution Research. 2018. **25**. P.31101–31112. https://doi.org/10.1007/s11356-018-3109-5

Stietiya M.H., Wang J.J. (2011) Effect of Organic Matter Oxidation on the Fractionation of Copper, Zinc, Lead, and Arsenic in Sewage Sludge and Amended Soils. J. Environ. Qual. 2011. **40**. P.1162–1171. https://doi.org/10.2134/jeq2011.0008

Singh R.P., Agrawal M. (2008). Potential benefits and risk of land application of sewage sludge. Waste Management. **28**(2). P.347–358. https://doi.org/10.1016/j.wasman.2006.12.010

Is bioaugmentation a successful strategy to manipulate biopolymer production from wastewater?

K. Khatami*, Z. Cetecioglu*

* Department of Industrial Biotechnology, KTH Royal Institute of Technology, AlbaNova University Center, SE-10691 Stockholm, Sweden,
kasrakm@kth.se, zeynepcg@kth.se

Abstract
Bio-based plastic production can be a prominent contributor to the development of a circular economy. Using volatile fatty acids acquired from anaerobic digestion of municipal wastes as substrate, two different strategies were compared for microbial polyhydroxyalkanoates (PHAs) production: 1) Long-term enrichment of activated sludge-161 days- with bioaugmentation of *Cupriavidus necator* and *Burkholderia cepacia* 2) Short-term enrichment of activated sludge-5 days- with bioaugmentation of *Cupriavidus necator* and *Burkholderia cepacia*. The highest PHA accumulation was obtained from bioaugmentation of *Cupriavidus necator* (52 % PHA/VSS) followed by bioaugmentation of *Burkholderia cepacia* (36 % PHA/VSS) after 154 days of enrichment (long-term enrichment). Whereas, maximal PHA content in the short-term enrichments was 17% PHA/VSS obtained from the non-bioaugmented activated sludge.

Keywords
Activated sludge; microbial community; polyhydroxyalkanoates; resource recovery; volatile fatty acids

INTRODUCTION

Environmental pollution such as the accumulation of plastic waste is a consequence of global population growth which needs to be addressed. Resource recovery from waste is deemed one of the pillars of transitioning into a circular economy and fulfilling the United Nation's environmental sustainability goals.
Polyhydroxyalkanoates (PHAs) are biodegradable intracellular biopolymers that are synthesized under environmental stress conditions. Having comparable characteristics, PHAs can be an alternative to conventional petrochemical plastics (Sohn et al., 2022). However, their commercial production is yet impeded due to the high costs of substrates, low yields, and downstream processing. Conversion of organic wastes into value-added materials such as PHAs not only presents an opportunity for waste management and resource recovery but can also, decreases the high production costs (Mannina et al., 2020).

Mixed microbial culture (MMC) production of PHAs requires three steps: substrate provision, biomass enrichment, and accumulation (Cakmak et al., 2021). One of the possible ways to increase the desired activity in the existing population of a microbial community is bioaugmentation; which is the introduction of particular consortia or microbial strains in the system (Khatami et al., 2020). In this study, we combined the conventional biomass enrichment for the PHA production process with the bioaugmentation of synthetic cultures of renowned PHA producers over both short (3 and 5 days) and long (161 days) periods, while using municipal waste (food waste and primary sludge) as the cheap substrate.

MATERIALS AND METHODS

LONG TERM EXPERIMENTS
In the long-term experiments, the activated sludge was taken from the Hammarby Sjöstadsverk wastewater facility in Stockholm, Sweden. The biomass was enriched in 5L sequencing batch reactors for 161 days with a cycle length of 12 h, and hydraulic (HRT) and solid retention (SRT) times of 1 day. The effluent of an anaerobic digester treating food waste and primary sludge, rich in volatile fatty acids (VFAs), was used as the substrate. The composition of the VFA effluent was adjusted to maintain the same composition of the feedstock throughout the experiments (Table 1).

Table 1- Composition of the utilized volatile fatty acids as the feedstock

Volatile fatty acid	Percentage (% w/w)
Acetic acid	67
Propionic acid	20
Butyric acid	5
Isovaleric acid	6.5
Valeric acid	0.75
Hexanoic acid	0.75

Each cycle initiated with the replacement of half of the reactor working volume with mineral medium and VFAs broth (2 g L^{-1}). The medium contained: K_2HPO_4 3.2 g/L; KH_2PO_4 1.6 g/L; 0.2 g/L $MgSO_4.7H_2O$ and 5 mM NH_4Cl and 2 ml/L of trace elements. Temperature and pH remained uncontrolled in the reactors. The contents of each bioreactor were continuously stirred. The dissolved oxygen level was kept above 20% through an air pump sparging into each bioreactor.
The wild-type species *Cupriavidus necator* and *Burkholderia cepacia* were grown separately in a minimal medium. These species were bioaugmented (10% v/v) as mono- and co-culture modes in the different MMC bioreactors biweekly throughout the enrichment at the beginning of every other cycle. During the enrichment period, three fed-batch PHA accumulations were performed for 55 h to determine the biopolymer production capacity after 91, 154, and 161 days.

SHORT TERM EXPERIMENTS
In the short-term experiments, three different activated sludges were collected from the aerated tanks of the Hammarby Sjöstadsverk wastewater facility, Käppala, and Henriksdal wastewater treatment plants in Stockholm, Sweden. The biomass was enriched in 2L sequencing batch reactors for only 5 days with a similar substrate, cycle conditions, and the bioaugmentation strategy as the long-term experiments. To comprehend the influence of bioaugmentation over short-term operations, fed-batch accumulations were conducted after 3 days of enrichment for the activated sludge obtained from the Hammarby Sjöstadsverk for 12 h. In the case of sludges taken from Käppala and Henriksdal wastewater treatment plants (WWTPs), two separate fed batches were performed for 48 h after 3 and 5 days of enrichment.

RESULTS AND DISCUSSION

In the long-term experiments, the highest PHA accumulations were obtained in the second fed batch; after 154 days of enrichment and bioaugmentation. Maximum PHA accumulation of 52% (PHA/VSS) was obtained from the *C. necator*-bioaugmented reactor after 52 h, followed by 36% (PHA/VSS) with *B. cepacia*-bioaugmented reactor after 49 h (Figure 1). The maximum PHA accumulation in the control and co-culture reactors were 34% and 28% (PHA/VSS), respectively (Figure 1).
Higher PHA accumulations were obtained from the *C. necator*-bioaugmented reactor in all three fed batches, increasing the PHA production capacity by 29%, 52%, and 53% compared to the control reactor in fed-batch one, two, and three, respectively. Meanwhile, the rate of PHA accumulations was faster in the *B. cepacia*-bioaugmented reactor. By prolonging the enrichment period from 98 to 154 and 161 days, the PHA accumulation capacity did not increase significantly (between 0.2-11 %) taking into account the reactor's operation and costs over longer periods.

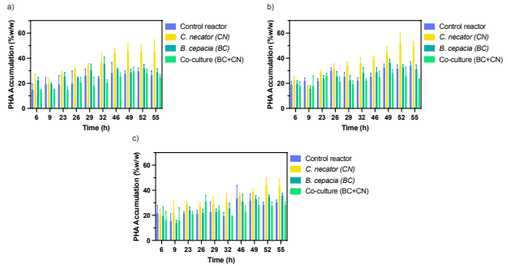

Figure 1-Polyhydroxyalkanoates production in the long-term experiments: fed batches (a) after 91 days of enrichment), (b) after 154 days of enrichment, and (c) after 161 days of enrichment

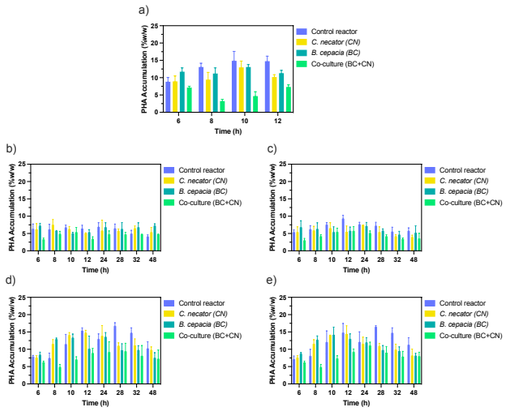

Figure 2-Polyhydroxyalkanoates production in short-term experiments: fed batches (a) after 3 days with activated sludge from the Hammarby Sjöstadsverk, (b) after 3 days of enrichment with activated sludge from the Käppala WWTP, (c) after 5 days of enrichment with activated sludge from the Käppala WWTP, (d) after 3 days of enrichment with activated sludge from the Henriksdal WWTP and (e) after 5 days of enrichment with activated sludge from the Henriksdal WWTP

In the short-term enrichments, the maximum PHA accumulations were acquired from the non-bioaugmented reactor for all the different setups regardless of the origin of the activated sludge (Figure 2). The highest PHA accumulations were 17% PHA/VSS after 28 h in the activated sludge from Henriksdal WWTP. Similar yields were obtained after 3 and 5 days of the enrichment. It is clear that the prolongation of the enrichment and bioaugmentation did not have any impact in the short-term period.

Waste-derived VFAs are suitable carbon sources that can be successfully utilized in MMC PHA production. PHA up to 52% cell dry weight was produced in the *C. necator* bioaugmented bioreactors; increasing approximately 1.6 times the accumulation capacity of the control bioreactors in the long-term enrichment experiments. In the short-term operations, the bioaugmentation did not have any influence on the PHA accumulation capacity of the activated sludges. This can probably be attributed to the short duration, meaning the synthetic cultures were not stabilized by the MMCs. The detailed results and discussions of the PHA production, VFA consumption, and changes in the microbial structure of the MMC will be presented at the conference.

This study indicated the successful influence of the bioaugmentation in MMC PHA production as a robust tool to manipulate the microbial community and to increase PHA production yield.

REFERENCES

Cakmak, E.K., Atasoy, M., Owusu-Agyeman, I., Khatami, K., Cetecioglu, Z., 2021. Circular City Concept for Future Biorefineries, in: Kumar Tyagi,Vinay. Kumar, Manish. Kj An, Alicia. Cetecioglu, Z. (Ed.), Clean Energy & Resource Recovery: Wastewater Treatment Plants Are Biorefineries. Elsevier.
Khatami, K., Perez-Zabaleta, M., Owusu-Agyeman, I., Cetecioglu, Z., 2020. Waste to bioplastics: How close are we to sustainable polyhydroxyalkanoates production? Waste Manag. https://doi.org/10.1016/j.wasman.2020.10.008
Mannina, G., Presti, D., Montiel-Jarillo, G., Carrera, J., Suárez-Ojeda, M.E., 2020. Recovery of polyhydroxyalkanoates (PHAs) from wastewater: A review. Bioresour. Technol. 297, 122478. https://doi.org/10.1016/j.biortech.2019.122478
Sohn, Y.J., Son, J., Lim, H.J., Lim, S.H., Park, S.J., 2022. Valorization of lignocellulosic biomass for polyhydroxyalkanoate production: Status and perspectives. Bioresour. Technol. 360, 127575. https://doi.org/10.1016/j.biortech.2022.127575

Fate of pollutants in overloaded Wastewater Stabilization Pond (WSP) system

Szymon Kilian*, Katarzyna Pawęska* and Aleksandra Bawiec*

* Institute of Environmental Engineering, University of Environmental and Life Sciences, 25 Norwida St. 50-375 Wrocław, Poland
(E-mail: *Szymon.kilian1@upwr.edu.pl; katarzyna.paweska@upwr.edu.pl; aleksandra.bawiec@upwr.edu.pl)*

Keywords
Abundance of biogenic compounds; Internal loading; Wastewater stabilization ponds; Wastewater reuse

INTRODUCTION

One of biggest challenges of our times is constantly growing water stress, induced by global climate crisis [UN - Water, 2019; EEA 2021, 2019]. In Europe in year 2021 the effects of drought and water scarcity affected 20% of its area and 30% of its population [EEA, 12/2021].
According to the European Environmental Agency (EEA) [EEA, 2021], we observe rapid decline in European biodiversity due to global climate change. [EEA, 2021]. Thus, there is a need to implement new solutions to mitigate water stress. EEA indicates Natural Based Solutions (NBS) as recommended solutions for global warming water stress mitigation, and reduction of its fallback on Earths biosphere [Almuktar i inni, 2018; EEA 2021, 01/2021].

Treated wastewater is seen as “endless”, reliable source of water, and as they contain number of organic material and biogenic compounds, they could also help limit usage of fertilizers.
One of possible NBSs consistent with Regulation EU 2020/741 goals are Waste Stabilization Ponds (WSPs). Wastewater stabilization ponds are widely described in literature [EPA, 2011; Butler i inni, 2017; Ratsey, 2017] However, there is lack of research done about WSPs in Central Europe climate conditions.
Researchers indicate that there is wide possibility of water reuse from wastewater, although there is need for solutions that would allow feasible fit-for-purpose treatment of wastewater, transportation, and storage of treated, ready for reuse wastewater [Ungureanu, Vlăduț i Voicu 2020; Hristov i inni, 2021; Hashem, Qi, 2021]. Wastewater stabilization ponds give good perspective for wastewater reuse, for crops irrigation, taking into account listed above limitations [Ungureanu, Vlăduț i Voicu 2020; Hristov i inni, 2021; Hashem, Qi, 2021].

MATERIALS AND METHODS

Scope of this paper is to evaluate changes of biogenic compounds concentrations in two stage waste stabilization pond (WSP) system, located in Sobótka wastewater treatment plant (WWTP). Sobótka is city located in lower Silesia voivodship. WWTP spatial plan is shown in Fig.1.

Sampling campaigns were carried out from 06.05.2021 to 14.10.2022, in month intervals (16 sampling campaigns). During sampling campaign samples were collected from sampling points shown on Fig.1 to 1.5L polyethylene containers and analysed in Environmental Engineering Institute Laboratory of Environmental Research using methods shown in Table.2.

Fig.1 Spatial plan of Sobótka WWTP

Table.2 Parameters and methods used in this research.

Parameter	Method
Nitrate nitrogen (N-NO_3^-)	Spectrophotometric method: PN-82C-04576/08
Ammonium nitrogen (N-NH_4^+)	Spectrophotometric method: PN-ISO 7150:2002
Nitrite nitrogen (N-NO_2^-)	Spectrophotometric method: PN-EN 26777:1999
Phosphates (P-PO_4)	Spectrophotometric method: ISO 6878/1:2006
pH	Potentiometric method: PN-90/C-04540.01
Turbidity	Nephelometric method: PN-EN ISO 7027-1:2016-09
Dissolved Oxygen (DO)	Insitu measurments (portable oxygen meter with galvanic probe)
Total Organic Carbon (TOC)	Supercritical Water Oxidation (SCWO) method, laboratory device TOC analyzer Sievers InnovOx by GE Analytical Instruments
Total suspended solids (TSS)	Weight method: PN-EN 872:2007

RESULTS

WSP system consist of two ponds, area of first pond is 0.47 ha and second pond area 1.35 ha, depth of both ponds is 1.1 m. Approximated HRT (Hydraulic Retention Time) of this WSP system is 8 days. As result of malfunction WSP I was skipped in treatment process and treated sewage from WWTP were directed directly into the WSP II in period 18.05.2021 to 26.07.2021 (Fig.1).
Performed statistical tests shown no difference on statistical importance level between sampling points on both waste stabilization ponds. As for turbidity and N-NO_3 differences between sampling points are on statistical importance level.
Ammonium nitrogen shows seasonal trends. With its maximal values in summer months (August 2021 – median 35.64, July 2022 – median 42.57, August 2022 -median 42.86), and minimal values in autumn and winter (November 2021– median 8.90, March 2022– median 6.28) (Fig.2).
Phosphates just like ammonium nitrogen shows seasonal trends, with maximal values in summer months. With their median values in July 2021 4.63 mg/dm^3 and 6.80 mg/dm^3 in July 2022. And minimal median values in January 2022 0.89 mg/dm^3 and after summer peak in October 2022 with median 2.29 mg/dm^3 (Fig.2). TOC concentrations raised at the beginning of sampling campaign as result of WWTP malfunction (Fig.3). Turbidity shows seasonal trends, as it raises in summer months, as result of raising sediments and WWTP malfunction (Fig.3).

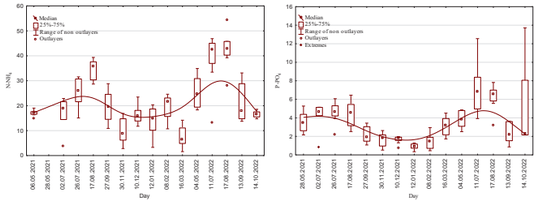

Fig. 2 Seasonal changes of ammonium nitrogen (N-NH_4) and phosphates (P-PO_4) in WSP treatment pond system

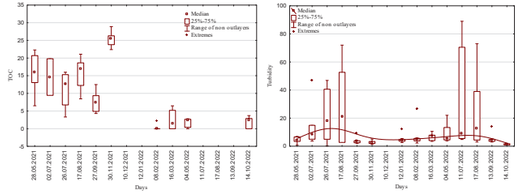

Fig.3 Seasonal changes of Total Organic Carbon (TOC) and turbidity in WSP treatment pond system

DISCUSSION

During sampling campaign at day 28.05.2021r. foamed activated sludge flowed out to the WSP I, and covered its surface with blanket like structure over sampling points no. 3 and 4. Created structure settled down in next few days. In seasons with higher temperatures, settled parts of “activated sludge blanked” emerged to the surface again.
Increased biological activity during spring and summer months connected with overload of organic material from WWTP malfunction depletes dissolved oxygen. Which changes redox potential, allowing reduction of compounds in sediments to dissolvable forms (internal loading), and intensification of methanogenic decomposition of organic matter [Søndergaard, Jensen, Jeppesen, 2001; EPA, 2011; Keffala, 2011; Butler i inni. 2017; Augustyniak i inni, 2017]. Moderate positive correlation between N-NH_4 and P-PO_4; moderate correlation between N-NH_4, P-PO_4 and temperature. High negative correlation between TOC and DO, high negative correlation between DO and mean temperature. All those correlations, and sampling point observations support occurrence of internal loading with methanogenic decomposition.
Due to described phenomenon’s there is degradation in quality of treated wastewater on ponds in terms of biogenic compounds due to processes described above. Although there is improvement in terms of turbidity and TSS due to the buffer capacities of ponds.

CONCLUSIONS

- Main factor shaping changes of phosphates concentrations (and thus, total phosphorus concentrations) in WSPs is phenomenon called internal loading in the period of biggest biological activity. Correlation between biological activity and temperature indicates seasonality of internal loading.
- Main source of ammonium nitrogen in ponds is effluent from WWTP. Although in period of increased biological activity, internal loading with methanogenic decomposition elevates ammonium nitrogen concentrations.
- Changes in N-NO_2 and N-NO_3 nitrogen forms is in line with the nitrification and denitrification intensity described by other researchers.
- Thanks to buffer capacities of WSPs limit shifts in quantity and quality of treated effluent, in case of turbidity and TSS there is improvement in quality of final effluent in comparison to WWTP effluent.

REFERENCES

Almuktar A, S.N., Scholz, M. 2018 Wetlands for wastewater treatment and subsequent recycling of treated effluent: a review, *Environmental Science and Pollution Research* **25**, 23595-23623
Augustyniak R., Neugebauer M., Kowalska J., Szymański D., Wiśniewski G., Filipkowska Z., Grochowska J., Łopata M., Parszuto K., Tandyrak R. 2017 Bottom deposits of stratified, seepage, urban lake (on the example of Tyrsko lake, Poland) as a factor potentially shaping lake water quality. *Journal of Ecological Engineering* **18** Issue 5, 55–62
Butler.E., 2017 Oxidation Pond for municipal wastewater treatment, *Applied Water Science, Springer* **7**, 31-51
EEA. 01/2021 Nature-based solutions in Europe: Policy, knowledge and practice for climate change adaptation and disaster risk reduction
EEA. 12/2021 Water resources across Europe — confronting water stress: an updated assessment
EEA. 2019 Climate change adaptation in the agriculture sector in Europe
EEA. 2021, Signals – Europe’s nature
Hashem M., Qi X. 2021 Treated Wastewater Irrigation—A Review *Water* **13**, 1527
Hristov J., Barreiro-Hurle J., Salputra G., Blanco M., Witzke P. 2021 Reuse of treated water in European agriculture: Potential to address water scarcity under climate change. *Agricultural Water Management* **251**, 106872
Ratsey H., 2017 Understanding oxidation ponds. Is dissolved oxygen profiling the key? *The Wastewater Specialists*,
Søndergaard, M., Jensen, J.P., Jeppesen, E. 2001 Retention and internal loading of phosphorus in shallow, eutrophic lakes. *The Scientific World* **1,** 427–442
Ungureanu N., Vlăduț V., Voicu G. 2020 Water Scarcity and Wastewater Reuse in Crop Irrigation. *Sustainability* **12**, 9055
United States Environmental Protection Agency (EPA) 2011 Principles of design and operations of wastewater treatment pond systems for plant operators, engineers, and managers
UN-Water Expert Group on Water and Climate Change, 2019 Climate Change and Water, UN-Water Policy Brief,

Effect of extracellular polymeric substances (EPS) content on sludge dewaterability using filter-press

S. J. Lee*, J. H. Kim**, H. Y. Choi*, S. G. Kim* and I. G. Byun***

* School of Civil and Environmental Engineering, Pusan National University, 2, Busandaehak-ro 63beon-gil, Geumjeong-gu, Busan, Republic of Korea (E-mail: *tnwls172@pusan.ac.kr, gydud9270@pusan.ac.kr, ksg584875@gmail.com*)
** School of Civil and Environmental Engineering, Pusan National University, 2, Busandaehak-ro 63beon-gil, Geumjeong-gu, Busan, Republic of Korea (E-mail: *hyeon@pusan.ac.kr*)
***Institute for Environment and Energy, Pusan National University, 2, Busandaehak-ro 63beon-gil, Geumjeong-gu, Busan, Republic of Korea (E-mail: *big815@pusan.ac.kr*)

Abstract
As the amount of sewage sludge continues to increase, sludge volume reduction through dewatering is essential. In sludge dewatering, EPS (Extracellular Polymeric substance) is known as a parameter that inhibits sludge dewatering. To evaluate the effect of EPS on the dewaterability of the sludge, two types of digested sludge (sewage sludge alone and sewage sludge mixed with food wastewater) were dewatered by the filter press method. As a result, the concentrations of LB-EPS and TB-EPS in the digested sludge of 'S' WWTP were lower than those of 'N' WWTP. In addition, as a result of filter press dehydration, the discharge rate of the dewatering filtrate of 'S' WWTP was faster than that of 'N' WWTP, and the water content after 30 minutes of dehydration was about 76%, which was lower than that of 'N' WWTP. It was confirmed that the higher the EPS content, the lower the dewatering.

Keywords: Dewaterability of sludge; Extracellular polymeric substances; Filter press

INTRODUCTION

According to domestic sewerage statistics in South Korea, the annual amount of sludge generated by sewage treatment plants is 4.22 million tons, a 71.7% increase over the past 10 years. As the amount of sewage sludge generated continues to increase every year, considerably high coasts are being spent on sludge treatment due to the limitation of sludge treatment capacity of local governments. In order to reduce sewage sludge treatment costs, sludge reduction is essential. Accordingly, many studies are being conducted to improve sludge dewatering.

Many studies have shown that the characteristics of extracellular polymeric substances (EPS) play an important role in the sewage sludge dewaterability. EPS is composed of a variety of organic substances including carbohydrates and proteins as the major constituents and humic substances, uronic acids and nucleic acids in smaller quantities. There are not many analyses on the EPS effect on dewaterability of digested sludge [1]. In addition, there is a possibility of EPS accumulation due to aboudant microbial residues in the organic waste digestive fluid after digestion [2].

In this study, we compared and analyzed the digested sludge of the two WWTPs to confirm the relationship between EPS content and dewaterability.

MATERIALS AND METHODS

Material

The sludge samples was collected from the 'N', 'S' wastewater treatment plant (WWTP) in the Busan, South Korea. In case of "S" WWTP, food waste and process water are mixed in a ratio of 1:4, and treated food wastewater and sewage sludge are mixed in a ratio of 1:5. Table 2-1 shows the characteristics of sludge samples.

Experimental procedure

Prior to the experiment, sludge conditioning was conducted by a jar test and conditioned using following procedure: (1) Coagulants addition (PAC, 100 mg/g TS), (2) 200 rpm stirring for 1 min, (3) 50 rpm stirring for 10 min.
After conditioning, 300 mL of digested sludge was injected into the filter press device, and the compression pressure was 1 MPa.

Table 2-1. Characteristics analysis results of WWTPs sludge.

Samples		pH	TCOD (mg/L)	T-N (mg/L)	T-P (mg/L)	VS/TS (%)	Water content (%)
"S" WWTP	Mixed sludge	5.15 ± 0.03	32,536 ± 5235	904 ± 175	469 ± 98	75.73 ± 6.03	96.45 ± 0.06
	Digested sludge	6.95 ± 0.03	17,929 ± 458	1,534 ± 92	586 ± 42	46.50 ± 3.61	98.27 ± 0.01
"N" WWTP	Mixed sludge	5.61 ± 0.06	29,098 ± 5,894	1,328 ± 806	672 ± 201	94.95 ± 6.82	96.19 ± 0.01
	Digested sludge	7.08 ± 0.02	31,443 ± 3,355	2,368 ± 325	1,040 ± 74	40.58 ± 5.40	97.42 ± 0.01

EPS extraction

A thermal method was used to extract different fractions of sludge EPS. In this case, two types of EPS were separated: the loosely bound EPS (LB-EPS) and the tightly bound EPS (TB-EPS). The first one was extracted by adding an 0.05% NaCl buffer solution at 70°C and mixing it for 1 min. After the mixture was centrifuged, the tightly bound EPS was extracted by adding an 0.05% NaCl buffer solution at room temperature and placed in a water bath at 60 °C for 30 min.

Analysis

TCOD, SCOD, TS, and VS were analyzed according to Standard Methods. Total A polysaccharide (PS) was analyzed using the phenol-sulfuric acid method. Glucose was used as standard. Protein (PN) was determined to used Protein Kit (Sigma-Aldrich, TP 0330) based on Lowry's description, but modified by Peterson. The Kit includes a standard solution. For the determination of absorbance, a spectrophotometer (K-LAB, Optizen pop) was used. The pH was measure using a pH meter (HI 9124, HANNA, USA).

RESULTS AND DISCUSSION

Concentration change of mixed-disgested sludge

Table 3-1 shows the measured SCOD and extracted EPS content of proteins (PN), polysaccharide (PS) from two WWTPS of digested sludge. After mixed sludge digestion in 'S' WWTP, the removal rates of SCOD and TS were about 97% and 51%, respectively, and the removal rates in 'N' WWTP were about 78% and 32%, respectively. As a noteworthy feature, the concentrations of PN and PS in the thickened sludge of the 'S' WWTP were higher than those of the 'N' WWTP, and the concentrations of PN and PS in the digested sludge were lower in the 'S' WWTP than in the 'N' WWTP.

The concentrations of SCOD, PN, PS, and VS of the food wastewater (FWW) of 'S' WWTP were 94,721, 130,783, 11,791 and 151,291 mg/L, respectively, indicating a high biodegradable organic matter content. Many studies have reported that food wastewater is suitable for use as a common substrate for digesters due to its high biodegradable organic matter content [3]. Therefore, it is believed that the high PS and PN concentrations of 'S' WWTP are due to the soluble carbohydrates and proteins derived from FWW. The higher removal efficiency of SCOD and TS of the 'S' WWTP indicates a higher efficiency of the digester.

Table 3-1. Organic content of WWTPs sludge.

Samples		SCOD (mg/L)	VS (mg/L)	TS (mg/L)	PN (mg/L)	PS (mg/L)
"S" WWTP	Mixed sludge	10,957 ± 510	26,887 ± 2,574	35,475 ± 556	979 ± 46	9,218 ± 1,403
	Digested sludge	289 ± 8	8,016 ± 611	17,275 ± 63	179 ± 10	57 ±2
"N" WWTP	Mixed sludge	2,389 ± 14	36,130 ± 2,592	38,053 ± 116	751 ± 95	201 ± 69
	Digested sludge	532 ± 32	10,474 ± 1,357	25,820 ± 102	257 ±12	127 ± 36

Concentration change of LB-EPS and TB-EPS

Figure 3-1 shows the concentrations of LB-EPS and TB-EPS in the digested sludge of the two WWTPs. The concentrations of LB-EPS and TB-EPS in the digested sludge of 'S' WWTP were lower than that of 'N' WWTP. In previous studies, the concentrations of LB-EPS and TB-EPS tended to gradually decrease with the increase of HRT in the early stage of digestion (1–17 days). The contents of PN and PS were decreased by the activity of hydrolase and the growth of bacteria decomposing organic matter. In 'S' WWTP, it is judged that the digester efficiency was high by FWW, so the reduction of PN and PS contents was more pronounced.

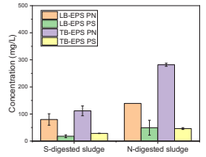

Figure 3-1. EPS content extracted from two WWTPs of digested sludge.

Dewaterability evaluation

Figures 3-2 and 3-3 shows the water content and filtrate discharge rate measured by the filter press system for two types of digested sludge. The rate of discharge of dewatering filtrate in 'S' WWTP was faster than that of 'N' WWTP, and the water content after 30 minutes was about 76%, which was lower than that of 'N' WWTP.

It is known that high EPS content can trap water molecules inside the EPS floe, increasing polymer demand and reducing dehydration [4]. This is because when the content of LB-EPS or TB-EPS is high, the relative hydrophilicity of the digestive fluid is strengthened by generally covering the bound water, resulting in low dehydration and coagulation effects [5].

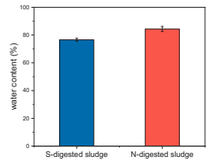

Figure 3-2. Water content of two type of digested sludge according to filter press system dewatering.

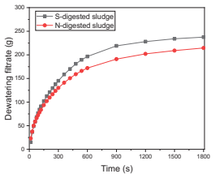

Figure 3-3. Cumulative dewatering filtrate amount of two types of digested sludge using filter press system.

CONCLUSION

The results of EPS extraction and dewaterability evaluation by two WWTPs of digested sludge are as follows. The concentrations of LB-EPS and TB-EPS in the digested sludge of 'S' WWTP were lower than those of 'N' WWTP. In addition, as a result of filter press dehydration, the discharge rate of the dewatering filtrate of 'S' WWTP was faster than that of 'N' WWTP, and the water content after 30 minutes of dehydration was about 76%, which was lower than that of 'N' WWTP. It was confirmed that the higher the EPS content, the lower the dewatering.

ACKNOWLEDGMENTS

This work supported by the Korea Environment Industry & Technology Institute (KEITI) through the Development of Demonstration Technology for Converting Unconventional Waste Biomass to Energy, funded by the Korea Ministry of Environment (MOE) (2022003480001).

REFERENCES

[1] Comte, S., Guibaud, G., & Baudu, M. (2006). Relations between extraction protocols for activated sludge extracellular polymeric substances (EPS) and EPS complexation properties: Part I. Comparison of the efficiency of eight EPS extraction methods. *Enzyme and microbial technology*, *38*(1-2), 237-245.
[2] Lü, F., Hao, L., Guan, D., Qi, Y., Shao, L., & He, P. (2013). Synergetic stress of acids and ammonium on the shift in the methanogenic pathways during thermophilic anaerobic digestion of organics. *Water research*, *47*(7), 2297-2306.
[3] Xu, R., Yang, Z., Chen, T., Zhao, L., Huang, J., Xu, H., ... & Li, M. (2015). Anaerobic co-digestion of municipal wastewater sludge with food waste with different fat, oil, and grease contents: study of reactor performance and extracellular polymeric substances. *Rsc Advances*, *5*(125), 103547-103556.
[4] Liang, J., Luo, L., Li, D., Wang, H., & Wong, J. W. (2022). Conductive materials supplement alters digestate dewaterability during anaerobic co-digestion of food waste and sewage sludge and promotes follow-up indigenous peroxides activation. *Chemical Engineering Journal*, *431*, 133875.
[5] Xie, S., Higgins, M. J., Bustamante, H., Galway, B., & Nghiem, L. D. (2018). Current status and perspectives on anaerobic co-digestion and associated downstream processes. *Environmental Science: Water Research & Technology*, *4*(11), 1759-1770.

Temperature effect over the PHA:TAG accumulation ratio with mixed microbial cultures and oily substrates

J.R. Lorenzo-Llarena*, J. García-González*, D. Correa-Galeote**, B. Rodelas**, A. Val del Rio*, A. Pedrouso*, A. Mosquera-Corral*

* Department of Chemical Engineering, CRETUS Institute, School of Engineering, Universidade de Santiago de Compostela, Rúa Lope Gomez de Marzoa, E-15782. Santiago de Compostela, Spain. (E-mail: *joseramon.lorenzo.llarena@usc.es; jennifergarcia.gonzalez@usc.es*; *mangeles.val@usc.es; alba.pedrouso@usc.es*; *anuska.mosquera@usc.es*)

** Microbiology Department, Faculty of Pharmacy and Institute of Water Research, University of Granada, Granada, 18071, SP.(E-mail: *dcorrea@ugr.es; mrodelas@ugr.es)*

Abstract

Two enrichment units with mixed microbial cultures (MMCs) were operated: R1 fed with oleic acid and R2 fed with the oily fraction of a fish-canning industry effluent from canned tuna. The reactors operated stable at 30 ºC for more than 60 days and then the temperature was increased to 35 ºC, to favour the hydrolysis of the oily substrates. This increase of temperature did not change the main characteristics of the reactor's effluent in terms of pH value and soluble COD. However, the ratio PHA:TAG changed from 77:23 to 9:91 in R1 and from 74:26 to 6:94 in R2, indicating that the increase of the temperature promotes the preferential growth of TAG producers over PHA ones.

Keywords

Biopolymers; enrichment; fat oil and grease; mixed microbial culture; waste; temperature.

INTRODUCTION

The fat, oil and grease (FOG) fraction present in wastewater is difficult to treat by conventional biological processes and for this reason it is normally separated in a first step in wastewater treatment plants (WWTPs), either municipal or industrial (Wallace et al., 2017; Frkova et al., 2020). This separated FOG fraction can then be valorised to obtain biopolymers like polyhydroxyalkanoates (PHA) and/or triacylglycerides (TAG). These biopolymers can be intracellularly accumulated by certain microorganisms using as carbon source the FOG fraction (Argiz et al., 2021). Normally the production of biopolymers by mixed microbial cultures (MMCs) requires two units: a first reactor to promote the enrichment of the MMC with the ability to accumulate PHA and a second reactor to maximize the accumulation of the biopolymers. Therefore, an adequate enrichment is crucial to have high accumulation percentages. In the case to use the FOG fraction as carbon source the uptake of the substrate by the accumulating microorganisms can be limited by its hydrolysis. As it is well known the increase of the temperature favours the hydrolysis of FOG compounds, however little is known about the effect over the microorganisms and their ability to accumulate preferentially PHA and/or TAG. Therefore, the objective of the present research work is to understand how an increase in the operational temperature from 30 to 35 ºC affects the process in two different enrichment units: one fed with a synthetic medium (oleic acid) and other fed with an industrial FOG residue.

MATERIALS AND METHODS

Two enrichment laboratory sequencing batch reactors (SBRs), R1 and R2, with a useful volume of 4 L were used for the experiments. The SBRs were fed with different oily carbon sources: R1 with oleic acid and R2 with the oily fraction of the industrial effluent from tuna cookers. These reactors were operated under the feast/famine (F/F) regime, in cycles of 12 hours and with the enrichment double growth limitation (DGL) strategy via separated C and N feedings. At the beginning of the cycle half of the volume (2 L) was removed and replaced by a single pulse of new culture media containing the carbon source (1.28 g COD/L in R1 and 0.83 g COD/L in R2). After 5 hours nitrogen source was introduced in the form of ammonium chloride (26 mg NH_4^+-N/L). The hydraulic and solids retention times (HRT and SRT) were of 24 h. Both SBRs operated stable at 30 ºC for more than 60 days and then the temperature was raised at 35 ºC.

RESULTS AND DISCUSSION

In both enrichment units (R1 and R2) the increase of the temperature neither affect the soluble COD concentration nor the pH value in the reactor's effluent, with values around 200-300 mg COD/L and 6.2-6.4, respectively. However, in R1 the nitrogen concentration increased from values close to zero (at 30 ºC) to 10 mg N/L (at 35ºC) indicating a decrease in the nitrogen consumption and, consequently, in the microbial growth. While in R2 the nitrogen concentration remained close to zero at both temperatures, except in punctual days when it reached values of 5-10 mg N/L. In this reactor after the increase of temperature to 35 ºC, an increase of the substrate's hydrolysis was observed in the first minutes after the carbon source feeding, as the soluble COD concentration rose up from 116,66 ± 3,93 to 169,43 ±3,93 mg/L. This increase was not observed at 30 ºC. In R1 the increase of soluble COD after carbon source addition was not observed neither at 30 nor at 35 ºC.

The improvement of the hydrolysis of the substrate resulted in a slight increase of the amount of active biomass and the percentage of compounds accumulated (Table 1). The active biomass raised in both systems; however, it was less significative in the case of R1, which correlates with the lower nitrogen consumption at high temperature. The maximum PHA storage capacity of the MMC increased in R1 from 34% to 41% and in R2 from 39 to 41%, at 30 and 35 ºC, respectively. Regarding the moment in which the maximum storage occurred (Figure 1) in R1 it was after 5 hours of carbon source feeding at both temperatures, that corresponds with the moment of nitrogen source addition. However, in R2 the maximum storage takes place at 4 and 2 hours for 30 and 35 ºC, respectively. The shorter feast phase in R2 can be correlated with the lower COD addition in the feeding and the higher amount of active biomass in comparison with R1. Regarding the compounds accumulated over the 12 hours of cycle in the enrichment units (Figure 1) the increase of temperature from 30 to 35 ºC promoted a higher accumulation of TAG in detriment of PHA (Table 1). The results showed that the PHA:TAG ratio changed from 77:23 to 9:91 in R1 and from 74:26 to 6:94 in R2. Despite that at 35 ºC the production of PHA is lower it is important to highlight that the ratio PHB:PHV changed (Table 2) and that the temperature increase favoured the production of PHV, which can be desirable for some PHA applications. Finally, despite using two different carbon sources (synthetic oleic vs industrial FOG waste) the behaviour of both enrichment units with the increase of the temperature was similar, mainly regarding the ratio of PHA:TAG accumulated, which indicates that the operational parameters, instead of the carbon source, can drive the preferent compound accumulated.

ACKNOWDLEGMENTS

This research was supported by the Spanish Government (AEI) through ECOPOLYVER (PID2020-112550RB-C21) and POLYGO1 (TED2021-130164B-I00) projects. Alba Pedrouso also acknowledges the Xunta de Galicia (Spain) for her postdoctoral fellowship (ED481B-2021-041). The authors belong to a Galician Competitive Research Group (GRC ED431C 2021/37), programme co-funded by FEDER (UE).

REFERENCES

Wallace, T., Gibbons, D., O'Dwyer, M., Curran, T.P. 2017. International evolution of fat, oil and grease (FOG) waste management: A review. *J. of Environmental Management.* **187**, 424-435.

Frkova, Z., Venditti, S., Herr, P., Hansen, J. 2020. Assessment of the production of biodiesel from urban wastewater-derived lipids. *Resources, Conservation and Recycling* **162**, 105044.

Argiz, L., González-Cabaleiro, R., Val del Río, A., González-López, J., Mosquera-Corral, A. 2021. A novel strategy for triacylglycerides and polyhydroxyalkanoates production using waste lipids. *Science of The Total Environment*, **763**(1), 142944.

Table 1. Summary of the accumulation of PHA and TAG in both SBRs at different temperatures.

	30 ºC	35 ºC
R1		
Active biomass (g/L)	0.14	0.16
Max. accumulation (%)	34.03	40.83
PHA:TAG	77:23	9:91
PHB:PHV	98:2	60:40
PALM:EST:OLE:LINO	13:5:77:5	0:1:92:7
R2		
Active biomass (g/L)	0.35	0.45
Max. accumulation (%)	38.6	41.2
PHA:TAG	74:26	6:94
PHB:PHV	95:5	55:45
PALM:EST:OLE:LINO	10:23:51:16	10:3:71:16

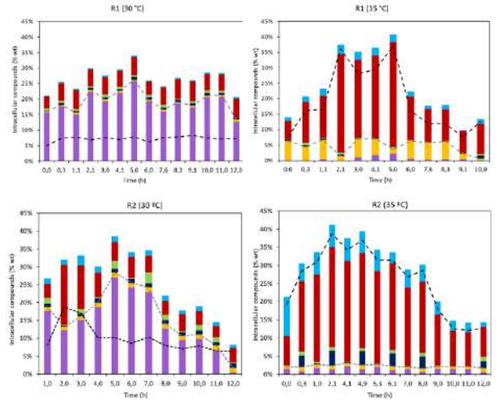

Figure 1. Profiles of intracellular compounds in R1 and R2 throughout a cycle of enrichment carried out at different temperatures. Percentage of intracellular TAG **(- - -)** and PHA (- - -) in the biomass. Composition expressed in percentages of PHB (■), PHV (■), palmitic acid (■), stearic acid (■), oleic acid (■) and linoleic acid (■).

Impact of high-rate activated sludge system on WWTP energy balance: Effect of HRT and dissolved oxygen

C. Martín-Medrano*, L. González-Gil**, J. M. Lema* and M. Carballa*

* CRETUS, Department of Chemical Engineering, Universidade de Santiago de Compostela, 15782 Santiago de Compostela, Spain (E-mail: cinta.martin.medrano@usc.es; juan.lema@usc.es; marta.carballa@usc.es)
** Defense University Center, Spanish Naval Academy, Plaza de España, 36920, Marín, Spain (E-mail: lorena.gonzalez@cud.uvigo.es)

Abstract
Next generation wastewater treatment plants (WWTPs) have to deal with energy scarcity. High-rate activated sludge (HRAS) processes produce higher amounts of sludge than conventional activated sludge systems, thus they offer an opportunity to increase the production of biomethane. The objective of this study is to find the operational conditions able to recover a higher fraction of organic matter into sludge to later determine the energy savings in comparison to conventional WWTPs. With this purpose, two HRAS reactors were operated at two levels of dissolved oxygen (DO), respectively, and four hydraulic retention times (HRT), keeping the sludge retention time at 4 d. Results suggest that low levels of DO do not impair the recovery of organic matter, and decreasing the HRT might slightly reduce the total removal of organic matter but not the recovered fraction, which was around 30% at a HRT of 8 h.

Keywords
Biomethane, COD mass balance, energy recovery, high-rate activated sludge, wastewater

INTRODUCTION

High-rate activated sludge (HRAS) processes are considered as an opportunity to transform the wastewater treatment plants (WWTPs) paradigm from energy consumers into producers, or at least self-sufficient facilities. Its main advantages, in comparison to the conventional activated sludge system, are the lower energy consumption in terms of aeration, no need of primary clarifier and the higher sludge production that can be anaerobically digested and converted into biomethane (Carrera et al., 2022). Therefore, HRAS should be operated under conditions that allow to meet the standards of effluent quality, but also a high production of sludge. To achieve both objectives the fraction of organic matter removed by oxidation into CO_2 should be restricted in benefit of a higher recovery into sludge. This study aims to determine the optimal conditions of dissolved oxygen (DO) and hydraulic retention time (HRT) that maximize the fraction of organic matter recovered into sludge. This will allow us to determine the energy savings of a WWTP configuration with a HRAS system in comparison with a conventional WWTP.

MATERIALS AND METHODS

Description and operational conditions of the HRAS units

Two HRAS lab-scale systems (2 L reactor + 1 L sedimentation tank) were inoculated with biomass from a conventional activated sludge reactor and operated for ~ 5 months at room temperature, which varied between 18 and 23 ºC. The sludge retention time (SRT) in both HRAS reactors (R1 and R2) was kept at around 4 d. Aeration was monitored and controlled so that the reactors operated at two different levels of DO, as shown in Figure 1. The 5-month operation of each HRAS system was divided in 4 periods with different HRT (12 h, 8 h, 4 h and 2 h) to assess the effect of this parameter and DO in COD recovery (Figure 1).

The biological reactors were continuously fed with real wastewater, taken from the municipal WWTP of Santiago de Compostela (Spain) after the pretreatment step (just before entering the primary clarifier). Due to dilution during rainy periods, a synthetic concentrate was additionally added to ensure a minimum COD concentration of 400 mg O_2/L (Table 1).

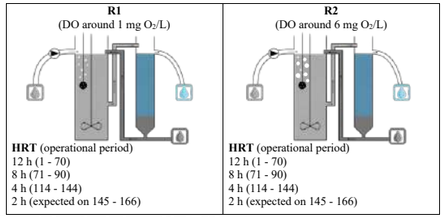

Figure 1. Operational scheme of the HRAS reactors

Table 1. Composition of the synthetic concentrate.

Compounds	mg/L
Sodium acetate ($CH_3COONa \cdot 3H_2O$)	84
Acetic acid (CH_3COOH)	36.2
Yeast extract	63.5
Ammonium chloride (NH_4Cl)	120.6
Potassium dihydrogen phosphate (KH_2PO_4)	6

Analytical methods

The reactor performance was monitored twice per week in terms of pH, TS, VS, TSS, VSS, COD, NH_4^+, NO_2^- and NO_3^- collecting samples from the influent and effluent and analysing them according to the Standard Methods by triplicate. Sludge from the purge and samples from the reactor were characterised every week in terms of TSS and VSS. Temperature and pH were daily monitored inside the reactor while DO was continuously monitored.

Calculations

Sludge purge flowrate was controlled daily to achieve a SRT of 4 days according to Table 2. The COD recovery and the COD mass balance (Table 2) was calculated in a five-day period assuming a ratio of 1.42 kg O_2/kgVSS (Carrera et al., 2022).

In order to address the implication of a HRAS system on energy recovery of a WWTP, an energy balance is conducted on an innovative WWTP scheme (HRAS + partial nitritation-anammox) in comparison with the conventional WWTP (primary clarifier + conventional activated sludge). Moreover, the influence of operational parameters, such as HRT or DO, on this energy balance is assessed.

Table 2. Definition and calculation of the COD mass balance and SRT.

COD in the influent (COD_{inf})	$mCOD_{inf} = Q_{inf} \cdot tCOD_{inf}$
COD in the effluent (COD_{eff})	$mCOD_{eff} = Q_{eff} \cdot tCOD_{eff}$
COD recovered (COD_{rec})	$mCOD_{rec} = \left(\sum Q_{sl} \cdot VSS_{sl} + \sum Q_r \cdot VSS_r\right) \cdot \frac{1.42\ mg\ O_2}{1\ mg\ VSS}$
COD balance	$mCOD_{inf} = mCOD_{eff} + mCOD_{ox} + mCOD_{rec}$

$$SRT = \frac{V_{reactor} \cdot VSS_{reactor}}{Q_{purge} \cdot VSS_{purge} + Q_{effluent} \cdot VSS_{effluent}}$$

m: mass flow rate (mg O_2/d); *Q*: volumetric flow rate (L/d); *tCOD*: total COD concentration (mg O_2/L); *sl*: sludge purge; *r*: reactor sampling

RESULTS

HRAS performance

The first two operational periods were carried out at a HRT of 12 h and 8 h. The third campaign (HRT 4 h) is ongoing and will be followed by the fourth and last period with an HRT of 2 h, which is expected to be finished by the end of February. From day 40 (Figure 2), real sewage was mixed with the synthetic concentrate due to the low COD observed during the previous rainy days. Therefore, from that moment 70-90% of the tCOD was soluble.

A stable operation was achieved in both reactors during the first two operational periods, reaching total and soluble COD removals of 80 – 90% and 75 – 95%, respectively, in both reactors (Figure 2). pH values varied between 6.5 – 7.5 and low nitrification values were observed through the operation (<1% NO_3^- and <5% NO_2^-). VSS were maintained during the first operational period at 1200 and 1500 mg/L in R1 and R2, respectively. During the second period, biomass concentration increased up to 1800 and 2400 mg/L in R1 and R2.

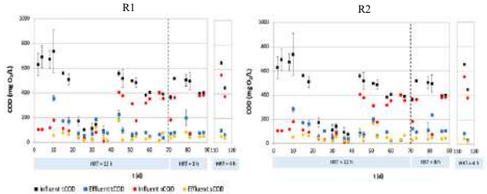

Figure 2. Total (t) and soluble (s) COD concentrations in influent and effluent on both reactors during the different operational periods.

Effect of HRT and DO in COD recovery

Figure 3 shows the distribution of the total COD among the different fractions at each operational period. During the first period (HRT = 12 h), DO seems to be a key parameter in COD recovered as sludge. Although a higher aeration appears to slightly increase COD removal from 87% in R1 to 93% in R2, this COD is not recovered but mineralised, as COD recovery decreases from 34% to 18%, respectively. During the second period of operation (HRT = 8 h), DO does not have a clear effect on COD recovery (27% in R1 versus 32% COD in R2). Therefore, these results suggest that higher DO levels in HRAS systems do not have a positive impact on COD recovery or COD removal.

Concerning the effect of HRT, it was observed that lower COD eliminations were achieved when reducing the HRT in both reactors (i.e., higher COD values were measured in the effluent, Figure 3). This might be due to biomass inability to completely metabolise the organic matter at such rate. The data from the next two operational periods will contribute to confirm these preliminary conclusions regarding the effect of HRT and DO on the COD recovery.

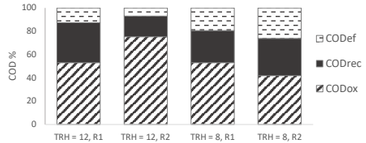

Figure 3. COD distribution (effluent, recovered into sludge and oxidized) in each operational period.

ACKNOWLEDGMENTS

This research was supported by the Spanish Research State Agency (AEI) through ANTARES (PID2019–110346RB-C21) project.

REFERENCES

Canals, J., Tor, J., Martin, M., Poch, M., & Ord, A. (2023). *High-rate activated sludge at very short SRT : Key factors for process stability and performance of COD fractions removal*. *231*(January).

Carrera, J., Carbó, O., Doñate, S., Suárez-Ojeda, M. E., & Pérez, J. (2022). Increasing the energy production in an urban wastewater treatment plant using a high-rate activated sludge: Pilot plant demonstration and energy balance. *Journal of Cleaner Production*, *354*(April).

Jimenez, J., Miller, M., Bott, C., Murthy, S., De Clippeleir, H., & Wett, B. (2015). High-rate activated sludge system for carbon management - Evaluation of crucial process mechanisms and design parameters. *Water Research*, *87*, 476-482.

Evaluation of the potential of carbon recovery from sewage sludge plus organic wastes by anaerobic co-fermentation in a region

M. Mauricio-Iglesias[1], M. L. Pérez Araújo[1], Iván Rodríguez-Verde[2], G. Corregidor-Garcia[1,2], J.M. Lema[1] and M. Carballa[1]

[1] CRETUS, Department of Chemical Engineering, Universidade de Santiago de Compostela, r/ López Gómez de Marzoa, Santiago de Compostela, ES
E-mail: miguel.mauricio@usc.es; marialuisaperez.araujo@usc.es; gabriel.corregidor@rai.usc.es; juan.lema@usc.es; marta.carballa@usc.es
[2] ICODA, Rúa Alfonso VII, 36650 Caldas de Reis, Pontevedra, ES
E-mail: ivan.rodriguez@icoda.es;

Abstract
Carbon recovery from sewage sludge by anaerobic fermentation is usually modest due to low volatile fatty acids yields. The potential of anaerobic fermentation in the wastewater treatment plants in a region was carried out, integrating the management of sewage sludge with possible co-substrates issued from local organic waste producers. The co-fermentation blends were defined using computer-aided methods and compared to sludge monofermentation, demonstrating the potential of co-fermentation to increase the yields of volatile fatty acids and their composition.

Keywords
Anaerobic co-fermentation; arrested methanogenesis; carboxylate platform; organic waste; sewage sludge; volatile fatty acids.

INTRODUCTION

While anaerobic digestion is the most common technology for recovery of organic carbon from sludge, other novel schemes based on anaerobic fermentation can lead to higher added-value products. The so-called carboxylate biorefinery is a set of processes whereby a substrate rich in organic carbon is first converted into volatile fatty acids (VFA) and, subsequently, into other products including medium-chain carboxylates, biopolymers or energy carriers.

Sewage sludge, produced annually at approximately 23 kg total solids (TS) per person-equivalent in wastewater treatment plants (WWTP) can be a substrate for the carboxylate platform. However, anaerobic fermentation of sewage sludge often leads to low VFA yields, e.g., between 10%-32% in mesophilic conditions (Esteban-Gutiérrez et al. 2018). A successful strategy aimed at increasing the conversion of sewage sludge to biogas consists of blending sludge with other organic wastes which are more readily degradable and may complement the composition of sludge. As other organic wastes are normally not produced or collected in municipal WWTPs, transporting large volumes of waste over long distances would offset the profit and possible environmental benefits of sludge co-fermentation. Therefore, candidates for co-fermentation should be collected at a limited distance from the WWTP.

In this study, an evaluation to the potential of carbon recovery by anaerobic co-fermentation was carried out for a number of WWTPs. First, the conversion to VFA was assessed in batch tests. To increase the VFA yield, a number of co-fermentation blends were proposed where the available wastes were selected using two different computer-aided methods.

MATERIALS AND METHODS

Approach. For each of the 7 WWTPs in the region that counts with anaerobic digestion on-site, an inventory of organic waste producers was elaborated based on available information on the net and direct inquiries. The inventory includes the distance to the WWTP, nature of the organic waste, volume of waste produced and potential seasonality. Wastes were characterized by measuring solid contents, chemical oxygen demand (COD), total Kjeldahl nitrogen, percentage of potassium and phosphorus and concentration of the main cations and anions.

Acidification tests. Sludge acidification tests were carried out in 0.5 L bottles at 37ºC gently mixed in orbital shakers. In each bottle, 5 g/L of volatile solids (VS) of anaerobic digester biomass was used as inoculum and mixed with 5 gVS/L of sewage sludge. Experiments were replicated with different inoculum to ensure the independence from the sampled biomass. Sewage sludge was sampled from the feed to the anaerobic digester. Methanogenesis was inhibited in these tests by addition of 0.5 g of 2-bromo-ethane sulfonate (BES) per g of substrate. At the beginning of the test, pH was adjusted to pH 7.5 and, if needed during the test, manually readjusted by addition of concentrated HCl or NaOH. Tests were carried out in duplicates, lasted for 11 days monitored by the following parameters: pH, alkalinity, total and soluble COD, VFA and total and volatile solids.

Co-fermentation tests. To increase the acidification yield, co-fermentation tests were carried out. The candidate wastes were selected for each WWTP out of those in the inventory located at less than 30 km from the WWTP. Then, two computer-aided tools were used to define the optimal mixture of sludge and organic wastes: the Optiblender (Garcia-Gen et al. 2014), which aims at defining the blend that maximizes the yield of methane (taken here as a proxy for VFA yield) and the method proposed by Saavedra del Oso et al (2022), specifically tailored to predict the VFA yield and spectrum of organic wastes mixtures, but limited to two substrates. Blends were required to have a minimum of 80% sludge (weight basis) as the main goal of the study is to assess alternatives to sludge valorisation. An additional constraint was not to exceed the available waste volume produced in the surroundings of the WWTP. To provide a fair comparison of the results, the sum of the sludge + organic wastes was kept at 5 gVS/L in all the experiments.

RESULTS AND DISCUSSION

The first acidification tests showed significant variability among the WWTPs (Figure 1) that could not be directly related to the WWTP process characteristics, with acidification yields ranging from 8% to 50% (COD basis). Testing different inocula, i.e. the biomass from each WWTP digester and as a common biomass the one from WWTP A digester, did not lead to significant differences in acidification yields.

To increase the acidification yield, co-fermentation blends were proposed and tested experimentally. As an example, the blends for WWTP C are shown here (Figure 2). The proposed blend by Optiblender for one of the WWTPs included (in weight basis) 89% of sludge, 4% of bread and pastry waste, 3.8 % of dairy sludge, 1.6% of dairy waste and 1.2% of slaughterhouse waste. This blend was appropriate as it would not exceed the production of each of the organic waste streams. It was seen that the VFA yield was more than doubled for the same amount of VS used in the substrate (although different substrate COD content). Even more, for the same VS, the concentration of VFA is higher than for the any of the individual substrates showing the goodness of co-fermentation for reaching higher conversions. Finally, substrate blending leads to higher fractions of longer chain VFA and branched VFA which may be of interest if VFA are to be further processes, e.g. to produce biopolymers such as polyhydroxyalkanotes.

As a conclusion, although VFA yield from sludge is, in general, modest, anaerobic co-fermentation with suitable substrates can lead to higher VFA yields and a spectrum richer in longer-chain VFA, demonstrating the potential of integrating sludge management together with other organic wastes.

ACKNOWLEDGMENTS. This work was supported by the Innovaugas 4.0 agreement with the public Galician Water Authority Augas de Galicia, co-funded by FEDER (EU)

REFERENCES

Esteban-Gutiérrez, M. et al. 2018. From sewage sludge and agri-food waste to VFA: Individual acid production potential and up-scaling, *Waste Management,* **77**, 203-12.
García-Gen, S., Rodriguez, J. Lema, J.M. 2014. Optimisation of substrate blends in anaerobic co-digestion using adaptive linear programming *Bioresource Technology,* **173**, 159–67.
Saavedra del Oso, M. et al. 2022. Fostering the valorisation of organic wastes into carboxylates by a computer-aided design tool, *Waste Management,* **142**, 101–10

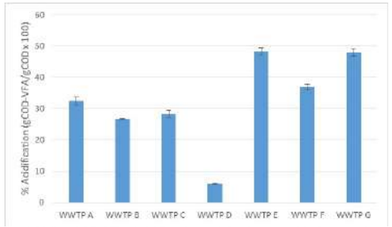

Figure 1. VFA yield (in gCOD-VFA /gCOD-substrate) for the anaerobic fermentation of sewage sludge of 6 WWTPs

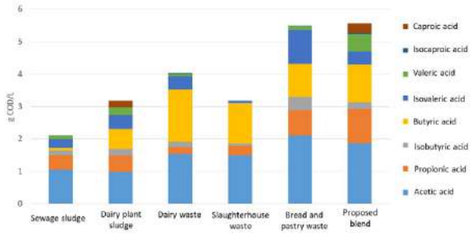

Figure 2. VFA obtained after co-fermentation tests for individual waste streams and proposed blend by Optiblender for WWTP C.

Mechanisms of Hexavalent Chromium Reduction by *Rhodococcus qingshengii* strain SC26

A. Melzi*, M. Colombo* and L. Cavalca*

* Department of Food, Environmental and Nutritional Sciences (DeFENS), University of Milan, Via Celoria 2, I-20133 Milan, Italy (E-mail: *lucia.cavalca@unimi.it*)

Abstract
Chromium represents a serious threat for both human health and ecosystems equilibrium. It is mainly present in two stable inorganic forms: trivalent (CrIII) and hexavalent (CrVI), the latter one being more toxic due to its high solubility and mobility in biological systems. The major pollution sources are electroplating and tannery industries. Among possible remediation strategies, the use of biological systems can be proposed since microorganisms interact with metals by passive adsorption processes and active enzymatic reactions.
In the present study, *Rhodococcus quingshengii* strain SC26 was characterized for its ability to resist Cr(VI) (MIC of 300 mg L^{-1}) and reduce Cr(VI) to Cr(III) in growing cells conditions. *R. quingshengii* strain SC26 was able to reduce Cr(VI) to Cr(III) up to 51.14 mg L^{-1} and the reduction was always paralleled by cell growth. Part of the metal was present on cell pellet (1.9 mg g^{-1}). Not proliferating cells were not able to reduce/adsorb Cr(VI), thus excluding passive adsorption processes. Trials conducted with contaminated wastewaters from the electroplating industry are ongoing to assess the bioremediation potential of *Rhodococcus qingshengii* strain SC26 in close-to-real scenarios.

Keywords (maximum 6 in alphabetical order)
Heavy metal removal; hexavalent chromium reduction; *Rhodococcus qingshengii*; wastewater bioremediation.

INTRODUCTION

Nowadays the presence of heavy metals in water bodies represents a serious environmental and human health threat. Chromium (Cr) is known for its widespread utility in various industrial processes such as industrial welding, dyes and pigments manufacturing, electroplating processes, leather tanning and wood preservation (Pushkar, *et al.,* 2021). Therefore, it is one of the most hazardous heavy metals discharged into surface water (Roşca, *et al.*, 2023). Cr is present in the environment mainly in two inorganic stable forms: trivalent (CrIII) and hexavalent (CrVI). Cr(VI) is the most hazardous one, being considered 1,000 times more toxic than Cr(III) (Diaconu, *et al.,* 2020). In some electroplating effluents, Cr(VI) concentration ranges from 6 to 887 mg L^{-1}, being the Cr(VI) and total Cr limits of 0.005 and 0.05 mg L^{-1}, respectively, in surface and ground waters (Directive 2000/60/CE). Therefore, the implementation of strategies to reduce Cr(VI) to Cr(III) and to remove total Cr from industrial wastewater is fundamental to reduce heavy metal pollution (Roşca, *et al.*, 2023). Among these strategies, the use of microorganisms can represent a sustainable alternative to conventional physico-chemical processes (Demarco, *et al.,* 2023). Beside Cr adsorption processes, bacteria can reduce Cr(VI) to the less toxic Cr(III) by intracellular or extracellular reduction mechanisms mediated, respectively, by aspecific ROS-scavenging and Cr(VI)-specific reductase systems (Diaconu, *et al.,* 2020).
The aim of the present study was to characterize Cr(VI) reduction and Cr adsorption mechanisms in *Rhodococcus qingshengii* bacterial strain SC-26, in order to envisage the most promising set-up for the development of a biological system useful to reduce Cr pollution in wastewater.

MATERIALS AND METHODS

Bacterial strains

Nine strains [As3-5a(1), As3-5a(3), As3-5a(4), As3-5a(5), SC5III, SC37, SC3I(2), SC23, and SC26] previously isolated from arsenic- (Cavalca *et al.,* 2010a) and petroleum hydrocarbon-(Cavalca *et al.,* 2010b) contaminated soils, were tested to assess their Cr(VI) resistance and reduction.

Determination of Cr(VI) Minimum inhibitory concentration

Cr(VI) Minimum inhibitory concentration (MIC) was determined on different minimum mineral media: M9 (Kunz and Chapman, 1981), DF (Dworkin and Foster, 1958) and TMM (Mergeay *et al.*, 1985). Na-gluconate (0.6 % *wt/vol*) was added as carbon and energy source. Increasing concentrations of Cr(VI) were tested between 25 and 500 mg L^{-1}, in the form of $K_2Cr_2O_7$ (VWR BDH Chemicals, Radnor, Pennsylvania, US) at pH of 5.67. Bacterial growth was determined by spectrophotometric analysis (OD_{600nm}).

Not-proliferating cell experiment in the presence of Cr(VI)

In biofilm-based system, 4 and 8 mL of bacterial suspensions (OD_{600nm} of 2), prepared in distilled water, were separately deposited onto 0.2 µm cellulose acetate filter (Millipore, Burlington, MA, USA). 50 mg L^{-1} Cr(VI) prepared as $K_2Cr_2O_7$ (VWR BDH Chemicals) solution added to MilliQ water, were vacuum-forced across the biomass-activated filter, with a few seconds of contact. Metal content of the flow through was analyzed by inductively coupled plasma spectrophotometry (ICP-MS).
In planktonic cell system, biomass was resuspended in 12 mL of 50 mg L^{-1} Cr(VI) solution added as $K_2Cr_2O_7$ (VWR BDH Chemicals) and stirred in plastic tubes (100 rpm at 23 °C). The effect of contact time on Cr(VI) reduction and biosorption was determined on cell biomass and supernatant after 0, 4, 72, and 168 h of incubation. Bacterial suspensions were centrifuged (15 min at 10,000 rpm) and the biomass total Cr and the supernatant Cr(VI) were analyzed by ICP-MS and by diphenyl carbazide (DPC) spectrophotometric methods, respectively. Each experiment was conducted in triplicate and the abiotic controls were always analyzed.

Growing cell experiment in the presence of Cr(VI)

R. qingshengii strain SC26 (inoculum 2% *vol/vol*, $OD_{600\ nm}$ of 2) was separately incubated for 7 days in DF mineral medium and in Luria Bertani (LB) rich medium, in the presence of approximately 50 mg L^{-1} Cr(VI) prepared from $K_2Cr_2O_7$ (VWR BDH Chemicals) solution. At subsequent incubation times, bacterial growth was determined (OD_{600nm}). Total Cr present on cell pellet was determined by ICP-MS analysis. Cr(VI) in the supernatant was determined by DPC spectrophotometric method (OD_{540nm}) according to Dean and Beverly (1958). Each experiment was conducted in triplicate and the abiotic controls were always analyzed.

RESULTS AND DISCUSSION

Cr(VI) MIC of isolated strains

Cr(VI) MIC was found to be 25 mg L^{-1} for most of the tested strains, the only exception being represented by *R. qingshengii* strain SC26 with a MIC of 300 mg L^{-1} Cr(VI). Resistance towards Cr is very variable in bacterial isolates. The MIC value of strain SC26 is consistent with Cr tolerance previously reported by Sevak *et al.* (2023) who found that only a few tested bacterial isolates were resistant to 300 mg L^{-1} Cr(VI) and only one isolate could tolerate up to 500 mg L^{-1}. Due to Cr resistance and the ability of the *Rhodococcus* genus to cope with different pollutants (Nazari, *et al.,* 2022), strain SC26 was chosen for further study.

Cr(VI) reduction to Cr(III) by SC26 not-proliferating cells

Not-proliferating cells didn't perform Cr removal or Cr(VI) reduction in biofilm-based and planktonic cell experiments (Table 1), being the amount of Cr present in abiotic solution always close to that of biotic ones. Total Cr biomass content was negligible.

Table 1. Cr (VI) concentrations in biofilm-based and planktonic cell experiments.

	SC26 biofilm		SC26 planktonic			
	OD_{600nm}=2	OD_{600nm}=4	0 h	4 h	72 h	168 h
Cr(VI) (mg L^{-1})	49.55 ± 1.01	49.88 ± 0.64	50.706 ± 3.737	51.065 ± 5.457	51.245 ± 4.609	49.807 ± 2.549

Cr(VI) reduction to Cr(III) by SC26 growing cells

Growing cell experiments performed in the presence of increasing concentrations of Cr(VI) from 32 to 146 mg L^{-1} (Figure 1) showed that Cr(VI) reduction to Cr(III) was inversely related to bacterial growth: increasing metal concentrations exerted cell toxicity thus affecting SC26 ability to reduce Cr(VI). These preliminary experiments evidenced that Cr(VI) transformation was strictly related to the growth of SC26 bacterial cells.

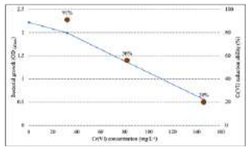

Figure 1. Cr(VI) reduction ability (%) ● of strain SC26 in growing cell experiment ⟷ at increasing Cr(VI) concentrations (32, 82 and 146 mg L^{-1}).

Analysis performed at increasing incubation times conducted in the presence of 50 mg L^{-1} Cr(VI) (Figure 2) confirmed that the reduction of the metal was parallel by cell growth, either in DF mineral minimal medium and in LB rich medium. After 7 d incubation, Cr(VI) present in the supernatant was 31.59 and 4.45 mg L^{-1} in DF and LB media, respectively, and the specific total Cr content of cell biomass was 7.62 and 1.92 mg g^{-1} cell d.w.. These data permit to determine that the strain was able to reduce 16.46 and 51.14 mg L^{-1} Cr(VI) to Cr(III), respectively. Abiotic controls did not show any Cr(VI) reduction. The ability of reducing Cr(VI) to Cr(III) while increasing in biomass and cell density was also reported by Guatam *et al.,* (2022), who observed the secretion of chromate reductase in the culture medium and intracellular enzyme activity.

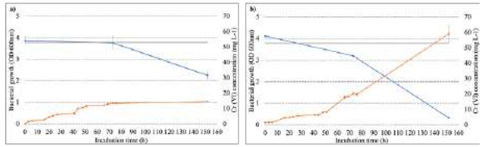

Figure 2. Cr(VI) reduction in *R. qingshengii* strain SC26 growing cell experiment performed in DF (a) and LB (b) media, in the presence of 50 mg L^{-1} Cr(VI) OD_{600nm} , Cr(VI) and total Cr concentrations — over seven days (152 h) of incubation.

The data obtained suggest that *R. qingshengii* strain SC26 is able to lower Cr toxicity either by reducing Cr(VI) to Cr(III) and by adsorbing Cr onto the cell biomass. Further analysis will determine the adsorbed Cr form. Experiments in the presence of real wastewaters are on-going.

REFERENCES

Roşca, M., Silva, B., Tavares, T., & Gavrilescu, M. (2023). Biosorption of Hexavalent Chromium by Bacillus megaterium and Rhodotorula sp. Inactivated Biomass. Processes, 11(1), 179.
Pushkar, B., Sevak, P., Parab, S., & Nilkanth, N. (2021). Chromium pollution and its bioremediation mechanisms in bacteria: A review. Journal of Environmental Management, 287, 112279.
Diaconu, M., Roşca, M., Cozma, P., Minuț, M., Smaranda, C., Hlihor, R. M., & Gavrilescu, M. (2020, October). Toxicity and Microbial Bioremediation of Chromium Contaminated Effluents. In 2020 International Conference on e-Health and Bioengineering (EHB) (pp. 1-4). IEEE.
Demarco, C. F., Quadro, M. S., Selau Carlos, F., Pieniz, S., Morselli, L. B. G. A., & Andreazza, R. (2023). Bioremediation of Aquatic Environments Contaminated with Heavy Metals: A Review of Mechanisms, Solutions and Perspectives. Sustainability, 15(2), 1411.
Cavalca, L., Zanchi, R., Corsini, A., Colombo, M., Romagnoli, C., Canzi, E., & Andreoni, V. (2010). Arsenic-resistant bacteria associated with roots of the wild Cirsium arvense (L.) plant from an arsenic polluted soil, and screening of potential plant growth-promoting characteristics. Systematic and applied microbiology, 33(3), 154-164.
Cavalca, L., Ciccazzo, S., Scotti, R., Rao, M. A., Colarieti, M. L., & Toscano, G. (2010). Propylene glycol-specific dehydrogenases as functional biomarkers for monitoring biodegradation in sites contaminated by de-icing chemicals. Journal of Biotechnology, 150, 293.
Kunz, D. A., & Chapman, P. J. (1981). Catabolism of pseudocumene and 3-ethyltoluene by Pseudomonas putida (arvilla) mt-2: evidence for new functions of the TOL (pWWO) plasmid. Journal of Bacteriology, 146(1), 179-191.
Dworkin, M., & Foster, J. (1958). Experiments with some microorganisms which utilize ethane and hydrogen. Journal of bacteriology, 75(5), 592-603.
Mergeay, M., Nies, D., Schlegel, H. G., Gerits, J., Charles, P., & Van Gijsegem, F. (1985). Alcaligenes eutrophus CH34 is a facultative chemolithotroph with plasmid-bound resistance to heavy metals. Journal of bacteriology, 162(1), 328-334.
Dean, J. A., & Beverly, M. L. (1958). Extraction and colorimetric determination of chromium with 1, 5-diphenylcarbohydrazide. Analytical Chemistry, 30(5), 977-979.
Sevak, P., Pushkar, B., & Mazumdar, S. (2023). Mechanistic evaluation of chromiumbioremediation in Acinetobacter junii strain b2w: A proteomic approach. Journal of Environmental Management, 328, 116978.
Nazari, M. T., Simon, V., Machado, B. S., Crestani, L., Marchezi, G., Concolato, G., ... & Piccin, J. S. (2022). Rhodococcus: A promising genus of actinomycetes for the bioremediation of organic and inorganic contaminants. Journal of Environmental Management, 323, 116220.
Gautam, A., Kushwaha, A., & Rani, R. (2022). Reduction of Hexavalent Chromium [Cr (VI)] by heavy metal tolerant Bacterium Alkalihalobacillus clausii CRA1 and its toxicity assessment through flow cytometry. Current microbiology, 79(1), 33.

Vinyl Chloride Biodegradation In Contaminated Aquifer Undergoing Stimulation Treatment

M. Bertolini*, S. Zecchin*, A. Melzi* and L. Cavalca*

* Dipartimento di Scienze per gli Alimenti, la Nutrizione e l'Ambiente (DeFENS), Università degli Studi di Milano, via Celoria 2, 20133 Milano, Italy, martina.bertolini@unimi.it, sarah.zecchin@unimi.it, lucia.cavalca@unimi.it

Abstract
Vinyl chloride is chloroethenes. It is very toxic for human because of its carcinogenicity. Vinyl chloride accumulations are widely present in chlorinated solvents contaminated area due to it hard transformation in anaerobic conditions by microorganisms. Nevertheless, it is efficiently biodegraded in microaerobic and aerobic conditions by bacteria. The first enzyme involved in its oxidation is alkene monooxygenase (AkMO), encoded by *etnABCD*.
In this work, aerobic oxidation activity of vinyl chloride present in a contaminated aquifer was investigated in order to trace microbial activities involved in the decrease of vinyl chloride. Laboratory scale experiment confirmed that vinyl chloride bacterial populations were active at the site. Molecular analyses conducted *in situ* allowed to monitoring oxidation activity and to determine the effects of biostimulation on microbial community present in the aquifer.

Keywords (maximum 6 in alphabetical order)
Chlorinated ethenes; Vinyl chloride; Aerobic oxidation;

INTRODUCTION

Chlorinated aliphatic hydrocarbons are the cause of soil and groundwater contamination due to a inadequate disposal. In Europe, chlorinated organic compounds are present in10% of contaminated water and 8% of contaminated soil (JRC, 2014). European directive indicated tetrachloroethene (PCE) and trichloroethene (TCE) as priority contaminant (Directive 2006/118/EC).
Chlorinated solvents are recalcitrant to traditional treatments, but they are efficiently transformed by microorganisms. Highly chlorinated ethenes (PCE and TCE) are dechlorinated in anaerobic conditions (organohalide respiration) by bacteria that use these compounds as energy source, organo-halide respiring bacteria, OHRB (Dolinová et al., 2017). This metabolic pathway is not efficient for lower chlorinated ethenes, dichloroethenes (DCE) and vinyl chloride (VC) (Abe et al., 2009), that can be oxidated in aerobic conditions by different bacteria (e.g. *Mycobacterium, Nocardioides, Rhodococcus*). These aerobic bacteria use VC (and similarly ethene) as sole carbon source, with production of water, CO2 and Cl-. In VC oxidation pathways, only the first two enzymes are known: alkene monooxygenase (AkMO), encoded by genes *etnA, etnB, etnC*, and *etnD*, and epoxyalkane:coenzyme M transferase (EaCoMT) encoded by *etnE* gene (Coleman & Spain, 2003). It has been hypothesized that the last compound of the degradative pathway enters into TCA cycle (Mattes et al., 2005).
Accumulation of VC in chloroethenes contaminated matrix results of incomplete anaerobic organohalide respiration turns out an important problem.
In this study, microbial community of contaminated aquifer was monitored to determine the efficiency of an aerobic biobarrier in sequence of an anerobic biobarrier on stimulation of VC oxidation.

MATERIALS AND METHODS

Ethene/VC degrading bacteria isolation from enrichment culture

Aerobic microcosms were set up in order to determine the presence of ethene/VC degrading bacteria in the contaminated aquifer. Vials were prepared with groundwater from piezometers near aerobic biobarrier with addition of ethene (3 mmol L^{-1}). Abiotic control samples were set up with sterile MSM and the addition of ethene. Enrichment cultures were incubated on an orbital shaker at 30°C in the dark. Enrichment cultures were monitored for 10 days, and ethene concentrations were analysed through gas chromatography with flame ionization detector (GC-FID). Bacterial strains were isolated from enrichment cultures according to their ability to use ethene as sole carbon source, and subsequently, they were identify.

Nucleic acid extraction methods and *etnC* quantification

Groundwater biomass was filtered by using a peristaltic pump apparatus. Filters were stored at -20°C until processed. Total DNA was isolated from the pellet using the DNA PowerSoil® Isolation kit (Qiagen, Germany) in triplicate for each sample.
16S rRNA genes of total bacteria and *etnC* (gene that encodes for one of subunit of AkMO) were quantified through real time quantitative PCR.

Microbial community characterization

Effects of biostimulation treatments on groundwater microbial community were investigated through Illumina sequencing of Bacteria 16S rRNA genes. Groundwater bacterial community was characterized at January 2021 and after one year (January 2022). Sequence analyses were performed with QIIME2 (Caporaso et al., 2010). Amplicon Sequence Variants (ASVs) were created in accordance with a similarity higher than 97% using UCLUST method. ASVs were aligned to the SILVA database.

RESULTS AND DISCUSSION

Ethene enrichment cultures showed growth highlighting the presence in the aquifer of bacteria that can use ethene/VC as sole carbon source. Isolated bacterial strains were identify as: *Mycobacterium frederiksbergense, Bacillus mobilis, Ralstonia pickettii, Ralstonia solanacearum, Simplicispira hankyongi*. Ethene degradation tests were set up with the 4 strains that showed a faster growth. *Mycobacterium frederiksbergense* strain 1.1 and *Ralstonia solanacearum* strain M4 degraded added ethene after 4 days of incubation, *Bacillus mobilis* strain 2 after 5 days, and *Simplicispira hankyongi* strain 6A after 7 days (Figure 1).

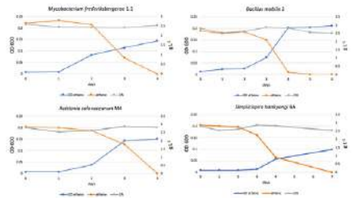

Figure 1. Growth and ethene degradation curves of isolated strain. *Mycobacterium frederiksbergense* ceppo 1.1, *Bacillus mobilis* ceppo 2, *Ralstonia solanacearum* ceppo M4, *Simplicispira hankyongi* ceppo 6A.

The gene for the first enzyme of VC oxidative pathway (alkene monooxygenase) was selected to monitoring VC mineralization activity for one year. Analysis showed that *etnC* was present in the aquifer with order of magnitude between 10^4 and 10^7 gene copies L^{-1} and it increased during the time. Statistical analysis of ratio *etnC*/16S rRNA showed that increase during the time was significant (ANOVA, $p<0.05$). At the end of monitoring year, the two piezometers downstream the biobarrier showed higher presence of *etnC* (Figure 2).

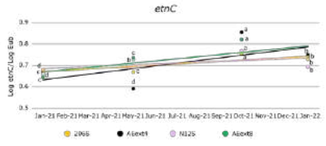

Figure 2. Ratio etnC/16S rRNA of all sampling points in biobarrier during one year. Lowercase letters indicate significant or not significant difference between different time (ANOVA, $p<0.05$).

Analysis of microbial community 16S rRNA genes sequencing in the aquifer showed that the biostimulation treatment induced a significant change in the microbial community composition (Permanova, $p < 0.05$). Indeed, β diversity of bacterial community of piezometers upstream the biobarrier were significant different than one of piezometers downstream the biobarrier (Figure 3).

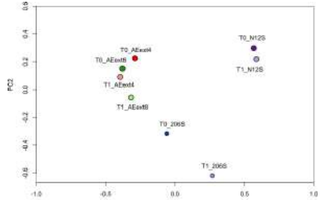

Figure 3. Analysis of bacterial community β diversity in the aquifer near the biobarrier

Treatment induced a high similarity between the bacterial community of downstream piezometers. This effect persisted after one year of treatment. The two piezometers upstream the biobarrier showed a significant diversity between them. Addition of air and nutrients induced after one year an increase of relative abundance of *Mycobacterium* and *Rhodoferax*, known VC-degrading bacteria, and *Simplicispira*, characterized for its VC/ethene degrading activity during this project (Figure 4).

Figure 4. Relative abundance significant variation at genus level in bacterial community between January 2021 and January 2022 in biobarrier.

CONCLUSIONS

In the aquifer, VC/ethene degrading bacteria were present. Presence of gene involved VC oxidative pathway was detected.
The addition of air and nutrients induced significant change in bacteria community with a selection of bacterial composition downstream the biobarrier. Treatment determined an increase of VC/ethene degrading bacteria in the aquifer.

REFERENCES

https://joint-research-centre.ec.europa.eu/publications/jrc-annual-report-2014_en

Dolinová, I., Štrojsová, M., Černík, M., Němeček, J., Macháčková, J., & Ševců, A. 2017. Microbial degradation of chloroethenes: a review. *Environmental Science and Pollution Research*, **24**, 13262-13283.

Abe, Y., Aravena, R., Zopfi, J., Parker, B., Hunkeler, D., 2009. Evaluating the fate of chlorinated ethenes in streambed sediments by combining stable isotope, geochemical and microbial methods. *J. Contam. Hydrol. 107,* 10–21. DOI:10.1016/j.jconhyd.2009.03.002

Coleman, N. V., Spain, J. C., 2003. Distribution of the Coenzyme M Pathway of Epoxide Metabolism among Ethene- and Vinyl Chloride-Degrading Mycobacterium Strains. *Appl Environ Microbiol* **69**, 6041–6046. DOI: 10.1128/AEM.69.10.6041–6046.2003

Mattes, T. E., Coleman, N. V., Spain, J. C., Gossett, J. M., 2005. Physiological and molecular genetic analyses of vinyl chloride and ethene biodegradation in Nocardioides sp. strain JS614. *Arch. Microbiol*. **183**, 95–106. DOI 10.1007/s00253-015-6771-2

Jin, Y. O., Mattes, T. E., 2010. A quantitative PCR assay for aerobic, vinyl chloride- and ethene-assimilating microorganisms in groundwater. *Environ. Sci. Technol.* **44**: 9036-9041.

Caporaso, J. G., Kuczynski, J., Stombaugh, J., Bittinger, K., Bushman, F. D., Costello, E. K., Fierer, N., Peña, A. G., Goodrich, J. K., Gordon, J. I., Huttley, G. A., Kelley, S. T., Knights, D., Koenig, J. E., Ley, R. E., Lozupone, C. A., McDonald, D., Muegge, B. D., Pirrung, M., Reeder, J., Sevinsky, J. R., Turnbaugh, P. J., Walters, W. A., Widmann, J., Yatsunenko, T., Zaneveld, J., Knight, R, 2010. QIIME allows analysis of high-throughput community sequencing data. Nat methods, **7(**5), 335-336.

Thermal treatment assessment to improve the phosphorus recovery as struvite from olive mill wastes

Mendoza M.*, Espejo L.**, Tey L.*, Viñas M.*, Fernández B.*

*IRTA Institute for Food and Agricultural Research and Technology, Torre Marimon, Road C59, km 12, E08140 Caldes de Montbui, Barcelona, Spain. **University of Barcelona, Barcelona, Spain. Email: marlene.mendoza@irta.cat; belen.fernandez@irta.cat.

Abstract

A thermal treatment at different pressures and temperatures was assessed for phosphorus solubilisation, before its recovery, contained in a mixture of olive oil mill pomace and olive oil mill wastewater. The highest increments of soluble phosphate, compared to the initial content were 55 % at 130 ºC & 10 bar (condition E), followed by 47 % at 100 ºC & 2.5 bar (condition C). Under any of these treatments, the soluble content of potassium and ammonium also increased thus allowing the recovery of 88-97% of the solubilised phosphate as a precipitate from hydrolysates or liquid fractions of treated mixtures; this precipitate was predominantly struvite ($MgNH_4PO_4.6H_2O$). Furthermore, mesophilic biomethanation tests of the remaining solid phase of the treated materials revealed an increment of methane production yield of +25% and +14% at conditions C and E, regarding the untreated mixture.

Keywords: olive pomace, phosphorus solubilisation, struvite, thermal treatment.

INTRODUCTION

A thermal treatment to improve the recovery of essential nutrients (N, P, K) required for olives production (Kolakovic, et al., 2021; Hadrami, et al., 2004), that were included in olive pomaces (OP) and olive mill wastewaters (OMWW), was developed as an improvement of the current valorisation strategy of a real olive oil cooperative that was already treating their mill wastes in a biogas plant. This work was designed as a proof of concept before implementing this strategy at field scale, to facilitate the closing of the olive oil production loop. Therefore, the main objectives of this study were (i) to improve the recovery of phosphorus as a salt from a mixture of OP and OMWW, and (ii) the production of biogas of the remaining material after the production of the phosphate salts.

MATERIALS AND METHODS

Two mixtures (initial-1 and initial-2) of OP:OMWW (wet weight ratio 56:44 %) were prepared. The mixture initial-1 was prepared with OP and OMWW collected in 2021 October, while mixture initial-2 contained OP and OMWW collected in 2022 January. All wastes were taken in the same industrial olive oil mill (Santa Bárbara, Tarragona, Spain) and were characterized similarly (TS, VS, COD, TN, TP, TK, pH, and soluble ions as phosphate, potassium, ammonium, nitrite, nitrate).

Both mixtures were submitted to a 60-minute thermal treatment in two ranges (Figure 1 and Table 1): low range or 50 - 75 - 100 °C at 2.5 bar (treatments A, B and C, respectively); high range or 100 – 130 - 180 °C at 10 bar (treatments D, E and F, respectively). After the thermal treatment, the treated mixtures were centrifuged (8,500 rpm, 10 °C, 20 minutes) to obtain a liquid and solid phases (L and S, respectively). The subsample L was characterised by its content in soluble ions, before the phosphorus recovery test, while all S subsamples were submitted to a biochemical methane production (BMP) test at 37 ºC for 34 days to determine their potential methane yield (Otero et al. 2021).

The solubilised phosphate was recovered by precipitation, adjusting the magnesium and phosphorus molar ratio (1:1 or 2:1), at ambient temperature (22ºC) and constant pH 10.5 (using a 40 % NaOH solution). The trials were made in batch in two steps: first, stirring at 200 rpm for 60 minutes (reaction and nucleation); then, no stirring for 60 minutes (crystal growth and precipitates settling).

The recovered phosphate as struvite was calculated based on the stoichiometric molar ratio of struvite precipitation (Eq. 1), after the experimental determination of the precipitated ions (Eq. 2). The initial and remaining content of soluble ions was determined by ion chromatography.

$$Mg^{2+} + NH_4^+ + PO_4^{3-} \rightarrow MgNH_4PO_4.6H_2O \quad Eq.\ 1$$

$$Ions_{initial} - Ions_{remaining} = Ions_{precipitated} \quad Eq.\ 2$$

RESULTS AND DISCUSSION

The mixtures initial-1 and initial-2 had a soluble phosphate content of 1,018 ±54 and 958 ±68 mg/kg, and an initial soluble potassium content of 3,923 ±67 and 3,771 ±81 mg/kg, respectively. Comparing the composition of soluble ions before and after the thermal treatments, the best phosphate solubilisation was attained with conditions C (100 ºC, 2.5 bar) and E (130 ºC, 10 bar) (Table 1), being the soluble phosphate a 47 and 55 % higher than the initial soluble phosphate respectively. Under these C and E conditions, the content of soluble potassium also increased (a 28 and 37 % higher than the initial soluble potassium in C and E, respectively) as well as the soluble ammonium content (17 and 18 % of the initial TN in C and E, respectively).

Based on the best results of phosphorus solubilisation, the hydrolysates or L phases of materials submitted to conditions C and E were selected to phosphorous recovery. The recovery assays were named C1, E1, C2, and E2, being the subscript equivalent to the Mg:P molar ratio (1:1 or 2:1) (Figure 2). In terms of phosphorus recovery, an 88% ±0 and 97% ±0 of soluble phosphate was recovered in C1 and E2 respectively. The recovery was 90% ±3 and 90% ±2 of soluble phosphate in the precipitates in C2 and E2, respectively, but some added magnesium remained not precipitated (Figure 2A); therefore, an optimisation of the combined processes of thermal treatment and precipitation would be done in a near future.

Considering the molar ratio for the formation of struvite (Eq.1), the amount of PO_4^{-3} and Mg^{+2} that precipitated under conditions C1 and E1 might indicate that struvite crystallization was completed (Figure 2B). The quantity of struvite obtained in each condition were 1.58, 1.74, 1.57 and 1.69 g-struvite/kg of initial mixtures in C1, E1, C2 and E2, respectively. Potassium struvite (K-struvite or MgKPO4.6H2O) could also be formed; however, ammonium ions competed and hindered the K-struvite precipitation based on the precipitation potential (p_{Ksp}) of struvite and of K-struvite (p_{Ksp} 12.5-13.6 and 12.2, respectively) (Xu et al., 2015).

Once the precipitates were extracted, a significant concentration of phosphate, potassium and ammonium remained available in hydrolysates (85-185 mg-PO_4^{-3}/kg, 143-193 mg-NH_4^+/kg and 3,398-4,396 mg-K^+/kg), which can be considered as hygienised liquid fertilisers due to the applied thermal treatment. The assessment as fertilisers of precipitates, and the remained fractions, through a phytotoxicity test are currently on-going.

Once the phosphorous was recovered, the S fraction of the treated mixture would be valorised in the biogas plant. The initial untreated mixtures had a methane yield of 219 and 316 NLCH4/kgVS (initial 1 and initial 2). After the thermal treatment, the methane yield was higher than methane yield of the untreated mixture for S fractions from treatments A (+16 %), C (+25 %) and E (+14 %). Other treatments showed negligible or no increment of the methane yield (+1 % from B solids; -5 and -6 % from D and F solids). The solubilisation of compounds such as polyphenols (Batista et al. 2014), or their intermediate compounds due to thermal decomposition, may have inhibited the methanogenic activity for B, D and F solids. Therefore, the best methane yield was obtained under treatment C, followed by treatments A and E (Table 1).

CONCLUSIONS

The recovery of essential nutrients NPK, together with biogas production, can be key to implement a circular economy model in the agricultural olive oil sector, obtaining non-fossil fertilisers and renewable energy from its own wastes. This study showed an improvement of soluble P (the soluble phosphate increased 47 - 55 % after the treatment under the best conditions C and E), soluble K and soluble N after the thermal treatment. This solubilisation, plus the adjustment of the Mg: P molar ratio to 1:1, allowed the recovered of the 88-97 % of the soluble phosphate, predominantly as struvite. Therefore, the best thermal treatment was C (100 ºC and 2.5 bar) considering its lower energy demand (compared with treatment E), the high phosphate recovery and the higher methane yield increment of its corresponding solid fraction (its methane yield was +25 % higher that the untreated mixture after treatment C).

Acknowledgements

This work was financed by Sustainolive project which is part of the PRIMA program supported by the European Union. IRTA thanks the financial support of CERCA program (Generalitat de Catalunya) and 2021 SGR 01568.

REFERENCES

Battista, F., Fino, D., Ruggeri, B. (2014). Chemical Engineering Transactions, Vol. 38. (M. B. Enrico Bardone, Ed.) doi:10.3303/CET1438063.

Hadrami, A. E., Belaqziz, M., Hassni, M. E., S. Hanifi, Abbad, A., Capasso, R., Hadrami, I. E. (2004). J. Agronomy 3(4), 247-254. doi: 10.3923/ja.2004.247.254.

Kolakovic, S., Santos, J. M., & A.M.Reis, M. (2021). Journal of Environmental Chemical Engineering, 9. doi: 10.1016/j.jece.2021.106261

Otero A., Mendoza M., Carreras R., Fernández B. (2021). Waste Management, 119-126. doi: 10.1016/j.wasman.2021.07.035.

Xu, K., Li, J., Zheng, M., Zhang, C., Xie, T., Wang, C. (2015). Water Research 80, 71-79. doi: 10.1016/j.watres.2015.05.026.

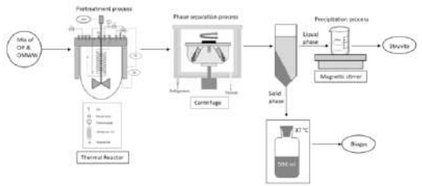

Figure 1. Phosphate recovery procedure.

Table 1. Thermal treatments: conditions and results. Notes: *Increment compared with the initial soluble content of the corresponding ion in the untreated initial mixture. **Increment of soluble ammonium, expressed as percentage of initial total nitrogen. ***Increment of the methane yield (NLCH4/kgVS) after the biodegradation of the solid phases obtained after the treatment, compared with the methane yield of untreated initial mixture. Nomenclature: L, S, liquid, and solid fraction; ww, wet weight.

Treatment	Temp (°C)	Pressure (bar)	L/S (%ww)	Soluble PO_4^{3-} inc* (% in)	Soluble K^+ inc* (% in)	Soluble NH_4^+ inc** (% TN)	Methane yield inc*** (% in)
A	50	2.5	52/48	+9.2	+46.3	+0.3	+16.0
B	75		52/48	+16.2	+16.0	+4.9	+0.7
C	100		55/45	+41.7	+27.7	+17.0	+25.1
D	100	10	60/40	-8.8	-10.7	+0.5	-5.1
E	130		57/43	+54.6	+37.0	+18.3	+13.5
F	180		69/31	+28.8	+30.5	+13.7	-5.7

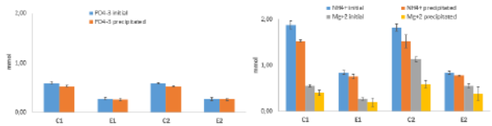

(a) **(b)**

Figure 2. Precipitation of struvite. (a) Initial and precipitated mmol of phosphate. (b) Initial and precipitated mmol of ammonium and magnesium. Nomenclature: C and E, hydrolysates from treatments C and E (table 1); 1 or 2, subscript equivalent to the Mg:P molar ratio (1:1 or 2:1). Colours: blue, initial phosphate and ammonium; orange, precipitated phosphate and ammonium; grey, initial magnesium; yellow, precipitated magnesium.

Starting points for the management of sewage sludge's digestate for phosphorus recovery in the concept of a circular economy

V. Mislej*, V. Zalar Serjun**, B. Novosel***, M. Vrbančič*, and N. Atanasova****

* JP Vodovod Kanalizacija Snaga d.o.o., Vodovodna c. 90, Ljubljana, Slovenia
(E-mail: *Vesna.Mislej@vokasnaga.si*; *Mojca.Vrbancic@vokasnaga.si*)
** The Slovenian National Building and Civil Engineering Institute, Dimičeva12, Ljubljana, Slovenia
(E-mail: *vesna.zalar@zag.si*)
*** Faculty of Chemistry and Chemical Technology, University of Ljubljana, Večna pot 113, Ljubljana, Slovenia
(E-mail: *barbara.novosel@fkkt.uni-lj.si*)
**** Faculty of Civil Engineering and Geodesy, University of Ljubljana, Hajdrihova 28, Ljubljana, Slovenia
(E-mail: *Natasa.Atanasova@fgg-uni-lj.si*)

Abstract
Because of high phosphorus content, the possibility of using treated anaerobically stabilised sewage sludge (digestate) as a fertiliser product is very ambiguous. The management of phosphorus in agriculture, as a critical raw material, begins at the urban wastewater treatment plant as phosphorus removal from wastewater (biological and chemical) and continues with the comprehensive characterisation of treated sewage sludge (pellets), expanded research of physico-chemical properties and the phase-mineralogical transformation of pellets' thermal residues, and researches of phosphorus bioavailability from resulted material. With a suitable technological pre-treatment of digestate and environmentally safe phosphorus recovery (preventing the unwanted possibility of heavy metals' leaching), new recycling strategies could be established to recover the valuable components of sewage sludge and strengthen the circular economy in waste processing.

Keywords
Bioavailability; pelletised digestate; phosphorus recovery; struvite; thermal residues; urban wastewater.

INTRODUCTION

In the European Union (EU), the use of sewage sludge in agriculture is regulated by the Sewage sludge framework Directive (SSD) (Directive, 1986), which is implemented differently by each EU Member State, reflected in the different limit values of critical parameters. The set of parameters for which the SSD prescribes limit values is short. It also does not specify a declaration for the content of C_{org} (organic carbon), primary nutrients (PN), secondary nutrients SN), macronutrients (MACN), and micronutrients. This shows the fact that there is an urgent need for the unification of the existing European market for fertilisers based on treated waste. In order to achieve this and to include as much recovered waste as possible in the raw material cycle, the EU has recently adopted a Fertilising Regulation (FR) (Fertilising Regulation, 2022). According to the vision of FR, the 'EU fertilising product' is a product labelled with the logo CE ("conformité européenne") when made available on the market. Also, it includes fertilisers from recovered or organic materials. The FR, which was entered in full into force on 16 July 2022, will not affect the implementation of SSD. Treated wastes that have the potential to be used as fertiliser according to the new FR are wastes that are composted or anaerobically stabilised (hygienic and with the content of polycyclic aromatic hydrocarbons below 6 mg/L), precipitated phosphate salts and derivates, thermal oxidation materials and derivates, together with pyrolysis and gasification materials. The possibility of using treated anaerobically stabilised sewage sludge (digestate) as a fertiliser product is still ambiguous. Considering the new possibilities of material utilisation of pelletised digestate, it also makes sense to reevaluate older research. A case study of the composition of treated sewage sludge generated at the Central wastewater treatment plant in Ljubljana (CWWTPL) (JP VOKA SNAGA 2006) has been performed. At the annual level, incorporated into the pellets, there are about 1,500 tons of organic matter expressed as total organic carbon (TOC), 230 tons of nitrogen, 80 tons of phosphorus, 13 tons of potassium and 16 tons of magnesium transported from the site of the plant to the location for final processing. Due to the impoverishment of natural sources of phosphorus, it is essential to find opportunities for recycling it.

MATERIALS AND METHODS

The yearly production of pellets at the CWWTPL is up to 4300 tons (designed capacity of 360,000 population equivalent) in the form of grain size diameter of 2 mm to 4 mm. We analysed non-treated digestate, centrate (technological wastewater after mechanical dehydration of digestate), pellets (annual representative samples of the years 2012 (sample Y2012), 2014 (sample Y2014), 2016 (sample Y2016), 2018 (sample Y2018), and 2021 (sample Y2021). Additionally, we prepared two types of residues, one simulating the bottom ash and a second type of residue simulating the biochar. We have used three kinds of techniques for the sample preparation: i) semi-pilot equipment for pyrolysis (sample BC 2014), ii) thermogravimetric analysis of the sample Y2012, using inert atmosphere (pyrolysis), TG/DTG in the range from 30 °C through 450 °C (sample "Pyrolysis 450 °C), iii) the ignition of pellets (sample Y2012) in the laboratory heating furnace at 450 °C (sample Ignition 450 °C), 550 °C (sample Ignition 550 °C), 700 °C (sample Ignition 700 °C), and 900 °C (sample Ignition 900 °C). In the resulting residues, we have determined the content of nutrients (TOC, P, K and Mg) and their mineralogical composition by XRD analysis and SEM-EDS technique; the proportion of water-soluble part of phosphorus with the EN 13652.

RESULTS AND DISCUSSION

The results in Table 1 show that the pellets have a reasonably reproducible composition and high nutrient content.

Table 1. Pellets characterisation according to Fertilising Regulation (2022)

		Y2012	Y2014	Y2016	Y2018	Y2021
		Declaration				
	% m/m	PN				
C_{tot}	C	36.6	36.1	35.9	38.5	no a.
C_{org}	C	34.8	36.1	30.1	32.3	30.1
P	P_2O_5	4.62	3.72	3.36	3.01	3.52
K	K_2O	0.326	0.430	0.309	0.344	0.239
		S MACN				
Ca	CaO	5.80	6.02	4.64	8.10	4.8
Mg	MgO	1.49	1.67		no a.	

Elements in granules can have the function of nutrients if they are water-soluble or if they are bioavailable. This is especially important for phosphorus and potassium recovery. In this process, emphasis is needed on preventing the re-entry of heavy metals into the environment. The paper will show the bioavailability of nutrients and the potential leaching of heavy metals from pellets.

ASH utilisation

Despite anaerobic stabilisation and biogas production, the pellets still contain enough organic matter to be used for the waste-to-energy (WtE) process. In addition to energy recovery, the WtE enables the material recovery of many inorganic compounds or elements in the granules (Figure 1). In addition to carbon, nitrogen, hydrogen, sulphur and phosphorus, the inorganic content presents the major elements in pellets. Some elements are also on the critical raw material list (Communication, 2017; Critical raw materials, 2012). To evaluate ash as a suitable fertiliser or as a fertiliser additive, it is essential to study the phase-mineralogical transformations that occur during the burning of pellets (Figure 1 and Figure 2) and the bioavailability of nutrients - especially phosphorus. The contribution will show the rate of bioavailability's loss of nutrients due to thermal treatment in oxidative conditions.

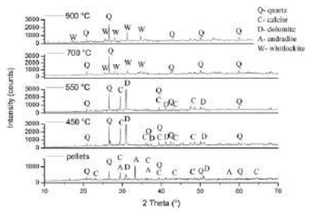

Figure 1. XRD analysis of pellets (Y2012) and their combustion residues.

PYROGEN MATERIAL utilisaton

The major part of the carbon content in pellets is bound in substances which, in an inert atmosphere when heated to 450 °C, are volatile or are thermo-chemically converted into volatile gaseous compounds. That makes sense to convert the pellets into pyrolytic products and then into fertiliser according to the FR (Figure 2), especially because the results show that phosphorus has better bioavailability in this case.

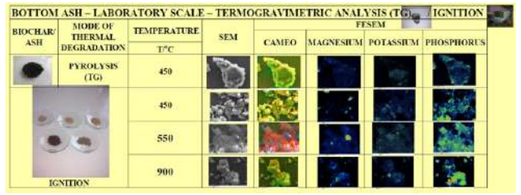

Figure 2. SEM analysis of combustion residues of sample Y2012 and its pyrogenic residue after thermal load at 450 °C.

NON-TREATED DIGESTATE utilisation

Non-treated digestate and centrate present valuable materials for struvite precipitation (Figure 3). As a spontaneous precipitation process, struvite is a disturbance, but it shows us the possibility of taking advantage of this chemical reaction. This is an essential strategy for phosphorus recovery.

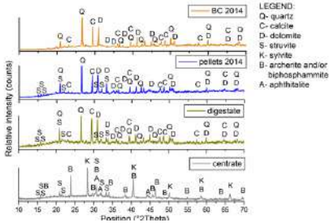

Figure 3. XRD patterns of centrate, digestate, pellets Y2014 and BC 2014.

CONCLUSION

Evaluation of the pellets and their solid combusted (ash) and pyrolytic residues according to FR is a complex procedure. New economically viable technologies need to be developed to recover the nutrients from digestate, centrate and treated sewage sludge's thermal residues to increase the extraction of essential components. Some materials recovered from treated sewage sludge are still considered as waste, even though they contain valuable nutrients that provide good market value [Position paper, 2021]. The example of the FR, explicitly defining the conditions or processes under which struvite or ashes and pyrolitic material from urban wastewater treatment plants would not longer be defined as waste and a product instead, would be a good starting point [Position paper, 2021]. In order to preserve natural sources to as large degree as possible it is especially important to find new recycling strategies.

REFERENCES

Central wastewater treatment plant Ljubljana. Available from: Centralna čistilna naprava Ljubljana | JP VOKA SNAGA [Accessed: 31.01.2023].
Directive 86/278/EEC on the protection of the environment, and in particular of the soil, when sewage sludge is used in agriculture, 1986, OJ L 181, 4.7.1986, p. 6–12.
Fertilising Resolution (FR) Regulation (EU) 2019/1009 of the European Parliament and of the Council of 5 June 2019 laying down rules on the making available on the market of EU fertilising products and amending Regulations (EC) No 1069/2009 and (EC) No 1107/2009 and repealing Regulation (EC) No 2003/2003, PE/76/2018/REV/1, OJ L 170, 25.6.2019, p. 1–114.
Communication from the Commission to the European Parliament, the Council, the European economic and social Committee of the Regions on the 2017 list of Critical Raw Materials for the EU, Brussels, 13.9.2017, COM(2017), 490 final.
Critical raw materials. Internal Market, Industry, Entrepreneurship and SMEs [Internet]. 2012. Available from: Critical raw materials | Internal Market, Industry, Entrepreneurship and SMEs (europa.eu) [Accessed: 31.01.2023].
Position paper, Enabling the circular potential of sewage sludge within the EU legislative framework, A critical analysis of the current urban waste water treatment sludge legislation with respect to the circular economy. EurEau 2021. Available from: file (eureau.org) [Accessed: 31.01.2023].

Gas-permeable membranes for the reduction of ammonia emissions in pig farms: A global approach.

B. Molinuevo-Salces*, B. Riaño*, M.C. García-González**, P. Calvo de Diego** and M. Sánchez Báscones**

* Agricultural Technological Institute of Castilla y León, Ctra. Burgos, km 119, 47071 Valladolid, Spain. (E-mail: ita-molsalbe@itacyl.es; beatriz.molinuevo.salces@gmail.com)
** Superior Technical School of Agricultural Engineering, University of Valladolid, Avenida de Madrid 57, 34004 Palencia, Spain (E-mail: mariacruz.garcia.gonzalez@uva.es)

Abstract
Gas-permeable membrane (GPM) technology is a N-recovery technology that could contribute to the mitigation of ammonia emissions while obtaining a fertilizing product. A global approach for the reduction of NH_3 emissions in a pig farm is reported in this study. Two pilot plants based on GPM technology were installed and evaluated on-farm, one plant for the N-capture in the atmosphere of the farm building and another for the capture of ammonia in the liquid manure of the manure storage tank. Nitrogen was successfully recovered as fertilizing product (i.e. ammonium sulphate) in both pilot plants. The temperature positively influenced TAN recovery rates in both systems.
Keywords
Ammonia recovery, Gas-permeable membranes, pig farm, swine manure

INTRODUCTION

Ammonia emissions reduction is of major importance for the competitiveness of the EU livestock sector. In the case of Spain, reductions of 16% are expected in 2030, in comparison to the 453 kt of NH_3 produced in 2005, the baseline year (NEC Directive (2016/2284). The agricultural sector was responsible for 3.6 million tons of NH_3 emissions in 2017, being released from the livestock buildings (44%), the manure storages (25%) and during land application (31%). Gas-permeable membrane (GPM) technology is a N-recovery technology that presents high recovery rates while not altering farm operations. Moreover, GPM technology transforms volatile NH_3 into a marketable fertiliser $(NH_4)_2SO_4$, so that this technology contributes to GHG reduction, since NH_3 production currently emits 1.5 ton of CO_2 per ton of NH_3. The LIFE Ammonia Trapping project demonstrated at on-farm pilot plant scale that the GPM technology successfully captures NH_3 from pig manure and from the air in animal buildings (TRL 6). The LIFE Green Ammonia aims at increasing the TRL of GPM technology through the design, evaluation and commercialization of improved models for N-capture. This study reports a global approach for the reduction of NH_3 emissions in a pig farm, both from the atmosphere of the farm building and from the liquid manure in the manure storage tank.

MATERIALS AND METHODS

Pilot plants configuration

Two pilot plants were designed, built and tested on farm: The NH_3-recovery pilot plant for gases (Soto-Herranz et al., 2021) and the NH_3-recovery pilot plant in liquids (Molinuevo-Salces et al., 2020). Both pilot plants were based on the GPM technology using tubular membranes made of ePTFE, with an outer diameter of 5.2 mm, a wall thickness of 0.64 mm and a polymer density of 0.95 g cm^{-3}. The NH_3-recovery pilot plant for gases consisted of a 2.6 m^3 steel structure with 32 membrane panels. The surface area of the membrane used was 7.7 m^2. The pilot plant contained a single-phase wall-mounted fan, two ammonia sensors, a recirculation pump for the acidic solution, a 0.25 m^3 tank for the storage of the acidic solution, a sealed distribution pipe connected to the 32 parallel membrane panels, a collecting pipe, pH and temperature probes, a pressure gauge to monitor the pressure of the acidic solution and a PLC system to control the equipment. The NH_3-recovery pilot plant in liquids was equipped as follows: A manure feeding pump, a 5.85 m^3 ammonia separation reactor tank with a module of 16 membrane panels, a blowing air pump for aeration, a manure recirculation pump for mixing the reactor, a 0.25 m^3 tank for ammonia concentration and for the trapping solution storage, a recirculation pump for the trapping solution, a heating blanket and a PLC control system. The surface area of the membrane used was 13.07 m^2, the ratio of membrane length per manure volume was 0.16 m L^{-1} and the ratio of the membrane area per volume of manure was 0.0026 m^2 L^{-1}.

Location

The experiments were carried out in Guardo (Palencia, Spain). The pilot plants were located in a sow farm with 2800 animals, generating a volume of swine manure of approximately 17,136 m^3 per year. More specifically, the NH_3-recovery pilot plant for gases was located inside a gestating sow house with 912 places, with a natural ventilation system. The NH_3-recovery pilot plant in liquids was installed inside a mobile shipping container, which was placed outside the farm building, next to a manure storage pit.

Experimental procedure and sampling

The NH_3-recovery pilot plant in liquids was evaluated during seven months in 2018. First, a setup period of 56 days was carried out to optimize the pilot plant operation and then the pilot plant was operated in batch mode. Five batch experiments (B1-B5) were carried out to evaluate the performance of the pilot plant at real environmental conditions. The NH_3-recovery pilot plant for gases was evaluated for eight-months in 2019. A two-month trial was first performed to optimize the performance of the equipment. Then, the plant was operated in continuous mode. Analyses of total ammonia nitrogen (TAN) were performed once per week both in the acidic solutions and in the manure. pH and temperature were daily monitored.

RESULTS AND DISCUSSION

Ammonia gas reacts with the acid of the trapping solution (sulphuric acid in this case) to form $(NH_4)_2SO_4$, that remains in the liquid phase. Ammonium sulphate is a valuable fertilizer. The TAN recovery in the acidic solution was 4108 g in 232 days for the NH_3-recovery pilot plant for gases and it was in the range of 1357-5457 g in batch experiments of 7 to 20 days for the NH_3-recovery pilot plant in liquids (Table 1). As it can be seen from the results, the amount of N that was recovered was in the same range, both in the liquids and from the atmosphere, but the latter in much lower time. This is due to the higher concentration of TAN in the manure than in the atmosphere of the farm building. In this way, and as it was previously reported by Soto-Herránz et al., (2021), the capture of nitrogen gas directly from the atmosphere would be only effective if the TAN concentration is high. So that, it seems appropriate to install GPM technology after the forced ventilation systems of the animal buildings.

Table 1. TAN recovery in the acidic trapping solution.

	Unit	Gas-recovery pilot plant	Pilot plant for ammonia recovery in liquids				
			B1	B2	B3	B4	B5
TAN acidic solution	g	4108	2198	5457	3296	1357	2301
Experimental time	days	232	11	7	20	14	20

Regarding TAN recovery rates a high variation between summer and winter months was observed. In the case of the NH_3-recovery pilot plant for gases, an average rate of 1.6 g TAN m^{-2} day^{-1} was obtained during the summer season and an average rate of 3.9 g TAN m^{-2} day^{-1} was registered during the winter season (Table 2). These results are in accordance with the higher ammonia concentrations registered in the farm house during winter, in comparison with the summer months. This is a consequence of an increase in ventilation in the animal houses during the summer season due to the harmful gases accumulated in the buildings with the high temperatures of summer. In the case of the gas pilot plant, operating the pilot plant would be more useful in winter months or in periods without natural ventilation. This it would contribute to reduce NH_3 emissions inside the buildings while recovering N in the form of ammonium sulphate.

Table 2. TAN recovery rates related to temperature.

	Unit	Gas-recovery pilot plant		Pilot plant for ammonia recovery in liquids				
		Summer	Winter	B1	B2	B3	B4	B5
TAN recovery rate	g TAN m^{-2} day^{-2}	1.6	3.9	25.2	38.2	16.1	8.4	10.9
Temperature	ºC	17.9*	5.8*	26.8**	28**	24.6**	20**	21.5**

*Temperature is referred to outdoor ambient temperature
**Temperature is referred to temperature in pig manure

On the other hand, in the NH_3-recovery pilot plant in liquids the TAN recovery rates during the different batch experiments were in the range of 8.4 and 38.2 g TAN m^{-2} day^{-1} (Table 2). These differences were in accordance with seasonal variations in manure temperature, so that a positive exponential relationship between temperature and TAN recovery (R^2=0.87) was found in this case. The higher temperature in the manure, the better TAN recovery rate.

CONCLUSIONS

Nitrogen was successfully recovered as ammonium sulphate both in the liquids and from the atmosphere using GPM technology. The temperature positively influenced TAN recovery rates in both systems. For N-recovery in gases, 1.6 g TAN m^{-2} day^{-1} were obtained during summer and 3.9 g TAN m^{-2} day^{-1} during winter. In the N-recovery in liquids, the rates ranged between 8.4 and 38.2 g TAN m^{-2} day^{-1}.

AKNOWLEDGEMENTS

This work has been funded by the European Union under the Project Life+ GREEN AMMONIA (LIFE20-ENV/ES/000858), and Project Life+ AMMONIA TRAPPING (LIFE15 ENV/ES/000284). B. Molinuevo-Salces thanks AEI for funding, through RYC-2020-029030-I/AEI/10.13039/501100011033.

REFERENCES

Directive, E. U. (2016). Directive (EU) 2016/2284 of the European Parliament and of the Council of 14 December 2016 on the reduction of national emissions of certain atmospheric pollutants, amending Directive 2003/35/EC and repealing Directive 2001/81. Official Journal of the European Union: Brussels, Belgium.

Molinuevo-Salces, B., Riaño, B., Vanotti, M.B., Hernández-González, D., García-González, M.C., 2020. Pilot-Scale Demonstration of Membrane-Based Nitrogen Recovery from Swine Manure. *Membranes*, **10**, 270.

Soto-Herranz, M.; Sánchez, M; Antolín-Rodríguez, J.M; Martin-Ramos, P. 2021. Pilot Plant for the Capture of Ammonia from the Atmosphere of Pig and Poultry Farms Using Gas-Permeable Membrane Technology. Membranes, **11**, 859

Production of Volatile Fatty Acids and Kinetic Study of the Anaerobic Digestion of Cheese whey

da Silva-Lacerda, V.*, Riaño, B.*, García-González, M. C.**, Molinuevo-Salces, B*.

* Agricultural Technological Institute of Castilla y Léon. Ctra. Burgos, km. 119 47071 Valladolid (Spain) (E-mail: *silfacvl@itacyl.es; rianrub@itacyl.es; ita-mosalbe@itacyl.es)*
** Department of Agricultural and Forestry Engineering, University of Valladolid, Avenida de Madrid 44, 34004 Palencia, Spain (E-mail: *mariacruz.garcia.gonzalez@uva.es)*

Abstract
The use of cheese whey for VFA production through anaerobic fermentation is being widely studied as a green and renewable alternative for whey valorisation. The study of kinetic models helps to predict the results of this process. Cheese whey was fermented in batch, at pH 5.5 and pH 10, and at constant temperature of 38ºC. VFA production from cheese whey shows great results. The highest production of VFA was at pH 5.5, with a yield of 9.11 g COD L^{-1}. The experimental results were analysed using two kinetic models and it was observed that to the Modified Gompertz model fits better to the pH 5.5 while the First Order model fits better to the pH 10. The best fit is for pH 5.5 using the Gompertz model, where an r^2 value of 0.9936 and a BIC value of -8.31 were found.

Keywords (maximum 6 in alphabetical order)
Anaerobic digestion; cheese whey; kinetic study; VFA production

INTRODUCTION

Cheese whey (CW) contains a high organic load, resulting in one of the main wastes to dairy industry. The cheese industry generates an average of 9L of whey for every kg of produced cheese (Guimaraes et al., 2010). CW contains mostly sugars (lactose), fat and proteins, so it is a great source of carbon and nitrogen. The current uses and management strategies for CW include animal feeding, biogas production and conversion of CW into valuable products as whey powder, lactose powder or protein concentrate (Asunis et al., 2020). The development of the dairy sector is highly dependent on the Environmental legislation, due to the GHG emissions of dairy activities (FAO and OECD, 2020). In this manner, innovative and sustainable solutions are necessary to ensure the competitiveness of dairy sector. Anaerobic digestion (AD) has proven to be a green alternative with great potential to reduce, recycle and recover various organic industrial wastes (Nguyen et al., 2019). Traditionally, investigation has been focused on maximizing methane production. However, and due to the value of the intermediate compounds, this technology is shifting to the production of volatile fatty acids (VFA) in the frame of a circular economy approach. VFA are value added molecules with a high price in the market and they are mostly produced by transformation of petrochemicals or via fermentation. Several factors influence the VFA yields and composition obtained from AD like pH (Greses et al., 2020, Yu et al. 2021), temperature, type of substrate (or inoculum), among others.
The main objectives of this study were to evaluate the influence of pH in the production and composition of VFA using CW as substrate and appling and evaluating two kinetic models (i.e. a first order kinetic model and the modified Gompertz model) to describe the kinetics and mechanisms of VFA production. A kinetic study was carried out to estimate which model presents the best adjustment and a better prediction of VFA production.

MATERIALS AND METHODS

Substrate and inoculum

Cheese whey (CW) from local cheese factories (Palencia, Spain) was used as a substrate to produce VFA. This by-product was collected and maintained frozen to avoid organic degradation. Thereafter, when was necessary, the substrate was thawed and stored at 4ºC. The inoculum was anaerobic sludge (AS) obtained from urban wastewater treatment plant of Valladolid, Spain. The CW and AS were characterized according to volatiles solids (VS), total solids (TS), total chemical oxygen demand (COD) and pH.

Experimental procedure

The experiments were conducted in a reactor with 1L of mixture substrate/inoculum (1:1, in VS proportions). The assays were performed in batch under two different conditions of pH, acidic (pH 5.5) and basic (pH 10), and at constant temperature (38ºC). The reactors were below constant mixing and the pH was adjusting every day by using 1M NaOH and 1M HCl. The temperature was maintained on the reactor glass jacket by circulation water. The VFA production assays were carried out for 14 days.

Kinetic study

Two types of kinetic model (First Order and Gompertz) were selected to predict the maximum production of VFA. The first order model Eq. (1) was selected to report the hydrolysis rate constant, while the Gompertz model Eq. (2) provides the lag phase time and the maximum VFA production rate.

First Order Kinetic model: $VFA = VFA_{max} \times [1 - exp(-kt)]$ (1)

Modified Gompertz model: $M = VFA_{max} \times exp\left\{-exp\left[\frac{VFA_{p}e}{VFA_{max}}(\lambda - t) + 1\right]\right\}$ (2)

where VFA is yield with respect to time t, VFAmax is the maximum VFA potential of the substrate, k is the hydrolysis rate constant, t is the time, VFAp is the maximum VFA production rate (g COD L^{-1} d^{-1}), λ is the lag phase time (days) and "e" is Euler's function equal to 2.7183.
The Bayesian information criterion (BIC) test Eq. (3) were used to compare the models and to determine the model that is more likely to be correct.

$$BIC = N\ ln\left(\frac{RSS}{N}\right) + K\ \ln\ (N) \quad (3)$$

where N is the number of data points, K is the number of parameters fit by the regression model, and RSS is the residual sum of the square.

RESULTS AND DISCUSSION

Production and composition of VFA

Figure 1 shows the VFA production and composition in mesophilic conditions (38ºC) and under two pH (5.5 and 10). The production of VFA was higher under acidic conditions than basic conditions, with a yield of 9.11 g COD L^{-1} and 7.01 g COD L^{-1}, for pH 5.5 and 10 respectively. The highest variety of VFA was in pH 5.5, with higher yield of propionic (2.79 g COD L^{-1}), acetic (2.58 g COD L^{-1}) and butyric acid (1.40 g COD L^{-1}). On the other hand, when operating at pH 10, the production was basically composed of acetic acid (5.78 g COD L^{-1}). Similar results, at basic conditions and using cheese whey as substrate was found in Iglesias-Iglesias et al (2020), where a higher production of acetic and butyric acid was observed. Khatami et al. (2021) corroborate the results found in this assay, where under acidic conditions also found that higher VFA produced was propionic acid and under basic condition was acetic acid.

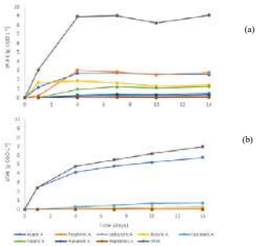

Figure 1. VFA production and composition, under pH 5.5 (a) and pH 10 (b) conditions.

Kinetic study

Figure 2 shows the graphical representation of the models indicated in equations 1 and 2. The kinetic parameters and the BIC test results are show in Table 1. High r^2 values confirm that all the models fit the experimental data. The values of k correspond to the hydrolysis rate constant. The constant k is higher for pH 5.5 than pH 10, with 0.53 and 0.33, respectively. Low k values indicate that there is a lower rate of biodegradability of the substrate and that more time is needed for VFA production to be maximum (Nguyen et al., 2019). As a result, it indicates that at pH 10 the reaction is slower than at pH 5.5. For both models, the VFA yield is higher for pH 5.5, with 9.21 g COD L^{-1} (First Order model) and 8.84 g COD L^{-1} (Modified Gompertz model), even though the first order model is closer to the experimental data.

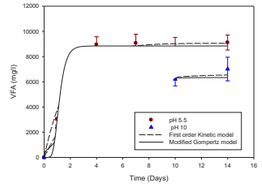

Figure 2. VFA yield from the First Order Kinetic model and Modified Gompertz model.

The VFAp is higher for pH 5.5 (9.40 g COD L^{-1} d^{-1}) than pH 10 (1.43 g COD L^{-1} d^{-1}). It indicates that the production of VFA is faster at acidic conditions than at basic conditions. The adaptation of microorganisms and the digestion response time is expressed by the lag phase (λ). The value of λ was lower for pH 10 (0 day) than at pH 5.5 (0.53 day) indicating that there is a higher adaptability of microorganisms to produce VFA at basic conditions (Pramanik et al., 2019).

Table 1. Estimated kinetic parameters for the two models.

Kinetic Model	Parameter	Units	pH 5.5	pH 10
First Order	k	day^{-1}	0.53	0.33
	VFA yield	g COD L^{-1}	9.21	6.59
	r^2	-	0.9732	0.9788
	BIC	-	-0.76	-6.34
Modified Gompertz	λ	days	0.67	0
	VFA yield	g COD L^{-1}	8.84	6.36
	VFAp	g COD L^{-1} d^{-1}	9.40	1.43
	r^2	-	0.9936	0.9437
	BIC	-	-8.31	-1.86

BIC is a statistical indicator that helps to determine the best fit between the kinetic model and the experimental data. The lowest BIC values show the most suitable kinetic model (Pramanik et al., 2019). According to BIC data, for pH 10 the best fit is for the First Order model presenting lowest values (-6.34). For pH 5.5 and using the Gompertz model, the highest value of r^2 (0.9936) and the lowest value of BIC (-8.31) were found, indicating that the Gompertz model is the best fits the experimental data at these conditions. All results of BIC are corroborated by r^2 values.

CONCLUSION

VFA production through anaerobic digestion is a sustainable way of valorization of cheese whey, using sewage sludge as inoculum. Anaerobic digestion of whey produces up to of 9 g COD L^{-1} and 7.01 g COD L^{-1}, for acidic and basic pH conditions, respectively. Under basic conditions VFA are mainly acetic acid while under acidic conditions VFA composition is more varied. First order and Gompertz kinetic models can be used to indicate the best conditions and predict the maximum production of VFA. The Modified Gompertz model fits better for pH 5.5 while the First Order model fits better for pH 10.

Aknowledgements: This study was funded by the European Union and the Rural Development Program for Castilla y León through the FEADER project LACTOCyL "Applying bioeconomy to the valorization of cheese whey for feeding, sustainable energy production and bioproducts obtention". B. Molinuevo-Salces thanks AEI for funding, trough RYC-2020-029030-I/AEI/10.13039/501100011033.

REFERENCES

Asunis, F., De Gioannis, G., Dessì, P., Isipato, M., Lens, P.N., Muntoni, A., Polettini, A., Pomi, R., Rossi, A. and Spiga, D., 2020. The dairy biorefinery: Integrating treatment processes for cheese whey valorisation. Journal of Environmental Management **276**, 111240.
Greses, S., Tomás-Pejó, E. and Gónzalez-Fernández, C., 2020. Agroindustrial waste as a resource for volatile fatty acids production via anaerobic fermentation. Bioresource technology **297**, 122
Guimaraes, P.M., Teixeira, J.A., Domingues, L. 2010. Fermentation of lactose to bioethanol by yeasts as part of integrated solutions for the valorization of cheese whey. Biotechnology Advances **28** (3), 375-384.
Iglesias-Iglesias, R., Kennes, C., Veiga, M.C. 2020. Valorization of sewage sludge in co-digestion with cheese whey to produce volatile fatty acids. Waste Management **118**, 541-551.
Nguyen, D.D., Jeon, B-H., Jeung, J.H., Rene, E. R., Rajesh Banu, J., Ravindran, B., Vu, C. M., Ngo, H. H., Guo, W., Chang, S.W. 2019 Thermophilic anaerobic digestion of model organic wastes: Evaluation of biomethane production and multiple kinetic model analysis. Bioresource Technology **280**, 269-276.
Khatami, K., Atasoy, M., Ludtke, M., Baresel, C., Eyice, O., Cetecioglu, Z. 2021. Bioconversion of food waste to volatile fatty acids: Impact of microbial community, pH and retention time. Chemosphere **275**, 129981.
Pramanik, S.K., Suja, F. B., Porhemmat, M., Pramanik, B. K. 2019. Performance and Kinetic Model of a Single-Stage Anaerobic Digestion System Operated at Different Successive Operating Stages for the Treatment of Food Waste. Processes **7**, 600.
OECD/Food and Agriculture Organization of the United Nations (2020), "Dairy and dairy products", in OECDFAO Agricultural Outlook 2020-2029, OECD Publishing, Paris/Food and Agriculture Organization of the United Nations, Rome.
Orhan Yenigün, Burak Demirel. 2013. Ammonia inhibition in anaerobic digestion: A review. Process Biochemistry **48**, 901-911
Yu, P., Tu, W., Wu, M., Zhang, Z., Wang, H. 2021. Pilot-scale fermentation of urban food waste for volatile fatty acids production: The importance of pH. Bioresource Technology **332** (2021), 125116.

Treatment of pickling waste liquors using a thraustochytrid for removal of organic carbon and nitrogen and simultaneous production of polyunsaturated fatty acids

S. Nakai*, T. Suenaga*, A. Umehara**, W. Nishijima**, T. Gotoh*

* Department of Chemical Engineering, Hiroshima University, Higashi- Hiroshima, 739-8527 Hiroshima, Japan
(E-mail: *sn424762l@hiroshima-u.ac.jp; suenagat@hiroshima-u.ac.jp; tgoto@hiroshima-u.ac.jp*)
** Environmental Research and Management Center, Hiroshima University, Kagamiyama, Higashi- Hiroshima, 739-8527 Hiroshima, Japan
(E-mail: *umehara@hiroshima-u.ac.jp; wataru@hiroshima-u.ac.jp*)

Abstract
The thraustochytrid, *Aurantiochytrium* sp. strain L3W was applied to treat the 3 pickling (*Shisohijiki, Hiroshimana*, and *Akimurasaki*) waste liquors to remove dissolved organic carbon (DOC) and dissolved nitrogen (DN) and to produce valuable polyunsaturated fatty acids (PUFAs) such as docosahexanoic acid (DHA) and eicosapentanoic acid (EPA). The strain L3W grew on the liquid waste liquors, while adjustment of the initial pH but not sterilization was carried out as pretreatment of the waste liquors. The removal efficiencies of DOC and DN were respectively about 35-80% and 35-80%. The produced biomass contained DHA and EPA, and the DHA and EPA contents, and the *Hiroshimana* waste liquor with the initial pH7 demonstrated the highest DHA and EPA contents of 75 mg/g and 1.1 mg/g, respectively. This study provided the evidence that the thraustochytrid can be used to treat the pickling waste liquors and to produce PUFAs.

Keywords: *Aurantiochytrium* sp., pickling waste liquors, polyunsaturated fatty acid.

INTRODUCTION

Pickling waste liquors are abundant in organic compounds but hypersaline. Because of this nature, new methodologies are required to treat pickling waste liquors. Therefore, this study focused on use of thraustochytrids. Thraustochytrids are heterotrophic and halophilic microorganisms that can produce valuable polyunsaturated fatty acids (PUFAs) such as docosahexanoic acid (DHA) and eicosapentanoic acid (EPA) (Nakai et al., 2021). DHA and EPA are contained in fish oil and essential for cultured fish such as salmon (Shepherd et al., 2017). Because of issues relating to the sustainability of wild fisheries and constraints on aquaculture systems (Cadillo-Benalcazar et al., 2020), cultivation of thraustochytrids using pickling waste liquors may be beneficial via satisfying both of removal of dissolved organic carbon (DOC) and dissolved nitrogen (DN) and production of valuable PUFAs. This study aims at investigating usability of a thraustochytrid for treatment of pickling waste liquors and production of PUFAs.

MATERIALS AND METHODS

The 3 waste liquors generated from the production processes of *Shisohijiki, Hiroshimana,* and *Akimurasaki* pickles (Table 1) were collected from the pickling factory in Hiroshima, Japan. The *Shisohijiki, Hiroshimana, and Akimurasaki* pickling waste liquors were diluted with sand filtered seawater at twice, 20 times and 5 times, respectively to attain about 10000 mg/L of DOC. Adjusting to pH4 and pH7, the thraustochytrid, *Aurantiochytrium* sp. strain L3W was inoculated. To confirm whether sterilization is necessary, both autoclaved and unsterile media was tested for cultivation of the strain L3W. Growth of strain L3W was monitored by microscopic observation, and the resultant biomass was analysed by a gas chromatograph equipped with a flame ionization detector (GC/FID).

Table 1. Characteristics of the pickling waste liquors.

	Shisohijiki	*Hiroshimana*	*Akimurasaki*
pH	4.0	4.0	3.5
Salinity [PSU]	30	38	48
DOC [mg/L]	20253	192120	54970
DN [mg/L]	814	1015	7701

RESULTS AND DISCUSSION

Growth of the strain L3W

The strain L3W did grow on the unsterile *Hiroshimana* pickling waste liquor, and no difference of the growth was confirmed between the sterile and unsterile conditions at the initial pH7 (Fig. 1). This indicates that sterilization was unnecessary for treatment of the *Hiroshimana* pickling waste liquor using the strain L3W. The strain L3W grew on the tested 3 pickling waste liquors (Fig. 2), though the measured biomass may include contaminating microorganisms such as yeasts.

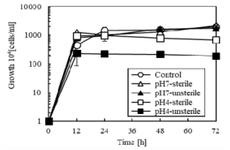

Figure 1. Growth curve of the strain L3W in the diluted *Hiroshimana* pickling waste liquor (n=3).

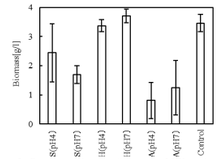

Figure 2 Biomass production of the strain L3W on the diluted *Shisohijiki* (S), *Hiroshimana* (H), and *Akimurasaki* (A) pickling waste liquors under nonsterile condition (n=3).

Removal of DOC and DN

The DOC and DN concentrations before and after cultivation of the strain L3W are compared in Fig. 3, where about 35-80% of DOC and 35-80% of DN were removed. Because the remaining DOC and DN concentrations were high, further treatment may be necessary. Possible reason for the lowest DOC and DN removal from the *Akimurasaki* waste liquor might be containment of polyphenols that can inhibit growth of the strain L3W.

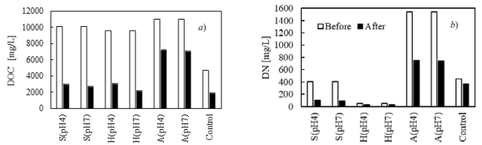

Figure 3 Dissolved organic carbon (DOC) and dissolved nitrogen (DN) concentrations before and after treatment using the strain L3W under nonsterile conditions.

PUFAs contents in the biomass of strain L3W

DHA and EPA production on the pickling waste liquors at pH7 was 15 mg/g and 0.37 mg/g for *Shisohijiki,* 75 mg/g and 11 mg/g for *Hiroshimana,* and 21 mg/g and 0.37 mg/g for *Shisohijiki,* though the cultural media were unsterile.

REFERENCES

Cadillo-Benalcazar, J.J., Giampietro, M., Bukkens, S.G.F., Strand, R. 2020 Multi-scale integrated evaluation of the sustainability of large-scale use of alternative feeds in salmon aquaculture. *J Clean. Prod.* 248, 119210

Nakai S., Das A., Maeda Y., Humaidah N., Ohno M., Nishijima W., Gotoh T., Okuda T. 2021 A novel strain of Aurantiochytrium sp. strain L3W and its characteristics of biomass and lipid production including valuable fatty acids. *J Water Environ Tech* 19, 24–34.

Shepherd, C.J., Monroig, O., Tocher, D.R. 2017 Future availability of raw materials for salmon feeds and supply chain implications: The case of Scottish farmed salmon. *Aquac* 467, 49–62.

Metabolic network reconstruction providing insights into the metabolism relevant for resource recovery in *Rhodobacter sphaeroides*

Akhila George*, Gabriel Capson-Tojo** and Adrian Oehmen*

* The School of Chemical Engineering, The University of Queensland, St. Lucia, QLD 4072, Australia (E-mail: akhila.george@uq.edu.au; a.oehmen@uq.edu.au)
** INRAE, University Montpellier, LBE, 102 Avenue des Etangs, Narbonne 11100, France (E-mail: gabriel.capson-tojo@inrae.fr)

Abstract
Rhodobacter sphaeroides is a versatile purple non-sulfur bacteria that can be used in resource recovery to produce hydrogen, polyhydroxyalkanoates, single-cell protein and other value-added products. We developed a genome-scale metabolic model representing the primary metabolism of a denitrifying strain *R. sphaeroides* ATCC 17025. This metabolic model predicted growth, production of hydrogen and polyhydroxybutyrate, and was in better agreement with literature-based experimental values as compared to predictions from existing models for *R. sphaeroides*. We evaluated the growth, production rates and product distribution under different metabolisms and using different organic substrates. In addition, it allowed to assess the metabolic mechanisms governing the preferential generation of different products. This model can be a valuable tool to optimize the generation of value-added products.

Keywords
Hydrogen production; metabolic modelling; polyhydroxybutyrate; resource recovery; *Rhodobacter sphaeroides*

INTRODUCTION

Purple phototrophic bacteria (PPB) can be used in the resource recovery of value-added products from waste streams. The versatility, high efficiency of removal of organics and the capability of PPB to utilize sunlight as its energy source for its growth and metabolism makes wastewater treatment using PPB economically feasible. *Rhodobacter sphaeroides* is one of the commonly observed PPB and was found dominant in mixed cultures cultivated outdoor (Hülsen, Stegman, et al., 2022; Hülsen, Züger, et al., 2022). A genome-scale metabolic model facilitates better understanding of the flexible metabolism of PPB and prediction of its varying physiological behaviour with different substrates and environmental conditions. Integration of this model with the bioprocess model would improve the reliability of the model and needs less recalibration with varying composition of wastewater feedstock or operational parameters.

To the best of our knowledge, there is no curated metabolic pathway database available for *Rhodobacter sphaeroides*, that would allow integration and visualization of the metabolic pathways, reactions, enzymes, proteins and genes and other evolving information related to transcript, protein and metabolite profiling. There are genome-scale metabolic models representing the photoheterotrophic growth of *Rhodobacter sphaeroides* strain 2.4.1 (Imam, Yilmaz, et al., 2011; Imam, Noguera, et al., 2013), *Rhodopseudomonas palustris* (Alsiyabi, Immethun, et al., 2019) that were applied to study the aspects of photosynthesis, hydrogen production, different substrate uptake and redox state. However, more study is needed to understand the substrate preferences of cells for growth and production of value-products and their distribution towards different products that are relevant to resource recovery. In the current study, a curated metabolic pathway database and a genome-scale metabolic model of *Rhodobacter sphaeroides* ATCC 17025 is developed, showing better predictions than that of existing models. The model was validated with experimental data under different trophic conditions like photoautotrophic, aerobic heterotrophic and anaerobic photoheterotrophic conditions. The metabolic model was employed to study the product distribution of hydrogen, polyhydroxybutyrate, CO_2 fixation and growth under different light uptake rates.

MATERIALS AND METHODS

Development of pathway database & metabolic model

A genome-pathway database of *R. sphaeroides* ATCC 17025 was retrieved from the biochemical database, BioCyc. Pathways and reactions involved in the central carbon and nitrogen metabolism were curated by adding 111 modifications that were based on studies gathered from 42 scientific articles/reviews and genome-based evidence. The curation of the database was guided by analysis using the Metaflux module of Pathway Tools software (Latendresse, Krummenacker, et al., 2012) and thus a draft metabolic model was developed from the database. Compartments of cytoplasm, membrane space, periplasmic space, and extracellular space were also included in the Rba_sphCyc database. The metabolic model was validated qualitatively and quantitatively by comparing the predictions of the model under various trophic conditions with the experimental observations or conclusions published in 17 articles.

RESULTS AND DISCUSSION

Curation and validation of the metabolic model

The details of the curated pathway-database, RbaSphCyc, which will be published in MetaCyc, are given in

Table 1. A genome-scale metabolic model was generated from the curated pathway database. As a part of the qualitative assessment of the metabolic model, growth of *R. sphaeroides* was simulated under photoautotrophic, aerobic heterotrophic, anaerobic heterotrophic, anaerobic photoheterotrophic condition. The validation of the model was carried out by conducting quantitative assessment of flux under photoautotrophic, aerobic heterotrophic and anaerobic photoheterotrophic conditions. The predicted values along with experimental data (gathered from literature) used for validation of the model under these conditions are shown in Figure 1, Figure 2 and Figure 3, respectively.

The photoheterotrophic growth of *R. sphaeroides* on different substrates (succinate-glutamate, succinate-ammonia, glucose-glutamate and glutamate only) were simulated using the uptake rates reported by Imam et al. (2011). In the first step, fluxes were optimized to produce maximum biomass and the specific growth rates predicted by RbaSphCyc model were in agreement with that observed in the reported experiments (Imam, Yilmaz, et al., 2011)(Imam, Noguera, et al., 2013). In the second step, a light constraint was applied and the production rates for polyhydroxybutyrate, hydrogen and CO_2 were predicted, which were in good agreement with the experimental values obtained by Imam et al. (2011).

Under photoheterotrophic and NH_3 limited conditions, when the light uptake rate is above the minimum rate that is needed for maximum growth, concomitant H_2 and PHB production was predicted (shown in Figure 4). An increase in light uptake rate increases ATP production and thus increases the rate of H_2 production, thereby affecting other electron sink pathways such as PHB production and CO_2 fixation inversely. This pattern was found similar in all the four cases mentioned, but the range of light uptake rate differs based on substrate. When the activity of nitrogenase is not limited by ammonia, the main factors that affect H_2 production were found to be light and redox condition of substrate.

CONCLUSION

We developed a genome-scale metabolic model representing primary metabolism of *R. sphaeroides* ATCC 17025, that can be used to simulate photoautotrophic, anaerobic heterotrophic, anaerobic photoheterotrophic growth and predict flux distribution towards production. Under photoheterotrophic and ammonia-limited condition, a light uptake rate higher than that needed for growth, is required to produce hydrogen. Under this condition, light uptake rate plays a major role in defining the flux distribution through electron sink pathways like production of hydrogen, PHB and CO2 fixation.

Table 1: Details of genome-pathway database, RbaSphCyc

Model Field	Values
Pathways	252
Enzymatic reactions	1587
Transport reactions	91
Enzymes	1237
Compounds	1220
Genes	1020
Compartments	4

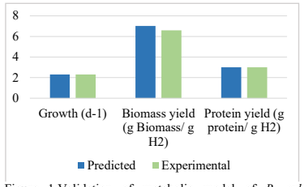

Figure 1:Validation of metabolic model of *R. sphaeroides* for photoautotrophic growth. Experimental data is taken from (Spanoghe, Vermeir, et al., 2021).

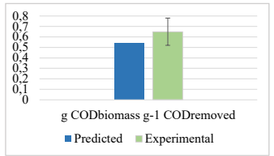

Figure 2: Validation of metabolic model of R. sphaeroides for photoautotrophic growth. Experimental data is taken from (Alloul, Muys, et al., 2021).

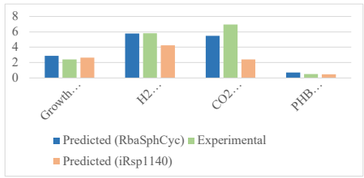

Figure 3:Validation of RbaSphCyc model for photoheterotrophic growth of *R. sphaeroides* growing on succinate as carbon source and glutamate as nitrogen source. iRsp1140 is a model developed for *R. sphaeroides* strain 2.4.1. by Imam et al. (2013).

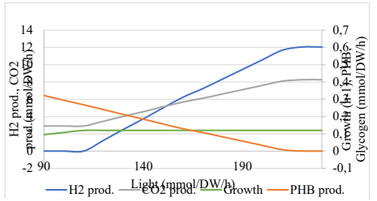

Figure 4: Growth of *R. sphaeroides* along with production of hydrogen, polyhydroxybutyrate (PHB) and CO2 with varying light uptake rate under photoheterotrophic condition. Succinate and glutamate were used as carbon source and nitrogen source.

REFERENCES

Alloul, A., Muys, M., Hertoghs, N., Kerckhof, F.-M., and Vlaeminck, S. E. 2021 Cocultivating aerobic heterotrophs and purple bacteria for microbial protein in sequential photo- and chemotrophic reactors. Bioresource Technology, **319**(August 2020), 124192.

Alsiyabi, A., Immethun, C. M., and Saha, R. 2019 Modeling the Interplay between Photosynthesis, CO2 Fixation, and the Quinone Pool in a Purple Non-Sulfur Bacterium. Scientific Reports, **9**(1), 12638.

Hülsen, T., Stegman, S., Batstone, D. J., and Capson-Tojo, G. 2022 Naturally illuminated photobioreactors for resource recovery from piggery and chicken-processing wastewaters utilising purple phototrophic bacteria. Water Research, **214**(February), 118194.

Hülsen, T., Züger, C., Gan, Z. M., Batstone, D. J., Solley, D., Ochre, P., Porter, B., and Capson-Tojo, G. 2022 Outdoor demonstration-scale flat plate photobioreactor for resource recovery with purple phototrophic bacteria. Water Research, **216**(March), 118327.

Imam, S., Noguera, D. R., and Donohue, T. J. 2013 Global insights into energetic and metabolic networks in Rhodobacter sphaeroides (G. Tucker-Kellogg, ed.). BMC Systems Biology, **7**(1), 89.

Imam, S., Yilmaz, S., Sohmen, U., Gorzalski, A. S., Reed, J. L., Noguera, D. R., and Donohue, T. J. 2011 iRsp1095: a genome-scale reconstruction of the Rhodobacter sphaeroides metabolic network. BMC systems biology, **5**(1), 116.

Latendresse, M., Krummenacker, M., Trupp, M., and Karp, P. D. 2012 Construction and completion of flux balance models from pathway databases. Bioinformatics, **28**(3), 388–396.

Spanoghe, J., Vermeir, P., and Vlaeminck, S. E. 2021 Microbial food from light, carbon dioxide and hydrogen gas: Kinetic, stoichiometric and nutritional potential of three purple bacteria. Bioresource Technology, **337**(June), 125364.

Waligórska, M., Seifert, K., Górecki, K., Moritz, M., and Laniecki, M. 2009 Kinetic model of hydrogen generation by Rhodobacter sphaeroides in the presence of NH4+ ions. Journal of Applied Microbiology, **107**(4), 1308–1318.

Onsite Sanitation Disinfection: A Modeling Approach for Lime Treatment of Fecal Matter Containing Viruses

W. Oishi* and D. Sano*,**

* Department of Civil and Environmental Engineering, Graduate School of Engineering, Tohoku University, Aoba 6-6-06, Aramaki, Aoba-ku, Sendai, Miyagi 980-8597, Japan (E-mail: *wakana.oishi.d1@tohoku.ac.jp*)
** Department of Frontier Sciences for Advanced Environment, Graduate School of Environmental Studies, Tohoku University, Aoba 6-6-06, Aramaki, Aoba-ku, Sendai, Miyagi 980-8597, Japan
(E-mail: *daisuke.sano.e1@tohoku.ac.jp*)

Abstract
Lime is a commonly used disinfectant for fecal matters generated in a resource-oriented nonsewered sanitation system. Here, we presented a modeling approach to estimate the minimum treatment time and lime dosage to raise matrix's pH. The estimated treatment time for 3 log inactivation of RNA mammalian viruses was less than 1 h at > pH 11.5, while it was more than 12 h at < pH 10.5. This study provided practitioners with the better guidance of the lime treatment of fecal matter containing viruses for the safe reuse and disposal.

Keywords
Sanitation disinfection; slake lime; alkaline treatment; virus

INTRODUCTION

On-site excreta disinfection is needed in a resource-oriented nonsewered sanitation system to secure the microbiological safety of workers and consumers who are directly exposed to viruses by oral transmission. Lime is commonly used as a base disinfectant for high organic loading waste because it can raise the matrix pH above 10, at which most microorganisms, including surrogate phages cannot survive (Kohn et al., 2017). Requirements on disinfectant dosage and treatment time are determined based on the quantitative relationship between the disinfectant dosage and the extent of virus inactivation. This study aimed to estimate the treatment time and lime dosage to achieve certain log-inactivation values of virus, using machine learning algorithms.

MATERIALS AND METHODS

In order to collect peer-reviewed papers that contain the time-course change of virus infectivity and quantitative information on physicochemical parameters of matrices, we conducted a systematic review following the PRISMA guidelines (Moher et al., 2009). Google Scholar and Web of Science were used as search engines to collect related articles from 1950 to July 2022. The keywords were (lime OR alkali OR calcium hydroxide) AND (pathogen OR virus) AND (inactivation OR disinfection) AND (biosolids OR sludge). The time for 3 LRVs (T99.9) was then calculated by a single reviewer. In short, the Hom model (Hom, 1972) was fit to the time series data of surrogate inactivation identified through the systematic review. T99.9 was then back calculated using the fitted Hom model. We also collected the quantitative and qualitative information on matrices' properties, virus types, and experimental settings.

We employed three machine learning algorithms to estimate T99.9: random forest, light GBM, and Automatic Relevance Determination (ARD) (scikit-learn version 1.2, in Python). The features used for prediction of T99.9 were: structure of virus genome (RNA or DNA), virus type (phage or virus), matrix type (natural or synthesized), suspended solid contents, pH, temperatures, and initial concentration of virus. Eighty percent of the whole datasets were used to train a model, while the rest 20% of datasets were used to evaluate the prediction accuracy of the model. We conducted this set of data allocation and cross validation for ten times, and the mean square values of test data (MSEtest) and training data (MSEtrain) were calculated in each time. We also calculated the ratio of those MSE indicative of the degree of overfitting to training data. The better model was selected based on the mean value of MSE of the ten-time calculation.

RESULTS AND DISCUSSION

Systematic Review

We identified 1,599 records by searching in Google Scholar and Web of Science. Fourteen articles which reported the time-series decay of viruses, types of matrices, and physicochemical properties were identified. Tested alkali additives were; slaked lime, burnt lime, sodium hydroxide, alkaline buffer, and ash. The matrix's pH after alkali addition ranged from pH 8.4 to pH 13.4.

Estimation of the lime dosage and T99.9

The better prediction accuracy was obtained based on the ARD model (**Figure 1**). The pH value was the most important factor on the treatment time compared to the structure of virus genome and the abundance of suspended solids. The coefficients were positive for the variables of virus type, matrix type, and virus initial concentration, which indicated that estimated treatment time was longer for the inactivation of phage compared to mammalian virus in a natural matrix with higher initial concentration. We found a linear relationship between the pH values and the maximum dose of slaked lime (p <0.05 by nonzero slope t test).

We finally simulated the appropriate T99.9 and lime dosage on fecal matter using the better model. The estimated T99.9 was less than 1 h at > pH 11.5, and exponentially prolonged at lower pH: more than 12 h at < pH 10.5. At least 2.5%(wt) of slaked lime was needed to yield higher pH. These results indicated that precise measurement of pH and record keeping of treatment time at lower pH are critical.

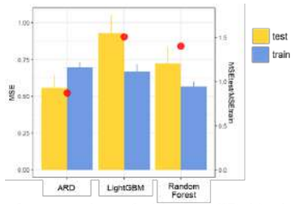

Figure 1. Mean value of mean squared error of training data (MSEtrain) and test data (MSEtest) by the three models for T99.9. Red plots represent the ratio of MSE values indicative for overfitting to training data.

REFERENCES

Kohn, T., Decrey, L., Vinnerås, B. 2017 Chemical Disinfectants, in: Jiménez-Cisneros, B., Rose, J.B. (Eds.), Water and Sanitation for the 21st Century: Health and Microbiological Aspects of Excreta and Wastewater Management (Global Water Pathogen Project). Michigan State University, E. Lansing, MI, UNESCO. https://doi.org/10.14321/waterpathogens.71

Moher, D., Liberati, A., Tetzlaff, J., Altman, D.G. 2009 Preferred reporting items for systematic reviews and meta-analyses: The PRISMA statement. BMJ (Online). https://doi.org/10.1136/bmj.b2535

Hom, L.W. 1972 Kinetics of chlorine disinfection in an ecosystem. *Journal of the Sanitary Engineering Division* **98**, 183–194.

Insights on the Agronomic Potential of Structural Extracellular Polymeric Substances (sEPS) from Aerobic Granular Sludge

B. Pagliaccia*, R. Campo*, J. P. Czellnik*, E. Carretti** - ***, M. Severi**, C. Lubello*, T. Lotti*

* Dept. of Civil and Environmental Engineering, University of Florence, Via di S. Marta 3, 50139 Florence, IT
(E-mail: *benedetta.pagliaccia@unifi.it; riccardo.campo@unifi.it; janpietro.czellnik@unifi.it; claudio.lubello@unifi.it; tommaso.lotti@unifi.it*)
** Dept. of Chemistry "Ugo Schiff", University of Florence, Via della Lastruccia 3, 50019 Sesto Fiorentino (Florence), IT
(E-mail: *emiliano.carretti@unifi.it; mirko.severi@unifi.it*)
*** CSGI Consortium, Via della Lastruccia 3, 50019 Sesto Fiorentino (Florence), IT

Abstract
This contribution aimed to study the agronomic potential of AGS-extracted sEPS and derived hydrogels. The recovery/gelation processes were fine-tuned based on agriculture-related criteria, highlighting that the chemicals used can influence the elemental composition of sEPS and derived hydrogels. The extracted sEPS formed hydrogels having high water-binding capacity (up to 15 gH_2O/gTS_{sEPS} adsorbed by 50°C-dehydrated hydrogels upon swelling) and nutrient holding/release ability (up to 103 mgK^+ and 147 $mgNO_3^-$ per gTS_{sEPS} released in water by KNO_3-swollen sEPS hydrogels). Together with compositional properties in line with the regulatory framework, these features suggested the feasible application of AGS-derived sEPS in sustainable agro-practises.

Keywords (maximum 6 in alphabetical order)
Aerobic granular sludge; agriculture; hydrogel; resource recovery; structural extracellular polymeric substances; water and nutrient adsorption/release

INTRODUCTION

In aerobic granular sludge (AGS) microorganisms produce large quantities of highly hydrated extracellular polymeric substances (EPS) to form a hydrogel matrix (mainly consisting of polysaccharides, proteins, nucleic acids, (phospho)lipids, humic substances, etc.) in which they are self-immobilized (Flemming and Wingender, 2010; Seviour et al., 2019). Part of the AGS-derived EPS, the so-called structural EPS (sEPS), have the ability to form hydrogels which is considered well linked to the structural integrity of granules (Felz et al., 2016). sEPS can be extracted from AGS and converted into value-added biomaterials, thus contributing to a circular economy-based wastewater sector (Lin et al., 2015). In this regard, this contribution aimed to explore the agronomic potential of AGS-derived sEPS and derived hydrogels combining a fine-tuning of the extraction/gelation processes based on agriculture-oriented criteria with an integrated assessment of key properties like elemental composition, water sorption ability and nutrient release capacity.

MATERIALS AND METHODS

sEPS were extracted from AGS adapting the method reported by Felz et al. (2016) (i.e., thermo-alkaline solubilization of EPS followed by acidic precipitation of sEPS). The hydrogel-formation was carried out by Ca^{2+} diffusion from a 2.5% (w/w) Ca^{2+} cross-linking aqueous solution into the sEPS matrix through a dialysis membrane (3.5 kDa MWCO) (Campo et al., 2022). The effect of distinct chemicals on the qualitative/quantitative properties of the extractable sEPS was addressed (**Figure 1**): the agro-based methods used reagents that potentially promoted the sEPS enrichment in nitrogen and potassium, avoiding phytotoxic elements (e.g., Na, Cl). The sEPS extraction yields were determined by gravimetry, measuring Total Solids (TS) and Volatile Solids (VS) according to standard methods (APHA/AWWA/WEF, 2017). Elemental analysis of sEPS and derived hydrogels were performed through CHN-S Analyzer and Inductively Coupled Plasma-Atomic Emission Spectroscopy. sEPS hydrogels from the agro-based method were characterized in terms of swelling and nutrient uptake/release properties. To this aim, sEPS hydrogels (3 wt% sEPS concentration) were dehydrated at 50 °C and then rehydrated in both demineralized water and 0.2 M KNO_3 aqueous solution, monitoring the swelling ratio over time as gram of H_2O adsorbed per gram of 50°C-Dehydrated Weight (50°C-DW) of hydrogel. The K^+/NO_3^- release kinetics in demineralized water of KNO_3-swollen sEPS hydrogels were evaluated by means of ion chromatography and fitted by pseudo-first-order (PFO) and pseudo-second-order (PSO) models (Wang et al., 2018).

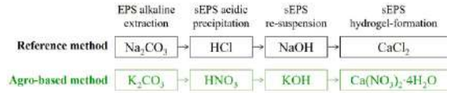

Figure 1. Chemicals used for the sEPS extraction and hydrogel-formation.

RESULTS AND DISCUSSION

As reported in **Table 1**, the agro-based protocol favoured a higher sEPS enrichment in potassium with respect to the reference method (K = 11.2 vs. 0.02 wt% as dry weight) without significantly reducing the extraction yield. By replacing Na_2CO_3 with K_2CO_3, the sodium content in sEPS considerably decreased, while the H/C, N/C and S/C molar ratios were kept almost constant and in agreement with literature data (Campo et al., 2022). Despite the extraction method applied, sEPS formed hydrogels storing up to 99 gH_2O/gTS_{sEPS}. The Ca/C molar ratio significantly increased upon gelation from 0.003 to 0.075-0.152 mol Ca/C-mol, thus indicating the inclusion of Ca^{2+} ions inside the polymeric matrix during the cross-linking reaction. The N/C molar ratio was kept almost constant from sEPS to hydrogels using $CaCl_2$ as cross-linking agent (0.187 vs. 0.134 mol N/C-mol) and considerably increased upon hydrogel-formation applying the agro-oriented method ($Ca(NO_3)_2{\cdot}4H_2O$ as Ca^{2+} source) from 0.163 to 0.972 mol N/C-mol. This evidence suggested that both Ca^{2+} and related counter ions diffused from the aqueous medium inside the polymeric matrix during gelation. The chemicals applied in the recovery and gelation processes should be hence properly selected based on application-related criteria: the use of reagents not containing phytotoxic elements is recommended for agricultural uses. The sEPS and derived hydrogels thus obtained respected the heavy metal concentrations limits of Regulation (EU) 2019/1009 on fertilizers.

Table 1. sEPS extraction yields of reference and agro-based methods and comparative elemental analysis of the recovered sEPS.

	Reference method	Agro-based method
Extraction yield ($mgVS_{sEPS}/gVS_{AGS}$)	231 ± 14	206 ± 9
VS/TS (% gVS_{sEPS}/gTS_{sEPS})	87.5 ± 1.3	84.2 ± 1.0
H/C (mol/C-mol_{sEPS})	1.620	1.702
N/C (mol/C-mol_{sEPS})	0.187	0.163
S/C (mol/C-mol_{sEPS})	0.022	0.029
Na/C (mol/C-mol_{sEPS})	0.020	0.002
K/C (mol/C-mol_{sEPS})	0.0001	0.080

Figure 2 shows the increase of the swelling ratio over time for swelling experiments carried out in demineralized water. The 50°C-dehydrated sEPS hydrogels were able to sorb up to 11 $gH_2O/g50°C$-DW upon swelling (15 gH_2O/gTS_{sEPS}). These high water-binding capacity and swelling ability are typical of superabsorbent polymers (SAPs) having high potential in sustainable agro-practises.

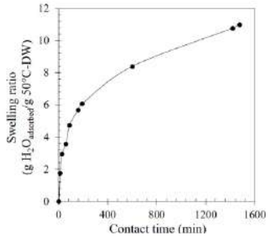

Figure 2. Experimental swelling kinetics in demineralized water of sEPS hydrogels.

Applying the agro-based method, potassium in sEPS was largely released in the cross-linker solution upon gelation likely due to ion exchange mechanisms in binding Ca^{2+}: this resulted in hydrogels poor in K (0.01 wt% as dry weight). The 50°C-dehydrated sEPS hydrogels were hence swollen in KNO_3 aqueous solution: in this case, the extent of swelling was lower (up to 5 $gH_2O_{adsorbed}/g50°C$-DW) because of the higher ionic strength of the surrounding medium. The 50°C-dehydrated sEPS hydrogels adsorbed up to 116 mgK/gTS_{sEPS} upon swelling in KNO_3: this suggested that the hydrogel elemental composition might be tuned acting on the type of swelling solution (thus providing nutrient enrichment upon hydrogel rehydration). As depicted in **Figure 3**, the KNO_3-swollen hydrogels released in demineralized water up to 103 mgK^+ and 147 $mgNO_3^-$ per gTS_{sEPS} within 8 hours (80-90% of their nutrient content): the release kinetics were better described by a pseudo-first order model (R^2=0.944), as reported for alginate gel beads (Wang et al., 2018).

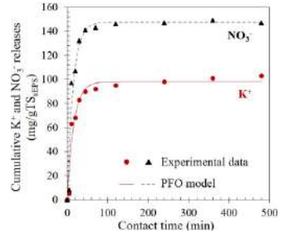

Figure 3. Experimental K^+ and NO_3^- release kinetics in demineralized water of KNO_3-swollen sEPS hydrogels and related fitting through pseudo-first-order (PFO) model.

In conclusion, paying attention to the chemicals used in the recovery process, AGS-extracted sEPS can form hydrogels having high water-binding and nutrient sorption/release properties suitable in agriculture for improving the soil water-holding capacity and/or as nutrient carriers/release agents.

ACKNOWLEDGEMENTS

This research was funded by ROP-ESFR Toscana 2014-2020 – IDRO.SMART project (CUP: 3647.04032020.157000040).

REFERENCES

APHA/AWWA/WEF 2017 Standard methods for the examination of water and wastewater. American Public Health Association, Washington, DC, USA, 23rd ed.

Campo, R., Carretti, E., Lubello, C., Lotti, T. 2022 Recovery of structural extracellular polymeric substances (sEPS) from aerobic granular sludge: Insights on biopolymers characterization and hydrogel properties for potential applications. *Journal of Environmental Management* **324**, 116247.

Felz, S., Al-Zuhairy, S., Aarstad, O.A., van Loosdrecht, M.C.M., Lin, Y. 2016 Extraction of Structural Extracellular Polymeric Substances from Aerobic Granular Sludge. *Journal of Visualized Experiments* (115) e54534, 1-8.

Flemming, H.C., Wingender, J. 2010 The biofilm matrix. *Nature Reviews Microbiology* **8**, 623-633.

Lin, Y., Nierop, K.G.J., Girbal-Neuhauser, E., Adriaanse, M., van Loosdrecht, M.C.M., 2015 Sustainable polysaccharide-based biomaterial recovered from waste aerobic granular sludge as a surface coating material. *Sustainable Materials and Technologies* **4**, 24–29.

Seviour, T., Derlon, N., Dueholm, M.S., Flemming, H.C., Girbal-Neuhauser, E., Horn, H., Kjelleberg, S., van Loosdrecht, M.C.M., Lotti, T., Malpei, M.F., Nerenberg, R., Neu, T.R., Paul, E., Yu, H., Lin, Y., 2019 Extracellular polymeric substances of biofilms: Suffering from an identity crisis. *Water Research* **151**, 1–7.

Wang, B., Gao, B., Zimmerman, A.R., Zheng, Y., Lyu, H., 2018 Novel biochar-impregnated calcium alginate beads with improved water holding and nutrient retention properties. *Journal of Environmental Management* **209**, 105-111.

Influence of system geometry and substrate on the removal of linalool and geraniol in zero-liquid discharge unplanted-NBS

K. M. Takahashi*, C. M. Passoni*, J. B. G. de Souza**, N. C. Yoshida**, C. G. Morandi***, H. Steinmetz***, M. A. Boncz*, P. L. Paulo*†

* Faculty of Engineering, Architecture and Urbanism and Geography, ** Institute of Chemistry, Federal University of Mato Grosso do Sul, Av. Costa e Silva, S/N, Cidade Universitária, Campo Grande, MS, Brazil, *** Department of Civil Engineering, Resource-Efficient Wastewater Technology, Technische Universität Kaiserslautern, Paul-Ehrlich-Str., 14/313, D- 67663 Kaiserslautern, Germany.

†*E-mail: paula.paulo@ufms.br*

Abstract Personal and home care products (PHCPs) are a potential source of micropollutants in greywater. The objective of this study was to select 2 perfuming compounds and assess their removal behaviour in a nature-based solution operating with zero-liquid discharge using different geometries and substrates. The reduced scale mesocosms showed removal of up to 72 and 64% for geraniol and linalool, respectively, using a rectangular geometry, and expanded clay as substrate.

Keywords
Greywater; emerging pollutants; nature-based solutions; reuse; treatment wetlands

INTRODUCTION

Greywater (GW) is a potential source of micropollutants (MP) due to the chemical compounds present in personal and home care products (PHCPs). Although the direct reuse, without treatment, of greywater at household level is not recommended, it seems to be a common informal practice in several countries. This raises concerns about the impact on human health and the environment. Several studies using treatment (constructed) wetlands for the removal of micropollutants have been conducted, both for conventional domestic sewage (DS) and GW (Sossalla et al. 2021 and 2022; Ramprasad and Philip, 2016, Ávila et al, 2014). Studies focusing on the selection of chemical compounds for monitoring programmes, based on consumption habits of personal care and home care products have been conducted (Paulo et al., 2018; Garcia-Hidalgo et al., 2017). For the HCPs database we screened the labels of 34 softeners (16 Brazil-BR and 18 European Union-EU) and 60 laundry detergents (liquid, powder, capsules, gel and tablets), from which 18 BR and 42 EU. Considering that 6% of the population is sensitive to ingredients present in PCPs and HCPs, especially to fragrances and preservatives (Pastor-Nieto et al., 2017), we selected linalool and geraniol, two compounds commonly used as perfuming agents in PHCPs, that are present in 17 out of 60 of the products mentioned above.

Table 1. Chemical compounds commonly used as perfuming agents in home and personal care products.

Compound	toxicological threshold value[a] (mg/kg bw[d] d)	Maximum detected value (µg.L^{-1}) greywater[a)(b)]	domestic sewage[(b)]	Possible effects on human health / environment[(c)]
Geraniol	0.030	0.8[(f)]	1.0[(e)] (influent)	allergies & immunotoxicity suspected to be an environmental toxin
Linalool	0.5	15.4	11.6 (effluent)	allergies & immunotoxicity

(a) Etchepare & van der Hoek, 2015; (b) Montes-Grajales, et al., 2017; (c) https://www.ewg.org/skindeep/; (d) bw: body weight; (e) Paxéus & Schröder, 1996; (f) https://pubchem.ncbi.nlm.nih.gov

The information shown in Table 1 is based on data retrieved from EWG Skin Deep®, which compiles a series of references used to disseminate information on ingredients regarding their effects on health and the environment. In spite of the low concentrations detected in GW and DS, studies indicate possible effects on human health and the environment. The selected products present an allergy and immunotoxicity indication, with geraniol suspected of environmental toxicity. On the other hand, none of these compounds is suspected of persistence or bioaccumulation. Considering the little information in literature regarding the removal of perfuming compounds in treatment wetlands, the objective of this study was to assess the removal behaviour of linalool and geraniol during treatment in a zero-liquid discharge system using different geometries and substrates.

MATERIALS & METHODS

The experiment was performed in reduced-scale units of CEvaT (evapotranspiration and treatment tank) which is fully described elsewhere (Magalhães & Paulo, 2021). Eight units, of which 4 square (0.5m H x 0.5m W x 0.5m L) and 4 rectangular (0.25m H x 0.5m W x 1.0m L), were built, filled with 2 different substrates: fine gravel and expanded clay. These 8 units were fed with onsite produced laundry GW and operated as zero liquid discharge systems during 1 month. The units were provided with piezometers (Figure 1) from where the samples were collected until day 7. Afterwards, samples were taken at the outlet of each unit.

Figure 1. Left: Experimental setup. Right: View of the anaerobic chamber inside the square and rectangular shaped mesocosms.

Analytical grade linalool (3,7-dimethyl-1,6-octadien-3-ol) and geraniol (3,7-dimethyl-2(E),6-octadien-1-ol) were diluted into laundry greywater to provide an inlet concentration of around 6 mg.L^{-1} for linalool and 2 mg.L^{-1} for geraniol. Concentrations were chosen based on the analysis of 4 laundry products of different brands (Table 2). For the analysis of monoterpenes, 4 mL of sample was used for extraction using 200 mg C18 solid phase extraction (SPE) cartridges (Strata® Phenomenex). The cartridge was conditioned with 4 mL of chloroform, 4 mL of methanol (MeOH) and 4 mL of 1% H_2O/MeOH, washed with 6 mL of H_2O and eluted with 1.5 mL of chloroform. The extract was analysed in a gas chromatograph (GC) with mass spectrometry (GCMS-QP2010, Shimadzu). The identification was performed based on the NIST20 mass spectra database.

Table 2. Concentration of linalool and geraniol in 3 softeners and 1 powder detergent from 4 different brands as commercialised in Brazil (BR) and in the European Union (EU).

Product type	Product	Linalool (mg.L^{-1})	Geraniol (mg.L^{-1})
Powder detergent	Brand A - EU	-	1.19
Softener	Brand A - BR	-	1.67
Softener	Brand B - EU	7.30	0.67
Softener	Brand C - EU	4.52	1.03

RESULTS AND DISCUSSION

Figure 2 shows the decrease on the concentrations of linalool and geraniol during the first 7 days of the experiment. Samples were collected until day 25, showing no further decrease in concentration for both compounds (data not shown). The total volume for both geometries is the same. In the square units, no removal occurred before day 4, however, the length of the rectangular units is twice length of the square units (1 m vs. 0.5 m), whereas their depth is half the depth of the square units (0.25 m for the rectangular units vs. 0.5m for the square units). Although the hydraulic retention time is about the same for both geometries (and actually slightly higher for the square units), the length of the units seems to play a role in the process. Possibly, in the shallower rectangular units, the less anoxic environment might favour the degradation mechanism of monoterpenes.

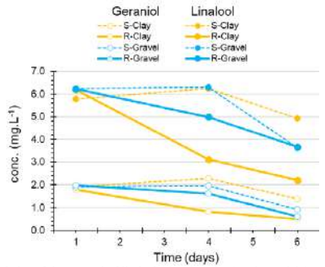

Figure 2 The evolution of the removal of linalool (closed markers) and geraniol (opened markers) in reduced scale Evapotranspiration and Treatment tanks (CEvaT) with square (dotted lines) and rectangular (solid lines) geometries, using fine gravel and expanded clay.

The rectangular shaped units (solid lines) showed the best performance when the substrate is clay, independent of the compound to be removed from the liquid phase. However, when using gravel, the removal was similar for both geometries, especially for Linalool (Figure 2 and Table 3). Thus, expanded clay seems not to be a good choice as filtering media for use in square geometry NBSs. When comparing the removal using expanded clay for both geometries, the removal in absolute values for rectangular mesocosms were 2.3 and 4.5 times higher for geraniol and linalool, respectively.

Table 3. Average concentration of linalool and geraniol at the sampling points inside the mesocosms (piezometers) and total removal for the 4 combinations tested with different geometries and substrates.

Geometry (substrate)	Geraniol P1 (mg.L^{-1})	Geraniol P2 (mg.L^{-1})	Geraniol Removal (mg.L^{-1})	Geraniol Removal %	Linalool P1 (mg.L^{-1})	Linalool P2 (mg.L^{-1})	Linalool Removal (mg.L^{-1})	Linalool Removal (%)
Square								
Gravel	1.90	0.92	0.98	51.6	6.25	3.63	2.62	41.9
Expand. Clay	1.92	1.38	0.54	28.1	5.79	4.92	0.87	15.0
Rectangular								
Gravel	1.98	0.61	1.37	69.2	6.22	3.67	2.55	41.0
Expand. Clay	1.79	0.50	1.29	72.1	6.19	2.21	3.98	64.3

The experiment was carried out 3 weeks after the start-up of the mesocosms, before introducing the plants to the system. This approach allowed to compare the two substrates before biofilm formation and without the interference of the plants. Therefore, the removal of linalool and geraniol within the mesocosms can be attributed mainly to physical and chemical removal mechanisms, with limited biological degradation. A more extensive discussion of the removal mechanisms, based on further physico-chemical monitoring, will be included in the oral presentation.

CONCLUSIONS

Linalool and geraniol were chosen to represent perfuming compounds that can pose health and environmental risks when reusing greywater. Greywater treatment can be performed in NBSs, like the CEvaT, for which the usual geometry is the square one, as it provides a higher volume, expected to result in better pollutant removal, using less area. However, the preliminary results for the removal of the tested monoterpene compounds showed a better performance of the rectangular systems, especially when using fine gravel as the substrate. Further long-term studies will allow to assess the contribution of the microbial and biochemical processes, and determine the most appropriate system configuration to deliver a better quality of treated greywater for a safer reuse.

ACKNOWLEDGEMENTS

The authors acknowledge the support received from: PROBRAL Programme - CAPES/DAAD project N° 88881.371339/2019-01, National Council for Scientific and Technological Development - CNPq, Coordination for the Improvement of Higher Education Personnel - CAPES, FAPEMIG and the INCT Sustainable Wastewater Treatment Plants.

REFERENCES

Ávila, C.C, Matamoros, V., Reyes-Contreras, C., Piña, B., Casado M., Mita, L. Rivetti, C., Barata, C., García, J., Bayonaet, J.M. 2014. Attenuation of emerging organic contaminants in a hybrid constructed wetland system under different hydraulic loading rates and their associated toxicological effects in wastewater. *Science of The Total Environment*, **470**, 1272–80.

Etchepare, R.; van der Hoek, J.P. 2015. Health risk assessment of organic micropollutants in greywater for potable reuse. *Water Research*, **72**, 186-98. DOI: 10.1016/j.watres.2014.10.048

Montes-Grajales, D.; Fennix-Agudelo, M.; Miranda-Castro, W. 2017. Occurrence of personal care products as emerging chemicals of concern in water resources: A review. *Science of The Total Environment*, **595**, 601-14. DOI: 10.1016/j.scitotenv.2017.03.

Magalhães Filho, F.J.C.; Paulo, P.L. 2022. Phytoremediation as the modular approach for wastewater treatment. In: Satinder Kaur Brar; Pratik Kumar; Agnieszka Cuprys. (Org.). Modular Treatment Approach for Drinking Water and Wastewater. 1st ed. Amsterdam: Elsevier, **1**, 1-300.

Pastor-Nieto, M.A.; Alcántara-Nicolás, F.; Melgar-Molero, V. Pérez-Mesonero, R., Vergara-Sánchez, A.; Martín-Fuentes, A.; González-Muñoz, P.; Eusebio-Murillo, E. 2017. Preservatives in Personal Hygiene and Cosmetic Products, Topical Medications, and Household Cleaners in Spain. *Actas Dermo-Sifiliográficas*, **108**(8), 758-70.

Paulo, P.L; Mamedes, I.M.; Boncz, M.A.; van Lier, J.B. 2018. A method to select organic micropollutants potentially present in greywater for integrated risk assessment studies aiming at non-potable reuse. In: 15th IWA specialized conference on Small Water & Wastewater Systems and 8th IWA specialized conference on Resources Oriented Sanitation, Haifa, Israel.

Paxéus, N.; Schröder, H.F. 1996. Screening for non-regulated organic compounds in municipal wastewater in Göteborg, Sweden. *Water Science and Technology*, **33**, 9-15.

Ramprasad, C.; Philip, L. 2016. Surfactants and personal care products removal in pilot scale horizontal and vertical flow constructed wetlands while treating greywater. *Chemical Engineering Journal*, **284**, 458–68.

Sossalla N.A., Nivala J., Escher B.I., Schlichting R, van Afferden M, Müller R.A., Reemtsma T. 2022. Impact of various aeration strategies on the removal of micropollutants and biological effects in aerated horizontal flow treatment wetlands. *Science of the Total Environment* **828**, 154423. DOI: 10.1016/j.scitotenv.2022.154423

Sossalla N.A., Nivala J., Reemtsma T., Schlichting R., König M., Forquet, N., van Afferden M., Müller, R.A., Escher B.I. 2021. Removal of micropollutants and biological effects by conventional and intensified constructed wetlands treating municipal wastewater. *Water Research* **201**, 117349.

Reclaimed wastewater reuse impacts: from literature data gaps to integrated risk modelling

L. Penserini*, B. Cantoni*, M. Antonelli*

* Department of Civil and Environmental Engineering (DICA) - Environmental Section, Politecnico Milano, Piazza Leonardo da Vinci 32, 20133 Milano, Italy
(E-mail: *luca.penserini@polimi.it; beatrice.cantoni@polimi.it; manuela.antonelli@polimi.it*)

Abstract
The complexity and the inherent interconnection of the reclaimed wastewater reuse (RWW) system requires the proper quantification of its advantages and drawbacks. In this context, water utilities and decision makers would benefit from a comprehensive risk-based framework of models aimed at the assessment of its associated impacts.
In this work, a critical literature review on the models available for the assessment of RWW reuse impacts is performed to highlight which gaps need to be filled and indicate the future research directions. A simplified approach for evaluating and integrating different type of risks was proposed to address the prioritization of critical endpoints and contaminants within regulations.

Keywords (maximum 6 in alphabetical order)
Antibiotic resistant bacteria; Impacts modelling; Literature Gaps; ONE-health approach; Risk assessment; Reclaimed wastewater reuse

INTRODUCTION

Given the interest on water as a renewable resource, the reuse of reclaimed wastewater (RWW) has been recognized as a fundamental alternative source for irrigation and is increasingly applied (de Santiago-Martín et al., 2020). Based on where the wastewater treatment plant (WWTP) effluent is discharged, the reuse can be (i) indirect, when the effluent is discharged into the surface water and irrigation water is derived downstream the point of discharge, or (ii) direct, when the effluent is directly used for crops irrigation, through a dedicated distribution network.
In both cases, it emerges that RWW reuse practices inherently connect water in numerous environmental compartments (e.g. surface water, groundwater, soil), leading to a series of impacts, either positive or negative, which need to be evaluated. As for positive impacts, besides alleviating the water stress, the reuse of RWW provides a reliable source of nutrients. On the other hand, the cross-contamination of the different environmental matrices is favored, due to the unavoidable presence of contaminants in the effluent, even after extensive treatment. RWW might be loaded with contaminants such as organic matter, suspended solids, salts, heavy metals, contaminants of emerging concern (CECs), disinfection by-products (DBPs), pathogenic microorganisms and antibiotic resistant bacteria (ARB). Besides, all these contaminants could have different effects depending on the compartment in which they occur. In fact, they can accumulate in soil, causing salinization and changes to the soils properties. From soil, contaminants can either be uptaken and accumulated by plants, negatively affecting their growth, or contaminate groundwater, where aquifers are present. Finally, the consumption of crops contaminated with, above all, pathogens, heavy metals and CECs implies a not negligible risk for human health (Delli Compagni et al., 2020). Given this system complexity, it emerges the need for a framework of models that allows a comprehensive assessment of the RWW reuse impacts, capable of quantitatively accounting and comparing all the related advantages and drawbacks, to support decision-makers and water utilities in planning, design and prioritizing the different alternatives to determine the optimum solution that minimize risks and costs.
Regarding the regulation, RWW quality aimed at direct reuse for irrigation is regulated in the European Union, and the common practice to establish minimum quality requirements is shifting towards preventive risk analysis aimed at minimizing risks (EU Commission, 2020). In this context, it becomes fundamental to define an integrated risk assessment approach, which considers all the impacts throughout all the steps of the RWW reuse chain in terms of quantitative risk for both human health and environment.
In this work, an overview of the models available for the evaluation of RWW reuse impacts is presented and a simplified approach to estimate and compare different risk assessment procedures applied to RWW reuse case studies is proposed.

MATERIALS AND METHODS

A comprehensive literature review was conducted in the field of municipal RWW reuse in agriculture, focusing on the related impacts and the models available to evaluate them. Scopus was used as database for the period 2017–2022 (documents published in 2023 were not included considering only complete annual periods). A sample of 252 articles was selected for a detailed analysis.
The RWW reuse framework was conceptualised based on four characteristics: (i) the type of RWW reuse, (ii) the analysed compartments, (iii) the models applied to evaluate the impacts, and (iv) the targeted variables in the models. For each characteristic, several categories were identified, and one or more of them were assigned to every article. Studies without at least one category from each characteristic were discarded. Ultimately, 139 articles were selected, to review the current state of the art on the available models for the evaluation of RWW reuse impacts, highlighting the gaps to be filled.
Finally, a simplified approach for comparing and prioritizing the available risk assessment procedures is proposed, focusing here on human health risk assessment due to CECs presence in crops irrigated through indirect RWW reuse. In detail, CECs concentration data in the WWTP effluent, in the receiving water body used for crops irrigation and in the irrigated crops were collected. Then, environmental risk quotient (RQ_E) and antibiotic resistance risk (RQ_R) were calculated comparing the Measured Environmental Concentrations (MEC) in rivers with the Predicted No-Effect Concentration, respectively for environmental ($PNEC_E$) and antibiotic resistance ($PNEC_R$), according to the following equations (Zhang et al., 2019):

$$RQ_E = MEC/PNEC_E \qquad RQ_R = MEC/PNEC_R$$

Details on the only 4 articles available for the comparison of human health, environmental and antimicrobial resistance risk in indirect RWW reuse practices are reported in Table 1.

Table 1. Summary of the studies used for the comparison of human health, environmental and antimicrobial risk: number of analysed CECs and antibiotics, concentration in WWTP, river and crops, indicated as average and range in brackets.

Study	# of CECs	# of antibiotics	WWTP effluent concentration [µg/L]	River concentration [µg/L]	Crop concentration [µg/g]
De Santiago-Martin et al., 2020	57	10	0.21 (<LOQ-1.5)	0.34 (<LOQ-6.5)	0.04 (<LOQ-0.25)
Delli Compagni et al., 2020	13	2	Not available	0.21 (<LOQ-0.8)	0.009 (<LOQ-0.08)
Liu et al., 2020	11	3	Not available	0.007 (<LOQ-0.025)	0.005 (<LOQ-0.03)
Meffe et al., 2021	25	3	Not available	0.25 (<LOQ-12.9)	0.001 (<LOQ-0.01)

RESULTS AND DISCUSSION

The selected studies were classified based on their characteristics and categories as shown in Figure 1, differentiated per type of RWW reuse, being (i) direct and (ii) indirect. The compartments correspond to the boundaries within which the impact is modelled and they were differentiated in (i) WWTP, (ii) environment (intended as the groundwater or surface water receiving the WWTP effluent), (iii) irrigation system, (iv) soil, (v) crops and (vi) humans. The models were differentiated between quantity- and quality-based models. Quantity-based models evaluate the impacts in terms of volumes of water available for irrigation; model as (i) water mass balances, (ii) Life Cycle Assessment (LCA), (iii) economic, (iv) energy, (v) sustainability and (vi) social assessments belong to this category. While quality-based models evaluate the impacts in terms of RWW quality, thus, concentrations or risks, and are usually specific for single compartments; here there are models assessing (vii) treatment removal, (viii) crop uptake, (ix) environmental risk and the (x) human health risk. Finally, the variables targeted by the applied models were divided again in quantity-based variables, affecting the volume of water, namely (i) water itself, and quality-based variables, affecting the water quality, such as (ii) nutrients, (iii) conventional contaminants (i.e., organic matter and suspended solids), (iv) salts, (v) heavy metals, (vi) CECs, (vii) DBPs, (viii) microbials and ARBs (ix).

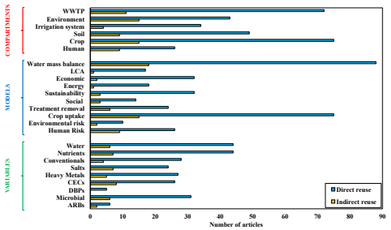

Figure 1. Number of articles mentioning the analyzed categories, differentiated per direct or indirect reuse.

Analysing Figure 1, it emerges that, on average for all the considered categories, the 85% of the studies deals with direct reuse, being the only type of reuse which is regulated so far, and being a process easier to replicate even in pilot-scale conditions, compared to indirect RWW reuse. However, there are a lot of RWW streams that are used *de facto* for indirect irrigation. Thus, studies in this field are a gap which need to be filled. Moreover, among articles addressing indirect RWW reuse practice, there are no studies considering how the dilution factor between the WWTP effluent and the receiving surface water affects the environmental impact, although the growing concern on the consequneces on the natural aquatic environment of climate change stress the importance of this evaluation.

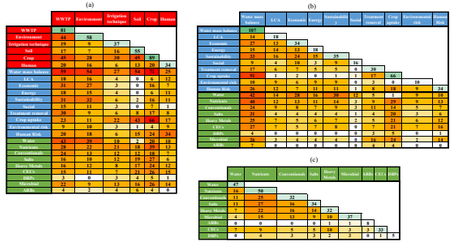

Figure 2. Heatmap reporting the paired correlations between the considered categories, differentiated per (a) compartments, (b) models and (c) variables.

Three heatmaps are reported in Figure 2 visualluy showing the paired correlations between all the considered categories, differentiated per compartments, models and variables. This visualization supports in analysing how the different characteristics (i.e., compartments, models and variables) are combined together to model the RWW reuse practice, and also permits to assess which fields are more consolidated and which ones need further research.
In particular, it is pointed out a lack of model application on ARBs, which are microrganisms of emerging concern inherently related to WWTP discharges. Regarding risk assessment models, LCA assesses human health and environmental risks through generalized standard values; if LCA studies are not considered, it emerges that only a single study applied an environmental risk assessment to a RWW reuse practice, while no studies consider both environmental and human health risk together.
In this context, given the importance of risk-based approaches to assess the impacts of RWW reuse practices, as stressed by the revision of the WW reuse Directive, the absence of studies simultaneously evaluating the environmental, antibiotic resistance and human health risks when indirect RWW reuse is applied is an important literature gap.
The analysis performed on studies dealing with human health risk assessment highlighted that environmental and antibiotic resistance risks have significant contribution to the overall risk, being higher than the human health risk for some of the CECs. This evidence stresses the importance of an holistic risk assessment, with a ONE-Health approach, to evaluate the most critical endpoint for each CEC, useful to prioritize their regulation.
To conclude, this work gave an overview of the models currently available for the evaluation of the impacts of RWW reuse practices, highlighting which are the associated literature gaps, and it might be useful in indicating future research directions, as well as to suggest which impact need to be prioritized when a comprehensive assessment is performed.

ACKNOWLEDGEMENTS

The authors greatly acknowledge the water utility Acque Bresciane S.r.l., for funding the Ph.D. scholarship of Luca Penserini.

REFERENCES

de Santiago-Martín, A., Meffe, R., Teijón, G., Martínez Hernández, V., López-Heras, I., Alonso Alonso, C., Arenas Romasanta, M., de Bustamante, I., 2020. Pharmaceuticals and trace metals in the surface water used for crop irrigation: Risk to health or natural attenuation? Sci. Total Environ. 705. https://doi.org/10.1016/j.scitotenv.2019.135825

Delli Compagni, R., Gabrielli, M., Polesel, F., Turolla, A., Trapp, S., Vezzaro, L., Antonelli, M., 2020. Risk assessment of contaminants of emerging concern in the context of wastewater reuse for irrigation: An integrated modelling approach. Chemosphere 242, 125185. https://doi.org/10.1016/j.chemosphere.2019.125185

EU Commission, 2020. Regulation (EU) 2020/741 of the European Parliament and of the Council of 25 May 2020 on minimum requirements for water reuse. Off. J. Eur. Union 2019, 32–55.

Liu, Xianjing, Liang, C., Liu, Xiaohui, Zhao, F., Han, C., 2020. Occurrence and human health risk assessment of pharmaceuticals and personal care products in real agricultural systems with long-term reclaimed wastewater irrigation in Beijing, China. Ecotoxicol. Environ. Saf. 190, 110022. https://doi.org/10.1016/j.ecoenv.2019.110022

Meffe, R., de Santiago-Martín, A., Teijón, G., Martínez Hernández, V., López-Heras, I., Nozal, L., de Bustamante, I., 2021. Pharmaceutical and transformation products during unplanned water reuse: Insights into natural attenuation, plant uptake and human health impact under field conditions. Environ. Int. 157. https://doi.org/10.1016/j.envint.2021.106835

Zhang, Y.P., Li, W.P., 2019. Blending antibiotic resistance into environmental risk assessment of antibiotics: a case study in coastal waters of the Bohai Bay, China. *Hum. Ecol. Risk Assess.* 25 (6), 1406–1421.

LIFE HIDAQUA: Sustainable water management in high water demanding industries

M. Mesas[1], S. Seršen[2], C. Pérez[3], P. Oprčkal[2], S. Markežič[4], J. Hočevar[5] and R. Milačič[6]

[1] Eurecat, Technological Centre of Catalonia, Water Air and Soil Unit, Plaça de la Ciència 2 - 08243 - Manresa, Catalonia, Spain (E-mail: *mireia.mesas@eurecat.org*)
[2] Slovenian National Building and Civil Engineering Institute (ZAG), Dimičeva ulica 12, 1000 Ljubljana, Slovenia (E-mail: *sara.sersen@zag.si; primoz.oprckal@zag.si*)
[3] Hidroquimia Tractaments i Química Industrial, Parc Audiovisual de Catalunya, Edifici Nord. 2ª Planta. Local O22. Autovía Orbital 40, Crta. BV-1274, Km. 1 - 08225 - Terrassa, Catalonia, Spain (E-mail: *cperez@hidroquimia.es*)
[4] Hidria d.o.o., Ulica Istrskega odreda 3, 6000 Koper, Slovenia (E-mail: *Sanja.Markezic@hidria.com*)
[5] Geologija d.o.o. Idrija, geološke raziskave in projektiranje, Prešernova ulica 2, 5280 Idrija, Slovenia (E-mail: *jure.hocevar@geologija.si*)
[6] Jožef Stefan Institute, Jamova cesta 39, 1000 Ljubljana, Slovenia (E-mail: *radmila.milacic@ijs.si*)

Keywords (maximum 6 in alphabetical order)
Sustainable water management, "Zero-Liquid-Discharge", "Zero-Waste" technology, industrial wastewater recycling.

Abstract
The LIFE HIDAQUA project aims to demonstrate a sustainable water management approach in high water demanding industries, such as the EU automotive industry, by decreasing the emission of pollutants from industry and preserving the quality of natural water bodies and natural drinking water resources.

The project addresses water management in industrialized EU areas by tackling the following environmental problems: i) the depletion of natural drinking water sources, especially in areas facing water scarcity, ii) the low ecological and chemical status of natural water bodies due to the emissions of pollutants in industrial wastewater discharge, iii) burdening of the environment, especially natural water bodies, with the discharging of liquids and the landfilling of wastes from water treatment processes.

The proposed integrated management strategy is based on the following priorities for the exploitation of alternative water sources: i) industrial recycled/reclaimed water, ii) harvested rainwater, and iii) brackish groundwater. Moreover, the innovative solution focuses on a sustainable water management approach by applying the Zero-Liquid-Discharge and the Zero-Waste concepts through the recycling of all wastes generated during the water treatment process.

The system can establish recycling of highly polluted industrial wastewater (high content of oils and grease - containing on average Chemical Oxygen Demand (COD) values of 20,000 mg O_2/L). Approximately 4000 m^3 of polluted water per year with the exploitation of alternative water sources (brackish water and rainwater) can be treated simultaneously on site and produce cca 24 m^3 of cleaned water per day (with conductivity less than 0.6 mS/cm).

The incorporation of an advanced solar evaporation (ASE) pond designed as a greenhouse collects the heat for intensive evaporation of the brines. This results in production of salt products, while the waste sludge and suspensions can be recycled into building composites and produced as a ready-for-use construction products (cca 0.5 tons of salt and 1 ton of construction composites).

The involvement of an innovative interactive "Decision-Making Tool" that is being developed, will help users to decide which water needs to be treated at any time, taking into consideration the relevant technical aspects as well as the results of Life Cycle Assessment, Life Cycle Costs, Social Life Cycle Assessment and Water Footprint. In general, the Tool has integrated measures to lower the environmental impacts as much as possible.

In the initial stages of the project, the different technologies that constitute the completely innovative water treatment scheme for the automotive industry were tested and optimized at bench scale at EURECAT facilities in Spain. Figure 1 shows the proposed treatment scheme and results obtained at bench scale. Bench scale tests were carried out using real industrial wastewater (IWW) and brackish water (BW) samples provided by HIDRIA.

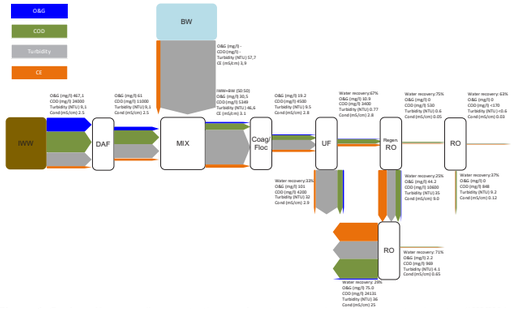

Figure 1. Sunkey diagram of concentrations and water recoveries of main contaminants of IWW in the treatment scheme at bench scale

Regarding the pre-treatment, it was decided to combine the pre-treatment steps of brackish water and industrial wastewater streams to improve the overall Oil and Grease (O&G) removal prior to continue with the rest of the treatment. The strategy chosen was to treat the industrial wastewater with Dissolved Air Flotation (DAF) to remove most of oils and COD present and then, combine this stream with the brackish water stream in a 1:1 ratio. Once both streams were mixed, a coagulation/flocculation treatment was applied to remove most of the turbidity and metals. With this pre-treatment, a removal higher than 90% was achieved for O&G and higher than 80% for COD and turbidity. The optimal pre-treatment conditions that were found were: 6 bar and 60% recirculation and no flocculant in DAF process; 5 ppm of coagulant and 0.5 ppm of flocculant for the coagulation/flocculation step with the mixed water.

The water stream resulting from the coagulation/flocculation was treated with ultrafiltration (UF) as a previous step before using a reverse osmosis (RO) with regenerated membranes to remove most of the pollutants. The UF step was able to reduce the turbidity to less than 1 NTU and a 67% of recovery rate was achieved. It is expected that higher recoveries will be obtained at larger scales due to the limitations by the dead volume of the experimental set up.

In the RO with regenerated membranes a high quality permeate was obtained with a recovery rate of 75%. A conductivity of 0.05 mS/cm was achieved, which was much less than the original goal of 0.6 mS/cm. For water reutilization purposes in HIDRIA's processes, the concentration of COD of the regenerated RO permeate was too high (~0.5 g/L COD). Different regenerated membrane modules were tested, and the results obtained where slightly different regarding the rejection of COD and final conductivity. To lower the concentration of COD in the regenerated RO permeate, a refining RO step was studied to treat the permeate achieving 87% COD removal efficiency and a 63% water recovery. The optimal regeneration conditions for RO membranes were also defined so that the RO modules for the pilot plant could be regenerated until obtaining the same NaCl and $MgCl_2$ rejection. The proposed treatment scheme would lead to a final COD concentration <70 mg COD/L in the refining RO permeate.

Finally, electrodialysis reversal (EDR) reversal was able to successfully treat the RO concentrate recovering 78% of the water in form of a dilute stream with the same conductivity as the RO influent (around 2.2-2.8 mS/cm) applying 330 Ah/m^3 (implying an electric consumption of 8 kWh/m^3). Anyway, the impossibility of treating the COD with EDR represent a limitation when using this technology for the studied wastewater. To decrease the volume of final concentrate to be sent to the ASE pond and increase the quality of the recovered water, other technologies were considered (Membrane Distillation (MD) and RO). Among these, RO gave the best results in terms of both COD, O&G and ions removal.

Afterwards, the demonstrated system at bench scale was up scaled to a pilot plant which was installed in HIDRIA factory in Koper (located in the NE part of the Adriatic Sea) in December of 2022. The results from the operation and optimization of the pilot plant are expected to be obtained during 2023.

Valorizing Methane: Methanotrophs based Biorefinery for Extracellular Biopolymers Production (CH4-BIOPOL)

D. Primo-Catalunya*,**, A. Aranda*,**, J.L. Balcazar*,**, M. Pijuan*,**

* Catalan Institute for Water Research (ICRA-CERCA), C. Emili Grahit 101, 17003 Girona, Spain.
** Universitat de Girona, Girona, Spain (E-mails: dprimo@icra.cat; aaranda@icra.cat; jlbalcazar@icra.cat; mpijuan@icra.cat)

Abstract
Methane (CH_4) is the second most abundant greenhouse gas (GHG) after carbon dioxide (CO_2), but it has much higher global warming potential with a heat retentive capacity over 34 times more than CO_2 in a century timeframe. Consequently, cutting off CH_4 emissions is considered the most effective strategy against the global warming. A significant amount of CH_4 is produced in the form of biogas and, due to energy increasing demands, it has been proposed as more sustainable energy source. Biogas potential, nonetheless, is currently hindered by its low conversion efficiencies. Nowadays, novel technologies are being developed to connect the reduction of methane emissions and the production of added-value substances such as designed proteins, additives, or biopolymers, in the frame of Circular Economy. Biological conversion of methane into biopolymers is highly attractive due to its efficiency under mild operating conditions and its adaptability. Also, CH_4 offers some advantages as carbon source when compared with sugars, which compete with human food supply for agricultural land and are experimenting a rapidly increasing production cost. Despite the theoretical advantages of methanotrophs for biopolymer production, this field is still very recent, with only a significant research outcome in polyhydroxyalkanoates (PHA) and its potential is impeded by intrinsic complications during the PHA extraction process. To overcome this obstacle and stablish methanotrophs as a good platform for biopolymers production, extracellular biopolymers (EPS) may emerge as an alternative. EPS possesses a structural diversity unmatched by other polymers, which makes its chemical production unprofitable, but displays interesting properties suitable for water-resistant paper coatings or fire retardants. The absence of research regarding EPS biological production, characterization and its diversity in chemical and mechanical properties encourages the approach as a potential cost-effective way for biopolymer production of this project.

Keywords: Biogas, biopolymers, biorefineries, EPS, MBfR, methane.

OBJECTIVES

The major objective of CH4-BIOPOL is to verify the feasibility of EPS production with methanotrophs. In doing so, it is expectable to understand the different pathways related to this production and how to control and optimize it. Also, characterizing methanotrophs' EPS will be key in determining whether it will be suitable for biopolymer production or not. These main aims are divided into others more specific, which constitute the different steps for them.

Proof of Concept

Until now, the different configurations for methanotrophs cultivation have encountered mass transfer limitations due to the low solubility of CH_4 in water. In this project, a different approach will be tested which is based on biofilm promotion around hollow fibres membrane, resulting in a membrane biofilm bioreactor (MBfR). Methane will be supplied through these membranes while oxygen by regular aeration to the aqueous column. Hence, CH_4 will be fed with two different streams at different concentrations: one of them will emulate natural gas so it will supply great quantities of CH_4, while the other one will mimic biogas CH_4 concentrations. This experimental set-up aims to elucidate the role of methanotrophs in the Circular Economy frame.

Identification of Key Genes

Despite methanotrophs research has already identified many genes, these findings are capitalized by the methane assimilation pathway and related ones, so EPS production genes are still quite unknown. To address this point, *Methylotuvimicrobium alcaliphilum* 20Z and *Methylomonas rubra* 15sh, two model microorganisms, have been selected and their EPS production genes will be characterized with genomics and transcriptomics techniques.

Impact of Operational Factors

There are several operational parameters that can be modified to increase cell growth, EPS biosynthesis or CH_4 uptake, according to literature in methanotrophs. Specifically, physicochemical properties of the EPS may change due to variations in such factors and these properties will be evaluated to initially characterize EPS.

EPS Regulation

Based on the conclusions reached in previous objectives, special emphasis will be placed on those genes that affects EPS production under the different operational parameters. Hence, a meta-transcriptomics analysis will show the metabolic pathway activity at the whole mixed cultures. Together with metagenomics and bioinformatics, a reconstruction of genomes and other genetic structures involved in EPS biosynthesis can be done.

METHODOLOGY

The project will last for 2 years, and it is structured into three connected Work Packages (WP). WP1 comprises those activities related to the cultivation of methanotrophs in a mixed aerobic community and will report results for the first and third sub-objectives. Within this package, it is included the design and set-up of two MBfRs, its operation to obtain enriched methanotrophic cultures, testing of different operational conditions and EPS physicochemical characterization. WP2 is only planned for the first year and addresses the second sub-objective, mainly, at unravelling the genomic expression of the two model microorganisms when producing EPS in pure cultures. Genes studies in WP2 are classified according to their major functional role in the EPS biosynthesis: NDP-sugar synthesis, glycotransferases and protein polymerization and export. For this purpose, pure cultures subjected to different operational factors will be subject to whole-genome sequencing (WGS), information from which will be used for further transcriptomic and bioinformatic analysis. Lastly, WP3 takes the knowledge generated in the previous packages to conduct several metanalysis in the mixed methanotrophic cultures.

ACKNOWLEDGEMENTS

This research is funded by the Agencia Estatal de Investigación (Spanish Government) through project TED2021129501B-I00 (Proyectos Estratégicos Orientados a la Transición Ecológica y a la Transición Digital. Convocatoria 2021). The authors acknowledge the support from the Economy and Knowledge Department of the Catalan Government through a Consolidated Research Group (ICRA-TECH - 2021 SGR 01283).

Monitoring and thorough behaviour of volatile methylsiloxanes through a wastewater treatment plant

F. Sánchez-Soberón*†, G.F. Pantuzza*, M. Fernandes*, N. Ratola*‡.

* LEPABE - Laboratory for Process Engineering, Environment, Biotechnology and Energy, Faculty of Engineering, University of Porto, Rua Dr. Roberto Frias, 4200-465 Porto, Portugal.
§ ALiCE - Associate Laboratory in Chemical Engineering, Faculty of Engineering, University of Porto, Rua Dr. Roberto Frias, 4200-465 Porto, Portugal. (E-mail: *nrneto@fe.up.pt)*
†Institute of Health Carlos III, Department of Atmospheric Pollution. Ctra. Majadahonda - Pozuelo, Km. 2. 28220 Madrid, Spain.

Abstract
Volatile methylsiloxanes (VMSs) are a group of compounds used as additives in personal care products and cosmetics. Once used, part of them ends up in wastewater treatment plants (WWTP), where they can migrate to biogas, hindering the quality of this renewable resource by corroding and blocking engines powered by this fuel upon combustion. The main objective of this work is the analysis of VMSs in sludge, water, air and biogas from a municipal WWTP located in Portugal. To accomplish that, different sampling strategies were carried out to collect the above-mentioned matrices for 14 days in August 2020. Subsequently, these samples were extracted following low-impact methodologies based on green chemistry approaches, and analysed by means of GC-MS (for air, sludge, and wastewater) and GC-IMS-SILOX in case of biogas. These results were later used in conjunction with mass flows provided by the management board of the WWTP to study the fate of the different compounds in the plant. Regardless of sampling point, D3 is the prevalent VMSs in wastewater. This result is likely caused by punctual releases rather than base levels. In sludge, D5 is the predominant compound, due to its higher lipophilicity and high use as additive in cosmetics and personal care products. Air showed different VMSs profiles depending on assessed environment. Thus, outdoor samples are characterized by a prevalence of D5, while indoor samples show a predominance of D3 and D4. This phenomenon is caused by differential VMSs sources between these two environments, and the installation of air filtering systems in indoor locations. Biogas was characterized by a prevalence of D5 showing concentrations up to 8 mg/m^3, which is higher than recommended by some internal combustion engines manufacturers. By studying the WWTP as a whole, it is possible to see a reduction of VMSs levels of 81% along the wastewater treatment. Most of this VMS mass migrates to sludge and air, with some plausible degradation of D3 and D6 once volatilized. This is a giant first step to help WWTP managers to deal with the current issue of VMSs interference in the energy production from anaerobic digestion that often takes place in these facilities.

Keywords (maximum 6 in alphabetical order)
biogas; mass balance; sludge; volatile methylsiloxanes; wastewater; WWTP

INTRODUCTION

Formed by Si-O bonds with aliphatic chains attached to silicon atoms, volatile methylsiloxanes (VMSs) are cyclic or linear compounds that exhibit low chemical reactivity and high thermal stability [1]. These characteristics make them widely used chemicals in industrial processes and a vast array of consumer products such as detergents, adhesives, paints, and personal care products. Being semi-volatile, VMSs are mainly emitted to the atmosphere after use, but a considerable part enter wastewater treatment plants (WWTPs) in the untreated wastewater [2]. There, they partition among wastewater, sludge, biogas and air and can generate technical problems in internal combustion engines powered with biogas, from blockage to corrosion of parts [3]. Knowing the behaviour of VMSs in WWTPs is the first step to reduce these negative impacts and ensure the use of biogas as renewable resource to the maximum potential. Thus, this pilot study relied on an unprecedent sampling campaign to investigate 4 cyclic (D3-D6) and 4 linear (L2-L5) VMSs in a WWTP. To do so, samples of wastewater, sludge, indoor and outdoor air, and biogas were collected for two weeks and analyzed by different environment-friendly protocols to obtain the levels and mass balance of VMSs and elucidate the fate of the different VMSs.

MATERIALS AND METHODS

Wastewater, sludge, air, and biogas were collected during 14 consecutive days in August 2020 (see details in Table 1) in a municipal WWTP (about 40,000 m^3/day and 160,000 population equivalent) located in Portugal. Several points along the WWTP were chosen to collect daily 250 mL composite samples of sludge (5 points) and wastewater (4 points) were taken, plus six-hours composite wastewater samples in the first week. Point samples of biogas were collected in five days with Tedlar bags. Air samples were collected at 3 indoor, 2 semi-indoor and 4 outdoor points using two mesh cylinders with 10 g of XAD-2 resin protected with a stainless-steel case and exposed for 14 days. The analytical protocol for wastewater and sludge consisted of liquid-liquid extraction protocols, the former with n-hexane as extraction solvent under sonication and the latter with n-hexane and acetone (1:1) as extraction solvent, followed by orbital shaking for 2 h. For the passive air samples, a solid-phase extraction in separation funnels was used with three n-hexane extractions. These matrices were quantified in GC-MS. Biogas was directly analyzed by a GC-IMS-SILOX chromatograph. In order to calculate mass balances, flows from the analyzed matrices were provided by the WWTP management board.

Table 1: Sampling sites, characteristics and periodicity according to each matrix studied

Matrix	Sampling type	Number of points	Sites	Periodicity
Wastewater	Collection in 250 mL polypropylene flasks	4	Entry, Post-preliminary treatment, Post-primary decanter, Treated effluent	Daily composite samples (two weeks), Six-hours composite samples (one week)
Sludge	Collection in 250 mL polypropylene flasks	5	Primary decanter, Secondary decanter, Thickener, Pre-digester, Post-digester	Daily composite samples (two weeks)
Air	Passive sampling with 2 x 10 g of XAD-2	9	Canteen, Laboratory, Office, Workshop, Sludge thickener, Preliminary treatment, Aeration tank, Centrifuge, Background (outside the plant)	Exposure for two weeks
Biogas	Collection in 1 L Teflon bags	1	After biogas production	Every 2-3 days

RESULTS AND DISCUSSION

The level of ∑VMSs (23 ± 25 µg/L) and profiles in entry water for the sampling period as a whole were similar to results found in the literature, except for D3, which had concentrations one order of magnitude higher than reported [4]. From the daily concentrations, it was observed that this result could be related to punctual releases of this compound instead of base levels. No specific hourly-dependent pattern of VMSs was detected entering the WWTP. Regarding the wastewater mass balance, the higher losses happened in the primary decanter and the secondary treatment (31% and 29%, respectively), as a consequence of the partition between water and sludge (
Figure *1*)

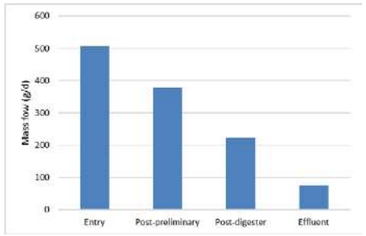

Figure 1: Mass flows of total VMSs in wastewater line

Primary and secondary sludge concentrations of ∑VMSs (8 ± 4 and 8 ± 3 µg/g dw respectively) and profiles were in line with values reported in the literature. Sludge profile was dominated by D5, followed by D6, regardless of sampling point. This outline is expectable if having into consideration the high use of D5 and the greater lipophilicity of D5-6. Concerning the mass balance of VMSs in sludge, it is possible to see a reduction along the sludge line (
Figure *2*). The digester is the treatment exerting the highest VMSs reduction in the sludge line (7% of entry levels). This result is caused by the migration of VMSs to biogas, favoured by the specific conditions in this treatment step (*i.e.*, 21 days of retention time and 37 ºC).

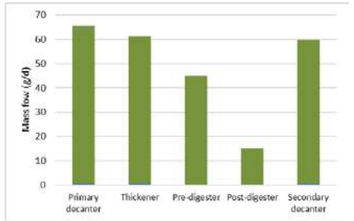

Figure 2: Mass flows of total VMSs in the sludge line

As a consequence of this migration from sludge, biogas concentrations for ∑VMSs (8 ± 0 mg/m^3) were above the limits for internal combustion engines recommended by some manufacturers (5 mg/m^3). D5 contributed with 89%, and D4 the remaining 11%.

VMSs profile in air is location-dependent, since in outdoor samples D5 was the major congener, but not indoors, where D3 and D4 prevailed. This trend, already observed in previous studies [5], is probably caused by two main reasons. On one hand, different sources are expectable between these two environments. While outdoor air is highly influenced by wastewater VMSs content, indoors may be more impacted by cosmetics and personal care products used by workers. On the other hand, the indoor air filtering systems installed in the office buildings are more prone to retain high molecular weight VMSs, such as D5 and D6.

The overall mass balance indicates a reduction of 81% in VMSs total mass is achieved along the WWTP (∑VMSs mass flows of 508 ± 530 and 96 ± 115 g/d for inputs and outputs respectively). Most of this reduction is achieved in the wastewater line, due to air migration of the VMSs. However, when comparing the observed results in air with those expected having into consideration the water/sludge partition, a lack of D3 and D6 is air is observed. This result could be indicative of atmospheric degradation and transformation processes of these compounds [2].

CONCLUSIONS

The present study highlights the importance of increased sampling periods in order to improve the representativity and time-sensitivity of VMSs monitoring and analysis. Equally, biogas and indoor air have shown their relevance as matrices to be sampled in WWTPs mass balance exercises. Future studies should aim to understand the seasonal effect on WWTP of VMSs influents and emissions.

REFERENCES

[1] K. Gaj, A. Pakuluk, Polish Journal of Environmental Studies, 24, 937–943 (2015).
[2] A.A. Bletsou, A.G. Asimakopoulos, A.S. Stasinakis, N.S. Thomaidis, K. Kannan, Environmental Science & Technology, 47, 1824–1832 (2013).
[3] I. Bragança, F. Sánchez-Soberón, G.F. Pantuzza, A. Alves, N. Ratola, Biomass and Bioenergy, 143, 105878 (2020).
[4] Y. Horii, K. Nojiri, K. Minomo, M. Motegi, K. Kannan. Chemosphere, 233, 677-686 (2019).
[5] F. Sánchez-Soberón, N. Ratola. Environmental Pollution, 315, 120423 (2022).

ACKNOWLEDGEMENTS

This work was financially supported by: (i) Projects LA/P/0045/2020 (ALiCE – Associated Laboratory in Chemical Engineering) and UIDB/00511/2020 and UIDP/00511/2020 (LEPABE – Laboratory for Process Engineering, Environment, Biotechnology and Energy), funded by national funds through FCT/MCTES (PIDDAC); (ii) Project LANSILOT (PTDC/CTA-AMB/32084/2017; POCI-01–0145-FEDER-032084), funded by FEDER through COMPETE2020—Programa Operacional Competitividade e Internacionalização (POCI) and by national funds (PIDDAC) through FCT/MCTES; (iii) Project "HealthyWaters – Identification, Elimination, Social Awareness and Education of Water Chemical and Biological Micropollutants with Health and Environmental Implications" (NORTE-01-0145-FEDER-000069), co-financed by Programa Operacional Regional do Norte (NORTE 2020), through Portugal 2020 and FEDER; (iv) G. Pantuzza thanks FCT PhD programme for Grant 2020.07815.BD, supported under the Portugal 2020 Partnership Agreement and European Social Fund (ESF). The authors wish to thank the help of the staff at the WWTP in the design of the sampling strategy and the collection of the samples.

Volatile methylsiloxanes (VMSs) in biogas generation in WWTPs – a mass balance

F. Sánchez-Soberón*†, M. Fernandes*, N. Ratola*§

* LEPABE - Laboratory for Process Engineering, Environment, Biotechnology and Energy, Faculty of Engineering, University of Porto, Rua Dr. Roberto Frias, 4200-465 Porto, Portugal.
§ ALiCE - Associate Laboratory in Chemical Engineering, Faculty of Engineering, University of Porto, Rua Dr. Roberto Frias, 4200-465 Porto, Portugal. (E-mail: *nrneto@fe.up.pt)*
†Institute of Health Carlos III, Department of Atmospheric Pollution. Ctra. Majadahonda - Pozuelo, Km. 2. 28220 Madrid, Spain.

Abstract
Despite it is well demonstrated that the presence of volatile methyl siloxanes (VMSs) in biogas hinders the quality of this renewable fuel, nowadays it is not well defined the dynamics of these compounds in methanogenic digesters. Therefore, the present work aims to study, for the first time, the distribution of VMSs within biogas digesters in different wastewater treatment plants (WWTP). Samples of sludge (both pre and post digested) and biogas were collected in five different WWTPs in Portugal. VMSs from sludges were extracted by liquid-liquid extraction with n-hexane, before GC-MS quantification. Biogas was directly analyzed from sampling bags by means of a GC-IMS-SILOX. Results show that the difference in VMSs mass between entry and digested sludge reach average values around 50%, being very variable among different congeners. Consequently, some locations showed levels of total VMSs above 5 mg/m^3 (limit recommended by some internal combustion engine manufacturers). Decamethylcyclopentasiloxane (D5) was the prevalent VMSs regardless of matrix and WWTP analyzed.

Keywords (maximum 6 in alphabetical order)
biogas; green chemistry; mass balance; sludge; volatile methylsiloxanes; WWTP

INTRODUCTION

Volatile methylsiloxanes (VMSs) are synthetic substances with a Si-O backbone saturated with methyl groups used in numerous consumer products [1]. Largely emitted to the environment, an important fraction of these compounds reaches wastewater treatment plants (WWTPs) where, depending on the congener physical and chemical properties, they can end up in biogas, often produced to fuel energy cogeneration systems. The combustion of biogas produces SiO_2 particles that settle and damage engine parts, decreasing the efficiency of the process [2]. The presence of VMSs in WWTPs has been reported in literature focusing on wastewater and sludge [3], but their behaviour in anaerobic digestors still lacks appropriate knowledge. Consequently, the objective of the present work is to study the distribution of VMSs within digesters in different WWTPs producing biogas.

MATERIALS AND METHODS

The sampling campaign occurred in 5 municipal WWTPs in Portugal in September 2021, targeting linear (L2-L5) and cyclic (D3-D6) VMSs. 250 mL of 24-hour composite samples of input and output sludge from methanogenic digesters. Biogas from every digester was taken at the same time using 1 L Tedlar® bags. Sludge and biogas flows were obtained from the WWTPs management boards. Biogas was directly injected and quantified on a GC-IMS-SILOX chromatograph. For sludge, 20 mL aliquots were mixed with 20 mL of hexane:acetone and spiked with 500 ppb M4Q (IS). Subsequently, the mixture was vortexed, orbital-shaken and centrifuged. The organic supernatant was collected, reduced to 1 mL, and injected into a GC-MS for quantification.

RESULTS AND DISCUSSION

Sludge concentrations

The ∑VMSs input concentrations (values ranging from 67.0 ± 1.76 to 395 ± 11.3 µg/L) were higher than in the output sludge (values ranging from 30.8 ± 15.1 to 94.7 ± 10.4 µg/L) concentrations in every WWTP, reflecting the partition to biogas. Cyclic VMSs were predominant in the sludge of every WWTP, with D5 representing more than 85% of the ∑VMSs regardless of the plant. L5 was the only linear VMS detected, maybe due to its more frequent use and higher lipophilicity [3].

Biogas concentrations

Cyclic VMSs were also prevalent in the biogas profile of every WWTP. D5 was the prevalent compound (representing in all cases above 78% of the ∑VMSs). L2 was the only linear VMSs detected, but only in one plant. Three of the facilities studied showed levels of ∑VMSs above 5 mg/m^3, the limit recommended as safe by some engine manufacturers [4].

Mass balance

The mass balance of all the WWTPs suggests that high molecular weight VMSs (L5, D4-D6) present a better consistency between input and output values in methanogenic digesters than low molecular weight compounds, as can be seen in Figure 1. D4 presented a total recovery of 73 ± 49%. Most of this mass partitioned to the biogas (47 ± 33%) while a smaller portion (26 ± 19%) remained in the sludge. An opposite trend was shown by D5, which yielded total recoveries of 71 ± 19%, with most mass remaining in the sludge (45 ± 24%) while approximately 26 ± 8.4% is transferred to biogas. This different behaviour can be explained by the differences in their boiling points (176 and 211 °C for D4 and D5 respectively) [3].

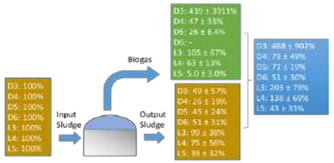

Figure 1. Overall relative mass distribution (mean ± standard deviation) of the different VMSs within the five biogas digesters

CONCLUSIONS

Cyclic VMS, and more specifically, D5 were predominant in both biogas and sludge. This outcome is a consequence of the intensive use of this compound in PCPs and cosmetics. The levels of total VMSs in biogas of three WWTPs were above the threshold proposed by some internal combustion engine manufacturers. The concentrations of total VMSs were higher in the digesters input sludge, suggesting a migration of VMSs from sludge to biogas, which was confirmed by the mass balance for most VMSs.

REFERENCES

[1] C. Rücker, K. Kümmerer, Chemical Reviews, 115, 466-5244 (2014).
[2] I. Bragança, F. Sánchez-Soberón, G.F. Pantuzza, A. Alves, N. Ratola, Biomass and Bioenergy, 143, 105878 (2020).
[3] D. Capela, N. Ratola, A. Alves, V. Homem, Environmental International, 102, 9-29 (2017).
[4] N. de Arespacochaga, C. Valderrama, J. Raich-Montiu, M. Crest, S. Mehta, J. L. Cortina, Renewable and Sustainable Energy Reviews 52 366–381 (2015).

ACKNOWLEDGEMENTS

This work was financially supported by:
(i) LA/P/0045/2020 (ALiCE), UIDB/00511/2020 and UIDP/00511/2020 (LEPABE – Laboratory for Process Engineering, Environment, Biotechnology and Energy), funded by national funds through FCT/MCTES (PIDDAC); (ii) Project LANSILOT (Ref. PTDC/CTA-AMB/32084/2017; POCI-01-0145-FEDER-032084), funded by FEDER funds through COMPETE2020 – Programa Operacional Competitividade e Internacionalização (POCI) and by national funds (PIDDAC) through FCT/MCTES; (iii) Project "HealthyWaters – Identification, Elimination, Social Awareness and Education of Water Chemical and Biological Micropollutants with Health and Environmental Implications", Ref. NORTE-01-0145-FEDER-000069, co-financed by Programa Operacional Regional do Norte (NORTE 2020), through Portugal 2020 and FEDER. The authors wish to thank the management boards and staff of the different WWTPs that collaborated in the present study.

Green roofs and green walls for greywater treatment and reuse: a review of design and operational conditions

F. Masi*, A. Rizzo*, E. Costamagna**, S., Fiore**, and F. Boano**

* IRIDRA Srl, via Alfonso La Marmora 51, Florence 50121, Italy
(E-mail: masi@iridra.com)
** Dept. Of Environment, Land and Infrastructure Engineering. Politecnico di Torino, Corso duca degli Abruzzi 24, 10129 Torino (Italy)

Abstract
Green walls and vegetated rooftops are emerging techniques for urban reconciliation ecology, and they are becoming more frequent in modern architecture. This work presents the results of the literature review done within the NICE H2020 project, regarding the state of the art of current applications of green walls and green roofs for treatment and reuse of greywater (i.e., domestic wastewater excluding toilet flush). A specific focus is adopted on the operational conditions (e.g., inflow rate of greywater), on the implementation schemes, and in the materials used as filter medium, considering that these factors are highly relevant for the treatment of greywater.

Keywords
Nature-based Solution; green wall; green roof; greywater reuse; non-conventional water.

INTRODUCTION

Green walls are vertical systems that provide vegetation cover to the external – and possibly internal – walls of buildings. According to the structure used to support vegetation growth and the classification given by Bustami et al (2018), green walls are generally classified in: Living walls, vegetation is planted in containers attached to the wall or is rooted to a supporting structure (e.g., geotextile) attached to the wall; green facades: vegetation is planted at the base of the wall and climbs either on a supporting structure (e.g., steel or plastic mesh) or directly on the wall itself. These structures can provide many valuable ecosystem services. For example, they enhance thermal regulation and increase economic value of buildings scale, and they also favour biodiversity preservation and improve air quality at urban scale (Boano et al., 2020). Moreover, they provide psychological and social benefits by lowering stress levels and enhancing people interactions. However, the implementation of green walls must take into account their water requirements, and the use of greywater has been proposed as an alternative water source to mitigate the water footprint of green walls. Moreover, green walls can also be adapted to become greywater treatment systems, becoming Nature-based Solutions that generate reclaimed water resources for non-potable reuse.

Green roofs are vegetated surfaces built on building roofs, composed of a medium layer where vegetation grows, a waterproof membrane and a vegetation layer. Green roofs are generally classified in: Extensive green roofs: medium depth up to 100 mm; Intensive green roofs: medium depth over 300 mm. Extensive green roofs are generally planted with smaller plants, usually Sedum, while intensive green roofs can be planted with larger plants and bushes, which results in heavier structures. When green roofs are integrated in buildings, they enhance thermal regulation through insulation and evapotranspiration. Biodiversity and air quality are also preserved and improved, increasing the economic value of the area in which green roofs are installed. Furthermore, rainwater can be collected, treated and reused with these systems instead of been discharged in the municipal drainage network, thus helping with the management of both extreme rain events and dry periods. Similarly to green walls, the irrigation of green roofs with greywater can support it during periods with limited rainfall and can generate treated greywater for non-potable reuse.

According with the aim of this work, the state of art of green walls and green roofs for greywater treatment and reuse is discussed in relation to new information and technologies involving these systems. For this aim, some case studies from the literature were used to derive some important data. Subsequently, statistical analyses were performed on these data to identify patterns between the relationships of different parameters in the performance of each case.

MATERIALS AND METHODS

Different literature types were investigated to obtain a suitable dataset to discuss the state of art of green walls and green roofs used for greywater treatment and reuse. Specifically, peer-reviewed and grey literature have been considered with the following rationale:

- Peer-reviewed literature – green walls: the analyzed articles were selected in cooperation with the Green Wall Cluster of the Circular City COST Action (https://circular-city.eu/) in which, POLITO and IRIDRA, partners of NICE, were involved. Eleven peer-reviewed papers have been selected and analyzed in this deliverable (for the full list of papers see section 4); all these papers consider the application of living walls for grey water treatment and reuse in real conditions. In addition, the paper of Kotsia et al. (2020) was also considered in the analysis, in order to include also the possibility to implement green wall for greywater treatment with green facades planted with climbing plants.
- Grey literature – green walls: IRIDRA experience has also been included as grey literature. Considering the design of green walls for greywater treatment and reuse for the demonstration pilots of the NAWAMED project made by IRIDRA, the data from these systems were obtained for this report. These data were presented in the 17th International Conference on Environmental Science & Technology, CEST2021, in Athens, Greece (Martinuzzi et al., 2021).
- Peer-reviewed literature – green roofs: the literature on green roofs for greywater treatment and reuse is quite limited, as reported by Boano et al. (2020); therefore, the articles have been selected considering the works citing and referred by a few key papers as Zapater-Pereyra et al. (2016); Boano et al. (2020); Cross et al. (2021); Thomaidi et al. (2022). Thirteen peer-reviewed papers have thus been selected and considered suitable for the analyses of this deliverable (for the full list of papers see section 4).
- Grey literature – green roofs: IRIDRA experience has been also included by the design approach of green roofs for greywater treatment and reuse for an installation on the roof of a resort built in Tanzania, reported in Masi et al. (2015).

The dataset obtained from the peer-reviewed and grey literature was systematized and structured according, collecting performance (e.g. TSS, BOD_5, COD, nutrients) and design values. Particular attention has been paid to collecting data in line with design parameters typical of treatment wetland technology (e.g. area, weight, HLR – Hydraulic Loading Rate, OLR – Organic Loading Rate, OTR – Oxygen Transfer Rate). When not directly reported in the papers, the parameters have been calculated from information given in the paper or from literature values (e.g., weight of the filling media).

Statistical analysis of the design parameters found in the different articles was performed to evaluate the variability of the design values within the samples. Moreover, regression analyses were performed between some key design parameters, to verify the relationship between the design and performance of green walls and green roofs.

RESULTS

The statistical analyses of the design parameters found in the different articles for green walls and green roofs are reported in Table 1 and 2, respectively.

According to the statistic parameters calculated from the literature dataset it was noted that the treatment surface per row and the medium volume per row show great variability, from 0.01 m2 to 53 m^2 (Table 1). This is due to the different scales of the green walls (laboratory scale vs. full scale) and to the different configurations of green walls, for example, from single columns of small pots to large troughs. Regarding the depth of the medium, they showed values of the order of tens of centimeters (10 – 80 cm), with an average of 40 cm. The weight per square meter of the green walls medium remained below 100 kg, with a minimum of 5 kg to a maximum of 78 kg, depending on the type of material used and the system configuration, with an average of 38 kg. The total weight per square meter, including medium and water, varied between 7 kg and 158 kg (avg. 81 kg). The observed average inflow rate was 1.4 m^3/d, with a range of 0.004 to 10.4 m^3/d. The average HLR on the first row was 411 L/m^2/d, while the average OLR on the first row was 91.5 gCOD/m^2/d with a range of 100 – 1111 L/m^2/d and 20 – 218 gCOD/m^2/d respectively. The retention time remained below two days, with an average of a day and a half (1.6 d), and with a single sample that exceeded three days (3.35 d). The OTR values varied between 3.2 and 68 gO2/m^2/d, with an average of 30 gO2/m^2/d. Green walls showed a good performance in BOD_5 and COD removal, with an average percentage removal of 87% and 73% respectively (range: 25 – 99% BOD_5, 18 – 97% COD).

Table 1. Statistical parameters of green walls design and performance from literature data.

	Unit of measure	Avg.	St.dev.	Min.	Q1	Q2	Q3	Max.	no. samples
Treatment surface per row	m^2	5.5	12.9	0.01	0.1	1.0	2.6	53	18
Medium volume per row	m^3	1.9	4.6	0.006	0.026	0.216	0.55	16.8	17
Depth per row	m	0.4	0.3	0.12	0.15	0.335	0.6	0.8	12
Medium weight	kg/m^2	37.8	25.9	5.6	14.8	44.3	55.9	78.2	16
Total weight	kg/m^2	81.2	57.7	6.9	21.9	111.8	127.4	158.2	16
Inflow rate	m^3/d	1.4	2.4	0.004	0.05	0.78	1.55	10.4	20
HLR first row	L/m^2/d	410.8	337.1	100	143.2	250	597.3	1111.1	17
OLR first row	gCOD/m^2/d	91.5	63.9	20.5	47	70.2	131.1	218.2	17
HRT	d	1.6	1.1	0.55	1	1.4	1.9	3.35	5
OTR	gO_2/m^2/d	29.9	18.5	3.2	18.4	30	39.8	67.9	11
BOD5 removal	%	87	19	25	88	95	96	99	25
COD removal	%	73	26	18	45	90	93	97	29

According to the literature dataset, in general green roofs exhibit a relatively good removal of BOD_5 and COD, with an average of 70% for BOD5 and 77% for COD. BOD_5 removal ranges from a minimum of 35% to a maximum of 97%, while COD removal ranges from 39% to 99% (Table 2). The depth of the medium layer of the green roofs in the analyzed papers varied from a minimum of 9 cm (extensive green roofs) to a maximum of 62 cm (intensive green roofs), with an average of 20 cm. The average weight of the medium layer per square meter was 203 kg/m^2, and 274 kg/m^2 with the addition of the weight of water. The observed weight range was very wide, as it depends on the depth of the medium layer and the type of filling material used, and so these values varied from a minimum of 28 kg/m^2 (88 kg/m^2 with water) to a maximum of 930 kg/m^2 (1180 kg/m^2 with water). The inflow rate varied between 0.003 m^3/d to 4 m^3/d, with an average of 0.3 m^3/d. The average hydraulic loading rate and organic loading rate that correspond to these rates are 39.2 L/m^2/d and 9.3 gCOD/m^2/d, respectively. The HRT values generally remained below two days, except for two samples, which showed an average of 1.4 days (minimum 0.5 d, maximum 3.8 d). Finally, the Oxygen Transfer Rate on average was equal to 14 gO_2/m^2/d, with a minimum of 1.1 gO_2/m^2/d and a maximum of 50.3 gO_2/m^2/d.

Other results of the statistical analyses and the regression analyses will be presented at the conference.

Table 2. Statistical parameters analysis of green roofs design and performance from literature data.

	Unit of measure	Avg.	St.dev.	Min.	Q1	Q2	Q3	Max.	no. samples
Depth	m	0.2	0.1	0.09	0.15	0.24	0.29	0.62	14
Medium weight	kg/m^2	202.7	208.9	28.2	100	134.5	205.5	932	19
Total weight	kg/m^2	274.2	254.1	88.2	145	202	303	1180	19
Inflow rate	m^3/d	0.3	0.9	0.003	0.02	0.03	0.04	4	20
HLR	L/m^2/d	39.2	38.8	3.9	21.9	28.4	45.15	173.9	20
OLR	gCOD/m^2/d	9.3	12	1.2	3.6	5.2	6.1	48.4	21
HRT	d	1.4	1	0.54	0.8	1	1.8	3.8	9
OTR	gO_2/m^2/d	14	15.6	1.1	2.3	8.7	18.5	50.3	47
BOD5 removal	%	70	20	35	55	67	90	97	21
COD removal	%	77	19	39	66	80	93	99	55

Acknowledgement. This has received funding from the European Union's Horizon 2020 research and innovation programme under grant agreement No. 101003765 (NICE - Innovative and enhanced nature-based solutions for sustainable urban water cycle).

REFERENCES

Boano, F., Caruso, A., Costamagna, E., Ridolfi, L., Fiore, S., Demichelis, F., Galvão, A., Pisoeiro, J., Rizzo, A. and Masi, F., 2020. A review of nature-based solutions for greywater treatment: Applications, hydraulic design, and environmental benefits. *Science of the Total Environment*, **711**, p.134731.

Bustami, R.A., Belusko, M., Ward, J. and Beecham, S., 2018. Vertical greenery systems: A systematic review of research trends. *Building and Environment*, **146**, pp.226-237.

Cross, K., Tondera, K., Rizzo, A., Andrews, L., Pucher, B., Istenič, D., ... & Mcdonald, R. (2021). *Nature-Based Solutions for Wastewater Treatment*. IWA Publishing.

Kotsia, D., Deligianni, A., Fyllas, N. M., Stasinakis, A. S., & Fountoulakis, M. S. (2020). Converting treatment wetlands into "treatment gardens": Use of ornamental plants for greywater treatment. *Science of The Total Environment*, **744**, 140889.

Martinuzzi N., Rivai K., Rizzo A., Masi F., Sarnari B. And Bousselmi L. (2021). Green walls for greywater treatment and reuse in Mediterranean countries. *17th International Conference on Environmental Science and Technology*, Sept. 2021.

Masi, F., Rizzo, A., & Bresciani, R. (2015). Green architecture and water reuse: examples from different countries. *Sustainable Sanitation Practice*, **23**, 4-10.

Thomaidi, V., Petousi, I., Kotsia, D., Kalogerakis, N., & Fountoulakis, M. S. (2022). Use of green roofs for greywater treatment: Role of substrate, depth, plants, and recirculation. *Science of The Total Environment*, **807**, 151004.

Zapater-Pereyra, M., Lavrnić, S., Van Dien, F., Van Bruggen, J.J.A. and Lens, P.N.L., 2016. Constructed wetroofs: A novel approach for the treatment and reuse of domestic wastewater. *Ecological Engineering*, **94**, pp.545-554.

Protein and carbohydrate recovery from secondary sludge biomass generated in wastewater treatment plant.

Alejandro Filipigh**, Elena.M. Rojo** and Silvia Bolado**

* Department of Chemical Engineering and Environmental Technology, School of Industrial Engineering, University of Valladolid, Dr. Mergelina s/n, 47011 Valladolid, Spain
** Institute of Sustainable Processes, University of Valladolid, Dr. Mergelina s/n, 47011 Valladolid, Spain.

(E-mail: *silvia.bolado@uva.es*)

Abstract
Secondary sludge biomass (or WAS) produced in wastewater treatment plants is an interesting renewable resource that accumulates nutrients from these waters in the form of proteins and carbohydrates, among others. Despite recent interest in valorizing this biomass to improve the economics of wastewater treatment plants, there is still very little research focused on fractional resource recovery from this biomass. In this study, different hydrolysis processes such as chemical (acidic, AC and alkaline, ALK), hydrothermal (HT), biological (autohydrolysis, AH), physical (ultrasound, US) and sequential (US-AH) and assisted (US+ALK, HT +ALK, HT +AC) combinations were used to recover proteins in the form of peptides and carbohydrates in the form of fermentable monosaccharides from WAS biomass. The combined US+ALK treatment provided the highest solubilization yields (SY) of proteins (97.2%) with losses of less than 25%, resulting in peptide recovery yields of 75.1% with sizes ranging from 70-215 kDa. The combination HT +ALK resulted in almost complete solubilization of proteins but lower solubilization of carbohydrates (SY ≈75%) with high loss factors (47%). The combination HT +AC achieved high carbohydrate SY (94.2% 1M HCl) but lower protein SY (≈72%). The low yields obtained with the HA treatment were improved by the addition of acid, which increased protein SY by 82% and carbohydrates by 130% (0.5 M HCl) and 144% (1 M) under the same temperature (50°C) and time (180 min) conditions.
Keywords
Biorefinery, peptide, pretreatments, monosaccharide, valorization, waste

INTRODUCTION

Secondary sludge is an abundant and problematic waste biomass, which accumulates nutrients from wastewater in the form of proteins and carbohydrates, among others. The handling or disposal of this sludge represents currently almost 50-60% of the total cost of wastewater treatment plants (WWTP) (Capodaglio & Olsson, 2019). In recent years, studies have been addressed to the uses of this waste biomass as source of renewable energy through processes such as anaerobic digestion. However, the fractional recovery of the biomass components could be more economically advantageous. The biomass generated in WWTPs contains various microorganisms and extracellular polymeric substances (EPS), the main component of which is protein, which accounts for about 50% of the dry weight of bacterial cells (Xiang et al., 2017). This biomass could be an important source of peptides useful in multiple applications (Zhou et al., 2017). On the other hand, the carbohydrate fraction can be used to produce different value-added products such as polyhydroxyalkanoates (PHAs), or biofuels. However, research dedicated to the fractional valorization of sludge components is very limited and this knowledge is crucial for the development of new biorefinery processes that can considerably improve the economic balance of wastewater treatment plants. In this context, the present work evaluates and compares different types of hydrolysis as chemical methods (acid, AC and alkaline, ALK), hydrothermal methods (HT), biological methods (autohydrolysis, AH), physical methods (ultrasound, US) and sequential physical-biological combinations (ultrasound-autohydrolysis, US-AH), and thermal+chemical (HT+ALK and HT+AC), physical+chemical (US+ALK) methods assisted on solubilization yield (SY) and recovery (RY) of the main components of this biomass: proteins as peptides and carbohydrates as fermentable monosaccharides (glucose and xylose).

MATERIALS AND METHODS

Raw sludge (RS) biomass used in this study was collected from local urban WWTP in Valladolid, Spain. The samples of RS were taken after the secondary settler unit of the urban WWTP. The moisture content and pH of raw sludge were 98% and 6.8. The RS was concentrated by centrifugation to achieve a concentration of total solid (TS) of 11.7% with a volatile solid fraction of 76.9 % in the centrifuged raw sludge biomass (CRS). All CRS fractions were homogenized, and the chemical composition of CRS was as follows: 43 % protein, 17.1% carbohydrates (composed by 13.6% glucose, 3.6% xylose, 1.5% cellobiose, and 1.1% arabinose), 14.3% lipid, 12.8% humic acid (percentages based on ash-free dry mass). The extraction operation conditions shown in Table 1 were selected according to the previous experience of this team working with algal biomass grown in wastewater (Martin Juárez et al., 2021) and the scarce references about WAS (Xiang et al., 2017) focused on component solubilization. After each treatment, the hydrolysate was centrifuged to separate the liquid and solid fractions. The residual solids were weighted and analyzed to calculate by difference the solubilized macro-components. The recovery as peptides and monosaccharides was calculated from the analysis of the liquid phase. Protein fraction in solid fraction was determined using the Total Kjeldahl Nitrogen (TKN) and applying the nitrogen to protein ratio (N:P) of 4.0, calculated from the amino acid profile of the CRS, determined by HPLC-UV. The size of peptides recovered from all the assays were characterized by using SDS-PAGE according to Rojo et al., (2021). The monosaccharides and amino acids recovered, in the liquid fraction, were determined by HPLC-IR and HPLC-UV, respectively. Carbohydrates, in the exhausted solid, were determined using the modified NREL protocol of hydrolysis and HPLC-IR according to Rojo et al., (2021).

RESULTS AND DISCUSSION

Figures 1 and 2 show the SY (%) and RY (%) of proteins and carbohydrates for the different treatments tested in relation to the initial mass of each component in CRS. The highest protein SY were obtained with the alkaline-based methods. Single alkaline hydrolysis (ALK, 50°C, 0.5 M and 1 M, 180 min) resulted in protein SY of 75% at both NaOH concentrations. With increasing NaOH concentration, the carbohydrate SY decreased from 65.5% at 0.5 M NaOH to 56.8% at 1 M, and the recovery of monosaccharides was slightly lower than 30%. Almost complete solubilization of proteins (≈ 97.2%) were achieved when combining thermal (HT +ALK) or ultrasonic (US+ALK) methods with alkaline medium (0.5 M or 1 M). The combination of HT +ALK conditions resulted in almost complete solubilization of proteins but lower solubilization of carbohydrates (≈78%) and high loss factors (47%) of both components. In spite of the high protein SY, HT+ALK resulted in peptide recoveries of 58.5% (1 M NaOH) and 63.5 (0.5 M NaOH) with peptide sizes around 100-150 kDa in both cases. For the US+ALK method, losses were less than 25%, resulting in a peptide recovery yield of 75.1% with sizes between 70-215 kDa and 40% essential amino acids (Eaa). No differences were observed with NaOH concentration (0.5 and 1 M). Assisted alkaline hydrolysis (US+ALK, 60 min) also achieved the highest carbohydrate SY (94.4%, NaOH 1 M) but with high carbohydrate losses, resulting in monosaccharide recovery yields of only 30%.

Even, as a single treatment, without alkali support, ultrasound (US, 60 min, 50°C) resulted effective achieving SY of 43.7% for proteins and 44.6% for carbohydrate, values much higher than the 19.6% and 24% SY for proteins and carbohydrates, respectively, obtained in the 180 min AH assay at identical pH (6.5) and temperature (50°C) conditions. The application of 20 minutes of US also improved the autohydrolysis results (US-AH, 20 min), remarkably for proteins, reaching SY of 35.1% for proteins and 25.2% for carbohydrates. In both assays (US and US-AH), protein recovery was 46.5%, but with peptide sizes lower than 70 kDa.

The effect of temperature as single hydrolysis method (HT) was also notable, especially for proteins. The solubilization yield after 60 min under hydrothermal conditions was 184% higher for proteins and 55% higher for carbohydrates than that after 180 min of autohydrolysis at pH 6.5 and 50°C. Finally, combined acid and hydrothermal hydrolysis conditions (HT +AC, 60 min) achieved high carbohydrate SY (94.2% 1 M HCl and 81.4% 0.5 M HCl) but lower protein SY (≈72%). The HT+AC treatment provided 44% of peptide recovery, with so small size peptides than they were not detected in electrophoresis analysis.

REFERENCES

Capodaglio, A. G., & Olsson, G. (2019). Energy Issues in Sustainable Urban Wastewater Management: Use, Demand Reduction and Recovery in the Urban Water Cycle. *Sustainability 2020, Vol. 12, Page 266*, *12*(1), 266. https://doi.org/10.3390/SU12010266

Lorenzo-Hernando, A., Ruiz-Vegas, J., Vega-Alegre, M., & Bolado-Rodríguez, S. (2019). Recovery of proteins from biomass grown in pig manure microalgae-based treatment plants by alkaline hydrolysis and acidic precipitation. *Bioresource Technology*. https://doi.org/10.1016/j.biortech.2018.11.068

Martin Juárez, J., Martínez-Páramo, S., Maté-González, M., García Encina, P. A., Muñoz Torre, R., & Bolado Rodríguez, S. (2021). Evaluation of pretreatments for solubilisation of components and recovery of fermentable monosaccharides from microalgae biomass grown in piggery wastewater. *Chemosphere*, *268*. https://doi.org/10.1016/j.chemosphere.2020.129330

Rojo, E. M., Piedra, I., González, A. M., Vega, M., & Bolado, S. (2021). Effect of process parameters on the valorization of components from microalgal and microalgal-bacteria biomass by enzymatic hydrolysis. *Bioresource Technology*, *335*(May). https://doi.org/10.1016/j.biortech.2021.125256

Xiang, Y., Xiang, Y., & Wang, L. (2017). Disintegration of waste activated sludge by a combined treatment of alkaline-modified eggshell and ultrasonic radiation. *Journal of Environmental Chemical Engineering*, *5*(2), 1379–1385. https://doi.org/10.1016/j.jece.2017.02.034

Zhou, K., Barjenbruch, M., Kabbe, C., Inial, G., & Remy, C. (2017). Phosphorus recovery from municipal and fertilizer wastewater: China's potential and perspective. *Journal of Environmental Sciences (China)*, *52*, 151–159. https://doi.org/10.1016/j.jes.2016.04.010

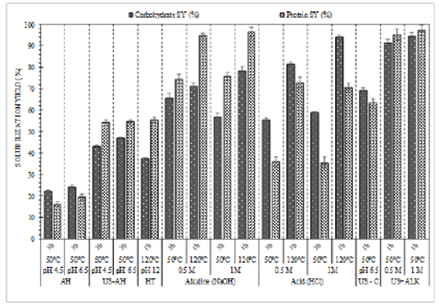

Figure 1: Protein and carbohydrate solubilization yields (%) in reference to the initial amount of carbohydrates and proteins in the centrifuged initial biomass (CRS)

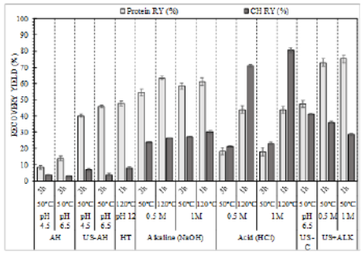

Figure 2:Peptide and monosaccharide recovery yields (%) in reference to the initial amount of carbohydrates and proteins in the centrifuged initial biomass (CRS)

Table 1: Operational condition using a 3.7% (w/w) biomass concentration

Type of hydrolysis	Condition	Time (min)	Temperature (°C)
Autohydrolysis (AH)	pH 4.5	180	50
	pH 6.5		
Ultrasound (US)-Autohydrolysis (AH)	20 kHz, 140 W, 50% amplitude	20	50
	pH 4.5	180	50
	pH 6.5		
Hydrothermal (HT)	pH 6.5	60	121
Alkaline (ALK)	NaOH 0.5 M	180	50
	NaOH 1 M		
Hydrothermal + Alkaline (HT+ALK)	NaOH 0.5 M	60	121
	NaOH 1 M		
Acid (AC)	HCl 0.5M	180	50
	HCl 1 M		
Hydrothermal + Acid (HT+AC)	HCl 0.5M	60	121
	HCl 1 M		
Ultrasound (US)	20 kHz, 140 W, 50% Amplitude	60	50
Ultrasound + Alkaline (US+ALK)	20 kHz, 140 W, 50% Amplitude + NaOH 0.5 M	60	50
Ultrasound + Alkaline (US+ALK)	20 kHz, 140 W, 50% Amplitude + NaOH 1 M	60	50

Acknowledgements: This work was supported by "Ministerio de Ciencia, Innovación y Universidades", Spain (PID2020-113544RB-I00). The authors also thank the regional government of Castilla y León (UIC 338, CLU 2017-09) and the EU-FEDER (CLU 2017-09) for financial support of this work. Filipigh. A (PRE2021-10017) and Rojo. E (PRE2018-083845) would like to thank the "Ministerio de Ciencia, Innovación y Universidades" for their PhD scholarships.

Towards a more sustainable water treatment and reuse through brines valorisation

A.Romero*, E.Santos-Clotas*, I.Casals**, E.Mena***, B. Lefèvre\, C.Echevarria*, J.Tobella*

* Cetaqua, Water Technology Centre, Carretera d'Esplugues 75, 08940 Cornellà de Llobregat, Barcelona, Spain
** Aguas Municipalizadas de Alicante,E.M, Avenida Catedrático Soler, 14, 03007, Alicante, Spain
*** Empresa Municipal de Aguas y Saneamiento de Murcia, S.A. Plaza Circular, 9,30008 Murcia, Spain
\AQUATEC, Proyectos para sector agua, S.A.U. Passeig Zona Franca, 48. 08038 Barcelona, Spain

Abstract
Environmental impact and costs related to the management of membrane concentrates are the main challenges from Drinking Water Treatment Plants and Reclaimed Water Treatment Plants. These types of facilities are at the same time large consumers of chlorine-based disinfectants. Two processes for brine valorisation will be demonstrated in two real case studies in Spain. Two semi-industrial prototypes have been designed using the results of laboratory scale tests and simulations for ionic and mass balances, chemicals, and energy consumption calculations based on Nanofiltration (NF), Selective Electrodialysis (SED) and Electrochlorination (EC) technologies. The prototypes will be operated until January 2024 to assess the feasibility of the solutions to produce N-rich reclaimed water and sodium hypochlorite.

Keywords
brine; chlorine; electrodialysis; electrochlorination

INTRODUCTION

Coastal areas affected by groundwater overexploitation may suffer high content of salts in groundwater and wastewater due to marine intrusion. To overcome this issue, Drinking Water Treatment Plants (DWTP) and Water Reclamation Plants (WRP) commonly rely on advanced treatments to produce desalinated water through Reverse Osmosis (RO). These technologies concentrate the salts in brines that are either managed as a waste or discharged to natural bodies, with its consequent environmental impact and high costs associated that may increase up to 0.7 €/m3. Moreover, intense agricultural activity has increased the concentration of nitrates in water bodies leading to the discharge of nitrate-rich brines and thus to eutrophication-related problems. These reasons increase the need of developing cost-effective solutions that reduce the environmental impact of membrane processes.

The present study is based on the demonstrative cases of Zarandona WRP (Murcia) and Rincon de León WRP (Alicante), where brine valorisation technologies will be applied to produce disinfectants from membrane concentrates and to benefit from nitrates as fertilizers. Current results include simulations and lab-scale trials carried out for the design of the nanofiltration, selective electrodialysis, and electrochlorination units, as well as calculation of the ionic and mass balances, and chemicals and energy consumption of the solution.

MATERIALS AND METHODS

Both proposed Brine Valorisation Treatments are shown in Figure 1.1. In Rincón de León WRP, concentrates from RO go through a SED that concentrates monovalent ions (mainly NaCl), followed by a 2D EC reactor to produce sodium hypochlorite (NaClO) in-situ. In Zarandona WRP, contaminated water with salinity and nitrates goes through a NF, producing N-rich reclaimed water: monovalent ions (mainly NaCl) from NF concentrate go through a concentration train followed by a novel 3D EC reactor to produce sodium hypochlorite.

Software design tools, such as Winflows®, were used to design the 2-stage NF for an 85% of water recovery. Lab-scale tests were performed on a set-up of 140 cm2 of active membrane area allowing determination of rejection profiles of NaCl, nitrates, and other ions.

Lab-scale tests of SED were performed on a set-up of 64 cm2 of active membrane area and a tension range of 0-36 V allowing continuous monitoring of current intensity, voltage, pressure, temperature, conductivity, flow and pH in the electrode, dilute and concentrate streams. The 2D EC setup works with one or two cells in parallel with an electrical current from 2 to 20 A that allows evaluation of active chlorine production under different conditions.

RESULTS AND DISCUSSION

Main compositions in feed streams are chloride (>88 mg/L), sodium (>500 mg/L), sulphates (>1-8 g/L), calcium (>0.3-1.7 g/L), and ammonia (>42-315 mg/L), for NF feed in Zarandona WRP and RO brines in Rincon de León WRP, respectively. Also, NF feed has nitrates (35 mg/L) and conductivity >3.5 dS/cm, while RO brines have a conductivity >8.7 dS/cm.

NF rejection values of 50-70% of dissolved monovalent salts (NaCl), 99% of divalent salts ($MgSO_4$) and 5-10% of dissolved nitrates were obtained for the membrane selected, producing a N-rich reclaimed water with conductivity below 3 dS/cm, suitable for irrigation.

SED was able to concentrate NaCl 5-10 times, whilst maintaining Ca^{2+} and Mg^{2+} below 100 mg/L for both ions, minimising the needs for pre-treatments to reduce scaling risk in the electrochlorination unit. Energy consumption of SED unit varied from 1.8 to 4.9 kWh/m^3, depending on the concentration factor, with overall energy consumption including 2D EC of 10.3 kWh/kg of active chlorine.

In Zarandona WRP, 0.2 hm^3/y of partially desalinated N-rich reclaimed water will be injected to Murcia Urban Irrigation Network, avoiding the discharge of 0.62 ton N_{eq}/y, and 26 ton/y of NaClO will be produced. In Rincon de León, up to 110 ton/y of NaClO will be produced from RO brines.

The proposed processes appear to be a cost-effective, circular economy-based alternative to conventional brine management strategies, reducing environmental impact related to brines management and N discharge, and producing in-situ sodium hypochlorite disinfectant.

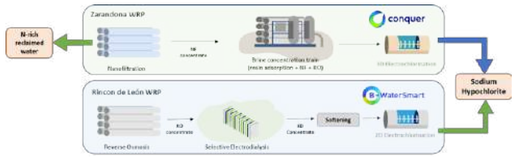

Figure 1. Flow diagram of the brine valorisation treatments

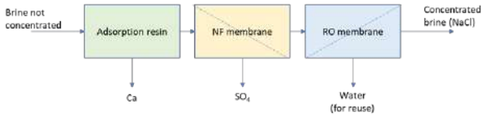

Figure 2. Scheme of brine concentration train after Nanofiltration at Zarandona WRP

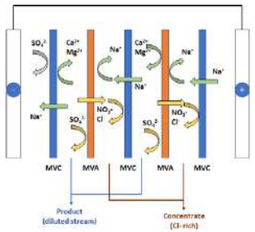

Figure 2. Scheme of the selective electrodialysis unit at Rincón de León WRP

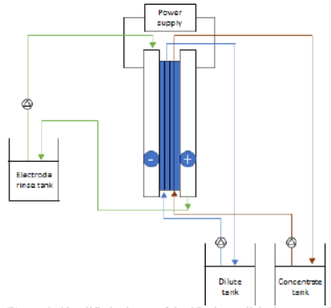

Figure 3. Simplified scheme of the 2D electrodialysis setup at Rincón de León WRP

REFERENCES

LIFE CONQUER Project (LIFE19 ENV/ES/000226 LIFE CONQUER)
H2020 B-WaterSmart (H2020-SC5-2019-2 869171 B-WaterSmart)

Proteins: How electrochemistry can drive the food future of Microbial Protein production

L. Rovira-Alsina*, N. Pous, M. Balaguer, S. Puig.

* LEQUiA, University of Girona, Catalonia (Spain)
(E-mail: *l.rovira@udg.edu; narcis.pous@udg.edu; dolors.balaguer@udg.edu; sebastia.puig@udg.edu*)

Abstract
Proteins are essential for the structure, function and regulation of tissues and organs in the human body. Proteins are ingested from meat, dairy products, nuts and some grains, but conventional methods to provide the ever-increasing demand are no longer sustainable. Microbial electrochemical technologies can arise as an alternative to generate protein-rich edible biomass by feeding it with recycled carbon dioxide and nitrogen-contaminated streams, while using the reducing power of water electrolysis. In this context, the control of the operating variables is of utmost importance. Different parameters (oxygen concentration, current supply and cell retention time) were tested, monitored and controlled to find the best conditions to maximise microbial growth. Yet, will humans be able to overcome conceptual barriers and benefit from a resource that has been a waste?

Keywords
Bioelectrosynthesis; CO_2 recycling; microbial food; nitrogen cascade effect; operating control

INTRODUCTION

We live in a world that no longer supports our pace. However, until we learn that de-growth is not poverty but consuming less to live better, we will need the help of technology to prevent malnutrition. Microbial electrochemical technologies (METs) normally use microbes as catalysts. Given that microbes are protein-rich organisms (content of 60-80%), METs could also be used as a platform to generate microbial biomass. A promising example is the production of hydrogen-oxidising bacteria (HOBs) from the reducing power of water electrolysis (H_2:O_2), carbon dioxide (CO_2) and reactive nitrogen (N), which in turn could be recycled from exhaust gases and N-contaminated streams. When growing HOBs in conventional fermenters, the need for external H_2 supply and the use of deionised water, certainly increase the operational costs (60% in electricity; Pikaar, de Vrieze, et al., (2018)) and the water footprint. Whereas the use of renewable energy might mitigate the first impact in the near future, METs could emerge as an attractive method capable of producing H_2 in the same medium where HOBs are cultivated (Pous, Balaguer, et al., 2022). Therefore, the main objective would be to maximise the production rate of protein-rich biomass at the same time as ensuring an efficient C and N assimilation. To this end, balancing the stoichiometry of water electrolysis and biomass production (Reactions 1 and 2, respectively) represents the key challenge.

Reaction 1. $2\ H_2O \rightarrow O_2 + 2\ H_2$
Reaction 2. $4\ H_2 + O_2 + CO_2 + 0.24\ NH_3 \rightarrow CH_{1.68}N_{0.24}O_{0.46} + 3.54\ H_2O$

MATERIALS AND METHODS

Two 1L membrane-less methacrylate reactors were designed, constructed and inoculated with a previously enriched HOBs mixed culture, while dissolved H_2 and O_2 profiles were monitored under variable current densities. The gas phase composition, pH, electric conductivity and optical density of the bulk liquid were measured daily. Meanwhile, 70 % of the medium containing urea (CH_4N_2O) as N source was periodically replaced to assay different cell retention times, and the dry cell weight (DCW), N-species and total Kjeldahl nitrogen (TKN) were determined to calculate the volumetric biomass productivity rate and close the nitrogen balance. The protein content was analysed through the N content of biomass relative to the DCW.

RESULTS AND DISCUSSION

Increased current densities led to faster gas production rates (Table 1) and subsequent microbial growth, but H_2 and O_2 profiles had to be closely monitored to guarantee a high N assimilation efficiency while providing the right amount of CO_2. The importance of retaining sufficient gases concentration in the liquid media yet ensuring a proper purge of excess O_2 was highlighted, allowing the settlement of upper and lower limits of H_2 and O_2 concentrations.

Table 1. Stoichiometric H_2 and O_2 production rates as a function of the applied current.

Current density (mA/cm²)	H_2 production (mg/Lh)	O_2 production (mg/Lh)
0.04	0.81	6.45
0.08	1.61	12.91
0.13	2.42	19.36

So far, higher percentages (>43%) of edible proteins compared to traditional routes (4-14%) have been achieved (Pikaar, Matassa, et al., 2017; Pikaar, de Vrieze, et al., 2018; Matassa, Verstraete, et al., 2016; Pous, Balaguer, et al., 2022) by reducing water use, avoiding the use of pesticides and recycling carbon and nitrogen streams.

The knowledge that this work provides in terms of the operational parameters required to enhance bacterial growth is a fundamental tool to increase the readiness level of the technology. However, the development of a stable microbiome, mass-transfer limitations and the public acceptance of the final product are still some challenges that need to be addressed. After all, it is a matter of closing cycles, and this means having to feed on what was once a waste product.
How far will we, humans, be prepared to go?

REFERENCES

Matassa, S., Verstraete, W., Pikaar, I., and Boon, N. (2016) Autotrophic nitrogen assimilation and carbon capture for microbial protein production by a novel enrichment of hydrogen-oxidizing bacteria. Water Research, **101**, 137–146. [online] http://dx.doi.org/10.1016/j.watres.2016.05.077.

Pikaar, I., Matassa, S., Rabaey, K., Bodirsky, B. L., Popp, A., Herrero, M., and Verstraete, W. (2017) Microbes and the Next Nitrogen Revolution. Environmental Science and Technology, **51**(13), 7297–7303.

Pikaar, I., de Vrieze, J., Rabaey, K., Herrero, M., Smith, P., and Verstraete, W. (2018) Carbon emission avoidance and capture by producing in-reactor microbial biomass based food, feed and slow release fertilizer: Potentials and limitations. Science of the Total Environment, **644**, 1525–1530. [online] https://doi.org/10.1016/j.scitotenv.2018.07.089.

Pous, N., Balaguer, M. D., Matassa, S., Chiluiza-Ramos, P., Bañeras, L., and Puig, S. (2022) Electro-cultivation of hydrogen-oxidizing bacteria to accumulate ammonium and carbon dioxide into protein-rich biomass. Bioresource Technology Reports, **18**(March), 1–9.

Low-cost natural by-products: an efficient way to improve emerging contaminants removal in Nature-based Solutions

D. T. Ruwer*, S. Arufe*, M. Rama*, A. Fernandez*, I. Fernandez*, C. Martinez-García*

* CETIM Technological Centre, Parque Empresarial de Alvedro, calle H, 20, 15180 Culleredo, A Coruña, Spain (E-mail:dtrevisan@cetim.es)

Abstract

Removal of emerging contaminants (ECCs) from wastewater has received a lot of attention because of the hazard potential of these pollutants. Different treatment techniques have been used to remove ECCs, and the low-cost and versatility of the adsorption processes has been advantageous compared to other techniques. However, due to certain limitations, the selection of adsorbents is in many cases not done properly. For that reason, this work aimed to select the best reactive media to adsorb four common emerging contaminants through different interconnected perspectives (economic, environmental, and adsorption efficiency). Therefore, adsorption kinetics tests, life cycle assessment, and life cycle cost analysis were performed to evaluate the best material as ECCs adsorbent. Among seven tested materials, coco coir and biochar SS showed most promising results. In addition, the overall results have revealed a great potential of the combination of different approaches for selecting appropriate substrate material for low-cost natural treatment systems.

Keywords: Adsorption; emerging contaminants; LCA; LCC; Nature-based Solutions

INTRODUCTION

Nowadays, the removal of emerging contaminants (ECCs) from wastewater has received a lot of attention because of the toxicities and carcinogenic nature of these pollutants. While conventional treatment methods can be effective for the removal of ECCs, adsorption is supposed as one of the best methods due to its low cost and ease of operation (Yousef *et al.* 2020). In addition, adsorption, in conjunction with biodegradation, is one of the key processes of pollutant elimination in Nature-based Solutions, which encompasses efficient treatment technologies, which due to their innovation, reliability, and economics have been increasingly applied (Castellar *et al.* 2022). However, there are many points to consider to choose a substrate as an ideal adsorbent, such as the cost, the feedstock, the hydraulic and engineering feasibility, the capacity to adsorb a large list of contaminants, the safety, and their useful life (Wang *et al.* 2020). Therefore, there is an increasing need for studies dedicated to knowledge on various adsorbents to remediate many pollutants, such as ECCs. For that reason, this work aimed to use different approaches to select the best reactive media to adsorb four common emerging contaminants, according to their physical characteristics, environmental risks, cost, and adsorption performance. Thus, this preliminary study essentially focussed on identifying the best material for ECCs adsorption through adsorption kinetics tests, physical characteristics (particle size, porosity and BET-specific surface area), and life cycle assessment (LCA), life cycle cost (LCC) perspectives. The results of this study will be helpful for selecting and identifying appropriate substrate material which can be used in an adsorption system, or as a matrix in natural treatment systems like Nature-based Solutions where the adsorption processes help to eliminate emerging contaminants (ECCs) from wastewater.

MATERIALS AND METHODS

Reactive adsorbent materials were selected according to their feedstock content and to previous adsorption performance from bibliographies. Seven low-cost materials, natural ones and by-products, were chosen to evaluate physical characteristics, environmental risks, cost, and adsorption performance, which are: chitosan, sewage sludge biochar (SS biochar), softwood pellets biochar (SWP biochar), coco coir, perlite, zeolites, and titanium dioxide. Due to the low molecular weight of chitosan and the low particle size of titanium dioxide, these materials were supported by zeolites in order to prevent their release.

Adsorption tests

To evaluate and select the best adsorbent material, concerning the adsorption of emerging contaminants, adsorption kinetics tests were performed. In these tests, aqueous samples with 400µg/L of four emerging contaminants (diclofenac, imidacloprid, estrone, and 17-β-estradiol) and ~0.1-0.5 g of each adsorbent substrate are mixed using a stirrer, and during this process, the supernatant is sampled for the evaluation of the adsorbate concentration until an equilibrium is reached. Specifically, the bottles were shaken at an orbital mixer and the supernatants from the bottles were sampled at the time intervals of 0, 0.5, 1, 2, 4, 8, and 24 hours. Determination of the concentration of emerging contaminants was performed by an LC-MS/MS following the Standard Methods for the Examination of Water and Wastewater.

Adsorbents characterization

Considering the importance of evaluating some physical parameters to choose the best adsorbent material analysis of particle size, porosity and BET specific surface area of each material was performed. These parameters were analysed through Standard Methods.

Life Cycle Assessment and Life Cycle Cost

To carry out these analyses, the stages established according to ISO 14040 and 14044 (ISO 2006a; ISO 2006b), which define the methodological steps, were followed. In this way, considering the adsorption process, through LCA and LCC the environmental impacts and the direct and indirect costs of the production of the adsorption materials used in this studied were quantified, as well as the impacts and costs associated to discharge the effluent water treated after the adsorption process. The quantities of materials that were used were listed in the Life Cycle Inventory (LCI) in which the materials were reported per tests (50 g of synthetic wastewater), that was established as Functional Unit (FU).

The process consumption data and the characterization of the treated wastewater were obtained through the adsorption experiments performed and the production data of the adsorbent materials were taken from the ecoinvent® 3.8 database (Frischknecht *et al.* 2005). The analysis was performed using the software SimaPro in which there are different characterization methods that transform the material inputs listed in LCI into environmental or economic impacts. The characterization methods selected in this study were ReCiPe Midpoint with the Hierarchy perspective for the characterization and normalization in LCA (Huijbregts *et al.* 2016), and the Environmental Prices method to the LCC (de Bruyn *et al.* 2018). In this way, regarding economic impacts, Environmental Prices method allows to quantify the economic costs as a consequence of the environmental burdens of the process. Additionally, to complete the LCC, direct costs data (price of materials, reagents and electricity) were taken into consideration.

RESULTS AND DISCUSSION

In order to choose the best adsorbent material according to kinetics results, biochar SS and coco coir showed the greatest potential to adsorb most of the emerging contaminants (Figure 1). For instance, coco coir and biochar SS presented the higher values adsorption capacity for estrone, 125 mg/g and 33 mg/g, respectively. Furthermore, biochar SS also shows a high potential to adsorb diclofenac (DFC), with a maximum adsorption capacity of 27 mg/g. While, the materials with lower adsorption capacity values were perlite, zeolite, and titanium dioxide-modified zeolite.

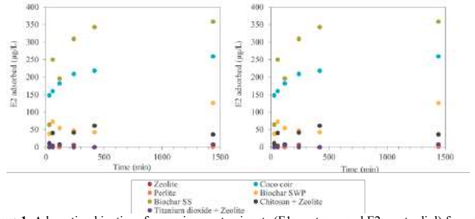

Figure 1. Adsorption kinetics of emerging contaminants (E1 – estrone and E2 – estradiol) for seven adsorbent materials (zeolite, coco coir, perlite, biochar SWP, biochar SS, chitosan modified zeolites and titanium dioxide-modified zeolites), representing the adsorbed concentration by the time.

These results could be attributed mainly to material granulometry properties. Coco coir was the material with a wider particle size range, including wide micro to macro particles, while biochar SS was the material with a higher BET-specific surface area. As expected, the material with more porosity and a variety of particle sizes has more active sites for adsorbed pollutants with different molecule sizes, which may explain the relation found. This relation was also observed for the negligible adsorbent results, the materials with the lowest adsorption capacity for most of the contaminants were the ones with the lowest BET-specific surface area.

With regard to the LCA results, Figure 2 shows the main results obtained with the 6 different adsorbents analysed in this study, after using the characterization and normalization method to quantify the environmental impact. The materials composed of zeolites and titanium and chitosan nanoparticles showed the worst values when quantifying the environmental loads. On the other hand, the material with the lowest environmental loadings was the Biochar SS. This is mainly due to the ability of Biochar SS to adsorb the contaminants used in these tests, which is generally superior to other materials. This makes the quality of the effluent (treated wastewater) better, and therefore the discharge is less harmful to the environment.

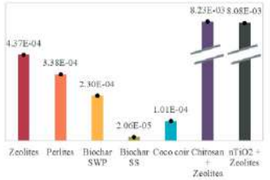

Figure 2. Results with normalized values corresponding to the environmental burdens for each adsorbent using ReCiPe midpoint method

In the case of LCC results, the direct costs were calculated on the one hand, taking into account the price of the materials, although in the case of the composite materials (Chitosan + zeolites and $nTiO_2$ + zeolites) the costs derived from their production were also considered. In this case, the materials with the highest direct costs were the composite material chitosan + zeolites ($8.77 \cdot 10^{-2}$ €/FU) and the material identified as having the lowest direct cost was coco coir ($6.21 \cdot 10^{-4}$ €/FU). However, considering the indirect costs, calculated using Environmental Prices, the material with the lowest cost was Biochar SS ($2.38 \cdot 10^{-4}$ €/FU), due to its quality as an adsorbent for the elimination of contaminants. Finally, considering the total cost, coco coir is the material with the lowest cost ($1.25 \cdot 10^{-3}$ €/FU), due to the fact that Biochar SS ($3.78 \cdot 10^{-2}$ €/FU) has a higher price.

In conclusion, with the observed results, it was possible to analyse seven materials and select the best adsorbents for removal of different emerging contaminants using economic, environmental, and adsorption efficiency perspectives. Coincidentally, the adsorption kinetics, and the LCA and LCC results indicated the same best reactive media. Coco coir and biochar SS were the materials with the lower cost, the lowest environmental loadings and with the best adsorption performance. Despite that, through a proper analysis of all factors that could affect the adsorbent choice, and consequently the efficiency of the adsorption process, this study highlights the importance of a detailed analysis of these aspects before a proper selection.

ACKNOWLEDGMENTS

This work was supported by the NICE project (grant agreement 101003765) from European Union's Horizon 2020 research and innovation programme.

REFERENCES

Castellar, J. A. C., Torrens, A., Buttiglieri, G., Monclús, H., Arias, C. A., Carvalho, P. N., Galvao, A., and Comas, J. (2022) Nature-based solutions coupled with advanced technologies: An opportunity for decentralized water reuse in cities. Journal of Cleaner Production, **340**.

de Bruyn, S.; Bijleveld, M.; de Graaff, L.; Schep, E.; Schroten, A.; Vergeer, R.; Ahdour, S. (2018). Environmental Prices Handbook. CE Delft.

Frischknecht, R.; Jungbluth, N.; Althaus, H.-J.; Doka, G.; Dones, R.; Heck, T.; Hellweg, S.; Hischier, R.; Nemecek, T.; Rebitzer, G.; Spielmann, M. (2005) The ecoinvent Database: Overview and Methodological Framework. The International Journal of Life Cycle Assessment **10**, 3–9.

Huijbregts, M.A.J.; Steinmann, Z.J.N.; Elshout, P.M.F.; Stam, G.; Verones, F.; Vieira, M.; Zijp, M.; Hollander, A.; van Zelm, R. (2017) ReCiPe2016: A harmonised life cycle impact assessment method at midpoint and endpoint level. The International Journal of Life Cycle Assessment **22**, 138–147.

ISO (2006a) ISO 14040: Environmental management – Life cycle assessment – Principles and framework. International Organization for Standardization (ISO).

ISO (2006b) ISO 14044: Environmental Management – Life cycle assessment – Requirements and guidelines.

Wang, Y., Cai, Z., Sheng, S., Pan, F., Chen, F., and Fu, J. (2020) Comprehensive evaluation of substrate materials for contaminants removal in constructed wetlands. Science of the Total Environment, **701**.

Yousef, R., Qiblawey, H., and El-Naas, M. H. (2020) Adsorption as a process for produced water treatment: A review. Processes, **8**(12), 1–22.

Preliminary study of anaerobic digestion of olive oil industry wastewaters in a conical spouted bed digester

M. J. San José*, S. Alvarez and R. López

* Departamento de Ingeniería Química, Universidad del País Vasco UPV/EHU, Bilbao, 48080, Spain
(E-mail: *mariajose.sanjose@ehu.eus)*

Abstract
An experimental study on operativeness of beds consisting of olive oil wastewaters was conducted in conical spouted beds reactors for anaerobic digestion of wastewater from the olive oil industry with at a temperature range of 40-55 ºC. The anaerobic digestion process of olive oil wastewater was studied in conical spouted beds digesters.

Keywords
Anaerobic digestion; biogas; conical spouted beds; olive wastewaters

INTRODUCTION

The olive oil extraction process produces a substantial amount of waste, such as olive mill solid waste, vegetable water, olive pomace, and other wastewaters. Anaerobic digestion is regarded as a sustainable way for the treatment of olive industry wastes because of the high organic matter concentration of these wastes, which converts the organic material to methane and carbon dioxide as well as a digestate (Messineo et al., 2020). Biogas generation is a major technology for promoting energy from renewable sources according to Directive (EU) 2018/2001 and is crucial to the decarbonization process (European Green Deal, (COM(2019) 640 final)).
Conical spouted bed reactors have been previously applied for thermal treatment of waste biomass (San José et al., 2013, 2014, 2018, 2019, 2021, 2023) and for anaerobic digestion of paper industry sludge (San José et al., 2015a), sewage sludge (San José et al., 2015b, 2017), and wine production waste (San José et al., 2018, 2021b). A conical spouted bed digester was developed for anaerobic digestion of beds consisting of olive waste.

MATERIALS AND METHODS

In order to design a conical spouted bed reactor for anaerobic digestion of olive industry waste, a hydrodynamic study of beds consisting of waste was conducted in an experimental plant equipped with conical spouted beds reactors of various geometric factors, Figure 1. The plant consists of an impulsion system, an electrical resistance for heating the fluid, and thermocouples to monitor bed temperature. The effect of temperature on the operating maps was determined in the spouted bed regime.
The anaerobic digestion was conducted in a battery of conical spouted beds digesters under thermophilic conditions (40-55 ºC) for 60 days. Different amounts of substrate/inoculum of methanogenic anaerobic bacteria were fed to each digester. Olive oil wastewater was obtained during the olive-oil extraction process at an olive oil processing plant. During the digestion, the biogas produced was measured by means of a gasometer through water displacement, and the biogas production was quantified by a Geotech Biogas-5000 analyzer. The characteristic parameters were quantified according to the standard methods.

RESULTS AND DISCUSSION

The proper geometric factors of the inlet diameter/particle diameter ratio and contactor angle for anaerobic digestion of olive oil wastewaters were established. Likewise, the operating conditions for beds consisting of olive oil wastewaters were determined from room temperature (25 ºC) to 55 ºC displays. by increasing fluid flow, the bed passes from the fixed bed to the spouted bed regime, which is characterized by a cyclic movement of particles and a clear distinction between the spout zone of ascending solids and the annular zone of descending solids. The system is stable for all of the stagnant bed heights studied, and an increase in bed mass leads to a higher minimum spouting velocity.

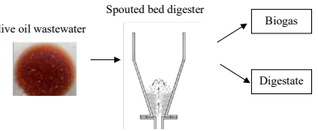

Figure 1. Scheme of anaerobic digestion of olive oil wastewater in conical spouted beds digesters.

Based on the volatiles removal and biogas production, conical spouted beds digesters are appropriate for industrial anaerobic degradation of olive oil wastewater under autothermal conditions.

Acknowledgement. This work is part of the project Grant PID2021-126331OB-I00 funded by MCIN/AEI/10.13039/501100011033 and by "ERDF A way of making Europe" and Grant TED2021-130150B-I00 MCIN/AEI funded by MCIN/AEI/10.13039/501100011033 and by EU NextGenerationEU/PRTR.

REFERENCES

Messineo, A., Maniscalco, MP, Volpe R. 2020 Biomethane recovery from olive mill residues through anaerobic digestion: A review of the state of the art technology. *Sci. Total Environ*. 703, 35508.
San José, M.J., Alvarez, S., García, I., Peñas, F.J. 2013. A novel conical combustor for thermal exploitation of vineyard pruning wastes. *Fuel* 110, 178–184.
San José MJ, Alvarez S, Peñas FJ, García I. 2013 Cycle time in draft tube conical spouted bed dryer for sludge from paper industry. *Chem Eng Sci* 100, 413–420.
San José, M.J., Alvarez, S., Peñas, F.J. García, I. 2014 Thermal exploitation of fruit tree pruning wastes in a novel conical spouted bed combustor. *Chem. Eng. J.,* 238(15), 227-233.
San José, M.J., Alvarez, S., López, R. 2018 Catalytic combustion of vineyard pruning wastes in a conical spouted bed combustor. *Catal Today* 305, 13-18.
San José, M.J., Alvarez, S., López, R. 2019 Drying of Industrial Sludge Waste in a Conical Spouted Bed Dryer. Effect of air temperature and air velocity. *Drying Technol* 37, 118-128.
San José, M.J., Alvarez, S., López, R. 2021a. Drying kinetics of sawdust in conical spouted beds: Influence of geometric and operational factors. *Fuel Process Technol* 221, 106950.
San José, M.J., Alvarez, S., López, R. 2023 Conical spouted bed combustor to obtain clean energy from avocado waste. *Fuel Process Technol*, 239, 107543.
San José, M.J., Alvarez, S., López R. 2015 Preliminary study of anaerobic digestion process of biomass waste sludge in a Conical Spouted Bed reactor. *Int Conf Industrial Waste & Wastewater Treatment Valorisation*, Athens (Greece).
San José, M.J., Alvarez, S., López, R. 2015 Performance of Draft-Conical Spouted Beds technology for anaerobic digestion process of sewage sludge. *Int Conf Chem Biochem Eng*, 170. Paris (France).
San José, M.J., Alvarez, S., López, R. 2017 Anaerobic digestion of sewage sludge in Conical Spouted Beds. *Eur Cong App Biotechnol*. Barcelona (Spain).
San José, M.J., Alvarez, S., López, R. 2018 Performance of conical spouted beds technology for anaerobic digestion of wastes from wine production. *Natural Gas Utilization Work*. Texas (USA).
San José, M.J., Alvarez, S., López, R. 2021b Co-digestion of sewage sludge with sludge from the Paper industry and digestate remediation. *Int Symp Environ Catal Process Eng*. Morocco.

Dietary exposure and human health risk assessment of wastewater-derived organic contaminants in leafy vegetables irrigated with treated wastewater under real agricultural field conditions

L.H.M.L.M. Santos*,**, S. Semitsoglou*,**, S. Rodriguez-Mozaz*,**, G. Buttiglieri*,**

* Catalan Institute for Water Research (ICRA-CERCA), C/ Emili Grahit, 101, 17003 Girona, Spain (E-mail: *lhsantos@icra.cat; ssemitsoglou@icra.cat; srodriguez@icra.cat; gbuttiglieri@icra.cat*)
** University of Girona, Girona, Spain

Abstract
Irrigation with treated wastewater is a growing practice to surpass water scarcity in agriculture. However, this practice might pose a risk to human health allowing the entrance of wastewater-derived organic contaminants, like pharmaceuticals, in the food chain. In this work, the dietary exposure and human health risk assessment to pharmaceuticals from chronic consumption of lettuce irrigated with treated wastewater under real agricultural field conditions were estimated. All detected pharmaceuticals showed Hazard Quotient (HQ) < 0.1 and would not represent a threat to human health in terms of pharmaceuticals intake.

Keywords
Hazard Quotient; Pharmaceuticals; Risk Assessment; Treated wastewater

INTRODUCTION

Agriculture is among the sectors more threatened by water scarcity, due to an increasing demand for water in agricultural production. Different integrated water resource management measures are needed, especially in what concerns to the use of non-conventional water resources, such as treated wastewater. The reuse of treated wastewater for irrigation of agricultural fields can surpass the problem of water scarcity and compensate for nutrients needs of crop plants (Christou et al., 2019). However, emerging contaminants, such as pharmaceuticals, may persist in treated wastewater, and these practices may represent a serious threat to human health and food safety by facilitating the entrance of emerging contaminants into the food chain. Currently there is a gap of knowledge in the dietary exposure to wastewater-derived organic contaminants and their potential risks for human health due to the chronic consumption of contaminated agricultural products. In this work, exposure and human health risk from pharmaceuticals (PhACs) related to the ingestion of lettuce irrigated with treated wastewater under real agricultural field conditions were assessed.

MATERIALS AND METHODS

Lettuce sampling, sample preparation and analysis of pharmaceuticals

The experiment was performed in an agricultural field in Lesvos Island (Greece). Lettuce was drip irrigated with treated wastewater resulting from: a) Treatment 1, consisting of a UASB unit followed by saturated wetland, unsaturated wetland, and UV disinfection; b) Treatment 2, comprising a UASB unit plus tertiary treatment by UV disinfection. At the harvesting time, lettuces were collected, rinsed with deionized water, dried, and stored at -20 ºC until analysis.
At the laboratory, lettuce samples were separated into leaves and roots, freeze-dried and then lettuce leaves were extracted by QuEChERS (adapted protocol from Montemurro et al., 2020). The final extracts were analyzed by UHPLC-MS/MS (Castaño-Trias et al., 2023).

Dietary exposure and Human health risk assessment

The estimated daily intake (EDI) (ng/kg bw/day) for each PhAC was calculated by multiplying the daily intake of lettuce leaves (g/day) for the Spanish population (98.67 g/day) by the mean concentration of PhAC in the lettuce leaves, in wet weight (ng/g, ww)), and dividing by the average body weight of an adult (18-64 years) (70 kg).
The potential human health risk was estimated using the Hazard Quotient (HQ) approach. The HQ was calculated by the ratio between the EDI and the acceptable daily intake (ADI). For that, the ADI (ng/kg bw/day) was estimated by dividing the lowest therapeutic dose (mg/day) by a safety factor of 1000 and a body weight of 70 kg. A HQ > 0.1 suggests a potential human health risk due to the chronic exposure to a certain PhAC.

RESULTS AND DISCUSSION

A total of 6 PhACs were detected in lettuce leaves at concentrations ranging from 0.12 to 7.54 ng/g, ww, and from 0.70 to 7.12 ng/g, ww, for Treatment 1 and Treatment 2, respectively (Table 1).
Human exposure to each PhAC was assessed for the two tested treatments and all the detected pharmaceuticals showed a HQ < 0.1 (Table 1), indicating no human health risk due to the chronic consumption of lettuce irrigated with treated wastewater in terms of PhACs intake. In general, both wastewater treatment approaches had similar HQ.

Table 1. Estimated daily intake (EDI) of the detected pharmaceuticals based on the mean concentration detected in lettuce leaves and its associated hazard quotients (HQ)

PhAC	Treatment 1				Treatment 2			
	Conc. (ng/g, ww)	EDI (ng/kg bw/day)	ADI (ng/kg bw/day)	HQ	Conc. (ng/g, ww)	EDI (ng/kg bw/day)	ADI (ng/kg bw/day)	HQ
Acetaminophen	1.31	1.86	28,571	0.00007	0.96	1.35	28,571	0.00005
Indomethacin	0.12	0.17	857	0.0002	1.92	2.70	857	0.0032
Naproxen	7.54	10.6	7143	0.0015	7.12	10.0	7143	0.0014
Ciprofloxacin	3.79	5.34	3571	0.0015	4.03	5.68	3571	0.0016
Furosemide	4.52	6.36	286	0.022	5.38	7.58	286	0.027
Paroxetine	1.54	2.17	107	0.020	0.70	0.99	107	0.0092

REFERENCES

Castaño-Trias, M., Rodriguez-Mozaz, S., Buttiglieri, G. 2013 10 years water monitoring in a Mediterranean region: pharmaceutical prioritisation for analytical methodology upgrade. *Journal of Environmental Management,* under review.
Christou, A., Papadavid, G., Dalias, P., Fotopoulos, V., Michael, C., Bayona, J.M., Piña, B., Fatta-Kassinos, D. 2019 Ranking of crop plants according to their potential to uptake and accumulate of contaminants of emerging concern. *Environmental Research* **170**, 422-432.
Montemurro, N., Orfanioti, A., Manasfi, R., Thomaidis, N.S., Pérez, S. 2020 Comparison of high resolution mrm and sequential window acquisition of all theoretical fragment-ion acquisition modes for the quantitation of 48 wastewater-borne pollutants ion lettuce. *Journal of Chromatography A* **1631**, 461566.

ACKNOWLEDGMENTS

This work was funded by the European Union's Horizon 2020 Research and Innovation programme (HYDROUSA project, GA N° 776643). G. Buttiglieri acknowledges Spanish State Research Agency of the Spanish Ministry of Science, Innovation and Universities for the Grant to the Creation of a permanent position Ramon y Cajal 2014 (RYC-2014-16754).

Biofiltration of odorous emissions in WWTPs through the reuse of by-products of the integral water cycle

L. Terrén*, S. Doñate*, M.D. Esclapez*, R. Lebrero**, R. Muñoz**, S. Sáez-Orviz**, L. Saúco*

* Depuración de Aguas del Mediterráneo, Av. Benjamín Franklin, 21, 46980 Paterna, Valencia, Spain.
(E-mail: *lidia.sauco@dam-aguas.es)*
** Institute of Sustainable Processes, University of Valladolid, Mergelina s/n., 47011 Valladolid, Spain;
(E-mail: *raquel.lebrero@iq.uva.es; mutora@iq.uva.es; ssaezo@funge.uva.es)*

Abstract
The project proposes an innovative approach based on the circular economy in the integral water cycle. The optimised design of a bioreactor for waste air treatment is investigated first at a laboratory scale and later at an industrial scale. The potential of waste by-products from wastewater treatment plants (WWTPs) as packing materials, such as plastics and sludge turned into compost and enriched with iron, was investigated. In addition, the development of innovative configurations of bioreactors (step-feed biofilters or two-stage systems) is proposed with the aim of improving deodorization efficiency and reducing the operating costs of odour treatment in WWTPs.

Keywords
Air Treatment; bioreactor; compost; packing material; two-stage systems, wastewater treatment plant

INTRODUCTION

The treatment of urban wastewater is well known and extended. Different technologies or strategies can be used for treating the wastewater, but all with the inherent drawback of generating solid and gaseous wastes during treatment. The emission of off-gases associated with wastewater treatment causes unpleasant nuisances for plant workers and people living nearby. Some of them can be toxic and cause adverse health effects. Furthermore, malodours have negative social economic effects by reducing the price of the surrounding properties and prospects for tourism, and can also cause damage to the facilities due to corrosion.

Nowadays, there is enough experimental evidence of the potential of biofilters and biotrickling filters to achieve high removal efficiencies of air pollutants at both trace levels (Lebrero et al., 2014, 2012) and industrial concentrations with reduced environmental impacts. Estrada et al. (2012) demonstrated that biological techniques were the most cost efficient alternatives with lower sensitivity to design parameters and lower operating cost than physical/chemical treatments at typical odour concentrations.

Despite the significant advances in biological odour removal technologies in the past 20 years, packing material selection still represents the most uncertain and critical design variable in biofiltration systems. This is paradoxical since packing material ultimately determines odorant removal efficiency and process operating costs (i.e., pressure drop across the bed and frequency of packing replacement). Therefore, there is still an incipient need for research to increase the sustainability and robustness, and decrease the capital and operating costs of these biotechnologies.

This research focuses on the development of cheaper, more sustainable packing materials, with better adsorption and reactivity properties, and that provide enhanced environmental conditions for the attachment of odour-degrading biofilms. These packing materials will be obtained from by-products produced in the WWTP itself, thus reducing wastes and promoting circularity within the wastewater treatment sector. In addition, the optimization of hybrid technologies composed of biotrickling filters and biofilters will be investigated in terms of their configuration, packing material, design parameters and operation.

MATERIALS AND METHODS

The investigation will be carried out through the following stages:
1. Obtaining the materials and residues available in the wastewater treatment plants that can be used as support for the biological deodorization system, together with the assessment of the modifications required for their reuse as packing material.
2. Development and optimization of the different bioprocesses at laboratory scale (Institute of Sustainable Processes of the University of Valladolid). For this purpose, three 2.5 L biofilters packed with the plastic materials under study and 3 biofilters of 8L of packed bed volume filled with the materials derived from compost will be used. Innovative bioreactor configurations involving two-state and step fed systems will be also optimized.
3. Field validation of a pilot plant with the optimal process configuration.

RESULTS AND DISCUSSION

This research proposes an innovative concept based on circular economy within the integral water cycle that allows the retrofitting of chemical scrubbers to innovative biological systems with a moderate investment, using reused and recycled packing materials.

The project also aims at developing improved packing materials for biofilters and new bioreactor configurations for the deodorization of WWTP, waste management facilities and certain industries. The product derived from this research project is an innovative biological deodorization system with packing materials made of by-products of the integral water cycle (plastic waste and compost produced with WWTP sludge).

ACKNOWLEDGEMENT

This research is financed by The Centre for the Development of Industrial Technology (CDTI)

REFERENCES

Alfonsín, C.; Lebrero, R.; Estrada, J.M.; Muñoz, R.; Kraakman, N.J.R.; Feijoo, G.; Moreira, M.A.T. Selection of odour removal technologies in wastewater treatment plants: A guideline based on Life Cycle Assessment. *J. Environ. Manag.* 2015, 149, 77–84.

Estrada, J.M.; Lebrero, R.; Quijano, G.; Kraakman, N.J.R.; Muñoz, R. Strategies for Odour Control. In Odour Impact Assessment Handbook; Belgiorno, V., Naddeo, V., Zarra, T., Eds.; John Wiley & Sons: New York, NY, USA, 2012; ISBN 9781119969280.

Estrada, J.M.; Lebrero, R.; Quijano, G.; Kraakman, B.; Muñoz, R. Odour abatement technologies in WWTPs: Energy and economic efficiency. In Sewage Treatment Plants: Economic Evaluation of Innovative Technologies for Energy Efficiency; Tsagarakis, K., Stamatelatou, K., Eds.; IWA Publishing: London, UK, 2015; pp. 163–187.

Lebrero, R.; Gondim, A.C.; Pérez, R.; García-Encina, P.A.; Muñoz, R. Comparative assessment of a biofilter, a biotrickling filter and a hollow fiber membrane bioreactor for odor treatment in wastewater treatment plants. Water Res. 2014, 49, 339–350.

Lebrero, R., Rodríguez, E., Collantes, M., De Juan, C., Norden, G., Rosenbom, K., Muñoz, R. 2021 Comparative Performance Evaluation of Commercial Packing Materials for Malodorants Abatement in Biofiltration. *Appl Sci.* 2021, 11, 2966.

LIFE REPTES - Renewable bio-hydrogen production technologies from lignocellulosic waste and sewage sludge co-fermentation

C. Bretas[1], M.D. Esclapez[1], L. Saúco[1], P. Roda[2], S. Mehdizadeh[2], G. Silvestre-Tormo[3], P. Gómez-Pérez[3], P. Madramany[4], A. Madrid[4] and S. Doñate [1]

[1]Depuración de Aguas del Mediterráneo, Av. Benjamin Franklin, 21, 46980 Paterna, Valencia (Spain)
(E-mail: *silvia.donate@dam-aguas.es*)
[2]Genia Bioenergy, Avinguda Ronda Nazaret, 9 Bajo, 46024, Valencia (Spain)
[3]AINIA, c/ Benjamín Franklin, 5-11, 46980 Paterna, Valencia (Spain)
[4]Consorci de la Ribera, C/ de la Safor, 22 - 46680 Algemesí, Valencia, (Spain)

Abstract
Currently, residues generated in rice agriculture are burned in several locations in Spain. Considering that the burning process contributes significantly to global warming through the emission of greenhouse gases (GHG), the development of a strategy to manage this waste in an appropriate and sustainable way is paramount. The LIFE REPTES project aims to demonstrate a new circular model that will integrate the production of biohydrogen from pretreated lignocellulosic substrate and sewage sludge through a dark fermentation process. In a second phase, the fermented stream - produced in the dark fermentation - will be used for improving biogas production in a conventional anaerobic digester. Finally, the project will provide an alternative for the efficient management of this bio-waste.

Keywords
Anaerobic digestion, biohydrogen, dark fermentation, energy, wastewater

INTRODUCTION

Huge amounts of rice straw are burned annually in the rice fields situated close to Albufera Natural Park (Valencia, Spain), meaning massive emissions GHGs and particulate matter that affect the quality of life of surrounding populations with an important environmental impact. The project LIFE REPTES will allow the valorisation of the rice straw, together with sewage sludge, by the production of renewable gas biofuels (biohydrogen and biogas).

The most innovative and the core technology of the project is the dark fermentation process (DF) to produce biohydrogen, but the technical and economic success of the model is backed by an innovative methodology for pre-treating the rice straw prior to DF. Furthermore, the project will demonstrate the potential of the fermented streams as co-substrate when used in anaerobic digestion in WWTPs. The project will allow, not only improving the welfare of the citizens surrounding areas of lignocellulosic extensive cultivations, thus avoiding GHGs emissions and the bio-waste valorisation, but also creating a new profitable and bioenergy efficient business model.

MATERIALS AND METHODS

For this project, rice straw from agricultural field and sewage sludge from a WWTP, both collected in Valencia (Spain), will be used to demonstrate the viability of producing biohydrogen and biomethane in a two-stage process (Figure 1).

Before entering in the dark fermentation, the rice straw passes through a pretreatment of bioextrusion. This process is required since the presence of lignin in the structure of lignocellulosic feedstock adds to it rigidity and impermeability. Moreover, the production of fermentable sugars from cellulose and hemicellulose is extremely difficult without a suitable pretreatment (Saha et al., 2022). Regarding the sewage sludge, this matrix has to be treated in order to reduce the presence of methanogenic bacteria, which would use the hydrogen produced on their metabolic route. In this sense, a pasteurization process (70ºC) will be applied.

After the treatment of the substrates, both streams will be mixed to obtain a homogeneous content to feed the DF. The DF will operate under thermophilic conditions (55ºC) with a hydraulic retention time of around 3 days. In order to avoid the stagnation of biohydrogen production, the reactor has been specifically designed to facilitate the desorption of the gas from the liquid to gas phase. The fermented product from the DF will be used in an anaerobic digestor to produce biogas, which will be increased thanks to the pretreatment step. Then, the biogas will be used for the production of electrical energy for the WWTP.

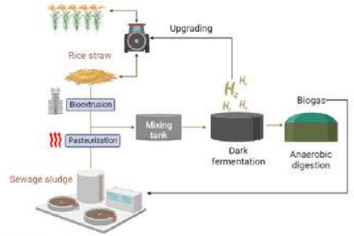

Figure 1. LIFE REPTES scheme

RESULTS AND DISCUSSION

The main expected results from this project are:

- It is expected to transform 252 tonnes of this lignocellulosic bio-waste during the demonstration, thus avoiding the inappropriately management of this waste.
- The gas stream produced by the dark fermentation process is expected to be composed of a mixture of H_2 (20-40%), CO_2 (50-60%) and CH_4 (10- 20%).
- In this innovative solution, the biohydrogen produced would be subjected to an upgrading process and later compressed for its use in agricultural machinery, or even directly used in the WWTP.
- It is expected to demonstrate an increase of the biogas production of at least 35 % in the pilot anaerobic digester module ($2m^3$) by using the fermented stream as a co-substrate.

ACKNOWLEDGEMENT

This project received funding from LIFE programme under grant agreement Nº 101074329. Funded by the European Union. Views and opinions expressed are however those of the author(s) only and do not necessarily reflect those of the European Union or CINEA. Neither the European Union nor the granting authority can be held responsible for them.

REFERENCES

Saha, R., Bhattacharya, D., & Mukhopadhyay, M. 2022. Enhanced production of biohydrogen from lignocellulosic feedstocks using microorganisms: A comprehensive review. *Energy Conversion and Management: X*, *13*. https://doi.org/10.1016/j.ecmx.2021.100153

New advanced applications of compost from sewage sludge. Compost-UP! Project

M. Bofi*, S. Doñate*, M.D. Esclapez * , L. Saúco*, E. Cubas-Cano**, and M. de la Cruz**

*Depuración de Aguas del Mediterráneo, Av. Benjamin Franklin, 21, 46980 Paterna, Valencia (Spain)
(E-mail: silvia.donate@dam-aguas.es)
**ITENE, Calle d'Albert Einstein, 1, 46980 Paterna, Valencia (Spain)

Abstract
The Compost-UP! research project improves traditional sewage sludge composting processes, establishing a new process for the management and valorisation of this bio-waste in a more efficient, profitable and sustainable way by means of bioaugmentation techniques. The process is based on the enhancement of consortia of microorganisms specially selected for their potential to degrade volatile compounds that cause bad smells, mainly VOCs, NH_3 and H_2S. The compost obtained is valorised in compost-based bed biofilters, and when its filtering capacity is exhausted, it is reused as an improved agricultural amendment, due to its enrichment in nutrients during the filtering process.

Keywords (maximum 6 in alphabetical order)
Compost; sewage sludge; biofilter; ammonia; VOCs; H_2S

INTRODUCCION

Waste recovery is one of the most complex environmental challenges facing modern societies. Around 1,200,000 tonnes of sewage sludge are produced annually [1] and its proper management is essential to avoid its negative impacts on ecosystems, biodiversity and human health. Under this premise, Compost-UP! focuses on the development of advanced applications based on the bio-increment of compost from sewage sludge, which helps to mitigate the environmental impact and social rejection generated by the bad smell of composting plants. As a result of the process, a compost with agronomic potential is obtained, which allows improving current agricultural production systems and reducing the amount of chemical fertilisers used.

During the project, a microbial consortium was studied and selected to obtain bio-enhanced compost capable of degrading the most frequent odorous gases in the composting process (NH_3, H_2S and VOCs). The selected microbial consortium must be able to reproduce in the compost and mineralise the odorous compounds in order to give the compost improved agronomic properties. In the second phase, a pilot plant consisting of a biofilter based on a bio-augmented compost bed for odour removal was designed and constructed. This validation, in turn, is carried out using the deodorisation of a composting plant as a use case. Gas flow measurements were carried out to establish the critical operating parameters of the pilot prior to design and construction.

MATERIALS Y METHODS

Compost characterization. Compost samples were collected during October-December 2021 at different stages of maturation (from weeks 0 to 10) and characterised, analysing ammoniacal nitrogen content, conductivity, pH, moisture, organic matter, C/N ratio and presence of heavy metals. Isolation tests were then carried out, obtaining between 8-10 microbial colonies per odorant agent (NH_3, H_2S and VOCs). Subsequently, colony compatibility tests were carried out, studying the adaptation and implantation of microorganisms in mesophilic (35ºC) and thermophilic (55ºC) conditions. Finally, nutrient deprivation tests were carried out for more than 48 hours to evaluate the performance of the consortium in intermittent feed for energy savings or operational shutdowns

Gas emissions characterization in the use-case plant. Gas samples were collected and measured following the methodology detailed in UNE 13725 [2]. This method is used to determine the odour concentration in an open space using the Lindal box method, which has a wind tunnel setup. During the test, XAM 7000 equipment was used to enable the concentration of NH_3, H_2S and VOCs (isobutylene) to be measured. Chromatography was used to identify the VOCs.

RESULTS AND CONCLUSIONS

The physicochemical characterisation of the compost samples has allowed evaluation of the suitability as a filter bed of the samples from weeks 2-6, being critical parameters for this purpose are moisture (50-70%), organic matter content (higher than 55%) and particle size (particle size, higher than 5 mm). Isolation tests showed more than 200 different genera of microorganisms identified, with Firmicutes representing 96% of the microbial diversity in the thermophilic phase of the composting process (week 3), and Chloroflexi, Patescibacteria, Actinobacteriota and Bacteroidota as common phyla in the composting process.

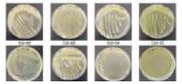

Figure 1. Microbial consortium formed by colonies of ammonia (Col A6-Col A8), hydrogen sulphide (Col S4-Col S5) and VOCs (Col-But4-Col DMDS2-DMDS5-DMDS7).

Nutrient deprivation tests performed after selecting colonies with the highest removal potential showed that ammonia-degrading colonies reduced performance insignificantly (<10%), while some VOC-degrading colonies not only withstood the test but increased their performance by 89%. Hydrogen sulphide-focused colonies did not withstand the nutrient deprivation test.

The results of the gas flow from the composting plant showed the presence of ammonia as the main compound with 40 ppm and reaching peak concentrations of 90 ppm (during turning of the compost piles), followed by H_2S and VOCs reaching concentrations of 0.6 and 15 ppm respectively during turning of the compost piles. In addition, chromatography identified 16 VOC compounds, including limonene and phenol, as a result of the degradation of organic compounds.

The results of the tests have made it possible to establish the design parameters of the biofilter, which will be able to treat a flow of 1,000 m^3/h (representing 1% of the flow of gases generated in the composting plant) and a useful surface area of $8m^2$ (4 x 2m). Finally, the validation of the bio-filter and the evaluation of its efficiency in an industrial environment will be carried out throughout 2023.

ACKNOWLEDGMENT

Compost-UP! is a project co-funded by the European Union through the Operational Program of the European Regional Development Fund (FEDER) of the Valencian Community 2014-2020 through the Business Value Chain Consolidation Program, by the Valencian Innovation Agency (AVI).

REFERENCES

[1] Spanish Ministry for the ecological transition and the demographic challenge. (Visited in January 2023). *https://www.miteco.gob.es/es/calidad-y-evaluacion-ambiental/temas/prevencion-y-gestion-residuos/flujos/lodos-depuradora/*

[2] EN 13725:2022 *Stationary source emissions - Determination of odour concentration by dynamic olfactometry and odour emission rate.*

Micropollutant uptake in lettuce irrigated with UASB-CW reclaimed wastewater in a water scarce area

S. Semitsoglou Tsiapou*,**, M. Salvoch*,**, S. Rodriguez-Mozaz*,**, G. Buttiglieri*,**

* Catalan Institute for Water Research (ICRA-CERCA), C/ Emili Grahit, 101, 17003 Girona, Spain
** University of Girona, Girona, Spain
(E-mail: ssemitsoglou@icra.cat; msalvoch@icra.cat; srodriguez@icra.cat; gbuttiglieri@icra.cat)

Abstract
Reclaimed water fertigation of crops is an increasingly considered solution to water scarcity. The advantage of water and nutrients reclamation can be mitigated by the possible introduction of organic contaminants in the fertigated, edible crops, posing a health risk. This work investigated the uptake of a variety of organic micropollutants by the leaves and roots of lettuce irrigated with either tap or reclaimed water. Overall, analgesics/anti-inflammatories, psychiatric drugs and β-blockers were the most detected compounds. Reclaimed water irrigation resulted in slightly higher concentrations of the same contaminants in the leaves, whereas root composition was largely different and involved compounds absent in the tap water treatment.

Keywords
fertigation; crop uptake; pharmaceuticals; endocrine disrupting compounds; water reuse

INTRODUCTION

The Mediterranean region faces significant challenges due to dry zones, increased tourist activity and wasted water resources. Water scarcity leads to new non-conventional practices that close the loops and lead towards a circular economy. In the agricultural sector, an important practice is the reuse of treated wastewater in the irrigation systems of crops, where both water and valuable nutrients can be reclaimed. However, organic contaminants of various sources are removed to different extents in wastewater treatment plants and can persist in the treated water used for fertigation (Calderon-Preciado et al., 2011). Uptake of these micropollutants by fertigated edible crops needs to be investigated, to assess their levels that correlate with food safety and ultimately human health. Most of the current studies use laboratory conditions that do not reflect field conditions. This work assessed the uptake of a variety of micropollutants, including pharmaceuticals, antibiotics and endocrine disrupting compounds, by the roots and leaves of lettuces irrigated by reclaimed wastewater.

MATERIALS AND METHODS

Lettuce sampling, micropollutants extraction and analysis

Samples from the HYDRO2 wastewater reclamation demo-site of the HYDROUSA project (www.hydrousa.org) on the island of Lesvos (Greece) involved lettuce fertigated with either: 1) tap water (TW) as a control experiment, or 2) water discharged from the wastewater treatment plant (i.e., Full Treatment, FT), which consists of an upflow anaerobic sludge blanket coupled to a constructed wetland. After harvesting, the lettuces were separated into leaves and roots, rinsed with deionized water, freeze-dried, extracted by QuEChERS (adapted protocol, Montemurro et al., 2020) and analyzed by UHPLC-MS/MS (Castaño-Trias et al., 2023) for a range of micropollutants.

RESULTS AND DISCUSSION

When lettuce was irrigated with tap water (TW), mostly analgesics/anti-inflammatories (acetaminophen, ibuprofen, indomethacin and naproxen) were detected in the leaves, with naproxen presenting the highest concentration at 121.22 ng/g extracted mass. Ciprofloxacin, an antibiotic, came second (79.55 ng/g extracted), and paroxetine, a psychiatric drug, third (53.45 ng/g extracted). 1-OH-ibuprofen, an ibuprofen metabolite, was found to be retained in the roots, whereas it was absent in the leaves.

Under reclaimed water irrigation (FT), the types of contaminants found in the leaves were the same as with the TW, with the total concentration slightly higher, mainly due to an increase in the levels of paroxetine, naproxen and caffeine. The composition of the roots for the FT treatment was largely different than in the TW one (Figure 1), with irbesartan, an anthelmintic drug, showing high retention in the roots (203.63 ng/g extracted), followed by mainly metoprolol and hydrochlorothiazide. This finding demonstrates that contaminants absent in tap water but present in the reclaimed water showed affinity for the lettuce roots rather than the edible part of the plant.

The levels of the organic micropollutants detected in this work are in line with available literature. Even though health-related risk is expected to be low, next steps of the ongoing project include dietary exposure and human health risk assessment.

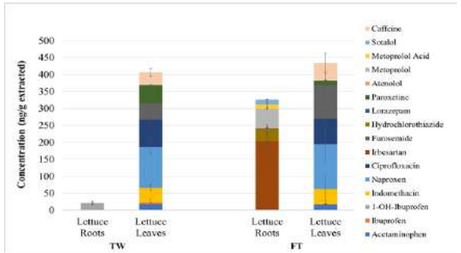

Figure 1. Concentration of micropollutants detected in lettuce leaves and roots. Irrigation type: TW: Tap Water, FT: Full Treatment

REFERENCES

Calderon-Preciado, D., Jimenez-Cartagena, C., Matamoros, V., Bayona, J.M., 2011. Screening of 47 organic microcontaminants in agricultural irrigation waters and their soil loading. *Water Research* **45**, 221-231.

Castaño-Trias, M., Rodriguez-Mozaz, S., Buttiglieri, G. 2013 10 years water monitoring in a Mediterranean region: pharmaceutical prioritisation for analytical methodology upgrade. *Journal of Environmental Management,* under review.

Montemurro, N., Orfanioti, A., Manasfi, R., Thomaidis, N.S., Pérez, S. 2020 Comparison of high resolution mrm and sequential window acquisition of all theoretical fragment-ion acquisition modes for the quantitation of 48 wastewater-borne pollutants ion lettuce. *Journal of Chromatography A* **1631**, 461566.

ACKNOWLEDGMENTS

This work was funded by the European Union's Horizon 2020 Research and Innovation programme (HYDROUSA project, GA N° 776643).

Soil contamination due to reuse of ZnO nanoparticles contaminated wastewater effluent

R. Sharma*, T. Watanabe** and A. Kumar*

* Department of Civil Engineering, Indian Institute of Technology Delhi, Hauz Khas, New Delhi, India
(E-mail: *r.bwn24@gmail.com*; *arunku@civil.iitd.ac.in)*
** Department of Food, Life & Environmental Sciences, Faculty of Agriculture, Yamagata University, Tsuruoka, 1-23Wakaba-machi, Yamagata, Japan
(E-mail: *to-ru(at)tds1.tr.yamagata-u.ac.jp*)

Abstract
The presence of nanoparticles in the environment is increasingly becoming common, with their wide-ranging application today. This theoretical study conducted an ecological risk assessment for the soil due to non-potable urban reuse of nanoparticle contaminated treated wastewater for irrigation of Spinach. A thorough search of the literature was carried out to gather data relevant to this work. Lognormal distribution of collected ZnO nanoparticles concentration in wastewater effluent was made as part of Monte Carlo analysis. Plant uptake models based on existing data were derived to compute uptake of Zn in the plant. Simple mass balance was used to find soil contamination. Contamination Factor, Potential Ecological Risk Factor, and Geo-accumulation index were found to be well within their respective contamination limits. This study found no risk to soil in such a hypothetical scenario. The framework demonstrated here could be well utilized again to find risk for such reuse.

Keywords
Ecological risk assessment; Nanoparticles; Wastewater irrigation

INTRODUCTION

Nanoparticles (NPs) are now being used in a variety of products and industries. ZnO nanoparticles are deployed in cosmetics, paints, etc. (Kumar Dey, Das, et al., 2018). It hence becomes inevitable that their presence has been found in different environmental compartments (Baranidharan and Kumar, 2018). Their toxicity has been documented in various in-vitro studies.

There are many studies observing the interaction of edible plant with nanoparticles containing irrigation water. But the potential of nanoparticles to contaminate soil while being irrigated with wastewater effluent contaminated with nanoparticles is not well documented. Hence this work attempts to present a framework and compute soil contamination indices as part of ecological risk assessment with respect to Zinc ion for the hypothetical scenario of Spinach plant being irrigated with Zinc Oxide nanoparticle contaminated wastewater effluent. The framework so developed could be utilised again for soil-based risks calculations in reuse for irrigation.

MATERIALS AND METHODS

Deriving log-normal distribution for ZnO NPs concentration in wastewater effluent

In the literature, ZnO NPs concentrations reported or predicted in the wastewater effluent were thoroughly searched for using scientific electronic databases. As environmental contaminants usually exist in lognormal concentration, this data was then pooled together to compute lognormal distribution for ZnO NPs concentration in wastewater, and hence 10,000 values were generated as part of Monte Carlo analysis.

Development of Plant Uptake Models

In the next step, plant uptake models to predict the uptake of Zinc ion in the shoot (C_{shoot}) and root (C_{root}) of the Spinach plant (upon its maturity) using ZnO NPs concentration in the irrigation water, were derived using literature work. It was decided to use log- logistic distribution for the plant uptake models. For this, the study by Singh and Kumar, 2020 was used as their work provides essential data on observing uptake in Spinach plant on irrigating it with ZnO NPs contaminated media for its maturity period (Singh and Kumar, 2020).

Computation of Soil Contamination Indices

Using simple mass- balance equations, remaining Zinc in the soil (C_{soil}) after the maturity of the Spinach plant was computed then. Corresponding to each of the 10,000 values of ZnO NPs concentration in irrigation water generated earlier, C_{shoot}, C_{root} and C_{soil} values were calculated. Using these values, the soil contamination indices were computed, namely Contamination Factor (CF), Potential Ecological Risk Factor (E_r) and Geo-Accumulation index (I_{geo}).

RESULTS AND DISCUSSION

The indices as part of ecological risk assessment are presented in Table 1.2. The value of the indices CF & E_r is the same here in all respect as $E_r = 1$ for Zinc element. The 99th percentile values for CF and E_r were found to be less than 1, suggesting no contamination to soil due to irrigation of Spinach with river water or STP effluent contaminated with ZnO nanoparticles. A negative value of I_{geo} denotes practically unpolluted soil, which has also been found in this study with the average value of the index varying as -14.42. Hence, no soil contamination would occur if wastewater effluent containing ZnO NPs are utilized for Spinach irrigation.

Table 2. Descriptive statistics for the computed soil contamination indices

Parameter	Average Value	90% Confidence Interval	99th percentile
CF	8.09×10^{-4}	2.48×10^{-3}	1.36×10^{-2}
E_r	8.09×10^{-4}	2.48×10^{-3}	1.36×10^{-2}
I_{geo}	-14.42	10.43	-6.79

CONCLUSIONS

This work developed plant uptake models & log-normal distribution for ZnO nanoparticle contamination in wastewater, to carry out ecological risk assessment for the hypothetical scenario of wastewater effluent containing ZnO nanoparticles being reused for irrigation of Spinach plants. At current ZnO NPs levels in the wastewater effluent, no contamination was found to occur in soil. The detailed stepwise framework developed could easily be applied to carry out ecological risk assessment due to metal that may occur due to nanoparticles-based wastewater effluent reuse, and hence making the reuse of non-potable urban water safe & informed.

REFERENCES

Baranidharan, S. and Kumar, A. 2018 Preliminary evidence of nanoparticle occurrence in water from different regions of Delhi (India). Environmental Monitoring and Assessment, **190**(4).

Kumar Dey, J., Das, S., and Mawlong, L. G. 2018 Nanotechnology and its Importance in Micronutrient Fertilization. International Journal of Current Microbiology and Applied Sciences, **7**(05), 2306–2325.

Singh, D. and Kumar, A. 2020 Quantification of metal uptake in Spinacia oleracea irrigated with water containing a mixture of CuO and ZnO nanoparticles. Chemosphere, **243**, 125239.

Innovative and versatile integrated solution to remove contaminants of emerging concern in water treatment systems

Aina Soler-Jofra *, Miriam Pérez-Cova *, Yolanda Lucía Solano Martos **, Carlos Lardín Mifsut***, Ana Maria Jimenez-Banzo*, Enrique Ferrero *, María M. Micó*

* ACCIONA, Innovation Department, Av. Les Garrigues, 22, 08820, El Prat de Llobregat, Barcelona, Spain (E-mail: *aisoler@acciona.com; mcperez@acciona.com; anamaria.jimenez.banzo@acciona.com; enrique.ferreo.polo@acciona.com; mariamar.mico.reche@acciona.com*)
** ACCIONA, Paraje de la Virgen, s/n, 30562, Ceutí, Murcia, Spain (E-mail: *yolandalucia.solano.martos@acciona.com*)
***Entidad Regional de Saneamiento y Depuración de la Región de Murcia. C/Santiago Navarro 4. 30.100, Espinardo, Murcia. Spain (E-mail: carlos.lardin@esamur.com)

Abstract
Contaminants of emerging concern (CECs) are present in water bodies, even though most of them are not regulated yet, they might bestow a risk for human health or the environment. The PRISTINE Integrated Solution aims to remove CECs in both wastewater and drinking water real scenarios using a combination of innovative and sustainable solutions. To design and optimize such solution an extensive real site characterization is needed. Thus, in the present study the occurrence and distribution of CECs in a wastewater treatment site is presented.

Keywords
Pharmaceuticals; pesticides; antibiotic resistance genes; Adsorbent; nanofiltration; UV-LED

INTRODUCTION

Water scarcity is a current problem in many EU regions, and it is expected to be one of the main health and climate related issues in the coming years (Zal et al., 2012). Thus, water reclamation and reuse are needed to be widely implemented and are considered a priority within EU. At the same time, since drinking water will be directly impacted by water scarcity, safe drinking water must be also ensured from conventional or alternative sources. Both reclaimed water and drinking water must fulfil quality requirements that ensure both human and environment safety. Apart from the parameters already gathered for example at the Regulation (EU) 2020/741 or the Directive (EU) 2020/2184 for reclaimed water and drinking water, respectively (European Commission 2020 and European Commission 2020b), the elimination of Contaminants of emerging concern (CECs), should also be tackled in the near future.

Despite the numerous references to their negative impact, CECs presence in water bodies is not regulated yet, as their distribution, accumulation and effect are not fully understood, and there are not standard protocols affordable and available to keep detailed track of them. Still, it is generally agreed that their monitoring and elimination from the environment and water bodies will be crucial in the coming years, specially to achieve safe drinking and reclaimed water.

PRISTINE project (LIFE21-ENV-ES-PRISTINE -101074430) aims to develop an Integrated Solution to remove CECs from the water cycle. The project focuses on the elimination of pesticides, pharmaceuticals, personal care products (PPCPs), toxins, antibiotic resistance genes (ARG) and microplastics, as main CECs families, from drinking water but also to polish treated wastewater for reclamation. The proposed PRISTINE Integrated Solution consists of 3 modular technologies: i) encapsulated adsorbents, ii) hollow-fibre nanofiltration and iii) UV-LED combined with advanced oxidation processes (AOP). As depicted in Figure 1, the modular technologies that could be applied in series or individually, will be supported by a virtual artificial intelligence (AI) soft sensor and a decision support system to optimize operation parameters. The system will be adaptable, tested and optimized in both real drinking water (DW) treatment and wastewater (WW) reclamation scenarios.

OBJECTIVES

PRISTINE Integrated Solution will effectively remove >80% of the monitored CECs in wastewater and drinking water scenarios, while reducing 30% the operational costs compared of similar treatment trains based on conventional technologies (i.e., reverse osmosis), while avoiding CECs concentrated streams to be handled separately.

Parallel monitoring campaigns of both demonstration sites are crucial to design, adapt and properly estimate the performance of the PRISTINE Integrated Solution. Thus, the characterization of the water quality and occurrence and distribution of CECs is currently being performed for a full year (November 2022-October 2023). Up to date, preliminary information has been gathered for both sites. However, in the present abstract only WW results are presented.

MATERIALS AND METHODS

The wastewater demo site is located at a wastewater treatment plant (WWTP) facility in Murcia region (Spain). It serves ca. 30.600 p.e., and has a pre-treatment, a biological treatment based on prolonged aeration activated sludge followed by a tertiary treatment. A 2-month intensive campaign (November and December 2022) was performed with high sampling frequency to obtain preliminary data to start the development of the AI soft-sensor and the demonstration site characterization. During the intensive campaign, punctual samples were withdrawn from the influent (once per week) and effluent (4 times per week) of the WWTP. The river, before the discharge point of the WWTP, was sampled twice per month. 134 CECs (38 drugs, 79 pesticides, 6 haloacetic acids, 4 PFAS, 3 surfactants, 1 toxin, 3 hormones) were analysed by means of solid phase extraction and liquid chromatography coupled to tandem mass spectrometry with a triple quadruple mass spectrophotometer. Physicochemical parameters in the WW site were measured simultaneously using the applicable Hach Lange test-kit and the appropriate sensor or probe for pH, conductivity, and turbidity determination. Volatile suspended solids were measured according to standard protocols (Baird, 2012).

RESULTS AND DISCUSSION

The effluent of the secondary clarifier will be the application point of the PRISTINE Integrated solution in the WW site. Consequently, the occurrence and concentration of the CECs detected will directly impact the design and optimization of the technology. The influent of the WWTP is also another point of interest, to understand if the CECs presence in the effluent is preceded by a certain removal within the conventional treatment. Furthermore, the actual state of the Segura River upstream of the WWTP discharge point is also another factor to consider, to understand the real contribution of the WWTP itself to the general conditions of the recipient water mass.

Figure 2 shows results of CECs concentration and their detection frequencies during November 2022 in the presented points. Preliminary results of the analytical campaign showed that a total of 24 compounds were detected at least once in one of the sampled points. From the 134 analyzed, 16 were present in the secondary clarifier effluent. Drugs such as salicylic acid, ibuprofen, caffeine and ampyrone, and pesticides such as glyphosate and pyrimethanil were detected at an average concentration higher than 1 µg/L (**Figure 2A**). Other pharmaceuticals like naproxen, ofloxacin, ciprofloxacin, sulfamethoxazole, venlafaxine, diclofenac and ketoprofen, and the surfactant nonylphenol were detected at mid concentrations ranging from 0,1 µg/L to 1 µg/L (**Figure 2A**). Furthermore, most of the previously mentioned compounds (except for nonylphenol, pyrimethanil, sulfamethoxazole, salicylic acid and diclofenac) had a high occurrence, with a detection frequency over 40% in the effluent of the secondary clarifier (**Figure 2B**). In the river, ampyrone, caffeine, ibuprofen, naproxen, salicylic acid, glyphosate, imzalil and pyrimethanil were detected, as they were in the effluent of the secondary clarifier of the WWTPs. Finally, since the water quality that will need to be treated will also impact the design of PRISTINE Integrated solution, **Table 1** summarizes solids concentrations, turbidity, and concentration of UV scavengers such as COD nitrite, nitrate, among others, from all three sampling point discussed.

CONCLUSIONS AND FURTHER WORK

Preliminary results showing the persistence and occurrence of 24 CECs in a wastewater treatment site have been collected up to date. From January 2023 onwards, a reduced frequency CECs sampling campaign will take place, while microplastics and ARG will also be analyzed, gathering insight on their elimination, distribution and potential seasonal fluctuations. Furthermore, similar analysis as those presented here will be performed in a drinking water site. Results from both scenarios will be considered in PRISTINE Integrated Solution design and optimization.

ACKNOWLEDGMENTS

The LIFE21-ENV-ES-LIFE PRISTINE Project (Num. 101074430) is funded by the European Union under the LIFE-2021-SAP-ENV call. However, the views and opinions expressed are solely those of the authors and do not necessarily reflect those of the European Union or the European Executive Agency for Climate, Infrastructure and Environment (CINEA). Neither the European Union nor the granting authority can be held responsible for them.

REFERENCES

Baird, R. B., Eaton, A. D., & Clesceri, L. S. 2012 Standard methods for the examination of water and wastewater. *American public health association*, E. W. Rice (Ed.). Washington, DC

European Commission. 2020. Directive (EU) 2020/2184 of the European Parliament and of the Council of 16 December 2020 on the quality of water intended for human consumption. *Official Journal of the European Union*.

European Commission. 2020b. Regulation (EU) 2020/741 of the European Parliament and of the Council of 25 May 2020 on minimum requirements for water reuse. *Official Journal of the European Union*, 177, 32-55.

Zal, N., Wolters, H., Psomas, A., Anzaldua, G., Bariamis, G., Rouillard, J., & Birk, S. 2021. Water Resources across Europe—Confronting Water Stress: An Updated Assessment. *European Environment Agency: Copenhagen, Denmark*.

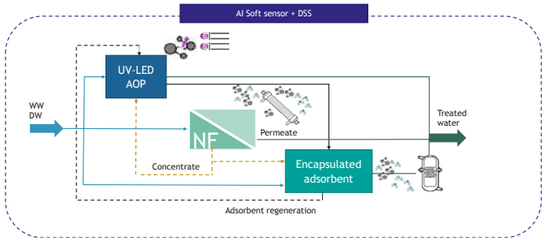

Figure 1. PRISTINE versatile and innovative integrated solution. WW – wastewater, DW – drinking water, AI – artificial intelligence, DSS- decision support system, NF – nanofiltration, UV-LED – LED ultraviolet light, AOP- advanced oxidation process.

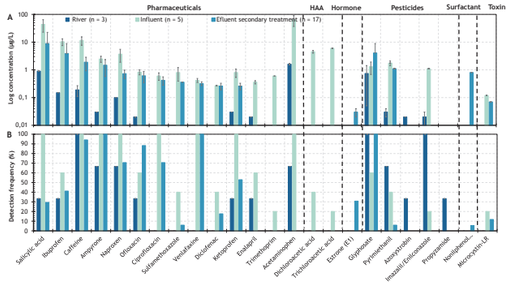

Figure 2. Preliminary results of CECs characterization in the wastewater treatment site during November 2022. Samples were withdrawn from the river before the WWTPs discharge point, the influent and effluent of the secondary clarifier of the WWTP. A) Logarithmic average concentration of different CECs, error bar represents the standard deviation, B) Percentage of detection of each compound in each sampling point.

Table 1. Preliminary physicochemical characterization of the WW site. VSS – volatile suspended solids, N – nitrogen, P – Phosphorous, COD – Chemical Oxygen Demand, TKN –Total Kjeldahl Nitrogen, *Calculated.

	River	Influent	Effluent secondary clarifier
Parameter	Average ± St. Dev	Average ± St. Dev	Average ± St. Dev
Num. Samples (n)	4	6	22
Turbidity (NTU)	125.5 ± 17.5	542.2 ± 248.3	8.2 ± 8.3
Conductivity (µS/cm)	1518 ± 184	3247 ± 310	2808 ± 121
pH	7.9 ± 0.2	7.2 ± 0.2	7.5 ± 0.2
VSS (mg/L)	97 ± 48	404 ± 230	9 ± 3
CODtotal (mg/L)	20 ± 7	2438 ± 1113	39 ± 5
$N\text{-}NO_3^-$ (mg/L)	1.4 ± 0.2	0.9 ± 0.6	0.5 ± 0.3
$N\text{-}NO_2^-$ (mg/L)	< 0.015	0.3 ± 0.2	0.1 ± 0
$N\text{-}NH_4^+$ (mg/L)	< 2	22 ± 3	3.4 ± 2.5
TKN (mg/L) *	1.8 ± 0.8	42.7 ± 8.1	5.6 ± 2.2
Ntotal (mg/L)	3.2 ± 0.8	43.3 ± 8.2	6 ± 2
Ptotal (mg/L)	0.3 ± 0.2	6.6 ± 4.6	1.6 ± 1.3

Can Peracetic Acid disinfect wastewater? A Portuguese pilot installation in a WWTP says it can

D. Sousa*, R. Dias*, R. Lourinho** and R. Maurício*

*CENSE – Center for Environmental and Sustainability Research & CHANGE - Global Change and Sustainability Institute; NOVA School of Science and Technology, NOVA University Lisbon, Portugal
(E-mail: db.sousa@campus.fct.unl.pt; ra.dias@campus.fct.unl.pt; rmr@fct.unl.pt);
** Águas do Tejo Atlântico, AdP—Grupo Águas de Portugal
(E-mail: rita.lourinho@adp.pt)

Abstract
Peracetic Acid (PAA) is an organic peracid with a high oxidation potential, with by-products less harmful than chlorine or ozone. The main goal pilot-scale study was to evaluate the PAA disinfection efficiency in secondary effluents in a Portuguese wastewater treatment plant (WWTP). To this end, six disinfection conditions were studied, three PAA doses (5, 10, and 15 mg/L) and three contact times (Tr) (5, 10, and 15 minutes). After the disinfection it was observed a BOD_5 and COD increase, however, it was not proportional to the PAA dose. The PAA performance showed that doses of 10 and 15 mg/L achieved log reduction higher than 2. Results also showed that the Tr was not a determining factor for the PAA disinfection performance, however, it was considered a minimum of five minutes. This study showed that PAA can be used as an alternative wastewater disinfectant, namely if wastewater reuse is an option.

Keywords
Peracetic acid; pilot study; wastewater disinfection alternative; wastewater reuse

INTRODUCTION

Wastewater disinfection is a key treatment for the elimination or inactivation of pathogenic microorganisms (Antonelli et al., 2006), and is essential since it protects the environment and public health from pathogenic infections (Blanco-Canella et al., 2022). Peracetic acid (PAA) is an organic peracid, with a high oxidation potential, larger than chlorine or chlorine dioxide (Kitis, 2004). PAA is a wide-spectrum disinfectant with efficacy against bacteria and viruses (Cavallini et al., 2013). PAA is classified as a safe and environmentally friendly disinfectant (Freitas et al., 2021), since it has less toxic disinfection by-products than chlorine or ozone (Deng et al., 2022) There are other advantages of using PAA as a disinfectant, such as the low pH dependence, easy implementation, low corrosivity, and reasonable cost (Chen & Pavlostathis, 2019). Recent studies show promising results regarding the use of PAA in the degradation of micropollutants present in treated wastewater (Deng et al., 2022; Maurício et al., 2020). According to the latter, it seems that PAA can be the new widespread disinfectant, however, there are still uncertainties among studies that must be clarified. To do so, more studies are needed to create new knowledge to support a safe and efficient shift between the disinfection processes. The main goal of this pilot-scale study was to evaluate, in a significant and representative period, the PAA disinfection efficiency of six disinfection conditions in secondary effluents in a Portuguese wastewater treatment plant (WWTP) in the Lisbon region.

MATERIALS AND METHODS

The pilot-scale installation was set in a conventional large-scale municipal WWTP located in Lisbon area (Portugal). This WWTP has a flow above 50 000 m^3/day (more than 200 000 equivalent inhabitants) and includes preliminary, primary, and secondary treatment with conventional activated sludge and nitrogen removal. Within the WWTP, the pilot-scale installation (Figure 1) was settled after the secondary clarifiers. The pilot installation had a 5 m^3 capacity tank equipped with a vertical mixer. A 15% PAA solution was dosed to the wastewater. The work was performed during six months, from April to September, (two different weather seasons) and six disinfection conditions (Table 1) were tested. Each condition was analysed for five days (three samples per day) in which the water quality parameters and the PAA residual concentration were determined. The samples were collected before and after disinfection and the main control parameters were: Biological Oxygen Demand (BOD_5), Chemical Oxygen Demand (COD) Escherichia coli, temperature, pH, and PAA residual concentration (only after disinfection). A statistical evaluation of the results was performed using one-way ANOVA and Tukey test. The significance level was set at 5% ($p \leq 0.05$) using the software SPSS v20.ea.

RESULTS AND DISCUSSION

The statistical analysis of the results before the disinfection showed significant differences in the E. coli content between conditions. The conditions C15T10 and C5T10 had significant differences from the conditions C15T15, C10T10 and C10T15 (Tukey, $p<0.022$). These two conditions had an E. coli content lower than the other studied conditions. The disinfection with PAA increased the BOD_5 and the COD in all conditions, which was to be expected since this behaviour was already reported in the literature (Cavallini et al., 2013). According to Luna-Pabello et al. (2009) this increase is due to the organic component of PAA. Statistical analysis showed that for different PAA doses (10 and 15 mg/L), with the same Tr, there were no significant differences (Tukey, $p>0.05$). Although PAA increases the BOD_5 (Figure 2) and the COD (Figure 3), this was not proportional to the PAA dose. The disinfection with PAA resulted in a slight decrease of pH, except in the condition C5T10, in which was verified a minor pH increase. PAA is a weak acid, when combined with an alkaline effluent the impact on pH is not significant (Cavallini et al., 2013), which may explain the results obtained.

The PAA performance showed that doses of 10 and 15 mg/L achieved E. coli log reduction (LR) higher than 2, and even higher than 3 when 15 mg/L were tested with 10 and 15 minutes of Tr (Figure 4). As reported in the study of Bonetta et al. (2017), PAA doses lower than 2 obtained the E. coli LR were lower than 2. Those results were equivalent to the ones obtained with condition C5T10, which may suggest that PAA doses lower than 5 mg/L may be not efficient. However, in the pilot study performed by Pileggi et al. (2022), 4 mg/L of PAA and 35 minutes of Tr achieved an E. coli LR of 2.6, comparable with the results of the condition C10T10, C10T15 and C15T5. Those results may indicate that lower PAA needs more Tr to achieve higher LR. In the study made by Freitas et al. (2021), using the C15T15 disinfection conditions, in an effluent of a similar type of wastewater treatment, was verified a LR of 3.9, similar to the results obtained in this study. No significant differences were found between the conditions with the same PAA dose, which may suggest that the Tr was not determinant for the PAA performance, at least for the Tr used in this study. It was also observed that even with a longer Tr, a 5 mg/L of PAA would not be enough to achieve higher LR of E. coli, since almost the PAA was consumed (Figure 5). According to Chen and Pavlostathis (2019), the temperature is a parameter that may affect the PAA decay rate, and this could explain the differences verified, since those conditions on which occurred a lower PAA consumption, were the ones with lower temperatures.

Overall, the results obtained with this pilot-scale study support the use of PAA as an alternative wastewater disinfectant. The independence of this disinfectant from the Tr may be an advantage for the implementation of this disinfectant in a WWTP. Also, the residual PAA concentration, after disinfection, turns out to be an operational advantage, when considering treated wastewater storage and reuse by avoiding bacteria regrowth. Such consideration is central when countries reusing policies are in action, which is the Portuguese situation.

REFERENCES

Antonelli, M., Rossi, S., Mezzanotte, V., & Nurizzo, C. (2006). Secondary effluent disinfection: PAA long term efficiency. *Environmental Science and Technology*, *40*(15), 4771–4775. https://doi.org/10.1021/es060273f

Blanco-Canella, P., Lama, G., Sanromán, M. A., & Pazos, M. (2022). Disinfection through Advance Oxidation Processes: Optimization and Application on Real Wastewater Matrices. *Toxics 2022, Vol. 10, Page 512*, *10*(9), 512. https://doi.org/10.3390/TOXICS10090512

Bonetta, S., Pignata, C., Lorenzi, E., de Ceglia, M., Meucci, L., Bonetta, S., Gilli, G., & Carraro, E. (2017). Peracetic Acid (PAA) Disinfection: Inactivation of Microbial Indicators and Pathogenic Bacteria in a Municipal Wastewater Plant. *Water 2017, Vol. 9, Page 427*, *9*(6), 427. https://doi.org/10.3390/W9060427

Cavallini, G. S., de Campos, S. X., de Souza, J. B., & de Sousa Vidal, C. M. (2013). Evaluation of the Physical–Chemical Characteristics of Wastewater After Disinfection with Peracetic Acid. *Water, Air, & Soil Pollution*, *224*(10), 1752. https://doi.org/10.1007/s11270-013-1752-5

Chen, J., & Pavlostathis, S. G. (2019). Peracetic acid fate and decomposition in poultry processing wastewater streams. *Bioresource Technology Reports*, *7*, 100285. https://doi.org/10.1016/j.biteb.2019.100285

Deng, J., Wang, H., Fu, Y., & Liu, Y. (2022). Phosphate-induced activation of peracetic acid for diclofenac degradation: Kinetics, influence factors and mechanism. *Chemosphere*, *287*, 132396. https://doi.org/10.1016/J.CHEMOSPHERE.2021.132396

Freitas, B. de O., Leite, L. de S., & Daniel, L. A. (2021). Chlorine and peracetic acid in decentralized wastewater treatment: Disinfection, oxidation and odor control. *Process Safety and Environmental Protection*, *146*, 620–628. https://doi.org/10.1016/j.psep.2020.11.047

Kitis, M. (2004). Disinfection of wastewater with peracetic acid: a review. *Environment International*, *30*(1), 47–55. https://doi.org/10.1016/S0160-4120(03)00147-8

Luna-Pabello, V. M., Ríos, M. M., Jiménez, B., & Orta De Velasquez, M. T. (2009). Effectiveness of the use of Ag, Cu and PAA to disinfect municipal wastewater. *Environmental Technology*, *30*(2), 129–139. https://doi.org/10.1080/09593330802422506

Maurício, R., Jorge, J., Dias, R., Noronha, J. P. P., Amaral, L., Daam, M. A. A., Mano, A. P., & Diniz, M. S. S. (2020). The use of peracetic acid for estrogen removal from urban wastewaters: E2 as a case study. *Environmental Monitoring and Assessment*, *192*(2), 114. https://doi.org/10.1007/s10661-020-8079-7

Pileggi, V., Bicudo, J. R., Nowierski, M., Manoharan, M., Lai, G., Fletcher, T., & Simhon, A. (2022). Side-Stream Comparison of Peracetic Acid and Chlorine as Hypochlorite for Disinfection of Municipal Wastewater Effluent at a Full-Scale Treatment Facility, Ontario, Canada. *ACS ES&T Engineering*. https://doi.org/10.1021/ACSESTENGG.2C00005

Table 1. Tested conditions

Condition (CT)	PAA concentration (mg/L)	Contact time (min.)
C15T15	15	15
C15T10	15	10
C10T10	10	10
C10T15	10	15
C5T10	5	10
C15T5	15	5

C - PAA concentration
T - Contact time

Figure 1. Pilot installation

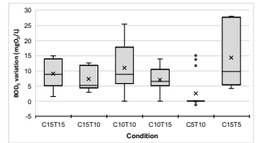

Figure 2. BOD_5 variation

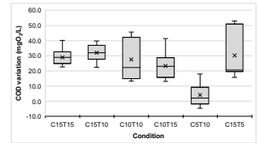

Figure 3. COD variation

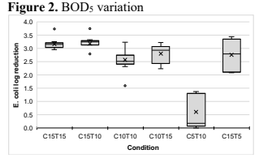

Figure 4. E. coli log reduction

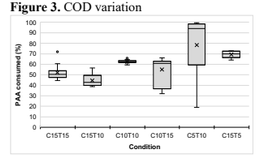

Figure 5. PAA consumed

Enhancing purple phototrophic bacteria granulation by size classification

S. J. Stegman, T. Huelsen, P. D. Jensen, D. J. Batstone

The Australian Centre for Water and Environmental Biotechnology, The University of Queensland, Gehrmann Building, 60 Research Road, Brisbane, 4067, QLD, Australia
(E-mail: *x.stegman@uq.edu.au)*

Abstract
Recently, large granular purple phototrophic bacteria (PPB) with good settling characteristics has been investigated. However, a sizeable flocculent component was still present. In anammox granular sludge, size classification (via hydro-cyclones) can be used to promote a larger, consistent granular biomass, and may apply to granular PPB. In this study, the effect of fortnightly size classification (biomass <200 µm) on the granular fraction was investigated. The granular fraction (~80 vol%) was high compared with previous studies (due to increased illumination) however the flocculent component regularly returned after size classification. Particle size was proportional with calcium phosphate content which suggests ballasting agents like ions are one precursor for granular PPB. Particle size was inversely proportional to organic biomass fraction (VSS/TSS ~0.53 for >1 mm diameter, VSS/TSS ~0.76 for <200 µm), and PPB relative abundance. Sieving significantly affected the PPB *Rhabdochromatium* (p=0.025), *Rhodobacter* (p=0.0218) and *Allochromatium* (p=0.052) and the non-PPB clades Desulfobacterota (p=0.0451) and Planctomycetota (p=0.0173). The change of microbial community with size was also reflected in the biomass activity which decreased with increasing particle size (e.g., biomass activity of large (>1 mm), medium (<250 µm, <1 mm), and small (<250 µm) granules were 0.63 gCOD, 1.8, and 2.8 gCOD $gVSS^{-1}$ d^{-1}, respectively)). Settling characteristics were comparable (SVI30 ~ 10 – 20 mL g^{-1}) between the different size classifications. The technology does not seem analogous to anammox as the size classification did not promote the granular fraction.

Keywords
Biological wastewater treatment; circular economy; granules; purple phototrophic bacteria; resource recovery

INTRODUCTION

The benefits of granular sludge for wastewater treatment (against conventional activated sludge) - lower capital and operational expenses and single-step removal of organics and nutrients - are well documented (Pol 1989, van der Star et al. 2007). Granular sludge mainly comprises aerobic, anaerobic and/or anammox bacteria and the high sludge disposal costs persist (Kroiss 2004). Aggregating purple phototrophic bacteria (PPB) (a promising technology in the resource recovery sphere) is incipient with only three studies performed (Blansaer et al. 2022, Cerruti et al. 2020, Stegman et al. 2021). Stegman et al. (2021) reported high flocculent biomass content, despite the growth of large (>3 mm), well-settling PPB granules. Removing the predominant flocculent fraction could be important in order to produce well-settling PPB granules with a consistent size profile. Some granular sludge technologies, such as anammox, improve the granulation rate and granule population using hydro-cyclones to select for larger granules (Wett et al. 2013). For example, in anammox systems, the anammox activity and biomass fraction increases (to an extent) as the granule size (and settling ability) increases and allows the anammox bacteria to outcompete the nitrite oxidising bacteria (Volcke et al. 2012). It is a provoking thought: could this technology translate to granular PPB? This study investigated the impact of the suspended fraction on PPB granulation and the treatment efficiency. This was tested in two PBRs on synthetic wastewater which underwent regular size classification. The physical and microbial structures of the sieved and non-sieved granular biomass' (from the two reactors and from the different particle sizes in the sieved reactor), as well as comparative performance were compared periodically.

MATERIALS AND METHODS

Two, 7 L (5 L working liquid volume), acrylic upflow photobioreactors (PBRs) were operated under anaerobic conditions. A liquid recirculation line from the 4 L to the 0 L port provided mixing in the form of liquid upflow. Synthetic media (wastewater proxy) was pumped into the reactor at the 0 L port and left the reactor at the 5 L port. The carbon source was pumped via syringe pump into the recirculation line. The reactors were covered in UV-VIS absorbing foil as per Stegman et al. (2021). Each reactor was constantly illuminated by two 150 W m^{-2} floodlamps located 15 cm from the reactor and five infrared (IR) lamps located 10 cm from reactor. The reactors were inoculated with granular PPB sludge (40 % PPB relative abundance). In the experimental reactor, undersized particles (<250 µm) were removed by sieve classification fortnightly while in the control reactor the biomass was not controlled.

RESULTS AND DISCUSSION

The PSD of the inoculum was dominated by granules (D_{50} of ~200 µm) but the reactors' biomass inventories – in terms of oversized granules (>200 µm) – increased from ~55 vol% to ~80 vol% within 60 days;**Error! No se encuentra el origen de la referencia.**. A predominantly granular system (oversized biomass >70 vol%) was maintained for the first 160 d in the control reactor, which reduced from day 174. The sieved reactor (pre-sieve biomass) contained on average ~60 vol% granular (despite fluctuations) biomass until day 160, after which the oversized granular fraction decreased to 25-35 vol%. At the HRTs used, the clear light column allowed for suspended biomass to rapidly regrow after each size classification preventing the formation of a pure granular system.

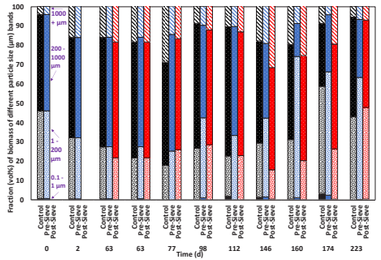

Figure 1. Volume fraction (%) of size bands of granular biomass in two reactors with time (d). The control reactor is black; the pre-sieved reactor is blue; the post-sieved reactor is red. The solid filled bar represents the biomass 0.1-1 µm; the confetti bar represents the biomass 1-200 µm; the dotted bar represents the biomass 200-1000 µm; the diagonal striped bar represents biomass >1000 µm.

Activity tests of differently sized granules (Figure 21) identified that the smaller sized particles/granules have higher SCOD removal rates compared to medium and large sized granules. Particles smaller than 250 µm had a specific COD removal rate of 2.80 gCOD $gVSS^{-1}$ d^{-1}, comparable with previously reported activities of suspended PPB (Puyol et al. 2017). The activity of medium sized PPB granules (250 µm<granules< 1 mm) was 1.83 gCOD $gVSS^{-1}$ d^{-1}, and PPB granules greater than 1 mm in diameter removed 0.63 gCOD $gVSS^{-1}$ d^{-1}. Due to the larger surface area to volume ratio, the undersized PPB have a higher activity and are more suited to phototrophic wastewater treatment.

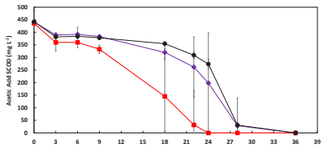

Figure 2. Activity test on consumption of acetate SCOD by granular PPB biomass of different size distributions. (-●-) undersized biomass < 250µm; (⊟) 250µm < granules < 1mm; (◆) granules > 1mm. Note: one data outlier was removed from the undersized and medium sized granules.

The undersized biomass had the lowest ash content (~20 %) and the control biomass and oversized biomass had higher ash fractions (56 ± 2.7 % and 47 ± 7.4 %, respectively). The Ca/P molar ratios of the control, oversized, and pre-sieved granular sludges were between 1-1.2, which is in line with the Ca/P molar ratios found in calcium phosphate precipitate in excess biological phosphorous removal processes (Carlsson et al. 1997) (Ca/P molar ratio of undersized biomass was ~0.8). This suggests that the calcium phosphate precipitation was a key factor in the production of large granules, likely due to it being a ballasting agent or bridging cations in EPS.

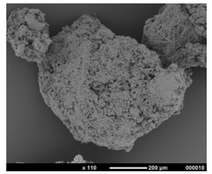

Figure 3. Ionic (calcium phosphate) compound within large PPB granules.

Inoculum was dominated by the purple sulfur bacteria (PSB) *Allochromatium* (20 %), the purple non-sulfur bacteria (PNSB) *Rhodopseudomonas* (15 %) and by a mixed group of other phyla including *Euryarcheota, Halobacterota* (*Methanobacteria*), and *Bacteroidota*. The PNSB *Blastochloris* – initially 0.3 % relative abundance in the inoculum – established itself in both reactors and persisted throughout the duration of the experiment with relative abundances of 10-20 %. The total relative abundance of PPB genera in both reactors represented on average ~50 % of the microbiota with peaks up to ~80 % and ~90 % in the control and the sieved reactors. ANOVAN indicated that the relative abundances of the PPB and non-PPB profile were not impacted by the reactor (PPB p=0.378; non-PPB p=0.532) but by time (p=0.0000 for both PPB and non-PPB) and sieving (PPB p=0.0152; non-PPB p=0.0187). Sieving significantly affected the PPB *Rhabdochromatium* (p=0.025), *Rhodobacter* (p=0.0218) and *Allochromatium* (p=0.052) and the non-PPB clades *Desulfobacterota* (p=0.0451) and *Planctomycetota* (p=0.0173) (it was potentially significant with *Chloroflexi* (p=0.056)) as the undersized biomass had a higher proportion of PPB.

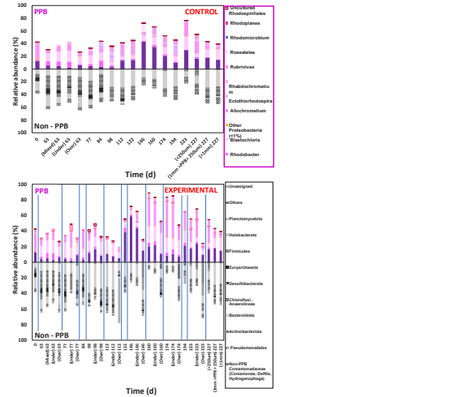

Figure 3. Relative abundance (%) of microbial communities in the biomass from the control (A) and experimental reactor (B) with time (d). PPB clades are shown with positive values (above the x-axis) in pink/purple colours and patterns and other non-PPB clades are shown with negative values (below the x-axis) in muted colours and patterns.

REFERENCES

Blansaer, N., Alloul, A., Verstraete, W., Vlaeminck, S.E. and Smets, B.F. (2022) Aggregation of purple bacteria in an upflow photobioreactor to facilitate solid/liquid separation: Impact of organic loading rate, hydraulic retention time and water composition. Bioresource Technology 348, 126806.
Carlsson, H., Aspegren, H., Lee, N. and Hilmer, A. (1997) Calcium phosphate precipitation in biological phosphorus removal systems. Water Research 31(5), 1047-1055.
Cerruti, M., Stevens, B., Ebrahimi, S., Alloul, A., Vlaeminck, S.E. and Weissbrodt, D.G. (2020) Enrichment and Aggregation of Purple Non-sulfur Bacteria in a Mixed-Culture Sequencing-Batch Photobioreactor for Biological Nutrient Removal From Wastewater. 8.
Kroiss, H. (2004) What is the potential for utilizing the resources in sludge? J Water Science Technology 49(10), 1-10.
Pol, L.H. (1989) The phenomenon of granulation of anaerobic sludge.
Puyol, D., Barry, E., Hülsen, T. and Batstone, D.J.W.r. (2017) A mechanistic model for anaerobic phototrophs in domestic wastewater applications: Photo-anaerobic model (PAnM). 116, 241-253.
Stegman, S., Batstone, D.J., Rozendal, R., Jensen, P.D. and Hülsen, T. (2021) Purple phototrophic bacteria granules under high and low upflow velocities. Water Research 190, 116760.
van der Star, W.R.L., Abma, W.R., Blommers, D., Mulder, J.-W., Tokutomi, T., Strous, M., Picioreanu, C. and van Loosdrecht, M.C.M. (2007) Startup of reactors for anoxic ammonium oxidation: Experiences from the first full-scale anammox reactor in Rotterdam. Water Research 41(18), 4149-4163.
Volcke, E., Picioreanu, C., De Baets, B., Van Loosdrecht, M.J.B. and bioengineering (2012) The granule size distribution in an anammox-based granular sludge reactor affects the conversion—Implications for modeling. 109(7), 1629-1636.
Wett, B., Omari, A., Podmirseg, S.M., Han, M., Akintayo, O., Gómez Brandón, M., Murthy, S., Bott, C., Hell, M., Takács, I., Nyhuis, G. and O'Shaughnessy, M. (2013) Going for mainstream deammonification from bench to full scale for maximized resource efficiency. Water Science and Technology 68(2), 283-289.

Evaluation of emerging micropollutants presence in laundry greywater facilities for recycling

M. Turull[*,**], G. Buttiglieri[*,**], S. Insa[*,**], D. Alvarez[*,**], L.H.M.L.M. Santos[*,**], P. Moretti[***], B. Mathon[***], B. Cedat[***], D. Barceló[*,**,****], S. Rodriguez-Mozaz[*,**]

* Catalan Institute for Water Research (ICRA-CERCA), C/ Emili Grahit 101, 17003 Girona, Spain.
(E-mail: *mturull@icra.cat; gbuttiglieri@icra.cat; sinsa@icra.cat; dalvarez@icra.cat; lhsantos@icra.cat; dbarcelo@icra.cat; srodriguez@icra.cat*)
** University of Girona, Girona, Spain.
***IDAEA-CSIC, Department of Environmental Chemistry. C/ Jordi Girona 18-26, 08034 Barcelona, Spain.
****Treewater, 61 rue de la Republique, 69002 Lyon, France
(E-mail: *pmoretti@treewater.fr; bmathon@treewater.fr; bcedat@treewater.fr*)

Abstract
The aim of this work is to characterize and monitor emerging pollutants in laundry greywater in the perspective of internal laundry water recycling. Specifically, 33 pharmaceuticals and 21 endocrine disrupting compounds were analysed in laundry greywater of three laundries of different size, clients, and services, located in France, Luxemburg, and Spain. Additionally, a novel analytical methodology was specifically developed for DEHP analysis in laundry greywater. Several pharmaceuticals were detected, including analgesics, psychiatric drugs, and antibiotics, as well as some hormones, preservatives, plasticizers, chemical biomarker (caffeine), alkylphenolic compounds, organophosphorus flame retardants compounds and DEHP at ng/L to µg/L levels. A prototype based on UV/H_2O_2 is being set-up to treat the water and remove pollutants, including organic micropollutants from laundry greywater. In this way, the effectiveness of the prototype will be determined and evaluated to establish a closed circuit and reuse 100% treated water in the same laundry.

Keywords (maximum 6 in alphabetical order)
DEHP; Endocrine disrupting compounds; Laundry greywater; Pharmaceuticals; Plasticizer; Recycled water.

INTRODUCTION

Greywater, once discharged into public sewage systems, represents a major source of pollutants in the urban wastewater. Europe has around 11,000 laundries, through which some 2,700 million kg of textile materials pass each year (Hloch *et al.*, 2012). This kind of water may contain softeners, plasticizers, emulsifiers, fatty acids, preservatives, antioxidants, surfactants, antioxidants, phthalates, phenols and solvents, pharmaceuticals and microplastics, along with many other emerging and priority contaminants (Shaikh and Ahammed, 2020; Le *et al.*, 2022). Many of these emerging contaminants are also considered endocrine disrupting compounds, carcinogens, and mutagens, representing a risk to the environment. As a specific case, DEHP and nonylphenol are currently considered priority substances under the Water Framework Directive (WFD) (EC, 2013), being limited to 25 µg/L in laundry effluents. Nevertheless, very limited information is currently available on the presence of several emerging pollutants in laundry greywater (Glover *et al*., 2021).
In addition, wastewater treatment plants are not designed for the removal of many of these substances contained in laundry greywater and these contaminants might end up in the environment. Although at low concentrations, they may have a negative impact on the ecosystems and ultimately on the human health as well.
Thus, the aim of this work is to monitor emerging contaminants in greywater of selected laundries of different size, and characteristics. In addition, greywater samples will be analyzed after an advanced oxidation treatment for the elimination of emerging pollutants for its subsequent re-use in the same establishment.

MATERIALS AND METHODS

Sampling

Greywater characterization was carried out to determine the level of pollutants in the water of three laundries located in France, Luxemburg, and Spain, differing in terms of water flow rate (25 m^3/d, 10 to 15 m^3/d and 2-3 m^3/d, respectively). Samples were collected on a weekly basis. Automatic refrigerated samplers were used to collect composite and homogenized greywater samples. Then, the water samples were kept at -20ºC till analysis. Additionally, samples were daily collected during a week in the laundry of Spain, to evaluate the inter-day variability throughout the week.

Contaminants of interest

The target pollutants assessed in this study are grouped into three groups:
- Pharmaceuticals (PhACs), including the antibiotics and psychiatric drugs from the Watch List 2020 (WL 2020/1161). Besides, clindamycin and ofloxacin included in the current Watch list (WL 2022/1307) were also considered in the analytical method.
- Endocrine disrupting compounds (EDCs), including hormones, antimicrobial, preservatives, plasticizers, chemical biomarkers, alkylphenolic compounds, anticorrosives, and organophosphorus flame retardants.
- Di(2-ethylhexyl) phthalate (DEHP), the most common phthalate which is used in hundreds of products (detergents, lubricating oils, pharmaceuticals…) and regulated by the Directive 2013/39/EU.

Analysis

For the extraction of PhACs and EDCs, laundry greywater samples were filtered (0.45 µm PVDF membrane filters). Then, the extraction was performed with a procedure adapted from Gros *et al.*, (2012) based on solid-phase extraction, followed by specific analytical methodologies for PhACs and EDCs using UHPLC-MS/MS adapted from Gros *et al.*, (2012) and Jakimska *et al.*, (2013) respectively. The analytical methodologies were validated for laundry greywater.
For the analysis of DEHP, a novel analytical methodology, based on on-line headspace solid-phase microextraction coupled to gas chromatography tandem mass spectrometry (HS-SPME-GC-MS/MS), was specifically developed for laundry greywater.

RESULTS AND DISCUSSION

Method validation in laundry greywater

In the process of analytical method development and validation for laundry greywater samples, confirmation analyses of composite laundry samples were performed. Quality parameters were assessed for each target compound in the 3 analytical methods validated, including limits of detection (LOD), limits of quantification (LOQ), and the percentage of recovery (Table 1).

Table 1. Concentration of the target pollutants in laundry greywater, LOD, LOQ and recovery (%).

Class	Compounds	Concentration (ng/L)	LOD (ng/L)	LOQ (ng/L)	Recovery (%)
Analgesics/anti-inflammatories	Acetaminophen	1,885	3	10.2	56
	Diclofenac	73	1.2	4	80
	Ibuprofen	570	3.2	10.6	72
	2OH-ibuprofen	366	10.8	36.4	120
	Ketoprofen	640	32	108	69
	Codeine	66	9	30	54
β-Blocking agents	Sotalol	18	16	54	67
	Metoprolol	4	0.3	0.9	23
Psychiatric drugs	Alprazolam	46	0.9	3	114
	O-desmethyl-venlafaxine	<LOQ	16	54	39
Lipid regulators	Fluvastatin	15	9	28	121
	Bezafibrate	38	0.2	1.0	71
Antibiotics	Sulfamethoxazole	26	0.7	2.2	47
Hormones	Levonorgestrel	1,608	79.3	381.8	119
Preservatives	Ethylparaben	25	0.2	0.8	40
	Methylparaben	636	5.5	18.4	74
	Propylparaben	164	0.16	0.53	27
Plasticizer	Bisphenol A	<LOQ	25.0	83.4	100
Chemical biomarker	Caffeine	9,285	26.4	87.8	89
Alkylphenolic compound	Nonylphenol	<LOQ	6.7	22.4	70
Organophosphorus flame retardants	Tris(2-chloroethyl) phosphate (TCEP)	767	7.3	24.8	111
Phthalates	DEHP	133,599	15.5	51.6	100

Acceptable recovery results (40-120%) were observed for all the selected contaminants, except for metoprolol (23%) and propylparaben (27%). Thus, LOD and LOQ for PhACs were found between 0.3-32 ng/L and 0.9-108 ng/L, respectively. For EDCs, values ranged between 0.2-79.3 ng/L for LOD and 0.8-381.8 ng/L for LOQ.

Characterization of laundry greywater

Greywater samples from the Spanish laundry were analyzed to validate and optimize the analytical method and allowed to have an overview of the level of contaminants (Table 1). Considering the detected concentrations in laundry greywater, caffeine (9.3 µg/L), levonorgestrel (1.6 µg/L), acetaminophen (1.9 µg/L) and DEHP (133.6 µg/L) were found at higher concentrations, while the other analytes were at ng/L level.
The concentration of contaminants in laundry greywater samples may vary depending on the day of the week, from week to week, and the period of the year because of their different cleaning treatments, different clients, and habits of the clients. Therefore, for its characterization, daily samples have been collected in a total of five samples in one week. A weekly composite sample was also analyzed to determine the variation that may exist in comparison to the collected daily samples.

FUTURE WORK

The characterization of greywater of the selected laundries will help in the further implementation of an advanced water treatment system on-site. This prototype system, based on advanced oxidation processes will allow the water reuse of laundry water by water recirculation as a water source.
Influent and effluent from the laundry will be sampled to evaluate the effectiveness of the prototype device in terms of removal of the emerging contaminants of interest.

ACKNOWLEDGMENTS

The authors would like to thank project LIFE-RECYCLO (LIFE20 ENV/FR/000205), with the contribution of the LIFE financial instrument of the European Community. G. Buttiglieri acknowledges Spanish State Research Agency of the Spanish Ministry of Science, Innovation and Universities for the Grant to the Creation of a permanent position RYC-2014-16754.

REFERENCES

EC. 2013 Directive 2013/39/EY of the European Parliament and of the Council of 12 August 2013 amending Directives 2000/60/EC and 2008/105/EC as regards priority substances in the field of water policy. *Official Journal of the European Union* L 226/1.
Glover, CM., Liu, Y., Liu, J. 2021 Assessing the risk from trace organic contaminants released via greywater irrigation to the aquatic environment. *Water Research* **205**, 117664.
Gros, M., Rodríguez-Mozaz, S., Barceló, D. 2012 Fast and comprehensive multi-residue analysis of a broad range of human and veterinary pharmaceuticals and some of their metabolites in surface and treated waters by ultra-high-performance liquid chromatography coupled to quadrupole-linear ion trap tandem mass spectrometry. *Journal of Chromatography A* **1248**, 104-121.
Hloch, H., Tokos, M., Spettmann, D., den Otter, W.A.J.L., Groosman, M., Vanderhoeven, M., Pušiü, T.,Šostar, S., Fijan, S. & Seite, M. 2012. Sustainable measures for industrial laundry expansion strategies: SMART-laundry-2015. SMILES Report, *European seventh framework programme*.
Jakimska, A., Huerta, B., Bargańska, Kot-Wasik, A., Rodríguez-Mozaz, S., Barceló, D. 2013 Development of a liquid chromatography-tandem mass spectrometry procedure for determination of endocrine disrupting compounds in fish from Mediterranean rivers. *Journal of Chromatography A* **1306**, 44-58.
Le, L., Nguyen, KN., Nguyen, P., Duong, HC., Bui, X., Hoang, NB., Nghiem, LD. 2022 Microfibers in laundry wastewater: Problem and solution. *Science of the Total Environment* **852,** 158412.
Shaikh, IN., Ahammed, M. 2020 Quantity and quality characteristics of greywater: a review. *Journal of Environmental Management* **261**, 110266.

Aerobic biodegradability of fat, oil and grease wastes

C. Ucha*, Y. López-Garabato*, A. Val del Rio*, A. Pedrouso*, J. Gonzalez-Lopez**, A. Mosquera-Corral*

Department of Chemical Engineering, CRETUS, School of Engineering, Universidade de Santiago de Compostela, Rua Lope Gomez de Marzoa, E-15782. Santiago de Compostela, Spain.
(E-mail: *carlota.ucha.munoz@usc.es; yolandalopez.garabato@usc.es; mangeles.val@usc.es; alba.pedrouso@usc.es; anuska.mosquera@usc.es)*

** Microbiology Department, Faculty of Pharmacy and Institute of Water Research, University of Granada, Granada, 18071, Spain. (E-mail: *jgl@ugr.es*)

Abstract
The biodegradability of an organic waste is a parameter that defines its possible valorisation by aerobic biological processes like those of biopolymer production. In the present study a respirometric technique was used to determine the biodegradable organic fraction (as % of the chemical oxygen demand (COD)) of four fat, oil and grease (FOG) wastes: olive pomace (78.74%), waste cooking oil (58.48%), tuna cooker oil fraction (35.24%) and FOG from municipal wastewater (11.91%). The time required for the total consumption of the biodegradable fraction of the wastes varied widely, ranging from 1.27 h (FOG from municipal wastewater) to 8.34 h (olive pomace). Considering biodegradability, the most suitable substrate for biopolymers production seems to be the olive pomace although the time required for the degradation is the longest. The less biodegradable one was the FOG from municipal sewage.

Keywords
Activated sludge; biodegradability; FOG waste; respirometry.

INTRODUCTION

The fat, oil and grease (FOG) fraction is a lipid-rich waste from private households, food industries and restaurants. It is mainly composed for free fatty acids, triacylglycerols, esters, waxes, phospholipids, sterols and sterol esters. The discharge of this fraction on the wastewater collectors provokes their complete blockage or overflow. With the proper management valuable products, like bioenergy and/or biomaterials, could be obtained from FOG wastes (Abomohra et al., 2020). One interesting possibility of valorisation is to use the FOG waste to produce biopolymers, like polyhydroxyalkanoates (PHA) and/or triacylglycerides (TAG), by a biotechnological process which certain microorganisms use this residue as carbon source to accumulate the PHA and TAG intracellularly. However, the low and/or slow biodegradability attributed to the FOG fraction may be a limiting step due to the difficulty to hydrolyse this type of substrates by microorganisms. For this reason, it is useful to first determine the biodegradable organic fraction of each FOG waste in order to select the most suitable one for this biological recovery process. Aerobic biodegradability of organic substrates is easily determined by respirometric experiments based on the measurement of the dissolved oxygen consumption (OC) rate of an aerobic microbial culture (Argiz et al., 2020; Surcis 2022). With the results obtained it is possible to control, design and protect a biological process such as the biopolymer accumulation one.

This study is part of the project ECOPOLYVER that aims to determine the biodegradability of four FOG wastes, olive pomace, waste cooking oil, tuna cooker oil fraction and FOG from municipal wastewater, to identify the best substrate to be used in a subsequent process for the production of biopolymers.

MATERIALS AND METHODS

The respirometric tests were carried out on a BM-T + analyser (Surcis, S.L) at 25 °C. Activated sludge (AS) samples used as inoculum, collected from a municipal wastewater treatment plant (WWTP), were aerated for 12 - 24 hours before the tests to remove any residual organic matter. First, the heterotrophic yield (Y_H), for the AS used as inoculum, was determined using equation 1 to check its suitability for sample degradation. *OC* is the oxygen consumed (mg O_2/L) and *COD* (mg COD/L) is the chemical oxygen demand of the sodium acetate used as substrate (325 mg COD/L).

$$Y_H = 1 - \frac{OC}{COD} \quad (1)$$

The biodegradability assays were carried out with 1 L of AS at a concentration of 1 - 3 g VSS/L, which was first aerated for approximately 20 - 60 min until oxygen saturation conditions of 7.5 - 8.0 mg O_2/L were reached. The FOG waste to be tested was then added to give a concentration of 0.14 g COD/L. During the experiments, the dissolved oxygen concentration measured with the oxygen probe was registered online to determine the oxygen uptake rate (OUR) and the analyser displayed the OC value over time (Figure 1). Four different FOG residues (Table 1) were assayed in triplicate: olive pomace (S1), waste cooking oil (S2), tuna cooker oil fraction (S3) and FOG from municipal wastewater (S4). The OC obtained was used to calculate the Biodegradable Chemical Oxygen Demand (COD_b) and the biodegradability of the substrate studied according to equation (2).

$$\%Biodegradability = \frac{COD_b}{COD} = \frac{\frac{OC}{1-Y_H}}{COD} \quad (2)$$

The AS samples used for S2, S3 and S4 were from the same collected batch, while for S1 it was collected in a different day (same origin but with different Y_H, Table 1).

RESULTS AND DISCUSSION

The respirometric assay results for the tested substrates are shown in terms of oxygen consumed (*OC*) (Figure 1). The time required to reach a stable *OC* value indicates how fast the biodegradable fraction of the substrate is degraded, with S4 being the fastest (1.27 hours) and S1 the slowest (8.34 hours). With these results the percentage of biodegradability can be calculated (equation 2). The most biodegradable substrate is the olive pomace (S1, 78.74 %), followed by waste cooking oil (S2, 58.48 %), tuna cooker oil fraction (S3, 35.24 %) and finally the less biodegradable was the FOG from municipal wastewater (S4, 11.91 %) (Figure 2). Comparing the biodegradability of olive pomace with the other food-derived substrates, its higher value may be due to the fact that it is "crude vegetable oil". However, cooking oil waste may contain recalcitrant compounds formed by the high temperatures reached during its use and similarly the tuna cooker oil fraction biodegradability is low due to the thermic process. The FOG fraction removed from municipal wastewater was collected from the supernatant of the dissolved air floatation unit, where coagulants and flocculants are used, and it has a complex composition which corresponds to its low biodegradability.

The results obtained in this study for the olive pomace are similar to those obtained for dairy wastewater from condensed milk production (79.68%) (Argiz et al., 2020) and the biodegradability of the waste cooking oil is close to that of the mixture of primary and secondary sludge from urban WWTP (63.31%) (Argiz et al., 2020). A study with different concentrations of oil and grease in fish canning wastewater shows a maximum biodegradability of 80%, lower than the maximum obtained with S1 (Cristóvão et al., 2016). A test with oily sludge showed a biodegradability of 90.7% (Cerqueira et al., 2011), higher than all the wastes evaluated in the present study. These wastes from previous studies have been already used for biopolymer production.

To conclude, biodegradability values of olive pomace and waste cooking oil are high enough to propose these wastes as substrate for biopolymer production. However, further research is needed to evaluate the possibility to decrease the biodegradation of olive pomace using an inoculum adapted to this substrate.

Acknowledgements

This research was supported by the Spanish Government (AEI) through the ECOPOLYVER project [PID2020-112550RB-C21]. Alba Pedrouso also acknowledge the Xunta de Galicia (Spain) for her postdoctoral fellowship (ED481B-2021-041). The authors belong to a Galician Competitive Research Group (GRC ED431C 2021/37), programme co-funded by FEDER (EU).

Table 1. Summary of the characteristics of the FOG wastes and activated sludge samples used in the respirometric assays.

	Substrate						Activated sludge	
	Origin	Density	COD	TS	VS	VS/TS	VSS	Y_H
Assay		(g/L)	(g/g_s)	(g/g_s)	(g/g_s)	(%)	(g/L)	(mg O_2/mg COD)
S1	Olive pomace	1200	0.33	0.313	0.298	95.27	1.98±0.25	0.49±0.097
S2	Waste cooking oil	844.3	2.42	0.937	0.917	97.85	2.67±0.14	0.47±0.020
S3	Tuna cooker oil fraction	870.8	2.47	0.847	0.835	98.61	2.60±0.13	0.47±0.020
S4	FOG of wastewater	913.8	0.10	0.081	0.060	74.47	2.66±0.07	0.47±0.020

COD: Chemical Oxygen Demand; TS: Total Solids; VS: Volatile Solids; VSS: Volatile Suspended Solids; Y_H: heterotrophic biomass yield.

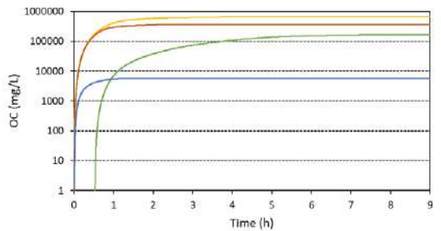

Figure 1. Evolution of the dissolved OC (mg O_2/L) concentration throughout the respirometric assays carried out with S1(•), S2 (•), S3 (•) and S4 (•), on logarithmic scale.

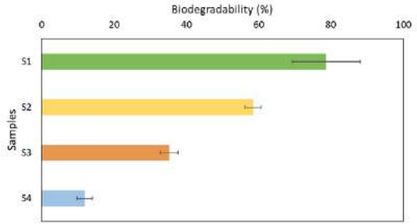

Figure 2. Biodegradability percentage with the corresponding error bar for the different wastes.

REFERENCES

Abomohra, A. E. F., Elsayed, M., Esakkimuthu, S., El-Sheekh, M., Hanelt, D. 2020 Potential of fat, oil and grease (FOG) for biodiesel production: A critical review on the recent progress and future perspectives. *Progress in Energy and Combustion Science*, **81**, 100868.

Argiz, L., Reyes, C., Belmonte, M., Franchi, O., Campo, R., Fra-Vázquez, A., Val del Río, A., Mosquera-Corral, A., Campos, J. L. 2020. Assessment of a fast method to predict the biochemical methane potential based on biodegradable COD obtained by fractionation respirometric tests. *Journal of Environmental Management*, 269, 110695.

Cerqueira, V. S., Hollenbach, E. B., Maboni, F., Vainstein, M. H., Camargo, F. A., Maria do Carmo, R. P., Bento, F. M. 2011 Biodegradation potential of oily sludge by pure and mixed bacterial cultures. *Bioresource technology*, 102(23), 11003-11010.

Cristóvão, R. O., Pinto, V. M., Martins, R. J., Loureiro, J. M., & Boaventura, R. A. 2016 Assessing the influence of oil and grease and salt content on fish canning wastewater biodegradation through respirometric tests. *Journal of Cleaner Production*, 127, 343-351.

Surcis, S. L. Respirometría BM en la depuración biológica de aguas residuales. (accessed 22 January 2023). https://www.surcis.com/es/respirometr%C3%ADa-bm-b%C3%A1sico_16576.pdf

Optimization of high rate algal ponds design and operation to enhance biomass production for biofertilizer application

E. Uggetti*, A. Ortiz*, A. Álvarez-González*, R. Díez-Montero*, N. Khalil, García, J.***

* GEMMA-Group of Environmental Engineering and Microbiology, Department of Civil and Environmental Engineering, Universitat Politècnica de Catalunya BarcelonaTech, Barcelona, Spain, enrica.uggetti@upc.edu
** Department of Civil Engineering, Z H College of Engineering & Technology, Aligarh Muslim University, Aligarh 202001 UP India

Abstract: This study aims at: 1) optimizing and validating the design and operation of High Rate Algal Ponds (HRAP) for wastewater treatment and biomass production and 2)assessing the effect of microalgal biomass as a biofertilizer. The design and operation of the HRAP (to be built in Aligarh, India) have been optimized and validated through a computational modelling and simulation technique. Wastewater treatment efficiency and biomass production were assessed by using a biokinetic model and hydrodynamic conditions evaluated by means of Computational Fluid Dynamics approach. Results indicate that the HRAPs with a total surface of 667m^2 at hydraulic retention time of 4 days enhanced wastewater treatment and biomass production. Agronomic bioassays were conducted on basil crop. The tests compared microalgae biofertilizers, inorganic fertilizers and a mixture of both. Results suggested that the combination of inorganic and microalgae fertilizers is suitable to reduce the use of inorganic fertilizers.

Keywords: Computational Fluid Dynamics, wastewater treatment, microalgae biomass, biofertilizers, India.

Introduction

PAVITR H2020 EU-India project (www.pavitr.net) aims to validate, deploy and/or develop cost-effective and sustainable solutions to tackle wastewater treatment challenges in India, ensuring also the provision of safe water reuse. Among the technologies considered, high rate algal ponds (HRAPs) are shallow raceways promoting the interaction between microalgae and bacteria to assimilate nutrients and organic matter present in wastewater. The low energy requirement compared to conventional wastewater treatment systems makes this solution particularly interesting for developing countries where climatic conditions are favourable. The advantages of such systems are especially evident in warm climate, with conditions extremely suitable for microalgae growth. Indeed, apart from the high efficiency in nutrients and organic matter removal, the great interest in such systems lies in the by-products that can be obtained from microalgae biomass grown in HRAPs (Yasir Arafat Siddiki et al., 2022).

In spite of the increasing interest on these systems, the optimum design of HRAPs is still not consolidated. Moreover, only few studies have been conducted on the properties of microalgae biomass as biofertilizer providing nutrients to the crops and encouraging circular economy with zero waste generation (Ronga et al., 2019).

Therefore, this study has two main objectives: 1) to optimize and validate the design and operation of HRAPs for wastewater treatment and biomass production and 2) to assess the effect of microalgal biomass as biofertilizer on basil crop.

Materials and Methods

To respond to the first objective, computational modelling and simulations were used to optimize and validate the design and operation of HRAPs to be built at one of

The GAIA project: Bioelectroconversion of orGAnic waste streams and CO_2 into sustaInAble fuels

Maria Vega*, Daniele Molognoni*, Paolo Dessì**, Meritxell Romans-Casas**, Lluís Bañeras***, Sebastià Puig**, Núria Zamorano-López**** and Eduard Borràs*

* Leitat Technological Center , C/ de la Innovació 2, 08225 Terrassa, Spain
(E-mail: mvega@leitat.org; dmolognoni@leitat.org; eborras@leitat.org)
** LEQUiA, Institute of the Environment, University of Girona, Carrer Maria Aurèlia Capmany 69, 17003, Girona, Spain.
(E-mail: paolo.dessi@udg.edu; meritxell.romans@udg.edu; sebastia.puig@udg.edu)
*** Grup d'Ecologia Microbiana Molecular, IEA, Universitat de Girona, Carrer Maria Aurèlia Capmany 40, 17003, Girona, Spain
(E-mail: lluis.banyeras@udg.edu)
**** FACSA, Sociedad de Fomento Agrícola Castellonense, S.A., C/Mayor 82-82, 12001 Castellón de la Plana, Spain
(E-mail: nuria.zamorano@grupogimeno.com)

Abstract
Microbial Electrochemical Technologies are promising Carbon Capture and Utilization technologies toto achieve decarbonization and revalorization of carbon dioxide. Within the frame of the GAIA project, it is intended to develop a reliable, robust, and resilient electro-driven biotechnology to produce butanol and methane from feedstocks rich in organic matter, such as wastewater, and CO_2-rich gas streams.

Keywords
Butanol production; Carbon Capture and Utilization; Electromethanogenesis; Microbial Electrochemical Technology; P2G/F; Wastewater Treatment

INTRODUCTION

The bioelectrochemical conversion of renewable feedstocks such as wastewater and CO_2 into sustainable fuels is an attractive alternative to achieve decarbonization and a circular economy. These bioconversion processes embrace a power-to-gas/fuel (P2G/F) approach. Besides, they represent a remarkable option to balance the electricity grid in the forthcoming scenario of a high renewable energy source (RES) penetration. Implementation of RES is indeed required to achieve the European Green Deal objective of lowering carbon emissions from electricity supply to nearly zero by 2050. This RES deployment will require high energy storage capacity, covered by batteries and flywheels for short-term storage and P2G/F technologies for medium-long term storage. The development of innovative production routes for renewable fuels, based on energy-efficient technologies, is required.

In this context, the GAIA project aims to develop novel, energy-efficient solutions for obtaining both liquid (butanol) and gaseous (methane) biofuels using bioelectroconversion technologies. The project concept is based on the principles of Circular Economy as depicted in Figure 1. It proposes the use of electricity as the driving force (used as a source of reduction equivalents) to convert wastewater and CO_2 into green fuels promoting toto close the circle[1]. This will also ease energy transport and storage while having a positive impact on water treatment and reuse.

Within this framework, novel energy-efficient solutions based on Microbial Electrochemical Technologies (METs) are used. METs benefit from (electro)-autotrophic microorganisms that use CO_2 as the sole carbon source for the production of organic compounds, such as butanol (microbial electrosynthesis) or methane (electromethanogenesis). METs' main advantages compared to conventional CCU and P2G/F technologies rely on their innovative biocatalytic process: (i) high process efficiency under mild operation conditions; (ii) adaptability to a variety of CO_2-rich gas streams from different decentralized sources (iii) resilience to the presence of impurities; (iv) high flexibility in terms of plant size and operation power fluctuation; (v) seasonal energy storage of electricity surpluses as fuels; and (vi) positive social recognition and environmental impact due to the promotion of a circular economy. Besides, economic, social and environmental aspects are important to ensure an effective future implementation. However, principal technological challenges to tackle prior to the release of METs to the market are: (i) not competitive capital and operational costs, (ii) lack of successful upscaling attempts and (iii) low production yields even when pure substrates are used.

Figure 1. GAIA project concept.

GAIA consortium is constituted of three partners (Leitat, University of Girona and FACSA). The key contribution of Leitat is based on management and coordination activities, development of 3D metal electrodes, design of electromethanogenesis reactors with improved hydrodynamics and promoting start-up, optimization, and deep characterization of MET reactors for the conversion of CO_2 to CH_4. UdG's contributions to the project are focused on the design, development and construction of microbial electrosynthesis reactors, the start-up process and further optimization for butanol production, and the study of electrode-microorganisms interaction. Lastly, the role of FACSA in the project is to provide its expertise in the management of biogas production facilities in Wastewater Treatment Plants (WWTP). This allows us defining the best scalability and replicability in different facilities and identifies possible synergies to integrate MET into WWTPs streams and processes.

All in all, MET, the central CCU technology in GAIA, is a technology of major interest because it successfully links biofuels production, RES (and its surpluses), wastewater treatment and CO_2 emissions abatement.

ACKNOWLEDGEMENTS

The GAIA project has been funded under the framework of the call " Proyectos de I+D+i en Líneas Estratégicas 2021" financed by the Ministerio de Ciencia e Innovación (MICINN), Agencia Estatal de Innovación (AEI) (file number: PLEC2021 -007802), and by the European funds Next Generation EU/PRTR. MR-C is grateful for the support of the Spanish Government (FPU20/01362). PD is supported by the European Union's Horizon 2020 research and innovation programme under the Marie Sklodowska-Curie grant agreement, project ATMESPHERE, No 101029266. S.P. is a Serra Hunter Fellow (UdG-AG-575) and acknowledges the funding from the ICREA Academia award. LEQUIA and EcoAqua have been recognized as "consolidated research groups" (Ref 2021 SGR01352 and 2021 SGR01142) by the Catalan Agency of Research and Universities.

REFERENCES

1 R. Blasco-Gómez, S. Ramió-Pujol, L. Bañeras, J. Colprim, M. D. Balaguer and S. Puig. 2019. Unravelling the factors that influence the bio-electrorecycling of carbon dioxide towards biofuels. *Green Chemistry* 21, 684.

Determination of microplastics in three wastewater treatment plants in north-western Spain

C. Vijande*, M. Lazzari**, JM. Lema*, S. Balboa***,
* CRETUS, Department of Chemical Engineering, Universidade de Santiago de Compostela, 15782 Santiago de Compostela, Spain;
**CIQUS, Department of Physical Chemistry.Universidade de Santiago de Compostela, 15782
*** CRETUS, Department of Microbiology and Parasitology, Universidade de Santiago de Compostela, 15782 Santiago de Compostela, Spain

Abstract
The presence of microplastics in the environment has become a worrisome issue in recent years. In this context, wastewater treatment plants could be considered microplastics hotspots, since they are not designed for their removal. However, the literature regarding their determination in the different points of these facilities is not consistent, primarily due to the lack of a standard methodology for sampling and identification. The aim of this work was to assess the occurrence of microplastics in different wastewater treatments in Galicia, Spain. For this, the optimization of a sampling and cleaning protocol was optimized, and three samplings were carried out in different wastewater treatment plants. The results show the presence of microplastics in water and sludge lines, being polystyrene, polypropylene and polyethylene the most abundant polymers.

Keywords
Microplastics, Sewage sludge, Wastewater

INTRODUCTION

In recent years, microplastics (MPs) released to different aquatic systems has aroused great interest. MPs are plastic particles with size ranging between 1 µm and 5 mm, that can be potentially harmful once released into the environment. MPs can be classified into primary MPs (those that enter the environment in small sizes, like microbeads in cosmetics) and secondary MPs (those that are produced by the degradation of larger fragments) (El Hayani et al., 2022).

Nowadays, many studies have focused on MPs in different environments. In addition, Wastewater Treatment Plants (WWTPs) have been identified as an important source of MPs since the occurrence of them in the effluent and sludge has been clearly demonstrated. However, a standard protocol for cleaning and identifying MPs has not been developed yet, and the methodology followed varies within authors (Löder et al., 2017).

Because of this, the main objectives of this work were 1) to develop an efficient protocol for determine the presence of MPs in wastewater and sludge 2) to assess the occurrence of MPs in various WWTPs.

MATERIALS AND METHODS

Optimization of sampling and cleaning protocol

An essay was performed to assess the efficiency and recovery rates of the sampling method. Particles of different size (50-100 µm; 100-500 µm; 500 µm -1 mm) of high-density polyethylene, polypropylene and polystyrene were added to distilled water and filtered using sieves of different mesh size (1 mm, 500 µm, 100 µm and 50 µm). The weight loss for each fraction of plastics was registered after filtering.

The first step of sampling treatment is the removal or organic matter and other materials that could interfere with the identification methods. Some of the most common protocols were tested: use of hydrogen peroxide, Fenton reagent (El Hayani, 2022) and enzymatic solutions (Löder et al., 2017).

Sampling campaign

Three samplings were carried out in three WWTPs in Galicia, Spain. The WWTPs were chosen considering each of them as an example of different size facilities, as well as for being representative of different treatment systems.

Samples from different points of water and sludge lines were taken and filtered using sieves as previously explained. For cleaning the samples, the optimized protocol developed was applied. Fourier-transform infrared and Raman spectroscopy were applied for polymer identification.

RESULTS AND DISCUSSION

Optimization of sampling and cleaning protocol

The recovery rate for the sampling method was 54,9 ± 3,9 %. It is important to note that the recovery efficiency was nearly 100 % for the fraction between 500 µm and 1 mm, and diminished with particle size. These results evidence the need of large volumes of sample, especially for water line samples. Liu et al., 2021 indicated that a limited sample volume in those cases could lead to experimental errors.

Regarding the cleaning protocol, the Fenton reagent was discarded since it resulted in a degradation of some polymers. Complete enzymatic protocol was discarded due to the high cost and time required even though it demonstrated to be effective. Therefore, the samples were treated in several steps with an SDS 10 % solution (24 h, 50 °C) and a hydrogen peroxide 30 % solution (24 h, 65 °C) to remove organic matter, and the enzyme cellulase (several incubations, 24 h, 40 °C), to remove cellulose from toilet paper.

Occurrence of MPs in WWTPs

Different polymers were identified in water and sludge line. The most abundant polymers determined were polypropylene, polyethylene and polystyrene. MPs ranging from 500 µm to 1 mm were easier to determine and were more abundant, which can be explained by the sampling methodology used.

The methodology applied was more effective for sludge samples, with 1.2 * 10^3 MPs/kg_{dw} for mixed sludge in the larger WWTP. This is consistent with literature since sedimentation processes are reported as the main cause of removal of MPs from the water line. The presence of large number of plastics in sludge can be potentially harmful, due to its use as fertilizer (El Hayany et al., 2022). The bibliography regarding water line is less consistent, but MPs presence in effluents implies a risk for the environment and reuse methodologies (Liu et al., 2021).

REFERENCES

Liu, W., Zhang, J., Liu, H., et al. 2021 A review of the removal of microplastics in global wastewater treatment plants: Characteristics and mechanisms. *Environmental International* 146, 106277

Löder, GJ., Imhof, HK., Ladehoff, M., et al. 2017. Enzymatic purification of microplastics in Environmental Samples. *Environmental Science and Technology 51*, 14283-14292

El Hayany, B., Rumpel, C., Hafidi, M., El Fels, L. 2022 Occurrence, analysis of microplastics in sewage sludge and their fate during composting: A literature review. *Journal of Environmental Management* 317, 115364

Synergistic cytotoxicity of specific combination of water disinfection by-products assessed by bacterial reverse mutation tests

J. M. Alcaide-Hidalgo*, L. Vinardell**, G. Chomiciute*, R. Pérez-Magrané**,***, I. Jubany** and X. Escoté*

* Eurecat, Centre Tecnològic de Catalunya, Unitat de Nutrició i Salut, Reus, Spain.
(E-mail: juanmaria.alcaide@eurecat.org; gertruda.chomiciute@eurecat.org; xavier.escote@eurecat.org)
** Eurecat, Centre Tecnològic de Catalunya, Unitat de Sostenibilitat, Manresa, Spain.
(E-mail: laura.vinardell@eurecat.org; irene.jubany@eurecat.org)
*** 2acs2ac, Universitat Politècnica de Catalunya, Terrassa, Spain
(E-mail: ramon.perez@upc.edu)

Abstract

Regenerated water will be highly used in water scarcity regions such as Catalonia (Spain). Currently, disinfectants aimed at the selective inactivation of pathogenic or undesirable organisms generate disinfection by-products (DBPs) when they react with organic matter. Unfortunately, little information is known about toxic and mutagenic DBPs synergies. This study aimed to compare the toxicity and mutagenesis of a DBP mixture, to the individual species values. The potential mutagenicity was assessed following the Organisation for Economic Co-operation and Development (OECD) guideline 471. Results obtained showed the toxic and mutagenic synergism between trihalomethanes and haloacetic acids present in drinking water when they are at very high concentration levels.

Materials and Methods

Chlorine-disinfected water was obtained from a drinking water distribution system in Catalonia (Spain) in March 2021. DBPs were analyzed by LC-MS/MS for HAA and GC/MS for THMs. Results (Table 1) were used to define the DBPs mix to test for synergism regarding toxicity and mutagenesis.

This study was undertaken following OCDE Guideline 4712, using S. typhimurium TA98, TA100, TA102, TA1535 and TA1537 strains in the presence and absence of metabolic activation (Fig. 1). The principle of this bacterial reverse mutation test is based on the detection of those mutations which revert mutations present in the test strains and restore the functional capacity of the bacteria to synthesize an essential amino acid 3–5. Each condition had a positive control, a negative control and six different concentrations of the sample. All of them were evaluated in triplicate. The toxicity of the sample was assessed from the reversion results.

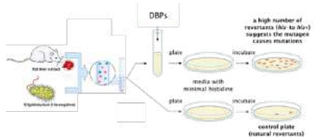

Figure 1. *Bacterial reverse mutation test (AMES) under OECD guidelines.*

Table 1. *Concentrations of the different dilutions tested for each DBP in the toxicity and mutagenicity tests, EC20 values 6, DBPs legal threshold 7 and site DBPs concentration.*

µg/mL	P1	P2	P3	P4	P5	P6	Sample	EC20 (95% CI)	Legal threshold
TCM	9.125	2.884	0.913	0.288	0.091	0.029	0.073	83.566	
BDCM	2.000	0.632	0.200	0.063	0.020	0.006	0.016	27.846	THM4 < 100 ppb
DBCM	0.375	0.119	0.038	0.012	0.004	0.001	0.003	22.911	
MCAA	0.625	0.198	0.063	0.020	0.006	0.002	0.005	-	
DCAA	2.500	0.790	0.250	0.079	0.025	0.008	0.019	2849.574	HAA5 < 100 ppb
TCAA	3.750	1.185	0.375	0.119	0.038	0.012	0.030	>6992.6	

Results and Discussion

The results are shown in Figure 2. The highest concentration (P1) showed signs of toxicity in most strains with and without metabolic activation since the number of reverted colony-formed units (CFUs) was significantly lower than in the case of the negative control or had a value of zero. Concerning the mutagenicity effects, the only concentration that showed significant differences with the negative control, despite not exceeding the threshold of twice the CFUs with respect to this control, was the P2 concentration for the TA100 strain in the absence of metabolic activation 4,8. Therefore, this concentration should be considered mutagenic for the conditions assessed in the bacterial reverse mutation test.

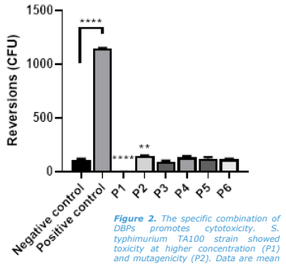

Figure 2. *The specific combination of DBPs promotes cytotoxicity. S. typhimurium TA100 strain showed toxicity at higher concentration (P1) and mutagenicity (P2). Data are mean ± SEM. ** p < 0.01, **** p < 0.0001 vs. negative control. CFU; colony forming unit.*

Conclusions

The potential mutagenicity of the DBP1 test item has been evaluated. The results obtained indicate that the concentration of 5.0 µL/plate is toxic to bacteria. In addition, the concentration of 1.6 µL/plate is the only presenting potential mutagenicity in one condition (TA100 without metabolic activation) which could be considered mutagenic in this test. Therefore, due to this result, the sponsor is recommended to confirm this result in an additional experiment. M2 DBPs' individual concentrations are not supposed to be mutagenic accordingly to their respective EC20 threshold, indicating a possible synergic effect between the mixture DBPs.

This work was financially supported by:

The Catalan Government through the funding grant ACCIÓ-Eurecat (Project SQUARE 2020-2022).

And by the European Union under grant agreement No 101081980

www.safecrew.org/

Enantioselective uptake, distribution, and biotransformation of chiral pharmaceuticals venlafaxine and O-desmethylvenlafaxine in hydroponic lettuces

Z. Wang[1,3], L.L Alonso[1,2], J. Vosse[1,2], D. Barceló[1,2,4], G. Buttiglieri[1,2], S. Rodriguez-Mozaz[1,2]

[1] ICRA-Catalan Institute for Water Research, Girona, Catalonia, 17003, Spain
[2] University of Girona (UdG), Girona, Spain
[3] Department of Pesticide Science, College of Plant Protection, Nanjing Agricultural University, Nanjing 210095, China
[4] Institute of Environmental Assessment and Water Research (IDAEA-CSIC), Barcelona, 08034, Spain

(E-mail: *2020202059@stu.njau.edu.cn*, *lalonso@icra.cat*, *jvosse@icra.cat*, *dbarcelo@icra.cat*, *gbuttiglieri@icra.cat*, *srodriguez@icra.cat*)

Abstract
Wastewater reuse for vegetable crops irrigation is regularly applied all over the world, which might introduce numerous pharmaceutical and personal care products into agro-food systems. Among marketed pharmaceuticals, over 50% are chiral. Despite their identical physicochemical properties, pharmaceutical stereoisomers may have distinct environmental toxicity and fate. In this study, an enantioselective method is being established for the analyses of the chiral venlafaxine and its main metabolite O-desmethylvenlafaxine and applied to study their enantioselectivity in lettuce under laboratory hydroponic conditions; i.e., enantioselective uptake, distribution, and transformation. Comprehensive data about the environmental fate of relevant pharmaceutical compounds such as venlafaxine and O-desmethylvenlafaxine in agro-food systems are needed to assess the feasibility of water reuse for irrigation purposes.

Keywords
Chiral pharmaceutical; enantioselectivity; distribution; bioaccumulation; biotransformation; reclaimed water.

INTRODUCTION

Due to climate change, urbanization, regional drought, and pollution, the issue of water shortage is becoming serious in many countries. Thus, agriculture is increasingly relying on treated wastewater as a vital irrigation source. In order to assess environmental and human impact of such practices, the plant uptake of chemical pollutants present in wastewater such as pharmaceuticals (e.g., antibiotics, non-steroidal anti-inflammatories, sulfonamides, and β-blockers) needs to be evaluated. However, there are no studies focusing on the enantioselective profiling of chiral pharmaceuticals in the agro-food system during irrigation. The different bioactivity, metabolism, and bioaccumulation between stereoisomers may pose distinct environmental risks. Thus, in this study, we focus on the enantiomeric fraction change of venlafaxine (VFX) and O-desmethylvenlafaxine (ODVFX) in lettuces through a laboratory hydroponic system. The aim of this study is to provide a chiral view on contaminants' fate in agri-food system to evaluate the opportunities and potential risks of the use of reclaimed water for irrigation of plants and crops.

MATERIALS AND METHODS

Laboratory hydroponic study

Lettuce seedlings of uniform size were selected, rinsed with Milli-Q water, and transferred to the hydroponic channels filled with half-strength nutrient solutions (Hoagland). The hydroponic channels were placed in a controlled environment, with a daily photoperiod of 14 h at an average light intensity of 2,700 Lux, temperature of 20−22 °C, and humidity of 50%. As shown in Figure 1, two exposure groups were spiked at a nominal individual concentration of 100 μg/L Rac-VNF and Rac-ODVFX. Control experiments without seedlings, and non-spiked seedling control were also set up. The spiked exposure solution was renewed twice per week, to keep the exposure concentration constant. The lettuces and solutions were sampled at time points, 0, 7, 14, 21, 28 d. The lettuce samples were washed with Milli-Q water and divided into two functional groups, including roots and edible parts (stems and leaves). Each part of the tissue was freeze-dried for 48 h in a lyophilizer, weighed, homogenized by grinding into fine powder, and stored at −20 °C.

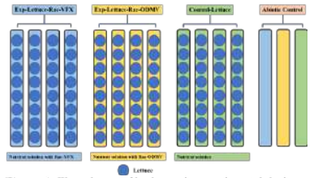

Figure 1. The scheme of hydroponic experimental designs.

Analytical methods

The lettuce roots, edible parts and water samples were collected in the laboratory experiments and analysed by liquid chromatography coupled with a hybrid mass spectrometry detector (UPLC-QqLIT) based on a method from Gros et al. (2012) and Santos et al. (2019). A Chirobiotic V column (250 × 2.1 mm, 5 μm) was applied for chromatographic separation (Liu et al., 2007). 50 mg of freeze-dried lettuce tissues were extracted with 1 mL of citric buffer pH 4: ACN (1:1, v/v) using a mini bead beater. Then samples were centrifuged (8,000 g, 15 min, 4 °C). This extraction procedure was repeated three times. All the supernatants were combined, evaporated until dryness, and reconstituted in 50mL ultrapure water with 0.1% formic acid. A solid phase extraction (SPE) using Oasis HLB (3cc, 60 mg) (Waters) was performed for sample clean-up.

RESULTS AND DISCUSSION

A chiral analytical method for VFX and ODVFX is being established, with acceptable LODs and recoveries in all the matrices. Further, the enantiospecific uptake and distribution in lettuce were found and the difference in bioaccumulation between VFX and ODVFX were obtained. Risk to human health (through dietary exposure) was not evaluated since the spiking concentrations were higher than usual environmental values. A field study is foreseen, where the enantiomeric fraction of VFX and ODVFX will be studied in lettuce grown in agricultural plots irrigated with reclaimed wastewater. More realistic data will thus be obtained, which will be used to evaluate human health risks.

Acknowledgements: Authors acknowledge funding from the Spanish State Research Agency of the Spanish Ministry of Science and Innovation for ReUseMP3 project (PID2020-115456RB-I00 /MCIN/AEI / 10.13039/501100011033) and the China Scholarship Council oversea PhD study program (No. 202206850021).

REFERENCES

Gros M, Rodríguez-Mozaz S, Barceló D. 2012 Fast and comprehensive multi-residue analysis of a broad range of human and veterinary pharmaceuticals and some of their metabolites in surface and treated waters by ultra-high-performance liquid chromatography coupled to quadrupole-linear ion trap tandem mass spectrometry. *Journal of Chromatography A* **1248**, 104-121.

Liu W, Wang F, Li H. 2007 Simultaneous stereoselective analysis of venlafaxine and O-desmethylvenlafaxine enantiomers in human plasma by HPLC-ESI/MS using a vancomycin chiral column. *Journal of Chromatography B* **850**(1-2), 183-189.

Santos L H, Freixa A, Insa S, et al. 2019 Impact of fullerenes in the bioaccumulation and biotransformation of venlafaxine, diuron and triclosan in river biofilms. Environmental Research 169, 377-386.

Contactless membrane distillation for effective ammonia recovery from waste sludge

Lei Wen and Xiao-yan Li*

Department of Civil Engineering, The University of Hong Kong, Pokfulam, Hong Kong, China
(E-mail: *wenlei17@connect.hku.hk)*

Abstract
Serious membrane fouling caused by direct contact between the hydrophobic membrane and feed hinders the ammonia (NH_3) recovery from waste fermented sludge via MD. In this study, a contactless MD system was developed by introducing an air gap and subtly solved the problem. Results showed the overall NH_3 transfer coefficient by contactless MD was $(1.49 \pm 0.05) \times 10^{-5}$ m/s, 7 times greater than that of conventional MD ($(0.20 \pm 0.01) \times 10^{-5}$ m/s). In continuous operation with a short retention time of 20 min, a high NH_3 recovery (greater than 80 %) and a clean membrane without foulant attachment were maintained, while the conventional MD system had failed in 12 h due to formation of a thick fouling layer on the membrane surface. This contactless MD can be an innovative technology to treat multiple NH_3-rich waste liquids.

Keywords
Ammonia recovery; mass transfer coefficient; membrane distillation; membrane fouling; sludge

NTRODUCTION

Through fermentation, sewage sludge can release more than 1,000 mg/L of NH_3-N and should be recovered. By means of MD, ammonia is vaporized as NH_3 and passes through the hydrophobic membrane, which rejects water, solutes, and solids in the sludge liquor. The penetrating NH_3 is then absorbed by acid on the other side of the membrane. However, the membrane often suffers from pollution by organic, salt, and solid impurities owing to its direct contact with the sludge. Since gaseous NH_3 is the transport species, ammonia removal and recovery do not require direct contact between the membrane and the NH_3-containing feed solution. Therefore, an air phase may be kept between the feed and membrane to avoid their direct contact. In this study, a contactless MD system with feed-air-membrane-acid compartments was introduced to realize efficient and fouling-free NH_3 recovery from sludge liquor.

MATERIALS AND METHODS

Two different MD modules and open evaporation were tested (Figure 1). In the conventional MD configuration, the MD feed chamber had a depth of 2.2 mm and was fully filled with the feed solution (fermented sludge liquor). The feed solution was in complete contact with the PTFE membrane. Serving as the absorbent of NH_3, 0.5 M H_2SO_4 was circulated at the top; In the contactless MD system introduced in this study, the same MD module was used, except the feed chamber had a depth of 15.0 mm. The air gap avoided the contact between feed solution and membrane; Open evaporation makes the upper free space a large dilution pool, which represents the minimal resistance to NH_3 transport.

The flux of NH_3 transport (J) through the interface of the two phases follows Fick's law of diffusion, i.e., $J = -D\frac{dC}{\delta n}$, where D is the diffusion coefficient of NH_3 molecules and $\frac{dC}{\delta h}$ is the concentration gradient at the interface. For an actual two-phase system such as the feed liquid phase (L) and phase A (referring to air, acid, or absorbent), the flux may be approximated to $J = -K(C_L - C_A)$, where K is the mass transfer coefficient.

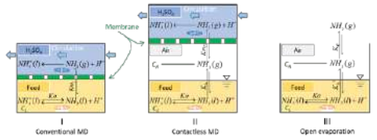

Figure 1. Schematics of ammonia transport in different MD modules and open evaporation.

RESULTS AND DISCUSSION

NH_3 recovery from sludge liquor via different MD modules

NH_3 removal from the fermented sludge liquor by contactless MD reached 95 % after 12 min, close to the open evaporation result, whereas the removal by conventional MD was only 50 % for a fresh membrane (Figure 2A). The calculated overall NH_3 transfer coefficient was $K_I = (0.20 \pm 0.01) \times 10^{-5}$ m/s for conventional MD and $K_{II} = (1.49 \pm 0.05) \times 10^{-5}$ m/s for contactless MD, which was significantly enhanced by more than 7 times. Contactless MD maintained a stable NH_3 recovery of 80 ± 2 % during the 12 h continuous test with a sludge retention time of 20 min, while conventional MD has totally failed after 12 h (Figure 2B).

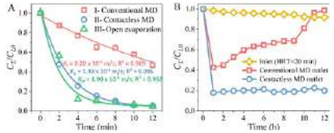

Figure 2. Ammonia removal via different MD modules in the batch (A) and continuous (B) tests.

Membrane fouling in different MD modules

In the contactless MD module, the membranes were kept fresh and maintained their original appearance throughout the 12-h test (Figure 3). Membrane fouling was observed in the conventional MD module. Impurities or foulants continued to adhere to the membrane surface on the feed side during the MD process. The thick fouling layer on the membrane surface significantly increased the resistance to NH_3 transport for the conventional MD.

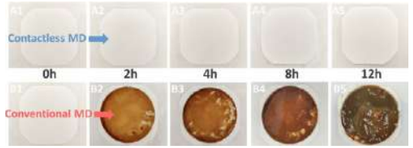

Figure 3. Photographs of the membranes from the contactless MD (A) and conventional MD (B).

Gravity-driven Membrane Filtration Primary Wastewater Effluent for Irrigating Soil-plants and Hydroponic-plants

Sif Guðjónsdóttir, Megan Wiegmann, Selina Hube, Bing Wu

Faculty of Civil and Environmental Engineering, University of Iceland, Hjardarhagi 2-6, IS-107, Reykjavik, Iceland; (E-mail: sig108@hi.is; mew@hi.is; seh34@hi.is; wubing@hi.is)

Abstract
In this study, gravity-driven membrane (GDM) systems packed with Icelandic lava stones were employed to treat primary wastewater for water reclamation and nutrient recovery. The results revealed that (1) Compared with non-cleaning condition, periodic physical or chemical-enhanced physical cleaning improved water productivity without compromising water quality. (2) In soil-based systems (tomato and basil), plant growth profiles or non-essential heavy metal contents in soils were comparable (p>0.05) when tap water, commercial fertilizer, and permeate water were used as irrigation water. (3) In hydroponic-based systems (lettuce and basil), insignificant difference of lettuce growth using permeate water and fertilizer solution was noticed (p>0.05), while basil plants could grow better in fertilizer solution. More heavy metals were accumulated in lettuce plants than those in basil plants. However, the hazard quotient indexes of heavy metals in the plants were less than 1, indicating negligible human health risk.

Keywords (maximum 6 in alphabetical order)
Gravity-driven membrane filtration; Nutrient recovery; Periodic membrane cleaning; Permeate quality; Water reclamation

INTRODUCTION

Globally, the recovery of nutrients and water from wastewater is crucially important for achieving circular economy and coping with the challenges of water scarcity and fertilizer shortage. However, the potential presences of pathogens and chemical contaminants in the reclaimed wastewater raise major concerns for its reuse (Hube and Wu, 2021). The recently reported gravity-driven membrane (GDM) filtration process utilizes hydrostatic force and naturally developed biofilm, combined with microfiltration (MF)/ultrafiltration (UF) membrane separation to obtain superior permeate water (Pronk et al., 2019), offering an alternative solution for municipal wastewater reclamation. However, the feasibility of using GDM permeate water as irrigation water to culture plants in soil-based and hydroponic-based systems has not been well investigated.

In this study, we aim to (1) illustrate the effects of biocarrier packing ratio and cleaning protocols on GDM performance, especially water quality; and (2) examine the applicability and feasibility of low-cost, easy-maintenance GDM systems in reclaiming primary wastewater for cultivating vegetables in both soil-based and hydroponic-based systems.

MATERIALS AND METHODS

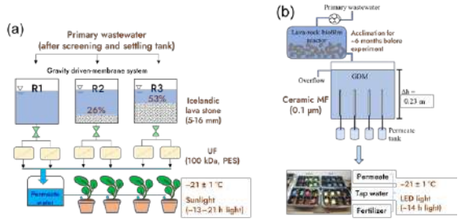

Figure 1. Schematic diagram of the GDM systems and (a) soil-based cultivation system and (b) hydroponic-based cultivation system.

RESULTS AND DISCUSSION

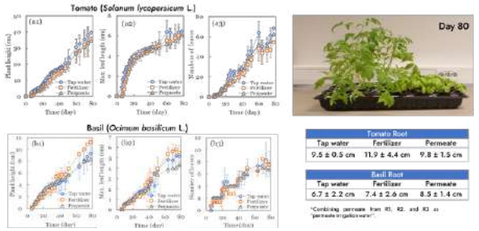

Tomato Root		
Tap water	Fertilizer	Permeate
9.5 ± 0.9 cm	11.9 ± 4.4 cm	9.8 ± 1.5 cm

Basil Root		
Tap water	Fertilizer	Permeate
6.7 ± 2.2 cm	7.4 ± 2.6 cm	8.5 ± 1.4 cm

Figure 2. The growth profiles of the plants in the soil-based systems.

REFERENCES

Pronk, W., Ding, A., Morgenroth, E., Derlon, N., Desmond, P., Burkhardt, M., Wu, B., Fane, A.G. 2019 Gravity-driven membrane filtration for water and wastewater treatment: A review. *Water Research* **149**, 553-565.

Hube S, Wu B. 2021 Mitigation of emerging pollutants and pathogens in decentralized wastewater treatment processes: A review. *Science of the Total Environment* **779**, 146545.

Regeneration of high-quality water for reuse by forward osmosis-reverse osmosis system treating urban wastewater

X. Yang*, I. Fernández* and C. Martínez García*

* CETIM Technological Centre, 15180, Culleredo, A Coruña, Spain
(E-mail: *xyang@cetim.es)*

Abstract
3.5 million people worldwide will face water scarcity by 2025 due to climate change. Wastewater reuse is one of the most important alternatives to traditional water sources to solve the problem of water shortage. Conventional municipal wastewater treatment plants (WWTPs) are ineffective at removing most of the emerging contaminants and pathogens. These pollutants can cause some concerns for the environment and human health, especially if WWTPs effluents are intended to be reused for agricultural irrigation. Osmosis membrane-based technologies are at the forefront of tackling this problem. Treatment of urban wastewater through osmosis membranes can produce high-quality treated water for reuse, because most of the bacteria, viruses, salt, emerging pollutants and refractory organic matter will be intercepted in the filtration unit. Hence, this study aims to investigate the feasibility of reusing the treated water for agricultural irrigation by a Forward Osmosis (FO)-Reverse Osmosis (RO) system according to the upcoming Regulation (EU) 2020/741 on the minimum requirements for the reuse of treated water. The results showed that the FO-RO system had a 100% removal efficiency for pathogens, a high removal rate for COD and TSS, and a removal rate higher than 90% for 92% of related emerging pollutants. Subsequently, values of the treated water regarding to *E. coli*, BOD_5, TSS and turbidity were verified as meeting the criteria for reuse at least in Class B agricultural irrigation according to Regulation (EU) 2020/741.

Keywords (maximum 6 in alphabetical order)
Biomimetic membranes; Forward osmosis; Reverse osmosis; Sustainability; Urban wastewater; Water reuse

INTRODUCTION

The scarcity of water resources is influenced by factors such as population growth, urbanization, per capita consumption, water pollution and climate change (Ungureanu et al., 2020). According to the estimates of the World Resources Institute in water sector, with 2025 as the reference year, about 3.5 million people in the world may face water shortages (World Resources Institute. Water, 2020). In order to overcome this problem, wastewater reuse is one of the most important alternatives. Reuse of treated wastewater for agricultural irrigation is by far the most defined end use of reclaimed water (Rizzo et al., 2020). Growing concerns about wastewater reuse for agricultural irrigation mainly include microbial risks and emerging contaminants such as pesticides, pharmaceuticals, illicit drugs, synthetic and natural hormones, etc. The recent EU Regulation 2020/741 is expected to be effective from June of 2023 on the minimum requirements for the reuse of treated water for agricultural irrigation (EU Regulation 2020/741, 2020).

To meet the criteria for water reuse, osmosis membrane-based technologies are at the forefront of tackling this problem. In recent decades, forward osmosis (FO) has gained attention as a novel membrane process for urban wastewater treatment. Unlike pressure-driven membrane processes, forward osmosis is driven by an osmotic pressure gradient between feed solution (wastewater) and draw solution (DS), which has the advantages of high product water quality, low energy consumption, and low tendency to membrane fouling (Liu et al., 2015). However, FO requires a DS recovery procedure to maintain the osmotic pressure gradient. A followed reverse osmosis (RO) process can re-concentrate the diluted DS while providing a second barrier to ensure the treated water with high quality for agricultural reuse.

Considering the above background, the objective of the present study is to validate the behavior of FO process with biomimetic membranes followed by RO process for DS recovery in treating urban wastewater and to evaluate the feasibility of reusing the treated water in agricultural irrigation.

MATERIALS AND METHODS

The FO-RO pilot system (treatment capacity up to 12 m^3/d) consists of a FO unit as the first barrier for wastewater purification, and a RO unit for the DS re-concentration as well as the second barrier to obtain the high-quality water for reuse. The pilot diagram of the system is shown in Figure 1.

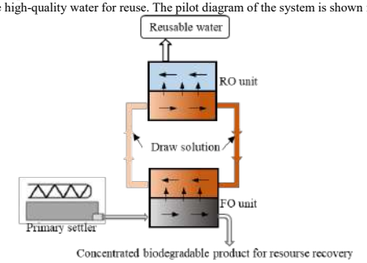

Figure 1. Pilot diagram of the FO-RO system

In this study, the biomimetic hollow fibre membranes (Aquaporin) were selected for the FO unit because of their higher performance. 3.5% NaCl was selected as the DS after testing the permeate flowrate. Toray TM810V RO membranes were considered for the RO unit due to their high salt rejection, which can minimize the DS salinity loss in the permeate (i.e., producing a permeate of higher quality). Water characteristics of influent and effluent were measured periodically following the Standard Methods for the Examination of Water and Wastewater (E.W. Rice et al., 2017).

RESULTS AND DISCUSSION

After 10 months operation of the FO-RO pilot plant at an urban WWTP, the validation of the treating performance is concluded in the following content. The average chemical oxygen demand (COD) and total suspended solids (TSS) removal rate of the system were 88.2% and 97%, respectively. In addition, the system obtained 100% removal of pathogens (*E. coli*, total coliforms and nematodes), and 92% of the relevant emerging pollutants were removed with removal rate higher than 90%.

In order to evaluate the reuse feasibility of the treated water, the upper part of Table 1 shows the value limits established by the upcoming Regulation (EU) 2020/741 on the minimum requirements for the reuse of treated water for agricultural irrigation. In the meanwhile, the last row of Table 1 shows the corresponding values of each parameter of the treated water to determine if they meet the reuse standards.

Table 1 Requirements for water reuse for agricultural irrigation of Regulation (EU) 2020/741and corresponding average values for the treated water

Reclaimed water quality class	***Escherichia Coli***	**BOD_5**	**TSS**	**Turbidity**
A: Raw consumption, contact with water	≤ 10 UFC / 100 ml	≤ 10 mg/l	≤ 10 mg/l	≤ 5 NTU
B: Raw consumption, without contact with reclaimed water	≤ 100 UFC / 100 ml	In accordance with Directive 91/271/EEC	In accordance with Directive 91/271/EEC	-
C: Raw consumption, without contact with reclaimed water. drip irrigation	≤ 1000 UFC / 100 ml			-
D: Destination industry, seed production, energy	≤ 10000 UFC / 100 ml			-
FO-RO treated water	0.04 UFC/100 ml	8 mg/l	3 mg/l	6 NTU

After comparing the standard and values of the treated water regarding to *E. coli*, BOD_5, TSS and turbidity, FO-RO treated water can be reused for Class A agricultural irrigation, except that turbidity was not complaint with the limit. Therefore, in general, the FO-RO system obtained reusable water for Class B agricultural irrigation, with high potential to meet Class A requirements.

REFERENCES

E.W. Rice, R.B. Baird, and A.D. Eaton (2017) Standard Methods for the Examination of Water and Wastewater, 23rd edition, American Public Health Association, American Water Works Association, Water Environment Federation.

Liu, P., Zhang, H., Feng, Y., Shen, C., and Yang, F. (2015) Integrating electrochemical oxidation into forward osmosis process for removal of trace antibiotics in wastewater. *Journal of Hazardous Materials*, **296**, 248–255.

Regulation (EU) 2020/741 (2020) Regulation (EU) 2020/741 of the European Parliament and of the Council of 25 May 2020 on minimum requirements for water reuse (Text with EEA relevance), [online] https://eur-lex.europa.eu/legal-content/EN/TXT/?uri=CELEX:32020R0741 (Accessed January 17, 2023).

Rizzo, L., Gernjak, W., Krzeminski, P., Malato, S., McArdell, C. S., Perez, J. A. S., Schaar, H., and Fatta-Kassinos, D. (2020) Best available technologies and treatment trains to address current challenges in urban wastewater reuse for irrigation of crops in EU countries. *Science of The Total Environment*, **710**, 136312.

Ungureanu, N., Vlăduț, V., and Voicu, G. (2020) Water Scarcity and Wastewater Reuse in Crop Irrigation. *Sustainability*, **12**(21), 9055.

World Resources Institute. Water. (2020) Mapping, Measuring, and Mitigating Global Water Challenge. [online] https://www.wri.org/our-work/topics/water (Accessed January 30, 2023).

ACKNOWLEDGEMENTS

LIFE GREEN SEWER is a European Project co-funded by the European Union under the LIFE Programme. Grant Agreement No. LIFE17 ENV/ES/000341.

Exploring the potential of olive by-products: antioxidants, sugars, contaminants and energy

V.M Ramos*, M. Ortega*, J.M Espinosa*, F.G Fermoso*, G. Rodríguez-Gutiérrez*, **S. Zahedi***,**
* Instituto de La Grasa, Spanish National Research Council (CSIC), Campus Universitario Pablo de Olavide–Ed. 46, Ctra. de Utrera, Km. 1, Seville, 41013, Spain.
(**corresponding: *szahedi@ig.csic.es*)

Abstract

The olive sector is one of the main sectors of the agri-food system in the Mediterranean basin and other producer countries, due to its economic, social, environmental and public health importance. Olive leaves are one of by-products of the olive oil and olive table products and they are produced in large quantities, although it is underutilised. These by-products can be used for animal feed, but generally without application of industrial interest, but currently olive industry waste is generating a great deal of interest within the framework of biorefineries. From olive by-products high number of added-value compounds can be obtained for energy, pharmaceutical, food and cosmetics use. The present study was undertaken to investigate the effect of different pre-treatment procedures to recover sugars, metals and natural antioxidants from Andalusian olive tree leaves. After the different pre-treatments the bioenergy generation potential will be evaluated and compared to the potential of the untreated leaf.

Keywords
Anaerobic digestion; contaminants; methane production; olive by-products.

INTRODUCTION

The olive sector is one of the main sectors of the agri-food system, due to its economic, social, environmental and public health importance. Olive cultivation is present and its cultivation area exceeds 11.6 million hectares and most of it is located in the countries of the Mediterranean basin (Figure 1).

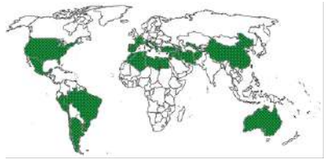

Figure 1. Olive cultivation around the world.

The most important products from the olive sector are the olive oil and olive table industries. Spain is the worldwide largest olive oil producer, reaching a production of more than 1.3 million of tons in the season 2021/2022. This amount corresponds around 65% of the European production (1.97 million) and 42% of the world production (3.1 million) (IOC, 2022). More than 80% of the Spanish production is located in Andalusia. Regarding to the olive table, the average production of table olives in Spain in the last five seasons was 561,100 tons, which represents 19.7% of world production of this product (Ruiz-Barba et al., 2023). Olive leaves are one of by-products of the olive oil and olive table products and they overcomes one million tonnes (Romero-García et al., 2016). Olive leaves occasionally can be used for animal feed, but currently olive industry waste is generating a great deal of interest within the framework of biorefineries. From olive by-products high number of added-value compounds can be obtained for energy, pharmaceutical, food and cosmetics use. As prominent examples as sugar, flavonoids and phenolic compounds can be highlight.

Other important point is because of the use of the extended use of metals, specially, Cu-derived compounds as antifungals in olive tree agricultural, Cu is expected to be detected in high amounts in the olive leaves and this should be removed from the leaves. The first reason for its great interest as a raw material, secondly for its oxidative potential in bioactive compounds and thirdly for its toxic potential in soils when the leaf is used as a soil amendment or soil improver.
As global energy consumption continues to grow and in order to mitigate global warming and he current energy crisis more eco-friendly researches are necessary. For this reason, the bioenergy generation potential is evaluated and compared to the potential of the untreated leaf.

MATERIAL AND METHODS

The leaf samples were collected and manually cleaned of twigs, insects, soil, etc. Once the material not coming from the leaves was removed and in order to reduce the particle size of the sample, the leaves were passed through a Yazicilar shredder, model DIV Line Countertop Cutter-Mixer, L9DIV. The samples were stored refrigerated (4 ºC) while characterisation and extraction tests are carried out. C/N, organic matter, ammonia, metals and bioactive compounds are being determined in both pre-treated and untreated olive leaves. Total polyphenols are being be determined through the Folin-Ciocalteau method, after extraction with an 80% methanol/water solution and the individual phenols concentration will be measured by liquid chromatography using a Hewlett-Packard 1100 HPLC-system using a C-18 column and a diode array detector. Trace elements will be measured using Inductive Coupled Plasma Mass Spectrometry (ICPMS-Agilent-7800.
To investigate the biochemical methane potential of the olive leaves and the effect of different pre-treatment on the methane production potential of PS, BMP tests will be evaluated. The BMP tests will be carried out in 250 mL bottles.

Each BMP test contained an inoculum to olive leave ratio of 2 on a dry VS basis. All the bottles will be closed and maintained in a mesophilic temperature controlled (at 35-37 ºC) regulated with a thermostat, and continuously stirring (300 rpm). Methane production will be measured using 0.5 and 1.0 L gasometers immersed in a solution of NaOH 2 N. Owing to the NaOH property of chemically absorbing the CO_2 present in the biogas, a correct measurement of the methane volume can get by liquid displacement and they will be maintained until biogas production will be totally exhausted, approximately 30 days.

RESULTS AND DISCUSSION

We are currently carrying out leaf characterisation and pre-treatments for the extraction of high added value compounds and next week we will set up the BMP tests. The most relevant results will be presented at the ECOSTP conference.

ACKNOWLEDGEMENTS

We thanks to 2022701040_CSIC project: Explorando el uso de subproductos del olivar para mejorar la generación de bioproductos y reducir microcontaminantes en purines. Also, thanks to the incentives for agents of the Andalusian knowledge system, aid under the Andalusian research, development and innovation plan (PAIDI 2020) (project P18-TP-616).

References

1. *IOOC, 2022. HO-W901-17-12-2021-P.pdf (internationaloliveoil.org) [WWW Document].*
2. *Romero-García, J. M., Lama-Muñoz, A., Rodríguez-Gutiérrez, G., Moya, M., Ruiz, E., Fernández-Bolaños, J., & Castro, E. (2016). Obtaining sugars and natural antioxidants from olive leaves by steam-explosion. Food chemistry, 210, 457-465.*
3. *Ruiz-Barba, J. L., Sánchez, A. H., López-López, A., Cortés-Delgado, A., & Montaño, A. (2023). Microbial community and volatilome changes in brines along the spontaneous fermentation of Spanish-style and natural-style green table olives (Manzanilla cultivar). Food Microbiology, 104286.*

Exploring veterinary drug and resistance genes in livestock manure and their removal by biomethanisation

S. Zahedi*,**, M. Gros**, O. Casabella**, J.L. Balcazar**, M. Pijuan**
* Instituto de La Grasa, Spanish National Research Council (CSIC), Campus Universitario Pablo de Olavide–Ed. 46, Ctra. de Utrera, Km. 1, Seville, 41013, Spain.
**Catalan Institute for Water Research (ICRA), C. Emili Grahit 101, 17003, Girona, Spain
(E-mail: *szahedi@ig.csic.es*)

Abstract
The mesophilic (35ºC) and thermophilic (55ºC) biomethanization of poultry, swine and cattle manures were investigated using biochemical methane potential (BMP) tests. Pasteurization pretreatment and post treatment was also investigated in combination with anaerobic treatment at 35 °C. Specific methane production (SMP), 24 pharmaceutical compounds (PhACs) and four antibiotic resistance genes (ARGs) (*qnrS*, *tetW*, *ermB* and *sul1*) were analyzed. The results showed that swine and poultry manure had higher methane productivities in mesophilic range (380 mL CH_4/g VS and 248 mL CH_4/g VS, respectively) than in thermophilic range (356 mL CH_4/g VS and 202 mL CH_4/g VSS, respectively), while for cattle manure an increase from 258 mL CH_4/g VS (mesophilic range) to 273 mL CH_4/g VS (thermophilic range) was observed. Several PhACS were detected in the manures. Most of these compounds were partially degraded. Tylosin was completely removed. Chlortetracycline (at thermophilic) and sulfamethoxazole presented removals higher than 50%. On the contrary, enrofloxacin, sulfadizine, sulfapyridine and flunixin showed poor removals (< 25%) indicating that anaerobic treatment can only partially remove these micropollutants which remain in the solid phase after treatment. The best removals were obtained at high temperatures indicating that thermophilic digestion is better suited for the removal of these compounds. This general trend was contrary to that observed in the study of antibiotic resistance genes, as the relative abundance of most of the genes studied (tetracycline, sulphonamide, fluoroquinolone and macrolide resistance genes) and of the horizontal transfer indicator of resistance genes (*IntI1*) not showed a lower relative abundance after thermophilic treatment. Finally, we studied the presence of potentially pathogenic bacteria and the most abundant genera were Streptococcus, Clostridium, Corynebacterium, Acinetobacter and Pseudomonas. All these genera were reduced after anaerobic treatment, except Clostridium which increased after thermophilic treatment.

Keywords
Anaerobic digestion; Antibiotic resistance genes; Methane production; Veterinary drugs.

INTRODUCTION

Intensive livestock farms are growing worldwide, leading to an increase on the production of different types of manures that, if untreated, can lead to a major environmental problem. Anaerobic digestion (AD) of organic manures offers an opportunity for energy recovery, making their treatment more attractive and economically more favourable. A part of the high content of conventional pollutants, manures are characterized also for containing relatively high concentrations of emerging pollutants such as pharmaceutical compounds (PhACs) and antibiotic resistance genes (ARGs). It is necessary to study the fate of these emerging pollutants in different types of manure as well as the capacity of AD to remove some of them. It is known that mesophilic (MAD) is not sufficient to reduce the content of pathogens, while thermophilic (TAD) present a higher removal efficiency, but it is more unstable and expensive for this type of waste. To overcome this limitation, interest in thermal pre-treatment before mesophilic digestion has increased. Sterilization of pathogenic microorganisms from wastewater can be achieved via a thermal pretreatment (70 °C for 1 h) before AD.

The fate of 24 PhACs, four ARGs (*qnrS, tetW, ermB and sul1*) and the gene *IntI1* were investigated in this study. The biogas production potential of swine, poultry and cattle manure under different anaerobic treatment conditions including the sanitation effect of pasteurization as pre or post treatments was also evaluated, as well as the effect of both temperatures on the degradation of the emerging pollutants.

The three substrates investigated were swine, cattle and poultry manure, which were obtained from a swine, cattle and poultry farms with a capacity of 600 pigs, 400 cows and 12,000 chickens.

RESULTS AND DISCUSSION

Biogas production

Mesophilic BMP tests displayed methane production from the first day with both substrates while the BMP performed under thermophilic temperature showed a delay. This is probably due to the adaptation of the inoculum to 35ºC as it was withdrawn from an anaerobic digester working at this temperature. The exponential increase in the specific methane production under thermophilic conditions was detected after 3-4 days indicating that the inoculum also had microorganisms able to work at 55ºC. The BMP tests conducted with poultry and swine showed significant differences in the average SMP values obtained under both temperatures, with 248 mL CH_4/ g VS and 202 mL CH_4/ g VS and 350 and 380 mL CH_4/g VS at thermophilic and mesophilic conditions, respectively. In the tests conducted with cattle manure (Fig. 1B) higher SMP was obtained at 55ºC.

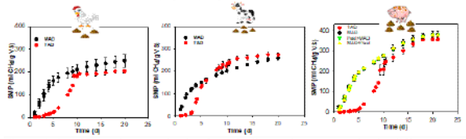

Figure 1. Specific methane production from the livestock manure under the different conditions tested.

Pharmaceuticals and antibiotic resistance genes

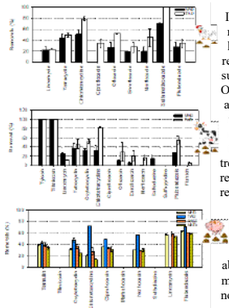

In general, general, all groups of PhACs showed higher removal in TAD as compared to MAD (except for lincomycin) (Figure 2). Tylosin was completely removed. Chlortetracycline (at thermophilic) and sulfamethoxazole presented removals higher than 50%. On the contrary, enrofloxacin, sulfadizine, sulfapyridine and flunixin showed poor removals (< 25%) indicating that anaerobic treatment can only partially remove these micropollutants which remain in the solid phase after treatment. Regarding the effect of pasteurization treatment in combination with AD on PhACs removal, results suggest that this treatment does not influence the removal of PhACs.

Four ARGs (*ermB, qnrS, sul1 and tetW), intI*1 and 16S rRNA genes were quantified in the biomass used as inoculum, in the livestock manures and at the end of the BMP tests. When comparing the relative abundance of ARGs at the end of each treatment, the most significant removal was found for *qnrS* which was not detected after most of the anaerobic treatment.

Figure 2. Removals of PhACs in the BMP tests conducted.

ACKNOWLEDGEMENTS

S. Zahedi thanks to 2022701040_CSIC project: Explorando el uso de subproductos del olivar para mejorar la generación de bioproductos y reducir microcontaminantes en purines.

Implementation of a municipal wastewater treatment technology to eutrophic environments: Ammonium nitrogen dosing strategy for developing phosphorus recovery from marine sediments

Fengyi Zhu*, Ece Kendir Cakmak*, Federica D'Amico**, Silvia Turroni**, Zeynep Cetecioglu*

* Department of Industrial Biotechnology, KTH Royal Institute of Technology, AlbaNova University Center, SE-11421 Stockholm, Sweden
** Unit of Microbiome Science and Biotechnology, Department of Pharmacy and Biotechnology, University of Bologna, 40126 Bologna, Italy
(E-mail: *fengyiz@kth.se; ece2@kth.se; federica.damico8@unibo.it; silvia.turroni@unibo.it; zeynepcg@kth.se*)

Abstract

The implementation of municipal wastewater treatment technology for phosphorus (P) recovery from marine sediments can be a promising strategy for P resource recovery and eutrophic ecology remediation. Currently, few studies explored the role of ammonia nitrogen (NH_4-N) in affecting P internal release under anaerobic eutrophic environments, although NH_4-N serves as an essential nutrient that can influence the metabolic activity of microorganisms. In our study, acetic acid and glucose, as prevailing carbon sources studied in the biological P removal system, were chosen, and the effects of different carbon/nitrogen on P release from marine sediment were investigated. Results showed that extra NH_4-N loading significantly impeded the decomposition of P ($p<0.05$), during the 24-day anaerobic operation, the maximum P release was 4.07 mg/L and 7.14 mg/L in acetic acid and glucose-fed system without extra NH_4-N addition. When glucose was fed as the carbon source, in addition to P releasing, volatile fatty acids were produced simultaneously.

Keywords
Alkaline phosphatase activity; ammonia loading; anaerobic reactor; marine sediments; microbial community; phosphorus release

INTRODUCTION

Phosphorus (P) present in eutrophic seawater and sediment could probably be a promising source for recovery, which can simultaneously address the burden of excess nutrient loading. The municipal technology for recycling P from waste streams has been well established; for example, the process of P removal/uptake relies on polyphosphate accumulating organisms (PAOs) under alternating anaerobic and aerobic conditions. In anaerobic conditions, PAOs can use organic carbons, hydrolysis of stored poly-P, and subsequently release orthophosphate to the environment (Cakmak et al., 2022). However, the feasibility of applying relevant processes to recover P from marine sediments has not been reported.

Ammonia nitrogen (NH_4-N), an influential bioavailable N in the sediment, however, studies on its role in influencing P internal release in anaerobic eutrophic environments are lacking. In this study, to clarify the overall influence of NH_4-N loading on P decomposition from anoxic sediments and to reach the goal of P recycling simultaneously, we conducted batch experiments using sodium acetate and glucose as external carbon sources under anaerobic conditions with different ratios of C/N (chemical oxygen demand, COD/NH_4-N).

MATERIALS AND METHODS

A serial of batch experiments was conducted in 120-mL serum bottles in triplicate, in acetic acid-fed system, 16 g of fresh sediments were dispensed in 80-mL synthetic seawater prepared with NaCl (6.5 psu) which is the average salinity of the Baltic Sea. Later, acetate (1 g/L acetic acid) and NH_4Cl were added to the serum bottles to provide carbon and nitrogen source, and different C/N loading groups were studied as no NH_4-N addition, COD/N=100, COD/N=5, and COD/N=10. The corresponding NH_4-N concentrations are around 0, 14, 28 and 140 mg/L. The bioreactors were operated for 3, 6, 9, 12, 18 and 24 days with daily manual mixing at 20°C. The experimental bottles were set up under initial pH of 7.2 and sealed with septa and aluminum caps. Each bottle was flushed with nitrogen gas for at least 5 min to provide anaerobic conditions. We repeated the above batch operation for the glucose-fed system using the same initial COD. PO_4-P, NH_4-N, acetic acid/glucose concentrations in the bioreactors, alkaline phosphatase (AP) activity, and microbial community structure of marine sediments were monitored with 24-day bioreactor operation.

RESULTS AND DISCUSSION

(1) Effects of C/N loading on phosphorus release

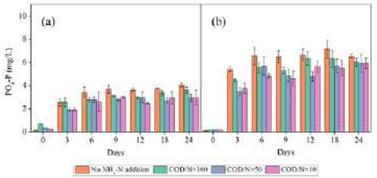

Figure 1. Variations of PO_4-P in two different carbon-fed systems under different C/N loading: (a) acetic acid system; (b) glucose system

The dissolved PO_4-P released from sediments with different NH_4-N loadings is shown in Figure 1. The concentration of PO_4-P increased considerably during the first 6 days, with 3.41 mg/L and 6.55 mg/L of P solubilization in acetic acid- and glucose-fed systems without extra NH_4-N addition. Although an increasing trend was observed in both systems, the maximum P release only increased by 19.35% (4.07 mg/L at day 24) and 8.26% (7.14 mg/L at day 18), respectively. The results exhibited that the release of P was significantly inhibited when more NH_4-N was dosed in the anaerobic system. With the increase of NH_4-N level from low (COD/N=100) to high (COD/N=10), the concentration of PO_4-P in supernatant of acetic acid-fed system decreased from 3.62 mg/L to 2.95 mg/L at the end of 24 days, while in supernatant of glucose-fed system, it decreased from 6.32 mg/L to 5.5 mg/L on the day 18.

(2) Variations of carbon in the acetic acid/glucose-fed system

Acetate consumption under different N loading is shown in Figure 2(a). Acetic acid concentrations remained stable in all groups, while only in no extra NH_4-N and COD/N=100 group exhibited slight consumption of 8.5% and 6.8% of acetate, respectively. However, unlike the acetic acid-fed system, the glucose was rapidly consumed in the glucose-fed system, for instance, over 95% of glucose was consumed in all groups in 6 days. Meanwhile, a large amount of biogas (data not available) and volatile fatty acids (VFA) were produced in the glucose-fed system (seen in Figure 2(c)-(f)), the dominant VFA types were acetic and butyric acids, the maximum VFA production was observed in no extra NH_4-N addition group on day 24 with 795.56 mg/L of total VFA, and 528.82 mg/L of acetic acid, 235.54 mg/L of butyric acid and 31.20 mg/L of propionic acid were generated, respectively.

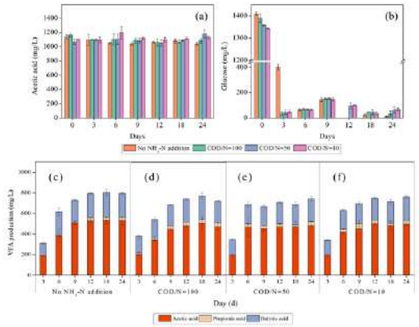

Figure 2. Variations of (a) acetic acid consumption in the acetic acid-fed system, (b) glucose consumption, and (c)-(f) VFA production in the glucose-fed system

(3) Variations of alkaline phosphatase activity

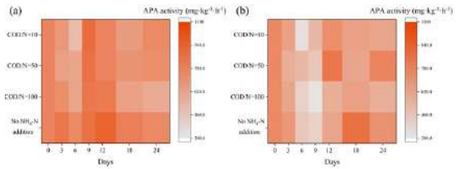

Figure 3. Variations of alkaline phosphatase activity of marine sediment: (a) acetic acid-fed system; (b) glucose-fed system

Ammonia acts as an essential nutrient for the growth of microorganisms; however, it may promote/inhibit the P release from sediment by influencing metabolic processes/activity (Li et al., 2016; Ma et al., 2018). For instance, Xie et al. (2010) investigated the correlation between phosphatase activities and P in activated sludge during the wastewater treatment process, and a negative correlation between phosphatase activities and ortho-phosphate in anaerobic bioreactors was reported. However, the contrary finding has been found by Ma et al. (2018), in the mesocosm experiment, extra NH_4-N loading stimulated AP activity and led to the promotion of lake sediment P release. Therefore, AP of marine sediments as a key enzyme in organic P mineralization, the role of its activity P decomposition under anaerobic conditions should be explored.

In this study, the activity of AP was measured during a 24-day bioreactor operation. As illustrated in Figure 3(a), the activity of AP in the acetic acid-fed system firstly increased then decreased, a maximum of 1046.97 mg/(kg·h) was reached on the day 12 in the group of no NH_4-N addition group. The opposite phenomenon was observed in the glucose-fed system, where the activity of AP was initially decreasing and lowest at day 6, with the AP activity of no NH_4-N addition, COD/N=100, COD/N=50, and COD/N=10 group was 490.67 mg/(kg·h), 447.86 mg/(kg·h), 584.45 mg/(kg·h) and 354.75 mg/(kg·h), respectively. However, the enzyme activity of the no NH_4-N addition group increased up to 967.79 mg/(kg·h) on day 18, the value was higher than that of the initial (day 0, 838.11 mg/(kg·h)).

(4) Analysis of microbial community structure

The analysis of microorganisms can help clarify the mechanism of microbial activity in the P release. The microbial community data will come later and will be presented at the conference.

CONCLUSION

Our study adopted the technology and theory of municipal wastewater treatment and investigated the feasibility of P recycling by anaerobic batch reactors from marine sediments. The influence of NH_4-N dosing on P decomposition was clarified. Our results can provide information for P release and recycling from marine sediments. Based on the findings of anaerobic batch experiments, conclusions are as follows:

(1) Additional NH_4-N loading can significantly inhibit P release from marine sediments.
(2) In terms of promoting P release, the glucose-fed system performed better compared to the acetate-fed system, up to 7.12 mg/L P can be obtained through 18-day anaerobic batch reactors.
(3) Stimulated AP activity derived by different NH_4-N loading could be the underlying reason for sediment P release.

REFERENCES

Cakmak, E., Hartl, M., Kisser, J., Cetecioglu, Z. 2022. Phosphorus mining from eutrophic marine environment towards a blue economy: The role of bio-based applications. Water Research. 219, 118505.

Li, H., Song, C.L., Cao, X.Y., Zhou, Y.Y. 2016. The phosphorus release pathways and their mechanisms driven by organic carbon and nitrogen in sediments of eutrophic shallow lakes. Sci. Total Environ. 572, 280-288.

Ma, S.N., Wang, H.J., Wang, H.Z., Li, Y., Liu, M., Liang, X.M., Yu, Q., Jeppesen, E., Sondergaard, M. 2018. High ammonium loading can increase alkaline phosphatase activity and promote sediment phosphorus release: A two-month mesocosm experiment. Water Res. 145, 388-397.

Xie, C., Lu, R., Huang, Y., Wang, Q., Xu, X. 2010. Effects of ions and phosphates on alkaline phosphatase activity in aerobic activated sludge system. Bioresource Technology. 101(10), 3394-3399.

Application of electrocoagulation treatment to meat industry wastewater

N. Duduković*, A. Leovac Maćerak *, N. Slijepčević*, M. Bečelić-Tomin*, V. Pešić*, D. Tomašević Pilipović*, Đ. Kerkez*

*Department of Chemistry, Biochemistry and Environmental Protection, University of Novi Sad, Trg Dositeja Obradovica 3, Republic of Serbia
(E-mail: *natasa.varga@dh.uns.ac.rs*)

Abstract

In recent years, a large number of researchers believe that electrocoagulation (EC) treatment has a future in wastewater treatment. In this work, we investigate the possibility of applying the EC process for the purification of meat industry wastewater. The experimental removal efficiencies for COD, BOD, total P, total N, and turbidity were 46%, 50%, 95%, 97%, and 99%, for aluminum electrodes and for iron electrodes removal efficiencies were 48%, 52%, 94%, 99%, and 98%, respectively. The next step is to optimize and improve the treatment to obtain water as a product that we can use for irrigating the surrounding agricultural areas or for reuse in the production process, which is very important from the point of view of the circular economy.

Keywords
wastewater, electrocoagulation, water reuse

INTRODUCTION

The meat industry generates wastewater highly loaded with organic matter. According to the United States Environmental Protection Agency (US EPA), this wastewater is one of the most damaging wastewaters for the environment (Štefanac et al., 2021). Application of traditional methods generally requires high investment and operation expenses can be a substantial hurdle to their implementation, particularly in small enterprises or developing nations. Therefore, it is necessary to find a treatment that is both, sustainable and environmentally friendly. In the last few years, electrocoagulation (EC) has attracted increasing attention in wastewater treatment. The main advantages of the EC process are flexibility, efficiency, ease of setup, does not require any chemical additives, lower production of sludge, and no representative copollution (Pinedo-Hernández et al., 2015). During EC treatment due to the application of low-voltage direct electric current and by the action of sacrificial metal electrodes, which are usually made of aluminum or iron, coagulants and metal hydroxides are electrochemically generated, in situ, which causes the destabilization and aggregation of contaminants (Morales-Rivera et al., 2020). In this work, we investigate the possibility of the application EC process for the purification of meat industry wastewater.

MATERIALS AND METHODS

Two sets of the EC experiments have been performed: (1) two aluminum electrodes Al(-)/Al(+)(EC1), (2) two iron electrodes Fe(+)/Fe (-) (EC2). The treatments were done in an EC unit which was made of borosilicate glass with a volume of 600 ml. For treatments aluminum and iron electrodes with the same dimensions of 10 cm x 5 cm x 0.1 cm were used. During the treatments the distance between the electrodes were 3 cm, the current strength were 3.33 mA/cm2, the rotation speed were 280/min, the surface of the immersed electrodes were 30 cm2, with the treatment time were 1 hour, and the volume of treated water was 0.5 l. The raw meat industry wastewater was characterized before and after each EC treatment determined: chemical oxygen demand (COD), biochemical oxygen demand (BOD), total phosphorous (P), total nitrogen (N), pH, and turbidity.

RESULTS AND DISCUSSION

The effects of electrocoagulation on meat industry wastewater were present in Table 1. To assess the effects of EC determining the pH value is the most appropriate step. Based on the obtained results, it is observed that the pH value increased by ~1 pH unit. We can explain this by a significant amount of ion OH− released by the electrochemical reaction of the hydrolysis of water at the cathode. The change in pH during EC was also observed by other researchers (Tahreen et al., 2020). The experimental removal efficiencies for COD, BOD, total P, total N, and turbidity were 46%, 50%, 95%, 97%, and 99%, for aluminum electrodes and for iron electrodes removal efficiencies were 48%, 52%, 94%, 99%, and 98%, respectively. We can explain the reduction of COD, BOD, P, and N in treated water by the adsorption onto the surfaces of hydroxide precipitates, which are released by the electrodes. The high percentage of turbidity reduction is in accordance with the previously mentioned efficiencies of the tested treatments. The presented results show that there is no big difference in the achieved efficiencies between EC1 and EC2, therefore our recommendation is EC2 because Fe electrodes are cheaper.

Table 1. Parameters of wastewater characterization, before and after electrocoagulation

Parameters	E0	EC1	EC2
COD (mg O_2/l)	846	454	443
BOD (mg O_2/l)	433	215	206
Total P (mg/l)	2.26	0.12	0.14
Total N (mg N/l)	64.8	2.13	0.86
pH	6.66	7.93	7.82
Turbidity (NTU)	210	2.85	5.06

Based on the above conclusions, it can be noted that EC holds immense potential to replace conventional wastewater treatment methods. In the future, we will focus on the optimization and improvement of the treatment in order to obtain water as a product that we can use for irrigating the surrounding agricultural areas or for reuse in the production process, which is very important from the point of view of the circular economy.

REFERENCES

Morales-Rivera, J., Sulbarán-Rangel, B., Gurubel-Tun, K.J., del Real-Olvera, J., Zúñiga-Grajeda, V. 2020. Modeling and optimization of COD removal from cold meat industry wastewater by electrocoagulation using computational techniques. *Processes*, **8**,1139.

Pinedo-Hernández, J., Núñez, Y., Sánchez, I., Marrugo-Negrete, J. 2015. Treatment of meat industry wastewater using electrochemical treatment method. *Portugaliae Electrochimica Acta*, **33**, 223–230.

Štefanac, T., Grgas, D., Landeka Dragičević, T. 2021. Methods of processing waste water from the meat industry. *Meat*, **23**, 54–66.

Tahreen, A., Jami, M.S., Ali, F. 2020. Role of electrocoagulation in wastewater treatment: A developmental review. *Journal of Water Process Engineering*, **37**, 101440.

This project has received funding from the *European Union's Horizon Europe research and innovation programme, Horizon Europe - Work Programme 2021-2022 Widening participation and strengthening the European Research Area, HORIZON-WIDERA-2021-ACCESS-02,* under grant agreement No [101060110], SmartWaterTwin

Application of electrocoagulation treatment to meat industry wastewater

N. Duduković*, A. Leovac Maćerak *, N. Slijepčević*, M. Bečelić-Tomin*, V. Pešić*, D. Tomašević Pilipović*, Đ. Kerkez*

*Department of Chemistry, Biochemistry and Environmental Protection, University of Novi Sad, Trg Dositeja Obradovica 3, Republic of Serbia
(E-mail: natasa.varga@dh.uns.ac.rs)

Abstract

In recent years, a large number of researchers believe that electrocoagulation (EC) treatment has a future in wastewater treatment. In this work, we investigate the possibility of applying the EC process for the purification of meat industry wastewater. The experimental removal efficiencies for COD, BOD, total P, total N, and turbidity were 46%, 50%, 95%, 97%, and 99%, for aluminum electrodes and for iron electrodes removal efficiencies were 48%, 52%, 94%, 99%, and 98%, respectively. The next step is to optimize and improve the treatment to obtain water as a product that we can use for irrigating the surrounding agricultural areas or for reuse in the production process, which is very important from the point of view of the circular economy.

Keywords
wastewater, electrocoagulation, water reuse

INTRODUCTION

The meat industry generates wastewater highly loaded with organic matter. According to the United States Environmental Protection Agency (US EPA), this wastewater is one of the most damaging wastewaters for the environment (Štefanac et al., 2021). Application of traditional methods generally requires high investment and operation expenses can be a substantial hurdle to their implementation, particularly in small enterprises or developing nations. Therefore, it is necessary to find a treatment that is both, sustainable and environmentally friendly. In the last few years, electrocoagulation (EC) has attracted increasing attention in wastewater treatment. The main advantages of the EC process are flexibility, efficiency, ease of setup, does not require any chemical additives, lower production of sludge, and no representative copollution (Pinedo-Hernández et al., 2015). During EC treatment due to the application of low-voltage direct electric current and by the action of sacrificial metal electrodes, which are usually made of aluminum or iron, coagulants and metal hydroxides are electrochemically generated, in situ, which causes the destabilization and aggregation of contaminants (Morales-Rivera et al., 2020). In this work, we investigate the possibility of the application EC process for the purification of meat industry wastewater.

MATERIALS AND METHODS

Two sets of the EC experiments have been performed: (1) two aluminum electrodes Al(-)/Al(+)(EC1), (2) two iron electrodes Fe(+)/Fe (-) (EC2). The treatments were done in an EC unit which was made of borosilicate glass with a volume of 600 ml. For treatments aluminum and iron electrodes with the same dimensions of 10 cm x 5 cm x 0.1 cm were used. During the treatments the distance between the electrodes were 3 cm, the current strength were 3.33 mA/cm2, the rotation speed were 280/min, the surface of the immersed electrodes were 30 cm2, with the treatment time were 1 hour, and the volume of treated water was 0.5 l. The raw meat industry wastewater was characterized before and after each EC treatment determined: chemical oxygen demand (COD), biochemical oxygen demand (BOD), total phosphorous (P), total nitrogen (N), pH, and turbidity.

RESULTS AND DISCUSSION

The effects of electrocoagulation on meat industry wastewater were present in Table 1. To assess the effects of EC determining the pH value is the most appropriate step. Based on the obtained results, it is observed that the pH value increased by ~1 pH unit. We can explain this by a significant amount of ion OH^- released by the electrochemical reaction of the hydrolysis of water at the cathode. The change in pH during EC was also observed by other researchers (Tahreen et al., 2020). The experimental removal efficiencies for COD, BOD, total P, total N, and turbidity were 46%, 50%, 95%, 97%, and 99%, for aluminum electrodes and for iron electrodes removal efficiencies were 48%, 52%, 94%, 99%, and 98%, respectively. We can explain the reduction of COD, BOD, P, and N in treated water by the adsorption onto the surfaces of hydroxide precipitates, which are released by the electrodes. The high percentage of turbidity reduction is in accordance with the previously mentioned efficiencies of the tested treatments. The presented results show that there is no big difference in the achieved efficiencies between EC1 and EC2, therefore our recommendation is EC2 because Fe electrodes are cheaper.

Table 1. Parameters of wastewater characterization, before and after electrocoagulation

Parameters	E0	EC1	EC2
COD (mg O_2/l)	846	454	443
BOD (mg O_2/l)	433	215	206
Total P (mg/l)	2.26	0.12	0.14
Total N (mg N/l)	64.8	2.13	0.86
pH	6.66	7.93	7.82
Turbidity (NTU)	210	2.85	5.06

Based on the above conclusions, it can be noted that EC holds immense potential to replace conventional wastewater treatment methods. In the future, we will focus on the optimization and improvement of the treatment in order to obtain water as a product that we can use for irrigating the surrounding agricultural areas or for reuse in the production process, which is very important from the point of view of the circular economy.

REFERENCES

Morales-Rivera, J., Sulbarán-Rangel, B., Gurubel-Tun, K.J., del Real-Olvera, J., Zúñiga-Grajeda, V. 2020. Modeling and optimization of COD removal from cold meat industry wastewater by electrocoagulation using computational techniques. *Processes*, **8**,1139.

Pinedo-Hernández, J., Núñez, Y., Sánchez, I., Marrugo-Negrete, J. 2015. Treatment of meat industry wastewater using electrochemical treatment method. *Portugaliae Electrochimica Acta*, **33**, 223–230.

Štefanac, T., Grgas, D., Landeka Dragičević, T. 2021. Methods of processing waste water from the meat industry. *Meat*, **23**, 54–66.

Tahreen, A., Jami, M.S., Ali, F. 2020. Role of electrocoagulation in wastewater treatment: A developmental review. *Journal of Water Process Engineering*, **37**, 101440.

This project has received funding from the *European Union's Horizon Europe research and innovation programme, Horizon Europe - Work Programme 2021-2022 Widening participation and strengthening the European Research Area, HORIZON-WIDERA-2021-ACCESS-02,* under grant agreement No [101060110], SmartWaterTwin

4. Digitalization

Modelling salinity effects on aerobic granular sludge treating fish-canning wastewater

P.Carrera [1,2], L.Strubbe [1], A. Val del Rio [2], A. Mosquera-Corral [2], E.I.P. Volcke [1]

[1] BioCo Research Group, Department of Green Chemistry and Technology, Ghent University, Coupure Links 653, 9000 Gent, Belgium
[2] CRETUS Institute. Department of Chemical Engineering, Universidade de Santiago de Compostela. E-15782, Santiago de Compostela, Spain
* Corresponding author: Eveline.Volcke@UGent.be

Abstract
The effect of salinity on aerobic granular sludge treating fish-canning wastewater was evaluated through a one-dimensional biofilm model. Salt inhibition was described by a non-competitive inhibition term, for which the value of the half-saturation coefficient was estimated based on data from literature. The model was calibrated and validated with experimental lab-scale data regarding COD and nitrogen removal from industrial wastewater. Two dynamic operating periods with salinities of 13 and 5 g NaCl L^{-1} were used for calibration and validation, respectively. The presence of salt caused nitrite accumulation, as well as unusually low estimated maximum growth rates of nitrifying bacteria. The addition of a salinity inhibition term to the model accurately described the COD and nitrogen species experimentally measured along the cycles with different salinities.

Keywords
Aerobic granular sludge; ASM3; industrial wastewater; salinity

INTRODUCTION

The Aerobic Granular Sludge (AGS) technology is nowadays regarded as an established way to treat both municipal and industrial wastewater. In addition, there has been an increasing interest to also treat saline wastewater with AGS. This includes municipal wastewater from treatment plants located in coastal areas, as well as from different industrial sectors, such as petrochemical or seafood processing. However, the presence of salt is known to affect the physical properties of the granules and hinder the biological activity of the bacterial populations. In this study, a model was set-up to describe the operation of an AGS reactor treating saline wastewater and evaluate the effect of salinity on reactor performance. The model was calibrated and validated under dynamic (cyclic) reactor operation, treating influent with different salt concentrations. In addition, the need to consider an inhibition term to include the effect of salinity was investigated.

MATERIALS AND METHODS

The operating conditions of a lab-scale AGS reactor (1.7 L) fed with fish-canning wastewater, described by Carrera et al. (2019), were taken as a reference scenario. The cycle length was 4 h, including 5 min of feeding, 227 min of aeration, 1 min of settling and 7 min of effluent withdrawal. During the aeration phase, the dissolved oxygen concentration reached saturation values of 8.6 g O_2 m^{-3}. Two independent datasets corresponding to operational periods with different salinities of 13 g NaCl.L^{-1} (0.61 kg soluble COD.m^{-3}, 73 g NH_4-N.m^{-3}) and 5 g NaCl.L^{-1} (0.90 kg soluble COD.m^{-3}, 106 g NH_4-N.m^{-3}), were used for model calibration and validation, respectively.
A one-dimensional ASM3 model was implemented in AQUASIM. Three modifications were applied to ASM3 for an accurate description of the process: simultaneous growth and storage processes of heterotrophs, two-step nitrification and addition of a non-competitive inhibition term to express the effect of salinity (Table 1). This term was added to all the growth processes of the different bacterial groups. The values of the half-saturation constants were estimated based on activity tests from literature reporting a reduction of the biological activity with the increase of salinity. Simulations were done for constant influent composition, corresponding to the measured average values.

Table 1. Estimated values for the half-saturation constant of the inhibition term

Inhibition term	**$K_{Inh,50}$ (g NaCl/L)**		
$\frac{K_{Inh,50}}{K_{Inh,50} + S_{Inh}}$	Ammonia oxidizing Bacteria	Nitrite oxidizing bacteria	Heterotrophic organisms
	24.8	21.7	44.3

RESULTS AND DISCUSSION

The calibrated kinetic parameters of heterotrophic bacteria ($\mu_{max,H}$ of 6 d^{-1} and storage rate constant (k_{STO}) of 8 d^{-1}) were similar to those from previous research works modelling AGS with ASM3. However, the calibrated values of nitrifying bacteria ($\mu_{max,A}$ of 0.18 and $\mu_{max,N}$ of 0.10 d^{-1} for AOB and NOB, respectively) were lower than the reported ranges of 1.1 – 1.3 and 0.9 – 1.3 d^{-1} for $\mu_{max,A}$ and $\mu_{max,N}$, respectively (Ni et al., 2008; Zhao et al. 2016). This difference was mainly attributed to the presence of salt, combined with other factors such as a high biomass retention in the reactor, which can cause a shift in the community composition towards slow-growing nitrifiers.

The addition of the non-competitive inhibitory term to the model could accurately predict the effluent concentrations of organic matter and nitrogen compounds with different salinities during calibration (13 g NaCl.L^{-1}) and validation (5 g NaCl.L^{-1}) (Figure 1, 2). Regarding the biological activity inhibition, heterotrophic bacteria were the least affected by the presence of salt. The biological activity was reduced with 23 and 10 % under salinity conditions corresponding to calibration and validation, respectively. The activity of both AOB and NOB suffered higher reductions, especially with salt concentrations of 13 g NaCl.L^{-1} (34 and 27% reduction for AOB and NOB, respectively), showing a higher sensitivity to the increase of salinity.

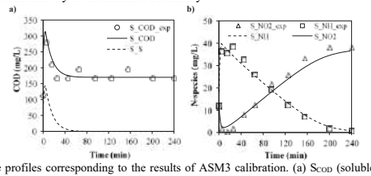

Figure 1. Cycle profiles corresponding to the results of ASM3 calibration. (a) S_{COD} (soluble COD) and S_S (soluble readily biodegradable COD) profiles predicted with ASM3; and S_{COD} profile from experimental data. (b) S_{NH} and S_{NO2} profiles predicted with ASM3; and S_{NH} and S_{NO2} profiles from experimental data.

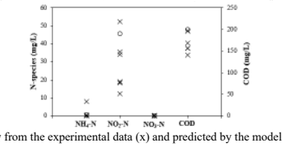

Figure 2. Effluent quality from the experimental data (x) and predicted by the model (○) during validation.

Nevertheless, the model was tested with low- to moderate salinities (< 15 g NaCl.L^{-1}), and further research is needed to validate it with a wider range of salt concentrations (20-40 g NaCl.L^{-1}).

REFERENCES

Carrera, P., Campo, R., Méndez, R., Di Bella, G., Campos, J.L., Mosquera-Corral, A., Val del Rio, A. (2019). Does the feeding strategy enhance the aerobic granular sludge stability treating saline effluents? Chemosphere, 226, 865-873
Ni, B.J., Yu, H.Q., Sun, Y.J. (2008). Modeling simultaneous autotrophic and heterotrophic growth in aerobic granules. Water Research, 42:6-7, 1583-1594
Zhao, J., Huang, J., Guan, M., Zhao, Y., Chen, G., Tian, X. (2016). Mathematical simulating the process of aerobic granular sludge treating high carbon and nitrogen concentration wastewater. Chemical Engineering Journal, 306, 676-684

SADAR: a digital predictive system with photonic pathogen biosensors for safe water reclamation in WWTP.

N. Zamorano-López*, A. Fernández**, S. Simón**, A. Fresneda**, I. Solís***, E. Ferrer-Caraco***, F. D. Bellvís*, L. García*, I. Beltrán****, C. Badenes****, M. García*.

*FACSA, SOCIEDAD DE FOMENTO AGRÍCOLA CASTELLONENSE, S.A. Calle Mayor, 82-84, 12001, Castelló de la Plana, Spain; nuria.zamorano@grupogimeno.com; fbellvis@facsa.com; lgarcia@facsa.com; mairena.garcia@facsa.com.
** LUMENSIA SENSORS S.L. Camino de Vera, 8F, 46022, València, Spain; afernandez@lumensia.com; ssimon@lumensia.com; afresneda@lumensia.com
*** EUROFINS- IPROMA, Camino de la Raya, 46, 12006, Castelló de la Plana, Spain. eferrer@iproma.com; isolis@iproma.com.
**** Ajuntament de Castelló. Plaza del Ayuntamiento, 8, 46270, Castelló de la Plana, Spain. ines.beltran@castello.es; cribad@castello.es.

Abstract
Safe water reuse requires the development and implementation of new strategies for microbial risk control in WWTP. Digitalisation and implementation of pathogen sensors are potential tools for WWTP operators to ensure safe water reclamation practices from public health and environmental perspectives. A machine learning model trained by real-time and analytical data has been developed to predict changes in the quality of reclaimed water. Local microbial risk control has been improved through the development of photonic biosensors for *Escherichia coli* and *Cryptosporidium* targets. Removal rates of pathogens in WWTP, including virus, are close to the values requested in the new regulation for safe water reuse in agriculture but further treatment is required for full viral particle removal.

Keywords (maximum 6 in alphabetical order)
digitalisation; machine learning; photonic; reclaimed water; sensors; WWTP.

INTRODUCTION

Water scarcity is among the top of the consequences of climate change and the increase of worldwide population. By 2030 the demand of freshwater will be 2680 km^3 over the available volume for supplying purposes on Earth (WRI, 2020). Also, in some regions such as the Mediterranean a 11% reduction of water resources by 2060 is expected (IPCC, 2022). In Europe, the Regulation on minimum requirements for water reuse will apply from June 26th, 2023, on. Microbial risk control will require measurement of bacteria, virus, and protozoa. Besides, risk management plans are required to protect health and environment. However, current methods for microbial control in WWTP are slow (2-3 days) and data management of reclaimed water quality is still at a low digitalisation level.
Alternative strategies for water reuse management are required. The aim of this work is to develop an innovative digital platform for managing the quality of reclaimed water based on microbiological parameters combining artificial intelligence and new microbial sensors. The novelty of this project relies on (i) the use of photonic technology in combination with immunoassays for high-specificity detection of pathogens in treated water and (ii) the application of artificial intelligence techniques to develop indicators of reclaimed water quality decay for WWTP managers.

MATERIALS AND METHODS

WWTP plant and microbial quality monitoring

The project was carried out in Castelló de la Plana WWTP which treats 45,000 m^3/d of urban wastewater. Five monitoring points were established: (P01) WWTP influent, (P02) Reclaimed water, (P03) UV influent, (P04) UV effluent and (P05) chlorination labyrinth. A probe for indirect measurement of E. coli (Proteus, UK) was installed in P05 for data analysis and machine learning model development. Microbial risks are being evaluated against UNE-EN-ISO 9308-1-2-3; UNE-EN ISO 10705-2; and EPA Method 1622 standards for *E. coli*, bacteriophages, and *Cryptosporidium*, respectively.

Photonic sensor

An IoT-sensor based on photonic technology has been developed for simultaneous detection of specific viable bacteria (*E. coli*) and protozoa (*Cryptosporidium*) in WWTP inlet and outlet samples (Figure 1). The sensor implements photonic readings over Photonic Integrated Circuits (PIC) with fixed antibodies for pathogen targets detection and quantification. The photonic system consists of: (i) a microfluidic cartridge that integrates the biofunctionalized PIC and the microfluidic structures; (ii) a biosensing platform that includes the read-out subsystem, optoelectronics and fluidic elements, the signal processing software and user interface. This system carries out the full measurement procedure automatically without any human intervention and is connected to the data lake for later analysis.

Data treatment and Machine Learning

Along with the analytical data from laboratory or biosensor, 7 years real-time operational data has been collected for the development of predictive analysis using machine learning techniques. Summarizing, 47 variables have been analysed. The stated hypothesis was that combination of real-time and laboratory data could predict changes reclaimed water quality in terms of *E. coli* indirect measurement (turbidity, tryptophan parameters). Retrieved data was filtered and transformed before linear and order correlation analysis. Models such as Ridge, SVM or XGBoost were applied. The resulting prediction was dockerized and implemented in the data lake for data exploitation.

RESULTS AND DISCUSSION

Predictive digital platform for water reuse management

A data model for water reuse management combining real-time from WWTP and analysis data from the photonic sensor and laboratory was established. The geospatial reference of the inputs and data allowed the application of artificial intelligence analysis combining both datasets. Several significant correlations were obtained. Best predictive model for reclaimed water quality in terms of turbidity was based on XGBoost algorithms (R2=0.41) (Figure 2). But predictions were not accurate for *E.coli* (R2=-0.04). It can be concluded that establishing a predictive model is possible but higher accuracy is required for predicting *E. coli*. This would be possible through the increase of *E. coli* measurements in WWTP effluent with the developed photonic sensor. However, high sensitivity of this biosensor for effluent would be required (below 10UFC/100mL).

Microbial risk monitoring and photonic biosensor

Microbial risk control in treated water was performed through log10 removal values as shown in Figure 3 for *E. coli*. Treated water quality meets the legal requirements (*E. coli*<200 UFC/100mL and log10 removal>5). The sensor could detect this pathogen in values with a difference of 1 or 2 log10 values compared to the laboratory measurements. Further training of the sensor is needed and will be performed in the following months to increase accuracy. Also, further work is being carried out to evaluate detection of *Cryptosporidium* oocytes (data not shown).
The extended analysis of virus revealed different levels of coliphages, rotavirus, norovirus (GI and GII) and crAssphage in WWTP effluent (Table 1). Highest removal rates were observed for coliphagues (log10=4) meeting the legal requirements. It should be highlighted that the rest of the virus were analysed using DNA/RNA detection techniques. Thus, infectivity capacity complementary analysis should be carried out to fully evaluate the risk of viral presence in reclaimed water after WWTP treatments.

ACKNOWLEDGEMENTS

This project has been co-financed by the Valencian Innovation Agency (AVI), under file number INNCAD/2021/95-96-101 and the entities of the Valencian Community participate in it: Sociedad de Fomento Agrícola Castellonense S.A. (FACSA), Lumensia Sensors S.L. and Eurofins Iproma and has the collaboration of the Castelló de la Plana City Council. PhD Gloria Sánchez research team from IATA-CSIC (Spain) is fully acknowledged for extended virus analysis in samples. Joan García Esquerdo from Instituto Tecnológico de Informática (ITI) Valencia (Spain) is also acknowledged for data analysis.

REFERENCES

World Resource Institute, 2020. Reckoning and Recovery. WRI ANNUAL REPORT, available at files.wri.org/s3fs-public/wri-2020-21-annual-report.pdf.
Intergovernmental Panel on Climate Change, 2022. Climate Change 2022: Impacts, Adaptation and Vulnerability, available at https://report.ipcc.ch/ar6/wg2/IPCC_AR6_WGII_FullReport.pdf.

Figure 1. Biosensor prototype for microbial risk monitoring.

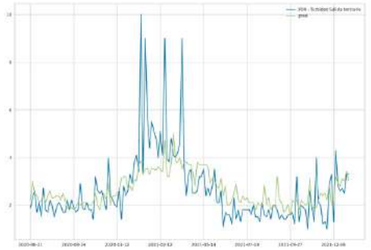

Figure 2. Predictive model for the quality of reclaimed water based on turbidity.

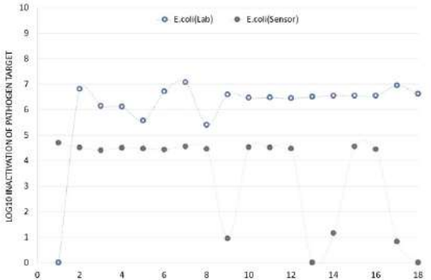

Figure 3. Log10 removal in WWTP for microbial risk control with laboratory analysis and new photobiosensor developed in the project.

Table 1. Virus concentration mean values detected by real-time qPCR of selected samples in WWTP.

	log10 value of concentration in samples				
	Coliphages	**Norovirus GI**	**Norovirus GII**	**Rotavirus**	**Crassphage**
WWTP influent (P01)	6,34±0,48	4,16±0,67	8,09±1,02	7,99±0,50	8,42±0,90
WWTP effluent (P02)	2,05±1,32	2,43±1,66	4,81±3,25	6,88±0,66	6,21±0,91
Log10 removal	4	2	3	1	2

Real-time, *in-situ* nitrite and nitrate analyser for process control within wastewater treatment facilities

M. Grau Butinyac[1], E. Murray[1,2]

1. Research & Development, T.E. Laboratories Ltd. (TelLab), Tullow, Carlow, Ireland
(E-mail: *mgraubutinyac@tellab.ie*)
2. Research & Development, Aquamonitrix Ltd. Tullow, Carlow, Ireland
(E-mail: *emurray@tellab.ie*)

Abstract
Nutrient pollution is the most prevalent global water quality issue. Nitrite (NO_2^-) and nitrate (NO_3^-) are considered nutrient pollutants and they play a key role in wastewater treatment. The established approach for the monitoring of these nutrients is manual sampling and laboratory analysis. Up to this point, real-time selective and accurate monitoring data of NO_2^- and NO_3^- in the sector has not been available. Using Aquamonitrix, a novel real-time *in-situ* NO_2^- and NO_3^- monitoring analyser, a new set of data can be obtained from activated sludge (AS) and final effluent from wastewater facilities. The system delivers lab-based analytical performance in the field. In this work, we report real-time *in-situ* nitrite and nitrate data from aeration tanks and final effluents of several wastewater treatment facilities. This level of *in-situ* analysis performance had not been previously available within the wastewater treatment sector. The delivery of this new dataset creates opportunities to control processes in a way that has not been possible before. Using this data there is potential for processes to be optimised to achieve energy savings by improved understanding of the aeration process, to potentially reduce nitrous oxide (N_2O) emissions and to improve management of nutrient pollution from wastewater treatment facilities.

Keywords (maximum 6 in alphabetical order)
Activated Sludge, *In-situ* monitoring, Process Control, Wastewater Treatment

INTRODUCTION

Environmental water quality has been heavily impacted due to growing global population and development of anthropogenic activities and industry. The most prevalent global water quality problem is nutrient pollution [1]. These pollutants are key parameters when considering wastewater treatment and management. At present, their monitoring predominantly consists of manual sample collection which is then transported for laboratory analysis. This method has drawbacks including cost and results are only available typically several days after sampling. This leads to the possibility of pollution events being missed and provides only limited information on the real time status of processes.

In recent years, significant progress has taken place in the field of *in-situ* analysers to improve established approaches. In this work, for the first time, a new set of data which has not been previously available in the sector is provided using Aquamonitrix, a novel technology platform for real-time selective *in-situ* monitoring of NO_2^- and NO_3^-. The system delivers lab-based analytical performance in the field and examples of this performance are reported. The system was deployed in several facilities were it successfully delivered real-time *in-situ* NO_2^- and NO_3^- data from activated sludge (AS) and final effluent.

MATERIALS AND METHODS

Automated *in-situ* nitrite and nitrate analyser

The Aquamonitrix deployable nitrite and nitrate analyser (Figure 1) was utilised in this work. The system employs rapid ion chromatography with a 235 nm LED-based absorbance detector module for selective detection of both nitrite and nitrate [2, 3]. The portable ion chromatography (IC) configuration used an eluent of 120 mM sodium chloride, so the analyser is environmentally friendly and does not use or generate any hazardous materials. The analyser included an internet-of-things (IoT) module to allow for real-time communication of concentration data and remote management of the system. Several systems were deployed within the aeration tank of a wastewater treatment facility in Ireland and within the aeration tank and final effluent of a wastewater treatment facility located in the UK.

Figure 1. Aquamonitrix real-time *in-situ* NO_2^- and NO_3^- analyser. The exterior dimensions of the unit are 60 × 37 × 27 cm and the unit weighs ~ 11 kg.

RESULTS AND DISCUSSION

The *in-situ* analyser has been assessed and verified for application within wastewater treatment facilities through analytical performance trials designed according to ISO 14034:2016 Environmental Technology Verification (ETV) standards. The analyser was deployed within septic tank water for a one-month trial led by the US EPA. The analyser was also deployed within final effluent of a Scottish Water facility for 3 months. An example of the typical analytical performance of the system in wastewater applications is illustrated in Figure 2. The average accuracy achieved by the system is ca.95% and an average precision of ± 5% is typically achieved.

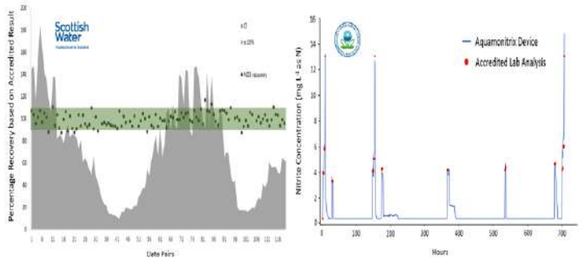

Figure 2. Demonstration of Aquamonitrix accuracy and precision in wastewaters. (Left) Accuracy assessment for Nitrate monitoring in wastewater effluent carried out by Scottish Water. The salinity of the wastewater varied yet accuracy was >90% throughout the 3-month deployment. (Right) Nitrite performance results from one-month verification monitoring within septic tank water performed by the US EPA. An accuracy of >95% for nitrite in septic tank water was obtained for the one-month deployment.

The real-time *in-situ* nitrite and nitrate analyser was deployed in a wastewater treatment plant in Ireland and in the UK for the analysis of AS and final effluent. An example of the real-time data generated is shown in Figure 3. The deployment delivered a level of *in-situ* analytical performance that has not previously been available within the wastewater treatment sector. No other analyser to this point has provided real-time nitrite and nitrate data which can be remotely accessed from ASP. The system provides advantages over the established approach of manual sampling and laboratory analysis, including the use of non-hazardous or toxic solutions; real-time *in-situ* data while delivering laboratory-analytical performance results.

The availability of this new set of data creates opportunities to optimise processes within the sector. The monitoring of final effluents in real time will aid to identify pollution events and mitigate or prevent them by taking immediate action. Aeration consists of a multi-step biological conversion of ammonia to nitrogen gas in which nitrite and nitrate are intermediates. Through real-time nitrite and nitrate data, an improved understanding of the nitrification and denitrification status within the aeration process could be enabled. This could facilitate improved process control towards the mitigation of N_2O emissions from wastewater treatment plants. Also, automation and linkage between aeration and NO_2^- is key to maximise energy savings. Monitoring of these nutrients in real time in ASP could potentially help to optimise the aeration process and save energy costs since up to 50% of energy consumption in wastewater treatment plants is attributed to aeration in ASP, being the single-most energy-intensive operation of the treatment.

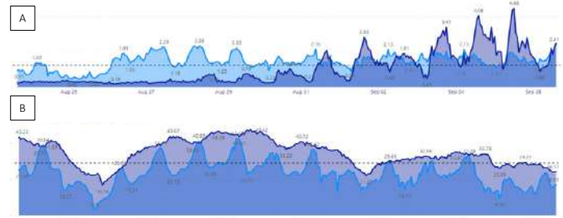

Figure 3. Real-time nitrite and nitrate data from portable analyser deployed in wastewater treatment plant in activated sludge process (light blue) and final effluent (dark blue). **3A**. Nitrite concentrations (mg/L as N) from wastewater treatment plant deployment. **3B**. Nitrate concentrations (mg/L as N) from wastewater treatment plant deployment.

REFERENCES

[1] United Nations, International Decade for Action "Water for Life", 2014
[2] Murray, E., Roche, P., Harrington, K., McCaul, M., Moore, B., Morrin, A., Diamond, D., Paull, B. 2019. Low-cost 235 nm ultra-violet light-emitting diode-based absorbance detector for application in a portable ion chromatography system for nitrite and nitrate monitoring. *Journal of Chromatography A* **1603**, 8-14.
[3] Murray, E., Roche, P., Briet, M., Moore, B., Morrin, A., Diamond, D., Paull, B. 2020 Fully automated, low-cost ion chromatography system for in-situ analysis of nitrite and nitrate in natural waters. *Talanta* **216**, 120955.

Prediction of methane production of co-digestion of pig manure in WWTP based on metabolic and machine learning models

M. J. Tárrega*, C. Lafita** and D. Aguado***

* Gran Vía Marqués del Turia, 17, 46005 Valencia, Spain; Universitat Politècnica de València, Camí de Vera s/n, 46022, Valencia, Spain
(E-mail: mjtarrega@globalomnium.com; mjotarma@postgrado.upv.es)
** Gran Vía Marqués del Turia, 17, 46005 Valencia, Spain
(E-mail: carlalo@globalomnium.com)
***Universitat Politècnica de València, Camí de Vera s/n, 46022, Valencia, Spain
(E-mail: daaggar@hma.upv.es)

Abstract
The search of appropriate predictive methane production models is a high priority to optimize anaerobic co-digestion in wastewater treatment plants. The methodology involved included the comparison between two regression machine learning models (Random Forest and Support Vector) and one metabolic model (Modified Gompertz) applied using pig manure as co-substrate in laboratory scale digesters fed discontinuously. The use of machine learning models allows predicting biogas production in systems with pig manure co-digestion The model with the best fit in this study was the Vector Support Regression model with 77% adjustments.

Keywords (maximum 6 in alphabetical order)
Anaerobic digestion; co-digestion; machine learning; methane prediction; pig manure

INTRODUCTION

In Europe about of 216 million tonnes of pig manure are produced yearly (Foged et al., 2011). This waste is estimated to have a potential methane production rate by anaerobic digestion around 0.25-0.5 Nm^3CH_4 per kg of volatile matter (Steffen et al., 1998), which results in an energy production of 165 GWh that is enough for supplying energy to 30 million people. The digestion of pig manure can be done in wastewater treatment plants (WWTP) as co-substrate in order to make good the existing digesters.

Machine learning (ML) is a data driven method for modelling that considers processes as a black-box models from input and output measurements, thereby facilitating prediction capability based on observations (Rudin, 2019). Thus, the implementation of this type of models is an effective way to predict and determine biogas production (Tufaner and Demirci, 2020) and, therefore, to optimize anaerobic co-digestion process (Jeong et al., 2021) by facilitating the decision-making process (De Clercq et al., 2019). Despite this, automated control strategies have not yet been successful implemented, so ML-based models have emerged as promising tools for prediction and decision-making for anaerobic co-digestion process.

The goal of this study is to develop a model based on ML for the improvement of methane production in the co-digestion of pig manure and sewage sludge in WWTP by the prediction of biogas production. To achieve this, Modified Gompertz, Random Forest (RF) and Support Vector (SVR) regressions were applied to a data set obtaining from discontinuous laboratory scale reactors and compared.

MATERIALS AND METHODS

Raw data collection

Every quarter of hour methane production was collected from six 1 L digesters (35 °C), three inoculated with adapted digestate to pig manure as co-substrate (SA) and three with non-adapted one (SNA). Organic matter (COD and volatile solids) and ammonia concentration were measured twice a week. All digesters were fed three times a week with a mixture of primary and secondary sludge (weekly total of 0.8 $kgVS/m^3$ digester), one SA and another SNA were fed three times a week with pig manure to a weekly total of 0.5 $kgVS/m^3$ digester and one SA and one SNA were fed once a week with pig manure at 0.5 $kgVS/m^3$ digester.

The data set obtained from the instantaneous flow produced in the laboratory digesters was 265 days

Models applied

The study applied both metabolic and regression models to predict methane output. To explore which models could most accurately predict methane production, the parameters of the Gompertz functions were based on empirical data from batch trials and tested. The ML algorithms (RF and SVR) were trained and tested with data recorded continuously and separated in training set and test set. Modified Gompertz assumed that the biogas production kinetics have a correspondence to specific growth rate of methanogens and in this study was evaluated based on root square error (R^2). On the other hand, RF is a non-parametric statistical method that permits regression and classification problems and SVR tries to find a hyperplane in the feature space that divides different categories of observations to the largest separation. Both, RF and SVR, were evaluated using the R^2 correlation coefficient.

RESULTS AND DISCUSSION

The application of the modified Gomperz model had an initial RMSE fit of 0.977, however, this fit decreased over time until 0.542, evidencing the need to recalculate the parameters frequently. The RFR model showed a fit of 0.756 and the fit obtained for the SVR model was 0.776.

REFERENCES

De Clercq, D., Jalota, D., Shang, R., Ni, K., Zhang, Z., Khan, A., Wen, Z., Caicedo, L., Yuan, K. 2019. Machine learning powered software for accurate prediction of biogas production: A case study on industrial-scale Chinese production data. *Journal of Cleaner Production* **218**, 390-399.

Foged, H.L., Flotats, X., Bonmati A., Palatsi, J., Magri, A. and Schelde K.M. 2011. Inventory of manure processing activities in Europe. Technical Report No. I concerning "Manure Processing Activities in Europe" to the European Commission, *Directorate-General Environment*. 138 pp.

Jeong, K., Abbas, A., Shin, J., Son, M., Kim, Y.M., Cho, K. H. 2021. Prediction of biogas production in anaerobic co-digestion of organic wastes using deep learning models. *Water Research* **205**(117697), 1-11.

Rudin, C. 2019. Stop explaining black box machine learning models for high stakes decisions and use interpretable models instead. *Nature Machine Intelligence* **1**(5), 206-2015.

Steffen, R., Szolar, O., Braun, R. 1998. Feedstocks for anaerobic digestion. *Institute of Agrobiotechnology Tulin, University of Agricultural Sciences, Vienna*.

Tufaner, F., Demirci, Y. 2020. Prediction of biogas production rate from anaerobic hybrid reactor by artificial neural network and nonlinear regressions models. *Clean Techenology Environment* **22**(3), 713-724.

ACKNOWLEDGMENTS

This research has been partly funded by the LIFE Program by the project LIFE ECOdigestion 2.0 'Innovative technology scale-up for the control and automation of co-digestion in WWTPs to produce energy on demand' under grant number LIFE19 ENV/ES/000098. María José Tárrega is partly funded by Agència Valenciana de la Innovació (AVI) and is likely to be co-financed by the European Union through the Operational Program of the European Regional Development Fund (ERDF) of Valencian Region 2021-2027 (Exp. INNTA3/2022/7). The authors are indebted to EPSAR, Entidad Pública de Saneamiento de Aguas Residuales de la Comunidad Valenciana from the Conselleria de Agricultura, Desarrollo Rural, Emergencia Climática y Transición Ecológica, Generalitat Valenciana.

Table 1. Parameter values of Modified Gompertz model for each digestate (SA and SNA) and feeding: only sewage sludge (0.8 $kgVS/m^3$ digester), sewage sludge + pig manure fed 3 times/week (total of 0.5 $kgVS/m^3$ digester/week) and sewage sludge + pig manure fed 1 time/week (total of 0.5 $kgVS/m^3$ digester/week).

Sample	Sludge	Rmax, LCH_4 /kgVS/d	λ, d^{-1}	BMPT, LCH_4 /kgVS	RMSE
Only sludge	SA	132±59	0.00±0.00	84±5	0.95±0.04
	SNA	98±87	0.00±0.00	59±30	0.03±0.98
Feeding 3 times/week	SA	171±136	0.10±0.06	124±8	0.99±0.00
	SNA	80±69	0.00±0.00	81±68	0.96±0.03
Feeding 1 time/week	SA	88±99	0.11±0.15	152±177	0.97±0.03
	SNA	80±87	0.07±0.10	152±177	0.97±0.04

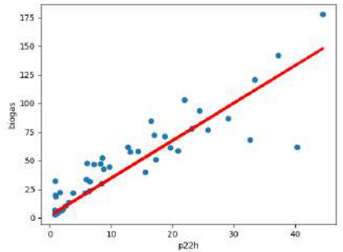

Figure 1. The figure shows the representation of the test data against the simulated data using the SVR model.

Aerial Mapping of Pollution and Odour in a Wastewater Treatment Plant: the SNIFFIRDRONE project

J. Alonso-Valdesueiro*, A. Benegiamo**, M.D. Esclapez***, L. Terrén***, L. Sauco***, S. Doñate***, S. Marco**, and A. Gutierrez-Galvez*

*Department of Electronics and Biomedical Engineering, University of Barcelona, Martí I Franquès 1, Barcelona, Spain. (E-mail: javier.alonsov@ub.edu, agutierrez@ub.edu)
**Signal and Information Processing for Sensing Systems, Institute for Bioengineering of Catalonia, Baldiri Reixac 10-12, Barcelona, Spain. (E-mail: abenegiamo@ibecbarcelona.eu, smarco@ibecbarcelona.eu)
*** Depuración de Aguas del Mediterráneo, Av. Benjamín Franklin, 21, 46980 Paterna, Valencia, Spain. (E-mail: silvia.donate@dam-aguas.es)

Abstract

This abstract introduces the advances to bring a drone-based chemical monitoring system to a more mature technological level within the framework of the SNIFFIRDRONE project. To improve the temporal resolution of our monitoring system we have reduced the chemical sensor chamber to a point of having only 25 mm^3 per single sensor cavity. This will dramatically reduce the air mixing effect of the chamber allowing for a better temporal resolution of the measurements. As a case study, we performed a measurement campaign in Torredembarra wastewater treatment plant. This preliminary results show the locations where the emissions of H_2S and NH_3 are higher.

Keywords
Drone-based monitoring, Chemical sensing, odour mapping, wastewater treatment plant

INTRODUCTION

In this work, we present a drone-based pollution and odour monitoring system for wastewater treatment plants. We will focus on the advances to bringing our current system [Burgués et al., 2022] to a more technologically mature status within the framework of the SNIFFIRDRONE project. The main objectives of the project are three. First, development of a high-performance multi-gas NDIR sensing unit that will allow a faster measurement of relevant chemicals such as H2S and NH3. Second, generation of a map of the environmental chemical emissions of the wastewater plant. Third, generation of a second map of the environmental odour within the plant. We use a machine learning model to predict the odour generated.

Our current system is composed by a Matrice 600 DJI drone equipped with a custom made IOMS with 21 chemical sensors and an air sampling system. The challenges we face to increase the Technology Readiness Level of the system to TRL7 are the following three: (1) Increasing the temporal resolution of measurements, (2) improving the system robustness, and (3) obtaining enough experimental data to train and validate the odour prediction models.

MATERIALS AND METHODS

We must consider two main factors that limit the temporal resolution of the measurements (1): the measuring time of the sensors and the volume of the sensor chamber. The measuring time of the sensors will be reduced with the new NDIR multi-gas sensor unit. On the other hand, the sensor chamber limits the temporal resolution of the measurements due to its air mixing effect. It mixes the air accumulated into the chamber in a certain time period before the measurement. As a result, we are measuring an accumulated concentration during this time period instead of the specific time measurement we are seeking. Considering that the length of this mixing time period is proportional to the volume of the chamber, we vanish this effect by reducing considerably the chamber volume. In Figure 1(b), we can see the design of the new sensor chamber where the volume has been reduced to 25 mm^3 of a single sensor cavity when in the previous chamber [Burgués et al., 2021] was 96 cm^3 for the total sensor chamber. The compact and design of the new chamber that includes all needed electronics attached to it makes the system much more robust (2).

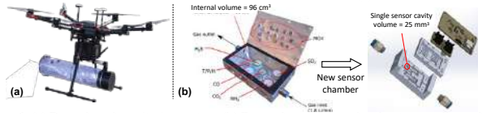

Figure 1. (a) Drone-based monitoring system. (b) From a larger sensor chamber to a smaller and more robust chamber design

RESULTS AND DISCUSSION

To collect enough data (3) within the SNIFFIRDRONE project we have planned 9 campaigns during the summer of 2022, 2023, and 2024. Figure 2 shows results obtained in measurements in Torredembarra WWTP during summer 2022. Overlaid on top of the plant map, we have the measuring path followed to cover the plant extension. The sensor responses show a clear increase on NH_3 and H_2S at $t \cong 1950$ s as we get close to the pre-treatment building (white building bottom left). There is also a lower-level signal, more noticeable in the MOX sensors, at $t \cong 1250$ s as we pass by the bioreactors. These preliminary results show that the concentration levels of H_2S and NH_3 are very low around all the plant except mostly in one location, around the pre-treatment building.

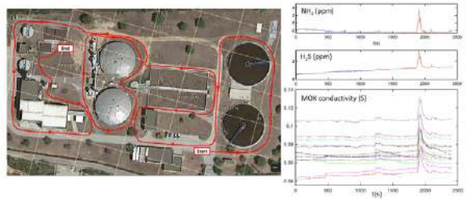

Figure 2. Measuring campaign in Torredembarra wastewater treatment plant

AGREEMENTS

This project has received funding from the European Union's Horizon 2020 research and innovation program under Grant Agreement No. 101004462.

REFERENCES

Burgués, J., Doñate, S., Esclapez M.D., Sauco, L., Marco, S., 2022 Characterization of odour emissions in a wastewater treatment plant using a drone-based chemical sensor system. *Science of The Total Environment* **846**, 157290

Burgués, J., Doñate, S., Esclapez M.D., Marco, S., 2021 RHINOS: A lightweight portable electronic nose for real-time odor quantification in wastewater treatment plants. *iScience* **24**(12), 103371

Study of atmospheric pollutants generated in wastewater treatment plants using Artificial Intelligence

L. Terrén*, M.D. Esclapez*, S. Doñate*, E. César*, M. Pignatelli**, X. Torret***, L. Saúco*

* Depuración de Aguas del Mediterráneo, Av. Benjamín Franklin, 21, 46980 Paterna, Valencia, Spain.
(E-mail*: lidia.sauco@dam-aguas.es; lara.terren@dam-aguas.es)*
**UTE Torredembarra, SORIGUÉ-DAM, 43761 Clará, Tarragona, Spain
*** BGEO Open GIS, SL. Carrer de Pinós, 1, 078402 Granollers, Barcelona, Spain.

Abstract
The monitoring of the emission of gases from wastewater facilities and their impact is a necessity to have preventive and corrective measures that are best adapted to each focus or nuisance, always seeking the greatest efficiency and sustainability. This study, carried out in the wastewater facilities of Torredembarra, in Catalonia, Spain, aims to predict the H_2S concentration using Artificial Intelligence (AI) and Machine Learning (ML) tools, such as Neural Networks, Linear and Nonlinear Regression.

Keywords
Artificial intelligence; hydrogen sulphide; machine learning; neural networks; prediction; wastewater treatment plant

INTRODUCTION

Wastewater treatment plants (WWTPs) are considered important sources of gaseous emissions, including greenhouse gases (GHG) and odorants (Shaw and Koh, 2018). Malodours causes several negative impacts such as: (i) complaints and discomfort around pumping stations, network sewages and WWTP; (ii) reduction in property and real estate value; (iii) labour risks for operators; (iv) corrosion of exposed equipment and facilities. Hydrogen sulphide (H_2S) is the most important of all odour compounds generated in WWTPs and sewage systems (Vincent y Hobson 1998).

Depuración de Aguas del Mediterráneo (DAM) participates together with BGEO in the analysis of odoriferous gases and how they are influenced by variables such as temperature, retention time, humidity and flow, among others.

The study aims to predict, through Artificial Intelligence (AI) and Machine Learning (ML) tools, the H_2S emissions in a particular section of the wastewater facilities (Zounemat-Kermania et al., 2019), in order to efficiently minimise the release of this pollutant downstream.

MATERIALS AND METHODS

The project will be carried out in the facilities of Torredembarra (Tarragona, Spain) through the following stages:

(i) Research of odoriferous gases, their generation and emission. This will allow finding out the main compounds that cause bad odours and the main gas emission points in the facility. At this stage, an optimal AI algorithm for this real case will be proposed.

(ii) Selection of the case study, variables to monitor and installation of the equipment for data collection (Table 1) and assembly of the database. A database will be generated with, at least, one month of data.

(iii) Design, assembly and train the prediction algorithm.

Table 1. Device and sources used for the study

Device/Source	Parameter	Units	Location
Kunak Air Lite	Env. temperature; humidity	ºC; %	EBAR General
Proline Prosonic Flow 93T	WW flow	m^3/h	Line EBAR-EDAR
Sulfilogger S1-1290	H_2S liq, water temperature	mg/L, ºC	EBAR General
Sulfilogger S1-1290	H_2S liq	mg/L	Pretreat. EDAR
Ijinus LOGAZPRO-200X-H2S-8X	H_2S gas	ppm	EBAR General
Ijinus LOGAZPRO-200X-H2S-8X	H_2S gas	ppm	EBAR General
National station	Sea level height	m	Tarragona station

RESULTS AND DISCUSSION

Predicting hydrogen sulphide generated in WWTPs and sanitation networks could be a challenge for Machine Learning algorithms, since a wide variety of interfering chemical compounds and other environmental factors are also involved. Currently, three weeks of data is being collected and a recurrent neural network will be used for the prediction of the gas between the last pumping station and the entrance of the WWTP.

At the end of this work, it is expected to achieve predictions of H_2S in liquid or gas at a given point, at least one hour earlier (less than the hydraulic retention time from the start to end point). It will be possible to optimise the actions to minimise the pollutant emissions and anticipate possible odorous impacts in the facility surroundings.

AGREEMENTS

The study described in this paper is part of a research project called atmosphAIr (AEI-010500-2022B-8), coordinated by the Catalan Water Partnership (CWP) and financed by the Ministry of Industry, Trade and Tourism of Spain under the Innovative Business Groups support program (AEI) in the frame of the NextGeneration EU - The Recovery and Resilience Plan.

The entire project seeks to predict and mitigate emissions of both odorous gases and greenhouse gases in sanitation networks and wastewater treatment plants. A consortium made up of the CWP itself, DAM, ACSA, Obras e Infraestructuras, SAU (Sorigué Group), BGEO OPEN GIS S.L, AERIS Tecnologías Ambientales S.L. and SPIN S.A participate in the project.

REFERENCES

Koh, S., Shaw, A. **2018** Gaseous Emissions from Wastewater Facilities. *Water Environment Research.*

Vincent A, Hobson J. **1998**. Odour control. CIWEM monographs on best practice no. 2. London, UK: Chartered Institution of Water and Environmental Management, 1998. pp. 31

Zounemat-Kermania M., Stephanb, D., Hinkelmannc, R. **2019**. Multivariant NARX neural network in prediction gaseous emission within the influent chamber of wastewater treatment plants. *Atmospheric Pollution Research.*

Effect of temperature on the kinetics of methane production in the co-digestion of manure and agri-food waste in WWTP

M. J. Tarrega*, C. Lafita**, P. Granell*** and T. Montoya****

* Gran Vía Marqués del Turia, 17, 46005 Valencia, Spain; Universitat Politècnica de València, Camí de Vera s/n, 46022, Valencia, Spain
(E-mail: mjtarrega@globalomnium.com; mjotarma@postgrado.upv.es)
** Gran Vía Marqués del Turia, 17, 46005 Valencia, Spain
(E-mail: carlalo@globalomnium.com)
** Gran Vía Marqués del Turia, 17, 46005 Valencia, Spain
(E-mail: pgranell@globalomnium.com)
** Gran Vía Marqués del Turia, 17, 46005 Valencia, Spain
(E-mail: tmontoya@globalomnium.com)

Abstract
The methane generation rate and the biodegradability index (BI) of agri-food residues and manure in digesters at different temperatures were determined. In this study the biochemical methanogenic potential (BMP) of the residue according to its composition was compared with the empirical BMP determined by batch tests. Subsequently, these empirical tests were modelled with two methodologies: first-order kinetic model to determine the degradation constant of the residue (obtaining kSA of 0.73-0.87 and kSNA of 0.80-2.07d-1) and through the use of sigmoidal model to calculate the lag phase (λ) and the maximum rate of methane production (Rmax), obtaining lag phase values λSA of 0.02-0.08 and λSNA 0.01-0.02d-1.
The results showed that this type of residue can be valorised in WWTP anaerobic digesters prior to acclimatization, obtaining BISA of 75.4-76.7% and that both modelling methodologies enable the simulation of methane production over time.
Keywords: anaerobic co-digestion; manure; modelling; kinetics; ammonia inhibition

Keywords (maximum 6 in alphabetical order)
Anaerobic co-digestion; agrifood waste; kinetics; manure; modelling; temperature

INTRODUCTION

The energy consumption in wastewater treatment plants (WWTPs) varies depending on volume of water treated, organic load and the type of treatment technology used and it is estimated to entail in typical WWTPs between 25 and 40 % of total operating costs (Panepinto et al., 2016). This value varies between the range of approximately 0.3-2.1 kWh/m3 of treated wastewater (Gandiglio et al., 2017). Albadalejo et al. (2014) concluded that the energy consumption increases in an exponential way while the size of WWTP decreases, from values of 0.286 kWh/m3 of wastewater treated in facilities for the treatment of 200,000 population equivalent (p.e.) to 2.807 kWh/m3 of wastewater treated for the treatment of 250 p.e. In addition to the economic costs for the use of energy, which in the current context are increasing, the use of energy in WWTP, mostly from fossil sources, causes the emission of 27 million tons of CO2 in the EU (Lotti, 2016). On the other hand, Spain produces 22% of all pig heads in the EU (Foged et al., 2011), which implies the need to manage approximately 36,083 miles of tons of manure per year, that have the potential production of 992 million cubic meters of biogas by anaerobic digestion, which represents 1.2% of the annual production of natural gas. This biogas production have to be summarized to the annual energy production from wastewater that it is estimated in 11,062 GWh. In this context, the present work proposes the application of the concepts of the circular economy in the treatment of agri-food waste and pig manure through their co-digestion in WWTP digesters. Thus, a circular solution is proposed for the waste generated while obtaining renewable energy.

The anaerobic digestion process can be carried out in a wide range of temperatures. Within the same system, methane generation rates will depend on the optimum temperature of the microbial population present. Despite the advantages of co-digestion in WWTP, co-digestion of agri-food waste can cause overloads and acidification of the system. On the other hand, the codigestion of manure presents a series of challenges, such as: i) inhibition due to a high concentration of ammonium, ii) high alkalinity content of the pig manure, iii) inhibition due to a high metal content and iv) inhibition of the process by the presence of antibiotics. For this reason, in this work the effect of the digestion temperature of agri-food waste and pig manure in WWTP digesters on the kinetics of methane production has been evaluated.

MATERIALS AND METHODS

Experiments were carried out in batch at laboratory scale in Automatic Methane Potential Test System, AMPTS II (Bioprocess Control, Sweden) using an inocula adapted to manure degradation from WWTP digester. The assays were conducted for the determination of kinetics constants with five replicates at four different concentrations (0.25, 0.5, 1 and 2 kg volatile solids (VS) of pig manure/m3) plus blank at mesophilic conditions (35 °C). The experiments were finished when the instantaneous methane production matched that of the blanks.

The determination of the theoretical methanogenic potential was carried out based on the nutritional composition of the pig manure, and for the determination of the degradation kinetics, first-order kinetics were assumed for hydrolysis and Monod kinetics for the semi-saturation constants. The determination of the lag phase was made using the modified Gompertz model.

The statistical indicators correlation coefficient (R2) and root mean square error (RMSE) were used to assess the mathematical adaptation of applied models and t-student tests were applied to evaluate the fitting of the results obtained for the different organic loads and parameters obtained with the studied models.

RESULTS AND DISCUSSION

Acknowledgements
This research has been partly funded by the LIFE Program by the project LIFE ECOdigestion 2.0 'Innovative technology scale-up for the control and automation of co-digestion in WWTPs to produce energy on demand' under grant number LIFE19 ENV/ES/000098.
The authors are indebted to EPSAR, Entidad Pública de Saneamiento de Aguas Residuales de la Comunidad Valenciana from the Conselleria de Agricultura, Desarrollo Rural, Emergencia Climática y Transición Ecológica, Generalitat Valenciana and

Table 1. This is an example of table layout. It shows the dimensions of the text area to be used for *Water Science and Technology* articles and of international and US paper sizes (and the consequent recommended margin settings). Note that a minimum number of horizontal rules and (usually) no vertical rules are used.

	Text area	A4 paper		US (Imperial) paper	
	(mm)	(mm)	(in)	(mm)	(in)
Depth	250	297	11.69	279.32	11.0
Top/bottom margin	-	25	1.0	15	0.6
Width	170	210	8.27	215.84	8.5
Left/right margin	-	20	0.8	23	0.9

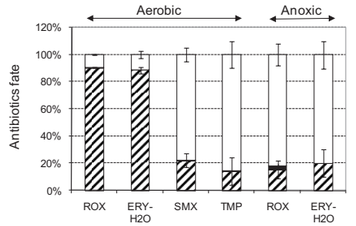

Figure 1. All figures should be embedded correctly positioned within your Word file.

REFERENCES

Albadalejo, A., Trapote, A., Simón, P. (2014). Energy consumption in an urban wastewater treatment plant: the case of Murcia Region (Spain). Civ. Eng. Environ. Syst. 31: 4.

Foged, Henning Lyngsø, Xavier Flotats, August Bonmati Blasi, Jordi Palatsi, Albert Magri and Karl Martin Schelde. 2011. Inventory of manure processing activities in Europe. Technical Report No. I concerning "Manure Processing Activities in Europe" to the European Commission, Directorate-General Environment. 138 pp.

Gandiglio, M., Lanzini, A., Soto, A., Leone, P., Santarelli, M. (2017). Enhancing the energy efficiency of wastewater treatment plants through co-digestion and fuel cell systems. Front. Environ. Sci. 5:70.

Lotti, T. (2016). Developing anammox for mainstream municipal wastewater treatment. PhD Thesis, Department of Civiele en Milieu Ingenieur. University of Florence, Italy.

Panepinto, D., Fiore, S., Zappone, M., Genon, G., and Meucci, L. (2016). Evaluation of the energy efficiency of a large wastewater treatment plant in Italy. Appl. Energy 161, 404–411.

Digital Water at Consorci Besòs Tordera

J. Tellez-Alvarez*,**, M. Centeno* and S. Riera*

* Department of Operations, Consorci Besòs Tordera, 241 Sant Julia Avenue, 08403, Granollers, Barcelona, Spain. (E-mail: jdtellez@besos-tordera.cat; mcenteno@besos-tordera.cat; sriera@besos-tordera.cat)
** Flumen Research Institute, Department of Civil and Environmental Engineering, Technical University of Catalonia, 0834 Barcelona, Spain (jackson.david.tellez@upc.edu)

Abstract
The purpose of the project "Digital Twin at Consorci Besòs Tordera (CBT) is to generate a single Centre of Operations to collect, organize and analyse all the information of the facilities in order to reproduce simulations, integrations, testing, monitoring and maintenance, etc. The develop of the operational decision support is focused to improve the control of combined sewer overflows (CSOs) in a sewer systems and proactive maintenance and process optimisation of a Waste Water Treatment Plant (WWTP).

Keywords
Digital Twin, BIM, Monitoring, modelling, sensors, sewers, Combined Sewer Overflow (CSO)

INTRODUCTION

Digital twins are a combination of models and real-time data that provide a digital representation of the behaviour of the water systems or part of its, being the main advantage of the digital twins is to improve the performance of the infrastructures.
The purpose of the project "Digital Twin at Consorci Besòs Tordera (CBT) is to generate a single Centre of Operations of all the facilities that be capable to collect, organize and analyse all the information in a single place through a digital model of the physicals installations for each sanitation system of CBT capable to reproduce simulations, integrations, testing, monitoring and maintenance, etc.
In this work, the develop of the operational decision support is focused to improve the control of combined sewer overflows (CSOs) in a sewer systems and proactive maintenance and process optimisation of a Waste Water Treatment Plant (WWTP).
The Consorci Besòs Tordera (CBT) is a Local Water Authority founded in 1988, with the main objective is to conserve the water quality of the Besòs river to guarantee the fish life on it. Among the activities of the CBT is the management, operation and maintenance of the water sanitation facilities, made up of a set of 27 WWTPs, 300 km of sewer pipes and 52 pumping stations.

METHODOLOGY

Since 2020, the CBT started the implementation of the Digital Twin, where was proposed a conceptual scheme as shown in the Figure 1, where the methodology was defined accord the process of the water cycle. Furthermore, once the structure of Digital Twin will be possible to optimization the systems, have energy saving, improve the quality of water and inform the citizen.
The implementation of the Digital Model was selected as a pilot case the WWTP located in Caldes de Montbui. The WWTP is designed to cover a population of 30,000 equivalent inhabitants, with a daily flowrate of 6,000 m³ and it collects the wastewater from the municipality of Caldes de Montbui that has 12,10 km long of sewer network.

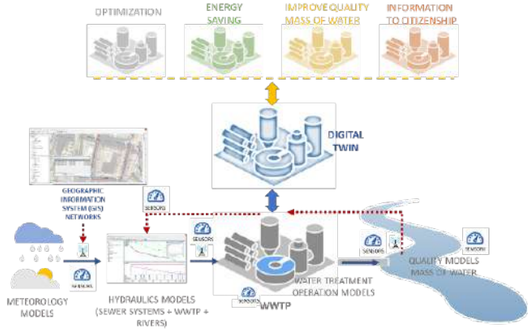

Figure 1. Basic Structure of Digital Twin Application in the ambit of CBT.

The first Digital model developed as BIM model was been the WWTP of Caldes de Montbui as shown in the Figure 2, where this model has a 3D repository of each element. In order to have a BIM model active to navigate, was necessary to generate a protocol of the general approach to combine different software's as asset management, management of sanitary systems, GIS, and SCADA (Riera i Llordella et al., 2022).
The use of 3D models will make it possible to have updated graphic information on the installations, which will include all the modifications/extensions made to the installation throughout its useful life.

Figure 2. Building Information Modelling (BIM) of WWTP of Caldes de Montbui.

In order to avoid using different software to obtain specific data, and to avoid having the same duplicate data in two different databases, the CBT has decided to create a digital twin through a middleware platform that ensures correct integration between the 3D models and management software (Figure 3). The middleware platform generates a central database and collects the information from all the software that is in the solution to feed said database. With this middleware platform, it will be possible to guarantee the bidirectionality of the information.

Figure 4. Relation of software's in the Digital Twin of CBT

The integration between BIM model and platform of Middleware was using the software ecodomus as shown in the Figure 5, with this result is possible to navigate and consult the characteristics and maintenance of each element.

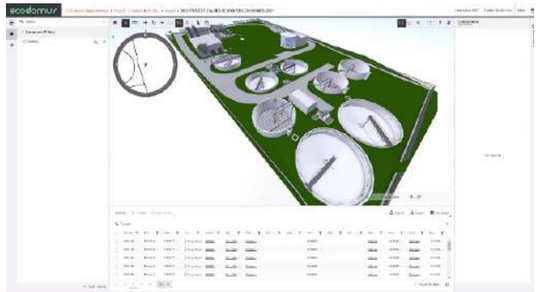

Figure 5. Relation of software's in the Digital Twin of CBT

In parallel, this study presents a methodology for outfalls' monitoring of Combined Sewer Systems (CSS) for the sewer network managed by Consorci Besòs Tordera (CBT), in the framework of the projects MIMER (Intelligent Discharge Monitoring to Receiving Environment using Overflow Sensors) and SewMo (Sewer network Modelling in rain events). The pollution of receiving water bodies resulting from Combined Sewer Overflows (CSO), especially in rain events, is a problem to tackle in the cities' sanitation facilities management, which have a dramatic impact in the environment and hence, the quantification of the spilled volume and water quality during these events, as well as their periodicity, is of paramount importance.
This technical study proposes the analysis of methodologies to determine, estimate, quantify, categorize and minimize the episodes of discharges into the river. The purpose of this study is the reduction of the impacts of these discharges in the framework of the public sanitation systems managed by CBT —about 300 km of sewer network— in order to improve the quality of the receiving water bodies when CSOs during rain events occur (Tellez-Alvarez, et al., 2022).
Spanish Royal Legislative Decree (RD) 1290/2012 (MAAMA, 2012) established that companies and public institutions involved in urban water drainage services are compelled to monitor, detect and quantify direct discharges into the environment (Cosco et al., 2018). For this reason, methodologies such as the one presented here are essential, in order to fulfil the requirements of RD 1290/2012. Hence, for the last years CBT has been installing new sensors for monitoring and modelling the network in its ambit, especially in the outfall points [2], whilst also periodically reporting to the Catalan Water Agency (ACA) about instrumentation of the drainage network using overflows sensors (OS) and level sensors (LS), respectively, for several of the sanitation systems which manage.

RESULTS AND CONCLUSION

The digital twin is a tool for Decision Support for engineers and techniques capable to visualised quickly the effects of the systems, and generate real or future scenarios. Also, is possible to elaborate a comparison between model predictions and measured data which require particular attention by operators and maintenance staff, thus minimising their efforts.
In order to achieve the objective of reducing the impacts of the CSOs of CBT systems to the environment, the technical study presented here has been developed. Specifically, here the behaviour of sewer networks is studied in order to detect criticalities and reduce related additional pollution, thus improving the water bodies in the CBT ambit.
The objective of the Besòs Tordera Consortium is, sooner rather than later, to create the digital twins of all the managed infrastructures and gradually incorporate the other management software used by the organization (LIMS Labware, Eplan, etc.), so that all the information managed by this entity is in one place and is accessible from the digital twins.

REFERENCES

Riera i Llordella, S. and Casadellà Cayuela, C. (2022). La Gestión de activos en saneamiento mediante metodología BIM, XXXVI Congres AEAS 2022, Cordoba, Spain.
Tellez-Alvarez, J., Belda, J., Begoña, M., Sonia, O. (2022). Monitoreo de desbordamientos en los sistemas de saneamiento del ámbito del Consorci Besòs Tordera, XXXVI Congres AEAS 2022, Cordoba, Spain.
Ministerio de Agricultura, Alimentación y Medio Ambiente (2012) Modificación del Reglamento Público Hidráulico de España por el que se establecen las normas aplicables al tratamiento de las aguas residuales urbanas, RD 1290/2012.
Cosco, C., Cugueró, M., Tàsias, F., Aguiló, P., Gómez, M. (2018). Sensor Placement for combined Sewer System monitoring in the Besòs River Basin, IFAC PapersOnLine 51-24 (2018) 949-956.

Quantitative Image Analysis of Biosolids: Evaluating morphological parameters versus visual features

S. O. N. Topalian*, N. Nazemzadeh*, K. Kjellberg**, D. J. Batstone***, K. V. Gernaey*, X. Flores-Alsina*, P. Ramin*

* Process and Systems Engineering Centre (PROSYS), Department of Chemical and Biochemical Engineering, Technical University of Denmark. Building 228 A, 2800, Kgs. Lyngby, Denmark. (sebtop@kt.dtu.dk, mimnaz@kt.dtu.dk, kvg@kt.dtu.dk, xfa@kt.dtu.dk, pear@kt.dtu.dk)
** Novozymes A/S, Hallas Alle 1, DK- 4400, Kalundborg, Denmark. (kpkr@novozymes.com)
*** Australian Center for Water and Environmental Biotechnology, The University of Queensland, 4 Gehrmann Laboratories Building, Research Rd, St Lucia QLD 4067, Brisbane, Australia. (d.batstone@uq.edu.au)

Abstract
Quantitative image analysis can be used to predict dewatering related sludge properties such as settling velocities or sludge volume index. Morphological parameters such as particle length and area are common features extracted and used in predictive models such as partial least squares. Here we develop a framework where the particles are analysed by a pretrained convolutional neural network (CNN), reduced with principal component analysis, grouped with K-means clustering and used in a partial least squares or random forest model to predict reject suspended and total solids related to industrial decanters treating inactivated biosolids. The models with CNN features from the CNN model had an improvement of 8% and 15% for predicting SS and TSS respectively compared to clusters built on conventional morphological parameters.

Keywords
Biosolids; Industrial WWTP; Dewatering; Quantitive Image Analysis; Transfer-learning;

INTRODUCTION

Microscopy techniques have long been used within the field of wastewater analysis for identifying biomass characteristics, viability, and composition. However, often the analysis of the microscopy information is labour intensive and requires a trained expert to distinguish for instance between different morphologies that could cause sludge bulking [1]. To automate the analytical procedure quantitative image analysis (QIA) and tools from the field of chemometrics have been combined. QIA applies a wide set of mathematical tools to segment images and obtain morphological parameters such as the length, area and circumference of particles present in the image which can be used to estimate sludge properties such as the sludge volume index (SVI). In recent years models from the field of deep learning (DL) such as convolutional neural networks (CNN) have excelled at computer vision (CV) tasks such as segmentation and classification. DL models represent end-to-end learning in the sense that they take the raw input image, generate features internally and relate the features to the output of interest [2]. The aim of this paper is to compare traditional morphological features with features obtained from a pretrained DL model in a transfer-learning (TL) approach. The features are compared in terms of their ability to predict reject quality in terms of turbidity which is deemed the best performance indicator of dewatering for the centrifugal decanters investigated here.

MATERIALS AND METHODS

Most of the studies on image characterization of sludge deal with activated sludge from municipal plants. Variations with operational impact are commonly obvious and significant [1]. Here we attempt to characterize inactivated biosolids to construct a semi-automated workflow for process monitoring and performance optimization of decanters from the largest industrial WWTP in Northern Europe located in Kalundborg (Denmark) which treats the wastewater produced at two biotech companies (Novozymes and Novo Nordisk). For a thorough description of the plant layout the reader is referred to our previous works [3-5]. Two measurement campaigns were conducted: A fall campaign from the 21st of September to the 8th of October 2021 and a spring campaign from the 28th of April to the 16th of May 2022. For each batch investigated in the two campaigns one feed sample of the inactivated biosolids was obtained, and three reject samples corresponding to 3 different polymer dosages -25%, mean, +25% where the mean polymer dosage is determined by the operators working a given shift. To obtain images that are not overcrowded a volumetric dilution factor of 20:1 is used. Since the operating pH affects the interaction energies of the particles observed in the image a sodium hydroxide solution is added after dilution so the pH is equal to the pH before dilution. The images were collected and processed off-line using a ParticleTech flow cell system and its corresponding software [6]. The morphological parameters for each particle were then recorded including: area, equivalent circular diameter (ECD), the minimum Feret diameter, the maximum Feret diameter, the mean Feret diameter, the Feret ratio, perimeter length, compactness, and circularity. For generating feature vectors, a pretrained image model such as a convolutional neural network is required. The Xception model is selected as such, optimising the trade-off between a high accuracy and a low computational demand [7]. Some of these features may be redundant – as the Xception model was trained on colourised photos, and these images are black and white. Principal component analysis (PCA) is commonly used for dimensionality reduction and in this case, it can create a more compact representation for our feature vectors by eliminating redundant variables which will speed up the clustering in the next step. Each sample photo has a different number of particles in it, and segmenting each will therefore yield a different number of particles and consequently a different number of feature vectors for each sample. For developing a model to predict reject turbidity a standard data-format is desired with an equivalent number of inputs per sample, and as such a transformation is required to go from a variable number of feature vectors per sample to a set number of feature vectors per sample. Clustering is a technique that groups similar observations into clusters and a cluster participation vector can be formed for each sample where each position in the vector represents the fraction of the total sample belonging to that respective cluster. A large variety of clustering algorithms exist and here we use K-means clustering. To predict the continuous reject solids content a regression tool is required such as partial least squares (PLS) or Random Forest (RF). For sludge characterization PLS is a widely used technique for regression, while RF has not been used thus far to the knowledge of the authors. In comparison to PLS, RF is a non-linear technique which may be able to outperform PLS if non-linear relationships are present in the data. **Figure 1** illustrates the proposed methodology.

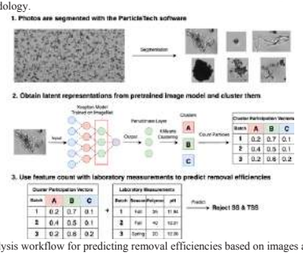

Figure 1. Analysis workflow for predicting removal efficiencies based on images and laboratory measurements.

RESULTS

Figure 2 shows the reject SS (g/kg) content for each polymer dosage for each batch. For each batch, a second order polynomial has been fit to visualize the apparent relationship between the polymer dosage and the reject quality in terms of SS. Theoretically all the response curves between polymer dosage and removal should be convex, since a concave curve implies that a negative SS measurement is possible, however since this is an empirical model with imperfect data that is not the case.

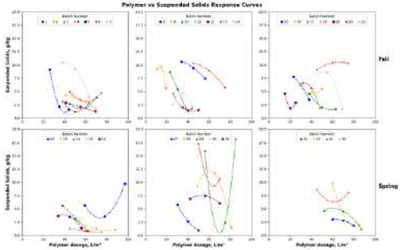

Figure 2. Measured suspended solids (g/kg) in the reject for a given polymer dosage. Each parabola corresponds to a polynomial fit between the three reject samples collected for each batch. The top and bottom plots are for fall and spring sampling campaigns respectively.

10.000 segmented photos randomly sampled from all the batches are fed through the Xception model to obtain a feature vector from the penultimate model layer for each. These feature vectors are reduced into principal components (PCs) by PCA. Before applying PCA the vectors are standardized by subtracting the mean and dividing by the standard deviation, and the variables in the obtained feature vector that are constant are removed reducing the size of the vectors from 2048 to 1731 elements. A threshold is selected where 99% of the variance is retained which corresponds to 1276 principal components, i.e., a dimensionality reduction of approximately 40% from 2048 to 1276. After the threshold of 1276 PCs is found K-means clustering is performed in conjunction with the supervised pipeline where the reject SS and TSS values are predicted. Three sets of independent variables are constructed. (i) the cluster participation vectors based on the Xception feature vectors, (ii) the mean of the morphological parameters for a sample, (iii) a cluster participation vector based on the morphological parameters. All three contain the laboratory measurements of pH of the sample taken, the adjusted pH after dilution, a continuous polymer dosage, a categorical polymer dosage, and a binary variable indicating which campaign the sample is taken from (seasonality). For each dataset a RF and PLS model is created which is trained and validated through leave-one-out cross-validation on a training set consisting of 24 of the 35 batches (covering both fall and spring campaigns) at random. This procedure is repeated 10 times with a different subset of batches each time. The performance is then evaluated in terms of a mean of root mean square errors (RMSE) on the 11 batches not used for training and validation over the 10 repetitions. This workflow is performed for different numbers of clusters to evaluate the best number of clusters for predicting reject SS and TSS. The number of clusters evaluated varies from 1 to 25. Figure 4 shows the RMSE for predicting SS and TSS in the reject as a function of the number of clusters used to characterize the obtained images.

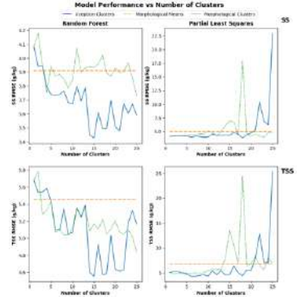

Figure 3. Performance of models as a function of the number of clusters used to characterize the images. Models predicting SS and TSS are depicted in the top and bottom row respectively, and RF and PLS models are depicted in the first and second column respectively.

Table 1. Average RMSE on an independent test set, standard deviation of RMSE, and the number of clusters associated with the given model. For predicting SS and TSS the models built on Xception clusters with RF and PLS are best respectively. The two best models are marked with asterisks.

	SS		TSS	
Reject	**RF**	**PLS**	**RF**	**PLS**
Xception Cluster	3.43 (0.51), 15*	3.82 (1.04), 18	4.55 (1.07), 15	4.33 (0.72), 10*
Morph. Mean	3.91 (0.47), 1	5.04 (1.73), 1	5.46 (1.01), 1	6.73 (3.51), 1
Morph. Cluster	3.73 (0.55), 25	3.98 (0.99), 23	4.83 (1.24), 25	5.08 (1.10), 2

Discussion

Estimating recovery in centrifugal decanters from laboratory measurements is difficult as the operation of the machine has a great influence and is unaccounted for in most methodologies that try to extrapolate from lab scale to full scale dewatering in decanters [8]. We postulate that the setup would see similar if not better results if applied to estimation of settling velocities or capillary suction time instead of reject quality in centrifugal decanters, and the methodology presented here can easily be adapted to other industrial or municipal systems for biomass characterisation and prediction of settling properties.

Conclusion

We present a new framework for utilising the power of DL vision models to extract features and track species in inactivated biosolids and relate said features for predicting reject quality in an industrial setting. The features outperform the conventional approach with morphological parameters, and we postulate that this can generalise to other QIA applications for predicting settling velocities or capillary suction time. An example of generating the utilised features from a sample of the used photos is freely available at the wwtmodels Github repository.

References

[1] Mesquita, D., Amaral, A., Ferreira, E. 2013 Activated sludge characterization through microscopy: A review on quantitative image analysis and chemometric techniques. *Analytica Chimica Acta* **802**, 14-28.

[2] Wang, J., Ma, Y., Zhang, R., Gao, X., Wu, D. 2018 Deep learning for smart manufacturing: Methods and applications. *Journal of Manufacturing Systems* **48**, 144-156.

[3] Topalian, S., Ramin, P., Kjellberg, K., Mbamba, C., Batstone, D., Gernaey, K., Flores-Alsina, X. 2023 A data analytics pipeline to optimise polymer dose strategy in a semi-continuous multi-feed dewatering system, *Preprint*

[4] Monje, V., Junicke, H., Batstone, D., Kjellberg, K., Gernaey, K., Flores-Alsina, X. 2022 Prediction of mass and volumetric flows in a full-scale industrial waste treatment plant, *Chemical Engineering Journal* **445**, 136774.

[5] Monje, V., Owsianiak, M., Junicke, H., Kjellberg, K., Gernaey, K., Flores-Alsina, X. 2022 Economic, technical, and environmental evaluation of retrofitting scenarios in a full-scale industrial wastewater treatment system, *Water Research* **223**(14), 118997.

[6] Image Equipment Utilised form ParticleTech, https://particletech.dk, visited 9th of January 9, 2023.

[7] Chollet, F., 2016 Xception: Deep Learning with Depthwise Separable Convolutions. *Proceedings of the IEEE conference on computer vision and pattern recognition*, 1251-1258.

[8] Ginisty, P., 2005 Laboratory tests to optimize sludge coagulation / floculation process before thickening or dewatering, *American Filtration and Separations Society 2005 – 18th Annual Conference*, Afs.

HADES: a digital twin for the optimization of WWTP performance

E. Muñoz-Cravioto*, C. Vázquez*,**, J. Colprim**, J. Comas**,***, M. Poch**, I. Rodríguez-Roda**, C. Koch-Ciobotaru*, M. M. Micó*

* ACCIONA, Innovation Department, Av. les Garrigues, 22, 08820, El Prat de Llobregat, Barcelona, Spain (E-mail: *edmunozc@acciona.com*)
** LEQUIA, Institut de Medi Ambient, Universitat de Girona, c/ Ma Aurèlia Capmany, 69, Campus Montilivi, 17003 Girona, Spain
*** Catalan Institute for Water Research (ICRA-CERCA), Emili Grahit 101, 17003 Girona, Spain.

Abstract
The optimization of treatment processes in wastewater treatment plants (WWTP) is crucial to achieve environmental goals and reducing energy and reagents consumptions, while preventing harmful biological events. While Industry 4.0 and proactive control approaches have shown promising potential, there is still a gap between the classical reactive solutions, still common in plants, and state-of-art developments. HADES is a project aiming to this gap with the development of a digital twin as a decision support tool for WWTP operation that includes advanced control features for the optimization in terms efficiency, reliability, and compliance, while preventing events such as foaming, bulking, deflocculation, and greenhouse gases emission. The HADES solution core combines mechanistic, hybrid, and heuristic models to perform as virtual sensor, bench test for optimized control strategies based on model predictive control, and prediction of biological events. In this paper the project HADES and the first findings are presented.

Keywords (maximum 6 in alphabetical order)
Decision support system; knowledge-based models; model predictive control; risk models; wastewater treatment

INTRODUCTION

Wastewater treatment plants (WWTP) are energy-intensive and consume notable amounts of reagents. Plants are also affected by weather conditions and hard to predict and revert biological events that can disrupt operation, such as deflocculation and foaming. Optimizing WWTP operation is crucial to meet environmental goals, lower costs, and maintain the process stability.

Despite the potential benefits of technological advancements and global trends around the digitalization of processes, the literature suggests a slow adoption of Industry 4.0 technologies and solutions with proactive approaches for optimizing WWTP operation. Among them, digital twins (DT), which popularity has exploded in the last few years (Pedersen et al., 2021) due to their wide range of applications and potential to change operational strategies for utilities and the design processes (Torfs et al., 2022), and optimize energy and resource consumption, environmental protection (effective and efficient treatment processes), and societal benefits (IWA 2021a).

Other solutions include the use of advanced control approaches, like model predictive control (MPC), and the use of heuristic models to predict risks of harmful biological phenomena and emissions of greenhouse gases. Classical control solutions, such as PI/PID, which are still the common practice in WWTP, struggle with the dynamic behaviour of influent, process changes and disturbances. Meanwhile, MPC-based solutions have shown to handle these conditions and interactions more effectively while optimizing WWTP operation, with promising results from previous studies (Steffens & Lant, 1999; Shen et al., 2009; Vrečko et al., 2011; Revollar et al., 2015; Zhang & Liu, 2019). The complexity of the microbiology of the activated sludge systems that cause solids separation problems of microbiological origin could be tackled through models integrating numerical models and knowledge-based systems (KBS) combining process and heuristic data (Comas et al., 2008). Despite having shown promising results in the literature (Rodriguez-Roda et al., 2002; Comas et al., 2003), heuristic methods such as KBS and case-based reasoning systems (CBRS) are still relatively uncommon in full scale WWTP. HADES is an ongoing project aiming to the gap between current WWTP control solutions and Industry 4.0 technologies by developing a DT that integrates the initiatives discussed above for decision support in operation.

OBJECTIVE

The objective of this paper is to present the HADES DT and features as a decision support tool for WWTP operators, composed of mechanistic, hybrid and heuristic models and MPC, oriented to optimize the treatment processes in terms of efficiency, reliability, and compliance. The main outcomes expected, once implemented in full scale WWTPs, are a reduction of 50% of effluent quality non-compliance episodes, a reduction of 15% of the energy consumption through advanced control (around 0,02 €/m3), and savings of 92.000 €/d for ACCIONA in chemicals for phosphorus removal and through the improvements of the sludge settleability and dewaterability.

MATERIALS AND METHODS

The HADES DT will be deployed, monitored, and validated at La Almunia WWTP, which serves the municipalities of La Almunia de Doña Godina, Almonacid de la Sierra, Alpartir, Calatorao, and Ricla. The plant has a capacity of 10.500 m3/d and an approximate load of 28.350 p.e. The treatment configuration consists of two oxidation ditches and two clarifiers. Waste sludge is thickened and dewatered before disposal. The plant already has a high level of instrumentation and automation, but additional sensors will be installed for monitoring key parameters for the DT. La Almunia WWTP has previously hosted digitalization-based projects, so the plant management is familiar with digital tools, making it a favourable environment for the HADES deployment. Since the DT will work as a decision support tool for the WWTP operation, it will be the responsibility of the plant manager, as final user, to close the control loop by using the optimized operational strategies suggested.

Figure 1 depicts the main elements of the HADES DT. The integrations of three complementary models, each of them using different approaches, is necessary to effectively address the complex challenges in the optimization of the treatment process and the prediction of harmful events.

The HADES project will develop a plant-wide model using the commercial modelling software GPS-X® which uses the widely known and validated activated sludge models (ASM). One instance of the model will work as a virtual sensor, another will validate operational strategies computed by the HADES control modules, and a third one will be user-dedicated. A CFD model extended with ASM, developed under ANSYS Fluent®, will be combined with other methods in a hybrid model to optimize the energy consumption of bioreactors mechanical equipment. A heuristic module combining KBS and CBRS will monitor the probability of risk of harmful events in real-time, while estimating the risk of using the optimized operation strategies suggested by the DT control modules.

The models will be back fed by a Data Centre that acquires data from external sources (SCADA, lab reports, weather monitoring databases, etc.), which may require validation and reconstruction before use. A Monitoring and Control Centre will also be part of the DT, fulfilling two functions: on one hand, MPC strategies and other control algorithms will be bench tested and validated over the mathematical models, in the other hand, relevant results of the models, and the conclusions derived from the tested control strategies, will be shown through a User Interface (UI), suggesting, if necessary, modifications to improve efficiency, prevent breaches and problematic events. User-dedicated instances for simulation will also be available through the UI.

RESULTS AND DISCUSSION

At the time of writing this document historical data from La Almunia WWTP was already gathered according to the project needs. A preliminary analysis of historical data revealed that due to agricultural activities in the region, irrigation water infiltrates the combined drainage network and arrives at the WWTP, without a clear pattern, mostly between April and November (Figure 2), so two different operational regimes are common in the plant (Figure 3). This is an additional challenge to consider for the development of data validation, reconstruction and prediction systems.

Data was analyzed and reconciled to detect, identify, and isolate outliers. A reconciled dataset was obtained for use in developing models such as statistical, machine learning (ML), or time series models (TSM) for reconstruction, prediction, and data transformation for the DT simulators. Preliminary models were developed on GPS-X® and ANSYS Fluent®. Software for data communication was developed for the inputs of the GPS-X® model, and reactor geometry and meshing were addressed in ANSYS Fluent® (Figure 4). For the MPC module, the Linear Parameter-Varying (LPV) framework was identified as a promising approach, and first steps have been taken with the development of a reduced linearized model with 6 variables, starting from ASM1.

FURTHER WORKS

Additional analytical measurements will be taken on the influent and additional sensors will be installed to monitor key parameters in influent and effluent. Clustering techniques will be applied to the dataset to separate data according to different operational conditions as a previous step to developing preliminary versions of reconstruction and prediction models using statistical models, ML, and TSM. Comparison and validation of reconstruction methods will be performed over different scenarios. Calibration tasks will be carried out for the GPS-X® model as well as the first multiphase simulations in the CFD model to study the overall hydrodynamics of the reactor in steady and transient state, as well as the interaction between the two phases. A state space model of the biological process will be developed as a Python library, reproducing the process dynamics described by ASM1 and will be used as a fundamental part of the MPC algorithm for computing the optimal sequence of set-points for the WWTP actuators. Historical data and event reports will be analyzed as first step in the development of heuristic models based on KBS and CBRS.

REFERENCES

Comas, J., Rodriguez-Roda, I., Sànchez-Marrè, M., Cortés, U., Freixó, A., Arráez, J., & Poch, M. (2003). A knowledge-based approach to the deflocculation problem: integrating on-line, off-line, and heuristic information. *Water research*, **37**(10), 2377-2387.

Comas, J., Rodriguez-Roda, I., Gernaey, K. V., Rosen, C., Jeppsson, U., & Poch, M. (2008). Risk assessment modelling of microbiology-related solids separation problems in activated sludge systems. *Environmental Modelling & Software*, **23**(10-11), 1250-1261.

IWA (2021a). Digital Water: Operational Digital Twins in the Urban Water Sector. *White Paper. London*, UK, p. 17.

Pedersen, A. N., Borup, M., Brink-Kjær, A., Christiansen, L. E., & Mikkelsen, P. S. (2021). Living and prototyping digital twins for urban water systems: towards multi-purpose value creation using models and sensors. *Water*, **13**(5), 592.

Revollar, S., Vega, P., & Vilanova, R. (2015, October). Economic optimization of wastewater treatment plants using Non Linear Model Predictive Control. In *2015 19th International Conference on System Theory, Control and Computing (ICSTCC)* (pp. 583-588). IEEE.

Rodriguez-Roda, I. R., Sànchez-Marrè, M., Comas, J., Baeza, J., Colprim, J., Lafuente, J., ... & Poch, M. (2002). A hybrid supervisory system to support WWTP operation: implementation and validation. *Water science and technology*, **45**(4-5), 289-297

Shen, W., Chen, X., Pons, M. N., & Corriou, J. P. (2009). Model predictive control for wastewater treatment process with feedforward compensation. *Chemical Engineering Journal*, **155**(1-2), 161-174.

Steffens, M. A., & Lant, P. A. (1999). Multivariable control of nutrient-removing activated sludge systems. *Water Research*, **33**(12), 2864-2878.

Torfs, E., Nicolaï, N., Daneshgar, S., Copp, J. B., Haimi, H., Ikumi, D., ... & Nopens, I. (2022). The transition of WRRF models to digital twin applications. *Water Science and Technology*, **85**(10), 2840-2853.

Vrečko, D., Hvala, N., & Stražar, M. (2011). The application of model predictive control of ammonia nitrogen in an activated sludge process. *Water Science and Technology*, **64**(5), 1115-1121.

Zhang, A., & Liu, J. (2019). Economic MPC of wastewater treatment plants based on model reduction. *Processes*, **7**(10), 682.

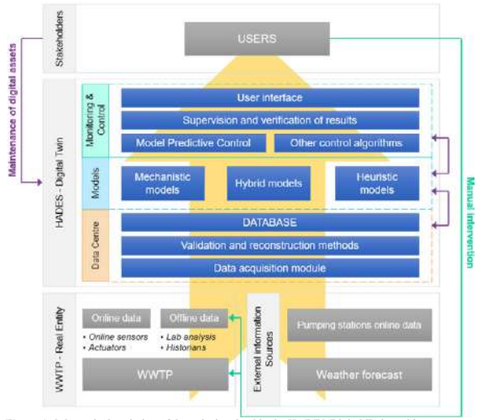

Figure 1. Schematic description of the units involved in the HADES Digital Twin and its implementation.

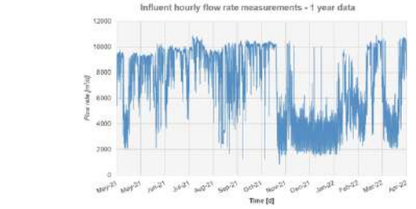

Figure 2. La Almunia WWTP influent flow rate from May 2021 to May 2022. Obtained from the plant SCADA database. The influence of irrigation infiltrations can be observed from May to November 2021.

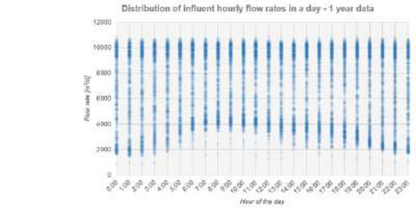

Figure 3. Distribution of hourly flow rate measurement of the La Almunia WWTP influent along a day, using 1 year of data. Two influent flow curves can be intuited corresponding to 'mostly urban wastewater influent' and 'high contribution irrigation infiltrations or rainwater influent'.

Figure 4. CFD related representations, a) Geometry of the carrousel reactor of La Almunia WWTP; b) Detail of surface mesh.

4SM PROJECT. SPREAD SEWER SENSING FOR SUSTAINABLE MANAGEMENT: ADVANCED TOOLS FOR OPTIMAL SEWER MANAGEMENT

O. Gutierrez[1,2], S. Busquets[1,2], Ll. Corominas[1,2], J. Radjenovic[1,2], M. Pijuan[1,2], S. Bergillos[1,2], J. García[3], I. Tormos[3], J. Climent[4], J. Vilarroig[4], P. Carratala[4], P.J. Martínez[3], O. Macías[3], J. Cayero[5]

[1] *ICRA, Catalan Institute for Water Research, Scientific and Technological Park of the University of Girona, Emili Grahit 101, E-17003 Girona, Catalonia, Spain*
[2] *University of Girona, 17003, Girona, Spain*
[3] *FACSA Ciclo Integral del Agua, C / Mayor, 82-84, 12001 - Castellón de la Plana, Spain*
[4] *Hydrens, Avda. del Mar. 53 bajo – 12003 Castellón de la Plana, Spain.*
[5] *EURECAT, Robotics & Automation Unit. C/ Bilbao, 72, 08005, Barcelona, Spain.*
(E-mail: ogutierrez@icra.cat)

Keywords: Sewer management, Digitalization, Resource and energy recovery, Smart sensors,

ABSTRACT:
The management of sewer systems is a critical aspect of urban infrastructure that faces numerous challenges. The 4SM project aims to address four key challenges in sewer management, namely:
(1) promoting the digitalization process of sewer networks,
(2) enhancing the capabilities of current tools,
(3) tapping into resource and energy recovery from sewers, and
(4) developing highly innovative methods for corrosion, toxicity, and odours control.
This poster provides an overview of the 4SM project and highlights the objectives and progress made in each of the six work packages.

Work Package 1 (WP1) focuses on the development of a digital platform for sewer management. The objective is to create an Internet of Things (IoT) based platform that collects, integrates, and visualizes data from the physical world. This platform will enable advanced standards for data analysis and decision-making in sewer management.

In WP2, the project aims to design a sulfide stripping process unit to extract and concentrate sulfide for recovery. Preliminary designs for a pilot plant have been proposed, and experiments are being conducted to determine the desorption velocity between gas and liquid phases. These efforts will contribute to the removal of Hydrogen sulfide from sewer systems.

WP3 explores a ground-breaking method for sulfide control that relies on electrocatalysis and low-cost nanomaterials. The objective is to test the effectiveness of this method in controlling sulfide gas without the use of chemicals. Initial evaluations of electrocatalytic sulfide removal from wastewater have been conducted, and further experiments using low-cost materials are planned.

The primary goal of WP4 is to develop a semi-autonomous drone for data collection and visual assessment in sewer systems. A prototype drone has been created, and initial tests have been conducted in real manholes. This drone will enable automatic data retrieval and inspection, improving the efficiency and accuracy of sewer management.

WP5 focuses on the integration of smart sensors for real-time wastewater quality control. The project aims to test wastewater quality sensors that can be incorporated into CSO (Combined Sewer Overflow) detection equipment. Online water quality sensors for COD (Chemical Oxygen Demand) and TSS (Total Suspended Solids) are being tested in the field, along with mechanisms for sensor protection against clogging and cleaning. Additionally, temperature sensors from the SENVES concept developed at ICRA are being tested in conjunction with a level sensor.

Work Package 6 (WP6) investigates energy recovery from sewers. Various options for energy recovery have been explored, with a focus on Pico-Hydraulic Turbines commonly used for energy recovery in water supply or irrigation tubes. However, the challenge lies in the presence of urban solids and fibers in sewer systems, which can obstruct the hydraulic flow. Efforts are underway to estimate the energy generated and optimize the design of the Pico-Hydraulic Turbine for sewer applications.

The 4SM project aims to revolutionize sewer management by leveraging advanced tools and sustainable approaches. Through digitalization, enhanced sulfide control, autonomous drones, smart sensors, and energy recovery, the project strives to connect the digital and physical worlds of sewer infrastructure. The results and findings from the project will contribute to the development of efficient, sustainable, and environmentally friendly sewer management practices.

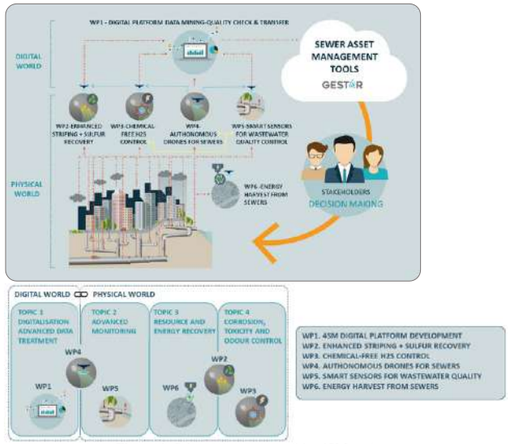

Figure 1. Schematic concept of the 4SM project.

Comparative modeling of SMP product/utilization on membrane fouling in submerged membrane bioreactor system using MES, PLS, MLR, PCA and ANN techniques

H. Benaliouche*, **, b, D. Abdessemed**, F. Benaliouche***, G. Lesage****, M. Heran****

* Laboratory of Environmental Process Engineering (LIPE), Faculty of Process Engineering, University Salah Boubnider Constantine 3, University City Ali Mendjli 25000 Constantine, Algeria (E-mail: hana.benaliouche@yahoo.fr)
** Laboratory of Industrial Sciences Process Engineering, University of Sciences and Technology, Houari Boumediene B.P., 32 El Alia, 16111 Bab Ezzouar, Algiers, Algeria
***UER Physico-Chimie des Matériaux Ecole Militaire Polytechnique Algiers, Algeria.
****Département Génie des Procédés Membranaires, Institut Européen des Membranes, Université Montpellier, 34095 Montpellier Cedex 05, France

Abstract
Membrane bioreactor (MBR) is one of the best solutions for wastewater treatment systems in producing high quality effluent that meets its standard regulations; The MBR has a broader prospect of its applications in wastewater treatment and reuse. However, the problem of membrane fouling restricts the application of MBR to a great extent resulting in pore clogging and reduced membrane permeability. The main objective of this study is to develop an overall SMP model applicable to a Membrane bioreactor (SMBR). A multivariate projection to latent structures (PLS) and artificial neural network (ANN) models are developed and analyzed to establish the Parameters limiting variables for predict SMP and membrane fouling. The proposed models account for the biological contribution of MBR and predict the SMP product. Regression models are subsequently trained to objectively predict the SMP product of submerged membrane bioreactor systems. Furthermore, this paper aimed to analyze biological parameters data in order to explore the most parameters influenced biomass activity and membrane fouling using statistical analysis. To establish the link between the dead mineral matter MOM, the concentration of the active biomass, the operating conditions and the subsequent fouling of the membrane, the heterotrophic and autotrophic bacteria are first quantified using respirometric measurements. The comparison of their evolution with the conditions and the operating parameters is carried out using the statistical analysis, and SRT, which is identified as the parameter having the greatest impact on active biomass concentration. A multivariate statistical analysis of the biomass activity parameters is performed, based on the data points of the MBR process. The parameters examined are: SOUR, SMP, MLVSS, XBH, XBAI, XBAA, COD, TOC and F/M. The methodology for characterization of MBR biomass activity is based on the above data combining the method of multiple linear regressions (MLR), principal component analysis (PCA)and structural equation modeling (SEM) method,

Keywords
Membrane bioreactor, principal compound analysis (PCA), Respirometric activity, soluble microbial products, structural equation modelling (SEM), Statistical analysis.

Smart sensor monitoring and prediction for safe wastewater reuse: Development of an early Warning System tool

N. Ciuccoli*, E. Marinelli*, S. Radini*, M.Sgroi*, L.Screpanti*, D. Scaradozzi*, A. L. Eusebi*, F. Fatone*

* Department of Science and Engineering of Materials, Environment and Urban Planning-SIMAU, Faculty of Engineering, Polytechnic University of Marche, Ancona, Italy
(E-mail: *l.desimoni@pm.univpm.it; s.radini@pm.univpm.it; a.foglia@univpm.it, a.l.eusebi@staff.univpm.it, f.fatone@staff.univpm.it)*

Abstract
Risk management can be supported and optimized using digital tools for assessment, monitoring, control and decision support. However, signals can give outlier data due to sensor faults, installation and maintenance issues or external conditions. When reliable data are not available, modelling can support providing simulated data of malfunction scenarios. In the context of the European H2020 project Digital Water City, an Early Warning System (EWS) has been developed to monitor effluent water quality and support decision making and risk management for water reuse applications. To carry out the development of this system a digital twin of a wastewater treatment plant was developed using a Multi Task neural network and a forecaster to predict the effluent water quality up to 6 hours later, via a Long Short-Term Memory network.

Keywords (maximum 6 in alphabetical order)
Artificial Neural Network; Digital tool; Early Warning System; risk management; soft sensor; water reuse.

INTRODUCTION

The transformation of the wastewater treatment sector to smart water treatment and reuse facilities is boosted by the process of digitalization of the wastewater treatment plants (WWTPS), improving process performance and reducing malfunctions. Digital technologies have the potential to develop predictive maintenance, extending the life of the infrastructure; to increase the efficiency in capital and operational management; to foster greater speed in decision-making due to the rapidity in data processing; and to detect malfunctions and anomalies in the WWTPs operation. Furthermore, digital tools can improve notably the management of water infrastructures, the quality of service provided to citizens and the levels of awareness and collaboration between utilities, authorities and citizens. However, the transition to a digital management of wastewater sector is often hammered by the low level of maturity and diffusion of innovative digital solutions; the commonly high investment needed to acquire digital tools, the efforts required to train the personnel and to keep digitals systems updated, other than a static regulatory landscape. Technological development, awareness on the benefits of digital tools as well as economic and political support to water utilities are thus expected to implement this digital transition in the water sector, which is essential to implement water reuse practices. In the framework of the European project Digital Water City, which aimed to boost digitalization in the water sector, an Early Warning System (EWS) has been developed in Peschiera Borromeo WWTP for safe wastewater reuse for agricultural purposes. The EWS provides warnings if in the plant are detected conditions where quality requirements for water reuse cannot be satisfied. The EWS represents a tool to support risk management, since it can receive real time information about effluent water quality WWTPs. In this way, decision making about water reuse can be supported and risk minimized allowing rapid reactions in case the occurrence of a hazardous event is detected by the EWS.

MATERIALS AND METHODS

Peschiera Borromeo WWTP

Peschiera Borromeo WWTP is located in the periurban area of Milan, in Italy. It has a treatment capacity of 500,000 P.E. and is divided in two treatment lines, of which the one selected to deliver reclaimed water is composed by pre-treatments, lamellar settler, biologic treatment combined with filtration and tertiary UV disinfection unit. The WWTP is equipped with a series of sensors for continuous monitoring of water quality, including ammonia, nitrates, pH, phosphates and suspended solids.

Development of an EWS for safe water reuse

The Early Warning System has been developed at Peschiera Borromeo WWTP to forecast water quality depending on sensors measurements and soft-sensing techniques. The EWS architecture includes the generation of warning and alarms related to measurements obtained by on-line sensors and from machine learning algorithms (i.e., soft sensors). Artificial Neural Networks (ANN) were developed for real-time and time-series prediction of parameters related to wastewater quality.
In particular, two neural networks have been developed. The first one is a MultiTask (MLT) neural Network that has to estimate the effluent Biochemical Oxygen Demand (BOD), the effluent Chemical Oxygen Demand (COD) and the effluent Total Suspend Solids (TSS), having as input influent flowrate, influent pH, temperature in the anoxic reactor, dissolved oxygen (DO) concentration in aerated reactor, effluent flowrate and effluent pH, which corresponded to the available sensors installed in the WWTP. MLT represents an implicit data augmentation strategy which allows to avoid model overfitting (Ruder, 2017).
Since microbial risk was highlighted as one of the most significant risks during wastewater reuse, particular attention has been addressed to TSS predict since solid particles may be vehicle of pathogens. With this aim, a Long Short-Term Memory network capable of predicting the behavior of TSS up to 6 hours later was developed. Predictive models require an affordable and large set of data to be trained and validated, including both periods of normal operation and periods with malfunctions occurrence, which are rarely available (Newhart et al., 2019). Hence, a model representing typical operational conditions of Peschiera Borromeo WWTP was created using a simulation software, also because sensor data were not always reliable and included outliers. Once the ANN models were generated, a procedure was elaborated to adapt its configuration using a real data set, made up by sensors data and lab measurements. The domain adaptation procedure allowed to fit the developed ANN to real data. Indeed, for the training procedure only 1000 data points were available. On the contrary, for ANN development using simulated data 6912 measurements were used for training, which represent the 80% of the simulated dataset.

RESULTS AND DISCUSSION

According to the WWTP operational conditions, the soft-sensing algorithms were able to forecast the quantitative values of target parameters and compare them with threshold limits for water reuse. Considering the first development using input data generated by model simulations, good performances of the ANN model were observed as shown in table 1.

A deviation was observed in correspondence of the simulated malfunction scenarios even if the network would still detect the presence of the malfunction as shown in Figure 1 in the case of the TSS (Figure 1).

Table 1. Statistical parameters calculated to evaluate the performance of the developed ANN model during the testing phase.

Predicted Parameter	CC	RMSE	SI	BIAS	Mean Absolute Percentage Differences (APD)	Std APD
Effluent BOD	0.963	1.235	0.228	-0.006	8.460	10.480
Effluent COD	0.961	2.388	0.147	-0.050	6.671	8.521
Effluent TSS	0.856	1.419	0.217	-0.105	5.630	11.966

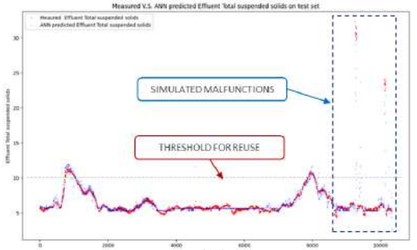

Figure 1. ANN predictions of effluent TSS using simulated data.

The second model was also able to forecast TSS with very high accuracy for the three different time offsets considered in this study, as reported in Table 2.

Table 2. Average of statistical parameters calculated to evaluate the performance of the forecasting models for TSS prediction.

Forecasting model	RMSE	SI	BIAS	Mean Absolute Percentage Differences (APD)	Std APD
1 h	0.224	0.025	-0.087	1.682	1.763
3 h	0.229442	0.0264834	-0.045	1.792	1.844
6 h	0.234	0.027	-0.099	1.855	1.661

Unlikely, results obtained during the test phase of the domain adaptation with the real sensors dataset were not consistent and the model was not able to produce stable outputs obtained for all the three target parameters. However, according to the scientific literature, in the case of real sensors installed on-line, acceptable errors in terms of APD values are assumed to be < 20% (Cecconi et al., 2019). In the case of the developed soft sensor in this work, the calculated mean APD was about 26 %for BOD, 22 for COD, and 19% for TSS, meaning that further steps are required to reach the convergence below the acceptable level. Nonetheless, it is expected that with the progressive increase of the dataset of sensors data, coupled with a deeper focus on maintenance and specific procedures designed to remove sensors outliers, the domain adaptation will be able to provide more affordable results.
The developed EWS follows a dynamic risk management approach and allows monitoring and control on health risks associated with the reuse of treated water, reducing the likelihood of the occurrence of hazardous outcomes and supporting risk minimisation.

REFERENCES

Cecconi, F., Reifsnyder, S., Ito, Y., Jimenez, M., Sobhani, R., & Rosso, D. (2019). ISE-ammonium sensors in WRRFs: field assessment of their influencing factors. Environ. Sci.: Water Res. Technol., 5, 737–746.
Fernandez de Canete, J., del Saz-Orozco, P., Gómez-de-Gabriel, J., Baratti, R., Ruano, A., Rivas-Blanco, I., 2021. Control and soft sensing strategies for a wastewater treatment plant using a neuro-genetic approach. Comput Chem Eng 144, 107146. https://doi.org/10.1016/j.compchemeng.2020.107146.
Ruder, S. (2017). An Overview of Multi-Task Learning in Deep Neural Networks. May. http://arxiv.org/abs/1706.05098
Newhart, K.B., Holloway, R.W., Hering, A.S., Cath, T.Y., 2019. Data-driven performance analyses of wastewater treatment plants: A review. Water Res. 157, 498–513. doi:10.1016/j.watres.2019.03.030.

5. Economics and environmental/ social footprint

5. Economics and environmental/social footprint

Lowering of groundwater levels and their effect on Water, Sanitation and Hygiene services in the Savelugu District, Northern Region of Ghana

Albert Acheampong, PE-GhIE, MGhIG, MIAH, MASCE
PhD Candidate, KNUST, World Vision Ghana, acheampongalbert@gmail.com

ABSTRACT

Of all the natural resources available to humankind, water holds a prominent place, particularly because of its importance for human livelihood. Savelugu district in northern Ghana is characterized by unpredictable rainfall patterns with periodic and perennial water shortages. The distance people travel to fetch water and the person-hours spent in search for water affect productivity, economic livelihood, and health and education benefits. Provision of potable water supply to these communities is expected to bring not only health, education benefits but also increase in sanitation and hygiene practices. Static water levels (SWLs) of 19 wells in the study area were collected, analyzed and compared to the initial SWLs measured when the wells were immediately drilled and constructed. The SWL data was subjected to paired samples T-test (with $\alpha = 0.05$). From the results, there was significant difference in the SWL immediately after drilling and construction ($\mu = 12.15$, $\sigma = 7.50$) and SWL after at least 10 years ($\mu = 17.81$, $\sigma = 10.29$); $t(18) = -3.7$, $P = 0.002$. Lowered groundwater levels were recorded in all wells measured. This can lead to drying up of some of the wells whose difference between the current SWL and well depth is close. There must be strong advocacy, development and implementation of IWRM plans to help address the problem of inadequate WASH in the study area.

INTRODUCTION

The provision of water through drilling of wells or boreholes helps to increase access to water. The availability of adequate water or increased water coverage promotes increased sanitation and good hygiene practices thereby reducing and preventing the myriad problems associated with inadequate water and sanitation infrastructure, and hygiene practices (WHO/UNICEF JMP progress report, 2018). The link between inadequate access to safe and affordable water and public health problems, cannot be over-emphasized. Water scarcity represents the single greatest threat to food security, human health, education and the natural ecosystem (WHO/UNICEF JMP progress report, 2017).

As high as 89.3 % of households in the Savelugu district are engaged in agriculture, 97.0 % out of this are involved in crop farming (Ghana Statistical Service, 2010). Savelugu district/AP is characterized by unpredictable rainfall patterns with periodic and perennial water shortages (Ghana Meteorological Agency, 2018), this serves as serious constraints to meeting the challenges to provide adequate water to all rural residents in the district. Wells were drilled by World Vision Ghana in Savelugu AP/district in the Northern region of Ghana to help provide adequate water and sanitation infrastructure and hygiene practices (Savelugu Nanton District Assembly, 2006). Some of these wells are drying up or have dried up over time, making them low yielding and even some non-functional/operational probably due to the lowering of the groundwater table with time and some environmental issues.

The study seeks to look at and address the possible causes of the drying up of these wells at Savelugu district and its associated cross cutting issues to Water, Sanitation and hygiene. Since WASH affects many other development sectors such as health and healthcare facilities, education, environment, agriculture and livelihood, etc. (WHO Guidelines on Sanitation and Health, 2018), the general wellbeing effect that arises out due to inadequate water and sanitation infrastructure, and hygiene practices needs to be looked at critically.

MATERIALS AND METHODS

Review of the works of one or two water committees, interviews, questionnaires and focus groups discussions – government officials, stakeholders/schools/clinics/CHPS and area mechanics were conducted. Static water levels (SWLs) of 19 wells in the study area as shown in Figure 1 were collected, analyzed and compared to the initial SWLs measured when the wells were immediately drilled and constructed. The SWL data was subjected to paired samples T-test (with $\alpha = 0.05$).

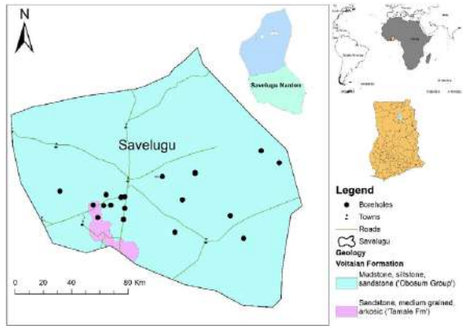

Figure 1. Map of study area showing drilled wells/communities

In addition, rainfall data were collected and analyzed. Also considered were land use information, river flows, geology within the area to determine the actual cause of lowering of the water table. Socio-economic parameters leading to the drying up of the wells and impact on WASH were analyzed to draw valid conclusions.

RESULTS AND DISCUSSION

The district is found in a region of the country with unfavourable natural environmental conditions. There is little tree-cover and it experiences harsh harmattan seasons, which results in many bush-fires caused by farmers clearing their lands and hunters searching for game (Yiran et al., 2016). The serious threat however, is the rate at which the tree vegetation is being cut down for fuel wood. The less tree-cover, harsh harmattan and rampant tree vegetation removal leads to desertification, increase surface runoffs, less percolation to recharge the underground waters after rainfall. This is mostly supplemented by hand-dug wells which dried up in the dry season. since most of the limited received rainfall would be trapped in the vadose zone, thereby impacting greatly on the water cycle of the district.

Lowered groundwater levels were observed and recorded in all the wells visited/measured with change in static water levels (SWL) range between 0.2 m to 26 m with an average of 6 m as shown in Table 1 and Figure 2. It is to be noted that, all current SWL measurements were taken in second (2nd) week of November, just after the main raining season. This point to the possible increase in the numbers/margins if taken in the dry season, potential increased lowered groundwater levels would be recorded. This can lead to drying up of some of the wells with time like Afayili, Tigu, Chehayili, etc where the difference between the current SWL and well depth is close (Figure 2). Longer and intense dry season period might compound the problem and enhance the chances of the drying up of these wells.

The SWL data was subjected to paired samples T-test (with $\alpha = 0.05$). From the results in Table 2, there was significant difference in the SWL immediately after drilling and construction ($\mu = 12.15$, $\sigma = 7.50$) and SWL after at least 10 years ($\mu = 17.81$, $\sigma = 10.29$); $t(18) = -3.7$, $P = 0.002$. Lowered groundwater levels were recorded in all wells measured. This can lead to drying up of some of the wells whose difference between the current SWL and well depth is close. The lowering of SWLs could be attributed to reducing tree-cover, the harsh harmattan and rampant vegetation removal, which contributes to desertification, increase surface runoffs, less percolation to recharge the underground waters after rainfall in the area.

Table 1. Change in SWL of drilled wells over time.

Community	District	Data drilled	GPS Coordinates		Grid elev	SWL (m)		Change in SWL	Depth
			(lat)	(long)	(m)	Original	Current	(m)	(m)
Kanshegu	S/N	2005	9.57469°	0.83397°	174	15.5	16.2	0.7	48.5
GIWASH Office	S/N	2002	9.60228°	0.83698°	163	5.5	9.2	3.7	40
Ligbu	S/N	2003	9.59251°	0.84990°	147	2.2	2.9	0.7	28
Zaazi-Kukuo	S/N	2005	9.57711°	0.86614°	166	20.3	21.0	0.6	40
Moglaa School	S/N	2005	9.59260°	0.87198°	172	15.4	19.7	4.3	40
Bulshie	S/N	2005	9.58860°	0.83240°	182	32.3	33.6	1.3	54.5
Yilkpani	S/N	2006	9.60982°	0.91332°	138	10.5	16.1	5.6	61
Zaazi	S/N	2003	9.59195°	0.85886°	150	4.1	5.3	1.2	31
Bilinnayili	S/N	2003	9.60561°	0.85565°	134	3.2	3.9	0.7	28
District Assembly	S/N	1999	9.60301°	0.83226°	169	7.9	10.5	2.6	40
Sanda	S/N	2005	9.63194°	0.74445°	155	15.1	20.5	5.4	40
Kpacelo	S/N	2004	9.55869°	0.76978°	158	22.1	28.5	6.4	43
Afayili	S/N	2004	9.59910°	0.76036°	159	12.5	38.0	25.5	40
Tigu	S/N	2005	9.66062°	0.66198°	160	12.9	25.4	12.4	31
Diga	S/N	2005	9.57941°	0.70069°	170	10.5	16.5	6.0	49
Chaakpem	S/N	2005	9.63310°	0.74447°	153	7.5	21.1	13.6	37
Zokuga	S/N	2007	9.64544°	0.63937°	150	4.4	6.1	1.7	36
Yong	S/N	2004	9.62811°	0.78542°	141	12.8	13.0	0.2	49
Chehyili	S/N	2004	9.55123°	0.68384°	168	16.1	31.1	15.0	34

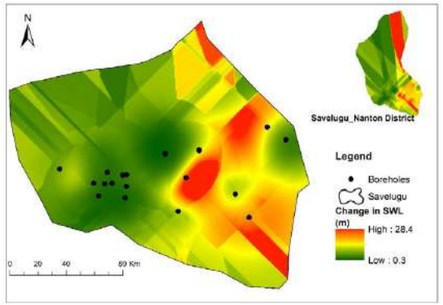

Figure 2: Spatial distribution of change in SWL of the study area

Table 2. Paired samples T-test results.

		Paired Differences				t	df	Sig. (2-tailed)
		Mean	Std. Deviation	95% Confidence Interval of the Difference Lower	Upper			
Pair 1	SWL Original - SWL Current	-5.67368E0	6.62184	1.51915	-8.86531	-3.735	18	.002

However, limited and unreliable access to water for domestic, industrial and irrigation use due to dried up wells and surface waters, affect time spent in accessing water, school attendance/enrolment and guinea worm eradication. The provision of potable water supply to these communities is expected to bring not only health and nutrition, education benefits but also a significant improvement in agricultural productivity, sanitation and hygiene practices. Hence a combination of decreased water availability and increased level of water use greatly imparts negatively on WASH. WASH is instrumental in achieving goals in: Poverty, food security, education, gender equality, health (child mortality, maternal mortality, and major diseases), environmental sustainability (loss of environmental resources, improving lives of slum dwellers) (WHO/UNICEF JMP progress report, 2019).

CONCLUSIONS AND RECOMMENDATIONS

Conclusions

The district experiences increased stream flow with high evaporation and transpiration due to high temperatures, low rainfall and landscape dominated by the savannah grasslands and less vegetation cover. The area experiences less base flow into the groundwater as a result of less percolation, since most of the limited received rainfall would be trapped in the vadose zone.

Lowered groundwater levels were observed and recorded in all the wells measured with change in static water levels (SWL) range between 0.2m to 26m with an average of 6m. This can lead to drying up of some of the wells whose difference between the current SWL and well depth is close.

The provision of potable water supply to these communities is expected to bring not only health, education benefits but also a significant improvement in agricultural productivity/economic empowerment, increase sanitation coverage and hygiene practices, and ecosystem sustenance.

Recommendations

There should be strong advocacy, development and implementation of IWRM and water efficiency strategies, plans, and programs at the study area to help address the problem of inadequate WASH in these communities in order to improve health and wellbeing in the study area.

Effective and efficient integrated land and water management needs to be instituted to prevent farming along river courses, reduce runoffs, increase water absorption and crust at the soil surface.

There is the need to replace or add up to existing wells that showed greater potential of drying up with time as disclosed by the results/findings from this study in the Savelugu Nanton district to address WASH in the district.

REFERENCES

District Profile Accessed (2006) at Savelugu Nanton District Assembly. www.ghanadistricts.com.
Ghana Meteorological Agency (2018). Weather Information, Northern Region, Ghana.
Population and Housing Census (2010). Regional Analytical Report of Ghana Statistical Service (2014).
Population and Housing Census (2010). National Analytical Report of the Ghana Statistical Service (2013).
World Health Organization Guidelines on Sanitation and Health (2018). Licence: CC BY-NC-SA 3.0 IGO.
World Health Organization/United Nations International Children Fund (2017). Joint Monitoring Programme progress report for water supply, sanitation and hygiene.
World Health Organization/United Nations International Children Fund (2018). Joint Monitoring Programme progress report for water supply, sanitation and hygiene.
World Health Organization/United Nations International Children Fund (2019). Joint Monitoring Programme progress report for water supply, sanitation and hygiene.
Savelugu Nanton District Assembly, Republic of Ghana (2006). Unpublished Technical Report, USAID funded program, Northern Region, Ghana.
Yiran, A.B., Stringer, L.C., Attua, E.M., Evans, A.J., Challinor, A.J., Gyasi, E.A., 2016. Mapping vulnerability to multiple hazards in the savannah Ecosystem in Ghana. Reg. Environ Change (2017) 17:665–676. https://doi.org/ 10.1007/s10113-016-1054-8.

Theoretical feasibility assessment of water loops in the Balearic Islands of Mallorca, Cabrera, and Formentera

G. Buttiglieri*,** and C. Amengual

* Catalan Institute for Water Research (ICRA-CERCA), C/ Emili Grahit, 101, 17003 Girona, Spain
** University of Girona, Girona, Spain
(E-mail: *caterina.am@gmai.com; gbuttiglieri@icra.cat*)

Abstract
The Balearic Islands, like many areas of the Mediterranean, are highly dependent on the tourism industry and environmental issues related to over tourism are widely reported. Natural groundwater bodies, for example, present severe problems of quality, due to wastewater contamination and marine intrusion. High efforts need to be done on water protection, and to find new water sources and water recycling systems. New water technologies and solutions are demanded to achieve a more sustainable level. The methodology designed and provided by UNIVPM in the context of the H2020 EU HYDROUSA project was applied to theoretically evaluate the feasibility of several wastewater, and rainwater harvesting nature-based solutions in the context of three islands of the Balearics: Mallorca, Cabrera, and Formentera.

Keywords
Rainwater, tourism; wastewater; water reuse; water scarcity.

INTRODUCTION

The Balearic Islands are highly dependent on the tourism industry (Pons, 2014). In 2019 they received 16.4 million tourists (54% in terms of GPD in 2019; AETIB, 2019). This high number reflects a heavy consumption of natural resources, especially water and energy, as well as waste production. Environmental issues related to over tourism are widely reported. The available drinking water supply sources for domestic uses are groundwater (71%), natural springs (9.6 %), water dams (5.6 %), and desalination (13.4 %; PHIB, 2019). Natural groundwater bodies present severe problems of quality, due to marine intrusion or wastewater contamination. High efforts need to be done on water protection, and to find new water sources and water recycling systems.

Regarding wastewater treatment, in all the archipelago there are 79 wastewater treatment plants (WWTPs) operating and treating 93 hm^3/year. These plants are designed for at least 400 PE and the public company responsible for the treatment has no or preliminary experience with small treatment systems. Scattered urbanizations and touristic urbanizations are an environmental issue/opportunity to deal with in the Balearic Islands, with a lack of sanitation system in some of these sites. It is estimated, in fact, that 55,000 houses in Mallorca are using only septic tanks or black wells (PHIB, 2019). Sewage sludge is another big problem on the islands. Each of the islands has different characteristics, and requirements, and the applicable solutions need to be carefully tailored. On the island of Cabrera, moreover, there is a lack of a proper wastewater treatment system, and the island is a National Park with specific legal binding and environmental requirements.

New water technologies and solutions are demanded to achieve a more sustainable level. The so-called HYDRO solutions of the H2020 EU HYDROUSA project improve the circular management of water, energy, and resources/waste. One advantage about living on an island is that when a new technology or operation strategy is implemented it becomes easily replicable, because on an island it is easy to create a connected network of innovators. Nonetheless, integrated water resources management is still largely in the theoretical body in the Balearic Islands, and there is not much experience right now. Different nature-based solutions were theoretically applied (in terms of wastewater treatment and irrigation, as well as to rainwater harvesting) to the island of Mallorca, Cabrera, and Formentera in the Balearic archipelago (Spain).

MATERIALS AND METHODS

The chosen nature-based solutions were the so-called HYDRO1 (wastewater) and HYDRO2 (irrigation) for the case of Mallorca Island; HYDRO1, HYDRO2, and HYDRO4 (rainwater harvesting) for the case of Cabrera Island; and HYDRO6 (small, decentralized tourist facility) for Formentera Island. The islands were theoretically analysed regarding social, legal, technical, and economic perspectives. In each of these areas, a group of theoretical feasibility criteria were defined that should be scored to obtain the feasibility of the feasibility study in that area (e.g., 80/100). The overall score of the project was calculated by giving a ponderation factor to 4 areas, that correspond to 30%, 30%, 20%, and 20%, to social, legal, technical, and economic areas, respectively. The methodology was completely designed and provided by UNIVPM (www.univpm.it).

RESULTS AND DISCUSSION

The three islands (Mallorca, Cabrera, Formentera) were theoretically evaluated in terms of potential applicability of the corresponding solutions (Table 1). The policy analyses considered European, National, and local (e.g., Cabrera National Park) legislation. Similarly, was done for the social analyses to highlight stakeholders that would act in favour or against the application of the chosen demonstration solutions. In terms of technical and economic feasibility, a preliminary design was drafted, as well as the CAPEX, OPEX, and payback periods were evaluated and compared for the installation of the wastewater reclamation and rainwater harvesting solutions.

Table 1. Theoretical feasibility results for Mallorca, Cabrera, and Formentera islands.

	Mallorca HYDRO 1, 2	Cabrera HYDRO 1,2,4	Formentera HYDRO6
Social Feasibility (30%)	77	69	74
Legal Feasibility (30%)	81	76	68
Technical Feasibility (20%)	76	43	40
Economic Feasibility (20%)	77	50	60
OVERALL FEASIBILITY	78/100	62/100	63/100

Confidence can be provided to the decision makers and lower the fears in front of new technologies and innovations. The proposed solutions can create a system that can close the loop on water and nutrients, reasons have been found under the laws related to agriculture, water, and waste treatment. The need for these decentralized systems is, in fact, high. Decentralized small towns and scattered facilities "off grid" do not have any wastewater treatment or water reuse system. When a first system is implemented and working in every island, the rest of the actors can learn and reply easily, and the public administration can adapt the procedures to allow and promote these systems.

REFERENCES

AETIB. Agencia de Turismo de las Islas Baleares ANUARIOS DE TURISMO: Datos informativos. 2019.Edita: Consejería de Modelo Económico, Turismo y Trabajo. https://www.caib.es/sites/estadistiquesdelturisme/es/anuarios_de_turismo-22816/

PHIB. Consejería de Medio Ambiente. Plan Hidrológico de las Illes Balears, 2019.

Pons, A.; Rullan, O. "The expansion of urbanisation in the Balearic Islands (1956–2006)" Journal of Marine and Island Cultures, Volume 3, Issue 2, 2014, Pages 78-88, ISSN 2212-6821, https://doi.org/10.1016/j.imic.2014.11.004

ACKNOWLEDGMENTS

This work was funded by the European Union's Horizon 2020 Research and Innovation programme (HYDROUSA project, GA N° 776643). Gianluigi Buttiglieri acknowledges Spanish State Research Agency of the Spanish Ministry of Science, Innovation and Universities for the Grant RYC-2014-16754 and ICRA-TECH (Tecnologies i avaluació del cicle integral de l'aigua)", Grup de Recerca de la Generalitat de Catalunya (2021 SGR 01283).

The uncertainty of N_2O emissions is underestimated and hampers accurate comparison of WWT technologies.

C. Domingo-Felez*,**, Marlene M. Jensen*, Anders Bang***, and Barth F. Smets**

* Department of Environmental and Resource Engineering, Technical University of Denmark, Miljøvej, Building 115, 2800 Kgs., Lyngby, DK (E-mail: *mmaj@dtu.dk*; *bfsm@dtu.dk)*
** Current address: Infrastructure and Environment, School of Engineering, University of Glasgow, University Avenue, Glasgow G12 8QQ, UK (E-mail: *carlos.domingo-felez@glasgow.ac.uk*)
*** Assens Forsyning A/S, 5610 Assens, DK (E-mail: *aba@assensforsyning.dk*)

Abstract
Critical validation of N_2O emission factor values is key to analyse the carbon footprint of WWT technologies. Current efforts to report N_2O emissions rely on approaches for NH_4^+, NO_3^-, or COD. However, the variability and uncertainty of N_2O production in WWT is significantly higher. Average values do not capture the intrinsic variability and propagated uncertainty associated to N_2O emissions. Here we analyse the error associated to all the measurements and model fitting efforts during a N_2O monitoring campaign and propagate them to the calculated Emission Factor. Gaussian distributions (average ± standard deviation) are not adequate and alternative probability distributions are necessary.

Keywords (maximum 6 in alphabetical order)
GHG; Nitrous oxide; Uncertainty; Nitrogen removal; Net-zero;

INTRODUCTION

Nitrous oxide emissions during biological nitrogen removal in wastewater treatment operations can compromise the environmental impact of the process. The carbon footprint of a WWTP is highly sensitive to N_2O emissions. However, reports of N_2O emissions focus on average emission factors (EF, N_2O emitted / TN removed), instead of accounting for the large uncertainty associated to N_2O emissions which depends on: technology, operational strategy, influent characteristics, spatial heterogeneity within reactors, etc. Hence, as the number of N_2O monitoring campaigns increases worldwide, accurate comparison between reports and technologies is necessary. In this study we:

- Propagate the uncertainty of every experimental value associated to N_2O EFs.
- Investigate more accurate methods compared to Gaussian distributions to report N_2O EFs.

MATERIALS AND METHODS

Experimental campaign: WWTP and N_2O monitoring: The Gummerup WWTP uses a Bio-Denitro technology with conventional activated sludge process for BNR and operates on alternating phases in the same reactor (Nitrification / Denitrification), with twin reactors interconnected. N_2O emissions were monitored for 110 days during spring and summer with 3 liquid sensors in one reactor and 1 in the twin reactor. Brush aerators at constant depth supply oxygen and operate in ON/OFF basis with varying aeration durations. The mass transfer coefficient for N_2O was estimated from a 2D-map of air flow measurements across the surface and linked to the oxygen mass transfer coefficient. The campaign accounts for daily variations but not for seasonal/yearly variations known to affect N_2O emission profiles (Gruber, Villez, et al., 2020) (**Figure 1**).

Data analysis: uncertainty propagation in N_2O emission factors: The experimental dataset considered to calculate the N_2O emission factor included measurement errors. The uncertainty of all the measurements was propagated via MC simulations assuming normal distributions in the parameter estimates maintaining correlation. The number of measurements for TN was significantly lower than for N_2O. The uncertainty associated to the calculation of emission factors was propagated throughout the study (**Figure 2**).

RESULTS AND DISCUSSION

Nitrous oxide emissions: Online measurements of N_2O emissions (gN/d) showed intrinsic variations due to diurnal, influent, and seasonal variations (Daelman, De Baets, et al., 2013) and were fitted to probability distributions. The distribution of daily or monthly N_2O emissions do not follow normal distributions and are highly skewed, with very few points being responsible for a large fraction of the total emissions. Still, in literature, the analysis of GHG from technologies relies mainly on average values. The calculated emission factor shows a large variability ($\sigma/\mu > 1$) and highlights the need for non-Gaussian distribution models for N_2O emissions. N_2O values differ from other WWT variables such as NH_4^+, NO_3^-, COD, whose dynamics are significantly lower compared to N_2O.

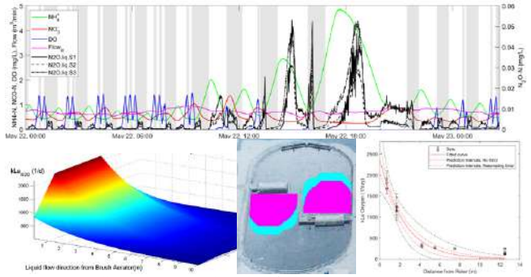

Figure 1. Top. Online liquid concentrations of NH_4^+, NO_3^-, DO, N_2O (x3 locations) and Flow rate. Shaded areas correspond to non-aerated periods. Bottom. Best-fit kLa.N2O for a brush-aerated bioreactor. Shaded areas for 90% and 95% of total N_2O emissions. Uncertainty associated to one step of the N_2O Emission Factor calculation.

$$N_2O_{Emission.Factor} = \frac{kL a_{N2O} \cdot \left(C.N2O_{liq} - C.N2O_{liq.air}\right) \cdot Vol_{BioT}}{TN_{removal}} \neq N(\mu, \sigma)$$

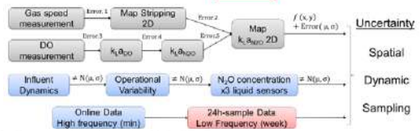

Figure 2. Equation describing the N_2O EF. Boxes show the sources and types of uncertainty associated to the N_2O EF.

REFERENCES

Daelman, M. R. J., De Baets, B., van Loosdrecht, M. C. M., and Volcke, E. I. P. (2013) Influence of sampling strategies on the estimated nitrous oxide emission from wastewater treatment plants. Water research, **47**, 3120–30. [online] http://www.ncbi.nlm.nih.gov/pubmed/23557698.

Gruber, W., Villez, K., Kipf, M., Wunderlin, P., Siegrist, H., Vogt, L., and Joss, A. (2020) N2O emission in full-scale wastewater treatment: Proposing a refined monitoring strategy. Science of the Total Environment, **699**, 134157. [online] https://doi.org/10.1016/j.scitotenv.2019.134157.

Re-thinking industrial wastewater treatment using advanced mathematical modelling.

Xavier Flores-Alsina[1], Vicente Monje[1], Elham Ramin[1], Pedram Ramin[1], Jens Abildskov[1], Krist V. Gernaey[1], Aleksandar Mitic[2], Laurent Lardon[2], Lana Wolmarans[3], Ilona Coremans[3]

[1]PROSYS Research center, Department of Chemical and Biochemical Engineering, Technical University of Denmark, Søltofts Plads, Building 228A, Kgs. Lyngby, 2800, Denmark
[2] BIOSCAVENGE ApS, Algade 2D, Gørlev, 4281, Denmark.
[3] ECCO leather, Vierbundersweg 11, Dongen, 5107 NL, The Netherlands

Abstract: Industrial water treatment facilities often treat multiple influents resulting from the different upstream production schemes. These streams may differ in quantity and quality, which will strongly affect the way they need to be managed. In this publication, a set of mathematical tools are used to assess the quality and quantity of industrial streams and re-think the way are handled. A full-scale site treating eight streams generated during leather processing is selected as case study. Reconciliation methods are applied to historical data to close mass and volumetric balances. Process simulation reproduces occurrence, transformation, recovery, and fate of organic (COD) and nitrogen (N) compounds (average deviation = 10 %). Hence, both data and model predictions reveal that 41 % of the incoming COD is converted into methane in the two anaerobic reactors (granular sludge and conventional). 16 % and 46 % of COD and N are biologically converted in the activated sludge reactor and 49 % and 36 % accumulated in the bio-solids (= cake). A scenario analysis suggests that it is possible to substantially increase the quantity of generated electricity (+82 %) and heat (+ 83 %) and reduce the quantity of sludge for disposal (-30 %) by modifying 1) upstream practices, and 2) carbon refluxing.

Keywords: Computer Aided Process Engineering, Mathematical Modelling, Multi-criteria evaluation, Plant Wide Optimization, Resource Recovery

INTRODUCION

The use of digital tools has revolutionized the way we design, operate and optimize industrial wastewater treatment plants (Müller-Czygan *et al.*, 2021). Digital tools provide engineers and operators with powerful assets to predict the behaviour of wastewater treatment processes, identify potential problems, and optimize the performance of the plant. One of the most widely used digital tools for predicting the behaviour of wastewater treatment plants is process simulation software (PSS) (Henze *et al.*, 2000, Batstone *et al.*, 2002). PSS allows engineers to create a digital model of the treatment process, which can be used to simulate the performance of the plant under different operating conditions. By simulating the treatment process, engineers can identify potential problems and optimize the performance of the plant to achieve better treatment efficiency.

The main objective of this paper is to show how mathematical modelling tools implemented in PSS can be used to re-think flow-diagrams treating industrial wastewater. An industrial site treating multiple streams coming from the leather processing industry is used as case study. The paper shows how to close mass balances in a data scarce environment, reproduce plant performance using process simulation, generate different re-design scenarios and assess the feasibility of these new proposals with the help of energy consumption / resource recovery criteria.

PLANT CONFIGURATION, MODELS, DATA & EVALUATED OPTIONS

The plant mainly treats effluents from the beam-house, which corresponds to the processing of raw hides into semi-finished leather (also called wet blue). The different transformation processes result in the following process wastewater streams (In): *In-S* soaking (1), *In-L* (2) liming (2) and deliming (4) water, *In-F* includes fleshings (3), In-*PC* includes pickling (6) and chrome water (7), *In-B* includes enzymatic treatment of the

hides (bating) (5). In addition, there are two additional streams containing rain water and polymer preparation (*In-RP*) and re-tanning, finishing water and R&D (*In-RD*). More info about tannery wastewater can be found in Jain et al., 2011.

The plant treats the previously described Process Waste Streams (*In*). The process layout consists of three buffer tanks (BFF1-3), 2 thickeners (THK, BT), 1 anaerobic granular sludge reactor (AnGSR), 1 biogas desulfurization tower (BDST), 1 tri-canter (TRI), 1 anaerobic digester (AD), 1 belt filter press (BF), 1 chrome treatment unit (CT), 1 activated sludge reactor (ASR), 1 secondary clarifier (SEC) and 1 belt thickener (BT). A schematic representation of the flow diagram can be found in **Figure 1**

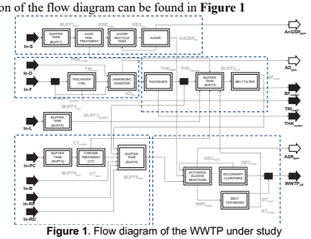

Figure 1. Flow diagram of the WWTP under study

Plant data used in this study comprises one year of measurements between January and December 2022 (1 to 3 measurements per week). Samples were taken from 7 locations: 1) BFF1 output, 2-3) AnGSR input & output, 4) AD2 output, 5) BFF2 output, 6) BFF3 output, 7) SEC output. There are some occasional measurements at *In-F*, *In-B*, *In-RF* and *In-RD*. Analytics involved the determination of: pH, total suspended solids (TSS), volatile suspended solids (VSS), chemical oxygen demand (COD) & total nitrogen (TN). These analyses were complemented with filtered (0.45 µm) samples for quantifying ammonium / ammonia (NH_x), nitrate/nitrite (NO_x) & sulfate/sulfite (SO_x) in selected points. Flow rate, COD & N (total concentrations) were balanced and adjusted using the approach proposed by Monje *et al.* (2022) where: 1) an identity matrix was defined, 2) data were cleansed and curated, 3) missing fluxes were estimated, 4) optimal flows were calculated and 5) the new data set was verified.

MATHEMATICAL MODELLING APPROACH

A full description of the plant-wide model used in this case study can be found in Monje et al., 2022a and b. In a few words, AnGSR and AD are approximated using the IWA Anaerobic digestion Model No 1 (Batstone *et al*, 2002). The syntrophic acetate oxidation pathway had to be included to correctly account for the absence of inhibition expected at these high ammonia concentrations on COD and N removal in the AD. The ASR is based on the ASM1 (Henze *et al.*, 2000), pH and liquid-gas transfer are modelled using the General Physicochemical Modelling (PCM) approach (Batstone and Flores-Alsina, 2022). Both interfaces (ADM-ADM and ADM-ASM) ensure COD and elemental (C, N) continuity. All separation units are modelled as ideal splitters. An empirical approach is used before belt and thickening filter in order to assume coagulation/flocculation. More info about the model can be found in Monje *et al.*, 2022a,b.

RESULTS

From the initial volumetric balance calculations, one may conclude that *In-L* (lime water) (25 %) is the main contributor, closely followed by *In-S* (Soaking) (19 %), *In-B* (Bating) (15 %) and *In-RP* (rain water + polymer preparation) (15%). With respect to COD and N loads, 32 + 30 % and 31 + 29 % comes with *In-L* (lime water) and *In-F* (fleshings) due to the high content of proteins and fats resulting from removal of hair and other keratinous material. When it comes to the outputs, the effluent (=overflow of the secondary clarifier) (SEC_{over}) carries most of the hydraulic load (98 %). The remaining 2 % is linked to bio-solids for post-digestion (THK_{under}) and/or disposal (BF_{under}). Around 31% of the incoming COD is transformed into methane and potentially recovered ($AnGSR_{gas}$ + AD_{gas}). The remaining COD is removed aerobically/anoxically (16%) in the activated sludge reactor (ASR_{gas}), ends up in bio-solids (49%) (BF_{under} + THK_{under}) or part of the effluent (> 1 %) (SEC_{over}). Regarding N, 46 % is biologically removed (ASR_{gas}). The second largest N outflow is in the biosolids (36%) (BF_{under} + THK_{under}) while another fraction leaves with the effluent (11%) (SEC_{over}). Detailed calculations can be found in **Figure 2**.

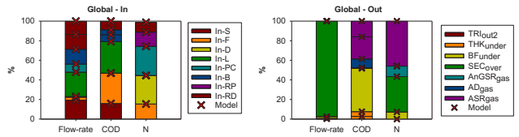

Figure 2. Relative contribution of flowrate, COD and N at the input (left) and output (right). Red crosses represent model predictions

All eight Influents (*In*) were fractionated using the principles described in Monje *et al.*, 2022a,b. Computer simulations reveal that the mathematical approach proposed in this study is capable of reproducing flow, mass and the main transformations (average deviation 10%) within the multiple units comprising the flow diagram (see **Figure 1**). In general, the model predicts the quantity of COD that, potentially, can be recovered in form of methane (AnGSR + AD), the COD and N that is biologically removed in the activated sludge reactors (ASR), the particulate material purged from dewatering units (THK + BF) and the energy demand (ED) in the aeration basin. More specifically, to better describe data: 1) the AnGSR model is assumed to function at less than half capacity, 2) Acetate oxidizers in the AD model had higher tolerance to ammonia inhibition than acetate degraders, 3) an empirical model assuming coagulation/flocculation was added at BF and BT in order to match under and overflow data (and mimic the effect of polymer addition), 4) a combined power and heat generator (CHP) assuming 40 and 42 % efficiency for electricity (EP) and heat (HP) production was assumed for both AnGSR and AD gas streams and 5) a factor of 1.4 kgO_2/kWh was used to estimate energy consumption (diffuser aerators) in the ASR. *More details about the model specific arrangement will be discussed in case the paper is selected for platform presentation*.

SCENARIOS & OUTLOOK

Two additional scenarios are simulated using the adjusted model. S1: *In-L* is redirected from ASR to AnGSR after Ca removal. This will remove the risk of intra-granule precipitation (Feldman *et al.*, 2017). In S2, *In-S*, *In-B* and *In-F* will be sent to a dissolved air flotation (DAF) unit. The underflow will be sent to the ASR. Two coagulation/flocculation efficiencies are assumed. The AnGSR will be decommissioned. Plant data, baseline simulation and the results of the two scenarios are summarized in **Table 1**. For a comprehensive description of operational cost indices quantification the reader is referred to Monje *et al.*, 2022a,b.

Table 1. Plant data and simulation results (Baseline, scenarios)

		Plant data	Baseline	S1	S2 (a)	S2 (b)
Biogas Production (BP)[1]	m^3/d	420 / 1700	450 / 1720	2028 / 1720	0 / 2000	0 /2600
Heat Demand (HD)[1]	kWh/d	2383 / 474	2383 / 474	5248 / 474	0 / 834	0 / 934
Heat Production (HP)[1]	kWh/d	-	2505 / 4465	8288 / 4465	0 / 5542	0 / 7079
Electricity Prod. (EP) [1]	kWh/d	-	2369 / 4228	7838 / 4228	0 / 5240	0 / 6694
Electricity Demand (ED)	kWh/d	1815	1837	2200	3998	3212
Disposed Sludge 1 (DS1)[2]	ton/d	4.7	4.7	4.7	8.6	11.8
Disposed Sludge 2 (DS2)[2]	ton/d	18.1	19.0	13.3	6.1	5.26

[1] The first value correponds to the AnGSR and the second value is the AD, [2] DS produced in THK. 3 DS produced in the BF

Model-based evaluation results (S1) show that diverting *In-L* to AnGSR (S1) substantially increases the quantity of COD recovered. This is reflected in 1) BP and 2) EP. Since *In-L* is treated anaerobically, sludge production (DS2) is also reduced. However, a comparatively higher COD (with respect to Baseline) leaving the AnGSR overloads the ASR and increases the energy needed for aeration (see ED values). These simulations were conducted assuming that :1) the AnGSR was operating at full capacity and 2) nitrification efficiency in the ASR was maintained. With respect to S2, the model suggests a substantial reduction in (total) BP and EP. In addition, a substantial increase of the EC. However, the higher the DAF capacity to capture more of the colloidal material part of CODs (= better coagulation/ flocculation), the lower the EC. However, DS1 is increased as trade-off (see S2b). These simulations are conducted assuming a DAF with 97 % TSS removal efficiency and 14 % TSS in the overflow.

The study has offered the preliminary results of a research study involving industry and academia. Additional information will be provided including more scenarios, accounting for water reclamation options and the use of chemicals for coagulation/flocculation (not added at this stage). Also better OPEX estimates (revenues versus costs). The mass balance analysis of the origin/transformations/fate of the different compounds gives a better picture of plant drawbacks and foresees potential optimization solutions. The possibility to generate and assess alternative retrofitting scenarios with the proposed plant-wide model will allow the scientist/process engineering to evaluate the feasibility of a new operational procedure/technology beforehand and only implement the solution with the highest chance of success.

REFERENCES

Batstone et al (2002). IWA STR n 9,
Batstone and Flores-Alsina (2022).. IWA STR n 29
Feldman et al. (2017). Water Research. 126, 488.
Henze et al., (2002). IWA STR N 9,
Monje et al., (2022a). Chemical Engineering Journal. 445.136774.
Monje et al., (2022b). Water Research. 223, 118997,
Müller-Czygan et al (2021). Energies. 14(22):7709

Distinct characteristic pollution and systematical ecological risk assessment of microplastic in the Yangtze River

Qian'en Huang, Ze Liu

* Lab of Contaminant process control and health effect (CPCHE), College of Resources and Environment, Northwest A&F University, Taicheng Road 3, 712100 Yangling, China
(E-mail: *ze.liu@nwafu.edu.cn)*

Abstract
Microplastic (MP) contamination in the river system has attracted widespread attention, whereas the abundance, characteristic and risk of microplastics in River remain poorly understood. Thereby, we develop a systematic assess framework to M. And the Yangtze River is taken for example. It is compiled a microplastic dataset, including 194 samples sites along the Yangtze River. It is found that MP abundance is from 2263.60±4231.77 particles/m³. According to MPs abundance and characteristic with a comprehensive risk assessment considering with all of these methods, the environmental risks of microplastics were partitioned into four classes, and Upstream and Midstream of Yangtze River were identified as potential high risk distinct. MPs risk assessment method and standard suggested that a unified standard is essential to further enhance our knowledge on the risk of microplastics in the river system.

Keywords
microplastics, Yangtze River, surface water, risk assessment

INTRODUCTION

There are of global concerns on plastic debris, and especially microplastics (MPs), in the aquatic environment over years. MPs are defined as plastic particles less than 5 mm in diameter, which can be derived from the breakdown of larger plastic items or deliberately manufactured for plastics productions (Xu, Chan, et al., 2021). MP has been considered as an emerging contaminant due to its recalcitrance, ubiquity and potentially adverse effects on the environment and human health (L. Zhang et al., 2020). Recent studies have reported that MPs are discovered in the digestive tract of aquatic organisms and accumulated in various plants (Biginagwa et al., 2016; Mercogliano et al., 2020; Mazurais et al., 2015), thus showing potential harmful impacts on ecosystems and agricultural sustainability (Ibrahim et al., 2021; Sun et al., 2020). MPs can be also exposed to humans through inhalation or ingestion (Biginagwa, Mayorna, et al., 2016; Takebira, Mondal, et al., 2021; Vethaak and Legler, 2021), and contained in the tissues and organs of the human body, which could cause specific toxicity by such as enhancing oxidative stress or further inducing inflammation and diseases (Liu et al., 2021; Noventa et al., 2021). After entering organisms, MPs are able to be transferred via the food web, leading to their widespread occurrence in the ecosystems.

Thus, it is urgent to build a systematic risk assessment framework for MP, in order to prophylaxis environmental pollution and human diseases better. Nowadays, there are PLI(Xu, Peng, et al., 2018), H(Xu, Peng, et al., 2018), SSD(Jung et al., 2021; Liu et al., 2022), ESI Rangel-Buitrago et al. (2021), and other risk assessment methods for the ecologic risk assessment of microplastics in rivers from a single characteristic of microplastics, but no method can comprehensively assess the environmental risk of microplastics in the river system. Therefore, we constructed a more comprehensive and convincing assessment method for the environmental risks of microplastics in the river system based on the Beta coefficient, a risk index commonly used for risk assessment in economics. And BetaMP coefficient, which is similar to Beta coefficient, was used for quantitative evaluation in the risk assessment of microplastics.

MATERIALS AND METHODS

The method what we called BetaMP that based on β, is firstly applied to the risk assessment of microplastics in the environmental field The BetaMP coefficient (BMPC) constructed by us calculated the comprehensive risk index of MPs in river system based on the formal risks index of PLI, H, SSD and ESI. In order to distinguish the influence factors of different risk assessment methods on the same region as well as comprehensively evaluate the risk of MPs in a region, we further subdivide BMPC into BMPC $_{method}$ and BMPC$_{distinct}$ Among them, BMPC $_{method}$ is used to evaluate the influence weight of different MP characteristics in a certain region on the regional risk index, so as to determine which MP characteristics in this region have a greater impact on the environmental risk of MPs. BMPC$_{distinct}$ is used to evaluate the environmental risk of MPs in different region in a wide range, so as to determine the harm of MPs in different regions to the environment. The calculation formula is as follows:

$$BMPC_{method} = \frac{\sum_{i=1}^{n} x_{ij} - x_{0j}}{\sum_{i=1}^{1-m,1-n} x_{ij} - \sum_{j=1}^{n} x_{0j}} \quad (1)$$

$$BMPC_{distinct} = \frac{\sum_{j=1}^{n} x_{ij} - x_{0j}}{\sum_{i=1}^{1-m,1-n} x_{ij} - \sum_{j=1}^{n} x_{0j}} \times \alpha \quad (2)$$

Where *i* presents MPs region (Source, Upstream, Midstream, Downstream, Estuary), that is, m=5, *j* presents the MP risk assessment method (PLI, H, SSD, ESI), that is, n=4, x_{0i} is risk-free value of a risk assessment index in each region after normalization, x_{0j} is the risk-free value of a normalized risk assessment index, x_i is the normalized actual risk value of a risk assessment index, x the normalized actual risk value of a region.

It is worth noting that in our analysis and assessment process, the risk assessment index ranges of existing risk assessment indexes PLI, H, ESI, and SSD are different, which brings great inconvenience to the comprehensive environmental risk assessment of microplastics in the river system. Therefore, we normalized each risk index before the comprehensive assessment. Differently from the formal risk assessment method, the normalization process first needs the support of experimental data.

RESULTS AND DISCUSSION

In order to verify the new risk assess framework for MP in the river system, MP pollution and exposure risk in different areas in the Yangtze River is analysed, calculated and compared. Based on the concentrations of MPs at the 147 sampling sites (Figure1).

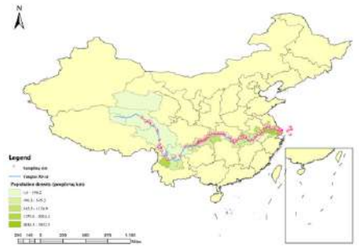

Figure 1. Sampling sites collected and screened from the relevant published articles. The colours represent the population density in the river basin in a range of 1.6-3922.5 people/km².

The risk index of PLI was firstly determined. The obtained results showed that 84.4% of sampling sites were with a risk level of V, suggesting that the entire watershed (from the source to the estuary) was at high risk of MP pollution (Figure 2). The values of PLI for the upstream, midstream and downstream were even significantly higher than those for the source and estuary, which was in consistent with the abundance distribution of MP in the basin. As known, the estuary area is affected by e.g., tides that may dilute the concentration of MPs in the surface water, making its abundance much lower than in other areas(Malli, Corella-Puertas, et al., 2022). Even if that, the PLI results suggested that the estuary area was still at an MP risk level of as high as VI, indicating that the risk of MP pollution in this area is high enough to pay more attention. For example, the PLI for Chongming, an island located in the estuary, was as high as 161.2, showing Chongming was at a risk level of V. Compared with the nearby downstream areas, e.g., Shanghai and Nanjing, Chongming in the estuary area has fewer human activities and industrial production there, so the amount of primary MPs discharging from the island is relatively small. Thus, it can be speculated that the high abundance of MPs occurred is likely to attribute to the effect of MPs emitted from surrounding areas (Liu, Lu, et al., 2018; Zhao, Zhu, et al., 2014).

For example, MPs discharge into the river from industrials area of the Yangtze River Delta via mainstream hydrological processes.(Luo, Su, et al., 2019).

Compared to the results of PLI-based risk assessment, the assessment based on ESI, H score and SSD index, were quite various (Figure 2). For example, the ESI-based assessment evaluated the source as "Unsatisfactory", while the other four areas were only at the level of "Mediocre". It suggested that the source was at relatively high risk of MP exposure from the perspective of the morphology, which was not consistent with the results of PLI-based. This may be explained by the high proportion of particle-shaped MPs in the surface water of the area of the source due to atmospheric deposition being the major source of MPs there. Furthermore, the downstream was assessed as an area with the same high-level MP exposure risk as the upstream and midstream based on the PLI assessment, while it was suggested to be a lower risk area by H-based assessment. This was supported by the fact that the uneven polymer types distribution of MPs in the Yangtze River, and the polymer types of MPs with high hazardous-score, e.g., PVC, were less contained in the downstream than in the upstream and midstream. Also, the midstream and downstream that were considered to have the highest level (level V) risk of MPs exposure based on the PLI assessment were viewed to have no toxic risk to the ecosystem in the assessment of the SSD approach. Therefore, the above confirms our hypothesis that evaluating the ecological risk of MPs exposure in the Yangtze River by single either the abundance or the characteristics and composition of MPs tends to make an underestimation or overestimation.

Notably, the upstream, which has ever been widely regarded as an area with low pollution risk (Zhang, Xu, et al., 2022) is surprisedly suggested as a high-level risk area of MPs exposure in the Yangtze River by not only PLI-based assessment but also H- and SSD-based assessment. Due to various driving factors, including the WWTPs discharging and the locations of dams on the river, causing the appearance of MP 'hotspot' in the region of upstream of the Yangtze River, in fact, it is reasonable to consider the risk of MPs exposure is at a high level in this region. Additionally, it is speculated that the 'hotspot' can be related to not only the high MPs concentration but also the high toxic effect of MPs.

Unlike other individual risk assessment method, BetaMP is to provide a quantitative recommendation on the risk level of different areas of the Yangtze River from an overall perspective. According to the results of BetaMP shown in Figure 2, the comprehensive risk of the different areas of the Yangtze River was in order as: Upstream (BMPC=0.34) > Midstream (BMPC=0.28) > Downstream (BMPC=0.19) > Estuary (BMPC=0.12) > Source (BMPC=0.07). Noteworthy, the obtained results show that the risk level of MP pollution in the areas of upstream and midstream is more serious than the average risk level (BMPC=0.2) of the entire river. It suggested that, for the Yangtze River, the upstream and midstream where are previously thought to be less polluted by MPs, should receive more attention on the MPs pollution than before. Furthermore, by means of BetaMP method, the influence of each individual MP risk assessment method on the comprehensive MP risk assessment is also able to be determined. As shown Table S7 in Supplementary Material 1, risk coefficients of each individual MP risk assessment method are in order as: H (0.77) > ESI (0.16) > PLI (0.05) > SSD (0.02). These obtained results indicate that the method of H index cause the highest effect on the result of the risk assessment, suggesting that polymer type may have the highest impact to MPs environmental risk in the Yangtze River. Although MP abundance is typically viewed as the most important impact factor on its risk in the river systems, abundance related indexes, i.e., PLI and SSD, show a relatively low impact on the final risk assessment results in this case. Therefore, it can be reasonably deduced that due to the differences of characteristics of MP pollution between different rivers or different areas of the river, the main factors that cause risk could be variable. However, given the MPs in the Yangtze River have only received attention in the past decade and related research is in its infancy, our analysis is certainly not fully representative. Nonetheless and to the best of our knowledge, it represents the most comprehensive study of spatial distribution and risk assessment of MPs in the riverine system, so far.

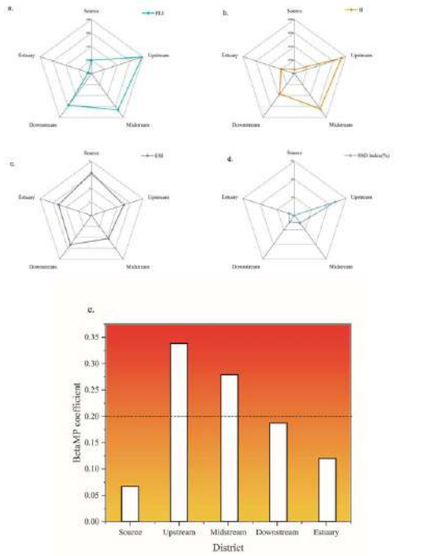

Figure 2. Comparisons of risk of MPs exposure in the different areas of the Yangtze River according to multiple evaluation methods, including assessment based on the (a).PLI, (b).H score, (c).ESI, and (d).SSD index of MPs presented in the five different regions, as well as the results of BetaMP method. (e).Dashed (BetaMP coefficient=0.2) in the figure presents the average BetaMP coefficient (0.2) of the Yangtze River.

This processing method can well avoid the differences caused by different data processing methods, and give a more convincing result for the research. To BetaMP coefficient (BMPC) coefficient as the evaluation index of the microplastic basin environmental risk comprehensive evaluation method not only can be flexible to change with different features of the microplastic evaluation method of risk assessment, species and amount can be compared to these evaluation methods compared, find out what kind of a greater role in the risk of micro plastic characteristics in this basin. In addition, the comprehensive environmental risk assessment method of microplastic watershed can also accurately assess the environmental risk values of microplastic in different regions of the whole watershed.

In conclusion, the microplastic watershed environmental risk comprehensive assessment method is a more comprehensive risk assessment method that integrates the existing microplastic risk assessment methods, and is suitable for the modified microplastic risk assessment articles in the Yangtze River system.

REFERENCES

Ahmed, M. B., Rahman, Md. S., Alom, J., Hasan, MD. S., Johir, M. A. H., Mondal, M. I. H., Lee, D.-Y., Park, J., Zhou, J. L., and Yoon, M.-H. (2021) Microplastic particles in the aquatic environment: A systematic review. Science of The Total Environment, **775**, 145793.

Biginagwa, F. J., Mayoma, B. S., Shashoua, Y., Syberg, K., and Khan, F. R. (2016) First evidence of microplastics in the African Great Lakes: Recovery from Lake Victoria Nile perch and Nile tilapia. Journal of Great Lakes Research, **42**(1), 146–149.

Jung, J.-W., Park, J.-W., Eo, S., Choi, J., Song, Y. K., Cho, Y., Hong, S. H., and Shim, W. J. (2021) Ecological risk assessment of microplastics in coastal, shelf, and deep sea waters with a consideration of environmentally relevant size and shape. Environmental Pollution, **270**, 116217.

Liu, Y., You, J., Li, Y., Zhang, J., He, Y., Breider, F., Tao, S., and Liu, W. (2021) Insights into the horizontal and vertical profiles of microplastics in a river emptying into the sea affected by intensive anthropogenic activities in Northern China. Science of The Total Environment, **779**, 146589.

Liu, Z., Huang, Q., Wang, H., and Zhang, S. (2022) An enhanced risk assessment framework for microplastics occurring in the Westerscheldt estuary. Science of The Total Environment, **817**, 153006.

Mercogliano, R., Avio, C. G., Regoli, F., Anastasio, A., Colavita, G., and Santonicola, S. (2020) Occurrence of Microplastics in Commercial Seafood under the Perspective of the Human Food Chain. A Review. Journal of Agricultural and Food Chemistry, **68**(19), 5296–5301.

Noventa, S., Boyles, M. S. P., Seifert, A., Belluco, S., Jiménez, A. S., Johnston, H. J., Tran, L., Fernandes, T. F., Mughini-Gras, L., Orsini, M., Corami, F., Castro, K., Mutinelli, F., Boldrin, M., Pantes, V., Sotoudeh, M., Mascarello, G., Tiozzo, B., McLean, P., Ronchi, F., Booth, A. M., Koelmans, A. A., and Losasso, C. (2021) Paradigms to assess the human health risks of nano- and microplastics. Microplastics and Nanoplastics, **1**(1), 9.

Rangel-Buitrago, N., Arroyo-Olarte, H., Trilleras, J., Arana, V. A., Mantilla-Barbosa, E., Gracia C., A., Mendoza, A. V., Neal, W. J., Williams, A. T., and Micallef, A. (2021) Microplastics pollution on Colombian Central Caribbean beaches. Marine Pollution Bulletin, **170**, 112685.

Sun, X.-D., Yuan, X.-Z., Jia, Y., Feng, L.-J., Zhu, F.-P., Dong, S.-S., Liu, J., Kong, X., Tian, H., Duan, J.-L., Ding, Z., Wang, S.-G., and Xing, B. (2020) Differentially charged nanoplastics demonstrate distinct accumulation in Arabidopsis thaliana. Nature Nanotechnology, **15**(9), 755–760.

Takebira, U., Mondal, M., and Habib, M. A. (2021) Microplastic Pollution and Human Body: Cause and Effect. International Journal of Polymer and Textile Engineering, **8**, 6–8.

Vethaak, A. D. and Legler, J. (2021) Microplastics and human health. Science, **371**(6530), 672–674.

Xu, P., Peng, G., Su, L., Gao, Y., Gao, L., and Li, D. (2018) Microplastic risk assessment in surface waters: A case study in the Changjiang Estuary, China. Marine Pollution Bulletin, **133**, 647–654.

Xu, Yuyao, Chan, F. K. S., Johnson, M., Stanton, T., He, J., Jia, T., Wang, J., Wang, Z., Yao, Y., Yang, J., Liu, D., Xu, Yaoyang, and Yu, X. (2021) Microplastic pollution in Chinese urban rivers: The influence of urban factors. Resources, Conservation and Recycling, **173**, 105686.

Case Study of Climate Change Countermeasures (Jeju Island in South Korea)

J. K. Kim*

* Department of Environmental Engineering, Jeju National University, 102 Jejudaehak-ro, Jeju-si, Jeju-do, Republic of Korea
(E-mail: *kjinkeun@jejunu.ac.kr)*

Abstract
Climate change adaptation strategies for 8 wastewater treatment plants(WWTPs) in Jeju, South Korea were investigated. Based on survey of 54 workers and risk assessment, climate change adaptation measures for heavy rains, strong winds, heat waves were proposed. Installation of equalization tank was proposed for heavy rain countermeasure to minimize impact of inflow surge. Dual power supply and flood prevention measures were proposed for strong wind. In the case of heat waves, it was suggested to improve responsiveness to toxic gases and reduce water use. This adaptation plan is a five-year plan, and the required budget is also calculated.

Keywords (maximum 6 in alphabetical order)
Abstract; adaption strategy; climate change; wastewater treatment plants

Climate change adaptation strategies for 8 wastewater treatment plants(WWTPs) in Jeju, South Korea were investigated following General process steps for adaptation planning (**Figure 1**.).

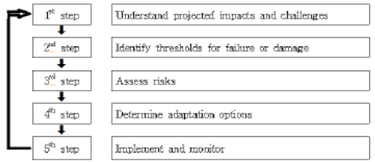

Figure 1. General process steps for adaptation planning

The climate change factors were evaluated on a 5-point scale (5 point means the negative impact is the largest) for 54 workers. Climate factors that negatively affect sewerage facilities are heavy rain (4.79), strong wind (3.46), heat wave (3.12), heavy snow (3.10), cold wave (2.67), and drought (2.12). If it is larger than 3.0 in the survey, it is a case where the negative impact on climate change is large. Therefore, this study established detailed climate change adaptation measures for heavy rains, strong winds, heat waves. Due to the warm climate of Jeju island, snow melts in a short period of time (e.g., less than 2 days), so the increase in sewage inflow becomes a problem, which is actually linked to heavy rain countermeasures. Therefore, in this study, adaptation measures were established by focusing on heavy rains (including heavy snow), strong winds, and heat waves.
Risk assessment for each climate change factor is calculated by calculating the probability of occurrence of climate impact factors (A) and the magnitude of impact (B) for climate impact vulnerable facilities when climate impact factors occur, and multiplying them (A×B).
In the event of heavy rain, a temporary increase in sewage inflow is expected in the case of combined sewer areas, and it is difficult to completely exclude the effect of precipitation even in separate sewer areas, so heavy rain can lead to an increase in sewage inflow. As an adaptation measure, installation of equalization tank was proposed.
In the case of strong wind, the risk of falling facilities increases. There is also a high risk of power outages. The risk of flooding due to waves increases in coastal pumping stations. Dual power supply and flood prevention measures were proposed as an adaptation measure
In the case of heat waves, the amount of tap water used increases, resulting in an increase in the amount of sewage generated. Increased sewage inflow in warm season may increase toxic gas generation in enclosed spaces and odor concentration in WWTPs, and eutrophication in discharged water areas are expected. As an adaptation measure, it was suggested to improve responsiveness to toxic gases and reduce water use.
This adaptation plan is a five-year plan, and the required budget is also calculated.

REFERENCES

American Water Works Association. 2021 Climate Action Plans-Adaptive Management Strategies for Utilities
USEPA. 2015. Adaptation Strategies Guide for Water Utilities

Social footprint evaluated within Chilean rural wastewater treatment plants.

Gatica[1] and C. A. Villamar-Ayala[1*]

[1]Facultad de Ingeniería, Departamento de Ingeniería Civil en Obras Civiles, Universidad de Santiago de Chile (USACH), Santiago, Chile (*email: cristina.villamar@usach.cl*)

Abstract
Wastewater treatment plants (WWTPs) correct operation can condition the public health risk of the surrounding population, generating strong resistance from nearby communities. The aim of this study was to measure the social footprint of five Chilean rural WWTPs over their social stakeholders, being these the workers and local community. The study included interviews to 8 operators and 4 administrators, as well as a total of 98 surveys to the local community. An Analytic Hierarchy Process (AHP) was used. Results demonstrated that natural-based WWTPs were un-valuated due to security and operational problems for worker and local community, respectively. Community engagement (0.56) and health and safety (0.27) were the best valuated subcategories for workers and local community, respectively. Better community engagement strategies and training could improve the performance of Chilean rural WWTPs.

Keywords
Activated sludge, local community, nature-based technologies, operation problems, workers.

INTRODUCTION

According to the 2019 Sustainable Development Goals Report (United Nations United, 2019), around 4 billion people in the world are affected by water scarcity, which represents more than 40% of the world population. It is so that water and sanitation are part of the Sustainable Development Goals as part of the 2030 Agenda. In relation to wastewater treatment, there are large gaps between developed and developing countries with percentages that average 75.6 and 18.5%, respectively (Malik et al., 2015). Rural areas tend to increase these gaps, with respect to urban zones, so Chile has sanitary urban coverage close to 100%, but in rural zones it does not reach 20% (Villamar et al., 2018). Moreover, the health risk in these sectors is increased by some factors, such as: frequent operational problems, little knowledge of workers and proximity of the population to WWTPs. There are few studies that evaluate the performance of WWTPs from the social footprint. Padilla-Rivera et al. (2016) compared rural and urban Mexican WWTPs considering 25 indicators, where urban WWTP was better evaluated than rural one, due to that urban population had not close WWTP. These precedents reveal the importance of measuring the social footprint in preventive and corrective decision-making inside WWTPs.

MATERIALS AND METHODS

Aim and scope of the study.

This study studied five Chilean rural WWTPs based on nature-based and conventional technologies, such, vermifilter (33°0'30.09"S 70°53'21.91"O), constructed wetland (33°10'5.68"S 70°53'13.90"O), aeration lagoon (33°44'43.42"S 70°52'17.32"O), activated sludge (33°49'59.63"S 70°38'50.28"O), and activated sludge + bio-discs (32°50'41.53"S 70°56'18.40"O), considering workers (operators and administrators) and local community. Moreover, only the operation phase was considered. Surveys in the local community considered a range between 15 and 2o interviews per WWTP within a radius of 500 metres.

Inventory analysis

The impact subcategories were defined based on the guidelines proposed by UNEP/SETAC (2019). Local communities considered subcategories, such as: safe and healthy living conditions, local comfort, community engagement, feedback mechanisms. Meanwhile, workers considered: fair wage, hours worked, equal opportunities and treatment, health, and security, working conditions and comfort, and child labour.

Impact assessment

Each stakeholder (workers, local community) was evaluated using Analysis Hierarchical Procedure (AHP) to obtain reference matrices, correlating it with multicriteria analysis between subcategories. This analysis considered Saaty-Gómez (2008) scale comparison using 5 levels (1, 3, 5, 7, and 9). The data obtained were considered valid if the consistency index ratio (CIR) is less than 0.1.

RESULTS AND DISCUSSION

Table 1 shows the AHP results per stakeholder and treatment technology for local community and workers. Local community mentioned that WWTPs using nature-based solutions (vermifilter and constructed wetland) had the worst performance in all subcategories. While that, conventional WWTPs (activated sludge) had the best behaviour. The best evaluated subcategory was safe and healthy living conditions (0.56) and the worst evaluated one was community engagement (0.06). In short, although there were differences between nature-based vs. conventional solutions, these were not related to the type of WWTP, but rather to the operation. WWTP who have ongoing dialogue with the community tend to have better perceptions than those who don't.

On the other hand, workers reported that WWTPs using nature-based solutions (vermifilter and constructed wetland) had the worst performance; while that, conventional WWTPs (activated sludge + bio-discs) showed the best behaviour. The best evaluated subcategory by workers was health and security (0,28) and the worst evaluated subcategory was opportunities equal opportunities and treatment (0.13). In conclusion, workers in rural WWTP often perceive negative aspects, when their safety and health are not prioritised. While salary was an important issue for them, it was only relevant when they had odd or part-time jobs. Working conditions are also reflected in less training, which could influence a better functioning of WWTPs.

Table 1. AHP results per stakeholder and technology (WWTP).

	Local community			Workers		
WWTP	Score (%)	Preference	Position	Score (%)	Preference	Position
Vermifilter	12	9.3	5th	6	6.0	5th
Constructed wetland	15	19.3	4th	8	11.8	4th
Aeration lagoon	17	23.6	2sd - 3th	13	28.5	
Activated sludge	17	23.6	2sd - 3th	17	40.8	1st
Activated sludge + bio-disks	17	23.4	1st	9	12.9	3th

Acknowledgements

This researcher was supported by the Fondecyt (project grant 11190352) and VIME 167-2022. Authors thank the facilities provided to this research by Chilean rural WWTPs. Moreover, authors thank the Interdisciplinary Lab of Water and Sciences Technology (KoYaku Lab, Chile).

REFERENCES

Malik, Hsu, A., Johnson, L. A., & de Sherbinin, A. (2015). A global indicator of wastewater treatment to inform the Sustainable Development Goals (SDGs). Environmental Science & Policy, 48, 172–185.

Padilla-Rivera, Morgan-Sagastume, J. M., Noyola, A., & Güereca, L. P. (2016). Addressing social aspects associated with wastewater treatment facilities. Environmental Impact Assessment Review, 57, 101–113.

Naciones Unidas. (2019). Informe de los Objetivos de Desarrollo Sostenible 2019.

Villamar, C. A., Vera-Puerto, I., Rivera, D., & De la Hoz, F. (2018). Reuse and recycling of livestock and municipal wastewater in Chilean agriculture: A preliminary assessment. Water, 10(6), 817.

UNEP-SETAC (2019). Guidelines for social life cycle assessment of products.

Stakeholders' attitudes towards acceptance in the use of nutrient reuse technologies and decentralised systems in four case studies in Europe.

Medina. B.*; Gómez-Román, C;**; Sabucedo, J.M.**

*WE&B, Water, Environment and Business for Development, Barcelona, Spain. (Email: *beatriz.medina@weandb.org*)
**CRETUS Institute and Department of Social Psychology, Basic and Methodology, Universidade de Santiago de Compostela, 15705 Santiago de Compostela, Spain (Email: cristina.gomez@usc.es, *josemanuel.sabucedo@usc.es)*

Abstract

Social acceptance is an important factor in terms of the success and feasibility of the technologies' implementation in relation to water and nutrient reuse systems. To implement these systems successfully, it is necessary not only to design this technology, but also to have social support and willingness among citizens to use it. In this study, after having conducted a social network analysis, we analyse the acceptance profiles for nutrient reuse technologies of the key stakeholders in four demo-sites in Europe. The demo-sites are located in Ghent (Belgium), Vigo (Spain), Helsingborg (Sweden), and Sneek (The Netherlands).
A qualitative approach for empirical data collection was used to analyse the acceptance profiles grounding in a thematic analysis of the focus groups conducted to different type of target groups: users's of technology, technology developers, farmers, fertiliser companies, environmental associations among others. According to the analysed data relating to the acceptance profiles, we addressed how perceived advantages and disadvantages from the stakeholders varies depending on the strength level of engagement to the systems development. Therefore, information about the technologies, needs to be used in a way that is most adapted to the audience so that relevant type of audiences are able to understand the added value of these technologies.This requires the development of communications that are part of a defined strategy and that are implemented with a two-way process of information integrating the behaviour and opinion of the users periodically gathered. Thus, we observed that the level of acceptance of the technologies and willingness to use the products from nutrient reuse is favourable around these four pilot decentralised systems.

Keywords (maximum 6 in alphabetical order)
Engagement, decentralised water technologies, nutrient reuse perception, qualitative analysis, social acceptance.

Monitoring of odorous emissions in WWTPs: proposal for a simple procedure

L. Palli*, D. Fibbi* and E. Coppini*

* G.I.D.A. Spa, Via di Baciacavallo 36, Prato, IT
(E-mail: l.palli@gida-spa.it; d.fibbi@gida-spa.it; e.coppini@gida-spa.it)

Abstract
The most commonly used technique worldwide to determine odor concentration is the dynamic dilution olfactometry, while in this paper we propose a simple and low-cost procedure for the monitoring of the evolution of odor emissions. The procedure consists in a sensory surveys based on the olfactory perception of odors by a selected group of people. A list of points in which to carry out the odor monitoring is decided. During the inspections, the subjects evaluate, at each point, the intensity, the hedonic tone and the nature of the odor. The collected intensity and hedonic tone data are multiplied (IxHT) and then the matrix of IxHT values is mapped, where the most odorous points are easily and immediately visualized. The proposed technique allowed to detect modifications in the nature and in the intensity of the odors, as well as seasonal changes. Furthermore, the simplicity and low cost of the procedure make it applicable to any system and with very high frequencies.

Keywords
Hedonic tone; Intensity of the odor; Nature of the odor; Sensory survey; Simple procedure; WWTP.

INTRODUCTION

Wastewater treatment plants (WWTPs) are considered to be one of the main causes of unpleasant odors noticed by the exposed population (Zarra et al., 2008). Odor emissions from WWTPs are characterized by the presence of a large number of volatile odorants (mainly sulfur and organic compounds) at trace level concentrations, which usually render them harmless from a toxicological point of view (Lebrero et al., 2011). However, monitoring odor emissions from WWTPs over time is important, especially if the plant is located near residential areas. The most commonly used technique worldwide to determine odor concentration is the dynamic dilution olfactometry, based on the concept of the detection threshold and the use of a set of human sensors (panelists) (Sneath, 2001). This technique, despite being the most reliable and reproducible for this type of measurement, is complex and very expensive and for this reason it cannot be performed very frequently. In this paper we propose a simple and low-cost procedure for the monitoring of the evolution of odor emissions from WWTPs which has been performed for over 5 years in two large WWTPs in Italy.

MATERIALS AND METHODS

The procedure consists in a sensory surveys based on the olfactory perception of odors by a selected group of people. The suitable subjects to carry out the inspections were selected excluding that any habits (e.g. cigarette smoke) or pathologies of the respiratory system could make their judgment unsuitable or ineffective. The surveys are carried out four times per year, in the months of March, June, September and December to cover any seasonal differences. A list of points in which to carry out the odor monitoring has been decided, both internally and externally to the plant, choosing internally the most odorous points (emission points) and externally sensitive points (e.g. presence of houses). During the inspections, the subjects evaluate, at each point, the following characteristics of the perceived odor: a) Intensity of the odor, expressed with a number ranging from 0 (perceptive threshold), up to 6 (irritation threshold); b) Hedonic tone of the odor, or unpleasantness (its acceptability), evaluated on scales from 0 to 6; c) Nature of the odor: represents the type and characteristics of the perceived odor. The collected intensity and hedonic tone data are then multiplied to calculate the average product intensity per hedonic tone (IxHT) for each season and each point, thus obtaining a matrix containing the values of the IxHT product. The implant surface was then divided into pertinent areas associated with each monitoring point using the Thiessen polygon method and finally the matrix of IxHT values was mapped, assigning a different color for different IxHT product ranges.

RESULTS AND DISCUSSION

An example of results is presented in figure 1. As can be seen, the most odorous points are easily and immediately visualized with darker colors and, in this example, are located near to the sewage inflows and to the septic tank sludge discharge point. Outside of the plant the odor is generally ten times lower and close to the perception threshold. As far as the nature of the odor is concerned, internally most odors are due to the existing treatment processes (such as sewage or ozone), while in the external monitoring, no odors whose nature can be traced back to the system were perceived.

Figure 1. Examples of mapping of the product IxHE (left) and nature of the odor (right).

CONCLUSIONS

The proposed technique has been performed for over 5 years in two large WWTPs in Italy managed by GIDA spa and it allowed to detect modifications in the nature and in the intensity of the odors, as well as seasonal changes. Furthermore, the simplicity and low cost of the procedure make it applicable to any system and with very high frequencies.

REFERENCES

Lebrero, R., Bouchy, L., Stuetz, R., Muñoz, R., 2011. Odor Assessment and Management in Wastewater Treatment Plants: A Review. Critical Reviews in Environmental Science and Technology **41**-10

Sneath, R.W. 2001. Olfactometry and the CEN standard. In R. Stuetz and F.B. Frechen (Eds.), Odours in wastewater treatment: Measurement, modelling and control (Chapter 7). IWA.

Zarra, T., Naddeo, V., Belgiorno, V., Reiser, M., Kranert, M. 2008. Odour monitoring of small wastewater treatment plant located in sensitive environment. *Water Science and Technology*, **58**(1), 89–.94

The effect of liquid wastes on a full-scale WWTP nitrogen removal performance

L. Palli*, E. Bacarelli*, F.F. Borchi* and D. Daddi*

* G.I.D.A. Spa, Via di Baciacavallo 36, Prato, IT
(E-mail: l.palli@gida-spa.it; e.bacarelli@gida-spa.it; f.borchi@gida-spa.it; d.daddi@gida-spa.it)

Abstract
In some regions most homes are equipped with septic tanks that remove most of the solids and organic matter from domestic wastewater. This habit drastically removes the organic matter content in the receiving system. Having a very low COD leads to a low COD/N ratio which negatively affect the removal of nitrogen. In this study we took as a case study a large plant (190·000 PE) treating municipal wastewater and liquid wastes and we evaluated the impact of septic tank sludge on nitrogen removal. In order to understand the effect of liquid waste on the efficiency of TN removal we evaluated the COD/N ratio of the actual influent of the WWTP and we compared to the COD/N ratio of the the influent of the plant in the absence of liquid wastes. This could be compared with the stoichiometric ratio which is generally considered equal to 4.2 gCOD/gN. However, this ratio is almost never sufficient in real conditions, and the critical COD/N ratio is considered to be about 7.6 gCOD/gN. In case of sewage only, out of 149 determinations, 32 have a ratio of less than 4.2 (21%) and 60 have a ratio of less than 7.6 (40%). We then calculate, day by day, the theoretical percentage of denitrification in the absence of liquid waste, assuming it equal to the real one when the COD/N ratio is greater than 7.6 and reducing it proportionally when the ratio is lower. We found out that the addition of liquid waste in the treatment helped increase the COD/N ratio and consequently increased the removal of nitrogen. We have estimated that without liquid wastes the TN discharged in the environment would be, on average, 18% higher than the real one leading to, considering the total volume of water discharged, almost 17 ton of N released in the environment. We can therefore conclude that, for the present case, the presence of liquid waste, in particular septic tank sludge is of crucial importance for the process of nitrogen removal.

Keywords
COD/N ratio; Denitrification; Liquid waste; Nitrogen; Septic tank sludge; WWTP.

INTRODUCTION

Municipal Wastewater Treatment Plants (WWTP) are designed to treat municipal wastewater and primarily remove solids, organic matter and nutrients such as nitrogen. In some regions, such as Tuscany (Italy), most homes are equipped with septic tanks that remove most of the solids and organic matter from domestic wastewater. This habit reduces the risks of odors and sediments in the sewage system, and reduce the risks linked to the combined sewer overflows, but also drastically removes the organic matter content in the receiving system (Bounds 1997). Consequently, most of the plants in the region receive low COD sewage (often below 125 mg/L which is the discharge limit into surface waters in Italy) (Campo et al., 2020). Having a very low COD leads to a low COD/N ratio which negatively affect the removal of nitrogen, therefore returning this COD to the plants could be useful for nitrogen removal. Some plants, in addition to sewage, also jointly treat liquid waste such as sludge from septic tanks. In this study we took as a case study a large plant (190 000 PE) treating municipal wastewater and liquid wastes and we evaluated the impact of septic tank sludge on nitrogen removal.

MATERIALS AND METHODS

The studied WWTP is located in Tuscany and treats urban wastewater and liquid wastes jointly. The wastewater treatment train is composed of bar screen, grit removal, primary sedimentation, equalization, denitrification, oxidation-nitrification, secondary sedimentation, clariflocculation and final ozonation. Liquid wastes are mainly composed by septic tanks sludge (about 100 000-115 000 ton per year) and landfill leachates (about 150·000-180·000 ton per year), while total sewage is about 9-11 millions of m^3 per year. Septic tank sludge (STS) is pre-treated in a separate line with screening and grit removal and then is pumped in the plant before grit removal, while landfill leachates (LFL) are pre-treated in an MBR plant and then pumped prior to primary sedimentation. In this study we collected for over a year daily samples of sewage, STS, LFL, primary influent (which is the actual mix of the above three components) and plant effluent. In these samples we evaluated COD, total nitrogen (TN) and the inorganic forms ($N\text{-}NH_4^+$, $N\text{-}NO_2^-$, $N\text{-}NO_3^-$) in order to evaluate the COD/N ratio and the removal efficiency of nitrogen in the plant.

RESULTS AND DISCUSSION

Table 1 depicts average values of COD and TN in the sampling points and clearly shows that sewage influent has a much lower COD content that the primary influent, which is enriched by the organic matter coming mainly from STS. The performance of the plant made it possible to comply with the TN discharge limit (which is 10 mg/L on the average value) with a total removal efficiency of 78%.

Table 1. Average values of COD and TN in all the sampling points.

Sampling point	Average COD value (mg/L)	Average TN value (mg/L)
Sewage	317	32
Septic tank sludge	20044	580
Pretreated LFL	1820	403
Primary influent	889	43
Plant effluent	70	9,7

In order to understand the effect of liquid waste on the efficiency of TN removal we evaluated the COD/N ratio of the primary influent (which is the actual influent of the WWTP) and we compared to the COD/N ratio of the sewage only, which would be the influent of the plant in the absence of liquid wastes. In order to understand if the sewage COD/N was sufficient for effective denitrification, this could be compared with the stoichiometric ratio which is generally considered equal to 4.2 gCOD/gN (inter alia Carrera et al, 2004). However, several experimental studies have shown that this ratio is almost never sufficient in real conditions, since it depends on the degree of reduction of the substrate. In fact, when the carbon source is not an easily degradable substance such as methanol or acetate normally used in laboratory experiments, the critical COD/N ratio is considered to be about 7.6 gCOD/gN (Carrera et al., 2004; Sobieszuk and Szewczyk 2006). Results, calculated for a year, are presented in figure 1.

As can be seen, actual plant influent is always well above both the stoichiometric and the experimental ratios, which means that the denitrification efficiency is always possible at its maximum rate. In case of sewage only, out of 149 determinations, 32 have a ratio of less than 4.2 (21%) and 60 have a ratio of less than 7.6 (40%). Taking these data info consideration, it can be stated that, when the ratio is lower than the minimum required, the denitrification can be affected. In particular, Carrera et al found out the denitrification percentage decrease linearly with the decrease in the COD/N ratio. Using this model, it is possible to calculate, day by day, the theoretical percentage of denitrification in the absence of liquid waste, assuming it equal to the real one (78%) when the COD/N ratio is greater than 7.6 and reducing it proportionally when the ratio is lower. Results are presented in Figure 2 and Table 2.

As can be seen, in the absence of liquid waste, the mean TN removal would decrease of about 17% and, even though the TN in the influent would be lower, the TN in the effluent would be higher and, in this case, would not allow the compliance of the discharge limit.

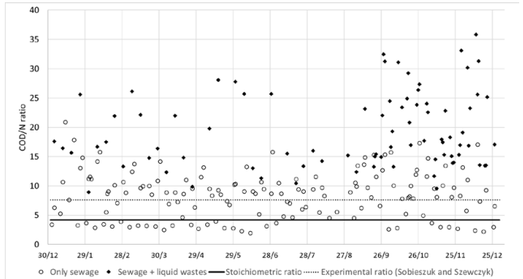

Figure 1. COD/N ratio of sewage and actual plant influent (sewage + liquid wastes) compared to stoichiometric ratio and experimental ratio.

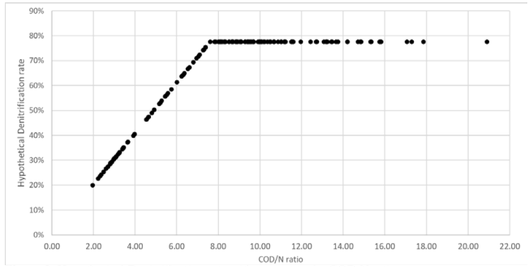

Figure 2. Hypothetical Denitrification rate with respect to the COD/N ratio

Table 2. TN in the influent and in the effluent in real condition and without liquid waste

	Real conditions	Without liquid waste
TN influent (mg/L)	43,1	32,2
Mean TN removal (%)	78%	64%
TN effluent (mg/L)	9,7	11,5

CONCLUSIONS

This study allowed to evaluate the effect of joint treatment of liquid waste such as septic tank sludge and urban wastewater in the removal of nitrogen. We found out that the addition of liquid waste in the treatment helped increase the COD/N ratio and consequently increased the removal of nitrogen. We have estimated that without liquid wastes the TN discharged in the environment would be, on average, 18% higher than the real one leading to, considering the total volume of water discharged, almost 17 ton of N released in the environment. We can therefore conclude that, for the present case, the presence of liquid waste, in particular septic tank sludge is of crucial importance for the process of nitrogen removal.

REFERENCES

Bounds, T.R., 1997. Design and performance of septic tanks, ASTM Special Technical Publication

Campo, R., Sguanci, S., Caffaz, S., Mazzoli, L., Ramazzotti, M., Lubello, C., Lotti, T., 2020. Efficient carbon, nitrogen and phosphorus removal from low C/N real domestic wastewater with aerobic granular sludge. *Bioresource Technology* **305**, 122961.

Carrera, J., Vicent, T., Lafuente, J., 2004. Effect of influent COD/N ratio on biological nitrogen removal (BNR) from high-strength ammonium industrial wastewater. *Process biochemistry* **39**, 2035-2041.

Sobieszuk, P., Szewczyk, K.W., 2006. Estimation of (C/N) ratio for microbial denitrification. *Environmental Technology* **27** (103-108)

Nature-based solutions in Europe and Latin America: A comparative analysis of regional situation and addressed challenges

Yarima Recalde*, Lucia Alexandra Popartán*, Manuel Poch*, Ignasi Rodríguez-Roda*

*LEQUIA, Laboratory of Chemical and Environmental Engineering (LEQUIA), University of Girona, C/Maria Aurèlia Capmany 69, 17003 Girona, Spain
(E-mail: *yarima.recalde@udg.edu; luciaalexandra.popartan@udg.edu; manuel.poch@udg.edu; ignasi.rodriguezroda.udg.edu)*

Abstract
Cities around the world face a number of challenges, including climate change and ecosystem degradation. Nature-based solutions (NbS) can help protect us from the impacts of climate change while also ensuring ecosystem services. However, NbS still face implementation barriers, mainly in developing countries. In order to identify and compare the state of NbS implementation and the main challenges to be addressed in European and Latin American cities, we reviewed and analyzed different case studies and projects published in peer-reviewed articles and gray literature. It was reported that NbS are still evolving as a concept and are not widely implemented in Latin America, mainly due to limited availability of financial resources. There is a marked imbalance in the distribution of studies, with most cases concentrated in the global north, although southern global countries are generally most vulnerable to the impacts of climate change. In Europe, the concept is more integrated into urban planning, however, there are also barriers such as limited understanding of the benefits of NbS by society. The main challenges that Latin American cities aim to address with NbS are agrobiodiversity and improved water management. On the other hand, in Europe, there is a priority to increase urban green infrastructure, as it plays an important role in carbon storage and mitigating the impacts of greenhouse gas emissions in cities.

Keywords
Climate change, Europe, Latin America, Nature-based solutions, Social challenges

INTRODUCTION

Nature-based solutions (NbS) are a concept that is currently gaining ground to address urban challenges. NbS mainly address 7 social challenges including climate change adaptation and mitigation, reduction of natural disaster risk, reversing ecosystem degradation and loss of biodiversity, human health, socio-economic development, food security and water security (IUCN, 2020). In regions with different economic and social realities than developed countries, nature-based solutions are a foreign concept, whose enforcement presents many challenges and limitations. This study aims to describe the state of implementation and challenges that NbS seek to address in Europe and Latin America through a comparative analysis.

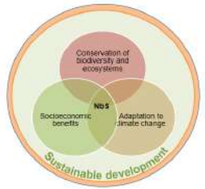

Figure 1. Challenges addressed by NbS

MATERIALS AND METHODS

This work involved a structured search of scientific and grey literature related to Nature-based Solutions (NbS) projects or studies in Europe and Latin America. The obtained literature was analyzed based on the review of the evolution of the NbS topic, its implementation level and the social and environmental challenges to be addressed in these two regions. In addition, limitations, knowledge gaps and opportunities for the implementation of NbS were identified by comparing the literature available in the north and south global. This qualitative method serves as an exploratory tool to achieve a clear picture of the development trajectory of NbS implementation.

RESULTS AND DISCUSSION

The EU has positioned itself as a world leader in NbS research and innovation. Increasingly, European cities are adopting NbS in their public policies, urban plans and programs and their implementation. On the other hand, Latin America society, in general, still does not perceive the importance and benefits of NbS. In this way, public works of another nature associated with the traditional infrastructure are prioritized. Thus, a large part of the projects that are being implemented are still in the phase of preparation and search for financing. One of the main limitations in both Europe and Latin America is the lack of information and data necessary to measure the potential benefits. However, since 2012 the EU has funded multisectoral projects with case studies in Europe and Latin America, which has boosted NbS research in this region as well (Davies et al., 2021). In general, most government objectives for NbS are focused on forests, therefore funding is currently channeled mainly towards tree planting (Seddon et al., 2021). However, this perception is different in Europe and Latin America. The low access of people to green areas is the main challenge in European cities. In Latin America, projects combining conservation and agriculture and solutions focused on improving water management, such as controlling runoff, floods, and rainwater, predominate (Ozment et al., 2021). In general, the social and environmental challenges that NbS are intended to address are different in the two regions. This depends on the local contexts in the environmental, political, economic and social spheres; therefore, more research is needed in terms of cost/benefit analysis and implementation opportunities.

REFERENCES

Davies, C., Chen, W. Y., Sanesi, G., & Lafortezza, R. (2021). The European Union roadmap for implementing nature-based solutions: A review. *Environmental Science & Policy*, *121*, 49–67. https://doi.org/10.1016/J.ENVSCI.2021.03.018

Ozment, S., Schumacher, A., Gonzalez, M., Oliver, E., Morales, G., Gartner, T., Silva, M., Grunwaldt, A., & Watson, G. (2021). Nature-Based Solutions in Latin America and The Caribbean: Regional Status and Priorities for Growth. *Washington, DC: Inter-American Development Bank and World Resources Institute.* https://www.wri.org/research/nature-based-solutions-latin-america-and-caribbean-regional-status-and-priorities-growth

Seddon, N., Smith, A., Smith, P., Key, I., Chausson, A., Girardin, | Cécile, House, J., Srivastava, S., & Turner, B. (2021). *Getting the message right on nature-based solutions to climate change.* https://doi.org/10.1111/gcb.15513

UICN. (2020). Orientación para usar el Estándar Global de la UICN para soluciones basadas en la naturaleza: primera edición. *Orientación Para Usar El Estándar Global de La UICN Para Soluciones Basadas En La Naturaleza: Primera Edición*. https://doi.org/10.2305/IUCN.CH.2020.09.ES

Emerging contaminants in sludge treatment reed beds: degradation or accumulation?

A. Martínez i Quer*, Gregor Plestenjak**, P. N. Carvalho*,***

* Department of Environmental Science, Aarhus University, Frederiksborgvej 399, DK-4000 Roskilde, Denmark (E-mail: alma@envs.au.dk, pedro.carvalho@envs.au.dk)
** University of Ljubljana, Biotechnical Faculty, Department of Agronomy, Jamnikarjeva 101, 1000, Ljubljana, Slovenia (E-mail: gregor.plestenjak@gmail.com)
*** WATEC - Centre for Water Technology, Aarhus University, Ny Munkegade 120, 8000 Aarhus, Denmark

Abstract
Sludge treatment reed beds (STRBs) are an interesting approach to dewater and mineralize sewage sludge. While these nature-based solutions are robust and efficient to dewater and stabilize activated sludge, they are also promising in providing as final product biosolids that can be used as fertilizer – if legislation allows for it. For this, the quality of the treated sludge is important from two angles: 1) the agricultural use potential based on dry content and nutrients composition, and 2) the content of harmful substances is below threshold limits. One of the critical steps to optimise STRBs performance, and therefore the quality of the final biosolid, is the operation regime which ensures proper sludge dewatering and mineralization. A larger study was carried to compare the performance and efficiency of three types of operation mode: passive aeration, draft aeration or forced aeration). The results herein focus on the different dynamics of degradation and/or accumulation of biocides and pharmaceuticals observed in one of the experiments carried out in Slovenia.

Keywords (maximum 6 in alphabetical order)
Circular economy, Emerging contaminants; Wastewater; Nature-based solutions

INTRODUCTION

Sludge treatment reed beds (STRBs) are an established technology for the management of sludge produced by wastewater treatment plants (Nielsen & Bruun 2015; Brix 2017). Reed beds were used for the first time in Denmark in 1988, when the first sludge processing system was introduced (Nielsen 2003). These systems are now a widespread and common sludge treatment practice in northern Europe, especially in Denmark, and are being used increasingly worldwide. Primary or secondary liquid sludge is loaded on the surface of the reed bed over several years, where long-term (10-12 years) sludge reduction takes place, partly due to dewatering and partly due to decomposition of the organic matter in the sludge (Matamoros et al. 2012).

It is known that the use of sewage sludge or biosolids as agricultural amendments can pose environmental and human health risks related to pathogens and/or antibiotic resistance. A study under Mediterranean climatic conditions demonstrated that the presence of ampicillin-resistant bacteria increased in amended soils 4 months after urban sludge application (Gondim-Porto et al. 2016). The long-term application of sewage sludge and chicken manure significantly increases the abundance and diversity of ARGs in soil (Chen et al. 2016).

In spite of the long-term of mineralization period (10-12 years), STRB operational procedures indicate that the ultimate load should be dewatered and stabilized for 6 months before sludge can be disposed as a biosolid for agriculture (Nielsen & Willoughby 2005). It is uncertain if this time period is enough to ensure the decay of antibiotics and other micropollutants to the environment.

The current project aims to evaluate for the first time the fate of micropollutants, including antibiotics, in STRBs.

MATERIAL AND METHODS

A pilot system was set up at Dragomer, Slovenia (Figure 1) and operated for several experiments until 2022. The pilot contains 9 basins in triplicates for the three of operation mode: passive aeration, draft aeration or forced aeration.

Experimental setup and sampling

Several bags containing the "initial" loading sludge of the beds were wrapped up with a permeable material to replicate natural conditions of water and micropollutant exchange. The bags were left while different sludge loading campaigns were performed onto the STRBs. After each loading campaign, three bags of each bed were pulled off and air dried. The air-dried sludge was used for organic micropollutant quantification.

Analysis

Sludge/biosolids samples were extracted by a two-step process, first water, second methanol, using an ultrasonic bath. The extracts were analysed by LC-MS/MS using two multi-compound methods, one targeting 13 biocides the other 36 pharmaceuticals (Thomsen et al. 2020). Concentrations are reported as dry weight of sludge.

Figure 1. Photo of the pilot at Dragomer, Slovenia in September 2019. The pilot contains 9 basins in triplicates for the three of operation mode: passive aeration, draft aeration or forced aeration.

RESULTS AND DISCUSSION

The biocides irgarol, pyraclostrobin and pirimicarb were detected in the initial sludge, while terbutryn (7 ± 1 ng/g) and the benzalkonium chloride 12-BAC (861 ± 83 ng/g), 14-BAC (210 ± 16 ng/g) and 16-BAC (28 ± 4 ng/g) were quantified. In terms of pharmaceuticals the occurrence was higher than for biocides. The pharmaceuticals tramadol, olmesartan and gabapentin were only detected in the initial sludge, while Azithromycin (75 ± 20 ng/g), Claritromycin (18 ± 4 ng/g), Ciprofloxacin (992 ± 151 ng/g), Propanolol (17 ± 3 ng/g), Carbamazepin (14 ± 1 ng/g), Citalopram (103 ± 13 ng/g), Diclofenac (38 ± 4 ng/g), Phenazone (2 ± 0.2 ng/g), Venlafaxine (21 ± 4 ng/g), Losartan (18 ± 1 ng/g) and Benzotriazole (274 ± 138 ng/g) were quantified.

In terms of fate, we observed three main behaviours of the compounds in time, decrease, no changes and increase in concentration, depending on the compounds (Figure 2). The pesticide terbutryin was stable, 12-BAC and 14-BAC shown a decrease trend, while 16-BAC concentration tended to increase. However, these variations were not significant. For the pharmaceuticals, several compounds showed decrease in concentration such as azithromycin ($p < 0.05$), propranolol, diclofenac ($p < 0.05$), venlafaxine ($p < 0.05$). Carbamazepine, citalopram, and losartan concentration did not change. An increase in concentration was observed for clarithromycin, ciprofloxacin, phenazone ($p < 0.05$) and benzotriazole ($p < 0.05$).

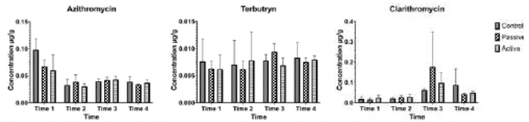

Figure 2. Selected results from representative organic micropollutants showing decrease, no changes and increase in concentration over time.

Statistical tests showed that time was the major variable affecting the micropollutants concentration, while operation mode did not provide any marked difference. It should be noted that the sludge samples in the bags were exposed to x new loadings, thus the increase in concentration. This also implies that a decrease in concentration implies not only biodegradation of the original sorbed compound, but potentially of new amounts that were inserted in the pilots. The experimental setup was considered interesting for understanding removal and accumulation rates in time, but does not allow to perform a mass balance, as the dynamics of a new load implies adding a liquid and a solid fraction and the potential percolation of compounds across de system. Nevertheless, the current results show that emerging contaminants have the potential to be both degraded and accumulated in STRBs in time. This means that it is very important in the future to characterize the stabilization of such systems during the last 6 months of operation without new loads.

REFERENCES

Brix, H. 2017. Sludge Dewatering and Mineralization in Sludge Treatment Reed Beds. *Water* **9**(3), 160

Chen, Q., An, X., Li, H., Su, J., Ma, Y., & Zhu, Y. G. 2016. Long-term field application of sewage sludge increases the abundance of antibiotic resistance genes in soil. *Environment International*, ***92–93***, 1–10.

Gondim-Porto, C., Platero, L., Nadal, I., & Navarro-Garcia, F. 2016. Fate of classical faecal bacterial markers and ampicillin-resistant bacteria in agricultural soils under Mediterranean climate after urban sludge amendment. *Science of The Total Environment*, ***565***, 200–210.

Matamoros, V., Nguyen, L. X., Arias, C. A., Nielsen, S., Laugen, M. M., & Brix, H. 2012. Musk fragrances, DEHP and heavy metals in a 20 years old sludge treatment reed bed system. *Water Research*, ***46***(12), 3889–3896

Nielsen, S. 2003. Sludge drying reed beds. *Water Science and Technology*, ***48***(5), 101–109

Nielsen, S., & Willoughby, N., 2005. Sludge treatment and drying reed bed systems in Denmark. Water and Environment Journal **19**, 296–305.

Nielsen, S., & Bruun, E. W. 2015. Sludge quality after 10–20 years of treatment in reed bed systems. *Environmental Science and Pollution Research*, ***22***(17), 12885–12891.

Silva Thomsen, L. B., Carvalho, P. N., dos Passos, J. S., Anastasakis, K., Bester, K., & Biller, P. (2020). Hydrothermal liquefaction of sewage sludge; energy considerations and fate of micropollutants during pilot scale processing. *Water Research*, ***183***, 116101.

Acknowledgements
AMQ PhD scholar in WETCYANO project granted by the Independent Research Council Denmark.

Effects of Environmental and Social Factors on Eutrophication in Tonle Sap Lake

Vouchlay Theng[a,b,*], Chihiro Yoshimura[c], Kong Chhuon[a]

[a]Faculty of Hydrology and Water Resources Engineering, Institute of Technology of Cambodia, Cambodia
[b]Research and Innovation Center, Institute of Technology of Cambodia, Cambodia
[c]Department of Civil and Environmental Engineering, Tokyo Institute of Technology, Japan
(Corresponding author: e-mail: vouchlay.theng@itc.edu.kh)

Abstract
This study aimed to elucidate the effects of environmental and social factors on eutrophication in Tonle Sap Lake and to propose effective countermeasures against lake eutrophication. The impact of environmental and social factors on eutrophication was analyzed based on Primary Production model sensitivity and scenario analysis. The results showed that the reduction or increase of dissolved inorganic phosphorus concentration in tributaries had highly influential on the percentage of their eutrophication area compared to the baseline eutrophication during 2016–2019 (*%EE*) more than the reduction or increase of particulate inorganic phosphorus and suspended solid concentration in tributaries. For the scenario of the population in 2080, *%EE* could increase by 6.5% in October. In the scenario of wind, Max. wind in 2000 had the highest impact on *%EE*. The countermeasures against eutrophication in less than 10 years are required to reduce phosphorus loading from bed sediment and external loading.

Keywords
Eutrophication, environmental and social factors, Tonle Sap Lake

INTRODUCTION

Tonle Sap Lake (TSL) is the largest tropical lake-floodplain system in Cambodia, being influenced by the seasonal flood pulse of Mekong River. TSL and its ecosystems are seriously threatened by anthropogenic activities such as the development of water infrastructure, population growth, and wastewater pollution, while they are poorly understood in most aspects. Thus, it is important to understand the impact of these environmental and social factors on eutrophication in this lake. Therefore, the objectives of this study are to elucidate the effects of environmental and social factors on eutrophication in TSL and to propose effective countermeasures against lake eutrophication for its short-term (i.e., shorter than 10 years) environmental management.

METHODOLOGY

The impacts of environmental and social factors including suspended solid (SS), dissolved inorganic phosphorus (DIP), and particulate inorganic phosphorus (PIP) concentration in the tributaries, population growth, and wind speed on eutrophication, were analyzed using Primary Production (PP) model of Theng et al. (2023) as illustrated in **Table 1**. Each condition was analyzed by comparing it to the baseline condition (**Table 1**). The indicator of this study was in terms of the percentage of eutrophication in each condition compared to the baseline eutrophication (*%EE*).

RESULTS AND DISCUSSIONS

The application of the PP model showed the reduction or increase of DIP concentration in tributaries by 50% from the baseline concentration had a higher influence on *%EE* than the reduction or increase of PIP and SS concentration in tributaries (**Fig. 1a**). Phytoplankton directly uptakes DIP for their growth. Thus, the increment and reduction of DIP concentration in the water directly impact phytoplankton growth. In the scenario of population growth, the *%EE* would be higher than the baseline by 0.7% – 1.8% for the scenario of Pop_2040, 1.5% – 3.9% for Pop_2060, and 2.4% – 6.5% for Pop_2080 (**Fig. 1b**). In the scenario of wind, Max. wind in 2000 had the highest wind speed in 1981 – 2019 and its impact on monthly *%EE* was 0.6% – 15.0% as it could increase sediment carrying capacity through wind-induced surface shear stress and net resuspension which directly increase SS and PIP concentration. According to spatial sensitivity analysis, the effective countermeasures against eutrophication in TSL in a short-term period (i.e., less than 10 years) are to reduce phosphorus internal loading, especially focusing on diffusion from bed sediments, in addition to the reduction of the external loadings from tributaries and villages (unshown figure).

CONCLUSION

The application of the PP model showed the reduction or increase of DIP concentration in tributaries had a higher influence on *%EE* than the reduction or increase of PIP and SS concentration in tributaries. In the scenario of population growth, the *%EE* would be higher than the baseline by 2.4% – 6.5% for Pop_2080. The wind data affect eutrophication as it could increase sediment carrying capacity. The effective countermeasures against eutrophication in TSL in a short-term period are to reduce phosphorus internal and external loadings.

Table 1. Conditions of environmental and social factors impacted eutrophication in TSL

Factors	Condition		
Baseline condition	Simulation of eutrophication and input data during 2016–2019 using PP model		
SS, DIP, PIP concentration in tributaries	-50%	+50%	
Population growth	2040 (Pop_2040)	2060 (Pop_2060)	2080 (Pop_2080)
Wind speed and direction	1981 (Average wind)	2000 (Max. wind)	2010 (Min. wind)

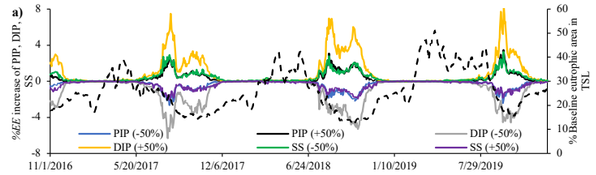

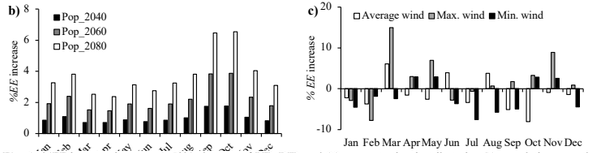

Fig. 1. *%EE* increase in case: **a)** 50% changes of PIP, DIP, and SS concentration in tributaries, **b)** population growth, and **c)** wind speed in 1981, 2000, and 2010 which is the average, maximum, and minimum wind speed during 1981–2019, respectively.

ACKNOWLEDGMENT

We would like to acknowledge the Japan Science and Technology Agency, Japan International Cooperation Agency, and INOWASIA project of the Erasmus Plus Programme.

REFERENCES

Theng, V., Hashimoto, K., Uk, S., Tanaka, T., Yoshioka, H., & Yoshimura, C. (2022). Hydrodynamics-based modeling of phosphorus balance and dynamics in a large tropical floodplain. *Environmental Advances*, **7**, 100176.
Theng, V., Sith, R., Uk, S., & Yoshimura, C. (2023). Phytoplankton productivity in a tropical lake-floodplain system revealed by a process-based primary production model. *Ecological Modelling*, **479**, 110317.

Monitoring and study of specified metals' behaviour in a large Italian wastewater treatment plant

F. Tuci*, A. Antal**, S. Doumett**, D. Fibbi**, R. Camisa**, E. Bettazzi**, E. Coppini**, D. Daddi**, and R. Gori*

*Department of Civil and Environmental Engineering, University of Florence, via S. Marta 3, Firenze 50139, Italy (E-mail: francesca.tuci@unifi.it; riccardo.gori@unifi.it)
**G.I.D.A. SpA, via di Baciacavallo 36, Prato 59100, Italy (E-mail: alexandra.antal@gida-spa.it; s.doumett@gida-spa.it; d.fibbi@gida-spa.it; r.camisa@gida-spa.it; e.bettazzi@gida-spa.it; e.coppini@gida-spa.it; d.daddi@gida-spa.it)

Abstract
The objective of this study is to analyse the removal of certain metals (Pb, Cd, Ni, Zn, Cu, Sn, Ba, B, Cr tot, and Sb) from a large wastewater treatment plant (WWTP) located in the Italian textile district of Prato. For this purpose, two monitoring campaigns were organized, collecting wastewater and sludge samples in some selected sections of the WWTP. It was found a good removal efficiency for Zn, Cu, Ba, Cr, and Sb. These metals are mainly present in a particulate form and leave the plant via the sludge stream. Finally, the good correlation between the influent load and the removed contaminant load demonstrates that the removal efficiency of the plant is not affected by the increasing influent load.

Keywords
Heavy metals; mass balance; metals removal mechanism; sustainability; textile wastewater

INTRODUCTION

Prato (Central Italy) is one of the biggest textile districts in Italy and the most relevant textile centre in Europe. It was the first textile district to create a centralized wastewater treatment plant (WWTP), managed by the company GIDA S.p.A., which treats both domestic and industrial wastewater (mainly originated by textile industries). According to Italian Law, textile industries must have an Integrated Environmental Authorization released upon the Best Available Techniques (BAT). It was necessary to verify the removal capacity of the WWTP for some chemical substances because of the new emission levels provided in the BAT conclusions recently published on the website of the European IPPC Bureau (European Union, 2023). The objective of this study is to analyse the behaviour of some specified metals mainly originating from industrial processes. For this purpose, two monitoring campaigns were organized to study the behaviour of the following metals: Pb, Cd, Ni, Zn, Cu, Sn, Ba, B, Cr tot, and Sb. The final goal is to verify that the removal of these contaminants is due to an effective treatment process and not just to a dilution effect with domestic wastewater.

MATERIALS AND METHODS

The Baciacavallo WWTP (designed for 900'000 PE) treats domestic and industrial wastewater with an average inflow of about 100'000 m^3/d. Industrial wastewater represents approximately 70% of the total influent flow (Muoio et al., 2019) and is partly collected by a separate sewer system. The treatment process (Figure 1) includes screening, grit removal, primary sedimentation, equalization, biological oxidation/nitrification, clariflocculation, and final ozonation. The final effluent is partly discharged into a surface water body and partly sent to the refining section for water recycling in the textile district. The secondary and tertiary sludges are recycled in primary sedimentation and removed together with the primary sludge. The sludge treatment consists of gravity thickeners, centrifuges, and final incineration. Thickener overflow and centrate are recycled into the primary sedimentation unit.

Wastewater sampling was carried out from October 2021 to October 2022. Samples were taken once a week and collected in the same sections of the plant. In this campaign, the composite samples of wastewater were taken simultaneously from the separate sewer system, the influent of the plant, the influent of the biological treatment, the effluent of the tertiary treatment, and the effluent of the plant (Figure 1), without considering the residence time of the WWTP (about 24 h). A further intensive monitoring campaign was carried out in May 2022. Wastewater samples were collected over eight consecutive days, including Saturday and Sunday, in the same sections mentioned above. 24-hour composite samples upstream of the biological treatment (sampling points A, B, C) were taken simultaneously, while those downstream of the tertiary treatment (sampling points D, E) were collected simultaneously but with a delay of 24 h. This sampling rate allowed enough correspondence between influent and effluent samples, a prerequisite for mass balance calculations. The total and dissolved concentrations of heavy metals were determined. In addition, grab samples of sludge were collected from the primary, secondary, and tertiary sludge, while grab samples of the final dewatered sludge were collected one day later, which is the retention time of the thickeners.

RESULTS AND DISCUSSION

Pb, Cd, Ni, and Sn concentrations were always under the Limit of Detection (LOD) both in the separate sewer system and in the total influent of the plant. For this reason, they are not worthy of further evaluations. Regarding the other species, the average removal efficiency of the mass load is higher than 50% for Ba, Cr, and Sb (Table 1). The intensive monitoring campaign confirms these results and shows average removal efficiencies of Zn, Cu, Ba and Sb different from the one obtained previously. Since these species are characterized by high concentration variability, results demonstrate the importance of the sampling procedure. Metal removal efficiencies in WWTPs are mainly related to metal partitioning between the liquid and the solid phase (Cantinho et al., 2016). As shown in Figure 2, most of the species are bound to the particulate matter (Zn, Cu, Cr, and Sb), Ba shows a half and a half distribution, and B is present in a soluble form (this could explain its low removal). The principal mechanism usually considered for metal removal is sorption. Thus, assuming no biodegradation, the total heavy metal load of untreated wastewater will end up in the sludge or remain in the treated effluent. For most metals, release via sludge is expected to be more relevant than via the treated effluent (Karvelas et al., 2003). In this study, the relative importance of the two release processes was calculated daily and mean values are reported in Figure 3. The amount of metal released from the WWTP via the sludge stream varies from 70% for Ba and Sb up to 84% for Cr. Regarding B, since it is mainly present in a soluble form, it is almost entirely released with the final effluent stream.

Finally, a linear correlation between the metal load removal and the metal load in the influent of the WWTP was found (Figure 4). Results demonstrate that the removal efficiency of the WWTP is not affected by the increasing influent load. It means that, at these observed contaminant loads, the sludge cannot achieve its saturation point, and it is still able to remove metals from the water.

CONCLUSIONS

A detailed characterization of the metal's influent on the Baciacavallo WWTP (Central Italy) was carried out. Pb, Cd, Ni, and Sn concentrations are almost always below the LOD. The most significant species are Zn, Cu, Ba, Cr tot, and Sb because they are typically associated with textile wastewater. The monitoring campaigns have demonstrated that the WWTP can remove these contaminants through an effective treatment process since Zn, Cu, Ba, Cr, and Sb are mainly present in a particulate form and thus released from the WWTP via the sludge stream. B is in a dissolved phase and almost entirely delivered with the final effluent stream. Finally, it was found that the removal efficiency of the plant is not affected by the increasing influent load.

Table 1. Removal efficiency (%) of metals' concentrations and mass load calculated for the one-year monitoring campaign and for the intensive one-week monitoring campaign (mean ± STD).

Removal efficiency	One-year monitoring campaign		One-week monitoring campaign	
	Concentration	Mass load	Concentration	Mass load
	Mean±STD	Mean±STD	Mean±STD	Mean±STD
Zn	37±19	39±18	76±12	75±19
Cu	39±20	42±20	57±8	63±11
Ba	58±3	62±5	63±3	68±9
B	19±17	25±15	13±6	27±10
Cr tot	81±6	81±7	78±11	80±11
Sb	68±15	71±13	58±21	61±28

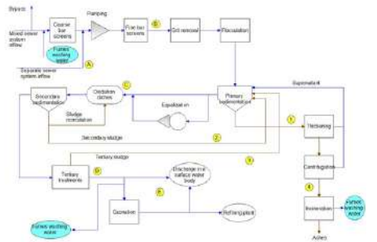

Figure 1. Flowchart of Baciacavallo WWTP. The yellow labels show the sampling points: A: separate sewer system inflow; B: influent of the WWTP; C: influent of the biological treatment; D: effluent of the tertiary treatment; E: effluent of the plant; 1: primary sludge; 2: secondary sludge; 3: tertiary sludge; 4: dewatered sludge.

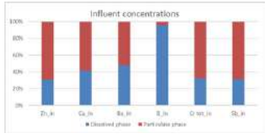

Figure 2. Distribution of the metals' influent concentration between the dissolved and the particulate phase.

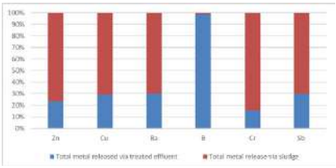

Figure 3. Release of metals from the WWTP via the treated effluent and the sludge streams.

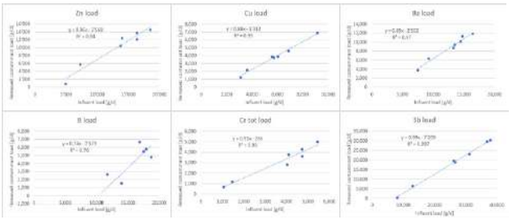

Figure 4. Correlation between the metal load removal and the WWTP's influent load.

REFERENCES

European Union, European IPPC Bureau 2023 *Textiles Industry*. EIPPCB. https://eippcb.jrc.ec.europa.eu/reference/textiles-industry

Muoio, R., Palli, L., Ducci, I., Coppini, E., Bettazzi, E., Daddi, D., Fibbi, D., Gori, R. 2019 Optimization of a large industrial wastewater treatment plant using a modelling approach: A case study. *Journal of Environmental Management* **249**, 109436.

Cantinho, P., Matos, M., Trancoso, M. A., Correia dos Santos, M. M. 2016 Behaviour and fate of metals in urban wastewater treatment plants: a review. *Int. J. Environ. Sci. Technol.* **13**, 359-386.

Karvelas, M., Katsoyiannis, A., Samara, C., 2003 Occurrence and fate of heavy metals in the wastewater treatment process. *Chemosphere* **53**, 1201-1210.

The challenges of the indigenous perspective on water security in the Amazon region

J. C. Cueva[1,3], A. Torrens[2], C.I. Villegas[3] and I. Rodriguez-Roda[4]

1 Faculty of Chemistry, University of Barcelona, Carrer de Martí i Franquès, 1-11, Barcelona
(E-mail: jcuevaor11@alumnes.ub.edu; jccuevaor@unal.edu.co)
2 Faculty of Pharmacy and Food Sciences, University of Barcelona, Campus Diagonal, Av de Joan XXIII, 27-31, 08028, Barcelona
(Email: antoninatorrens@ub.edu)
3 Facultad de Minas, Universidad Nacional de Colombia, Av. 80 #65 – 223, Medellin, Colombia.
(E-mail: civilleg@unal.edu.co)
4 LEQUiA, Institute of the Environment, University of Girona. Campus Montilivi, Carrer Maria Aurèlia Capmany 69, E-17003 Girona, Spain
(Email: ignasi.rodriguezroda@udg.edu)

Abstract
Water security can contribute positively to Sustainable Development Goals implementation and synergies. Indigenous perspective can complement to the original definition of water security with the incorporation of concepts such as indigenous culture and traditional knowledge. In this work, we describe the challenges of indigenous perspective on water security in the Amazon region: environmental threats, environmental biodiversity, water resources, drinking water, adaptation, spiritual and cultural, governance and institutional.

Keywords
Amazon, challenges; indigenous perspective; water security

INTRODUCTION

Water availability is of humanity interest given its character of essential resource for human activities, ecosystems, and life on the planet. Water security may be compromised due to climate crisis. The impacts of climate change could be manifested mainly through water, in particular by changes in extreme weather events, resulting in droughts, floods, and pollution. Given this, the 2030 Global Agenda has set Sustainable Development Goals (SDGs) for both water (SDG 6) and climate change (SDG 13), with strong linkages between the targets associated with these goals, emphasizing the climate change-water nexus (Babel et al., 2020). Improving water security with focus on vulnerable population can contribute to respond to the water-related challenges of climate change. However, there is still a long way to go to achieve SDGs.

Improving water security can contribute positively to SDGs implementation and synergies (Taka et al., 2021). Water security has been a relevant object of study for researchers in the world in the last decade (Chiluwe & Claassen, 2020), with multiple definitions (Zeitoun et al., 2016). For example, Grey & Sadoff (2007) define water security as "the availability of an acceptable quantity and quality of water for health, livelihoods, ecosystems, and production, coupled with an acceptable level of water-related risks to people, environments and economies". Few studies have focused on water security from an indigenous perspective, which could constitute a complement to the western science definition as mentioned by Grey & Sadoff (2007). The indigenous perspective enriches and diversifies water security discourse through the incorporation of concepts such as indigenous culture and traditional knowledge (Awume et al., 2020).

METHODS

This work aims to review the literature on the challenges of the indigenous perspective on water security in the Amazon region. We identified the most relevant scientific literature in Web of Science using the key words "water security", "indigenous perspective" and "Amazon", supplemented with an online search of the Amazon context.

RESULTS AND DISCUSSION

The indigenous communities from the Amazon have a combination of different environmental threats such as deforestation and water pollution by economic and urban activities, and also fires, floods, and droughts by extreme weather events (Esquivel-Muelbert et al., 2019; Rorato et al., 2021). It is a challenge to access affordable drinking water with good quality and quantity due to institutional policies that have been implemented without the Amazonian geographic, biodiversity, spiritual and cultural, social, governance, and economic context. Despite this, the indigenous communities in the Amazon have long adapted to the many water challenges by using indigenous culture and traditional knowledge. But, as the years go by, the adaptation will have to take greater efforts, and thus strengthening of water systems will become more and more necessary. Therefore, the challenges of indigenous perspective on water security in the Amazon region are environmental threats, environmental biodiversity, water resources, drinking water, adaptation, spiritual and cultural, governance and institutional (see Figure 1).

Figure 1. Challenges of indigenous perspective on water security in the Amazon region

ACKNOWLEDGEMENT

This project has been financed by Minciencias, Transnational Centre for Just Transitions in Energy, Climate and Sustainability – TRAJECTS from Colombia and the AMAZOMEM-IV from University of Girona.

REFERENCES

Awume, O., Patrick, R., & Baijius, W. (2020). Indigenous Perspectives on Water Security in Saskatchewan, Canada. Water, 12(3), Article 3. https://doi.org/10.3390/w12030810

Babel, M. S., Shinde, V. R., Sharma, D., & Dang, N. M. (2020). Measuring water security: A vital step for climate change adaptation. Environmental Research, 185, 109400. https://doi.org/10.1016/j.envres.2020.109400

Chiluwe, Q. W., & Claassen, M. (2020). Systems perspectives on water security: An applied review and conceptual framework. Environmental Policy and Governance, 30(6), 332-344. https://doi.org/10.1002/eet.1889

Esquivel-Muelbert, A., Baker, T. R., Dexter, K. G., Lewis, S. L., Brienen, R. J. W., Feldpausch, T. R., Lloyd, J., Monteagudo-Mendoza, A., Arroyo, L., Álvarez-Dávila, E., Higuchi, N., Marimon, B. S., Marimon-Junior, B. H., Silveira, M., Vilanova, E., Gloor, E., Malhi, Y., Chave, J., Barlow, J., … Phillips, O. L. (2019). Compositional response of Amazon forests to climate change. Global Change Biology, 25(1), 39-56. https://doi.org/10.1111/gcb.14413

Grey, D., & Sadoff, C. W. (2007). Sink or Swim? Water security for growth and development. Water Policy, 9(6), 545-571. https://doi.org/10.2166/wp.2007.021

Rorato, A. C., Picoli, M. C. A., Verstegen, J. A., Camara, G., Silva Bezerra, F. G., & Escada, M. I. S. (2021). Environmental Threats over Amazonian Indigenous Lands. Land, 10(3), Article 3. https://doi.org/10.3390/land10030267

Taka, M., Ahopelto, L., Fallon, A., Heino, M., Kallio, M., Kinnunen, P., Niva, V., & Varis, O. (2021). The potential of water security in leveraging Agenda 2030. One Earth, 4(2), 258-268. https://doi.org/10.1016/j.oneear.2021.01.007

Zeitoun, M., Lankford, B., Krueger, T., Forsyth, T., Carter, R., Hoekstra, A. Y., Taylor, R., Varis, O., Cleaver, F., Boelens, R., Swatuk, L., Tickner, D., Scott, C. A., Mirumachi, N., & Matthews, N. (2016). Reductionist and integrative research approaches to complex water security policy challenges. Global Environmental Change, 39, 143-154. https://doi.org/10.1016/j.gloenvcha.2016.04.010

Bioplastics accelerated degradation under simulated conditions: generating data for including their end-of-life in LCA studies

Brais Vázquez-Vázquez*, Jessica Pérez-García*, Massimo Lazzari** and Almudena Hospido*

* CRETUS, Department of Chemical Engineering, Universidade de Santiago de Compostela, 15782, Santiago de Compostela, Spain
(E-mail: brais.vazquez.vazquez@rai.usc.es; jessicaperez.garcia@usc.es, almudena.hospido@usc.es)
** CIQUS, Department of Physical Chemistry, Universidade de Santiago de Compostela, 15782, Santiago de Compostela, Spain
(E-mail: massimo.lazzari@usc.es)

Abstract
Fatty waste and wastewaters have been proved to be suitable for bioplastics production, but the development of the technology is still on its earlier stages. The national funded project ECOPOLYVER aims at taking the valorisation process to pilot scale as well as to develop the information required to include the bioplastics end-of-life (EoL) stage when evaluating the environmental performance of the complete value chain. In fact, EoL is normally excluded with the excuse of the bioplastics´ biodegradability and the lack of the required data for the inventory and impact assessment phases. Therefore, the main objective of this work is to obtain experimental data on accelerated degradation of bioplastics with the aim of filling such gap on the EoL of bioplastics.

Keywords (maximum 6 in alphabetical order)
characterization factor; fatty waste valorisation; life cycle assessment; marine litter; PHA; polyhydroxyalkanoates.

INTRODUCTION

The fish and seafood sector generates large volumes of wastewater rich in lipids. At the moment, several strategies are under development to valorise these fatty residual streams into value-added products such as bioplastics, i.e. polyhydroxyalkanoates (PHA) (Roibás-Rozas et al., 2020). PHA are biodegradable polymers that can substitute oil-based plastics, which are materials consumed by the companies that generate this waste. By doing so, the fish and seafood sector would be able to implement real circular economy strategies and reduce dependence on conventional plastic.

The national funded project ECOPOLYVER (https://biogroup.usc.es/ecopolyver) aims at developing and evaluating a robust biological system capable of transforming fatty residual streams into PHA, using mixed microbial cultures. Besides being technically feasible, the system should prove a better environmental performance and the main challenge there is the inclusion of the end-of-life (EoL) stage. Only by including it, the full picture that is required to validate the expected better environmental performance on any circular economy strategy will be achieved (Peña et al., 2021). According to Bremer (2022) approximately 22% of produced plastics are mismanaged, i.e. they reach the environment without going through any waste collection and management system, and it is generally assumed that oceans are the final environmental compartment where plastic waste will end up, regardless of where they were originally deposited (Wu & Su, 2020). How to include marine litter impact in the Life Cycle Assessment (LCA) framework is the aim of MarILCA (https://marilca.org/), where the models and methodologies under development require a significant amount of data on plastic degradation which, for bioplastics, is not yet available. The main objective of this work is then to generate that data to make the implementation of the EoL models possible for PHA-based bioplastics.

MATERIALS & METHODS

Degradation data are required to calculate the characterization factors which include the Fate Factor (FF), the Effect Factor (EE) and the Exposure Factor (XF). The FF (expressed in days) is associated to the plastic transport and its fragmentation and degradation, it represents the residence time of the plastic in the environmental compartments; the EF (expressed in Potentially Affected Fraction of species (PAF)·m^3·kg^{-1}) deals with the sensitivity of the species to the released pollutant; and the XF (dimensionless) measures the availability of the released plastic in the environmental compartment. The accelerated degradation data are related to bioplastics fragmentation and degradation under controlled conditions, so will feed the FF estimation. Besides, accelerated degradation experiments will also provide information on the dynamics of additives release.

Real samples of bioplastics manufactured from PHA and other additives will be used, and two different experiments are planned:

- Sun degradation with UV light cameras under controlled conditions of temperature and humidity (Sadi et al., 2010).
- Biodegradability in water (Romero et al., 2022) by means of a Rolling Biofilm Bioreactor (RBB), originally designed for biofilm selective growth for bacteria culture, for biodegradation of bioplastics present in water.
-

By combining both methods, the biodegradation study of bioplastics will cover different environmental compartments. Real samples of bioplastics will be placed in the RBB and their biodegradability will be studied in contact with bacteria; under controlled temperature conditions and with the type of water previously chosen (salt or fresh) to simulate the different aquatic compartments. Jointly analysing the results of the RBB experiment with those of sun degradation experiment will be key to covering the different degradation environmental compartments of bioplastics.

To evaluate the bioplastics bio- and photodegradation, measurements of its properties (i. e. molecular weight, functional groups, mass losses, …) will be carried out. Chemical techniques will be used to assess changes in functional groups [Proton nuclear magnetic resonance (^{1}H-NMR)], thermal properties [Differential scanning calorimetry (DSC) and Thermogravimetric analysis (TGA)] and molecular weight [Size exclusion chromatography (SEC)] (Sadi et al., 2010).

RESULTS & DISCUSSION

Data on the two accelerated degradation methods for two packaging materials will be presented (i.e. film and tray). The estimation of FF will be possible and the correspondent characterization factor calculated. This information together with the bioplastic leakages estimations will make possible the inclusion of the EoL on the environmental analysis of the bioplastic value chains.

REFERENCES

Bremer, C. (2022). https://www.oecd.org/environment/plastic-pollution-is-growing-relentlessly-as-waste-management-and-recycling-fall-short.htm
Peña, C., et al. (2021). https://doi.org/10.1007/s11367-020-01856-z
Roibás-Rozas, A et al. (2020). https://doi.org/10.1016/j.scitotenv.2020.140893
Romero, M., et al.(2022). https://doi.org/10.1111/1462-2920.15985
Sadi, R. K et al. (2010)https://doi.org/10.1016/J.POLYMDEGRADSTAB.2010.09.003
Wu, Y., & Su, D. (2020). https://doi.org/10.1007/978-3-030-39149-2

Development of methodologies and tools of risk assessment for wastewater and stormwater reuse

L. De Simoni[1], S. Radini[1], A. Foglia[1], M. Sgroi[1], D. J. Magna[1], B. Szelag[2], A. Kiczko[3], A. L. Eusebi[1], F. Fatone[1]

[1] Department of Science and Engineering of Materials, Environment and Urban Planning-SIMAU, Faculty of Engineering, Polytechnic University of Marche, Ancona, Italy
[2] Department of Geotechnics and Water Engineering, Kielce University of Technology, Kielce, Poland
[3] Department of Hydraulic and Sanitary Engineering, Warsaw University of Life Sciences, Warsaw, Poland
(E-mail: *l.desimoni@pm.univpm.it, s.radini@pm.univpm.it, a.foglia@univpm.it, m.sgroi@staff.univpm.it, debora.jaretamagna@phd.unict.it, bartoszszelag@op.pl, adam_kiczko@sggw.edu.pl, a.l.eusebi@staff.univpm.it, f.fatone@staff.univpm.it)*

Abstract
Climate change and environmental degradation increasingly represent a threat to the entire world, and therefore the safe recovery of resources is crucial in order to encourage the use of what is now considered as waste as a real resource. In this context, risk analysis is the main element to ensure the safe reuse of wastewater and grey water. For this purpose, a semi-quantitative approach was followed for risk assessment in wastewater reuse, while a QMRA calculation tool was developed for a quick assessment of the risk of re-use to support stakeholders in making decisions about possible restrictions.

Keywords (maximum 6 in alphabetical order)
FMEA; QMRA; risk assessment; run-off; stormwater management; water reuse.

INTRODUCTION

Water scarcity and water stress are issues of growing concern at international and European level (Delli Compagni et al., 2020). Freshwater availability is getting scarcer due to effects related to climate change issues, like heatwaves or drought periods. Apart from limiting water resources for human consumption, water scarcity implies some environmental impacts such as increasing contaminants concentration and water pollution. Potential contamination sources include also diffuse inputs, such as urban and agricultural run-offs, which may occur during precipitation and flooding events. Extreme rainfall events may impact on sewer overflows and thus on surface water quality, since they may increase bacterial loads and concur in environmental contamination, affecting both human health and ecosystem. Reclaimed wastewater and greywater can contribute to compensate water needs, providing regular supply (Deviller et al., 2020), reducing the exploitation of natural water resources and alleviating the pressures of wastewater treatment plants (WWTP) discharges into sensitive areas. In this context, risk assessment represents a crucial task to ensure health and environmental protection for water reuse applications. Regulatory frameworks are including this aspect, even if detailed procedures are still lacking, especially for alternative sources, such as greywater. The work carried out aimed to face risk assessment, both for wastewater and for run-off water reuse.
Considering wastewater reuse, a semi-quantitative risk assessment has been developed and detailed for a full-scale water reuse system in Italy. Moreover, a specific methodology has been developed for safe stormwater management and reuse of greywater, during the European project WATERUN.

MATERIALS AND METHODS

Risk assessment has been developed according to existing international guidelines, such as Australian Guidelines and WHO Manuals (QMRA 2016).

Table 1. QMRA methodology.

Step	Description	Formulas
1	**Dose-response relationship** (dose of pathogens with which the exposed group enter in contact)	*d = pathogen concentration × log reduction × exposure* *Exposure/event = volume (mL) with which people enter in contact in a single event of exposure during a certain activity*
2	**Probability of infection** (Pinf) related to each event of exposure to the target pathogen	$P_{inf} = 1 - (1-d/\beta)^{(-\alpha)}$ *Beta Poisson model* α,β = dose response constants
3	**Total probability of infection in one year** (of each pathogen)	$P_{inf\,(year)} = 1-(1-P_{inf})^{N}$ 1 activity N=number of exposures/year
4	**Probability of illness** (Pill) in one year	$P_{illness\,(year)} = P_{inf\,(year)}$ × ratio of illness to infection
5	**Disability-adjusted life years (DALYs)**	DALY/year = $P_{illness\,(year)}$ × DALY per case × susceptibility fraction

Risk assessment includes uncertainties, due to not reliable data or lack of information, which might lead to errors in the overall result (WHO, 2016). Data analysis may support the development of a robust dataset, which allows to increase the numerosity but also to include extreme events characterised by lower probability of occurrence, which are more difficult to detect by standard measures. Literature research may also be useful to define typical ranges of concentration and characteristic ratios between parameters, in case local measures are not available, not sufficient or not trustable. Models and analysis, such as multi-criteria decision analysis, fuzzy and stochastic analysis or Monte Carlo based models can help to deal with uncertainty, but their application requires specific skills. Simpler models, such as Failure Mode and Effects Analysis (FMEA) can also be used to assess water systems. FMEA analysis allows to identify the critical parameters that may have an impact on water quality, by comparing the 95th percentile with intervals defined between the lab detection limits and quality standards (ISS, 2019). The approach and the level of detail are strictly dependant from the site-specific characteristics, the available information and the required results. The methodology for risk assessment should thus be flexible and reshaped to be fitted with the specific application in exam.

Wastewater reuse

The water utility ACEA manages the territorial district of ATO2 in Lazio, Italy, and Fregene WWTP was selected to provide safe reclaimed water for irrigation purposes, since the surrounding area is voted to horticultural cultivation. The WWTP is characterised by pre-treatment, biologic CAS process, secondary sedimentation, sand filtration and UV disinfection. Data from the routinary lab analysis for the characterisation of influent and effluent wastewater were acquired, together with information on the design and operative parameters of each unit.

Run-off reuse

In order to support risk assessment for run-off water reuse, an innovative tool for stormwater management, based on a risk-based approach, is being implemented, in the context of the EU project WATERUN. Hence, a python tool (β -version) for QMRA calculation has been developed, which is able to calculate the microbiological risk for specific reuse scenarios (e.g., garden irrigation, toilet flushing) and for three different pathogens (Campylobacter, Rotavirus, Cryptosporidium). Furthermore, a preliminary version of a graphical user interface (GUI) has been created to allow the communication of a stormwater management model (SWMM) outputs with the phyton tool.

RESULTS AND DISCUSSION

Proposed methodology for risk assessment

A detailed and specific methodology for risk assessment has been developed to be implemented in water reuse applications.
The steps detailed for safe wastewater reuse (Figure 1) included a preliminary phase of system description and asset management, where the design and operative parameters of each operative unit were verified and compared with the literature working ranges, in order to define indicators for the resilience of the treatment layout. Then, a phase of data analytics was performed, in order to detect anomalies or critical conditions occurred in the plant. Once all the information was elaborated, risk assessment must be performed. A first semi-qualitative approach has been carried out, with the definition of a risk matrix that included all the hazardous events identified for each unit, according to the evaluations of the previous data analysis. A quantitative approach could be furtherly performed, in case from the previous phase a deeper analysis would be required. In that case, QMRA and QCRA could be performed to evaluate microbial and chemical risks, respectively. After that, control measures and digital support tools could be applied and implemented in the monitoring. Finally, communication and emergency procedures should be implemented.

Figure 1. Proposed methodology for risk assessment.

The presented approach has been followed to perform the risk assessment of Fregene water reuse system. Data from the WWTP has been analysed and the possible hazardous events have been identified. The FMEA has been then implemented, in order to evaluate effluent quality and identify the most critical parameters. A semi-quantitative approach was followed and a risk matrix has been developed. Scores have been attributed to the probability and the severity of each identified hazardous event, according to the results of data analysis, expertise judgement and considering the control measures applied in the plant.

A more detailed approach has been followed to assess the risks for run-off reuse. In order to provide a more quantitative information on the health outcomes from run-off water reuse and since information on pathogens in urban stormwater were available from literature, a quantitative assessment has been developed and implemented into a tool that could support users to perform a QMRA. More in detail, the developed tool allowed to perform QMRA for each pathogen and for each rainfall event that generate overflow (DWA A-118 (2006) guidelines), implementing Monte Carlo analysis for statistical reliability. This tool will provide information about water quality, indication for safe reuse practices and thus restrictions needed in the districts of the urban catchment for reuse or recreational activities after the simulated storm water event. Moreover, this risk-based tool will allow to evaluate the reduction of the health-risk after the implementation of different preventive measures through the application of different log removals.
This tool will enable stakeholders to quickly assess the risk for different activities following weather events and thus make decisions on possible reuse.

Figure 1. GUI interface for QMRA calculation.

REFERENCES

R. Delli Compagni, M. Gabrielli, F. Polesel, A. Turolla, S. Trapp, L. Vezzaro, M. Antonelli, 2020 Risk assessment of contaminants of emerging concern in the context of wastewater reuse for irrigation: An integrated modelling approach, *Chemosphere* 242. https://doi.org/10.1016/j.chemosphere.2019.125185.
G. Deviller, L. Lundy, D. Fatta-Kassinos, 2020 Recommendations to derive quality standards for chemical pollutants in reclaimed water intended for reuse in agricultural irrigation, *Chemosphere* 240. https://doi.org/10.1016/j.chemosphere.2019.124911.
World Health Organization, 2016 Quantitative Microbial Risk Assessment: Application for Water Safety Management. https://apps.who.int/iris/handle/10665/246195 (accessed January 10, 2023).
Lucentini L, Achene L, Fuscoletti V, Nigro Di Gregorio F, Pettine P (Ed.). Linee guida per la valutazione e gestione del rischio nella filiera delle acque destinate al consumo umano secondo il modello dei Water Safety Plans. Roma: Istituto Superiore di Sanità; 2014. (Rapporti ISTISAN 14/21).

SPONSORS

COLLABORATORS

With the support from the Department of Research
and Universities from Generalitat de Catalunya,
through SGR ICRA-TECH - 2021 SGR 01283